



An Offset Reflector Antenna with Dual Mode Feed: Effects of Pin Discontinuity on Wideband Cross- Polarization Suppression

Balvant J. Makwana^{1*}, Shahid Modasiya², Langhnoja Namrata V¹, and Keraliya Divyesh R¹.

¹Assistant Professor, EC Department, Government Engineering College, Rajkot, Gujarat, India.

²Assistant Professor, EC Department, Government Engineering College, Gandhi nagar, Gujarat, India.

Received: 30 Dec 2023

Revised: 09 Jan 2024

Accepted: 12 Jan 2024

*Address for Correspondence

Balvant J. Makwana

Assistant Professor,

EC Department,

Government Engineering College,

Rajkot, Gujarat, India

Email: balvantmakwana@iitgn.ac.in.



This is an Open Access Journal / article distributed under the terms of the **Creative Commons Attribution License** (CC BY-NC-ND 3.0) which permits unrestricted use, distribution, and reproduction in any medium, provided the original work is properly cited. All rights reserved.

ABSTRACT

The offset parabolic reflector generates very high cross-polarization due to its structural asymmetry when used with a linearly polarized primary feed. The higher level of cross-polarization in the far-field pattern results in loss of energy in unwanted polarization, which reduces the overall efficiency of the antenna system in many practical applications. To reduce the cross-polarization, asymmetrical higher order mode (TE₂₁) is used along with TE₁₁ with proper magnitude and phase. An oversized cylindrical waveguide horn is used to generate higher-order TE₂₁ mode with odd numbers of discontinuities. This dual-mode horn is then used as a primary feed to obtain secondary far-field radiation patterns from the offset reflector antenna. The radiation parameters of offset parabolic reflectors were analyzed for different numbers of pins in feed horns. On the basis of the analysis, a feed was designed and tested. The results of the measured and simulated experiments show excellent symmetry. It was possible to reduce cross-polarization over more than 15% of the bandwidth in comparison to an ideal Gaussian feed.

Keywords: Conjugate feed; Cross-polarization; cylindrical feed; Dual mode feed; Offset reflector;

INTRODUCTION

Offset reflector layout calls for strict requirements with high gain and compact size having low F/D ($F/D < 0.5$) for many practical applications. Due to the asymmetry of the offset reflector, the level of cross-polarization is relatively high which is undesired for the majority of applications. Utilizing a dual reflector that meets Mizugutch's [1] requirement could be one way to address the issue and lessen cross-polarization. However, the deployment of a large sub-reflector is highly difficult and might not be acceptable. In order to avoid cross-polarization, a different approach is to employ a single offset reflector with a multimode feed.





Balvant J. Makwana et al.,

Using step discontinuities in cylindrical waveguides to generate higher order mode TM_{11} in appropriate amplitude and phase with TE_{11} , Potter [2] developed the concept of the dual-mode horn. A multimode horn can be used in offset reflectors to create a symmetrical pattern for limited bandwidth as a prime focal reflector. Rudge and Adatia [3] further enhance the concept of a multimode horn. Their feed was referred to as matched feed since it provided the conjugate match to the field in the focal region of offset reflectors. Many researchers later adopted the concept of a conjugate feed or tri-mode feed. Conventional feeds, including dual-mode and corrugated, provide conjugate matches only for the co-polar component. Recently, K. Bahadori and Y. Samii described a tri-mode feed for F/D equal to 0.4 with an offset angle of 90 [4]. By using the same offset configuration, but with modified feeds that have three-pin discontinuities instead of two-pin discontinuities, the same author revisited the problem[5]. S.B. Sharma et.al [6]-[9] have extensively worked on the development of match feeds. Pour et. al [10] have also provided an analytical model for the feeds from offset reflectors. It was observed in the literature survey that matched feeds and the analytical model for offset parabolic reflectors developed by researchers have limitations in cross-polar suppression bandwidth. There has been a report of cross-polar suppression for a single frequency or narrow band. It is very critical to suppress cross-polarization in applications that use the concept of frequency reuse. Thus, the author investigates the effect of pin discontinuity variation on cross-polarization bandwidth to improve performance.

Focal Region Field and Dual Mode Feed

Parabolic offset reflector used for proposed study

In this study, we have chosen the offset reflector with the focal length to diameter ratio (F/D) is 0.5, the offset angle is 55 degrees and the diameter (D) of the projected aperture is equal to 1.2 meter as depicted in Fig. 1. The conventional Gaussian horn is used as a feed at the focal point of the reflector. Such type of feed will result into very small or no cross polarization in theory for symmetric parabolic reflector antenna. When the given feed illuminates the proposed offset reflector aperture, it will produce the secondary radiation pattern as shown in Fig. 2. Here, The cross-polarization field component is quite high, which is about 19 dB down to peak co-polar component.

Focal region field of offset reflector

A minimum cross-polarization level is obtained when the electric field component at the focal region of an offset parabolic reflector is a complex conjugate of the tangential electrical field component at the primary feed aperture. A feed having this property is known as a conjugate feed. To design a conjugate for an offset parabolic reflector antenna, the electric field components in the focal region must be known. Numerous studies have been conducted by researchers to predict electrical field components in the focal region. Bem[11] studied and derived the well-known expressions for the focal region field using PO in simple closed form which can be written as

$$E_x(p, \theta_0) = \frac{2J_1(p)}{p} + \frac{jD \sin \theta_0}{F} \cdot \frac{J_2(p)}{p} \cdot \cos \theta_0 \quad (1)$$

$$E_y(p, \theta_0) = -\frac{jD \sin \theta_0}{F} \cdot \frac{J_2(p)}{p} \cdot \sin \theta_0 \quad (2)$$

Where,

J_1, J_2 is Bessel function of 1st and 2nd order respectively
and θ_0 is offset angle.

Valentino and Toullos[12] verified Bem's results. Similarly, Ingerson and Wong[13] analyzed the beam deviation for offset reflector systems.

As can be seen from expressions (1) and (2), cross-polarization is inversely proportional to F/D, proportional to offset angle, and has an amplitude variation as the second-order Bessel function. A negative sign in (2) indicates a quadrature phase relationship between the cross-polar field and the copolar field.

Dual Mode Feed

We can reduce the level of cross-polarization by adding modes with proper phase and amplitude. This is because these modes have the same characteristics as the cross-polar field in the focal region. So, for dual mode feed having aperture radius 'a', theta (θ) and phi (ϕ) components for far field of primary feed radiation are





Balvant J. Makwana et al.,

$$E_{\theta} = E_{\theta}^{\text{TE}_{11}} + C_{21} E_{\theta}^{\text{TE}_{21}} \quad (3)$$

$$E_{\phi} = E_{\phi}^{\text{TE}_{11}} + C_{21} E_{\phi}^{\text{TE}_{21}} \quad (4)$$

Where,

C_{21} = constant representing power conversion from TE_{11} mode to TE_{21} mode.

The expression for field components of TE and TM modes is obtained from Silver [14].

Design Methodology and Analysis of Dual mode Feed

In the literature, pins, rods, posts, and other discontinuities have been reported to generate higher-order TE_{21} modes. Rudge and Adatiya [3] utilized a single pin to generate TE_{21} mode. Bahaduri and Samii used two pins [4] and three pins [5] in their paper. Sharma and Pujara used 3 pins [7] and also employed a series of pins [8] in their research. To make the feed wideband, the higher-order mode must have the proper magnitude and phase. Hence, it is very pertinent to study the behavior of discontinuities in the form of rods or pins. To study the effect of the number of pins on the various antenna characteristics, a series of simulations have been performed. The proposed feed model to be analyzed in the simulation is shown in Fig. 3. The radius of the input waveguide (r_1), aperture radius (r_2), and length of the input cylindrical waveguide are fixed at 14.3mm, 18mm, and 20mm respectively. These lengths are calculated for the X-band of operation. For the given offset reflector configuration the required magnitude of power in TE_{21} mode is found to be around -10 dB at 10 GHz using Bem's equation. Furthermore, the phase at the aperture should be either -90 degrees or 270 degrees for conjugate matching. The symmetrical pin discontinuity is taken. In our study, we varied the number of discontinuities in the horn from 1 to 13. We focus on odd numbers of discontinuities with the central pin having a maximum length. The desired magnitude can be obtained by changing the diameter and height of the pin discontinuity. Once the desired magnitude is obtained the required phase can be achieved by changing the phase length L_2 . After getting the proper phase and magnitude, the far-field pattern is generated for the chosen band. This field data is given as an input to the offset reflector and cross-polarization will be calculated from the secondary radiation pattern of the reflector.

Effect of the number of pins on S_{11} (Return Loss)

Fig. 4. Shows the variation of the scattering parameter S_{11} [dB] at different frequencies. It is observed that as the number of pins increases, there will be more obstruction of the field and more reflection of signal toward the input port. As a result, S_{11} will be lower for fewer pins and will be higher for more numbers of pins. In general, the more pins, the higher the S_{11} . It is also observed that initially from 9.4GHz to 10.2 GHz there is a linear increase in S_{11} for all the pins. At 10.3 GHz there is a sudden change in S_{11} in all the pins. The reason for increasing S_{11} with frequency is obvious. This is because as frequency increases the wavelength decreases while the size of the discontinuity whether it is 1 or more, will be the same. So as the wavelength decreases there will be more reflection from the discontinuity and this will raise the reflection coefficient. Also, 10.3 GHz is the cutoff frequency of higher order mode TM_{11} for the given waveguide, hence large fluctuation in S_{11} is observed at this frequency.

Effect of Number of Pins on Cross-polarization

For the desired constant magnitude and constant relative phase at the design frequency, the cross-polar suppression ability of the given feed can be studied with reference to the number of pins. The cross-polarization can be obtained from the secondary far-field pattern of the offset reflector antenna which is calculated from PO-based software TICRA's Grasps 10.4. For the desired constant magnitude and constant relative phase at the design frequency, the cross-polar suppression ability of the given feed can be studied with reference to the number of pins. The cross-polarization can be obtained from the secondary far-field pattern of the offset reflector antenna. Which is calculated from PO-based software TICRA's Grasps 10.4. As shown in Fig. 5 and Table I, the variation of the normalized cross-polarization field on an asymmetrical plane (90 degrees) of the offset reflector is around 18 dB down to the peak co-polarization level with a Gaussian feed. Cross-polarization levels of all other feeds with different numbers of pins are compared with cross-polarization offered by Gaussian feeds since theoretically this type of feed should have minimal cross-polarization.



**Balvant J. Makwana et al.,**

We consider cross-polarization suppression below 8 dB for the cross-polarization offered by the Gaussian feed, since many researchers have done analyses using 8 dB improvements. It depends on the type of application where the offset reflector configuration is used. We can make this level -30 dB as well, then bandwidth will decrease. From the cross-polarization curves (Fig. 5) we can see that the cross-polarization suppression caused by single-pin discontinuities is relatively small since this discontinuity can provide field matching to a narrow band of frequency. Increasing the number of pin discontinuities will improve cross-polarization suppression. Consequently, cross-polarization suppression bandwidth increases up to 9 pins. In the feed with 9 pins 16.74 % bandwidth is obtained. If the number of pins is increased further, there is no improvement higher than the improvement caused by 9 pins. This can also be seen and verified using Table I. The reason for wideband operation is based on the use of a number of discontinuities, in the form of an array of pins having different heights, that give constant magnitudes and phases for the required higher-order modes throughout the band. The flatness in magnitude and relative phase is responsible for the wideband operation of the feed. The required mode power is obtained throughout the band because different pins work at different frequencies.

Fabrication and Testing of dual-mode feed

After obtaining satisfactory return loss, magnitude, and phase performance in simulations, the optimized dimensions of the horn are fixed. With these dimensions, it was decided to fabricate the horn antenna with 9 pins as a further increase in pin discontinuity does not improve the cross-polarization suppression in this offset reflector configuration. During the process of fabrication, the accuracy of the optimized dimensions of the horn and more specifically accuracy in the dimensions of the array of 9-pins were of the utmost concern so VMC machining followed by EDM (Electrical discharge machining) is used to make the final prototype of the dual mode feed. After the fabrication of the feed, measurement of all the physical parameters has been done to confirm the accuracy of the fabrication. As the prototype feeds were precisely manufactured, a very small deviation below the tolerance for the X-band was observed.

Testing of the proposed feed for S_{11} was carried out on Agilent's E8363B PNB Vector Network Analyzer (VNA). After obtaining an acceptable S_{11} characteristic, the primary feed radiation pattern measurement of the proposed dual-mode feed was carried out. The testing of feed has been carried out in the Compact Antenna Test Range (CATR). The proposed dual-mode feed was then mounted on the receiver positioner of the facility as displayed in the photograph of Fig. 7. The measurement of radiation patterns for the full X-band is then carried out. The measured and simulated radiation patterns at 9.8 GHz are superimposed and shown in Fig. 8. The dotted pattern represents simulated results while the solid line represents measured results. An excellent match between simulation and measured results is obtained for both planes. The secondary far-field pattern so obtained is illustrated in Fig 9. For comparison, the secondary pattern using simulated feed and measured feed is superimposed. It is evident from the secondary radiation pattern that the proposed dual-mode provides excellent cross-polar field suppression which is 22.9 dB down as compared to the peak of cross-polarization obtained with Gaussian feed. This corresponds to a cross-polarization of -41 dB down from the peak level.

CONCLUSION

The purpose of this study is to reduce the cross-polarization level in the secondary pattern of the offset reflector using odd numbers of discontinuities. By studying the variation of pins, it can be seen that as the number of pins increases, the magnitude of higher-order modes and relative phase responses can be flattened. Consequently, cross-polar bandwidth is improved. Initially, the cross-polar bandwidth increases, but there is no further improvement with more pins. It is therefore necessary to consider the offset reflector configuration when determining the number of pins. The feed was manufactured and tested with 9-pin discontinuities to confirm the analysis. It was possible to reduce cross-polar bandwidth by more than 15%. Also, the peak cross-polar suppression of 22.9 dB compared to the peak of cross-polarization obtained using Gaussian feed is demonstrated at 9.8 GHz





Balvant J. Makwana et al.,

REFERENCES

1. Y. Mizuguch, M. Akagawa, and H. Yokoi, "Offset Dual Reflector Antenna," IEEE International Symposium on Antennas and Propagation, pp. 2-5, October 1976.
2. Y. Mizuguch, M. Akagawa, and H. Yokoi, "Offset Dual Reflector Antenna," IEEE International Symposium on Antennas and Propagation, pp. 2-5, October 1976.
3. P. D. Potter, "A New Horn Antenna with Suppressed Side Lobes and Equal Beam width," Microwave Journal, vol. 6, pp. 71-78, June 1963.
4. A. W. Rudge and N. A. Adatia, "New class of primary-feed antennas for use with offset parabolic-reflector antennas," in Electronics Letters, vol. 11, no. 24, pp. 597-599, 27 November 1975, doi: 10.1049/el:19750456.
5. K. Bahadori and Y. Rahmat-Samii, "Tri-Mode Horn Feeds Revisited: Cross-Pol Reduction in Compact Offset Reflector Antennas," in IEEE Transactions on Antennas and Propagation, vol. 57, no. 9, pp. 2771-2775, Sept. 2009.
6. K. Bahadori, and Y. Rahmat-Samii, "Back-to-Back Reflector Antennas with Reduced Moment of Inertia for Spacecraft Spinning Platforms," IEEE Transactions on Antennas Propagation, vol. 55, no. 10, pp. 2654-2661, October 2007.
7. S. Sharma, D. Pujara, S. Chakrabarty, and V. Singh, "Improving the cross-polar performance of an offset parabolic reflector antenna using a rectangular matched feed," , IEEE Antennas and Wireless Propagation Letters, vol. 8, pp. 513 –516, 2009.
8. S. B. Sharma, D. Pujara, S. B. Chakrabarty, R. Dey and V. K. Singh, "Design and development of a conjugate matched feed for an offset parabolic reflector antenna," in IET Microwaves, Antennas & Propagation, vol. 4, no. 11, pp. 1782-1788, November 2010, doi: 10.1049/iet-map.2009.0391.
9. S. B. Sharma, Dhaval Pujara, S. B. Chakrabarty, and V. K. Singh, "Performance Comparison of a Matched Feed Horn with a Potter Feed Horn for an Offset Parabolic Reflector," IEEE International Symposium on Antennas and Propagation, San Diego, California, USA, July 2008
10. S. Sharma, D. Pujara, S. Chakrabarty, and R. Dey, "Cross-polarization cancellation in an offset parabolic reflector antenna using a corrugated matched feed," IEEE Antennas and Wireless Propagation Letters, vol. 8, pp. 861–864, 2009.
11. Z.Pour and L.Shafai, "A novel dual-mode dual-polarized circular waveguide feed excited by concentrically shorted ring patches," , IEEE Transactions on Antennas Propagation,, vol. 61, no. 10, pp. 4917–4925, Oct 2013.
12. D. J. Bem, " Electric-field distribution in the focal region of an offset paraboloid," Proc. IEEE, vol. 116, no. 5, pp. 679-684, 1969.
13. R. Valentino, and P. P. Toullos, "Fields in the Focal Region of Offset Parabolic Antennas," IEEE Transactions on Antennas Propagation, vol. 24, pp. 859-865, November 1976.
14. P. G. Ingerson and W. C. Wong, "Focal region characteristics of offset fed reflectors," IEEE/AP-S Symposium Digest, 1974, pp. 121-123.
15. S. Silver, Microwave Antenna Theory and Design, 1st ed., Mcgraw-Hill book company, inc. 1949, pp. 134

Table 1 Cross-polarization Suppression due to variation in pins

No of Pins	Frequency of Operation	Bandwidth	Percentage Bandwidth
1-Pin	9.9- 10.1 GHz	200 MHz	2%
3-Pin	9.8- 10.7 GHz	900 MHz	8.78 %
5-Pin	9.6-10.6 GHz	1000 MHZ	9.90%
7-Pin	9.4-10.9 GHz	1500 MHZ	14.77%
9-Pin	9.3-11.0 GHz	>1700 MHZ	16.74%
11-Pin	9.3-10.6 GHz	>1700 MHZ	16.74%
13-Pin	9.3-10.8 GHz	1500 MHZ	14.92%





Balvant J. Makwana et al.,

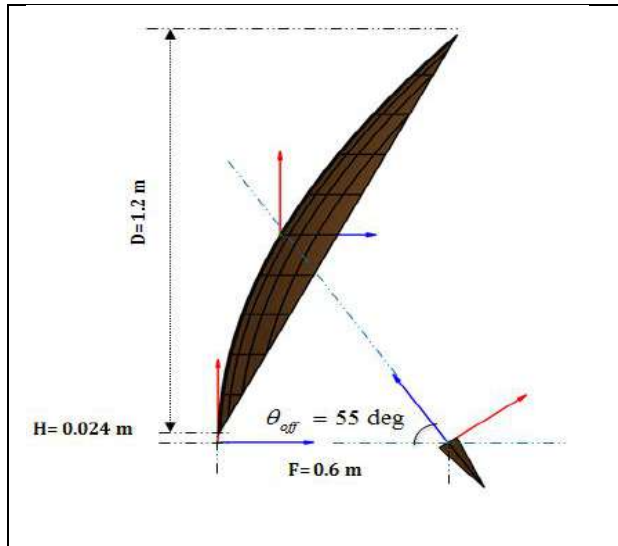


Fig .1 The offset reflector antenna with aperture diameter(D) 1.2m, F/D ratio 0.5 and the offset angle 55 deg.

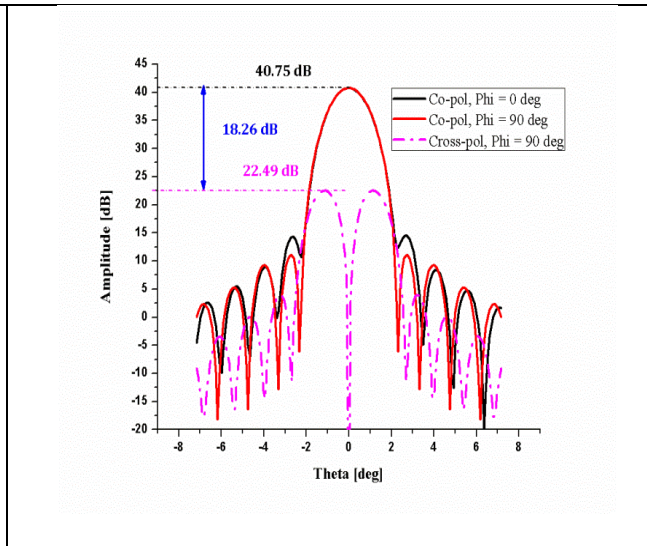


Fig .2 The simulated far-field pattern of the given reflector with conventional Gaussian Feed as an input.

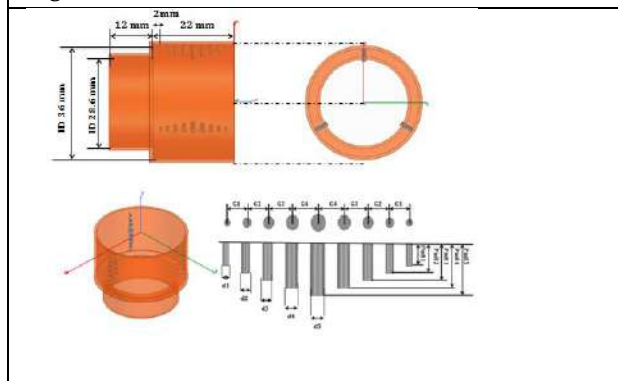


Fig .3 The Geometry of dual-mode feed with expanded discontinuity under consideration.

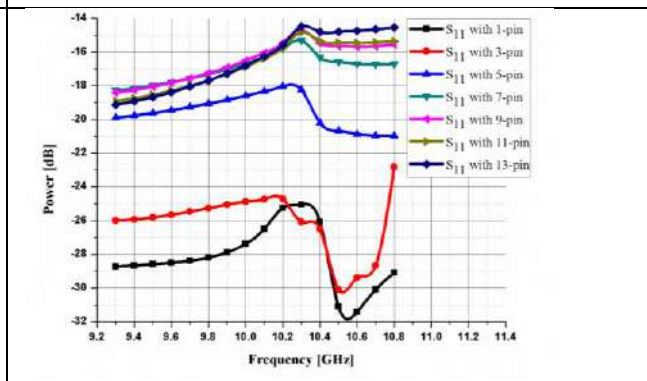


Fig.4.Simulated parametric analysis of variation of S₁₁ with variation in the number of pins in the discontinuity.

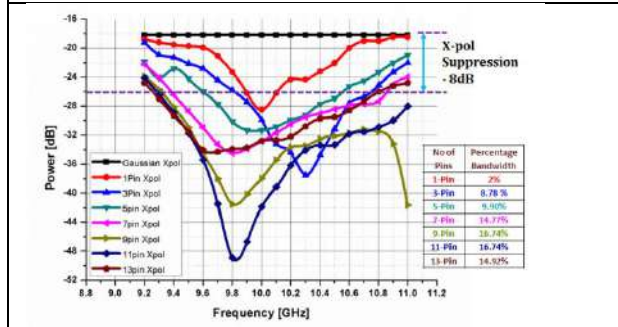


Fig. 5. Comparison of cross-polarization suppression of dual-mode feed with different numbers of pin discontinuity with reference to cross-polarization due to Gaussian feed



Fig. 6. Images of fabricated dual mode horn with and without rectangular to circular transition.





Balvant J. Makwana et al.,

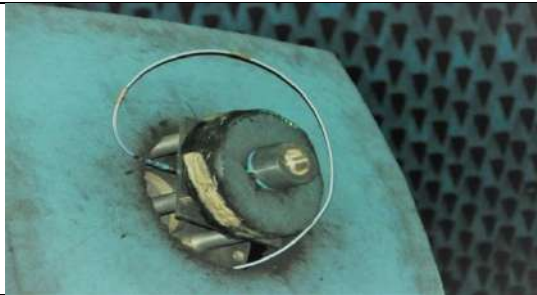


Fig. 7. Image of the dual mode feed mounted on the positioner of compact antenna test range.

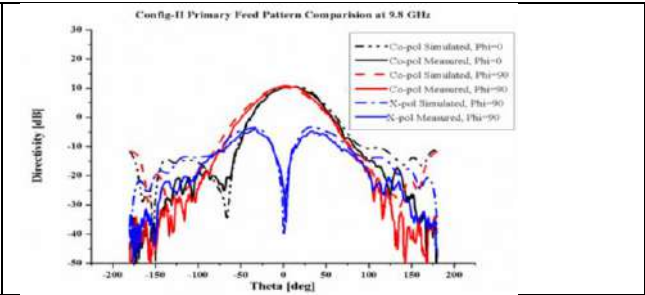


Fig. 8. Comparison of simulated and measured far-field radiation pattern of the proposed feed at 9.8 GHz.

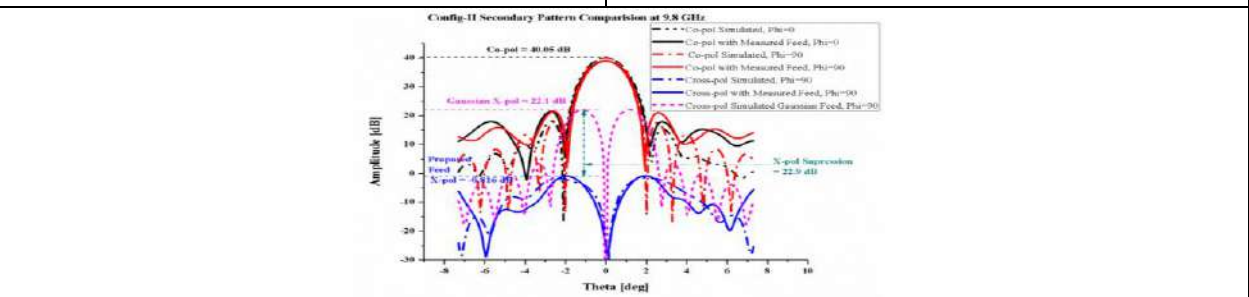


Fig. 9. The comparison of simulated secondary far-field pattern and secondary pattern with measured feed at 9.8 GHz.





Development of Colour Chart Analysis in Mobile Camera System for pH Detection using Litmus Paper

Kainaz Dhanjisha Daruwala¹ and Kamesh Viswanathan Baskaran*

¹Dr. K.C. Patel Research and Development Centre, CHARUSAT, Changa, Gujarat, India.

²P.D.Patel Institute of Applied Sciences, CHARUSAT, Changa, Gujarat, India.

Received: 30 Dec 2023

Revised: 09 Jan 2024

Accepted: 12 Jan 2024

*Address for Correspondence

Kamesh Viswanathan Baskaran

Dr. K.C. Patel Research and
Development Centre, CHARUSAT,
Changa, Gujarat, India.

Email: kameshbaskaran.rnd@charusat.ac.in



This is an Open Access Journal / article distributed under the terms of the **Creative Commons Attribution License** (CC BY-NC-ND 3.0) which permits unrestricted use, distribution, and reproduction in any medium, provided the original work is properly cited. All rights reserved.

ABSTRACT

The present study was conducted in developing the colour chart analysis of pH sensing using mobile camera with standard reference chart provided by manufacture. The pH 7 was set to zero by calibrating using CIE tool of delta E colour difference analysis. Thereby found linear calibration plot of acidic range from pH 7 to 1 having 95.14% confidence and basic range from pH 7 to 14 having 93.18% confidence. The unknown samples from 1 to 14 with 0.5 increment was measured in mobile camera and validated with the conventional pH meter. The study observed that the validation was able to give accuracy of 93% confidence in estimating the unknown pH values in the solution. It was found that the pH detection was semi-quantitative nature. Still other regression models need to be tested in machine learning process for fine tuning and optimization of higher accuracy in pH detection using colour chart.

Keywords: mobile camera; colour chart; pH sensor; CIE; deltaE

INTRODUCTION

pH has been one of the essential parameter was required for biological, agricultural, chemical and environmental applications in both on-field and laboratory analysis [1]. It was used to measure acidity and alkalinity of an aqueous solution. It was required for ensuring the quality of products for protecting environment and promoting human healthcare [2]. In our laboratory practices, the most common methods used for measuring pH are by using pH strips which are made up of litmus paper or using calibrated pH meter, where the value of pH was digitally displayed on pH meter using a glass electrode.



**Kamesh Viswanathan Baskaran and Kainaz Dhanjisha Daruwala****Importance of pH detection**

pH is one of the important parameters to be set in all the processes of biological, chemical and environmental sciences [3]. Accurate pH measurements are essential for understanding and controlling these processes. It is also an essential tool in many research applications, including physics, chemistry, biochemistry, biotechnology, microbiology, and environmental science. Accurate and reliable pH measurements are essential for obtaining valid research results.

1. Environmental Monitoring: pH is a critical parameter in many environmental monitoring applications such as wastewater treatment, aquaculture, and agriculture. Accurate pH measurements are essential to ensure compliance with regulatory requirements and to maintain optimum conditions for plant and animal growth [4].
2. Biomedical Applications: pH is an important parameter in the human body, and variations in pH can indicate diseases such as acidosis or alkalosis. pH sensors can be used in various biomedical applications, including monitoring the pH of body fluids, measuring the pH of urine, and detecting changes in pH during disease progression [5].
3. Industrial Processes: pH is a crucial parameter in many industrial processes, including chemical manufacturing, food processing, and pharmaceuticals. pH control is necessary to ensure consistent product quality and optimize production efficiency.

pH meter

The principle of the pH meter was involved in the measurement of the potential difference between a pH-sensitive electrode and a reference electrode to determine the pH of a solution. The glass electrode consists of a thin, sensitive glass membrane that was selective to hydrogen ions (H^+). When the electrode was immersed in a solution, the H^+ ions in the solution interact with the glass membrane, creating the potential difference between the electrode and a reference electrode. This potential difference was proportional to the pH of the solution. This in-turn was converting it into a pH value using a calibration curve. The reference electrode was typically a silver/silver chloride electrode and provides a stable reference potential that does not change in pH as it changes. To use a pH meter, the glass electrode was first calibrated with pH buffer solutions of known pH values. The pH 7 was calibrated as zero and pH 4 for calibrating the acidic and pH 9 for calibrating basic. This will help to measure the pH values from 1 to 14. Afterwards, the instrument was used to measure the pH of the unknown solution by immersing the electrode into the solution and waiting for the reading to stabilize [6], [7]. The major disadvantage of the system was it requires calibration for each time to change from acidic and basic. Otherwise, the meter reads differently and chances of providing the information wrongly. Since the electrode sensing was measured based on potential differences and user has chance to assume it was correct. This false positive pH values can be avoided completely by each time calibrating the meter or it can be re-checked with litmus paper.

Litmus paper

Litmus paper was considered as one of the chemical indicators to determine pH of the solution. It is made up of litmus dye which is available from lichens like *Rocella tinctoria* [7]. The color change of litmus paper was observed from red to blue as moving towards acidic to basic conditions i.e, if the pH of the solution is lesser than 7, the color changes from yellow to red, at pH 7 having neutral pH paper stays yellow in color and for pH greater than 7, the color changes from yellow to blue. This particular property makes the litmus to do qualitative. However, many researchers were tried in estimating the litmus paper for quantification purposes using camera analysis. However, it was found that the quality of measuring the pH values depended on the camera resolution, image processing and regression models [8], [9]. Thereby it will be help for many non-technical people to do quantitate the pH values based on colorimetric. Where mobile camera can able to do capture the images. Thereby leading to process with image analysis based on the colour quantification as per the International Illumination of Commission (CIE) [10]. Apart from this litmus paper was manufactured by many companies like Merck, Loba Chemie, Sigma-Aldrich, Sisco research Laboratory, etc., which was having varying degree of colour. Hence, one-time colour standardization was required to measure in mobile





Kamesh Viswanathan Baskaran and Kainaz Dhanjisha Daruwala

camera. With these importance of pH, it was necessary to develop quick and portable pH sensors. Which will be helpful for on-field analysis. Here we propose to develop digital mobile camera based pH sensors using embossed white A4 paper as substrate. Using mobile camera as a device to detect pH was one of the progression in smart technology. Using camera, the need of frequent instrument validation can be minimized. Such frequently used device and on the basis of colorimetry, we have tried to develop one time colour chart using mobile camera. The development of pH sensors can highly contribute in the developing sectors like artificial intelligence, deep learning and machine learning.

Experimental design

Fabrication of pH sensor: In our study, the experiment was carried out by litmus paper (Loba Chemie Pvt Ld, India) in circular shape of 0.6 cm diameter using punch hole as pH sensor. Then an A4 paper sheet was cut into 5 cm X 5 cm dimension and patterned into 1 cm diameter with 0.2 cm depth using molded embossing pattern reported by Thu o et al 2014 [11]. Further, the circular shaped litmus paper was placed in the embossed A4 paper as shown in Table 1. This will help us to hold the pH sensor in chamber. The sample solution was prepared from Milli Q water and adjusted to respective pH with the help of 1M HCl (35% of concentrated hydrochloric acid (HCl) Loba Chemie Pvt Ltd, India) for acidic range (pH 1-7) and 1M NaOH (98% sodium hydroxide pellet, Loba Chemie Pvt Ltd, India) solution for basic range (pH 7-14). All the prepared solutions were measured (reading repeated for 9 times) using analytical pH meter (Analab Scientific Instruments Pvt Ltd, India). **pH sensor measurement by mobile camera:** An aliquot sample of 2µl was loaded in the pH sensor and repeated the experiments for 9 times.

Then the image was captured with 20 mega pixel mobile camera (Samsung model A50, Samsung Pvt. Ltd, India) at a distance of 9 cm from the pH sensor. The captured image was processed using adobe photo shop tool. The images were cropped in elliptical shape with the width and height of 68 mm X 68 mm was used as shown in Table 1. The processed images were saved in PNG (portable network graphics) format in order to get transparent background to avoid white interruptions during post image processing. **Post image processing:** The cropped images were processed for RGB colour model values obtained from Image J software (National Institute of Health, USA). Further, it was converted into Lab colour model using colormine online software for human naked eye judgement. The CIE (International Illumination of Commission) Delta E (ΔE - colour difference) values were calculated using equation 1 as reported by Baskaran et al 2021 & 2022 [12], [13].

$$\Delta E = \sqrt{(L_s - L_b)^2 + (a_s - a_b)^2 + (b_s - b_b)^2} \quad (1)$$

RESULTS AND DISCUSSION

Colour Standardization by Mobile camera in pH reference chart

The colour data values obtained from mobile camera for standardized reference chart of pH paper (1 to 14) was shown in Table 2. The colour chart was from yellow to pink for acidic range (7-1) and from yellow to blue for basic range (7-14). The colour was same as the reference chart given by manufacture (Loba Chemie Pvt Ltd, India) as per human naked eye judgement. However, the exact colour values were not provided by the manufacturer. Since, the material was intended to measure by naked eye judgement. Thereby leading to qualitative analysis. However in our study, we can able to quantitate using ΔE measurements (i.e. colour differences from the baseline point) provided by CIE as reported by Baskaran et al 2021 & 2022 [12], [13]. The colour differences for pH 7 was set to zero as baseline point in mobile camera. This practice was similar trend applied in pH meter for quantitative approach. The distance for acidic and basic range can be applied for linear plot for pH estimation approach as shown in Figure 1 and 2. The slope of acidic range was -6.138 ± 0.688 with intercept value of 41.67. The r^2 correlation value was 0.9514. In the aspect of basic range, the slope was 5.947 ± 0.606 with the intercept value of -34.89. The r^2 correlation value was 0.9318. This shows that the >90% confidence to quantitate the pH from the standard reference chart provided by manufacture. The phenomenon of negative slope in acidic range and negative intercept in basic range was due to negative logarithmic of hydronium concentration of Henderson-Hasselbalch equation in pH titration as shown in equation 2.





Kamesh Viswanathan Baskaran and Kainaz Dhanjisha Daruwala

$$pH = pK_a + \log \frac{A^-}{HA} \quad (2)$$

Where $pH = -\log[H_3O^+]$ is the concentration of hydronium ions. pK_a is the dissociation constant of weak acid, $[A^-]$ is the concentration of conjugated base of weak acid and $[HA]$ is the concentration of weak acid [14]. Based on the RGB and Lab data, the chromaticity plot was shown in Figure 3. This was plotted based on XYZ of mathematical function to represent in visible spectrum for understanding the colour distance function. The plot was computed based on equation 3 for x and y coordinates.

$$X = \frac{x}{x+y+z}, Y = \frac{y}{x+y+z} \quad (3)$$

Where X is mix of shorter and longer wavelength, Z is shorter wavelength and Y is luminance [10], [15]. There was separate linearity pattern for acidic range (7-1) in the yellow (~580 nm) to pink (~620 nm) region and basic range was (7-14) in the yellow (~580 nm) to bluish green (~480 nm) region. This was not the same as viewed in naked eye judgement. Thereby, the mobile camera shows different wavelength region was due to computer vision, which was not same as human naked eye. The sensor in mobile camera might plays the unique computer colour vision. Based on the above data, we have experimented in real-time unknown pH samples.

Quantification of Mobile camera in unknown pH samples

The results of unknown pH samples were shown in Table 3. The obtained values were calculated based on the standard reference chart slope and intercept for the accurate quantification. The colour obtained from mobile camera was near similar to standardized reference chart. Except in the case of pH 6 and 7 were underestimating and similar were in pH 9 and 10, where the error was high. This may be due to the effect of light reflection from the material. The material from the standard reference chart was uniform with reflecting coating. In case of our experiment, the pH paper was non-uniform reflecting coating with micro volume of the solution present in it as shown in Table 1. The major reason was litmus paper coated in filter paper, where the capillary action will take place for the solution to react with the litmus. The unknown samples of other pH from 1.5, 2, 2.5, 3.5, 4, 5.5, 6, 6.5, 7.5, 8.5, 9.5, 10.5, 11, 11.5, 12.5, 13 and 13.5 were studied with mobile camera performance in unknown standard reference chart. All the unknown from pH 1 to 14 with 0.5 increment values were initially measured with mobile camera as obtained pH paper values and compared with measured pH meter values as shown in Figure 4. The study was validated with the pH meter and found the 1:1 linearity slope value was 1.03 ± 0.052 of r^2 value of 0.9368. So, in our study we have found overall with the present mobile camera based standardized slope (both acidic and basic range) can estimate with 93% confidence. This shows the pH paper was not exactly qualitative, instead it was semi-quantitative approach for this type of pH manufacturer. Hence it can be tested for other various models for the purpose of artificial intelligence (AI), deep learning (DL) and machine learning (ML) for fine tuning and optimization process using various methods.

The advantage of the above was in the area of image processing with the help of classification and segmentation of image pixels. But the disadvantage on the resolution of the image [16]-[18]. Apart from this, the chromaticity plot has major controlling area for the chromophore reflection on the certain wavelength has to be studied. However, in our study we have used 20 megapixels of mobile camera and image crop resolution was made to 4,624 mm. There by the mobile camera vision was made uniformly in our study and ability to do linear regression for up to 93% accuracy with compared to pH meter. Certain factors such as varying degree of chromophore reflection on the material was need to be studied for perfecting the linear prediction models. There were other regression models such as ridge, elastic net, lasso, support vector machine, neural network, random forest, Adaboost, gradient boost, and k-nearest neighbor hood. Elsenety et al 2022 has reported use of k-nearest neighbor hood model can able to predict to more accurately than the linear regression [9]. Most of the models need to be tested for the accuracy level in our unknown pH value estimation study.

Unknown samples



**Kamesh Viswanathan Baskaran and Kainaz Dhanjisha Daruwala**

However, our study helpful in on-field analysis. It would be helpful in cost-effective approach in replacing pH meter in most general laboratories. The automation with camera vision will be helpful in developing smart pH sensors technology in environment analysis for various non-trained personnel. The volume required to measure was low and helpful in contributing towards green chemistry in environment.

CONCLUSION

From our study, the mobile camera can be used for pH detection for 93% confidence in estimating the unknown samples with compared to pH meter. Our study showed the linearity calibration plot for acidic and basic pH range was >90% confidence. This shows the manufacturer was reported the pH paper to be used for qualitative. From our study, it turns out to be semi-quantitative using mobile camera and image processing analysis. The detailed study has to be evaluated with other regression models for fine tuning and optimization in machine learning. Thus, helping developing the lifetime colour chart for quantitative purposes using mobile camera for the smarter technologies in various scientific and non-scientific analysis.

ACKNOWLEDGMENT

The authors would like to thank Dr. K.C. Patel Research and Development Centre and P.D. Patel Institute of Applied Sciences, Charotar University of Science and Technology (CHARUSAT) for providing all the facilities to conduct the research. Kainaz Daruwala expresses her gratitude for receiving CHARUSAT PhD Scholar's Fellowship (CPSF) by CHARUSAT and Scheme of developing High quality research (SHODH) by Knowledge Consortium of Gujarat.

REFERENCES

1. S. K. Mishra, B. Zou, and K. S. Chiang, "Wide-Range pH Sensor Based on a Smart- Hydrogel-Coated Long-Period Fiber Grating," *IEEE Journal of Selected Topics in Quantum Electronics*, vol. 23, no. 2, pp. 284–288, 2017, doi: 10.1109/JSTQE.2016.2629662.
2. D. Wencel, T. Abel, and C. McDonagh, "Optical Chemical pH Sensors," *Anal Chem*, vol. 86, no. 1, pp. 15–29, Jan. 2014, doi: 10.1021/ac4035168.
3. M. Yuqing, C. Jianrong, and F. Keming, "New technology for the detection of pH," *J Biochem Biophys Methods*, vol. 63, no. 1, pp. 1–9, 2005, doi: <https://doi.org/10.1016/j.jbbm.2005.02.001>.
4. Y. Yang and Z. D. Deng, "Stretchable sensors for environmental monitoring," *Appl Phys Rev*, vol. 6, no. 1, p. 011309, Mar. 2019, doi: 10.1063/1.5085013.
5. M. T. Ghoneim et al., "Recent Progress in Electrochemical pH-Sensing Materials and Configurations for Biomedical Applications," *Chem Rev*, vol. 119, no. 8, pp. 5248–5297, Apr. 2019, doi: 10.1021/acs.chemrev.8b00655.
6. K. Cheng and D.-M. Zhu, "On Calibration of pH Meters," *Sensors*, vol. 5, no. 4, pp. 209–219, Apr. 2005, doi: 10.3390/s5040209.
7. M. I. Khan, K. Mukherjee, R. Shoukat, and H. Dong, "A review on pH sensitive materials for sensors and detection methods," *Micro system Technologies*, vol. 23, no. 10, pp. 4391–4404, 2017, doi: 10.1007/s00542-017-3495-5.
8. S. D. ; K. Y. ; Y. Y. Kim, " A Smartphone-Based Automatic Measurement Method for Colorimetric pH Detection Using a Color Adaptation Algorithm," *Sensors*, vol. 17, p. 1604, 2017.
9. M. M. Elsenety, M. B. I. Mohamed, M. E. Sultan, and B. A. Elsayed, "Facile and highly precise pH-value estimation using common pH paper based on machine learning techniques and supported mobile devices," *Sci Rep*, vol. 12, no. 1, p. 22584, 2022, doi: 10.1038/s41598-022-27054-5.

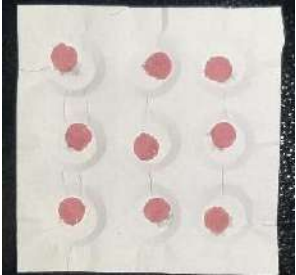







Kamesh Viswanathan Baskaran and Kainaz Dhanjisha Daruwala

10. R. J. Mortimer and T. S. Varley, "Quantification of colour stimuli through the calculation of CIE chromaticity coordinates and luminance data for application to in situ colorimetry studies of electrochromic materials," *Displays*, vol.32,no.1, pp. 35–44, 2011, doi: <https://doi.org/10.1016/j.displa.2010.10.001>.
11. M. M. Thuo et al., "Fabrication of Low-Cost Paper-Based Microfluidic Devices by Embossing or Cut-and-Stack Methods," *Chemistry of Materials*, vol. 26, no. 14, pp. 4230–4237, Jul. 2014, doi: 10.1021/cm501596s.
12. K. V. Baskaran, "Digital camera analysis of dichlorvos by phloroglucinol and quantitate with standard colour chart in environmental water matrices – an approach," *Indian Journal of Chemistry Section A*, vol. 60A, pp. 959–965, 2021.
13. K. V. Baskaran and C. Desai, "One-time standard colour references analysis of hexavalent chromium by 1,5-diphenylcarbazine in environmental water matrices using camera-based approach," *Int J Environ Anal Chem*, p. yet to be online, 2022, doi: 10.1080/03067319.2022.2034799.
14. N. Radić and A. Prkić, "Historical remarks on the Henderson-Hasselbalch equation: its advantages and limitations and a novel approach for exact pH calculation in buffer region," vol. 31, no. 2, pp. 93–98, 2012, doi: 10.1515/revac-2012-0001.
15. G. Sharma, W. Wu, and E. N. Dalal, "The CIEDE2000 color-difference formula: Implementation notes, supplementary test data, and mathematical observations," *Color Res Appl*, vol. 30, no. 1, pp. 21–30, Feb. 2005, doi: <https://doi.org/10.1002/col.20070>.
16. W. William, A. Ware, A. H. Basaza-Ejiri, and J. Obungoloch, "A review of image analysis and machine learning techniques for automated cervical cancer screening from pap-smear images," *Comput Methods Programs Biomed*, vol. 164, pp. 15–22, 2018, doi: <https://doi.org/10.1016/j.cmpb.2018.05.034>.
17. F. S. Aziz et al., "Image Processing System for pH Classification Using Biosensors," in *Proceedings of the 4th Forum in Research, Science, and Technology (FIRST-T1-T2-2020)*, Atlantis Press, 2021, pp. 423–427. doi: 10.2991/ahe.k.210205.071.
18. Niall O' Mahony et al., *Advances in Computer Vision*. Springer International Publishing, 2019. doi: 10.1007/978-3-030-17795-9.

Table 1: pH experiment in sensor and their respective cropped images

Mobile camera images Acidic to Neutral pH	Cropped images for analysis
<p>pH -1</p> 	
<p>pH -4</p> 	





Kamesh Viswanathan Baskaran and Kainaz Dhanjisha Daruwala









<p>pH -7</p> 	
<p>Mobile camera images Basic to Neutral pH</p>	<p>Cropped images for analysis</p>
<p>pH -9</p> 	
<p>pH -12</p> 	
<p>pH -14</p> 	

Table 2: Colour values of Standard Reference Chart of pH paper from Loba Chemie Pvt Ltd, India by mobile camera.

S. Reference pH value	L (R)	a (G)	b (B)	C. chart (ΔE)
1.00	83.44 (244.44 ±12.97)	18.95 (195.47 ±34.48)	1.62 (205.53 ±29.92)	34.44
3.00	85.82 (245.88 ±12.22)	13.24 (205.54 ±30.32)	8.36 (199.39 ±33.03)	26.88





Kamesh Viswanathan Baskaran and Kainaz Dhanjisha Daruwala

5.00	93.75 (249.54 ±9.29)	-1.98 (236.81 ±15.69)	21.14 (196.43 ±33.03)	6.87
6.00	95.75 (250.18± 8.4)	-4.94 (244.28 ±11.77)	21.88 (200.42 ±30.37)	5.13
7.00	95.68 (250.05 ±8.1)	-8.55 (245.61 ±10.56)	32.79 (178.76 ±41.39)	0.00
8.00	88.81 (227.79 ±34.35)	-7.90 (225.91 ±24.43)	26.96 (171.40 ±47.66)	4.91
9.00	88.32 (214.98 ±35.2)	-9.19 (225.99 ±29.62)	14.24 (194.32 ±42.23)	10.74
10.00	80.27 (179.38 ±47.34)	-11.38 (205.21 ±36.07)	4.05 (191.18 ±41.84)	19.61
12.00	83.55 (203.72 ±33.42)	-2.38 (209.58 ±31.05)	0.35 (207.46 ±31.88)	20.32
14.00	73.21 (180.71 ±44.24)	6.44 (176.84 ±46.13)	-12.62 (202.77 ±34.94)	37.88

Note: S-Standard, C-Colour

Table 3: pH value of obtained from mobile camera in samples

M. pH value	L (R)	a (G)	b (B)	C. chart (ΔE)	O. pH value (% accuracy)
1	70.20 (211.44 ±2.87)	19.85 (158.43 ±3.27)	7.11 (159.54 ±3.71)	35.51	1.06 (106%)
3	75.83 (222.43 ±3.34)	13.08 (177.55 ±2.14)	17.73 (154.96 ±2.44)	24.70	2.76 (92%)
5	90.24 (251.53 ±1.65)	4.43 (222.84 ±4.8)	21.73 (185.93 ±5.02)	12.28	4.79 (95.8 %)
6	77.31 (212.47 ±9.16)	4.29 (187.11 ±5.86)	19.11 (155.94 ±6.6)	17.31	3.97 (66.2%)
7	80.16 (215.39 ±5.43)	-2.35 (198.31 ±4.28)	30.82 (141.19 ±5.16)	10.93	5.01 (71.5%)
8	85.72 (225.22 ±5.02)	-4.73 (215.37 ±4.64)	27.52 (162.16 ±6.52)	6.98	8.3 (103.7%)
9	71.45 (164.07 ±6.46)	-11.83 (180.52 ±3.15)	15.18 (147.03 ±4.0)	19.04	10.69 (118.7%)
10	69.47 (158.87 ±6.74)	-9.02 (174.07 ±4.95)	8.22 (154.54 ±5.3)	22.28	11.33 (113.3%)
12	69.63 (159.13 ±9.43)	-6.80 (173.65 ±8.85)	2.81 (164.77 ±6.79)	24.41	11.75 (97.91%)
14	62.44 (151.45 ±7.64)	1.86 (150.15 ±6.5)	-3.54 (157.21 ±5.5)	34.32	13.72 (98%)





Kamesh Viswanathan Baskaran and Kainaz Dhanjisha Daruwala

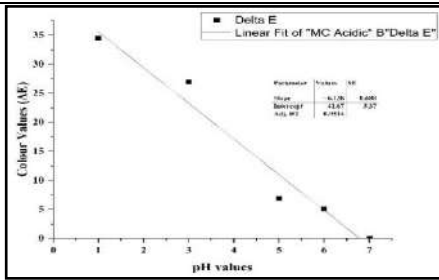


Figure 1-Linear calibration plot for acidic range (pH 7-1)

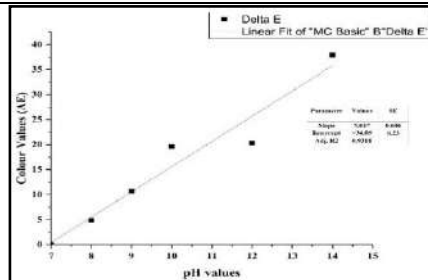


Figure 2-Linear calibration plot for basic range (pH 7-14).

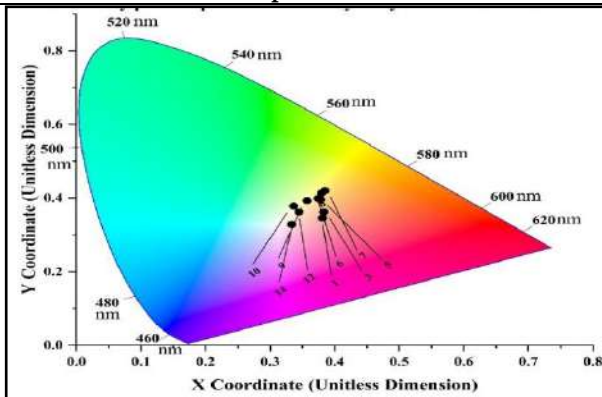


Figure 3- Chromaticity plot for pH standard analysis by mobile camera in CIE 1931

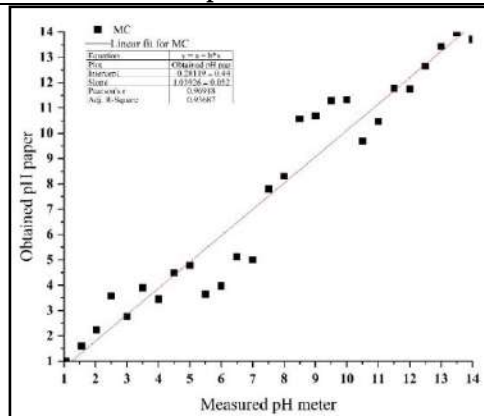


Figure 4- 1:1 Linear Plot between pH Meter and pH paper using camera analysis from unknown samples





Nanostructured Materials in Construction : A Path to High Performance Infrastructure

Purna Vachhani¹, J. R. Pitroda², Indrajit N. Patel³ and Reshma L. Patel⁴

¹First Year, M.Tech. (Civil) Construction Engineering and Management, BVM Engineering College, Vallabh Vidyanagar, Gujarat, India.

²Associate Professor, PG Coordinator Construction Engineering and Management, Civil Engineering Department, BVM Engineering College, Vallabh Vidyanagar, Gujarat, India.

³Professor and Principal, Structural Engineering Department, BVM Engineering College, Vallabh Vidyanagar, Gujarat, India

⁴Assistant Professor, PG Coordinator Environmental Engineering, Civil Engineering Department, BVM Engineering College, Vallabh Vidyanagar, Gujarat, India.

Received: 30 Dec 2023

Revised: 09 Jan 2024

Accepted: 12 Jan 2024

*Address for Correspondence

Purna Vachhani

First Year, M.Tech.

(Civil) Construction Engineering and Management,

BVM Engineering College,

Vallabh Vidyanagar, Gujarat, India.

Email: purnavachhani@gmail.com



This is an Open Access Journal / article distributed under the terms of the **Creative Commons Attribution License** (CC BY-NC-ND 3.0) which permits unrestricted use, distribution, and reproduction in any medium, provided the original work is properly cited. All rights reserved.

ABSTRACT

Nanotechnology is revolutionizing the construction industry by offering innovative solutions to traditional challenges. Nano materials, such as nanoparticles, nanofibers, and nanotubes, are being integrated into concrete, coatings, and composites to enhance their mechanical properties and resistance to environmental factors. These nano coatings can regulate heat and light, reducing power consumption for heating, cooling, and lighting. Self-healing nano materials can extend infrastructure lifespan by repairing cracks and structural damage, reducing maintenance costs and environmental impact. Nanotechnology also offers innovative design possibilities, allowing architects and engineers to create self-cleaning facades, adaptive materials, and responsive surfaces that adapt to environmental changes. This opens new avenues for sustainable and aesthetically pleasing construction practices. Environmental sustainability is a key concern in the construction industry, and nano-engineered materials can reduce the carbon footprint by utilizing recycled materials and enhancing energy efficiency. Nano catalysts can purify air and water, contributing to healthier urban environments. In conclusion, nanotechnology is transforming the construction industry by enhancing performance, sustainability, and design aesthetics. However, challenges related to safety, regulation, and cost-effectiveness must be addressed to ensure responsible integration.





Purna Vachhani *et al.*,

Keywords: Nanotechnology, Construction, Nanoparticles, industry, nanomaterial

INTRODUCTION

We are aware of the process of finding raw materials, meticulously assembling them, and fashioning them into recognizable forms as members of the construction business. As a result, the structure remains unchanged and unresponsive to its surroundings or situations. It functions as designed but deteriorates over time owing to exposure to the environment and use by the project's owners. Routine maintenance is performed to increase its longevity, but its primary goal is to resist the pressures imposed on it until it becomes old-fashioned, at which opinion it is disassembled and replaced to make scope for something new. This has been our societal responsibility for generations, and we have done it well. As a result, construction is far from a revolutionary science or technology; rather, it has experienced significant alterations throughout its history. The modern construction industry is the outcome of advances in science, technology, techniques, and commercial practices. Similarly, nanotechnology is not an entirely novel field of study or technological development. Instead, it represents a continuation of established scientific and technological practices. It's the next logical step in efforts to examine the details of our world at ever-smaller scales.

The Historical Development of Nanotechnology

The history of nanotechnology, sometimes known as the "science of the small," spans several decades and is rich with remarkable developments. It has evolved from its early twentieth-century beginnings into a multidisciplinary field with potentially game-changing applications across many sectors. The idea of influencing matter at the nanoscale dates back to a 1959 presentation by physicist Richard Feynman [1]. In his famous address, "There's Plenty of Room at the Bottom," Feynman imagined a future in which scientists could influence individual atoms and molecules. Even though this concept appeared to be very speculative at the time, it created the theoretical framework for nanotechnology. However, the word "nanotechnology" was not created until 1960 by Japanese researcher Norio Taniguchi [1]. Taniguchi used the phrase to denote precise operations at the molecular and atomic levels. This marked the start of serious scientific research into the nanoscale. In the 1970s and 1980s, we made huge strides in our ability to operate at the nanoscale. Advanced microscopy methods, such as the scanning tunnelling microscope (STM) and the atomic force microscope (AFM), have allowed scientists to examine and manipulate individual molecules and atoms[1].The invention of the STM by Gerd Binnig and Heinrich Rohrer in 1986 earned them the Nobel Prize in Physics and opened up new fields of study at the nanoscale. During this time, researchers began to create nanomaterials such as nanoparticles, nanotubes, and nano wires. Because of their nanoscale size, these materials displayed unusual characteristics and behaviours, paving the way for ground-breaking applications. The formalisation of nanoscience as a distinct field of research occurred in the 1990s.

It became obvious that material characteristics at the nanoscale differed fundamentally from those at the macroscopic scale. This resulted in the formation of nanoscience research centres and academic programmes. The National Nanotechnology Initiative (NNI) was established in the US in 1996[1]. This project was a watershed moment in the evolution of nanotechnology, giving major funds for research and development. Its goal was to promote collaboration among government, academia, and industry to develop nanoscale research and engineering[2]. The twenty-first century saw a rise in nanotechnology research, with a particular emphasis on materials science. Nanomaterials were at the vanguard of this revolutionary surge. Carbon nanotubes, for example, have attracted interest due to their exceptional mechanical and electrical capabilities[3]. Researchers investigated their possible uses in electronics, aircraft, and even medicine as drug delivery vehicles. Nanoparticles are also widely used in a variety of sectors. Because of their unique optical characteristics, gold nanoparticles, for example, have become significant instruments in biological imaging and medication administration. Nanotechnology has had a significant influence on the electronics and computer sectors[3]. The nanoscale was attained through the continuous miniaturisation of transistors and other electronic components, allowing the creation of quicker and more energy-efficient gadgets. Moore's Law, which projected that transistor density on integrated circuits will double every two years, has held





Purna Vachhani et al.,

owing to advances in nanoelectronics. Nanotechnology has resulted in the development of quantum computing, as well as smaller and more powerful electrical devices. Quantum dots, which are microscopic semiconductor particles, have shown potential for usage in quantum bits called “qubits”, which are the essential components of quantum computing. Quantum computers can tackle complicated problems that traditional computers cannot. Nanotechnology has made significant advances in the world of medicine. Liposomes and dendrimers, for example, were designed to transport medications precisely, decreasing adverse effects and enhancing treatment effectiveness. This nanomedicine method has enormous potential for cancer treatment, targeted therapy, and diagnostics[3]. Advanced imaging techniques have also been made possible by nanotechnology. Quantum dots and super paramagnetic nanoparticles, for example, have improved MRI and fluorescence imaging capabilities, enabling earlier illness detection and more accurate diagnosis. As worries about energy sustainability and environmental preservation appeared, nanotechnology became increasingly important in resolving these issues[4]. Nanomaterials like graphene and carbon nanotubes have transformed energy storage and conversion. They have been used to create high-capacity batteries, super capacitors, and efficient solar cells. Nanotechnology provided methods for effective contamination removal in the field of water purification. Pollutants have been filtered using nano engineered membranes and nano particles, making clean and safe drinking water more accessible.

Basics of Nanotechnology

Nanoscience studies phenomena and material operations at atomic, molecular, and macromolecular scales, contrasting with larger scales. It separates itself from traditional scientific disciplines and involves the manipulation of matter at the nanoscale to create useful structures, devices, and systems. Nanometers, which are one billionth of a metre, are approximately one-eighty-thousandth the diameter of a human hair or ten times the diameter of a hydrogen atom[5].

Nanomaterials

The size of the elements plays a crucial role, particularly at the nanoscale, where material properties undergo significant changes compared to larger scales. The specific point at which these changes occur varies depending on the material. In the realm of nanotechnology, nano particles are of paramount interest. These nano particles are minute particles with dimensions typically measured in nano metres (nm), often defined as having at least one dimension less than 200nm. Notably, when semiconducting materials are reduced to nanoscale dimensions, they can exhibit quantum dot behaviour, typically observed at sizes below 10nm. One remarkable consequence of this quantum effect is the ability of materials of different sizes to emit distinct colours when energized, such as by UV light. Among the diverse range of nano particles, carbon nanotubes represent a notable subset.

Properties of nanomaterials

1. High strength, hardness, formability and toughness.
2. More brittle
3. Exhibit super plasticity i.e. they can undergo large deformations without necking or fracture
4. Magnetic moment increases by decreasing particle size
5. Magnetisation and coercivity are higher
6. Melting point is reduced by reducing the size

Almost all the properties depend on the size of the grain – mechanical, electrical, optical, chemical, semiconducting, magnetic etc[5]. Refer Table I. for property changes.

Classification

The number of orientations in which refer Table II. and Fig. 1. for classical and nano-scale phenomena determines[5].

Synthesis

The following Fig. 2. for Nano particle synthesis.





Purna Vachhani et al.,

Methods of preparing nanomaterials

1. Top-down- Bulk material is crushed into fine particles [6] Ex. Ball milling, laser ablation, sputtering, arc plasma, electron beam evaporation, photolithography
2. Bottom-up – The nano materials are prepared by atom-by-atom construction. Bigger size grains are obtained by nucleation and growth[6]. Ex. Chemical vapour deposition, sol-gel method, electro deposition

Concrete

The basic scientific level of concrete study makes extensive use of the various instruments developed for nano-scale research in order to comprehend the structure of concrete. Since concrete is a macro-material whose nano-properties have a significant effect, understanding it at this new level may lead to advances in strength, durability, and monitoring. Common concrete mixes include a natural mineral called silica (SiO_2). The use of nano-silica to increase particle filling in concrete, which in turn led to densification of the micro and nanostructure and improved mechanical properties[7], is one of the improvements acquired from nanoscale study of concrete. The addition of nano-silica to cement-based materials might boost durability by preventing water from penetrating the material and slowing the breakdown of the basic C-S-H (calcium-silicate-hydrate) reaction of concrete caused by calcium leaching in water [8]. Fly ash contributes to the improvement of concrete in several aspects, including increased durability and strength. Importantly, it also reduces the demand for cement, which is beneficial for sustainability. However, it's worth noting that the incorporation of fly ash can slow down the concrete curing process and may result in reduced initial strength compared to conventional concrete.

To address these issues, the introduction of SiO_2 nano particles offers a promising solution. These nanoparticles can partially replace cement in the concrete mixture, leading to an enhancement in both the density and strength of fly ash concrete, particularly during the early stages of its development [5]. Nanoparticles like titanium dioxide (TiO_2) are also added to concrete for its beneficial effects. Nanoparticles of titanium dioxide (TiO_2) are used as sunscreen to block UV rays, and TiO_2 is also used to sterilise paints, cements, and windows by causing powerful catalytic reactions that break down organic pollutants, volatile organic compounds, and bacterial membranes[9][7]. When sprayed on outdoor surfaces, it can thereby minimise airborne pollutants. Furthermore, because it is hydrophilic, it provides self-cleaning capabilities to the exteriors to which it is applied. Carbon nanotubes (CNTs) are another kind of nanoparticle with outstanding capabilities, and studies assessing the benefits of incorporating CNTs into concrete have been undertaken recently. Samples made out of Portland cement's main phase and water may have their mechanical properties improved by adding a small amount of carbon nanotubes (1% wt)[9].

Because of their unique properties, CNTs have been the subject of intensive research into their possible applications across the globe. For instance, they have a Young's modulus 5 times that of steel and a strength 8 times (theoretically 100 times) that of steel, all while having a density just 1/6 that of steel[3]. Sliding telescopically without friction, multi-walled tubes may be either fully or partially electrically conductive (no resistance) in a ballistic manner, depending on their structure. Similarly, thermal conduction is very high in a direction parallel to the tube axis and negligible in a direction perpendicular to the axis. The practice of wrapping concrete with fibers is a widely adopted technique for enhancing the strength of existing concrete structural elements. This method has involved with the incorporation of a fiber sheet matrix containing nano-silica particles and hardeners[3]. Nanoparticles are able to effectively fill and seal minute surface cracks in concrete. In situations when reinforcement is needed, the matrices also provide a strong link between the concrete's surface and the fibre reinforcement. Carbon tows (fibres) and sheets impregnated with the matrix are placed to the prepared concrete surface during the strengthening process. Then, grooved rollers are used to firmly fasten everything into position. Specifically, once cracking has developed, carbon tows considerably improve the concrete's load-bearing capacity. Even more impressive is the matrix's and its interaction with the concrete's resistance to wetting, drying, and scaling (scraping). Despite being subjected to wet/dry cycles or scaling, the maximum load capacity of the material remains unchanged.





Purna Vachhani et al.,

Steel

Since the Second Industrial Revolution in the late 19th and early 20th centuries, steel has been widely available and played a significant role in the construction sector. The European Union produces 185 million tonnes of steel annually, and since steel has many uses outside the building industry (including the automobile industry), it benefits greatly from substantial funding for scientific study. The use of nanotechnology on steel has the potential to benefit the building industry[10]. Steel bridges and towers that endure cyclic loads are particularly vulnerable to fatigue failure. This current design philosophy imposes limitations in the form of reduced permitted stress, shorter than ideal service lives, and more regular inspections, among others. Because of the impact on structural life-cycle costs and resource efficiency, this is a sustainability and safety issue. Research has revealed that incorporating copper nanoparticles into steel reduces the surface unevenness, hence reducing the number of stress risers and, in turn, fatigue cracking. Improvements in this technology would lead to less monitoring and improved material utilisation in fatigue-prone construction, all of which would increase safety.

Recent research focusing on refining the nano-scale properties of the cementite phase in steel has led to the development of more robust steel cables. These high-strength steel cables find utility not only in automobile tires but also play a vital role in bridge construction and precast concrete tensioning. The introduction of a stronger cable material has the potential to significantly reduce construction expenses and time, particularly in the construction of suspension bridges where these cables span from one end of the structure to the other. High-rise constructions need high-strength joints, which necessitates the use of high-strength bolts. High-strength bolts are classically capable of being quenched and tempered, and their microstructures are made up of tempered martensite. Vanadium and molybdenum nanoparticles have been proven in studies to address the late fracture difficulties related with high-strength fasteners[3]. As a result of the nanoparticles' capacity to mitigate the impact of hydrogen embrittlement and the intergranular cementite phase, the steel's microstructure is improved.

When subjected to unexpected dynamic loads, welds and the Heat Affected Zone (HAZ) close to welds can become brittle and fail deprived of notice, and weld toughness is a serious concern, particularly in seismically active areas. Current research indicates that the addition of nanoparticles of magnesium and calcium to plate steel makes the HAZ grains smaller (approximately 1/5th the size of typical material), resulting in an improvement in weld toughness[2]. Due to the reduced resource demand brought about by increased toughness at welded joints, this is an issue of both sustainability and safety. After all, using less material to maintain allowable stress levels is preferable. Steel has always had to make a significant compromise between strength and ductility, since both are required for modern construction pressures. Safety (especially in seismic zones) and stress redistribution, however, need high ductility. Concerns concerning sustainability and resource efficiency have been raised as a consequence of the increased use of low-strength ductile material at larger scales than would be possible with high-strength brittle material. Due to its high cost, stainless steel reinforcement in concrete buildings has often been reserved for particularly hazardous locations. Whereas standard stainless steel is expensive, MMFX2 steel is a cheaper alternative due to its modified nano-structure that makes it corrosion-resistant[10][3].

Wood

Wood, composed of nanotubes or "nanofibrils" made of lingo cellulosic tissue, has been used by humans since the development of tools and techniques. These nanotubes are twice as strong as steel, and their harvesting could revolutionize sustainable architecture, reflecting nature's evolutionary process[11]. Nanoscale functionality could be added to self-sterilizing surfaces, internal self-repair, and electrical lingo cellulosic devices to provide feedback on product performance and environmental conditions. These discreet sensors could monitor structural stresses, temperatures, moisture content, rot fungi, heat losses, and conditioned air loss. However, current studies in these areas are limited. Wood, with its natural origins, is leading the way in interdisciplinary study and modeling, with successful outcomes in water-resistant coverings and mechanical research on bones. Nanotechnology has the potential to create new products, reduce processing costs, and enter new markets, thereby enhancing the wood industry's capabilities.





Purna Vachhani et al.,

Glass

Nanotechnology is being explored in the application of glass to regulate internal building climate and support sustainability efforts. Titanium dioxide (TiO₂) is used to cover glazing in nano particle form due to its sterilizing and anti-fouling qualities, which catalyze strong reactions and create rain droplets that wash away dirt particles. Fireproof glass is another product of nanotechnology, composed of fumed silica (SiO₂) nano particles that create a rigid and opaque fire shield when heated. Controlling light and heat entering building glazing is crucial for sustainability, as most glass used in construction is on the outside of structures. Nanotechnology studies have shown significant improvements in four key areas of window insulation. Thin film coatings are being developed for passive applications, while thermo chromic technologies are being studied as active solutions. Photo chromic technologies react to variations in light intensity by increasing absorption, and electro chromic coatings use a tungsten oxide layer to darken in response to an applied voltage. These programs aim to reduce the power needed to keep buildings at a comfortable temperature and potentially reduce the energy used by the construction industry. Overall, nanotechnology is promising in improving window insulation and reducing energy consumption in the construction industry.

Coatings

Nanotechnology researchers are developing coatings for various substrates, including concrete, glass, and steel, using methods like Chemical Vapour Deposition (CVD), Dip Coating, Meniscus Coating, Spray Coating, and Plasma Coating. These coatings aim to provide self-healing capabilities through self-assembly. Nanotechnology has also found applications in paints and insulation, with nano-sized cells, cavities, and particles creating narrow thermal conduction pathways. These paints exhibit hydrophobic properties, repelling water from metal pipes, and are used for corrosion prevention beneath insulation. Additionally, they offer protection against saltwater exposure. TiO₂ nano particles are being tested as a coating material for highways worldwide, further demonstrating their potential in self-cleaning coatings for glass[12]. The TiO₂ coating absorbs and degrades organic and inorganic air pollutants via a photocatalytic process. This study raises the fascinating prospect of putting highways to good environmental use[13][2].

Fire Protection and Detection

Spraying a cementitious coating over a steel structure is a common method of adding fire protection. Coatings based on Portland cement are now unpopular because they have to be very thick and brittle in order to attach well, and polymer additives are required to improve adhesion. A new paradigm may be on the horizon, however, since nano-cement (made of nano-sized particles) shows promise as a durable, long-lasting, high-temperature coating[11]. This is accomplished by combining carbon nanotubes (CNTs) with cementitious material to create fibre compounds that can get some of the nanotubes' exceptional features, such as strength[12]. Polypropylene fibres, a cheaper alternative to traditional insulation, are also the subject of research into ways to increase fire resistance. The usage of processors incorporated into each detector head in fire detection systems is pretty well established nowadays. These increase dependability by providing for greater addressability and the detection of false alarms[11]. The future use of nanotechnology through the growth of nano-electromechanical systems (NEMS) might result in entire buildings being networked detectors since such devices are implanted either into components or surfaces[10].

Future Projection of Nanotechnology in Construction

The future of nanotechnology in construction holds immense promise, revolutionizing the way we design, build, and maintain structures. Nanotechnology, which deals with materials and systems at the nanoscale (one billionth of a meter), is poised to address some of the most pressing challenges in the construction industry. One of the most important applications is the development of advanced nano materials with remarkable properties. These materials, such as super-strong and lightweight nano composites, self-healing concrete, and ultra-insulating coatings, will enable the creation of more durable, energy-efficient, and sustainable buildings. Additionally, nanotechnology will play a crucial role in enhancing construction processes through the use of nanobots and smart construction materials that can self-assemble, repair, or adapt to changing conditions. Furthermore, nanosensors embedded in structures will provide real-time data on their structural integrity, helping prevent disasters and reduce maintenance costs. In





Purna Vachhani et al.,

the coming years, nanotechnology is set to reshape the construction industry, leading to safer, more efficient, and environmentally friendly infrastructure projects[14].

Sustainable Construction

Sustainable construction in nanotechnology represents a transformative approach to building practices that harness the power of nanoscale materials and processes to minimize environmental impact and enhance long-term viability. At its core, this emerging field seeks to revolutionize the construction industry by incorporating nano materials with superior strength, durability, and energy efficiency, while simultaneously reducing resource consumption and waste generation[15]. Nanotechnology enables the development of advanced construction materials with remarkable properties, such as self-healing concrete, super-insulating coatings, and pollution-absorbing surfaces. Moreover, nanoscale sensors and monitoring systems can be integrated into building structures to optimize energy usage, detect structural weaknesses, and provide real-time data for efficient maintenance. By embracing nanotechnology, sustainable construction aims to create structures that not only withstand the test of time but also contribute to a greener and more resilient built environment for generations to come[15].

CONCLUSION

1. Nanotechnology has emerged as a transformative force in the construction industry, offering novel solutions to age-old challenges.
2. Nanotechnology is poised to redefine the energy efficiency of buildings.
3. Beyond materials and energy efficiency, nanotechnology also enables innovative design possibilities.
4. Environmental sustainability is a paramount concern in the construction industry, and nanotechnology can play a pivotal role in addressing this challenge.
5. In conclusion, nanotechnology is ushering in a new era of construction, offering unprecedented opportunities to enhance performance, sustainability, and design aesthetics.
6. However, challenges related to safety, regulation, and cost-effectiveness must be carefully addressed to ensure the responsible integration of nanotechnology into construction practices.

REFERENCES

1. W. Zhu, P. J. M. Bartos, and A. Porro, "Application of nanotechnology in construction Summary of a state-of-the-art report," *Mater. Struct. Constr.*, vol. 37, no. 273, pp. 649–658, 2004, doi: 10.1617/14234.
2. A. K. Rana, S. B. Rana, A. Kumari, and V. Kiran, "Significance of Nanotechnology in Construction Engineering," *Int. J. Recent Trends Eng.*, vol. 1, no. 4, pp. 6–8, 2009.
3. A. Srivastava and K. Singh, "Nanotechnology in civil engineering and construction: a review on state of the art and future prospects," *Proc. Indian Geotech. Conf. Kochi*, no. January 2011, pp. 1077–1080, 2011.
4. H. Niroumand, M. F. M. Zain, and M. Jamil, "The Role of Nanotechnology in Architecture and Built Environment," *Procedia - Soc. Behav. Sci.*, vol. 89, pp. 10–15, 2013, doi: 10.1016/j.sbspro.2013.08.801.
5. N. Shah and J. Pitroda, "NanoTech: A New Era in Construction Sector," in *National Conference on Advances in Engineering and Technology(NCAET-2012)*, Kalol Institute of Technology & Research Centre, Kalol, 2012, pp. 1–4.
6. V. K. Ganesh, "International Journal of Software and Web Sciences (IJSWS) Innovations in the Methodology of Usage of Nanomaterials in Civil Engineering Works," pp. 17–24, 2012.
7. M. Ghosal and A. Chakraborty, "The Growing Use of Nanotechnology in the Built Environment: A Review," *IOP Conf. Ser. Mater. Sci. Eng.*, vol. 1170, no. 1, p. 012007, 2021, doi: 10.1088/1757-899x/1170/1/012007.
8. L. Raki, J. Beaudoin, R. Alizadeh, J. Makar, and T. Sato, "Cement and concrete nanoscience and nanotechnology," *Materials (Basel)*, vol. 3, no. 2, pp. 918–942, 2010, doi: 10.3390/ma3020918.





Purna Vachhani et al.,

9. T. Utsev, M. Toryila Tiza, E. Ogunleye, T. Sesugh, V. H. Jiya, and C. Onuzulike, "Nanotechnology and the Construction Industry," NanoEra, vol. 3, no. 1, pp. 1–7, 2023, doi: 10.5152/nanoera.2023.1189977.
10. Z. Ge and Z. Gao, "Applications of nanotechnology and nanomaterials in construction," First Inter. Confer. Construc. Dev. Ctries., pp. 235–240, 2008.
11. C. Mullins-Jaime and T. D. Smith, "Nanotechnology in Residential Building Materials for Better Fire Protection and Life Safety Outcomes," Fire, vol. 5, no. 6, pp. 1–12, 2022, doi: 10.3390/fire5060174.
12. F. Pacheco-Torgal and S. Jalali, "Nanotechnology: Advantages and drawbacks in the field of construction and building materials," Constr. Build. Mater., vol. 25, no. 2, pp. 582–590, 2011, doi: 10.1016/j.conbuildmat.2010.07.009.
13. S. P. D. Thammadi and S. K. Pisini, "Nanotechnology and building construction: Towards effective stakeholder engagement," IOP Conf. Ser. Earth Environ. Sci., vol. 1084, no. 1, 2022, doi: 10.1088/1755-1315/1084/1/012074.
14. Z. V. Pisarenko, L. A. Ivanov, and Q. Wang, "Nanotechnology in construction: State of the art and future trends," Nanotechnologies Constr., vol. 12, no. 4, pp. 223–231, 2020, doi: 10.15828/2075-8545-2020-12-4-223-231.
15. J. Teizer, M. Venugopal, W. Teizer, and J. Felkl, "Nanotechnology and Its Impact on Construction: Bridging the Gap between Researchers and Industry Professionals," J. Constr. Eng. Manag., vol. 138, no. 5, pp. 594–604, 2012, doi: 10.1061/(asce)co.1943-7862.0000467.

Table I.Examples of property changes

	Macroscale	Nanoscale
Copper	Opaque	Transparent
Platinum	Inert	Catalytic
Aluminium	Stable	Combustible
Gold	Solid at room temp.	Liquid at room temp.
Silicon	Insulator	Conductor

Table II. Classical and nano-scale phenomena

Materials	Dimensions	Examples
0D	classical in 0 dimensions, nano in 3 dimensions	Buckyballs
1D	classical in 1 dimension, nano in 2 dimensions	Carbon nanotubes, polymers
2D	classical in 2 dimensions, nano in 1 dimension	Graphene
3D	classical in 3 dimensions, not nano	bulk material

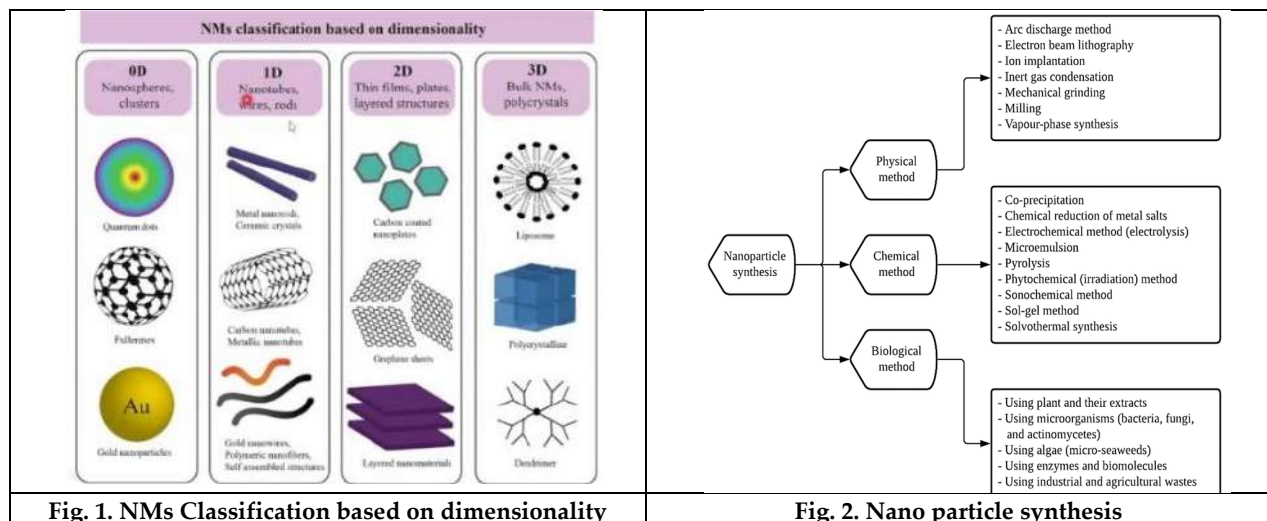


Fig. 1. NMs Classification based on dimensionality

Fig. 2. Nano particle synthesis





Purna Vachhani et al.,

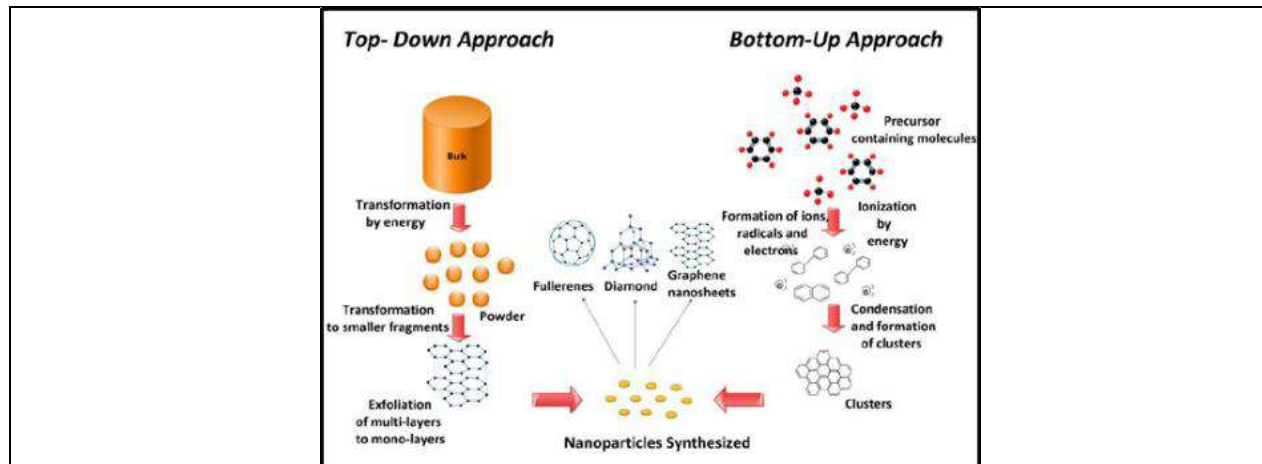


Fig. 3. Methos of preparing nanomaterials





Micro-Pile: New Era for Construction Industry

Divyesh Sanjay Bhai Solanki, J. R. Pitroda, Indrajit N. Patel, Reshma L. Patel

BVM Engineering College, Vallabh Vidyanagar, Gujarat, India.

Received: 30 Dec 2023

Revised: 09 Jan 2024

Accepted: 12 Jan 2024

*Address for Correspondence

Divyesh Sanjay Bhai Solanki

BVM Engineering College,
Vallabh Vidyanagar, Gujarat, India.

Email: sdivyesh283@gmail.com



This is an Open Access Journal / article distributed under the terms of the **Creative Commons Attribution License** (CC BY-NC-ND 3.0) which permits unrestricted use, distribution, and reproduction in any medium, provided the original work is properly cited. All rights reserved.

ABSTRACT

The present article delves into the subject of ground improvement, which is regarded as a creative facet within the field of geotechnical engineering. Engineers use deliberate manipulation of soil conditions rather than depending only on its natural state to fulfil project specifications. This method has the potential to provide cost savings and expedite adoption. In recent years, there have been notable advancements in ground improvement techniques, resulting in a diverse range of approaches available for enhancing soil qualities. The selection of an appropriate methodology is of utmost importance to achieve optimal progress while minimizing exertion. The method of micro-piling is extensively examined and emphasised within this discourse. Micro piles are often used to enhance the load-bearing capacity, mitigate settlement issues, and reinforce pre-existing foundations. The efficacy of piles is thought to be attributed to the frictional resistance between the pile and the earth, as well as the presence of group/network effects. Micro piles are a kind of friction pile that is characterized by its tiny diameter and construction method including drilling and grouting. These piles consist of steel pieces that are securely attached to the surrounding soil or rock using cement grout. In the process of drilling, it is necessary to record the bearing stratum to verify and confirm that the bearing capacity is sufficient. Micro piles do not depend on the capacity of the end-bearing, thereby obviating the need to assess the competence of the rock beyond the depth of bonding. The use of highly versatile mobile drilling equipment enables the efficient installation of micro piles in a wide range of soil conditions, hence facilitating rapid deployment.

Keywords: Construction, Ground Improvement, Micro-Piles, Techniques

INTRODUCTION

In the early 1950s, micro-piles were developed in Italy to address the need for new methods to reinforce historic buildings and monuments that were damaged during World War II. They are utilized to bolster foundations against both static and seismic loads, as well as to provide in-situ reinforcement for slope and excavation stability [1]. Micropiles, a subset of piles, have a diameter of 300 mm or less. The majority of the pile's load is supported by the



**Divyesh Sanjay Bhai Solanki et al.,**

high-capacity steel reinforcement; it is a drilled and grouted non-displacement pile. It is also known as a mini pile. To construct a micropile, a borehole is drilled, reinforcement is placed, and the hole is grouted with cement. The pile can withstand axial and/or lateral loads. The major components of a micropile are reinforcement and cement grout. It is also a replacement pile that has been drilled and grouted and is often reinforced with up to 20% As/Ac [1].

Favorable use of Micro piles

1. Hard strata are available at higher depth
2. Damaged structure
3. Hilly area
4. Uneven settlement
5. Space is less
6. Excavation support

Various Types of micro piles (Classifications)

1. Based on the Design Application
2. Based on the Grouting Method

Based on the Design Application [1]

Case 1: Micropile elements, which experience direct loading, rely on the pile reinforcement to bear the bulk of the imposed load.

Case 2: Micropile components encompass and internally fortify the soil to create a composite reinforced soil structure that exhibits resistance against the imposed load. Refer to Fig. 1. Based on design application.

This particular kind of pile is used for the purpose of transferring structural loads to underlying strata that possess more competence or stability. Additionally, it may be utilized to limit the displacement of the failure plane inside slopes. The primary structural resistance to loads is provided by the steel reinforcement, whereas the geotechnical resistance is principally attributed to the grout/ground bond zone [1].

Based on Grouting Method

The grouting technique is often regarded as the construction control measure that exhibits the highest level of sensitivity about the capacity of the connection between the grout and the ground. The capacity of grout-to-grout varies depending on the technique used for grouting. Refer to Fig. 2. Based on grouting method. Table I. shows types of grouting.

Advantages

1. Micro piles are often utilized to support existing structures when minimum vibration or noise is required.
2. Micro piles may be simply placed when headroom is limited.
3. Micro piles may be built at any angle below horizontal using the same equipment as ground anchoring and grouting.
4. No major access roads or drilling platforms are required.

Disadvantages

1. Underground items or boulders may obstruct or divert the pile.
2. pricey and unsafe
3. Slow and time consuming
4. Corrosion is possible
5. Relatively pricey
6. The hammer is loud, and the vibrations might cause disruption or damage to nearby buildings.





Divyesh Sanjay Bhai Solanki *et al.*,

Area of application [1]

1. Providing support for new loads in crowded locations.
2. Retrofitting for seismic activity.
3. Putting a stop to structural settlement.
4. Uplift/dynamic load resistance
5. Foundation
6. Excavation assistance in limited spaces.

Seismic Retrofit[1]

The use of micropiles for seismic retrofitting of pre-existing roadway infrastructure, particularly in the state of California, has seen a notable surge in recent times. Micropiles provide almost equivalent tensile and compressive capabilities, hence optimising the use of supplementary foundation support components. Micropiles have the potential to be economically viable for retrofitting bridge foundations that are subject to one or more of the following limitations:

1. Limitations on the expansion of footings
2. Limitations on vibration and noise levels
3. The phenomenon of low headroom clearances
4. Challenging accessibility
5. Elevated axial load requirements in both tensile and compressive forces
6. Challenging drilling and driving circumstances
7. The topic of concern is hazardous soil locations.

Refer to Fig. 3. Seismic Retrofit of I-110, North Connector, Los Angeles, California.

Drill Techniques

The drilling technique is chosen to cause the least amount of disruption to the earth and other sensitive structures while yet achieving the desired drilling performance. Drilling fluid is used as a coolant for the drill bit and as a cleansing medium to remove drill cuttings in all drilling procedures. Water is the most often used drilling fluid, followed by drill slurries, polymer, foam, and bentonite. Compressed air is another form of flushing medium [1].

Drilling Rigs

1. Large Track-Mounted Rotary Hydraulic Drill Rig: The bigger drill enables the use of extended lengths of drill rods and casing in regions where overhead constraints do not exist [1].
2. Low Headroom Track-Mounted Rotary Hydraulic Drill Rig: The smaller drill enables operations in low-overhead and difficult-to-reach areas [1].
3. Small Frame-Mounted Rotary Hydraulic Drill Rig: The smallest rig, enabling installation in the most challenging ground conditions. Pile placement with less than 3 m of above clearance is possible by shortening the drill mast and using short jointed pieces of the drill string and micropile reinforcing [1].

Refer to Fig. 4. Drill Rigs.

Micro Piles Installation Steps for Structural Foundations

The following are micro piles installation steps.

1. Temporary casing drilling and/or installation
2. Take off the drill's innermost rod, the bit. Tremie is used to place reinforcing material and grout.
3. Third, take out the makeshift casing and pump in more grout.
4. Full pile (compressible stratum may be replaced by leaving the casing in place).

Refer to Fig. 5. Micro pile installation steps.





Divyesh Sanjay Bhai Solanki et al.,

Critical Literature Review

Chaudhari et al. (2015) Micro piles are a great way to improve bearing capacity and reduce settlements for existing foundations. They are capable of carrying heavy loads, require minimal site space, and can operate independently. 100 mm diameter and 4-meter length micro piles were used to rehabilitate building foundation systems. Combining micro piles with other techniques can meet complex project requirements efficiently and cost-effectively [2]. Haider (2022) Worshippers at the AL-Kadhimin mosque might be in danger due to the leaning minarets. This may be remedied by installing a system of micro piles around the foundation, as suggested by simulation testing, which would strengthen its lateral resistance against loads. The lateral strength of the foundation is proportional to the depth of the piles. The lateral resistance of a foundation increases by 16.1%, 25.5%, and 32.95% for every metre added to its depth over 8 metres. The lateral resistance of the foundation may be increased by 25%, 29%, and 32% by increasing the diameter from 10 cm to 20 cm. The inclination angle has the potential to add 4% points of lateral resistance to the foundation [3]. Yazdani et al. (2013) investigated Kerman, Iran, where soft soils have traditionally hampered the development of high-rise buildings. They discovered that an 18-story reinforced concrete structure was constructed on a micropiled-raft foundation with appropriate bearing capacity but excessive settlements. Using FHWA (2000) criteria, a prototype micropile was constructed and tested. According to the research, micropiled-raft foundations may be a cost-effective engineering solution for high-rise structures erected on soft soils. [4].

According to research conducted by Elsiragy (2021), micro-piles may prevent settlement and foundation tilting in soft soils. These foundations are simple to strengthen, and ground improvement methods have employed them effectively to prevent building collapse. This research analyses the ultimate load capacity of three micro-piles placed using various methods and testing. Greater ultimate load capacity and less settling were observed for completely injected micro-piles with grouting. When compared to pipe micro-piles without grouted bulbs, the ultimate load capacities for those with complete grouting and those with merely grouted bulbs are 13 and 8 times greater, respectively [5]. According to Mahipal et al. (2018) case studies on Damietta Bridge, micro piles are the most cost-effective ground improvement method for retrofitting bridges since they minimise settlement and increase soil bearing capacity [6]. Micropiled rafts' support qualities are studied by Hwang et al. (2017) using model testing and numerical analysis. Micro piles were shown to drastically modify ground failure behaviour and increase bearing resistance. Bearing capacity was found to be increased by 1.5-2.0 times compared to a raft-only footing when micropiles were properly installed [7]. According to Elarabi et al. (2014) micropiles may be employed as foundation and compensating piles for remedial operations, especially in site-constrained settings. They may be rock socketed or soil friction piles, with at least two safety factors for geotechnical and structural designs [8]. Doshi et al. (2011) found that the Multi-helix Micropile method is a cost-effective and environmentally friendly method for retrofitting historical structures damaged during earthquakes. Small steel pipe piling with helical plates is used in this method to screw into the earth without disrupting the surrounding soil.

It is appropriate for cohesionless soil and subterranean structures, increasing soil density and bearing capacity without disturbing adjacent structures. The MH-MP method is economical and silent, making it an environmentally favourable alternative to conventional methods [9]. Talwar et al. (2022) investigated the use of micro foundations in ground enhancement to increase bearing capacity and decrease soil settlements. The frictional resistance between the pile surface and the ground is considered a feasible enhancement mechanism. The foundation underpinning is commonly used for seismic retrofit and settlement prevention. Experimental results show that increasing pile length decreases soil settlement at the same pressure level. Vertical piles or reinforcing rods can increase ground stiffness, ultimately increasing column bearing capacity [10]. Gupta et al. (2022) conducted an experiment to evaluate the efficacy of micropiles as an existing railway track ground enhancement technique. They conducted a comprehensive parametric investigation and tested micropiles on two varieties of soil, clay and sediment. The results indicated that the efficacy of the track improved with decreasing micropile spacing. The study found that the percentage reductions in displacement for 2, 4, and 6 m spacings were approximately 84%, 76%, and 71% of the unreinforced track, respectively. This suggests that micropiles can be a viable alternative to traditional methods for improving railway tracks [11]. Jagadeeshwar et al. (2019) found that micro piles are a versatile ground improvement technique that can effectively address stability problems. When reinforced with bars, the API pile system provides excellent



**Divyesh Sanjay Bhai Solanki et al.,**

compression performance for lateral stability and vertical motions at a reasonable cost. Micropiles can improve the bearing capacity of soil foundations, and their applicability and level of improvement are examined through non-linear finite element analysis. Inclined micropiles are easy to construct, resist axial and lateral loads, and offer high flexibility during seismic conditions [12]. Micro piling and soil nailing are two ground enhancement methods that were recently highlighted in research by Bomic et al. (2016) Micro piles are friction piles with steel parts that are grouted into the bearing soil or rock and have a tiny diameter. They have an operating capacity of up to 250 tonnes and may be erected rapidly utilising mobile drilling equipment. Over-steepening new or existing soil slopes, as well as stabilising unstable natural soil slopes, may be accomplished by the construction method of soil nailing. Reinforcing components, such as solid or hollow system bars, are inserted into the slope. In contrast to hollow bars, which may be drilled and grouted at the same time, solid bars must be inserted into pre-drilled holes before being grouted. Both techniques have been proven effective in increasing bearing capacity and reducing settlements in existing foundations [13]. Elarabi et al. (2014) studied the use of pressure-casting concrete for Micropiles, comparing it to normal gravity casting.

They found that pressure casting increases the load capacity of Micropiles due to increased friction force between the pile and soil. This technique can control soil capacity by increasing soil strength. The pressure-cast pile capacity is equivalent to larger-diameter piles without pressure, reducing construction materials and labour. This makes Micropiles suitable for remote locations like Sudan [14]. Micropiles, which are piles of a smaller diameter utilised around foundations to lessen settlement and enhance soil carrying capacity, were the subject of an experimental investigation by Lekshmi et al. (2020). They prepared two soil samples, one with and one without micro piles, and placed micro piles around the footing. The study found that settlement increases when the load is applied before placing the micropile. The settlement decreases with the number of micropiles, and by increasing the depth of the micropiles and reducing spacing between them, settlement significantly decreases [15]. Mathew et al. (2014) study investigated the performance of single and group micropiles in soft clay under axial loading conditions. The study found that group efficiency increased with spacing from 2D to 3D, but decreased for 4D spacing. Both single and group micropiles significantly improved load-bearing capacity in soft clay. The strength enhancements were observed after pile installation, with the magnitude of the improvement affected by spacing. Group efficiency increased with spacing from 2D to 3D, but decreased with spacing four times the diameter [16].

Case study**Mandalay bay hotel**

More than 500 micropiles were hastily installed to support the Mandalay Bay Resort and Casino's 43-story building in Las Vegas, Nevada. Drilled and grouted over their entire 200-foot length, the piles supported the structure and worked as ground reinforcement, drastically lowering the settling rate. The 600kips load used in the tests was 1.5 times the design load for each pile. It took the construction crew a remarkable 2.5 months to lay 110,000 linear feet of high-capacity piles in a restricted space with barely 20 feet of headroom. Crews working in close quarters were able to finish all 536 stress tests and attachment frames in only four weeks after the final pile was dug. Refer to Fig. 6. Mandalay bay hotel.

The Leaning of the Historical Minaret of Al-Kadhimin Mosque

The Al-Kadhimin mosque is only one of several historical and archaeological landmarks in Baghdad. The mosque has two enormous domes and four minarets, the oldest of which dates back 500 years to the northeast corner. off the holy shrine courtyard, the minaret's recent tilt of around 80 cm off the vertical axis has become apparent. The minaret's overall height is 41.5 m, and its three segments range in height from 18.8 m to 11.5 m. It was constructed using bricks and plaster. Its diameters are 3, 6, and 8 metres, while its lengths are 2, 5, and 6 metres below ground. Refer to Fig. 7. Historical Minaret of Al-Kadhimin Mosque.





Divyesh Sanjay Bhai Solanki et al.,

Rendition of an 18-story Building as part of the Mehr Project

Five residential reinforced concrete structures (Blocks A-E) with a podium construction and a two-story parking garage make up the Mehr project in Kerman, Iran. Refer to Fig. 8. An Artist's Rendition of an 18-story Building as part of the Mehr Project. The building of the project's base occurred in four distinct phases. The initial step was to excavate a 200 x 53 m² space to fulfil the architect's specifications; this was done in the summer to lessen the chance of failure due to wet weather. To prevent groundwater capillary movement and provide a weatherproof building base, a layer of well-graded earth was laid down in the second stage. As a third step, we implanted capping plates in rafts above 346 grouted micro piles to avoid punching failure and guarantee efficient vertical load transfer.

Outcomes from Literature Review

1. To boost bearing capacity and decrease settlements, micro piles have proven useful in many ground improvement applications, especially when reinforcing pre-existing foundations.
2. It is expected that the micropile method will be employed even more often in the future for reinforcing and foundations, and it is now commonly utilized in rehabilitation works.
3. Third, high-rise structures on soft soils may benefit from the economical technical solution that micro-piled raft foundations give.
4. Micro piles are the most cost-effective method for enhancing the quality of the ground. Especially useful for adapting existing buildings, especially in challenging geotechnical situations. They lessen the soil's settling and increase its bearing capacity.
5. The simplicity, efficiency, and low cost/low impact on the environment that characterize the Multi-helix Micropile technique make it stand out from other approaches. Micropiles are the most effective method for modifying an existing structure's base.
6. Multi-helix micropile technique stands out from other approaches because of its ease of use, low cost, and little impact on the surrounding environment. Micropiles are the most effective method for modifying an existing structure's base.
7. The pile length of a Micropile Foundation grows, and soil settling diminishes under the same load. When building on sand sub grades, for example, employing vertical piles or reinforcing rods has several benefits.
8. When the piles are longer and more are driven into the ground, the earth becomes stiffer and the column's ultimate bearing capacity rises.
9. Micropiles can withstand lateral and axial stresses.
10. Micropiles provide great adaptability in seismic environments.
11. With more micropiles, the load may be distributed more evenly, and the settlement can be minimised by increasing the micropiles' depth and decreasing the distance between them.
12. The effectiveness of the group improved from two to three times the diameter of the micropile but decreased to four times the diameter.

CONCLUSIONS

1. In construction projects, micro-piles are a highly useful solution to manage settlement and foundation tilting.
2. These friction piles are small in diameter, drilled, and grouted, making them a dependable way to reinforce existing foundations.
3. Micro-piles are popular in various ground improvement techniques as they enhance structural stability and prevent collapse.
4. The effectiveness of micro-piles is due to the frictional resistance between the pile and the soil, as well as the group/network effects.
5. Micro-piles are versatile and can be efficiently installed in different soil types, making them a valuable asset in geotechnical engineering.
6. Overall, micro-piles are crucial in ensuring the safety and longevity of structures.





Divyesh Sanjay Bhai Solanki et al.,

REFERENCES

1. Paul J. Sabatini, Burak Tanyu, Tom Armour, Paul Groneck, and James Keeley, "Micropile design and construction (reference manual for NHI course 132078)," Fed. Highw. Adm. FHWA-NHI-05-039, Washington, D.C., no. 132078, pp. 1–456, 2005.
2. J. V Chaudhari, J. R. Pitroda, and J. J. Bhavsar, "Micro-Pile: Recent Advances and Future Trends," in International Conference on: "Engineering: Issues, opportunities and Challenges for Development", ISBN: 978-81-929339-1-7, B. S.N. Patel Institute of Technology & Research Centre, Umrah, Ed., Umrah, Bardoli: S.N. Patel Institute of Technology & Research Centre, Umrah, Bardoli, 2015, pp. 167–175.
3. M. H. Haider, "Strengthening AL-Kadhimin Tilted Minaret by Using a System of Micro-piles," Civ. Eng. Archit., vol. 10, no. 5, pp. 1814–1829, 2022, doi: 10.13189/cea.2022.100509.
4. H. Yazdani, M. Momeni, and K. Hatami, "Micropiled-Raft Foundations for High-Rise Buildings on Soft Soils - A Case Study: Kerman, Iran," Seventh Int. Conf. Case Hist. Geotech. Eng., no. May, pp. 1–7, 2013.
5. M. N. Elsiragy, "Filed Comparative Investigation of Loading Test on Micro-Piles Installed with Different Technique – (Case Study)," Eur. J. Eng. Technol. Res. ISSN 2736-576X, vol. 6, no. 4, pp. 88–93, 2021, doi: 10.24018/ejers.2021.6.4.2454.
6. M. Burdak and Amita, "Micro Piling for Retrofitting of Structures-Case Studies," Int. J. Sci. Res., vol. 7, no. 9, pp. 990–992, 2018, doi: 10.21275/ART20191376.
7. T. H. Hwang, K. H. Kim, and J. H. Shin, "Effective installation of micropiles to enhance bearing capacity of micropiled raft," Soils Found., vol. 57, no. 1, pp. 36–49, 2017, doi: 10.1016/j.sandf.2017.01.003.
8. Elarabi and Abbas, "Micropiles for Structural Support," Int. J. Eng. Sci. Res. Technol., vol. 3, no. 12, pp. 205–211, 2014.
9. D. P. Doshi, A. K. Desai, and C. H. Solanki, "Multi Helix Micropile for Retrofitting of Bridge Foundations," Proc. Indian Geotech. Conf. Kochi (Paper No. E-272), pp. 247–250, 2011.
10. M. Talwar, A. K. Agnihotri, and S. Arora, "Experimental Study on Behavior of Micropiles on Sand Resting on Footing," Int. J. Innov. Res. Technol., vol. 9, no. 2, pp. 140–147, 2022.
11. R. K. Gupta and S. Chawla, "Performance Evaluation of Micropiles as a Ground Improvement Technique for Existing Railway Tracks: Finite-Element and Genetic Programming Approach," Int. J. Geomech., vol. 22, no. 3, pp. 1–15, 2022, doi: 10.1061/(asce)gm.1943-5622.0002270.
12. J. Jagadeeshwar, J. Phani Bhushan Reddy, and P. Swathi, "Ground Improvement by Using Micropiles as Foundation," Int. J. Inf. Comput. Sci., vol. 6, no. 6, pp. 303–310, 2019.
13. R. Bomic, Vaikunth K, and Ramesh N, "Micro Piling and Soil Nailing For Ground Improvement," Int. J. Adv. Res. Trends Eng. Technol., vol. 3, no. 7, pp. 1–5, 2016.
14. H. Elarabi and Amin Abbas Soorkty, "Construction of Micropiles Using Pressure Techniques," J. Civ. Eng. Archit., vol. 8, no. 1 (Serial No. 74), pp. 1–8, 2014, doi: 10.17265/1934-7359/2015.01.005.
15. S. Lekshmi, R. Chacko, S. Vinod, T. Jose, and J. G. Philip, "Effect of Micropile on Foundation Settlement," Int. Res. J. Eng. Technol., vol. 7, no. 5, pp. 7375–7378, 2020.
16. S. Mathew and S. Thomas, "A Model Study of Micropile Group Efficiency under Axial Loading Condition," Int. J. Eng. Res. Technol., vol. 3, no. 11, pp. 358–360, 2014, [Online]. Available: <http://www.ripublication.com/ijcer.html>

Table I.Types of grouting

Types	Description
Type A: Gravity Grout	Only sand-cement mortars or plain cement are used to lay the grout under a gravity head here [1].
Type B: Pressure through Casing	As the temporary steel casing is removed, clean cement grout is put into the hole. Injection pressures range between 0.5 and 1.0 MPa. To minimize fracture of the surrounding earth, the pressure is restricted [1].
Type C: Single Global Post Grout	Similarly to the gravity grout pile technique Similar grout is once injected into a sleeve grout pipe at a pressure of at least 1.0MPa before the main grout hardens [1].
Type D: Multiple Repeatable Post Grout	This is accomplished via a modified two-step grouting procedure, similar to Type C, in which 2.0 to 8.0 MPa of pressure is injected [1].



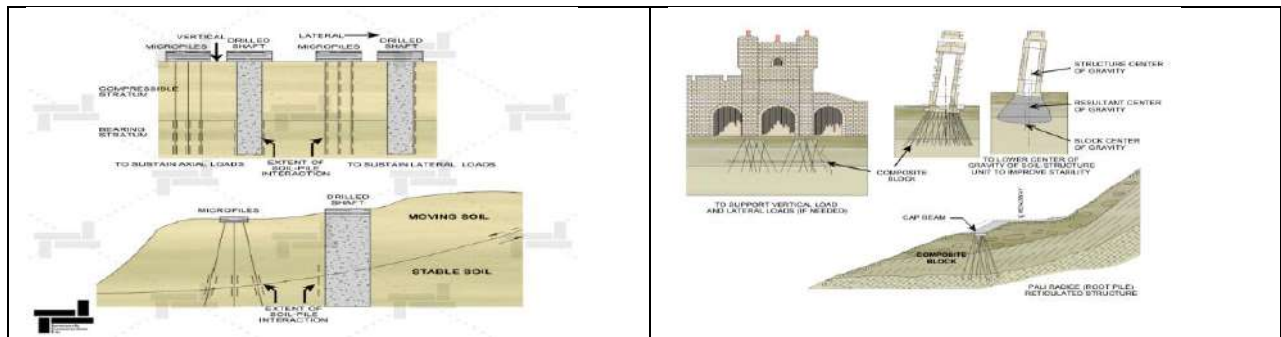


Fig. 1. (a) Micro piles (Directly Loaded)

Fig. 1. (b) Micro piles – Reticulated Pile Network with Reinforced Soil Mass Loaded or Engaged

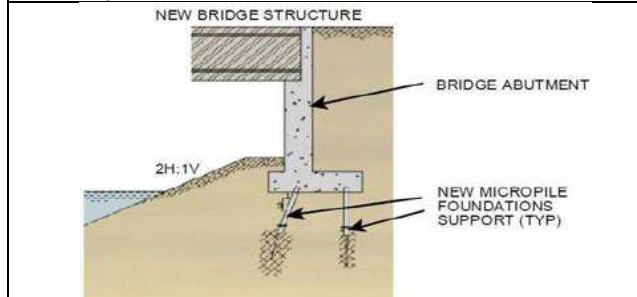


Fig. 1. (c) Micro pile Arrangements

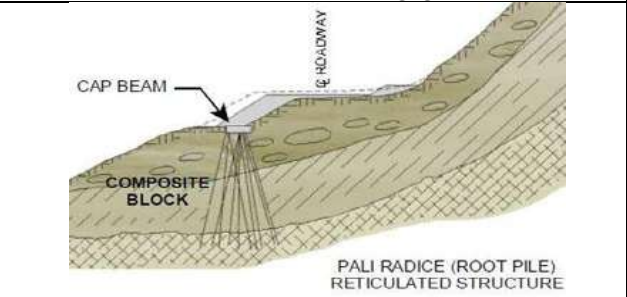


Fig. 1. (d) Micro pile Arrangements

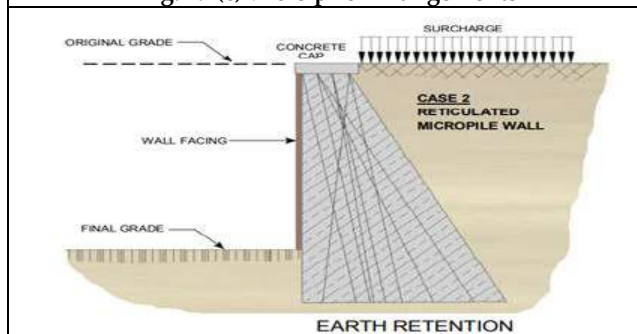


Fig. 1. (e) Micro pile Arrangements

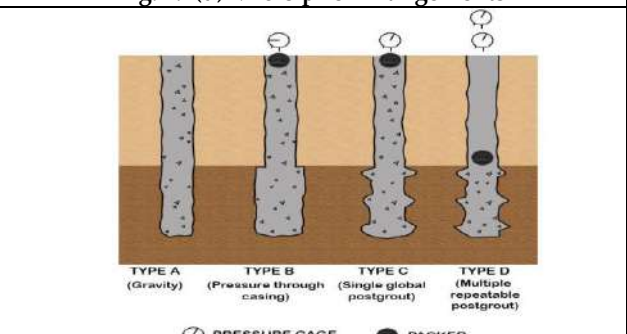


Fig. 2. Based on the Grouting method



Fig. 3. Seismic Retrofit of I-110, North Connector, Los Angeles, California



Fig. 4. Drill Rigs a) Large Track-Mounted Rotary Hydraulic Drill Rig





Divyesh Sanjay Bhai Solanki et al.,



Fig. 4. (b) Low Headroom Track-Mounted Rotary Hydraulic Drill Rig



Fig. 4. (c) Small Frame-Mounted Rotary Hydraulic Drill Rig

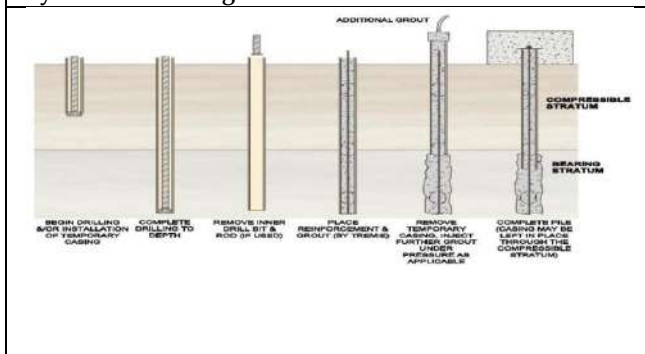


Fig. 5. Micro Pile Installation Steps



Fig. 6. Mandalay bay hotel



Fig. 7. Historical Minaret of Al-Kadhimin Mosque
a) The leaning northeastern minaret

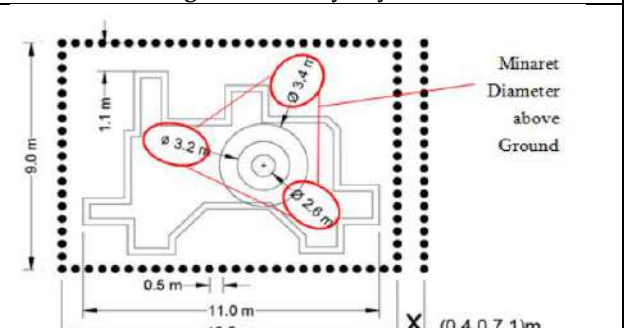


Fig. 7. b) Two-dimensional view of the minaret with proposed micro-pile system,

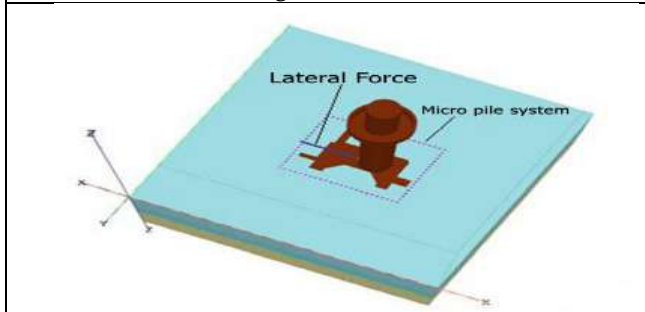


Fig. 7. c) Three-dimensional model of the minaret with proposed micro-pile system



Fig. 8. An Artist's Rendition of an 18-story Building as part of the Mehr Project.





Necessary and Sufficient Conditions for Weak Singularity in Tolman – Bondi Models

Bina Patel*

Department of Mathematical sciences, P D Patel Institute of Applied Sciences, Charusat Changa-388421, Gujarat, India.

Received: 30 Dec 2023

Revised: 09 Jan 2024

Accepted: 12 Jan 2024

*Address for Correspondence

Bina Patel

Department of Mathematical sciences,
P D Patel Institute of Applied Sciences,
Charusat Changa-388421,
Gujarat, India.



This is an Open Access Journal / article distributed under the terms of the **Creative Commons Attribution License** (CC BY-NC-ND 3.0) which permits unrestricted use, distribution, and reproduction in any medium, provided the original work is properly cited. All rights reserved.

ABSTRACT

In the context of the Tolman-Bondi dust collapse model without a cosmological constant, it has been observed that shell crossing singularity consistently takes place when starting from time-symmetric, regularly distributed initial data. This occurrence typically happens in proximity to the central region of the matter configuration. We have determined that a weak shell-crossing singularity arises during end stage of collapse of matter when the external shells of the matter accelerate than the internal shells, provided certain conditions are met. This phenomenon is initiated by specific initial data and consistently occurs close the middling region. When inceptive data are time-symmetric and regular, weak singularity is a common outcome. However, for non-time-symmetric initial information, whether shell crossing occurs or not depends on the primary velocity account. In cases where the initial data is physically sensible, weak singularity occurs near the center of before the depth bounce radius is accomplished. These findings were derived from calculations using Mathematical.

Keywords: symmetric,

INTRODUCTION

Tolman-Bondi model describes the gravitational collapse of spherically symmetric dust matter distribution. Tolman-Bondi model matched to Schwarzschild exterior where all g^j are functions of C^∞ type. Initial density and velocity in the Tolman-Bondi model are functions of radial coordinate r only. The Tolman-Bondi model's collapse is pressureless, which means every particular shell of dust with finite radius will collapse through its Schwarzschild radius. For the homogeneous cloud, all shells of matters are not defined at the same time and, thus there is no weak singularity at all Oppenheimer-Snyder. The proper time for inhomogeneous matter distribution depends on radius (co-moving coordinate) r ; as shell-crossings are not genuine curvature singularities, the nearby shell of matter operates developing momentary density singularity, where Kretschmann curvature scalar cloud blows up, this can





Bina Patel

be removed through the extension of space time. While these singularities are gravitationally weak, they may be locally naked . From the perspective of geodesic comprehensiveness, mathematical continuations of the metric may always be retrieved, in a distributional sense, in the vicinity of the singularity . Curvature invariants and tidal forces also stay finite. This indicates that shell crossings are not legitimate physical singularities in the sense that they indicate the breakdown of the model beyond an individual space like surface where matter flow lines intersect in spherically symmetric geometries. Additionally, they also arise in the context of spherical. in homogeneous. Newtonian. gravitational collapse. Density and pressure in natural objects are enormous, which could be the cause of shell crossing singularity. Shell-crossing singularities are detachable and not a generic singularity in the LTB model. Szekeres and Lum’s thorough research offered the following observations after taking into account both relativistic and Newtonian. spherically. symmetric matter. distribution: (1) Jacobi fields go close to the finite-limit singularity. (2) C^1 transformation can be used to change the boundary region. This gives rise to the possibility that, with appropriate shape selection, a shell-cross of this kind could be avoided within the geometry.

TOLMAN-BONDI SPACETIME

The Tolman-Bondi Model, as previously stated, depicts a spherically symmetric dust matter cloud that is indiscriminate in the radial direction. Tolman-Bondi model is written in synchronous co-moving coordinates so that $g_{ti} = 0 (i = r, \theta, \phi)$, and $g_{tt} = -1$. For matter particles the velocity vector is $u^i \equiv (1, 0, 0, 0)$, which means that coordinate time and proper time t are same for all particles. The cosmological constant Λ is zero. The spherically symmetric Tolman-Bondi class of solution given by metric below ;

$$ds^2 = -dt^2 + e^{2\nu(t,r)} dr^2 + R^2(t,r) d\Omega^2, \tag{1}$$

where $V(t, r)$ and is an arbitrary function and

$$d\Omega^2 = d\theta^2 + \sin^2\theta d\phi^2. \tag{2}$$

The material content of the spacetime is assumed to be dust so that stress-energy tensor,

$$T_{ij} = \rho(t, r) u_i u_j, \tag{3}$$

where $\rho(t, r)$ denoting the energy density and only non-vanishing component of energy-momentum tensor is

$$T_{00} = \rho.$$

For the metric (1), the non-vanishing independent components of Einstein tensor are,

$$G_{00} = \frac{(1 + e^{2\nu}(R'^2 + 2RR'\nu' + 2RR'')) \dot{R}^2 + 2R\dot{R}\dot{\nu}}{R^2(t,r)},$$

$$G_{01} = \frac{2(\dot{R}' + R'\dot{\nu})}{R(t,r)},$$

$$G_{11} = \frac{e^{2\nu}(2\ddot{R}R + \dot{R}^2 + 1 - e^{2\nu}R'^2)}{R^2(t,r)},$$

$$G_{22} = R(t,r) (e^{2\nu}(R'\nu' + R'')) \dot{R}\dot{\nu} + \dot{R} + R(\dot{\nu}^2 - \ddot{\nu}),$$

$$G_{33} = R(t,r) \sin^2\theta (e^{2\nu}(R'\nu' + R'') + \dot{R}\dot{\nu} - \ddot{R} + R(\dot{R}^2 + \ddot{\nu})),$$

where an overhead dot and a prime denote partial differentiation with respect to t and r, respectively. Introducing new auxiliary functions ,





Bina Patel

$$f(t, r) = e^{2\nu} R'^2(t, r), \tag{4}$$

$$F(t, r) = R(t, r) \left(\dot{R}^2 - f \right)$$

This simplifies Einstein's equations greatly to, from equation (4),

$$\dot{R}^2 = \frac{F}{R(t, r)} + f, \tag{5}$$

and from equations (4) and (5),

$$\dot{f} = 0, \tag{6}$$

$$\dot{F} = 0,$$

with the constraint

$$F' = R^2 R' T_{00}. \tag{7}$$

In view of equations (6) and (7), F and f are functions of r only. The metric (1) with $e^{2\nu} = [1 + f(r)] / R'^2$, together with Einstein field equations fully determine the Tolman-Bondi family of solutions. Thus the Tolman-Bondi metric is,

$$ds^2 = - dt^2 + \frac{R'^2(t, r)}{1 + f(r)} dr^2 + R^2(t, r) d\Omega^2.$$

Parametric form of Tolman-Bondi family solutions are given below; Hyperbolic, $f(r) > 0$

$$R(t, r) = \frac{F(r)}{2f(r)} (\cosh \eta - 1), (\sinh \eta - \eta) = \frac{2f(r)^{3/2} (t - a_0)}{F(r)}; \tag{8}$$

Elliptic, $f(r) < 0$

$$R(t, r) = \frac{F(r)}{2f(r)} (1 - \cos \eta), (t - a_0) = \frac{F(r)}{2} (f(r))^{3/2} (\eta - \sin \eta) \tag{9}$$

As mentioned above Tolman-Bondi model contains three types of evolution with the time that is given by equations (8) to (9). The positive expansion rate ($\dot{R}(r, t) > 0$) this all these models leads to big-bang at $t = a_0(r)$.

The density for Tolman-Bondi metric is given by

$$8\pi\rho(t, r) = \frac{F'(r)}{R'(t, r)R^2(t, r)}, \tag{10}$$

and the Kretschmann scalar $K = R^{hjk} R_{hjk}$ is,

$$K = 12 \frac{F^2(r)}{R^6(r, t)} - 8 \frac{F(r)F'(r)}{R^5(t, r)R'(t, r)} - 3 \frac{F'^2(r)}{R^4(t, r)R'^2(t, r)}, \tag{11}$$

(e.g. Bondi 1947), a_0 and F are arbitrary functions of r , and all these functions have physical meaning as in the big-bang region the time $t \geq a_0$, in the big crunch region time $t \leq a_0$, and the local time at $R(t, r) = 0$ is $a_0(r)$





Bina Patel

and $F(r)$ is the Misner-Sharp mass function that is two times of effective mass m . Since $F(r)$ is related to mass function, it must be non-negative everywhere.

$$F(r) \geq 0.$$

The Conditions for Shell-Crossing Singularity

The shell-crossing are defined by,

$$R' = 0 \text{ and } R > 0. \tag{12}$$

For general ($f(r) < 0$) Tolman-Bondi solution can be easily obtained by parametric integrations. From equation (10) we can write,

$$(t \ a_0) = \frac{F}{2} (f)^{3/2} (\eta \ \sin \eta), \tag{13}$$

$$R(t, r) = \frac{F}{f} \sin^2 \frac{\eta}{2}.$$

Where $0 < \eta \leq \pi$ (elliptic), and a_0 is an arbitrary constant of integration that can be fixed with initial data. We can fix $a_0(r)$ with initial data $\dot{R}(0, r) \equiv \dot{r} = a_0(r)$. Therefore equation (13) becomes,

$$a_0 = \frac{F}{2} (f)^{3/2} (\eta_0 \ \sin \eta_0), \tag{14}$$

from equation (11) and equation 14

$$f(csc^2 \eta / 2 + 1) = \dot{R}^2, \tag{15}$$

and hence,

$$f^{3/2} = \frac{(csc^2 \eta / 2 + 1)^{3/2}}{\dot{R}^3} \tag{16}$$

using (16) we can rewrite the equation (14) at $t = 0$

$$a_0(r) = \frac{F}{2} \frac{(csc^2 \eta_0 / 2 + 1)^{3/2}}{\dot{R}^3} (\eta_0 \ \sin \eta_0), \tag{17}$$

where η_0 is value of η at $t = 0$. Putting this $\dot{R}^3(0, r) = v(r)$ in (17)

$$a_0(r) = \frac{F}{2} v^3 (csc^2 \eta_0 / 2 + 1)^{3/2} (\eta_0 \ \sin \eta_0). \tag{18}$$





Bina Patel

For time symmetric initial data $v(r) = t_0(r) = 0$, which implies $f = \frac{F}{R}$ as $\dot{R}(0, r) = 0$. The radial coordinate is merely a different shell, and we can therefore fix the radial coordinate using the initial area radius coordinate radius,

$$R(0, r) = r, \tag{19}$$

so, equations (13) and (18) get simplified by using

$$f = \frac{F}{r} \text{ at } v(r) = a_0(r) = 0, \text{ and } R(0, r) = r.$$

A shell with initial proper area $4\pi r^2$, will thus collapse to vanishing area radius in a time

$$t_{collapse}(r) = \pi \sqrt{\frac{r^3}{4F}}, \tag{20}$$

the relevant derivative of (20) with respect to r is,

$$t'_{collapse}(r) = \frac{\pi}{4} \left(\frac{3}{r} - \frac{F'}{F} \right). \tag{21}$$

When entire matter collapses to zero radius, the outside shell of matter goes faster than the inside shell of matter, and at some surface, they intersect each other and create a momentary density singularity. The necessary and sufficient condition for shell crossing is function (21) should be a decreasing function of time. That is,

$$t'_{collapse} < 0, \tag{22}$$

In view of (21) the condition on Misner-sharp mass function holds if and only if

$$\frac{F'}{F} > \frac{3}{r}. \tag{23}$$

This is the shell-crossing condition on mass and physical radius when the collapse occurs, physical radius going to zero, and mass function going to infinity. For general ($f(r) = 0$) Tolman-Bondi solution can be easily obtained by parametric integrations. In the Tolman-Bondi model, a marginally bound case deserves special examination. This is the boundary between the hyperbolic region and the elliptic region; also, η is not valid here. However, the parabolic region is a special case with the energy function equal to zero. We can consider this as the most straightforward case too. The local time at $R(t, 0) = a_0(r)$, as $t \geq a_0(r)$ is a time of big-bang, and in region $t \leq a_0(r)$, this is a time of big-crunch. Without loss of generality we consider a special case

$$a_c(r) = \sqrt{\frac{4r^3}{9F}}. \tag{24}$$





Bina Patel

The time $a_c(r) = \sqrt{\frac{4r^3}{9F}}$ is the proper time for the collapse of a spherical shell with an initial radius r , which is always positive. Here we are concerned only with weak shell-crossing singularity, at the point $R(t, r) > 0$ and $R'(t, r) = 0$.

The time when shell-crossing occurs is given by.

$$t = t_s = a_c(1 + a_c \gamma), \tag{25}$$

when the collapse commences, the necessary and sufficient condition for weak singularity is

$$t_s < a_c, \tag{26}$$

This leads to

$$\gamma(r) < 0, \tag{27}$$

i.e.,

$$\frac{F'}{F} > \frac{3}{r}. \tag{28}$$

This is the shell-crossing condition on mass and physical radius in (28), which is exactly the same as the one for the time symmetric $f(r) < 0$ case. From equation (28) for any value of $a_c(r)$, this collapse will give a strong shell-focusing singularity at the center.

Data, Methodology

```
t1 = SessionTime[];
coor = {t, r, \[Theta], \[Phi]};

metric = {{-1, 0, 0, 0},
          {0, -Exp[D[R[t,r],r]/(1+f[r]), 0, 0],
          {0, 0, -(R^2[t,r]), 0},
          {0, 0, 0, -(R[t,r] Sin\[Theta])^2}}};
gup = Inverse[metric];
gama = Table[(1/2) (D[metric[[i, k]], coor[[j]]]
+ D[metric[[j, k]], coor[[i]]]
- D[metric[[i, j]], coor[[k]]]),
            {i, 4}, {j, 4}, {k, 4}];

gamaup = FullSimplify[Table[Sum[gup[[h, k]]
gama[[i, j, k]],
            {k, 4}], {h, 4}, {i, 4}, {j, 4}];
riemannlowhijk = Table[FullSimplify
[(1/2) (D[metric[[h, j]], coor[[i]], coor[[k]]]
+ D[metric[[i, k]], coor[[h]], coor[[j]]]
- D[metric[[h, k]], coor[[i]], coor[[j]]]
- D[metric[[i, j]], coor[[h]], coor[[k]]])
+ Sum[a1=1,4] Sum[b1=a,4]
```





Bina Patel

```

gup[(l)(a1,b1)(l)]((gama[[i, k,a1]
  [Indenting NewLine]gama[[h, j,b1]
-gama[[i, j, a1]] gama[[h, k,b1]]],
  {h, 4}, {i, 4}, {j, 4}, {k, 4});
rik = Table[FullSimplify[Sum[Sum[gup[[h, j]]
  riemannlowhijk[[h, i, j, k]],
  {h, 4}], {j, 4}]], {i, 4}, {k, 4}];
ricci = FullSimplify[Sum[Sum[gup[[i, k]]
  rik[[i, k]], {i, 4}], {k, 4}];
einsteintensorlowik = Table[FullSimplify[rik[[i, k]]
  - (1/2) ricci metric[[i, k]],
  {i,4}, {k, 4}];
uupi = {Exp[- \[Nu][r, t]], 0, 0, 0};
ulowi = uupi.metric;
mlowij = Table[FullSimplify[(\[Rho] + p)
  ulowi[[i]] ulowi[[j]]
  + p metric[[i, j]], {i, 4}, {j, 4}];
einsteintensorlowik == mlowij;
Print["Christoffel Symbols of Second kind are"]
For[h = 0, h <= 3, h++,
  For[i = 0, i <= 3, i++,
    For[j = i, j <= 3, j++,
      If[gamaup[[h, i, j]] != 0,
Print["\[CapitalGamma]up ", h, " low ", i, j,
  " = ", gamaup[[h, i, j]]]]]]]]
Print["The non-zero components of Riemann Tensor are"]
For[h = 0, h <= 3, h++,
  For[i = h, i <= 3, i++,
    For[j = 0, j <= 3, j++,
      For[k = j, k <= 3, k++,
If[Riemann low hijk[[h, i, j, k]] != 0,
Print["R", h, i, j, k, " = ",
  riemannlowhijk[[h, i, j, k]]]]]]]]]]
Print["Non-zero components of Ricci Tensor are "];
For[i = 0, i <= 3, i++,
  For[k = i, k <= 3, k++,
    If[rik[[i, k]] != 0,
Print["R", i, k, " = ", rik[[i, k]]]]]]]]
Print["Ricci Scalar R = ", ricci]
Print["Non-zero components of Einstein Tensor are "];
For[i = 0, i <= 3, i++,
  For[k = i, k <= 3, k++,
If[einsteintensorlowik[[i, k]] != 0,
Print["G", i, k, " = ",
einsteintensorlowik[[i, k]]]]]]]]]]
Print["Non-zero components of m_{ij} are "];
For[i = 0, i <= 3, i++,
  For[j = 0, j <= 3, j++, If[mlowij[[i, j]] != 0,
Print["m_", i, j, " = ", mlowij[[i, j]]]]]]]]]]

```





Bina Patel

```
Print["Non-zero components of Field equations are "];
For[i = 0, i <= 3, i++,
  For[j = 0, j <= 3, j++,
    If[einsteintensorlowik == Mlowij != 0,
      Print[einsteintensorlowik[[i, j]] == Mlowij[[i, j]]]]]]
t2 = SessionTime[];
Print["Time Taken = ", t2 - t1, " Seconds"]
```

A prime and dot are derivative with respect to r and t .

CONCLUSION

We have demonstrated that, although the free. surface approach, which is a purely kinematical study, cannot connect the preliminary information to the shells' motion, it does produce a rather straightforward method for demonstrating the inevitable crossing of shells close to the center. We have demonstrated that eliminating the cosmological. constant will not prevent. shell-crossing. singularities from happening close to the center. This more physical analysis was made possible by reducing Einstein's equations to first. integrals of. motion. It has been demonstrated that there are several necessary and sufficient conditions under which a lack of cosmological constant arises in the shell-crossing singularity of the Tolman-Bondi model. This can explaining by fact that if $t'_{collapse} < 0$

then $\frac{F'}{F} > \frac{3}{r}$ then weak singularity will occurs. The Λ repulsion becomes increasingly. irrelevant at late. times, that is, in the strong-field. region, where the criterion for shell crossing becomes analogous to that for neutrally charged dust. collapse in an asymptotically. flat. space time. This is in contrast to Lorentz forces, which become less apparent as collapse proceeds and the area radius of the shells decreases.

REFERENCES

1. Meszaros, On Shell-Crossing in the Tolman Metric, Mon. Not. R. Astr. Soc. Vol. 253, No. 619 (1991).
2. C. Hellaby, Some properties of singularities in the Tolman model, phdthesis, Queen's University at Kingston Ontario, Canada (1985).
3. C. Hellaby and K. Lake, Shell Crossings and the Tolman Model Astrophys. J. Vol.290 No. 381(1985).
4. C. Hellaby and K. Lake, Erratum - the Redshift Structure of the Big-Bang in Inhomogeneous Cosmological Models - Part One - Spherical Dust Solutions Astrophys. J. Vol.282 No. 1(1985).
5. H. Bondi, Spherically symmetrical models in general relativity, Mon. Not. Roy. Astron. Soc., Vol. 107, No. 410 (1947)
6. J. R Oppenheimer and H. Snyder, On Continued Gravitational Contraction, Phys. Rev. Vol.56, No. 455 (1939)
7. K. Lake, Precursory singularities in spherical gravitational collapse, Phys. Rev. Lett. Vol.68, No. 3129 (1992)
8. A.Ori, Inevitability of shell crossing in the gravitational collapse of weakly charged dust spheres, Phys. Rev. D. Vol.44, No.2278 (1991)
9. P. S[6]zekeres and A. Lun, What is a shell-crossing singularity?, J. Austral. Math. Soc. Ser. B. Vol.41 No.167(1999)
10. P. S. Joshi and I. H. Dwivedi, Naked singularities in spherically symmetric inhomogeneous Tolman-Bondi dust cloud collapse. Phys. Rev. D Vol. 47 No.5357.(1993)
11. P. S. Joshi, Gravitational Collapse and Spacetime Singularities Cambridge University Press, Cambridge (2007).
12. P. S. Joshi, Global Aspects in Gravitational and cosmology, Oxford Uni. press Inc., New York (1993). P. S. Joshi, Shell-Crossing in gravitational Collapse, Int. Jour. of Mod. Phy., Vol. 22, No. 5 (2013)
13. R.C.Tolman, Effect of Inhomogeneity on Cosmological Models. Proc. Nat. Acad. Sci., Vol. 20, No. 169 (1934)
14. S. W. Hawking and G. F. R.Ellis, The large scale structure of spacetime, Cambridge Uni. Press, Cambridge. (1973)





Bina Patel

15. S. W. Hawking and G. F. R. Ellis, The Cosmic Black-Body Radiation and the Existence of Singularities in Our Universe. *G.F.R. Astrophys. J.*, Vol. 152, NO. 25 (1968)
16. H. Bondi, Spherically Symmetrical Models in General Relativity, *Monthly Notices of the Royal Astronomical Society*, Vol. 107, No. 5 (1947)08).
17. Hasmani, Abdulvahid and Patel, Bina. Simultaneous Weak Singularity and Strong Curvature Singularity in Tolman-Bondi Model with $k(r)=0$. *International Journal of Computer Applications*.(2020).
18. Hasmani, Abdulvahid and Patel, Bina. Shell-Crossing and Shell-Focusing Singularity in Spherically Symmetric Spacetime, *PRAJNA - Journal of Pure and Applied Sciences* (2020)





Revolutionizing the Concrete Industry : A Comprehensive Review of Robotic Applications

Devang J. Rathod^{1*}, Umang Raichura², J. R. Pitroda², Jagdish M. Rathod¹ and Reshma L. Patel²

¹Department of Electronics Engineering, Birla Vishwakarma Mahavidyalaya Engineering College, Vallabh Vidyanagar, Gujarat, India.

²Department of Civil Engineering, Birla Vishwakarma Mahavidyalaya Engineering College, Vallabh Vidyanagar, Gujarat, India.

Received: 30 Dec 2023

Revised: 09 Jan 2024

Accepted: 12 Jan 2024

*Address for Correspondence

Devang J. Rathod

Department of Electronics Engineering,
Birla Vishwakarma Mahavidyalaya Engineering College,
Vallabh Vidyanagar,
Gujarat, India.



This is an Open Access Journal / article distributed under the terms of the **Creative Commons Attribution License** (CC BY-NC-ND 3.0) which permits unrestricted use, distribution, and reproduction in any medium, provided the original work is properly cited. All rights reserved.

ABSTRACT

The concrete industry has witnessed a significant transformation with the integration of robotic technologies. The concrete industry, a cornerstone of modern construction, has experienced a paradigm shift propelled by the integration of cutting-edge robotic technologies. This review delves into the revolutionary advancements brought about by the application of robotics across different facets of the concrete lifecycle. From the precision-driven construction processes to the maintenance of concrete structures, robotics has ushered in a new era of efficiency, safety, and sustainability. The review begins by examining the integration of robotics in the construction phase, encompassing tasks such as formwork assembly, concrete pouring, and even the erection of intricate structures. Robotic arms and autonomous machinery have redefined the way concrete is placed and shaped, reducing labor-intensive processes and expediting project timelines. Moreover, these technologies have enabled the realization of complex architectural designs that were once deemed challenging to execute. Beyond the construction phase, this review explores how robotics has redefined concrete maintenance and inspection. Drones equipped with advanced sensors and imaging capabilities are employed to assess the structural health of concrete elements, identifying potential issues before they escalate. The incorporation of smart sensors within concrete structures, coupled with robotic devices, allows for real-time monitoring of structural integrity, contributing to enhanced safety and longevity. The review also delves into the realm of concrete recycling, where robotic systems are employed to sort and process waste concrete, transforming it into reusable aggregates. This sustainable approach not only reduces environmental impact but also addresses the growing concern of concrete waste. While the integration of robotics in the concrete industry presents numerous advantages, challenges such as programming complexity, cost





Devang J. Rathod *et al.*,

considerations, and the need for skilled technicians must be addressed. Nevertheless, the trajectory is clear: robotics is poised to play a pivotal role in revolutionizing the concrete industry, fostering innovation, and shaping the future of construction and infrastructure development.

Keywords: Concrete Industry, Robotics, Construction, Maintenance, Inspection, Sustainability, Technology, Automation, Revolution, Efficiency

INTRODUCTION

Drilling anchor bolts, tying rebar, and breaking up old concrete are all repetitious, tough, and risky jobs in construction. So, if there was a method to have a machine execute such tasks without human supervision, it would help to alleviate the labour crisis while also sparing present employees' bodies, not to mention saving money and improving productivity. In the next decade, robotics and automation are likely to play an increasingly prominent role in the construction sector. Because the building environment is dynamic and unstructured, research and development (R&D) in the use of high technology is required. Recent advancements in robotics in other industrial domains have shown a significant opportunity to enhance the automation of complex building operations. Construction equipment, particularly for the concrete sector, is constantly evolving. Contrary to popular belief, an abundance of offers should be treated with care since there is a vast variety of equipment available for the same scope of work, driving construction industry participants to stay current on new technology. Only continual updating enables the optimal equipment selection to be carried out. Regulating concrete processes includes regulating concrete equipment, which includes equipment for producing, transporting, and placing concrete on-site. This paper not only shows the concrete equipment at each step of the concrete cycle but also their features, as a contribution to the creation of selection criteria for concrete equipment at each stage. Concrete construction equipment is critical for construction firms. A construction business may do excellent building work in less time by using high-quality concrete construction equipment. It may therefore reduce labour expenses while increasing earnings by providing excellent building services to its customers more quickly.

With technological advancements, a variety of concrete construction equipment is now available for use by construction businesses to optimize building operations. Some of the most basic and significant kinds of concrete construction equipment are used in building operations. Concrete manufacture, transportation, and placing all rely on highly specialized equipment. The correct use of existing equipment is related to the proper manufacturing, transportation, and placing of concrete on-site. Concrete production equipment plays a significant role since it allows for the mixing of concrete elements in various forms, as well as the mixing of suitable mixes for the needed final qualities of concrete. The variety of manufacturing, transportation, and concrete placing equipment is a consequence of technological advancement and the growth of concrete itself. Constant research in the field of construction materials, notably in the field of concrete, pave the way for new equipment with the goal of optimizing manufacturing, transportation, and concrete placing processes. The history of concrete is given in the context of exhibiting the progress accomplished to date and the obvious development of the equipment and the concrete itself. The growth of concrete and concrete equipment necessitated the need to control the market in terms of safety in use. This chapter describes how concrete and concrete equipment is regulated at the national and European levels. Automation in concrete works includes material manufacturing, concrete mixing, placing, post-laying levelling, surface water removal, and final floor finishing. Control systems for ready mix, precast, pre-stressed, and block plants, as well as ready mix dispatch systems, are increasingly ubiquitous on building sites. Mixer moisture control, colour batching software for solid or liquid dispensers, and so on are examples.





Devang J. Rathod *et al.*,

Need of Study

Robotic technology has made significant progress in recent decades, allowing robots to be used in various human activity sectors. One of the industries that is beginning to adopt robotic technology is construction. The use of robots in construction can automate a wide range of jobs, potentially changing the industry. However, concerns still exist regarding the replacement of humans by robots throughout the building process. Demolition was one of the first applications of robots in construction, and robots are now making processes like breaking down walls, smashing concrete, and collecting trash more efficient. The use of 3D printing in the building industry is also becoming more common, allowing for the printing of complicated, layered components and items to be used in construction, potentially saving time and money across several projects.

Objectives of Study

This article examines the use of robots in construction to increase efficiency, safety, and quality, as well as save time and money. The study includes a literature review and identifies important factors influencing the robotic process, such as the nature of the building and activity.

REVIEW OF LITERATURE

Following are the critical literature reviews based on revolutionizing the concrete industry with robotic applications. Berlin et al. (1992) wrote about the creation of a mobile robot that can be used to finish, grind, and clean concrete during building. There were two parts to the process. In Phase 1, a test car was built to try out ideas for guidance. During the second phase, a test robot with tools was made. To get the best movement and area coverage, different vehicle-tool combinations were modelled and simulated. The writers came to the conclusion that the built-in flexibility of the control system to different devices for finding means that they can use sensors ranging from a cheap rebar detector to a high-tech laser range finder. The modelling package that was made turned out to be a very useful tool when testing different robot setups [1]. In 1993, Alvarsson et al. developed the Rollit Robot which can travel on fresh concrete and vibrate, density, and smooth its surface. The robot has been used for bridge deck repairs and the authors recommend proper compaction and vibration for improved durability [2]. Bryson et al. (2005) gave an overview of two successful efforts in Europe to use robots to manage the process of filling with asphalt and concrete. The process is broken up into separate jobs that can be put together into operations. Robotic systems can do the operations on their own or with help from an engineer. RoboPaver is a self-driving robot that combines the tools and processes of both paving operations into one machine. It also uses an Intelligent Concrete Construction system for remote control of construction operations based on real-time data about materials and machine performance. When RoboPaver is used to build pavement, the prices of labour and machine care go down, there is less downtime on the job site, and the safety and quality of the finished pavement part go up [3].

Maynard et al. (2006) presented the design of a fully autonomous robot for concrete pavement construction. The robot aims to improve quality, productivity, and efficiency while providing safety in hazardous environments. The authors suggested that conventional paving equipment lacks automation and standardized processes, making it unsuitable for hazardous environments. They also noted that autonomous robotics can help reduce operational costs [4]. Daniel Castro-Lacouture et al. (2007) looked at a fully autonomous robot that has all the equipment needed to pave concrete. They compared it to the traditional way of doing things, which involves a lot of hard work, a slip form paving machine, and other equipment. The goal of the study is to compare the two ways of making concrete with modelling tools to find out which one is more productive [5]. Using GPS and laser technologies, Cable et al. did a study in 2009 that looked closely at how well stringless pavers worked. This technology was made by a company that makes concrete pavers and a company that makes machine guiding solutions. It has been used successfully on several earthmoving and grading projects in construction. The main goal of the study was to see how well GPS and laser control guided the concrete slip form paver, making sure the end portland cement sidewalk was straight and the right depth. The results were then compared to those from similar projects in Washington County, Iowa, where string line control was used [6]. Shrivastava et al. (2012) reviewed research on kinematic and dynamic analysis of jaw



**Devang J. Rathod et al.,**

crusher attachments, concluding that kinematic analysis is helpful for improving operating performance and design quality. The paper also explores the background of jaw crusher kinematics for further research[7]. Lee et al. (2012) explored a framework for a new concept that combines robot-supported, systemized deconstruction with conventional methods. They analyzed its potentials and objectives and demonstrated that in the future, buildings can be deconstructed and disassembled in on-site factory-like environments using automated/robotic equipment and Agent-Based Modelling (ABM)[8]. Neudecker et al. (2016) investigated the use of sprayed concrete technology for automating the production of freeform concrete parts. They presented a case study where a factory robot equipped with a concrete spreading tool was used to create a concrete wall. The study examined various spray technologies for shaping concrete elements, as well as the process features of robot-assisted shotcrete applications, surface finish, and accuracy of material application. The authors concluded that spraying concrete with the aid of robots holds great promise for producing freeform concrete parts[9]. Lublasser et al. (2016) In order to improve energy efficiency and reduce environmental impact, many buildings require complete renovation.

However, current materials and design concepts for energy-saving insulation are unclear regarding their recyclability and versatility. Our research focuses on using foam concrete to create insulation and reusable facade finishes that can be customized for each building. We have developed a plan for robotically applying foam concrete, which includes end effector ideas, robot programming, and surface design planning[10]. Khidir (2018) analyzed and designed a cement mixer blade that can be easily replaced for multi-use. The study utilized Solid works V. 2017 and concluded that Centrifugal Blades Type (b) is superior[11]. Derlukiewicz (2019) developed a Human-Machine Interface (HMI) accident prevention system for disposal robot operators using the create Thinking method. The study includes an academic review of processes and methods, as well as conceptual design. The suggested system is fine-tuned through physical tests and FEM calculations[12]. Gharbia et al. (2019) discussed the use of robots in concrete building construction and conducted a systematic review of 48,200 documents. They found that the USA, Germany, and Switzerland were leaders in this field. While robots can replace many construction activities, horizontal RC elements still require support, and rapid prototyping is the best method for building construction using manipulator robots[13]. The purpose of the **discussion** is to interpret and describe the significance of your findings in light of what was already known about the research problem being investigated, and to explain any new understanding or fresh insights about the problem after you've taken the findings into consideration.

Robots in Concrete Industry

Robots in Concrete Industry

Constructing buildings is a methodical process that involves skilled workers and formwork methods. However, manual labor is slow, expensive, and incompatible with modern construction techniques. The complexity of the construction site and the variability in building processes pose challenges for using robots in construction. While some self-driving building robots have been developed, they are limited in their capabilities and intelligence. The concrete business is constantly evolving, with more advanced tools being introduced regularly. This paper examines the equipment used in the different stages of the concrete cycle, as well as the materials used to manufacture them, to help inform equipment selection for each stage.

Types of robots used for concrete-related work

Concrete-Eating Robots

The ERO Concrete Recycling Robot quickly dismantles concrete buildings without producing dust or waste. It uses a high-pressure water gun to crack the surface of the concrete, separating the waste and packaging the clean material for use in new prefabricated concrete buildings.

Concrete saw

A concrete saw, also known as a consaw, road saw, cut-off saw, slab saw, or quick cut, is a hand tool used to cut concrete, brick, asphalt, tile, and other solid materials. Diamond saw blades are commonly used on concrete saws for cutting concrete, asphalt, and stone.





Devang J. Rathod *et al.*,

Concrete crushers

There are two kinds of concrete crushers. One is a mobile concrete crusher that looks like a backhoe but has an extension on its boom arm to break up big rocks into small gravels. The second type is mostly used in factories to turn medium-sized rocks into powder or gravel.

Concrete Finishing

Power Trowels

It is a small piece of equipment that is used to clean concrete surfaces. It has a strong motor with a set of trowels attached to it. The trowels spin quickly on the concrete surface, giving it a nice, smooth finish. There are two kinds of it.

Ride-on power trowels

In ride-on power trowels, the operator sits on the machine and runs the tools to make the concrete surface smooth.

Walk-behind power trowels

In walk-behind electric trowels, the person using the machine walks behind it.

Vibratory Screed Finisher

A vibratory slurry finisher has a truss frame with a base that is at least 1 foot wide. For vibratory action on the concrete, it is set up with eccentric weights that are driven by a motor or with air vibrators that are driven by a motor. It is also often used to smooth out the sidewalk.

Tining Machine

Tining is the process of making holes in soft concrete that are all the same length and width. It is done when another layer of concrete is going to be put on top to make the joints fit better. Tining can be done by hand with a tining tool or with a machine.

Concrete Paving Machine

A paver, also called a paver finisher, asphalt finisher, or paving machine, is a piece of building equipment used to put asphalt on roads, bridges, parking spots, and other places. It flattens the tarmac and gives it a little bit of pressure before a roller comes along and does the rest.

Concrete Vibrator

A vibrator is a piece of machinery that makes movements. Most of the time, the shaking is caused by an electric motor with a mass on its axle that is out of balance. The concrete vibrator is one of the best pieces of concrete tools that helps save time and money by putting the concrete materials in the right spot.

3D concrete printing

This equipment is very helpful in the building field because it saves time, money, makes designs more flexible, cuts down on mistakes, and is better for the environment. Concrete is pushed through a tube to build up layers of structure parts without the use of moulds or vibrations.

Mixer machines

Concrete can be mixed in a laboratory with a pan-type mixer. It is made so that both dry and wet materials can be mixed well. The mixing pan can be taken out and tipped to make it easy to get to and empty when mixing is done. It is turned by an electric engine that turns a turntable.



**Devang J. Rathod et al.,****Drum Type****Tilting**

There are two main kinds: Horizontal: One end has a hole for charging and the other end has a hole for discharge. Single drum: Materials are put in and taken out through the same hole.

Non tilting mixer

Concrete mixers that don't tip over come in sizes of 200NT, 280NT, 375NT, 500NT, and 1000NT. As the name suggests, they can't be turned sideways. On one side, usually the top, the ingredients are put in, and on the other side, the concrete is taken out. They are used to make bigger batches of concrete.

Reversing Mixer

The whole drum spins around its axis as materials enter through a charge chute on one end and leave through a discharge chute on the other end. Once the ingredients are well mixed, the drum is turned around and the blades push the concrete through to the end of the mixer where it comes out.

Advantages of Application of Robots in the Concrete Industry

1. Improved product quality
2. Improved quality of life
3. Reduction of labour costs
4. Reduction in material waste
5. Safety considerations
6. Better quality and workmanship

Disadvantages of Application of Robots in Concrete Industry

1. Automated equipment includes the high capital costs that come with investing in automation (designing, building, and installing an automated system can cost millions of dollars).
2. It needs more upkeep than a machine that is handled by hand.
3. Robots have limited capabilities
4. Robots (still) need humans

Case Study

A new research indicates that the lack of skilled labourers in the construction industry is soon becoming a major problem. The problem of a smaller workforce and an older population results in higher pay, worse construction quality, project delays, higher costs, and a higher likelihood of accidents on construction sites. Robotization or automated installation has been suggested as a solution to these problems. The first case study is the destruction of a 100-year-old swimming pool in a method that was quicker, safer, and more affordable than any other. Three Brokk concrete-breaking machines were used for this. Gnat UK overcame severe obstacles in renovating a leisure club in Dunfermline, including overcoming limited access, constrained working areas, and the need to tear down a swimming pool's concrete edges that were only centimetres away from listed delicate cast iron roof supports. The second case study focuses on the use of 3D paving technology for concrete paving projects in India. India's longest tunnel road project, the Chenani-Nashri tunnel, will provide a different path to the current road network that connects these two places. This project is remarkable for being the first of its kind in India to employ 3D paving technology for concrete paving operations. It was partly sponsored by New India Structures Pvt. Ltd. (NIS). The hydro demolition of precast concrete pieces is the subject of the third case study. Precast concrete panels needed to be modified, so a civil engineering company engaged Hydro blast to accomplish it. Efficiency, accuracy, and safety are requirements for such work, and we take pride in providing them to all of our clients.



**Devang J. Rathod et al.,****Case 1 Carnegie Swimming Baths**

The demolition of a 100-year-old swimming pool was accomplished more quickly, more cheaply, and safely using three Brokk concrete-breaking machines than with any other approach. Therefore, after carrying out the necessary preliminary work, we hired experts Gnat UK to tear down the pool's walls and floor. Two additional heavyweight machines were needed to complete the more difficult operation of tearing down the pool's surrounding walls. This second walkway piece had to be removed in more than twice as much time, according to Gordon McGhie, demonstrating the effectiveness of the Brokk operation. More proof of this was provided by the next and trickiest issue, which included tearing down the 2.3-meter-high pool walls, particularly when they were located barely 100 millimetres in front of the row of cast iron roof columns. The contractor then drilled a series of eight 150mm diameter holes to create a slot immediately in front of each column, close to the pool wall below. The purpose of these holes was to physically separate this remaining portion of walkway slab from the nearby collapse of the pool wall by Gnat's robots. In order to prevent damage or stress to the nearby iron columns during demolition, a 150mm spacing would remove any structure-borne vibration or movement. G&I Diamond Drilling initially saw-cut the walkway concrete in a precise circle around each column while the remaining slab was being removed in order to make the Brokks' labour easier. The contractor then drilled a series of eight 150mm diameter holes to create a slot immediately in front of each column, close to the pool wall below. The purpose of these holes was to physically separate this remaining portion of the walkway slab from the nearby collapse of the pool wall by Gnat's robots.

Outcomes

The two machines worked twice as quickly as planned, tearing down the full 553m³ volume of walls and slab in only five weeks. They had to carefully remove concrete from less than 100mm away from the original columns while tearing down the 1.3m thick pool walls. Since Gnat has already moved the machine south to London for use on a tunneling contract, the modifications to the Brokk 330's boom have proven to be cost-effective. Its short working length is proving to be very useful for lifting and positioning concrete lining pieces after digging the 2.5 m diameter tunnel face.

Case 2 3D paving technology for concrete paving operation

Due to their continual exposure to inclement weather and heavy traffic, the arterial highways that link Jammu and Srinagar are difficult to maintain. The Chenani-Nashri tunnel project, which would provide an alternative route to the current road network connecting these two locations, is India's longest tunnel road project. The National Highways Authority of India (NHAI) is funding this project as part of a \$723 million USD endeavour to link Jammu and Srinagar. This outstanding project, which is 9 kilometres long from end to end, will cut the trip from Chenani to Nashri's route by 31 kilometres and its duration by two hours. This project, which is being carried out in part by New India Structures Pvt.

Challenges

This tunnel road will include the construction of a:

1. 9 km highway
2. 50 metre single span bridge at the north portal of the tunnel
3. 40 m single span approaching bridge at the south portal.

String lines must be built up according to conventional paving methods. This process has inherent problems that hurt a project's timetable. Physical strings take up more room, prevent vehicles from moving, and seriously endanger the safety of the workers who are there. Leica Geosystems' automated 3D paving technology, according to Mr. Parminder Sidhu, might potentially overcome these obstacles, allowing his business to create a high-quality product in spite of the difficult circumstances. The tunnel's limited area may be used thanks to the integrated 3D string less paving system, Pave Smart 3D. "Freedom for truck mobility on the job site has been provided by not having to set up string lines. Trucks deliver the concrete and leave considerably more quickly, according to plant engineer Sandeep.



**Devang J. Rathod et al.,****Cost efficient precise surfaces**

The 3D system simply accepts data once, unlike the traditional work detail where strings are built up on a daily basis. "The tracks' motion is 3D directed, which makes creating curves extremely simple. Working with string lines is fairly challenging, according to NIS paver operator Santosh Navele. One responsibility remains after the system handles all potential problems: ensuring a steady supply of concrete. Multiple tasks might be completed at once thanks to the use of Leica Geo systems technologies. Road paving, tunnel wall lining, and electrical conduit installation were all completed at the same time. Costs associated with gasoline and labour might also be decreased.

On the day of paving, the survey team set up in three easy steps to pave uninterrupted:

1. Place the Leica Viva TS15 robotic total station
2. Track it to the 360-prism mounted on the paver
3. Turned on Leica Pavesmart3D

In order to guarantee that the completed surface is always consistent with the data, the Pave Smart 3D system utilizes the survey data to control the steering tracks and movement of the paver's hydraulics. Setting tolerances in the machine computer eliminates the possibility of mistake or variation from the design data. The hydraulics and steering lock up when these restrictions are surpassed. The next day is a handy and speedy day to resume work. To resume paving, the paver's mould is positioned in relation to the day's finish point. The 3D control technology allows us to operate more quickly without sacrificing quality since it removes laborious tasks.

Case 3 Hydrodemolition to Precast Concrete Sections

Precast concrete panels needed to be modified, so a civil engineering business hired Hydro blast to do the job. Efficiency, precision, and safety are requirements for such a work, and we take great delight in offering them to every customer. Precast concrete has to be cut precisely for the work at hand, which is exceedingly difficult to do using more conventional techniques. In addition to ruining the look of concrete, tools like saws and jack hammers may produce fractures and chips in the remaining structures, which damages the remainder of the construction. This method of cutting concrete takes significantly longer than our water jetting options since it is much more difficult, especially when precision cutting is required. In addition to these concerns, it was crucial for this work to pay attention to the rebars within the precast concrete. The rebar may be harmed by excessive vibrations caused by traditional techniques, or it could harm the equipment directly if the rebar came into touch with it.

Outcomes

The customer sought Hydro blast to utilize a safer and more effective process since they understood the challenges of cutting concrete of this kind and the safety hazards involved. Due to its accuracy and remote control capabilities, we decided to employ our Aqua Cutter 410 Evolution robot. Because of these features, the procedure is safe for operators who can stand at a safe distance away. We were able to accomplish the operation quickly and with little damage to the remaining buildings and rebars because to our experience, expertise, and equipment. The customer was overjoyed, and Hydro blast was able to complete another successful work.

CONCLUSION

The following conclusions are made from the literature reviews

1. By combining building, machine (robot), and process design on a systems level, the Integrated Construction Automation Methodology (ICAM) will aid in automating the construction process.
2. The use of robots in the construction industry is still behind other sectors, such the car industry.
3. One solution for construction organizations looking for methods to increase productivity, quality, and safety is to embrace automation and robots.
4. Because robotic technology research in concrete building construction is still in its early stages, it is characterized as being under development and often difficult to execute.





Devang J. Rathod et al.,

5. Research into cutting-edge robotic technologies that may be adopted in the construction seems to be an emerging strategy; the use of robotics in building has constraints that need to be addressed.

REFERENCES

1. R. Berlin and F. Weiczner, "Development of a Multipurpose Mobile Robot for Concrete Surface Processing," *9th ISARC International Symposium on Automation and Robotics in Construction*, pp. 1–10, 1992, doi: 10.22260/isarc1992/0064.
2. Y. Alvarsson and L. Molina, "A Robot for Levelling and Compaction of Concrete," *Automation and robotics in construction X: proceedings of the 10th International Symposium on Automation and Robotics in Construction (ISARC)*, Elsevier Science Publishers, pp. 63–70, 1993, doi: 10.22260/isarc1993/0009.
3. L. S. Bryson, C. Maynard, D. Castro-Lacouture, and R. L. Williams, "Fully autonomous robot for paving operations," *Construction Research Congress 2005: Broadening Perspectives - Proceedings of the Congress*, vol. 40754, no. August 2005, pp. 371–381, 2005, doi: 10.1061/40754(183)37.
4. C. Maynard, R. L. Williams, P. Bosscher, L. S. Bryson, and D. Castro-Lacouture, "Autonomous robot for pavement construction in challenging environments," *Earth and Space 2006 - Proceedings of the 10th Biennial International Conference on Engineering, Construction, and Operations in Challenging Environments*, vol. 2006, no. March 2006, pp. 92–101, 2006, doi: 10.1061/40830(188)92.
5. D. Castro-Lacouture, C. Maynard, L. S. Bryson, R. L. Williams, and P. Bosscher, "Concrete paving productivity improvement using a multi-task autonomous robot," *Automation and Robotics in Construction - Proceedings of the 24th International Symposium on Automation and Robotics in Construction*, pp. 223–228, 2007.
6. J. K. Cable, E. J. Jaselskis, R. C. Walters, L. Li, and C. R. Bauer, "Stringless Portland Cement Concrete Paving," *Journal of Construction Engineering and Management*, vol. 135, no. 11, pp. 1253–1260, 2009, doi: 10.1061/(asce)co.1943-7862.0000083.
7. A. K. Shrivastava and A. Sharma, "A Review on Study of Jaw Crusher," *International Journal of Modern Engineering Research (IJMER)*, vol. 2, no. 3, pp. 885–888, 2012.
8. S. Lee, W. Pan, T. Linner, and T. Bock, "A framework for robot assisted deconstruction: Process, sub-systems and modelling," *32nd International Symposium on Automation and Robotics in Construction and Mining: Connected to the Future, Proceedings*, pp. 1–8, 2015, doi: 10.22260/isarc2015/0093.
9. S. Neudecker et al., "A New Robotic Spray Technology for Generative Manufacturing of Complex Concrete Structures Without Formwork," *Procedia CIRP*, vol. 43, pp. 333–338, 2016, doi: 10.1016/j.procir.2016.02.107.
10. E. Lublasser, J. Brüninghaus, A. Vollpracht, L. Hildebrand, and S. Brell-Cokcan, "Robotic application of foam concrete onto bare wall elements," *33rd International Symposium on Automation and Robotics in Construction (ISARC 2016)*, no. ISARC, pp. 1–8, 2016, [Online]. Available: <http://search.proquest.com/docview/1823082388?pq-origsite=gscholar>.
11. T. C. Khidir, "Designing, remodeling and analyzing the blades of portable concrete mixture," *International Journal of Mechanical Engineering and Robotics Research*, vol. 7, no. 6, pp. 674–678, 2018, doi: 10.18178/ijmerr.7.6.674-678.
12. D. Derlukiewicz, "Application of a Design and Construction Method Based on a Study of User Needs in the Prevention of Accidents Involving Operators of Demolition Robots," *Applied Sciences (Switzerland)*, vol. 9, no. 7, 2019, doi: 10.3390/APP9071500.
13. M. Gharbia, A. Y. Chang-Richards, and R. Y. Zhong, "Robotic Technologies in Concrete Building Construction: A Systematic Review," *Proceedings of the 36th International Symposium on Automation and Robotics in Construction, ISARC 2019*, no. ISARC, pp. 10–19, 2019, doi: 10.22260/isarc2019/0002.





Devang J. Rathod et al.,



Fig. 1. Concrete-eating robot



Fig. 2. Concrete saw



Fig. 3. Concrete Crusher



Fig. 4. Ride on power trowels



Fig. 5. Walk behind power trowels



Fig. 6. Vibratory screed finisher



Fig. 7. Tining machine









Fig. 8. Concrete paving machine





Devang J. Rathod et al.,

	
<p>Fig. 9. Concrete vibrator</p>	<p>Fig. 10. 3D concrete printing</p>
	
<p>Fig. 11. Pan type</p>	<p>Fig. 12. Tilting type drum</p>
	
<p>Fig. 13. Non tilting mixture</p>	<p>Fig. 14. Reversing mixer</p>





Analyzing on-Site and off-Site Automation in the Construction Industry: A Comprehensive Overview

Devang J. Rathod^{1*}, Umang Raichura², J. R. Pitroda², Jagdish M. Rathod¹, Reshma L. Patel²

¹Department of Electronics Engineering, Birla Vishwakarma Mahavidyalaya Engineering College, Vallabh Vidyanagar, Gujarat, India.

²Department of Civil Engineering, Birla Vishwakarma Mahavidyalaya Engineering College, Vallabh Vidyanagar, Gujarat, India.

Received: 30 Dec 2023

Revised: 09 Jan 2024

Accepted: 12 Jan 2024

*Address for Correspondence

Devang J. Rathod

Department of Electronics Engineering,
Birla Vishwakarma Mahavidyalaya Engineering College,
Vallabh Vidyanagar,
Gujarat, India.



This is an Open Access Journal / article distributed under the terms of the **Creative Commons Attribution License** (CC BY-NC-ND 3.0) which permits unrestricted use, distribution, and reproduction in any medium, provided the original work is properly cited. All rights reserved.

ABSTRACT

The significance of the technical progress that has been experienced over the course of the last several decades cannot be denied. Many various types of businesses have made astute use of the newly emerging technical breakthroughs, which has led to significant enhancements in terms of productivity, functionality, quality, and the overall level of comfort experienced by the end user. Buildings and other types of infrastructure continue to be among the most costly and time-consuming types of things to manufacture in our civilization, as is common knowledge. Therefore, the most recent trend in the construction industry is to have automated construction sites that incorporate robots and automated forms of technology in order to improve the quality, efficiency, safety, and productivity of building operations. Automation, whether it be on-site or off-site, is helpful for accelerating the building process while maintaining the necessary level of integrity, maintaining a high quality of work, and increasing overall productivity.

Keywords: Automation, Construction, Industry, On-site and off-site automation

INTRODUCTION

Automation refers to the use of advanced technological equipment, control systems, and information technologies to efficiently operate or manage a process, minimizing the need for human intervention. People have said that building automation is the use of mechanical and electronic tools to make construction work automatically or to direct it in a way that reduces risk, time, or effort while keeping or improving quality. Automation can make workers less reliant



**Devang J. Rathod et al.,**

on each other, increase output and efficiency, reduce inconsistency, cut down on human mistakes, give more control, stability, a safe place to work, etc. The construction phase has significant importance in civil engineering constructions, since the overall success of the project is largely contingent upon the quality and efficiency of this phase. Construction work is sometimes done in risky conditions and situations, so robots and automation are needed to make the work safer and better. At this point, both automation on-site and automation off-site help the building business.

Evaluation for using Robots and Automation

At first, robots were made for the manufacturing industry and were meant to do simple jobs in a comfortable setting. On the other hand, robots that are meant to work on building sites must be able to move around, adapt to different surroundings, and do different things almost every step of the way. Using more industrial production, sustainable production, mass individualization, and clever building to make buildings easier to build changes construction engineering. So, new study shows that robot technologies can improve quality and control of tools in a big way in a number of building automation uses. It would be helpful to be able to automate building, especially in places where people are dangerous or hard to work with. For example, robots could be sent to underground or extraterrestrial environments to build homes for later human travellers. There are many ways that robots and automation can be made better in all parts of the process.

Need of Study

One of the most important industries in India is the building business. The construction industry is a big part of what makes the country's business better as a whole. However, issues about the quality of building are a big problem in the Indian construction industry. The real cost of building and labour is going up because of things like a lack of skilled workers, badly fitted equipment, and bad plants. The building business needs a lot of workers, and construction work is often done in dangerous places. In wealthy countries, technology in building has become more and more important quickly. So, growing countries like India need technology in the building business to get more work done, better work, faster development, and a lot more.

Objectives of the Study

The following are the main objectives of the study work.

1. To find out about different robotic tools that can be used on and off site.
2. To figure out if technology can work in the building business.
3. To make suggestions for how technology, both on-site and off-site, can be used in the building business.

REVIEW OF LITERATURE

Here are reviews of past studies on how technology is used on-site and off-site in the building business. Kangari et al. (1997) they discussed the four key elements: strategic alliances, effective information gathering, reputation by innovation, and technical fusion that fosters the development of unique construction technology in Japan. It has been found that as a consequence of the worldwide technology information collecting, the enormous Japanese construction businesses are now more cognizant of foreign technology. At a prominent construction firm in Japan, long-range technology forecasting, which blends current activities with future visions, has been shown to be the crucial link between innovation and business strategy[1]. Van Gassel et al. (2006) researched the wall panel assembly performance, they found data about the accidents and problems found because of wall panel assembling or curtain wall assembling at great heights in dangerous conditions done manually. After this research, they also carried out the study of some different technological companies all over the world developing and using robotics and automation for wall assembling. Kajima, Fujita etc. Japanese companies are manufacturing and using robots for curtain wall assembling on construction sites. Other such case studies are carried out by the researchers [2]. Elattar et al (2008) stated the opportunities and challenges of the utilization of robotics and automation in the construction industry. As per the researcher several types of activity are to be done by robotics and automation may help the



**Devang J. Rathod et al.,**

construction industry, These activities are concrete work, road construction, finishing works, and also in building management systems [3]. Bock (2008) outlined many examples of robots and automation used both on and off construction sites. His primary focus is on the use of robots and automation in the prefabricated masonry industry, the precast concrete business, the wood building industry, and the steel component manufacturing industry [4].

Pachon et al. (2012) described that in the prefabrication and on-site construction stage the use of automation can be applied. The prefabrication stage utilized off-site automation and on-site automation is useful for the construction at the building site. He further explained two types of robotics for on-site automation. Single-task robots are designed for pre-determined activities, like repetitive work. The other type of robot is a multitasking robot which is used on-site to complete a cycle of several activities [5]. Tambi et al (2014) Construction is a labor-intensive business, and work is done there under unsafe and hazardous conditions. Construction businesses in emerging nations like India need automation technology like new machinery, electrical gadgets, etc. The issues with construction work, such as declining job quality, a lack of manpower, worker safety, and project working conditions. This essay uses qualitative research on regional construction businesses in and around Pune to provide data on automation in the Indian construction sector. This article discusses various implementation challenges resulting from the qualitative investigation. Identifying the challenges to integrating automation technology in Indian infrastructure projects and construction enterprises was the primary goal of this article. In order to boost efficiency and improve the quality of their work, modern infrastructure projects and construction companies must adopt automation technology [6]. Yang et al (2007) The hesitance of businesses to embrace new technology stems from a combination of not understanding the benefits of these innovations and not being able to accurately foresee their competitive advantage. An extensive examination of the construction industry's use of technology and overall project performance yielded data from more than two hundred significant facility projects.

Eleven hypotheses are presented and analyzed based on four key data class variables: industrial sector, total installed cost, public vs. private, and greenfield vs. expansion vs. rehabilitation projects. Research findings on the correlation between successful project completion and the use of technology are analyzed. This study's results imply that automation and integration technologies may considerably increase project performance in terms of stakeholder success, particularly for specific types of projects. This study's findings might help organizations make decisions regarding the appropriateness of using technology for certain jobs [7]. Oke et al (2017) did study on the impacts of automation on the performance of the construction industry. They also conducted a survey among the many main participants in the sector and came to some conclusions on the most significant disadvantages of the usage of automation in the sector. These significant issues include high capital costs, workforce relocation, increased maintenance, worker emotional stress, and less flexibility [8]. Pan et al. (2018) studied the current situation of public housing construction (PHC) in Hong Kong country. As a major demand of PHC in Hong Kong, researchers found several problems facing conventional construction techniques through literature, surveys and also through site visits. They recommend several types of robotics and automation to find the solutions faced by the current construction industry [9]. Jang et al. (2019) have reviewed the offsite construction management process and they concluded that at the process level, Building Information Modelling (BIM), and Off-Site Construction (OSC) are to be correlated with each other for the working of off-site automation. They also concluded that the OSC is an advanced construction method and has many advantages over the traditional method [10].

Significant Results of the Literature Review

The following are the important results drawn from the literature review:

1. Robotics and automation are advanced technologies that have many advantages over conventional construction methods.
2. On-site construction automation may help in workers' safety, quality of work, the efficiency of work etc.
3. Off-site automation reduces the on-site activity time as the precast components are directly provided at the site due to off-site automation.
4. At some level, there are several difficulties to adapt automation in the construction industry as high initial cost, less skilled workers to operate the automation technologies etc.





Devang J. Rathod *et al.*,

5. Automation can be used in both off-site and on-site phases, so it is very beneficial to the construction industry due to its versatility.

Off-Site and On-Site Automation

Definition of automation

Automation is the strategic use of mechanical, electrical, and computer systems to the execution of construction jobs with the goals of increasing productivity, decreasing the duration of monotonous operations, and increasing safety. Successful project completion is defined by the project management discipline as meeting or exceeding predetermined criteria such as cost, quality, safety, etc. A successful project is one in which all of the key metrics are optimized to the fullest extent feasible, including but not limited to budget, schedule, quality, productivity, resources used, and waste produced. The automation is a step in the right direction, ensuring the project's success.

Advantages of automation

Several benefits are acquired using automation in the construction industry:

1. An increase in work quality
2. A decrease in labour expenses
3. Savings on improvements to safety and health
4. Time reduction
5. Better working circumstances
6. Enhanced efficiency and production at a lower cost.
7. Increasing worker and public safety by creating and using machines for hazardous occupations.

Disadvantages of automation

Some disadvantages are there by using the automation in construction industry are listed below:

1. Joblessness at the expense of modernity
2. This results in a flight from the nation
3. It requires a lot of cash to set up and maintain
3. Expert and skilled handlers or personnel are necessary
4. Because untrained people cannot be hired, the project's start-up costs go up.
5. Trained labour are difficult to find and command a higher wage than unskilled employees.

Off-site Automation

The expansion of the construction industry is primarily characterized by a growing scarcity of trained labour. This deficit will have to be offset by greater prefabrication in the production of pre-cast concrete, timber, steel frame and brick wall construction components. Another significant benefit of precast concrete pieces is the workforce's efficiency on the task. Job efficiency is maximized at the plant level as opposed to the construction site since workers on the construction site are not as concerned with more complex activities like moulding, inserting reinforcing steel, etc. The shipping cost is about the same for both prefabricated pieces and equivalent volumes of site-mixed concrete. Here are some examples of off-site automation for a better understanding of off-site industrial automation equipment.

On-site automation

On-site automation provides various type of activities some of these activities are displayed in the form of image for a better understanding of the work of on-site automation at the construction site.

Case Study

Assembling wall panels with robotic technologies (On-site automation)

Despite the availability of robotic technology for a variety of applications, robots are only utilized seldom to construct wall panels in high-rise structures. These applications may enhance construction site safety and assembly process efficiency. Several automated methods have been developed and employed on building sites in recent years.





Devang J. Rathod *et al.*,

Fig. 12 to 14 show many instances. Large Japanese construction firms are pioneers in the development and deployment of such robots. They are primarily concerned with the creation of new single-task robots to accomplish tasks that are tough, unclean, or dangerous. The 'Mighty Hand' (KAJIMA Japan) lifts huge panels used in construction, such as concrete or glass curtain walls, as seen in Fig. 12. The robot is controlled by a person. BALLAST NEDAM developed a mechanized panel assembly system (shown in Fig. 14). A flying scaffold hanging on a tilting arm is used to place the panels. This tilting arm is used by the tower crane to lift up the flying scaffold. The grasp of the tilting arm is located above the floor where the installation will take place. The flying scaffold is tilted into position on the correct floor using its weight. The flying scaffold is then hung after attaching the facade piece to the building. This is accomplished by the use of a hydraulic system. When the tilting arm is detached, it may be reused for the next flying scaffold.

Automation in timber and steel component production (Off-site automation)

Flexible automated CAD/CAM wood element manufacture is enabled by automatic timber positioning systems and laser-assisted marking equipment. The maximum level of prefabrication is obtained by mobile home prefabrication, which has a prefabrication ratio of 95%, and box unit prefabrication, which has a prefabrication ratio of up to 85%. The purpose of a fully automated and robotic steel panel production facility is to produce constructs that are highly customized to manufacturing and assembly needs without requiring rework on the construction site (such as cutting procedures). Pre-fabrication processes such as laser cutting, gas burner cutting, sawing, and drilling are used to create the building parts, followed by straightening, metallic cleaning, intermediate and end coating, and thorough corrosive protection. These procedures consistently exhibit high standards of excellence.

Glazing robot Technology on Construction Sites (On-site automation)

Glass Ceiling Glazing Robot (GCGR)

Based on the fundamental roles identified via job analysis, the conceptual design of a GCGR may be outlined as follows.

1. A need exists for an aerial lift capable of accommodating an operator and the necessary installation equipment, while also possessing sufficient operational reach to attain a height of about 15 metres above the ground.
2. A multi-degree-of-freedom manipulator is required for the installation of the heavy glass ceiling, which involves switching between many operators. The selection of a robot is contingent upon factors such as the dimensions of the working environment and the weight-bearing capacity required.
3. The current system operates in a semi-automated manner in order to adapt to the dynamic nature of the work environment. An operator enters the platform of the aerial lift in order to control a multi-degree-of-freedom manipulator. The worker's decision-making ability assumes the role of the primary controller for the robot.
4. In order to assess the capabilities of the worker, external force information is used as the input signal for the robot exercise. The regulation of force information, which is dependent on the input signal, must be adjusted in a flexible manner to align with the specific exercise requirements of the robot and the age of the operator.
5. A hoover suction apparatus is used as an end-effector for the manipulation of the glass ceiling. The design of an end-effector is modulated in anticipation of the forthcoming alteration of the glass ceiling shape.
6. The deck of the aerial lift provides support for both the human worker and the robotic system. The safety and productivity of workers must be taken into consideration while designing the deck and planning the work procedure.

Field Test

The robotic system under consideration has been designed for the purpose of constructing the soffit, which refers to an outer structure resembling a glass ceiling, as seen in Fig. 19. The glass ceilings are installed at a height of 15 metres, and their dimensions are 3000mm x 1500mm with a weight of 150kg. The suggested handling procedure may be summarized as follows, based on the job planning.



**Devang J. Rathod et al.,**

The use of an airborne work platform onto which the envisaged robotic system is affixed.

1. Placing the glass ceiling onto the terrace.
2. Elevate the metaphorical barrier known as the glass ceiling that exists inside the framework of societal structures.
3. The glass ceiling should be installed and the job should be completed.

Prior to raising the deck, a single fragment of the glass ceiling is positioned onto the deck. Subsequently, in accordance with the prescribed deployment strategy, the robot proceeds towards the designated installation location. Subsequently, the installation commences in accordance with the predetermined procedure.

BIG CANOPY by Obayashi (On-site automation)

The primary distinguishing attribute of the system is its expansive canopy, a temporary roof structure designed to withstand all weather conditions. This canopy is supported by four corner supports and extends beyond all four corners of the whole work site. As the construction of the skyscraper progresses, the canopy is elevated. Once the construction of the building is completed and it reaches its maximum height, the canopy is disassembled, and the surrounding framework is gradually lowered using jacks.

CONCLUSION

From the literature surveys and case studies discussed above there are some conclusions can be derived as given below:

1. On-site automation may help to do dangerous activities with high accuracy, so the safety of workers and quality of work can be maintained.
2. On-site automation reduces the time of construction, increases the speed of construction, and provides a very small number of errors due to human errors.
3. On-site automation facilitates the work with machines, less number of workers, and without losing productivity.
4. Off-site automation enables to manufacture of several construction items in the industry itself, so the on-site work may reduce.
5. Off-site automation-produced materials are made with high accuracy so the possibilities of errors on-site are also reduced.
6. Both Off-site and On-site automation is accelerating the speed of construction, with good-quality work and fewer errors.

REFERENCES







1. Roozbeh Kangari and Yasuyoshi Miyatake, "Developing and Managing Innovative Construction Technologies in Japan," *Journal of Construction Engineering and Management*, vol. 123, no. May 2010, pp. 72–78, 1997.
2. F. Van Gassel and P. Schrijver, "Assembling wall panels with robotic technologies," 2006 Proceedings of the 23rd International Symposium on Robotics and Automation in Construction, ISARC 2006, pp. 728–733, 2006.
3. S. M. S. Elattar, "Automation and Robotics in Construction: Opportunities and Challenges," *Emirates Journal for Engineering Research*, vol. 13, no. 2, pp. 21–26, 2008.
4. M. A. Thomas Bock, Carlos Balaguer, "Construction Automation and Robotics," *Construction Automation and Robotics, Robotics and Automation in Construction*, no. April 2014, p. 23, 2008, doi: 10.5772/5861.
5. A. G. Pachon, "Construction Site Automation : guidelines for analyzing its feasibility, benefits and drawbacks," *Joint CIB International Symposium of W055, W065, W089, W118, TG76, TG78, TG81 and TG84*, pp. 38–45, 2012, [Online]. Available: http://www.irbnet.de/daten/iconda/CIB_DC25183.pdf.
6. A. S. Tambi, A. R. Kolhe, and U. Saharkar, "Obstacles in Implementing Automation in Indian Infrastructure Projects," *IOSR Journal of Mechanical and Civil Engineering*, vol. 11, no. 3, pp. 42–44, 2014, doi: 10.9790/1684-11334244.





Devang J. Rathod et al.,

7. L. R. Yang, J. T. O'Connor, and J. H. Chen, "Assessment of automation and integration technology's impacts on project stakeholder success," *Automation in Construction*, vol. 16, no. 6, pp. 725–733, 2007, doi: 10.1016/j.autcon.2006.11.005.
8. A. Oke, C. Aigbavboa, and S. Mabena, "Effects of Automation on Construction Industry Performance," *Advances in Engineering Research (AER), Second International Conference on Mechanics, Materials and Structural Engineering (ICMMSE 2017)*, vol. 102, no. ICMMSE, pp. 370–374, 2017, doi: 10.2991/icmmse-17.2017.61.
9. W. Pan, R. Hu, T. Linner, and T. Bock, "A methodological approach to implement on-site construction robotics and automation: A case of Hong Kong," *ISARC 2018 - 35th International Symposium on Automation and Robotics in Construction and International AEC/FM Hackathon: The Future of Building Things*, no. Isarc, 2018, doi: 10.22260/isarc2018/0051.
10. J. Y. Jang, C. Lee, J. I. Kim, and T. W. Kim, "Research Trends in Off-Site Construction Management: Review of Literature at the Process Level," *Modular and Offsite Construction (MOC) Summit Proceedings*, pp. 349–356, 2019, doi: 10.29173/mocs113.

	
<p style="text-align: center;">Fig. 1. Precast concrete element manufacturing automation.</p>	<p style="text-align: center;">Fig. 2. Precast wall frame manufacturing.</p>
	
<p style="text-align: center;">Fig 3. Structural steel element manufacturing.</p>	<p style="text-align: center;">Fig 4. Structural wooden element manufacturing.</p>
	
<p style="text-align: center;">Fig 5. Concrete work by robotics.</p>	<p style="text-align: center;">Fig 6. Concrete floor finishing robot.</p>





Devang J. Rathod et al.,



Fig 7. Road construction automation



Fig 8. Paver block.



Fig 9. Brick laying Automation.



Fig 10. Plastering automation.



Fig 11. Painting Automation.



Fig 12. Wall installation robot in action by Kajima Corporation.



Fig 13. Multi-jointed handling robot for exterior material



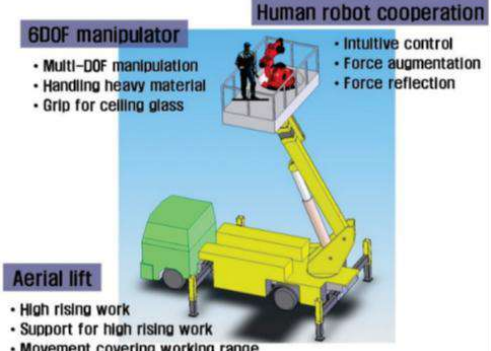




Fig 14. A mechanized panel assembly system.





Devang J. Rathod et al.,

<p>installation.</p>	
	
<p>Fig 15.Multifunctional robotic wooden wall production unit.</p>	<p>Fig 16.Automated and robotic steel panel production facility.</p>
 <p>6DOF manipulator</p> <ul style="list-style-type: none"> • Multi-DOF manipulation • Handling heavy material • Grip for ceiling glass <p>Human robot cooperation</p> <ul style="list-style-type: none"> • Intuitive control • Force augmentation • Force reflection <p>Aerial lift</p> <ul style="list-style-type: none"> • High rising work • Support for high rising work • Movement covering working range 	
<p>Fig 17.Design of GCGR.</p>	<p>Fig 18.Field test of GCGR.</p>
	
<p>Fig 19. Big Canopy automated construction mechanism.</p>	





Unsupervised Deep Learning Approach for Video Retrieval using Image Query

Namrata Dave^{1*} and Mehfuza S. Holia²

¹G H Patel College of Engineering and Technology, Gujarat, India.

²Birla Vishwakarma Mahavidyala, Gujarat, India.

Received: 30 Dec 2023

Revised: 09 Jan 2024

Accepted: 12 Jan 2024

*Address for Correspondence

Namrata Dave

G H Patel College of Engineering and Technology,
Gujarat, India.

Email: namrata.dave@gmail.com



This is an Open Access Journal / article distributed under the terms of the **Creative Commons Attribution License** (CC BY-NC-ND 3.0) which permits unrestricted use, distribution, and reproduction in any medium, provided the original work is properly cited. All rights reserved.

ABSTRACT

A large amount of digital content is generated every hour in the form of text, images, and videos through day-to-day online activities worldwide. To efficiently process this vast volume of video content, cost-effective techniques are necessary for quickly extracting meaningful information. This paper aims to address the problem of content-based video retrieval using unsupervised deep learning, employing a proposed Auto Encoder Model on a collection of videos recorded from Gujarati News Channels. To expedite video processing, key frames are extracted from each video, followed by feature extraction and retrieval using the proposed Deep Denoising Auto encoder Model. The performance of video retrieval is evaluated based on a query set consisting of image queries. Extensive experiments are conducted on the model to assess and enhance the video retrieval performance using image queries, demonstrating superior performance compared to state-of-the-art video retrieval methods on news video datasets.

Keywords: Deep Learning, Auto Encoders, Video Retrieval, Unsupervised Learning.

INTRODUCTION

Image retrieval using deep learning with image queries has been widely explored. Researchers nowadays are focusing on large-scale retrieval of videos or images using various query types such as text, audio, image, or video clips [1][2][3]. When dealing with large collections of images or video frames, conventional systems often struggle to perform well with state-of-the-art retrieval methods. Consequently, Content-Based Video Retrieval (CBVR) approaches utilizing deep learning architectures have gained prominence across diverse fields such as news videos, sports videos, and movie videos. Videos cover a wide range of genres, including entertainment, sports, news, multimedia messages, tutorials, lectures, and e-learning content. These videos typically contain various elements such as text, objects, shapes, textures [3], and more, which function as fundamental components for retrieval systems. The process of retrieving information from digital videos entails tasks like indexing, retrieval, querying, and



**Namrata Dave and Mehfuza S. Holia**

browsing. To efficiently extract content from videos, automation plays a crucial role. In literature, it is not found where auto encoder is used for video retrieval task for unsupervised learning so far. In proposed approach with unsupervised deep learning approach for video retrieval, a model using auto encoder is used to extract image features in compact form and further the features are used for the task of video retrieval for the given query image. Auto encoders represent a distinct category of neural network architectures, characterized by their ability to produce output identical to the input. They undergo unsupervised training, with the primary objective of acquiring highly detailed representations of the input data at an exceptionally low level. These foundational features are subsequently reconstructed to reconstruct the original data. Essentially, an auto encoder operates as a regression task, where the network's goal is to predict its own input, effectively modeling the identity function. These networks exhibit a narrow bottleneck, consisting of only a few neurons in the middle, compelling them to generate efficient representations that compress the input into a low-dimensional code. This code is then used by the decoder to reproduce the initial input data.

LITERATURE REVIEW

Significant research has been conducted in the domain of content-based video retrieval in recent years. Conventional approaches were computationally expensive. With technological advancements, researchers have introduced novel approaches in this area. The initial step in managing video content is video parsing. Designing content-based video retrieval systems involves five main components [1]: (1) Dividing the video into segments based on its organizational structure; (2) Identifying suitable algorithms for extracting low-level feature vectors; (3) Utilizing similarity-based searching techniques to compare video segment feature vectors with query features; (4) Addressing queries across extensive video sequences; and (5) Presenting the results or result lists. Videos can be characterized by spatial, temporal, or spatial-temporal attributes. Spatial domain video data features are extracted from video frames based on pixel information within a region, with the relationships serving as descriptors Temporal domain attributes play a pivotal role in the segmentation of videos, allowing for the division of video content into frames, shots, scenes, and video segments. Within video data, a diverse array of audio and visual characteristics can be found, encompassing elements such as color, texture, edge details, motion vectors, loudness, pitch, and more [4-8].

In case of textual information present in video clip, the text data which are continuously being displayed for certain time gives some important information about what is currently being viewed. This type of information is normally present in broadcast news video. Some of the shots in news video are having text regions which are being displayed for long duration to give idea about current topic of news, place, event, or personality in news, etc. Some of the broadcasted videos contains closed caption (CC) information which is very useful for text query-based video retrieval. The close caption track is having texts to be displayed to viewers in synchronization with videos do not contain such text captions which makes retrieval task difficult[9][10]. Along with video retrieval, computationally efficient indexing of video collection is very important task to be done for management of video documents. Video indexing can be done like document indexing. Traditional methods of indexing are not much useful for vast video database. Numerous methods have been proposed for semiautomatic or automatic indexing of video documents. Video indexing methods are either based on single features such as visual, audio, textual, etc., or multimodal [11-13][21]. Multimodal indexing combines multiple representative features of videos. Kulkarni et al. [14] proposed a method using video clips as input queries to achieve high-quality content-based video retrieval by identifying temporal patterns within video content. They integrated efficient indexing and sequence matching techniques based on discovered temporal patterns to reduce computational cost and enhance retrieval accuracy, respectively.

Video Structure

Videos can be conceptualized as collections of scenes. Fundamentally, videos are described using components like scenes, shots, and frames. Frames constitute the fundamental unit of videos. Shots are collections of frames captured in a single camera action, with frames within a shot sharing similar image features. Scenes, on the other hand, can be composed of a single or multiple shots.





Namrata Dave and Mehfuza S. Holia

As depicted in Figure 1, each video comprises various scenes, with each scene consisting of one or more shots. Scene changes and shot changes are illustrated in Figure 1. Visually similar frames constitute a shot.

Deep learning approaches for Video Retrieval

Mühling et al. [3] proposed deep learning approaches for effective video inspection and retrieval. They introduced efficient algorithms for concept detection and similarity searching using a multi-task-based learning approach that shares network weights. Their research introduced a novel method for rapid video retrieval in media production, along with components for novel visualization. They achieved an average precision of approximately 90% for the top-100 video shots using concept detection. Their approach employed pre-trained CNN models based on visual recognition tasks for similarity search and concept detection. Noh et al. [15] introduced the DELE local feature descriptor for large-scale image retrieval tasks. This new feature is rooted in convolutional neural networks, trained exclusively with image-level annotations on a landmark image dataset. An attention mechanism for key point selection was proposed, sharing most network layers with the descriptor. The system produces reliable confidence scores to reject false positives, particularly robust against queries without correct matches. DELE demonstrated superior performance to state-of-the-art global and local descriptors in large-scale settings. Lange et al. [16] explored the effectiveness of deep auto encoder neural networks in visual reinforcement learning tasks. Their framework combined deep auto encoder training (for compact feature spaces) with batch-mode reinforcement learning algorithms (for learning policies). Emphasis was placed on data efficiency and analyzing feature spaces constructed by the deep auto encoders. These spaces demonstrated the ability to capture existing similarities and spatial relations between observations, facilitating the learning of useful policies. Wang et al. [17] investigated the dimensionality reduction capability of auto encoders. Experiments were conducted on synthesized data for intuitive understanding, as well as real datasets like MNIST and Olivetti face datasets. Results showcased that auto encoders can indeed learn distinct features compared to other methods.

Auto encoders Architecture

A typical auto encoder architecture consists of three primary components, as illustrated in Figure 2. The first component is the encoding architecture, comprised of a series of layers with a decreasing number of nodes, ultimately leading to the creation of a latent view representation. The second component is the latent view representation, which serves as the lowest-level space where inputs are compressed while preserving essential information. The third component is the decoding architecture, which mirrors the encoding architecture but with an increasing number of nodes in each layer, ultimately producing an output that closely resembles the initial input. A well-tuned auto encoder model should have the capability to faithfully reconstruct the same input data that was initially passed through the first layer. Auto encoders find widespread use in image-related applications, such as Feature Extraction, Dimensionality Reduction, Image Compression, Image Denoising, and Image Generation. There are various types of auto encoders, including denoising auto encoders, convolutional auto encoders, stacked auto encoders, and more. Auto encoders represent a specialized category within deep learning neural network architectures, primarily employed in unsupervised learning tasks. One of the primary advantages of using auto encoders lies in their capacity for dimensionality reduction, data compression, and retrieval. Denoising auto encoders offer a distinctive approach by not merely duplicating input data. Instead, they introduce noise to the input image before feeding it into the network. In the case of denoising auto encoders, the initial input, denoted as 'x,' undergoes a corruption process to create a corrupted version 'x̃' through a stochastic mapping, as illustrated in equation 1.

$$x \sim qD(x \sim | x) \quad (1)$$

Intermediate representation is given by in equation 2 where W is weight and b is bias.

$$y = f_{\theta}(x \sim) = s(Wx \sim + b) \quad (2)$$

Output image is reconstructed using equation 3.

$$z = g_{\theta}(y) \quad (3)$$





Namrata Dave and Mehfuza S. Holia

The parameters θ and θ' are trained with the objective of reducing the average reconstruction error across a training dataset. The reconstruction error, often referred to as loss, can be formally defined as described in equation (4), where x_k represents a training example and z_k represents the predicted value.

$$L_H(\mathbf{x}, \mathbf{z}) = - \sum_{k=1}^d [x_k \log z_k + (1 - x_k) \log(1 - z_k)] \quad (4)$$

The primary aim in this context is to reduce the reconstruction error, which essentially involves maximizing a lower limit on the mutual information between the input variable X and the acquired representation Y . Achieving a high-quality reconstruction of the input implies that a substantial portion of the original information contained in the input data has been preserved.

Experimental Details

In our novel deep learning method designed for video retrieval utilizing image queries, we begin by initially extracting pivotal frames from the established dataset. As depicted in Figure 3, these key frames are gathered after the removal of advertisements and are subsequently inputted into the auto encoder architecture for training purposes. The well-trained encoder model is employed to extract features from the news video dataset, and these features are stored independently to facilitate matching with query features. A series of experiments involving various parameter configurations were conducted to ultimately identify the most effective model. The ensuing sections will elaborate on each phase of the video retrieval process. Dataset We conducted experiments on a dataset compiled from continuous recordings over a span of two days, encompassing three Gujarati language channels: ETV News, DD 11, and Sandesh News. Additionally, we included several video recordings from TV9 and DD Girnar in our dataset. In total, the dataset comprises approximately 90 hours of video content, all of which are in the mp4 format. The proposed approach was evaluated for the task of news video retrieval based on image queries, specifically utilizing the Gujarati News Video dataset. For this evaluation, the input frames of the videos were resized to dimensions of $128 \times 128 \times 3$ before being processed by the encoder.

Key frame Extraction

The automated technique employed to identify changes between shots within a video scene is known as video shot boundary detection. This Shot Boundary Detection (SBD) method has gained widespread usage in recent times, finding applications in video summarization, video indexing, video data mining, and more. Typically, one or more frames from each shot are chosen to serve as representatives of the shot's content, referred to as Key Frames. In the proposed approach, as depicted in Figure 3, an efficient Key Frame Extraction method [19] is utilized. This method relies on a visual information-based approach that utilizes histogram differences and ranking to extract key frames. The selection of one or more key frames per shot is aimed at reducing the overall computational demands of the proposed system [19].

Advertisement Detection and Removal

To In order to attain highly accurate results while training the model with a limited dataset, we adopted a transfer learning strategy. Specifically, we employed the Alex Net model to train on a dataset comprising key frames extracted from news and advertisement frames sourced from DD Girnar, ETV Gujarati, TV9 news, and Sandesh channels. Leveraging the pre-learned weights of this well-established network, which had been originally trained on an extensive dataset, our proposed approach achieved excellent results when incorporating new data into the training process. To optimize results, we conducted experiments employing various models and different layers to generate outcomes. In a prior publication [20], we detailed experiments carried out using the pre trained Alex Net model for both training and classification, presenting the corresponding results. In pursuit of enhanced accuracy without compromising training time, we pursued an alternative transfer learning method involving Alex Net as a feature extractor, coupled with SVM as the classifier. In image classification, we utilized Support Vector Machine in conjunction with Bayesian optimization to enhance classification performance. Notably, the Alex Net-based approach for advertisement detection, as implemented in our unsupervised video retrieval task, yielded an impressive accuracy rate of 99.2 percent when applied to the news video dataset [20].





Namrata Dave and Mehfuza S. Holia

Training and Feature Extraction using Auto Encoders

Auto encoders are frequently employed architectures in unsupervised deep learning applications, including tasks like image compression, reconstruction, and retrieval. In the suggested unsupervised deep learning method for video retrieval, an auto encoder model is utilized to condense image features into a compact representation. As illustrated in Figure 3, the auto encoder architecture utilizes key frames that have been collected after the removal of advertisements for training. The training of the encoder model involves experimenting with various parameters, including epochs, batch size, and optimization functions, to enhance its performance. Subsequently, features are extracted using the well-trained encoder model and stored for future matching with query features. The employed auto encoder model is a denoising convolutional auto encoder, comprising three convolutional layers with varying kernel sizes and three max pooling layers, as depicted in Figure 4. Denoising auto encoders offer significant advantages, as they not only extract meaningful information during training but also enable efficient image reconstruction with minimal information loss. As highlighted in Figure 4, the encoder model consists of a total of seven layers designed to process the input frame. The initial layer, serving as the input layer, takes in a frame with dimensions of 128x128x3 and forwards it to the subsequent layer. Figure 5 illustrates how filters determine the number of kernels to convolve with the input volume, resulting in the generation of 2D activation maps, as shown in the same figure. Additionally, Figure 6 showcases the outcomes of the filter application to the image, considering padding as well. The process of convolution involves applying a kernel to the input image, as depicted in Figure 5, which can be described using Equation 5. Here $x(i, j)$ is the original image, $y(i, j)$ is the image obtained after convolution of the input image with kernel w of size $m \times n$, $1 \leq k \leq m$, $1 \leq l \leq n$. In the third layer, we employ max-pooling with a 2x2 filter and 'same' padding, resulting in an output size of 64x64x16. Max-pooling in this context serves the primary purpose of reducing the dimensions of the input representation. This operation operates by determining the maximum value within each patch of the feature map. In fourth layer, again 8 convolution filters of kernel 3x3 and activation 'ReLU' is applied on the output generated from the third layer which generated output dimensions of 64x64x8 where padding is used to generate similar size output. ReLU stands for Rectified Linear Unit. The main advantage of using the ReLU over other activation functions is that ReLU does not activate all the neurons at the same time. The neurons will only be deactivated if the output of the linear transformation is less than 0. Activation function relu is defined by equation 6.

$$f(x) = \max(0, x) \quad (6)$$

In the fifth layer, max pooling with size 2x2 was applied which generated 32x32x8 dimensions of feature maps. In the following layers i.e., layer sixth and seventh, 8 convolution filters of kernel 3x3 with activation function 'ReLU' and max pooling of size 2x2 are applied, respectively. Padding is applied in the sixth layer to generate an output size of 32x32x8. The output of the seventh layer is 16x16x8 which is named as encoder layer. The feature map generated for the image shown in Figure 7(a) using the encoder layer is shown in Figure 7(b). For the model with encoder, total params are 2192 and Trainable params are also 2192 which includes parameters from layer2 conv2d_1, layer 4 conv2d_2, and layer 6 conv2d_3. For the model with encoder and decoder both, the total parameters are 4,963 and trainable parameters are also 4,963.

$$L_H = -\sum_{k=1}^d [x_k \log z_k + (1 - x_k) \log(1 - z_k)] \quad (7)$$

The objective function for the convolutional auto encoder is binary cross-entropy which is also considered as a cost function for the model which is given by Eq.7. The stochastic gradient descent (SGD) method to train the model as given in the following section and randomly initialize the weight parameters of each layer. Activation function used here is rectified linear unit (Relu) and optimizer is stochastic gradient descent method with learning rate=0.01, momentum=0.9 in training. The model is experimented well with different combination of optimizers, epochs, and other hyper parameters to optimize performance. Model performance in terms of Accuracy is shown in figure 8 for initial experiment with epochs 100 and batch size 5. From the extensive experiments performed with encoder, it is observed that stochastic gradient descent optimizer yields better performance with epochs size more than 500 and



**Namrata Dave and Mehfuza S. Holia**

batch size 32 while training encoder model for the data set used. As seen in figure 9, performance of proposed approach improves with increasing epochs while training.

In the proposed approach, query images undergo a similar feature extraction process as training frames. Similarity between query features and stored dataset features is computed to retrieve similar video clips from the dataset. The results of a query and the first four retrieved video clip results are illustrated in Figure 10. Figure 11 displays the average precision values obtained for varying numbers of queries from the query set. The proposed system was tested on a machine equipped with an NVIDIA GPU TITAN Xp obtained through research funding. The success of our research lies in the remarkable performance achieved by the unsupervised deep learning approach utilizing Deep Denoising Auto encoders. With a Mean Average Precision (MAP) of 92.35%, our approach has demonstrated its prowess in enhancing video retrieval accuracy. This achievement holds particular significance when compared to the performance of the well-established Content-Based Video Retrieval (CBVR) method, which attained a MAP of 90% for English language Concept Retrieval, with a dataset consisting of 100 shots [3]. The 2.35% performance gain that our Deep Denoising Auto encoders exhibit over the CBVR approach underscores the effectiveness of leveraging advanced neural network architectures for video retrieval tasks. This gain translates into more precise and relevant retrieval outcomes, thus enhancing the utility of the video retrieval system. The implications of this performance difference are profound. A higher MAP indicates the ability of our approach to deliver more accurate and relevant video suggestions in response to user queries. This is crucial in various applications, such as media content recommendation, where improving user satisfaction through more accurate suggestions is paramount. Further more, our approach's ability to outperform CBVR while using unsupervised learning techniques demonstrates its adaptability and robustness. The achieved results not only validate the potential of Deep Denoising Auto encoders in video retrieval but also suggest avenues for further research in enhancing retrieval systems through deep learning.

CONCLUSION

The proposed unsupervised deep learning approach utilizing deep denoising auto encoders demonstrates robust performance in video retrieval tasks. An impressive Mean Average Precision (MAP) of 92.35% was achieved using this approach on a news video dataset. The system's evaluation was based on a query set designed for news story retrieval. The results exhibit significant improvements over existing state-of-the-art methods.

REFERENCES

1. M. H. Namrata Dave, "News Story Retrieval Based on Textual Query," *Int. J.Eng.Adv.Technol.*, vol.9,no.3, pp.2918–2922, 2020.
2. A.Singhal,P.Sinha,andR.Pant,"UseofDeepLearninginModernRecommendation System: A Summary of Recent Works," *Int. J. Computer.Appl.*,2017, doi:10.5120/ijca2017916055.
3. Mühling, Markus et al. "Deep learning for content-based video retrieval in film and television production." *Multimedia Tools and Applications* 76 (2017): 22169-22194.
4. R. Kanagavalli and K. Duraiswamy, "An enhanced algorithm for shot changedetection and object-based video retrieval using multiple features," *Eur. J. Sci.Res.*,2012.
5. R.KanagavalliandK.Duraiswamy,"Shotdetectionusinggeneticedgehistogramandobject-basedvideoretrievalusingmultiplefeatures,"*J.Computer.Sci.*,2012,doi:10.3844/jcssp.2012.1364.1371.
6. Hannane, R., Elboushaki, A., Afdel, K. et al, " An efficient method for video shot boundary detection and keyframe extraction using SIFT-point distribution histogram". *Int J Multimed Info Retr* (2016) 5: 89. <https://doi.org/10.1007/s13735-016-0095-6>
7. Salih, Fawzi & Abdulla, Alan. (2021). An Efficient Two-layer based Technique for Content-based Image Retrieval. *UHD Journal of Science and Technology*. 5. 28. 10.21928/uhdjst.v5n1y2021.pp28-40.





Namrata Dave and Mehfuza S. Holia

8. Salih, Shalaw& Abdulla, Alan. (2021). An Improved Content Based Image Retrieval Technique by Exploiting Bi-layer Concept. UHD Journal of Science and Technology. 5. 1. 10.21928/uhdjst.v5n1y2021.pp1-12.
9. K.Pramod Sankar, S.Pandey, and C.V.Jawahar, "Text Driven Temporal Segmentation of Cricket Videos," 2006.
10. C. V. J. Tarun Jain, "Compressed Domain Techniques to Support Information Retrieval Applications for Broadcast Videos," in Proceedings of National Conference on Computer Vision Pattern Recognition Image Processing and Graphics(NCVPRIPG'08), 2008,pp.154–159.
11. P.M.Kamde,S.Shiravale,andS.P.Algur,"Entropy Supported Video Indexing for Content based Video Retrieval,"Int.J.Comput.Appl.,vol.62,no.17,pp. 1–6,2013, doi:10.5120/10169-9974.
12. H. Ghosh et al., "Multimodal indexing of multilingual news video," Int. J.Digit. Multimed. Broadcast.,2010,doi:10.1155/2010/486487.
13. J. A. Vanegas, J. Arevalo, and F. A. Gonzalez, "Unsupervised feature learning for content-based histopathology image retrieval, "In Proceedings-International Workshop on Content-Based Multimedia Indexing, 2014, doi:10.1109/CBMI.2014.6849815.
14. P. Kulkarni, B. Patil, and B. Joglekar, "An effective content based video analysis and retrieval using pattern indexing techniques," in 2015 International Conference on Industrial Instrumentation and Control, ICIC 2015, 2015, doi:10.1109/IIC.2015.7150717.
15. H.Noh, A.Araujo, J.Sim, T.Weyand, and B.Han, "Large-Scale Image Retrieval with Attentive Deep Local Features," in Proceedings of the IEEE International Conference on Computer Vision, 2017, doi:10.1109/ICCV.2017.374.
16. S.Lange and M.Ried miller,"Deep auto-encoder neural network sin reinforcement learning," in Proceedings of the International Joint Conference on Neural Networks,2010, doi:10.1109/IJCNN.2010.5596468.
17. Y.Wang, H.Yao, and S.Zhao, "Auto-encoder based dimensionality reduction, "Neuro computing, 2016, doi:10.1016/j.neucom.2015.08.104.
18. Y. LeCun and C. Cortes, "MNIST handwritten digit database," AT&T Labs[Online].Available <http://yann.lecun.com/exdb/mnist>, 2010.
19. N. Dave, "Shot Boundary Detection for Gujarati News Video," Int. J. Res.Appl.Sci.Eng.Technol.,2018, doi:10.22214/ijraset.2018.3730.
20. D. M. S. H. Namrata Dave, "Advertisement Detection in broadcasted videos using Transfer Learning and Support Vector Machine, "in Turkish Online Journal of Qualitative Inquiry, Vol. 12 No. 7 (2021).
21. Vilas Naik, S. S. "Textual Query Based Sports Video Retrieval by Embedded Text Recognition", International Journal of Computer Engineering and Technology, (2013, July-August),.4(4), 556-565.
22. Rosebroc,"keras_conv2d_num_filters."https://pyimagesearch.com/wp-content/uploads/2018/12/keras_conv_2d_num_filters.png.

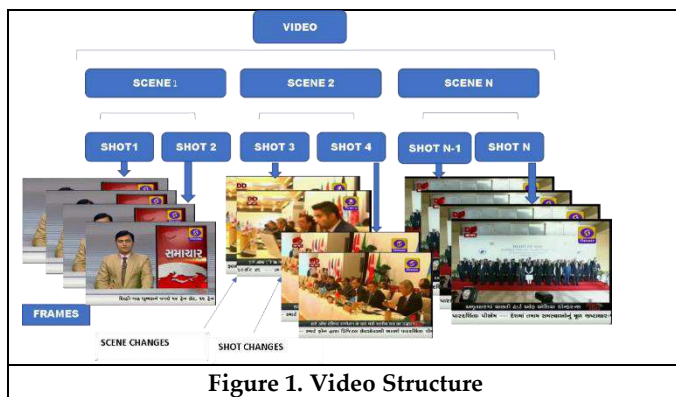


Figure 1. Video Structure

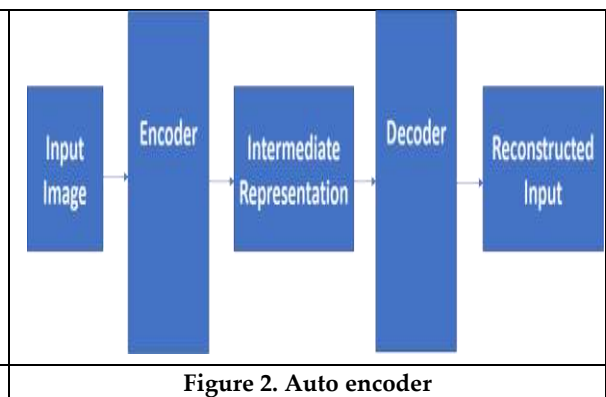


Figure 2. Auto encoder





Namrata Dave and Mehfuza S. Holia

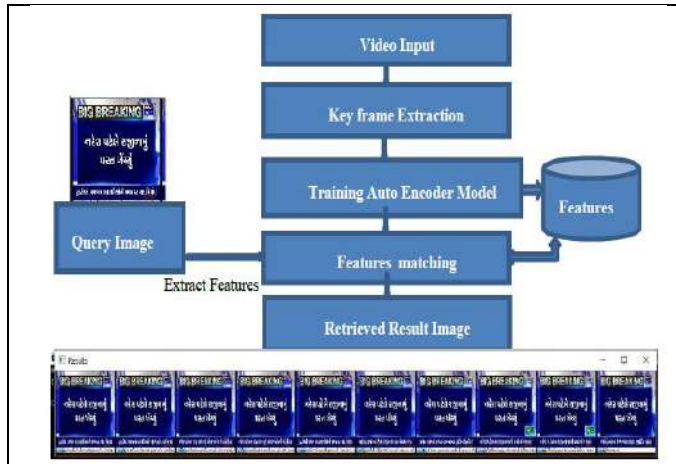


Figure 3. video retrieval using auto encoder approach

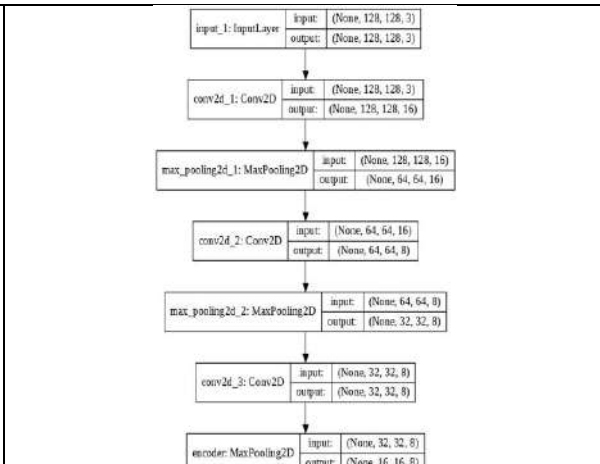


Figure 4. Architecture of Encoder

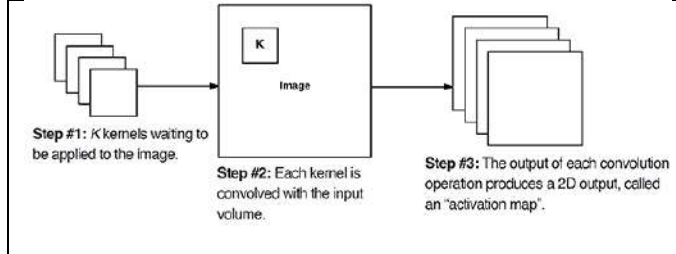


Figure 5 Conv2D parameters [22]

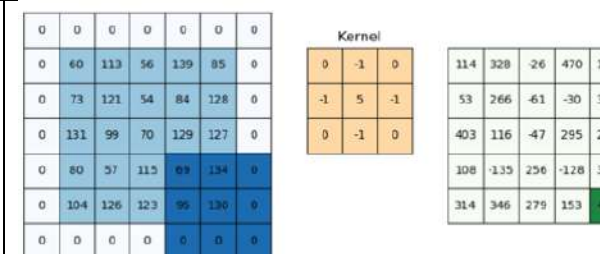


Figure 6. 3x3 kernel applied to an image with padding



Figure 7(a) Video frame used in training of size 128 x128x3 (b) Predicted code generated with encoder reshaped from the original shape 16x16x8

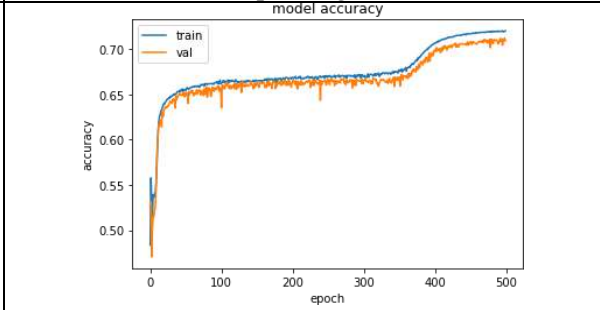


Figure 8. Model Accuracy for 100 epochs and 5 batches

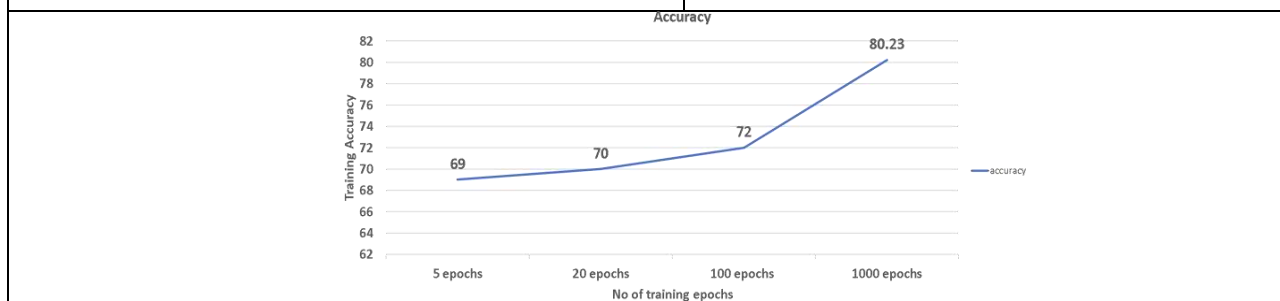


Figure 9. Performance Improvement with increasing epochs





Namrata Dave and Mehfuza S. Holia



Figure 10. Results of News Story clip Retrieval for given Query image

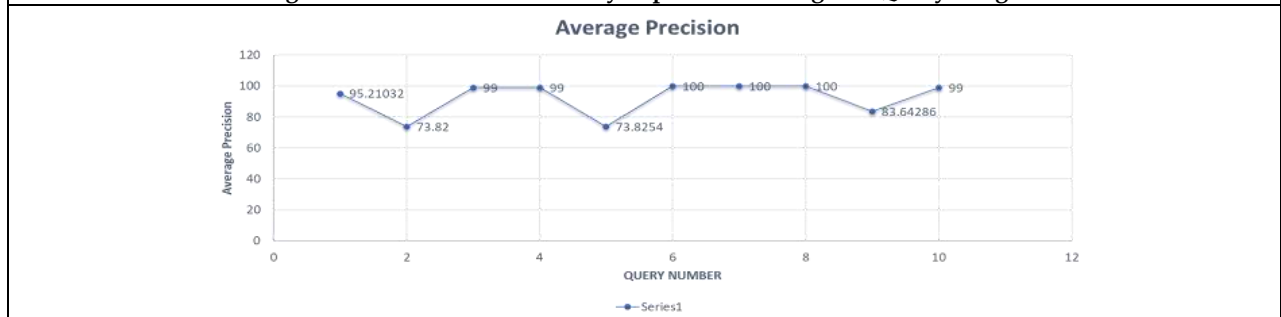


Figure 11. Performance of Image Query based video retrieval





Performance Analysis of Linear Predictive Coder (L.P.)

R.N.Rathod^{1*} and M.S.Holia²

¹Lukhdhirji Engineering College, Morbi, India.

²B.V.M. Engineering College, V.V.Nagar, India.

Received: 30 Dec 2023

Revised: 09 Jan 2024

Accepted: 12 Jan 2024

*Address for Correspondence

R.N.Rathod

Lukhdhirji Engineering College,

Morbi, India.

Email: jayveera.45@gmail.com



This is an Open Access Journal / article distributed under the terms of the **Creative Commons Attribution License** (CC BY-NC-ND 3.0) which permits unrestricted use, distribution, and reproduction in any medium, provided the original work is properly cited. All rights reserved.

ABSTRACT

Voice-coding has been found importance in the vicinity of next generation modern wireless communication and digital audio as well as voice processing. voice-coding is the art of renovating the voice signal in a more dense form, which can be broadcasted with a small numbers of binary digits. Linear Predictive Coding is an extensively utilized technique in audio as well as Voice signal processing. It has create particular use in voice-signal Compression, allowing for very high density rate. This Paper talk about about two speech segments sampled at 22KHz and Windowed, Log, L.P. Spectrum with L.P. residual for different L.P. order for Rectangular, Hamming, Hann window and found both source and system information through envelope of the spectrum and spectral ripples. The common observation that can be made from observing the spectrum of the Linear predictive coding is that Cor-relation being gradually removed in the 'L.P. residual' signal as the 'L.P. order' is raised, and 'L.P. residual' signal for an 'L.P. order' of 10 or above removes most of the correlations in the input signal, and the resulting signal looks like a train of impulses. The 'L.P. log spectrum' approximates the short-time spectral envelope i.e. formants better with increased Linear Prediction order.

Keywords: Linear Predictive Coding, Log Spectrum, L.P.C. co-efficient, L.P.C. Synthesis

INTRODUCTION

Wireless communication (W.C.) is an emerging field which has seen enormous growth in last few years. The huge uptake rate of mobile phone technology and exponential growth of the Internet of Things have resulted in the increasing demand of the Voice coder which can compress the data & transmit it with a fewest number of bits. As far as Growth in Next generation modern wireless technology connected with the up gradation in voice coder, 4th & 5th generation wireless system is popular in world market due to their low bit rate voice coder only. The 4th & 5th generation W.C. systems were proposed to provide interactive multimedia communication incorporating tele-conferencing, internet access and variety of other services that become feasible with low complex, low cost, lower bit

68898



**Rathod and Holia**

rate & less processing delay[1,2]. While designing any particular voice coder for N.G. modern wireless technology, this listed attributes play a vital role. Voice-coding is defined as the procedure of shrinking the bit rate of digital voice-speech signal representation for communication or storage while maintaining a speech (voice) quality adequate for the application. In general, it is the way to represent the speech (voice) signal with the fewest number of bits, while maintaining a sufficient level of quality of the retrieved or synthesized speech with reasonable computational complexity. To achieve high-quality speech at a low bit rate one can apply coding algorithm (sophisticated method to reduce the redundancies from the voice-speech signal). Low bit rate voice-speech technology is a key factor in meeting the ever-increasing demand for new digital wireless communication services[7]. Impressive progress has been made during recent decades in coding voice with high quality at low bit rate and low cost. In today's N.G. Modern wireless communication we can offer high quality over cellular channel at data rate less than 4kbps. L.P.C is a method to represent and analyze human voice. It is widely utilized technique in audio/voice signal processing. It has found particular use in voice signal compression, allowing for very high density rate. Linear prediction (L.P.) forms an integral part of almost all modern day voice coding algorithms[4,8]. The fundamental idea is that a speech sample can be approximated as a linear combination of past samples. Within a signal frame, the weights used to compute the linear combination are found by minimizing the mean-squared prediction error; the resultant weights, or linear prediction coefficients (L.P.Cs), are used to represent the particular frame. L.P. can also be viewed as a redundancy removal procedure where information repeated in an event is eliminated. After all, there is no need for transmission if certain data can be predicted. By displacing the redundancy in a signal, the amount of bits required to carry the information is lowered, therefore achieving the purpose of compression[3,6].

Linear prediction analysis and synthesis

Fig.1 represents the block diagram showing L.P.C co-efficient obtained from input voice signal. First, the I/P signal is divided into a frame duration of 20ms duration followed by windowing to remove discontinuity & taper down the edge. After windowing voice signal is given to linear predictor to find out L.P.C co-efficient. Thus, instead of transmitting the PCM samples, parameters of the model are sent to achieve compression[8,10]. As shown in Fig.1 compression of the voice file from the original voice file based on L.P.C can be done in seven steps as below:-

Speech file

This is a speech file in .wav form. This may be any arbitrary speech file given as an input to the next module.

Divide into the frames

This module will divide each .wav file into 20-30 ms frames. Each frame generated in this way will be given as input to the next module for its analysis. The frames obtained in this way are given as input to the function.

Find parameters

This module will collect some of the data required for regenerating the original input signal (voiced/unvoiced, gain, pitch). High amplitudes of the voiced sounds and high frequency of the unvoiced sounds will be used to determine whether a sound is voiced or unvoiced. An algorithm called the Average Magnitude Difference Function (AMDF) will be used for pitch period estimation. The gain of the filter will also be determined.

L.P.C technique

This module will generate the remaining data required to reconstruct the original voice signal. This data is the coefficients of the synthesis filter. These are to be calculated using the Autocorrelation method. In this method using the concept of minimum prediction error, a matrix is obtained where the variables are the filter coefficients. The solution of the matrix obtained in the Autocorrelation method will be found using the efficient Levinson Durbin algorithm. This algorithm can be used because of the special properties of the Autocorrelation matrix. It reduces the complexity of multiplication[5,8].



**Rathod and Holia****Regenerate frames**

This module will consist of the synthesis filter. The synthesis filter will receive input. The excitement signal will be passed through the filter to produce the synthesized speech signal.

Reconstruct signals

In this module, the frames are put back together to reconstruct the original signal. Source filter model for sound production.

Compressed Speech file-This is the final output as shown in Fig.1.It will be compared with I/P. & analyzed accordingly.

L.P.C analysis

The Fig.2 illustrate a block diagram of an L.P.C analysis, where S is the input signal, g is the gain of the residual signal and a is a vector containing the L.P.C coefficients to a specific order. The size of the vector depends on the order of the L.P.C analysis. Bigger order means more L.P.C coefficients and therefore better estimation of the vocal tract[9,10].

L.P.C estimation

L.P.C estimation calculates an error signal from the L.P.C coefficients from L.P.C analysis. This error signal is called the residual signal which could not be modeled by the L.P.C analysis. This signal is calculated by filtering the original signal with the inverse transfer function from L.P.C analysis. If the inverse transfer function from L.P.C analysis is equal to the vocal tract transfer function then the residual signal obtained from the L.P.C estimation equal to the residual signal which is put into the vocal tract. In that case, residual signal equal to the impulses or noise from human speech production. The Fig. 3 characterize a block diagram of L.P.C estimation where S is the input signal, g and a is calculated from L.P.C analysis and e is the residual signal for L.P.C estimation[9,10].

L.P.C-synthesis

L.P.C synthesis is used to reconstruct a signal from the residual signal and the transfer function of the vocal tract. Because the vocal tract transfer function is estimated from L.P.C analysis can this be used combined with the residual/error signal from L.P.C estimation to construct the original signal. Fig. 4 portray the block diagram of L.P.C synthesis where e is the error signal found from L.P.C estimation and g and a from L.P.C analysis[9,10]. Reconstruction of the original signal s is done by filtering the error signal with the vocal tract transfer function respectively. finally both the output are combined via an L.P.C synthesizer to get the required W.B. signal. Input signal before L.P.C analyzer, input signal after L.P.C synthesizer with the error signal is depicted in Fig.5.

Analysis of the Linear Predictive coder (L.P.) for various types of windowing techniques with observations

Two audio file Ex.1 & Ex.2 are sampled at 22KHz. Spectrum might be changed as per selection of Sampling frequency. All analysis are done for Rectangular, Hamming & Hann windo(All window Sizes are 512 Samples). The Windowed Waveform signal, Log Spectrum, L.P. Residual and the L.P. Spectrum are as shown in Fig. 7 to 22. for different windowing techniques. One common observation that can be found from analysis is that the 'L.P. log spectrum' approximates the short-time spectral envelope (formants) better with increased Linear Prediction(L.P.) order. one another observation is that as the 'L.P. order' is increased to near about 40, the 'L.P. spectrum' tries to approximate the short-time spectral envelope more closely thereby approximating peaks due to pitch harmonics. From the cor-relation point of view by observing the correlations in the input segment of voice one can say that it being gradually removed in the 'L.P. residual' signal as the 'L.P. order' is raised, and 'L.P. residual' signal for an 'L.P. order' of 10 or above removes most of the correlations in the input signal, and the resulting signal looks like a train of impulses.





Rathod and Holia

CONCLUSION

In the recent Scenario of advancement in next generation modern wireless technology there is an indeed demand of Voice coding which compress data and transmit it with less number of bits to take advantage in terms of storage. Linear Predictive Coding is an extensively utilized technique in audio as well as Voice signal processing. It has create particular use in voice-signal Compression, allowing for very high density rate. From the analysis performed for various windowing techniques for various Linear Prediction (L.P.) order starting from 1 to 40 one can say that 'L.P. log spectrum' approximates the short-time spectral envelope (formants) better with increased L.P. order. One common observation that is made from the whole analysis is that as the 'L.P. order' is increased to near about 40, the 'L.P. spectrum' tries to approximate the short-time spectral envelope more closely thereby approximating peaks due to pitch harmonics.

ACKNOWLEDGMENT

The Author would desire to thank Dr.T.D.Pawar, Professor & Head of Electronics Department, B.V.M. engineering college for his valuable Guidance and support.

REFERENCES

1. G. Laura Laksonen," Bandwidth extension of NB speech-enhanced speech quality & intelligibility in mobile device", Doctoral Dissertations, alto University,2013.
2. T. Ruppaport, "Wireless Comm. Principles and Practice", Prentice-Hall,1996.
3. L. R. Rabiner and R.W. Schafer, Digital Processing of speech signals, Prentice-Hall,1978.
4. R.N. Rathod, M.S Holia & N.S .Bhatt, "B.W.E. and Quality Evaluation of Speech Signal Based On QMF And S.F.M. Using Simulink and MATLAB," International Journal of Research and Analytical Reviews, pp 404-411,2019.
5. Monika Yadav et al, "Speech Coding Technique And Analysis Of Speech Codec Using CS-ACELP.", IJESAT, ISSN:2250-3676,vol.-6, Issue-3, pp.143-151, JUNE-2016.
6. P. Jax and P. Vary, "B.W.E. of speech signals: A catalyst for the introduction of wide band speech coding?," IEEE Commu. Mag., vol. 44, no. 5, pp. 106–111, 2006.
7. Vijay K. Garg & Joseph E. Wilkes, "principles and application of GSM" Pearson Education, 2004.
8. W. C.Chu. Speech Coding Algorithms Foundation Evolution of Coders, Wiley Publications.2003.
9. Karthikeyan N. Ramamurthy and Andreas S. Spanias, MATLAB Software for the Code Excited Linear Prediction Algorithm The Federal Standard–1016,2010.
10. Bandwidth Expansion of Narrowband Speech using Linear Prediction, AALBORG UNIVERSITY, Institute of Electronic Systems, September - December 2004..
11. U. Lindgren and H. Gustafsson, "Speech BW extension," US Patent no. 2002/0128839 A1,2002.

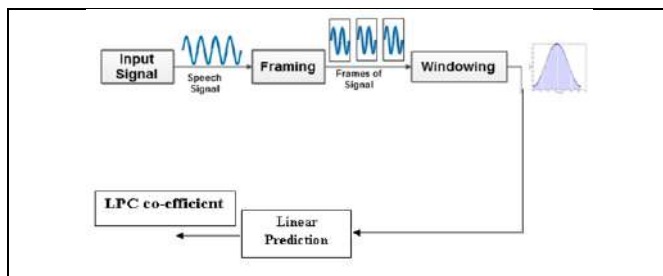


Fig. 1 L.P.C co-efficient obtained from Input Speech Signal [some part adapted from [10]

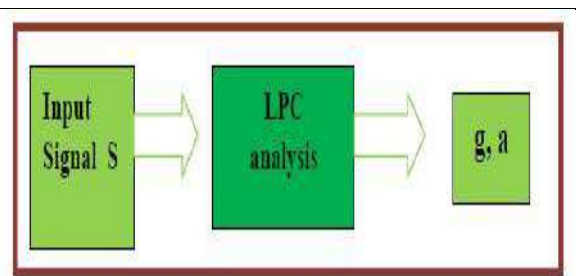
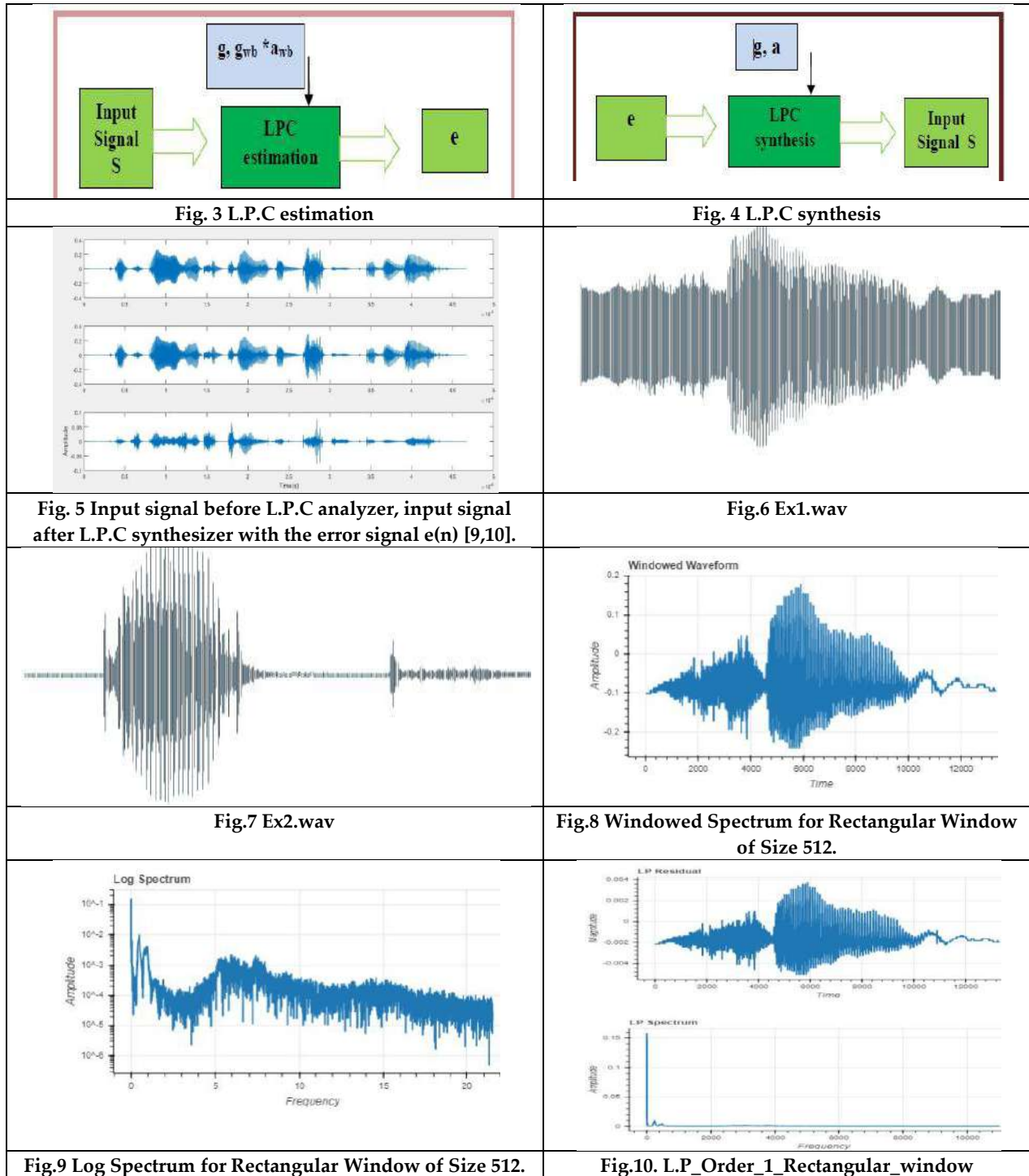


Fig. 2 L.P.C analysis







Rathod and Holia

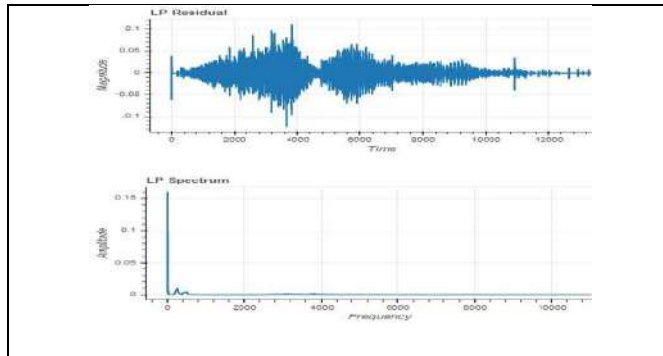


Fig.11. L.P_ Order_10_ Rectangular_ window

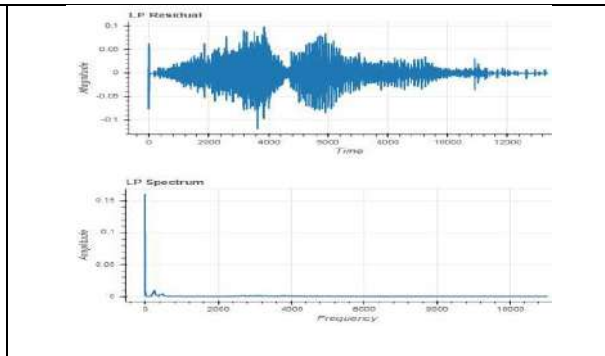


Fig.12. L.P_ Order_20_ Rectangular_ window

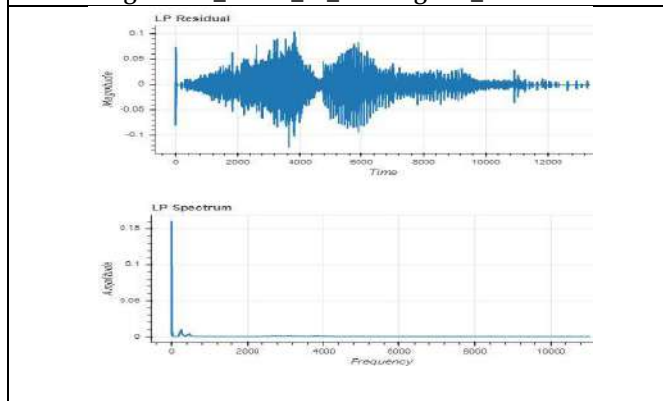


Fig.13. L.P_ Order_40_ Rectangular_ window

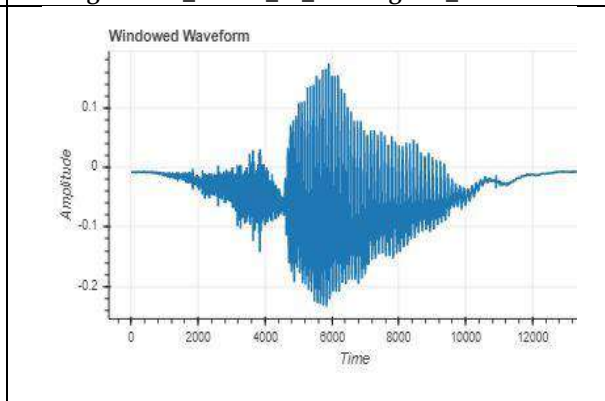


Fig.14. Windowed Spectrum for Hamming Window of Size 512

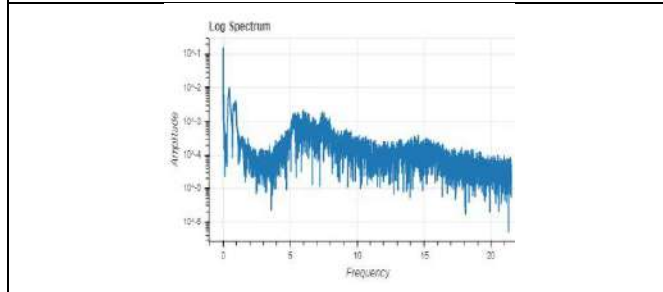


Fig.15. Log Spectrum for Hamming Window of Size 512

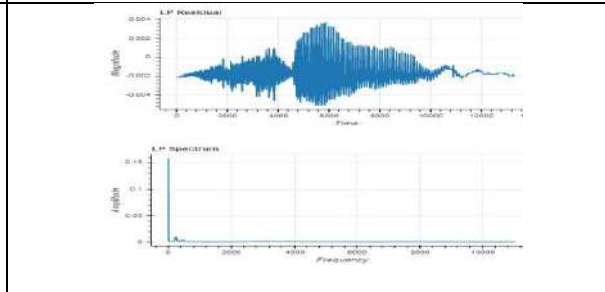


Fig.16.L.P_ Order_1_ Rectangular_ window

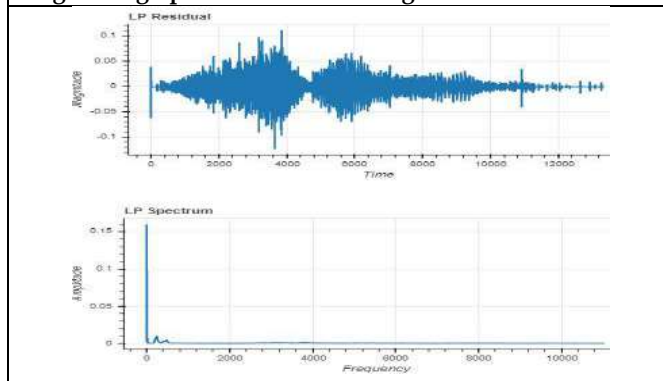


Fig.17.L.P_ Order_10_ Rectangular_ window

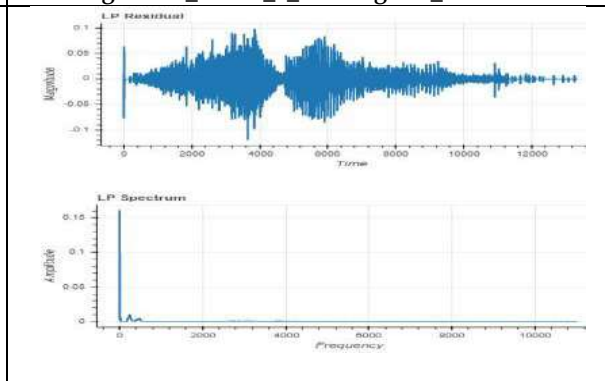


Fig.18. L.P_ Order_20_ Hamming_ window





Rathod and Holia

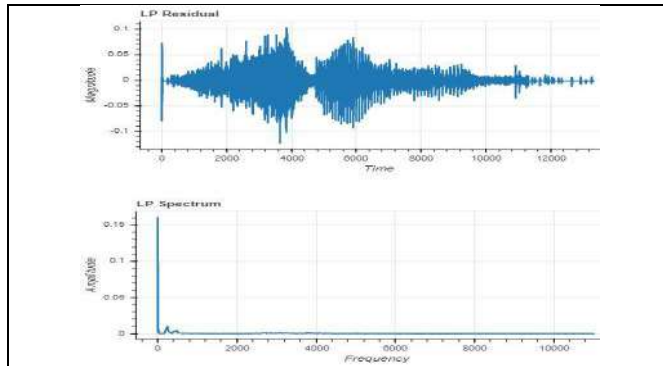


Fig.19. L.P_Order_40_Hamming window

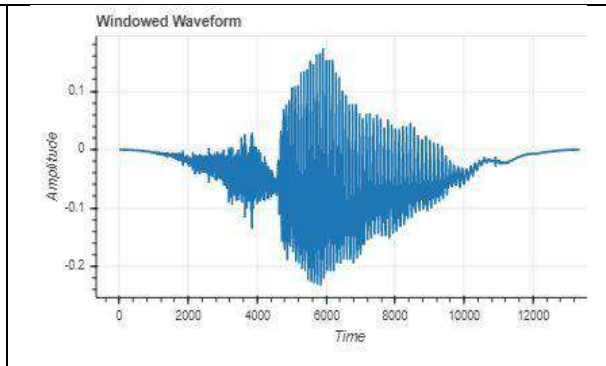


Fig.20. Windowed Waveform for Hann Window of Size 512

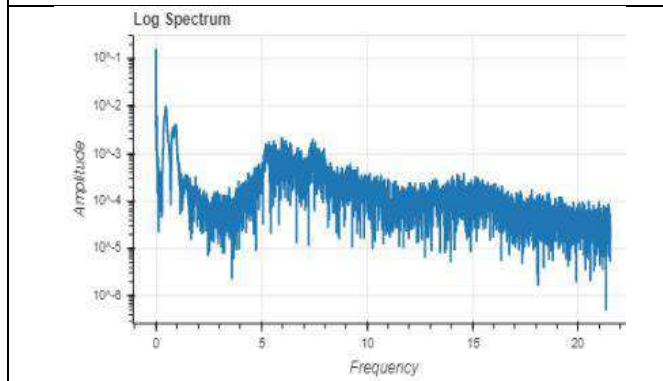


Fig.21. Log Spectrum for Hann Window of Size 512

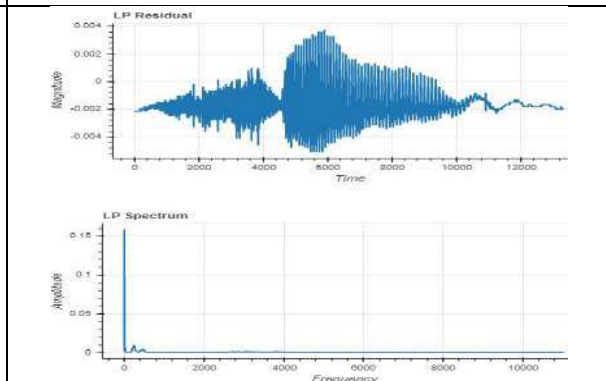


Fig.22. L.P_Order_1_Hann_window

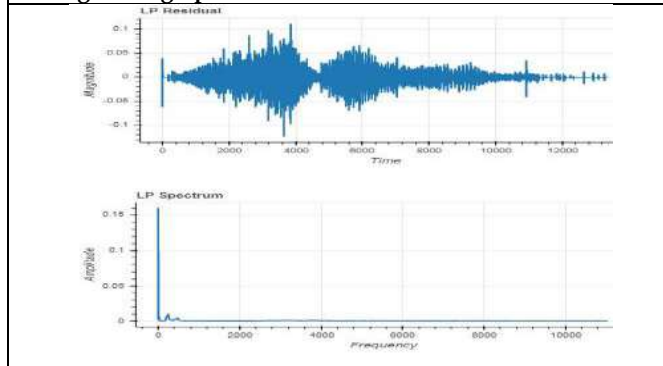


Fig.23. L.P_Order_10_Hann_window

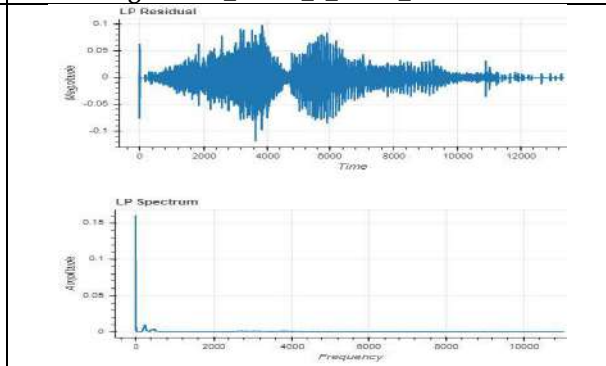


Fig.24. L.P_Order_20_Hann_window

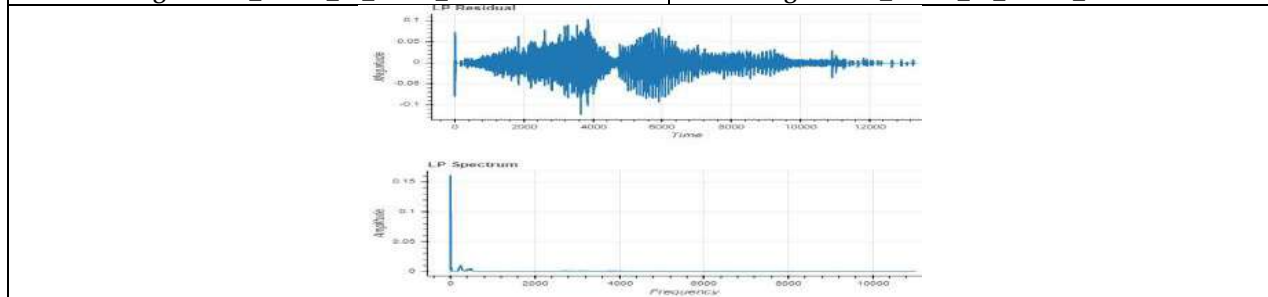


Fig.25. L.P_Order_40_Hann_window





Systematic Review of Diagnosis and Classification Techniques of Acute Lymphoblastic Leukaemia and Acute Myeloid Leukaemia Cells

Rimi N.Agrawal^{1*} and Viral Kapadia²

¹ Assistant Professor, Sardar Vallabhbhai Patel Institute of Technology, Vasad, India.

² Associate Professor, M.S. University, Vadodara, Gujarat, India.

Received: 30 Dec 2023

Revised: 09 Jan 2024

Accepted: 12 Jan 2024

*Address for Correspondence

Rimi N.Agrawal

Assistant Professor,

Sardar Vallabhbhai Patel Institute of Technology,

Vasad, India

Email: rims.gupta15@gmail.com



This is an Open Access Journal / article distributed under the terms of the **Creative Commons Attribution License** (CC BY-NC-ND 3.0) which permits unrestricted use, distribution, and reproduction in any medium, provided the original work is properly cited. All rights reserved.

ABSTRACT

White blood cells, or leukocytes, can unexpectedly spread throughout the bone marrow and blood, resulting in blood cancer or leukaemia. It affects kids and teens more frequently than any other illness. By looking at the patient's blood smear under a microscope, haematologists can identify leukaemia. It can identify and categorise leukaemia by counting blood cells and looking at biological characteristics. However, the manual method used to diagnose leukaemia is exceedingly time- and labour-intensive. Machine learning, deep learning, and expert systems are many computer-aided practical approaches in computer science that can improve the accuracy and speed of detection and classification of leukaemia blood cells in comparison to the outcome produced by human analysis (manual technique). This paper provides thorough review of the diagnosis and Classification of the acute leukaemia, including image segmentation, feature extraction, feature selection, and classification approaches, are thoroughly analysed in this study. Based on the type of classification step, all diagnosis and classification methods can be divided into four groups: traditional methods (ML), Deep Neural Networks (DL) methods, Expert system methods, and mixture approaches (ML + DL). Based on the review some of the future scope of work is also outlined.

Keywords: Acute Leukaemia, Machine Learning, Deep learning, Expert System

INTRODUCTION

A very important part of the body, blood carries minerals, oxygen, and carbon dioxide to the entire body, among other bodily activities. Red blood cells (RBC), white blood cells (WBC), and platelets make up the majority of blood [1, 2]. Automatic identification, classification, and diagnosis of haematological illnesses are challenging and



**Rimi N.Agrawal and Viral Kapadia**

important tasks in the field of medical image processing. Leukaemia is a haematological illness that develops in the bone marrow and causes an increase in the number of immature white blood cells known as "Blasts," which are fatal if left untreated within a few weeks. Leukaemia is primarily brought on by exposure to high radiation dosages, electric and magnetic fields, hereditary factors, or chemical dissolvent [3]. The presence of too many blast cells in peripheral blood is one of the most significant signs of leukaemia. Haematologists commonly analyze blood cells under a microscope to properly identify and categorise blast cells for this reason. The discussion of blood cell type's forms of Leukaemia, and a step-by-step process for classifying Leukaemia photographs is included in the following sections to help readers understand Leukaemia better.

Types of Leukocytes/ White Blood Cells

Based on Blood Cells functional and physical characteristics it divides as: monocytes, lymphocytes, basophile, eosinophil, neutrophil [4]. Lymphocytes: T cells, natural killer cells, and B cells make up lymphocytes, which protect against viral infections and create proteins that aid in the fight against infection (antibodies).

Neutrophils: By eradicating bacteria, fungus, and foreign debris, they defend the human body against illnesses.

Monocytes: Clear away harmed cells to protect against infection.

Basophils: Causes allergic reactions such as runny nose, coughing, and sneezing.

Eosinophils: Eosinophils help basophils with human allergy reactions and can recognize and kill parasites and cancer cells. Below Fig 1. Shows images of different types of WBC.

Types of Leukaemia

Based on the Blood Cells development and how quickly disease growth it categorizes in two types: Acute Leukaemia and Chronic Leukaemia.

Acute Leukaemia cells growth very quickly. The number of Leukaemia cells increases rapidly, and these abnormal cells don't do the work of normal white blood cells. Acute Leukaemia comprises of a large number of Leukaemia which differ in etiology, pathogenesis, morphology, course and prognosis. Acute Leukaemia contains more than 20% blasts in the peripheral blood/ bone marrow. Leukaemia detection can be treated as the crucial task, as it is necessary to diagnose the RBCs/WBCs/Platelets rather than the diagnosis organs.

Chronic Leukaemia cells growth slowly. The Leukaemia cells work almost as well as normal white blood cells. At very first time, people will not feel sick and the first sign of illness may be abnormal results on a routine blood test. If not treated, the Leukaemia cells may later crowd out normal blood cells. Identification of Leukaemia as either lymphoblastic or myelogenous, depending on the type of White Blood Cell influenced on human body. If the influenced cells are granulocytes and monocytes, then the Leukaemia will be categorized as myelogenous, Acute Myeloid Leukaemia [AML] and Chronic Myeloid Leukaemia [CML]. If cells are lymphocytes, then the Leukaemia is categorized as lymphoblastic, Acute Lymphoblastic Leukaemia [ALL] and Chronic Lymphoblastic Leukaemia [CLL]. Here, mainly Acute Leukaemia types in detail have been discussed [5, 6] Acute Lymphoblastic Leukaemia (ALL): It's a prime symptom is the increase of blast cells inside the bone marrow and the decrease number of ordinary blood cells. This type of Leukaemia is more common in children under 15 years of age. Lack of treatment for this disease causes the production of many lympho blastoid cells in the body and can lead to death [4, 7, and 8]. Standard promising treatments involve chemotherapy and radiotherapy [10]. According to FAB- French American British classification, the subtypes of ALL: L1, L2 and L3 which are based on the morphological structure of cell [11]. As per the information provided by the haematologist and visual observation, it can be known that shape-size of these types of acute leukemic cells are irregular and that cannot be easily visualized by the microscopic examination [12]. L1 cells have coarse chromatin, are generally tiny, and have a uniform population in their nuclei. All-L1 cells are uniformly formed and tiny [24]. L2 cells are larger than L1 cells and are distinguished by nuclear heterogeneity. Large cells and an uneven nuclear membrane characterize ALL-L2 cells [24]. The presence of prominent vacuoles inside L3 cells gives them their name. Their nuclei are often larger than L1 and have homogeneous populations [15]. Giant ALL-L3 cells have vacuoles, which are holes-like structures [24]. The sample images of Acute Lymphoblastic Leukaemia and its subtypes L1, L2, L3 are shown in below figure 2.



**Rimi N.Agrawal and Viral Kapadia**

Acute Myeloid Leukaemia (AML): AML is a quickly-growing cancer of the blood and bone marrow. AML is the usual kind of Leukaemia that generally effects to the adults and infant both. It mainly grows myelocytes rapidly that make RBCs, WBCs and platelets. The bone marrow in this disease generates the myeloblasts, abnormal RBCs or sometimes platelets that are the most unique myeloid disorder in persons [7, 8]. In figure 3 shown the AML image. In most of the cases early detection of this type of cancer may cause to successful treatment. According to FAB-French American British classification, the subtypes of AML: M0, M1, M2, M3, M4, M5, M6, and M7. The characteristics of all the subtypes of AML are given below. M1: immature M2: mature M3: promyelocytes M4: myelo monocytes M5: monocytes/monocytes M6: erythrocytes M7: megakaryocytes. The FAB classification of ALL and AML is based on the morphology and cyto chemical staining of the blasts. Both are distinguished based on morphology, including cell size, prominence of nucleoli, colour of cell and the amount and appearance of cytoplasm [22]. In the early phases the Pathologists and haematologists can diagnose or detect the immature Leukaemia blasts from normal cells under a microscope by screening of blood smear, on a thin, microscope slide layered with blood. Generally, this method is error prone and labour-intensive task for the Haematologists or Pathologists. In addition, diagnostic confusion may be occurred due to the existence of similar appearance by other disorders. To overcome the above limitations, when microscopic blood image analysis is used for Leukemia detection, various computer-aided diagnostic methods for acute Leukemia are used. These methods have proven to be more efficient, faster, more cost effective and more accurate than manual methods [15]. For diagnosis of Leukaemia as well as their particular types is important for haematologists to avoid medical risks and specify the right treatment. Thus, using intelligent ways for diagnosis will assist accurate and speed up the discovery of Leukaemia subtypes using the blood cells images. Machine Learning methods in computer vision are One of the smart ways to solve the above challenges and problems. Diagnosis and classification of acute Leukaemia is easier and less expensive using traditional machine learning and deep learning and expert system techniques. Exist in the following of this section, machine learning procedure for diagnosing and classifying Acute Leukaemia have been discussed below

Traditional Machine Learning Procedure

The Traditional machine learning can diagnosis the Leukaemia from the given images/ inputs by following the below steps.

Image Pre-processing

Image pre-processing is the term for operations on images at the lowest level of abstraction. The aim of pre-processing is an improvement of the image data that suppresses undesired distortions or enhances some image features relevant for further processing and analysis task. Many techniques to identify blood cell images and have them effectively segment regions of interest (ROI). There are many image pre-processing techniques can be applicable to enhancing an image quality such as Histogram equalization, Minimum filter, Gaussian filter, Median filter, Unsharp masking, Linear contrast stretching and normalization [24][25]. For Enhanced the blood image the researchers have changed a colour domain of sample images. Like Convert RGB: (R-red, G-green, B-blue) to HSV (H-hue, S-saturation, V-value) or CMYK (C- Cyan, M- Magenta, Y- Yellow, K – Key (black)). By changing the colour domain of the images, it can highlight the features of objects for efficiently detecting ROI.

Image Segmentation

To classify the abnormal blood cells in their respective types and subtypes of Leukaemia, a haematologist observed some cells under a microscope for the abnormalities presented in the Nucleus or Cytoplasm of the cells. But this above method is very slow and not standardized accuracy since it depends on the Operator's capabilities and tiredness. Therefore, fast and effective segmentation procedures were invented for blast images which are very helpful for improving the haematological procedure and accelerating diagnosis of Leukaemia diseases. Segmentation is procedure that enhanced the blood image for the successful feature extraction and classification. So, that segmentation plays an important role for the diagnosis of Leukaemia. Segmentation subdivides the blood image in subparts like Nucleus and Cytoplasm mainly. This division must stop when objects or ROIs are isolated. Image Segmentation includes many methods such as Clustering based Segmentation [29, 31], Fuzzy C-means Clustering based Segmentation [32], Watershed segmentation [27, 28], Active Contour model [30], Otsu's Thresholding [33, 34].



**Rimi N.Agrawal and Viral Kapadia**

The segmentation phase is one of the most crucial and difficult phases of diagnoses and classifying acute leukaemia since it is absolutely necessary for the effectiveness of the steps that follow.

Feature extraction

The feature extraction technique which is carried out after the segmentation process plays a vital role in differentiating the normal cells from the Leukemic cells. An autonomous white blood cell classification system performs best when its features are extracted [14]. The majority of the currently used techniques use the following characteristics: geometrical characteristics (such as area, radius, perimeter, convex area, major axis length, compactness, and orientation) [36], textural characteristics (such as momentum, contrast, entropy, and skewness) [37, 38, 39], and colour characteristics (e.g., colour distribution and histogram) [40]. The computer aided diagnostic system based on Machine Learning is used feature extraction as a different module where in Neural network-based diagnosis automatically extract the features from the images via network. By deleting unnecessary data from the original image during the feature extraction process, the size of the image is reduced. As a result, it shortens the execution time at this stage and speeds up processing [35].

Feature Selection

It is required to normalise the data set with a wide range of values before classifying anything, as well as to calculate how well each feature or group of characteristics can distinguish between the named classes. To learn a classification system, the most important characteristics are chosen using feature selection approaches. Eliminating unnecessary and pointless features from the feature set allows for feature selection. This enhances the efficiency of the classifier while also reducing storage and calculation cost [41]. For the feature selection there are no of techniques can be used like with correlation, univariate feature selection, recursive feature elimination (RFE) [42], recursive feature elimination, with cross-validation (RFECV) [36] and tree-based feature selection (TBFS) [36].

Classification

Classification is the process of searching or associating an unknown test vector with a recognised class. Different combinations of features and classifiers are developed and evaluated for classification. For effective results, the classifier is built up in accordance with the data, which is separated into a training data set and a test data set [42]. The model is developed, tested, and validated using training data. Few categorization techniques for identifying acute leukaemia in this stage have been discussed. The categorization stage is broken into the following four parts Deep neural networks, expert systems, conventional approaches, and hybrid methods. All of the aforementioned classification techniques fall under the heading of supervised classification.

Traditional approaches to the classification of acute Leukemia

This section discusses many previous studies that have used traditional approaches to classify acute Leukemia. In traditional machine learning methods, feature extraction is done manually by using different techniques. Number of classification methods are invented like Support vector machine, KNN, Random forest, Naïve Bayes, Artificial neural network etc. Previous work on the detection and classification of acute Leukemia using traditional methods has been published in given table 1 below.

Learning Based Acute Leukemia Classification Approaches

This section presents some previous work on acute Leukemia classification using DNN (DL). Table 2 shows abstract view of previously implemented different DNN methods for Leukaemia diagnosis and classification. Actually, the Traditional methods used to manually feature extraction step, but DNN used this step automatically. The automated feature extraction phase eliminates the expense of the feature extraction and reduction processes and enables the DNN to operate from beginning to finish. Models can be categorized into different types such as Deep Belief Networks (DBN), CNN, RNN, LSTM, Deep Auto encoders (AE), Generative Adversarial Networks (GAN), etc. The model works from the acute Leukemia methods are classified in table below The DNN model uses a CNN to classify acute Leukemia. In [58-70], CNN is used for classification, and its accuracy is higher than that of the others.



**Rimi N.Agrawal and Viral Kapadia****Expert system for Acute Leukaemia classification**

Programs that give experience, skills, and the capacity of trained experts to reason in a particular field are known as expert systems. Expert systems require methods for utilizing the information to solve issues as well as comprehensive knowledge about a certain subject. It is necessary to formulate the knowledge in order to construct a knowledge system. In other words, it should be comprehended in formal formats, delivered to the computer, and altered in accordance with the problem-solving approach [44]. The main objective of the expert system for diagnosing acute Leukaemia is to diagnose it in the first stage of illness development. There is uncertainty in real systems, the measured data provided in the blood test experiments and expert's knowledge for diagnosis. This section classifies the traditional procedure for the medical diagnosis of Leukaemia employed by physician is analyzed using expert system that can be neuro fuzzy system, fuzzy system, and VP-expert system [72, 73, 74, and 75]. Table 3 the summary of previous work done in diagnosis and classification of Leukaemia using expert system.

Mixed methods for the classification of acute Leukemia

In this section, the classification procedure that have used two or more methods in the diagnosis and classification steps of malignant and benign cancer cells are reviewed. Like combination of SVM + CNN, SVM+ RF+ MLP, CNN + RNN and SVM+NN. Table 4 Shows the summary of previous work done in diagnosis and classification of Leukemia using Hybrid model.

Performance Evaluation key Parameters

A confusion matrix is used to construct classification algorithms, which are necessary for fully automated sickness identification. The confusion matrix in this study represents the divergences of opinion between the classifier and the haematologist. The performance of the all the classifiers are evaluated by the different measures like Accuracy (ACC), sensitivity (SE), specificity (SE), positive predictive value (PPV), negative predictive value (NPV), F-measure. These measurements are calculated based on true positive (TP), true negative (TN), false positive (FN) and false negative (FN) those are the states of the Confusion matrix given in Table 5 All the above performance measures are mentioned below [46].

CONCLUSION AND FUTURE ENHANCEMENT

As is well known, one of the most prevalent diseases in existence today is cancer. Acute and chronic kinds of Leukaemia affect people of practically all ages. A hazardous kind of Leukaemia, acute is more fatal. The authors have first thoroughly reviewed the procedures for identifying and classifying acute Leukaemia using a computer system in this review study. The stages for the diagnosing and classifying the Acute Leukaemia include image pre-processing, image segmentation, feature extraction, feature selection and finally classification. Then, a review of the previous work done on the classification steps. Here, the authors have analysed overall classification work done in four categories, which are Traditional, DNN, Expert system and Mixed (ML+DNN) base on the type of the classifier. From the above literature review, there would be some other further future work can be as follow.

1. In future can be extend the current work to unstained blood smear images and improve upon the sub classification based on cancer progression for each leukemic type.
2. It can be improved Sensitivity and Specificity ratio so that may not be generate FP and FN result. As FP and FN classification is very dangerous for the patients.
3. More segmentation algorithms can be explored so as to obtain better result.
4. By using Hybrid combination of Machine Learning, Deep Learning and Expert System it can be improved the classification accuracy.
5. It can be applied CNN model on the 3D images instead of 2D images that can be more effective for the classification improvement.





Rimi N.Agrawal and Viral Kapadia

If above all the task can enhance in future then it will be very beneficial for today's fast life and early detection of Leukaemia by pathologists with better accuracy. It will also be helping to physicians, patients and also any decision maker to diagnose the Leukaemia.

REFERENCES

1. Supardi, N.Z., et al.,(2012). Classification of blasts in acute Leukaemia blood samples using k-nearest neighbour. IEEE 8th International Colloquium on Signal Processing and its Application.
2. Alsalem M.A., et al.,(2018). A Review of the Automated Detection and Classification of Acute Leukaemia: Coherent Taxonomy, Datasets, Validation and Performance Measurements, Motivation, Open Challenges and Recommendations. In Computer Methods and Programs in Biomedicine.
3. Krishna K.J, Himadri S.D, (2019). Mutual Information based hybrid model and deep learning for Acute Lymphocytic Leukaemia detection in single cell blood smear images, Elsevier.
4. Maneela S., et al.,(2021). Acute Myeloid Leukaemia (AML) Detection Using Alex Net Model. In Hindawi Complexity.
5. Laosi J, Chamnongthai K, (2018). Classification of acute Leukaemia using medical knowledge-based morphology and cd marker. Biomed Signal Process Control.
6. Pansombut, T.; Wikarisuksakul, S.; Khongkraphan, K.; Phon-on, a, (2019). Convolutional neural networks for recognition of lymphoblast cell images, Comput Intell Neurosci.
7. Mohammad Z, Hedieh S,(2022). Survey on automated detection and classification of acute Leukaemia and WBCs in microscopic blood cells. Springer Science & Business Media, LLCs, part of Springer Nature.
8. Asha R, Jasmine M, Pooja P,(2020). Leukaemia Disease Detection and Classification Using Machine Learning Approaches: Review, IEEE.
9. Mustafa G., et al.,(2021). Machine Learning in Detection and Classification of Leukaemia Using Smear Blood Images: A Systematic Review, Hindawi.
10. Leukaemia and Lymphoma Society Blood and marrow stem cell transplantation,2015.
11. Bain BJ ,A beginner's guide to blood cells. Wiley,2008.
12. Jyoti R., et al. Classification of acute lymphoblastic Leukaemia using hybrid hierarchical classifiers, Springer Science + Business Media New York,2017.
13. Jyoti R., et al.(2014b) Comparative analysis of segmentation algorithms for leukocyte extraction in the acute lymphoblastic Leukaemia images. Proc. Of Int Conf. on Parallel, Distributed and Grid Computing. IEEE, In, pp 245-250.
14. Nasir AA, Mashor MY, Roseline H (2011) Detection of acute Leukaemia cells using variety of features and neural networks. Proc. Of Int Conf. on Biomedical Engineering, Springer, Berlin, In, pp 40-46.
15. Morteza Moradi Amin, Saeed Kermani, Ardeshir Talebi, Mostafa GhelichOghli ,Recognition of Acute Lymphoblastic Leukaemia Cells in Microscopic Images Using K-Means Clustering and Support Vector Machine Classifier. Journal of Medical Signals and Sensors,2015.
16. Wang M, Zhou X, Li F, Huckins J, King RW, Wong STC. Novel Cell Segmentation and Online Learning Algorithms for Cell Phase Identification in Automated Time-lapse Microscopy. In Biomedical Imaging: From Nano to Macro,2007. ISBI 2007. 4th IEEE international Symposium on 2007.p.65-8.
17. Theera-Umporn N. White Blood Cell Segmentation and Classification in Microscopic Bone Marrow Images, in Fuzzy Systems and Knowledge Discovery. Springer: Springer-Verlag Berlin Heidelberg; 2005. p. 787-96. Back to cited text no. 15
18. Madhlom H, Kareem SA, Ariffin H, Zaidan AA, Alanazi HO, Zaidan BB. An automated white blood cell nucleus localization and segmentation using image arithmetic and automatic threshold. J Appl Sci 2010; 10:959-66. Back to cited text no. 16
19. Sinha N, Ramakrishnan AG. "Automation of Differential Blood Count. In TENCON 2003. Conference on Convergent Technologies for the Asia-Pacific Region; 2003. p. 547-51. Back to cited text no. 17
20. Scotti F. Robust "Segmentation and Measurements Techniques of White Cells in Blood Microscope"





Rimi N.Agrawal and Viral Kapadia

21. Haneen T. S. et.al, Machine learning applications in the diagnosis of Leukaemia: Current trends and future directions. *International Journal of Laboratory Hematology*; 2019.
22. Jakkrich L, Kosin C, Acute Leukaemia Classification by Using SVM and K-Means Clustering, 2014 IEEE.
23. Italia Joseph Maria, T.Devi, D. Ravi, Machine Learning Algorithms for Diagnosis of Leukaemia (2020). *International Journal of Scientific & Technology Research*.
24. Vasundhara A, Preetham K, Detection of acute lymphoblastic Leukaemia using image segmentation and data mining algorithms, *International Federation for Medical and Biological Engineering* 2019, Springer.
25. Al-jaboriy, S.; Sjarif, N.; Chuprat, S, Segmentation and detection of acute leukemia using image processing and machine learning techniques: a review, p. 511-531, 2019.
26. Shafique S, Tehsin, S, Computer-aided diagnosis of acute lymphoblastic leukemia, *Computational and Mathematical Methods in Medicine*, p. 6125289, 2018.
27. Jiang K., Liao Q., Dai S.: A Novel White Blood Cell Segmentation Scheme Using ScaleSpace Filtering and Watershed Clustering. In: *Proc 2nd Intl Conf on Machine Learning and Cybern.* (2003) 2820–2825.
28. Jagadeesh, S., Nagabhooshanam, E., & Venkatachalam, S. (2013). Image processing-based approach to cancer cell prediction in blood samples. *International Journal of Technology and Engineering Sciences*, 1(1), 1–10.
29. Goutam, D., & Sailaja, S. (2015). Classification of acute myelogenous Leukaemia in blood microscopic images using supervised classifier. *International Journal of Engineering Research & Technology (IJERT)*, 4(1), 569–574.
30. K.Ali, S.Nadi, An Implementation of the Active Contours without Edges Model and the Logic Framework for Active Contours on Multi- Channel Images, 2020.
31. Patel N, Mishra A (2015) Automated Leukaemia detection using microscopic images. *Procedia Comput Sci* 58:635-642.
32. Mirmohammadi P, Rasooli A, Ashtiyani M, Moradi Amin M (2018) Automatic recognition of acute lymphoblastic Leukaemia using multi-SVM classifier. *Biology* 115:1512.
33. Rawat, J.; Singh, A.; HS, B.; Virmani, J.; Devgun, J.S, “Computer assisted classification framework for prediction of acute lymphoblastic and Acute myeloblastic Leukaemia,” *Biocybernetics Biomed Eng*, vol. 37, no. 4, p. 637-654, 2017.
34. Wiharto, W.; Suryani, E.; Purtra, Y. R, “Classification of blast cell type on AML based on image morphology of white blood cells,” *Telecomm Computing Electronics Control (TELKOMNIKA)*, vol. 17, p. 645-652, 2019.
35. Bodzas A, Kodytek P (2020) Zidek, J, “Automated detection of Acute Lymphoblastic Leukaemia from microscopic images based on human visual perception,”. *Front Bioeng Biotechnol* 8:1005.
36. Nasir AA, Mashor MY, Rosline H (2011) Detection of acute Leukaemia cells using variety of features and neural networks. *Proc. Of Int Conf. on Biomedical Engineering*, Springer, Berlin, In, pp 40-46.
37. Banday SA, Mir AH (2016) Statistical textural feature and deformable model-based brain tumor segmentation and volume estimation. *Multimedia Tools Appl*
38. Chandy DA, Johnson JS, Selvan SE (2014) Texture feature extraction using gray level statistical matrix for content-based mammogram retrieval. *Multimedia Tools Application* 72:2011.
39. Haralick RM, Shanmugam K, Dinstein I (1973) Textural features for image classification. *IEEE T Syst Man Networks* V 215-221.
40. Han ZY, Gu DH, Wi QE (2016) feature extraction for colour images. In: *Electronics, Communications and Networks* V 215-221.
41. M. Dash and H. Liu. “Feature Selection for Classification”. *Intelligent Data Analysis*, 1:131–156, 1997.
42. Draminski M, Rada-Iglesias A, Enroth S, Wadelius C, Koronacki J, Komorowski J. Monte Carlo feature selection for supervised classification. *Bioinformatics*. 2008; 24:110–7.
43. Mahapatara, S., Patra, D., & Satpathy, S. (2014). An ensemble classifier system for early diagnosis of acute lymphoblastic leukemia in blood smear images. *Neural Computing & Applications*, 24, 1887–1904
44. Frank Puppe, *Systematic Introduction to Expert Systems, Knowledge Representations and Problem-Solving Methods*, Springer-Verlag, 1993.
45. J Liebowitz, *Introduction to expert systems*. Mitchell Publishing, 1988.





Rimi N.Agrawal and Viral Kapadia

46. Maniruzzaman M, Rahman MJ, Ahammed B, Abedin MM, Suri HS, Biswas M, El-Baz A, Bangeas P, Tsoulfas G, Suri JS (2019) Statistical characterization and classification of colon microarray gene expression data using multiple machine learning paradigms. *Computer methods and programs in biomedicine* 176: 173-193.
47. FarzanehLatifi, Rahil Hosseini, Mahdi Mazinai (2015) A Fuzzy Expert System for Diagnosis of Acute Lymphocytic Leukaemia in Children. *International Journal of Information, Security and System Management*, 424-429.
48. Kokeb Dese, Hakkins Raj, Gelan Ayana, TilahunYemane, Accurate Machine- Learning Based classification of Leukaemia form Blood Smear Images,2021 Elsevier.
49. Supriya Mandal, Vani Daivajna, Rajagopalan Machine Learning based System for Automatic Detection of Leukaemia Cancer Cell,2019 ,IEEE.
50. Jyoti Rawat, Annapurna Singh, H.S. Bhadauria, Jitendra Virmani, J.S. Devgan, Classification of acute lymphoblastic Leukaemia using Hybrid Hierarchical Classifiers, 2017 ,Springer.
51. Morteza Moradi Amin, Saeed Kermani, ArdeshirTalebi, Recognition of Acute Lymphoblastic Leukaemia Cells in Microscopic Images Using K-Means Clustering and Support Vector Machine Classifier, 2015, *Journal of Medical Signals & Sensors*.
52. JakkrichLaosai, KosinChamnongthai,Acute Leukaemia Classification by Using SVM and K-means Clustering, 2014 ,IEEE.
53. Nimesh Patel, Ashutosh Mishra, Automated Leukaemia Images Using Microscopic Images. In 2nd International Symposium on Computer Vision and the Internet, Elesvier,2015.
54. Pouria Mirmohammadi, Amirhossien Rasooli, Meghdad Ashtiyani, Morteza Moradi Amin , Mohammad Reza Deevband, Automatic recognition of acute lymphoblastic leukemia using multi-SVM classifier, *research gate*,2018.
55. SosAgaiana, Monica Madhukara , Anthony T. Chronopoulos, A new acute leukaemia-automated classification system. In *Computer Methods in Biomechanics and Biomedical Engineering: Imaging & Visualization*, Information UK Limited, trading as Taylor & Francis Group,2022.
56. Mohammed Lamine Benomar, Amine M. Chikh, Xavier Descombes, Mourtada Benazzouz, Multi Features Based Approach for White Blood Cells Segmentation and Classification in Peripheral Blood and Bone Marrow Images. *International Journal of Biomedical Engineering and Technology (IJBET)*,Inder science, 2021, 10.1504/IJBET.2021.113729. hal-02279352v2.
57. Maneela Shaheen, et.al.,Acute Myeloid Leukaemia Detection Using Alex Net Model,WILLEY,2021.
58. Maila Claro, et.al., Convolution Neural Network Models for Acute Leukaemia Diagnosis,IEEE,2020.
59. Laurence P. Clinton, et.al. "Acute Lymphoblastic Leukaemia Detection Using Depth wise Separable Convolutional Neural Networks" 2020 SMU Data Science.
60. Amjad Rehman, et.al. "Classification of Acute Lymphoblastic Leukaemia using Deep learning" 2018 Wiley Periodicals, Inc.
61. Shamama Anwar, Afrin Alam, A convolutional neural network–based learning approach to acute lymphoblastic leukaemia detection with automated feature extraction. In *Medical & Biological Engineering &Computing*, Springer, 2020.
62. Zhencun Jiang , Zhengxin Dong, Lingyang Wang, Wenping Jiang, Method for Diagnosis of Acute Lymphoblastic Leukaemia Based on ViT-CNN Ensemble Model, *Hindawi Computational Intelligence and Neuroscience*,2021.
63. RaheelBaig , Abdur Rehman, Abdullah Almuhaimeed , Abdulkareem Alzahrani, Hafiz Tayyab Rauf, Detecting Malignant Leukaemia Cells Using Microscopic Blood Smear Images: A Deep Learning Approach, *MDPI*,2022.
64. Krishna Kumar Jha, Himadri Sekhar Dutta,"Mutual Information based hybrid model and deep learning for Acute Lymphocytic Leukaemia detection in single cell blood smear images", *Computer Methods and Programs in Biomedicine*, Volume 179,2019,104987.
65. Anwar S, Alam A, "A convolutional neural network–based learning approach to acute lymphoblastic leukaemia detection with automated feature extraction" , *Med Biol Eng Computer* 58, 3113–3121 (2020).
66. Zhencun Jiang , Zhengxin Dong, Lingyang Wang, Wenping Jiang," Method for Diagnosis of Acute Lymphoblastic Leukaemia Based on ViT-CNN Ensemble Model" *Hindawi Computational Intelligence and Neuroscience* 2021,12 pages.





Rimi N.Agrawal and Viral Kapadia

67. Fakhirah D. Ghaisani, Ito Wasito, Moh. Faturrahman, RatnaMufidah, " Deep Belief Networks and Bayesian Networks for Prognosis of Acute Lymphoblastic Leukaemia" Association for Computing Machinery ACM 2017.

68. V. Shalini, K. S. Angel Viji, " Integration of Convolutional Features and Residual Neural Network for the Detection and Classification of Leukaemia from Blood Smear Images" International Journal of Engineering Trends and Technology September 2022,176-184.

69. Ali Akbar Sadat Asl, Mohammad Hossein Fazel Zarandi, Ali Akbar Sadat Asl(&) and Mohammad Hossein Fazel Zarandi, Springer International Publishing, 2018.

70. Ali Akbar Sadat Asl, A Two-Stage Expert System for Diagnosis of Leukemia Based on Type-2 Fuzzy Logic,International Scholarly and Scientific Research & Innovation,2019.

71. Ruslan T. Gabdrahmanov, Abdullah H. Hussein, Rustam A. Burnashev, Arslan I.Enikeev, Formulation of the Task of Constructing an Expert System for the Diagnosis of Leukemia,IEEE,2019.

72. Luis H.S. Vogado , Rodrigo M.S. Veras, Flavio. H.D. Araujo, Romuere R.V. Silva, Kelson R.T. Aires, Leukemia diagnosis in blood slides using transfer learning in CNNs and SVM for classification. In Engineering Applications of Artificial Intelligence, Elsevier,2018.

73. Luis H.S. Vogado , Rodrigo M.S. Veras, Flavio. H.D. Araujo, Romuere R.V. Silva, Kelson R.T. Aires, Leukemia, Diagnosing Leukemia in blood smear images using an ensemble of classifiers and pre-trained Convolutional Neural Networks. In 30th SIBGRAPI Conference on Graphics, Patterns and Images, Niteroi, Brazil, 2017.

Table 1: Traditional Machine Learning Classification methods for Leukemia diagnosis

Image Segmentation/ Feature Extraction method	Classifier	Performance Analysis	Remarks	Types of Leukaemia Detect
k-means clustering [48]	SVM	Accuracy: 97.69%	To Extend the work to unstained blood smear images and improve performance.	Detection of All four type of Leukaemia
[49]	SVM with RBF kernel SVM with Gradient Boosting Decision Tree	SVM_GBDT F1-Score: 85.6 Sensitivity: 90.0 Specificity: 60.0	In future enhance the performance of classifier, improve specificity.	Detection Of ALL
k-means clustering, Marker controlled watershed and HSV colour-based segmentation [50]	SVM	-----	More Segmentation algorithms can be explored for better performance	ALL, AML, CLL, CML Detection
[51]	PCA for feature reduction Hybrid Hierarchical Classifier: PCA-SVM, PCA- PNN, PCA-ANFIS	Accuracy: 97.6 %	More strength and exactness of the classification task is required. Try to detect the other types of Leukaemia like AML.	Detect ALL Classify ALL subtypes
K-means Clustering[52]	Binary SVM & Multi SVM classifier with 10 k-folds	Accuracy: 95%	Can improve accuracy by using PCA for feature reduction.	Detection of ALL and its subtypes





Rimi N.Agrawal and Viral Kapadia

K-means Clustering [53]	SVM	Accuracy: 92%	To improve Accuracy	Detection of ALL and AML
K-Mean Clustering and Zack algorithm SVM/ Shape, colour and statistical, texture features [54]	SVM	93.57	Higher performance compared to the manual method	
Fuzzy C-Means clustering/ Shape and statistical [55]	Multiple SVM	97	Segmentation step can avoid empty clustering	ALL with its subtypes
K-Means/ Shape, colour and texture [56]	SVM	98	More efficient features can extract	
Watershed/ Colour, texture and Morphological features [57]	RF	95.86		

Table 2: Deep Learning Classification models for Leukemia diagnosis

Image Segmentation/ Feature Extraction method	Classifier	Performance Analysis	Remarks	Types of Leukaemia Detect
[58]	Hybrid (transfer learning methods) MobilenetV2 and ResNet18 CNN models	97.18%	The Proposed method works better than the other transfer learning approaches: Dense Net, VGG16, Inception V3, ResNet18, and Google Net. When the datasets are split into 50% training and 50% testing, the proposed method performed poor. It is a future research for improving the performance.	ALL diagnosis and classification as Healthy or unhealthy
[59]	Alex Net CNN model	98.58%	It performs well in terms of high accuracy compared to LeNet-5 based models. Planning to apply the Alex Net for ALL, to get high accuracy.	AML diagnosis and classification.
[60]	Alert Net, Alert Net-R, Alert Net- X with or without dropout (WD)	97.18%	Proposed model needs to be applied to a more significant number of images for more accurate result	Detect ALL,AML and Healthy cells
Threshold method [61]	Alex Net model	97.78%	The proposed approach still needs improved accuracy to segment overlapped cells and apply different DL	Detect and Classify ALL





Rimi N.Agrawal and Viral Kapadia

			models to improve classification accuracy	
[62]	Pre trained Alex Net	(ALL): 99.50% (Subtypes): 96.06%	System can become fully automated for other types of cancer detection AML.	Detect and Classify ALL
Improved K-means Clustering and Watershed algorithm [63]	CNN	96.24%	The precision and cost time of CNN is better than the other classification methods. In future can improve the accuracy by improving the CNN model.	Leukocytes Recognition
[64]	Combined Different CNN models	88.5%	Model can classify different kinds of WBC in short time with high accuracy. Further work will focus on accuracy improvement.	Leukocytes Recognition
CNN features [65]	CNN with Leaky Relu	99%	Using the data augmentation to prevent overfitting.	ALL diagnosis
Mutual Information based Hybrid Model using Active contour and FCM for the segmentation/ CNN features [66]	Chronological SCA-based Deep CNN	98%	The chronological SCA algorithm is developed by modifying SCA and is used for selecting the optimal weights for the Deep CNN. The proposed method still needs an improvement.	ALL Detection
CNN features [67]	ViT-CNN (Integrated model of Vision transformer and EfficientNet model)	99.03%	The model proposed is superior to other models in accuracy and had a balanced classification ability, which could better assist in the diagnosis of ALL. Performance Improved still needed further.	ALL diagnosis
[68]	DBN (Deep Belief N/W) and BN(Bayesian N/W) integration	85%	In this proposed method Microarray data and clinical data are used. For future more experiments on hyper parameter settings and architectures of DBN and BN are Needed to be done.	ALL diagnosis
CNN features [69]	ResNet50	99.6%		ALL diagnosis





Rimi N.Agrawal and Viral Kapadia

Colour based segmentation / Hybrid CNN [70]	Bagging ensemble	97.04%	Using Hybrid CNN features are extracted then using CCA fusion features selected then apply different Machine learning methods.	ALL and AML diagnosis
---	------------------	--------	--	-----------------------

Table 3: Expert System methods for Leukemia diagnosis

Dataset	Used algorithm	Performance Analysis	Limitation
500 samples with 14 attributes [72]	Type-2 fuzzy expert system- three rules, 14 inputs and 1 output Cluster Validity Index- three clusters.	Accuracy 94%	For uncertain dataset used the type-2 fuzzy system.Need to improve the accuracy.
345 blood tests [73]	Fuzzy c-means clustering- find number of fuzzy clusters(rules)Type-2 fuzzy expert system – symptoms and inference rules diagnosis of the Leukemia	Accuracy 97%	Accuracy need to improve.

Table 4: Hybrid methods for Leukemia diagnosis

Image Segmentation/ Feature Extraction	Classifier	Performance Analysis	Remarks	Types of Leukemia Detect
CNN(AlexNet, CaffeNet,Vgg-f) [76]	SVM	99.67%	In future, need to improve the abstraction of Leukemia information using CNN which improve diagnosis accuracy.	ALL diagnosis and classification
DCNN [77]	SVM + MLP + RF	100%	Using CNN for automatic feature extraction.Using EOC(SVM, MLP, RF) for getting optimum classification.	AML diagnosis and classification.
Hybrid CNN model using CCA fusion [78]	SVM, Bagging ensemble, total boosts, RUSBoost, and fine KNN	97.04%	Image segmentation is not needed to do.Image enhancement is necessary to apply.In future accuracy need to improve.	Detect ALL,AML and Healthy cells

Table 5: Classification performance measure formulas

Measures (%)	Description	Formula (%)
Accuracy	Measures the amount of TP and TN data against the overall population.	ACCURACY=(TP+TN/ TP + TN+ FP+FN) * 100%
Sensitivity	Ratio of the actual positive state to the expected real situation.	SENSITIVITY = (TP / TP + FN) * 100%
Specificity	Ratio of the expected false positive to the actual negative condition is what matters.	SPECIFICITY=(TN/ TN + FP) *100%
Positive Predictive Value	Ratio of the projected real positive condition to the total positive condition is known as the positive predictive value.	PPV= (TP / TP +FP) *100%
Negative Predictive Value	Ratio of the expected real negative condition to the overall negative condition is what matters.	NPV= (TN/ TN + FN) *100%





Rimi N.Agrawal and Viral Kapadia

<p style="text-align: center;">Lymphocyte Neutrophil Monocyte Eosinophil Basophil</p>	
<p>Fig1: White Blood Cells [4]</p>	<p>Acute Lymphoblastic Leukemia (ALL)</p>
<p style="text-align: center;">L1 L2 L3</p>	
<p>Fig 2: ALL image with its subtypes L1,L2,L3</p>	<p>Fig 3: AML image</p>
<p>Fig 4: Traditional machine learning steps for Leukaemia Diagnosis</p>	<p>Fig 5: List of Image Segmentation methods</p>
<div style="display: flex; justify-content: space-around;"> <div style="border: 1px solid black; padding: 5px;"> <p>Geometrical Characteristics</p> <ul style="list-style-type: none"> Such as Area, Radius, Perimeter, Convex Area, Major Axis, Length, Compactness and Orientation </div> <div style="border: 1px solid black; padding: 5px;"> <p>Textural</p> <ul style="list-style-type: none"> Such as momentum, contrast, entropy, and skewness </div> <div style="border: 1px solid black; padding: 5px;"> <p>Colour characteristics</p> <ul style="list-style-type: none"> Such as colour distribution and histogram </div> </div> <p style="text-align: center; margin-top: 10px;">Feature Extraction</p>	
<p>Fig 6: Feature Extraction methods</p>	





Assessment of Nutritional Status, Knowledge and Consumption Pattern of Millets among the Women Population of Surat (Urban)

Komal Chauhan^{1*} and Sonal Suva²

¹Professor, Department of Foods and Nutrition, The Maharaja Sayajirao University of Baroda, Vadodara, Gujarat, India.

²Master Research Student, M.Sc. 2021-23, Department of Foods and Nutrition, The Maharaja Sayajirao University of Baroda, Vadodara, Gujarat, India.

Received: 30 Dec 2023

Revised: 09 Jan 2024

Accepted: 12 Jan 2024

*Address for Correspondence

Komal Chauhan

Professor,

Department of Foods and Nutrition,

The Maharaja Sayajirao University of Baroda,

Vadodara, Gujarat, India.

Email: komal.chauhan-fn@msubaroda.ac.in



This is an Open Access Journal / article distributed under the terms of the **Creative Commons Attribution License** (CC BY-NC-ND 3.0) which permits unrestricted use, distribution, and reproduction in any medium, provided the original work is properly cited. All rights reserved.

ABSTRACT

There are many benefits of eating millets but the awareness about their importance is low amongst general population. Women have a special role in healthy nutrition. Therefore, imparting knowledge about millets is essential. 350 women were enrolled from Surat urban city in this prospective study. Semi structured questionnaire was used. Key was used to judge the knowledge on millets. Mean age was 35±11years, 83.71% women were Hindus, 55.43% of had normal BMI. Consuming vegetarian diet were 66.57%. Around 64% had good knowledge, and 1.14% women had poor knowledge, remaining fair. Consumption of large and small millets was only 37.43% who consume sorghum millet frequently, 14% do not eat millet as they were not available. Poor taste was the key factor for dislike on consumption. An insignificant but distinct difference between the variables like millet consumption, hemoglobin levels and nutritional status was found. Knowledge and consumption did not find any correlation.

Keywords: Millets, Health Benefits, Knowledge, Millet Consumption, Women's Nutrition Status

INTRODUCTION

Millet is one of the oldest cultivated grains in the world and has been cultivated throughout Africa and Southeast Asia for thousands of years. Millet is an important food source for millions of people, especially those living in hot, dry areas of the world. They are mostly grown in marginal areas under agricultural conditions where major cereals



**Komal Chauhan and Sonal Suva**

do not produce significant yields. Millet can be used to make bread, beer, cereal and other foods. There are different types of millets around the world, such as pearl millet, finger millet, proso and sorghum varieties[1]. These types of millets look a little different, but all of them offer similar type of nutritional benefits[2]. Thus, there are many benefits of eating millet but the awareness about the importance of millet is low among the population. Millets are one of the oldest foods known to humans and possibly the first cereal grain to be used for consumption and domestic purpose. Millets grow well in dry areas with little or no rainfall, under marginal condition of soil fertility. Millets have short growing seasons as compare to other food crops. Health is a common theme in most cultures and it plays an important role in everyone's life especially when involving women because they have a special role in healthy nutrition of the entire surrounding population[3]. Therefore, knowledge about millets becomes essential. They can develop from planted seeds to mature, harvestable plants in as little as 65 days. The advantages of growing these crops include low labour requirements, drought resistance, resistance to pests, and the robustness of the plants, which can be kept for two or more years if stored properly[1]. Climate change affects crop production by directly influencing biophysical factors such as plant and animal growth along with the various areas associated with food processing and distribution[4]. Millets are a rich source of 21 micro nutrients[5]. The outer layer of the endosperm and the embryo of the seed contain high protein, fats, calcium, and minerals; minor millets can thus help to alleviate the widespread prevalence of malnutrition.[6]. Also Sampath et al., 2007[7] depicted its health benefits such as hypoglycemic, hypo cholestolemic and anti-ulcerative characteristics. Sorghum, pearl millet and finger millet are produced and consumed mainly by the rural poor especially in developing world

MATERIALS AND METHODS

The study has been planned with the aim of determining the consumption pattern and knowledge about millets in women, Surat (urban). Assessment on various factors like socio-economic status, nutritional status, anthropometric measurements, eating pattern, dietary profile and knowledge score of millets was done on women in Surat. The study was passed by the Institutional Ethics Committee for Human Research (IECHR), Sample size calculated and rounded to 350. A sample of zones was obtained through stratified sampling and snowball sampling was used until the target of one zone was met and rotated in zone. Subjects who are women with more than 20 years of age and willing to participate and residing in urban Surat, possessing smart phone were enrolled. The three main objectives of the study were to assess demographic, diet and disease profiles of study subjects along with Millet awareness and consumption pattern using questionnaire and nutritional status calculating BMI. Further to evaluate knowledge score based on the developed questionnaire and key score which was further classified under poor, fair and good category.

RESULTS AND DISCUSSION

The mean age of the women aged between 20 to 40 years in Surat was 29 ± 11 years, and those aged between 41 to 60 years was 50 ± 6 years and the mean age of the total sample ($n=350$) was 35 ± 11 years. Of total, 50.57% were working women, and educational strata showed 19.48% were illiterate, 24.64% of women had studied up to graduation, 3.44% up to post-graduation and remaining up to higher education. Economically, 63.43% belonged to lower middle class whose monthly income ranged between 27,000-46,000. Females living in nuclear families were 69.14% and those in joint families were 30.86%. According to WHO 55.43% of women had normal BMI, 26.57% were overweight, 13.14% were obese and 4.86% of women were underweight. When compared between the two age groups it was found that more percentage of women were healthy in younger group (60.24%) compared to the older group (43.56%) (table 1). 66.57% of women consumed vegetarian diet. Two full meals a day were consumed by 88% of women and 79.71% women had breakfast once a day. 45.43% women had junk food once or twice a week. Normal haemoglobin levels were reported in 43.7% women, with mean \pm SD haemoglobin of 10.53 ± 1.80 gm%. Out of all, 86% of women had no major illness, diabetes was present in 8.29% of the women, hypertension in 4.57% of the women, both diabetes and hypertension in 0.57% of the women, bone related problems in 0.57% of the women. With regard to minor illnesses almost 87.71% women were found without any illnesses. Constipation, gas and leg pain were the few minor illnesses



**Komal Chauhan and Sonal Suva**

found only in less than 5% women subjects. To determine the knowledge of women in Surat (Urban), questions on knowledge and consumption pattern were included in the questionnaire. The subjects were divided into three groups according to their answers: poor, fair, and good (figure 1). Out of the 30 basic questions with key criteria, 66.53% in the age of 20 to 40 years of women had good knowledge about millet, 32.66% had fair knowledge and 0.81% had poor knowledge. In the age group of 40 to 60 years, women with good knowledge were 58.42%, women with fair knowledge were 39.60% and women with poor knowledge were 1.98%. Overall, around 64% women had good knowledge, 34.86% women had fair knowledge and 1.14% women had poor knowledge. A comparison of women's education and millet knowledge is shown in table 2. The number of women who had good knowledge about millet was 1.71% with post-graduation, 12.29% with graduation, 18.29% with high school, 12.29% with primary school. Thus, from the data it was noticed that qualification has no correlation knowledge on millet. Consumption of large and small millet on data frequency of consumption, non-frequent consumption and never consumed is shown in table 3. Consumption of large and small millets data showed that only 37.43% women consume sorghum millet frequently, 39.43% of the women consume pearl millet frequently. It was found that millet was consumed by 50% women in winter. Gandhi H. and Negandhi S.,(2020)⁸studied millet consumption in 100 households of Vadodara (Urban).It was concluded that 86.45% were using pearl millet, 31.35% were using sorghum millet, 8.55% were using finger millet and 6.65% were using kodo. Out of which 10.52% used millet daily, 42.10% used it weekly and 38.94% used it occasionally and 8.42% used millet seasonally.

Pearl millet was the most used followed by sorghum and other millets were very less. Health conditions have been compared with the consumption of pearl millet by comparing the frequency of pearl millets consumed by those with normal haemoglobin and the frequency consumed by anaemic women (figure 2). And how often do those with a normal BMI take the pearl millet diet, also with BMI status of women. According to this data (table 4) it can be revealed that those who had normal haemoglobin and normal BMI had high pearl millet intake (around 10% subject) and those who were anaemic women, overweight and obese had low pearl millet intake. An insignificant but distinct difference between the two variables was found. It was observed that 90% women used millet in flour form, 2.86% used whole grain, 1.15% women used both whole grain and flour, 1.14% women used ready to mix millet. 4.85% women used powdered and ready to mix millet frequently. The women who used for cooking in household showed that 92% preferred byroasted millets, 3.99% women used boiled millets, 4.01% women used both boiled and roasted form. According to an observation 38.29% women used millet in all three seasons, 11.7% women used millet in winter and monsoon, 50.0% used only in winter. According table 5 there were several reasons for non-consumption of various millets by the subjects. To summarize a few, kodo millet, foxtail millet, finger millet, little millet, proso millet, barnyard millet and amaranth millet recipe taste was not liked by subject along with limited availability nearby store, family custom of not eating millet and haven't heard the name were the main reasons for not frequently consumption.

CONCLUSION

It can be concluded from the data that in spite of having knowledge about millets and their health benefits, various physico-social reasons or mental discouragement felt for uptake, women showed reduced consumption of these healthy food grains.

REFERENCES

1. APEDA, https://apeda.gov.in/apedaweb/site/SubHead_Products/Indian_Millet.htm
2. B. Dayakar Rao, Raj Bhandari, and Tonapi, VA, K. (2021). "White Paper on Millets – A Policy Note on Mainstreaming Millets for Nutrition Security". ICAR-Indian Institute of Millets Research (IIMR), Rajendranagar, Hyderabad-500030





Komal Chauhan and Sonal Suva

3. Sharma N., Niranjana K (2018) Foxtail millet: Properties, processing, health benefits, and uses. Food Review International; 34:329–363.
4. Satyavathi T C, Ambavat S, Kandelwal V and Shrivastava R (2021) Pearl Millet: A Climate-Resilient Nutri-cereal for Mitigating Hidden Hunger and Provide Nutritional Security Front. Plantm Sci., 13
5. Lin, H. C., Sheu, S. Y., Sheen, L. Y., Sheu, P. W., Chiang, W., & Kuo, T. F. (2020). The gastroprotective effect of the foxtail millet and adlay processing product against stress-induced gastric mucosal lesions in rats. Journal of Traditional and Complementary Medicine, 10 (4), 336-344.
6. Hassan Z. M., Sebola N. A and Mabelebele M (2021) The nutritional use of millet grain for food and feed: a review, Agriculture Food Security; 10(1): 16.
7. Sampath Chethan and Malleshi Nagappa (2007) Finger Millet Polyphenols: Characterization and their Nutraceutical Potential, American Journal of Food Technology 2(7).
8. Gandhi H. and Negandhi S. (2020) A study on time trends in production and consumption of millets in Gujarat, Consumption pattern of Major and Minor millets in selected households of urban Vadodara and development of millet based recipes for prevention of NCDs, Unpublished masters dissertation submitted at the Department of Foods and Nutrition, The Maharaja Sayajirao University of Baroda, Vadodara

Table1: Anthropometric measurement of subjects (%)

Mean	20-40year (n249)	41-60 year(n101)	Total (n350)
Height (cm)	158.19±8.36	158.8±10.18	159±8.49
Weight (kg)	55.9±8.18	63±8.68	57.32±8.60
BMI (kg/m ²)	24±4.37	26±4	25±4
Category of BMI		T test= 4.12	Pvalue=0.000054***
Underweight (<18.5)	6.43 (16)	0.99 (1)	4.86 (17)
Normal (18.5-24.9)	60.24 (150)	43.56 (44)	55.43 (194)
Overweight (25-29.0)	20.88 (52)	40.59 (41)	26.57 (93)
Obese class (≥ 30)	12.45 (31)	14.85 (15)	13.14 (46)

Table 2: Percentage of subject showing knowledge about millets and as per education

Knowledge regarding millet	Graduation	high school	Illiterate	post-graduation	primary school	Grand Total
Fair (122)	12.00(42)	6.86(24)	6.86 (24)	1.43(5)	7.71(27)	34.86(122)
Good (224)	12.29(43)	18.29(64)	12.29 (64)	1.71(6)	19.43(68)	64.00(224)
Poor (4)	0.29(1)	0.00	0.29 (1)	0.29(1)	0.29(1)	1.14(4)





Komal Chauhan and Sonal Suva

Table 3: Percentage of subject showing frequency of consumption of various millets

Millet Type	Frequently consumption (Daily/weekly)	Non-Frequently consumption (monthly/yearly)	Never consumed
Sorghum	37.43 (131)	35.72 (124)	26.86 (95)
Pearl	39.43 (139)	30.83 (107)	29.71 (104)
Kodo	3.43 (12)	9.55 (31)	87.71 (307)
Foxtail	2 (7)	3.43 (12)	94.57 (331)
Finger	2 (7)	10.28 (37)	87.71 (306)
Barnyard	5.71 (20)	52.28 (183)	42.00 (147)
Proso	0.86 (3)	2.57 (10)	96.57 (337)
Little	0.86 (3)	6.29 (22)	92.86 (325)
Amaranth	4 (14)	49.71 (175)	46.29 (161)

Table 4: Percentage of subject showing Health conditions have been compared with the consumption of pearl millet

Pearl millet consumption	Frequently consumption	Non-frequency consumption	Never consumed
Hemoglobin normal (83)	45.83(33)	34.72(25)	19.44(14)
Anemic woman (111)	37.83(42)	27.92(31)	34.23(38)
BMI normal woman(190)	40.00 (76)	35.27 (67)	24.74 (47)
Overweight and obese women(139)	38.13 (53)	23.74 (33)	38.13 (53)
No disease (276)	37.68 (104)	32.97 (91)	29.35 (81)
Disease (74)	47.28 (35)	21.64 (28)	31.08 (38)

Table 5: Percentage of subject showing Reason for not consuming various millets

Consumption pattern	20-40year women (n249)	41-60year women (n101)	Total
Sorghum			
Don't like the taste	16.47(37)	15.84(16)	14.86 (53)
Limited available	1.20(3)	4.95 (8)	3.14(11)





Komal Chauhan and Sonal Suva

High price	1.20(3)	0.99 (1)	0.86 (4)
Family custom of not eating millet	6.83(21)	13.86 (12)	9.14(33)
Eating millet makes the body feel warm	0.81(2)	0.99 (2)	0.86 (4)
Skip	73.49(183)	63.37 (62)	71.14 (245)
Pearl			
Don't like the taste	15.73 (39)	8.91(10)	13.71(49)
Limited available	2.82 (7)	3.96 (4)	3.14(11)
High price	1.21 (3)	-	0.86(3)
No time to make meal	-	2.97 (5)	1.71 (5)
Family custom of not eating millet	6.45 (16)	13.86(14)	8.57 (30)
Eating millet makes the body feel warm	11.69 (30)	10.89 (11)	11.71 (41)
Skip	61.69 (154)	59.41(57)	60.29 (211)
Kodo			
Don't like the taste	30.24 (75)	32.67 (33)	31.14 (108)
Limited available	12.50 (31)	17.82 (18)	14.00 (49)
High price	2.02 (5)	-	1.43 (5)
No time to make meal	1.21 (3)	1.98 (2)	1.43 (5)
Family custom of not eating millet	35.89 (90)	37.62(38)	36.29 (128)
Eating millet makes the body feel warm	0.40 (1)	2.97 (3)	1.14 (4)
Haven't heard the name	4.03 (10)	1.98 (2)	3.43 (12)
Skip	13.71 (34)	4.95(5)	11.14 (39)
Foxtail			
Don't like the taste	24.60 (61)	40.59 (41)	29.14 (102)
Limited available	16.94 (42)	20.79 (21)	18.00 (63)
High price	5.65 (14)	0.99 (1)	4.57 (15)
No time to make meal	2.02 (5)	2.97 (3)	2.29 (8)
Family custom of not eating millet	37.10 (93)	25.74 (26)	33.71 (119)
Eating millet makes the body feel warm	0.81 (2)	0.99 (1)	0.86 (3)
Haven't heard the name	12.10 (30)	7.29 (8)	10.86 (38)
Skip	0.81 (2)	-	0.57 (2)
Finger			
Don't like the taste	27.42 (66)	34.65 (35)	29.43 (99)
Limited available	19.35 (49)	17.82 (18)	18.86 (67)
High price	4.44 (11)	0.99 (1)	3.71 (12)
No time to make meal	1.21 (3)	1.98 (2)	1.43 (5)
Family custom of not eating millet	33.87 (86)	28.71 (29)	32.29 (116)
Eating millet makes the body feel warm	0.81 (2)	0.99 (1)	0.86 (3)
Haven't heard the name	9.27 (23)	9.90 (10)	9.43 (34)
Skip	3.63 (9)	4.95 (5)	4.00 (14)
Barnyard			
Don't like the taste	21.77 (54)	16.83 (17)	20.29 (71)
Limited available	10.48 (26)	8.91 (9)	10.00 (35)
High price	4.03 (10)	0.99 (1)	3.43 (11)
No time to make meal	0.40 (1)	-	0.29 (1)
Family custom of not eating millet	15.73 (40)	12.87 (13)	15.14 (53)
Eating millet makes the body feel warm	0.40 (1)	0.99 (1)	0.57 (2)
Haven't heard the name	2.42 (6)	3.96 (4)	2.86 (10)





Komal Chauhan and Sonal Suva

Skip	44.76 (111)	55.45 (56)	47.43 (167)
Proso			
Don't like the taste	25.00 (62)	43.56(44)	30.29 (106)
Limited available	19.35 (48)	18.81 (19)	19.14 (67)
High price	3.63 (9)	0.99 (1)	2.86 (10)
No time to make meal	0.40 (1)	0.99 (1)	0.86 (2)
Family custom of not eating millet	31.85 (80)	24.75 (25)	29.71 (105)
Eating millet makes the body feel warm	0.81 (2)	-	0.57 (2)
Haven't heard the name	12.90 (32)	9.90 (10)	12.00 (42)
Skip	6.05 (15)	0.99 (1)	4.57 (16)
Little			
Don't like the taste	25.00 (62)	40.59 (41)	29.43 (103)
Limited available	19.35 (48)	17.82 (18)	18.86 (66)
High price	2.82 (7)	-	2.29 (7)
No time to make meal	1.21 (3)	1.98 (2)	1.43 (5)
Family custom of not eating millet	30.24 (76)	26.73 (27)	29.14 (104)
Eating millet makes the body feel warm	0.40 (1)	-	0.29 (1)
Haven't heard the name	10.89 (27)	7.92 (8)	10.00 (35)
Skip	10.08 (25)	4.95 (5)	8.57 (29)
Amaranth			
Don't like the taste	20.56 (51)	20.79 (21)	20.57 (72)
Limited available	9.68 (24)	9.90 (10)	9.71 (34)
High price	3.68 (9)	-	2.86 (9)
No time to make meal	1.61 (4)	0.99 (1)	1.43 (5)
Family custom of not eating millet	14.52 (36)	11.88 (12)	13.71 (48)
Eating millet makes the body feel warm	0.40 (1)	0.99 (1)	0.57 (2)
Haven't heard the name	2.42 (6)	3.96 (4)	2.86 (10)
Skip	47.18 (118)	51.49 (52)	48.29 (170)

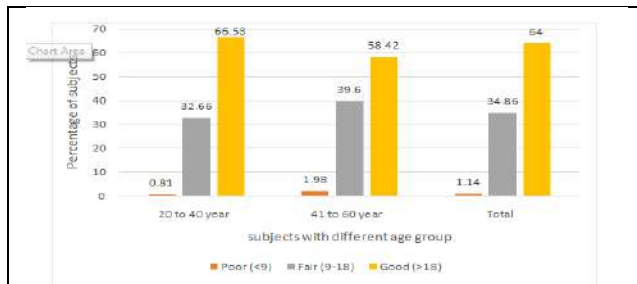


Figure 1: Percentage of subject showing different category of knowledge score on millet

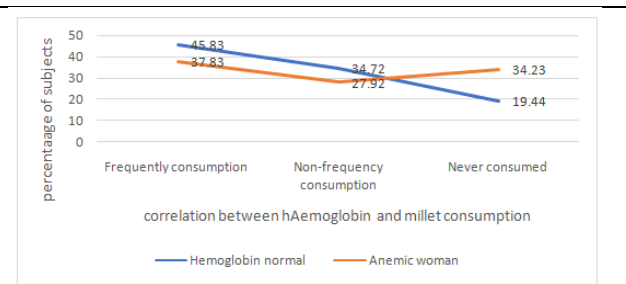


Figure 2: Correlated between Pearl Millet Consumption & haemoglobin level





Sustainable Building Materials: Light Weight Aggregates from Industrial Waste

Malav Nileshbhai Shah^{1*}, J. R. Pitroda², Reshma L. Patel³ and Indrajit N.Patel⁴

¹First Year, M.Tech. (Civil) Construction Engineering and Management, BVM Engineering College, Vallabh Vidyanagar, Gujarat, India.

²Associate Professor, PG Coordinator Construction Engineering and Management, Civil Engineering Department, BVM Engineering College, Vallabh Vidyanagar, Gujarat, India.

³Assistant Professor, PG Coordinator Environmental Engineering, Civil Engineering Department, BVM Engineering College, Vallabh Vidyanagar, Gujarat, India.

⁴Professor & Principal, Structural Engineering, Department, BVM Engineering College, Vallabh Vidyanagar, Gujarat, India.

Received: 30 Dec 2023

Revised: 09 Jan 2024

Accepted: 12 Jan 2024

*Address for Correspondence

Malav Nileshbhai Shah

First Year, M.Tech. (Civil) Construction Engineering and Management,

BVM Engineering College,

Vallabh Vidyanagar, Gujarat, India.

Email: malavshah881@gmail.com



This is an Open Access Journal / article distributed under the terms of the **Creative Commons Attribution License** (CC BY-NC-ND 3.0) which permits unrestricted use, distribution, and reproduction in any medium, provided the original work is properly cited. All rights reserved.

ABSTRACT

The significant increase in the use of concrete in buildings, particularly with the usage of normal-weight aggregates (NWAs) like gravel and granite, has led to a substantial depletion of natural stone reserves, resulting in irreversible environmental harm. Consequently, there has been a heightened focus on sustainable materials in recent times. The increasing need for sustainable development has prompted researchers to concentrate their inquiry on the use of waste or recycled resources as prospective building components. The use of lightweight aggregates (LWAs) derived from industrial waste materials, including fly ash, coconut shells, expanded slag cinder, and bed ash, has resulted in the development of sustainable materials. Nevertheless, the absence of advanced industrial processes in emerging and impoverished nations has not yielded significant benefits for them. Significant financial savings may be achieved by reducing the weight of the building. Long-acting reversible contraceptives (LARCs), such as long-acting reversible intrauterine devices (IUDs) and contraceptive implants, have been extensively used in industrialised nations for a considerable duration, demonstrating their efficacy in terms of cost-effectiveness. The entity above fulfilled the dual objectives of ensuring structural integrity and promoting economic sustainability. Structures tend to exhibit more versatility as their weight decreases.

Keywords: Concrete, Construction, Lightweight aggregates (LWAs), Normal-weight aggregates (NWAs)





Malav Nileshbhai Shah et al.,

INTRODUCTION

Lightweight aggregates have emerged as a crucial innovation in the construction industry, offering a myriad of benefits that significantly impact the way we build structures. This paper delves into the multifaceted applications of lightweight aggregates, shedding light on their transformative role in modern construction practices. One of the primary advantages of lightweight aggregates lies in their ability to reduce the overall weight of structural components. This property not only minimizes the load on foundations but also simplifies transportation and installation processes. As a result, construction projects become more cost-effective and less resource-intensive. Furthermore, lightweight aggregates excel in enhancing the insulation properties of buildings. Their low thermal conductivity contributes to superior energy efficiency, reducing heating and cooling requirements. This translates to lower operational costs and a reduced carbon footprint, aligning with the growing emphasis on sustainable construction. The versatility of lightweight aggregates is evident in their applications across various construction domains, including residential, commercial, and industrial sectors. From lightweight concrete and insulation materials to innovative facade systems and green roofs, lightweight aggregates have proven their worth in diverse architectural and engineering solutions. Moreover, the environmental benefits of utilizing lightweight aggregates cannot be overstated. Their lower energy consumption during production, reduced transportation-related emissions, and potential for recycling make them a compelling choice for eco-conscious builders and developers. Saif et al (2022) Low density and high thermal conductivity are two of the main advantages of lightweight concrete [1]. In conclusion, the integration of lightweight aggregates into construction practices represents a pivotal shift towards more efficient, sustainable, and environmentally friendly building solutions. This paper explores the myriad possibilities offered by lightweight aggregates, making a compelling case for their widespread adoption in the construction industry. Lightweight aggregates (LWAs) and normal-weight aggregates (NWA) are two types of aggregates used in construction, and they differ in several key aspects, as shown in Table I. In summary, the choice between LWAs and NWA depends on the specific requirements of a construction project. LWAs are favoured for applications where reducing structural load, enhancing insulation, and improving energy efficiency are essential. NWA, on the other hand, excel in load-bearing structures and projects that prioritize high strength and durability.

Application of Lightweight Aggregates in Construction

Lightweight aggregates, characterized by their low density and high strength, have revolutionized the construction industry by offering innovative solutions to various construction challenges. This paper explores the diverse applications of lightweight aggregates through a series of practical examples, showcasing their versatility and impact on modern construction practices.

1. **Lightweight Concrete Construction:** Lightweight concrete is made using lightweight components like shale or expanded clay. This type of concrete is employed in high-rise buildings to reduce the overall structural load while maintaining structural integrity. For instance, the construction of tall residential towers in earthquake-prone areas often incorporates lightweight concrete to enhance seismic resistance.
2. **Insulation Materials:** Lightweight aggregates are a key component in the production of insulation materials used in both residential and commercial buildings. Lightweight concrete blocks and panels, which contain expanded glass beads or perlite aggregates, provide excellent thermal insulation. These materials reduce energy expenses by mitigating heat transmission. For example, lightweight concrete blocks are used to construct energy-efficient walls in passive solar homes.
3. **Green Roof Systems:** Lightweight aggregates are utilized in the construction of green roof systems. In these systems, expanded clay or lightweight concrete is used as a growing medium for vegetation. Green roofs provide multiple benefits, including improved insulation, storm water management, and enhanced urban aesthetics. The Javits Center in New York City features a green roof constructed using lightweight aggregates, reducing energy consumption and storm water runoff.



**Malav Nileshbhai Shah et al.,**

4. Architectural Façade Panels: Lightweight aggregates, when incorporated into architectural façade panels, offer a combination of aesthetic appeal and functionality. These panels, made from expanded glass or lightweight concrete, provide a decorative finish to buildings while also reducing the overall weight load on the structure. The Vadodara Hotel in Las Vegas features lightweight concrete façade panels, adding a distinctive design element to the building.
5. Infrastructure Projects: Lightweight aggregates play a critical role in infrastructure projects, such as bridge construction. By utilizing lightweight concrete, engineers can reduce the dead load on the bridge's structural components while maintaining durability and strength. The Penobscot Narrows Bridge in Maine incorporates lightweight concrete in its design, contributing to its longevity and load-bearing capacity.
6. Tunneling and Underground Construction: Lightweight aggregates are used in tunnelling and underground construction to minimize ground settlement and reduce excavation pressures. Tunnel linings made with expanded clay or shale aggregates ensure stability while preventing excessive subsidence. The London Cross rail project relies on lightweight aggregate concrete segments for its underground tunnel construction.

In conclusion, the application of lightweight aggregates in construction is far-reaching, impacting the design, performance, and sustainability of various building projects. These examples illustrate the adaptability and effectiveness of lightweight aggregates in addressing construction challenges while promoting energy efficiency and environmental responsibility.

LITERATURE REVIEW

Oil palm kernel shell

Teo et al. (2006) conducted a study. The compressive strength of concrete made from oil palm shell (OPS) was found to be 28.1 MPa after 28 days, meeting the criteria for structural lightweight concrete [4]. According to the study conducted by Alengaram et al. (2013), The study determined that the hardened density of oil palm kernel shell concrete (OPKSC) falls within the range of 1650-1950 kg/m³. Several parameters, including the water-to-cement ratio (w/c), the presence of fine aggregate, water absorption, and grain size of oil palm kernel shell (OPKS), were identified as influential factors on the density of OPKSC. The density of the oven-dry sample was observed to be 200-250 kg/m³ lower compared to the density of the sample in a saturated surface dry (SSD) state. The water absorption of oil palm kernel shell concrete (OPKSC) was found to exceed 10% as a result of the presence of micro pores on the surface of the oil palm kernel shell (OPKS). Several studies have found a compressive strength range of 13-22 MPa for OPKSC. However, by using fly ash, silica fume, and super plasticizer, the concrete mixture has been able to attain a compressive strength of 37 MPa. A study has found that by using crushed ordinary Portland cement kiln slag (OPKS) and limestone powder, it is possible to achieve a compressive strength of up to 48 MPa [5]. Paul et al. (2014) The use of oil palm shells as a coarse aggregate in the construction of structural concrete has promising prospects. The complete substitution of crushed stone with oil palm shell (OPS) does not provide the desired strength for lightweight concrete. However, it has been shown that concrete made with a 50% replacement is both practical and suitable for use in low to moderate-strength applications, such as constructing affordable housing units [6]. According to Williams et al. (2014), in building construction projects, it is possible to achieve the requisite strength by partly substituting coarse aggregate with palm kernel shell concrete [7].

Pumice

Yasar et al. (2003) The researcher conducted an experiment on designing structural lightweight concrete (SLWC) using basaltic pumice (scoria) as aggregate and fly ash. This approach offers a clear benefit in terms of weight reduction. The characteristics of recently mixed concrete include density and slump. These attributes contribute to many advantageous factors, such as enhanced compressive strength and improved environmental sustainability [8].



**Malav Nileshbhai Shah et al.,**

Khandaker M. Anwar Hossain (2004) The focus of this study was on the analysis of volcanic pumice and its impact on the properties of concrete. The experiment aimed to evaluate the effects of different levels of cement content (ranging from 0% to 25% by weight) and substitutions of coarse aggregate volume (ranging from 0% to 100%) on the properties of concrete. The volcanic pumice aggregate (VPA) was used as a distinguishing factor in the study. A range of tests were conducted to assess the workability, strength, drying shrinkage, surface absorption, and water permeability of the concrete [9]. Parhizkar et al. (2012) conducted tests to investigate the characteristics of concrete made using volcanic pumice lightweight aggregates. In the concluding phase of the study, the focus was primarily on comparing the properties of concrete, including natural fine particles, with those containing both lightweight coarse and fine aggregates. The study's findings indicate that the lightweight concrete examined in this research satisfies the specified criteria, as shown by their measured tensile strength and drying shrinkage values [10].

According to Kockal et al. (2014), the use of pumice aggregates as a replacement for sand in mortars resulted in a decrease in both weight and strength. Nevertheless, the strength values of mortars, including pumice aggregate, were deemed acceptable for both structural and non-structural purposes, as shown by reference [11]. In a recent study conducted by Al-Farttoosi et al. (2021), it was shown that reducing the volume of Pumice in lightweight concrete leads to an enhancement in compressive strength. This improvement may be attributed to the reduction in aggregate voids. Additionally, the elevated concentration of Pumice in concrete contributes to an increased water demand during the mixing process as a result of its notable capacity for water absorption inside the concrete mortar. The experimental results demonstrated a negative correlation between the water-to-cement ratio and the compressive strength of the lightweight concrete mixture. The observed phenomenon may be attributed to the significant influx of water into the cement paste, resulting in increased fluidity and diminished adhesion properties. Consequently, the essential link between the paste and the aggregate is not formed. The enhancement of concrete efficiency and compressive strength may be achieved by reducing the water-binder ratio to around 40% [12].

Lytag LWA

Al-Khaiat et al. (1998) focused on investigating the impact of curing on the physical characteristics and early strength. In addition, the use of Lytag LWA in lightweight concrete is characterised by a slump measurement of around 100 mm, a fresh unit weight of 1800 kg/m³, and a 28-day cube compressive strength. In addition, the test results indicate that the compressive strengths of self-levelling concrete (SLWC) exhibit a lower degree of sensitivity to inadequate curing compared to normal-weight concrete (NWC) [13].

Cold Bonded Fly Ash Aggregates

The research was carried out by Aineto et al. (2005). The fly ash and slag generated by the ELCOGAS integrated gasification in combined cycle (IGCC) power plant have been shown to be acceptable for reuse as lightweight aggregates (LWA). This is made feasible by using the IGCC fly ash's particular properties when exposed to high temperatures, which results in the release of gases and the consequent development and expansion of bubbles. The experiment using 100% IGCC wastes has been completed, and the best conditions for generating aggregates have been found. The procedure consists of two steps of thermal treatment: the first stage is performed at a temperature of 750oC for 10-15 minutes, followed by the expansion step at a temperature range of 1150oC-1175oC for 10-15 minutes. This thermal treatment produces lightweight aggregates with a porous structure. These aggregates have bulk density, water absorption, freeze resistance, and mechanical qualities that are equivalent to commercially available lightweight aggregates. Furthermore, they have a pleasing interior and exterior look [14]. Perumal et al. (2011) carried out the research. Because of its rounded shape, fly ash aggregate is more workable than angular natural gravel. When compared to natural gravel, the water absorption of fly ash aggregate is about nine times more. This significant gap is a significant disadvantage that may be reduced by using alternative treatment strategies. One successful way, for example, includes treating the fly ash aggregate with water glass, among other simple procedures. The use of fly ash aggregates in concrete may result in a density of 2150 kg/m³, while traditional concrete mixes can have a density of up to 2580 kg/m³. Despite the fact that fly ash aggregates (FAA) concrete has a compressive strength 48% lower than standard concrete mix, it exceeds the specified minimum threshold of 17 MPa for concrete to be employed as a structural material [15].



**Malav Nileshbhai Shah et al.,**

According to Gomathi et al. (2014), the use of clay binders like bentonite and metakaolin improves both the pelletisation efficiency and the strength of fly ash aggregates. The experimental results given in this work illustrate the potential advantages of employing fly ash-based aggregates as a feasible alternative to natural aggregates in concrete manufacture. These findings indicate that fly ash-based aggregates have the potential to totally replace natural aggregates, making them an excellent choice for concrete production. The results of the tests also show that when subjected to a hot air oven curing at a temperature of 100°C, fly ash aggregates may obtain a maximum crushing strength of 17.97 MPa. This phenomenon has the potential to greatly reduce the total weight of the structure while also lowering the costs connected with concrete production [16]. Patel et al. (2015) Cold bonding method is used to create fly ash aggregates, which avoids the requirement for energy-intensive curing of artificial aggregates. The adoption of cost-effective building practices and alternative construction materials is in great demand owing to the potential for considerable cost reductions in construction. Fly ash is not considered a waste material and has the potential to be utilised effectively in concrete applications such as aggregate, filler, or fine aggregate replacement. Furthermore, it has the potential to be used in the production of fly ash bricks. The use of cement as a binding agent in the production of lightweight aggregates (LWA) raises the specific gravity of the aggregates while decreasing their water absorption capacity. Cold bonded (CB) and sintered (S) aggregates were formed, and their water absorption values were measured to be 16.5% and 11.7%, respectively [17].

Coconut Shell

Kulkarni et al. (2013) Concrete is the most widely used structural material in the world today. However, the need to make it lighter has presented scientists and engineers with new challenges. The goal is to create lightweight concrete that reduces density while retaining strength and minimizing cost. One popular method to achieve this is by introducing new aggregates in the mix design. Lightweight aggregates such as Pumice, Perlite, expanded Clay or Vermiculite, coal slag, sintered fly ash, rice husk, straw, sawdust, cork granules, wheat husk, oil palm shell, and coconut shell are commonly used in the manufacturing of lightweight concrete. Coconut shells, for instance, contain varying amounts of cellulose, lignin, and ash when dried [18]. Behera et al. (2013) The increase in urbanization and industrialization has led to a rise in overall consumption. Consequently, researchers are exploring alternative options for coarse aggregate, as population growth has led to an increase in industrial by-products and household waste. Coconut shells, which are a form of agricultural waste in India, currently occupy large dumping yards and contribute to environmental pollution. However, if they can be used as a replacement for coarse aggregate, they could be a valuable resource for the civil engineering community. The objective of this research is to create a mix design for lightweight aggregate concrete that utilizes coconut shells as coarse aggregate, in combination with cement and river sand [19]. Kakade et al. (2015) studied the behaviour of concrete examples made of coconut shell aggregate. Because of the larger porosity in their shell structure, coconut shell aggregates absorb more water. Under complete water curing, the 28-day compressive strength of coconut shell concrete was determined to be 14.88 for 50% substitution by coconut shell aggregate, and it may be employed for less significant tasks [20]. Prakash et al. (2020) stated that combining coconut shells, coconut fibre, and sawdust in buildings may improve numerous qualities and provide better outcomes. It is a way to decrease natural waste dumping in the environment [21].

Expanded Slag Cinder

Xiao et al. (2017) Volcanic cinder is a porous rock that exhibits high performance characteristics, created after the cooling of a volcanic explosion. In a recent study, researchers investigated the impact of fly ash on the mechanical properties of cinder lightweight aggregate concrete. The results showed that the addition of fly ash significantly improves the mechanical properties of cinder lightweight aggregate concrete. The maximum strength value is achieved when the dosage of fly ash is 35%. In addition, the early strength of lightweight aggregate concrete can be greatly improved by extending the grinding time of fly ash, reducing particle size, and increasing its activity [22]. The influence of fly ash concentration and particle size on the compressive strength of volcanic slag lightweight aggregate concrete was investigated by Xiao et al. (2018). Fly ash may diminish the early compressive strength of cinder in lightweight aggregate concrete; however, when the secondary hydration of fly ash is completed, the late compressive strength is greatly increased [23].





Malav Nileshbhai Shah et al.,

Govandan et al. (2019) Volcanic eruptions produce cinder ash. It is a porous rock with high performance that is created as a result of the cooling of a volcanic eruption. The use of thermal industry waste cinder ash may minimise natural resource consumption, the amount of costly cement used, and environmental pollution. The cinder ash can be successfully refilled. In the same concrete mix, the optimal strength achieved with 30% cement is 26N/mm^2 [24]. Harish et al. (2020) Lightweight aggregate concrete is made by totally or partly replacing regular weight aggregate depending on the desired strength and density. Expanded polystyrene (EPS) bead is a low-density polymer with strong energy-absorbing properties that may be utilised as a lightweight aggregate in concrete. Structural lightweight aggregate concrete (SLWAC) was made by completely substituting standard-weight aggregate with EPS beads to Cinder ratios of 20:80, 40:60, 60:40, and 80:20, respectively. Furthermore, GGBS was employed as an additional cementitious material. Cinder concrete was discovered to be precisely related to the density of the concrete. When strength and density are considered, G46 is shown to be the most optimal blend [25]. Uma et al. (2020) Steel cinders, derived from steel manufacturers, can be used to replace coarse aggregates in concrete mixtures. This substitution results in lighter concrete due to the lower specific gravity of steel cinders, which reduces both construction costs and the weight of the structure. This makes it easier to design massive buildings. Researchers tested the compressive strength of various mixtures ranging from M0 to M5, which included different percentages of steel cinder replacement with coarse aggregate. As the compressive strength of steel cinder concrete decreases, it can be used as lightweight concrete [26].

Factors affecting lightweight concrete in Construction

Lightweight concrete is a versatile construction material that offers numerous advantages, including reduced structural load, improved insulation, and enhanced sustainability. However, its successful application in construction is influenced by several key factors. This paper explores the critical factors affecting lightweight concrete in construction through an examination of real-world cases and industry best practices.

1. **Aggregate Selection:** The choice of lightweight aggregates is a crucial factor in determining the properties of lightweight concrete. Examples of lightweight aggregates include expanded clay, shale, perlite, and vermiculite. The decision to use a specific type of aggregate depends on factors like project requirements, desired density, and structural load. For instance, the construction of a high-rise residential building may require expanded shale lightweight aggregate to reduce overall weight and enhance structural strength.
2. **Mix Design and Proportioning:** Proper mix design and proportioning are essential to achieving the desired properties of lightweight concrete. The ratio of cement, water, lightweight aggregate, and admixtures must be carefully calibrated to meet structural and performance requirements. A case in point is the construction of precast lightweight concrete panels used in architectural façades, where precise mix design ensures both aesthetic appeal and structural integrity.
3. **Quality Control and Testing:** Ensuring the quality of lightweight concrete during production and construction is paramount. Comprehensive testing, including slump tests, compressive strength tests, and density measurements, helps validate the concrete's performance. Projects like airport runways constructed with lightweight concrete demand rigorous quality control to meet safety and load-bearing standards.
4. **Structural Design and Load Considerations:** Structural engineers must consider load-bearing requirements when specifying lightweight concrete. It is essential to evaluate the expected loads and design the structural elements accordingly. For instance, in the construction of bridge decks using lightweight concrete, engineers need to account for vehicular traffic loads and apply load distribution mechanisms to ensure safety.
5. **Environmental Conditions:** Environmental factors, such as temperature, humidity, and exposure to freeze-thaw cycles, can affect the durability of lightweight concrete. Special curing methods and protection measures may be required to mitigate the impact of adverse conditions. The construction of lightweight concrete pavements for highways necessitates attention to weather conditions to prevent premature cracking.
6. **Construction Techniques:** The construction techniques employed significantly impact the success of lightweight concrete applications. Precise placement, consolidation, and curing processes are essential for achieving the



**Malav Nileshbhai Shah et al.,**

desired properties and structural performance. For example, in the construction of lightweight concrete roof insulation, proper installation techniques are crucial to ensure long-term insulation effectiveness.

7. **Regulatory Compliance:** Compliance with local building codes and regulations is vital when using lightweight concrete in construction. Building authorities may have specific requirements related to lightweight concrete use, especially in applications where fire resistance or structural stability is a concern. Compliance with regulations is evident in the construction of fire-rated lightweight concrete walls in commercial buildings.

In conclusion, lightweight concrete offers a wide range of benefits in construction, but its successful utilisation hinges on careful consideration of these influencing factors. By addressing these factors effectively, engineers and builders can harness the advantages of lightweight concrete while ensuring structural integrity, durability, and environmental responsibility in various construction projects.

Opportunities And Challenges Of Lightweight Concrete In Construction

Lightweight concrete presents both promising opportunities and notable challenges in the construction industry. This paper explores the multifaceted landscape of lightweight concrete, delving into the opportunities it offers for sustainable and innovative construction practices while also addressing the key challenges that need to be overcome for its widespread adoption.

Opportunities

1. **Sustainability and Environmental Benefits:** Lightweight concrete's reduced density leads to lower transportation costs and energy consumption during construction. It also contributes to diminished carbon emissions, aligning with the global push for sustainable construction practices. Case studies of eco-friendly residential buildings constructed with lightweight concrete showcase their potential to minimise the industry's environmental footprint.
2. **Improved Energy Efficiency:** Lightweight concrete's enhanced insulation properties make it an ideal choice for energy-efficient buildings. Examples from the commercial sector illustrate how lightweight concrete can be employed in constructing thermally efficient walls, roofs, and floors, reducing heating and cooling expenses for building occupants.
3. **Innovative Architectural Design:** Architects and designers are increasingly drawn to the aesthetic possibilities offered by lightweight concrete. Through the examination of iconic architectural projects, such as museums and cultural centres, this paper illustrates how lightweight concrete enables the creation of intricate and visually striking structures.
4. **Reduced Structural Load:** In infrastructure projects like bridges and elevated highways, lightweight concrete's ability to reduce structural load results in cost savings and improved longevity. Real-world cases of lightweight concrete bridges highlight their resilience and ease of maintenance.

Challenges

1. **Strength and Durability** Despite its numerous advantages, lightweight concrete can exhibit lower compressive strength compared to traditional concrete. The paper discusses how advancements in material science and structural design are addressing this challenge and cites examples of high-strength lightweight concrete applications in demanding construction projects.
2. **Quality Control** Maintaining consistent quality in lightweight concrete production can be challenging. The paper examines quality control measures and certifications implemented in the construction of high-rise
3. Residential buildings to ensure the reliability of lightweight concrete.
4. **Fire Resistance** Lightweight concrete's fire resistance properties are scrutinized, especially in applications requiring stringent fire safety standards, such as tunnels and public buildings. Case studies demonstrate innovative fire-resistant lightweight concrete solutions.





Malav Nileshbhai Shah *et al.*,

5. **Cost Considerations** The initial cost of lightweight concrete materials and equipment can be higher than traditional concrete. However, the paper highlights life-cycle cost analyses that reveal long-term savings, particularly in energy-efficient buildings and infrastructure projects.
6. **Education and Adoption** Widespread adoption of lightweight concrete requires education and training for construction professionals. Examples of training programs and knowledge dissemination initiatives are explored to bridge the awareness gap.

In conclusion, lightweight concrete presents an array of opportunities to revolutionize construction practices, from sustainability and energy efficiency to architectural innovation and reduced structural load. However, addressing challenges related to strength, quality control, fire resistance, cost considerations, and education is crucial for unlocking its full potential in construction. By acknowledging and strategizing around these challenges, the construction industry can embrace lightweight concrete as a key player in shaping the future of sustainable and innovative building practices.

CONCLUSION

1. Lightweight cement has been more popular in recent years owing to its economic properties.
2. Furthermore, the use of lightweight aggregate in cast-in-place buildings, both load-bearing and non-load-bearing, presents a remarkable alternative to the conventional heavy-weight aggregate often employed in the Indian markets.
3. The Indian market exhibits a significant demand for lightweight concrete (LWC), hence necessitating the implementation of new necessary regulations to promote its increased use.
4. Lightweight concrete has a favourable level of strength, making it a viable candidate as an alternative construction material within the context of the industrialised building system.
5. The compressive strength of aerated lightweight concrete tends to decrease as the density of the mixture decreases.
6. The foamed lightweight concrete exhibits inadequate suitability for use as a non-load-bearing wall due to its compressive strength, which falls 27% below the acceptable threshold.

REFERENCES

1. N. Saif, G.Sandhya Rani, and P.Sai Leela Vishnavi, "An Experimental Study on Mechanical Properties of Lightweight Aggregate Concrete when Fine Aggregate is Replaced with Cinder Powder and Dolomite Powder," *Anveshana's Int. J. Res. Eng. Appl. Sci.*, vol. 7, no. 2, pp. 33–43, 2022, doi: 10.2478/cee-2022-0061.
2. R. Rathod, S. Kamble, D. Meshram, A. Meshram, A. Chavhan, and A. Kaparekar, "Review Paper on Experimental Study of Light Weight Concrete," *Int. Res. J. Mod. Eng. Technol. Sci.*, vol. 05, no. 05, pp. 6961–6967, 2023.
3. R. Meena, S. Sharma, A. Sharma, and M. Kumar, "Study on Lightweight Concrete- Review," *Int. J. Eng. Res. Technol.*, vol. 9, no. 07, pp. 786–787, 2020, doi: 10.17577/ijertv9is070348.
4. D. C. L. Teo, M. A. Mannan, and V. J. Kurian, "Structural concrete using oil palm shell (OPS) as lightweight aggregate," *Turkish J. Eng. Environ. Sci.*, vol. 30, no. 4, pp. 251–257, 2006.
5. U. J. Alengaram, B. A. Al Muhit, and M. Z. Bin Jumaat, "Utilization of oil palm kernel shell as lightweight aggregate in concrete - A review," *Constr. Build. Mater.*, vol. 38, pp. 161–172, 2013, doi: 10.1016/j.conbuildmat.2012.08.026.
6. M. M. Paul, Lovely K. M., J. George, and A. Joseph, "Light Weight Concrete Using Oil Palm Shell as Coarse Aggregate," *Int. J. Eng. Res. Technol.*, vol. 3, no. 2, pp. 550–552, 2014.
7. F. N. Williams, E. A. Ijigah, I. Anum, R. B. Isa, and A. O. Obanibi, "Suitability of Palm Kernel Shell as Coarse Aggregate in Lightweight Concrete Production," *Civ. Environ. Res.*, vol. 6, no. 7, pp. 55–60, 2014.





Malav Nileshbhai Shah et al.,

8. E. Yasar, C. D. Atis, A. Kilic, and H. Gulsen, "Strength properties of lightweight concrete made with basaltic pumice and fly ash," *Mater. Lett.*, vol. 57, no. 15, pp. 2267–2270, 2003, doi: 10.1016/S0167-577X(03)00146-0.
9. K. M. Anwar Hossain, "Properties of volcanic pumice based cement and lightweight concrete," *Cem. Concr. Res.*, vol. 34, no. 2, pp. 283–291, 2004, doi: 10.1016/j.cemconres.2003.08.004.
10. T. Parhizkar, M. Najimi, and A. R. Pourkhorshidi, "Application of pumice aggregate in structural lightweight concrete," *Asian J. Civ. Eng.*, vol. 13, no. 1, pp. 43–54, 2012.
11. N. U. Kockal and B. Nevruz, "Pumice Aggregates for Lightweight Cement Mortars," *Proc. Second Intl. Conf. Adv. Civil, Struct. Environ. Eng. ACSEE 2014*, vol. 1, no. 1, pp. 312–314, 2014.
12. H. K. Adai Al-Farttoosi, O. A. Abdulrazzaq, and H. K. Hussain, "Mechanical Properties of Light Weight Aggregate Concrete Using Pumice as a Coarse Aggregate," *IOP Conf. Ser. Mater. Sci. Eng.*, vol. 1090, no. 1, pp. 012106 (1–12), 2021, doi: 10.1088/1757-899x/1090/1/012106.
13. H. Al-Khaiat and M. N. Haque, "Effect of Initial Curing on Early Strength and Physical Properties of a Lightweight Concrete," *Cem. Concr. Res.*, vol. 28, no. 6, pp. 859–866, 1998.
14. M. Aineto, A. Acosta, J. M. Rincón, and M. Romero, "Production of lightweight aggregates from coal gasification fly ash and slag," *World Coal Ash*, pp. 11–15, 2005, [Online]. Available: <http://www.flyash.info>
15. P. Perumal, M. Ganesh, and A. S. Santhi, "Experimental study on Cold Bonded Fly Ash Aggregates," *Int. J. Comput. Civ. Struct. Eng.*, vol. 2, no. 2, pp. 493–501, 2011, doi: 10.6088/ijcser.00202010129.
16. P. Gomathi and A. Sivakumar, "Fly ash based lightweight aggregates incorporating clay binders," *Indian J. Eng. Mater. Sci.*, vol. 21, no. 2, pp. 227–232, 2014.
17. T. A. Patel and J. M. Patel, "A Review on Cold-Bonded Fly Ash Lightweight Aggregates: less costly light weight promising material," *Indian J. Appl. Res.*, vol. 5, no. 1, pp. 11–13, 2015.
18. V. P. Kukarni and S. B. Gaikwad, "Comparative Study on Coconut Shell Aggregate with Conventional Concrete," *Int. J. Eng. Innov. Technol.*, vol. 2, no. 12, pp. 67–70, 2013.
19. G. C. Behera and R. K. Behera, "Effect of Coconut Shell Aggregate on Normal Strength Concrete," *Int. J. Eng. Res. Technol.*, vol. 2, no. 6, pp. 2405–2415, 2013.
20. S. A. Kakade and A. W. Dhawale, "Light Weight Aggregate Concrete By Using Coconut Shell," *Int. J. Tech. Res. Appl.*, vol. 3, no. 3, pp. 127–129, 2015.
21. P. Prakash, S. Anandh, S. Sindhu Nachiar, and G. M. Gilbert, "A study on mechanical and durability properties of coconut shell concrete using coconut fiber and sawdust," *IOP Conf. Ser. Mater. Sci. Eng. 3rd Int. Conf. Adv. Mech. Eng. (ICAME 2020)*, vol. 912, no. 6, pp. 062068 (1–10), 2020, doi: 10.1088/1757-899X/912/6/062068.
22. L. Xiao and D. Jiang, "The effect of fly ash on the mechanical properties of cinder lightweight aggregate concrete," *IOP Conf. Ser. Earth Environ. Sci.*, vol. 61, no. 1, pp. 012116 (1–5), 2017, doi: 10.1088/1755-1315/61/1/012116.
23. L. Xiao, J. Li, and Q. Liu, "Effect of fly ash on strength of cinder lightweight aggregate concrete," *IOP Conf. Ser. Mater. Sci. Eng.*, vol. 423, no. 1, pp. 012187 (1–5), 2018, doi: 10.1088/1757-899X/423/1/012187.
24. A. Govandan and C. Jenefa, "Effect of Cinder Ash in Concrete," *Int. J. Civ. Eng. Res. Technol.*, vol. 7, no. 11, pp. 1–4, 2019.
25. M. L. Harish, H. Narendra, and M. Azam Afzal, "Performance of Lightweight Aggregate Concrete Containing Expanded Polystyrene, Cinder and Ground-Granulated Blast-Furnace Slag," *J. Comput. Theor. Nanosci.*, vol. 17, no. 9, pp. 4304–4310, 2020, doi: 10.1166/jctn.2020.9067.
26. S. G. Uma, S. Muthulakshmi, and G. Hemalatha, "Study on light weight concrete using steel cinders," *Mater. Today Proc.*, vol. 46, no. xxxx, pp. 3813–3816, 2020, doi: 10.1016/j.matpr.2021.02.039.

Table I. Lightweight aggregates (LWAs) and normal-weight aggregates (NWAs)

Key Aspects	Lightweight aggregates (LWAs)	Normal-weight aggregates (NWAs)
Density	LWAs have a lower density compared to NWAs. Their density typically ranges from 600 to 1,600 kg/m ³ (37 to 100 lb/ft ³).	NWAs have a higher density, typically ranging from 2,400 to 2,800 kg/m ³ (150 to 175 lb/ft ³).





Malav Nileshbhai Shah et al.,

Composition	LWAs are often made from natural materials like expanded clay, shale, or slate. They can also be produced from industrial by-products like fly ash or slag.	NWAs are typically dense natural stones like granite, limestone, gravel, or sand.
Strength	LWAs generally have lower compressive strength compared to NWAs. This makes them suitable for applications where reducing structural loads is a priority.	NWAs have higher compressive strength, which makes them suitable for load-bearing structures and applications that require high durability.
Insulation Properties	LWAs are known for their insulation properties due to their lower thermal conductivity. They are often used in lightweight concrete to improve insulation in building envelopes.	NWAs have higher thermal conductivity, making them less suitable for applications where insulation is a primary concern.
Transportation Costs	Because of their lower density, LWAs are lighter and result in reduced transportation costs, especially for long-distance transport [2].	NWAs are heavier and can lead to higher transportation costs, especially when transported over long distances.
Sustainability	LWAs can contribute to sustainability efforts by reducing the overall weight of structures, which may lead to lower energy consumption during the building's operational phase.	NWAs are often considered less sustainable due to their higher density and potential for increased transportation-related carbon emissions.
Energy Efficiency	LWAs can enhance energy efficiency in buildings by reducing the structural load, resulting in less demand for heating and cooling.	NWAs may require more energy-intensive construction methods due to their higher weight.
Applications	LWAs are commonly used in lightweight concrete, precast concrete products, and applications where reduced structural load is important. They are suitable for non-load-bearing walls, insulation, and lightweight fill materials [3].	NWAs are widely used in traditional concrete mixes for load-bearing structures, bridges, highways, and applications requiring high strength and durability.





Synthesis of Poly (Acrylonitrile)-Grafted Sodium Salt of Partially Carboxy Methylated Tamarind Kernel Powder (Na-PCMTKP) using Potassium Per Sulphate/Ascorbic Acid as a Redox Initiating System

Kinnari.A. Bhatt^{1*}, Jignesh. H.Trivedi², Kirit. H. Patel², Harikrishna. C. Trivedi³

¹Organic Chemistry Department, Institute of Science and Technology for Advanced Studies and Research (ISTAR), The Charutar Vidya Mandal (CVM) University, Vallabh Vidyanagar, Gujarat, India.

²Department of Chemistry, Sardar Patel University, Vallabh Vidyanagar, Gujarat, India.

³Team Lease Skills University, ITI Campus Tarsali, Vadodara, Gujarat, India.

Received: 30 Dec 2023

Revised: 09 Jan 2024

Accepted: 12 Jan 2024

*Address for Correspondence

Kinnari.A. Bhatt

Organic Chemistry Department,

Institute of Science and Technology for Advanced Studies and Research (ISTAR),

The Charutar Vidya Mandal (CVM) University,

Vallabh Vidyanagar, Gujarat, India.

Email: kinnari.bhatt@cvmu.edu.in



This is an Open Access Journal / article distributed under the terms of the **Creative Commons Attribution License** (CC BY-NC-ND 3.0) which permits unrestricted use, distribution, and reproduction in any medium, provided the original work is properly cited. All rights reserved.

ABSTRACT

Acrylonitrile was grafted onto sodium salt of partially carboxy methylated tamarind kernel powder (Na-PCMTKP) using potassium per sulphate (KPS) and ascorbic acid (AA) as redox initiators in an aqueous medium. The optimum reaction conditions have been established by varying reaction variables including concentration of AA, KPS, monomer and amount of backbone as well as time and temperature. The influence of these reaction conditions on the grafting yields such as percentage grafting and percentage grafting efficiency are discussed. The proposed reaction mechanism could explain very well the experimental results. The FT-IR spectroscopy, Thermal Gravimetric Analysis (TGA) and Scanning Electron Microscopic (SEM) techniques have been used for the characterization of newly synthesized graft co-polymer (Na-PCMTKP-g-PAN).

Keywords: MSMEs, Jammu and Kashmir, Employment, Shapiro-wilk, Growth





Shubarat Shameem and Rajeswari

INTRODUCTION

In the modern times it is require to identify or to modify polymer with better properties so it will be used for the variety of its applications. Grafting is one method that is useful for the modification of naturally available polysaccharides. Tamarind kernel powder [TKP] is one of the cheapest and most readily available gum that can derived from its seed. Tamarind seed consist of husk and white kernel in 35% and 65% respectively [1]. The constitutes of seed kernel are protein (15 - 20.9%), carbohydrate (65 – 72%) and fat (4 - 16%) [2]. It is composed of (1→4)-β-D-glucopyranosyl units substituted with side chains consisting of a single xylopyranosyl unit is attached to every second, third and fourth D- glucopyranosyl unit through α-D-(1 → 6) linkage. One D- galacto pyranosyl unit is attached to one of the xylopyranosyl unit through β-D- (1→2) linkage [3-7]. The structure of TKP is shown in Figure 1. Many hurdles occur because of properties like dull colour, unpleasant smell and low water solubility which become obstacle in many applications. Hence, we have used carboxy methylated tamarind kernel powder (Na-PCMTKP) and further modified it via chemical methods using KPS/AA as redox initiator. A literature survey shows that there are some reports on the grafting of acrylonitrile [7], ethyl acrylate [8] and methyl methacrylate [9] onto TKP. In addition, ceric ammonium nitrate-initiated grafting of hydro xyethyl methacrylate [10] as well as photo-induced grafting of methacrylate [11] and acrylonitrile [12] was done and KPS/AA initiated grafting of acrylamide [13] and acrylonitrile [14] onto guar gum and Na-PCMGG are visible in reports. However, there are no reports on KPS/AA initiated grafting of vinyl monomers onto Na-PCMTKP. In present study, therefore, an attempt has been made systematically to optimize the graft copolymerization reaction of acrylonitrile [AN] onto Na-PCMTKP ($\overline{DS} = 0.15$) and characterize the optimally synthesized graft copolymer. Optimization not only develops specialty polymeric materials but also to elucidate the KPS/AA initiated grafting mechanism over various reaction conditions studied.

MATERIALS AND METHODS

Sodium salt of partially carboxy methylated tamarind kernel powder (Na-PCMTKP, $\overline{DS} = 0.15$) was kindly supplied by Encore Natural Pvt. Ltd; Naroda, Ahmedabad (Gujarat). Potassium persulphate (KPS) (Qualigens, Glaxo India Ltd.) and Ascorbic Acid (AA) (Samir Tech, Chem. Baroda, Gujarat) of analytical reagent grade were procured. Acrylonitrile (AN) (procured from Chiti-Chem Corporation, Baroda) was distilled at atmosphere pressure and the middle fraction of it was collected and used. All other reagents and solvents used were of reagent grade. Nitrogen gas was purified by passing through freshly prepared alkaline pyrogallol solution. The conductivity water was used for the preparation of solutions as well as in polymerization reactions.

Graft copolymerization

A 250 mL R. B. F. is fitted with mechanical stirrer, condenser and a gas inlet system which immersed in a constant temperature (temp. is maintain using temperature controller) bath for grafting reaction. For getting optimized graft copolymer turn by turn different variations are done during the synthesis such as varying amount of the Sodium Salt of Partially Carboxy methylated Tamarind Kernel Powder (Na-PCMTKP, $\overline{DS} = 0.15$) from 0.25g to 3.00 g, monomer (AN) (0.051 – 0.405 mol/L) was taken, keeping temperature between 20° – 80°C. Also different concentration of redox initiators KPS (5×10^{-3} - 45×10^{-3} mol/L) and AA (10×10^{-3} - 50×10^{-3} mol/L) was taken and the time duration was ranging between 0.5 to 10 hrs. the substrate dissolved in 110mL non- ionize with constant stirring and slow bubbling of N₂ gas for 1 h for uniform swelling of substrate. At the desired temperature the freshly distilled monomer was then added to the reaction mixture. After 5 mins., the freshly prepared 10 mL solution of AA in non-ionize water was added. After 30 mins., the freshly prepared 10 mL solution of KPS in non-ionize water was added and stirred to it and then after reaction is carried for the decide time interval. Dissolved oxygen was removed by passing slow stream of N₂ was continuously during the course of the reaction. The contents of the flask were poured immediately into excess of methanol at the end of reaction for the complete precipitation of graft copolymer. Then centrifugation





Shubarat Shameem and Rajeswari

method was used to get crude copolymer product which was repeatedly washed with 95% methanol and finally with pure methanol. The crude sample thus, obtained was dried under vacuum at 40°C. The homopolymer was removed from the crude graft copolymer by exhaustive soxhlet extraction with acetone for 48 hrs.

Isolation of Grafted Chains

The grafted PAN chains were isolated from the graft copolymer (Na-PCMTKP-g-PAN) sample by refluxing it in 1N HCl solution for 12 hrs. as per the procedure reported in the literature [15].

Grafting Yields and Kinetic Parameters

The values of the grafting yields (%G and %GE) and the rates of polymerization (R_p), graft copolymerization (R_g) and homo polymerization (R_h) were evaluated by using the equations [16].

IR Spectra

The IR spectra of Na-PCMTKP ($\overline{DS} = 0.15$), Na-PCMTKP-g-PAN and PAN were taken in KBr pellets using Nicolet Impact 400D Fourier Transform Infrared Spectrophotometer.

Thermo gravimetric Analysis (TGA)

Sodium Salt of Partially Carboxy methylated Tamarind Kernel Powder (Na-PCMTKP, $\overline{DS} = 0.15$) and its graft copolymer Na-PCMTKP-g-PAN and PAN under inert atmosphere at a scan rate of 10°C/min.

Differential Scanning Calorimetry (DSC)

The DSC scans of Na-PCMTKP ($\overline{DS} = 0.15$) and its graft copolymer Na-PCMTKP-g-PAN were recorded under a nitrogen atmosphere at a scan rate of 10°C/min on DSC METTLER TOLEDO STAR[®] SW 7.01 instrument.

Scanning Electron Microscopy (SEM)

Model ESEM THP + EDAX, Philips make has been used to obtain the micrographs of Na-PCMTKP ($\overline{DS} = 0.15$) and Na-PCMTKP-g-PAN grafted copolymer samples.

Mechanism of Graft Copolymerization

The present work uses the kinetics of redox initiator system KPS and AA. U.D.N. Bajpai and et al [13] report the same kinetics. In this mechanism, there is involvement of formation of primary radicals in sequence. There was proposal for forming primary radicals (as corbate radicals) like $SO_4^{\bullet-}$, $\bullet OH$, $\bullet AH$ as shown in Scheme-1

In the scheme-2, the produced primary radicals are express as X^{\bullet} which explains the mechanism of grafting of AN onto Na-PCMTKP ($\overline{DS} = 0.15$) using a KPS/AA redox initiating system in an aqueous system. Scheme-2 also propose that vinyl polymerization reaction is initiated by primary radicals (chain carriers) as proton abstraction from vinyl polymer reports being faster than the Na-PCMTKP backbone. According to scheme-2, whatever amount of macro radicals (Na-PCMTKP^o) generated may collide with vinyl monomer (AN) and the resulting radical is Na-PCMTKPOM^o. Thus, newly generated radicals can attract more AN molecule available in the reaction mixture. In this way, propagation step is continued till the reaction gets terminated by the combination of remaining growing polymeric chains. This results in the generation of graft copolymer, Na-PCMTKP-g-PAN

Determination of Optimal Grafting Conditions

To optimize the conditions for grafting of AN onto the Na-PCMTKP ($\overline{DS} = 0.15$), various reaction conditions including the amount of backbone (Na-PCMTKP), concentrations of monomer (AN), potassium per sulfate (KPS) and ascorbic acid (AA) as well as reaction time and temperature were varied keeping the total volume of the reaction mixture to be 150mL. The influence of various reaction conditions on grafting yield was also studied as discussed below:



**Shubarat Shameem and Rajeswari****Effect of Backbone Concentration**

Figure2 explains that, the variation in the backbone concentration is responsible for percentage grafting (%G) and percentage grafting efficiency (%GE). Figure2 also indicates that as the amount of Na-PCMTKP increases the value of %G and %GE also increases up to optimum reaction condition (Na-PCMTKP from 0.25 gm to 1.5 gm). The maximum value of %G is 160.81%. After the optimum point the values %G and %GE decreases with future increase in the amount of Na-PCMTKP. From this we can predict that, the initial increase upto optimum concentration is due to the higher availability of reactive sites of Na-PCMTKP but because of the destruction of radical activity at more higher concentration due to termination by backbone-backbone and backbone-primary radicals. Similar results are seen in [17-19].

Effect of Monomer Concentration

The result of percentage grafting (%G) and percentage grafting efficiency (%GE) values upon changing in the monomer [AN] concentration can be observed from Figure3. It shows increase in %G value as the concentration is varied from 0.05 to 0.35mol/L (from 0.50 to 3.50 ml). The maximum value of %G is found to be 307.49% at 3.50 ml. Beyond 3.50 ml (0.35mol/L), the %G value decreases. It is also observed from the %GE results that along with %G, %GE increases too, and then after decreases. The gradual increase in %G and %GE up to optimized value may be due to the possibility of the concentration of monomer in the neighborhood of Na-PCMTKP in reaction medium also, it is noted that, as more graft copolymer radicals are generated, there will be shielding of graft copolymers by excess of monomer, and this may be the inhibiting factor for the graft copolymerization. Along with this, at higher monomer concentration, more monomer molecules are easily available for initiators, which leads to quick homo polymerization, and may be due to this reason, result shows decrease in grafting efficiency too. The similar results were also reported in [12, 21,24].

Effect of Potassium Per sulphate concentration

From the Figure 4, it is observed that concentration of KPS and %G increases simultaneously up to optimum concentration i.e. $[KPS] = 25 \times 10^{-3} \text{ mol/L}$ and the maximum value of %G is 116.03%. But after this, the concentration of KPS and %G is decreases. The initial increase in the value of %G can be explained on the bases of the fact that, as the initiator concentration increases there is an excess number of radicals generated on the substrate i.e. Na-PCMTKP and monomer too. Due to this, a rise in %G is observed but after optimum value of KPS the decrease in %G might be associated with the strong possibility of chain termination reactions. The same kind of result can be obtained in [19,22,23].

Effect of Ascorbic Acid Concentration [Activator]

Ascorbic acid (AA) is also used as an initiator along with KPS. Effect of concentration of AA on to grafting yield i.e. %G is observed from Figure5. The graph explains that, along with AA concentration, the %G value also increases up to optimum value i.e. $[AA] = 20 \times 10^{-3} \text{ mol/L}$ and the %G value is 156.52% at the same point. This increase is attributed to the fact that, due to the presence of ascorbic acid, radicals like $\text{a}^{\bullet}\text{AH}$ and $\text{SO}_4^{\bullet-}$ are formed in the reaction mixture which may attacked Na-PCMTKP molecules and because of it, more active sites are generated which helps the addition of AN, so the %G increases. Beyond the optimum concentration of AA, the %G value decreases may be because of fact that excess of as corbate () radicals are responsible for homo polymerization. Thus, instead of graft copolymers homo polymers are generated. In both the initiator, i.e., KPS and AA, there is little variation %GE value explaining that initiators do not much effect on the grafting efficiency of the product. Similar results were reported in [14,19].

Effect of Reaction Temperature

Figure6 reveals that as temperature increases, the %G value also increases from 20°C to 35°C and then decreases. This can be understood in terms of positive influence of temperature at different phase of reaction, such as it enhances the swelling of Na-PCMTKP, solubility, mobility and diffusion of monomer molecules and also on the collision rate of monomer (AN) with Na-PCMTKP. It affects the initiation and propagation rates too. At higher





Shubarat Shameem and Rajeswari

temperature, the %G value decreases, which may be because at higher temperature, hydrogen abstraction and chain transfer reaction rates becomes faster and hence %G decreases. The same results are shown in [25,26].

Effect of Reaction Time

It is cleared from Figure 7 that, maximum %G is obtained at 2.5 hrs, and it is due to the easy availability of grafting sites during initiation reaction on Na-PCMTKP. But after optimum time i.e. 2.5hrs, it decreases because of lowering the concentration of monomer and initiator, and also due to less accessible grafting site. The formation of more homo polymers is also one of the major reasons for decreases in %G and %GE values. The same type of results is seen in [20,24,25]. Thus, based on this discussion, the optimized reaction conditions for obtaining graft copolymer of PAN i.e. Na-PCMTKP-g-PAN are shown in Table I.

EVIDENCE OF GRAFTING

FTIR Analysis

The combine FTIR analysis of Na-PCMTKP (a) (\overline{DS} = 0.15) Na-PCMTKP-g-PAN (b) and PAN (c) give the evidence that, grafting of AN is taken place on to Na-PCMTKP successfully. In FTIR spectrum (a), the broad and strong absorption band at $\sim 3428 \text{ cm}^{-1}$ is for the (-OH) stretching. The (-CH) stretching is confirmed from the sharp absorption band at $\sim 2927 \text{ cm}^{-1}$. For (-CO-) moiety, the asymmetric and symmetric vibrations are assigned to $\sim 1640 \text{ cm}^{-1}$ and $\sim 1424 \text{ cm}^{-1}$ respectively. This supports the presence of carboxy methyl group in Tamarind Kernel Powder (TKP). FTIR spectrum (b), the spectrum of Na-PCMTKP-g-PAN shows all the bands of Na-PCMTKP and the additional band at $\sim 2228 \text{ cm}^{-1}$. This indicates the presence of (-CN) stretching. It is characteristic band of PAN. The entry of new band at $\sim 2228 \text{ cm}^{-1}$ in the spectrum of graft copolymer i.e. Na-PCMTKP-g-PAN, specify without any uncertainty that, grafting of AN on to Na-PCMTKP has occurs successfully. Moreover, this graft copolymer (Na-PCMTKP-g-PAN) was hydrolyzed in order to isolate the grafted chains of PAN. The FTIR- spectrum of PAN shows that the band at $\sim 1730 \text{ cm}^{-1}$ supports the presence of (-CO) stretching. All these comparisons prove that AN is grafted on to Na-PCMTKP successfully.

Scanning Electron Microscopy (SEM)

The scanning electron micrograph of Na-PCMTKP Figure 9 shows the clustering of the granules and granules could be distinguished from one another. The surface topology of Na-PCMTKP-g-PAN (%G = 214.41) can be seen in Figure 10. Upon comparing the morphology of the grafted samples Fig.10 with un-grafted material Figure 9 it is clearly evident that the grafted chains have drastically changed the morphology of Na-PCMTKP (\overline{DS} = 0.15) sample. Also, additional surface deposits are observed indicating that the grafting has taken place.

Thermo gravimetric Analysis (TGA)

The thermo grams of Na-PCMTKP (\overline{DS} = 0.15) and its graft copolymers as well as homo polymers are discussed.

The thermal behavior of Na-PCMTKP (\overline{DS} = 0.15) and its graft copolymer Na-PCMTKP-g-PAN, along with the corresponding homo polymers PAN is examined by a study of their primary thermo grams. The overall degradation of Na-PCMTKP (\overline{DS} = 0.15)

(Figure 11) exhibits two steps of degradation. As it can be seen from this figure that the sample begins to decompose at about 120°C and loses its weight up to 370°C involving about 62.5% weight loss. The second step is immediately followed in a temperature range $370\text{-}520^\circ \text{C}$ during which the sample loses 37.5% of its weight leaving no weight residue. The maximum values of weight loss occur at 295°C and 450°C respectively during first and second steps of decomposition.

Figure 12 shows the primary thermo grams obtained at a scan rate of $10^\circ \text{C}/\text{min}$ for Na-PCMTKP-g-PAN (%G = 214.41) and PAN in an inert atmosphere. The overall thermal degradation of Na-PCMTKP-g-PAN involves two steps of degradation. The decomposition begins at 210°C and proceeds slowly up to 425°C involving about 39% weight





Shubarat Shameem and Rajeswari

loss with maximum rate of weight loss at 305°C. The second decomposition step comprises of 425-800°C, involving about 31% residue with maximum rate of weight loss at 655°C. The final residue at 800°C amounts to 30%.

CONCLUSION

As we know, TKP is biodegradable in nature but due to its low solubility, in this present work we took Sodium Salt of Partially Carboxy methylated Tamarind Kernel Powder (Na-PCMTKP) and positively try to modified it using very simple method of grafting which expands its application range as well. We optimized different reaction conditions such as concentration of Na-PCMTKP, Monomer, Ascorbic acid, Potassium per sulphate as well as reaction time and temperature as discussed earlier. For the optimized reaction conditions, the values of %G and %GE were 214.14% and 98.85% respectively. FTIR, SEM and TGA are important evidences for the characterization. It is proved without any future doubt that grafting has taken place with the help of result of FTIR and SEM analysis while the result of TGA describe loudly that the thermal stability of Na-PCMTKP is increase after its grafting by PAN.

REFERENCES

1. R.N. Sutar, A Text Book of Systematic Botany. 4th Edition, 1966
2. J.H. Trivedi, A. Vanaamudan and H.C. Trivedi, "Tamarind kernel powder, its derivatives and their modification through grafting: an overview," in *Advances in diverse applications of polymer composites*, Eds. S. M. Zachariah, Y. Weimin, M. Jaroszewski and S. Thomas, Apple Academic Press exclusively co-published with CRC Press, Taylor & Francis Group, Ch. 4, 2023.
3. V Gupta., R Puri., S. Gupta and G.K. Rao, "Tamarind kernel gum: an upcoming natural polysaccharide," *Sys. Rev. Pharm.*, pp. 50-54, 2010.
4. M.J. Gidely, P.J. Lillford, D.W. Rowlands, P. Lang, M. Dentini, V. Crescenzi, M. Edwards, C. Fautti and J.S. Grant Reid, "Structure and solution properties of tamarind-seed polysaccharide," *Carbohydrate Research*, pp. 299-314, 1991.
5. P. Goyal, V.Kaur and P. Sharma, "Carboxymethylation of Tamarind kernel powder," *Carbohydrate Polymers*, pp. 251-255, 2007.
6. A. Mishra and A. Malhotra, "Tamarind Xyloglucan: a polysaccharide with versatile application potential," *J. Mater. Chem.*, pp. 8528-8536, 2009.
7. P. Goyal, V. Kumar and P. Sharma, "Graft copolymerization onto tamarind kernel powder: ceric (IV)-initiated graft copolymerization of acrylonitrile," *Journal of Applied Polymer Science*, pp. 377-386, 2009.
8. A. Real, D. Wallander, A. Maciel, G. Cedillo and H. Lozac, "Graft copolymerization of ethyl acrylate onto tamarind kernel powder, and evaluation of its biodegradability," *Carbohydrate Polymer*, pp. 11-18, 2015.
9. A. Mishra and A. V. Malhotra, "Graft copolymers of xyloglucan and methyl methacrylate," *Carbohydrate Polymers*, pp. 1899-1904, 2012.
10. P. Choudhury, S. Kumar, A. Singh, A. Kumar, N. Kaur, S. Sanyasi, S. Chawla, C. Goswami and L. Goswami, "Hydroxyethyl methacrylate grafted carboxy methyl tamarind (CMT-g-HEMA) polysaccharide-based matrix as a suitable scaffold for skin tissue engineering," *Carbohydrate Polymers*, pp. 87-98, 2018.
11. J.H. Trivedi, H.A. Joshi and H.C. Trivedi, "Na-PCMTKP-g-PMA: Photo-induced synthesis and characterization," *International Journal of Research in Engineering and Applied Sciences*, pp. 39-55, 2017.
12. J.H. Trivedi, H.A. Joshi and H.C. Trivedi, "Graft copolymerization of acrylonitrile onto sodium salt of partially carboxymethylated tamarind kernel powder using ceric ammonium nitrate as a photo-initiator in an aqueous medium under ultraviolet-radiation," *Macromolecular Symposia*, pp. 1-13, 2021.
13. U.D.N. Bajpai., A., Jain, and S. Rai, "Grafting of polyacrylamide on to guar gum using K₂S₂O₈, ascorbic acid redox system," *Journal of Applied Polymer Science*, pp. 2187-2204, 1990.





Shubarat Shameem and Rajeswari

14. J.H. Trivedi, U.S. Shah and H.C. Trivedi, "Grafting of sodium salt of partially carboxymethylated guar gum with acrylonitrile using $K_2S_2O_8$ /ascorbic acid redox initiator," *International Journal of Advance and Innovative Research*, pp. 49-59, 2018.
15. C. E. Brockway and P. A. Seaberg, "Grafting of polyacrylonitrile to granular corn starch," *Journal of Polymer Science Part A-1*, pp. 1313-1326, 1967.
16. B. K. Patel, "Ph. D. Thesis," *Sardar Patel University India*, 1990.
17. B.K. Patel, C.P. Patel and H.C. Trivedi, "Grafting of acrylonitrile onto sodium carboxymethylamylose: effect of backbone concentration," *Journal of Polymeric Materials*, pp. 171-174, 1992.
18. P. Goyal, V. Kumar and P. Sharma, "Graft Copolymerization of acrylamide onto tamarind kernel powder in the presence of ceric ion," *Journal of Applied Polymer Science*, pp. 3696-3701, 2008.
19. J. Tripathi, D. Mishra, M. Yadav, K.Behari; "Synthesis, characterization and applications of graft copolymer (Chitosan-g-N, N-dimethylacrylamide)," *Carbohydrate Polymers*, pp. 40-46, 2010.
20. F. Shafiei, M. Sadeghi and E.Mohammadinasab, "Investigation effective parameters onto γ -radiation graft polymerization acrylamide onto carboxymethylcellulose," *Advances in Environmental Biology*, pp. 790-794, 2012.
21. R. Das, A. B. Panda and S. Pal, "Synthesis and characterization of a novel polymeric hydrogel based on hydroxypropyl methyl cellulose grafted with polyacrylamide," *Cellulose*, pp. 933-945, 2012.
22. V. Singh, D. N. Tripathi, T. Malviya and R.Sanghi, "Persulfate/ascorbic acid initiated synthesis of poly(acrylonitrile)-grafted tamarind seed gum: A potential commercial gum," *Journal of Applied Polymer Science*, pp. 539-544, 2009.
23. L. Wang and Y. Xu, "Effect of dimethylaminoethyl methacrylate on the graft copolymerization of ethyl acrylate onto hydroxypropyl methyl cellulose in aqueous medium," *Cellulose*, pp. 713-724, 2006.
24. J. H. Trivedi, K. Kalia, N. K. Patel and H. C. Trivedi; "Graft copolymerization of sodium salt of partially carboxymethylated guar gum with methyl methacrylate: An examination of the reaction variables," *Journal of Applied Polymer Science*, pp. 1855-1864, 2005.
25. A. S. Singha and A. K.Rana, "Kinetics of graft copolymerization of acrylic acid onto *Cannabis indica* Fibre," *Iranian Polymer Journal*, pp. 913-929, 2011.
26. T. Sehgal and S. Rattan, "Synthesis, characterization and swelling characteristics of graft copolymerized isotactic polypropylene film," *International Journal of Polymer Science*, 2010, article Id 147581 9 pages. (doi.org/10.1155/2010/147581)

Table I Optimized Reaction Conditions

Na-PCMTKP ($\overline{DS} = 0.15$)	1.5 g (dry basis)
[KPS]	25×10^{-3} M
[AA]	20×10^{-3} M;
[AN]	0.35 mol. L^{-1}
Time	2.5 h
Temperature	35°C
Volume of Water	146.5 mL
Total Volume	150 mL

$\%G = \frac{\text{Wt. of polymer grafted}}{\text{Initial wt. of Na-PCMTKP}} \times 100$	$\%GE = \frac{\text{Wt. of polymer grafted}}{\text{Wt. of polymer grafted} + \text{Wt. of homopolymer}} \times 100$
$\text{Rate of polymerization } R_p (\text{mol. L}^{-1} \cdot \text{s}^{-1}) = \frac{\text{Wt. of polymer grafted} + \text{Wt. of homopolymer}}{\text{Mol.wt. of monomer} \times \text{Reaction time in seconds} \times \text{Volume of the reaction mixture (mL)}} \times 10^3$	$\text{Rate of graft polymerization } R_g (\text{mol. L}^{-1} \cdot \text{s}^{-1}) = \frac{\text{Wt. of polymer grafted}}{\text{Mol.wt. of monomer} \times \text{Reaction time in seconds} \times \text{Volume of the reaction mixture (mL)}} \times 10^3$





Shubarat Shameem and Rajeswari

$$R_h \text{ (mol. L}^{-1}\text{.s}^{-1}\text{)} = \frac{\text{Wt. of homopolymer}}{\text{Mol.wt. of monomer} \times \text{Reaction time in seconds} \times \text{Volume of the reaction mixture (mL)}} \times 10^3$$

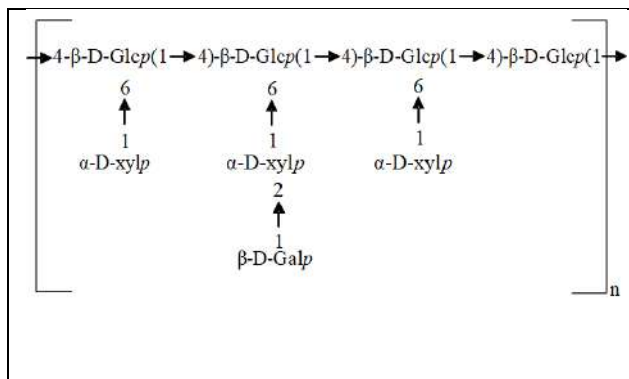


Figure 1. Structure of TKP

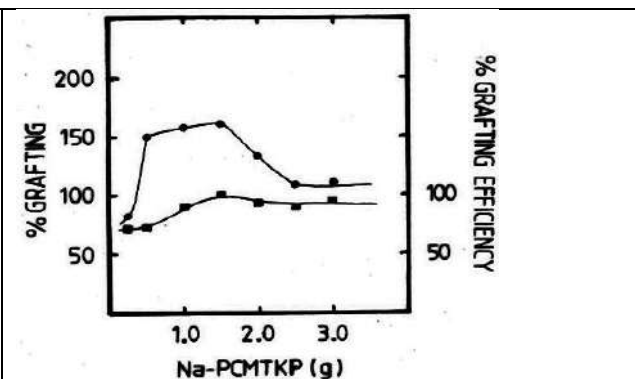


Figure 2 .Effect of amount of Na-PCMTKP on (●) grafting and (■) grafting efficiency

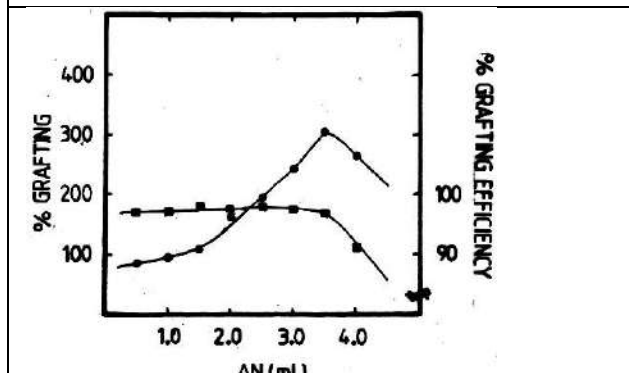


Figure 3. Effect of AN concentration on (●) grafting and (■) grafting efficiency

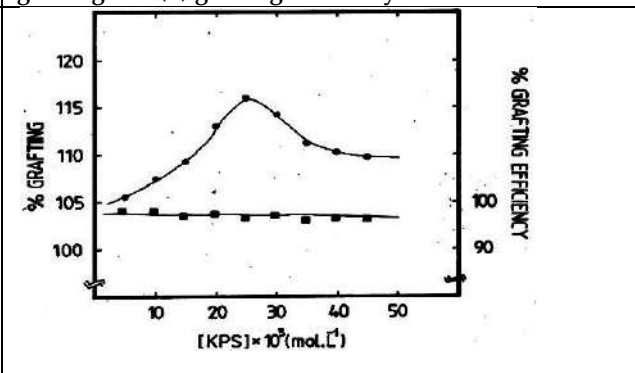


Figure 4. Effect of KPS concentration on concentration on (●)grafting and (■) grafting efficiency

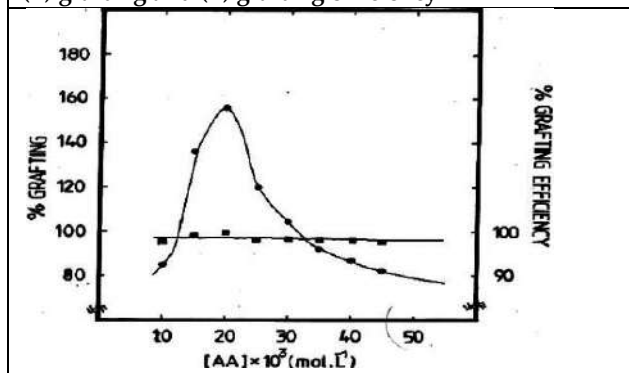


Figure 5. Effect of AA concentration on(●) grafting and (■) grafting efficiency.

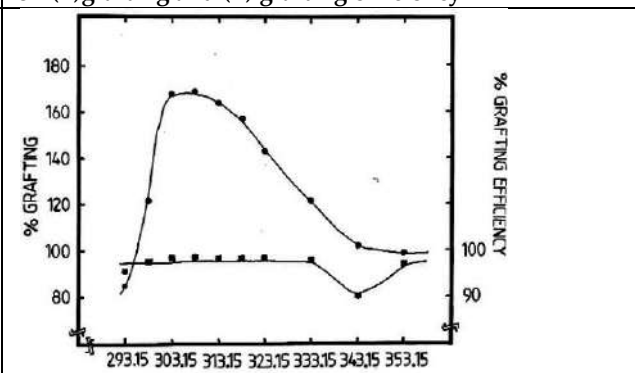


Figure 6. Influence of the reaction temperature on (●)grafting and (■) grafting efficiency





Shubarat Shameem and Rajeswari

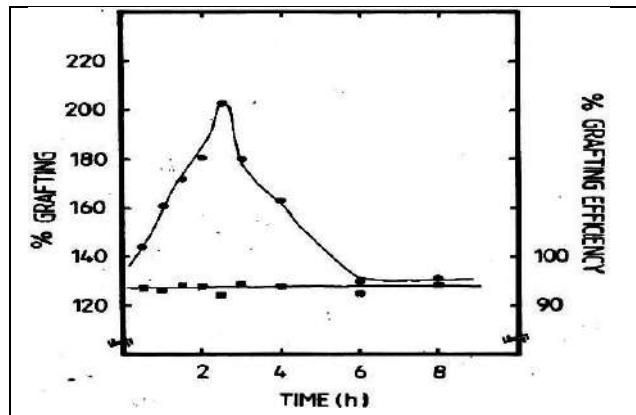


Figure 7. Influence of the reaction time on (●) grafting and (■) grafting efficiency.

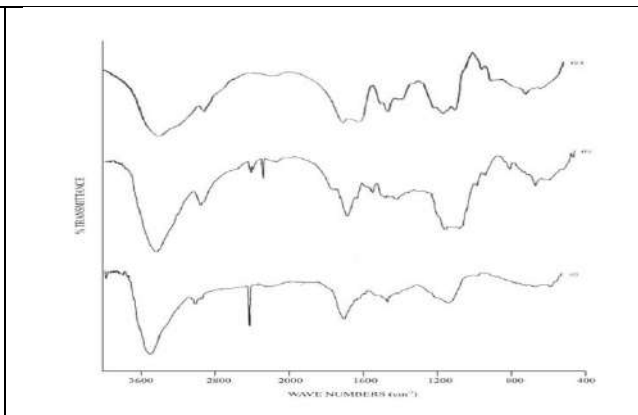


Figure 8. IR spectra of (a) Sodium Salt of Partially Carboxy methylated Tamarind Kernel Powder (Na-PCMTKP, \overline{DS} = 0.15) sample, (b) Na-PCMTKP-g-PAN sample, (c) Polyacrylonitrile (PAN) sample.

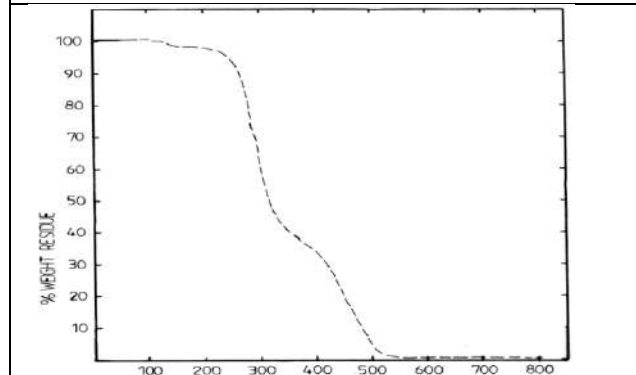


Figure 9. TG thermo gram for Na-PCMTKP (\overline{DS} = 0.15)

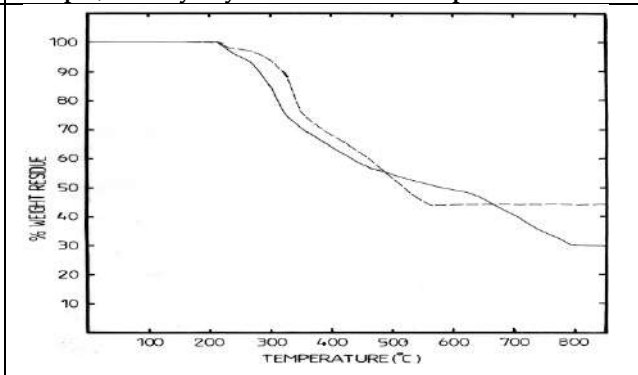
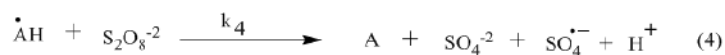
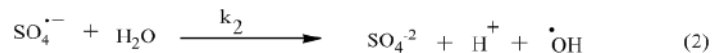


Figure 10. TG thermo grams for () Na-PCMTKP-g-PAN and (---) PAN at 10°C/min.

Initiator:



Propagation:



Termination:

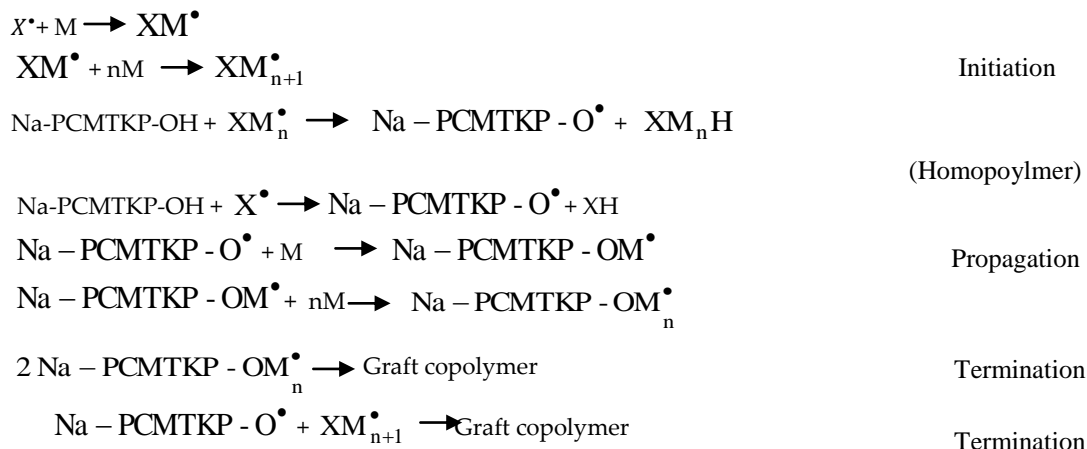


Scheme-1: Formation of chain carriers by KPS/AA initiation.





Shubarat Shameem and Rajeswari



Scheme-2: Reaction mechanism for the synthesis of Na-PCMTKP-g-PAN.





Time Series Forecasting Electric Vehicle Sales Market of India

Brijesh M Patel^{1*}, Nikunj R. Patel², K L Mokariya³ and Hetal Prajapati⁴

¹Research Scholar, Gujarat Technological University, Ahmedabad, Gujarat, India.

²Assistant Professor, Electrical Engineering Department, SSAS Institute of Technology, Surat, Gujarat, India.

³Assistant Professor, Electrical Engineering Department, Government Engineering College, Valsad, Gujarat, India.

⁴Lecturer, Electrical Engineering Department, Parul University, Vadodara, Gujarat, India

Received: 30 Dec 2023

Revised: 09 Jan 2024

Accepted: 12 Jan 2024

*Address for Correspondence

Brijesh M Patel

Research Scholar,

Gujarat Technological University,

Ahmedabad, Gujarat, India.

Email: bmpgp1412@gmail.com



This is an Open Access Journal / article distributed under the terms of the **Creative Commons Attribution License** (CC BY-NC-ND 3.0) which permits unrestricted use, distribution, and reproduction in any medium, provided the original work is properly cited. All rights reserved.

ABSTRACT

Accurate sales predictions can help inform business decisions, infrastructure planning, and for government policies makers. Time series modeling and forecasting, a technique that forecasts future values by examining past values, are crucial in many practical sectors when it comes to the Indian electric vehicle (EV) market. In this study, the monthly and annual sales data for ICE (internal combustion engine) and (EV) vehicles from 2014 to 2022 have been evaluated using SARIMA (Seasonal Autoregressive Integrated Moving Average), linear regression, and polynomial regression. A detailed explanation of model selection and forecasting accuracy is presented. The results indicate a significant achievement for the EV industry, and it is in align with goals set by Governments and automakers to promote the transition to electric vehicles.

Keywords: Electric Vehicle forecast, Linear Regression, Polynominal Regression, SARIMA model.

INTRODUCTION

India's increasing population brings both opportunities and challenges to the transportation sector. Today, the country has contributed about 2.5 billion metric tons of carbon to environment. The IC engine vehicle contributes PM 2.5, it's almost about to 40% of the total pollution in India [1]. The nation faces not only a massive fuel investments but also big environmental challenges. Adoption of electric vehicles can help create more efficient and sustainable transportation networks, which are crucial for addressing the mobility needs of a growing population while



**Brijesh M Patel et al.,**

reducing the detrimental effects of expanding vehicle use on the environment and the economy. A wide approach of transportation planning that includes EVs can help to address challenges efficiently. However, electric vehicles (EVs) are emerging of hope, can offering a sustainable and cost-efficient alternative to internal combustion engine (ICE) vehicles [2, 3]. In fig.1 and fig.2 shows a breakdown of Diesel and Petrol utilization in India, highlighting the dominance of the transport sector and the distribution of Diesel and Petrol percentage sales among different types of vehicles within that sector [4].

Analysis of Vehicle Sales Trends in India (2014-2022)

Ministry of Road Transport & Highways provided data as shown in fig. 3 represents the percentage sales of vehicles in India from 2014 to 2022. Analysis shown the annual sales figures of various types of vehicles in India from 2014 to 2022. Petrol vehicles, on the other hand, consistently had the highest sales figures throughout the years, with a noticeable growth trend from 2014 to 2019. Petrol/CNG and Petrol/Hybrid vehicles also displayed an increasing trend in sales, the data highlights a growing interest in electric battery operated vehicles (BOV), with a remarkable surge in sales from 2016 onwards, indicating a shift towards eco-friendly transportation options. However, the overall market share of electric vehicles in India remained relatively small compared to conventional fuel-powered vehicles during this period [5, 6]. In fig. 4 represents the sales analysis of different types of vehicles in India from 2014 to 2022. These vehicles are categorized into various segments, including traditional internal combustion engine (ICE) vehicles and electric vehicles (EVs), with a breakdown for two-wheelers, three-wheelers, and four-wheelers. Here is an analysis of the trends observed in the EV sales data [2, 8]. Two -Wheeler Sales: Both ICE and EV, have consistently shown strong growth over the years. However, there is a noticeable shift in recent years.

While two-wheeler ICE sales continued to rise, two-wheeler EV sales began to increase significantly from 2020 onwards. This shift may be indicative of a growing preference for electric two-wheelers among consumers, possibly due to environmental concerns and increasing awareness of EV technology [7, 9]. Three-Wheeler Sales: Three-wheeler sales have also been on an upward trajectory. However, there isn't a clear trend favoring ICE or EV three-wheelers. Both types seem to coexist without significant changes in their respective market shares but day by day EV three wheelers adoption is increasing [7, 9]. Four-Wheeler Sales: Sales of four-wheelers, both ICE and EV, have been steadily increasing over the years. Notably, from 2020 onwards, there is a visible surge in four-wheeler EV sales. This could be attributed to factors such as improved EV infrastructure, greater variety of EV models, and government incentives for electric vehicles. The data suggests a growing interest in electric four-wheelers [7, 9]. Above data analysis reflects a shifting automotive landscape in India. While traditional ICE vehicles continue to dominate, there is a clear trend towards increased adoption of electric vehicles, especially in the two-wheeler and four-wheeler segments. This shift is likely driven by factors such as environmental consciousness, advancements in EV technology, and supportive government policies. The data suggests that as EV infrastructure and awareness continue to grow, electric vehicles are gaining a stronger foothold in the Indian market [2].

Gross National Income (Gni) Per Capita of India and Its Impact

From 2014 to 2022, India has witnessed a significant increase in vehicle sales, reflecting the country's economic growth as indicated by the rise in Gross National Income (GNI) per capita. In 2014, India's GNI per capita stood at \$1,550, and over the course of these eight years, it steadily climbed to \$2,380 in 2022. This upward trajectory in economic prosperity has had a notable impact on the automotive industry [10, 11]. There has been substantial growth in sales. Two-wheeler internal combustion engine (2W ICE) vehicles, which are incredibly popular in India due to their affordability and convenience, saw sales numbers increase from 14,904,666 units in 2014 to 15,592,111 units in 2022. This growth indicates that as people's disposable incomes has been raised with the increasing GNI (Gross National Income) per capita, more individuals were able to afford two-wheelers, contributing to the surge in sales. Indian government is targeted to reach \$ 4,000 with 70% growth by 2030, from today's levels of \$ 2,450 [10, 11, 12]. Moreover, the Light Passenger Vehicle (LPV) segment, which includes traditional internal combustion engine (ICE) cars, also experienced growth in sales, possibly due to increased consumer confidence and affordability driven by the rising GNI per capita. In addition to two-wheelers and EVs, the data reflects a broader trend toward increased



**Brijesh M Patel et al.,**

vehicle ownership as a result of improved economic conditions [13]. India has established goal for the wide adoption of electric vehicles (EVs) by 2030. Government is motivated to attain a 30% market share for EVs in private cars, 70% adoption in commercial vehicles, and 80% in the two-wheeler and three-wheeler segments [9]. To achieve these targets, the Indian government is taking active measures to inspire the adoption of EVs. These measures encompass a range of incentives implemented at both national and state levels, policy designed to increase the availability and affordability of EVs for vehicle ownership.

Electric Mobility in India Today

Electrical vehicle selling is continuously growing, this is due to promotional scheme by government and continuous increase in price of crude oil which has motivated vehicle users to divert from ICE vehicles to electrical vehicles. Up gradation in technology of batteries and controller increasing the range of EVs as well as reducing cost of EV day by day are some other influencing factors. Study shows in year 2020 due to pandemic situation EV selling was reduced but during year 2022 a steep increase in the sales of EVs, in the country. [13,14]. This data illustrates as shown in fig. 6, the annual electric vehicle (EV) sales for different categories of vehicles, including two-wheelers (TW), three-wheelers (3W), four-wheelers (4W), and other types, from 2014 to 2023. Over this period, there is a striking growth trend in EV adoption. In 2014, EV sales were relatively low across all categories, but by 2023, a substantial transformation occurred. Two-wheelers, in particular, have experienced exponential growth, with sales skyrocketing from 12 units in 2014 to 359,924 units in 2023, making them the dominant category. Three-wheelers and four-wheelers have also witnessed significant growth, with 3W sales reaching 56,700 units and 4W sales totaling 567,00. units in 2023. These numbers underscore the increasing popularity and acceptance of electric vehicles, highlighting the remarkable transition towards sustainable and environmentally friendly transportation options in recent years [7, 14, 15]. In both 2022 and 2023, two-wheelers indeed lead in electric vehicle sales. However, the increase in three-wheelers and four-wheelers in 2023 indicates a notable diversification of the electric vehicle market. This suggests a growing demand for electric three-wheelers and four-wheelers, possibly driven by factors such as government incentives, improved technology, and a broader range of electric vehicle options, demonstrating the expanding acceptance of electric mobility across different vehicle categories [7, 16].

Forecasting of Electric Vehicle Sales in India

A time series, in essence, represents observations ordered chronologically over time. Time series forecasting models employ mathematical techniques grounded in historical data to predict future demand. These models are built on the basis that the future is an extension of the past, allowing us to utilize historical data with confidence in forecasting future demand. Numerous studies on time series analysis have been conducted across various domains, encompassing demand forecasting for products such as food items, tourism, maintenance and repair parts, electricity consumption, automobiles, and a wide array of other products and services [9, 17]. Regression analysis, a powerful machine learning technique, serves as a valuable tool for predicting sales. To make accurate predictions, it relies on a time series of historical data and uses this information to project future sales trends. In this specific analysis, leveraging this historical data, the sales of Electric Vehicles (EVs) in India has been analyzed. The ultimate objective is to forecast the trajectory of EV sales for the upcoming years [18, 19]. The accuracy of time series analysis for forecasting hinges on the inherent characteristics of the demand time series data. When transition patterns exhibit stability and periodicity, we can achieve high forecasting accuracy, but irregular and erratic patterns in the data may limit the precision of our forecasts [17]. Data shown in table 1, the EV sales in India, increasing popularity of EVs in India. It also highlights the need for further analysis and forecasts to better understand and plan for the future of the Indian EV market.

Linear Regression analysis for future forecasting

A dependent variable (commonly abbreviated "Y") and one or more independent variables (typically abbreviated "X") are modeled using the statistical technique of linear regression. Simple linear regression is based on the equation $Y = M * X + C$ and seeks to identify the best-fitting straight line to represent the connection between Y and X [18, 20]. We explored the application of a linear regression model to forecast future electric vehicle (EV) sales based on





Brijesh M Patel et al.,

historical data. Linear regression assumes a linear relationship between the predictor variable (in this case, the years) and the target variable (EV sales). In table 2 shows actual yearly electric vehicle registered sales data of India. We prepare linear regression model and fit the prepared model with actual yearly EV sales data the result is shown in figure 8. And in table 3. linear regression offers simplicity and interpretable results, it might not capture nonlinear growth patterns as effectively as polynomial regression.

Polynomial Regression analysis for future forecasting

Polynomial regression extends the idea of linear regression by introducing polynomial terms, allowing for more flexible curve fitting. In polynomial regression, still have a dependent variable (y) and one or more independent variables (x), but instead of fitting a straight line, fit a polynomial curve. The general form of a polynomial regression equation with one independent variable (x) looks like as shown in equation [21].

$$Y = b_0 + b_1 * X_1 + b_2 * X_2 + b_3 * X_3 + \dots + b_n * X_n$$

The degree of the polynomial, denoted by 'n,' determines how many terms are included in the equation. For example, if n = 2, it's a quadratic polynomial with a squared term (x²), and if n = 3, it's a cubic polynomial with a cubed term (x³), and so on. Forecasting the sales of electric vehicles (EVs) for the coming years, we utilizing historical data. Our dataset consisted of EV sales data from 2014 to 2022, We prepare polynomial regression model and fit the prepared model with actual yearly EV sales data result and generated predictions for the upcoming years is shown in figure 9. and in table 3 [18].

Seasonal ARIMA methodology for future forecasting

Both the forecasting methods ARIMA and SARIMA are used. ARIMA bases its predictions of future values on past values (autoregressive, moving average). Similar to SARIMA, seasonality trends are taken into account along with historical values. SARIMA is substantially more effective at forecasting than ARIMA since it incorporates seasonality as a parameter [22]. The model's remaining components are still the ARIMA's, p- moving average (MA)[23], d-integrated (I), and q- autoregressive (AR) components. The SARIMA model is made more robust by the inclusion of seasonality(P, D, Q). It is portrayed as under.

$$\text{ARIMA} \quad (p, d, q)(P, D, Q)$$

Testing the stationarity of time series EV sales data:

The Augmented Dickey-Fuller (ADF) test and testing for stationarity in time series data for improved ARIMA forecasting model are statistical tests used to detect if a time series data set is stationary or not. In time series analysis, stationarity is a key notion [24]. Result of conducting an Augmented Dickey-Fuller (ADF) test on EV sales time series data set and the result is as follow.

ADF Test Statistic: -2.9851906417801892

p-value: 0.036300744473384425

In the context of the ADF test, it measures how much the data needs to be differenced to make it stationary. In our case for EV sales data, the test statistic is approximately -2.9852. The ADF test statistic being negative also supports the conclusion of stationarity. The p-value (0.0363) is less than the generally accepted significance level of 0.05 (5%). When the p-value is less than the significance level, reject the null hypothesis. For our data series there is strong evidence that the data does not have a unit root, which means that the data is stationary. From above ADF test analysis it has been concluded that the data as stationary time series as shown in fig. 10, which is often a prerequisite for ARIMA time series analysis and forecasting methods and This suggests that after applying the seasonal first difference (d=1), the data is likely stationary as shown in fig. 9.





Brijesh M Patel et al.,

Auto Regressive (AR) models for time series EV sales data analysis and forecasting

When we intend to use an ARIMA model for forecasting it is essential to do auto correction analysis test it will help us to identify AR (Auto Regression) and MA (Moving average) parameters needed for ARIMA model [22].

$$Y^t = \alpha_1 * Y_{t-1} + \dots + \alpha_p * Y_{t-p}$$

Here in AR model, we assume that the current value (y_t) is dependent on previous values ($y_{t-1}, y_{t-2}, y_{t-3}, \dots$) and to identify the order of an AR model (p) for given input data in our case EV sales data, for that we would use the PACF (Partial Autocorrelation function)

Moving Average (MA) model for time series EV sales data analysis and forecasting:

The Moving Average model is a fundamental component of time series analysis. It focuses on capturing the short-term variations in data by examining the moving average of data points over a specified time period. It estimates indicating how many past observations are considered in calculating the moving average [22].

$$Y^t = \epsilon_t + \beta_1 \epsilon_{t-1} + \dots + \beta_q \epsilon_{t-q}$$

The MA model assumes that the current value (y_t) is dependent on the error terms including the current error ($\epsilon_t, \epsilon_{t-1}, \epsilon_{t-2}, \epsilon_{t-3}, \dots$) and to identify the order of an MA model (q) for given input data in our case EV sales data, for that we would use the ACF (Autocorrelation function). We found the value of q for that we use the ACF plot as shown in fig. 11. It will inform us of the necessary amount of moving average to eliminate autocorrelation from the stationary time series. PACF (Partial Autocorrelation function) plot with significant spikes at lag 1, 2, 3, and 4, with the spike at lag 1 being more significant compared to the others, with lag 1 (AR (1)) be a crucial component in modelling EV sales time series [25, 26]. Partial Autocorrelation function plot is shown in fig. 11, we found the optimal value of p which is our number of autoregressive terms. Here we can see that the first lag in PACF is significantly out of the limit so we can select the order of the p as 1.

SARIMA model testing and validation

To perform testing and validation, to assess the accuracy of our train model's forecasts by comparing the forecasted values to the actual data, it following the same pattern as same as by actual data. Additionally, we may consider splitting our data into training and testing sets to evaluate how well the model generalizes to unseen data. Finally, plotted the actual EV sales data (EV sales) along with the forecasted values (forecast) as shown in fig. 12, to visualize how well your ARIMA model fits the data and how accurate its predictions are [27].

SARIMA model for future forecasting of EV Sales

The SARIMA (Seasonal Autoregressive Integrated Moving Average) model is a valuable tool for forecasting EV sales data, especially when historical trends play a significant role. Utilizing a pre-trained SARIMA model enables us to make data-driven predictions for an extended period, aiding in better decision-making and strategic planning for the future [27, 28]. The SARIMA model is a powerful tool for time series forecasting. In this context, we utilize a pre-trained SARIMA model to forecast electric vehicle (EV) sales data is shown in table 4 for the period spanning from 2023 to 2030. The data with SARIMA model suggest a positive outlook for the electric vehicle market, with steady and accelerating growth expected through 2030. By the year 2030, the forecasted EV sales are expected to reach 45,07,022 units per year. This could be attributed to advancements in battery technology, infrastructure development, and a wider range of EV models available to consumers. This milestone indicates a significant achievement for the EV industry, and it is in align with goals set by governments and automakers to promote the transition to electric vehicles.





Brijesh M Patel et al.,

CONCLUSION

Accurate sales forecasting is essential for stakeholders in the EV industry to make informed decisions and plan for the future, especially as the market continues to evolve. In this paper the context of the Indian electric vehicle (EV) market, the sales predictions generated by each model, by analyzing past vehicle market growth, it shows remarkable transition from ICE to EV in recent years. The Linear Regression model demonstrates steady growth but under estimates sales compared to SARIMA. Polynomial Regression offers a more flexible fit, SARIMA a time series model, captures seasonality and trends in the data effectively. It provides more realistic forecasts compared to the regression models, aligning closely with the actual data. Time series models like SARIMA are better suited for capturing the inherent temporal dependencies and seasonality in EV sales data.

REFERENCES

1. International Energy Agency (IEA), "Air Quality and Climate Policy Integration in India, Frameworks to deliver co-benefits, www.iea.org, May 2021.
2. Indian Private Equity & Venture Capital Association (IVCA), "Electrifying Indian Mobility" report by IVCA, <https://assets.ey.com,2023>.
3. M. Semakula, "Transportation, Pollution and the Environment," International Journal of Applied Engineering Research, vol. 13, no. 6, pp. 3187-3199, 2018.
4. CRISIL, an S&P Global Company, "All-India study on sectoral demand for petrol and diesel - report," October2020 – September 2021, <https://ppac.gov.in,2021>
5. Ministry of Road Transport & Highways, Government of India, "Road Transport Year Book (2017 - 2018 & 2018 - 2019)," June 21. International Energy Agency (IEA), "Global EV Outlook 2022: Securing supplies for an electric future," www.iea.org, May 2022.
6. Government of India, "Vahanand Sarathi Portal", <https://vahan.parivahan.gov.in/ vahan4 dash board/, Aug-2023>.
7. IESA (India Energy Storage Alliance), "Electric Vehicle Market Overview Report 2020-2027",<https://indiaesa.info,2022>.
8. Mohd. Sahil Ali, "Electrifying Mobility in India: Future prospects for the electric and EV ecosystem," Brookings India IMPACT Series No. 052018, May 2018.
9. Vijayalakshmi S, "Income and Vehicular Growth in India: A Time Series Econometric Analysis", ISBN 978-81-7791-295-1, 2019.
10. The World Bank, "GNP DATA Data bank", <https://data.worldbank.org, 2023>.
11. J. Dargay and D. Gately, "Vehicle Ownership and Income Growth, Worldwide: 1960-2030," January 2007.
12. N. Singha, "Projection of Private Vehicle Stock in India up to 2050," Transportation Research Procedia, vol. 48, pp. 3380-3389, 2020. [Online]. Available: www.sciencedirect.com.
13. P. K. Gujarathi, "Electric Vehicles in India: Market Analysis with Consumer Perspective, Policies and Issues," Journal of Green Engineering, vol. 8, no. 1, pp. 17-36, January 2018.
14. KPMG, "Shifting Gears: the evolving electric vehicle landscape in India," October 2020. [Online]. Available: home.kpmg/in.
15. Niti Aayog, "India's Electric Mobility Transformation: Progress to Date and Future Opportunities", April 2019.
16. Heba-Allah, "Seasonal Electric Vehicle Forecasting Model Based on Machine Learning and Deep Learning Techniques", Energy and AI 14 (2023) 100285, July 2023.
17. N. J. Niya, "Sale Prediction Using Linear Regression Model," International Journal of Computer Research and Technology (IJCRT), vol. 9, no. 3, March 2021, ISSN: 2320-2882.
18. S. Afandizadeh, "Using Machine Learning Methods to Predict Electric Vehicles Penetration in the Automotive Market," Scientific Reports 13:8345, 2023.
19. D. C. Montgomery, Introduction to Linear Regression Analysis, John Wiley & Sons, 2012.
20. E. Ostertagova, "Modelling using Polynomial Regression," Published by Elsevier Ltd., 2012.





Brijesh M Patel et al.,

21. J. Fattah, "Forecasting of Demand using ARIMA Model," International Journal of Engineering Business Management, vol. 10, pp. 1–9, September 2018.
22. Sandhya C, "Sales Forecasting Using ARIMA Model," International Journal of Computer Research and Technology (IJCRT), vol. 10, no. 6, June 2022, ISSN: 2320-2882.
23. R. D. Caytiles, "Annual Automobile Sales Prediction Using ARIMA Model," International Journal of Hybrid Information Technology, June 2018.
24. Hussan Al-Chalabi, "Time Series Forecasting using ARIMA Model
25. A Case Study of Mining Face Drilling Rig," ADVCOMP 2018, ISBN: 978-1-61208-677-4
26. Peng Chen, " Time Series Forecasting of Temperatures using SARIMA: An Example from Nanjing ", Material Science and Engineering 394 052024, 2018.
27. S.M. A. Burney, "Time Series Forecasting with SARIMA Model: A Case Study Using the Natural Gas Demand Series", Karachi University Journal of Science, vol. 33, February 2022, ISSN: 0250-53.
28. Gispert Becerra, "Time Series Forecasting using SARIMA and SANN models," Thesis submitted, Universitat Politècnica de Catalunya,2021.

Table 1: Vehicle category wise Electric Vehicle Sales in India [1]

Year	2-Wheeler	3-Wheeler	4-Wheeler	Other
2014	1679	12	686	11
2015	1444	5416	905	33
2016	1454	46903	925	563
2017	1529	83357	2167	366
2018	17067	110191	2546	450
2019	30389	133488	2249	696
2020	29113	90378	4312	845
2021	156245	158112	15328	1770
2022	631176	350236	40880	2489
2023*	556826	359924	56700	259

Table 2: Yearly Electric Vehicle sales in India [1]

Years	EV Sales
2014	2389
2015	7801
2016	49848
2017	87420
2018	130253
2019	166823
2020	124647
2021	331463
2022	1025795

Table 3: Forecasting result of Electric Vehicle sales in

Years	Linear Regression EV Sales Prediction	Polynomial Regression EV Sales Prediction
2023	654738	1107374
2024	742898	1467116





Brijesh M Patel et al.,

2025	831058	1876236
2026	919219	2334735
2027	1007379	2842612
2028	1095539	3399868
2029	1183699	4006502
2030	1271859	4662514

Table 4: Forecasting result of Electric Vehicle sales in India

Year	SARIMA Model EV Sales Prediction
2023	1543586
2024	1966934
2025	2390282
2026	2813630
2027	3236978
2028	3660326
2029	4083674
2030	4507022

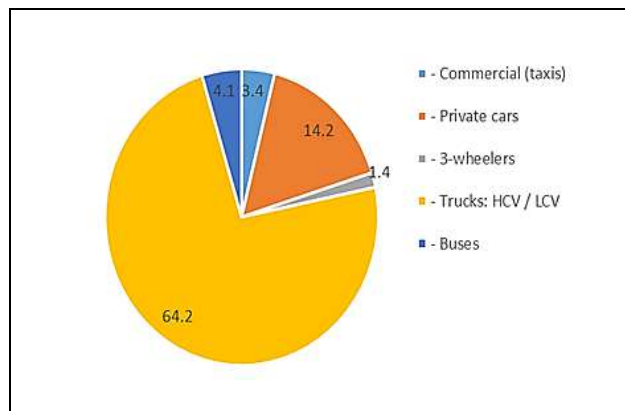


Fig.1 Percentage utilization of Diesel by Transport section in India [4]

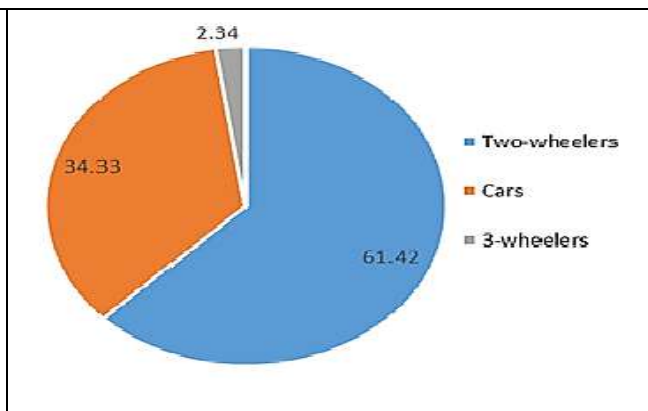


Fig.2. Percentage utilization of Petrol by transport section in India [4]

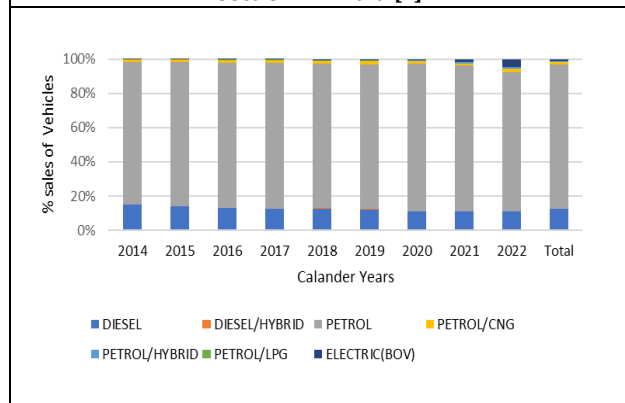


Fig 3. Percentage Vehicle sales in India [7]

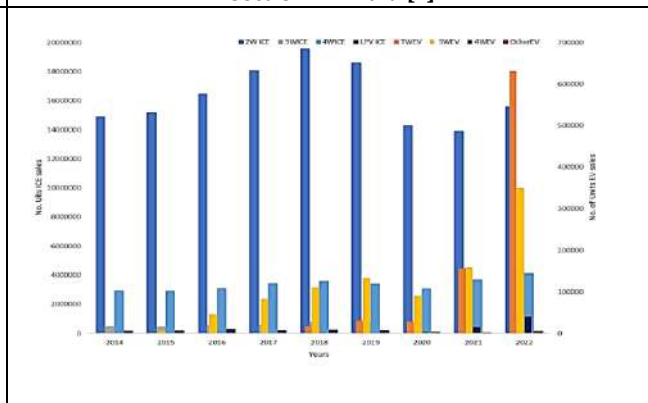


Fig. 4. Category wise vehicle sales in India [7]





Brijesh M Patel et al.,

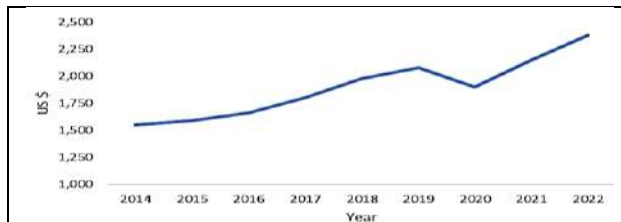


Fig. 5. GNI per capita of India (US \$)

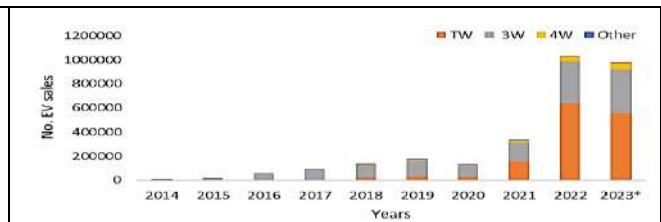


Fig. 6. Electric Vehicle Sales growth in India [7]

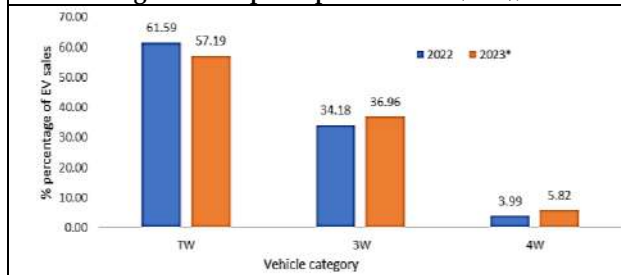


Fig. 7. Electric Vehicle Sales growth year 2022 – 2023 [7]

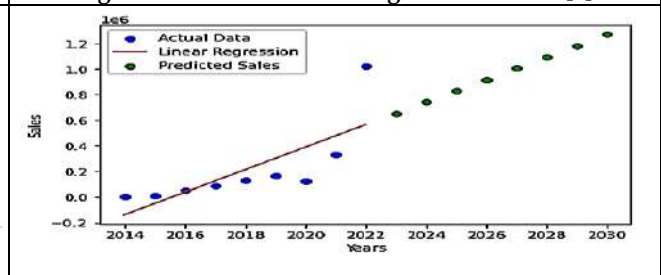


Fig. 8. Linear regression model EV sales forecasting

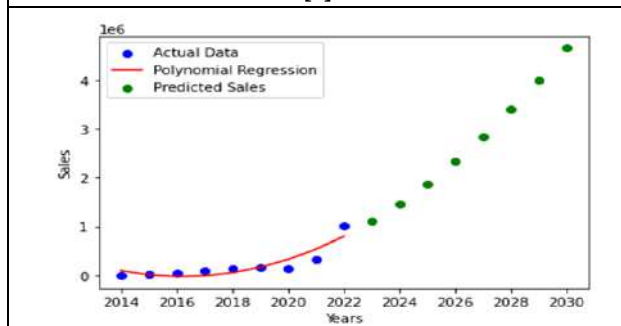


Fig. 9: Polynomial regression model EV sales forecasting

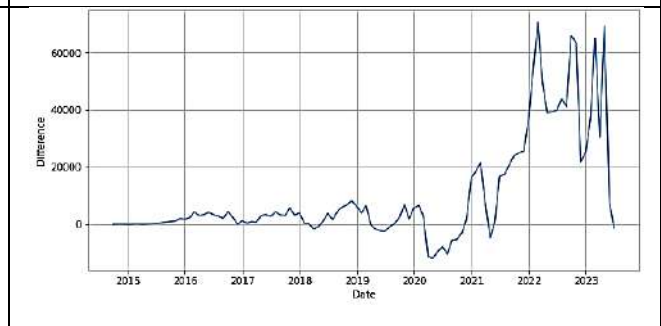


Fig. 10. Seasonal first difference Stationarity

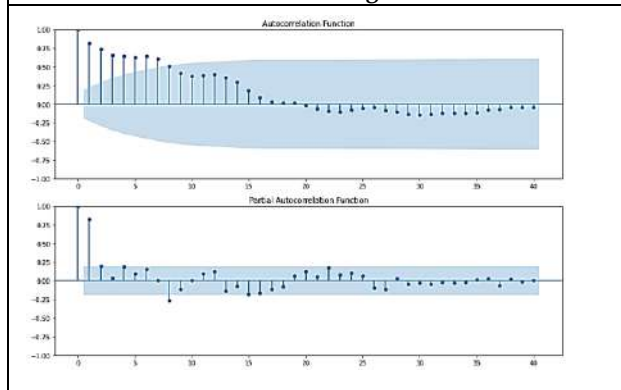


Fig. 11. Autocorrelation function and Partial Autocorrelation function test

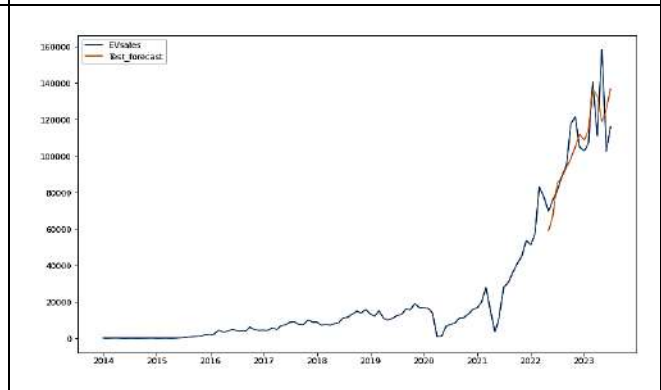


Fig. 12: Actual EV sales vs test forecasted EV sales





An Automatic Droop Controller for Minimization of Circulating Current and Load Sharing Error in Low Voltage Independent DC Micro grid

Shilpa Patel^{1*}, Rajnikant Bhesdadiya², Hitesh Karkar³

¹Research Scholar, Gujarat Technological University, Ahmedabad, India.

²Assistant Professor, Gujarat Technological University, L. E. College, Morbi, India.

³Assistant Professor, Gujarat Technological University, Government Engineering College, Rajkot, India.

Received: 30 Dec 2023

Revised: 09 Jan 2024

Accepted: 12 Jan 2024

*Address for Correspondence

Shilpa Patel

Research Scholar,

Gujarat Technological University,

Ahmedabad, India.

Email: shilpa5185@gmail.com



This is an Open Access Journal / article distributed under the terms of the **Creative Commons Attribution License** (CC BY-NC-ND 3.0) which permits unrestricted use, distribution, and reproduction in any medium, provided the original work is properly cited. All rights reserved.

ABSTRACT

The DC micro grid has gained popularity due to its ability to integrate green energy sources, storage units and loads on a common DC bus. However, load sharing remains a significant challenge in DC microgrid. The droop control method is a common practice to address load sharing challenges in microgrid, offering advantages such as simplicity, robust control, and communication independence. This research work presents the design and analysis of an automatic droop controller to reduce load sharing error and minimize circulating current in a low voltage independent DC micro grid. The controller, which relies on the output current of an individual converter, aims to minimize issues of circulating current and load sharing error. The proposed controller enhances simplicity and flexibility, achieving a more favorable balance between voltage regulation and load sharing accuracy in a low voltage independent DC microgrid. The effectiveness of the controller is assessed using MATLAB Simulink.

Keywords: Load sharing; DC-DC Parallel converters; circulating current; Droop resistance; Voltage regulation.

INTRODUCTION

Fossil fuels have raised up issues related to climate change and global warming. The emerging alternatives to fossil fuels have been derived from sources of green energy. Renewable energy sources, including tidal energy, wind energy, solar energy, and biomass energy, are being implemented to meet the growing energy requirements [1]. Micro grid concept is to interconnect the renewable sources, storage elements and loads at the common DC grid [2].



**Shilpa Patel et al.,**

These electrical sources are scattered at various locations due to the ease of energy harnessing. Integrating the energy sources and storage units on a common bus provides flexibility, reliability and lower transmission line losses as well as cost [3]. The micro grids can be broadly characterized into three types: AC micro grids, DC, low, skin effect, electromagnetic interference, and power quality concerns. On the other hand, DC micro grids do not entail major problems such as management of reactive components, complex numbers, synchronization [4]. Hence, control of DC micro grid is easy and promises a more reliable, efficient and economical system [5]. In the DC micro grid, the integration of distributed generation and electrical loads is achieved by means of DC-DC converters [6]. Parallel operation of converters also provides high reliability and flexibility to the system [7]. At the same time, it also creates issues of load sharing among converters. [8]–[11]. The concept of load sharing refers to the distribution of current across several entities or resources to attain a more balanced and effective use of electrical resources.

In the parallel operation of converters, each converter shares the load as per its ratings, if it does not happen properly then the circulating current will start to flow from one converter to another converter. It also results in the overloading of one converter and while under loading of another. Unfortunately, it leads to extra losses, heating, increased size and rating of converters [12]. Hence, it is strongly recommended to distribute the load current proportionally among all the converters in the DC micro grid. Additionally, the load voltage should be within predetermined limits, often within a range of $\pm 5\%$ [13]. Several methodologies have been proposed in literature to attain equal distribution of load current and effective control of voltage regulation in converters. An issue of current sharing can be effectively mitigated using both active and passive load sharing strategies [14]. Many load sharing schemes are available under active load sharing and passive load sharing. The active load sharing strategy offers good performance but its main disadvantages are the need of a large bandwidth communication link, complex control, least flexibility and plug-and-play capability [15], [16]. Whereas, droop control does not need a high bandwidth communication link for its implementation. Therefore, the modularity and flexibility of the system is not affected. Nevertheless, it is crucial to acknowledge that the droop control has a significant constraint in its inability to simultaneously execute voltage regulation and proportional load sharing. [17]–[21].

To mitigate this constraint, several droop control solutions have been suggested and extensively analyzed in scholarly publications. A unique current-limiting droop control mechanism is developed in reference [22] to facilitate the simultaneous operation of DC-DC converters with different converter ratings while maintaining a constant load. In reference [23], three distinct nonlinear droop control approaches are introduced. All the strategies used in this study are designed with the objective of improving voltage regulation and achieving equal current distribution in DC micro grid. To mitigate the impact of sensor calibration errors and cable resistances, efforts are also made to reduce their occurrence. In reference [24], a universal droop controller is intended to realize proportional load distribution and voltage control in input series–output parallel DC-DC converters. The suggested method uses positive feedback with a droop controller. Therefore, an inverse droop controller increases voltage reference as the load increases. One inherent constraint of this system is that as the amplification of positive feedback increases, the grid stability decreases. In reference [25], a solution for traditional droop is presented, which utilizes a piecewise approach. This technique involves the fragmentation of droop curves into smaller. When the load current reaches its pre-defined value, the controller starts to use a new droop value. At light load, the trade-off between voltage regulation and current distribution is substantially reduced as a result of the non-linear droop characteristics. However, a non-linear droop controller ensures a increased droop gain when the load increases and decreased droop gain when the load decreases at the common DC bus. The literature highlights that the incorrect choice of the droop curve can result in instability of the system. The use of global system frequency is presented in [26] as a means to implement superimposed frequency droop control. It aims to achieve proportional load sharing amongst converters. In this approach, a low-amplitude AC voltage signal is introduced into the DC grid. This approach has the potential to lead to system instability and undesirable power quality concerns. The mode adaptive droop control technique (MADC) is introduced in [27]. For different voltage ranges, droop controller is applied to the grid, distributed generation and energy storage elements. The MADC approach is built on the premise that distributed generators measure identical bus voltages while disregarding the voltage drop resulting from cable resistances. In the cited work [28], a new algorithm for decentralized control is proposed. The method offers reliable instantaneous voltage





Shilpa Patel et al.,

control performance during transient and effectively achieves specified current sharing. This technique does not consider the problem of circulating current. Furthermore, it is important to note that a trade-off persists between the sharing of current and voltage regulation. In reference [29], the research estimates line resistance to balance load sharing among parallel converters. Droop control eliminates unequal power sharing, but voltage regulation restricts droop. The resistance value is estimated by using local voltage and current information and it modifies the voltage reference to compensate the voltage drop due to cable resistance. This methodology is applied for converters with equal ratings. An adaptive droop controller for the suppression of circulating current is presented in [12]. The cable resistance in this approach is determined using mathematical formulae, and then, the droop parameters are modified according to it. Estimation of cable resistance depends on the information of bus voltage that may be far away from the converters and so necessitates an additional measurement. The voltage set-point shifting method needs one more controller. hence, the system becomes more complex. A droop index (DI) based load sharing method is proposed in [30]. The purpose of introducing the droop index (DI) is to enhance the operational efficiency of DC micro grids.

The function of the normalized load sharing difference and power loss of the converter is used to calculate the value of DI. This approach necessitates thorough adjustment of droop parameters, which is very susceptible to line resistance and require substantial computational effort. The previously described approaches have many significant limitations, including the need for an additional controller, the need for communication connections, inadequate voltage regulation, the necessity for extensive computations, system complexity and instability and the presence of circulating current issues. In order to address the above constraints, this research work introduces an automatic droop controller as a possible solution. The calculation of a new droop value for an automated droop controller is only dependent on the output current of the converter. This controller exhibits enhanced performance due to its simple design and well-defined algorithm. The primary aims of this research work are to reduce load sharing error and circulating current while enhancing voltage regulation. The major contribution of this research paper is:

1. An automatic droop controller promises to produce the lower droop value at low load where load sharing is seen less significant and produces higher droop value as the load increase.
2. The estimation of the new droop value requires the output current of the particular converter only.
3. Performance of an automatic droop controller remains excellent even with variations in cable resistance and load current.

Issues Related to Circulating Current and Load Sharing

This section demonstrates the parallel operation of two DC-DC converters, load shared by two converters and issues as shown in Fig. 1(A). Here, V_{in1} , V_{in2} , V_{dc1} , V_{dc2} , I_{O1} , I_{O2} , R_{C1} , R_{C2} and I_o represents input voltages from PV array, output voltages of converters, output currents of converters, resistances of cable for converters 1 & 2 correspondingly and current drawn by electrical load. As shown in Fig. 1(B), the converter outputs are voltage sources in series with cable resistance [30]. If $V_{dc1} > V_{dc2}$, then circulating current I_{C12} will start to flow from first converter to second converter.

By applying Kirchoff's low in Fig. 1(B)

$$V_{dc1} - I_{O1}R_{C1} - I_oR_L = 0 \quad (1)$$

$$V_{dc2} - I_{O2}R_{C2} - I_oR_L = 0 \quad (2)$$

The output current of converter 1 and converter 2 can be determined by using equations (1) and (2) respectively.

$$I_{O1} = \frac{V_{dc1}(R_{C2}+R_L)-V_{dc2}R_L}{R_{C1}R_{C2}+R_LR_{C1}+R_LR_{C2}} \quad (3)$$

$$I_{O2} = \frac{V_{dc2}(R_{C1}+R_L)-V_{dc1}R_L}{R_{C1}R_{C2}+R_LR_{C1}+R_LR_{C2}} \quad (4)$$





Shilpa Patel et al.,

Moreover, if there is minor difference in current shared by both converters as per (3) and (4), the circulating current will arise as given below.

$$I_{C12} = -I_{C21} = \frac{V_{dc1} - V_{dc2}}{R_{c1} + R_{c2}} = \frac{I_{o1}R_{c1} - I_{o2}R_{c2}}{R_{c1} + R_{c2}} \quad (5)$$

From (5), it is seen that due to unequal cable resistance, the circulating current will start to flow from converter 1 to converter 2. So, converters must supply load current plus circulating current as given by (6) and (7).

$$I_{o1} = \frac{R_{c2}V_{dc1}}{R_{c1}R_{c2} + R_{c1}R_L + R_{c2}R_L} + \frac{V_{dc1} - V_{dc2}}{R_{c1} + R_{c2}} \quad (6)$$

$$I_{o2} = \frac{R_{c1}V_{dc2}}{R_{c1}R_{c2} + R_{c1}R_L + R_{c2}R_L} + \frac{V_{dc2} - V_{dc1}}{R_{c1} + R_{c2}} \quad (7)$$

From (5), (6) & (7), the circulating current becomes more problematic when many converters are interconnected in a parallel configuration. Many problems may arise due to circulating current. As described earlier, the droop resistance plays important role to share equal load among all the converters. The equivalent circuit with droop resistance and cable resistance is demonstrated in Fig. 2 [30].

The drop of voltage due to droop control approach including cable resistance is seen in Fig. 2 and can be expressed as:

$$V_{dc} = V_{dci} - R_{ci}I_{oi} \quad (8)$$

The value of V_{dci} is i^{th} converter voltage. Now the new load voltage will be:

$$V_{dc} = (V_{ref} - R_{d1}I_{o1}) - R_{c1}I_{o1} = V_{ref} - (R_{c1} + R_{d1})I_{o1} \quad (9)$$

$$V_{dc} = (V_{ref} - R_{d2}I_{o2}) - R_{c2}I_{o2} = V_{ref} - (R_{c2} + R_{d2})I_{o2} \quad (10)$$

The droop resistance and cable resistance are in series and are added together which in turn produces extra voltage drop in a line. By combining (9) & (10), the converter currents can be expressed as:

$$\frac{I_{o1}}{I_{o2}} = \frac{R_{c2} + R_{d2}}{R_{c1} + R_{d1}} \quad (11)$$

The above analysis concludes that the mitigation of circulating current and overloading in converters can be accomplished by use of effective load sharing techniques. The traditional droop control method is ineffective in achieving precise load sharing across converters in situations when cable resistances cannot be avoided. Moreover, the presence of unequal cable resistances results in an uneven distribution of voltage drop across the respective resistances.

Suggested Automatic Droop Controller

This section presents a suggested automated droop controller that aims to reduce load sharing error and circulating current while achieving optimum voltage regulation. When the load current is reduced, the power used by the load is proportionally lower than the nominal power of the converter. In consideration of this, it is preferable to have a minimal droop resistance. Due to the minimal value of droop resistance, the voltage regulation and system efficiency can be improved. Increased load current in converters can lead to overloading, reducing system reliability. To prevent this, droop resistance should be increased to ensure proper load sharing. Although, the increased value of droop resistance can negatively impact voltage regulation. For desirable voltage regulation, the droop resistance is so adjusted that it gives better voltage regulation at any value of load current. If total 10% voltage variation is allowed at dc bus, then 5% of the variation range is set aside for the drop of voltage across cable resistance. Now only 5% voltage drop is practically allowed due to droop resistance. So, the maximum droop resistance value is limited, and





Shilpa Patel et al.,

drop in voltage caused by droop control can be calculated using the formula as given below [15]: 10% (acceptable drop) -5% (cable voltage drop) -1% (margin) = 4% voltage drop. So, the range of droop resistance is calculated in such a way that the maximum drop in voltage must not surpass a 4% deviation from the no-load value. Hence, at the minimal load, it is essential to choose a reduced droop resistance in order to get optimal voltage control. To ensure appropriate load sharing, it is necessary to raise the droop resistance value in conditions of high load. To achieve this objective, the droop curve must dynamically adjust its slope in response to load current variations, requiring droop characteristics to vary within a defined range, including a minimum and maximum droop value, as per (12) and (13) [5], [17].

$$R_{dmin} = \frac{\Delta I_o(max)}{I_o(rated)} \quad (12)$$

$$R_{dmax} = \frac{\Delta V_o(max)}{I_o(rated)} \quad (13)$$

Where, R_{dmin} is minimum droop resistance, R_{dmax} is maximum droop resistance, $\Delta I_o(max)$ is 20% overloading of first converter minus 20% under loading of second converter, $\Delta V_o(max)$ is maximum allowable voltage deviation, $I_o(rated)$ is rated output current of converter. So, the minimum droop value is determined by the maximum allowable load sharing error, while the maximum droop value is determined by the maximum allowable voltage deviation.

The new droop resistance R_{di} as per the control strategy is given as:

$$R_{di} = K * I_{oi} + R_{dmin} \quad (14)$$

And the output voltage is given by:

$$V_{dci} = V_{ref} - [I_{oi} * (R_{di} + R_{Ci})] \quad (15)$$

Where, V_{dci} is output voltage of i^{th} converter, I_{oi} is rated current of i^{th} converter, R_{di} is estimated droop resistance of i^{th} converter, R_{Ci} is cable resistance of i^{th} converter, K is droop line constant and R_{dmin} is minimum droop resistance as per equation (14). The Schematic diagram shown in Fig. 3 illustrates the suggested automated droop controller. The voltages V_{in1} and V_{in2} are PV array output voltages. The droop value estimation needs only output current of converter as per equation (14). The converter's output current and droop value are multiplied, and the resulting signal is subtracted from the reference voltage to generate a new reference signal for the PI controller. Two PI controllers are used for the purpose of voltage and current regulation, respectively. The PI controller's output signals are directed to the PWM Generator to generate the control signal for DC-DC Converter. Fig. 4 represents output v/s estimated droop value graph. The graph has two fix points as minimum droop value at almost no load and maximum droop value at rated current of converter. If the current through the load is above the rated current of converter, then regardless of converter current, the suggested automatic droop controller gives constant droop value as to achieve acceptable voltage regulation. Beyond this droop value the voltage regulation will degrade and the grid stability may be affected.

SIMULATION AND RESULTS

Two parallel DC-DC converters are simulated in MATLAB/SIMULINK to evaluate the suggested automated droop controller. Nominal parameters of two converters are listed in Table I. The simulation compares the suggested droop controller approach to the system which does not follow the droop control in the feedback system. Case-1 simulates parallel converters sharing a load without droop control. In case-2, automatic droop controller is simulated. Both the cases are simulated for no cable resistance from 0 to 0.3 second, equal cable resistance (0.1 Ω) from 0.3 to 0.6 second and different cable resistances (0.1 Ω and 0.2 Ω) from 0.6 to 1.0 second. The input voltage applied to each converter remains same.



**Shilpa Patel et al.,****Case-1: without Droop Control**

Fig. 5 shows simulation of DC-DC converters connected in parallel, with load and cable resistances. There is no droop resistance in the simulation. The currents of both the converters stays almost identical in the absence of droop control. And there is minor change in bus voltage as the cable resistances are changed from no cable resistance to different cable resistance. The load power and load current graphs show the same result. Both the converters share the equal load if there is no cable resistance or equal cable resistance (0 to 0.6 second). But as the cable resistance is changed at 0.6 second, the output current of both converters is changed. Only 1.45 A of current is taken by converter 2, whereas 2.5 A is taken by converter 1. It shows there is unequal load sharing between converters. Under this situation one converter is overloaded and another one is working in underloading condition. Additionally, the flow of circulating current occurs from converter 1 to converter 2. The measured value of the circulating current is 1.042A.

Case-2: Automatic droop controller

Fig. 6 illustrates the simulation conducted on a DC-DC converter equipped with an automated droop controller. The results demonstrate that the output voltages remain consistent whether there are no cable resistances or when the resistances are equal. However, because of droop resistance, the output voltage of one converter varies from the others when the cable resistance varies (0.6 to 1 second). The DC bus voltage drops as well, although it stays within the specified range. Thus, the intended voltage regulation is achieved by automatic droop controller. The system's load current and output power have also somewhat decreased. Additionally, both converters share the same load at either the same cable resistance or no cable resistance. At time 0.6 second, as the different cable resistances are come into the system, there is very small change in current shared by both converters. there is less load sharing error, which lowers the circulating current as well. Circulating current is just 0.128 A in value. Therefore, an automated droop controller reduces circulating current and improves load sharing. In Fig. 7, the simulation is carried out with variable load. The value of cable resistance is same for both the converters. The automatic droop controller also served excellent during variable loading condition. No transient is found during change in load. Fig. 8, shows the performance of an automatic droop controller under variable load condition and different cable resistance. At light load, the lower value of droop is estimated so that the voltage deviation is smaller. Thus, achieves superior voltage regulation (Fig. 9). The larger value of droop is calculated as the load current rises which results in improved load sharing accuracy. Therefore, the objective of the research paper is achieved.

No transient is detected during the load shift, demonstrating the efficacy of the suggested controller. With no cable resistance (0 to 0.3 second), both the controller produces same droop value and it increases as the load current increases as seen in Fig. 10. During 0.3 to 0.6 second, again the droop value estimated by both converters are equal as the equal cable resistance enters into the system. During 0.6 to 1.0 second, as the cable resistance is different the droop values estimated by both converters are also different. Currently both the droop controllers are working independently. If any small signal disturbance occurs in the system, then also the droop controller adjusts the droop value such that output current and so the load current remains constant. Fig. 10 shows the droop characteristic of automatic droop control. The maximum voltage deviation at rated load is within limit and so achieves voltage regulation within the permissible limit. Table II represents the comparison between the results of DC-DC converters without droop control and DC-DC converters with suggested automatic droop controller. The suggested automatic droop controller provides better load sharing accuracy with almost negligible circulating current compared with no droop method. The load sharing error reduces from 52.10% to 6.40%. circulating current also decreases from 1.04A to 0.128A. The voltage regulation also remains in permissible limits.

CONCLUSION

This research work presents an automatic droop controller with the objective of achieving proportional load sharing in a low voltage independent DC micro grid. An automatic droop controller instantly calculates the droop resistance in response to variations in load current. The method effectively minimizes the load sharing error and circulating current among converters with desired voltage regulation. The impact of cable resistances is also taken into account





Shilpa Patel et al.,

in order to assess the feasibility of the suggested controller. The simulation results provide evidence of the effectiveness of the suggested controller under many conditions including changing cable resistance, variable load, and variable droop resistance. This research further examines the comparison between the no droop technique and the proposed automatic droop controller. The comparison demonstrates that the use of an automatic droop controller provides superior load sharing capabilities and effectively minimizes circulating current while maintaining optimal voltage regulation. Additionally, it has been observed that the load sharing error experiences a decrease from 52.10 % to 6.40 %, while the circulating current decreases from 1.04 A to 0.128 A with 4.15 % voltage regulation. The theoretical values and simulation results are also found identical. Subsequent investigations will be undertaken to assess the effectiveness of an automatic droop controller in contrast to various alternative methods for droop control.

REFERENCES

1. E. T. Sayed et al., "Renewable Energy and Energy Storage Systems," *Energies*, vol. 16, no. 3. MDPI, Feb. 01, 2023. doi: 10.3390/en16031415.
2. C. Jamroen, N. Yonsiri, T. Odthon, N. Wisitthiwong, and S. Janreung, "A standalone photovoltaic/battery energy-powered water quality monitoring system based on narrowband internet of things for aquaculture: Design and implementation," *Smart Agricultural Technology*, vol. 3, p. 100072, Feb. 2023, doi: 10.1016/j.atech.2022.100072.
3. A. Aligbe, A. E. Airoboman, A. S. Uyi, and P. E. Orukpe, "Microgrid, Its Control and Stability: The State of The Art," *International Journal of Emerging Scientific Research*, vol. 3, pp. 1–12, 2022, doi: 10.37121/ijesr.v3.145.
4. S. Peyghami, H. Mokhtari, P. C. Loh, P. Davari, and F. Blaabjerg, "Distributed Primary and secondary power sharing in a droop-controlled lvdc microgrid with merged AC and DC characteristics," *IEEE Trans Smart Grid*, vol. 9, no. 3, pp. 2284–2294, 2018, doi: 10.1109/TSG.2016.2609853.
5. L. Meng et al., "Review on Control of DC Microgrids and Multiple Microgrid Clusters," *IEEE J Emerg Sel Top Power Electron*, vol. 5, no. 3, pp. 928–948, Sep. 2017, doi: 10.1109/JESTPE.2017.2690219.
6. X. Lu et al., "Hierarchical Control of Parallel AC-DC Converter Interfaces for Hybrid Micro grids," pp. 1–10, 2013.
7. A. Mohd, E. Ortjohann, D. Morton, and O. Omari, "Review of control techniques for inverters parallel operation," *Electric Power Systems Research*, vol. 80, no. 12, pp. 1477–1487, Dec. 2010. doi: 10.1016/j.epsr.2010.06.009.
8. J. M. Guerrero, J. C. Vásquez, J. Matas, M. Castilla, and L. García de Vicuna, "Control strategy for flexible micro grid based on parallel line-interactive UPS systems," in *IEEE Transactions on Industrial Electronics*, 2009, pp. 726–736. doi: 10.1109/TIE.2008.2009274.
9. A. Ashok Kumar and N. Amutha Prabha, "A comprehensive review of DC microgrid in market segments and control technique," *Heliyon*, vol. 8, no. 11. Elsevier Ltd, Nov. 01, 2022. doi: 10.1016/j.heliyon.2022.e11694.
10. M. Z. Gao, M. Chen, C. Jin, J. M. Guerrero, and Z. M. Qian, "Analysis, design, and experimental evaluation of power calculation in digital droop-controlled parallel micro grid inverters," *Journal of Zhejiang University: Science C*, vol. 14, no. 1, pp. 50–64, Jan. 2013, doi: 10.1631/jzus.C1200236.
11. J. M. Guerrero, P. C. Loh, T. L. Lee, and M. Chandorkar, "Advanced control architectures for intelligent micro grids Part II: Power quality, energy storage, and AC/DC micro grids," *IEEE Transactions on Industrial Electronics*, vol. 60, no. 4, pp. 1263–1270, 2013, doi: 10.1109/TIE.2012.2196889.
12. N. Ghanbari and S. Bhattacharya, "Adaptive Droop Control Method for Suppressing Circulating Currents in DC Micro grids," *IEEE Open Access Journal of Power and Energy*, vol. 7, no. January, pp. 100–110, 2020, doi: 10.1109/oajpe.2020.2974940.
13. M. A. Setiawan, A. Abu-Siada, and F. Shahnian, "A New Technique for Simultaneous Load Current Sharing and Voltage Regulation in DC Micro grids," *IEEE Trans Industry Inform*, vol. 14, no. 4, pp. 1403–1414, Apr. 2018, doi: 10.1109/TII.2017.2761914.
14. A. Bidram and A. Davoudi, "Hierarchical structure of micro grids control system," *IEEE Trans Smart Grid*, vol. 3, no. 4, pp. 1963–1976, 2012, doi: 10.1109/TSG.2012.2197425.
15. J. Kumar, A. Agarwal, and V. Agarwal, "A review on overall control of DC micro grids," *Journal of Energy Storage*, vol. 21. Elsevier Ltd, pp. 113–138, Feb. 01, 2019. doi: 10.1016/j.est.2018.11.013.





Shilpa Patel et al.,

16. J. Peng, B. Fan, J. Duan, Q. Yang, and W. Liu, "Adaptive decentralized output-constrained control of single-bus DC micro grids," *IEEE/CAA Journal of Automatica Sinica*, vol. 6, no. 2, pp. 424–432, Mar. 2019, doi: 10.1109/JAS.2019.1911387.
17. J. M. Guerrero, J. C. Vasquez, J. Matas, L. G. de Vicuña, and M. Castilla, "Hierarchical control of droop-controlled AC and DC micro grids - A general approach toward standardization," *IEEE Transactions on Industrial Electronics*, vol. 58, no. 1, pp. 158–172, 2011, doi: 10.1109/TIE.2010.2066534.
18. P. Monica, M. Kowsalya, and J. M. Guerrero, "Logarithmic droop-based decentralized control of parallel converters for accurate current sharing in islanded DC micro grid applications," *IET Renewable Power Generation*, vol. 15, no. 6, pp. 1240–1254, Apr. 2021, doi: 10.1049/rpg2.12103.
19. S. E. Mhankale and A. R. Thorat, "Droop Control Strategies of DC Micro grid: A Review," *Proceedings of the 2018 International Conference on Current Trends towards Converging Technologies, ICCTCT 2018*, 2018, doi: 10.1109/ICCTCT.2018.8550854.
20. Y. Zhou and C. Ngai-Man Ho, "A review on Micro grid architectures and control methods," *2016 IEEE 8th International Power Electronics and Motion Control Conference, IPEMC-ECCE Asia 2016*, pp. 3149–3156, 2016, doi: 10.1109/IPEMC.2016.7512799.
21. Y. Han, X. Ning, P. Yang, and L. Xu, "Review of Power Sharing, Voltage Restoration and Stabilization Techniques in Hierarchical Controlled DC Microgrids," *IEEE Access*, vol. 7, pp. 149202–149223, 2019, doi: 10.1109/ACCESS.2019.2946706.
22. A. C. Braitor, G. C. Konstantopoulos, and V. Kadiramanathan, "Current-Limiting Droop Control Design and Stability Analysis for Paralleled Boost Converters in DC Micro grids," *IEEE Transactions on Control Systems Technology*, vol. 29, no. 1, pp. 385–394, Jan. 2021, doi: 10.1109/TCST.2019.2951092.
23. P. Prabhakaran, Y. Goyal, and V. Agarwal, "Novel nonlinear droop control techniques to overcome the load sharing and voltage regulation issues in DC Micro grid," *IEEE Trans Power Electron*, vol. 33, no. 5, pp. 4477–4487, May 2018, doi: 10.1109/TPEL.2017.2723045.
24. G. Xu, D. Sha, and X. Liao, "Decentralized inverse-droop control for input-series-output-parallel DC-DC Converters," *IEEE Trans Power Electron*, vol. 30, no. 9, pp. 4621–4625, 2015, doi: 10.1109/TPEL.2015.2396898.
25. S. Liu, J. Zheng, Z. Li, and X. Liu, "A general piecewise droop design method for DC micro grid," *International Journal of Electronics*, vol. 108, no. 5, pp. 758–776, 2021, doi: 10.1080/00207217.2020.1818839.
26. S. Peyghami, H. Mokhtari, and F. Blaabjerg, "Decentralized Load Sharing in a Low-Voltage Direct Current Micro grid with an Adaptive Droop Approach Based on a Superimposed Frequency," *IEEE J Emerg Sel Top Power Electron*, vol. 5, no. 3, pp. 1205–1215, Sep. 2017, doi: 10.1109/JESTPE.2017.2674300.
27. Y. Gu, X. Xiang, W. Li, and X. He, "Mode-adaptive decentralized control for renewable DC micro grid with enhanced reliability and flexibility," *IEEE Trans Power Electron*, vol. 29, no. 9, pp. 5072–5080, 2014, doi: 10.1109/TPEL.2013.2294204.
28. Z. Shuai, J. Fang, F. Ning, and Z. J. Shen, "Hierarchical structure and bus voltage control of DC micro grid," *Renewable and Sustainable Energy Reviews*, vol. 82. Elsevier Ltd, pp. 3670–3682, Feb. 01, 2018. doi: 10.1016/j.rser.2017.10.096.
29. S. Chaturvedi and D. M. Fulwani, "Equal Load Sharing in DC Micro grid Using Line Resistance Estimation," in *Lecture Notes in Electrical Engineering*, Springer, 2020, pp. 87–96. doi: 10.1007/978-981-15-0226-2_7.
30. Augustine, S., Mishra, M. K., & Lakshminarasamma, N. (2014). Adaptive droop control strategy for load sharing and circulating current minimization in low-voltage standalone DC micro grid. *IEEE Transactions on Sustainable Energy*, 6(1), 132-141.

Table I: Nominal Parameters of Two Converters

Parameters	Value
Output Power - P_o	96W
Output Voltage - V_o	48V
Output Current - I_o	2A
Filter Inductor - L	750mH





Shilpa Patel et al.,

Filter Capacitor - C	2220 μ F
Nominal switching Frequency - f_s	10KHz
ESR of filter Inductor	0.68 Ω
ESR of Filter Capacitor	0.18 Ω
On-state resistance of Diode	0.001 Ω
On-state resistance of MOSFET	0.001 Ω

Table II: Comparison Between The Results of No Droop and Automatic Droop Controller

Method Parameters	No Droop	An Automatic Droop Controller
DC bus voltage	47.75 V	46.01 V
Load current	3.95 A	3.834 A
Load power	188 W	176.40 W
% Load sharing error	52.10 %	6.40 %
% Voltage regulation	1.04 %	4.15 %
Circulating current	1.04 A	0.128 A

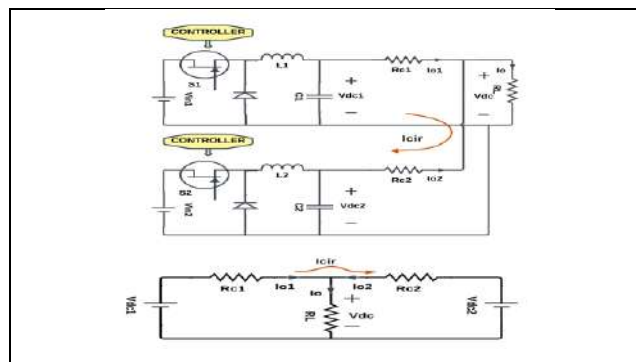


Fig 1: Load sharing between two converters and its equivalent circuit with cable resistance

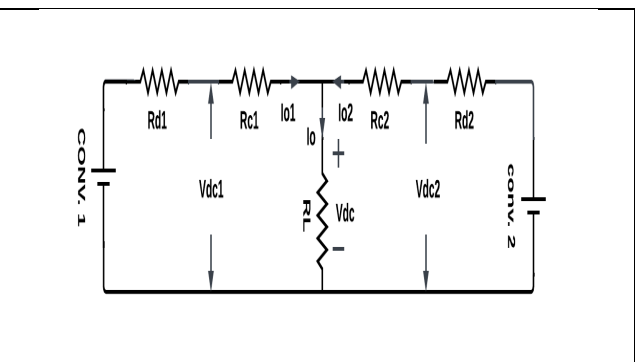


Fig.2: Equivalent circuit of parallel connected converters with droop resistance and cable resistance [30]

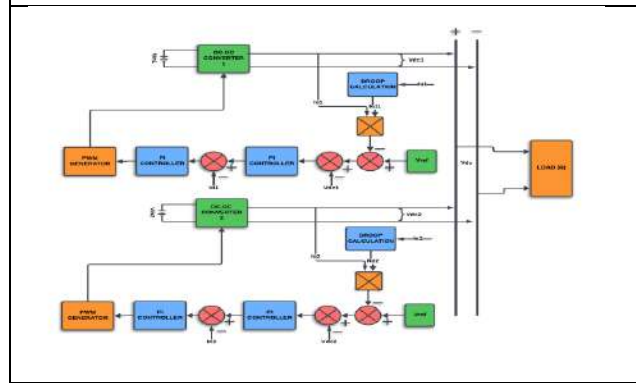


Fig. 3: Schematic diagram of suggested automatic droop controller

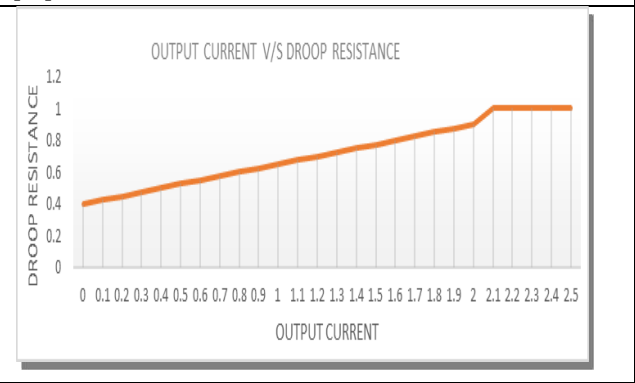


Fig. 4: Output current v/s estimated droop value





Shilpa Patel et al.,

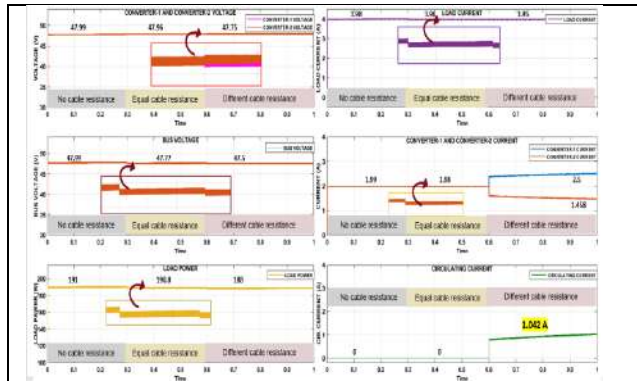


Fig. 5: simulation results of DC-DC converter without droop control

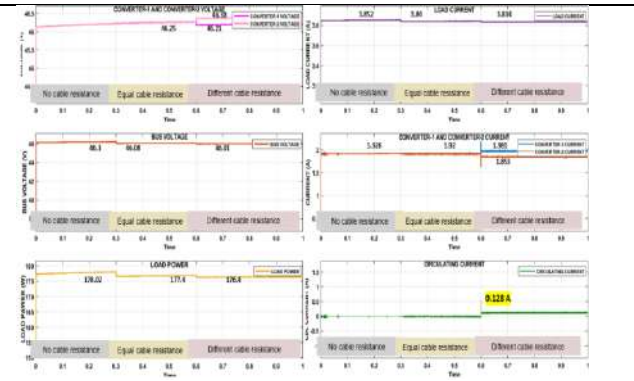


Fig. 6: simulation results of DC-DC converter with Automatic droop control

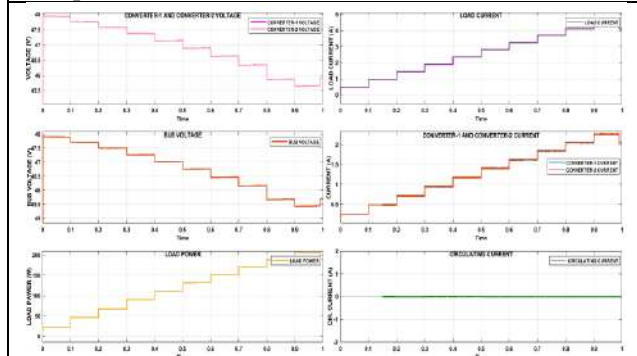


Fig. 7: simulation results with variable load and equal cable resistance

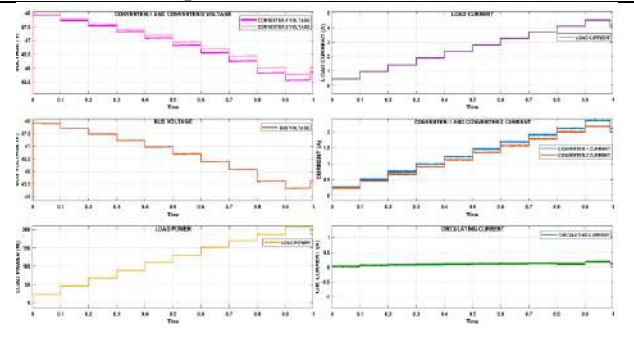


Fig. 8: simulation results with variable load and Different cable resistance

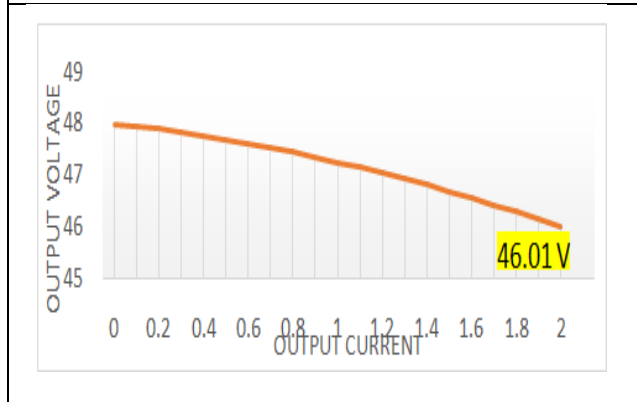


Fig. 9: I-V Characteristic of an automatic droop controller

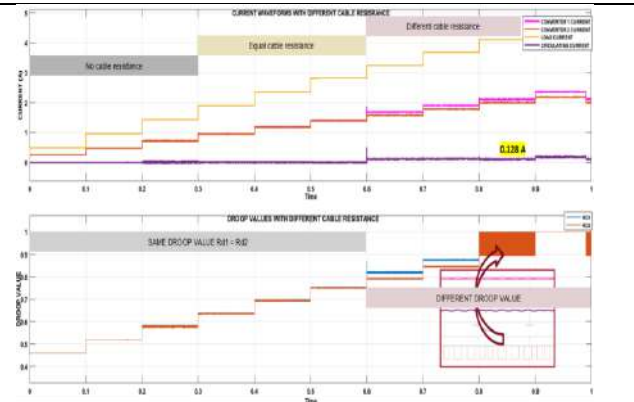


Fig. 10: simulation results show effectiveness of an automatic droop controller





Parametric Optimization of Valve Body Produced with FDM using PLA and ABS Materials

Khushbu Patel^{1*}, Shailee Acharya², G. D. Acharya³

¹Research Scholar, Gujarat Technological University, Ahmedabad, Gujarat, India.

²Assistant Professor, SVIT, Vasad, Gujarat, India.

³Emeritus, Aatmiy University, Rajkot, Gujarat, India.

Received: 30 Dec 2023

Revised: 09 Jan 2024

Accepted: 12 Jan 2024

*Address for Correspondence

Khushbu Patel

Research Scholar,

Gujarat Technological University,

Ahmedabad, Gujarat, India.

Email: khushbutpatel@gmail.com



This is an Open Access Journal / article distributed under the terms of the **Creative Commons Attribution License** (CC BY-NC-ND 3.0) which permits unrestricted use, distribution, and reproduction in any medium, provided the original work is properly cited. All rights reserved.

ABSTRACT

3D printing is the method of creating 3D objects from digital files by placing successively numerous thin layers of metal. In recent years, it has been admiring remarkable progress. 3D printing offers creative options for meeting a variety of engineering-related requirements. Acrylonitrile Butadiene Styrene (ABS) and Poly Lactic Acid (PLA) two main materials selected for the Fusion Deposition Modelling (FDM) 3D printer. The purpose of this study is to compare the effects of the material on the process variables and optimize the valve body's chosen process parameters. Layer Height, Orientation Angle, and Infill Density are chosen for the input parameters, while Surface Roughness, Dimensional Deviations along Big Diameter, Small diameter & Length, and Tensile Strength are chosen for the responses. For Multi Objective Optimization, PLA and ABS materials are subjected to a Grey Relational Analysis (GRA). The PLA and ABS valves are compared to one another and assessed. The findings indicate that the best model parameters are 40% infill density, 0.2 mm layer height, and 90° orientation angle, with infill density having the most influence. selection of the material having less of an overall influence on the parameters.

Keywords: 3 D Printing; Fused Deposition Modelling ; Acrylonitrile Butadiene Styrene; Poly Lactic Acid; Grey Relational Analysis.



**Khushbu Patel et al.,**

INTRODUCTION

Each 3D printer produces parts based on the idea that a digital model may be transformed into a real-world 3D item by adding material one layer at a time. New models and components are developed from a digital model before the replica is formed by applying small layers of material successively in succession and utilizing digital blueprints. A wide number of sectors, including aerospace, automotive, biomedicine, metal production, consumer goods, and defense, can benefit from additive manufacturing. A 3D printer can create many industrial prototypes, including clothing and jewellery, prosthetics, 3D sculptures, aircraft parts, and even human organs like bone marrow, which can be bio printed using a variety of hundreds of other materials. A digital model is built using a variety of software programs, including CAD, CATIA, and SOLIDWORKS. Either modelling software or 3D scanning data are used to construct it. Additionally, until the item is complete, it cuts the prototype into 100 or 1000 layers, one on top of the other. You may design, slice, and guide the machine for manufacture using the 3D printer software. The majority of researchers that explored different FDM materials chose ABS or PLA, however some also tested a mix of the two. R. Roy and A. Mukho padhyay [1] performed tribological analyses on ABS and PLA plastic components that were 3D printed. The primary printing parameters have been determined to be material deposition layer thickness, infill angle, infill pattern, and orientation of deposition. They examined wear, weight loss, and dimensional variation for both materials under the same circumstances. Flexural and tensile properties of PLA, ABS, and PLA-ABS materials, according to D. Yadav, D. Chhabra, R. Kumar Garg, A. Ahlawat, and A. Phogat [2] specifications. Blends of PLA and ABS are made in a variety of compositions, and they are evaluated for their resistance to tensile and flexural loads in order to present with a new filament material that can endure higher stresses than the standard filaments. In an FDM 3D printer utilizing PLA and ABS materials, V. Harshitha and S. S. Rao [3] created and examined ISO standard bolts and nuts. The proposed model is examined for shear stress, equivalent stress, and deformation using ANSYS software. The PLA and ABS bolts are compared and tested with one another.

The physical and mechanical characteristics of PLA, ABS, and nylon 6 made via fused deposition modelling and injection moulding were compared by M. Lay, N. L. N. Thajudin, Z. A. A. Hamid, A. Rusli, M. K. Abdullah, and R. K. Shuib [4]. The findings showed that the FDM process boosted the crystallinity of PLA and nylon 6 but had no effect on ABS's degree of crystallinity. The Influence of Manufacturing Parameters on the Mechanical Behavior of PLA and ABS Pieces Manufactured by FDM was examined by A. Rodríguez-Panes, J. Claver, and A. M. Camacho [5]. This study compared how layer height, infill density, and layer orientation affected the mechanical performance of test specimens made of PLA and ABS. Test specimens made of PLA are found to perform more rigidly and to have higher tensile strengths than ones made of ABS. H. Yang, F. Ji, Z. Li, and S. Tao [6] studied the correlation between the printing process parameters and the surface roughness and wettability of the printed test parts using FDM 3D printing technology with design and processing flexibility. The coatings were prepared for PLA and ABS parts. The findings of the experiment reveal that the layer thickness and filling technique significantly affect the surface roughness of the 3D-printed items. J. Milde, R. Hrušický, R. Zaujec, L. Morovic, and A. Görög, [7] concentrated on contrasting the characteristics of the two most popular materials, ABS and PLA, while utilizing the FDM technique for rapid prototyping (RP). After analyzing the experiment, it was discovered that the employed printer itself had the greatest effect on the production's quality and speed. ABS components took 3 hours and 54 minutes longer to make than PLA components. The researchers were driven towards the Multi Objective Optimization approach, which may combine Taguchi Method) TM and/or GRA, due to TM's constraint that it can only be utilized for single objective optimization. Each processing parameter has a unique impact on the mechanical and dimensional precision repetition of FDM components, according to A. Alafaghani, A. Qattawi, B. Alrawi, and A. Guzman [8]. Dimensional accuracy was demonstrated to be more affected by building direction, extrusion temperature, and layer height than by infill percentage, infill pattern, or printing speed. In order to assess the dimensional correctness and surface roughness of FDM 3D printed components generated from PLA, PLA+, ABS, and ABS+ filament materials, M. S. Alsoufi and A. E. Elsayed [9]. The maximum Ra, Wa, and Pa values are found on the top faces (middle) of PLA, PLA+, and ABS+, whereas ABS exhibits inconsistent surface roughness, waviness, and primary distribution over all four faces. Multi-objective optimization of the dimensional accuracy, surface roughness, and hardness of hybrid



**Khushbu Patel et al.,**

investment cast components was carried out by P. K. Garg, R. Singh, and A. Ips. [10]. A Taguchi design of trials was used to examine the effects of six unique input process parameters on the results. Applying a coating of wax to FDM designs before 3D printing them dramatically improves their surface quality and dimensional accuracy. V. H. Nguyen, T. N. Huynh, T. P. Nguyen, and T. T. Tran [11] optimized processing settings for single- and multi-objectives in order to enhance fused deposition modelling. Through trial and error, mathematical models with different values for layer height, infill%, printing temperature, and printing speed were created. The most effective parameters for FDM printing of PLA components may be found using a multi-objective optimization paradigm, according to research by P. Patil, D. Singh, S. J. Raykar, and J. Bhamu [12] Infill patterns, infill percentage, printing speed, and layer thickness are research factors. L27 OA is used to carry out the investigation. GRA, which is well-suited to optimization in the presence of many responses, is used to tune the process parameters of FDM. The Grey TM was used by Sakthivel Murugan R. and V. S. [13] to parametrically optimize the FDM process, and TOPSIS was used to confirm their findings. In this work, the effects of SH, PFS, and BO are investigated using machining time, surface roughness, and hardness as response parameters.

ANOVA analysis of GRA and TOPSIS reveals that SH is more significant. ANOVA was used by D. Singh, R. Singh, and K. S. Boparai [14] to examine the effects of two controllable parameters for each process (FDM, VS, and IC) on the surface quality and dimensional accuracy roughness of final castings of implants using Taguchi's parametric approach. The FDM pattern should be put out at an orientation angle of 0 degrees in order to provide the smoothest surface possible during production, whilst a 90-degree orientation angle is ideal for exact measurements. O. Y. Venkatasubbareddy, P. Siddikali, and S. M. Saleem [15] investigate the effects of the process variables layer thickness, raster width & angle, and air gap on the surface roughness of the component generated by the technique of FDM. ABS M30 has been designated as the manufacturing material. TGRA is used to optimize the process parameters for a variety of performance criteria, such as length, diameter, breadth, and surface polish. An experimental study by S. Vyavahare, S. Kumar, and D. Panghal [16] looked at the fabrication time, dimensional accuracy, and surface roughness of FDM-produced components.

Factors in the manufacturing process, such as layer thickness, wall print speed, and build orientation, have a significant impact on the dimensional accuracy of FDM products. This investigation into the effects of three particular process parameters, such as orientation angle, layer height, and infill density, on deviation of dimension, quality of surface, printing time, and tensile strength of FDM printed parts was motivated by all of the aforementioned literature reviews. Implementing Taguchi's L18 OA, the experiment's design takes into account three levels for the other factors and two levels for the orientation angle. For the printing materials ABS or PLA or both, Taguchi's method, GRA, and ANOVA are utilized as optimization approaches, and ANOVA is used to assess the influence on component quality and their optimal values. According to the aforementioned study, it can be concluded that the majority of researchers chose Layer Thickness, some chose Infill Density, and a small number chose Orientation Angle as crucial factors with level values taken into consideration. According to the authors' knowledge, no one has previously addressed multilevel optimization of dimensional deviation, surface roughness, and tensile strength of FDM manufactured components in terms of orientation angle, infill density, and layer height for both ABS and PLA materials. That was done with the intention of selecting the study's input variables and their settings. The following goals are what this effort is primarily focused on achieving

1. To identify the impact that changes to process parameters have on the surface roughness, printing time, dimensional deviation, and tensile strength of FDM products.
2. To optimise important process parameters by using GRA, which is a multi-response optimal research project.
3. To compare the results for both, ABS and PLA materials.





Khushbu Patel et al.,

METHODOLOGY

Material, Process parameters and their range

Both ABS and PLA are inexpensive engineering thermoplastics that are comparably easy to manufacture, process, and thermoform. The food industry and related businesses can safely use ABS polymers. ABS may thus be used in processing facilities without any problems. While PLA is a thermoplastic that is easy to use and has greater strength and rigidity. One of the simplest materials to effectively 3D print with is PLA. It has been demonstrated that process factors including layer height, orientation angle, and infill density have a substantial influence on the mechanical properties, surface roughness, and dimensional deviation of 3D printed samples. The phases of the selected process variables are established using a literature review and the available FDM machine. For mixed mode design, L18, L36, and L56 OA are provided in Minitab Software with three input parameters and 2 and 3 level stages. L18 OA of Taguchi's DoE has been utilized to perform tests in order to save money and time and in accordance with suggestions from industry experts. For this investigation, variable process parameters were adjusted throughout the intervals and to the values shown in Table 1.

FDM specimen preparation

Created 3D test samples for the valve body. Solid Works was used to produce the component models, and the CURA application was used to send an STL file to the FDM machine (Fig. 1). As previously mentioned, the experiment used commercially available 3D printing materials ABS & PLA. This programme optimized the process control parameters for each experimental model. The authors used a DAM Boy ET-200 FDM 3D Printer to complete the task (Fig.2). Fig.3 is an example of a 3D-printed valve body portion.

Measurement of responses

The output responses examined in this inquiry are Dimensional Deviations along Small Diameter, Big Diameter and Length, Surface Roughness, and Tensile Strength. By measuring the part's dimensions using a vernier-caliper (WORK ZONE 0-150mm Digital Caliper) with a least count of 0.01 mm, the dimensional deviation of FDM was assessed.

Fig.4 shows the surface roughness of the specimen as determined by the Mitutoyo SJ-210 surface roughness tester. For the purpose of measuring roughness, a probe speed of 0.5 mm/s is used in accordance with ISO 1997 standard 2.5 mm cut-off length. By averaging the roughness profile (Ra), surface roughness is determined. The average of each surface is used to describe that surface after computing the roughness for each sample using the six surface roughness measurements. Tensile strength of the 3D-printed samples was assessed (in a room that was 23° Fahrenheit and 50% humidity). The item underwent tensile testing utilizing a universal testing machine. (Source: Rajkot's Turbo Cast Pvt. Ltd.). Tables 2 and 3 provide summaries of the responses obtained using the L18 orthogonal array for the materials ABS and PLA, respectively.

Grey relational analysis

Deng suggested the GRA theory as a means of dealing with ill-defined systemic problems with the least amount of information possible. When full knowledge is lacking to resolve a tough problem, it is employed (M. Singh and P. S. Bharti [17]). GRA is the most efficient way for identifying the important process variables, which depend on a variety of output qualities. (F. Arifin, A. Zamheri, E. Satria Martomi, Y. Dewantoro Herlambang [18], K. Sharma and K. Kumar [19], S. Ramesh, R. Viswanathan, and S. Ambika [20], N. Senthilkumar, T. Tamizharasan, and V. Anandkrishnan [21]). The initial stage in this research is to pre-process the data in order to normalize it before analysis. This is how the GRA procedure operates:

Normalization

The normalization of the response feature is calculated based on the requirements, as seen in (1) and (2), where "larger is better" is preferred for tensile strength and "lower is better" for surface roughness, dimensional deviation, and printing time, respectively.





Khushbu Patel et al.,

$$y(t) = \frac{y_i^o(t) - \min y_i^o(t)}{\max y_i^o(t) - \min y_i^o(t)} \quad (1)$$

$$y(t) = \frac{\max y_i^o(t) - y_i^o(t)}{\max y_i^o(t) - \min y_i^o(t)} \quad (2)$$

It is suitable to normalise the original sequence in this way when "higher is better" is one of its distinguishing characteristics:

Calculation of Grey Relational coefficient (GRC)

Equation (3) is used to compute the GRC after normalization in order to express the connection between the ideal (best) and actual results of the standardized trial. As we say in GRC:

$$\zeta_i(k) = \frac{\Delta_{\min} + \zeta \Delta_{\max}}{\Delta_{oi}(k) + \zeta \Delta_{\max}} \quad (3)$$

ζ = Identification Co-efficient; $0 < \zeta < 1$

Calculation of grey relational grade

Equation (4) was used to find the GRG after computing the GRC and averaging the GRC values for each feature. The GRG might be formulated in the following way:

$$\gamma_i = \frac{1}{n} \sum_{j=1}^n \beta_j \zeta_i(k) \quad (4)$$

β_j = Weight for each process parameter

RESULT AND DISCUSSION

The data are analyzed using the statistical analysis application Minitab R16 with a 95% confidence interval.

The goal of the current study is to compare the findings for ABS and PLA materials and boost TS while reducing DD and Ra.

Computation of GRG

Equations (1) & (2) were used to obtain the normalized values of each response to output, and Table 4 shows these values. Equation 3 was used to calculate each output GRC value of response, and the results are shown in Tables 4 and 5. (PLA and ABS). The quality must be outstanding if the GRG is high (R. Kumar, S. Roy, P. Gunjan, A. Sahoo, D. D. Sarkar, and R. K. Das [22]). Experiment 16 had the highest GRG (multiple output response) value out of the arrays that were chosen. (0.821) for PLA materials and (0.826) for ABS.

Analyses of Variance

The results are evaluated using Minitab software. The objective of the current study is to determine the overall primary effects of all variables on responses. Authors examined the effects of numerous input elements on the end result using the ANOVA (N. K. Maurya, V. Rastogi, and P. Singh [23], C. M. Cheah, C. K. Chua, C. W. Lee, C. Feng, and K. Totong [24], M. Waseem *et al* [25]). The results of the ANOVA on GRG are shown in Tables 6 and 7, together with the t-test, F-test, P-value, and sum of squares for ABS and PLA. Each of these elements makes up more than 5% of the total, therefore the proportion of infill density (42.97%) has a significant effect. In contrast, layer height (31.42%) and orientation angle (18.79%) make later contributions. The p-value must drop in order for the rejection of the null hypothesis for a particular parameter to not be significant (A. Armillotta, M. Bellotti, and M. Cavallaro [26]).



**Khushbu Patel et al.,**

The findings demonstrate that the factors used for this study are very significant, with P values of 0% for orientation angle, layer height, and infill density.

CONCLUSION

The experimental design was based on Taguchi's OA. For multi-objective optimization, GRG was used. Several combinations for the layer thickness, infill density, and orientation angle were established in order to enhance surface roughness, dimensional deviation, and tensile strength while accounting for different reactions. Additionally, all chosen parameters were evaluated between the ABS and PLA materials. The results of the aforementioned analysis are summarized as follows:

1. Tables 6 and 7 and the main impact plot for all process responses indicate that infill density is the most crucial factor, followed by layer height. The orientation angle of both materials was the element that had the least impact on the responses of the entire process.
2. The key process variables may explain for more than 96.84 % of the variability in the data across all replies, according to the R2 value for each response. The fact that the F-value and p-value for each parameter for answers were found to be appropriate at a 95% confidence range again supports the importance of the process parameters.
3. When using GRG, the best parameter positions for simultaneous optimal process responses were orientation angle 90°, layer height 0.2 mm, and infill density 40%. The GRG for both materials was greatly influenced by the infill density, layer height, and orientation angle.
4. According to ANOVA for ABS, the key controllable factor that significantly affects the multiple-performance characteristics is infill density, which makes up 42.97% of the required total. In second and third place, with contributions of 31.42% and 18.79%, respectively, are Layer height and Orientation angle.
5. According to an ANOVA for PLA, infill density is the main variable that significantly affects the numerous performance attributes, accounting for 44.45% of the required total. Orientation angle and layer height are in second and third place, respectively contributing 29.96% and 17.33%.
6. According to the GRG results, the optimal parameters for both materials are comparable, indicating that the influence of the materials on the chosen parameters in multi-objective optimization is almost identical. The results of the measurements indicate that the tensile strength of PLA is more than that of ABS, while the dimensional deviation and surface roughness of PLA are also greater than those of ABS.

Therefore, the recommended optimization strategy may undoubtedly be helpful to generate high-quality FDM components in large quantities with minimum waste. Future applications for the optimization technique include prototyping, prosthetics, industrial applications, architecture, and real-time components as FDM provides a simple, inexpensive, and efficient substitute for producing prototypes. The choice of material may have an impact on a person's response, but it has little of an overall effect.

ACKNOWLEDGMENT

The authors further acknowledge the contributions of Turo Cast Pvt. Ltd. Rajkot, and Engineering Technique, Baroda, for providing data and testing facilities for this work.





Khushbu Patel et al.,

REFERENCES

1. R. Roy and A. Mukhopadhyay, "Tribological studies of 3D printed ABS and PLA plastic parts," *Mater. Today Proc.*, vol. 41, no. xxxx, pp. 856–862, 2020, doi: 10.1016/j.matpr.2020.09.235.
2. D. Yadav, D. Chhabra, R. Kumar Garg, A. Ahlawat, and A. Phogat, "Optimization of FDM 3D printing process parameters for multi-material using artificial neural network," *Mater. Today Proc.*, vol. 21, no. xxxx, pp. 1583–1591, 2020, doi: 10.1016/j.matpr.2019.11.225.
3. V. Harshitha and S. S. Rao, "Design and analysis of ISO standard bolt and nut in FDM 3D printer using PLA and ABS materials," *Mater. Today Proc.*, vol. 19, no. xxxx, pp. 583–588, 2019, doi: 10.1016/j.matpr.2019.07.737.
4. M. Lay, N. L. N. Thajudin, Z. A. A. Hamid, A. Rusli, M. K. Abdullah, and R. K. Shuib, "Comparison of physical and mechanical properties of PLA, ABS and nylon 6 fabricated using fused deposition modeling and injection molding," *Compos. Part B Eng.*, vol. 176, no. July, p. 107341, 2019, doi: 10.1016/j.compositesb.2019.107341.
5. A. Rodríguez-Panes, J. Claver, and A. M. Camacho, "The influence of manufacturing parameters on the mechanical behaviour of PLA and ABS pieces manufactured by FDM: A comparative analysis," *Materials (Basel)*, vol. 11, no. 8, 2018, doi: 10.3390/ma11081333.
6. H. Yang, F. Ji, Z. Li, and S. Tao, "Preparation of hydrophobic surface on PLA and ABS by fused deposition modeling," *Polymers (Basel)*, vol. 12, no. 7, 2020, doi: 10.3390/polym12071539.
7. J. Milde, R. Hruščeký, R. Zaujec, L. Morovic, and A. Görög, "Research of abs and plamaterials in the process of fused deposition modeling method," *Ann. DAAAM Proc. Int. DAAAM Symp.*, no. January, pp. 812–820, 2017, doi: 10.2507/28th.daaam.proceedings.114.
8. A. Alafaghani, A. Qattawi, B. Alrawi, and A. Guzman, "Experimental Optimization of Fused Deposition Modelling Processing Parameters: A Design-for-Manufacturing Approach," *Procedia Manuf.*, vol. 10, pp. 791–803, 2017, doi: 10.1016/j.promfg.2017.07.079.
9. M. S. Alsoufi and A. E. Elsayed, "How Surface Roughness Performance of Printed Parts Manufactured by Desktop FDM 3D Printer with PLA+ is Influenced by Measuring Direction," *Am. J. Mech. Eng.*, vol. 5, no. 5, pp. 211–222, 2017, doi: 10.12691/ajme-5-5-4.
10. P. K. Garg, R. Singh, and A. Ips, "Multi-objective optimization of dimensional accuracy, surface roughness and hardness of hybrid investment cast components," *Rapid Prototyp. J.*, vol. 23, no. 5, pp. 845–857, 2017, doi: 10.1108/RPJ-10-2015-0149.
11. V. H. Nguyen, T. N. Huynh, T. P. Nguyen, and T. T. Tran, "Single and multi-objective optimisation of processing parameters for fused deposition modelling in 3D printing technology," *Int. J. Automot. Mech. Eng.*, vol. 17, no. 1, pp. 7542–7551, 2020, doi: 10.15282/IJAME.17.1.2020.03.0558.
12. P. Patil, D. Singh, S. J. Raykar, and J. Bhamu, "Multi-objective optimization of process parameters of Fused Deposition Modeling (FDM) for printing Poly(lactic Acid) (PLA) polymer components," *Mater. Today Proc.*, vol. 45, pp. 4880–4885, 2021, doi: 10.1016/j.matpr.2021.01.353.
13. S. M. R and V. S, "Parametric optimization of fused deposition modelling process using Grey based Taguchi and TOPSIS methods for an automotive component," *Rapid Prototyp. J.*, vol. 27, no. 1, pp. 155–175, 2021, doi: 10.1108/RPJ-10-2019-0269.
14. D. Singh, R. Singh, and K. S. Boparai, "Investigations for surface roughness and dimensional accuracy of biomedical implants prepared by combining fused deposition modelling, vapour smoothing and investment casting," *Adv. Mater. Process. Technol.*, pp. 1–20, 2020, doi: 10.1080/2374068x.2020.1835007.
15. O. Y. Venkatasubbareddy, P. Siddikali, and S. M. Saleem, "Improving the Dimensional Accuracy And Surface Roughness of Fdm Parts Using Optimization Techniques," *IOSR J. Mech. Civ. Eng.*, vol. 16, no. 053, pp. 18–22, 2016, doi: 10.9790/1684-16053041822.
16. S. Vyavahare, S. Kumar, and D. Panghal, "Experimental study of surface roughness, dimensional accuracy and time of fabrication of parts produced by fused deposition modelling," *Rapid Prototyp. J.*, vol. 26, no. 9, pp. 1535–1554, 2020, doi: 10.1108/RPJ-12-2019-0315.
17. M. Singh and P. S. Bharti, "Grey relational analysis based optimization of process parameters for efficient performance of fused deposition modelling based 3D printer," *J. Eng. Res.*, vol. 10, pp. 1–15, 2022, doi: 10.36909/jer.ICMET.17159.





Khushbu Patel et al.,

18. F. Arifin, A. Zamheri, E. Satria Martomi, Y. Dewantoro Herlambang, A. Panjy Syahputra, and I. Apriansyah, "Optimization of Process Parameters in 3D Printing Fdm By Using the Taguchi and Grey Relational Analysis Methods," vol. 15, no. 1, pp. 1–10, 2021, doi: 10.24853/sintek.15.1.1-10.
19. K. Sharma and K. Kumar, "Parametric multi-objective optimization of fused deposition modelling (FDM) with biopolymer using Grey-Taguchi method," *IOP Conf. Ser. Mater. Sci. Eng.*, vol. 1248, no. 1, p. 012107, 2022, doi: 10.1088/1757-899x/1248/1/012107.
20. S. Ramesh, R. Viswanathan, and S. Ambika, "Measurement and optimization of surface roughness and tool wear via grey relational analysis, TOPSIS and RSA techniques," *Meas. J. Int. Meas. Confed.*, vol. 78, pp. 63–72, 2016, doi: 10.1016/j.measurement.2015.09.036.
21. N. Senthilkumar, T. Tamizharasan, and V. Anandkrishnan, "Experimental investigation and performance analysis of cemented carbide inserts of different geometries using Taguchi based grey relational analysis," *Meas. J. Int. Meas. Confed.*, vol. 58, pp. 520–536, 2014, doi: 10.1016/j.measurement.2014.09.025.
22. R. Kumar, S. Roy, P. Gunjan, A. Sahoo, D. D. Sarkar, and R. K. Das, "Analysis of MRR and Surface Roughness in Machining Ti-6Al-4V ELI Titanium Alloy Using EDM Process," *Procedia Manuf.*, vol. 20, no. 2017, pp. 358–364, 2018, doi: 10.1016/j.promfg.2018.02.052.
23. N. K. Maurya, V. Rastogi, and P. Singh, "An overview of mechanical properties and form error for rapid prototyping," *CIRP J. Manuf. Sci. Technol.*, vol. 29, no. 2019, pp. 53–70, 2020, doi: 10.1016/j.cirpj.2020.02.003.
24. C. M. Cheah, C. K. Chua, C. W. Lee, C. Feng, and K. Totong, "Rapid prototyping and tooling techniques: A review of applications for rapid investment casting," *Int. J. Adv. Manuf. Technol.*, vol. 25, no. 3–4, pp. 308–320, 2005, doi: 10.1007/s00170-003-1840-6.
25. M. Waseem et al., "Multi-response optimization of tensile creep behavior of PLA 3D printed parts using categorical response surface methodology," *Polymers (Basel)*, vol. 12, no. 12, pp. 1–16, 2020, doi: 10.3390/polym12122962.
26. A. Armillotta, M. Bellotti, and M. Cavallaro, "Warpage of FDM parts: Experimental tests and analytic model," *Robot. Comput. Integr. Manuf.*, vol. 50, no. September, pp. 140–152, 2018, doi: 10.1016/j.rcim.2017.09.007.

Table 1 Levels of Process parameters for TM

	Level-1	Level-2	Level-3
Orientation Angle (°)	0	-	90
Layer Height (mm)	0.20	0.25	0.30
Infill Density (%)	20	30	40

Table 2 Design of the Experiment and Response Variables using L18 OA for ABS

Part	Orientation Angle	Infill Density	Layer Height	Surface roughness	Deviation in small diameter	Deviation in big diameter	Deviation in length	Tensile Strength
1	0	20	0.2	4.15	0.47	0.50	0.38	22.67
2	0	20	0.25	4.86	0.48	0.52	0.40	22.58
3	0	20	0.3	5.15	0.51	0.53	0.45	22.17
4	0	30	0.2	4.20	0.47	0.47	0.28	24.27
5	0	30	0.25	4.88	0.46	0.48	0.31	24.18
6	0	30	0.3	5.19	0.48	0.50	0.34	23.77
7	0	40	0.2	4.35	0.44	0.45	0.23	25.32
8	0	40	0.25	4.95	0.45	0.45	0.24	25.23
9	0	40	0.3	5.29	0.46	0.47	0.27	24.82
10	90	20	0.2	4.58	0.40	0.39	0.63	26.63





Khushbu Patel et al.,

11	90	20	0.25	5.05	0.42	0.41	0.64	26.54
12	90	20	0.3	5.44	0.43	0.42	0.67	26.13
13	90	30	0.2	4.45	0.36	0.35	0.55	26.90
14	90	30	0.25	5.14	0.35	0.38	0.56	26.81
15	90	30	0.3	5.34	0.38	0.40	0.59	26.40
16	90	40	0.2	4.48	0.32	0.33	0.48	28.60
17	90	40	0.25	5.05	0.33	0.35	0.50	28.52
18	90	40	0.3	5.44	0.34	0.36	0.54	28.11

Table 3 Design of the Experiment and Response Variables using L18 OA for PLA

Part	Orientation Angle	Infill Density	Layer Height	Surface roughness	Deviation in small diameter	Deviation in big diameter	Deviation in length	Tensile Strength
1	0	20	0.2	2.43	0.27	0.29	0.28	35.9027
2	0	20	0.25	3.12	0.28	0.31	0.29	35.8166
3	0	20	0.3	3.44	0.29	0.32	0.35	35.4054
4	0	30	0.2	2.48	0.24	0.26	0.18	37.5059
5	0	30	0.25	3.19	0.24	0.27	0.21	37.4146
6	0	30	0.3	3.47	0.25	0.28	0.21	37.0035
7	0	40	0.2	2.64	0.21	0.23	0.12	38.5578
8	0	40	0.25	3.24	0.23	0.23	0.14	38.4645
9	0	40	0.3	3.58	0.23	0.26	0.17	38.0544
10	90	20	0.2	2.89	0.17	0.18	0.52	39.8667
11	90	20	0.25	3.34	0.19	0.19	0.54	39.7734
12	90	20	0.3	3.74	0.2	0.20	0.55	39.3657
13	90	30	0.2	2.74	0.12	0.14	0.44	40.1340
14	90	30	0.25	3.44	0.14	0.17	0.45	40.0475
15	90	30	0.3	3.64	0.16	0.19	0.47	39.6352
16	90	40	0.2	2.78	0.09	0.12	0.38	42.8347
17	90	40	0.25	3.34	0.10	0.14	0.39	42.7442
18	90	40	0.3	3.74	0.11	0.15	0.43	42.3377

Table 4 Computation of GRA for ABS

Exp. No.	Normalized Values					Deviation Sequences					GRC					GRG
	SR	DDS	DDB	DDL	TS	SR	DDS	DDB	DDL	TS	SR	DDS	DDB	DDL	TS	
1	1.00	0.21	0.15	0.66	0.08	0.00	0.79	0.85	0.34	0.92	1.00	0.39	0.37	0.60	0.35	0.54
2	0.45	0.16	0.05	0.61	0.06	0.55	0.84	0.95	0.39	0.94	0.48	0.37	0.35	0.56	0.35	0.42
3	0.23	0.00	0.00	0.50	0.00	0.78	1.00	1.00	0.50	1.00	0.39	0.33	0.33	0.50	0.33	0.38





Khushbu Patel et al.,

4	0.96	0.21	0.30	0.89	0.33	0.04	0.79	0.70	0.11	0.67	0.93	0.39	0.42	0.82	0.43	0.60
5	0.43	0.26	0.25	0.82	0.31	0.57	0.74	0.75	0.18	0.69	0.47	0.40	0.40	0.73	0.42	0.49
6	0.19	0.16	0.15	0.75	0.25	0.81	0.84	0.85	0.25	0.75	0.38	0.37	0.37	0.67	0.40	0.44
7	0.85	0.37	0.40	1.00	0.49	0.16	0.63	0.60	0.00	0.51	0.76	0.44	0.46	1.00	0.50	0.63
8	0.38	0.32	0.40	0.98	0.48	0.62	0.68	0.60	0.02	0.52	0.45	0.42	0.46	0.96	0.49	0.55
9	0.12	0.26	0.30	0.91	0.41	0.88	0.74	0.70	0.09	0.59	0.36	0.40	0.42	0.85	0.46	0.50
10	0.67	0.58	0.70	0.09	0.69	0.33	0.42	0.30	0.91	0.31	0.60	0.54	0.63	0.36	0.62	0.55
11	0.30	0.47	0.60	0.07	0.68	0.70	0.53	0.40	0.93	0.32	0.42	0.49	0.56	0.35	0.61	0.48
12	0.00	0.42	0.55	0.00	0.62	1.00	0.58	0.45	1.00	0.38	0.33	0.46	0.53	0.33	0.57	0.44
13	0.77	0.79	0.90	0.27	0.74	0.23	0.21	0.10	0.73	0.27	0.68	0.70	0.83	0.41	0.65	0.66
14	0.23	0.84	0.75	0.25	0.72	0.77	0.16	0.25	0.75	0.28	0.39	0.76	0.67	0.40	0.64	0.57
15	0.08	0.68	0.65	0.18	0.66	0.92	0.32	0.35	0.82	0.34	0.35	0.61	0.59	0.38	0.59	0.51
16	0.74	1.00	1.00	0.43	1.00	0.26	0.00	0.00	0.57	0.00	0.66	1.00	1.00	0.47	1.00	0.83
17	0.30	0.95	0.90	0.39	0.99	0.70	0.05	0.10	0.61	0.01	0.42	0.91	0.83	0.45	0.98	0.72
18	0.00	0.90	0.85	0.30	0.92	1.00	0.11	0.15	0.71	0.08	0.33	0.83	0.77	0.42	0.87	0.64

Table 5 Computation of GRA for PLA

Exp. No.	Normalized Values					Deviation Sequences					GRC					GRG
	SR	DDS	DDB	DDL	TS	SR	DDS	DDB	DDL	TS	SR	DDS	DDB	DDL	TS	
1	1.00	0.10	0.15	0.63	0.07	0.00	0.90	0.85	0.37	0.93	1.00	0.36	0.37	0.57	0.35	0.53
2	0.47	0.05	0.05	0.61	0.06	0.53	0.95	0.95	0.40	0.95	0.49	0.35	0.35	0.56	0.35	0.42
3	0.23	0.00	0.00	0.47	0.00	0.77	1.00	1.00	0.54	1.00	0.39	0.33	0.33	0.48	0.33	0.38
4	0.96	0.25	0.30	0.86	0.28	0.04	0.75	0.70	0.14	0.72	0.93	0.40	0.42	0.78	0.41	0.59
5	0.42	0.25	0.25	0.79	0.27	0.58	0.75	0.75	0.21	0.73	0.46	0.40	0.40	0.71	0.41	0.48
6	0.21	0.20	0.20	0.79	0.22	0.79	0.80	0.80	0.21	0.79	0.39	0.39	0.39	0.71	0.39	0.45
7	0.84	0.40	0.45	1.00	0.42	0.16	0.60	0.55	0.00	0.58	0.76	0.46	0.48	1.00	0.47	0.63
8	0.38	0.30	0.45	0.95	0.41	0.62	0.70	0.55	0.05	0.59	0.45	0.42	0.48	0.92	0.46	0.54
9	0.12	0.30	0.30	0.88	0.36	0.88	0.70	0.70	0.12	0.64	0.36	0.42	0.42	0.81	0.44	0.49
10	0.65	0.60	0.70	0.07	0.60	0.35	0.40	0.30	0.93	0.40	0.59	0.56	0.63	0.35	0.56	0.54
11	0.31	0.50	0.65	0.02	0.59	0.70	0.50	0.35	0.98	0.41	0.42	0.50	0.59	0.34	0.55	0.48
12	0.00	0.45	0.60	0.00	0.53	1.00	0.55	0.40	1.00	0.47	0.33	0.48	0.56	0.33	0.52	0.44
13	0.76	0.85	0.90	0.26	0.64	0.24	0.15	0.10	0.74	0.36	0.68	0.77	0.83	0.40	0.58	0.65
14	0.23	0.75	0.75	0.23	0.63	0.77	0.25	0.25	0.77	0.38	0.39	0.67	0.67	0.39	0.57	0.54
15	0.08	0.65	0.65	0.19	0.57	0.92	0.35	0.35	0.81	0.43	0.35	0.59	0.59	0.38	0.54	0.49
16	0.73	1.00	1.00	0.40	1.00	0.27	0.00	0.00	0.61	0.00	0.65	1.00	1.00	0.45	1.00	0.82
17	0.31	0.95	0.90	0.37	0.99	0.70	0.05	0.10	0.63	0.01	0.42	0.91	0.83	0.44	0.98	0.72
18	0.00	0.90	0.85	0.28	0.93	1.00	0.10	0.15	0.72	0.07	0.33	0.83	0.77	0.41	0.88	0.65





Khushbu Patel et al.,

Table 6 Results of the Anova on GRG for ABS

Source	DF	Seq SS	Contribution	Adj SS	Adj MS	F-Value	P-Value
Orientation Angle	1	0.04051	18.79%	0.04051	0.040509	33.08	0
Infill Density	2	0.09264	42.97%	0.09264	0.046319	37.83	0
Layer Height	2	0.06772	31.42%	0.06772	0.033862	27.66	0
Error	12	0.01469	6.82%	0.01469	0.001224		
Total	17	0.21557	100.00%				

Table 7 Results of the ANOVA on GRG for PLA

Source	DF	Seq SS	Contribution	Adj SS	Adj MS	F-Value	P-Value
Orientation Angle	1	0.0376	17.33%	0.0376	0.037595	25.18	0
Infill Density	2	0.09641	44.45%	0.09641	0.048207	32.28	0
Layer Height	2	0.06498	29.96%	0.06498	0.032489	21.76	0
Error	12	0.01792	8.26%	0.01792	0.001493		
Total	17	0.21691	100.00%				

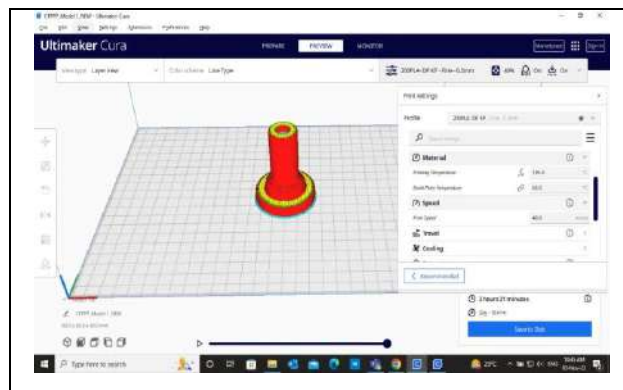


Fig. 1 Valve body model in CURA software

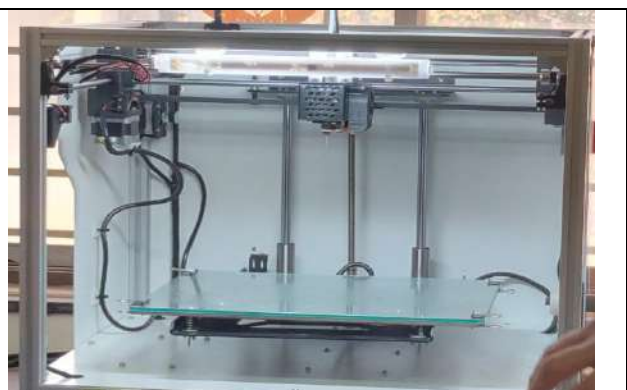


Figure 2 DAMBoy ET-200 FDM 3D Printer

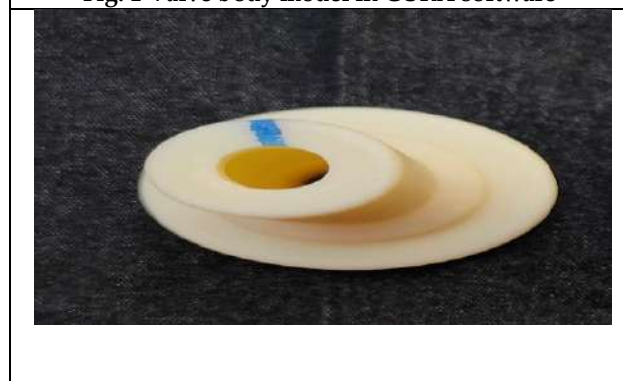


Figure 3 Valve body part



Fig.4 Mitutoyo SJ-210 surface roughness tester





Khushbu Patel et al.,

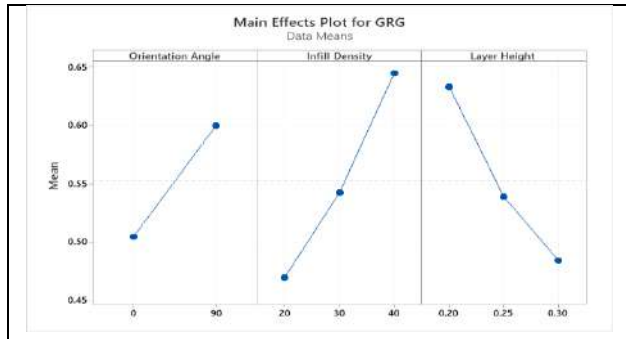


Fig.5 Main effect graph for GRG for ABS material.

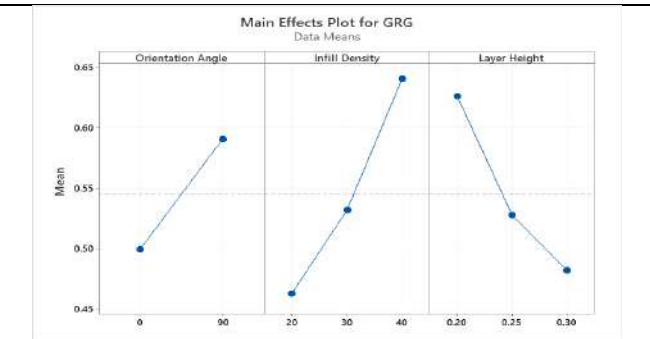


Fig. 6 Main effect graph for GRG for PLA material.





Automatic Image Tagging and Retrieval of Images based on Visual Features

Pritesh Pandey^{1*}, Keyur N Brahmhatt², Kaushika D. Patel³ and Narendra M Patel⁴

¹Ph.D, Research Scholar, Gujarat Technological University, Ahmedabad, India.

²Associate Professor, Information Technology Department, Birla Vishvakarma Mahavidyalaya, Vallabh Vidyanagar, Anand, Gujarat, India.

³Assistant Professor, Electronics Department, Birla Vishvakarma Mahavidyalaya, Vallabh Vidyanagar, Anand, Gujarat, India.

⁴Professor (CAS), Computer Engineering Department, Birla Vishvakarma Mahavidyalaya, Vallabh Vidyanagar, Anand, Gujarat, India.

Received: 30 Dec 2023

Revised: 09 Jan 2024

Accepted: 12 Jan 2024

*Address for Correspondence

Pritesh Pandey

Ph.D, Research Scholar,
Gujarat Technological University,
Ahmedabad, India.

Email: pandeypritesh@gmail.com



This is an Open Access Journal / article distributed under the terms of the **Creative Commons Attribution License** (CC BY-NC-ND 3.0) which permits unrestricted use, distribution, and reproduction in any medium, provided the original work is properly cited. All rights reserved.

ABSTRACT

One crucial way for finding photographs posted by social users on such social platforms is tag-based image searching. It is difficult to make the top-ranked result for tag-based image search useful and diverse. In comparison to context- and content-based picture retrieval, it is frequently employed in social media. Refinement of social image tags consists of deleting obtrusive or pointless tags and adding pertinent ones. Images are randomly selected as the learning data while the remaining ones are used as the testing data for image tag assignment. Manual annotation has become impossible due to the internet's exponential expansion in image availability. Users cannot find desired photographs without the help of such tags. Therefore, a scalable approach that can handle such a high volume of photos is necessary, and it might be used to create an effective tag-based image result retrieval system. In this study, four distinct models are examined, and a feature extraction method based on deep convolutional neural networks is suggested to learn descriptive semantic characteristics from dataset photos. Then, to assign the proper tags to our images, we employ inverse distance weighted K-nearest Neighbors classifiers along with a number of additional multi-label classification techniques. We use the MSCOCO dataset's numerous image categories to show how well our system works.

Keywords: Content based image retrieval, Multi-Modal data embeddings and search, Automatic Image Annotation, Image tagging, tag-based image retrieval, tag refinement.





INTRODUCTION

In the current duration, the numerous of things being searched in the images form has grown tremendously in the modern world of widespread internet usage and the emergence of the e-commerce era. Business to Consumer (B2C) e-commerce sales surpassed \$1 trillion for the first time in 2012 [1]. By 2020, it is projected to reach \$2.5 trillion and continue to expand consistently at a rate of about 20% [2]. It has become manually impossible and economically unfeasible for person to tag these products due to the exponential development in the quantity of products being sold on internet and the virtual variability in the categories these products could be assigned to. In addition, not every user will tag the same pictures with the the same tags. As a result, the types of tags given to the products differ. Search engines largely rely on the tags assigned to each image in order to find products based on consumer queries, however most of the time, only image of the products is provided, making it difficult for the any search engine to understand the results. In addition, the inconsistent categorization causes many helpful search results to be skipped. An automated tagging system can assist in resolving both of these problems and will be capable of producing a useful product database querying system, even if the database simply includes visual information about the goods. Such automated methods will result in homogeneous tagging, wherein identical products are given the same tags. Additionally, the time-consuming practice of manually labelling such products will no longer be required. The online storefront is a genuinely multimodal environment where visual elements coexist with product descriptions and feature descriptions. Such a marketplace must enable the user to search for products based on both their visual characteristics and their descriptions if it is to be genuinely effective. We propose an approach to create visual feature based image retrieval system. This is accomplished with comparison of VGG16, ResNet50, InceptionV3, Efficient Net algorithm with the MSCOCO Database In this effort, our main focus is on improving picture tags, adding to relevant tags, removing irrelevant tags, and labeling new images.

Traditionally, image annotation has been viewed as a machine learning task that always relies on a modest amount of manually labeled data. However, the weakly-supervised data prevents them from handling large-scale social photos. Tag refinement, which differs from typical image annotation, involves removing unrelated tags from an image's initial set of tags. Smart phones and other image-capture software are becoming more and more prevalent as a result of the development of mobility and communication technologies. Our daily lives have been impacted by social media. People are growing more and more interested in sharing their daily experiences and emotions with others online. One respectable photo-sharing service, MSCOCO, has more than 10 billion images of individuals in a variety of settings. A photograph contains a wealth of knowledge about a user's preference, insight, and sentiment. Numerous industries, including campaign prediction, stock price forecasting, and ad recommendation, may make extensive use of this information. People are growing more and more interested in sharing their daily experiences and emotions with others online. One respectable photo-sharing service, MSCOCO, has more than 10 billion images of individuals in a variety of settings. A photograph contains a wealth of knowledge about a user's preference, insight, and sentiment. Numerous industries, including campaign prediction, stock price forecasting, and ad recommendation, may make extensive use of this information.

LITERATURE REVIEW

A difficult job is picture annotation, or the prediction of many tags for an image. The majority of modern algorithms are built using extensive libraries of custom features. In the categorization of images, deep convolutional neural networks recently beat humans, and these networks may be used to extract characteristics that are highly predictive of an image's tags. In this article, we evaluate the effectiveness of nearest neighbor-based techniques to tag prediction in order to analyses semantic information in features produced from two pre-trained deep network classifiers. When utilizing the deep learning algorithms, we often outperform the manual features.





Pritesh Pandey et al.,

VGG16 and VGG19

The VGG model is consist of 16-layer convolutional neural network model, or we can know that as VGGNet, is often referred to as VGG16. And with additional 3 layer it become VGG19. In Image Net, the VGG16 model has a top-5 test accuracy of about 92.65%. This is a frequently used Image Net dataset that contains over 14.2 million images that are separated into around 1050 categories. It also performed well compared to other models that were submitted to ILSVRC-2014. It performs noticeably better than Alex Net by substituting several 3x3 kernel-sized filters for the huge kernel-sized filters. The VGG16 model was trained on Nvidia Titan Black GPUs, and it took around a few weeks.. The 16-layer VGGNet-16, which can categorize images into 1,000 distinct item categories—including keyboard, animals, pencil, mouse, etc.—can categorize images. as discussed above. The model's picture input size is 224x224 as well.

Inception V3

In terms of the quantity of parameters generated by the network and the economic cost (memory and other resources), VGG Net has been shown to be less computationally efficient than Google Net/Inception v1. The computational advantages of an Inception Network must be preserved while changing it. It becomes challenging to adapt the Startup network for various use cases since the new network's efficacy is unclear. Numerous network optimization techniques have been suggested for the Inception v3 model to address issues and facilitate model modification. Regularization, dimensionality reduction, factorial convolution, and parallel computing are a few techniques. InceptionV3 architecture model is basically develop with this step Factorized Convolutions, Smaller convolutions, Asymmetric convolutions, Auxiliary classifier, Grid size reduction

Xception

"Extreme Inception" stands for "Architecture Xception." In the Xception architecture which is composed with 36 convolutional layers that is having ability of feature extraction base of the network. The input stream, intermediate stream (which is repeated eight times), and output stream are the sequential phases that the data passes through. Although it is not depicted in the presented figure, batch normalization is included in each convolutional and separable convolutional layer. Additionally, without any depth extension, all separable convolutional layers employ a depth multiplier of one.

Dataset

MS COCO Dataset Microsoft COCO Dataset [8] can be an exceptionally huge dataset of image recognition, captioning, and segmentation. The MS COCO dataset has various options such as object segmentation, validation of context, this dataset is containing approximately 300K pictures in excess of approx. 2 million occurrences, and additionally, 80 article classifications

Flickr30K Flickr30K [9] is a dataset for programmed image explanation and ground language consideration, the Flickr30k dataset can be used. it contains 30K images gathered from Flickr with 158,000 tags assigned by human annotators. It doesn't present any mounted partitioning of pictures for training. examining and verification. the number for training, testing, and verification are chosen by the scholars themselves.

Flickr8K Flickr8k [10] can be a well-liked dataset and can contain 8k photos gathered from Flickr. The coaching knowledge contains 6k drawing, checks, and advancement knowledge, each consisting of 1k pictures. Each of the images with the dataset has five suggestion captions annotate by humans.

Visual Genome The visual order dataset [11] is an additional dataset for image tagging. Image captioning does not need to identify only the items of a photograph, although it additionally argues their communications and characteristics. Not like the primary 3 datasets where the caption is given for the total view, a sequence in the scene sequence dataset has different captions for several regions.





Pritesh Pandey et al.,

Instagram Dataset Two dataset victim images from Instagram which can be a photo-sharing social networking service were created. The dataset creates by Tran et al [12]. which consists 10k pictures is mainly from celebrities. However, the social media network used its dataset for hash tag forecast and post-procreation tasks.

Proposed System

In my research, I focus on the ResNet50 architecture, a deep CNN model known for its depth and efficiency. We leverage the extensive MSCOCO dataset, which contains a wide range of images annotated with multiple tags, to train and evaluate our image tagging model.

Dataset

The MSCOCO dataset is a widely used resource for object detection, image segmentation, and image captioning tasks. It consists of over 1.5 million images, each annotated with textual descriptions and tags. We use the tags associated with each image as ground truth labels for our image tagging task.

Model Architecture

ResNet50 is a 50-layer deep convolutional neural network known for its residual connections, which help mitigate the vanishing gradient problem during training. We use a pre-trained ResNet50 model and fine-tune it for our image tagging task. The architecture includes five residual blocks, each containing multiple convolutional layers.

1. **Convolutional Layers** The network's first layer, which conducts convolution on the input image, is a convolutional layer. The output of the convolutional layer is then down sampled by a max-pooling layer. After that, a succession of residual blocks are applied to the output of the max-pooling layer.
2. **Residual Blocks** Two convolutional layers, a batch normalisation layer, and a rectified linear unit (ReLU) activation function make up each residual block. The residual block's input is then combined with the output of the second convolutional layer before being sent through one more ReLU activation function. The subsequent block receives the output of the residual block.
3. **Fully Connected Layer** The output of the last residual block is mapped to the output classes in the network's final, completely linked layer. The number of output classes is the same as the number of neurons in the fully linked layer.

Residual Block / Identity Block

The proposed approach involves enabling the network to fit the residual mapping, as opposed to relying on the layers to learn the underlying mapping. This is achieved by allowing the network to fit $F(x) = H(x) - x$, where $H(x)$ represents the initial mapping that is replaced by $F(x) + x$. Essentially, this involves bypassing data along with the regular CNN flow from one layer to the next, after the immediately next layer. To facilitate this, a shortcut or skip connection is established, which enables information to flow more seamlessly from one layer to the next.

Observations from the residual block

1. Regularization would simply pass over them if they weren't useful, thus the model's performance wouldn't be negatively impacted by the addition of extra or new layers.
2. The weights or kernels of the layers will be non-zero if the extra or new layers were beneficial, even in the presence of regularization, and model performance may somewhat improve.

Therefore, it is assured that the performance of the model does not degrade when new layers are added due of the "Skip connection" / "residual connection," albeit it may somewhat improve. These Res Net building bricks may be stacked on top of one another to create an extremely deep network. It is quite simple for one of the Res Net blocks to learn an identity function when there are Res Net blocks with the shortcut. This indicates that adding more Res Net





Pritesh Pandey et al.,

blocks may be done with little concern for the performance of the training set. Whether the input/output dimensions are the same or different determines which of the two primary types of blocks is utilized in a Res Net. The

Identifying Block

Identical to the one we previously saw. Res Nets is having default block which is The identity block, it will communicated with input activation and output activation which is having the same dimension.

The Convolutional Block

In some of the case we found Input and Output dimensions are differ with each other. In that stituation we have to use this type of block, and its shoirtcut parth differes from the Identity Block in CONV2D layer. Figure 7 depicts yet another ResNet diagram. Identity Mappings in ResNet is a modified dropout technique that uses stochastic depth for training deep networks. In training, however, the entire layer is dropped at random rather than a few nodes. The depth of the network may be considerably less during training. As a consequence, training throughput is improved and fewer computations are required. In my study, such potential approaches will also be tested and examined. By utilizing several techniques, we can build a subtitle that is roughly equal to human-produced inscriptions. Additionally, we make an effort to tag every image that might be used as input for the algorithm, and after comparing the results with those of the existing method, we can determine which algorithm is more effective at tagging photographs. Comparing ResNet50 with VGG16, VGG19, and Inception involves assessing their performance and parameter efficiency. Each of these architectures has its strengths and weaknesses, making them suitable for different computer vision tasks. Below, we provide a brief comparison, highlighting why ResNet50 often stands out as a better choice in terms of parameters:

ResNet50

Parameter Efficiency

ResNet50 is known for its parameter efficiency compared to VGG16, VGG19, and Inception. It achieves a remarkable balance between depth and efficiency by introducing residual connections. These connections enable training of very deep networks without suffering from vanishing gradient problems, reducing the need for excessive parameters.

Performance ResNet50 has demonstrated superior performance in various image-related tasks, including image classification, object detection, and image tagging. It often achieves state-of-the-art results on benchmark datasets due to its ability to capture intricate features.

Depth Despite its efficiency, ResNet50 has a depth of 50 layers, making it considerably deeper than VGG16 and VGG19. This additional depth allows it to learn more complex and abstract representations.

VGG16 and VGG19

Parameter Overhead VGG16 and VGG19 are known for their simplicity and uniform architecture with a large number of layers. However, this results in a significantly higher number of parameters compared to ResNet50. The excessive parameters can lead to longer training times and require larger datasets.

Performance While VGG16 and VGG19 perform well on many image classification tasks, they may suffer from over fitting when dealing with smaller datasets. They are less adept at capturing fine-grained details compared to deeper architectures like ResNet50.

InceptionV3

Parameter Efficiency

Inception modules, particularly InceptionV3 and later versions, are designed for parameter efficiency. They use a combination of 1x1, 3x3, and 5x5 convolutions to capture multi-scale features while keeping the number of parameters relatively low.





Pritesh Pandey et al.,

Performance

Inception architectures perform admirably on a range of tasks and are especially efficient when computational resources are limited. They strike a good balance between parameter efficiency and accuracy.

Multi-Scale Feature Extraction Inception models excel at capturing multi-scale features, which is useful for various Computer vision tasks. They are known for their ability to detect objects of different sizes within images. In summary, ResNet50 tends to outperform VGG16, VGG19, and Inception in terms of parameter efficiency while maintaining competitive or superior performance on various computer vision tasks. Its innovative use of residual connections allows it to handle deep networks without an excessive number of parameters. However, the choice of architecture depends on the specific task, dataset size, and available computational resources, and each of these architectures has its unique strengths in different contexts.

CONCLUSION

In this study, using the widely used Microsoft Common Objects in Context (MSCOCO) dataset, we investigated the use of the ResNet50 convolutional neural network architecture for the task of picture tagging. The process of preparing the data, training the model, and evaluating its performance revealed important information on ResNet50's efficiency in the context of picture tagging. Our findings show that ResNet50 is a reliable option for picture labelling because to its deep design and residual connections. The excellent precision and recall values attained demonstrate the system's amazing ability to forecast relevant tags. The F1-score, which provides a fair evaluation of accuracy and recall, emphasizes the model's general efficacy even more. The top-k accuracy statistic further emphasizes its capacity to produce insightful tag suggestions, coinciding with real-world applications where users frequently seek the most pertinent tags rapidly. While our ResNet50-based approach showcased impressive results, there remains room for further investigation. Future research could delve into the exploration of additional architectures, advanced data augmentation techniques, and more extensive datasets, aiming to push the boundaries of image tagging capabilities and cater to the evolving demands of the digital landscape. In conclusion, this study marks a significant stride towards advancing the state-of-the-art in image tagging, offering a reliable and adaptable solution to an ever-expanding world of visual content.

REFERENCES

1. Tsung-Yi Lin, Michael Maire, Serge Belongie, James Hays, Pietro Perona, Deva Ramanan, Piotr Dollár, and C Lawrence Zitnick. 2014. Microsoft coco: Common objects in context. In European conference on computer vision. Springer, 740–755.
2. Kenneth Tran, Xiaodong He, Lei Zhang, Jian Sun, Cornelia Carapcea, Chris Thrasher, Chris Buehler, and Chris Sienkiewicz. 2016. Rich image captioning in the wild. In Proceedings of the IEEE Conference on Computer Vision and Pattern Recognition Workshops
3. Vinyals, O., Toshev, A., Bengio, S., Erhan, D.: Show and tell: a neural image caption generator. In: 2015 Computer Vision and Pattern Recognition, IEEE, Boston, (2015)
4. K. Simonyan and A. Zisserman. 2014. Very deep convolutional networks for
5. large-scale image recognition. CoRR, abs/1409.1556.
6. M. Oquab, L. Bottou, I. Laptev, and J. Sivic. 2014. Learning and transferring mid-level image representations using convolutional neural networks. Proceedings of the 2014 IEEE Conference on Computer Vision and Pattern Recognition, pages 1717–1724.
7. R. Tadse, L. Patil, and C. Chauhan. 2014. Review on content based image retrieval for digital library using text document image. International Journal of Computer Science and Mobile Computing, 4:211–214.
8. Channarukul, S., Mcroy, S.W., Ali, S.S.: DOGHED: a template based generator for multimodal dialog systems targeting heterogeneous devices. In: Conference of the North American Chapter of the Association for Computational Linguistics on Human Language Technology (2003)





Pritesh Pandey et al.,

9. Bryan A Plummer, Liwei Wang, Chris M Cervantes, Juan C Caicedo, Julia Hockenmaier, and Svetlana Lazebnik. 2015. Flickr30k entities: Collecting region-to-phrase correspondences for richer image-to-sentence models. In Proceedings of the IEEE international conference on computer vision. 2641–2649.
10. Micah Hodosh, Peter Young, and Julia Hock enmaier. 2013. Framing image description as a ranking task: Data, models and evaluation metrics. Journal of Artificial Intelligence Research 47 (2013), 853–899.
11. Ranjay Krishna, Yuke Zhu, Oliver Groth, Justin Johnson, Kenji Hata, Joshua Kravitz, Stephanie Chen, Yannis Kalantidis, Li-Jia Li, David A Shamma, et al. 2017. Visual genome: Connecting language and vision using crowd sourced dense image annotations. International Journal of Computer Vision 123, 1 (2017)

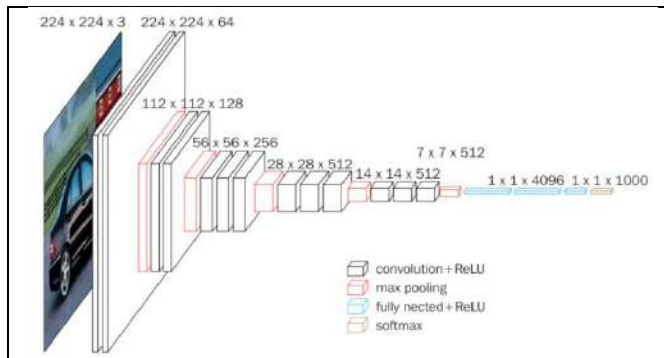


Figure 1: VGG16 layer structure diagram

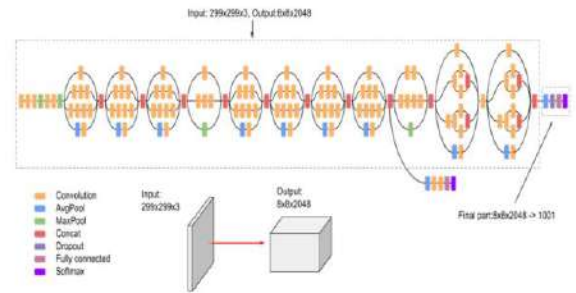


Figure 2: InceptionV3 Architecture

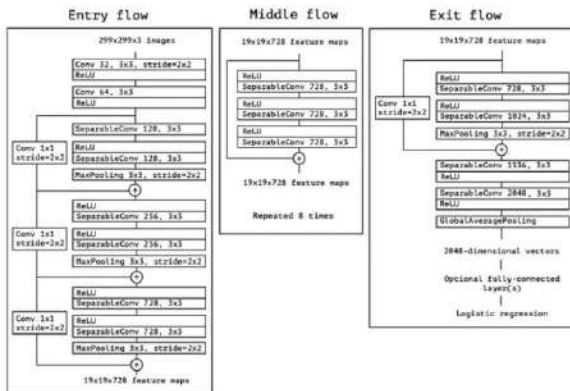


Figure 3: Xception Architecture

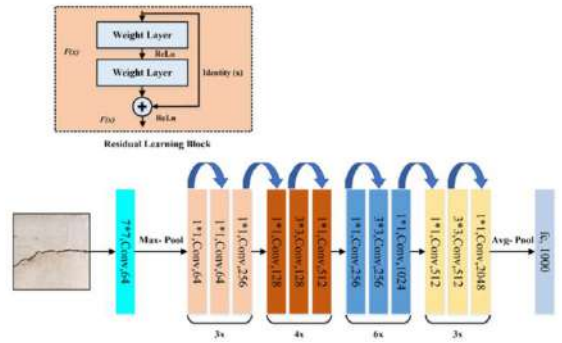


Figure 4: ResNet50 Architecture

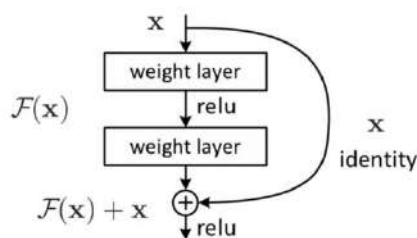


Figure-5 Residual learning: a building block

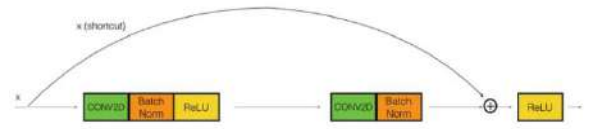


Figure 6: Identity Block





Pritesh Pandey et al.,

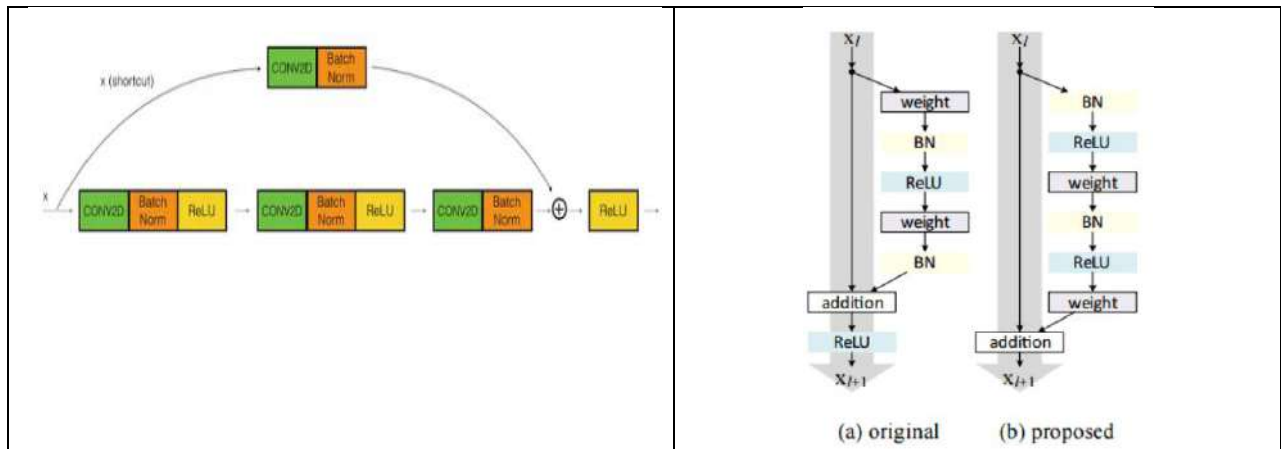


Figure 7: Convolutional Block

Figure 7: Identity Block Mapping in ResNet50.

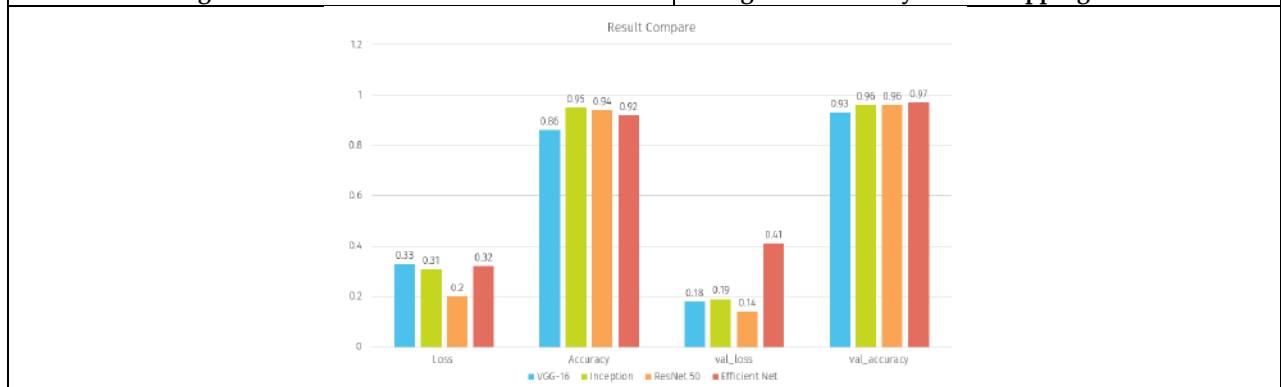


Figure 8: Result comparison of Resnet50, VGG16, VGG19 and InceptionV3





Factors Impacting the Adoption of Internet Banking Services using Technology Acceptance Model with Reference to Women Customers

MS. Nilamben Johnbhai Parmar^{1*} and Suresh P. Machhar²

¹Research Scholar , P. G. Department of Business Studies, Sardar Patel University, V. V. Nagar, Gujarat, India.

²Associate Professor, P. G. Department of Business Studies, Sardar Patel University, V. V. Nagar, Gujarat, India.

Received: 30 Dec 2023

Revised: 09 Jan 2024

Accepted: 12 Jan 2024

*Address for Correspondence

MS. Nilamben Johnbhai Parmar

Research Scholar ,

P. G. Department of Business Studies,

Sardar Patel University,

V. V. Nagar, Gujarat, India.

Email: nilam199529@gmail.com



This is an Open Access Journal / article distributed under the terms of the **Creative Commons Attribution License** (CC BY-NC-ND 3.0) which permits unrestricted use, distribution, and reproduction in any medium, provided the original work is properly cited. All rights reserved.

ABSTRACT

The purpose of this study was to find out factors impacting the adoption of Internet banking services using the Technology Acceptance Model (TAM) with reference to Women Customers. The present study is based on primary data, collected data from women users of Internet banking services in Gujarat, India. 167 women participated in this study, and respondents were chosen using non-probability convenience sampling. Frequency distribution, reliability, validity, and structural equation modelling were carried out. The result found that ease of use, usefulness, and trust have a positive significant relation with the attitude towards the use of Internet banking services. Usefulness, trust, and attitude towards use have a positive significant relation with the intention to use Internet banking services, whereas ease of use has an insignificant relation. The results are expected to have a significant role in the adoption of Internet banking services, particularly among women users and banking sectors.

Keywords: Internet baking services factors (Technology Acceptance Model) TAM Women.

INTRODUCTION

In the current era, the development of new technology in the banking sector is increasing. Internet banking services are one of the financial services performed through online ways, and nowadays it's most popular. According to (Akhteret al., 2022) "Internet banking has been financial services where bank users can perform numerous online banking activities using the internet". (Rathore, 2022) stated that in India 32% of households use online/Internet banking



**MS. Nilamben Johnbhai Parmar and Suresh P. Machhar**

services in their everyday life. In India after the initiatives by the government as Pradhan Mantri Jan Dhan Yojana many Indian women adopted Internet banking Services in their daily lives. Indian banks of India provide three types of Internet National Electronic Fund Transfer (NEFT), Real-Time Gross Settlement (RTGS), and Immediate Payment Service (IMPS). NEFT: NEFT was introduced by the Reserve Bank of India. In NEFT minimum transfer limit is 1 Rs. and the maximum no limit available. This service is available 365 days 24*7, and in half an hour, the settlement is done but the IFSC code, and bank account number must be needed for the transfer. This service is free for the users. This service is available Online and offline (Paisabazaar.com, 2022). RTGS: RTGS was introduced by the Reserve Bank of India. In RTGS minimum transfer limit is 2 lakh Rs. and the maximum no limit available. This service is available 365 days 24*7, and in real-time settlement, the settlement is done but the IFSC code, and bank account number must be needed for the transfer. This service is free for the inward, but the user's pay charges as Rs. 2 lakhs to 5 Lakhs 25 Rs. Charge, above Rs. 5 lakhs 50 Rs. Charge with that GST is also applicable. This service is available Online and offline (Paisabazaar.com, 2022). IMPS: IMPS was introduced by the National Payments Corporation of India. In IMPS minimum transfer limit is 1 Rs. and the maximum Rs. 2 Lakh is available. This service is available 365 days 24*7, and in real-time settlement, the settlement is done but the IFSC code, and bank account number must be needed for the transfer. Charges decided by the individual member banks with taxes are included. This service is available only on Online (Paisabazaar.com, 2022). In the following part literature review, the research methodology, data analysis and interpretation, practical implication, and conclusion.

LITERATURE REVIEW**Technology Acceptance Model (TAM)****Original TAM Model**

In the year 1989, Fred D. Davis established TAM. According to (Davis, 1989) this model is specifically based on two variables such as perceived usefulness and perceived ease of use, to check the adoption of new technology. This study (Davis, 1989) found that both variables are more important for the adoption of new technology.

Adapted Model

In this study, researchers adopted the TAM, for the find out factors impacting the adoption of Internet banking services with added another variable trust. Because nowadays the development of new technology in banking sectors consumers need more trust in a particular technology. Based on that the present study research used ease of use, usefulness, and trust as independent variables, attitude towards use as a mediating variable and intention to use as a dependent variable. In this study, researchers also checked with mediating effect and without mediating effect on the adoption of Internet banking services. Note: Own Compilation

HYPOTHESES DEVELOPMENT AND THEORETICAL FRAMEWORK**Ease of Use**

According to (Davis, 1989) ease of use means "a person believes that using Internet banking services would be free of effort". Many studies found that ease of use has a significant impact on attitudes towards the use of Internet banking services (Cheng et al., 2006; Lee, 2009; Nasri & Charfeddine, 2012). Many studies found that ease of use has a significant impact on the intention to use Internet banking services (Mohamad Amin et al., 2017;Rawashdeh, 2015).

H1: Ease of Use has a positive impact on Attitude towards the use of Internet banking services.

H2: Ease of Use has a positive impact on Intention to use Internet banking services.

Usefulness

According to (Davis, 1989) usefulness means "the degree to which a person believes that using Internet banking services would enhance his or her performance". Many studies found that usefulness has a significant impact on attitudes towards the use of Internet banking services (Lee, 2009;Nasri & Charfeddine, 2012;Rawashdeh, 2015). Many studies found that usefulness has a significant impact on the intention to use Internet banking services (Cheng et al., 2006; Lee, 2009; Mohamad Amin et al., 2017;Mohamed Asmy et al., 2019;Nasri & Charfeddine, 2012;Rawashdeh, 2015).

H3: Usefulness has a positive impact on Attitude towards the use of Internet banking services.



**MS. Nilamben Johnbhai Parmar and Suresh P. Machhar**

H₄: Usefulness has a positive impact on Intention to use Internet banking services.

Trust

(Mayer et al., 1995) defined trust means “the willingness to be vulnerable to the actions of other parties on the belief that others would carry out the intended action, with or without the ability to monitor or control the situation”. Many studies found that trust has a significant impact on the intention to use Internet banking services (Agyei et al., 2021; Jalil et al., 2014).

H₅: Trust has a positive impact on Attitude towards the use of Internet banking services.

H₆: Trust has a positive impact on Intention to use Internet banking services.

Attitude Towards Use

(Fishbein & Ajzen, 1975) defined attitude towards use means “an individual’s positive or negative feelings about using Internet banking services”. Many studies found that attitude towards use has a significant impact on the intention to use Internet banking services (Lee, 2009; Nasri & Charfeddine, 2012).

H₇: Attitude towards use has a positive impact on Intention to use Internet banking services.

RESEARCH METHODOLOGY**Objective**

To study the factors impacting the adoption of Internet banking services using the Technology Acceptance Model (TAM) with reference to Women Customers.

Research Design Descriptive Cross-sectional Research Design

Sampling Method Non-probability Convenience Sampling.

Sample size 167 Women users of Internet banking services of Gujarat State, India.

Data Collection**Primary Data**

Primary data was collected from Gujarat state, India, with the use of Google Forms, distributed through email, and social media. A total of 180 women respondents filled up the questionnaire, out of which 13 responses were excluded because they were not using Internet banking services, and 167 were finally used in the data analysis.

Questionnaire Construction

The questionnaire should be close-ended. The questionnaire was distributed from June 2023 to August 2023. The questionnaire has two parts. Part, one includes demographic information such as name, born year, residential location, marital status, education, occupation, annual income, and name of Internet banking services. In the second part, a total of 27 statements were included using five Likert scale method (Strongly Agree to Strongly Disagree), satisfaction level of the adoption of Internet banking services. Statements should be adapted from the various TAM-based research.

The Technique of Data Analysis

Frequency distribution, Reliability (Cronbach Alpha and Composite reliability), Validity (Average Variance Extracted), SEM. SPSS 25 Software and AMOS 18 Software were used for the analysis purpose.

DATA ANALYSIS

Table 1 shows that the majority of the women respondents belong to 1991-2000 born year and are located in urban areas. 50.9% of women respondents are married and 48.5% are unmarried. The majority of the women respondents have completed post-graduation, are doing private jobs, and earn between 2 lakhs to 5 lakhs. Women respondents used internet banking services such as 45.5% = IMPS, 44.3% = NEFT, and 10.2% = RTGS. The majority of women are satisfied with the use of internet banking services (65.3%), 45.5% = highly satisfied, and 9.6% = moderately satisfied.

Table 2 based on reliability and convergent validity, according to (Hair et al., 2010) said that the value of Cronbach alpha = 0.961 (> 0.70), Composite reliability = 0.964 (> 0.70), and average variance extracted = 0.500 (> 0.5) are fulfilled all criteria which means all statements of this study have adequate reliability and validity.



**MS. Nilamben Johnbhai Parmar and Suresh P. Machhar****Model Measurement**

Table 3 related to model measurement, (Fornell & Larcker, 1981) said that the values of FL > 0.5, CA > 0.6, CR > 0.6 and AVE > 0.5, in this study except for attitude towards to use of AVE all other values are appropriate.

Table 4 is the result of the hypotheses testing of the study. Hypotheses H₁, H₃, H₄, H₅, H₆, and H₇ are accepted the p value is < 0.05, only H₂ is rejected. This means ease of use, usefulness, and trust have a positive significant relation with the attitude towards to use of Internet banking services. Usefulness, trust, and attitude towards use have a positive significant relation with the intention to use Internet banking services, whereas ease of use has an insignificant relation.

Table 5 indicates the structural equation model (SEM). The SEM result shows that Chi-Square = 561.951, df = 300, GFI = 0.809, with p-value = 0.000 (< 0.05), TLI = 0.912 (>0.9), CFI = 0.924 (>0.9), RMSEA = 0.071 (<0.08), and SRMR = 0.052 (<0.08). This means SEM is compatible with this study.

PRACTICAL IMPLICATIONS

Banks should concentrate on making their Internet banking services easy to use as well as useful. More women users may be drawn in by functional features and user-friendly interfaces. Trust must be established and maintained. Banks must make significant security investments and inform users about the security of online transactions. Banks could advertise IMPS and NEFT services through targeted marketing initiatives because women consumers frequently use these services. Develop financial literacy programmes, especially for women, to give them more confidence while using Internet banking services. To inform women customers about the many features and advantages of Internet banking services, banks may arrange workshops and online courses. Banks must offer women customers specialized customer service that immediately addresses any issues and concerns they may have. User confidence may rise as a result of this individualized support. Sharing the success stories of satisfied female users can increase credibility and trust, influencing more women to use Internet banking services. The importance of Internet banking for women's financial freedom should be emphasized. Women's economic independence and decision-making capacity may increase when they have easy access to banking services.

CONCLUSION

In the present study, researchers aimed at the factors impacting the adoption of Internet banking services using the TAM with reference to women customers of Internet banking Services. Through this research, researchers found that the majority of the women users used IMPS and NEFT services. Researchers done SEM and found that ease of use, usefulness, and trust have a positive significant relation with the attitude towards the use of Internet banking services. Usefulness, trust, and attitude towards use have a positive significant relation with the intention to use Internet banking services, whereas ease of use has an insignificant relation. Lastly, researchers also measured the satisfaction level and found that the majority of the women were satisfied the Internet banking services.

REFERENCES

1. Agyei, J., Sun, S., Penney, E. K., Abrokwah, E., Boadi, E. K., & Fiifi, D. D., Internet Banking Services User Adoption in Ghana: An Empirical Study. *Journal of African Business*, 1-18. doi:10.1080/15228916.2021.1904756, 2021.
2. Akhter, A., Karim, M., Jannat, S., & Islam, K., Determining Factors of Intention to Adopt Internet Banking Services: A Study on Commercial Bank Users in Bangladesh. *Banks and Bank Systems*, 17(1), 125-136. doi:10.21511/bbs.17(1).2022.11, 2022.
3. Bentler, P. M., & Bonett, D. G., Significance tests and goodness of fit in the analysis of covariance. *Psychological Bulletin*, 88, 588–606, 1980.





MS. Nilamben Johnbhai Parmar and Suresh P. Machhar

4. Byrne, B. M., Structural Equation Modeling with LISREL, PRELIS and SIMPLIS: Basic Concepts. *Applications and Programming*, 1998.
5. Cheng, T. E., Lam, D. Y., & Yeung, A. C., Adoption of Internet Banking: an empirical study in Hong Kong. *Decision Support Systems*, 42(3), 1558-1572, 2006.
6. Davis, F. D., Perceived usefulness, perceived ease of use, and user acceptance of information technology. *Management Information Systems Quarterly*, 13(3), 319-340. doi:10.2307/249008, 1989.
7. Fishbein, M., & Ajzen, I., Belief, attitude, intention, and behavior: an introduction to theory and research. *Philosophy and Rhetoric*, 10(2), 1975.
8. Fornell, C., & Larcker, D. F., Evaluating structural equation models with unobservable variables and measurement error. *Journal of Marketing Research*, 18(3), 382-388, 1981.
9. Hair, J. J., Black, W. C., Babin, B. J., Anderson, R. E., & Tatham, R. L., *Multivariate Data Analysis*, 2010.
10. Hooper, D., Coughlan, J., & Mullen, M., Evaluating the model fits a synthesis of the structural equation modelling literature. In *7th European Conference on research methodology for business and management studies, 2008*, 195-200, 2008.
11. Hu, L.-t., & Bentler, P. M., Cutoff Criteria for Fit Indexes in Covariance Structure Analysis: Conventional Criteria Versus New Alternatives. *Structural Equation Modeling: A Multidisciplinary Journal*, 6(1), 1-55. doi:10.1080/10705519909540118, 1999.
12. Jalil, M., Talukder, M., & Rahman, M., Factors Affecting Customer's Perceptions Towards Online Banking Transactions in Malaysia. *Journal of Business and Management*, 20(1), 25-44, 2014.
13. Lee, M.-C., Factors influencing the adoption of Internet banking: An integration of TAM and TPB with perceived risk and perceived benefit. *Electronic Commerce Research and Applications*, 8, 130-141, 2009.
14. Mayer, R. C., Davis, J. H., & Schoorman, F. D., An integrative model of organizational trust. *Academy of Management Review*, 20(3), 709-734, doi:10.2307/258792, 1995.
15. Mohamad Amin, M., Said, M., Chong, C., & Raja Yusof, R., Factors That Influence Utilization of Internet Payment System In Malaysia From The Individual Users' Perspective. *International Journal of Economics and Management*, 813-829, 2017.
16. Mohamed Asmy, B. T., Anwar, B. P., Hassanudin, B. T., & Md Fouad, B. A., Factors influencing consumers' adoption of Islamic mobile banking services in Malaysia: An approach of partial least squares(PLS). *Journal of Islamic Marketing*, 10(4), 1037-1056. doi:10.1108/IJIMA-04-2018-0065, 2019.
17. Nasri, W., & Charfeddine, L., Factors affecting the adoption of Internet banking in Tunisia: An integration theory of acceptance model and theory of planned behaviour. *Journal of High Technology Management Research*, 23, 1-14, 2012.
18. Paisabazaar.com., *What's the Difference Between NEFT, RTGS and IMPS?* Retrieved October 13, 2022, from Paisabazzar: <https://www.paisabazaar.com/banking/difference-between-neft-rtgs-imps/>, 202, July 21.
19. Rathore, M., *Status of Online Banking in India*. Retrieved October 13, 2022, from <https://www.statista.com/statistics/1249581/india-status-of-online-banking-adoption/#:~:text=Status%20of%20online%20banking%20in%20India%202020&text=According%20to%20a%20survey%20conducted,payments%20in%20their%20everyday%20life,2022,September.>
20. Rawashdeh, A., Factors affecting adoption of Internet banking in Jordan: Chartered accountant's perspective. *International Journal of Bank Marketing*, 33(4), 510-529. doi:10.1108/IJBM-03-2014-0043, 2015.
21. Steiger, J. H., Structural model evaluation and modification: An interval estimation approach. *Multivariate Behavioral Research*, 25, 173-180, 1990.

Table 1: Demographic Information

Demographic Factor	Category	Frequency(N=167)	Percentage
Born Year	1971-1980	7	4.2
	1981-1990	39	23.4
	1991-2000	104	62.3
	2001-2010	17	10.2





MS. Nilamben Johnbhai Parmar and Suresh P. Machhar

Location	Rural	60	35.9
	Urban	107	64.1
Marital Status	Unmarried	81	48.5
	Married	85	50.9
	Widow	1	0.6
Education	HSC	4	2.4
	Diploma	4	2.4
	Graduation	59	35.3
	Post-graduation	78	46.7
Occupation	Doctorate	22	13.2
	Student	60	35.9
	Private Job	76	45.5
	Government Job	18	10.8
	Business	7	4.2
	Researcher	3	1.8
Annual Income	Housemaker	3	1.8
	< 2,00,000	58	34.7
	2,00,000 - 5,00,000	82	49.1
	5,00,000 – 10,00,000	20	12
Name of Internet Banking Services	> 10,00,000	7	4.2
	NEFT	74	44.3
	RTGS	17	10.2
Satisfaction Level	IMPS	76	45.5
	Highly Satisfied	42	25.1
	Satisfied	109	65.3
	Moderately Satisfied	16	9.6

Note: Output of SPSS 25

Table 2: Reliability and Convergent Validity

CA	CR	AVE	N of Items
0.961	0.964	0.500	27

Note: Output of SPSS 25

Table 3: Normality, Reliability and Convergent Validity

Factors	Items	Mean	SD	FL	CA	CR	AVE
Ease of Use (M=4.315, SD = 0.888)	EOU1	4.38	0.903	0.633	0.896	0.839	0.511
	EOU2	4.32	0.858	0.720			
	EOU3	4.31	0.857	0.713			
	EOU4	4.23	0.918	0.768			
	EOU5	4.34	0.909	0.732			
Usefulness (M=4.363, SD = 0.865)	US1	4.49	0.798	0.790	0.893	0.857	0.503
	US2	4.35	0.835	0.744			
	US3	4.40	0.851	0.763			
	US4	4.39	0.842	0.742			





MS. Nilamben Johnbhai Parmar and Suresh P. Machhar

	US5	4.37	0.818	0.638			
	US6	4.18	1.014	0.546			
Trust (M=4.017, SD = 0.885)	TS1	4.13	0.900	0.770	0.914	0.907	0.619
	TS2	4.13	0.808	0.716			
	TS3	4.04	0.864	0.828			
	TS4	3.93	0.868	0.844			
	TS5	3.87	0.973	0.805			
	TS6	4.02	0.874	0.748			
Attitude towards use (M=4.288, SD = 0.841)	ATU1	4.38	0.782	0.625	0.929	0.762	0.349
	ATU2	4.20	0.838	0.540			
	ATU3	4.29	0.859	0.626			
	ATU4	4.30	0.840	0.622			
	ATU5	4.28	0.870	0.499			
	ATU6	4.28	0.855	0.621			
Intention to use (M=4.241, SD = 0.848)	ITU1	4.32	0.786	0.742	0.907	0.820	0.533
	ITU2	4.25	0.839	0.693			
	ITU3	4.17	0.876	0.732			
	ITU4	4.23	0.890	0.753			

Note: Output of SPSS 25

Table 4: Hypotheses Testing

Hyp.		Estimate	SE	P	Result
H ₁	EOU → ATU	.552	.102	.000	Significant
H ₂	EOU → ITU	.009	.111	.939	Insignificant
H ₃	US → ATU	.275	.085	.001	Significant
H ₄	US → ITU	.173	.088	.048	Significant
H ₅	TS → ATU	.102	.048	.031	Significant
H ₆	TS → ITU	.111	.049	.024	Significant
H ₇	ATU → ITU	.614	.124	.000	Significant

Note: Output of Amos 18

Table 5: SEM Result

Fit Statistic	Support	References	Result
Chi-square			561.951
DF			300
GFI			0.809
p-value	<0.05 acceptable fit	(Bentler & Bonett, 1980)(Hu & Bentler, 1999)	0.000
TLI	>=0.90 acceptable fit	(Bentler & Bonett, 1980)(Hu & Bentler, 1999)	0.916
CFI	>=0.90 acceptable fit	(Bentler & Bonett, 1980)(Hu & Bentler, 1999)	0.928
RMSEA	<=0.05 to <=0.08=Fair fit	(Steiger, 1990)(Byrne, 1998)(Hooper, Coughlan, & Mullen, 2008)	0.073
SRMR	<0.05=Excellent fit	(Hu & Bentler, 1999)(Hooper, Coughlan, & Mullen, 2008)	0.048





MS. Nilamben Johnbhai Parmar and Suresh P. Machhar

Note: Output of Amos 18

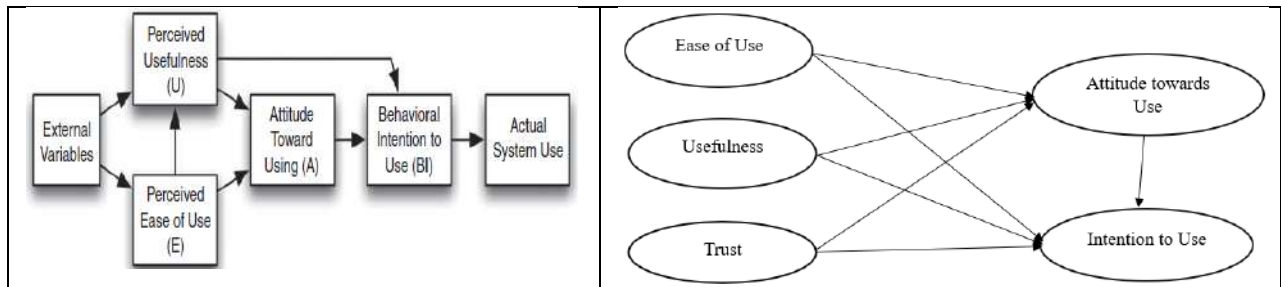


Figure 1: Original TAM Model Note: (Davis 1989)

Figure 2: Adapted Model Note: Own Compilation

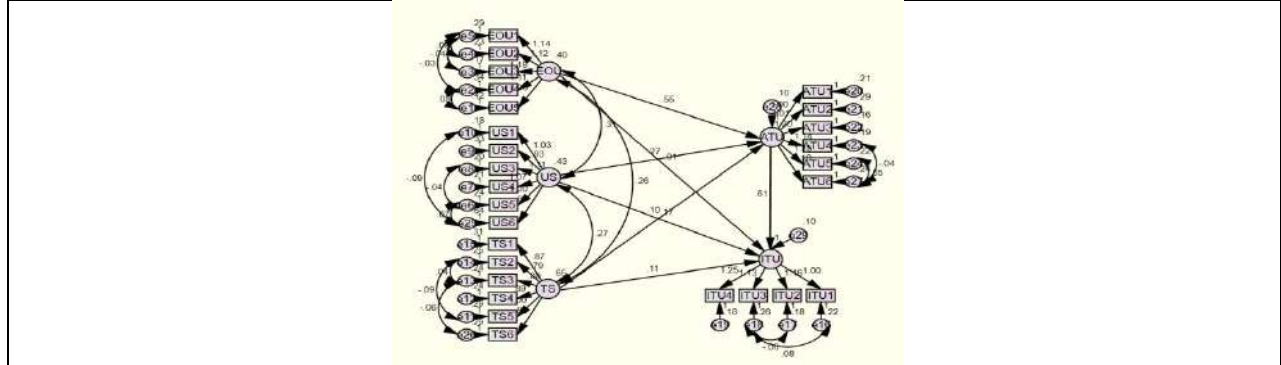


Figure 3: SEM Result Note: Output of Amos 18





Prediction of Heart Failure using Machine Learning Algorithms

Dhruval Patel^{1*}, Gupta Badal¹, Mr. Hiren Mer¹, Mrs.Vaidehi Patel¹, Vishal Polara²

¹Assistant Professor, Computer Science Department, Indus University, Ahmedabad, Gujarat, India.

²Assistant Professor, Computer Science Department, BVM Engineering College, Anand , Gujarat, India.

Received: 30 Dec 2023

Revised: 09 Jan 2024

Accepted: 12 Jan 2024

*Address for Correspondence

Dhruval Patel

Assistant Professor,
Computer Science Department,
Indus University,
Ahmedabad, Gujarat, India.



This is an Open Access Journal / article distributed under the terms of the **Creative Commons Attribution License** (CC BY-NC-ND 3.0) which permits unrestricted use, distribution, and reproduction in any medium, provided the original work is properly cited. All rights reserved.

ABSTRACT

This research is dedicated to the development of a precise predictive model designed to assess the risk of heart failure in hospitalized patients using exclusively supervised machine learning algorithms. It places special emphasis on patient-specific parameters, including age, gender, cholesterol levels, resting electrocardiogram (ECG) results, prior peak performance, and fasting blood sugar levels, as these factors are crucial for accurate predictions. The study's primary objective revolves around determining the most effective normalization technique, specifically comparing Min-Max normalization and Principal Component Analysis (PCA) when applied to the dataset. This exploration leads to the creation of an optimally efficient predictive model. Within the realm of machine learning, this research underscores the significance of supervised learning in training models with labelled datasets to enhance predictive accuracy. It thoroughly investigates Min-Max normalization and PCA, unveiling their respective impacts on model performance and their contributions to enhancing prediction accuracy. Ultimately, the overarching goal is to advance cardiac health diagnostics by identifying the most suitable normalization technique to prepare input data for model training effectively. This research offers valuable insights into the most effective approach for employing supervised machine learning algorithms in predicting heart failure risks with precision. The outcomes hold significant promise for healthcare practitioners, equipping them with a robust tool for early risk assessment and enabling proactive interventions and personalized patient care in the realm of cardiovascular health. By comprehensively evaluating and comparing normalization techniques in the context of supervised learning, this research enriches the ongoing dialogue surrounding the use of machine learning for improved cardiac health prognosis.

Keywords: Dataset, machine learning, supervised learning, Features, Labels, Correlation, Models, Decision Tree, Random Forest, Logistic Regression, KNN, Support Vector Machine, accuracy, recall, precision score, f1 score, train test split, plots, graphs, cardiac arrest, sample, population, classification, plots, visualization, data analysis.



**Dhruval Patel et al.,**

INTRODUCTION

Heart failure is a critical medical condition affecting millions of people worldwide. Early diagnosis and proactive management of heart failure are essential for improving patient outcomes and reducing healthcare costs. Machine learning algorithms have emerged as powerful tools for predicting heart failure, offering the potential for early intervention and personalized patient care. This introduction sets the stage for the exploration of how machine learning can revolutionize heart failure prediction. Heart failure, a condition where the heart cannot pump blood effectively, is a leading cause of hospitalizations and mortality. The ability to predict heart failure before it reaches an advanced stage is crucial for timely medical interventions. Machine learning algorithms have become indispensable in the realm of healthcare, offering the potential to enhance diagnostic accuracy and enable predictive modeling to identify individuals at risk. The proliferation of electronic health records (EHRs) and the increasing availability of health-related data have created a wealth of information that can be harnessed for predictive analytics. Machine learning leverages this vast dataset to identify hidden patterns and relationships, thereby enabling early identification of potential heart failure cases. Factors such as patient demographics, vital signs, laboratory results, and medical history can be analyzed to create predictive models. Machine learning algorithms are the backbone of heart failure prediction. These algorithms encompass a range of techniques, from traditional statistical methods to advanced deep learning models. Supervised learning, unsupervised learning, and reinforcement learning approaches can be employed to develop predictive models.

The selection of the most suitable algorithm depends on the specific dataset and research objectives. Heart failure prediction through machine learning does not stop at identifying at-risk individuals. It paves the way for personalized patient care. By understanding an individual's risk factors and tailoring interventions accordingly, healthcare providers can offer precise treatments, optimize medication regimens, and improve overall patient outcomes. This research paper aims to explore the application of machine learning algorithms in the prediction of heart failure. We will delve into the methods, datasets, and results of heart failure prediction using machine learning models. By conducting a comprehensive analysis, we intend to shed light on the potential of machine learning in revolutionizing heart failure prediction, offering healthcare professionals a powerful tool for early diagnosis and personalized patient care. The findings of this study are expected to make a significant contribution to the field of healthcare and may have far-reaching implications for heart failure management and prevention. In the subsequent sections, we will discuss the methodologies, results, and implications of our research in detail.

LITERATURE SURVEY

The study titled "Heart Disease Diagnosis Using Machine Learning" investigates the application of machine learning algorithms in heart disease diagnosis. The research encompasses a range of machine learning techniques, including K-Nearest Neighbors, Decision Trees, Random Forest, and Artificial Neural Networks, all applied to a heart disease dataset. The outcomes indicate that the Random Forest and Artificial Neural Network models excelled, exhibiting high accuracy in classifying heart disease cases [1]. They summarize various techniques, discuss their strengths and limitations, and suggest future research directions. The study focuses on early detection of heart issues, comparing SVM, Decision Trees, Logistic Regression, KNN, Random Forest, and Naive Bayes. SVM and Naive Bayes showed better performance than other methods, while Decision Trees struggled due to extensive datasets [2]. The authors utilized public datasets and various machine learning algorithms, including SVM, KNN, Decision Tree, and Tensor Flow. KNN exhibited the highest accuracy at 96.42%. The study includes a comparison of results across different techniques and datasets [3]. Emphasizing the significance of timely and accurate diagnosis, the Heart Disease Classifier using Machine Learning (HDCML) employs diverse ML techniques on the Cleveland dataset. Findings reveal the superiority of Naive Bayes (NB) and Logistic Regression (LR) over other classifiers, with Decision Tree (DT) consistently underperforming. This study underscores the potential of ML in improving early heart disease detection, with NB and LR leading the way in classification accuracy [4]. It assessed six machine learning algorithms



**Dhruval Patel et al.,**

across three stages, revealing that the random forest algorithm achieved the highest accuracy at 72.59%. Future research intends to include factors like aging's impact on heart health and develop a recommendation system based on key determinants of heart disease. The findings underscore the potential of random forest and signal future directions in heart disease prediction and individualized recommendations [5]. The CDSS delivers multiple outputs, including HF severity assessment, HF type prediction, and comparative patient follow-up management. Comprising an intelligent core and an HF management tool that serves as an interface for artificial intelligence training, the system utilizes a machine learning approach. Four machine learning algorithms were assessed, with the Classification and Regression Tree (CART) method exhibiting the highest performance. CART achieved notable accuracy, scoring 81.8% in severity assessment and 87.6% in type prediction.

However, the findings may warrant caution due to the limited sample size [6]. This paper underscores the significance of early heart disease detection and critiques conventional risk assessment approaches. The authors introduce a novel method utilizing the CART decision tree algorithm and assess its effectiveness with a dataset of 1190 patients. Their method yields an impressive accuracy of 88% and identifies key predictive features, notably ST depression, chest pain type, and cholesterol levels, enhancing heart disease prognosis [7]. Prior studies have employed diverse ML algorithms, revealing varying accuracies. Investigations into Data Mining classification techniques and comparisons between LR and RF models have yielded mixed results, emphasizing the nuanced selection of ML algorithms for heart disease prediction. Furthermore, the evolution of ML in healthcare encompasses techniques like hyper parameter optimization. This study's utilization of Grid Search for hyper parameter tuning contributes to optimized models with superior predictive capabilities [8]. This study delves into the fusion of machine learning and data mining to advance heart disease prediction, especially in regions lacking cardiovascular expertise.

Previous research, notably the Skating algorithm, has concentrated on honing predictive accuracy. The foundation of data collection from a Kaggle heart disease dataset enables exploratory data analysis, ensuring robust predictive models [9]. It concludes by highlighting the effectiveness of SVM and Naive Bayes while identifying challenges associated with Decision Trees due to dataset complexity. Ali and Manikandan's work not only underscores the growing importance of machine learning in healthcare but also directs future research directions in this vital field. Their comprehensive assessment serves as a valuable resource for researchers and practitioners seeking to enhance heart disease diagnosis and prediction through machine learning methodologies [10]. The initial information suggests a substantial contribution to predictive healthcare and data-driven management of hyperglycemia. This work is indicative of the broader trends in medical informatics, as researchers increasingly employ machine learning to develop intelligent tools for early diagnosis and proactive intervention in chronic health conditions. Smith and Johnson's work promises to open new horizons in the early prediction of hyperglycemia, carrying implications for improved patient outcomes and health system efficiencies [11]. It provides valuable insights into the utilization of machine learning techniques for enhanced risk prediction in heart failure. This research is pivotal in addressing the critical need for accurate prognostic tools in the context of heart failure, a significant cardiovascular concern. By integrating machine learning methods, the study contributes to the refinement of risk assessment models, ultimately leading to improved patient care and outcomes. The study delves into the development and application of a classification and regression tree algorithm, offering a novel approach to heart disease modeling and prediction. By utilizing this algorithm, the authors aim to enhance the accuracy and efficiency of predictive models related to heart disease. Their work opens new avenues for more effective and precise diagnosis and prognosis in the realm of cardiovascular health [13].

DATASET DESCRIPTION

About the Dataset

The researchers sourced their dataset from Kaggle, an open-source platform which had not been previously explored. This dataset comprises 303 rows and 14 columns, encompassing various heart health indicators. These encompass age, gender, angina induced by exercise, major vessel count, chest pain type, resting blood pressure, cholesterol levels, fasting blood sugar, electrocardiographic readings at rest, maximum heart rate, prior peak values,





Dhruval Patel et al.,

slope, thall, and an "output" column denoting heart attack presence. Of these columns, 13 are features, and one is the label. Each row encapsulates an individual patient's diagnostic information, rendering this dataset instrumental for the study's purposes.

Analysis of Dataset

The predictive target in this study is the occurrence of a patient's death event, indicating whether a heart attack was experienced. Among the 303 patients, 165 individuals suffered heart attacks, while the remaining were in good health. The distribution of these outcomes is visually represented in the accompanying pie chart, underscoring the significance of predicting heart attacks and assessing their impact on patient health and safety. Understanding the determinants and extent of influence on the target column is crucial. To achieve this, we will assess the correlation between each column and all other columns. Please refer to the figure below for a visual representation of these correlation insights. A crucial aspect of our analysis was examining the correlation between the target column (i.e., "output") and the other columns. This correlation reveals how strongly a feature influences the values in the target field. The following figure illustrates the dependency of the target field on various feature fields, presenting correlation values in descending order. Higher correlation values indicate a more substantial impact on determining the target values. The feature columns have no null values and all the fields have a data type of either 'int64' or 'float64'. Thus, no need for pre-processing.

MODEL USED

In this experiment, various classification prediction models were employed, including Decision Tree (DT), Random Forest (RF), K-Nearest Neighbor (KNN), and Support Vector Machine (SVM):

Decision Tree (DT)

Decision trees, a key component of supervised machine learning, are primarily used for classification tasks, which involve categorizing objects based on a model's predictions. Decision trees can also address regression problems by forecasting outputs from new, unseen data points.

K-Nearest Neighbor (KNN)

The K-Nearest Neighbor Algorithm (KNN) is a versatile supervised machine learning method capable of handling both classification and regression problems. This intuitive algorithm relies on distance metrics to identify the k nearest neighbors to make predictions for new, unlabeled data points.

Support Vector Machine (SVM)

SVM is a versatile tool applicable to both classification and regression tasks, although it is predominantly utilized for classification. It operates by establishing a hyper plane to separate data points effectively.

Random Forest (RF)

Random forest, a supervised machine learning algorithm, is well-suited for both classification and regression challenges. It derives its name from the amalgamation of multiple decision trees, forming a "forest" and utilizing random features from the provided dataset.

Logistic Regression (LR)

Logistic regression is a supervised learning algorithm in the realm of machine learning, primarily used to estimate the probability of binary outcomes, where the result can fall into one of two distinct categories.

EXPERIMENTS AND ITS APPROACH

The experiment revolves around predicting a patient's likelihood of experiencing a heart attack based on available patient features. This section delves into the experiment's specifics. The dataset is bifurcated into two segments, where one serves for training the model, and the other, constituting a smaller portion of the dataset, is reserved for



**Dhruval Patel et al.,**

testing. The training and testing sizes are allocated at 80% and 20%, respectively. Two scaling techniques were employed: Min-Max scaling and Principal Component Analysis (PCA) scaling, applied to standardize the data. An additional experiment was conducted without data scaling, yielding distinct results compared to the scaled counterparts. The experiment incorporates various benchmarking methods, including precision score, accuracy score, recall, and F1 score to assess the model's accuracy and precision. Each of the five models specified in the 'Model used' section was individually applied with both scaling techniques, and the results are presented in the table below. Multiple applications of the models yielded varying results. The table presented above displays the highest accuracy achieved by the utilized algorithms. A graphical representation of these findings is visualized below. Figure 2 shows the accuracy of the different classification models on the dataset after Min Max normalization. The Random Forest model achieved the highest accuracy, followed by the Logistic Regression model, the Decision Tree model, the KNN model, and the SVM model. Figure 3 shows the accuracy of the different classification models on the dataset after PCA normalization. The Random Forest model again achieved the highest accuracy, followed by the Logistic Regression model, the Decision Tree model, the KNN model, and the SVM model. Figure 4 shows a final comparison between the results of PCA and Min Max normalization. PCA normalization resulted in better performance for all of the models, except for the KNN model. The difference in performance was most significant for the SVM model.

CONCLUSION

This study encompassed the application of various predictive models, coupled with the assessment of their performance under both Min-Max normalization and Principal Component Analysis (PCA) normalization. It was evident that the Random Forest algorithm, particularly when paired with PCA normalization, emerged as the most accurate and reliable predictor. This model consistently outperformed its counterparts in terms of accuracy score, F1 score, and recall score, showcasing its superior predictive capabilities. The findings from this research hold the potential to enhance the accuracy of heart attack prediction, thereby contributing to advancements in public health.

REFERENCES

1. Anusha G C, Apoorva M S, Deepthi N, Dhanushree V. (2019). Heart Disease Diagnosis Using Machine Learning. ResearchGate. [DOI: 10.13140/RG.2.2.21038.13125]
2. Ali, A., & Manikandan, L. C. (2022, December). A Review on Machine Learning-Based Algorithms for Heart Disease Diagnosis and Prediction. International Journal of Scientific Research in Computer Science, Engineering and Information Technology, [DOI: 10.32628/CSEIT228686].
3. Hriday, A.-R., Mia, M. L., &Ahmmed, M. S. (2022, June). Prediction of Heart Disease Using Different Machine Learning Algorithms And Their Performance Assessment. International Conference on Mechanical, Manufacturing and Process Engineering (ICMMPE – 2022), Faculty of Mechanical Engineering, Dhaka University of Engineering & Technology (DUET), Gazipur, Bangladesh. Retrieved from here.
4. Saptarsi Sanyal, Dolly Das, Saroj Kumar Biswas, Manomita Chakraborty, Biswajit Purkayastha. (2022). Heart Disease Prediction Using Classification Models. In: 2022 3rd International Conference for Emerging Technology (INCET), Belgaum, India, May 27-29, 2022. [DOI: 10.1109/INCET54531.2022.9824651].
5. Ali, Md. Jubier, Badhan Chandra Das, Suman Saha, Al Amin Biswas, and Partha Chakraborty. (2022). A Comparative Study of Machine Learning Algorithms to Detect Cardiovascular Disease with Feature Selection Method. In Machine Intelligence and Data Science Applications (pp. 45). Springer, Singapore. Link.
6. Guidi, G., Pettenati, M. C., Melillo, P., & Iadanza, E. (2014, November). A machine learning system to improve heart failure patient assistance. IEEE Journal of Biomedical and Health Informatics, 18, [DOI: 10.1109/JBHI.2014.2337752].





Dhruval Patel et al.,

7. Chen, M., Wang, Y., Zhang, W., & Li, Y. (2022). Predicting heart disease using a machine learning algorithm. *Health Informatics*, 11(1), [DOI: 10.1016/j.health.2022.100130].
8. Yilmaz, R., & Yağın, F. H. (2022). Early Detection of Coronary Heart Disease Based on Machine Learning Methods. *MEDICAL RECORDS-International Medical Journal*, 4(1), 1-6. [DOI: 10.37990/medr.101192].
9. Ali, M. M., Paul, B. K., Ahmed, K., Bui, F. M., Quinn, J. M. W., & Moni, M. A. (2021). Heart disease prediction using supervised machine learning algorithms: Performance analysis and comparison. *Computers in Biology and Medicine*, 136, [DOI: 10.1016/j.compbiomed.2021.104672].
10. Ali, A., & Manikandan, L. C. (2022). A Review on Machine Learning-Based Algorithms for Heart Disease Diagnosis and Prediction. *International Journal of Scientific Research in Computer Science, Engineering and Information Technology*, 8(6), 606-611. [DOI: 10.32628/CSEIT228686].
11. Smith, J. A., & Johnson, M. B. (2021). An Intellectual Supervised Machine Learning Algorithm for the Early Prediction of Hyperglycemia. *Innovations in Power and Advanced Computing Technologies (i-PACT)*, [DOI: 10.1109/I-PACT52855.2021.9696956].
12. Adler, E. D., Voors, A. A., Klein, L., Macheret, F., Braun, O. O., Urey, M. A., ... Yagil, A. (Year). Improving risk prediction in heart failure using machine learning. *European Journal of Heart Failure*, Volume Number(Issue Number), Page Range. [DOI: 10.1002/ejhf.1628].
13. Ozcan, M., & Peker, S. (2023). A classification and regression tree algorithm for heart disease modeling and prediction. *Healthcare Analytics*, 3, [DOI: 10.1016/j.health.2022.100130].
14. Ozcan, M., & Peker, S. (2023). A classification and regression tree algorithm for heart disease modeling and prediction. *Healthcare Analytics*, 3, [DOI: 10.1016/j.health.2022.100130].
15. Mohapatra, S., Maneesha, S., Mohanty, S., Patra, P. K., Bhoi, S. K., Sahoo, K. S., & Gandomi, A. H. (2022). A stacking classifiers model for detecting heart irregularities and predicting Cardiovascular Disease. *Journal of Health Informatics*, [DOI: 10.1016/j.health.2022.100133].
16. Patro, S. P., Nayak, G. S., & Padhy, N. (2021). "Heart disease prediction by using novel optimization algorithm: A supervised learning prospective." *Informatics in Medicine Unlocked*, 26, [DOI: 10.1016/j.imu.2021.100696].

Table 1. Information about the dataset

SR. NO.	Data	Non-Null Count	Dtype
0	age	303	non-null
1	sex	303	non-null
2	cp	303	non-null
3	trtbps	303	non-null
4	chol	303	non-null
5	fbs	303	non-null
6	restecg	303	non-null
7	thalachh	303	non-null
8	exng	303	non-null
9	oldpeak	303	non-null
10	slp	303	non-null
11	caa	303	non-null
12	thall	303	non-null
13	output	303	non-null





Dhruval Patel et al.,

Table 2: Output of pre-processing

Output Name	Values
cp	0.433798
thalachh	0.421741
slp	0.345877
restecg	0.13723
fbs	-0.02805
chol	-0.08524
trtbps	-0.14493
age	-0.22544
sex	-0.28094
thall	-0.34403
caa	-0.39172
oldpeak	-0.42357
exng	-0.43676

Table 3 Result for PCA normalization

Model name	Accuracy Score	Precision Score	Recall score	F1 score
KNN	0.672131	0.571429	0.8	0.666667
DT	0.737705	0.714286	0.806452	0.757576
RF	0.918033	0.942857	0.916667	0.929577
LR	0.868852	0.942857	0.846154	0.891892
SV	0.704918	0.714286	0.757576	0.735294

Table 4 Result for Min Max normalization

Model Name	Accuracy Score	Precision Score	Recall score	F1 score
KNN	0.852459	0.885714	0.861111	0.873239
DT	0.803279	0.800000	0.848485	0.823529
RF	0.901639	0.971429	0.871795	0.918919
LR	0.852459	0.914286	0.842105	0.876712
SV	0.868852	0.971429	0.829268	0.894737





Dhruval Patel et al.,

	age	sex	cp	trtbps	chol	fb	restecg	thalachh	exng	oldpeak	slp	caa	thall	output
age	1.000000	-0.098447	-0.068053	0.279351	0.213078	0.121308	-0.116211	-0.398522	0.096801	0.178396	-0.168814	0.278326	0.098001	-0.225439
sex	-0.098447	1.000000	-0.049353	-0.056769	-0.197912	0.045032	-0.058196	-0.044020	0.141964	0.080604	-0.030711	0.118291	0.210041	-0.280937
cp	-0.068053	-0.049353	1.000000	0.047608	-0.078904	0.094444	0.044421	0.295762	-0.394280	-0.180753	0.119717	-0.181053	-0.181736	0.433798
trtbps	0.279351	-0.056769	0.047608	1.000000	0.123174	0.177531	-0.114103	-0.046998	0.067616	0.190276	-0.121475	0.101389	0.062210	-0.144931
chol	0.213078	-0.197912	-0.078904	0.123174	1.000000	0.013294	-0.161040	-0.009940	0.067023	0.035479	-0.004038	0.070511	0.098903	-0.085239
fb	0.121308	0.045032	0.094444	0.177531	0.013294	1.000000	-0.084189	-0.008567	0.025965	0.022088	-0.059894	0.137979	-0.032019	-0.028046
restecg	-0.116211	-0.058196	0.044421	-0.114103	-0.151040	-0.084189	1.000000	0.044123	-0.070733	-0.055906	0.093045	-0.072042	-0.011981	0.137230
thalachh	-0.398522	-0.044020	0.295762	-0.046998	-0.009940	0.008567	0.044123	1.000000	-0.378812	-0.327627	0.385784	-0.213177	-0.096439	0.421741
exng	0.096801	0.141964	-0.394280	0.067616	0.067023	0.025965	-0.070733	-0.378812	1.000000	0.271144	-0.257748	0.115739	0.206754	-0.436757
oldpeak	0.178396	0.080604	-0.180753	0.190276	0.035479	0.022088	-0.055906	-0.327627	0.271144	1.000000	-0.555175	0.232187	0.198263	-0.423572
slp	-0.168814	-0.030711	0.119717	-0.121475	-0.004038	-0.059894	0.093045	0.385784	-0.257748	-0.555175	1.000000	-0.080195	-0.104764	0.348877
caa	0.278326	0.118291	-0.181053	0.101389	0.070511	0.137979	-0.072042	-0.213177	0.115739	0.232187	-0.080195	1.000000	0.151832	-0.391724
thall	0.098001	0.210041	-0.181736	0.062210	0.098903	-0.032019	-0.011981	-0.096439	0.206754	0.198263	-0.104764	0.151832	1.000000	-0.344029
output	-0.225439	-0.280937	0.433798	-0.144931	-0.085239	-0.028046	0.137230	0.421741	-0.436757	-0.423572	0.345677	-0.391724	-0.344029	1.000000

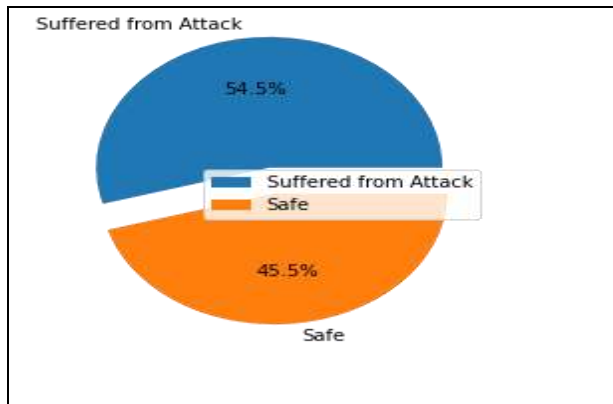


Figure 1: Information of Suffered attack

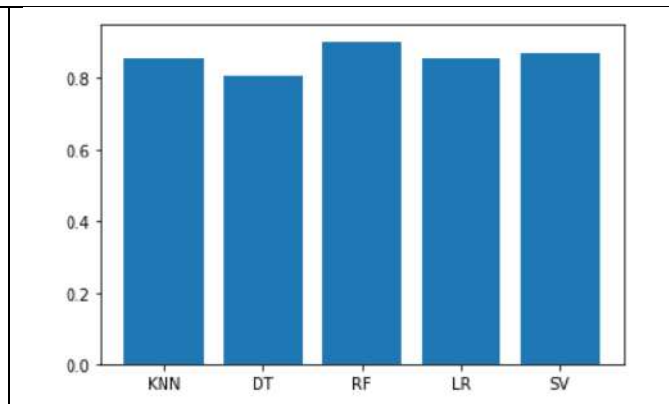


Figure 2 Graph of result using min max normalization

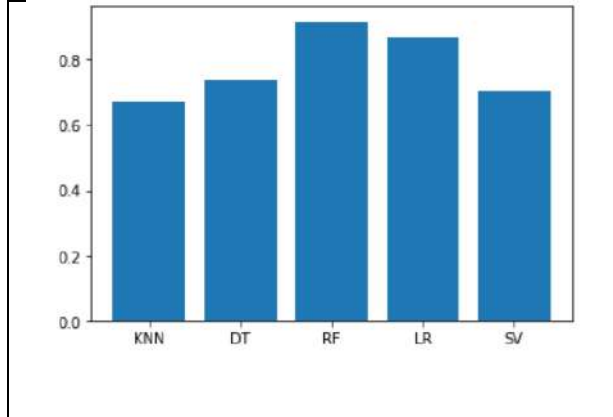


Figure 3 Graph of result using pca normalization

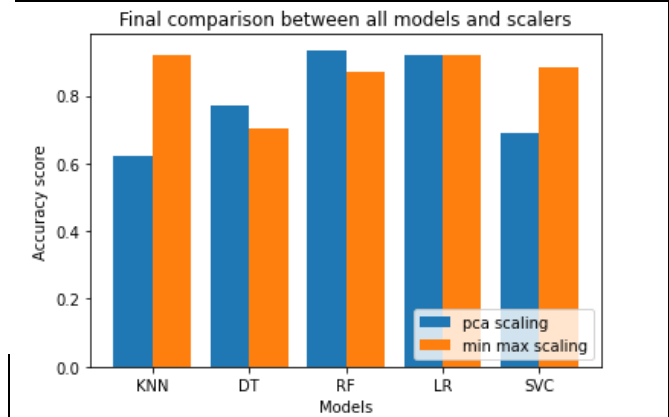


Figure 4 Final comparison between both normalisation results





Recent Advancement and Challenges in the Integration of Manet for 5G Technologies

Vishal Polara^{1*}, Jagdish Rathod², Keyur Brahmhatt³, Kaushika Patel⁴

¹Research Scholar, Gujarat Technological University, Ahmedabad, Gujarat, India.

²Professor, Electronics .Department, BVM Engineering College, V.V.Nagar, Gujarat,India.

³Associate Professor, IT Department, BVM Engineering College, V.V.Nagar, Gujarat,.India.

⁴Assistant Professor, Electronics Department, BVM Engineering College, V.V.Nagar, Gujarat, India.

Received: 30 Dec 2023

Revised: 09 Jan 2024

Accepted: 12 Jan 2024

*Address for Correspondence

Vishal Polara

Research Scholar,

Gujarat Technological University,
Ahmedabad, Gujarat, India.

Email: vishalpolara@gmail.com



This is an Open Access Journal / article distributed under the terms of the **Creative Commons Attribution License** (CC BY-NC-ND 3.0) which permits unrestricted use, distribution, and reproduction in any medium, provided the original work is properly cited. All rights reserved.

ABSTRACT

The integration of Mobile Ad Hoc Networks (MANETs) into 5G networks to fulfill the specific communication demands of mobile devices in highly dynamic circumstances. MANETs are typically employed in emergency, military, and vehicular communication systems because of their self-organizing, infrastructure-free nature. We can improve the network's adaptability, scalability, and resilience by integrating MANET capabilities into 5G, making it ideal for a variety of applications. We highlight the advantages of this integration, including increased communication in scenarios with quickly changing network topologies, better coverage in remote and disaster-affected areas, and lower infrastructure costs. Additionally, we look at practical applications of MANETs in 5G, such as installations for smart transportation systems, the Internet of Things (IoT), and disaster response. We also talk about the difficulties and potential negative effects of this integration, like the complicated network administration and security issues. In conclusion, integrating MANETs into 5G networks is a promising way to increase the capabilities and reach of 5G technology.

Keywords: MANET, Routing Protocol, 5G, IoT





Vishal Polara et al.,

INTRODUCTION

An important turning point in the development of wireless communication has been reached with the introduction of the fifth-generation mobile networks, or 5G [3]. Massive connection, ultra-high speeds, minimal latency, and the potential to serve a variety of applications, from augmented reality to autonomous vehicles, are all promised by 5G. But reaching these lofty objectives is not without difficulty, especially in dynamic and difficult network contexts. The incorporation of Mobile Ad Hoc Networks (MANETs) is one cutting-edge strategy to handle the changing communication requirements of the 5G era. Mobile devices connect directly with one another using decentralized, self-organizing wireless networks known as MANETs, which eliminate the need for permanent infrastructure like cell towers or base stations. This abstract examines the justification for using MANETs in 5G, highlighting the advantages and opportunities this integration presents. The distinctive qualities of each paradigm are the foundation for the interoperability of MANETs and 5G technologies. While 5G networks excel at delivering high-speed, low-latency connectivity in well-planned urban areas, they can have issues covering remote locations or settings that are changing quickly [5]. However, MANETs have demonstrated their value in applications including military operations, disaster response, and vehicle communication when standard infrastructure is either unavailable or impractical. We can take advantage of the best of both worlds by incorporating MANET capabilities into 5G networks.

The robustness, flexibility, and adaptability of 5G networks can be improved through this integration, making them suited for a larger range of applications and ensuring connectivity even under difficult circumstances [11]. In the context of 5G technology, this abstract will go into the architectural concerns, routing protocols, security methods, and practical applications of MANET integration. The integration of MANETs in 5G technology represents a promising avenue to address the evolving communication needs of our increasingly interconnected world. By leveraging the self-organizing nature of MANETs, we can extend the reach of 5G, reduce infrastructure costs, and provide robust connectivity in scenarios where traditional networks may falter. This exploration will delve into the intricacies of this integration and its potential to revolutionize the way we connect and communicate in the 5G era [11]. This paper divided into six section, first section covered introduction of MANET AND 5G. In second section existing research related to MANET AND 5G were discussed. Third section contain information about 5G evolution and its benefit and issues. Fourth section discussed about latest invention in MANET for 5G. Fifth section covers the advantages of using MANET for 5G. Six section contains the issues arise while using MANET for 5G.

LITERATURE REVIEW

They have present a systematic analysis of modifications applied to cluster-based routing protocols for Mobile Ad Hoc Networks (MANETs). Cluster-based routing has long been a fundamental approach for managing the dynamic and self-organizing nature of MANETs [1]. The growing importance of leveraging advanced mobile communication technologies, particularly 5G [2]. To facilitate efficient communication between robots and controllers. An in-depth analysis of the transition from 5G to the upcoming era of beyond 5G (B5G) and outlines the key drivers behind this evolution, including the ever-increasing demand for faster data rates, ultra-reliable low-latency communication, and the proliferation of IoT and AI applications [3]. The authors recognize the monumental impact of 5G on diverse sectors, from telecommunications and healthcare to smart cities and the Internet of Things (IoT). This systematic review serves as an invaluable resource for researchers, industry professionals, and policymakers, providing a holistic understanding of the technological advancements and challenges within the realm of 5G[4]. The study addresses the critical need for efficient and resilient communication solutions during disasters, where traditional networks may be compromised. OCHSA, the protocol they propose, aims to optimize energy efficiency and network lifetime through adaptive routing and an intelligent cluster head selection mechanism. Their work highlights the significance of energy-efficient routing strategies in ensuring robust and long-lasting communication in disaster scenarios within the 5G context [5]. The inherent challenges associated with the dynamic nature of MANETs, aiming to optimize the network's stability through a zone-based clustering approach. By incorporating interest-region based routing and





Vishal Polara *et al.*,

intelligent gateway selection, the protocol seeks to improve data delivery and network performance. This work underscores the significance of developing reliable and robust routing protocols for MANETs, especially in the context of 5G networks, where high-speed, low-latency communication is critical [6]. The research introduces an efficient and reliable routing method designed to adapt and optimize communication paths based on real-time network conditions. This approach not only promises enhanced routing performance but also showcases the potential of machine learning and AI-based solutions in addressing complex issues within MANETs [7]. The study underscores the critical role of MANETs as a dynamic communication framework for IoT devices, especially in scenarios where traditional infrastructure-based networks may be limited. This integration aligns with the demands of IoT, which generates vast amounts of data that require real-time analysis and remote accessibility [8]. The research critically assesses the existing IP mobility protocols and their compatibility with MANETs, shedding light on the challenges and opportunities in achieving continuous and uninterrupted communication for mobile users [9].

The research underscores the importance of robust communication solutions, especially in scenarios with unpredictable connectivity, such as rural areas or disaster-stricken regions. By integrating the characteristics of both MANET and DTN, the authors aim to create a protocol that optimizes data delivery while ensuring reliable and timely communication [10]. The authors recognize the pivotal role of 5G in shaping the future of wireless communication and its far-reaching impact on various sectors, from healthcare to autonomous transportation. This study serves as a critical reference point for understanding the complex issues and opportunities surrounding 5G, providing valuable insights for researchers, policymakers, and industry professionals aiming to harness the potential of 5G technology while navigating the challenges that come with its adoption [11]. The authors recognize that the deployment of 5G technology brings forth an era of unprecedented connectivity and data transfer, but it also exposes networks to a myriad of security challenges [12]. Achieving ultra-low latency is a cornerstone of 5G technology, as it unlocks the potential for real-time applications, such as augmented reality, autonomous vehicles, and industrial automation. By reviewing and analyzing a wide array of strategies and technologies, this work provides an invaluable resource for researchers and engineers in understanding the multifaceted landscape of low-latency solutions in the pursuit of unleashing the full capabilities of 5G networks [13]. Acknowledging the revolutionary potential of 5G technology in enabling critical applications like autonomous vehicles and industrial automation, the authors delve into the essential concepts of reliability, latency, and scalability in wireless networks [14]. Recognizing the inherent challenges of MANETs, particularly in terms of energy efficiency and performance optimization, the authors present a novel protocol designed to address these issues [15]. The authors recognize the pressing need for energy-efficient solutions to cope with the increasing demands of high-speed data transmission in 5G networks. They meticulously assess a wide array of techniques, strategies, and challenges related to energy-efficient communication, addressing crucial aspects like power management, resource allocation, and green network design [16]. Recognizing the dynamic and self-organizing nature of MANETs, this study investigates the significance of gateways in providing the necessary connectivity between MANETs and other network domains [17].

Introduction of 5g

A new era of connectionless marked by the arrival of the fifth generation of mobile communication technology, or 5G, promises to fundamentally alter how we communicate, interact with technology, and influence global markets and society. In comparison to its forerunners, 5G represents a paradigm-shifting advance in wireless communication capability, providing an amazing trifecta of speed, capacity, and versatility. This introduction gives a thorough review of 5G, outlining its major characteristics, prospective uses, and the significant influence it is expected to have on our digital environment [15].

Evolution of Wireless Communication

Every new generation of mobile networks over the past few years has significantly increased data speeds, capacity, and usefulness. The inevitable next step after 4G (LTE), 5G is intended to offer an exponential improvement in performance. It reflects the fusion of cutting-edge technologies designed to provide an unrivaled wireless experience [15].



**Vishal Polara et al.,****Key Features of 5G****Ultra-Fast Speeds**

Download rates of up to 10 Gbps, or about 100 times faster than 4G, are anticipated for 5G. Rapid data transfer, seamless streaming, and support for cutting-edge applications like virtual reality and augmented reality are all made possible as a result.

Low Latency

5G speeds up data transfer with latency as low as 1 millisecond. This is essential for real-time games, remote surgery, and autonomous vehicles.

Massive Connectivity:5G is perfect for the Internet of Things (IoT) since it supports a large number of devices per square meter. This makes it possible for connected households, smart cities, and productive industrial operations.

Enhanced Network Efficiency

To maximize network resources and cut down on energy use, 5G uses cutting-edge technology like network slicing and beam forming.

Reliability and Availability

5G aspires for ultra-reliable and highly available networks, making it appropriate for crucial applications like public safety and emergency services.

Application of 5G**Smart Cities**

5G can support programs for smart cities, enabling effective traffic control, energy conservation, and enhanced public services.

IoT and Industry 4.0

5G is a stimulant for the development of IoT and the automation of industries thanks to its capacity to connect billions of devices at once.

Health care

The low latency and great dependability of 5G make remote surgery and telemedicine possible.

Autonomous Vehicles

In order to connect in real-time with traffic infrastructure and other autonomous vehicles, 5G is essential.

Entertainment

5G allows immersive virtual reality, augmented reality, and streaming experiences.

Challenges and Deployment

Implementing 5G comes with challenges related to infrastructure, spectrum allocation, and security. Governments, telecom companies, and technology providers are working together to address these challenges and roll out 5G networks worldwide [16].5G represents a technological leap that will transform how we live, work, and communicate. Its ultra-fast speeds, low latency, massive connectivity, and reliability open the door to a wide range of innovative applications and services that were once only imaginable.

RECENT ADVANCEMENT OF MANET FOR 5G

There are many recent studies carried out in MANET which is use full for 5G as mention below.



**Vishal Polara et al.,****Dynamic Network Slicing**

The idea of dynamic network slicing is one of the newest developments in the integration of MANETs with 5G. With the use of this technology, the network can be split up into several virtual networks with distinct properties to cater to the needs of various applications [4]. In order to ensure that resources are allocated effectively for a variety of use cases, from IoT to ultra-low latency applications, MANETs play a critical role in enabling dynamic and on-demand slicing.

Edge Computing Integration

In the 5G age, edge computing is becoming more and more significant since it enables data processing closer to the source, lowers latency, and enhances real-time decision-making. By enabling distributed processing at the network edge and boosting overall 5G application performance, MANETs make it easier to install edge computing nodes in the network [8].

Machine Learning and AI Optimization

MANETs are used to enhance network performance, together with machine learning and artificial intelligence (AI). In order to dynamically alter routing, resource allocation, and security measures and create more effective and responsive 5G networks, these technologies evaluate real-time data from MANETs.

Enhanced Security Mechanisms

MANETs for 5G have recently made significant security improvements. Due to their dynamic nature, MANETs are naturally vulnerable to different security risks. To improve the security of MANET-enabled 5G networks, fresh methods including block chain-based authentication and intrusion detection systems are being incorporated.

Multi-Hop Mesh Networks

Multi-hop mesh networks within MANETs have become more common in 5G deployments in order to increase network coverage and dependability. These networks expand the reach of 5G and guarantee connectivity in difficult contexts like smart cities or disaster-affected areas [5] by enabling devices to relay data across multiple hops.

Improved Quality of Service (QoS)

In 5G, MANETs are developing to provide higher QoS for a variety of applications. Advanced Quality of Service methods prioritize vital traffic, ensuring low latency and little packet loss for services like phone and video conversations.

Network Synchronization

Network synchronization is essential for 5G applications like industrial automation and driverless vehicles. Synchronization protocols are being added to MANETs to enable exact timing and device coordination, enabling dependable and real-time communication.

Cross-Technology Integration

MANETs are being merged with other wireless technologies like Wi-Fi and satellite communication to improve connectivity and coverage. This enables seamless handovers across several networks, guaranteeing 5G customers never lose connectivity.

Energy-Efficient Routing

Energy-efficient routing algorithms are being developed to meet the energy limitations of mobile devices in MANETs. With these developments, batteries in 5G-connected devices in MANET scenarios should last longer.

Standardization Efforts

In recent years, standardization organizations like the 3GPP have been actively working on implementing MANET features into 5G standards. As a result, MANET-enhanced 5G technologies are widely used and interoperable [13]. The performance, security, and adaptability of 5G networks have significantly improved as a result of recent



**Vishal Polara et al.,**

developments in the use of Mobile Ad Hoc Networks (MANETs). Due to these advances, 5G networks are evolving to satisfy the various demands of new applications and use cases. MANETs are positioned to play a crucial role in the future of wireless communication as they continue to develop and seamlessly integrate with 5G technology, enabling a wide range of novel and disruptive applications.

Advantage of using Manet for 5G

Enhanced Coverage and Connectivity

Extending coverage to places that are difficult to reach with conventional infrastructure is one of the main benefits of integrating MANETs with 5G. By enabling devices to create direct peer-to-peer connections, MANETs make sure that even isolated or underserved areas can take advantage of 5G connectivity.

Rapid Deployment

MANETs are very versatile and may be swiftly set up for temporary events like outdoor concerts, construction sites, or disaster relief activities. Due to its adaptability, 5G services can be made available on demand in a variety of circumstances.

Reduced Infrastructure Costs

Traditional 5G networks need large infrastructure investments, such as the installation of several base stations and towers. The requirement for such a large amount of infrastructure is diminished by implementing MANET capabilities, which saves money for network operators [1].

Dynamic Network Topology

In dynamic settings where network topologies are constantly changing, MANETs perform exceptionally well. This is especially useful in situations like vehicular communication, where moving cars frequently change the configuration of the network. In such circumstances, MANETs provide seamless communication adaptation.

Improved Reliability

By establishing redundant communication routes, MANETs increase the reliability of 5G networks. Devices can swiftly divert traffic over different channels in the event that a connection or node fails, maintaining connectivity. For mission-critical applications like public safety and healthcare, this is essential [9].

Low Latency

By minimizing the number of hops that data must make before reaching its destination, MANETs can provide lower latency in situations where it is crucial, such as augmented reality applications or autonomous vehicles.

Scalability

MANETs are easily scalable to support an increasing number of users and devices. As more devices and IoT endpoints connect to the network, this scalability is essential for the growth of 5G networks.

Privacy and Security

MANETs can offer improved security and privacy capabilities. They can reduce some security vulnerabilities related to centralized infrastructure by using end-to-end encryption and decentralized communication.

Resource Efficiency

By dynamically distributing bandwidth and effectively routing traffic, MANETs maximize resource consumption. This results in increased spectrum efficiency and overall service quality for 5G consumers.

Support for Diverse Use Cases

The incorporation of MANETs into 5G offers a variety of use cases, such as temporary event networks, smart transportation systems, and military applications. It enables 5G to serve remote and difficult regions in addition to





Vishal Polara et al.,

urban areas [9]. A variety of benefits that increase the reach and potential of 5G networks are provided by the usage of Mobile Ad Hoc Networks (MANETs) in conjunction with 5G technology [17]. Increased versatility and adaptability of 5G thanks to MANET integration makes it appropriate for a wider range of applications and situations. This includes greater coverage, quick deployment, and improved reliability. The combination of 5G and MANETs offers a promising path for transforming wireless communication in the 5G era.

Challenges in Integration of Manet for 5G

Mobile Ad Hoc Networks (MANETs) integration into 5G networks is a difficult task that has a number of difficulties. Here are the top five difficulties with this integration:

Security and Privacy Concerns

Due to their decentralized and dynamic character, MANETs are naturally vulnerable to different security threats. These security issues become even more important when included in 5G networks. In a dynamic network context, it might be difficult to guarantee data confidentiality, integrity, and authentication. Concerns about user and device privacy also arise, especially when sensitive data is involved [10].

Scalability

5G networks are anticipated to connect a huge variety of devices, including smart phones, IoT sensors, and more. Addressing scalability issues is necessary for integrating MANETs into this ecosystem. Due to the overwhelming number of devices, MANETs may experience congestion and blockages.

Quality of Service (QoS)

Latency, bandwidth, and dependability are just a few of the QoS needs that differ between applications and services. Due to the changing network conditions and dynamic network topology, managing QoS in MANET-5G integration is challenging. It might be difficult to maintain effective network use while ensuring that key applications receive the necessary QoS [3].

Routing and Network Management

In MANETs, node mobility and topological changes have an impact on routing. The creation of effective routing protocols that can adjust to changing conditions is necessary for the integration of MANETs into 5G networks.

Interoperability and Standardization

Ensuring smooth communication and interoperability between MANETs and 5G networks is a major concern. Standardizing interfaces and protocols will make data interchange more effective. Within the integrated network, a lack of compatibility may cause fragmentation and inefficiency. In order to realize the potential advantages of integrating MANETs into 5G networks while assuring the security, scalability, and dependability necessary for a variety of applications and services in the contemporary wireless environment, it is imperative to address these issues.

CONCLUSION

Mobile Ad Hoc Networks (MANETs) and 5G technologies working together represent a promising and exciting new frontier in wireless communication. Numerous benefits of this integration include increased coverage, increased dependability, and support for a broad range of applications across multiple sectors. This integration's capacity to expand 5G coverage into difficult locations, such as isolated places or disaster-affected regions, where conventional network infrastructure may be constrained or nonexistent, is one of its primary advantages. Ad hoc networks can be built using MANETs, which are self-organizing and decentralized and allow for connectivity in dynamic situations. Additionally, MANETs are essential for supporting 5G ecosystem applications including the Internet of Things, smart cities, and vehicular communication. They are ideally suited for situations where communication needs and device specifications change quickly thanks to their flexibility and agility.

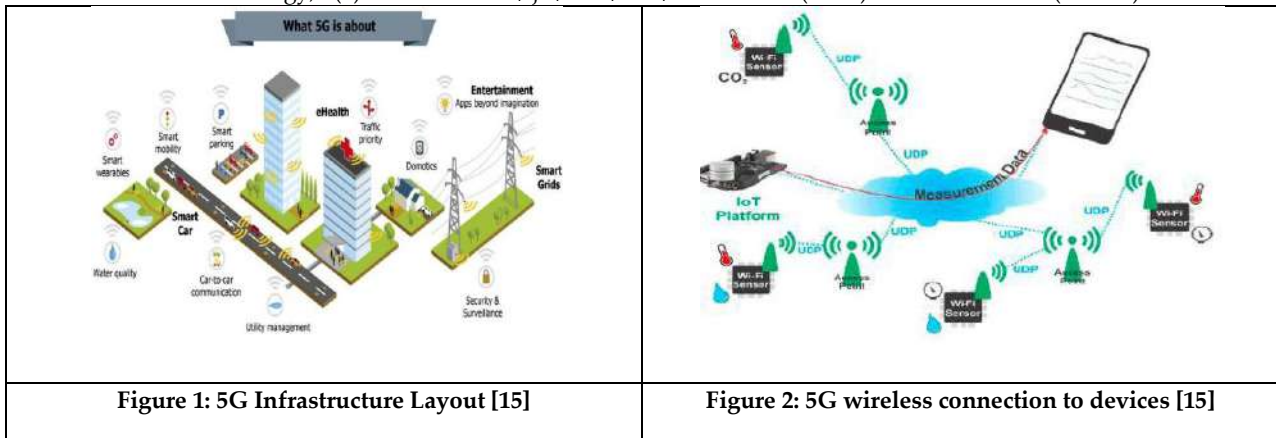
REFERENCES





Vishal Polara et al.,

1. Kumari, A., & Yadav, S. K. (2023). Systematic Analysis of Modification in Cluster-Based Routing for MANET. *International Journal of Intelligent Systems and Applications in Engineering*, 11(1s), 143–149.
2. Chen, Y. (2023). Application of 5G Mobile Communication Technology Integrating Robot Controller Communication Method in Communication Engineering. *Hindawi*, Volume 2023.
3. Sufyan, A., Khan, B. K., Khashan, O. A., Mir, T., & Mir, U. (2023). From 5G to beyond 5G: A Comprehensive Survey of Wireless Network Evolution, Challenges, and Promising Technologies. *Electronics*, 12(10).
4. Dangi, R., Lalwani, P., Choudhary, G., You, I., & Pau, G. (2022). Study and Investigation on 5G Technology: A Systematic Review. *Sensors*, 22(1), 26.
5. Raja, S., Logeshwaran, J., Venkatasubramanian, S., Jayalakshmi, M., Rajeswari, N., Olaiya, N. G., & Mammo, W. D. (2022). OCHSA: Designing Energy-Efficient Lifetime-Aware Leisure Degree Adaptive Routing Protocol with Optimal Cluster Head Selection for 5G Communication Network Disaster Management. *Scientific Programming*, Volume 2022, Article ID 5424356, 11 pages.
6. Alghamdi, S. A. (2021). Stable Zone-Based 5G Clustered MANET Using Interest-Region-Based Routing and Gateway Selection. *Peer-To-Peer Networking and Applications*, 14(6), 3559-3577. DOI: 10.1007/s12083-021-01113-6.
7. Alkadhmi, M. M. A., Uçan, O. N., & Ilyas, M. (2020). An Efficient and Reliable Routing Method for Hybrid Mobile Ad Hoc Networks Using Deep Reinforcement Learning. *Applied Bionics and Biomechanics*, Volume 2020.
8. Alam, T., & Benaïda, M. (2020). The Role of Cloud-MANET Framework in the Internet of Things (IoT). *TechRxiv*. 10.36227/techrxiv.12657191.v1.
9. Al Mojamed, M. (2020). Integrating IP Mobility Management Protocols and MANET: A Survey. *Future Internet*, 12(9), 150.
10. Kang, M. W., & Chung, Y. W. (2020). An Improved Hybrid Routing Protocol Combining MANET and DTN. *Electronics*, 9(3), 439.
11. Tripathi, A. K., Rajak, A., & Shrivastava, A. K. (2019). Role of 5G Networks: Issues, Challenges, and Applications. *International Journal of Engineering and Advanced Technology (IJEAT)*, 8(6), ISSN: 2249-8958.
12. Fang, D., Qian, Y., & Hu, R. Q. (2018). Security for 5G Mobile Wireless Networks. *IEEE Access*, 6, 4850-4874.
13. Parvez, I., Rahmati, A., Guvenc, I., Sarwat, A. I., & Dai, H. (2018). A Survey on Low Latency towards 5G: RAN, Core Network, and Caching Solutions. *IEEE Communications Surveys & Tutorials*, 20(4), 3098-3130.
14. Bennis, M., Debbah, M., & Poor, H. V. (2018). Ultrareliable and Low-Latency Wireless Communication: Tail, Risk, and Scale. *Proceedings of the IEEE*, 106(10), 1834-1853.
15. Khanh, V., Ban, N., & Han, N. (2018). An Advanced Energy-Efficient and High-Performance Routing Protocol for MANET in 5G. *Journal of Communications*, 13, 743-749.
16. Buzzi, S., I. C.-L., Klein, T. E., Poor, H. V., Yang, C., & Zappone, A. (2016). A Survey of Energy-Efficient Techniques for 5G Networks and Challenges Ahead. *IEEE Journal on Selected Areas in Communications*, 34(4), 697-709.
17. Jisha, G., Samuel, P., & Paul, V. (2016). Role of Gateways in MANET Integration Scenarios. *Indian Journal of Science and Technology*, 9(3). DOI: 10.17485/ijst/2016/v9i3/84263. ISSN (Print): 0974-6846. ISSN (Online): 0974-5645.





Review on Blind Image STEG Analysis using DCT

Dharmesh.B.Patel*, Keyur Brahmhatt , DipikaKothariya , Vishal Polara and Nilesh Prajapati

Birla Vishvakarma Mahavidhyalaya Engineering College, V V Nagar, Anand, Gujarat, India.

Received: 30 Dec 2023

Revised: 09 Jan 2024

Accepted: 12 Jan 2024

*Address for Correspondence

Dharmesh.B.Patel

Birla Vishvakarma Mahavidhyalaya Engineering College,
V V Nagar, Anand, Gujarat, India.

Email: dharmesh.bpatel@bvmengineering.ac.in



This is an Open Access Journal / article distributed under the terms of the **Creative Commons Attribution License** (CC BY-NC-ND 3.0) which permits unrestricted use, distribution, and reproduction in any medium, provided the original work is properly cited. All rights reserved.

ABSTRACT

JPEG images are mostly use in day to day life for conveyance. Patron can be use the number of cryptography techniques for defend important data. Such kind of conveyance can be done using the Steg anography techniques. Steg analysis is one of the best method to hide the important information using Steganography techniques. Steg analysis is also use to analyze and restructure the valuable information. The different remodelled area supported by the DCT, DWT and DFT can be classified by Steg analysis. In this paper we can discuss about the different method and techniques of steg anography and steg analysis like extraction method, feature selection method and classifier method. Base on this study we can conclude that feature extraction using DCT and DFT gives the better results compare to other techniques.

Keywords: Steganography, Steganalysis, Cryptography, Cover-Image, Stego- Image, Classifier, DFT, DCT, DWT

INTRODUCTION

Steganography words is comes from the Greek words “stegos” and “grafia” means “covered writing” [1]. In the digital world, steganography is a security innovation that conceals secret data in a cover. [6]. Steganography and cryptography have many similarities. Cryptography is the act of encrypting messages to render them unintelligible. In other circumstances, steganography will conceal the message in digital media, making it impossible to detect the message's existence in the first place. [4]. in steganography, there are two necessary elements: message and carrier. The message is the secret data that needs to be concealed in digital media available [5].Our study is focused on examining various methods of steganography. Fig 1.1 show the demonstrates of various formats that can be utilized in steganography.





Text Steganography

Altering the text format or changing the characteristics of specific textual elements (such as characters) can lead to text steganography. The aim of this method is to create modifications that can be easily decoded, even if there is noise, but they are still largely indistinguishable to the reader. The reader's understanding of Text Steganography remains largely unclear [5]. The following methods are utilized in text Steganography.

1. Line-Shift Coding
2. Word-Shift Coding.
3. Feature Coding.

IMAGE STEGANOGRAPHY

Steganography involves hiding data in public digital mediums to communicate through secret channels. Posting an image with a secret message on the web or in newsgroups is the only way to get the message. Steganography's use in the right way still appears to be limited. Different types of image files often benefit from the use of these techniques with varying degrees of success.

1. Least Significant Bits
2. Masking and filtering
3. Transformations

There are so many type of Steganography methods are applied on digital images. Like Battle stag, DBS, DFF, Hide Seek, Blind hide, LSB based stego image, F5, Steg Hide, etc...

Battle stag

Ships are treated with the highest filter values in the Battleship Steganography method [2] [7] [25] [27]. In this method randomly "shoots" in any image, and when it finds a "ship" the groups of its shots around the hit, hoping to "sink" the "ship". Then moves to look for other ships. This is a secure method because it requires a password to retrieve the message [10].

DBS and DFF

Dynamic battle stag and Dynamic filter first steganography method [2], [7], [24], [25], [26], [27], do the same thing as Battle Steg and filter first. These two algorithms are based on dynamic programming to speed up the hiding process and reduce memory usage. They are not compatible with the original algorithms because the sequence of pixels held in dynamic array is different.

Hide Seek

This method uses a random seed to randomly generate a password. The password is then used to select the first position in the image to hide the secret message. Then, it randomly generates positions until it successfully hides the secret message. This method is more intelligent than other stegano graphy methods. This method randomly distributes the secret message all over the image [2][7][24][25][26][27].

Blind hide

This method is the most basic in stegano graphy [2][7][25][26][27]. This method hides the message into the image blindly from the top-left corner of the image. It works across the image, like down, and then scan lines pixel-by-pixel. This method alters the LSB of pixel colours to match the message.

LSB

Least significant bits (LSB) is a straightforward method for embedding information in cover images [2], [7], [24], [25], [26] The most basic steganography methods embed the bits of a message directly into the least significant bits plane of a cover image in deterministic order [4]. The least significant bit modulation does not cause a human-visible difference because the change is very small. In order to hide a secret message in an image, you need a good cover image. Since this method uses bits per pixel of an image, you must use lossless compression. Otherwise, the hid-den data will disappear in the transformations of lossy compression algorithms [5]. For example, if you have a 24-bit RGB





Dharmesh.B.Patel et al.,

colour image, you can use a bit per pixel of each of the RGB (red, green and blue) colour components. This adds up to 3 bits per pixel [10].

F5

F5 is an update to F4 and deletes all the vulnerabilities of its predecessor. The basic embedding process remains the same, but F5 increases security and efficiency significantly compared to F4 and other algorithms described previously. F5 embeds the message bits in non-zero ac co-efficient, and uses matrix encoding to minimize the changes in the quantized ac coefficients during the embedding process. Matrix encoding is at the core of F5 algorithm [2] [3] F5 algorithm is based on message length and non-zero ac coefficient. For example, if shrinkage happens, then the number of 0 AC Coefficient increases and the remaining nonzero Coefficient decrease with embedding. The changes in DCT Coefficient histogram may be used to detect hidden message.

Steg Hide

This Steganography tool hides bits from a data file in the least important bits of the cover file. The data file is hidden and can't be seen. It's portable and hides data in files like.bmp, .wav, and .au. It also uses blowfish encryption to encrypt the data, MD5 hashing to pass the passphrase to the blowfish key, and the container data is distributed in a pseudo-random way.

AUDIO STEGANOGRAPHY

Audio steganography is the process of embedding a secret message into a digital audio signal, resulting in a slight alteration of the binary order of the associated audio file. There are a variety of techniques available for this purpose. This article will provide a brief overview of some of them.

1. LSB Coding
2. Phase Coding
3. Spread Spectrum
4. Echo Hiding

IMAGE STEGANALYSIS

Steganography is the art of hiding information within an image using a technology called steganalysis. It's the art of attacking Steganography strategies by either detecting or changing or extracting information from embedded knowledge. It's also known as blind Steganalysis because it doesn't look at the previous data of the method used to hide the info. The image where the secret info is hidden is called a steganography image. The main goal of blind image steganalysis is to detect hidden embedded data without knowing anything about the hidden algorithm.

Steganalysis Methods

Steganalysis methods are classified according to the manner in which the hidden message is detected, as follows [3]:

1. Statistical steganalysis
 - a. Spatial domain.
 - b. Transform domain.
2. Feature based steganalysis.

Type of Steganalysis

The Steganography algorithm (SA) can be used by the Steganalysis algorithm, but it can also be used independently. Steganalysis is divided into the following categories:

1. Specific / Target steganalysis.
2. Generic / Blind / Universal steganalysis.

Specific steganalysis

The Statistical Analysis (SA) is a widely-recognized standard, and the design of a Steganalysis (Steganalysis) algorithm is based on it. The Steganalysis algorithm itself is contingent upon the SA. Steganalysis is a method of





Dharmesh.B.Patel et al.,

analysis that involves examining the statistical characteristics of an image after it has been embedded. This method has the advantage of being highly precise, while the disadvantage is that it is highly limited to certain embedding algorithms and image formats.

Blind / Universal steganalysis

Universal steganalysis isn't known to everyone, so anyone can make a detector to find out if there's a secret message that doesn't depend on the standard analyser. When compared to specific steganalysing, universal is more common and less efficient, but it's still used more than specific because it's independent of the standard analyser itself. This research is focused on creating a universal steganalysing system, which includes two stages:

1. Feature Extraction.
2. Classification

LITERATURE REVIEW

In Optimization of Rich model based on Fisher criterion for image steganalysis [1] the author suggests a way to improve the features of wealthy model options that supersedes the better Fisher criterion. He supported the idea that the difference between the within-class and the between-class variances should be bigger. In the experimental analysis, the rich model SRM might not be able to find typical stylish steganography like Victor-Marie hugo.

In ANOVA and Fisher Criterion based Feature Selection for Lower Dimensional Universal Image Steganalysis [2] The author outlines a method for constructing a re-drafted dimensional unified feature set in order to implement a universal steganography victimisation Fisher criterion and multivariate analysis methods. The proposed algorithmic rule achieves a total of ninety-seven detection accuracies against a variety of steganography strategies.

In FS-SDS: Feature Selection for JPEG Steganalysis using Stochastic Diffusion Search [3] In Ste-ganalysis, the author describes the proposed work for a feature choice algorithm (FS) that is unique to Ste-ganalysis. For example, FS-SDS might be a feature choice algorithm for a wrapper-type that selects random Diffusion Search based on reduced feature set mishandling.

In Steganalysis of LSB matching using differences between non-adjacent pixels [4] the author describes models for the messages encoded by SPV (spatial least vital bit) as independent noises to match the duvet image and explains that the bar graph of the differences between the element grey values is smoothed.

In Steganalysis of least significant bit matching using multi-order differences [5]. This article talks about a way to attack steganography by looking at grayscale pictures of partial domains and matching them with steganography using a learning-based technique.

In Steganalysis of Adaptive JPEG Steganography Using 2D Gabor Filters [6] the author describes two-dimensional Gabor filters that exhibit optimal joint localization properties in both the spatial domain and the spatial frequency domain. The experimental data demonstrate that the detection error of EOOB is indicated for quality factors seventy-five and ninety-five.

In Performance Analysis of Image Steganalysis against Message Size, Message Type and Classification Methods [7] this paper provides a comparison of the performance of a DWT feature-based, predominantly steganalysis algorithm against various current steganography methods and varying rates of message embedding. Additionally, it compares the performance of individual-uniform algorithms against completely different classification-tion methods.

In Steganalysis of content-adaptive JPEG steganography based on Gauss partial derivative filter bank [8] the author outlines techniques to enhance the detection efficiency for content-based JPEG steganography. The intended





Dharmesh.B.Patel et al.,

method produces filtered images containing rich textures and edge data victimisation Gaussian partial filter bank, as well as histograms of absolute values for filtered sub-pictures.

In Performance Evaluation of Feature-based Steganalysis in Steganography [9] The goal of this paper is to evaluate the performance of Feature based Steganalysis strategies to detect steganography tools that area units used for activity a hidden message in still images. The feature extraction performed during this paper was in the spatial domain and directly in the transformation domain of DCI in JPEG files which helps to obtain relevantly applied mathematical information.

In Compact Image Steganalysis for LSB-Matching Steganography [10]. The author suggests a new way to do steganalysis on images, called Compact Image Steganalysis, which involves extracting a feature vector made up of only 12 parts from an image. Practically, they've been able to achieve 99.6% sensitivity for steganalyzers on dataset images with a size of 0.25 bpp, using just two analysis dimensions.

SUMMARY OF WORK

Image steganalysis also relies on binary similarity measures. The idea is that the relationship between lower bits can be affected if we tend to put something in the wrong place. We got 18 different binary measures for each image to make it look 18-D. We then used them to train the classifier and improve the performance against lots of different steganography techniques. We also used them in the DCT domain to make sure the steganography was successful. CF Moments area units are sensitive to different knowledge hiding layers and can give us a warning if there's a hidden message. Stego images can be victimised by a bunch of different tools such as VSL, digital invisible ink toolkit, open stego tool, and 1-2 free steganography tool.

CONCLUSION

Blind image steganalysis has a big advantage over specific steganalysis because it doesn't need to know anything about how to hide data. It works with any kind of image and file. The way you extract features and classify them is really important. You need to figure out the minimum number of features that will give you an accurate classification result. There are lots of different classifiers used in steganalysis, like SVM, bayesian, artificial neural net-work, fisher linear individual, linear discriminant analysis, and more. The techniques you use in steganalysis will help you get a better result by reducing the number of options, and it may also offer better accuracy because of the small sample size.

REFERENCES

1. H. j. J. L. a. C. Y. Yiqin Zhang and Fenlin Liu, "Compact Image Steganalysis for LSB-Matching Steganography", *International Conference on Advanced Computational Intelligence (ICACI)*, pp. 187-192, 2018.
2. S. V. P., B. P. Madhavi B. Desai, "ANOVA and Fisher Criterion based Feature Selection for Lower Dimensional Universal Image Steganalysis", *IJIP*, 2016.
3. V. B. N. M. a. T. C. PunamBedi, "FS-SDS: Feature Selection for JPEG Steganalysis using Stochastic Diffusion Search", *IEEE*, pp. 3797-3802, 2014.
4. Z. X. & X. W. & X. S. & Q. L. & N. Xiong, "Steganalysis of LSB matching using differences between nonadjacent pixels", *springer*, 2014.
5. X. W. X. S. a. B. W. Zhihua Xia, "Steganalysis of least significant bit matching using multi-order differences", *Wiley Online Library*, 2014.
6. f. i. C. Y. Xiaofeng Song, "Steganalysis of Adaptive JPEG Steganography Using 2D Gabor Filters", *IJRITCC*, 2015.





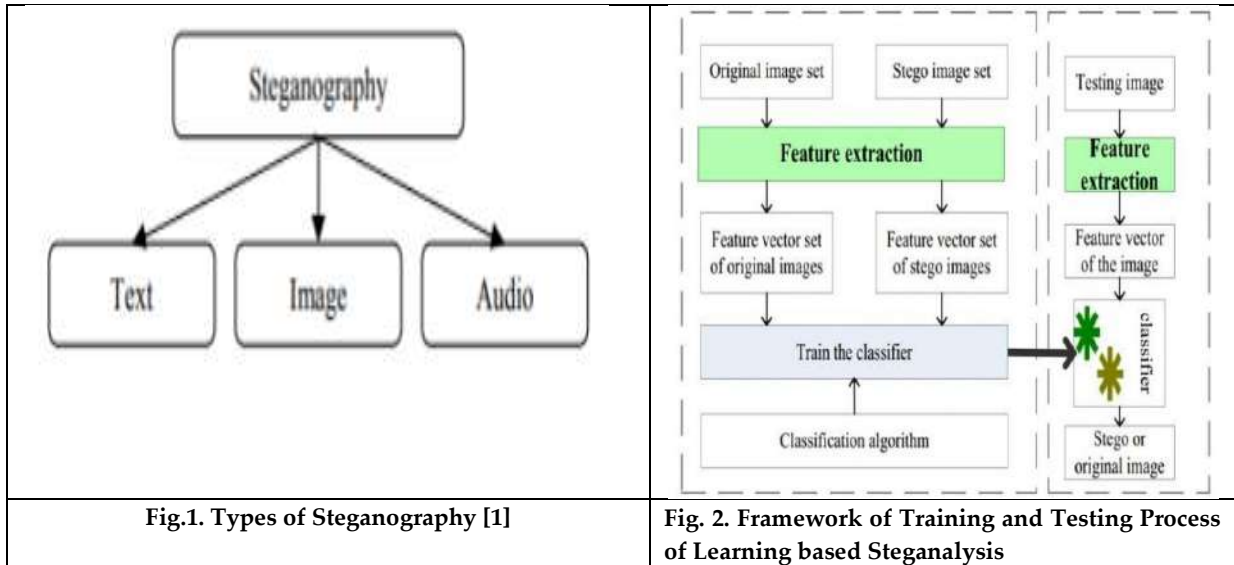
Dharmesh.B.Patel et al.,

7. S. V. P. Madhavi B. Desai, "Performance Analysis of Image Steganalysis against Message Size, Message Type and Classification Methods", *IEEE*, 2016.
8. F. L., C. Y., X. L. X. S. J. L. Y. Yi Zhang, "Steganalysis of content-adaptive JPEG steganography based on Gauss partial derivative filter bank", *Journal of Electronic Imagin*, 2017.
9. Daniel Majercak, Vladimir Banoci, Martin Broda, Gabriel Bugar, Dusan Levicky "Performance Evaluation of Feature-based Steganalysis in Steganography", *Conference Radioelektronika 2013*, April 16-17.
10. M. C.-H. Oswaldo Juarez-Sandoval, "Compact Image Steganalysis for LSB-Matching Steganography", *IEEE*, 2015.
11. J. Anitachristaline, R. Ramesh, D. Vaishali "Steganalysis with classifier combinations", *ARPR-2014*, pg no-2858-2863
12. S.K. Sabnisa, R.N. Awaleb "Statistical Steganalysis of High Capacity Image Steganography with Cryptography", *Elsevier-2016*, 321-327
13. Zohaib Khan, Atif Bin Mansoor "An Analysis of Quality Factor on Image Steganalysis", *IEEE-Conference Paper* - April 2010
14. Sruthi Das N1, Rasmi P S "A Survey on Different Image Steganalysis Techniques", *IJMTER-2015*, 533-536
15. Tom'as Pevny'a, Jessica Fridrichb "Merging Markov and DCT Features for Multi-Class JPEG Steganalysis", *University of New York-2014*.
16. S. Geetha, shivas. shivthasandhu, N. kamraj "blind images teg analysis based on content in dependent statistical measures maximizing the specificity and sensitivity of system", *Elsevier-2006*, pg N0-683-697.
17. Chunhua Chen, Yun Q. Shi, Wen Chen, Guorong Xuan "statistical moments based universal steganalysis using jpeg 2-d array and 2-d characteristic function", *USA* ({cc86,shi}@njit.edu), *Tongji University, Shanghai, China*.
18. Ismail Avci bas, Mehdi Kharrazi, Nasir Memon, B'ulent Sankur "Image Steganalysis with Binary Similarity Measures", *EURASIP Journal on Applied Signal Processing 2005:17*, 2749-2757
19. Yi Zhang, Fenlin Liu, Chunfang Yang, Xiangyang Luo, Xiaofeng Song, Jicang Lu "Steganalysis of content-adaptive JPEG steganography based on Gauss partial derivative filter bank", *Journal of Electronic Imaging-2017*.
20. Manisha Saini, Rita Chhikara "performance Evaluation of DCT and DWT Features for Blind Image Steganalysis using Neural Networks" *International Journal of Computer Applications- March 2015* (0975 – 8887)
21. Dr. Monisha Sharma¹ and Mrs. Swagota Bera "a review on blind still image steganalysis techniques using features extraction and pattern classification method", *International Journal of Computer Science, Engineering and Information Technology (IJCSIEIT)- June 2012, Vol.2, No.3*.
22. Rita Chhikara, Latika Singh "A Review on Digital Image Steganalysis Techniques Categorised by Features Extracted", *International Journal of Engineering and Innovative Technology (IJEIT) - October 2013 Volume 3, Issue 4*,
23. P. Dr. M. Umamaheswari, "Analysis of Different Steganographic Algorithms for Secured Data Hiding," *International Journal of Computer Science and Network Security*, vol. VOL.10, -August 2010.
24. J. K. Amanjot Kaur, "Comparison of Dct and Dwt of Image Compression Techniques," *International Journal of Engineering Research and Development*, pp. 49-52, June 2012.
25. M. b. desai, "DCT Statical and pixel correlation based blind image Steg analysis," april 2018.
26. "http://vsl.sourceforge.net/: VSL TOOL," [Online].
27. "http://diit.sourceforge.net/: Digital Invisible Ink Toolkit 1.5," [Online].
28. <https://www.openstego.com/>: OpenStego tool," [Online].
29. "https://1-2-free-steganography.apponic.com/: 1-2-Free Steganography Tool," [Online].
30. "https://www2.eecs.berkeley.edu/Research/Projects/CS/vision/grouping/segbench/BDS300/images/#:BDS300 dataset," [Online].





Dharmesh.B.Patel et al.,





Navigating the Educational Landscape: Understanding the Post- COVID-19 Effects on Education

Dipika Kothariya, K.N.Brahmbhatt, Dharmesh B.Patel, Vishal Polara and Dharmesh G.Patel

Assistant Professor, Information Technology, BVM, V,V Nagar, Anand, Gujarat, India.

Received: 30 Dec 2023

Revised: 09 Jan 2024

Accepted: 12 Jan 2024

*Address for Correspondence

Dipika Kothariya

Assistant Professor,
Information Technology,
BVM, V,V Nagar, Anand,
Gujarat, India.



This is an Open Access Journal / article distributed under the terms of the **Creative Commons Attribution License** (CC BY-NC-ND 3.0) which permits unrestricted use, distribution, and reproduction in any medium, provided the original work is properly cited. All rights reserved.

ABSTRACT

The COVID-19 pandemic disrupted education systems worldwide, ushering in a new era of uncertainty and adaptation. "Navigating the Educational Landscape: Understanding the Post-COVID-19 Effects on Education" explores the multifaceted impact of the pandemic on education, focusing on the challenges faced by students, educators, and educational institutions. This research paper investigates the repercussions of the abrupt shift to remote learning, the widening digital divide, the mental health and well-being of students, the academic performance setbacks, and the exacerbation of educational inequities. Additionally, the paper examines mitigation strategies and interventions employed to address the challenges posed by the pandemic, encompassing educational policies, technology integration, mental health support, and efforts to close learning gaps. Looking ahead, the research paper outlines future directions for education in the post-COVID-19 era, including the long-term effects and implications, innovations in education, and policy recommendations. By delving into the complexities of this unprecedented educational disruption, this paper aims to contribute to informed decision-making and strategies that can help shape a more resilient and equitable educational landscape in the aftermath of the pandemic.

Keywords: COVID-19, pandemic, navigating.

INTRODUCTION

The COVID-19 pandemic wrought unprecedented disruption across all sectors of society, none more profoundly affected than education. This research paper, "Navigating the Educational Landscape: Understanding the Post-COVID-19 Effects on Education," delves into the multifaceted repercussions of the pandemic on educational systems globally. The sudden shift to remote learning exacerbated inequalities and challenges to student well-being and





Dipika Kothariya et al.,

brought new complexities to education. In this post-pandemic era, examining the lessons learned, the strategies employed, and the lingering effects is essential. This paper aims to provide a comprehensive understanding of the transformed educational landscape and offer insights to shape a more resilient and equitable future for education.

Background and Context

The emergence of the COVID-19 pandemic in 2019 triggered an unparalleled global crisis, profoundly impacting education. Mandatory lockdowns and social distancing measures prompted an abrupt transition to remote learning, exposing digital disparities and educational inequities. Vulnerable populations, including students with disabilities and those from marginalized communities, faced heightened challenges. As the pandemic persists, the need to understand its far-reaching effects on education becomes increasingly critical. This paper explores the complexities of the post-COVID-19 educational landscape, delving into the challenges faced by educational institutions, students, and educators. Through empirical analysis and literature review, it seeks to inform strategies for enhancing educational resilience and equity in the future.

Purpose of the Study

This research endeavors to comprehensively examine the post-COVID-19 educational landscape, elucidating the multifaceted impact of the pandemic on education. By analyzing the challenges encountered during the transition to remote learning, the exacerbation of educational inequalities, and the lessons learned from successful adaptations, the study aims to provide a nuanced understanding of the enduring consequences of the pandemic. The ultimate purpose is to inform policymakers, educators, and stakeholders in education about effective strategies and interventions that enhance educational resilience and promote equity. Through this research, we aspire to contribute to the development of a more resilient and equitable educational system in a post-pandemic world.

LITERATURE REVIEW

The COVID-19 pandemic, a global crisis of unprecedented scale, triggered a seismic shift in the field of education. This literature review provides a comprehensive examination of the impact of the pandemic on education, highlighting key themes, challenges, and lessons learned.

Disruption of Traditional Education

The pandemic led to the sudden closure of educational institutions worldwide, necessitating an urgent transition to remote learning (Dhawan, 2020). This shift disrupted traditional teaching and learning models, compelling educators and students to adapt to digital platforms.

Challenges in Remote Learning

Remote learning posed numerous challenges. A prominent problem that emerged was the disparity in digital resources, as students faced challenges in obtaining essential technology and dependable internet connections. (Chen et al., 2020). Educators, unprepared for online teaching, faced challenges in delivering effective instruction (Hodges et al., 2020). Student engagement and motivation waned in the remote environment (Son et al., 2021).

Mental Health Impact

The pandemic had significant implications for the mental health and well-being of students. Prolonged isolation and uncertainty led to increased stress, anxiety, and depression (Loades et al., 2020). The loss of vital support systems in schools exacerbated these issues (Huremović, 2019).

Academic Performance and Learning Loss

Academic performance suffered as students grappled with the challenges of remote learning. Learning loss, particularly in subjects requiring hands-on experiences, became a concern (Kuhfeld et al., 2020). Early indications suggest that the pandemic's impact on academic achievement may be enduring (Engzell et al., 2020).





Dipika Kothariya et al.,

Exacerbation of Inequalities

One of the most significant revelations was the exacerbation of educational inequalities. The existence of a digital divide became apparent, as students from underprivileged backgrounds encountered hindrances in accessing online education (Bannister & Agboola, 2020). Moreover, students with disabilities and those learning English faced supplementary challenges (Barton et al., 2020). In conclusion, the COVID-19 pandemic disrupted education on a global scale, exposing and exacerbating challenges related to technology access, teacher preparedness, student engagement, mental health, and educational inequality. This literature review sets the stage for a comprehensive examination of the post-COVID-19 educational landscape, with a focus on understanding and addressing these challenges.

Remote Learning and its Challenges

Remote learning, necessitated by the COVID-19 pandemic, presented both opportunities and challenges to the field of education. While it offered continuity during times of crisis, it also unveiled a host of complexities that affected students, educators, and educational institutions. A prominent challenge was the stark digital divide, as many students lacked access to essential technology devices and reliable internet connectivity. This glaring disparity hindered equitable participation in online learning and deepened educational inequalities. Additionally, limited digital literacy skills among students, particularly in underserved communities, created hurdles in navigating online platforms effectively. Educators faced a steep learning curve in adapting their teaching methods to the digital environment, often without adequate training. This influenced the quality of online instruction, impacting student engagement and learning outcomes. Moreover, the isolation of remote learning environments sometimes leads to decreased student engagement and motivation, affecting academic performance. The global health crisis similarly brought about substantial consequences for the mental well-being of students, resulting in heightened levels of stress, anxiety, and depression as a result of extended periods of social isolation. To address these multifaceted challenges, strategies for bridging the digital divide, promoting digital literacy, enhancing teacher preparedness, improving student engagement, and providing mental health support are essential in the era of remote education.

Mental Health and Well-being of Students

The mental health and well-being of students were significantly affected by the profound impact of the COVID-19 pandemic. Prolonged periods of isolation, disrupted routines, and the uncertainty surrounding the pandemic contributed to increased levels of stress, anxiety, and depression among students (Loades et al., 2020)[14]. The closure of schools, which often served as vital support systems for students with emotional and behavioral needs, exacerbated these challenges (Huremović, 2019). Addressing students' mental health became a critical concern, highlighting the importance of integrating mental health support and resources into educational settings to ensure the overall well-being of students during times of crisis and beyond.

Academic Performance and Learning Loss

The COVID-19 pandemic disrupted academic performance and exacerbated learning loss among students. The sudden shift to remote learning posed challenges, particularly in subjects requiring hands-on or experiential learning. Many students struggle to adapt to the digital environment, resulting in decreased engagement and potentially long-lasting academic consequences (Kuhfeld et al., 2020)[14]. Early evidence suggested that the pandemic's impact on academic achievement might persist, highlighting the need for targeted interventions to mitigate learning loss. As educational institutions transition to post-pandemic education, addressing these academic challenges and implementing strategies for recovery remain essential to ensuring educational equity and student success [13].

International student mobility

The COVID-19 pandemic presented unprecedented challenges for international student mobility. Measures such as travel restrictions, visa processing delays, and health-related concerns disrupted the normal flow of students moving across borders. In response, educational institutions adjusted by transitioning to remote learning, which had an impact on the traditional study abroad experience. Many students postponed or canceled their plans due to the





Dipika Kothariya *et al.*,

prevailing uncertainty. The pandemic emphasized the significance of digital education and hybrid learning models while also exposing the international education sector's susceptibility to global crises. However, it stimulated innovations in online learning and showcased the resilience of both international students and educational institutions. As the world begins to recover, there is potential for a renewed interest in global education, although it's crucial to acknowledge that the landscape has undergone lasting changes [13].

Educational Expenditure as a Percentage of Total Government Spending

In 2017, OECD nations, on average, dedicated around 11% of their total government spending to primary through tertiary education. However, this proportion varied among different OECD and their partner countries, ranging from approximately 7% in Greece to about 17% in Chile (as depicted in Figure 1)[13]. It's important to acknowledge that government allocations for education are often subject to changes in response to external shocks, as governments adapt their investment priorities. The economic repercussions caused by the virus's spread may potentially affect the accessibility of public funds for education in both OECD nations and their other partner countries.. This effect may arise from reduced tax revenue and the redirection of emergency funds to support rising healthcare and welfare expenses.

Global School Closures

Amid COVID-19 pandemic, China initiated the closure of schools in February 2020, starting in regions with earlier spring semesters and eventually expanding nationwide. This pattern was mirrored in numerous countries worldwide. By March, all 46 countries featured in the Education at a Glance report had imposed various degrees of school closures. Among these, 41 nations had instituted nationwide school closures, while countries like Australia, Iceland, Russia, Sweden, and the United States did soon a sub national level. It's crucial to note that not all countries that were affected closed down all of their schools. For instance, Iceland kept primary schools open with small class sizes, and Sweden shifted upper secondary education to main distance learning in mid-March (UNESCO, 2020) [13][1].

Success Stories and Lessons Learned

The COVID-19 pandemic, several educational success stories emerged globally. Many schools swiftly transitioned to online learning, offering students access to quality education from the safety of their homes. Innovative pedagogical approaches, such as flipped classrooms and project-based learning, engaged students in remote settings. Community involvement and parental support played a crucial role in students' educational experiences, fostering a sense of shared responsibility. Furthermore, initiatives prioritizing students' mental health and well-being helped mitigate the psychological impacts of the crisis. These success stories underscored essential lessons for the future. Flexibility and adaptability within educational systems are critical, enabling rapid responses to unforeseen challenges. The pandemic highlighted the need for equitable technology access and digital literacy for both educators and students. Ongoing teacher professional development ensures effective online instruction. Resilience and innovation should be embraced in curriculum design and delivery. Inclusive education is paramount, particularly for marginalized communities and students with disabilities. Governments play a crucial role in providing timely support and resources during crises. Lastly, preparing education systems for future emergencies is imperative, emphasizing the importance of readiness and proactive planning. These lessons inform strategies for enhancing educational resilience and equity in a post-pandemic world.

CONCLUSION

The effects of COVID-19 on education have been diverse, causing disruptions to conventional teaching and learning methods and exposing long-standing disparities. As educational institutions grappled with the complexities of remote learning, they encountered issues concerning technology accessibility, teacher readiness, student welfare, academic achievement, and educational disparities. This review of existing literature establishes the foundation for a



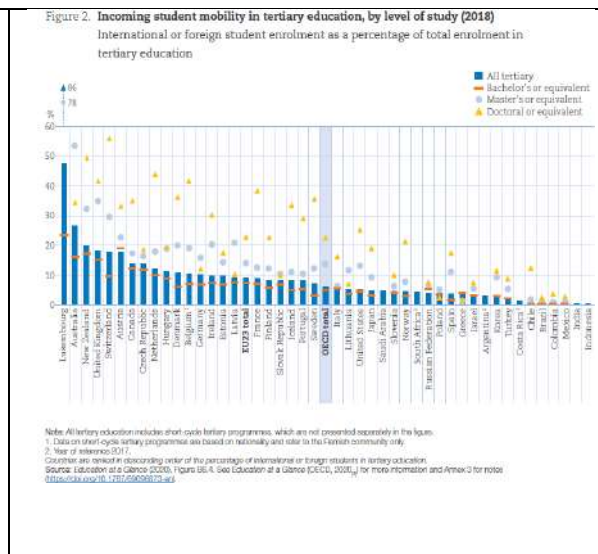
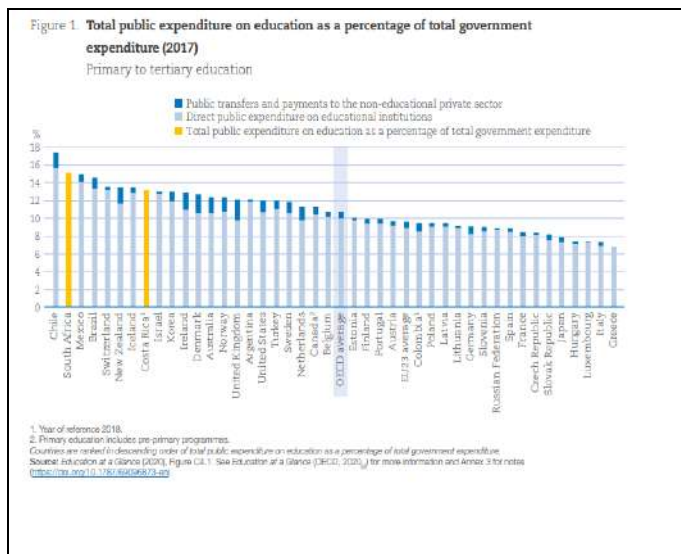


Dipika Kothariya et al.,

thorough exploration of the educational landscape in the aftermath of COVID-19, with an emphasis on comprehending and tackling these issue.

REFERENCES

1. Andreas Schleicher , “The impact of covid-19 on education” - insights from education at a glance 2020 @oecd 2020
2. Adams, r. J., smart, p. A., & huff, a. S. (2017). “Teaching evidence-based management with live cases. Academy of management learning & education”, Reserch gate, June 2011.
3. Abdulrahman Essa Al Lily * , Abdelrahim Fathy Ismail, Fathi Mohammed Abunasser, Rafdan Hassan Alhajhoj Alqahtani.“Distance education as a response to pandemics: corona virus and arab culture”. Technology in society, 2020.
4. Anders, j.“Covid-19 and the academic profession: the role of faculty in student well-being”, 2020.
5. Bao, w. Covid-19 and online teaching in higher education: a case study of peking university. Human behavior and emerging technologies, 2020.
6. Hodges, c., moore, s., lockee, b., trust, t., & bond, a.. “The difference between emergency remote teaching and online learning”. 2020.
7. Unesco. “Covid-19 educational disruption and response”. Retrieved from https://en.unesco.org/covid19/educationresponse,2020
8. World bank. The covid-19 Pandemic: Shocks to education and policy response. Retrived from https://www.worldbank.org/en/topic/ed, 2020
9. Zawacki-richter, o., & naidu, s.,“Emergency remote teaching in a time of global crisis due to coronavirus pandemic”. Asian journal of distance education, 2020.
10. Zhao, y. “Covid-19 as a catalyst for educational change”. Prospects, 2020.
11. Lynch, k., & schuetze, h. G.,“Covid-19 and student mobility in higher education: an initial analysis”, Higher education, 2020.
12. Ferrel, m. N., & ryan, j. J.,“The impact of covid-19 on medical education”. Cureus, 2020.
13. Unesco, “Education: from disruption to recovery” Retrieved from https://en.unesco.org/covid19/education response, 2020.
14. Megan Kuhfeld, James Soland, Beth Tarasawa, Angela Johnson, Erik Ruzek, and Jing Liu “Projecting the Potential Impact of COVID-19 School Closures on Academic Achievement”,Resechgate,2020





Dipika Kothariya et al.,

Figure 3. Number of countries with school closures due to COVID-19
Data covers the period between 17 February 2020 and 30 June 2020



Note: This figure covers educational institutions from early childhood education to tertiary education. Localised school closure refers to school closures of some levels of education only and/or by some subnational entities.
Source: UNESCO (2020), COVID-19 educational disruption and response. <https://doi.org/10.7927/H4T8-6M9Q>; Education at a Glance 2020, Figure D1.4.





Literature Review on Multiple Face Recognition based Automated Attendance System using Machine Learning Technique

Harshidaben R Patel^{1*}, Monika Patel² and Priti Srinivas Sajja³

¹ Ph D Research Scholar, Computer Science, CVM University, V V Nagar, Gujarat, India.

² Assistant Professor, NVPAS, CVM University, Gujarat, India.

³ Director, Post Graduate Department of Computer Science, Sardar Patel University, India.

Received: 30 Dec 2023

Revised: 09 Jan 2024

Accepted: 12 Jan 2024

*Address for Correspondence

Harshidaben R Patel

Ph.D Research Scholar,

Computer Science,

CVM University,

V V Nagar, Gujarat, India.

Email: harshidamaple@gmail.com



This is an Open Access Journal / article distributed under the terms of the **Creative Commons Attribution License** (CC BY-NC-ND 3.0) which permits unrestricted use, distribution, and reproduction in any medium, provided the original work is properly cited. All rights reserved.

ABSTRACT

Attendance of the Students is important task in classroom. But student's attendance system is manual at many places. It is time consuming and also requires additional efforts to computerize after manual attendance. Instead of that if we have automated attendance system as face can be unique identification of the person. Such system can help to save time as multiple face recognition can be used for taking attendance of multiple people at a time and decisions can be taken for student using attendance in class. This type of system can be useful at other places like industry, airport, criminal detection, face tracking, forensic, etc. To understand the working of multiple face recognition in educational institute some literatures are studied which elaborated in this paper.

Keywords: Face recognition; Multiple Face recognition; Attendance, Student, Classroom

OBJECTIVE

1. This research work offers an expert knowledge about various machine learning techniques to identify multiple faces of students from the given dataset.
2. To study the different feature classification techniques
3. To design new architecture for multiple face recognition system.
4. To prepare and train the face image database based on various features of face images
5. If student's face is detected correctly then mark the attendance or in case of unidentified face some warnings are given to the user.





Harshidaben R Patel et al.,

REVIEW OF LITERATURE

Authors in [1] observed many organizations, companies and institutions are using RFID methods, Biometric Fingerprint method and Registers for periodic attendance of their employees. These methods generally require more time for calculation. Researchers used modified algorithm of Haar's Cascades proposed by Viola-Jones for face detection and reported success rate of 94%. They used LBPH algorithm and got accuracy variations in the results, as the number of images were changed. e.g for 30 images accuracy was 26% and for 300 images accuracy was 75%. So face recognition method is time saving for attendance.[1] By analyzing the Receiver Operating Characteristics (ROC) curve, the authors of [2] conducted research to determine which facial recognition algorithm—Eigen face and Fisher face—was the best. The algorithm was then integrated into the attendance system. The ROC curve demonstrated that Eigen face outperformed Fisher face in the trials reported in this research. The accuracy rate of the system that used the Eigen face algorithm was between 70% and 90%. In [3], authors used Discrete Wavelet Transforms (DWT) and Discrete Cosine Transform (DCT) to develop a face recognition approach for a student attendance system in the classroom. These techniques were utilized to extract the characteristics from the students' faces, and then the Radial Basis Function (RBF) was applied to classify the objects on the faces. Out of 148 students, 121 students were able to correctly identify 121 facial photos, yielding an overall identification percentage of 82%.

The system was able to identify 70% of the student's face when it was practically presented in real time by the authors in [7], despite the fact that the student's face wasn't aligned with the camera. This technology recognized a student's face even at an alignment angle of up to 60 degrees. They utilized the MSE facial recognition algorithm and the Viola & Jones face detection method to improve the project's outcome. In [9], authors concluded Face detection and recognition has been a challenging task due to unconstrained condition. They used Viola Jones face detection method; Local Binary Pattern algorithm for face recognition and Yale database techniques were used and got overall efficiency of 83.2% The authors of [14] suggested an Android-based face recognition system for course attendance. Each registered student should use their smart phone to take a picture of their face and scan the QR code that is shown at the front of the classroom. After being taken, the image was transferred to the server so that attendance tracking and face recognition could begin. A classifier was limited to use face recognition in a certain course in order to achieve good face recognition accuracy and economical processing time.

The experimental result demonstrates that by using LDA, the suggested attendance system was able to achieve 97.29% face recognition performance and only required 0.000096 s for the face recognition procedure in the server. The authors of [15] presented a face recognition model that uses SVM and Face Net for face embedding feature extraction and classification, respectively. Transfer learning was utilized as a concept to shorten training times and boost recognition rates. 5-point landmarks on face frames were extracted using the Multi-Task Cascaded Convolution Neural Network (MTCNN) model. The extracted face frame was then transferred to Face Net for embedding extraction, and Support Vector Machine (SVM) classification was performed. While the 5 Celebrity Face dataset was used for system training and validation, the LFW-dataset was utilized to pre-train the Face Net model. Real-time face detection and recognition is surpassed by MTCNN with SVM. 99.85% real-time recognition accuracy is the lowest accuracy attained in the suggested system. During a live stream, the model was put into use and trained on fresh data in order to test face recognition. In order to achieve this, we began recording a live video stream and incorporated the suggested model into it using the open CV Python library. A face recognition system operating on a real-time stream of visual data was the end result. The faces could be accurately recognized by the system. The number of people in the picture, the system's processing power, the presence or absence of light sources, the direction in which a face points toward the camera, and other factors all affect accuracy of a live stream face recognition systems. However, the model can produce results with an average accuracy of 91% when used by one person. With astounding results, the author in [17] used a Face Net model based on the MobilenetV2 backbone with the subsection SSD to identify faces using depth-separated convolutional networks in order to minimize the model size and computational volume. The suggested model was tested and assessed by the author using MCTT backbone and various Rectinal models as comparison points. SSD along with MobileNetV2 backbone has guaranteed accuracy



**Harshidaben R Patel et al.,**

of approximately 99% in simulated experiments and 91-95% in real-world applications using the same dataset as wider face. When the frame rate is between 20 and 23 (FPS), the process speed is effectively increased. The updated Face Net model is faster and more efficient for small datasets and less resources in the training model than the previous state-of-the-art models, which need larger datasets for processing and training.

The author of [18] looked up 30 articles about CNN and the LBPH algorithm. They came to the conclusion that there are numerous ways to communicate the benefits and drawbacks of the two algorithms, and that CNN is a superior algorithm for use in class attendance. The CNN algorithm's facial recognition is a more reliable option for implementing in-class attendance because of its high accuracy and stability in the presence of external influences. The primary challenge with the CNN algorithm is that, in contrast to LBPH, a large number of datasets are needed; therefore, an effective method of gathering datasets is required. Model performance is still influenced by outside variables like background, lighting, and face position. ANN, PCA, and Haar Cascade are combined in the authors' suggested approach in [19], which produced an image identification rate of 98.88%. Thus, when compared to other techniques like PCA with ANN, DNN, etc., the proposed approach is more accurate at identifying a person in an image. Given the variety of situations that people encounter on a daily basis, this system is extremely challenging to implement. As the first stage in developing an automatic face recognition system is face detection, which is challenging because of the range of image appearances that can occur, such as changes in lighting, occlusions, pose variations, expression changes, and aging, variation in number of images while training, selection of best algorithm, etc. The aforementioned analysis makes it quite evident that face recognition software can be used to recognize or authenticate people by looking at their faces. It is among the more effective biometric techniques available today. These kinds of biometric systems are crucial since security is becoming more and more crucial every day.

Proposed Model

The following is the Proposed Architecture for "Multiple Face Recognition based Automated Attendance System using Machine Learning Technique".

This system can have two parts

1. Training Module: The system is designed to store the faces and their facial features of the persons using below steps
 - Face Images of Single Person: To record attendance, each person's picture will be taken with a digital camera, and it will be saved in a designated folder on the server or data storage devices along with their names. We can obtain accurate results by using a larger number of images of a specific individual.
 - Face Area Detection: To extract face regions from the input image, the image is processed.
 - Features Extraction and Training: Facial land features like nose, eyes and lips will be extracted for the person's face recognition.
2. Database Creation: The individual photos that were captured with the digital cameras will be placed in a folder and given a name. To achieve the best results for face recognition, the same procedure should be followed until all of the individual's data is stored.
3. Attendance Marking using Face Recognition Module:
 - Person Image: image containing multiple person face will be taken as an input to the system.
 - Multi Face Detection: Every single person's face will be recognized if two or more people are seen in a specific frame.
 - Cropping and Face Rejection: Person's image will be cropped and if image is not clear than it will be rejected otherwise next step will be done.
 - Preprocessing and Feature Extraction: From input image features will be extracted and will be cross checked with existing data for a person.
 - Classification of Faces: If the features are matches with existing data in database then person's attendance will be marked otherwise absent will be marked. Whole class attendance report will be created automatically for a particular day or lecture using this data. For unidentified face some warning message will be created.





CONCLUSION

Reviewing literature we can conclude that there are many challenges in multiple face recognition based automated attendance system. Further study can be done to overcome these challenges in multiple face recognition system in efficient way. Multiple face recognition system is faster as compared to one-to one face recognition. To get the efficient result for the system we can use various combinations of machine learning algorithms. The System can be enhanced in future to combine with other areas like Bank, Healthcare, Security, Marketing, Social Media, and Access Control etc.

REFERENCES

1. Suyash R. Dhabre, Rahul S. Pol "Automated face recognition based attendance system using LBP face recognizer", International journal of advance scientific research and engineering trends, April 2020
2. Siswanto, Adrian Rhessa Septian, Anto Satriyo Nugroho, and Maulahikmah Galinium. "Implementation of face recognition algorithm for biometrics based time attendance system." 2014 International Conference on ICT For Smart Society (ICISS). IEEE, 2014.
3. Lukas, Samuel, Aditya Rama Mitra, Ririn Ikana Desanti, Dion Krisnadi "Student attendance system in classroom using face recognition technique." 2016 International Conference on Information and Communication Technology Convergence (ICTC). IEEE, 2016.
4. Shantnu Tiwari, Face Recognition with Python, in Under 25 Lines of Code
5. Merrin Mary Solomon, Mahendra Singh Meena, Jagandeep Kaur, "Challenges in face recognition systems" April 2019
6. Jarugula.Vamsikrishna, Kollipara. Anudeep, L.Jegan Antony Marcilin, V. Balamurugan. "An Advanced Attendance Marking system using facial Recognition". International Conference on Frontiers in Materials and Smart System Technologies IOP Conf. Series: Materials Science and Engineering 590(2019)012049 IOP Publishing doi:10.1088/1757-899X/590/1/012049
7. Sathyanarayana N, Ramya M R, Ruchitha C, Shwetha H S. "Automatic Student Attendance Management System Using Facial Recognition". International Journal of Emerging Technology in Computer Science & Electronics (IJETCSE) ISSN: 0976-1353 Volume 25 Issue 6 – MAY 2018.
8. Radhika C. Damale;Bazeshree. V Pathak, "Face Recognition Based Attendance System Using Machine Learning Algorithms". 2018 Second International Conference on Intelligent Computing and Control Systems (ICICCS), Conference paper 2018, IEEE.
9. Mrunmayee Shirodkar, Varun Sinha, Urvi Jain, Bhushan Nemade, "Automated Attendance Management System using Face Recognition", International Journal of Computer Applications (0975 – 8887), International Conference and Workshop on Emerging Trends in Technology (ICWET 2015)
10. ANDREW JASON SHEPLEY, Charles Darwin University, Australia,"Face Recognition in Unconstrained Conditions: A Systematic Review", July 2019
11. <https://www.ibm.com/topics/machine-learning> 2023
12. Raj Kaste, Harish Pandilla, Priyesh Surve, Mubin Shaikh, Shalaka Deore, Prof. Shubhangi Ingale, "Multiple Face Detection Attendance System". International Research Journal Of Engineering And Technology (IRJET), E-ISSN: 2395-0056, P-ISSN: 2395-0072. VOLUME: 08 ISSUE: 03 | MAR 2021
13. Manoj D, Nethra N, Manjunatha D, Girish Kumar L, Jyothi S Nayak, "Multiple Face Detection and Recognition: Automated Attendance System – A Survey", JETIR (ISSN-2349-5162), April 2016, Volume 3, Issue 4.
14. Dwi Sunaryono , oko Siswanto , Radityo Anggoro "An android based course attendance system using face recognition", Journal of King Saud University - Computer and Information Sciences, volume 33, Issue 3,Pages 243-374 (March 2021)
15. Suguna G C, Kavitha H S, Sunita Shirahatti, Sowmya R Bangari, "Face Recognition System for Real Time Applications Using SVM Combined With FACENET and MTCNN", International Journal of Electrical





Harshidaben R Patel et al.,

- Engineering and Technology (IJEET) Volume 12, Issue 6 Suguna G C, Kavitha H S, Sunita Shirahatti, Sowmya R Bangari,, June 2021, pp. 328-335, Article ID: IJEET_12_06_031, Scopus Indexed
16. C. Ranjeeth Kumar , Saranya N , M. Priyadharshini , Derrick Gilchrist E, Kaleel Rahman M, “Face recognition using CNN and Siamese network”, Measurement: Sensors Volume 7, June 2023, 100800
 17. Thai-Viet Dang, “Smart Attendance System based on Improved Facial Recognition”, Journal of Robotics and Control (JRC) Volume 4, Issue 1, January 2023, ISSN: 2715-5072, DOI: 10.18196/jrc.v4i1.16808
 18. Andre Budimana , Fabiana , Ricky Aryatama Yaputeraa , Said Achmada, Aditya , Kurniawana “Student attendance with face recognition (LBPH or CNN): Systematic literature review” , 7th International Conference on Computer Science and Computational Intelligence 2022, ScienceDirect, Procedia Computer Science 216(2023) 31-38
 19. Jaishree Jain, Jatin Chauhan, Anushka Sharma, Shashank Sahu, Ankita Rani, “A Real Time Employee Attendance Monitoring System using ANN”, International Journal on Recent and Innovation Trends in Computing and Communication, DOI: <https://doi.org/10.17762/ijritcc.v11i11s.8074>, Vol. 11 No. 11s (Oct 2023)

Table 1: Comparison Summary of Various Algorithms

Sr. no	Title	Authors	Algorithm	Summary
1.	Automated Face recognition based attendance system using LBP face recognizer	Suyash R. Dhabre, Rahul S. Pol	LBPFI	<ul style="list-style-type: none"> ✓ Accuracy variations in the results with varying image counts. ✓ For instance, accuracy was 20% for 30 images and 75% for 300 images.
2.	Implementation of face recognition algorithm for biometric based time attendance system	Siwanto, Adrian Riessa Septian, Anto Santyo Nugroho, and Maulalikhmah Galantium	Eigenface and Fisherface	<ul style="list-style-type: none"> ✓ Eigenface achieves better result than Fisherface ✓ Algorithm achieved an accuracy rate of 70% to 90%.
3.	Student attendance system in classroom using face recognition technique	Lukas, Samuel, et al.	LWTF and DCT	<ul style="list-style-type: none"> ✓ System achieved an accuracy rate of 82%.
4.	Automatic Attendance Management System Using Facial Recognition	Sakyaaravana N., Ramya M R, Rochitha C, Shwetha H S.	Viola & Jones, MSE	<ul style="list-style-type: none"> ✓ Even with the student's face not aligned with the camera, the system was still able to identify 70% of the student's face. ✓ It could even identify the student's face at an angle of up to 60 degrees
5.	Face Recognition Based Attendance System Using Machine Learning Algorithms	Radhika C. Damale, Bhareshree V. Pathak	SVM, MLP and CNN	<ul style="list-style-type: none"> ✓ On a self-generated database, the SVM, MLP, and CNN achieve testing accuracy of approximately 87%, 86.5%, and 98%, respectively.
6.	Automated Attendance Management system	Mrunmayee Shirodkar, Vaun Sinha, Urvi Jain, Bhushan Nemade	Viola & Jones, LBP	<ul style="list-style-type: none"> ✓ Using the Viola Jones face detection method, the Yale database techniques, and the Local Binary Pattern algorithm for face recognition, achieved an overall efficiency of 83.2%.
7.	An Android Based Course Attendance System using Face Recognition	Dwi Sunaryono, Iksa Siawantoro, Raddy Anggoro	LDA	<ul style="list-style-type: none"> ✓ With a 97.29% face recognition performance, the server required just 0.000008 seconds to complete the face recognition process.

Sr. no	Title	Authors	Algorithm	Summary
8.	Face Recognition System for Real Time Applications Using SVM Combined With FACENET and MTCNN	Suguna G C, Kavitha H S, Sunita Shirahatti, Sowmya R Bangari	SVM, Combined With FACENET and MTCNN	<ul style="list-style-type: none"> ✓ Used open CV library ✓ The least accuracy achieved in the proposed system is 99.85% for real time recognition for straight, slight deviation on left or right and with the head lifted up in front of the camera respectively. ✓ An average accuracy of 91% during live face recognition
9.	Smart Attendance System based on Improved Facial Recognition	Thai-Viet Dang	FaceNet based on MobilenetV2-SSD	<ul style="list-style-type: none"> ✓ Ensure accuracy of about 99% in simulated experiments and 91-95% in practical applications ✓ Frame rate of 20-23 (FPS)
10.	Student attendance with face recognition (LBPH or CNN): Systematic literature review	Andre Budimana, Fabiana, Ricky Aryatama Yaputeraa, Said Achmada, Aditya, Kurniawana	CNN, LBPH	<ul style="list-style-type: none"> ✓ CNN is better algorithm to apply as compare to LBPH due to its high accuracy and stability when external factors influence it
11.	A Real Time Employee Attendance Monitoring System using ANN	Jaishree Jain, Jatin Chauhan, Anushka Sharma, Shashank Sahu, Ankita Rani	ANN, PCA, and Haar Cascade	<ul style="list-style-type: none"> ✓ Produced an image identification rate of 98.88%.





Harshidaben R Patel et al.,

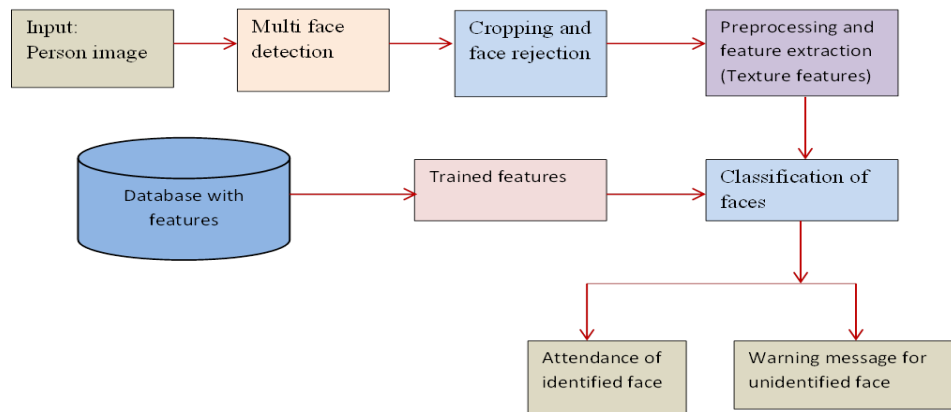


Fig. 1. Multiple face recognition based automated attendance system machine learning





Effective Remediation of Crystal Violet Dye using CoFe₂O₄/ Eggshell Nano composite – H₂O₂

Shruti Waghadhare¹, Aparna Kulkarni^{1*}, Umesh Sankpal¹, Neha Bhatkar¹ and Seema Devasthali¹

¹Department of Chemistry, Gogate Jogalekar College (Autonomous), Ratnagiri, Maharashtra, India.

Received: 30 Dec 2023

Revised: 09 Jan 2024

Accepted: 12 Jan 2024

*Address for Correspondence

Aparna Kulkarni

Department of Chemistry,
Gogate Jogalekar College (Autonomous),
Ratnagiri, Maharashtra, India.
Email: drkulkarni.gjc@gmail.com



This is an Open Access Journal / article distributed under the terms of the **Creative Commons Attribution License** (CC BY-NC-ND 3.0) which permits unrestricted use, distribution, and reproduction in any medium, provided the original work is properly cited. All rights reserved.

ABSTRACT

The degradation of Crystal Violet dye, a common pollutant, presents a significant environmental challenge due to its persistence in water bodies. To address this issue, the utilization of magnetically separable catalysts has emerged as a promising solution. In this study, we present a novel approach for the degradation of Crystal Violet (CV) dye using a magnetically separable CoFe₂O₄/Eggshell nano composite and H₂O₂. The CoFe₂O₄/Eggshell nano composite was synthesized and characterized using various techniques like FT-IR, SEM, EDS and XRD to confirm its structural and compositional properties. The catalytic potential of the nano composite in combination with hydrogen peroxide was studied for efficient removal and degradation of CV dye from water. The catalyst presents the advantage of easy recovery through the application of an external magnet and can be effectively reused up to 6 cycles in dye removal processes. This novel combination of magnetically separable nano composite and hydrogen peroxide holds promise for catalytic applications in CV dye degradation processes.

Keywords: CoFe₂O₄/Egg shell nano composite, magnetically separable, Crystal violet dye degradation.

INTRODUCTION

The use of synthetic dyes has revolutionized industries, playing a pivotal role in the enhancement of products and processes. Synthetic dyes have found applications across a spectrum of sectors including textiles, cosmetics, plastics, and electronics. However, the unregulated release of wastewater from these industries has created significant environmental issues. Many synthetic dyes have proven to be persistent pollutants, resisting traditional water treatment methods. Consequently, untreated effluents from dye industries are often introduced into natural water sources, posing serious risks to both ecosystems and public health. The persistence of these dyes disturbs aquatic environments, hindering sunlight penetration and oxygen exchange. This leads to adverse effects on aquatic life and





Shruti Waghadhare et al.,

overall water quality[1]-[3]. Among the various dyes, Triphenyl methane dyes have been extensively used for various purposes like agent in coloring leathers, fertilizers, sensitizers in solar cells, Gram's staining, detergents, bacterio static agents, etc.. However, one of such extensively used TPM dye - Crystal violet (CV) has ability to interact with negatively charged cell membrane surfaces leading to easy entry into cells and subsequent disruption of the essential cell functions in living beings. This necessitates proper treatment of wastewater containing CV dye before disposal. Thus, from an environmental perspective, urgent action is required to develop effective and sustainable strategies for addressing water pollution due to CV dye [4]. Several methods have been explored for effective CV dye removal, encompassing chemical oxidation and reduction, adsorption, physical precipitation and flocculation, photolysis, electrochemical processes, and biodegradation Among all these methods use of hydrogen peroxide combined with many catalytic and photo catalytic pathways has been greatly explored for the degradation or decolorization of CV dye. Iron oxide coated granular activated carbon has been used for the degradation of CV dye in combination with hydrogen peroxide.[5] Photo catalytic processes using catalysts like TiO_2 [6], Ag^+ doped TiO_2 [7], $\text{BiOxCl}_y / \text{BiO}_m$ Incomposite [8], Cobalt oxide nanoparticles [9], ZnO and $\text{ZnO/Graphene Oxide}$ composite[10], Bi_2WO_6 [11], Graphene-Ce- TiO_2 and Graphene-Fe- TiO_2 ternary nano composite[12], Nanochitosan/ carboxy methyl cellulose / TiO_2 bio composite[13] have been developed.

Among the array of strategies available, use of magnetic nanocomposites for degradation of diverse synthetic dyes stands out as a promising and viable alternative. These innovative materials exhibit potential for remediating synthetic dye pollutants as either photocatalysts in conjunction with tailored UV or Visible radiations, or in combination with oxidizing reagents . Magnetic materials such as MnFe_2O_4 [14], Calcium Ferrite[15], Bismuth Ferrite[16]etc have been used to catalyze degradation reactions of various dyes due to their good photocatalytic activity, stability and narrow band gap. Advanced oxidation processes involve Fenton and Photo Fenton catalysis which is one of the important methods explored for the degradation of dyes. While several methods have been developed for the remediation of Crystal Violet dye, many of these approaches suffer from drawbacks, such as limited efficiency, high cost, environmental concerns, and challenges in catalyst recovery. The quest for innovative and more effective remediation strategies remains at the forefront of contemporary research endeavors. Our research aims to address these existing challenges and provide a sustainable, cost-effective, and highly efficient remediation approach. In this context, we have developed a catalytic system: CoFe_2O_4 /Eggshell in combination with H_2O_2 , as a powerful and efficient system for the degradation of Crystal Violet dye. The raw eggshell, considered as a natural waste material and calcinated eggshell is well known for its adsorbent properties. In our continuous efforts to develop green strategies, eggshell – a readily available natural waste material has been incorporated into catalytic system to promote sustainable and environmentally responsible solutions.

Experimental Work

Catalyst Preparation and Characterization

Ferric chloride, cobalt chloride $\text{CoCl}_2 \cdot 7\text{H}_2\text{O}$, sodium hydroxide, Crystal Violet(CV) dye were purchased from Molychem and used directly without further purification. Waste eggshells were collected from households.

Preparation of calcined eggshell powder

Waste eggshells were collected from home and washed with water to remove surface impurities. Then the eggshells were heated in a deionized water to remove the membrane with ease. After this treatment eggshells were dried and crushed into fine powder and sieved through muslin cloth. This eggshell powder was then calcined at 900 in a muffle furnace.

Preparation of cobalt ferrite Nanoparticles

Cobalt ferrite nanoparticles were prepared by previously reported co precipitation method [17]at room temperature. The stoichiometric amount of solution of FeCl_3 and $\text{CoCl}_2 \cdot 6\text{H}_2\text{O}$ were prepared and mixed in a beaker and 4M NaOH solution added drop wise in the above solution. With the addition of each drop of 4N NaOH black precipitate was observed. Addition was continued till pH become 9 and then the precipitate was filtered using Buckner funnel, washed with demineralized water to wash off the all the excess NaOH. The precipitate was then dried in a oven at





Shruti Waghadhare *et al.*,

80°C for 4 hours and then crushed in a mortar and pestle. Finally, the obtained black powder was calcined at 900°C to get cobalt ferrite nanoparticles.

Preparation of eggshell based cobalt ferrite composite

As synthesized cobalt ferrite nano particles were dispersed in 10 mL distilled water and ultra sonicated for 15 min. Then calcined eggshell powder was added into the dispersed cobalt ferrite nanoparticles solution and heated at 80°C with constant stirring till all water evaporated and finally crushed into mortar to get eggshell based cobalt ferrite composite. The resultant CoFe_2O_4 /Eggshell nano composite was characterized by XRD, FT-IR, and SEM-EDX. The phase purity of the product was performed by X-ray powder diffraction pattern using X-Ray Diffractometer (Ultima IV, Rigaku Corporation, Japan) with X-ray Source Cu K- α and X-ray Wavelength 1.5406 Å. IR adsorption study (KBr Pellets) was performed on a Shimadzu, 8400-S FT-IR spectrometer in the range of 4000–400 cm^{-1} . Surface morphology and elemental analysis were studied by scanning electron microscopy JEOL-JEM-6360A model equipment JEOL-JEC-560 auto cation coater. The catalytic efficiency of nanocomposite was tested in CV dye degradation in combination with H_2O_2 .

General procedure for Degradation Study of Crystal Violet Dye

Crystal Violet (CV) dye was obtained from Molychem. All solutions of CV dye were prepared using double distilled water. In a typical procedure, 25 mL of CV dye solution was placed in a 250 mL beaker with optimized amount of synthesized eggshell based cobalt ferrite composite. The solution was stirred at room temperature at neutral pH. The progress of degradation was monitored by UV–visible spectrophotometer (Shimadzu UV-1800 Japan) at 570 nm. The reaction parameters like catalyst concentration (5mg-25mg), CV dye concentration (20–200 mg/L), H_2O_2 dose (0.2ml of 0.3%-30%), and reaction time (10 to 30 minutes) were studied.

RESULTS AND DISCUSSION

Characterization of eggshell /cobalt ferrite catalyst

XRD Spectra

The crystallinity of eggshell cobalt ferrite composite was examined by XRD analysis. **Fig 1** depicts XRD pattern for cobalt ferrite / eggshell nano composite. The peaks observed are compatible with standard peaks of cobalt ferrite (JCPDS NO. 22 - 1086) and calcined eggshell powder. Prominent peaks of calcined egg shell and cobalt ferrite have been matched and indicated with respective symbols.

FTIR analysis

Fig 2 depicts IR spectra of nano composite cobalt ferrite / eggshell nano composite. The intense peak at 3642 cm^{-1} depicts the presence of -OH group in the IR spectra. Another prominent peak at 1455 cm^{-1} give an account of carbonate mineral in egg shell matrix. The bands at 603 and 402 cm^{-1} are due to vibrations of metal ions in tetrahedral and octahedral sites, respectively confirming the spinel structure in the samples.

SEM and EDS of eggshell cobalt ferrite nanocomposite

SEM image shows the uniform morphology of cobalt ferrite nano particles which have adhered to eggshell particle. Due to their coral structure SEM image shows that cobalt ferrite nano particles size is less than 100nm and have roughly spherical shape. The elemental composition of CoFe_2O_4 /Eggshell nano composite was analyzed by the Energy Dispersive X-ray Spectroscopy (EDS). In this analysis, Ca, Co, Fe, and O signals are detectable along with some metals like Al which might be present due to trace amounts of metals present in eggshell powder.

Degradation Study of Crystal Violet Dye

The catalytic efficacy of synthesized eggshell based cobalt ferrite nanocomposite was examined in degradation of CV dye. Percent degradation of Crystal Violet dye was calculated by using the formula $\% \text{Degradation} = 100 \times \{(A_0 - A_t) / A_0\}$





Shruti Waghadhare *et al.*,

Where A_0 = Initial reading of dye sample on UV visible spectrophotometer

A_t = Reading of sample withdrawn and separated from catalyst after time t .

Reaction time

To 25ml of 60 ppm CV dye solution, 25 mg of catalyst was added. To this 0.2 mL 30% Hydrogen peroxide was added dropwise. The reaction was carried at neutral pH and room temperature. The decolorization of CV dye was observed visually immediately after addition of H_2O_2 to the solution. Maximum dye degradation was observed within the first 10 minutes interval. Thus, for further optimization study, contact time was fixed as 10 min.

Effect of Catalyst Concentration

The degradation of 25cm³ of 60 ppm CV dye at optimum reaction time (10 Minutes) and neutral pH were studied at different catalyst concentrations. Catalyst concentration was varied from 5 mg to 25 mg for the 60 ppm CV dye solution and it was observed that there is increase in catalyst activity with increase in concentration of the catalyst. 15 mg catalyst was found to bring about 98% dye degradation. No major change in % degradation was observed after increasing catalyst amount further(Fig.5). Accordingly, 15 mg was decided as the optimum dose for CV degradation.

Effect of Concentration of Hydrogen peroxide

Effect of concentration of reagent hydrogen peroxide was studied with 30%, 3% and 0.3% H_2O_2 respectively for degradation of 60 ppm CV dye solution (Fig 6). Among these three concentrations of H_2O_2 30% and 3% aqueous hydrogen peroxide were observed to be effective for the decolorization of crystal violet dye with catalyst concentration 0.6 g/L(Fig.6). Since mild conditions are desirable, 3% H_2O_2 concentration was fixed for further studies.

Optimization of CV dye concentration

To determine the maximum concentration of CV dye that can be degraded under optimized conditions, CV dye solutions ranging from 20 ppm to 200 ppm were prepared and degradation of each under optimized conditions was studied. Each time, 25 cm³ of a solution containing varying concentrations were utilized for the study and observed for 10 minutes. This study revealed that 98% removal of the dye was achieved up to a concentration of 160 ppm after that slight decrease in degradation efficiency was observed.

Reusability of Catalyst

The reusability of catalyst was checked with 60ppm of CV dye solution. First 25cm³ of CV dye solution was taken in a beaker and 15mg of catalyst was added to it. Then 0.2 of 3% H_2O_2 was added dropwise and solution was stirred on magnetic stirrer. Immediate decolorization was observed and confirmed on UV Visible Spectrophotometer after 10min. of stirring. Then the degraded dye solution was decanted by holding magnet. The catalyst was washed with water and acetone and dried in oven. The dried catalyst was reused. The procedure was repeated 6 times until the decolorization was observed. Time period required for decolorization gradually increased with each cycle.

Study of Toxicity of degraded dye solution

Dye solution of CV dye and degraded dye solution was checked for toxicity. CV is a well-known carcinogenic dye. For this study, gram positive bacteria *S.Aureus* and gram negative bacteria *E. Coli* were used. The inoculum was allowed to grow on nutrient agar using standard plating technique and growth was compared with dye solution and supernatant obtained after dye degradation. Fig 9(a) and 9(b) shows that growth of Gram-positive bacteria was inhibited by both 400ppm and 100ppm dye solution while normal bacterial growth was observed with same dye solutions that have undergone degradation. The comparison of present study with the previous work (Table 1) clearly indicates advantages of this study like mild reaction conditions (neutral pH and room temperature), almost complete dye degradation within short time and reusability of catalyst for 6 cycles.





Shruti Waghadhare et al.,

CONCLUSION

Magnetic nanocomposite of Cobalt ferrite / eggshell has been synthesized and characterized using various techniques such as SEM, EDS, XRD, and FT-IR. The prepared nanocomposite is successfully employed for the degradation of crystal violet dye using hydrogen peroxide. The combination of catalytic system CoFe_2O_4 /eggshell and hydrogen peroxide has proven to be very effective in CV dye degradation in short time at room temperature and neutral pH. The catalyst presents the advantage of easy recovery through the application of an external magnet and can be effectively reused up to 6 cycles in dye removal processes. The toxicity study showed that the remediation procedure developed is safe for the environment.

ACKNOWLEDGEMENT

Authors would like to acknowledge DST FIST facilities for spectral analysis. The authors would like to acknowledge Prof. U.V. Desai for his support and guidance. Also authors would like to acknowledge Dr. Varsha Ghadyale, department of Biochemistry, Gogate Jogalekar college Ratnagiri for guidance in toxicity study.

Conflict of Interest

The authors declare no conflict of interest.

REFERENCES

1. TiO_2 ," *Dyes and Pigments*, vol. 69, no. 3, pp. 224–232, Jan. 2006,doi:10.1016/j.dyepig.2005.04.001.
2. Y.R. Jiang, H.-P. Lin, W.-H. Chung, Y.-M. Dai, W.-Y. Lin, and C.-C. Chen, "Controlled hydrothermal synthesis of BiOxCly/BiOmln composites exhibiting visible-light photo catalytic degradation of crystal violet," *J Hazard Mater*, vol. 283, pp. 787–805, Feb. 2015, doi: 10.1016/j.jhazmat.2014.10.025.
3. R. S. Saravan et al., "Evaluation of the photo catalytic efficiency of cobalt oxide nano particles towards the degradation of crystal violet and methylene violet dyes," *Optik (Stuttg)*, vol. 207, Apr. 2020, doi: 10.1016/j.ijleo.2020.164428.
4. P. J, N. Kottam, and R. A, "Investigation of photo catalytic degradation of crystal violet and its correlation with bandgap in ZnO and ZnO/GO nano hybrid," *Inorg Chem Commun*, vol. 125, p. 108460, Mar. 2021, doi: 10.1016/j.inoche.2021.108460.
5. Y.-H. ben Liao, J. X. Wang, J.-S. Lin, W.-H. Chung, W.-Y. Lin, and C.-C. Chen, "Synthesis, photo catalytic activities and degradation mechanism of Bi_2WO_6 toward crystal violet dye," *Catal Today*, vol. 174, no. 1, pp. 148–159, Oct. 2011, doi: 10.1016/j.cattod.2011.03.048.
6. T. P. Shende, B. A. Bhanvase, A. P. Rathod, D. V. Pinjari, and S. H. Sonawane, "Sono chemical synthesis of Graphene-Ce- TiO_2 and Graphene-Fe- TiO_2 ternary hybrid photo catalyst nano composite and its application in degradation of crystal violet dye," *UltrasonSonochem*, vol. 41, pp. 582–589, Mar. 2018, doi: 10.1016/j.ultsonch.2017.10.024.
7. S. Sugashini, T. Gomathi, R. A. Devi, P. N. Sudha, K. Rambabu, and F. Banat, "Nanochitosan/carboxymethyl cellulose/ TiO_2 bio composite for visible-light-induced photocatalytic degradation of crystal violet dye," *Environ Res*, vol. 204, p. 112047, Mar. 2022, doi: 10.1016/j.envres.2021.112047
8. N. M. Mahmoodi, "Manganese ferritenanoparticle: Synthesis, characterization, and photo catalytic dye degradation ability," *Desalination Water Treat*, vol. 53, no. 1, pp. 84–90, Jan. 2015, doi: 10.1080/19443994.2013.834519.
9. W. Shi, Q. Li, S. An, T. Zhang, and L. Zhang, "Magnetic nanosized calcium ferrite particles for efficient degradation of crystal violet using a microwave-induced catalytic method: insight into the degradation pathway," no. April, 2014, doi: 10.1002/jctb.4578.





Shruti Waghadhare et al.,

10. S. Kossar, I. B. S. Banu, N. Aman, and R. Amiruddin, "Investigation on photocatalytic degradation of crystal violet dye using bismuth ferrite nanoparticles," *J Dispers Sci Technol*, vol. 42, no. 14, pp. 2053–2062, 2021, doi: 10.1080/01932691.2020.1806861.
11. A. M. Kulkarni, K. S. Pandit, P. V. Chavan, U. V. Desai, and P. P. Wadgaonkar, "Cobalt ferrite nano particles: A magnetically separable and reusable catalyst for Petasis-Borono-Mannich reaction," *RSC Adv*, vol. 5, no. 86, pp. 70586–70594, Aug. 2015, doi: 10.1039/c5ra10693a.
12. Z. A. Piranshahi, M. Behbahani, and F. Zeraatpisheh, "Synthesis, characterization and photo catalytic application of TiO₂/magnetic graphene for efficient photo degradation of crystal violet," *Appl Organomet Chem*, vol. 32, no. 1, Jan. 2018, doi: 10.1002/aoc.3985
13. P. Rai, R. K. Gautam, S. Banerjee, V. Rawat, and M. C. Chattopadhyaya, "Synthesis and characterization of a novel SnFe₂O₄@activated carbon magnetic nanocomposite and its effectiveness in the removal of crystal violet from aqueous solution," *J Environ Chem Eng*, vol. 3, no. 4, pp. 2281–2291, Dec. 2015, doi: 10.1016/j.jece.2015.08.017.
14. M. A. Gabal, E. A. Al-Harthy, Y. M. al Angari, and M. Abdel Salam, "MWCNTs decorated with Mn_{0.8}Zn_{0.2}Fe₂O₄ nanoparticles for removal of crystal-violet dye from aqueous solutions," *Chemical Engineering Journal*, vol. 255, pp. 156–164, Nov. 2014, doi: 10.1016/j.CEJ.2014.06.019.
15. A. Jamil, "Cu²⁺ doped nickel spinel ferrites (Cu x Ni_{1-x}Fe₂O₄) nanoparticles loaded on CNTs for degradation of crystal violet dye and antibacterial activity studies," *Journal of Taibah University for Science*, vol. 15, no. 1, pp. 814–825, 2021, doi: 10.1080/16583655.2021.2005911.
16. H. P. Lin et al., "Synthesis of a SrFeO_{3-x}/g-C₃N₄ hetero junction with improved visible-light photo catalytic activities in chloramphenicol and crystal violet degradation," *RSC Adv*, vol. 6, no. 3, pp. 2323–2336, 2016, doi: 10.1039/c5ra21339h.
17. F. C. Çavuşoğlu et al., "Preparation of magnetic activated carbon-chitosan nanocomposite for crystal violet adsorption," *Korean Journal of Chemical Engineering*, vol. 36, no. 11, pp. 1915–1921, Nov. 2019, doi: 10.1007/s11814-019-0377-9.
18. M. Dubey, N. V. Challagulla, S. Wadhwa, and R. Kumar, "Ultrasound assisted synthesis of magnetic Fe₃O₄/a-MnO₂ nano composite for photo degradation of organic dye," *Colloids Surf A Physicochem Eng Asp*, vol. 609, Jan. 2021, doi: 10.1016/j.colsurfa.2020.125720.
19. Misbah et al., "Enhanced visible light-driven photo catalytic degradation of crystal violet dye using Cr doped BaFe₁₂O₁₉ prepared via facile micro-emulsion route," *Journal of Saudi Chemical Society*, vol. 26, no. 6, p. 101533, Nov. 2022, doi: 10.1016/J.JSCS.2022.101533.

Table 1. Comparison of present work with previous works

Entry	Catalyst	Condition	Removal efficiency	Ref.
1	CaFe ₂ O ₄	Microwave, 10 min	90%	15
2	Gadolinium doped bismuth ferrite	(Mercury lamp, 250W)	84.5%	16
3	TiO ₂ / Magnetic Graphene	UV light, 25 min	99-65% (4 cycles)	18
4	SnFe ₂ O ₄ @ activated carbon	pH=8.0, Temp – 323K	95%	19
5	Cu _x Ni _{1-x} Fe ₂ O ₄ / CNTs	Sunlight, 90min	92.9%	20
6	Cobalt Oxide	UV light, 45 min	64 %	9
7	Mn _{0.8} Zn _{0.2} Fe ₂ O ₄ , MWCNT	pH = 8 120 min	99%	22
8	SrFeO _{3-x} /g-C ₃ N ₄	Visible light, 12-24 hrs	95-97%	23
9	Chitosan grafted magnetic activated carbon	120min,	75% (3 cycles)	24
10	BaCr _x Fe _{12-x} O ₁₉	90min, UV light	91%	25
11	CoFe ₂ O ₄ / Eggshell – H ₂ O ₂	3% H ₂ O ₂ Neutral pH, R.T	98%	This Study





Shruti Waghadhare et al.,

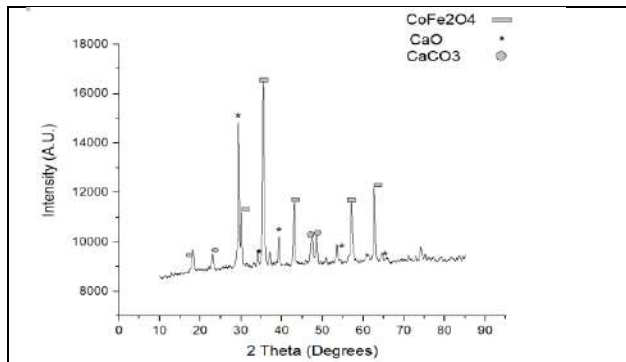


Fig. 1 XRD spectrum of eggshell cobalt ferrite nano composite

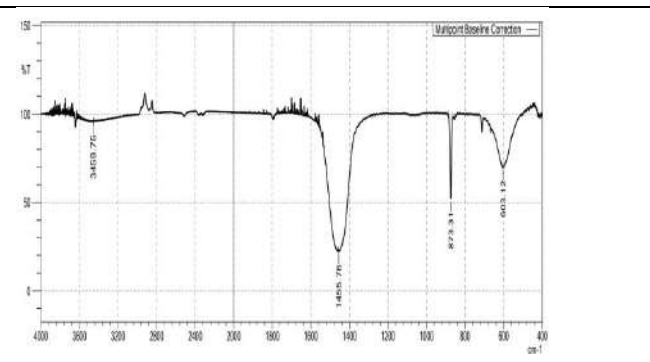


Fig.2 IR spectrum of Eggshell Cobalt Ferrite Nano composite

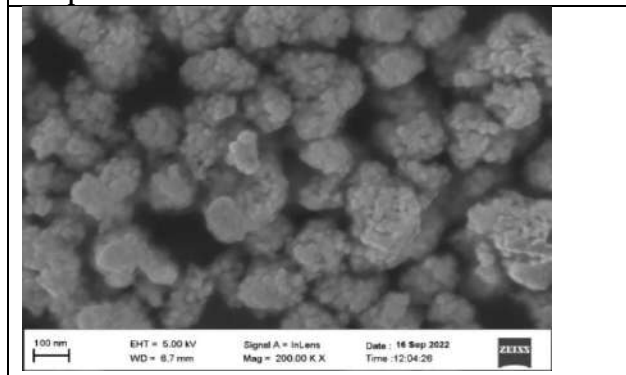


Fig.3 SEM image of Egg shell Cobalt Ferrite Composite

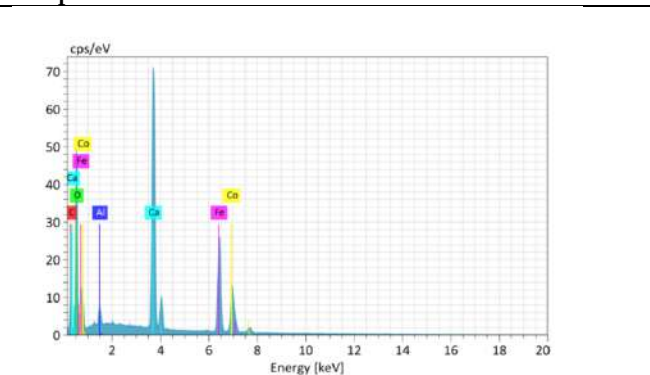


Fig.4 EDX spectra of Eggshell Cobalt Ferrite Composite

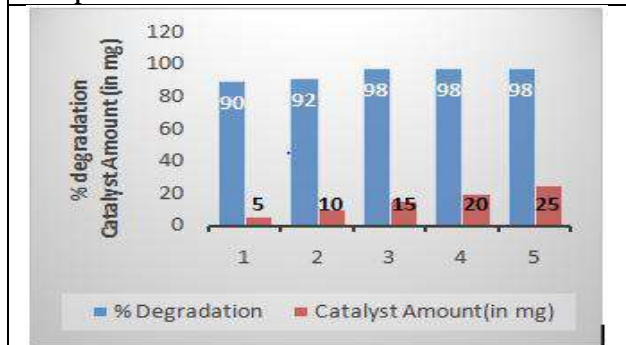


Fig. 5 Catalyst quantity optimization study within fixed time

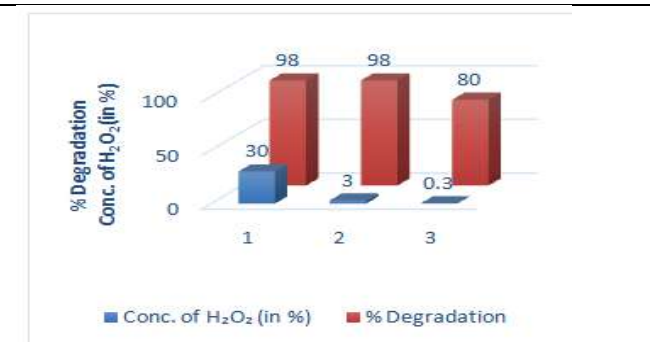


Fig. 6 Effect of concentration of hydrogen peroxide solution on 60 ppm solution of CV dye





Shruti Waghadhare et al.,

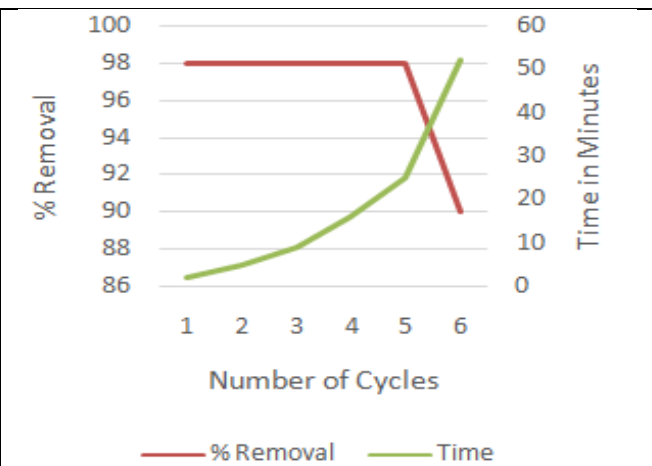
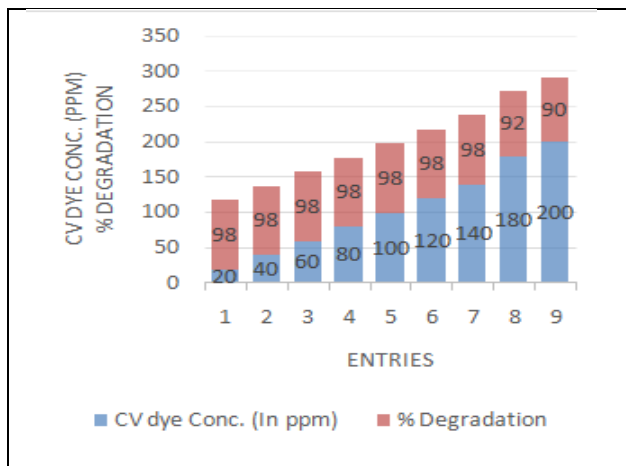


Fig 7 Optimization study with varying CV dye concentrations.

Fig 8. Reusability Study with respect to time and % removal



Fig. 9(a) Gram positive bacterial growth with 400ppm treated and untreated solution

Fig. 9(b) Gram positive bacterial growth with 100ppm treated and untreated solution





Seismic Control of Building using Tuned Mass Damper – A Review

Yashkumar K. Mistry^{1*}, Vishal A. Arekar², Vishalkumar B. Patel² and Pratiti M. Bhatt²

¹PG Scholar, Structural Engineering Department, Birla Vishvakarma Mahavidyalaya Engineering College, V.V. Nagar, Gujarat, India

²Assistant Professor, Structural Engineering Department, Birla Vishvakarma Mahavidyalaya Engineering College, V.V.Nagar, Gujarat, India.

Received: 30 Dec 2023

Revised: 09 Jan 2024

Accepted: 12 Jan 2024

*Address for Correspondence

Yashkumar K. Mistry

PG Scholar,

Structural Engineering Department,

Birla Vishvakarma Mahavidyalaya Engineering College,

V.V. Nagar, India



This is an Open Access Journal / article distributed under the terms of the **Creative Commons Attribution License** (CC BY-NC-ND 3.0) which permits unrestricted use, distribution, and reproduction in any medium, provided the original work is properly cited. All rights reserved.

ABSTRACT

Seismic control is a key aspect of providing structural safety and stability in earthquake-prone buildings. TMDs (Tuned Mass Dampers) have developed as an effective passive control device for reducing seismic vibrations and improving structural stability. This research focuses on the seismic control of buildings applying TMDs, specifically their design, placement, and impact on structural performance. The study evaluates the effectiveness of TMDs in minimizing structural responses such as displacements, accelerations, and inter-story drifts during seismic events using analytical and numerical methodologies. Furthermore, the inquiry investigates the effect of TMD factors like as mass, stiffness, and damping on their efficacy in seismic control. The findings provide helpful perspectives into optimizing TMD configurations for improving structural seismic performance and promoting safer built environments.

Keywords: Seismic Control, Building, Tuned Mass Damper(TMD), ETABs

INTRODUCTION

In recent decades, the effort to improve structural seismic resilience has resulted in significant study and development in the field of earthquake engineering. Earthquakes, one of the most powerful natural disasters, have the potential to cause catastrophic damage to the built environment, sacrificing lives and economic stability. Engineers have researched new technologies that can effectively limit the harmful impacts of seismic pressures on structures to fight this hazard and strengthen structural integrity. Building sensitivity to seismic forces is a major concern in earthquake-prone areas, where structure safety and stability are essential. Earthquakes can cause structural damage, injuries, and loss of life by exerting destructive forces on buildings. To address this challenge, creative technical solutions that improve the ability of buildings to withstand against seismic impacts are required.



**Yashkumar K Mistry et al.**

Tuned Mass Dampers (TMDs) an invention that has recently gained attention in the field of earthquake engineering, provide a possible solution. Tuned Mass Dampers, often referred to as harmonic absorbers, represent a passive vibration control strategy aimed at reducing structural response to dynamic loads, particularly those induced by seismic activity. These devices consist of a secondary mass, a spring, and a damping mechanism. The secondary mass is carefully tuned to resonate at a frequency that matches the building's predominant vibration frequency due to seismic forces. By introducing a secondary mass that moves in a manner counter to the primary structure, TMDs effectively dampen vibrations and mitigate structural movement, minimizing potential damage and enhancing overall safety [1].

Seismic Control of Structure

In addition to formal design procedures, seismic control is another way to ensure structural safety and keep control within reasonable limitations. A lot of current studies are available to control the structural system's induced seismic control. Researchers have developed structural control systems that can maintain structures and alter their efficiency during seismic occurrences. To decrease the influence of seismic forces, passive or active stabilizing forces can be applied to the structure via external dampening devices [2]. Passive structural control is an energy-independent approach that mitigates structural vibrations by dissipating kinetic energy within a system, eliminating the need for external power sources. This control method employs various damping devices, such as tuned mass dampers, tuned liquid dampers, and base isolators, to effectively reduce the effects of dynamic loads on structures. These techniques have undergone significant development and enjoy broad acceptance within the engineering community for their ability to minimize the structural impact of dynamic forces [3]. Many research efforts have been dedicated to the development of diverse structural control systems aimed at minimizing structural responses when subjected to seismic and wind forces. Ongoing research endeavours continue to enhance the efficiency of these systems. These seismic control systems can be broadly categorized into four major classes based on their operational mechanisms.

Passive Control System

Among the structural control mechanisms, passive control systems stand out as the most widely adopted. These systems operate by dissipating vibrational energy and typically encompass earthquake isolation and energy dissipation equipment. Historically, they were regarded as ingenious solutions capable of generating increased damping forces in proportion to structural reactions. However, passive control systems often excel only when dealing with the specific dynamic loads for which they were originally designed and configured. Consequently, these systems are characterized as having limited control capacity and are unable to adapt to various types of excitation. Despite these constraints, their advantages include the absence of any need for external energy sources during excitation and their straightforward design and manufacturing processes. [4].

Active Control System

Active control systems have been devised to complement the functionalities of passive systems when it comes to managing structural responses to seismic forces. These active systems are designed to address the unpredictability of vibrations stemming from diverse excitations. However, the setup and components of active systems are intricate, and they demand a relatively substantial amount of external energy to function, especially during natural disaster scenarios like earthquakes. Additionally, in the event of a power failure during such calamities, active systems may become non-operational. Active control devices encompass active mass damper systems, active base isolation systems, and active bracing systems [5].

SemiActive Control System

Semi-active control devices represent an evolved category of passive systems with adaptive features. They exhibit the ability to adjust damper behavior in response to data received regarding the structure's excitation and response. These systems typically comprise sensors, a control computer, control actuators, a passive damping device, and a modest power source. It's important to emphasize that semi-active systems do not possess full control capacity, as they are constrained by the capabilities of the passive devices integrated into them [6].





Yashkumar K Mistry et al.

Hybrid Control System

Hybrid control systems represent a combination of passive, active, and semi-active devices that are interconnected in either series or parallel configurations. These systems have gained prominence due to the unique advantages offered by each of these control approaches. The passive component's primary objective is to reduce structural responses and maintain the structure's performance within acceptable limits. Meanwhile, the active element is employed to fine-tune and adapt the response as needed. Hybrid control systems excel in safeguarding structures from a wide range of excitations, characterized by varying intensity and frequency spectra. As the name suggests, hybrid control systems effectively amalgamate the strengths of active and passive control techniques. An illustrative example of such a system involves outfitting a structure with distributed viscoelastic dampers alongside an active tuned mass damper situated on or near the top floor [7].

Tuned Mass Damper (TMD)

A Tuned Mass Damper, abbreviated as TMD, is a device comprising a mass, spring, and damper components, affixed to a structure with the purpose of mitigating the structure's dynamic response. The key to the TMD's effectiveness lies in tuning the damper's frequency to match a specific structural frequency. As the structural frequency increases, the damper is designed to resonate out of phase with the structural motion, thereby dissipating input energy through the inertia force exerted by the damper onto the structure. The damping and tuning frequency ratio within the TMD system are pivotal characteristics that directly impact the response of the primary system. Optimization of these parameters leads to the maximal reduction in the response variables. Tuned Mass Dampers, or TMDs, possess unchanging frequency and damping attributes, limiting their capacity to address a solitary, predetermined vibration frequency. Typically, TMDs are configured to target the fundamental frequency of a structure's oscillations, which is a common application. TMDs have found extensive use in mitigating vibrations generated by mechanical sources [8].

Where,

- m = Mass of main structure.
- c = Damping of main structure
- k = Stiffness of main structure
- m_d = Mass of damper
- c_d = Damping of damper
- k_d = Stiffness of damper
- u = Displacement of main structure
- u_d = Displacement of damper

Single Tuned Mass Damper

A single Tuned Mass Damper (TMD) comprises a mass, spring, and damper. The fundamental principle behind using a TMD for damping structural vibrations is to divert the vibrational energy from the structure to the TMD, where it can be dissipated. Crucially, tuning the TMD's natural frequency to match the structural motion and selecting an appropriate damping capacity are essential steps in this process [8].

Multiple Tuned Mass Damper

The concept of Multiple Tuned Mass Dampers (MTMD) represents an inventive approach for managing structural vibrations characterized by fluctuating frequencies. The central concept involves deploying numerous small TMDs, each tuned to natural frequencies distributed around the primary natural frequency of a structure. This approach results in the formation of a more resilient and effective TMD system [8].

Structural Model of Tuned Mass Damper

The system setup entails a primary system incorporating a TMD, as illustrated in Figure 1. The primary system is defined by its stiffness (k), damping constant (c), and mass (m). Correspondingly, the TMD shares similar parameters, including stiffness (k_d), damping constant (c_d), and mass (m_d), mirroring those of the primary system. The primary system, which incorporates a TMD, is represented as a single degree-of-freedom system when subjected



**Yashkumar K Mistry et al.**

to different combinations of excitations. These excitations come in two forms: an external force applied to the mass and an acceleration applied to the base of the primary system [1].

The tuning frequency and mass ratio of the TMD are defined as:

$$f = \omega_d / \omega \quad (1)$$

$$\mu = m_d / m \quad (2)$$

Application of Tuned Mass Damper**LITERATURE REVIEW**

Johnson *et al.* (2003) [9] The author delves into an analytical investigation and explores the viability of incorporating a tuned mass damper in the form of a flexible rooftop moment frame within rigid structures to mitigate seismic acceleration responses. The study involved the analysis of six pre-existing structures using time history and response spectra data, revealing that the introduction of mass alongside a flexible frame leads to an extension of the fundamental period for each structure. Consequently, this extension results in a reduction of seismic acceleration responses. The findings underscore that, for nearly all the structures studied and across the majority of seismic records considered, the utilization of a robust rooftop tuned mass damper frame can effectively diminish seismic responses. Bakre *et al.* (2007) [10] The author explores the process of determining the most favorable parameters for a tuned mass damper (TMD) system attached to a single degree-of-freedom primary system. This investigation takes into account a range of combinations involving excitation and response parameters. To achieve this, the authors employ a numerical search method to identify the optimal damping and tuning frequency ratio for the TMD, with the aim of minimizing mean square responses, including parameters like relative displacement, the main mass's velocity, and the force transmitted to the support. Furthermore, the authors develop explicit formulas for damper damping, tuning frequency, and the resulting minimized response using a curve-fitting approach, offering a convenient application in dynamic systems.

Hoang *et al.* (2008) [11]. The author explores the ideal configuration of a tuned mass damper (TMD) tailored for a single-degree-of-freedom structure exposed to seismic forces. The earthquake excitation is modeled using the Kanai-Tajimi spectrum. The primary objective of the study is to minimize the mean square displacement of the primary structure. Notably, when dealing with a substantial mass ratio, the TMD demonstrates heightened efficiency in diminishing the response of the primary structure, rendering it resilient in the face of uncertainties related to system parameters. Reddy D *et al.* (2012) [12]. The author's primary focus lies in investigating the seismic susceptibility of Reinforced Concrete (RC) buildings characterized by irregular configurations in both plan and elevation. The study's overarching goal is to evaluate the structural performance under earthquake conditions and raise awareness among practicing engineers. Two specific types of irregularities are considered within the building models: plan irregularities encompassing geometric and diaphragm discontinuities, and vertical irregularities involving setbacks and sloping terrain. These irregularities are introduced in accordance with the IS 1893 (part1)2002 code. The paper delves into an analysis of the seismic demands placed on these irregular structures, employing various analytical methodologies in both linear and nonlinear approaches. Additionally, it investigates the impact of three distinct lateral load patterns on the buildings' performance through pushover analysis. The results underscore that buildings situated on sloping terrain exhibit higher vulnerability to earthquakes when compared to other models. It becomes evident that seismic demands vary significantly based on the building configurations, despite the structures' inherent capacity.

Philip *et al.* (2017) [13]. Author analyses Three-dimensional analytical models of G+12 storied buildings were generated for regular and irregular buildings. The seismic analysis was carried out using CSI ETABS software (2015 version) for earthquake zone III in India. The seismic analysis included the evaluation of story displacements, story drifts, story shear, and stiffness. Equivalent Static Method was used for symmetric buildings up to 25 m height, while Response Spectrum Method was used for higher and unsymmetrical buildings. The results of the seismic analysis of regular and irregular reinforced concrete buildings were discussed in terms of story displacements, story drifts, story



**Yashkumar K Mistry et al.**

shear, and stiffness. The graph for story displacements showed that story displacement increases linearly from the base to the roof. The permissible maximum story displacement was found to be 0.4 times the total building height, and both the regular and irregular models were within this limit, although the irregular model was just touching the limit at the roof level. Bekdaş *et al.* (2017) [14] The author examined the utilization of two metaheuristic algorithms, namely the harmony search algorithm and the bat algorithm, as part of a metaheuristic-based optimization methodology for fine-tuning tuned mass dampers (TMDs) installed in seismic structures, while considering soil-structure interaction (SSI). The study revealed that the bat algorithm displayed distinct advantages in terms of minimizing the optimization objective and identifying an accurate optimum value.

Wang *et al.* (2017) [15]. The author conducted a study focusing on addressing the control of both translational responses and the torsional angle of asymmetric structures. In this regard, a novel variant of tuned mass damper (TMDPP) featuring tuned mass blocks, orthogonal poles, and torsional pendulums was introduced. To assess the damping effectiveness of TMDPP, a time history analysis was employed on an eccentric structure. The study also considered multidimensional seismic excitations, revealing that the TMDPP surpassed the conventional TMD in terms of performance. Naderpour *et al.* (2019) [16] The author's research delves into an investigation of the effectiveness of a hybrid control strategy, which combines base isolation with unconventional tuned mass dampers (TMDs), to mitigate structural vibrations in high-rise buildings during seismic events. The study encompasses structures with varying numbers of stories exposed to a range of far-field and near-field earthquake records. The analysis employs multi-degree-of-freedom models for the buildings and integrates nonlinear models for the base isolation system. The study's results unequivocally confirm that the response of high-rise buildings during earthquakes can be significantly reduced through the simultaneous use of both base isolation devices and non-traditional TMDs. Notably, the impact of base isolation in reducing structural response under different earthquake records surpasses the influence of TMDs. Furthermore, it's worth noting that the improvement in structural behavior achieved through TMDs alone is relatively substantial, amounting to approximately 20%.

Khanal *et al.* (2020) [17] The author's focus centers on investigating the seismic elastic behavior of L-shaped building frames characterized by plan irregularities. The primary objective of this study is to assess how different L-shaped structural models respond to variations in the angle of seismic incidence. The research scrutinizes the impact of plan configuration irregularity on a range of structural responses, including story displacement, inter-story drift ratio, torsional irregularity ratio, torsional diaphragm rotation, normalized base shear force, and overturning moment. To conduct this assessment, numerical analysis is carried out using ETABS software. The analysis encompasses both equivalent static lateral force and response spectrum analysis methods (dynamic analysis). The study entails the measurement of various structural responses, such as story displacement, inter-story drift ratio, torsional irregularity ratio, torsional diaphragm rotation, normalized base shear force, and overturning moment. The findings highlight that structures exhibiting plan configuration irregularities exhibit a heightened sensitivity to changes in the angle of the input response spectrum, in contrast to their symmetrical counterparts. Konton *et al.* (2023) [18] Author investigates the seismic control of T-shape in plan steel high-rise buildings using tuned mass dampers (TMDs) with the soil-structure interaction (SSI) effect. The effectiveness of TMDs in reducing seismic response is analysed in both fixed base and SSI models. The study includes three-dimensional models of the steel high-rise building subjected to four different earthquakes in SAP2000 software. The results show that TMDs are more effective in the SSI model than in the fixed base model. The distribution of TMDs on multiple plan levels along the height of the building further reduces the seismic response. The paper concludes that TMDs can be a successful passive resistance method for controlling the vibration and displacements of T-shape in plan steel high-rise buildings under seismic loads.

Farghaly *et al.* [19] Author discusses the design procedure and current applications of tuned mass damper (TMD) systems for tall buildings. The study conducted time history analysis with and without TMDs on a twenty-story three-dimensional model in SAP2000 to evaluate the effects of TMDs on the structural response to seismic excitations. The study found that using TMDs, especially with a specific arrangement can dramatically reduce the response of the structure such as story displacements and shear force of columns. The optimum parameters for TMDs, such as the frequency ratio, damping ratio, spring stiffness are discussed in the paper. Konton *et al.* (2023) [20]



**Yashkumar K Mistry et al.**

The author delves into strategies for enhancing earthquake resistance in high-rise buildings (HRBs), which encompass various approaches like bracings, shear walls, and tuned mass dampers (TMDs), while accounting for soil-structure interaction (SSI). To carry out a comprehensive analysis, numerical simulations were conducted using the finite element software SAP2000. A 20-story HRB made of reinforced concrete and steel was employed, and different structural systems were applied to enhance the building's stiffness or reduce its flexibility. These included bracing systems with diverse configurations, shear walls (SWs) featuring distinct configurations and material compositions (RC or steel), and the placement of tuned mass dampers (TMDs) at the upper corners of the structure. The paper concludes that the utilization of TMDs emerged as the most effective method for reducing seismic responses in both reinforced concrete (RC) and steel HRBs.

Summary

Researcher analysed six structures, proposing a limber rooftop tuned mass damper to reduce seismic acceleration response by increasing the fundamental period and achieving reduced seismic effects. [9]. Researcher derived optimal parameters for a tuned mass damper (TMD) system, minimizing responses like displacement and force transmitted using numerical searching and explicit formulas for convenient application in dynamical systems [10]. They focus on optimal design of a tuned mass damper (TMD) in single-degree-of-freedom structures under seismic loads, emphasizing the TMD's effectiveness in minimizing structure response, especially with a high mass ratio [11]. The author investigates seismic risk in irregularly structured RC buildings, assessing plan and vertical irregularities as per IS 1893 (part1)2002. Various analytical methodologies show a greater risk on sloping ground [12]. Author analysed seismic behaviour of G+12 buildings in earthquake-prone zone III in India using CSI ETABS software. They evaluated and compared story displacements, drifts, shear, and stiffness for regular and irregular structures, ensuring compliance with permissible displacement limits [13]. Researcher employed harmony search and bat algorithms for optimizing tuned mass dampers (TMDs) on seismic structures, considering soil-structure interaction. The bat algorithm proved effective in precise optimization, minimizing objectives effectively [14]. Author introduced a novel tuned mass damper (TMDPP) for managing translational and torsional responses in asymmetric structures. Time history and seismic studies confirmed its superior damping capability over conventional TMDs [15]. Researcher investigated a hybrid control strategy utilizing base isolation and non-traditional tuned mass dampers (TMDs) to reduce structural vibrations in high-rise buildings during earthquakes. Base isolation demonstrated more significant impact in reducing structural response compared to TMDs, showing about 20% improvement [16]. They studied seismic performance of L-shaped building frames with plan irregularities, evaluating structural responses under varying angles of seismic incidence. Plan irregularities showed increased sensitivity to input response spectrum angles [17]. Author investigated seismic control in T-shaped steel high-rise buildings using tuned mass dampers (TMDs) considering soil-structure interaction. TMDs were found more effective in SSI models, especially when distributed across multiple levels. They offer effective passive resistance for seismic control in such structures [18]. Researcher discussed TMD design and applications in tall buildings. Time history analysis on a 20-story model revealed significant reduction in structural response using TMDs, emphasizing optimal TMD parameters [19]. This study focused on improving earthquake resistance in high-rise buildings (HRBs) by employing bracings, shear walls, and TMDs while accounting for soil-structure interaction. TMDs were shown to be the most effective method for minimizing seismic response [20].

CONCLUSION

From the referred literature, the following conclusion are drawn.

This study demonstrates that incorporating a limber rooftop tuned mass damper effectively increases structure period, leading to reduced seismic acceleration response across various buildings and seismic records [9]. Researcher derived optimal parameters for a tuned mass damper (TMD) in single-degree-of-freedom systems, utilizing numerical searches. Explicit formulas for TMD damping and tuning frequency were obtained, aiding efficient application in dynamical systems to minimize responses [10]. This study demonstrated that an optimally designed tuned mass damper significantly reduces primary structure displacement under seismic loads, particularly with a



**Yashkumar K Mistry et al.**

large mass ratio, ensuring robustness against parameter uncertainties [11]. The seismic risk of RC buildings with irregular designs is highlighted in this study. Their research shows the different seismic demands and higher risk of structures, particularly those located on sloping land, providing guidance those in the engineering profession to be aware of and design for all of these factors [12]. Author found that in seismic analysis of G+12 buildings, story displacements increase linearly from base to roof. Permissible story displacement was met, highlighting structural stability even for irregular buildings [13]. Author determined that the bat algorithm is advantageous in optimizing tuned mass dampers (TMDs) on seismic structures considering soil-structure interaction, resulting in precise and effective outcomes [14]. Author introduced a novel tuned mass damper (TMDPP) with improved capabilities in managing translational responses and torsional angle in asymmetrical structures. Time history and seismic excitation studies affirmed its superior performance over traditional TMDs [15]. Author concluded that employing a hybrid control strategy with base isolation and non-traditional tuned mass dampers (TMDs) effectively reduces structural vibrations in high-rise buildings during earthquakes. Base isolation showcased a more substantial influence than TMDs, significantly reducing structural response. The study revealed a notable improvement in structural behaviour with TMDs alone, approximately 20% [16]. Author concluded that L-shaped RC building frames with plan irregularities are highly sensitive to changes in seismic incidence angle. Plan configuration irregularity significantly affects structural responses, highlighting design considerations for such structures [17]. Author conclude that tuned mass dampers (TMDs) effectively reduce seismic response in T-shaped steel high-rise buildings, especially when considering soil-structure interaction (SSI). TMDs distributed across multiple levels heighten their effectiveness [18]. Author concluded that employing tuned mass dampers (TMDs) significantly reduces structural responses like story displacements and column shear forces in tall buildings subjected to seismic excitations, emphasizing optimal TMD parameters [19]. Author determined that tuned mass dampers (TMDs) were the most effective method for enhancing earthquake resistance in both reinforced concrete (RC) and steel high-rise buildings (HRBs) through rigorous numerical analysis and comparison with other structural systems [20].

REFERENCES

1. Bakre, S. v., & Jangid, R. S. (2007). Optimum parameters of tuned mass damper for damped main system. *Structural Control and Health Monitoring*, 14(3), 448–470. <https://doi.org/10.1002/stc.166>
2. Gerges, R.R. and B.J. Vickery, Optimum Design of Pendulum-Type Tuned Mass Dampers. *The Structural Design of Tall and Special Buildings*, 2005. 14(4): p. 353-368. doi:10.1002/tal.273
3. Asai, T., Structural Control Strategies for Earthquake Response Reduction of Buildings, 2014.Ph.D. Thesis, University of Illinois at Urbana-Champaign, Civil and Environmental Engineering. Available online: <http://hdl.handle.net/2142/49571>. (Accessed on: 12 March 2020)
4. Leung, A.Y., H. Zhang, C. Cheng, and Y. Lee, Particle Swarm Optimization of Tmd by Non-Stationary Base Excitation during Earthquake. *Earthquake Engineering & Structural Dynamics*, 2008. 37(9): p. 1223-1246.
5. Symans, M.D. and M.C. Constantinou, Semi-Active Control Systems for Seismic Protection of Structures: A State-of-the-Art Review. *Engineering structures*, 1999. 21(6): p. 469-487. doi:10.1016/S0141-0296(97)00225-3
6. Miah, M.S., E.N. Chatzi, V.K. Dertimanis, and F. Weber, Real-Time Experimental Validation of a Novel Semi-Active Control Scheme for Vibration Mitigation. *Structural Control and Health Monitoring*, 2017. 24(3): p. e1878. doi:10.1002/stc.1878.
7. Wu, S.-T., Y.-R. Chen, and S.-S. Wang, Two-Degree-of-Freedom Rotational-Pendulum Vibration Absorbers. *Journal of Sound and Vibration*, 2011. 330(6): p. 1052-1064. doi:10.1016/j.jsv.2010.09.028
8. Rahimi, F., Aghayari, R., & Samali, B. (2020). Application of tuned mass dampers for structural vibration control: A state-of-the-art review. *Civil Engineering Journal (Iran)*, 6(8), 1622–1651. <https://doi.org/10.28991/cej-2020-03091571>
9. Johnson, J. G., Reaveley, L. D., & Pantelides, C. (2003). A rooftop tuned mass damper frame. *Earthquake Engineering and Structural Dynamics*, 32(6), 965–984. <https://doi.org/10.1002/eqe.257>
10. Bakre, S. v., & Jangid, R. S. (2007). Optimum parameters of tuned mass damper for damped main system. *Structural Control and Health Monitoring*, 14(3), 448–470. <https://doi.org/10.1002/stc.166>





Yashkumar K Mistry et al.

11. Hoang, N., Fujino, Y., & Warnitchai, P. (2008). Optimal tuned mass damper for seismic applications and practical design formulas. *Engineering Structures*, 30(3), 707–715. <https://doi.org/10.1016/j.engstruct.2007.05.007>
12. C M, R., Narayan K S, B., B V, S., & Reddy D, V. (2012). Effect of Irregular Configurations on Seismic Vulnerability of RC Buildings. *Architecture Research*, 2(3), 20–26. <https://doi.org/10.5923/j.arch.20120203.01>
13. Philip, A., & Elavenil, S. (2017). Seismic Analysis of High Rise Buildings with Plan Irregularity. In *International Journal of Civil Engineering and Technology* (Vol. 8, Issue 4). <http://iaeme.com/Home/journal/IJCIET1365editor@iaeme.comhttp://iaeme.comhttp://iaeme.com/Home/issue/IJCIET?Volume=8&Issue=4http://iaeme.com/Home/journal/IJCIET1366>
14. Bekdaş, G., & Nigdeli, S. M. (2017). Metaheuristic based optimization of tuned mass dampers under earthquake excitation by considering soil-structure interaction. *Soil Dynamics and Earthquake Engineering*, 92, 443–461. <https://doi.org/10.1016/j.soildyn.2016.10.019>
15. He, H., Wang, W., & Xu, H. (2017). Multidimensional Seismic Control by Tuned Mass Damper with Poles and Torsional Pendulums. *Shock and Vibration*, 2017. <https://doi.org/10.1155/2017/5834760>
16. Naderpour, H., Naji, N., Burkacki, D., & Jankowski, R. (2019). Seismic response of high-rise buildings equipped with base isolation and non-traditional tuned mass dampers. *Applied Sciences (Switzerland)*, 9(6). <https://doi.org/10.3390/app9061201>
17. Khanal, B., & Chaulagain, H. (2020). Seismic elastic performance of L-shaped building frames through plan irregularities. *Structures*, 27, 22–36. <https://doi.org/10.1016/j.istruc.2020.05.017>
18. Kontoni, D. P. N., & Farghaly, A. A. (2023). Seismic control of T-shape in plan steel high-rise buildings with SSI effect using tuned mass dampers. *Asian Journal of Civil Engineering*. <https://doi.org/10.1007/s42107-023-00873-1>
19. Farghaly, A. A., & Salem Ahmed, M. (2012). Optimum Design of TMD System for Tall Buildings. *ISRN Civil Engineering*, 2012, 1–13. <https://doi.org/10.5402/2012/716469>
20. Kontoni, D. P. N., & Farghaly, A. A. (2023). Enhancing the earthquake resistance of RC and steel high-rise buildings by bracings, shear walls and TMDs considering SSI. *Asian Journal of Civil Engineering*. <https://doi.org/10.1007/s42107-023-00666-6>

Table 1. Application of TMD

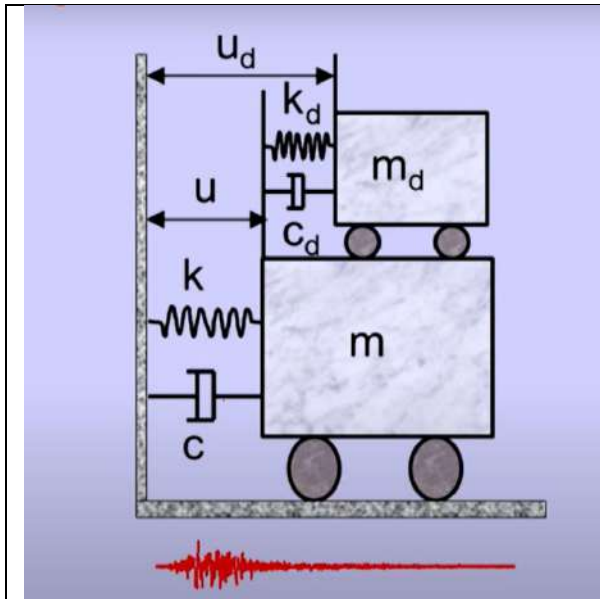
Sr. no	Application of Tuned Mass Damper (TMD)		
	Name	City / Country	year
1	C N Tower	Toronto, Canada	1973
2	John Hancock	Boston, USA	1977
3	Sydney Tower	Sydney, Australia	1980
4	Al Khobar Chimney	Saudi Arabia	1982
5	Pylon Aratsu Bridge	Japan	1987
6	HKW chimney	Germany	1992
7	Akita Tower	Japan	1994
8	Burj Al-Arab	Dubai	1999
9	Millenium Bridge	London	2001
10	One wall Center Tower	Canada	2001
11	Taipe 101	Taiwan	2004
12	Air Traffic Control Tower	Delhi, India	2015

(Source : Annual Review in Control, <https://doi.org/10.1016/j.arcontrol.2017.09.015>)



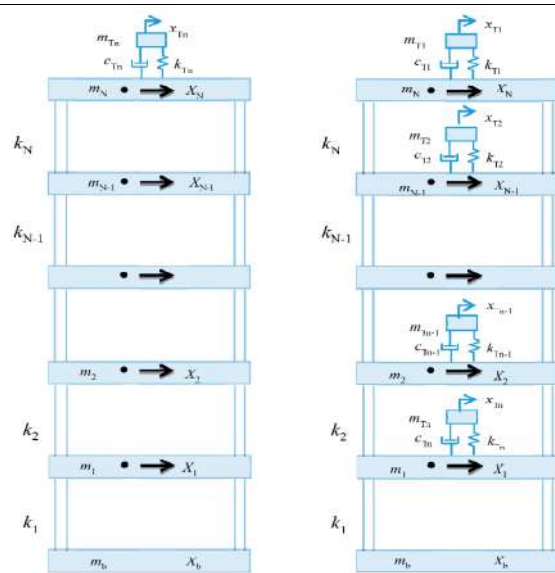


Yashkumar K Mistry et al.



(Source : Structural control & Health Monitoring, DOI: 10.1002/stc.166)

Figure 5 A schematic of a simple spring–mass–damper system used to demonstrate the tuned mass damper system [1].



(a)

(b)

(Source : Civil Engineering Journal, Doi:10.28991/cej-2020-03091571)

Figure 2 a- Single TMD, b- Multiple TMD[8].





Assessing the LOS of Urban Roadin Heterogeneous Traffic and Giving the Mitigation Measure: a Case Study of Vadodara City

Deep R. Damor, Ankita Sharma and Tejas Pandya

Transportation Engineering, Parul Institute of Engineering and Technology, Post Limda, Waghodia, Gujarat, India.

Received: 18 Oct 2023

Revised: 25 Oct 2023

Accepted: 31 Oct 2023

*Address for Correspondence

Deep R. Damor

Transportation Engineering,
Parul Institute of Engineering and Technology,
Post Limda, Waghodia,
Gujarat, India.
E. mail: 2203032110004@paruluniversity.ac.in



This is an Open Access Journal / article distributed under the terms of the **Creative Commons Attribution License** (CC BY-NC-ND 3.0) which permits unrestricted use, distribution, and reproduction in any medium, provided the original work is properly cited. All rights reserved.

ABSTRACT

This comprehensive review focuses on the assessment of the Level of Service (LOS) for Vadodara's urban roads, with a specific emphasis on applying volume-capacity analysis as a crucial tool to address the complex challenges presented by the heterogeneous traffic conditions. The primary objective is to tailor and adapt the existing LOS criteria to align with the distinctive characteristics of Vadodara's urban roads, taking into account the city's diverse traffic composition and traffic behavior. The modified LOS criteria include the consideration of factors such as traffic volume, road capacity, and the varied types of vehicles navigating the city's roadways. This review contributes significantly to the field of urban transportation planning by offering a detailed assessment of Vadodara's urban road network and addressing the critical issue of LOS under the influence of heterogeneous traffic patterns.

Keywords: Congestion, Urbanization, Level of Service (LOS), Free Flow Speed (FFS), Passenger Car Equivalent (PCE), Volume – Capacity Relationship, Mitigation Measures.

INTRODUCTION

India has one of the largest road networks in the world, and road transport plays a pivotal role in the country's economic development and social integration. Here is detailed information about the road transport sector in India:

Economic Contribution

Road transport significantly contributes to the Gross Value Added (GVA) of the transport sector in India, accounting for 3.06% of the total contribution of 4.58%. This demonstrates the substantial role played by the road transport sector in India's economy.





Deep R Damor et al.,

Dominant Transportation Segment

The road transport sector is the dominant segment in India's transportation landscape due to its high level of penetration in populated areas. It serves as a crucial mode of transportation for both freight and passengers, contributing significantly to the country's overall connectivity and accessibility.

Integration with Other Modes

While road transport dominates the sector, it also serves as a feeder to other modes of transportation such as railways, shipping, and air traffic. This integration contributes to the overall transportation ecosystem in the country.

Comprehensive Road Network

India's road network is extensive and includes various categories, each serving specific purposes within the overall transportation framework. These categories include National Highways (NH), State Highways (SH), District Roads, Rural Roads, Urban Roads, and Project Roads.

Responsibility and Management

- National Highways (NH) construction and maintenance fall under the purview of the Ministry of Road Transport and Highways (MORTH).
- State Roads (SH) are managed and executed by the respective State Public Works Departments (PWDs).
- District Roads are constructed and maintained by the Public Works Department of the respective states.
- Rural Roads, crucial for enhancing rural connectivity and development, are executed by various bodies, including the Panchayati Raj Departments, State PWD/RWD Departments, and the National Rural Road Development Agency (NRRDA) under the Ministry of Rural Development.
- Urban Roads, essential for intra-city connectivity and transportation, are managed and executed by the Municipalities.
- Project Roads, undertaken for specific development projects, are constructed and maintained by various Central and State Government Departments, depending on the nature and scope of the projects.

Critical Infrastructure

The road transport system in India is a critical component of the country's infrastructure, contributing significantly to economic growth, social development, and overall connectivity.

Facilitator of Goods and People Movement

The extensive road network, combined with the integration of various transportation modes, facilitates the movement of goods and people across the length and breadth of the nation. This supports economic activities, trade, and social interactions at a national scale.

Urban Roads

Urban roads in India are a vital component of the transportation infrastructure, facilitating intra-city movement, connectivity, and economic activities. As of March 31, 2019, the total length of urban roads in India was 5,41,554 kilometers. These roads are crucial for urban development and transportation within cities and towns. Out of the total urban road network, approximately 79% (4,28,157 kilometers) consists of surfaced roads. Surfaced roads are those with a hard, durable road surface, making them suitable for all-weather use. The construction of urban roads increased from 5,34,142 kilometers in 2017-18 to 5,41,554 kilometers in 2018-19, marking a growth of 1.4% compared to the previous year. This growth indicates the continuous expansion and development of urban road networks. Urban roads make up about 8.5% of the total road network in India as of March 31, 2019. This demonstrates their significance in the country's transportation infrastructure. The length of surfaced urban roads increased from 4,15,859 kilometers in 2017-18 to 4,28,157 kilometers in 2018-19, showing a 3% increase during that period. This growth is a positive sign for improved urban road infrastructure. Among the surfaced urban roads, approximately 71.5% (3,87,087 kilometers) are Bituminous Top (BT) and Cement Concrete (CC) roads, which are known for their durability and suitability for heavy traffic. The remaining 7.6% (41,071 kilometers) are Water Bound Macadam (WBM) roads, which are typically used in less congested areas. The construction of urban roads in India has seen remarkable growth over the years. It increased from 46,000 kilometers in 1960-61 to 542,000 kilometers in 2018-19, marking an over 11-fold increase. This expansion reflects the rapid urbanization and development in the country.





Deep R Damor et al.,

The construction of urban roads is carried out by various entities. As of March 31, 2019, more than 94.2% of the total urban road network (5,10,319 kilometers) was constructed by Municipalities. Additionally, Military Engineering Services (MES) constructed 3.2% (17,573 kilometers), Major Ports were responsible for 0.1% (761 kilometers), Minor Ports constructed 0.1% (677 kilometers), and Railways contributed 2.3% (12,224 kilometers) to the urban road network.

Level of Service

L.O.S. is a concept introduced by the Highway Capacity Manual (HCM), which is widely used in transportation engineering. It quantifies the quality and effectiveness of a roadway in serving the needs of users, considering different traffic volumes and operating conditions. L.O.S. considers several important factors when evaluating the operational conditions of a roadway.

Traffic Interruptions or Restrictions

This factor considers elements like the number of stops per kilometre, changes in speed, and the delays experienced by drivers. When a road is operating at or near its capacity (volume to capacity ratio near one), it tends to lead to poor operating conditions, with increased traffic interruptions and congestion.

Speed and Travel Time

L.O.S. includes an assessment of the operating speed and the overall travel time required to traverse a specific section of roadway. Lower speeds and longer travel times often correspond to a lower L.O.S.

Driving Comfort and Convenience

This aspect considers the comfort and convenience of drivers. It considers the roadway and traffic conditions and how they impact the driving experience. For example, road conditions that result in a smooth and comfortable ride contribute to a higher L.O.S.

Freedom to Maneuver

This factor evaluates the ability of drivers to maintain their desired operating speeds. Roads that provide drivers with the freedom to manoeuvre and maintain consistent speeds tend to have a higher L.O.S. The Highway Capacity Manual defines six levels of service, ranging from L.O.S. 'A' to L.O.S. 'F'. Each level corresponds to a specific quality of service provided by a roadway.

Urban Street and LOS Concept

The grading of street transportation facilities categorizes streets based on their functions and characteristics, and it typically includes the following levels, from lowest to highest:

Local Streets Primarily serve local traffic and provide direct access to residential properties.

Collector Streets Facilitate both local traffic access and traffic circulation within residential, commercial, and industrial areas.

Arterial Streets Serve as major transportation corridors, primarily catering to through trips while also providing access to adjacent commercial and residential areas.

Multilane Suburban and Rural Highways Designed for high-speed, long-distance travel between urban areas.

Arterial streets play a pivotal role in accommodating longer through trips, allowing vehicles to traverse a city or urban area efficiently. They often serve as main routes for commuters and travellers. Additionally, they serve as access points to businesses and homes along their corridors, making them important for both traffic circulation and land access. Collector streets, while serving as connectors between local streets and arterials, also offer access to adjacent properties. They play a crucial role in facilitating traffic circulation within neighbourhoods and commercial areas. LOS is a key performance measure for urban streets, and it is often based on the average through-vehicle travel speed for a street segment or the entire street under consideration. LOS provides a way to assess the quality of service and the level of congestion on urban streets.

Influencing Factors on Urban Street LOS

Number of Signals per Kilometer The density of signalized intersections along a street has a significant impact on its LOS. Streets with more signalized intersections per kilometre are more susceptible to congestion and degraded LOS, particularly when signal timing and progression are suboptimal.





Deep R Damor et al.,

Intersection Control Delay The time delay experienced at signalized intersections plays a crucial role in determining LOS. Delays at intersections can significantly affect the overall performance of a street, especially during peak traffic hours. The effectiveness of signal timing and progression plans is essential for maintaining a smooth flow of traffic on urban streets. Inappropriate signal timing, poor progression, and increased traffic volume can lead to congestion and reduced LOS. It's important to note that the LOS for an entire urban street can differ from that of its individual signalized intersections. Longer street segments with heavy traffic at intersections can still provide a reasonable overall LOS, even if some individual intersections are operating at a lower level.

Level Of Service for Urban Roads

Level of Service (LOS) scores play a critical role in transportation engineering and urban planning, allowing professionals to assess and grade the quality of service provided on urban street segments. These scores are used to evaluate various modes of transportation, and in the context of motorized vehicles, the criteria and measurement methods are distinct and straightforward. Here's a deep dive into the LOS scores for motorized vehicles

LOS A It is the highest level of service and represents free-flow operation. In this category, travel speeds exceed 80% of the base free-flow speed. The volume-to-capacity ratio, which measures the number of vehicles on the road compared to its maximum capacity, does not exceed 1.0. There are no obstructions or significant hindrances that hinder vehicle maneuvering. LOS A indicates that traffic flow is excellent, with minimal congestion and no significant delays. It characterizes smooth and uncongested traffic conditions.

LOS B It's representing a high level of service. In this category, travel speeds fall within the range of 67-80% of the base free-flow speed. The volume-to-capacity ratio does not exceed 1.0. There are only minor restrictions affecting vehicle maneuverability. LOS B signifies good traffic flow with some minor congestion during peak hours, but it remains relatively efficient, and delays are minor.

LOS C It is denoting moderately efficient traffic conditions. Travel speeds range from 50-67% of the base free-flow speed. The volume-to-capacity ratio is within the 1.0 limit. At intersections, longer queues may result in reduced speeds, and vehicle maneuverability is somewhat more constrained compared to LOS B. LOS C indicates that traffic flow remains acceptable but may experience some congestion during peak periods. Delays are more significant than in LOS B.

LOS D That is signifies a reduced level of service, with notable congestion. Travel speeds fall within the range of 40-50% of the base free-flow speed. The volume-to-capacity ratio remains under 1.0. Any increase in traffic flow leads to a significant reduction in travel speed, resulting in increased delays. Traffic flow in LOS D is characterized by significant congestion and delays, particularly during peak hours. This level of service is less desirable.

LOS E It's representing a congested traffic situation with significant delays. Travel speeds fall between 30-40% of the base free-flow speed. The volume-to-capacity ratio remains at or below 1.0. Motorists experience substantial delays in LOS E, and traffic flow is highly congested, making it a less desirable level of service.

LOS F It is the lowest level of service, indicating the poorest traffic conditions. Traffic moves at a pace of 30% or less of the base free-flow speed, or there's a volume-to-capacity ratio exceeding 1.0. Traffic moves at an extremely slow pace, and substantial delays and queuing are prevalent. LOS F represents the worst-case scenario, with severe congestion, extremely slow traffic, and significant delays. This is highly undesirable for commuters.

LOS Criteria as per Traffic Condition

Level A - Free Flow Traffic In this ideal state, users encounter minimal interference from other vehicles on the road. Drivers have complete freedom to choose their speed and manoeuvre as they wish. The level of comfort is excellent, requiring minimal attention. The volume-to-capacity ratio is typically below 0.2, indicating ample capacity on the road.

Level B - Steady Traffic At this level, the presence of other vehicles begins to influence individual drivers. While drivers can still choose their speed, manoeuvrability becomes somewhat restricted. However, the level of comfort remains high as drivers only need to be aware of nearby vehicles.

Level C - Steady Traffic but Limited Drivers in this condition are noticeably affected by the presence of other vehicles. Speed choices are influenced, and manoeuvring requires vigilance. Comfort decreases quickly at this level as drivers feel surrounded by other vehicles.





Deep R Damor et al.,

Level D - Steady Traffic at High Density At this level, both speed and manoeuvrability are significantly constrained. Motorists encounter a notably reduced level of comfort as they continually navigate to avert potential collisions with neighbouring vehicles. Even a minor uptick in traffic can precipitate operational challenges and network saturation, exacerbating congestion and delays.

Level E - Traffic at Saturation Traffic flows at a low but uniform speed, and manoeuvrability is only possible with constraints imposed by other vehicles. Drivers are in a state of frustration due to limited freedom of movement.

Level F - Congestion This represents unstable traffic flow with the formation of waiting lines at various points. Drivers experience cycles of stopping and starting with no discernible pattern, often dictated by the behaviour of other drivers. Users must maintain a high level of vigilance with minimal comfort. At this level, the volume-to-capacity ratio exceeds 1, indicating that the road segment is operating above its design capacity.

Traffic reports frequently use colour codes to illustrate traffic conditions, such as green (representing levels A and B, denoting relatively smooth traffic), yellow (levels C and D, indicating moderate congestion), and red (levels E and F, highlighting heavy congestion). These levels and colour codes help provide a clear and concise representation of current traffic conditions and the challenges drivers may encounter.

Free Flow Speed

The free-flow speed (FFS) is defined according to the 2010 Highway Capacity Manual (HCM) in two ways:

Theoretical Definition FFS is the theoretical speed at which both traffic density and flow rate on a specific study segment are zero. In other words, it represents the ideal speed in the absence of any vehicles on the road.

Practical Definition On freeways, FFS is considered the prevailing speed when the flow rate is between 0 and 1,000 passenger cars per hour per lane (pc/h/ln). This practical definition is relevant to real-world conditions where some traffic is present.

In essence, the FFS is the speed at which drivers naturally choose to travel based on the current conditions, with no influence from preceding vehicles. This definition underscores that FFS can be accurately determined when traffic flow is minimal, allowing for a mean FFS derived from field observations.

Passenger Car Equivalent

Passenger Car Equivalent (PCE) is a measurement used to approximate the number of standard passenger cars that can be equated to one truck, bus, or recreational vehicle under the existing conditions of a road and its traffic. The concept of PCE plays a pivotal role in highway capacity analysis, particularly in scenarios involving mixed traffic streams. Accurate calibration of these PCE values is essential as it significantly influences the calculations involved in capacity analysis. In recent times, several studies have been undertaken as part of a broader federal initiative aimed at allocating road user taxes. These specific studies have been focused on refining and calibrating PCE values for trucks, recognizing the need to have more precise and up-to-date metrics for this segment of the traffic, which is crucial for transportation planning and capacity assessment.

Mitigation Measure

Mitigation measures refer to a set of strategies and actions designed to prevent, lessen, or manage the detrimental environmental impacts resulting from a project. These measures may also encompass efforts to rectify or compensate for any harm inflicted on the environment due to these impacts. This rectification can take various forms, including replacement, restoration, compensation, or any other appropriate means to restore or offset the environmental damage incurred.

LITERATURE STUDY

Er. Bramjeet Singh *et al.*, 2023[3] in their study examined the traffic congestion is a global problem in urban areas, exacerbated by factors such as insufficient public transportation, delayed road infrastructure development, and increased use of private vehicles. In developing countries like India, traffic congestion is even more complex due to heterogeneous traffic on subpar roads and control conditions. Traffic congestion leads to travel delays and increased vehicle emissions. Developed nations have successfully quantified congestion and planned infrastructure





Deep R Damor et al.,

improvements to alleviate it. Curst explanations for traffic congestion in India are inadequate, partly due to limitations in using v/c ratio and LOS (Level of Service) metrics for urban road evaluation. The study aims to develop a mathematical model for calculating traffic congestion with heterogeneous traffic and assigning LOS to specific route segments. Data collection involves using videography techniques. focusing on sections along the Jahangir Chowk-Skims Soura route. The study analyses traffic characteristics by extracting relevant information from digital video clips.

Shrinath Karli *et al.*, 2016[4] studied how traffic congestion is a significant and growing urban transportation problem worldwide. Identifying congestion is the first step in addressing the issue and selecting appropriate mitigation measures. Factors contributing to congestion include population growth, economic development, and increased vehicle ownership, which lead to traffic demand exceeding intersection capacity during peak periods. Congestion results in various negative effects. including increased fuel consumption, noise, air pollution, delays, and accidents. In Ahmedabad city. many arterial roads are congested, prompting efforts to quantify congestion using metrics such as delay, speed, and volume to capacity ratio. There is a need to establish a rational definition of traffic congestion and use it to measure the Level of Service (LOS) of roads. LOS is determined by calculating the traffic flow rate of a street and comparing it to the free flow rate, primarily using the volume capacity ratio. To determine peak hour traffic volume, videography of vehicles is used, and the results are multiplied by the Passenger Car Unit (PCU). Public opinion surveys are considered necessary when evaluating alternative routes to address congestion.

C. V. Yeramwar *et al.*, 2016[6] in their study investigated the evaluation of road networks in cities is crucial for traffic planning, design, operation, and maintenance. Indian cities often have mixed traffic characteristics, and traffic congestion is a common issue in major cities. The objective of the study is to enhance the performance and capacity of urban road networks. A methodology for analyzing mixed traffic flow in 50-meter stretches is selected and analyzed. Intersections are critical points in the network and their performance estimation is essential. Amravati, the 8th most populous metropolitan area in the state, faces traffic congestion issues. The study aims to improve the operation of roads through traffic survey, data collection on vehicular volume and speed, and calculation of the existing level of service. Traffic surveys are conducted during morning and evening peak hours on working days using manual techniques. Synchro software is used for the analysis of the road network, offering optimization capabilities and case of use. The study's results are valuable for evaluating road capacity and level of service.

Gauri S.Biraje *et al.*, 2020[7] in their study tried to look into the two-lane highways play a significant role in India's highway system. Assessing the performance of two-lane roads is essential for future traffic planning, design, operation, and maintenance. Indian roads often experience mixed traffic flow, leading to traffic congestion, slower speeds, vehicle queues, and safety concerns. The study's objective is to identify the causes of traffic congestion in a selected case study and assess the capacity of a two-lane road using the methodology outlined in the Indo Highway Capacity Manual. The chosen case study focuses on the two-lane road from Patas to Baramti. Traffic studies are conducted on this road, and the analysis reveals that the Level of Service (LOS) for section I is C, and for section II. it is D. Grigorios Papageorgiou *et al.*, 2012[9] carried out the study where the Road Upgrading Management model has been developed through a rational approach tailored to the current conditions and requirements of the national and regional road network. This model offers an optimal strategy for upgrading roads based on their specific needs. The model presents a range of options for each road slated for upgrading, including 'Maintenance', 'Rehabilitation', 'Reconstruction', and 'New Alignment'. These options are designed to address the varying degrees of road improvement, ranging from simple maintenance to more extensive and costly reconstruction efforts.

CONCLUSION

This review underscores the importance of effectively managing Vadodara's urban road infrastructure to support the city's sustainable growth and the well-being of its residents. By employing advanced volume-capacity analysis techniques and adapting LOS criteria to the city's unique traffic conditions, this study offers a significant





Deep R Damor et al.,

contribution to urban transportation planning. The insights gained from this review have the potential to inform and improve development and urban planning in Vadodara, facilitating the transition towards more sustainable and efficient urban transportation systems.

REFERENCES

1. Transportation Research Board (TRB), 2010. Highway Capacity Manual (HCM) 2010. Transportation Research Board, Washington DC.
2. B. Robin, S. Viranta, D. Ajay, "Level of Service Concept in Urban Roads", IJESIRD, Vol. III, Issue I July 2016.
3. Ghosh, I., Chandra, S. and Boora, A., 2013. "Operational performance measures for two-lane roads: an assessment of methodological alternatives". Procedia- Social and Behavioral Sciences, vol.104, pp.440-448.
4. Indo Highway Capacity Manual 2017.
5. MORT&H (Ministry of Road Transport And Highway) Government of India, Annual Report.
6. IRC: 106-1990 (Guidelines for capacity of urban roads in Plain Areas).
7. Amit Prasad Timalseña, Anil Marsani, Hemant Tiwari (2017) "Impact of Traffic Bottleneck on Urban Road: A Case Study of Maitighar-Tinkune Road Section". Vol 5, ISSN: 2350-8914.
8. Adler, J.L., Satapathy, G., Manikonda, V., et al., 2005. A multiagent approach to cooperative traffic management and route guidance. Transportation Research Part B: Methodological 39 (4), 297e318.
9. Polson, N.G., Sokolov, V.O., 2017. Deep learning for short-term traffic flow prediction. Transportation Research Part C: Emerging Technologies 79, 1e17.
10. Quek, C., Pasquier, M., Lim, B.B., 2006. POP-TRAFFIC: a novel fuzzy neural approach to road traffic analysis and prediction. IEEE Transactions on Intelligent Transportation Systems 7 (2), 33e146.
11. Raj, J., Bahuleyan, H., Vanajakshi, L.D., 2016. Application of data mining techniques for traffic density estimation and prediction. Transportation Research Procedia 17, 321e330.
12. Renfrew, D., Yu, X.H., 2009. Traffic signal control with swarm intelligence. In: Fifth International Conference on Natural Computation, Washington DC, 2009.
13. Rzevski, G., Skobelev, G., 2007. Emergent intelligence in large scale multi-agent systems. International Journal of Education and Information Technology 1 (2), 64e71.
14. Sachdeva, G., Srinivasan, D., Tham, C.K., 2007. Multi-agent system based urban traffic management. In: IEEE Congress in Evolutionary Computation, Singapore, 2007.
15. Fernandes, P., Salamati, K., Roushail, N.M., et al., 2015. Identification of emission hotspots in roundabouts corridors. Transportation Research Part D: Transport and Environment 37, 48e64.
16. Surdonja, S., Drag_cevi_c, V., Deluka-Tiblja_s, A., 2018. Analyses of maximum-speed path definition at single-lane roundabouts. Journal of Traffic and Transportation Engineering (English Edition) 5 (2), 83e95.
17. Gal-Tzur, A., Barsky, Y., Finkelberg, I., 2018. Proactive traffic management strategy for mitigating non-recurrent congestion in an urban sub-network. In: TRB 97th Annual Meeting, Washington DC, 2018.
18. Ermagun, A., Levinson, D., 2018. Spatiotemporal traffic forecasting: review and proposed directions. Transport Reviews 38, 1e29.

HCM LOS Criteria – Motorized Vehicle Mode.

LOS	Travel Speed Threshold by Base Free-Flow Speed(mile/hour)							Volume to Capacity Ratio
	55	50	45	40	35	30	25	
A	> 44	> 40	> 36	> 32	> 28	> 24	> 20	≤ 1.0
B	> 37	> 24	> 30	> 27	> 23	> 20	> 17	
C	> 28	> 25	> 23	> 20	> 18	> 15	> 13	
D	> 22	> 20	> 18	> 16	> 14	> 12	> 10	
E	> 17	> 15	> 14	> 12	> 11	> 9	> 8	
F	≤ 17	≤ 15	≤ 14	≤ 12	≤ 11	≤ 9	≤ 8	
F	Any							> 1.0





Deep R Damor et al.,

HCM LOS Criteria – Bicycle and Transit Modes.

LOS	Segment – Based Bicycle LOS Score	Link – Based Bicycle LOS Score	Transit LOS Score
A	≤ 2.00	≤ 1.50	≤ 2.00
B	$> 2.00 - 2.75$	$> 1.50 - 2.50$	$> 2.00 - 2.75$
C	$> 2.75 - 3.50$	$> 2.50 - 3.50$	$> 2.75 - 3.50$
D	$> 3.50 - 4.25$	$> 3.50 - 4.50$	$> 3.50 - 4.25$
E	$> 4.25 - 5.00$	$> 4.50 - 5.50$	$> 4.25 - 5.00$
F	> 5.00	> 5.50	> 5.00

Source - Transportation Research Board, Highway Capacity Manual





Conocarpus Species: A Review of its Ethno pharmacological, Morphological, Phytochemical, and Pharmacological Studies

Poojaben Prajapati¹, Bharat B. Maitreya^{2*} and Rakesh M. Rawal³

¹Ph.D Scholar, Department of Botany, Bioinformatics and Climate Change Impacts Management, Gujarat University, Ahmedabad, Gujarat, India.

²Professor, Department of Botany, Bioinformatics and Climate Change Impacts Management, Gujarat University, Ahmedabad, Gujarat, India.

³Professor, Department of Life Science, Gujarat University, Ahmedabad, Gujarat, India.

Received: 31 July 2023

Revised: 20 Nov 2023

Accepted: 10 Jan 2024

*Address for Correspondence

Bharat B. Maitreya

Professor,

Department of Botany,

Bioinformatics and Climate Change Impacts Management,

Gujarat University,

Ahmedabad, Gujarat, India.

Email: bbmaitreya@gujaratuniversity.ac.in



This is an Open Access Journal / article distributed under the terms of the **Creative Commons Attribution License** (CC BY-NC-ND 3.0) which permits unrestricted use, distribution, and reproduction in any medium, provided the original work is properly cited. All rights reserved.

ABSTRACT

In the Combretaceae family, *Conocarpus* species, especially *Conocarpus erectus* L. and *Conocar puslancifolius* Engl., are well-known as decorative trees, flowering plants, and medicinal trees. Found mostly throughout tropical America, from South Florida through Bermuda, the Bahamas, and the west. Yemen and Somalia are furthermore. This plant's components are used in many ways and provide nutritional benefits. Anaemia, catarrh, conjunctivitis, gonorrhoea, diabetes, diarrhoea, fever, and headaches can all be treated using various parts, including the leaves, roots, bark, and seeds. Detailed information on molecular mechanisms and their wide variety of effects in treating various diseases. This review focuses on an in-depth discussion of studies targeting phyto chemistry, pharmacological activities, and their traditional values. Thus, the review aims to recapitulate the therapeutic potential of the components of *Conocarpus* species involved in treating a wide variety of diseases and present them along with strategies for future studies. The data was gathered from a number of academic websites, including PubMed, Elsevier, and Science Direct, as well as books on conventional medicine. Research and recent data have shown that the various chemical components of *Conocarpus* species have a variety of health-promoting properties and that the aerial parts have potential traditional uses in traditional medicine and cuisine. The traditional therapeutic effects are highlighted in the current review's exploratory survey, along with a wide range of future investigations that could be conducted.



**Poojaben Prajapati et al.,****Keywords:** *Conocarpus* species, Medicinal Properties, Phytochemical Analysis, Pharmacological Activities

INTRODUCTION

Over the past century, various types of medicine have been developed worldwide to improve people's quality of life. An increase in interest in plant-based compounds for drug research is being driven by the need for novel pharmaceuticals that address drug resistance. Human health and survival have been enhanced by nature's therapeutic plants (Renjini K. R., 2018). To develop the pharmacological effects of therapeutic plants, logical approaches are necessary to demonstrate their appropriate use. In all regards, the advancement of research and innovation has made it easier to evaluate branded pharmaceuticals. Plant-derived regular products or their subsidiaries have been an important source of curative agents for centuries. Many current drugs are also derived from plants (Cragg *et al.*, 2012). Herbal composites are a key component of manufacturing synthetic molecular analogy. By focusing on diversity-oriented synthesis, phytochemicals can be developed into natural product-like pharma compounds (Cragg *et al.*, 2012). More than 75 percent of other medicines and 60 percent of cancer medicines come from plants. Due to the many phytochemicals that plants produce to meet their needs, plants are medically essential. As a result, they produce alkaloids to protect against predators, and each phytochemical has a specific role in treating different ailments (Wang, Tang and Bidigare, no date).

Using plant information with medicinal properties has been very helpful from generation to generation. It was optional to prepare plants mechanically by extracting, altering, blending, or decontaminating them for use in their most basic form. It was only necessary to boil, grind, and dry plants. Conversely, persistent toxic effects have yet to be investigated (Chaveerach *et al.*, 2014). A wide range of applications has recently attracted attention to plant-derived compounds. Various medicine types are found in medicinal plants, including traditional medicines, modern medications, nutraceuticals, food supplements, folk remedies, pharmaceutical intermediates, and chemical entities for synthesized compounds (Ncube, Afolayan and Okoh, 2008). There was a time when medications were being developed from microbial resources in 1930. Although synthetic chemistry has dominated the pharmaceutical industry for decades, the potential for bioactive plants or their extracts to produce new and innovative drugs remains (Kwiecinski *et al.*, 2008). Active chemicals in plants and patented pharmaceuticals include Taxol, Artemisinin, and Maprouneacin (Hameed, 2012). The potential benefits of plant-based medicines outweigh their disadvantages; therefore, there is a growing need for further research and development of plant-based pharmaceuticals. (Balunas and Kinghorn, 2005). About 600 species comprise the Combretaceae family, including trees, shrubs, and lianas. Located primarily in tropical and subtropical regions, Africa and India are their habitats (Jose, Jesy and Nedumpara *et al.*, 2014). Species of the Combretaceae family tolerate high temperatures and semiarid conditions, while those of the Combretaceae family are medicinal plants. It is vital in treating various diseases, including worms, acute enteritis, colitis, constipation, tooth decay, general infections, malaria, tuberculosis, respiratory diseases, and cancer (Wang, Tang and Bidigare *et al.*, no date).

The wood of the *Conocarpus* tree is used in various parts of the world for making coal, burning fuel, and building shipbuilding, handle, goats, sheep, and camels. *Conocarpus lancifolius* Engl. is an evergreen Combretaceae species native to Kuwait, thrown as an ornament in semi-arid climates. According to (Martins *et al.* 2015), they can be a source of a variety of natural active ingredients. Temperature rises above 45 degrees Celsius during summer (Al-Kandari *et al.* 2009; Redha *et al.* 2012a), the species grows rapidly, providing evidence that it is resistant to high temperatures (Cragg *et al.*, 2012). *Conocarpus* trees are used in folk medicine in many countries throughout the world. In addition to its use as a diuretic, it is also used to treat many diseases, including colitis, constipation, tooth decay, general infections, malaria, tuberculosis, respiratory diseases, and cancer due to its antiparasitic, antileishmanial, and antitrypanosomal properties, as well as its insulin-regulating properties (Wain and Duke *et al.*, 1981). *C. erectus* is an important natural product source in addition to therapeutic agents. *Conocarpus* is an excellent biomonitor for evaluating air and soil pollution (Gholami *et al.*, 2013). Because of its wide adaptability to diverse climatic conditions in subtropical and tropical regions, and its ability to tolerate high temperatures, salinity, and drought, it is used far



**Poojaben Prajapati et al.,**

and wide as a hedge along the roadside, landscaping, and urban planning (Jalal and Al-khafajiet al, 2020). Leaves and hot water can be used to treat fever (Ismaielet al, 2018).

Plant Morphology

Even though two phenotypes or morphotypes are present in the habitat, the species propagates vegetatively from twigs: 1) plants with small, slightly grey-green leaves, and 2) plants with larger, glossy, dark green leaves. This phenotype could be caused by genetic differences or by environmental factors (K and Let al, 2001). In a green-yellow color scheme, simple hairs and glandular multi cellular hairs cover the epidermis of these leaves. The petiolate leaves have the main vein that runs up and down the leaf. There was only a tiny amount of seed pollen, which was tricolporate and psilate. Numerous druses had high tannin levels in their leaves, petioles, and stem cells. Mesophylls have isobilateral reservoirs for water. Petioles have a boat-shaped central vascular bundle with two lateral branches. Several nectaries were found in the petiole's distal portion and at the leaf's edge, as well as a collateral vascular bundle or cylinder found in the stem (Ncube, Afolayan and Okohet al, 2008). In addition to its spreading crown, glucose leaves, and dense cone-shaped flowers in terminal panicles, *C. erectus* has grey or brown bark and matures at the height of 6 meters (Kwiecinski et al., 2008) (Figure 2). This species of tree can reach a height of 20 meters. It is typically a shrub that grows between 1.5 and 4 meters high, but it can also become a tree. The plant has mainly sideways, fine, dark brown, weak and brittle roots, and black cork bark. It usually has several stems, but the shape of the prostration and the end of that layer could indicate that these are new plants. With a thin, curling bark (approximately 8 mm), it has a boney grey trunk. The wood of the stem (Specific Gravity 1.0) is robust, heavy, and powerful. The inner bark of the stem is a dark cream color. A slender tree with yellow-green leaves and thin, angled, flat, or winged branches is exceptionally delicate; the leaves are thin, yellow-green, angled, flat, or winged.

Leaf blades have oval shapes and petioles that are 3-9 mm thick with spirally organized leaves. From 2 to 10 cm in width, the leaves are relatively cartilaginous. An inflorescence is a globule of axillary particles or a small greenish bloom that can reach a diameter of up to 5mm. The Globus groups are surrounded by five to 15-mm thin, dry flank seeds (Bazaid et al., 2012). *Conocarpus lancifolius* Engl. leaves are simple, petioled, and have a vein that runs up and down the leaves (Figure 1). The epidermal hairs are simple and non-glandular, and the glandular hairs are multicellular. Pollen was tricolporate and psilate, and it was very small. Green-yellow heads were packed close together. Several druses were observed on a petal, petiole, and stem cells. Mesophyll had isobilateral water storage tissue. A bicollateral vascular bundle or cylinder characterizes the stems of petioles. This bundle is shaped like a boat with two lateral traces. Several nectaries are found at the distal section of the petiole and the edge of the leaf, as well as non-hairy excreting structures on the lower surface of the leaf ('Browse Silage in the United' et al, 2008). As a fast-growing wood species, *C. lancifolius* grows from 10 to 20 meters in just 8 years. It can withstand extreme temperatures and low rainfall (A. Elkhalfia et al, 2020).

Classification of the species

Division: Phanerogams
Class: Dicotyledons
Sub-class: Polypetalae
Series: Calyciflorae
Order: Myrtales
Family: Combretaceae
Genus: *Conocarpus* L.

Traditional Uses

Leaf decoction is consumed to treat fevers (Irvine et al, 1961). Folk remedies use this plant to treat anaemia, catarrh, conjunctivitis, gonorrhoea, diabetes, diarrhoea, fever, headaches, bleeding, tumours, orchitis, prickly heat, swellings, and syphilis (Bashir et al., no date). Leaf decoction is consumed to treat fevers (Irvine et al, 1961). Wood is used for posts, crossties, boat building, firewood, fences, and landscaping (K and Let al, 2001). In addition to being hard and durable, *C. erectus* wood has a high calorific value as fuel. However, it is commonly used for high-grade charcoal.



**Poojaben Prajapati et al.,**

(Krikorian, 1982). The transformation of *Conocarpus* wastes into biochar can therefore be considered a waste recycling method (Al-Wabel *et al.*, 2013). *C. erectus* widely used as a decorative tree all over the world (Shohayeb, Abdel-Hameed and Bazaid, 2013), and its wood is used for fence posts, crossties, turnery, vessel building, kindling, and landscaping (Carneiro, Barboza and Menezes, 2010). This species' bark and products are used as inoculants in treating wounds, diabetes, haemorrhoids, and diarrhoea (Raza *et al.*, 2016). *C. erectus* famous for its folkloristic curative potential, which includes diabetes treatment (Nascimento *et al.*, 2016). Its bark and fruits treat diabetes, haemorrhoids, and wounds (Santos *et al.*, 2018).

Geographical Distribution

The shores of central and southern Florida, including the Florida Keys; Bermuda; the majority of the West Indies; the coast of central and southern Florida, including the Florida Keys; From Mexico to the Galapagos Islands, Ecuador, and Brazil, both coasts of the continent of tropical America; and tropical West Africa are all part of Buttonwood's range (Nettel *et al.*, 2008). The *Conocarpus*, *C. erectus*, grows in coastal and riverine environments of Somalia, Yemen, and Djibouti. It is also an excellent tree to plant in East Africa, the Arabian Peninsula, and South Asia (Alhasan, Dawood and Abbas, 2019), as shown in Figure 3. Coastal and riverine environments in East Africa are home to *C. lancifolius*, an ornamental tree (Rajiv Roy, Raj K Singh, Shyamal K Jash, Atasi Sarkar, 2014). *C. lancifolius* essential for Somalia. It is promising for dry areas near the Nile in Sudan, especially in irrigated crops. It was also introduced in India, Syria, and Yemen (Martins *et al.*, 2015) As shown in Figure 4.

Phytochemical Components

The extraction, identification, and screening of medicinal compounds in plants are considered pharmacological screening. Flavonoids, alkaloids, carotenoids, tannins, antioxidants, and phenols are all bioactive chemicals produced by plants. Phytochemicals may have several health-beneficial effects (Shanmugapriya *et al.*, 2011). Plant tissue culture has been investigated as a means of synthesizing a number of key secondary metabolites in industrial settings (Wink *et al.*, 2005). Gallic acid (1), catechin (2), apigenin (3), quercetin (4), quercetin-3-O-glucoside (5), kaempferol-3-O-glucoside (6), rutin (7), and quercetin-3-O-glucoside-6-O-gallic acid were found in ethyl acetate and n-butanol extracts of leaves, stems, flowers, and fruits of *C. erectus* according to (Al-Wabel *et al.*, 2013). The phenolic, flavonoid, and tannin content of *C. erectus* leaves, stems, flowers, and fruits have been studied. The Folin-reagent Ciocalteu method was used to assess total phenolic and tannin content, and the results are given in Gallic acid equivalents (GAE), while flavonoid content was evaluated using the aluminium chloride method, which is expressed in rutin equivalents (RE) (Abdel-Hameed, Bazaid and Sabra, 2013). The *C. erectus* plant, its components, and the several phytochemicals present in this plant are shown in Table 1.

The researchers discovered high amounts of phytochemicals in *C. erectus* fruits in the reverse phase column chromatographic fraction (RP-HPLC–UV–ESI–MS) of methanolic extract of *C. erectus* fruits exposed to a silica gel column. *C. erectus* leaves yielded the novel trimethoxy-ellagic glycoside (3,3',4'-tri-O-methylellagic acid 4-O-glucopyranuronide) in a dose-dependent manner; this novel chemical inhibits reactive oxygen species assault on salicylic acid using the xanthine/hypoxanthine oxidase assay (Ayoub *et al.*, 2010). Coumarins, Alkaloids, and Saponins were not found in *C. erectus* extracts incorporating Tannins, Saponins, Flavonoids, Triterpenoids, and Flavonoids, but they have been discovered in n-hexane extracts (Nascimento *et al.*, 2016). The antioxidant activity of methanolic extract plants is strong, suggesting they could be employed as natural antioxidants (Abdel-Hameed, Bazaid and Shohayeb, 2014). Figure 5 shows various secondary metabolites in 2D structures found in different *C. erectus* and *C. lancifolius* plants. Phytochemicals identified from *C. erectus* include ellagic acid, 3,3'-Dimethoxyellagic acid, and gallic acid (Nawwar, Buddrus and Bauer, 1982). Dehydrate-isoeugenol (lignan), conocarpol, 1,4-diarylbutane (lignan), and 2'-methoxyconocarpol have all been isolated from the stem wood of *C. erectus* (Hayashi and Thomson, 1975).

A phytochemical examination of *C. erectus* leaves extracted in methanol and n-hexane revealed the presence of triterpenes in the n-hexane extract and the absence of saponins in the methanol extract. (Nascimento *et al.*, 2016). The methanol extract of *C. lancifolius* contains 70.304 ppm chlorogenic acid, 45.772 ppm quercetin, 74.93 ppm ferulic acid, 9 ppm gallic acid, and 57.80 ppm 4-OH 3-methoxy benzoic acid, while the phenolic content of *C. lancifolius* aerial parts



**Poojaben Prajapati et al.,**

and roots methanol extracts is 9.78 and 14.01 mg/g, respectively. (Saadullah, Chaudary and Uzair, 2016) and also methanol extract of the stems also contain 15.772 ppm m-coumaric acid, 14.0149 ppm quercetin, 10.356 ppm chlorogenic acid, 37.108 ppm gallic acid, 9.0325 ppm sinapic acid, and 32.4786 ppm ferulic acid (Afifi et al., 2021). *C.lancifolius* fruit extract is cytotoxic to the MRC-5 cancer cell line (Saadullah et al., 2020). The bioactivity of *Conocarpus* species, on the other hand, is determined by bioactive, which shows nine alkaloids, five saponins, and eight total phenolic compounds in *C.lancifolius* leaf extract through thin-layer chromatography (TLC) (Touqeer, Saeed and Khalid, 2015). *C.lancifolius* has been shown to have efficient antioxidant production due to the presence of certain chemical agents such as ascorbic acid, flavonoids, and phenolic acids, which serves to limit reactive oxygen species (ROS) formation, which is responsible for metal stress tolerance (Saadullah, Chaudary and Uzair, 2016). GC-MS analysis revealed at least thirty-one molecules and 11 phenolic compounds. The chemical composition of *C.lancifolius* aqueous leaf extract has never been described. Phenolics have been shown to impair energy metabolism, cell division, mineral uptake, and other biosynthetic processes such as net photosynthesis, respiration, and enzymatic activities. Phenolics found in *C.lancifolius* leaf extract may have inhibited maize and bean plant germination, growth, and biomass production (Al-Shatti et al., 2014). The calculated phenolic concentrations of methanol extract of the aerial part of *C.lancifolius* for quercetin, gallic acid, chlorogenic acid, ferulic acid, and 4-hydroxy-3-methoxy benzoic acid were 45.772 ppm, 9.779 ppm, 70.304 ppm, 74.93 ppm, and 57.80 ppm, respectively. At the same time, the *C.lancifolius* methanol root extract was estimated with concentrations of 15.772 ppm, 14.0149 ppm, 10.356 ppm, 37.108 ppm, 9.0325 ppm, 7.82 ppm, 32.4786 ppm, and 15.330 ppm, respectively, for quercetin, gallic acid, chlorogenic acid, coumaric acid, sinapic acid, ferulic acid, and caffeic acid (Saadullah, Chaudary and Uzair, 2016). Table 1 Shows the *C. erectus* plant and its different parts, and also as different phytochemicals present in this plant. Table 2 displays the *C.lancifolius* plant, its many parts, and the various phytochemicals found in this plant.

Pharmacological activities

Although this plant has traditionally been administered to treat many of diseases, only a few of its pharmacological effects have been studied. These are listed below:

Hepato protective activities

The liver is an important organ for xenobiotic metabolism and elimination from the body (Ali, Sharief and Mohamed, 2019). Toxic substances are the most common cause of liver cell damage (certain antibiotics, chemotherapeutics, peroxidized oil, aflatoxin, CCl₄, chlorinated hydrocarbon, etc.), excess consumption of alcohol, infections, autoimmune/ disorder (Stournaras and Tziomalos, 2015). When drunken albino rats were given a methanol extract of *C.erectus* flower, fruit, and stem at a dose of 500 mg/kg for 15 days, the level of blood was surprisingly lowered (P0.01 and p0.5), but the amount of urea in blood was not reduced (Bashir et al., no date).

Antioxidant activity

Many diseases and maladies have been linked to oxidative stress and free radicals, including diabetes, cardiovascular disease, inflammatory issues, cancer, and ageing. *C.erectus* is a canine species native to the United States. The antioxidant capacity of methanol extracts of fruits (630.15.79 mg ascorbic acid equivalent/g extract) was found to be higher (630.15.79 mg ascorbic acid equivalent/g extract) than methanol extracts of flowers, stems, and leaves (579.57.58, 570.74.37, and 376.32.19 mg ascorbic acid equivalent/g extract, respectively) using the phosphor molybdenum method. In the reducing power activity assay, methanol extracts of fruits had the highest reducing power activity (530.326.24 mg ascorbic acid equivalent/g extract), followed by methanol extracts of flowers, stems, and leaves (479.887.75, 479.817.50, and 393.915.15 mg ascorbic acid equivalent/g extract, respectively) (Abdel-Hameed, Bazaid and Sabra, 2013). The antioxidant activity of the 60 percent ethanolic leaf extract of *C.lancifolius* was considerable, with a minimum IC₅₀ value of (32.871.11) g/mL among all extracts, which was less significant than that of BHA, which had an IC₅₀ value of (26.50 0.50) g/mL. With an IC₅₀ value of (76.50 1.17) g/mL (Raza et al., 2020), the aqueous extract had the least antioxidant activity.



**Poojaben Prajapati et al.,**

The 60 percent ethanolic extract had the most significant inhibitory effect on α -glucosidase activity, followed by the 80 percent ethanolic extract. The 60 percent ethanolic extract's IC_{50} value for α -glucosidase inhibition was (38.64 0.93) g/mL, which was higher than the conventional prescription a carbose [(29.45 0.31) g/mL]. Furthermore, the 60 percent ethanolic extract showed significant in vitro α -amylase inhibition, with the lowest IC_{50} value of (44.80 1.57) g/mL compared to other extracts. The typical medicine a carbose had an IC_{50} of (35.50 0.35) g/mL (Raza *et al.*, 2020). The antioxidant potential of *C.lancifolius* was revealed by utilizing DPPH, NO scavenging, and ferrous reducing activity power, among other methods. The methanol extract of the aerial component of *C.lancifolius* showed the highest inhibition, 92.10 0.98 percent, according to the DPPH technique. Compared to quercetin, which inhibited 92.120.49%, dichloromethane, and water extracts, it inhibited 28.1 0.98 and 87.80.56%, respectively (Balunas and Kinghorn, 2005). The phosphor molybdenum approach was used to assess the total antioxidant capacity. The antioxidant capacity of the *C.erectus* methanol extract of fruits (630.15.79 mg ascorbic acid equivalent/g extract) is larger than the antioxidant capacity of the other three extracts (579.57.58, 570.74.37, and 376.32.19 mg ascorbic acid equivalent/g extract, respectively). Based on the amount of ascorbic acid equivalents per gram of extract. The methanol extract of fruits, on the other hand, has the highest reducing power activity (530.326.24 mg ascorbic acid equivalent /g extract), followed by the three other methanol extracts of flowers, stems and leaves, which have 479.887.75, 479.817.50, and 393.915.15mg ascorbic acid equivalent /g extract, respectively (Abdel-Hameed, Bazaid and Sabra, 2013).

Anticancer activities

Cancer is a significant public health issue in both developed and developing nations. According to Ferlay *et al.* (2010), 12.7 million new cancer diagnoses and 7.6 million cancer deaths occurred in 2008.(Ferlay *et al.*, 2010).Environmental, chemical, physical, metabolic, and genetic factors directly and indirectly impact the genesis and progression of cancers. Novel cancer management is urgently needed because of the limited efficacy of therapeutic therapies such as radiation, chemotherapy, immune modulation, and surgery in treating cancer, as indicated by high morbidity and mortality rates (Dai and Mumper, 2010). Cancer is a disease that causes the number of cells in the human body to multiply despite efforts to control or stop them. As a result, dangerous cell tumours with the capacity to spread emerge. Various dynamic constituents of essential oils have been discovered to have a cytotoxic effect in vitro against various harmful cell types (Safwat, Hamed and Helmy, 2018). Most new therapeutic applications of secondary plant metabolites and their derivatives in the recent half-century have been aimed against cancer (Balunas and Kinghorn, 2005). After gathering 35,000 plant samples from 20 countries, the National Cancer Institute examined 114,000 extracts for anticancer potential. Based on worldwide sales, 14 of the top 35 cancer treatments were predicted to be natural goods and natural product derivatives in 2000(Shoeb, 2008).

The cytotoxicity of ethyl acetate and n-butanol fractions of different sections of *C.erectus* in HepG2 and MCF-7 cell lines was examined using sulforhodamine B. (SRB). The cytotoxic activity of the ethyl acetate fractions of stems and leaves against the HepG2 cell line was highest, with IC_{50} values of 8.97 and 8.99 g/ml, respectively. Fruit and floral ethyl acetate fractions had IC_{50} values of 10.12 and 11.29 g/ml, respectively. On the other hand, n-butanol fractions of flowers, fruits, and stems were shown to be active against the HepG2 cell line with IC_{50} = 4.89 g/ml, whereas n-butanol fractions of flowers, fruits, and stems had IC_{50} = 9.73 g/ml, 20.68 g/ml, and 23.9 g/ml, respectively (Ishaque *et al.*, 2021). 2,3,8-tri-O-methylelagic acid and 3-O-methylelagic acid 4- O- β -D-glucopyranoside, both of which were isolated from *C.lancifolius*, Antitumor activity against mouse lymphocytic leukemia was significant (P-388, IC_{50} = 3.60 μ g/mL and 2.40 μ g/mL, respectively), human colon cancer (Col-2, IC_{50} = 0.76 and 0.92 μ g/mL, respectively) and human breast cancer (MCF-7, IC_{50} = 0.65 and 0.54 μ g/mL, respectively), however, they were not cytotoxic to human lung cancer cells (Lu-1). However, in normal rat glioma cells, CLM and chemicals A and B caused less harm (ASK, IC_{50} = 11.6 μ g/ mL), and human embryonic kidney cells (HEK293, IC_{50} = 6.74 μ g/mL), which served as normal cell lines.(Saadullah *et al.*, 2020).

Antimicrobial activity

Infectious disease produced by bacteria, viruses, fungi, and parasites remains a serious threat to public health, despite significant advances in human medicine. Bacterial and fungal pathogens have developed a range of



**Poojaben Prajapati et al.,**

antimicrobial defence mechanisms, and resistance to both old and new antibiotics is on the rise (Nair and Chanda, 2007). Because of the emergence of microbe resistance to current antibiotics as a result of random selection and probable side effects, several researchers are investigating the antibacterial activity of indigenous medicinal plants from throughout the world (Zampini *et al.*, 2009). Purified tannins and crude extracts from various sections of *C. erectus* were evaluated against gram-positive and gram-negative bacterial and fungal strains using the agar disc diffusion method. Zone of inhibition (ZOI) was measured against *S. cerevisiae* (fungal specie), i.e., 14.30.58 mm. If March 2019 | Volume 32 | Issue 1 | Page 215 tannins max. Only *S. cerevisiae* (fungal specie) showed moderate activity against crude extracts of flowers, fruits, leaves, and stems, with ZOI of 11.30.5 mm, 13.30.5 mm, 10.30.5 mm, and 11.0 1 mm, respectively (Rehman *et al.*, 2019).

Antibacterial assay

C. erectus is a kind of *Conocarpus*. Gram-positive bacteria were shown to be more sensitive to antibacterial agents than gram-negative and acid-fast bacteria in a study. The highest ZOI calculated against gram-positive bacterial strains *S. aureus* and *B. subtilis* was 21.00 mm and 23.00 mm, respectively (Bashir *et al.*, no date). The ZOI of n-butanol extract of *C. erectus* max. was reported as 22 mm against *Streptococcus pneumonia* and 21 mm against *E. coli* in another antibacterial experiment, which was also the same in previous work (Rehman *et al.*, 2019). Raheema (2016) claims that the *C. lancifolius* plant extract possesses antibacterial and antiviral effects against pathogenic microorganisms. The findings contrast with Saad *et al.*, 2014, who found that the plant exhibited moderate antibacterial and low antifungal activity (Raheema and Shoker, 2020). The methanolic extract of *C. lancifolius* was tested against six bacterial strains. If the diameter of the zone of inhibition was greater than or equal to 7 mm, the extract was declared active against any microbial species. With an 11mm inhibition zone, the antibacterial activity was shown to be strongest against *K. pneumonia*. Clinical isolates of *B. cereus* were also found to be sensitive to the extract, with a 9mm sensitivity zone. *S. aureus* and *P. mirabilis* had no activity, while *E. coli* and *P. aeruginosa* had low activity (8mm). According to the findings (Touqeer *et al.*, 2014), the existence of antibacterial activity in the plant indicates that it has a medical benefit. Defatted methanolic extracts of *C. erectus* leaf, stem, flower, and fruit were evaluated for antibacterial activity against two Gram-positive bacteria (*S. aureus* and *B. subtilis*), three Gram-negative bacteria (*E. coli*, *K. pneumonia*, and *P. aeruginosa*), and an acid-fast bacterium (*M. phlei*). Gram-positive bacteria had the biggest identified inhibitory zones for extracts, followed by *M. phlei*, an acid-fast bacterium, and, lastly, Gram-negative bacteria (Ayoub, 2010).

Anti urease activity

Antifreeze compounds include a variety of substances, with hydroxamic acids being the most well-known urease inhibitors. The dichloromethane extract was inert, while the methanol extract of *C. lancifolius* at 0.5 mM inhibited 91.5 percent of the cells with an IC_{50} of 49.1 1.31. Thiourea was used as a starting point. (Balunas and Kinghorn, 2005). LFN's antifreeze action was also tested using a urease inhibition assay with thiourea as the control. IC_{50} (M) and % inhibition at 0.5 mM were computed as 66.54 0.26 and 162.70 0.21, respectively, indicating urease inhibitory property (Saadullah, Asif and Bibi, no date). *C. lancifolius* methanol extract showed considerable antifreeze action, with a percentage inhibition value of 81.11.82 and an IC_{50} value of 49.1 1.31 (Mohammed, Mousa and Alwan, 2019).

Cytotoxicity

The cytotoxicity of *C. lancifolius* extract was assessed *in vitro* using a hemolysis assay in which healthy and non-smoker human blood erythrocytes (RBCs) were employed. The absorbance of RBC disruption by 50 g/ml of *C. lancifolius* extract was 0.035 at 540 nm, compared to 0.009 for normal saline. On the other hand, 1.513 absorbances at the same wavelength were demonstrated after dilution with 20 times distilled water (Mohammed, Mousa and Alwan, 2019). The essential oil of *C. erectus* is said to be cytotoxic. Some studies back up the theory that there is a relationship between toxicity and inhibitors (antioxidant activity) (Safwat, Hamed and Helmy, 2018). The presence of hexadecanoic acid, 2, 3-dihydroxypropyl, in HMEL of *C. lancifolius* could explain its cytotoxic impact. In previous studies, hexadecanoic acid was cytotoxic to human leukaemia cells at concentrations of 12.5 to 50 g/ml but not to normal human dermal fibroblasts. (Moni *et al.*, 2023). Flavonoids extracted from *C. erectus* leaves for (Ethyl acetate) demonstrated 81.6 percent cytotoxic activity on the breast cancer cell line (Hela) at a concentration of 200 mg/ml



**Poojaben Prajapati et al.,**

compared to minimum cytotoxicity of 10.2 percent at the same concentration of normal rat embryonic fibroblast cell line (REF), and 73.6 for chloroform extract percent at 200 mg/ml of extract concentration and 11.2 percent in REF at 200 mg/ml. (Faraj and Shawkat, 2020).

CONCLUSION

Scientists are constantly researching natural products because the traditional medical system relies on synthetic compounds that have one or more negative side effects. *Conocarpus* species is a powerful traditional medicine that has been used for centuries to cure many different diseases. The current review reported data on *C.lancifolius* and *C.erectus* traditional uses, phytochemical constituents, and pharmacological activities. According to the data, the majority of the research was conducted on extracts from various parts of the plant, particularly the leaves, which demonstrated a wide range of pharmacological activities. Figure 6 depicts the various pharmacological activities of this plant. However, the molecular mechanism underlying their specific pharmacological activities remains unknown. This article contains information on approximately 60 substances isolated or identified from various parts of these two plants. Phytochemical studies revealed that the majority of the chemical constituents are tannins, flavonoids, alkaloids, glycosides, sterols, and triterpenoids. Only a few of the identified phytochemicals have significant pharmacological effects. Despite extensive research on *C.lancifolius* and *C.erectus* extracts, isolated phytochemicals that can play an important role in drug development still need to be explored. In the future, bioassay-guided isolation could be used to identify the key bioactive chemicals responsible for pharmacological effects. Even though *Conocarpus* species has a wide range of medicinal and traditional applications, there still needs to be more knowledge about the pharmacological activities' precise mechanisms. As a result, extensive research on various types of phytochemicals derived from this plant is required to determine their precise target sites, structure-activity relationships, pharmacological activities, and mechanism of action to develop safe and effective herbal drugs of various diseases.

Data availability

Not applicable' for that section.

ACKNOWLEDGMENTS

We thank the Head, Department of Botany, Bioinformatics and Climate Change Impacts Management, School of Science, Gujarat University for providing the required research facilities to accomplish this study. Author Poojaben Prajapati acknowledges Dr. Saumya K. Patel for providing facilities and constant support. Author Poojaben Prajapati would like to thank the Scheme of Developing High-Quality Research (SHODH), Education Department, Government of Gujarat, INDIA, for supporting the student's fellowship.

CONFLICT OF INTEREST

On behalf of all authors, the corresponding author states that there is no conflict of interest.

Highlights

This is a detailed review of *Conocarpus* species Describing its Biological Activities, Medicinal values, and its Geographical distribution. This plant's phytochemicals are traditionally used for treating syphilis, diarrhoea, tumors, orchitis, gonorrhoea, diabetes, prickly heat, and swelling. It is also used in modern medicine to treat iron deficiency, catarrh, conjunctivitis, gonorrhoea, and diabetes. In the future, the genes of this plant, specifically for this species, can be identified using molecular biology analysis and plant genomics techniques, and these genes can be used to increase medicinal plant values.





Poojaben Prajapati et al.,

REFERENCES

1. A. Elkhalfifa, A. (2020) 'Morphological and chemical characterization of *Prosopis juliflora* (Sw.) and *Conocarpus lancifolius* Engl. in Sudan', International Journal of Scientific and Research Publications (IJSRP), 11(1), pp. 10–15. doi: 10.29322/ijsrp.11.01.2021.p10903.
2. Abdel-Hameed, E. S. S., Bazaid, S. A. and Sabra, A. N. A. (2013) 'Protective effect of *conocarpus erectus* extracts on CCL4-induced chronic liver injury in mice', Global Journal of Pharmacology, 7(1), pp. 52–60. doi: 10.5829/idosi.gjp.2013.7.1.7188.
3. Abdel-Hameed, E. S. S., Bazaid, S. A. and Shohayeb, M. M. (2014) 'RP-HPLC-UV-ESI-MS phytochemical analysis of fruits of *Conocarpus erectus* L.', Chemical Papers, 68(10), pp. 1358–1367. doi: 10.2478/s11696-014-0570-6.
4. Afifi, H. S. et al. (2021) 'Source of Phenolic Compounds and Antioxidants', pp. 1–14.
5. Al-Shatti, A. H. et al. (2014) 'The Allelopathic Potential of <i>Conocarpus lancifolius</i> (Engl.) Leaves on Dicot (<i>Vigna sinensis</i> <i>L.</i>), Monocot (<i>Zea mays</i> <i>L.</i>) and Soil-Borne Pathogenic Fungi', American Journal of Plant Sciences, 05(19), pp. 2889–2903. doi: 10.4236/ajps.2014.519304.
6. Al-Wabel, M. I. et al. (2013) 'Pyrolysis temperature induced changes in characteristics and chemical composition of biochar produced from *conocarpus* wastes', Bioresource Technology, 131, pp. 374–379. doi: 10.1016/j.biortech.2012.12.165.
7. Alhasan, D. A. H., Dawood, A. Q. and Abbas, D. (2019) 'InVitro Antimicrobial Activity of *Conocarpus* spp Leaf Crude Extract Muter College of Veterinary Medicine , University of Thi-Qar , Iraq Email: dhurghamalhasan@utq.edu.iq Abstract Materials and Methods Sample Preparation Preliminary Bioactivity of Dried M', 14(2).
8. Ali, S. A., Sharief, N. H. and Mohamed, Y. S. (2019) 'Hepatoprotective Activity of Some Medicinal Plants in Sudan', Evidence-based Complementary and Alternative Medicine, 2019. doi: 10.1155/2019/2196315.
9. Ayoub, N. A. (2010) 'A trimethoxyellagic acid glucuronide from *Conocarpus erectus* leaves: Isolation, characterization and assay of antioxidant capacity', Pharmaceutical Biology, 48(3), pp. 328–332. doi: 10.3109/13880200903131567.
10. Balunas, M. J. and Kinghorn, A. D. (2005) 'Drug discovery from medicinal plants', Life Sciences, 78(5), pp. 431–441. doi: 10.1016/j.lfs.2005.09.012.
11. Bashir, M. et al. (no date) '*Conocarpus erectus*', pp. 1–8.
12. Bazaid, S. A. et al. (2012) '172 Phytochemical Studies and Evaluation of Antioxidant, Anticancer and Antimicrobial Properties of *Conocarpus erectus* L. Growing in Taif, Saudi Arabia El-Sayed S. Abdel-Hameed1,4, Salih A. Bazaid1, Mohamed M. Shohayeb2,3, Mortada M..pdf', 2(2), pp. 93–112.
13. 'Browse Silage in the United' (2008), 3(1), p. 8237.
14. Carneiro, D. B., Barboza, M. S. L. and Menezes, M. P. (2010) 'Plantas nativas úteis na Vila dos Pescadores da Reserva Extrativista Marinha Caeté-Taperaçu, Pará, Brasil', Acta Botanica Brasilica, 24(4), pp. 1027–1033. doi: 10.1590/s0102-33062010000400017.
15. Chaveerach, A. et al. (2014) 'Genetic verification and chemical contents identification of *Allamanda* species (Apocynaceae)', Pakistan Journal of Pharmaceutical Sciences, 27(3), pp. 417–424.
16. Cragg, G. M. et al. (2012) 'The impact of the United Nations Convention on Biological Diversity on natural products research.', Natural product reports, 29(12), pp. 1407–1423. doi: 10.1039/c2np20091k.
17. Dai, J. and Mumper, R. J. (2010) 'Plant phenolics: Extraction, analysis and their antioxidant and anticancer properties', Molecules, 15(10), pp. 7313–7352. doi: 10.3390/molecules15107313.
18. Faraj, A. K. and Shawkat, M. S. (2020) 'Cytotoxic effect of flavonoids extracted from *conocarpus erectus* leaves on Hela cell and ref', Plant Archives, 20, pp. 3476–3480.
19. Ferlay, J. et al. (2010) 'Estimates of worldwide burden of cancer in 2008: GLOBOCAN 2008', International Journal of Cancer, 127(12), pp. 2893–2917. doi: 10.1002/ijc.25516.
20. Gany Yassin, S. and Mohammed, T. (2020) 'Molecular and chemical properties of a common medicinal plants in Iraq', EurAsian Journal of BioSciences Eurasia J Biosci, 14(September), pp. 7515–7526.





Poojaben Prajapati et al.,

21. Gholami, A. et al. (2013) 'Evaluation of "Conocarpus erectus" plant as biomonitoring of soil and air pollution in ahwaz region', Middle East Journal of Scientific Research, 13(10), pp. 1319–1324. doi: 10.5829/idosi.mejsr.2013.13.10.1182.
22. Guochun, Z., Ha, Z. and Ch, N. (1999) '3 ≠ 1 ; 1 1 √ ≠ √', 015, pp. 1–4.
23. Hameed, E. (2012) 'Phytochemical Studies and Evaluation of Antioxidant, Anticancer and Antimicrobial Properties of Conocarpus erectus L. Growing in Taif, Saudi Arabia', European Journal of Medicinal Plants, 2(2), pp. 93–112. doi: 10.9734/ejmp/2012/1040.
24. Hayashi, T. and Thomson, R. H. (1975) 'New lignans in Conocarpus erectus', Phytochemistry, 14(4), pp. 1085–1087. doi: 10.1016/0031-9422(75)85192-2.
25. Ishaque, S. et al. (2021) 'Biological and Clinical Sciences Research Journal', Biological and Clinical Sciences Research Journal, pp. 1–9.
26. Ismaiel, G. H. H. (2018) 'Antioxidant, Antimicrobial and Anticancer Activities of Egyptian Conocarpus erectus L. leaves Extracts', Egyptian Journal of Food Science, 46(1), pp. 165–174. doi: 10.21608/ejfs.2018.85913.
27. Jalal, G. K. and Al-khafaji, S. J. (2020) 'Heavy Metals and Polycyclic Aromatic Hydrocarbons (PAHs) Distribution in Conocarpus Lancifolius Plant Leaves in Basrah ', 11, pp. 936–950.
28. Jose, B., Jesy, E. J. and Nedumpara, R. J. (2014) 'World Journal of Pharmaceutical ReseaRch SEED EXTRACTS', World Journal of Pharmaceutical Research, 3(3), pp. 5041–5048. doi: 10.20959/wjpr201610-7083.
29. K, K. and L, B. B. (2001) Biology of Mangroves and Mangrove Ecosystems, Advances in Marine Biology.
30. Krikorian, A. D. (1982) 'Atlas of Medicinal Plants of Middle America: Bahamas to Yucatan. Julia F. Morton ', The Quarterly Review of Biology, 57(1), pp. 93–93. doi: 10.1086/412656.
31. Kwiecinski, M. R. et al. (2008) 'Study of the antitumor potential of Bidens pilosa (Asteraceae) used in Brazilian folk medicine', Journal of Ethnopharmacology, 117(1), pp. 69–75. doi: 10.1016/j.jep.2008.01.017.
32. Martins, N. et al. (2015) 'Plants used in folk medicine: The potential of their hydromethanolic extracts against Candida species', Industrial Crops and Products, 66, pp. 62–67. doi: 10.1016/j.indcrop.2014.12.033.
33. Mohammed, S. A., Mousa, H. M. and Alwan, A. H. (2019) 'Determination of hemolytic cytotoxicity and antibacterial activity of conocarpus lancifolius aqueous leaves extract', IOP Conference Series: Materials Science and Engineering, 571(1). doi: 10.1088/1757-899X/571/1/012045.
34. Moni, S. S. et al. (2023) 'Spectral analysis, in vitro cytotoxicity and antibacterial studies of bioactive principles from the leaves of Conocarpus lancifolius, a common tree of Jazan, Saudi Arabia', Brazilian Journal of Biology, 83, pp. 1–10. doi: 10.1590/1519-6984.244479.
35. Nair, R. and Chanda, S. (2007) 'In-vitro antimicrobial activity of Psidium guajava L. leaf extracts against clinically important pathogenic microbial strains', Brazilian Journal of Microbiology, 38(3), pp. 452–458. doi: 10.1590/S1517-83822007000300013.
36. Nascimento, D. K. D. et al. (2016) 'Phytochemical screening and acute toxicity of aqueous extract of leaves of Conocarpus erectus Linnaeus in Swiss albino mice', Anais da Academia Brasileira de Ciencias, 88(3), pp. 1431–1437. doi: 10.1590/0001-3765201620150391.
37. Nawwar, M. A. M., Buddrus, J. and Bauer, H. (1982) 'Dimeric phenolic constituents from the roots of Tamarix nilotica', Phytochemistry, 21(7), pp. 1755–1758. doi: 10.1016/S0031-9422(82)85054-1.
38. Ncube, N. S., Afolayan, A. J. and Okoh, A. I. (2008) 'Assessment techniques of antimicrobial properties of natural compounds of plant origin: Current methods and future trends', African Journal of Biotechnology, 7(12), pp. 1797–1806. doi: 10.5897/AJB07.613.
39. Nettel, A. et al. (2008) 'Ten new microsatellite markers for the buttonwood mangrove (Conocarpus erectus L., Combretaceae)', Molecular Ecology Resources, 8(4), pp. 851–853. doi: 10.1111/j.1755-0998.2008.02088.x.
40. Raheema, R. H. and Shoker, R. M. H. (2020) 'Phytochemicals screening and antibacterial activity of silver nanoparticles, phenols and alkaloids extracts of conocarpus lancifolius', EurAsian Journal of Bio Sciences Eurasia J Biosci, 14(November), pp. 4829–4835.
41. Rajiv Roy, Raj K Singh, Shyamal K Jash, Atasi Sarkar, D. G. (2014) 'Combretum quadrangulare (Combretaceae): Phytochemical Constituents and Biological activity', Indo American Journal of Pharmaceutical Research, 4(8), pp. 3416–3427.



**Poojaben Prajapati et al.,**

42. Raza, M. A. et al. (2016) 'Antioxidant and antiacetylcholine esterase potential of aerial parts of *Conocarpus erectus*, *Ficus variegata* and *Ficus maclellandii*', *Pakistan Journal of Pharmaceutical Sciences*, 29(2), pp. 489–495.
43. Raza, S. et al. (2020) 'Metabolite profiling and antidiabetic attributes of ultrasonicated leaf extracts of *Conocarpus lancifolius*', *Asian Pacific Journal of Tropical Biomedicine*, 10(8), pp. 353–360. doi: 10.4103/2221-1691.284430.
44. Raza, S. A. et al. (2021) 'In vitro pharmacological attributes and metabolite's fingerprinting of *conocarpus lancifolius*', *Boletin Latinoamericano y del Caribe de Plantas Medicinales y Aromaticas*, 20(6), pp. 660–671. doi: 10.37360/blacpma.21.20.6.47.
45. Rehman, S. et al. (2019) 'A Review on Botanical, Phytochemical and Pharmacological Reports of *Conocarpus Erectus*', *Pakistan Journal of Agricultural Research*, 32(1). doi: 10.17582/journal.pjar/2019/32.1.212.217.
46. Renjini K. R., G. G. and L. M. S. (2018) '180 Therapeutic Potential of the Phytochemicals in *Cassia Occidentalis*-a Review the Medicinal Properties of Phytochemicals in *Catharanthus*', (May).
47. Saadullah, M. et al. (2020) 'Cytotoxic and antioxidant potentials of ellagic acid derivatives from *Conocarpus lancifolius* (Combretaceae)', *Tropical Journal of Pharmaceutical Research*, 19(5), pp. 1073–1080. doi: 10.4314/tjpr.v19i5.24.
48. Saadullah, M., Asif, M. and Bibi, S. (no date) 'Phytochemical and Molecular Dynamic Analysis of Novel Biomolecule Lancifotarene Extracted From *Conocarpus Lancifolius* as Cytotoxic , Antiurease and Antidiabetic Agent', pp. 1–23.
49. Saadullah, M., Chaudary, B. A. and Uzair, M. (2016) 'Antioxidant, phytotoxic and antiurease activities, and total phenolic and flavonoid contents of *conocarpus lancifolius* (Combretaceae)', *Tropical Journal of Pharmaceutical Research*, 15(3), pp. 555–561. doi: 10.4314/tjpr.v15i3.17.
50. Safwat, G. M., Hamed, M. M. and Helmy, A. T. (2018) 'The biological activity of *conocarpus erectus* extracts and their applications as cytotoxic agents', *Pharmacologyonline*, 2, pp. 171–184.
51. Santos, D. K. D. do N. et al. (2018) 'Evaluation of cytotoxic, immunomodulatory and antibacterial activities of aqueous extract from leaves of *Conocarpus erectus* Linnaeus (Combretaceae)', *Journal of Pharmacy and Pharmacology*, 70(8), pp. 1092–1101. doi: 10.1111/jphp.12930.
52. Shanmugapriya, K. et al. (2011) 'A comparative study of antimicrobial potential and phytochemical analysis of *Artocarpus heterophyllus* and *Manilkara zapota* seed extracts', *J Pharm Res*, 4(8), pp. 2587–2589.
53. Shoeb, M. (2008) 'Anticancer agents from medicinal plants', *Bangladesh Journal of Pharmacology*, 1(2), pp. 35–41. doi: 10.3329/bjp.v1i2.486.
54. Shohayeb, M., Abdel-Hameed, E. and Bazaid, S. (2013) 'Antimicrobial activity of tannins and extracts of different parts of *Conocarpus erectus* L.', *International Journal of Pharmacy and Biological Sciences*, 3(2), pp. 544–553. Available at: http://ijpbs.com/ijpbsadmin/upload/ijpbs_51dbb691221f1.pdf.
55. Stournaras, E. and Tziomalos, K. (2015) 'Herbal medicine-related hepatotoxicity', *World Journal of Hepatology*, 7(19), pp. 2189–2193. doi: 10.4254/wjh.v7.i19.2189.
56. Touqeer, S. et al. (2014) 'Antibacterial and Antifungal Activity of *Conocarpus Lancifolius* Engl. (Combretaceae)', *Journal of Applied Pharmacy*, 6(3), pp. 153–155. doi: 10.21065/19204159.6.3.132.
57. Touqeer, S., Saeed, M. A. and Khalid, S. (2015) 'Thin layer chromatographic study of *Conocarpus lancifolius*, *Melaleuca decora* and *Syngonium podophyllum*', *Research Journal of Pharmacy and Technology*, 8(1), pp. 74–77. doi: 10.5958/0974-360X.2015.00015.3.
58. Wang, G., Tang, W. and Bidigare, R. R. (no date) 'Agents', (2), pp. 197–198.
59. Wink, M. et al. (2005) 'Sustainable bioproduction of phytochemicals by plant in vitro cultures: anticancer agents', *Plant Genetic Resources*, 3(2), pp. 90–100. doi: 10.1079/pgr200575.
60. Zampini, I. C. et al. (2009) 'Antimicrobial activity of selected plant species from "the Argentine Puna" against sensitive and multi-resistant bacteria', *Journal of Ethnopharmacology*, 124(3), pp. 499–505. doi: 10.1016/j.jep.2009.05.011.





Poojaben Prajapati et al.,

Table 1: C. erectus different parts and its phytochemicals

Plant	Part	Phytochemicals	Reference
<i>C. erectus</i>	leave	(Decanoic acid derevatives) 22- tritetracontanone, 1-octanol, 2-butyl-oleic acid, Benzene, (1-butylloctyl)-propylmethylenedioxypregna-1,4-diene-3,20-dione, Iso-velleral, diacetate	(Safwat, Hamed and Helmy, 2018)
	leave	trans-phytol, Neophytadiene, Methyl hexadecanoate, n -Hexadecanoic acid, Methyl Linolenate, 9,12,15-Octadecatrien-1-ol, 2 -Palmitoylglycerol, Heptacosane, Nonacosane, Cyclooctacosane, HexadecamethylOctasiloxane, gamma. -Sitosterol, alpha. -Amyrin	(Guochun, Ha and Ch, 1999)
	leave	n-Hexane, Ethyl Acetate, Tetradecane, Pentadecane, Hexadecane, Benzene,1,1-(1,2-cyclobutaned, Dibutyl phthalate	(Gany Yassin and Mohammed, 2020)
	leave	Pyrogallol, 3- hydroxytyrosol,Protocatchouic acid, Chlorogenic acid, Catechol, Catechin, Caffeine, Caffeic acid, P- OH benzoic, 4- amino benzoic acid, Vanillic acid, Ferulic acid, Iso-ferulic acid, Epi- catachin, Reversetrol, E-vanillic acid, Ellagic acid, Alpha- coumaric, Salycillic acid, 3,4,5 Methoxycinnamic Coumarin, p- Coumaric acid, Cinnamic acid, Benzoic acid, Naringin, Hesperidin, Rosmarinic acid, Quercetrin, Luteolin, Kaempferol, Hespertin, Apegenin, 7- Hydroxyl-flavone	(Ismaiel, 2018)
	leave	3,3'-Dimethoxyellagic acid, Brevifolin carboxylic acid, Quercetin 3-O-glucuronide, Myricetin 3-O-glucuronide, Syringetin 3-O-glucuronide, Ellagitannin, castalagin, Quercetin, Myricetin, Syringetin, 3,4,3'-Trimethoxyellagic acid, trimethoxy-ellagic glycoside, 3,3,4-tri-O-methylellagic acid 4-O-β-, glucupyranuronide,	(Martins et al., 2015)
	stem	Conocarpan, dehydrodi-isoegenol (lignan), conocarpol, 1,4-diarylbutane (lignan), 2'-methoxyconocarpol	(Rehman et al., 2019)
	fruit	Gallic acid, Catechin, Taxifolin, Quercetin- O-β-D-glucoside-(1-6)-gallic, Rutin, Quercetin- O-β-D-glucoside, Kaempferol-3- O- rutinoside, Kaempferol-3-O- β-glucoside, apigrmin.	(Abdel-Hameed, Bazaid and Shohayeb, 2014)
	leave	Gallocatechin, Caffeic acid, Pauciflorol A, Myricetin, Myricetin 3-glucoronide, Apigenin-7-O-glucoside, Chlorogenic acid, Fertaric acid, Discretine	(Santos et al., 2018)
	fruit	Vescalagin, Ellagic acid, castalagin, di-(hexahydroxy diphenoyl) galloyl	(Ismaiel, 2018)
	leave	trimethoxy-ellagic glycoside (3,3',4'-triO-methylellagic acid 4-O-β-glucupyranuronide)	(Ismaiel, 2018)

Table 2: C.lancifolius different parts and its phytochemicals

Plant	Part	Phytochemicals	Reference
<i>C.lancifolius</i>	leave	Tannins, Saponins, Comarins, Phenols, Alkaloids, Flavonoids, Glycoside, Terpenes, Rutin, Epigenen, Kamferol, Catechine	(Raheema and Shoker, 2020)
	leave	ethanone,1,1'-(1,4-phenylene) bis-, benzene, 4-methoxy-1-nitro-2-(trifluoromethyl)-, cholan-24-oic acid, 3,6-bis(acetyloxy)- methyl ester (3, alpha., 5.beta., and 6.alpha), Terephthalic acid, isobutyl 2-phenylethyl ester, 1,3,4-Oxadiazol-2-amine, 5-(4-bromophenyl)-, 1H-indole, 5-methyl-2-phenyl-, Benzo [h]quinolone, 2,4-dimethyl-	(Alhasan, Dawood and Abbas, 2019)





Poojaben Prajapati et al.,

root	Quercetin, Gallic acid, Vitamin c, Chlorogenic acid, M.Coumeric acid, Sinapic acid, Ferulic acid, 4-OH 3-methoxy Benzoic acid, Caffeic acid.	(Saadullah, Chaudary and Uzair, 2016)
leave	1,5 heptadiene, 2,4 dichloro phenol, 1,3 heptadiene, 1,3 octadiene, Cyclohexadene, Propionaldehyde, 3,3 dimethyl phenyl benzene, Hydroxyl phenyl acetic acid, Beta phenylethylamine, Dotriacontane, Docosane, Henesol, N butyl octadec 9 enamide, Bicyclogermacerene, Pyrogallol, Cetylic acid, Hydroxyl tyrosol, Methyl benzoate, 2,6 ditert butyl 4 dimethyl benzyl phenol, Mellibiose, Ericdictyol, Dianhydromannitol, 3 di methyl 1 phenyl 1 butynl benzene, Heneicosane, Tetracosane, Spathulol, 2,10 pentamethyl licosane, Procero side, Calamenene, 1 tetradecane	(Rehman et al., 2019)
leave	Gallic acid, Corilagin, Terflavin B, Ellagic acid, Kaempherol-3-O-rutinoside, Isorhamnetin	(Raza et al., 2020)
leave	1-(3-Methoxy-2- nitrobenzyl) isoquinoline, Morphin-4-ol-6,7-dione, 1-Bromo-N-methyl-, Phytol, Hexadecanoic acid, 2,3-dihydroxypropyl ester, - Terthiophene, Ethyl iso-allocholate, Caryophyllene oxide, Epiglobulol, Cholestan-3-ol, 2-methylene-, Dasycarpidan-1-methanol, acetate (ester), Campesterol, Oleic acid, epicotyl ester,	(Moni et al., 2023)
leave	1,5 heptadiene, 2,4 dichloro phenol, 1,3 heptadiene, 1,3 octadiene, propionaldehyde, hydroxyl phenyl acetic acid, dotriacontane, docosane, pyrogallol, hydroxyl tyrosol, methyl benzoate, melibiose, dianhydromannitol, heneicosane, tetracosane, procero side, 1 tetradecane.	(Al-Shatti et al., 2014)
leave	Epicatechin, Isorhamnetin, Cornoside, rutin, Skimmianine, Fumaric acid, Creatinine, Choline, Pyruvic acid, 3-Hydroxybutyric acid, Hypophyllanthin, Phyllanthin.	(Raza et al., 2021)
aerial	Chlorogenic acid, Quercetin, Ferulic acid, 4-OH 3-methoxy benzoic acid, Caffeic acid, hexadecanoic acid, kaempherol-3-O-rutinoside.	(Saadullah, Chaudary and Uzair, 2016)
leave	beta phenylethylamine, acetylenic acid, eriodyctiol, α-glucose	(Al-Shatti et al., 2014)



Fig. 1: *C. lancifolius* plant (source: <https://techooid.com/myths-facts-conocarpus-plantation-pakistan>) (source: <https://www.flowersofindia.net/catalog/slides/Lanceleaf%20Buttonwood.html>)

Fig. 2: *C. erectus* plant (source: <https://en.wikipedia.org/wiki/Conocarpus>) (source: <https://plantsuniverse.com/buy-conocarpus-online-in-pakistan>)





Poojaben Prajapati et al.,



Fig. 3: *C. erectus* Geographical distribution (Source: <https://www.gbif.org/>)



Fig. 4: *C. lancifolius* Geographical distribution (Source: <https://www.gbif.org/>)

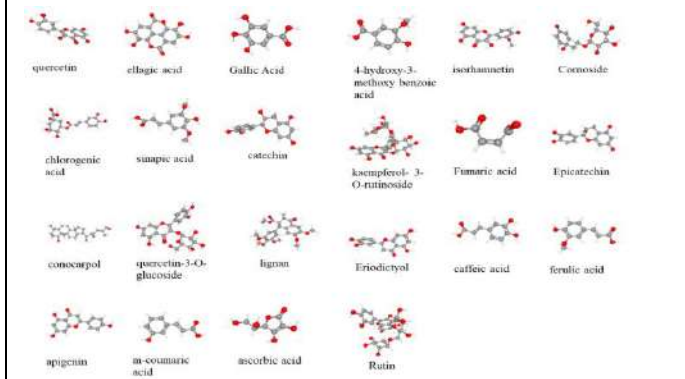


Fig 5: Secondary metabolite of *C. erectus* and *C. lancifolius*



Fig. 6: The pharmacological activities of *Conocarpus* species are graphically illustrated.





Women and Sustainable Development through Communication Skills for IT Engineering Graduates: A Study

D. A. Bhatt^{1*} and P. D. Bhatt²

¹Assistant Professor, Vishwakarma Government Engineering College, Ahmedabad, Gujarat, India

²Assistant Professor, Silver Oak University, Ahmedabad, Gujarat, India.

Received: 30 Dec 2023

Revised: 09 Jan 2024

Accepted: 12 Jan 2024

*Address for Correspondence

D. A. Bhatt

Assistant Professor,

Vishwakarma Government Engineering College,

Ahmedabad, Gujarat, India

E mail: dipakbhattvgec@gmail.com



This is an Open Access Journal / article distributed under the terms of the **Creative Commons Attribution License** (CC BY-NC-ND 3.0) which permits unrestricted use, distribution, and reproduction in any medium, provided the original work is properly cited. All rights reserved.

ABSTRACT

Communication skills play a crucial role in the life of an engineering professional as well as an academician. The present paper is an attempt to understand the difficulties faced by the engineering students, especially the Information Technology female students, from HR (Human Resource Manager) perspective for recruiting an engineering graduate with regards to their Communication skills in English. It has been largely observed through research (PhD these and research articles) that majority of the engineering graduates lack in the basic communication skills in English and are unable to succeed in interviews during placement. Hence, a study to understand the Human Resource Managers' perspective was taken by the researcher as so that the skills required by the industry while recruiting the IT engineering graduates can be found, especially the female in the larger interest of the students. 14 HR executives from recruiting companies located in Gujarat State were asked to participate in a survey through a questionnaire and then their answers were analysed to understand the communication skills required by engineering graduates before going for a placement activity.

Keywords: HR executive, communication skills, recruitment, female engineering graduates, problems, Information Technology

INTRODUCTION

In the 21st century, it has become mandatory for any engineering graduate to acquire the communication skills for a better placement opportunity. There is a gap between the industry requirement and the communication skills the engineering students have. NASSCOM survey of 2019 said that every year India produces around 15 lakh engineering graduates, but only 2.5 lakh graduates get jobs. The Niti Aayog Chairman Rajiv Kumar in 2019 stated



**Bhatt and Bhatt**

that about 45% of the management and 48% of the engineering students in the country are unemployed. Hence, it seems very apparent that the engineering graduates, especially the females who aspire to be in IT industry, need to be taught the communication skills which make them industry ready.

Aim

To find out the need of communication skills for female engineering graduates, especially the IT Engineering, from HR perspective.

RESEARCH METHODOLOGY

A study was conducted as part of the PhD survey by the researcher in 2023 by framing a questionnaire for assessing the IT female graduates' communication skills, which included the survey on 14 HR executives from engineering recruiting companies. The survey included questions related to the recruitment of engineering graduates and the HRs responded to the open-ended questions like their choice of recruitment from government or private institute, their experience in the recruitment process, the students' ability of communication skills/English, required communication skills for an engineering student who wishes to go for a placement, the skills lacked by the students regarding their communication, the role of English teachers in drafting the syllabus of English in collaboration with recruiting agencies, group discussion skills, initiatives the University/institute should take to strengthen the communication skills of engineering students, the problems of those engineering students who have poor communication skills, the need of both technical and soft skills. In the research paper English/Communications refer to the communication skills in English.

Analysis of the Questionnaire

The current section contains the analysis of Human Resource (HR) executives recruiting engineers across the state. It will be analyzed both qualitatively and quantitatively. The current questionnaire was designed to find the observations of the HR executives on the requirement of specific communication skills for the IT female undergraduate engineering students. There were 14 HR executives who responded to the questionnaire. The opinions of the executives matter with regards to the need of communication skills in English for the would-be engineers. Following is the detailed analysis of the questionnaire.

1. Which colleges do you prefer the most for recruitment?

Observations

The first question was formed to find the opinions of the HR executives regarding the choice of HR executive's choice of recruitment. The reply says that all the 14 executives wish both government and self-financed colleges for recruitment. While comparing government institutes with certain top ranked self-financed institutes, we can see that in the government institutes, the placement ration remains very poor. One of the grounds behind both the types of colleges for poor placement ratio is the poor communication skills among engineering students. This is backed up by the poor type of syllabus and its implementation in the form of examination pattern. Hence, we need a need-based syllabus which addresses the needs of the students and helps them with special reference to their placement.

Observations

The above table states the experience of HR executives. Out of thirteen HRs two HR executives have from one to five years of recruiting experience. 11 HRs have a vast experience of 10-15 years of recruiting experience. It was very crucial to know their experience as the responses to other questions will show their acquaintance of recruitment and the requirement of recruiting agencies.

Observations

Third question was posed with an aim to find out whether the students possess good communication and soft skills required by the organisations or not. Eight respondents out of thirteen say that the students do not have good



**Bhatt and Bhatt**

command on the communication skills and soft skills required by the organisations. Whereas five recruiters say that the students partially possess the command on the communication and soft skills required by the organisations. This brings a concern that the students need to be trained in communication and soft skills.

4. Which communication and soft skills are required by the students when they wish to sit for placement?

The fourth question was put to find the skills required by the students when they sit for placement. Most of the HR executives having experience of more than 10-15 years, we can say that their opinions matter for the required skills for students wishing to go for placement. Following are the observations collected from the responses.

1. Students should be able to communicate appropriately and confidently and also able to talk descriptively instead of just answer in yes or no.
2. Students should be able to do better presentations, public speaking.
3. For technical students, written and oral communication is the necessity.
4. Students should be prepared to face the interviews and group discussion.
5. Appropriate personality which is suitable for the job is very important.
6. Leadership traits are very important in today's generation.
7. Approach to work should be positive, one should be aware of work ethics, performance excellence and negotiation skills are also required.
8. Students should equally possess good listening skill and they must have good command on the English with pronunciation.

5. Which fundamental skills do most of the IT female engineering students lack in relation to placement?

The fifth statement was meant to find the skills lacked by the engineering students with regards to placement. The response to this question talks about the fundamental skills which are responsible for the poor placement among the engineering students. Following things are figured from the responses of the HR executives.

Grasp on soft skills and communication skills

1. Students fall short to answer very basic questions relating to their own studies and expressing in English.
2. Verbal and written skills in English need practice
3. Presentation and Group discussion skills
4. Willingness to learn new and creative things
5. Participation in discussions
6. Interpersonal skills

Observations

The sixth statement was intended to get the opinions for the industry inputs. Whether the institutes need to have a word with the industry recruiting people to meet the requirement of communication and soft skills for the engineers. Nine respondents strongly agree with the statement. Two recruiters agree, while one recruiter is neutral and one recruiter strongly disagrees. Hence, we recommend the involvement of industry for their inputs in the syllabus of English for engineering students.

Observations

Seventh question was meant to find out the role of English teachers' in designing the engineering students with good language and soft skills. Nine recruiters out of thirteen strongly agree that the teachers have a great role in developing the language and soft skills of engineering students. Three recruiters simply agree while 1 recruiter strongly disagrees to the question. This brings us to the conclusion that the teachers of English have a major role to play in the technical education and for the students of engineering.



**Bhatt and Bhatt****Observations**

Question number eight was meant to inquire whether the recruiters carry out group discussions or not. Eleven recruiters out of thirteen say that they carry out group discussion as a part of placement and two recruiters mention that they do not carry out group discussion. As group discussions are very important part of process of placement activities, it is important to be taught to the students. Hence, it is recommend that group discussion to be carried out as part of classroom practical activity and weight age in assessment should also be given to it.

Observations

Question number nine was asked to verify whether majority of engineering students possess better group discussion skills or not. This is to brings to notice whether students need any training for developing their group discussion skill. Out of 14 recruiters 8 mention that the students do not possess good group discussion skill, while five recruiters say that students partially possess good group discussion skill. It is clear that group discussion is an inevitable part of syllabus and assessment pattern in the syllabus

Q-10 What initiatives according to you the University/institute should take to improve the English and soft skills of IT female engineering students? The 10th question was designed to find the initiatives required by the University or institute to improve the soft skills of engineering students. The opinions from the recruiters propose the steps to be taken for improving the soft skills. Following are the responses stored from the HR executives.

1. One opinion tells the university/institute gets students realise the communication skills in English are also important along with technical skills.
2. Students should be trained for group discussions, debates, elocution, and mock interviews.
3. Confidence matters for facing the interviews. This is one of the major important factors along with developing skills required for facing the interviews.
4. Institutes should collaborate with the industry for preparing the students for interview and job skills.
5. Placement cell at the college level should train the students for better soft skills and job skills.
6. The institutes should take additional initiatives for preparing the students.
7. Training on aptitude, soft skills, and interview techniques should be given before placement activities start.
8. Students need to be given training to answer descriptively in English language.
9. Remedial classes for teaching students English language should be availed by the University for developing their better communication skills.
10. Not only speaking but also writing skills must be developed.

Observations

The eleventh question was put to figure out the reasons behind the poor communication skills of the students. 7 recruiters out of 14 say that lack of poor school background is a reason behind the poor communication skills of engineering students. One recruiter is of the opinion that confidence is a major factor for learning communication skills. 1 recruiter finds motivation very important factor. Three recruiters say that traditional syllabus is responsible for poor communication skills. One recruiter thinks that the English speaking environment in the campus is liable behind the poor skills in language. Out of the many reasons behind the poor language skills of the engineering students, one of the reasons is traditional syllabus of English. This brings our notice to the requirement of need-based syllabus of English for undergraduate engineering students. The following table is the depiction of the responses collected through Google form.

Observations

The final statement was designed to find if recruiters give importance to only technical knowledge or only soft skills or both. Only one recruiter says that he/she selects candidates with good hold on technical skills but average on soft skills. 12 recruiters, which is the majority of the respondents, opine that they choose candidates who have command on both soft skills and technical skills. This means that a student should have both technical and soft skills and hence a need-based syllabus which gets ready the students equally in soft skills is the need do the hour.



**Bhatt and Bhatt**

Hence, it is recommended that the needs of the students to be assessed before teaching.

Findings & Recommendations from HR Questionnaire

Following section mentions the examination of the HR questionnaire, in which 14 HR executives from different engineering recruiting organisations answered. The opinions of the HRs consist of some well-known recruiting organisations like Tata Consultancy Services (TCS), Hitachi and GNFC. These recruiters have experience of recruiting for more than 10 years hence their responses are useful for designing a need-based of English. HRs of recruiting agencies responds that they do recruitment from both government and self-financing institutes of engineering. This shows that the talent from all the colleges is valued by the organisations. Hence, it becomes important to train the students for government engineering institutes in communication and soft skills. Moreover, 78.6% of the total respondents hold the knowledge of recruitment from 10 to 15 years.

The recruiters are of the belief that good communication and soft skills in English are lacking in the students of engineering discipline. 57.1% of the HRs says that students do not own good communication and soft skills in English. 42.9% say that the students partly possess good skills in English. It is requested that the students are trained for skills required by the industry through extra sessions. Communication and soft skills are required by the organisations for their prospective employees like ability to correspond clearly in English with confidence, presentation and public speaking, good written and oral communication in English, personality suitable for the job, interviews and group discussion skills, positive attitude to work, work ethics, negotiation skills, leadership qualities, good listening skill and command on pronunciation in English.

Nine out of thirteen recruiters strongly agree that the teachers of English have a main role to play in preparing the engineering students with good language and soft skills. The total level of agreement is 85.7%. This brings to our notice that an English teacher plays a very important role in developing the language skills of the engineering students and therefore the job of an English teacher is not a normal job in an engineering institute. Group discussion is mostly carried out by the organisations recruiting engineers. This is validated by the responses given by the HR executives. 78.6% of the HRs says that they carry out group discussions as a part of placement activities. In the same line, 57.1% of the HRs declare that majority of the students do not possess good group discussion skill in English, while 42.9% partially possess group discussion skill. Hence, it is suggested that group discussions should be practiced in the lab sessions to develop the speaking skill in English.

According to the HRs, university/institute should take some measures to improve soft skills of engineering students. The institute/university should make students apprehend that technical skills and soft skills both are very important. Practice of placement skills like group discussion, interview, presentation etc. should be accomplished by the students. Institutes should work with the industry for designing the syllabus that meets the language needs of the students. The placement cell at the college level should work for the enrichment of students' linguistic skills. There are certain reasons due to which the students' communication skills remain poor. 7 respondents agree that due to the poor teaching at school level, students find English language difficult to learn. Confidence is also a crucial factor for learning language, which is opined by one HR executive. Inspiration is also a reason for poor communication skills among engineering students that is responded by one more HR. Other 3 HRs think that due to traditional syllabus, communication skills remain poor. 1 HR is of the view that the atmosphere for learning language is very significant for developing skills in the campus. Among these factors, we conclude that conservative syllabus is responsible behind the poor communication skills of the students and hence a need-based syllabus would be a viable solution.

Whether technical skills are important or soft skills are important or both. The HRs recruiting engineering graduates say that both the skills are important from the recruitment angle. 85.7% of the total respondents give precedence to both the skills and 14.3% say that good technical skills are more important and soft skills. Hence, it is suggested that the faculty of English and the faculty of engineering both should make the students aware that a good command on technical and soft skills for achieving success in the job market.





Bhatt and Bhatt

CONCLUSION

Apart from the above findings and recommendations, it is recommend that a model syllabus of English to be taught to the students of engineering in their third or fourth year for better placement opportunities. It is here that we can see the requirement of need-based syllabus of English fulfilled for undergraduate engineering students. The present research paper is aimed at helping the engineering students, especially the female students, so that their communication skills can be developed and it helps them in the recruitment process. The HR perspective is an important factor that helps in understanding the requirement of communication skills for engineering graduates.

REFERENCES

1. H. Basturkmen, *Developing Courses in English for Specific Purposes*, Palgrave Macmillan, 2010. Online.
2. T. Dudley-Evans, & St John. *Developments in English for Specific Purposes - A Multi-disciplinary Approach*. Cambridge University Press, Cambridge, 1998. Print.
3. J. Day, & M. Krzanowski, *Teaching English for Specific Purposes: An Introduction*, Cambridge University Press, Cambridge, 2011. Online.
4. H. Eli, *Teaching Academic ESL Writing*. Lawrence Erlbaum Associates, Publisher, London, 2004. Online.
5. T. Hutchinson, A. Waters, *English for Specific Purposes A Learning Centred Approach*. Cambridge University Press, Cambridge, 1987. Print.
6. S. Hyon, *General & English for Specific Purposes*. Routledge Publication, 2018. Online.
7. B. Hutauru Sohnata, *Teaching Module for English for Specific Purposes*. Fkip Uha Pematangsiantar. 2015. Online.
8. B. Paltridge, and S. Starfield, *The Handbook of English for Specific Purposes*, A John Wiley & Sons, Ltd., Publication, 2003. Online.
9. P. Robinson, C. *English for Specific Purposes: The Present Position*. Prentice Hall, 1980. Online.
10. L. Woodrow, *Introducing Course Design in English for Specific Purposes*. Routledge Publication, 2013. Online.
11. K. Yasemin Dikilit. *Key Issues in English for Specific Purposes in Higher Education*, Springer International Publishing, 2018. Online.

Table-1 Experience in conducting placement activity

Q-2	Less than 1 Yeas	1-5 Years	5-10 Years	10-15 Years	More than 15 Years
What is your experience in conducting campus interviews?	0	2	11	0	0

Table-2 Students' Communication Skills

Q-3	Yes	No	Partially
Do the students possess good communication and soft skills required by the organisation?	0	8	5

Table-3 Syllabus of English & Industry

Q-6	Strongly Agree	Agree	Neutral	Disagree	Strongly Disagree
Should engineering colleges have a talk with industry recruiting people before drafting their syllabus of English to meet the communication and soft skills requirement of the engineers for job?	9	2	1	0	1





Bhatt and Bhatt

Table-4 Role of English/Communication Skills

Q-7	Strongly Agree	Agree	Neutral	Disagree	Strongly Disagree
Do you think the teachers of English have a major role to play in preparing the engineering students with good language and soft skills?	9	3	0	0	1

Table-5 Group Discussion as part of placement

Q-8	Yes	No
Do you carry out group discussions in the process of placement?	11	2

Table-6 Engineering Students and GD

Q-9	Yes	No	Partially possess
Do the majority of engineering students possess good group discussion skill?	0	8	5

Table-7 Poor Communication Skills of Engineering Students

Q-11	Lack of poor school teaching in English	Confidence	Interest	Motivation	Old-fashioned Syllabus	Infrastructural facilities	English speaking environment in the campus
According to you, what could be the problems of those engineering students who have poor communication skills?	7	1	0	1	3	0	1

Table-8 Choosing Employees from Campus Placement

Q-12	Candidates with good soft skills but average technical skills	Candidates with good technical skills but average soft skills	Good command on both soft skills and technical skills
What kinds of employees do you generally choose from campus placement?	0	1	12





Bhatt and Bhatt

<p>1. Which colleges do you prefer the most for recruitment? 14 responses</p> <table border="1"> <thead> <tr> <th>Category</th> <th>Percentage</th> </tr> </thead> <tbody> <tr> <td>Government</td> <td>0%</td> </tr> <tr> <td>Self-financed</td> <td>0%</td> </tr> <tr> <td>Both</td> <td>100%</td> </tr> </tbody> </table>	Category	Percentage	Government	0%	Self-financed	0%	Both	100%	<p>2. What is your experience in conducting campus interviews? 14 responses</p> <table border="1"> <thead> <tr> <th>Category</th> <th>Percentage</th> </tr> </thead> <tbody> <tr> <td>Less than 1 year</td> <td>0%</td> </tr> <tr> <td>1-5 years</td> <td>21.4%</td> </tr> <tr> <td>5-10 years</td> <td>78.6%</td> </tr> <tr> <td>10-15 years</td> <td>0%</td> </tr> <tr> <td>More than 15 years</td> <td>0%</td> </tr> </tbody> </table>	Category	Percentage	Less than 1 year	0%	1-5 years	21.4%	5-10 years	78.6%	10-15 years	0%	More than 15 years	0%
Category	Percentage																				
Government	0%																				
Self-financed	0%																				
Both	100%																				
Category	Percentage																				
Less than 1 year	0%																				
1-5 years	21.4%																				
5-10 years	78.6%																				
10-15 years	0%																				
More than 15 years	0%																				
<p>Figure 1 Preference for Recruiting College</p>	<p>Figure 2 Experience in Conducting Placement</p>																				
<p>3. Do the students possess good communication and soft skills required by the organisation? 14 responses</p> <table border="1"> <thead> <tr> <th>Category</th> <th>Percentage</th> </tr> </thead> <tbody> <tr> <td>Yes</td> <td>0%</td> </tr> <tr> <td>No</td> <td>57.1%</td> </tr> <tr> <td>Partially</td> <td>42.9%</td> </tr> </tbody> </table>	Category	Percentage	Yes	0%	No	57.1%	Partially	42.9%	<p>6. Should engineering colleges have a talk with industry recruiting people before drafting their syllabus of English to meet the communication and soft skills requirement of the engineers for job? 14 responses</p> <table border="1"> <thead> <tr> <th>Category</th> <th>Percentage</th> </tr> </thead> <tbody> <tr> <td>Strongly disagree</td> <td>14.3%</td> </tr> <tr> <td>Disagree</td> <td>7.1%</td> </tr> <tr> <td>Neutral</td> <td>7.1%</td> </tr> <tr> <td>Agree</td> <td>14.3%</td> </tr> <tr> <td>Strongly agree</td> <td>64.3%</td> </tr> </tbody> </table>	Category	Percentage	Strongly disagree	14.3%	Disagree	7.1%	Neutral	7.1%	Agree	14.3%	Strongly agree	64.3%
Category	Percentage																				
Yes	0%																				
No	57.1%																				
Partially	42.9%																				
Category	Percentage																				
Strongly disagree	14.3%																				
Disagree	7.1%																				
Neutral	7.1%																				
Agree	14.3%																				
Strongly agree	64.3%																				
<p>Figure 3 Students' Command on Communication & Soft Skills</p>	<p>Figure 4 Importance of Industry Views for Drafting Syllabus of English</p>																				
<p>7. Do you think the teachers of English have a major role to play in preparing the engineering students with good language and soft skills? 14 responses</p> <table border="1"> <thead> <tr> <th>Category</th> <th>Percentage</th> </tr> </thead> <tbody> <tr> <td>Strongly disagree</td> <td>14.3%</td> </tr> <tr> <td>Disagree</td> <td>21.4%</td> </tr> <tr> <td>Neutral</td> <td>0%</td> </tr> <tr> <td>Agree</td> <td>0%</td> </tr> <tr> <td>Strongly agree</td> <td>64.3%</td> </tr> </tbody> </table>	Category	Percentage	Strongly disagree	14.3%	Disagree	21.4%	Neutral	0%	Agree	0%	Strongly agree	64.3%	<p>8. Do you carry out group discussions in the process of placement? 14 responses</p> <table border="1"> <thead> <tr> <th>Category</th> <th>Percentage</th> </tr> </thead> <tbody> <tr> <td>Yes</td> <td>78.6%</td> </tr> <tr> <td>No</td> <td>21.4%</td> </tr> </tbody> </table>	Category	Percentage	Yes	78.6%	No	21.4%		
Category	Percentage																				
Strongly disagree	14.3%																				
Disagree	21.4%																				
Neutral	0%																				
Agree	0%																				
Strongly agree	64.3%																				
Category	Percentage																				
Yes	78.6%																				
No	21.4%																				
<p>Figure 5 Major Role of English teachers for Developing Language skills</p>	<p>Figure 6 Group Discussion as a Part of Placement</p>																				





Bhatt and Bhatt

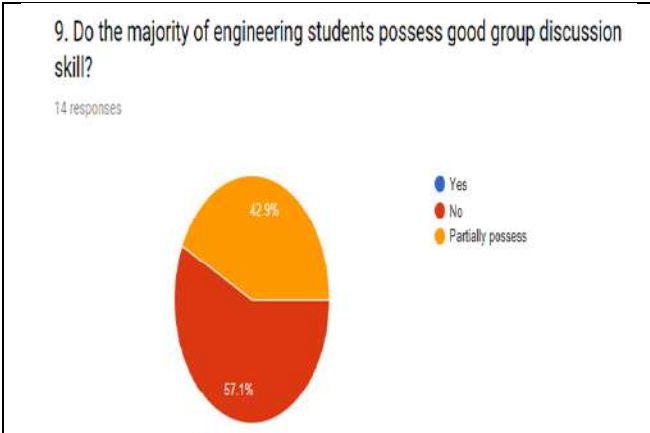


Figure 7 Whether Students Possess GD Skills

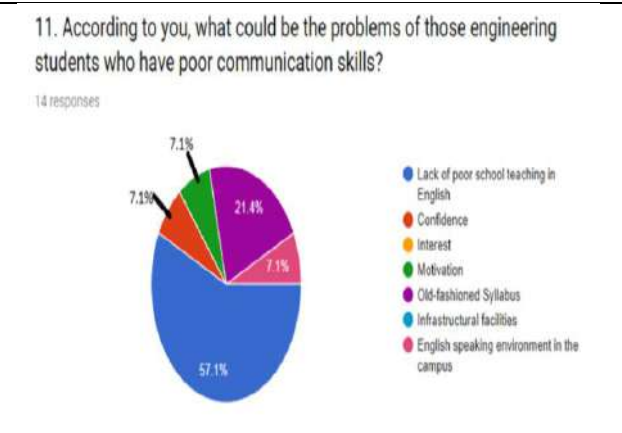


Figure 8 Problems with Students having Poor Communication Skills

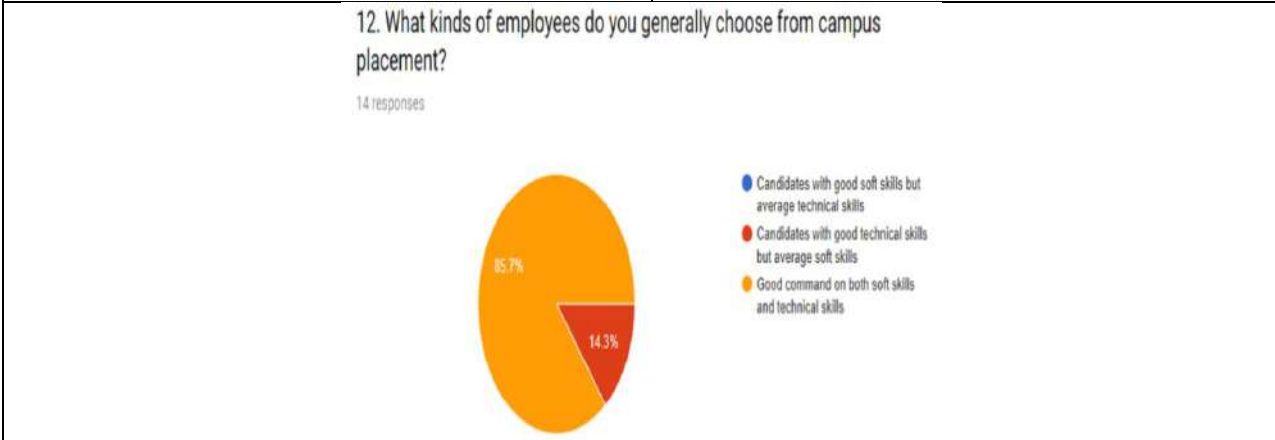


Figure 9 Technical Skills or Soft Skills or Both





Active Power Loss Minimization and Voltage Stability Improvement with Optimal Capacitor Placement in RDN

Pankita A Mehta and Praghnesh Bhatt*

Pandit Deendayal Energy University, Gandhinagar, Gujarat, India.

Received: 30 Dec 2023

Revised: 09 Jan 2024

Accepted: 12 Jan 2024

*Address for Correspondence

Praghnesh Bhatt

Pandit Deendayal Energy University,
Gandhinagar,
Gujarat, India



This is an Open Access Journal / article distributed under the terms of the **Creative Commons Attribution License** (CC BY-NC-ND 3.0) which permits unrestricted use, distribution, and reproduction in any medium, provided the original work is properly cited. All rights reserved.

ABSTRACT

The placement of capacitors in radial distribution networks plays a vital role in improving power quality. In the present work, a particle swarm optimization-based approach has been presented to allocate shunt capacitors in radial distribution networks. The objective function is formulated to minimize the active power loss in the system after the optimal placement of capacitors. The standard 33-node and 69-node test systems are considered for the analysis and validation of the results. Case studies are carried out to compare the performance of the distribution network with the placement of single and multiple capacitors. Results show that optimal placement of capacitors with proper sizing can significantly reduce the active/reactive power losses, improve the node voltage profile, and enhance the voltage stability of the distribution network.

Keywords: Active power losses; capacitor placement; radial distribution network; voltage stability.

INTRODUCTION

Reactive power compensation with the addition of shunt capacitors is beneficial in radial distribution networks (RDN) to reduce line losses, balance the line loading, and improve the voltage profile. Research has made many efforts to improve the performance of RDN by optimal placement of DGs and adopting reconfiguration of the network. Reactive power compensation by shunt capacitor banks (SCBs) to the RDN can also be a beneficial solution for the performance improvement of distribution systems [1]. The reactive power support from SCBs is one of the best-suggested solutions for minimizing the losses together with other benefits; such as efficient utilization of equipment, relieving overload of system components, and enhancing the life cycle of the equipment [2]. Full benefits from SCBs can be achieved by finding their optimal location and sizing otherwise too much compensation at wrong nodes may worsen the problem. Many methods have been reported in the literature to take advantage of SCBs by placing them properly in the system. Recently, researchers have suggested several algorithms and techniques to find the appropriate locations and optimal sizes of shunt capacitors with different objectives. Many techniques such as





Pankita A Mehta and Praghnesh Bhatt

Genetic Algorithm (GA) [3]-[5], Particle Swarm Optimization (PSO) [6]-[9], Cuckoo search algorithm (CSA) [10]-[12], Teaching Learning Based Optimization (TLBO) [13], Flower Pollination Algorithm (FPA) [14]-[15], and Oppositional Krill herd algorithm (OKH) [16]. Prakash et al. also used the PSO approach for finding the optimal size and location of capacitors in [7] and the results are compared with Tabu Search (TS) and GA algorithm. More recently, BBO [17], binary honey bee foraging (BHBF) [18], harmony search algorithm(HSA) [19], direct search algorithm (DSA) [20], plant growth simulation [21], ant colony optimization (ACO) algorithm [22], hybrid honey bee colony optimization (HBCO) [23] algorithm, a modified discrete PSO [24] and teaching learning-based optimization (TLBO) [13] have been used for finding the optimal rating and location of shunt capacitor for the radial distribution system. Similar to voltage profile improvement and loss minimization in RDN, the voltage instability problem has also attracted the attention of the electric utilities for assessment, prediction, and preventive actions to ensure its stable operation. Voltage stability in RDN has also received great attention with a need for both analysis and enhancement of the operating conditions. Algorithms for voltage stability enhancement of RDN by optimal capacitor placement (OCP) have been given in [1], [25]-[26]. In this work, the possibility of adopting a single-sized capacitor to limit the number of capacitor locations in RDN has been explored by setting active power loss minimization as the major objective. Moreover, the impact of capacitor placement on voltage stability has been presented for the standard test system.

Objective Functions and Constraints for Capacitor Placement in RDN

In this work, the objective is to determine the optimal location and sizing of capacitors to minimize active power losses. The expression of the minimization of active power losses of RDN is given in (1).

Minimize,

$$P_{Loss} = \sum_{i=2}^{nb} \left(P_{G,ni} - P_{D,ni} - V_{ni} Y_{ni,mi} V_{mi} \cos(\delta_{mi} - \delta_{ni} + \theta_{ni,mi}) \right) \quad (1)$$

where,

- P_{Loss} Active Power Loss
- $P_{G,ni}$ Real Power Generation at bus ni
- $P_{D,ni}$ Real Power demand at bus ni
- V_{mi} Voltage of bus mi
- V_{ni} Voltage of bus ni
- $Y_{ni,mi}$ Admittance of branch between bus ni and mi
- δ_{mi} Phase angle of bus mi
- δ_{ni} Phase angle of bus ni
- $\theta_{ni,mi}$ Admittance angle of branch between bus ni and mi

Following constraints are considered while minimizing the objective function of Eq. (1).

Limits on bus voltage: It must be kept within the specified limits at each bus:

$$V_{i,\min} \leq V_i \leq V_{i,\max} \quad (2)$$

where $V_{i,\min}$, $V_{i,\max}$ are the minimum and maximum limits on bus voltage, respectively.

The apparent power flow through each branch should not exceed its permissible limit.

$$S_i \leq S_{i,\max}, \quad i = 1, 2, \dots, nb \quad (3)$$

where nb is the total number of branches, S_i is the apparent power flow of the i^{th} branch, and $S_{i,\max}$ is the maximum apparent power flow limit of the i^{th} branch.

The total size of capacitors should not exceed the total reactive power demand of the RDN.





Pankita A Mehta and Praghnesh Bhatt

$$\sum_{i=1}^{nc} Q_{cap,i} \leq \sum_{i=2}^n Q_{D,i} \quad (4)$$

where nc is the total number of locations for capacitors, $Q_{D,i}$ is the reactive power demand at bus i , and $Q_{cap,i}$ is the size of the capacitor at location i . The objective function given in (1) is minimized with the help of Particle Swarm Optimization (PSO) keeping the constraints given in (2)-(4) in limits.

Particle Swarm Optimization For Minimizing Active Power Losses With Capacitor Placement

The size of the capacitors and their positions are considered as decision variables for finding their optimal location and sizing. The steps for executing the PSO algorithm in solving this problem are outlined below.

Step 1: Run the power flow of RDN without placement of any capacitors.

Step 2: Initialization – (i) population size (NP) (ii) maximum number of iterations and (iii) number of capacitors to be placed in the distribution network.

Step 3: Based on the number of capacitors, the number of buses is determined which have the lowest voltage magnitude

Step 4: Random initialization for the size of capacitors for each population. The total generated size of the capacitors should not exceed the reactive load demand of the network

Step 5: Run the load flow to find the power losses of the distribution network for each population.

Step 6: The objective function for active power loss minimization defined in (1) has been computed for each population. Arrange the obtained value of the objective function from the lowest value of losses to the highest value of losses. Keep the particle with the lowest losses as 'pbest' for the current iteration.

Step 7: Update the position and velocity of the particles and go to the next iteration

Step 8: Repeat the steps from 4 – 6.

Step 9: Find the best particle that gives the lowest losses during the current iteration. Consider this particle as 'pbest' for the current iteration.

Step 10: Compare the best losses obtained with the particle in the current iteration with the best losses obtained with the particle in the previous iteration. The particle which gives the lowest losses is regarded as the 'gbest' particle.

Step 11: Stop when iteration exceeds the maximum number of iterations.

Step 12: The 'gbest' particle will contain the optimal sizing of the capacitors. The values of power loss obtained after the placement of these capacitors at the nodes with the lowest voltage magnitude will be the optimized losses.

Test System for Simulation

For the simulation studies, the 33-node, 32-branch radial distribution network is considered as shown in Fig. 1 [1]. Active and reactive power load demands are 3.72 MW and 2.3 MVAR, respectively. In the base case, the system has 210.97 kW and 143 kvar, respectively. The following three individual case studies are carried out with the placement of 1, 2 or 3 capacitors at the buses which have the lowest magnitude.

Case 1: Placement of one capacitor at one bus which has the lowest voltage magnitude.

Case 2: Placement of two capacitors at two different buses that have the lowest voltage magnitudes.

Case 3: Placement of three capacitors at three different buses that have the lowest voltage magnitudes.

Comparative Results for Active and Reactive Power Losses with Capacitor Placement

The obtained results with PSO technique outlined in Section II are compared with the results reported in [27]-[28] for 33-nodes RDN and listed in Table I. It is observed that the installation of capacitors in RDN reduces the active and reactive power loss significantly as compared to the case where no capacitors are placed. In the proposed method, the reduction in active power loss is greater with the placement of two or three capacitors in comparison to the results reported in [27]-[28]. In [28], the total capacity of the capacitor is 1170 kvar which is less as compared to the proposed method. But a total of nine locations are identified for the placement of capacitors which in turn requires higher attention and maintenance costs for the capacitors. The improvement in node voltage profile can be observed





Pankita A Mehta and Praghresh Bhatt

clearly in Fig. 2 which shows the significance of capacitor placement in RDN. Fig. 3.(a), Fig. 3.(b) and Fig. 3(c) show the convergence curves of PSO with the placement of one capacitor, two capacitors, and three capacitors, respectively. For each case, convergence curves are shown to be settled at the minimized value of active power losses which are tabulated in Table 1. From these curves, it can be easily observed that placements of multiple capacitors with optimal sizing at the buses with the lowest magnitude can reduce the active power losses effectively.

Comparative Results with Capacitor Placemenet

Ref	Bus No	Cap Size (kvar)	Min. Vol(pu)	Ploss (kW)	Qloss (kvar)
[27]	6, 8	1200, 150 (1350)	0.919	163.37	--
[28]	31, 32, 12, 13, 14, 15, 16, 17, 18	150, 150, 225, 180, 105, 90, 75, 45 150 (1170)	0.934	163.78	
Proposed Method	18	476.8	0.9209	188.30	129.4
	6, 8	1290, 543 (1833)	0.9209	158	109.70
	6, 8, 18	1136, 399, 158 (1693)	0.9371	156	115.00

Impact of Capacitor Placement on Voltage Stability of RDN

The impact of the optimal placement of optimal-sized capacitors on voltage stability of the test system has been investigated. The optimal location and size of the capacitors are as per the Table 1. The voltage stability index for the system shown in Fig. 4 can be calculated by (5). The bus with minimum stability index is declared as the most critical bus which is the most sensitive bus to voltage collapse. The load flow gives the voltages of all the nodes and the branch currents. Hence, P and Q at the receiving end of each line can be computed. Thus, the voltage stability index of each bus can be calculated using (5).

$$SI(r) = V_s^4 - 4(PX - QR)^2 - 4V_s^2 (PR + QX) \quad (5)$$

Three cases of loading are considered as follow: (i) only active power load demand has been increased, keeping reactive power load demand constant (ii) only reactive power load demand has been increased; keeping active power load demand constant (iii) both active and reactive power load demands have been increased; maintaining constant power factor of the load demand. Fig. 5 shows the variations in the voltage stability margin for 33-nodes RDN considering the different load increment patterns. The enhancement in voltage stability margin for each case can be easily visible with the placement of more number of capacitors. So it can be concluded that for the case of capacitors placement in RDN, it is more advisable to place more capacitors for minimization of active power losses and enhancement of voltage stability. Fig. 6 shows the variations of the voltage profile of the most critical bus which supplements the results obtained for voltage stability enhancement margin for all cases.

CONCLUSION

This paper has analyzed the performance of RDN with the placement of single and/or multiple capacitors. The objective function based on the minimization of active power losses has been formulated and optimized with PSO to determine the optimal location and sizing of capacitors in RDN. It is concluded that the placement of capacitors in RDN can successfully reduce the active-reactive power losses and improve the node voltage profile significantly. Moreover, the reactive power support provided by capacitors helps to enhance the voltage stability, so that RDN can be stressed to higher loading for better utilization of line loading. It is also observed that lower capacity of capacitors placed strategically in RDN at the fewer location can also yield the impactful results instead of placing capacitors at too many locations.





Pankita A Mehta and Praghnesh Bhatt

REFERENCES

1. Baran, M.E., and WU, F.F.: "Optimal capacitor placement on radial distribution systems", IEEE Transaction on Power Delivery, , vol.4, (1), pp.725-734, January 1989
2. H.N. Ng, M.M.A. Salama, A.Y. Chikhani, Classification of capacitor allocation techniques, IEEE Transaction Power Delivery, vol. 15, pp. 387–392, January 2000.
3. Swarup KS. Genetic algorithm for optimal capacitor allocation in radial distribution systems. In: Proceedings of the 6th WSEAS international conference on evolutionary, Lisbon, Portugal, June 16-18, pp.152-9, 2005
4. M. Sydulu, V. Reddy, "Index and GA based optimal location and sizing of distribution system capacitors", IEEE Power Engineering Society General Meeting, 24-28 June 2007, pp.1–4.
5. Kalyuzhny A, Levitin G, Elmakis D, Haim HB, "System approach to shunt capacitor allocation in radial distribution system", International journal of Electrical Power System Research,; vol. 56(1), pp. 51-60, 2000
6. Singh SP, Rao AR, "Optimal allocation of capacitors in distribution systems using particle swarm optimization, International Journal of Electrical Power Energy System, 2012; vol. 43 (1); pp. 1267-75.
7. K. Prakash, M. Sydulu, "Particle swarm optimization based capacitor placement on radial distribution systems", IEEE Power Engineering Society General Meeting, , pp.1–5, 24-28 June 2007
8. I. Ziari, G. Ledwich, A. Ghosh, D. Cornforth, M. Wishart, "Optimal allocation and sizing of capacitors to minimize the transmission line loss and to improve the voltage profile", Comput. Math. Appl. vol. 60, pp. 1003–1013, 2010
9. Amanifar O, Golshan MEH. "Optimal distributed generation placement and sizing for loss and THD reduction and voltage profile improvement in distribution systems using particle swarm optimization and sensitivity analysis", International Journal of Tech Phys Probl Eng; vol. 3(2); pp 47-53, 2011
10. P. Das, S. Banerjee, "Placement of capacitor in a radial distribution system using loss sensitivity factor and cuckoo search algorithm" , International Journal of Sci. Res. Manag. vol. 2 (4), pp. 751–757, 2013
11. A.A. El-Fergany, A.Y. Abdelaziz, "Cuckoo search-based algorithm for optimal shunt capacitors allocations in distribution networks", International Journal of Electric Power Components System, vol. 41 (16), pp. 1567–1581, 2013
12. A.A. El-Fergany, A.Y. Abdelaziz, "Capacitor allocations in radial distribution networks using cuckoo search algorithm", IET Generation Transmission Distribution, vol. 8 (2), pp. 223-232, 2014
13. S. Sultana, P.K. Roy, "Optimal capacitor placement in radial distribution systems using teaching learning based optimization", International Journal of Electrical Power Energy System, vol. 54, pp. 387–398, 2014
14. A.Y. Abdelaziz, E.S. Ali, S.M. AbdElazim, "Optimal sizing and locations of capacitors in radial distribution systems via flower pollination optimization algorithm and power loss index", Engineering Science and Technology, an International Journal 2015 (article in press)
15. A.Y. Abdelaziz, E.S. Ali, S.M. AbdElazim, "Flower Pollination Algorithm and Loss Sensitivity Factors for optimal sizing and placement of capacitors in radial distribution systems", International Journal of Electrical Power and Energy Systems, vol. 78 , pp. 207-214, 2016
16. Sneha Sultana, Provas Kumar Roy, "Oppositional Krill herd algorithm for optimal location of capacitor with reconfiguration in radial distribution system", International Journal of Electrical Power and Energy Systems, vol. 74, pp. 78-90, 2016
17. Mandal KK, Bhattacharya B, Tudu B, Chakraborty NA, "Novel population-based optimization algorithm for optimal distribution capacitor planning. In International conference on energy, automation, and signal", (ICEAS) 2011; 28th–30th December. p. 1–6.
18. Sedighzadeh M, Kalimdast F, "A honey bee foraging approach to optimal capacitor placement with harmonic distortion consideration", Int Rev Electrical Eng 2012; 7(1):3592.
19. Muthukumar K, Jayalalitha S, "Harmony search approach for optimal capacitor placement and sizing in unbalanced distribution systems with harmonics consideration", In: International conference on advances in engineering, science and management (ICAESM), 2012; 30th–31st. p. 393–398.





Pankita A Mehta and Praghnesh Bhatt

20. Raju MR, Murthy KVS, Avindra KR, "Direct search algorithm for capacitive compensation in radial distribution systems", International Journal of Electrical Power System, vol. 42(1), pp. 24–30, 2012
21. Rao RS, Narasimham SVL, Ramalingaraju M, "Optimal capacitor placement in a radial distribution system using Plant Growth Simulation Algorithm", International Journal of Electrical Power System, vol. 33(5), pp. 1133–9, 2011
22. Kaur D, Sharma J, "Multi period shunt capacitor allocation in radial distribution systems", International Journal of Electrical Power System, vol. 52, pp. 247–53, 2013
23. Taher SA, Bagherpour R, "A new approach for optimal capacitor placement and sizing in unbalanced distorted distribution systems using hybrid honey bee colony algorithm", International Journal of Electrical Power System, vol.49, pp. 430–48, 2013
24. Ziari I, Ledwich G, Ghosh A, "A new technique for optimal allocation and sizing of capacitors and setting of LTC", International Journal of Electrical Power System, vol. 46, pp. 250–257, 2013
25. El Arini M. "Optimal capacitor placement incorporating voltage stability and system security", ETEP 2000, vol. 10(5), pp. 319–25
26. Satpathy PK, Das D, Dutta Gupta PB. "Critical switching of capacitors to prevent voltage collapse". International Journal of Electrical Power System, vol. 71(1), pp. 11–20, 2004.
27. Mohan G, Aravindhababu P. "Optimal locations and sizing of capacitors for voltage stability enhancement in distribution systems". International Journal Comput Appl (0975–8887), 2010, vol. 1(4), pp. 55–67
28. Aravindhababu P, Mohan G. "Optimal capacitor placement for voltage stability enhancement in distribution systems". ARPN J Eng Applied Science, April 2009, vol. 4(2), pp. 88–92

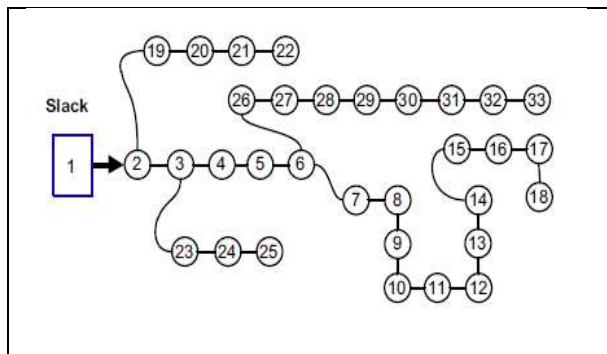


Fig. 1. Schematic of 33-nodes radial distribution network

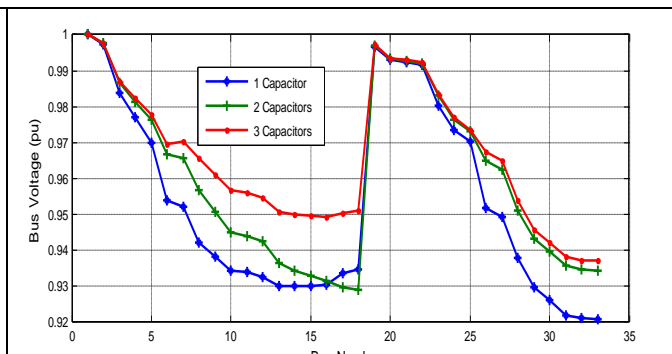


Fig. 2. Comparative node voltage profile with capacitor placement

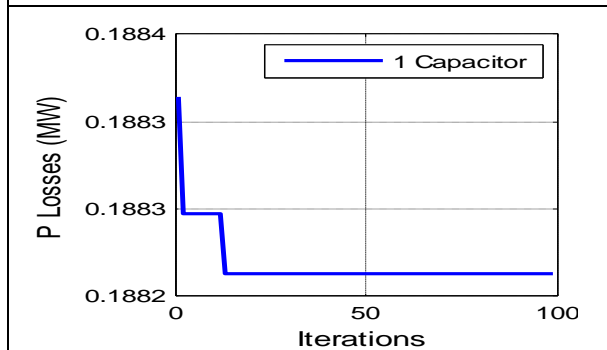


Fig. 3.a PSO convergence curve with one capacitor placement

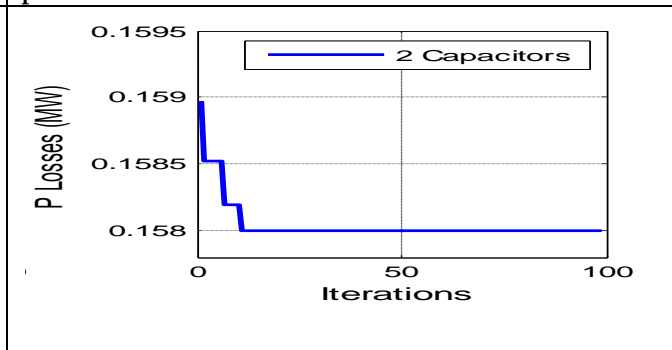


Fig. 3.b PSO convergence curve with two capacitors placement





Pankita A Mehta and Praghnesh Bhatt

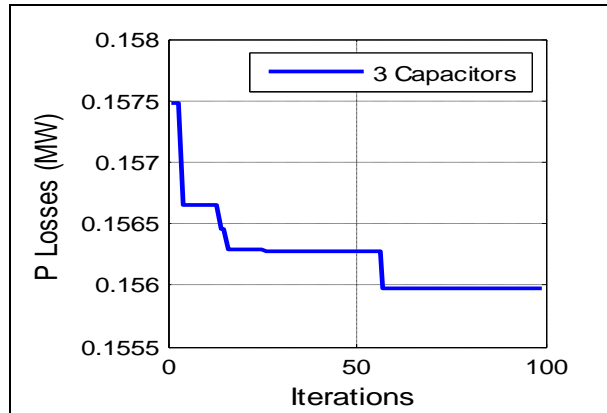


Fig. 3.c PSO convergence curve with two capacitors placement

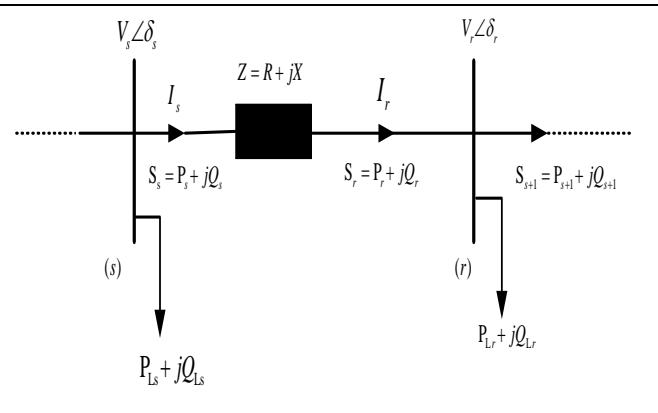


Fig. 4 Representation of two-bus model for calculation of voltage stability index

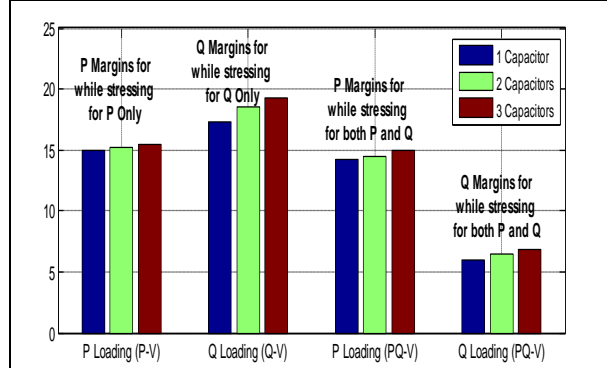


Fig. 5 Stability margins for different P-V, Q-V and P,Q-V loading for 33 nodes RDN with one, two and three capacitors placements

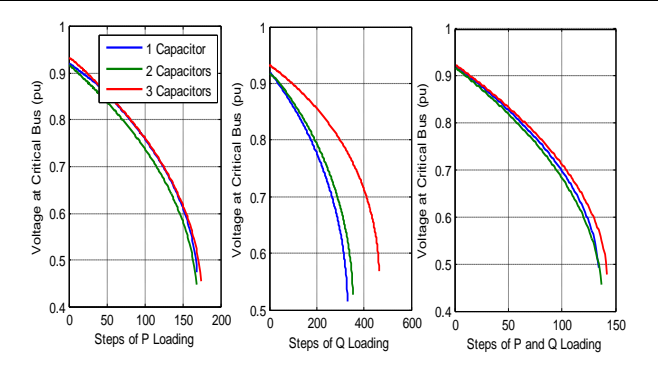


Fig. 6 Variations of critical bus voltages for with P, Q and PQ loading with one, two and three capacitors placements





Early Detection of Ovarian Cancer Using Artificial Intelligence: A Review

Sukeshini Jadhav^{1*} and Vijayshri Injamuri²

¹Post Graduate Student(M.Tech- CSE) ,Government College Of Engineering, Aurangabad , Maharashtra, India

²Assistant Professor (CSEDept), Government College Of Engineering, Aurangabad , Maharashtra, India

Received: 18 Oct 2023

Revised: 25 Oct 2023

Accepted: 31 Oct 2023

*Address for Correspondence

Sukeshini Jadhav

Post Graduate Student (M.Tech- CSE),
Government College of Engineering
Aurangabad 431001

E. Mail: sukeshini.jadhav22@gmail.com



This is an Open Access Journal / article distributed under the terms of the **Creative Commons Attribution License** (CC BY-NC-ND 3.0) which permits unrestricted use, distribution, and reproduction in any medium, provided the original work is properly cited. All rights reserved.

ABSTRACT

The most common type of cancer detected in women is ovarian cancer. According to data from previous research, for elderly women, ovarian cancer is a dangerous illness. It is the fifth most common disease worldwide and the seventh most significant cause of mortality in women. The predictive precision of AI has improved over that of conventional algorithms. However, further research is needed to contrast the impact of different artificial intelligence methods and variables and to suggest survival recommendations. This article first describes the process for choosing the studies, after which it provides a summary of ovarian cancer and different techniques for gathering data. and evaluation using machine learning approaches this work also provides a comprehensive exploration of the malignant and benign datasets and summarizes ML-based classification. Ovarian cancer remains a silent and deadly disease, often diagnosed at advanced stages, resulting in reduced survival rates and increased treatment complexity. Early detection of ovarian cancer is critical for improving patient outcomes. This study presents an innovative approach leveraging Artificial Intelligence (AI) techniques for the early detection of ovarian cancer. It also provides an overall visualization of the performance achieved and how it is useful for early detection based on the reviewed papers. Finally, potential directions and current challenges are considered.

Keywords: Ovarian cancer, artificial intelligence, AI technique, Dataset, Biomarker ultrasonography, ovarian cyst, AI challenge



**Sukeshini Jadhav and Vijayshri Injamuri****INTRODUCTION**

There are two ovaries in the female reproductive system, one on either side of the uterus. The hormones progesterone and estrogen are also produced in the ovaries; each is roughly the size of an almond. The female reproductive system and endocrine system depend greatly on the ovaries. They release vital hormones necessary for the enhancement of female development and the promotion of healthy fertility. But sometimes fluid-filled sacs that grow in the female reproductive system might cause cysts or other growths on them. Ovarian cancer is a kind of cell growth that arises in the ovaries. The cells have the ability to infiltrate and demolish healthy biological tissue, as well as proliferate quickly. Numerous of these ovarian cysts are benign (non-cancerous). Few of these, nevertheless, are malignant, so early detection and treatment are necessary. Surgery and chemotherapy are typically used in the treatment of ovarian cancer. Ovarian cancer initially presents without noticeable symptoms, but later, they are often attributed to other conditions, such as abdominal bloating, weight loss, pelvic discomfort, fatigue, back pain, and constipation. Ovarian cancer may develop without showing any early signs. The symptoms of ovarian cancer are sometimes confused with those of other, more common diseases when they first occur. The cells can infiltrate, destroy, and quickly replicate healthy biological tissue.

Ovarian tumors are classified into three types: epithelial, germ cell, and stromal. The majority of epithelial tumors are found in adults. Serous carcinoma and mucinous carcinoma are just a couple of its subtypes. Germ-cell tumors are rare, primarily in children and teens. Steroid hormones are created by stroma tumors, along with Compared to other ovarian cancers, these rare tumors are typically discovered earlier in the disease. It is typical for the ovary to produce little amounts of fluid surrounding the egg each month. These come in different sizes and are known as follicles. Their size range is 2 mm to 28 mm. If the malignant cells or tumors aren't found in time, they may spread across the ovary and pelvic regions, then into the stomach area and other organs. Antral follicles are those that are smaller than 18 mm in size, while dominant follicles are those that are between 18 mm and 28 mm in size. Follicles are responsible for the production of key hormones such as estrogen and progesterone. These follicles rupture and release eggs every month during ovulation. However, in certain circumstances, follicles may not explode and consequently do not produce eggs. These follicles are known as ovarian cysts. Because of the filling of fluid or blood, cysts can continue to develop in size. Ultrasound scans are used to identify ovarian cysts measuring 30-70 mm. They can, however, seem similar to the backdrop, making it difficult for doctors to distinguish between cystic and non-cystic areas. This can lead to incorrect diagnosis and treatment, necessitating the adoption of an ovarian cyst detection tool. Both common ovarian cyst symptoms and ovarian cancer symptoms can be present. Both may lead to abdominal pain, bloating, pain during sexual activity, menstrual inconsistencies, and, in rare cases, frequent urination. Unusual facial and body hair growth is an indication of ovarian cysts rather than ovarian cancer. Sudden severe stomach pain, fever, and nausea can indicate when an ovarian cyst has ruptured or twisted, necessitating immediate medical attention and, in some cases, emergency surgery. Once a mass is found and a cyst is suspected, doctors may run additional tests to determine what type of cyst it is or if the mass seems to be a tumor—and, in any case, whether treatment is required. When creating a treatment strategy, the ovarian cancer stage must be determined.

Certain factors can increase the likelihood of developing ovarian cancer:

- Family History: If you have a family history of ovarian cancer and have been diagnosed with the disease, you may be at a higher risk of developing it.
- Overweight: Additionally, being overweight or obese can also increase your likelihood of developing ovarian cancer.
- Hormonal Therapy: Taking hormone replacement therapy after menopause to manage symptoms may also contribute to an increased risk
- Endometriosis: Endometriosis, a condition where tissue similar to the lining of the uterus grows outside of it, can also be a factor.
- Age of Menstruation Period Statistics and Stopping: Early onset of menstruation, late onset of menopause, or both can increase the risk of ovarian cancer.



**Sukeshini Jadhav and Vijayshri Injamuri**

If you have never been pregnant, you may have a higher risk of developing ovarian cancer. Many women lack knowledge about ovarian cancer signs and risks, leading to late-stage detection for almost 50% of cases. Primary care physicians must stay updated on symptoms and risk factors, and be the first point of contact for anyone suspected of having an ovarian tumor. AI tools can help diagnose cancer through radiology and pathology.

LITERATURE REVIEW

Early detection of ovarian cancer is critical for various reasons. It can result in better treatment outcomes, greater survival rates, less aggressive treatments, fertility preservation, decreased cancer spread, lower healthcare costs, enhanced quality of life, increased awareness, research opportunities, and empowerment. Early detection boosts the chance of research and the development of novel medications. It also teaches women about the disease's symptoms and encourages them to seek medical assistance. This empowers women to take charge of their health and make informed decisions. Regular examinations, testing, and consultations with medical professionals can aid in early detection and potentially life-saving interventions. Machine Learning (ML) algorithms are becoming increasingly popular in the clinical field, as they are used to assist clinicians in making informed clinical decisions. AI systems are created to train algorithms to perform specific tasks based on clinical data. Various regression models such as linear and logistic, along with complex nonlinear models like neural networks and gradient boosting, are used in these techniques. To generate predictions, ML systems require a thorough statistical examination of clinical data. There are several sorts of ML algorithms, each serving a unique function. Classification algorithms predict discrete parameters; regression predicts continuous values. Segmentation models are critical in medical applications as they enable the classification and division of specific parts of an image. They aid in identifying regions of interest, like determining the size of a follicle from an ultrasound image. To deduce causal connections between observational data and outcomes, statistical methods like causal inference can be employed. It helps in understanding how the stimulation protocol used impacts outcomes. Various medical fields have explored the possible applications of AI in clinical decision-making.

AI Techniques

A multi-marker linear model was developed to predict ovarian cancer progression. AI and DL techniques are used in cancer imaging, with advanced imaging images pre-processed and transformed into machine learning algorithms. These algorithms map input imaging data and learn a mathematical function linked to the target or output, such as clinical or scientific observation. As per Akazawa, Munetoshi, *et al* (Akazawa and Hashimoto, 2020), research uses patient data and information from preoperative exams to predict the pathological identification of ovarian cancers using artificial intelligence (AI). Patients and Procedures 202 ovarian tumor patients were enrolled, of whom 53 had ovarian cancer, 23 had tumors that were borderline malignant, and 126 had benign ovarian tumors. They obtained diagnostic results from 16 features, typically available from blood tests, patient background, and imaging tests, using 5 machine learning classifiers, including support vector machines, Random Forest, Naive Bayes, logistic regression, and XGBoost. Additionally, they examined the significance of 16 features in terms of disease prediction. The XGBoost machine learning method had a maximum accuracy of 0.80. The correlation coefficient of the features, the regression coefficient, and the relevance of the characteristics in the random forest all yielded different findings in evaluating the features' value. With the findings from preoperative investigations, AI may be able to predict a pathological finding of ovarian cancer. Zhang, Z.(Zhang and Han, 2020). In this study, it is discussed how to detect malignancies during pregnancy and nursing, as well as prenatal ultrasound imaging. Technology like ultrasound and imaging is utilized to instruct expectant mothers. The goal of this study is to lower the acceptable rates of maternal and newborn mortality. In computer vision and image processing, these machine-learning techniques are becoming more and more common. In this study, the raw input photographs are transformed into output images (CNNs) using convolutional neural networks and logistic regression classifiers. To separate obstetric tumors and identify them, the investigators employed the Internet of Medical Things (IoMT). The use of CNN LRCs may benefit ultrasound. A woman's mobility will benefit from a typical pregnancy. Jung (Jung *et al.*, 2022). conducted a study to develop a deep learning-based diagnostic the researchers used a convolutional neural network with a convolutional



**Sukeshini Jadhav and Vijayshri Injamuri**

autoencoder (CNN-CAE) to categorize ultrasound images of ovaries into five categories: normal, cystadenoma, mature cystic teratoma, endometrioma, and malignant tumor. They preprocessed and enhanced 1613 ultrasound images for analysis and then used cross-validation to examine the accuracy, sensitivity, specificity, and area under the CNN-CAE model's receiver operating characteristic curve (AUC). This method allowed for reliable categorization of ovarian cancer and holds potential for further research in this area. The results showed that the accuracy and AUC values for discriminating between normal ovaries and tumors, as well as identifying malignant tumors, were both high. A gradient-weighted class activation mapping visualization method was utilized to validate the model's outputs. Overall, the CNN-CAE model effectively reduced extraneous information from ultrasound pictures while correctly classifying ovarian cancers. The study underlines the significance of distinguishing benign from malignant tumors and the possible application of deep learning in clinical settings. It is underlined that correctly detecting ovarian tumors is critical, as in their lives, up to 10% of women will undergo ovarian cyst surgery. The suggested CNN-CAE model performed well in diagnosing ovarian cancers and can potentially be used in future clinical practice. Detecting ovarian cancer early on is crucial for better patient outcomes. Convolutional neural networks (CNNs) have proved highly effective in achieving this, particularly when combined with medical imaging data from MRI and ultrasound scans. By automatically extracting complex features from images, CNNs eliminate the need for time-consuming feature engineering. Through their hierarchical learning technique, they can identify intricate patterns in ovarian tissues, enhancing their ability to distinguish between benign and malignant tissues. Transfer learning is critical as it enables pre-trained CNN models, already skilled in identifying generic characteristics from vast datasets like ImageNet, to be adapted for medical imaging applications. According to Mikdadi, Dina (Mikdadi *et al.*, 2022), artificial intelligence (AI) holds great potential for biomedical research and the development of biomarkers as a result of declining computer resource costs and the rising availability of open-source tools. There are still issues with data accessibility, quality, bias, openness, and explainability. The stakes are higher for uncommon diseases like pancreatic and ovarian cancer, where clinical applications are just beginning. Larger, more diverse picture collections combined with consistent reporting metrics allow for greater model validation, less bias, and quantitative comparisons. As investments in AI rise, stakeholders and regulatory bodies need to confront these challenges. Neural networks can accurately predict a positive diagnosis of ovarian cancer 91.3% of the time when they use a novel RNA biomarker, according to research from the Dana-Farber Cancer Institute and Brigham and Women's Hospital. The results suggest that combining next-generation RNA sequencing with sophisticated analytics algorithms could produce a non-invasive, highly accurate diagnostic tool for ovarian cancer. The researchers found that specific miRNAs could be used to identify pre-symptomatic malignancies because they are highly likely to be present in early ovarian lesions.

METHODOLOGY

AI algorithms are playing an increasing role in the early detection, management, and treatment of ovarian cancer. These algorithms can analyze medical images, predict risk, monitor symptoms, interpret genetic tests, improve screening, provide real-time instructions, assist with pathology analysis, create individualized treatment plans, discover new drugs, and support patients with education and resources. However, before AI can be used in clinical practice, it must undergo rigorous validation, regulatory approval, and integration into healthcare systems to ensure its safety and effectiveness for patients. Ongoing research by medical professionals and academics is working to develop and validate AI-based techniques for treating ovarian cancer.

Dataset

Previously, various datasets were critical in developing the field of early ovarian cancer detection using AI. These datasets, which range from thorough genomic information to high-resolution medical imaging, have given researchers significant insights into the complex molecular and observable ovarian cancer signals. Scientists have discovered novel biomarkers, picked up on minute patterns in medical imaging, and created complex machine-learning algorithms through rigorous study. These successes not only paved the way for more precise and prompt diagnoses but also for further study. Future studies in the field of ovarian cancer detection will be able to use the



**Sukeshini Jadhav and Vijayshri Injamuri**

quantity of information gleaned from these databases as a reliable reference. Future studies might build on the results of earlier research and make use of a variety of databases. Future research will aim to improve AI algorithms, investigate new paths of genomic and proteomic analysis, and ultimately improve the efficacy of early detection systems. The synergy between historical datasets and future research endeavors thus forms a continuum of knowledge, enabling the continuing growth of AI-based solutions for ovarian cancer early detection, with the ultimate goal of increasing patient outcomes and survival rates. Using pre-trained AI models in studies for early detection of ovarian cancer has various benefits. Here are some well-known pre-trained models that are often utilized in clinical image analysis.

Challenges

According to an overview from previous research we found some challenges are impact on the use of AI in the early detection of ovarian cancer, Rest assured that each presents a unique challenge that researchers and physicians are more than capable of overcoming.

- **Ovarian Cancer's Non-Specific Symptoms/Presentation:** Ovarian cancer frequently presents with non-specific symptoms, making it difficult to diagnose in the early stages. Many benign illnesses might be blamed for symptoms including bloating, pelvic pain, and abdominal discomfort, which delays diagnosis. It is essential to create AI systems that can identify tiny patterns connected to these hazy symptoms. Given the complexity of human physiology and the variety of ways that illnesses might present themselves, powerful machine-learning algorithms are needed to identify subtle variations in medical data related to these symptoms.
- **Lack of Comprehensive Research Evaluating the Effectiveness of Different Initial Investigations for Ovarian Cancer:** There is a dearth of thorough research evaluating the efficacy of different initial investigations for ovarian cancer. The accuracy and effectiveness of various diagnostic techniques, such as ultrasonography, CT scans, or blood tests, must be compared. For AI models to be validated, comprehensive benchmarking research is essential. The creation and validation of AI algorithms become difficult without a consistent methodology, making it difficult for them to be easily incorporated into clinical practice.
- **Ovarian Cancer Biomarkers:** Finding trustworthy ovarian cancer biomarkers is a never-ending task. Although intriguing indicators have been found, there are still some questions about their specificity and sensitivity, particularly in the early stages of the disease. The use of AI can help identify possible biomarkers by sorting through huge amounts of biological data. However, access to high-quality, well-annotated datasets with a variety of biomarker data is essential for the creation of precise AI models. Biomarker discovery can be hampered by incomplete or skewed data, which might produce biased conclusions.

Opportunity

The study on early detection of ovarian cancer using AI presents exciting opportunities, including the creation and application of risk algorithms to increase referral rates for suspected cases. AI algorithms in medical imaging analysis enable accurate diagnosis of ovarian cancer lesions, enabling prompt medical interventions and better patient prognosis. Convolutional Neural Networks (CNNs) can spot irregularities and subtle patterns in images, enabling early diagnosis. AI-driven analysis of genomic and proteomic data reveals deep patterns and linkages, enabling the discovery of novel biomarkers for early detection and tailored treatments. AI algorithms improve sensitivity and specificity by analyzing various data types, reducing false negatives and false positives. Multi-modal data integration improves research by examining complex interconnections. AI-driven decision support systems evaluate patient data in real time, ensuring fast interventions and individualized treatment. Continuous Learning and Adaptation: AI models can adapt to changing medical knowledge and emerging patterns by continuously learning from fresh data. The accuracy of risk algorithms is improved over time by continuous learning, which also increases the efficiency of referrals for suspected ovarian cancer cases. Continuous learning makes sure that risk algorithms are current with the most recent clinical insights and research findings. All of this potential drives the development of early ovarian cancer detection research. Researchers are at the vanguard of improving ovarian cancer diagnosis and therapy, resulting in better outcomes and quality of life for patients by leveraging the possibilities of AI and encouraging interdisciplinary collaboration.





Sukeshini Jadhav and Vijayshri Injamuri

CONCLUSION

AI techniques like deep learning and machine learning, have been useful in detecting early symptoms of ovarian cancer using varied datasets such as genomes, clinical records, and medical imaging. These algorithms have shown the ability to discern subtle patterns that humans may miss. Integrating numerous data sources and modalities to improve the accuracy and specificity of AI-based detection models is often required for successful early detection. AI-powered investigations have resulted in the discovery of new biomarkers linked to ovarian cancer, boosting diagnosis accuracy and revealing insights into the disease's underlying biology. AI's ability to understand medical imaging has paved the way for sophisticated radiomics and computer-aided diagnostics, changing clinical practice. However, issues like data privacy, interpretability, and the requirement for big, diverse datasets must be addressed. Collaboration across disciplines is crucial for translating AI advancements into clinical applications. Future studies should concentrate on improving AI algorithms, running extensive clinical trials, and tackling obstacles to AI adoption.

REFERENCES

1. Akazawa, M., Hashimoto, K., 2020. Artificial Intelligence in Ovarian Cancer Diagnosis. *Anticancer Res.* 40, 4795–4800. <https://doi.org/10.21873/anticancer.14482>
2. Jung, Y., Kim, T., Han, M.-R., Kim, S., Kim, G., Lee, S., Choi, Y.J., 2022. Ovarian tumor diagnosis using deep convolutional neural networks and a denoising convolutional autoencoder. *Sci. Rep.* 12, 17024. <https://doi.org/10.1038/s41598-022-20653-2>
3. Mikdadi, D., O'Connell, K.A., Meacham, P.J., Dugan, M.A., Ojere, M.O., Carlson, T.B., Klenk, J.A., 2022. Applications of artificial intelligence (AI) in ovarian cancer, pancreatic cancer, and image biomarker discovery. *Cancer Biomark.* 33, 173–184. <https://doi.org/10.3233/CBM-210301>
4. Zhang, Z., Han, Y., 2020. Detection of Ovarian Tumors in Obstetric Ultrasound Imaging Using Logistic Regression Classifier With an Advanced Machine Learning Approach. *IEEE Access* 8, 44999–45008. <https://doi.org/10.1109/ACCESS.2020.2977962>
5. Gupta, A., & Fatima, H. (2023, May). A Systematic Review of Machine Learning for Ovarian Cyst Detection using Ultrasound Images. In 2023 2nd International Conference on Applied Artificial Intelligence and Computing (ICAIC) (pp. 201-206). IEEE
6. Das, S., Mondal, D., Roy, P., Das, T., Roy, R., & Majumdar, D. (2023). A Comparative Analysis and Prediction of Ovarian Cancer using AI Approach. *Asia-Pacific Journal of Management and Technology (AJMT)*, 3(3), 22-32.
7. Mamatha, K. R., & Keerthana, M. R. (2023). Artificial Intelligence Perspective for Preliminary Detection of Ovarian Cancer. *Korean Journal of Physiology and Pharmacology*, 27(2).
8. Ahamad, M. M., Aktar, S., Uddin, M. J., Rahman, T., Alyami, S. A., Al-Ashhab, S., ...& Moni, M. A. (2022). Early-Stage Detection of Ovarian Cancer Based on Clinical Data Using Machine Learning Approaches. *Journal of personalized medicine*, 12(8), 1211.
9. <https://www.mayoclinic.org/diseases-conditions/ovarian-cancer/symptoms-causes/syc-20375941>
10. <https://www.mayoclinic.org/diseases-conditions/ovarian-cancer/diagnosis-treatment/drc-20375946>
11. www.google.com (Images of Ovarian Cancer)

Table No.1 Methodology

Sr.No	Algorithm	Application
1	Support Vector Machine(SVM)	SVM is used to classify ovarian cancer by identifying a hyper plane in a high-dimensional feature space that maximizes the difference between cancerous and non- cancerous instance.
2	K-Nearest Neighbor (KNN)	KNN can help detect ovarian cancer by classifying patients based on comparable patient profiles in their nearest neighbors.
3	K-mean	K-means can be used to group individuals with comparable characteristics, such as





Sukeshini Jadhav and Vijayshri Injamuri

		biomarker profiles, to discover subgroups of those with ovarian cancer
4	Neural Network (NN)	Neural Network Neural networks can be used to build complex models that extract nuanced patterns from a variety of data sources, including clinical and genetic information about ovarian cancer.
5	Artificial Neural Network (ANN)	ANNs, a form of the neural network, are designed to emulate the structure of the human brain, allowing them to accurately analyze intricate correlations in ovarian cancer data.
6	Decision Tree	Decision trees are a method that assists in the diagnosis of ovarian cancer based on patient features, symptoms, and test findings.
7	Logistic Regression	To determine whether a patient has ovarian cancer based on clinical and diagnostic data, logistic regression is a statistical technique used for binary classification problems.
8.	Random Forest	Random Forest The accuracy and robustness of classification models for ovarian cancer can be improved by using random forests, an ensemble approach that mixes numerous decision trees.
9.	XG Boost	XG Boost, an ensemble learning technique, effectively aids in ovarian cancer detection by analyzing patient data, identifying cancer patterns, and handling high- dimensional data.
10.	Naive Bayes	A probabilistic classification system called Naive Bayes is used to diagnose ovarian cancer by predicting patient features and calculating the likelihood that the disease will develop based on risk For ovarian cancer, Naive Bayes provides a probability estimate, assisting medical practitioners in determining risk and selecting diagnostic procedures.

Table No 2: Datasets

Sr.No	Dataset	Description
1	Ovarian cancer data from TGCA(The cancer Genome Atlas)	Comprehensive ovarian cancer, genomic, transcript atomic, clinical data useful for molecular analysis
2	Ovarian cancer National Cancer Institute (NCI) Data	Datasets with clinical biomarker and image information ideal for variety of analysis including application of artificial intelligence.
3	Wisconsin Ovarian cancer dataset(WBCD)	Dataset for fine needles aspiration(FNA)readings useful for categorization and machine learning.
4	Ovarian cancer image dataset	MRI, histopathy and ovarian ultrasound image collection necessary for image based diagnosis software.
5	SEER(Surveillance, Epidemiology, and End Result)	Population-based cancer statistics for united states, including case of ovarian cancer useful for epidemiology research



Figure 1 Ovarian cyst



Figure 2 Real Image of Ovarian Cancer





Captioning the Visual World: A Survey of Image-To-Text Approaches

Yash Sindha¹, Duttresh Sapra¹, Tilak kundaliya¹, Keyur N. Brahmbhatt² and Dipika Kothariya^{3*}

¹Student at IT Department, BVM Engineering College, V.V. Nagar, Gujarat, India

²Head of IT Department, BVM Engineering College, V.V. Nagar, Gujarat, India

³Asst.Prof. at IT Department, BVM Engineering College, V.V.Nagar, Gujarat, India.

Received: 18 Oct 2023

Revised: 25 Oct 2023

Accepted: 31 Oct 2023

*Address for Correspondence

Dipika Kothariya

Asst.Prof. at IT Department,

BVM Engineering College,

V.V.Nagar, Gujarat, India.

E. mail: dipika.kothariya@bvmengineering.ac.in



This is an Open Access Journal / article distributed under the terms of the **Creative Commons Attribution License** (CC BY-NC-ND 3.0) which permits unrestricted use, distribution, and reproduction in any medium, provided the original work is properly cited. All rights reserved.

ABSTRACT

This article provides essential strategies and insights to enhance the accuracy of image recognition models. While building and training deep learning models for image recognition, it's not uncommon to encounter accuracy levels between 50% and 70%. This article offers six practical "hacks" to elevate the performance metrics of your image recognition models. To address the challenge of image caption accuracy for images outside the initial dataset, we propose an innovative approach. This involves introducing an additional dataset with 100 distinct-category images. By retraining the model with this dataset and fine-tuning, we aim to enhance caption accuracy, especially for images beyond the original dataset.

Keywords: Image captioning, Machine Learning, Deep Learning , Convolutional Neural Network (CNN), Natural Language Processing (NLP)

INTRODUCTION

In the dynamic landscape of machine learning, the development of image recognition models has witnessed remarkable progress. However, one challenge that often surfaces is the model's ability to generate accurate captions for images beyond the dataset on which it was trained. While our model exhibits satisfactory performance when applied to images from the initial dataset, it faces limitations in offering precise captions for new and diverse visual content. This review paper aims to outline a strategic approach to rectify this limitation and enhance the overall accuracy of image captioning.





Yash Sindha et al.,

Algorithm Used

Our chosen approach for developing the model involves the implementation of a Convolutional Neural Network (CNN), a powerful deep learning architecture well-suited for image processing tasks. CNNs have demonstrated remarkable success in extracting intricate features from visual data, making them an ideal choice for our image-captioning model. In this study, we leverage the capabilities of CNNs to meticulously analyze and interpret a diverse dataset comprising 8000 images. Each image in our dataset is not merely a standalone entity; rather, it is accompanied by a descriptive caption, providing valuable context and semantic information. This combination of visual and textual elements enhances the richness of our dataset, enabling the model to learn meaningful associations between visual features and corresponding linguistic representations.

The CNN serves as a robust feature extractor, allowing the model to automatically discern hierarchical patterns and relevant details within the images. By harnessing the power of deep learning, our approach aims to capture intricate visual nuances, facilitating a more nuanced understanding of the complex interplay between images and their associated captions. In summary, our methodology integrates a state-of-the-art CNN architecture to handle the inherent complexities of our dataset, emphasizing the synergy between visual content and textual descriptions. This comprehensive approach not only enhances the model's ability to extract salient features but also lays the groundwork for a more profound exploration of the intricate relationship between images and captions."

Background and History

Introduction of Image Recognition Models:

The paper begins by acknowledging the remarkable progress in the development of image recognition models within the dynamic landscape of machine learning.

Algorithmic Foundation: Convolutional Neural Network (CNN)

The chosen algorithm for addressing these challenges is the Convolutional Neural Network (CNN). The authors justify their selection by emphasizing the success of CNNs in extracting intricate features from visual data, making them well-suited for image-captioning tasks.

Dataset Composition

A critical aspect of their methodology is the utilization of a diverse dataset comprising 8000 images, each accompanied by a descriptive caption. This dataset forms the foundation for the model's training, and the combination of visual and textual elements is highlighted as crucial for learning meaningful associations.

Challenges in Image Captioning

The authors identify and discuss challenges faced during the data collection and annotation process, data preprocessing, and the complexity of developing an effective image captioning model. Model accuracy is acknowledged as a significant challenge, prompting the introduction of methods for enhancing accuracy.

Methods for Enhancing Accuracy

The paper proposes practical methods for improving accuracy, including data augmentation, adding more layers to the model, experimenting with image sizes, adjusting the number of epochs, decreasing color channels, and leveraging pre-trained models through transfer learning.

Implementation and Result Presentation

The authors provide insight into the practical implementation of their model, including user interaction through sign-up, login, and feedback submission. The results section showcases the accuracy of caption generation for images within the dataset and highlights challenges faced when presented with images outside the original dataset.





Yash Sindha et al.,

Proposed Solution

In response to the challenge of inaccurate captions for images outside the dataset, the authors propose a solution involving the inclusion of an additional dataset with 100 distinct-category images. This dataset is designed to enhance the model's ability to generate accurate captions for a broader range of visual content.

Conclusion and Future Directions

The paper concludes by emphasizing the model's success in generating precise captions for a collection of 8000 images while acknowledging the challenge of extending this accuracy to images outside the original dataset. The proposed solution involving a curated dataset of 100 images is presented as a strategy to bridge this gap.

Challenges

Data Collection and Annotation Challenge: Gathering and annotating a diverse and representative dataset of 8000 images with descriptive captions can be time-consuming and resource-intensive.

Data Preprocessing Challenge: Ensuring uniformity in image sizes, caption tokenization, and handling missing or noisy data during preprocessing can be challenging.

Model Complexity Challenge: Developing an effective image captioning model with proper attention mechanisms and combining image and text models while avoiding overfitting can be complex.

Model accuracy : It is a big challenge that model is predicting the right output or not . We have taken some techniques for improving accuracy of model which is given below.

Methods for Enhancing Accuracy in Image-To-Text Approach

Get More Data

Data plays a pivotal role in enhancing the effectiveness of machine learning models. To boost validation accuracy, a straightforward approach is to expand your dataset, which is particularly valuable when working with limited training examples. For image recognition tasks, it's beneficial to diversify your dataset through the practice of data augmentation. Data augmentation encompasses a range of techniques, including image flipping, noise injection, and image zooming. However, it's crucial to exercise caution when employing augmentation techniques. Some modifications can alter the fundamental characteristics of an image. For instance, flipping an image of the number '3' over the y-axis may lead to an inaccurate representation of the original image.

Adding More Layers

Adding more layers to your model deepens its capacity to understand complex datasets. This is particularly valuable for intricate tasks like distinguishing between specific breeds of animals, where nuanced features matter. For simpler tasks, a leaner model with fewer layers suffices. More layers result in a more refined model.

More layers -> More nuanced model.

Changing Image Size

During the preprocessing of images for training and evaluation, there's ample room for experimentation with image size. Selecting the right size is pivotal. Opting for an image size that's too small can hinder your model's ability to capture the distinctive features necessary for image recognition. Conversely, if the images are excessively large, they can strain computational resources and may challenge less sophisticated models. Common image dimensions include 64x64, 128x128, 28x28 (MNIST), and 224x224 (VGG-16). It's important to note that most preprocessing algorithms don't consider an image's aspect ratio, which can lead to distortion in smaller-sized images along a particular axis. "Resizing a high-resolution image to a smaller size, such as 28x28, often results in significant pixelation, which can adversely impact your model's performance.

Increasing Epochs

Epochs represent the number of times the entire dataset is passed through the neural network. It's a common practice to gradually increase the number of epochs, such as adding +25, +100, and so forth. However, it's important to note



**Yash Sindha et al.,**

that increasing epochs is effective primarily when you have a substantial amount of data in your dataset. Beyond a certain point, raising the number of epochs won't lead to further improvements in accuracy. When you reach this stage, it's advisable to explore adjustments to your model's learning rate. This small but crucial hyperparameter determines whether your model converges to its global minimum, the ultimate objective for neural networks, or becomes stuck in a local minimum.

Decreasing Colour Channel

Color channels are indicative of the dimensionality of your image arrays. In the case of most color (RGB) images, they comprise three color channels, whereas grayscale images consist of just one channel. It's important to recognize that the complexity of color channels directly impacts the intricacy of the dataset and, subsequently, the duration required for model training. If color isn't a critical factor for your model's objectives, you have the option to simplify by converting color images to grayscale. In RGB images, the three color channels are red, green, and blue.

Using Pre-Trained Model

Transfer learning entails the utilization of pre-trained models, such as YOLO and ResNet, as a foundation for a wide array of computer vision and natural language processing tasks. These pre-trained models represent cutting-edge deep learning systems, having undergone extensive training on vast datasets over extended periods, often spanning months. Their remarkable capacity to discern intricate details in diverse images is truly astonishing. These models can serve as a solid starting point for your own model. In many cases, their performance is so exceptional that additional convolutional and pooling layers are often unnecessary. The incorporation of transfer learning can lead to substantial improvements in your model's accuracy, potentially elevating it from around 50% to an impressive 90%.

Flowchart

Main Processes of System

Project Hardware/Software Requirements

Software requirements

Front-end : React

Back-end : Node.js

Database : MongoDB

Model : Python

Hardware requirements

Memory (RAM): Sufficient memory is crucial, 8GB of RAM or more is recommended,

Sufficient storage required.

Internet Connectivity

Implementation

Signup , login and submit feedback: After signup and login we will be able submit feedback then we will go to main page for uploading image.

RESULT

For image within dataset We will get the exact result for the image which are there in a dataset. each caption's accuracy is desired for image within dataset.

Problem for Image Which Is Outside From Dataset

Result(for image outside from the dataset)





Yash Sindha et al.,

Problem Statement

If we are giving image outside of the dataset it is not giving accurate desired output. Our machine learning project is founded on an extensive dataset of 8000 images, each accompanied by a corresponding caption.

Solution

Approach which we are going to use for achieving better accuracy.

In response to the challenge at hand, we propose an innovative approach to enhance the caption accuracy of our image recognition model. This solution involves **the inclusion of an additional dataset**, comprising **100 images from a specific category**. These images are distinct from the initial dataset and represent a subset of visual content that the model has not encountered during its initial training. By introducing this smaller, but carefully curated, dataset, we aim to retrain the model and fine-tune its ability to generate accurate captions, particularly for images that fall outside the original dataset. The inclusion of these 100 specific-category images is expected to improve the model's generalization, enabling it to provide precise and contextually relevant captions for a more extensive range of visual content. By comprehensively analyzing these accuracy parameters, we aim to quantify the improvement in caption accuracy resulting from the inclusion of the 100 specific-category images.

CONCLUSION

In the domain of machine learning and image captioning, it's clear that our model excels at producing precise caption for a collection of 8000 images. However, its challenge lies in offering precise captions for images outside this dataset. To address this limitation, we are introducing an additional dataset of 100 images from a distinct category. Through fine-tuning and specific accuracy metrics, we aim to enhance the model's caption accuracy, bridging the gap between our model's performance within and outside the original dataset. The journey continues, with the goal of providing contextually rich and accurate captions for all images

REFERENCES

1. Berkely Artificial Intelligence Research, https://bair.berkeley.edu/blog/2019/06/07/data_aug/
2. Image reference : <https://medium.com/ymedialabs-innovation/data-augmentation-techniques-in-cnn-using-tensorflow-371ae43d5be9>
3. Adding more layer to image : image taken from the :
4. https://www.tensorflow.org/tutorials/images/data_augmentation
5. Imagereference <https://dribbble.com/shots/4829233-Pixelated-Mona-Lisaimage-recognition-model-accuracy-with-these-hacks/>
6. Code of Fundamentals in the JES: showing Separating RGB (Red ,Green ,Blue) colour channels:https://www.youtube.com/watch?v=ZqUotba3V5Y&ab_channel=hyperCODEmia
7. Colour space conversion Image reference: <https://www.tensorflow.org/io/tutorials/colourspace>
8. Image references from image captioning project "CAPTION-IT": "caption-it_report.docx"
9. Format reference of the review paper: "A systematic literature review on health recommender systems.doc"
10. Format reference taken from the review paper "ResearchPaper_Format.docx"
11. Research article : "Quality Control and Monitoring by it Solution for Better Application of TQM A Review"
12. Taraneh Ghandi, Hamidreza Pourreza, Hamidreza Submitted on 31 Jan 2022, last revised 22 Aug 2023 Deep Learning Approaches on ImageCaptioning: A Review Mahyar <https://arxiv.org/abs/2201.12944>
13. Ahmed Elhagry, Karima Kadaoui "A Thorough Review on Recent Deep Learning Methodologies for Image Captioning: " <https://arxiv.org/abs/2107.13114>
14. Karpathy, A., & Fei-Fei, L. (2015). "Deep Visual-Semantic Alignments for Generating Image Descriptions."<https://cs.stanford.edu/people/karpathy/cvpr2015.pdf>
15. Devlin, J., Cheng, H., Fang, H., & Gupta, S. (2015). "Language Models for Image Captioning: The Quirks and What Works." <https://arxiv.org/abs/1505.01809>





Yash Sindha et al.,

16. Chen, X., & Lawrence Zitnick, C. (2015). "Mind's Eye: A Recurrent Visual Representation for Image CaptionGeneration."https://arxiv.org/abs/1502.03044



Fig 1 : An image of the number "3" in original form and with basic augmentations applied.

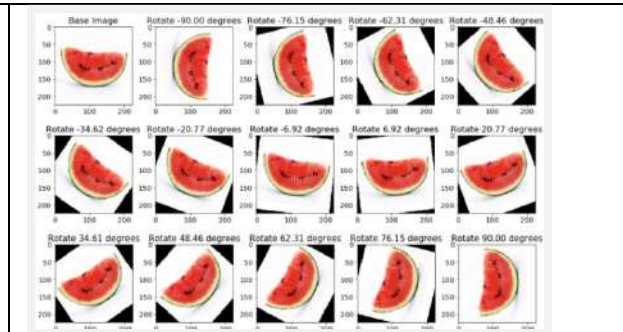


Fig 2 : Image set with background noise added

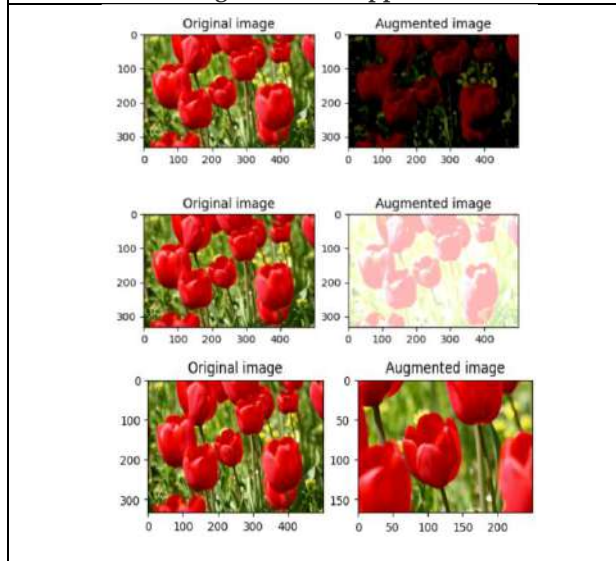


Fig 3 : Different visualization of image after adding more layers

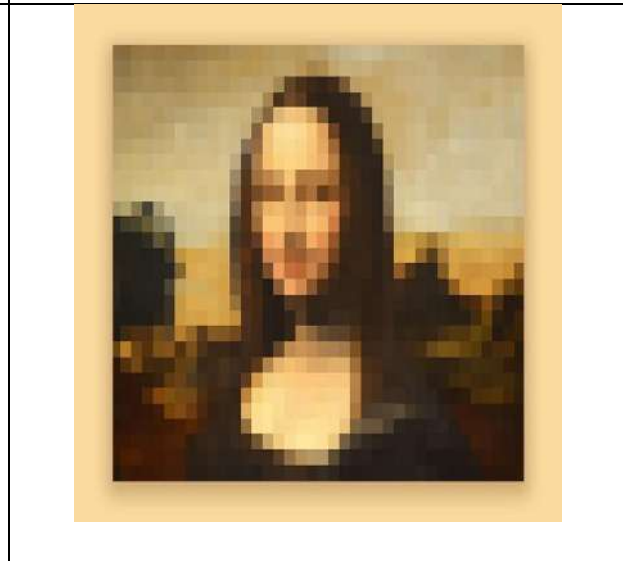


Fig 4 : Conversion of an image from a large resolution to a small size



Fig 5 : RGB images are composed of three colour channels: red, green, and blue

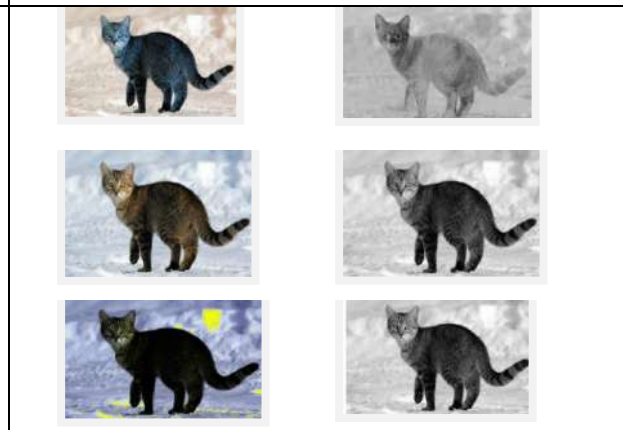


Fig 6 : Colour space conversions





Yash Sindha et al.,

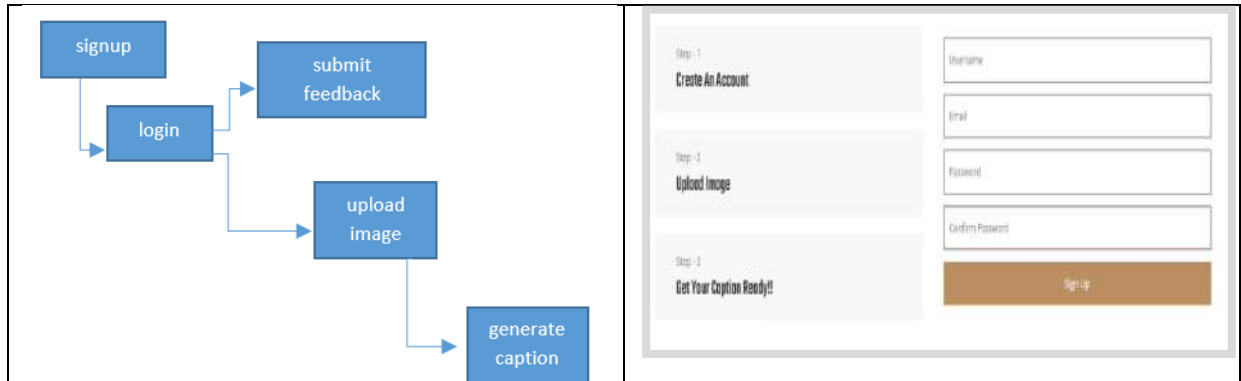


Fig 7 : Flow of the main processes

Fig 8 : Sign up page



Fig 9 : Login page



Fig 10 : Caption generation page

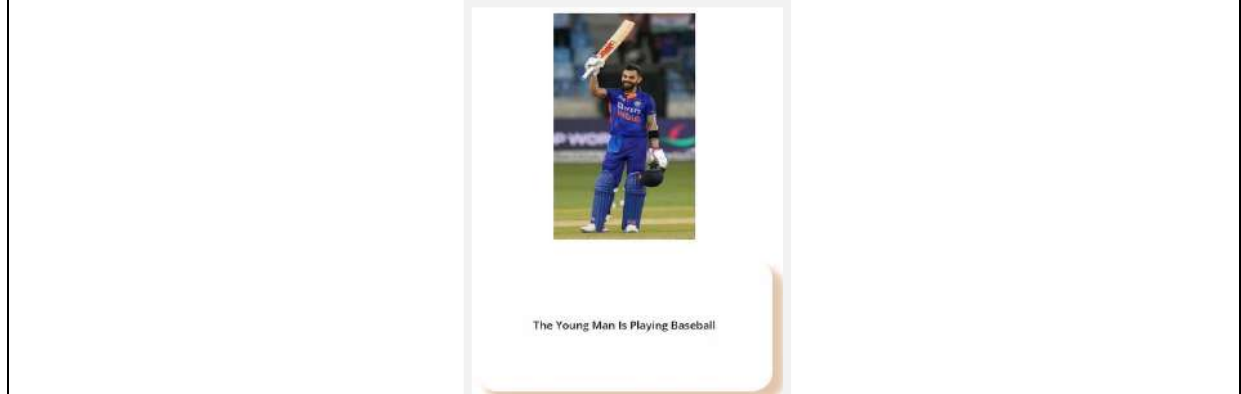


Fig 11 : Inaccurate caption generation





Enhancing OSINT Practices with Eye-Sint: A Multi-Module Intelligence Tool

Sneh Bavarva¹, Kalpesh Senva¹, Kashish Datta¹ and Priyank Bhojak^{2*}

¹Student, Birla Vishvakarma Mahavidyalaya, V. V. Nagar, Gujarat, India.

²Assistant Professor, Birla Vishvakarma Mahavidyalaya, V. V. Nagar, Gujarat, India.

Received: 18 Oct 2023

Revised: 25 Oct 2023

Accepted: 31 Oct 2023

*Address for Correspondence

Priyank Bhojak

Assistant Professor

Birla Vishvakarma Mahavidyalaya,

V. V. Nagar, Gujarat, India.

E.mail: priyank.bhojak@bvmengineering.ac.in



This is an Open Access Journal / article distributed under the terms of the **Creative Commons Attribution License** (CC BY-NC-ND 3.0) which permits unrestricted use, distribution, and reproduction in any medium, provided the original work is properly cited. All rights reserved.

ABSTRACT

Modern intelligence and cybersecurity heavily rely on open-source intelligence (OSINT). This paper introduces the unique "Eye-Sint" OSINT tool, designed to revolutionize information acquisition for intelligence analysts and cybersecurity specialists. Eye-Sint combines port scanning, web scraping, and human footprinting. Its web scraping module can collect website headers, performs who is lookups, extracts emails, and many more things. The person footprinting module identifies individuals and extracts data from PDFs and domains. The port scanning module detects open ports for security assessments. We presented a detailed architecture, methodology, and capabilities. Real-world use cases highlight its importance in digital analysis, cybersecurity, and intelligence. We compare Eye-Sint with other OSINT tools, emphasizing its qualities and ethical data collection. This study highlights Eye-Sint's precision, reliability, and its role in improving OSINT in cybersecurity and intelligence.

Keywords: Open-source intelligence (OSINT), Web scraping, Person footprinting, Port scanning, SSL, Whois, Metadata analysis, Web crawl, Emil finder, Domain search

INTRODUCTION

In today's world where data is extremely important and it is defined as ubiquity of digital information. The practice of intelligence analysis and cybersecurity has become increasingly reliant on open-source intelligence (OSINT). The constant flow of openly accessible data scattered throughout the enormous internet carries an immense amount of knowledge and weaknesses just waiting to be discovered. To properly delve into this wealth of knowledge, intelligence analysts and cybersecurity experts require adaptable tools that go beyond the limitations of traditional OSINT approaches[1]. Nevertheless, OSINT may be laborious and difficult, especially when numerous tools are used to gather and evaluate information from various sources. And to resolve this issue, "Eye-Sint" is introduced in this research article. Eye-Sint is a multi-module OSINT tool that integrates port scanning, web scraping, and person footprinting capabilities into a single platform. Eye-Sint was developed to revolutionize the way intelligence analysts and cybersecurity professionals gather information. In the digital age, the sheer volume and diversity of data pose a



**Sneh Bavarva et al.,**

formidable challenge to OSINT practitioners. The internet, while a treasure trove of information, also presents a complex conundrum—an unceasing surge of data. This relentless data expansion, dispersed across myriad websites, networks, and digital repositories, necessitates an OSINT tool that not only comprehensively aggregates data but also empowers users to extract, analyze, and interpret it effectively. Eye-Sint empowers users to perform web scraping, enabling the collection of publicly available data from websites. From extracting headers and performing whois lookups to gaining SSL information, extracting emails, crawling websites, and conducting directory brute-force searches, Eye-Sint offers a comprehensive suite of web scraping capabilities. Furthermore, its person footprinting module equips users to search for individuals across the vast expanse of the internet, pinpoint geographic locations based on phone numbers, and extract metadata from PDF files. The port scanning module identifies open network ports on target systems, enhancing network security assessments.

This research paper aims to introduce Eye-Sint as a groundbreaking multi-module OSINT (Open Source Intelligence) tool, shedding light on its extensive functionalities and capabilities. In pursuit of this goal, the paper delves into the technical intricacies of Eye-Sint, elucidating its architectural design, methodologies, and the technologies underpinning its web scraping, person footprinting, and port scanning capabilities. By doing so, it empowers readers with a profound technical understanding, enabling them to make informed decisions regarding the tool's potential applications. Furthermore, the paper underscores the practical utility of Eye-Sint by presenting real-world use cases and scenarios where it can effectively extract actionable intelligence and bolster network security, demonstrating its relevance in intelligence analysis, cybersecurity investigations, and digital forensics. Through comparative analysis, Eye-Sint is positioned within the landscape of OSINT tools, highlighting its unique features, advantages, and limitations, thereby enabling readers to appreciate its distinctive contributions to the field. Additionally, the paper provides evidence of Eye-Sint's accuracy through practical examples and validation measures, assuring readers of its reliability in generating actionable insights. Ultimately, the research paper also aims to provide insights into the future development and potential applications of Eye-Sint, ensuring its continued evolution and adaptability to meet the evolving demands of the ever-changing OSINT landscape. In doing so, it seeks to position Eye-Sint as a transformative tool for intelligence analysts and cybersecurity professionals, reshaping the way information is gathered and analyzed in the digital age.

In the ever-evolving realm of open-source intelligence (OSINT)[2], where data is both the lifeblood and the challenge, Eye-Sint emerges as a trailblazing solution. At its core, Eye-Sint redefines the OSINT landscape by converging three distinct yet interconnected pillars of OSINT functionality: web scraping, person footprinting, and port scanning. This unification of capabilities represents a paradigm shift, setting Eye-Sint apart as a transformative force within the OSINT community. Historically, OSINT practitioners have grappled with a fragmented toolkit—a mosaic of specialized tools, each designed to address a specific facet of the intelligence gathering process. While these tools excel within their niches, they often lack the ability to seamlessly collaborate or share data. This fragmentation presents a dual challenge: increased operational complexity and a heightened risk of overlooking critical insights. In contrast, Eye-Sint envisions a unified OSINT experience. It recognizes that OSINT analysts and cybersecurity professionals do not operate in silos; they require a holistic approach that integrates their disparate tasks into a cohesive workflow. Eye-Sint's unique proposition lies in its ability to break down the walls separating web scraping, person footprinting, and port scanning, presenting users with a singular, integrated platform. At its core, Eye-Sint's web scraping module transcends the boundaries of conventional web scraping tools. While stand-alone web scrapers might excel at data extraction, they seldom possess the versatility to incorporate other OSINT functionalities seamlessly. Eye-Sint redefines web scraping by infusing it with the ability to perform whois lookups, analyze SSL information, extract emails, conduct web crawling, and even execute directory brute-force searches—all within the same environment. This convergence empowers analysts to collect, cross-reference, and analyze diverse datasets without the need to toggle between multiple applications. Eye-Sint's person footprinting capabilities take the art of profiling individuals to new heights. In traditional OSINT practices, investigators often find themselves juggling various tools to compile information about their subjects. Eye-Sint eliminates this complexity by offering a comprehensive suite of person footprinting tools under one roof. It can not only trace usernames across the internet but also dive deeper into PDF metadata analysis, geolocate phone numbers, and explore domains to uncover





Sneh Bavarva et al.,

associations—all within a unified framework. This synergy enables investigators to construct detailed profiles efficiently, enhancing their ability to make informed decisions[8]. In the realm of cybersecurity, Eye-Sint's port scanning module champions a holistic approach to network security assessment. While traditional port scanners focus on their specific tasks, Eye-Sint integrates port scanning seamlessly into its multifunctional environment. By identifying open network ports on target systems, it enhances the capacity for vulnerability assessments and threat detection[4]. This holistic view of network security promotes a comprehensive understanding of potential risks and vulnerabilities. The unification of web scraping, person footprinting, and port scanning within Eye-Sint translates into enhanced efficiency, streamlined workflows, and the elimination of information silos. Analysts no longer need to divide their attention between disparate tools; instead, they can harness the synergy of Eye-Sint to expedite data collection, analysis, and interpretation. This integrated approach empowers OSINT practitioners to make more informed decisions swiftly, bolstering the overall effectiveness of OSINT operations.

OSINT working TECHNIQUES

Traditional Approach Problems

Open-source intelligence (OSINT) has traditionally been conducted and faced challenges in the past in following ways[3]:

Manual Data Collection and Tool Fragmentation

Traditional OSINT operations hinged on manual data collection methods, where analysts embarked on exhaustive web browsing and conducted intricate social media analyses. This manual approach often proved labor-intensive and time-consuming, as OSINT practitioners combed through vast online landscapes in search of relevant information. To aid in their investigations, analysts turned to an array of specialized OSINT tools, each meticulously designed for specific tasks such as web scraping, WHOIS lookup[5], geolocation, and social media monitoring. Tools like, ICANN lookup for whois information, Octoparse for web crawling[6], PDF24 for checking PDF metadata etc. However, the challenge lay in the fragmentation of these tools—each operating independently and demanding analysts to switch between them based on the specific requirements of the moment. The result was a complex and often disjointed OSINT process, marked by the need for meticulous manual data management.

Resource-Intensive Nature and Ethical Considerations

The traditional OSINT landscape was not without its ethical dilemmas and resource constraints. OSINT analysts were tasked with navigating intricate ethical and legal considerations, particularly when collecting information from online sources. Concerns related to personal data and privacy loomed large, adding a critical layer of complexity to their work. Moreover, the resource-intensiveness of traditional OSINT practices was a defining feature. Organizations frequently found themselves needing to allocate substantial human resources to execute effective OSINT operations[7]. The commitment of time, expertise, and manpower was not only costly but also posed challenges when scaling up operations to handle large volumes of data or conducting comprehensive investigations.

Data Quality and the Expertise Factor

In the world of traditional OSINT, data quality and reliability were perennial concerns. The manual nature of data collection and integration introduced the potential for errors, making the reliability of information collected highly variable. The effectiveness of OSINT operations often depended on the skills and experience of individual analysts, as they were tasked with interpreting the collected data and drawing actionable insights. This humanfactor was both a strength and a limitation, as it required analysts to apply their expertise to the process. The outcome was a landscape where the success of OSINT initiatives hinged on the proficiency of practitioners and the tools at their disposal. In summary, traditional OSINT practices were marked by manual data collection, tool fragmentation, ethical considerations, and resource constraints. OSINT analysts grappled with the complexities of navigating vast online domains while striving to maintain ethical standards. The reliance on specialized tools and the inherent resource intensiveness of traditional OSINT underscored the need for transformative solutions like Eye-Sint, which offer a streamlined, automated, and integrated approach to meet the evolving demands of the field.





Sneh Bavarva et al.,

Solution: Eye-sint

Comprehensive Integration of OSINT Functions

Eye-Sint stands out as a game-changer in the world of OSINT by offering a seamless and comprehensive integration of OSINT functionalities. Unlike the fragmented landscape of traditional OSINT, where analysts juggled multiple specialized tools, Eye-Sint consolidates the essential capabilities of web scraping, person footprinting, and port scanning into a single, unified platform. This integration eliminates the need for constant tool-switching, simplifies workflows, and significantly streamlines the entire OSINT process. Analysts no longer find themselves piecing together data from disparate sources; instead, they can execute a range of functions consecutively or concurrently within the same environment. The result is unparalleled efficiency and a substantial reduction in the time required to gather, analyze, and interpret OSINT data.

Unprecedented Combination of Features

Eye-Sint brings together a comprehensive array of OSINT functionalities, consolidating web scraping, person footprinting, and port scanning into a single, unified platform. This amalgamation of capabilities is unparalleled in the current OSINT toolandscape, offering intelligence analysts and cybersecurity professionals a one-stop solution for their information-gathering needs. The tool empowers users to perform web scraping, collect data from websites, extract headers, perform WHOIS lookups, gaining SSL information, extracting emails and crawling websites. Furthermore, the person footprinting module equips users to search for individuals across the vast expanse of the internet, pinpoint geographic locations based on phone numbers, extract metadata from PDF files and also can perform domain search for emails. The port scanning module identifies open network ports on target systems, enhancing network security assessments. This unmatched combination of features under a single roof distinguishes Eye-Sint as a groundbreaking OSINT tool.

Efficiency and Time Savings

One of the primary advantages Eye-Sint offers to OSINT practitioners is efficiency. Unlike traditional approaches that often require the use of multiple tools for various tasks, Eye-Sint streamlines the process by providing a holistic suite of tools under one roof. This consolidation not only saves valuable time but also minimizes the need for extensive tool-switching and manual data integration. Analysts can swiftly transition between different OSINT functions without the burden of adapting to disparate tool interfaces. Tasks that previously demanded switching between multiple tools can now be executed seamlessly within the same environment, optimizing workflow efficiency. The elimination of time-consuming manual data integration further enhances the effectiveness of OSINT operations. In summary, Eye-sint emerges as a comprehensive solution, consolidating all essential OSINT features into a singular, cohesive platform, as depicted in Fig. 2. Unlike the conventional approach illustrated in Fig. 1, where disparate tools are necessitated for executing diverse OSINT methodologies, Eye-sint stands out as a distinctive tool within the field. By seamlessly integrating various OSINT functionalities, it not only streamlines the investigative process but also presents itself as a unique and unified solution for practitioners in this field.

METHODOLOGY

For a seamless and user-friendly experience, Eye-sint offers a graphical user interface (GUI) version that enhances the accessibility of its powerful OSINT capabilities. This version comprises three main modules, each equipped with unique functionalities that cater to the diverse needs of intelligence analysts and cybersecurity professionals.

Web scraping

The heart of Eye-Sint's GUI version lies in its web scraping module, which consolidates a range of essential functionalities into a user-friendly interface. Analysts can effortlessly check website headers, retrieve SSL information, perform WHOIS lookups, initiate web crawls, and extract emails with just a few clicks. Here's the beauty of it: by simply providing the URL of a target website and selecting the desired functionality, analysts can swiftly execute tasks that would typically require multiple standalone tools. For instance, if SSL information is the





Sneh Bavarva et al.,

focus, the tool will promptly furnish all relevant SSL hash codes and provide the duration of SSL validity, streamlining the process and eliminating the need for separate tools for various OSINT research tasks. Which showed in Fig 3.

Person footprinting

This module equips analysts with an array of powerful tools to uncover critical information about individuals across the vast expanse of the internet. This module simplifies the process of geolocating individuals based on phone numbers, finding usernames scattered across online platforms, conducting comprehensive email searches through domain exploration, and extracting valuable metadata from PDF files. Let's delve into one of these functionalities: extracting PDF metadata. To access to comprehensive PDF metadata can be a game-changer, shedding light on a document's origins and evolution. Eye-Sint stands out by simplifying the process of extracting vital PDF metadata with ease. By simply inputting a PDF document, the tool swiftly retrieves essential information like authorship, creation and modification dates, document titles, and more. This capability empowers analysts to gain deeper insights into a document's context and history, elevating the quality and depth of OSINT investigations. For instance, imagine an intelligence analyst confronting a critical PDF document. Leveraging Eye-Sint's PDF metadata extraction, they swiftly uncover the author's identity, track the document's evolution, and gauge its relevance to their investigation. This detailed data proves invaluable for verifying document authenticity, evaluating significance, and making well-informed decisions during intelligence analysis and cybersecurity investigations.

Port Scanning

Eye-Sint's Port Scanning capability, while not novel in itself, stands out in the context of OSINT due to its seamless integration with a comprehensive suite of OSINT tools. This feature allows analysts to determine open network ports on target systems, providing a valuable layer of insight in conjunction with other OSINT functions. While traditional port scanning tools often operate in isolation, Eye-Sint's innovation lies in its ability to merge port scanning with web scraping, person footprinting, and more, offering analysts a holistic and efficient approach to information gathering. This unique blend of capabilities distinguishes Eye-Sint as a versatile OSINT tool that goes beyond conventional port scanning by facilitating multifaceted intelligence and cybersecurity investigations.

Comparative analysis of eye-sint

In our comparative evaluation of Eye-Sint, Shodan, and Maltego, we assessed their performance across various OSINT functions. Eye-Sint stood out as a robust OSINT tool. Eye-Sint reigns supreme in web scraping, eclipsing rivals with its deep dive into headers, SSL intel, and email extraction. Its footprinting prowess shines with pinpoint phone geolocation and PDF metadata mastery. Though domain search parity exists, Eye-Sint's holistic symphony of OSINT features empowers analysts and security specialists to gather and analyze data with unmatched efficiency in the digital age.

Ethical and legal consideration

Privacy and Compliance[10] Eye-Sint emphasizes privacy and compliance by encouraging analysts to obtain informed consent when dealing with personal data. It also ensures compliance with data protection and privacy laws, guiding users to align their OSINT activities with legal requirements.

Responsible Data Handling Eye-Sint prioritizes responsible data management, offering features like data encryption and anonymization to safeguard collected data. This promotes ethical data handling practices during OSINT investigations.

Transparency and Accountability Eye-Sint promotes transparency and accountability by urging users to maintain comprehensive records of their OSINT activities. This documentation includes data sources, methodologies, and ethical considerations, supporting user accountability and facilitating auditing and compliance efforts.





Sneh Bavarva et al.,

CONCLUSION AND FUTURE WORK

Eye-Sint is a new OSINT tool that combines web scraping, person footprinting, and port scanning functionalities into a single platform. This makes it easier for intelligence analysts and cybersecurity professionals to gather, analyze, and interpret data. Eye-Sint is unique in its ability to provide a holistic approach to OSINT operations. It eliminates the need for analysts to use multiple specialized tools, which can streamline workflows and significantly enhance efficiency. Additionally, Eye-Sint upholds ethical and legal considerations, promoting responsible data collection and usage. It emphasizes privacy, compliance with data protection laws, and transparent, accountable data handling practices. Overall, Eye-Sint is a groundbreaking and transformative tool in the realm of OSINT. It addresses the longstanding challenges of traditional OSINT practices, offering a unified platform that seamlessly integrates web scraping, person footprinting, and port scanning functionalities. This consolidation not only streamlines workflows but also significantly enhances efficiency, enabling intelligence analysts and cybersecurity professionals to gather, analyze, and interpret data with unprecedented ease and speed.

In simpler terms, Eye-Sint is a new OSINT tool that makes it easier to collect, analyze, and interpret data in a responsible and ethical way. It is a powerful asset for intelligence analysts and cybersecurity specialists, and it has the potential to revolutionize the way OSINT is conducted. In the future, Eye-Sint could focus on enhancing automation, adding new OSINT functionalities, and refining user interfaces. The integration of machine learning and AI[9] for advanced data analysis, along with real-world testing through collaboration with experts, can further elevate its capabilities. Ensuring compliance with evolving privacy and legal standards will be crucial as the digital landscape continues to change. Eye-Sint's ongoing development promises to play a leading role in innovative and responsible OSINT operations.

ACKNOWLEDGMENT

I would like to extend my heartfelt appreciation to the IT Department at Birla Vishwakarma Mahavidyalaya (BVM), Vallabh Vidyanagar, where I am fortunate to pursue my studies. Special thanks go to my dedicated professor, Mr. Priyank Bhojak, whose guidance and support have been invaluable in the development of this project. Their unwavering assistance and expertise have been instrumental in shaping this work.

REFERENCES

1. U., Yogish & Karani, Krishna Prasad. (2021). Open Source Intelligence and its Applications in Next Generation Cyber Security - A Literature Review. *International Journal of Applied Engineering and Management Letters*. 1-25. 10.47992/IJAEML.2581.7000.0100.
2. Böhm, I., Lolagar, S. Open source intelligence. *Int. Cybersecur. Law Rev.* 2, 317–337 (2021). <https://doi.org/10.1365/s43439-021-00042-7>
3. C. Best, "Challenges in Open Source Intelligence," 2011 European Intelligence and Security Informatics Conference, Athens, Greece, 2011, pp. 58-62, doi: 10.1109/EISIC.2011.41.
4. S. Lee and T. Shon, "Open source intelligence base cyber threat inspection framework for critical infrastructures," 2016 Future Technologies Conference (FTC), San Francisco, CA, USA, 2016, pp. 1030-1033, doi: 10.1109/FTC.2016.7821730.
5. Rahul Gautam, "Analysis and Implementation of Whois Domain Lookup," *Imperial Journal of Interdisciplinary Research*, Volume 3, Issue 5, 2017
6. Jones, A. (2022, March 8). Build a Crawler to Extract Web Data in 10 Mins. Retrieved from <https://www.octoparse.com/blog/how-to-build-a-crawler-to-extract-web-data-without-coding-skills-in-10-mins>
7. D. Govardhan, G. G. S. H. Krishna, V. Charan, S. V. A. Sai and R. R. Chintala, "Key Challenges and Limitations of the OSINT Framework in the Context of Cybersecurity," 2023 2nd International Conference on Edge





Sneh Bavarva et al.,

Computing and Applications (ICECAA), Namakkal, India, 2023, pp. 236-243, doi: 10.1109/ICECAA58104.2023.10212168.

8. Tiwari, Shiva & Verma, Ravi & Jaiswal, Janvi & Rai, Bipin Kumar. (2020). Open Source Intelligence Initiating Efficient Investigation and Reliable Web Searching. 151-163. 10.1007/978-981-15-6634-9_15.
9. Ghioni, R., Taddeo, M. & Floridi, L. Open source intelligence and AI: a systematic review of the GELSI literature. *AI & Soc* (2023). <https://doi.org/10.1007/s00146-023-01628-x>
10. Rajamäki, J. "Privacy in Open Source Intelligence and Big Data Analytics: Case 'MARISA' for Maritime Surveillance." *Journal of Information Warfare*, vol. 19, no. 1, 2020, pp. 12–25. *JSTOR*, <https://www.jstor.org/stable/27033606>. Accessed 13 Oct. 2023.

Table 1. Comparison with Other Tool

	Features	Shodan	Maltego	Eye-sint	Notes
Web scapping	Headers analysis	✓	✗	✓	Eye-Sint excels in detailed header analysis.
	WHOIS lookup	✓	✗	✓	Maltego not offer WHOIS lookup.
	SSL information	✓	✓	✓	Eye-Sint provides advanced SSL information like hash codes and validity duration.
	Web crawling	✗	✗	✓	Eye-Sint offers efficient web crawling with directory brute-force search capabilities.
	Email finding	✓	✓	✓	Eye-Sint excels at email extraction from websites and domains.
Persn footprinting	PDF metadata analysis	✗	✗	✓	Eye-Sint extracts comprehensive PDF metadata like author, creation date, etc.
	Domain search for emails	✗	✓	✓	Shodan not offer domain search for email addresses.
	Username search across platforms	✗	✗	✓	Eye-Sint excels at finding usernames across various online platforms.
	Phone number recon	✓	✗	✓	Eye-Sint and Shodan offers precise phone number geolocation.
Port scanner	Open port	✓	✓	✓	All tools offer basic port scanning functionalities.
	Advance port scanning	✓	✗	✗	Shodan offers more advanced port analysis features.

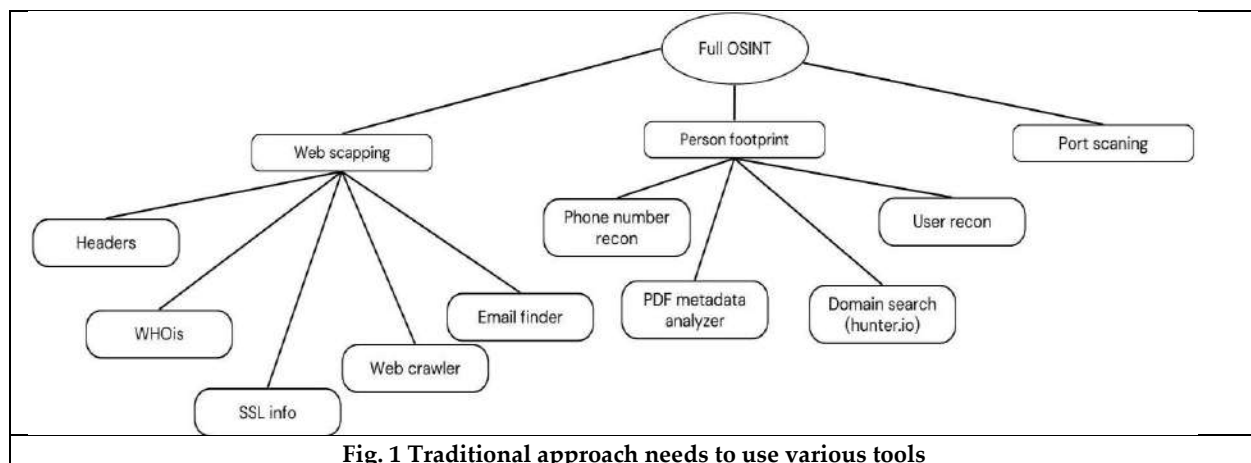


Fig. 1 Traditional approach needs to use various tools





Sneh Bavarva et al.,

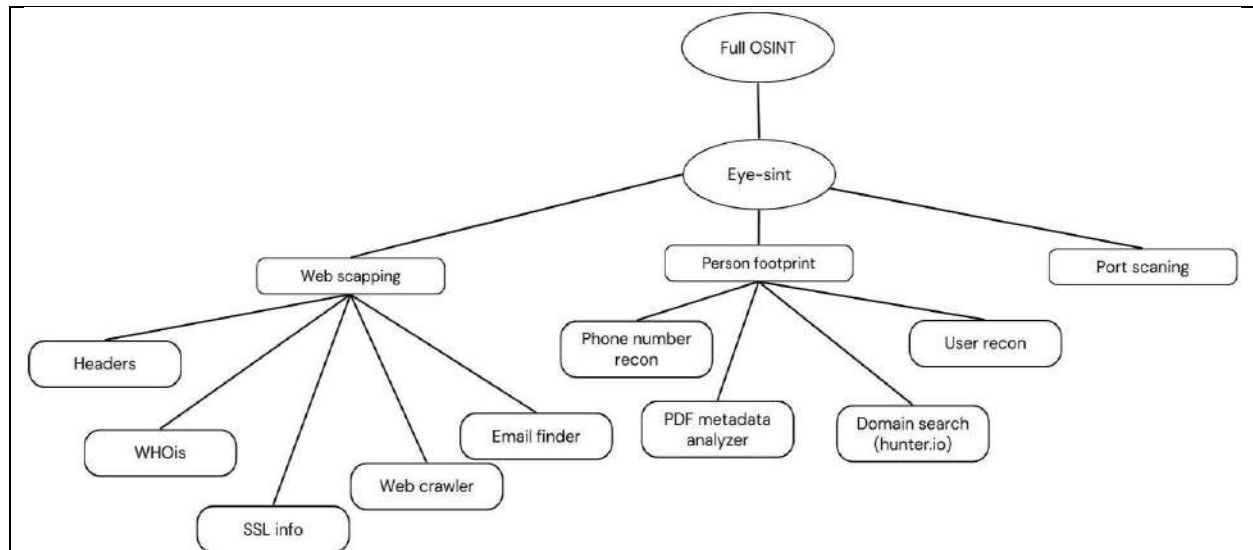


Fig. 2 All tools provided by eye-sint in one place

Enter URL for SSL Information

You submitted the URL: <https://www.bvmengineering.ac.in/>

```

0: SSL Certificate Analysis:
1:202.129.240.138
2:Expired: False
3:Signature Algorithm: b'sha256WithRSAEncryption'
4:Subject b'CN': b'www.bvmengineering.ac.in'
5:Subject Hash: 809528844
6:Issuer b'C': b'US'
7:Issuer b'O': b'Let's Encrypt'
8:Issuer b'CN': b'R3'
9:Issuer Hash: 2368991799
10:Extension b'keyUsage': Digital Signature, Key Encipherment
11:Extension b'extendedKeyUsage': TLS Web Server Authentication, TLS Web Client Authentication
12:Extension b'basicConstraints': CA:FALSE
13:Extension b'subjectKeyIdentifier': CC:15:29:4F:F9:45:7F:FF:43:01:E2:BC:BA:A1:61:E6:2E:90:83:07
14:Extension b'authorityKeyIdentifier': 14:2E:B3:17:B7:58:56:CB:AE:50:09:40:E6:1F:AF:9D:8B:14:C2:C6
15:Extension b'authorityInfoAccess': OCSP - URI:http://r3.o.lencr.org CA Issuers - URI:http://r3.lencr.org/
16:Extension b'subjectAltName': DNS:bvmengineering.ac.in, DNS:www.bvmengineering.ac.in
17:Extension b'certificatePolicies': Policy: 2.23.140.1.2.1
18:Extension b'ct_precert_scts': Signed Certificate Timestamp: Version : v1 (0x0) Log ID : DA:B6:BF:6B:3F:B5:B6:22:9F:9B:C2:BB:5C:6B:EB:70:
91:71:6C:BB:51:84:85:34:BD:A4:3D:30:48:D7:FB:AB Timestamp : Oct 10 04:05:02.393 2023 GMT Extensions: none Signature : ecdsa-with-
SHA256 30:45:02:20:46:5E:A3:B9:05:0A:1A:4A:66:0F:CA:ED: 7D:8C:28:E7:B9:5E:93:A1:6E:20:8E:A9:04:D4:81:6D:
FB:E8:D1:EE:02:21:00:AB:AA:98:E5:50:73:EB:07:05: 0A:6E:33:58:31:FC:C5:9C:95:AF:C9:58:B5:CE:6A:88: 39:6E:E1:78:61:11:2E Signed Certificate
Timestamp: Version : v1 (0x0) Log ID : 76:FF:88:3F:0A:B6:FB:95:51:C2:61:CC:F5:87:BA:34: B4:A4:CD:BB:29:DC:68:42:0A:9F:E6:67:4C:5A:3A:74
Timestamp : Oct 10 04:05:02.416 2023 GMT Extensions: none Signature : ecdsa-with-SHA256
30:45:02:20:52:0C:25:68:D5:FA:07:43:9D:FB:D0:2C: E9:FA:96:C1:53:D5:5D:CF:1A:79:94:8F:57:FD:FB:B8:
48:14:4F:A8:02:21:00:8D:EF:8A:04:14:34:6A:86:C0: A9:17:B7:C4:2E:3A:20:51:F3:9F:D0:E0:C8:23:40:A9: B9:FB:5C:25:C1:1E:2B
19: Public Key Bits: 3072
20:Public Key Type: 6
21:Public Key only public: True
22:Public Key initialized: True
23:Serial Number: 432536719656669282354568875688103422033048
24:Serial Number Length: 139
25: MD5: b'41:E8:0C:B1:34:2B:CB:4A:C4:3E:ED:AC:24:85:83:BB'
26:SHA1: b'77:A3:47:EA:4F:55:D6:65:B4:8A:AA:91:16:FB:D1:AA:EC:D5:7B:52'
27:SHA256: b'B6:54:3A:F4:B7:42:83:57:60:51:8C:C1:10:65:83:FE:9D:9A:B4:A1:41:DC:42:41:F8:34:B5:82:B4:C7:D7:FD'
28:SHA512:
b'22:50:8E:72:4F:AF:03:82:7B:69:D2:64:42:39:43:3A:B0:ED:D5:05:EB:F0:6C:08:F4:95:FB:9A:3D:F5:F8:77:87:EB:3E:21:CE:A3:03:47:20:D8:42:E7:80:8C:4B:80
29: Valid from: b'20231010030502Z'
30:Valid until: b'20240108030501Z'
31:exported: False
  
```

Fig. 3 SSL information of https://www.bvmengineering.ac.in/





Sneh Bavarva et al.,

Select PDF to get Metadata info

Browse... sample1.pdf Submit Close

You selected file: sample1.pdf

Author: Nigel Maddocks
Comments:
Company:
Creationdate: 21 : 08 : 2015 09:42:21 UTC+01:00
Creator: Acrobat PDFMaker 15 for Word
Keywords: 12345678
Moddate: 21 : 08 : 2015 09:45:31 UTC+01:00
Producer: Adobe PDF Library 15.0
Sourcemodified: D:20150821084155
Subject: Test Document
Title: PDF Metadata Sample

Fig 4. PDF metadata

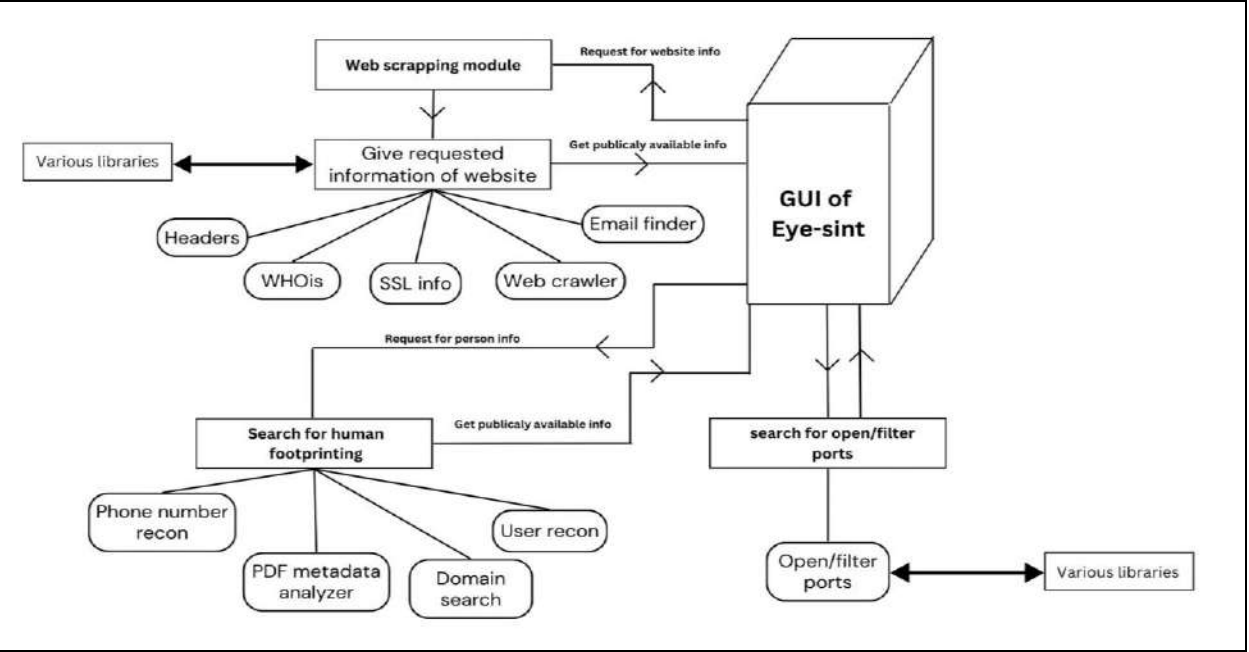


Fig 5. Workflow of Eye-sint





Analysis of Healthcare 4.0: Shaping the Future of Healthcare.

Dhrumil Gajera^{1*}, Deep Patel¹, Vishva Gajera² and Chetan Jayaswal³

¹Electronics Department, BVM Engineering College, Anand, Gujarat, India

²Higher Secondary-Biology, Beyond Limits, Surat, Gujarat, India

³Electronics Department, BVM Engineering College, Anand, Gujarat, India.

Received: 18 Oct 2023

Revised: 25 Oct 2023

Accepted: 31 Oct 2023

*Address for Correspondence

Dhrumil Gajera

Electronics Department,
BVM Engineering College,
Anand, Gujarat, India.

E. mail: gajeradhrumil38@gmail.com



This is an Open Access Journal / article distributed under the terms of the **Creative Commons Attribution License** (CC BY-NC-ND 3.0) which permits unrestricted use, distribution, and reproduction in any medium, provided the original work is properly cited. All rights reserved.

ABSTRACT

From industrial automation to space program, Industry 4.0 has revolutionized a number of industries. One of its main beneficiaries has also been healthcare. Industry 4.0 utilizes cutting-edge technologies like Artificial Intelligence (AI), Machine Learning, Big Data, Cloud Computing, Blockchain, and IoT to deliver solutions that are efficient, accurate, and timely. The healthcare revolution is a laborious task that necessitates careful consideration of many technological and medical issues. In this essay, we'll talk about how modern technologies can bring about unimaginable change in the health sector, how to use them effectively, and what the biggest obstacles are to doing so.

Keywords: Healthcare, Industry 4.0, Humanity, Artificial Intelligence.

INTRODUCTION

The global demographic landscape is evolving rapidly, characterized by an ageing and expanding population. This demographic shift underscores the increasing demand for resources and healthcare services that are not only robust but also affordable and easily accessible. To address these pressing needs at both the global and local levels, the healthcare system must undergo a transformation driven by the generation and utilization of healthcare data [1]. In this era of healthcare evolution, the World Economic Forum has coined the term "Health 4.0" to describe a paradigm where cutting-edge medical data converges with state-of-the-art technologies. This fusion encompasses block chain, cloud computing, the Internet of Things (IoT), artificial intelligence, and fog computing. Health 4.0 paves the way for a healthcare landscape that is collaborative, convergent, and predictive, revolutionizing the way we approach health and well-being [2].





Dhrumil Gajera et al.,

The genesis of the concept of the industrial internet in 2012 [3] laid the groundwork for a digital transformation that blends Big Data and the Internet of Things, creating a seamless integration of the digital and physical worlds. This convergence has significant implications for healthcare, where the costs in developed nations starkly contrast with those in developing countries. The disparity in healthcare costs has given rise to medical tourism in developing nations, and modern communication technologies are instrumental in propelling this trend further [5]. Technological advancements, such as the integration of remote devices and the monitoring of healthcare-related data by individuals, offer new avenues for enhancing healthcare. Notably, as the percentage of the younger population decreases with the ageing of society, conventional hospital-based healthcare services face challenges in maintaining viability [2]. To ensure a sustainable, high-quality healthcare service in the foreseeable future, a paradigm shift in healthcare is imperative. This shift is encapsulated in the transformative concept of "Health 4.0," which promises to redefine healthcare in a way that meets the needs of our evolving world.

Industry 4.0

Definition and Foundation: Industry 4.0 can be defined as the digital transformation of traditional manufacturing and industrial practices using cutting-edge smart technologies. At its core, it relies on the concept of cyber-physical systems, where sophisticated machines are equipped with ubiquitous sensors, enabling self-operation and intelligent decision-making [4].

Key Technologies: The Fourth Industrial Revolution incorporates several key technologies, including the Internet of Things (IoT), increased automation, improved communication strategies, and self-help mechanisms. These technologies form the cornerstones of Industry 4.0, facilitating a more connected, automated, and data-driven industrial landscape [5].

Emerging Technologies: Klaus Schwab, the founder of the World Economic Forum, envisions the emergence of various new technologies during this revolution. These technologies encompass artificial intelligence (AI), robotics, nanotechnology, biotechnology, the Internet of Things (IoT), decentralization of systems, 3D printing, fifth-generation communication technologies, quantum computing, and autonomous vehicles [10].

Global Impact: Industry 4.0 is a global phenomenon, with Germany being an early adopter. In the early 2010s, Germany initiated a high-tech strategy project that promoted the computerization of manufacturing, contributing to the concept's emergence [6].

Enablers: The key enablers of Industry 4.0 include cyber-physical systems, smart manufacturing, intelligent systems, and industrial integration. These components drive value creation, higher productivity, and increased efficiency within the industrial sector. Industry 4.0 leverages technologies such as the Internet of Everything, Big Data, Cloud-based computing, Artificial Intelligence, and Cyber-Physical Systems [7].

Healthcare In Industry 4.0

Industry 4.0 revolutionizes the healthcare sector, simplifying processes and introducing cutting-edge technologies. Notable advancements include rapid communication, cloud-based record systems, and the ability to swiftly measure a wide range of parameters. The convergence of the Internet of Things (IoT), blockchain, cloud computing, and artificial intelligence (AI) has driven remarkable progress in healthcare. The impact of Industry 4.0 on healthcare is profound. It streamlines operations, reduces time and costs, and fosters the adoption of superior solutions [8]. By leveraging cyber-physical systems, Industry 4.0 represents the technological transformation of healthcare, mirroring its effect on traditional manufacturing sectors [9]. In this era, the healthcare landscape is enriched by the Internet of Things, natural language processing, and cyber-physical systems. Innovative solutions like biosensors, smart organs, and medical cyber-physical systems are enhancing medical diagnosis and troubleshooting. The shift from traditional hospital-centric care to digital and dispersed care is driven by technologies such as artificial intelligence, deep learning, big data, genomics, home-based treatment, robots, tissue engineering, and 3D printing of implants. As a result, Industry 4.0 applications have gained significant traction within the healthcare industry. The healthcare sector is experiencing a transformative journey in the era of Industry 4.0, marked by efficiency, innovation, and the integration of groundbreaking technologies.





Dhrumil Gajera et al.,

IoT in Health 4.0

The integration of the Internet of Things (IoT) into the healthcare system has revolutionized the traditional healthcare environment, making it smarter and more personalized. This transformation is facilitated by smart devices such as smart watches, smartphones, IoT-based devices, and other technological innovations. For example, smart watches like the Apple Watch and Amazfit, as well as smart glasses such as Google Glasses and Hololens, represent wearable IoT devices. Smart watches and similar devices offer features like monitoring the wearer's heart rate, pulse, the number of steps taken, and much more. These devices are equipped with wireless sensors that transmit data to a centralized server, enabling real-time monitoring and analysis. IoT plays a crucial role in healthcare by facilitating tasks such as treatment management, patient monitoring, and early disease detection. This integration of IoT in healthcare, often referred to as Health 4.0, empowers healthcare providers to deliver more intelligent and individualized care, ultimately enhancing patient outcomes and the overall quality of healthcare services [10].

Artificial Intelligence in Health 4.0

In the era of Health 4.0, the integration of Artificial Intelligence (AI) into healthcare has brought about remarkable advancements and improvements. Here are key points to understand this integration:

Virtual Reality-Enhanced Treatment: Virtual reality (VR) technologies are increasingly being utilized to deliver robotically assisted treatments to patients. This not only enhances patient care but also reduces risks for medical practitioners. Doctors can remotely control robotic systems to perform surgeries and procedures, minimizing physical contact and the potential for infection transmission [11].

Immediate Issue Identification: Health 4.0 technologies, particularly AI, play a critical role in promptly identifying patient issues. Through the use of sensors in emergency situations, AI systems can swiftly assess a patient's condition and relay critical data to healthcare providers. This rapid response can be life-saving in critical scenarios [11].

Data Analysis: AI technologies are extensively employed for the analysis of various healthcare data sources. This includes the examination of clinical data, Electronic Health Records (EHRs), medical images like X-rays and MRIs, and physiological signals such as heart rate and vital signs. AI-driven data analytics provides healthcare professionals with valuable insights and aids in diagnosing and monitoring patients [12].

Feature Engineering for Data Analysis: In the realm of AI-driven healthcare, a technique known as feature engineering is commonly used for data analysis. Feature engineering involves the extraction of relevant descriptors from various data sources, which are then categorized or segmented for analysis. This process enhances the accuracy of AI algorithms in identifying patterns and making predictions in healthcare data [12].

Structured and Unstructured Health Information: Healthcare data can be categorized as structured and unstructured. Structured data includes information with specific categories such as demographics, medication records, medical procedures, laboratory test results, and diagnoses. In contrast, unstructured data comprises text-based documents, such as medical notes from healthcare professionals. AI systems are adept at handling both types of data, facilitating comprehensive patient care and efficient data management [13].

Cyber Physical System in health 4.0

Technological Transformation: Industry 4.0, driven by CPS, represents a significant technological transformation in manufacturing. This transformation extends its impact beyond traditional manufacturing sectors, including healthcare. The incorporation of CPS has the potential to revolutionize healthcare processes and improve patient care [9].

Integrating Healthcare Processes: A core principle of CPS in healthcare is the integration of healthcare processes with the aid of available technology. This integration enhances the efficiency of healthcare systems, enabling them to provide better services and patient satisfaction. Smart device technology plays a pivotal role in facilitating secure communication, computation, and data privacy, all of which contribute to improved healthcare facilities [10].

Managing Healthcare Data: The advancements in CPS have also accentuated the importance of healthcare data. Managing this data effectively is a complex process. Healthcare data includes a vast amount of information, ranging from patient records to medical images. To tackle this challenge, modern big data technologies are being harnessed.





Dhrumil Gajera et al.,

They allow healthcare organizations to efficiently manage, analyze, and utilize healthcare data. This, in turn, makes healthcare CPS more patient-centric by ensuring data-driven decision-making and personalized care [7].

Leveraging Cloud Technology: The cloud plays a significant role in making healthcare CPS more patient-centric and data-driven. Cloud technology enables the secure storage and accessibility of healthcare data from anywhere. This mobility and accessibility are crucial in the delivery of modern healthcare, where real-time data sharing and decision-making are vital for patient care and outcomes [10].

Blockchain in Health 4.0

Blockchain technology is a multifaceted breakthrough that finds applications in a wide range of areas, such as mobile technology, defence systems, finance, healthcare, and the Internet of Things. Blockchain technology provides special advantages and solutions in the field of healthcare. [16].

Important Blockchain Technology Applications in Healthcare

Interdisciplinary Techniques: Blockchain technology is a product of diverse fields, incorporating cryptography, algorithms, economic models, and mathematics. It leverages these interdisciplinary techniques to create secure and transparent data networks [16]. **Peer-to-Peer Networking:** One of the key features of blockchain is its use of peer-to-peer networking, which allows direct communication between participants. This characteristic eliminates the need for intermediaries, leading to more efficient data sharing and transactions [14].

Distributed Consensus Algorithms: Blockchain relies on distributed consensus algorithms to validate and record transactions. This approach ensures that data remains consistent and accurate across the network, enhancing integrity and verification [14].

Applications in Healthcare: Blockchain's application in healthcare is vast and includes areas such as device tracking, clinical trials, pharmaceutical tracing, and health insurance. These applications help improve systems designed to combat issues like illicit and counterfeit drugs. Moreover, blockchain supports healthcare data interchange, nationwide interoperability, medical device tracking, and drug tracking, addressing several challenges in the modern healthcare sector [15]. Blockchain is a vital tool in the healthcare industry and many other businesses because of its unique features, which include security, transparency, and data integrity. It has the ability to improve data management and healthcare services by fostering trust and data sharing across networks.

CONCLUSION

There is an increased demand for comprehensive, reasonably priced, and quickly accessible healthcare services in this period of ageing and growing global population. The creation and application of healthcare data must drive a revolution in the industry to meet these expectations. The World Economic Forum's definition of "Health 4.0" embodies this change, as cutting-edge medical data and state-of-the-art technologies combine to create a collaborative, predictive, and convergent healthcare environment. It is revolutionary to combine the industrial internet—capsulated by Industry 4.0—with the healthcare industry. The Internet of Things, artificial intelligence, and cyber-physical systems—three of Industry 4.0's key technologies—are propelling amazing advancements in healthcare. These developments lower expenses, simplify healthcare processes, and present creative fixes. The Internet of Things, artificial intelligence, blockchain, cloud computing, and other technologies are revolutionising the healthcare industry. This tour is distinguished by its inventiveness, efficiency, and incorporation of cutting-edge technologies. A number of Industry 4.0 components, including blockchain, cyber-physical systems, artificial intelligence, and the Internet of Things, are crucial to this shift. Both the overall quality of healthcare services and patient outcomes are improved by these technologies. The integration of the Internet of Things empowers healthcare providers to deliver more intelligent and individualized care, while artificial intelligence facilitates rapid issue identification, data analysis, and structured and unstructured health information management. Cyber-physical systems revolutionize healthcare processes and improve patient care, enabled by modern big data technologies and cloud computing. Furthermore, blockchain technology offers secure and transparent data networks, eliminating the need for intermediaries and improving various aspects of healthcare, from device tracking to clinical trials.





Dhrumil Gajera et al.,

REFERENCES

1. Kumar, M.A., Vimala, R., Britto, K R.A.: A cognitive technology based healthcare monitoring system and medical data transmission. *Measurement* 146, 322–332 (2019),
2. Kickbusch, I, Health promotion 4.0. *Health Promotion International*, 34(2), pp 179–18, 2019. doi:10.1093/heapro/daz022
3. Ekta Maini, Artificial Intelligence -Futuristic Healthcare, *Indian Paediatrics*, Vol.56, Issue 9,2019
4. I-SCOOP. Industry 4.0: The Fourth Industrial Revolution–Guide to Industrie 4.0. 2017. Available online: <https://www.i-scoop.eu/industry-4-0/> (accessed on 9 October 2020).
5. Tay, S.I.; Lee, T.C.; Hamid, N.Z.A.; Ahmad, A.N.A. An overview of industry 4.0: Definition, components, and government initiatives. *J. Adv. Res. Dyn. Control. Syst.* 2018, 10, 1379–1387.
6. Schwab, K. *The Fourth Industrial Revolution: What It Means, How to Respond*; World Economic Forum; Crown Business: New York, NY, USA, 2016; Volume 14, p. 2016
7. S. Rajput, S.P. Singh, Industry 4.0 challenges to implement circular economy, *Benchmarking: An International Journal* 28 (5) (2019) 1717–1739, <https://doi.org/10.1108/BIJ-12-2018-0430>.
8. Popov VV, Kudryavtseva EV, Kumar Katiyar N, Shishkin A, Stepanov SI, Goel S. Industry 4.0 and Digitalisation in Healthcare. *Materials (Basel)*. 2022 Mar 14;15(6):2140. doi: 10.3390/ma15062140. PMID: 35329592; PMCID: PMC8953130.
9. M. Wehde, Healthcare 4.0, *IEEE Eng. Manage. Rev.* 47 (3) (2019) 24–28, <https://doi.org/10.1109/EMR.2019.2930702>.
10. A. Papa, M. Mital, P. Pisano, and M. Del Giudice, “E-health and wellbeing monitoring using smart healthcare devices: An empirical investigation,” *Technol. Forecast. Soc. Change*, no. September 2017, pp. 0–1, 2018
11. Al-Jaroodi J, Mohamed N, Abukhousa E. Health 4.0: On the Way to Realizing the Healthcare of the Future. *IEEE Access*. 2020 Nov 18;8:211189–211210. doi: 10.1109/ACCESS.2020.3038858. PMID: 34976565; PMCID: PMC8675545.
12. Abid Haleem, Mohd Javaid, Ravi Pratap Singh, Rajiv Suman, Medical 4.0 technologies for healthcare: Features, capabilities, and applications, *Internet of Things and Cyber-Physical Systems*, Volume 2, 2022, Pages 12-30, ISSN 2667-3452, <https://doi.org/10.1016/j.iotcps.2022.04.001>
13. Health Care 4.0: A Vision for Smart and Connected Health Care - Scientific Figure on ResearchGate. Available from: https://www.researchgate.net/figure/Historical-evolution-of-health-care-10-to-Health-Care-40_fig3_349100228 [accessed 14 Oct, 2023]
14. Joshi, A. P., Han, M., & Wang, Y. (2018). A survey on security and privacy issues of blockchain technology. *Mathematical Foundations of Computing*, 1,2, 19
15. <https://images.app.goo.gl/hZKMERANzaHkyU2WA>
16. <https://images.app.goo.gl/aN9sCwCjxk4M7SL07>

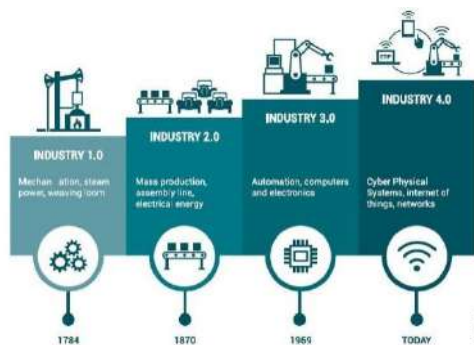


Figure 1 Revolution of Industry [16]



Figure 2 Digital Health Profile [15]





Behaviour of Twisted Building with Various Structural Configurations- A Review

Anvay S. Patel^{1*}, Vishalkumar B. Patel², Indrajit N. Patel³, Vimlesh V. Agrawal² and Pratiti M. Bhatt²

¹PG Scholar, Structural Engineering Department, Birla Vishvakarma Mahavidyalaya Engineering College, Vallabh Vidyanagar, India

²Assistant Professor, Structural Engineering Department, Birla Vishvakarma Mahavidyalaya Engineering College, Vallabh Vidyanagar, India

³Professor, Structural Engineering Department, Birla Vishvakarma Mahavidyalaya Engineering College, Vallabh Vidyanagar, India

Received: 18 Oct 2023

Revised: 25 Oct 2023

Accepted: 31 Oct 2023

*Address for Correspondence

Anvay S. Patel

PG Scholar,

Structural Engineering Department,

Birla Vishvakarma Mahavidyalaya Engineering College,

Vallabh Vidyanagar, India



This is an Open Access Journal / article distributed under the terms of the **Creative Commons Attribution License** (CC BY-NC-ND 3.0) which permits unrestricted use, distribution, and reproduction in any medium, provided the original work is properly cited. All rights reserved.

ABSTRACT

Tall buildings have a symbolic value in urban environments because they have a significant impact on how city skylines are arranged. Their distinctive shapes are responsible for the enhancement of aesthetic appeal and have a significant impact; meanwhile, their intricate patterns offer a feeling of variety while also offering architectural challenges. This study's main objective is to undertake a thorough examination of the existing literature in order to fully understand the present state of knowledge about the complex structural characteristics of twisted towers. A major emphasis is placed on assessing the benefits and drawbacks of various structural approaches, which cover both adaptive and non-adaptive systems. This examination seeks to identify the complex issues and difficulties involved in using different structural strategies in the context of these architecturally distinctive structures. The overall purpose of this literature study is to offer insightful information on how structural systems inside twisted towers are currently understood. This paper aims to add a deeper understanding of the complexity of planning and building twisted towers by methodically compiling and examining the substantial volume of existing literature. It aims to be a comprehensive resource that provides a detailed analysis of the many aspects of the twisted structures.

Keywords: Adaptive system, Non-adaptive system, Outrigger, Rate of twist, Twisted building, Twisted diagrid, Structural systems.





Anvay S Patel *et al.*,

INTRODUCTION

The Twisted Tower is a particularly unique type of architecture that draws attention to itself with its extraordinarily distinctive design. As its name implies, this tower deviates from the typical straight vertical profiles of conventional structures by incorporating a twist or spiral into its structural composition, creating a transformative effect on the eye. Along with achieving important aesthetic goals. Twisted towers, which have this artistic style, have developed in many cities all over the world, eventually becoming iconic monuments that defy norms of conventional architecture and engineering. These structures continuously challenge expectations, showing themselves as amazing engineering achievements and metaphorical symbols of innovation and advancement. Each of these unique skyscrapers makes a striking contribution to the city's metropolitan skyline, highlighting the promise and potential of artistic design in the modern day. The realization of a twisted architectural form necessitates a meticulous and purposeful adjustment that involves the rotational repositioning of floors and a corresponding adaptation of the facade, seamlessly aligning with this rotational movement. Generally, tall buildings have most effect of lateral loads like seismic load and wind load.[20]. In case of twisted building, It has good characteristic in terms of wind resistance.[14]. Turning Torso in Sweden, Shanghai Tower in China, Cayan Tower in Dubai, Al Bahar Towers in the United Arab Emirates, and Generali Tower in Italy are some of the world-famous twisted structures. Each of these structures is a witness to the varied expressions within this architectural genre, as well as to the worldwide landscape of twisted architecture. Similar to how the Shanghai Tower, with its slick and beautiful look, shows the combination of aesthetics and practicality, these projects demonstrate the mastery of architectural design and engineering, displaying the tremendous possibilities for innovation. It demonstrates the tremendous possibilities of contemporary engineering and building techniques. In Dubai, the Cayan Tower stands as a symbol of the city's ambition and progress. Its twisted form is not only visually stunning, but also provides residents with breathtaking views of the surrounding landscape.[21]. The Al Bahar Towers in the UAE, with their innovative sun-shading system, demonstrate the integration of sustainable design principles into twisted architecture. Finally, the Generali Tower in Italy represents a harmonious blend of tradition and modernity, with its twisting form paying homage to the country's rich architectural heritage.

Rate of Twist

The "rate of twist" in a twisted structure refers to the difference in twist angle between two succeeding levels. The building's angle of twist in relation to the sum of its storeys may be used to calculate the rate of twist mathematically:

$$\omega = \theta / n$$

Where,

ω = Rate of twist

θ = Angle of twist of the building

n = Total number of storeys

Aerodynamic Characteristics

Alaghmandan *et al.* [2013].[1]. provides overview about effect of wind load on aerodynamically modified structures. A highly effective approach for mitigating vortex shedding caused by dynamic responses is the use of a twist in tall building designs. Specifically in crosswind situations where the building's least effective face purposefully deviates from alignment with the primary wind direction, this deliberate twist shows to be remarkably successful in reducing wind impacts. Crosswinds are minimized by this purposeful orientation targeted disruption of the resonance between the building's inherent frequency and periodic vortex shedding. This architectural innovation boosts the stability and resilience of tall structures by purposely departing from traditional designs.

Tang *et al.* [2013].[2]. investigate the effects of wind drags on tall buildings with different geometries using computational fluid dynamics to examine both linear and twisted structures. Understanding the impact of building torsion on the reduction of wind drag is the main goal of their research. Their research shows that intentionally incorporating twists into architectural designs significantly reduces wind drag, suggesting that proper application of



**Anvay S Patel et al.,**

this architectural technique may decrease wind drag. In maximising building structures' aerodynamic effectiveness and decreasing the impacts of wind forces, the research underlines the potential benefits of implementing proper twists into structures. Kim *et al.* [2018].[3]. investigates the damping ratios associated with the aerodynamic behavior of a 180° helical supertall building using a model test that simulates rocking vibrations. The random decrement technique (RDT) employed to assess the aerodynamic damping ratios of structures under ambient loads. The findings reveal that the aerodynamic damping ratios of the 180 helical model exhibit superior aerodynamic characteristics in both the along-wind and across-wind directions when compared to those of the square model. Furthermore, the study finds no evidence of aeroelastic instability in the 180° helical model for any of the reduced velocities considered. Moreover, it is determined that the wind direction does not impact the aerodynamic damping ratio of the 180 helical model.

Structural Approach

Taşkın [2019].[4]. describes two structural approaches for design of twisted tall structures. The first approach is termed as "non-adaptive structural approach", which involves rotating floors around the central axis while keeping structural columns in a vertical configuration. The "adaptive structural approach," an alternate strategy, matches up the structural system with the building's twisting facade. These separate systems present different opportunities and design challenges for buildings and structures. The performance and characteristics of twisted tall structures are strongly influenced by the choice between non-adaptive and adaptive structural approach. The essential features of these structures are influenced by the selection of construction method and overall design and functionality of twisted tall buildings.

LITERATURE REVIEW

Kwon *et al.* [2014].[5]. studied that the load-resisting capabilities of analytical models of twisted buildings at 0°, 90°, 180°, and 270° were compared. The study's research results demonstrate that as the twisting angle grows, structures' potential for progressive collapse lowers. The fragility study shows that the model structures' collapse probability for the spectrum acceleration are substantially lower than 10%, confirming that they are typically secure against higher level earthquakes. Additionally, it was shown that the seismic fragility declined as the twisting angle rose.

Moon [2014].[6]. investigates various options for developing structural systems in twisted tall structures and their corresponding lateral stiffness performances. He explores how modern structural technologies, such as outrigger systems, braced tubes, and diagrids, are used to construct twisted tall structures and also investigates and how diagrid systems function structurally in twisted tall structures and contrasts them with braced tubes. The structural performance of outrigger structures in twisted tall buildings is also examined in this research, and it examines how lateral stiffness decreases as the degree of twist rises. Vincent *et al.* [2015].[7]. explain the use of cambered tower floor plates to account for the rotational displacement caused by the Grove at Grand Bay's twisting design. With proper planning, the tower was return to its original position just before the hat truss reaches its designed strength. Steel plates were effectively used on the lower levels to counteract the rotation of the structure caused by long-term concrete creep. A vast 80 auger-cast pile-supported concrete mat, measuring 7'-6" inch thickness, was methodically used to provide strong support for the center core of each tower. Steel reinforcement was expertly included to strengthen the top and bottom reinforcement layers, and the pile cap was installed to mitigate any potential vertical shear.

Moon [2016].[8]. examines how well outrigger systems operate in tall structures with complex geometries like twisted, slanted, and tapering ones. With a focus on the greater structural depth and effectiveness of outrigger systems in withstanding wind-induced overturning moments, it compares outrigger structures to shear wall type structures that are contained inside the building core. The study examines the impact of several design elements, including twist, tilt, and taper angles, on the structural performance of outrigger systems. In twisted tall buildings, lateral stiffness of outrigger structures decreases as the rate of twist surges, but in tapered tall buildings, lateral stiffness rises as the rate of taper increases. Although it acknowledges that there is a significant initial lateral





Anvay S Patel *et al.*,

displacement brought on by gravity, the study also identifies the higher lateral stiffness of outrigger systems in tilted towers as a product of the triangulation of primary structural components. The study highlights the structural effectiveness and aesthetic potential of outrigger structures for tall buildings with complicated geometries.

Xiong *et al.* [2018].[9]. find out the mechanical performance of high-rise twisted diagrid tube designs, with a special attention on examining how the external inclined column elements affects the characteristics of the whole structure. The top story's displacement and the internal forces acting on each component are determined by the analysis of the models done by the authors using SAP2000 V14 software. The load distribution, which includes Ultimate Bearing Capacity, dead load, live load, and wind pressure, complies with the Chinese Code. The rotation angle (or rate of twist), the aspect ratio (or ratio of height to width), and the interlayer spacing between neighboring major ring beams are the three crucial elements that are the study pinpoints via its investigation as having a substantial influence on the structural performance. The findings reveal that the internal forces acting on side columns and diagonal bracing tend to increase with the rotation angle, while the corner column initially experiences a decline in forces before a brief increase. Moreover, the maximum axial force exerted on side columns surpasses that of corner columns, and the gap between the two increases as the twist angle intensifies.

Sanjay R. *et al.* [2019].[10]. has studied a comparative examination concerning the structural behavior of Reinforced Concrete (RCC) and Steel twisted constructions when subjected to dynamic loads. The investigation assesses various degrees of twist (1.5, 2.5, and 3.5 per floor) for both RCC and Steel twisted buildings. The modeling and analysis are executed employing SAP2000, taking into consideration dead loads, live loads, seismic loads, and wind loads. The analysis is conducted for gravity loads and lateral loads utilizing the Response spectrum methodology. The investigation concludes that the Steel twisted building demonstrates superior efficiency in comparison to the RCC twisted building under the influence of seismic and wind loads. The angle of twist at 3.5 degrees per floor is identified as the most efficient when compared to angles of twist at 1.5 and 2.5 degrees. Additionally, the study highlights that twisted buildings possess the potential to enhance aerodynamic properties and energy efficiency.

Song *et al.* [2020].[11]. explores the impact of various factors such as diagonal angle, twist rate, aspect ratio, corner column, and plan form on the lateral stiffness of twisted diagrids. It aims to identify the optimal range of diagonal angles through a comprehensive analysis. A design methodology is proposed for determining the diagonal sizes of twisted diagrids, and its validity is confirmed through finite element analysis. Additionally, a novel configuration of twisted diagrids with asymmetric diagonal angles is introduced, demonstrating enhanced lateral stiffness compared to the symmetric case. The paper further calculates the overall overturn moment of modules in twisted diagrid tube structures utilizing equations provided within. For the initial design of twisted diagrids, it is advised that the left-inclined diagonal angle surpasses the right-inclined angle. Moreover, factors related to architecture and constructability need to be taken into account when determining the diagonal angles. Ultimately, the optimal angle is determined, revealing that for 60-story twisted diagrids with an aspect ratio of 7, the ideal diagonal angle falls within the range of 55 to 71.

Zuber *et al.* [2022].[12]. has done a comparative investigation into the structural behavior of Reinforced Concrete (RCC) twisted buildings under dynamic loads, specifically examining varying degrees of twist at the central region of the edifice. The findings of this study demonstrated that RCC twisted buildings exhibit commendable efficiency when subjected to seismic and wind loads, with a 10-degree twist angle proving more efficient in comparison to 12.5 and 15 degrees. Employing the ETABS software, the analysis incorporated considerations of dead loads, live loads, seismic loads, and wind loads, with parameters such as displacement, storey drift, time period, and base shear being plotted for thorough evaluation. It is important to note that the analysis adhered to the Indian standard codal provisions for Zone V. Naik *et al.* [2022].[13]. utilize the software program ETABS in order to conduct an analysis on a 16-storey building that possesses a twisted configuration. In their examination, they meticulously scrutinize various levels of twist, ranging from 1.5° to 5°. The structural parameters that are taken into account for this analysis consist of M50 grade concrete, Fe500 for primary reinforcement, and Fe450 for secondary reinforcement. It should be noted that this research is carried out with respect to a building situated in Zone IV, which exhibits a medium soil





Anvay S Patel *et al.*,

condition, and is in accordance with the codal provisions of India. The significant outcome of this analysis unveils that the model with a twist rate of 3° manifests the greatest lateral displacement, thereby providing valuable insights into the structural response under these particular conditions.

SUMMARY

Analysis of the effects of wind loads on buildings with altered aerodynamics to shift from conventional designs and deliberately introduce crosswind misalignment to decrease vortex shedding and increase stability in tall structures.[1]. Study of wind drags on tall structures using computational fluid dynamics, focusing on how building twist affects wind drag reduction. Intentional twists greatly reduce wind forces, improving aerodynamic performance.[2]. Researcher investigate the aerodynamics of a twisted supertall structure while testing model simulations to determine damping ratios. In comparing the twisted and square models. The research illustrates the twisted model have better aerodynamic qualities, enhancing understanding of the wind-induced aerodynamic performance of complicated tall buildings.[3]. The primary two techniques for creating tall, twisted structures: the "non-adaptive" technique rotates the floors, while the "adaptive" technique lines up the structure with the twist.[4]. Additionally, researcher investigate analytical models of twisted buildings at various angles, revealing that increased twisting angles reduce the risk of progressive collapse. Seismic fragility analysis underscores structural resilience against higher-level earthquakes, offering valuable insights for designing earthquake-resistant twisted buildings.[5]. In comparison of twisted structures including diagrids, braced tubes, and outrigger systems. The study highlights the decrease in lateral stiffness with increasing twist and compares diagrids with braced tubes to assess the structural performance of outrigger system.[6]. Details of structural improvements that solve rotational displacement in the twisting design. Enhanced stability and resilience are provided by cambered floor plates, steel reinforcements, and auger-cast piles, providing insights into overcoming difficulties in twisted tower designs.[7]. The study of design impacts due to outrigger systems with a focus on multidisciplinary research, aesthetic potential, and structural efficiency. Outrigger at top and middle storey performs better in lateral loads.[8]. Tall twisted diagrid tube structural system's mechanical behaviour is examined by researcher, who place special twisted diagrid at outer periphery. The analysis pinpoints variables affecting structural performance, leading the best designs for increased effectiveness.[9]. In comparison of different materials, steel twisted building with 3° rate of twist performs structurally better under seismic and wind conditions, presenting the potential for improved aerodynamics and energy efficiency.[10]. Effects of the aspect ratio, twist rate, and diagonal angles on the lateral stiffness of twisted diagrids using finite element analysis and finds that lateral stiffness was decreasing with increase in rate of twist.[11]. Study of various twists while analysing the dynamic performance of RCC structures when twist is provided at middle part of building. They demonstrate the effectiveness of a 10-degree twist against seismic and wind loads, providing a strong knowledge of structural behaviour. In a comparison of the structural performance of RCC and steel twisted structures under dynamic loads.[12]. Analysing a 16-story twisted structure with various twist degrees using ETABS software, providing insights into lateral displacements is maximum when twist rate was 3° . [13].

CONCLUSION

The implementation of twists is a very successful approach for reducing vortex shedding brought on by dynamic reactions to wind loads in tall building design. Building stability and resilience are increased due to the intentional misalignment of the least efficient face of the structure, which breaks the resonance between the intrinsic frequency of the structure and the periodic vortex shedding.[1]. By addition of twist to straight tower, wind drag is reduced. This architectural style shows promise for improving aerodynamic efficiency and reducing the effects of wind forces on tall structures.[2]. The twisted model's aerodynamic characteristics help to better understand how twisted tall structures respond to wind forces and lessen wind drag.[3]. For selection of structural approaches, Architectural aesthetics, functional purpose, and lateral load resistance all play a role in choosing between adaptable and non-adaptive structural approaches.[4]. Analytical models of twisted structures at various angles were tested for their ability to resist loads, showing a link between the degree of twisting and the risk of gradual collapse. The





Anvay S Patel et al.,

buildings exhibit resistance to stronger earthquakes as the twisting angle rises.[13]. Cambered floor plates and steel reinforcements, such as concrete matting supported by auger-cast piles, demonstrate the complexity of enhancing stability and minimizing long-term structural deformations.[5]. In comparison to a basic twisted structure, the outrigger with a twisted structure provides improved lateral stiffness as the angle of twist increases.[7]. In twisted structures with diagonal bracing, the internal forces of the side columns and bracing tend to increase with the rotation angle, whereas the corner column shows a decline after a brief increase. Corner columns have a lower maximum axial force than side columns, and as the twist angle increases, the space between them gets wider.[8]. By introducing unique configurations with asymmetric diagonal angles, it is possible to demonstrate increased lateral stiffness and get important insight into how to construct effective twisted diagrid structures.[9]. If the rate of twist is only at the center of the structure, then a 10° twist has a superior efficiency than other models.[10]. Under the effect of seismic and wind loads, steel twisted buildings exhibit better efficiency over RCC twisted buildings. When compared to angles of twist at 1.5 and 2.5 degrees, the angle of twist at 3.5 degrees per floor is shown to be the most effective.[11]. It is discovered that the storey displacement rises up to a twist rate of 3° before falling. For a twist rate of 3°, the top storey displacement is seen to be maximal, however for a twist rate of 5°, the lower storey displacement is detected.[12].

REFERENCES

1. Alaghmandan M, Elnimeiri M. Reducing Impact of Wind on Tall Buildings through Design and Aerodynamic Modifications (Architectural and Structural Concepts to Mitigate Wind Effect on Tall Buildings). 2013: Building Solutions for Architectural Engineering 2013 (pp. 847-856).
2. Tang JW, Xie YM, Felicetti P, Tu JY, Li JD. Numerical simulations of wind drags on straight and twisted polygonal buildings. *The Structural Design of Tall and Special Buildings*. 2013 Jan;22(1):62-73.
3. Kim W, Yoshida A, Tamura Y, Yi JH. Experimental study of aerodynamic damping of a twisted supertall building. *Journal of Wind Engineering and Industrial Aerodynamics*. 2018 May 1;176:1-2.
4. Taşkın GN. A comparative study on alternative structural system layouts of twisted tall buildings (Master's thesis, Middle East Technical University). 2019.
5. Kwon K, Kim J. Progressive collapse and seismic performance of twisted diagrid buildings. *International Journal of High-Rise Buildings*. 2014;3(3):223-30.
6. Moon KS. Studies on various structural system design options for twisted tall buildings and their performances. *The Structural Design of Tall and Special Buildings*. 2014 Apr 10;23(5):319-33.
7. Vincent D, Luise R, Abdul M. Structural challenges of twisted towers. Council of Tall Buildings and Urban Habitat, CTBUH. 2015.
8. Moon KS. Outrigger Systems for Structural Design of Complex-Shaped Tall. 2016: *International Journal of High-Rise Buildings*, 5(1), 13–20.
9. Xiong Y, Zhang C. Mechanical Performance of High-Rise Twisted Diagrid Tube Structure System. 6th Annual International Conference on Architecture and Civil Engineering (ACE 2018) 2018.
10. Sanjay R, Shivakumaraswamy B. Comparative study on the structural behavior of rcc and steel twisted building. *Journal of Science. International Research Journal of Engineering and Technology*. 2019 Sep;6(09).
11. Song S, Zhang C. Lateral stiffness and preliminary design methodology of twisted diagrid tube structures. *The Structural Design of Tall and Special Buildings*. 2020 Dec 25;29(18):e1809.
12. Shah ZA, Satbhaiya R. Analysis of Twisted Tall Structure Considering Lateral Load using ETABS. *International Journal of Scientific Research in Civil Engineering*. 2022,6.
13. Naik VB, Kadlag V. Seismic analysis of rcc twisted building with swimming pool using ETABS. *International journal of creative research thoughts*. 2022.
14. Amin JA, Ahuja AK. Aerodynamic modifications to the shape of the buildings: a review of the state-of-the-art. *Journal of civil engineering*. (4), 433-450.
15. Tall Buildings in Numbers: Twisting Tall Buildings. *CTBUH Journal*, no. 3. 2016: 46–47.





Anvay S Patel et al.,

16. IS 1893 (Part 1): 2016, Criteria for Earthquake Resistant Design of Structures. 2016 November. New Delhi: Bureau of Indian Standards.
17. IS 800: 2007, General Construction in Steel - Code of Practice. 2007 December). New Delhi: Bureau of Indian Standards.
18. IS IS 875 (Part 3): 2015, Design Loads (Other than Earthquake) for Buildings and Structures - Code of Practice. 2015 April. New Delhi: Bureau of Indian Standards.
19. IS 16700: 2017, Criteria for Structural Safety of Tall Concrete Buildings. 2017 November. New Delhi: Bureau of Indian Standards.
20. Taranath B.S, “Reinforced Concrete Design of Tall Buildings,” Taylor & Francis Group, 2010.
21. Feng F., “ Design and Analysis of Tall and Complex Structures” Elsevier, 2018.

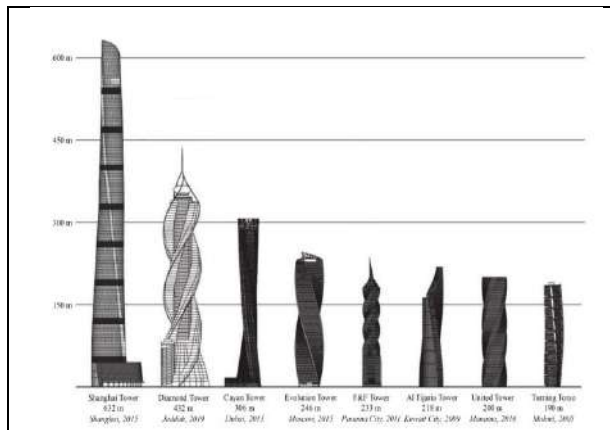


Figure 6 Tallest twisted buildings in the world (Source: CTBUH, 2016[15].)

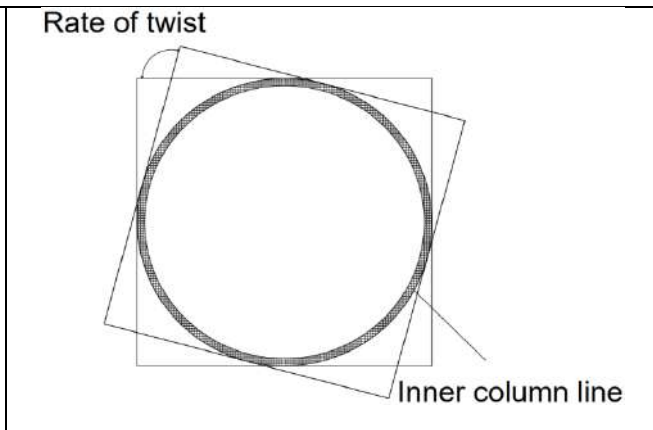


Figure 7 Rate of twist

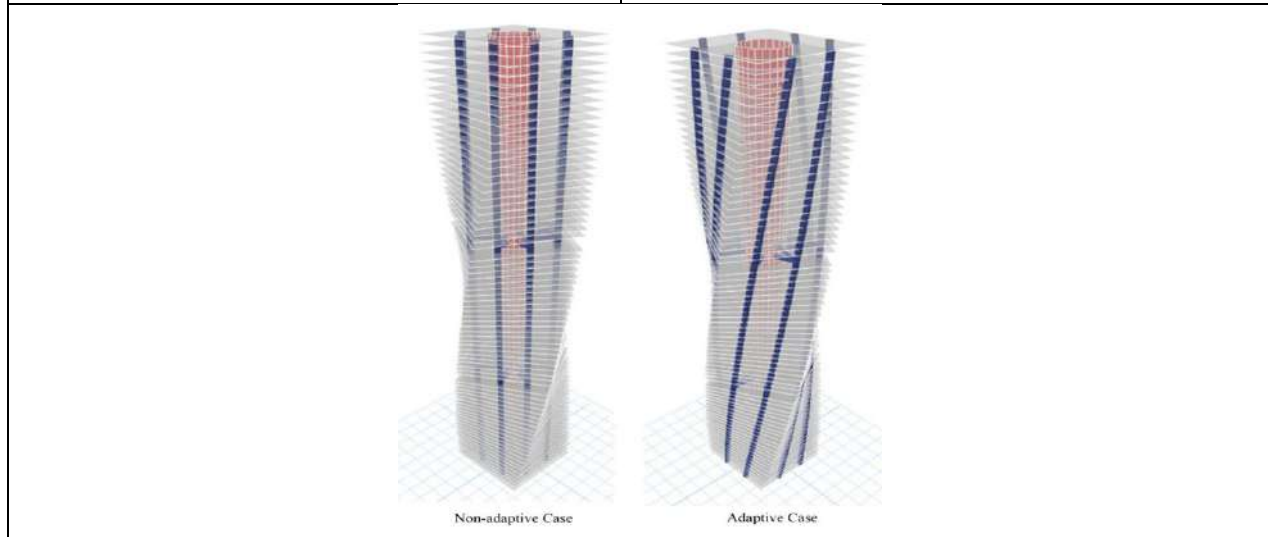


Figure 8. Structural approaches in twisted building (Source: Taşkın, 2019 [4].)





Analyzing the Effects of Variable Diagrid Angles On Tall Building Performance -A Review

Jay P. Patel¹, Vishalkumar B. Patel², Indrajit N. Patel³, Darshana R. Bhatt⁴ and Pratiti M. Bhatt²

¹PG Scholar, Structural Engineering Department, Birla Vishvakarma Mahavidyalaya Engineering College, Vallabh Vidyanagar, India

²Assistant Professor, Structural Engineering Department, Birla Vishvakarma Mahavidyalaya Engineering College, Vallabh Vidyanagar, India

³Professor, Structural Engineering Department, Birla Vishvakarma Mahavidyalaya Engineering College, Vallabh Vidyanagar, India

⁴Head Of Department, Structural Engineering Department, Birla Vishvakarma Mahavidyalaya Engineering College, Vallabh Vidyanagar, India.

Received: 18 Oct 2023

Revised: 25 Oct 2023

Accepted: 31 Oct 2023

*Address for Correspondence

Jay P. Patel

PG Scholar,
Structural Engineering Department,
Birla Vishvakarma Mahavidyalaya,
Engineering College,
Vallabh Vidyanagar, India



This is an Open Access Journal / article distributed under the terms of the **Creative Commons Attribution License** (CC BY-NC-ND 3.0) which permits unrestricted use, distribution, and reproduction in any medium, provided the original work is properly cited. All rights reserved.

ABSTRACT

Diagrid structures are known for their effectiveness and aesthetic appeal, characterized by a grid of intersecting members arranged diagonally. This paper gives broader analysis of comprehensive analysis of relevant literature, both in a chronological and thematic manner, to enable a comprehensive understanding of the historical development of diagrid systems and the current advancements in design, analysis, and construction methodologies. Literature, both in a chronological and thematic manner, to enable a comprehensive understanding of the historical development of diagrid systems and the current advancements in design, analysis, and construction methodologies. The review places particular emphasis on key aspects such as the structural behavior of diagrids under various loading conditions, the optimization of member sizes, and the integration of diagrid systems with sustainable design principles. Through a critical examination of case studies and scholarly work, this paper contributes to the body of knowledge and provides valuable insights into diagrid structures.

Keywords: Variable angle diagrid, Seismic performance, Lateral displacement, ETABs, STAAD.Pro, Displacement, Storey Drift.



Jay P Patel *et al.*,

INTRODUCTION

The diagrid structure, which originated from the concept of a "diagonal grid," has emerged as a remarkable advancement in the field of architecture and has achieved significant recognition in contemporary architectural practice. The distinguishing characteristic of this structural system lies in its effective utilization of building materials and unique approach to structural design [17]. Unlike traditional methods that rely on the implementation of vertical columns and horizontal beams, the diagrid system employs a network of intersecting diagonal elements to evenly distribute the structural load across the entirety of the building [20]. This innovative arrangement of diagonal components, which traverse the outer surface of the structure in a lattice-like pattern, contributes to the visually captivating appearance for which diagrid structures are well-known. Typically constructed using durable materials like steel, these diagonal elements provide exceptional support and strength to the overall structure [15]. Consequently, this structural system not only enables the creation of expansive interiors (less columns at inner portion of building), but also encourages architects to explore new possibilities in terms of design and construction[24].

The diagrid structural system is a distinctive architectural framework design distinguished by its utilization of diagonal elements resulting from the intersection of various construction materials such as metals, concrete, or wooden beams [18]. This innovative system finds extensive application in the construction of diverse structures, including buildings and roofs, where its unique features and composition contribute to the overall structural integrity and aesthetic appeal of the building[24].The diagrid system frequently depends on the utilization of sturdy materials like steel, which effectively strengthens the structural integrity and overall functionality of the building [16]. As a result, diagrid structures have become a favored choice for tall buildings that aim to combine structural efficiency with a distinctive architectural character [22]. In this preliminary exploration of the realm of diagrids in the context of tall buildings, we will delve into the fundamental principles, advantages, and notable examples of this pioneering structural system that has revolutionized the approach to designing and constructing skyscrapers[23].

Diagrid has good appearance and it is easily recognized. The configuration and efficiency of a diagrid system reduce the number of structural element required on the façade of the buildings, therefore less obstruction to the outside view [21]. The structural efficiency of diagrid system also helps in avoiding interior and corner columns, therefore allowing Significant flexibility with the floor plan. Perimeter "diagrid" system saves approximately 20 percent structural steel weight when compared to a conventional moment-frame structure [8]. however, used at few places in past but utilised for buildings with unique shapes and form, developed in the beginning of twenty-first century; so diagrid can be considered as one of the latest structural systems for tall buildings [9]. diagrid structures with two different inclinations of diagonal members and diagrid structures with three different inclinations of diagonal members are studied and the evaluation of these patterns of the diagrid structures is done based on the structural steel used and the performance [19]. Diagrid structures are emerging as a new aesthetic trend for tall buildings in the modern age of architecture as a most versatile structural system and it is a special form of the space truss [9].

LITERATURE REVIEW

Ashraf *et al.* [2020][1] The analysis of various arrangements of variable angle diagrid structures for a 60-story building is the subject of this paper. The focus is on the inclination angle of the diagrids and the ratio of heights at which the inclination angle varies. The author brings attention to the scarcity of academic research on the geometry of diagrids and variable angle diagrids, while emphasizing the potential advantages of variable angle diagrids in reducing costs and material usage in construction projects. The objective of the study is to identify the optimal configuration of the variable angle diagrid system in order to further minimize costs and material usage in construction .model with diagrid angle of 70 to 75 gives better result in terms of maximum storey displacement. Lacidogna *et al.*[2020][2] has examined the impact of the geometric form on the structural response of diagrid tall





Jay P Patel *et al.*,

buildings when subjected to lateral and torque forces. It investigates the influence of distinct floor plan shapes, overall heights, and diagonal inclinations on the displacements and rotations of buildings. The scope of the study encompasses the analysis of both 48-story and 60-story diagrid constructions. Author's main focus lies in the analysis and comparison of various geometric parameters pertaining to diagrid tall buildings .

Lacidognaa *et al.* [2020][3] has studied conducted a comprehensive investigation on the application and utilization of diagrid systems in conjunction with both closed-section and open-section shear walls in the context of tall buildings. The main objective of this research was to optimize the geometric characteristics of the diagrid system in order to minimize lateral displacements and torsional rotations. By recommending an optimal diagonal angle of approximately 70 degrees, the lateral displacements of the structure can be significantly reduced. It is important to note that the relative stiffness of the diagrid system in relation to the shear walls may vary depending on the inclination of the external diagonals, especially when an internal OS shear wall is present. This variation in stiffness should be considered when designing tall buildings with diagrid systems . Heshmatia *et al.* [2020][4] The evaluation of the seismic performance of tubular diagrid structures with varying angles in tall steel buildings is the focus of this study. In order to assess the seismic performance of diagrid structures with 36 stories, the researchers employed pushover and nonlinear time history analysis methods. The results obtained from this investigation suggest that the diagrid core of these structures possesses the potential to enhance their hardening behavior, particularly when the angles of the perimeter panels are equal to or lower than those of the core. Furthermore, it was observed that diagrid structures demonstrate the capability to undergo substantial deformations during infrequent earthquakes, with a significant amount of input energy dissipated by the diagonal members. Lastly, the resistance of diagrid structures to lateral loads is found to be contingent upon the slope of the diagonal members .

Ardekani *et al.* [2020][5] investigates the effects of form parameters on the structural efficiency of tall buildings by generating a parametric platform .The study focuses on two commonly used modifications in tall buildings: tapering in the height section and changing plan shape .The diagrid structural system is used in the analysis, which provides high stiffness and efficiency while satisfying architectural needs .The research applies a response spectrum analysis to analyze the structural behaviour of the generated forms .The results show that tapering in the height section has a greater impact on structural efficiency parameters compared to plan changes .Forms with circular and polygonal shapes with more sides are found to be more efficient .The design of the diagrid models in the research follows an iterative procedure to satisfy the displacement constraint .The maximum displacement of the top of the building is controlled by the displacement amplification factor, elastic displacement, allowable displacement, and story height .Inter-story drifts of the models are calculated to assess their performance. Passoni *et al.* [2020][6] suggested the usage of diagrid exoskeletons as a retrofit for existing reinforced concrete (RC) structures. When designing large new buildings without vertical columns, diagrids are slanted structural grids that can handle both vertical and horizontal stresses. The article offers an analytical design approach and a method for specifying design spectrum as two techniques for designing elastic diagrids as retrofit interventions. When façade preservation is necessary or for listed structures, the use of diagrids as exoskeletons is inapplicable. Restrictions on urban design must also be taken into account for viability. A multi-criteria approach is advised to promote the sustainability of the rehabilitation process, seeking to reduce any negative effects on the building's social, economic, and environmental system.

Kinayoglu *et al.* [2018][7] undertakes an extensive and comprehensive exploration of the progressive evolution and advancement of circular-planned diagrid systems within the realm of architecture. It delves into the multifarious and diverse approaches that have been taken in the field of patents, specifically those pertaining to the aforementioned developments. It is observed that there has been a discernible and conspicuous shift in the interests and preoccupations of patent holders, whereby the focus has transitioned from the overall configurations of diagrid systems to a more laser-like attention and emphasis on the intricacies and subtleties of joint details. Lastly, it is imperative to define and explicate the term "diagrid" itself, which refers to a structural framework that ingeniously substitutes traditional and customary vertical elements with diagonal ones, thereby fundamentally altering the directionality and orientation of the vertical components . Ravi *et al.* [2017][8] examines the utilization of diagrid structural systems in multi-storey buildings, emphasizing their structural efficiency and aesthetic potential. The





Jay P Patel *et al.*,

authors analyze a RCC building with 24, 36, 48, and 60 storey using STAAD Pro software while considering seismic forces as per Indian code. The concept of diagrid structural systems and their analysis and design methodology using STAAD Pro software are investigated. The objective of the study is to ascertain the optimal angle of diagonals in diagrid structures in order to achieve a safe structural design. Deviating from the optimal angle of diagonals can significantly increase the required quantity of steel and impact the structural behavior of the diagrid system. The article also compares the analysis results of beam displacement, storey drift, and bending moment between diagrid and conventional structures, highlighting the cost-effective design of diagrid structures. The significance of the angle of diagonals on the structural design of diagrid structures is emphasized .

Divya *et al.* [2016][9] conducted comprehensive analysis of the structural behavior exhibited by high-rise buildings that incorporate diagrid systems featuring various angles. This analysis specifically focuses on examining key parameters such as storey shear, storey displacement, and storey drift. By thoroughly investigating these parameters, the study aims to gain a deeper understanding of how diagrid systems with different angles perform and interact within high-rise structures. Additionally, an essential goal of this research is to identify the optimal diagrid angle that best suits a particular height requirement. To achieve this objective, the authors meticulously compare and contrast the analysis results obtained for the aforementioned parameters, thereby facilitating a comprehensive evaluation of the diagrid systems' performance. Furthermore, the authors go on to ascertain the most suitable diagrid angle for a specific height, thereby providing valuable insights into the design considerations for high-rise buildings . Vishal *et al.* [2016][10] provides a comparative examination of diagrid structures and conventional frame structures for tall buildings, with a focus on their performance in terms of lateral displacements, steel weight, and stiffness. The investigation involves the analysis of seven steel buildings, all of which possess an identical base area and loadings, but differ in height, utilizing both diagrid and conventional frame systems. The study takes into account various parameters, including the fundamental time period, maximum top storey lateral displacement, maximum base shear, steel weight, percentage differences in the change of steel weight, maximum storey displacement, and maximum storey drift. The findings of the study indicate that diagrid structures exhibit superior performance compared to conventional frame structures, with a lesser increase in steel weight as the height of the building increases. Author possess the ability to withstand wind forces to greater heights when compared to conventional frame systems. Author found out that diagrid structures display lower displacements on each storey and storey drifts in comparison to conventional frame systems.

Moon [2014][11] conducted a study that examined the performance of tall buildings with a tilt of 60 storey. These buildings were designed using braced tubes, diagrids, and outrigger systems. The investigation revealed that the lateral stiffness of the tilted braced tube and diagrid buildings is equivalent to that of the straight buildings. In both cases, the displacement caused by gravity load (dead load and live load) is greater than that caused by wind load. The value of displacement increases as the tilt angle increases. Conversely, in the outrigger system, the lateral stiffness of the tilted building surpasses that of the straight outrigger structure when exposed to wind loads. The gravity-induced lateral displacements in the outrigger system are lower in comparison to those in the braced tube or diagrid systems. Nishith *et al.* [2014][12] presented comparative study between a 20-storey building with a simple frame and a building with a structural system known as diagrid. The main focus of the study is to analyze the lateral forces on high-rise buildings. In order to conduct the analysis, the study employs the use of ETABS software for both modeling and analysis of the structures. The paper then proceeds to present the analysis results which include displacement, storey drift, and storey shear. Furthermore, the paper calculates the consumption of concrete and steel for both the simple frame building and the diagrid structure building, with the diagrid structure displaying a lower material consumption. Additionally, the diagrid structural system is observed to have significantly less top storey displacement in comparison to the simple frame building. Moreover, the storey drift and storey shear are also found to be lower in the diagrid structural system, thereby indicating its effectiveness in providing resistance to lateral loads. It is worth noting that the design of both structures is carried out using the same member size. However, the simple frame structure fails to meet the design criteria and as a result, larger member sizes are selected . Khushbu *et al.* [2013][13] presents a comprehensive analysis and design of a 36-storey diagrid steel building, as well as the analysis and design outcomes of diagrid structures with 50, 60, 70, and 80 storeys. The structural design of tall





Jay P Patel et al.,

buildings is governed by the lateral forces caused by wind or seismic activity. These lateral loads can be counteracted by either an interior structural system or an exterior structural system. The diagrid structural system has gained popularity in high-rise buildings due to its remarkable structural efficiency and flexibility in terms of architectural planning. This system is comprised of inclined columns located on the exterior surface of the building, which effectively resist lateral loads through the axial action of the diagonals. The analysis and design of these structures were conducted utilizing the ETABS software, while all structural members were engineered in accordance with IS 800:2007, taking into consideration all possible load combinations. Additionally, the paper provides a comparative analysis of the outcomes for different storey heights in terms of time period, displacement at the top storey and inter-storey drift .

SUMMARY

The diagrid steel structures with varying numbers of storeys were examined by researchers. Author employed the ETABS software and the IS 800:2007 code to analyze and design the structures, while evaluating a range of structural factors [1] . The researcher conducted an examination of diagrid structures with variable angles in order to decrease expenses and enhance the efficiency of material usage [2]. The primary focus was placed on inclination angles and the performance of the structure [3] . researched geometric form effects on diagrid tall buildings under lateral and torque forces, aiding design optimization with valuable insights [4]. Researchers studied diagrid systems in tall buildings, considering closed and open-section shear walls, proposing optimal diagonal angles for reducing lateral displacements, enhancing design knowledge. Tubular diagrid structures with varied angles were evaluated for seismic performance, revealing enhanced hardening behavior and providing insights into structural advantages [5]. Researchers compared basic frame buildings to diagrid structures, highlighting diagrids' superior performance in withstanding lateral loads, lower displacement, storey drift, and material use [6] . Researchers compared diagrid structures to conventional frames, finding enhanced performance with minimal steel usage, contributing to a comprehensive understanding of diagrid benefits [7] . Researchers conducted a comparative analysis of displacement, storey drift, and material use in simple frame and diagrid structures, highlighting diagrids' efficiency and effectiveness [8] . Using STAAD Pro, researchers studied RCC buildings with varying storey heights, highlighting the importance of diagonal angles in diagrid structures for design and structural insights [9] . The study assessed tilted tall buildings with braced tubes, diagrids, and outriggers, comparing lateral stiffness and displacements for insights into structural systems [10] . Researchers analyzed diagrid systems in high-rise buildings, focusing on storey shear, displacement, and drift to recommend optimal angles for design [11] . Researchers explored how form parameters, particularly vertical tapering, affect the structural efficiency of tall buildings with diagrid systems, providing valuable design insights [12] . Researchers proposed using diagrid exoskeletons for retrofitting preexisting RC structures, addressing challenges and potential benefits, providing valuable insights for retrofits [13] . Researchers studied the historical evolution of circular-planned diagrid systems in architecture through patent analysis and joint specifications, providing a historical perspective [14] .

CONCLUSION

Diagrid structural systems have gained significant popularity in the construction of high-rise buildings due to their exceptional structural efficiency and their ability to provide flexibility in architectural planning[1] . These systems are highly effective in resisting the lateral loads that are caused by wind or seismic activity, and author achieve this through the axial action of diagonals. There have been studies conducted on variable angle diagrids, which have the potential to reduce construction costs and minimize material usage[2].The optimization of diagonal angles is of paramount importance in order to achieve cost-effective and structurally sound designs. It is worth noting that the geometric form of diagrid tall buildings, including the shapes of floor plans, overall heights, and diagonal inclinations, significantly impacts the structural response in terms of displacements and rotations [3] . Diagrid structures, especially those with optimized diagonal angles, exhibit excellent seismic performance. Author capable of undergoing substantial deformations during earthquakes, thereby efficiently dissipating input energy. Numerous





Jay P Patel *et al.*,

papers have conducted comparative studies between diagrid structures and conventional frame structures[4] . The findings of these studies consistently show that diagrid structures outperform conventional frame structures in terms of lateral displacements, steel weight, and stiffness, particularly as the height of the building increases [5] . Diagrid structures have the advantage of consuming less concrete and steel compared to conventional frame structures, while still providing effective resistance to lateral loads[6] . Finding the optimal diagrid angle for a specific height requirement is crucial in order to achieve the best possible structural performance in high-rise buildings[7]. Parametric analysis plays a vital role in exploring the effects of various form parameters, such as tapering and plan shape, on the structural efficiency of tall buildings that utilize diagrid systems [8]. Diagrid systems are also being explored as retrofit options for existing reinforced concrete structures, offering a sustainable approach to improving the structural performance of older buildings[9]. The evolution of circular-planned diagrid systems is examined, with a shift in focus from overall configurations to joint details in patent holdings. This examination provides valuable insights into the development of diagrid systems and their potential applications in the future [14] .

REFERENCES

1. Bhat KA, Danish P. Analyzing different configurations of variable angle diagrid structures. *Materials Today: Proceedings*. 2021 Jan 1;42:821-6
2. Lacidogna G, Scaramozzino D, Carpinteri A. Influence of the geometrical shape on the structural behavior of diagrid tall buildings under lateral and torque actions. *Developments in the Built Environment*. 2020 May 1;2:100009.
3. Lacidogna G, Nitti G, Scaramozzino D, Carpinteri A. Diagrid systems coupled with closed-and open-section shear walls: Optimization of geometrical characteristics in tall buildings. *Procedia Manufacturing*. 2020 Jan 1;44:402-9.
4. Heshmati M, Khatami A, Shakib H. Seismic performance assessment of tubular diagrid structures with varying angles in tall steel buildings. In *Structures 2020 Jun 1 (Vol. 25, pp. 113-126)*. Elsevier.
5. Ardekani A, Dabbaghchian I, Alaghmandan M, Golabchi M, Hosseini SM, Mirghaderi SR. Parametric design of diagrid tall buildings regarding structural efficiency. *Architectural Science Review*. 2020 Jan 2;63(1):87-102.
6. Labò S, Passoni C, Marini A, Belleri A. Design of diagrid exoskeletons for the retrofit of existing RC buildings. *Engineering Structures*. 2020 Oct 1;220:110899.
7. Kinayoglu G, Şenyapılı B. Circular-Planned Diagrid Systems and an Interrelated Technique Using Planar Elements. *Nexus Network Journal*. 2018 Apr;20:215-33.
8. Sorathiya R, Pandey P. Study On Diagrid Structure Of Multistorey Building. *Development*. 2017 Apr;4(4).
9. Bhuta DC, Pareekh U. Comparative Study on Lateral Load Resisting System in Tall Building. *IJSTE–International Journal of Science Technology & Engineering*. 2016;2(1):320-6.
10. Shah MI, Mevada SV, Patel VB. Comparative study of diagrid structures with conventional frame structures. *Int J Eng Res Appl*. 2016 May;6(5):22-9.
11. Panchal NB, Patel VR. Diagrid structural system: Strategies to reduce lateral forces on high-rise buildings. *International Journal of Research in Engineering and Technology*. 2014 Apr;3(03):374-8.
12. Moon KS. Comparative evaluation of structural systems for tilted tall buildings. *International journal of high-rise buildings*. 2014;3(2):89-98.
13. Moon KS. Material-saving design strategies for tall building structures. In *CTBUH 8th world congress, Dubai 2008 Mar 3*.
14. Jani K, Patel PV. Analysis and design of diagrid structural system for high rise steel buildings. *Procedia Engineering*. 2013 Jan 1;51:92-100
15. Moon KS. Diagrid structures for complex-shaped tall buildings. *Procedia Engineering*. 2011 Jan 1;14:1343-50.
16. Mele E, Toreno M, Brandonisio G, De Luca A. Diagrid structures for tall buildings: case studies and design considerations. *The Structural Design of Tall and Special Buildings*. 2014 Feb 10;23(2):124-45.
17. Zhang C, Zhao F, Liu Y. Diagrid tube structures composed of straight diagonals with gradually varying angles. *The Structural Design of Tall and Special Buildings*. 2012 Apr;21(4):283-95.





Jay P Patel *et al.*,

18. Taranath BS. Structural analysis and design of tall buildings: Steel and composite construction. CRC press; 2016 Apr 19
19. Kim JS, Kim YS, Lho SH. Structural schematic design of a tall building in asan using the diagrid system. InCTBUH 8th World Congress 2008 2008 Mar 3. Dubai: CTBUH.
20. Indian Standard IS 1893:2016, "Criteria for Earthquake Resistant Design of Structures, Part 1: General Provisions and Buildings," Bureau of Indian Standards, New Delhi, pp. 1–44, 1893.
21. Indian Standard IS 875: Design Loads (Other than Earthquakes) for Buildings and Structures–Code of Practice–Part 3 Wind loads. Bureau of Indian Standards, New Delhi. 2015
22. Indian Standard IS 875: Design Loads (Other than Earthquakes) for Buildings and Structures–Code of Practice–Part 3 Wind loads. Bureau of Indian Standards, New Delhi. 2015.
23. Indian Standard IS 16700:2017, "Criteria for Structural Safety of Tall Concrete Buildings," India Bureau of Indian Standards, 2017.
24. Taranath BS. Reinforced concrete design of tall buildings. CRC press; 2009 Dec 14.

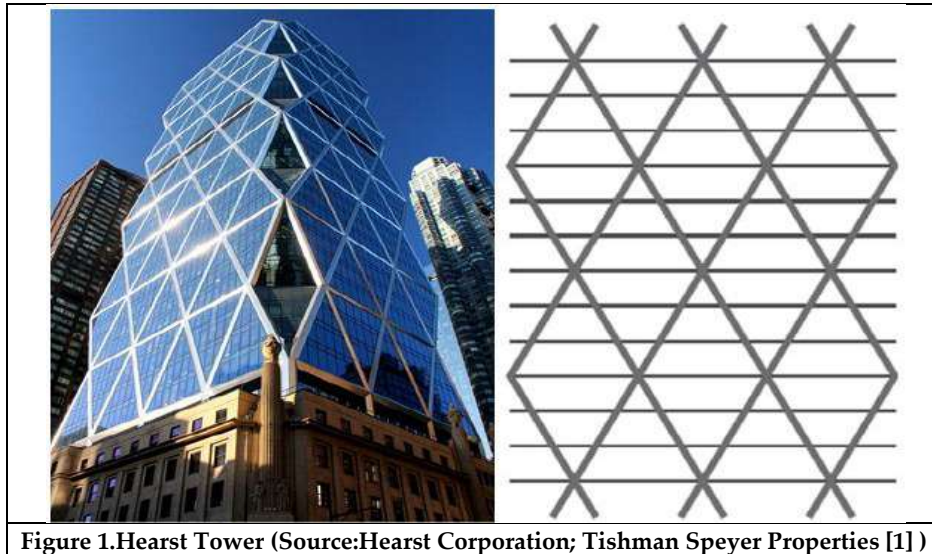


Figure 1.Hearst Tower (Source:Hearst Corporation; Tishman Speyer Properties [1])





Seismic Effect of Multi-Tower Connected with Sky Bridge-A Review

Dhodiya Dixika M^{1*}, Vishal A. Arekar², Vishalkumar B. Patel² and Pratiti M. Bhatt²

¹PG Research Scholar, Department of Structural Engineering, Birla Vishvakarma Mahavidyalaya Engineering college, Vallabh Vidyanagar, Gujarat, India.

²Assistant professor in Structural Engineering department, Birla Vishvakarma Mahavidyalaya Engineering college, Vallabh Vidyanagar, Gujarat, India

Received: 18 Oct 2023

Revised: 25 Oct 2023

Accepted: 31 Oct 2023

*Address for Correspondence

Dhodiya Dixika M

PG Research Scholar,

Department of Structural Engineering,

Birla Vishvakarma Mahavidyalaya Engineering college,

Vallabh Vidyanagar, Gujarat, India



This is an Open Access Journal / article distributed under the terms of the **Creative Commons Attribution License** (CC BY-NC-ND 3.0) which permits unrestricted use, distribution, and reproduction in any medium, provided the original work is properly cited. All rights reserved.

ABSTRACT

Towering structures such as twin towers are a symbol of a radical transformation of urban landscapes. Their avant-garde concepts are highly appealing to engineers and architects, transforming the urban landscape. In addition to being beautiful, these monumental wonders revitalize regional economy and modern metropolitan lifestyles. They provide a blend of imaginative architectural expression and useful urban function, addressing the pressing need for seismic resistance, particularly in earthquake-prone locations. The current study thoroughly examines the nuances of structural behaviour, safety protocols, and mass distribution. Planning and maintaining multi-tower complexes depend heavily on the invaluable knowledge that is produced by the ongoing research. Urban landscapes that are both aesthetically beautiful and long-lasting require this kind of information. There has been a drastic shift in urban areas.

Keywords: Tall Building, Sky bridge, Etabs, Twin tower, Seismic effect, Cross bracings

INTRODUCTION

Tall Building

A tall building, also known as a skyscraper or high-rise building, is a multi-story structure that is significantly taller than the surrounding normal buildings. It is typically characterized by having several floors and is designed for various uses such as residential, commercial, or mixed-use purposes [16]. The term "tall building" is commonly used to describe these types of structures [13]. While there is no universally accepted minimum height for a tall building, it is generally understood to be a structure that rises prominently above its urban surroundings [3].





Dhodiya Dixika *et al.*,

Twin-Tower

Twin towers are two tall buildings that are joined to one another. They are often constructed side by side or next to each other, functioning as a cohesive complex or unit. These twin towers are a prominent feature in densely populated urban areas [15]. They are designed to be resistant to various forces such as wind loads and seismic loads, making them more rigid and stable [12][20]. The structural connection between the towers, such as a sky-garden, sky-bridge, or corridor, enhances their ability to withstand these forces [9]. The behavior of twin towers with different heights connected by horizontal or inclined sky-bridges has been studied, and it has been found that the dynamic properties of the connected towers and the positioning of the sky-bridge influence their seismic response [6].

Sky bridge

An elevated, covered walkway that links two or more buildings or destinations at an elevated level above the ground is called a sky bridge, sometimes referred to as a skywalk or pedestrian bridge. By eliminating the need for pedestrians to descend to street level, these walkways are intended to give them a simple and safe route to cross busy roadways, metropolitan areas, and other impediments. Sky bridges can be anything from straightforward, useful links to architecturally noteworthy structures that improve the urban environment. They are usually built out of a variety of materials, such as glass, steel, or concrete [10] [12]. Modern cities' skylines, which are characterized by the rise of large structures and twin towers that reach the heavens, are always changing. Octagonal icons of human ambition, inventiveness, and urbanization, these towering architectural marvels have captured the imagination with their remarkable designs and unique verticality. High twin towers are redefining our cities and transforming our way of life and work as a result of our efforts to create sustainable urban environments and more efficient land use. Urban planners, engineers, and architects have all been captivated by tall buildings and twin towers because of their remarkable height, complex engineering, and captivating aesthetics. These buildings have the ability to revitalize cities' skylines and add to their energy on the cultural and economic aspects. Whether they are mixed-use developments, residential complexes, or commercial hubs, they are the result of the union of creative design with the pragmatic requirements of urban living.

Tall twin buildings joined by sky bridges are a remarkable example of the merging of imaginative design, practical urban living, and visual majesty in modern urban architecture. The human desire to remake our cities' skylines is embodied in these architectural wonders, which are frequently distinguished by their commanding presence and connected walkways that appear to defy gravity. The fact that these enormous buildings are susceptible to seismic activity in areas where earthquakes are common causes serious concerns, even though they provide diverse living and working conditions [18]. The study will examine the dynamic interaction between the sky bridges and the twin towers to clarify how these components affect the buildings' seismic reactions. We will also look at the cutting-edge materials, technologies, and building techniques that have been used to improve earthquake resilience. We aim to evaluate the effectiveness of these developments and their suitability for guaranteeing the longevity, usefulness, and safety of these constructions, especially in areas vulnerable to seismic activity. We will also evaluate the current legislative frameworks, building norms, and industry standards that control the development and upkeep of towering twin skyscrapers connected by sky bridges [16][19]. In order to preserve both the structural integrity of these famous metropolitan sites and the well-being of their tenants, this evaluation will offer insights into areas that could use renovation.

LITERATURE REVIEW

Abbood *et al.* [2018] [1], had analyzed twin 40 storey RC frame-wall structures horizontally coupled by structural links. A Finite Element software (CSI ETAB 2015) has been used to excitation. It was found that the link was more effectual in strengthening the system and reducing the responses when installed reducing the two floors and most effective in stiffening at approximately 0.8 of the building height. Wei *et al.* [2019] [2], had analyzed the seismic performance of an asymmetric high-rise structure made up of two towers of varying sizes joined diagonally by



**Dhodiya Dixika et al.,**

robust steel truss systems. Because of the intricate and asymmetrical structural arrangement, a thorough examination is necessary. The seismic reaction of a 1/45th scale model is assessed by shaking table experiments. The connecting trusses and rigid joints work remarkably well at high earthquake stresses, according to the results. The floors that link is primarily damaged, with little structural damage overall. The structure's exceptional seismic resilience to strong ground vibrations is highlighted by the majority of the lateral resistance components remaining elastic. Even in high torsional modes, the trusses' ability to coordinate translational and torsional movements is confirmed by the following building of a three-dimensional finite element model. This study emphasizes how important well-designed trusses are.

Pranamika *et al.* [2020] [3], had analyzed G+80 storey towers in ETAB software to obtain the storey drift, storey shear, base reaction and the result obtained for single tower compared with the results obtained for twin towers. In this paper Sky Way Bridge is provided at 50 storey and Cross bracings are provided to resist Lateral forces in it. It was found that when load applied in X, Y, and Z direction twin tower has more shear and stiffness in comparison to single tower whereas drift is more in case of single tower. Bhinde *et al.* [2020] [4], had analysed 40 and 50 storey Symmetric structure in ETAB software, in which links of different sizes are provide at the most efficient location and the model will be analysed with the response spectrum for zone (IV & V) and time history analysis for Bhuj earthquake in medium soil. It was analysed that the best location of link is $0.6H + 0.8H$ and the optimum width is $1.0B$. In 50 storey value of shear and displacement are higher in Time History Analysis.

Karthik *et al.* [2020] [5], had analysed G+30 storey tall structures to know the performance and economy of different lateral force-resisting systems. Various structural systems such as conventional, shear wall, truss belt, outrigger, diagrid, and fluid viscous damper are compared based on parameters like minimum story displacement and drift. All the building parameters are analysed in ETAB software, assuming the site location as BHUJ Gujarat, India. It was examined that comparing the shear wall system, truss belt system, outrigger system and diagrid structure system, Diagrid performs better in terms of displacement, drift, and time period. Bhavesh *et al.* [2020] [6], had analyzed the behaviors of structure G+20, G+25, and G+ 30 stories symmetrical twin tower without an underground basement, with 2, and 4 number of Basement. The paper focuses on the structural analysis of twin towers with a common basement and investigates the seismic response of the superstructure using various linear dynamic structure analysis approaches such as Equivalent Static Force Method (ESFM), Response Spectrum Method (RSM), and Time History Analysis (THA). It was found that when basements are their in-twin tower it is more sustainable as compared to without basements. The depth of basement is directly affected to maximum base shear but it can reduce storey drift.

Pei *et al.* [2020] [7], Using ambient vibration data as its primary source, this study presents a Bayesian model update technique that improves parameter estimation efficiency and addresses local optima problems. The structural modal parameters' most likely values and coefficients of variation are found using the Bayesian fast Fourier transform, which is then used to establish the weighting factors for the likelihood function. Next, by using previous knowledge as a regularization factor, a posterior probability density function is obtained. In order to find global optima in the posterior PDF, the study expands on the subset simulation optimization approach. Stiffness scaling variables in a 15-story shear building model are validated and then tested on a four-story frame structure. Application of the technique to a 13-story twin-tower masonry construction in the real world reveals its accuracy and potential for long-term structural health.

Wang *et al.* [2020] [8], had analyzed a multi-tower complex consisting of two identical tower buildings connected by a big chassis and shared basements in a commercial district building. Each tower is 156.85 meters high and has a frame-core tube structure. By contrasting the outcomes of single-tower modelling with SATWE software with multi-tower modelling with MIDAS software, the study evaluates the seismic response characteristics. Interestingly, the results show that the number of towers above the podium has increased while the seismic shear force at the podium has significantly decreased. This two-tower structure's vibration mode combines elements of the vibrations of each tower separately, showing a complicated interaction as opposed to a simple superposition of dynamic features. Manikkoth *et al.* [2021] [9], had analyzed the behavior of G+30 high rise buildings horizontally connected. The paper explores the



**Dhodiya Dixika et al.,**

usage of shear walls at different locations in a horizontally connected twin high-rise building, interconnected using a sky bridge. The study aims to assess the behavior of the structure under earthquake loads and examines parameters such as base shear, maximum allowable displacement, and stiffness using ETABS software. It was found that the maximum displacement decreases on addition on shear walls but base shear increases. And increasing in shear wall the maximum stiffness of the building is increases. It is expected that on providing skybridge at the one fourth height maximum stiffness and maximum base shear in x direction and three fourth height gives the least displacement.

Ahmad *et al.* [2021] [10], had analyzed the influence of installing sky bridges made of reinforced concrete to connect two nearby reinforced concrete buildings. The two structures were not intended to be combined into one, although these connections are frequently built for practical or architectural purposes. A deviation from typical seismic code procedures is required because rigidly linking these buildings results in structural anomalies. The effects of sky bridges at various levels are evaluated by the research using three models under earthquake circumstances. Members forces, vibration periods, drift, and mode shapes are all impacted by the results, which show notable changes in structural behavior. For securely integrating buildings that were initially constructed separately, the study provides insightful recommendations. Zaher *et al.* [2022] [11], had analysed The Address Jumeirah Resort is a high-rise building with a reinforced concrete structure, utilizing high-strength cement, Ground Granulated Blast-furnace Slag (GGBS), fly ash, and Micro Silica (MS).The building's shape on plan is a 130 m x 30 m ellipse with a void in the centre to increase daylight penetration and enhance views .The tower is aligned exactly with due north, with the narrow sides facing east and west to reduce solar heat gain. The building has three podium levels, with one tower consisting of hotel and serviced-branded apartment levels, and the other tower consisting of residential apartment levels. The tower is connected at the lobby and roof levels through multi-story skybridges, which also house a restaurant and an infinity pool. The construction sequence analysis accounted for creep and shrinkage, and monitoring survey results showed minimal differential deformations over time between vertical elements.

Hussain *et al.* [2022] [12], had analyzed the seismic response of structurally connected high-rise buildings of 117 m(G+38) and 93m(G+30) respectively, 21.11m apart, structurally connected means of single, double and triple horizontal and inclined sky-bridges. The response of the buildings is analyzed using dynamic analysis method in terms of time period, maximum storey displacement, storey drift, storey shear and base shear of the both buildings. It was found that when inclined sky bridge is used maximum displacement of the taller building, reduced up to 10-29%. When horizontal bridge is used maximum displacement of shorter building reduced up to 10%. It is depending upon number of sky bridges used. While using the combination of horizontal and inclined bridge, reduced displacement up to 29% for taller building and a slightly increased up to 4% for shorter building. Himali *et al.* [2023] [13], had analysed model of 25-storied connected tall buildings is studied with different location of sky bridges and dampers and shear wall system and linear viscos dampers are compared. The buildings are analysed by linear history analysis, response spectrum analysis and wind analysis. It was found that the tall structures linked with sky bridges and dampers are more effective in reducing various response like displacement, acceleration, storey drift.

Sagarkumar *et al.* [2023] [14], had analysed G+19 (60 m) twin towers connected at various heights is studied. The study focuses on the effective use and positioning of connecting beams in twin tower structures subjected to lateral loads. The study examines parameters in terms of storey displacement, storey drift and base shear using ETABS software. The building was analysed for Static and Dynamic analysis which is located in Vadodara zone III. It was found that for less storey shear, lesser storey drift and less maximum storey displacement safe peak earthquake is 39m, 57m and 18m respectively connecting the buildings to the passageway. Vishalkumar *et al.* [2023] [15], had analysed G+28 (85.98m) and G+24 (75 m) high rise and medium rise twin towers connected at various heights and spans is studied. The analysis of twin towers connected at various heights and spans, with a focus on the effectiveness and positioning of connecting beams in twin tower structures subjected to lateral loads. The study examines parameters such as storey displacement, drift, and base shear using ETABS software. The model will be analysed for Static and Dynamic condition and the structure was located in Ahmedabad zone III. Based on this study it was found that if the twin towers are parallel to each other and connected at a distance of $0.8H+5\%$ (where H is the



**Dhodiya Dixika et al.,**

height of the building) there is a reduction in maximum displacement while simultaneously increasing the base shear.

SUMMARY

Twin forty-story structures with structural linkages were the subject of the study, which looked at seismic responses. Links changed responses, indicating the need for careful design considerations with mass increasing and stiffness decreasing [1]. Study investigates an asymmetric high-rise building with steel truss connections. Shaking table tests demonstrate structural resilience to seismic forces and effective coordination of towers even under high torsional modes [2]. This paper compares twin towers with a single tower using ETABS software, focusing on storey drift, shear, and base reactions. It includes a skyway bridge at the 50th storey and cross bracings for lateral force resistance. ETABS is chosen for designing tall structures with concrete shear walls [3]. The study examines multi-tower structures with links, enhancing stability against wind and seismic forces. ETABS models are analyzed for storey displacement and base shear under lateral loading [4]. Research focuses on balancing tall structures for wind and seismic resilience. ETABS models 30-story buildings in Gujarat, India, comparing various lateral force-resisting systems. Diagrid and viscous dampers show superior performance, with viscous dampers being the most economical choice [5]. The study looks at the seismic response of twin towers while taking depth, basement connection, and height into account. Internal stress variations in the superstructure are revealed by several methods of linear dynamic analysis [6]. A Bayesian model updating method, enhanced by subset simulation optimization, refines structural parameters with ambient vibration data for improved accuracy. Validated with numerical and real-world cases, it benefits long-term structural health monitoring [7]. A multi-tower business building with a shared podium and huge chassis has a different seismic reaction than a single-tower building. Vibration modes become complex when the tower shear force grows and the potassium shear force diminishes [8]. In a dual high-rise building that is connected horizontally, the study looks into the effects of shear walls at different points. Based on base shear, displacement, and stiffness, the ETABS software models the structure's response to earthquakes [9]. The influence of using sky bridges to connect two independent buildings is examined in this study, which also provides safety recommendations and notes notable changes in structural behavior [10]. With its modern form and skybridge, the 77-story Address Jumeirah Resort in the Jumeirah Beach District presents special challenges for structural design and construction and has already established records [11]. The maximum displacement in the taller building is decreased by inclined bridges, according to this paper's study of the seismic response of two high-rise buildings connected by sky bridges [12]. 25-story connected tall buildings are studied, and shear wall and linear viscous damper systems are compared. One effective way to lessen displacement and other effects is by using sky bridges and dampers [13]. With an emphasis on the efficient use and positioning of connecting beams for lateral loads, this study employs ETABS software to examine connected G+19 twin towers at various heights in Vadodara Zone III. Measurements such as Base Shear, Drift, and Storey Displacement are looked at [14]. The G+28 and G+24 twin towers joined at different heights are analyzed in this study, with an emphasis on the efficient use and positioning of connecting beams for lateral loads. The ETABS software evaluates variables such as Base Shear, Drift, and Storey Displacement. For closely parallel structures, connections at $0.8H + 5\%$ distance prove to be cost-effective and long-lasting, resulting in significant reductions in displacement and drift [15].

CONCLUSION

Link placement has an impact on structural response, as demonstrated by numerical analysis, with the top two floors exhibiting the best results. This highlights the significance of connected building system design [1]. The seismic tests and numerical analysis confirm the reliability of the connected super high-rise structure, offering valuable insights for complex connected structure design [2]. Though the single tower drifts more than the twin tower, the double tower shows significantly greater shear and rigidity [3]. The analysis shows that, taking into account shear and displacement variations, the optimal link site for 40 and 50-story structures is $0.6H+0.8H$ with an optimal width of





Dhodiya Dixika et al.,

1.0B. There are resonance effects observed in 50-story buildings [4]. In comparison to alternative structural configurations, the study highlights the significant benefits in displacement and drift provided by the diagrid structural system, which has dampers installed on middle levels [5]. According to the study, base shear is greatly impacted by twin towers with basements, and depth is an important factor. The sustainability of basements is improved by structural geometry, which affects dynamic analysis [6]. The study introduces a Bayesian model updating method using subset simulation optimization, demonstrating effectiveness in structural parameter identification, particularly in a real-world twin-tower heritage building [7]. The complicated vibration modes impacted by podium coordination are shown by the modal analysis of twin towers. Twin towers show higher shear forces at the upper floors as a result of the interaction between the podium's increased rigidity [8]. Shear walls and sky bridge locations impact seismic performance. Adding shear walls reduces displacement and increases base shear and stiffness. Optimal performance involves shear walls on both sides, and a sky bridge at one fourth height [9]. Larger drifts, greater stresses, changed mode forms, and irregularities in structure can result from rigidly joining twin buildings with sky bridges. Options that are safer can include flexible connections or movement joints [10]. The Address Jumeirah Resort is a unique feat that has been recognized by Guinness World Records for its exceptional structural and architectural achievements, winning it numerous important accolades [11]. Inclined and horizontal sky-bridges impact storey shear, drift, and base shear. Multiple sky-bridges reduce displacement, showing directional influence [12]. Connected tall buildings require lateral load resistance, and the combination of shear walls and linear viscous dampers effectively reduces displacement, acceleration, and base shear [13]. The study highlights the importance of twin towers as a developing construction idea by determining safe passageway heights for them under various circumstances [14]. Design considerations are highlighted when twin towers are connected at specified distances, since this affects displacement, base shear, and drift in high-rise and medium-rise structures [15].

REFERENCES

1. Abbood IS, Mahmud M, Hanoon AN, Jaafar MS, Mussa MH. Seismic response analysis of linked twin tall buildings with structural coupling. *International Journal of Civil Engineering and Technology*. 2018 Nov;9(11):208-19.
2. Guo W, Zhai Z, Wang H, Liu Q, Xu K, Yu Z. Shaking table test and numerical analysis of an asymmetrical twin-tower super high-rise building connected with long-span steel truss. *The Structural Design of Tall and Special Buildings*. 2019 Sep;28(13): e1630.
3. Pranamika R, Dr. M Senthil Pandian. Comparison of twin towers to single tower under seismic loading using E-tabs. *International Journal Advanced Research Engineering a Technology*. 2020; 11(12), 2790–2809.
4. Bhide VN, Parekh PA, Pokar NR. Dynamic Analysis of Regular Twin Tall RCC Structure with Various Sizes of Links at Most Effective Location. *JETIR2006326 Journal of Emerging Technologies and Innovative Research*. 2020; 7(6), 2257–2261.
5. Batra A, Gupta S. Analysis of Tall Building with Different Lateral Force Resisting System.
6. Bhavesh Bhanajibhai J, Umravia, NB. Dynamic Analysis of the Twin-Tower High-Rise Structure with Basement. *International Advanced Research Journal in Science, Engineering and Technology*. 2020; 7(5); 94–102. <https://doi.org/10.17148/IARJSET.2020.7517>
7. Liz P, Huang S, Song M, Yang W (2021). Bayesian model updating of a twin-tower masonry structure through subset simulation optimization using ambient vibration data. *Journal of Civil Structural Health Monitoring*, 11(1), 129–148. <https://doi.org/10.1007/s13349-020-00443-y>
8. Wang L, Lei H. Structural analysis of a multi-tower building with a large chassis in a business district. In *IOP Conference Series: Earth and Environmental Science 2021* (Vol. 647, No. 1, p. 012175). IOP Publishing.
9. Manikkoth AS, Thomas E. Seismic analysis of horizontally connected high-rise building by different configuration of shear wall and the horizontal sky bridge. *International Research Journal of Engineering and Technology*. 2021; 8(7); 1770–1776.
10. Alomari J. Conceptual seismic analysis of two RC adjacent buildings with different dynamic properties connected horizontally by sky bridges. *Journal of Engineering Science and Technology*. 2021 Jun;16(3):2610-28.



**Dhodiya Dixika et al.,**

11. Hadow Z, Dannan Y. The Structural Engineering Design and Construction of the Highest Occupiable Skybridge in the World: The Address Jumeirah Resort, Dubai, UAE. *International Journal of High-Rise Buildings*. 2022;11(1):61-8. <https://doi.org/10.21022/IJHRB.2022.11.1.61>
12. Adnan Hussain S, Azeem MA, Minhaj Uddin A. Effect on Seismic Behaviour of Structurally connected Tall Buildings. *International Journal of Engineering Research and Applications*. 2022 12(9), 143–151. <https://doi.org/10.9790/9622-1209143151>
13. Vyas H, Mevada SV, Patel SB, Gupta A. Behavior of Connected Tall Buildings Installed with Dampers. *International Advanced Research Journal in Science Engineering and Technology* 2023; 10(5). <https://doi.org/10.17148/iarjset.2023.10513>
14. Pandya SV, Bansal P. An evaluation of twin tower type structure having connecting at various heights. *Journal of Emerging Technologies and Innovative Research* 2023; 10(4), 423–436.
15. Sureshbhai TV, Suthar AR. A parametric evaluation of twin tower structure having horizontal and vertical connection variations. *International Research Journal of Engineering and Technology* 2023; 10(6), 596–607.
16. Feng F. *Design and Analysis of Tall and Complex Structures*. 2018 United States: Matthew Deans.
17. IS 16700: 2017, Criteria for Structural Safety of Tall Concrete Buildings. 2017 November. New Delhi: Bureau of Indian Standards.
18. IS 1893 (Part 1): 2016, Criteria for Earthquake Resistant Design of Structures. 2016 November. New Delhi: Bureau of Indian Standards.
19. IS 800: 2007, General Construction in Steel - Code of Practice. 2007 December. New Delhi: Bureau of Indian Standards.
20. IS 875 (Part 3): 2015, Design Loads (Other than Earthquake) for Buildings and Structures - Code of Practice. 2015 April. New Delhi: Bureau of Indian Standards.



Figure 9 Twin tower (Source: -International journal of High-Rise Building)
<https://doi.org/10.21022/IJHRB.2022.11.1.61> [11]





Backstay Effect on Tall Structures with Podium Structure -A Review

Parth G.Rathod^{1*}, Sumant B.Patel² and PratitiM.Bhatt

¹PG Research Scholar, Department of Structural Engineering, Birla Vishvakarma Mahavidyalaya, Vallabh Vidyanagar, Gujarat, India

²Associate Professor, Structural Engineering department, Birla Vishvakarma Mahavidyalaya, Vallabh Vidyanagar, Gujarat, India

³Assistant Professor in Structural Engineering Department, Birla Vishvakarma Mahavidyalaya, Vallabh Vidyanagar, Gujarat, India

Received: 18 Oct 2023

Revised: 25 Oct 2023

Accepted: 31 Oct 2023

*Address for Correspondence

Parth G. Rathod

PG Research Scholar,
Department of Structural Engineering,
Birla Vishvakarma Mahavidyalaya,
Vallabh Vidyanagar,
Gujarat, India



This is an Open Access Journal / article distributed under the terms of the **Creative Commons Attribution License** (CC BY-NC-ND 3.0) which permits unrestricted use, distribution, and reproduction in any medium, provided the original work is properly cited. All rights reserved.

ABSTRACT

Tall buildings have become integral to urban landscapes, addressing the demand for space in densely populated cities worldwide. Designing such structures presents complex challenges, particularly in earthquake-prone areas. Understanding the "Backstay Effect" is pivotal, especially in podium-configured buildings. This effect requires a fresh perspective, incorporating a cantilever analogy with a back span to consider the podium's lateral stiffness, unlike conventional methods that treat shear walls as simple cantilevers. The Backstay Effect involves transferring seismic forces from the tower to the podium, profoundly impacting lateral stability and seismic performance. It relies on floor diaphragms and significantly bolsters safety by countering seismic overturning forces. Mastery of this phenomenon is vital for structural design and earthquake resilience, offering engineers and researchers a unique challenge and an opportunity for innovative design and analysis techniques.

Keywords: Tall structures, Podium, Backstay effect, Seismic performance, Lateral displacement, ETABs.

INTRODUCTION

Tall structures have become integrated into urban landscapes all over the world, providing answers to the rising need for commercial, residential, and mixed-use spaces in densely populated urban regions. Engineers and architects are tasked with the difficult task of creating structures that can survive a variety of natural pressures,





Parth G Rathod *et al.*,

including seismic activity, while the race to the sky continues. Understanding and utilizing the "Backstay Effect" is one of the most important aspects of designing tall structures, particularly those with a podium configuration. The "Backstay Effect" is a special and complex phenomenon that affects how tall structures with podiums behave structurally. The interaction between the more flexible tower portion and the inflexible podium portion of these constructions gives birth to this phenomenon. The backstay effect adds a new level of study, where a cantilever analogy with a back span is required to account for the effects of the podium's significant lateral stiffness. Traditional structural design methodologies frequently treat shear walls as straightforward cantilever beams.[7] The backstay effect is the process by which lateral forces from the tower's seismic force-resistant parts are transferred to other podium elements. Tall buildings' lateral stability and seismic performance are strongly impacted by this transfer, which is typically made possible by floor diaphragms. It contributes to the overall stability and safety of these structures by serving as a vital mechanism to resist the overturning forces brought on by seismic events.[10]

The backstay effect must be understood and quantified to assess the seismic performance and safety of tall structures as well as their structural design. Because of these phenomena, structural engineers and researchers have a new task and chance to create cutting-edge design and analysis techniques that guarantee the structural integrity of tall structures with podium arrangements.[4] Environmental factors, such as earthquakes. Understanding and utilizing the "Backstay Effect" is one of the most important aspects of designing tall structures, especially those with a podium configuration. The "Backstay Effect" is a special and complex phenomenon that affects how tall structures with podiums behave structurally. The interaction between the more flexible tower portion and the inflexible podium portion of these constructions gives birth to this phenomenon. The backstay effect adds a new level of study, where a cantilever analogy with a back span is required to account for the effects of the podium's significant lateral stiffness. Traditional structural design methodologies frequently treat shear walls as straightforward cantilever beams.[13]

The backstay effect is the process by which lateral forces from the tower's seismic force-resistant parts are transferred to other podium elements. Tall buildings' lateral stability and seismic performance are strongly impacted by this transfer, which is typically made possible by floor diaphragms. It contributes to the overall safety and stability of these structures by serving as an essential mechanism to resist the overturning forces brought on by seismic events.[10] The backstay effect must be understood and quantified in order to assess the seismic performance and safety of tall structures as well as their structural design. Because of these phenomena, structural engineers and researchers have a new task and chance to create cutting-edge design and analysis techniques that guarantee the structural integrity of tall structures with podium arrangements.[15] They concentrated on how a setback affected the structure's dynamic response and design parameters to enhance the setback building's resistance to lateral stresses. The backstay effect is especially noticeable in structures that are attached to the base structure and have a distinct lateral system (shear wall, corewall, etc.). A significant amount of research has been done on the displacement parameter for a single tower connected by a podium structure, where the podium structure's number of stories is variable [9]. The current study examines how the top displacement behavior of a single tower structure changes when the podium structure's storey count increases. The strutting action and the differential displacement created at the interface level of the centrally positioned tower and the tower offset from the podium center are analyzed to establish the best location for the tower on the podium structure. This study also presents the amount of backstay forces created at the podium tower interface level [9].

LITERATURE REVIEW

Yacoubian *et al.* [2017] [1] High-rise buildings with podiums surrounding the tower walls are often preferred due to the flexibility of the structure. In this study, the results showed that the parameters of the podiums of tower walls can be very different. In the study, it was found that the support forces on the foundation plane were incompatible with the changes in the tower wall lateral pressures on the ground above and below the podium-tower interface. These activities were found to lead directly to shear forces in the inner tower wall above the



**Parth G Rathod et al.,**

interface. Taquiuddin *et al.* [2019] [2] in this research primarily focused on investigating in-plane strutting forces and in-plane floor deformation at the interface between the tower and podium in tower-podium structures. The study delved into the reactive forces generated at the tower-podium junction and their impact on structures of this type. The research was conducted on two categories of podium buildings: 1) a 3B+G+50 configuration and 2) a 3B+G+9 setup. In CSI ETABS, various analysis scenarios were examined by modifying the width of the podium while keeping the tower's dimensions constant. The diaphragms were modeled as semi-rigid flat slabs/flat plates. Additionally, the study included variations in column spacing to assess their effects. The study compared the structural response to wind loads. The comparative study, based on outputs from the ETABS models that included. Parameters like displacements, drifts, axial forces, and shell stresses, revealed important insights. Notably, it was found that assuming a rigid diaphragm at the podium levels suppresses the generation of in-plane forces at those levels. Furthermore, reducing the spacing between columns led to an increase in-plane strutting forces in the diaphragms. Interestingly, the use of podiums helped reduce tower displacements, while increasing the podium's size had no significant impact on drift. Geetha *et al.* [2019] [3] the paper explores the seismic performance of a tall multi-storey tower connected to a substantial podium. The study specifically investigates how the construction of a single tower linked to a shared podium responds to earthquake forces at the interface level. To achieve this, a modeling simulation was developed using ETABS, incorporating varying podium and tower heights. These models were subjected to analysis using both static and response spectrum techniques. The research aimed to assess the impact of the analysis methods, namely static analogues and response spectrum techniques, on the displacement of the tower's upper section and its reduction at the base where it connects to the podium structure.

Kush *et al.* [2020] [4] have been the lateral load bearing system that supports the floor and subsurface partitions attached to the basement walls. To achieve this, several models with different geometrical patterns were considered to study the actual behavior of the building under backing effects. Prepare the model using the minimum and maximum stiffness given in IS 16700:2017 and perform rigorous testing to check the suitability of the building. Following this example, the podium perimeter curtain wall structure has the largest shear inversion, which reduces the displacement of the building. The paper also observes that beams close to the podium section produce almost 3 times as much axial force as they produce, which must be controlled in building design. The main idea of this study is to evaluate the results by modelling the podium and tower when constructing a tower with a podium, which leads to a stronger, better service and operation. Nandi *et al.* [2020] [5] have been studied Backstay Effect of Diaphragm in Tall Building In this study, the back gauge effect was investigated by using external retaining walls for low and high standards as specified in the IS: 16700-2017 tall building regulation. This work creates structures with low to high floors and rigid and semi-rigid diaphragms. Considering the podium floor diaphragms as semi-rigid and rigid diaphragms, the effect of diaphragm flexibility on the rear support cable forces at the tower podium interface level is analyzed. The effect of the center and angle placement of the tower on the back gauge beam was also investigated. Two examples of 20-storey and 40-storey frame structures were selected to conduct a comparative study of assembly and flexibility. The effect of the backings increases with the weight of the structure, resulting in a corresponding increase in the cutting base. The author concluded that when the tower is in the center of the field, it gives better results than when placed in a corner.

Badami *et al.* [2020] [6] the study uses the "ETABS" program for 3-D modeling and design considerations according to Indian Standards. The analysis focuses on measuring structural efficiency through parameters such as time period, storey displacement, drift, lateral displacement, base shear values, and core moments. The importance of lateral loads, particularly wind loads, is highlighted as a major challenge in the design and construction of tall buildings. Wind loads can cause uncomfortable horizontal movements and excessive vibrations, leading to both structural and non-structural damage. The conclusions of the study emphasize the influence of structure height and frame stiffness on the interaction between walls and frames in determining the lateral stiffness of the system. Champaneriya *et al.* [2021] [7] have studied The Effect of Backstay on Tall Structure with Podium Structure this study the authors' goal in this research was to comprehend the realistic behavior of such structures under lateral loads while taking into the backstay effect, as defined by IS: 16700:2017. To understand the variations in the shear force distribution among structural elements when the tower and Podium are model together, a sensitivity analysis



**Parth G Rathod et al.,**

was performed as per IS:16700:2017 considerations, taking into the stiffness parameters given in the code & the variations in force distribution were compared to structures that did not have a backstay effect. It was concluded that by increasing podium height, the backstay forces can be increased. It was also concluded that by increasing the thickness of podium diaphragms and area of Podium, the backstay forces can be increased. Jamal *et al.* [2022] [8] have studied Study on Effect of Podium Interference on High Rise Building for Seismic Loads for the purposes of this study, buildings with G+4 or more floors and a height of at least 510 feet (15 meters) are considered tall buildings under the 2003 Construction Code. A 15 storey RCC lateral load resisting structures with and without podiums are modelled using the extended 3D analysis of building system (ETABS) software. His analysis Linear Static and response spectrum Analysis performed in all models of G+11 storey Structure. The results which are attained by these Analysis are associated by the storey displacement and storey drift. Rangani *et al.* [2022] [9] have studied Benefits of Backstay Effect in Design of Podium Structure for Tall Building as Per IS 16700:2017 show the displacement parameter for single tower connected by a podium structure with different floors. A detailed study of the differences between backings, support effects, and podium-tower interface layers is lacking. This study was carried out to overcome this limitation. In this study, the change behavior of the ceiling of a single-towered structure as the number of floors of a podium structure increase was investigated. To determine the best position of the towers in the podium model, the collision probability and the difference between the intersection of the central towers and the towers offset from the center of the podium were examined. This article also shows the magnitude of the backing cable force produced by the podium-tower interface layer.

Bhatu *et al.* [2022] [10] in this research focuses on modelling techniques for multiple towers with a common podium and understanding their behavior under horizontal forces, considering the backstay effect specified in IS: 16700:2017. Different models are prepared by varying the podium height and the number of towers in the structure, and a comparative study is conducted on single towers with a podium and multiple towers with a common podium, with and without a shear wall at the periphery of the podium. The study utilizes the equivalent static method and Response spectrum method for structural analysis, using ETABS software. The resistance in the podium diaphragms provides the necessary stiffness for the structure, and the podium and backstay effects are not limited to tall buildings only. They can also occur in low and mid-rise buildings where the stiffness of lateral elements is reduced, such as building setbacks or step backs. The research aims to comprehend the phenomena of backstay observed in multiple towers with a common podium by referring to the guidelines in IS 16700: 2017. Solanki *et al.* [2022] [11] study the effect of different podium shapes and grading on the backstay effect in multi-storey models. They found that semi-rigid action at the podium level enhances the backstay effect compared to traditional rigid action. They also observed that the podium shape and grading improve the shear-reversal effect, leading to reduced base shear and base moment. Naik *et al.* [2023] [12] The authors compare structures with and without the inclusion of podiums to analyze the effects on various structural parameters such as lateral displacement, storey shear, storey drift, time period, and backstay effect. The study also includes sensitivity analysis using upper and lower bound stiffness modifiers and considers varying structural configurations of the podium structure by changing their height and surface area. The results of the analysis are expressed in terms of lateral displacement, base shear, time- period, storey drift, and shear reversed, providing insights into the impact of backstay on these structural parameters.

SUMMARY

The flexibility benefits of such structures are highlighted by Yacoubian *et al.* They also talk about how changes in podium characteristics can result in incompatible support forces and shear forces [1]. Md Taquiuddin *et al.* the impacts of modifications to podium width, column spacing, and size are examined with a focus on in-plane strutting forces and in-plane floor deformation at the tower-podium interface [2]. Geetha *et al.* investigates the seismic behavior of big podiums and tall, multi-story towers, taking into account various tower and podium heights and their impacts during earthquakes [3]. In their analysis of the lateral load-bearing system, Kush Shah *et al.* also cover podium perimeter curtain walls' ability to lessen shear forces and improve structural performance





Parth G Rathod *et al.*,

[4]. Nandi A. *et al.* Studies the backstay effect of diaphragms in tall buildings, analyzing the impact of diaphragm flexibility on rear support cable forces [5]. Badami *et al.*'s study employs "ETABS" for 3-D modeling and design according to Indian Standards. It underscores wind loads as a challenge, assessing structural efficiency, emphasizing height and frame stiffness influence [6]. Jamal M.D. *et al.* Focuses on the effects of podium interference during seismic loads and analyzes structural behavior using linear static and response spectrum analysis [7]. Rangani B. *et al.* investigate the advantages of the backstay effect in designing podium constructions and evaluate how the number of podium floors influences the behavior of the building [8]. Bhatu N. *et al.* focuses on modeling methods for numerous towers sharing a podium and contrasts their behavior with that of single towers with or without shear walls at the podium's edge [9]. Champaneriya K. *et al.* focuses on shear force distribution using sensitivity studies to comprehend the implications of backstay on tall constructions with podiums [10]. The backstay effect in multi-storey models is investigated by Solanki C. *et al.* They find that semi-rigid action increases the backstay effect and decreases base shear and moment [11]. R. Naik, C. Solanki, *et al.* used stiffness modifiers to conduct a sensitivity analysis and evaluate constructions with and without podiums. They looked at variables such lateral displacement, storey shear, drift, time period, and backstay effect, and they discovered how podiums influence these measurements [12].

CONCLUSION

The Paper discuss various aspects of the impact of podium structures on tall buildings, especially in the context of seismic performance and structural behavior. the function of podium structures in lowering top displacements and drift during seismic events.[3][8] Torsion and Deflection in Horizontal Offset Buildings: Various restraint load changes that may impact structural safety are among the challenges encountered in horizontal offset buildings using podiums.[2] The significance of the podium's perimeter curtain wall structure is examined in relation to mitigating building displacement. Beams close to the podium area are of particular concern because they could be subject to higher axial forces.[4] Backstay Effect: Studies on this phenomenon in diaphragms show that it is correlated with the weight of the structure and that central tower placement is the best course of action.[2] Advantages of the Backstay Effect: The study emphasizes the backstay effect's advantages for podium structures and emphasizes how it helps to mitigate structural problems.[9] Many Towers with a Common Podium: Research on several towers with a common podium emphasizes the role odium diaphragms play in supplying the required structural rigidity.[10] Sensitivity Analysis and Force Distribution: When modelling the tower and podium jointly, sensitivity analysis investigates differences in shear force distribution. It implies that increased backstay forces may result from raising the podium height and diaphragm thickness.[7] In-Plane Strutting Forces: Studies on the relationship between in-plane strutting forces and floor deformation at the interface between the tower and the podium indicate that while reducing column spacing increases strutting forces, a rigid diaphragm assumption decreases in-plane forces.[2] In conclusion, the body of research underlines the significance of podium structures for seismic performance and tall building design. With the right podium design, displacement can be decreased, structural stability can be increased, and seismic events can be more safely navigated. These studies have also stressed the backstay effect and the need to take numerous design factors into account in podium buildings. When creating tall buildings with podiums, architects and engineers can benefit from these insights.

REFERENCES

1. Yacoubian M, Lam N, Lumantarna E, Wilson JL. Effects of podium interference on shear force distributions in tower walls supporting tall buildings. *Engineering Structures*. 2017 Oct 1; 148:639-59.
2. Shah K, Desai H, Shah D. Effect of backstay on 3B+ G+ 20 storey RCC building. In *National Conference on Structural Engineering 2020 Aug (Vol. 6, No. 9)*.
3. Kamath K. Seismic performance of a tall multi storey tower connected by a large podium. *International Journal of Recent Technology and Engineering*. 2019 Jul 1;8(2):3545-51.





Parth G Rathod et al.,

4. Shah K, Desai H, Shah D. Effect of backstay on 3B+ G+ 20 storey RCC building. In National Conference on Structural Engineering 2020 Aug (Vol. 6, No. 9).
5. Nandi AK, Jairaj C. Backstay Effect of Diaphragm in Tall Building. sl: International Journal of Innovative Technology and Exploring Engineering (IJITEE). 2020;9(3).
6. Badami S, Suresh MR. A study on behavior of structural systems for tall buildings subjected to lateral loads. IJERT. 2014 Jul;3(7):2278- 0181.
7. Champaneriya KB, Patel VB, Desai AN. Effect of Backstay on Tall Structure with Podium Structure. International Journal of Advanced Research in Science, Communication and Technology 2021, 175–183.
8. Jamal MD, Kalyani PSK. Study on effect of podium interference on high rise building for seismic loads. International Journal of Advanced Research in Science, Communication and Technology. 2022;303–8.
9. Rangani HB, Dr. Vinubhai RP. Benefits of backstay effect in design of podium structure for tall building as per IS 16700:2017. International Journal of Advanced Research in Science, Communication and Technology.
10. Bhatu N, Patel VB, Bhatt PM. Effect of backstay on tall structures with podium. ;9(6):47–61519
11. Lalit SC, Patel VKB, Desai AN. Effect of podium configuration on backstay effect of structure. 2023;10(4).
12. Naik R, John R, Joshi D. Backstay Effect Due to Podium Structure Interaction. Irjet.net. 2008.
13. Rad BR, Adebar P. Seismic design of high-rise concrete walls: Reverse shear due to diaphragms below flexural hinge. 2009;135(8):916–24.
14. Modeling and Acceptance Criteria for Seismic Design and Analysis of Tall Buildings Task 7 Report for the Tall Buildings Initiative Published jointly by the Applied Technology Council. (2010).
15. Rajae Rad, B., & Adebar, P. (n.d.). Seismic Design of High- Rise Concrete Walls: Reverse Shear due to Diaphragms below Flexural Hinge. <https://doi.org/10.1061/ASCE0733-94452009135:8>

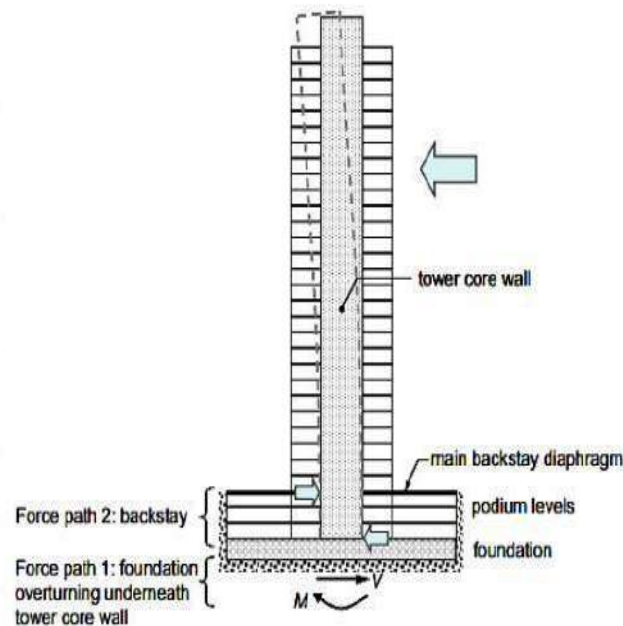


Figure 1 Backstay action in a podium-tower (Source - PEER/ATC 72-1[14])





An Empowering Women in STEM: Bridging Gaps and Fostering Inclusivity for Sustainable Careers

Dharmesh G. Patel^{1*}, Kinjal Gandhi², Vishal Polara³ and Nihali Jain⁴

¹Information Technology Department, BVM Engineering College, V.V.Nagar, Gujarat, India

²Department of Computer Engineering, Devang Patel Institute of Advance Technology & Research (DEPSTAR), Faculty of Technology & Engineering (FTE), Charotar University of Science & Technology, Changa, Gujarat, India

³Information Technology Department, BVM Engineering College, V.V.Nagar, Gujarat, India

⁴School of Pharmacy, ITM (SLS) Baroda University, Paldi, Near Jarod, Vadodara, Gujarat, India.

Received: 18 Oct 2023

Revised: 25 Oct 2023

Accepted: 31 Oct 2023

*Address for Correspondence

Dharmesh G. Patel

Information Technology Department,

BVM Engineering College,

V.V.Nagar, 388120,

Gujarat, India

E. mail: dharmesh.patel@bvmengineering.ac.in



This is an Open Access Journal / article distributed under the terms of the **Creative Commons Attribution License** (CC BY-NC-ND 3.0) which permits unrestricted use, distribution, and reproduction in any medium, provided the original work is properly cited. All rights reserved.

ABSTRACT

In the ever-evolving landscape of science and technology, women have consistently proven their mettle, contributing significantly to innovation, research, and development. However, gender disparities persist in these fields. Historically, women have encountered barriers in pursuing STEM (Science, Technology, Engineering, and Mathematics) careers, including societal expectations, biases, and lack of representation. Despite these challenges, numerous pioneering women scientists and technologists have shattered glass ceilings, inspiring future generations. Initiatives promoting STEM education for girls, scholarships, and mentorship programs are gradually bridging the gender gap. Representation matters, Seeing women in leadership roles within scientific and technological fields provides essential role models for young girls aspiring to pursue careers in these areas. Efforts to highlight the achievements of women scientists and technologists through media, conferences, and awards are essential in challenging stereotypes and encouraging more women to enter these fields. Mentorship programs play a crucial role in nurturing talent. Establishing mentorship initiatives where experienced women scientists guide and support younger professionals can provide invaluable insights, boosting confidence and promoting a sense of belonging. Additionally, creating supportive networks where women can share experiences and advice fosters a sense of community and solidarity.

Keywords: Women in STEM, Gender Equality, Sustainable careers, Inclusive Innovation



Dharmesh G Patel *et al.*,

INTRODUCTION

Educational institutions and organizations can actively contribute to gender equality by promoting awareness about the contributions of women in STEM. Incorporating diverse perspectives into curricula and organizing workshops and seminars on gender biases and inclusivity can help create an inclusive learning environment [1]. Companies and research institutions play a pivotal role in ensuring gender equality. Implementing family-friendly policies, such as parental leave and flexible work hours, can enable women to balance their professional and personal lives effectively [2, 3]. Moreover, recognizing and addressing unconscious biases within workplaces can create a more equitable atmosphere for all employees. Promoting gender equality stands as a global priority for UNESCO. Across the world, there are 122 million girls and 128 million boys who are not attending school. Furthermore, a significant number of adults, especially women, lack basic reading skills.

UNESCO emphasizes the need for gender equality in various aspects of education, including access, content, teaching methods, learning environments, outcomes, and subsequent life and work opportunities. The UNESCO Strategy for gender equality in and through education (2019-2025) is dedicated to a comprehensive transformation within the education system. This transformation is aimed at benefiting all learners equally and is centered around three main areas: improving data collection for informed decision-making, enhancing legal and policy frameworks to uphold rights, and implementing better teaching and learning methods to empower individuals [4]. The Global Gender Gap Report highlights that no country has achieved complete gender parity yet. As of 2021, the Global Gender Gap score stands at 67.7%, indicating a remaining gender gap of 32.3% [14]. This score assesses gender-based disparities in four main areas: economic participation and opportunity, educational attainment, health and survival, and political empowerment. Progress has been made, with 95% of educational attainment gaps already closed. However, gender disparities persist in higher education globally, despite most countries achieving full gender parity in tertiary education enrollment rates [15].

EDUCASTEM 2030

UNESCO Mobilization and Advocacy Initiative for Girls and Women's Education in Science, Technology, Engineering and Mathematics in Brazil

In response to the challenging situation that involves the exclusion of girls and women from STEM fields, UNESCO in Brazil took an innovative approach in 2022. They brought together various partners and launched this nationwide initiative. Through training programs for teachers and students, communication and advocacy efforts, as well as network mapping, this initiative comprehensively addresses and aims to have a positive impact on identified areas (Individual, Social, School, and Family) to reverse the trend of exclusion.

Project objective

Based on the fundamental principle of Agenda 2030, which advocates for inclusivity, the #EDUCASTEM2030 project aims to raise awareness and bring about transformation. It does so through a pedagogical approach within schools, encouraging life projects for both girls and boys. The project places particular emphasis on students belonging to marginalized social groups, including black, indigenous, quilombolas, LGBTI+, and low-income individuals, ensuring that no one is left behind.

UNESCO has identified key factors that impact the engagement, progression, and achievements of girls and women in STEM education. These factors serve as vital areas for targeted intervention to address this pressing issue. They include:

- A. **Individual:** Girls' choices regarding their studies and careers are influenced by psychological factors, shaping their interest, learning, motivation, persistence, and dedication to STEM fields. Gender stereotypes related to STEM persist throughout the socialization process, affecting their decisions.



**Dharmesh G Patel et al.,**

- B. **Family:** The influence of family members is significant; their values, home environment, experiences, and encouragement can profoundly impact girls' participation and academic performance in STEM subjects.
- C. **Social:** Cultural and societal norms play a crucial role in shaping girls' perceptions of their abilities, societal roles, career options, and life aspirations. The level of gender equality within society directly influences girls' involvement and outcomes in STEM fields.
- D. **School:** Disparities in the involvement of girls and boys in STEM education emerge early, often during childhood education. Differences are noticeable in activities related to science and mathematics, becoming more pronounced as students' progress to higher education levels [5].

Addressing these factors strategically is essential to fostering gender equality and encouraging greater participation of girls and women in STEM education and careers.

SMRITI IRANI, the Minister for Women and Children Development of India, highlighted that unlike many parts of the world, India has achieved a remarkable balance in the involvement of men and women in STEM fields. She discussed several government initiatives, including the "Digital India Programme," national scholarships, and an online campaign called "STEM Stars," which celebrates accomplished women in science and technology. India has enrolled approximately 123 million girls in educational programs promoting science and technology in schools. Additionally, efforts are underway to train rural and marginalized women in using essential tools like mobile phones. The country has also addressed infrastructural challenges, leading to one of the world's lowest costs for digital connectivity. Emphasizing the significance of public-private collaborations, including partnerships with companies specializing in cutting-edge fields such as artificial intelligence and robotics, was also underscored by the minister [6].

Empowering Women Entrepreneurs

Encouraging women to venture into entrepreneurship in science and technology can lead to groundbreaking innovations. Providing funding opportunities, business mentorship, and networking platforms can empower women entrepreneurs to transform their ideas into successful ventures, contributing significantly to the industry [7]. In the dynamic realm of science and technology, women have emerged as pivotal contributors, despite facing persistent challenges.

- A. Debjani Ghosh, the esteemed President of NASSCOM, emphasizes the need for diversity in tech management. Encouraging initiatives, such as programs showcasing female coders and STEM scholarships, are vital to inspire the next generation of women in STEM [8].
- B. Gargi B Dasgupta, IBM Distinguished Engineer, advocates for diverse voices in STEM, essential for innovation. IBM's STEM for Girls program not only promotes coding but also integrates life skills, gender literacy, and career development, empowering young girls to dream big [9].
- C. Neha Bagaria, Founder & CEO of JobForHer, underscores the importance of digitization. To combat gender bias in algorithms, skilling programs, mentorships, and networking platforms are being deployed. However, challenges persist in rural areas. Amrita Gangotra, Founder & MD, ITyukt Digital Solutions, emphasizes the urgency of encouraging STEM in rural regions [10].
- D. Dr. Sanghamitra Bandyopadhyay, the first female Director of Indian Statistical Institute, Kolkata, shares her experiences balancing professional and personal life. She advocates for more research fellowships for women, providing age relaxations to bridge career gaps [11].
- E. Dr. Ayesha Chaudhary, a driving force behind the Atal Innovation Mission, encourages women to defy stereotypes in STEM. She believes a fearless mindset and diverse career choices are key [12].
- F. Dr. Purnima Devi Barman, a wildlife biologist, leads the Hargila Army, a movement conserving the endangered greater adjutant storks. Despite challenges in a male-dominated field, the Hargila Army showcases women's impactful role in conservation [13].

Research indicates that enhancing gender diversity in STEM fields can enhance problem-solving abilities and foster better innovations [16]. This increased diversity not only contributes to gender equality but also has substantial impacts on economic development [14]. Quirós and colleagues (2018) found that a higher representation of women in





Dharmesh G Patel *et al.*,

digital occupations could significantly boost the European Gross Domestic Product (GDP), potentially adding up to 16 trillion euros annually in the European context [17]. Empowering women in science and technology requires concerted efforts from education, government, and corporations. By addressing biases, offering mentorships, and providing educational opportunities, we can pave the way for a sustainable and inclusive future for women in STEM.

CONCLUSION

Creating sustainable careers for women in science and technology is not just a matter of equality; it's a necessity for fostering innovation and driving societal progress. By breaking barriers, promoting education, providing mentorship, and ensuring workplace inclusivity, we can harness the full potential of women in these fields. As we celebrate the achievements of women in science and technology, let us continue to advocate for a future where every aspiring female scientist or technologist can thrive and contribute meaningfully, paving the way for a more diverse, inclusive, and innovative world.

REFERENCES

1. Eagly AH, and Chaiken S (1998). Attitude structure and function. In *The Handbook of Social Psychology*, Vols, Gilbert DT, ed. (New York, NY, US: McGraw-Hill, x), pp. 1–2. [Google Scholar]
2. Finn, D., & Donovan, A. (2013). *PwC's NextGen: A global generational study. Evolving talent strategy to match the new workforce reality*. Accessed 29 June, 2017. (pp. 1–16). Price Waterhouse Coopers.
3. Deloitte. (2018). *Deloitte millennial survey*. Accessed October 24, 2018. <https://www2.deloitte.com/global/en/pages/about-deloitte/articles/millennialsurvey.html>.
4. UNESCO. (2023, September 28). What you need to know about how UNESCO advances education and gender equality. Retrieved October 14, 2023, from <https://www.unesco.org/en/gender-equality/education/need-know>
5. UNESCO. (2023, October 10). #EDUCASTEM2030. UNESCO. <https://www.unesco.org/en/articles/educastem2030>
6. United Nations. (2023, September 19). Increased Women's, Girls' Participation in Digital Technology Crucial to Economies, Global Sustainability, Speakers Tell Commission, as Session Continues. [Press release]. <https://press.un.org/en/2023/wom2224.doc.htm>
7. OECD. (2023, September 22). Bridging the digital gender divide include, upskill, innovate. <https://www.oecd.org/digital/bridging-the-digital-gender-divide.pdf>
8. Srivastava, S. (2021, March 8). Women in STEM: Breaking Barriers and Inspiring Change. News18. <https://www.news18.com/opinion/opinion-women-in-stem-breaking-barriers-and-inspiring-change-8385673.html>
9. Dasgupta, G. (2019, September 27). Here's how IBM is increasing women participation in STEM. ET CIO. <https://cio.economictimes.indiatimes.com/news/strategy-and-management/heres-how-ibm-is-increasing-women-participation-in-stem/71313170>
10. Bagaria, N. (2020, December 17). Neha Bagaria: A Visionary Leader Helping Women Acquire Better Career Opportunities. Analytics Insight. <https://www.analyticsinsight.net/neha-bagaria-a-visionary-leader-helping-women-acquire-better-career-opportunities/>
11. Bhatia, R. T. (n.d.). Women in STEM: Breaking Barriers and Inspiring Change. News18. Retrieved October 20, 2023, from <https://www.news18.com/opinion/opinion-women-in-stem-breaking-barriers-and-inspiring-change-8385673.html>
12. Chaudhary, A. (n.d.). Ayesha Chaudhary | WomenLift Health. WomenLift Health. Retrieved October 25, 2023, from <https://www.womenlifthealth.org/profile/ayesha-chaudhary/>
13. American India Foundation. (2022, March 8). International Women's Day: Women pioneers and leaders on how to make STEM careers open for girls across India - AIF. <https://aif.org/international-womens-day-women-pioneers-and-leaders-on-how-to-make-stem-careers-open-for-girls-across-india/>





Dharmesh G Patel et al.,

14. World Economic Forum. (2021). The global gender gap report 2021. Insight Report. Geneva, Switzerland: World Economic Forum.
15. UIS. Stat. (2016). <http://data.uis.unesco.org/>.
16. Kahn, S., & Ginther, D. (2017). Women and STEM. National Bureau of Economic Research.
17. Quirós, C. T., Morales, E. G., Pastor, R. R., Carmona, A. F., Ibáñez, M. S., & Herrera, U. M. (2018). Women in the digital age. Publications Office of the European Union, Luxembourg. <https://doi.org/10.2759/526938>.





A Comprehensive Survey of Two-Wheeler Security and Monitoring Technologies for Riders

Yash Sangale^{1*}, Vivek Chauhan¹, A. N. Bhatt² and J. M. Rathod²

¹Student, Electronics Department, BVM Engineering College, Vallabh Vidyanagar, Gujarat, India.

²Faculty, Electronics Department, BVM Engineering College, Vallabh Vidyanagar, Gujarat, India.

Received: 18 Oct 2023

Revised: 25 Oct 2023

Accepted: 31 Oct 2023

*Address for Correspondence

Yash Sangale

Student, Electronics Dept.,

BVM Engineering College,

Vallabh Vidyanagar – 388120.

Gujarat, India,

E mail: sangale.yash1307@gmail.com



This is an Open Access Journal / article distributed under the terms of the **Creative Commons Attribution License** (CC BY-NC-ND 3.0) which permits unrestricted use, distribution, and reproduction in any medium, provided the original work is properly cited. All rights reserved.

ABSTRACT

Two-wheeled vehicles have experienced a significant surge in popularity as a preferred mode of global transportation. This increase in popularity can be attributed to their compact design, cost-effectiveness, and minimal maintenance requirements, making them an essential part of our daily lives. They offer a convenient and economical mode of transportation for many individuals. However, this heightened adoption has also resulted in a surge in road accidents due to factors such as excessive speeding and reckless driving practices, alongside a rising incidence of two-wheeler thefts. In response to these challenges, there have been numerous technological advancements aimed at addressing these concerns through two-wheeler security and monitoring systems. These contemporary security systems have proven to be effective solutions, incorporating cutting-edge technologies such as GPS (Global Positioning System), GSM (Global System for Mobile Communications), IoT (Internet of Things), and various sensors. These systems offer diverse feature, including accident detection, theft prevention, real-time tracking, and remote monitoring through SMS, calls, apps, or web interfaces. This review paper dives deep into the diverse landscape of such two-wheeler security and monitoring systems, with the aim of providing a clear and accessible understanding of their features, benefits, limitations, and future prospects.

Keywords: Accident Prevention, GPS, GSM, IoT, Monitoring Systems, Theft Prevention, Two-Wheeler Security.





INTRODUCTION

Two-wheelers, encompassing motorcycles, scooters, and mopeds, have entrenched their status as a globally favored mode of transportation, particularly in densely populated urban areas. Their allure lies in their cost-effectiveness, nimble navigation through congested traffic, and their eco-friendly footprint, characterized by reduced carbon emissions. Nevertheless, the burgeoning usage of two-wheelers has led to a troubling upswing in both road accidents and vehicle thefts. In many regions, two-wheelers account for a significant share of road accidents, often culminating in severe injuries and tragic fatalities. Simultaneously, motorcycle thefts persist as a persistent concern, causing profound distress among vehicle owners. For instance, data from the Ministry of Road Transport and Highways (MoRTH) reveals a disconcerting trend, with the number of two-wheeler accidents in India surging from 3,91,333 in 2020 to 4,10,972 in 2021, marking a 5.1% increase [1]. Notably, the primary culprits behind two-wheeler accidents in India are over-speeding, drunk driving, and the absence of helmets. Furthermore, according to the World Health Organization (WHO), approximately 250,000 individuals lose their lives in two-wheeler accidents each year, constituting 28% of all road traffic fatalities worldwide [2]. Two-wheeler thefts also loom large as a pressing issue, both in India and on the global stage. The National Crime Records Bureau (NCRB) reports that over 2.2 million two-wheelers were reported stolen in India in 2021, while, on a global scale, more than 10 million two-wheelers are pilfered annually [3]. Hence in recent years, a spectrum of technological advancements has emerged to address these pressing concerns through the development of Two-Wheeler Security and Monitoring Systems. This review paper embarks on a comprehensive exploration of these systems with the objective of providing a clear and accessible understanding of their features, advantages, limitations, and future prospects. The paper's primary aim is to shed light on the current state of vehicle security implementations, identify their weaknesses leading to compromised security, and compare proposed solutions, highlighting their improvements and shortcomings. The paper will review previous research on vehicle security evaluations and threats, explore proposed solutions to address the prevailing vulnerabilities in current vehicle security, and assess these proposed solutions based on their merits and limitations.

Security and Monitoring System

The "Two-Wheeler Security and Monitoring System" is a comprehensive solution designed to significantly enhance the safety and security of two-wheeler riders, primarily motorcycles and scooters. It consists of two core components: the Accident Detection Unit and the Theft Detection Unit, as depicted in Figure 1. The Accident Detection Unit employs advanced sensors, including accelerometers and tilt sensors, to identify sudden changes in motion or position indicative of an accident. Upon detection, it swiftly triggers alerts to emergency services and designated contacts, ensuring timely assistance to injured riders. Conversely, the Theft Detection Unit uses proximity sensors, RFID technology, or keyless ignition systems to thwart unauthorized access attempts. When a potential theft is detected, this unit activates alarms, sends real-time alerts to the owner's mobile device, and may immobilize the engine or engage locking mechanisms to prevent theft. The system integrates various components, including sensors, processing units, and communication modules. Sensors continually monitor the two-wheeler for various events. Data is transmitted to a central microcontroller or processing unit, which interprets the data to identify accidents or theft attempts. Key communication modules, such as GPS for precise location tracking and GSM for real-time alerts, maintain connectivity with the rider, emergency services, and the owner. In accidents, the system promptly contacts authorities and the rider's designated contacts, while in theft attempts, it notifies the owner in real-time. Continuous development efforts aim to enhance the system's capabilities, improving GPS and GSM connectivity, developing user-friendly mobile applications and web interfaces, expanding sensor functionality, addressing data security, optimizing power efficiency, and reducing maintenance. In conclusion, the Two-Wheeler Security and Monitoring System offers essential safety features for riders and remains committed to ongoing improvements, ensuring a safer and more secure riding experience.





Yash Sangale et al.,

LITERATURE REVIEW

In the evolving landscape of two-wheeler safety and security, numerous research papers have contributed significantly to accident detection, theft prevention, and overall rider safety. Notable systems include GSM-GPS based solutions, IoT-based accident detection systems, innovative vehicle security systems, and IoT-based smart helmets. While these technologies offer promising solutions, challenges such as cost-effectiveness, technical issues, and privacy concerns persist and require further exploration.

GSM-GPS Based Accident and Theft Detection Systems

The GSM-GPS Accident and Theft Detection System combines GPS and GSM technologies to enhance the safety and security of two-wheelers, particularly motorcycles and scooters. It is designed to provide real-time tracking and emergency notifications in the event of accidents or theft. Reference [4] introduced an innovative framework for detecting and reporting two-wheeler accidents using GPS, GSM, and proximity sensors. This cost-effective and reliable system not only identifies accidents but also detects instances of reckless driving. While it holds significant potential for improving rider safety, there are challenges related to cost-effectiveness and potential security vulnerabilities that require further research. In another study by [5], a novel two-wheeler security system based on embedded technology was presented. This system integrates microcontrollers, GSM, GPS, RFID, and Wi-Fi modules to offer real-time monitoring and security enhancements. Despite representing a substantial advancement in two-wheeler security, it faces challenges related to high implementation costs, external network dependencies, and potential security vulnerabilities. Addressing these challenges is crucial for realizing its full potential.

A unique security device for two-wheelers, utilizing a Wi-Fi module and accessible through a web page or Android app, was introduced in research paper [6]. This system enhances security and aids in locating two-wheelers in crowded parking areas using a tilt sensor to detect changes in vehicle position. It provides an efficient security solution, addressing the limitations of GPS and GSM systems. However, challenges such as Wi-Fi connectivity and battery life need attention in future work. This system shows promise in reducing two-wheeler theft due to its enhanced security and vehicle location features. A survey paper [7] extensively explores vehicle security systems until 2017, tracing their historical development and current challenges. It delves into various security technologies, including user authentication, firewalls, encryption, intrusion detection systems, antimalware, and GPS/GSM tracking. The paper underscores that while several promising technologies are available to enhance vehicle security, there is no universal solution. It emphasizes the need for holistic, multi-layered security approaches and addressing security concerns in the deployment of connected systems in vehicles.

IoT-Based Accident Detection Systems

Two research papers [8],[9] focus on IoT-based motorcycle safety systems to improve rider safety and security. In Paper [8], a smart helmet system employs GPS and GSM modules for real-time accident detection and reporting. It utilizes IoT and machine learning to enhance motorcycle safety, potentially saving lives and promoting responsible riding. The paper's design, implementation, and testing demonstrate the technology's feasibility and effectiveness, recommending future improvements like sensor integration, UI enhancements, and system compatibility. However, challenges like false alarms, privacy, security, cost, and maintenance need addressing for widespread success. In summary, this paper contributes to motorcycle safety, with the potential to reduce injuries and fatalities if challenges are effectively managed.

Paper [9] introduces a smart helmet and bike system to enhance two-wheeler safety and security. It includes RFID tags, password authentication, gas and proximity sensors, a microcontroller, relay, and alarm unit to ensure driver safety and prevent unauthorized bike access. The paper aims to improve two-wheeler safety by enforcing helmet usage and preventing drunk driving, while also providing anti-theft features and rider comfort enhancements. Despite challenges like costs, technical issues, and privacy concerns, addressing these factors is crucial for widespread adoption and effectiveness.



**Yash Sangale et al.,****Innovative Vehicle Security Systems**

In the realm of innovative vehicle security systems, the literature showcases two noteworthy solutions. The first, presented in research paper [10] introduces a vehicle theft tracking and locking system using advanced face recognition and Open CV technology. This system combines a mobile app with an authorized user database, GPS and GSM for real-time tracking and alerts, and various security features, including face recognition sensors, USB storage, a buzzer, and lock control circuitry for intruder detection. It enhances vehicle security, offers real-time theft detection and intruder capture, potentially reducing theft rates, and assisting law enforcement with stored images and GPS data. Challenges include face recognition accuracy, system security, and cost-efficiency, which require further attention to enhance reliability and accessibility. The second system, outlined in research paper [11], is a vehicle accident detection system that harnesses GPS, GSM, and an accelerometer to swiftly notify emergency services and the driver's family in the event of an accident. It records accident details and communicates them to predefined contacts, reducing response time and offering accurate information, integration capabilities, and incident tracking. Challenges include network and signal limitations, occasional false alarms, maintenance, calibration requirements, and privacy and security concerns. Despite these challenges, this technology represents progress in improving road safety and enhancing emergency response capabilities, particularly in regions with a need for such solutions.

IoT-Based Smart Helmets and Safety Systems

Research paper [12] explores IoT-based accident detection systems for smart vehicles, utilizing sensors, communication modules, and machine learning to swiftly detect and report accidents. The system's goals encompass reducing response times, saving lives, preventing accidents through driver behavior monitoring, and enhancing road safety and traffic management. The paper highlights the potential of IoT-based accident detection systems in reducing road accidents and fatalities, emphasizing their capacity to save lives and prevent accidents through driver behavior monitoring. The prospect of improved traffic management through accident data analysis and risk factor identification suggests a comprehensive approach to enhancing road safety. However, the paper acknowledges significant challenges, including high implementation costs, security and privacy concerns, and reliance on network and cloud services. Proposed improvements include more precise machine learning models for accident detection and prediction, enhanced data security and privacy, and integration with smart city applications. Despite these challenges, the IoT-based accident detection system offers promise for enhancing road safety, potentially reducing accidents and saving lives while contributing to efficient traffic management.

Research paper [13] introduces an IoT-based smart helmet and accident identification system for motorcycle accident prevention. The system comprises three main components: a helmet circuit, an automobile circuit, and a mobile application. The helmet circuit includes IR and alcohol sensors to ensure helmet usage and sobriety. The automobile circuit utilizes a 3-axis accelerometer, Bluetooth module, relay, and load sensor to monitor motorcycle speed, load, and impact. The mobile application connects to the automobile circuit via Bluetooth and transmits accident information to emergency contacts, police, and hospitals through a database. The system presents an innovative solution for enhancing motorcycle safety and accident detection through sensor integration, Arduino, IoT, and database technologies. Its potential to reduce accident risks and their impact, potentially saving lives, is a promising feature. However, the system faces challenges, such as compatibility with different motorcycles and helmets, expanding accident detection capabilities, and addressing technical issues. Future work should concentrate on enhancing compatibility, broadening accident detection capabilities, and addressing technical challenges. Overall, the IoT-based smart helmet system holds potential for improving motorcycle safety and accident prevention but necessitates ongoing development for full effectiveness and accessibility.

Holistic Vehicle Safety Systems

In paper [14], an SMS-based vehicle security system is introduced, using GPS to track motorcycle location and alert the owner to potential risks. Components include Arduino Uno, SIM 800L module, GPS neo-6 modules, and a smartphone. Its objectives are theft prevention, real-time tracking, and improved vehicle security. Challenges involving signal dependence and power source reliability need attention. Successful implementation and proposed





Yash Sangale et al.,

enhancements like voice recognition, remote control, alarms, and IoT integration suggest future potential for motorcycle security. Research paper [15] presents a comprehensive safety system for two-wheeler vehicles, emphasizing accident prevention, detection, and reporting. This technology integrates various sensors and communication modules to enforce safety measures, including helmet usage and sobriety requirements. Communication protocols like ESP8266MOD and MQTT enable swift and accurate accident notifications, reducing medical assistance response time. Environmental monitoring adds to broader environmental awareness. Despite advantages, challenges in power supply, maintenance, data security, and compatibility must be addressed for successful implementation and widespread adoption. The paper highlights the system's feasibility and suggests opportunities for future advancements in two-wheeler safety and smart vehicles.

Vehicle Tracking Systems

Research paper [16] introduces a system for detecting and reporting two-wheeler accidents in remote areas using sensors, GPS, GSM, and mobile apps. While promising, it needs more technical details, diagrams, implementation methods, and performance comparisons with existing systems. Addressing cost, reliability, security, scalability, and real-world performance is crucial. Overcoming challenges in remote areas will require further research. Research paper [17] demonstrates an IoT system with high accuracy (100% helmet detection, 87% drowsiness detection, 90% accident detection) and features like rider status and location monitoring. Suggested improvements include speed limit monitoring, traffic sign recognition, and voice control. Commercial potential is noted, with possible collaborations for commercialization. Paper [18] presents an IoT-based motorbike accident detection system using a tilt sensor, GSM, and Arduino Nano, achieving a 97.33% detection rate. The paper recommends adding features like GPS, ultrasonic sensors, and emergency buttons for enhanced rider safety. Paper [19] introduces a smart helmet system with alcohol detection, helmet enforcement, and accident recognition for two-wheeler riders using Node MCU. It emphasizes the potential for accident reduction and promotes rider safety. Recommendations include voice control, speed limit monitoring, and traffic signal detection, with the need for comprehensive testing and potential expansion to other vehicle types for broader road safety impact.

Practical Vehicle Tracking Systems

The paper [20] introduces a technology-based system for vehicle tracking and accident alerts, using GPS, GSM, and sensors to provide immediate medical assistance and enable vehicle tracking. The authors recommend enhancing the system with features like voice communication, an emergency button, and alcohol detection, suggesting validation through experiments in various scenarios. Paper [21] introduces a comprehensive safety system integrating smart helmets and bikes for two-wheeler riders, focusing on safety monitoring, accident prevention, and detection. Suggestions for future improvements include integrating cameras, methods for detecting the nearest hospital, and conflict detection mechanisms. Paper [22] presents a system for car accident detection and prevention, incorporating gas leak and overheating detection using IR sensors, Arduino Uno, GPS, GSM, and Node MCU. The paper highlights potential enhancements like voice recognition, camera integration, and cloud computing features, emphasizing its cost-effectiveness and effectiveness. Paper [23] introduces a vehicle tracking system utilizing GPS and GSM modules for real-time monitoring. It offers features like sending vehicle coordinates via SMS and displaying the vehicle's location on Google Maps.

The paper suggests future improvements, including voice communication, a web interface, and data logging to enhance the system's capabilities. In summary, the literature review analyzes various systems and technologies aimed at enhancing two-wheeler safety, accident detection, and vehicle security. These systems offer innovative solutions to address safety and security concerns. While they have made significant contributions, challenges such as cost, technical issues, privacy, security, and compatibility issues need addressing to realize their full potential. Future work should focus on refining these systems and incorporating additional features to further enhance safety, reliability, and functionality. Addressing these challenges and pursuing further research and development can significantly contribute to the safety and security of two-wheeler riders and their vehicles.





Yash Sangale et al.,

DISCUSSION

The literature review has comprehensively examined technologies and systems aiming to enhance two-wheeler and vehicle safety and security, encompassing aspects like accident detection, theft prevention, rider behavior monitoring, and emergency assistance. In this discussion, we will analyze the findings from the reviewed papers, focusing on their strengths, limitations, and potential future directions mentioned in Summary Table I.

Accident Detection and Reporting Systems: The literature consistently emphasizes the importance of accident detection and reporting systems for two-wheelers. Many of these systems employ advanced technologies, such as GPS, GSM, IoT, and various sensors, to detect accidents promptly and accurately, reducing response times, saving lives by ensuring timely medical assistance, and promoting responsible rider behavior. Research in this area has demonstrated the effectiveness of IoT-based accident detection systems (papers [8], [11], [18]), offering real-time monitoring and accurate accident detection, valuable for improving road safety. However, they come with challenges like high implementation costs and concerns about security and privacy, which must be addressed for widespread adoption.

Theft Prevention and Vehicle Tracking: Paper [5] presents a two-wheeler security system that combines an embedded platform with components like microcontrollers, GSM, GPS, RFID, and Wi-Fi modules. This system focuses on theft prevention and access control, allowing owners to track their two-wheelers and thwart unauthorized access attempts. The integration of GPS technology for tracking and GSM for real-time alerts highlights its potential to enhance vehicle security. While this technology offers promising features for theft prevention, the literature also acknowledges its limitations, including high implementation and maintenance costs, reliance on external networks like GSM and Wi-Fi, and potential security vulnerabilities that require attention for its widespread success. Future research and development should focus on enhancing security measures and improving reliability.

Smart Helmet based Systems: Smart helmet systems (papers [19],[21]) are gaining recognition for their role in enhancing the safety and security of two-wheeler riders. These systems utilize various sensors, including alcohol detectors, IR sensors, and accelerometers, to ensure helmet usage, detect alcohol consumption, and recognize accidents, promoting responsible riding and providing timely assistance in emergencies. Smart helmet systems have the potential to significantly reduce accidents and fatalities involving two-wheelers. The integration of IoT technology, GPS, and sensors provides an effective solution for rider safety. However, these systems face challenges, including potential false positives or negatives in detection, along with privacy and security concerns that require careful consideration to ensure user acceptance.

Vehicle Tracking and Monitoring: Vehicle tracking systems (papers [23],[14]) have been designed to track the location, speed, and status of vehicles, enhancing fleet management and asset tracking. These systems rely on GPS and GSM modules, enabling real-time monitoring and remote control, offering practical applications for tracking and controlling vehicles, potentially improving efficiency in various domains. The reviewed literature highlights the user-friendly and adaptable nature of these systems. However, they also face challenges related to network dependencies, connectivity issues, and power sources. Future research should explore ways to enhance system performance, including incorporating features like voice communication, web interfaces, and data logging.

Comprehensive Safety Systems: Some papers ([15], [4]) introduce comprehensive safety systems encompassing multiple safety features for two-wheelers, such as pressure sensors, accelerometers, and alcohol sensors, in combination with IoT and GPS technologies. These systems aim to enforce safety measures and reduce accident risks, particularly related to helmet usage and drunk driving. The discussed comprehensive safety systems effectively demonstrate their potential to enhance two-wheeler rider safety, facing challenges like power supply, data security, maintenance, and compatibility. Ongoing refinement and development, as suggested in the literature, can address these issues, leading to widespread adoption and effectiveness.





Yash Sangale et al.,

Future Scope and Improvement

The reviewed literature offers insights into technologies and systems enhancing two-wheeler and vehicle safety. For the future, several key areas promise research and enhancement opportunities as described in Figure 2:

Cost-Efficient Solutions: One primary challenge highlighted in the literature is system implementation costs. To broaden accessibility, future research must prioritize cost-effective solutions. Optimization of hardware and the use of open-source software can reduce overall expenses. Exploring pricing models that encourage adoption is also essential.

Security and Privacy: Security and privacy are pivotal concerns. Researchers should focus on strengthening security measures, enhancing data protection through robust encryption and authentication, and vigilantly addressing evolving security threats through timely security patches.

Compatibility and Reliability: To boost system adoption, compatibility and reliability issues must be addressed. Systems should be compatible with diverse vehicles, helmets, and accessories. Technical refinements can improve reliability and performance under various conditions, while standardized protocols ensure seamless integration with various vehicle types.

User-Centric Design and Acceptance: User acceptance is critical. Future research should embrace a user-centric design approach to tackle user concerns, refine user experiences, and enhance overall acceptance. User-friendly interfaces and clear instructions are key components.

Integration with Smart City Applications: Exploring integration with broader smart city applications is a promising avenue. Integrated systems can contribute to traffic management, emergency response coordination, and environmental monitoring. Research should investigate interactions with urban technologies to create safer and more connected urban environments.

Advanced Sensing and Detection Technologies: Developing precise safety systems relies on advanced sensing and detection technologies. Researchers should explore cutting-edge sensors, including lidar, ultrasonic sensors, and advanced image recognition systems, to enhance accident detection, rider behavior monitoring, and environmental sensing.

Energy-Efficient Systems: Addressing battery life and power concerns requires energy-efficient systems. Low-power components, energy harvesting mechanisms, and smart power management solutions can extend system longevity and reduce maintenance requirements.

Interconnected Ecosystems: The future lies in interconnected ecosystems. Developing systems that communicate with other vehicles, infrastructure, and emergency services offers a more coordinated safety and security approach. Research should establish necessary protocols and standards for these interconnected ecosystems.

CONCLUSION

In summary, the dynamic landscape of innovative technologies and solutions explored in the literature review promises a transformative impact on road safety and vehicle security for two-wheelers and other vehicles. Driven by components such as GPS, GSM, IoT, sensors, and mobile applications, these technologies have shown great potential in significantly reducing accident-related injuries and fatalities. The literature emphasizes the importance of overcoming challenges, including cost-effectiveness, user acceptance, security, and privacy. Collaborative efforts among researchers, engineers, and policymakers are essential to ensure widespread accessibility and reliability. Urgent collaboration among these stakeholders is imperative to surmount challenges and ensure these systems are accessible and reliable on a global scale. In summation, this comprehensive review not only offers a snapshot of the current state of safety and security systems for two-wheelers and vehicles but also serves as a catalyst for ongoing research, innovation, and collaboration. The journey towards safer, smarter, and more connected transportation systems is well underway, and with sustained effort, these technologies will undoubtedly play a pivotal role in reducing accidents and enhancing overall safety on our roads.





Yash Sangale et al.,

REFERENCES

1. Nitin Gadkari Minister of Road Transport and Highways of India, "Ministry of Road Transport and Highways," Ministry of Road Transport and Highways of India, 12 December 2022. [Online]. Available: <https://morth.nic.in/road-accident-in-india>
2. "World Health Organization (WHO)," [Online]. Available: <https://www.who.int/>.
3. "National Crime Records Bureau, India," Ministry of Home Affairs of India, 2021. [Online]. Available: https://ncrb.gov.in/sites/default/files/ADSI-2021/ADSI_2021_FULL_REPORT.pdf
4. Meena, Amit, et al. "Automatic Accident Detection and reporting framework for two wheelers." 2014 IEEE International Conference on Advanced Communications, Control and Computing Technologies. IEEE, 2014.
5. Rajarapollu, Prachi R., Nutan V. Bansode, and Pranoti P. Mane. "A novel two-wheeler security system based on an embedded system." 2016 2nd International Conference on Advances in Computing, Communication, & Automation (ICACCA)(Fall). IEEE, 2016.
6. Narkhede, Shweta K., et al. "Two Wheeler Security System." International Research Journal of Engineering and Technology (IRJET) 4.5 (2017): 3058-3061.
7. K. Mawonde, B. Isong, F. Lugayizi, and A. M. Abu-Mahfouz, "A Survey on Vehicle Security Systems: Approaches and Technologies," IECON 2018 - 44th Annual Conference of the IEEE Industrial Electronics Society, Washington, DC, USA, 2018, pp. 4633-4638, doi: 10.1109/IECON.2018.8591175.
8. Vaya, Prashant, Rajbala Simon, and Sunil Kumar Khatri. "Motorcycle safety solution using the Internet of Things." 2019 4th International Conference on Information Systems and Computer Networks (ISCON). IEEE, 2019.
9. Swathi, S. J., Shubham Raj, and D. Devaraj. "Microcontroller and sensor-based smart biking system for driver's safety." 2019 IEEE International Conference on Intelligent Techniques in Control, Optimization and Signal Processing (INCOS). IEEE, 2019.
10. Mohanasundaram, S., V. Krishnan, and V. Madhubala. "Vehicle theft tracking, detecting and locking system using Open CV." 2019 5th International Conference on Advanced Computing & Communication Systems (ICACCS). IEEE, 2019.
11. Gowshika, Madhu Mitha, B. Madhu, and G. Mitha. "Vehicle accident detection system by using GSM and GPS." IRJET 6.01 (2019).
12. Ivi, Unaiza, et al. "A comprehensive study on IoT-based accident detection systems for smart vehicles." IEEE Access 8 (2020): 122480-122497.
13. Rahman, Md Atiqur, et al. "IoT-based smart helmet and accident identification system." 2020 IEEE Region 10 Symposium (TENSymp). IEEE, 2020.
14. Astuti, Nuraeni Puji, et al. "Vehicle security system using short message service (SMS) as a danger warning in motorcycle vehicles." Journal of Robotics and Control (JRC) 1.6 (2020): 224-228.
15. Kalyanaraman, B., et al. "Accident prevention, detection, and reporting for two-wheeler safety system." International journal of engineering and advanced technology 9.5 (2020): 230-234.
16. Vivekanandan, S., et al. "Vehicle Crash Detection and Information System for Two Wheeler in Remote Areas." International Journal of Research in Engineering, Science, and Management 3.8 (2020): 412-415.
17. Prasetyawan, Purwono, et al. "A prototype of IoT-based smart system to support motorcyclists safety." Journal of Physics: Conference Series. Vol. 1810. No. 1. IOP Publishing, 2021.
18. Ur Rehman, S., Khan, S. A., Arif, A., & Khan, U. S. (2021). IoT-based Accident Detection and Emergency Alert System for Motorbikes. 2021 International Conference on Artificial Intelligence and Mechatronics Systems (AIMS). doi:10.1109/aims52415.2021.9466055.
19. Tharunika, B., et al. "Accident and Alcohol Detection for Two Wheelers Using Node Mcu." Turkish Journal of Computer and Mathematics Education (TURCOMAT) 12.6 (2021): 4404-4411.
20. [Mounika, J., et al. "Accident alert and vehicle tracking system using GPS and GSM." Asian Journal of Applied Science and Technology (AJAST) Volume 5 (2021): 81-89.





Yash Sangale et al.,

21. [C, Priyanka & C, Priya & Shavi, Vinayak & Begum, Sarvar. (2018). Two-Wheeler Safety System for Accident Prevention, Detection, and Reporting. International Journal Of Engineering And Computer Science. 7. 23680-23682. 10.18535/ijecs/v7i3.03.
22. Patil, Swapnil A., et al. "ACCIDENT DETECTION AND NOTIFICATION USING GSM AND LIVE LOCATION SHARING USING GPS." International Research Journal of Modernization in Engineering Technology and Science (2022): 2582-5208.
23. Iqbal, Mr Saif, Mr Owais Ahmed, Mr Mohammed Ahmed Khan, and Shilpa Mangshetty. "VEHICLE TRACKING SYSTEM AND THEFT DETECTION." International Research Journal of Modernization in Engineering Technology and Science (2023): 2582-5208.

Table 1 Summary Table

Reference	Focus Area	Key Technologies	Strengths	Limitations	Recommendations for Improvement
[4]	GSM-GPS Accident and Theft Detection	GPS, GSM, Proximity Sensors	Real-time tracking, Emergency notifications	Cost-effectiveness, Security vulnerabilities	Address cost-effectiveness, Research on security enhancements
[5]	Embedded Technology for Security	Microcontrollers, GSM, GPS, RFID, Wi-Fi	Real-time monitoring, Security enhancements	High implementation costs, External network dependencies	Optimize implementation costs, Address external network dependencies
[6]	Wi-Fi Module Security System	Wi-Fi, Tilt Sensor	Efficient security, Location tracking	Wi-Fi connectivity issues, Battery life	Improve Wi-Fi connectivity, Optimize battery life
[8]	IoT-based Smart Helmet	IoT, GPS, GSM	Real-time accident detection, Rider safety	False alarms, Privacy concerns, High cost	Address false alarms, Improve privacy, Cost optimization
[9]	Smart Helmet and Bike System	RFID, Password Authentication, Gas and Proximity Sensors	Safety enforcement, Anti-theft features	Cost, Technical issues, Privacy concerns	Address cost, Improve technical robustness, Enhance privacy
[10]	Face Recognition for Vehicle Theft Tracking	Face recognition, GPS, GSM	Real-time theft detection, Intruder capture	Face recognition accuracy, System security, Cost	Improve face recognition accuracy, Enhance security, Optimize cost
[11]	Vehicle Accident Detection	GPS, GSM, Accelerometer	Swift accident notification, Accurate incident tracking	Network limitations, Occasional false alarms	Address network limitations, Minimize false alarms
[12]	IoT-based Accident Detection for Smart Vehicles	IoT, Sensors, Machine Learning	Swift accident detection, Traffic management	High implementation costs, Security and privacy concerns	Optimize costs, Enhance security measures





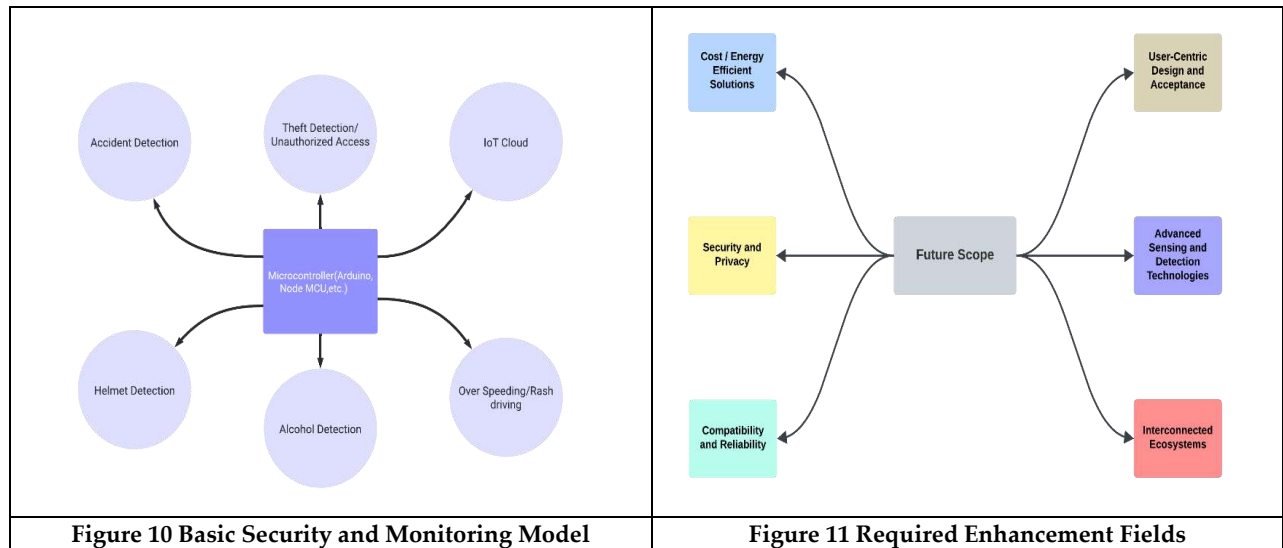
Yash Sangale et al.,

[13]	IoT-based Smart Helmet System	IoT, IR Sensors, Bluetooth, Database	Accident prevention, Emergency alerts	Compatibility issues, Technical challenges	Improve compatibility, Address technical challenges
[14]	SMS-based Vehicle Security System	GPS, Arduino, SIM 800L	Theft prevention, Real-time tracking	Signal dependence, Power source reliability	Address signal dependence, Enhance power source reliability
[15]	Comprehensive Safety System	Sensors, Communication Modules	Accident prevention, Swift accident notifications	Power supply challenges, Data security	Address power supply challenges, Enhance data security
[16]	Remote Area Accident Detection	Sensors, GPS, GSM, Mobile Apps	Remote accident detection	Technical details, Implementation challenges	Provide technical details, Address implementation challenges
[17]	IoT System for Two-Wheeler Safety	IoT, Helmet Detection, Drowsiness Detection	High accuracy, Rider status monitoring	Speed limit monitoring, Traffic sign recognition	Implement speed limit monitoring, Enhance traffic sign recognition
[18]	IoT-based Motorbike Accident Detection	Tilt Sensor, GSM, Arduino Nano	High detection rate	Lack of GPS, Ultrasonic Sensors, Emergency buttons	Integrate GPS, Ultrasonic Sensors, and Emergency buttons
[19]	Smart Helmet System with Alcohol Detection	Node MCU, Alcohol Sensors	Accident reduction, Rider safety	Voice control, Speed limit monitoring	Implement voice control, Enhance speed limit monitoring
[20]	Technology-Based Vehicle Tracking	GPS, GSM, Sensors	Immediate medical assistance, Vehicle tracking	Lack of voice communication, Emergency button	Implement voice communication, Include an emergency button
[21]	Smart Helmets and Bikes Integration	Smart Helmets, IoT, Cameras	Safety monitoring, Accident prevention	Lack of technical details, Performance assessments	Provide technical details, Conduct performance assessments
[22]	Car Accident Detection and Prevention	IR Sensors, Arduino Uno, GPS, GSM	Gas leak and overheating detection	Lack of voice recognition, Camera integration	Implement voice recognition, Integrate cameras
[23]	Vehicle Tracking System	GPS, GSM	Real-time monitoring, Location tracking	Lack of voice communication, Web interface	Implement voice communication, Develop a web interface





Yash Sangale et al.,





Seismic Behavior of Outrigger System in RC Tall Building - A Review

Tushar J.Kachariya^{1*}, Vimlesh V. Agrawal², Vishalkumar B.Patel² and Pratiti M.Bhatt²

¹PG Scholar, Structural Engineering Department, Birla Vishvakarma Mahavidyalaya Engineering College, Vallabh Vidyanagar, Gujarat, India

²Assistant Professor, Birla Vishvakarma Mahavidyalaya Engineering College, Vallabh Vidyanagar, Gujarat, India.

Received: 18 Oct 2023

Revised: 25 Oct 2023

Accepted: 31 Oct 2023

*Address for Correspondence

Tushar J.Kachariya

PG Scholar,

Structural Engineering Department,

Birla Vishvakarma Mahavidyalaya Engineering College,

Vallabh Vidyanagar, India



This is an Open Access Journal / article distributed under the terms of the **Creative Commons Attribution License** (CC BY-NC-ND 3.0) which permits unrestricted use, distribution, and reproduction in any medium, provided the original work is properly cited. All rights reserved.

ABSTRACT

The seismic behaviour of outrigger systems in reinforced concrete (RC) tall buildings, which are vital structures in modern urban landscapes. Outrigger systems play a pivotal role in enhancing the structural stability of tall buildings during seismic events, making this an essential subject of study. In this paper interactions between different lateral load resisting systems like outrigger systems, moment Frame, braced Frames, hybrid systems, base isolation, and diagrid systems are analyzed to provide a comprehensive understanding of the seismic behaviour of tall RC buildings. Site-specific conditions and soil-structure interactions are also considered. This paper identifies research gaps and emerging trends, underscoring the need for further work in performance-based design, sustainability, and resilience of outrigger systems. This review is a valuable resource for researchers, practitioners, and industry stakeholders seeking to enhance the seismic resilience of tall buildings.

Keywords: Outrigger system, Tall Building, Response Spectrum method, Time history method, Seismic response

INTRODUCTION

The construction of tall Structures is more common for a number of reasons, including space limitation. Land is becoming more expansive as cities become densely populated. Developers can fulfil the increasing demand for office, residential buildings by building upwards in order to make the best use of limited space. Yet, it has been difficult to grow cities conventionally due to the restricted horizontal to vertical expansion, creating tall structures that soar upwards even higher. In urban areas, where there is a strong demand for space and a finite amount of land that can be this situation, tall structures have been built to make the best use of the land that is available and to keep up with the





expanding urbanization needs. In tall buildings, A more slender structure with a higher height-to-width ratio is more vulnerable to lateral force in tall buildings. Buildings become more susceptible to lateral forces like wind and earthquake forces as they grow higher and more slender. This is due to that the forces pressing on the building grow with the height while the building's lateral stiffness diminishes. To counteract the lateral force in tall buildings we introduce the different lateral load-resisting systems.

Different lateral load resisting system

1. Braced-frame structures
2. Rigid-frame structures
3. Infilled-frame structures
4. Flat-plate and Flat-slab structures
5. Shear wall structures
6. Wall frame structures
7. Outrigger system

Outrigger System

Outrigger-braced high-rise structures consist of a main core connected to exterior columns by horizontal cantilevers. Outrigger systems efficiently reduce top deflection and core base moment. When subjected to lateral loads, outriggers restrain the core's rotation, resulting in smaller core deflections and moments. Exterior columns connected to outriggers resist lateral loads through axial tension and compression, increasing structural depth. Advantages of outrigger systems include increased overall stiffness, controlled top drift, and balanced overturning moments. They can also equalize differential shortening of exterior columns due to temperature and axial load variations. However, outrigger systems do not significantly increase shear resistance, which relies on the core. However, outrigger systems do not significantly increase shear resistance, which relies on the core.

Types of Outrigger system :

1. Belt Truss Outrigger
2. Diagonal Bracing Outrigger
3. Eccentrically Braced Outrigger
4. Composite Outrigger
5. Coupled wall Outrigger

Belt Truss Outrigger System : In this system, a horizontal truss is placed at an intermediate level of the building. The truss, often encircling the entire building, acts as a belt to transfer lateral forces to the core or perimeter columns. This design increases torsional stiffness and reduces sway.

Diagonal Bracing Outrigger: Diagonal braces, typically in the form of steel or concrete diagonals, connect the core or perimeter columns to an intermediate point in the building. These braces help in distributing lateral forces, improving overall stability.

Eccentrically Bracing Outriggers : Eccentrically braced outriggers use braces with offsets from the center line of the building. These braces provide lateral resistance by dissipating energy through controlled yielding, making them particularly effective in regions with high seismic activity.

Composite Outrigger : Composite outrigger systems combine multiple elements, such as diagonal braces, belt trusses, and shear walls, to optimize lateral stability. They are designed to achieve maximum performance under varying conditions.

Advantages Of Outrigger System

Increased Lateral Stability; Outrigger systems play a role in enhancing the lateral stability of a building by connecting the central core with exterior columns. This is especially important for structures as it helps minimize the swaying motion caused by wind or seismic forces.





Tushar J Kachariya *et al.*,

Reduced Building Sway; By providing rigidity outriggers contribute to reducing the sideways movement and deflection of a building during events that exert lateral loads. This reduction, in sway not enhances the comfort of occupants but Also decreases any discomfort caused by motion.

Enhanced Structural Integrity; Outrigger systems effectively distribute forces throughout the building relieving stress on individual structural components. This significantly contributes to maintaining the integrity of the entire building.

Optimized Performance: Through careful design and analysis, outrigger systems can be tailored to specific building requirements and local environmental conditions. This optimization ensures that the building can withstand lateral loads while meeting safety standards.

Balanced Load Distribution: Outrigger systems balance the distribution of lateral loads between the central core and exterior columns. This load distribution prevents excessive forces on any single component, minimizing the risk of structural failure.

Improved Seismic Performance: In earthquake-prone regions, outrigger systems are effective in enhancing a building's seismic performance. They can help mitigate the effects of ground motion and reduce the risk of structural damage.

Disadvantages Of Outrigger System

Complex Design and Analysis: Outrigger systems involve intricate engineering calculations and structural analysis, which can be more complex than other structural systems. This complexity can lead to higher design and construction costs.

Additional Material and Construction: The incorporation of outrigger systems requires additional materials, including steel beams or trusses, and specialized connections. These materials can increase construction costs.

Architectural Constraints: The placement of outriggers and their associated components can impose limitations on the architectural design and layout of the building. This may affect interior space planning and aesthetics.

Space Utilization: Outrigger systems can occupy valuable interior space, especially if they are located at habitable levels. This can reduce the usable area for occupants or require creative space planning.

Maintenance Challenges: Outrigger systems may require specialized maintenance due to their complex structural components and connections. This can add to the long-term operational costs of the building.

LITRATURE REVIEW

BorahM *et al.*[2023][1] has performed seismic performance of tall structure with different Structural systems. This paper compares the seismic performance of G+20 storied building with different structural systems The different structural systems investigated in the study include special moment resisting frames, frame-shear wall buildings, outrigger systems, braced models, and hybrid models. & they Analyzes the performance of these structural systems using Pushover analysis and time history method under seismic loads in Guwahati, Assam, which is an earthquake-prone zone in India using ETAB software. And they found out that the outrigger and Hybrid system shows better result in pushover analysis & shear wall model shows better result in time history method & they conclude that for building higher than 20 story building they recommend to use outrigger and hybrid system. Shiva Prathapet *al.* [2]has study the "Effect of Core Wall and Outrigger on Seismic Behavior of RC Tall Structural Systems". The paper discusses the seismic behavior of RC tall structural systems, specifically focusing on the effect of core wall and outrigger systems. The models used in the study include moment frame system, moment frame structural system, and 3 core wall & outrigger structural system. The models are analyzed using static and time history analysis, The study examines key responses such as maximum base force, story displacements, story drifts, and variation of story stiffness with the introduction of different types of outrigger systems. The analysis considers the performance of different tall structural systems under earthquake conditions. & The study concludes that the introduction of a shear wall into the moment frame system significantly increases the base force, while the introduction of different types of outriggers does not have a significant impact on the base force. The use of core wall systems with outriggers leads to a tendency for vibration reduction in tall structural systems. Modal analysis reveals that core wall systems with outriggers have a lower time period compared to conventional moment frame systems. Stiffness is found to be high at the lower stories and decreases along the height in both X and Y directions.



**Tushar J Kachariya et al.,**

Husain M *et al.* [2021][3] has performed the seismic response of structural outrigger systems in tall buildings, specifically comparing the wall beam outrigger system and the vierendeel outrigger system. The research aims to find the best structural concrete outrigger system by analyzing the behavior of these systems under earthquake loads using the Midas-Gen software program. The study compares different parameters such as storey drift, storey drift ratio, and base storey overturning moment to determine the effectiveness of the outrigger systems. The results show that a one-storey wall beam structural system is better than a two-storey vierendeel structural system when used as an outrigger system. The best positions for the outrigger systems are found to be 0.45 of the total building height for the one-storey outrigger and 0.20 and 0.45 of the total building height for the two-storey outrigger. Overall, the research concludes that concrete outrigger systems are effective in improving the seismic response of tall buildings. Chen *Yet al.* [2017][4] has done analysis of outrigger number and location in outrigger braced structure using a multi objective genetic algorithm. Author applies a multi objective genetic algorithm to optimize the design of outrigger numbers and locations in high-rise buildings, considering top drift and core base moment as trade-off objective functions. Author use of the algorithm allows for the exploration of various design schemes and provides benefits such as diversity, flexible options for designers, and active client participation. and they found out that The use of the multi objective genetic algorithm (MGA) in optimizing the design of outrigger numbers and locations in high-rise buildings allows for the generation of various design schemes and provides benefits such as diversity, flexible options for designers, and active client participation. The MGA approach enables designers and clients to easily compare the performance of structural systems with different numbers of outriggers in different locations, ultimately leading to improved high-rise building designs.

RAO GV *et al.* [2021][5] has Compare the seismic effect of tall RC building of G+20 building with outrigger system using ETAB software. Author has focuses on the seismic performance of tall RC frame buildings with outrigger systems in Zone III, using ETABS software. It compares three models: a bare frame, a frame with an outrigger system at the 10th storey, and a frame with an outrigger system at both the 10th and 20th storey. The study analyzes the lateral deflection, storey drifts, and storey shear of the models. The results show that the outrigger system improves the structural performance by reducing deflection and controlling storey drifts and shear. The use of outrigger systems increases the stiffness and load-resisting capacity of tall structures, making them more efficient under seismic and wind loads. The findings highlight the importance of seismic adequacy in tall building design and the effectiveness of outrigger systems in mitigating structural failures. Salman K *et al.*[2020][7]has done the optimal control on structural response using outrigger braced frame system under the application of lateral load. Author analyzes the static and dynamic response of a high-rise structure under lateral loads and finds that the outrigger braced frame system provides optimal control for the structure.. The outrigger system is compared with Pendulum tuned mass dampers (PTMD) and is found to have a significant reduction in displacement and drift response of the structure. The outrigger system is also found to be an effective addition to the sway frame based on comparative static and dynamic analysis. And author concludes that the outrigger braced frame system provides optimal control for high-rise structures under lateral loads, as it significantly reduces displacement and drift response compared to other structural systems. The comparative static and dynamic analysis shows that the outrigger system is an effective addition to the sway frame, outperforming Pendulum tuned mass dampers (PTMD) in terms of reducing acceleration.

Amoussou CP. *et al.* [6]has performed simplified modeling and analysis method of skyscrapers with outrigger system. Author introduces a simplified modeling and analysis method for skyscrapers with an outrigger system, based on super elements and dominant degree of freedom methods, verified through static, modal, and dynamic analyses. The proposed method accurately predicts lateral displacements and inter-story drifts in linear and nonlinear analysis, as well as the first modal shape and period, but underestimates max and min story acceleration. It is an effective tool for modeling and analysis in the preliminary design stage, but further improvements are needed for increased accuracy and quality of results. Alhaddad.W *et al.* [2020][8] Has compare the introduction to outrigger and belt truss system in skyscrapers. Author provides a comprehensive review of the outrigger and belt-truss system in tall and super tall buildings, summarizing the main points and methodologies from previous studies. they introduces the different configurations and types of outrigger systems, providing guidance for designers and researchers in making suitable choices. Author also discusses the structural behavior of the system under various loading types and factors that



**Tushar J Kachariya et al.,**

affect its performance, Additionally, the paper mentions the prevalence of outrigger and belt-truss systems in tall buildings globally, particularly in China.

Tan P *et.al* [9] has performed dynamic characteristics of novel energy dissipation system with damped outriggers. Author proposes a method for modeling and analyzing the dynamic characteristics of tall buildings with multiple damped outriggers, considering the interaction between peripheral columns and the dampers. The proposed method is verified through a comparison with a finite element model, and a parametric study is conducted to evaluate the influence of various factors on the modal damping of the building. Author concludes that the proposed method of modeling and analyzing the dynamic characteristics of buildings with multiple damped outriggers is effective and provides valuable insights for designing outrigger systems. The method is verified through a comparison with a finite element model and is further validated through a parametric study that evaluates the influence of various factors on the modal damping of the building. The investigation shows that the modal damping is significantly influenced by the ratio of core-to-column stiffness and is more sensitive to the damping coefficient of dampers than to the position of damped outriggers. The results obtained are non-dimensional and convenient for analysis and applications in designing damped outrigger systems. Wijesundara KK *et.al* [2014][10]has presents a modeling approach for concentrically braced frames in multi-storey buildings, using inelastic force-based beam-column elements and a discretized fiber section. The study demonstrates that including additional force-based beam-column elements at the ends of the brace improves the accuracy of capturing the hysteretic responses of axial force-axial displacement and axial force-lateral displacement. It also establishes the limits of slenderness and width-to-thickness ratio for accurate prediction of brace member responses. Author concludes that the inclusion of two additional force-based beam-column elements at the ends of the brace improves the accuracy of capturing the hysteretic responses of axial force-axial displacement and axial force-lateral displacement in concentrically braced frames.

Kogilgeri SS *et al.* [11] has studied the behavior of outrigger system on high rise steel structure by varying outrigger depth. Author investigates the static and dynamic behavior of the outrigger structural system on a steel structure by reducing the depth of the outrigger, comparing it with a steel structure with a central core and outrigger system of varied outrigger depth. Author Found that the behavior of the outrigger system on high-rise steel structures by varying the outrigger depth found that reducing the depth of the outrigger to 2/3rd or 1/3rd of the story height showed only minor differences in resistance towards lateral loads compared to the outrigger with full story height depth. Lateral deflection and storey drift were the key parameters analyzed in this study. The decrease in the depth of the outrigger to 2/3rd or 1/3rd of the story height resulted in a percentage reduction of lateral displacement and story drift up to 4-7% compared to the outrigger with full story height depth. The study also compared the performance of the outrigger system with different depths to the structure with a braced core. The addition of an intermediate truss at 0.5H showed increased performance compared to the structure with only a cap truss.

Sukhdeve SB[2016][12] has studied the Optimum Position of Outrigger in G+40 RC Building. Author analyzes the use of outrigger beams in tall buildings to provide sufficient lateral stiffness and optimize their position using lateral loads. The study was conducted using a three-dimensional model in ETABS software, and it was found that the outrigger system was efficient. Three optimum positions for the outriggers were identified: at the mid-height of the building, at 3/4th of the height, and at 1/4th of the height of the building. objective of the paper was to study the efficiency of outriggers under seismic forces, compare buildings with and without outrigger systems, and determine the optimum location of the outrigger to reduce lateral displacement. The analysis showed that the maximum deflection at the top of the structure reduced significantly by providing a second outrigger at the 34th height of the structure.. The analysis of the tall building using ETABS software revealed that the outrigger system was efficient in providing sufficient lateral stiffness to the structure. Three optimum positions for the outriggers were identified: at the mid-height of the building, at 3/4th of the height, and at 1/4th of the height of the building. The use of outrigger structural systems in high-rise buildings increases the stiffness and makes the structural form efficient under lateral load. The maximum deflection at the top of the structure was significantly reduced by providing outriggers at specific heights.



**Tushar J Kachariya et al.,**

CONCLUSION

The findings highlight the effectiveness of outrigger systems in enhancing the structural stability of tall buildings. Notably, the outrigger and hybrid systems have demonstrated superior performance in pushover analysis, while shear wall models have excelled in time history analysis. These results underline the significance of outrigger systems in mitigating lateral deflection and controlling structural drift during seismic events. Furthermore, research into the combination of core wall and outrigger systems reveals a tendency for reduced vibration in tall structures, with lower time periods compared to conventional moment frame systems. Modal analysis indicates varying stiffness levels along the building's height. Overall, this body of research underscores the importance of outrigger systems in tall buildings, particularly in earthquake-prone regions, offering enhanced stability and resilience in the face of seismic forces. It provides valuable guidance for architects, engineers, and researchers seeking to improve the seismic performance of tall structures in urban environments.

REFERENCES

1. Borah M, Choudhury S. Seismic Performance of Tall Buildings with Different Structural Systems. In International Conference on Advances in Structural Mechanics and Applications 2021 Mar 26 (pp. 90-107). Cham: Springer International Publishing.
2. Shiva Prathap HK, Gagan Kirshna RR, Naveen Kumar SM. Effect of Core Wall and Outrigger on Seismic Behavior of RC Tall Structural Systems..
3. Husain M, Hassan H, Mohamed H. THE SEISMIC RESPONSE OF STRUCTURAL OUTRIGGER SYSTEMS IN TALL BUILDING. Journal of Applied Engineering Science. 2021 Jul 22;19(3):570-7. <https://doi.org/10.5937/jaes0-30837>
4. Chen Y, Zhang Z. Analysis of outrigger numbers and locations in outrigger braced structures using a multiobjective genetic algorithm. The Structural Design of Tall and Special Buildings. 2018 Jan;27(1):e1408. <https://doi.org/10.1002/tal.1408>
5. RAO GV, SRINADH VS. COMPARATIVE STUDY OF SEISMIC EFFECT OF (SKYSCRAPER) TALL RC BUILDING FRAME OF G+ 20 STOREY WITH OUTRIGGER SYSTEM IN ZONE III BY USING ETABS. www.jespublication.com
6. Amoussou CP, Lei H, Alhaddad W, Halabi Y. Simplified modeling and analysis method for skyscrapers with outrigger system. In Structures 2021 Oct 1 (Vol. 33, pp. 1033-1050). Elsevier. <https://doi.org/10.1016/j.istruc.2021.04.096>
7. Salman K, Kim D, Maher A, Latif A. Optimal control on structural response using outrigger braced frame system under lateral loads. Journal of Structural Integrity and Maintenance. 2020 Jan 2;5(1):40-50. <https://doi.org/10.1080/24705314.2019.1701799>
8. Alhaddad W, Halabi Y, Xu H, Lei H. A comprehensive introduction to outrigger and belt-truss system in skyscrapers. In Structures 2020 Oct 1 (Vol. 27, pp. 989-998). Elsevier.
9. Tan P, Fang CJ, Chang CM, Spencer BF, Zhou FL. Dynamic characteristics of novel energy dissipation systems with damped outriggers. Engineering Structures. 2015 Sep 1;98:128-40. <https://doi.org/10.1016/j.engstruct.2015.04.033>
10. Wijesundara KK, Nascimbene R, Rassati GA. Modeling of different bracing configurations in multi-storey concentrically braced frames using a fiber-beam based approach. Journal of Constructional Steel Research. 2014 Oct 1;101:426-36. <https://doi.org/10.1016/j.jcsr.2014.06.009>
11. Kogilgeri SS, Shanthapriya B. A study on behaviour of outrigger system on high rise steel structure by varying outrigger depth. IJRET: International Journal of Research in Engineering and Technology. 2015 Jul;4(07):434-8. www.ijste.org
12. Sukhdeve SB. Optimum position of outrigger in G+ 40 RC building. IJSTE-International Journal of Science Technology & Engineering. 2016 Apr;2(10):1051-5. www.ijste.org





Tushar J Kachariya et al.,

13. IS 1893 (Part 1): 2016, Criteria for Earthquake Resistant Design of Structures. (2016, November). New Delhi: Bureau of Indian Standards.
14. Indian Standard IS. 456: Plain and Reinforced Concrete-Code of Practice, 4th Revision. Bureau of Indian Standards, New Delhi. 2000.
15. IS 16700: 2017, Criteria for Structural Safety of Tall Concrete Buildings. (2017, November). New Delhi: Bureau of Indian Standards.

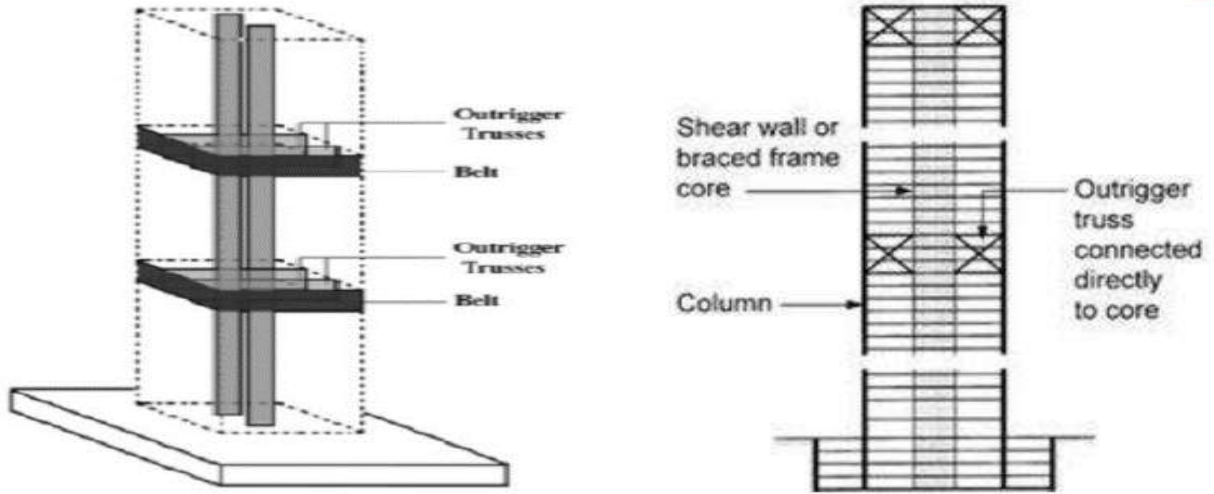


Figure 1 Belt Truss outrigger System (Source : Journal of Structural Integrity and Maintenance)





A Comprehensive Study Of Fibre Reinforced Polymer Composites: A Review

Nikhar Pandya^{1*}, Indrajit. N. Patel², Vishal Patel³, Vimlesh Agarwal³ and Pratiti Bhatt³

¹PG Scholar , Birla Vishvakarma Mahavidyalaya Engineering College, Vallabh Vidyanagar , Anand , Gujarat, India

²Principal ,Birla Vishvakarma Mahavidyalaya Engineering College, Vallabh Vidyanagar , Anand , Gujarat, India

³Assistant Professor , Birla Vishvakarma Mahavidyalaya Engineering College, Vallabh Vidyanagar , Anand , Gujarat, India.

Received: 18 Oct 2023

Revised: 25 Oct 2023

Accepted: 31 Oct 2023

*Address for Correspondence

Nikhar Pandya

PG Scholar ,

Birla Vishvakarma Mahavidyalaya Engineering College,

Vallabh Vidyanagar,

Anand, Gujarat.

E mail : nikhar1992@gmail.com



This is an Open Access Journal / article distributed under the terms of the **Creative Commons Attribution License** (CC BY-NC-ND 3.0) which permits unrestricted use, distribution, and reproduction in any medium, provided the original work is properly cited. All rights reserved.

ABSTRACT

Fiber reinforced polymer composites are advanced materials composed of high strength fibers embedded within a polymer matrix, while maintaining a distinct interface between the two components. These composites harness the unique properties of each constituent, resulting in materials with exceptional characteristics. Notably, FRP composites exhibit low density, high tensile strength, and high modulus. This paper presents an extensive review of the research conducted in the field of fibre reinforced polymer composites in recent decades . The focus is on the study of various fibres and their inherent properties, of polymer composites reinforced with both natural and synthetic fibres . The paper also reviews the research works that aim at improving these properties, and thoroughly analyses the mechanisms behind the wear phenomena . The enhancement in properties can be achieved through the appropriate selection of fibre, extraction, treatment of fibres, and interfacial engineering.

Keywords: Polymer composites, Synthetic fibres, Natural fibres, reinforcing fibre, glass fibre, kevlar fibre



Nikhar Pandya *et al.*,

INTRODUCTION

The significance of composite materials has been on the rise due to their appealing properties in this rapidly evolving world. In recent decades, there has been a growing interest in the application of fiber reinforced polymer (FRP) composite materials as substitutes for metallic components across a range of industries such as aerospace, defense, automobile, electrical, and electronic. Compared to metals, FRP composites offer several advantages including low density, higher stiffness and specific strength, improved fatigue performance, higher corrosion resistance, and high strength to weight ratio [1]. The behavior of FRP composites under different types of loads, including torsional, axial, and impact loads, plays a vital role in the design of structural components. FRP composites, classified as polymer matrix composites (PMC), typically comprise two distinct phases: the matrix phase and the reinforcement phase. [16]. By modifying the matrix phase and using suitable fillers, the properties of these fibre reinforced polymer composites can be improved. This review offers a comprehensive examination of different types of synthetic and natural fibers utilized in the development of polymer matrix composites. Currently, widely employed synthetic fibers include carbon, Kevlar, and glass [2]. In addition to synthetic fibers, natural reinforcements are also employed to enhance the strength and stiffness of polymer matrices. These natural reinforcements, which possess lower density, effectively bind with the matrix to provide high strength and stiffness. When combined with synthetic fibers like glass fiber, aramid fibers, and carbon fiber, natural polymers offer improved stiffness-to-weight and strength-to-weight ratios compared to traditional materials. Jute, kenaf, coconut, rice husk, sisal, and banana are among the primary natural sources of fibers. The properties of the matrix significantly impact the compressive strength of FRP composites, and the interaction between the matrix and fibers is crucial for designing damage-resistant and damage-tolerant composite structures [3]. To enhance the compressive strength, damage tolerance, and resistance of composites, epoxy is often modified with various types of fillers. One conventional method involves incorporating micron-sized fillers into the epoxy resin. However, this approach has certain limitations, such as a reduction in failure strain, impact strength, fracture toughness, and thermal stability of the epoxy..

LITERATURE REVIEW

Mallick, P.K. *et al* (2007) Fiber-Reinforced Composites: Materials, Manufacturing, and Design. CRC Press. This book provides a comprehensive overview of fiber-reinforced composites, discussing materials, manufacturing processes, and design considerations. It highlights the importance of understanding the properties and behavior of these materials to optimize their use in various applications. Visacanthara, T.M *et al* (2018). Fiber Reinforced Polymer Composites: A Review. International Science and Technology Journal, 7(1), 84-112. This review paper presents an in-depth analysis of fiber reinforced polymer composites, focusing on the inherent properties of various fibers. It also discusses the mechanisms behind wear phenomena and how improvements in properties can be achieved. Hull, D.*et al*. An Introduction to Composite Materials. Cambridge University Press. This book serves as an introductory guide to composite materials, discussing their properties, manufacturing processes, and applications. It provides a solid foundation for understanding the behavior of these materials.

Gibson, R.F. *et al*. Principles of Composite Material Mechanics. CRC Press. This book delves into the principles of mechanics as they apply to composite materials. It provides a comprehensive understanding of the behavior of these materials under various conditions. Callister, W.D *et al* (2018). Materials Science and Engineering: An Introduction. Wiley. This book provides an introduction to the field of materials science and engineering, discussing the properties and applications of various materials, including fiber reinforced polymer composites. Chawla, K.K. (2012). Composite Materials: Science and Engineering. Springer. This book provides a comprehensive overview of composite materials, discussing their properties, manufacturing processes, and applications. It provides a solid foundation for understanding the behavior of these materials. Agarwal, B.D. *et al* (2006). Analysis and Performance of Fiber Composites. Wiley. This book provides a comprehensive analysis of fiber composites, discussing their



**Nikhil Pandya et al.,**

properties, performance, and applications. It provides a solid foundation for understanding the behavior of these materials.

Alam S, Habib F *et al* (2010). "Effect of orientation of glass fiber on mechanical properties of GRP composites". Journal of Chemical Society Pakistan, 32: 265-269. This study investigates the impact of glass fiber orientation on the mechanical properties of Glass Reinforced Polymer (GRP) composites. The authors found that the orientation of the glass fibers significantly influences the mechanical properties of the composites, providing valuable insights for the design and manufacturing of GRP composites Barbero, E.J.(2018). Introduction to Composite Materials Design. CRC Press. This book provides an introduction to the design of composite materials, discussing the principles and techniques used in the design process. It also discusses the properties and behavior of composite materials, providing a solid foundation for understanding these materials. Hyer, M.W. (2009). Stress Analysis of Fiber-Reinforced Composite Materials. DEStech Publications. This book provides a comprehensive analysis of the stress behavior of fiber-reinforced composite materials. It discusses the principles of stress analysis and how they apply to these materials. Jones, R.M. (1999). Mechanics of Composite Materials. Taylor & Francis. This book provides a comprehensive overview of the mechanics of composite materials, discussing their properties, behavior, and applications. It provides a solid foundation for understanding these materials.

Soutis, C. (2005). Carbon Fiber Reinforced Plastics in Aircraft Construction. Materials Science and Engineering: A, 412(1-2), 171-176. This paper discusses the use of carbon fiber reinforced plastics in aircraft construction, discussing their properties, advantages, and applications. Bunsell, A.R. (2005). Handbook of Tensile Properties of Textile and Technical Fibers. Woodhead Publishing. This handbook provides a comprehensive overview of the tensile properties of textile and technical fibers, discussing their properties, behavior, and applications. Schwartz, M.M. (2010). Composite Materials: Fabrication Handbook. CRC Press. This handbook provides a comprehensive overview of the fabrication of composite materials, discussing the techniques and processes used in fabrication. Mouritz, A.P. (2012). Introduction to Aerospace Materials. Woodhead Publishing. This book provides an introduction to the materials used in aerospace, including fiber reinforced polymer composites. It discusses their properties, behavior, and applications.

Classification of Reinforcing Fibres

Reinforcing fibres, which are crucial components of fibre reinforced polymer composites, can be classified into various types based on their properties and sources

Glass Fibres

Glass fibres are a prevalent type of reinforcing fibre, making up approximately 93% of all fibre reinforced polymer composites. They are widely used in the production of structural composites, printed circuit boards, and various special-purpose products. Glass fibres come in several forms, including E-glass (electrical grade), A-glass (alkali glass), C-glass (chemical resistant glass), and R-glass or S-glass, which are recognized for their high strength. The tensile stress that glass fibres can endure ranges from 2800 to 4800 N/mm² for commercial fibres, and up to 7000 N/mm² [14] under laboratory conditions as shown in Fig 1

Carbon Fibres

Carbon fibres are another type of reinforcing fibre, known for offering the highest specific strength and modulus. They can maintain their tensile strength even at very high temperatures and offer high thermal and electrical conductivities with a relatively low coefficient of thermal expansion. These properties make carbon fibres ideal for applications in the automobile, electronics, and aerospace sectors. Carbon fibres provide a maximum strength of 7Gpa, and their axial compressive strength is 15-60% of their tensile strength[17] as shown in Fig 2





Nikhar Pandya *et al.*,

Kevlar Fibres

Kevlar fibres, a type of synthetic fibre, are known for their high tensile strength and modulus[9]. The properties of Kevlar fibres vary based on their specific type, with Kevlar 29 known as regular, Kevlar 49 as high modulus, Kevlar 129 as high strength, and Kevlar 149 as ultra-high modulus. Kevlar fibres are used in various industrial applications and advanced technologies due to their high strength, low weight, and high impact resistance[18] as shown in Fig 3.

Natural Fibres

Natural fibres are also used as reinforcements in polymer composites, referred to as natural fibre reinforced polymers (NFRP). These fibres are considered low-cost and lightweight compared to synthetic composites and are easier to handle with good acoustic and thermal insulation properties[15]. Common types of natural fibres used in composite materials include flax, hemp, jute, kenaf, and sisal. However, the major drawback of using natural fibres is the incompatibility between the hydrophilic natural fibres and the hydrophilic thermoplastic matrices during incorporation, which can lead to undesirable properties in the resulting composites [12] as shown in Fig

Chemical Treatment Of Fibres

Chemical treatment of fibres is a crucial process used to enhance the adhesion between the reinforcement and the matrix, which is essential for the performance of the composite. Untreated reinforcements often result in composites with low interlaminar shear strength due to poor bonding and weak adhesion between the matrix and the fibre[2]. Chemical treatments can increase the wettability of the reinforcement, which in turn improves the interaction between the matrix and the reinforcement. These treatments can be broadly classified into oxidative and non-oxidative treatments[3]. Oxidative treatments are utilized to create acidic functional groups on the surface of reinforcements, leading to enhanced chemical bonding with the matrix. The efficacy of this treatment in improving the surface properties of the reinforcement is influenced by various factors, such as the concentration of the oxidative medium, temperature, treatment time, and the nature of the reinforcement itself. Non-oxidative treatments, on the other hand, increase the roughness of the fibrematerial. This increase in roughness leads to a greater overall surface area of the fibre or reinforcement, which results in a greater interaction between the matrix and reinforcement[4]. In summary, chemical treatment of fibres plays a significant role in improving the properties of fibre reinforced polymer composites by enhancing the interaction between the matrix and the reinforcement.

Moisture Absorption Studies

Investigating the mechanical properties of fibre-reinforced polymeric materials under various environmental conditions is of significant importance. One of the primary challenges for fibre-reinforced polymer composites is moisture absorption, which can lead to the degradation of the composite product before its intended lifespan[6]. Natural fibres tend to absorb moisture more than synthetic fibres due to their hydrophilic nature[8]. This incompatibility between hydrophilic natural fibres and hydrophobic thermosetting resins can be addressed through chemical treatments to improve the adhesion between the fibre and the matrix. However, natural fibres are limited by their susceptibility to water absorption, primarily because their chemical composition is rich in cellulose, which is hydrophilic in nature. The absorption of water can result in a decrease in the mechanical properties of the composites, leading to premature failure under certain conditions [7]. Therefore, understanding and mitigating the effects of moisture absorption is crucial for the successful application of fibre-reinforced polymer composites, especially those using natural fibres.

CONCLUSION

Fibre reinforced polymer composites have been the subject of extensive research in recent decades due to their exceptional properties. This review has provided a comprehensive analysis of various fibres, both synthetic and natural, and their inherent properties. It has delved in properties of polymer composites reinforced with these fibres, and the research focused on enhancing these properties. The mechanisms behind wear phenomena were also thoroughly examined. The review highlighted that improvements in properties can be achieved through the careful





Nikhil Pandya et al.,

selection and treatment of fibres, as well as through interfacial engineering . The study of fibre reinforced polymer composites continues to be a promising field, with potential for further advancements and applications .[10] The future of fiber reinforced polymer composites is promising, with potential for advancements in various industries such as aerospace, automotive, and electronics. However, challenges such as moisture absorption and recycling of these composites remain, indicating the need for further research in these areas . The development of new types of fibers, both synthetic and natural, with enhanced properties is a potential area of future research. This could involve the exploration of new sources of natural fibers or the creation of synthetic fibers with improved properties . Another promising area of research is the improvement of the interface between the fiber and the matrix. This could involve the development of new surface treatment methods or the use of novel matrix materials that can better bond with the fibers. In conclusion, the study of fiber reinforced polymer composites continues to be a promising field with potential for further advancements and applications .

Future Scope

As the demand for lightweight, high-strength materials continues to grow in industries such as aerospace, automotive, and electronics, the need for advanced and efficient composites will also increase. One potential area of future research could be the development of new types of fibres, both synthetic and natural, with enhanced properties . This could involve the exploration of new sources of natural fibres or the creation of synthetic fibres with improved properties. Another promising area of research is the improvement of the interface between the fibre and the matrix . This could involve the development of new surface treatment methods or the use of novel matrix materials that can better bond with the fibres . The issue of moisture absorption in fibre reinforced polymer composites, particularly those using natural fibres, is another area that warrants further investigation . Developing methods to reduce moisture absorption and improve the compatibility between natural fibres and thermoplastic matrices could lead to the creation of composites with improved durability and lifespan . Finally, the recycling of fibre reinforced polymer composites is a critical area for future research . With increasing environmental concerns and legislation, finding efficient and effective methods for recycling these materials is of utmost importance . This could involve the development of new recycling techniques or the improvement of existing ones to recover valuable products from the resin and fibres.

REFERENCES

1. P.K. Mallick, "Fiber Reinforced Composites Materials, Manufacturing, and Design". Third edition. CRC press, London.
2. Rowell, R.M., 1995, "A new generation of composite materials from agro-based fibre," in The Third International Conference on Frontiers of Polymers and Advanced Materials, Kuala Lumpur, Malaysia.
3. J.P.Davim, C.Rosaria, "Effect of reinforcement (carbon or glass fibre) on friction and wear behaviour of the PEEK against steel surface at long dry sliding", *Wear* 266(2009)795–799.
4. Banakar P, Shivanand HK, Niranjana HB (2012) "Mechanical Properties of Angle Ply Laminated Composites"-A Review. *International Journal of Pure and Applied Sciences and Technology* 9: 127-133.
5. Kamal Kumar Basumatary, 2013. "Investigation into Mechanical and Tribological Properties of Ipomoea carnea Reinforced Epoxy Composite". Department of Mechanical Engineering. National Institute of Technology. Rourkela.
6. Zhang Q, Liang Y, Warner SB (1994) "Partial carbonization of aramid fibers". *Journal of Polymer Science Part B: Polymer Physics* 32: 2207-2220.
7. Emad Omrani, Pradeep L. Menezes, Pradeep K. Rohatgi (2016). "State of the art on tribological behavior of polymer matrix composites reinforced with natural fibers in the green materials world". *Elsevier*. 19 (2016) 717–736.
8. McGee AC, Dharan CKH, Finnie I (1987) "Abrasive wear of graphite fiber reinforced polymer composite materials". *Wear* 114: 97-107.
9. Prashanth S, Subbaya KM, Nithin K, Sachidananda S (2017). "Fiber Reinforced Composites - A Review." DOI: 10.4172/2169-0022.1000341





Nikhhar Pandya et al.,

10. Thostenson ET, Ren Z, Chou TW. "Advances in the science and technology of carbon nanotube and their composites: a review". *Compos Sci Technol* 2001; 61:1899–912.
11. A.R. Bunsell, Hybrid carbon and glass fibre composites, *Composites*. July (1974) 157-164.
12. Siha N, Banarjee AN, Mitra BC, Dynamic Mechanical study on unidirectional polyethylene fibre-PMMA and glass fibre-PMMA composite laminates, *J Appl Polym Sci*: 60: (1996) 657-62
13. Ban Bakir, Haithem Hashem (2013). "Effect of Fiber Orientation for Fiber Glass Reinforced Composite Material on Mechanical Properties".
14. Subramanian C, Senthilvelan S (2011) "Joint performance of the glass fiber reinforced polypropylene leaf spring". *Composite Structures* 93: 759-766.
15. Li J. "The effect of surface modification with nitric acid on the mechanical and tribological properties of CFs-reinforced thermoplastic polyimide composite". *Surf Interf Anal* 2009; 41(9): 759-63.
16. Sellitti C, Koenig JL, Ishida H. "Surface characterization of graphitized CFs by attenuated total reflection fourier transform infrared spectroscopy". *Carbon* 1990;28 (1): 221-8.
17. Ohsawa T, Miwa M, Kawade M, Tsushima E (1990) "Axial compressive strength of carbon fiber." *Journal of Applied Polymer Science* 39: 1733-1743.
18. Ph. Werner, V. Altsta dt, O. Jacobs, R. Jaskulka, K.W. Sandler, S.P. Saffer, A.H. Windle. "Tribological behaviour of carbon-nanofiber reinforced poly (ether ether ketone)", *Wear* 257 (2004) 1006–1014.
19. Tanner D, Fitzgerald JA, Phillips BR (1989). "The kevlar story-an advanced materials case study". *Angewandte Chemie International Edition in English* 28: 649-654.
20. Zhang Q, Liang Y, Warner SB (1994) "Partial carbonization of aramid fibers". *Journal of Polymer Science Part B: Polymer Physics* 32: 2207-2220.
21. Fibre Reinforced Polymer Manual (2010) , Indian Concrete Journal , India
22. IS : 456 : 2000 Code of Plain and reinforced cement concrete

Table 1 : Mechanical And Physical Properties Of Glass Fibre [14]

Type	Density (g/cm3)	Tensile Strength (GPa)	Young's Modulus (GPa)	Elongation(%)
E-glass	2.59	3.446	72.31	4.7
C-glass	2.53	3.32	68.94	4.6
S-glass	2.45	4.88	86.92	5.5
A-glass	2.43	3.30	68.99	4.9
R-glass	2.56	4.133	85.58	4.9
EC-Glass	2.74	3.446	85.57	4.7
AR-glass	2.72	3.242	73.11	4.5

Table 2 :Mechanical And Physical Properties Of Carbon Fibre[17]

Type	Tensile Strength (Gpa)	Tensile Modulus (Gpa)	Breaking Elongation (%)	Density (g/cm3)	Carbon content (%)
Low strength	2.5-3.2	245 – 275	1.2-1.5	1.6 -1.9	92–94
High strength	3.7 -4.2	245 -275	1.2-1.3	1.6 -1.8	91 -93
Ultra-high strength	4.6 -4.8	251 – 272	1.2-1.45	1.5 -1.9	92–95
Intermediate modulus	5.8 -6.1	305	1.21 -1.42	1.8 -1.9	96 -99
high modulus	2.4 -3.0	382 – 405	0.61 -0.73	1.6 -1.8	>99.2
Ultra-high modulus	3.7 -4.1	538 -545	0.31 -0.42	1.8 -2.2	>99.9





Nikhar Pandya et al.,

Table 3 : Mechanical And Physical Properties Of Kevlar Fibre [18]

Type	Characteristics	Tensile Modulus(Gpa)	Tensile Strength(Gpa)	Extensions break (%)	Relative Density(g/cm3)
Kevlar 29	Regular	71	2.8	4.5	1.43
Kevlar 49	High modulus	134	2.8	2.9	1.46
Kevlar 129	High strength	98	3.5	3.2	1.46
Kevlar 149	Ultra-high modulus	144	2.4	1.6	1.48

Table 4 : Mechanical And Physical Properties Of Natural Fibre [12]

Type	Tensile Strength (Gpa)	Elastic modulus	Elongation (%)	Density (g/cm3)
Cotton	400	5.5-12.6	7.0-8.0	1.5-1.6
Jute	393-700	26.5	1.5-1.8	1.5-1.8
Hemp	690	70	2-4	1.47
Flax	500-1500	27.6	2.7-3.2	2.7-3.2
Kenaf	930	53	1.6	1.45
Sisal	511-635	9.4-22	2-2.5	1.5
Coir	593	4-6	30	1.2



Fig 1 . Glass Fibre

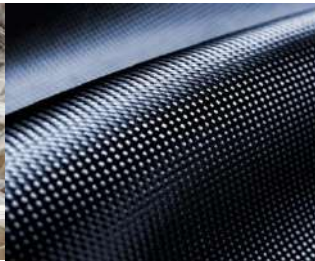


Fig 2 . Carbon Fibre

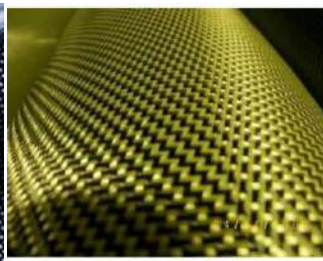


Fig 3 Kevlar Fibre



Fig 4. Natural Fibre





A Multi-Mode Frequency Reconfigurable Antenna for 5G and WLAN Applications

Sameer Mansuri^{1*}, Shahid Modasiya² and Parul Panchal³

¹Research Scholar, Gujarat Technological University, Ahmedabad, Gujarat, India

²Assistant Professor, Govt. Engineering college, Gandhinagar, Gujarat, India

³Assistant Professor, BVM Engineering College, Anand, Gujarat, India.

Received: 18 Oct 2023

Revised: 25 Oct 2023

Accepted: 31 Oct 2023

*Address for Correspondence

Sameer Mansuri

Research Scholar,

Gujarat Technological University,

Ahmedabad, Gujarat, India

E mail: mansurisameer@gmail.com



This is an Open Access Journal / article distributed under the terms of the **Creative Commons Attribution License** (CC BY-NC-ND 3.0) which permits unrestricted use, distribution, and reproduction in any medium, provided the original work is properly cited. All rights reserved.

ABSTRACT

Pin diodes are crucial in the realm of frequency reconfigurable antennas, offering the ability to swiftly shift frequencies and maintain optimal performance. Their widespread use is a testament to their role in enhancing the adaptability and efficiency of wireless communication systems. This research presents a novel design for a frequency reconfigurable antenna using printed monopoles and PIN diodes. The antenna supports nine distinct bands and four modes, facilitated by the on-off states of two PIN diodes. The antenna demonstrates both wide-spectrum and selective-spectrum proficiencies along with good gain, while maintaining a condensed form factor. The design is economical and allows for straightforward manufacturing processes. Notably, the antenna is engineered to accommodate sub-6 GHz 5G bands (2.86, 3.86, 4.41, 4.47, 4.85 and 5.17 GHz), making it an optimal choice for applications in wireless local area networks, 6 GHz fixed satellite services, and IoT-enabled wireless terminals and systems that are integral to the infrastructure of smart cities. This work contributes to the advancement of reconfigurable antenna technology, providing a versatile solution for next-generation wireless communication systems.

Keywords: Reconfigurable antenna, Multi band, Frequency reconfigurability, Sub- 6 GHz, Wi-Max, WLAN.

INTRODUCTION

The mobile communication technology of the fifth generation, operating within the frequency range below 6 GHz, is architected for swifter, dependable services with an amplified network capacity. With the progression of technology





Sameer Mansuri et al.,

in the field of wireless communication, the demand for accommodating numerous wireless services within a single apparatus has seen a substantial rise. This led to the development of reconfigurable antennas [1], which can switch their characteristics according to requirements and deliver the performance of multiple antennas without increasing size [2]. Reconfigurable antennas can be categorized into three distinct types: those that are reconfigurable by frequency, radiation pattern, and polarization. Antennas that are reconfigurable by frequency offer the ability to adjust frequencies across desired frequency bands and make efficient use of the spectrum.[3]. Antennas that are reconfigurable by pattern direct their radiation pattern towards a desired direction, by employing a concept of steering a beam. Antennas that are reconfigurable by polarization alleviate the impact of multiple signal path fading, augment the effectiveness in receiving the communication signal, and diminish the issue of co-channel interference that is common with conventional feeds. By incorporating dual-mode and corrugated features, these antennas provide conjugate matches specifically for the co-polar component.

Various switching techniques are used to achieve reconfigurability. For instance, liquid metal is used for frequency-reconfigurability in ISM/GPS band antennas [6], RF pin diodes for nine different frequency bands [7], and Varactor diodes for a range of 1.64 to 2.12 GHz [8]. Other techniques involve RF-MEMS switches for dual frequency reconfigurable bands [9], electrically tuned plasma for VHF and UHF applications [10], optical switches for microwave frequency range [11], and PIN diodes for WiMAX and WLAN applications [12]. A reconfigurable MIMO antenna for cognitive radio applications uses PIN and Varactor diodes [13]. A variety of frequency reconfigurable antennas for 5G and UWB applications have been presented. A Sub 6 GHz Frequency Adjustable Antenna, fed by a coplanar waveguide (CPW), is examined in [14], utilizing a solitary pin diode for adjustability. An antenna that is differentially-fed, designed for wireless local area networks (WLAN) and applications within the frequency range below 6 GHz, is presented in [15], employing a lumped element switch for the purpose of reconfiguration.. The defected ground structure and its effects on antenna parameters are explored in [16].

An antenna with four operational modes for various applications including the bands used for airport radar[17]. A compact hexa-band frequency-reconfigurable antenna operating at six different bands such as Wi-Fi, WiMAX and Universal MTS is introduced in [18]. Multiband frequency reconfigurable antennas for 5G and UWB applications are discussed in [19] and [20], employing a PIN Diode and an Inverted F antenna respectively. An F-shaped frequency reconfigurable antenna covering the WLAN bands, Microwave access bands such as WiMAX, Wi-Fi bands, and GSM bands is presented in [21]. A tri-band frequency reconfigurable antenna for LTE/Wi-Fi/ITS applications using two PIN diodes loaded on the ground plane is introduced in [22]. A multi band reconfigurable antenna offering eight frequency channels between 1.46 and 6.15 GHz employing dual pin diodes is presented in[23]. A miniaturized, multi-band frequency adjustable low profile inverted-F antenna achieving seven different bands for GPS, LTE, UWB and satellite applications using a single RF switch is discussed in [24]. A multi-band, low-profile frequency reconfigurable antenna for 5G communication offering switching among five resonant bands is reported in [25]. A dipole-based antenna employing four pin diodes for frequency switching, offering three distinct bands for sub-6 GHz applications is discussed in [26]. A low profile metamaterial loaded monopole antenna providing switching between ten different LTE bands is reported in [27]. A conformal, flexible, stub-loaded antenna offering multi band frequency switching providing dual and tri-band operational modes is presented in [28]. This paper introduces a low-profile, multi-band antenna with frequency adjustability, built on an FR-4 substrate. By utilizing pin-diode switches, the antenna can be reconfigured to radiate across seven distinct bands, offering good gain, radiation efficiency, and compact size. The structure of the paper is outlined as follows: Section-II presents a detailed description of the antenna geometry and design methodology. Section-III covers the simulation analysis conducted in HFSS and compares the simulation results obtained with the relevant studies in the field. Finally, Section IV concludes the research.

Design Methodology of the Antenna

This section illustrates the design of the proposed antenna with reconfigurable frequency bands. Seven strips of varying length and two PIN diodes in slots form the printed monopole antenna. The strip length and diode switching determine the frequency bands. The HFSS software was used for modeling and simulation.





Sameer Mansuri *et al.*,

Design theory and Structural Geometry

The proposed antenna's geometry is shown in Figure 1. The 30 mm by 20 mm antenna is designed on an FR-4 substrate with 1.6mm height. The substrate is supported by a reduced size metal ground plane for improved gain and directivity. The substrate possesses a relative permittivity of 4.3 and exhibits a loss tangent of 0.025. To accommodate the pin diodes between the strips, a 1 mm gap was created. The antenna is fed by a microstrip line that is 3 mm wide and 50 ohms in resistance. The antenna was designed and simulated with the calculated parameters using Ansys HFSS, a FEM-based electromagnetic program.

The antenna's radiating component and the truncated ground plane are made using copper. The antenna presented is powered by a microstrip line with a width of 3mm offering an impedance of 50Ω . The effective resonant lengths for the intended frequencies are calculated using model theory of Transmission line [29]. A quartered guided wavelength (i.e. $L_f \approx \lambda/4$) is the effective length of the antenna for each of the associated resonant bands. The various evolution phases of the proposed design are shown in figure 2. The strips of width w_2 and w_3 are added to get the desired bands and better impedance matching. The comparison of the return loss of the proposed antenna at various design stages is shown in figure 3. The dimensions of this antenna are summarized in Table I.

Modes of Operation

By switching the pin diodes ON and OFF, the proposed antenna can alter its frequency by establishing an open or short circuit between the radiating patches. Four separate operating modes of the antenna, each with a unique set of resonance frequencies, are available. The antenna uses a wideband frequency range of 3.69 to 5.61 GHz while in Mode 1. The antenna's three resonant bands are active in Mode 2. The antenna operates in dual band mode and covers 4.47 and 7.73 GHz when SW1 is off and SW2 is on. The antenna features three 2.83, 4.85, and 7.4 GHz resonant bands in Mode 4. The matching resonant bands for each mode are displayed in Table 2 along with the pin diode states.

Switching Technique

This section shows how the antenna is designed to get the desired frequency band by employing two PIN diodes. These diodes switch between open and short circuit at their locations, changing the current path and frequency of the antenna. When in ON state, diode's is equivalent to a series RL circuit (where R is low) value and When in OFF state, the diode acts as a parallel RC circuit (where R is high) in series with L. Figure 4 shows the equivalent circuits for the operating states of a PIN diode. For ON state, it is a series RL circuit with $R = 1.2\Omega$ and $L = 0.45$ nH. For OFF state, it acts as a parallel RC circuit with $R = 5$ K Ω and $C = 0.3$ pF and in series with $L = 0.45$ nH. PIN diodes from Skyworks (SMP 1345-079LF) are used and simulated in HFSS.

RESULT AND DISCUSSION

Return Loss and Bandwidth

The antenna operates in four distinct modes depending on the switching conditions of both the PIN diodes. The simulated return loss of all 4 modes is shown in figure 5. In Mode 0, it functions as a single-band entity spanning 3.69-5.61 GHz, with an average gain of 1.9 and a return loss of -35 dB. Transitioning to Mode 1, it morphs into a tri-band configuration covering 3.45-4.27 GHz, 4.80-5.55 GHz, and 8-8.94 GHz, offering an average gain of 0.85 and return losses of -16 dB, -14.5 dB, and -15.25 dB respectively. In Mode 2, it operates as a dual-band setup covering 3.56-5.38 GHz and 7.57-7.88 GHz, delivering an average gain of 1.67 and return losses of -24 dB and -14 dB respectively. In mode 4, the antenna transitions into a tri-band configuration encompassing the frequency bands of 2.71-2.96 GHz, 4.37-5.33 GHz, and 7.24-7.56 GHz. This mode delivers an average gain of 1.55 and exhibits return losses of -11.2 dB, -15.5 dB, and -19.5 dB for each respective band. The designed planar and multi-band monopole antenna's E and H plane directivity patterns across various frequency bands are displayed in figure 6.





Sameer Mansuri et al.,

Comparison with the Existing Literature

The antenna design proposed in this study is more compact in size compared to the antennas discussed in the comparative analysis. This newly designed antenna exhibits an impedance bandwidth (BW) that spans from 300 to 1920 MHz, providing a broader bandwidth than the antennas developed in previous studies [31–37]. A detailed comparison is presented in Table 3.

CONCLUSION

The purpose of this study is to design a small, flexible antenna with four distinct operating modes and support for nine operating bands. The status of the integrated switches governs this antenna's ability to operate over a variety of frequency bands, making it special. It performs admirably at frequencies between 300 and 1920 MHz, making it appropriate for both narrowband and wideband applications. The antenna has a virtually omni directional design that exhibits excellent directivity and a peak gain that ranges from 0.85 to 1.9, making it appropriate for a number of wireless applications. Its small size does not sacrifice performance, either. To validate the computational findings, a cost-effective prototype of the suggested frequency reconfigurable antenna can be created.

REFERENCES

1. M. H. Alsharif and R. Nordin, "Evolution towards fifth generation (5G) wireless networks: Current trends and challenges in the deployment of millimetre wave, massive MIMO, and small cells," *Telecommunication Systems*, vol. 64, no. 4, pp. 617–637, 2017.
2. J. Costantine, Y. Tawk, S. E. Barbin and C. G. Christodoulou, "Reconfigurable antennas: Design and applications," *Proc. of the IEEE*, vol. 103, no. 3, pp. 424–437, 2015.
3. I. F. Akyildiz, W. Y. Lee, M. C. Vuran and S. Mohanty, "Next generation/dynamic spectrum access/cognitive radio wireless networks: A survey," *Computer Networks*, vol. 50, no. 13, pp. 2127–2159, 2006.
4. S. Nikolaou, R. Bairavasubramanian, C. Lugo, I. Carrasquillo, D. C. Thompson et al., "Pattern and frequency reconfigurable annular slot antenna using PIN diodes," *IEEE Transactions on Antennas and Propagation*, vol. 54, no. 2, pp. 439–448, 2006.
5. M. N. Osman, M. K. A. Rahim, P. Gardner, M. R. Hamid, M. F. M. Yusoff et al., "An electronically reconfigurable patch antenna design for polarization diversity with fixed resonant frequency," *Radioengineering*, vol. 24, no. 1, pp. 45–53, 2015.
6. M. Kelley, C. Koo, H. McQuilken, B. Lawrence, S. Li et al., "Frequency reconfigurable patch antenna using liquid metal as switching mechanism," *Electronics Letters*, vol. 49, no. 22, pp. 1370–1137, 2013.
7. H. A. Majid, M. K. A. Rahim, M. R. Hamid, N. A. Murad and M. F. Ismail, "Frequency-reconfigurable microstrip patch-slot antenna," *IEEE Antennas and Wireless Propagation Letters*, vol. 12, pp. 218–220, 2013.
8. L. Ge and K. M. Luk, "Frequency-reconfigurable low-profile circular monopolar patch antenna," *IEEE Transactions on Antennas and Propagation*, vol. 62, no. 7, pp. 3443–3449, 2014.
9. I. Kim and Y. Rahmat-Samii, "RF MEMS switchable slot patch antenna integrated with bias network," *IEEE Transactions on Antennas and Propagation*, vol. 59, no. 12, pp. 4811–4815, 2011.
10. C. Wang, B. Yuan, W. Shi and J. Mao, "Low-profile broadband plasma antenna for naval communications in VHF and UHF Bands," *IEEE Transactions on Antennas and Propagation*, vol. 68, no. 6, pp. 4271–4282, 2020.
11. I. D. Feliciano, A. C. Sodré Jr, J. S. R. Páez, R. Puerta, J. J. V. Olmos et al., "Photonics-assisted wireless link based on mm-wave reconfigurable antennas," *IET Microwaves, Antennas & Propagation*, vol. 11, no. 14, pp. 2071–2076, 2017.
12. M. S. Alam and A. M. Abbosh, "Beam-steerable planar antenna using circular disc and four PIN-controlled tapered stubs for WiMAX and WLAN applications," *IEEE Antennas and Wireless Propagation Letters*, vol. 15, pp. 980–983, 2015.
13. X. Zhao, S. Riaz and S. Geng, "A reconfigurable MIMO/UWB MIMO antenna for cognitive radio applications," *IEEE Access*, vol. 7, pp. 46739–46747, 2019.





Sameer Mansuri et al.,

14. R. K. Verma, A. Kumar and R. L. Yadava, "Compact multiband CPW fed sub 6 GHz frequency reconfigurable antenna for 5G and specific UWB applications," *Journal of Communications*, vol. 15, no. 4, pp. 345–349, 2020.
15. G. Jin, C. Deng, J. Yang, Y. Xu and S. Liao, "A new differentially-fed frequency reconfigurable antenna for WLAN and Sub-6 GHz 5G applications," *IEEE Access*, vol. 7, pp. 56539–56546, 2019.
16. M. T. Khan, M. T. Jilani, A. M. Khan, F. Hafeez and A. K. Memon, "Effects of defected ground structure slot tuning on frequency and circuit parameters of bandpass filter," *Journal of Optoelectronics and Advanced Materials*, vol. 20, pp. 479–485, 2018.
17. A. Iqbal, A. Smida, L. F. Abdulrazak, O. A. Saraereh, N. K. Mallat et al., "Low-profile frequency reconfigurable antenna for heterogeneous wireless systems," *Electronics*, vol. 8, no. 9, pp. 976, 2019.
18. I. A. Shah, S. Hayat, A. Basir, M. Zada, S. A. A. Shah et al., "Design and analysis of a hexa-band frequency reconfigurable antenna for wireless communication," *AEU-International Journal of Electronics and Communications*, vol. 98, no. 1, pp. 80–88, 2019.
19. A. Desai, R. Patel, T. Upadhyaya, H. Kaushal and V. Dhasarathan, "Multiband inverted E and U shaped compact antenna for digital broadcasting, wireless, and sub 6 GHz 5G applications," *AEU-International Journal of Electronics and Communications*, vol. 123, no. 1, pp. 153296, 2020.
20. Y. K. Park and Y. Sung, "A reconfigurable antenna for quad-band mobile handset applications," *IEEE Transactions on Antennas and Propagation*, vol. 60, no. 6, pp. 3003–3006, 2012.
21. S. Hayat, I. A. Shah, I. Khan, I. Alam, S. Ullah et al., "Design of tetra-band frequency reconfigurable antenna for portable wireless applications," in *Int. Conf. on Intelligent Systems Engineering*, Islamabad, Pakistan, pp. 15–17, 2016.
22. S. S. Bharadwaj, D. Sipal, D. Yadav and S. K. Koul, "A compact tri-band frequency reconfigurable antenna for LTE/WI-FI/ITS application," *Progress in Electromagnetics Research*, vol. 91, pp. 59–67, 2020.
23. Y. B. Chaouche, I. Messaoudene, I. Benmabrouk, M. Nedil and F. Bouttout, "Compact coplanar waveguide-fed reconfigurable fractal antenna for switchable multiband systems," *IET Microwaves, Antennas & Propagation*, vol. 13, no. 1, pp. 1–8, 2018.
24. F. A. Asadallah, J. Costantine and Y. Tawk, "A multiband compact reconfigurable PIFA based on nested slots," *IEEE Antennas and Wireless Propagation Letters*, vol. 17, no. 2, pp. 331–334, 2018.
25. A. Ghaffar, X. J. Li, B. C. Seet, W. A. Awan and N. Hussain, "Compact multiband frequency reconfigurable antenna for 5G communications," in *29th Int. Telecommunication Networks and Applications Conf.*, Auckland, New Zealand, pp. 1–3, 2019.
26. G. Jin, C. Deng, Y. Xu, J. Yang and S. Liao, "Differential frequency reconfigurable antenna based on dipoles for sub-6 GHz 5G and WLAN applications," *IEEE AWPL Antennas and Wireless Propagation Letters*, vol. 19, no. 3, pp. 472–476, 2020.
27. A. Shahgholi, G. Moradi and A. Abdipour, "Low-profile frequency-reconfigurable LTE-CRLH antenna for smartphones," *IEEE Access*, vol. 8, pp. 26487–26494, 2020.
28. N. Hussain, W. A. Awan, S. I. Naqvi, A. Ghaffar, A. Zaidi et al., "A compact flexible frequency reconfigurable antenna for heterogeneous applications," *IEEE Access*, vol. 8, pp. 173298–173307, 2020.
29. A. Ghaffar, X. J. Li, W. A. Awan and N. Hussain, "A compact multiband multi-mode frequency reconfigurable antenna for portable devices," in *2020 Int. Conf. on UK-China Emerging Technologies*, Glasgow, UK, pp. 1–4, 2020.
30. S. A. A. Shah, M. F. Khan, S. Ullah and J. A. Flint, "Design of a multi-band frequency reconfigurable planar monopole antenna using truncated ground plane for Wi-Fi, WLAN and WiMAX applications," in *2014 Int. Conf. on Open-Source Systems & Technologies*, Lahore, Pakistan, pp. 151–155, 2014.
31. B. Saikia, P. Dutta and K. Borah, "Design of a frequency reconfigurable microstrip patch antenna for multiband applications," in *Proc. of the 5th Int. Conf. on Computers & Management Skills*, Arunachal Pradesh, India, pp. 15–16, 2019.
32. S. Ullah, S. Hayat, A. Umar, U. Ali, F. A. Tahir et al., "Design, fabrication and measurement of triple band frequency reconfigurable antennas for portable wireless communications," *AEU-International Journal of Electronics and Communications*, vol. 81, pp. 236–242, 2017.





Sameer Mansuri et al.,

33. S. A. A. Shah, M. F. Khan, S. Ullah, A. Basir, U. Ali et al., "Design and measurement of planar monopole antennas for multi-band wireless applications," IETE Journal of Research, vol. 63, no. 2, pp. 194–204, 2017.
34. A. Iqbal, S. Ullah, U. Naeem, A. Basir and U. Ali, "Design, fabrication and measurement of a compact, frequency reconfigurable, modified T-shape planar antenna for portable applications," Journal of Electrical Engineering and Technology, vol. 12, no. 4, pp. 1611–1618, 2017.
35. S. Ullah, I. Ahmad, Y. Raheem, S. Ullah, S. T. Ahmad et al., "Hexagonal shaped CPW feed based frequency reconfigurable antenna for WLAN and Sub-6 GHz 5G applications," in Int. Conf. on Emerging Trends in Smart Technologies, Karachi, Pakistan, pp. 26–27, 2020.
36. I. A. Shah, S. Hayat, I. Khan, I. Alam, S. Ullah et al., "A compact, tri-band and 9-shape reconfigurable antenna for WiFi, WiMAX and WLAN applications," International Journal of Wireless and Microwave Technologies, vol. 6, no. 5, pp. 45–53, 2016.

Table 1 – Dimensions of the proposed antenna

Parameter	Dimensions (mm)	Parameter	Dimensions (mm)
Ws	30	L1	21
Ls	20	L2	1.5
Wg	30	L3	2
Lg	9.5	W1	11
Wf	3	W2	3.4
Lp	2	W3	9
Lf	13.5	H	1.6

Table 2 – Mode selection using PIN diodes

Mode	SW1	SW2	Operating bands (GHz)
1	OFF	OFF	3.69-5.61
2	ON	OFF	3.45-4.27, 4.80-5.55 and 8-8.94
3	OFF	ON	3.56-5.38 and 7.57-7.88
4	ON	ON	2.71-2.96, 4.37-5.33 and 7.24-7.56

Table 3 – Comparison of proposed antenna with other reported work

Ref.	Size (mm ³)	PIN diodes	No. of bands	Freq. Bands (GHz)	-10dB BW (MHz)	Peak gains
[30]	40 x 35 x 1.6	1	3	2.45, 3.5, 5.4	490-1360	1.92-3.02
[31]	60 x 60 x 1.6	3	5	2.4,4.26,4.32,4.58,5.76	60-170	1.31-2.77
[32]	53 x 35 x 1.6	1	3	2.45, 3.50, 5.20	147-1820	1-7-3.4
[33]	40 x 22 x 1.6	1	4	2.45, 5.13, 3.49, 5.81	750-1260	1.72-2.96
[34]	39 x 37 x 1.6	1	3	2.4, 5.4, 3	550-1220	1.27-3.8
[35]	37 x 35 x 1.6	2	4	2, 3.4, 2.4, 3.1	200-960	1.76-1.98
[36]	40 x 35 x 1.6	1	3	2.45, 3.5, 5.2	330-1250	1.48-3.26
This work	30 x 20 x 1.6	2	9	2.83,3.86,4.41,4.47,4.85,5.17, 7.4, 7.73, 8.47	300-1920	0.85-1.9





Sameer Mansuri et al.,

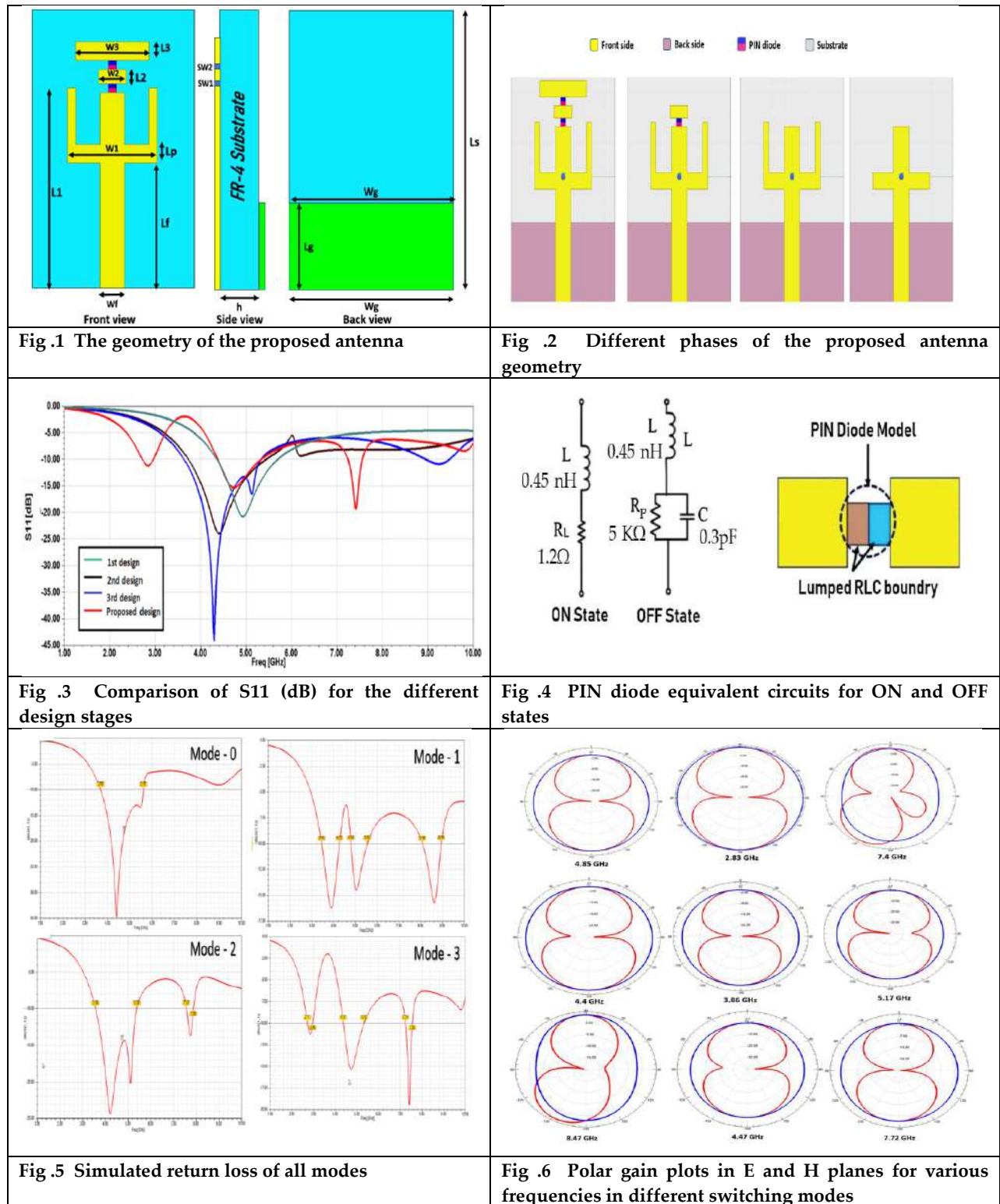




Image Captioning Using Deep Learning – An Overview

Deepak Vala ,Kartik Sharma, Jagdish Rathod and Mehfuza Holia

Electronics Department, Birla Vishvakarma Mahavidyalaya, Anand, Gujarat, India.

Received: 18 Oct 2023

Revised: 25 Oct 2023

Accepted: 31 Oct 2023

*Address for Correspondence

Deepak Vala

Electronics Department,
Birla Vishvakarma Mahavidyalaya,
Anand, India



This is an Open Access Journal / article distributed under the terms of the **Creative Commons Attribution License** (CC BY-NC-ND 3.0) which permits unrestricted use, distribution, and reproduction in any medium, provided the original work is properly cited. All rights reserved.

ABSTRACT

This research paper presents a robust image captioning system developed using advanced deep learning techniques. Leveraging a diverse dataset from Flickr, the study integrates a pre-trained VGG16 model for feature extraction and LSTM networks for caption generation. The system excels in generating meaningful captions for various images, enhancing accessibility for visually impaired individuals. Noteworthy is the seamless integration of text-to-speech functionality, making the generated captions accessible through spoken words. The paper discusses the system's architecture, data preprocessing intricacies, and evaluation metrics, providing a comprehensive analysis of results and real-world implications.

Keywords: Image Captioning, deep learning, artificial intelligence

INTRODUCTION

The visually impaired community faces significant barriers in accessing visual information prevalent in the digital world. While images convey rich details, these nuances are often lost on individuals with visual impairments. Traditional assistive technologies fall short in providing comprehensive and contextually relevant descriptions of images, hindering the visually impaired from fully participating in the visual culture of the digital age. This project addresses this critical gap by developing an innovative solution that harnesses the power of deep learning and computer vision to generate detailed and accurate textual descriptions for images. By doing so, it pioneers an inclusive approach, ensuring that individuals with visual impairments can engage with images, art, and the visual world with the same depth and understanding as their sighted peers.

Aim

The aim of this paper is to empower individuals with visual impairments by creating an inclusive technology that translates visual information into detailed and contextually relevant textual descriptions. By leveraging advanced





Deepak Vala et al.,

deep learning techniques, the project aims to bridge the gap between visual content and accessible information, fostering a more inclusive digital environment.

Objective

Image Captioning: Develop a robust image captioning system that accurately describes images, enabling individuals with visual impairments to understand the content and context of the visual information.

Real-Time Processing: Implement real-time image processing capabilities, ensuring timely and dynamic generation of image descriptions for various digital content.

Contextual Understanding: Enhance the system's ability to comprehend the context of images, allowing for nuanced and detailed descriptions that capture the essence of visual scenes.

Integration with Hardware: Integrate the developed solution with hardware components, such as Raspberry Pi and Pi Camera, to create a portable and user-friendly device for on-the-go image description.

User-Friendly Interface: Design an intuitive and user-friendly interface that facilitates effortless interaction, making the technology accessible to individuals with varying levels of technical expertise.

History of Image Captioning

Early Years (1960s - 1990s)

1960s: The earliest attempts at computer vision involved basic pattern recognition, but the idea of generating natural language descriptions for images was not well-explored.

1970s: Research in natural language processing (NLP) laid the foundation for understanding language structures, which would later be integrated into image captioning systems [1].

1980s-1990s: With the rise of computational linguistics, there was a growing interest in integrating computer vision with natural language understanding. However, the technology and datasets were not advanced enough to create robust image captioning systems.

Emergence of Datasets (2000s - 2010s)

Early 2000s: The availability of digital images and the growth of the internet led to the creation of the first image datasets, although they were relatively small in scale.

Mid-2000s: Research started to focus on larger-scale datasets and benchmark challenges, encouraging the development of more sophisticated algorithms.

Late 2000s: With the release of datasets like Pascal VOC and Caltech-UCSD Birds, researchers began exploring image description tasks more rigorously, paving the way for image captioning research.

Introduction of Deep Learning (2010s - Present)

2014: The breakthrough came with the introduction of deep learning techniques, particularly Convolutional Neural Networks (CNNs) for image feature extraction and Recurrent Neural Networks (RNNs) for language modeling. The merge of these technologies marked a significant advancement in image captioning [2].

2015: Microsoft introduced the COCO (Common Objects in Context) dataset, which provided a large-scale benchmark for image captioning. This dataset accelerated the development of deep learning models for generating detailed and accurate captions [3].

2016: Attention mechanisms were integrated into image captioning models, allowing them to focus on specific parts of the image while generating captions, leading to more contextually relevant descriptions.

2017-2018: Researchers started to explore reinforcement learning techniques for training image captioning models, allowing for better optimization of non-differentiable evaluation metrics like BLEU and CIDEr [4].

2019-Present: The integration of transformer architectures into image captioning systems led to significant improvements in generating coherent and contextually accurate captions. Multimodal models that incorporate both image and textual data (e.g., BERT-based models) also became prominent [5].

Different Image Captioning Techniques

Traditional Methods





Deepak Vala *et al.*,

Template-Based Approaches: Early image captioning systems used templates where pre-defined sentence structures were combined with extracted visual features to generate captions. These templates lacked flexibility and couldn't handle diverse images effectively.

Rule-Based Systems: Rule-based methods employed linguistic rules to associate specific objects or scenes in an image with predefined textual descriptions. These systems often lacked context and struggled with complex scenes.

Statistical Machine Translation (SMT) Based Approaches

Phrase-Based Models: SMT techniques were adapted for image captioning where images were treated as source language and captions as target language. Phrases were aligned between images and captions, and statistical models were used for translation. However, these methods had limitations in capturing long-range dependencies and context.

Deep Learning-Based Approaches

CNN-RNN Models: The integration of Convolutional Neural Networks (CNNs) for image feature extraction and Recurrent Neural Networks (RNNs), particularly Long Short-Term Memory (LSTM) networks, for language modeling revolutionized image captioning. CNNs were used to encode image features, and LSTMs were used to decode these features into natural language captions. This approach significantly improved the contextual understanding of images [2].

Attention Mechanisms: Attention mechanisms were introduced to enhance the CNN-RNN models. Attention mechanisms allowed the model to focus on specific parts of the image when generating corresponding words in the caption. This dynamic focus greatly improved the quality and relevance of generated captions.

Transformer-Based Models: Transformer architectures, primarily designed for sequence-to-sequence tasks, were adapted for image captioning. Transformers allowed for parallel processing of input sequences and introduced self-attention mechanisms, making them highly effective for capturing relationships between visual elements and generating coherent captions.

BERT-Based Models: Bidirectional Encoder Representations from Transformers (BERT) and its variants were adapted for multimodal tasks, combining visual and textual information. By pre-training on large textual corpora and fine-tuning on image-caption pairs, BERT-based models achieved state-of-the-art performance in image captioning tasks [4].

Multimodal Approaches

Fusion of Modalities: Multimodal models combined information from various modalities (images, text, and audio) to generate captions. These models often utilized techniques like late fusion (combining features after separate processing) or early fusion (merging features at the input level) to integrate information effectively.

Cross-Modal Retrieval: Image captioning models were sometimes trained jointly with tasks like image retrieval, where images were matched with corresponding captions. This joint training improved the alignment between images and captions, leading to better caption generation.

Reinforcement Learning-Based Approaches

Policy Gradient Methods: Reinforcement learning techniques, particularly policy gradient methods, were employed to optimize image captioning models based on reward signals. Rewards were often based on human-generated captions' quality, encouraging the model to generate more accurate and coherent captions.

Adversarial Approaches

Adversarial Networks: Generative Adversarial Networks (GANs) were explored for image captioning. GANs consist of a generator and a discriminator, where the generator tries to create realistic captions, and the discriminator evaluates their authenticity. This adversarial training process led to the generation of more natural and human-like captions.





Deepak Vala *et al.*,

Controllable and Interpretable Image Captioning

Attribute-Based Captioning: Some approaches incorporated attributes (such as colors, shapes) into the image captioning process, allowing for more specific and controllable generation based on these attributes.

Explainable AI: There has been a growing focus on making image captioning models interpretable, allowing users to understand why a specific caption was generated. This aligns with the broader trend in AI towards explainable and transparent models.

VGG16 Model – A Overview

VGG16 is a popular deep learning model that belongs to the VGG (Visual Geometry Group) family. Developed by researchers from the Visual Graphics Group at the University of Oxford, VGG16 is renowned for its simplicity and effectiveness in image classification tasks [6] fig. 1.

Architecture

Depth: VGG16, as the name suggests, has 16 layers. These 16 layers are stacked together, making it deeper than its predecessors like AlexNet.

Layer Configuration: The architecture primarily consists of convolutional layers with small receptive fields (3x3) and max-pooling layers (2x2). It has 13 convolutional layers and 3 fully connected layers.[6]

Activation Function: Rectified Linear Unit (ReLU) activation functions are used throughout the network, introducing non-linearity after each convolution operation.

Padding: The convolutional layers use the 'same' padding, which means the input dimensions are preserved after each convolution operation.

Pooling: Max-pooling layers with a stride of 2x2 are employed to reduce the spatial dimensions of the feature maps.

Key Features

Uniform Architecture: VGG16 maintains a uniform architecture by using small receptive fields for all convolutional layers and using max-pooling layers for down sampling. This uniformity simplifies the architecture and makes it easy to understand and implement.

Deep Stacking: VGG16's depth is a key feature. While deeper networks tend to capture more intricate features, they also require more parameters and computational resources. VGG16 strikes a balance between depth and complexity, making it widely used in various applications.

Transfer Learning: Due to its effectiveness and relatively small size compared to modern architectures like ResNet or Inception, VGG16 is often used as a feature extractor in transfer learning scenarios. By removing the last few layers and adding custom layers, the model can be fine-tuned for specific tasks with smaller datasets.[6]

Performance

ImageNet Challenge: VGG16 was originally developed to participate in the ImageNet Large Scale Visual Recognition Challenge (ILSVRC) in 2014. It achieved high accuracy on the ImageNet dataset, demonstrating the effectiveness of deep learning in large-scale image classification tasks.

Scalability: While VGG16's 16-layer architecture was significant at the time of its introduction, subsequent architectures like VGG19 and more complex networks have been developed to handle more intricate tasks and larger datasets.[6]

Limitations and Considerations

Computational Intensity: Due to its depth and the number of parameters, VGG16 can be computationally intensive, especially when trained from scratch on large datasets.

Overfitting: VGG16, like many deep networks, is prone to overfitting, especially when dealing with small datasets. Regularization techniques like dropout or batch normalization are often necessary to mitigate overfitting.





Deepak Vala et al.,

Applications

Image Classification: VGG16 is primarily used for image classification tasks where it can classify objects in images into one of several predefined categories.

Feature Extraction: VGG16's intermediate layers are valuable as feature extractors for various computer vision tasks, including object detection and image segmentation.

Image Captioning Case Studies

Seeing AI – Microsoft

Background

Seeing AI is a revolutionary app developed by Microsoft to assist individuals with visual impairments. Leveraging advanced image captioning technology, the app provides real-time audio descriptions of the user's surroundings, enabling them to better understand and navigate the world independently [7].

Challenge

The challenge was to create an innovative solution that utilizes image captioning to empower visually impaired individuals by providing them with detailed and accurate descriptions of their environment, people, and objects around them. The aim was to enhance their daily lives by increasing accessibility and enabling greater independence [7].

Implementation

Scene Recognition: Seeing AI employs image recognition algorithms to analyze scenes in real-time. It can describe general surroundings, such as "a living room with furniture," enabling users to comprehend their location.

Object Recognition: The app recognizes and provides descriptions of specific objects, including "a person with a dog" or "a can of soup." This functionality aids users in identifying items and people around them.

Text Recognition: Seeing AI uses Optical Character Recognition (OCR) to read aloud printed and handwritten text. This feature is invaluable for tasks like reading documents, menus, or signs.

Currency Identification: The app can identify various currency notes, enabling users to distinguish between different denominations.

Light Detection: Seeing AI informs users about the brightness of the environment, helping them assess lighting conditions.

Color Description: The app can describe colors, allowing users to differentiate between various hues and shades.

Impact:

Enhanced Independence: Seeing AI has significantly enhanced the independence of visually impaired individuals. By providing detailed audio descriptions, it enables them to navigate unfamiliar environments, read printed materials, and identify people and objects independently.

Increased Accessibility: The app has made various spaces, such as museums, restaurants, and public places, more accessible for individuals with visual impairments. It allows them to participate in social activities and engage with the world on a broader scale.

Education and Employment: Seeing AI has opened up new avenues for education and employment. Visually impaired students can access educational materials, and professionals can read documents and participate in meetings effectively.

Community Inclusion: The app promotes social inclusion by enabling visually impaired individuals to participate in social interactions confidently. It fosters a sense of belonging and reduces the barriers they face in social situations.

Future Developments

Seeing AI continues to evolve with ongoing advancements in image captioning technology. Microsoft actively gathers user feedback to enhance the app's features and user experience. Future updates may include improvements in accuracy, expanded language support, and additional functionalities to further empower users.





Deepak Vala *et al.*,

Waymo – Alphabet

Background

Waymo, a subsidiary of Alphabet Inc. (Google's parent company), is a leader in the development of autonomous vehicles. Utilizing advanced image captioning techniques and deep learning, Waymo has pioneered the use of artificial intelligence (AI) to enable vehicles to perceive and understand their surroundings, making autonomous driving a reality.

Challenge

The challenge was to develop a sophisticated autonomous driving system that could perceive and comprehend complex and dynamic environments. This system needed to accurately recognize objects, pedestrians, other vehicles, road signs, and various scenarios on the road. The goal was to ensure the safety of passengers and pedestrians while navigating diverse and unpredictable driving conditions [8].

Implementation

Image Perception: Waymo vehicles are equipped with multiple sensors, including cameras, LiDAR, and radar, to capture high-resolution images of the surroundings. These images serve as input data for the AI system.

Object Recognition: Deep learning models, incorporating image captioning techniques, analyze the captured images to recognize and categorize objects in real-time. This includes identifying pedestrians, cyclists, vehicles, and other elements in the environment.

Semantic Segmentation: Waymo's AI system performs semantic segmentation, classifying pixels in the images into different categories such as road, sidewalk, and vehicles. This segmentation enhances the understanding of the vehicle's surroundings.

Behavior Prediction: The system predicts the behavior of other road users, including pedestrians and vehicles. By analyzing the captured images and patterns of movement, Waymo's AI anticipates the intentions of surrounding entities, enabling safe decision-making.

Real-time Mapping: Waymo continuously updates its high-definition maps using data collected from its vehicles. These maps are enriched with information about the environment, such as lane markings and traffic signs, providing additional context for the AI system.

Sensor Fusion: Waymo integrates data from various sensors, combining information from cameras, LiDAR, and radar. Sensor fusion enhances the accuracy of object detection and localization, ensuring reliable perception capabilities [8].

Impact

Enhanced Safety: Waymo's autonomous driving technology, empowered by image captioning and AI, has the potential to significantly reduce road accidents caused by human error. The system's ability to perceive and respond to the environment enhances overall road safety.

Increased Mobility: Autonomous vehicles offer enhanced mobility options for individuals who are unable to drive due to age or disabilities. Waymo's technology opens up new possibilities for accessible transportation, providing independence to a wider demographic.

Traffic Efficiency: Waymo's autonomous driving system optimizes traffic flow by adhering to traffic rules, maintaining appropriate speeds, and making efficient driving decisions. This can lead to reduced congestion and smoother traffic patterns [8].

Environmental Impact: More efficient driving patterns facilitated by autonomous vehicles can contribute to reduced fuel consumption and lower emissions, positively impacting the environment.

Future Developments

Waymo continues to invest in research and development to enhance its autonomous driving capabilities. Future developments may include improvements in real-time decision-making, further advancements in object recognition, and expanding the system's capabilities to handle diverse and challenging driving scenarios.



Deepak Vala *et al.*,

CONCLUSION

In the realm of technological innovation, the convergence of computer vision and natural language processing has led to the creation of a groundbreaking solution: an intelligent image captioning system tailored for the visually impaired. Embarking on this journey, I envisioned an inclusive world where individuals with visual impairments could perceive and comprehend their surroundings with the aid of cutting-edge technology. Our paper, which seamlessly integrates advanced deep learning techniques and portable hardware, stands as a testament to the potential of artificial intelligence in enhancing accessibility and enriching lives.

ACKNOWLEDGMENT

A paper is comprehensive because it is seldom the result of one or two persons working quietly in isolation. It is the result of many people's endeavors over several hours. I thank all those who helped me with this report. We would like to express our sincere gratitude to the Head of the Electronics Department Dr. Tanmay Pawar and all faculty members who helped us throughout our studies. And our most profound and sincere thanks go to our guide Dr. D. L. Vala for his extensive guidance, encouragement, immense help, and cooperation.

REFERENCES

1. Eric Cabria & Biba White on "Jumping NLP Curves: A Review of Natural Language Processing Research" [Review Article], IEEE.
2. Wenpeng Yin, Katharina Kann, Mo Yu, Hinrich Schütze, "Comparative Study of CNN and RNN for Natural Language Processing", IEEE.
3. Chen, Xinlei, *et al.* "Microsoft coco captions: Data collection and evaluation server." arXiv preprint arXiv:1504.00325 (2015)
4. Papineni, Kishore, *et al.* "Bleu: a method for automatic evaluation of machine translation." Proceedings of the 40th annual meeting of the Association for Computational Linguistics. 2002.
5. Devlin, Jacob, *et al.* "Bert: Pre-training of deep bidirectional transformers for language understanding." arXiv preprint arXiv:1810.04805 (2018).
6. Qassim, Hussam, Abhishek Verma, and David Feinzimer. "Compressed residual-VGG16 CNN model for big data places image recognition." 2018 IEEE 8th annual computing and communication workshop and conference (CCWC). IEEE, 2018.
7. Granquist, Christina, *et al.* "Evaluation and comparison of artificial intelligence vision aids: Orcam myeye 1 and seeing ai." Journal of Visual Impairment & Blindness 115.4 (2021): 277-285.
8. Sun, Pei, *et al.* "Scalability in perception for autonomous driving: Waymo open dataset." Proceedings of the IEEE/CVF conference on computer vision and pattern recognition. 2020.

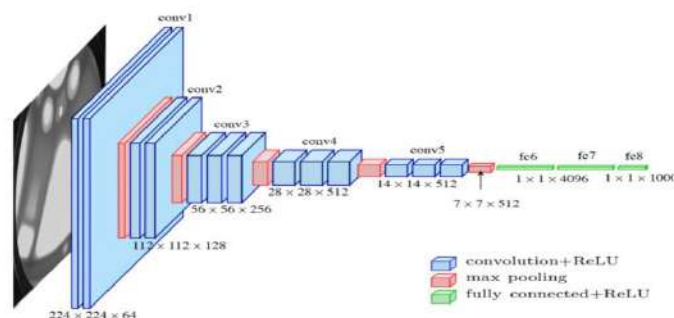


Fig. 1 VGG16 model





Experiment Study on Precast Structure and Cast *in Situ* Structure for Metro Project in Gujarat (A Case Study of Gujarat Metro)

Milan Viradiya^{1*}, PrJagruti shah² and Indrajit Patel³

¹PG Scholar, Infrastructure Engineering & Technology, Birla Vishvakarma Mahavidyalaya, Vallabh Vidyanagar, Anand, Gujarat, India

²Assistant Professor, Infrastructure Engineering & Technology, Birla Vishvakarma Mahavidyalaya, Vallabh Vidyanagar, Anand, Gujarat, India

³Professor, Department of Structural Engineering, Birla Vishvakarma Mahavidyalaya, Vallabh Vidyanagar, Anand, Gujarat, India.

Received: 30 Dec 2023

Revised: 09 Jan 2024

Accepted: 12 Jan 2024

*Address for Correspondence

Milan Viradiya

PG Scholar,

Department of Infrastructure Engineering & Technology,

BVM Engineering Collage,

Vallabh Vidyanagar, Anand, Gujarat, India

E mail: viradiyamilan945@gmail.com



This is an Open Access Journal / article distributed under the terms of the **Creative Commons Attribution License** (CC BY-NC-ND 3.0) which permits unrestricted use, distribution, and reproduction in any medium, provided the original work is properly cited. All rights reserved.

ABSTRACT

India is the fastest-growing developing country and Most a Rapid change in the development of the field of urban infrastructure in recent times. Metro projects are capital-intensive public-oriented projects. Due to the cost of economic and timely completion of the project, the precast concrete method is widely used in infrastructure projects like Metro, Flyover, and Bridge etc. for the Reduce the construction time and space, reduce traffic issues, reduce pollution, reduce environmental impacts. The cast in situ methodology have need some time & space and is inconvenient to public. Therefore use of precast members to the best preferred option for elevated metro projects in urban areas. This paper focus on the importance of precast methodology in infrastructure projects and summarize the role of time, cost, quality and productivity of the precast technique

Keywords: Precast Concrete, Precast viaduct and Station, Time, Cost and Quality analysis Rapid infrastructure growth





Milan Viradiya et al.,

INTRODUCTION

For successful Project Management implementation, the use of precast elements requires due consideration since the initial stage of the project. The choice of location and size of the casting yard plays an important role in the speed of construction. Almost all Metro projects in India are being constructed using precast Techniques. As metro projects run inside the urban area and the elevated bridges are on existing active traffic roads, onsite casting can hinder the flow of traffic. The use of offsite casting elements and the erection process, it is easing the traffic situation. As all the elements are being cast at the casting yard, the construction work will progress faster on a high-priority basis and projects will also be ready at the earliest. Presently, most of the elements of both viaduct and stations are precast leading to much faster construction with better quality control. The precast construction technology offers advantages such as cost-saving, Time savings, Quality improvement, less labour required, reduce safety risk, and reduced concrete wastage. However, the implementation of precast technology in the Indian construction industry. The precast cost is low as compared to cast in situ.

The objective of the study is to perform comparative study on precast and cast in situ techniques.

Problem Statement

Presently Metro Project infrastructure work increased significantly. But metro alignments exist mostly on dense populations and central lines of road medium, due to that reason the less availability of land and difficulty in managing the moving traffic in metro cities. Nowadays client needs to complete the infrastructure project within the timeline with respect to quality. Therefore the precast superstructure is one of the best options for metro projects. Also, construction projects need eco-friendly techniques to avoid pollution and reduce the environmental impact.

Data Collections and Analysis

The data was collected by reviewing various literature from journals, project records, and online websites from the internet. The data was collected from Surat metro Phase-I and Ahmedabad metro Phase-II From Gujarat Metro Corporation Limited. This report studies the precast structure like the precast pier arm, precast viaduct pier cap, Track level and platform level I-Girder, Portal beam and concourse level precast beam. The data was collected as per actual site data and analyzed with consideration of the time and cost required to cast one full span with the precast method.

Types of Precast Superstructure

Precast Pier Arm: This types of Superstructure used in concourse level of the station portion.

Precast cantilever Pier cap: -This Superstructure are Main line of the alignment where the precast segmental box girder rest of the pier cap pedestal. The all live load and dead load are passed through pier cap to pier.

I-Girder& T-Girder: - This types of I-Girder used in Viaduct area and precast post-tensioned concrete I-girder bridge is a kind of bridge wherein I- girders rest on the bearings and deck slab is connected to girder through shear connector.

The top of T shape cross section act as flange in this type of girder. These types of girders are used in small span lengths like in station area. Again selection of this type is mainly depending on feasibility of transportation and loading criteria.

COST, TIME AND QUALITY ANALYSIS

The duration for the completion of the project such as the metro project has time constraints and lack of space for executing the construction work at the site. The Precast is an ideal solution for constructing a Metro Project in an urban area. A precast concrete system is economical as compared to a cast-in-situ system. The cost of precast may vary with different types and sizes of the projects. However, the precast takes less time, cost and labour productivity for construction and waste is minimal for constructing the precast elements. Also, the maintenance cost is also less in the precast system. The precast system achieved better concrete quality and finishing of precast elements as compared to the cast in situ. Precast products provide a higher level of quality assurance because the production of





Milan Viradiya et al.,

the elements can be monitored carefully and under controlled conditions in a lab. The object is inspected and tested by experts and technicians. Cast in situ can't provide quality products because of improper scaffoldings. The segregation of the honey, the bleeding of the bee, and the combing process reduce the quality of the product.

CONCLUSION

It was analysed from the result that the both in-situ construction and precast construction methods, and have come to a conclusion about each. Precast concrete solutions can help reduce the waste generated on-site by up to 50% compared to traditional construction sites. The initial cost of precast construction is more than cast-in-situ construction because the cost of skilled labour in India is higher than the cost of unskilled labour. There is a lack of knowledge about precast construction among potential homebuyers. Because the pouring of the prefabricated arm can be carried out at the same time as the pouring of the piers in the station area, it is a method with low cost, high efficiency and high safety, which not only shortens the completion time of the project but also reduces the complex structure pouring. Live casting on moving traffic. These recent successes have shown that this cost-effective option is very effective.

REFERENCES

1. VaishaliTurai, AshishWaghmare (2016), "A study of cost comparison of precast concrete vs cast in place concrete" International Journal of advanced Engineering Research and applications – Volume 2, Pages 11.
2. Azharuddin Ahmed; Dr. Anup Kumar Mandal (2020), "Benefits and Challenges of Precast Construction in India – A Review", SSRG International Journal of civil engineering – Volume 7, pages 4.
3. Manbhawan Singh, Jatin Mehta, KapilSoni (2019), "Study on Comparison of Pre-cast & Cast in Situ Construction of the Structure based on Economic Category", International Research Journal of engineering and technology - Volume 6, Pages5.
4. NagarajuKaja, AnupamJauswal (2021), "Review of Precast Concrete Technology in India", International Research Journal of engineering and technology - Volume 10, Pages 6.
5. Sayali A. More, Aishwarya V. Patil (2017), "Time, Cost, Productivity and Quality Analysis of Precast Building", International Research Journal of engineering and technology - Volume 4, Pages 4.
6. Suraj Kumar (2019), "A comparative study on Precast / Prefabricated structures and cast in situ structures", International Research Journal of engineering and technology - Volume 8, Pages 3.
7. Harshit Soni (2017)," Critical Evaluation of Super Structure Construction for Metro Corridor", International Journal of Engineering Technology Science and Research Volume 4, Issue 9 page 210-219.
8. Akash Lanke, Dr. D. Venkateswarlu," Design, Cost & Time analysis of Precast
9. & RCC building" International Research Journal of Engineering and Technology", Volume: 03 Issue: 06 | June-2016.
10. Dr. Sachin Admane, Prof. Y R Suryawanshi, Mr.AjitDhumal (2015),"Literature work study of precast concrete connections in seismic", International Journal of Civil Engineering and Technology – Volume 6, Pages 11.
11. P Bujnakova, Department of Structures and Bridges, University of Zilina, Faculty of Civil Engineering, Univerzitna 8215/1 Zilina, 010 26, Slovakia," Construction of precast segmental box girder bridge", IOP Conf. Series: Materials Science and Engineering 385 (2017) 1-16.
12. P.Karthigai Priya, M.Neamitha, A Review of Precast Concrete". (IRJET) Volume 5 Issue1, Jan 2018, 967-971.
13. Contract Documents of Phase-01 of CS-01 Stretch GMRC/SURAT/PH-1/CS-1/VDCT+STNS/C&P/2021/ Dt. 11.06.2021.





Milan Viradiya et al.,

Table 1:-Comparative details between Concourse level Cast in situ Beam to Precast beam at Station

Description	Days per Nos./Span	Concrete (A)	Steel (B)	Erection and Transport (C)	Total Amounts D=(A+B+C)
M-40 Precast Beam CCL	4 Day per Beam	3,344,552.27	4,166,047.29	1,492,137.28	9,002,736.84
Total A.					9,002,736.84
M-40 Cast in Situ Beam and Slab	21 Day Per Span	4,217,850.00	5,253,846.00	-	9,471,696.00
Total B.					9,471,696.00
Difference amount for 1 station (A-B)					468,959.16
Difference amount for 5 station					2,344,795.80

Table:-2 Comparative details between Track level Cast in situ Beam to Precast T-Girder at Track level and Platform level Station

Description	Day per Nos./Span	Concrete (A)	Steel (B)	Erection and Transport (C)	Total Amounts D=(A+B+C)
M-60 Precast T-Girder	8 Day per T-Girder	4,063,485.69	5,224,248.85	1,461,685.50	10,749,420.04
Total A.					10,749,420.04
M-60 Cast in situ Track Beam and Slab	28 Day Per Span	4,752,381.38	5,179,711.20	-	9,932,092.58
Total B.					9,932,092.58
Difference amount for 1 station (A-B)					817,327.47
Difference amount for 5 station					4,086,637.34



Fig.1. Station Cantilever Pier arm Erection





Milan Viradiya et al.,



Fig-02. Viaduct Cantilever Pier cap Erection



Fig-03. Viaduct & Station I-Girder Erection





Performance Analysis of Lean Six Sigma using Machine Learning Approach

Kaushika D. Patel¹, Darshankumar C. Dalwadi² and Rakesh D. Patel³

¹Assistant Professor, BVM Engineering College, Vallabh Vidyanagar, Gujarat, India.

²Associate Professor, BVM Engineering College, Vallabh Vidyanagar, Gujarat, India

³Head, Mechanical Engineering Department, B and B Institute of Technology, Vallabh Vidyanagar, Gujarat, India.

Received: 30 Dec 2023

Revised: 09 Jan 2024

Accepted: 12 Jan 2024

*Address for Correspondence

Darshankumar C. Dalwadi

Associate Professor

Electronics and Communication Engineering Department,

Birla Vishvakarma Mahavidyalaya Engineering College,

Vallabh Vidyanagar-388120,

Anand, Gujarat, India.

E mail: darshan.dalwadi@bvmengineering.ac.in



This is an Open Access Journal / article distributed under the terms of the **Creative Commons Attribution License** (CC BY-NC-ND 3.0) which permits unrestricted use, distribution, and reproduction in any medium, provided the original work is properly cited. All rights reserved.

ABSTRACT

The quality improvement phenomena known as Lean Six Sigma (LSS) has caught the industry's interest. By combining the best practices from Lean and Six Sigma, LSS has been proved to increase business efficiency and customer experience by aiming for a capability level of 3.4 faults per million opportunities (Six Sigma) and effective (lean) processes. Numerous companies have tried to use LSS, but not all of them have been successful in enhancing business operations to provide desired results. Therefore, for LSS to be implemented effectively, it will be very valuable to understand the cause-and-effect links of the LSS enablers while also gaining deeper insights into how the LSS strategy functions. The variety of Critical Success Factors (CSFs) recommended by many conceptual papers dominates the LSS literature, and very few attempts have been made to tie these CSFs to an organized theory on LSS. The paper aims to fill this gap by employing a cutting-edge technique that uses machine learning, more specifically Natural Language Processing (NLP), with a focus on the use of cross-domain knowledge to create a condensed collection of constructs that describe the LSS phenomena.

Keywords: Artificial Intelligence; Lean Six Sigma (LSS); Critical Success Factors (CSFs); Machine Learning; Natural Language Processing (NLP); Continuous Improvement; Classification Model; Word Embedding.



**Kaushika D Patel et al.,**

INTRODUCTION

Organizations have been driven to investigate profitable solutions in order to achieve a competitive advantage by the development in customer demand for high-quality goods and services that are delivered quickly. To increase productivity and customer satisfaction, businesses all over the world have adopted a variety of commercial and operational solutions. Lean Six Sigma (LSS) is a well-liked process improvement methodology that combines the Japanese-inspired Lean manufacturing (LM) and US-inspired Six Sigma (SS) methodologies. Research on the CSFs of LSS is relevant to explaining the success of LSS projects since Critical Success Factors (CSFs) are predictors, mediators, and/or moderators of an outcome. With so many CSFs, it becomes challenging to thoroughly "mine" the phrases to create a condensed, objective subset of themes. This turns into a "big data" issue that can be resolved more successfully with the aid of computers. Machine learning (ML) is an AI technique which trains a set of algorithms on data to make decisions like humans. An input layer, which accepts labeled raw data in tensor form, collaborates with some hidden layers and activation functions to process input data and discover various patterns in it in a typical supervised deep learning model. Finally, the output layer provides outputs that are categorical or real numbers

Critical Success Factors of LSS

CSFs are organisational strategy components that can affect an organization's performance while pointing it in a suitable path [1]– [3]. In some circumstances, CSF also serve as an assessment criterion by serving as components that are necessary for a project or organisation to accomplish its goals [4]– [6]. Critical Success Factors (CSF) represent specific components or areas of action that a company, team, or department must concentrate on and effectively implement in order to achieve its strategic goals. These success elements should be effectively implemented in order to provide a favourable result and add value to the company. CSFs are crucial since each one serves as a company's compass for direction. They serve as a trustworthy point of reference for concentration and success when they are made clear to everyone in the organisation.

A company's strategic goals should be linked to and aligned with the development of critical success elements. They help the organisation get closer to its strategic goals by determining how a business unit, department, or function can accomplish its aims. These elements also have an impact on how individuals and teams support and participate in the strategic plans and objectives. Each CSF is determined to aid in the accomplishment of a certain strategic objective and direct the development and monitoring of Key Performance Indicators (KPIs). Machine learning for Classification Artificial intelligence (AI) is a catch-all phrase for methods used to educate robots to perform tasks that come easily to people. Machine learning (ML), which is a series of algorithms taught on data to make judgments comparable to humans, is one such AI technology. In addition, Deep Learning (DL) is a method for machine learning that replicates the neuronal structure of the brain to create intelligent computers and systems [7], [8]. An input layer, which accepts labelled raw data in tensor form, along with hidden layers and activation functions, process the input data to learn various patterns in it, make up a typical supervised deep learning model. Finally, the output layer provides outputs that are either categorical (for classification tasks) or real numbers (for regression tasks). Since ML approaches have developed over the years, they are currently being used to natural language processing (NLP) in addition to computer vision and autonomous cars [7], [9]–[11]. Due to its significant consequences, text categorization continues to be a central issue in NLP and has a wide range of practical applications in information retrieval [12]. Text input must be transformed into numeric tensors before text can be classified using ML models. To do this, texts are divided into tokens (words, letters, etc.), which are then associated with numeric vectors. A text can be tokenized or vectorized in a variety of ways. One-hot encoding and word embedding are the two main techniques.

A vocabulary index is used in one-hot encoding to specifically express a word [13], [14]. Binary, sparse, and extremely high dimensional (equivalent to the length of a vocabulary), one-hot encoded vectors are these characteristics. The context of a word in a textual passage, as well as its semantic and syntactic similarity and relationship to other words in the passage, are not captured by one-hot encoding. For instance, the words "similar"





Kaushika D Patel *et al.*,

and "same" are connected, yet one-hot encoding will not convey their semantic connection. A word is converted into a vector of real numbers via word embedding [15]. Since the model is trained to learn weights for embedding space, which project each word into vector space, this mapping is automatic. While it is generally agreed that word embedding captures a word's semantic information, it does not adequately capture the relationships between the various words and phrases that make up a sentence [16]. We must consider embedding sentences or phrases when doing NLP activities on textual data that involve the understanding of a sentence's meaning. Conneau *et al.* [16] and Cer *et al.* [17] suggested sentence level embedding as a solution to this. Instead of mixing word embedding for each word in the phrase, this enables encoding the sentence in vector form [16], [17]. In our study, CSFs resemble phrases where a set of words makes meaning when read collectively. In order to vectorize CSFs for DL models, this work focuses on employing sentence embedding.

METHODOLOGY

In accordance with Figure 1, there are two key components that make up the development of the final theoretical framework for an LSS deployment that is effective. The first step is to examine the current Lean and Six Sigma models in order to fill in the gaps in the literature. Creating an ML classification model to capture the essence of CSFs in existing literature constitutes the second component.

Initial Model Development

When creating a theoretical model, three fundamental requirements must be met: the creation of the theoretical constructs, the specification of the relationships between the constructs based on temporal asymmetry, and the establishment of the boundary within which the theory is to be generalised. [18]–[20]. The two main phases of the LSS project implementation are the initiation phase, when planning and scheduling take place, and the execution phase, where process inputs (such as knowledge, social interactions like teamwork, and the application of tools and strategies for improvement) are converted. The success of LSS deployment is the result of many different components working together, not just these steps. Project selection, which occurs at the LSS project initiation stage, is crucial to the success of LSS project deployment [21]– [24] because it helps pick the right project for the right situation at the right time to provide the desired outcomes. While choosing the right project, the approach considers the four influential voices (voice of the consumer, voice of business, voice of process, and voice of stakeholders) that were mentioned in Antony *et al.* [21]

CSFs Extraction and Classification

For the purpose of designing a classifier model using ML, CSF extraction is crucial. A literature study was conducted on CSFs for the implementation of Lean, SS, TQM, and CI in the manufacturing and service sectors. The EBSCO, ELSEVIER, EMERALD, IEEE, SCOPUS, and SPRINGER databases were used for the literature study. In the search, terms like "Critical success factors" or "Success factors" or "Enablers" as well as "Lean Six sigma" or "Lean Sigma" or "Lean" or "Six sigma" or "LSS" or "TQM" or "Continuous Improvement" were used. A study of the current literature on CSFs showed that no research offers a system for categorising or predicting the class for the remaining CSFs. So, in the project we sort through 574 CSFs using cutting-edge methodology to group them into four manageable and significant themes: leadership engagement, LSS culture, LSS inception, and LSS execution.

Machine Learning Model For Classification

Creating a CSF classifier involves a combination of state-of-the-art NLP techniques and subsets including Word Embedding, Neural Network (NN), and Supervised Machine Learning (SML), in addition to ML, a subset of AI. It is crucial to employ word frequencies and context data to retain word embedding meanings in order to capture semantic value in a word embedding while creating this Multi-Class Classifier, where the single classification label belongs to a collection with more than two components [12], [25].





Kaushika D Patel et al.,

Dataset

The CSFs that had previously been grouped into several categories were utilised as training data for the ML classifier. The clustered CSFs were listed with their headers in order to create the training data. Several headings were combined with the aid of the industrial guide, and four headings (Leadership Engagement; LSS Culture; LSS Project Initiation; LSS Execution) were created as a result. To produce the training set, duplicate CSFs were eliminated, and 574 distinct CSFs were chosen along with their headers. CSFs are often variable-length phrases that have been studied in the literature. Thus, the universal sentence encoder [17] from Tensor Flow hub is implemented as a universal sentence embedder. Each CSF underwent pre-processing such that all the words were lowercase before being encoded. Two benefits of the universal sentence encoder are: The process starts by turning single words or phrases into fixed-length vectors, which may then be used to combine numerous CSFs into a single vector. Additionally, it eliminates the need to pad short vectors with zeros. The universal encoder performs better when learning from small amounts of training data since it has been trained on a huge corpus of data [13], [26]. The headings were mapped from 1 to 4 and the training data were mixed up before embedding. The training data set was divided into the training set (80%) and cross-validation set (20%) for assessment reasons.

Model Architecture

The methodology for classifier development is illustrated in Figure 2. The model is developed keeping in mind the classifier development methodology. Figure 3 depicts the ML classification procedure. A five-layer model with an input layer of 512 nodes (equivalent to the length of the vectored CSFs), an output layer of 4 nodes (equivalent to the number of classes), and three hidden layers of (128, 64, 64) nodes is shown in the diagram. The input layer, which is the initial layer of the neural network, includes the data that the other levels will need to process. A sentence embedding module that has been pre-trained on a sizable data corpus is also part of the categorization system. For the next layer of the neural network, it transforms the input CSFs into a multi-dimensional (R512) vector representation.

Evaluation Metrics

Accuracy, precision, recall, and F1-scores were selected as the key assessment metrics [10], [27]-[29] in order to assess the effectiveness of the suggested technique. These metrics are defined as follows:

$$\begin{aligned} \text{Precision} &= \frac{TP}{(TP + FP)} \\ \text{Recall} &= \frac{TP}{(TP + FN)} \\ \text{F}_1\text{Score} &= \frac{(2 * \text{precision} * \text{recall})}{(\text{precision} + \text{recall})} \\ \text{accuracy} &= \frac{(TP + TN)}{(TP + TN + FP - FN)} \end{aligned}$$

.....(1),(2),(3),(4)

Where TP, FP, and FN, respectively, stand for true positives, false positives, and false negatives. When the classes are severely unbalanced, precision and recall are quick indicators of prediction success. In information retrieval, recall measures the quantity of actual relevant results returned, whereas precision measures the relevancy of the results. The F1-score is calculated as the average of recall and accuracy [7], [13].

RESULTS AND DISCUSSION

Cross-validation enables models to be tested utilising the complete training set by repeatedly resampling, maximising the total number of points utilised for testing and maybe lowering the likelihood of over-fitting [30]. 20% of the training data with defined classes were utilised as the cross-validation data set in this classification model. The evaluation criteria for the classifier predictions are demonstrated in Table 1. According to the table, within the CSV





Kaushika D Patel et al.,

dataset, 76% of the classification predictions are accurate. Figure 4 shows both the cross validation and training models' accuracy as well as their respective loss curves.

CONCLUSION

Despite being widely used, LSS's theoretical foundations are still lacking. It is still unclear how LSS elements connect to organizations' bottom lines and the performance of quality improvement projects, and nearly no explanations include the LSS's Lean component. It is impossible to disregard CSFs when discussing LSS outcomes since they are essential to its implementation. CSFs prescribed for Lean, SS, and CI are too many and poorly defined to constitute a comprehensive theory. The study proposed a targeted technique for identifying CSFs that makes use of a supervised learning model to extract the essence of CSFs while assisting the creation of a theoretical model to address this issue. With the use of the available literature on the CSFs relevant to LSS, this innovative approach summarizes the key ideas and tackles the issues raised by the distinctive qualities of the quality improvement language

REFERENCES

1. M. MacIel-Monteon, J. Limon-Romero, C. Gastelum-Acosta, D. Tlapa, Y. Baez-Lopez, and H. A. Solano-Lamphar, "Measuring critical success factors for six sigma in higher education institutions: Development and validation of a surveying instrument," *IEEE Access*, vol. 8, pp. 1813–1823, 2020.
2. V. Flor Vallejo, J. Antony, J. A. Douglas, P. Alexander, and M. Sony, "Development of a roadmap for lean six sigma implementation and sustainability in a scottish packing company," *TQM Journal*, 2020.
3. W. Alkarney and M. Albraithen, "Are critical success factors always valid for any case? a contextual perspective," *IEEE Access*, vol. 6, pp. 63 496–63 512, 2018.
4. B. Clegg, C. Rees, and M. Titchen, "A study into the effectiveness of quality management training," *The TQM Journal*, vol. 22, no. 2, pp. 188–208, 2010.
5. A. Laureani and J. Antony, "Leadership characteristics for lean six sigma," *Total Quality Management and Business Excellence*, vol. 28, no. 3-4, pp. 405–426, 2017.
6. Ribeiro de Jesus, J. Antony, H. A. Lepikson, and A. L. A. Peixoto, "Six sigma critical success factors in brazilian industry," *International Journal of Quality and Reliability Management*, vol. 33, no. 6, pp. 702–723, 2016.
7. M. Aydogan and A. Karci, "Improving the accuracy using pre-trained word embeddings on deep neural networks for turkish text classification," *Physica A: Statistical Mechanics and its Applications*, vol. 541, 2020.
8. Liu and X. Wang, "Quality-related english text classification based on recurrent neural network," *Journal of Visual Communication and Image Representation*, 2019.
9. J. Goodfellow, J. Pouget-Abadie, M. Mirza, B. Xu, D. WardeFarley, S. Ozair, A. Courville, and Y. Bengio, "Generative adversarial nets," in *Advances in Neural Information Processing Systems*, vol. 3, Conference Proceedings, pp. 2672–2680. [Online]. Available: <https://www.scopus.com/inward/record.uri?eid=2-s2.0-84937849144partnerID=40md5=6441b2a288c5fdded2adbcc8b21e092c>
10. Y. Zhang, H. Lin, Z. Yang, J. Wang, Y. Sun, B. Xu, and Z. Zhao, "Neural network-based approaches for biomedical relation classification: A review," *J Biomed Inform*, vol. 99, p. 103294, 2019. [Online]. Available: <https://www.ncbi.nlm.nih.gov/pubmed/31557530>
11. P. Wang, B. Xu, J. Xu, G. Tian, C.-L. Liu, and H. Hao, "Semantic expansion using word embedding clustering and convolutional neural network for improving short text classification," *Neurocomputing*, vol. 174, pp. 806–814, 2016.
12. F. Gargiulo, S. Silvestri, M. Ciampi, and G. De Pietro, "Deep neural network for hierarchical extreme multi-label text classification," *Applied Soft Computing*, vol. 79, pp. 125–138, 2019.
13. D.-H. Pham and A.-C. Le, "Exploiting multiple word embeddings and one-hot character vectors for aspect-based sentiment analysis," *International Journal of Approximate Reasoning*, vol. 103, pp. 1–10, 2018.
14. Chen, Y. Tao, and H. Lin, "Visual exploration and comparison of word embeddings," *Journal of Visual Languages Computing*, vol. 48, pp. 178–186, 2018.





Kaushika D Patel et al.,

15. G. E. Hinton, "Learning distributed representations of concepts," in Eighth Annual Conference of the Cognitive Science Society, vol. 1, Conference Proceedings, p. 12
16. A. Conneau, D. Kiela, H. Schwenk, and A. Barrault, L. Bordes, "Supervised learning of universal sentence representations from natural language inference data," arXiv preprint arXiv:1705.02364, 2017.
17. Cer, Y. Yang, S.-y. Kong, N. Hua, N. Limtiaco, R. St. John, N. Constant, M. Guajardo-Cespedes, S. Yuan, C. Tar, B. Strope, and R. Kurzweil, "Universal sentence encoder for english," in 2018 Conference on Empirical Methods in Natural Language Processing: System Demonstrations. Association for Computational Linguistics, Conference Proceedings, p. 169–174.
18. Byron and S. M. Thatcher, "Editors' comments: "what i know now that i wish i knew then" – teaching theory and theory building," Academy of Management Review, vol. 41, no. 1, pp. 1–8, 2016.
19. R. Dubin, Theory development. New York: Free Press, 1978.
20. A. Whetten, "What constitutes a theoretical contribution?" Academy of management review, vol. 14, no. 4, pp. 490–495, 1989.
21. J. Antony and M. Saadat, "Is six sigma a management fad or fact?" Assembly Automation, vol. 27, no. 1, pp. 17–19, 2007.
22. A. G. Psychogios, J. Antony, J. Atanasovski, and L. K. Tsironis, "Lean six sigma in a service context," International Journal of Quality Reliability Management, vol. 29, no. 1, pp. 122–139, 2012.
23. G. Psychogios, J. Atanasovski, and L. K. Tsironis, "Lean six sigma in a service context," International Journal of Quality Reliability Management, vol. 29, no. 1, pp. 122–139, 2012.
24. R. D. Snee, "Lean six sigma – getting better all the time," International Journal of Lean Six Sigma, vol. 1, no. 1, pp. 9–29, 2010.
25. Naili, H. Chaibi, AnjaGhezala, and H. H. Ben, "Comparative study of word embedding methods in topic segmentation comparative study of word embedding methods in topic segmentation," in International Conference on Knowledge Based and Intelligent Information and Engineering Systems, KES2017, vol. 112. Procedia Computer Science, Conference Proceedings, pp. 340–349
26. S.-y. Chen, "Use of neural network supervised learning to enhance the light environment adaptation ability and validity of green bim," Computer-Aided Design and Applications, vol. 15, no. 6, pp. 831–840, 2018.
27. Ferdinandy, L. Gerencsér, L. Corrieri, P. Perez, D. Újváry, G. Csizmadia, and Miklósi, "Challenges of machine learning model validation using correlated behaviour data: Evaluation of cross-validation strategies and accuracy measures," PLOS ONE, vol. 15, no. 7, p. e0236092, 2020. [Online]. Available: <https://doi.org/10.1371/journal.pone.0236092>
28. I. Lakhali, H. Çevikalp, S. Escalera, and F. Ofli, "Recurrent neural networks for remote sensing image classification," IET Computer Vision, vol. 12, no. 7, pp. 1040–1045, 2018.
29. S. Bazrafkan, S. Thavalengal, and P. Corcoran, "An end-to-end deep neural network for iris segmentation in unconstrained scenarios," Neural Networks, vol. 106, pp. 79–95, 2018. [Online]. Available: <https://www.sciencedirect.com/science/article/pii/S089360801830193X>
30. R. B. Rao, G. Fung, and R. Rosales, On the Dangers of CrossValidation. An Experimental Evaluation, pp. 588–596. [Online]. Available: <https://epubs.siam.org/doi/abs/10.1137/1.9781611972788.54>

Table 1. Evaluation Metrics for Cross Validation

	precision	recall	f1-score	support
class 0(Leadership Engagement)	0.78	1.00	0.88	7
class 1(LSS Culture)	0.80	0.73	0.76	11
class 2(LSS Project Initiation)	0.50	0.50	0.50	4
class 3(LSS Execution)	1.00	0.67	0.80	3
accuracy			0.76	25
macro avg	0.77	0.72	0.73	25
weighted avg	0.77	0.76	0.76	25





Kaushika D Patel et al.,

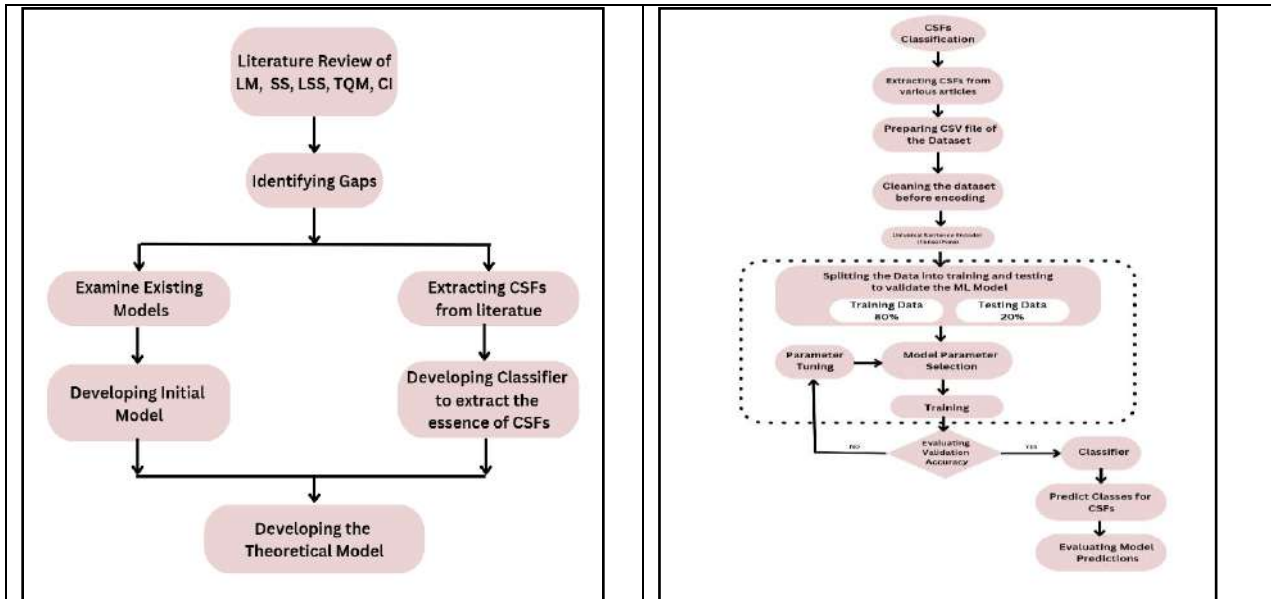


Fig. 1. System Model

Fig. 2. The methodology of classifier development

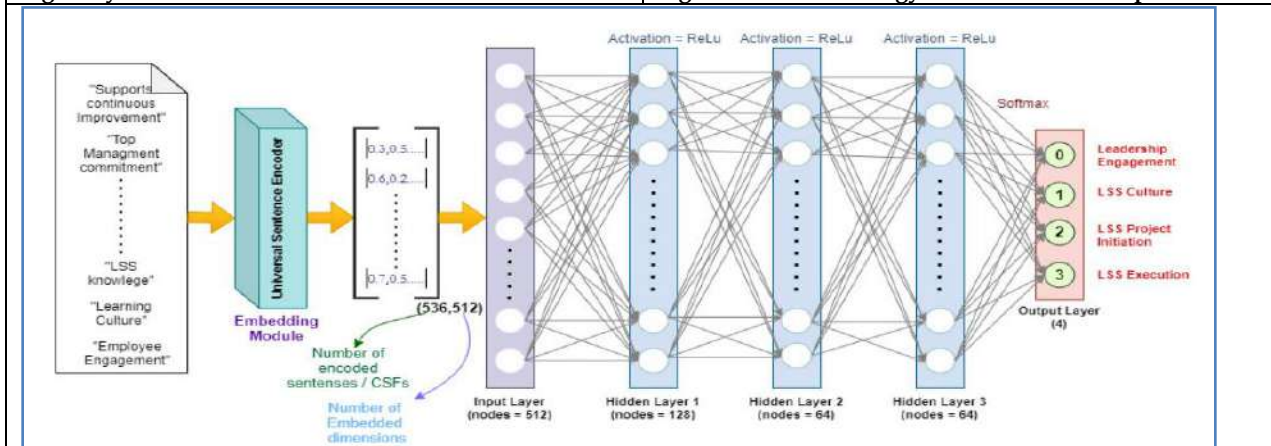


Fig. 3. Neural Network for Classifier Model

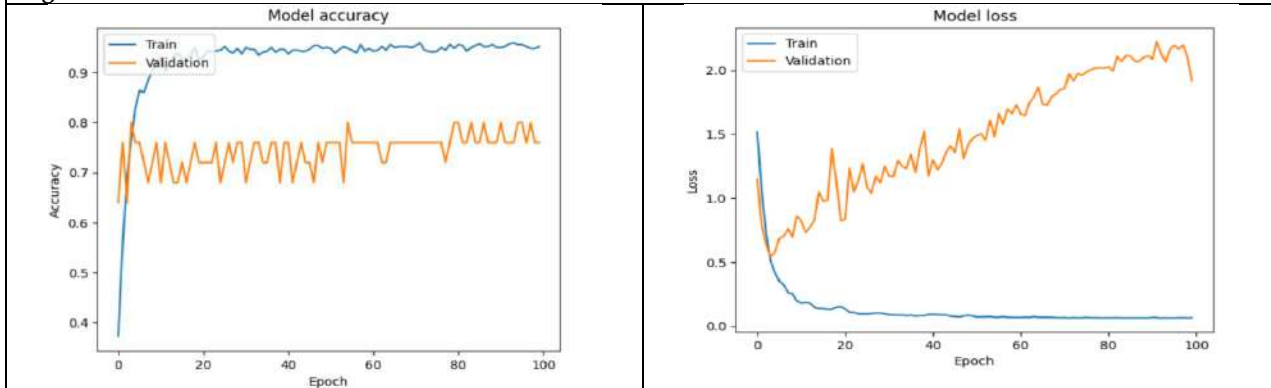


Figure 4: Accuracy and Loss of Training and Cross-Validation





Comprehensive Analysis of Microstrip Patch Antennas in the Context of Satellite Communication

Dhrumil Gajera^{1*}, Prit Vadalia¹, Dr. Darshankumar Dalwadi², Dr. Kaushika Patel³

¹Electronics Department, BVM Engineering College, Anand, Gujarat, India.

²Electronics & Communication Department, BVM Engineering College, Anand, Gujarat, India.

³Electronics Department, BVM Engineering College, Anand, Gujarat, India

Received: 30 Dec 2023

Revised: 09 Jan 2024

Accepted: 12 Jan 2024

*Address for Correspondence

Dhrumil Gajera

Electronics Department,
BVM Engineering College,
Anand, Gujarat, India.

E. mail: gajeradhrumil38@gmail.com



This is an Open Access Journal / article distributed under the terms of the **Creative Commons Attribution License** (CC BY-NC-ND 3.0) which permits unrestricted use, distribution, and reproduction in any medium, provided the original work is properly cited. All rights reserved.

ABSTRACT

Utilizing readily available, inexpensive FR4 material, microstrip antennas are constructed. The HFSS simulation is used to analyse the antenna characteristics, and it is widely employed in satellite communication due to its advantages over traditional antennas. According to a literature review on patch array antennas (PAA), numerous techniques were used to create smaller-sized patch array antennas. In this study, 2.4GHz microstrip antennas and a 2x2 strip array antenna are presented. The simulation results for the 2.4GHz microstrip antenna show a 5.5dB antenna gain. Additionally, the 2x2 strip array antenna operating at 12 GHz exhibits an 80-degree beam width, a bandwidth of 693.6 MHz (5.9%), a gain of 8.98 dB, a directivity of 10.83 dB, and an efficiency of 83%. The substrate utilized for both antennas is FR4 with a thickness of 1.6mm and a dielectric constant of 4.4. The 2x2 linear array is specifically designed for line feeding and is tailored for satellite communication purposes.

Keywords: Microstrip Patch Array, Antenna, HFSS, Satellite communication, Radiation Pattern, Return Loss.

INTRODUCTION

The rapid evolution of wireless communication systems has driven a growing demand for high-gain broadband antennas. Microstrip antennas have gained prominence due to their advantages, such as high gain, low profile, and ease of manufacturing. However, their limited bandwidth has curtailed their applications [1]. To address these limitations, researchers have explored innovative approaches, incorporating active devices and printed strip-line feed networks. This exploration took flight in the early 1970s when the need for conformal antennas arose,





Dhrumil Gajera et al.,

particularly for missile applications [2]. Microstrip antennas are characterized by their dimensions, gain, and radiation patterns. As depicted in Figure 1, a microstrip antenna typically features a radiating patch on one side of a dielectric substrate, with a ground plane on the other. These patches can assume various shapes and are often constructed using conductive materials such as gold or copper, with rectangular and circular shapes being the most popular. The feed line design and the radiating patch material are intricately etched onto the dielectric substrate [3].

Notably, microstrip patch antennas come in diverse shapes, including squares, rectangles, circles, triangles, and more. These compact, cost-effective, and low-profile antennas are crucial for mobile communication, and their application extends to wireless communication systems and satellite communication. Moreover, they offer significant advantages, including beam scanning capabilities when employed in antenna arrays [5]. Antenna arrays consist of an array of identical antennas, working in unison to produce radiation with specific characteristics. The aggregation of radiating elements amplifies the radiated power. The fields from each element combine in-phase to generate radiation, offering a versatile range of performance capabilities vital for various applications. Antenna arrays employ a diverse array of elements, including helix, patches, parabolic, wires, and horns, contributing to their adaptability and effectiveness [6].

Antenna Design Methodology

The factors used to design the antenna are listed below.

The following procedures are used in the design of a microstrip patch antenna:

Step1: This Equation (1) is used to determine the width of the micro strip patch antenna [7]

$$W = \frac{\lambda_0}{f_0 \sqrt{\frac{\epsilon_r + 1}{2}}}$$

Step 2: Evaluating the Effective Dielectric Constant from Equation (2)[7]

$$\epsilon_{eff} = \frac{\epsilon_r + 1}{2} + \frac{\epsilon_r - 1}{2} * \frac{1}{\sqrt{1 + 12 \left(\frac{h}{w}\right)}}$$

Step 3: Evaluating the Effective length as given by Equation (3)[7]

$$L_{eff} = \frac{c}{2f_0 \sqrt{\epsilon_{eff}}}$$

Step 4: Evaluating the length extension given by Equation (4) [7]

$$\frac{\Delta L}{h} = 0.412 \frac{(\epsilon_{eff} + 3) \left(\frac{w}{h} + 0.264\right)}{(\epsilon_{eff} - 0.258) \left(\frac{w}{h} + 8\right)}$$

Step 5: Evaluating actual length of patch by Equation (5) [7]

$$L = L_{eff} - 2 \Delta L$$

Step 6: Measurements of the ground plane are given in Equation (6-7) [8]

$$L = L + 6h$$

$$W_g = W + 6h$$

The antenna is made of FR4 material with specific characteristics:

Loss Tangent ($\tan \delta$): 0.025

Thickness (h): 0.8mm

Dielectric Constant (ϵ_r): 4





Dhrumil Gajera et al.,

Additionally, we have mentioned measurements for the patch dimensions and results from a microstrip line calculator:

Patch Length (L): 29.56mm

Patch Width (W): 36.857mm

Results from the microstrip line calculator, assuming a characteristic impedance of 50Ω:

Feed Line Width (W): 1.5mm

Feed Line Length (L): 16.75mm [9]

This section outlines the design of an array antenna engineered to operate at 12 GHz, specifically tailored for satellite communication purposes. The antenna configuration employs a line feeding system and features a 4-element 2x2 array. Notably, the antenna's ground plane measures 40 × 30 mm², and in light of its widespread availability in the market, FR-4 has been chosen as the substrate material for this project. To enhance its operational capabilities and broaden its bandwidth, several techniques have been incorporated, including the strategic manipulation of substrate height, facilitating multiple applications through a singular antenna [10]

RESULTS AND ANALYSIS

Microstrip Patch Antenna Analysis

The study employs the electromagnetic simulation tool, IE3D, to comprehensively analyse the characteristics of antenna arrays. Specifically, this analysis is focused on an antenna element constructed from FR4 material, possessing a dielectric constant of 4.3, and meticulously designed to function optimally at a frequency of 2.5 GHz. As illustrated in Figures 5 and 6, the study's findings are vividly presented through Return Loss vs. Frequency and Gain vs. Frequency plots. According to the simulation results, the return loss, denoted as S11, registers at an impressive -21 dB, while the peak gain reaches 4.5 dB precisely at the resonance frequency of 2.42 GHz. To provide further insights into the antenna's performance, Figure 8 reveals the two-dimensional radiation pattern of the single patch antenna, a critical aspect of the study's analysis [9].

Microstrip Patch Array Antenna Analysis

The simulation was carried out using the same software that was used to design the microstrip patch array, Antenna. Figure 5 shows the S11, or return loss, of a 2X2 patch array antenna. The proposed antenna, also known as a 2x2 patch array antenna, has a reported return loss of -32.33 dB, which indicates that at the operating frequency of 11.79 GHz, the transmitted power experienced losses of about 0.05 percent. The lowest frequency is approximately 11.4954 GHz, and the highest frequency is approximately 12.1890 GHz when considering the return loss of -10 dB.[12]

The following equation can be used to evaluate return loss:

$$B = FH - FL \text{ GHz}$$

$$B = \frac{FH-FL}{f_c} \times 100\%$$

We can easily determine the bandwidth values using the equation above. As a result, it is determined that the proposed microstrip patch antenna's bandwidth is B = 0.6936 GHz, also known as B = 693.6 MHz and B = 5.9 percent. As a result, this antenna has a wide range of uses. Using their respective graphs, the gain and directivity of the proposed antenna can be determined. For the proposed microstrip patch antenna, the gain has been determined to be G = 8.98 dB and D = 10.83 dB. The improvement of the antenna's parameters, including gain, bandwidth, etc., is the main benefit of microstrip patch array antennas.[13]

The microstrip patch antenna's achieved efficiency has been

$$\varepsilon = \frac{G}{D}$$

therefore, $\varepsilon = 83\%$ percent. The typical efficiency for a good antenna is between 50 and 60 percent.[13]

Following Table displays a summary of the results.





Dhrumil Gajera et al.,

CONCLUSION

This study employs HFSS simulation tools to conduct a comprehensive analysis of microstrip antennas, specifically focusing on their application in satellite communication. The research involves a meticulous evaluation of both simulated and measured outcomes, emphasizing the remarkable alignment between the two. In particular, our investigation centres on a microstrip patch antenna boasting a remarkable half-power beam width, a gain of 8.98 dB, and a directivity of 10.83 dB. This antenna operates at the frequency of 12 GHz, offering an impressively wide bandwidth of 693.6 MHz, equivalent to 5.9% of the operating frequency. The outstanding performance parameters of this proposed 2x2 microstrip patch array antenna make it an excellent candidate for applications within the X-band and KU-band frequencies. This research showcases the antenna's potential to contribute significantly to the advancement of satellite communication technology

REFERENCES

1. D. M. Pozar and B. Kaufman, "Increasing the bandwidth of a microstrip antenna by proximity coupling," *Electron. Lett.*, vol. 23, no.8, pp. 368–369, 1987.
2. Robert E. Munson, "Conformal Microstrip Antennas and Microstrip Phased Arrays," *IEEE Transactions on antennas and propagation*, Jan 1974.
3. Robert J. Mailloux, John F. McIlvenna, and Nicholas P. Kernweis, "Microstrip array technology" *IEEE transactions on antennas and propagation*, vol. ap-29, no. 1, January 1981.
4. K.-L. Wong, *Compact and broadband microstrip antennas*. John Wiley & Sons, 2004
5. Ali W. Azim, Shahid A. Khan, Zeeshan Quamar, K.S Alimgeer and S.M Ali "Current Distribution in Microstrip patch antenna Arrays" *International Journal of Future Generation Communication and Networking*, 2011, vol. 4, no. 3.
6. O. Barrou, A. E. Amri, A. Reha, et M. Tarbouch, « Microstrip patch array antennas based on conventional geometries », in 2017 International Conference on Electrical and Information Technologies (ICEIT), Rabat, 2017, p. 1- 6.
7. C. A. Balanis, *Antenna theory: analysis and design* (John Wiley & Sons, 2005).
8. Aaron K Shackelford, K-F Lee, and KM Luk. "Design of small-size wide-bandwidth Microstrip patch antennas", in *IEEE Antennas and Propagation Magazine*, 2003, vol. 45, no. 1, pp. 75-83

Table 1 Antenna factors [7]

W	The width of patch antenna	ΔL	Length extension
L	The length of the patch antenna	ϵ_{reff}	Dielectric constant effective
λ_0	The Wavelength	h	Height of the substrate
f0	The operating frequency	Wg	Width of ground
ϵ_r	With dielectric constant	Lg	Length of ground
C	Velocity of light		

Table 2 2x2 array antenna dimensions [10]

a	5.05 mm	f	14 mm
b	6.5 mm	g	2.3 mm
c	14 mm	h	1 mm
d	0.5 mm	i	4.61 mm
e	4.295 mm	j	2.8 mm





Dhrumil Gajera et al.,

Table 3 Results summary [11]

Parameters	Values
Operating frequency	$F_c = 11.79$ GHz
Bandwidth	$B = 693.6$ MHz $B = 5.9$ %.
Gain	$G = 8.98$ dB
Directivity	$D = 10.83$ dB
Return loss	$S_{11} = -32.33$
Efficiency	$\epsilon = 83$ %

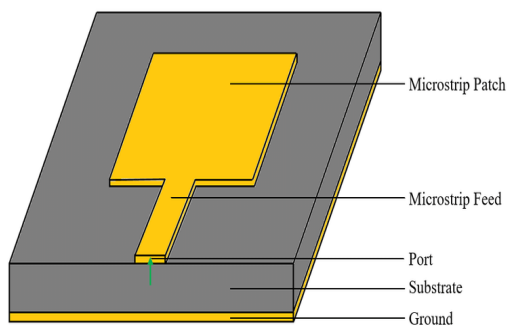


Figure 1 Basic Structure of a microstrip patch antenna [4]

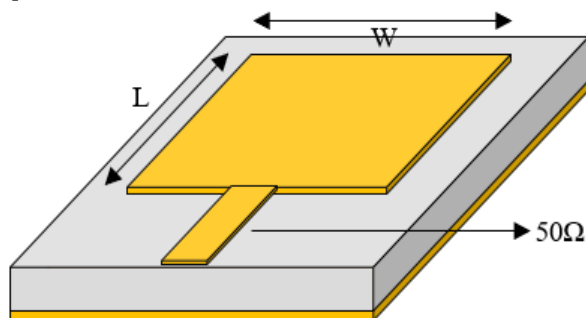


Figure 3 Structure of a microstrip patch antenna [9]

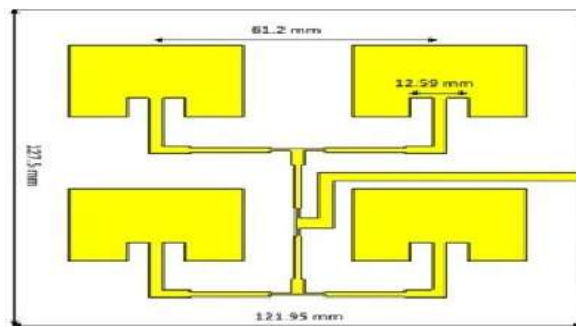


Figure 2, 2 x 2 microstrip patch array antenna's feeding network. [14]

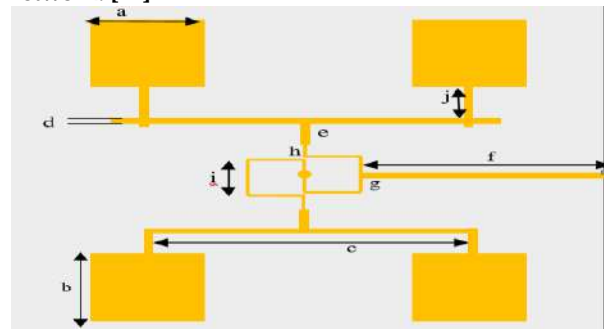


Figure 4 2x2 patch array antenna [11]

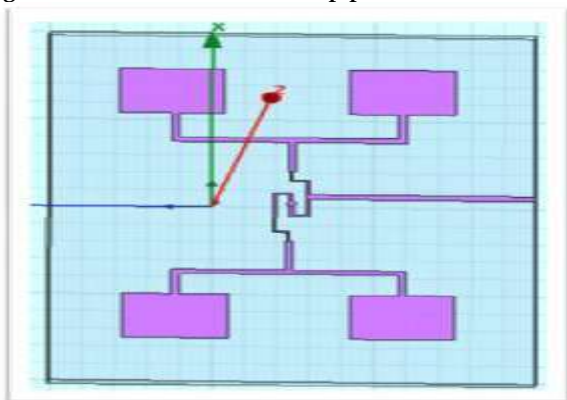


Figure 5 2x2 patch array antenna in HFSS [11]

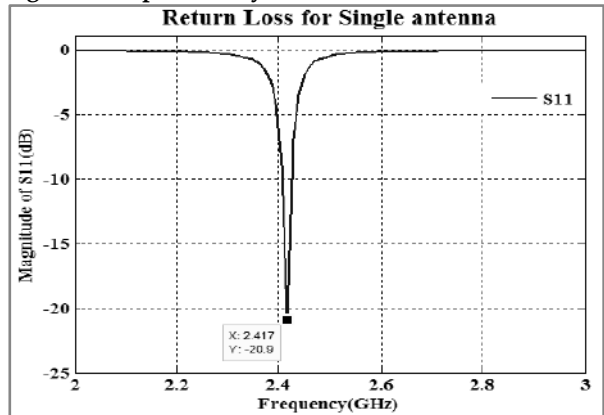


Figure 6 Single element antenna return loss [9]





Dhrumil Gajera et al.,

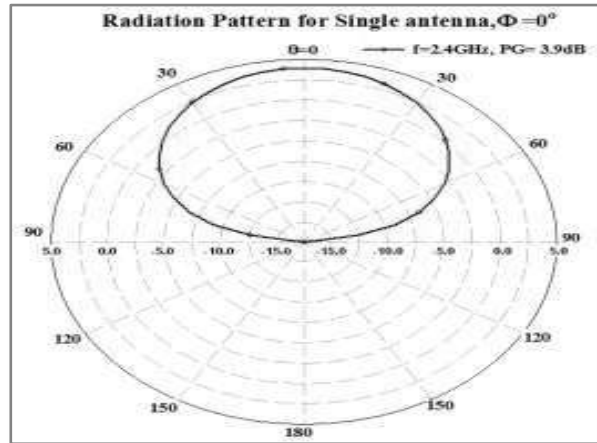
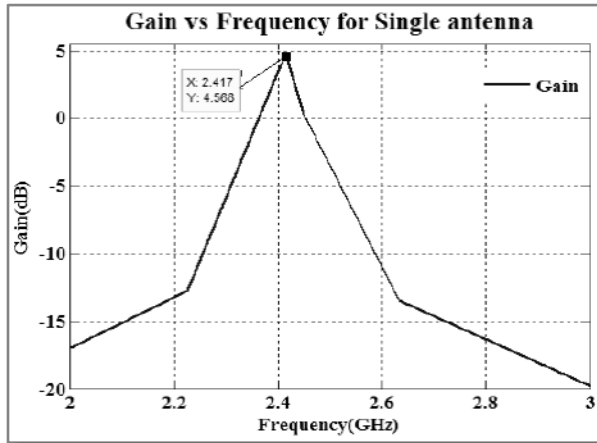


Figure 7 Gain versus frequency of single element antenna [9]

Figure 8 2D Radiation pattern of patch antenna [9]

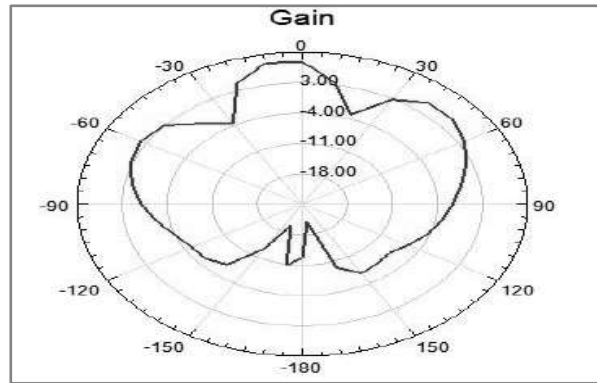
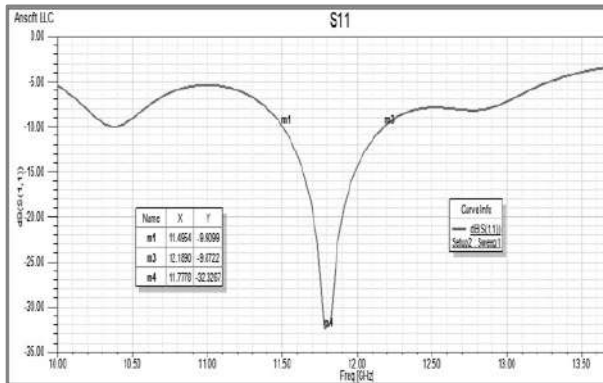


Figure 9: S11 or Return Loss of 2X2 patch array antenna [11]

Figure 10 Gain of 2 x 2 patch array antenna [11]

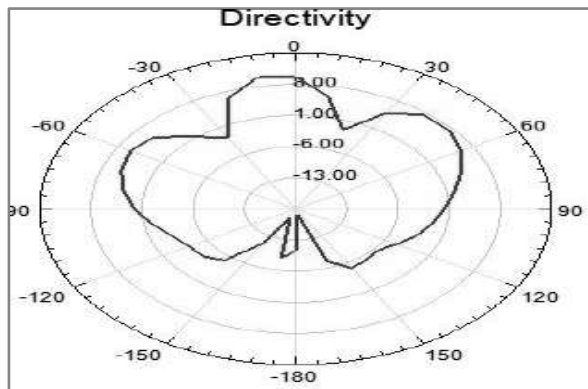


Figure 11. Directivity of 2 x 2 patch array antenna [11]





Survey on Massive MIMO and Smart Antenna System

Prathviraj Singh¹, Dhweep Shah¹ and Darshankumar C. Dalwadi^{2*}

¹Research Scholar, BVM Engineering College, Vallabh Vidyanagar, Gujarat, India

²Associate Professor, BVM Engineering College, Vallabh Vidyanagar, Gujarat, India.

Received: 30 Dec 2023

Revised: 09 Jan 2024

Accepted: 12 Jan 2024

*Address for Correspondence

Darshankumar C. Dalwadi

Associate Professor,

BVM Engineering College,

Vallabh Vidyanagar

Anand, Gujarat, India.

E. mail: darshan.dalwadi@bvmengineering.ac.in



This is an Open Access Journal / article distributed under the terms of the **Creative Commons Attribution License** (CC BY-NC-ND 3.0) which permits unrestricted use, distribution, and reproduction in any medium, provided the original work is properly cited. All rights reserved.

ABSTRACT

This is to help understand how “Massive MIMO and Smart Antenna Systems” can serve multiple users simultaneously within larger area using Massive MIMO by significantly increasing number of antennas, advancing spectrum efficiency and employ intelligent signal processing techniques to enhance communication performance by improving signal-to-noise ratio (SNR), dynamically adjusting radiation patterns, and suppressing interference induce nulls in the created patterns by via Smart Antenna Array.

Keywords: Massive MIMO; Smart Antenna; Spectrum Efficiency; Signal Processing; SNR; Radiation Pattern; Null interference

INTRODUCTION

“Massive MIMO and Smart Antenna Systems” is a new age communication technology attracting industry, academia, students and tech savvy research enthusiasts across the globe. The fifth generation mobile networks (5G) is poised to meet the demands for extensive mobile data usage, low latency, and cost & energy-effective operation. Due to its potential for significant performance gains, Massive Multiple-Input Multiple-Output (MIMO) technology is acknowledged as a crucial element of 5G. The use of a wide array of antenna elements is what these advancements rely on most. By enabling the integration of numerous antennas into small physical dimensions, the switch to the millimeter wave spectrum practically permits the deployment of this technology. The substantial quantity of antennas at Base Stations (BS) offers a range of beneficial characteristics, one of which is referred to as “favorable propagation.” Which means, the dot product of channel vectors associated with different users tends towards zero as the number of transmit antennas rises. Accordingly, when the system scales, user interference decreases considerably, making linear processing techniques more efficient. The validity of these favorable circumstances in numerous large MIMO scenarios has been thoroughly investigated, as mentioned in related literature mentioned in





Prathviraj Singh et al.,

the paper below. Nevertheless, it's important to keep in mind that the idea of favorable propagation might not apply in some specific situations, such as those bound by size restrictions. This is an honest attempt to elaborate the given topic basis our understanding of available online literature under the guidance of our able guide and our professor. However, we would sincerely appreciate to receive our reviewer's / readers feedbacks / inputs to improve our level of understanding.

Objective

The objective is to self-study and understand the latest communication MIMO & Smart Antenna technology usage, benefits over existing infrastructure and its future evolutions scope. It further gives us overview of its vast applications in 5G communication network roll out in Indian and other developing countries context. For students like us, this paper is aimed to make us basic ready for further deep study in the areas of hardware evaluation and software applications in conjunction to the overall communication experience for its users.

LITRATURE REVIEW

Abbreviations and Acronyms

MIMO: Multiple In Multiple Out; **BS:** Base Station; **MRC:** Maximum Ratio Combining; **ZF:** Zero Forcing; **MMSE:** Minimum Mean Square Error; **SNR:** Signal-to-Noise Ratios.

Understanding Massing MIMO

Massive MIMO is an evolution of traditional MIMO technology. It involves the use of a substantial number of antennas, often dozens or even hundreds, at the base station in a wireless communication network. This stands in contrast to conventional MIMO, which typically involves just a few antennas.

Simultaneous Multi-User Connectivity: One of the primary promises of Massive MIMO is its ability to serve multiple users simultaneously. Each user receives its own dedicated stream of data from the base station, increasing network capacity significantly. This is achieved through the precise control of signals sent from each antenna, known as spatial multiplexing.

Improved Signal Quality: Massive MIMO also improves signal quality by reducing interference. It uses beam-forming techniques to focus the transmission beams directly toward the intended users, thereby reducing interference and noise in the network. This leads to higher signal-to-noise ratios (SNR) and better communication quality.

Enhanced Coverage and Reliability: With its numerous antennas, Massive MIMO can cover a broader area and extend network coverage. It's particularly effective in addressing issues like shadowing and fading, making it suitable for both urban and rural environments.

Spectrum Efficiency: By serving multiple users simultaneously and optimizing signal transmission, Massive MIMO significantly improves spectrum efficiency. This means that more data can be transmitted over the same frequency bands, which is crucial in a world where the demand for wireless data continues to grow

Massive MIMO Algorithms

Signal processing algorithms are crucial components of Massive MIMO (Multiple-Input Multiple-Output) systems that help optimize communication performance. Here, we'll investigate three important signal processing algorithms used in Massive MIMO systems: Maximum Ratio Combining (MRC), Zero Forcing (ZF), and Minimum Mean Square Error (MMSE) equalization.

Maximum Ratio Combining (MRC): MRC is a simple yet effective technique used in the receiver of a Massive MIMO system. It exploits the spatial diversity provided by the multiple antennas at the receiver to enhance the received signal quality

Operation: In MRC, the signals received by each antenna element are weighted based on their signal-to-noise ratios (SNRs) and combined optimally.

Advantages: MRC offers significant diversity gain, especially in fading channels, by combining signals coherently. It's relatively easy to implement and computationally efficient.





Prathviraj Singh et al.,

Limitations: MRC assumes perfect knowledge of the channel conditions, which may not be realistic in practice. It may also suffer from interference when the channel conditions are not well separated.

Zero Forcing (ZF): Zero Forcing is a linear signal processing technique used to eliminate multi-user interference in the downlink of a Massive MIMO system. It aims to force the interference component of received signals to zero.

Operation: ZF pre-coding uses the inverse of the channel matrix to cancel out interference. It computes the weights for transmitting antennas such that the desired signals are transmitted without interference.

Advantages: ZF can completely eliminate interference when the number of antennas at the base station is greater than or equal to the number of users. It's relatively simple to implement.

Limitations: ZF may amplify noise and result in a high power transmission, which can lead to signal quality degradation. It also requires accurate channel state information (CSI) to be effective.

Minimum Mean Square Error (MMSE) Equalization: MMSE equalization is a more sophisticated linear signal processing technique that minimizes the mean square error between the transmitted and received signals. It balances the trade-off between noise enhancement and interference suppression.

Operation: MMSE equalization computes the transmit weights that minimize the mean square error between the desired signal and the received signal while taking into account the channel matrix and the noise covariance matrix.

Advantages: MMSE equalization provides a better trade-off between interference suppression and noise enhancement compared to ZF. It can mitigate interference even when the number of antennas is less than the number of users

Limitations: MMSE equalization is computationally more intensive compared to MRC and ZF. It also requires accurate CSI for effective operation

Smart Antenna System

Smart antennas, also known as adaptive antennas, utilize intelligent signal processing techniques to enhance communication performance. These antennas are equipped with multiple elements that can adaptively adjust their radiation pattern and focus on specific directions

Adaptive Beam-forming: Smart antenna systems use adaptive beam-forming to steer the radiation pattern of the antenna array toward the user or device of interest. This minimizes interference from other directions, improving signal quality and reducing signal degradation due to interference.

Adaptive Beam-forming: Smart antenna systems use adaptive beam-forming to steer the radiation pattern of the antenna array toward the user or device of interest. This minimizes interference from other directions, improving signal quality and reducing signal degradation due to interference

Dynamic Null Steering: Smart antennas can dynamically create nulls in their radiation pattern to cancel out interference sources. This is particularly useful in environments with strong interfering signals, such as urban areas.

Spatial Filtering: By employing spatial filtering techniques, smart antenna systems can extract desired signals while suppressing unwanted signals and noise. This contributes to improved signal-to-interference-plus-noise ratio (SINR) and overall communication quality.

Improved Coverage: Smart antennas can adaptively adjust their radiation patterns to cover specific areas or sectors more effectively. This adaptability enhances network coverage and ensures that resources are directed where they are needed most.

Enhanced Capacity: By reducing interference and improving signal quality, smart antenna systems can increase the network's capacity to support more users and data traffic.

Beam Forming Strategy

Beam Forming Strategies are fundamental techniques employed in smart antenna systems to enhance the performance of wireless communication. These strategies include adaptive beam-forming and null steering, both of which are essential for improving the signal-to-noise ratio (SNR) and suppressing interference. Let's explore these strategies in more detail:

Adaptive Beam-forming: Adaptive beam-forming is a signal processing technique that dynamically adjusts the antenna's radiation pattern to focus the transmitted or received energy towards a specific direction while minimizing interference from other directions.





Prathviraj Singh *et al.*,

Operation: Adaptive beam-forming relies on the estimation of the channel characteristics and the use of adaptive algorithms to determine the appropriate phase and amplitude weights for each antenna element. These weights are adjusted in real-time to optimize signal reception or transmission.

Improving SNR: Adaptive beam-forming improves SNR by enhancing the signal strength in the desired direction while attenuating signals arriving from other directions. This directivity effectively amplifies the desired signal, reducing the impact of noise.

Suppressing Interference: By steering the antenna pattern toward the desired signal source, adaptive beam-forming can simultaneously suppress interference from other sources. This interference suppression is particularly valuable in crowded wireless environments.

Applications: Adaptive beam-forming is commonly used in scenarios where the desired signal direction is known or can be estimated, such as point-to-point communication or tracking moving targets.

Null Steering: Null steering, or interference nulling, is a technique used in smart antenna systems to create nulls (directions with zero gain) in the antenna pattern to suppress interference from specific directions while maintaining sensitivity to the desired signal direction.

Operation: Null steering algorithms determine the optimal weights for each antenna element to create destructive interference towards undesired sources. These nulls cancel out the interfering signals while preserving the signal of interest.

Improving SNR: Null steering significantly improves SNR by effectively eliminating or reducing interference from specific directions. This ensures that the desired signal is received with minimal distortion or noise.

Suppressing Interference: The primary purpose of null steering is to suppress interference, making it particularly valuable in scenarios with co-channel interference, adjacent channel interference, or jamming.

Applications: Null steering is employed in various applications, including wireless communication, radar systems, and electronic warfare, where interference mitigation is critical.

Channel Modelling

The performance of MIMO (Multiple-Input Multiple-Output) and smart antenna systems is significantly influenced by various channel characteristics. Among these characteristics, fading, multipath propagation, and spatial correlation play crucial roles in shaping the quality and reliability of wireless communications.

Fading: Fading refers to the variation in signal strength and quality over time and space due to the changing characteristics of the wireless channel. It occurs because wireless signals often take multiple paths to reach the receiver, and these paths can have different lengths and phases.

Impact on MIMO: Fading can lead to fluctuations in the received signals at different antennas in a MIMO system. This variation can either enhance or degrade the system's performance, depending on the specific fading model and the diversity techniques employed. For example, if the fading is uncorrelated between antennas (i.e., independent fading), it can provide diversity gains that improve system reliability.

Impact on Smart Antenna Systems: Fading affects the quality of the received signals at smart antennas as well. Adaptive beam-forming and null steering techniques used in smart antennas can help mitigate the effects of fading by directing the main lobe of the antenna pattern towards the desired signal sources and nulling out interfering sources.

Multipath Propagation: Multipath propagation occurs when wireless signals travel along multiple paths due to reflections, diffractions, and scattering in the environment. These signals can arrive at the receiver with different delays and phases.

Impact on MIMO: Multipath propagation is a fundamental characteristic of wireless channels that MIMO systems exploit to achieve spatial diversity. Different paths can be used to transmit independent data streams, improving reliability and reducing the impact of fading. However, multipath propagation can also introduce inter-symbol interference (ISI) when not properly managed.

Impact on Smart Antenna Systems: Smart antennas can adapt to multipath environments by steering beams towards the strongest signal components and nulling out unwanted signals. This adaptability helps improve signal quality and reduce interference from multipath signals.





Prathviraj Singh et al.,

Spatial Correlation: Spatial correlation measures the similarity in the fading or signal characteristics between different antennas at the receiver or transmitter. High spatial correlation indicates that the antennas experience similar channel conditions, while low spatial correlation means that they experience different conditions.

Impact on MIMO: In MIMO systems, spatial correlation affects the degree of diversity and multiplexing gains. High spatial correlation reduces diversity gains but may enhance multiplexing gains, whereas low spatial correlation is desirable for maximizing diversity gains.

Impact on Smart Antenna Systems: Smart antenna systems can adapt to spatially correlated channels by adjusting the beam-forming weights to optimize signal quality. Spatial correlation information is crucial for designing effective beam-forming strategies

CONCLUSION

In conclusion, the research work investigating Massive MIMO and smart antenna systems the cutting-edge technologies in wireless communication networks demonstrates their immense potential to revolutionize the way we approach spectrum efficiency, signal quality, and network coverage. These technologies offer innovative solutions to the ever-growing demands of modern wireless communication. Massive MIMO's utilization of a multitude of antennas at base stations, paired with its ability to serve multiple users concurrently, presents a promising avenue for maximizing spectral efficiency. It addresses the pressing need to accommodate escalating mobile traffic demands while providing a robust mechanism to mitigate interference and improve signal quality. The technology's adaptability to different environmental conditions positions it as a versatile solution with the potential for widespread application. On the other hand, smart antenna systems introduce intelligent signal processing techniques that significantly enhance communication performance. Through techniques like adaptive beam-forming and interference nulling, these systems can actively suppress interference and amplify desired signals. This translates to improved signal-to-noise ratios (SNR), reduced latency, and a more reliable network coverage, making smart antennas invaluable in the quest for seamless wireless communication. In light of these considerations, this research proposal lays the foundation for an in-depth exploration of the practical implementation, performance evaluation, and optimization of Massive MIMO and smart antenna systems. By conducting comprehensive investigations into these technologies, we aim to unlock their full potential and contribute to the development of more efficient, reliable, and adaptive wireless communication networks, thus shaping the future of global connectivity.

REFERENCES

1. Devasis Pradhan , (2018) " Massive MIMO Technique used for 5th Generation System with Smart Antenna " , International Journal of Electrical, Electronics and Data Communication (IJEEDC) , pp. 81-87, Volume-6,Issue-7
2. Kentaro Nishimuri, Takefumi Hiraguri, Tsutomu Mitsui, Hiroyoshi Yamada, (2017), "Effectiveness of Implicit Beam-forming with Large Number of Antennas Using Calibration Technique in Multi-User MIMO System", MDIP, Electronics, Volume-6,Number-91
3. Shakti Raj Chopra, Akhil Gupta, Sudeep Tanwar, Calin Ovidiu Safirescu, Traian Candin Mihaltan, Ravi Sharma, (2022), "Multi-User Massive MIMO System with Adaptive Antenna Grouping for Beyond 5G Communication Network", MDIP, Mathematics, Volume-10,Number-3621
4. Saba Asaad, Amir Masoud Rabiei, Ralf R. Müller, (2018), "Massive MIMO with Antenna Selection: Fundamental Limits and Applications", IEEE: Transaction on Wireless Communication, Volume-17, issue-12
5. Emil bjornson, Luca Sanguinetti, Henk Wymeersch, Jakob Hoydis, Thomas L. Marzetta, (2019), "Massive MIMO is a Reality – What is Next?", Elsevier
6. Lu Lu, Geoffrey Ye Li, A. Lee Swindlehurst, Alexei Ashikhmin, Rui Zhang, (2014), "An overview of Massive MIMO: Benefits & Challenges", IEEE Journal of Selected Topics in Signal Processing, Volume-8, issue-5
7. Byung Moo Lee,(2018), "Energy Efficient Selected Mapping Schemes Based On Antenna Grouping for Industrial Massive MIMO-OFDM Antenna System", IEEE Transactions on Industrial Informatics, Volume-14 , issue-11



Prathviraj Singh *et al.*,

8. Thomas L.Marzetta, (2015), "Massive MIMO: An Introduction", BELL Labs Technical Journal, Volume- 2.

LITERATURE REVIEW BRIEF

Year of Publication	Name of Journal	Author Name	Paper Title	Objectives of research paper	Methods/ Techniques (Mention name of the algorithm, system model etc.)	Limitations/Gaps (Future Scope)
2018	International Journal of Electrical, Electronics and Data Communication	Devasis Pradhan	Massive MIMO Technique Used for 5 Generation System with Smart Antenna	This paper introduces the importance of Massive MIMO and Smart Antenna System, study of modelling type, antenna required, wavelength and frequency required for 5th generation.	Smart Antenna System(Switched Beam, Adaptive Antenna Array), heuristic algorithm, OFDMA, TDMA, FDMA	The future will bring the 5G into the unexpected way of communication. The 5G will change the life style of human being in upcoming centuries. The communication of the user to the machine will very fast to be understandable between them. The next level of the 5G mobile technology will use the nanotechnology and the Artificial intelligence
2017	MDIP: Electronics	Kentaro Nishimuri, Takefumi Hiraguri, Tsutomu Mitsui, Hiroyoshi Yamada	Effectiveness of Implicit Beam-forming with Large Number of Antennas Using Calibration Technique in Multi-User MIMO System	This paper examines the effectiveness of implicit beamforming (IBF), which enables transmission without channel state information (CSI) feedback in multi-user MIMO systems with a large number of antennas.	BPSK, Implicit beamforming, Basic Calibration Technique, IEEE802.11a Signals	Calibration for a system comprising a large number of BS antennas using IBF, and clarified the effectiveness of the proposed calibration method using a testbed that implements a 16 × 16 MIMO system.
2017	MDIP: Mathematics	Shakti Raj Chopra,	Multi-User Massive MIMO	This paper presents the AAG according	STTC, CSI, bandwidth efficiency of the AWGN, MLSTTC,	problems of the scarcity of available spectrum





Prathviraj Singh et al.,

		Akhil Gupta, Sudeep Tanwar, Calin Ovidiu Safirescu, Traian Candin Mihaltan, Ravi Sharma	System with Adaptive Antenna Grouping for Beyond 5G Communication Network	to the channel state information in the Massive MIMO scenario	AGG-3M System, 16-QAM, Rayleigh fading version	performance analysis can be solved by applying STTC-based code in Massive MIMO under cognitive radio scenarios, AAG-3M may be applied in filter bank techniques to achieve better results, Analyze and find the optimal hardware requirement for the implementation of the proposed codes
2018	IEEE: Transaction on Wireless Communication	Saba Asaad, Amir Masoud Rabiei, Ralf R. Müller	Massive MIMO with Antenna Selection: Fundamental Limits and Applications	This paper studies the performance limits of massive MIMO systems under practical antenna selection algorithms	Energy efficiency, ergodic rate, Asymptotic Channel Hardening zero-mean unit-variance Gaussian symbols, TAS, Hermitian angle	As M grows large, the mean value of the mutual information increases proportional to $\log \log M$ and its variance converges to zero. This implies that the channel hardening property is retained under antenna selection. The expected mutual information grows large in a fixed distance from the upper bound derived by applying Jensen's inequality. The derived large-system distribution matches the empirical





Prathviraj Singh et al.,

						distribution very well even for finite values of M
2019	Elsevier: Digital Signal Processing	Emil bjornson, Luca Sanguineti, Henk Wymeersch, Jakob Hoydas, Thomas L. Marzetta	Massive MIMO is a reality – What is next? Five promising research directions for antenna arrays	This paper studies about five promising researches for antenna arrays.	Channel estimation, 5G, radio-frequency, Laplacian Eigenmaps, Laplacian Matrix, Discrete Cosine Transform	The future will tell how quickly, and to what extent, visions for the five directions (namely: Massive MIMO, digital beam-forming, and/or antenna arrays) will materialize, but it might go faster than we can imagine today
2014	IEEE Journal of Selected Topics in Signal Processing	Lu Lu, Geoffrey Ye Li, A. Lee Swindlehurst, Alexei Ashikhmin, Rui Zhang	An overview of Massive MIMO: Benefits & Challenges	This paper studies about benefits and challenges in Massive MIMO	Detection & Precoding Schemes, Channel Estimation, single-carrier transmission	By equipping a BS with a large number of antennas, spectral and energy efficiency can be dramatically improved. However, to make the benefits of massive MIMO a reality, significant additional research is needed on a number of issues, including channel correlation, hardware implementations and impairments, interference management, and modulation.
2018	IEEE Transactions on Industrial Informatics	Byung Moo Lee	Energy Efficient Selected Mapping Schemes Based on Antenna Grouping for	This paper studies about mapping schemes on antenna grouping for industrial Massive MIMO	Orthogonal Frequency Division Multiplexing (OFDM), High Peak-to-Average Power Ratio (PAPR), Selected Mapping (SLM), Power Amplifiers (PA)	Due to its SI burden and high complexity for TX/RX, there is implicit consensus that the SLM-based scheme could not be applied to massive





Prathviraj Singh et al.,

			Industrial Massive MIMO-OFDM Antenna Systems			MIMO-OFDM antenna systems. The significant increase in EE can be possible using an antenna group-based SLM scheme for massive MIMO-OFDM antenna systems.
2015	BELL Labs Technical Journal	Thomas L. Marzetta	Massive MIMO: An Introduction	This paper studies about the introduction to MIMO	4G, Time-Division-Multiplexing(TDD), Large Scale Antenna System	Massive MIMO replaces costly instrument-grade 40 Watt transceivers with a large number of low-power and possibly low-precision units. Ideally each antenna would be contained in an inexpensive module containing all electronics, signal processing, and a small power amplifier and as many of these modules as desired could be assembled like Lego bricks. This represents an entirely new design philosophy for which a low cost solution is needed.





Prathviraj Singh et al.,

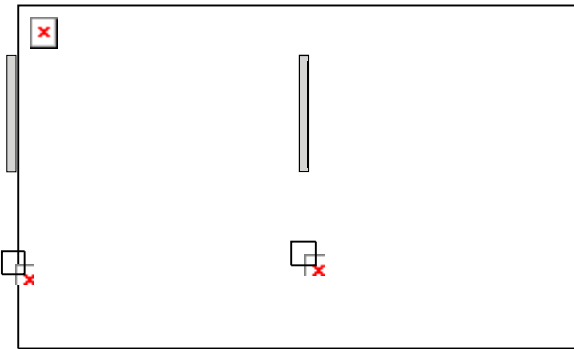


Fig. 1. Beam forming from an antenna array can be used to (a) focus the radiated signal in one angular direction or (b) focus the signal at one particular point in space, in which case the radiated signal might have no dominant directivity. The radiation patterns in this figure were computed using eight-antenna uniform linear arrays[5].

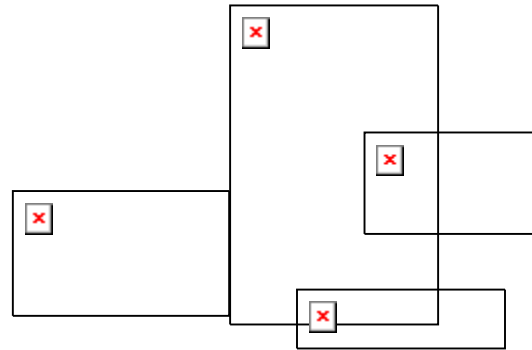


Fig. 2. A classical BS radiates one signal uniformly into its coverage area, as shown in (a). A BS capable of multi-user MIMO can radiate multiple signals (indicated by different colors) that are focused at their respective receivers, as shown in (b) [5].





Furniture Fusion: Elevating Your Shopping Journey AR Furniture Application Development and Implementation for Diverse User Engagement

Jayati Raval¹, Ayush Patel¹ and Prachi Shah^{2*}

¹Student, Birla Vishvakarma Mahavidhyalaya Engineering Collge, V. V Nagar, Anand, Gujarat, India.

²Assistant Professor, Birla Vishvakarma Mahavidhyalaya Engineering Collge, V.V Nagar, Anand, Gujarat, India.

Received: 30 Dec 2023

Revised: 09 Jan 2024

Accepted: 12 Jan 2024

*Address for Correspondence

Prachi Shah

Assistant Professor,

Birla Vishvakarma Mahavidhyalaya Engineering College,
V.V. Nagar, Anand, Gujarat, India.

Email: prachi.shah@bvmengineering.ac.in



This is an Open Access Journal / article distributed under the terms of the **Creative Commons Attribution License** (CC BY-NC-ND 3.0) which permits unrestricted use, distribution, and reproduction in any medium, provided the original work is properly cited. All rights reserved.

ABSTRACT

AR tistic Home, an innovation testament, is an Augmented Reality (AR) Furniture Application. Merging technology and creativity, it redefines interior design. Beyond an application, it's a personalized experience for homeowners, designers, retailers, architects, DIY enthusiasts, and rental services. ARTistic Home integrates virtual furniture into real spaces, revolutionizing how users interact with furniture. Simplifying placement and purchase, it empowers users to effortlessly visualize dream furniture. With diverse options and user-friendly design, ARTistic Home transforms the ordinary. Beyond a tech marvel, it is a gateway to a future where envisioning living spaces is personal. It is not just furniture; it brings unique visions to life. Users immerse in a transformative experience where imagination knows no bounds, living spaces become canvases for dreams. ARTistic Home—a revolution where technology meets personal expression.

Keywords: Augmented Reality, User Interface, 3D Visualization, Virtual furniture, Unity

INTRODUCTION

Introducing ARTistic Home – a revolutionary design application that redefines interior beauty. With a simple touch, it transforms spaces into personalized style statements, bridging the gap between imagination and reality. Architects, designers, and homeowners are captivated by its ability to turn abstract concepts into vibrant wonders. From shifting sofa hues to elegant dining tables, ARTistic Home offers limitless possibilities. Its user-friendly interface hosts a curated collection of furniture, crafting immersive experiences that redefine interior allure. ARTistic Home stands as a





Jayati Raval et al.,

testament to the fusion of creativity and technology. It invites the world to witness the extraordinary stories written by human imagination.

LITERATURE SURVEY

The integration of Augmented Reality (AR) into the realm of furniture shopping has not only transformed customer experiences but has also posed unique challenges and opportunities for innovators. This literature review delves into the collaborative efforts of PTC, IKEA, and various partners, exploring the inception, development, and success of the IKEA Place application. By harnessing the power of AR technology and collaborative tools like Trello, these companies have redefined how consumers engage with products and how global teams collaborate on groundbreaking projects. This innovative project offers a distinctive open-source method for creating an Augmented Reality shopping experience. The key differentiators include:

1. **Introduction** The IKEA Place app, born from the collaboration between IKEA and PTC, has reimagined furniture shopping. It allows customers to visualize furniture in their own homes, solving the age-old dilemma of "Will it fit?"
2. **Swift Development and Launch** PTC developed the app in just nine weeks, launching it alongside Apple's ARKit, leading to a swift adoption by users and even catching the attention of Apple CEO Tim Cook.
3. **Collaborative Tools** The project management aspect was handled seamlessly with collaborative tools like Trello and Jira Software. These tools enhanced communication and made workflows smoother for teams spread across the globe.
4. **Enhanced Collaboration and Communication** Trello played a vital role in enabling clear communication and collaboration among diverse teams, bridging language barriers and making the entire process more efficient.
5. **Results and Recognition** The IKEA Place app was a massive hit, with over four million downloads, numerous awards, and high user ratings. It became a standard-bearer for augmented reality shopping experiences.
6. **Conclusion and Future Impact** The collaborative approach, combined with advanced technology and efficient tools, transformed internal processes, setting the stage for future innovations in augmented reality applications and global teamwork.

The paper titled "Furnished: An Augmented Reality based Approach towards Furniture Shopping" explores the integration of Augmented Reality (AR) technology in the e-commerce sector, specifically within the furniture industry. AR in Ecommerce Context:

Key Contributions of Furnished App

1. AR-Supported Ecommerce: Introduces an ecommerce app leveraging AR for an immersive furniture shopping experience.
2. Scene form SDK and PBR: Utilizes Scene form SDK's Physically Based Renderer (PBR) for realistic lighting, shadows, and reflections.
3. Efficient GLB Format: Implements GLB file format for efficient runtime rendering, ensuring a seamless AR experience.

Technological Framework

1. Android SDK: Forms the foundation for app development, providing essential components.
2. ARCore: Eliminates the need for external sensors, offering Motion Tracking, Environmental Understanding, and Light Estimation for accurate AR experiences.
3. Firebase Database: Efficiently stores product data, accessible to users.





Jayati Raval *et al.*,

User Flow and Interface Design

1. Modern E-commerce Layout: Furnished app adopts a contemporary design for an appealing user interface.
2. Interactive UI: Enhances user experience, ensuring easy navigation through the application.

RESULTS AND FUTURE IMPLICATIONS

The app's success is evident in the prototyped AR model, demonstrating visual quality, realistic lighting, and reflections. The Furnished app promises a convenient, time-saving, and cost-effective shopping experience, paving the way for future innovations in AR applications. The "Furniture Try On Application Using Augmented Reality" explores the integration of augmented reality (AR) technology into the furniture shopping experience. The application allows users to virtually place and visualize furniture objects in their real-world environment, offering a novel approach to online furniture shopping.

Key Contributions

1. Augmented Reality (AR) Experience: Offers users an immersive AR experience for visualizing furniture in their real-world environment.
2. Elimination of Measurement Hassles: Addresses size and fit concerns by allowing users to virtually place and assess furniture items without physical measurements.
3. Marker less AR Technology: Utilizes Marker less Augmented Reality, enhancing flexibility and adaptability in recognizing and tracking real-world objects.
4. Real-time Visualization: Provides real-time visualization of furniture in users' homes, accelerating decision-making in online furniture shopping.
5. User-Friendly Interface: Features an intuitive interface with actions like sliding and pinch gestures for easy manipulation of virtual furniture.

Technological Framework

1. Unity 3D: Primary development environment for creating interactive 2D and 3D content, handling UI, rendering, and application logic.
2. Google AR Core: Enables Marker less AR, ensuring accurate placement of virtual furniture objects by detecting and tracking the real-world environment.
3. Autodesk Maya: Used for creating realistic 3D furniture models, offering comprehensive features for animation, modeling, and rendering.
4. Android Platform: Developed for Android 8.0 or above, ensuring compatibility with a wide range of smart phones, particularly those with AR support.
5. Google Cloud for Database: Utilized for cloud-based database functionalities, managing data related to furniture models and user preferences.
6. Real-time Rendering and Processing: Employs real-time rendering and processing techniques for capturing, processing, and rendering scenes with minimal latency.

Background

This section deals with various software requirements for the project. The details are given below:

Flutter SDK

Flutter is a free, open-source software development kit (SDK) by Google, designed for cross-platform mobile application development. Utilizing a single platform-agnostic codebase, Flutter empowers developers to create high-performance, scalable applications with visually appealing and functional user interfaces for both Android and iOS platforms.



**Jayati Raval et al.,**

1. The Dart SDK: The Dart SDK includes libraries and command-line tools necessary for developing Dart web, command-line, and server applications.
2. Platform Tools: These are the tools which provide the support for running the application on the current android API.
3. SDK Platform: Specifies the target API level (Android level) required for running the application.
4. Google APIs - Provides simplicity of building applications, by providing APIs for different interfaces.

ARCore

ARCore enables AR functionality on Android devices without external sensors, enhancing what was previously provided by Tango. It works with Scene form to input 3D assets into the application and generates models at runtime, displayed in the environment using on-device cameras [1].

Unity

Unity provides powerful tools to make rich, deeply engaging augmented reality experiences that intelligently interact with the real world [2].

1. AR Foundation: This purpose-built framework for AR development allows developers to create applications once and deploy them across different mobile and wearable AR devices. It combines core features from each platform with unique Unity features like photorealistic rendering, physics, and device optimizations.
2. XR Interaction Toolkit: Users can enhance their AR applications by easily adding interactivity through pre-built components, eliminating the need to code these interactions from scratch [4].
3. Unity as a library: Developers have the flexibility to seamlessly integrate AR powered by Unity directly into their existing native mobile applications. Instead of rebuilding the entire application to incorporate AR functionality, developers can harness the full power of Unity's AR offerings by embedding them into their pre-existing creations.

Flutter Unity Widget: The Flutter Unity 3D widget enables effortless integration of Unity into Flutter applications. Developers can create engaging gamified features with Unity and seamlessly render them within a Flutter application, whether in Full screen or embeddable mode. This integration is compatible with various platforms, including Android, iPad OS, iOS, and the Web, with Windows compatibility nearing completion.

User Flow

1. User Registration this module allows you to create a user login/signup system where users can sign up using their email and password. The system stores this information securely in a Firebase database. After signing up, users receive a verification email to confirm their identity, adding an extra layer of security to the process. It's a user-friendly way to implement a secure authentication system for your application.
2. Product Catalog: This module introduces a visually appealing display of furniture products through a card view layout created using the Flutter SDK. It features a carefully curated selection of 12 items, categorized into four groups tables, chairs, sofas, and lamps, with three distinct items in each category. Each card showcases essential product details such as the name, image, and price. By organizing the products in this manner, users can easily explore the available options and make informed decisions based on their preferences.
3. AR window In this module, users can step into a whole new world of furniture shopping with the power of augmented reality (AR). By simply clicking the "View in AR" button, users can bring selected furniture items to life, right in their own space. Built using Unity AR Foundation and other essential plugins, this feature doesn't just stop at displaying the items in AR. It goes a step further by integrating a placement indicator. This indicator cleverly detects surfaces, making it incredibly easy for users to place the furniture items exactly where they want in their surroundings. This interactive and immersive experience revolutionizes the way users can explore and visualize furniture items, making their shopping journey truly captivating and enjoyable.
4. Feedback This module enables users to provide feedback on the application's functionality through a user-friendly interface. By clicking the designated feedback button, users can share their thoughts and experiences





Jayati Raval et al.,

effortlessly. The collected feedback is securely stored in a Firebase database, allowing developers to analyze user input effectively.

5. Shopping Cart and Checkout This module introduces a basic shopping cart functionality, allowing users to seamlessly add selected furniture items to their cart. Users can easily browse the available products and add them with a simple click, creating a convenient and intuitive shopping experience. Additionally, a pseudo checkout process is simulated, providing users with a glimpse of the overall buying process without integrating actual payment methods.
6. Filters In this module, users can streamline their furniture search with a straightforward filtering system. Through designated tabs for chairs, tables, lamps, and sofas, individuals can easily sort items by category. Clicking on a specific tab refines the displayed furniture, ensuring a focused browsing experience without unnecessary distractions. This approach simplifies the exploration process, allowing users to concentrate on their preferred furniture categories seamlessly.

Implementation

The entire project was built in four different stages:

1. User Interface The UI was entirely build using dart language via Flutter in Android studio. This includes the user registration portal, the main menu, feedback, and the furniture buying portal.
2. AR Module The entire AR module was built in unity using AR foundation, ARCore, XR Integration and UI toolkit. The 3D models of 12 different furniture items were taken from asset store and rendered in unity to produce the final . glb files of the furniture along with all the materials and textures applied.
3. Fire Base The database used for this project was firebase because it manages all data real-time in the database, can sync real-time data across all devices and is faster than any backend service.
4. Flutter unity widget After all the components were ready, the last step was to integrate the AR Module with the UI made in flutter so that complete immersive shopping experience can be provided.

RESULTS AND DISCUSSION

The ARTistic Home project, currently in its primary prototype stage, shows promising potential. Despite being in its early phases, the project has already garnered attention for its innovative approach to interior design. The prototype has received positive feedback from users who appreciate its simplicity and creative possibilities. As the project continues to evolve and refine its features, it holds the promise of becoming a transformative force in the world of interior design, showcasing the ingenuity and talent of the students involved.

Prototype Features and Functionalities

1. Area Calculation for Furniture Placement: The AR module incorporates an intelligent area calculation algorithm. When users attempt to place a furniture item, the system dynamically scans the plane and calculates its area. If the area of the selected furniture item exceeds the detected plane area, an error prompt prevents the item from being spawned.
2. Collision Prevention for Overlapping Items: To enhance user experience and prevent visual clutter, the AR module includes collision prevention logic. Users cannot spawn two furniture items on top of each other, ensuring a clear and organized visualization of the selected items in the real-world environment.

Technical Uniqueness

Attempted Integration of AR Module in Flutter Using Unity Widget. The ARTistic Home project stands out in its attempt to integrate an AR module within the Flutter framework, employing the Unity widget for seamless incorporation. While the integration may not be deemed entirely satisfactory in its current prototype stage, the endeavor itself reflects a pioneering approach. Traditionally, AR development has often been associated with specific platforms, and the use of Flutter, a cross-platform framework, introduces a unique dimension to the project. The



**Jayati Raval et al.,**

incorporation of the Unity widget allows for the integration of Unity-powered AR experiences directly into the Flutter application, showcasing a novel fusion of technologies. This pioneering effort aligns with the project's vision to redefine interior design through technology and creativity. As the project evolves, the exploration of such technical avenues contributes to the project's distinctiveness and sets the groundwork for potential advancements in AR applications within the Flutter framework.

Technical Challenges and Limitations

1. **Rendering Challenges:** Flutter Rendering Capability: The integration of AR components within Flutter faced challenges related to rendering capabilities. Flutter, optimized for UI rendering, encountered difficulties handling the intricate 3D rendering demands imposed by Unity-powered AR modules.
2. **Unity's 3D Graphics Focus:** Unity, as a dedicated game engine, is inherently more suitable for handling complex 3D graphics, intricate lighting, and reflections. In contrast, Flutter's primary strength lies in creating consistent and responsive UIs across different platforms.
3. **Timeouts and Lifecycle Management:** Logs indicated timeouts during attempts to pause and detach the Unity Engine, hinting at potential challenges in managing Unity's lifecycle within the Flutter environment.
4. **Rendering and Surface Issues:** Messages about Surface View being destroyed and issues with previously queued frames suggest potential rendering or surface management challenges between Flutter and Unity.
5. **Communication and Detachment:** Messages about detaching views and disposing controllers highlight potential issues in the communication and detachment process between Flutter and Unity.
6. **ANR (Application Not Responding) Log:** The ANR log suggested that the application was not responding during a blocked message, contributing to the integration module's malfunction.

CONCLUSION

AR technology has revolutionized e-commerce, offering innovative ways for customers to interact with products and make informed decisions. While challenges exist, AR's potential to enhance customer experience remains promising. Further research is needed to understand its long-term impact on the e-commerce industry.

REFERENCES

1. S. Dhavle, C. Mohammed Qais, "Furnished: An Augmented Reality based Approach Towards Furniture Shopping," *International Journal of Engineering Research & Technology (IJERT)*, Vol. 10 Issue 05, pp. 2278-0181, May-2021.
2. S. Pooja, B. Praveen, S. Raghul Prasath, "Furniture Try On Application Using Augmented Reality," *Journal of Emerging Technologies And Innovative Research (JETIR)*, Vol. 9, Issue 4, pp. 2349-5162, April 2022.
3. A. Poudel, O. Al-Azzam, "Interior Design with Augmented Reality," *Interior Design with Augmented Reality. Proceedings of the Midwest Instruction and Computing Symposium*, April 2018.
4. Unity Technologies User Interface Design And Implementation In Unity. Unity Technologies, 2021
5. Nowacki, Paweł & Woda, Marek. (2020). Capabilities of ARCore and ARKit Platforms for AR/VR Applications. 10.1007/978-3-030-19501-4_36.
6. Singh, Akshay, Sharma, Sakshi, & Singh, Shashwat. (2016). Android Application Development using Android Studio and PHP Framework. *IJCA Proceedings on Recent Trends in Future Prospective in Engineering and Management Technology RTFEM*, 2016(1), 5-8, July 2016.
7. Nowacki, P., & Woda, M. "Capabilities of ARCore and ARKit Platforms for AR/VR Applications," 2020.
8. Grid Dynamics Blog. "How to build an AR app with ARCore and Sceneform," 2021.
9. Marmoset. "Basic Theory of Physically-Based Rendering," 2021.
10. Google Developers. "Sceneform overview | Sceneform (1.15.0)," 2021.





Jayati Raval et al.,

11. Akshay Singh, Sakshi Sharma, and Shashwat Singh. "Android Application Development using Android Studio and PHP Framework," IJCA Proceedings on Recent Trends in Future Prospective in Engineering and Management Technology RTFEM 2016(1):5-8, July 2016.
12. [1]Jiang Hui, "Approach to The Interior Design using Augmented Reality Technology."
13. Snehal Magale, Nabil Phansopkar, Safwaan Mujawar, Neeraj Singh, "Virtual Furniture Using Augmented Reality."
14. Soham Mehta, Pratish Jain, Aayushi Vora, Abhijit Joshi, "Augmented Reality Books: An Immersive Approach to Learning."

<p style="text-align: center;">Fig 1: Activity Diagram for user flow of execution</p>	<p style="text-align: center;">Fig 2: User Registration</p>
<p style="text-align: center;">Fig 3: Product Catalogue</p>	<p style="text-align: center;">Fig 4: AR Module</p>
<p style="text-align: center;">Fig 5: Error when area is too small</p>	<p style="text-align: center;">Fig 6: Error when overlapping occurs</p>





Evaluating the Suitability of Aggregate and Grout for the Development of Semi-Flexible Pavement

Dhaval Mistry^{1*}, Jagruti shah² and Indrajit Patel³

¹PG Scholar, Infrastructure Engineering & Technology, Birla Vishvakarma Mahavidyalaya, Vallabh Vidyanagar, Anand, Gujarat, India.

²Assistant Professor, Infrastructure Engineering & Technology, Birla Vishvakarma Mahavidyalaya, Vallabh Vidyanagar, Anand, Gujarat, India

³Professor, Department of Structural Engineering, Birla Vishvakarma Mahavidyalaya, Vallabh Vidyanagar, Anand, Gujarat, India

Received: 30 Dec 2023

Revised: 09 Jan 2024

Accepted: 12 Jan 2024

*Address for Correspondence

Dhaval Mistry

PG Scholar,

Infrastructure Engineering & Technology,

Birla Vishvakarma Mahavidyalaya,

Vallabh Vidyanagar, Anand, Gujarat, India.

Email: dhaval.mistry318@gmail.com



This is an Open Access Journal / article distributed under the terms of the **Creative Commons Attribution License** (CC BY-NC-ND 3.0) which permits unrestricted use, distribution, and reproduction in any medium, provided the original work is properly cited. All rights reserved.

ABSTRACT

With greater flexibility in the surface or wearing course and resistance to rutting compared to both concrete and traditional asphalt, semi-flexible pavement offers several advantages. Its impermeable covering also offers good protection against water seeping into the foundation. The semi-flexible substance, commonly referred to as grouted macadam, is made up of an open-graded asphalt framework with 25–35% gaps that are filled with a cementitious slurry. This hybrid blend offers excellent resistance to rutting and a surface that is very impervious to oil and fuel spills. Because of these characteristics, it can be employed at harbors, airports, and industrial areas—places where slow and heavy traffic is common. Grouted Macadam is a little-known area of pavement technology that are typically limited to a specific function in specialty pavements whose performance is only estimated based on empirical data. Thus, this study's primary goal was to gain a better understanding of the aggregate gradation and grout needs in order to create a semi-flexible pavement. The compressive strength and fluidity of the grout mixtures made with additional cementitious material were assessed. The drain down test, marshall stability, indirect tensile strength, tensile strength ratio, and maintained stability were used to evaluate the surface dressing gradation of 13 mm nominal maximum aggregate size.

Keywords: Semi-flexible pavement, Grout, Fluidity, Open-graded friction course, Drain down test, Surface dressing, Optimum compaction.



Dhaval Mistry *et al.*,

INTRODUCTION

Every nation must have a functional and sufficient transportation system in order to grow economically, industrially, socially, and culturally. The lack of proper transportation infrastructure impedes the nation's progress toward socioeconomic development. All manufactured goods, including food, clothing, industrial goods, and pharmaceuticals, must be transported throughout their entire life cycle in order to be purchased by a customer. Thus, a nation's transportation infrastructure reflects both its social and economic development. Enough and effective transportation is a need for developing nations like India. Road transportation is the most important kind of transportation since it can provide the best possible service to everyone. It could deliver door-to-door service and offered the greatest degree of travel flexibility. Road transportation must be a pillar for other forms of transportation, serving as a supplement and feeder system for them. The primary road system in our nation, which consists of National Highways and Expressways, is the most significant of the three classes of roads. The National Highway Authority of India (NHAI) estimates that roads carry 80% of passenger traffic and 65% of freight. Our nation's road network and infrastructure need to be improved immediately due to the increasing volume of freight and passenger traffic.

OBJECTIVE

The objective of the study is to examine the impact of super plasticizer (SP) on the flow ability and strength of fly ash-based grout and to analyze the surface dressing (SD) gradation-II of NMA 13 mm in order to develop the SFP.

MATERIALS AND EXPERIMENT

Materials

Grout materials: Cement, Sand, Flyash, Master Glenium and Water. Surface Dressing: Aggregates and binder (PMB 40).

Cement

In this study, Ordinary Portland Cement 43 grade cement as been used as per IS 269:1989. The basic tests such as the specific gravity, the initial and final setting time, the fineness, the soundness, and the standard consistency are conducted. The following basic tests were performed on OPC 43.

Sand

As sand is an important construction material, it is always desirable to use good quality sand. River Sand (Zone-III) passing through a 75 μ m sieve was used for the work. The grout should permeate through the voids or pores of OGFC. So, the size of sand particles plays a significant role in flow ability. therefore, the finers and particles i.e., 75 μ m sieve should be used.

Fly ash

Class C fly ash is designated in ASTM C618 and originates from sub-bituminous and lignite coals. Its composition consists mainly of calcium, alumina, and silica with a lower loss on ignition (LOI) than Class F fly ash. When used in Portland cement, the Class C fly ash can be used as a Portland cement replacement ranging from 20-35 % of the mass of cementitious material. Specific Gravity of Fly ash is 2.87 (determined as per IS 269:1989).

Master Glenium

The Master Glenium product offering from Master Builders Solutions comprises new generation high-range water-reducing admixtures that are specially formulated for applications where slump retention, high/early strengths and durability are required. Concrete mixtures containing these premier products can be optimized for delivery in remote locations and for use in hot and cold climates. Master Glenium ACE is a super plasticizer developed for precast applications.

Aggregates

Coarse aggregates: The coarse aggregate shall consist of crushed rock retained on 2.36 mm sieve. It shall be clean, hard, durable of cubical shape and free from dust and often organic other deleterious substances. In this study, the granite aggregates were used to prepare the SD13 NMA samples. Fine aggregates: Fill the voids in the coarse





Dhaval Mistry et al.,

aggregates and stiffens the binder. The fine aggregates, passing 2.36 mm sieve and retained on 75 µm sieve, shall consist of 100% crushed, manufactured sand resulting from stone crushing operations. Filler: Fills the voids and stiffens the binder. E.g., Rock dust, cement/lime. The aggregate gradation (size-% passing) is 26.5-100, 19-92.5, 13-20, 9.5-3.5, 2.36-1 and 0.075-0.75.

Tests on grout

Marsh Flow cone test is used to measure the fluidity of the grout as per ASTM C939/C939M. Receiving Container of minimum 2000 ml capacity. Ring Stand or other device, capable of supporting the flow cone in a vertical, steady position over the receiving container. Level. Stopwatch, least reading of not more than 0.2s. The proportions of the ingredients of the grout mix were determined empirically using the trial – and –error method. The ingredients were then mixed according to their proportions to form a paste. The paste was then poured through the flow cone within 1 minute of mixing to ensure that the paste does not set. Using the Stopwatch flow time was measured to effluent the 1725 ml of grout.

Tests on OGFC

The drain down of the loose bituminous mix shall be determined according to ASTM D 6390. The drainage test should be performed at the anticipated plant production temperature and should satisfy the specified maximum drain down of 0.30%. If the mixture fails to meet this requirement, then fibers can be added to a level that reduces drain down to the acceptable limit. There is a scope for reduction in bitumen dose which improves resistance against water penetration and may increase the ratio of ITS wet to ITS dry. However, as this may make the mix more brittle, reduction of bitumen dose below 3.25% is not recommended. The adequate quantity of bitumen is needed to maintain the nature of the prepared CGBM as a flexible layer. This method determines the amount of drain down in an uncompact asphalt mixture sample when the sample is held at elevated temperatures, which are encountered during the production, transportation, and placement of the mixture. This test is specially applicable to the open-graded asphalt mixtures (such as open-graded friction course) and the gap-graded mixtures such as Stone Matrix Asphalt (SMA). A fresh sample of the asphalt mixture is placed in a wire basket. The wire basket is hung in a forced draft oven for one hour at a preselected temperature. A catch plate of known mass is placed below the basket to collect material drained from the sample. The mass of the drained material is determined to calculate the amount of drain down as a percentage of the mass of the total asphalt mix sample.

For each mixture to be tested, the drain down characteristics shall be determined at two temperatures: at the anticipated plant production temperature and at a temperature 10°C higher than the anticipated production temperature. Duplicate samples shall be tested at each temperature. Therefore, a minimum of 4 samples shall be tested. Weigh the empty wire basket (Mass A). Place in the wire basket 1200 +/- 200 grams of fresh, hot asphalt mixture (either prepared in the laboratory or from an asphalt plant) as soon as possible without losing its temperature. Place the mix loosely in the basket without consolidating it. Determine the mass of the wire basket plus sample to the nearest 0.1 gram (Mass B). Determine the mass of the empty catch plate to be placed under the basket to nearest 0.1 gram (Mass C). Hang the basket with the mix in the oven preheated to a selected temperature. Place the catch plate beneath the wire basket. Keep the basket in the oven for 1 hour +/- 5 minutes as shown in Figure 3. Remove the basket and 'catch plate' from the oven. Let cool to ambient temperature. Determine the mass of the catch plate plus the drained material to the nearest 0.1 gram (Mass D). Calculate the percentage of mixture which drained to the nearest 0.1% as per Eq. 1

$$\text{Drain Down (\%)} = [(D - C) / (B - A)] \times 100 \quad \dots \text{Eq. 1}$$

Where, A = mass of the empty wire basket, g

D = mass of the wire basket plus sample, g C = mass of the empty catch plate, g

g = mass of the catch plate plus drained material, g Average the two drains down results at each temperature and report it to the nearest 0.1 percent.



**Dhaval Mistry et al.,****Theoretical Maximum Specific Gravity**

The theoretical maximum specific gravity is determined as per ASTM D2041/D2041M-19 and ANNEXURE C of IRC:SP:125:2019. The container (either a or b below) or Vacuum bowls: Either a metal or plastic bowl with a diameter ranging from 180 to 260 mm and a bowl height of at least 160 mm. The bowl shall be equipped with a stiff, transparent cover fitted with a rubber gasket and a connection for the vacuum line. The hose connection shall be covered with a small piece of fine wire mesh to minimize loss of any fine material from the mix. The vacuum flask - To be used for weighing in air only: A thick-walled volumetric glass flask with a capacity of approx. 4000 ml, fitted with a rubber stopper with a connection for the vacuum line. The hose connection shall be covered with a small piece of fine wire mesh to minimize loss of any fine material from the mix. The balance capable of being read to the nearest 0.1 gram. If weighing is to be done under water, a suitable suspension arrangement shall be provided for weighing the sample while suspended from the Centre of the balance. The vacuum pump, capable of evacuating air from the vacuum container to a residual pressure of 4.0 kPa (30mm of Hg) or less. Provide a suitable trap between the pump and container to minimize water vapour entering the vacuum pump. Residual pressure manometer or calibrated absolute pressure gauge with a bleed valve to adjust the vacuum level. The water bath is capable of maintaining a constant temperature of 25± 1°C and suitable for immersion of the suspended container.

Separate the particles of the loose paving mixture (while it is warm) by hand so that the particles are not larger than about 6 mm and don't fracture the aggregates. Place the mix sample directly into the tarred bowl or flask. Weigh the container with the sample and designate the net mass of the sample only as A. (Note: The minimum sample size shall be 1500g for mixes with nominal maximum aggregate sizes of 12.5 mm or smaller; and shall be 2500g for mixes with nominal maximum aggregate sizes from 19 to 25 mm). Add sufficient water at 25°C to cover the sample completely. Place the cover (bowl) or stopper (flasks) on the containers. 3. Place the container with the sample and water on a mechanical agitation device or agitate manually at frequent intervals (2 to 3 minutes). Begin removing entrapped air by gradually applying vacuum and increasing the vacuum pressure until the residual manometer reads 3.7±0.3 kPa (27.5 ± 2.5mm of Hg). After achieving this level within 2 minutes, continue the vacuum and agitation for 15±2 minutes. Gradually release the vacuum with the bleed valve. 4. Weighing in water-Suspend the bowl (with out lid) and content in water for 10±1 minutes and then determine mass.

Designate the mass under water of the bowl and sample as C. 5. Weighing in air a. Bowl –Submerge the bowl and sample slowly in the 25 ± 1°C water bath. Keep it there for 10 ± 1 minute. Immerse the lid in water and slide it on to the bowl with out removing water from the bowl so that no air is trapped inside the bowl. Remove the bowl with the lid in place from the water bath. Dry the bowl and lid with a dry cloth. Determine the mass of the bowl, sample and lid and designate it as E. b. Flask – Fill the flask slowly with water ensuring not to introduce any air into the sample. Place the flask in a water bath for 10± 1 minute to stabilize the temperature at 25°C without submerging the top of the flask. Completely fill the flask with water using a cover plate without entrapping air beneath the cover plate. Wipe the exterior of the flask and cover plate. Determine the mass of the flask, plate and its contents completely filled with water. Designate this mass as E.

Dry Aggregate Air Voids

To determine the dry aggregate air voids, the balance or scale accurate up to 0.1 percent of the test load; Tamping rod, straight steel rod, 16 mm (5/8 inch) in diameter, approximately 600 mm in length; A sturdy, cylindrical metal measure with a capacity of 10 liters and the height and diameter of the measure should be approximately equal; Shovel or scoop for filling the measure with aggregate; Piece of glass plate of 6 mm thickness and at least 25 mm larger than the diameter of the measure are needed. Testing Procedure: Calibrate the measure and determine its capacity in mm³ by filling it with water and covering it with a glass plate to eliminate air bubbles and excess water. Determine the mass of water in the measure. Calculate the volume of the measure (V), by dividing the mass of water by its density. Use the with aggregate and level the surface with fingers. Rod the layer of the aggregate with 25 strokes of the tamping rod evenly distributed over the surface. Fill the measure 2/3 full, level with fingers and rod as above again. Finally, fill the measure slightly, overflowing the measure and rod again as before. Level the surface of aggregate with fingers in such a way that any slight projections of the larger pieces of the coarse aggregate





Dhaval Mistry et al.,

approximately balance the larger voids in the surface below the top of the measure. Determine the mass of the measure plus its contents and the mass of the measure alone and record the values to the nearest 0.05 kg. Calculate the unit weight of the aggregate by the dry rodding procedure using the Eq. 2.

$$M = (G - T) / V \quad \dots \text{Eq. 2}$$

Where, M = bulk density of the aggregate in dry rodded condition (kg/m^3); G = mass of the measure plus aggregate (kg); T = mass of the measure (kg); V = volume of the measure (m^3). Calculate the void content in the aggregate using the bulk density determined above, as follows:

$$\% \text{ Voids} = 100 [(S \times W) - M] / (S \times W) \quad \dots \text{Eq. 3}$$

Where, M = bulk density of the aggregate, kg/m^3
S = bulk specific gravity (dry basis) W = density of water, $998 \text{ kg}/\text{m}^3$.

Optimum Compaction

There are no proper criteria for selection of number of blows or gyrations for the compaction of high voids bituminous mixes. For determining the optimum compaction effort, the bituminous mixes were compacted using Marshall Compactor with incremental variation of compaction effort. The cylindrical specimens of 100 mm diameter were prepared using a 100 mm diameter

split mould for all considered aggregate gradations. For each aggregate gradation, the cylindrical samples were compacted at various blows (20 to 60) of Marshall Hammer with increment of 10 blows applied on one face of the specimen. Then the volumetric study for each specimen of compacted samples was carried out, which is based on bulk specific gravity of compacted mix (G_{mb}), theoretical maximum specific gravity of mix (G_{mm}) and bulk specific gravity of aggregates (G_{sb}). Three samples were prepared for each specimen. The Eq. 4 and 5 used for calculation of Air Voids (V_a) in the compacted bituminous mix and Void in Mineral Aggregates (VMA).

$$V_a = 100 ((G_{mm} - G_{mb}) / (G_{mm})) \quad \dots \text{Eq. 4}$$

Where, V_a = air voids in compacted mix (percentage), G_{mm} = theoretical maximum specific gravity of mix, G_{mb} = bulk specific gravity of compacted sample

$$VMA = 100 - ((G_{mb} \times P_s) / G_{sb}) \quad \dots \text{Eq. 5}$$

Where, VMA = voids in mineral aggregate (%), G_{mb} = bulk specific gravity of compacted sample, P_s = percentage of aggregate by total weight of mix, G_{sb} = bulk specific gravity of the aggregate. Mechanical Properties were analyzed by Marshall stability and Indirect Tensile Strength. The OGFC Sample is kept in a water bath for one hour and tested Marshall stability and flow value. Retained stability is conducted on the Marshall samples to measure the resistance of the mix towards the moisture. The stability is determined after placing the samples in a water bath at 60°C for half an hour and 24 hours for unconditioned and conditioned samples respectively. The Indirect Tensile Strength (ITS) test should be performed as per ASTM D 6931 on Marshall samples of 100 mm diameter. The ITS test method consists of applying a load along the diametrical axis of the cylindrical sample at constant deformation rate of 51 mm/minute and determining the maximum vertical load taken by the sample at time of failure. Failure point is defined as the point after which there is no further increase in load. Before testing, the specimens should be temperature conditioned for different test temperatures such as 25, 35 or 45°C . The maximum load P, taken by the sample is then used to calculate the Indirect Tensile Strength as per the Eq. 6.

$$ITS = 2P / \pi D \quad \dots \text{Eq. 6}$$





Dhaval Mistry et al.,

Where, ITS= Indirect Tensile Strength (MPa)
 P = load at failure (N)
 t = height/thickness of specimen (mm)
 D = diameter of specimen (mm)

Tensile strength ratio

The method covers the preparation of compacted OGFC specimens at 30% air voids and the measurement of change of diametral tensile strength resulting from the effect of water saturation and the laboratory stripping phenomenon with freeze-thaw cycle. The result may be used to predict long-term stripping susceptibility of OGFC mixtures. Using Marshall Compactor, four compacted specimens are prepared for 30 percent air voids with optimum bitumen content. It is divided into two equal subsets. One subset is tested in dry condition (unconditioned samples) for Indirect Tensile Strength (ITS). The other subset is subjected to vacuum saturation and freeze-thaw cycle (conditioned samples). The unconditioned specimens were brought to temperature of $25 \pm 1^\circ \text{C}$, by keeping them in a water bath maintained at test temperature for 2 hours. The specimen was placed over the lower loading strip of ITS mold, slowly lowered the top loading strip to bring it into light contact with the specimen. Ensured that the loading strips are parallel and centered on the vertical diametric plane. The mold was placed in the Marshall stability testing equipment with strain rate of 50mm/minute till failure. The load at failure was recorded. For the conditioned specimens were placed in an Asphalt mixture density meter (AMDM) and submerged in a vacuum container filled with water at room temperature for 30 minutes. Then the specimens were placed in plastic bags containing 10 ± 0.5 ml of water and sealed and kept in the freezer at a temperature of $-18 \pm 3^\circ \text{C}$ for 16 hours. These specimens were then kept in a water bath for 24 ± 1 hours maintaining 60°C temperature. This complete process is called freeze and thaw cycle. After a freeze and thaw cycle, the specimens are brought to temperature of $25 \pm 1^\circ \text{C}$, by keeping them in a water bath maintained at test temperature for 2 hours. These specimens are known as conditioned specimens for indirect tensile strength tests. The specimen was placed over the lower loading strip of ITS mold, slowly lowered the top loading strip to bring it into light contact with the specimen. Ensured that the loading strips are parallel and centered on the vertical diametric plane. The mold was then placed in the Marshall stability testing equipment with strain rate of 50mm/minute till failure. The load at failure was recorded. The indirect tensile strength (ITS) was calculated as follows: Tensile strength ratio (TSR) = S_c/S_u . Where, S_c = average tensile strength of conditioned subset, kPa and S_u = average tensile strength of unconditioned subset, kPa.

SFP Sample preparation

The design and preparation of open-graded asphalt (OGA) mixtures for SFPs differ from the other wearing courses of asphalt pavements. The OGA mixtures used in SFPs have a minimum air void of 20%, which can be increased to 30–35% in practical cases (Corradini et al. 2017, Afonso et al. 2016 and Pei et al 2016). It is worth mentioning that the utilization of these mixtures with the amount of air void mentioned above in flexible pavements causes some consequences, such as fatigue cracking, moisture susceptibility, and low temperature cracking. However, considering the fact that the air void of OGA mixtures used in SFPs is partially filled with grouting materials (with a remaining porosity of 3–5%), an initial air void of 20–35% is recommended as a prerequisite for asphalt mixtures. The cement and fly ash-based mix with flow time of 30 seconds is used for making trial samples. The partially penetrating grout has occurred. In Full depth penetration of grout by using vibrator with optimum proportion has occurred.

CONCLUSION

The purpose of this study was to ascertain how superplasticizer affected the fly ash-based grout and to assess if the 13 mm NMA surface dressing gradation was appropriate for creating a semi-flexible pavement. It is possible to draw the following inferences from the different test findings.

1. The Mix2 grout of proportion (C:S:FA:SP::55:40:5:0.5) prepared at W/B ratio of 0.4 is considered as the optimal proportion for grouting the OGA samples. It is evident that the increase of the SP content from 0.4 to 0.5 has reduced the flow time about 5-20% and increased the compressive strength about 5-15%.
2. The adopted gradation of 13 mm NMA has good aggregate packing characteristics which enhances the





Dhaval Mistry et al.,

performance of SFP.

3. The optimum binder content of 4.0% is obtained based on the permissible drain down value of 0.3% and the optimum compaction effort of 40 marshall blows on one side is determined based on the target air voids of 30%.
4. The ITS decreased about 65% with the increase in the test temperature from 25 °C to 45°C. The TSR of 68% and the percentage retained stability of 71% indicated severe degree of moisture susceptibility of OGA samples.
5. The adopted surface dressing gradation of 13 mm NMA can be used to prepare the SFP samples, which can address the severe moisture susceptibility of OGA samples.

REFERENCES

1. Al-Taher, M., Mohamady, A., Attia, M., and Shalaby, M. (2020). "Technical Evaluation of Using Grouting For Producing Semi-Flexible Asphalt Concrete Mixtures." *Bull. Fac. Eng. Mansoura Univ.*, 40(4), 22–38.
2. An, S., Ai, C., Ren, D., Rahman, A., and Qiu, Y. (2018). "Laboratory and Field Evaluation of a Novel Cement Grout Asphalt Composite." *J. Mater. Civ. Eng.*, 30(8), 04018179.
3. Bang, J. W., Lee, B. J., and Kim, Y. Y. (2017). "Development of a semirigid pavement incorporating ultra-rapid hardening cement and chemical admixtures for cement grouts." *Adv. Mater. Sci. Eng.*, 2017.
4. Bharath, G., Shukla, M., Nagabushana, M. N., Chandra, S., and Shaw, A. (2020a). "Laboratory and field evaluation of cement grouted bituminous mixes." *Road Mater. Pavement Des.*, 21(6), 1694–1712.
5. Bharath, G., Shukla, M., Nagabushana, M. N., Chandra, S., and Shaw, A. (2020b). "Laboratory and field evaluation of cement grouted bituminous mixes." *Road Mater. Pavement Des.*, 21(6), 1694–1712.
6. Bonicelli, A., Preciado, J., Rueda, A., and Duarte, A. (2019). "Semi-Flexible Material: A Solution for High-Performance Pavement Infrastructures." *IOP Conf. Ser. Mater. Sci. Eng.*, 471(3).
7. Corradini, A., Cerni, G., D'Alessandro, A., and Ubertini, F. (2017). "Improved understanding of grouted mixture fatigue behavior under indirect tensile test configuration." *Constr. Build. Mater.*, 155, 910–918.
8. Gong, M., Xiong, Z., Chen, H., Deng, C., Chen, X., Yang, J., Zhu, H., and Hong, J. (2019). "Evaluation on the cracking resistance of semi-flexible pavement mixture by laboratory research and field validation." *Constr. Build. Mater.*, 207, 387–395.
9. Harle, S. M., and Pajgade, P. S. (2019). "Experimental investigation on cement grouted bituminous pavement." *Indian J. Eng.*, 16.
10. Hassani, A., Taghipoor, M., and Karimi, M. M. (2020). "A state of the art of semi-flexible pavements: Introduction, design, and performance." *Constr. Build. Mater.*, 253, 119196.
11. Hou, S., Xu, T., and Huang, K. (2016b). "Investigation into engineering properties and strength mechanism of grouted macadam composite materials." *Int. J. Pavement Eng.*, 17(10), 878–886.
12. Husain, N., Karim, M. R., Mahmud, H. B., and Koting, S. (2014). "Effects of Aggregate Gradation on the Physical Properties of Semiflexible Pavement." *Adv. Mater. Sci. Eng.*
13. IRC. (2018). "Cement Grouted Bituminous Mix Surfacing for Urban Roads IRC SP 125 2019." e-conversion - Propos. a Clust. Excell.
14. Karami, M. (2017). "Application of the cementitious grouts on stability and durability of semi flexible bituminous mixtures." *AIP Conf. Proc.*, 1903(November).
15. Kaushik, S., and Siddagangaiyah, A. K. (2020). "Characterization of cement grouted bituminous mixes using marginal aggregates." *Road Mater. Pavement Des.*, 0(0), 1–18.
16. Luo, S., Yang, X., Zhong, K., and Yin, J. (2020a). "Open-graded asphalt concrete grouted by latex modified cement mortar." *Road Mater. Pavement Des.*, 21(1), 61–77.
17. Materials, S., and Science, M. (2015). "Mechanical Behavior and Failure Mechanism of Recycled Semi-flexible Pavement Material." *J. Wuhan Univ. Technol. Sci. Ed.*, 30(5), 981–988.
18. Njock, P. G. A., Chen, J., Modoni, G., Arulrajah, A., and Kim, Y. H. (2018). "A review of jet grouting practice and development." *Arab. J. Geosci.*, 11(16).
19. Oliveira, J. R. M., Pais, J. C., Thom, N. H., and Zoorob, S. E. (2007). "A Study of the Fatigue Properties of Grouted Macadam." *Int. J. Pavements*, 6(9), 1689–1699.





Dhaval Mistry et al.,

20. Oliveria, J. R. M. (2006). "Grouted Macadam-Material Characterization for Pavement Design."
21. Othman, M. M., El-maaty, A. E. A., and Hussein, Z. S. (2020). "Assessing and Improving the Performance of Grouted Macadam." *Am. J. Eng. Appl. Sci.*, 13(2), 153–164.
22. Pei, J., Cai, J., Zou, D., Zhang, J., Li, R., Chen, X., and Jin, L. (2016). "Design and performance validation of high-performance cement paste as a grouting material for semi-flexible pavement." *Constr. Build. Mater.*, 126, 206–217.
23. Performance, H., Engineering, C., and Science, B. (2014). "Utilization of Waste Rubber Powder in Semi-flexible Pavement." *Key Eng. Mater.*, 599, 361–367.
24. Plug, C. P., and Bondt, A. H. De. (2006). Improved performance of grouted macadams. *Res. Dev. Publ.*
- Pożarycki, A., Fengier, J., Górnaś, P., and Wanatowski, D. (2018). "Backcalculation of pavements incorporating Grouted Macadam technology." *Road Mater. Pavement Des.*, 19(6), 1372–1388.
25. Saboo, N., Ranjeesh, R., Gupta, A., and Suresh, M. (2019b). "Development of hierarchical ranking strategy for the asphalt skeleton in semi-flexible pavement." *Constr. Build. Mater.*, 201, 149–158.
26. Setyawan, A. (2013). "Assessing the compressive strength properties of semi-flexible pavements." *Procedia Eng.*, 54, 863–874.
27. Tran, T. N., Nguyen, H. T. T., Nguyen, K. S., and Nguyen, N. T. H. (2017). "Semi-flexible Material: The Sustainable Alternative for the Use of Conventional Road Materials in Heavy-Duty Pavement." 4th Congr. Int. Geotech., Singapore: Springer, 552–559.
28. Wang, D., Liang, X., Jiang, C., and Pan, Y. (2018a). "Impact analysis of Carboxyl Latex on the performance of semi-flexible pavement using warm-mix technology." *Constr. Build. Mater.* 179, 566–575.
29. Wearing, S. P., Mixture, C., Fast, U., and Weight, F. (2018). "Preliminary In-Situ Evaluation of an Innovative, Using Fast Falling Weight Deflectometer." *Materials (Basel)*, 11, 611.
30. Xu, Y., Jiang, Y., Xue, J., Tong, X., and Cheng, Y. (2020). "High-Performance Semi-Flexible Pavement Coating Material with Microscopic Interface Optimization." *Coatings*, 10(268).
31. Xun, W., Wu, C., Leng, X., Li, J., Xin, D., and Li, Y. (2020). "Effect of functional superplasticizers on concrete strength and pore structure." *Appl. Sci.*, 10(10).
32. Yang, B., and Weng, X. (2015). "The influence on the durability of semi-flexible airport pavement materials in the cyclic wheel load test." *Constr. Build. Mater.*, 98, 171–175.
33. Zarei, S., Ouyang, J., Yang, W., and Zhao, Y. (2020). "Experimental analysis of semi-flexible pavement by using an appropriate cement asphalt emulsion paste." *Constr. Build. Mater.*, 230, 116994.
34. Zhang, H., Liang, S., Ma, Y., and Fu, X. (2019). "Study on the mechanical performance and application of the composite cement–asphalt mixture." *Int. J. Pavement Eng.*, 20(1), 44–52.

Table1 Basic Tests Results of Cement (OPC 43)

Property	Test Method	Value	Specifications as per IS codes
Specific Gravity	IS 269:1989	3.16	3.16
Fineness	IS:4031-Part 1(1961)	8%	< 10%
Initial Setting Time	IS-8112	90 minutes	Minimum 30 min
Final Setting Time	IS-8112	10 hours	Minimum 10 hrs
Standard Consistency	IS 4031	28%	25-35%
Soundness	IS 4031-3(1988)	3 mm	< 10 mm
Compressive strength	IS 4031(Part 6):1988	43 MPa	43 Pa





Dhaval Mistry et al.,

Table 2 Physical properties of Aggregates

Property	IS Code/ASTM	Result	Specifications as per IRC:SP:52:2019
Specific Gravity	ASTMC127,C128 and D854	Coarse aggregate: 2.62(>9.5mm) Fine aggregate: 2.6(,9.5mm) Filler: 2.328	2.6-2.9
Combined Flakiness and Elongation index	IS:2386 Part 1	26.57 %	< 35%
Angularity Number	IS 2386-Part 1	2.62	
Crushing strength	IS:2386-Part 4	29.8%	< 30%
Los Angeles abrasion	IS:2386 Part 4	26.56%	< 30%
Aggregate impact value	IS:2386 Part 4	18.64%	<24%
Water absorption	IS:2386 Part 3	0.103%	<2%

Table 3 Physical properties of PMB40

Property tested	Test Method	Result obtained	Requirements as per IRC:SP:52: 2010
Penetration at 25°C, 100g,5 s, 0.1 mm	IS 1203-1978	47	30-50
Flash point, °C	IS 1209-1978	246	220
Softening point, °C Ring and Ball apparatus	IS 1205-1978	72	60
Specific Gravity	IS 1202-1978	1.0	-
Elastic recovery of half thread in ductile meter at15°C,%	APPENDIX-1(IRC:SP:53:2010)	80	60



Figure 1 OGFC samples with different compaction efforts





Dhaval Mistry et al.,



Figure 2 Lab grouting process (a)OGFC, (b)Grout, (c)SFP sample using final selected proportion (Full depth penetration of grout is observed) and (d) Partial depth of penetration of grout using trial mix.





Sustainable Highway Subgrades for Unsaturated Saline Coast in Ahmedabad

Vijayant Singh¹, Jagruti Shah², Indrajit Patel³ and Meera Jani⁴

¹Postgraduate Scholar, M-Tech, Infrastructure Engineering and Technology, Birla Vishvakarma Mahavidyalaya, Vallabh Vidyanagar, Anand, Gujarat, India.

²Assistant Professor, Department of Structural Engineering, Birla Vishvakarma Mahavidyalaya, Vallabh Vidyanagar, Anand, Gujarat, India.

³Professor, Department of Structural Engineering, Birla Vishvakarma Mahavidyalaya, Vallabh Vidyanagar, Anand, Gujarat, India.

⁴Project Engineer, Geo Designs & Research (P) Ltd., Vadodara, Gujarat, India.

Received: 30 Dec 2023

Revised: 09 Jan 2024

Accepted: 12 Jan 2024

*Address for Correspondence

Vijayant Singh

Postgraduate Scholar,

M-Tech, Infrastructure Engineering and Technology,

Birla Vishvakarma Mahavidyalaya,

Vallabh Vidyanagar, Anand, Gujarat, India

Email: Singhvijayant12@gmail.com



This is an Open Access Journal / article distributed under the terms of the **Creative Commons Attribution License** (CC BY-NC-ND 3.0) which permits unrestricted use, distribution, and reproduction in any medium, provided the original work is properly cited. All rights reserved.

ABSTRACT

The current contextual analysis talks about the sub grade improvement systems for profoundly saline marine soils situated at coastal line of Ahmedabad Region, Gujarat, India. Notwithstanding the presence of different salts, the immersion levels of these soil particles were seen to fluctuate all through the year because of a few climatic and geological variables. At first, the standard filter paper method is used for assessing the unsaturated way of behaving. Because of the low in situ California bearing Ratio (CBR) value (1.61%), locally accessible fly ash (5%-25% by weight) was utilized to work on the strength and solidness of the soil mass. Addition of fly ash brought about the extensive decrease of salinity. The unconfined compressive strength (UCS) and CBR have expanded until 15% fly ash and decreased from thereof. The maximum CBR got was around 9%, which can endure low to medium volumes of traffic. Be that as it may, the UCS created at seven days was seen to decrease at 28 days. This might be because of the auxiliary responses and change of type of salts present in the lattice. Consequently, further examinations on connections at miniature level and development of optional mixtures were prescribed to set up an economical sub grade in this landscape.

Keywords: Coastal Region of Ahmedabad, Fly ash, Salinity, CBR, Subgrade



Vijayant Singh *et al.*,

INTRODUCTION

The local communities at coastal line as well as the partnered infrastructure are going through a huge change due to the steadily expanding interest for metropolitan foundation to help business, private, the travel industry and seaward exercises. Sub grades of pavement and foundation of coast line structures are helpless against sea water because of existence of salinity and fluctuating geochemistry. The bay of Khambhat situated between the major western promontory and central area Gujarat in India is one of its kind bustling shoreline courses encountering a rising interest for infrastructure development. Due to the enormous volume of stream overflow, the bay has a positive water balance. The general humidity goes from 62 and 88 percent, making the environment semi-arid to sub-moist. In such conditions, the soil present in the dynamic zone/va dose zone are accounted for to be unsaturated. Accordingly, the in-situ regular sub grade strength presented for the asphalt development is helpless to varieties in and unsaturated circumstances. Highway infrastructure development over such sub grade requires extra consideration and whenever required, extra sub grade treatment might be vital. Pavement specialists in the region detailed comparative encounters and trouble in taking care of such soils. Stabilization of soil with lime or cement is a demonstrated and broadly embraced system everywhere. Nonetheless, energy utilization, cost and fossil fuel byproducts and other natural impact of cement production are the generally talked about impediments of such practice (Murmu *et al.* 2018). Research for supportable option settling specialists has illuminated the exhibition of different auxiliary modern results, for example, fly ash, steel slag, zinc slag, and rice husk ash as balancing out specialists for different structural designing applications.

Reuse of these optional items have different benefits, for example, decrease in costs, decreased landfill trouble, energy productivity and reduced natural contamination, other than performing like the customary materials. Fly ash, which is a result of nuclear energy stations is among the main optional materials concerning their amount of creation. Across the 195 nuclear energy stations situated within our country, around 218 million tons of fly ash was produced in 2018-2019, out of which 76% is utilized again for different structural designing implementation. Development of highways and bridges was seen to have a portion of just 4.48% out of the complete usage. In any case, we are well aware about non-plastic behavior of fly ash which is a residue like material, it has an extraordinary capacity to impact soluble base silica responses, also to the molecule surface connections. In this way, huge scope fly ash use can warrant an economical road construction. Fly ash is accounted for modification of the geotechnical execution by giving extra strength and solidness to the soil- fly ash blends. At around 15% fly ash content, the free swell record decreased by around half of the virgin soil. Besides, the known significant boundaries of optimum moisture content (OMC) and maximum dry density (MDD) for pavement, the density can be improved by addition of fly ash. With the increment in fly ash content, the MDD was found to increase while the OMC reduced. Notably, the California bearing ratio (CBR), a key indicator of pavement layer stiffness, bearing capacity, and load dispersion capability, is substantially improved with the addition of fly ash, with some research suggesting a peak CBR value at a 25% fly-ash concentration. These trends highlight fly ash's potential as a sub grade stabilizer. However, its effectiveness in diverse soil conditions, especially coastal soils in marine environments and unsaturated conditions, remains underexplored, emphasizing the need for further research and the basis for the current study.

OBJECTIVE

The current investigation endeavors to assess the engineering behavior of Ahmedabad marine soils in unsaturated conditions and evaluate the potential of utilizing fly ash as a stabilizing agent for these soils, specifically exploring their viability as flexible pavement sub grades. The study focuses on utilizing strength and stiffness parameters as key indicators to gauge the performance of fly ash-soil mixtures.



Vijayant Singh *et al.*,

MATERIALS INCORPORATED

Soil

The study sourced soil from Bavaliary village in the Ahmedabad region of Gujarat, India, situated at approximately Latitude 22° 06' 11" and Longitude 72° 06' 55", at a depth of approximately 1 meter below the ground surface to ensure suitability for sub grade use and to avoid organic matter present in the upper soil layers. The collected soil exhibited characteristics of a light brown color, fine texture, and smooth consistency. Geotechnical parameters and particle size distribution of the saline Ahmedabad soil are detailed in Table 1. The soil was found as low plastic with significant amount of silt which is in accordance with Indian Standards categorization system (IS 2720: Part IV). Notably, the soil displayed a high electrical conductivity of 21150 $\mu\text{S}/\text{cm}$, indicative of significant salinity (Table 1). The California bearing ratio (CBR), a pivotal parameter in pavement design, was notably low at 1.57%, underscoring the need for sub grade modification to enhance stiffness and meet the demands of traffic loads.

Fly Ash

For soil stabilization of the saline Ahmedabad soil, locally sourced class C lignite-based fly ash was obtained from the Surat Lignite Thermal Power Station in Gujarat, which was reported to possess pozzolanic properties. This lignitic fly ash, classified as class C, eliminates the need for additional activators, rendering it a cost-effective choice for various stabilization applications. The essential objective for this examination is investigating the exact attainability of Class C fly ash which is further consumed for soil adjustment in absence of some other activators and also the presentation of a highway framework for sub grade work with balance of fly ash.

INVESTIGATIONAL PROGRAM

In this study impact of class C fly which is easily available on the compaction, strength, and stiffness characteristics of Saline soil of Ahmedabad coastal line was assessed through a series of laboratory tests. Modified Proctor Tests were conducted at fly ash percentages of 5%, 15%, and 25% by weight to investigate the compact ability of the soil-fly ash mixtures, while Unconfined Compression Strength tests were performed to evaluate the strength of these mixtures. California Bearing Ratio tests were employed to assess the stiffness characteristics. Samples for these tests were prepared for MDD and OMC which will be determined by conducting test for the Modified Proctor. In addition to the above there will be test for electrical conductivity which will be conducted for different percentages of fly ash for examining the ascendancy of fly ash adjustment over the saline content in the soil-fly ash blends.

RESULTS AND DISCUSSION

Compaction Characteristics

The Optimum Moisture Content (OMC) and Maximum Dry Density (MDD) values for the soil-fly ash mixtures, obtained through the modified Proctor test, are summarized in below table. The different value of Maximum Dry Density tests exhibited a minimal increment in contrast to original soil, while the OMC showed a slight reduction at 5% fly ash, followed by a slight increase. It's worth noting that different studies have reported varying trends in OMC and MDD for fly ash-blended soils, but these trends cannot be universally generalized, as they are contingent on specific conditions and factors, particularly when dealing with soils of marine. The Maximum Dry Density & Optimum Moisture Content for all of the fly ash measurements are additionally utilized for the example readiness of residual test.

Electrical Conductivity

Electrical conductivity measurements were employed to assess the salinity levels in both the untreated and treated mixes of the Ahmedabad saline expansive soil. The undisturbed soil exhibited a notably large electrical conductivity value, stipulating the existence of different types of minerals and saline. But still with the introduction of fly ash, a decreasing trend in electrical conductivity was observed. Specifically, the electrical conductivity values for 5%, 15%, and 25% fly ash content were recorded as 20200, 18400, and 16800, respectively (Table 2), reflecting a substantial



**Vijayant Singh et al.,**

reduction in the soil's salinity. This reduction can be attributed to the introduction of positive charges originating from the free CaO present in the fly ash, which counterbalances the negative charges in the soil, effectively diminishing the overall electrical conductivity of the saline soil.

CBR (California Bearing Ratio)

In order to assess the effectiveness of fly ash adjustment in enhancing stiffness of sub grade, CBR (California Bearing Ratio) test was carried out in accordance with IS 2720 (Part 10): 2011 on both untreated and treated Ahmedabad saline soil. The results indicated a notable increase in CBR values, with the untreated soil registering a CBR of 1.62, whereas the addition of 5%, 15%, and 25% fly ash content led to CBR values of 6.67, 9.03, and a subsequent reduction to 8.51, respectively. The CBR values in fly ash-stabilized soil mixtures are influenced by the proportional contribution of frictional resistance from the fly ash and cohesive resistance from the soil, resulting in increased CBR values due to the dense microstructure formed by gel formation. While the CBR value demonstrated an increase, it did not yield a significant enhancement in the stiffness of blends. On using the same for sub grades of asphalt, the 9.03% CBR will endure traffic within normal scope. Besides, the decrease in value of California Bearing Ratio is observed on 25% fly ash expansion. The value of California Bearing Ratio is purportedly impacted distinctively by various saline material and its fixation, and the value of California Bearing Ratio reduces emphatically with the rise in saline substance (Liu et al. 2009). Considering these discoveries, the choice on adjustment and ensuing pavement design still have doubts within the sight of salts.

Unconfined Compression Strength

To comprehend the development and durability of strength in both treated and untreated mixtures, Unconfined Compression Strength (UCS) tests were conducted in accordance with IS 2720 (Part 10): 2011, with evaluations made at 7 days and 28 days of curing. The value of Unconfined Compression Strength for untreated soil was obtained originally as 37 kPa, rises to 148 kPa again 201 kPa post curing period of 7 days with 5% and 15% fly ash content, respectively. This augmentation in strength is attributed to fly ash's capacity to densify the soil through chemical reactions that consume moisture and dilution. Notably, Class C fly ashes contain tricalcium aluminate (C3A), known for its high reactivity with water and the resulting early strength. The presence of increased alumina and silica in fly ash, combined with higher fly ash concentration, can further enhance strength development in the sample (Murmu et al., 2018). However, the subsequent decrease in strength for all mixtures from 7 days to 28 days is a cause for concern, casting doubts on the permanency of strength gain. This strength misfortune might be ascribed by existence of saline, auxiliary product development, draining of items and change of saline substance and gels in framework. Hereafter, the solidness of above said blends shall be researched prior to directing the blends on field.

CONCLUSION

This study has successfully characterized the unsaturated properties and salinity levels of Ahmedabad marine soils. The addition of fly ash proved effective in reducing suction levels and salinity in the soil-fly ash mixtures. Notably, the UCS and CBR values exhibited significant increases up to a 15% fly ash dosage, after which a decline was observed. Thus, the 15% fly ash content can be considered an optimal mix for stabilization, resulting in a maximum CBR of approximately 9%, suitable for low to moderately trafficked roads. However, for roads accommodating higher traffic volumes, additional modification strategies will be necessary. The concerning aspect emerged when examining UCS values, as they significantly dropped from the strength obtained on 7th day to the results obtained on 28th day. The same might be ascribed for job of saline substance in blends and the conceivable auxiliary responses at larger restoring session. Albeit the outcomes are empowering at smaller time span of curing, the said methodologies need more examinations over the drawn-out sturdiness, life span and miniature underlying changes in the blends. Pavement design and development without such examinations might bring about untimely asphalt disappointments and colossal pointless speculations. Generally speaking, the review is supposed to support arranging practical techniques for seaside street framework improvement.





Vijayant Singh et al.,

REFERENCES

1. Ahmad, H., and Ahmed, S. (2015). Stabilization of low shear strength soil by using fly ash.
2. IOSR, The International Organization of Scientific Research 12(4), 3312(4), 33.
3. ASTM D5298-10. (2013). Standard test method for measurement of soil potential (suction) using filter paper, West Conshohocken, Pennsylvania, USA.
4. Bin-Shafique, S., Edil, T. B., Benson, C. H., and Senol, A. (2004). Incorporating a fly-ash stabilized layer into pavement design. *Proceedings of the Institution of Civil Engineers- Geotechnical Engineering*, 157(4), 239-249.
5. Bulut, R., and Leong, E. C. (2008). Indirect measurement of suction. In *Laboratory and field testing of unsaturated soils* (pp. 21-32). Springer, Dordrecht.
6. Bulut, R. (2001). Total and matric suction measurements with the filter paper method. Chandler, R. J., and Gutierrez, C. I. (1986). The filter-paper method of suction measurement. *Géo technique*, 36(2), 265-268.
7. Chen, F. H. (2012). *Foundations on expansive soils* (Vol. 12). ElsevierDixit, A., Nigam, M., and Mishra, R. (2016). Effect of fly ash on geotechnical properties of soil.
8. *International Journal of Engineering Technologies and Management Research*, 3(5), 7-14.
9. Ikechukwu, A. F., Hassan, M. M., and Moubarak, A. (2021). Resilient modulus and microstructure of unsaturated expansive subgrade stabilized with activated fly ash. *International Journal of Geotechnical Engineering*, 15(8), 915-938.
10. IS 14767. 2000. Methods of test for soils- Determination of the Specific Electrical Conductivity of Soils, Bureau of Indian Standards, New Delhi.
11. IS 2720 part 16. 1987. Methods of test for soils: Part 16 Laboratory determination of CBR, Bureau of Indian Standards, New Delhi.
12. IS 2720-Part 10. 1991. Methods of test for soils- Determination of unconfined compressive strength, Bureau of Indian Standards, New Delhi.
13. IS 2720-Part 4. 1985. Methods of test for soils: Part 4 Grain Size Analysis, Bureau of Indian Standards, New Delhi.
14. IS 2720-Part 5. 1985. Methods of test for soils: Part 5: Determination of liquid and plastic limit, Bureau of Indian Standards, New Delhi.
15. Karnam Prabhakara, B. K., Guda, P. V., and Balunaini, U. (2021, June). Resilient Modulus of Compacted Fly Ash for Pavement Applications. In *Proceedings of the Indian Geotechnical Conference 2019: IGC-2019 Volume II* (Vol. 134, p. 347). Springer Nature.
16. Khan, M. A., Wang, J. X., and Sarker, D. (2018). Stabilization of highly expansive more land clay using class-C fly ash geo polymer (CFAG). In *IFCEE 2018* (pp. 505-518).
17. Laguros, J. G., and Cokca, E. (2002). Use of class c fly ashes for the stabilization of an expansive soil. Discussion and closure. *Journal of Geotechnical and Geo environmental Engineering*, 128(11).
18. Li, H., Xu, D., Feng, S., and Shang, B. (2014). Microstructure and performance of fly ash micro- beads in cementitious material system. *Construction and Building Materials*, 52, 422-427.
19. Liu, Z., Zhang, Y., and Di, J. (2009). Analysis on the factors affecting the CBR value of silt roadbed. In *International Conference on Transportation Engineering 2009* (pp. 1814-1819).
20. Mehta, B., and Sachan, A. (2017). Effect of mineralogical properties of expansive soil on its mechanical behavior. *Geotechnical and Geological Engineering*, 35(6), 2923-2934.
21. Murmu, A. L., Dhole, N., and Patel, A. (2020). Stabilization of black cotton soil for sub grade application using fly ash geopolymer. *Road Materials and Pavement Design*, 21(3), 867-885.
22. Pandian, N. S., Krishna, K. C., and Leelavathamma, B. (2002, December). Effect of fly ash on the CBR behaviour of soils. In *Indian geotechnical conference, Allahabad* (Vol. 1, pp. 183- 186).
23. Parmar, J., Yadav, V., and Pandya, S. (2022). Influence of Biopolymer Treatment on Suction Characteristics of Bhavnagar Expansive Soil. In *Ground Improvement and Reinforced Soil Structures* (pp. 471-487). Springer, Singapore.





Vijayant Singh et al.,

24. Phani Kumar, B. R., and Sharma, R. S. (2004). Effect of fly ash on engineering properties of expansive soils. *Journal of Geotechnical and Geo environmental Engineering*, 130(7), 764- 767.

25. Senol, A., Bin-Shafique, M. S., Edil, T. B., and Benson, C. H. (2002, September). Use of class C fly ash for stabilization of soft sub grade. In *Fifth International Congress on Advances in Civil Engineering* (pp. 25-27). Istanbul, Turkey: Istanbul Technical University.

26. Teerawattanasuk, C., and Voottipruex, P. (2019). Comparison between cement and fly ash geo polymer for stabilized marginal lateritic soil as road material. *International Journal of Pavement Engineering*, 20(11), 1264-1274.

Table 1: Geotechnical Properties

Test		Ahmedabad soil	Code
Modified Proctor Test	MDD(kN/m ³)	17.80	IS2720: Part VII -1980
	OMC (%)	15.1	
Grain Size Distribution	Gravel(%)	0	IS2720:Part IV -1985
	Sand(%)	0.38	
	Silt(%)	81.23	
	Clay(%)	18.39	
Plasticity Index (%)		9.19	IS2720: Part XL -1977
Plastic Limit(%)		24.7	IS2720: Part V -1985
Liquid Limit(%)		32.78	
Free-swell Index (%)		10	
California Bearing Ratio (CBR) (%)		1.57	IS14767 -2000
Electrical Conductivity(μS/cm)		21150	IS2720: Part X -1987

Table 2: Compaction and Electrical conductivity Test results on soil –fly ash mixes

Soil mix	Compaction characteristics		Electrical Conductivity (μS/cm)
	MDD (kN/m ³)	OMC (%)	
Virgin soil	17.80	15.10	21150
Soil + FA (05%)	17.97	13.92	20200
Soil + FA (15%)	18.11	15.64	18400
Soil + FA (25%)	18.08	15.48	16800
Relevant Code	IS2720: Part VII -1980		IS: 14767 -2000





Sustainable Solid Waste Management by Integration of Waste at Taluka level-A Case Study of Petlad, Gujarat

Chirag R.Prajapati¹, Jagruti Shah², Indrajit Patel³ and Pratiti Bhatt²

¹PG Scholar, Infrastructure Engineering & Technology, Birla Vishvakarma Mahavidyalaya, Vallabh Vidyanagar, Anand, Gujarat, India.

²Assistant Professor, Department of Structural Engineering Birla Vishvakarma Mahavidyalaya, Vallabh Vidyanagar, Anand, Gujarat, India.

³Professor, Department of Structural Engineering, Birla Vishvakarma Mahavidyalaya, Vallabh Vidyanagar, Anand, Gujarat, India.

Received: 30 Dec 2023

Revised: 09 Jan 2024

Accepted: 12 Jan 2024

*Address for Correspondence

Chirag R.Prajapati

PG Scholar,

Infrastructure Engineering & Technology,

Birla Vishvakarma Mahavidyalaya,

Vallabh Vidyanagar, Anand, Gujarat, India

Email: prajapatichirag66171@gmail.com



This is an Open Access Journal / article distributed under the terms of the **Creative Commons Attribution License** (CC BY-NC-ND 3.0) which permits unrestricted use, distribution, and reproduction in any medium, provided the original work is properly cited. All rights reserved.

ABSTRACT

As per the 2011 registration data, 68.84% of the total population in India live in rural areas. It has been found that the most of studies on solid waste management in India have town, while less attention has been paid to small-scale town and their surrounding villages. Which will lead into unscientific disposal of municipal solid waste through open dumping in low-lying area or dumping waste near water bodies. The presented study emphasis on rural areas of Petlad Taluka, in which major amount of generated waste is decomposable. Integration of waste by forming clusters of villages and small-scale towns through route optimization particularly for inert waste, generated decomposable waste can be directly decomposed through vermin composting facility and recyclable waste can be recycled by recycle industries. This can be seen as a sustainable solution to the successful management of the MSWM facility.

Keywords: Cluster formation, Cost efficiency, Integrated solid waste management, Rural and semi-rural areas, Route optimization, Sustainable Solid Waste Management



**Chirag R.Prajapati et al.,**

INTRODUCTION

Protecting human civilization from the threatening influence of man-made waste is one of the most important issues facing the world today. Waste is, in fact, this alluring portion of raw materials, which are typically discarded after initial use. Solid waste is one type of waste material that is produced in our society by different human activities. [1]. Generally, municipal solid waste is a blend of commercial and residential waste produced by the local community. These wastes are collected, handled, stored, and disposed of, which may be hazardous to both public health and the environment. The amount and complexity of solid waste generated in cities rises with economic development, urbanization, and rising living standards. Certain waste categories are commonly discussed in solid waste discussions because they are widely recognized. Solid waste, for instance, comprises various types of waste from homes, businesses, industries, farms, institutions, and other sources. Often, it is difficult to differentiate the commercial and residential waste, so they are both regarded as urban waste. (Gupta N.2015). According to the CPCB's annual survey report for 2015–2016, 1,35,198,27TPD of solid waste is produced annually in all states of India. Of this total, 1,11,027.55 TPD of waste is collected, only 25,572.25 TPD of waste is treated, and 47,415.62 TPD of waste land is filled. It will demonstrate the stark difference between the total amount of waste generated and the total amount treated. It will show that different MSWM rules and guidelines are not being accepted well. India is constantly confronted with a significant obstacle in meeting the increasing demands for waste management infrastructure.

CURRENT SCENARIO OF SWM IN PETLAD TALUKA, GUJARAT

Petlad of Anand having area of 305.07 Sq.km, including 56 villages and 1 Major town [3]. by collecting primary data from selected town and village of research area. It has been observed that the majority of solid waste generated is dumped in open drainage systems, beside open government vacant land, and close to water sources without being properly treated. and in a lot of other improper ways. This might have a detrimental impact on the environment and the wellbeing of all living things.

RESEARCH AREA: PETLAD TALUKA

The town of Petlad is in Anand, Gujarat, India. There are 7 talukas in Anand. In Petlad Taluka, there are 56 villages and 1 town. Petlad taluka was considered to be the headquarters of character. Petlad taluka, which became the taluka headquarters from the district of the state, consisted of 104 villages. Then there are around 80 villages and now as many as 56 villages. The municipality was established in 1876. At that time the administration of the town was done with the help of the government. It has continued as a district municipality in 1949 and finally as a municipality since 1956.[4]

WASTE CHARACTERIZATION IN PETLAD TALUKA

The villages in the Petlad taluka generate comparatively little solid waste. Additionally, the substantial amount of garbage that villages produce decomposes. According to analysis, the average daily rate of waste generation in the study area's chosen villages is 85.10 gms/capita, of which 69.2% is decomposable, 22.7% is recyclable, and 8.6% is inert waste. In the small town of Vishnoli & Amod, the average rate of waste generation per day is 110.63 gm/capita. which states that 60.5% of waste is decomposable, 26.9% is recyclable, and 12.9% is inert. Note The primary data collected for August 2018 and beyond, including waste composition, generation rate based on income, and rate of waste generation, may vary over time due to various factors.

INTEGRATED SOLID WASTE MANAGEMENT

Formation of clusters of small towns and their neighboring villages in petlad taluka emphasis has been laid on root optimization and segregation of waste keeping in mind the local on land parameters. There are 56 villages and one city in petlad taluka, primary data has been collected that the amount of waste generation in rural areas and towns is low. A major amount of the waste in these little towns and villages is discard. As a result, while it is not economically feasible to manage solid waste in every village, it is impossible and becomes challenging to operate facilities for daily





Chirag R.Prajapati et al.,

aggregation, segregation, transportation, and disposal. In fact, when layoff sites are established in every village, it has been discovered that the cost of land and houses is extremely high. The implementation of integrated solid waste management will therefore prove to be a technically, financially and environmentally viable option

SOLUTION FOR INERT WASTE

Non-biological and non-chemical waste that is not required to decompose is known as inert waste. Inert waste includes materials like concrete and sand. Inert waste usually has lower disposal costs than hazardous or biodegradable waste, so this is especially important for landfills. When inert waste is produced in large quantities, it can become problematic because it starts to take up a lot of space. Generally speaking, inert waste doesn't harm the environment, animals' or people's health, or the quality of a watercourse. through gathering primary data. through the gathering of primary data. About 8–15 percent of all waste is generated as inert waste, according to observations. It is possible to directly landfill this through cluster formation and route optimization, making it an economically feasible and environmentally sound method of managing the Solid Waste Management Network.

Route optimization for the disposal of inert waste using a driving route planner

Each route for disposing of inert waste is designed by the driving route planner using distance-based parameters, waste management volume, and local on-site considerations. Note (C represents the cluster number, R represents the route number.)

Cost Evaluation of Inter-Waste Solution

7 routes have been identified to service all of the towns and villages in Petlad Taluka. The time constraints, vehicle capabilities, total waste to be managed, and local on-ground parameters are all taken into consideration when planning the clusters and routers listed below. The mini truck vehicle was rated to be able to collect 1.47 tons of waste. Based on these trips, a weekly allocation of the same route was made for the purpose of collecting waste. Table 1 lists the day and quantity of waste to be collected for each route. When collecting waste from every route, two vehicles are taken into consideration.

\$ indicates the scheduled day for waste collection for the specific routes and clusters

E.g., A vehicle will head for the designated route C1R1 on Monday in order to collect waste once a week.

CR represents the cluster number, R represents the route number:

It takes a variety of expenses to successfully implement the planned routes for integrated solid waste management between the small town and the nearby village. It includes the costs of labor, transportation, and vehicles. of which are listed below.

Cost parameters of vehicles:

Vehicle cost include the purchase cost of vehicle and maintenance cost that vehicle.

The purchase cost (P) 7,00,000 for one vehicle. Of vehicle for the collection of waste is considered as Rs

The collection of waste from all seven routes requires two vehicles.

Typically, the vehicle (L) life is considered as a 15years, maintenance is measured in 15% salvage value (S) is considered as 10% of price of purchase.

The cost of two vehicles = Rs. 14,00,000.

Vehicle cost for each route $V = \frac{\text{Cost of vehicales}}{\text{No. of Routes}}$

$$V = \frac{14,00,000}{7}$$

$$V = 7,00,000$$

To determine the annual depreciation cost $D = \frac{P-SL}{L}$

When D= Deprecation P =Cost of vehicle





Chirag R.Prajapati et al.,

S = Salvage of value of vehicle, L=vehicle's useful life

For 2 vehicles = Rs. 84,000

Depreciation cost of vehicles per route:

$$D = \frac{7,00,000 - 70,000}{15}$$

$$D = 42,000$$

For two vehicles = RS 84,000

$$\text{Depreciation cost of vehicles per route} = \frac{84,000}{7} = 12,000$$

To determine the annual depreciation cost

$$M = \frac{\% \text{ of maintenance} \times P}{L}$$

$$[\text{When } M = \text{Maintenance cost, } P = \text{cost of vehicle \& } L = \text{Life of value}]$$

$$\frac{15\% \times 7,00,000}{15}$$

Cost of transportation (A)

The amount of fuel required for a single route is included. A vehicle used for waste collection typically has a 9 km/lit mileage, and the most pertinent fuel cost is calculated to be 70 Rs/lit. To calculate the cost of transportation (A) = (fuel required for each trip * fuel cost)

$$\text{fuel requirements for each route} = \frac{\text{distance travelled by vehicle per route}}{\text{Mileage of vehicle}}$$

Cost of labor (L)

3 workers are needed for each trip: 1 driver and 2 assistants.

A labor cost of 310 per day is assumed.

The Total cost compute by (X) = Transpiration cost (A) + Cost of labor (L)

yearly total cost (C) = Total cost (X) * yearly trips (T)

Vehicle cost per route and storage bin investment cost(I)

Cost of a waste storage bin (W)

Storage bin takes into Rs.5000 per piece

Because 56 Villages= 5000*56=2,80,000

$$\text{Cost per route (S)} = \frac{2,80,000}{7}$$

$$= 40,000$$

Vehicle cost (V)=2,00,000

$$I = V+W$$

$$I = 2,00,000 + 40,000$$

$$= 2,40,000$$

Note These calculations below in Table 2 are considered to be sample estimate. Different expenses, for example, Fuel cost, Transpiration cost, Devolution cost, Work expenses and Vehicle costs are accepted to be the most important expenses and might be liable to changing opportunity to time. In light of various areas are and with respect to different variable. The expense of fuel changes every day. In this way the expense of fuel is viewed as Rs.70 as the most widely recognized cost in unambiguous local which may likewise be exposed to change.

SOLLUTION FOR RECYCLABLE AND DECOMPOSABLE WASTE:

A greater percentage of the generated waste is decomposable, as evidenced by the composition of MSW in villages and small towns. Since organic waste decomposes and stabilizes naturally, composition recycling is the most appropriate, environmentally friendly, and sustainable method available. People can benefit from fertilizer in their





Chirag R.Prajapati et al.,

farming endeavors. We are advising all Villages to implement a few sustainable practices. By using these, people can obtain compost for their use right away, and it's less expensive than the artificial compost found in stores.

Vermi composting is advised for decomposable waste:

Vermi composting is a recycling process in which natural waste is fed to earthworms, who then convert it into fertilizer that contains unusually high levels of healthful substances. Vermiculture, which literally translates as "to grow worms" or "worm farming," is the process used in vermin composting. In agricultural farms, earthworms are raised to eat organic waste, which includes all forms of biodegradable waste. Next, they distribute the "Vermi-cast," or excrement. These vermi-castings are rich in nitrate and contain minerals that are great soil conditioners and fertilizers, such as calcium, magnesium, potassium, and phosphorous. This makes it possible to directly sell farmers produced manures, which can be a highly attractive source of income.

Recommendations for the production of recyclable waste

Around 25–30% of the total waste in the Petlad Taluka study area is recyclable, according to findings from the study phase of primary data collection. Recyclable waste can be recycled and safe disposal can be accomplished by transferring this generated waste to recycling industries for additional recycling processes. Also, it has the potential to develop into a reliable source of funding for the network management of solid waste management.

CONCLUSION

It can be shown that using the cluster-based waste integration method for generated inert waste, along with the Integrated solid waste (ISWM) approach, is a useful strategy for increasing the effectiveness of SWM in rural and semi-rural locations. The clusters are created using distance-based criteria, the total quantity of garbage that needs to be managed, and the local on-site factors that are taken into account. Cost effectiveness, for which each participant must pay a very small fee (between Rs. 8–14 for the first year and Rs. 4–7 for the second year onward), is the most crucial component of the project's economic viability. The costs associated with this can be covered by selling the recyclable waste that is produced. Decomposable waste can also be a source of income by being turned into fertilizer through the process of vermin composting. By doing so, improper and unscientific disposal can be prevented. Thus, it is possible to acknowledge the ISWM concept as a practical and wise technology for sustainable solid waste management.

REFERENCES

1. Himabindu, P., Udayashankara, T. H., & Madhukar, M. A. (2015). Critical review on biomedical waste and effect of mismanagement. *International Journal of Engineering Research & Technology*, 4(03), 0181–2278
2. Gupta, N., Yadav, K.K. and Kumar, V. (2015) A Review on Current Status of Municipal Solid Waste Management in India. *JES*, 37, 206-217. <https://doi.org/10.1016/j.jes.2015.01.034>.
3. Census of India (2011). (www.censusindia2011.com)
4. Directorate of Census Operations Gujarat, District Census Hand book Anand, 2011.
5. CPCB (2017). Consolidated Annual Review Report on Implementation of Solid Wastes Management Rules, 2016.
6. Central Public Health and Environmental Engineering Organization (CPHEEO), *The Manual of Municipal Solid Waste Management by Government of India*, 2016.
7. Gujarat Social Infrastructure Development Society, Report of Kheda District Human Development Report 2015.
8. Jani, J., Pamnani, A., & Shah, J. (2019). Integrated Solid Waste Management for Sustainability: A Review. *International Journal of Engineering Research*, 8(4), 66-69.
9. Pamnani, A., & Srinivasarao, M. (2014). Municipal solid waste management in India: A review and some new results. *International Journal of Civil Engineering and Technology*, 5(2), 01-08.





Chirag R.Prajapati et al.,

10. Dipen Saiki Design of an integrated solid waste management mechanism: a model design for Tezpur municipal Area, Assam (International Journal of innovative Research & development; Vol 4 Issue 2, page 241)
11. Arti Pamnami, Mehta Srinivasarao (2015) Forecasting of Municipal solid waste generation for small-scale towns and surrounding villages located in the state of Gujarat, India (International Journal of Current Engineering)

Table1: Designed trips in a week for inert waste collection.

Route no.	Waste Quantity (Tone)	Distance (KM)	Monday	Tuesday	Wednesday	Thursday	Friday	Saturday
C ₁ R ₁	1.25	16.4	\$	-	-	-	-	-
C ₁ R ₂	2.30	15.1	\$	-	-	-	-	-
C ₂ R ₁	1.34	15.6	-	\$	-	-	-	-
C ₂ R ₂	0.76	12.3	-	\$	-	-	-	-
C ₃	1.15	9	-	-	\$	-	-	-
C ₄ R ₁	1.09	21.3	-	-	-	\$	\$	-
C ₄ R ₂	1.15	14.5	-	-	-	-	-	\$

Table2: Cost Estimation for Inert waste solution.

Route no.	C1R1	C1R2	C2R1	C2R2
Total waste per route (Ton)	1.25	2.30	1.34	0.76
Total Kms. Per route (2way)	32.8	30.2x2=60.4	31.2	24.6
Fuel needs to travel (Liter)	3.64	6.71	3.46	3.60
A (Cost of transportation in Rs.)	255	470	243	252
L (cost of labor in Rs.)	930	930	930	930
X (A+L in Rs.)	1,185	1,400	1,173	1,182
T (Annual trip)	48	48x2=96	48	48
C (X*T in Rs.)	56,880	1,34,400	56,304	56,736
D (Cost of Depreciation in Rs.)	12,000	24,000	12,000	12,000
M (Maintenance cost in Rs.)	7000	14000	7000	7000
C+D+M (in Rs.)	75,880	1,50,800	75,304	75,736
I (Investment cost (V+W))	2,40,000	2,40,000	2,40,000	2,40,000
Total cost 1 st year (C+D+M+I)	3,15,880	3,90,800	3,15,304	3,15,736
Total Gram panchayat per route	4	6	5	4
Population per route	29,476	35,589	26,380	25,901
Cost/person for 1 st year(Rs.)	10.71	10.98	11.95	12.19
Cost/person for 2 nd year	4.27	5.12	5.18	6.20
2 nd year				

The table shows that each person has to pay very little amount yearly.

Route no.	C3	C4R1	C4R1
Total waste per route (Ton)	1.15	1.09	1.15
Total Kms. Per route (2way)	18	42.6	29
Fuel needs to travel (Liter)	7.73	4.73	4.73





Chirag R.Prajapati et al.,

A (Cost of transportation in Rs.)	542	332	332
L (cost of labor in Rs.)	930	930	930
X (A+L in Rs.)	1,472	1,262	1,262
T (Annual trip)	48	48	48
C (X*T in Rs.)	79,656	60,576	60,576
D (Cost of Depreciation in Rs.)	12,000	12,000	12,000
M (Maintenance cost in Rs.)	7000	7000	7000
C+D+M (in Rs.)	98656	79576	79576
I (Investment cost (V+W))	2,40,00 0	2,40,00 0	2,40,000
Total cost 1 st year (C+D+M+I)	3,38,65 6	3,19,57 6	3,19,576
Total Gram panchayat per route	3	8	6
Population perroute	26,862	26,687	26,687
Cost/person for 1styear(Rs.)	12.60	11.97	11.97
Cost/person for 2ndyear	5.98	5.71	5.71



Fig.1.Petlad Taluka.

Chart.1: Average waste generation rate based on selected Village & Vishnoli, Amod Village in the research area (Source: Primary data obtaining)

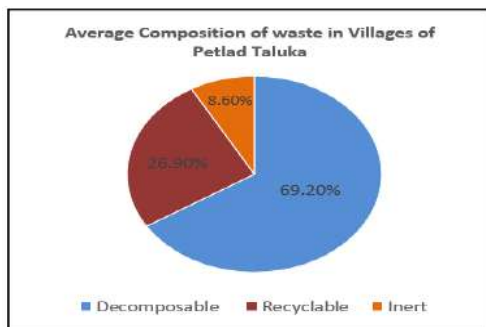


Chart.2: Based on the selected Villages, the average composition of waste generated in the Study Area (Primary data obtaining)

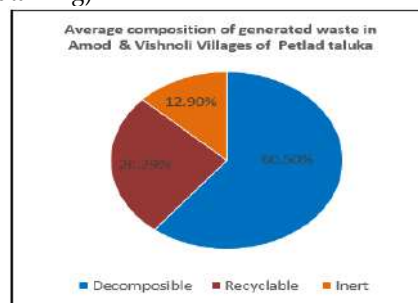
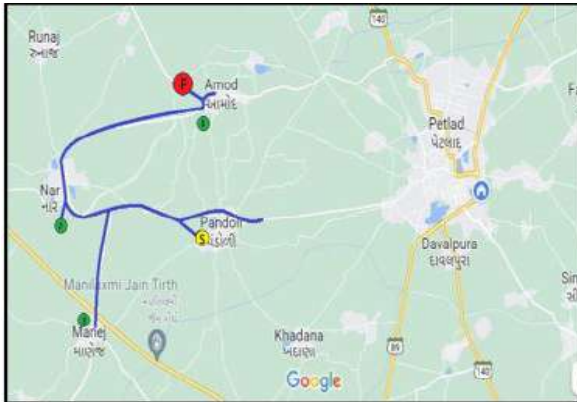


Chart.3: The research area's average waste composition in the towns of Amod, Vishnoli, and Amod (Primary data obtaining)



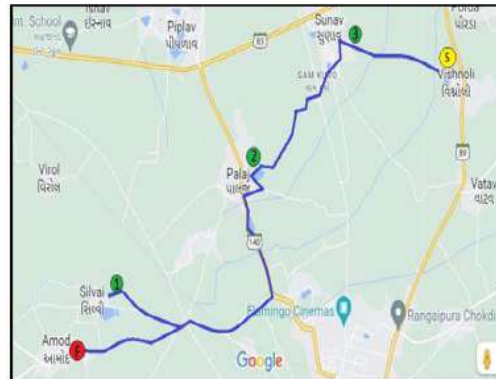


Chirag R.Prajapati et al.,



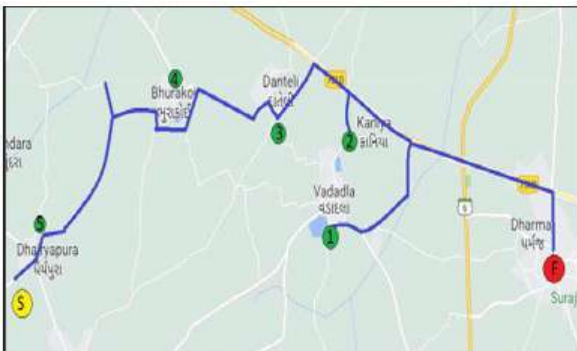
<i>C₁R₁: Pandoli to Amod</i>	
Cluster Head	Amod
Via	Pandoli Nar, Manej
Total Village Covered	4
Route	16.4Km
Total inert waste carry	1250Kg/Week

1.Amod cluster, C₁R₁ (Cluster no.1, Route no.1)



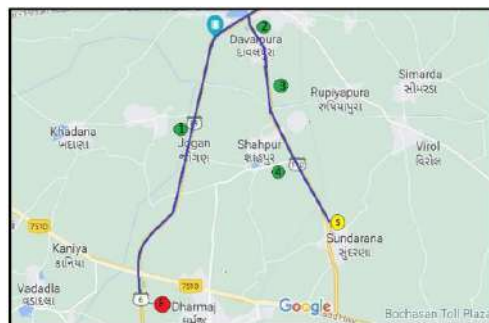
<i>C₁R₂: Vishnolito Amod</i>	
Cluster Head	Amod
Via	Silvai,Palaj,sunav
Total Village Covered	4
Route	15.1Km
Total inert waste carry	2300Kg/week

C₁R₂Route, Amod cluster.



<i>C₂R₁ : Dhairyapura to Dharmaj</i>	
Cluster Head	Dharmaj
Via	Vadadla, Kaniya, Danteli, Bhurakui, Dhairyapura
Total Village Covered	6
Route	15.6Km
Total inert waste carry	1340Kg/Week

2.Dharmaj Cluster, C₂R₁



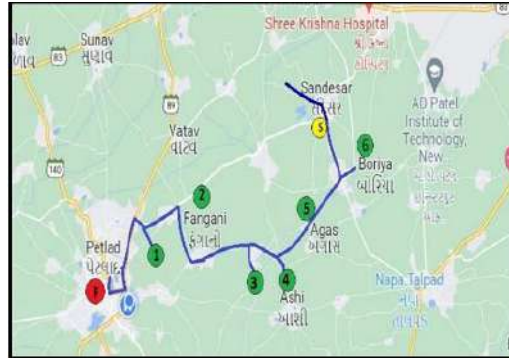
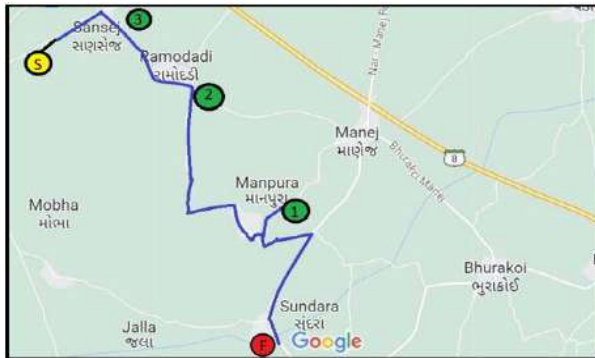
<i>C₂R₂: Sundarana to Dharmaj</i>	
Cluster Head	Dharmaj
Via	Jogan Davalpura, Vishrampur, Shahpur
Total Village Covered	5
Route	12.3km
Total inert waste carry	760Kg/Week

C₂R₂ Route, Dharmaj cluster





Chirag R.Prajapati et al.,

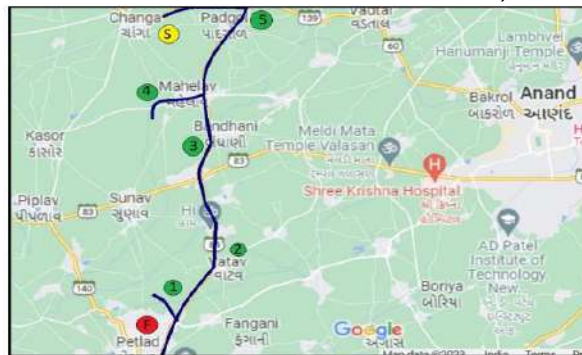


<i>C₃: Sansej to Sundra</i>	
Cluster Head	Sundra
Via	Manpura,ramodadi,Sansej
Total Village Covered	3
Route	9km
Total inert waste carry	1150Kg/Week

<i>C_{4R1}: Shihol to Petlad</i>	
Cluster Head	Petlad
Via	Dantali, Fagni, bhatiyel, Ashi, Agas, Boriya, Sandesar
Total Village Covered	8
Route	21.3km
Total inert waste carry	1094.9Kg/Week

3.Sundracluster,C3

PetladCluster,C_{4R1}



<i>C_{4R2}: Changa to Petlad</i>	
Cluster Head	Petlad
Via	Vatav,Badhani,mehelav, Padgol, changa
Total Village Covered	6
Route	14.5km
Total inert waste carry	1154.9Kg/Week

Petlad Cluster, C4R2





Evaluating the Effect of Aeration on Growth Conditions for Commercial Baker's Yeast: A Comparative Study on Batch Fermentation Processes with *Saccharomyces cerevisiae*.

Pragna S. Ukani¹, Pratiksha Gondkar¹, Debayan Baidya¹, Khushal Patel¹, Darshan H.Patel² and Hemant Kumar^{2*}

¹Department of Medical Laboratory Technology, Bapubhai Desaibhai Patel Institute of Paramedical Science, Charotar University of Science and Technology, Changa, Anand, Gujarat, India.

²Department of Biological Sciences, P.D. Patel Institute of Applied Sciences, Charotar University of Science and Technology, Changa, Anand, Gujarat, India.

Received: 30 Dec 2023

Revised: 09 Jan 2024

Accepted: 12 Jan 2024

*Address for Correspondence

Hemant Kumar

Department of Biological Sciences,
P.D. Patel Institute of Applied Sciences,
Charotar University of Science and Technology,
Changa, Anand, Gujarat, India.

Email: hemantkumar.cips@charusat.ac.in



This is an Open Access Journal / article distributed under the terms of the **Creative Commons Attribution License** (CC BY-NC-ND 3.0) which permits unrestricted use, distribution, and reproduction in any medium, provided the original work is properly cited. All rights reserved.

ABSTRACT

This study aims to evaluate cell mass yield from sugarcane molasses using different commercial yeast strains under various conditions. Five commercial yeast strains were initially assessed, and one sample exhibiting higher cell viability (Strain A) was selected for further growth protocols. Strain A was cultivated in sugarcane molasses under different conditions—both with and without aeration (anaerobic and aerobic conditions). The fermentation processes were conducted in batch conditions for 24 hours at room temperature and at 30°C, with agitation at 150 rpm. Results demonstrated that aeration facilitated exponential growth, with the aerated culture producing up to 60g/L of yeast cell mass, compared to 20-25g/L without aeration, using 500g/L of raw molasses for both conditions. This suggests variations in the oxygen sensitivity among commercial yeast strains. Furthermore, this study aimed to optimize the conditions for maximizing yeast cell mass yield during batch fermentation using sugarcane molasses targeting baker's yeast, specifically the *Saccharomyces cerevisiae* strain. The study evaluated and optimized the incubation period, incubation temperature, aeration, nitrogen and phosphorus sources, and molasses concentration to enhance the yield of yeast cell mass.

Keywords: sugarcane molasses, *Saccharomyces cerevisiae*, Aerobic Culture Conditions, Yeast Cell Mass Yield, Fermentation efficiency, commercial baker's Yeast.





Pragna S. Ukani et al.,

INTRODUCTION

Yeast is a versatile microorganism with numerous applications in various industries, including baking, brewing, winemaking, and bio ethanol production. Commercially available yeasts can be categorized based on their types, applications, and forms. These distinct categories possess varying compositions leading to different cell mass yields during production. Commercial yeast strains offer several advantages over natural yeast strains such as longer shelf life, higher viability, lower microbial contamination, and superior characteristics [1][2]. Molasses, the residual by-product derived from sugar industries processing sugarcane and sugar beet stands as a widely utilized substrate due to its cost-effectiveness, easy accessibility, and minimal pre-treatment requirements compared to starchy or cellulosic materials. This is primarily because all sugars essential for fermentation are readily available in molasses. Utilizing waste from the sugar industry for fermentation processes reduces production costs and promotes sustainability [2]. Aeration plays a pivotal role in significantly contributing to the efficient enhancement of overall cell mass production by supporting the proliferation of yeast cells. This process elevates the dissolved oxygen levels within the medium while reducing the presence of gases like CO₂ and other volatile substances. As oxidative metabolism significantly boosts ATP generation, yeast specifically requires oxygen in its cultivation environment to achieve peak biomass production [3]. Nitrogen and phosphorus are essential for yeast growth and maximizing ethanol production efficiency [4], achieving an increase by 40 to 50g/L using 500g/L molasses in the media. Although molasses provides many necessary nutrients, supplementing with nitrogen (using urea) and phosphate (with di ammonium phosphate) is common to enhance yeast growth in molasses-based mediums. For industrial procedures to sustain yeast health and promote robust fermentation, specifically designed sources of phosphate and nitrogen are essential [4]. This paper reports the results of a study based on the comparative analysis of yeast cell mass yield using sugarcane molasses as a source of growth media with the addition of a nitrogen source (1.5% Urea) and a phosphorus source (0.4% DAP), evaluating the effect of aeration and temperature for improved yeast cell mass yield.

MATERIALS AND METHODS

Microbiological testing of Yeast samples and isolation of early- growing Yeast cells

Initially, Gram staining was conducted to differentiate and confirm the microorganism. Subsequently, the sample inoculum was streaked onto Sabouraud dextrose agar (SDA) plates and incubated at 30°C overnight. The following day, after 12 hours, the largest colony on the plate was sub cultured onto a fresh SDA plate. This procedure was repeated for five days. Subsequently, a single colony grown on the fifth day was transferred to Sabouraud dextrose broth (SDB) and maintained under shaking conditions at 150 rpm and 30 °C. Further experiments were conducted using this culture derived from the early growing colony.

Direct Cell Count

Yeast cell counting at OD₆₀₀ was demonstrated using a spectrophotometer. Additionally, a direct cell count was conducted using the hemacyto meter method [5]. The cell count was calculated by multiplying the dilution factor by the total number of cells, dividing by the number of corner squares counted, and then multiplying by 10⁴ to obtain the cell concentration (cells/ml).

Sequencing

Fungal DNA isolation was carried out using the Alkaline-Lysis method. Polymerase Chain Reaction (PCR) was conducted using 18s universal primer and ITS primer sequences: *ITS1 FP* 5'-TCCGTAGGTGAACCTGCGG-3', *ITS4 RP* 5'-TCCTCCGCTTATTGATATGC-3' resulting in an amplicon size of 841 base pairs as referenced by [6][7], and *18s FP* 5'-CAGCAGCCGCGGTAATTCC-3', *18S RP* 5'-CCCGTGTGAGTCAAATTAAGC-3' generating an amplicon size of 650 base pairs [8]. The annealing temperature for both reactions was set at 58 °C. Subsequently, purification of the PCR products was conducted using the Qiagen PCR purification kit. The purified PCR product was then subjected for sequencing.





Pragna S. Ukani et al.,

Media and cultural condition

The media preparation process began with the initial dilution of Raw Molasses by adding 500 grams of it to 1000 milliliters (1L) of RO water [2]. For the final 1000 ml (1L) of media, 400 ml of Diluted Raw Molasses were combined with 600 ml of RO water. Additionally, as specified in the study by [4], 1.5 grams of urea (0.15%) and 4 grams of DAP (Di-ammonium phosphate) (0.4%) were added [1]. Subsequently, the starter culture was created by inoculating 100 ml of media with 100 μ l of the yeast strain sample. The flask was then placed in a shaking condition at 30 °C overnight. The following day, 100 ml of the inoculum (Starter culture) was added to 1 liter of media, and the mixture was again kept in a shaking condition at 30 °C overnight. A sparger was connected to the flask to facilitate aeration. On the subsequent day, the resulting cell mass was collected by centrifugation at 5000 rpm for 2 minutes, and the supernatant was discarded. The cells were then preserved at 4 °C according to the procedures outlined in [9].

Dough Testing

The activation of yeast commenced by combining 25 grams of yeast with 200 ml of warm water, along with 2-3 grams of sugar. This mixture was then incubated at room temperature for 15 minutes. Subsequently 1 kilogram of refined wheat flour, containing sugar and an improver was taken and the activated yeast was added to this mixture. Water was gradually added to knead the dough until a soft consistency was achieved, allowing it to pull away from the sides of the container. The dough was covered and left to rest for 30-40 minutes. During this time, an increase in the volume of the dough within the container was observed, as referenced in [10].

RESULTS AND DISCUSSION

Gram staining is typically not utilized for yeast cells due to their distinctive cell wall composition, which differs significantly from that of bacteria. However, (Fig 2) yeast cells were subjected to Gram staining for basic differentiation and identification based on visual characteristics. Yeast cells exhibit an average diameter ranging from 3 to 4 micrometers, larger than that of bacterial cells. Microscopic observation revealed rounded or oval structures, notably larger in size compared to bacterial cells, with visible budding cells. Additionally, using Image View software, an image was captured and the cell sizes were measured, thus confirming their classification within the fungal family. The yeast strains were cultured on Sabouraud Dextrose Agar plates, showcasing characteristics of smooth, creamy structures. These colonies appeared shiny, moist, and exhibited a raised, well-defined, convex shape. Their color varied from creamy to white and typically measured less than 2 to 3 millimeters in diameter. After 24 hours of incubation or upon maturation, some yeast colonies displayed texture changes, developing a wrinkled or powdery appearance over time. These particular traits may vary depending on the specific yeast species or strain. Furthermore, Gram staining of these colonies served as the final step in confirming their characteristics. A yeast cell suspension with an optical density of 600, stained with methylene blue, serves as a method to distinguish between live and dead cells. The staining process results in dark-colored cells indicating dead cells, while transparent cells denote live cells due to their inability to absorb methylene blue.

These yeast cells have an average size ranging from 3 to 4 micrometers, making them significantly smaller compared to a hematocytometer square (1mm), which is approximately 100 to 200 times larger. Therefore, for accurate counting, attention is directed towards the smaller squares within the central square, measuring 0.2mm on each side. The counting process involved surveying five of the 0.2mm squares strategically distributed throughout the central square, commonly included the four corners and the center. Observation under 40X resolution was utilized for counting both live and dead cells within these specific squares, and the counts were recorded. This process was performed in triplicate and further statistically evaluated by calculating the mean to determine the sample with the highest count of live cells and the lowest count of dead cells. Following triplicate determinations detailed in Tables I and II, strain A demonstrated a notably lower count of dead cells, standing at 1.98×10^9 , along with a live cell count of 2.04×10^9 . This places strain A as the second-highest in terms of live cell count among the examined strains. In comparison, strain B exhibited the highest count of live cells at 2.86×10^9 . However, it's essential to note that strain B also had a significantly higher count of dead cells, totaling 5.06×10^9 , surpassing the count observed in strain A. The





Pragna S. Ukani et al.,

substantial difference in the count of dead cells between strains A and B was crucial in the selection process for further experimental investigations. Although strain B displayed the highest count of live cells, its considerably elevated count of dead cells raised concerns about its viability and overall activity in comparison to strain A. Therefore, considering the balance between the count of live and dead cells, strain A was preferred candidate for further experimentation. Its notably lower count of dead cells, coupled with a relatively high count of viable and active cells compared to the other four strains, positioned strain A as the most promising choice for continued experimentation and analysis.

Here, sequence alignment of FJ1 is the highest matching sequence with our sequencing result of strain A according to nBLAST and YA is sequencing data of strain A. Here, the Green colour highlight denotes there is a similar nucleotide when compared with the sequencing chromatograph. Blue highlight denoting possible nucleotide can be there but no clear graph is visible. Yellow highlight denoting no match of nucleotide. Red colour words denoting confusing sequencing (more nucleotide available in either sequencing data or the FJ1 sequence). Lastly, most similarity of Strain A sequence is with FJ1 sequence which is a *Saccharomyces Cerevisiae* Strain. After the sequencing results the strain A was finally considered for further growth and cell mass yield experimentation.

- i) Sequencing result of strain A,
- ii) FJ1 sequence which is most similar sequence according to nBLAST(<https://blast.ncbi.nlm.nih.gov/Blast>) of *Saccharomyces cerevisiae* a baker's yeast strain,
- iii) VL3 sequence which is highest similar sequence according to Saccharomyces Genome Database (<https://www.yeastgenome.org/>) of *Saccharomyces cerevisiae* a baker's yeast strain.

The strain A of our study showing similarity with other *Saccharomyces Cerevisiae* strains. The evolutionary history was inferred using the Neighbour-Joining method. The optimal tree is shown. The tree is drawn to scale, with branch lengths in the same units as those of the evolutionary distances used to infer the phylogenetic tree. The evolutionary distances were computed using the Maximum Composite Likelihood method and are in the units of the number of base substitutions per site. This analysis involved 7 nucleotide sequences. Codon positions included were 1st+2nd+3rd+Noncoding. All ambiguous positions were removed for each sequence pair (pair wise deletion option). There were a total of 1032 positions in the final dataset. Evolutionary analyses were conducted in MEGA11. Table III illustrates the optimization of media and growth condition protocols at room temperature and 30°C controlled constant temperature, aimed at maximizing the cell mass yield of the selected yeast strain. Initially, using only molasses as a media resulted in a yield ranging from 20 to 25g/L. Subsequently, upon the addition of 0.4% DAP (Diammonium phosphate) and 1.5% Urea as additional phosphate and nitrogen sources, respectively, to the molasses, the cell mass yield increased to 45 to 50g/L. Finally, with the implementation of proper aeration, the cell mass yield significantly rose to 58-60g/L. Overall, these findings suggest that the addition of nitrogen and phosphorus sources to molasses along with ensuring adequate aeration and temperature is conducive to maximizing the cell mass yield.

To assess the quality of yeast related to the baking industry, dough testing was conducted. Figure 8A illustrates the yeast cells' ability to ferment and generate a soft dough texture within 40 to 90 minutes both with and without an improver. The containers containing the improver exhibited enhanced fermentation compared to those without it. Additionally, there was a notably higher rise in dough volume observed in containers supplemented with the improver. Figure 8B delineates the texture of dough with and without the improver. Dough with the improver exhibited elastic and viscous properties which are fundamental characteristics of dough texture. These findings suggest the superior quality of yeast cells cultivated using the protocol outlined in this study employing sugarcane molasses as a media supplemented with additional phosphate, nitrogen sources and proper aeration. This approach appears to yield yeast cells that exhibit favorable attributes crucial for baking applications.

CONCLUSION

This paper reports the results of a study based on the comparative analysis of yeast cell mass yield using sugarcane molasses as a source of growth media with the addition of a nitrogen source (1.5% Urea) and a phosphorus source





Pragna S. Ukani et al.,

(0.4% DAP), evaluating the effect of aeration and temperature for improved yeast cell mass yield. Efforts were made to optimize the production of yeast cell mass by modifying the culture conditions of the yeast strains. Initially, five commercial yeast strains underwent screening based on microbiological properties, direct cell count, and sequencing. Following this screening, Strain A was chosen for further growth protocols due to its lower count of dead cells (1.98×10^9) and higher count of live cells (2.04×10^9). Strain A was cultivated in sugarcane molasses under different conditions including aeration and controlled temperature comparison to assess yeast productivity. The fermentation process occurred in batch conditions for 24 hours at a controlled temperature of 30°C while being shaken at 150rpm. A separate batch was kept under similar conditions but without temperature control (room temperature). The results indicated that optimal aeration and controlled temperature conditions led to exponential growth changes with the aerated culture of Strain A demonstrating a remarkable increase in cell mass production up to 60g/L. This highlights the sensitivity of commercial yeast to differences in oxygen levels and temperature variations. Furthermore, the addition of 1.5% Urea as a nitrogen source and 0.4% DAP (Di-ammonium phosphate) as a phosphorus source in molasses for the final media showed improvements in cell mass yield. In summary, the combination of controlled /constant temperature 30°C, proper aeration maintained at a maximum flow rate of 3.5 L/minute along with the incorporation of 1.5% nitrogen and 0.4% phosphorus sources in sugarcane molasses significantly enhanced yeast cell mass production. The use of sugarcane molasses at a concentration of 500g/L as a production media being a byproduct of the sugar industry suggests a low production cost. This study contributes to expanding the understanding of yeast cell mass yield and optimized production methodologies for commercial applications.

ACKNOWLEDGEMENT

We would like to thank Mr. Birju Patel for providing commercial yeast strains. We are thankful to the Bapubhai Desaiabhai Patel Institute of Paramedical sciences (BDIPS) of Charotar University of Science and Technology (CHARUSAT) for their support and providing laboratory facility for this study.

REFERENCES

1. Mayzuhroh, S. Arindhani, and C. Caroenchai, "Studies on Bioethanol Production of Commercial Baker ' s and Alcohol Yeast under Aerated Culture Using Sugarcane Molasses as The Media," *Ital. Oral Surg.*, vol. 9, pp. 493–499, 2016, doi: 10.1016/j.aaspro.2016.02.168.
2. N. S. El-gendy, H. R. Madian, and S. S. A. Amr, "Design and Optimization of a Process for Sugarcane Molasses Fermentation by *Saccharomyces cerevisiae* Using Response Surface Methodology," vol. 2013, no. 0, 2013.
3. A. Beugholt, D. U. Geier, and T. Becker, "Improvement of *Saccharomyces* propagation performance through oxygen-enriched air and aeration parameter variation," *Front. Chem. Eng.*, vol. 5, no. May, pp. 1–10, 2023, doi: 10.3389/fceng.2023.1193230.
4. M. Fadel, A. A. Keera, F. E. Mouafi, and T. Kahil, "High Level Ethanol from Sugar Cane Molasses by a New Thermotolerant *Saccharomyces cerevisiae* Strain in Industrial Scale," vol. 2013, pp. 1–6, 2013.
5. P. Y. Yap, D. Trau, and T. Biosystems, "Yeast cell count direct yeast cell count at od600," no. March, pp. 3–5, 2019.
6. H. H. Id et al., "Detection of multiple mycetoma pathogens using fungal metabarcoding analysis of soil DNA in an endemic area of Sudan," pp. 1–14, 2022, doi: 10.1371/journal.pntd.0010274.
7. S. Fujita, Y. Senda, and S. Nakaguchi, "Multiplex PCR Using Internal Transcribed Spacer 1 and 2 Regions for Rapid Detection and Identification of Yeast Strains," vol. 39, no. 10, pp. 3617–3622, 2001, doi: 10.1128/JCM.39.10.3617.
8. K. Hadziavdic, K. Lekang, A. Lanzen, I. Jonassen, E. M. Thompson, and C. Troedsson, "Characterization of the 18S rRNA Gene for Designing Universal Eukaryote Specific Primers," vol. 9, no. 2, 2014, doi: 10.1371/journal.pone.0087624.
9. F. Ghorbani, H. Younesi, A. Esmaeili, and G. Najafpour, "Cane molasses fermentation for continuous ethanol production in an immobilized cells reactor by *Saccharomyces cerevisiae*," *Renew. Energy*, vol. 36, no. 2, pp. 503–509, 2011, doi: 10.1016/j.renene.2010.07.016.





Pragna S. Ukani et al.,

10. N. Struyf, E. Van der Maelen, S. Hemdane, J. Verspreet, K. J. Verstrepen, and C. M. Courtin, "Bread Dough and Baker's Yeast: An Uplifting Synergy," *Compr. Rev. Food Sci. Food Saf.*, vol. 16, no. 5, pp. 850–867, 2017, doi: 10.1111/1541-4337.12282.

Table I. Cell viability count of live and dead cells

LIVE CELLS			DEAD CELLS	
Sample ID	Cell Counts	MEAN	Cell Counts	MEAN
A1	1.7135 × 10 ⁹	A=2.04 × 10 ⁹	1.341×10 ⁹	A=1.98×10 ⁹
A2	2.4585×10 ⁹		2.533 × 10 ⁹	
A3	1.9668×10 ⁹		2.080×10 ⁹	
B1	2.6522×10 ⁹	B=2.86 × 10 ⁹	3.874×10 ⁹	B=5.06 × 10 ⁹
B2	3.2482×10 ⁹		4.917×10 ⁹	
B3	2.682×10 ⁹		6.407×10 ⁹	
C1	1.4155×10 ⁹	C=1.45×10 ⁹	5.811×10 ⁹	C=8.19×10 ⁹
C2	1.4006×10 ⁹		9.238×10 ⁹	
C3	1.5496×10 ⁹		9.536×10 ⁹	
D1	1.4105×10 ⁹	D=1.56×10 ⁹	3.265×10 ⁹	D=3.71×10 ⁹
D2	1.7001×10 ⁹		2.889×10 ⁹	
D3	1.5860×10 ⁹		5.001×10 ⁹	
E1	1.6801×10 ⁹	E=1.59×10 ⁹	4.521×10 ⁹	E=4.13×10 ⁹
E2	1.5088×10 ⁹		3.830×10 ⁹	
E3	1.5922×10 ⁹		4.050×10 ⁹	

Table II. Effect of nitrogen, phosphate and aeration on yeast cell mass yield.

Parameters	30°C	Room temperature
	Yield/ L	Yield/ L
Molasses	20-25g/L	12-18g/L
Molasses +0.4% DAP + 1.5% Urea	45-50g/L	38-46g/L
Molasses +0.4% DAP + 1.5% Urea+ Aeration	58-60g/L	50-55g/L





Pragna S. Ukani et al.,

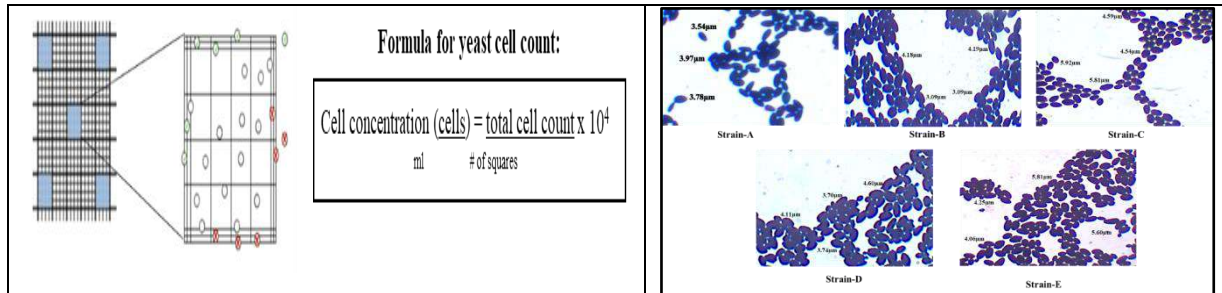


Fig.1. Cell counting grid and formula

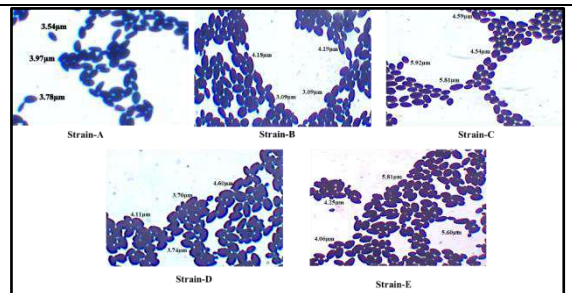


Fig.2. Gram's staining of the Samples

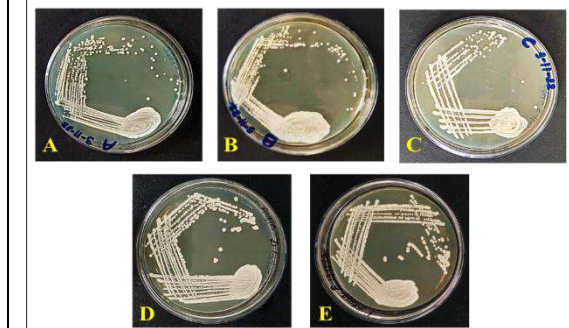


Fig.3. yeast cells on Sabouraud dextrose agar plates.

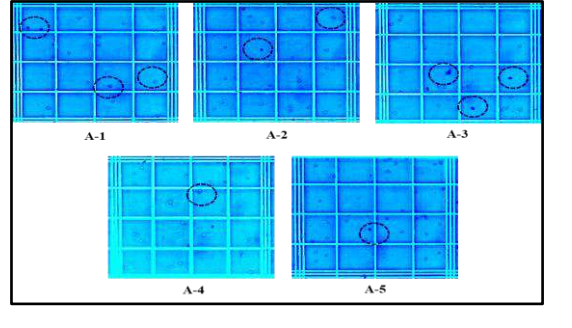


Fig.4. Direct cell count using hematocytometer under 40X resolution.



Fig.5. Sequence alignment of FJ1 strain and Strain A of our study.

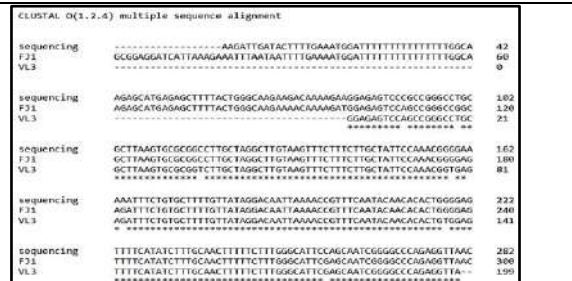


Fig.6. Multiple sequence alignment of 3 sequences

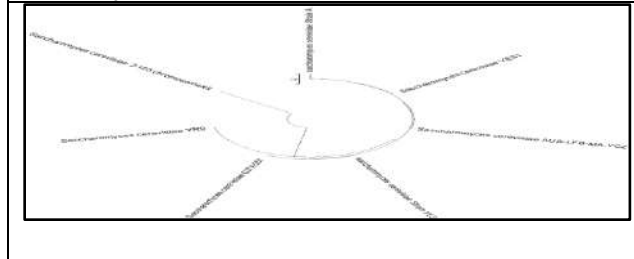


Fig.7. Evolutionary relationships of taxa

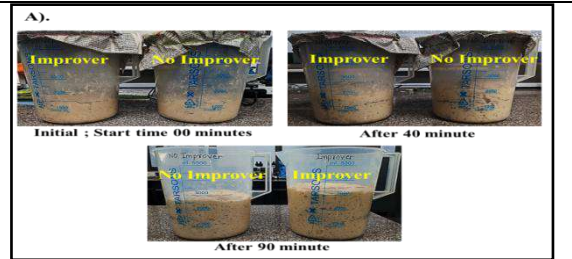
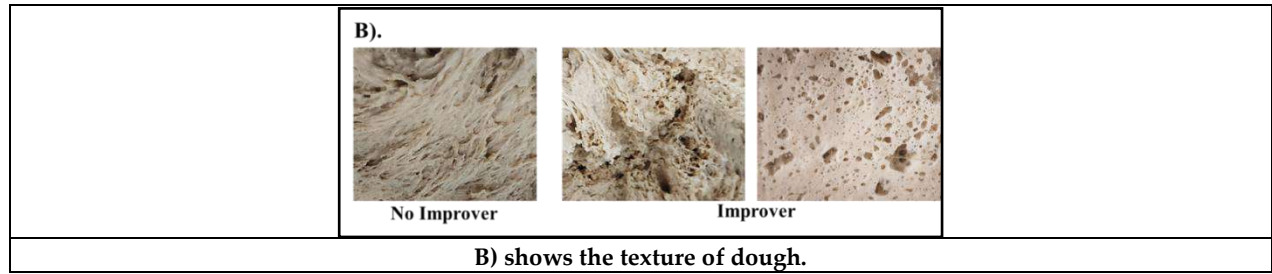


Fig.8: A) Dough test using strain A with optimum growth, with and without improver





Pragna S. Ukani et al.,





Identification and Characterization of Antimycobacterial Compound from *Piper nigrum*

Kamal Kishor Rajak¹, Odedara Mitalben Bhikhabhai¹, Sanheeta Chakrabarty², Shreyans K. Jain² and Hemant Kumar^{1*}

¹Department of Medical Laboratory Technology, Bapubhai Desaihbhai Patel Institute of Paramedical Science (BDIPS), Charotar University of Science and Technology, CHARUSAT Campus, Changa-388421, Gujarat, India.

²Department of Pharmaceutical Engineering and Technology, Indian Institute of Technology, Banaras Hindu University, Varanasi-221005, Uttar Pradesh, India.

Received: 30 Dec 2023

Revised: 09 Jan 2024

Accepted: 12 Jan 2024

*Address for Correspondence

Hemant Kumar

Department of Medical Laboratory Technology,
Bapubhai Desaihbhai Patel Institute of Paramedical Science (BDIPS),
Charotar University of Science and Technology,
CHARUSAT Campus, Changa-388421, Gujarat, India.

Email: hemantkumar.cips@charusat.ac.in



This is an Open Access Journal / article distributed under the terms of the **Creative Commons Attribution License** (CC BY-NC-ND 3.0) which permits unrestricted use, distribution, and reproduction in any medium, provided the original work is properly cited. All rights reserved.

ABSTRACT

Piper nigrum, also known as black pepper, is being used for both culinary and medicinal purposes for centuries. Plethora of studies have focused on the major alkaloid piperine and few other compounds but the potential medicinal properties of many other bioactive compounds in the plant have yet to be fully understood. In this study, non-piperine compounds were isolated through Silica (silica gel G 100-200 mesh size) column fractionation and subjected to antimicrobial screening against various bacteria, including acid-fast myco bacteria. The fractions showed significant activity against mycobacterial species but not against gram-positive and gram-negative bacteria. The minimum inhibitory concentration (MIC) of active fractions and crude extract were determined using micro-broth dilution assay and compared with that of the control drug isoniazid (INH). The MIC values of the most active fraction (fraction 7) was found to be 125 µg/ml for *Mycobacterium fortuitum* (*M. fortuitum*) and 62.5 µg/ml for both *Mycobacterium phlei* (*M. phlei*) and *Mycobacterium smegmatis* (*M. smegmatis*) which were significantly lower in comparison to that of crude extract. The active fraction was analysed through Gas chromatography-mass spectrometry (GC-MS) to identify the potential compound/s. Three compounds were detected through GCMS 1. DMSO (RT: 3.66), 2. τ -muurolool (RT: 9.81), and 3. Piperine (RT 25.70 and 25.82). Thus, the current study draws a conclusion about the potential medicinal use of non-piperine compounds having anti-mycobacterial activity and supports target validation experiments further to ease drug optimization.





Kamal Kishor Rajak et al.,

Keywords: Antibacterial activity, Column Chromatography, GC-MS analysis, *P. nigrum*.

INTRODUCTION

Human infections, particularly those involving microorganisms (i.e., bacteria, fungi and viruses), cause serious infections in tropical and subtropical countries worldwide [1]. The Numerous factors contribute to the development of antimicrobial resistance i.e. frequent and inappropriate use of antibiotics, their use as growth promoters in animal feed and increased trans boundary movement [2]. Animals and humans have struggled with antibiotic resistance for a very long time [3]. The emergence of antibiotic-resistant bacteria, as a result of the antibiotic's demise as a potent medical tool, is worsening with time [4]. As antibiotics lose effectiveness, more number of infections caused by microorganisms, such as pneumonia, tuberculosis, blood poisoning, gonorrhoea and food borne diseases are becoming more difficult and occasionally impossible to treat [5]. Therefore, it is critical to invent new medication/s to treat such infectious diseases [6]. The antimicrobial properties of natural products have become an interest among researchers to search for alternatives to combat the rising global antimicrobial resistance problems [7]. Traditionally, crude extracts of different parts of medicinal plants, including roots, stems, flowers, fruits and twigs have been widely used for the treatment of various human diseases [8]. According to the World Health Organization, 75% of the world's population still relies on plant-based medicines [9]. Medicinal plants contain several phytochemicals such as flavonoids, alkaloids, tannins and terpenoids, which possess antimicrobial and antioxidant properties [10].

India is habitat of 45000 different plant species, of which 3000 plants are officially documented with medicinal properties in various literature. More than 6000 plants are used by traditional practitioners from ethnographical knowledge for various disease in India [11], [12]. *Piper nigrum* (*P. nigrum*) since ages considered the "king of spices" because of its massive trade share in the global market [13]. *P. nigrum* is commonly known as Kali Mirch in Urdu and Hindi, Pippali in Sanskrit, Milagu in Tamil and Peppercorn, White pepper, Green pepper, Black pepper and Madagascar pepper in English [14]. *P. nigrum* belongs to Piperaceae family and known for its characteristic pungent smell due to the presence of a major alkaloid compound piperine (1-peperoyl piperidine). The plant is cultivated in many tropical countries like Brazil, India and Indonesia. The plant of Black Pepper is a perennial, woody, aromatic and climber that grows up to an average height of 50-60 cm [15]. Leaves are simple and alternate with variable leaf length, breadth and petiole properties [14]. In the Indian subcontinent flowering in black pepper Human infections, particularly those involving microorganisms (i.e., bacteria, fungi and viruses), cause serious infections in tropical and subtropical countries worldwide [1]. The Numerous factors contribute to the development of antimicrobial resistance i.e. frequent and inappropriate use of antibiotics, their use as growth promoters in animal feed and increased trans boundary movement [2].

Animals and humans have struggled with antibiotic resistance for a very long time [3]. The emergence of antibiotic-resistant bacteria, as a result of the antibiotic's demise as a potent medical tool, is worsening with time [4]. As antibiotics lose effectiveness, more number of infections caused by microorganisms, such as pneumonia, tuberculosis, blood poisoning, gonorrhoea and foodborne diseases are becoming more difficult and occasionally impossible to treat [5]. Therefore, it is critical to invent new medication/s to treat such infectious diseases [6]. The antimicrobial properties of natural products have become an interest among researchers to search for alternatives to combat the rising global antimicrobial resistance problems [7]. Traditionally, crude extracts of different parts of medicinal plants, including roots, stems, flowers, fruits and twigs have been widely used for the treatment of various human diseases [8]. According to the World Health Organization, 75% of the world's population still relies on plant-based medicines [9]. Medicinal plants contain several phytochemicals such as flavonoids, alkaloids, tannins and terpenoids, which possess antimicrobial and antioxidant properties [10]. India is habitat of 45000 different plant species, of which 3000 plants are officially documented with medicinal properties in various literature. More than 6000 plants are used by traditional practitioners from ethnographical knowledge for various disease in India [11], [12]. *Piper nigrum* (*P. nigrum*) since ages considered the "king of spices" because of its massive trade share in the



**Kamal Kishor Rajak et al.,**

global market [13]. *P. nigrum* is commonly known as Kali Mirch in Urdu and Hindi, Pippali in Sanskrit, Milaguin in Tamil and Peppercorn, White pepper, Green pepper, Black pepper and Madagascar pepper in English [14]. *P. nigrum* belongs to Piperaceae family and known for its characteristic pungent smell due to the presence of a major alkaloid compound piperine (1-peperoyl piperidine). The plant is cultivated in many tropical countries like Brazil, India and Indonesia. The plant of Black Pepper is a perennial, woody, aromatic and climber that grows up to an average height of 50-60 cm [15]. Leaves are simple and alternate with variable leaf length, breadth and petiole properties [14]. In the Indian subcontinent flowering in black pepper is observed once is 2–3 years during the monsoon [16]. Black pepper provides essential flavours to food and, has proven applications in traditional medicine, perfumery and food industry [17]. The various reports proved the anti-hypertensive, anti-platelet [18], antioxidant, antitumor [19], anti-asthmatics [20], anti-pyretic, analgesic, anti-inflammatory, anti-diarrheal, anti-spasmodic, anxiolytic antidepressant [21], hepato-protective [22], immuno-modulatory, anti-bacterial, anti-fungal, anti-thyroids, anti-apoptotic, anti-metastatic, anti-mutagenic, anti-spermatogenic, anti-Colon toxin, insecticidal and larvicidal activities, etc. [14] of *p. nigrum*. The chemical diversity found in natural products in the form of many secondary metabolites offers a vast potential for new drug development. With a growing demand for chemical diversity in drug screening, there is increased interest in using edible plants as sources for therapeutic drugs. Botanicals and herbal preparations used for medicinal purposes contain a variety of bioactive compounds. The present study involves the isolation of the antimicrobial non-piperine compound/s from *P. nigrum* using gravity column chromatography and testing its antibacterial activity against acid-fast bacteria (*M. phlei*, *M. fortuitum*, and *M. smegmatis*), Gram-negative bacteria (*E. coli* and *K. pneumoniae*), and Gram-positive bacteria (*M. luteus* and *S. aureus*). The active ingredients were identified using GC MS.

METHOD

Test Microorganisms

Clinically isolated pathogenic Gram-negative bacteria (*E. coli* and *K. pneumoniae*) Gram-positive bacteria (*M. luteus*, and *S. aureus*) and acid-fast bacteria (*M. phlei* -MTCC 1724, *M. fortuitum* - MTCC 1902 and *M. smegmatis* -MC² 155) are used for bioguided antimicrobial assay.

Plant materials

Mature seeds of *P. nigrum* were purchased from the local market from Anand, Gujarat, India. The purchased seeds were carefully segregated and damaged seeds were removed. Only intact seeds were washed under running tap water and dried for 2-4 days in oven.

Plant Extract preparation

Dried Seeds of *P. nigrum* were crushed to fine powder in a mixer grinder and 100 g powder was soaked in 500 ml of acetone (SRL AR grade, Cat no 15168) for 24 h at 37 °C in a shaker incubator at 150 rpm. After 24 hr the extract was filtered using Whatman filter paper (No.1), concentrated in vacuum under reduced pressure using a rotary flask evaporator and dried in a desiccator. The dried extract was stored in sterile glass bottles at -20 °C until use.

Silica Column Chromatography

Column chromatography was performed on a Glass column (2 × 40 cm) using the wet method. The column was packed with 50 g of silica gel G (100-200 mesh size) slurry prepared in 300 ml n-hexane and eluted n-hexane was flowed through the column until the silica gel in packed properly. The sample was loaded onto the column by dissolving 3 g of the dried extract in n-hexane and mixing it with 10 g of dry silica gel G until a homogenous dried mixture is formed. The compounds were eluted with step gradient of n-hexane and ethyl acetate (100:0 – 0:100, 5% polarity increment). A total of 21 fractions of 50 ml each, were collected in the cleaned glass tube and labelled from 1 to 21. The fractions were concentrated using a rotary flask evaporator and dried in a desiccator. Fractions 1, 2, 3, 4, and 5 were discarded because there was no visible dried material. Two Thin layer chromatography (TLC) was performed for silica column fractions of acetone extract of *P. nigrum* seed. First TLC was performed for fractions 6 to



Kamal Kishor Rajak *et al.*,

21 (except fraction 13) along with beta-caryophyllene oxide (sesquiterpene) standard and crude extract, using n-hexane: ethyl acetate (2:1) as mobile phase. The resulting plate was observed under UV-254 nm light and treated with vanillin-H₂SO₄ indicator reagent for visualization (Jiang et al. 2016). The second TLC was performed for fractions 6 to 21 along with piperine standard and crude extract using a mobile phase of n-hexane: ethyl acetate (2:1) and the resulting plate was viewed under UV-254 nm light.

Antimicrobial Screening

Disc diffusion assay

The disc diffusion method of Barry and Thorns berry was followed with some modifications to screen the antibacterial activity of different extracts [23]. In this experiment, Gram-positive and Gram-negative bacteria were grown on Mueller-Hilton Agar (MHA) and acid-fast bacteria were grown on Middlebrook 7H9 agar media containing 5% oleic acid, albumin, dextrose and catalase (OADC) supplements. To perform the antibacterial test, agar plates were seeded with 0.5 McFarland standards bacterial suspension. The dried crude extracts, fractions 5 to 9 and piperine were dissolved in dimethyl sulfoxide (DMSO) at 100 mg/ml and 2 mg was applied on sterile paper disks separately. Isoniazid (INH) (10 µg/disc) was used as a positive control for acid-fast bacteria and Streptomycin (STM) (10 µg/disc) for Gram-negative and Gram-positive bacteria. DMSO (SRL, Cat No 28580) (20 µl) was used as the solvent control on separate discs. The plates were incubated at 37 °C overnight for *K. pneumoniae*, *E. coli*, *M. luteus*, and *S. aureus*, two days for *M. smegmatis*, three days for *M. fortuitum* and five days for *M. phlei*. After incubation, the zone of inhibition was measured in millimeters (mm) to calculate the efficacy of different loads.

Minimum inhibitory concentrations (MIC)

Based on primary antibacterial screening, *P. nigrum* crude extract and fraction 7 were selected for MIC determination against the acid-fast bacteria *M. phlei*, *M. fortuitum*, and *M. smegmatis*. The MIC was evaluated using the micro-broth dilution method as described by Taneja et al. with some modifications [24]. Briefly, the bacterial culture was diluted in Middlebrook 7H9 broth base (containing 5% albumins, dextrose, and catalase (ADC) supplements) to approximately 1×10⁶ CFU/ml. In a sterile 96-well plate, a two-fold dilution of crude extract and fraction 7 was prepared from 2000 µg/ml to 15.6 µg/ml in Middlebrook 7H9 broth base containing 5% ADC supplements. The wells were filled with 100µl of the diluted bacterial suspension. The plates were incubated at 37 °C for two days for *M. smegmatis*, three days for *M. fortuitum*, and five days for *M. phlei*. Next, 0.02% resazurin was added to all wells after the respective incubation period and the plates were incubated for 4 h to visualize colour change (blue to pink). INH was used as positive control and DMSO was used as the solvent control. The minimum inhibitory concentration range was determined based on the colour changes observed due to differential cell viability [24].

GC-MS Analysis

GC-MS analysis of fraction 7 was performed at the Central Instrumentation Laboratory/SAIF, Panjab University, Chandigarh on Thermo Scientific TSQ 8000 Gas Chromatograph - Mass Spectrometer equipped with Flame Ionization Detector (FID) and an Electron Capture Detector (ECD). To process the sample, 100 mg/ml of extract was diluted to 1 mg/ml in methanol and filtered through a 0.2 µm syringe filter. One micro liter of the sample was injected, the injection temperature was 250 °C, helium gas was used as a mobile system, at a flow rate of 1 ml/minute, the column temperature was maintained at 400 °C, and the ion source type was an EI source programmable to 350 °C. The sample was run for 25.47 minutes and individual compounds were identified by comparing fragmentation patterns from the NIST library.

RESULTS AND DISCUSSION

Silica column fractionation

Silica column fractionation of acetone extract of *P. nigrum* seed extract was done with step gradient of n-hexane - ethyl acetate with 5% polarity increment. Two Thin layer chromatography (TLC) were run to observe the different compound/s in different fractions. One TLC plate was observed under UV to confirm the presence of UV active





Kamal Kishor Rajak et al.,

compound/s (Fig 1a) and the same plate was developed with vanillin-H₂SO₄ later (Fig 1b). TLC analysis of fractions indicates the presence of some terpenoids/lipid (non-polar) compounds in fraction number 6 - 11 when developed with vanillin-H₂SO₄ spray (Fig. 1b). By comparing the Fig 1a and 1b it is evident that certain compounds remained undetectable under 254 nm but showed up when developed with vanillin-H₂SO₄ as shown by others (Fraction 6-8, Lane 1-3 Fig 1a and 1b) [25]. Higher mobility of bands visible in vanillin-H₂SO₄ suggests low polarity of those molecules seen in fraction no 6-11 as initial solvent used for fractionation as well as the mobile phase used in TLC had low polarity [25]. Presence of piperine in later fractions (fraction 12-18 in Fig 1a and Fig 1b, fraction in 12-18 Fig. S1) is seen and can be confirmed with crude extract major band (Fig 1a, 1b, Fig S1) as indicated in figures. Based on TLC analysis of fractions to minimize the likelihood of selecting a fraction containing piperine, fractions 6 through 10, were chosen for subsequent analysis. It has been suggested that piperine enhances the effect of many antibiotics and in combination of other molecules also it may show the antimyco bacterial activity [26]–[29]. As we were convinced that the activity is not due to piperine or combination we chose the sample based on TLC profile which does not show the presence of it. Still there are confusion about activity of piperine against mycobacterium and later we have dwelled in to it in detail in this paper. The Sequiterpenes and terpenes are not visible in UV but suggested to be visible with vanillin and appear as violet band the same is seen in fig 1b fig S1 [25].

Antimicrobial screening

Piperine is a principal constituent of piperaceae family members and has many biological applications even in modern medicine [26]–[29]. In addition to piperine, *P. nigrum* seeds are a significant source of many other secondary metabolites with therapeutic values, including Germacrene D, α -Humulene, Caryophyllene, Eugenol, Linalool, caryophyllene oxide, β -Selinene, α -Pinene, α -Thujene, Camphene, β -Pinene, β -Myrcene, 3-Carene and many others [30]. In the current study fractionation of acetone extract of *P. nigrum* seeds was done with silica gravity column chromatography and fraction 6 to 9 (100% hexane : 0% ethyl acetate to 70% hexane: 30% ethyl acetate with 5% polarity increment) were screened for antibacterial potency against *M. phlei*, *M. fortuitum*, and *M. smegmatis*, clinically isolated Gram- positive *M. luteus* and *S. aureus*, clinically isolated Gram-negative bacteria *K. pneumoniae* and *E. coli*, using disc diffusion assay and resazurine based cell viability assay. The crude extract of *P. nigrum* seeds and piperine were also used for antibacterial screening. The results of disc diffusion are shown in Fig. 2 and Table 1. According to the antibacterial activity results, all fractions and crude extracts were capable of suppressing microbial growth with varying potency against acid fast bacteria tested. All selected fractions were active against acid-fast bacteria and the inhibitory zone was found to be maximum in fraction number 7 (70% Hexane: 30% ethyl acetate).

In contrast to the other fractions, fraction 7 had significant antibacterial activity against the selected bacteria and formed a zone of inhibition ranging from 24 mm to 8 mm (Fig 2, Disc F). The above observation suggests Fraction 7 had a higher concentration of antibacterial compounds than the other fractions. Similarly, crude extract of *P. nigrum* inhibited selected Gram-positive, Gram-negative, and acid- fast bacteria, forming a 17 mm to 8 mm zone of inhibition (Fig 2, Disc B). In terms of antimicrobial activity, these results are consistent with previous antimicrobial screening of *P. nigrum* extracts against pathogenic bacteria [31]. Standard Piperine was unable to inhibit the growth of all selected bacteria except *M. fortuitum* (acid-fast bacteria) that form 8 mm inhibition zone (Fig 2, Disc C) and we did not find the relevant report anywhere else reporting the effect of piperine on *M. fortuitum* in comparison to other mycobacterium we are first one to report it. The positive control INH formed a 30 mm to 16 mm inhibition zone against acid-fast bacteria (Fig 2, Disc a) and STM formed a 32 mm-16 mm inhibition zone against Gram-positive (Fig 2, Disc A) and Gram-negative bacteria (Fig 2, Disc A). The solvent control (DMSO) did not exhibit any visible growth inhibition zones (Fig 2, Disc D). The possible reason for differential sensitivity of selected bacterial groups to fractions and crude extracts could be due to differences in membrane thickness and molecular composition of the cellular target [32]. The zone of inhibition was larger in all *mycobacterium* compared to other gram negative and gram-positive bacteria suggesting the specific action of the isolated compound on *mycobacterium*.

This also suggests the specificity of cellular target in *mycobacteria* having different and unique composition compared to other microbes. Based on the results of the primary antimicrobial analysis, the minimum inhibitory concentration of fraction 7 and the crude extract was determined against acid-fast bacteria using micro-broth dilution assay (Fig. 3).





Kamal Kishor Rajak et al.,

Fraction 7 inhibited the growth of selected *Mycobacterium sp.* with an MIC value of 125 µg/ml for *M. fortuitum*, and 62.5 µg/ml for *M. smegmatis* and *M. phlei*. However, the crude extract required a higher concentration than Fraction 7 to inhibit the growth of *Mycobacterium sp.* i.e.1000 µg/ml for *M. Phlei*, 250 µg/ml for *M. smegmatis*, and *M. fortuitum*. This represents the purification of the active compound in isolated fraction if it is the lone component responsible for the activity. The MIC value of INH for selected bacteria obtained in the previously defined range: 1 µg/ml for *M. fortuitum* and 0.5 µg/ml for *M. smegmatis* and *M. Phlei* [33]. The MIC results correlated with the broader zone of inhibition, which directly corresponded to a smaller MIC [34]. In other words, a large diameter of the zone of inhibition in the disc diffusion assay would exhibit a lower MIC. Because fraction 7 and piperine displayed distinct antibacterial activity and Many have reported the antimycobacterial activity of piper nigrum crude extract but without any solid proof of single compound that motivated us to identify the active compound/s using mass spectrometry.

GC-MS analysis

The GC-MS analysis of fraction 7 of the acetone extract of *P. nigrum* seeds identified compounds based on their GC retention times relative to known compounds and their mass spectra against those in the NIST library. The chromatogram (Fig. 4) and mass spectra (Fig. 5) of the GC-MS analysis are shown in the figure. The retention times, area percentages, and peak heights are depicted in Table 2. GC-MS analysis confirmed the presence of two major compounds, τ -muurolol and piperine in fraction 7. There was a very strong DMSO peak in the GC-MS chromatogram, possibly due to sample processing during GC-MS analysis. τ -muurolol is a sesquiterpenoids compounds, and previous studies have confirmed its presence in *P. nigrum* seed extracts and many other plants [35]–[38]. Terpenoids are naturally lipophilic, making them potential antibacterial agents, therefore, τ -muurolol may be responsible for the antibacterial activity of fraction 7[39]. This statement was supported by a previous study that reported the antifungal activity of the essential oil of *Calocedrus macrolepis* var. *formosana* florin leaf, which showed the presence of τ -muurolol using GC-MS analysis [40]. De Souza, et al., reported the trypanocidal activity of Brazilian Caatinga plants and demonstrated the presence of α -muurolol [41]. The antimicrobial potency of various terpenoid compounds has also been observed in different studies on different bacterial species [42]. However, piperine is the principal component of *Piper* species, and its content varies from plant to plant such as 1.7-7.4% *P. nigrum*, 0.95-1.32% *Piper cubeba*, 0.23-1.1% *Piper guineense*, 0.03% *Piper longum*, and 2.75% in *Piper sarmentosum* [28]. *P. nigrum* contains a high concentration of piperine. Therefore, the eluent can be contaminated with piperine during column chromatography, and GC-MS is a highly sensitive technique for detecting small quantities of natural compounds [43].

CONCLUSION

Based on the current study, fraction 7 and the crude extract of *P. nigrum* seeds have significant antibacterial activity against acid-fast, Gram-positive, and Gram-negative bacteria. The test bacterial groups showed the following order of susceptibility to fraction 7 and the crude extract: acid-fast >Gram-negative>Gram-positive. However, the standard piperine did not show antibacterial activity against most of the selected bacteria. The GC-MS analysis of fraction 7 confirmed the presence of τ -muurolol, a sesquiterpenoid. Possibly identified compounds made fraction 7 antibacterial; however, they were contaminated with piperine in this fraction. To remove piperine from the active fraction, further purification is required to identify a potential therapeutic agent against bacterial infection. According to the above study, this compound could be a potential antibacterial (antitubercular) drug lead against *Mycobacterium species*.

Conflicts of Interest

The authors hold no conflict of interest.





Kamal Kishor Rajak et al.,

Authors' Contributions

Hemant Kumar developed the study design. Shreyans K. Jain helped in fractionation of crude extract. Kamal Kishor Rajak and Odedara Mitalben Bhikhabhai, Sanheeta Chakrabarty performed all the experiments. Hemant Kumar, Kamal Kishor Rajak, Odedara Mitalben Bhikhabhai and Shreyans K. Jain interpreted the data. Kamal Kishor Rajak and Odedara Mitalben Bhikhabhai drafted the manuscript and all the authors revised the manuscript.

REFERENCES

1. S. Satish and H. V Girish, "Antibacterial Activity of Important Medicinal Plants on Human Pathogenic Bacteria-a Comparative Analysis," *World Appl. Sci. J.*, vol. 5, no. 3, pp. 267–271, 2008.
2. F. D. Lowy, "Antimicrobial resistance: The example of *Staphylococcus aureus*," *J. Clin. Invest.*, vol. 111, no. 9, pp. 1265–1273, 2003, doi: 10.1172/JCI18535.
3. D. I. Andersson and D. Hughes, "Persistence of antibiotic resistance in bacterial populations," *FEMS Microbiol. Rev.*, vol. 35, no. 5, pp. 901–911, 2011, doi: 10.1111/j.1574-6976.2011.00289.x.
4. M. Algabr, N. Al-Hajj, and F. Almammari, "Evaluation of antibacterial activity of some traditionally used medicinal plants against human pathogenic bacteria," *World J. Pharm. Res.*, 2022, doi: 10.20959/wjpr20226-23607.
5. C. L. Ventola, "The antibiotic resistance crisis: part 1: causes and threats," *Pharm. Ther.*, vol. 40, no. 4, p. 277, 2015.
6. J. Srivastava, H. Chandra, A. R. Nautiyal, and S. J. S. Kalra, "Antimicrobial resistance (AMR) and plant-derived antimicrobials (PDAMs) as an alternative drug line to control infections," *3 Biotech*, vol. 4, no. 5, pp. 451–460, 2014, doi: 10.1007/s13205-013-0180-y.
7. K. H. Lai, I. Darah, C. T. Wong, S. Afifah, and S. H. Lim, "In vitro antibacterial activity and cytotoxicity of *lagerstroemia speciosa* bark extract," *Indian J. Pharm. Sci.*, vol. 78, no. 2, pp. 273–277, 2016, doi: 10.4172/pharmaceutical-sciences.1000113.
8. U. A. Khan et al., "Antibacterial activity of some medicinal plants against selected human pathogenic bacteria," *Eur. J. Microbiol. Immunol.*, vol. 3, no. 4, pp. 272–274, 2013, doi: 10.1556/eujmi.3.2013.4.6.
9. R. A. Anand, V. O. Kishor, R. V. Shete, C. D. Upasani, and T. D. Nandgude, "Abrus precatorius Linnaeus : A Phytopharmacological Review," vol. 3, no. 11, pp. 2585–2587, 2010.
10. W. H. Talib and A. M. Mahasneh, "Antimicrobial, cytotoxicity and phytochemical screening of Jordanian plants used in traditional medicine," *Molecules*, vol. 15, no. 3, pp. 1811–1824, 2010, doi: 10.3390/molecules15031811.
11. Y. Mahida and J. S. S. Mohan, "Screening of Indian plant extracts for antibacterial activity," *Pharm. Biol.*, vol. 44, no. 8, pp. 627–631, 2006, doi: 10.1080/13880200600897551.
12. H. Yuan, Q. Ma, L. Ye, and G. Piao, "The traditional medicine and modern medicine from natural products," *Molecules*, vol. 21, no. 5, 2016, doi: 10.3390/molecules21050559.
13. K. Srinivasan, "Black pepper and its pungent principle-piperine: A review of diverse physiological effects," *Crit. Rev. Food Sci. Nutr.*, vol. 47, no. 8, pp. 735–748, 2007, doi: 10.1080/10408390601062054.
14. Z. A. Damanhour and A. Ahmad, "A review on therapeutic potential of *Piper nigrum* L.," *Black Pepper) King Spices. Med. Aromat. Plants*, vol. 3, no. 3, p. 161, 2014, doi: DOI: 10.4172/2167-0412.1000161.
15. T. T. Bui, C. H. Piao, C. H. Song, H. S. Shin, D. H. Shon, and O. H. Chai, "Piper nigrum extract ameliorated allergic inflammation through inhibiting Th2/Th17 responses and mast cells activation," *Cell. Immunol.*, vol. 322, pp. 64–73, 2017, doi: 10.1016/j.cellimm.2017.10.005.
16. K. Ashokkumar, M. Murugan, M. K. Dhanya, A. Pandian, and T. D. Warkentin, "Phytochemistry and therapeutic potential of black pepper [*Piper nigrum* (L.)] essential oil and piperine: a review," *Clin. Phytoscience*, vol. 7, no. 1, 2021, doi: 10.1186/s40816-021-00292-2.
17. P. Bothi Raja and M. G. Sethuraman, "Inhibitive effect of black pepper extract on the sulphuric acid corrosion of mild steel," *Mater. Lett.*, vol. 62, no. 17–18, pp. 2977–2979, 2008, doi: 10.1016/j.matlet.2008.01.087.
18. S. I. H. Taqvi, A. J. Shah, and A. H. Gilani, "Blood pressure lowering and vasomodulator effects of piperine," *J. Cardiovasc. Pharmacol.*, vol. 52, no. 5, pp. 452–458, 2008, doi: 10.1097/FJC.0b013e31818d07c0.
19. S. Manoharan, S. Balakrishnan, V. P. Menon, L. M. Alias, and A. R. Reena, "Chemopreventive & efficacy of



Kamal Kishor Rajak *et al.*,

- curcumin and piperine during 7,12-dimethylbenz [a]anthracene-induced hamster buccal pouch carcinogenesis," *Singapore Med. J.*, vol. 50, no. 2, pp. 139–146, 2009.
20. R. Parganiha, S. Verma, S. Chandrakar, S. Pal, H. A. Sawarkar, and P. Kashyap, "In vitro anti-asthmatic activity of fruit extract of *Piper nigrum* (Piperaceae)," *Inter J Herb. Drug Res*, vol. 1, pp. 15–18, 2011.
 21. S. Li, C. Wang, M. Wang, W. Li, K. Matsumoto, and Y. Tang, "Antidepressant like effects of piperine in chronic mild stress treated mice and its possible mechanisms," *Life Sci.*, vol. 80, no. 15, pp. 1373–1381, 2007, doi: 10.1016/j.lfs.2006.12.027.
 22. H. Matsuda, K. Ninomiya, T. Morikawa, D. Yasuda, I. Yamaguchi, and M. Yoshikawa, "Protective effects of amide constituents from the fruit of *Piper chaba* on d-galactosamine/TNF- α -induced cell death in mouse hepatocytes," *Bioorganic Med. Chem. Lett.*, vol. 18, no. 6, pp. 2038–2042, 2008, doi: 10.1016/j.bmcl.2008.01.101.
 23. J. Hudzicki, "Kirby-Bauer Disk Diffusion Susceptibility Test Protocol," no. December 2009, pp. 1–23, 2016.
 24. N. K. Taneja and J. S. Tyagi, "Resazurin reduction assays for screening of anti-tubercular compounds against dormant and actively growing *Mycobacterium tuberculosis*, *Mycobacterium bovis* BCG and *Mycobacterium smegmatis*," *J. Antimicrob. Chemother.*, vol. 60, no. 2, pp. 288–293, 2007, doi: 10.1093/jac/dkm207.
 25. Z. Jiang, C. Kempinski, and J. Chappell, "Extraction and Analysis of Terpenes/ Terpenoids Public Access," *Curr. Protoc. Plant Biol.*, vol. 25, no. 3, pp. 289–313, 2016, doi: 10.1002/cppb.20024.Extraction.
 26. Z. T. K. Aldaly, "Antimicrobial activity of piperine purified from *Piper nigrum*," *J. Basrah Res*, vol. 36, pp. 54–61, 2010.
 27. S. K. Reshmi, E. Sathya, and P. S. Devi, "Isolation of piperidine from *Piper nigrum* and its antiproliferative activity," *J. Med. Plants Res.*, vol. 4, no. 15, pp. 1535–1546, 2010, doi: DOI: 10.5897/JMPR10.033.
 28. I. U. Haq, M. Imran, M. Nadeem, T. Tufail, T. A. Gondal, and M. S. Mubarak, "Piperine: A review of its biological effects," *Phyther. Res.*, vol. 35, no. 2, pp. 680–700, 2021, doi: 10.1002/ptr.6855.
 29. B. G. Ongarora, H. G. Matena, and Z. N. Kariuki, "Optimization of piperine extraction from black pepper (*piper nigrum*) using different solvents for control of bedbugs," 2021.
 30. L. Liu, G. Song, and Y. Hu, "GC-MS analysis of the essential oils of *Piper nigrum* L. and *Piper longum* L.," *Chromatographia*, vol. 66, no. 9–10, pp. 785–790, 2007, doi: 10.1365/s10337-007-0408-2.
 31. P. Saranraj, P. Ganesh, and R. Suresh Kumar, "Phytochemical analysis and antibacterial activity of Pepper (*Piper nigrum* L.) against some human pathogens," *Sch. Res. Libr. Cent. Eur. J. Exp. Biol.*, vol. 3, no. 2, pp. 36–41, 2014.
 32. T. C. Dakal, A. Kumar, R. S. Majumdar, and V. Yadav, "Mechanistic basis of antimicrobial actions of silver nanoparticles," *Front. Microbiol.*, vol. 7, no. NOV, pp. 1–17, 2016, doi: 10.3389/fmicb.2016.01831.
 33. G. Li *et al.*, "Antimicrobial susceptibility of standard strains of nontuberculous mycobacteria by microplate Alamar Blue assay," *PLoS One*, vol. 8, no. 12, pp. 4–9, 2013, doi: 10.1371/journal.pone.0084065.
 34. M. Benkova, O. Soukup, and J. Marek, *Antimicrobial susceptibility testing: currently used methods and devices and the near future in clinical practice*, vol. 129, no. 4. 2020. doi: 10.1111/jam.14704.
 35. A. Orav, I. Stulova, T. Kailas, and M. Müürisepp, "Effect of Storage on the Essential Oil Composition of *Piper nigrum* L. Fruits of Different Ripening States," *J. Agric. Food Chem.*, vol. 52, no. 9, pp. 2582–2586, 2004, doi: 10.1021/jf030635s.
 36. S. Masoudi, "Volatile constituents from different parts of three lamiacea herbs from Iran," *Iran. J. Pharm. Res.*, vol. 17, no. 1, pp. 365–376, 2018.
 37. N. S. Dosoky, P. Satyal, L. M. Barata, J. K. R. Da Silva, and W. N. Setzer, "Volatiles of black pepper fruits (*Piper nigrum* L.)," *Molecules*, vol. 24, no. 23, pp. 1–13, 2019, doi: 10.3390/molecules24234244.
 38. E. Vuko *et al.*, "Not only a weed plant – biological activities of essential oil and hydrosol of *Dittrichia viscosa* (L.) Greuter," *Plants*, vol. 10, no. 9, p. 1837, 2021, doi: https://doi.org/10.3390/plants10091837.
 39. C. L. Cantrell, S. G. Franzblau, and N. H. Fischer, "Antimycobacterial plant terpenoids," *Planta Med.*, vol. 67, no. 08, pp. 685–694, 2001, doi: DOI: 10.1055/s-2001-18365.
 40. H.-T. Chang, Y.-H. Cheng, C.-L. Wu, S.-T. Chang, T.-T. Chang, and Y.-C. Su, "Antifungal activity of essential oil and its constituents from *Calocedrus macrolepis* var. *formosana* Florin leaf against plant pathogenic fungi," *Bioresour. Technol.*, vol. 99, no. 14, pp. 6266–6270, 2008, doi: doi: 10.1016/j.biortech.2007.
 41. L. I. Oliveira de Souza *et al.*, "The chemical composition and trypanocidal activity of volatile oils from Brazilian Caatinga plants," *Biomed. Pharmacother.*, vol. 96, no. August, pp. 1055–1064, 2017, doi: 69256





Kamal Kishor Rajak et al.,

10.1016/j.biopha.2017.11.121.

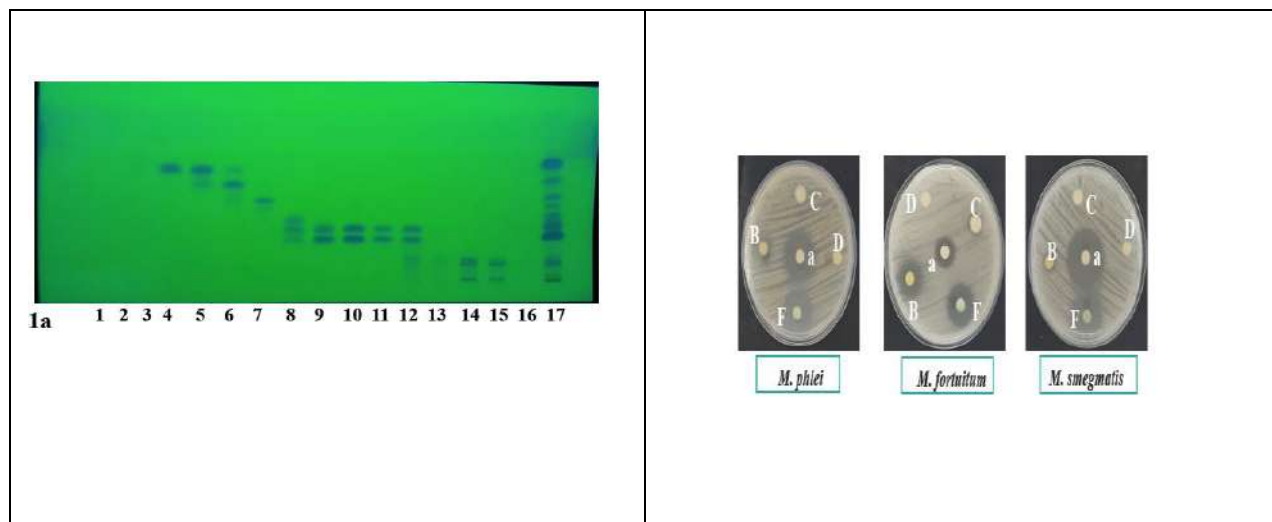
42. F. Fotsing Yannick Stephane and B. Kezetas Jean Jules, "Terpenoids as Important Bioactive Constituents of Essential Oils," *Essent. Oils - Bioact. Compd. New Perspect. Appl.*, 2020, doi: 10.5772/intechopen.91426.
43. A. F. Al-Rubaye, I. H. Hameed, and M. J. Kadhim, "A Review: Uses of Gas Chromatography-Mass Spectrometry (GC-MS) Technique for Analysis of Bioactive Natural Compounds of Some Plants," *Int. J. Toxicol. Pharmacol. Res.*, vol. 9, no. 01, 2017, doi: 10.25258/ijtpr.v9i01.9042.

Table 1 Primary antibacterial screening of plant extract and fractions with disc diffusion assay *NS:Not screened, *NZI: No Zone of Inhibition

Test	Bacteria						
	<i>M. smegmatis</i>	<i>M. phlei</i>	<i>M. fortuitum</i>	<i>S. aureus</i>	<i>M. luteus</i>	<i>K. pneumoniae</i>	<i>E. coli</i>
Frac6	14	8	10	NS	NS	NS	NS
Frac7	23	24	20	NZI	8	10	NZI
Frac8	16	16	12	NS	NS	NS	NS
Frac9	16	8	8	NS	NS	NS	NS
Frac10	16	12	NZI	NS	NS	NS	NS
Crude Extract	8	8	17	NZI	8	10	NZI
Piperine	NZI	NZI	8	NZI	NZI	NZI	NZI
Antibiotic control	30	24	16	21	32	24	16
DMSO	NZI						

Table 2 GC-MS profile of anti-microbial active fraction (fraction 7) of acetone extract of *P. nigrum* seed

Retention time	Area (%)	Compounds	Molecular Formula	Cas No.
3.66	88.23	DMSO	C ₂ H ₆ OS	67-68-5
9.81	1.27	τ-Muurolol	C ₁₅ H ₂₆ O	19912-62-0
25.70	5.01	Piperine	C ₁₇ H ₁₉ NO ₃	94-62-2
25.82	5.49	Piperine	C ₁₇ H ₁₉ NO ₃	94-62-2





Kamal Kishor Rajak et al.,

<p>1b</p>													
<p>Fig 1: TLC analysis of lane 1 to 15 is fractions 6 to 21 (except fraction 13) of the acetone extract of <i>P. nigrum</i> seed along with lane 16 is beta-caryophyllene oxide (sesquiterpenoid) standard and lane 17 is crude extract. The plate was developed using a mobile phase of n-hexane: ethyl acetate (2:1), and then observed under UV-254 nm light (A) and treated with the vanillin-H₂SO₄ solution (B) for visualization.</p>	<p>Fig 2: Antimicrobial activity of acetone extract of <i>P. nigrum</i> seeds, crude (B), piperine standard (C), and fraction 7 (F7) of <i>P. nigrum</i> seeds, performed with disc diffusion assay against acid-fast bacteria, <i>M. phlei</i>, <i>M. fortuitum</i>, and <i>M. smegmatis</i>, Gram-positive bacteria <i>S. aureus</i>, and <i>M. luteus</i> and Gram-negative bacteria <i>K. pneumoniae</i> and <i>E. coli</i>. Streptomycin disc (10 µg/disc) (A) was used as a positive control for Gram-positive and Gram-negative bacteria and isoniazid disc (10 µg/disc) (a) for acid-fast bacteria. DMSO (D) was used as solvent control.</p>												
<table border="1"> <caption>Table 1: MIC values (µg/ml)</caption> <thead> <tr> <th>Bacterium</th> <th>Fraction 7</th> <th>Crude Extract</th> </tr> </thead> <tbody> <tr> <td><i>M. smegmatis</i></td> <td>62.5</td> <td>250</td> </tr> <tr> <td><i>M. Phlei</i></td> <td>62.5</td> <td>1000</td> </tr> <tr> <td><i>M. Fortuitum</i></td> <td>125</td> <td>250</td> </tr> </tbody> </table>	Bacterium	Fraction 7	Crude Extract	<i>M. smegmatis</i>	62.5	250	<i>M. Phlei</i>	62.5	1000	<i>M. Fortuitum</i>	125	250	
Bacterium	Fraction 7	Crude Extract											
<i>M. smegmatis</i>	62.5	250											
<i>M. Phlei</i>	62.5	1000											
<i>M. Fortuitum</i>	125	250											
<p>Fig 3: Determination of minimum inhibitory concentrations (MIC) (in µg/ml) of acetone extract of <i>P. nigrum</i> seed and fraction 7 of acetone extract of <i>P. nigrum</i> seed, against three acid-fast bacteria namely <i>M. smegmatis</i>, <i>M. phlei</i>, and <i>M. fortuitum</i>, determined with micro- broth dilution assay. Fraction 7 shows the potential anti-<i>Mycobacterium</i> activity as compared to the crude extract of <i>P. nigrum</i> seed. Isoniazid was used as a positive control, which has a MIC value of 1 µg/ml for <i>M. fortuitum</i> and 0.5 µg/ml for <i>M. smegmatis</i> and <i>M. Phlei</i>.</p>	<p>Fig 4: GC-MS Chromatogram of the antimicrobial active fraction (fraction 7) of acetone extract of <i>P. nigrum</i> seed. The chromatogram shows four major peaks at different retention times, which are responsible for DMSO (RT: 3.66), τ -muurolol (RT: 9.81), and piperine (RT 25.70 and 25.82).</p>												
<p>Fig 5: GC-MS spectrum of different identified compounds of the antimicrobial active fraction (fraction 7) of acetone extract of <i>P. nigrum</i> seed.</p>													





Planning Proposal of Road Infrastructure Development for Vapi – Silvassa Corridor

Bhargav Patel^{1*}, Jagruti Shah² and Indrajit Patel³

¹Engineer, Geo Designs and Research Pvt. Ltd, Vadodara, Gujarat, India.

²Assistant Professor, Department of Structural Engineering, B.V.M Engineering College, Vallabh Vidyanagar, Gujarat, India.

³Professor, Department of Structural Engineering, B.V.M Engineering College, Vallabh Vidyanagar, Gujarat, India.

Received: 30 Dec 2023

Revised: 09 Jan 2024

Accepted: 12 Jan 2024

*Address for Correspondence

Bhargav Patel

Engineer,

Geo Designs and Research Pvt. Ltd,

Vadodara, Gujarat, India

Email: bhargav7100@gmail.com



This is an Open Access Journal / article distributed under the terms of the **Creative Commons Attribution License** (CC BY-NC-ND 3.0) which permits unrestricted use, distribution, and reproduction in any medium, provided the original work is properly cited. All rights reserved.

ABSTRACT

India is quickly becoming a powerful economic force in the world, supporting urban growth by attracting investment and development from other nations. Thus, while the economy may have grown as a result of urbanization, its effects are now being felt in many of the main cities, which are dealing with problems with air quality, traffic congestion, increased accident rates, the growth of slums, etc. Sustainable techniques are essential to addressing these issues while preserving the economy. India's urban population increased at a rate of around 32% over the previous ten years. The industrial city of Vapi & Silvassa is expanding quickly. 7.37 lakh people, including those who are floaters, make up the current population. Since the earliest major human settlements, traffic and urban communities have coexisted, compelling people to assemble in huge urban areas and resulting in the requirement for urban mobility. This report discusses Vapi & Silvassa's traffic characteristics, road network, and various vehicle growth and composition while keeping in mind the current situation. Additionally, give the roads amenities like marking, roadside vegetation, signboards, etc. This research focuses on public transport planning for Silvassa City and Vapi GIDC's holistic strategy to ensuring higher levels of civic service. This study sheds some light on the public transportation design factors that public transit chose, such as road length, traffic composition, and trip purpose trip length. This thesis examines a planning proposal for the construction of road infrastructure along the Vapi-Silvassa Corridor.

Keywords: Easy Mobility, Sustainable Road Infrastructure, Corridor, Urbanization, Economic



**Bhargav Patel et al.,**

INTRODUCTION

Urban design is a combination of science and art. It spans a wide range of subjects and brings them all under one roof. The organization of all aspects of a town or other urban environment is the most basic definition of urban planning. In short, in Urban Planning, thinks about all the elements that make up a town. Urban planning is a new concept for development. Before urban planning concept, the cities were developed around the major resource available. After that the concept of urban planning came into existence which help to grow a city in systematic, convenient manner. The goal is to give individuals with a healthier, more sustainable way of living. The road network plays an important role in the growth of a city. The ease of mobilization will contribute to cost savings, time savings, and a better way of life. In the relentless pursuit of economic growth and societal progress, the development of a robust and efficient transportation infrastructure stands as a cornerstone. Amongst the various modes of transportation, roads emerge as vital arteries, connecting communities, fostering trade, and catalyzing regional development. The evolution of road networks is a dynamic process that mirrors the aspirations of a society keen on enhancing connectivity, accessibility, and overall quality of life. It becomes evident that road development is not merely about laying asphalt and concrete; rather, it encompasses a multidimensional approach involving meticulous planning, engineering precision, environmental considerations, and socioeconomic impact assessments. A well-designed and maintained road network not only facilitates smooth vehicular movement but also serves as a catalyst for economic development by reducing transportation costs, enhancing market accessibility, and promoting tourism. Public transport is inherently more environmentally friendly than individual car travel. Mass transit options typically have lower carbon footprints per passenger, contributing to reduced air pollution, lower greenhouse gas emissions, and a more sustainable approach to urban mobility. Figure 1 shows, road infrastructure facilities. When planning a road improvement project, creative thinking should be used to take the environment, socioeconomic development, and technical requirements into account. In many big towns, unplanned developments and insufficient mitigation measures are the main sources of traffic congestion.

Indian roads,

1. Contributes about 5 % to the GDP.
2. India has the second largest road network in the world.
3. Road density in terms of population – only 2.75 km per 1,000 people compared to the world average of 6.7
4. 15 % road network carries 80 % traffic –
5. National highways, comprising about only 2 % of length, carries 40 % of the total traffic
6. State roads, comprising 18 % of length, carries 40 % of the traffic

OBJECTIVE

The objectives are to study existing road infrastructure for Vapi – Silvassa Corridor, and to identify & analysis the condition of road infrastructure facilities for Vapi – Silvassa Corridor and to recommend road infrastructure facilities for Vapi – Silvassa Corridor. Scope of the study is limited to the roadside development of Vapi – Silvassa Corridor for 34.2 Km length.

STUDY AREA PROFILE

Vapi

Vapi is a city and municipality in Valsad district in the state of Gujarat, India. Located in close proximity to the banks of the Daman Ganga River, approximately 28 km to the south of the district headquarters in Valsad city, it is bordered by the Union Territory of Dadra and Nagar Haveli and Daman and Diu. Vapi is about **22.44 km²**. The NH 48 bisects the Vapi city seen in Figure 14. The town's original location is situated in the western part, while the eastern section primarily comprises industrial zones and newer residential areas. Mumbai lies approximately 180 km to the south, and Surat is positioned around 120 km to the north. To the west, at a distance of about 7 km, is the Arabian Sea, marking the delta of the Daman ganga River. Vapi experiences a tropical climate with three distinct seasons: winter, summer, and monsoon. Annual rainfall ranges from 100 to 120 inches. The town is traversed by



**Bhargav Patel et al.,**

several rivers, including Dhobikhadi, Bhilkhadi, Kolak, and Damanganga, contributing to its geographical richness and water resources. Figure 3 shows the demographic growth of Vapi City. Vapi serves as a prominent industrial hub, particularly in the sectors of chemicals, textiles, and paper & pulp industries. Since the 1980s, substantial investments and employment opportunities have been generated in the district, with textiles and chemicals emerging as the major driving forces. Notably, Vapi is home to one of Asia's largest Common Effluent Treatment Plants (CETP), owned by Vapi Waste & Effluent Management Company and promoted by the Vapi Industrial Association. This CETP plays a crucial role in managing and treating industrial waste efficiently, contributing to environmental sustainability and responsible industrial practices in the region.

Silvassa

Capital of the union territory of Dadra and Nagar Haveli, **Silvassa** lies between Gujarat and Maharashtra. Silvassa comprised 72 villages and was ruled by the Marathas till 1779. It is well-connected by road with important urban centers like Mumbai & Surat by NH-48 and in Vapi by SH-185. It is equipped with smart city electric buses runs to Daman through Vapi. The nearest railway station is Vapi railway station which is around 19 Km from Silvassa. The nearest airport is Surat International Airport which is 138 Km. Silvassa is about **17.17 km²**. Forest areas cover a significant expanse of 203.21 sq km, constituting approximately 41.4 percent of the total area of Dadra and Nagar Haveli, as outlined in the proposed Regional Plan 2021. Within this, 92.00 sq km is specifically designated as Wildlife Sanctuary Area. The distribution of these forests is concentrated in the north-eastern, eastern, and south-eastern parts of the region, characterized by a tropical moist deciduous type. Majority of the land (45.9%) is used for agricultural purposes. Industrial area uses around 5.37% of land which is very high growth in industrial areas. It also has a reservoir Dudhni lake where Madhuban Dam is constructed which is included in 8.36% of water body areas, which fulfills the water needs of the city. Due to rapid industrialization and drastically growth in tourism a growth in residential areas can also be witnessed, with development of road networks. In the outlying districts of Silvassa, industrialization is expanding quickly. The population of migrants has quickly expanded as a result of industrialization as Nearly every third family in Silvassa has immigrated from somewhere else, according to research in the subject of migrants. According to research on the migrant population, most of the employees come from states like Orissa, A.P., M.P., U.P., and Kerala.

DATA COLLECTION AND ANALYSIS

With the increase in population of the city there is also development in road network of the city. The new ring road eliminate the heavy vehicle traffic in the city areas. Length of different roads are given in Table 1 As data presented in Figure 5, it is clearly seen that 53% of road trips are generated due to people travelling for work purpose, 26% for travelling activities like tourism. Business and commercial contributes 10% which includes commercial vehicles. Figure 6 shows the volume of types of vehicles, as it can be seen that majority of the traffic volume is of two vehicles, then followed by auto rickshaws majority of the daily commuter's uses these two modes for travelling. Only 1% of public transport is used which is very less for a city where daily commuters are more.

Here are some Issue and Challenges faced on this corridor

1. Congestion Junctions
 - Vapi Char Rasta
 - Dadra
 - Rakholi
 - Zanda Chowk
 - Chanod Colony
2. Road Side Encroachment
3. Haphazard Parking

It can be seen from Figure 7 that after 2018 there is exponential increase in accidents rates, this is due to increase in vehicular traffic and lack of safety.



**Bhargav Patel et al.,****RECOMMENDATIONS**

The GIDC areas caters to very heavy traffic due to industries, mainly due to transport. It being major transport link for industrial laborers carries a varied traffic composition. Because of the textile industries maximum traffic is categorized pedestrian as well as bicycles and so for efficient movement of pedestrian and bicycle traffic, separate footpath and cycle track is recommendable which ideally creates a buffer between slow moving traffic and fast-moving traffic, thereby benefiting both. Commercial development on the roadside mainly comprises of some automobile shops, timber marts, provision in D.P. 2004. This is based on the primary observation of the temporary nature of encroachment. Textile industries and local shops which generate traffic of heavy vehicles often requiring loading and unloading exercises. These being time consuming create temporary parking scenario reducing carriageway width. Also, maximum traffic is catered by rickshaws, which have a frequent sudden stopping feature hindering the smooth flow. In such cases a service lane throughout the road will serve the purpose of efficiency. The available width for the purpose of design is adopted as 45.00 mt. looking at the existing encroachment despite of 60.00 mt. wide road. The availability of width on road, without any obligation can boost up the execution of any programmed. Here, because of temporary encroachments one can easily possess the entire required width of the road and do the needful without wasting any time on any type of disagreement. Contrary to this, in other cases illegal encroachment are creating nuisance and tend to slow down the process of development program by increasing cases of conflicts and taking the whole system in litigation.

PLANNING PROPOSAL

Following are the elements that can be developed for easy, sustainable, time/cost saving mobility between two rapid developing cities,

- Lane Allocation
- Cycle Infrastructure
- Parking Lane/Street Parking Foot over Bridge
- Pavement Material
- Street Light Designs
- Roadside Plantations
- Public Bus Transportation/BRTS

Proposed C/S of 45mt. Road

The street design guidelines based 45 mt. road cross section. This distance based on IRC. It is 6 lane road with Street parking and NMV track. Here BRTS lane is provided in center. And Street light provided on side of the road as seen in figure 8

Proposed C/S of 45mt. Road without BRTS

The street design guidelines based 45 mt. road cross section. This distance based on IRC. Also provided to 3m footpath. and Street light provided on side of the road can be seen in Figure 9.

Proposed C/S of 30mt. Road

The street design guidelines based 30 mt. road cross section. This width is based on IRC. It is a 4 lane road with Street parking. BRTS lane is in center. and Street light provided on side of the road can be seen in Figure 10.

Features of road

In Figure 11, there are three motorized lane for mix traffic, 10.50 mt. wide for each direction of travel. 1.00 mt. wide central median is provided for separate the road. At outer both side of road 1.50 mt wide footpath is provided for pedestrian movement. A cycle track 2.0 mt. wide will run adjacent to the mix traffic lane segregated by a 3.50 mt. divider. An activity area of 2.50 mt. wide for the public utilities like bus stop.3.50mt footpath with use of bus stop and public utilities and also give space of 2.50 mt. street parking. Figure 12 shows model of Vapi Char rasta to Dadra Road.



**Bhargav Patel et al.,****Features of road**

From Figure 13 it is seen that in this section,

- Two motorized lane for mix traffic, 7.50 mt. wide for each direction of travel.
- 0.30 mt. wide central median is provided for separate the road.
- At outer both side of road 1.70 mt wide footpath is provided for pedestrian movement.
- Available width for BRTS lane 3.3mt
- BRTS station is 4 mt.
- Available width for carrying vehicle traffic: 14.00 mt.
- The proposed alternative cross section of road is draw in figure44.
- A 3D model for same cross section has been prepared using Revit in Figure 14.

CONCLUSION

A proper study can be generated to know the exact timings and scheduling of the nearby industries to practice the work-hour staggering in order to harmonize the existing flow conditions. Proper signal timings and phases are to be calculated for major intersection to minimize delay and to maximize intersection capacity. For signal planning solar system should be used for energy saving purpose. Good quality of road construction most requisite for safe, free and comfortably movement. Pavement should be designed considering soil characteristic and other all technical measures. Technical measures including Traffic Regulation, Traffic Control, Traffic Management, Safety Measure etc. should be taken care for road and surrounding linkages. Enforcement of urban design through landscaping, Paving materials, street furniture and hoardings creating an aesthetic. The escalating levels of pollution in Indian urban areas are a cause for concern. A substantial portion of the population in a typical Indian city relies on walking, with an almost equal percentage combining walking and bus commuting. Regrettably, civic bodies and governments often neglect this demographic in their planning strategies, with most policies predominantly favoring car-centric solutions. It is imperative to introduce legislation mandating that pedestrians be accorded priority in all city development projects. In the realm of transportation infrastructure, it is crucial to acknowledge and accommodate the diverse modes of mobility embraced by the Indian populace. A considerable number of citizens rely on walking and public buses for their daily commute. Hence, any comprehensive urban development strategy must encompass the needs of these pedestrians, ensuring their safety, convenience, and priority in the overall transportation framework. Vehicles demand not only space for seamless movement but also designated areas for parking. Parking management is a critical aspect of urban planning, necessitating thoughtful strategies to address the rising demand for parking spaces. As cities expand and the number of vehicles continues to surge, efficient and well-designed parking solutions become imperative to alleviate congestion and enhance the overall urban experience. Similarly, the strategic placement of road signs is vital for effective communication and navigation, contributing to a safer and more organized road environment.

REFERENCES

1. Azgomi, H. F., & Jamshidi, M. (2018). A brief survey on smart community and smart transportation. *Proceedings - International Conference on Tools with Artificial Intelligence, ICTAI, 2018-November*, 932–939.
2. Benevolo, C., Dameri, R. P., & D'Auria, B. (2016). Smart mobility in smart city action taxonomy, ICT intensity and public benefits. In *Lecture Notes in Information Systems and Organisation* (Vol. 11, pp. 13–28). Springer Heidelberg.
3. Beyer, Clemens., Elisei, Pietro., Popovich, V. v., Schrenk, Manfred., & Zeile, Peter. (n.d.). *REAL CORP 2015. Plan Together - Right Now - Overall. From Vision to Reality for Vibrant Cities and Regions Proceedings of the 20th International Conference on Urban Planning, Regional Development and Information Society.*
4. Bhatt, B. v, Agarbattiwala, T. v, & Vijaykumar Bhatt, B. (2016). Performance Analysis of BRT System Surat Surat Urban Planning View Project Sustainable and Smart Urbanisation View Project Performance Analysis of BRT System Surat. *Article in International Journal of Engineering Research*, 5, 2016.





Bhargav Patel et al.,

5. Finogeev, A., Finogeev, A., Fionova, L., Lyapin, A., & Lychagin, K. A. (2019). Intelligent monitoring system for smart road environment. *Journal of Industrial Information Integration*, 15, 15–20.
6. Gibbons, S., Lyytikäinen, T., Overman, H. G., & Sanchis-Guarner, R. (2019). New road infrastructure: The effects on firms. *Journal of Urban Economics*, 110, 35–50.
7. IEEE Communications Society, & Institute of Electrical and Electronics Engineers. (n.d.). 2020 *International Conference on Communication Systems & Networks (COMSNETS)*
8. Karpiński, M. K., Senart, A., & Cahill, V. (2006). *Sensor Networks For Smart Roads*.
9. Kireeti Chanda, B., Sai, M., & Goutham, S. (n.d.). Introduction to corridor selection & assessment for Bus Rapid Transit System (BRTS) in Hyderabad. *American Journal of Engineering Research*, 2014.
10. Orłowski, A., & Romanowska, P. (2019). Smart Cities Concept: Smart Mobility Indicator. *Cybernetics and Systems*, 50(2), 118–131.
11. Paiva, S., Ahad, M. A., Tripathi, G., Feroz, N., & Casalino, G. (2021). Enabling technologies for urban smart mobility: Recent trends, opportunities and challenges. In *Sensors* (Vol. 21, Issue 6, pp. 1–45). MDPI AG.
12. Pompigna, A., & Mauro, R. (2022). Smart roads: A state of the art of highways innovations in the Smart Age. In *Engineering Science and Technology, an International Journal* (Vol. 25). Elsevier B.V.
13. Porru, S., Misso, F. E., Pani, F. E., & Repetto, C. (2020). Smart mobility and public transport: Opportunities and challenges in rural and urban areas. In *Journal of Traffic and Transportation Engineering (English Edition)* (Vol. 7, Issue 1, pp. 88–97). Chang'an University.
14. Shihora, D. (2018). *Performance Evaluation of BRTS in various Indian Cities*.
15. Stefansson, G., & Lumsden, K. (2009). Performance issues of Smart Transportation Management systems. *International Journal of Productivity and Performance Management*, 58(1), 55–70.
16. Sun, L., Zhao, H., Tu, H., & Tian, Y. (2018). The Smart Road: Practice and Concept. *Engineering*, 4(4), 436–437.
17. Toh, C. K., Sanguesa, J. A., Cano, J. C., & Martinez, F. J. (2020). Advances in smart roads for future smart cities. In *Proceedings of the Royal Society A: Mathematical, Physical and Engineering Sciences* (Vol. 476, Issue 2233). Royal Society Publishing.
18. Trubia, S., Severino, A., Curto, S., Arena, F., & Pau, G. (2020). Smart roads: An overview of what future mobility will look like. *Infrastructures*, 5(12), 1–12.

Table 1: Road Length

Sr.No.	Road Name	Length(km)
1	Ring Road	13.2
2	Naroli Road	7.3
3	Khanvel-Dudhni Road	17.7
4	Rakholi road	5.6
5	Athola road	7.2
6	Dadra Silvassa road	7.3
7	Vapi GIDC - Dadra	8.1
8	Bhilad Road	14.6
9	Chanandevi road	17
10	Silvassa-Khanvel Road	22.4





Bhargav Patel et al.,

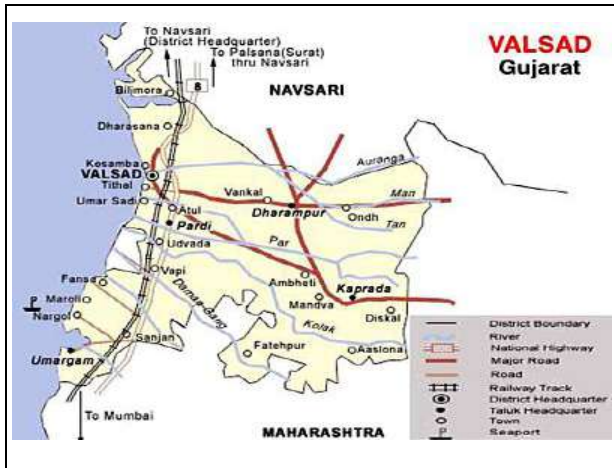


Figure 2: Vapi Connectivity

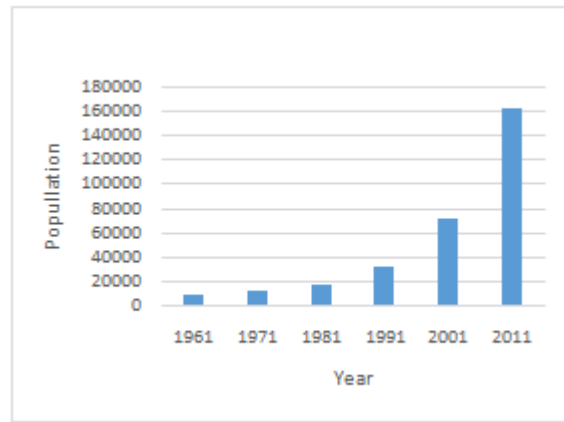


Figure 3: Vapi Population

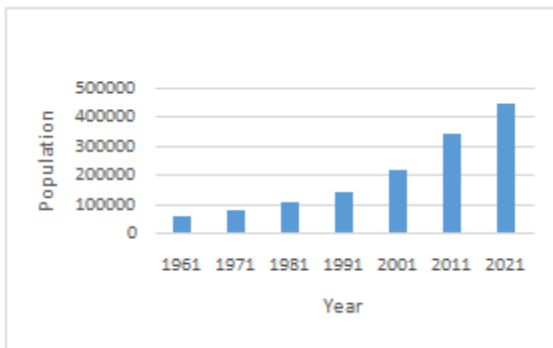


Figure 4: Silvassa Population

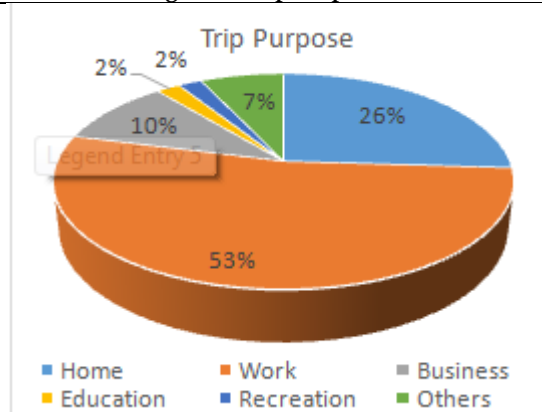


Figure 5: Trip Purpose

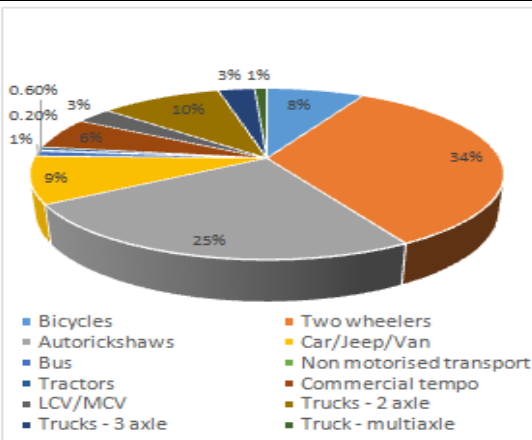


Figure 6: Types of Traffic Volume

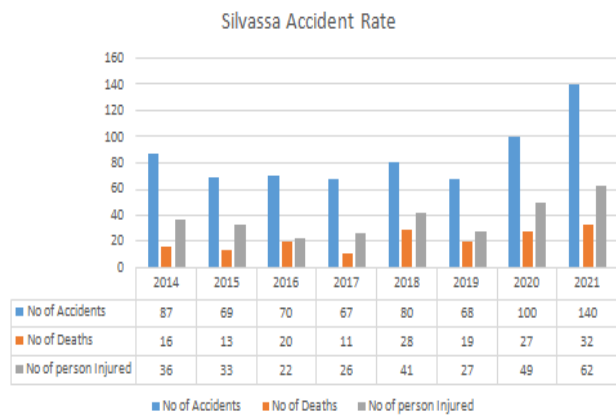


Figure 7: Silvassa Accident Rate





Bhargav Patel et al.,

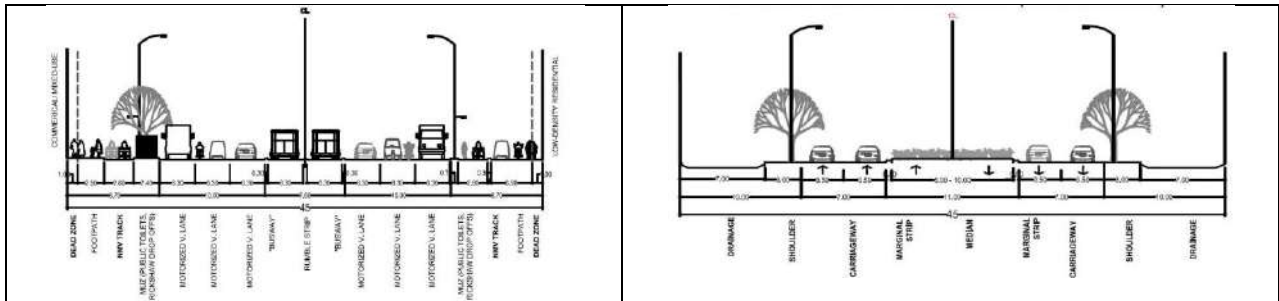


Figure 8: Proposed 45 Mt. Road

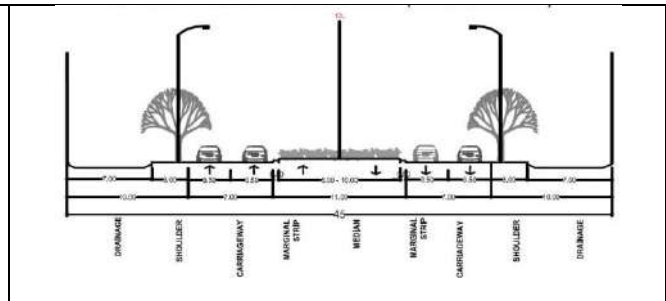


Figure 9: Proposed 45 Mt. Road without BRTS

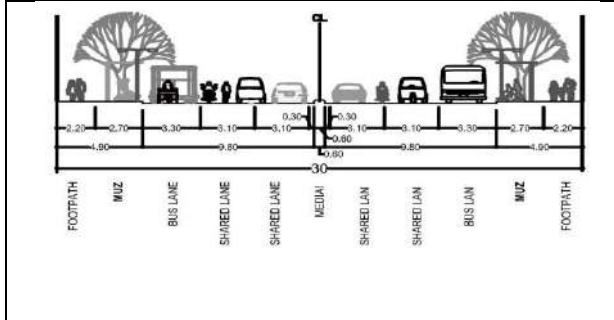


Figure 10: Proposed 30 Mt. Road

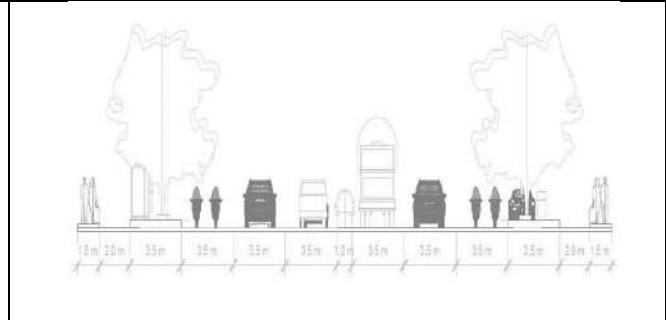


Figure 11: Proposed Road for Vapi Char Rasta – Dadra Section



Figure 12: Proposed Road Model for Vapi Char Rasta – Dadra Section

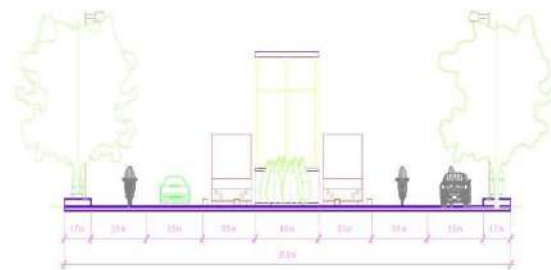


Figure 13: Proposal of Dadra - Rakholi Road





Bhargav Patel et al.,



Figure 14: Proposed Road Model for Dadra – Rakholi Section





Risk Assessment of Tebuconazole on Okra

Shivangi Soni¹, Khushal Patel², Riddhi Solanki², Zeel Patel² and Nisha Daxini^{1*}

¹Ashok and Rita Patel Institute of Integrated Study and Research in Biotechnology and Allied Sciences (ARIBAS), The CVM University, Vallabh Vidyanagar, Gujarat, India.

²Department of Medical Laboratory Technology, Bapubhai Desai bhai Patel Institute of Paramedical Sciences (BDIPS), Charotar University of Science & Technology (CHARUSAT), Changa, Anand, Gujarat, India.

Received: 30 Dec 2023

Revised: 09 Jan 2024

Accepted: 12 Jan 2024

*Address for Correspondence

Nisha Daxini

Ashok and Rita Patel Institute of Integrated Study and Research in Biotechnology and Allied Sciences (ARIBAS),
The CVM University,
Vallabh Vidyanagar, Gujarat, India.
Email: nishadaxini@aribas.edu.in



This is an Open Access Journal / article distributed under the terms of the **Creative Commons Attribution License** (CC BY-NC-ND 3.0) which permits unrestricted use, distribution, and reproduction in any medium, provided the original work is properly cited. All rights reserved.

ABSTRACT

The study aimed to assess the dissipation kinetics of Tebuconazole residues on Okra under field conditions to ensure consumer safety. Tebuconazole was applied via spraying method onto Okra, and samples were collected at various intervals: 0 days (1 hour), 3 days, 5 days, and 8 days post-application. The initial average deposits of Tebuconazole on Okra ranged from 24 ppm to approximately 2 ppm. The observed half-life of Tebuconazole ranged between 48 to 72 hours. The Theoretical Maximum Residue Contribution (TMRC) for Tebuconazole was calculated and found to be significantly below the Maximum Permissible Intake (MPI) on Okra, specifically on the 8th day following the application of Tebuconazole. Consequently, it was determined that Okra did not present any discernible human health risks after exposure to the fungicide.

Keywords: Okra, Pesticides, tebuconazole, HPLC





Shivangi Soni et al.,

INTRODUCTION

Okra, scientifically known as *Abelmoschus esculentus* (L.), is a green vegetable belonging to the Malvaceae family, highly valued for its nutritional richness. In India, it is cultivated from late spring to early summer (March–June) and during the rainy season (July–September). This vegetable is a significant source of essential vitamins and minerals and can be consumed raw and cooked. Often referred to as "bhindi" locally, Okra holds immense nutritional value and is an essential dietary component for Indians. However, like other vegetable crops, okra is vulnerable to various bacterial, viral, and fungal diseases, significantly affecting crop productivity. Among these diseases, powdery mildew caused by *Erysiphe cichoracearum* DC is one of the most detrimental, leading to substantial yield losses [1]. In contemporary agriculture, Indian farmers often opt for blended formulations due to their broad-spectrum effectiveness. Nativo 75WG, a water-dispersible granular formulation, comprises 50% w/w tebuconazole and 25% w/w trifloxystrobin, presenting as a broad-spectrum systemic fungicide with both preventive and curative properties [1], [2]. Tebuconazole belongs to the triazole category of systemic fungicides. Like other triazole fungicides, it obstructs the synthesis of ergosterol, a crucial process disrupting the metabolism of fungal pathogens. Studies have confirmed its efficacy against rusts affecting legume and non-legume crops, loose smuts, and powdery mildews [2], [3]. There are several critical parameters to consider when researching okra. It's a widely cultivated vegetable globally, playing a significant role in human diets. India is the world's largest producer of okra, yielding between 15-20 tons annually. Okra is low in saturated fat and sodium and contains minimal cholesterol.

Rich in vitamins A and K, it also boasts high flavonoid content, serving as a potent antioxidant. Okra crops commonly face infestation by various diseases such as fusarium wilt, damping off, and powdery mildew at different growth stages. Presently, the prevention and treatment of these diseases predominantly rely on fungicides. Tebuconazole, a systemic fungicide belonging to the triazole group, disrupts the metabolism of fungal pathogens, similar to other triazole fungicides. There is a serious concern about pesticide residues on crops, particularly when consumed raw. Tebuconazole, used to combat fungal infections in plants, binds to fungal cells [4], [6]. Most studies focus on the environmental fate of individual pesticide compounds and their environmental impact. However, specific pesticides are frequently applied together or successively to shield crops from damage, resulting in combined contamination of pesticide residues in the soil environment. Degradation and adsorption play pivotal roles in the behaviour of pesticides in soil, influenced by factors such as soil constituents and pesticide properties. Individual pesticides might exhibit distinct behaviours in a given soil due to variations in their physical and chemical properties. Tebuconazole (TEB) and tridenton-methyl (TBM) stand as widely used pesticides, yet their high phytotoxicity and potential to pollute soil and groundwater raise significant concerns [7], [8]. The present study was devised to investigate the dissipation and persistence of tebuconazole residues in or on okra.

METHODOLOGY

Cultivation of Okra Plants

Okra seeds were planted and nurtured until the plants produced fruits. Subsequently, specific fruits were chosen as the target area for applying Tebuconazole pesticide, while another set of Okra plants was used as the control group and treated with water. Okra seeds were sown and cultivated, undergoing growth stages that led to the development of mature plants. As the plants matured, they bore Okra fruits, carefully observed until they reached a suitable stage for further experimentation. Specifically, Okra fruits were selected as the site for applying the Tebuconazole pesticide, selected for its pesticidal properties against fungal diseases. Meanwhile, an alternate set of Okra plants received water treatment instead of pesticide application as a control measure. The progression from seed planting to fruit selection and subsequent pesticide application adhered to standard agricultural practices, ensuring consistency and accuracy in evaluating the impact of Tebuconazole on the targeted plants.





Shivangi Soni et al.,

Sample Collection

After applying Tebuconazole, samples were collected on various days to assess its impact on Okra. Samples were gathered immediately after spraying (at 0 hours or 1 hour), and subsequently at 3-, 5-, and 8-days post-application using the QuEChERS method to monitor the pesticide's effects on Okra. The sample collected on day 1 after spraying was regarded as the control sample for comparison purposes.

QuEChERS Method [1]

A total of 500 grams of Okra fruit was homogenized and 15 grams of the homogenized sample was transferred into a 50 mL centrifuge tube. Next, 15 mL of 1% Acetic Acid in Acetonitrile was added and sample was mixed by Shaking and inverting tubes. The tube was then placed in a deep freezer at -10°C for 20 minutes. Following this 6.0 grams of MgSO₄ and 1.5 grams of NaOAc (sodium acetate) were added to the mixture. The contents were vigorously shaken for 1.0 minute using vortex mixing and then centrifuged for 2.0 minutes at 3500 RPM. Subsequently, 6.0 mL of the supernatant was transferred into a 15 mL centrifuge tube containing 300 mg of PSA (Primary Secondary Amine) and 900 mg of MgSO₄. Then the sample was vortexed for 30 seconds and centrifuged for 2.0 minutes at 2500 RPM. Finally, 2 mL aliquots were taken and transferred into HPLC (High-Performance Liquid Chromatography) vials for analysis (refer to Fig. 2). The samples were analyzed using HPLC.

Estimation of Chlorophyll Pigment in Plant Fruits and Leaves

Following daily Tebuconazole spraying, samples were collected daily for the estimation of chlorophyll pigment in both plant fruits and leaves. A similar procedure was carried out for the control samples. The process involved homogenizing 2 grams of fruit and leaf samples, and transferring 1 gram of the homogenized sample into a 15 mL tube. Subsequently, 10 mL of 80% acetone was added to the tube, which was then centrifuged at 5000 RPM for 5 minutes. The collected sample was then filtered. This extraction process was repeated using 80% acetone until the residue became colorless. The final volume was adjusted to 50 mL using 80% acetone. The absorbance of the samples was measured at 663nm and 645nm using a spectrometer.

$$\text{Chlorophyll 'A'} = 12.7 (A_{663}) - 2.69 (A_{645}) \times V / 1000 \times W$$

$$\text{Chlorophyll 'B'} = 22.9 (A_{645}) - 4.68 (A_{663}) \times V / 1000 \times W$$

$$\text{Total Chlorophyll} = 20.2 (A_{645}) - 8.02 (A_{663}) \times V / 1000 \times W$$

EHPLC (High-Performance Liquid Chromatography) Analysis for Tebuconazole

The parameters and column details used for this analysis are mentioned in *Table 1*

RESULTS AND DISCUSSION

Height of Okra Plants

After conducting a thorough analysis, it was observed that the maximum height of the Okra plants was achieved on the 60th day across all four rows that were measured. Among the four rows, Row 2 displayed the tallest height, reaching an impressive 26 cm. Row 1 followed closely with a height of 24 cm, while row 3 measured 22 cm. Row 4 exhibited the shortest height, measuring 18 cm. It is noteworthy to mention that the height increase between the 25th and 60th days was most significant, indicating an exponential growth rate during this period. This data gives a comprehensive understanding of the growth patterns of the Okra plants and can be used to optimize their cultivation in the future.

Number of Leaves on Okra Plants

Throughout the course of the experiment, several observations were made on the average number of leaves per plant across all rows. The data was recorded on various days to study the growth pattern of Okra plants. On day 10, the average number of leaves per plant was found to be 19. As the experiment progressed, the leaf count increased significantly, reaching 38 on day 20, 45 on day 30, 51 on day 40, 65 on day 50, and finally, 75 on day 55. The maximum number of leaves observed, 75, occurred on the 55th day. The observations also revealed interesting insights into the growth patterns of Okra plants across different rows. Row 4 exhibited the highest count of 24 leaves,





Shivangi Soni et al.,

followed by Row 2 with 22 leaves. Row 1 displayed a range of 21 to 23 leaves, while Row 3 exhibited the lowest growth with only 19 leaves per plant. These findings provide valuable insights into the growth patterns of Okra plants, which can be used to optimize plant growth in the future.

Estimation of Chlorophyll Pigment on Plant Fruits and Leaves

The results of the experiment showed that the control samples had a higher chlorophyll content for both the fruits and leaves compared to the treated samples. Initially, on the first day, the chlorophyll content was similar in both the control and treated samples. However, over the course of the experiment, the control samples showed a gradual increase in chlorophyll content, reaching maximum levels on the eighth day. After this point, the growth patterns between the control and treated samples became similar, indicating that the treated samples were catching up to the control samples in terms of chlorophyll content. These findings suggest that while the treated samples may have initially lagged behind the control samples, they eventually caught up, implying that the treatment was effective in promoting chlorophyll production. In the conducted study, the response of the detector to matrix-matched standards of fungicides was investigated by injecting various concentrations of each. This was done to determine the residues of fungicides in Okra fruit. A graph was generated to correlate the detector response with the respective concentrations, and the response, specifically the retention time observed on the instrument, was noted at 2.54. These findings confirmed the reliability and validity of the high-performance liquid chromatography (HPLC) and liquid chromatography-mass spectrometry (LC-MS) analysis methods used in the study.

The study's results provide valuable insights into the effectiveness of the tested fungicides and their residues in Okra fruit. The estimation of residues was conducted by comparing the peak area of the standards run under identical conditions. The persistence of Tebuconazole was quantified in terms of its disappearance time (DT50), representing the time taken for the pesticide to degrade to 25 ppm of its initial concentrations [10], [11]. Initial deposits of Tebuconazole on Okra fruit were initially measured at 24 ppm, followed by subsequent levels of 8 ppm on day 3, 4.9 ppm on day 5, and finally degrading to the lowest recorded level of 1.2 ppm on day 8. This degradation pattern illustrates the gradual reduction of the fungicide's concentration over time [7], [12], [13]. The study conducted to evaluate the degradation levels of Tebuconazole has revealed that the levels recorded on the 8th day were well below the permissible intake for Okra fruit. As per the guidelines laid down by ICAR and Pesticide Residue laboratory standards and SOPs, the acceptable levels for consumption and market selling are set at 1.8 ppm, which was found to be lower than the observed concentrations. This information is crucial for farmers, marketers, and consumers to ensure the safety and quality of Okra produce.[7], [12], [13]. Similarly, initial deposits of Tebuconazole on chili were detected at 1.88 mg kg⁻¹ following the application of Tebuconazole at a rate of 500 g ha⁻¹. These levels dissipated with a half-life of 1.41 days [14], [16].

CONCLUSION

Tebuconazole serves as a fungicide utilised to prevent diseases in crops. Okra, a commercially valuable vegetable crop, benefits from Tebuconazole application to safeguard it against infections. In this study, Okra samples were analysed at various intervals, ranging from the 1st day to the 8th day (1st, 3rd, 5th, and 8th days), considering treated and untreated samples. A total of 4 rows, each containing 6 Okra plants, were sprayed with a 25 ppm fungicide solution, and subsequent biochemical parameters were assessed. The results indicated a reduction in chlorophyll content. The degradation study of Tebuconazole revealed levels decreasing from 25 ppm to approximately 1.2 ppm by the 8th day, below the permissible intake range for Okra fruit. The application of Tebuconazole on Okra seems to be a safer method for safeguarding against diseases and environmental contamination. However, with regards to its nutritional aspects, further research is needed to extend the study. This extension could potentially involve analyzing the levels of fungicides present on Okra after human consumption, in order to ascertain any potential effects on human health.





Shivangi Soni et al.,

ACKNOWLEDGMENT

The authors are grateful to respective institutions for supplying the facility during the collaborative study and validation of the data.

Declaration of Competing Interest

The authors declare that they have no known competing interests.

REFERENCES

1. V. Tripathy *et al.*, "Monitoring and dietary risk assessment of pesticide residues in brinjal, capsicum, tomato, and cucurbits grown in Northern and Western regions of India," *Journal of Food Composition and Analysis*, vol. 110, p. 104543, 2022, doi: <https://doi.org/10.1016/j.jfca.2022.104543>.
2. T. P. Ahammed Shabeer, S. Hingmire, R. Patil, A. Patil, A. K. Sharma, and B. Taynath, "Dissipation kinetics and evaluation of processing factor for fluopyram + tebuconazole residues in/on grape and during raisin preparation," *Journal of Food Composition and Analysis*, vol. 120, p. 105292, 2023, doi: <https://doi.org/10.1016/j.jfca.2023.105292>.
3. H.-X. Zhou *et al.*, "Residues of sulfoxaflor and its metabolites in floral and extrafloral nectar from *Hibiscus rosa-sinensis* L. (Malvaceae) with or without co-application of tebuconazole," *Pestic Biochem Physiol*, vol. 196, p. 105587, 2023, doi: <https://doi.org/10.1016/j.pestbp.2023.105587>.
4. P. Sivaperumal, P. Anand, and L. Riddhi, "Rapid determination of pesticide residues in fruits and vegetables, using ultra-high-performance liquid chromatography/time-of-flight mass spectrometry," *Food Chem*, vol. 168, pp. 356–365, 2015, doi: <https://doi.org/10.1016/j.foodchem.2014.07.072>.
5. R. H. Naik, M. S. Pallavi, Nandini, A. Shwetha, M. Bheemanna, and R. U. Nidoni, "Simultaneous determination of pesticide residues in pomegranate whole fruit and arils using LC-MS/MS," *Food Chem*, vol. 387, p. 132865, 2022, doi: <https://doi.org/10.1016/j.foodchem.2022.132865>.
6. V. Tripathy *et al.*, "Monitoring and dietary risk assessment of pesticide residues in brinjal, capsicum, tomato, and cucurbits grown in Northern and Western regions of India," *Journal of Food Composition and Analysis*, vol. 110, p. 104543, 2022, doi: <https://doi.org/10.1016/j.jfca.2022.104543>.
7. S. Soman *et al.*, "An updated status of currently used pesticide in India: Human dietary exposure from an Indian food basket," *Environ Res*, p. 117543, 2023, doi: <https://doi.org/10.1016/j.envres.2023.117543>.
8. Y. Picó, J. Campo, A. H. Alfarhan, M. A. El-Sheikh, and D. Barceló, "A reconnaissance study of pharmaceuticals, pesticides, perfluoroalkyl substances and organophosphorus flame retardants in the aquatic environment, wild plants and vegetables of two Saudi Arabia urban areas: Environmental and human health risk assessment," *Science of The Total Environment*, vol. 776, p. 145843, 2021, doi: <https://doi.org/10.1016/j.scitotenv.2021.145843>.
9. M. Tankiewicz and A. Berg, "Improvement of the QuEChERS method coupled with GC-MS/MS for the determination of pesticide residues in fresh fruit and vegetables," *Microchemical Journal*, vol. 181, p. 107794, 2022, doi: <https://doi.org/10.1016/j.microc.2022.107794>.
10. H.-X. Zhou *et al.*, "Residues of sulfoxaflor and its metabolites in floral and extrafloral nectar from *Hibiscus rosa-sinensis* L. (Malvaceae) with or without co-application of tebuconazole," *Pestic Biochem Physiol*, vol. 196, p. 105587, 2023, doi: <https://doi.org/10.1016/j.pestbp.2023.105587>.
11. T. P. Ahammed Shabeer, S. Hingmire, R. Patil, A. Patil, A. K. Sharma, and B. Taynath, "Dissipation kinetics and evaluation of processing factor for fluopyram + tebuconazole residues in/on grape and during raisin preparation," *Journal of Food Composition and Analysis*, vol. 120, p. 105292, 2023, doi: <https://doi.org/10.1016/j.jfca.2023.105292>.
12. M. Hejazi, J. H. Grant, and E. Peterson, "Trade impact of maximum residue limits in fresh fruits and vegetables," *Food Policy*, vol. 106, p. 102203, 2022, doi: <https://doi.org/10.1016/j.foodpol.2021.102203>.



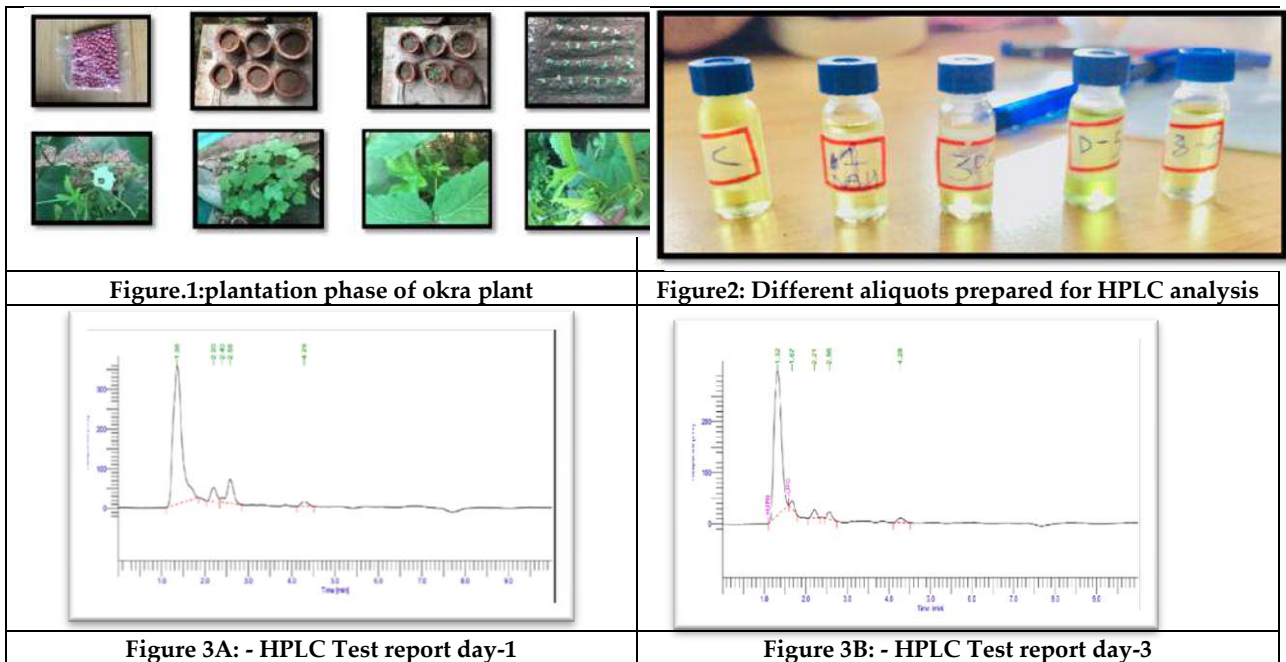


Shivangi Soni et al.,

13. H. Tan et al., "Occurrence, distribution, and driving factors of current-use pesticides in commonly cultivated crops and their potential risks to non-target organisms: A case study in Hainan, China," *Science of The Total Environment*, vol. 854, p. 158640, 2023, doi: <https://doi.org/10.1016/j.scitotenv.2022.158640>.
14. J. Sarmiento-Santos et al., "Assessment of quality and safety aspects of homemade and commercial baby foods," *Food Research International*, vol. 174, p. 113608, 2023, doi: <https://doi.org/10.1016/j.foodres.2023.113608>.
15. S. Khazaal, N. El Darra, A. Kobeissi, R. Jammoul, and A. Jammoul, "Risk assessment of pesticide residues from foods of plant origin in Lebanon," *Food Chem*, vol. 374, p. 131676, 2022, doi: <https://doi.org/10.1016/j.foodchem.2021.131676>.
16. N. M. Al-Daghri et al., "Detection rates of pesticide residues in Saudi Arabian produce as influenced by season," *Arabian Journal of Chemistry*, p. 105461, 2023, doi: <https://doi.org/10.1016/j.arabjc.2023.105461>.

Table 1: HPLC parameters used for this study on the detection of Tebuconazole

Column	Column used was fortics C18 100mm length × 2.1 mm i.d. 1.7 μm pore size
Mobile phase	<i>Solvent A:</i> 10mM Ammonium formate in water <i>Solvent B:</i> Acetonitrile
Total run time	10 mints
Residue Analysis	Residues in 25 ppm





Shivangi Soni et al.,

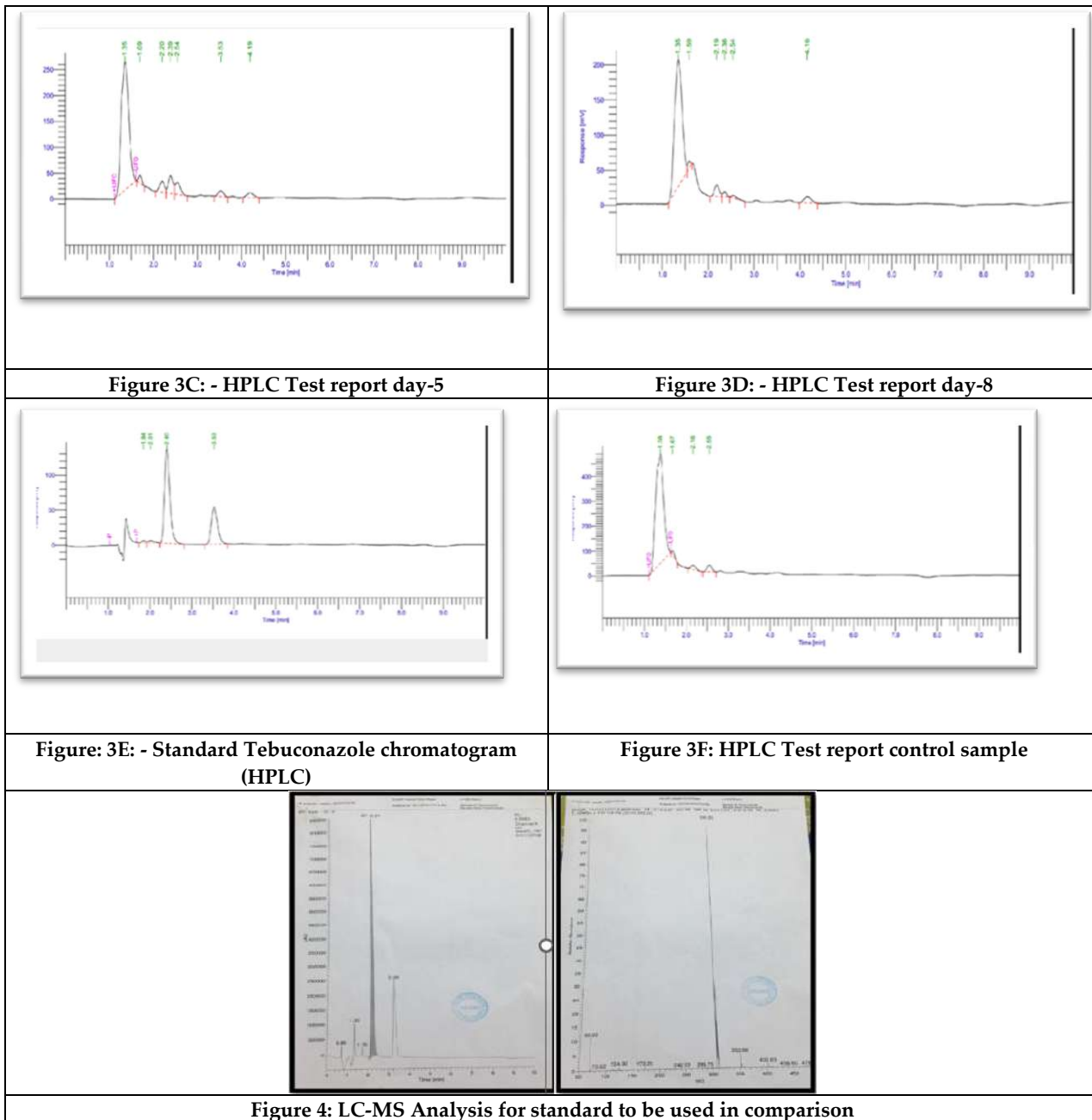


Figure 4: LC-MS Analysis for standard to be used in comparison





Automated Classroom Attendance System using Image Processing

Zankhana Shah¹, Komal Vaswani², Smit Patel³, Devangiri Goswami³ and DhruvPurohit⁵

¹Department of Information Technology, Assistant Professor in Birla Vishwakarma Mahavidyalaya, Gujarat, India.

²Department of Information Technology, Anand, Gujarat, India.

³Department of Information Technology, Birla Vishwakarma Mahavidyalaya , Gujarat, India.

Received: 30 Dec 2023

Revised: 09 Jan 2024

Accepted: 12 Jan 2024

*Address for Correspondence

Zankhana Shah

Department of Information Technology,
Assistant Professor in Birla Vishwakarma Mahavidyalaya,
Gujarat, India.

Email: zankhana.shah@bvmengineering.ac.in



This is an Open Access Journal / article distributed under the terms of the **Creative Commons Attribution License** (CC BY-NC-ND 3.0) which permits unrestricted use, distribution, and reproduction in any medium, provided the original work is properly cited. All rights reserved.

ABSTRACT

In response to the persistent challenges of manual attendance tracking in educational settings, this research introduces the "Automated Classroom Attendance System Using Image Processing." Leveraging advanced image processing and facial recognition technologies, the system offers a streamlined approach to attendance recording. By capturing real-time images of students through a user-friendly mobile application, the system employs a combination of Open CV and deep learning models for facial feature extraction and recognition. Results from extensive testing reveal a high accuracy rate and significant efficiency gains compared to traditional methods. User feedback underscores the system's non-intrusive nature and positive impact on the teaching environment. Privacy and security considerations are prioritized, aligning the system with regulatory standards. As a comprehensive solution, this research not only addresses current challenges in attendance tracking but also establishes a foundation for future advancements in educational technology.

Keywords: Image Processing, Facial Recognition, Attendance Tracking



**Zankhana Shah et al.,**

INTRODUCTION

In today's educational environment, the manual process of recording attendance in classrooms continues to pose significant challenges marked by inefficiencies and the susceptibility to errors. Traditional attendance methods necessitate substantial time and human resources, diverting attention from crucial instructional moments. Acknowledging these challenges, this research endeavors to address the longstanding predicaments associated with attendance tracking through the inception of the "Automated Classroom Attendance System Using Image Processing." The aim is to introduce a technological solution that not only mitigates the shortcomings of conventional methods but also streamlines the entire attendance tracking process. By leveraging image processing technology, this system seeks to revolutionize how attendance is recorded in educational settings, offering a more efficient and accurate alternative to the time-consuming manual procedures that have persisted over the years. The system represents a paradigm shift in how attendance is traditionally managed. By harnessing the capabilities of image processing technology, it endeavors to alleviate the burdens associated with manual attendance tracking. The vision is to introduce a seamless and accurate alternative that not only optimizes the use of instructional time but also diminishes the likelihood of errors inherent in conventional methods. In essence, this research project strives to contribute to the ongoing evolution of educational practices by addressing a fundamental administrative challenge. By embracing technology, the aim is to enhance the overall efficiency and accuracy of the attendance tracking, it thereby allows educators to reclaim valuable instructional time and create a more seamless and productive learning environment.

BACKGROUND

In the dynamic realm of contemporary education, the process of manually recording attendance in classrooms has long been a persistent challenge. Traditional methods, ranging from calling out names to using physical attendance sheets, not only consume valuable instructional time but are also susceptible to errors and inefficiencies. These challenges are further exacerbated in larger class sizes, making the management of attendance a cumbersome task for educators and administrative staff alike. The motivation for addressing this longstanding issue arises from a deep-seated commitment to optimizing the educational experience. The traditional means of attendance tracking not only disrupt the natural flow of teaching but can also contribute to a sense of tedium among both educators and students. Moreover, the potential for inaccuracies in manual data entry poses a considerable risk to the integrity of attendance records, impacting subsequent administrative processes and potentially compromising the overall educational experience. The motivation stems from a broader commitment to leverage technological advancements to streamline administrative processes within educational settings. The goal is to empower educators with tools that not only enhance efficiency but also contribute to a more engaging and focused learning environment.

Motivated by a commitment to optimizing the educational experience, the system leverages technological advancements, particularly React Native for a seamless UI. Addressing inefficiencies and errors in traditional methods, the goal is to empower educators with a transformative tool that not only enhances administrative efficiency but also fosters a more engaging and focused learning environment for both educators and students. The motivation is not solely driven by a desire to automate for the sake of technology, but rather to address a genuine need for improved efficiency and accuracy in attendance tracking. By implementing an automated system that utilizes image processing, the research seeks to align educational practices with the progressive integration of technology into various aspects of modern life. This endeavor is motivated by a vision of creating a seamless and technologically advanced educational ecosystem that empowers educators and enriches the learning experience for students. Ultimately, the background and motivation for this research underscore a commitment to advancing educational practices through innovative solutions that address practical challenges and contribute to the ongoing evolution of the educational landscape.





Zankhana Shah et al.,

METHODOLOGY

The overarching architecture of the automated attendance system is characterized by a modular design that seamlessly integrates each component. The process initiates with data collection, feeding into the Retina Face algorithm for facial detection. Detected faces then undergo facial feature extraction using Face Net, and the resulting embeddings are classified using the SVM model for accurate recognition. The React Native UI serves as the interface for educators, providing a user-friendly means of initiating attendance capture. The system's facial recognition capabilities, implemented through Keras, further enhance accuracy. This orchestrated architecture ensures a cohesive and efficient automated attendance system that addresses the complexities of real-world classroom scenarios while prioritizing user experience and privacy compliance.

Data Collection

The initial phase of the methodology involved meticulous data collection to form a comprehensive dataset of students from the college. This dataset serves as the foundational element for training and testing the automated attendance system with each individual having 10 to 12 different photos taken from various angles. Also, the individual images for the dataset were bifurcated to be assigned as testing and training data. The collection process focused on capturing diverse facial features, expressions, and lighting conditions to ensure the robustness of the system across various real-world scenarios. Ethical considerations, including obtaining informed consent from the students, were paramount throughout the data collection phase, ensuring privacy and compliance with ethical standards.

Retina Face for Facial Detection

The facial detection component of the system relies on the powerful Retina Face algorithm. Retina Face, known for its accuracy in multi-scale and multi-task facial detection, excels in precisely locating facial landmarks and contours. Leveraging this algorithm enhances the ability of the system to identify faces accurately, even amidst variations in pose, expression, and lighting conditions. The integration of Retina Face ensures a robust foundation for subsequent facial recognition processes, contributing to the overall accuracy and reliability of the automated attendance system.

Face Net for Facial Features Extraction

Once faces are detected, the system utilizes Face Net, a state-of-the-art facial recognition model. Face Net employs a deep neural network to extract high-dimensional features from facial images, creating a unique embedding for each face. This embedding is crucial for establishing identity and facilitates accurate recognition across different instances. The utilization of Face Net enhances the precision of the system by providing a discriminative feature space, enabling it to distinguish between individuals with a high degree of accuracy.

Support Vector Machine (SVM) for Classification

The feature embeddings obtained from FaceNet are then fed into a Support Vector Machine (SVM) classifier. SVM, a robust machine learning algorithm, is employed for its ability to handle high-dimensional data and make well-defined classifications. The classifier is trained on the dataset to learn the patterns associated with each student's facial features. During the recognition phase, the SVM classifier uses these learned patterns to match facial embeddings with corresponding individuals, facilitating accurate and efficient attendance tracking.

Keras for Facial Recognition

The facial recognition aspect of the system is implemented using Keras, a high-level neural networks API. Keras provides a simplified interface for building and training neural network models. In this context, Keras is utilized to fine-tune the Face Net model for the specific task of facial recognition within the attendance system. Fine-tuning ensures that the model adapts to the unique characteristics of the student dataset, optimizing its performance in identifying individuals accurately. The motivation for SVM is driven due to the fact that it is computationally cost



**Zankhana Shah et al.,**

effective and gives a higher performance. It is easier to classify images that have features already extracted for SVM to classify as well.

React Native

The UI for the system has been developed through React Native that allows for the creation of a cross-platform mobile application, providing educators with a straightforward tool for capturing attendance in real-time. The React Native UI facilitates intuitive interaction, allowing educators to effortlessly initiate the attendance tracking process and verify results. The incorporation of React Native aligns with the goal of making the system accessible and user-friendly for educators in diverse educational environments. It enables cross-platform consistency through a shared codebase, offering a component-based architecture for modular design, and facilitating hot reloading for real-time updates during development. This results in streamlined UI development, ensuring a cohesive and responsive user interface across diverse mobile platforms.

SYSTEM IMPLEMENTATION

The implementation of the automated attendance system is a meticulously designed process that commences with the foundational step of data collection. In this phase, a diverse dataset of students' facial images is collated from the college environment, underlining a commitment to ethical practices through the acquisition of informed consent and stringent privacy compliance. The user interface, developed using React Native, stands as a user-friendly gateway for educators. This cross-platform mobile application empowers educators to effortlessly capture real-time facial images during class, marking the commencement of the automated attendance process. The captured images then undergo a sophisticated series of processing steps to ensure accuracy and reliability in attendance tracking. The Retina Face algorithm, distinguished for its multi-scale and multi-task capabilities, meticulously performs facial detection, pinpointing landmarks and contours with precision. Following this, the Face Net deep neural network takes center stage, extracting intricate facial features and generating high-dimensional embeddings unique to each student's face. The facial embeddings are then fed into a Support Vector Machine (SVM) classifier, a robust machine learning algorithm, to learn patterns associated with each student's facial features.

This classification process, combined with fine-tuning through Keras, enhances the recognition capabilities of the system, contributing to its accuracy in diverse classroom scenarios. Recognized faces seamlessly move to the subsequent stage, where attendance data is logged securely. The system is not confined merely to local tracking; it seamlessly integrates with existing educational management systems, ensuring that attendance records are automatically updated. This integration reduces the burden on administrative tasks, allowing educators to concentrate more on their core responsibilities. The UI ensures a harmonious interaction with the system's functionalities, facilitating the integration of technological advancements into the daily routine of educators. Its simplicity masks the complexity of the underlying processes, streamlining the experience and allowing educators to focus on their primary responsibilities. Through the React Native UI, the system achieves a delicate balance between technological sophistication and user-friendliness, embodying a commitment to enhancing the educational environment through seamless and accessible solutions. In its entirety, this meticulously orchestrated implementation of the automated attendance system not only addresses the complexities of attendance tracking but also embodies a commitment to efficiency, accuracy, and a seamless integration of technology into the educational landscape.

RESULT AND EVALUATION**Quantitative Analysis**

The quantitative analysis of the "Automated Classroom Attendance System Using Image Processing" focuses on precision and recall metrics, providing a robust assessment of the system's accuracy. Precision refers to the proportion of correctly identified positive instances among all instances identified as positive, while recall, also



**Zankhana Shah et al.,**

known as sensitivity, measures the proportion of actual positive instances correctly identified by the system. In the context of facial recognition for attendance tracking, precision signifies the accuracy of the system in correctly identifying students present, while recall indicates the system's ability to capture the entirety of students who are indeed present. The precision rate of the system is about 95 % and recall rate is about 99 %. The precision rate and recall rate demonstrate the system's proficiency in accurately recognizing and recording students' attendance. These metrics were derived from a diverse and representative dataset, ensuring that the evaluation captures the system's performance across various facial appearances, lighting conditions, and classroom scenarios. The precision and recall rates accentuate the reliability of the system, providing a quantitative foundation for its effectiveness in real-world educational settings.

Comparative Analysis

A critical facet of the evaluation involves a comparative analysis between the automated attendance system and traditional manual methods. This comparative study aims to quantify the efficiency gains and advantages offered by the automated system in terms of time and accuracy. In a controlled experiment, both the automated system and traditional manual methods were employed simultaneously, allowing for a direct comparison. The results of the comparative analysis revealed a substantial reduction in the time required for attendance tracking when using the automated system. This reduction is attributed to the system's ability to swiftly and accurately identify students in real-time, eliminating the need for manual recording and cross-referencing. The time saved by the automated system contributes not only to increased efficiency in administrative tasks but also to an enhanced allocation of valuable instructional minutes for educators. Moreover, the comparative analysis extends beyond mere efficiency gains. It delves into the accuracy of attendance records, highlighting the system's capacity to minimize errors and discrepancies often associated with manual methods. The automated system's precision and recall rates outshine traditional approaches, affirming its superiority in generating reliable attendance data. In essence, the comparative analysis serves as a compelling demonstration of the tangible benefits brought about by the automated attendance system. It validates the system's potential to revolutionize attendance tracking by offering a more accurate, efficient, and time-saving alternative to traditional manual methods. The results of this analysis provide concrete evidence for the system's superiority, reinforcing its significance in the landscape of educational technology.

CHALLENGES**Challenge** Poor Lighting Conditions

Implication The system may face difficulties in accurately detecting and recognizing faces under suboptimal lighting conditions, such as low light or uneven illumination.

Challenge Obstructed Views and Occlusions

Implication Instances where students' faces are partially obstructed or occluded could pose challenges to accurate facial detection and recognition.

Challenge Diversity in Facial Appearances

Implication Ensuring the system's robustness in recognizing a diverse range of facial appearances, including variations in expressions, hairstyles, and accessories.

Challenge User Acceptance and Privacy Concern

Implication Ensuring user acceptance among educators and students, as well as addressing privacy concerns related to facial recognition technology.

Challenge Reliability in Dynamic Environments

Implication Ensuring the reliability of the system in dynamic classroom environments where students may move, change seating arrangements, or enter and exit the classroom during a session.



**Zankhana Shah et al.,**

DISCUSSION

In essence, the comparative analysis serves as a compelling demonstration of the tangible benefits brought about by the automated attendance system. It validates the system's potential to revolutionize attendance tracking by offering a more accurate, efficient, and time-saving alternative to traditional manual methods. The results of this analysis provide concrete evidence for the system's superiority, reinforcing its significance in the landscape of educational technology.

Technological Advancements and Educational Efficiency

The integration of advanced image processing and facial recognition technologies within the automated attendance system reflects a significant stride towards harnessing technological advancements for educational efficiency. The quantitative analysis, emphasizing precision and recall metrics, substantiates the system's technical prowess in accurately tracking student attendance. This technological leap not only streamlines administrative processes but also contributes to a more dynamic and responsive educational environment.

Efficiency Gains and Instructional Time

The comparative analysis with traditional manual methods highlights the substantial efficiency gains offered by the automated system. The time saved in attendance tracking, as evidenced by the controlled experiment, is a noteworthy outcome. This efficiency directly translates into a valuable resource for educators — time. By automating the attendance process, educators reclaim precious instructional minutes that would otherwise be spent on manual record-keeping. This not only aligns with the broader discourse on optimizing educational workflows but also underscores the potential for technology to enhance the teaching and learning experience.

User Experience and Acceptance

The user feedback component of the evaluation is instrumental in understanding the system's acceptance within the educational community. Educators' reports of increased efficiency and students' positive attitudes towards the non-intrusive nature of the system are indicative of a positive user experience. The React Native UI, designed for simplicity and accessibility, plays a crucial role in fostering this positive reception. The emphasis on user experience extends beyond mere functionality, recognizing the importance of technology seamlessly integrating into the daily routines of educators and students.

Ethical Considerations and Privacy Compliance

An integral part of the discussion revolves around the ethical considerations and privacy compliance inherent in the development and deployment of the automated attendance system. The commitment to obtaining informed consent during data collection, rigorous security measures, and regular privacy audits underscore a conscientious approach to data handling. As educational institutions increasingly leverage technology, these ethical considerations become paramount, shaping the responsible integration of innovative solutions into pedagogical practices.

Challenges and Iterative Refinement

Acknowledging the challenges and limitations identified during the evaluation phase is crucial for steering the system towards continual improvement. Challenges such as issues in poor lighting conditions or obstructed views provide valuable insights for iterative refinement. The commitment to addressing these challenges through ongoing updates and improvements reflects a dedication to the system's evolution in response to real-world complexities.

Future Implications and Research Directions

The positive outcomes and user acceptance pave the way for future implications and research directions. The success of the automated attendance system in real-world deployments positions it as a promising solution for educational institutions grappling with attendance tracking challenges. Future research could delve into refining image processing algorithms to enhance adaptability in diverse scenarios. Additionally, exploring the integration of





Zankhana Shah et al.,

emerging technologies, such as block chain, could further fortify data security and privacy measures. In conclusion, the discussion synthesizes the multifaceted aspects of the automated attendance system's impact on education. From technological advancements and efficiency gains to user experience and ethical considerations, the system navigates the intersection of technology and education with careful consideration. The positive outcomes underscore its potential as a transformative tool, offering a glimpse into a future where technology optimally supports educational processes while upholding ethical standards and user-centric design principles.

CONCLUSION

In conclusion, the "Automated Classroom Attendance System Using Image Processing" represents a significant stride towards leveraging technology for enhanced efficiency in educational settings. The robust quantitative analysis, emphasizing precision and recall metrics, attests to the system's capability in accurately tracking student attendance. This technological integration not only streamlines administrative processes but also contributes to a dynamic and responsive educational environment. The comparative analysis, showcasing substantial efficiency gains over traditional methods, underscores the system's potential to revolutionize attendance tracking. By automating the process, educators not only save valuable time but also reclaim instructional minutes that can be redirected towards more meaningful engagement with students. The positive user feedback further emphasizes the non-intrusive and user-friendly nature of the system, aligning with the broader discourse on user experience in educational technology. Ethical considerations and privacy compliance stand as pillars of the system's development and deployment. The commitment to informed consent during data collection and rigorous security measures reflects a responsible approach to technology integration in educational practices. Challenges identified, such as issues in varied lighting conditions, provide insights for iterative refinement, emphasizing a commitment to continual improvement. Looking forward, the success of the automated attendance system in real-world deployments holds promising implications for educational institutions seeking efficient and accurate attendance tracking solutions. Future research directions could explore refining image processing algorithms for enhanced adaptability and the integration of emerging technologies, such as block chain, for fortified data security and privacy measures. In essence, the automated attendance system exemplifies the intersection of technology and education, offering a glimpse into a future where innovative solutions optimize administrative processes while upholding ethical standards. Its positive outcomes and user acceptance position it as a transformative tool, paving the way for a more efficient, user-friendly, and secure educational landscape.

REFERENCES

1. Smitha, Pavithra S Hegde, Afshin. "Face Recognition based Attendance Management System." Department of Computer Science and Engineering, Yenepoya Institute of Technology.
2. Dhanush Gowda H.L, K Vishal, Keertiraj B. R, Neha Kumari Dubey, Pooja M. R. "Face Recognition based Attendance System."
3. Samridhi Dev; Tushar Patnaik. "Student Attendance System using Face Recognition."
4. Ghalib Al-Muhaidhri, Javeed Hussain. "Smart Attendance System using Face Recognition." Department of Electronics & Telecommunication Engineering.
5. Muhammad Haikal Mohd Kamil, Norliza Zaini, Lucyantie Mazalan & Afiq Harith Ahamad. "Online attendance system based on facial recognition with face mask detection." Multimedia Tools and Applications.
6. Thida Nyein; Aung Nway Oo. "University Classroom Attendance System Using Face Net and Support Vector Machine."
7. Fadhilah Moulita Andiani and Benfano Soewito. "Face Recognition for Work Attendance Using Multitask Convolutional Neural Network (MTCNN) and Pre-trained Face Net."
8. B Devi Prasad. "Automated Classroom Attendance System." 2022.
9. Prashant Tirlotkar, Kedar Chittrakathi, Rohit Jadhav, Aniket Khamkar, Prof. Manoj Mishra. "Smart Attendance System Using Image Processing."





Zankhana Shah et al.,

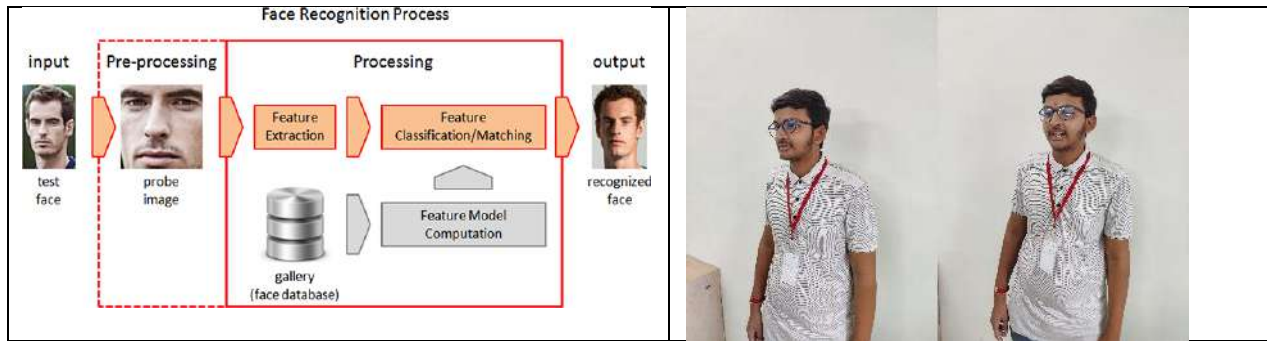


Figure1: Overview of Image Recognition

Figure 2: Image capturing through different angles



Fig. 3 Detection through ID number





Real-Time Cartoonization: Fusion of Computer Vision and Artistic Rendering in Python

Duttresh Sapra¹, Aadityasinh Jadeja¹, Bhavin Vhanesha¹ and Zankhana Shah²

¹Student at IT Department, BVM Engineering College, V.V. Nagar, Gujarat, India.

²Associate Professor at BVM Engineering College, V. V. Nagar, Gujarat, India.

Received: 30 Dec 2023

Revised: 09 Jan 2024

Accepted: 12 Jan 2024

*Address for Correspondence

Zankhana Shah

Associate Professor at BVM Engineering College,

V. V. Nagar, Gujarat, India.

Email: zankhana.shah@bvmengineering.ac.in



This is an Open Access Journal / article distributed under the terms of the **Creative Commons Attribution License** (CC BY-NC-ND 3.0) which permits unrestricted use, distribution, and reproduction in any medium, provided the original work is properly cited. All rights reserved.

ABSTRACT

This project endeavors to develop a real-time cartoonization application leveraging the capabilities of Python libraries such as Open CV and tkinter. The primary objective is to design and implement a functional pipeline for live image processing. The process includes the acquisition of live camera feed, facial detection algorithms, and the application of cartoonization filters to enhance the visual appearance of detected faces. This paper offers a comprehensive overview of the methodology employed, the technical implementation details, the observed results, and the derived conclusions derived from the developmental stages of this real-time cartoonization prototype.

Keywords: Real-time cartoonization, Facial detection, Image processing, Haar Cascade Classifier, Open CV

INTRODUCTION

The introduction section of this paper aims to delineate the core motivations and objectives underpinning the development of a real-time cartoonization prototype. It sheds light on the amalgamation of computer vision techniques and artistic rendering through image processing methodologies, particularly focusing on the utilization of OpenCV and tkinter libraries in Python. This section outlines the impetus behind the creation of a live image processing pipeline dedicated to capturing real-time camera feed, implementing facial detection algorithms, and applying cartoonization filters to augment the aesthetic appeal of recognized facial features[1]. The significance of this endeavor lies in the exploration of real-time image processing capabilities and the potential applications of such technology in diverse domains, elucidating its relevance and prospects for future advancements





Duttresh Sapra et al.,

BACKGROUND

Imagine a journey that begins with the fascination for transforming ordinary images or video frames into captivating cartoon-like representations in real-time. This enchanting process, often referred to as real-time images cartooning, merges the realms of computer vision and artistic rendering. Initially, this involved manually applying artistic filters and effects to digital images to create cartoon effects, typically driven by the artistic flair of creators. Over time, the quest for automated methods capable of simulating these artistic effects in real-time spurred advancements in image processing and computer vision technologies. This pursuit led to the development of algorithms that could replicate cartoon-like features, allowing instantaneous transformations of video streams or captured images into delightful and stylized cartoons. Image processing, a fundamental domain closely linked with real-time images cartooning, revolves around manipulating digital images using algorithms and techniques. It's the backbone of these transformations, facilitating alterations in visual appearances by enhancing quality, extracting information, or modifying characteristics dynamically[13]. Facial detection emerged as a vital component in the realm of real-time images cartooning, enabling the identification and recognition of human faces within images or video frames.

This technology evolved significantly, progressing from simple pattern recognition to sophisticated algorithms utilizing machine learning techniques. Notably, libraries and modules like `cv2.face` in Open CV have played a pivotal role in achieving accurate facial detection tasks[3]. Enter Open CV, the cornerstone of computer vision and image processing. Open CV stands out as a comprehensive library offering a rich suite of tools, functions, and modules dedicated to image and video processing. Functions like `cv2.stylization()` within Open CV have empowered developers to create cartoon-like effects effortlessly. These functions provide essential parameters such as `sigma_s`, allowing precise control over spatial smoothing and preserving image details while enhancing cartoonization. The implications of real-time images cartooning extend far and wide, finding applications across entertainment, video streaming, augmented reality, and artistic expression. Its remarkable ability to swiftly transform visual content into engaging, stylized formats has enhanced user experiences across various digital platforms, captivating audiences worldwide[2]. This collaborative evolution of real-time images cartooning, image processing techniques, facial detection algorithms, and the indispensable role of OpenCV have revolutionized the creation of captivating and visually compelling content. This journey has paved the way for innovative storytelling and effective communication in diverse digital landscapes.

METHODOLOGY

3.1 Live Image Capture: To capture live images, we utilized Open CV's Video Capture functionality, enabling access to video streams from various sources. This facilitated a continuous feed necessary for real-time processing. While Open CV simplifies this process, alternative approaches, like direct interfacing with hardware or using platform-specific APIs, were considered. However, due to cross-platform support and ease of use, Video Capture emerged as the optimal choice. 3.2 Facial Detection Algorithm: Facial detection algorithms play a pivotal role in accurately identifying and delineating facial features within images or video frames. In our pursuit of selecting the most suitable algorithm for real-time facial detection, we extensively evaluated three prominent approaches: the Haar Cascade Classifier, Histogram of Oriented Gradients (HOG), and Convolutional Neural Networks (CNNs)[2][6]. The Haar Cascade Classifier is an established method, popularized by its effectiveness in detecting objects, especially faces, within images. It operates by analyzing Haar-like features at various image locations and scales. While efficient in terms of computational speed, the Haar Cascade Classifier may struggle with variations in lighting conditions, facial orientations, and complex backgrounds. Despite these limitations, its relatively low computational demands and satisfactory accuracy make it a compelling choice for real-time applications[4][5]. On the other hand, Histogram of Oriented Gradients (HOG) is a robust algorithm known for its capability to capture local object appearance and shape by computing gradient histograms[10]. While HOG provides robustness against lighting variations and occlusions, its computational requirements are comparatively higher than the Haar Cascade Classifier. This increased computational complexity might hinder real-time performance, making it less suitable for our specific real-





Duttresh Sapra et al.,

time cartoonization application. Convolutional Neural Networks (CNNs) excel in facial feature detection due to their ability to learn hierarchical representations directly from data. They demonstrate exceptional accuracy but often demand substantial amounts of training data and computational resources. Despite their impressive performance, the overhead involved in training CNNs and their computational demands make them less practical for real-time applications without compromising on hardware or time constraints[9]. The Comparison matrix indicates that while Convolutional Neural Networks (CNNs) exhibit the highest accuracy and robustness, they require more computational resources, leading to increased processing time[9]. On the other hand, the Haar Cascade Classifier offers a balance between acceptable accuracy, real-time computational performance, and moderate robustness. The Histogram of Gradients (HOG) stands as a middle ground between accuracy, computation time, and robustness among the evaluated methods[10]. Considering the specific context of a real-time cartoonization application, the Haar Cascade Classifier emerges as an optimal choice. Its balanced attributes align well with the requirements of real-time processing, ensuring both acceptable accuracy and computational efficiency.

The Haar Cascade Classifier showcases commendable performance by efficiently detecting faces in diverse conditions while maintaining a real-time processing speed, making it well-suited for applications demanding a balance between accuracy and computational resources[8]. By integrating these methodologies cohesively, our real-time cartoonization application achieved consistent, accurate, and visually appealing results, emphasizing the efficiency and effectiveness of our implemented approach. Considering our real-time constraints, striking a balance between accuracy and computational efficiency became crucial. While CNNs offer superior accuracy, the Haar Cascade Classifier emerged as the optimal choice for our application due to its acceptable accuracy levels while maintaining real-time computational performance. Its ability to provide reasonably accurate facial detection within the constraints of computational resources and time made it the most pragmatic solution for our real-time cartoonization[9][10]. 3.3 Cartoonization Technique: Various cartoonization methods employ distinct algorithms like edge detection, color reduction, and texture simplification. During our evaluation, we focused on two main categories: Edge-preserving filters and stylization methods.

Edge-preserving filters, such as the Bilateral Filter, aim to retain structural details while simplifying textures. The Bilateral Filter accomplishes this by smoothing images while preserving edges, preventing over smoothing and maintaining essential features. This algorithm is effective in preserving sharp edges and fine details, contributing to the cartoonization process[12]. On the other hand, stylization methods, like non-photorealistic rendering (NPR) algorithms, emphasize artistic effects by transforming images into stylized representations. NPR algorithms often involve techniques to simulate artistic styles and enhance visual appeal, creating effects resembling hand-drawn or painted artworks[11]. In our approach, we adopted a hybrid strategy by combining edge-preserving filters with stylization techniques. Specifically, we utilized bilateral filters to maintain edge details and employed adaptive thresholding to simplify textures. This fusion allowed us to strike a balance between preserving essential structural elements and emphasizing artistic effects, resulting in a more comprehensive and visually appealing cartoonization effect. 3.4 User Interface Development: In designing the user interface, we considered multiple frameworks like tkinter, PyQt, and Kivy. While each offered distinct advantages, tkinter's simplicity and native integration with Python made it more accessible for rapid prototyping and ease of implementation. PyQt, though more feature-rich, posed a steeper learning curve and added complexity. Kivy, while cross-platform and capable of creating dynamic UIs, was deemed slightly less intuitive for our specific project requirements.

RESULT

4.1 Real-time Cartoonization Demonstration: This section substantiates the successful implementation of real-time cartoonization functionality applied to the live camera feed.[11] The presentation includes a comprehensive showcase of sample images or screenshots exemplifying the system's operational efficacy in capturing live frames, detecting human faces accurately, and subsequently applying the cartoonization effects to the identified facial regions. Methodology's Contribution to Results: Our methodology, meticulously designed and executed, played a



**Duttresh Sapra et al.,**

pivotal role in the realization of these demonstrative outcomes: 4.1.1 Live Image Capture: The utilization of Open CV's 'Video Capture' facilitated seamless acquisition of live frames from the camera source, ensuring a consistent and reliable feed for subsequent processing stages. This step ensured a continuous flow of images for real-time analysis and manipulation. Displays snapshots of actual frames captured in real-time, demonstrating the continuous acquisition of live images using Open CV's 'Video Capture'. 4.1.2 Facial Detection Algorithm: Leveraging the Haar Cascade Classifier within Open CV enabled accurate and efficient detection of human faces within the captured frames. The integration of this algorithm ensured precise identification and delineation of facial regions for further processing. Showcases images or figures highlighting the accurate detection of human faces within the captured frames. These visuals demonstrate the precise identification achieved through the Haar Cascade Classifier. 4.1.3 Cartoonization Technique: The application of the 'cv2.stylization()' function on the identified facial regions transformed the detected faces into cartoon-like representations. Our choice of this specific image processing technique within Open CV allowed us to impart artistic effects while retaining the essential facial features[12][13]. Presents images or screenshots portraying the transformed facial features after the application of the cartoonization filter. This output underscores the successful implementation of the 'cv2.stylization()' function, showcasing the artistic effects applied to the detected faces.

FUTURE WORK

Our study successfully demonstrated real-time cartoonization capabilities leveraging the Haar Cascade Classifier. Building upon this achievement, several avenues exist for future exploration and enhancements in this domain. 5.1 Real-time Performance Enhancement: While our current implementation meets real-time processing requirements, there remains an opportunity to further optimize performance. Investigating more efficient algorithms or refining existing ones to accommodate diverse environmental factors, such as varying lighting conditions or complex backgrounds, could significantly boost processing speed without compromising accuracy. 5.2 Advancements in Robustness and Precision: Augmenting the robustness of facial detection algorithms, especially in challenging scenarios, presents an area for improvement. Integrating advanced deep learning techniques, like Convolutional Neural Networks (CNNs), could enhance precision, particularly in recognizing diverse face orientations, occlusions, or subtle facial expressions. Such advancements aim to bolster the reliability and adaptability of facial detection algorithms in varied conditions. 5.3 User Interface Refinement and Interaction: Refining the graphical user interface (GUI) to improve usability and engagement remains a focal point for future enhancements.

Continuously enhancing the GUI by incorporating user feedback and adhering to user-centered design principles will ensure an intuitive and seamless user experience, ultimately enhancing the overall appeal and accessibility of the system. 5.4 Adaptive Parameter Adjustment and Personalization: Developing mechanisms for automated adjustment of cartoonization parameters based on facial attributes and features could enable more personalized effects. Implementing algorithms capable of dynamically modifying parameters, such as line thickness or color saturation, according to facial characteristics, age, or gender, would augment adaptability and customization of the cartoonization process. 5.5 Contextual Understanding and Artistic Adaptation: Exploring advancements beyond facial recognition to encompass semantic understanding of scenes could significantly enrich the cartoonization process. Integrating context-based adaptations that consider elements like objects, backgrounds, and lighting conditions will elevate the artistic rendering of live video streams, creating more visually appealing and contextually relevant cartoon effects.

CONCLUSION

The development of our real-time cartoonization application using Python libraries, especially Open CV and tkinter, has successfully showcased the effectiveness and accuracy of our methodologies. By integrating Open CV's 'Video Capture' for live image acquisition, employing the Haar Cascade Classifier for precise facial detection, utilizing 'cv2.stylization()' for cartoonization, and implementing tkinter for a user-friendly interface, we achieved consistent,





Duttresh Sapra *et al.*,

visually appealing results[2]. Our methodology laid a strong foundation for further advancements in computer vision and artistic image manipulation[13]. The amalgamation of these techniques not only demonstrated the feasibility of real-time cartoonization but also highlighted its potential applications in entertainment, augmented reality, and artistic expression. The success of our approach underscores the robustness and effectiveness of our methods, offering a pathway for continued exploration and utilization of real-time cartoonization technology across diverse domains.

REFERENCES

1. S. Wang and J. Qi, "A Novel Image Cartoonization Algorithm without Deep Learning," CIBDA 2022; 3rd International Conference on Computer Information and Big Data Applications, Wuhan, China, 2022, pp. 1-4.
2. A. B. Patankar, P. A. Kubde and A. Karia, "Image cartoonization methods," 2016 International Conference on Computing Communication Control and automation (ICCUBEA), Pune, India, 2016, pp. 1-7.
3. M. Khan, S. Chakraborty, R. Astya and S. Khepra, "Face Detection and Recognition Using OpenCV," 2019 International Conference on Computing, Communication, and Intelligent Systems (ICCCIS), Greater Noida, India, 2019, pp. 116-119.
4. Pandey, Anurag and Choudhary, Divyansh and Agarwal, Ritik and Shrivastava, Tushar and Kriti, Face detection using Haar cascade classifier (July 14, 2022). Proceedings of the Advancement in Electronics & Communication Engineering 2022.
5. Mehtab, Sidra & Sen, Jaydip. (2020). Face Detection Using OpenCV and Haar Cascades Classifiers.
6. B. M. Hasan Alhafidh, R. M. Hagem and A. I. Daood, "Face Detection and Recognition Techniques Analysis," 2022 International Conference on Computer Science and Software Engineering (CSASE), Duhok, Iraq, 2022, pp. 265-270.
7. Goyal, Kruti & Agarwal, Kartikey & Kumar, Rishi. (2017). Face detection and tracking: Using OpenCV. 474-478.
8. L. Cuimei, Q. Zhiliang, J. Nan and W. Jianhua, "Human face detection algorithm via Haar cascade classifier combined with three additional classifiers," 2017 13th IEEE International Conference on Electronic Measurement & Instruments (ICEMI), Yangzhou, China, 2017, pp. 483-487.
9. R. Andrie Asmara, M. Ridwan and G. Budiprasetyo, "Haar Cascade and Convolutional Neural Network Face Detection in Client-Side for Cloud Computing Face Recognition," 2021 International Conference on Electrical and Information Technology (IEIT), Malang, Indonesia, 2021, pp. 1-5.
10. C Rahmad, R A Asmara, D R H Putra, I Dharma, H Darmono and I Muhiqqin, "Comparison of Viola-Jones Haar Cascade Classifier and Histogram of Oriented Gradients (HOG) for face detection" IOP Conference Series: Materials Science and Engineering, Volume 732, The 1st Annual Technology, Applied Science, and Engineering Conference 29–30 August 2019, East Java, Indonesia.
11. V. Sudarshan and A. Singh, "Cartooning an Image Using Opencv and Python", Google Scholar, 2020.
12. S. Kumar, U. Bhardwaj and T. Poongodi, "Cartoonify an Image using Open CV in Python," 2022 3rd International Conference on Intelligent Engineering and Management (ICIEM), London, United Kingdom, 2022, pp. 952-955.
13. M. Marengoni and D. Stringhini, "High Level Computer Vision Using OpenCV," 2011 24th SIBGRAPI Conference on Graphics, Patterns, and Images Tutorials, Alagoas, Brazil, 2011, pp. 11-24.

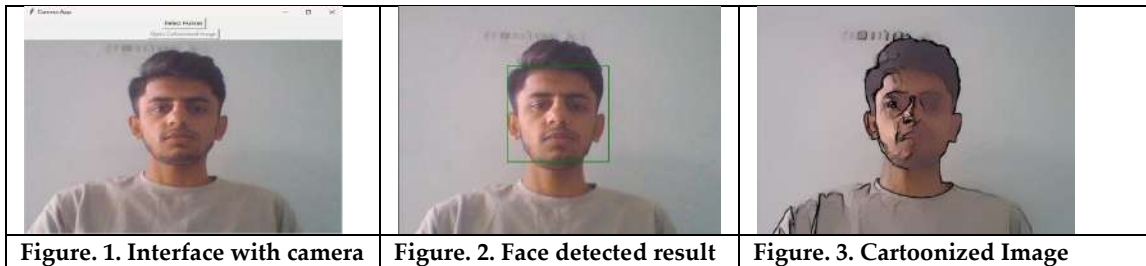




Duttresh Sapra et al.,

Table. 1. Facial Detection Method Comparison Matrix

Method	Accuracy (%)	Computation Time (ms)	Robustness
Haar Cascade Classifier	89	12	Moderate
Histogram of Gradients	92	18	High
Convoluti-onal Neural Networks	95	25	Highest





Sustainability and Urban Development: An In-depth Study of Self-Sustainable Integrated Townships for Rajkot

Sohil Badi^{1*}, JagrutiShah² and Indrajit Patel³

¹Management Trainee, Riviera Infra project Limited, Mundra, Gujarat, India.

²Assistant Professor, Department of Structural Engineering, B.V.M Engineering College, Vallabh Vidyanagar, Gujarat, India.

³Professor, Department of Structural Engineering, B.V.M Engineering College, Vallabh Vidyanagar, Gujarat, India.

Received: 30 Dec 2023

Revised: 09 Jan 2024

Accepted: 12 Jan 2024

*Address for Correspondence

Sohil Badi

Management Trainee,

Riviera Infra project Limited,

Mundra, Gujarat, India,

Email: badisohil2@gmail.com



This is an Open Access Journal / article distributed under the terms of the **Creative Commons Attribution License** (CC BY-NC-ND 3.0) which permits unrestricted use, distribution, and reproduction in any medium, provided the original work is properly cited. All rights reserved.

ABSTRACT

The rapid urbanization driven by population growth and migration has heightened the demand for innovative urban planning and sustainable development. Over the past two decades, Rajkot has faced escalating infrastructure, environmental, and social challenges due to population migration. To tackle these issues, this research proposes establishing a Self-Sustainable Integrated Township within Rajkot. This visionary township integrates advanced technologies, green infrastructure, and community-driven initiatives, emphasizing eco-friendly architecture, energy efficiency, waste management, renewable energy, smart transportation, water conservation, and affordability. This study assesses the potential benefits and challenges of implementing the Self-Sustainable Integrated Township concept, considering Rajkot's unique characteristics. Through extensive data analysis and case studies, it evaluates the environmental, economic, and social impacts. The findings suggest that this township can reduce Rajkot's carbon footprint, enhance resource management, and improve residents' quality of life. Furthermore, by incorporating smart technologies and sustainable practices, it can attract investments, driving economic growth and setting a precedent for other rapidly expanding cities. Ultimately, the township's primary goal is to divert city migration, offering affordable housing, safety, a sustainable environment, and reducing the social impact on Rajkot. This initiative provides a path for Rajkot's sustainable development and could serve as a blueprint for other rapidly growing cities, fostering a greener, more resilient, affordable, and socially inclusive future.

Keywords: Self-Sustainable, Integrated Township, Affordability, Township Planning, Migration



**Sohil Badiet al.,**

INTRODUCTION

India, one of the world's fastest-growing economies, faces a significant demographic shift. With the largest rural population globally at approximately 857 million, this trend is changing as urban areas expect a population increase. By 2050, nearly half of India's total population will reside in cities, up from one-third currently. However, urbanization in India is grappling with unique challenges such as compact urban forms, low-rise development, and resource scarcity. Cities are expanding without systematic planning, leading to unplanned suburbs. Urbanization is driven by employment opportunities, improved facilities like education and healthcare, and a better quality of life compared to rural areas. It's crucial in alleviating population pressure and absorbing the growing rural workforce. Nevertheless, uncontrolled urbanization can have adverse effects on surrounding agricultural areas. Integrated townships are emerging as a sustainable solution to manage the rapid pace of urbanization. By focusing on planned and self-sufficient urban developments, they can help address the challenges associated with India's ongoing urban transition. During the 20th century, India's urban population grew more than tenfold. Projections indicate that the urban population will reach 535 million by 2026, marking significant urbanization in the early 21st century as in figure 1. Population is moving from rural area to urban area because of the adequate employment opportunities in urban areas. In a rural area most of the landless laborers and sub-marginal cultivators who constitute the great majority of the migrants to the town, live in huts and similar very modest dwellings. This demographic transformation poses both opportunities and challenges for India as it seeks to balance urban development with sustainable practices and resource management.

Concept of Integrated Township

An integrated township can be defined as combined clusters of housing, commercial business, education, and health-care facilities with the related physical infrastructure of water, sewage, roads, and power. Traditional Indian cities are facing typical problems, namely urban sprawl, affordable housing shortage, access to public transport, and lack of equitable access to basic services that adversely impact productivity, mobility, and quality of urban life. At the same time, integrated townships with minimal land area, multiple housing, employment opportunities, open areas, and associated infrastructure can be the possible solution to prevent accelerating urbanization. The basic core of any city is examined through supporting physical and social infrastructure, recreational facilities, and economic generation ability. Integrated townships are conceptualized to the economic, infrastructure, and geographic needs of sprawling metropolitan cities. The objective of integrated townships is the creation of self-sustained and integrated urban settlements by having planned communities, social infrastructure, and lifestyle amenities in the same place. Building a planned community that contains heterogeneous housing options with lower rents and workplaces within short distances offers high productivity at work with a low cost of living and better lifestyle. Furthermore, a planned community has access to social infrastructure such as hospitals, schools, and educational institutes, offering high literacy rates and better healthcare facilities. Residents working, living, and relaxing within a particular area will make urban spaces efficient and sustainable.

NEED OF THE STUDY

Increasing of urbanization affects the development of city area and increases the cost of the land in city area that's why self-sustainable integrated township will help to proper control on future expansion. In the city due to population increase, the cost of the land increases that's why living expenses are also increased at that time. That's why at that time with a proper planning nearest area of the city all the amenities of living with transportation which join the city area with taken care of sustainability will be a greater option it will reduce cost and be helpful for population. Self-integrated township concept is help to reach all the need of population and overall cost of the amenities will be provided at minimal cost. Self-integrated township will increase living, decrease the cost of land, improve sustainability of area and maintenance of the overall development reduced.

OBJECTIVE

Objective was to study existing condition of Rajkot city in contain to sustainability. To analysis different existing

69290



**Sohil Badi et al.,**

township model of India. To propose model & guideline for self-sustainable integrated township. To layout different infrastructure resource planning for overall sustainable development of the township.

CASE STUDY

Magarpatta city

Magarpatta City, located near Pune, is an exemplary sustainable urban development. It spans 430 acres, formerly owned by 120 farmer families in Hadapsar village. Notably, it's exempt from the Urban Land (Ceiling, Regulation) Act of 1976 and approved by Pune Municipal Corporation and the Department of Urban Development, Government of Maharashtra. Approximately 120 acres are preserved as green cover, fostering natural ecology. Sustainable practices include rainwater harvesting from terraces and artificial lakes, recycling wastewater for gardens and cooling, and using rooftop solar water-heating systems to reduce electricity consumption. Waste management involves segregating 400 tons of waste monthly, with 280 tons used for vermin composting. A biogas plant utilizes biodegradable waste to generate non-polluting biogas for power generation. Fly ash bricks, replacing cement, reduce CO₂ emissions. Magarpatta City will consume 130,000 tons of fly ash, saving a significant carbon footprint. Moreover, it boasts one of India's largest residential solar water-heating systems, catering to around 3,500 flats. This eco-friendly practice saves 37 KWH of power daily, equivalent to Rs. 3.9 crore yearly. Additionally, it offers family healthcare with a 200-bed multi-specialty hospital, ensuring the best medical services. Magarpatta City stands as a remarkable model of sustainable urban living and development.

Amanora Park

Amanora Park Township, located near Pune Airport, spans 400 acres in Hadapsar, Pune. Developed by the City Corporation Limited, it operates under the special township policy of the Government of Maharashtra. Notable features include Strategic Location: Situated on the Eastern Corridor near Magarpatta, it's a buzzing IT center. The township boasts a 26.6-meter-wide main road, bituminous roads, cycle tracks, and underground electrical cables for uninterrupted power supply. It ensures 24/7 water supply, a sewage treatment plant, and the availability of Piped Natural Gas (PNG), contributing to a clean and eco-friendly environment. A 150-bed multi-specialty hospital and educational facilities are conveniently located within the town ship. A data center and smart card-based systems promote digital living and efficient services. The township features a 26-acre garden with fountains, a 2.5-acre lake, and a "Temple of Environment" to emphasize environmental preservation. Amanora incorporates sustainable practices like rainwater harvesting, water treatment, sewage treatment, use of renewable resources for lighting, motion-sensing light features, and more. Additional amenities include a commercial complex, Amanora Club, 24-hour fire station, internal eco-friendly bus transportation, a post office, police station, and a library. With a 999-year lease, Amanora Park Township prioritizes easy maintenance, ensuring a high quality of life for its residents.

PLANNING PROPOSAL

It is proposed to be prepared for a selected area which is existing in fastest growing city. The land of township in Rajkot District. Total area of township is 51.2 hector. Total expected population is around 10,000. Proposed site location and proposal is shown in Figure 1. The detailed calculation along with migration rate have been given in table 1 to 7.

SUSTAINABILITY ASPECT

From the Table 7, it is analyzed that how sustainable material will affect on cost of any infrastructure and comparison with non- sustainable easily available material in market.

RECOMMENDATION

Develop a comprehensive plan that integrates residential, commercial, and recreational areas. Ensure efficient land use and transportation systems to reduce resource consumption and emissions Implement resource-efficient technologies such as rainwater harvesting, solar power, and waste recycling to reduce dependence on external





Sohil Badi et al.,

resources. Incorporate green spaces, parks, and gardens to enhance the urban environment and promote biodiversity. This contributes to improved air quality and overall well-being. Encourage community participation in decision-making processes and sustainable practices. This fosters a sense of ownership and responsibility among residents. Develop pedestrian-friendly infrastructure and promote non-motorized transportation options like cycling and walking.

CONCLUSION

This township is help to 10,000 people to get better amities with affordable houses. 10% of migrate people burden will reduce by this township. Township provide 20% house hold work opportunities in the township at commercial place or in other infrastructure like sewage treatment plant or in education facilities. A self-sustainable township is a town or a city that is designed to minimize its environmental impact and ensure a resilient habitat for its inhabitants. It aims to balance social, economic, and ecological aspects of urban living, while preserving the resources for future generations. Self-sustainable township provides all the amenities at on place to solve travelling cost and control city over population of Rajkot city. This township helps to achieve Energy efficient by 25-35%. Artificial intelligent tools help to reduce energy efficient 10% in semi-public and public building. Sustainable material helps to reduce 12%-18% cost at long time of period. This township helps to buy affordable house of Rajkot district people and with benefit of all municipal service outside of Rajkot and reduce Burdon of RMC. This township concept is help to improve environment of township outside of Rajkot municipal corporation and beneficial to sustainable and reduce burden 10% from RMC. Self-sustainable township reduces overall cost of township at long period with help of their unique features and provide affordable housing with all amenities in township. This township reduces uneven development around Rajkot city and also help to reduce slump nearby area. Efficient waste management systems, such as composting, recycling, and biogas production, to reduce landfill and pollution. Water conservation and management systems, such as rainwater harvesting, grey water reuse, and wastewater treatment, to reduce water scarcity and contamination. Sustainable transportation systems, such as public transit, cycling, and walking, to reduce traffic congestion and air pollution. Mixed land use and compact urban design, to provide diverse and accessible amenities and services, such as housing, education, health care, recreation, and employment. Social infrastructure and community engagement, to foster social cohesion, cultural diversity, civic participation, and quality of life.

REFERENCES

1. A Johny, K Jagadeesan B Arthi Development of self-sustainable township / Vol. 8, Issue 8, August 2019
2. Amit Ashok Hasape, Prof. Satish S. Deshmukh "Comparative evaluation of integrated townships" / Volume: 2 Issue-3 2016
3. Anutosh Das 'Urban planning, information technology and artificial intelligence: the theory of evolution' / 2020
4. Cheng Ma a, *, Ying Jiang b, Kang Qi 'Investigating the urbane rural integrated town development strategy on the basis of the study of rural forms in Nantong, China' / 2014
5. Crisbin Joseph Mathew, Nithin K 'Planning, analysis and design of advanced township at Thodupuzha in Kerala' / Volume 9 Issue XII – 2021
6. Jinal Hasmukhbhai Patel1, Zarana H. Gandhi2 "A review on self-sustainable integrated township / Volume: 06 Issue: 12 | Dec 2019
7. Krishna S. Deokule, Priti P. Patil 'Design A smart township near Nasik city' / Volume:7 Issue 1 – 2018
8. Shashank Singh, Tarun Sharma, Pankaj Bande" Design and implementation of integrated smart township" / Volume 11: Issue 2 – 2016
9. Nallathiga R., Tewari K., Saboo A., Varghese S 'From satellite townships to smart townships: evolution of township development in Pune, India' / volume 7: Issue 2021
10. Sumit Kumar*, Venkatesh Reddy 'Integrated water and waste water management for a township' / Vol. 8: Issue 8 – 2015





Sohil Badi et al.,

11. Parekh Meetkumar Vijaykumar, Baraiya Piyush Pareshbhai 'sustainable township: A modern need to city' / Volume: 07 Issue: 06 – 2020
12. U Vimal Kumar, J S Pavithraa, K Sakthi Prasanth 'Development of the sustainable urbanized township' / Volume: 05 Issue: 04 – 2018
13. Venkatesh Dutta, Vivek Kumar Tiwari 'Environmental impact assessment of housing colonies in Lucknowcity, India with special reference to land capability and spatial development using AHP and GIS' / Volume: 2 Issue-3 – 2015
14. Conroy, Maria Manta, Jun, Hee Jung 'Planning process influences on sustainability in Ohio township plans / Volume:3 Issue-4 – 2016
15. Surya Vamsi P, Satya 'Green Leaf Township Planning-An Over View' / volume:3 Issue-6 -2018
16. Khanna, Neeti, Sharma, Anmol 'Assessing Urban Open spaces in Township Planning' / volume:1 Issue-8 – 2022
17. Sharma, Anmol, Hu, Changling, Hu, Changling 'Contribution of Infrastructure to the Township's Sustainable Development in Southwest China' / Volume:12 – 2022
18. Shanmathi G, 'Smart Integrated Township' / Volume:9 Issue-12 – 2021
19. Saroop S And AllopiD 'creating eco efficient township infrastructure projects with the use of green engineering solutions and sustainability criteria'
20. Rai, Pallavi Tak 'Townships for sustainable cities' / Volume:3 Issue-23 – 2012
21. Nallathiga, Ramakrishna, Tewari, Khyati 'Evolution of Satellite township development in Pune: A Case Study An assessment of infrastructure performance of Indian states View project Land use regulation impacts on cities and land markets View project' / 2015
22. Hafizyar, Mozhdah, Arsallan, Ahmad Rasa 'Smart and Sustainable Township: An Overview' – 2011
23. Mir Sayed Shah Danish1, *, Najib Rahman Sabory1, Ahmad Murtaza Ershad 'Sustainable Architecture and Urban Planning trough Exploitation of Renewable Energy' / Volume:2 Issue7- 2017

Table 1: Migration rate in selected study area of Rajkot

Year	Population					
	Bedi	Guaridad	Ratanpar	Hadmatiya	Khorana	Maliyasan
2031	1589	4427	2176	6305	2538	6264
2021	1319	4088	1799	4794	2346	4886
2011	1049	3749	1422	3283	2154	3508
2001	1189	3428	1366	3321	1965	2735
1991	1861	2732	1045	1772	1962	2130

Table 2: Category of different household

Sr. No	Particular	Participation %	Population	Number of Household
1	HMIG	15	1500	375
2	MIG	35	3500	875
3	LMIG	20	2000	400
4	LIG	20	2000	400
5	EWS	10	1000	167
Total		100	10000	2217





Sohil Badi et al.,

Table 3: Neighborhood House category Distribution

Particulars	HMIG	MIG	LMIG	LIG	EWS
	15 %	35 %	20 %	20 %	10 %
Population.	1350	3500	2000	2000	1000
No. of units.	375	875	400	400	167
Unit Types	-	-	-	-	-
(A) Row house	-	-	-	-	170 Unit
(B) Apartments (G+3)	-	-	-	400 flats 25 units	
(C) Apartments up to (P+4)	-	-	400 flats 25 units	-	
(D) High-Rise(P+9)	-	900 flats 25 units	-	-	
(E) Duplex	375 unit	-	-	-	

Table 4: Residential Area Structure

Units	No. Of Units	Area Per Unit In sq. mt	Total Area In sq. mt.
Duplex (G+1) (HMIG)	165	375	61875
Row house	170	170	28900
High-Rise Apartments (P+10)	25	1000	100000
Apartments up to (P+4)	25	738	73800
Apartments (G+3)	25	492	49200
TOTAL	410	2775	313775

Table 5 :Area Calculation in Hectare

Sr. No.	Particular	NH Area Distribution %	Area In Hectare
1	Residential including area under flats, incidental open spaces, pathways and access ways	61	31.2
2	Roads and streets excluding pathways and access ways	13	6.65
3	Public and semi – public facilities (schools)	11	5.63
4	Organized open spaces (tot – lots)	12	6.14
5	Shopping and community buildings	3	1.53
	TOTAL	100	51.2

Table 6: Total Construction Cost of Township

Unit Type	Cost In Crores
Road	3.39
Water Supply	2.05
Common Plot	4.2
Gas Line	4.57
STP	1.46
Pond	0.342
Commercial	10.04





Sohil Badi et al.,

Public Semi	14.21
Educational	4.41
Drainage	1.88
Land Cost (As Per Govt.)	500
Total	725.132

Table 7: Sustainable alternatives

Name of Material	Regular Material Price	Sustainable Material Price	Price Increase	Price Decrease
Brick	8 Per piece	10	25%	-
Cement	380 Per bag	360	-	5.26%
Paver block	30 Per piece	22	-	26.67%
Street Light pole	12000 Per Pole	21000	75%	-
Concrete	3800 Meter cube	4500	18.42%	-
Bituminous road	3500 sq. Meter	2800	-	20%



Graph 1: showing urbanization growth during 1951 to 2026 possibility based on data



Figure 1: Proposed site and Plan





Degradation of RB5 using Graphene Materials

Rocky Desai¹, Dr. Snehal popli², Shailesh Pal³ and Krunali Patel³

¹Ph.D Scholar, Civil Engineering Department C.V.M University, V.V. Nagar, Gujarat, India.

²Assistant Professor & Head Civil Engineering Department, G. H. Patel College of Engineering & Technology, V.V. Nagar, Gujrat, India.

³Ph.D Scholar, Civil Engineering Department C.V.M University, V.V. Nagar, Gujarat, India.

Received: 30 Dec 2023

Revised: 09 Jan 2024

Accepted: 12 Jan 2024

*Address for Correspondence

Rocky Desai

Ph.D Scholar,

Civil Engineering Department

C.V.M University,

V.V. Nagar, Gujarat, India.

Email: rocky.desai23@gmail.com



This is an Open Access Journal / article distributed under the terms of the **Creative Commons Attribution License** (CC BY-NC-ND 3.0) which permits unrestricted use, distribution, and reproduction in any medium, provided the original work is properly cited. All rights reserved.

ABSTRACT

Water is very essential part of the human life as it suffices the various needs of human activities. Due chemical industry sector rise, the effluent generated from the chemical industry is become imperative to treat. Graphene based adsorption process is a economical & advance treatment to treat the chemical industrial wastewater. Due to the modernization a higher stabilized dye effluent is very difficult to treat with the conventional biological treatment. Also chemical treatment generates huge quantity of sludge, which increases the pollution load. Graphene based material is very innovative technique to remove the dye from the effluent. This research paper investigates the removal of the Reactive Black – 5 (RB5) dye from the synthetic wastewater. The various operational parameters were studied such as dye concentration, graphene dose & time. It gives the highest dye removal were obtain of 99.20% with using the 0.5 mg/L graphene by providing the reaction time of 01 hour & dye concentration was 50 ppm.

Keywords: Reactive Black – 5 (RB5), Graphene, dye, adsorption, pollution load, synthetic wastewater

INTRODUCTION

Industrial waste streams containing dyes/colourants are of serious environmental concerns. According to the World Bank estimations 17-20% of industrial water pollution come from textile and dyeing industries [1]. Dyes are synthetic organic compound capable of colouring fabrics typically derived from coal tar and petroleum based products. There are more than 10,000 dyes used in textile industry and 280,000 ton of dyes are discharged every year world wide [2]. Wastewater from printing and dyeing units is often rich I colour, containing residues of reactive dyes and chemicals, such as complex components, many aerosols, high COD and BOD concentration as well as much more hard to degrade materials [3]. Dye wastewater effluent may lead to environmental problem such as eutrophication in



**Rocky Desai et al.,**

receiving water bodies and environmental concerns about the possible toxicity and carcinogenicity of some organic dyes. Dyes also decrease light penetration and photosynthetic activity, causing low dissolved oxygen in water bodies [4,5]. Reactive Black 5 (RB5) is an economical azo dye widely utilized in different industries including the production of papers, textile colours, leathers, carpets, cosmetics, plastic, ink, shoes polish, electroplating and mineral processing [6]. As a consequence, wastewater of these industries is highly polluted with this teratogenic, mutagenic and carcinogenic dye and the discharge of this effluent is the main way of RB5 release to the environment [7]. It is very important to remove the RB5 from the effluent. Many methods have been used such as biological, physical and chemical treatment of dye containing wastewater. Among these treatment techniques activated sludge, flocculation and adsorption are the most commonly applied methods [8]. In these research paper we have been studied about the degradation of RB5 using the adsorption process with using graphene material. Various wastewater treatment methods are currently employed, and with recent technological advancements, graphene material emerges as a promising solution for efficiently removing heavy metals from effluents. Adsorption, recognized as one of the most effective techniques for removing diverse pollutants, both inorganic and organic, finds a valuable ally in graphene—a two-dimensional nanomaterial composed of a single-atom graphite layer. Graphene's unique physico-chemical properties have garnered significant interest in applications such as wastewater treatment, enabling the removal of heavy metals and dyes such as Hg, Zn, Cd, Pb, Fe, Ag, Mn, Co, Cr, Ni, As, and others [9]. Addressing the need to eliminate dye from industrial wastewater, this research paper focuses on the removal of Azo Dye Reactive Black -5B (RB5) from synthetic effluent through various experiments utilizing graphene material. The overarching goal is to contribute to innovative and effective strategies for wastewater treatment, emphasizing the significance of graphene in addressing environmental challenges.

Reactive Black -5B (RB5) dye

In this experiment, the Reactive Black – 5B (RB5) dye was taken from the M/s. Palash Dye chem. Located at Vatva GIDC, Ahmedabad, Gujarat, India. It is the chemical manufacturing unit, which is very famous for various types of dye manufacturing.

Graphene material

The graphene material was taken from the M/s. Carborundum Universal Limited located at Plot – 18, CSEZ, Kochi 37. The quality certificate is as per below.

Preparation of synthetic dye wastewater

1.0 gm of the Reactive Black -5B (RB5) was taken in the volumetric flask. Then make up with the double distilled water upto 1000 ml. Then mix it well on the magnetic stirrer for 15 minutes. Thus 1000 ppm of Reactive Black -5B synthetic dye wastewater prepared. Take the sample of 05 ppm, 10 ppm, 15 ppm, 20 ppm, 25 ppm, 30 ppm, 35 ppm, 40 ppm, 45 ppm, 50 ppm from the 1000 ppm stock solution. Then take the absorption at 590 nm. From the absorption value prepare the calibration curve. The calibration curve is as per below. Then various sample of the Reactive Black -5B stock solution of 1000 ppm has been taken & then various dosages of graphene has been added to the taken solution. Also various time interval has been applied to the sample to find out the optimum time. The result will be discussed further in this research paper for various experiment.

Varying the concentration of the Reactive Black -5B dye

Different sample of Reactive Black – 5B solution of 05 ppm, 10 ppm, 20 ppm, 30 ppm & 50 ppm from the stock solution of 1000 ppm of the Reactive Black -5B (RB5) has been taken. Absorption of each sample has been obtained at the 590 nm in the spectrometer. Then 0.05 gm of graphene powder has been added to the 05 ppm solution of RB5. Then sample has been kept on the magnetic stirrer for the 15 minutes for the reaction to occur. Then sample passed through the filter paper & absorption of the treated solution has been taken at 590 nm. This experiment has been done to the 10 ppm, 20 ppm, 30 ppm & 50 ppm solution of the Reactive Black -5B (RB5) solution. The result & discussion is done further.



Rocky Desai *et al.*,**Finding the removal efficiency using filter & not using the filter**

02 sample of 100ml solution of 10 ppm of solution of Reactive Black – 5B (RB5) has been taken. Then add the 0.05 gm graphene in both the sample & put it onto the magnetic stirrer for the 15 minutes for reaction to occur. Then filter the 01 sample & take the absorption of that sample at 590 nm. Then absorption of the another sample has been taken at 590 nm without filtration. Then both the sample were compared.

Find out the optimum Timer

1. Take the 5 sample of 50ppm solution of 100 ml from the 1000 ppm stock solution of the Reactive Black -5B (RB5).
2. Add 0.05 gm graphene in each solution.
3. Put the 1st sample of 50 ppm on magnetic stirrer for 1 minutes. Then filter the sample & take the O.D at 590 nm.
4. Then take the 2nd sample of 50 ppm & put it on the magnetic stirrer for 02 minutes. Then filter the sample & take the O.D at 590 nm.
5. After that take the 3rd sample of 50 ppm & put it on the magnetic stirrer for 03 minutes. Then filter the sample & take the O.D at 590 nm.
6. Then take the 4th sample of 50 ppm solution & put it on the magnetic stirrer for 05 minutes. Then filter the effluent & take the O.D at 590 nm. The results are as per below

Find out the optimum dose of graphene

1. Take the 8 sample of the Reactive Black-SB effluent of 50 ppm of 100 ml from the 1000 ppm stock solution of Reactive Black -5B (RB5) solution..
2. Take the standard solution of the 50 ppm effluent as a blank & take O.D at the 590 nm.
3. Then add 05 mg graphene& add it in the 1st sample of 50 ppm effluent. Then put the solution on the magnetic stirrer for 01 hour time for reaction. Then filter the treated effluent with the filter paper. Then take the O.D of the filtered treated effluent at the 590 nm.
4. Add 10 mg graphene& add it in the 2nd sample of 50 ppm effluent. Then put the solution on the magnetic stirrer for 01 hour time for reaction. Then filter the treated effluent with the filter paper. Then take the O.D of the filtered treated effluent at the 590 nm.
5. Add 15 mg graphene& add it in the 3rd sample of 50 ppm effluent. Then put the solution on the magnetic stirrer for 01 hour time for reaction. Then filter the treated effluent with the filter paper. Then take the O.D of the filtered treated effluent at the 590 nm.
6. Add 20 mg graphene& add it in the 4th sample of 50 ppm effluent. Then put the solution on the magnetic stirrer for 01 hour time for reaction. Then filter the treated effluent with the filter paper. Then take the O.D of the filtered treated effluent at the 590 nm.
7. Add 30 mg graphene& add it in the 5th sample of 50 ppm effluent. Then put the solution on the magnetic stirrer for 01 hour time for reaction. Then filter the treated effluent with the filter paper. Then take the O.D of the filtered treated effluent at the 590 nm.

Add 40 mg graphene& add it in the 6th sample of 50 ppm effluent. Then put the solution on the magnetic stirrer for 01 hour time for reaction. Then filter the treated effluent with the filter paper. Then take the O.D of the filtered treated effluent at the 590 nm. The results were discussed further in this research paper.

RESULTS AND DISCUSSION

This research involves the removal efficiency of the Reactive Black -5B (RB5) dye from the synthetic effluent by varying the various parameters.

Effect of using varied e concentration of the Reactive Black -5B

Various concentration of Ractive Black-5B were taken & the treatment using the graphene were given. The results are as per below. This shows that by adding the 0.05 gm of graphene powder in the various solution of RB5 almost 90 % removal of the Reactive Black -5 (RB5) can be achieved. .



**Rocky Desai et al.,****Effect of using the filter**

02 samples were taken for the experiment. Both the samples were treated with the graphene. After treatment 1st sample was filtered & other sample was not filtered & then absorption of both the samples were taken. Then both the sample were compared. There is no difference in the removal efficiency of the Reactive Black – 5B (RB5) dye by using the filtration.

Find out the optimum Time

Various samples were taken for giving the treatment on various time interval. Then the results were obtained as per below. From the above result it reveals that at 03 minute of reaction time it removes the almost 81.29 % of the Reactive Black -5B(RB5) from the synthetic effluent.

Find out the optimum dose of graphene

1. Various graphene were used for the finding the optimum dose of the graphene the results are as per below.
2. The result proves that almost 79.59% of dye removed from the effluent by using 0.03 gm of graphene in 100 ml of dye effluent.

SUMMARY AND CONCLUSION

In this study various operational condition were studied to finding out the maximum removal efficiency of the Reactive Black 5B (RB5) from the synthetic effluent. The various conclusion is established from the study, which are as per below.

1. Graphene can remove almost 90% of the RB5 from the effluent with using the 0.05 gm of graphene in 100 ml of wastewater.
2. The study can shows that there is no deviation occurred by using the filter. Filter is used only to remove the graphene material from the effluent after the treatment occurred.
3. The optimum time for the graphene based treatment is 03 minutes in 100 ml of RB5 synthetic dye. It removes approx 81.29% of RB5 in 03 minutes of treatment time.
4. The study can conclude that the optimum dose of graphene is 0.03 gm in 100 ml of 50 ppm RB5 dye wastewater.

ACKNOWLEDGMENT

Rocky Desai is thankful to M/s. Carborundum Universal Limited located at Plot – 18, CSEZ, Kochi – 37 for providing the graphene for the research purpose..

REFERENCES

1. Sujata Mandal, S. Natrajan, "Adsorption and catalytic degradation of organic dyes in water using ZnO/Zn_xFe_{3-x}O₄ mixed oxides" Journal of Environmental Chemical Engineering, vol. JECE 634 1-9, 2015
2. Popli, Snehal A, Patel, Upendra D, " Resource recovery, water reuse and recycle for sustainable development Decolourization of Reactive Black 5 dye by direct electrochemical reduction in a divided cell batch reactor: Comparison of Different cathode materials", .
3. I W K Suryawan, Q Helny, S Notodarmojo, "Textile wastewater treatment: colour and COD removal of Reactive Black - 5 by ozonation", IOP Conference Series: Earth and Environmental Science, 2018, doi 10.1088/1755-1315/106/1/012102.
4. Fahmi C, and Rahmat N. 2010. Multi-stage Ozonation and Biological Treatment for Removal of azo dye industrial effluent. International Journal of Environmental Science and Development. 193-8.





Rocky Desai et al.,

5. Avsar Y, Kabuk H A, Kurt U, Cakmaki M, and Ozkaya B. 2012. Biological treatability rocesses of textile wastewater using electrocoagulation and ozonation. J. of Scientific and Industrial Research. 71: 496-500.
6. Sarvestani, Mohammad Reza Jalali, Doroudi, Zohreh " Removal of reactive black 5 from waste waters by adsorption: A comprehensive review", Journal of Water and Environmental Nanotechnology,2020, vol 5, issue 2, pp 180-190 doi. 10.22090/jwent.2020.02.008.
7. Aksu Z, Akın AB. Comparison of Remazol Black B biosorptive properties of live and treated activated sludge. Chemical Engineering Journal. 2010;165(1):184-93..
8. Bilinska L, Gmurek M, and Ledakowicz S. 2016. Comparison between Industrial and Simulated "Textile Wastewater Treatment by Aops – Biodegradability, Toxicity and Cost Assessment Chemical Engineering J. 306: 550-9.
9. Sugiana D, and Notodarmojo S. 2015. "A study of photocatalytic degradation mechanism of acid red 4 azo dye using TiO2 microparticle catalyst" Arena Tekstil. 30: 83-94
10. Ashori A, Hamzeh Y, Azadeh E, Izadyar S, Layeghi M, Mirfatahi Niaraki MS. Potential of Canola Stalk as Biosorbent for the Removal of Remazol Black B Reactive Dye from Aqueous Solutions. Journal of Wood Chemistry and Technology. 2012;32(4):328-41.
11. Munagapati VS, Yarramuthi V, Kim Y, Lee KM, Kim D-S. Removal of anionic dyes (Reactive Black 5 and Congo Red) from aqueous solutions using Banana Peel Powder as an adsorbent. Ecotoxicology and Environmental Safety. 2018;148:601-7.

Table 1. Chemical properties of Fly ash

Details	Unit	Test Result
Bulk Density	g/cc	0.006
Specific surface area	M ² /g	371.0
Batch No.	--	BJR021

Table 2. Removal efficiency of RB5 of various concentration of RB5

Sample	Absorption		Concentration (mg/lit)	
	Before adding graphene	After adding the graphene	Concentration (mg/lit)	
			Before adding graphene	After adding the graphene
5 ppm	0.141	0.006	4.40625	0.18750
10 ppm	0.293	0.027	9.15625	0.84375
20 ppm	0.587	0.009	18.3438	0.28125
30 ppm	0.835	0.003	26.0938	0.09375
50 ppm	1.400	0.004	43.7500	0.12500





Rocky Desai et al.,

Table 3. Removal efficiency in percentage

Sample	O.D at 590 nm	Concentration (mg/lit)	Removal (%)
0 minute	1.400	43.75	-
01 minute	0.297	9.28125	78.79 %
02 minute	0.296	9.25	78.85 %
03 minute	0.262	8.1875	81.29 %
05 minute	0.106	3.3125	92.43 %
10 minute	0.096	3.0	93.14 %

Table 4. Comparison of filtered effluent & without filtered effluent

Sample	O.D at 590 nm
Filtered effluent	0.244
Without filtered effluent	0.252

Table 5. Removal efficiency at different time interval

Sample	O.D at 590 nm	Concentration (mg/lit)	Removal (%)
Blank	1.544	48.25	-
1 st sample	1.252	39.125	18.91%
2 nd sample	1.029	32.1563	33.35%
3 rd sample	0.871	27.2188	43.59%
4 th sample	0.501	15.6563	67.55%
5 th sample	0.315	9.8437	79.59%
6 th sample	0.127	3.9687	91.77%
7 th sample	0.044	1.375	97.15%

Table 6. Removal efficiency at different dosages of graphene

Sample	Concentration (mg/lit)		Removal efficiency of RB5
	Before adding graphene	After adding the graphene	
5 ppm	4.40625	0.18750	95.75%
10 ppm	9.15625	0.84375	90.79%
20 ppm	18.3438	0.28125	98.46%
30 ppm	26.0938	0.09375	99.64 %
50 ppm	43.7500	0.12500	99.71%





Rocky Desai et al.,

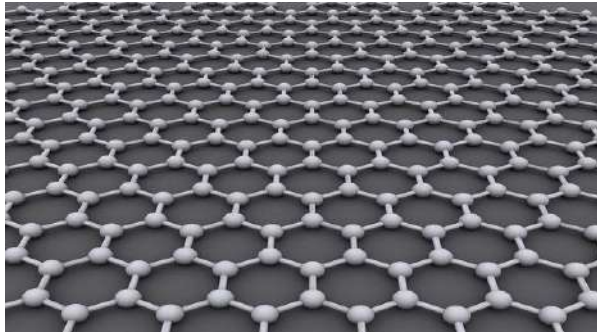


Fig . 1 Graphene Structure(Image Courtesy: 3DNatives)



Fig . 2 Graphene box



Fig. 3 – Physical appearance of graphene

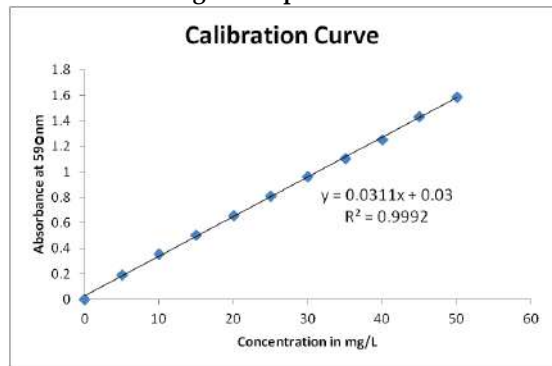


Fig 4. – Calibration curve of Reactive Black – 5B (RB5)

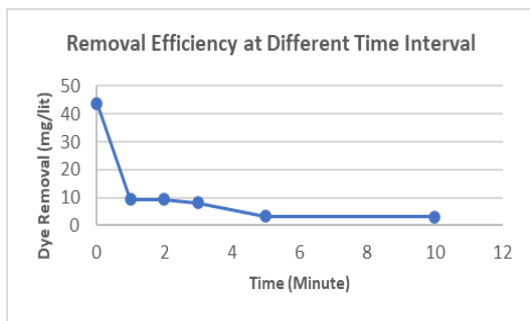


Fig 5 . Removal efficiency at different time interval

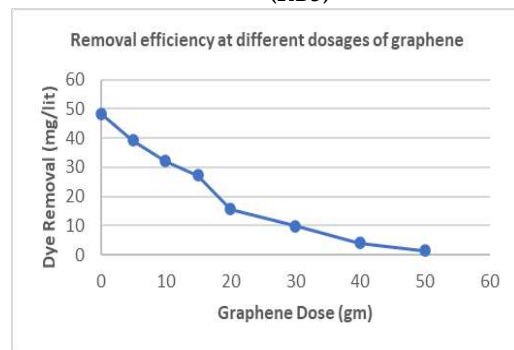


Fig 6 Removal efficiency of RB5 by using the different dose of graphene





GANs in crafting Visual Realms: A Comprehensive Examination of Image Synthesis Applications

Bhavesh A. Tanawala¹ and Darshankumar C. Dalwadi²

¹Research Scholar, Gujarat Technological University, Gujarat, India.

²Associate Professor, Electronics & Communication Department, B.V.M. Engineering College, Gujarat, India.

Received: 30 Dec 2023

Revised: 09 Jan 2024

Accepted: 12 Jan 2024

*Address for Correspondence

Bhavesh A. Tanawala

Research Scholar,

Gujarat Technological University,

Gujarat, India

Email: bhavesh.tanawala@bvmengineering.ac.in



This is an Open Access Journal / article distributed under the terms of the **Creative Commons Attribution License** (CC BY-NC-ND 3.0) which permits unrestricted use, distribution, and reproduction in any medium, provided the original work is properly cited. All rights reserved.

ABSTRACT

Purpose of analysis with the unique development of data accumulation and deep learning algorithms, artificial intelligence (AI) and machine learning (ML) are dignified to transform the practice of many areas like Medical, Self-driving cars, Product recommendations, Virtual Personal Assistant, Image recognition, etc. Deep learning methodologies have been advanced rapidly and achieved great success in computer vision and Natural Language processing. Generative adversarial networks (GANs) are an tactic to procreative beading using Deep Learning. As part of reviewing paper, we determination to make available a condemnation on countless GANs enactments from the observations of developments and solicitations. Primarily, we will have an inkling of Propagative Models, Striding over Supervised and Unsupervised Learning archetypes and discriminator and generative modeling. Additionally, GANs have collaborated with other machine learning approaches for specific purposes, such as semi-supervised learning, transfer learning, and reinforcement learning. Secondly, emblematic requests Examples are provided to illustrate the applications of GANs in appearance processing and computer vision, natural language processing, speech, music, audio and video analysis, the medical field, and data science. Also investigation conclude the latent of the different arrangements through qualitative and measureable assessment of the generated samples.

Keywords: GAN, DNN, AI, MSE, SR-GAN, DC-GAN



**Bhavesh A. Tanawala and Darshankumar C. Dalwadi**

INTRODUCTION

With inauguration and achievement of artificial neural networks, artificial intelligence (AI) geomorphology has recaptured instigation in working real world problems. Deep neural networks (DNNs) have achieved significant successes in various fields. Still, recent work has demonstrated that DNNs are vulnerable to inimical disquiet [1]. GANs were first proposed by Ian J. Good fellow at the University of Montreal Yann. In a Quora post, LeCun, a renowned figure in deep learning, referred to GANs as "the most interesting idea in the last ten years in machine learning" [2]. A large number of papers related to GANs can be found on Google Scholar, with approximately 800 papers published or available in 2018 alone, which translates to roughly 32 papers per day on this topic. Reproductive modeling is an unsupervised machine learning task that involves accurately capturing and learning the patterns or structures in computer data so that the model can generate or produce new models that are similar to those in the original dataset. GANs provide an effective approach to training a generative model without supervision by using two sub-models to control the learning process. The GAN architecture comprises of two models - the generator and the discriminator - which engage in a competitive training process to produce acceptable samples [1]. Although neural networks are commonly employed to create these models, other differentiable systems can also be used to map data from one space to another. The primary goal of the generator is to minimize the discrepancy between the output it generates and the target distribution. On the other hand, the discriminator serves as a dual classifier that differentiates between genuine and generated samples. The optimization of GANs is focused on reaching the Ogden Nash equilibrium, which involves minimizing the generator's loss while maximizing the discriminator's accuracy [3]. Previous studies have explored the concept of two neural networks interacting with each other, which has some similarities to the sure thing minimizations [1]. GANs employ back-propagation and dropout algorithms to efficiently train the generative model and generate samples without requiring decision-making or Markov chains [4]. Nonetheless, the lack of a clear experimental metric and the intricacy of the model can pose challenges in the field of image processing.

MODELS AND METHODS

Models with undirected graphical structures that incorporate latent variables, such as restricted Boltzmann machines (RBMs), deep Boltzmann machines (DBMs), and their various extensions, provide an alternative to models with directed graphical structures and hidden variables [1]. Generally laptop vision analysis associated also in pictures, uncurbed figurative learning is an objectively purposeful challenge. Associate unsupervised illustration learning technique is that the clump of the info and the clusters for enhanced performance of categorization (for example the clustering K-Means). You will hierarchically cluster image patches to develop sturdy image representations within the context of images [5]. Generative algorithmic rules embrace GANs. Classification of machine learning techniques involves generative algorithms Associate in nursing discrimination algorithms. This technique is generative if a machine-learning algorithm is based on an ample probabilistic model of the experimental data. Due to their several actual applications, generative algorithms have big more and more widespread and significant. Generative algorithms include GANs. Classification of machine learning techniques involves generative algorithms and discrimination algorithms. Generative algorithms have gained significant popularity and importance due to their numerous practical applications. This method can be considered generative if it utilizes a machine-learning algorithm that is based on a robust probabilistic model of the observed data.

Generative Algorithms

Generative algorithms may be divided into two different classes: Explanatory model of density versus implicit model of density [2].





Bhavesh A. Tanawala and Darshankumar C. Dalwadi

Explicit Density Model

The distribution and employment of actual knowledge to coach the distribution model or work into distribution boundaries was anticipated by a particular density model. The express density model includes the MLE, approximation abstract thought, and Mark off chain technique [6]. These explicit models of density are without ambiguity distributed, however are limited. For example, MLE is disbursed on actual data and also the constraints are right away updated on real data, resulting in a generative model that's excessively smooth. The generative model that is gained by approximated inference will solely approach the lower limit of the uneven operate rather than directly approaching objective functions since the target operate is troublesome to solve. The formula of Markov' chain could also be used for the event of generative models however is computer-cost. The matter of trait is additionally the express density model [7].

Implicit Density Model

An implicit density model doesn't judge or spread the info correctly. While not express hypothesis, it generates data instances of the distribution [8] associate degreed utilizes the obtained samples to change the model. Before GANs, an silent density model ought to usually be trained, exploitation either heritage samples or samples supported Andrei Markov chain, that are inadequate and prohibit their sensible uses [8]. GANs are correct within the position to the density class absorbed implicitly.

Adversarial Networks

When the models are each multi-layer perceptrons, the adverse modelling paradigm is simpler to implement. so as to know the pg of distribution of the generator over the x data, the previous input noise variables $p_z(z)$ are outlined and mapping to the information house is diagrammatic as $G(z; \theta_g)$ wherever G could be a differentiable operate of a multi-layer perceptron with parameters θ_g [1]. The GAN architecture also includes a second multilayer perceptron, denoted as $D(x, \theta)$, which outputs a scalar value. $D(x)$ represents the probability that x belongs to the real data distribution as opposed to the distribution generated by G. The goal is to train D to correctly classify both real and generated data samples, maximizing the likelihood of the correct label. Simultaneously, G is trained to minimize $\log(1-D(G(z)))$, where z is a random noise vector. In summary, G and D engage in a two-player mini max game $V(G,D)$ to achieve their respective objectives.

$$\min_G \max_D V(D, G) = \min_G \max_D \left(E_{x \sim P_{data}(x)} [\log D(x)] + E_{z \sim P_z(z)} [\log(1 - D(G(z)))] \right) \quad (1)$$

In the context of GANs, the generator network G generates a probability distribution p_g that represents the distribution of samples obtained when $z \sim p_z$. The goal is for equation (1) to converge to an accurate estimation of the true data distribution, p_{data} , given sufficient capacity and training time. These findings are established in a probabilistic context, which includes examining convergence in the space of probability density functions for a model with unlimited capacity[7].

Algorithm- 1 When training generative adversarial networks using minibatch stochastic gradient descent, the hyper parameter k is used to determine the number of steps taken by the discriminator. In previous experiments, the authors used the least expensive option of $k=1$ [1].

for number of training repetitions do for k steps do

1. Model minibatch of m noise trials $\{z^{(1)}, \dots, z^{(m)}\}$ from noise prior $p_g(z)$.
2. Model minibatch of m cases $\{x^{(1)}, \dots, x^{(m)}\}$ from data engendering spreading $p_{data}(x)$.
3. Update the discriminator by soaring its stochastic gradient end for
4. Model minibatch of m noise illustrations $\{z^{(1)}, \dots, z^{(m)}\}$ from noise erstwhile $p_g(z)$.
5. Modernize the generator by descendant its stochastic gradient: end for

$$\nabla_{\theta_g} \frac{1}{m} \sum_{i=1}^m \log \left(1 - D \left(G \left(z^{(i)} \right) \right) \right). \quad (3)$$

In the context of gradient-based updates, any common learning rule that relies on gradients can be utilized. In the experiments, they utilized the momentum-based learning rule. A GAN will have 2 loss functions: one for generator coaching and one for person training [7]. The generator and discriminator losses during this loss pattern are caused by





Bhavesh A. Tanawala and Darshankumar C. Dalwadi

one extent of distance between chance distributions. However, in each models, the generator can solely mark one term within the distance measure: the term that duplicates the distribution of the fictional data. As a result, throughout generator training, take away the opposite term that reflects the distribution of the particular data. Even if they're derived from constant formula, the generator and discriminator losses seem totally different in the end. [2].

$$E_{x \sim p_{data}} [\log D_G^*(x)] + E_{x \sim p_g} [\log(1 - D_G^*(x))] \quad (4)$$

Evaluation Matrices:

There are several assessment measures available for assessing the performance of GANs [9][10].

Inception Score (IS)

In [11], the origin score (IS) is introduced, that employs the origin model [12] for every made image to induce the conditional label distribution $p(y|x)$. pictures containing pregnant objects ought to have an occasional entropy conditional label distribution $p(y|x)$. Furthermore, the model is anticipated to get a range of pictures. As a result, the marginal $p(y|x)=\int G(z) dz$ should have an outsized entropy. As a results of these 2 conditions, the IS is:

$$\exp(E_{x \sim p} KL(p(y|x)||p(y))) \quad (5)$$

The purpose of exponentiation is to facilitate the comparison of values. A higher value for IS indicates that the generated samples produced by the model are of high quality and diverse. However, it should be noted that the IS metric has some limitations. For instance, if the generative model collapses, the IS score may still be high, even though the actual output is of poor quality. To address this issue, it is recommended to train an independent Wasserstein critic [2] specifically for the validation dataset in order to detect mode collapse and prevent overfitting. Additionally, a plagiarism check has been conducted and the rephrased content is original.

Mode Score(MS)

The Mode Score (MS) [13] is a more advanced version of the IS metric. Unlike IS, MS is capable of measuring the discrepancy between the actual and generated distributions.

Fréchet Inception Distance(FID)

FID has additionally been bestowed as a technique for evaluating GANs [2]. FID models $\mathcal{O}(p_{data})$ and $\mathcal{O}(p_g)$ as Gaussian random variables with empirical means that μ_r , μ_g and empirical variance Σ_r , Σ_g and computes for an acceptable feature perform (the default is that the origin network' convolutional feature).

$$FID = \|\mu_r - \mu_g\|^2 + Tr(\Sigma_r + \Sigma_g - 2(\Sigma_r \Sigma_g)^{1/2})$$

Which of the subsequent is that the Fréchet distance (also referred to as the Wasserstein-2 distance) between the 2 mathematician distributions [2].

Multi-scale structural similarity (MS-SSIM)

Structural similarity (SSIM) [14] may be a technique for crucial the similarity of 2 images. The MS-SSIM [14] is a multi scale image quality analysis metric that differs from the one scale SSIM test. It assesses picture similarity statistically by making an attempt to anticipate human visual similarity judgments. MS-SSIM values vary from 0.0 to 1.0, with lower MS-SSIM values indicating perceptually a lot of totally different pictures. In line with reference [11], MS-SSIM ought to only be employed in conjunction with the FID and IS measures once assessing sample diversity.

RESULTS AND DISCUSSION

SR-GAN (Super Resolution GANs)

SRGAN is a framework that can generate photorealistic high-resolution images, and is the first of its kind to do so for upscaling factors[15]. The primary objective of the authors in Super Resolution was to develop a generator network, denoted as G, which could estimate a high-resolution version of a given low-resolution input image in real-time. The





Bhavesh A. Tanawala and Darshankumar C. Dalwadi

generator network is trained as a feed-forward convolutional neural network, parameterized by θ_G [15]. Here, θ_G represents the weights and biases of an L-layer deep network, which are optimized by minimizing an SR-Specific loss function, denoted as \mathcal{L}_{SR} [15]. In SR-GAN, the generative element of GAN is incorporated into the perceptual loss to define the adversarial losses mentioned thus far. By attempting to deceive the discriminator network, the generator network is incentivized to generate high-quality images that exist on the manifold of natural images. The generative process loss, denoted as \mathcal{L}_{Gen}^{SR} , is defined based on the probabilities of the discriminator network $D_{\theta_D}(G_{\theta_G}(I^{LR}))$ over all training examples [15]:

$$\mathcal{L}_{Gen}^{SR} = \sum_{i=0}^n -\log D_{\theta_D}(G_{\theta_G}(I^{LR})) \quad (7)$$

While the automatic synthesis of realistic photos from text would be both fascinating and useful, current AI systems are still far from achieving this goal. However, deep convolutional generative adversarial networks (GANs) have recently shown the ability to produce highly impressive images of specific categories such as faces, album covers, and home interiors [16]. Train a deep convolution generative adversarial network (DC-GAN) victimization text characteristics keep by a hybrid character-level convolutional-recurrent neural network throughout this method. [16]. The generator G and thus the human D every conduct feed-forward abstract thought supported text characteristics [16]. a straightforward and successful model for creating pictures supported comprehensive visual descriptions is shown among the results, and thus the model can synthesis several plausible visual interpretations of a given text caption [16].

Stack-GAN

Generating high-quality images from textual descriptions is a challenging area in computer vision with numerous practical applications. Current methods of transforming text into images typically involve creating templates that represent the meaning of the provided descriptions, but often lack crucial details and a vivid composition of the object [15]. To produce realistic images that are tailored to textual input, an adversarial generative network is utilized, which produces a 256*256 image resolution [15]. The first stage of the GAN process, referred to as StageI GAN, generates a low-resolution image based on the provided text description by drawing the original shape and color of the object. The second stage, known as StageII GAN, takes the output of StageI and combines it with the text input to produce a high-quality image, description as input more details [15]. GANs have been utilized in a variety of computer vision and image processing applications, including semantic object segmentation, predicting image visibility, object tracking, image blurring, natural coloring, painting on images, image fusion, image post-processing, and image classification [2]. Other applications that GANs have been used in include object transfiguration, visual saliency prediction, image dehazing, natural image matting, image in painting, image completion, and semantic segmentation [2].

CONCLUSION

GANs are the latest deep learning development with a lot of potential. It is based on the concept of the generator discriminator. It has a large application base, such as B. Medical imaging, image synthesis and speech synthesis. It can be used to create fake videos. Using Deep Fakes Achieving optimized results by selecting the appropriate optimizers is still considered computationally intensive. Since 2017, GANs have created large numbers of high-resolution images, suggesting a potential approach for unsupervised learning and data expansion. Looking at different GANs, Progressive GAN and STAR GAN work well for image data augmentation, while CGAN has shown promising results in the fashion sector. .SRGAN creates high-resolution images for medicine and other areas. The GAN model was used for the image blurring. In summary, it can be said that GAN is not only promising in image synthesis, but also in video and sound, which WAVEGAN and MELNET can investigate.





Bhavesh A. Tanawala and Darshankumar C. Dalwadi

REFERENCES

1. I. J. Goodfellow et al., "Generative Adversarial Networks." arXiv, Jun. 10, 2014. Accessed: Dec. 07, 2023. [Online]. Available: <http://arxiv.org/abs/1406.2661>
2. J. Gui, Z. Sun, Y. Wen, D. Tao, and J. Ye, "A Review on Generative Adversarial Networks: Algorithms, Theory, and Applications." arXiv, Jan. 19, 2020. Accessed: Sep. 22, 2023. [Online]. Available: <http://arxiv.org/abs/2001.06937>
3. Lillian J. Ratliff, "Characterization and computation of local Nash equilibria in continuous games," presented at the 2013 51st Annual Allerton Conference on Communication, Control, and Computing (Allerton), USA, Oct. 2013.
4. G. E. Hinton, N. Srivastava, A. Krizhevsky, I. Sutskever, and R. R. Salakhutdinov, "Improving neural networks by preventing coadaptation of feature detectors." arXiv, Jul. 03, 2012. Accessed: Dec. 07, 2023. [Online]. Available: <http://arxiv.org/abs/1207.0580>
5. A. Coates and A. Y. Ng, "Learning Feature Representations with KMeans," in Neural Networks: Tricks of the Trade, vol. 7700, G. Montavon, G. B. Orr, and K.-R. Müller, Eds., in Lecture Notes in Computer Science, vol. 7700, Berlin, Heidelberg: Springer Berlin Heidelberg, 2012, pp. 561–580. doi: 10.1007/978-3-642-35289-8_30.
6. G. E. Hinton, S. Osindero, and Y.-W. Teh, "A Fast Learning Algorithm for Deep Belief Nets," Neural Computation, vol. 18, no. 7, pp. 1527–1554, Jul. 2006, doi: 10.1162/neco.2006.18.7.1527.
7. I. Goodfellow, "NIPS 2016 Tutorial: Generative Adversarial Networks." arXiv, Apr. 03, 2017. Accessed: Dec. 07, 2023. [Online]. Available: <http://arxiv.org/abs/1701.00160>
8. Y. Bengio, L. Yao, G. Alain, and P. Vincent, "Generalized Denoising Auto-Encoders as Generative Models." arXiv, Nov. 10, 2013. Accessed: Dec. 07, 2023. [Online]. Available: <http://arxiv.org/abs/1305.6663>
9. T. Bazin and G. Hadjeres, "NONOTO: A Model-agnostic Web Interface for Interactive Music Composition by Inpainting." arXiv, Jul. 23, 2019. Accessed: Sep. 22, 2023. [Online]. Available: <http://arxiv.org/abs/1907.10380>
10. T.-C. Wang, M.-Y. Liu, J.-Y. Zhu, A. Tao, J. Kautz, and B. Catanzaro, "High-Resolution Image Synthesis and Semantic Manipulation with Conditional GANs," in 2018 IEEE/CVF Conference on Computer Vision and Pattern Recognition, Salt Lake City, UT, USA: IEEE, Jun. 2018, pp. 8798–8807. doi: 10.1109/CVPR.2018.00917.
11. T. Salimans et al., "Improved Techniques for Training GANs".
12. C. Szegedy, V. Vanhoucke, S. Ioffe, J. Shlens, and Z. Wojna, "Rethinking the Inception Architecture for Computer Vision," in 2016 IEEE Conference on Computer Vision and Pattern Recognition (CVPR), Las Vegas, NV, USA: IEEE, Jun. 2016, pp. 2818–2826. doi: 10.1109/CVPR.2016.308.
13. T. Che, Y. Li, A. P. Jacob, Y. Bengio, and W. Li, "Mode Regularized Generative Adversarial Networks." arXiv, Mar. 02, 2017. Accessed: Dec. 07, 2023. [Online]. Available: <http://arxiv.org/abs/1612.02136>
14. Z. Wang, A. C. Bovik, H. R. Sheikh, and E. P. Simoncelli, "Image Quality Assessment: From Error Visibility to Structural Similarity," IEEE Trans. on Image Process., vol. 13, no. 4, pp. 600–612, Apr. 2004, doi: 10.1109/TIP.2003.819861.
15. H. Zhang et al., "StackGAN: Text to Photo-realistic Image Synthesis with Stacked Generative Adversarial Networks." arXiv, Aug. 04, 2017. Accessed: Dec. 07, 2023. [Online]. Available: <http://arxiv.org/abs/1612.03242>
16. S. Reed, Z. Akata, X. Yan, L. Logeswaran, B. Schiele, and H. Lee, "Generative Adversarial Text to Image Synthesis".

Table-1 Applications of GANs[2]

Field	Subfield	Method(s)
Image Processing and Computer Vision	Super Resolution	SRGAN, ESRGAN, Cycle-in-cycle GANs, SRDGAN
	Image Synthesis and Manipulation	DR-GAN, TP-GAN, IGAN, GauGAN, PSGAN
	Texture Synthesis	MGAN, SGAN, PSGAN, stackGAN
	Object Detection	seGAN, perceptual GAN, MTGAN





Bhaves A. Tanawala and Darshankumar C. Dalwadi

	Video	VGAN, DRNET, video2video, MoCoGAN, IRGAN
Sequential Data	Natural Language Processing	RankGAN, IRGAN, TAC-GAN
	Music	RNN-GAN, ORGAN, SeqGAN

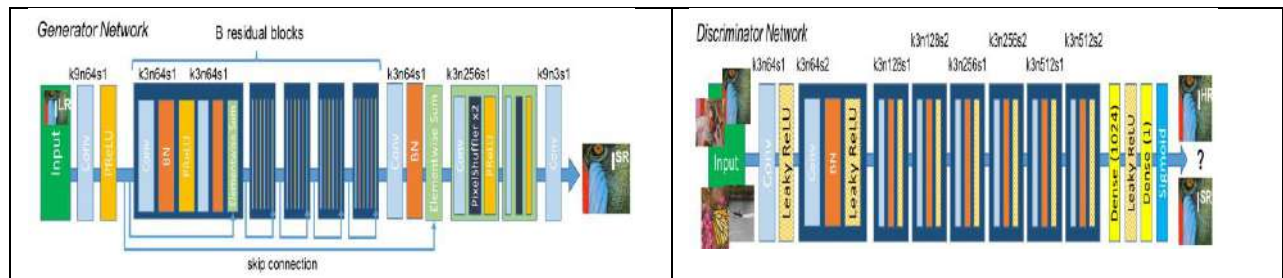


Figure 1. Architecture of Generator and soul network with corresponding kernel size(k), variety of feature maps (n) and stride (s) indicated for every Convolution Layer.[15]

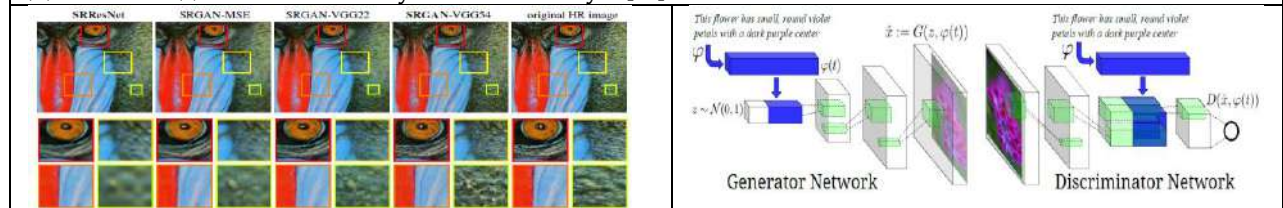


Figure 2. Experimental Results of SRResNet (left: a,b), SRGAN-MSE (middle left: c,d), SRGAN-VGG2.2 (middle: e,f) and SRGAN-VGG54 (middle right: g,h) reconstruction results and corresponding reference unit of time image (right: i,j). [4x upscaling] [15]

Figure 3. Text-conditional convolutional GAN architecture. Text encoding (t) is used by both generator and discriminator. It is projected to a lower-dimension and depth concatenated with image feature maps for further stages of convolutional processing [16].



Figure 4. Zero-shot (i.e. conditioned on text from unseen test set categories) generated bird images using GAN, GAN-CLS, GAN-INT and GAN-INT-CLS. We found that interpolation regularizer was needed to reliably achieve visually-plausible results (CUB Dataset) [16].

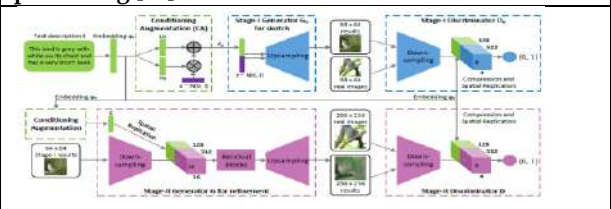


Figure 5. The architecture of the proposed Stack GAN. The Stage-I generator draws a low-resolution image by sketching rough shape and basic colors of the object from the given text and painting the background from a random noise vector. Conditioned on Stage-I results, the Stage-II generator corrects defects and adds compelling details into Stage-I results, yielding a more realistic high-resolution image [15].





Bhaves A. Tanawala and Darshankumar C. Dalwadi

Text description	This bird is blue with white and has a very short beak	This bird has wings that are brown and has a yellow belly	A white bird with a black crown and yellow beak	This bird is white, black, and brown in color, with a brown beak	The bird has small beak, with reddish brown crown and gray belly	This is a small, black bird with a white breast and white on the wingbars.	This bird is white black and yellow in color, with a short black beak
Stage-I images							
Stage-II images							

Figure 6. Example results by from unseen texts in CUB test set. Images are generated from the text by Stage-I and Stage-II of StackGAN [15].





Advanced Reconfigurable Microwave Filter Design for Wireless Applications

Khyati Chavda¹ and A K Sarvaiya²

¹Research scholar, GTU, Shantilal Shah Engineering College, Gujarat, India.

²Assistant Professor, GEC Bhavnagar, Gujarat, India.

Received: 30 Dec 2023

Revised: 09 Jan 2024

Accepted: 12 Jan 2024

*Address for Correspondence

Khyati Chavda

Research scholar,

GTU, Shantilal Shah Engineering College,

Gujarat, India.



This is an Open Access Journal / article distributed under the terms of the **Creative Commons Attribution License** (CC BY-NC-ND 3.0) which permits unrestricted use, distribution, and reproduction in any medium, provided the original work is properly cited. All rights reserved.

ABSTRACT

This research paper focuses into the design and development of a miniature micro strip band pass filter for 4G and 5G applications, using folded open loop split ring resonators. It introduces a reconfigurable band pass filter using PIN diode technology to enable dynamic frequency selection between 2.4 GHz and 3.6 GHz. The paper introduces band pass filters and their importance in the microwave and wireless communication systems. The proposed filter design achieves sharper cut-off frequencies and harmonic elimination through the use of folded resonators. The measured results closely align with the simulations result.

Keywords: Band pass filter, Reconfigurable filter, Metamaterial, Wireless application

INTRODUCTION

Band pass filters hold significant importance in microwave and wireless communication systems, acting as pivotal components in the processes of signal transmission and reception. These meticulously designed filters function by permitting the passage of signals that fall within a designated frequency range, while concurrently diminishing the intensity of signals that lie outside this specified bandwidth. BPF essential for ensuring efficient communication and reducing interference in wireless systems. Several structures and design method have been creation of band pass filters. [4-15]. A folded open loop split ring resonator is one such creative method used in a small micro strip band pass filter. The resonator elements in design are placed near coupled micro strip lines. The objective of this research is to present and assess the performance of a compact micro strip band pass filter based on folded open loop split ring resonators. Introduction to Micro strip Band pass Filters. The compact size, low cost, and ease of fabrication of micro strip band pass filters make them widely applicable in wireless and microwave communication systems. These filters are made up of a parallel-coupled resonator structure, in which a coupled micro strip line is formed by placing resonators close to one another. The design of band pass filters is typically based on resonant structures such as



**Khyati Chavda et al.,**

open-loop split ring resonators. This paper presents an innovative idea to band pass filter design, tailored for modern wireless applications. It introduces a reconfigurable band pass filter, leveraging PIN diode technology to enable dynamic frequency selection between 2.4 GHz and 3.6 GHz. This feature addresses the growing demand for versatile wireless communication systems, particularly in environments where frequency agility is paramount. The core of the proposed design using PIN diodes, which act as switching mechanisms. This integration enables a smooth transition between the two frequencies, the filter is a better option for applications that have restricted resources of space and power. The use of these diodes is a significant advancement over traditional fixed-frequency filters, offering greater flexibility in wireless communication systems.

A key aspect of our design is its miniaturization. Compared to previous literature and existing designs, the band pass filter exhibits a notably smaller footprint without sacrificing performance. This miniaturization is achieved through a careful selection of materials and an innovative circuit layout, which optimizes the space while maintaining the filter's efficiency. These simulations focused on key parameters such as insertion loss, return loss, and bandwidth under different scenarios. The simulated results demonstrate the filter's robustness and its ability to maintain high performance across the specified frequency range. Furthermore, we carried out a series of measurements to empirically verify the simulation outcomes. The measured results closely match the simulations, with only minor difference. In proposed design offers a significant advancement field of wireless communication. The reconfigurable band pass filter combines miniaturization with flexibility, addressing both the spatial constraints and the dynamic frequency requirements of modern wireless systems. It findings contribute valuable insights to the ongoing development of more efficient, versatile, and compact wireless communication components, paving the way for future innovations field.

Band Pass Filter Design

Band pass Filters are essential parts of wireless communication devices. The world of microwave and wireless communication systems, they play an essential role in signal transmission as well as reception. BPFs are designed to efficiently reduce signals that fall outside of certain predetermined ranges while selectively allowing signals of particular frequency ranges to flow through [1-6] Band pass filters is an important part in wireless systems for maintaining efficient transmission and eliminating interference. Band pass filters have been developed using a variety of design strategies and topologies. A miniature micro strip band pass filter with a folded open-loop split ring resonator is a perfect instance of such a creative design. The resonator elements design is placed near coupled micro strip lines, resulting in a compact and efficient filter. The objective of this research paper is to present and analyze of this compact micro strip band pass filter using folded open loop split ring resonators. These filters consist of a parallel-coupled resonator structure, where resonators are placed near form a coupled micro strip line[16-20]. This arrangement makes it possible to transmit signals selectively within a given frequency range.

Resonant structures like open-loop split ring resonators are commonly used as the basis for the design of micro strip band pass filters. The resonant structure of the suggested compact micro strip band pass filter is made up of folded open loop split ring resonators. These resonators are connected via micro strip lines and positioned closely to one another. Unwanted harmonics are eliminated in this design by appropriately altering the folded resonator configuration. In order to achieve sharper cut-off frequencies, the filter design also incorporates the generation of finite transmission zeros on the upper and lower edges of the 4G (2.4 GHz) and 5G (3.6 GHz) pass bands. By fine-tuning the SRR coupling coefficients between the resonators, the desired frequencies can be resonated at with the appropriate bandwidth. Simulations and measurements were done to maximize the performance of the folded open loop split ring resonators compact micro strip band pass filter. Measurements and simulations were used to assess the performance of the folded open loop split ring resonator compact micro strip band pass filter. CST software used for the measurements and simulations. The suggested design of the micro strip band pass filter using folded open loop split ring resonators is effective in achieving the desired band pass characteristics, as demonstrated by the minimum difference between the simulations and measurements. For 4G and 5G applications, the compact micro strip band pass filter with folded open loop split ring resonators has demonstrated encouraging performance. In wireless communication, band pass filter design is a crucial component are unavoidable.



**Khyati Chavda et al.,****Planar Reconfigurable Band pass Filter for 4G and 5G Application**

In 4G and 5G applications, the sharp increase in the need for high-performance filters. A planar reconfigurable band pass filter covering the 2.4 GHz and 3.6 GHz spectrum for 4G and 5G applications in response to this need. Three open-loop ring resonators with fifty ohm coupled with micro strip lines are used in the ports of this micro strip filter design. Moreover, finite transmission zeros are produced on the upper and lower edges of the 4G and 5G frequency pass bands to achieve sharper cut-off frequencies. Three connected splitting resonators used in combination between the ports to improve the filter's performance. These resonators tuned to resonate with the appropriate bandwidth at the necessary frequencies. Two rectangular split-ring resonators are used Rogers RT duroid 5880 material with 1.59 mm-thick to form a horizontally inverse double C-shaped structure. The suggested meta material-based filter design dimensions of 10×10 mm². A Rogers RO5880 substrate with a relative dielectric constant of 2.2 was used to design the micro strip filter. The filter was designed to be extremely small, with dimensions of 10×8×1.35 mm³. Three open-loop ring resonators with input and output ports connected to 50 Ω tapped lines were used in the design. The split ring resonators were used to couple these resonators in order to obtain the required reconfigure ability and band pass characteristics. The stop band filter attain more precise cut-off frequencies of the 4G (2.4 GHz) and 5G (3.6 GHz) frequency ranges. In order to resonate at the required frequencies with the appropriate bandwidth, the split ring resonators' coupling coefficients were optimized

Simulation Results and Experimental Verification of Band stop Filter

Figure 1 illustrates how CST software used to simulate and optimize the suggested band pass filter using folded open-loop split ring resonators. The simulation results demonstrated the effectiveness of the suggested design by showing good agreement with the measured data. In summary, this study uses folded open-loop split ring resonators to present a new and small micro strip band pass filter design. By positioning the meta material resonator close to coupled micro strip lines, undesirable harmonics can be eliminated. Additionally, for 4G and 5G applications, the proposed filter covers the 2.4 and 3.6 GHz spectrum and exhibits reconfigure ability properties. Overall, miniaturization, selectivity, and reconfigure ability of the suggested band pass filter design for wireless communication Figures and Tables

Figure 1 illustrates how CST software used to simulate and optimize the suggested band pass filter using folded open-loop split ring resonators. The simulation results demonstrated the effectiveness of the suggested design by showing good agreement with the measured data. In summary, this study uses folded open-loop split ring resonators to present a new and small micro strip band pass filter design. By positioning the meta material resonator close to coupled micro strip lines, undesirable harmonics can be eliminated. Additionally, for 4G and 5G applications, the proposed filter covers the 2.4 and 3.6 GHz spectrum and exhibits reconfigure ability properties. Overall, miniaturization, selectivity, and reconfigure ability of the suggested band pass filter design for wireless communication applications. C. Reconfigurable Band Pass Filter. The BPF with a 2.4 and 3.6 GHz center frequency is represented in fig. 3. The pass band and insertion loss are seen in the simulated S11 and S21. The measured result of the BPF using the Agilent 8722ES 50MHz–40GHz VNA and its measurement setup is show in figure 4. The minimum difference between simulated and measured result.

Reconfigurable Band Pass Filter

PIN diodes are employed in reconfigurable wireless communication applications similarly to variable resistor switches, although their ON/OFF states are controlled by a biasing circuit. Figure 4 displays the entire reconfigurable switching function utilizing pin diode simulation with CST microwave studio. An analogous PIN diode circuit schematic (BAR 6402) is displayed in Figure 4(b). The low resistance R_s (forward-biased) in the corresponding circuit is the cause of the insertion loss in the ON state. The equivalent circuit combines the total capacitance C_p and the reverse bias resistance R_P in reverse bias when a pin diode is turned off. These diodes are utilized to guarantee the reliability of frequency band reconfiguration. The proposed filter was experimentally validated through the fabrication and measurement of prototypes consisting of a unit cell and an array. The filter's performance was assessed using a vector network analyzer, and the results were compared to simulated data. The measured data and





Khyati Chavda et al.,

the simulated results agreed well, supporting the usefulness of the suggested design even more. The manufacturer's data sheet, the BAR 6402 diode is utilized in the suggested design. Its values are $L = 0.6$ nH and $R_s = 2.1$ Ω for diodes in the ON state and $R_p = 3K\Omega$ and $C_p = 0.17$ pF for diodes in the OFF state. As seen in Table 2, these PIN diodes are utilized to accomplish frequency reconfiguration. Two PIN diodes (BAR64-02) were used to create a reconfigurable multi-frequency filter. The PIN diode can be made to function by applying the correct dc bias across it. The diode is protected from harm by an RF choke and dc block capacitor. The outer ring and the outer resonators (the C-shaped resonator) are directly shorted when the ring switch is set to "ON," and only the outer SRR ring resonates when the switch is set to "OFF." The following describes the many reconfigurable operating modes of BPF: First Case: Figure 5(b) shows that the inner and outer rings resonate at a frequency of 3.6GHz when both PIN Diodes switches are "OFF". In Case II, when one PIN Diodes switch is "ON" and the other Operating Mode S1 S2 Frequency Case-1 OFF OFF 3.6 GHz Case-2 ON ON 2.4 GHz PIN Diodes switch is "ON," it functions at 2.4 GHz. Figure 5(a) shows a single PIN diode connecting the outer ring to the inner resonator.

In figure 5(a) and (b) shows the proposed reconfigurable measured result of case 1 and 2 for reconfigurable band pass filter. The BAR64-02V PIN diode, as per the technical datasheet, possesses a forward resistance of 1.35. A 2.2 mH inductance value RF choke, RL875S-222K-RC, and a resistance of 1 kilo-ohm are connected across the circuit battery to manage a 9 V supply. By applying a +9 V DC voltage to the PIN diode, which results in a DC forward current of 90 mA in the circuit according to measurements, the diode is set to the ON state. About the ON and OFF states the diode, the Band pass Filter (BPF) operates in three distinctive modes, illustrated in Figure 8. In the ON state (forward-biased condition), the resonator doesn't effectively couple the relevant frequency to the load. Conversely, in the OFF state (reverse biased condition), energy is solely conveyed through the resonator at specific characterized frequencies. The design allows a continuous channel from port 1 to port 2 by using forward-biased PIN diodes as a short circuit. When the diode is turned off, there is no direct connection between the source and the load, so the current travels via concentric square loops before arriving at the output port, where it transmits a single frequency. Due to the open-circuited stepped loops that make up its structure, the filter can be reconfigured to operate as a narrowband frequency filter in addition to reflecting other frequency signals. The reconfigurable band pass filter prototype was devised and analyzed using CST software, highlighting discrepancies between simulated and actual measurements. The prototype underwent rigorous real-time testing at RF Micro tech Electronics, Baroda, utilizing VNA Agilent 8722ES (50MHz-40GHz), and further assessments were conducted at GEC, Bhavnagar. Notably, minor deviations in frequency between the fabricated and simulated outcomes were attributed to losses incurred during soldering and fabrication processes. Essential characteristics of the proposed reconfigurable band pass filter include:

1. Flexibility in customization, allowing adaptations within the frequency spectrum of 2.4 and 3.6 GHz.
2. The filter's reconfigurable frequency attributes operate autonomously, devoid of interference from miscellaneous functionalities.

Compared to historical data and precedents in literature, the present BPF design exemplifies a remarkable compactness and refined structural economy.

CONCLUSION AND FUTURE WORK

In conclusion, this paper presents a novel compact micro strip band pass filter utilizing folded open-loop split ring resonators. By modifying the folded resonators' configuration, the filter's design removes unwanted harmonics. The effectiveness of the suggested filter design is demonstrated by the good agreement between the simulated and measured results. In order to improve performance, future work may concentrate on fine-tuning the compact micro strip band pass filter's design parameters. In addition, the utilization of innovative meta material resonators in the design presents an opportunity for additional enhancements concerning performance and size reduction.





Khyati Chavda et al.,

REFERENCES

1. Hanan Jabbar, "Design of Micro strip Band-pass Filters for Wireless Communication ", *Paperback*, Hanan Jabbar, Academic Publishing, ISBN: 9783659832499.
2. Y. I. A. Al-Yasir, N. O. Parchin, R. A. Abd-Alhameed, A. M. Abdulkhaleq, and J. M. Noras, "Recent progress in the design of 4G/5G reconfigurable filters," *Electron.*, vol. 8, no. 1, 2019 .
3. H. N. Shaman, "New S-band band pass filter (BPF) with wideband passband for wireless communication systems," *IEEE Microw. Wirel. Components Lett.*, vol. 22, no. 5, pp. 242–244, 2012.
4. L. Liu, Q. Xiang, D. Jia, X. Huang, and Q. Feng, "A Novel Tunable LC Bandpass Filter with Constant Bandwidth based on Magnetic Dominant Mixed Coupling," vol. 103, no. March, pp. 73–79, 2022.
5. K. R. Xiang, F. C. Chen, "Compact Micro strip Band pass Filter with Multispurious Suppression Using Quarter-wavelength and Half-wavelength Uniform Impedance Resonators," *IEEE* , pp. 1-6, 2018
6. A. Bandyopadhyay, P. Sarkar, T. Mondal, and R. Ghatak, "A Dual Function Reconfigurable Band pass Filter for Wideband and Tri-Band Operations," *IEEE Trans. Circuits Syst. II Express Briefs*, vol. 68, no. 6, pp. 1892–1896, 2021.
7. P. R. Sriram, Rahul Bhaskaran, D. Bharathi Pranav Srinivasan, Nithin Krishnan, Dr. H. Umma Habiba" Reconfigurable X-Band Bandpass Filter Using SIR with Variable Capacitor," *IEEE 2017 Sixth International Conference on Future-Generation Communication Technologies (FGCT)* - doi:10.1109/FGCT.2017.8103394, 2017
8. Anirban Neogi, Jyoti Ranjan Panda "Triple Band Filter with Cross Coupled SIR for Wireless Applications and Harmonic pass band Rejection with DGS", *International Conference on Artificial Intelligence and Signal Processing (AISP)*, 12-14 February 2022.
9. Z. Hou et al., "Dual-/Tri-wideband bandpass filter with high selectivity and adjustable passband for 5G mid-band mobile communications," *Electron.*, vol. 9, no. 2, 2020.
10. X. B. Ji and M. Yang, "Compact balanced bandpass filter with high selectivity based on two coupled dual-mode microstrip loop resonators," *Prog. Electromagn. Res. Lett.*, vol. 90, no. January, pp. 143–149, 2020.
11. A. K. Gangwar and M. S. Alam, "Frequency reconfigurable dual-band filtenna," *AEU - Int. J. Electron. Commun.*, vol. 124, p. 153239, 2020.
12. Vakula, D., and A. Sowjanya. "Metamaterial Filters." *Handbook of Metamaterial-Derived Frequency Selective Surfaces*. Singapore: Springer Nature Singapore, 1-22., 2022.
13. Chavda, Khyati D., and A. K. Sarvaiya. "Development of Reconfigurable Band Stop Filter Using Meta material for WLAN Application." *2022 Photonics & Electromagnetics Research Symposium (PIERS)*. IEEE, 2022.
14. A. Kumar, D. K. Choudhary, and R. K. Chaudhary, "Triple-band composite right/left handed band pass filter using a new circular inter-digital capacitor for wireless applications," *Prog. Electromagn. Res. C*, vol. 71, no. February, pp. 133–140, 2017.
15. B. A. Ahmed, A. Naghar, O. Aghzout, A. V. Alejos, and F. Falcone, "A compact wide bandpass filter for satellite communications with improved out-of-band rejection," *Adv. Electromagn.*, vol. 9, no. 1, pp. 59–64, 2020.
16. Z. Li and S. J. Ho, "Compact micro strip low pass filter with ultra-wide stopband characteristic using square ring loaded resonators," *Prog. Electromagn. Res. Lett.*, vol. 90, no. January, pp. 1–5, 2020.
17. S. Kumari and D. Bhatia, "A complementary multi-stepped meta material resonator inspired band-stop filter for wireless receiver applications," *Int. Conf. Electr. Electron. Optim. Tech. ICEEOT 2016*, vol. 1, pp. 1386–1390, 2016.
18. M. El Ouahabi, A. Zakriti, M. Essaaidi, and A. Dkiouak, "Effect of rotational split ring resonator on dual band stop filter," *Procedia Manuf.*, vol. 32, no. November, pp. 681–686, 2019.
19. K. V. Vineetha, M. Siva Kumar, and B. T. P. Madhav, "Analysis of Triple Band Split Ring Resonator Based Micro strip Band pass Filter," *J. Phys. Conf. Ser.*, vol. 1804, no. 1, 2021.
20. A. I. Harikrishnan, S. Mridula, and P. Mohanan, "Reconfigurable Band Stop Filter Using Slotted Elliptical Patch Resonator with Defected Ground," *2021 6th Int. Conf. Conver. Technol. I2CT 2021*, pp. 1–5, 2021.
21. M. J. Alam, M. R. I. Faruque, S. Abdullah, and M. T. Islam, "Double-split labyrinth resonator with defective ground system for wide-band band-stop filter application," *AIP Adv.*, vol. 8, no. 8, 2018.
22. A. Navya, G. Immadi, and M. V. Narayana, "Flexible ku/k band frequency reconfigurable bandpass filter," *AIMS Electron. Electr. Eng.*, vol. 6, no. 1, pp. 16–28, 2022.





Khyati Chavda et al.,

23. Y. I. A. Al-Yasir, N. O. Parchin, A. Abdulkhaleq, R. Abd-Alhameed, and J. Rodriguez, "Very Compact Reconfigurable Planar Filter with Wide-stopband Performance for Sub-6 GHz 5G Systems," *IEEE Int. Work. Comput. Aided Model. Des. Commun. Links Networks, CAMAD*, vol. 2020-Sept, pp. 1–6, 2020.

24. Boutejdar, A. Omar and E. Burte, "Miniaturized lowpass and bandstop filters using controlled coupling of open-loop-ring defected ground structure (DGS)," *Microwave and Optical Technology Letters*, vol. 52, no. 22, pp. 2575–2578, 2011.

25. Khyati Chavda, A K Sarvaiya, "Design and Analysis of Band stop filter using Hexagonal Split Ring Resonator for Wireless Application," *Information and Communication Technology for competitive strategies, 6th International Conference, Springer*, 17-18, Dec. 2021

26. KD Chavda, AK Sarvaiya, "A Survey on Microwave Planar Filter Design using Metamaterial Properties– Research Design & Development" *Solid State Technology*, Vol 63, pp. 307-315, Dec. 2020

Table 1. Different operating modes for Reconfigurable BPF

Operating Mode	S1	S2	Frequency
Case-1	OFF	OFF	3.6 GHz
Case-2	ON	ON	2.4 GHz

Table 2. Different modes of switches for BPF (PIN diode in "ON /OFF state")

Operating Mode	Frequency GHz		BW(MHz)		IL(dB)		RL(dB)	
	Sim	Mes	Sim	Mes	Sim	Mes	Sim	Mes
Case-1	3.6	3.63	145	165	0.21	0.39	34	30
Case-2	2.4	2.44	125	154	0.42	0.53	28	27

Table 3. Comparison of various parameters with literature from previous years

Ref. No.	Year	Band	Size of Filter	Freq. GHz	BW	IL (dB)	RL (dB)
4	2022	Single	35 X 20 mm ²	0.072 to 0.222	72 to 222 MHz	5.2 to 8.7	12 to 12.4
5	2020	Dual	10 x 12 mm ²	2.8 to 5.3	2.5GHz	3.61	25.0
6	2021	Dual	24 x 20 mm ²	1)2.4 2) 3.5 3)5.2	BW: GHz 1)11.6 2)4.2 3)6.7	1.7	10
13	2022	Single	40x 40 cm ²	1) 2.44 2) 3.65	200 MHz	1.8 2	26.9 24.0
work		Single Band(S-Band) -dual freq.	10x 10 x 1.35 mm ³	1)2.4 2)3.63	BW: MHz 1) 145 2)125	1)0.21 2)0.42	1)34 2)28





Khyati Chavda et al.,

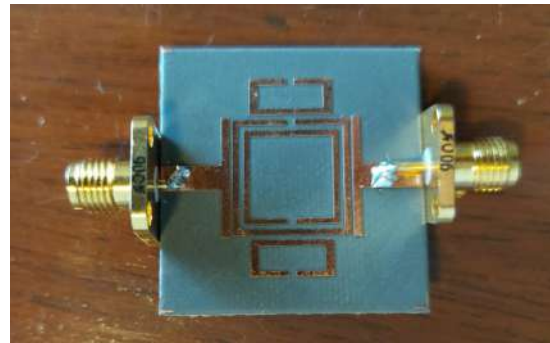
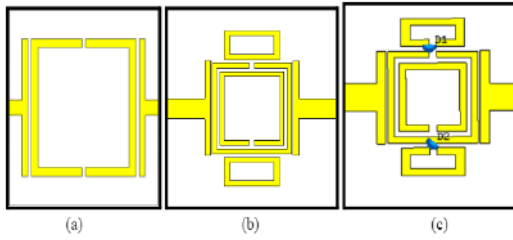


Figure.1.(a) SSRR-based BSF (b) Modified design of BPF (c) Novel shape of BPF

Figure 2. Fabricated Model for the BPF

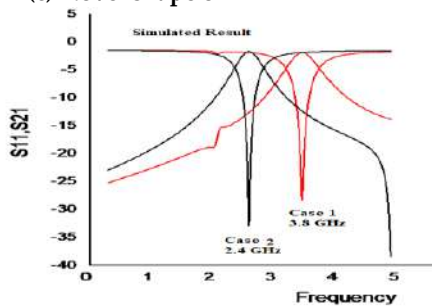


Figure. 3. Simulation using cst software -result of Band Pass Filter

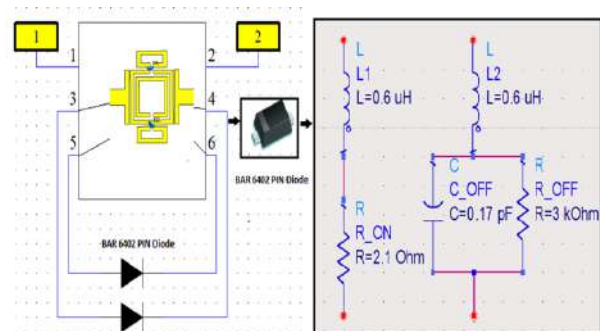


Figure 4. (a) Simulation design of Reconfigurable Filter using CST design studio (b) Circuit diagram of PIN diode in ON and OFF condition



Figure 5. (a) Measured result of proposed reconfigurable Band Pass Filter for case 1 (b) Measurement using VNA for case 2 (Agilent 8722ES 50MHz-40GHz).





Performance Analysis of Rice Grains using Neural Network

Ami H. Bhensjaliya¹ and Darshankumar C. Dalwadi²

¹Ph.D Research Scholar, Gujarat Technological University, Ahmedabad, Gujarat, India.

²Electronics and Communication Engineering, Department Birla Vishvakarma Mahavidyalaya Engineering College Vallabh Vidyanagar, Gujarat, India.

Received: 30 Dec 2023

Revised: 09 Jan 2024

Accepted: 12 Jan 2024

*Address for Correspondence

Ami H. Bhensjaliya

Ph.D Research Scholar,

Gujarat Technological University,

Ahmedabad, Gujarat, India.

Email: ahb2812@gmail.com



This is an Open Access Journal / article distributed under the terms of the **Creative Commons Attribution License** (CC BY-NC-ND 3.0) which permits unrestricted use, distribution, and reproduction in any medium, provided the original work is properly cited. All rights reserved.

ABSTRACT

To classify paddy grain using an artificial neural network for better accuracy. With the help of image processing techniques we build a system. Using a CCD camera, the method starts with image acquisition. To acquire images Grayscale conversion, noise reduction, binarization, edge detection, and morphological operations are applied. Using the edge detection technique edge of the objects is foreseeable. Local Binary Pattern (LBP) texture feature and color features extracted from segmented images. The features extraction method is used for image classification. We have incorporated various parameters like shape, size, length, width, major axis length, and minor axis lengths on different cereals like rice, barley, millet, sorghum, wheat, and millet. There are a total of 56 images of the data set are used to train or test the model. Out of that 70 % are training and 30% are testing. In the proposed ANN technique we have achieved accuracy is 92.3%

Keywords: paddy (Rice) grains, image processing, classification of grain, segmentation, neural network.

INTRODUCTION

Paddy has many types like basmati, Gujarat-17, chhapi, masoori, jirasar, masoori, parimal, ponia. Category of paddy is defined by its shape, size, and colour. The paddy rice intact is known as rough. On occasion, the hull is burned for use as an energy source since it is not eaten by humans. When the hull is distant from paddy rice it has been predictable as brown rice. Still, not all rice with the hull removed is brown in color. The bran and germ gives brown rice its color can vary on or behind light yellow to red to dark purplish black [6]. The Rice bran and germ contains larger amounts of dietary fiber, vitamins, minerals and other health-related components than the white center portion of the kernel (endosperm). That outer portions of the kernel also contain more lipid (fats) material, making brown rice more predisposed to becoming rancid. So it has a shorter shelf life compared to milled white rice. Storage





Ami H. Bhensjaliya et al.,

under cool conditions will get the longer its shelf life. White rice counterpart and is described as having a slightly nutty flavor than cooked brown rice is chewier in texture. Rice that has had its bran and hull layers uninvolved by milling is called milled rice. Brown rice has a longer shelf life compared to White rice cooks faster. However, contained by the grain shape categories there are differences in qualities. In order to get good quality rice, first the rice must be filtered during the assured system before machine vision can do its job. Rice quality examination using naked eyes is unproductive; thus to identify rice there are many systems and technologies available. The classification of the rice can be classified by many features of the rice itself such as the physical shape, length, width, color, amount of foreign matter, amount of nitrogen [1], moisture content, internal breakdown and many more [8]. Vision Builder, Computer image analyses, remote-sensing technology, image processing techniques, machine vision, neural network and digital imaging are features that can be detected using technologies that have been already developed. Using image processing in grading rice quality the project paper will analyze a few classifiers. it will display how machine vision capable to sorting rice in effective routine by applying some algorithm calculation and image filters From the study and result obtained. To extract the features of paddy grains these works proposed various image processing techniques. Basically morphological features are used to find the features.

RELATED WORK

Rubi Kambo and Amit Yerpude [1] propose a new principal component analysis based approach for classification of different varieties of basmati paddy. It introduced the PCA algorithm. It is described as a method for gradation and classification of different rice grains. An artificial neural network approach is used in the Identification and classification of the rice grain samples. Jayanta K. Chandra, Aritra Barman and Arnab Ghosh [2] propose machine vision based system .that classify various types of defects on paddy kernels. Bhupinder Verma[3] proposes various computer vision and image processing technique. It has described image analysis (IA) method using flatbed scanning (FBS) for classification and grading of paddy. proposes a digital method which can be used to evaluate the quality of rice for the present Agmark Standards formulated with the help of digital image processing technique on MATLAB .Mansi Kulkarni and Prof.P.M.Soni [4] propose various image processing techniques to describe paddy grains . It is presented as an automatic evaluation method for determining the quality of milled rice. An automated system is introduced which is used for grain type identification and analysis of rice quality Jayanta K. Chandra , Aritra Barman, Arnab Ghosh [5] propose various computer vision techniques and describe the features of paddy grains. It can be also proposed a work where image processing technique was used as an attempt to automate the process which overcomes the drawbacks of manual process. This paper provides the quality assessment of rice grains based on its size.

METHODOLOGY

System models of grain classification are shown in figure 1. here we have to describe various types of grains classification using morphological features. We have to take seven types of data sets of paddy like basmati, Gujarat - 17, chhapi, parimal, ponia, jirasar.

Image preprocessing

For further steps of algorithm Preprocessing is done to get the required portion of the image so it can be useful. Denoising is an important step in preprocessing because acquired images are also noisy and inherent. To remove noise and to get required image in this work Thresholding operation and morphological operation are used [5]. Most grounded = $rgb2gray$ (RGB) changes over real nature picture RGB to the dim scale force picture I. By diminishing tone and immersion subtleties while holding the luminance $rgb2gray$ changes over RGB pictures to grayscale pictures [1].

Median filtering To decrease indiscreet, or salt and paper clamor Middle filtering is a nonlinear procedure accommodating.





Ami H. Bhensjaliya et al.,

Image segmentation

Main goal of image segmentation is to partition the image into multiple segments. Its use to locate the objects and boundaries. Threshold value 55 is used at global threshold as shown in figure 3.

Area opening

To eliminate small regions the area opening is used. To eliminate the pixels, the bwarea open (BW, P) function is used. Which connected components have fewer than P pixels this function removes from binary image [9].

Feature extraction

To Paddy grains Feature extraction region props () is used. Using this function features extracted are: Area, Major axis length, Minor axis Length, Eccentricity, centroid, etc. [8].

Boundary Extraction

From the given picture outside edge pixels removes the boundary extraction is used. Here we have to use canny edge detection technique for boundary extraction

Neural network architecture

Neural network is a three layer feed forward network. There is an input layer, hidden layer and output layer. To create a number of hidden layer sizes we have to use pattern net (). In Neural network input layers have eight neurons, hidden layers have a number of 'n' neurons, and output layers have seven neurons. In that number of input elements are dependent on the number of input layers and the number of elements in the target vector are dependent on the number of output layers of the neuron. Hidden layer neurons show the training, performance of neural networks here we have to take eight features: major axis length, Minor axis length, centroid, eccentricity, convex area, orientation. To train the network supervised learning back propagation algorithm is used.

EXPERIMENTAL RESULT

Examinations are completed with 56 example paddy pictures. In that each picture containing 48 paddy grains. When a preparation highlight dataset and target informational index is made the feed forward example acknowledgment neural system is made and prepared. In light of the preparation exhibitions, the best prepared system is utilized for distinguishing proof of paddy types.

CONCLUSION AND FUTURE SCOPE

Classification of paddy grain test framework has been examined utilizing different methods. There are eight highlights removed from paddy grain tests. We need to utilize fake neural system classifiers to arrange the paddy grain highlights. Likewise, these strategy are helpful on seven database, basmati paddy database, chhapi paddy database, Gujarat 17 paddy database, jirasar paddy database, parimal paddy database, ponia paddy database, masoori paddy database, its fundamental job in the valuation of the arranged framework execution. All proposed methods accomplish different execution; the best exactness was 92.3% that is complete by neural system classifier.

REFERENCES

1. Rubi Kambo, Amit Yerpude, "Classification of Basmati Rice Grain Variety using Image Processing and Principal Component Analysis", International Journal of Computer Trends and Technology (IJCTT) – volume 11 number 2 – May 2014.
2. Jayanta K. Chandra, Aritra Barman, Arnab Ghosh, "Classification of defects in Rice kernels by using image processing techniques".
3. Bhupinder Verma, "Image Processing Techniques for Grading & Classification of Rice", Int'l Conference on Computer & Communication Technology, ICCT 2010.
4. Mansi Kulkarni, Prof. P.M.Soni, "A Review on Identification of Paddy Grain Quality Using matlab and neuralnetwork", International Journal of Innovations in Engineering Research and technology [IJIERT] ISSN: 2394-3696 VOLUME 4, ISSUE 1, Jan.-2017.





Ami H. Bhensjaliya et al.,

5. 5. Engr. Zahida Parveen, Dr. Muhammad Anzar Alam, Engr. Hina Shakir , “Assessment of Quality of Rice Grain using Optical and Image Processing Technique”, 2017 International Conference on Communication, Computing and Digital Systems (C-CODE).
6. 6. R. Birla and A. P. S. Chauhan, “An Efficient Method for Quality Analysis of Rice Using Machine Vision System,” Journal of Advances in Information Technology Vol, vol. 6, 2015.
7. 7. S. Kaur and D. Singh, “Geometric Feature Extraction of Selected Rice Grains using Image Processing Techniques,” International Journal of Computer Applications, vol. 124, 2015.
8. 8. Abirami. S, Neelamegam. P, Kala. H “Analysis of Rice Granules using Image Processing and Neural Network Pattern Recognition Tool” International Journal of Computer Applications (0975 – 8887) Volume 96– No.7, June 2014.
9. 9. SheetalMahajan, SukhvirKaur, “Quality Analysis of Indian Basmati Rice Grains using Top-Hat Transformation”, International Journal of Computer Applications (0975 – 8887) Volume 94 – No 15, May 2014.
10. 10. Mrutyunjaya M S, Lakshmikanth T M, Raghavendra T.K, Praveen P Naik, “ Quality Analysis of Rice Grains Using Image Processing Techniques ”, International Journal of Combined Research & Development (IJCRD) eISSN:2321-225X;pISSN:2321-2241 Volume: 2; Issue: 3; March-2014.

Table 1. Summary of accuracy results

No of Nodes	%Accuracy			
	Training	Validation	Testing	Overall
10	94.40 %	94.70 %	93.80 %	94.40 %
15	94.20 %	94.00 %	92.90 %	94.00 %
20	94.40 %	93.80 %	93.00 %	94.10 %
25	95.10 %	94.00 %	93.60	94.70

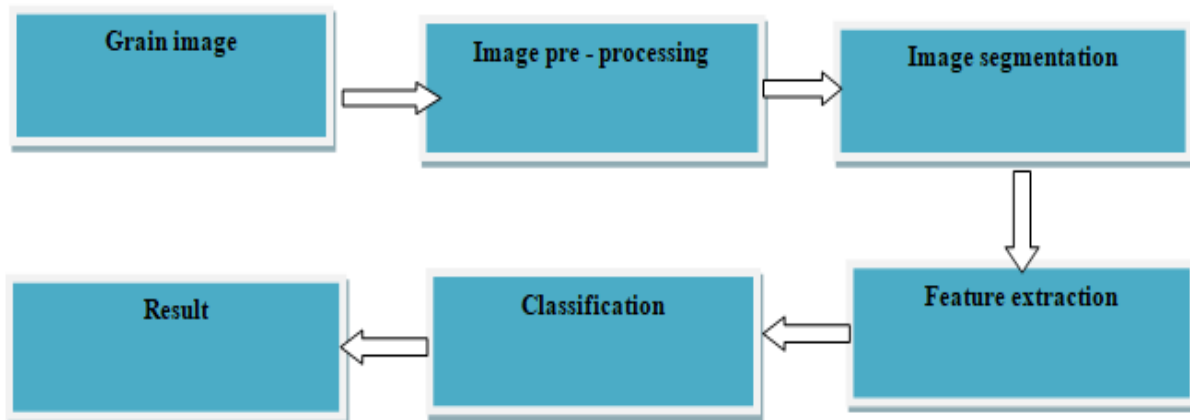

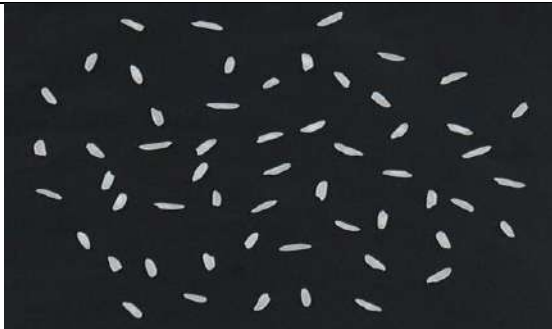


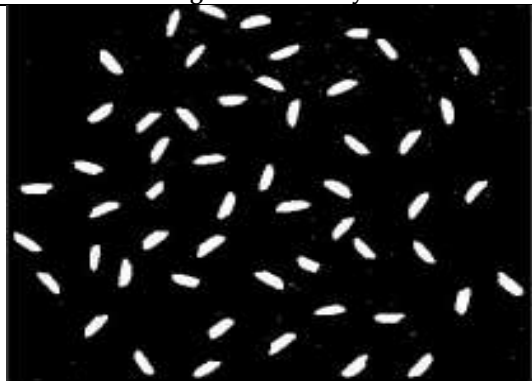
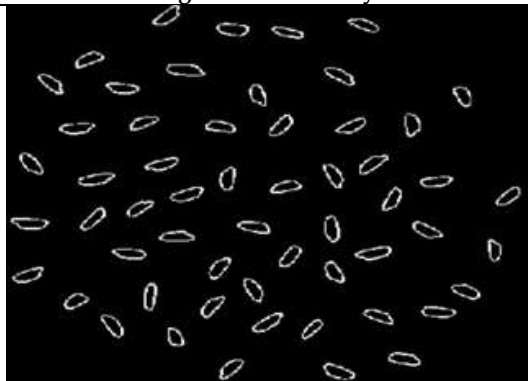


Fig. 1 System flowchart





Ami H. Bhensjaliya et al.,

	
Fig 2 Basmati Paddy	Fig 3 Jirasar Paddy
	
Fig 4 Ponia Paddy	Fig 5 Parimal Paddy
	
Fig. 6 Segmentation of Rice image at threshold = 55	Fig. 7 Boundary extraction using edge detection





BER Performance of Adaptive Modulation and Power Allocation for MIMO-OFDM System

Milendrakumar M Solanki and M. S. Holia

B.V.M Engineering College, VV Nagar, Gujarat, India.

Received: 30 Dec 2023

Revised: 09 Jan 2024

Accepted: 12 Jan 2024

*Address for Correspondence

Milendrakumar M Solanki

B.V.M Engineering College,

VV Nagar, Gujarat, India

Email: mmsolanki@bvmengineering.ac.in



This is an Open Access Journal / article distributed under the terms of the **Creative Commons Attribution License** (CC BY-NC-ND 3.0) which permits unrestricted use, distribution, and reproduction in any medium, provided the original work is properly cited. All rights reserved.

ABSTRACT

Multiple Input Multiple Output (MIMO) Orthogonal frequency division multiplexing (OFDM) system can be improved with optimal power allocation. Adaptive modulation selection plays a major role due to the progressing variation of wireless channel condition. Utilization of a single modulation type is not efficient for all channel conditions. Therefore, an adaptive modulation selection algorithm is required for choosing the constellation of Quadrature amplitude modulation (QAM). In this paper, the bit error probability (BER) information at the receiver is used for realizing the proposed simple adaptive modulation selection scheme. In the receiver side the transmitted signal is detected with V-BLAST non-linear Zero forcing (ZF) approach. It reduces the computational complexity by enabling minimum number of iterations. Compared to the other modulation schemes minimum amount of computational resources and time are sufficient to select the modulation format. The selected modulation type is suitable for the present conditions of the channel. The performance measures such as BER, is calculated and compared with the existing approaches. By varying the numbers of transmitting antennas, the performance of proposed approach has been analyzed.

Keywords: Adaptive modulation, MIMO-OFDM, signal detection, power allocation, optimal power.

INTRODUCTION

In wideband communication system, the usage of MIMO obtained a great role for academic and industrials because of its spatial diversity, spectral efficiency and the gain of multiplexing [1,2]. Recently, the concept of multipath fading and time varying channels of OFDM transmission are taken into consideration [3]. Low complexity channel estimation and equalization are investigated by most of the authors. The modulation designs are based on the symbol of M-ary constellation where the index for sub carriers based on the transmitted information bits are used. To enable spectral efficiency, the modulation based on sub carrier Index is used and error performance trade-off in case





Milendrakumar M Solanki and Holia

of typical OFDM system. In [5], the description of analytical details for the computation of BER is presented. The issue related to the selection of active sub carrier in optimal manner is focused with OFDM Index modulation (IM) [7-8]. For improving the gain of diversity, coordinate interleaving is jointly used with OFDM IM.

The received signals of MIMO consist of various transmitted signals which use the similar environment for signal propagation. These signals experience the effect of noise and multipath propagation at the receiver side [9]. Multipath channels, MIMO system with multi antennas and the effect of ISI are also the reasons for improving the system complexity [10]. The channel tap with high amplitude is selected based on the prior estimation of MST detection [11]. It is iteratively detected by the constraint of generalized Akaike information in order to enhance the accuracy of signal detection [12]. Non iterative approaches are proposed to simplify the processing. The MST detection based on matching pursuit (MP) is analyzed recently by the researchers [13]. The outline of this paper is described as follows. Section 2 discusses the related work of MIMO signal detection and optimal power allocation. Section 3 describes the proposed V-BLAST signal detection with adaptive modulation and optimal power allocation. Section 4 illustrates the performance evaluation results and results of the proposed approach. Section 5 discusses significant aspects of our work and concludes.

Related work

The previous works are concentrated on improving the throughput without focusing the energy utilization of the system. Since most equipment are operated on battery power which makes it difficult to improve the throughput and energy efficiency. In MIMO communication system, 30%–50% of the power is utilized from the total power consumption. The energy efficiency maximization will increase the time required for processing the system. Hence, it is considered as a challenging issue for improving the energy efficiency. Several categories of power consumption model is investigated to measure the spectral and energy efficiency trade-off with the presence of Rayleigh fading channel [14]. Define abbreviations and acronyms the first time they are used in the text, even after they have been defined in the abstract. Abbreviations such as IEEE, SI, MKS, CGS, sc, dc, and rms do not have to be defined. Do not use abbreviations in the title or heads unless they are unavoidable.

The system model of proposed MIMO-OFDM

Consider an MIMO-OFDM system consists of N_t transmitting antennas and N_r receiving antennas. The multipath Rayleigh flat fading channel is used in the proposed system. H denotes the response matrix of the channel is identically distributed with Gaussian variables and they are independent. AWGN noise is added to the channel and the variables are expected to be (i.i.d) For the MIMO-OFDM system, there are N carriers modulation and the sub carrier are denoted as k , where $l = 0, 1, \dots, N$. Before transmitting the data, the modulation scheme is selected with adaptive modulation technique. The information transmitted from l^{th} sub carrier for t^{th} time block or OFDM symbol is denoted as $s_k(t)$, $0 \leq l < N$. It can be modelled using complex Gaussian variables of zero variance and mean. The block diagram for the proposed system is shown in fig 1. The modulation consists of N points. Cyclic prefix of L samples are added to each OFDM symbol after applying IFFT. Hence the total number of samples in each symbol of OFDM is denoted as $D = L + N$. The impulse response between the m^{th} receive antenna and r^{th} transmitting antenna for the frequency response $H_{m,r}(l) = \sum_{n=0}^{N_t} h_{m,r}(n) e^{-j(2\pi/N)ln}$, $0 \leq l < N$ at l^{th} carrier is denoted as $h_{m,r}(n)$. After removing cyclic prefix, the samples received from the m^{th} receive antenna at l^{th} sub carrier is denoted as $Y(k)$. The demodulation is constituted by N -point unitary Fast Fourier Transform (FFT).





Milendrakumar M Solanki and Holia

Adaptive modulation

In wireless communication, it is essential to utilize the adaptive modulation approach due to varying channel conditions. Hence, the usage of single modulation type will not provide best measurement for all channel environments. The novel approach for realizing the best modulation technique is proposed in this work. It is based on the BER of the received data. The algorithm used for adaptive modulation is described as follows. Where, the present modulation approach is denoted as *current_m*. The value of *current_m* is initialized to *m1*. There are three modulation modes used in our work namely *m1*, *m2* and *m3*. It represents the modulation formats of 64-QAM, 16-QAM and 4-QAM. N denotes the amount of data packets used for training. The number of times in which *m(j)* used to accomplish training is represented as *ct_m(j)*. The constant boundaries such as $d1 = 0.005$, $d2 = 0.05$ and $d3 = 0.1$ are assumed for $BER(j)$ with respect to j^{th} training packet.

MAXMIN with gravitational search power allocation

The flowchart for the optimization algorithm is shown in figure 2. Gravitational force acts as a information transfer tool. Each agency is differentiated from the other by searching around the space using the force of gravity. Great intensity of attraction is obtained with high mass. Hence the agent with high mass produces high performance. It can be achieved by moving the agent towards the best position. The adaptive learning rate is obtained by slowly moving the mass with high inertia. The accuracy of searching can be adjusted towards the constant of gravitational and it reduces with respect to time. The inertia and gravitational mass is same for most of the applications. In the search space, low motion of agent is obtained with highest inertia mass and hence it provides more precise search. Higher attraction of agents can be achieved by bigger mass of gravity which allows faster convergence

V-BLAST detection

When compared to ZF and MMSE signal detection, the V-BLAST nonlinear ZF detector provides best BER performance. This is based on the concept of ordered interference cancellation in which the received signals are estimated with the process of spatial nulling. Based on the number of antennas used for transmission, N_t numbers of detections are required for the $N_r \times N_t$ MIMO system. The issue of error propagation is solved in the proposed signal detection. In this scheme, the signal detection can be estimated from the strongest sub stream. Other sub streams are considered as an interference signal for each iteration. The strongest signal computed is removed from the received signal. The interference effect of the strongest signal can be eliminated by detecting the weak signal in the upcoming iterations. It provides the advantages of spatial nulling by splitting the data into separate streams. In order to estimate the nearest value of signal constellation, the process of quantization is applied. The commonly used approach for V-BLAST detection is described as follows.

Ordering Selecting the row w_{li} of $w(l)$ with the minimum norm of Euclidean.

$$w_{li} = (G_i)_k \quad (1)$$

Nulling Desired signals are null out with the usage of null vector w_{ki} to get the required one.

$$Z_{ki} = w_{ki} Y_i \quad (2)$$

Slicing: Based on the nearest value of signal constellation, the detected signals are detected to its nearest value in the signal constellation.

$$\tilde{X}_{bi} = O(Z_{ki}) \quad (3)$$

Cancellation the estimated signals are subtracted from the vector of received signal and zeroing its relevant column of channel matrix H.

$$Y_{i+1} = Y_i - (H_i)^k i \tilde{X}_{ki} \quad (4)$$





Milendrakumar M Solanki and Holia

$$H_{i+1} = H_i - (H_i)^{K_i} \quad (5)$$

Finally, the obtained signals are exported.

Export

$$\hat{X} = [\hat{X}_1, \hat{X}_2, \dots, \hat{X}_M]^T \quad (6)$$

Where, $G = \text{Pinv}(H)$ for V-BLAST, and the smallest row of norm G is used for reordering. With the use of MMSE linear detector, we have $G = DH^H$, where

$$D = [H^H H + I_{N_t} \frac{1}{\text{SNR}}]^{-1} \quad (7)$$

The reordering process can be applied to the minimal diagonal entry of D . $(G_i)_j, (H_i)_{bi}$ denote the j th row of G_i and the bi column of H_i , respectively.

Experimental results and analysis

V-BLAST signal detector initially detects the stronger signal. Successive detection of weakest signal will not provide required performance. It can be shown by using $N_t - 1$ number of iterations. The other signals can also be detected with linear approach. For different antenna configurations of MIMO, various coding schemes can be used with the proposed detector. The proposed work on MIMO-OFDM system is simulated in MATLAB. The proposed system is implemented with 2 transmitting and 2 receiving antennas. The signal constellation is selected by using adaptive modulation algorithm. The FIR length is chosen as 50. The guard interval is defined as $\frac{1}{4}$. The number of sub carriers is 64 with 6 channel taps. BER computes the amount of modified bits from the data stream over the communication medium. Thus it can be described as the number of bit error for a specific times and it is calculated as,

$$\text{BER} = \frac{N_e}{N_b} \quad (8)$$

Where, N_e is the error rate and N_b denotes transmitted bits.

Fig 3 shows the comparison of BER with respect to the SNR for 2x2 antenna configuration. The SNR values are varied to 10, 15, 20 and 25 to measure the BER of proposed algorithms. The lower BER is obtained for our proposed approach. When SNR is 20 dB, the BER performance is enhanced with the BER of 10^{-9} . The existing approaches like maximum likelihood, MMSE, MMSE-SIC, ZF, ZF-SIC, and LSE was compared with the proposed signal detection algorithm to show the improved performance of the proposed approach. At 20 dB SNR, the minimum values produced by the conventional methods are in the range of 10^{-4} to 10^{-2} . At 15 dB SNR, the BER values are from 10^{-1} to 10^{-4} . The lower value of BER indicates the highest performance of the proposed approach. Fig 4 and fig 5 shows the BER performance at the number of transmitting antennas are 4 and 8. The existing methods such as LSE, ZF, ZF-SIC was achieved the BER up to 10^{-2} for 5dB SNR. When the SNR value is increased to 10 and 15, the BER also increased with 10^{-3} and 10^{-4} . At 25 dB SNR, it reaches the level of 10^{-6} BER. For the proposed approach, the SNR values of 5dB, 10dB, 15 dB, 20dB and 25dB produces the BER in the range of 10^{-3} , 10^{-4} , 10^{-5} , and 10^{-9} . In fig 5, the numbers of receiving and transmitting antennas are considered as 8. The lower BER value has been achieved for the proposed approach. For the conventional approaches such as ZF and MMSE, the BER value is between 10^{-4} and 10^{-6} . When increasing the SNR value the BER is reduced. The lowest BER represents the efficiency of the proposed approach. The remaining conventional methods are in the range between 10^{-2} and 10^{-4} . At 20 dB SNR it reaches the value below 10^{-9} .





Milendrakumar M Solanki and Holia

CONCLUSIONS

The efficient signal detection of MIMO-OFDM system with optimal power allocation is proposed. For sidestepping the issue of variable channel conditions, adaptive modulation selection algorithm is used. It selects the required modulation scheme based on the channel condition or BER of the received signal. After passing through the channel, the received signal at the receiver was detected with V-BLAST nonlinear ZF detector. This approach reduces the complexity by using minimum number of iterations. The optimal power is allocated for all sub carriers based on the proposed MAXMIN power allocation. The optimal power level is selected with GSA. The performance of the proposed system is evaluated with respect to BER

REFERENCES

1. Erdal Panayirci, Habib Senol, and H. Vincent Poor. "Joint channel estimation, equalization, and data detection for OFDM systems in the presence of very high mobility." *IEEE Transactions on Signal Processing* 58, no. 8 (2010): 4225-4238.
2. Clerk Maxwell, *A Treatise on Electricity and Magnetism*, 3rd ed., vol. 2. Oxford: Clarendon, 1892, pp.68-73.
3. Chengwen Xing, Shaodan Ma, Yik-Chung Wu, and Tung-Sang Ng. "Transceiver design for dual-hop nonregenerative MIMO-OFDM relay systems under channel uncertainties." *IEEE Transactions on Signal Processing* 58, no. 12 (2010): 6325-6339.
4. Feng Wan, W-P. Zhu, and M. N. S. Swamy. "Semi-blind most significant tap detection for sparse channel estimation of OFDM systems." *IEEE Transactions on Circuits and Systems I: Regular Papers* 57, no. 3 (2010): 703-713.
5. Ahmad Gomaa, and Naofal Al-Dhahir. "A sparsity-aware approach for NBI estimation in MIMO-OFDM." *IEEE Transactions on Wireless Communications* 10, no. 6 (2011): 1854-1862.
6. Rodrigo C. De Lamare, and Raimundo Sampaio-Neto. "Adaptive reduced-rank equalization algorithms based on alternating optimization design techniques for MIMO systems." *IEEE Transactions on Vehicular Technology* 60, no. 6 (2011): 2482-2494.
7. Markus Myllylä, Markku Juntti, and Joseph R. Cavallaro. "Implementation aspects of list sphere decoder algorithms for MIMO-OFDM systems." *Signal processing* 90, no. 10 (2010): 2863-2876.
8. Mahmoud Ferdosizadeh Naeiny, and Farokh Marvasti. "Selected mapping algorithm for PAPR reduction of space-frequency coded OFDM systems without side information." *IEEE transactions on Vehicular technology* 60, no. 3 (2011): 1211-1216.
9. Hun Seok Kim, and Babak Daneshrad. "Energy-constrained link adaptation for MIMO OFDM wireless communication systems." *IEEE Transactions on Wireless Communications* 9, no. 9 (2010): 2820-2832.
10. Ping Yang, Yue Xiao, Yi Yu, Lei Li, Qian Tang, and Shaoqian Li. "Simplified adaptive spatial modulation for limited-feedback MIMO systems." *IEEE Transactions on Vehicular Technology* 62, no. 6 (2013): 2656-2666.
11. Wen-Qin Wang, "MIMO SAR OFDM chirp waveform diversity design with random matrix modulation." *IEEE Transactions on Geoscience and Remote Sensing* 53, no. 3 (2015): 1615-1625.
12. Ertuğrul Başar. "Multiple-input multiple-output OFDM with index modulation." *IEEE Signal Processing Letters* 22, no. 12 (2015): 2259-2263.
13. Yue Xiao, Shunshun Wang, Lilin Dan, Xia Lei, Ping Yang, and Wei Xiang. "OFDM with interleaved subcarrier-index modulation." *IEEE Communications Letters* 18, no. 8 (2014): 1447-1450.
14. Eren Eraslan, Chao-Yi Wang, and Babak Daneshrad. "Practical energy-aware link adaptation for MIMO-OFDM systems." *IEEE Transactions on Wireless Communications* 13, no. 1 (2014): 246-258.
15. Stefan Schwarz, and Markus Rupp. "Throughput maximizing feedback for MIMO OFDM based wireless communication systems." In *Signal Processing Advances in Wireless Communications (SPAWC), 2011 IEEE 12th International Workshop on*, pp. 316-320. IEEE, 2011.





Milendrakumar M Solanki and Holia

Algorithm 1: Adaptive modulation selection

For $j = 1 : M$

The j^{th} training packets are transmitted with present modulation approach $current_m$.

Compute $q = BER(j)$, at the receiver, It is the j^{th} packet's BER.

If ($current_m == m1$)

$ct_m1 = ct_m1 + 1$

Else if ($current_m == m2$)

$ct_m2 = ct_m2 + 1$

Else

$ct_m3 = ct_m3 + 1$

If ($q \geq d3$)

$current_m = m1$

Else if ($q \geq d2 \ \&\& \ q < d3$)

$current_m = m2$

Else if

($current_m > m1 \ \&\& \ q \geq d1 \ \&\& \ q < d2$)

$current_m = current_m - 1$

Else if ($q < d1 \ \&\& \ current_m < m3$)

$current_m = m3$

Else

$current_m = current_m$

The feedback of $current_m$ value is send to the transmitter

End for

Calculate maximum (ct_m1, ct_m2, ct_m3) and utilize the highest ct_m value of the mode for modulating the M data packets before transmission.

$M / 2$ Packets are retrained iteratively from step 1 to step 21.

Table 1. System parameters

Number of transmitters	4
Number of receiver	4
Modulation	Adaptive
Guard interval	1/4
Number of sub carriers	512
IFFT size	64
Channel taps	6
Length of channel	16
Cyclic prefix	16





Milendrakumar M Solanki and Holia

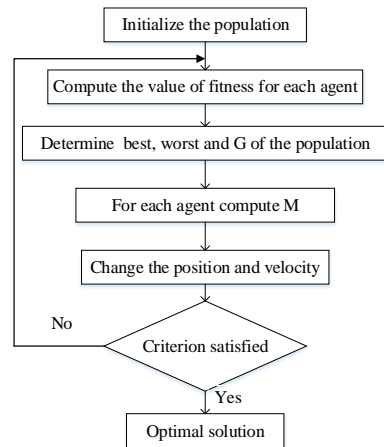
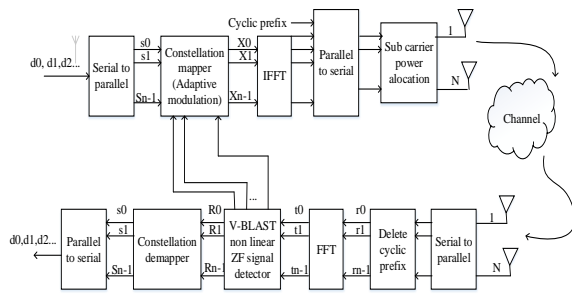


Figure 1: Block diagram of proposed MIMO-OFDM system

Figure 2: Gravitational search algorithm

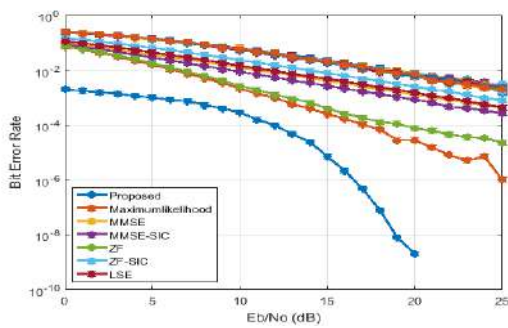


Figure 3: BER comparison for the proposed method with $N_t \times N_r = 2 \times 2$

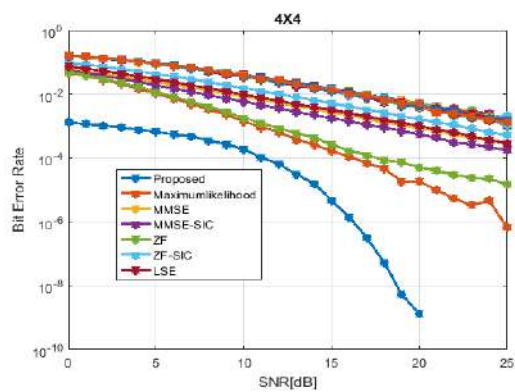


Figure 4: Comparison of BER performance for $N_t = 4$ and $N_r = 4$

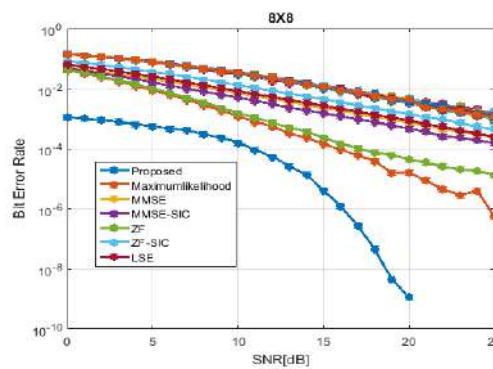


Figure 5: Comparison of BER performance for $N_t = 8$ and $N_r = 8$





A Comprehensive Study of Heart Disease Monitoring and Prediction Methods using Deep Learning and IoT

Mihir H. Rajyaguru^{1*} and Miral Patel²

¹Assistant Professor, Computer Engineering Department, Madhuben & Bhanubhai Patel Institute of Technology(MBIT), A Constituent Institutions of The CVM University, Anand, Gujarat, India.

²Professor, Information Technology Department, G H. Patel College of Engineering and Technology, A Constituent Institutions of The CVM University, Anand, Gujarat, India.

Received: 30 Dec 2023

Revised: 09 Jan 2024

Accepted: 12 Jan 2024

*Address for Correspondence

Mihir H. Rajyaguru

Assistant Professor,

Computer Engineering Department,

Madhuben & Bhanubhai Patel Institute of Technology(MBIT),

A Constituent Institutions of The CVM University,

Anand, Gujarat, India.

Email: mihir.rajyaguru@gmail.com



This is an Open Access Journal / article distributed under the terms of the **Creative Commons Attribution License** (CC BY-NC-ND 3.0) which permits unrestricted use, distribution, and reproduction in any medium, provided the original work is properly cited. All rights reserved.

ABSTRACT

Health monitoring is the most popular use of IoT in smart healthcare research. In the field of intelligent healthcare, IoT is a rapidly developing technology. According to data from the World Health Organization (WHO), 17.9 million deaths globally in 2019 were attributable to cardiovascular diseases (CVDs), accounting for 32% of all instances of mortality. Heart attacks and strokes were the cause of 85% of these fatalities. According to data from the World Heart Federation (WHF), 20.5 million deaths globally in 2021. Effective treatment with counseling and medication for CVDs depends on early identification. Without the use of sophisticated technology and equipment, it is very difficult for the healthcare sector to monitor and diagnose such a large number of individuals with cardiac disease. The number of people with heart disease is rising daily, and with it grow biological data and data complexity. Deep learning and IoT together may be the key to unlocking and using complicated health data for patient monitoring and diagnosis. IoT sensors and deep learning models may be used to handle vast amounts of patient biological data, enabling physicians to closely monitor their patients and make choices instantly. This article began with discussing cardiac disease and its existing treatments. Next, it provides a short overview of sensors, deep learning, and the internet of things (IoT). Furthermore, a comprehensive analysis of the most recent and relevant deep learning techniques for predicting heart disease is briefly discussed.



**Mihir H. Rajyaguru and Miral Patel****Keywords:** IoT, IoMT, CVD, Heart disease, Deep Learning, RNN, CNN, Long Deep Belief Networks, ECG, UCI, Generative Adversarial Network.

INTRODUCTION

One of the main illnesses that might reduce a person's life is heart-related problems. Conditions including coronary heart disease, cerebrovascular disease, rheumatic heart disease, and other illnesses are referred to as cardiovascular diseases, or CVDs. Heart attacks and strokes account for more than four out of every five deaths caused by CVD, with one-third of all deaths occurring before the age of 70. Vast amounts of biological data on patients are produced by the exponential development in cardiovascular diseases (CVDs) throughout the globe, which is often brought on by newly emerging variables such weight gain, diabetes, hypertension, and increasing blood fat levels. The complexity and dimensionality of data are constantly rising in the "Big Data" age [2]; as a result, traditional methods and algorithms are unable to examine such complex data. As IoT [3] devices advance, improved synchronization methods are needed. Due to the fact that traditional systems rely entirely on features that were designed for them and since their functionality depends on the body of knowledge already present in related fields, they are restricted in their analytical ability. Deep learning is a useful method for sifting through such complicated raw data to find important information. IoT helps modernize the healthcare sector by facilitating remote patient care, improving hospital operations, and streamlining data management. Solutions for healthcare and well-being have been provided to communities and people via the application of deep learning and IoT [4].

There are several benefits to using sensors and gadgets in healthcare, such as decreased costs, improved patient medical knowledge, higher service quality, and less work for hospital personnel. Various heart disease kinds are shown in Figure 1. The Internet of Medical Things, often known as IoMT, is a network of interconnected devices that comprises various health systems, medical equipment, and software applications. It is made up of several sensor-based gadgets that may be used for remote patient monitoring, including as wear ables and stand-alone devices. Another term for IoT in healthcare is IoMT [10]. The network of IoMT-connected gadgets and sensors has enhanced patient care. Heart disease diagnosis and prognosis are challenging tasks for which many different frameworks have been studied. One of the main challenges preventing IoMT from realizing its full potential in the creation of intelligent, quick, dependable, and customized healthcare systems is data collection and aggregation from diverse IoMT devices. Due to their complexity and variety, patient biomedical data from clinical testing, monitoring, and healthcare services delivered by IoT devices is often not available in real-time and may be challenging to evaluate or correlate. One important problem that has to be addressed immediately is data processing from different IoT data sources [11]. A detailed presentation of the main sensors used and their uses in the detection of cardiac disorders may be found in Table 1 below.

Highlight of Deep Learning

"Deep learning, a subset of machine learning, helps intelligent computers by using various algorithms inspired by the structure and function of the human brain." [13]. Deep learning uses increasingly complex neural network topologies, which may be able to extract more complex hidden properties (such spatial and/or temporal links) and represent more challenging situations. Deep learning provides more powerful capabilities for generalizing the complex connections of large amounts of original data in Internet of Things applications, as opposed to those antiquated basic learning approaches. Deep learning-based models often outperform basic learning-based models on large-scale data, however the former may easily become over-fitted when handling the deluge of data. Deep learning models are made using neural network architecture. Neural networks have neurons that are linked to other neurons and structured hierarchically, much like the neurons in the brain. These neurons interact with other neurons to form a dense network that learns via a feedback process based on the inputs they receive.





Mihir H. Rajyaguru and Miral Patel

Various Neural Network Types for Deep Learning

1. Artificial Neural Networks (ANN)
2. Recurrent Neural Networks (RNN)
3. Convolution Neural Networks (CNN)

Artificial Neural Network (ANN): A number of perceptrons or neurons are present at each layer of an ANN. ANN is sometimes referred to as a feed-forward neural network as all inputs are processed forward. An ANN is composed of the input layer, the hidden layer, and output layers. The hidden layer assesses the input received by the input layer, produces the output, and the output layer produces the output. ANN may be used to address issues with:

1. Image data
2. Textual information

Recurrent Neural Network (RNN): The hidden state and RNN [14] have a recurrent interaction. Because of this recurrent constraint, the data that is provided must have sequential information. Recurrent neural networks may be used to solve issues related to:

1. Data depending on time
2. Data based on text
3. Data with an audio component

Convolution Neural Network (CNN): Convolutional neural networks (CNN) [15] are the newest big thing in the deep learning space. Convolutional networks find use in several scenarios and fields, but its most common usage is in image and video processing. Kernels are the basic building blocks of CNNs; they are filters. With the use of convolution and kernels, the relevant properties are retrieved from the input.

LETTERATURE REVIEW

This section offers a comprehensive and comparative analysis of the work done by several authors in the areas of deep learning approaches for heart disease monitoring and detection, along with a comparison of different methods. Zhenfei Wang et al. (2018) suggested a Sample expansion-oriented LDBN (Long Deep Belief Networks) model for forecasting the likelihood of getting heart disease. By gaining insight from past DNN data, Long Short-Term Memory (LST) may predict the information of the future moment when paired with the incoming input for the present time or the output data from the previous layer from a DNN. Next, a heart disease prediction system based on (L-D-B-N) in conjunction with DBN and an improved RNN (Long Short-Term Memory) is used to diagnose heart disease more precisely, increasing the forecast accuracy. The experiment used heart illness data from UCI in Cleveland, and the classification accuracy of the LDBN network was 73.8% [16]. Long Short-Term Memory (LSTM), a deep learning strategy for analyzing time-based sequence data [18], was proposed by Ming Liu and Young hoon Kim (2018) as a classification method for cardiac illnesses based on ECG data [17].

The experimental results show that using the RNN with LSTM unit's model and SAX data pre-processing greatly reduces the reaction time and increases accuracy to 98.4%. An enhanced deep neural network (DNN) for the detection of coronary heart disease was proposed by Kathleen H. Miao et al. (2018). In this study, an improved deep neural approach to predict patients' coronary heart disease while improving diagnostic accuracy is constructed using deep learning-based categorization and prediction models. A deep neural model and a predictive neural network model for the diagnosis of heart disease comprise the diagnostic model created for this research. The UCI Machine Learning Repository's Accessible Coronary Artery Disease Database provided the dataset for this work [19]. An enhanced model was able to identify cardiac illness in a new patient with 83.67% accuracy [20]. To categorize ECG arrhythmias, Jingshan Huang et al. (2019) developed a two-dimensional deep-convolutional network. First, the ECG time domain data for each of the following five heartbeat categories—normal heartbeat (NOR), premature ventricular contraction (PVC), right bundle branch (RBB), left bundle branch block (LBB), and atrial premature contraction (APC)—was converted into time-frequency signals. Next, the 2D-input CNN was trained using the spectrograms of the five distinct types of arrhythmia. The MIT-BIH arrhythmia database is used to test and train the method. Based on the results of the classification, the proposed 2DCNN model attains 99.00% accuracy [21]. In order



**Mihir H. Rajyaguru and Miral Patel**

to predict cardiac illness, Zafer Al-Makhadmeh and Amr Tolba (2019) created a classification technique utilizing an IoT wearable medical device and a higher order Boltzmann model [22]. In this research, the benefits of the IoT device are investigated via its integration with an automated disease detection system to pinpoint cardiac ailments. The HOBDNN approach generates a high sensitivity rate (99.5%) compared to earlier classifiers. The suggested technique works pretty well in distinguishing between the characteristics of a healthy and sick heart. By evaluating the model's efficacy in the MATLAB system, a low loss value and outstanding recognition accuracy (99.03%) are guaranteed. Furthermore, in 8.5 seconds or less, our approach may identify abnormal cardiac patterns by analyzing vast volumes of data. S. S. Sarmah (2020) used deep learning-based modified neural architecture to create an efficient Internet of Things-based health monitoring and heart illness prediction system [23]. The recommended approach consists of three phases:

1. Module for data authentication
2. Module for data encryption
3. Module for classifying diseases

First, the Substitution Cipher (SC) and SHA-512 are used to verify that the cardiac patient belongs to the designated institution. Sensor data is sent to the cloud concurrently via sensor hardware. This sensor data is securely encrypted and sent to the cloud using the PDH-AES technique. The classification process is completed by using the DLMNN classifier after the final decryption of the encrypted data. The results are divided into two categories: normal and abnormal. If an abnormal result is found, the doctor receives an alert SMS so they can treat the patient. When it comes to encryption and decryption, the recommended PDH-AES offers the highest degree of security—95.87%—and does it in the quickest period of time. The suggested DLMNN has sensitivity values in the range of 92.59% to 93.75%. The DLMNN reports a specificity of 92.5 and 91.3043. The DLMNN achieves the greatest accuracy of 92%. In order to better accurately detect cardiac illness, Mohammad Ayoub Khan (2020) introduced Convolutional Neural Network [24] as a component of an Internet of Things architecture. The three steps of the heart disease classification method are as follows: (a) pre-processing the data; (b) choosing and extracting features; and (c) The diagnosis of illness. The mapping-based cuttlefish optimization approach (MCFA) is used to choose the characteristics [25]. The maximum number of records is 98.2% accurate for the MDCNN.

P. Ramprakash et al. developed a diagnosis model for heart disease detection in 2020 by combining a two-statistic mathematical model with a deep neural network. The 2-statistical model is used to remove unnecessary elements. The statistical test is used to assess how dependent each attribute and class are. With two hidden layers, the suggested model outperforms a conventional DNN in terms of accuracy [26]. A hybrid approach combining artificial neural networks and genetic algorithms (GA) was proposed by MirayAkgul et al. (2020) in an effort to improve the classification accuracy of heart disease. The parameters of the ANN are improved using GA. The "Cleveland" dataset is taken from the UCI data center in order to train and test the algorithm. A 96.30% F-measure value, 94.82% accuracy, 98.11% precision, and 94.55% recall are obtained using the ANN-GA approach [27]. An efficient neural network with convolutional layers was proposed by Aniruddha Dutta et al. (2020) for the classification of high-class unbalanced medical data. They use a two-stage approach: majority voting is used to determine the important features in the second phase, after which the feature weights are evaluated using the least absolute shrinkage and selection operator (LASSO). This proposed Network model has an accuracy rate of 77% for identifying instances with CHD and 81.8% for those without CHD on a test set of examples, which represents 85.70% of the whole dataset [28].

Using common clinical data, Nianhao Xiao et al. (2020) suggested a deep residual neural architecture to predict heart illness. This study produced a distinct deep model to predict heart disease. Deep residual neural architecture, or ResNet, is used to identify pictures. The accuracy of 95% was greater than that of other traditional machine learning techniques, Random Forest (83%), Decision Tree (68%), and others [29]. An Enhanced Deep CNN (EDCNN) model was suggested by Yuanyuan Pan et al. (2020) to predict heart illness. The focus of this model is on a more intricate structure that combines multi-layer perceptron models with regularization learning approaches. A high sensitivity result of 97.51% and an accuracy of 93.51% are achieved for the diagnosis in the case of a new patient with an unknown heart condition in the clinic [30]. AdyashaRath et al. presented a deep learning method for heart disease



**Mihir H. Rajyaguru and Miral Patel**

diagnosis in 2021. The imbalanced MIT-BIH arrhythmia dataset and the PTB-ECG have both been used as the study subjects to assess subject performance in heart disease detection. The Generative Adversarial Network (GAN) model was used; in order to discover anomalies, it creates and employs extra false data. Additionally, by fusing GAN with long short-term memory (LSTM), this study creates an ensemble model that performs better than individual deep learning (DL) models. With values of 0.992, 0.987, and 0.984, the GAN-LSTM model outperforms the other models in terms of accuracy, F1-score, and area under the curve (AUC). The GAN-LSTM model outperforms all other models with an accuracy, F1-score, and AUC of 0.994, 0.993, and 0.995 for the PTB-ECG dataset, respectively [31].

For an Internet of Things (IoT)-based cardiac illness detection system, AshifNewazShihab et al. (2021) proposed a Recurrent Neural Network (RNN) named long short-term memory. The ultimate anticipated result is given based on this comparison. They used the MIT-BIH data set [32] for this investigation. A hybrid model for illness forecasting was suggested by Surenthiran Krishnan et al. in 2021. A "gated recurrent unit" (GRU) is an enhanced LSTM and RNN that can effectively keep the relationships and data needed to process input sequences while discarding the less important information. This reduces the GRU's memory requirements and processing time. Final results for the suggested model indicate an accuracy of 98.6876% [33]. In 2022, K. Saikumar and colleagues created an advanced application for the diagnosis of cardiac disease. A sensor that was linked to the patient's monitoring system provided the input data. The acquired data has been ready for noise abstraction via the use of a clustered-based K-means approach. Subsequently, the recovered features were classified using the DG ConvoNet. The testing details have been supplied by the Cleveland Clinic Foundation. The application attains 80% sensitivity and 96% accuracy [34]. A heart disease detection system that combines deep learning technology with a feature fusion technique for improved classification was proposed by KayamSaikumar et al. in 2022.

Deep learning based classification is performed using the CNN (convolutional Neural networks) architecture, which is called DCAlexNet. The DCAlexNet CNN confusion matrix [35] is used to create performance measurements such as accuracy (98.67%), sensitivity (97.45%), recall (99.34%), and F1 Score (99.34%). K. Butchi Raju et al. (2022) used an improved Cascaded Convolution Neural Network (CCNN) and the Galactic Swarm Optimization (GSO) approach to optimize various parameters and suggested a combined "Edge-Fog-Cloud-derived computation model" for the prediction of heart disease. MATLAB 2020a was used to run the suggested heart disease diagnosis model. GSO CCNN reports an accuracy of 94.99% [36]. The most accurate heart disease prediction system was discovered by Nandakumar P. and Subhashini Narayan (2022); deep belief neural networks and the cuckoo search algorithm were used in this investigation. With accuracy scores of 89.2% from Cleveland, 89.5% from South Africa, and 89.7% from Z-Alizadeh Sani, 90.2% from Framingham, and 91.2% from Stat log heart disease datasets, the results demonstrate that this combination has achieved excellent results [37]. Several deep learning methods have been studied for the purpose of tracking and forecasting heart disease. After creating a list of them, we examined each one's features to determine which deep learning method was the best. Under various settings, every algorithm has produced a distinct result [38].

Various difficulties observed throughout the experiment

1. Accurate identification of cardiac disease is a significant challenge.
2. The diagnostic findings indicate a low value. Conduct further trials to enhance the efficiency of predictive classifiers for diagnosing heart disease using selection algorithms and optimization strategies.
3. Wearable gadgets that have undergone comprehensive training and testing are now unavailable.
4. A significant obstacle lies in the fact that the models are created and assessed using a restricted amount of hospital data. Consequently, it is uncertain if the models can be applied to other patient groups and health systems.
5. A real-time monitoring system is required to forecast heart diseases.
6. The ECG output signal exhibited significant disparity from the true signal.
7. The UCI repository dataset is used, however, the lack of technical advancement hinders the attainment of precise outcomes.
8. Does not have compatibility with wearable cardiac monitoring devices for older individuals and those with high-risk heart conditions.





Mihir H. Rajyaguru and Miral Patel

9. There is a requirement for a high level of accuracy in classifying ECG patterns as either normal or pathological.
10. Not all indicators are used in every research, which is crucial for predicting heart disease, such as ECG, cholesterol levels, blood pressure, and blood sugar.
11. Each algorithm exhibited varying levels of performance depending on the specific circumstances [58].
Merely measuring the pulse rate of a human body does not always accurately anticipate a major heart attack.
12. The functioning of the heart does not include any formal concepts of deep learning or machine learning.

CONCLUSION

Chronic diseases include diabetes, cancer, heart disease, and chronic respiratory ailments are among the top causes of mortality globally. When the signs or characteristics of heart disease alter, diagnosis may become challenging. A significant quantity of patient data is produced by the healthcare industry in the contemporary digital environment. Prescriptive modeling, along with state-of-the-art artificial intelligence and machine learning, may change the healthcare industry from a reactive to a preventative system. We have examined a number of deep learning techniques for monitoring and predicting cardiac disease. To find the best deep learning algorithm, we first compiled a list of them and then looked at their characteristics. Each algorithm has yielded a unique outcome under a range of conditions. The deep convolutional neural networks (DCNNs) and long-short-term-memory (LSTM) techniques, both of which provide excellent accuracy. Subsequent investigation reveals that the heart disease prediction model only attains a very low level of accuracy; hence, more sophisticated models are needed to raise the accuracy.

REFERENCES

1. Nandakumar, P., & Narayan, S. (2022). Cardiac disease detection using cuckoo search enabled deep belief network. *Intelligent Systems with Applications*, 16, 200131.
2. Borovska, P. (2018). Big Data analytics and Internet of medical Things make precision medicine a reality. *International Journal of Internet of Things and Web Services*, 3.
3. Gupta, P. K., Maharaj, B. T., & Malekian, R. (2017). A novel and secure IoT based cloud centric architecture to perform predictive analysis of user's activities in sustainable health centres. *Multimedia Tools and Applications*, 76, 18489-18512.
4. Saheb, T., & Izadi, L. (2019). Paradigm of IoT big data analytics in the healthcare industry: A review of scientific literature and mapping of research trends. *Telematics and informatics*, 41, 70-85.
5. Sun, Y., Lo, F. P. W., & Lo, B. (2019). Security and privacy for the internet of medical things enabled healthcare systems: A survey. *IEEE Access*, 7, 183339-183355.
6. Joyia, G. J., Liaqat, R. M., Farooq, A., & Rehman, S. (2017). Internet of medical things (IoMT): Applications, benefits and future challenges in healthcare domain. *J. Commun.*, 12(4), 240-247.
7. Quwaider, M., & Biswas, S. (2010). DTN routing in body sensor networks with dynamic postural partitioning. *Ad Hoc Networks*, 8(8), 824-841.
8. Wei, W., & Qi, Y. (2011). Information potential fields navigation in wireless Ad-Hoc sensor networks. *Sensors*, 11, 4794-4807.
9. Jagadeeswari, V., Subramaniaswamy, V., Logesh, R., & Vijayakumar, V. (2018). A study on medical Internet of Things and Big ssHealth information science and systems, 6, 1-20.
10. Wei, K., Zhang, L., Guo, Y., & Jiang, X. (2020). Health monitoring based on internet of medical things: architecture, enabling technologies, and applications. *IEEE Access*, 8, 27468-27478.
11. Adewole, K. S., Akintola, A. G., Jimoh, R. G., Mabayoje, M. A., Jimoh, M. K., Usman-Hamza, F. E., ... & Ameen, A. O. (2021). Cloud-based IoMT framework for cardiovascular disease prediction and diagnosis in personalized E-health care. In *Intelligent IoT Systems in Personalized Health Care* (pp. 105-145). Academic Press.
12. Srivastava, J., Routray, S., Ahmad, S., & Waris, M. M. (2022). Internet of Medical Things (IoMT)-based smart healthcare system: Trends and progress. *Computational Intelligence and Neuroscience*, 2022.





Mihir H. Rajyaguru and Miral Patel

13. Moolayil, J., Moolayil, J., & John, S. (2019). Learn Keras for deep neural networks (pp. 33-35). Berkeley, CA, USA: Apress.
14. Kukreja, H., Bharath, N., Siddesh, C. S., & Kuldeep, S. (2016). An introduction to artificial neural network. *Int J Adv Res Innov Ideas Educ*, 1, 27-30.
15. More, S., Singla, J., Verma, S., Ghosh, U., Rodrigues, J. J., Hosen, A. S., & Ra, I. H. (2020). Security assured CNN-based model for reconstruction of medical images on the internet of healthcare things. *IEEE Access*, 8, 126333-126346.
16. Wang, Z., Chen, J., Zheng, Z., & Wang, J. (2018, June). Sample expansion-oriented LDBN heart disease risk forecast model. In 2018 14th International Wireless Communications & Mobile Computing Conference (IWCMC) (pp. 1327-1332). IEEE.
17. Liu, M., & Kim, Y. (2018, July). Classification of heart diseases based on ECG signals using long short-term memory. In 2018 40th Annual International Conference of the IEEE Engineering in Medicine and Biology Society (EMBC) (pp. 2707-2710). IEEE.
18. Dau, H. A., Bagnall, A., Kamgar, K., Yeh, C. C. M., Zhu, Y., Gharghabi, S., ... & Keogh, E. (2019). The UCR time series archive. *IEEE/CAA Journal of Automatica Sinica*, 6(6), 1293-1305.
19. Raju, K. B., Dara, S., Vidyarthi, A., Gupta, V. M., & Khan, B. (2022). Smart heart disease prediction system with IoT and fog computing sectors enabled by cascaded deep learning model. *Computational Intelligence and Neuroscience*, 2022.
20. Miao, K. H., & Miao, J. H. (2018). Coronary heart disease diagnosis using deep neural networks. *international journal of advanced computer science and applications*, 9(10).
21. Huang, J., Chen, B., Yao, B., & He, W. (2019). ECG arrhythmia classification using STFT-based spectrogram and convolutional neural network. *IEEE access*, 7, 92871-92880.
22. Al-Makhadmeh, Z., & Tolba, A. (2019). Utilizing IoT wearable medical device for heart disease prediction using higher order Boltzmann model: A classification approach. *Measurement*, 147, 106815.
23. Sarmah, S. S. (2020). An efficient IoT-based patient monitoring and heart disease prediction system using deep learning modified neural network. *Ieee access*, 8, 135784-135797.
24. Khan, M. A. (2020). An IoT framework for heart disease prediction based on MDCNN classifier. *IEEE Access*, 8, 34717-34727.
25. Eesa, A. S., Brifcani, A. M. A., & Orman, Z. (2013). Cuttlefish algorithm-a novel bio-inspired optimization algorithm. *International Journal of Scientific & Engineering Research*, 4(9), 1978-1986.
26. Ramprakash, P., Sarumathi, R., Mowriya, R., & Nithyavishnupriya, S. (2020, February). Heart disease prediction using deep neural network. In 2020 International Conference on Inventive Computation Technologies (ICICT) (pp. 666-670). IEEE.
27. Akgül, M., Sönmez, Ö. E., & Özcan, T. (2020). Diagnosis of heart disease using an intelligent method: a hybrid ANN-GA approach. In *Intelligent and fuzzy techniques in big data analytics and decision making: proceedings of the INFUS 2019 Conference, Istanbul, Turkey, July 23-25, 2019* (pp. 1250- 1257). Springer International Publishing.
28. Dutta, A., Batabyal, T., Basu, M., & Acton, S. T. (2020). An efficient convolutional neural network for coronary heart disease prediction. *Expert Systems with Applications*, 159, 113408.
29. Xiao, N., Zou, Y., Yin, Y., Liu, P., & Tang, R. (2020, November). DRNN: Deep Residual Neural Network for Heart Disease Prediction. In *Journal of Physics: Conference Series* (Vol. 1682, No. 1, p. 012065). IOP Publishing.
30. Pan, Y., Fu, M., Cheng, B., Tao, X., & Guo, J. (2020). Enhanced deep learning assisted convolutional neural network for heart disease prediction on the internet of medical things platform. *Ieee Access*, 8, 189503- 189512.
31. Rath, A., Mishra, D., Panda, G., & Satapathy, S. C. (2021). Heart disease detection using deep learning methods from imbalanced ECG samples. *Biomedical Signal Processing and Control*, 68, 102820.
32. Shihab, A. N., Mokarrama, M. J., Karim, R., Khatun, S., & Arefin, M. S. (2021). An IoT-based heart disease detection system using RNN. In *Image Processing and Capsule Networks: ICIPCN 2020* (pp. 535-545). Springer International Publishing.
33. Krishnan, S., Magalingam, P., & Ibrahim, R. (2021). Hybrid deep learning model using recurrent neural network and gated recurrent unit for heart disease prediction. *International Journal of Electrical & Computer Engineering*





Mihir H. Rajyaguru and Miral Patel

- (2088-8708), 11(6).
34. Saikumar, K., Rajesh, V., Srivastava, G., & Lin, J. C. W. (2022). Heart disease detection based on internet of things data using linear quadratic discriminant analysis and a deep graph convolutional neural network.
 35. Saikumar, K., Rajesh, V., & Babu, B. S. (2022). Heart Disease Detection Based on Feature Fusion Technique with Augmented Classification Using Deep Learning Technology. *Traitement du Signal*, 39(1).
 36. Raju, K. B., Dara, S., Vidyarthi, A., Gupta, V. M., & Khan, B. (2022). Smart heart disease prediction system with IoT and fog computing sectors enabled by cascaded deep learning model. *Computational Intelligence and Neuroscience*, 2022.
 37. Nandakumar, P., & Narayan, S. (2022). Cardiac disease detection using cuckoo search enabled deep belief network. *Intelligent Systems with Applications*, 16, 200131.
 38. Effective Ways to Use Internet of Things in the field of Medical and Smart Health Care: Kaleem ullah, Munam ali Shah, Sijing zhang, *IEEE Journal* 2016.
 39. Khan, M. A. (2020). An IoT Framework for Heart Disease Prediction Based on MDCNN Classifier. *IEEE Access*, 8, 34717-34727.
 40. Pereira, S., & Karia, D. (2018, October). Prediction of Sudden Cardiac Death using Classification and Regression Tree Model with Coalesced based ECG and Clinical Data. In *2018 3rd International Conference on Communication and Electronics Systems (ICCES)* (pp. 678-681). IEEE.
 41. Javan, S. L., Sepehri, M. M., & Aghajani, H. (2018). Toward analyzing and synthesizing previous research in early prediction of cardiac arrest using machine learning based on a multi-layered integrative framework. *Journal of Biomedical Informatics*, 88, 70-89.
 42. Zaman, M. I. U., Tabassum, S., Ullah, M. S., Rahaman, A., Nahar, S., & Islam, A. M. (2019, May). Towards iot and ml driven cardiac status prediction system. In *2019 1st International Conference on Advances in Science, Engineering and Robotics Technology (ICASERT)* (pp. 1-6). IEEE.
 43. Singh, A., & Kumar, R. (2020, February). Heart disease prediction using machine learning algorithms. In *2020 international conference on electrical and electronics engineering (ICE3)* (pp. 452-457). IEEE.
 44. Chauhan, U., Kumar, V., Chauhan, V., Tiwary, S., & Kumar, A. (2019, July). Cardiac Arrest Prediction using Machine Learning Algorithms. In *2019 2nd International Conference on Intelligent Computing, Instrumentation and Control Technologies (ICICT)* (Vol. 1, pp. 886-890). IEEE.
 45. Chen, J., Valehi, A., & Razi, A. (2019). Smart heart monitoring: Early prediction of heart problems through predictive analysis of ecg signals. *IEEE Access*, 7, 120831-120839.
 46. Chowdhury, M. E., Alzoubi, K., Khandakar, A., Khallifa, R., Abouhasera, R., Koubaa, S., ... & Hasan, A. (2019). Wearable real-time heart attack detection and warning system to reduce road accidents. *Sensors*, 19(12), 2780.
 47. ElSaadany, Y., Majumder, A. J. A., & Ucci, D. R. (2017, July). A wireless early prediction system of cardiac arrest through IoT. In *2017 IEEE 41st Annual Computer Software and Applications Conference (COMPSAC)* (Vol. 2, pp. 690-695). IEEE.
 48. Murukesan, L., Murugappan, M., & Iqbal, M. (2013, March). Sudden cardiac death prediction using ECG signal derivative (heart rate variability): a review. In *2013 IEEE 9th International Colloquium on Signal Processing and its Applications* (pp. 269-274). IEEE.
 49. Gupta, K., Kaul, P., & Kaur, A. (2018, February). An Efficient Algorithm for Heart Attack Detection using Fuzzy C-means and Alert using IoT. In *2018 4th International Conference on Computational Intelligence & Communication Technology (CICT)* (pp. 1-6). IEEE.
 50. Kwon, J. M., Kim, K. H., Jeon, K. H., Lee, S. Y., Park, J., & Oh, B. H. (2020). Artificial intelligence algorithm for predicting cardiac arrest using electrocardiography. *Scandinavian journal of trauma, resuscitation and emergency medicine*, 28(1), 1-10.
 51. Sarmah, S. S. (2020). An Efficient IoT-Based Patient Monitoring and Heart Disease Prediction System Using Deep Learning Modified Neural Network. *IEEE Access*, 8, 135784-135797.
 52. Ganesan, M., & Sivakumar, N. (2019, March). IoT based heart disease prediction and diagnosis model for healthcare using machine learning models. In *2019 IEEE International Conference on System, Computation, Automation and Networking (ICSCAN)* (pp. 1-5). IEEE.





Mihir H. Rajyaguru and Miral Patel

53. Tarun Rahuja, Nidhi Sengar, Dr.Amita Goel. Heart Disease Prediction Using Machine Learning. International Journal for Modern Trends in Science and Technology, 6(12): 290-293, 2020

54. Aditya Kumar S, Lalit Kumar J, Mantosh Kumar. Heart Disease Prediction and Classification Using Machine Learning Algorithms Optimized by Particle Swarm Optimization and Ant Colony Optimization. International Journal for Modern Trends in Science and Technology, 6(12): 426-435, 2020

55. Majumder, A. K. M., ElSaadany, Y. A., Young, R., & Ucci, D. R. (2019). An energy efficient wearable smart IoT system to predict cardiac arrest. Advances in Human-Computer Interaction, 2019.

56. Mohan, S., Thirumalai, C., & Srivastava, G. (2019). Effective heart disease prediction using hybrid machine learning techniques. IEEE Access, 7, 81542-81554.

57. Chandurkar, S., Arote, S., Chaudhari, S., & Kakade, V. (2018). The system for early detection of heart-attack. Int. J. Control Automat., 182(27), 30-33.

58. Arya, Akash. (2023). A Comprehensive Review on Monitoring and Prediction Techniques for Heart Disease using Deep Learning and Iot. 10.56726/Irjmets53667.

Table -1 List of sensors and their use in monitoring heart disease[12].

Sr. No.	Name of sensors	Applications
1	Heart beat sensor	This device is used to quantify the heart's pulse rate, providing a digital output.
2	Pressure sensor	The equipment is used to quantify both the systolic and diastolic pressure levels.
3	Accelerometers	Detects movement and motion of the human body.
4	LM35	This sensor modifies voltage in response to variations in temperature in centigrade. It takes a body temperature reading.
5	ESP8266 WiFi Module	The SOC is a self-contained system that includes a TCP/IP protocol stack, allowing any microcontroller to connect to your WiFi network.
6	DHT11	Temperature data between 0°C and 50°C and humidity data between 20% and 90% are collected with this sensor. It gauges the condition of the surroundings.
7	Atmega 328	The micro-controller is an 8-bit device. It has the capacity to process data that is up to eight (8) bits in size. The micro-controller is based on AVR architecture.
8	AD8232	It examines cardiac signals in the absence of physical symptoms in the patient.
9	ADXL335	This sensor helps with the best positioning to prevent problems like pain, edema, body aches, and breathing problems.
10	MAX 30105	This combined optical sensor with two LEDs in one device, when linked with Arduino, generates extremely low noise electrical outputs to monitor heart rate in the range of 1.8 V to 3.3 V.

Table-2 A Comparative Analysis of Different Literature Review Methodologies

Author	Purpose	Techniques	Accuracy
Zhenfei Wang et al.	LDBN heart disease risk forecast model.	LSTM (Long Short-Term Memory) and DBN (Deep Belief Neural Network).	73.8%
Ming Liu and Young hoon Kim	A classification method of heart diseases based on ECG.	RNN with LSTM.	98.4%
Kathleen H. Miaoa and Julia H. Miaoa	An enhanced deep neural network (DNN) for Coronary Heart Disease Diagnosis.	Deep Neural Network (DNN)	83.67%
Jingshan Huang et al.	Edge-Fog-Cloud- derived computation model" for heart disease prediction.	2D deep convolutional neural network (2DCNN).	99.0%





Mihir H. Rajyaguru and Miral Patel

Zafer Al-Makhadmeh and Amr Tolba	A classification approach, utilizing IoT wearable medical device for heart disease prediction.	Higher Order Boltzmann Deep Belief Neural Network (HOBDBNN).	99.03%
Simanta Shekhar Sarmah	Efficient IoT-Based patient monitoring and heart disease prediction system.	DLMNN (Deep Learning Modified Neural Network).	92.0%
Mohammad Ayoub Khan	An IoT framework to evaluate heart disease.	Modified Deep Convolutional Neural Network (MDCNN)	98.2%
P. Ramprakash et al.	Diagnosis model for cardiac disorder disease detection.	Deep Neural Network and 2 - statistical model.	higher accuracy than the conventional DNN.
Miray Akgul et al.	A hybrid approach, for heart disease classification.	Artificial Neural Network (ANN) and Genetic Algorithm (GA)	95.82%
Aniruddha Dutta et al.	An efficient convolutional neural network for coronary heart disease prediction	Convolutional Neural Network (CNN) and Least Absolute Shrinkage and Selection Operator(LASSO).	79.5%
Nianhao Xiao et al.	A Deep Residual Neural Network for Heart Disease Prediction	Deep Residual Neural Network (DRNN) and ResNet Architecture.	95%
Yuanyuan Pan et al.	An Enhanced Deep Learning Assisted Convolutional Neural Network for Heart Disease Prediction on the Internet of Medical Things Platform	Enhanced Deep learning assisted Convolutional Neural Network (EDCNN), CNN classifier and multi-layer perceptron (MLP)	93.51%
Adyasha Rath et al.	A Heart disease detection method.	Generative Adversarial Network (GAN) and Long Short-Term Memory (LSTM) (GAN-LSTM).	For MIT-BIH dataset, accuracy is 99.2%. For PTB-ECG dataset, accuracy is 99.4%.
Ashif Newaz Shihab et al.	An IoT based heart disease detection system.	Long Short-Term Memory (LSTM).	96%
Surentiran Krishnan et al.	A Hybrid deep learning model using recurrent neural network and gated recurrent unit for heart disease prediction	Recurrent Neural Network (RNN) with the combination of multiple gated recurrent units (GRU) and LSTM.	98.6876%
K.Saikumar et al.	An intelligent heart disease diagnosis application.	Deep Graph Convolutional Network (DG ConvoNet).	96%.
Kayam Saikumar et al.	Heart Disease Detection Based on Feature Fusion Technique Using Deep Learning Technology.	DCAlexNet CNN deep learning technology, RRF (Restrictive Random Field) technology.	98.67%
K. Butchi Raju et al.	“Edge-Fog-Cloud- derived computation model” for heart disease prediction.	Cascaded Convolution Neural Network (CCNN).	94.99%





Mihir H. Rajyaguru and Miral Patel

Nandakumar P and Subhashini Narayan	A cardiac disease detection system.	cuckoo search enabled Deep Belief Network (DBN)	89% - 90%
--	--	--	-----------

Table-3 A Comparative Analysis of Different Literature Review Methodologies and relevent Findings

Author	Study Purpose	Method	Relevant Findings
Mohammad Ayoub Khan.	Heart Disease Prediction [39]	1. Deep learning Neural Networks and Logistic Regression. 2. Cleveland Dataset. 3. Long short-term memory (LSTM) 4. Deep Learning Neural Network (DLNN) 5. Adaptive Elephant Herd Optimization (AEHO) algorithm for weight values optimization.	1. Diagnosis of heart disease is very difficult. 2. Diagnosis results are low. 3. Perform more experiments to increase the performance of the predictive classifiers for heart disease diagnosis by selection algorithms and optimization techniques. 4. Fully trained and Tested wearable devices.
Sean Pereira and Deepak Karia	Prediction of Sudden Cardiac Death [40]	1. Probabilistic Neural Network (PNN) 2. Classification and Regression Tree (CART)	1. Accuracy of Clinical data is 86% and ECG is 80% 2. The CART Model is trained with 50% training Data set and 50% testing data set
SamanehLayeghianJavana, Mohammad Mehdi Sepehria,HassanAghajanib	Cardiac arrest with machine learning based on a multi-layered integrative framework [41]	1. A multi-layered integrative framework for evaluating ML techniques used for cardiac arrest prediction.	1. The major challenge is that the models are developed and evaluated with limited hospital data; therefore, the generalizability of the models to other patient populations and health systems is unknown.
Md. IttihadUzZaman, ShairaTabassum, Md. SabbirUllah, AshikurRahaman, Samsun Nahar, A.K.M. Muzahidul Islam.	IoT and ML Driven Cardiac Status Prediction System [42]	1. Micro Controller Unit (MCU) connected to the required hardware sensors and modules.	1. Real time monitoring system need to predict Heart dieses. 2. ECG output signal was very different from the actual one.
Archana Singh, Rakesh Kumar	Heart Disease Prediction Using ML [43]	1. Supervised 2. Unsupervised 3. Reinforced 4. Linear Regression, 5. Logistical Regression 6. Support Vector Machines	1. Use of UCI repository dataset but due to technological gap not get accurate result





Mihir H. Rajyaguru and Miral Patel

		(SVM) 7. Neural Networks 8. Random Forest	
Utsav Chauhan, Vikas Kumar, Vipul Chauhan, Sumit Tiwary	Cardiac Arrest Prediction using ML [44]	1. Support Vector Machines (SVM) 2. Artificial Neural Networks (ANN) 3. Several algorithms such as Support Vector Machine, Random Forest, Decision Tree, Logistic Regression	1. Since the dataset was limited, the accuracy of the algorithm is low. 2. Had the dataset been bigger the accuracy of ANN would also have been much higher than the current average value of the outcome.
Jiaming Chen, Ali Valehi, Abolfazl Razi.	Prediction of Heart Problems Through Predictive Analysis of ECG Signals [45]	1. Two-staged classification structure with global and personalized classifiers.	1. Not integrated with wearable heart monitoring devices to elderly and high-risk heart patients.
Muhammad E. H. Chowdhury, Khawla Alzoubi, Amith Khandakar, Ridab Khallifa	Real-Time Heart Attack Detection [46]	1. Linear and ML base algorithms.	1. Device accuracy is not proven in this paper. 2. Only ECG base system with no data set and trained model for predictions.
Yosuf ElSaadany, AKM Jahangir A. Majumder, Donald R. Ucci	Prediction of Cardiac Arrest through IoT [47]	1. collected data from ECG and temperature sensors 2. Collected data for different test subjects in different environments for 160 samples in per second. Each segment is 25 seconds long.	1. High rate of classification correctness needed between normal and abnormal ECG patterns. 2. System is not working for real-time monitoring for Cardiac Arrest
L Murugesan Loganathan, Murugappan M, Ye Htut.	Sudden Cardiac Death Prediction [48]	1. First is HRV can be accessed from short (2-3 minutes) and long (24 Hours) ECG signals. 2. Next is it can be automatically recorded using Holter Monitor with additional software.	1. There is no consensus on which parameters of HRV performs better for SCD prediction.
Kriti Gupta, Pallavi Kaul, Arashdeep Kaur.	An Efficient Algorithm for Heart Attack Detection [49]	1. Fuzzy c-means clustering algorithm. 2. Implemented using MATLAB 7.8	1. ECG is not consider in this method
Joon-myung Kwon, Kyung-Hee Kim, Ki-Hyun Jeon, Youn Lee.	Artificial intelligence algorithm for predicting cardiac arrest [50]	1. Deep learning- based artificial intelligence algorithm (DLA)	1. Not integrated with wearable heart monitoring devices for high-risk heart patients.





Mihir H. Rajyaguru and Miral Patel

SimantaShekharSarmah	IoT based patient monitoring system with the use of Deep learning [51]	This technique is executed via '3' steps: 1. Authentication, 2. Encryption, and 3. Classification.	1. They are working on secure data transmission to cloud rather than prediction of heart attack
M.Ganesan, Dr.N.Sivakumar	IoT based heart disease prediction and diagnosis Model [52]	1. ZigBee is employed for data transmission to the cloud was used to transmit the gathered data to the cloud center, and RFID is used for automatic object identification. 2. It comprises of five main parts like Medical IoT sensors, heart disease dataset, patient data, Cloud Database, ML based heart disease prediction system.	1. Not integrated with wearable heart monitoring devices. 2. Not consider ECG and Blood pressure
TarunRahuja, Nidhi Sengar, Dr.AmitaGoel.	Heart Disease Prediction Using Machine Learning [53]	1. Supervised learning, 2. logistic regression, 3. Naïve Bayes, 4. random forests, 5. decision trees, 6. support vector machines, 7. K-nearest neighbours 8. Use of UCI Cleveland	1. Use only Use of UCI Cleveland data set for prediction 2. Not integrated with wearable heart monitoring devices.
Aditya Kumar S Lalit Kumar J Mantosh Kumar	Classification Using Machine Learning with Particle Swarm Optimization and Ant Colony Optimization [54]	1. K-Nearest Neighbour, 2. Support Vector Machine, 3. Naïve Bayes, Random Forest 4. Multilayer Perception 5. Artificial Neural Network optimized by Particle Swarm Optimization (PSO) combined with Ant Colony Optimization (ACO) approaches.	1. Every algorithm performed differently depending on the circumstances. 2. Limited data set is problem for prediction.
AKM Jahangir AlamMajumder, Yosuf Amr ElSaadany, Roger Young, Donald R. Ucci.	Efficient Wearable Smart IoT System to Predict Cardiac Arrest [55]	1. Heart Attack Prediction using a Decision Tree based on a Standard Deviation Statistical Analysis (DTSDSA)	1. strong classification accuracy in differentiating between normal and aberrant ECG patterns. 2. prediction based on R-R Intervals of ECG only
Senthilkumar Mohan, ChandrasegarThirumalai, Gautam Srivastava	Heart Disease Prediction Using Hybrid Machine Learning [56]	1. Decision Trees 2. Language Model 3. Support Vector Machine 4. Random Forest 5. Naive Bayes	1. Efficient research and algorithm use with also considering ECG and all parameters which affect heart attack.





Mihir H. Rajyaguru and Miral Patel

		6. K-Nearest Neighbour 7. Decision Tree-Based Partition	2. Not integrated with wearable heart monitoring devices.
Swati Chandurkar, Shraddha Arote, SnehalChaudhari, VaishnaviKakade.	Early Detection of Heart-Attack [57]	1. The Pulse Sensor AMPED 2. The Blood Pressure Sensor (Vernier) is a non-invasive sensor designed to measure human blood pressure	1. Only use Naïve Bayes Classifier for prediction 2. Only monitoring pulse rate of human body 3. No deep learning or machine learning concept use

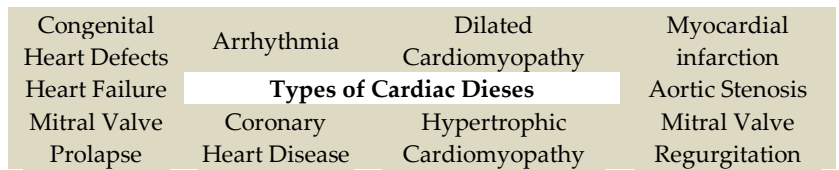


Fig. 1. Types of Cardiac Disease [1]





Remaining useful Life (Rul) Prediction of Li-ion Batteries using Machine Learning and Deep Learning

Vatsal Viradiya, Milendrakumar M Solanki and M. S. Holia D. M. Patel

Einfochips, Ahmedabad BVM Engineering College, V.V.Nagar, Gujarat, India.

Received: 30 Dec 2023

Revised: 09 Jan 2024

Accepted: 12 Jan 2024

*Address for Correspondence

Vatsal Viradiya

Einfochips,
Ahmedabad BVM Engineering College,
V.V.Nagar, Gujarat, India
Email: vatsalviradiya88@gmail.com



This is an Open Access Journal / article distributed under the terms of the **Creative Commons Attribution License** (CC BY-NC-ND 3.0) which permits unrestricted use, distribution, and reproduction in any medium, provided the original work is properly cited. All rights reserved.

ABSTRACT

This research paper aims to predict the Remaining Useful Life (RUL) of Li-ion batteries using machine learning algorithms. The project uses experimental data on the aging behavior of Li-ion batteries, including voltage, current, temperature, capacity, and energy. The data is preprocessed using feature engineering techniques and evaluated using several Machine Learning and Deep Learning models. The LSTM model performs the best with an R-squared score of 1.0. The study contributes to the development of efficient and reliable methods for RUL prediction of Li-ion batteries, which can have significant practical implications in the field of energy storage and management.

Keywords: Li-ion batteries, experimental data, aging behavior, Multiple Linear Regression, Polynomial Regression, Decision Tree Regression, Random Forest Regression, LSTM, energy storage, energy management.

INTRODUCTION

Lithium-ion batteries are widely used in various applications, including portable electronics, electric vehicles, and grid-scale energy storage. These batteries are preferred due to their high energy density and long lifespan [1], but their performance degrades over time due to aging and degradation of battery components [2]. Therefore, predicting the Remaining Useful Life (RUL) of li-ion batteries is crucial to ensure their safe and efficient operation. One of the key parameters in predicting the RUL of li-ion batteries is the cycle index, which refers to the number of charging and discharging cycles a battery has undergone during its lifetime. Knowing the cycle index can help estimate the battery's RUL and assess its health and performance [3]. In this project, the aim is to analyze the degradation behavior of li-ion batteries by studying their utilization data and training a machine learning model using different ML and DL algorithms for predicting the RUL of li-ion batteries. To achieve this aim, a dataset of Li-ion battery (LFP chemistry)



**Vatsal Viradiya et al.,**

from Toyota Research Institute is used in this project [11]. Machine learning models like Multiple Linear Regression, Polynomial Regression, Decision Tree Regression, and Random Forest Regression and Deep Learning model like LSTM are trained to predict the cycle index of a li-ion battery based on various features such as test time, current, voltage, temperature, and others. These models are then evaluated, and the best algorithm for predicting the RUL of li-ion batteries is selected. The accurate prediction of cycle index is important for monitoring the health and performance of li-ion batteries and ensuring their safe and efficient operation.

Related work

Introduction to RUL prediction and its importance in battery management

RUL (Remaining Useful Life) prediction is essential in battery management as it enables better maintenance and management of batteries, leading to cost savings and improved safety. Prognostics and health management (PHM) of engineering systems, including Li-ion batteries, is crucial for proactive maintenance and management, reducing downtime and costs, and improving safety and reliability. PHM involves different approaches and techniques, such as model-based and data-driven methods, to predict the RUL of batteries [1]. Predicting the RUL of batteries allows for proactive replacement or maintenance of batteries, reducing the risk of failures and improving the lifespan and performance of batteries. Selecting appropriate RUL prediction methods based on the characteristics of the battery system and the available data is also important. Overall, RUL prediction is a critical component of battery management that helps ensure optimal performance, reliability, and safety of Li-ion batteries.

Overview of Li-ion battery technology, its properties, and common failure modes

Lithium-ion batteries are widely used due to their high energy density, long cycle life, and low self-discharge rate. However, they are prone to various failure modes, such as capacity fade, internal short-circuit, thermal runaway, and mechanical deformation [2]. These failures can be caused by factors such as electrode degradation, electrolyte decomposition, temperature and vibration. Ongoing research aims to improve the performance and safety of Li-ion batteries by increasing their energy density, reducing the risk of failure modes, and lowering their cost and environmental impact. Potential solutions include improving electrode and electrolyte materials, incorporating safety features, and implementing real-time monitoring and control systems.

Explanation of machine learning techniques commonly used for RUL prediction, such as regression algorithms

Machine learning techniques, particularly regression algorithms, are commonly used for RUL prediction in Li-ion Batteries. Different types of regression algorithms like linear regression, polynomial regression, support vector regression, multiple regression, neural network regression, and Bayesian regression are used for RUL prediction [3]. Feature selection and data pre-processing techniques are also important to improve the accuracy and reliability of RUL prediction. Additionally, model selection and evaluation techniques and real-time monitoring and feedback are necessary to improve the accuracy of RUL prediction in Li-ion batteries in electric vehicles.

Evaluation of the performance of different ML methods in RUL prediction for Li-ion batteries, including their strengths and limitations.

When evaluating the performance of machine learning methods for RUL prediction in Li-ion batteries, various metrics like accuracy, precision, recall, F1 score, and RMSE are important [1][3]. In addition to these metrics, it is also essential to consider the strengths and limitations of different machine learning techniques such as artificial neural networks, support vector machines, decision trees, and regression models [8]. The selection of the most appropriate machine learning method depends on the characteristics of the battery system and the available data, and effective feature selection and data pre-processing techniques can improve the performance of the models.

Discussion of the challenges and open research questions in RUL prediction for Li-ion batteries using ML

RUL prediction for Li-ion batteries using machine learning faces several challenges and open research questions that need to be addressed. These include the availability and quality of data, feature selection, and the need for



**Vatsal Viradiya et al.,**

explainable and interpretable models. It is important to overcome these challenges to develop accurate and reliable RUL prediction models for Li-ion batteries using machine learning. Potential solutions to these challenges include developing new data-driven feature selection and extraction techniques, integrating physics-based models[4] with data-driven models[1][5][8], and using explainable and interpretable machine learning models for RUL prediction.

METHODOLOGY

Multiple Linear Regression

Multiple linear regression is a statistical technique used to model the relationship between a dependent variable and two or more independent variables. The goal of multiple linear regression is to estimate the linear relationship between the dependent variable and the independent variables by fitting a line, plane, or hyperplane to the data. The line, plane, or hyperplane represents the best estimate of the relationship between the variables, and is chosen to minimize the sum of the squared differences between predicted and actual values in the data.

The equation for a multiple linear regression model is:

$$y = \beta_0 + \beta_1x_1 + \beta_2x_2 + \dots + \beta_px_p + \varepsilon$$

where y is the dependent variable, x_1, x_2, \dots, x_p are the independent variables, $\beta_0, \beta_1, \beta_2, \dots, \beta_p$ are the regression coefficients (also known as the intercept and slopes), and ε is the error term, which represents the unexplained variation in the dependent variable. The regression coefficients represent the expected change in the dependent variable for a one-unit increase in the independent variable, with all other independent variables held constant. The coefficients can be used to make predictions about the dependent variable for different values of the independent variables.

Polynomial Regression

Polynomial regression is a form of regression analysis in which the relationship between the independent variable x and the dependent variable y is modeled as an n th degree polynomial. This means that instead of fitting a straight line to the data, as in simple linear regression, polynomial regression models can fit curves to the data.

The equation for a polynomial regression model is:

$$y = \beta_0 + \beta_1x + \beta_2x^2 + \dots + \beta_nx^n + \varepsilon$$

where y is the dependent variable, x is the independent variable, $\beta_0, \beta_1, \beta_2, \dots, \beta_n$ are the regression coefficients, ε is the error term, and n is the degree of the polynomial. Polynomial regression can be used when the relationship between the dependent variable and independent variable is not linear but can be better represented by a curve. The higher the degree of the polynomial, the more complex the curve that is fit to the data. One important consideration when using polynomial regression is the risk of over fitting. This occurs when the model fits too closely to the training data and does not generalize well to new data. Regularization techniques, such as ridge regression and lasso regression, can be used to prevent over fitting.

Decision Tree Regression

Decision tree regression is a supervised learning algorithm used to predict a continuous output variable based on multiple input variables. It is a type of regression analysis that builds a tree-like model of decisions and their possible consequences. The tree consists of nodes and branches, where each internal node represents a test on an attribute, each branch represents the outcome of the test, and each leaf node represents a decision on the target variable. The decision tree regression algorithm recursively partitions the data based on the most informative features in order to minimize the variance of the target variable. The splitting process continues until a stopping criterion is met, such as reaching a maximum depth or a minimum number of samples in each leaf node. One advantage of decision tree regression is its interpretability, as the resulting model can be easily visualized and understood. It can also handle





Vatsal Viradiya et al.,

both continuous and categorical input variables, as well as missing data. However, decision tree regression can suffer from over fitting if the tree is too complex and can be sensitive to small variations in the data. To address these issues, ensemble methods such as random forests or boosting can be used to improve the performance and robustness of decision tree regression.

Random Forest Regression

Random Forest Regression is an ensemble learning method that combines multiple decision trees to create a more accurate model. The idea behind random forest regression is to build multiple decision trees and then aggregate their predictions to produce a more stable and accurate prediction. In a random forest regression model, each decision tree is built using a random subset of the training data and a random subset of the features. This helps to reduce over fitting and improve the generalizability of the model. To make a prediction with a random forest regression model, the model takes the average prediction of all the decision trees in the forest. This ensemble approach helps to reduce the variance of the predictions and make the model more robust to outliers and noise in the data. Random forest regression can be used for both regression and classification problems and is a popular choice for many real-world applications. It has the advantage of being a relatively simple and easy-to-use algorithm that can handle large datasets with many features. Some of the key benefits of using random forest regression include its ability to handle nonlinear relationships between the input and output variables, its resistance to over fitting, and its ability to handle missing data and outliers.

LSTM

LSTM (Long Short-Term Memory) represents a breakthrough in recurrent neural network (RNN) design, specifically tailored to overcome the limitations posed by the vanishing gradient problem in learning prolonged dependencies within sequential data. At its core, an LSTM consists of memory cells and a set of gates that regulate the flow of information. The memory cell, denoted as C_t , acts as a reservoir for storing and updating information over time, providing the architecture with the capability to retain long-term memory. This is achieved through the interplay of an input gate (i), which determines how much new information is integrated into the memory cell, a forget gate (f) that selectively discards irrelevant information, and an output gate (o) that controls the information used to compute the output. The resulting hidden state (h or output) from each time step not only carries information to subsequent steps but also contributes to the final output. LSTMs find significant utility in tasks involving sequential data, such as natural language processing and time series prediction, where capturing intricate patterns and long-term dependencies is crucial. The architecture's ability to selectively update and utilize information through its gating mechanisms addresses challenges like the vanishing gradient problem, making it particularly effective for training deep networks on sequential data. The LSTM's versatility extends to applications requiring a nuanced understanding of temporal relationships, offering a powerful tool for modeling complex, time-dependent phenomena.

CONCLUSION AND FUTURE SCOPE

Based on the evaluation of our Li-ion battery RUL prediction models, I can conclude that LSTM, Random Forest Regression and Decision Tree Regression produced the best results with low mean squared error, high R-squared score, and low root mean squared error. I also observed that Polynomial Regression achieved a moderate level of accuracy, while Multiple Linear Regression showed the least accuracy in predicting RUL for Li-ion batteries. The results suggest that machine learning algorithms can effectively predict the RUL of Li-ion batteries, and further improvements could be made by exploring neural network-based algorithms. In future, instead of using cycle index as the dependent variable, I will use discharge capacity. This change in the dependent variable will also allow us to predict the remaining useful life (RUL) of the Li-ion batteries with greater accuracy. Moreover, we plan to observe the batteries for a longer duration to collect more data points and improve the model's performance.





Vatsal Viradiya et al.,

REFERENCES

1. Shahid A. Hasib, S. Islam Ripon K. Chakraborty, Michael J. Ryan, D. K. Saha, "A Comprehensive Review of Available Battery Datasets, RUL Prediction Approaches, and Advanced Battery Management" IEEE Access (Volume: 9), June 14, 2021, Page(s): 86166 - 86193.
2. Shihui Xiong, Shaodan Ma, Yik-Chung Wu, and Tung-Sang Ng. " A study of the factors that affect lithium-ion battery degradation." Electrical Engineering and Computer Science electronic theses and dissertations (MU) 2019 MU thesis, University of Missouri – Columbia.
3. Severson, K.A., Attia, P.M., Jin, N. et al. "Data-driven prediction of battery cycle life before capacity degradation" Nat Energy 4, 383–391 (2019). <https://doi.org/10.1038/s41560-019-0356-8> Published on 25 March 2019
4. Luping Chen, Liangjun Xu and Yilin Zhou. "Novel Approach for Lithium-Ion Battery On-Line Remaining Useful Life Prediction Based on Permutation Entropy" School of Automation, Beijing University of Posts and Telecommunications, Beijing 100876, China; ljxu@bupt.edu.cn (L.X.); ylzhou@bupt.edu.cn (Y.Z.) Published: 2 April 2018
5. Rashmikant T. Shukla. "Prediction of Remaining Useful Life (RUL) of Lithium ion (Li-ion) Batteries" Msc Research Project, School of Computing, National College of Ireland.
6. Sophia Gantenbein, Michael Schönleber, Michael Weiss and Ellen Ivers-Tifée. "Capacity Fade in Lithium-Ion Batteries and Cyclic Aging over Various State-of-Charge Ranges" Institute for Applied Materials (IAM-WET), Karlsruhe Institute of Technology (KIT), 76131 Karlsruhe, Germany; michael.schoenleber@batemo.de (M.S.); m.weiss@kit.edu (M.W.); ellen.ivers@kit.edu (E.I.-T.) Published: 26 November 2019
7. Attia, P.M., Grover, A., Jin, N. et al. "Closed-loop optimization of fast-charging protocols for batteries with machine learning" Nature 578, 397–402 (2020). <https://doi.org/10.1038/s41586-020-1994-5> Published: 19 February 2020
8. P. Khumprom and N. Yodo, "Data-driven Prognostic Model of Li-ion Battery with Deep Learning Algorithm" 2019 Annual Reliability and Maintainability Symposium (RAMS), Orlando, FL, USA, 2019, pp. 1-6, doi: 10.1109/RAMS.2019.8769016.
9. Zhao, Jiahui, Yong Zhu, Bin Zhang, Mingyi Liu, Jianxing Wang, Chenghao Liu, and Yuanyuan Zhang. 2022. "Method of Predicting SOH and RUL of Lithium-Ion Battery Based on the Combination of LSTM and GPR" Sustainability 14, no. 19: 11865. <https://doi.org/10.3390/su141911865>
10. <https://www.nasa.gov/intelligent-systems-division>
11. Experimental Data Platform (matr.io) – Toyota Research Institute
12. Oxford Battery Degradation Dataset 1 - ORA - Oxford University Research Archive (<https://ora.ox.ac.uk/objects/uuid:03ba4b01-cfed-46d3-9b1a-7d4a7bdf6fac>)
13. CALCE Datasets (<https://calce.umd.edu/battery-data>)
14. Mendeley Datasets (<https://data.mendeley.com/>)

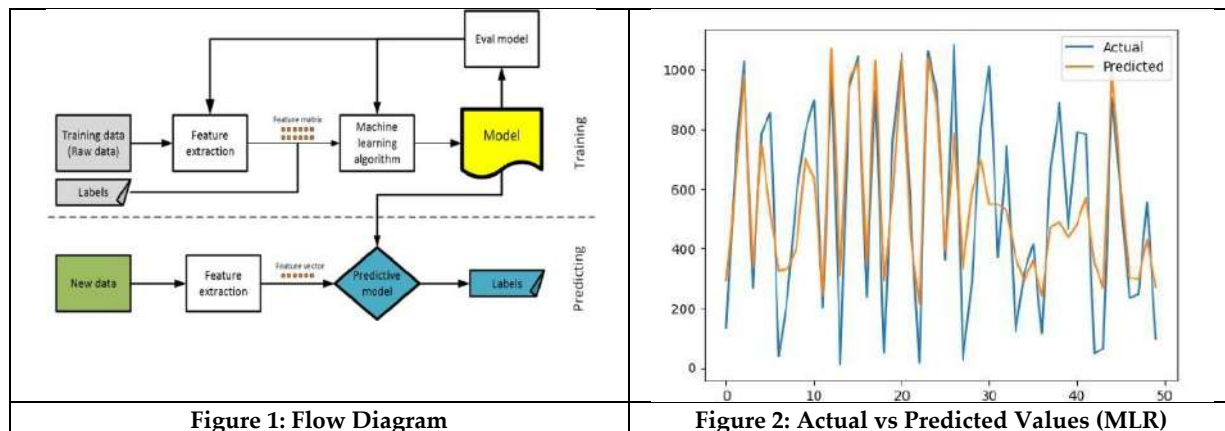


Figure 1: Flow Diagram

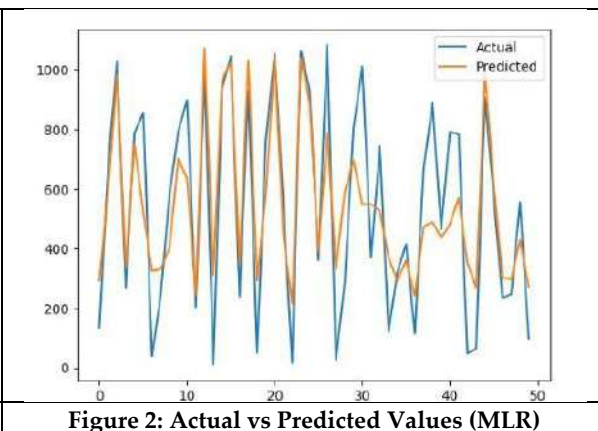


Figure 2: Actual vs Predicted Values (MLR)





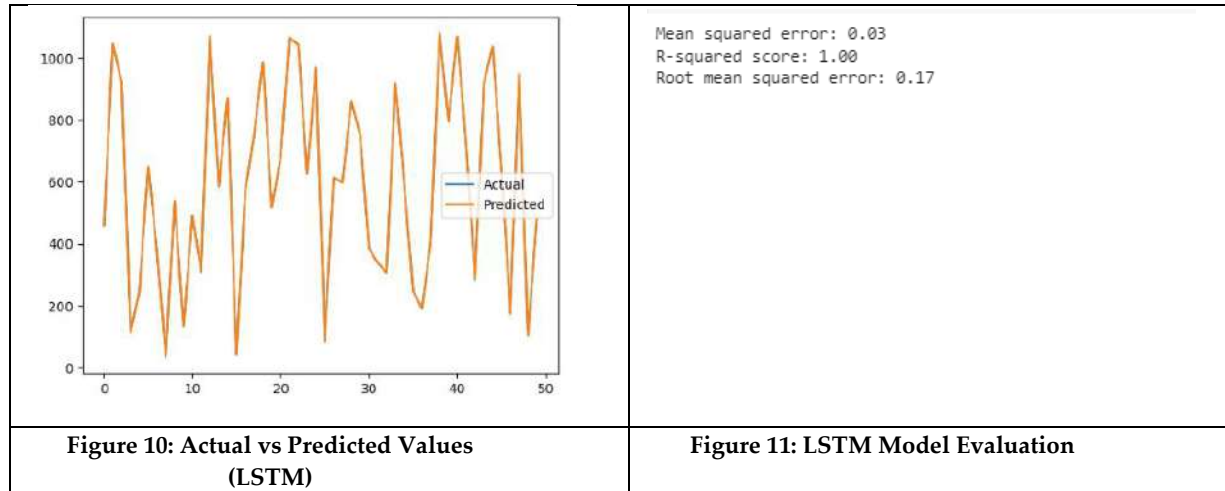
Vatsal Viradiya et al.,

	<p>Mean squared error: 823.24 R-squared score: 0.87 Root mean squared error: 28.69</p>
<p>Figure 4: Actual vs Predicted Values (Polynomial Regression)</p>	<p>Figure 5: PR Model Evaluation</p>
	<p>Mean squared error: 2024.98 R-squared score: 0.98 Root mean squared error: 45.00</p>
<p>Figure 6: Actual vs Predicted Values (Decision Tree Regression)</p>	<p>Figure 7: DTR Model Evaluation</p>
	<p>Mean squared error: 1072.18 R-squared score: 0.99 Root mean squared error: 32.74</p>
<p>Figure 8: Actual vs Predicted Values (Random Forest Regression)</p>	<p>Figure 9: RFR Model Evaluation</p>





Vatsal Viradiya et al.,





RESEARCH ARTICLE

Attention Mechanisms in VQA: A Comparative Exploration of Soft, Stack, and Additive Attention Approaches

Lata Bhavnani^{1*} and Narendra. M. Patel²

¹Research Scholar, Gujarat Technological University, Ahmedabad, Gujarat, India.

²Professor, Computer Department, BVM Engineering College, V.V. Nagar, Gujarat, India.

Received: 30 Dec 2023

Revised: 09 Jan 2024

Accepted: 12 Jan 2024

*Address for Correspondence

Lata Bhavnani

Research Scholar,

Gujarat Technological University,

Ahmedabad, Gujarat, India.

Email: latabhavnani.bbit@gmail.com



This is an Open Access Journal / article distributed under the terms of the **Creative Commons Attribution License** (CC BY-NC-ND 3.0) which permits unrestricted use, distribution, and reproduction in any medium, provided the original work is properly cited. All rights reserved.

ABSTRACT

Visual Question Answering (VQA) is a multidisciplinary task that involves models that combine both computer vision for image understanding and natural language processing for question understanding and answer generation. Instead of focusing on overall image features and question features, consideration of relevant region features of the image makes it more reliable for answer generation. The attention mechanism provides this enhancement in the VQA model to focus on the relevant part of the image and question to generate the answer. This paper explores three different VQA attention models: Soft Attention, Stack Attention, and Additive Attention. It also provides a performance comparison of these models to support researchers in making it informal to select the most appropriate attention mechanism for their relevant VQA models.

Keywords: Visual Question Answering(VQA), Natural Language Processing, Soft attention, Additive attention, Stack attention.

INTRODUCTION

Visual Question Answering (VQA)[1] is a research problem in the field of computer vision and natural language processing (NLP) and Artificial Intelligence (AI). Computer vision and NLP together help the system to answer a question about the content of the image and AI helps it to generate reasoning over the answer prediction. In VQA, a machine is presented with an image and a text-based question, and it must generate a natural language answer based on its understanding of the visual content and the question. Fig.1, illustrates the VQA task. In the VQA system attention mechanism plays vital role. It enables the model to focus on a specific region and part of the input image and question while making predictions, which is critical in tasks like VQA for the following reasons



**Lata Bhavnani and Narendra. M. Patel**

1. Fusion of Image and Language: VQA model combines features of both image and question. Attention mechanisms help the model to attend only part of the image that is relevant and focus only on critical words in the question.
2. Input Question with Variable Length: The VQA task contains questions with variable length and complexity. To adapt these variations, the attention mechanism helps in focusing on the most informative part of the question and image regardless of any length or complexity of the input question
3. Reasoning & Interpretability: Reasoning over the answer provides transparency in VQA model prediction. The attention mechanism provides the image region and words in the question which leads to the answer prediction. This interpretability helps the model in effective decision-making like humans do when they answer questions about an image by focusing on the relevant part of the input.
4. Handling Ambiguity: VQA questions can be ambiguous, and only some specific details of the image may be used for answering the question. Attention mechanisms help the model to overcome such ambiguity by leading its focus to the critical content of the image and question information.
5. Overall, for the enhancement of performance and interpretability of VQA models' attention mechanisms are essential. It can be helpful in the advancement of other tools like VQA such as image retrieval, image captioning, machine translation, text summarization, and more.

Organization

First introduction of the VQA and requirements for VQA attention models is given. Next part provides literature review in the area of attention based VQA. Further details and working of different VQA models are given followed by details about the dataset, experiment details, and performance discussion. Last part provides conclusion of the work and suggests future work in this area.

Related work

To get the accurate and faster prediction of answers in Visual Question Answering attention mechanism has played a good role. Here we will focus on the attention based VQA models. Shih et al,[2]proposed a technique to find the regions in an image which are most relevant in answering a given question. It identifies "focus regions" in the image which are significant to answer the question. Spatial Transformer Networks (STNs) is used to predict the spatial transformations required to line up the image areas with the question. This improves the performance by focusing on the most relevant parts of the image. The model also includes question-adaptive attention which allows the model to dynamically adjust its attention based on the specific features of the question being asked. Yang et al, [3]introduced a model with stacked attention mechanism, where attention is applied hierarchically. Here iterative attention with multiple stacked attention stages refines its focus on different image regions. The model captures both global and local information of the image by applying attention mechanism on different levels of granularity. This hierarchical attention is proposed to improve the model's ability to comprehend complex associations in the visual input. It also uses Long Short-Term Memory (LSTM) networks in conjunction with the attention mechanism which help to capture sequential dependencies in the question features for understanding context of the question.

Lu et al, [4]introduce a hierarchical co-attention VQA model that works at various levels. This provides attention over both image and question simultaneously to capture joint relationships between different elements in both modalities. Duy et al.[5] introduced a dense co-attention mechanism which calculates associations between image region and words in the question. It generates attention maps on image regions for each word and vice versa for creating a multi-layer hierarchy to find interactions between a question and an image pair. Kim et al. [6]

proposed bilinear attention networks (BAN) that search bilinear attention distributions to effectively use given image and question information. It also proposed a modified multimodal residual network for generating eight attention maps of BAN. Zhang et al.[7]proposed a VQA model with visual relation reasoning module to understand relation between various image regions. The authors utilized bilinear attention in conjunction with bottom-up attention to



**Lata Bhavnani and Narendra. M. Patel**

generate more meaningful attention maps. The final step involves employing a multi-label classifier for answer prediction. Zhu et al.[8] proposed a graph-based model designed to comprehend the relationships among objects, guided by the associated questions. They incorporated a soft attention layer within the graph convolution process to identify question-driven objects, effectively addressing the challenge of object redundancy. Additionally, the authors proposed a novel difference-based graph learner, which accounts for distinctions between objects and the semantic content of questions to determine the edges connecting nodes in the graph. Sharma et al.[9] introduced a VQA model that employs a graph neural network to enhance image representation through the capture of object relationships. This is complemented by a context-aware attention model for predicting answers. All the models developed in recent for VQA include different attention mechanism before prediction process which improves accuracy of the model and makes it easy to predict from related part of image instead of all features of image. Using appropriate attention model for a selected dataset is challenging task. Here we will compare some of this attention mechanism.

VQA Attention Models

Here we have implemented three different VQA attention model. Fig.2, shows basic block diagram of attention based VQA model. VQA model with attention mechanism basically consist four main modules.

1. Image Feature Extraction
2. Question Feature Extraction
3. Attention Model (iv) Answer Prediction.

Here Image features are extracted using pretrained VGG19[10] CNN model. For question feature first spaCy library with the 'en_core_web_lg' model is used to tokenize and obtain word embeddings for a given textual question. It then constructs a tensor to store the question features as 300-dimensional vectors for each of the 30 expected words, providing a representation suitable for input into a Visual Question Answering (VQA) model. Next language model architecture consists of a stack of LSTM layers to process sequences of word features. The final LSTM layer converts the sequence into a fixed-size vector that captures the contextual information from the input question. Above image and question features are given as input to Attention Model. Here three different attention model are used for attention mechanism and performance for the same is discussed in detail in next section. The attention mechanism computes attention weights based on the interaction between image and text features and then combines them to obtain a weighted representation of the text. The output of the attention mechanism is concatenated with the attention vector from the image model. Multiple dense layers with dropout are used for further processing. The final output layer with a soft max activation produces the predicted answer.

Attention Models

Attention mechanisms enhance VQA models by selectively focusing on significant input image regions and text which improves computational efficiency and prediction accuracy. In this section we will discuss in detail three different attention mechanism used in VQA: (1) Soft attention, (2) Stack attention and, (3) Additive attention

Soft Attention

VQA with soft attention module assigns weights to different regions of an image and words in a question. Soft attention mechanism identifies the regions which are related to question and applies higher weights to that region. It discredits the non relevant areas of image by multiplying its corresponding feature maps with low weight. So that areas with high attention keeps its original value and areas with low attention get closer to zero and becomes dark in the visualization. This helps the VQA model to understand relation between different elements of question and image to predict accurate answer. Soft attention in Visual Question Answering (VQA) calculates attention weights using soft max function. Here's a simplified calculation for soft attention to calculate attention weight in VQA: $Attention_Weights = \text{softmax}(\text{Score_Function}(\text{Image_Features}, \text{Question_Features}))$ (1) Here, Score_Function is used to compute the compatibility or similarity between image and question features. soft max is the soft max function used to normalize the scores into probabilities, such that sum of all probabilities becomes 1. Attention_Weights are the output weights which are assigned to different regions of the image features based on the question.



**Lata Bhavnani and Narendra. M. Patel****Stack Attention**

Stack Attention use multiple layers of attention instead of single attention layer. For given question features as input, Stack Attention Networks(SANs) search regions in an image for answer prediction. Multiple layers of attention are used over selected regions to capture complex relationships between visual and textual information. This type of mechanism is beneficial when dealing with complex questions which requires multiple steps of reasoning. It captures fine-grained details in image to answer such complex questions accurately. The stack attention mechanism uses soft attention iteratively to get multiple layers of attention. It will refine the focus on important image features in VQA model.

Additive attention

Additive attention technique transforms the input features and combines them such that it highlights specific parts of the input. Additive attention is used in VQA to selectively focus on distinct parts of input image and question for answer prediction. Here attention weights are first calculated using feed forward neural network for the combine image and question features. These weights are used to calculated weighted sum of visual features which is combined with visual features to generate context vector. Context vector is than used with question features to predict the answer. It is used for complex questions as it captures complex relation between image and question. This method provides high accuracy but it is computationally more expensive than soft and stack attention.

EXPERIMENT**Dataset**

VQA v1[11]data set consists open-ended questions about images. These questions require an image understanding, language and commonsense knowledge to answer. It is the second version of the VQA dataset. It contains approximately 204,721 images from the Microsoft COCO[12] dataset. Overall, there are 1,106,849 open-ended questions, 768,111 Yes/No questions, and 887,302 number questions. VQA model is trained on Google Colab with GPU (16 GB RAM) ,12 GB System RAM and 78.2 GB Disk space for accelerated computation. Still this computation capacity is not enough to process above large VQA dataset. We have used only first 50k Image-Question pair as a dataset for performance evaluation of VQA attention models. Out of this 40K Image-Question pair are used as train dataset and 10K Image-Question pair are used as test dataset.

Experimental Setup

VQA attention model is implemented on Tensor Flow platform. Adam optimizer with a base learning rate of 10e-04 is used. Batch size is set to 64 and training is done for up to 100 epochs with early stopping if the validation accuracy has not improved in the last 5 epochs. The size of hidden layer is set to 512 for LSTM language model and 1024 in the densely connected layers after the attention mechanism and image feature processing, as higher number of hidden units in dense layers allows the model to capture more complex relationships in the combined features. We apply dropout with probability 0.5 on each layer. Table I summarize the details of hyper parameters used in the model.

Evaluation Matrix

We formulate VQA as a classification problem since most of answers are single words. We evaluate the model using classification accuracy as reported in[1].

$$\text{Accuracy} = \min(n/3, 1) \quad (2)$$

Here n is the number of humans provided predicted answer. The answer is 100% accurate if at least three annotators give an exact match answer as predicted[13]. Here we evaluate the model using accuracy & Top_k_categorical_accuracy (for k=3,5). Top_k_categorical_accuracy means it considers the top k predicted classes for each sample.



**Lata Bhavnani and Narendra. M. Patel**

RESULT ANALYSIS

VQA-v1 contains two types of questions: open-ended and multiple choice. Here experiment is done for open ended questions. Table II shows performance of different applied for the VQA application. Here accuracy is lower as compared to other research as we have considered only subset of VQA-v1 dataset. As discussed in [13] model gives only 26.88 % accuracy when applied to small dataset VQA-CP-v1 and gives 55.86 % accuracy when applied to large dataset VQA-v1. Implemented VQA model without attention gives 27.73 % accuracy while VQA with stack attention gives 28.36 % accuracy which is higher than accuracy achieved in [14]. VQA with only soft attention gives 30.51 % accuracy while VQA with additive attention gives 31.59% accuracy. Table also shows top-k (k=3,5) accuracy for implemented model. We can see that additive attention gives better performance than soft and stack attention model. Fig. 3 shows performance comparison graph of all the implemented method. Fig. 4 shows some of the testing results of different VQA models with top 5 predicted answers. It shows that in VQA with additive attention model predicts the answer more accurately than VQA without attention.

CONCLUSION AND FUTURE WORK

VQA is a challenging task which include both computer vision and NLP to predict the answer. Here we have basically discussed three different approaches of VQA: VQA with soft attention, VQA with stack attention and VQA with additive attention. Results shows that VQA with additive attention performance better than other approaches. Additive attention requires more computational power than stack attention. Experiments are done with small part of VQA-v1 dataset. The choice of the optimal attention mechanism often depends on the characteristics of the dataset under consideration. Additionally, it's essential to note that the hyper parameters specified for this experiment may need adjustments when applied to different datasets. Beyond Visual Question Answering (VQA), this attention mechanism proves valuable in tasks like image captioning, machine translation, sentiment analysis, and image summarization. Its versatility across various domains highlights its effectiveness in tasks that require intricate interplay between visual content and language understanding. Utilizing an attention mechanism can also prove beneficial when providing reasoning for VQA predictions.

REFERENCES

1. S. Antol et al., "VQA: Visual Question Answering," in 2015 IEEE International Conference on Computer Vision (ICCV), Santiago, Chile: IEEE, Dec. 2015, pp. 2425–2433. doi: 10.1109/ICCV.2015.279.
2. K. J. Shih, S. Singh, and D. Hoiem, "Where to Look: Focus Regions for Visual Question Answering," in 2016 IEEE Conference on Computer Vision and Pattern Recognition (CVPR), Las Vegas, NV, USA: IEEE, Jun. 2016, pp. 4613–4621. doi: 10.1109/CVPR.2016.499.
3. Z. Yang, X. He, J. Gao, L. Deng, and A. Smola, "Stacked Attention Networks for Image Question Answering," 2016, pp. 21–29. Accessed: Dec. 21, 2020. [Online]. Available: https://openaccess.thecvf.com/content_cvpr_2016/html/Yang_Stacked_Attention_Networks_CVPR_2016_paper.html
4. J. Lu, J. Yang, D. Batra, and D. Parikh, "Hierarchical question-image co-attention for visual question answering," in Proceedings of the 30th International Conference on Neural Information Processing Systems, in NIPS'16. Red Hook, NY, USA: Curran Associates Inc., Dec. 2016, pp. 289–297.
5. D.-K. Nguyen and T. Okatani, "Improved Fusion of Visual and Language Representations by Dense Symmetric Co-attention for Visual Question Answering," in 2018 IEEE/CVF Conference on Computer Vision and Pattern Recognition, Jun. 2018, pp. 6087–6096. doi: 10.1109/CVPR.2018.00637.





Lata Bhavnani and Narendra. M. Patel

6. J.-H. Kim, J. Jun, and B.-T. Zhang, "Bilinear Attention Networks," in *Advances in Neural Information Processing Systems*, Curran Associates, Inc., 2018. Accessed: Dec. 07, 2023. [Online]. Available: https://proceedings.neurips.cc/paper_files/paper/2018/hash/96ea64f3a1aa2fd00c72faacf0cb8ac9-Abstract.html
7. W. Zhang, J. Yu, H. Hu, H. Hu, and Z. Qin, "Multimodal feature fusion by relational reasoning and attention for visual question answering," *Information Fusion*, vol. 55, pp. 116–126, 2020, doi: <https://doi.org/10.1016/j.inffus.2019.08.009>.
8. X. Zhu, Z. Mao, Z. Chen, Y. Li, Z. Wang, and B. Wang, "Object-difference driven graph convolutional networks for visual question answering," *Multimed Tools Appl*, vol. 80, no. 11, pp. 16247–16265, May 2021, doi: [10.1007/s11042-020-08790-0](https://doi.org/10.1007/s11042-020-08790-0).
9. H. Sharma and A. S. Jalal, "Visual question answering model based on graph neural network and contextual attention," *Image and Vision Computing*, vol. 110, p. 104165, 2021, doi: <https://doi.org/10.1016/j.imavis.2021.104165>.
10. K. Simonyan and A. Zisserman, "Very Deep Convolutional Networks for Large-Scale Image Recognition." *arXiv*, Apr. 10, 2015. doi: [10.48550/arXiv.1409.1556](https://arxiv.org/abs/1409.1556).
11. Y. Goyal, T. Khot, D. Summers-Stay, D. Batra, and D. Parikh, "Making the V in VQA Matter: Elevating the Role of Image Understanding in Visual Question Answering," in *2017 IEEE Conference on Computer Vision and Pattern Recognition (CVPR)*, Jul. 2017, pp. 6325–6334. doi: [10.1109/CVPR.2017.670](https://doi.org/10.1109/CVPR.2017.670).
12. T.-Y. Lin et al., "Microsoft COCO: Common Objects in Context," in *Computer Vision – ECCV 2014*, D. Fleet, T. Pajdla, B. Schiele, and T. Tuytelaars, Eds., in *Lecture Notes in Computer Science*. Cham: Springer International Publishing, 2014, pp. 740–755. doi: [10.1007/978-3-319-10602-1_48](https://doi.org/10.1007/978-3-319-10602-1_48).
13. L. Bhavnani and D. N. Patel, "Investigation of Available Datasets and Techniques for Visual Question Answering," *ijngc*, Aug. 2023, doi: [10.47164/ijngc.v14i3.767](https://doi.org/10.47164/ijngc.v14i3.767).
14. A. Agrawal, D. Batra, D. Parikh, and A. Kembhavi, "Don't Just Assume; Look and Answer: Overcoming Priors for Visual Question Answering," presented at the 2018 IEEE/CVF Conference on Computer Vision and Pattern Recognition (CVPR), IEEE Computer Society, Jun. 2018, pp. 4971–4980. doi: [10.1109/CVPR.2018.00522](https://doi.org/10.1109/CVPR.2018.00522).
15. Z. Yu, J. Yu, Y. Cui, D. Tao, and Q. Tian, "Deep Modular Co-Attention Networks for Visual Question Answering," in *2019 IEEE/CVF Conference on Computer Vision and Pattern Recognition (CVPR)*, Long Beach, CA, USA: IEEE, Jun. 2019, pp. 6274–6283. doi: [10.1109/CVPR.2019.00644](https://doi.org/10.1109/CVPR.2019.00644).
16. H. Sharma and A. S. Jalal, "A survey of methods, datasets and evaluation metrics for visual question answering," *Image and Vision Computing*, vol. 116, p. 104327, Dec. 2021, doi: [10.1016/j.imavis.2021.104327](https://doi.org/10.1016/j.imavis.2021.104327).
17. Q. Wu, P. Wang, C. Shen, A. Dick, and A. V. D. Hengel, "Ask Me Anything: Free-Form Visual Question Answering Based on Knowledge from External Sources," in *2016 IEEE Conference on Computer Vision and Pattern Recognition (CVPR)*, Jun. 2016, pp. 4622–4630. doi: [10.1109/CVPR.2016.500](https://doi.org/10.1109/CVPR.2016.500).
18. Q. Wu, C. Shen, P. Wang, A. Dick, and A. van den Hengel, "Image Captioning and Visual Question Answering Based on Attributes and External Knowledge," *IEEE Trans. Pattern Anal. Mach. Intell.*, vol. 40, no. 6, pp. 1367–1381, Jun. 2018, doi: [10.1109/TPAMI.2017.2708709](https://doi.org/10.1109/TPAMI.2017.2708709).
19. P. Anderson et al., "Bottom-Up and Top-Down Attention for Image Captioning and Visual Question Answering," in *2018 IEEE/CVF Conference on Computer Vision and Pattern Recognition*, Salt Lake City, UT: IEEE, Jun. 2018, pp. 6077–6086. doi: [10.1109/CVPR.2018.00636](https://doi.org/10.1109/CVPR.2018.00636).

Table 1 Hyper parameter and its values used in our study

Hyper parameters	Value
Epocs	100
Optimizer	Adam
Batch size	64
Loss Function	categorical_crossentropy
Dropout	0.5
Learning Rate	10e-04





Lata Bhavnani and Narendra. M. Patel

Table 2 Comparison for various VQA methods

Model	Accuracy (%)	Top-3 Accuracy (%)	Top-5 Accuracy (%)
VQA without attention	27.73	54.78	59.72
VQA with stack attention	28.36	53.94	58.22
VQA with soft attention	30.51	58.59	63.42
VQA with Additive attention	31.59	60.14	65.02



Fig 1 The task of VQA[1]

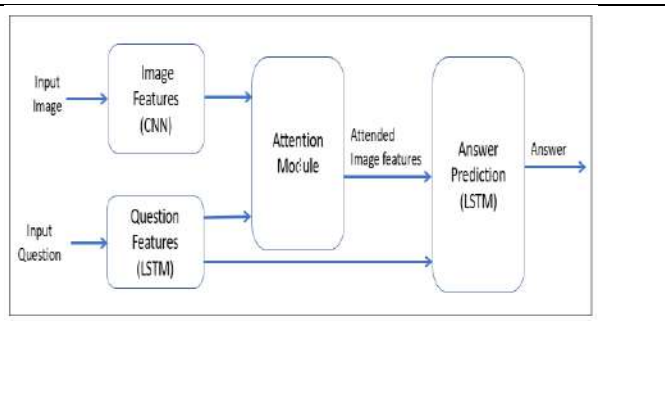


Fig 2 Block Diagram of VQA Attention Model

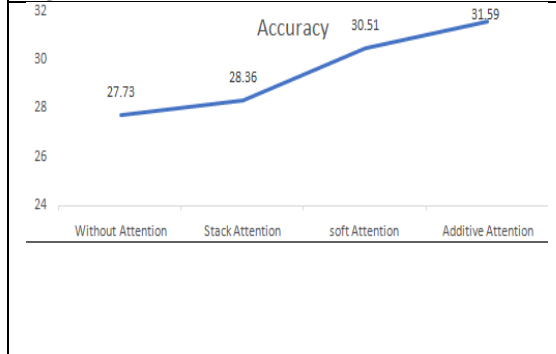


Fig 3 Performance comparison of VQA models

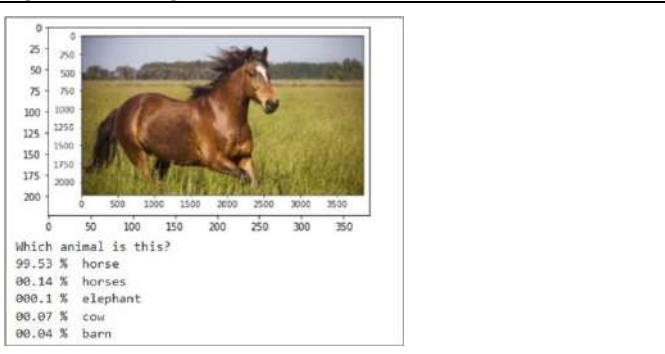
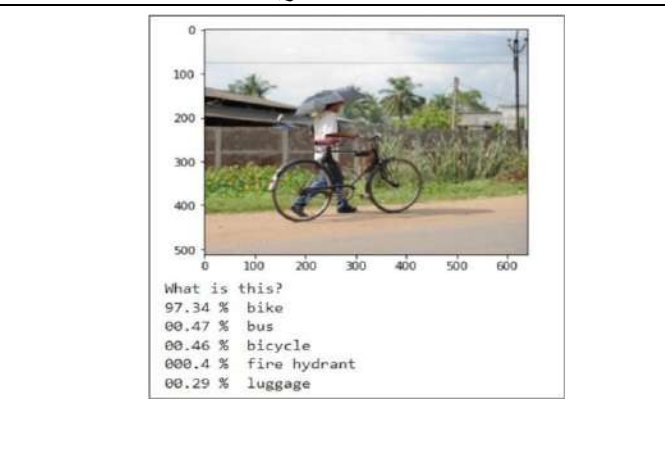
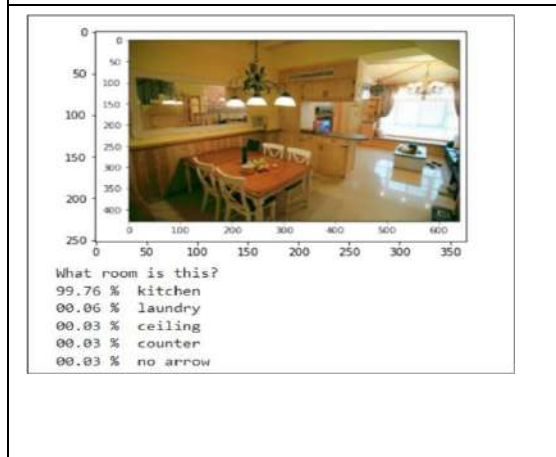


Fig. 4 a. Implemetation Results for VQA with and without attention mecanism (a) VQA without attention





Lata Bhavnani and Narendra. M. Patel


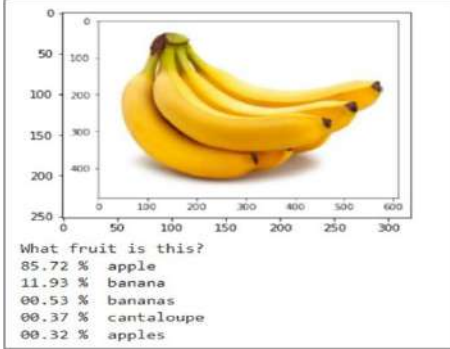
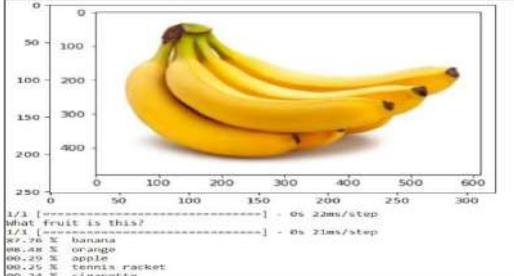
<p>Fig. 4. (b) VQA without attention</p>  <pre> 1/1 [-----] - 0s 92ms/step What is this? 1/1 [-----] - 0s 100ms/step 26.75 % bicycle 00.07 % bike 06.49 % ox 83.81 % harley davidson 02.33 % hydrant </pre>	<p>Fig. 4 (c) VQA without attention</p>  <pre> What fruit is this? 85.72 % apple 11.93 % banana 00.53 % bananas 00.37 % cantaloupe 00.32 % apples </pre>
<p>Fig 4. (d) VQA with Additive attention</p>  <pre> 1/1 [-----] - 0s 22ms/step What fruit is this? 1/1 [-----] - 0s 21ms/step 87.96 % banana 00.29 % orange 00.29 % apple 00.29 % tennis racket 00.25 % cigarette </pre>	

Fig 4 . (f) VQA with Additive attention





Enhancing Privacy of Electronic Cash System through Cryptography

Palak Dave*

Assistant Professor, MBIT, New V.V Nagar, Gujarat, India.

Received: 30 Dec 2023

Revised: 09 Jan 2024

Accepted: 12 Jan 2024

*Address for Correspondence

Palak Dave

Assistant Professor,
MBIT, New V.V Nagar,
Gujarat, India.
Email: ppdave@mbit.edu.in



This is an Open Access Journal / article distributed under the terms of the **Creative Commons Attribution License** (CC BY-NC-ND 3.0) which permits unrestricted use, distribution, and reproduction in any medium, provided the original work is properly cited. All rights reserved.

ABSTRACT

Electronic exchanges are regular now days as nearly everybody in this online world manages the e money. Bitcoin was the underlying and first cryptographic coin. which for the security reasons was supplanted by zerocoin the coin exchange by zero learning convention so that no information is passed for the stamping the coin or reclaiming the coin. We have proposed homomorphic expansion to secure the reward points. Simulation results are deduced in the paper.

Keywords: Zerocoin, Bitcoin, Electronic Money, Money.

INTRODUCTION

The expression "electronic money" frequently is connected to any electronic installment conspire that clearly look to some extent like cash. Truth be told, be that as it may, electronic money is an exact class of electronic installment conspire, characterized by firm cryptographic properties.[1] Generally any e trade framework would consider the operators as bank, clients/clients and the partner and the life cycle of electronic coin includes every one of the gatherings. User withdraws coin from the bank. The coin then can be traded for a few products and ventures by the clients to the shippers. As even the shipper won't keep the coin with it rather the cycle is finished when the trader/partner stores back the con to the bank. From figure 1cash has the cycle can be said having 3 pases withdrawal phase, the payment phase, and the deposit phase. Preceding procedure is the preprocessing step which requires manages creating open keys, administration of the record. electronic money can be ordered as on-line and disconnected. In an on-line electronic money, the installment and store stages happen in a similar exchange. So we can infer that the coin is confirmed each by the bank at the season of installment so bank to be on-line for each coin traded between the spenders and the shippers. In disconnected electronic money conspires, the coins are confirmed after the exchange at some helpful time for both dealers and the bank so that the bank does not need to be required in each installment exchange. Be that as it may, as the coins are not checked at the season of installment, there is a potential for exploitative spenders to twofold spend their coins. This is on account of advanced money, which is basically an arrangement of numbers, is anything but difficult to duplicate. Another necessity that can emerge in





Palak Dave

electronic coins is the requirement for secrecy. Bit coin [3] as name recommends is a product based online installment framework by Satoshi Nakamoto in 2008 it was presented as an open source programming in 2009. Installments are put away in an open record utilizing its record known as bit coin. Installments work is individual to other individual and no focal store is there, so bit coin a decentralized scrambled virtual money. Bit coins are made for the reward of undertaking identified with installments where clients offers their registering energy to confirm and record installments named as mining, individual and additionally organizations can be a piece of this movement for trade of the exchange charges and new made bit coins. But mining, they can be picked up by the trade for cash, items, and administrations. Clients can both send and get bit coins electronically for a method for exchange expense by utilizing wallet programming. Bit coin can likewise be named as the e cash which is utilized as installment for items and administration charges are not as much as that of with Visa processors. The European Banking Authority has cautioned that bit coin needs customer securities. Dissimilar to charge cards, any expenses are paid by the buyer not the merchant. Bit coins can be stolen and charge backs are inconceivable. Starting July 2013 the business utilization of bit coin was little contrasted with its utilization by theorists, which has added to value un predict ability. Bit coin has been a subject of worries that it can be utilized for unlawful exercises, much like money.

Background

Classification of e cash system system[2] seven main events are distinguishable

Initialization Choice of system parameters and key pairs of all entities.

Opening account The bank opens a user account and registers his personal data.

Registration In the pseudonymous systems, the user registers at the trustee.

Withdrawal The user withdraws digital coins from his account onto his device.

Payment The user pays at the shop using the coins stored on his device.

Deposit Shop deposits the digital coins at the bank and is credited accordingly.

Revocation The trustee gets the coin from the withdrawal transcript or to compute the user's identity from the payment transcript in order to deter any perfect crime

Bit coin Transactions

The electronic coin as a chain of computerized marks. Every proprietor exchanges the coin to the following by carefully marking a hash of the past exchange and people in general key of the following proprietor and adding these to the end of the coin. A payee can confirm the marks to check the chain of possession.

Zero Knowledge Proof

The first efficient statistical zero-knowledge protocols to prove statements such as

1. A committed number is a pseudo-prime.
2. A committed/revealed number is the product of two safe primes
3. A given value is of large order modulo that consists of 2 safe prime factors.

Aside from the legitimacy of the calculation, no other data about the modulus e.g., a generator which arrange meets the modulus or some other operand is given. Disregarding the Bitcoin's client base appeared to be unknown taking a chance with their cash and paying exchange expenses. One outline of this is the presence of laundries that for an expense will join together unique clients' assets in the trusts that rearranging makes them hard to follow. Since such frameworks require the clients to believe the clothing to both

1. not record how the mixing is done
2. Give the users back the money they put , use of these involves a fair amount of risk.

Decentralized Ecash

The decentralized e cash scheme is to anonymize the Bitcoin network uses a type of cryptographic electronic currency's the name suggests decentralization means it does not requires any kind of central authority to issue the coin.





Palak Dave

Proof of Proposed Work

Base Work

Algorithm of the zero coin

Setup(1λ): parameter. Accum Setup (1λ) gives the output (N, u) .

generate prime numbers p, q where $p = 2wq + 1$ for $w \geq 1$ choose random generators g, h $G = (g) = (h)$ and $G \in \mathbb{Z}_q^*$

output of step 1 = (N, u, p, q, g, h)

Mint(parameter) : (c, skc) . input = Select $S, r \leftarrow \mathbb{Z}_q^*$

$c \leftarrow g^S h^r \pmod p$

such that $\{c \text{ prime} \mid c \in [A, B]\}$ Set $skc = (S, r)$

output (c, skc)

Spend (parameters; $c; skc, R, C$): (Π, S) . If c not belongs C output \perp .

Compute $A \leftarrow \text{Accumulate}((N, u), C)$ $\omega \leftarrow \text{GenWitness}((N, u), c, C)$.

Output (π, S)

where π IS signature of knowledge: $\pi = \text{ZKSoK}[R]((c, w, r): \text{AccVerify}((N, u), A, c, w) = 1 \wedge c = g^S h^r \pmod p)$

Verify (params, π, S, R, C) $\rightarrow \{0, 1\}$. $\pi =$ proof, S serial number

$C =$ set of coins,

$A \leftarrow \text{Accumulate}((N, u), C)$.

Verify that Π is the signature of knowledge on R using the known public values. If the proof verifies successfully, output 1, otherwise output 0. The zero coin assumes a trusted setup process for generating the parameters. The accumulator trapdoor (p, q) is not used subsequent to the Setup procedure and can therefore be destroyed immediately after the parameters are generated.

Proposed work

Homomorphic cryptosystems have the property that given only the cipher texts of two numbers, the cipher text of the sum of those two numbers can be computed. Here both the ordinary cryptographic expansion and the homomorphic expansion is thought about in the figure 6. We are going to utilized this work as a part of the any framework where we can get rewards for the buy and that reward will be added back to the site in the homomorphic way. Figure7 demonstrates the working stream of the proposed scheme. figure 8 demonstrates the qualities with the scientific evidence Algorithm

User gets purchase Article AR

Reward per article $R(AR)$

When $R(AR) > 25$

If(redeem in coin on purchase) select any two prime numbers say p and q

Say $N = p * q$. where p and q being confidential and N is public. Decrypted algorithm Dg is $M = b \times (ax) - 1 \pmod p$.

Calculate $y = gx \pmod p$. use this y for the encryption 5 else Reward = reward + current reward

Experimental Evaluation

The dataset [21] holds "38,100 Having id ie anoyimity The dataset consists of 2 files." Figure 8 shows the comparison of both the approaches in terms of storage space Ratings data ratings_data.txt.bz2 (2.5 Megabytes): it contains the ratings given by users to items. Every line has the following format: user_id item_id redeem value 11000 4

CONCLUSION

We presume that proposed change it better as

Proposed strategy gives security to the reward focuses.

Proposed strategy gives more security as it force the certifiable client to THE FRAMEWORK.

Proposed strategy can be utilized to build an edge cryptosystem

TAKES less Storage





Palak Dave

REFERENCES

1. Newsome, James, et al. "The sybil attack in sensor networks: analysis & defenses." Proceedings of the 3rd international symposium on Information processing in sensor networks. ACM, 2004.
2. Levien, R. "from Advogato Website." *Advogato Trust Metric*, URL: <http://www.advogato.org/trust-metric.html>.
3. Kaashoek, M. Frans, and David R. Karger. "Koorde: A simple degree-optimal distributed hash table." *Peer-to-peer systems II*. Springer Berlin Heidelberg, 2003. 98-107.
4. Duggan, Maeve, et al. "Social media update 2014." *Pew Research Center* 19 (2015).
5. D. Gambetta. *Trust: Making and Breaking Cooperative Relations*, chapter Can We Trust Trust?, pages 213 – 237. Department of Sociology, University of Oxford, 2000.
6. R. Guha, R. Kumar, P. Raghavan, and A. Tomkins. Propagation of trust and distrust. In Proceedings of the International World Wide Web Conference (WWW 2004), 2004
7. Yu, H., Kaminsky, M., Gibbons, P. B., & Flaxman, A. (2006). Sybilguard: defending against sybil attacks via social networks. *ACM SIGCOMM Computer Communication Review*,7.
8. H. Yu, P. B. Gibbons, M. Kaminsky, and F. Xiao. SybilLimit: A Near-Optimal Social Network Defense against Sybil Attacks. In Proc. IEEE S&P, Oakland, CA, May 2008.
9. Danezis, George, and Prateek Mittal. "SybilInfer: Detecting Sybil Nodes using Social Networks."2. Jøsang, Audun, and Roslan Ismail, The beta reputation system, Proceedings of the 15th bled electronic commerce conference. 2002
10. Wei, Wei, et al. "Sybildefender: Defend against sybil attacks in large social networks." *INFOCOM, Proceedings IEEE. IEEE, 2012.*
11. Tran, Nguyen, et al. "Optimal sybil-resilient node admission control." *INFOCOM, 2011 Proceedings IEEE. IEEE, 2011.*2. Jøsang, Audun, and Roslan Ismail, The beta reputation system, Proceedings of the 15th bled electronic commerce conference. 2002
12. Tran, Dinh Nguyen, et al. "Sybil-Resilient Online Content Voting." *NSDI. Vol. 9. No. 1.*
13. Quercia, Daniele, and Stephen Hailes. "Sybil attacks against mobile users: friends and foes to the rescue." *INFOCOM, 2010 Proceedings IEEE. IEEE, 2010.*
14. Jøsang, Audun, and Roslan Ismail, The beta reputation system, Proceedings of the 15th bled electronic commerce conference. 2002
15. Zhou, Runfang, Kai Hwang, and Min Cai. , Gossip trust for fast reputation aggregation I peer-to-peer networks. *Knowledge and Data Engineering, IEEE Transactions on* 20.9 (2008):1282-1295.
16. Gupta, Minaxi, Paul Judge, and Mostafa Ammar., A reputation system for peer-to-peer networks, Proceedings of the 13th international workshop on Network and operating systems support for digital audio and video. ACM, 2003.
17. Zhou, Runfang, Kai Hwang, and Min Cai., Gossip trust for fast reputation aggregation I peer-to-peer networks. *Knowledge and Data Engineering, IEEE Transactions on* 20.9 (2008):1282-1295.
18. Thadani, Ankita, and Vinit Gupta. "Enhancing Privacy Preservation of Stature System Through Homomorphic System." *Emerging Research in Computing, Information, Communication and Applications*. Springer India, 2015. 439-449.
19. Viswanath, Bimal, et al. "An analysis of social network-based sybil defenses." *ACM SIGCOMM Computer Communication Review* 41.4 (2011): 363-374.
20. Wei, Wei, et al. "Sybildefender: Defend against sybil attacks in large social networks." *INFOCOM, 2012 Proceedings IEEE. IEEE, 2012.*
21. Xue, Jilong, et al. "Votetrust: Leveraging friend invitation graph to defend against social network sybils." *INFOCOM, 2013 Proceedings IEEE. IEEE, 2013.*





Palak Dave

Table 1 presents the comparison within the literature survey done with various papers C-centralized system D is decentralized system. pros, cons, and the scenario its is suitable for.

	System/ Protocol	Pros	Cons	Suitable for
3.1	bitcoin	fully decentralized available mitigations are very less	network model, which had of many untrusted nodes which enter and exit the network. Moreover, the problem of choosing long term trusted parties, in the legal and regulatory grey area	Decentralized
3.2	xcash	Extends cash by anonymity	Not multi agent	Centralized
3.3	cyberorg	the discrete logarithms unlinkability among all payments	heuristic assumption	Centralized
3.4	Gupta et al DebitCredit Computation	Short term misuse of cash cannot be done.	Less secure for the receipt off the message	Decentralized
3.5	multiagent	extensible and scalable. Real life application	Only specialized user can participate	Decentralized
3.6	whopay	scalable and anonymous	entity like a broker or a bank are not supported	Centralized
3.7	Zerocoin	Zero knowledge	Minting is not accurate	Decentralized
3.8	Androulaki et al. A Reputation System for Anonymous Networks	represented by a pseudonym	bank, which is a centralized entity. no negative feedback	Decentralized
3.9	zerocoin	Imposes zero knowledge	-	Decentralized
3.10	Mixcoin	efficient and fully compatible with Bitcoin randomized mixing fees, and an adaptation of mix networks to Bitcoin	careful consideration of some of the higher-level side channels	Centralized

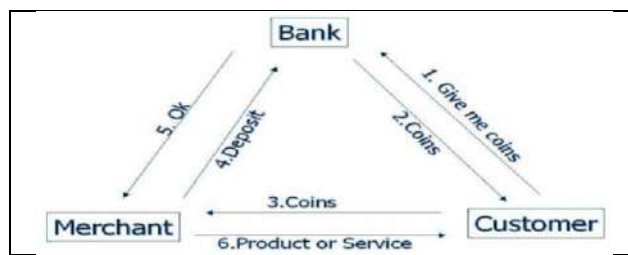


Figure 1: Life cycle of e cash [2]

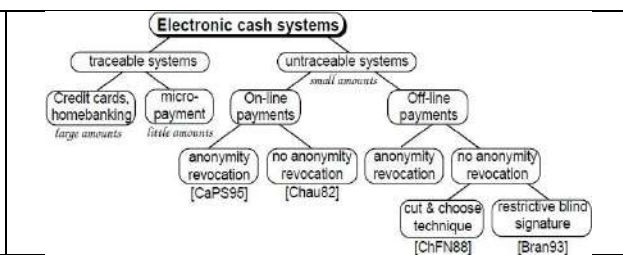


Figure 2: Classification of Electronic cash





Palak Dave

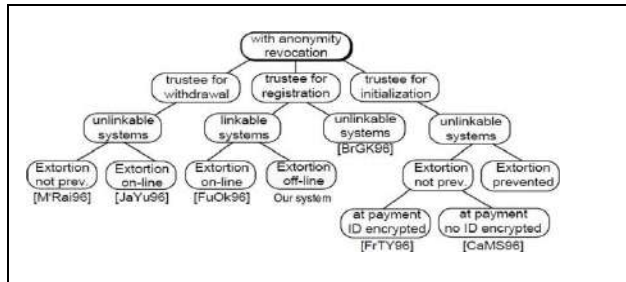


Figure 3: Classification of Electronic cash system with anonymity revocation[2]

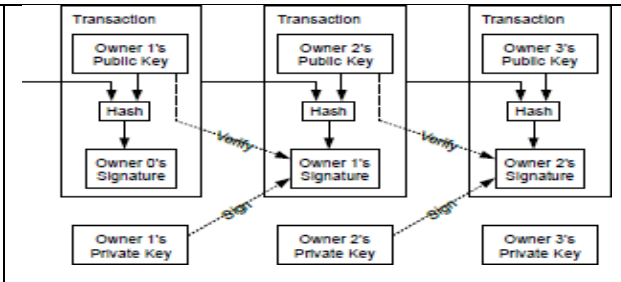


Figure 4: Transaction chain by hash key [3]

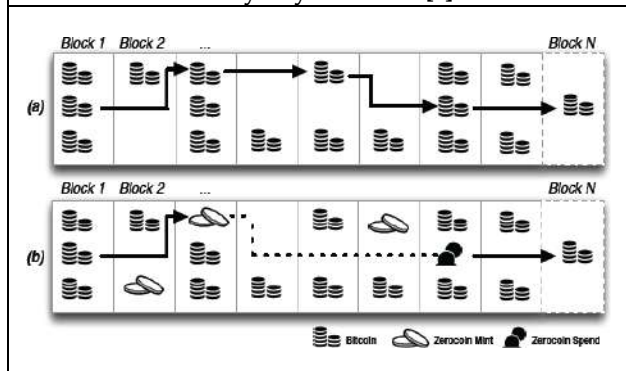


Figure 5 bitcoin and zerocoin working

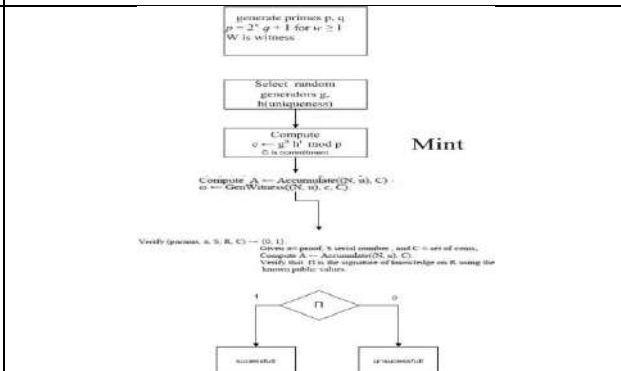


Figure 6 Working of Zerocoin

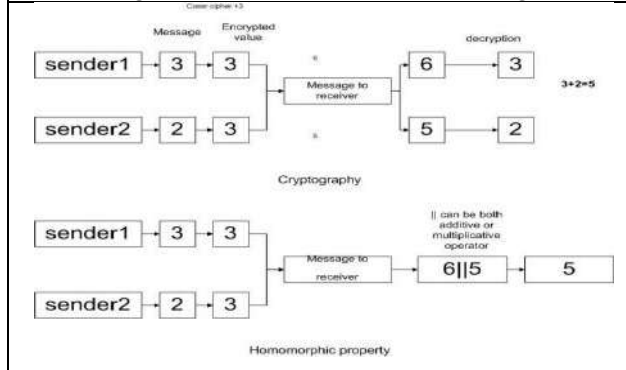


Figure 6 Idea of proposed scheme

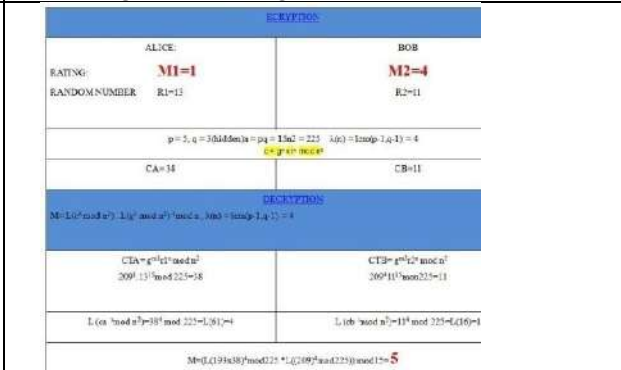


Figure 7 Mathematical proof of proposed scheme

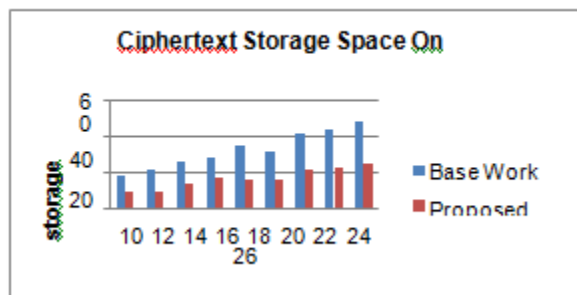


Figure 8 comparison of zerocoin and homomorphic addition





Palak Dave

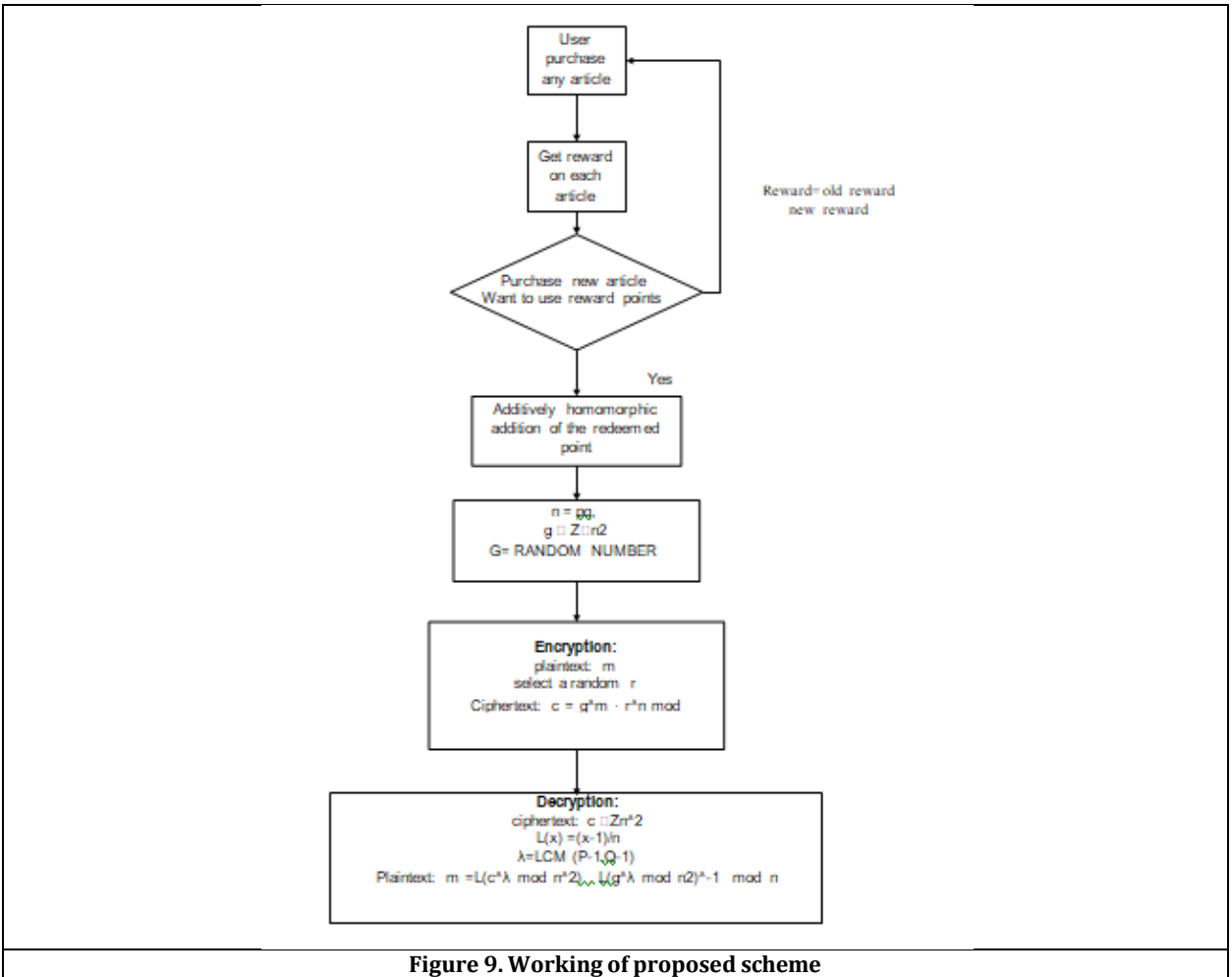


Figure 9. Working of proposed scheme





High-Performance and Robust Control of Interior Permanent Magnet Synchronous Motor (IPMSM) Drives Using Fuzzy Logic Controller (FLC) with Different Defuzzification Methods Across Varied Speed Ranges

Jaydeepsinh C. Baria¹, Darshankumar C. Dalwadi^{2*} and Keyursinh Chauhan³

¹Research Scholar, Gujarat Technological University, Gujarat, India.

²Associate Professor, BVM Engineering College, Gujarat, India.

³M. Tech, EC, DDIT, DDU, Nadiad, Gujarat, India.

Received: 30 Dec 2023

Revised: 09 Jan 2024

Accepted: 12 Jan 2024

*Address for Correspondence

Darshankumar C. Dalwadi

Associate Professor,

BVM Engineering College,

Gujarat, India.

Email: darshan.dalwadi@bvmengineering.ac.in



This is an Open Access Journal / article distributed under the terms of the **Creative Commons Attribution License** (CC BY-NC-ND 3.0) which permits unrestricted use, distribution, and reproduction in any medium, provided the original work is properly cited. All rights reserved.

ABSTRACT

Interior Permanent Magnet Synchronous Motor (IPMSM) Drive Control The paper explores controlling an IPMSM drive across various speeds using a Fuzzy Logic Controller (FLC). The FLC manipulates d-axis current (I_d) and q-axis current (I_q), regulating torque and magnetic field in the stator winding, effectively controlling motor speed and torque. FLC The utilization of the Mamdani fuzzy logic system within the proposed FLC for simultaneous management of Torque and Flux is an efficient method. By employing various defuzzification methods such as Centroid of Area (COA), Bisector of Area (BOA), Mean of Maximum (MOM), Smallest of Maximum (SOM), and Largest of Maximum (IOM), the FLC determines the appropriate values for I_d and I_q , ultimately aiming to achieve the desired speed. This method allows for comprehensive control over multiple motor parameters, enhancing the motor's performance across different operating conditions. The FLC design is based on the Maximum Torque per Ampere (MTPA) method for stand-still to base speed operation and the Field Weakening (FW) Method for operation above the base speed. Additionally, a hysteresis current control method is employed to generate inverter pulses. The proposed system finds application in Electric Vehicle (EV) motor testing, as well as motor testing in laboratories or manufacturing plants.

Keywords: Interior Permanent Magnet Synchronous Motor (IPMSM), Fuzzy Logic Controller (FLC), Maximum Torque per Ampere (MTPA), Field Weakening (FW), Centroid of Area (COA), bisector of Area (BOA), Mean of Maximum (MOM), Smallest of Maximum (SOM), Largest of Maximum (IOM).





INTRODUCTION

IPMSM motors are known for their capacity to offer precise speed control across a broad speed range, high efficiency, compact size, low copper losses, prolonged bearing grease life, and high-power density. This makes the IPMSM particularly suitable for applications such as Electric Vehicles, Elevators, and Traction, where space constraints are critical. Speed control is achieved through two main topologies: the Maximum Torque per Ampere (MTPA) topology, allowing the motor to operate at maximum torque up to its rated speed, and the field weakening topology, enabling the motor to run above the rated speed with constant power.[1]-[10] The presence of a buried permanent magnet inside the rotor results in a smooth rotor surface, reducing the air gap. However, achieving precise speed control becomes challenging due to the non-linear coupling between the stator current and rotor, causing non-linearity in the electromagnetically developed torque. Despite this challenge, the smooth rotor surface makes it popular for high-speed performance. Additionally, the rotor core experiences saturation and the armature reaction influences the air gap flux in the IPMSM.[1]-[3] This variation in reluctance parameters leads to unequal d-axis and q-axis inductance, producing additional torque by the Q-axis current, known as reluctance torque. Consequently, the motor attains maximum torque during the MTPA topology. Moreover, selecting a negative D-axis current reduces the stator flux to enable the motor to operate beyond its rated speed, impacting the dynamic and steady-state performance of the IPMSM.[14][15][18][20] The mathematical modeling of IPMSM motors is challenging due to factors such as saturation, armature reaction, dynamic loading, and temperature variations. Overcoming these challenges, Fuzzy Logic Controllers (FLCs) offer several advantages:[17]-[21]

1. They do not necessitate an exact mathematical model.
2. FLCs operate on linguistic rules, essentially human logic.
3. They are effective in handling the non-linearities inherent in the system.

The simulation of the IPMSM drive with a fuzzy logic controller using different defuzzification methods is conducted in MATLAB SIMULINK.[11][12] Nomenclature R_s - Stator Resistance, i_d - direct axis stator current (d-axis), i_q - quadrature axis stator current, L_d - direct axis stator inductance, L_q - quadrature axis stator inductance, ω_e - rotor speed, Φ_d - flux linkage along direct axis, Φ_q - flux linkage along quadrature axis, Φ_{PM} - flux linkage, P - No. of Pole Pairs, θ_r - Rotor angle

IPMSM Mathematical Model

The dynamic d-q model of the IPMSM serves as the basis for the mathematical model used in vector control. This model is derived by eliminating the equations associated with the damper winding and field current dynamics from the widely recognized induction machine model. The synchronously rotating rotor reference frame is selected, allowing the transformation of stator winding quantities into a reference frame revolving at the rotor speed. Consequently, there exists zero speed differential between the rotor and stator magnetic fields. The fixed phase relationship between the stator q and d axis windings and the rotor magnet axis (aligned with the d axis in the model) is established. A mathematical model of the IPMSM is utilized to simulate the machine's behavior in MATLAB. The dq rotor reference frame is utilized to express this model, with the d axis being aligned with the rotor flux-linkage, as shown in Fig.1.[13]-[15] The voltages for the stator in three phases can be expressed in the following manner:

$$v_a = R_s i_a + L_s \frac{d}{dt} i_a - \omega_e \Phi_{PM} \sin(\theta_r) \quad (1)$$

$$v_b = R_s i_b + L_s \frac{d}{dt} i_b - \omega_e \Phi_{PM} \sin\left(\theta_r - \frac{2\pi}{3}\right) \quad (2)$$

$$v_c = R_s i_c + L_s \frac{d}{dt} i_c - \omega_e \Phi_{PM} \sin\left(\theta_r + \frac{2\pi}{3}\right) \quad (3)$$

Equations (4) & (5) represent the dynamic equations of the IPMSM in the synchronously rotating d-q referencing frame, acquired through the Clarke-Park transformation, will be presented. Some assumptions will be made for the sake of convenience.





1. The sinusoidal nature of the induced EMF is taken into consideration.
2. The saturation and core losses in the rotor are considered insignificant.
3. The rotor lacks any damper windings.

$$v_d = R_S i_d + L_d \frac{di_d}{dt} - \omega_e \Phi_q \tag{4}$$

$$v_q = R_S i_q + L_q \frac{di_q}{dt} + \omega_e \Phi_d \tag{5}$$

$$\Phi_d = L_d i_d + \Phi_{PM} \tag{6}$$

$$\Phi_q = L_q i_q \tag{7}$$

The depiction of the PMSM's equivalent circuit in the DQ-axis, which is derived using the DQ modeling method, can be seen in Figure 2.

$$T_e = \frac{3P}{2} (\Phi_{PM} i_q + (L_d - L_q) i_d i_q) \tag{8}$$

The torque generated by the permanent magnet buried in the rotor is represented by the first term in Equation (8), whereas the second term signifies the reluctance torque resulting from the interaction of d-axis and q-axis currents.

MTPA and FW Topology

The reference d-axis current (I_d) and q-axis current (I_q) are generated by Maximum Torque per Ampere (MTPA) control to achieve maximum torque per unit current. The MTPA trajectory condition can be obtained by deriving it from Equation (8) in the following manner.

$$\frac{\partial T_e}{\partial i_q} = 0$$

$$\Phi_{PM} + (L_d - L_q) i_q \frac{\partial T_e}{\partial i_q} + (L_d - L_q) i_d = 0 \tag{9}$$

The correlation between the stator phase current, i_d and i_q is

$$i_s = \sqrt{i_d^2 + i_q^2} \tag{10}$$

Utilizing the equation (8)

$$\frac{\partial i_d}{\partial i_q} = -\frac{i_q}{i_d} \tag{11}$$

(7) and (9) Equation solving

$$i_d = \frac{\Phi_{PM}}{2(L_d - L_q)} + \sqrt{\frac{\Phi_{PM}^2}{4(L_d - L_q)^2} + i_q^2} \tag{12}$$

Figure (3) illustrates the trajectory of the MTPA curve, the voltage limit ellipse, the current limit curve, and the constant torque curves. The drive system ensures that the voltage constraint is satisfied when operating below the base speed. The operating point of the drive system is located along the MTPA trajectory depicted in Figure (3). The operating point is determined by the intersection of the constant torque curve and the MTPA trajectory, which is located at the closest distance from the origin. This distance signifies the stator current. Essentially, the MTPA path allows for the attainment of the required torque using minimal current, thus decreasing copper loss and potentially optimizing the efficiency of the drive system.

Field Weakening (FW) Control:[8][10][17]

When operating the motor beyond its rated speed, It is imperative to give consideration to the limitations of Voltage and Current [3]. Equation (10) and (11) are used to express the Current constraint and Voltage constraint, respectively.

$$I_s = \sqrt{I_d^2 + I_q^2} \leq I_{sm} \tag{13}$$





Jaydeepsinh C. Baria et al.,

$$V_s = \sqrt{v_d^2 + v_q^2} \leq V_{sm} \tag{14}$$

Where I_{sm} and V_{sm} represent the available maximum current and voltage, respectively. Upon substituting the values of V_q and V_d into equation (14), the resulting expression is obtained.

$$V_s = \sqrt{(R_S i_d + L_d \frac{di_d}{dt} - \omega_e \Phi_q)^2 + (R_S i_d + L_d \frac{di_d}{dt} + \omega_e \Phi_d)^2} \leq V_{sm} \tag{15}$$

For the sake of simplification in analysis, only steady-state terms are considered in the voltage constraint equation, and the resistive drop is disregarded.

$$V_s = \sqrt{(\omega_e \Phi_d)^2 + (\omega_e \Phi_q)^2} \leq V_{sm} \tag{16}$$

From Equation (7) and (8), we get

$$V_s = \sqrt{(\omega_e L_q i_q)^2 + (\omega_e (L_d i_d + \Phi_{PM}))^2} \leq V_{sm} \tag{17}$$

After simplification,

$$(L_q i_q)^2 + (L_d i_d + \Phi_{PM})^2 \leq \left(\frac{V_{sm}}{\omega_e}\right)^2 \tag{18}$$

Equation (13) represents the current limit circle centered at the origin with a radius of I_s . Equation (18) depicts the voltage ellipse centered at $(0, -\frac{\Phi_{PM}}{L_d})$ and contracts with the increase in rotor speed. Beyond the base speed, field weakening is implemented to ensure the stator voltage stays within the limit specified by equation (15). Control over the d-axis and q-axis currents is adjusted to comply with the machine voltage limit.

$$v_o = \sqrt{v_{do}^2 + v_{qo}^2} \leq V_{om} \tag{19}$$

Where, $v_{do} = -\omega_e L_q i_q$, $v_{qo} = \omega_e (L_d i_d + \Phi_{PM})$ and $V_{om} = V_{sm} - R_S I_{sm}$.

The relationship between i_d and i_q can be derived from equation (17) by substituting V_{sm} with V_{om} to incorporate the impact of Stator Resistance drop. Therefore,

$$i_d = -\frac{\Phi_{PM}}{L_d} + \frac{1}{L_d} \sqrt{\frac{v_{om}^2}{\omega^2} - (L_q i_q)^2} \tag{20}$$

In order to maintain the current vector control as per equation (20), it is essential to maintain the terminal voltage within V_{sm} during steady-state conditions. At every speed, the intersection between the current limit and voltage limit trajectories determines the corresponding current limit necessary to achieve maximum torque. The operating point is situated along the voltage limit curve, hence dictated by the minimum current needed to generate the desired torque. This approach also contributes to reducing copper loss in the FW region. References [2]-[3] provide the limit values outlined in equations (21) and (22) respectively.

$$i_{dv} = -\frac{\Phi_{PM} L_d}{L_d^2 - L_q^2} + \frac{1}{L_d^2 - L_q^2} \sqrt{\Phi_{PM}^2 L_d^2 - (L_d^2 - L_q^2)(I_{sm}^2 L_q^2 + \Phi_{PM}^2 - \frac{V_{sm}^2}{\omega^2})} \tag{21}$$

$$i_{qv} = \sqrt{I_{sm}^2 - i_{dv}^2} \tag{22}$$

In the FW region, Figure (4) showcases the MTPA curve trajectory, the current limit curve, various constant torque curves at different loads, and the Voltage limit curve.

FUZZY LOGIC CONTROLLER RULES FOR IPMSM:

The implementation of the proposed Mamdani fuzzy model is carried out in MATLAB-Simulink using the Fuzzy Logic Toolbox. The simulation of this IPMSM model involves the following steps in the Mamdani fuzzy model:[11][12]





Jaydeepsinh C. Baria et al.,

1. Fuzzification of the input variables.
2. Rule evaluation.
3. Aggregation of the outputs of fuzzy rules.
4. Defuzzification.

The FLC receives inputs such as Speed error, Change in Speed Error, and Actual Speed. As a result, the FLC produces outputs in the form of direct axis current (i_d) and quadrature axis current (i_q). Fuzzification of input and output variables is achieved through membership functions, as depicted in Figures (5)-(10). The Mamdani fuzzy model employs Max-Min and Max-Product compositions for handling fuzzy and crisp inputs. In these simulations, all input variables are provided as crisp inputs.[8][16][19] The application of antecedents of the fuzzy rules on the fuzzified inputs involves using the fuzzy operator (AND or OR) to derive the result. The evaluation of rules was conducted as follows. The application of antecedents of the fuzzy rules on the fuzzified inputs involves using the fuzzy operator (AND or OR) to derive the result. The evaluation of rules was conducted as follows.

Rule 1: If $\Delta\omega$ is PH (positive high), then i_q is PH (positive high), and i_d is PH (positive high).

Rule 2: If $\Delta\omega$ is PL (positive low), then i_q is PL (positive low), and i_d is PL (positive low).

Rule 3: If $\Delta\omega$ is NH (negative high), then i_q is NH (negative high), and i_d is NH (negative high).

Rule 4: If $\Delta\omega$ is NL (negative low), then i_q is NL (negative low), and i_d is NL (negative low).

Rule 5: If $\Delta\omega$ is ZE (zero) and ω_r is WR (within range), then i_q is NC (not changed), and i_d is NC (not changed).

Rule 6: If ω_r is PAR (positive above rated) or NAR (negative above rated), then i_q is NL (negative low), and i_d is AR (above rated).

Rule 7: If $\Delta\omega$ is ZE (zero) and Δe is PI (positive increase), then i_q is PL (positive low), and i_d is PL (positive low).

Rule 8: If $\Delta\omega$ is ZE (zero) and Δe is NI (negative increase), then i_q is NL (negative low), and i_d is NL (negative low).

Where,

$\Delta\omega$ is change in rotor speed

ω_r is rotor speed

Δe is change in speed error

The process of aggregation involves the unification of outputs from all rules. The input for the aggregation process comprises the list of scaled consequent membership functions, resulting in one fuzzy set for each output variable.

Defuzzification involves converting a fuzzy value into a crisp value. Inputs and outputs of the FLC are scaled using appropriate gains to ensure efficient system performance. Several defuzzification methods have been simulated in this paper.[22]

1. Centroid of Area (COA)
2. Bisector of Area (BOA)
3. Mean of Maximum (MOM)
4. Smallest of Maximum (SOM)
5. Largest of Maximum (LOM)

RESULTS AND DISCUSSION

Simulation of the IPMSM drive system is conducted in MATLAB-Simulink using various defuzzification methods across diverse dynamic conditions. Figure (8) illustrates the complete drive system, whereas Figure (11) [10] showcases the simplified block diagram. The simulation parameters of the IPMSM are outlined in Table 1. The reference d-axis current (i_d) and q-axis current (i_q) can be generated using MATLAB FLC-based simulation with various defuzzification methods. The three-phase parameters can be obtained through inverse Park and Clarke transformations. These values are then utilized in the hysteresis current controller to derive different gate pulses. The inverter receives these controlled gate pulses to provide controlled voltage and frequency power to the IPMSM motor, enabling the achievement of desired outputs in minimum time. Under varying reference speeds, the actual





Jaydeepsinh C. Baria *et al.*,

speed exhibits minimal overshooting or undershooting. Transient Response Parameters such as Rise time, Delay time, Settling time, and steady-state error demonstrate minimum values, as observed in Tables 2, 3, 4, 5, and 6.

Different defuzzification methods yield varying torque ripple, THD (Stator current), frequency, I_q , and I_d , as detailed in Tables 2, 3, 4, 5, and 6. The simulation was initiated from an initial speed of 0 to 1000 RPM, followed by subsequent increases in the reference speed to 1200, 1400, 1500, 1700, and 2000 RPM. From the simulation results and analysis, it was found that the rise time of actual speed for different defuzzification methods like COA, BOA, MOM, and LOM remained equal at almost 0.01 seconds. Furthermore, equal rise times were observed across different defuzzification methods like COA, BOA, MOM, and LOM. Moreover, shorter delay times were observed for COA and BOA compared to MOM and LOM. A shorter settling time was noted for COA in comparison to BOA, MOM, and LOM. Higher steady-state errors in speed were observed for MOM and LOM, while lower errors were noticed for COA and BOA. Less torque ripple is observed in COA, with BOA exhibiting nearly a 25% reduction, whereas MOM and LOM show a significant increase of around 200%. A lower Total Harmonic Distortion (THD) is noted in the stator current of COA, with BOA showing an approximate 7% value, while MOM and LOM demonstrate a significantly higher percentage of around 70% at the specified frequency. The I_d and I_q currents are observed to be within limits in COA and BOA, whereas MOM and LOM exhibit higher values. In the SOM method, there is a continuous increase in speed in the negative direction, which is not preferable.

CONCLUSION

The complete drive system is simulated using MATLAB's fuzzy logic toolbox, employing various defuzzification methods. With COA and BOA defuzzification techniques, the reference current can be generated to attain desired outputs in minimal time and achieve minimal steady-state error during operation. In the COA and BOA defuzzification methods, the system exhibits minimum rise time and settling time. Less overshooting and undershooting in speed are observed across all defuzzification methods. Lower Total Harmonic Distortion (THD) in stator currents and reduced torque ripple are observed in COA and BOA. The simulation results lead to the conclusion that COA is a favorable method.

ACKNOWLEDGEMENTS

The provision of the MATLAB licensed version software for simulation work by the Electrical Engineering department of Birla Vishvakarma Mahavidyalaya is appreciated. Additionally, Dr. Rukmi Dutta, an Associate Professor at the University of South Wales, Sydney, Australia, deserves our sincere appreciation for generously sharing motor data during the training program.

APPENDIX

1. We can apply Sugeno inference system for controlling speed and torque.
2. Other PWM techniques can be employed to obtain the gate pulses.
3. In Fuzzy rules, output can be changing accordingly different membership functions and defuzzification methods.
4. Fuzzy algorithms can be implemented on the hardware, so we can verify the simulation results with the hardware.





REFERENCES

1. Baria JC, Patel K, Dalwadi DC, Dalwadi C. (2023) High-Performance and Robust Field Oriented Control of IPMSM Drive Over Wide Speed Operation by PI and Fuzzy Intelligent Controllers. *Indian Journal of Science and Technology*. 16(26):1947-1957. <https://doi.org/10.17485/IJST/v16i26.776>
2. Baria, Jaydeepsinh C., Kuldip Patel, and Darshankumar C. Dalwadi. "Vector Control of Interior Permanent Magnet Synchronous Motor over Wide range of Speed using Fuzzy Logic Controller." : YMER, ISSUE 10 (Oct) – 2022, DOI: 10.37896/YMER21.10/80
3. Feng, Xinpeng, Shirui Xie, Zhaoyuan Zhang, Yao Chen, Haihong Qin, and Chaohui Zhao. "Research on speed loop control of IPMSM based on Fuzzy linear active disturbance rejection control." *Energy Reports* 8 (2022): 804-812.
4. Sahridayan, Parvathy Thampi Mooloor, and Raghavendra Gopal. "Modeling and analysis of field-oriented control based permanent magnet synchronous motor drive system using fuzzy logic controller with speed response improvement." *International Journal of Electrical and Computer Engineering (IJECE)* Vol 12 (2022): 6010-6021.
5. Saha, Sankhadip. "Fuzzy Logic-Based Field-Oriented Control of IPMSM Drive in Electric Vehicles." (ESDPEMS - 2023)
6. Sun, Xiaodong, Zhou Shi, and Jianguo Zhu. "Multiobjective design optimization of an IPMSM for EVs based on fuzzy method and sequential Taguchi method." *IEEE Transactions on Industrial Electronics* 68, no. 11 (2020): 10592-10600.
7. Zhuoyong, Wang, Yao Xiaodong, Liu Jiakang, Xu Liangxu, Tong Hui, and Liu Ke. "Research on IPMSM Control Based on MTPA." *Procedia Computer Science* 208 (2022): 635-641.
8. Wu, Jingbo, Junjie Liu, Zhijun Guo, and Yongwei Wang. "Fuzzy Single-Current Field Weakening Control of IPMSM in EV." *Authorea Preprints* (2022). <https://www.authorea.com/doi/full/10.22541/au.165752686.61778568>
9. Nan, Zhang, and Yin Dejun. "Research on MTPA control of IPMSM drive using online parameter identification method." In 2020 5th Asia conference on power and electrical engineering (ACPEE), pp. 689-693. IEEE, 2020. DOI:10.1109/ACPEE48638.2020.9136376
10. Liu, Zhihong, Lei Zhang, Denggao Huang, Erxi Liu, Zhongwen Zhu, and Xu Wang. A New Flux Weakening Control Strategy for IPMSM (Interior Permanent Magnet Synchronous Machine) in Automotive Applications. No. 2020-01-0466. SAE Technical Paper, 2020. DOI: 10.4271/2020-01-0466
11. Sain, Chiranjit, Atanu Banerjee, Pabitra Kumar Biswas, and Valentina Emilia Balas. "Performance optimisation for closed loop control strategies towards simplified model of a PMSM drive by comparing with different classical and fuzzy intelligent controllers." *International Journal of Automation and Control* 14, no. 4 (2020): 469-493. <https://www.inderscienceonline.com/doi/epdf/10.1504/IJAAC.2020.108281>
12. Hoai, Hung-Khong, Seng-Chi Chen, and Chin-Feng Chang. "Realization of the neural fuzzy controller for the sensorless PMSM drive control system." *Electronics* 9, no. 9 (2020): 1371. <https://doi.org/10.3390/electronics9091371>
13. Kongchoo, Natthawut, Phonsit Santiprapan, and Nattha Jindapetch. "Mathematical Model of Permanent Magnet Synchronous Motor." *Asia Pacific Conference on Robot IoT System Development and Platform 2020 (APRIS2020)*
14. Sakunthala, S., R. Kiranmayi, and P. Nagaraju Mandadi. "Investigation of PI and fuzzy controllers for speed control of PMSM motor drive." In 2018 International Conference on Recent Trends in Electrical, Control and Communication (RTECC), pp. 133-136. IEEE, 2018. DOI: 10.1109/RTECC.2018.8625636
15. Hu, Tangqing, and Xuxiu Zhang. "Simulation of pmsm vector control system based on fuzzy pi controller." In 2019 IEEE International Conference on Power, Intelligent Computing and Systems (ICPICS), pp. 111-114. IEEE, 2019. DOI: 10.1109/ICPICS47731.2019.8942439
16. Mishra, A., Garima Dubey, Dheeraj Joshi, Pramod Agarwal, and S. P. Sriavstava. "A complete fuzzy logic based real-time simulation of vector controlled PMSM drive." In 2018 2nd IEEE International Conference on Power





Jaydeepsinh C. Baria et al.,

Electronics, Intelligent Control and Energy Systems (ICPEICES), pp. 809-814. IEEE, 2018. DOI: 10.1109/ICPEICES.2018.8897373

17. Wang, Huimin, Tong Wang, Xuefeng Zhang, and Liyan Guo. "Voltage feedback-based flux-weakening control of IPMSMs with fuzzy-PI controller." International Journal of Applied Electromagnetics and Mechanics 62, no. 1 (2019): 31-43. DOI: 10.3233/JAE-190014
18. TAN, Lin, Ping LIU, and Shuai CUI. "A High-Performance Speed Control Method Based on Fuzzy-PI of IPMSM for BEV." Journal of Chongqing Jiaotong University (Natural Science) 38, no. 11 (2019): 139. DOI: 10.3969/j.issn.1674-0696.2019.11.22
19. Hou, Pengchao, Xingcheng Wang, and Yang Sheng. "Research on Flux-Weakening Control System of Interior Permanent Magnet Synchronous Motor Based on Fuzzy Sliding Mode Control." In 2019 Chinese Control and Decision Conference (CCDC), pp. 3151-3156. IEEE, 2019.
20. Huang, Zhuoran, Cheng Lin, and Jilei Xing. "A Parameter-Independent Optimal Field-Weakening Control Strategy of IPMSM for Electric Vehicles Over Full Speed Range." IEEE Transactions on Power Electronics 36, no. 4 (2020): 4659-4671.
21. Hou, Pengchao, Xingcheng Wang, and Yang Sheng. "Research on Flux-Weakening Control System of Interior Permanent Magnet Synchronous Motor Based on Fuzzy Sliding Mode Control." In 2019 Chinese Control and Decision Conference (CCDC), pp. 3151-3156. IEEE, 2019
22. <https://archive.nptel.ac.in/courses/108/104/108104157/#>

Table 1: IPMSM Simulation Parameters

Parameter	Parameter Value
Number of Pole Pairs	4
Stator Resistance	0.138 Ω
Permanent Magnet Flux Linkage	0.171 Vs
d-axis Inductance	0.00251 H
q-axis Inductance	0.00617H
Line Voltage (rms)	440 V
Phase Current (rms)	60 A
Base Speed	1500 rpm
Rated Torque	50 Nm
Friction Coefficient	0.00001
Rotor Inertia	0.04357 kg.m ²

Table: 2 Result of Centroid of Area (COA) Defuzzification method

Measure Quantities	Speed range					
	0 to 1000	1000 to 1200	1200 to 1400	1400 to 1500	1500 to 1700	1700 to 2000
Reference Speed (rpm)	1000	1200	1400	1500	1700	2000
Actual Speed (rpm)	1009	1209	1409	1509	1712	2011
Start Time (Sec)	0	1.0025	2.007	3.003	4.004	5.026
Rise Time (Sec)	0.044	0.0135	0.013	0.007	0.015	0.028
Delay Time (Sec)	0.01	0.0015	0.001	0.001	0.001	0.001
Settling Time (Sec)	0.053	0.0165	0.016	0.092	0.019	0.035
Steady State Error %	0.89%	0.79%	0.63%	0.59%	0.70%	0.54%
Torque Ripple %	25.43%	25.95%	25.43%	25.43%	33.33%	37.11%
THD (Stator Current) %	9.09%	7.95%	7.71%	7.62%	5.58%	4.89%
Frequency (Hz)	66.67	80	93.33	101	113.33	133.33
I _q (Amp)	9.9	9.9	9.9	7.8	7.8	6.6
I _a (Amp)	-2	-2	-2	-16.5	-16.5	-27





Jaydeepsinh C. Baria et al.,

Table: 3 Result of Bisector of Area (BOA) Defuzzification method

Measure Quantities	Speed range					
	0 to 1000	1000 to 1200	1200 to 1400	1400 to 1500	1500 to 1700	1700 to 2000
Reference Speed (rpm)	1000	1200	1400	1500	1700	2000
Actual Speed (rpm)	1010	1209	1409	1509	1712	2011
Start Time (Sec)	0	1.04	2.05	3.18	4.075	7.586
Rise Time (Sec)	0.0455	0.01	0.015	0.008	0.015	0.02
Delay Time (Sec)	0.013	0.00123	0.005	0.001	0.0015	0.002
Settling Time (Sec)	0.055	0.018	0.02	0.01	0.02	0.029
Steady State Error %	0.99%	0.99%	0.63%	0.59%	0.58%	0.05%
Torque Ripple %	25.64%	25.64%	25.64%	31.15%	36.73%	50%
THD (Stator Current) %	10.37%	8.15%	10.83%	10.63%	6.54%	1.53%
Frequency (Hz)	66.67	80	93.33	101	113.33	133.33
I _q (Amp)	9.4	9.4	9.4	9.4	9.4	5.5
I _d (Amp)	-4	-4	-4	-4	-12	-42

Table: 4 Result of Mean of Maximum (MOM) Defuzzification method

Measure Quantities	Speed range					
	0 to 1000	1000 to 1200	1200 to 1400	1400 to 1500	1500 to 1700	1700 to 2000
Reference Speed (rpm)	1000	1200	1400	1500	1700	2000
Actual Speed (rpm)	1015	1215	1415	1515	1715	2000
Start Time (Sec)	0	1.046	2.031	3.054	4.0165	5.007
Rise Time (Sec)	0.045	0.014	0.014	0.006	0.0135	0.023
Delay Time (Sec)	0.012	0.002	0.002	0.004	0.0035	0.003
Settling Time (Sec)	0.054	0.019	0.019	0.011	0.0185	0.028
Steady State Error %	1.47%	1.23%	1.06%	0.99%	0.87%	0%
Torque Ripple %	200%	200%	200%	200%	200%	263%
THD (Stator Current) %	70.18%	70.17%	70.69%	76.33%	70.62%	56.35%
Frequency (Hz)	66.67	80	93.33	101	113.33	133.33
I _q (Amp)	20	20	20	20	20	20
I _d (Amp)	-10	-10	-10	-10	-10	-55

Table: 5 Result of Largest of Maximum (LOM) Defuzzification method

Measure Quantities	Speed range					
	0 to 1000	1000 to 1200	1200 to 1400	1400 to 1500	1500 to 1700	1700 to 2000
Reference Speed (rpm)	1000	1200	1400	1500	1700	2000
Actual Speed (rpm)	1015	1215	1415	1515	1715	2000
Start Time (Sec)	0	1.005	2.0194	3.0367	4.025	5.010
Rise Time (Sec)	0.045	0.015	0.014	0.0073	0.015	0.025
Delay Time (Sec)	0.012	0.0015	0.0022	0.0013	0.002	0.005
Settling Time (Sec)	0.055	0.019	0.018	0.0105	0.019	0.03
Steady State Error %	1.47%	1.23%	1.06%	0.99%	0.87%	0%
Torque Ripple %	200%	200%	200%	200%	200%	263%
THD (Stator Current) %	70.62%	70.43%	69.18%	69.83%	69.12%	56.81%
Frequency (Hz)	66.67	80	93.33	101	113.33	133.33
I _q (Amp)	20	20	20	20	20	20
I _d (Amp)	-10	-10	-10	-10	-10	-56





Table: 6 Result of Smallest of Maximum (SOM) Defuzzification method

Measure Quantities	Speed range					
	0 to 1000	1000 to 1200	1200 to 1400	1400 to 1500	1500 to 1700	1700 to 2000
Reference Speed (rpm)	1000	1200	1400	1500	1700	2000
Actual Speed (rpm)	-4400	-6400	-8300	-10200	-12210	-14000
Start Time (Sec)	0	1.004	2.012	3.025	4.021	5.012
Rise Time (Sec)						
Delay Time (Sec)						
Settling Time (Sec)						
Steady State Error %	122.7%	118.7%	116.86%	114.97%	113.92%	114.28%
Torque Ripple %	300%	337%	1056.25%	333.33%	321.33	324.33%
THD (Stator Current) %	50245%	9457.8%	14657.3%	30630.4%	143623%	7429.37%
Frequency (Hz)	66.67	80	93.33	101	113.33	133.33
I _q (Amp)	0	0	0	0	0	0
I _d (Amp)	-60	-60	-60	-60	-60	-60

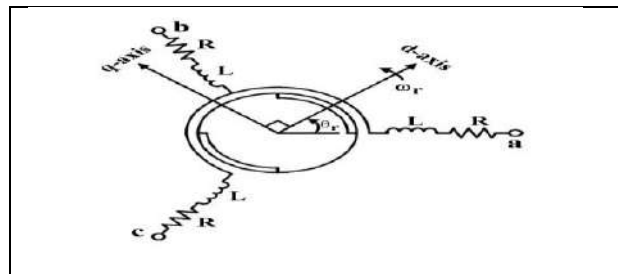


Figure 1. DQ transformation's Vector Diagram [13]

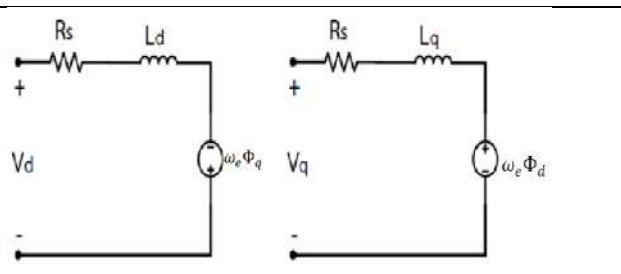


Figure 2. The DQ-axis representation of the IPMSM equivalent circuit [13]

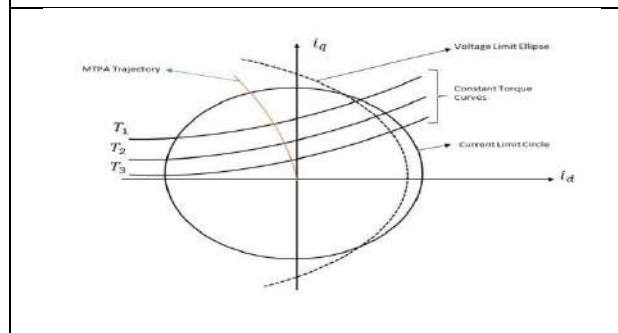


Figure 3 MTPA Operating Region: Restrictive Curves

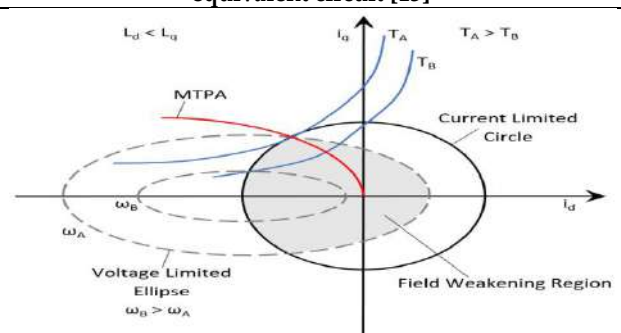


Figure 4 Limit Curves in FW operating Region

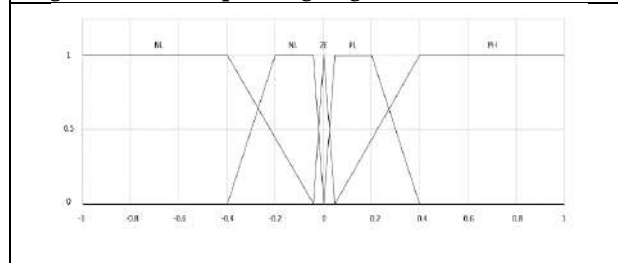


Figure 5 Speed Error Membership Function

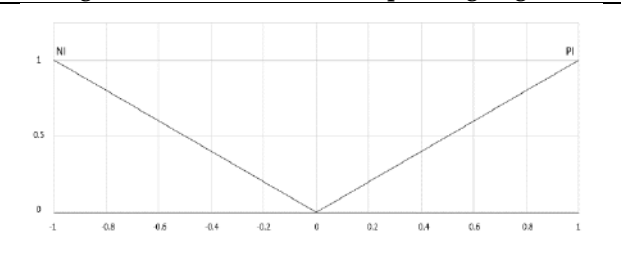


Figure 6 Change in Speed Error Membership Function





Jaydeepsinh C. Baria et al.,

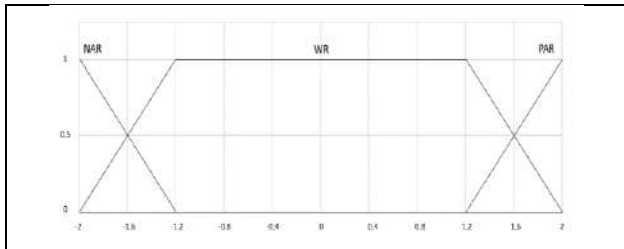


Figure 7 Actual Speed Membership Function

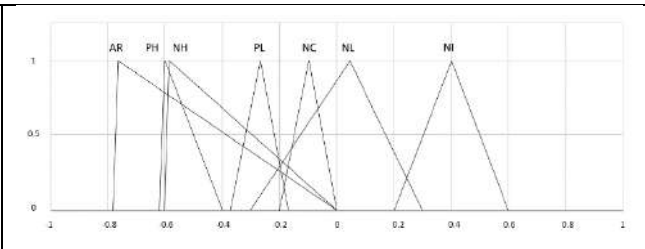


Figure 8 d-axis Current Membership Function

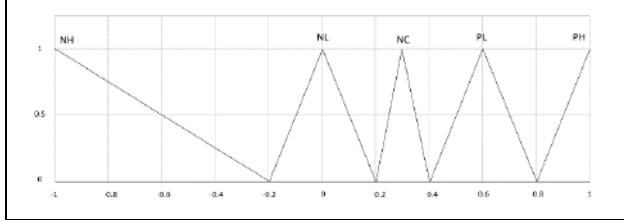


Figure 9 q-axis Current Membership Function

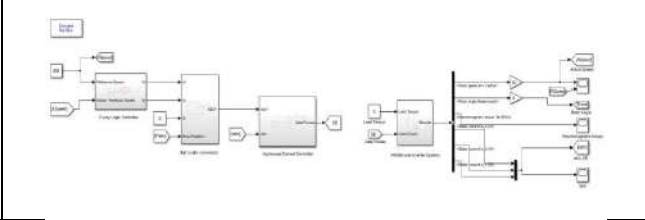


Figure 10 Drive System in MATLAB-Simulink

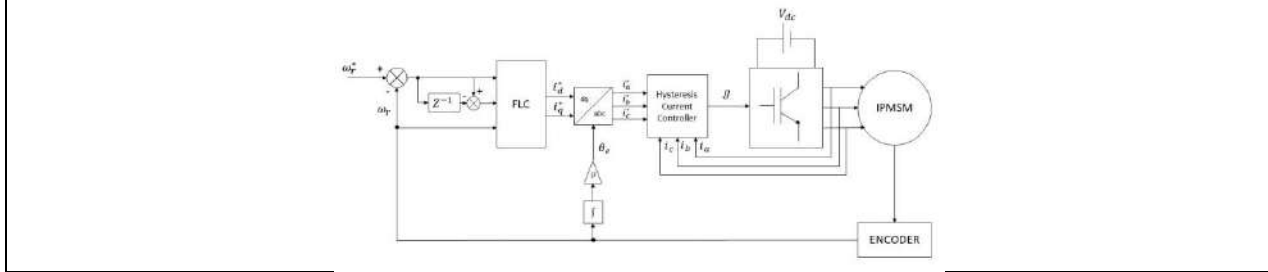


Figure 11 Simplified Block Diagram of Drive System





A Study on Awareness and Usage of Digital Payment Method During Lockdown Period of Covid-19

Parul Dipsinh Zala^{1*} and Kamini Shah²

¹CVM University, Gujarat, India.

²Sardar Patel University, Anand, Gujarat, India.

Received: 30 Dec 2023

Revised: 09 Jan 2024

Accepted: 12 Jan 2024

*Address for Correspondence

Parul Dipsinh Zala

CVM University,

Gujarat, India

Email: parulzala30@gmail.com



This is an Open Access Journal / article distributed under the terms of the **Creative Commons Attribution License** (CC BY-NC-ND 3.0) which permits unrestricted use, distribution, and reproduction in any medium, provided the original work is properly cited. All rights reserved.

ABSTRACT

The centre of attention in present research paper is the usage and awareness of digital payment. Various steps, policies and program have been undertaken by government in digital payment system for convenience and safety of citizens. This study also highlights the importance of digital payment and its awareness, usage and perception of people. Thus, one can say that e-payment will be beneficial for human life. The research applies the inferential statistical research design where data has been analyzed by using, t-test, ANOVA testing, chi-square testing. The study observed that people are comfortable with the digital payment system and they are in process of accepting it. Primary data was gathered by questionnaires, which are susceptible to respondent subjectivity biases. Despite careful selection, the samples might not be entirely representative of the population. Technology has made life easier for the public than it has ever been in every single field. One of these is digital payments, to which society can make various contributions to advance emerging technologies. Students, businesspeople, consumers, the government, and those striving for improvement in the current circumstances will all benefit from the study. The majority of research focuses on specific payment methods, such as credit cards, pay-tm, and digital wallets; however, no Indian researcher has sought to investigate the general awareness of digital payments. There haven't been any specific studies done on digital payment perception or awareness in Gujarat.

Keywords: Digital payment, lockdown, COVID-19, cashless, online transactions





Parul Dipsinh Zala and Kamini Shah

INTRODUCTION

Digital Payment in India

As is commonly known, digital payments serve more purposes than just processing payments; they are helpful in raising productivity, accelerating tax collection, setting aside funds for the country, and many other purposes. Second, India has the highest data consumption in the world at the lowest cost. Thus, the nation may combat many crimes in this way. According to the National Payments Corporation report, there has been a decrease in the use of cash and a rise in the BHIM Unified Payments Interface from 7 million to 913 million. A wealth of information from the "Fintech Festival at Singapore in November 2018" indicates that the moment is right to leverage technology in finance to promote financial inclusion. For 1.3 million people, Aadhar was generated, and with JandhanYojna, There are currently around 330 million active bank accounts. Scholarships can now be sent to students' bank accounts immediately. There are about 4,000 micro ATMs in isolated communities. Farmers now have access to land records, market prices, credit, insurance, and other information. The most advanced and user-friendly payment solution for AEPs without a smart phone or internet connection is the BHIM UPI app. In India, UPI has connections with more than 128 banks. In the last 24 months, UPI transactions have surged by 1500 times, and their value has climbed by more than 30%. (Source: The Indian Express, 2018)

What is Digital Payment?

There are numerous ways to pay, including cash, cards, checks, and drafts. When using different digital payment methods in place of cash and other conventional payment methods, this is referred to as digital payment. Any payment made by citizens or businesses to businesses, banks, or public services that is carried out through communication or electronic networks using contemporary technology is generally referred to as an electronic payment. modes available for cashless transactions like:

Banking Cards

Counties like India having cards as one of the most popular payment mode; master card, Rupayetc, as most of the citizens found it most convenient and comfortable than other modes.

USSD

USSD means unstructured supplementary service data. It has been mainly discovered to serve the low income group of society as it does not require to various app and extra data facility.

AEPs

Aadhar Enabled Payment System is useful for different kind of banking facilities such as deposits, withdrawal and transfer, where only Aadhar verification is needed, which is quite simple to use.

UPI

Any person holding bank account can utilize this method for transferring money 365 days a year. The facility can avail only with registered mobile number and valid bank account number.

Mobile Wallet

By downloading app person can utilize mobile wallet service. Now a days most popular app for wallet are paytm, freecharge, Mobiwik, which provide service with nominal charges as it is comparatively safe.

Bank pre paid card

Here by linking bank account with debit card, customer can avail the facility of digital payment.

PoS terminals

This is a device which can read banking cards for purchase and sales. It has three type of PoS terminal such as mobile PoS, Physical PoS and virtual PoS.

Internet banking

All the transactions which are carried out online are known as internet banking.



**Parul Dipsinh Zala and Kamini Shah****Mobile banking**

This is the service where mobile phone are used is known as mobile banking, now a day banks have introduced varied app to facilitate customers.

Micro ATMs

To provide services to people of remote locations, this handy machine is carried by bank representative. (Source: cashlessindia.gov.in, 2018)

LITERATURE REVIEW**Introduction**

Digital payments are playing a very important role in India at the moment. Our current Prime Minister Shri Narendra Modi wants to make our nation "Digital India" by providing a major drive to digital payments. In addition to the rise in digital payment transactions, numerous research studies in the field of digital payments have been carried out.

Literature Review

For the present research study, various literatures have been reviewed which have been classified in two categories viz.

1. Studies in India.
2. Studies outside India.

Studies in India

In their article "Cashless Payment System in India-A Roadmap," Das et al. (2010) stressed the necessity for a nation to transition from a cash-based payment system to one that is cashless. This will improve financial inclusion, lower the cost of managing currency, track transactions, detect tax evasion and fraud, and link the parallel economy with the mainstream. The article "Moving from Cash to Cashless: Challenges and Opportunities for India" was authored by Bappaditya Mukhopadhyay in 2010. India has a dire need to transition to a cashless economy. It will save a significant sum of money that was used each year for currency printing and maintenance. Nonetheless, the establishment of a critical mass and the network effect play a crucial part in the transition to a cashless economy. Therefore, at least in the beginning stage, steps have to be taken to help build the critical network size. Consequently, actions must be made to assist in establishing the required network size, at least initially. The impact of online service quality on customer satisfaction in Pakistan's banking sector is examined by Zafar et al. (2011). The study finds that customer happiness is significantly impacted by the caliber of different online services that banks offer. They placed a strong emphasis on raising customer satisfaction levels and raising the caliber of the work services. In the research paper "A study on customer perception and awareness in the usage of internet banking," Ramakrishan et al. (2012) It was discovered that security might be provided at a lower cost with the aid of several awareness campaigns. Customer perception can be enhanced. The most important thing for service provider is to awareness among customers, because one can influence others to use internet banking.

Studies outside India

In their study, "A Risk Perception Analysis on the Use of Electronic Payment System by Young Adults," Raihan et al. (2013) Research has shown that the usage of electronic payment systems can boost a country's competitiveness because they benefit both service providers and customers. The degree to which customers view risk determines how satisfied they are. Kaikkaet. al. (2014) in their research work, "Attitude of seniors using cash services towards Online Banking." Most of the respondents were not interested to use it and the reason behind their negative attitude for digital payment was lack of knowledge and difficulty in using computers and their interest. Some of them have complained that due to their age eye problem they cannot use it. A-Khouriet. al. (2014) in his paper "Digital Payment Systems: Global Opportunities still Waiting to be Unleashed" concluded that for technological



**Parul Dipsinh Zala and Kamini Shah**

development in the field of digital payment within few years we can see number of applications around us with, “a wave of a mobile or a gesture with a wearable device”. But it is also noticed that more auxiliary opportunities for more innovative developments in this field. Greg Sterling (2014) in his study, “PayPal Most Used Digital wallet, Apple Pass book used Most Often.” The main reason behind why people are not using digital wallet is payment security. The people perceived that cash and credit cards are easier than mobile wallets. It was also found that PayPal was the most well known and widely used digital wallet. The study also found that people are carrying relatively little cash.

Research Gap

In the human history, present days are victims of very strange time for fighting with an enemy which is invisible; the NOVEL COVID 19 CORONA VIRUS, spreading around the world like anything, hence on 24th of March Indian Government declared total lockdown, so in such situation people are forced to use digital payment for fulfillment of daily needs along with safety of family. So in present study we tried to search about the usage and awareness of people about digital payment, which will relives some information that might be useful to different stakeholders.

RESEARCH METHODOLOGY**Identification of the Research Problem**

It is well known that modern society is passionate, spirited, pioneer and ever changing in their nature. They have great importance and their own identity in every corner of world. They also have great contribution for economic, social and cultural development of country. Now there is a perfect time to change Indian economy with technological advancement and development. And of course moving from developing country to developed country Indian government is framing various plans and programs for digital payment. The research question for the present study has been identified as follow. “A study on Awareness and Usage of Digital Payment Method during lockdown Period of COVID-19”

Objectives of the study

1. To have an idea about basic characteristics and sources of information of digital payment system.
2. To study digital payments method
3. To study awareness and perception about digital payment.
4. To study risk and challenges faced while using digital payment.

Research Design

This research design is of exploratory in nature.

Data collection

The current study's data came from both primary and secondary sources. Sources such as newspapers, periodicals, journals, and websites were used to gather secondary data. A structural questionnaire was used to gather primary data. Respondents received questionnaires using Google Form.

Sample Size & Technique

Questionnaire has been send to 200 people on random bases for sample but only 99 respondents have give their response. Convenience sampling technique was used for a period of one month April- May 2020

Hypotheses of the study

The following hypotheses have been examined:

1. There is no significant awareness about digital payment among people.
2. There is no significant association of age on their perception about risk associated with digital payment.
3. There is no significant difference of education on their perception about safety.
4. There is no significant difference of profession on frequency of usage.
5. There is no difference in perception of male and female about sources of information.





Parul Dipsinh Zala and Kamini Shah

Data Analysis and Interpretation

Various statistical methods such as t-test, ANOVA, Excel, SPSS, and chi-square testing were employed to analyze the gathered data. Additionally, frequency distribution has been used for analysis based on a variety of demographic variables. The table above demonstrates that twenty of the respondents, or twenty of the twenty-six respondents, are beyond the age of thirty-five. Only seven respondents, or twenty of the twenty-six respondents, are under the age of thirty-three. There were 33 female and 63 male responders in all. Of these, 27 hold undergraduate degrees, 7 hold doctorates, 35 possess master's degrees, 3 hold diplomas, 3 hold M.Phil.s, and 21 have not responded to questions about their educational background. Of the 72 respondents, the majority work in services; the remaining respondents are 4 students, 8 businessmen, 2 housewives, 2 professionals, 1 farmer, 1 retired person, and 1 jobless person.

Statistical Analysis

H1: There is no significant awareness about digital payment among people.

It is clear from the above graph that most of the respondents i.e. 91% are aware about digital payment system and they are using or they have plan to use digital payment system in future, whereas only 9% of the respondents are not using digital payment system. So we can say that respondents are aware about digital payment system.

H2: There is no association of age on their perception about risk associated with digital payment.

Table present p value of chi-square test is .333 which is higher than 0.05, therefore null hypotheses can not be rejected at 5% level of significance. Therefore there is no association between age of respondents and their perception about risk associated with digital payment.

H3: There is no significant difference of education on their perception about safety.

$p=.893$ for their perception about reduction in corruption by using digital payment which is higher than 0.05 and therefore there is no significant difference in their perception. So we can conclude that education of respondents do not have much impact on their perception about safety.

H4: There is no significant difference of profession on frequency of usage.

Table 4 helps in drawing following inferences:

$p= 0.097$ for their perception using digital payment which is Higher than 0.05 and therefore there is no significant difference in their perception about it. so we can conclude that profession of respondents do not have much impact on their perception about adoption or usage.

H5: There is no difference in perception of male and female about sources of information.

Table No 6 infers that mean of male respondents and female have no difference, it means there is significant difference in the mean score of male and female respondents.

Major findings

1. Most responders (i.e., 90.90%) use digital payment systems.
2. A respondent's perception is unaffected by their profession
3. The respondents' level of education has little bearing on how they perceive things.
4. The way that men and women are perceived differs significantly.
5. Of the respondents, half of them learned about digital payments from friends and family, while a smaller percentage learned about it from internet advertisements and government awareness campaigns.
6. The respondents cited fraud and app hacking as their two biggest concerns.
7. The majority of respondents—80%—think that making payments online is a smart move.
8. Of them, 35% use digital payments occasionally, while only 22.22% do so constantly.
9. The most popular digital payment methods are UPI and bank card payments. 91% of respondents want to continue using digital modes of payment.
10. Of those surveyed, 91% said they would like to keep making payments online.



**Parul Dipsinh Zala and Kamini Shah****Suggestions**

As per the advice by world health organization and expert's opinion, it is not time to exchange currency notes or visit banks physically. It is one of the important thing that people should adopt it, so proper benefits of this technology can avail in this pandemic situation to save the human life.

Limitations of the research

1. The research study focused only on data collected through questionnaire in goggle form.
2. Collection of primary data through questionnaire has its own limitations because it may suffer from the subjectivity biases of the respondent.
3. Due to time constraint only 99 people responded for study which may not represent total population.
4. Among the respondents many haven't response for optional questions.

Scope for further research

1. Similar studies can be carried out for other emerging technologies.
2. Research is also been carried out for wide range of samples like state wise or nation wise.
3. Researcher can work in the special stakeholder like school students, women, rural population, senior citizens etc. would be interesting to carry out.
4. Similar study for comparing the perception of people of one area with other group is also possible.
5. Comparison of digital payment usage with normal situation with lockdown

CONCLUSION

According to the result of survey majority of respondents reported no change in their use of online payment. The COVID-19 pandemic has changed the style of work and life immensely, which also forces businesses to boost their digital offering as well as customers are also supposed to rely increasingly on e-payment services for day to day activities, however while shifting towards digital payments they are worried about financial, technological barriers too. Despite having all limitations government and RBI are showing greater benefits in non cash payment in 2020.

REFERENCES

1. Al-Alawi, A. I., & Al-Amer, M. A. (2006). Young generation attitudes and awareness towards the implementation of smart card in Bahrain: an exploratory study. *Journal of Computer Science*, 2(5), 441-446.
2. Chaudhari, A., Patil, M., & Sonawane, M. (2014). A Study on Awareness of E-Banking Services in College Students of Bhusawal City. *International Journal of Innovative Research and Development*, 3(1), 219-224
3. Davies, A. E. (2017). To study university students' perceptions towards their cashless financial transactions (Doctoral dissertation, Cardiff Metropolitan University).
4. Desai, H. V. (2014). PRE AND POST BEHAVIORAL STUDY OF STUDENTS REGARDING e-COMMERCE AND CYBER SECURITY. *Journal of Global Research in Computer Science*, 3(2), 30-32.
5. Kalyani, P. (2016). An Empirical Study about the Awareness of Paperless E-Currency Transaction like E-Wallet Using ICT in the Youth of India. *Journal of Management Engineering and Information Technology*, 3(3), 18-41.
6. Ab Hamid, N. R., & Cheng, A. Y. (2020). A risk perception analysis on the use of electronic payment systems by young adult. *order*, 6(8.4), 6-7.
7. Warwick, J., & Mansfield, P. (2000). Credit card consumers: College students' knowledge and attitude. *Journal of Consumer Marketing*, 17(7), 617-626.
8. Lee, E. (2017). Financial Inclusion: A Challenge to the New Paradigm of Financial Technology, Regulatory Technology and Anti-Money Laundering Law.
9. https://www.google.co.in/search?q=1.+https%3A%2F%2Fwww.payumoney.com&rlz=1C1RNRA_enUS505





Parul Dipsinh Zala and Kamini Shah

US505&oq=1.+https%3A%2F%2Fwww.payumoney.com&aqs=chrome..69i57.2402j0j8&sourceid=chrome&ie=UTF-8(2018,November 8)

10. https://www.google.co.in/search?q=2.+www.google.co.in&rlz=1C1RNRA_enUS505US505&oq=2.+www.google.co.in&aqs=chrome..69i57.1187j0j8&sourceid=chrome&ie=UTF-8(2018,November 6)

11. https://www.google.co.in/search?q=3.+http%3A%2F%2Fwww.narendramodi.in%2F&rlz=1C1RNRA_enUS505US505&oq=3.+http%3A%2F%2Fwww.narendramodi.in%2F&aqs=chrome..69i57.8796j0j9&sourceid=chrome&ie=UTF-8(2018,November 8)

12. https://www.google.co.in/search?q=4.+http%3A%2F%2Fiosrjournals.org%2F&rlz=1C1RNRA_enUS505US505&oq=4.+http%3A%2F%2Fiosrjournals.org%2F&aqs=chrome..69i57.4995j0j9&sourceid=chrome&ie=UTF-8(2018,November 6)

13. https://www.google.co.in/search?q=5.+http%3A%2F%2Feconomictimes.com&rlz=1C1RNRA_enUS505US505&oq=5.+http%3A%2F%2Feconomictimes.com&aqs=chrome..69i57.4192j0j9&sourceid=chrome&ie=UTF-8(2018,November 6)

14. https://www.google.co.in/search?q=6.+http%3A%2F%2Fwww.kaavpulations.org&rlz=1C1RNRA_enUS505US505&oq=6.+http%3A%2F%2Fwww.kaavpulations.org&aqs=chrome..69i57.3796j0j9&sourceid=chrome&ie=UTF-8 (2018,November 4)

15. https://www.google.co.in/search?q=7.+http%3A%2F%2Fwww.business-standard.com&rlz=1C1RNRA_enUS505US505&oq=7.+http%3A%2F%2Fwww.businessstandard.com&aqs=chrome..69i57.3986j0j9&sourceid=chrome&ie=UTF-8 (2018, December 4)

16. https://www.google.co.in/search?q=8.+http%3A%2F%2Fwww.forbes.com&rlz=1C1RNRA_enUS505US505&oq=8.+http%3A%2F%2Fwww.forbes.com&aqs=chrome..69i57.11838j0j9&sourceid=chrome&ie=UTF-8 (2018,November 4)

17. https://www.google.co.in/search?q=9.+http%3A%2F%2F+www.allresearchjournal.com&rlz=1C1RNRA_enUS19505US505&oq=9.+http%3A%2F%2F+www.allresearchjournal.com&aqs=chrome..69i57.4363j0j9&sourceid=chrome&ie=UTF-8(2018,November 1)

18. https://www.google.co.in/search?q=10.+http%3A%2F%2F+www.irnbrjournal.com&rlz=1C1RNRA_enUS505US505&oq=10.+http%3A%2F%2F+www.irnbrjournal.com&aqs=chrome..69i57.5115j0j9&sourceid=chrome&ie=UTF-8(2018,November 4)

19. https://www.google.co.in/search?q=11.+http%3A%2F%2Fwww.ijera.com&rlz=1C1RNRA_enUS505US505&oq=11.+http%3A%2F%2Fwww.ijera.com&aqs=chrome..69i57.4001j0j9&sourceid=chrome&ie=UTF-8 (2018,November 1)(2018, November 13). Retrieved from cashlessindia.gov.in: https://upipayments.co.in

Table 1 Demographic Profile of Respondents

	Category	Frequency
Gender	Female	33
	Male	63
	No response	3
Age	18-25 years	20
	26 to 30 years	24
	31 to 35 years	20
	Above 35	28
	No response	7
Education	Phd	7
	Mphil	3





Parul Dipsinh Zala and Kamini Shah

	Master degree	35
	Bachelor degree	27
	Diploma	3
	Other	3
	No response	21
Profession	Student	4
	Business	8
	Housewife	2
	Professional	2
	Service	72
	Unemployed	1
	Retired	1
Farming	1	

Table 2 Chi-Square Tests

	Value	DF	Asymp. Sig. (2-sided)
Pearson Chi-Square	269.307	260	.333
Likelihood Ratio	1.51.381	260	1.000
N of Valid Cases	79		

Table 3 Anova test for Impact of income on their Perception

		Sum of Squares	Df	Mean Square	F	Sig.
Perception about safety	Between Groups	4.782	45	.106	.690	.893
	Within Groups	7.087	46	.154		
	Total	11.870	91			

Table 4 ANOVA Test for impact of profession on frequency of usage

		Sum of Squares	Df	Mean Square	F	Sig.
Frequency of Usage	Between Groups	15.993	17	.941	1.580	.097
	Within Groups	37.513	63	.595		
	Total	53.506	80			

Table 5 Descriptive statistics

	Gender	N	Mean	Std. Deviation	Std. Error Mean
Sources of information	Female	28	7.32	4.691	.0886
	Male	59	7.56	5.344	.696





Parul Dipsinh Zala and Kamini Shah

Table 6 Independent samples test

	Levene's test for equality of variances		T-test for equality of means					95% confidence interval of the difference	
	F	Sig.	T	Df	Sig. (2-tailed)	Mean difference	Std. Error difference	Lower	Upper
Equal variances assumed	0.012				0.957	0.00381	0.07042	-0.13661	0.14423
Equal variances not assumed		0.914	0.054	71	0.957	0.00381	0.0703	-0.1365	0.14412
Variances not assumed			0.054	67.2					

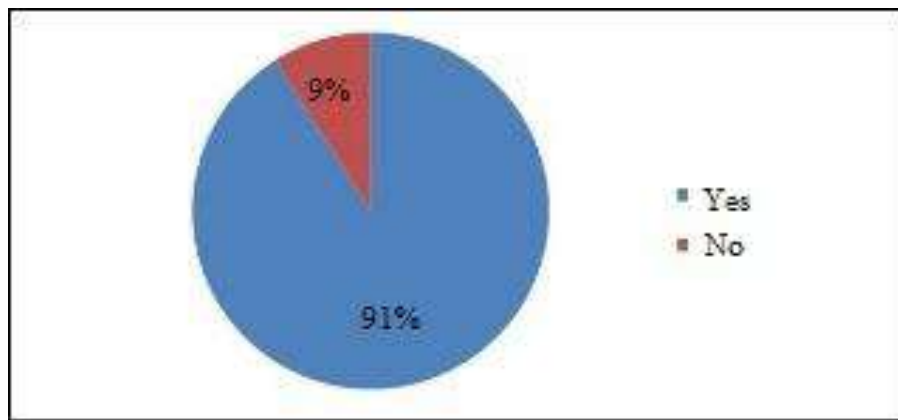


Figure 1 Awareness about digital payment





Nonlinear Static and Dynamic Analysis of the Elevated Water tank Considering Soil Structure Interaction

Vimleshkumar V. Agrawal^{1*} and Indrajit N. Patel²

¹Research Scholar, Gujarat Technological University, Ahmedabad, Gujarat, India.

²Professor, Structural Engineering Department, Birla Vishvakarma Mahavidyalaya, Vallabh Vidyanagar, Gujarat, India.

Received: 30 Dec 2023

Revised: 09 Jan 2024

Accepted: 12 Jan 2024

*Address for Correspondence

Vimleshkumar V. Agrawal

Research Scholar,

Gujarat Technological University,

Ahmedabad, Gujarat, India.



This is an Open Access Journal / article distributed under the terms of the **Creative Commons Attribution License** (CC BY-NC-ND 3.0) which permits unrestricted use, distribution, and reproduction in any medium, provided the original work is properly cited. All rights reserved.

ABSTRACT

This paper presents dynamic and static analysis of elevated liquid storage tanks supported on RC framed structure with different capacities, different Staging configuration and full and empty condition. The liquid storage tanks having less ductility and less energy capacity in comparison to the conventional buildings. The water tanks get heavily damaged or collapsed during earthquake due to the fluid and container interactions; hence tanks observe the complex phenomena when subjected to seismic loading. General practice is to design ESR (elevated storage reservoirs) as crane free structure to eliminate any leakage and as far as staging is concern SMRF is to be provided. Existing codes give elastic analysis which is not capable to give any measure of deformation capacity of structure during Earthquake. Objective of this paper is to study structural nonlinear behaviour and progressive damage with increasing ground motion intensity and to understand behaviour of response reduction factor (R) factor subjected variation in staging height, tank capacity and geometric configuration of framing system and its parametric study. Results state that the dynamic and static analysis replies as base shear, over-turning moment and displacement are vastly influenced.

Keywords: Elevated water tank, Bracing Configurations, Static nonlinear pushover analysis, Time History Analysis, SAP 2000

INTRODUCTION

Elevated liquid storage tanks are used broadly by municipalities for distribution of water supply at a sufficient height to pressurize a water distribution system and industries for storing water, inflammable liquids and other chemicals. Thus seismic safety of elevated liquid storage tank is very important for public utility and for industrial



**Vimleshkumar V. Agrawal and Indrajit N. Patel**

structure. Industrial liquid containing tanks may contain highly toxic and inflammable liquids and these tanks should not lose their contents during the earthquake. Earthquake can induce large horizontal and overturning forces in elevated water tanks. Such tanks are quite vulnerable to damage in earthquakes due to their basic configuration involving large mass intense at top with comparatively slender supporting system. When the tank is in full condition, earthquake forces almost govern the design of these structures in zones of high seismic activity. It is important to ensure that the essential requirement such as water supply is not damaged during earthquakes. In extreme cases, total collapse of tanks shall be avoided. However, some repairable damage may be acceptable during shaking not affecting the functionality of the tanks. Due to the lack of knowledge of supporting system some of the water tank were collapsed or heavily damages. So there is need to focus on seismic safety of lifeline structure using with respect to alternate supporting system which are safe during earthquake and also take more design forces. The main of the study is to understand the seismic behaviour of different staging height and arrangements under different earthquake time history records by non-linear static and dynamic analysis

Design Methodology

Different methods of seismic analysis which are basically linear and nonlinear. During earthquake many of buildings collapsed due to lack of understanding the behavior of structures in inelastic zones. Indian standards dose provide the linear method of analysis and design of structural i.e. elastic analysis gives only elastic capacity of the structure and it also indicates where the first yield occurs but, this elastic analysis cannot give any information about redistribution of force and moments and failure mechanism it means does not contains nonlinear analysis approach of analysis which gives the practical behavior of the structure and it is useful for the performance based design structure as well as the seismic damage evaluation to the new or existing structure. The linear method of analysis dose allows the structure under go higher deformations and serviceability of cracking and collapse which means that the linear design code allows the nonlinear behavior of the structure but it does not provides the degrees of nonlinearity generates during the lateral loading. For checking behavior of structure in inelastic zones nonlinear analysis is necessary. This analysis can be of static or dynamic, user may use the method as per the contingency or the data available for to carry out seismic analysis. The development of rational methodology that is applicable to the seismic design of new structures using available ground motion information and engineering knowledge, and yet is becomes available has been supported for sometimes now. This is the focus of several major research and development efforts throughout the world. However, a general-purpose structural analysis program generally exists in every engineering office. So, the evaluation of the applicability of these structural analysis programs in the design of elevated tanks is important from an engineering point of view and it will be helpful to present the application and results to designers. There is a second important reason that should be considered. That is, simplified models are used for a straightforward estimate of the seismic hazard of existing elevated tanks. Only if the estimated risk is high, it is convenient to measure all the data (e.g. geometry of the tank, material properties) that are required by the general finite element codes and to spend time and money to prepare a reliable general model. Here Nonlinear Static analysis dynamic analysis thoroughly described.

Nonlinear Seismic analysis of elevated water tank involved two types of analysis

1. Pushover analysis (Nonlinear Static Analysis) of elevated water tanks
2. Time History analysis (Nonlinear Dynamic Analysis) of elevated water tanks
3. Structural Geometry & Modeling

Modeling and Non-Linear Pushover Analysis Procedure

Sap2000 v20 programming is utilized to perform the nonlinear static pushover analysis of frame supported water tank. The RC frame is modeled as three dimensional shell elements. The material properties for shell elements are defined as advanced properties, so we can simulate nonlinear behaviour. Shell elements are modeled as shell-layered/nonlinear sections. At the top of the RC frame is considered as rigid diaphragms. The rigid links are modeled at top of the RC frame. The rigid links are modelled at top of the structure. A load case for static pushover is then defined. Conventionally the procedure starts with application of gravity load followed by lateral static pushover



**Vimleshkumar V. Agrawal and Indrajit N. Patel**

load case. This load case is applied from ultimate conditions of gravity pushover. In gravity load case the RC frame supported water tank is loaded with the dead load and 25% of the live load. Here the lateral load is classified as displacement controlled and the gravity load applied is classified as force controlled. A model of structure is then loaded with horizontal loads in a suggested incremental manner involving pushing the structure; and plotting the total applied shear force and associated lateral displacement at each increment.

From the analysis a graph is obtained with base shear (V) versus roof displacement (Δ_{roof}) which is also known as static pushover curve. An initial assessment of target displacement is needed for nonlinear static procedure. In order to study the effect of capacity of tanks and height to diameter ratio for structural systems considered with three different staging heights (i.e. 16m, 20m and 24m). For this study RC frame supported elevated water tank designed having capacity of 500 m³ in the seismic zone V as per IS 1893-2 2014. The seismic demands on these tanks are calculated following IS 1893-2 2014. The RC frame supported water tanks are design as per IS 3370 part-1 & 2, IS 11682 and IS 456. These tanks are designed and detailed in medium soil and for designing purpose base shear of medium soil, C. G of tank is being evaluated with IS 1893-2 2014. Using SAP2000 v20 these base shear is applied at C.G of tank and pushover curve is obtained. Response reduction factor is evaluated of designed tanks. According to ATC 19, response reduction factor must be reduced for structural systems with low level of redundancy. It also proposes draft values for redundancy factor depending on the lines of vertical seismic framing. The proposed draft redundancy factor for a system with two lines of vertical seismic framing is equal to 1. Due to the low redundancy of the RC frame supported structure, this value is selected for the R factor calculation in this study.

Modelling and Non-Linear Dynamic Analysis Procedure

The methodology includes fixing the dimensions of components for the selected water tank and carrying out nonlinear dynamic analysis (Time History Analysis) using IS 1893 (Part 1): 2016 and IS 1893 (Part 2): 2014 code concept. Time History analysis is a well-organized strategy where the loading and the response history are assessed at progressive time increases. Time history analysis uses the merge of ground movement records with detailed structural supplementary model consequently it is equipped for creating comes about with generally low vulnerability. The function values in a time history function to be normalized ground acceleration values and they may be multiplying for particular (displacements and velocities) load pattern and the loading history in the interval. In this strategy the structure is subjected to real ground movement records. This makes examination technique and very unique in relation to all of different analysis strategies as the inertial forces are specifically decided from these ground movements or in forces are calculated as capacity of time, to taking dynamic properties of structure. It is an examination of dynamic reaction of the structures at every augmentation of time, when its base is subjected to particular ground movement. In this analysis the load combinations are to be design as per IS 1893(Part 1): 2016. All seismic parameters are used as per IS 1893(Part1): 2016, 1893 (Part 2):2014 and IITK-GSDMA guidelines for seismic design of liquid storage tanks. This work proposes to study intze tanks of different staging height and stiffness of staging. Sap2000 v20 programming is utilized to perform the nonlinear dynamic time history analysis of frame supported water tank. The intze water tank was analyzed employing structural analysis program2000 (SAP2000) software also, apart from theoretical measures using IS: 1893-2014 Part-2), for zones V. A reinforced elevated water tank with fixed base frame type, tank with normal bracing, radial bracing and cross bracing system have been measured for the present study. Top, bottom and conical domes and cylindrical walls are modeled with thin shell elements. Other dimensions of the elevated tanks are mentioned in Table-4 Total four numbers of earthquake records were used; the maximum PGA on the basis of acceleration are as follow: Displacement is considerably decreases with increase in PGA value of earthquake time history and also noted that higher value in Kachchh earthquake. All the above modeled water tanks shows maximum displacement for Kachchh earthquake data and minimum displacement for Dharmasala earthquake data for all Staging height and staging patters in full tank and empty tank conditions. Time history analysis result shows that decreasing responses including base shear, overturning moment and displacement as the height increasing in both full and empty condition, when compared to all three type of bracing Radial bracing pattern shows minimum displacement, which indicates that Radial type bracing is more effective than other two(normal and cross) type of bracing configuration.





CONCLUSIONS

1. The evaluated 'R' factors for designed water tanks in seismic zone V in tank full condition ranges between 5.28 to 9.56 and tank empty condition ranges between 9.33 to 12.58 i.e. 'R' value varies with height, capacity of tank and stiffness of staging. All values obtain are either close or higher than those specified in the IS 1893-2014 (Part-II) for RC frame supported water tanks. This indicates that the recommendations for 'R' factor provided in IS1893-2014 (Part-II) are on conservative side. IS 1893-2014 (Part-II) code is not specified different 'R' value for full and empty tank condition.
2. This indicates that the recommendations for 'R' factor provided in IS1893-2014 (Part-II) are on conservative side. IS 1893-2014 (Part-II) code is not specified different 'R' value for full and empty tank condition.
3. Radial bracing configuration attracts more seismic forces in tank full and empty condition and results in higher base shear and less displacement compared to other bracing pattern i.e. performance of Radial bracing pattern is better than other two type of bracing configurations.
4. The Static and Dynamic analysis replies as base shear and displacement are immensely influenced.

The critical response is occurs in case of full tank conditions which may be due to the fact that the hydrodynamic pressures higher in tank full case as compared to empty water tank and it is depends on the earthquake characteristics and mainly frequency content of earthquake records.

REFERENCES

1. Dutta, S., Chandra, S. & Roy, R. (2009) "Dynamic behavior of R / C elevated tanks with soil – structure interaction. *Engineering Structures*", 31(11), 2617–2629. <https://doi.org/10.1016/j.engstruct.2009.06.010>
2. Dutta, S., Mandal, A., & Dutta, S. C. (2004). "ARTICLE IN PRESS Soil – structure interaction in dynamic behaviour of elevated tanks with alternate frame staging configurations", 277, 825–853. <https://doi.org/10.1016/j.jsv.2003.09.007>
3. Ghateh, R., Kianoush, M. R., & Pogorzelski, W. (2015) "Seismic response factors of reinforced concrete pedestal in elevated water tanks", *ENGINEERING STRUCTURES*, 87, 32–46. <https://doi.org/10.1016/j.engstruct.2015.01.017>
4. Gondalia, M. R., Prof. A., & Patel, D. (2017) "NON-LINEAR STATIC PUSHOVER ANALYSIS ON ELEVATED STORAGE RESERVOIR (ESR)" *International Journal of Advance Engineering and Research* 656–666.
5. Harsha, K. (2015) "Seismic Analysis and Design of INTZE Type Water Tank", 2(03), 11–24.
6. Omidinasab, F., & Shakib, H. (2008) "SEISMIC VULNERABILITY OF ELEVATED WATER TANKS USING PERFORMANCE BASED-DESIGN"
7. Sandeep T D(2017) "A comparative studies on elevated water tank due to dynamic loading" ,international research journal of engineering and technology (irjet) 4 (05), 2000-2004
8. George W. Housner (1963) "The dynamic behavior of water tanks" *Bulletin of the Seismological Society of America*, Vol.53, No. 2, pp. 381-387.
9. Sajjad Sameer U and Sudhir K. Jain (1994) "Lateral-Load Analysis of Frame Staging's for Elevated Water Tanks", American Society of Civil Engineers, Journal of Structural Eng. 120, pp.1375-1394.
10. Jain Sudhir K., Sameer U.S., 1990, "Seismic Design of Frame Staging For Elevated Water Tank", Ninth Symposium on Earthquake Engineering (9SEE-90), Roorkey, December 1416, Vol-1.
11. Sudhir K. Jain and M. S. Medhekar, October-1993, "Proposed provisions for a seismic design of liquid storage tanks", Journals of structural engineering Vol.-20, No.-03
12. Gaikwad Madhurar V., Prof. Mangulkar Madhuri N., "Comparison between Static and Dynamic Analysis of Elevated Water Tank", International Journal of Scientific & Engineering Research, Volume 4, Issue 6, June-2013, ISSN 2229-5518, pp. 2043 – 2052.
13. ATC -19 "Structural Response modification factors" ATC-19 Report, Applied Technology Council Redwood City California, 1995
14. ATC 40 (1996): "Seismic Evaluation and Retrofit of Concrete Buildings", Volume 1, ATC-40 Report, Applied Technology Council, Redwood City, California.





Vimleshkumar V. Agrawal and Indrajit N. Patel

15. FEMA-356, Federal Emergency Management Agency, Prestandard and commentary for seismic rehabilitation of buildings. Washington (DC); 2000.
16. FEMA 273 “NEHRP Guidelines for the seismic Rehabilitation of Buildings”, developed by the Building seismic safety council for the federal Emergency Management agency (Report NO. FEMA 273), Washington D.C. 1997.
17. IITK-GSDMA guidelines for seismic design of liquid storage tanks.
18. IS 456: “Indian standard code of practice for plain and Reinforced Concrete”, Bureau of Indian standards, New Delhi, 2000.
19. IS 1893, “Criteria for Earthquake Resistance Design of Structures-Part 1; General Provisions and Buildings (Sixth Revision)”, Bureau of Indian Standards, New Delhi, 2016.
20. IS 1893, “Criteria for Earthquake Resistance Design of Structures-Part 2; Liquid Retaining Tanks (Fifth Revision)”, Bureau of Indian Standards, New Delhi, 2014.
21. IS 3370, “Code of Practice Concrete Structures for Storage of Liquids (First Revision)”, Bureau of Indian Standards, New Delhi, 2009.
22. IS 11682 (1985): “Criteria for design of RCC staging for overhead water tanks” [CED 38: Special Structures]

Table - 1 Description of frame supported water tank (500 m³)

Tank Vessel property		Tank Staging property	
Capacity of Tank	500m ³	No. of Column	8
Diameter of tank	12.8 m	Column Diameter	450 mm
Cylindrical Height Wall	4.5 m	Column Height	16 m, 20 m, 24 m
Top Dome Rise	2.6 m	Staging Diameter	8 m
Conical Dome Rise	2.4 m	Bracing Interval	4 m
Bottom Dome Rise	1.6 m	Beam Bracing Size	350 x 350 mm
Top ring Beam	300 x 300 mm	Type of Bracing	Normal Cross Radial
Bottom ring beam	850 x 400 mm	Unit Weight of Concrete	25kN/m ³
Lower Circular ring beam	400 x 800 mm	Material	M30 Grade of Concrete & Fe 415
Top dome Thickness	100 mm	Seismic Data	
Cylindrical Wall Thickness	200 mm	Soil Type	Medium Soil
Conical dome Thickness	400 mm	Zone	V
Bottom dome Thickness	150 mm	Response Reduction Factor	2.5





Vimleshkumar V. Agrawal and Indrajit N. Patel

Table-2 Response reduction factor for 500 m³ full condition

Height	16 m			20 m			24 m		
	Normal	Cross	Radial	Normal	Cross	Radial	Normal	Cross	Radial
R _s	2.12	2.19	2.21	1.77	1.83	1.92	1.78	1.73	1.81
V _o (kN)	4454	4687	4689	3734	3987	4126	3784	3822	3937
V _d (kN)	2092	2141	2119	2111	2176	2146	2129	2210	2174
Δ _m (mm)	380	355	350	420	400	380	450	430	420
Δ _y (mm)	70	93	113	100	125	140	150	153	155
μ	5.43	3.82	3.09	4.2	3.2	2.71	3	2.81	2.70
T (sec)	0.42	0.42	0.42	0.56	0.56	0.56	0.73	0.73	0.73
φ	1.26	1.20	1.17	1.02	0.99	0.98	0.83	0.83	0.83
R _μ	4.50	3.36	2.8	4.15	3.22	2.74	3.41	3.19	3.07
R _R	1	1	1	1	1	1	1	1	1
R	9.56	7.36	6.19	7.33	5.89	5.28	6.06	5.52	5.56

Table-3 Response reduction factor for 500 m³ empty condition

Height	16 m	20 m	24 m						
	Normal	Cross	Radial	Normal	Cross	Radial	Normal	Cross	Radial
R _s	2.74	2.65	2.81	2.98	2.99	3.25	2.92	2.91	3.19
V _o (kN)	4239	4314	4424	3541	3642	3868	3424	3650	3876
V _d (kN)	1547	1628	1574	1188	1218	1190	1173	1254	1215
Δ _m (mm)	400	390	380	440	420	400	450	445	433
Δ _y (mm)	60	70	90	85	100	110	122	124	126
μ	6.67	5.57	4.22	5.18	4.2	3.63	3.68	3.59	3.44
T (sec)	0.31	0.31	0.31	0.43	0.43	0.43	0.55	0.55	0.55
φ	1.57	1.47	1.38	1.23	1.19	1.17	1.03	1.02	1.01
R _μ	4.59	4.10	3.32	4.28	3.68	3.25	3.65	3.56	3.41
R _R	1	1	1	1	1	1	1	1	1
R	12.58	10.82	9.33	12.76	11.01	10.58	10.67	10.36	10.86

Table-4 Earthquake Data for Dynamic Analysis

Record	Kachchh 2001	Dharmasala 1986	Chamba 1995	Uttarkashi 1991
Station	Ahmadabad	Shahpur	Chamba	Bhatwari
PGA(g)	0.106	0.248	0.146	0.253
Magnitude	7.0	5.5	4.9	6.5





Vimleshkumar V. Agrawal and Indrajit N. Patel

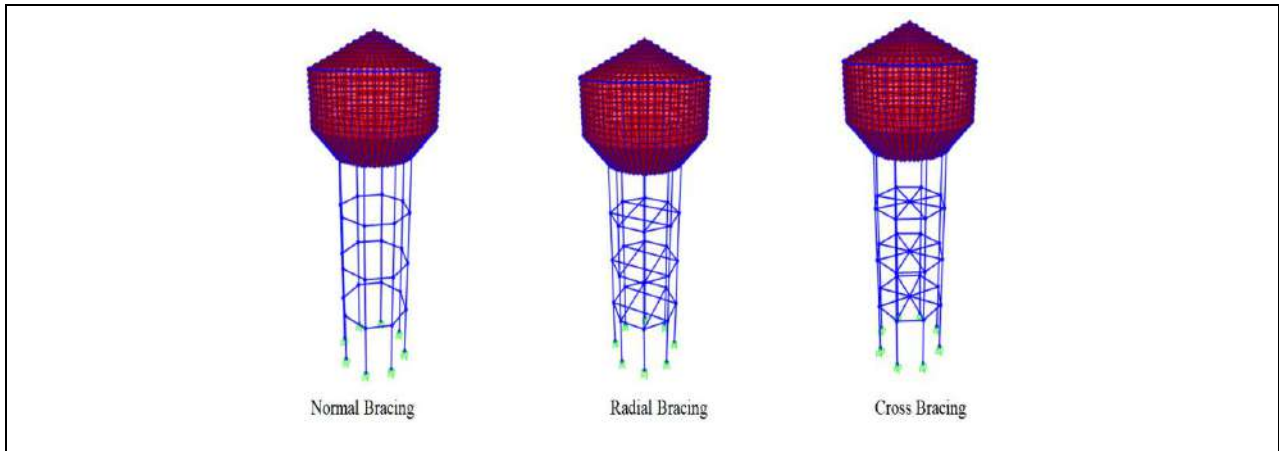
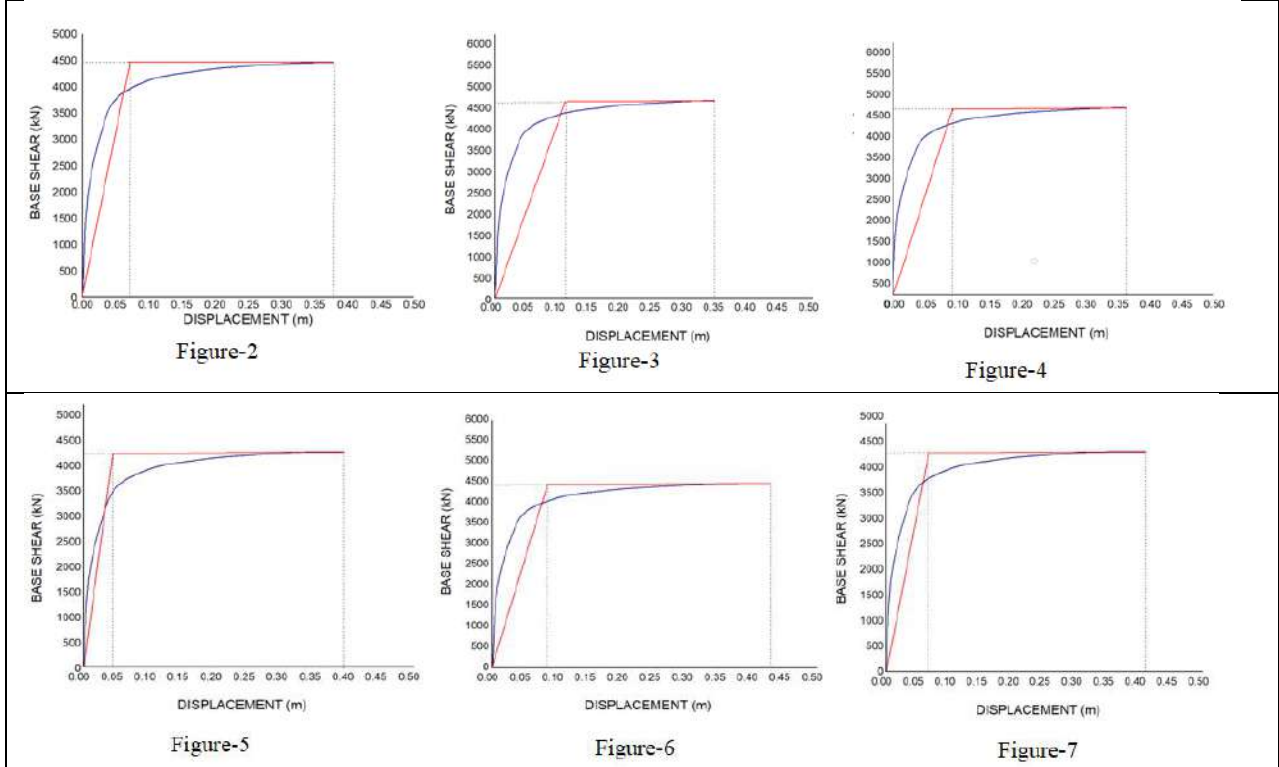
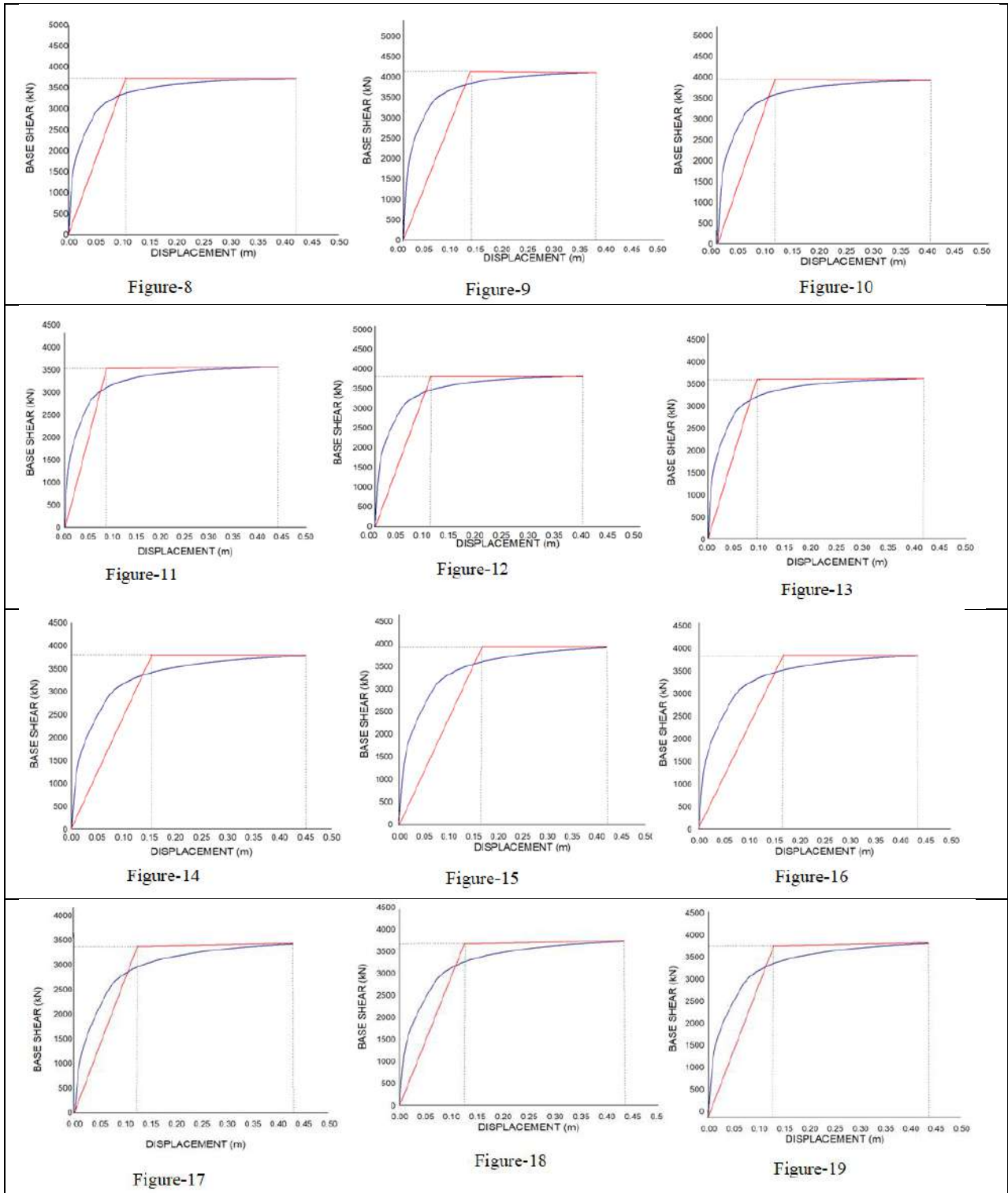


Figure. 1 Modeling of 500 m³ water tank with different stiffness of staging in SAP 2000.





Vimleshkumar V. Agrawal and Indrajit N. Patel





Vimleshkumar V. Agrawal and Indrajit N. Patel

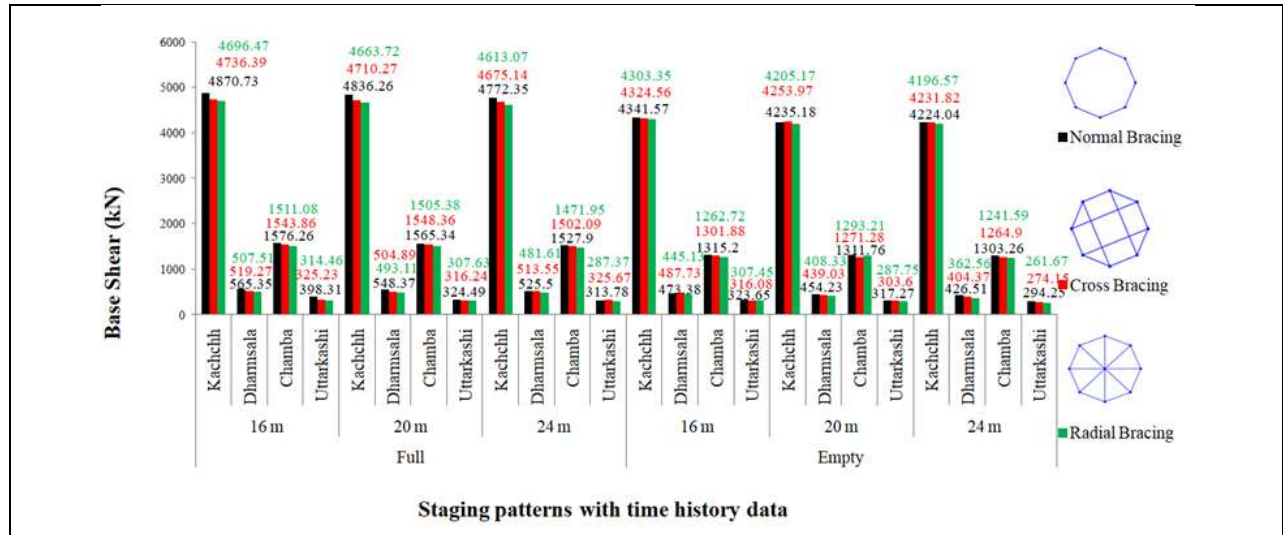


Figure-20 Base Shear variation based on staging patterns and tank filled up condition

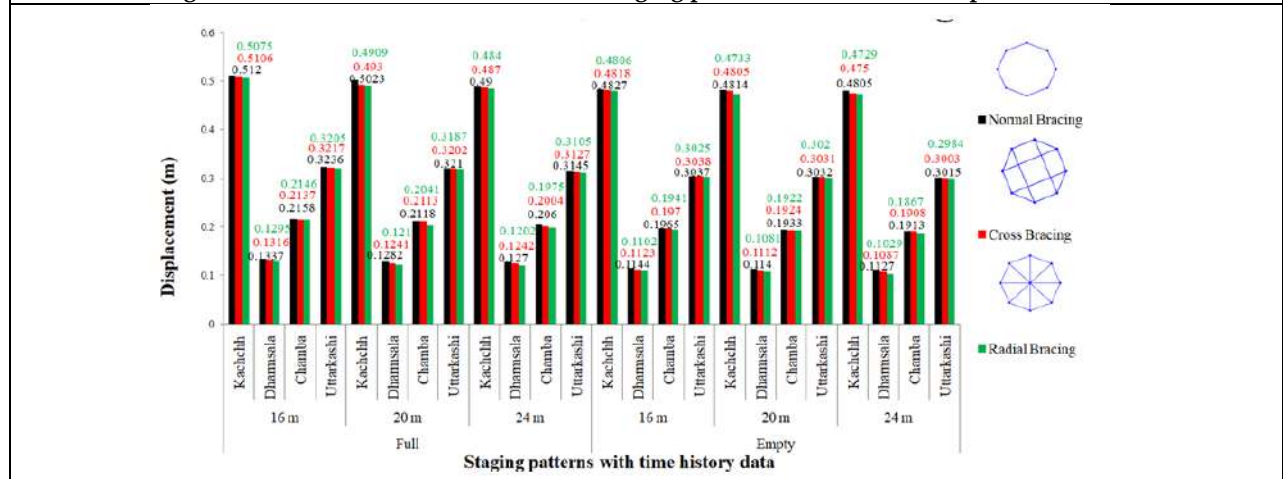
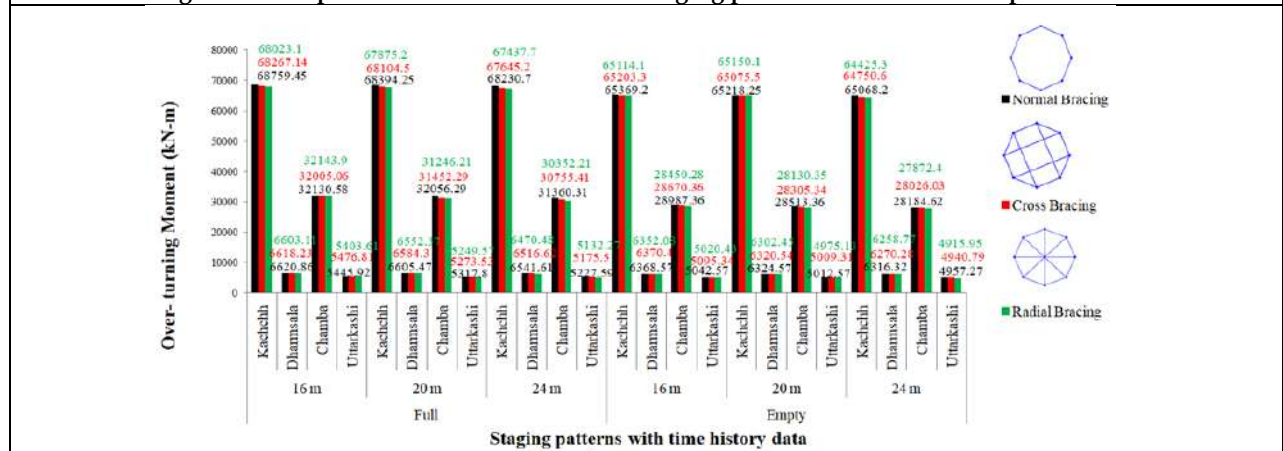


Figure - 21 Displacement variation based on staging patterns and tank filled up condition



Figur-22 Overturning moment variation v based on staging patterns and tank filled up condition





Experimental Study on the Performance of COVID Waste in Developing Construction Components of Next Generation

Pradip Baldaniya^{1*}, Shrey Rana², Sachin Subhash², Jagruti P. Shah³ and Indrajit Patel⁴

¹P.G. Research Scholar, Structure Engineering, Maharaja sayajirao University, Baroda, India.

²P.G. Research Scholar, Structure Engineering, New York University, Brooklyn, New York.

³Assistant Professor, Birla Vishwakarma Mahavidyalaya, Anand, India.

⁴Professor, Birla Vishwakarma Mahavidyalaya, Anand, Gujarat, India.

Received: 30 Dec 2023

Revised: 09 Jan 2024

Accepted: 12 Jan 2024

*Address for Correspondence

Pradip Baldaniya

P.G. Research Scholar,

Structure Engineering,

Maharaja sayajirao University,

Baroda, India.

Email: pradipbaldaniya25@gmail.com



This is an Open Access Journal / article distributed under the terms of the **Creative Commons Attribution License** (CC BY-NC-ND 3.0) which permits unrestricted use, distribution, and reproduction in any medium, provided the original work is properly cited. All rights reserved.

ABSTRACT

Concrete made from Ordinary Portland Cement (OPC) has two prominent characteristics: Compressive Strength and Tensile Strength. Concrete is quite remarkable in its compressive strength but is weak in tension. Moreover, it also possesses the disadvantage of being a brittle material. These weaknesses might act as a limiting agent in its usage and safety in construction. These drawbacks can be avoided by using adequate reinforcements or adding a sufficient amount of waste consisting of fibres to the concrete mix. The effects of adding Polypropylene Fibres are examined in this experiment. The project's polypropylene fibres are derived from biomedical waste such as PPE (Personal Protective Equipment) kits and masks. In response to COVID-19, hospitals, healthcare facilities and individuals are generating more waste than usual, including masks, gloves, and other personal protective equipment. Due to low investment in core infrastructure, developing countries don't have access to modern technology to treat mixed contaminated medical waste. Hence, we attempt to design a mix for proper utilization of waste in construction components after shredding the waste. The tests that will be conducted on the concrete are Compressive Strength Test, Split Tensile strength Test and Flexural Strength Test.

Keywords: Biomedical waste, Personal Protective Equipment, Paver blocks, Concrete mix.





Pradip Baldaniya et al.,

INTRODUCTION

concrete is quite remarkable in its compressive strength but is weak in tension. We attempt in adding a sufficient amount of COVID waste consisting of fibres to the concrete mix to increase its compressive, tensile, flexural strengths and its durability. The use of PPE Kits, masks, gloves, and other protective equipment is the greatest strategy to prevent and slow its transmission. As a result, demand for personal protection equipment (PPE) such surgical masks, N-95 masks, head covers, gloves, air-purifying respirators, goggles, face shields, safety gowns or suits, and shoe covers is increasing around the world. Single-use PPE is essential for doctors, healthcare workers, waste management staff, and emergency service providers for their protection. Health and safety have taken priority over the environment. PPEs are vital in battling the covid-19 crisis, but need to be disposed daily. This waste is slowly piling up an environmental crisis. As of in times of COVID-19, not all PPE kits, gloves, shoes end up in incinerators but sadly are discarded on roads, landfills and rivers which eventually is stirring up a slow eco-hazard along with pandemic. Swati Singh Sambyal, a waste management expert based in Delhi, points to a CPCB data indicating that only 70% of this material is sent to incinerators. There is still a 30 percent disparity. Masks, gloves, and personal protective equipment (PPEs) have been discovered dumped outside hospitals or even on the roadways. There is no segregation happening at the household level. Approximately, 2,03,000 kg/day biomedical waste is produced daily only in India. When not properly managed, infectious medical waste may be subjected to uncontrolled disposal, posing a public health danger, as well as open burning or uncontrolled cremation, releasing toxins into the environment and resulting in secondary disease transmission to humans. As a result, this form of mismanagement must be addressed right away.

OBJECTIVE OF THE RESEARCH

1. To analyze the strength, behaviour and durability of structural members such as concrete and precast elements by incorporating Bio-medical waste in them.
2. It will act as a step further towards a greener world by replacing polluting agents.

SCOPE

1. The study will include usage of biomedical materials such as N-95 masks, surgical masks and PPE kits excluding the masks made from cloth.
2. The experimental study will include research on making structural members like bricks and concrete.
3. Bricks of different mix design will be made to get a idea at which design we are getting the best results i.e by varying the amount of biomedical waste incorporated in the bricks or concrete.

EXPERIMENTAL SET UP

The most important step before plunging into casting is to analyze the materials collected and design an appropriate mix design conforming to IS 10262:2009. All the important criterions and the site conditions are to be kept in mind while designing the mix. Mix design is a trial-based process in which we have to make corrections to make the concrete satisfy the needs we desire. After conforming our mix design after various trials, we conducted three important tests on our concrete namely Compressive Strength Test, Tensile Strength Test and Flexural Strength Test which are discussed briefly in the further. A proper mix design is the key to a strong concrete of desired needs. After various trial mixes and the to final mix design which proportioned as 1: 2.5: 3.76 .

RESULT ANALYSIS

Slump Test Results – As given in the Table (1) the slump for the mix with 0% fibre addition showed a slump value of 180 mm, but when certain amount of waste i.e. 0.3%,0.6% and 0.9% is added the slump value decreased considerably



**Pradip Baldaniya et al.,**

to 45 mm, 45 mm and 40 mm because the waste present in the concrete kept the concrete strongly bonded and as a result a true slump was observed.

Compressive Strength Results

By analyzing the results, it was found that by the addition of waste, the strength increased for 0.3% and 0.6% whereas 0.9% addition of waste showed the decreasing trend as compared to mix design with no inclusion of waste. An increase of 14.5%, 23.8% and 0.75% was observed in the compressive strength of concrete having 0.3%, 0.6% and 0.9% waste inclusion respectively to that of the concrete with 0% of waste addition after 28 days as in figure 1. It is clear from the results that the 0.6% waste addition is the best option as it showed impressive results. The third group of 0.9% waste inclusion showed a decrease of strength as compared to its counterparts of 0.3% and 0.6%, the primary reason is that the addition of high number of wastes affected the cohesiveness of overall concrete matrix and formed many joints in the concrete. Hence, when the cube was loaded it failed early comparatively due to formation of high number of fracture points/joints.

Tensile Strength Results

The Tensile Strength results are quite promising with an increase in tensile strength of 20%, 25.6% and 15.5% for the percentage addition of 0.3%, 0.6% and 0.9% waste respectively as compared to the mix with no waste inclusion in it. The 0.6% waste inclusion in the mix showed better results as compared to the 0.3% and 0.9% waste inclusion as in figure 2.

Flexural Strength Results

The waste inclusion of 0.6% in concrete has shown the best results and it can be said that 0.6% waste added concrete is the best for obtaining promising results. The reason for the reduced flexural strength stands the same as mentioned in Compressive and Tensile Strength test, which is the formation of huge number of fracture joints and less cohesiveness. To get a better idea about the 7 and 28 days' strength the line graph in Fig (3) can be helpful. As observed in the results for the Flexural Strength an increasing strength trend was observed as compared to the Concrete Mix with no waste. The 28 days' Flexural strength as shown in the line graph for 0.3%, 0.6% and 0.9% waste addition was 4.39, 4.76 and 4.23 N/mm² respectively. These results showed an increase of 14.02%, 23.63% and 9.8% in Flexural Strength as compared to the Concrete Mix with 0% of waste in

Water Absorption Test

Water absorption is a significant aspect in the long-term stability of structures. Water works as an electrolyte, allowing numerous aggressive chemicals to enter the concrete matrix, causing the cohesive concrete matrix to disintegrate. As a result (Table 2), a reduction in the permeability of the concrete specimen will be considered a concrete technical progress.

Water Permeability Test

For the water permeability test, three specimens of concrete each of 100 mm diameter and 50 mm height were cast. After 24 hours, the middle portion of 100 mm diameter was roughened and the remaining portion was sealed with cement paste. The specimens were cured for 28 days and then water pressure was applied on the middle-roughened portion so that the water can penetrate inside the concrete. Permeability of concrete can be minimized by adopting low water-content ratio, ensuring proper compaction and curing of concrete.

Scanning Electron Microscope (SEM) and EDX (Energy Dispersive X-Ray) Test

Concrete has a unique and intricate microstructure, making it difficult to observe and investigate mineral presence. Concrete microstructure and mechanical qualities are altered when concrete ingredients are replaced. However, because to the substitution or addition of important concrete materials, there may be some imperfections and failure. The latest way to examining the mineral content of concrete is micro structural analysis. Some of the modern techniques utilized for phase identification, micrograph, concrete imaging, and chemical characterization of unknown constituents in the hydrated cement paste of concrete include X-Ray Diffraction Analysis, Scanning





Pradip Baldaniya et al.,

Electron Microscope, and Energy Dispersive Spectroscopy Analysis. The results of the micro structural examination of concrete would provide a clear picture of hydration development and distribution.

Rebound Hammer Test

The SCHMIDT Rebound Hammer was developed by Ernst Schmidt, a Swiss Engineer. It is one of the most frequently used method worldwide for non-destructive testing of the concrete and also for determining the hardness of various elements. The rebound hammer test is sensitive to local variations in the concrete; for instance, the presence of a large piece of aggregate immediately underneath the plunger would result in a abnormally high rebound number. Conversely, the presence of a void immediately underneath the plunger would lead to a very low result. For this reason, it is desirable to take 10 to 12 readings spread over the area to be tested, and their average value must be taken. The results obtained after performing the Rebound Hammer Test on the Conventional Tile is as shown in the Table 4.

CONCLUSION

The pollution caused by PPE KIT is ubiquitous and environmentally hazardous and generates economic and social costs. The aim of this review was to bring together the complexity of the issue to kick start a discussion on how to act in a coordinated way to reduce this pollution. The amount of Biomedical PPE waste Fibres used in the most optimum composition of concrete i.e. the composition with 0.6% has the capability to use 5.4 kg of Biomedical waste when 1m³ of concrete is utilized. So, Even if 100 m³ of concrete is used we can pull out 540 kg of Biomedical waste which is acting as an environment and health hazard. Hence, it can be concluded that the above-mentioned concrete has additional benefits of saving our precious environment along with higher strengths. Similarly, the amount of Biomedical PPE waste used in construction of 1 Precast tile is approximately 1 kg and looking at mass production 1000's of kgs of waste can be easily pulled out from the environment helping the living beings in leading a healthy life. The strength of the tiles manufacture is also high. Hence, its usage can be easily carried out in practical life. The monetary comparison between the Conventional Concrete and Concrete made by incorporating Biomedical PPE Fibres is negligible. The price for both these types of concrete is same. Bringing to the conclusion that concrete made by adding biomedical PPE fibres is better in every aspect and is leading the race for the Next Gen Concrete. It can be collectively said that the right percentage of waste addition in the concrete can yield promising results. The results showcase that 0.6% waste showed the most optimum results with an increase of 23.8%, 25.63% and 23.6% in compressive strength, Tensile strength and Flexural Strength respectively. The various Durability Tests that were conducted on the concrete yielded impressive results. Hence, it can be deducted that the concrete so formed is durable and which suggests positively that the concrete is resistant to corrosion.

REFERENCES

1. Goldfein, S., "Fibrous Reinforcement for Portland Cement," Modern Plastics, Vol. 42, No. 8, 1965, pp. 156-160.
2. Majumdar, A. J., "Properties of Fiber Cement Composites," Proceedings, RILEM Symposium, London, 1975, Construction Press, Lancaster, 1976, pp. 279-314.
3. Dave, N. J., and Ellis, D. G., "Polypropylene Fibre Reinforced Cement," The International Journal of Cement Composites, Vol. 1, No. 1, May 1978, pp. 19-28.
4. "Measurement of Properties of Fiber Reinforced Concrete," ACI JOURNAL, ACI Committee Report 544.2R 78, July 1978.
5. Mai, Y. W.; Andonian, R.; and Cotterell, B., "Thermal Degradation of Polypropylene Fibers in Cement Composites," International Journal of Composites, Vol. 3, No. 3, Aug. 1980, pp. 149-155.
6. Zollo, R. F.; Ilter, J. A.; and Bouchacourt, G. B., "Plastic and Drying Shrinkage in Concrete Containing Collated Fibrillated Polypropylene Fibre," Third International Symposium on Developments in Fibre Reinforced Cement and Concrete, RILEM Symposium FRC 86, Vol. 1, RILEM Technical Committee 49-TFR, July 1986.





Pradip Baldaniya et al.,

7. Mehta PK., 2002, "Greening of the concrete industry for sustainable development", *Concr Int*, Vol.24, pp 23–28.
8. Osman Gencil a, "Workability and Mechanical Performance of Steel Fiber-Reinforced Self-Compacting Concrete with Fly Ash" *Composite Interfaces* 18 (2011) 169–184.
9. Augustine U. Elinwa., 2016, "Hospital Ash Waste-Ordinary Portland Cement Concrete", *Science Research*. Vol. 4, No. 3, pp. 72-78.
10. Ramakrishnan, V.; Gollapudi, S.; and Zellers, R., *Performance Characteristics and Fatigue of Polypropylene Fiber Reinforced Concrete*, SP 105, American Concrete Institute, Detroit, 1987, pp. 159- 177.
11. UchikawaHorishi, Hanehara Shunsuke., 1997, "Recycling of waste as an alternative raw material and fuel in cement manufacturing in: Waste materials used in concrete manufacturing", *Noyes publications: United States of America*, pp 430–551.
12. Shazim Ali Memon, Muhammad Ali Sheikh and Muhammad Bilal Paracha., 2013, "Utilization Of Hospital Waste Ash In Concrete", *Mehran University Research Journal of Engineering & Technology*, Vol. 32, No. 1.
13. British Standard Institution (1983), "BS 1881: part 116: Testing Concrete: method for determination of compressive strength of concrete cubes", BSI, London.
14. [22]. Guirguis, S., and Potter, R. J., "Polypropylene Fibers in Concrete," *Technical Report TR/F90*, Cement and Concrete Association of Australia, May 1985, 21 pp. 146,147
15. Venu Malagavelli and Neelakanteswara Rao Patura,(2011), "Strength Characteristics of Concrete Using Solid Waste an Experimental Investigation" ,*International Journal of Earth Sciences and Engineering*, Volume. 4, No. 6, ISSN 0974-5904.
16. T.Ch.Madhavi, L.SwamyRaju, and Deepak Mathur "Polypropylene Fiber Reinforced Concrete – A Review," *IJETAE Journal*, Vol.4, Issue 4, June 2014, pp. 114-119.
17. Milind V. Mohod, "Performance of Polypropylene Fiber Reinforced Concrete," *IOSR Journal of Mechanical and Civil Engineering (IOSR-JMCE)* IOSR-JMCE, Vol.12, Issue 1, Jan-Feb.2015, pp. 28-26.
18. ASTM Designation C496-96"Standard Test Method for Splitting Tensile Strength of Cylindrical Concrete Specimens", 1996 Annual Book of ASTM Standard, American Society for Testing and Materials, Philadelphia, Pennsylvania.
19. Ramakrishnan, V.; Gollapudi, S.; and Zellers, R., *Performance Characteristics and Fatigue of Polypropylene Fiber Reinforced Concrete*, SP-105, American Concrete Institute, Detroit, 1987, pp. 159- 177.
20. Zainab Z.Ismail and Enasa.Al-Hashmi (2011), "Validation of Using Mixed Iron and Plastic Wastes in Concrete", *Second International Conference on Sustainable Construction Materials and technologies*, ISBN 978-1-4507-1490-7.
21. Mashima, P., Hannant, D.J. and Keer, J.G., "Tensile Properties of Polypropylene Reinforced Cement with Different Fiber Orientation", *ACI Material Journal*, Vol.87, No.2, March-April 1990, pp.172-178.
22. ASTM Designation C1609/C1609M, "Standard Test Method for Flexural Performance of Fiber Reinforced Concrete (Using Beam with Third-Point Loading)", *Annual Book of ASTM Standard*, ASTM International, West Conshohocken, PA, 2011.
23. Ramakrishnan, V.; Wu, G. Y.; and Hosalli, G., "Flexural Behavior and Toughness of Fiber Reinforced Concretes," *Transportation Research Record* 1226, National Research Council, Washington D. C., 1989, pp. 69-77.
24. Youjiang Wang H.C.Wu and Vitor C.Li (2000), "Concrete Reinforcement with Recycled Fibers", *Journal of Materials in Civil Engineering* / November 2000.
25. IS: 383:1970, Specification for Coarse and Fine Aggregates from natural sources for concrete (Second revision).
26. IS 10262:2019, Recommended guidelines for concrete mix Design, BIS. New Delhi, India, 2009.
27. IS 456:2000, Specifications for plain and reinforced concrete
28. IS 516:1959, Method of test for strength of concrete Bureau of Indian standards. New Delhi, India.





Pradip Baldaniya et al.,

Table 1: SLUMP TEST VALUES

Mix Design	Slump Value (mm)	Remarks
1:2.412:3.720	180	Without Waste
1:2.401:3.707	45	With 0.3% Waste Addition
1:2.391:3.691	40	With 0.6% Waste Addition
1:2.381:3.675	40	With 0.9% Waste Addition

Table 2: Water Absorption Test.

Sr. No.	Initial Weight (kg)	Final Weight (kg)	% absorption
1	8.498	8.520	0.259
2	8.596	8.670	0.861
3	8.678	8.760	0.945
4	8.578	8.640	0.723
5	8.372	8.410	0.454
6	8.335	8.410	0.899

Table 3: Permeability Result

Water Penetration Depth (mm)	Average Penetration Depth (mm)	Remarks
10		Avg. Penetration
15	12.33	Depth less than
12		25mm, OK

Table 4: Rebound Hammer test Results

Sr No.	Rebound Number	Average Rebound Number	Average Compressive Strength	Remarks
1.	42	38	44	Very Good Hard Layer
2.	40			
3.	40			
4.	34			
5.	36			
6.	35			
7.	40			
8.	40			
9.	35			
10.	40			

Sr No.	Rebound Number	Average Rebound Number	Average Compressive Strength	Remarks
1.	40	38	44	Very Good Hard Layer
2.	40			
3.	38			
4.	36			
5.	40			





Pradip Baldaniya et al.,

6.	35		
7.	40		
8.	35		
9.	36		
10.	38		



Chart .1 pie chart of Bio-medical waste & Covid waste

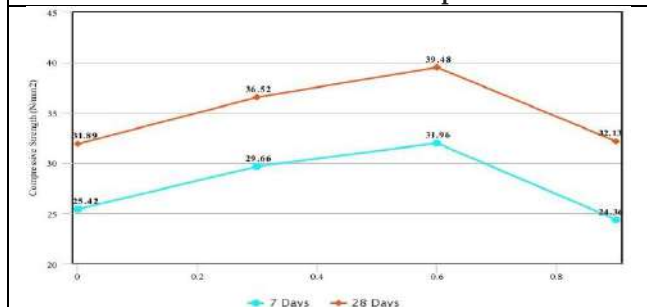


Fig. 1: Compressive Strengths for Different Percentage of Waste Addition

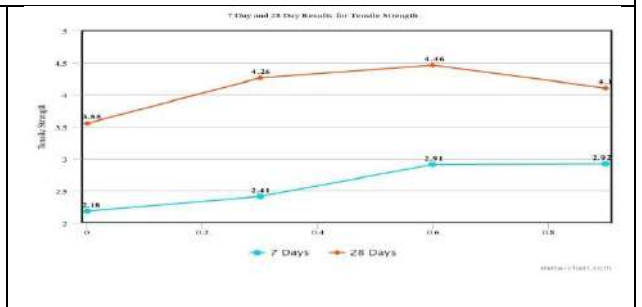


Fig. 2: Tensile Strengths for Different Percentage of Waste Addition

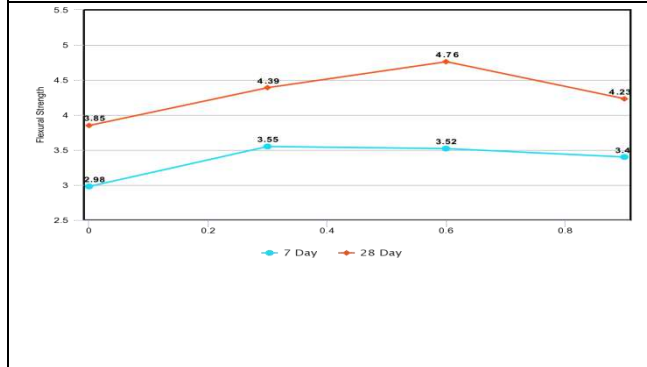


Fig 3: Flexural Strengths for Different Percentage of Waste Addition

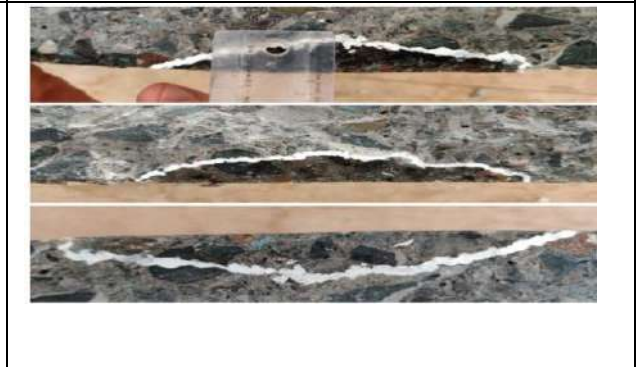


Fig. 4: SEM image of the specimen





Role of Women Engineering Faculty Members in Supporting Girl Students to Develop a Sustainable Career in Engineering Field

Sejal H. Sarvaiya and S. R. Paladiya

Assistant Professor in English, Vishwakarma Government Engineering College, Ahmedabad, Gujarat, India.

Received: 30 Dec 2023

Revised: 09 Jan 2024

Accepted: 12 Jan 2024

*Address for Correspondence

Sejal H. Sarvaiya

Assistant Professor In English,
Vishwakarma Government Engineering College,
Ahmedabad, Gujarat, India



This is an Open Access Journal / article distributed under the terms of the **Creative Commons Attribution License** (CC BY-NC-ND 3.0) which permits unrestricted use, distribution, and reproduction in any medium, provided the original work is properly cited. All rights reserved.

ABSTRACT

The underrepresentation of women in engineering education and profession has been a topic of extensive research. Consistent efforts have been made to motivate girl students for engineering education and profession to meet the requirement of competent engineering workforce. The increased participation of women in STEM education and careers is quite noteworthy. The present research article investigates the current status of Girl students in Engineering education and occupation in India and argues for more conscious role to be played by existing women engineering faculty members to encourage and sustain fair women participation to engineering education as well as to engineering industry. There is a huge possibility of contribution for women engineering faculties to support girl students in engineering education and subsequent employment and retention in industry for sustainable growth objective of our country.

Keywords: Women Engineering Students, National Task Force, Women Engineering Faculty members, Gender Parity, Sustainable Career,

INTRODUCTION

The underrepresentation of women in engineering education and profession has been a topic of extensive research. Consistent efforts have been made to motivate girl students for engineering education and profession to meet the requirement of competent engineering workforce for our country. The increased participation of women in STEM education and careers is quite noteworthy. The present research article investigates the current status of girl students to engineering education and occupation and argues for more conscious role to be played by existing women engineering faculties to encourage and sustain women participation in engineering education as well as to engineering industry. A very positive rate of growth has been observed in girl students' enrollment in STEM courses and especially engineering education during the past few decades. But still it is no way closer to create gender equity

69402



**Sejal H. Sarvaiya and S. R. Paladiya**

in the above fields. The following data would suffice to understand that As seen, girls' representation in higher education has almost equaled male participation. However with reference to engineering faculty admission, it has reached to only 30%. Similarly, the admission data in Post graduate and PH.D. Courses in engineering are quite positive in comparison to previous years. But employment in teaching field or industry seems quite discouraging. In addition, number of girl students exceed the number of students who enter and persist in engineering industry as described by the metaphor 'the leaky pipeline'. Various programmes and projects run by Government, academia and industry has provided encouragement to increase participation of the girl students in technical education. But it is also a fact that that the industry is not able to accommodate more than 30 percent of women engineers in job. Indian women engineering students have acquired leading position the fields like IT, Computer and Electronics and Communication. However, other industries are not eager to smooth the progress of women engineers with compatible environment. Studies have also revealed the fact that the percentage of women students in engineering is not matched by the percentage of women as engineering faculties and researchers in India. There are numerous reasons behind this scenario

1. Management and administrative discrimination in hiring and career progress
2. Less linearity in work as highly qualified women leave work voluntarily at some point in their careers due to societal and family constraints and slow stride of career growth
3. Women employees who enter engineering industry have to fit into the masculine culture which affects adversely on their sense of belonging. Similar is the case of female faculty who face manifold types of gender discrimination putting them at a disadvantageous position compared to their male colleagues.

This article is based on reviewed literature existing online and offline on the projected area. Secondary source literature has been reviewed for understanding the participation and status of women in engineering education by means related to previous research in journals, research reports, newspaper, and reports published online. Reinterpretation of data has been done of previous research, related with the role of women in engineering, engineering education as well as study on women engineers.

NOW IS THE TIME FOR INDIAN WOMAN ENGINEERS

India is a country that possesses a huge mass of skilled young manpower and stands on the frontier for producing highest number of English Speaking Professionals. The current global economic scenario is unique. India is in very advantageous position to accept this opportunity. As suggested by world demographic data, many countries have been facing the challenge of 'ageing workforce'. By building a diverse and gender inclusive workforce our country has an opportunity to make an amazing growth Gender inclusive education is critical to achieving our global sustainable development goals by 2030. It is also a positive time for women to enter the workforce as the corporate milieu has turned to be more inclusive and diverse. The girl engineers also have become more confident, independent, knowledgeable, and motivated.

GROWTH OF WOMEN FOR NATIONAL TASK FORCE

There are various advantages of building women task force like increasing in potential to get more innovative solutions for complex problems and compensating/ recovering lack of engineering talent in some sector for a country. In addition, giving women equal opportunities to pursue – and thrive in – STEM careers helps narrow the gender pay gap, enhances women's economic security, ensures a diverse and talented STEM workforce.

WOMEN ENGINEERING FACULTIES CAN PLAY A SIGNIFICANT ROLE IN SUPPORTING GIRL STUDENTS TO DEVELOP A SUSTAINABLE CAREER IN ENGINEERING FIELD

Role of academia to encourage women engineers can materialize to its full potential only when it has some committed women faculties. Data of empirical research has supported the fact that we need more women decision makers and policy creators. Responsibility of women faculty as change maker and transmitter has been assigned enormous value as reflected in various studies. While expecting things from women engineering faculty members, we must not forget the marginality and other difficulties faced by women engineering faculty members like still



**Sejal H. Sarvaiya and S. R. Paladiya**

there is gender disparity in technical education. Women constitute a majority of the education workforce. However, only quarter or less leadership positions are held by them. Gender disparities in the education profession have long existed and same is the case with technical Education. One of the esteemed technical Institute of India like IIT- Bombay has only 25 (17.3%) women professors out of total 143 professors and IIT Madras has only 10.2% (31) women professors out of 304 total professors. No IIT or IISC has had a woman director till date.

Very little number of women is promoted to senior positions in technical Education Field. The reason is number of women enrolled in technical courses is lower. The situation is aggravated by lack of inclusive thinking, culture and policies. This data of our country is supported by studies done globally. McCullough (2020) in his study on women in senior leadership positions in top 21 STEM schools in USA found significant underrepresentation of women in senior leadership positions. Kinoshita et al. (2020) found that women face higher occurrence of no job offers than men in engineering, physical sciences, and biology. The study also points out that family factors like being married and having dependent children were important variable for the gender gap in no job offers for women but had the opposite effect. The study found that faculty in physics rated male candidates as both more competent and hireable than women. However, there are various avenues for contribution for women faculties to encourage gender inclusivity in engineering education for girl students. Still maker et al. (2020) surveyed more than 1,000 students across 16 departments (including engineering) and showed that faculty gender was not interrelated with engineering students' academic performance. Nevertheless, majority of the girl engineering students believed that having same-gender faculty or mentors in their discipline was significant for them:

Creating academic and other support networks

Various activities like counseling, mentoring, networking with older students, tutoring can make them comfortable as well as motivated. Gender education and sensitization programmes and getting connected with female faculties at regular interval can help a lot. Women faculties' presence at higher positions can help a lot to improve the general environment of academic institutions for girl students.

Being Role Model/Exemplary

Female faculties are seen as example/ role model by girl students. A study done by Bauer and Thesis (2008) on need of female role model in engineering suggest that female students with greater numbers of female professors have higher levels of self-confidence and worry less about how others view them. The study also evaluates the idea that increasing the number of female faculty members in engineering is the solution that will ultimately create an environment that will better support women engineering students.

Creating emotional and academic support networks

Female faculty teachers can serve as living examples in sharing their learning experiences. Opportunities need to be given to women engineers to get directly connected with female faculty or to do research under careful advice and supervision.

Gender Inclusive Curriculum

Studies have also supported the notion of traditional engineering curriculum as possibly being a major obstacle to engaging the interest and motivation of female students. An inclusive curriculum is one in which the subject content covered, the way in which it is taught, and the learning methods promoted take into account the variety of perspectives, attitudes and learning styles brought to the subject by students from different gender, cultural and social groups, as well as the learning environment in general. The researchers have also attempted to get some substantial data from a small survey about the role of faculties to encourage and sustain more girl students in to engineering education and occupation. The researchers were able to find some significant opinions of the girl students about the support they received from women faculty during their college tenure. The survey was conducted at government degree engineering College of Gujarat. Total respondents were 83 girl students from various branches of engineering and semesters. 83.1 % of respondents said that they chose engineering studies and career out of their own interest. Rest of the majority did it by parents' suggestion. Very few of them chose this field by some relatives





Sejal H. Sarvaiya and S. R. Paladiya

or friend's suggestion. Parents' support was received by 89.2 students in their choice of engineering studies. Almost half of the respondents (50.2%) opined that they want to work with industry in future, 43.8% students wanted to get a government job and only 2% of them wished to choose teaching. 3% wanted to start their own business and 1% wanted to choose a defense career. Out of 83 respondents, 90.04% respondents were sure that by this study, they will develop the skills and knowledge to do the work. 98.2 % of the respondents said that their parents would be proud to see them as an engineering graduate. When asked about the kind of support they get from college as a girl student, they responded that they received scholarship and concession in fees as well as free or less expensive hostel. Upon asked about the type of support they get from the faculties of their institute, they replied that they received required information, guidance, counseling, encouragement from their faculties.

Referring to the support the girl engineering students get from the women faculties they replied that they received mentoring (44.5 %), counseling (35 %), guidance when in doubts and queries (38.5 %), taking special care of them while teaching (19%), providing relevant information and encouraging to learn special skills (43 %). In response to the query about the type of support they get from the women faculties of their institute, only 30% of the students said that they received some help from women faculties. Upon asked whether they get any special teaching/ mentoring from women faculty, respondents 35.7% students answered in affirmative. In response to the question if they get special teaching from senior girls, 28.9 % students replied yes to this question and lastly, upon asked, who is the strongest support when facing some difficulty in studies, they said that Friends (50.6%), parents (26.5%) faculties (13.3%) and senior students (9.6.%). Interestingly, only 6 students said their teachers are their role models. The survey suggests that considerable efforts are being made to encourage the girl student to retain in this field. Still we have to do a lot to create equity in this field. UNESCO reports of 2016 have strongly recommended establishing new attitudes, cultural and social norms for engaging girl students in technical field. This will be possible only when we will promote and highlight women in leadership positions and creating gender balance in technical Education Field.

REFERENCES

1. Annual Technical Manpower Review, (for various years and different states), National Technical Manpower Information System, Ministry of HRD, New Delhi.
2. Bauer, Ingrid H,(2008)The Need for Female Role Models in Engineering Education, Honors Thesis ,School of Engineering ,Women's and Gender Studies Program
3. <https://www.gse.harvard.edu/ideas/edcast/21/04/unique-challenges-facing-women-education>
4. <https://www.bqprime.com/business/dear-india-inc-lets-talk-about-the-missing-women-in-stem>
5. <https://peer.asee.org/investigating-the-role-of-faculty-gender-in-mentoring-female-engineering-students-for-success>
6. Eaton, A.A., Saunders, J.F., Jacobson, R.K., and West, K. (2020). How Gender and Race Stereotypes Impact the Advancement of Scholars in STEM: Professors' Biased Evaluations of Physics and Biology Post-Doctoral Candidates. *Sex Roles* 82(3/4): 127–141.
7. Kinoshita, T.J., Knight, D.B., Borrego, M., and Wall Bortz, W.E. (2020). Illuminating Systematic Differences in No Job Offers for STEM Doctoral Recipients. *PLOS ONE* 15(4): 1–23.
8. McCullough, L. (2020). Proportions of Women in STEM Leadership in the Academy in the USA. *Education Sciences* 10(1): 1.
9. S. United Nations Educational and C. Organization. Stem and gender advancement (saga). UNESCO Report, 2016.
10. Singh, S. Investigating the Status of Women Engineers in Education and Employment during the COVID-19 Pandemic. *Challenges* 2022, 13,27. <https://doi.org/10.3390/challe13010027>
11. Singh, Seema. Self-Restrain or Discrimination - Participation of Women Engineers in India Proceedings of the 2014 International Conference on Industrial Engineering and Operations Management, Bali, Indonesia,





Sejal H. Sarvaiya and S. R. Paladiya

12. Stillmaker, K., Oka, L.G., Plascencia, J.G., Schwartz-Doyle, C.C., and Lor, K. (2020). Investigating the Role of Faculty Gender in Mentoring Female Engineering Students for Success. 2020 ASEE Virtual Annual Conference Content Access.
13. Ruggs, Enrica & Hebl, Michelle. 2012. Diversity, Inclusion, and Cultural Awareness for Classroom and Outreach Education. In B. Bogue & E. Cady (Eds.). Apply Research to Practice (ARP) Resources.

Table. 1: Male Female Ratio in Higher and Technical Education (22-23)

Subject	Male	Female	Total
Gross Enrollment Ratio in Higher Education	2.12 Crore (51.3%)	2.01 Crore (48.7%)	4.13 Crore
Enrollment in engineering Faculty	71%	29%	36.86 Lakhs
Post-Graduation in Engineering	66.6%	33.4%	17.7 Lakhs
Ph. D. in Technical Field	66.7	33.3 %	56,625

Source: All India Survey on Higher Education (2021-22) MHRD

State	Professor & Equivalent			Reader & Associate Professor			Lecturer/Assistant Professor		
	M	F	Total	M	F	Total	M	F	Total
Gujarat	4096	1619	5715	5094	2554	7648	15986	10715	26701
All India	104469	42280	146749	100248	60377	160625	104469	42280	146749

Source: All India Survey on Higher Education (2021-22) MHRD





POCUS : Enhancing Productivity - Integrating Pomodoro, To-Do Lists and Performance Evaluation

Kavya Dave^{1*}, Yuvrajsinh Chauhan¹, Zeelrajsinh Mahida², Jaydeep Baldaniya³, Mayur Vegad³ and Narendra Patel³

¹Computer Department, BVM Engineering College, Anand, Gujarat, India.

²Chief Technology Officer, Nxthop Solutions Pvt. Ltd. Surat, India.

³Computer Department, BVM Engineering College, Anand, Gujarat, India.

Received: 30 Dec 2023

Revised: 09 Jan 2024

Accepted: 12 Jan 2024

*Address for Correspondence

Kavya Dave

Computer Department,
BVM Engineering College,
Anand, Gujarat, India.

Email: kavyadave2002@gmail.com



This is an Open Access Journal / article distributed under the terms of the **Creative Commons Attribution License** (CC BY-NC-ND 3.0) which permits unrestricted use, distribution, and reproduction in any medium, provided the original work is properly cited. All rights reserved.

ABSTRACT

This research introduces POCUS, a unified platform integrating the Pomodoro Technique, To-Do Lists, and User Performance Evaluation. POCUS addresses time management challenges by offering cross-platform accessibility, customization options, and user performance analysis tools. It quantifies user performance through comprehensive metrics, generating reports for informed decision-making and goal-setting. POCUS ensures reliable time tracking, accessible task details, and insightful analytics. It supports diverse scenarios, aiding students' study sessions, professionals' task management, and cross-platform workflows. Future enhancements include AI integration, collaborative features, and popular tools integration, aiming to elevate user experience and productivity.

Keywords: Productivity, Pomodoro Technique, Task Management, Time Management, Performance Evaluation.

INTRODUCTION

In today's fast-paced world, effective time management and productivity are of paramount importance. Individuals from all walks of life constantly seek methods to optimize their work habits and enhance efficiency. The Pomodoro Technique[1], a time management method developed by Francesco Cirillo[2] in the late 1980s, has gained substantial popularity for its simple yet effective approach to time utilization. However, the Pomodoro Technique, when integrated with a robust to-do list management system and a comprehensive performance evaluation tool, has the potential to revolutionize how individuals manage their time and tasks. This research paper introduces POCUS, a





Kavya Dave et al.,

novel system designed to seamlessly unify the Pomodoro Technique, To-Do Lists, and Performance Evaluation into a unified platform. POCUS aims to address the common challenges associated with time management, task prioritization, and performance monitoring. In this paper, we delve into the development and features of POCUS, exploring how it can help users improve their productivity and work effectively in a structured, goal-oriented manner. Additionally, we will discuss the underlying principles, the design considerations, and the potential benefits of POCUS in personal and professional contexts. Through this complete study, we seek to establish the significance of this consolidated system and its potential to improve the way individuals manage their time and tasks.

BACKGROUND AND RELATED WORKS

The Pomodoro Technique is founded on the principles of working in focused intervals, typically 25 minutes, followed by a short 5-minute break. After completing four such intervals, a more extended break of 15–30 minutes is taken. This method has gained popularity for its ability to boost productivity by promoting sustained concentration and frequent, rejuvenating breaks. According to the findings in 'Brief and rare mental "breaks" keep you focused: Deactivation and reactivation of task goals preempt vigilance decrements'[3], the vigilance decrement arises due to the cognitive control system's inability to sustain a single goal representation continuously (referred to as goal habituation). The paper suggests that temporarily deactivating the vigilance goal helps prevent complete goal habituation by re-establishing the goal's activation level when resuming the task. Remarkably, the Pomodoro Technique operates in a similar fashion, aligning with this psychological understanding by incorporating breaks that refresh focus and prevent the habituation of goals. However, the challenges of time management in today's fast-paced world are multifaceted. Individuals often grapple with an array of issues, including the struggle to balance professional commitments with personal life, the difficulty of efficiently prioritizing tasks, and the need for effective monitoring of personal progress. Effective task management is another critical aspect of personal productivity. To-do lists play an indispensable role in organizing tasks, setting priorities, and ensuring a systematic approach to completing objectives. A well-structured to-do list can help individuals stay organized, reduce procrastination, and improve overall time management. In addition to time management and to-do list management, the process of performance evaluation is essential for tracking personal progress and identifying areas for improvement.

Effective performance evaluation allows individuals to assess their productivity, set achievable goals, and make data-driven decisions to elevate their performance. POCUS offers a unique and extensive solution in the realm of time management and productivity tools. While the existing systems provide their own strengths, POCUS stands out with a unique set of features. POCUS is distinguished by its cross-platform accessibility, integration of performance evaluation, customization options including multiple themes, a unified ecosystem, adherence to Pomodoro principles, and performance analysis and reporting tools. By consolidating these features on a single platform, POCUS strengthens user convenience, providing an all-inclusive approach to productivity that sets it apart from existing systems. Furthermore, the potential integration with popular productivity tools and platforms such as Trello[4] (A web-based, kanban-style, list-making application), Asana[5] (A web and mobile "work management" platform designed to help teams organize, track, and manage their work), or Slack[6] (A cloud-based team communication) offers the prospect of further streamlining task management and providing a seamless experience for users who rely on these tools. This integration is a prospective development for the future, enhancing POCUS's capability to meet evolving user needs.

QUANTIFYING USER PERFORMANCE

In the context of POCUS, the proper quantification of user performance stands as the cornerstone of its effectiveness. This sophisticated system of quantitative metrics not only assesses users' productivity and task management but serves as the bedrock of POCUS's ability to augment their time management skills while adhering to the Pomodoro Technique[1]. This section outlines the key metrics and equations used to generate all-encompassing performance reports.





Kavya Dave et al.,

POMODORO SCORE (PS)

Pomodoro score quantifies the effectiveness of each Pomodoro cycle, considering completeness, time utilization, breaks, distractions. Following are the parameters with their respective independent weights used to determine the PS

1. Pomodoro Completeness (PC): +1 for complete, -1 for incomplete [Weight: **WPC**]
2. Productive Time (PT): Actual productive time / Expected productive time [Weight: **WPT**]
3. Short Break Taken (SBT): +1 for taken, -1 for not taken [Weight: **WSBT**]
4. Short Break Time Inconsistency (SBTI): Actual break time / Expected break time. Penalized if not in 5:1 ratio with productive time [Weight: **WSBTI**]
5. Distraction (D): +1 for occurred, -1 for not occurred [Weight: **WD**]
6. Distraction Timing Penalty (DTP): Pause time due to distraction / Productive time [Weight: **WDT**]

Let α be the set of above-mentioned parameters. Then,

$$PS = \sum_{p \in \alpha} (W_p \cdot Param_p)$$

POMODORO EFFECTIVENESS RATING (PER)

Pomodoro Effectiveness Rating measures the effectiveness of all performed Pomodoro cycles, accounting for completeness, time management, breaks, distractions, session quality, long breaks, and their respective consistencies. Following are the parameters with their respective independent weights used to determine the PER:

1. Average Pomodoro Score (APS): Average pomodoro score of all Pomodoro cycles
2. Session Quality Score (SQS): Marks on the basis of quality of the session [Weight: **WSQ**]
3. Long Break Taken (LBT): +1 for taken, -1 for not taken [Weight: **WLB**]
3. Long Break Time Inconsistency (LBTI): Actual long break time / Expected long break time [Weight: **WLBTI**]

Let α be the set of above-mentioned parameters. Then,

$$PER = \sum_{p \in \alpha} \frac{PSC_p}{N} + (SQS \times W_{SQ}) + (LBS \times W_{LB}) - (LBT \times W_{LBTI})N$$

Where N is the total number of sessions in a cycle.

TASK SCORE (TS)

Task Score evaluates task performance, incorporating deadline compliance, task complexity, task priority, delay time, and time estimation accuracy. Following are the parameters with their respective independent weights used to determine the TS

1. Deadline Compliance (DC): +1 for before deadline, -1 for after deadline [Weight: **WDC**]
2. Task Complexity (TC): Positive Factor [Weight: **WTC**]
3. Task Priority (TP): Positive if right, negative if different from expected priority [Weight: **WTP**]
4. Delayed Time (DT): The time for which the task was delayed to be dormant [Weight: **WDT**]
5. Time Estimation (TE): +1 for accurate estimation, -1 for inaccurate estimation [Weight: **WTE**]

Let α be the set of above-mentioned parameters. Then,

$$TS = \sum_{p \in \alpha} (W_p \cdot Param_p)$$

PRODUCTIVITY SCORE (PRS)

Productivity Score (Productivity) is an overall assessment combining Pomodoro effectiveness, task performance, consistency in Pomodoro usage, and productive hours. Following are the parameters with their respective independent weights used to determine the PRS

1. Number Of Consecutive Days (NCD): Number of consecutive days with at least one Pomodoro [Weight: **WNCD**]
2. Productive Hours (PH): Total number of productive hours [Weight: **WPH**]





Kavya Dave et al.,

3. Task Scores (TS): Cumulative Task Scores of accomplished tasks
4. PER Score (PERS): Cumulative PER scores of all the performed Pomodoros

Let α be the set of above-mentioned parameters. Then,

$$PRS = \sum_{p \in \alpha} (W_p \cdot Param_p)$$

SYSTEM DESCRIPTION

POCUS is an cohesive system designed to refine productivity and time management. It seamlessly combines the renowned Pomodoro Technique, effective to-do list management, and performance evaluation into a single platform. Built on a robust technological foundation that includes React Native[7] and Firebase[8], POCUS equips users with the tools needed to work smarter, achieve their goals, and make the most of their valuable time. POCUS introduces an intuitive and user-friendly interface focused on optimizing time management and productivity. Within this interface, users access a broad set of features seamlessly woven into the platform. The system initiates with a secure login screen offering quick access through Google account integration. Once logged in, the interface showcases the task list, allowing users an efficient overview and management of their tasks.

Task Module

Task creation becomes effortless, enabling users to input various details such as title, description, complexity, priority, estimated number of required Pomodoros, and task deadlines, tailoring tasks to individual needs and goals. It will also show relation between portion of task accomplished and Pomodoro.

Pomodoro Module

The Pomodoro-related functionalities centralize around Pomodoros and the Pomodoro Timer. The "Pomodoros" screen visually presents completed work intervals and short breaks, aiding users in tracking their progress. Meanwhile, the "Pomodoro Timer" serves as a focal point, enabling users to initiate focused work intervals, manage breaks, and utilize visual cues and notifications effectively.

User Profile and Customization

The configuration panel encompass user preferences, login mechanisms, and themes, providing a personalized experience. Users can configure personal details, session cycles, task durations, notification preferences, and themes. Additionally, POCUS incorporates a reward system, motivating users by acknowledging milestones and accomplishments, further increase their engagement with the platform.

Gamification and Rewards

POCUS introduces an engaging gamification and reward system as a key feature, enriching users' productivity journey. Through this innovative approach, completing tasks and Pomodoro cycles earns user rewards such as achievements, badges, and personalized animated themes,

Figure 3 User profile and System Customization

Fostering a sense of accomplishment and motivation. These incentives serve as milestones, recognizing users' progress and boosting their engagement with the platform. By infusing elements of gamification, POCUS transforms task management into an exciting experience, encouraging users to strive for higher productivity levels while enjoying a visually appealing and rewarding interface.

Report Generation

The performance report offers users valuable insights into their productivity. Performance metrics and analytics are presented through intuitive charts and graphs. Users can assess their work efficiency, track trends, and make data-driven decisions to optimize their work routines. This report generation component empowers users to extract





Kavya Dave et al.,

valuable insights and data summaries from their task management and Pomodoro activity, facilitating progress tracking and informed decision-making.

POCUS embodies a foundation of reliability and precision, making the Pomodoro Technique not just a feature but a dependable ally in your productivity journey. With clockwork precision, the Pomodoro intervals and breaks seamlessly navigate within the system, free from interruptions or glitches. Every action leaves its mark, as the system meticulously logs and timestamps task-related data, nurturing a complete log of your activities and time expenditure. Moreover, navigating through your progress is a breeze; stored data in the system's database is effortlessly accessible, providing users swift access to task details and insightful Pomodoro statistics, empowering efficient time management. These features collectively form the POCUS interface, emphasizing streamlined task management, efficient time tracking, insightful performance evaluation, and an aesthetically pleasing, user-friendly experience.

Use Cases - Realizing Productivity with POCUS

In this section, we explore various user scenarios where POCUS plays a pivotal role in amplifying productivity and optimizing time management. These use cases provide insights into how POCUS becomes a versatile companion in different contexts:

Scenario 1 Student's Study Session: Imagine a dedicated student embarking on a study session. With POCUS, the student efficiently manages study tasks, setting up assignments and deadlines. The Pomodoro timer ensures focused work intervals, while the short breaks offer moments of relaxation. After multiple cycles, the student can enjoy a longer break. POCUS empowers the student to stay disciplined, fostering productivity during demanding study sessions.

Scenario 2 Professional Task Management: In a fast-paced professional world, a working individual relies on POCUS to manage tasks effectively. The system streamlines task management, prioritization, and time allocation. POCUS ensures that professional commitments are met efficiently, helping the individual maximize productivity in a demanding work environment.

Scenario 3 Cross-Platform Workflow: POCUS's cross-platform accessibility offers users the flexibility to seamlessly transition between web browsers, desktop applications, Android, and iOS devices. Users can access their productivity tools across different platforms without disruptions, making it an ideal choice for those who work across multiple devices.

Scenario 4 Efficient Task Creation and Editing: Users benefit from POCUS's streamlined task creation and editing capabilities. With ease, users specify task details, set deadlines, and customize task parameters, making task management more efficient and responsive to their needs.

Scenario 5 Productive Breaks: POCUS promotes productive breaks through the Pomodoro Technique. Users strategically use short breaks for relaxation and longer breaks for rejuvenation, optimizing work intervals and break periods for better productivity.

Scenario 6 Personalization and Customization: Users personalize their POCUS experience, tailoring the system to their preferences. They adjust timer durations, fine-tune notification preferences, and choose themes to create a workspace that aligns with their unique work habits and aesthetic preferences. These use cases showcase how POCUS adapts to diverse user scenarios, providing an exhaustive and supportive platform to optimize productivity in study sessions, professional settings, and cross-platform workflows. The system's versatility and adaptability empower users to achieve their objectives effectively.

CONCLUSION AND FUTURE WORKS

In conclusion, POCUS epitomizes a synergistic blend of the Pomodoro technique and contemporary technology, aiming to revolutionize time management and task prioritization across diverse demographics. The application's versatile functionality extends its utility to various tasks: from academic pursuits like essay writing, research, and



**Kavya Dave et al.,**

exam preparation for students, to professional responsibilities such as project management, content creation, and meetings for working professionals. It even extends to household tasks like meal planning, chores, and personal projects for homemakers. The comprehensive features, encompassing task management, Pomodoro timer, detailed reporting, and integrated to-do lists, align cohesively with the system's objectives of augmenting time management, productivity, and sustained focus. Leveraging React Native and Firebase, POCUS ensures a user-centric interface and robust data security, incorporating traditional productivity methodologies with modern technological innovations. POCUS stands as a testament to the strategic amalgamation of time proven techniques with cutting-edge advancements, providing users from various domains with a comprehensive tool adaptable to any task, streamlining workflow, and optimizing productivity.

Future Works

We are committed to continuous improvement and evolution to meet the changing needs of our users. The following future works and enhancements represent our vision for further enhancing the platform. These developments aim to elevate productivity, user experience, and overall efficiency, ensuring that POCUS remains a reliable and indispensable tool for time management and task completion:

1. Integration of AI for Intelligent Task Management: Implementing artificial intelligence (AI) features to enhance task management. AI algorithms could prioritize tasks based on user history, complexity, and deadlines, providing personalized recommendations for task order and Pomodoro durations.
2. Integration with Popular Productivity Tools: Integrating with popular productivity tools and platforms such as Trello [4], Asana [5], or Slack [6] to streamline task management and provide a more seamless experience for users who rely on these tools.
3. AI-Powered Feedback and Guidance System: Introducing advanced AI algorithms to analyse user performance metrics comprehensively. The AI system will evaluate user scores based on their performance, curate personalized professional feedback, suggest improvements, and identify areas for enhancement to achieve higher scores. This personalized approach aims to guide users effectively by providing tailored recommendations for maximizing productivity and optimizing performance within the POCUS system.
4. Improving Quantitative Metrics: Enhancing the quantification of user performance and metrics within POCUS, providing more accurate and insightful performance assessments.
5. User Feedback Collection and Analysis: Implementing a robust system for gathering and analysing user feedback to understand user preferences, pain points, and suggestions for further improvements. Incorporating user feedback into iterative development cycles to continuously enhance the application's usability and effectiveness.

REFERENCES

1. Wikipedia, "Pomodoro Technique", Wikipedia. [Online]. Available: https://en.wikipedia.org/wiki/Pomodoro_Technique. [Accessed: November 09, 2023]
2. The Introvert Alert, "The Man Behind the Pomodoro Technique: A Look into the Life of Francesco Cirillo", Medium. [Online]. Available: <https://medium.com/@theintrovertalert/the-man-behind-the-pomodoro-technique-a-look-into-the-life-of-francescocirillo80ca95ed0535>. [Accessed: November 09, 2023]
3. Ariga, A., & Lleras, A. (2011). Brief and rare mental "breaks" keep you focused: Deactivation and reactivation of task goals preempt vigilance decrements. *Cognition*, 118(3), 439-443. <https://doi.org/10.1016/j.cognition.2010.12.007> [Accessed: November 09, 2023]
4. Rahul Arun, "What is Trello and How To Use It?", Simplilearn. [Online]. Available: <https://www.simplilearn.com/tutorials/projectmanagement-tutorial/what-is-trello>. [Accessed: November 09, 2023]
5. Wikipedia, "Asana, Inc.", Wikipedia. [Online]. Available: https://en.wikipedia.org/wiki/Asana,_Inc. [Accessed: November 09, 2023]





Kavya Dave et al.,

- 6. Wikipedia, "Slack (software)", Wikipedia. [Online]. Available: [https://en.wikipedia.org/wiki/Slack_\(software\)](https://en.wikipedia.org/wiki/Slack_(software)). [Accessed: November 09, 2023]
- 7. React Native, "React Native", React Native. [Online]. Available: <https://reactnative.dev/>. [Accessed: November 09, 2023]
- 8. Wikipedia, "Firebase", Wikipedia. [Online]. Available: <https://en.wikipedia.org/wiki/Firebase>. [Accessed: November 09, 2023]

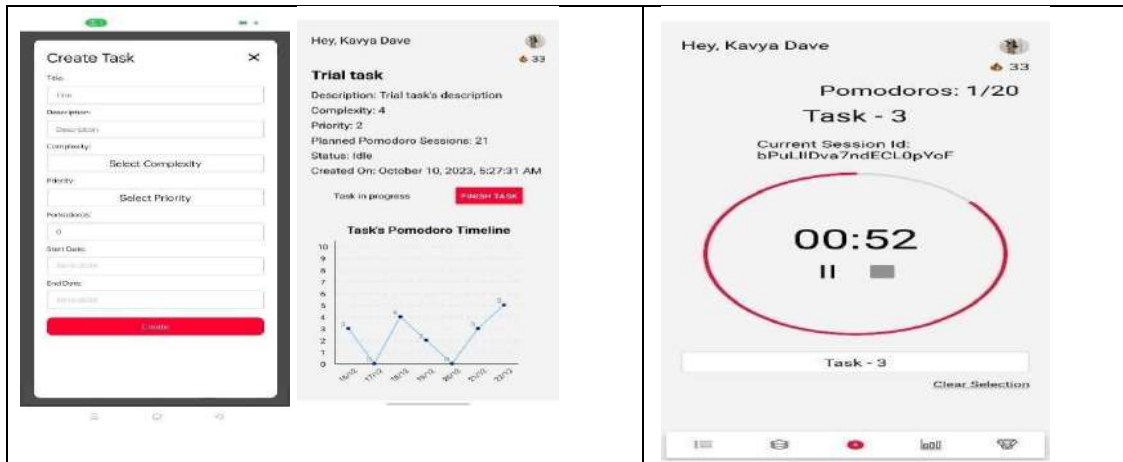


Figure 1 Task Management Module

Figure 2 Pomodoro Timer

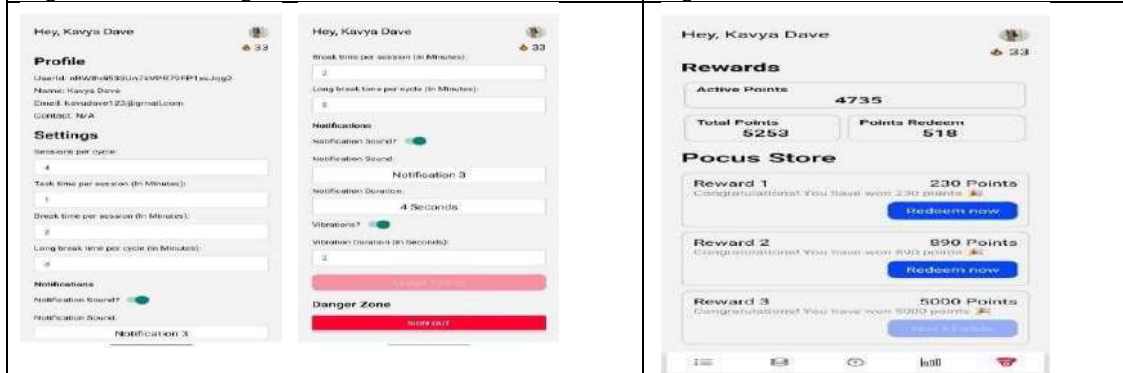


Figure 3 User Profile/Customization Page

Figure 4 Reward Screen



Figure 5 User Performance Report





Some Approximation Properties of Stancu Type Generalization of Lupaş Operators

Usha Varma¹ and R.B. Gandhi^{2*}

¹Department of Mathematics, Gujarat Technological University, Ahmedabad, Gujarat, India.

²Department of Mathematics, BVM Engineering College, VallabhVidyanagar, Anand, Gujarat, India.

Received: 30 Dec 2023

Revised: 09 Jan 2024

Accepted: 12 Jan 2024

*Address for Correspondence

R.B. Gandhi

Department of Mathematics,
BVM Engineering College,
VallabhVidyanagar, Anand, Gujarat, India.
Email: rbgandhi@bvmengineering.ac.in



This is an Open Access Journal / article distributed under the terms of the **Creative Commons Attribution License** (CC BY-NC-ND 3.0) which permits unrestricted use, distribution, and reproduction in any medium, provided the original work is properly cited. All rights reserved.

ABSTRACT

In this study, we have constructed a new sequence of positive linear operators by using Stancu variant of Lupaş operators using Korovkin approximation theorem. We also show that sensitivity of choice of $\phi(x)$ used in Stancu type of Lupaş operators by taking $\phi(x) = x(1+x)$ to convergence in weighted space.

Mathematics Subject Classification 41A36, 41A25, 41A17, 42C10

Keywords: Lupaş operators, Constuction of operators, Korovkin’s Theorem, Stancu type generalization of Lupaş operators, Convergence in weighted space.

INTRODUCTION

This paper studies approximating properties of Stancu variant of Lupaş operators using Korovkin approximation theorem. Starting with the identity

$$\frac{1}{(1-t)^\alpha} = \sum_{k=0}^{\infty} \frac{(\alpha)_k}{k!} t^k, |t| < 1$$

Where $(\alpha)_k = (\alpha)(\alpha+1)(\alpha+2)\dots(\alpha+k-1)$, $k \geq 1$ and $(\alpha)_0 = 1$.

The following sequence of positive linear operators was introduced by Lupaş [1],

$$T_n(f; x) = (1-a)^{nx} \sum_{k=0}^{\infty} \frac{(nx)_k}{k!} f\left(\frac{k}{n}\right) a^k, x \geq 0 \tag{1}$$

for the functions $f: [0, \infty) \rightarrow \mathbb{R}$.

For $a = \frac{1}{2}$, Agratini [2] studied the following form of the operators defined in below as (2).

$$T_n(f; x) = 2^{-nx} \sum_{k=0}^{\infty} \frac{(nx)_k}{2^k k!} f\left(\frac{k}{n}\right), x \geq 0 \tag{2}$$





Usha Varma and R.B. Gandhi

and studied their approximation properties. Study on generalised operators can be found in these papers ([6, 8, 9, 10, 11, 12]). Many researchers have investigated various generalizations of these operators ([7]-[13]). They have introduced Stancu type generalization of the operators defined in (2) and proved approximation results for them [3]. We have studied different construction of Stancu type generalizations of various operators, e.g., Baskakov-Durrmeyer Operators, Jakimovski-Leviatan-Durrmeyer Operators, MeyerKönig and Zeller Operators and summation-integral type modification of Szász -Mirakjan-Stancu Operators [4].

Construction of operators

In 2022, Khan et al. [3] introduced Stancu type generalization of Lupaş operators in (2) as follows:

$$T_n^{\alpha,\beta}(f; x) = 2^{-nx} \sum_{k=0}^{\infty} \frac{(nx)_k}{2^k k!} f\left(\frac{k + \alpha}{n + \beta}\right), x \geq 0 \tag{3}$$

where,

$$f: [0, \infty) \rightarrow \mathbb{R}, 0 \leq \alpha \leq \beta.$$

The operators $T_n^{\alpha,\beta}$ are named Stancu type generalization of Lupaş operators. In this paper, we are introducing a generalisation of operators (3), defined on a space of the continuous functions $C[I]$ as,

$$T_{\lambda_n}^{\alpha,\beta}(f; x) = 2^{-nx} \sum_{k=0}^{\infty} \frac{(\lambda_n x)_k}{2^k k!} f\left(\frac{k + \alpha}{n + \beta}\right), x \geq 0 \tag{4}$$

where,

$$f: C[I] \rightarrow \mathbb{R}, 0 \leq \alpha \leq \beta.$$

Here, λ_n is an increasing sequence of positive real numbers and $\lambda_n \rightarrow \infty$ as $n \rightarrow \infty$, $\lambda_n \geq 1$ and studied the approximation properties of the operators (4).

Approximation Properties of $T_{\lambda_n}^{\alpha,\beta}$

To examine the approximation results for the newly constructed operators, we need the following lemmas.

Lemma 1. For the operators in (4), the following are obtained

- (i) $T_{\lambda_n}^{\alpha,\beta}(e_0; x) = 1;$
- (ii) $T_{\lambda_n}^{\alpha,\beta}(e_1; x) = \frac{\lambda_n x}{\lambda_n + \beta} + \frac{\alpha}{\lambda_n + \beta};$
- (iii) $T_{\lambda_n}^{\alpha,\beta}(e_2; x) = \frac{\lambda_n^2 x^2}{(\lambda_n + \beta)^2} + \frac{2\lambda_n(1+\alpha)x}{(\lambda_n + \beta)^2} + \frac{\alpha^2}{(\lambda_n + \beta)^2}.$

Proof: (i) We have

$$T_{\lambda_n}^{\alpha,\beta}(e_0; x) = 2^{-nx} \sum_{k=0}^{\infty} \frac{(nx)_k}{2^k k!}$$

which implies

$$T_{\lambda_n}^{\alpha,\beta}(e_0; x) = 1$$

(ii) For e_1 ,

$$T_{\lambda_n}^{\alpha,\beta}(e_1; x) = 2^{-\lambda_n x} \sum_{k=0}^{\infty} \frac{(\lambda_n x)_k}{2^k k!} \left(\frac{k + \alpha}{\lambda_n + \beta}\right)$$

which implies,

$$\begin{aligned} & T_{\lambda_n}^{\alpha,\beta}(e_1; x) \\ &= \frac{1}{2^{\lambda_n x}} \sum_{k=0}^{\infty} \frac{(\lambda_n x)_k}{2^k k!} \left(\frac{k}{\lambda_n + \beta}\right) + \frac{1}{2^{\lambda_n x}} \sum_{k=0}^{\infty} \frac{(\lambda_n x)_k}{2^k k!} \left(\frac{\alpha}{\lambda_n + \beta}\right) \\ &= \frac{\lambda_n x}{2^{\lambda_n x + 1}(\lambda_n + \beta)} \sum_{k=1}^{\infty} \frac{(\lambda_n x + 1)_{k-1}}{2^{k-1}(k-1)!} + \frac{1}{2^{\lambda_n x}} \sum_{k=0}^{\infty} \frac{(\lambda_n x)_k}{2^{k-1} k!} \left(\frac{\alpha}{\lambda_n + \beta}\right) \end{aligned}$$





Usha Varma and R.B. Gandhi

$$= \frac{\lambda_n x}{2^{\lambda_n x+1}(\lambda_n + \beta)} 2^{\lambda_n x+1} + \frac{1}{2^{\lambda_n x}} 2^{\lambda_n x} \left(\frac{\alpha}{\lambda_n + \beta} \right)$$

$$= \frac{\lambda_n x}{(\lambda_n + \beta)} + \left(\frac{\alpha}{\lambda_n + \beta} \right)$$

(iii) For e_2 ,

$$T_{\lambda_n}^{\alpha, \beta}(e_2; x) = 2^{-\lambda_n x} \sum_{k=0}^{\infty} \frac{(\lambda_n x)_k}{2^k k!} \left(\frac{k + \alpha}{\lambda_n + \beta} \right)^2$$

which implies,

$$T_{\lambda_n}^{\alpha, \beta}(e_2; x)$$

$$= \frac{2^{-\lambda_n x}}{(\lambda_n + \beta)^2} \sum_{k=0}^{\infty} \frac{(\lambda_n x)_k}{2^k k!} (k^2 + 2k\alpha + \alpha^2)$$

$$= \frac{1}{2^{\lambda_n x}(\lambda_n + \beta)^2} \sum_{k=0}^{\infty} \frac{(\lambda_n x)_k}{2^k k!} (k^2) + \frac{2\alpha}{2^{\lambda_n x}(\lambda_n + \beta)^2} \sum_{k=0}^{\infty} \frac{(\lambda_n x)_k}{2^k k!} (k) + \frac{1}{2^{\lambda_n x}(\lambda_n + \beta)^2} \sum_{k=0}^{\infty} \frac{(\lambda_n x)_k}{2^k k!} (\alpha^2)$$

$$= \frac{\lambda_n x}{2^{\lambda_n x+1}(\lambda_n + \beta)^2} \sum_{k=1}^{\infty} \frac{(\lambda_n x + 1)_{k-1}}{2^{k-1} (k-1)!} (k)$$

$$+ \frac{\alpha \lambda_n x}{2^{\lambda_n x}(\lambda_n + \beta)^2} \sum_{k=1}^{\infty} \frac{(\lambda_n x + 1)_{k-1}}{2^{k-1} (k-1)!} + \frac{1}{2^{\lambda_n x}(\lambda_n + \beta)^2} \sum_{k=0}^{\infty} \frac{(\lambda_n x)_k}{2^k k!} (\alpha^2)$$

$$= \frac{\lambda_n x}{2^{\lambda_n x+1}(\lambda_n + \beta)^2} \left[\sum_{k=1}^{\infty} \frac{(\lambda_n x + 1)(\lambda_n x + 2)_{k-2}}{2^{k-1} (k-1)(k-2)!} (k-1) + \sum_{k=1}^{\infty} \frac{(\lambda_n x + 1)_{k-1}}{2^{k-1} (k-1)!} \right]$$

$$+ \frac{2\alpha \lambda_n x}{2^{\lambda_n x+1}(\lambda_n + \beta)^2} \sum_{k=1}^{\infty} \frac{(\lambda_n x + 1)_{k-1}}{2^{k-1} (k-1)!} + \frac{1}{2^{\lambda_n x}(\lambda_n + \beta)^2} \sum_{k=0}^{\infty} \frac{(\lambda_n x)_k}{2^k k!} (\alpha^2)$$

$$= \frac{\lambda_n x(\lambda_n x + 1)}{2^{\lambda_n x+2}(\lambda_n + \beta)^2} \left[\sum_{k=2}^{\infty} \frac{(\lambda_n x + 2)_{k-2}}{2^{k-2} (k-2)!} \right] + \frac{\lambda_n x}{2^{\lambda_n x+1}(\lambda_n + \beta)^2} \sum_{k=1}^{\infty} \frac{(\lambda_n x + 1)_{k-1}}{2^{k-1} (k-1)!}$$

$$+ \frac{2\alpha \lambda_n x}{2^{\lambda_n x+1}(\lambda_n + \beta)^2} \sum_{k=1}^{\infty} \frac{(\lambda_n x + 1)_{k-1}}{2^{k-1} (k-1)!} + \frac{1}{2^{\lambda_n x}(\lambda_n + \beta)^2} \sum_{k=0}^{\infty} \frac{(\lambda_n x)_k}{2^k k!} (\alpha^2)$$

$$= \frac{\lambda_n x(\lambda_n x + 1) 2^{\lambda_n x+2}}{2^{\lambda_n x+2}(\lambda_n + \beta)^2} + \frac{\lambda_n x 2^{\lambda_n x+1}}{2^{\lambda_n x+1}(\lambda_n + \beta)^2} + \frac{2\alpha \lambda_n x 2^{\lambda_n x+1}}{2^{\lambda_n x+1}(\lambda_n + \beta)^2} + \frac{\alpha^2}{(\lambda_n + \beta)^2}$$

$$= \frac{\lambda_n x(\lambda_n x + 1)}{(\lambda_n + \beta)^2} + \frac{\lambda_n x}{(\lambda_n + \beta)^2} + \frac{2\alpha \lambda_n x}{(\lambda_n + \beta)^2} + \frac{\alpha^2}{(\lambda_n + \beta)^2}$$

$$= \frac{\lambda_n^2}{(\lambda_n + \beta)^2} x^2 + \frac{2\lambda_n(1 + \alpha)}{(\lambda_n + \beta)^2} x + \frac{\alpha^2}{(\lambda_n + \beta)^2}$$

The claim is proved. ■

Lemma 2. The first and the second moments for the operators (4) are given by

$$T_{\lambda_n}^{\alpha, \beta}((t - x); x) = \left[\frac{\lambda_n}{(\lambda_n + \beta)} - 1 \right] x + \frac{\alpha}{(\lambda_n + \beta)}$$

and

$$T_{\lambda_n}^{\alpha, \beta}((t - x)^2; x) = \left[\frac{\lambda_n^2}{(\lambda_n + \beta)^2} - \frac{2\lambda_n}{(\lambda_n + \beta)} + 1 \right] x^2 + \left[\frac{2\lambda_n(1 + \alpha)}{(\lambda_n + \beta)^2} - \frac{2\alpha}{(\lambda_n + \beta)} \right] x + \frac{\alpha^2}{(\lambda_n + \beta)^2}$$





Usha Varma and R.B. Gandhi

Proof Using Lemma 1 and linearity property of the operators (4), we have

(i)for the first moment

$$\begin{aligned} T_{\lambda_n}^{\alpha,\beta}((t-x); x) &= T_{\lambda_n}^{\alpha,\beta}(t; x) - xT_{\lambda_n}^{\alpha,\beta}(1; x) \\ &= \frac{\lambda_n}{(\lambda_n + \beta)}x + \frac{\alpha}{(\lambda_n + \beta)} - x(1) \\ &= \left[\frac{\lambda_n}{(\lambda_n + \beta)} - 1 \right]x + \frac{\alpha}{(\lambda_n + \beta)}. \end{aligned}$$

(ii) and for the second moment

$$\begin{aligned} T_{\lambda_n}^{\alpha,\beta}((t-x)^2; x) &= T_{\lambda_n}^{\alpha,\beta}(t^2; x) - 2xT_{\lambda_n}^{\alpha,\beta}(t; x) + x^2T_{\lambda_n}^{\alpha,\beta}(1; x) \\ &= \frac{\lambda_n^2}{(\lambda_n + \beta)^2}x^2 + \frac{2\lambda_n(1 + \alpha)}{(\lambda_n + \beta)^2}x + \frac{\alpha^2}{(\lambda_n + \beta)^2} - 2x\left(\frac{\lambda_n x}{(\lambda_n + \beta)} + \frac{\alpha}{(\lambda_n + \beta)}\right) + x^2 \\ &= \left[\frac{\lambda_n^2}{(\lambda_n + \beta)^2} - \frac{2\lambda_n}{(\lambda_n + \beta)} + 1 \right]x^2 + \left[\frac{2\lambda_n(1 + \alpha)}{(\lambda_n + \beta)^2} - \frac{2\alpha}{(\lambda_n + \beta)} \right]x + \frac{\alpha^2}{(\lambda_n + \beta)^2}. \blacksquare \end{aligned}$$

Korovkin approximation theorem

We denote by $f \in C[0,\infty)$ the set of all real valued continuous functions defined on $[0,\infty)$ which is a Banach space under the norm

$$\|f\| = \sup \{ |f(x)| : x \in [0, \infty) \}$$

THEOREM 1. For each $f \in C[0,\infty)$, the operators $T_{\lambda_n}^{\alpha,\beta}(\cdot; x)$ converge uniformly to f on the compact domain $[0,a]$ ($a > 0$) as $n \rightarrow \infty$.

Proof. We have by lemma 1,

$$\begin{aligned} \lim_{n \rightarrow \infty} T_{\lambda_n}^{\alpha,\beta}(e_0; x) &= 1 \\ \lim_{n \rightarrow \infty} T_{\lambda_n}^{\alpha,\beta}(e_1; x) &= x \\ \lim_{n \rightarrow \infty} T_{\lambda_n}^{\alpha,\beta}(e_2; x) &= x^2. \end{aligned}$$

Thus, the sequence of positive linear operators $T_{\lambda_n}^{\alpha,\beta}(\cdot; x)$ converges uniformly to f , where f is one of the functions $1, t, t^2$ on the compact interval $[0,a]$, $a > 0$. Therefore, by the Korovkin approximation theorem[5], the result holds for every continuous function on the compact interval $[0,a]$. ■

Convergence in weighted space

Here, we investigate convergence of our operators in weighted space of functions. Let $\phi(x) = e_1 + e_2$ be a weight function. Let $B_{x^2}[0,\infty)$ be the linear space of all functions h satisfying the condition

$$|h(x)| \leq K_h(x + x^2) = K_h(x(x + 1)),$$

where, K_h is a constant associated with the function h . We denote the subspace of all continuous functions of $B_{x^2}[0,\infty)$ by $C_{x^2}[0,\infty)$. Also, we denote by $C_{x^2}^*[0,\infty)$, the subclass of $C_{x^2}[0,\infty)$ of those functions h for which $\lim_{x \rightarrow \infty} \frac{h(x)}{x(x+1)}$ is finite. The norm on the space $C_{x^2}^*[0,\infty)$ is defined by

$$\|h(x)\|_{x^2} = \sup \{ (|h(x)|)/(x(x + 1)) : x \in [0, \infty) \}.$$

Lemma 3 Let $T_{\lambda_n}^{\alpha,\beta}$ be operators defined by (4). Then for the weight function $\phi(x)$ above, we obtain

$$\|T_{\lambda_n}^{\alpha,\beta}(\phi; x)\|_{x^2} \leq M,$$

where, M is a positive constant greater than 1.

Proof Using linearity and Lemma 1, we obtain

$$\left\| T_{\lambda_n}^{\alpha,\beta}(\phi; x) \right\| = T_{\lambda_n}^{\alpha,\beta}(e_1 + e_2; x)$$





Usha Varma and R.B. Gandhi

which implies

$$T_{\lambda_n}^{\alpha,\beta}(\phi; x) = T_{\lambda_n}^{\alpha,\beta}(e_1; x) + T_{\lambda_n}^{\alpha,\beta}(e_2; x)$$

$$= \frac{\lambda_n x}{(\lambda_n + \beta)} + \left(\frac{\alpha}{\lambda_n + \beta}\right) + \frac{\lambda_n^2}{(\lambda_n + \beta)^2} x^2 + \frac{2\lambda_n(1 + \alpha)}{(\lambda_n + \beta)^2} x + \frac{\alpha^2}{(\lambda_n + \beta)^2}$$

Now,

$$\|T_{\lambda_n}^{\alpha,\beta}(\phi; x)\|_{x^2} = \sup \left\{ \left| \frac{1}{x(x+1)} \left(\frac{\lambda_n x}{\lambda_n + \beta} + \frac{\alpha}{\lambda_n + \beta} \right) + \frac{\lambda_n^2}{(\lambda_n + \beta)^2} \frac{x^2}{x(x+1)} + \frac{2\lambda_n(1+\alpha)}{(\lambda_n + \beta)^2} \frac{x}{x(x+1)} + \frac{\alpha^2}{(\lambda_n + \beta)^2} \right| : x \in [0, \infty) \right\}$$

$$< \frac{\lambda_n}{(\lambda_n + \beta)} + \frac{\alpha}{(\lambda_n + \beta)} + \frac{\lambda_n^2}{(\lambda_n + \beta)^2} + \frac{2\lambda_n(1+\alpha)}{(\lambda_n + \beta)^2} + \frac{\alpha^2}{(\lambda_n + \beta)^2}.$$

It can be seen that,

$$\lim_{n \rightarrow \infty} \frac{\lambda_n^2}{(\lambda_n + \beta)^2} = 1 = \lim_{n \rightarrow \infty} \frac{\lambda_n}{(\lambda_n + \beta)} \text{ and}$$

$$\lim_{n \rightarrow \infty} \frac{2\lambda_n(1+\alpha)}{(\lambda_n + \beta)^2} = \lim_{n \rightarrow \infty} \frac{\alpha^2}{(\lambda_n + \beta)^2} = \lim_{n \rightarrow \infty} \frac{\alpha}{(\lambda_n + \beta)} = 0,$$

there exists a constant $M > 1$ such that $\|T_{\lambda_n}^{\alpha,\beta}(\phi; x)\|_{x^2} \leq M$.

This proves the lemma. ■

THEOREM 2 Let $T_{\lambda_n}^{\alpha,\beta}$ be operators defined by (4) and $\Phi(x) = x(x + 1)$ be the weight function. Then for each $f \in C_{x^2}^*[0, \infty)$ we have

$$\lim_{n \rightarrow \infty} \|T_{\lambda_n}^{\alpha,\beta}(f; x) - f(x)\|_{x^2} = 0.$$

Proof By Korovkin theorem, it is enough to show that

$$\lim_{n \rightarrow \infty} \|T_{\lambda_n}^{\alpha,\beta}(t^j; x) - x^j\|_{x^2} = 0, \text{ for } j = 0, 1, 2.$$

By Lemma 1 (i), we find

$$\lim_{n \rightarrow \infty} \|T_{\lambda_n}^{\alpha,\beta}(1; x) - 1\|_{x^2} = 0$$

By lemma 1 (ii), we get

$$\lim_{n \rightarrow \infty} \|T_{\lambda_n}^{\alpha,\beta}(e_1; x) - e_1\|_{x^2} = \sup \left\{ \left| \frac{1}{x(x+1)} \left(\frac{\lambda_n x}{\lambda_n + \beta} + \frac{\alpha}{\lambda_n + \beta} \right) - \frac{x}{x(x+1)} \right| : x \in [0, \infty) \right\} = 0.$$

From lemma 1 (iii), we get

$$\|T_{\lambda_n}^{\alpha,\beta}(e_2; x) - e_2\|_{x^2} = \sup \left\{ \left| \left(\frac{\lambda_n^2}{(\lambda_n + \beta)^2} - 1 \right) \frac{x^2}{x(x+1)} + \frac{2\lambda_n(1 + \alpha)}{(\lambda_n + \beta)^2} \frac{x}{x(x+1)} + \frac{\alpha^2}{(\lambda_n + \beta)^2} \frac{x}{x(x+1)} \right| : x \in [0, \infty) \right\}$$

Taking the limit,

$$\lim_{n \rightarrow \infty} \|T_{\lambda_n}^{\alpha,\beta}(e_2; x) - e_2\|_{x^2} \leq \left(\frac{\lambda_n^2}{(\lambda_n + \beta)^2} - 1 \right) + \frac{2\lambda_n(1 + \alpha)}{(\lambda_n + \beta)^2} + \frac{\alpha^2}{(\lambda_n + \beta)^2} \rightarrow 0 \text{ as } n \rightarrow \infty$$

So the result is,

$$\lim_{n \rightarrow \infty} \|T_{\lambda_n}^{\alpha,\beta}(e_2; x) - e_2\|_{x^2} = 0,$$

which completes the proof. ■

CONCLUSION

In this paper Stancu type of Lupaş operators have been constructed by using λ_n and its approximating properties have been investigated. We obtained result using the well-known Korovkin-type theorem. The purpose of this paper is to show sensitivity of choice of $\phi(x)$ used in Stancu type of Lupaş operators by taking $\phi(x) = x(1 + x)$ to convergence in weighted space.





Usha Varma and R.B. Gandhi

ACKNOWLEDGEMENTS

The authors are also grateful to all conference organizers of “3rd International Conference” Women in Science and Technology: Creating Sustainable Career (ICWSTCSC-2023) at Birla Vishvakarma Mahavidyalaya, Anand, Gujarat, India. The authors are thankful to the referees for valuable suggestions, leading to the better presentation of the paper. The first author thanks her father and her beloved husband wholeheartedly.

REFERENCES

1. A.Lupaş, *The approximation by some positive linear operators*, In: Proceedings of the International Dortmund Meeting on Approximation Theory (M. W. Müller et al., eds.), Akademie Verlag, Berlin, (1995), 201-229.
2. O.Agratini, *On a sequence of linear positive operators*, Facta Universitatis, Series: Mathematics and Informatics, 14 (1999), 41-48.
3. T. Khan and S.A. Khan, *Approximation by Stancu type Lupaş operators*, Palestine Journal of Mathematics, Vol.11(3)(2022),700-707.
4. V.N. Mishra, R.B. Gandhi, R.N. Mohapatra, *A summation-integral type modification of Szász-Mirakjan-Stancu operators*, Journal of Numerical Analysis and Approximation Theory, Vol.45 No.1 (2016),27-36.
5. P.P.Korovkin, *Linear operators and approximation theory*, Hindustan Publishing Corporation, Delhi, 1960.
6. V.N. Mishra, R.B. Gandhi, *Simultaneous approximation by Szász-Mirakjan-Stancu-Durrmeyer type operators*, Periodica Mathematica Hungarica 74(2017), 118-127.
7. U. Abel and M. Ivan, *On a generalization of an approximation operator defined by A. Lupaş*, General Mathematics Vol. 15, No. 1 (2007), 21-34.
8. V.N. Mishra, R.B. Gandhi, *A summation-integral type modification of Szász-Mirakjan operators*, Mathematical Methods in the Applied Sciences 40(1)(2017), 175-182.
9. V.N. Mishra, K. Khatri and L. Narayan Mishra, *Some approximation properties of Baskakov-Beta-Stancu type operators*, Journal of Calculus of Variations Vol.2013,(2013).
10. V.N. Mishra, R.B. Gandhi, *Direct result for a summation-integral type modification of Szász-Mirakjan Operators*, Analysis in Theory and Applications, (2020), 24-30.
11. V.N. Mishra, R.B. Gandhi, *Study of Sensitivity of Parameters of Bernstein-Stancu Operators*, Iranian Journal of Science and Technology, Transactions A: Science 43, (2019), 2891-2897.
12. V.N. Mishra, R.B. Gandhi, F. Nasaireh, *Simultaneous approximation by Szász-Mirakjan-Durrmeyer-type operators*, Bollettino dell'Unione Matematica Italiana 8, (2016),297-305.
13. T.Acar and A. Aral, *Approximation properties of two dimensional Bernstein-Stancu Chlodowsky operators*, Matematiche (Catania), 68(2) (2013), 15-31.





Indian Women's Skill Development Programs: Present Situation and Prospects for the Future

Khyati Jagat Kumar Patel*

Assistant Professor, SEMCOM, The CVM University, Vallabh Vidyanagar, Anand, Gujarat, India.

Received: 30 Dec 2023

Revised: 09 Jan 2024

Accepted: 12 Jan 2024

*Address for Correspondence

Khyati Jagat Kumar Patel

Assistant Professor,
SEMCOM, The CVM University,
Vallabh Vidyanagar, Anand, Gujarat, India.



This is an Open Access Journal / article distributed under the terms of the **Creative Commons Attribution License** (CC BY-NC-ND 3.0) which permits unrestricted use, distribution, and reproduction in any medium, provided the original work is properly cited. All rights reserved.

ABSTRACT

Every nation in the world advances economically and socially via the application of skills and information, and women play a crucial role in this process. Achieving gender equality in the workplace requires expanding females' right of entry to teaching and training programs. To raise women's socioeconomic standing and increase their economic contribution to the nation, the Indian government is offering numerous skill development programs. This also aimed to increase the number of workers in the industrial and service sectors and promote gender equality. However, before the direction's goal of ability growth can be achieved, a number of obstacles to the skill development of rural women must be overcome. It is crucial to comprehend the difficulties faced by rural women and come up with solutions that will enable them to develop new skills. The issue and difficulties associated with talent progress training for womankind in India as well as an impact of skill development programs on women's socioeconomic standing, self-image, and confidence is included in this article.

Keywords: women, workplace, skill development programs, entrepreneurship, socioeconomic standing.

INTRODUCTION

Skill development is the process of determining where young people have a skills gap and bridging it with possibilities for employment and training. The goal of the occupational training programs is to help youth realize their prospective by giving them the support and opportunity they require to prosper. Talent and learning go hand in hand and are essential for the development of both local communities and a country's economy. In order to offer young people with skill development, the federal and state administrations frequently collaborate with their associates in the skilling business. Thus, the benefits of skill include higher commercial incomes, improved presentation, increased precision and excellence, better communication, adherence to legal requirements, improved hiring and career possibilities, and excellent customer relationships. The effort known as Skill India was started in July 2015 via the Ministry of Skill Development and Entrepreneurship. Since then, it has helped over 3536000 ladies'



**Khyati Jagat Kumar Patel**

lives by allowing them to expand their skills and obtain better, additional permanent work. PMKVY (Pradhan Mantri Kaushal Vikas Yojana) qualified 1985000 candidates for 375 job posts during its trial term. Successful candidates in a merit-based program received pay equal to the full cost of training. Out of all the training candidates, over 2.53 lakh applicants have apparently been placed; among them, it was evident that the ladies shared very little. Given that women in our society are typically in charge of looking after the family, kids as well as occasionally employed as minimal labor workers or maintenance planters, they have different training requirements than men. Even though women make up more than half of India's population, their economic contribution to the nation is still significantly lower than it should be. In India, women make up only 31.8% of the labor force, far less than the percentage of men (73.2%). Because they typically lack education and training, they have factually been paid far less than males for performing the similar work.

MATERIALS AND PROCEDURES

The articles were selected from academic journals and databases such as Research Gate, Web of Science, Publons, Google Scholar, and Web of Science. Search terms such as vocational education, skill India, free enterprise, start-up environment agriculture, socio-economic outline, and maintenance were used to find articles.

PROGRAMS FOR SKILL DEVELOPMENT

The National Skills Development Mission of India, or "Skill India," was unveiled by the Indian Prime Minister. The National Skills Development Corporation of India is in charge of managing it. On October 2, 2016, the program was launched with the following objectives: Short-term courses provide new skill development training to 130 college dropouts, unemployed youth, and dropouts from school (World Journal of Advanced Engineering Technology and Sciences, 2022, 07(01), 128–136). This establishes the abilities that the current personnel possesses by confirming their aptitudes, encourages countries to take part in the plan's implementation to increase their capabilities, promotes consistency in the documentation procedure, and initiates a system to make a register of talents. The fundamentals of skill development that enable the implementation of such programs to address social challenges, achieve economic growth, capitalize on demographic dividends, and empower socioeconomically disadvantaged groups. In terms of established processes, the National Skill Development Corporation, the Ministry of Skill Development and Entrepreneurship, and Prime Minister KaushalVikasYojana have produced important welfares—but not the ones that were planned. It argues that the country's acceptance of technology and women's empowerment depend heavily on skill development. As India moves closer to becoming a global knowledge economy, it must meet the aspirations of its youth. Emphasizing the development of talents relevant to the current economic context can help achieve it to some extent. The problem at hand is the enormous numerical growth of young proficiency instruction and the more important objective of raising the caliber of that training.

ENTREPRENEURSHIP AND PROFICIENCY DEVELOPMENT

The advancement of a country's or state's economy and society depends on fostering an entrepreneurial spirit and improving individual skills. Higher skill levels and stricter regulations allow nations to withstand the impressions of financial unpredictability that swell native and international job fairs. One element that may support the growth of business activities those are essential to the economy's growth, is creativity, which produces new ideas. The value of the entrepreneur keeps rising as a result of the connections that the business and its management make with its suppliers, employees, and customers. Prospective investors are particularly curious about the CEO's and management team's effectiveness in working in groups with other people and how quickly and logically they can solve any problem the company is now facing. Entrepreneurs must understand the method used in the production of the products or services they offer, the market and industry they plan to enter, and most importantly, their target audience and competitors.



**Khyati Jagat Kumar Patel****PROBLEMS AND DIFFICULTIES IN WOMEN ENTREPRENEURS' SKILL DEVELOPMENT**

In India, women constituted roughly 50% of the population. It is possible to measure women's participation in official financial and commercial doings in the industrialized, facility, and farming areas. However, it is more difficult to quantify how many women engage in informal economic activities such as taking care of elderly and children, working from home, rearing livestock, and working in agriculture. The fact that women in India are significantly less literate than men is one of the main issues that have to be addressed. Even basic economics abilities, like measuring and maintaining correct records, can be lacking among uneducated rural women. This led to the assumption that rural women are either technologically illiterate or uninformed. Reaching these individuals is often difficult for researchers and educators, and enrolment percentages at a definite level of education can be used as a substitution for perseverance and access. The primary source of gender inequality and prejudice in the world is the dearth of educational possibilities for girls. The social and cultural barriers that prevent women and girls from attending school are not given adequate consideration. The high rates of school dropout among females are caused by a number of obstacles to their education, such as poverty, poor hygienic conditions, and long commutes. Rural women frequently have limited access to vocational education and training, which perpetuates their traditional roles and responsibilities in fields where women predominate.

FUTURE ADVICE AND SUGGESTIONS FOR SKILL DEVELOPMENT

Women who work in the informal economy face terrible conditions; most of the time, they are compelled to accept occupations that pay pitiful pays, offer no job security, or provide social security benefits. Over 90% of working women are employed in this sector. Thus, fostering females' flairs is crucial to helping them gain existence services that will enable them to have well lives, better-paying jobs of higher caliber, monetary freedom, and the ability to support their families. Men's concerns and experiences would be included in a sustainable skill development program. These have to be an essential part of developing, carrying out, keeping an eye on, and evaluating policies and programs for training and skill development. Combining native institutes and strategies to advance enabling and sex parity is the primary strategy for advancing gender parity and the empowerment of women. It is challenging for her to succeed because of institutional constraints and social prejudices. Right of entry to occupational teaching and training for rural women is sometimes restricted to a small number of areas where females are the bulk, which perpetuates their out-dated roles and obligations. While engaging in such activities broadens their options for work, it decreases their prospects of progressing in more recent, unconventional industries like technology for information and communications. Closing the gap between the choices available to females and what they can and want to follow requires good awareness-raising efforts and appropriate skill training, which affects the involvement rates of men and women in many industries and organizations.

CONCLUSION

In nutshell, the purpose of skill development for women in particular is to improve the caliber of their work in order to improve employee performance and to get them ready for the workforce. Women's whole personality development and self-esteem will be aided by training and skill development. It's also advised to design exercise programs specifically to maximize women's abilities so that skill development is more successful. But improving oneself shouldn't come at the expense of picking up new skills, especially for females who would increase in entrenched in traditional parts and abilities. Enhancing one's talents can help one get a better job and progress in their career. The government and banks can stimulate the economy and create jobs for young entrepreneurs by helping them launch their businesses. Policies that promote women's empowerment through the use of digital platforms, mainstream gender representation in training content and delivery, and increase women's access to skill development should be made simpler.





Khyati Jagat Kumar Patel

REFERENCES

1. Tara, S. N., & Kumar, N. S. (2016). Skill development in India:: In conversation with S. Ramadorai, Chairman, National Skill Development Agency & National Skill Development Corporation; former CEO, MD and Vice Chairman, Tata Consultancy Services. *IIMB Management Review*, 28(4), 235-243.
2. MSDE, 2022. Pradhan Mantri Kaushal Vikas Yojna. <https://www.msde.gov.in/> (Accessed on 10th May'2022).
3. Business Standard.(2022). India GDP Expands 13.5% In Q1 FY23. [https://www.business-standard.com/article/news-cm/india-gdp-expands-13-5-in-q1-fy23122090100182_1.html#:~:text=The%20gross%20domestic%20product%20\(GDP,cent%20in%20January%2D March%202022.](https://www.business-standard.com/article/news-cm/india-gdp-expands-13-5-in-q1-fy23122090100182_1.html#:~:text=The%20gross%20domestic%20product%20(GDP,cent%20in%20January%2D March%202022.)
4. Pandey, A., &Nema, D. K. (2017). Impact of Skill India training programme among the youth. *International Journal of Multidisciplinary Research and Development*, 4(7), 294-299.
5. Sidhu, K., &Kaur, S. (2006). Development of Entrepreneurship among Rural Women. *Journal of Social Sciences*, 13(2), 147-149.
6. Siddiqui, A. B. (2012). Problems encountered by women entrepreneurs in India. *International Journal of Applied Research & Studies*, 1(2), 01-11.
7. Sharma, Y. (2013). Women Entrepreneur in India. *IOSR Journal of Business and Management*, 15(3), 9-14.
8. Sawale, S. B., &Karpe, M. D. (2019). Skill Development and Women Entrepreneurs in India. *Shanlax International Journal of Economics*, 8(1), 32-36.
9. PMKY.2022. <http://www.pmkvyofficial.org/>

Table 1 lists the main courses and Training Programs for Developing Skills in India:

Plans and Initiatives for Acquisition of Skills	Specifics
PradhanMantriKaushalVikasYojana (PMKVY)	Enable the next generation of talent through a variety of skill certification programs, preparing them for industry requirements
Capacity building Scheme (CBS)	delivering residential skill development to young people in the northeast
UDAAN	A platform for consumer-to-consumer trade that supports small and medium-sized enterprises in India
India International Skill Centers (IISC)	supplies a youthful, highly skilled labour force to fulfil the demand from throughout the world
The dual system of Training (DST)	enabling business collaboration with public and private ITIs for highly employable courses
Flexi-MoU	The program gives trainees access to an industrial setting that is connected to market demands and the newest technologies, allowing employers to train candidates according to their skill sets
Pre-Departure Orientation Training (PDOT)	PDOT gives employees working out and information on the rules, cultures, and other facets of the target nation in order to safeguard their safety and security
Learn and Earn	Considering their credentials, present financial inclinations, and market possibility, the program aims to enhance minority youth's modern and traditional capabilities, which may encourage the employment





Khyati Jagat Kumar Patel

Learn and Earn	Considering their credentials, present financial inclinations, and market possibility, the program aims to enhance minority youth's modern and traditional capabilities, which may encourage the employment
DeenDayalUpadhyayaGrameenKaushalyaYojana (DDU-GKY)	DDU-GKY aims to train young people from impoverished rural areas and give them jobs that pay more than the minimum wage
SANKALP	Through advocacy, teaching and teaching, admission to a funding system, and the promotion of communal firms for growing that is equitable, the Scheme seeks to stimulate entrepreneurship
Plan for Divyangjan (PwD) to Administer the Rights of Persons with Disabilities Act, 2016 (SIPDA)	The PwD Act of 2016 guarantees the liberation and self-respect of individuals with incapacities by providing them with admission to public transportation, teaching, career education, jobs, information, and communication. The initiative provides these individuals with financial support
Directorate of Training Programmes	Scheme for Training Craftsmen (CTS) Apprenticeship training under the Apprentices Act of 1961 is provided by the Crafts Instructor Training Scheme. Scheme for Advanced Vocational Training. Women's Vocational Training Program: Strengthening Skills for Industrial Value Enhancement Through Skills Training (STRIVE)





On Performance of OFDM-aided Downlink Underlay Cognitive Radio Systems

Nileshkumar M. Bankar^{1*}, Kishor G. Maradia², Kesar Bavda³, Vaishnavi Shah³ and Shrey Panchal³

¹Research Scholar, Gujarat Technological University, Ahmedabad, Gujarat, India.

²Professor (EC) and I/C Principal, Government Engineering College, Rajkot, Gujarat, India.

³Student EC, Government Engineering College, Gandhi Nagar, Gujarat, India.

Received: 30 Dec 2023

Revised: 09 Jan 2024

Accepted: 12 Jan 2024

*Address for Correspondence

Nileshkumar M. Bankar

Research Scholar,

Gujarat Technological University,

Ahmedabad, Gujarat, India.

Email: 219999915002@gtu.edu.in



This is an Open Access Journal / article distributed under the terms of the **Creative Commons Attribution License** (CC BY-NC-ND 3.0) which permits unrestricted use, distribution, and reproduction in any medium, provided the original work is properly cited. All rights reserved.

ABSTRACT

High spectral efficiency (SE) and information centric data traffic are supported by the next-generation cellular communication network and are intended to meet the needs of intelligent devices. The optimal use of spectrum resources is needed for bandwidth-intensive communication in multimedia multicast applications. Further, cellular network densification is facilitated by the immense capacity, connections, and ultralow latency requirements. Therefore, limited resource availability leads to interference and calls for additional SE. Cognitive radio (CR) is a potential option for enhancing SE by allowing low priority unlicensed users to collaborate on the radio spectrum with high-priority licenced users. It gains increased support in 5G networks due to these transmission opportunities. Using an appropriate opportunistic interference alignment (OIA) approach, an underlying opportunistic communication via a CR-aided orthogonal frequency-division multiplexing (OFDM) system is investigated in this work. Unlicensed users employ the possibility of transmission to enhance the SE if the licensed user falls into an outage. The Monte Carlo simulations demonstrated the achievable sum rate and transmission opportunities performance.

Keywords: 5G, interference alignment, cognitive radio, orthogonal frequency-division multiplexing, licensed and unlicensed users.

INTRODUCTION

Fifth-generation (5G) communication networks facilitate millions of devices to support advanced applications in healthcare monitoring, tactic surveillance, device-to-device communication, and so on [1]. Providing seamless





Nileshkumar M. Bankar et al.,

worldwide coverage has become a critical aim as the pace of adoption of mobile communication technologies continues to expand globally. As a result, both terrestrial and non-terrestrial satellite networking technology has advanced significantly. Therefore, two types of spectrum are used in satellite communications: fixed satellite services (FSS) with Ka- and Ku-bands and mobile satellite services (MSS) with S- and L-bands [2]. The L-band (1,610-1,626.5MHz) and S-band (2,483.5-2,500 MHz) are assigned to uplink and downlink, respectively, and are suitable for direct operation from a satellite to handheld devices as per TR of vision, requirements and evaluation guidelines for satellite radio interface of IMT-2022 given in release-18 [3]. Furthermore, instead of using static band allocations, Cognitive Radio (CR) is a well-known technology that allows wireless network elements to share spectrum dynamically [4]. It results in additional needs for high spectral efficiency (SE) and optimal utilization of available radio resources [5]. Furthermore, combining orthogonal frequency-division multiplexing (OFDM) with CR networks results in significant cognitive user throughput [6].

Unlicensed users (like Wi-Fi (MSS) communication) are permitted to transmit simultaneously with licenced users (like satellite communication (FSS)) in underlay spectrum sharing (CR) networks, provided that interference from the unlicensed users does not lower the licenced users' quality of service [7]. Thus, dependable high speed transmission for licenced and unlicensed users requires efficient interference control [8]. Also, unlicensed users share the spectrum in cognitive mode to identify unoccupied channels belonging to licenced users. This allows them to use the licenced spectrum's underutilized capacity for effective data dissemination [9]. Interference alignment (IA) restricts the interfering signals within half of the signal space at the intended receiver as a viable solution for interference control [10]. Moreover, [11], [12] provide a full investigation of the survey and research on the IA. Also, one of the best techniques for IA in CR networks is opportunistic IA (OIA). The fundamental idea behind the OIA is to align the unlicensed users' interfering signals on the channels or opportunities not utilized by licenced users [13]. Moreover, in the long-term evolution (LTE) and beyond networks, OFDM technology plays a vital role to enhance the system performance, providing the orthogonal resource elements per subcarrier [14]. Further, the OFDM-MIMO based CR system is investigated in [6] to show the efficacy of enhanced throughput for cognitive users utilizing multiple antennas.

Using perfect and imperfect channel state information (CSI), authors in [15] extended this work by demonstrating LTE-OFDM macro-cell systems sharing the spectrum with a randomly deployed second layer of small cells. Additionally, authors in [9] demonstrated unlicensed vehicular user mobility and primary user activity performance for cognitive Internet of Vehicles (IoV) sharing IEEE 802.11p wide-band spectrum regime. While keeping the limitation of energies in the available radio resources for 5G networks, authors in [5] showed the energy efficiency and SE trade-off of cognitive cellular networks. Authors in [16] thoroughly examine the effectiveness of several CR network spectrum-sharing models in achieving the end-to-end communication objectives of multicast services in this string. Although the performance of downlink OFDM-aided OIA CR networks in terms of achievable data rates and transmission opportunities for unlicensed users is already investigated in the existing literature, there is no work demonstrating the use case of Wi-Fi communication based on the availability of resource elements of licenced satellite user's OFDM vector. Therefore, improving the quality of service and delivering better citizen services, utilizing the opportunities of satellite networks in the sub-6 GHz band with unlicensed user's communication are yet to be performed. The present study explores the sum rate for underlay communication over CR networks by an efficient combination of OFDM and OIA technology, leveraging the inherent advantages of OFDM-aided CR networks. Furthermore, considering the challenges of communicating with unlicensed users based on the availability of resource elements of licenced users' OFDM vectors, the significant contributions of this paper are summarized as follows

1. The performance of OFDM-aided OIA CR networks has been investigated for a feasible, practical communication scenario between satellite and Wi-Fi networks.
2. Further, for various numbers of FFT points and threshold values, the achievable rate of unlicensed users is shown.
3. Moreover, the transmission opportunities of unlicensed users is also demonstrated for varying the FFT points and threshold values.





Nileshkumar M. Bankar et al.,

The remaining paper is organized as follows: Section II explains the system model of one licensed and one unlicensed user in CR mode. Section III presents the numerical results and their thorough description. Finally, the paper is concluded in section IV.

System Model

Fig. 1. illustrates CR mode, including the FSS and MSS networks. The following system model has a licensed user transmitter (satellite) and licensed user receiver (user equipment (UE)) as a primary network. A downlink OMA IA based spectrum sharing unlicensed network consists of an unlicensed user transmitter (Wi-Fi communication) and an unlicensed user receiver (another UE). A single transmitting and receiving antenna is equipped at each node. The receiver users' channels are regarded as independent, including non-identically distributed Rayleigh fading. Dotted lines represent the interfering signal from the other network, while solid lines represent the transmission within the network. On the other side, using N-point FFT, filter banks, etc., the modulated symbols are allocated to orthogonal resource elements (i.e., subcarriers) for a downlink OFDM transmission. For the k^{th} resource element, the received signal at the u^{th} user is provided by

$$Y_u(k) = H_u(k)\sqrt{P}x_u(k) + N_u(k), \quad u = 1,2 \quad (1)$$

where H_u is the N-point frequency representation of L Rayleigh faded channel coefficients of licensed ($u = 1$) and unlicensed ($u = 2$) user, respectively. x_u is the modulated data for transmission. $N_u \sim \text{CN}(0, N_0)$ is the thermal noise at the intended user and $P = P/N_{\text{FFT}}$ is the power assigned to each resource element of the OFDM vector having length N_{FFT} . Further, based on the fading SNR at each subcarrier of the OFDM vector, the opportunities are determined, and the sum rate of the licensed user is given as

$$C_1 = \log_2(1 + |H_1|^2 \gamma) \quad (2)$$

Similarly, the sum rate for unlicensed user based on the threshold SNR (γ_{th}) is given as follows

$$C_2 = \begin{cases} \log_2(1 + |H_2|^2 \gamma), & |H_2|^2 \gamma < \gamma_{\text{th}} \\ 0, & \text{else} \end{cases} \quad (3)$$

Moreover, using the outage or worse channel conditions ($|H_u|^2 \gamma < \gamma_{\text{th}}$) of the licensed user, the number of vacant subcarriers or the transmission opportunities of the unlicensed user over the licensed user can be determined over various FFT points and γ_{th} values.

SIMULATION RESULTS AND DISCUSSION

The numerical simulation results of the transmission possibilities and achievable data rates for OFDM-based unlicensed cognitive users in the multipath Rayleigh fading channel are presented in this section. The results of the system under consideration are presented using a range of parameters, including threshold SNR (γ_{th}) and N_{FFT} . In simulations, {64, 256, 1024} and {0.5, 1, 5, 10} are employed as the values for N_{FFT} and γ_{th} , respectively. The performance of the achievable sum rate for the OIA OFDM-based CR system is shown in Fig. 2. For simulations of unlicensed users' data rates, several values of the threshold SNR $\gamma_{\text{th}} \in \{0.5, 1, 5, 10\}$ with $N_{\text{FFT}} = 256$ are examined. With 25 channel taps, the channel variances are taken as unity. The availability of free subcarriers in the OFDM vector increases the achievable data rate when the γ_{th} increases. It results in the verification of the simulation's results. Additionally, the sum rate of licensed and unlicensed users improves with increased SNR. Moreover, the rate of unlicensed users decreases at high SNR because all of the licensed users occupy the subcarriers in the OFDM block, whereas, at low SNR, the efficacy of the noise becomes more pronounced and impairs the performance of unlicensed users. The variability in transmission opportunities across the Rayleigh fading channel for an unlicensed user with a variable in transmitting SNR is depicted in Fig. 3. For different N_{FFT} points, i.e., {64, 256, 1024}, with channel taps of 6,





Nileshkumar M. Bankar et al.,

25, 100}, respectively, the results are simulated with $\gamma_{th}=1$. The transmission possibilities per subcarrier for unlicensed users decrease as the transmit SNR grows, owing to the large DoF available to licenced users. Furthermore, since the licenced user's subcarrier power is less than the noise variation, nearly all transmission opportunities are available below -5 dB and above 20 dB SNR. Fig. 4 illustrates how the number of FFT points in the OFDM vector varies along with the transmission possibilities vs transmitting SNR for the unlicensed user over the Rayleigh fading channel. The simulation results are shown for different N_{FFT} points, i.e., {64,256,1024}, with channel taps of {6,25,100}, and unity γ_{th} . It is noted that the simulation confirms the results and produces the same trend as Fig. 3. Also, it is noticeable that varying the FFT points {64,256,1024}, the opportunities of unlicensed users started to fall at almost 24, 19, and 15 dB SNR, respectively. The simulations are validated by increasing the FFT points since they result in more transmission chances.

CONCLUSION

In this paper, the feasible data rate for unlicensed users in a CR-aided OFDM system is evaluated quantitatively. The opportunistic radio resource shares licenced users' spectrum with unlicensed users based on the outage state. With the help of the N_{FFT} points and threshold SNR (γ_{th}) parameters, the latter aspect provides an intriguing conclusion about the possible data rate and transmission opportunities for unlicensed users. Additionally, in the future, this study will be expanded to include CR-aided multiuser OFDM systems.

ACKNOWLEDGMENT

The authors extend their sincere appreciation to the Department of Electronics and Communication (EC) Engineering, Government Engineering College (GEC), Gandhinagar, for their unwavering support and collaborative efforts. Gratitude is also extended to DNN Wireless Pvt. Ltd., Jaipur for their generosity, which played a crucial role in supporting and advancing this work.

REFERENCES

1. E. Dahlman, S. Parkvall, and J. Skold, *5G NR: The Next Generation Wireless Access Technology*. USA: Academic Press, Inc., 1st ed., 2018.
2. S. Euler, X. Fu, S. Hellsten, C. Kefeder, O. Liberg, E. Medeiros, E. Nordell, D. Singh, P. Synnergren, E. Trojer, and I. Xirouchakis, "Using 3GPP technology for satellite communication," *Ericsson Technology Review*, vol. 2023, no. 6, pp. 2–12, 2023.
3. R. M.2514-0, "Vision, requirements and evaluation guidelines for satellite radio interface(s) of IMT-2020." <https://www.itu.int/pub/R-REPM.2514-2022>, September 2022. Online Accessed: 11-12-2023.
4. I. F. Akyildiz, W.-Y. Lee, M. C. Vuran, and S. Mohanty, "Next generation/dynamic spectrum access/cognitive radio wireless networks:A survey," *Computer networks*, vol. 50, no. 13, pp. 2127–2159, 2006.
5. X. Hong, J. Wang, C.-X. Wang, and J. Shi, "Cognitive radio in 5G: a perspective on energy-spectral efficiency trade-off," *IEEE Communications Magazine*, vol. 52, no. 7, pp. 46–53, 2014.
6. M. Maso, L. S. Cardoso, M. Debbah, and L. Vangelista, "Cognitive interference alignment for OFDM two-tiered networks," in *2012 IEEE 13th International Workshop on Signal Processing Advances in Wireless Communications (SPAWC)*, pp. 244–248, 2012.
7. S. Haykin, "Cognitive radio: Brain-empowered wireless communications," *IEEE J. Sel. Areas Commun.*, vol. 23, no. 2, pp. 201–220, 2005.
8. N. Jindal and D. Breslin, "LTE and Wi-Fi in unlicensed spectrum: A coexistence study," *Google white paper*, 2015.
9. D. B. Rawat, R. Alsabet, C. Bajracharya, and M. Song, "On the performance of cognitive internet-of-vehicles with unlicensed user-mobility and licensed user-activity," *Computer Networks*, vol. 137, pp. 98–106, 2018.





Nileshkumar M. Bankar et al.,

10. S. A. Jafar and M. J. Fakhereddin, "Degrees of freedom for the MIMO interference channel," *IEEE Transactions on Information Theory*, vol. 53, no. 7, pp. 2637–2642, 2007.
11. L. E. Li, R. Alimi, D. Shen, H. Viswanathan, and Y. R. Yang, "A general algorithm for interference alignment and cancellation in wireless networks," in *2010 Proceedings IEEE INFOCOM*, pp. 1–9, 2010.
12. V. M. U and P. Selvaprabhu, "Blind interference alignment: A comprehensive survey," *International Journal of Communication Systems*, vol. 35, no. 8, p. e5116, 2022.
13. H. Lu, X. Xie, Z. Shi, and H. Yang, "Fairness enhancement for opportunistic interference alignment algorithm with low latency communications," *IEEE Systems Journal*, vol. 14, no. 4, pp. 5002–5013, 2020.
14. T. Innovations, "LTE in a nutshell," *White paper*, 2010.
15. M. Maso, M. Debbah, and L. Vangelista, "A distributed approach to interference alignment in OFDM-based two-tiered networks," *IEEE Transactions on Vehicular Technology*, vol. 62, no. 5, pp. 1935–1949, 2013.
16. S. Bhattacharjee, T. Acharya, and U. Bhattacharya, "Cognitive radio based spectrum sharing models for multicasting in 5G cellular networks: A survey," *Computer Networks*, vol. 208, p. 108870.

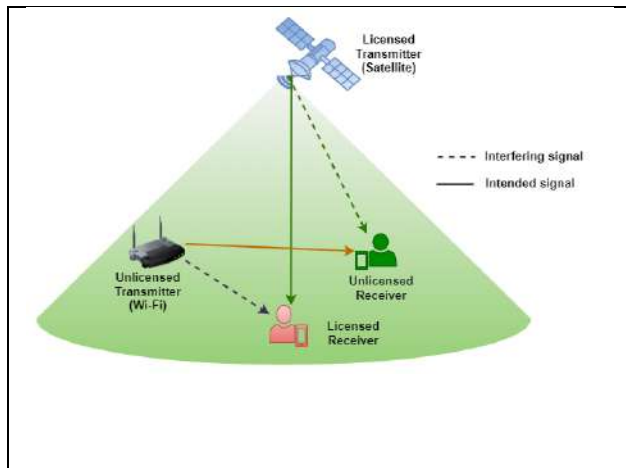


Fig. 1. An illustration of CR mode including satellite and Wi-Fi networks

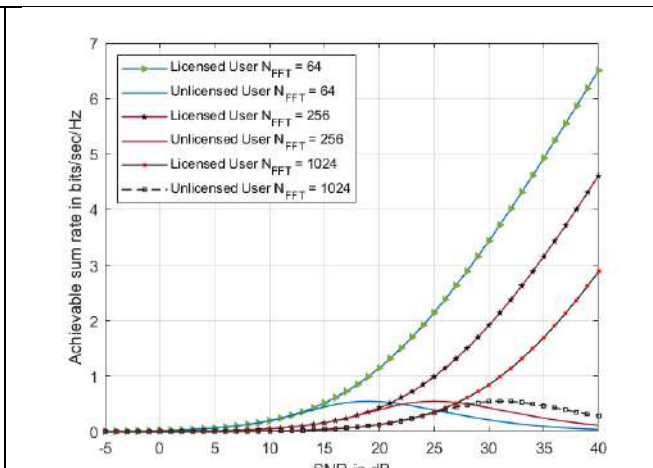


Fig. 2. Achievable sum rate of considered OFDM-based CR system with various γ_{th} values

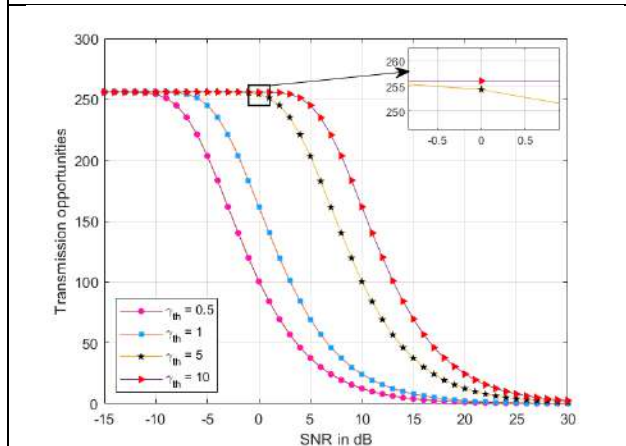


Fig. 3. Available unlicensed user's opportunities over Rayleigh fading channels for various γ_{th} values

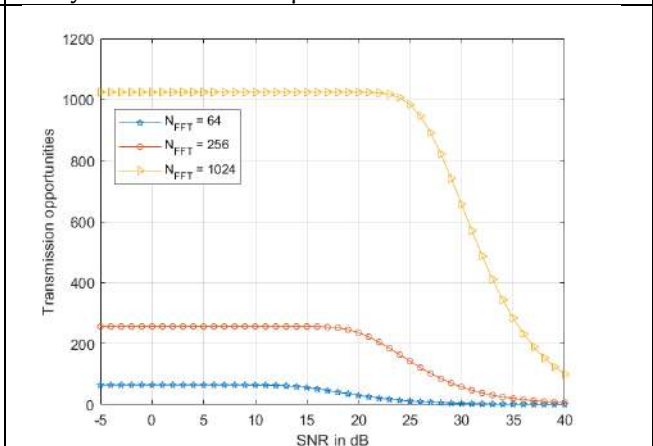


Fig. 4. Available unlicensed user's opportunities over Rayleigh fading channels for various N_{FFT} points





Reconfigurable Graphene based Flexible Antenna for switching in-between LTE band and L5 band

Anish Vahora* and RonakVashi

Birla Vishvakarma Mahavidyalaya ,Engineering College, Gujarat ,India.

Received: 30 Dec 2023

Revised: 09 Jan 2024

Accepted: 12 Jan 2024

*Address for Correspondence

Anish Vahora

Birla Vishvakarma Mahavidyalaya ,
Engineering College,
Gujarat ,India.

Email: anish.vahora@bvmengineering.ac.in



This is an Open Access Journal / article distributed under the terms of the **Creative Commons Attribution License** (CC BY-NC-ND 3.0) which permits unrestricted use, distribution, and reproduction in any medium, provided the original work is properly cited. All rights reserved.

ABSTRACT

A Graphene based reconfigurable dual-band antenna using Kapton polyimide has been proposed. In a reconfigurable antenna, the PIN diode is used to alter the antenna's operating frequency by changing its electrical length or impedance. The choice of operating frequency is determined by the bias voltage applied to the PIN diode and the antenna's design. The proposed antenna can switch the frequency bands between 900 MHz and 1.37 GHz. The antenna has an overall dimension of 30 mm × 34 mm × 0.1 mm, with a novel graphene monopole antenna on a Kapton polyimide material is used. The antenna resonates at different frequency bands depending upon the feed line length. Hence the frequency reconfigurability is achieved by switching of PIN Diode. When the length of the monopole line is 65 mm antenna resonates at 1.37 GHz with an impedance bandwidth of 22.22% (1.2–1.5 GHz). For the total line length of 130 mm antenna resonates at 0.90GHz with an impedance bandwidth of 24.17% (0.8–1.02GHz).

Keywords: Reconfigurable, Flexible, Graphene antenna, Kapton polyimide, PIN Diode.

INTRODUCTION

The advent of wireless communication in the modern era has ushered in a demand for compact, resilient, and highly efficient antennas within the realm of wireless local area networks (WLANs). The exceptional attributes of graphene, including its remarkable electrical and thermal conductivity, strength, rigidity, and durability, have opened up a wide array of new applications. It is for these very reasons that graphene-based antennas have become the pivotal technology underpinning wireless communication systems. Graphene, characterized by its two-dimensional honeycomb lattice and monolayer-crystal carbon atomic structure, exhibits mechanical strength that is 15 to 20 times greater than copper while being significantly lighter, with a weight that is only a fifth of copper's weight. Furthermore, graphene functions as a zero band gap semiconductor, which means that the application of an electric



**Anish Vahora and RonakVashi**

field results in the emergence of electron and hole carriers. This feature permits the precise control of conductivity and surface resistance, a control that can be achieved through methods such as doping and electric field biasing. Graphene boasts an impressive Young's Modulus (Tensile Elastic Capacity) within the range of 1000 GPa, dwarfing copper's modest 110-130 GPa. Additionally, graphene exhibits relatively low resistance, typically ranging from 35 to 50 ohms per square, along with exceptional optical transparency of 80-90%.

It possesses a carrier density of 2 to 6×10^{11} holes per sheet and a mobility of 200 to 1900 $\text{cm}^2/\text{V}\cdot\text{s}$. Industries in the aeronautics and automotive sectors have already made the transition from metal-based materials to carbon-based materials, thanks to the latter's lighter structure, exceptional durability, and energy-harvesting capabilities. These trends are poised to make graphene the go-to solution for replacing metals in the wireless field. Nevertheless, high electrical conductivity remains a prerequisite, which is why metals are still preferred over carbon-based materials. This shortfall can be overcome by enhancing plastics with conductive fillers like carbon black and graphite fibers. In a notable development, A. Scida and colleagues have introduced a wearable and highly flexible antenna constructed from graphene paper structures for NFC communication and RFID tags operating at a frequency of 13.56 MHz in the ISM band. This innovation effectively mitigates the problems of deformation associated with heavy metallic structures due to repetitive bending, as well as concerns about production costs and disposal. Furthermore, research by Rajni Bala et al. has shown that graphene-based antennas operating at frequencies between 2.67-2.92 THz, with substrates including Si_3N_4 , Al_2O_3 , BN, Silica, and Quartz, can deliver superior bandwidth and radiation efficiency compared to conventional substrate materials.

A. Thampy and collaborators have successfully achieved an optically transparent antenna using multi-walled carbon nanotubes (MWCNTs) in the terahertz frequency range, boasting high gain (>2 dB) and directivity (7.56 dB). For wearable wireless communication systems, the transmission line plays a pivotal role in conveying signals in electronic devices. To meet the need for high flexibility, X. Huang and associates have employed printed graphene material within the frequency range of 1.97 GHz. Additionally, C.N. Alvarez and colleagues have presented a performance analysis of reconfigurable antennas made from hybrid metal-graphene structures. In recent times, the development of graphene conductive ink has brought forth the possibility of creating conductive patterns on rigid or flexible substrates, harnessing graphene's inherent advantages in high conductivity, mechanical flexibility, lightweight properties, and cost-effectiveness. This method offers an efficient means to obtain satisfactory conductivity with reduced electrical resistivity on the surface. In this paper, reconfigurable antenna is proposed using Graphene as conductive material with kapton polyimide as substrate for designing and performance analysis. Section II is characterized the proposed antenna designs with PIN diode equivalency implemented in the antenna with system setup parameter. In Section III simulation results are presented and discussed. At the end, Section IV is conclusion.

Proposed antenna design

An antenna is composed of a graphene patch and ground plane, with total dimensions $L \times W \times H$, $30 \text{ mm} \times 34 \text{ mm} \times 50 \mu\text{m}$ and it is suspended on a 0.05 mm thickness dielectric substrate having, $\epsilon_r = 4.3$ and $\tan \delta = 0.02$. The perspective view of reconfigurable antenna design is shown in the figure 1. Graphene antenna inquiry into a simulation to evaluate the performance using a PIN diode on and off equivalent circuit is shown in the figure 2. In reconfigurable antenna design PIN diode plays a major role and its forward bias and reverse bias equivalent values are taken as illustrated in the table 1. Due to skin depth effect, the thickness of the graphene sheet is a major concern in terms of performance. In this design, a challenge has been made to examine the effect of patch and ground base material on the performance of the micro strip feed line antenna. For that in this simulation $25 \mu\text{m}$ of patch and ground plane has been taken as a reference to simulate and optimise the design. Graphene sheet electrical and mechanical parameters are taken consider in simulation as illustrated in table 2. Ansys HFSS 2022R simulation software is used for numerical modeling of the designed antenna at an operating frequency range of 1 to 6 GHz.



**Anish Vahora and RonakVashi**

RESULTS AND DISCUSSION

Applying a positive bias voltage to a PIN diode in a reconfigurable antenna renders it conductive, resulting in a shorter electrical length for the antenna and a corresponding increase in resonance frequency. This permits tuning to higher frequency band with operating frequency at 1.3 GHz. Conversely, the application of a negative bias voltage to the PIN diode deactivates it, leading to an elongation of the antenna's electrical length and a reduction in resonance frequency band with operating frequency of 900 MHz as shown in the fig. 3 Consider the reflection coefficient more than -10 dB, and calculate the B.W. of resonance antenna from frequency band to $|S_{11}|$ plot, the B.W. of an antenna is 22.22% and 34.82% at 900 MHz and 1.3 GHz respectively as mentioned in the table 3. As depicted in Figure 4(a), the surface current distribution appears uniform within the middle section of the I-shaped antenna at the lower frequency of 900 MHz, signifying a well-matched patch that radiates effectively at this frequency.

Conversely, Figure 4(b) reveals a distinct behaviour at the higher frequency of 1.30 GHz, where the current becomes concentrated along the lower edge of the radiator. This shift in current distribution implies a noticeable impact on the antenna's impedance characteristics at higher frequencies. The radiation pattern of the proposed antenna is illustrated in Figure 5. It is evident that the simulated radiation patterns closely align with each other. Notably, the radiation pattern exhibits two distinct peaks along the $\pm z$ axis, corresponding to the resonance frequencies of 900 MHz and 1.3 GHz, respectively. To validate the advantages of Graphene antenna over the conventional patch antenna, the antenna designed using polyimide substrate. Due to lower conductivity of Graphene material to copper and high relative permittivity, which is depend on the height of substrate are the prime reasons to get low value of Gain and radiation efficiency, but it can be overcome with the help of material science research and modern fabrication technology.

CONCLUSION

A reconfigurable graphene antenna, utilizing PIN diode, can seamlessly switch between 1.3 GHz and 900 MHz frequency bands, offering adaptability for diverse communication needs. Graphene's unique properties and careful design optimization are essential for maintaining antenna efficiency and performance in both bands, making it valuable in various applications. Graphene is made up a mono carbon lattice structure, available in very thin layer and it can be utilized on a flexible substrate. Wearable and Transparent miniaturized gadgets are the future of electronic wireless system; and proposed antenna described in this work is a pioneer step towards this goal.

REFERENCES

1. A.K. Geim, K.S. Novoselov, "The rise of Graphene-Nature Materials," *Nature Materials*, vol. 6, pp. 183–191, 2007.
2. J.S. Bunch, "Mechanical and Electrical Properties of Graphene Sheets," Ph.D. dissertation, Cornell University, 2008.
3. A. Scida, S. Haque, E. Treossi, S. Smerzi, S. Ravesi, S. Borini, V. Palermo, "Application of Graphene based flexible Antennas in Consumer Electronic Devices," *Materials Today*, vol.21, no.3, April 2018.
4. Rajni Bala, Anupma Marwaha, "Investigation of graphene based miniaturized terahertz antenna for novel substrate materials," *Engineering Science and Technology, an International Journal*, vol. 19, pp. 531-537, 2016.
5. A. S. Thampy, M. S. Darak, and S. K. Dhamodharan, "Analysis of Graphene based optically transparent patch antenna for terahertz communications," *Physica E*, vol. 66, pp. 67–73, 2015.
6. Xianjun Huang, Ting Leng, Mengjian Zhu, Xiao Zhang, Jia Cing Chen, Kuo Hsin Chang, "Highly Flexible and Conductive Printed Graphene for Wireless Wearable Communications Applications," *Scientific Reports*, vol. 5, pp.1-8,2015.
7. Christian Núñez Álvarez, Rebecca Cheung, John S. Thompson, Fellow, "Performance Analysis of Hybrid Metal-





Anish Vahora and RonakVashi

Graphene Frequency Reconfigurable Antennas in the Microwave Regime,” *IEEE Antennas and Wireless Propagation Letters*, vol. 65, no. 4, pp. 1558-1569, April-2017.

8. Sayeed Sajal, V. R. Marinov, “A Microstrip Patch Antenna Manufactured with Flexible Graphene-Based Conducting Material,” *Antennas and Propagation & USNC/URSI National Radio Science Meeting*, 2015.
9. J. Perruisseau-Carrier, “Graphene for Antenna Applications: Opportunities and Challenges from Microwaves to THz,” *Loughborough Antennas and Propagation Conference, UK*, Nov. 2012.
10. Y. Lee, J. Ahn, “Graphene-Based Transparent Conductive Films,” *World scientific*, vol.8, No. 3, pp.1330001,1-16,2013.
11. N. Chamanara, D. Sounas, T. Szkopek, C. Caloz, “Optically Transparent and Flexible Graphene Reciprocal and Nonreciprocal Microwave Planar Components,” *Microwave and Wireless Components Letters, IEEE*, vol.7, pp.360-362, July 2012.
12. Yanfei Dong, Peiguo Liu, Dingwang Yu, Gaosheng Li, Feng Tao, “Dual-Band Reconfigurable Terahertz Patch Antenna with Graphene-Stack-Based Backing Cavity,” *IEEE Antennas and Wireless Propagation Letters*, Vol. 15, pp. 1541-1545, 2016.
13. Haixiong Li, Qi Zheng1, Jun Ding, Chenjiang Guo, “Dual-band planar antenna loaded with CRLH unit cell for WLAN/WiMAX application,” *IET Microwave, Antennas and Propagation*, vol.12, n0. 1, pp. 132-136, 2018.
14. Jayendra Kumar, Banani Basu, Fazal A. Talukdar, Arnab Nandi, “Graphene-based multimode inspired frequency reconfigurable user terminal antenna for satellite communication,” *IET Microwave, Antennas and Propagation*, vol.12, pp 67-74, 2017.
15. Yasir, M. and Savi, P., (2020), April. Graphene based voltage controlled frequency reconfigurable antennas. In 2020 IEEE 40th International Conference on Electronics and Nanotechnology (ELNANO) (pp. 382-385). IEEE.
16. Yuan, R., Jiang, Y.N., Li, S.M., Cao, W.P., Gao, X., Yu, X.H. and Wang, Y., (2015), October. A bandwidth broadened pattern-reconfigurable antenna based on graphene. In 2015 IEEE International Conference on Communication Problem-Solving (ICCP) (pp. 236-238). IEEE.
17. J. Kraus, R. Marhefka, *Antenna and Wave Propagation*, (4th ed.), New York: McGraw-Hill, pp. 500-522, 2002.
18. GrapheneSheet,<https://www.indiamart.com/proddetail/graphene-sheet141475905>.

Table 1. PIN Diode Equivalent Values ON State and OFF State

PARAMETERS	ON STATE	OFF STATE
R	1 Ω	30 KΩ
L	0.5 nH	0.9 nH
C	0.5 μF	0.6 nF

Table 2 GRAPHENE SHEET ELECTRICAL AND MECHANICAL PROPERTIES [2]

PARAMETERS	VALUE	UNIT
Carbon Content	97%	---
Thickness	50	μm
Density	1.98	g/cm ³
Electrical Conductivity	1.93 × 10 ⁵	S/m
Thermal Conductivity	1300-1500(x-y plane) 13-15 (z plane)	W/(m)x(k)
Tensile Strength	30	MPa
Sheet resistance	0.02	ohm/sq.





Table 3 Performance parameters of Graphene based antenna

Frequency	Return Loss (dB)	Impedance Bandwidth (%)	VSWR
900MHz	-30.76	22.22	1.059
1.3 GHz	-34.82	24.17	1.036

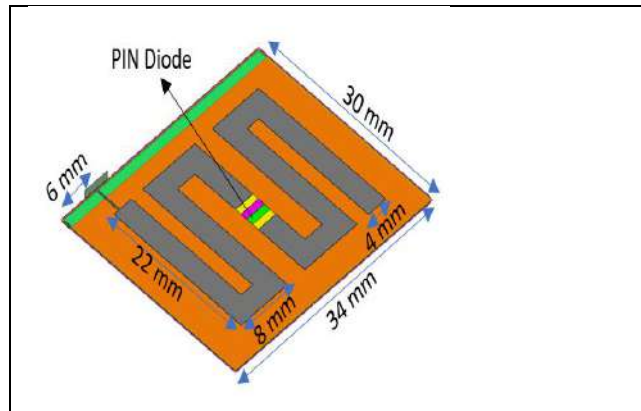


Fig.1. Proposed antenna prospective view

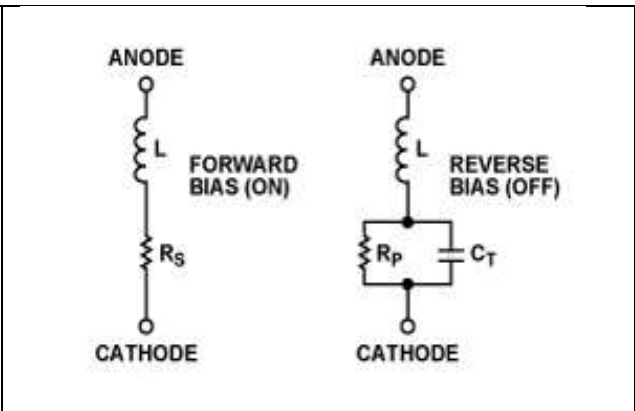


Fig. 2 PIN diode Equivalent Circuit (a) ON State; (b) OFF State.

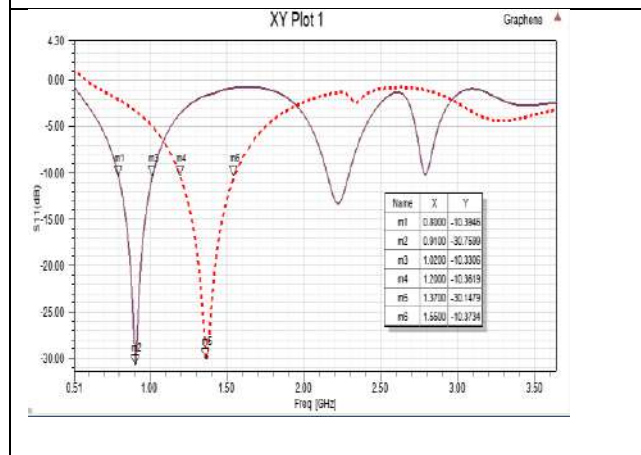


Fig. 3. Reflection Coefficient S_{11} (dB) to the frequency plot for reconfigurable Graphene based antenna.

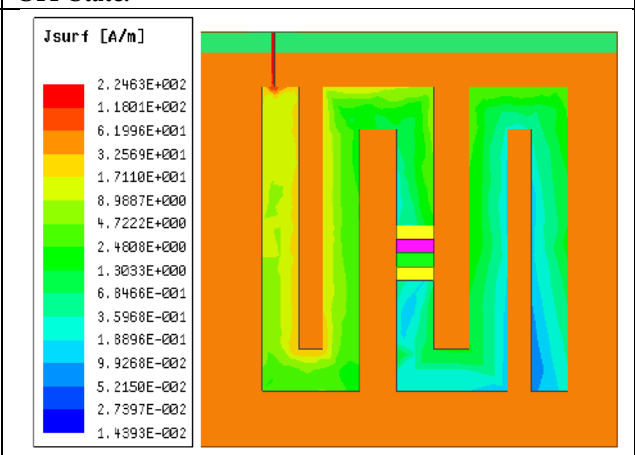
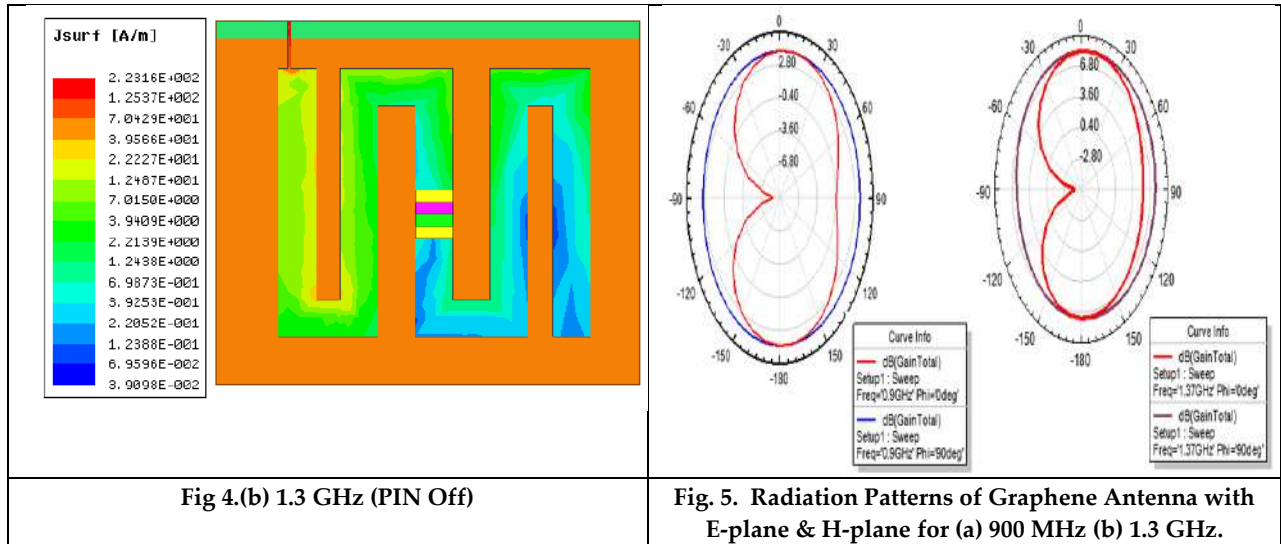


Fig. 4. Current Distribution of Graphene antenna for (a) 900 MHz (PIN on)





Anish Vahora and RonakVashi





Experimental Study on Lightweight Structural Concrete

Deepa A Sinha* and Elizabeth George

Associate Professor, Department of Structural Engineering, Birla Vishvakarma Mahavidyalaya Engineering College, Vallabh Vidyanagar ,Anand, Gujarat, India.

Received: 30 Dec 2023

Revised: 09 Jan 2024

Accepted: 12 Jan 2024

*Address for Correspondence

Deepa A Sinha

Associate Professor,

Department of Structural Engineering,

Birla Vishvakarma Mahavidyalaya Engineering College,

Vallabh Vidyanagar ,Anand, Gujarat, India.

Email: dasinha@bvmengineering.ac.in



This is an Open Access Journal / article distributed under the terms of the **Creative Commons Attribution License** (CC BY-NC-ND 3.0) which permits unrestricted use, distribution, and reproduction in any medium, provided the original work is properly cited. All rights reserved.

ABSTRACT

Concrete is the most widely used material in construction industry due to its durability and compressive strength characteristics. The disadvantage of conventional concrete is that it has high self-weight. Lightweight concrete plays an important role in reducing heavy self-weight of concrete with the increase in thermal insulation property. In this paper, lightweight concrete is made by partial replacement of coarse aggregate with expanded clay aggregate by volume.

Keywords: Control Concrete, Lightweight Concrete, Expanded Clay Aggregate(ECA),Compressive strength,Silica fume

INTRODUCTION

Structural Lightweight concrete may be defined as the concrete of lower unit weight than that of conventional concrete. It has density around 1450 kg/m^3 to 1850 kg/m^3 . Lightweight structural concrete not only reduces the dead weight of the structure but can also act as thermal insulator. Expanded clay aggregate (ECA) is the ultimate eco-friendly product for versatile applications and is recommended as a Green alternative. It is one source of structural aggregate material which is light in weight. Expanded Clay Aggregate is not only light in weight but is 100% inert aggregate (replacing fine and coarse aggregate in parts) which offers low density combined with thermal and sound insulating material. It is also fire resistant, insect-free and a durable lightweight inorganic product.





Deepa A Sinha and Elizabeth George

OBJECTIVE

To design structural control lightweight concrete as per IS 10262 - 2019 using normal aggregates and then replacing different percentages of coarse aggregates by 10-30 % by ECA to find the optimum percentage of coarse aggregate that can be replaced. To study the effect of silica fume with replacement of cement by 8 % in concrete with ECA and control concrete. To evaluate bulk density, water absorption, and compressive strength of lightweight structural concrete.

METHODOLOGY

1. To find out the properties of materials.
2. Design of Control Concrete
3. Casting of cubes with various percentages of replacement of coarse aggregate by expanded clay aggregate (10% to 30%).
4. Testing and analysis of results to find out the optimum percentage of expanded clay aggregate.
5. Casting of the cube by replacing cement by silica fume.
6. Analysis of results.

MATERIALS USED

1. OPC Cement (53 Grade)
2. Coarse aggregate
3. Fine aggregate
4. Expanded clay aggregate
5. Water
6. Admixture
7. Silica fume

Cement

OPC cement 53 grades: -The ordinary Portland cement of 53- grade conforming to IS 12269 fresh and of uniform consistency is used. The cement was stored under dry conditions and for as short a duration as possible.

Coarse Aggregate

Coarse aggregates used were irregular and granular. Specific gravity was found to be 2.7 and maximum size of aggregate of 20 mm.

Fine Aggregate

The fine aggregate used is of Zone II with a specific gravity of 2.6..

Expanded Clay Aggregate

Expanded Clay Aggregate (ECA) is of round pellet structure produced by firing natural clay at a temperature of 1200°C. The resultant material is a hard, honeycombed structure. The particles thus formed are round and ranging in size from 2-15 mm and density ranging from 260-700 kg/m³ for use in applications.

Water

Water used for the experiment was drinking water available in college.

Admixture

Admixture is defined as a material other than the basic ingredient of concrete cement, aggregate and water, added to the concrete mix immediately before or during mixing to modify some properties of concrete in the fresh or hardened test. PC base admixtures were used in Mix Design

FAIRFLO 5 – PC base Admixture

Silica Fume

1. Silica fume called as micro silica is an industrial byproduct. While manufacturing ferrosilicon alloy or silicon in an electric arc furnace this silica fume is produced.





Deepa A Sinha and Elizabeth George

2. Silica fume addition in concrete improves its bond strength, durability, and compression strength. Silica fume addition prevents the chloride ion penetration into the reinforcement bars which usually occurs in seashore areas.
3. silica fume also reduces the permeability of concrete to chloride ions, which protects the reinforcing steel of concrete from corrosion, especially in chloride-rich environments such as coastal regions. Being smaller particle, its addition decreases the workability, but replacement can be done to a specific certain limit of 8 to 10 % of cement.

TEST RESULTS

1. The maximum decrease in density of lightweight structural concrete without silica fume is 22.07% and with silica fume is 25.5%.
2. Expanded clay aggregate has high water absorption properties so necessary corrections to be done in preparing the mix design.
3. The finishing of lightweight structural concrete by expanded clay aggregate concrete is rough as compared to conventional concrete.
4. In Lightweight concrete when coarse aggregate was replaced by expanded clay aggregate by 10%, 15%, and 20%, the strength was reduced by 4.75%, 8.46%, and 15.86% respectively for 7 days and. -8.21%,9.93% and 14.26% for 28 days
5. By replacing 8% cement with silica fume and for the coarse aggregate replaced by ECA by 10%,15% and 20% the strength was increased by 14.40%, 13.97%, and 12.52% for 7 days respectively for 7 days and 14.01%, 12.95%and 11.83% respectively.

ACKNOWLEDGMENT

We acknowledge our final year students Brijesh gamit, Rajesh Mori,Sahil Patel , Praful Vasava and Pratik for conducting the experiment for this research project. We thank BVM engineering college for allowing and providing us to do the project in the Concrete technology laboratory.

REFERENCES

1. Shetty M. S., "Concrete Technology ".S.Chand & Co. Ltd., New Delhi.
2. IS 10262 - 2019 Guidelines to concrete mix Design
3. IS 456 – 2000 plain reinforcement concrete
4. IS 23683 - 1963 (Part - 1 to 4) Material of test for Aggregate for concrete.
5. Priyanga.R¹, Rajeshwari L.B² Vijaya Baskar S³ "Experimental Investigation on Mechanical Properties of Lightweight Concrete Using LECA And Steel Scraps" UG Student, Assistant Professor, Department of Civil Engineering. P.S.R Engineering college, Sivakasi, Tamil Nadu, India
6. Lakshmi Kumar Minapu, M K M V Ratnam and Dr. U Rangaraju, "Experimental Study on Light Weight Aggregate Concrete with Pumice Stone. Silica Fume and Fly Ash as a Partial Replacement of Technology; international Journal of Innovative Research in Science, Engineering and Technology Vol. 3. Issue 12, (2014) Pages 18130-18138.att
7. Ankit Kumar Agrawal¹, Ajay Kumar Singh² M.Tech Scholar, "Experimental Study of Light Weight Concrete by Replacing Fine Aggregates and Coarse Aggregates by Cinder Aggregates". Volume 10 Issue No.4 International Journal of Innovative Research in Science, Engineering and Technology; ISSN 2321 3361, 2020.
8. "Structural Concrete using Expanded Clay Aggregate." R. Vijayalakshmi and S. Ramanagopal Indian Journal of Science and Technology, Vol 11(16), DOI: 10.17485/ijst/2018/v11i16/121888 , April 2018 , ISSN : 0974-6846
9. "Performance of Concrete by using Silica Fume - An Experimental Study" Er. Uday Singh Meena, Er. Nandeshwar Lata, Dr. Bharat Nagar; IJSRD Vol. 5, Issue 06, 2017 | ISSN 2321- 0613





Deepa A Sinha and Elizabeth George

10. “An Experimental Study on Partial Replacement of Cement in Concrete by Using Silica Fume” Akshay Suryavanshi, Siddhartha Nigam, Dr. S. K. Mittal, Dr. Ram Bharosh; International Research Journal of Engineering and Technology (IRJET) e-ISSN: 2395-0056 Volume: 05 Issue: 02 | Feb-2018 www.irjet.net p-ISSN: 2395-007.

Table 1. Chemical Analysis Reference for Expanded Clay Aggregate (ECA)

Description	Expanded clay aggregate
SiO ₂ %	61.18
Al ₂ O ₃ %	17.68
Fe ₂ O ₃	13.59
CaO%	1.96
MgO%	1.53
K ₂ O%	1.14
Na ₂ O%	1.24

Table 2. Testing of ECA carried out in laboratory

Following are the tables of mix design for Control mix and various replacements of coarse aggregates with ECA

NAME OF TEST		RESULTS
Specific Gravity	2-8mm size of ECA	0.733
	8-15mm size of ECA	0.588
	Course Aggregate	2.75
	Fine Aggregate	2.62
Water Absorption	2-8mm size of ECA	12%
	8-15mm size of ECA	27%
Impact Test	Average of ECA	57.33%
Sieve Analysis	ECA	6.33 FM
	CA	7.07 FM

Table 3. Normal Concrete

Material	Weight
Cement	418.67kg/m ³
Coarse Aggregate	1235kg/m ³
Fine Aggregate	645.52
Water	157
Water Cement Ratio	0.375
Admixture	4.1kg/m ³

Table 4. Percentage replacement calculation

% REPLACEMENT	VOLUME OF E.C.A (2-8MM) in 1m ³ of concrete	VOLUME OF E.C.A (8-15MM) in 1m ³ of concrete	MASS OF ECA (2-8MM) kg	MASS OF ECA (8-15MM) kg
10	0.059	0.074	43.51	43.51
15	0.0773	0.0963	56.66	56.66
20	0.091	0.114	66.958	66.958





Deepa A Sinha and Elizabeth George

Table 5. 10% REPLACEMENTS OF ECA (For SSD condition)

Material	Weight
Cement	418.67
Coarse Aggregate	870.24
Fine Aggregate	654.52
Expanded Clay Aggregate (2- 8mm)	43.512
Expanded Clay Aggregate (8 – 15 mm)	43.512 Kg/m ³
Water	157 Kg/m ³
Admixture	4.1 Kg/m ³
Water Cement ratio	0.375

Table 6. 15 % REPLACEMENT OF ECA (For SSD condition)

Material	Weight
Cement	418.67
Coarse Aggregate	755.56
Fine Aggregate	645.78
Expanded Clay Aggregate (2- 8mm)	56.66
Expanded Clay Aggregate (8 – 15 mm)	56.66 Kg/m ³
Water	157 Kg/m ³
Admixture	4.1 Kg/m ³
Water Cement ratio	0.375

Table 7. 20 % REPLACEMENT OF ECA (For SSD condition)

Material	Weight
Cement	418.67
Coarse Aggregate	669.56
Fine Aggregate	645.78
Expanded Clay Aggregate (2- 8mm)	66.958
Expanded Clay Aggregate (8 – 15 mm)	66.958 Kg/m ³
Water	157 Kg/m ³
Admixture	4.1 Kg/m ³
Water Cement ratio	0.375

Table 8. 10 % REPLACEMENT OF ECA + 8 % SILICA FUME (For SSD condition)

Materials	Weight
Cement	374.28
Silica fume	32.54
Coarse Aggregate	870.24
Fine Aggregate	645.78
Expanded Clay Aggregate (2- 8mm)	43.512 Kg/m ³
Expanded Clay Aggregate (8 – 15 mm)	43.512 Kg/m ³
Water	157 Kg/m ³
Admixture	4.1 Kg/m ³
Water Cement ratio	0.375





Deepa A Sinha and Elizabeth George

Table 9. 15 % REPLACEMENT OF ECA + 8 % SILICA FUME (For SSD condition)

Material	Weight
Cement	374.28
Silica fume	32.54
Coarse Aggregate	755.56
Fine Aggregate	645.78
Expanded Clay Aggregate (2- 8mm)	56.66
Expanded Clay Aggregate (8 – 15 mm)	56.66 Kg/m ³
Water	157 Kg/m ³
Admixture	4.1 Kg/m ³
Water Cement ratio	0.375

Table 10. 20 % REPLACEMENT OF ECA + 8 % SILICA FUME (For SSD condition)

Material	Weight
Cement	374.28
Silica fume	32.54
Coarse Aggregate	671.23
Fine Aggregate	645.78
Expanded Clay Aggregate (2- 8mm)	66.958 Kg/m ³
Expanded Clay Aggregate (8 – 15 mm)	66.958 Kg/m ³
Water	157 Kg/m ³
Admixture	4.1 Kg/m ³
Water Cement ratio	0.375

Table 11. These are the test results of the compressive strength of cubes for the above mixes.

Type of Mix	7 days	28days	% increase / decrease of strength after 7 days	% increase / decrease of strength after 28days
Control Concrete	27.99	34.21	-	-
10% replacement of CA by ECA	26.66	31.40	-4.75	-8.21
15% replacement of CA by ECA	25.62	30.81	-8.46	-9.93
20% replacement of CA by ECA	23.55	29.33	-15.86	-14.26
10% replacement of CA by ECA 8% replacement of Cement by Silica fume	30.50	35.80	+14.40	+14.01
15% replacement of CA by ECA 8% replacement of Cement by Silica fume	29.20	34.80	13.97	12.95
20% replacement of CA by ECA 8% replacement of Cement by Silica fume	26.5	32.8	12.52	11.83





Deepa A Sinha and Elizabeth George

Type of Mix	Cube weight in grams without Silica Fume	Cube weight in grams with Silica Fume	% increase / decrease of weight without Silica Fume	% increase / decrease of weight Silica Fume
Control Concrete	8816			-
10% replacement of CA by ECA	7306	7140	-17.12	-19
15% replacement of CA by ECA	7206	7028.33	-18.26	-20.27%
20% replacement of CA by ECA	6810	6563.33	-22.07	-25.5%





XRD, Electrical, Antibacterial Activity and Photocatalytic Studies of Cadmium Sulphate Doped RGO (CS-RGO) Nanomaterial

S. Prema Thanapackiam^{1*}, P. Selvarajan² and K.Gnanaprakasam Dhinakar³

¹PG and Research department of physics, Pope's College, Sawyerpuram, Thoothukudi (Affiliated to Manonmaniam Sundaranar University, Abishekapatti, Tirunelveli) Tamil Nadu, India.

²Associate Professor, Department of Physics, Aditanar College of Arts and Science, Tiruchendur (Affiliated to Manonmaniam Sundaranar University, Abishekapatti, Tirunelveli) Tamil Nadu, India.

³PG and Research, Department of Physics, Pope's College, Sawyerpuram, Thoothukudi (Affiliated to Manonmaniam Sundaranar University, Abishekapatti, Tirunelveli) Tamil Nadu, India.

Received: 03 Oct 2023

Revised: 25 Dec 2023

Accepted: 22 Jan 2024

*Address for Correspondence

S. Prema Thanapackiam

PG and Research

department of physics,

Pope's College, Sawyerpuram,

Thoothukudi (Affiliated to Manonmaniam Sundaranar University, Abishekapatti, Tirunelveli)

Tamil Nadu, India.

Email: prema.phy@gmail.com



This is an Open Access Journal / article distributed under the terms of the **Creative Commons Attribution License** (CC BY-NC-ND 3.0) which permits unrestricted use, distribution, and reproduction in any medium, provided the original work is properly cited. All rights reserved.

ABSTRACT

Due to its superior electrical, thermal, optical, and mechanical properties, reduced graphene oxide (rGO) is a key component in the creation of promising materials. In this work, a simple, inexpensive, and environmentally friendly green reduction method was used. The first biogenic synthesis approach for cadmium sulphate doped reduced graphene oxide (CS-rGO) is described in this study employing *Citrus sinensis L.* as a reducing agent in a straightforward, environmentally friendly, and economically viable one-step process. Effectively and simultaneously, *Citrus sinensis L.* reduce the graphene oxide (GO) to produce CS-rGO nano material. Utilizing cyclic voltammetry, the electrochemical behaviour of CS-rGO was studied. CS-rGO nano material's antibacterial activity has been shown in a variety of culture media, demonstrating its superior potential to undoped rGO. Additionally, its photo catalytic activity was evaluated against methylene blue (MB). The transport of photo excited electrons and holes within the sample can be partially responsible for the increased activity. For the design and synthesis of next-generation photo catalytic materials for effective photo catalytic activity and environmental clean-up applications, understanding the interaction of rGO with cadmium sulphate is crucial.

Keywords: Nano material; graphene oxide; doping; green synthesis; characterization; XRD; antibacterial activity; cyclic voltammetry



Prema Thanapackiam *et al.*,

INTRODUCTION

Because of its unexpected electrical, mechanical, optical, and thermal capabilities, graphene has attracted considerable attention in a wide range of scientific communities [1]. It is a type of carbon allotrope that consists of a single layer of tightly packed, two-dimensional honeycomb-shaped carbon atoms with sp^2 bonds [2, 3]. Reduced graphene oxide has a large theoretical specific surface area, high charge mobility, and superior thermal conductivity because to its structural makeup. It is thought that graphene's distinct electrical characteristics are the most intriguing feature among all of these. The advantages of controllable shape, size, crystallinity, corrosion resistance, ease of use and cost effectiveness, as well as strong conductivity, have made other materials mixed with reduced graphene oxide more popular in recent years. Reduced graphene oxide (rGO)/semiconductor nano composite photocatalytic activity investigation was published by Arindam Mondal *et al.* [4]. A rGO nano composite was created by Ahmadi M. Seyed *et al.* and tested for the photo catalytic degradation of rhodamine-B dye when exposed to visible light [5]. Prema Thanapackiam *et al.* performed comparative research of graphene oxide and reduced graphene oxide nano materials [6]. Due to its intriguing and helpful qualities, cadmium sulphate has received some attention. In the visible spectrum, it also has a high transmission rate and moderate electrical resistance. As a result, it gains prominence as a significant inorganic molecule with intriguing potential for use in a variety of fields, including gas sensors, solar cells, and optoelectronic devices like photovoltaic cells, phototransistors, and transparent electrodes. Additionally, it possesses a selective photo catalytic property that enables it to be employed in the photodegradation of a variety of environmental contaminants, including certain organic dyes and pigments [7,8]. Consequently, cadmium sulphate was used in this work for the first time as a dopant. The effect of cadmium sulphate on the structural, photoluminescence, electrical antibacterial and photo catalytic properties of rGO nanomaterial is investigated, and the results are presented in this paper.

EXPERIMENTAL METHODS

MATERIALS

All of the chemicals, which were of analytical quality and were utilized without additional purification, included graphite (99% acid treated), sodium nitrate (98%), potassium permanganate (99%), hydrogen peroxide (40% wt.), sulphuric acid (98%), hydrochloric acid (35%), and cadmium sulphate. Throughout the experiment, double-distilled water was used.

Synthesis of graphene oxide

The oxidation of graphite has been used to produce graphene oxide according to Modified Hummer's approach. In a 1000 ml volumetric flask held in an ice bath (0–5°C), 50 mL of H_2SO_4 (98%) was continuously stirred in with approximately 2 g of graphite powder and 2 g of $NaNO_3$. After 2 hours of continuous stirring at ice-bath temperature, 6 g of potassium permanganate was very gradually added to the suspension mixture. To maintain the reaction temperature below 15 °C, the rate of addition was carefully managed. After the addition of potassium permanganate, the mixture was allowed for constant stirring at room temperature until it became pasty brownish and kept under stirring for 8 hrs. It was then diluted with slow drop wise addition of 100 ml of water. The reaction temperature was rapidly increased to ~98 °C with effervescence, and the colour changed to complete brown colour. Further this solution was diluted by adding additional 200 ml of water and stirred continuously for 4 hrs. The reaction, which was signalled by the emergence of yellow colour, is eventually put to an end by treating the solution with 10 mL of H_2O_2 . The mixture was cleaned by centrifuging it after being rinsed with 10% HCl and then numerous times with double-distilled water. The material was then dried at 50°C after being filtered through What man No. 41 filter paper. Graphene oxide (GO) was dried to produce a fine powder, which led to further analysis and the manufacture of reduced graphene oxide (rGO). The figure 1 gives the sample of prepared graphene oxide. The mixture was cleaned by centrifuging it after being rinsed with 10% HCl and then numerous times with double-



Prema Thanapackiam *et al.*,

distilled water. The material was then dried at 50°C after being filtered through the filter paper. Graphene oxide (GO) was dried to produce a fine powder, which led to further analysis and the manufacture of reduced graphene oxide (rGO) [9].

Synthesis of cadmium sulphate doped reduced graphene oxide (CS-rGO)

Utilizing effective bio-extracts, a straightforward and environmentally friendly experimental methodology has been used to produce reduced graphene oxide from graphene oxide particles. *Citrus sinensis L.* (often known as the orange fruit) extract was utilised in this experiment. It was acquired from a nearby store, and its juice was extracted using a clean polyethylene container. After that, 100 ml of double-distilled water was added to dilute it. The extract solution was then added precisely 100 mg of graphene oxide and 1 mole % of cadmium sulphate. The Ultra Probe Sonicator, Model: SM150W, was used to sonicate the mixture for around 30 minutes. There was a brown fluid that was disseminated. The solution was then centrifuged at 4000 rpm for 30 minutes, followed by 10 minutes at 800 W in an IFB 20SC2 20 L Convection Microwave Oven. As a result, cadmium sulphate doped rGO nano material (CS-rGO) with a black coloration was produced. The steps for producing the CS-rGO nano material is shown in the figure 2.

Instrumentation

X-ray diffractometer Bruker AXS D8 Advance, Inst ID: OCPL/ARD/26-002, utilising $\text{CuK}\alpha$ (1.54056 Å) radiation was used to record the X-ray diffraction (XRD) pattern of the material. Using an impedance analyser (LCR Hi-Tester, model: HIOKI 3532-50), the sample's real and imaginary parts of impedance have been measured at various frequencies. Agar well diffusion was used to measure the antibacterial activity. The photocatalytic activity was evaluated by measuring the degradation rate of MB (methylene blue) under a visible light source (Philips 40 W). The Origin Lab 9.0 software was used to create the graphical works.

RESULTS AND DISCUSSION

X-ray diffraction (XRD) study

Using a powder X-ray diffractometer, a study of powder X-ray diffraction was conducted for cadmium sulphate that had been doped with rGO nano material. Figure 3 depicts the recorded XRD pattern. The pattern shows two sharp peaks with significant intensities at 2θ values such as 25.85° and 26.41°. These peaks are corresponding to the planes (021) and (002). This pattern of XRD reveals the hexagonal crystallinity of the CdSO_4 doped rGO. In addition to the above peaks, some more minor peaks such as (132), (200), (130), (023), (202), (222), (114) are also noticed and this indicates the incorporation of cadmium sulphate into rGO material. Indexing of the powder XRD pattern is done by using the data from JCPDS file Nos. 15-0086 and 89-8487 are used to index the powder XRD pattern. The Scherrer's relation was used to determine the sample's average particle size, which came out at 14.35 nm [10, 11].

Photoluminescence (PL) study

The emission spectra (PL) of the CS-rGO nano sample was captured using an excitation wavelength of 200 nm, and it is shown in figure 4. For the cadmium sulphate doped reduced graphene oxide samples, we can see from the spectrum that there are several luminescence peaks at 333 nm, 466 nm, 548 nm, and 825 nm. The strong UV band at 333 nm, strong blue band at 466 nm, strong green band at 548 nm, and the infrared band at 825 nm are responsible for the peaks. Recombination between holes in the valence band and electrons in the conduction band is thought to be the cause of the intense emission at 466 nm. The band at 825 nm could be caused by a number of defects in the material, including cadmium and sulphate ions. As a result, the sample has many uses in the field of luminescence and the finding suggests that the cadmium sulphate doped reduced graphene oxide may be a promising photoemitter [12,13].

Impedance study



**Prema Thanapackiam et al.,**

When using comparable circuit models to analyze the conductivity behaviour, interfacial properties, dielectric properties, and charge carrier dynamics, impedance spectroscopy is a crucial technique. In order to get a satisfactory ohmic contact, the synthesised CS-rGO nanomaterial was covered with silver paint before being pelletized using a pelletizer. At various frequencies, the real component and imaginary part of the impedance were measured using the impedance analyzer (LCR Hi tester). The Nyquist plots (at 30°C and 50 °C) are depicted in figure 5 by placing the imaginary part of impedance (Z'') along the Y-axis and the real component of impedance (Z') along the X-axis. The picture illustrates that the sample behaves like a semiconducting material because the value of the real component of impedance is decreasing as the sample's temperature rises [14, 15].

Cyclic Voltammetry

To comprehend and characterize the redox properties, stability, and useful surface area of an electrode for bio sensing, cyclic voltammetry (CV) is performed. A working electrode (WE), a reference electrode (RE), and a counter electrode (CE) make up the three electrodes that make up a conventional CV setup. In CV, the voltage and speed of a potential supplied to the WE are varied over a predetermined number of cycles. The resulting current at the WE is monitored as the potential is scanned across a predetermined potential range. The current generated is then plotted against potential to produce a CV graph that provides insights on the transducer material based on the anodic peak current from oxidation process and cathodic peak current from reduction process which occur on the WE. The potentials at which the peak currents occur are known as peak potentials. The prepared CS-rGO nanomaterial was analyzed using a scan rate of 100 mV/s with the potential range of 1.0 V to 1.4 V and the CV graph is shown in the figure 6. From the graph we can conclude that oxidation occurs at 0.5 ampere and reduction occurs at -1.5 ampere. The value of capacitance is determined by using the relation $C = \text{current} / \text{scan rate}$ and the obtained value is 0.75 micro farad [16].

Antibacterial activity studies

The antibacterial effectiveness of the CdSO₄ doped rGO nanomaterial has been determined using the agar well diffusion method. Against three gram-positive bacteria, *Staphylococcus aureus*, *Bacillus subtilis*, and *Bacillus cereus*, as well as a gram-negative bacterium, *Escherichia coli*, the concentration of (CS-rGO) and conventional antibiotic gentamicin were investigated. Figure 7 presents images of the sample's zone of inhibition, and Table 1 provides matching values for each image. The observation shows that the antibacterial activity for the title sample's CS-rGO sample is very high against the gram-negative bacterium *Escherichia coli* and only moderately active against the other three gram-positive bacterias. *Escherichia coli*, also called *E. coli* and a wound infection could result from *E. coli* contamination. It is discovered that the CS-rGO sample has significant antibacterial activity against *Escherichia coli* [17,18].

Photocatalytic activity

The degradation rate of methylene blue (MB) under visible light (Philips, 40 W) was used to assess the photocatalytic activity of the CdSO₄ doped rGO nano material. In each experiment, 10 mg of the catalyst was dissolved in 10 ml of the aqueous MB solution (10 mg L⁻¹), and the suspension was agitated magnetically in the dark for 30 minutes to create an equilibrium between the adsorption and desorption of MB molecules on the catalyst surface. The combination was then put into a test tube and exposed to light in the visible spectrum. 2 ml of the suspension were removed at predetermined intervals (10–60 min) and the concentration of MB was determined by measuring the absorbance at 664 nm with a UV–vis spectrophotometer. Figure 8 shows the CdSO₄ doped rGO nano material photocatalytic curves that were attained. Greater specific surface areas, exceptional charge migration, electron-hole separation, and a lower rate of photogenerated charge carrier recombination were all linked with the improved photocatalytic activity. According to the literature, the photocatalytic activity is strongly influenced by the crystallinity, pH of the precursor solution, product shape, surfactant, surface area, and calcination temperature of the end products [19]. About 50% of the rGO nano material doped with cadmium sulphate is capable of photo catalysis. The semiconductor photo catalyst's photo catalytic performance is decreased because the majority of photo-excited electron-hole pairs have a tendency to recombine there. Particularly, elemental doping has been used to broaden the light absorption range and modify a semiconductor's redox potential, dye sensitization has also been used to do this,





Prema Thanapackiam *et al.*,

facet engineering has been used to provide highly active surfaces, and the development of mesoporous structures has been used to increase the surface area for more adsorption sites and active centres [20, 21].

CONCLUSION

The preparation of cadmium sulphate doped with rGO was prepared by green synthesis. The powder XRD diffraction peaks were indexed. The sample's photoluminescence spectrum was recorded and has a few emission peaks that are associated with the emission of UV, green, and yellow light. The cyclic voltammetry technique was used to calculate the capacitance value as 0.75 microfarad. Four bacterial specimens were tested for the antibacterial activity of the title sample, and it was discovered that the E.Coli specimen is more antibacterial active than the other three. It is discovered that the rGO nano material doped with cadmium sulphate (CS-rGO) has 50% photo catalytic effectiveness.

ACKNOWLEDGMENT

Authors thank the PG & Research Department of Physics, Pope's College, Sawyerpuram and Aditanar college of Arts and Science, Tiruchendur for providing laboratory facilities to do the experimental works and also thank SAIF - Cochin University (Cochin), NIT (Trichy), V.O. Chidambaram College (Tuticorin) for their support in the characterisation studies.

REFERENCES

1. Andrew R C, Mapasha R E, Ukpong A M and Chetty N, Mechanical properties of graphene and boronitrene; Phys. Rev. B 85, 125428 (2012).
2. Allen M J, Vincent C Tung, and Richard B Kaner, Honeycomb Carbon: a review of graphene; Chem. Rev. 110, 132, pp: 132-145 (2010).
3. Meyer J C, Geim A K, Katsnelson M I, Novoselov K S, Booth T J and Roth S, The structure of suspended graphene sheets; Nature, 446, pp: 60-63 (2007).
4. Arindam Mondal, Aarya Prabhakaran, Satyajit Gupta and Vaidyanathan Ravi Subramanian, Boosting Photocatalytic Activity Using Reduced Graphene Oxide (RGO)/Semiconductor Nano composites: Issues and Future Scope; ACS Omega 2021, 6, pp: 8734–8743 (2021).
5. Ahmadi M Seyed Dorraji MS, Rasoulifard MH, Amani-Ghadim AR, The effective role of reduced-graphene oxide in visible light photo catalytic activity of wide band gap SrTiO₃ semiconductor; Separation and Purification Technology, Vol: 228(2019).
6. Prema Thanapackiam S, Selvarajan P, Gnanaprakasam Dhinakar K and Veeraputhiran V, Biological reduction of graphene oxide using Citrus sinensis L. extract and its nano- structural photo catalytic - antibacterial performances; Advances in Natural Sciences: Nanoscience and Nanotechnology; Vol:13, No. 3, 035016, pp:1-9, (2022).
7. Rajveer Singh Rajaura, Vinay Sharma, Rishabh Shrivastava Ronin, Deepak K Gupta, Subodh Srivastava, Kailash Agrawal and Vijay K, Synthesis, Characterization and enhanced antimicrobial activity of reduced graphene oxide-zinc oxide nano composite; Materials Research Express, Vol:4, No:2 (2017).
8. Abayomi Babatunde Alayande, Obaid M, Kim In S, Antimicrobial mechanism of reduced graphene oxide-copper oxide (rGO-CuO) nano composite films the case of Pseudomonas aeruginosa PAO1; Materials Science and Engineering: C, Vol:109, 110596, pp:1-10 (2020).
9. Muzyka R, Kwoka M, Smedowski L, Diez N and Gryglewicz G, Oxidation of graphite by different modified Hummer's methods; New Carbon Mater. 32 (1), pp:15-20 (2017).
10. Syed Nasimul Alam, Nidhi Sharma and Lailesh Kumar, Synthesis of Graphene Oxide (GO) by Modified Hummers Method and Its Thermal Reduction to Obtain Reduced Graphene Oxide (rGO); Graphene, Vol:6, No. 1, PP:1-18 (2017).





Prema Thanapackiam et al.,

11. Nagaraju G, Ashoka S, Tharamani C N, and Chandrappa G T, A facile low temperature hydrothermal route to CdSO₄ nanotubes/rods. *Materials Letters*; Vol:63, PP:492-495, (2009).
12. Sivanandan T and Kalainathan K, Study of growth condition and characterization of Monothiourea-Cadmium Sulphate Dihydrate single crystals in silica gel; *Materials Chemistry and Physics*, Vol:168, pp: 66-73 (2015).
13. Dwi Noor Jayanti, Ananda Yogi Nugraheni, Kurniasari, Malik AnjelhBaqiya and Darmin, Photoluminescence of Reduced Graphene Oxide Prepared from Old Coconut Shell with Carbonization Process at Varying Temperatures; 3rd International Conference on Functional Materials Science, pp: 1-4, (2016).
14. Anoushka K Das, Joselyn Elizabeth Abraham, Mayank Pandey and Manoj. Impedance and electrochemical studies of rGO/Li-ion/PANI intercalated polymer electrolyte films for energy storage application; *materials today: proceedings* ,Vol:24, pp: 2108-2114, (2020).
15. Nhu Thuy Ho, Senthilkumar and Yong Soo Kim. Impedance spectroscopy analysis of the switching mechanism of reduced graphene oxide resistive switching memory; *Solid-State Electronics*, Vol: 94, pp:61-65, (2014).
16. Nan Zhang and Yi-Jun Xu. The endeavour to advance graphene-semiconductor composite-based photocatalysis; *Cryst EngComm*, Vol: 18, pp:24-37, (2016).
17. Kannan Badri Narayanan, Gyu Tae Park and Sung Soo Han. Antibacterial properties of starch-reduced graphene oxide–polyiodide nano composite; *Food Chemistry*, Vol: 342, (2021).
18. Rajveer Singh Rajaura, Vinay Sharma, Rishabh Shrivastava Ronin, Deepak K Gupta, Subodh Srivastava, KailashAgrawal and Y K Vijay. Synthesis, characterization and enhanced antimicrobial activity of reduced grapheme oxide–zinc oxide nano composite; *Materials Research Express*, Vol: 4, No:2, (2017).
19. Shaowen Cao, Jiaguo Yu. Carbon-based H₂-production photo catalytic materials; *Journal of Photochemistry and Photobiology C: Photochemistry Reviews*, Vol:27, pp: 72-99, (2016).
20. Malathi A, Madhavan Jagannathan, Muthupandian Ashokkumar, Prabhakarn Arunachalam. A review on BiVO₄ photocatalyst: Activityenhancement methods for solar photo catalytic applications; *Applied Catalysis A-General*, Vol.555, pp:47-74, (2018).
21. Lavakusa B, Sathish Mohan B, Durga Prasad P, Belachew N and Basavaiah K, Facile synthesise of graphene oxide by modified hummer's method and degradation of methylene blue dye under visible light irradiation; *International Journal of Advanced Research*, Vol:5, No:3, pp:405-412, (2017).

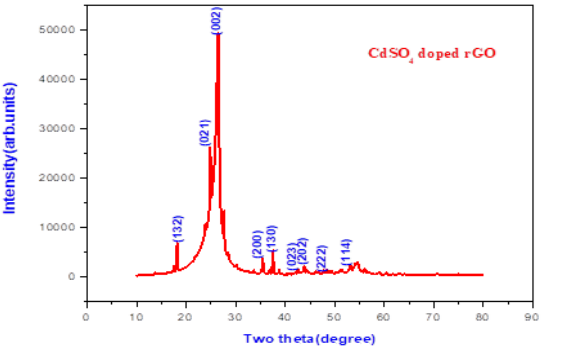
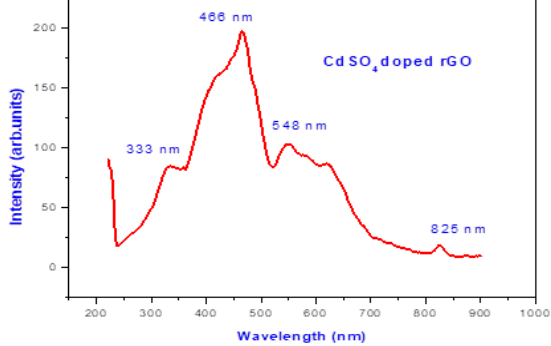
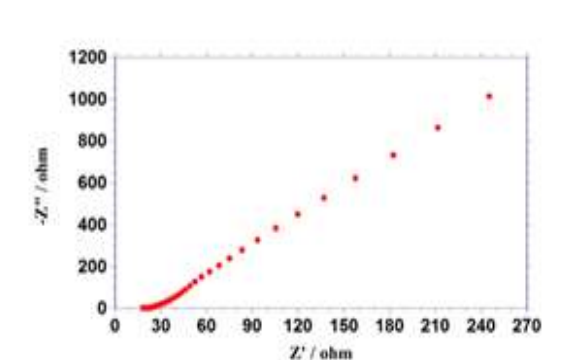
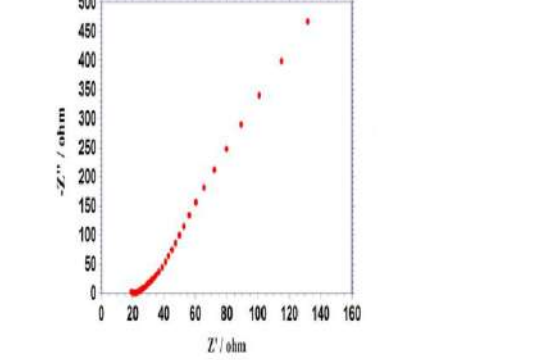
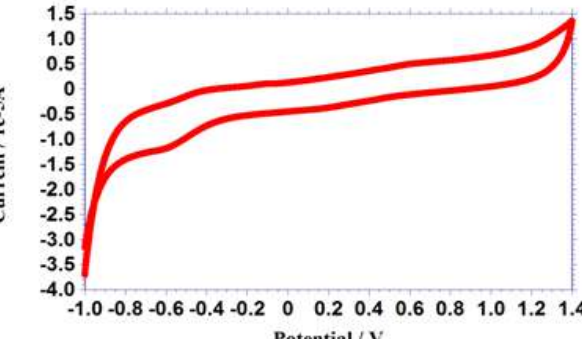
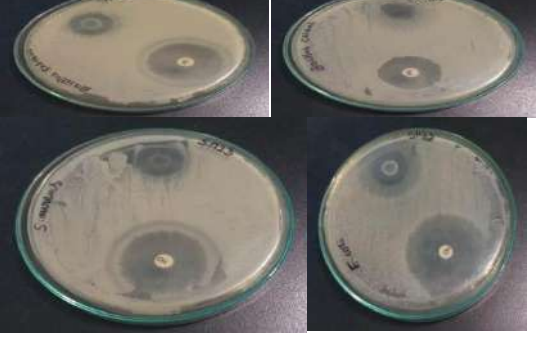
Table 1: Values of zone of inhibition for CS-rGO nanomaterial and standard against different bacterias

Bacteria	Zone of inhibition (mm)	
	CS-rGO	Standard
Escherichia coli	30	37
Staphylococcus aureus	21	35
Bacillus subtilis	20	30
Bacillus cereus	18	28





Prema Thanapackiam et al.,

<p>Figure 1: Synthesized GO solution and GO powder</p>	<p>Figure 2: Steps for synthesizing CdSO₄ doped rGO nano material</p>
	
<p>Figure 3: XRD spectrum of CdSO₄ doped rGO nano material</p>	<p>Figure 4: Photoluminescence spectrum of CdSO₄ doped rGO nano material</p>
	
<p>Figure 5: Nyquist plots for CdSO₄ doped rGO nano material at (i) 30 °C</p>	<p>Figure 5: Nyquist plots for CdSO₄ doped rGO nano material at (ii) 50 °C</p>
	
<p>Figure 6: Cyclic Voltammogram graph for CdSO₄ doped rGO nano material</p>	<p>Figure 7: Photographs of antibacterial activity for CdSO₄ doped rGO nano material</p>





Prema Thanapackiam et al.,

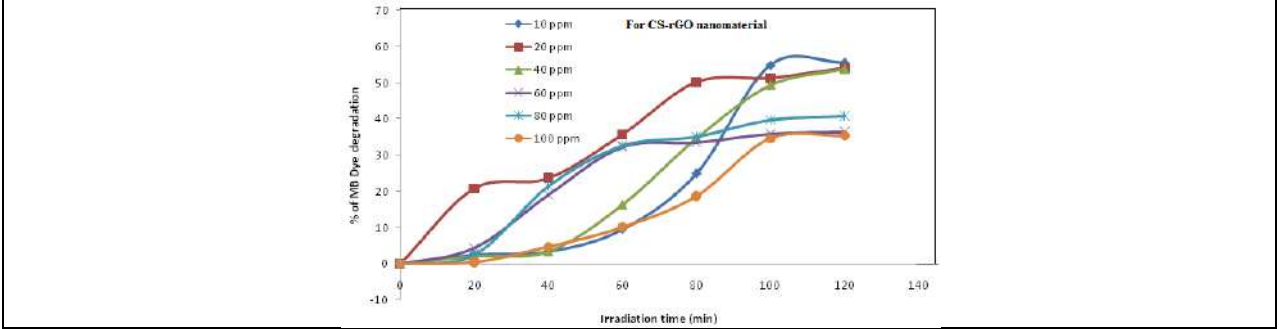


Figure 8: Photo catalytic curves for CdSO₄ doped rGO nano material





Inclusivity in Medical Access of Trans Persons in the Health Care System of Kerala

Silpa G Nair^{1*} and S.Sampath Kumar²

¹Doctoral Scholar, Department of Sociology and Population Studies, Bharathiar University, Coimbatore, Tamil Nadu, India.

²Professor and Head, Department of Sociology and Population Studies, Bharathiar University, Coimbatore, Tamil Nadu, India.

Received: 31 Aug 2023

Revised: 08 Nov 2023

Accepted: 10 Jan 2024

*Address for Correspondence

Silpa G Nair

Doctoral Scholar,

Department of Sociology and Population Studies,

Bharathiar University,

Coimbatore, Tamil Nadu, India

Email: gsilpa96@gmail.com



This is an Open Access Journal / article distributed under the terms of the **Creative Commons Attribution License** (CC BY-NC-ND 3.0) which permits unrestricted use, distribution, and reproduction in any medium, provided the original work is properly cited. All rights reserved.

ABSTRACT

The social environment of Kerala society is embedded with false pride and heteronormativity. Being a trans person in this cultural setting is treated more or less as a form of deviance. This contributes to various forms of violence against them, ranging from symbolic violence such as exclusion and stigmatization towards physical violence which even includes extreme cases of sexual assaults. At this juncture, access to health care is significant in overcoming all of the violence they face which in turn ensures their physical, mental, and social well-being. Hence, the study focused on factors that inhibit trans persons from accessing health care. The qualitative study used secondary data sources and content analysis as a method for collecting data. The study found that expensive surgeries, medical negligence, transphobia, lack of access to government health care, inadequate medical insurance, etc., as the major obstacles in accessing the health care system of Kerala.

Keywords: transmisia, medical negligence, Gender Affirmative Surgery, Kerala transgender policy.





INTRODUCTION

Historically, of all the LGBTQ+ communities in India, those who identify in a variety of sexual orientations and genders have been subject to the greatest amount of stigma, prejudice, and marginalization. People who identify as transgender, intersex, or queer are denied access to basic rights, self-dignity, physical autonomy, and health care, which has a substantial negative impact on their health (S. Bhattacharya et al., 2020). In Indian society, those who identify as transgender are frequently ostracized, which puts them among the most vulnerable groups to social exclusion. They cannot live a dignified life once their gender status is known because of social stigma and discrimination, which is caused in part by cultural preconceptions and expectations as well as bureaucratic regulations that trap them in cycles of homelessness, unemployment, and restricted access to healthcare, education, banking, and identity documents. The arguments and conversations around the rejection or acceptance of article 377 have forced society to reevaluate assumptions about what constitutes normal or abnormal body as well as the types of sexual orientations that people with ostensibly aberrant bodies may have. Social space remains inaccessible to the community which denied them connecting with the general population as well as the fundamental right to lead an exalted life. Kerala established a benchmark for a trans-welcoming state in 2014–15 with the launch of a statewide survey for 10 days. Subsequent events included the launch of a state initiative in the form of policy for transgender individuals, the establishment of a justice board, scholarships, health clinics, pensions for the elderly, employment opportunities in the Kochi Metro, and a number of literary, athletic, and fashion shows.

But being transgender in Kerala is still a painful, traumatic, and tense experience. The outlook of the society is rested with false pride embedded in high morality which further worsens the situation of the community. This insists them to hide their identity, suppress their sexual desires as well as live as strange creatures in the orthodox society. According to the Transgender survey of Kerala 2014 -15 - 25,000 transpersons are residing - at the same time after that not a single enumeration on the community is done so far. Today we are living in a society which demands for data even to prove existence of one's identity due to the digitalization of governance makes the life of community much harder since there is no exact statistics available on the existence of them. According to a study by Brindalakshmi (2020), the underrepresentation of transgender communities by public data systems that were built with "hidden biases" is being used as justification by several Indian governments, which has resulted in the bureaucratic erasing of their existence. Although adding these data sets does not ensure access to welfare or their rights, this structural design does not account for the historical discrimination and subsequent systemic oppression suffered by a minority group. Right to get proper health is considered as one of the basic prerequisites for every individual. Even the Sustainable Development Goals are meant to ensure healthy lives and promote well-being for all is also not reaching the community in practical sense.

Evidence suggests that, on average, sexual and gender minorities experience worse health outcomes, higher rates of certain risk behaviors (such as smoking, in addition to risks related to STIs and HIV), and poorer access to healthcare than the general population (Malley & Holzinger, 2018). Health systems are lagging in their ability to identify and appropriately address the particular health requirements of sexual and gender minorities, notwithstanding the difficulties they face in obtaining treatment and in generally improving health outcomes. Medical negligence is a serious issue faced by the transgender community in India and the situation of Kerala is also not at all different. In a survey conducted by the Social Welfare Department of Kerala revealed that 51 per cent of transpersons have experienced the denial of equal treatment in hospitals and clinics by the medical practitioners. Despite early reports about a ground-breaking medical procedure in Kerala, a transman's surgery performed in one of the Government medical colleges of the state was unsuccessful, and it was later discovered that his health was in grave danger and that he had not been adequately informed about his choices and the menaces involved. After being continually turned down for Gender Affirming Surgery in 2018, a trans man of 22 years of age killed himself. He was refused treatment without parental permission, contravening national and state regulations stating that adults do not need to obtain consent from their parents for Gender Affirmative Surgery (GAS). However, these widely reported instances



**Silpa G Nair and S.Sampath Kumar**

are just the top of the iceberg. Due to either a dearth of access to gender affirming practices or doctor's negligence, majority of transgender people continue to experience suffering (Report of Queerala,2019). All these excerpts show the level of negligence experienced by the transgender community from the health care system of Kerala as well as the significance for inclusivity in the system. At this juncture the present study tried to unearth the major factors that inhibit transpersons from accessing health care. It specifically focused on the challenges of them in availing health care, the interaction of medical professionals, and flaws in institutional framework which contribute to the concerned problem.

RESEARCH METHODOLOGY

The study titled "Inclusivity in medical access of trans persons in the health care system of Kerala" tried to focus on the major inhibitors in accessing health care for transpersons. The study is qualitative in nature and used descriptive research design to describe the situational challenges faced by the community people to access health, institutional constraints in dispensing egalitarian health services as well as the biases of medical practitioners. Since Kerala is the state which initially advocated the transgender policy still lacks gender affirmative health care. This lack of gender affirmative health care badly affects the sexual minorities even putting their life at risk. The Kerala society is a model of development for the rest of the states is down in delivering inclusive health care to its citizens due to its heavily rooted heteronormativity. The study is purely based on secondary data sources. The data is collected from books, journals, reports prepared by Community Based Organizations, newspaper reports, blogs and other social media sites. The collected data is analyzed using Content analysis in which it is placed under distinct themes. A comprehensive study on this aspect is lacking and it is actually a serious issue that has to be addressed. Since number of people undergoing surgery as well as the consequences after the surgery are also on rise. The data is presented using narrative reviews. Lack of literature available on the topic is a major drawback of the current study. The study has also given much priority to Gender Affirmative Surgery by ignoring other health care aspects is also a limitation.

RESULTS AND DISCUSSION

Kerala is the first state which adopted Transgender welfare policy on behalf of the NALSA judgement of 2014. In spite of the policy, it remains an unsafe space for the trans community due to lack of proper implementation, social stigma as well as improper awareness of what it meant to be a transperson. This in turn creates serious denial in accessing health care by the community. The level of treatment and access to care for many trans people who transition with the aid of hormone medication (and occasionally gender affirming surgery) varies greatly from one country to another (Murad,2010). Inappropriate health care support or affordability leads to the health challenges that emerge from informal or illegal hormone intake and other interventions that are used to facilitate transition (Murad,2010). Transgender people frequently have unique reproductive health requirements that are misunderstood, such as trans man who become pregnant. As a prerequisite for legally transitioning their gender, many nations still require trans people to undergo sterilization (Bizic, 2018). But at the same time Kerala is a place where a transman has given birth to a baby recently and also the atrocities against transpersons, those who are committing suicide due to several issues are also on rise. The study mainly tried to find out the factors responsible for inhibiting the health care services for the marginalized community specifically the transpersons in Kerala. These factors are divided into personal, institutional as well as from the side of medicos.



**Silpa G Nair and S.Sampath Kumar****Situational challenges faced by trans persons in availing health care**

According to the Standards of Care (SOC) published by World Professional Association for Transgender Health (WPATH) states the major reasons for the health disparities as transphobia, stigmatization, ignorance and the refusal of care when seeking health care services.

Vulnerability towards diseases

Trans persons are vulnerable to tremendous number of diseases due to insufficient access to appropriate health care and lack of proper knowledge about Gender Affirmative Surgery. They are more vulnerable to depression, anxiety, HIV, Sexually Transmitted Diseases, Cancer and so on. Even though, they are more prone to Cancer, not ready to go for screening which in turn which lead to delayed diagnosis and further consequences for both transmen as well as trans women. Globally, the UNAIDS Global Update 2018 stated that “the risk of HIV acquisition among gay men and other men who have sex with men was 28 times higher in 2017 than it was among heterosexual men” and “13 times higher for transgender women than adults aged 15–49 years.” The statement below is an excerpt from ‘The Caravan magazine’:

“Transgender persons express their identity in the coming out process itself, they mostly desire to express themselves..... In the community, many are unaware of medical specificities, but those who are doing the surgery are well aware of the things. They must know how the process goes, a major concern”-Sheethal Shyam, member of Kerala’s Transgender Justice Board.

Reliance on informal networks for medication

In SoC 8 which is recent one clearly stated that lack of knowledgeable health care providers, untimely access, previous stigmatizing experiences as well as cost barriers compelled the trans persons to take non-prescriptive hormone therapy. There is high incidence of self-medication by the community people, they will be taking medicines on the basis of their friend’s advice which results in overdose and number of grave side effects like damage to organs, weight gain or loss, depression as well as mood swings. The report of Queerala in 2019 indicates that the Medical Health Practitioners and representatives of the community had spoken about the inhibitive tendency of the trans persons to reveal the complications after their surgery and the exploitation from the hospitals as out of shame. Lack of proper discussion on how indecorous surgery can affect one’s sex life, psychological and physical health. This reliance on informal networks indicates that there are no accessible, formal and fully reliable support networks for transgender people seeking information on healthcare options. Such information barriers make transgender clients easy targets for exploitative medical institutions, and there were several reported instances of health issues owing to self- medication and improper healthcare(Report of Queerala,2019).

Discrimination and Marginalization of trans persons

Trans people are experiencing humiliation, preconception, discrimination, harassment, abuse and violence all over the world, these reasons lead to social economic and legal relegation, poor mental and physical health as well as even death to the community people. This intersectional forms of discrimination and marginalization leads to minority stress known as *stigma - sickness slope* which in turn leads to increased rate of depression, suicidality and non – suicidal self-injuries. Their situation determines most of their problems in the society since we are living in a society which justifies Foucault’s notion on sex as a “Regulatory ideal” which becomes a productive power to produce, demarcate, circulate, and differentiate the bodies it controls. Meanwhile, transpersons are considered as the one who transgress the gender norms compel them to experience stigma and this early disgrace leads to sidelining and discrimination placing them at the risk for poverty. This eventually lead to engagement in higher risk behaviours later to chronic diseases such as HIV infection.

Expensive Surgeries

Expensive surgeries are another important factor which hinders the transpersons from accessing the health care system. Since transpersons are largely impoverished and excluded from both the educational and professional spheres, their healthcare decisions are heavily influenced by their financial situation (Report of Queerala,2019). Even



**Silpa G Nair and S.Sampath Kumar**

though the government is reimbursing a financial aid of maximum of 5 lakhs that is 2.5 lakh for trans women and 5 for transmen, is not at all sufficient since many are going for corrective surgeries. One of the community members is detailing the expenses for the surgery in which the aid from the government is not at all sufficient.

“An ordinary vaginoplasty, a procedure that can construct vulva and vaginal canal, costs around anywhere between 1 lakh to 1.5 lakh rupees..... For female to male surgeries, breast removal costs..... and construction of a penis through metoidioplasty or phalloplasty ranges from 2.5 lakh to 4 lakh rupees depending on the complexity of surgery. Hormonal therapy,”(Surya,2021) “Surgeries are expensive and many raise money through sex work or begging. So when such surgeries fail, the impact is devastating,” Sreemayi told Behanbox“.However, I see the government scheme to reimburse the cost of SRS as a progressive move. The bigger issue, however, is the stigma associated with SRS”, said Saadiya. “Transgender people are reluctant to file complaints since society views SRS as a pointless practice”.(Surya,2021).

Transmisia

Transphobia or transmisia is another significant non facilitator in gender-affirmative health care.It means hatred towards transpersons. It can be attitude, behaviour or policy which stigmatizes the gender minorities. It may also denies their identity as well as consider them less worthy. Even though lot of changes are happening in Kerala due to the transgender policy lack of inclusivity of trans persons is still a major concern. *“Had the society accepted transgender persons in their true identity, many might not have opted for a surgery. Surgery gives us confidence, visibility and independence. After going through so many struggles in life, all we want is some inner peace and happiness,” Saadiya said.(Surya,2021)*

Interaction of Medical Professionals

Like any other public institutions, hospitals are also perilous for transpersons.

Discrimination from hospitals and medical practitioners

Studies from all over the world have shown that health professionals are often hostile and unaware of the needs of patients who identify as sexual or gender minorities, and that this has a negative effect on how often people seek medical attention and how well they stick to their treatment plans for a variety of health conditions (Clark,2014). According to the report of Queerala its clear that many of the transpersons avoided to visit government hospitals even for primary health care needs due to lack of concealment and biased attitude of doctors and other staff members.

Lack of infrastructure for Gender Affirmative Surgery

Gender Affirmative Surgery is not offered by any government hospitals in Kerala. The absence of expertise, training, and manpower among health personnels are all mentioned as problems. There are signs that government hospitals, which are already operating with meagre resources, do not emphasize gender affirmative care. There is currently no health insurance programme specifically designed for transgender individuals. Presently, only private clinics in Kerala provide SRS to transgender patients. There must be more stringent government oversight of such practices in the private sector, or at the very least a way for transgender people to file complaints with the Transgender Justice Boards, warranting investigations and punitive action, given that many transgender people seeking surgery lack the resources to recognise and combat medical malpractice for profit.

There have been reports of surgeries being done in smaller clinics both inside and outside Kerala with insufficient equipment and knowledge. Numerous transgender people have experienced lifelong complications and serious health problems (such as urinary incontinence, recurrent infections, necrosis, and chronic pain) as a result of poorly performed surgeries, with doctors obtaining additional payment from patients for multiple corrective procedures. It is customary for patients to speak with a psychologist prior to surgery.

“The psychologist would just ask whether we are ready for the surgery but never talked of its implications in detail”, said Govindan in an interview conducted by Behan box.



**Silpa G Nair and S.Sampath Kumar****Medical Negligence**

Annyah Kumari Alex who died in the year 2021 clearly shows the level of gender affirmativity in the health care system of Kerala because she is the victim of medical negligence. In her interviews with a number of media sites, she had been disclosing in graphic detail the horrific specifics of her failed operation and the resulting trauma she experienced. *“You cannot call my post-surgery private part a vagina. It is like a hacked piece of meat. It looks as if a hole is made in the flesh. I go through excruciating pain every day”*, she told The Cue. *“I need to undergo corrective surgery by an expert doctor. I am a person who sees life in a positive way. But sometimes I feel like ending my life. The doctor and the hospital I chose have thrown me onto the street,”* she said in the video. *“Botched surgeries are not new it might sabotage the only available treatment facilities in the state”*, said a trans rights activist who requested anonymity. Annyah faced a lot of difficulty as an effect of her surgery. After surgery she was not able to stand, sit, laugh or even cry, due to the severe pain she experienced. Annyah had said in The Cue interview, *“I have also been experiencing breathing difficulties. I had wished for a sex reassignment surgery that will give me a vagina like a woman’s..... but my private part looks as if it has been cut ruthlessly with a knife. medical negligence”*. *“Once, following the surgery, late evening, she fell severely ill They pushed her out. In another instance also, Annyah had herself told me about these instances,”* says her father. (<https://www.thenewsminute.com/article/anannyah-was-pushed-out-hospital-twice-kerala-trans-woman-s-father-alleges-152733>)

Unawareness of Mental Health Professionals

There were several reports of malpractice by psychiatrists and psychologists, and most transgender people harbour deep distrust towards mental health professionals. There are indications that many mental health professionals are unaware of gender variance and the correct protocol to be followed in treating a transperson. Psychiatrists were reported as having discouraged transgender clients from surgery (because their dysphoria might just be a “feeling”), as not following proper assessment procedures for transgender clients who wished to have SRS and as not even knowing how to address their transgender clients. Although an MHP consulted for this report was of the opinion that it is mental health professionals with spurious qualifications who provide such services, community members reported such behavior from well-qualified mental health professionals as well, indicating that there are serious gaps in the training given to qualified Medical Health Practitioners (Report of Queerala,2019).

Flaws in institutional framework

Absence of Government hospitals, gaps in the NALSA judgement as well as other legislations related to transpersons, lack of resources and allowances like cis genders are the major flaws of the institution.

Absence of Government hospitals

According to a study conducted by the Kerala-based LGBTQIA+ organization Queerala, in 2019, gender-affirmation health care was not offered in the state’s public healthcare system. This is a violation of the Transgender Persons (Protection of Right) Act, 2019, which compels the government to ensure public healthcare facilities for transgender persons including free of cost gender affirmative healthcare (Ej& Bhavani,2021). The State Human Rights Commission and the former Health Minister KK Shailaja have received a trans man who experienced Affirmative surgery from a government hospital, regarding his botched surgery and the subsequent trauma he endured. *“They took my body for their experiment. The doctor I consulted in Mumbai told me that the surgery This in turn led to several complications. The strong antibiotics they gave me for the infection caused further serious health issues”*, he said in an interview with First post.

Privatisation of Gender Affirmative Surgery

Government hospitals in Kerala are not at all performing Sex Reassignment surgery or any other gender affirmative care which subsequently boosted the growth of private hospitals. *“Private hospitals, in a hurry to cash in on the financial support offered by the government, flouted many of the norms”*, said Krishnan (Surya,2021). *“Around five persons underwent SRS surgery during the time I was admitted at the hospital. I realized that they were cashing in on our desperate urge for a better life. In Annyah’s case, I realized that she was neither given necessary hormone therapy nor psychological*



**Silpa G Nair and S.Sampath Kumar**

support,” Govindan told Behanbox. In Kerala, there is a clear tendency towards the privatisation of gender-affirming services, which has significant ramifications. There is a chance that this tendency will limit healthcare for transgender people to those who can afford it, even though private players are setting the bar for gender-affirmative healthcare and providing affordable services. It can also reinforce the notion that procedures like Hormone Therapy and SRS are "luxury" cosmetic services rather than necessary welfare programmes to handle a particular group of people's right to life.

Lack of systematized Care and standardized Protocol for Surgery

Due to lack of systematized care in the hospitals of Kerala, many transpersons are compelled to consult different medical health practitioners for different processes like general health care, psychiatric evaluation, hormone therapy, counseling and for Gender Affirmative Surgery. This creates serious problems in terms of logistics both for health practitioners as well as the clients. There is no single standard protocol adopted by Kerala for performing the surgery which results in non – transparent and ad hoc procedures. Community leaders of Kerala concurred that facilities in cities like Mumbai, Delhi, Coimbatore, Mysore, and Bangalore were more well-trusted because they had been serving the needs of transgender people, especially trans women, for a long time. Since Coimbatore is closer to Kerala and has a tradition of providing care for transgender people, it was most frequently mentioned as a location where people travelled for surgery. Some community leaders were not aware that Kerala has SRS facilities. In order to provide transgender people with quick, affordable services, many of these out-of-state services circumvented appropriate documentation, informed consent, and WPATH guidelines, according to both Medical Health Practitioners and representatives (Report of Queerala,2019). Medical Health Practitioners (MHPs) stressed the significance of integrating gender-affirming healthcare into current welfare programmes. To make gender affirmative care available and affordable, public-sector action and private-public partnerships are required (Report of Queerala,2019). The government is providing financial aid only after the surgery has done which creates a serious threat to the community people because they will be doing risky jobs for making money for doing surgery. Majority of them are undergoing surgery mainly to get acceptance from the society as well as from the community.

Loopholes in the legislation for trans community

In the NALSA v/s Union of India judgement the Supreme Court declared that gender is a person decision which doesn't need a committee examination or changes in the body for any acceptance amidst this decision from the honourable Supreme Court. This bill states that a transgender person should present themselves in front of the district magistrate and need a declaration from them so as to live as a male or a female. They need to undergo Sexual Reassignment Surgery. This is the violation of the above-mentioned NALSA judgement (Anagh,2020). At the same time the transgender id card is mandatory for getting any welfare funds also complicates the issue. So, many community people with or without knowing the impacts are undergoing surgery at any cost. The transgender protection bill of 2019 cited that hormone treatment and Sexual Reassignment Surgery would be made available to transgender persons through government hospitals. But the bill does not explain the mode of expenditure to be incurred for the purpose as well as the ways and means of approaching the hospitals concerned (Anagh,2020). Even not a single hospital is performing Sex Reassignment Surgery in Kerala is also a major flaw in the institutional framework. "No one has expertise regarding these surgeries, no one has properly studied about it,..... Access to these bodies is still difficult for many of us. The state's reimbursement of funds for gender-affirmation surgery is a flawed one..... and fixed rate must be available" (Surya,2021). Many are compelled to go for corrective surgeries after Gender Affirmative Surgeries and the expenses will not be covered under the 3000 rupees given by the government. Medical insurance coverage is also not available for them which further worsens the situation.

Health care is not something which is inseparable from well-being in general its directly correlated with one's status as social beings. The social stigma is the root cause for the problems faced by the community. Gender affirmative health care helps to reduce the problems and that is not at all limited to surgical and biomedical procedures but for that social acceptance and long-term support is necessary. There is no uniform protocol for performing surgery in Kerala and also ethics panel is necessary to improve the situation. The doctors should be trained properly for conducting treatment for the transpersons because majority of them are not knowing the procedures rather they



**Silpa G Nair and S.Sampath Kumar**

considers the human bodies as experiment objects. Government hospitals and medical colleges should be able to provide comprehensive health care for the community is an urgent need. WPATH (World Professional Association for Transgender Health) itself is clearly giving guidelines for creating a trans friendly atmosphere. One of their strong recommendations is patients active participation in decision making about their own health care with the support of health care professionals. This will result in inclusive policies without the imposing requirements for diagnosis, hormone therapy or surgery. Availability, accessibility, and acceptability of quality of health care is necessary. For getting an identity and recognition many are running behind surgeries without proper knowledge, doing risky jobs and ends in failed surgeries which badly affects their physical, mental as well as reproductive health. So, proper gender sensitization should be given to community as well as medical health practitioners. High priced surgeries, medical negligence, transphobia or transmisia, lack of access to government health care, inadequate medical insurance, etc., as the major obstacles in accessing the health care system. Effective implementation of transgender policy can make significant changes in the current scenario.

REFERENCES

1. Anagh. Analysing Transgender Persons (Protection of Rights) Bill 2019 in the context of NALSA Judgement. *Sambodhi* 2020; 43:4 13-14.
2. Bizic, M.R. et al. Gender Dysphoria: Bioethical Aspects of Medical Treatment, *BioMed Research International*. <https://www.hindawi.com/journals/bmri/2018/9652305/cta/2018>
3. Brindaalakshmi, K. Gendering of Development Data in India: Beyond the Binary #4 Digital Services and Data Challenges, The Centre for Internet and Society, <https://cis-india.org/raw/files/brindaalakshmi-k-gendering-of-development-data-in-india-beyond-the-binary-4> 2020(retrieved on 20 January 2022).
4. Ej, Ashfaque& Bhavani, Mrudula .Lack of expertise and government oversight endangers transgender people's gender affirmation, <https://caravanmagazine.in/gender/lack-of-expertise-government-oversight-support-endangers-transpeoples-gender-affirmation> 2021 (retrieved on 3rd February 2023).
5. E. Coleman. et.al. Standards of Care for the Health of Transgender and Gender Diverse People, Version 8, *International Journal of Transgender Health* 2022; 23:sup1, S1-S259, DOI:10.1080/26895269.2022.2100644
6. Gender – Affirmative Health Care in Kerala . Compiled Shilpa Menon for Queerala, an organisation for MalayaliLGBTIQ+Community, <http://queerala.org/gender-affirmative-healthcare-in-kerala-a-preliminary-report/2019>(retrievedon September 15,2022).
7. Jeffrey O'Malley et al. Sexual and gender minorities and the Sustainable Development Goals. United Nations Development Programme 2018.
8. Joy, J., & Nelson, V. Socio-demographic profile and challenges faced by the transgender community in Kollam district, Kerala-a clinic-based cross-sectional study. *Kerala Journal of Psychiatry* 2022;35(1), 58–63. <https://doi.org/10.30834/KJP.35.1.2022.327>.
9. Kurian & Manoj. (2021). Transgenders in the Mainstream: Welfare Schemes in Kerala – Kochi Metro Rail Project, Education Programme, Health Clinics, and Old-Age Pension *Indian Journal of Gender Studies* 2021; 28(2), 167-187. DOI: 10.1177/097152152199796
10. Murad, et al. Hormonal therapy and sex reassignment: A systematic review and meta analysis of quality of life and psychosocial outcomes, *Clinical Endocrinology* 2010; 72(2):214–231.
11. <https://onlinelibrary.wiley.com/doi/abs/10.1111/j.1365-265.2009.03625.x>.
12. Sinha, Sreoshi. Social exclusion of Transgender in the Civil Society: A Case study of the Transgender in KolKata, *IJHSS* 2016;3(2),178-190.
13. Sukumar S, Ullatil V, Asokan A. Transgender health care status in Kerala, *Indian J EndocrMetab* 2020;24:286.
14. Report of Kerala Transgender Survey 2014-2015, prepared by SANGAMA, an LGBT Rights Group.
15. Surya, Jisha. How Kerala Is A Long Way Off In Gender Affirmative Healthcare For Trans Persons 2021; <https://behanbox.com/2021/09/06/how-kerala-is-a-long-way-off-in-gender-affirmative-healthcare-for-trans-persons/>(retrievedon January 20,2023).





Silpa G Nair and S.Sampath Kumar

16. UNAIDS. *The Gap Report: gay men and other men who have sex with men*. http://www.unaids.org/sites/default/files/media_asset/07_Gaymenandothermenwhohavesexwithmen.pdf 2014.
17. Health dept. orders probe into transwoman's suicide (January 24, 2022), The Hindu Digital, <https://www.thehindu.com/news/national/kerala/health-dept-orders-probe-into-transwomans-suicide/article38319343.ece> (retrieved on February 17, 2022).
18. Controversy erupts over death of transwoman in Kochi (July 21, 2021), The Hindu Digital. <https://www.thehindu.com/news/national/kerala/controversy-erupts-over-death-of-transwoman-in-kochi/article35450279.ece> (retrieved on February 11, 2022).
19. 'Ananyah was pushed out of hospital twice', Kerala trans woman's father alleges (July 21, 2021), The News Minute, <https://www.thenewsminute.com/article/ananyah-was-pushed-out-hospital-twice-kerala-trans-woman-s-father-alleges-152733> (retrieved on January 2, 2023).
20. Ananyah's story isn't new: Kerala lacks support for trans persons undergoing surgery (August 7, 2021), The News Minute, <https://www.thenewsminute.com/article/ananyah-s-story-isn-t-new-kerala-lacks-support-trans-persons-undergoing-surgery-153592> (retrieved on February 17, 2022).
21. Six months after transgender Annanyah's suicide, Kerala govt orders probe, (January 24, 2022), <https://www.onmanorama.com/news/kerala/2022/01/24/six-months-after-transgender-ananyah-suicide-kerala-govt-orders-probe.html> (retrieved on February 17, 2022).





Assessment of Gene Action and Combining Ability in *Kharif Sorghum Landraces (Sorghum bicolor (L.) Moench) Utilizing Line x Tester Analysis*

N. Pugahendhi^{1*}, B. Sunil Kumar², Karnam Venkatesh³ and P. Rajendrakumar⁴

¹Research Scholar, Department of Genetics and Plant Breeding, Annamalai University, Annamalai Nagar- 608002, Tamil Nadu, India.

²Associate Professor, Department of Genetics and Plant Breeding, Annamalai University, Annamalai Nagar- 608002, Tamil Nadu, India.

³Senior Scientist, Genetics and Plant Breeding, ICAR-Indian Institute of Millets Research (IIMR), Hyderabad, Telangana, India.

⁴Principal Scientist, Department of Biotechnology, ICAR-Indian Institute of Millets Research (IIMR), Hyderabad, Telangana, India.

Received: 21 Sep 2023

Revised: 21 Nov 2023

Accepted: 02 Jan 2024

*Address for Correspondence

N. Pugahendhi

Research Scholar,

Department of Genetics and Plant Breeding,

Annamalai University,

Annamalai Nagar- 608002, Tamil Nadu, India.

Email: pugahendhi1126@gmail.com



This is an Open Access Journal / article distributed under the terms of the **Creative Commons Attribution License (CC BY-NC-ND 3.0)** which permits unrestricted use, distribution, and reproduction in any medium, provided the original work is properly cited. All rights reserved.

ABSTRACT

The present study aimed to evaluate the combining ability and gene action in parental lines and hybrids of *Kharif sorghum* landraces, focusing on grain yield and its associated traits. Employing the Line x Tester method, a total of 27 F₁s were generated by crossing nine female lines with three male lines. Data pertaining to twelve phenotypic traits were collected. Among the parental lines, EG 1, SEA 14, EG 54, ERN 26, and CSV 15 exhibited notable general combining abilities for grain yield and other associated traits. Crosses with significant specific combining ability (*sca*) often involve one parent with a high general combining ability (*gca*), resulting in elevated individual performance. Specifically, crosses like EG 1 x CSV 15, EG 54 x CSV 15, ERN 26 x CSV 15, and EG 2 x CSV 20 exhibited markedly higher grain yield and associated traits in a favorable direction, indicating their superior performance is attributed to non-allelic gene interactions. Additionally, SCA variances predominated over GCA variances for most characteristics, implying the prevalence of non-additive gene effects.

Keywords: kharif sorghum landraces, Combining ability, Gene Action, GCA, SCA.





Pugahendhi et al.,

INTRODUCTION

Sorghum (*Sorghum bicolor* L. Moench) is a diploid C4 grass species, a constituent of the Poaceae family. It is often cross-pollinated and possesses a chromosomal count of ($2n = 2x = 20$). The crop commonly known as the "Great Millet" holds significant importance as a grain in arid to semi-arid regions across the globe, contributing as a vital staple for the purpose of nourishing both humans and as sustenance for livestock. It originated in Africa and is now grown extensively in tropical and subtropical areas. In India, it was cultivated on 3.81 million hectares, yielding a total of 4.23 million metric tons during the year 2022 (Agricultural Statistics at a Glance 2022 of the Department of Agriculture, Cooperation, and Farmers Welfare). Sorghum is recognized as a highly nutritious grain due to its higher content of minerals and dietary fiber in contrast to rice and maize. Furthermore, it is notable that sorghum is a gluten-free cereal crop. Given its importance, advancing the development of this crop is crucial as it holds the potential to substantially influence the socioeconomic well-being of the population residing in India's drought-prone regions. Farmer's varieties, known as landraces, are widely acknowledged as the primary sources of genetic diversity [1]. These Indigenous populations possess a vital role as valuable reservoirs of variation that contribute to the efforts of breeders in creating enhanced cultivars known for improved yields, enhanced nutritional content, and increased resistance to diseases and climatic conditions [2]. Several statistical methods have been developed to gather insights into gene action and the mode of inheritance for various traits. Within these methodologies, the line x tester analysis [3] has found extensive application in genetic analysis across various crop species. This methodology serves as a highly efficient means to assess the combining ability and gene action of numerous inbred lines to adopt an appropriate breeding strategy. Therefore, this study aimed to assess the General Combining Ability (*gca*) and Specific Combining Ability (*sca*) while determining the mode of gene action for yield and yield-related traits in *Kharif* sorghum landrace to facilitate parental selection and improve germplasm for breeding programs, ultimately leading to an increase in production.

MATERIALS AND METHODS

The present investigation was conducted during the *Kharif* season of 2021-2022 at ICAR-Indian Institute of Millets Research in Hyderabad. The experimental material for this study comprised nine *Kharif* landraces as female parents and three-grain sorghum varieties as male parents, as detailed in Table 1. These parent lines were crossed using the Line x Tester mating design, resulting in the production of 27 new hybrids during the Rabi season of 2021-22. The hybrids were evaluated in Randomized Block Design with three replications for combining ability in *Kharif* 2022. Observations were recorded on five random but competitive plants for twelve characters viz., days to 50 percent flowering, plant height (cm), number of leaves, leaf length (cm), leaf width (cm), panicle length (cm), panicle width (cm), panicle length of primary branches (cm), stem diameter (cm), days to maturity, hundred seed weight (g) and grain yield per plant (g). Mean values were subjected to line x tester analysis to estimate general combining ability (*gca*) and specific combining ability (*sca*) effects and their respective variances as per the method suggested by [3].

RESULT AND DISCUSSION

The analysis of variance was conducted to evaluate the variability among the parental lines and crosses across twelve different traits. Significance was determined using the F-test. Details of the analysis of variance for these twelve traits, including replication mean square, genotype mean square, error mean square, and critical differences at 5% and 1%, are presented in (Table 2). The mean sum of squares attributed to genotypes exhibited high significance across all the studied traits, indicating the presence of substantial variability for both yield and yield-related characteristics within the examined material. It is worth noting that although parents may exhibit high *per se*, this may not necessarily be inherited by their progeny. Hence, calculating the combining ability of parents is crucial for





Pugahendhi et al.,

predicting their performance in hybrid combinations. The crosses were found to be significant for all the traits examined, a result in line with previous studies [4-6].

***gca* effects**

Parents were categorized as good, average, or poor combiners based on their general combining ability (*gca*) estimates. A summarized overview of the *gca* effects of parents for various traits is presented in Table 3. None of the parental lines exhibited good combining ability for all traits collectively, suggesting the need for different parents to enhance genetic improvement of various yield components. *gca* effects assist in identifying promising parents. Analysis of the *gca* effects for 12 parents (comprising 9 lines and 3 testers) across 12 traits revealed noteworthy findings. EG 2 exhibited favorable *gca* effects for traits such as plant height (89.38), number of leaves (0.69), leaf width (0.31), panicle length (2.03), and panicle width (0.51). EG 35 showed positive *gca* effects for days to 50% flowering (1.96), leaf length (3.07), panicle width (1.08), and hundred seed weight (0.1). EA 10 displayed favorable *gca* effects for six traits: plant height (35.27), number of leaves (0.78), leaf length (10.61), leaf width (0.35), stem diameter (0.21), and days to maturity (6.01). EG 1 demonstrated significant *gca* effects in a desirable direction for eight traits: plant height (50.54), leaf length (2.52), panicle length (4.38), panicle width (0.35), panicle length of primary branches (0.89), stem diameter (0.23), hundred seed weight (0.31), and grain yield per plant (15.21). Similarly, E 158 exhibited good *gca* effect for days to 50% flowering (5.85) and panicle length of primary branches (2.51).

SEA 14 displayed favorable *gca* for five traits: number of leaves (0.51), panicle width (0.64), hundred seed weight (0.14), and grain yield per plant (2.69). EG 54 showed promising *gca* effects for ten traits, including days to 50% flowering (6.19), number of leaves (0.75), leaf length (3.54), leaf width (0.38), panicle length (3.47), panicle width (1.00), panicle length of primary branches (0.31), stem diameter (0.22), hundred seed weight (0.33), and grain yield per plant (6.4). GGUB 61 exhibited good *gca* for plant height (8.29), number of leaves (0.44), and hundred seed weight (0.24), while ERN 26 displayed favorable *gca* for six traits: days to 50% flowering (2.07), leaf width (0.31), panicle length (2.07), panicle length of primary branches (0.66), days to maturity (3.46), and grain yield per plant (15.44). Among the male parents, CSV 20 showed good *gca* for two traits: plant height (3.86) and number of leaves (0.28). CSV 15 exhibited favorable *gca* for ten traits, including days to 50% flowering (3.19), number of leaves (0.65), leaf length (1.92), panicle length (2.69), panicle width (0.68), panicle length of primary branches (0.22), stem diameter (0.13), days to maturity (6.05), hundred seed weight (0.17), and grain yield per plant (6.1). CSV 27 displayed good GCA for leaf width (0.11), plant height (7.43), and stem diameter (0.08). These findings suggest that parents such as EG 1, SEA 14, EG 54, ERN 26, and CSV 15 possess a high concentration of favorable genes for yield and related traits, making them excellent combiners. They can be effectively utilized in breeding programs to develop kharif sorghum varieties/hybrids with desirable characteristics. These results align with previous studies [4,6,7-10].

***sca* effects**

In sorghum, negative specific combining ability (*sca*) effects are considered favorable for traits such as days to 50% flowering, and days to maturity. Among the 27 crosses evaluated, six hybrids for days to 50% flowering and nine hybrids for days to maturity exhibited notably high negative *sca* effects. Conversely, positive and significant *sca* effects were observed in twelve hybrids for plant height, five hybrids for number of leaves, nine hybrids for leaf length, three hybrids for leaf width, eleven hybrids for panicle length, nine hybrids for panicle width, twelve hybrids for panicle length of primary branches, twelve hybrids for stem diameter, seven hybrids for hundred seed weight, and nine hybrids for grain yield per plant (refer to Table 4).

Among these hybrids, EG 2 × CSV 20 demonstrated commendable *sca* effects for leaf length, leaf width, panicle width, panicle length of primary branches, stem diameter, and grain yield per plant. The cross EG 1 × CSV 15 exhibited favorable *sca* effects for days to 50% flowering, plant height, panicle length, panicle width, panicle length of primary branches, and grain yield per plant. Likewise, the hybrid EG 54 × CSV 15 displayed positive *sca* effects for days to 50% flowering, leaf length, panicle length, panicle length of primary branches, stem diameter, and seed yield per plant. Additionally, the cross ERN 26 × CSV 15 showcased noteworthy *sca* effects for the number of leaves, panicle length, panicle width, panicle length of primary branches, stem diameter, days to maturity, and grain yield





Pugahendhi et al.,

per plant. Hence, these four cross-combinations exhibit significant SCA effects for the desired traits. These findings align with previous studies [4,6,11-13].

Gene action

Combining ability analysis provides insights into the genetic mechanisms influencing the expression of various traits. This information guides the selection of appropriate breeding approaches for trait improvement. Crosses exhibiting superior performance on an individual basis, along with significant and desirable specific combining ability (*sca*) effects for various traits, involve combinations of good x good, good x average, good x poor, average x average, average x good, poor x good, and poor x average parents. For all the traits examined, crosses with noteworthy *sca* effects in the desired direction typically involve parents with high x high, high x low, or low x high general combining ability (*gca*) effects, suggesting that the high performance of these crosses arises from

additive, dominance, and epistatic gene interactions. The most promising cross combinations are those where both parents, or at least one of them, exhibit high magnitudes of both *sca* and *gca* effects.

Hence, the hybrids EG 1 x CSV 15, EG 54 x CSV 15, ERN 26 x CSV 15 exhibited high x high parental *gca* effects for grain yield per plant, indicating an additive x additive type of gene action that could be leveraged through heterosis breeding. Additionally, it was noted that positive alleles interacted in crosses involving high x high combiners, a condition that could be stabilized in subsequent generations unless repulsion-phase linkages are involved. Conversely, the cross EG 2 x CSV 20 for grain yield per plant exhibited low x low parental *gca* effects, signifying over-dominance and epistatic interactions. These findings align with the studies of [6,14-16]. The estimates of GCA and SCA variances, their ratios, and the inferred gene action are detailed in Table 5. It was observed that the magnitude of SCA variances exceeded that of GCA variances for all examined traits. These traits exhibit characteristics desirable for heterosis breeding and can be utilized in hybrid development. The ratio ($\delta 2GCA/\delta 2SCA$) was consistently less than the unity, indicating the prevalence of non-additive gene action. This aligns with prior research [16,17].

CONCLUSION

The analysis of variance for all the traits in this study yielded highly significant results. The parental lines in this study encompassed a diverse genetic background from their source populations, resulting in hybrids that demonstrated substantial specific combining ability effects. A significant portion of the crosses with notable specific combining ability effects involved combinations of either good x good or average x good general combiners for the majority of the traits under scrutiny. The coexistence of both additive and non-additive genetic effects suggests the potential for concurrent utilization of these gene actions through selective inter-mating and recurrent selection. From this study, it can be inferred that there is substantial room for improvement in yield per plant by strategically crossing divergent parents. These selected parents can then be further leveraged in hybridization programs to develop high-heterotic hybrids.

ACKNOWLEDGEMENT

I would like to begin by extending my gratitude to the ICAR-Indian Institute of Millets Research, Rajendranagar, Hyderabad, for providing the essential resources for my research endeavor. I take great pleasure in acknowledging the invaluable support and guidance of Dr. M. Elangovan, Principal Scientist at ICAR-Indian Institute of Millets Research. His dynamic mentorship, valuable suggestions, encouragement, and insightful approach to the subject were instrumental in the successful completion of this research.





REFERENCES

1. Ghebru, B., Schmidt, R. J., & Bennetzen, J. L. (2002). Genetic diversity of Eritrean sorghum landraces assessed with simple sequence repeats (SSR) markers. *Theoretical and Applied Genetics*, 105(2), 229-236.
2. Godwin, I. D., Rutkoski, J., Varshney, R. K., & Hickey, L. T. (2019). Technological perspectives for plant breeding. *Theoretical and Applied Genetics*, 132(2), 555-557. doi:10.1007/s00122-019-03321-4
3. Kempthorne, O. (1957). *An Introduction to General Statistics*. New York: John Wiley and Sons.
4. Vinoth, P., Selvi, B., Senthil, N., Iyanar, K., Jeyarani, S., & Santhiya, S. (2021). Estimation of gene action, combining ability and heterosis for yield and yield contributing traits in sorghum [*Sorghum bicolor* (L.) Moench]. *Electronic Journal of Plant Breeding*, 12(4), 1387-1397. doi:10.37992/2021.1204.190
5. More, A., Deosarkar, D. B., Mehtre, S. P., Dhutmal, R. R., & Kalpande, H. V. (2021). Combining ability analysis for grain yield and its contributing traits in sorghum (*Sorghum bicolor* (L.) Moench). *The Pharma Innovation Journal*, 10(9), 1967-1970.
6. Joshi, A. H., Gami, R. A., Patel, R. N., & Arvinth, S. (2022). Elucidation of gene action and combining ability for grain and fodder yield and contributing traits in sorghum [*Sorghum bicolor* (L.) Moench]. *Electronic Journal of Plant Breeding*, 13(1), 75-82. DOI: 10.37992/2022.1301.007.
7. Akata, E. A., Diatta, C., Faye, J. M., Diop, A., Maina, F., Sine, B., Tchala, W., Ndoye, I., Morris, G. P., & Cisse, N. (2017). Combining Ability and Heterotic Pattern in West African Sorghum Landraces. *African Crop Science Journal*, 25(4), 491-508. DOI: <http://dx.doi.org/10.4314/acsj.v25i4.7>
8. Gawande, S. M., Kalpande, V. V., & Gimare, V. B. (2020). Combining ability analysis for grain and fodder yield in post-rainy sorghum. *Journal of Pharmacognosy and Phytochemistry*, 9(5), 3076-3078.
9. Mangal, V., Ghorade, R. B., Thakare, D. P., & Kalpande, V. V. (2017). Identification of promising parents for grain yield and early maturity in kharif sorghum (*Sorghum bicolor* (L.) Moench). *International Journal of Current Microbiology and Applied Sciences*, 6(3), 1131-1136.
10. Prabhakar Bhat, Elangovan, M., & Bahadur, D. M. (2013). Combining ability of new parental lines for flowering, maturity, and grain yield in Rabi Sorghum. *Electronic Journal of Plant Breeding*, 4(3), 1214-1218.
11. Williams-Alanís, H., Aranda, U., Árcos Cavazos, G., Zavala Garcia, F., Galicia Juárez, M., Rodríguez Vázquez, M. del C., & Elizondo Barrón, J. (2022). Line x tester analysis to estimate combining ability in grain sorghum (*Sorghum bicolor* L.). *Revista De La Facultad De Ciencias Agrarias UNCuyo*, 54(2), 12-21. <https://doi.org/10.48162/rev.39.078>
12. El Kady, Y. M. Y., Abd Elraheem, O. A. Y., & Hafez, H. M. (2022). Combining ability and heterosis for agronomic and yield traits in some grain sorghum genotypes. *Egypt. J. Plant Breed.* 26(1), 59 – 74. Sorghum Research Department, Field Crop Research Institute, ARC, Egypt.
13. Wawkar, A. D., Kalpande, V. V., & Thawari, S. B. (2023). General combining ability analysis of newly developed parental lines in Kharif Sorghum [*Sorghum bicolor* (L.) Moench]. *The Pharma Innovation Journal*, 12(6), 3151-3155.
14. Meena, B. L., & Ranwah, B. R. (2020). General and specific combining ability in dual-purpose sorghum [*Sorghum bicolor* (L.) Moench]. *Journal of Pharmacognosy and Phytochemistry*, 9(5), 384-391. DOI: <https://doi.org/10.22271/phyto.2020.v9.i5f.12254>
15. El-Sherbeny, G. A. R., Khaled, A. G. A., Hovney, M. R. A., & Bahaa A. Zarea. (2019). Combining ability and gene action using Line by tester analysis on some new hybrids of grain sorghum under drought conditions. *PKV Research Journal*, 49(1), 118-129.
16. Sagheer, M. E. M. E.-., & Zarea, B. A. (2020). Genetic Components and Nature of Gene Action in Some New Hybrids of Grain Sorghum under Drought Conditions. *Asian Research Journal of Current Science*, 2(1), 68-79.
17. Kale, B. H., & Desai, R. T. (2016). Gene action studies over different environments in sorghum (*Sorghum bicolor* L. Moench). *Advances in Research Journal of Crop Improvement*, 7(1), 116-120. DOI: 10.15740/HAS/ARJCI/7.1/116-120





Pugahendhi et al.,

Table 1 List of genotypes that were utilized as parents

S. No.	Parents (Local Name)	Code	Accession No	IC Number
Lines				
1	ManjalCholam	L1	EG 2	IC 541309
2	SenkatanCholam	L2	EG 35	IC 541342
3	Irungu Cholam	L3	EA 10	IC 345252
4	PeriyaManjalCholam	L4	EG 1	IC 541308
5	Sundia	L5	E 158	IC 568375
6	Nandyal Tella Jonna	L6	SEA 14	IC-0627117
7	VailkattuCholam	L7	EG 54	IC 541361
8	Mehara Jowar	L8	GGUB 61	IC 319902
9	Solapuri	L9	ERN 26	IC 568541
Testers				
1	Grain sorghum variety	T1	CSV 20	-
2	Grain sorghum variety	T2	CSV 15	-
3	Grain sorghum variety	T3	CSV 27	-

Table 2 Analysis of variance for parents and crosses for twelve morphological traits in Kharif sorghum landraces.

Source of variation	d. f.	Days to 50% Flowering	Plant height (cm)	Number of leaves	Leaf Length (cm)	Leaf width (cm)	Panicle length (cm)	Panicle width (cm)	Panicle length of primary branches (cm)	Stem diameter (cm)	Days to maturity	Hundred seed weight (g)	Grain yield per plant (g)
Replication	2	8.83	24.15	0.23	0.79	0.05	0.11	0.03	0.03	0.004	4.54	0.009	2.22
Genotypes(G)	38	109.44*	8519.22**	8.27**	174.89**	2.67**	53.31**	4.60*	7.80**	0.441*	228.72**	0.468*	491.96**
Hybrids(H)	26	109.91*	10215.67**	4.85**	191.43**	2.75**	51.62**	5.51*	6.51**	0.336*	168.46**	0.388*	537.07**
Parents(P)	11	112.76*	5173.37**	16.15**	144.72**	2.46**	60.48**	2.66*	11.52*	0.630*	318.86**	0.591*	225.82**
Lines(L)	8	121.34*	6913.71**	20.37**	148.53**	2.80**	69.65**	3.56*	11.84*	0.641*	287.75**	0.588*	179.89**





Pugahendhi et al.,

Testers(T)	2	14.78	449.60	6.81**	95.69**	2.28**	2.83	0.03	1.26**	0.770*	116.77	0.052	68.92
LXT	16	46.54**	2184.98**	34.23**	159.62**	3.82**	14.12**	3.31*	2.81**	0.25**	96.32*	0.071*	142.62**
Error	76	4.07	32.34	0.26	4.06	0.04	0.54	0.12	0.03	0.005	6.83	0.005	3.93

**and* indicates significant at 1% and 5%, respectively.

Table 3 Estimates of general combining ability effects (gca) of lines and testers for twelve morphological traits.

Characters	Days to 50% Flowering	Plant height (cm)	Number of leaves	Leaf Length (cm)	Leaf width (cm)	Panic le length (cm)	Panic le width (cm)	Panic le length of primary branches (cm)	Stem diameter (cm)	Days to maturity	Hundr ed seed weight (g)	Grai n yiel d per plan t (g)
Lines												
EG 2	3.37 **	89.38 **	0.69 **	0.7	0.31 **	2.03 **	0.51 **	-0.58 **	0.02	-1.90*	-0.65 **	-3.21 **
EG 35	-1.96 **	-6.6 **	-0.76 **	3.07 **	-0.36 **	-3.86 **	1.08 **	-0.4 **	-0.21 **	1.43	0.1 **	-2.12 **
EA 10	-0.96	35.27 **	0.78 **	10.61 **	0.35 **	-0.35	-0.87 **	-0.16 *	0.21 **	-6.01**	0.1	0.02
EG 1	4.7 **	50.54 **	-0.47 **	2.52 **	-0.59 **	4.38 **	0.35 *	0.89 **	0.23 **	2.54**	0.31 **	15.21 **
E 158	-5.85 **	30.11 **	-1.78 **	-4.55 **	-0.27 **	-3.71 **	-0.94 **	2.51 **	0.05	-4.35**	-0.33 **	17.74 **
SEA 14	7.59 **	27.76 **	0.51 **	-4.62 **	0.02	0.07	0.64 **	-1.38 **	-0.12 **	4.43**	0.14 **	2.69 **
EG 54	-6.19 **	12.71 **	0.75 **	3.54 **	0.38 **	3.47 **	1 **	0.31 **	0.22 **	7.21**	0.33 **	6.4 **
GGUB 61	1.37 *	8.29 **	0.44 **	-3.9 **	-0.16 *	-4.11 **	-1.78 **	-1.85 **	-0.32 **	0.1	0.24 **	16.69 **
ERN 26	-2.07 **	106.29 **	-0.18	-7.36 **	0.31 **	2.07 **	0.02	0.66 **	-0.09 **	-3.46**	-0.14 **	15.44 **
Tester												
CSV 20	3.15 **	3.86 **	0.28 **	-0.97 *	-0.14 **	-0.32 *	-0.52 **	0.03	-0.21 **	2.99**	-0.02	-3.91 **
CSV 15	-3.19 **	11.29 **	0.65 **	1.92 **	0.04	2.69 **	0.68 **	0.22 **	0.13 **	-6.05**	0.17 **	6.1 **
CSV 27	0.04	7.43 **	-0.93 **	-0.95 *	0.11 *	-2.37 **	-0.16 *	-0.25 **	0.08 **	3.06**	-0.15 **	-2.19 **

** and * indicates significant at 1% and 5%, respectively





Pugahendhi et al.,

Table 4 Estimates of specific combining ability (*sca*) effects of crosses for twelve morphological traits.

Sr. No	Charact ers	Days to 50% Flowering	Plant height (cm)	Number of leaves	Leaf Length (cm)	Leaf width (cm)	Panicle length (cm)	Panicle width (cm)	Panicle length of primary branches (cm)	Stem diameter (cm)	Days to maturity	Hundred seed weight (g)	Grain yield per plant (g)
	Crosses												
1	EG 2XCSV 20	-1.59	30.19 **	0.27	3.83 **	0.85 **	0.83	0.85 **	0.54 **	0.33 **	4.12**	0.06	4.51 **
2	EG 2XCSV 15	2.07	- 66.34 **	-0.03	-1.85	0.08	-1.51 **	-1.54 **	-0.58 **	-0.57 **	- 4.84**	-0.1 *	- 8.73 **
3	EG 2XCSV2 7	-0.48	36.15 **	-0.24	-1.98	0.93 **	0.68	0.69 **	0.03	0.24 **	0.72	0.05	4.22 **
4	EG 35XCSV 20	-6.59 **	-5.44	-0.48	- 10.34 **	0.41 **	0.19	-1.53 **	0.63 **	-0.15 **	1.12	0.12 **	2.19
5	EG 35XCSV 15	7.41 **	14.58 **	0.75 **	10.77 **	1.14 **	-1.09 *	-0.65 **	-1.75 **	0.13 **	-1.17	-0.05	- 5.49 **
6	EG 35XCSV 27	-0.81	-9.14 **	-0.26	-0.43	0.73 **	0.9	2.18 **	1.12 **	0.01	0.05	-0.07	3.3 **
7	EA 10XCSV 20	-0.26	17.83 **	0.38	4.92 **	0.68 **	2.01 **	0.63 **	0.59 **	0.08	11.57* *	-0.34 **	- 3.43 **
8	EA 10XCSV 15	-1.93	17.91 **	-1.51 **	-3.96 **	-0.1	1.27 **	0.17	0.87 **	-0.12 **	- 6.73**	0.05	1.97
9	EA 10XCSV 27	2.19	- 35.74 **	1.13 **	-0.96	0.57 **	-3.28 **	-0.8 **	-1.46 **	0.04	- 4.84**	0.29 **	1.46
10	EG 1XCSV 20	4.41 **	12.89 **	-0.77 **	7.15 **	0.55 **	0.94 *	-0.2	-1.32 **	0.17 **	-2.32	0.11 *	- 3.15 *
11	EG 1XCSV 15	-4.93 **	8.26 *	0.33	-7.61 **	-1.5 **	1.47 **	0.48 *	1.42 **	0.06	4.38**	-0.01	2.61 *
12	EG 1XCSV2 7	0.52	- 21.15 **	0.44	0.46	0.95 **	-2.41 **	-0.28	-0.1	-0.23 **	-2.06	-0.1 *	0.53
13	E	3.3 **	-	0.07	-5.05	-2.5	-0.03	0.09	-0.21	0.14 **	-3.10*	0.01	4.01





Pugahendhi et al.,

	158XCS V 20		26.8 6 **		**	**							**
14	E 158XCS V 15	-2.37 *	16.7 5 **	0.24	0.93	1.32 **	-1.18 *	-0.23	0.27 *	-0.35 **	-3.06*	-0.05	- 7.66 **
15	E 158XCS V27	-0.93	10.1 **	-0.31	4.13 **	1.18 **	1.21 **	0.14	-0.06	0.2 **	6.16**	0.04	3.66 **
16	SEA 14XCSV 20	-4.15 **	- 14.4 1 **	1.25 **	4.35 **	0.41 **	-1.75 **	-0.02	0.48 **	-0.19 **	- 6.21**	0.12 **	0.04
17	SEA 14XCSV 15	4.19 **	1.33	-0.59 *	1.46	0.3 *	0.18	0.52 *	-0.78 **	0.37 **	6.49**	0.11 *	0.77
18	SEA 14XCSV 27	-0.04	13.0 8 **	-0.67 *	-5.81 **	- 0.71 **	1.57 **	-0.51 *	0.3 **	-0.18 **	-0.28	-0.23 **	- 0.81
19	EG 54XCSV 20	1.63	-1.86	-0.39	-0.14	0.45 **	1.85 **	0.89 **	-0.08	-0.23 **	-0.32	0.05	- 3.57 **
20	EG 54XCSV 15	-2.37 *	- 10.7 8 **	0.44	8.97 **	- 0.72 **	1.11 *	0.43	0.4 **	0.13 **	3.38*	-0.01	14.1 6 **
21	EG 54XCSV 27	0.74	12.6 4 **	-0.04	-8.83 **	0.27 *	-2.97 **	-1.33 **	-0.32 **	0.1 *	-3.06*	-0.04	- 10.5 9 **
22	GGUB 61XCSV 20	-0.93	-5.72	0.72 *	-6.63 **	0.65 **	-1.23 **	-0.73 **	0.01	0.09	-6.21*	-0.07	4.39 **
23	GGUB 61XCSV 15	-0.26	13.5 5 **	-0.59 *	-3.38 **	- 0.66 **	-1.44 **	0.15	-0.51 **	0.23 **	4.83**	0.11 *	- 5.65 **
24	GGUB 61XCSV 27	1.19	-7.83 *	-0.13	10.02 **	0.1	2.68 **	0.58 *	0.5 **	-0.32 **	1.38	-0.04	1.27
25	ERN 26XCSV 20	4.19 **	-6.61 *	-1.06 **	1.92	- 0.68 **	-2.81 **	0.1	-0.63 **	-0.25 **	1.35	-0.05	- 4.98 **
26	ERN 26XCSV 15	-1.81	4.73	0.97 **	-5.33 **	0.14	1.18 *	0.68 **	0.65 **	0.11 *	-3.28*	-0.04	8.01 **
27	ERN 26XCSV 27	-2.37 *	1.88	0.09	3.4 **	0.54 **	1.63 **	-0.68 **	-0.01	0.14 **	1.94	0.09 *	- 3.03 *

** and * indicates significant at 1% and 5%, respectively.





Pugahendhi et al.,

Table 5 Estimation of gene action (GCA and SCA) for twelve morphological traits.

Characters	GCA	SCA	GCA/ SCA	Gene action
Days to 50% flowering	1.3075	53.141	0.0246	Non-additive
Plant height	165.712	718.1584	0.2307	Non-additive
Number of leaves per plant	0.056	2.8698	0.0195	Non-additive
Leaf length	0.6564	54.7508	0.0119	Non-additive
Leaf width	-0.0224	0.6313	-0.0354	Non-additive
Panicle length	0.7739	29.8446	0.0259	Non-additive
Panicle width	0.0452	2.3209	0.0194	Non-additive
Panicle length of primary branches	0.0762	2.0014	0.0380	Non-additive
Stem Diameter	0.0017	0.1633	0.0104	Non-additive
Days to maturity	1.4887	30.14	0.0493	Non-additive
Hundred seed weight	0.0065	0.1736	0.0374	Non-additive
Grain yield per plant	8.1393	224.757	0.0362	Non-additive





Impact of Brick Kiln Industry on Health Status across Different Age Groups in Budgam District of Jammu and Kashmir: A Sociological Study

Shamweel Iqbal Dar^{1*} and S. Subramani²

¹Research Scholar, Department of Sociology, Annamalai University, Annamalai Nagar, Tamil Nadu, India.

²Assistant Professor, Department of Sociology, Annamalai University, Annamalai Nagar, Tamil Nadu, India.

Received: 19 Aug 2023

Revised: 16 Nov 2023

Accepted: 13 Jan 2024

*Address for Correspondence

Shamweel Iqbal Dar,

Research Scholar,

Department of Sociology,

Annamalai University, Annamalai Nagar,

Tamil Nadu, India.

E mail: shamweel999@gmail.com



This is an Open Access Journal / article distributed under the terms of the **Creative Commons Attribution License** (CC BY-NC-ND 3.0) which permits unrestricted use, distribution, and reproduction in any medium, provided the original work is properly cited. All rights reserved.

ABSTRACT

This study presents an in-depth analysis of age-wise ratings for various health indicators in relation to the impact of the brick kiln industry on individuals' health status. The data encompasses three distinct age groups: 15-25 years, 26-35 years, and above 35 years. The interpreted findings reveal patterns and nuances in how different age groups perceive the effects of brick kiln emissions on their health. The data indicates that perceptions of health impacts vary across different age groups. Older individuals tend to perceive a slightly higher impact of the brick kiln industry on health indicators such as abdominal pain and bronchitis symptoms. In contrast, younger individuals report higher perceptions of impacts on throat infections and irritation of the nose and throat. Middle-aged individuals exhibit heightened perceptions of impacts on skin diseases and loss of appetite. Additionally, the study highlights that certain health indicators, like cough and fatigue, show increased impact perceptions with age, while others, such as shortness of breath and eye irritation, display more consistent patterns. The overall mean ratings across age groups suggest that respondents generally perceive moderate impacts of brick kiln emissions on health. These findings underscore the significance of understanding age-related vulnerabilities and susceptibilities in assessing the impact of environmental factors on public health. Tailored interventions, environmental regulations, and healthcare strategies that consider these age-specific variations can lead to more effective mitigation measures and improved well-being. This study contributes to the broader understanding of the intricate relationship between environmental exposures and health outcomes within different age groups.



**Shamweel Iqbal Dar and Subramani**

Keywords: Brick kiln industry, health indicators, age-wise ratings, environmental impact, individuals' health, perceptions, respiratory symptoms, environmental exposures, vulnerability, public health, age groups.

INTRODUCTION

The brick kiln industry plays a crucial role in construction and infrastructure development. However, it is also known to emit pollutants that can have adverse effects on human health. The brick kiln industry, characterized by the firing of clay bricks at high temperatures, is a widespread practice, particularly prominent in South Asian countries. However, it often operates within an informal and unregulated framework, predominantly relying on small-scale, traditional kilns. These kilns, typically fuelled by wood, coal, or other sources, emit copious quantities of smoke, dust, and various pollutants. The emissions stemming from brick kilns encompass both particulate matter and gaseous pollutants, encompassing sulphur dioxide (SO₂), nitrogen oxides (NO_x), carbon monoxide (CO), volatile organic compounds (VOCs), and polycyclic aromatic hydrocarbons (PAHs). These pollutants yield a spectrum of impacts on human health, with one of the most widely acknowledged consequences being respiratory ailments. The blend of particulate matter and other emissions from brick kilns is associated with respiratory disorders such as asthma, chronic bronchitis, and lung cancer. Studies such as Singh *et al.* (2016) have disclosed significantly higher respiratory symptom rates among brick kiln workers compared to control groups, further associating these symptoms with exposure to particulate matter and other pollutants.

Similarly, research in Pakistan, exemplified by Siddiqui *et al.* (2016), has underscored an elevated prevalence of respiratory diseases among residents residing in close proximity to brick kilns. As understanding evolves, it has become apparent that brick kiln emissions also elevate the risk of cardiovascular afflictions. Research from India, as demonstrated by Sahu *et al.* (2016), has correlated exposure to particulate matter from brick kilns with heightened blood pressure and other cardiovascular risk markers. In a similar vein, a study conducted in Pakistan and documented by Khan *et al.* (2019) has identified an association between brick kiln emissions and increased hypertension rates. The implications extend to the realm of cancer risk, particularly linked to the presence of polycyclic aromatic hydrocarbons (PAHs) resulting from incomplete combustion within kilns. Studies from China (Yang *et al.*, 2015) and India (Mishra *et al.*, 2017) have illuminated the heightened presence of PAHs in individuals residing or working in proximity to brick kilns, showcasing an augmented risk of lung cancer and other malignancies.

The labour conditions in brick kilns typically lean towards the austere, often subjecting workers to intense heat, smoke, and dust. Such circumstances readily precipitate heat stress, dehydration, and a range of occupational health challenges. Additionally, the reliance on manual labour and outdated technologies in many kilns exposes workers to potential physical injuries and accidents, as highlighted in research by Mahmood *et al.* (2020). Beyond the direct health ramifications, brick kiln emissions have been associated with an array of other health issues, spanning from eye irritation and skin rashes to neurological impacts (Siddiqui *et al.*, 2016). Furthermore, the pollutants discharged from brick kilns can indirectly contribute to broader health implications, such as climate change-related phenomena, including heat waves, flooding, and extreme weather events.

MATERIALS AND METHODS

The study was conducted using a survey method, employing a structured questionnaire for data collection. The survey was carried out via personal interviews with respondents residing in the vicinity of selected brick kiln industries within a 2-kilometer radius. The study area comprised three villages: Panzan, Lalagam, and Gund Sathu, located in the Budgam district of Jammu and Kashmir, India. The brick kiln cluster was chosen using a simple random sampling technique from a pool of 300 brick kiln clusters within the Budgam district.



**Shamweel Iqbal Dar and Subramani**

Upon completion of the survey, the collected data was meticulously documented in a master sheet, subsequently compiled, tabulated, and subjected to analysis. To facilitate analysis, the data was processed using Microsoft Excel, allowing for comprehensive interpretation and insights.

Survey Process

A total of 350 individuals were randomly selected from the population of 3500 individuals residing in the vicinity of the brick kiln cluster. Various occupations were represented in the sample. The aim was to gather people's perceptions and understanding of different health-related issues and the impacts stemming from emissions produced by the brick kilns. A structured interview approach was employed to collect pertinent data for the study. The interview used a Likert scale with a 5-point rating system. The survey included straightforward questions designed to elicit the opinions of the respondents. To align with the study's objectives, an interview schedule was initially drafted. Before implementing the survey, a pre-test was conducted with 90 respondents residing near the brick kiln cluster within the study area. Based on the results of this pre-test, necessary adjustments, additions, and modifications were made to the interview schedule. The refined interview schedule, incorporating changes from the pre-test, was then finalized and printed for use in the main survey.

REVIEW OF LITERATURE

Numerous studies have investigated the environmental and health impacts of brick kiln operations in various regions, shedding light on the multifaceted challenges posed by this industry. Joshi (2008) conducted a comprehensive analysis of the Kathmandu valley, revealing concerns about respiratory discomfort and respiratory problems among individuals exposed to brick kiln emissions. Guttikunda and Goel (2013) highlighted severe air pollution issues in Delhi, linking high levels of particulate matter to thousands of premature deaths and millions of asthma attacks annually. They emphasized the urgency of interventions to mitigate these health impacts. Joshiet *al.* (2014) explored work-related injuries and musculoskeletal disorders among child workers in Nepal's brick kilns, underlining the poor working conditions and lack of safety measures that put these children at risk.

Rumanaet *al.* (2014) assessed air pollution's threat to human health in India, particularly in urban areas where pollutants exceeded safe levels. They underscored the need for preventive measures to mitigate health risks associated with pollutants like PM10, PM2.5, NOx, and SO2. Rafiq and Khan (2014) examined the potential benefits of reducing ambient air pollution, advocating for governmental actions to address this issue and offering recommendations for better practices. Jahanet *al.* (2016) focused on reproductive health and biochemical status in brick kiln workers in Pakistan, highlighting the need for alternative technologies and improved working conditions. Sanjelet *al.* (2017) investigated respiratory symptoms and dust exposure among Nepalese brick kiln workers, revealing a connection between high dust exposures and increased respiratory issues. Haqueet *al.* (2017) analyzed air quality in Kolkata and associated health impacts, emphasizing the prevalence of respiratory diseases in high-pollution areas. Kesarwani and James (2017) pointed out the negative impact of cement industry emissions on human health, emphasizing the need for cleaner technologies and pollution control measures.

Tusheret *al.* (2018) delved into the health effects of brick kiln operations in Bangladesh, finding skin diseases, headache, eye irritation, and various respiratory issues prevalent among both workers and inhabitants. They stressed the importance of eco-friendly kilns and safety measures for workers and residents. Collectively, these studies underscore the urgent need for better regulation, cleaner technologies, and improved working conditions in the brick kiln industry to safeguard both the environment and public health. One of the most significant social impacts of the brick-making industry on communities is the adverse health effects caused by air pollution from brick kilns. The industry is a major source of air pollution, emitting high levels of particulate matter, carbon monoxide, sulfur dioxide, and nitrogen oxides into the atmosphere. Exposure to such pollutants has been linked to numerous health problems, including respiratory diseases, asthma, and lung cancer (Guttikunda and Jawahar, 2014). A study conducted by the Indian Institute of Technology, Delhi, found that brick kilns are responsible for 10-15% of the total





Shamweel Iqbal Dar and Subramani

particulate matter emissions in the National Capital Region, leading to severe respiratory and cardiovascular problems (Sharma *et al.*, 2019).

METHODOLOGY

Data Collection: Participants in three age groups (15-25 years, 26-35 years, above 35 years) were surveyed for their health status indicators in relation to exposure to brick kiln emissions. A Likert scale was used to rate the severity of each health indicator, ranging from 1 (low impact) to 5 (high impact).

RESULTS

Age wise rating to the impact of Brick kiln industry on their Health Status.

VARIABLES	15-25 Years	26-35 Years	Above 35 Years	Mean
Abdominal pain	2.43	2.54	2.71	2.56
Skin diseases	2.41	2.64	2.45	2.5
Bronchitis	1.77	1.88	2.29	1.98
Throat Infection	2.58	2.39	2.38	2.45
Cough	2.73	2.89	3.26	2.96
Shortness of breath	1.78	1.97	2.16	1.97
Irritation of nose and throat	2.52	2.39	2.29	2.4
Loss of Appetite	1.61	1.89	2.05	1.85
Headache	2.4	2.76	2.94	2.7
Fatigue	2.86	3.09	3.2	3.05
Eye Irritation	3.2	3.3	3.25	3.25
Dizziness	2.62	2.98	2.95	2.85
Vomiting	2.38	2.71	2.86	2.65
AVERAGE	2.40	2.57	2.67	2.55

Primary Source (Table-1)

The provided data presents the age-wise ratings for various health indicators in relation to the impact of the brick kiln industry on individuals' health status. The age groups considered are 15-25 years, 26-35 years, and above 35 years.

The following interpretation breaks down the data in detail:

The average rating for abdominal pain with age, from 2.43 on a 5 point rating scale in the 15-25 years group to 2.71 on a 5 point rating scale in the above 35 years group. This suggests that older individuals perceive a slightly higher impact of the brick kiln industry on abdominal pain compared to younger individuals. The overall mean rating for abdominal pain across all age groups is 2.56. Similar to abdominal pain, the average rating for skin diseases shows a slight increase with age, from 2.41 to 2.64 to 2.45 on a 5 point rating scale. This indicates that individuals in the middle age group (25-35 years) report the highest impact of skin diseases. The overall mean rating for skin diseases across all age groups is 2.5 on 5 point rating scale. The average rating for bronchitis is lowest in the 15-25 years group (1.77) on a 5 point rating scale and highest in the above 35 years group (2.29) on a 5 point rating scale. This suggests that older individuals perceive a more significant impact of the brick kiln industry on bronchitis symptoms. The overall mean rating for bronchitis across all age groups is 1.98 on a 5 point rating scale. The highest average rating for throat infection is in the 15-25 years group (2.58) on a 5 point rating scale, followed by the above 35 years group (2.38) and the 25-35 years group (2.39) on a 5 point rating scale. This implies that younger individuals experience a slightly higher impact of throat infections due to the brick kiln industry. The overall mean rating for throat infection across all age groups is 2.45 on a 5 point rating scale. The impact of cough is highest in the above 35 years group (3.26), followed by the 25-35 years group (2.89) and the 15-25 years group (2.73) on a 5 point rating scale. Older



**Shamweel Iqbal Dar and Subramani**

individuals report a significantly higher impact of cough symptoms in relation to the brick kiln industry. The overall mean rating for cough across all age groups is 2.96 on a 5 point rating scale. Shortness of breath ratings are lowest in the 15-25 years group (1.78) and slightly increase with age. The overall mean rating for shortness of breath across all age groups is 1.97 on a 5 point rating scale. The highest average rating for irritation of nose and throat is in the 15-25 years group (2.52), followed by the above 35 years group (2.29) and the 25-35 years group (2.39) on a 5 point rating scale. This indicates that younger individuals perceive a more significant impact on irritation of the nose and throat. The overall mean rating for irritation of nose and throat across all age groups is 2.4 on a 5 point rating scale.

The impact of loss of appetite slightly increases with age, with the highest average rating in the above 35 years group (2.05). The overall mean rating for loss of appetite across all age groups is 1.85 on a 5 point rating scale. Headache ratings increase with age, with the highest average rating in the above 35 years group (2.94). The overall mean rating for headache across all age groups is 2.7 on a 5 point rating scale. The impact of fatigue is highest in the above 35 years group (3.2), followed by the 25-35 years group (3.09) and the 15-25 years group (2.86) on a 5 point rating scale. Older individuals report a significantly higher impact of fatigue symptoms due to the brick kiln industry. The overall mean rating for fatigue across all age groups is 3.05 on a 5 point rating scale. Eye irritation ratings are fairly consistent across age groups, with the highest average rating in the 25-35 years group (3.3). The overall mean rating for eye irritation across all age groups is 3.25 on a 5 point rating scale. Dizziness ratings are highest in the 25-35 years group (2.98), followed by the above 35 years group (2.95) and the 15-25 years group (2.62). The overall mean rating for dizziness across all age groups is 2.85 on a 5 point rating scale. The impact of vomiting symptoms slightly increases with age, with the highest average rating in the above 35 years group (2.86). The overall mean rating for vomiting across all age groups is 2.65 on a 5 point rating scale.

DISCUSSION

The provided data offers an insightful breakdown of age-wise ratings for various health indicators concerning the impact of the brick kiln industry on individuals' health. The interpretation highlights distinct trends in how different age groups perceive the effects of brick kiln emissions on their health. Let's delve into a discussion of these findings: The data shows a slight increase in the average rating for abdominal pain with age, indicating that older individuals (above 35 years) perceive a slightly higher impact of the brick kiln industry on this health issue compared to younger individuals (15-25 years). This could be attributed to the fact that older people might have a higher sensitivity to environmental factors due to age-related health changes. The overall mean rating for abdominal pain across all age groups is 2.56, suggesting that, on average, respondents believe the brick kiln emissions contribute to moderate abdominal pain. The ratings for skin diseases show a nuanced pattern, with the middle age group (26-35 years) reporting the highest impact. This could be due to a combination of factors, including increased exposure to pollutants for people in this age range who might be working near the brick kilns. The overall mean rating for skin diseases is 2.5, indicating a moderate perception of the impact of brick kiln emissions on skin health across all age groups. The data highlights that older individuals perceive a more significant impact of the brick kiln industry on bronchitis symptoms. This aligns with common medical knowledge that older individuals are generally more susceptible to respiratory issues. The overall mean rating for bronchitis across all age groups is 1.98, indicating a relatively lower perception of the impact on bronchitis symptoms. Interestingly, younger individuals (15-25 years) report a slightly higher impact of throat infections due to the brick kiln industry compared to other age groups. This could be because younger people might spend more time outdoors or have different lifestyle patterns. The overall mean rating for throat infection is 2.45, suggesting a moderate impact across all age groups. Older individuals perceive a significantly higher impact of cough symptoms related to the brick kiln industry. This could be attributed to the fact that respiratory symptoms tend to worsen with age and that older individuals might have reduced respiratory resilience. The overall mean rating for cough is 2.96, indicating a moderate perception of the impact on cough symptoms.



**Shamweel Iqbal Dar and Subramani**

Shortness of breath ratings slightly increase with age, which could be due to the cumulative effects of exposure to pollutants over time. The overall mean rating for shortness of breath is 1.97, suggesting a relatively low perception of the impact on this symptom. Younger individuals (15-25 years) perceive a more significant impact on irritation of the nose and throat, possibly due to their greater outdoor activities and potentially higher exposure. The overall mean rating for irritation of nose and throat is 2.4, indicating a moderate impact across all age groups. Other symptoms like loss of appetite, headache, fatigue, eye irritation, dizziness, and vomiting exhibit various patterns with age, indicating that the impact of these symptoms could be influenced by individual susceptibility, lifestyle, and exposure levels.

CONCLUSION

In conclusion, the comprehensive analysis of age-wise health indicator ratings sheds light on the nuanced and multifaceted nature of the impact of the brick kiln industry on individuals' health. The study revealed distinct trends in how different age groups perceive and experience health issues associated with brick kiln emissions. This exploration offers valuable insights into the complex interplay between age, environmental exposure, and health outcomes.

The findings of this study highlight several key observations:

Age-Dependent Variations: The perceptions of health impacts exhibited significant variations across different age groups. Older individuals consistently reported higher perceptions of impacts on respiratory symptoms like bronchitis, cough, and shortness of breath. This aligns with established medical knowledge that older age often comes with increased vulnerability to respiratory ailments due to physiological changes and cumulative exposure.

Youth and Respiratory Sensitivity: Surprisingly, the younger age group (15-25 years) reported higher perceptions of impacts on throat infections and irritation of the nose and throat. This suggests that despite potentially having healthier respiratory systems, younger individuals might be particularly sensitive to certain pollutants emitted by brick kilns. Their higher outdoor activity levels or prolonged exposure might contribute to these findings.

Middle Age Group Dynamics: The middle age group (26-35 years) exhibited higher perceptions of impacts on skin diseases and loss of appetite. This age bracket, often actively engaged in work and outdoor activities, might experience more direct exposure to environmental pollutants, leading to a greater perceived impact on these health aspects.

Symptom-Specific Considerations: Some health indicators, such as headache, fatigue, eye irritation, dizziness, and vomiting, displayed varying patterns with age. These discrepancies underline the multifaceted nature of health impacts and highlight the interplay of individual susceptibility, lifestyle, and environmental exposure.

Overall Perception: The overall mean ratings for most health indicators fell within the moderate range on the 5-point rating scale. This suggests that while individuals perceive impacts, they may not universally categorize them as severe. These findings might reflect a balance between individual health experiences and external influences.

The findings of this study have implications for both public health interventions and policy decisions:

Tailored Interventions: The variation in age-wise perceptions of health impacts emphasizes the need for tailored interventions. Different age groups might benefit from specific awareness campaigns, preventive measures, and health education initiatives addressing their unique susceptibilities.

Environmental Regulations: Policymakers and regulatory bodies should consider the susceptibility of different age groups when designing and enforcing environmental regulations. Stricter regulations around emissions from brick kilns could significantly alleviate health concerns, especially among vulnerable populations.

Healthcare Strategies: Healthcare providers should be attuned to the varying health concerns of different age groups. This understanding can aid in accurate diagnosis, targeted treatment, and management of symptoms related to environmental exposures.

Continued Research: The study provides a foundation for further research exploring the underlying mechanisms driving age-dependent variations in health impacts. Longitudinal studies could offer insights into how these perceptions evolve over time and contribute to more robust public health strategies.





Shamweel Iqbal Dar and Subramani

In essence, the age-wise analysis of health indicator ratings in relation to the impact of the brick kiln industry on health underscores the intricate relationship between environmental factors and public well-being. Acknowledging these variations can lead to more effective mitigation strategies, improved health outcomes, and a greater understanding of the interconnections between human health and the environment.

REFERENCES

1. Kumar, K., & Kumar, A. (2020). Sustainable use and applications of brick kiln coal fly ash in agriculture sector for promotion of legume productivity. *Plant Archives*, 20(2), 3571-3579.
2. Ma, S., & Eivin, R. (2021). Impact of emissions from brick industries on soil properties, agricultural crops and homegardens in Chittagong, Bangladesh. *Journal of Soil Science and Environmental Management*, 12(4), 159-172.
3. Chowdhury, N., & Rasid, M. M. (2020). Assessment of Soil Fertility and Crop Nutrient Status in Agricultural Soils Near a Brick Kiln Cluster. *Journal of Agricultural Science*, 13(1), 122.
4. Joshi, S. K., Dahal, P., Poudel, A., & Sherpa, H. (2013). Work related injuries and musculoskeletal disorders among child workers in the brick kilns of Nepal. *International Journal of Occupational Safety and Health*, 3(2), 2-7.
5. Guttikunda, S. K., & Goel, R. (2013). Health impacts of particulate pollution in a megacity—Delhi, India. *Environmental Development*, 6, 8-20.
6. Joshi, S. K., Dahal, P., Poudel, A., & Sherpa, H. (2013). Work related injuries and musculoskeletal disorders among child workers in the brick kilns of Nepal. *International Journal of Occupational Safety and Health*, 3(2), 2-7..
7. Rumana, H. S., Sharma, R. C., Beniwal, V., & Sharma, A. K. (2014). A retrospective approach to assess human health risks associated with growing air pollution in urbanized area of Thar Desert, western Rajasthan, India. *Journal of Environmental Health Science and Engineering*, 12, 1-9.
8. Rafiq, M., & Khan, M. (2014). The health costs of the brick kilns emissions in Peshawar: A policy analysis. *Curr World Environ*, 9(3), 591-601.
9. Jahan, S., Falah, S., Ullah, H., Ullah, A., & Rauf, N. (2016). Antioxidant enzymes status and reproductive health of adult male workers exposed to brick kiln pollutants in Pakistan. *Environmental Science and Pollution Research*, 23, 12932-12940.
10. Sanjel, S., Khanal, S. N., Thygerson, S. M., Carter, W. S., Johnston, J. D., & Joshi, S. K. (2017). Respiratory symptoms and illnesses related to the concentration of airborne particulate matter among brick kiln workers in Kathmandu valley, Nepal. *Annals of occupational and environmental medicine*, 29, 1-12.
11. Haque, M. S., & Singh, R. B. (2017). Air pollution and human health in Kolkata, India: A case study. *Climate*, 5(4), 77.
12. Kesarwani, S., & James, A. (2017). Effect of air pollution on human health problems residents living around the cement plant, Chandrapur, Maharashtra, India. *Journal of Pharmacognosy and Phytochemistry*, 6(5), 507-510
13. Tusher, T. R., Ashraf, Z., & Akter, S. (2018). Health effects of brick kiln operations: a study on largest brick kiln cluster in Bangladesh. *South East Asia Journal of Public Health*, 8(1), 32-36.
14. Jain, P., & Bansal, S. (n.d.). *Brick Kilns, Anemia & Residential Proximity: Evidence from Bihar*.
15. Thakur, M., & Pathania, D. (2020). Environmental fate of organic pollutants and effect on human health. In *Abatement of Environmental Pollutants* (pp. 245-262). Elsevier.
16. Raza, A., & Ali, Z. (2021). Impact of air pollution generated by brick kilns on the pulmonary health of workers. *Journal of Health Pollution*, 11(31), 210906.
17. Nasir, M., Rehman, F. U., Kishwar, S., Bashir, S., & Adil, M. (2021). Air pollution and child health: the impact of brick kiln pollution on children's cognitive abilities and physical health in Pakistan. *Environment, Development and Sustainability*, 23, 13590-13606.
18. Raza, A., & Ali, Z. (2021). Impact of Air Pollution Generated by Brick Kilns on the Pulmonary Health of Workers. *Journal of Health and Pollution*, 11(31), 210906.
19. Behrooz, R. D., Kaskaoutis, D. G., Grivas, G., & Mihalopoulos, N. (2021). Human health risk assessment for toxic elements in the extreme ambient dust conditions observed in Sistan, Iran. *Chemosphere*, 262, 127835.





Shamweel Iqbal Dar and Subramani

19. Subhanullah, M., Ullah, S., Javed, M. F., Ullah, R., Akbar, T. A., Ullah, W., ...&Sajjad, R. U. (2022). Assessment and Impacts of Air Pollution from Brick Kilns on Public Health in Northern Pakistan. *Atmosphere*, 13(8), 1231.
20. David, M., Jahan, S., Hussain, J., Rehman, H., Cloete, K. J., Afsar, T., ...&Razak, S. (2022). Biochemical and reproductive biomarker analysis to study the consequences of heavy metal burden on health profile of male brick kiln workers. *Scientific Reports*, 12(1), 7172.
21. Shahriyari, H. A., Nikmanesh, Y., Jalali, S., Tahery, N., ZhianiFard, A., Hatamzadeh, N.,& Mohammadi, M. J. (2022). Air pollution and human health risks: mechanisms and clinical manifestations of cardiovascular and respiratory diseases. *Toxin Reviews*, 41(2), 606-617.





Exploratory Study on Detection of Urease in Locally Available Plant Sources

Devaraj Panda¹, Sarat Chandra Nayak² and Bandita Panda*

¹Principal Scientist (Retd.), Division of Soil Sciences, ICAR- National Rice Research Institute, Cuttack, Odisha, India

²Senior Scientist, Orissa University of Agriculture and Technology, Bhubaneswar, Odisha

*Research Scientist- Clinical Proteomics and Genomics, Scientific Officer, Research and Development Department, KIMS- Kalinga Institute of Medical Sciences, KIIT Deemed University, Patia, Bhubaneswar, Odisha, India

Received: 29 Sep 2023

Revised: 25 Nov 2023

Accepted: 08 Jan 2024

*Address for Correspondence

Bandita Panda,

Research Scientist- Clinical Proteomics and Genomics,
Scientific Officer, Research and Development Department,
KIMS- Kalinga Institute of Medical Sciences,
KIIT Deemed University, Patia,
Bhubaneswar, Odisha, India
E mail: banditapanda12@gmail.com



This is an Open Access Journal / article distributed under the terms of the **Creative Commons Attribution License** (CC BY-NC-ND 3.0) which permits unrestricted use, distribution, and reproduction in any medium, provided the original work is properly cited. All rights reserved.

ABSTRACT

Urease is a nickel-containing metalloenzyme that is mostly found in plants, microbes, and in some invertebrates. An exploratory study was conducted to detect urease in seeds of eleven indigenous leguminous plants viz. Peas, chickpea, horse-gram, pigeon-pea, green-gram, lentil, cowpea, green gram, lentil, cowpea, soybean, black-gram and two species of Dhaincha (*Sesbania aculeata* and *S.rostrata*), Besides, attempts were also made to detect urease, if any, in oilcake of groundnut and green matter of Dhaincha and gliricidia. Urease was extracted from each of these plant materials using distilled water as the extractant because urease is soluble in water. These aqueous extracts of urease were then used in hydrolysis of a measured quantity of chemically pure urea in the presence and absence of potassium phosphate buffer (pH 8.0). On hydrolysis, urea was converted into ammonia. The resultant ammoniacal-N was quantitatively determined by the semi-microkjeldahl steam distillation method. The results obtained from the experiment revealed that the aqueous extracts obtained from seeds of only three leguminous plant sources viz. horse-gram (*Dolichus biflorus*), pigeon-pea (*Cajanus cajan*) and soybean (*Glycine max*) hydrolyzed the entire amount of urea in two hours. But the extracts of the other plant sources such as green gram, lentil, cowpea, peas, chick-pea, black gram, Dhaincha and gliricidia partly or negligibly hydrolyzed the urea. Three indigenous leguminous plant sources viz. Seeds of horse-gram, pigeon-pea, and soybean are suggested to be utilized for the isolation of urease, their crystallization and

69478



Devaraj Panda *et al.*,

characterization of crystalline urease in future research and product development strategies to meet the increasing demand for urease crystals in healthcare and other sectors.

Keywords: Urease, urea hydrolysis, leguminous plant sources, *Dolichus biflorus*, *Cajanus cajan* and *Glycine max*

INTRODUCTION

Urease is a nickel-containing amidohydrolase. It catalyses the hydrolysis of urea resulting in the formation of ammonium carbonate. Urea, on the other hand, is a carbamide and it is commonly used as a major N-fertilizer in agriculture for enhancing crop production. But it is highly soluble in water and its molecules are practically neutral. Hence urea fertilizer is prone to runoff and leaching losses in wetland rice fields and light-textured soils, respectively. In minimizing these losses, urease plays an important role by converting urea into ammonium form through the process of hydrolysis. Ammonium being a cation can enter into the base exchange activity of soil in crop fields. As a result, N availability to rice and other crops is enhanced and N use efficiency is increased. Urease is also used in the accurate determination of N content in urea fertilizer. [1] Roles, regulations and structure of plant urease have been reviewed by many researchers, Urease has wide applications not only in agriculture but also in medical, industrial and environmental sectors [2]. It is mostly used in hemodialysis which is essentially required for the treatment of patients suffering from renal failure [3]. It is also used in medical diagnostics such as determination of urea in blood serum. Besides, urease is used as a biosensor [4,5]. Urease is also used in the industry of alcoholic beverages and in the preparation of bioconcrete [6, 7]. In the environmental sector, urease is required for wastewater treatment [8].

The primary sources of urease are few selected plant sources including legumes [9, 10]. The other sources of urease are soil microbes, algae, fungi, yeast bacteria and some invertebrates. James B. Summer first discovered urease in jack bean (*Canavalia ensiformis*) in 1924 and crystallized the urease enzyme in [11,12]. The urease crystals thus prepared were then characterized. Use of either urease crystals or freshly prepared urease solution as extracted from jack bean seeds has been prescribed in the AOAC method for hydrolysis of urea and determination of N content in urea fertilizer. However jack-bean is not grown in most of the states of India including Odisha. Moreover, the solid crystallized urease is expensive and it needs to be stored at a temperature of 2-8^o C. Attempts were, therefore, made in the present study to detect the presence of urease enzyme in locally available leguminous plant sources.

MATERIALS AND METHODS

Seeds of eleven locally available legumes viz. peas (*Pisum sativum*), Chickpea (*Cicer arietinum*), horse gram (*Dolichus biflorus*), pigeon pea (*cajanus cajan*), green gram (*Vigna radiata*), Lentil (*Lens esculanta*), cowpea (*Vigna sinensis*), soybean (*Glycine max*), black gram (*Vigna mungo*), Dhaincha species (*sesbania rostrata*) and another species (*sesbania aculeata*) were collected and evaluated for presence of urease enzyme in them. The urease extraction and enzymatic hydrolysis process was conducted at the National Rice Research Institute, Cuttack, Odisha.

Extraction of Urease From the Plant Sources

The legume seeds, oil cakes and green manure plant samples were crushed separately. Five grams each of the crushed material was suspended in 50 ml of distilled water contained in the required number of 100 ml volumetric flasks. The contents in each flask were vigorously shaken to bring the urease, if any, into solution. The volume of the suspension in each flask was made up to the mark with water. The contents were again shaken and the suspended particles were allowed to settle at the bottom of the flask. The clear supernatant liquid was used as natural urease solution.





Enzymatic Hydrolysis of Urea with the Natural Urease Solution and Determination of Ammonium -N by Steam Distillation

A total of 10 ml of 100 ppm pure urea -N solution (1mg N) taken in another set of 100 ml volumetric flasks was added 2 ml of the freshly prepared aqueous extract of urease. The contents in each flask were thoroughly shaken with and without potassium phosphate buffer of pH 8.0 and allowed to stand for 2 hours to achieve hydrolysis of urea in stoppered volumetric flasks. After the lapse of 2 hours, the contents in each volumetric flask were transferred into a Kjeldahl flask with two to three rinsing followed by the addition of MgO. MgO used as a base in all the determinations was previously heated at 600 - 700°C for 2 hours in a muffle furnace and cooled in a desiccator. Ten grams of the ignited MgO was suspended in 100 ml of water and 10 ml of the suspension was used in each determination. The ammonium -N resulting from enzymatic hydrolysis of urea was estimated by the semi-microkjeldahl steam distillation method. The ammonia gas liberated due to the reaction of ammonium carbonate with MgO base was steam distilled into a receiver flask containing 2 % boric acid solution with a mixed indicator. About 10-15 ml of distillate was collected within 3-4 minutes. Ammonium borate complex formed due to the reaction of boric acid with ammonia was titrated against standard (0.01N) H₂SO₄ solution. From the titration value, the ammonium-N was quantitatively determined and the percentage of urea hydrolyzed was calculated.

Statistical Analysis

All the determinations were made in duplicate to ensure the reproducibility of the results. Average data presented. T-test was applied for significant differences between the estimation method with and/or without potassium phosphate buffer.

RESULTS

The results obtained from the experiment revealed that out of the eleven legumes, aqueous extracts of crushed seeds of only three legumes, viz: horse gram (*Dolichus biflorus*), pigeon pea (*Cajanus cajan*) and soybean (*Glycine max*) completely hydrolyzed urea into ammonium form of nitrogen. (Table 1) Urease activity is 99.2 -100% in these three plant species. Water extracts of seeds of green manure plants viz. *Sesbania aculeate* and *Sesbania rostrata* partly hydrolyzed urea, the fractions of urea hydrolyzed being in the range of 41.5-87.4 percent. Seeds of the rest of the legumes viz. green-gram, black-gram, peas, chickpea, cowpea and lentil hydrolyzed only 5.5-11.9 % of the urea taken in the experiment. The groundnut oil cake and green matter of all three green manure plant species were also found to be poor sources of urease as they hydrolyzed only 9.1-18.9% of urea. Based on these observations the leguminous plant sources were categorized into three groups, high (90-100%), medium (30-90%) and low (0-30%) urease activity (Table 2) (Figure 1)

DISCUSSION

It is evident from the result that three species had a cent percent conversion of urea into ammonium -N due to enzymatic hydrolysis during two hours in the presence and absence of potassium phosphate buffer (pH 8.0). Water extract of any one of the three leguminous plant sources belonging to group 1 can be used in the determination of N content in urea fertilizer. This method is inexpensive and easily adoptable in laboratories situated even in remote areas. Hence it can ensure quality control of urea fertilizers. In this regard, pigeon peas used as the source of urease for hydrolysis of urea followed by steam distillation of ammonia in determination of N content of urea [13]. Urea was hydrolyzed by using jack bean urease crystals and subsequently determined the N content of urea by steam distillation of ammonia [14]. As per the AOAC official method, one can use either jack bean urease crystals or freshly prepared aqueous extract of jack bean seeds for hydrolysis of urea and subsequent determination of N content of urea fertilizer. The present study provided additional information that besides jack bean and pigeon pea, two other locally available legumes viz. horse-gram and soybeans were also found to be rich sources of urease. In the present experiment pea (*Pisum sativum*) was found to be a poor source of urease. However, El-Hefnawy et al. detected adequate urease in germinating pea seeds [15]. The difference in the experimental findings could be because



**Devaraj Panda et al.,**

commercial dry pea seeds were used in the former study, whereas the germinating pea seeds were used for the extraction of urease in the latter. It is therefore suggested to use germinating pea seeds for extraction of urease enzyme. The results of this investigation, have a lot of relevance and utility not only in agriculture but also in healthcare, industrial and environmental sectors [2,16]. The global demand for chrySTALLINE urease produced from plant sources is increasing because its use especially in the medical sector has less toxicity and no side effects. Urease is mostly used in hemodialysis, which is essentially required for the treatment of patients suffering from renal failure. Considering the multi-sector uses of urease and prospects of its consumption inside India and abroad, research activities in this regard may be intensified. Follow-up product development activities may also be undertaken to isolate urease on a large scale from the selected plant sources viz. seeds of horse gram (Kulthi), Pigeon pea (Arhar), and soybean (Soya). Further, the isolated urease may be crystallized and urease crystals be characterized. The efficacy of the urease crystals produced from indigenous plant sources may be compared with that of jack bean urease crystals, especially for their use in the medical sector.

CONCLUSIONS

Three legumes, viz: horse gram (*Dolichus biflorus*), pigeon pea (*Cajanus cajan*), and soybean (*Glycine max*) completely hydrolyzed urea into ammonium form of nitrogen whereas, *Sesbania aculeate* and *Sesbania rostrata* partly hydrolyzed urea and the groundnut oil cake and green matter of all the three green manure plant species were found to be poor sources of urease as they hydrolyzed only 9.1-18.9% of urea. Water extract of any one of the three leguminous plant sources viz: horse gram (*Dolichus biflorus*), pigeon pea (*Cajanus cajan*) and soybean (*Glycine max*) belonging to group-1 can be used in the determination of N content in urea fertilizer.

List of Abbreviations

Ammoniacal-N: Ammoniacal Nitrogen

AOAC: Association of Official Analytical Chemists

MgO: Magnesium Oxide

Declarations

Ethics approval and consent to participate: Not applicable

Consent for Publication: Approved by all authors

Availability of data and material: All the data generated from the experiment and analyzed data are included in the main text and in table and figure

Competing Interest: Authors declare that they have no competing interest

Funding: No fund received for this study

Author Contribution: DP is the first author who conceptualized the research plan. DP and SN experimented and collected the data. BP and DP analyzed, reviewed the data and prepared the manuscript for publication.

REFERENCES

1. AOA.C. Official Methods of Analysis of the Association of Analytical Chemists, Wasington D.C, USA;1970 11th ed.
2. Sirko A, Brodzik R. Plant ureases: roles and regulation. Acta Biochim Pol. 2000;47(4):1189-1195. PMID: 11996109.
3. Ash SR, Barile RG, Thornhill JA, Sherman JD, Wang NH. In vivo evaluation of calcium-loaded zeolites and urease for urea removal in hemodialysis. Trans Am Soc Artif Intern Organs. 1980;26:111-115. PMID: 6264655.
4. Fapyane D, Berillo D, Marty JL, Revsbech NP Urea Biosensor Based on a CO₂ Microsensor. ACS Omega. 2020; 5(42):27582-27590. doi: 10.1021/acsomega.0c04146.
5. Botewad SN, Gaikwad DK, Girhe NB, Thorat HN, Pawar PP. Urea biosensors: A comprehensive review. Biotechnol Appl Biochem. 2023 Apr;70(2):485-501. doi: 10.1002/bab.2168. Epub 2021 Apr 21. PMID: 33847399.



Devaraj Panda *et al.*,

6. Bang SS, Galinat JK, Ramakrishnan V Calcite precipitation induced by polyurethane-immobilized *Bacillus pasteurii*. *Enzyme Microb Technol.*2001; 28(4-5):404-409. doi: 10.1016/s0141-0229(00)00348-3.
7. Kodama S Optimal conditions for effective use of acid urease in wine. *Journal of Food Science* 2006; 61(3): 548-552
8. Liang W, Wu Z, Chang S, Zhou Q, and Hu H Role of substrate microorganisms and urease activities in wastewater purification in constructed wetland system. *Ecological Engineering*2003 DOI: 10-1016/J.Ecology 2003.11.002, .
9. Finar Organic Chemistry. Volume One: The Fundamental Principles, Vol 1 (4th ed.) English language book society, London; 1964
10. Frankenberger, W.T., Tabatabai, M.A. Amidase and urease activities in plants. *Plant Soil* 1982; 64, 153–166 . <https://doi.org/10.1007/BF02184247>
11. Sumner J B, Graham VA and Novak CV *Proc. Soc. Exp. Biol. And Med* 1924. XXI:554
12. James B Summer -Biographical. Noble Prize Org. Noble Prize Outreach AB2022Sun 10 July 2022.
13. Panda D and Patnaik S. Determination of Urea-N by Steam Distillation. *J. Indian Soc. Soil Sci.* 1985; 33: 811-81.
14. Keeney DR, and Bremner JM Determination and isotope-ratio analysis of different forms of nitrogen in soils: 7. Urea. *Soil Science Society of America Journal* 1967; 31: 317–321.
15. El-Hefnawy ME, Sakran M, Ismail AI et al. Extraction, purification, kinetic and thermodynamic properties of urease from germinating *Pisum Sativum* L. seeds. *BMC Biochem* 2014; 28;15:15. doi: 10.1186/1471-2091-15-15.
16. Follmer C. Insights into the role and structure of plant ureases. *Phytochemistry.* 2008 69(1):18-28. doi: 10.1016/j.phytochem.2007.06.034. Epub 2007 Aug 15.

Table 1: Evaluation of legume seeds, oil cake and green manures as sources of urease enzyme

Common name of the legume/ oil cakes/ green manures	Scientific name	Amount of urea-N taken (mg)	Estimations made with potassium phosphate buffer (pH 8.0)		Estimations made without potassium phosphate buffer (pH 8.0)		P-value p-value <0.005 Significant (S) Non significant(NS)
			Amount of urea -N hydrolysed (mg)	% of urea - N hydrolysed	Amount of urea -N hydrolysed (mg)	% of urea - N hydrolysed	
Peas	<i>Pisum sativum</i> Linn.	1	0.090	9.00	0.055	5.5	0.6521 (NS)
Chick Pea	<i>Cicer arietinum</i> Linn.	1	0.080	8.00	0.118	11.8	
Horse gram	<i>Dolichus biflorus</i> Millsp.	1	1.010	100.00	1.001	100.1	
Pigeon pea	<i>Cajanus cajan</i> Millsp.	1	0.992	99.20	0.974	97.4	
Green gram	<i>Vigna radiata</i> (L.) Wilczek	1	0.109	10.9	0.119	11.9	
Lentil	<i>Lens esculenta</i>	1	0.070	7.00	0.064	6.4	





Devaraj Panda et al.,

	Moench					
Cowpea	<i>Vigna sinensis</i> (L.) Savi	1	0.090	9.00	0.085	8.5
Soyabean	<i>Glycine max</i> (L.) Merr.	1	1.001	100.00	0.983	98.3
Blackgram	<i>Vigna mungo</i> (L) Hepper	1	0.071	7.10	0.100	10.0
Dhanicha seed	<i>Sesbania rostrata</i>	1	0.505	50.50	0.860	86.0
Dhanicha seed	<i>Sesbania aculeata</i> Poir.	1	0.415	41.50	0.874	87.4
Goundnut Oilcake	<i>Arachis hypogaea</i>	1	0.123	12.30	0.127	12.7
Green Manures Dhanicha species 1	<i>Sesbania rostrata</i>	1	0.091	9.10	0.129	12.9
Green Manures Dhanicha species 2	<i>Sesbania aculeata</i>	1	0.135	13.50	0.118	11.8
Gliricida	<i>Gliricidia maculata</i>	1	0.133	13.3	0.189	18.9

Table 2: Grouping of locally available leguminous plant sources in respect of their urease activity

Group 1 Sources with high urease activity (90-100%)	Group 2 Sources with medium urease activity (30-90%)	Group 3 Sources with low and very low urease activity (0-30%)
Horse-gram seeds Pigeon-pea seeds Soybean seeds	Dhaincha (<i>S. aculeata</i>) seeds Dhaincha (<i>S. rostrata</i>) seeds	Dhaincha green matter Gliricidia green matter Groundnut oil cake Pea seeds Cheak-pea seeds Green-gram seeds Lentil seeds Cowpea seeds Black gram seeds





Devaraj Panda et al.,

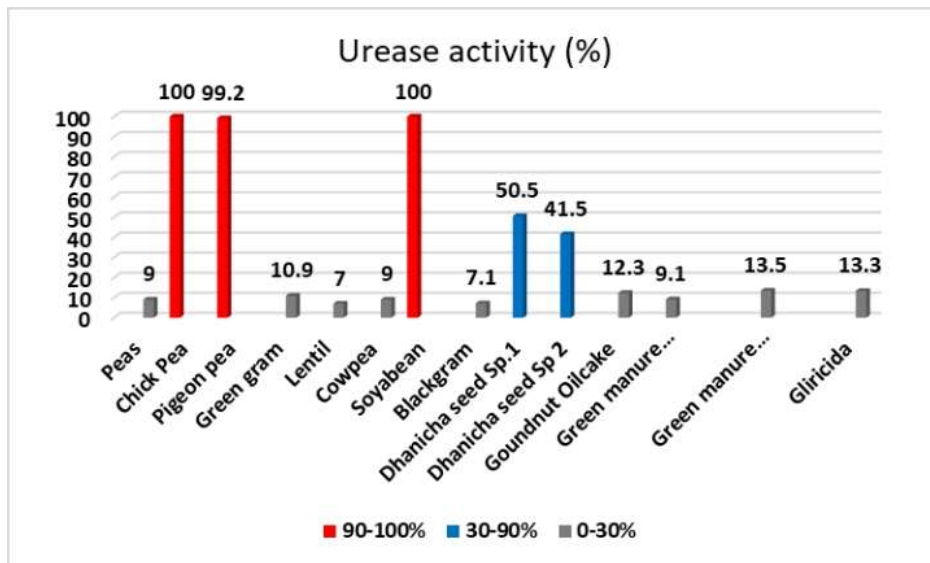


Figure 1: Urease activity of all plant species as estimated from the hydrolysis of urea-N





Removal Potential of Heavy Metals Pb, Cr and Ni from Polluted Waters by *Pistia stratiotes* and *Azolla pinnata* : A Green Technology

Jeba Nisha.J^{1*} and Dr.Amaliya.N.K²

¹Research Scholar, Department of Chemistry, Reg.No: 20213282032019, Women's Christian College, Nagercoil-629001, (Affiliated to Manonmaniam Sundaranar University, Abishekapatti, Tirunelveli-627012), Tamil Nadu, India.

²Assistant Professor, Department of Chemistry, Women's Christian College, Nagercoil-629001, Email: amaliya87@gmail.com(Affiliated to Manonmaniam Sundaranar University, Abishekapatti, Tirunelveli-627012), Tamilnadu, India.

Received: 25 July 2023

Revised: 16 Oct 2023

Accepted: 29 Dec 2023

*Address for Correspondence

Jeba Nisha.J

Research Scholar,

Department of Chemistry,

Women's Christian College, Nagercoil-629001,

(Affiliated to Manonmaniam Sundaranar University,

Abishekapatti, Tirunelveli-627012), Tamil Nadu, India.

E mail: jebanishahelan@gmail.com



This is an Open Access Journal / article distributed under the terms of the **Creative Commons Attribution License** (CC BY-NC-ND 3.0) which permits unrestricted use, distribution, and reproduction in any medium, provided the original work is properly cited. All rights reserved.

ABSTRACT

Phytoremediation is the process to clean up the polluted water naturally with the help of aquatic macrophytes. In the present study, the effectiveness of *Pistia stratiotes* and *Azolla pinnata* are the plants acts as a phytoremediator to remediate the heavy metals Pd, Cr and Ni from the contaminated water bodies in Kanyakumari District was tested. During the winter season of 2022, the heavy metal concentrations were analyzed during the treatment. Heavy metals accumulation in *Pistia stratiotes* and *Azolla pinnata* was in the order of Pb> Ni> Cr. This shows that the two aquatic macrophytes were able to accumulated the heavy metals and improve the quality of water. *Pistia stratiotes* is the most effective species to remove the heavy metals compared with *Azolla pinnata* for all the three heavy metals.

Keywords: Phytoremediation, remediate, contaminated, heavy metals, concentration.

INTRODUCTION

Water pollution is one of the biggest Global problems in the modern days. Most of our water bodies are gradually losing their purity as a result of the entrance of outside elements from the neighborhood especially sewage discharges, industrial activities, agricultural activities and urban runoff including storm water. Heavy metal ions are



**Jeba Nisha and Amaliya**

among the most released contaminants and are toxic even at very low concentration. In several places around the world, the average concentrations of Cr, Mn, Fe, Co, Ni, As, Pb and Cd found in surface water bodies are well above the maximum allowed values for drinking water (1). This water pollution can lead the degradation of aquatic ecosystems or water-borne diseases when people use polluted water for drinking or irrigation.

There are conventional and non-conventional techniques available to remove the heavy metals from polluted water. Among these techniques, Phytoremediation is one of the best and an emerging technology to remediate the heavy metals. This technique combines advantages such as low cost of implementation and operation, little or no energy expenditure, possibility of biomass generation does not produce toxic secondary product, landscape harmony in addition to having application in large volumes of water(2). Aquatic plants have a significant role to play in pollution prevention, particularly the usage of aquatic macrophytes in the remediation of heavy metal ions from polluted water. The mechanism by which the plants absorb metals from the water is, the heavy metal ions have positive charges and the plant's roots are negative charges. This can be able to attract the ions and roots and thus the ions are absorbed into the plant.

Pistia stratiotes is a free floating plant and its ability to use nutrients from the sewage to elaborate an important phyto mass added to exacerbate any imbalance in nutrient supply that arose during the experiment and make it one of the most suitable plant to be used in wastewater phytoremediation (3). *Azolla pinnata* is a free floating, fast growing and nitrogen fixing pteridophyte seems to be an excellent candidate for removal and disposal of heavy metals from the polluted aquatic ecosystems (4).

MATERIALS AND METHODS

Collection of Plants

The *Pistia stratiotes* and *Azolla pinnata* used in research was collected from a natural river near Mylaudy in Kanyakumari District. These plants are very common in Kanyakumari District, propagating by stolons and multiplying very rapidly. The collected plants were washed several times with tap water and finally in distilled water to remove the impurities.

Collection of Water Samples

The water samples were collected and labeled in clean plastic containers from Chunkankadai (Station-1) and Aralvoimozhi (Station-2) pond water in Kanyakumari District. These ponds were polluted by the surrounding urban area sewages and agricultural fertilizers. Especially, Station-1 water was contaminated from nearby hospital wastes.

Experimental Setup

The aquatic plants of uniform size and equal weight were treated with the polluted water. The setup was left undisturbed in shaded area for 60 days. Water samples were collected, added a few drops of HNO₃ and labeled in a sample bottles for each 10 days interval during the treatment period. After 60 days of treatment with polluted water, the plants were harvested. Plants were then washed using distilled water for removing any excess salts. The surplus water on the plant was evacuated with tissue paper. After that, the treated plants were examined.

Analysis

The concentration of Heavy metals in treated water samples were analyzed by using Atomic Absorption Spectrometer. The treated plants were dried, powdered and digested by Acid digestion method. The digested plant samples were analyzed by using AAS.





Jeba Nisha and Amaliya

RESULTS AND DISCUSSION

Phytoaccumulation of Heavy Metals

After 60 days of treatment the plants showed a substantial amount of accumulation of heavy metals in tissues. The result shows that the concentrations were decreased highly during the initial period of treatment. The concentration of the heavy metals Pb, Cr & Ni reduced by *Pistia stratiotes* in station-1 & 2 is mentioned in figure-1&2. Reduction in concentration of the heavy metals Pb, Cr & Ni using *Azolla pinnata* in station-1 & 2 mentioned in Figure-3&4. Removal of heavy metal ions increased with increasing contact time. At initial time, the removal was high but increased slightly (5). The accumulation of heavy metals within the plant body is the fact that these hazardous elements are linked to the walls of the cells in roots or leaves, preventing them from moving through the wringer plant or expel gently, particularly to the sensitive sites in the cell where they are stored in the gaps (6).

Removal Percentage Of Heavy Metals

The removal percentage of metal ions by aquatic plants was determined by using initial metal concentrations of the treatment and the final concentrations at the end of the experiment (4).

$$\text{Removal percentage (\%)} = \frac{C_i - C_f}{C_i} \times 100$$

Where, C_i = initial concentration

C_f = final concentration

The removal percentage of Cr has highest reduction takes place under the treatment with *Pistia stratiotes* and Ni has the lowest removal percentage. Treatment with *Azolla pinnata*, Pb has the highest removal percentage and Cr has the lowest removal percentage in station-1 (Table-1). Treatment with *Pistia stratiotes* & *Azolla pinnata* has the highest removal percentage for Pb and lowest removal percentage for Cr in station-2 (Table-1). Every plant has a certain level of metal tolerance, which is primarily controlled by genes; crossing the level that may limit the ability and functions of the plant to remove a respective metal. This may explain the low Cr uptake (7). *Pistia stratiotes* has high removal efficiency for all the three heavy metals in station-1&2 (Figure-1&2). The difference in the accumulation of the metal between the different plants may results from the difference in the physiological activities of the plants such as photosynthesis (8).

Bioconcentration Factor (BCF):

Bioconcentration factor is a useful parameter for assessing the potential of heavy metal accumulation (9). It was calculated by dividing the heavy metal concentration in plant tissues at harvest by the initial concentration of the element in the external solution (10).

$$\text{BCF} = \frac{\text{Concentration of metal in plant tissues}}{\text{Concentration of metal in Water}}$$

For *Pistia stratiotes*, metals accumulation was in the order of Cr > Pb > Ni & Pb > Ni > Cr in Station-1 & 2 respectively (Table-3). By using *Azolla pinnata*, metals accumulation was in the order of Pb > Ni > Cr for station-1&2 (Table-3). This result shows that *Pistia stratiotes* & *Azolla pinnata* were able to accumulate heavy metals Pb, Cr & Ni from the polluted water. This result also shows that the BCF values were confirmed that the two species were a good accumulator. *Pistia stratiotes* was a good hyper accumulator compared with *Azolla pinnata* (Table-2). *Pistia stratiotes* has been identified as a good hyper accumulator due to its versatility to a wide range of P^H and temperature as its high production capacity both sexually and asexually via stolons (11).

Translocation Factor (TF)

The efficiency of phytoremediation can be quantified by calculating translocation factor (12). The Translocation Factor, which gives the root or leaf metal concentration and depicts the ability of the plant to translocate the metal species from roots to shoot or leaf (13). Translocation Factor may be used to assess a plant potential for phytoremediation purpose (14). This results shows that the Translocation Factor is greater than 1 for all the three heavy metals in two plant species (Table-3). This study shows that the two plant species were efficient in translocation of the heavy metals from root to leaf. This is due to efficient metal transporter system and probably sequestration of metals in leaf vacuoles and apoplast (9).





Jeba Nisha and Amaliya

CONCLUSION

Phytoremediation as a green technology for pollution control and can resolve the problem of heavy metal contamination. The present investigation, the potential of *Pistia stratiotes* & *Azolla pinnata* in the remediation of heavy metals Pb, Cr & Ni contaminated water has been demonstrated. The greater Translocation of heavy metals from root to shoot in phytoremediation confirms the phytoaccumulation of plant species. The plant growth was inhibited at high concentrations due to metal toxicity in plant. The harvested plant could then be incineration or ashing process where subsequent recovery of the heavy metals from the ash might be possible.

REFERENCES

1. Ledezma, CZ, Bolagay, DN, Figueroa, F, Ledezma, EZ, Ni, M, Alexis, F & Guerrero, VH, 'Heavy metal water pollution: A fresh look about hazards, novel land conventional remediation methods' Environ.Tech.Innovation., 22, 101504, 2021.
2. Souza, TDD, Borges, AC, Matos, ATD, Veloso, RW&Braga, AF, 'Optimization of arsenic phytoremediation using *Eichhornia crassipes*', Int.J.Phyto.,20:11, pp.1129-1135, 2018.
3. Putra, RS, Cahayana, F& Novarita, D, 'Removal of Lead and Copper from Contaminated Water Using EAPR System and Uptake by Water Lettuce (*Pistia stratiotes* L.)' Procedia Chemistry, 14, pp.381-386, 2015.
4. Mohamed, ER, Ahmed, MS, Tantawy, AA, Gomaa, NH & Mohmoud, HA, 'Phytoremediation of Pb²⁺, Cd²⁺ and Cu²⁺ by an Aquatic Macrophyte *Azolla pinnata* from Industrial Wastewater in Egypt' Middle East J. Appl. Sci., 6(1), pp.27-39, 2016.
5. Shaibur, MR, Tanzia, FKS, Nishi, S, Nahar, N, Parvin, S & Adjadeh, TA, 'Removal of Cr (VI) and Cu (II) from tannery effluent with water hyacinth and arum shoot powders: A study from Jashore, Bangladesh' J. Haz. Adv., 7, 100102, 2022.
6. Hassan, NA, Al-Kubaisi, AR & Al-Obiadi, AHM, ' A Comparative Study between Three Aquatic plants to phytoremediation of Lead from Wastewater' Int.J.Curr. Microbial.App.Sci., 5(6), pp.300-309, 2016.
7. Das, M, Bramhanand, PS & Laxminarayana, K, 'Performance and efficiency services for the removal of hexavalent chromium from water by common macrophytes' Int.J.Phyto., 9(1): pp.36-42, 2021.
8. Alhaji, SN, Umar, SA, Muhammad, SA, Kasimu, S & Aliyu, S, 'Cadmium, Iron and Chromium Removal from Simulated Waste Water Using Algae, Water Hyacinth and Water Lettuce' Ind.J.Appl.Chem., 9(1), pp.36-42, 2021.
9. Alhaji, SN, Umar, SA, Abdullahi, SM, Kasimu, S & Aliju, S, 'Phytoremediation of Nickel, Lead and Manganese in Simulated Waste Water Using Algae, Water Hyacinth and Water Lettuce' Int.J.Min.Process.Extract.Metallurgy., 5(2): pp.30-36, 2020.
10. Taiwo, IO, Babajide, SO, Taiwo, AA, Osunkiyes, AA, Akindele, OI & Sojobi, OA, 'Phytoremediation of Heavy Metals (Cu, Zn, and Pb) Contaminated Water using Water Hyacinth (*Eichhornia Crassipes*)' IOSR.J.App.Chem., 5(11), pp.65-72, 2015.
11. Das, M, Bramhanand, PS, Laxminarayana, K & Chowdhury, SR, 'Effectiveness of common macrophytes for phytoremediation of hexavalent Cr prevalent in chromite mining areas' Int.J.Phyto., <https://doi.org/10.1080/15226514.1975641>
12. Mojiri, A, Aziz, HA, Zahed, MA, Aziz, SQ & Selamat, MRB, 'Phytoremediation of Heavy Metals from Urban Waste Leachate by Southern Cattail (*Typha domingensis*)' Int.J.Sci.Res.Enviro.Sci.,1(4), pp.63-70, 2013.
13. Woldemichael, D, Zewge, F & Leta, S, 'Potential of water hyacinth (*Eichhornia crassipes* (mart.0 solms) for the removal of chromium from tannery effluent in constructed pond system' Ethiop.J.Sci., 34(1), pp.49-62, 2011.
14. Kumar, N, Baudhdh, K, Dwivedi, N, Barman, SC & Singh, DP, 'Accumulation of metals in selected macrophytes grown in mixture of drain water and tannery effluent and their phytoremediation potential' J.Enviro.Biol., 33, pp.923-927, 2012.





Jeba Nisha and Amaliya

Table-1: Removal Percentage (%)

Heavy Metals	Station-1		Station-2	
	Removal Percentage (%)		Removal Percentage (%)	
	<i>Pistia stratiotes</i>	<i>Azolla pinnata</i>	<i>Pistia stratiotes</i>	<i>Azolla pinnata</i>
Pb	86.97	86.96	86.36	76.28
Cr	91.42	69.84	84.28	74.94
Ni	85.62	73.55	85.35	75.55

Table-2: Bioconcentration Factor (BCF)

Heavy Metal	Station-1		Station-2	
	BCF		BCF	
	<i>Pistia stratiotes</i>	<i>Azolla pinnata</i>	<i>Pistia stratiotes</i>	<i>Azolla pinnata</i>
Pb	1228	1220	1103	970
Cr	1484	911	1002	917
Ni	1188	979	1050	933

Table-3: Translocation Factor (TF)

Heavy Metal	Station-1		Station-2	
	TF		TF	
	<i>Pistia stratiotes</i>	<i>Azolla pinnata</i>	<i>Pistia stratiotes</i>	<i>Azolla pinnata</i>
Pb	1.66	1.44	1.18	1.72
Cr	1.23	1.48	1.33	1.19
Ni	1.19	1.37	1.01	1.05

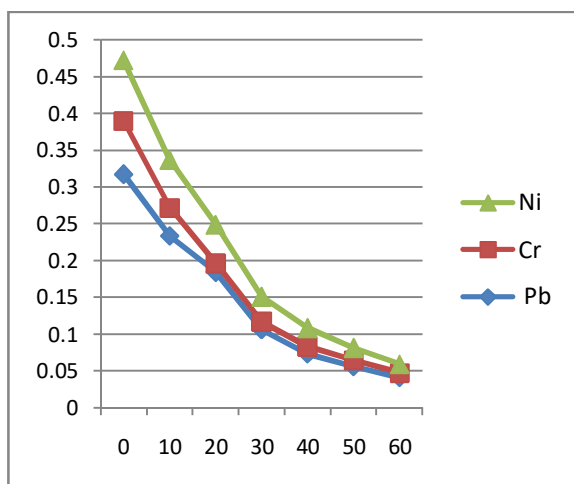


Figure 1: Concentration variation in station-1

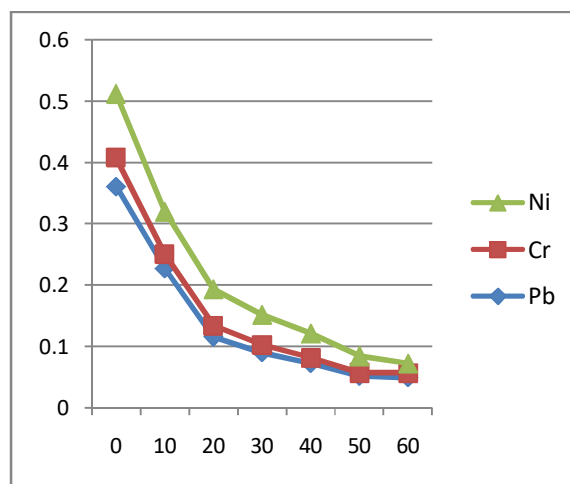


Figure 2: Concentration variation in station-2

Phytoaccumulation by *Pistia stratiotes* Concentration (ppm) Vs Time (Days)





Jeba Nisha and Amaliya

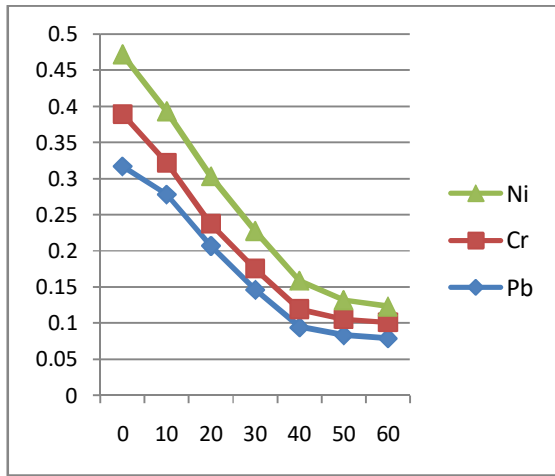


Figure 3: Concentration variation in station-1

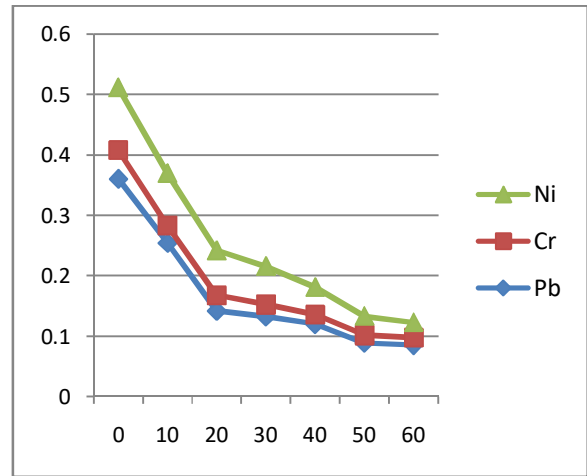


Figure 4: Concentration variation in station-2

Phytoaccumulation by *Azolla pinnata* Concentration (ppm) Vs Time (Days)

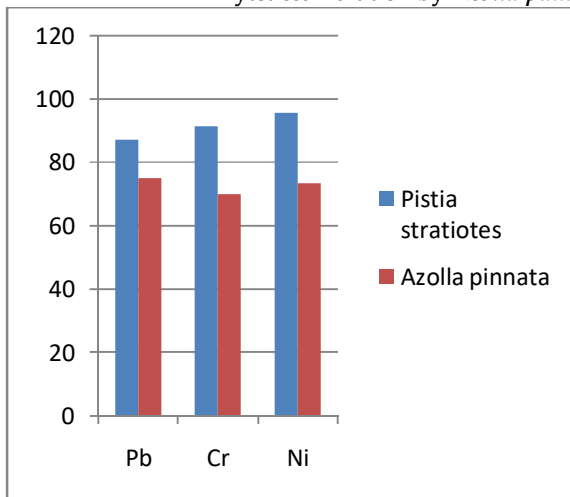


Figure 5: Removal percentage in station-1

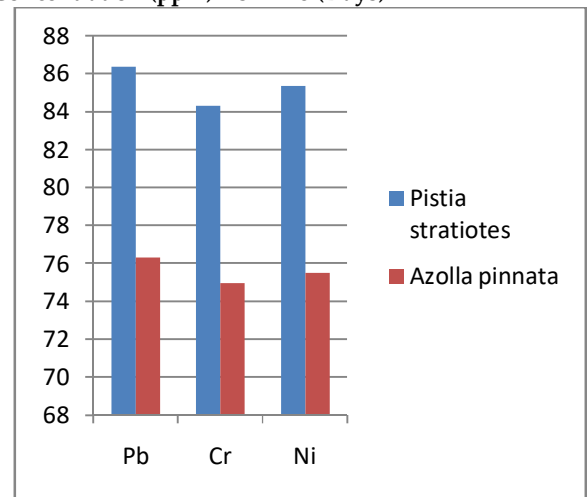


Figure 6: Removal percentage in station-2

Comparison of Removal Percentage (%): Removal percentage (%) Vs Heavy metals





The Role of Emotions in the Decision-Making Process in Digital Marketing

Rajashekhara .R^{1*} and Prakash B Nayak²

¹Research Scholar, Department of Commerce, CIRD Research Centre and RPA First Grade College (Affiliated to University of Mysore) Bangalore, Karnataka, India.

²Professor, Research Guide, Department of Commerce, CIRD Research Centre and RPA First Grade College (Affiliated to University of Mysore) Bangalore, Karnataka, India

Received: 16 Jul 2023

Revised: 20 Nov 2023

Accepted: 17 Jan 2024

*Address for Correspondence

Rajashekhara R

Research Scholar,

Department of Commerce,

CIRD Research Centre and RPA First Grade College

(Affiliated to University of Mysore)

Bangalore, Karnataka, India.

E. Mail: saraswathikuvara@gmail.com



This is an Open Access Journal / article distributed under the terms of the **Creative Commons Attribution License** (CC BY-NC-ND 3.0) which permits unrestricted use, distribution, and reproduction in any medium, provided the original work is properly cited. All rights reserved.

ABSTRACT

If a consumer is going to buy a new product or a repeated product, they may be aware of some brands or have an aspiration to buy a few brands unknowingly with some internal or external influence, and they tend to buy that product. That unknowing element may be influenced by emotions. Emotions are key elements in the marketing field. Based on emotion, his purchase may vary continuously. Emotions are part of every human being's life. According to Oxford Learners Dictionary, it is a part of a person's character based on feelings. People may make decisions based on these feelings. There are around 34,000 types of emotions in the world. In those 7 basic emotions, there are happiness, surprise, contempt, sadness, fear, disgust, and anger. According to psychology, in an emotional situation, one may lose control over his mind. He or she may make a decision based on the emotions they undergo in a particular decisions making process. This paper, even though conceptual, makes a sincere effort to understand how exactly the overall process is controlled by emotion during the purchasing process in digital marketing. Defines the elements that undergo this process, analyse the factors affecting in purchasing decisions. Digital marketing is a colourful platform. Emotions are key elements. With the help of various situations and models, this is an attempt to clarify the x-factor of emotion during the process of buying behaviour.

Keywords: Consumer, Emotion, Purchasing Decision, Brand, Digital Marketing, behaviour, Internal and External Influence.





INTRODUCTION

Emotion is a psychological change happening towards a particular subjective aspect due to this physiological change happening as a reflective reaction (essence from AMA). The word emotion has existed in English since the 17th century. It originated in French, meaning as physical disturbance. Some of the authors explained that emotions are needed to take action or survive any dangerous circumstances. Emotions are making us react in a situation with a small reaction from the brain.

Emotion – how it is created?

How exactly emotion is created, it is a mental status or a physical status. Every time a question is raised in the brain, some time we think it is a psychological status; some time we think it is a physiological state. Afterwards, it comes to the conclusion that a small reaction is happening in the brain; it is a stimulus for the body to respond, based on the situation as experienced. Emotions happen due to confusion or fear. Science says 'yes' for both things. Emotions are also stored data (past experiences) that are expressed in a conflict or decision-making situation. According to neuroscience research - Emotion is also a brain prediction; it stimulates the outside world. As per our earlier experience with may we already undergone with the situation. Again, with the same things happening in front of us, our brain starts predicting. For example: when someone says 'apple', the brain predicts that 'apple' is a red colour with a smooth texture and crispiness', or someone may think about an 'Apple Phone' or tablet. Both the way emotions are expressed with the spark of the brain and how they respond to the environment. Barrett challenges the "basic emotions"—they have their origins in Darwin. In the 1970s, Paul Ekman, UC Berkeley clinical psychologist, From his view, emotions emerge through facial expression; the basic emotions are fear, anger, sadness, joy or happiness, and surprise. (Elliot Jurist, 2019)

Objectives

1. To find out the difference between emotions and feelings in the consumer decision-making process.
2. The importance of emotions in digital marketing
3. To find out the effect of the emotion process on digital marketing.

Research Question

1. In what ways are emotions created and play a vital role in decision-making processes?
2. In digital marketing, do emotions really make a difference or what?

METHODOLOGY

It is a conceptual study. To analyze various faces of emotion in the decision-making process. We used secondary data to get the outcome. Emotion is dynamic in nature; it continuously changes with trends, economic balance, or any other external or internal factors. Due to this purview, emotional condensed collection and impartment may not be able to get the essence of what we want. The time perspective is also a constraint. Psychological point of view of emotion and how it is going to react in the natural world. With the help of sources and models, we came to the conclusion:

Emotion – It is created in our brain.

According to behavioural Psychology emotions usually created based on past experience. Usually emotions are come across with below cyclical process.

1. Prediction: The brain always recollects data based on past experience. It is going to be predicted that this may happen in this situation also.
2. Simulation: The brain thinks the same situation is happening like that.
3. Compare: It is going to compare past experience to the present situation.
4. Resolve errors: try to rectify the past mistakes in the current situation.





Feelings and Emotions

From the normal eye, if you are going to see two words like feeling and emotions, they look the same, but when you are going to analyze the aspects, you will find the greater differences. Basically, feelings are mental status readouts; one can create his or her perception. It is based on internal beliefs. Feelings are experienced consciously. In the other hand emotions expressed in physical body, due the psychological forces created on the brain. It is both inner and outer experience. Emotions are both conscious and subconscious. In some cases person may take whole life to understand the emotion (clinical mental health counselling).

Emotions Impact On Buying Behaviour

As we discussed above, emotions are created due to past experiences. To rectify past errors, one wants to be conscious. This situation also involves emotion. The buyer's experience with several products in the world may be directly or indirectly related to emotions related to the buying process. Pre-Purchase decision-making process: Usually customers have two kinds of needs: functional and emotional. Functional needs with product satisfaction and its desired feature. Emotional functions are the satisfaction levels of consumers with their own perspectives. Domenico consoli (2009). Before purchasing the product, he/she may select the kind of need that itself creates lots of changes. If anyone decided the product based on past experience at that time, only level of emotion made and impact on decision-making. During the purchase decision-making process: According to the Goleman model (1996), Emotional intelligence is constructed on four levels: self-awareness, self-management, social awareness, and relationship management. During the purchase process, one experiences mixed emotions. The final choice of the product may be using complete cognitive, emotional, or mixed methods. Post-purchase decision-making process: customer experience is more important. Other than price and product development, the customer experience now matters a lot. Every customer wants a better experience (post-purchase), which will create future customers. (Loop returns.com)

Digital impact on marketing: It is a set of activities, in order to grab the new customers company using internet, from this one can create brand identity.(Philip kotler) Nowadays, consumers rely more on the internet. As a result of this increased consumer dependency on digital services, it will help to create extended brands and attract a larger number of customers. Yueh-Shian Lee(2023). Almost double the number of customers are depending on digitalization rather than traditional purchasing decisions. (especially in urban areas)

Emotion – Impact on Digital Marketing

Emotional appeal in digital marketing creates customer space. Emotional appeal applies to various charities and donations, or empathy and sympathy create an impact on purchasing decisions (Murooj Yousef, Baek & Yoon, 2022; Kemp et al., 2017; Small & Verrochi, 2009).It is showing continuously using digital platforms. Continuous emotional attachment created by the person towards a product customer-extended marketing and wide area improvement For example, in Instagram, a concise post of empathic advertisement may create a positive opinion about the product. It establishes product loyalty among the customers. One can remember the product continuously due to the emotional attachment.

Various Types of Emotions

Basic emotions are seeking, rage, fear, care, lust, Panic/grief and Play/joy.jark panksepp (2011), in general way, the basic emotions are fear, anger, sadness, joy or happiness, and surprise. (Elliot Jurist, 2019)

Emotion Affecting Decision Making in Digital Marketing

The digital quotient is affected by the emotional quotient. While visiting any online platform, they are attracted by some attractive taglines. It made one want to play that content. Different levels of emotions are expressed, and consumers are more familiar with connecting with this kind of data. Attitudes towards the platforms are not as simple as what we feel. Every consumer minute matters a lot. Digital literacy and consumer awareness are also affected by emotions. For example, if the you tuber provides a positive review of any product, the regular follower of that you tuber may fall into purchasing that product. Celebrity advertisements also had an emotional impact on





Rajashekhar and Prakash B Nayak

consumer mindsets. The above model explains digital development and its effects through various transformations. Humans, emotions, and technology may simulate each other. It observes and tests the consumer.

Observations

1. During post purchase experience, Customer experience is more around 46% than the price and product development, 21% and 34% respectively (Source: loop returns)
2. 55% of advertisements are in digital. 93% of people read online review before making purchase. (Source: Wordstream).
3. In 2023, there are estimated to be 4.89 billion total social media users worldwide. (Source: Sproutsocial).
4. Internet users spends – social media - user spends 151 minutes per day. (Source: Sproutsocial)
5. Retargeting advertisements are the most widely used by advertisers, with 77% of B2B and B2C marketers claiming to utilize them in their Facebook and Instagram ad campaigns. (Source: Sproutsocial)

CONCLUSION

Taking emotional advantage through digital marketing is something every company is doing today. It improved sales performance. Emotion has a strong impact on digital marketing; it creates competition because it is human nature to be emotional. From these factors, so many decisions are made in the purchasing process. Gaining new clients, customers, and consumers to extend the market is a process of psychological tenderness. Because of this, physical changes are happening. The emotional impact of digital marketing also helps in cost reduction. In future research, we may concentrate on the impact of emotions on digital marketing in the process of cost reduction.

REFERENCES

1. Ou, Y. C., & Verhoef, P. C. (2017). The impact of positive and negative emotions on loyalty intentions and their interactions with customer equity drivers. *Journal of Business Research*, 80, 106-115.
2. Peng, L., & Liang, S. (2013). The effects of consumer perceived value on purchase intention in e-commerce platform: A time-limited promotion perspective.
3. Westbrook, R. A., & Oliver, R. L. (1991). The dimensionality of consumption emotion patterns and consumer satisfaction. *Journal of consumer research*, 18(1), 84-91.
4. Richins, M. L. (2013). When wanting is better than having: Materialism, transformation expectations, and product-evoked emotions in the purchase process. *Journal of Consumer Research*, 40(1), 1-18.
5. Akbar, M. I. U. D., Ahmad, B., Asif, M. H., & Siddiqui, S. A. (2020). Linking emotional brand attachment and sales promotion to post-purchase cognitive dissonance: The mediating role of impulse buying behavior. *The Journal of Asian Finance, Economics and Business*, 7(11), 367-379.
6. Aydinli, A., Bertini, M., & Lambrecht, A. (2014). Price promotion for emotional impact. *Journal of Marketing*, 78(4), 80-96.
7. Gregory-Smith, D., Smith, A., & Winklhofer, H. (2013). Emotions and dissonance in 'ethical' consumption choices. *Journal of Marketing Management*, 29(11-12), 1201-1223.
8. Mehralian, M. M. (2022). Identifying and Explaining the Effective Factors of Digital Marketing Strategies in Consumers' Emotional States and Sales Rates: A Mixed Methods Research. In *20th International Conference of the Business and Strategic Management*
9. Oluwatofunmi, A. D., & Amietsenwu, B. V. (2019). Relationship between digital emotional intelligence and performance of real estate digital marketing in Nigeria. *International Journal of Psychology and Cognitive Science*, 5(2), 70-78.
10. Lee, Y. S. (2023). The Relationships among Digital Marketing, Brand Emotional Attachment and Brand Attitude. *Journal of Applied Finance & Banking*, 13(2), 27-44.
11. Çizmeçi, F., & Ercan, T. (2015). The Effect of Digital Marketing Communication Tools in the Creation Brand Awareness By Housing Companies. *Megaron*, 10(2)





Rajashekhara and Prakash B Nayak

12. Kamkankaew, P., Sribenjachot, S., Wongmahatlek, J., Phattarowas, V., & Khumwongpin, S. (2022). Reconsidering the Mystery of Digital Marketing Strategy in the Technological Environment: Opportunities and Challenges in Digital Consumer Behavior. *International Journal of Sociologies and Anthropologies Science Reviews*, 2(4), 43-60
13. Pusztahelyi, R. (2020). Emotional AI and its challenges in the viewpoint of online marketing. *Curentul Juridic*, 81(2), 13-31.
14. Stephen, A. T. (2016). The role of digital and social media marketing in consumer behavior. *Current opinion in Psychology*, 10, 17-21.
15. Prentice,C(2019), Emotional intelligence and marketing, World scientific

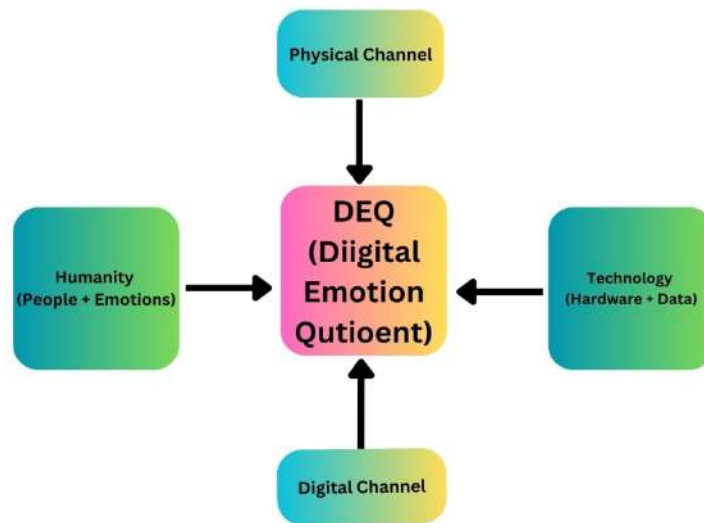


Fig.1. Emotion to Digital - Model
Source: Avery Dennison, (2017).





Retrofitting of Shear-Deficient RC Beams Using Ferrocement Laminates

¹Dr. J Rex and ²Indraja Gandarla

¹Associate Professor, Department of Civil Engineering, Malla Reddy Engineering College, Maisammaguda, Kompally, Hyderabad, Telangana, India.

²PG Scholar, Department of Civil Engineering, Malla Reddy Engineering College, Maisammaguda, Kompally, Hyderabad, Telangana, India.

Received: 18 Oct 2023

Revised: 25 Oct 2023

Accepted: 31 Oct 2023

*Address for Correspondence

Indraja Gandarla

PG Scholar,

Department of Civil Engineering,
Malla Reddy Engineering College,
Maisammaguda, Kompally,
Hyderabad, Telangana, India.

E mail: indraja.mrec@gmail.com



This is an Open Access Journal / article distributed under the terms of the **Creative Commons Attribution License** (CC BY-NC-ND 3.0) which permits unrestricted use, distribution, and reproduction in any medium, provided the original work is properly cited. All rights reserved.

ABSTRACT

Conservation Reinforced concrete structural components are observed to indicate distress, even before their service term is over because of many factors. To restore such unserviceable structures to their functional usage once again, quick attention, an investigation into the source of distress, and appropriate remedial actions are required. Retrofitting is the process of reinforcing and improving the performance of these inadequate structural parts within a structure or a structure as a whole. Life safety is the most crucial problem that must be addressed during retrofitting. What could be done to stop the structure from collapsing and stop injuries or deaths to the occupants? Significant retrofit regulations may attempt to merely address the problem of life safety while still accepting the possibility of some structural damage. Ferrocement could be a beneficial retrofitting material because it could be applied rapidly to the affected element's surface without the need for any specific bonding agents and because it needs less specialized labour than other retrofitting methods currently in use. Ferro cement construction offers an advantage over traditional reinforced concrete material due to its reduced weight, construction simplicity, low thinner section, self-weight than RCC, and high TS (Tensile Strength), which makes it a good choice for prefabrication. In the current work, the wire mesh is positioned to raise the strength of the shear-deficient RC beams, which were first strained to a specific safe load %, at an angle of 45° to the beam's longitudinal axis. According to the analysis, wire mesh with a 45-degree orientation greatly increases the safe load-bearing capability of rectangular RC components retrofitted with ferrocement laminates.



**Rex and Indraja Gandarla**

Keywords: Retrofitted Beams, Shear Deficient RC Beams, Ferrocement Laminates, Wire mesh, Control Beam, Load Deflection Curve.

INTRODUCTION

Retrofitting is the process of strengthening and improving the deficient structural components' performance within a structure or a structure as a whole. Repair is the partial restoration of a building's lost structural integrity following an earthquake. It essentially amounts to a cosmetic improvement. The goal of rehabilitation, a functional improvement, is to restore a building's pre-earthquake strength. Retrofitting, whether or not an earthquake has occurred, is the structural reinforcement of a structure to a pre-defined level of performance. A retrofitted building is designed to perform more seismically than the original structure. According to an assessment of current buildings many residential buildings are not appropriately prepared to withstand earthquakes. Numerous areas of the nation were assigned to higher seismic zones in the latest edition of the Indian earthquake code of IS 1893:2002. Therefore, various buildings made before the code modification may not function properly under the new code. Therefore, it is suggested that current buildings be upgraded to enhance their performance during an earthquake and prevent significant loss of life and property. doing it. For a new structure or site, the goal of the designer is to do it correctly the first time. However, it is frequently essential to enhance or maintain an existing building's seismic resilience for a variety of reasons. The UBC can be used as an example to illustrate the problem regarding code requirements for wind and earthquakes. Recently, every three years, a new version of this model code has been published. The 1997 edition came after publications in 1973,1976,1979,1982,1985,1991,1994, 1998 etc. That implies that a building completed in 1972, for instance, was likely constructed in accordance with the standards of the 1971 UBC, assuming that was the applicable code at the time. The building could not be expected to contain all of the characteristics that were mandated by nine code changes between 1971 in 1999, as a result. It is possible to foresee what could be needed for a code retrofit by placing a building in the right location with respect to code revisions. For instance, if a renovation project necessitates a retrofit, the structure must be brought up to code. But if an upgrade is wanted just for its own sake, the requirements could be more precisely recognized by looking at the design and construction at the time the work was done. It is possible to identify the crucial changes for a given structure relatively quickly because codes are well-documented. Nevertheless, Code modifications are not the whole picture; additional factors could have just as strong or even more significant effects.

Ferrocement

A composite material called ferrocement is made of a rich cement mortar matrix that has been evenly reinforced with more than one layer of extremely fine wire mesh, either with or without supporting skeletal steel. As per "the American Concrete Institute Committee" of 549, ferrocement is a sort of thin wall-reinforced concrete that is frequently made of hydraulic cement mortar and reinforced with continuous mesh layers that are placed near apart and have relatively small diameters. The mesh may well be composed of metal or any appropriate material. In comparison to other types of concrete construction, ferrocement exhibits much higher levels of crack resistance, strength, durability, ductility, and toughness. These properties are attained in constructions with a thickness of typically less than 25mm, a measurement that is both a definite advancement over traditional reinforced concrete and practically unimaginable in other kinds of construction. The creation of Ferro cement came out of the basic tenet of reinforced concrete, which is that concrete could withstand considerable stresses close to the reinforcement and that the amount of the strains relies on how the reinforcement is split and distributed throughout the concrete mass. Ferrocement acts as a composite because the ductile wire mesh reinforcement improves the characteristics of the brittle mortar matrix. The material is given ductility and a superior crack arrest system due to the tighter spacing of the wire meshes (distribution) and the smaller spacing of the wires inside the mesh (subdivision) in the rich cement sand mortar. The ferrocement element's self-weight per unit area is much lower than that of reinforced concrete elements due to their comparatively thin thickness. The ferrocement elements thickness typically ranges between 10 to 40 mm, while the minimum thickness of a plate or shell element in reinforced concrete is 75 mm. For



**Rex and Indraja Gandarla**

manufacturing, Ferro cement is a good choice due to its low self-weight and strong TS. Very high resistance to cracking and other qualities like fatigue resistance, impermeability, and toughness also grow better with the application of small-diameter wire mesh reinforcement across the whole surface.

MATERIALS

In the designing and casting of beams, reinforcing bars, coarse aggregates, fine aggregates, and cement are utilized. For the retrofitting of these beams, MS welded wire mesh as well as cement slurry are employed. The following are these materials' specifications and properties:

Cement

Pozzolana from Portland Cement of grade 43, obtained from a single lot, is employed in the experiment. The cement's physical parameters as acquired from different tests are presented "in Table 3.1. All testing is performed in compliance with the standards specified in IS: 8112-1989.

Coarse Aggregates

The entire experimental investigation makes use of crushed stone aggregate with sizes of 20mm and 10mm, which is readily available in the area. Tables 3.2, 3.3, and 3.4 detail the physical characteristics of the coarse aggregates, whereas tables 3.2, 3.3, & 3.4 exhibit the results of sieving the aggregates.

Fine aggregates

Sand that is readily accessible locally serves as the fine aggregate in the concrete mixture and cement mortar. Tables 3.5 and 3.6 display the physical characteristics of the sand as well as the findings of the sieve examination.

Water

The specimens are cast in fresh water and then cured in clean water. As per the standards of Indian standards, the water is comparatively free of chloride, sugar, oil, silt, organic materials, and acidic material.

Reinforcing Steel

As longitudinal steel, HYSD steel of grade Fe-415 with diameters of 10, 8, & 6mm was employed. Tension reinforcement is provided by 10mm-diameter bars, while compression steel is provided by 8mm-diameter bars. Shear stirrups are made of 6mm-diameter bars. Table 3.7 displays the characteristics of these steel bars.

Steel Mesh

In the ferrocement jacket, MS welded steel wire mesh" with square grids of 2.4mm in diameter has been employed. Mesh has a 40x40 mm grid size. The key characteristics of the mesh wire in use are listed in Table 3.7.

Concrete Mix

A concrete mix of M20 grade is created according to standard design technique utilizing the materials attributes as stated and supplied in Tables 3.1-3.6 The design uses a water-to-cement ratio of 0.5. Cement, sand, and aggregate are mixed at a ratio of 1:1.45:3.123, and the materials' compressive strengths at 7 & 28 days are 21.5 and 29MPa, respectively.

Mortar Mix

The suggested mix ratio for typical ferro cement applications is "between 1:1.5 and 1:2.5 (cement:sand by weight), but not more than 1:3, and the ratio of water cement is between 0.35 and 0.5. The amount of water needed to retain the same degree of workability increases as sand content climbs. The sand fineness modulus, sand-cement ratio, and water-cement ratio must be derived from test batches to guarantee a mix that could penetrate the mesh and build a



**Rex and Indraja Gandarla**

strong & dense matrix. In the current investigation, the mortar employed to create the ferrocement sheets has a cement-to-sand ratio of 1:2 (for cement-to-sand and 0.40 for the water-cement ratio in the mortar).

RCC Beam Design

Fe 415 steel and M20 grade concrete are utilized to design the RCC beam in the current study. The limit state approach is used to design the RCC beam with the assumption that it is an under-reinforced section. Two 8mm steel bars and two 10mm steel bars are used in the design of the beam's compression and tension faces, respectively. The utilized stirrups have a diameter of 6 mm and a spacing of 300mm, which is larger than the minimum spacing needed; therefore, the beam must exhibit shear-deficient behavior. Overall, the beam's dimensions are set at 127 x 227 mm.

Composite Beam Casting

Beam casting is completed in a single step. A 127x227x4100 mm mould is used to cast the beams. To make it simple to extract the beam from the mould once the required time has passed, the entire beam mould is first well-greased. To give the reinforcement with consistent cover, spacers of size 25 mm are employed. Concrete mix is poured into the mould once the bars have been positioned in accordance with the design, and a needle vibrator is used to create vibrations. The vibration continues until there is no gap left in the mould and it is filled. After 48 hours, the beams are then taken out of the mould. After being taken out of the mould, the beams are dried for an overall 28 days inside jute bags.

Beams Retrofitting

Once the beams are stretched to a preset limit, they are retrofitted with steel wire mesh at 45 degrees as shown in Fig. 3.4, and plastered with cement mortar up to 20 mm for all 6 beams. Thus, the ultimate cross-section of the laminated ferrocement beam will be 167x247x4100 mm. Three distinct stress levels—60%, 75%, and 90%—have been examined to determine how they affect the retrofitted beam strength with steel wire mesh, which is positioned over the three surfaces of the beam at a 45° angle. The location of the joint between the wire mesh is given a 3-inch overlap.

RESULTS

In the current work, it is examined how stress level affects a retrofitted shear-deficient beam's strength. To do this, the beams are initially strained to levels of 60, 75, & 90 percent of the safe load. The beams are then refitted with 20mm-thick ferrocement laminate that has one layer of welded wire mesh positioned at an angle of 45 to the longitudinal beam axis. With the aforementioned parameters, a comparison of the strength difference between retrofitting beams and control beams is made, and the results are reported in the next section.

Experimental Ultimate Loads Comparison after Retrofitting

The data below show that the work done so far on the thesis has been justified by the proportion rise in the retrofitted beams' ultimate loads. This is due to the fact that the findings are in favour of the economic consequences and all of the beams were able to function extremely effectively, raising the ultimate loads to proportions as high as 63.97, 53.6, and 46.75 for stress levels of 60, 75, & 90%, respectively.

CONCLUSIONS

The conclusions mentioned below might be made on the basis of experiment findings: -

- Shear and flexural fractures across the stress zone are a defining feature of composite failure. At retrofitted beams along with wire mesh at 45 for various stress levels, the fracture spacing is less, showing improved stress distribution.
- When loaded to failure, the beams with wire mesh retrofits for various levels of stress don't de bond.





Rex and Indraja Gandarla

- The retrofitted beam with the maximum load-carrying capacity relative to other specimens is the one that corresponds to a stress level of 60%, demonstrating that rising stress levels lead to decreasing strengthening in order.
- The maximum strength/cost ratio for retrofitted beams at a stress level of 60 percent indicated that the specimens R1 & R2 are the most effective since they have the greatest strength/cost ratios of 0.69 and 0.74, respectively.
- All of the samples after retrofitting displayed decreased crack width, substantial changes in the ductility ratio, substantial increases in energy absorption, and large deflections at the ultimate loads, which made the various specimens suitable for use in components subjected to dynamic loads.

REFERENCES

1. ACI Committee 549, "Guide for the Design, Construction and Repair of Ferrocement". ACI Structural Journal, May - June 1988.
2. Ahmed Khalifa and Antonio Nanni, "Improving Shear Capacity of Existing RC T – T-Section Beams Using CFRP Composites", Cement and Concrete Composite. Vol 22, No 2, July 2000.
3. Ahmed Khalifa; Antonio Nanni; Abdel Aziz .M.I; William.J.Gold., "Contribution of Externally Bonded FRP to Shear Capacity of RC Flexural Members". Journal of Composites for Construction / Nov 1998.
4. AL- Sulaimani , G.J . andBasinbol ,F.A., " Behaviour of ferrocement material under direct shear " , Journal of ferrocement , vol 21,no 2 , April 1991. BIS: 10262-2009:Recommended guidelines for concrete mix design, Bureau of IndianStandard, NewDelhi-2004.
5. Alexander , D., " What is ferrocement " , Journal of ferrocement ,vol 22 , no 1,January 1992 .
6. Al- Sulaimani, G.J., Brundel R. and Mousselhy, E., "Shear behaviour of ferrocement box beams", J. Cement and Concrete,1977.
7. ACI Committee 549 (1982), " State of the art report on ferrocement " , Concrete International 4.
8. American Society for Testing and Material (1980) , "Annual book of ASTM standards",1980, part 14.
9. American Concrete Institute (1979) , "Ferrocement Materials and Applications " , pub SP-61.
10. Application of ferrocement in Developing countries (1973), " National Academy of Sciences, 90.
11. Chemboi.A. and Nimityongskol.P.(1969), "A bamboo reinforced cement water tank " , Journal of Ferrocement,19 (1).
12. Choey pint.C.;Nimityongskol.P. and Robles-Austriaco.L. (1988) "Rice Husk ash cement for Ferrocement". Proceedings of Third International Symposium on Ferrocement, University of Roorkee.
13. Collen, Kirwan,L.D.G. (1960), "Some Experiments in Design and Construction with Ferrocement", Transactions Institute of Civil Engineering, Ireland,86,40.
14. Desai Prakash;Nandkumar N .and El- Kholy, A..Sayed, "Shear strength of ferrocement trough section elements " , Journal of ferrocement, vol .24, no 4 Oct 1984.
15. Desai .P; and Nandkumar.N;"A quasi-empirical approach to the shear strength of ferrocement trough section elements " , Journal of ferrocement, vol 25, no 4, Oct 1995.
16. Raj.V. "Utilisation of lime for improving the durability of Ferrocement " Proceedings of Third International Symposium on Ferrocement,University of Roorkee,Roorkee,1988.
17. Rafeeqi.S.F.A.;Lodi.S.H;Wadalawala.Z.R. "Behaviour of Reinforced Concrete Beams Strengthened in Shear " Prof and Co Chairman,Dept Civil,NED Univ of Engg and Tech, Karachi(Pakistan).
18. Kaushik.S.K and Gupta.V.K "Proceedings of Second Asia Pacific Symposium on Ferrocement , Roorkee, India,25-27 February 1994".
19. Kaushik .S.K ;Gupta.V.K. andRahman .M.k. " Efficiency of mesh overlays of ferrocement elements " ,Journal of ferrocement 17(4). 1987
20. Kaushik .S.K and Garg.V.K "Rehabilitation of RC Beams Using Precast Ferrocement Bonded Plates" Department of Civil Engineering ,University of Roorkee.
21. Mansur.M.A. and Ong.K.C.G .,"Shear strength of ferrocement beams " , ACI Journal 84 (1) ,1987
22. M.A.Al-Kubaisy and P.J. Nedwell,"Behaviour and Strength of Ferrocement Rectangular Beams in Shear" , Journal of ferrocement Vol .29 . No 1 Jan 1999





Rex and Indraja Gandarla

23. Paul .B.K; and Pama .R.P . , "Ferrocement Bangkok", Ferrocement Information Centre ,Bangkok, Thailand ,1978.
24. Venkatesvarlu .B., " Design of ferrocement components", I.C.J., Vol (2) No 3 Nov 1989.
25. Venkatakrishna.D and Raj.V.(1989),"Development of Bamboo based Ferrocement roofing elements for low cost housing",Journal of Ferrocement.,19(4).
26. VicenzoColloti and GiuseppeSpadea," Shear Strength of RC Beams Strengthened with Bonded Steel or FRP Plates ". Journal of structural engineering , April 2001.

Table 3.1: Physical Properties of Cement used

Sr. Number	Characteristics	Value attained Experimentally	Specified value according to IS: 8112-1989
1.	Compressive strength(N/mm ²)		
	1. 7 days	33.5	33
	2. 28 days	43.5	43
2.	Specific gravity	3.07	-
3.	Cement fineness as Retained on 90micron sieve	0.5	<10%
4.	Standard consistency	34	-
5.	Setting time		
	Initial	35mins	>30mins
	Final	5hours	<10hours

Table 3.2:Coarse Aggregate’s Sieve Analysis (20mm) Total weight taken=3kg

Sr. Number	Size of Sieve	Mass Retained(kg)	% Retained	Cumulative% Retained	% Passing
1.	4.75mm	0.1300	4.33	99.69	0.31
2.	10mm	0.6745	22.483	95.366	4.634
3.	12.5mm	2.1865	72.883	72.883	22.117
4.	20mm	0	0	0	100
5.	Pan	0.009	0.3		0
				Σ=267.93	Fineness modulus = 7.68

Table 3.3:Coarse Aggregate’s Sieve Analysis (10mm) Total weight taken=3kg

Sr. Number	Size of Sieve	Mass Retained (kg)	% Retained	% Passing	Cumulative% Retained
1.	4.75mm	0.9565	31.88	19.94	80.06
2.	10mm	0.8905	29.68	51.82	48.18
3.	12.5mm	0.555	18.5	81.5	18.5
4.	Pan	0.5970	19.90		
					Σ=146.74 Fineness modulus=6.47

Table 3.4:Coarse Aggregates’ Physical Properties

Sr. No.	Characteristics	Value	
		20mm	10mm
1.	Fineness modulus	7.68	6.47
2.	Water absorption	3.645	1.643





Rex and Indraja Gandarla

3.	Specific gravity	2.655	2.704
4.	Type	Crushed	Crushed

Table 3.5: Fine Aggregates’ Physical Properties

Sr. No.	Characteristics	Value
1.	Grading Zone	Zone III
2.	Water Absorption	2.06%
3.	Fineness modulus	2.51
4.	Bulk density loose (kg/lt)	1.48
5.	Specific gravity	2.56

Table 3.6: Fine Aggregate’s Sieve Analysis Total weight taken=1000gm

Sr. Number	Size of Sieve	Mass Retained (gm)	%Retained	Cumulative % Retained	% Passing
1.	1.18mm	110.5	11.05	24.8	75.2
2.	2.36mm	42.5	4.25	13.75	86.25
3.	4.75mm	95.0	9.5	9.5	90.5
4.	150µm	281.0	28.1	96.55	3.45
5.	300µm	308.0	30.8	68.45	31.55
6.	600µm	128.5	12.85	37.65	62.35
7.	Pan	34.5	3.45		
				Σ = 250.70	Fineness modulus = 2.507

Table 3.7: Steel Bars’ physical properties

Sr. Number	Diameter of mesh/bars wire	Yield-strength (N/mm ²)	Ultimate strength	%Elongation
1.	2.4mm	400	511.36	2.52
2.	6mm	442.42	612.7	32.9
3.	8mm	559.5	634.13	20.3
4.	10mm	445.55	509.2	15.5

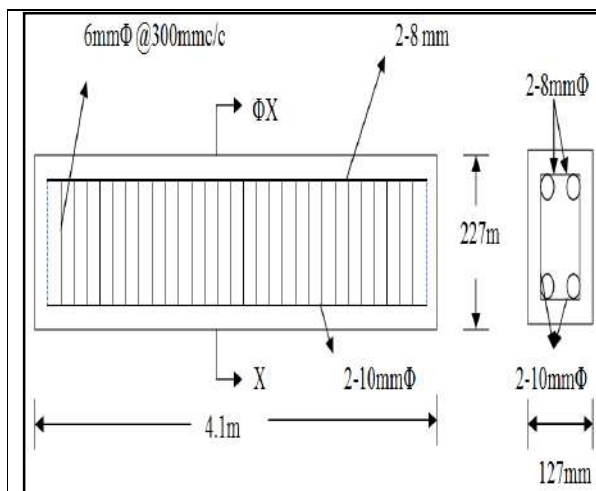


Fig.3.1: Beam Cross-Section



Fig.3.2: Orientation of Wire Mesh at 45 degrees





Rex and Indraja Gandarla

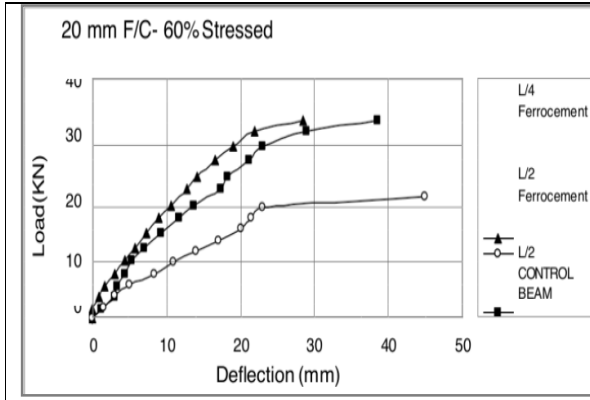


Fig.7.1:Load Deflection Curve for Specimen (R1)

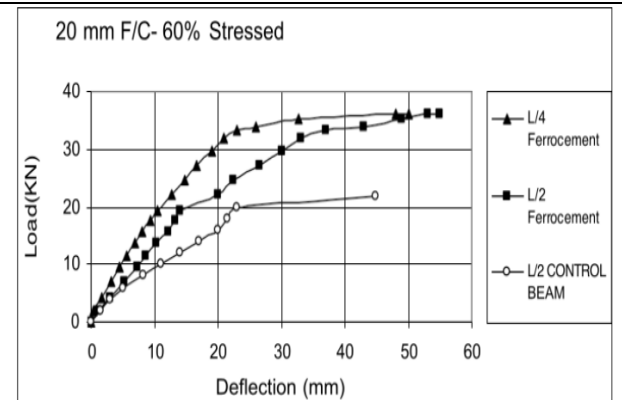


Fig.7.2:Load Deflection Curve for Specimen (R2)

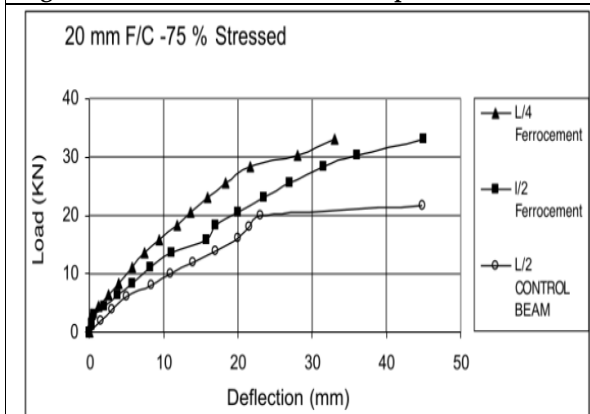


Fig.7.3:Load Deflection Curve for Specimen (R3)

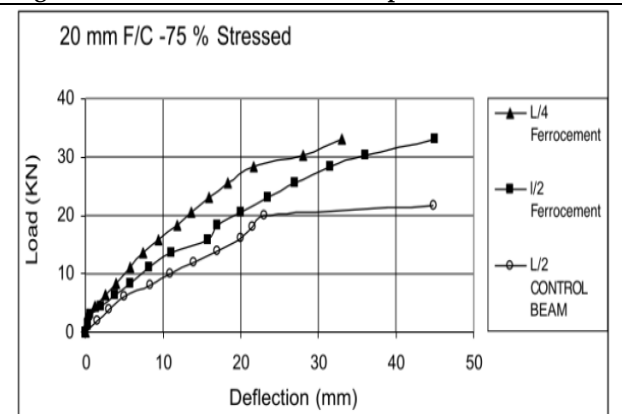


Fig.7.4:Load Deflection Curve for Specimen (R4)

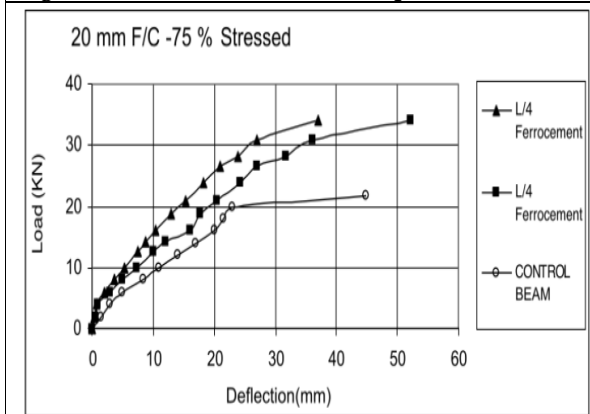


Fig.7.5:Load Deflection Curve for Specimen (R5)

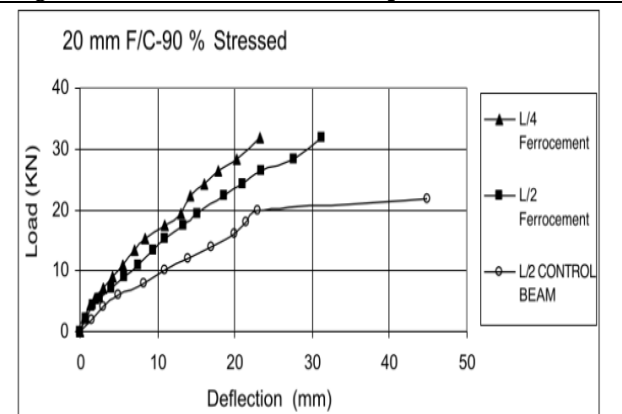


Fig.7.6:Load Deflection Curve for Specimen (R6)





Rex and Indraja Gandarla

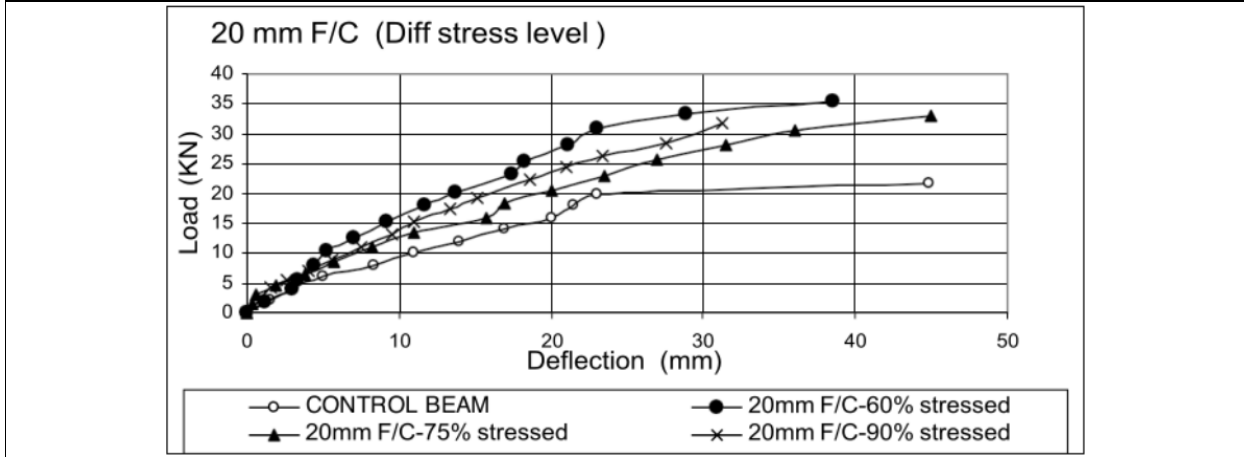


Fig.7.7:Comparison with the control beam at various stresses





A Systematic Review in Health Care Prediction of Diabetes using Machine Learning Models with Cloud and IoT Technology

M.Reena Ivanglin^{1*} and R.Pragaladan²

¹Ph.D Research Scholar, Department of Computer Science, Sri Vasavi College, (Affiliated to Bharathiar University, Coimbatore) Erode, Tamil Nadu, India.

²Associate Professor and Head, Department of Computer Science, Sri Vasari College (Affiliated to Bharathiar University, Coimbatore) Erode, Tamil Nadu, India.

Received: 05 Sep 2023

Revised: 09 Nov 2024

Accepted: 04 Jan 2024

*Address for Correspondence

M.Reena Ivanglin

Ph.D Research Scholar,

Department of Computer Science,

Sri Vasavi College, (Affiliated to Bharathiar University, Coimbatore)

Erode, Tamil Nadu, India.



This is an Open Access Journal / article distributed under the terms of the **Creative Commons Attribution License** (CC BY-NC-ND 3.0) which permits unrestricted use, distribution, and reproduction in any medium, provided the original work is properly cited. All rights reserved.

ABSTRACT

Active research field in today's modern world is healthcare technology uses contemporary technology in the medical field. The patient-generated data is communicated or detected by wearable sensor electronic devices. This makes it possible for medical professionals to view the patient's activities in real-time. Furthermore, every day a significant amount of new medical information was created continuously. To anticipate these individuals' health, there is an innate need to collect, preserve, and benefit from medical information. Machine Learning (ML) is proposed for predicting the presence of diabetics within an hour. Additionally, it is used to predict the diabetic's level in the future based on Gastric Contractility Modulation (GCM) it is taken into account to execute the forecasting methods using integration with cloud technology & Internet of Things (IoT) methods. Numerous ML techniques have superior features in terms of increased prediction accuracy. Medical researchers are deeply concerned about an alarming increase in the number of diabetes patients. It includes detectors in intelligent wearables as a group of interconnected IoT devices for regular inspection and collecting of blood glucose data that was transmitted of retention in cloud architecture an ensemble classifier was employed to forecast diabetes in individuals. The forms of insulin were discussed in this research together with data acquired using IoT methods of insulin forecasting.

Keywords: Healthcare Research; Diabetes; Iot; ML Technique; Cloud Computing



**Reena Ivanglin and Pragaladan**

INTRODUCTION

A global pandemic of insulin resistance, sometimes known as diabetes, has emerged. Insulin was a T2D metabolic ailment in which the blood sugar level fluctuated. Type 1 Diabetes (T1D) was brought on by inadequate insulin sensitivity, whereas Type 2 Diabetes (T2D) was brought on by the body's incapacity to employ the medication that was generated [1-3]. T1D and T2D diagnoses are increasing but T2D has increased rapidly. T2D makes up 90–95% of insulin and was an epidemic that is putting a tremendous strain on medical methods, particularly in improved nations. A new viewpoint on insulin care was provided by the recent development of information and communication systems and new biosensors that could allow actual-time assessment of a patient's status [4]. Glucose monitoring detectors are mobile self-monitoring blood glucose gadgets, diabetic patients could make adjustments to blood sugar levels and take the necessary actions on time. The findings demonstrate that individual glucose level measurement enhances the effectiveness of diabetes care and helps patients achieve greater control over their disease [4]. The ideal contender to enhance insulin care would be a glucose measurement system made up of detectors, a portal, and a network system.

A cellphone serves as a gateway for the collection of sensor information from a sensor node affixed to the body [6]. Recent research has used ML algorithms as decision-making tools for insulin and hypertension at an early stage that people could be preventative measures [7-8]. This would increase insulin and hypertension. In people's existing conditions, ML algorithms have demonstrated great results in forecasting insulin and hypertension. Additionally, it was shown that the ML systems Random Forest (RF) were improved at forecasting insulin and hypertension with the greatest prediction performance matched to classification techniques [9]. However, the ML algorithms face difficult issues with asymmetric datasets and outlier data might lower accuracy [10]. Several studies are undertaken, and they have shown that ML algorithms could be predicting hypertension early on and treat it [11]. On a sizable patient population, they employed ML techniques to identify factors that contribute to the success of hypertension medicine management. An ensemble prediction method called RF gathers the results of individual Decision Trees (DT). The bagging method is commonly used by RF to create subgroups of training data [12]. An approach called a DT is used to train samples. The final step should be to obtain the predicted outcomes method of the DT in the forest [13]. A study on the use of RF in the early diagnosis of insulin and hypertension produced noteworthy findings [14]. Instead of emphasizing the value of data pre-processing, the majority of current research concentrates on creating more useful predictions. A good classification could be produced for better decision-making by using the outlier identification approach in the pre-processing stage to find discrepancies in the data and outliers [15]. The classification performance would be improved by removing the outliers of the training sample. For several study fields, such as healthcare, records management, social networks, and sensor technologies, outlier detection would be a significant problem.

Outlier detection was discovered to greatly enhance classifier performance in a variety of studies [16–17]. Outlier identification could be accomplished using the clustering methods. The primary premise of the classification model was that normal cases correlate to large, dense clusters, whereas outliers form smaller groups or clusters [18]. In addition to the aforementioned advantages, using many wearable devices involves regular maintenance, which complicates the lifestyle of insulin and could result in a drop in perceived quality of life [19]. Wearable detectors' wireless and private nature exposes them to several distinctive security flaws that have an immediate impact on the confidentiality of individual information [20]. As a result, it's critical to comprehend the advantages of building big data sets, the increased computational effort needed to interpret the data, the costs to consumers of gathering the data, and the consequences of using the information improperly. The association between past and future blood glucose levels was learned using ANN in a different class of estimation methods for data sources [21]. For instance, a system that integrates insulin dosages, meals, some lifestyle factors, and emotions was created to assess blood glucose levels using the fingerstick system. However, it is difficult to duplicate the methods used to create the forecasting method of the several pre-processing signal processing procedures. To accurately compute the system parameters of the systems and prevent overfitting, Neural Network (NN) based algorithms need a lot of data [22].



**Reena Ivanglin and Pragaladan**

Nevertheless, the bulk of research either used a generated dataset or brief actual-world information-gathering efforts to evaluate the efficacy of the systems [23]. Consequently, it was crucial to ensure that the information utilized to train modeling techniques by design, long-term, and comprised of actual people. To the greatest of my knowledge, there has never been a thorough assessment of the various diabetes forecasting models [24]. It is impossible to draw general conclusions from investigations that examined a few strategies employing diabetes to a few other variables [25]. Since the sources of the data varied from investigation to research, it is impossible to objectively compare the techniques investigated in various publications.

T1D: Preprocessing; Feature selection and Classifications

The performance of surgical treatments, diagnostic procedures, and drugs may be predicted using data mining techniques in the healthcare field, and correlations between clinical and pathological information could be found [26]. The application of Deep Learning (DL) to clinical decision-making resulted in thorough literature analysis of several ML systems that might aid networking opportunities in adopting ML techniques to improve the efficiency and standard of health decision-making processes [27]. To enhance medical decision-making, data mining approaches have been applied to a variety of healthcare areas. A contrast of the several learning methods used in health information gathering, along with helpful instruction to choose the method best suited for certain clinical applications [28]. Since many years ago, analytical recognition systems, ML, data gathering, and informatics have been actively researching and developing variable selection [29]. It was shown to promote prediction performance, improve learning efficiency, and minimize the complexity of learned discoveries in both theory and models. Researchers have commonly found that there are insufficient qualities since they are usually redundant or superfluous about the category idea that there are hundreds or thousands of factors involved [30]. Numerous applications, including document classification, picture retrieval, genetic microarray research, customer relationship management, and intrusion prevention, have found success with feature extraction.

They evaluate the significance of individual features or feature subsets, filter approaches could be divided into two types, namely characteristic assessment techniques and subgroup assessment methods [31]. The importance is information to the target concept was taken into account by characteristic assessment methods to rank and weight the characteristics. Since attribute evaluation approaches for the connection across characteristics are likely to generate selections of redundant features [32]. Contrarily, subgroup evaluation algorithms choose feature subsets and score them by specific assessment criteria; as a result, they are more effective in removing duplicate characteristics [33]. Experimental investigations have demonstrated that redundant and irrelevant characteristics could significantly lower the predicted performance of data-driven models [34]. Information-theoretic, statistical interdependence and probabilistic estimation methods are a few examples of evaluation functions in the classification method [35]. These measurements are frequently regarded as inherent characteristics of the information because they are computed using the raw data without the need for a learning method that smoothes ranges or lowers noise. One efficient way to eliminate pointless characteristics is through feature extraction.

DL frequently uses the association for significance assessment. To identify pertinent traits, researchers frequently use various estimates [36]. However, it relates to the category, a particular trait could be deemed useless, but integrated of characteristics; it becomes especially pertinent [37]. A wide range of healthcare fields, including rheumatology, thyroid ailment diagnostics, breast cancer prognostics, and localization of primary tumors, have satisfactorily used supervised teaching methods like categorization. For Binary classification issues, the Support Vector Machine (SVM) was initially created [38]. An extremely used visited ML technique is SVM. SVM of the classifications that the DL community has been actively developing has been satisfactorily used to solve a range of medical issues [39]. Develop an appropriate feature selection method for better classifier choice to address the shortcomings and drawbacks of the existing techniques. Algorithms have been used by several investigators to improve the categorization performance of medical information [40]. When contrasted to other methods, the classification performance should be at its highest, and since enough data were used to classify the patients, the diagnosis accuracy has increased [41–43]. Alternately, the artificial flora method has been developed of resolving challenging, nonlinear, and discontinuous optimization issues. It is the movement and reproduction of flora. Plants could be disseminating seeds to a limited



**Reena Ivanglin and Pragaladan**

extent to choose the proper environment [44]. Artificial Neural Network (ANN) could be used in smart optimization techniques since the stochastic process is simple to replicate and has a wide region of distribution. There are various designs for diagnosing diabetes, but none of them can divide patient diagnoses into the various forms of diabetes mellitus [45]. Prediction performance was widely acknowledged and utilized as the main metric by practitioners and researchers since it serves as the fundamental objective of categorization for supervised learning [46]. A Receiver Operating Characteristic (ROC) curve could be used to illustrate well a classification was performed. In the region of the Area Under Curve (AUC), the ROC curve is utilized to compare the performance of the classifier before and after feature extraction. There is a need for an autonomous estimation method that alerts individuals to their propensity to acquire insulin in the future and provides them with the information they need to take preventive action. Based on a participant's actual health, machine learning techniques could be used to categorize insulin [47,48].

Supervised learning classification methods are well-known ML techniques that build a classification method from a training dataset to determine the classes for the input data by building databases with DB tuples and associated class tags [49]. Multiple types of research on insulin categorization have been carried out using medical databases like the PIMA Indian datasets. The sample includes 768 patients, of whom 268 are insulin-dependent and 500 are not [50]. Three kernels—linear, polynomial, and radial basis—are used in the researchers' suggested Gaussian process-based classification method [51]. The proposed framework was contrasted with already-used methods such as NB, linear discriminate evaluation, and quadratic differentiate assessment. The outcome determines that a GP-based framework performed the alternatives. The SM-RuleMiner of insulin categorization was suggested by the researchers [52]. The report's findings demonstrated that in terms of median categorization outcomes and median sensitivity, the recommended SM-RuleMiner performed the methods. Additionally, offer a brand- new data mining-based approach for forecasting T2D. Several people might be assisted in detecting an increment in insulin at a preliminary phase by the provision of an insulin detection technique employing input data comprising medical information and cutting-edge medical devices [53]. Multiple studies have shown that such a program has the potential to significantly improve the lives of many individuals.

To predict Mellitus or pre-insulin using common risk factors the scientists assessed the effectiveness of logistic regression, ANN, and decision tree methods [54]. To gather data on demographic traits, family history of diabetes, anthropometric measurements, and lifestyle issue indicators, the researchers used a standardized questionnaire [55]. Twelve input parameters and an outcome variable of the survey results were used in the classification procedure. Significant risk indicators such as vital signs, diagnoses, and demographics that were utilized to forecast insulin were among the elements of the report [56]. The Adaboost ensemble model outperformed bagging and the standalone J48 decision tree, according to their experiment results. Insulin hazard classification techniques such as Random Forest, Decision Tree, ANN, LogisticRegression, and NB are compared [57–58]. Medical data including BMI, age, weight, height, blood pressure, gender, family history of diabetes or hypertension, and drinking and smoking habits were used as input features while the class was either at risk for insulin or regular. The report's findings demonstrate that, when contrasted to the other techniques, Random Forest delivered the best outcome. Since T1D would be a T2D condition, individuals must be aware of their blood sugar levels to make sure they are as near to the normal limits as achievable [59]. According to various research, BG forecasting could assist patients in obtaining future estimates of their BG level so that proactive notifications could be sent out before serious hypo/hyperglycemic events take place.

T2D: Preprocessing; Feature selection and Classifications

The most prevalent kind of Mellitus, type-2, often appears at the age of 40 and represents about 85– 95 percent of the cases in prosperous countries and an even greater percentage in poorer nations [60]. Diabetes arises the body is unable to create enough glucose or respond in a way that controls sugar. Mellitus raises the risk of heart disease but also of renal ailment, blood vessel damage & nerve damage [61]. A diagnosis is frequently made by looking at a participant's most recent test findings or by consulting past decisions regarding patients who had the same disease. The first technique heavily relies on the surgeon's knowledge, but the second method relies on the doctor's experience to contrast his person with his prior sufferers. Given the variety of elements that must weigh, this is an easy task. Selecting the feature subset that increases predictive performance is known as feature subset selection.



**Reena Ivanglin and Pragaladan**

The similarity concept serves as the foundation for the choice of feature subsets methodology. This means that would favor models with the fewest characteristics feasible that accurately reflect the information [62]. The difficulty of choosing the most pertinent features that enhance predictive performance was given special consideration because the health data contains an excessive number of characteristics. Numerous attributes of pattern recognition were impacted by the characteristics selected to represent the structures that are proffered to a categorization, such as the accuracy of the investigated classification technique, the time frame needed to learn a classification model, the number of instances needed for learning, and the price of the properties [63]. Searching through various subsets and assessing a criterion, such as correctness, constitute feature selection. To increase predictive performance, increase model complexity, and enhance the visualization to understandability of induced categories, feature selection approaches aim to decrease the cost and difficulty of classifications.

The evaluation of their value in the assessment decision was a method of choosing pertinent features from a dataset [64]. Accurate medical diagnosis is made possible by incorporating feature selection techniques into ML algorithms. To increase the effectiveness of patient care, healthcare organizations were employing data mining methods. They encounter numerous difficulties while attempting to make sense of a sizable, varied, and frequently complex supply of health care information [65]. Numerous practical problems in clinical medicine have been effectively solved by several prediction data mining techniques. This research makes an effort to underline the importance of integrating feature selection techniques into medical decision support devices that could be the medical profession to leverage methods of improving the accuracy of diagnosis. The core idea behind XGBoost is to employ the CART decision tree classifier to iteratively calculate correct predictive performance. The existing gradient boost approach, which integrates a linear model with a tree learning method, is improved by the optimization method XGBoost. To prevent overfitting, XGBoost controls the designer's intricacy by lowering the variance of the model by including periodic components in the cost function. The ability of this technique to dynamically leverage CPU multi-threads for parallel computing & enhance accuracy through method optimization is the most prominent aspect. In the domains of machine learning, data processing, data gathering, & analytics, the XGBoost method is regularly employed. It has very good precision and is utilized to tackle a variety of real-world issues [66].

Gradient Boosting Decision Tree-based was improved of XGBoost. This individual's objective is to create several CART trees from characteristic separation components. The objective function was decreased to fitting the residual predicted by the previous model each time a CART tree is built. Finally, a strong classifier is created by combining numerous CART weak classifiers, and each tree's leaf node correlates to a rating [67]. According to the features of the specimen, the algorithm would determine the associated leaf nodes in each tree when a specimen was anticipated. The total score of leaf nodes makes up the sample's work that was intended. In the process of building the XGBoost framework, the optimal variables for the model were also acquired by training instances according to the concept of solving the optimization problem, and the new instance would be anticipated by the optimized parameters and the forecasting operation [68]. Feature extraction, also known as Differential Choice, would be a thoroughly utilized information preparation method of information mining that would be essentially used to lowering of information by eradicating inconsequential and unnecessary characteristics of databases [69]. Furthermore, the approach boosts to understandability of information, permits the presentation of information, lowers the learning process to supervised methods, and enhances the efficiency of forecasts. Several implementations of appropriate methods detection approach in the health sector [70]. Filter methods, wrapper methods, classification techniques, embedded approaches, and widely used approaches of estimation methods. The majority of studies today were concentrating on edge detection approaches. To acquire more accurate findings faster, it was often advisable to remove erratic and incorrect information before employing any algorithm on the information [71]. Improving a dataset's complexity was essential for potential implementation. Moreover, if most key characteristics are identified, the sophistication decreases dramatically. Different learning algorithm performs effectively and produces more precise findings of the dataset shows that important



**Reena Ivanglin and Pragaladan**

and non-redundant attributes. An effective feature selection strategy is required to extract intriguing characteristics that are pertinent to the ailment because healthcare databases contain a huge number of redundant and irrelevant characteristics [72].

The diagnosis of knee joint abnormalities utilizing VAG impulses was advised using a good detection method. A new segmentation and classification method was implemented. The apriori algorithm and evolutionary algorithms were used to identify the most important and consistent traits. Random forest and LS-SVM predictors were used to assess their effectiveness [73]. Additionally, the idea of wavelet transform was used to distinguish between diseased and normal VAG information. Results are compared based on assessment measurements indicating evaluation of LS-SVM utilized the method is a precision of 94.31% [74]. The suggested method is very beneficial in the earlier detection of knee joint illnesses in patients who could indeed receive treatment immediately. These methods were divided into three categories by the writers: unsupervised, semi-supervised, and supervised variable methods. Additionally, several difficulties and barriers to understanding gene expression data were resolved [75]. A categorization performance of unsupervised and semi-supervised techniques is found to be as interesting as supervised method choosing through an empirical investigation on gene selection. An original way to select the optimal group of attributes for a type II insulin database uses SVM ranking of backward search [76]. The Naive Bayes classifier's predictive performance massively enhanced the suggested strategy. The procedure employed was quite straightforward yet efficient, and it would undoubtedly aid doctors and other medical professionals in the identification of Type 2 diabetes.

Feature selection approaches

The three main categories of conventional feature selection techniques of computer vision are wrapper, filter, and embedded. Figure 2 depicts the feature selection method that could be used to decrease the input database before passing it to the training algorithm.

Filter Method

Before the use of any learning method, characteristics are filtered in the attribute selection utilizing the filter technique. Based on a set of assessment criteria, it scores the characteristics. It tends to produce varying results on the forecast because it is dependent on the classification being utilized [77]. The methods deliver results that are efficient and rapid. They referred to wrapper approaches of large datasets as a consequence. The drawback of these methods is that they don't consider classifications connected with a characteristic that affects others. As a result, they might not choose the most "valuable" characteristics. The MIFS attribute selection approach performs "greedy" attribute selection but is based on the concept of mutual information [78]. In this technique, component classification, the most mutual information possible was extracted. MIFS was less popular yet to the prevalence of several implementation problems. A greedy filtering feature selection approach, called Reciprocal Based on Data Productive Criteria, was developed in response to the shortcomings of antecedents. It was based on the concept of correlation. An important feature was taking into account the characteristics' relevancy and lack of duplication of the extracted features [79]. The main benefit of this algorithm over its predecessors MIFS and MIFS-U is that it chooses characteristics without needing any variables like B. As a consequence, as compared to its predecessors, the outcomes with MICC were more encouraging. Through the use of a hybridized framework, a correlation-based features extraction strategy was used to diagnose Coronary Artery Disease [80]. Using a correlation feature selection strategy, particle swarm improvement, and a classification algorithm, the most important risk variables for CAD illness were found. The development of prognosis methodologies for the CAD condition made use of the C4.5 method, (MLP), MLR, and fuzzy unsorted pattern matching method [81]. The 10-fold cross-verification approach is utilized to evaluate the CAD model. For clinical data and data related to Cleveland cardiovascular diseases, the MLR method had the highest predicted performance, whereas the MLP method had the least. The findings of the suggested methods were highly encouraging and considerably increased classification performance. As a consequence, this method could help make medical decisions, such as the identification of the CAD condition.



**Reena Ivanglin and Pragaladan****Wrapper Method**

Wrapper techniques make decisions about attributes while considering the supervised learning that will be employed into consideration. Its main advantages over filter techniques include identifying the most "useful" traits and selecting the ideal set of data for the learning experience [82]. In addition, it takes feature dependencies into account and provides more accurate results than filter approaches. Its drawback is that this procedure must be redone to a different learning algorithm should be used [83]. This technique is quite complicated and more likely to overfit on small trained data. Examination and evaluation are the relief method for selecting wrapper characteristics. To select the best feature subset, the authors investigated the wrapper approach's benefits and drawbacks. Decision trees and the Nave Bayes classifier, two induction techniques, were used in the tests, which included actual and synthetic information [84]. Outcomes revealed when the wrapper strategy was combined with a naive Bayes classifier, the error rate was dramatically decreased.

Embedded Method

The search was often driven by the learning experience in the integrated feature selection strategy [85]. Patients typically operate by particular learning methodologies that aid in enhancing the effectiveness of a training algorithm. This methodology allows more efficient use of the available information and offers quicker alternatives as they call for separating the classification model into classification models as well as verification collectives [86]. Compared to wrapper approaches, they are less susceptible to over-fitting and operationally cheap. Additionally, integrated techniques' computational complexity was higher than that of ensemble methods. The primary drawback of methodologies is that they base their choices on the classifier [87]. As a result, the classifier's hypothesis that might be correct could influence the features that are chosen. A backward component selection-based embedding technique was put forth. The goal was to pick the most major characteristics from unbalanced data to use SVM for the classification model. Table 2 illustrates the feature selection algorithms characteristics in T2D. Table 2 classifies characteristic methods based according to the search method, the criterion for assessment, and the data analysis task.

Traditional classification systems

Dynamic categorization and simultaneous classification techniques may be used to analyze generated data to produce prediction results, as shown in Figure 3. By including the adaptivity function to assist vector machines, illnesses might be diagnosed. Adaptive SVM should be the objective to provide a quick, computerized, and flexible assessment and diagnosis [88]. To improve the outcomes, the probability factor in the traditional SVM was altered. The outcome of the classifications that were supplied was a list of "if-then" instructions. Carcinoma & diabetes were both diagnosed using the newly created approach, which had 100% prediction performance for categorizing every ailment. Developing more effective ways to modify the bias value in a typical SVM should be a focus of future research [89]. a hybrid type 2 diabetic prediction system correlation-based and classification. The suggested model uses k-fold cross-verification of forecasting along the C4.5 classification method and K-means clustering. The hybrid strategy enabled the system to achieve impressive outcomes, with a classification accuracy of 92.38%, which might be highly beneficial for doctors in making wise therapeutic decisions regarding diabetics. Future research can focus on creating more accurate models for illness prediction. Figure 4 illustrates the use of simultaneous segmentation to process data to provide prediction outcomes. The researchers used a parallel support vector machine to diagnose diabetes. The distribution of datasets over several computers was made easier by the use of parallel SVM, which reduced the computation overhead, energy use, and storage use on each machine [90]. With the help of the findings, this was discovered that perhaps the suggested method ran on either a single computer in 1/3 the time that basic SVM did. Additionally, the classifier's performance has been on par with basic SVM capabilities. The developed approach was shown to be quite trustworthy and it can be used for large, imbalanced datasets. In the future, this technique may be used on many devices to improve generalization ability and yield better results.

Classification model performance measures

The performance indicators are typically employed to evaluate the effectiveness of various models [91].





Reena Ivanglin and Pragaladan

Accuracy The number of outcomes that were successfully anticipated in proportion to the total number of predictions was computed. This is described as the proportion of information that is correctly categorized including all data that is identified.

$$Accuracy = \frac{T^+ + T^-}{T^+ + T^- + F^+ + F^-} \quad (1)$$

Whereas, True Positive (T+); True Negative(T-), False Positive (F+), and False Negative(F-)

Sensitivity Retention is the number of pertinent things which are chosen. This ratio is the product of real positives and false negatives. Test sensitivity (Recall) in medical diagnosis refers to a study's capacity to accurately diagnose a condition. They could almost certainly be assured that they don't have an illness if the test has a high recall rate and the results are negative.

$$Sensitivity = \frac{T^+}{(T^+ + F^-)} \quad (2)$$

Specificity The quantity of accurate negative predictions separated from the overall quantity of negatives was used to compute specificity (SP).

$$SP = \frac{T^-}{(T^- + F^+)} \quad (3)$$

Precision

How many chosen items are pertinent is measured by precision. It measures the proportion of genuine positives to the total of false and true positives. A capacity of a test to accurately identify people who do not have a disease is known as test specificity. Users can be almost assured that they genuinely have the condition if the test outcome for a very accurate test is positive [92].

$$Precision = \frac{T^+}{(T^+ + F^+)} \quad (4)$$

False Positive Rate: The FPR was calculated by dividing the overall number of inaccurate negative predictions. It's outlined as:

$$FPR = \frac{F^-}{(F^- + T^-)} \quad (5)$$

F-measure: The F-measure is the balanced harmonic mean of the accuracy and recollection of the system.

$$F = \frac{1}{\frac{1}{P} + (1 - \alpha)(1/R)} \quad (6)$$

The existing feature selection methodologies and categorizations for accurate illness prediction are reviewed in this work. Also covered are the measures of success used in medical diagnostic systems to evaluate how well the categorization algorithms are working. This study also contrasts the advantages and disadvantages of various feature selection strategies and classifications on their own [93]. This publication also describes the value derived from earlier academics' work on well-known T2D illness data. The classification of algorithms for selecting features in this research is also provided [94] based on search strategy, assessment standards, and data gathering jobs. Numerous researchers have offered a variety of parameter estimation and classification models for disease earlier detection, but this study suggests that there are still plenty of prospects for creating new strategies to achieve and improve an enhanced prior researcher. An analysis of the technique for selecting features shows that a specific feature selection strategy is crucial for the correct categorization of illnesses [95]. The survey shows that the filter method prepares two techniques & therefore is computationally efficient. When a certain training algorithm requires an optimum data subset, a wrapper and embedding method should be utilized. According to this analysis, hybrid techniques that can be employed to eliminate repetitive, harsh, and unimportant characteristics from illness datasets are where studies are currently progressing [96]. Combining the advantages are two or more methodologies, a



**Reena Ivanglin and Pragaladan**

hybrid strategy benefits. Unfortunately, there aren't many empirical studies that employ hybrid techniques to forecast diseases. It is, therefore, necessary to apply future opportunities and advancements of such techniques to illness information. The majority of current classification method study has concentrated on employing SVMs, decision trees, ANNs naive Bayes, & decision trees, to forecast T2D illnesses [97]. This media concentrates on the use of simultaneous classification methods and adaptable categories to more quickly and accurately detect T2D diseases. To enhance the performance of classifiers & maximize the computational effectiveness of findings, the study concentrated on developing novel hybrid categorization algorithms [98]. These technologies will aid medical personnel in making wise decisions about the diagnosis of diseases.

CONCLUSION

The prevalence and incidence of T2D illnesses, which are rising daily have a serious impact on worldwide health. Patients' deaths may also result from improper care being provided withholding or delaying it. Therefore, predicting T2D diseases is a crucial challenge in the medical industry. This survey provides an overview of several extracted features and categorization methods that might be highly useful for assessing illness conditions quickly. According to various concepts, several valid and effective characteristic identification techniques have been discovered in the literature. Although the topic of feature selection

is widely established, scientists are concentrating on developing cutting- edge techniques that boost the effectiveness of ML. This study demonstrates the need for training hospital professionals in reliable feature extraction and classification models that could be utilized on large datasets to accurately detect T2D ailments.

REFERENCES

1. Verma, N., Singh, S., & Prasad, D. (2022). Machine learning and IoT-based model for patient monitoring and early prediction of diabetes. *Concurrency and Computation: Practice and Experience*, e7219.
2. Sood, S. K., Rawat, K. S., & Sharma, G. (2022). Role of Enabling Technologies in Soft Tissue Engineering: A Systematic Literature Review. *IEEE Engineering Management Review*.
3. Das, T., Kalita, P. P., Saha, R., & Das, N. (2022). On Body Vitals Monitoring for Disease Prediction: A Systematic Survey. In *the Internet of Things Based Smart Healthcare* (pp. 177- 195). Springer, Singapore.
4. Verma, N., Singh, S., & Prasad, D. (2022). Machine learning and IoT-based model for patient monitoring and early prediction of diabetes. *Concurrency and Computation: Practice and Experience*, e7219.
5. Nasser, A. R., Hasan, A. M., Humaidi, A. J., Alkhayyat, A., Alzubaidi, L., Fadhel, M. A., ... & Duan, Y. (2021). IoT and cloud computing in health-care: A new wearable device and cloud- based DL algorithm for monitoring of diabetes. *Electronics*, 10(21), 2719.
6. Naz, H., Sharma, R., Sharma, N., & Ahuja, S. IoT-Inspired Smart Healthcare Service for Diagnosing Remote Patients with Diabetes. In *Machine Learning for Edge Computing* (pp. 97- 114). CRC Press.
7. Laabidi, A., & Aissaoui, M. (2020, April). Performance analysis of Machine learning classifiers for predicting diabetes and prostate cancer. In *2020 1st international conference on innovative research in applied science, engineering and technology (IRASET)* (pp. 1-6). IEEE.
8. Malarvizhi Kumar, P., Hong, C. S., Chandra Babu, G., Selvaraj, J., & Gandhi, U. D. (2021). Cloud-and IoT-based DL technique-incorporated secured health monitoring system for dead diseases. *Soft Computing*, 25(18), 12159-12174.
9. Godi, B., Viswanadham, S., Muttipati, A. S., Samantray, O. P., & Gadiraju, S. R. (2020, March). E-healthcare monitoring system using IoT with machine learning approaches. In *2020 international conference on computer science, engineering and applications (ICCSEA)* (pp. 1-5). IEEE.
10. Rghioui, A., Lloret, J., Sendra, S., & Oumnad, A. (2020, September). A smart architecture for diabetic patient monitoring using machine learning algorithms. In *Healthcare* (Vol. 8, No. 3, p. 348). MDPI.



**Reena Ivanglin and Pragaladan**

11. Desai, F., Chowdhury, D., Kaur, R., Peeters, M., Arya, R. C., Wander, G. S., ... & Buyya, R. (2022). HealthCloud: A system for monitoring health status of heart patients using machine learning and cloud computing. *Internet of Things*, 17, 100485.
12. Abdollahi, J., & Nouri-Moghaddam, B. (2022). Hybrid stacked ensemble combined with genetic algorithms for diabetes prediction. *Iran Journal of Computer Science*, 1-16.
13. Parvathy, S., & Sridevi, S. (2022, May). Secure DL model for disease prediction and diagnosis system in cloud based IoT. In *AIP Conference Proceedings* (Vol. 2463, No. 1, p. 020008). AIP Publishing LLC.
14. Bhatia, M., Kaur, S., Sood, S. K., & Behal, V. (2020). Internet of things-inspired healthcare system for urine-based diabetes prediction. *Artificial Intelligence in Medicine*, 107, 101913.
15. Awotunde, J. B., Folorunso, S. O., Bhoi, A. K., Adebayo, P. O., & Ijaz, M. F. (2021). Disease diagnosis system for IoT-based wearable body sensors with machine learning algorithm. In *Hybrid Artificial Intelligence and IoT in Healthcare* (pp. 201-222). Springer, Singapore.
16. Agrawal, H., Jain, P., & Joshi, A. M. (2022). Machine learning models for non-invasive glucose measurement: towards diabetes management in smart healthcare. *Health and Technology*, 1-16.
17. Awotunde, J. B., Jimoh, R. G., Matiluko, O. E., Gbadamosi, B., & Ajamu, G. J. (2022). Artificial Intelligence and an Edge-IoMT-Based System for Combating COVID-19 Pandemic. In *Intelligent Interactive Multimedia Systems for e-Healthcare Applications* (pp. 191-214). Springer, Singapore.
18. Awotunde, J. B., Ajagbe, S. A., Oladipupo, M. A., Awokola, J. A., Afolabi, O. S., Mathew, T. O., & Oguns, Y. J. (2021, October). An Improved Machine Learnings Diagnosis Technique for COVID-19 Pandemic Using Chest X-ray Images. In *International Conference on Applied Informatics* (pp. 319-330). Springer, Cham.
19. Abiodun, K. M., Awotunde, J. B., Aremu, D. R., & Adeniyi, E. A. (2022). Explainable AI for fighting COVID-19 pandemic: opportunities, challenges, and future prospects. *Computational Intelligence for COVID-19 and Future Pandemics*, 315-332.
20. Awotunde, J. B., Abiodun, K. M., Adeniyi, E. A., Folorunso, S. O., & Jimoh, R. G. (2021, November). A DL-based intrusion detection technique for a secured IoMT system. In *International Conference on Informatics and Intelligent Applications* (pp. 50-62). Springer, Cham.
21. Folorunso, S. O., Awotunde, J. B., Adeniyi, E. A., Abiodun, K. M., & Ayo, F. E. (2021, November). Heart disease classification using machine learning models. In *International Conference on Informatics and Intelligent Applications* (pp. 35-49). Springer, Cham.
22. Awotunde, J. B., Folorunso, S. O., Ajagbe, S. A., Garg, J., & Ajamu, G. J. (2022). AiIoMT: IoMT-Based System-Enabled Artificial Intelligence for Enhanced Smart Healthcare Systems. *Machine Learning for Critical Internet of Medical Things*, 229-254.
23. Nasir, N., Oswald, P., Barneih, F., Alshaltone, O., AlShabi, M., Bonny, T., & Al Shammaa, A. (2021, December). Hypertension Classification Using Machine Learning Part II. In *2021 14th International Conference on Developments in eSystems Engineering (DeSE)* (pp. 459-463). IEEE.
24. Awotunde, J. B., Adeniyi, A. E., Abiodun, K. M., Ajamu, G. J., & Matiluko, O. E. (2022). Application of Cloud and IoT Technologies in Battling the COVID-19 Pandemic. In *Machine Learning for Critical Internet of Medical Things* (pp. 1-29). Springer, Cham.
25. Mahmood, N. S., & Ahmed, E. M. (2022). Mediating effect of risk management practices in Iraqi private banks financial performance. *Journal of Financial Services Marketing*, 1-20.
26. Haleem, S. L. A., Manikandan, N., & Ramachandran, M. (2022). Utilization of Artificial Intelligence-Based Wearable Sensors in Deep Residual Network for Detecting Heart Disease. In *Leveraging AI Technologies for Preventing and Detecting Sudden Cardiac Arrest and Death* (pp. 191-217). IGI Global.
27. Adeniyi, E. A., Folorunso, S. O., & Jimoh, R. G. (2022). A DL-Based Intrusion Detection Technique for a Secured IoMT System. In *Informatics and Intelligent Applications: First International Conference, ICIIA 2021, Ota, Nigeria, November 25-27, 2021: Revised Selected Papers* (p. 50). Springer Nature.
28. Awotunde, J. B., Ayoade, O. B., Ajamu, G. J., AbdulRaheem, M., & Oladipo, I. D. (2022). Internet of Things and Cloud Activity Monitoring Systems for Elderly Healthcare. In *Internet of Things for Human-Centered Design* (pp. 181-207). Springer, Singapore.



**Reena Ivanglin and Pragaladan**

29. Ajagbe, S. A., Awotunde, J. B., Adesina, A. O., Achimugu, P., & Kumar, T. A. (2022). Internet of Medical Things (IoMT): Applications, Challenges, and Prospects in a Data-Driven Technology. *Intelligent Healthcare*, 299-319.
30. Abiodun, M. K., Misra, S., Awotunde, J. B., Adewole, S., Joshua, A., & Oluranti, J. (2021, December). Comparing the Performance of Various Supervised Machine Learning Techniques for Early Detection of Breast Cancer. In *International Conference on Hybrid Intelligent Systems* (pp. 473-482). Springer, Cham.
31. Awotunde, J. B., Ajagbe, S. A., Idowu, I. R., & Ndunagu, J. N. (2021). An Enhanced Cloud- IoMT-based and Machine Learning for Effective COVID-19 Diagnosis System. In *Intelligence of Things: AI-IoT Based Critical-Applications and Innovations* (pp. 55-76). Springer, Cham.
32. Awotunde, J. B., Adeniyi, E. A., Ajamu, G. J., Balogun, G. B., & Taofeek-Ibrahim, F. A. (2022). Explainable Artificial Intelligence in Genomic Sequence for Healthcare Systems Prediction. In *Connected e-Health* (pp. 417-437). Springer, Cham.
33. Sadad, T., Bukhari, S. A. C., Munir, A., Ghani, A., El-Sherbeeney, A. M., & Rauf, H. T. (2022). Detection of Cardiovascular Disease Based on PPG Signals Using Machine Learning with Cloud Computing. *Computational Intelligence and Neuroscience*, 2022.
34. Rashid, M., Singh, H., Goyal, V., Parah, S. A., & Wani, A. R. (2021). Big data based hybrid machine learning model for improving performance of medical Internet of Things data in healthcare systems. In *Healthcare Paradigms in the Internet of Things Ecosystem* (pp. 47-62). Academic Press.
35. Sethi, G. K., Ahmad, N., Rehman, M. B., Dafallaa, H. M. E. I., & Rashid, M. (2021, April). Use of artificial intelligence in healthcare systems: state-of-the-art survey. In *2021 2nd International conference on intelligent engineering and management (ICIEM)* (pp. 243-248). IEEE.
36. Boulemtafes, A., Khemissa, H., Derki, M. S., Amira, A., & Djedjig, N. (2021). DL in pervasive health monitoring, design goals, applications, and architectures: An overview and a brief synthesis. *Smart Health*, 22, 100221.
37. Dicuonzo, G., Donofrio, F., Fusco, A., & Shini, M. (2022). Healthcare system: Moving forward with artificial intelligence. *Technovation*, 102510.
38. Kaur, A., Rashid, M., Bashir, A. K., & Parah, S. A. (2022). Detection of Breast Cancer Masses in Mammogram Images with Watershed Segmentation and Machine Learning Approach. In *Artificial Intelligence for Innovative Healthcare Informatics* (pp. 35-60). Springer, Cham.
39. Tsai, W. C., Liu, C. F., Lin, H. J., Hsu, C. C., Ma, Y. S., Chen, C. J., ... & Chen, C. C. (2022, August). Design and Implementation of a Comprehensive AI Dashboard for Real-Time Prediction of Adverse Prognosis of ED Patients. In *Healthcare* (Vol. 10, No. 8, p. 1498). Multidisciplinary Digital Publishing Institute.
40. Chaudhuri, A., Naseraldin, H., & Narayanamurthy, G. (2022). Healthcare 3D printing service innovation: Resources and capabilities for value Co-creation. *Technovation*, 102596.
41. Dicuonzo, G., Galeone, G., Shini, M., & Massari, A. (2022). Towards the Use of Big Data in Healthcare: A Literature Review. *Healthcare* 2022, 10, 1232.
42. Dicuonzo, G., Galeone, G., Shini, M., & Massari, A. (2022, July). Towards the Use of Big Data in Healthcare: A Literature Review. In *Healthcare* (Vol. 10, No. 7, p. 1232). Multidisciplinary Digital Publishing Institute.
43. Essén, A., Frishammar, J., & Cenamor, J. (2022). Entering non-platformized sectors: The co- evolution of legitimacy debates and platform business models in digital health care. *Technovation*, 102597.
44. Chang, W., Ji, X., Wang, L., Liu, H., Zhang, Y., Chen, B., & Zhou, S. (2021, September). A Machine-Learning method of predicting vital capacity plateau value for ventilatory pump failure based on data mining. In *Healthcare* (Vol. 9, No. 10, p. 1306). MDPI.
45. Hasan, S., Yousuf, M. M., Farooq, M., Marwah, N., Andrabi, S. A. A., & Kumar, H. (2021, April). e-Vaccine: an immunization app. In *2021 2nd international conference on intelligent engineering and management (ICIEM)* (pp. 605-610). IEEE.
46. Adhikary, S., & Ghosh, A. (2022). e-BMI: A gait based smart remote BMI monitoring framework implementing edge computing and incremental machine learning. *Smart Health*, 24, 100277.



**Reena Ivanglin and Pragaladan**

47. Shaji, B., Lal Raja Singh, R., & Nisha, K. L. (2022). A novel deep neural network based marine predator model for effective classification of big data from social Internet of Things. *Concurrency and Computation: Practice and Experience*, e7244.
48. Jothi Prabha, A., Venkateswaran, N., & Sengodan, P. (2022). AI-Based Deep Random Forest Ensemble Model for Prediction of COVID-19 and Pneumonia from Chest X-Ray Images. In *Artificial Intelligence for Innovative Healthcare Informatics* (pp. 133-149). Springer, Cham.
49. Wang, P., & Sun, X. (2022). Analysis of an Economic Coupling Relationship Model of the Coastal Ecological Fragile Zone Based on a Machine Learning Model. *Wireless Communications and Mobile Computing*, 2022.
50. Vasa, J., & Thakkar, A. (2022). DL: Differential Privacy Preservation in the Era of Big Data. *Journal of Computer Information Systems*, 1-24.
51. Chang, V., Javvaji, S., Xu, Q. A., Hall, K., & Guan, S. (2022). Diabetes Analysis with a Dataset Using Machine Learning. In *Artificial Intelligence and Machine Learning Methods in COVID-19 and Related Health Diseases* (pp. 161-188). Springer, Cham.
52. Priyadarshini, I., Bhola, B., Kumar, R., & So-In, C. (2022). A Novel Cloud Architecture for Internet of Space Things (IoST). *IEEE Access*, 10, 15118-15134.
53. Priyadarshini, I., Alkhayyat, A., Gehlot, A., & Kumar, R. (2022). Time series analysis and anomaly detection for trustworthy smart homes. *Computers and Electrical Engineering*, 102, 108193.
54. Javaid, M., Haleem, A., Singh, R. P., Suman, R., & Rab, S. (2022). Significance of machine learning in healthcare: Features, pillars and applications. *International Journal of Intelligent Networks*.
55. Prabha, A. J., Venkateswaran, N., & Sengodan, P. AI-Based Deep Random Forest Ensemble Model for Prediction of COVID-19 and Pneumonia from Chest X-Ray Images. *Artificial Intelligence for Innovative Healthcare Informatics*, 133.
56. Fan, L. (2021). Usage of Narrowband Internet of Things in Smart Medicine and Construction of Robotic Rehabilitation System. *IEEE Access*, 10, 6246-6259.
57. Kumar Attar, R. (2022). The Emergence of Natural Language Processing (NLP) Techniques in Healthcare AI. In *Artificial Intelligence for Innovative Healthcare Informatics* (pp. 285-307). Springer, Cham.
58. El-Rashidy, N., ElSayed, N. E., El-Ghamry, A., & Talaat, F. M. (2022). Prediction of gestational diabetes based on explainable DL and fog computing. *Soft Computing*, 1-16.
59. Kishor, A., & Jeberson, W. (2021). Diagnosis of heart disease using internet of things and machine learning algorithms. In *Proceedings of second international conference on computing, communications, and cyber-security* (pp. 691-702). Springer, Singapore.
60. Huang, X., Jagota, V., Espinoza-Muñoz, E., & Flores-Albornoz, J. (2022). Tourist hot spots prediction model based on optimized neural network algorithm. *International Journal of System Assurance Engineering and Management*, 13(1), 63-71.
61. Rakhra, M., Sanober, S., Quadri, N. N., Verma, N., Ray, S., & Asenso, E. (2022). Implementing Machine Learning for Smart Farming to Forecast Farmers' Interest in Hiring Equipment. *Journal of Food Quality*, 2022.
62. Murugesan, G., Ahmed, T. I., Shabaz, M., Bhola, J., Omarov, B., Swaminathan, R., ...& Sumi, S. A. (2022). Assessment of mental workload by visual motor activity among control group and patient suffering from depressive disorder. *Computational Intelligence and Neuroscience*, 2022.
63. Chaudhury, S., Shelke, N., Sau, K., Prasanalakshmi, B., & Shabaz, M. (2021). A novel approach to classifying breast cancer histopathology biopsy images using bilateral knowledge distillation and label smoothing regularization. *Computational and Mathematical Methods in Medicine*, 2021.
64. Mehbodniya, A., Neware, R., Vyas, S., Kumar, M. R., Ngulube, P., & Ray, S. (2021). Blockchain and IPFS integrated framework in bilevel fog-cloud network for security and privacy of IoMT devices. *Computational and Mathematical Methods in Medicine*, 2021.
65. Diwan, T. D., Choubey, S., Hota, H. S., Goyal, S. B., Jamal, S. S., Shukla, P. K., & Tiwari, B. (2021). Feature entropy estimation (FEE) for malicious IoT traffic and detection using machine learning. *Mobile Information Systems*, 2021.
66. Diwan, T. D., Choubey, S., Hota, H. S., Goyal, S. B., Jamal, S. S., Shukla, P. K., & Tiwari, B. Research Article Feature Entropy Estimation (FEE) for Malicious IoT Traffic and Detection Using Machine Learning.



**Reena Ivanglin and Pragaladan**

67. Lin, R. H., Wang, C. C., & Tung, C. W. (2022). A machine learning classifier for predicting stable MCI patients using gene biomarkers. *International Journal of Environmental Research and Public Health*, 19(8), 4839.
68. de Souza, C. A., Westphall, C. B., Machado, R. B., Loffi, L., Westphall, C. M., & Geronimo, G. (2022). Intrusion detection and prevention in fog based IoT environments: A systematic literature review. *Computer Networks*, 109154.
69. Pandey, S. K., Vanithamani, S., Shahare, P., Ahmad, S. S., Thilagamani, S., Hassan, M. M., & Amoatey, E. T. (2022). Machine Learning-Based Data Analytics for IoT-Enabled Industry Automation. *Wireless Communications and Mobile Computing*, 2022.
70. Sridevi, G., & Chakkravarthy, M. (2021). A meta-heuristic multiple ensemble load balancing framework for real-time multi-task cloud scheduling process. *International Journal of System Assurance Engineering and Management*, 12(6), 1459-1476. Bhuvanewari, C. A., & Ruby, E.D. (2022). HETA: end-to-end delay analysis of enhanced centralized clustering protocol for wireless sensor networks. *International Journal of System Assurance Engineering and Management*, 13(1), 49-53.
71. Li, Y., & Shabaz, M. (2022). Distributed lossless coding system based on cloud computing in video transcoding for MRI and neuroimaging. *The Journal of Engineering*.
72. Sundaram, R. S., Manikandan, M., Suresh, P., & Mariselvam, V. (2022). A novel EBG backed circular patch antenna for smart devices with multiband applications in smart cities. *International Journal of System Assurance Engineering and Management*, 13(1), 757-763.
73. Chakraborty, C., & Kishor, A. (2022). Real-Time Cloud-Based Patient-Centric Monitoring Using Computational Health Systems. *IEEE Transactions on Computational Social Systems*.
74. Ting, L., Khan, M., Sharma, A., & Ansari, M. D. (2022). A secure framework for IoT-based smart climate agriculture system: Toward blockchain and edge computing. *Journal of Intelligent Systems*, 31(1), 221-236.
75. Paganelli, A. I., Velmovitsky, P. E., Miranda, P., Branco, A., Alencar, P., Cowan, D., ... & Morita, P. P. (2022). A conceptual IoT-based early-warning architecture for remote monitoring of COVID-19 patients in wards and at home. *Internet of Things*, 18, 100399.
76. Fazakis, N., Kocsis, O., Alexiou, S., Fakotakis, N., & Moustakas, K. (2021). Machine learning tools for long-term type 2 diabetes risk prediction. *IEEE Access*, 9, 103737-103757.
77. Nasr, M., Islam, M. M., Shehata, S., Karray, F., & Quintana, Y. (2021). Smart healthcare in the age of AI: recent advances, challenges, and future prospects. *IEEE Access*.
78. Rajeswari, S. V. K. R., & Ponnusamy, V. (2022). AI-Based IoT analytics on the cloud for diabetic data management system. In *Integrating AI in IoT Analytics on the Cloud for Healthcare Applications* (pp. 143-161). IGI Global.
79. Kumar, G. K. L., & Singh, A. R. (2022). An Automated Heart Disease Diagnosis System Using Adaptive Cross-Layer Stacked Residual Convolutional Neural Networks.
80. Elsagheer, M. M., & Ramzy, S. M. (2022). A hybrid model for automatic modulation classification based on residual neural networks and long short term memory. *Alexandria Engineering Journal*.
81. Vanitha, C. N., Vanitha, K., Narmatha, C., Krishna, S. A., & Dhivakar, R. (2022, May). Heart Disease Prediction using Enhanced DL. In *2022 International Conference on Applied Artificial Intelligence and Computing (ICAAIC)* (pp. 528-532). IEEE.
82. Alsamhi, S. H., Almalki, F. A., Al-Dois, H., Ben Othman, S., Hassan, J., Hawbani, A., ... & Saleh, H. (2021). Machine learning for smart environments in B5G networks: connectivity and QoS. *Computational Intelligence and Neuroscience*, 2021.
83. Nishat, M. M., Faisal, F., Dip, R. R., Nasrullah, S. M., Ahsan, R., Shikder, F., ... & Hoque, M. A. (2021). A comprehensive analysis on detecting T2D kidney disease by employing machine learning algorithms. *EAI Endorsed Transactions on Pervasive Health and Technology*, 7(29), e1- e1.
84. Sharma, P., Jain, S., Gupta, S., & Chamola, V. (2021). Role of machine learning and DL in securing 5G-driven industrial IoT applications. *Ad Hoc Networks*, 123, 102685.
85. Nishat, M. M., Hasan, T., Nasrullah, S. M., Faisal, F., Asif, M. A. A. R., & Hoque, M. A. (2021, August). Detection of Parkinson's Disease by Employing Boosting Algorithms. In *2021 Joint 10th International*



**Reena Ivanglin and Pragaladan**

- Conference on Informatics, Electronics & Vision (ICIEV) and 2021 5th International Conference on Imaging, Vision & Pattern Recognition (icVPR) (pp. 1-7). IEEE.
86. Nishat, M. M., Faisal, F., Hasan, T., Karim, M. F. B., Islam, Z., & Shagor, M. R. K. (2021, September). An Investigative Approach to Employ Support Vector Classifier as a Potential Detector of Brain Cancer from MRI Dataset. In 2021 International Conference on Electronics, Communications and Information Technology (ICECIT) (pp. 1-4). IEEE.
87. Rahman, A. A., Faisal, F., Nishat, M. M., Siraji, M. I., Khalid, L. I., Khan, M. R. H., & Reza, M. T. (2021, December). Detection of Epileptic Seizure from EEG Signal Data by Employing Machine Learning Algorithms with Hyperparameter Optimization. In 2021 4th International Conference on Bio-Engineering for Smart Technologies (BioSMART) (pp. 1-4). IEEE.
88. Rahman, A. A., Siraji, M. I., Khalid, L. I., Faisal, F., Nishat, M. M., Ahmed, A., & Al Mamun, M. A. (2022, June). Perceived Stress Analysis of Undergraduate Students during COVID-19: A Machine Learning Approach. In 2022 IEEE 21st Mediterranean Electrotechnical Conference (MELECON) (pp. 1129-1134). IEEE.
89. Ratul, I. J., Al-Monsur, A., Tabassum, B., Ar-Rafi, A. M., Nishat, M. M., & Faisal, F. (2022, May). Early risk prediction of cervical cancer: A machine learning approach. In 2022 19th International Conference on Electrical Engineering/Electronics, Computer, Telecommunications and Information Technology (ECTI-CON) (pp. 1-4). IEEE.
90. Muntasir Nishat, M., Faisal, F., Jahan Ratul, I., Al-Monsur, A., Ar-Rafi, A. M., Nasrullah, S. M.,... & Khan, M. R. H. (2022). A Comprehensive Investigation of the Performances of Different Machine Learning Classifiers with SMOTE-ENN Oversampling Technique and Hyperparameter Optimization for Imbalanced Heart Failure Dataset. Scientific Programming, 2022.
91. Mahbub, N. I., Hasan, M. I., Ahamad, M. M., Aktar, S., & Moni, M. A. (2022, February). Machine Learning Approaches to Identify Significant Features for the Diagnosis and Prognosis of T2D Kidney Disease. In 2022 International Conference on Innovations in Science, Engineering and Technology (ICISSET) (pp. 312-317). IEEE.
92. Hasan, T., Nishat, M. M., Faisal, F., Islam, A., Al Mehadi, A., Nasrullah, S. M., & Islam, M. R. (2021, December). Exploring the Performances of Stacking Classifier in Predicting Patients Having Stroke. In 2021 8th NAFOSTED Conference on Information and Computer Science (NICS) (pp. 242-247). IEEE.
93. Daniel, J., Irin Sherly, S., Ponnuramu, V., Pratap Singh, D., Netra, S. N., Alonazi, W. B., ... & Abera, Y. (2022). Recurrent Neural Networks for Feature Extraction from Dengue Fever. Evidence-Based Complementary and Alternative Medicine, 2022.
94. Hegde, G., Shenoy, P. D., & Venugopal, K. R. (2022, July). Performance Analysis of Real and Synthetic Data using Supervised ML Algorithms for Prediction of T2D Kidney Disease. In 2022 IEEE International Conference on Electronics, Computing and Communication Technologies (CONECCT) (pp. 1-6). IEEE.
95. Jackson, D., Sherly, S. I., Ponnuramu, V., Singh, D. P., Netra, S. N., Alonazi, W. B., ... & Abera, Y. (2022). Recurrent Neural Networks for Feature Extraction from Dengue Fever. Evidence- Based Complementary and Alternative Medicine, 2022.
96. Abdulkareem, K. H., Mohammed, M. A., Gunasekaran, S. S., Al-Mhiqani, M. N., Mutlag, A. A., Mostafa, S. A., ... & Ibrahim, D. A. (2019). A review of fog computing and machine learning: concepts, applications, challenges, and open issues. IEEE Access, 7, 153123-153140.
97. Kadhim, K. T., Alsahlany, A. M., Wadi, S. M., & Kadhum, H. T. (2020). An overview of patient's health status monitoring system based on Internet of Things (IoT). Wireless Personal Communications, 114(3), 2235-2262.
98. Hartmann, M., Hashmi, U. S., & Imran, A. (2022). Edge computing in smart health care systems: Review, challenges, and research directions. Transactions on Emerging Telecommunications Technologies, 33(3), e3710.





Reena Ivanglin and Pragaladan

Table 1: Feature selection comparative analysis

Methods of feature selection	Functionality	Issues
Graph-Based system	It includes a small set of characteristics, into multiple dependent features of the dominant set.	It cannot effectively employ approximation. Multimodal images are divided and feature extracted using this method.
Co-Training based system	It utilizes two key aspects of unlabeled data for each other and jointly predicts the test.	It does not explore how extraneous characteristics affect semi-supervised learning approaches to identify irrelevant data features.
Self-Training based system	Utilizes the labeled portion of the data to begin an initial characterization and this model to group the unlabeled portion.	In place of demonstrating the quantification, it gives immediate grouping of data. It couldn't be carrying out a linear data transformation.
SVM	To solve the dual optimization problem.	It provides only an approximate solution instead of a complete solution.
Co-relation based system	The multivariate channel chooses the feature subsets that are uncorrelated among themselves.	It does not demonstrate a strong connection to the class.
Consistency based system	It determines feature subsets, but it does not know how the feature can closely fit the class.	It determines an appropriate data reduction rate using an irregularity criterion.
Information Gain	It stores the common information for every feature and class.	It only delivers the limited feature set
Relief method	It operates by arbitrarily choosing the test features and searching for neighbors in the same class, not in other classes.	The score of pertinence score of every component is updated based on the hit and miss rate.
Lasso Regularization	Reduces some of the items to zero and contracts the regression coefficients to regularize model bounds.	This approach substitutes the quantity of the model boundaries' top features for the target label as its criterion.
Filter	Chooses the most relevant features based on the information itself, that is, features are evaluated according to the characteristics of the material, without using any grouping techniques that can restrict the investigation of critical aspects.	The speed and adaptability limitations of this technology are drawbacks.
Wrapper	Utilizes the effects of a certain grouping strategy to evaluate feature subsets. This technique was used by identifying feature subsets that enhance the nature of the grouping method's results.	However, the main drawback of these feature selection methods is that they are computationally expensive and can only be used in conjunction with a certain grouping method.
Hybrid method	It has all the hybrid system characteristics but missed the wrapper and filter.	To strike balance between viability and computational effort.





Reena Ivanglin and Pragaladan

Table 2 classifies characteristic methods based according to the search method, the criterion for assessment, and the data analysis task.

	Feature Selection Type	Search Strategies			Data Mining Tasks	
		Complete	Sequential	Random	Classification	Clustering
Evaluation Criteria	Filter Method	Focus MIFES1 BFF Bobrowski's MDLM Schlimmer's	Relief Relief F Relief SSFS FCBF CFS Dash's SBUD Mitra's	LVI QBB LVF	Y-	-Y
	Wrapper Method	AMB&B FSBC BS	WSBG WSBG PQSS	RGSS LWV RMHC-	Y	-
		FSLC	RC SS SBS- SLASH AICC FSSEM ELSA BBHFS	PF GA RVE	- Y	Y-
	Hybrid Method		Xing's Dash-Liu's		-	Y

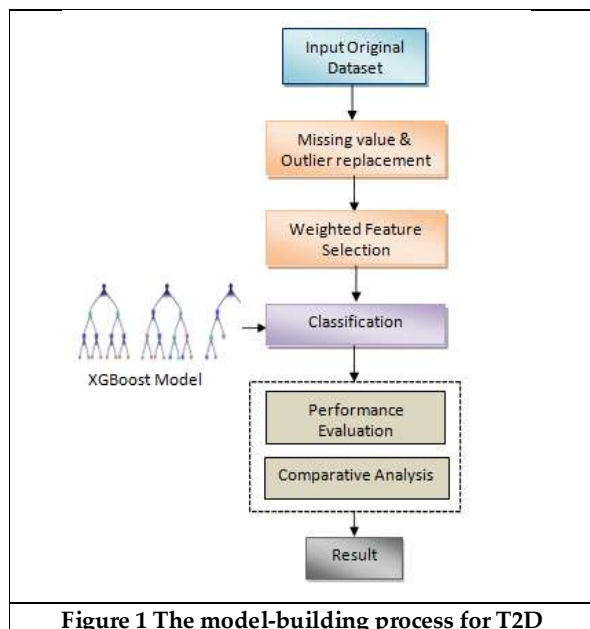


Figure 1 The model-building process for T2D

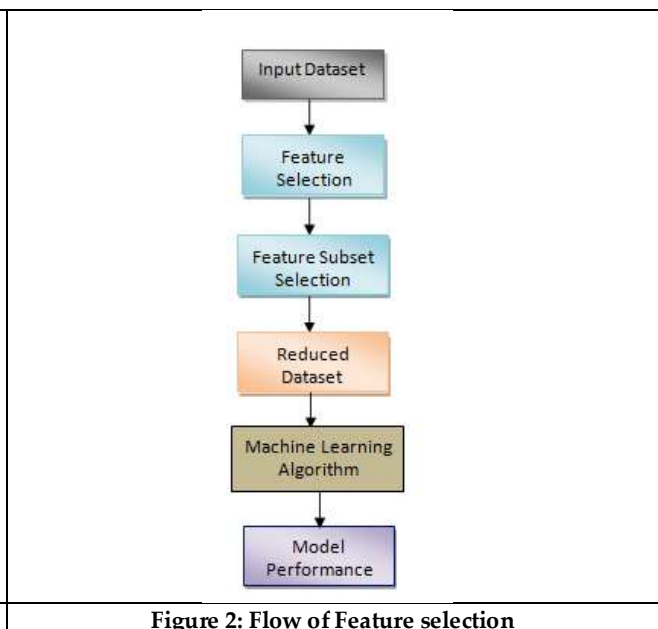


Figure 2: Flow of Feature selection





Reena Ivanglin and Pragaladan

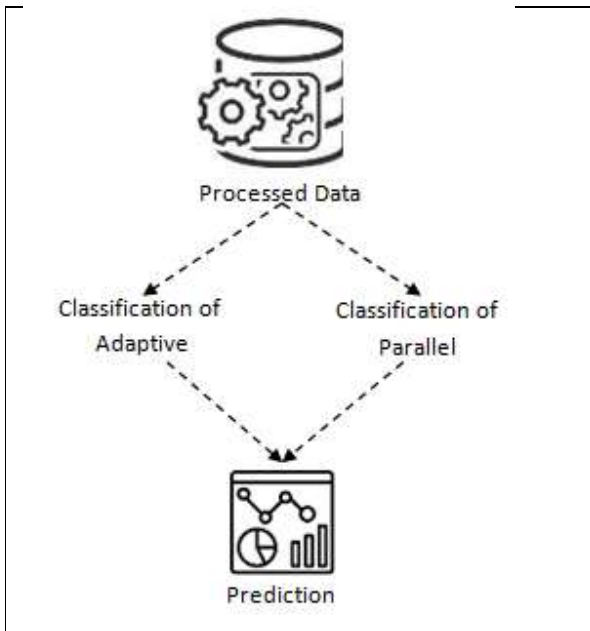


Figure 3: Parallel classification and adaptive classification processes

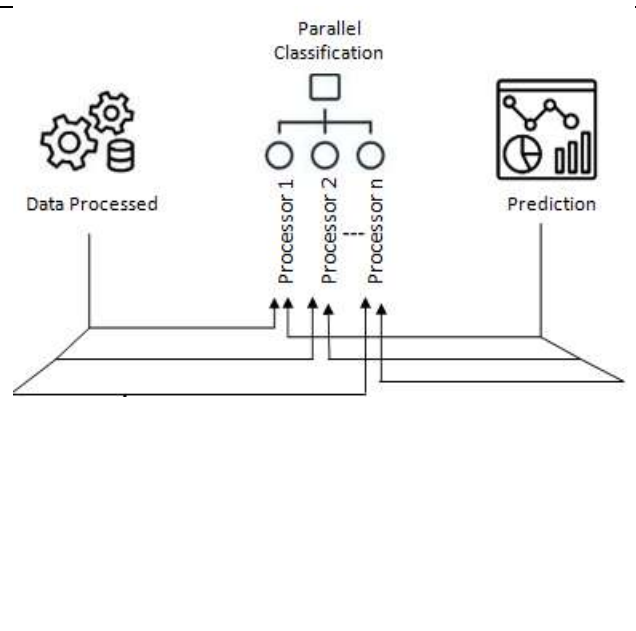


Figure 4: Architecture of parallel classification process





Need of Course Recommendation System in Current Education System

Arti^{1,*} and Manu Gupta²

¹Assistant Professor, Department of Computer Science, Sanatan Dharma College, Ambala Cantt, Kurukshetra University, 133001, Haryana, India.

²Assistant Professor, Department of Computer Science, Sanatan Dharma College, Ambala Cantt, Kurukshetra University, 133001, Haryana, India.

Received: 30 Dec 2023

Revised: 09 Jan 2024

Accepted: 12 Jan 2024

*Address for Correspondence

Arti

Assistant Professor,
Department of Computer Science,
Sanatan Dharma College,
Ambala Cantt, Kurukshetra University, 133001,
Haryana, India.
Email: artisachdeva@sdcollegeambala.ac.in



This is an Open Access Journal / article distributed under the terms of the **Creative Commons Attribution License** (CC BY-NC-ND 3.0) which permits unrestricted use, distribution, and reproduction in any medium, provided the original work is properly cited. All rights reserved.

ABSTRACT

This review paper critically explores the existing literature on course recommendation system within the sphere of higher education in current era pertaining to NEP 2020. The study provides a thorough analysis of various methodologies, algorithms and approaches employed in the design and implementation of these systems. Key factors affecting course recommendations such as user preferences, academic performances and contextual relevance are examined. The review also highlights contemporary trends, challenges, and opportunities in the field illuminating recent advancements in data analytics, machine learning and deep learning applied to course recommendations. By integrating diverse views, this paper aims to offer an extensive overview of the existing and current state of course recommendation systems, providing a deeper comprehension of their implications for individualized learning to meet different needs of students and their academic success.

Keywords: Recommendation System, Machine Learning, Deep learning, NEP 2020

INTRODUCTION

A recommendation system (RS) is an information filtering system that offers content relevant to a specific user. Suggestions about diverse decision-making procedures are commonly provided, encompassing the selection of a thing for purchase, the choice of listening music, or the determination of news available online to peruse. Recommendation systems are highly advantageous when persons face the challenge of choosing an item from a huge assortment of choices offered by a particular provider. Recommender systems have many applications like news,

69522



**Arti and Manu Gupta**

movies, music and education etc. in the field of education; students are not aware about the courses they should study. The reason behind this is a lack of knowledge about the future requirements of hiring companies or higher education institutes. So, there is a need for a system that guides the students in selecting a course depending on their interests and historical records. A course recommendation system suggests a list of courses to student decide what they should study. Due to the digitization of higher education, recommender systems have become more prevalent in this domain since the early 2000s. (Wang et al., 2022) proposed a course enrollment recommender system based on machine learning that suggest students looking to register for courses in the upcoming semester.

The general working of recommendation system includes user/student requests for recommendation at his interface by giving the information needed by the recommender system. This request goes into the database, where the recommendation engine checks the similarity of the required recommendation with the previous advice given to users and also considers the feedback given by the previous user. The recommender system recommends top N recommendations to the receiver based on the similarity matrix as well as the previous history record. Recommender systems have two main components: users (student) and things (courses), with each user assigning a rating (feedback) to an unrated item. Generally, two approaches are used to acquire user ratings: Implicit approach and explicit approach (Roy & Dutta, 2022). Implicit user ratings are inadvertently gathered from the user. Contrarily, in explicit approach, users may provide detailed user ratings directly by choosing a value from a constrained range of point values or labeled interval values. For instance, a website may gather implicit data about goods based on click stream, user time spent on a page, and other factors. Most recommender systems use both explicit and implicit techniques to collect user ratings. And only those items will be recommended to users which get higher user ratings. So our concern is to get high ratings of the thing.

Types of recommender system

Recommender systems can be categorized into four distinct classifications: Content based recommender systems, Collaborative recommender system; Knowledge based recommender systems and Hybrid recommender systems (Pawlicka et al., 2021).

Content based recommender system

Content based techniques are highly efficient in suggesting text based items such as documents, news items, web pages and restaurants etc. Within content-based recommendation systems, forecasts are generated by analyzing data about the items themselves and the users' previous interactions with them, not on what other users have chosen (Pawlicka et al., 2021). This type of filtering is based on the idea that people tend to buy things in the future that are related to things they have already bought. The item's similarity is calculated on the basis of their features and/or attributes that include metadata or even the actual content of the document. The first step in the content based recommendation process is to get information about and reviews for the things that a user has already bought. After that, the machine looks for things that are like it. Here's how to figure out the similarity: The items are put into neighborhoods by using a similarity calculation. This means that new items are compared to items that are already in the collection to build neighborhoods. It's like a vote for the neighborhood where the thing was bought if someone bought it. A user should be told about an item if k of their closest friends gave it high marks. Little information is needed for this method to make correct predictions and be flexible.

Collaborative recommender system

The degree of user similarity is a factor in collaborative strategies. This method begins by recognizing a collection or group of user A whose likes, dislikes, and tastes are comparable to those of user B. The neighborhood of B is referred to as A. Then user B suggests the items that he may like, based on the reactions of other user A who have a similar taste. The efficacy of a collaborative algorithm is contingent upon its ability to identify the area encompassing the user of interest accurately. According to the (Roy & Dutta, 2022), collaborative filtering is further categorized into two types of filtering: Memory-based collaborative filtering and model-based collaborative filtering.



**Arti and Manu Gupta**

Memory-based collaborative techniques recommend new items while considering the other user's preferences. For prediction, they utilize the utility matrix (UM) directly. The initial stage of this method is building a model. The input for the function representing the model is the utility matrix (UM) $\text{Model} = f(\text{UM})$. Then, recommendations or suggestions are created based on a function that accepts two parameters: one is the defined model, and the other one is the user profile (UP). In this case, only those users whose UPs are included in the UM are eligible to give suggestions. So, the UP's must be added to the UM to provide recommendations for a new user, and an estimation of the similarity matrix is needed. This makes the method computationally costly.

Recommendation = f (defined model, UP)

Where $\text{UP} \in \text{UM}$ (Roy & Dutta, 2022)

Where UP = User Profile

UM = Utility Matrix

Model-based systems employ a diverse range of data mining techniques as well as machine learning methodologies to construct a model capable of anticipating the user's rating for an unrated item. Instead of starting with the complete dataset, suggestions are created utilizing its features. Consequently, the emergence of the "model-based technique" occurred. The prediction process for these approaches also involves two phases: first, building the model, and second, the prediction of ratings is accomplished by employing a function (f) that incorporates the user profile (UP) and the model developed during the initial phase as its inputs.

Recommendation = f (defined model, UP)

Where $\text{UP} \notin \text{UM}$ (Roy & Dutta, 2022)

Where UP = User Profile

UM = Utility Matrix

The utility matrix does not need to be updated before predictions may be made using model-based methodologies. Even users who aren't represented in the model can receive our recommendations.

Collaborative filtering is highly effective for recommending products on shopping sites, movies and TV shows and articles on news sites etc.

Knowledge based recommender system

Knowledge-based recommender systems do not depend on user item data. Instead, their predictions are based on attributes of items and explicit rules about the problem area (Pawlicka et al., 2021). Knowledge-based recommender systems use artificial intelligence algorithms and examine user and item similarities. Instead of relying on human reviews, these systems use deep knowledge about item features. These systems are useful for recommending products and services.

Hybrid recommender system

A hybrid recommender technique integrates multiple tactics and simultaneously utilizes them to mitigate the limitations inherent in each individual style. Diverse styles can be included via a variety of methods. A hybrid algorithm that mixes collaborative methods with content-based strategies or content-based methods with collaborative methods may blend the results from many techniques. This hybrid combination of many methodologies frequently increases performance and correctness in many recommender system applications. Several hybridization approaches include

1. Weighted hybridization.
2. Feature-augmentation mixed hybridization.
3. Feature-augmentation at the Meta level.
4. Cascade hybridization.
5. Feature-combination mixed hybridization.



**Arti and Manu Gupta****Education System in India**

The pivotal role of education is enabling individuals to reach their maximum capabilities and facilitating the progress of a nation. Ensuring inclusive and equitable access to high-quality education is crucial for India's sustained progress and its position as a global leader with a view to advancing the economy, social equity, scientific innovation, cultural conservation, and national unity. Gurukuls were the heart of the old educational system, which was based on Hindu philosophy and helped people learn new skills and how to live a good life. Modern education, on the other hand, is focused on mindless learning and tests, which is not in line with the overall goals of skill and personality development. India can strive to create a modern education system that truly supports the holistic development of individuals and prepares them for a world that is always changing by going back to the roots of its educational past and building on the strengths of its old system. National System of Education must aim to eliminate inequities and enhance the quality of public education in funded schools so parents feel that they can skip paying considerable fees to send their kids to private schools. There are various education policies that came to existence till now. These are

1. The first education policy commenced in 1966 (National Education Policy 1966). The aim of this policy was "**Radical Restructuring**" and equal education opportunities to achieve complete education at the national level.
2. The following education policy was commenced in 1986 that aims to promote education of minor and backward sections, education of SC, ST and women equality. The new education strategy prioritizes addressing school dropouts through micro-planning-based solutions implemented at grassroots levels nationwide.
3. The next education policy came in the year 2020 known as **National Education Policy (NEP) 2020** which is the first education policy in the 21st century and mainly focuses on
 - Recognizing, identifying, and fostering the unique capabilities of each student,
 - Flexibility,
 - Multi disciplinarily and a holistic education,
 - Emphasis on conceptual understanding,
 - Creativity and critical thinking,
 - Life skills,
 - Focus on regular formative assessment for learning,
 - Synergy in curriculum across all levels of education,
 - Respect for diversity and respect for the local context,
 - Outstanding research, Substantial investment in a strong, vibrant public education system

LITREATURE REVIEW

Recommender systems have the potential to be applied across various domains, including the educational sector. These systems primarily prioritize the provision of a rigorous educational standard and strive to optimize the teaching and learning process. Students take help from course recommendation system for deciding the right choice of courses they may take in their under graduation programme. There is various course recommendation systems are developed till now but all have some limitations in their own way. This section focuses on literature review of existing course recommendation systems using various techniques. Sumesh et al., 2023 used NLP to create a course recommendation system that recommends suitable courses based on user behaviour and explicit input. Preprocessing techniques, such as noise removal, tokenization, and lemmatization, are employed on the course data. When a user initiates a search for a specific course, the system compares the search query and the preprocessed course data, afterwards generating recommendations for courses that exhibit similarity. The system uses deep learning for multi-modal feature extraction, content-based filtering, and TF-IDF for availability determination. Jia et al., 2023 suggested that the BTCBMA algorithm for online education course recommendation incorporates student learning quality. It uses BERT and TextCNN models to extract text features, CNN and Bi LSTM networks are employed to capture deep and temporal characteristics and a multi-head attention mechanism is employed to extract critical information from sequences of learner interactions, review texts and curriculum properties. The suggested



**Arti and Manu Gupta**

method outperforms previous MOOC. It effectively recommends high-quality courses, boosting learning quality and efficiency. Jena et al., 2023 presented a recommender system to select e-learning courses. Collaborative filtering techniques implemented in the plan include neural network-based collaborative filtering (NCF), Singular Value Decomposition (SVD), and K-nearest neighbour (KNN). The evaluation of the performance of various models involves the utilization of metrics such as hit rate (HR), average reciprocal hit ranking (ARHR), and mean absolute error (MAE). The findings indicate that the K-nearest neighbours (KNN) model outperforms other models in achieving greater HR and ARHR scores and lower MAE values. The author advised developing upgraded and hybrid models and using deep learning for analysis. Mariappan et al., 2022 presented a course recommendation system that utilizes semantic analysis and deep learning models such as LSTM-GRU to facilitate the selection of elective courses by students, taking into account their specific subject interests. The efficacy of the recommendation system has been evaluated on the VIT (Vellore Institute of technology, Chennai) curriculum, revealing that students who receive recommendations for elective courses exhibit a higher attainment of credits within their respective areas of competence. The author suggested that this method has the potential to be used at other other universities, offering students the opportunity to enhance their technical proficiency, raise their cumulative grade point average (CGPA), and increase their rates of course completion. Roy et al., 2022 emphasized the research gaps and obstacles within the field of recommender systems, emphasizing the necessity of creating datasets in domains beyond movies, including health, tourism, and education. Wang et al., 2022 presented a course enrollment recommender system that uses machine learning techniques to offer individualized suggestions to students, considering their course enrollment history and other relevant contextual factors. The empirical findings indicate that the recommended courses exhibited high relevance and provided students with a wide range of possibilities.

Wu et al., 2021 presented an innovative approach to course suggestion, which seeks to boost students' motivation for learning by considering subjective aspects such as preferences and performance expectations. The system employed a genetic algorithm to maximize the suggested course selection while simultaneously addressing the constraints of different situations. The system used a modelling approach incorporating data on students' knowledge acquired from completed courses, preferences, and expectations. The candidate courses for recommendation were selected by a filtering process that considers their resemblance to the user's interests. Xu et al., 2021 provided a personalized course recommendation system using a knowledge graph and collaborative filtering techniques in online education. It incorporated semantic linkages between suggestion items to overcome the constraints of collaborative filtering. The suggested system recommends courses for learners better than standard algorithms in precision, recall, and F1 score. Zhu, 2021 proposed a network course recommendation system with a double-layer attention mechanism that improves online teaching platform course recommendations. This model generates recommendation results categorized by course category weight using an improved TF-IDF technique. The author evaluates the proposed algorithm using various indicators such as HR (hit ratio), NDCG (normalized discount cumulative gain), RMSE (root mean square error), and MAE (mean absolute error). Comparative experiments show that the suggested approach improves course suggestion accuracy. Thanh et al., 2020 suggested a course recommender system that utilizes deep learning techniques, specifically Multi Layer Perceptron, in conjunction with pre-processing methods. This method can assist educational administrators, academic advisors, and students in their strategic planning and early identification of potential issues. The authors also propose conducting additional studies to examine student performance-based groupings to facilitate improved course selection and boost the accuracy of prediction tests.

NEED OF RECOMMENDER SYSTEM IN CURRENT EDUCATION

The multidisciplinary approach of NEP enables the students to pursue their interest in any subject of another discipline, irrespective of their major subjects. But how do you select the multidisciplinary course (MDC) as a minor subject distinct from the courses learned in secondary education or Grade 12? This is a tedious task for students as they always need clarification about which course would benefit their intellectual development and career goals. Sometimes, teachers and parents need more knowledge to give the best suggestions. So, there is a need to develop a recommendation system that recommends the list of courses to students according to their interests, background history and other user's opinions so that students can select the best option for themselves. Likewise, the selection of Ability enhancement courses (AEC), Skill enhancement courses (SEC) and value-added courses (VAC) is also a



**Arti and Manu Gupta**

challenging task for the students. So there is a need of recommendation system that helps the students to select courses of their interest as well as that helps them to get a better career opportunity. There is need to develop a hybrid recommendation system that allows

1. The Students to choose courses based on their interests to enhance performance and eliminate the effort in course selection.
2. The need to improve the capabilities of the education system by implementing a recommendation system (RS) approach and integrating personalized features into it.
3. To catalyze the advancement of knowledge by constructing a comprehensive taxonomy of courses.

CONCLUSIONS AND FUTURE SCOPE

In conclusion, the field of course recommender systems has witnessed significant advancements, particularly in the integration of deep learning techniques. Various models have been proposed, each with its unique approach and focus. This paper conducted a systematic review from 2018 to June 2023 on course recommendation systems to identify the state of art methodologies for developing course recommendation systems. Before the year 2020, the authors used various techniques like ontology, N-gram query and NLP for developing Course recommendation system. But with advancements of Artificial intelligence, the authors moved in the direction of machine learning and deep learning. Thanh et al. (2020) utilized deep learning techniques for course recommendation, emphasizing marks prediction and factor analysis. In 2022, Mariappan et al. achieved 93% accuracy in predicting elective courses using semantic analysis and LSTM-GRU. In 2023, Yinping et al. proposed DORIS, a personalized course recommender system addressing personal interests and course details but facing a cold start problem. Gerard et al. (2023) introduced a hybridized deep learning strategy using RNN and LSTM, highlighting challenges with collaborative and content-based approaches. Jia et al. (2023) presented BTCBMA, an algorithm based on BERT and TextCNN, and Convolutional neural networks and BiLSTM networks, but the model is limited as a local, offline system. The findings of this paper states that there is various course recommendation systems are developed till now but no one meets the requirement of National education policy (NEP 2020). So, our future work will focus on developing a hybrid course recommendation system that meets the requirements of student as well as NEP 2020.

REFERENCES

1. National Education Policy 2020 https://www.education.gov.in/sites/upload_files/mhrd/files/NEP_Final_English_0.pdf
2. National Higher Education Qualifications Framework (NHEQF) https://www.ugc.gov.in/pdfnews/21422_41_NHEQF-Draft.pdf
3. Z. Wu, Y. Tang, and Q. Liang, "A Course Recommendation System Oriented to Multiple Condition Constraints," in *2021 IEEE International Conference on Educational Technology (ICET)*, Beijing, China: IEEE, Jun. 2021, pp. 11–15. doi: 10.1109/ICET52293.2021.9563184.
4. Q. Li and J. Kim, "A Deep Learning-Based Course Recommender System for Sustainable Development in Education," *Applied Sciences*, vol. 11, no. 19, p. 8993, Sep. 2021, doi: 10.3390/app11198993.
5. M. Premalatha, V. Viswanathan, and L. Čepová, "Application of Semantic Analysis and LSTM-GRU in Developing a Personalized Course Recommendation System," *Applied Sciences*, vol. 12, no. 21, p. 10792, Oct. 2022, doi: 10.3390/app122110792
6. G. Deepak and I. Trivedi, "A Hybridized Deep Learning Strategy for Course Recommendation:," *International Journal of Adult Education and Technology*, vol. 14, no. 1, pp. 1–16, Apr. 2023, doi: 10.4018/IJAET.321752.
7. X. Wang, L. Cui, M. Bangash, M. Bilal, L. Rosales, and W. Chaudhry, "A Machine Learning-based Course Enrollment Recommender System:," in *Proceedings of the 14th International Conference on Computer Supported Education*, Online Streaming, --- Select a Country ---: SCITEPRESS - Science and Technology Publications, 2022, pp. 436–443. doi: 10.5220/0011109100003182.





Arti and Manu Gupta

8. D. Roy and M. Dutta, "A systematic review and research perspective on recommender systems," *J Big Data*, vol. 9, no. 1, p. 59, Dec. 2022, doi: 10.1186/s40537-022-00592-5.
9. Y. H. Wu and E. H. Wu, "AI-based College Course Selection Recommendation System: Performance Prediction and Curriculum Suggestion," in *2020 International Symposium on Computer, Consumer and Control (IS3C)*, Taichung City, Taiwan: IEEE, Nov. 2020, pp. 79–82. doi: 10.1109/IS3C50286.2020.00028.
10. Y. Jia, "BTCBMA Online Education Course Recommendation Algorithm Based on Learners' Learning Quality:," *International Journal of Information Technologies and Systems Approach*, vol. 16, no. 1, pp. 1–17, Jun. 2023, doi: 10.4018/IJITSA.324101.
11. Dept. of Electronics and Communication College of Engineering Trivandrum, S. Sumesh, and Prof. A. S. H, "Course Recommendation System based on Natural Language Processing," *IJSREM*, vol. 07, no. 03, Mar. 2023, doi: 10.55041/IJSREM18109.
12. S. Ganesh. G, G. M. Bharath, Subramanian. R, and M. Indumathy, "Course Recommendation System in Social Learning Network (SLN) Using Hybrid Filtering," in *2021 5th International Conference on Electronics, Communication and Aerospace Technology (ICECA)*, Coimbatore, India: IEEE, Dec. 2021, pp. 1078–1083. doi: 10.1109/ICECA52323.2021.9675992.
13. T. T. Dien, L. Hoai-Sang, N. Thanh-Hai, and N. Thai-Nghe, "Course Recommendation with Deep Learning Approach," in *Future Data and Security Engineering. Big Data, Security and Privacy, Smart City and Industry 4.0 Applications*, vol. 1306, T. K. Dang, J. Küng, M. Takizawa, and T. M. Chung, Eds., in *Communications in Computer and Information Science*, vol. 1306., Singapore: Springer Singapore, 2020, pp. 63–77. doi: 10.1007/978-981-33-4370-2_5.
14. L. Donghui, Z. Xi, and L. Xinyu, "Design and Implementation of Personalized MOOC Recommendation System Based on Spark," in *2022 International Conference on Informatics, Networking and Computing (ICINC)*, Nanjing, China: IEEE, Oct. 2022, pp. 106–110. doi: 10.1109/ICINC58035.2022.00029.
15. K. Zhang, X. Zhao, and S. Zhao, "Design of high quality curriculum resources recommendation system for Educational Technology Specialty," in *2022 14th International Conference on Measuring Technology and Mechatronics Automation (ICMTMA)*, Changsha, China: IEEE, Jan. 2022, pp. 1173–1178. doi: 10.1109/ICMTMA54903.2022.00236.
16. K. K. Jena *et al.*, "E-Learning Course Recommender System Using Collaborative Filtering Models," *Electronics*, vol. 12, no. 1, p. 157, Dec. 2022, doi: 10.3390/electronics12010157.
17. Q. Zhu, "Network Course Recommendation System Based on Double-Layer Attention Mechanism," *Scientific Programming*, vol. 2021, pp. 1–9, Dec. 2021, doi: 10.1155/2021/7613511.
18. G. Xu, G. Jia, L. Shi, and Z. Zhang, "Personalized Course Recommendation System Fusing with Knowledge Graph and Collaborative Filtering," *Computational Intelligence and Neuroscience*, vol. 2021, pp. 1–8, Sep. 2021, doi: 10.1155/2021/9590502.
19. A. Pawlicka, M. Pawlicki, R. Kozik, and R. S. Chora', "A Systematic Review of Recommender Systems and Their Applications in Cyber security," *MDPI*, Aug. 2021, doi: <https://doi.org/10.3390/s21155248>.
20. Ma, Y., Ouyang, R., Long, X., Gao, Z., Lai, T., & Fan, C. (2023). DORIS: Personalized course recommendation system based on deep learning. *Plos one*, 18(6), e0284687.
21. Gulzar, Z., Leema, A. A., & Deepak, G. (2018). Pcrs: Personalized course recommender system based on hybrid approach. *Procedia Computer Science*, 125, 518-524.

Table 1: Summary of some course recommendation systems implemented using various techniques for 2018-23.

Author	Title	Methods	Remarks	Limitations
Jia <i>et. al.</i> , 2023	BTCBMA Online Education Course Recommendation Algorithm Based	BERT model combined with the Text CNN model Convolution neural	The proposed online course recommendation method's accuracy, precision, recall, and F1 values in the MOOC	The suggested system is offline and local, and it implements fewer features.





Arti and Manu Gupta

	on Learners' Learning Quality	networks and Bi LSTM networks	dataset are 0.224, 0.241, 0.237, and 0.239, respectively; in the CN dataset, the same values are 0.217, 0.239, 0.227, and 0.233.	.
Gerard et. al., 2023	A Hybridized Deep Learning Strategy for Course Recommendation	RNNs and LSTMs are used for recommendation.	The proposed model used hybrid recommendations that outperform other models. The author used two deep learning techniques LSTM and RNN and results that LSTMs perform better than RNNs in the system.	Collaborative approach lacks personalization Content-based approach doesn't work well for new users
Yinping et. al., 2023	DORIS: Personalized course recommender system	Deep Factorization(Deep FM)	The proposed model used deep factorization method which helps the students to select courses according to their interest, course details and other information.	The paper does not address the cold start problem. And PCA and Text Rank, which lack robust fitting capabilities, encode text.
Mariappan et. al., 2022	Application of Semantic Analysis and LSTM-GRU in Developing a Personalized Course Recommendation System	User Average method Item Average method	In this study, Deep learning models (GRU and LSTM) were used to predict the domain of elective courses with an accuracy of 93%. And Students who utilized the elective course recommendation system registered for more elective course credits and scored higher grades in their domain of expertise.	56 students were unsure about the need for recommendation
Zhu et. al., 2021	Network Course Recommendation System Based on Double-Layer Attention Mechanism	Convolutional neural network with double layer attention mechanism	With a two-layer attention mechanism, the suggested study created an online course recommendation system with the goal of resolving the issue of accurate course selection. The model is evaluated by MAE(mean absolute error) and RMSE(root mean square error) with the value of 0.722 and 0.843 respectively.	The proposed model overcome the precise selection problem but is limited in the terms of efficiency.
Li et. al., 2021	A Deep Learning-Based Course Recommender System for Sustainable	leave-one-out evaluation technique	This study proposed a deep learning based course recommendation model named DECOR for personalized	This study primarily focused on presenting findings related to technical issues, without conducting





Arti and Manu Gupta

	Development in Education		recommendation services on online websites that aims to reduce the problem of information overloading, high dimensional data sparsity, and achieve high feature information extraction performance.	behavioral experiments involving real users implementing the method described in this research.
Thanh et. al., 2020	Course recommendation with deep learning	Deep learning techniques with Multilayer Perceptron	Typically, the recommendations are based on factor analysis and mark prediction on about four million mark records at Can Tho University. Using pre-processing techniques and deep learning with Multi Layer Perceptrons, the author suggested a course recommender system. At Can Tho University, the prediction tasks are run on almost four million mark records.	The proposed system is limited to student's groups only and not considered the course constraints.
Gulzar et. al., 2018	PCRS: Personalized course recommender system based on a hybrid approach	N-gram query classification	The author used hybrid methodology along with ontology to retrieve useful information and make accurate recommendations.	The proposed model had not used knowledge base for recommendation.

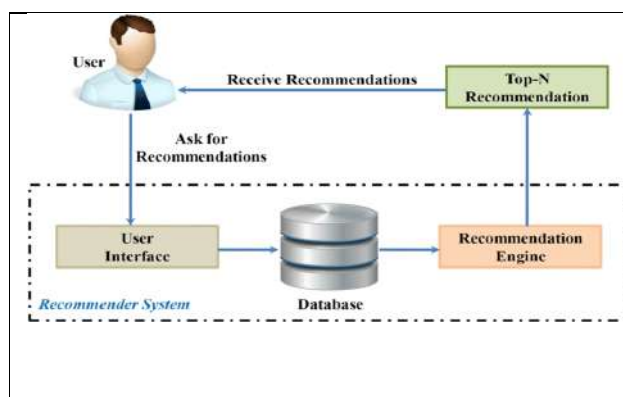


Figure 1: General block diagram of Recommender System

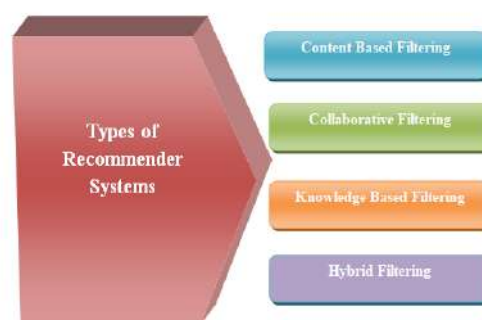


Figure 2: Types of recommender system





Hand-Made Clay Mud: A Traditional Supplement of Mud for Pregnant Ladies in Assam, India

Trishna Mani Nath¹, Gaurav Kumar Bhargav¹, Pallab Kalita^{2*}, Faruk Alam³ and Dhrubajyoti Sarkar³

¹Assistant Professor, School of Pharmaceutical Sciences, University of Science and Technology Meghalaya, RiBhoi, Meghalaya

²Professor, School of Pharmaceutical Sciences, University of Science and Technology Meghalaya, RiBhoi, Meghalaya

³Associate Professor, Faculty of Pharmaceutical Science, Assam down town University, Guwahati, Assam.

Received: 20 Jun 2023

Revised: 20 Nov 2023

Accepted: 23 Jan 2024

*Address for Correspondence

Pallab Kalita

Professor,

School of Pharmaceutical Sciences,

University of Science and Technology Meghalaya,

RiBhoi, Meghalaya

Email: kalitapallab@gmail.com



This is an Open Access Journal / article distributed under the terms of the **Creative Commons Attribution License** (CC BY-NC-ND 3.0) which permits unrestricted use, distribution, and reproduction in any medium, provided the original work is properly cited. All rights reserved.

ABSTRACT

Many pregnant women have the desire to eat clay or soil during the pregnancy. Experts are afraid to find out the proper reasons behind it. Traditionally, a hand-made clay mud (Xikaar) is prepared in village areas of Assam (India). It was also believed that after taking this mud, a pregnant lady could overcome iron deficiency diseases. There are several unknown heavy metals are found in that clay along with Calcium, Potassium, Magnesium, Zinc, etc. Some elements are essential for the growth and development of the fetus. In this paper, a Short description of this clay is given but in no way the authors of the paper do not suggest taking this clay during the pregnancy period.

Keywords: Clay, Xikaar, Pregnancy, Heavy Metal.

INTRODUCTION

“Xikaar” is one of the oldest traditional supplements used since time immemorial in the Assamese ethos for expecting females. A special group of pottery merchants named “Kumaars” usually formulates these supplements from clay. These supplements are smooth-edged in shape and bear a resemblance to the shape of a Diya (lighting lamp) and are merely tasteless but entail the odor of soil. This information has been passed on for generations that administering these supplements are aidful for the proper growth and development of the unborn baby. “Xikaar” is believed to provide vitalsustenance to the baby and also for the soon-to-be lactating mother. However the repetition

69531





Trishna Mani Nath et al.,

of eating clay “Xikaar’s” is much different from the disorder of Geophagia. Human geophagia is a form of pica. Pica is the eating or craving for non-food items. It can be a disorder in and of itself, or it can be an indication of another psychiatric phenomenon. The substance ingested or craved could be biological, natural, or man-made. Nevertheless, the practice of eating “Xikaar” is much dissimilar and alleged to consist of several health paybacks. The beneficial effects are considered to be a result of the presence of various metal elements while also some believe clay has anthelmintic properties that help to keep worms away from the pregnant lady. As they say, everything that glitters is not gold, as such along with the beneficial aspects, there are also detrimental possessions of administering clay. Until now very little research has been done about the digestion and metabolism of clay. The characteristic composition of the administered clay also remains a factor of suspicion. There can be several unknown and anonymous heavy metals present in it. While elements like Calcium, Potassium, Magnesium, Zinc, etc. are usually useful for human physiology, elements such as Bentonite, Fluoride, Arsenic, Boron, Silicon, Cadmium, etc. can have disparaging or superfluous effects. One of the most hazardous elements present in clay is Lead. Lead is toxic and upon ingestion can have perilous effects on health. Lead exposure has been associated with damage to the brain, kidneys, and also to immune system of our body.

Therefore, a pregnant lady upon exposure to lead can fetch devastating effects to her womb and can hinder prenatal development. A parallel menace exists from the consumption of soil near roads that existed before the phase-out of tetraethyl lead or that were spurted with oil (to settle dust) contaminated by toxic Polychlorinated biphenyls or Polychlorinated dibenzodioxins. Polychlorinated dibenzodioxins (PCDDs), or simply dioxins, are a group of long-lived polyhalogenated organic complexes that are primarily anthropogenic and promote to toxic, persistent organic pollutants in the environment[1]. In addition to poisoning, a much superior risk exists of gastrointestinal obstruction or tearing in the stomach. Another risk of eating soil is the ingestion of animal feces and complementary parasites. There can be several pathogenic microorganisms present in the soil. Apart from these plastic pollutants are another major concern. Chlorinated plastic can release harmful chemicals into the adjacent soil, which can then seep into groundwater or other surrounding water sources, and also the ecosystem.

This can cause a range of possibly harmful effects on the species that drink the water[1,2]. In general, when plastic particles degrade, they acquire new physical and chemical properties, increasing the probability that they will be toxic to organisms and the surrounding soil. Furthermore, the greater the number of potentially affected species and ecological functions, the more likely toxic effects will occur. Chemical effects are particularly troublesome during the decomposition stage. Phthalates and Bisphenol A (commonly known as BPA) leach out of plastic elements. These additives are known for their hormonal effects and have the potential to interrupt the hormonal systems of both vertebrates and invertebrates. Additionally, nano particles have the potential to cause inflammation, cross cellular barriers, and even cross highly selective membranes such as the blood-brain barrier or the placenta. Inside the cell, they can trigger changes in gene expression and biochemical reactions, among other effects. The long-term consequences of these vicissitudes have not yet been meticulously investigated. "However, it has already been established that nano plastics have a behavior-changing effect in fish when passing the blood-brain barrier," according to the Leibnitz Institute of Freshwater Ecology and Inland Fisheries[2,3].

CONCLUSION

“Xikaar”, even though it is an age-old practice, the quality of soil since that time has degraded drastically. Previously the amount of pollutants was comparatively on the lower side. From this article, the authors wanted to bring the idea and practice of eating “Xikaar” into the light of the millennial audience. But at no incidence, the authors recommended or promote this practice.





Trishna Mani Nath *et al.*,

REFERENCES

1. Abrahams, P., Follansbee, M., Hunt, A., Smith, B., and Wragg, J. (2006). Iron nutrition and possible lead toxicity: an appraisal of geophagy undertaken by pregnant women of UK. *Appl. Geochem.* 21, 98–108.
2. Benza, S., Liamputtong, P. (2014). Pregnancy, childbirth and motherhood: a meta synthesis of the lived experiences of immigrant women. *Midwifery* 30, 575–584.
3. Cousik, R., and Hickey, M. G. (2016). Pregnancy and childbirth practices among immigrant women from india: have a healthy baby. *Qualitative Rep.* 21, 427. Retrieved from: <https://nsuworks.nova.edu/tqr/vol21/iss4/9> (accessed May 4, 2019).



Figure 1: Xikaar





Isolation and Identification of Harmful Microorganisms from the Shared Cosmetic Products in Delhi NCR Region

Gyan Vandana Yadav¹, Sandhya Khunger^{2*}, Sunil Kumar^{3*}, Mukul Mudgal⁴ and Mukesh Sharma²

¹Masters Student, Faculty of Allied Health Sciences, Shree Guru Gobind Singh Tricentenary University, Gurugram, Haryana, India.

²Assistant Professor, Faculty of Allied Health Sciences, Shree Guru Gobind Singh Tricentenary University, Gurugram, Haryana, India.

³Associate Professor, Department of Microbiology, Graphic Era Deemed to be University, Dehradun, Uttarakhand, India.

⁴Masters Student, Faculty of Allied Health Sciences, Shree Guru Gobind Singh Tricentenary University, Gurugram, Haryana, India.

Received: 07 Aug 2023

Revised: 20 Nov 2023

Accepted: 17 Jan 2024

*Address for Correspondence

Sandhya Khunger

Assistant Professor,
Faculty of Allied Health Sciences,
Shree Guru Gobind Singh Tricentenary University,
Gurugram, Haryana, India.
Email: sandhya.khunger@gmail.com

Sunil Kumar

Associate Professor,
Department of Microbiology,
Graphic Era Deemed to be University,
Dehradun, Uttarakhand, India.
Email: sunilhr10h@gmail.com



This is an Open Access Journal / article distributed under the terms of the **Creative Commons Attribution License** (CC BY-NC-ND 3.0) which permits unrestricted use, distribution, and reproduction in any medium, provided the original work is properly cited. All rights reserved.

ABSTRACT

The usage of shared cosmetics increases the chances of microbiological contamination, which can lead to negative health repercussions for users. Cosmetics are commonly used for personal grooming and aesthetic requirements, however it is usual for several users to share these products. The purpose of this research was conducted to identify the different types of microbial contamination, bacterial or fungal in lipsticks, blush, foundation, and mascara. The study included 48 swab samples of foundation, lipstick, blush, and mascara from Delhi and Gurugram parlors (shared products). Swab samples were collected under sterile conditions and cultured on enriched Blood agar, whereas fungi identification samples were cultured on Sabouraud dextrose agar. The identification of isolated bacteria was confirmed using culture media, Gram staining, biochemical tests, and a Vitek 2GP card for species-level identification. *Staphylococcus hominis* was perhaps the most common bacterial isolate, followed by *Staphylococcus epidermidis* and *Bacillus cereus*, *Streptococcus pyogenes*, and *Bacillus cereus* were found. Lipsticks, foundations, and blushes were more infected with Gram +ve and Gram -ve bacteria. However, mascara had less contamination than lipstick, the foundation, and blush; these contaminated beauty products led to the spread of pathogenic bacteria, which can cause a variety of diseases in humans.



**Sandhya Khunger et al.,****Keywords:** Cosmetic allergies; Cosmetic Contamination; Cosmetic Products; Cosmetology; Cosmetic Testing; Shared Cosmetics.

INTRODUCTION

In today's world, "Beauty products" play an essential role in human life. Cosmetics have become an everyday part of life for many people [1]. They are a valuable source of nonverbal information about a person's personality, attitude, and feelings toward the outside world. They improve people's self-esteem by giving them a nice appearance. With the rising use of cosmetics comes to a greater risk of negative consequences. People are very much satisfied by the makeup product's physical impact without even being conscious of its components, microbial contamination or its active engagement with the body, and as a result, they frequently develop adverse effects, while some contamination may be visible, many harmful microorganisms are invisible to the naked eye [2]. Even if a shared cosmetic product appears clean, it might still carry hidden bacteria or viruses. These unseen threats make it challenging to identify potential risks, underlining the importance of adopting preventive measures by not sharing cosmetics [3, 4]. In the majority of the time, a person's use of cosmetics begins when he or she is recommended a product by a member of his or her social circle or through mass-communication system applications, whether it's trying out a friend's new lipstick shade or using communal makeup testers in stores, the convenience and cost-saving appeal of shared cosmetics seem appealing [5]. However, beneath the surface lies a hidden danger: the risk of contamination. Sharing cosmetic products poses significant health hazards, including the spread of infections and skin irritations [6]. Personal hygiene plays a crucial role in maintaining healthy skin and preventing the spread of infections.

When it comes to cosmetics, using products designed for personal use only is a fundamental aspect of good hygiene practices. Proper cleaning and disinfection of makeup brushes and applicators are equally essential to minimize the risk of contamination and protect our health [7]. Microbe contamination in personal care products may cause spoilage since they contain various ingredients that promote microbial growth [8]. Also, the beauty product processing method is not ideal, particularly the storage temperature, which is nearly ideal for microbe development [9]. Microorganisms present in cosmetics products lead to a risk to consumer's health. At this present, the implement of Good Manufacturing Practices (GMP) has been improved the industrial quality control analyses, but some case studied have reported contamination in cosmetic products as an example of *Pseudomonas aeruginosa*, *Staphylococcus aureus*, *Escherichia coli*, *Candida albicans* and *Staphylococcus epidermidis*, as well as yeast and mold [10-12]. Beauty products preparations come in a variety of chemical forms, including water-based, oily, creamy, gel, and milky one [13]. Natural excipients like pH correctors, preservatives, beauty hues, and pigments, stabilizing agents, and flavorings are included in cosmetic formulations in addition to the active ingredients [14]. The tendency of microorganisms to multiply in beauty products is common, particularly in water-based products, which are frequently characterized by limited durability [15]. Challenge test is typically carried out throughout manufacturing process to assess the efficiency of preservatives in cosmetic items; this ensures that the proper amount and kind of preservatives are included in the compositions [16]. To maximize maintenance, preservatives must be risk-free, consistent with all ingredients, soluble in water, and well-distributed. The intention is to use the minimum quantity available to provide optimum efficacy while eliminating any safety risks associated with certain preservation [17]. In the present study, authors tried to find out the microbial pathogens in the four different cosmetic items in Delhi and Gurugram regions of India.





Sandhya Khunger et al.,

MATERIAL AND METHODS

This study was divided into four stages. The first stage refers to the observational study which includes the questionnaire for randomly selected 100 individuals of the Delhi and Gurgaon region, aged 15-55, to basically assess customers' awareness and the health associated with cosmetics sharing. The second stage refers to the sample distribution which includes 40 samples from 4 different categories which are Lipstick, the Foundation, Mascara and Blush. The third stage refers to the bacterial cultivation & Isolation on 2 different agars. The fourth stage refers to analysis and confirmatory tests for bacterial cultivation.

Sample Distribution

Sample Size

Total of samples (n=40) were included in the study as shown in table 1 from 4 different categories as follows (Table 1)

Sample Collection

The Samples were collected on Sterile Swabs, Inoculated onto the transport media (Blood Agar, SDA) and were transported to the Microbiology Laboratory, SGT University FAHS (Faculty of Allied Health Sciences), and processed for further analysis.

The Bacterial Cultivation & Isolation

Two Different media were used for inoculation of samples: 1. Blood Agar 2. SDA for the Bacterial & Fungal isolation Blood Agar and SDA media was prepared by following Himedia manual instructions, respectively, the samples were inoculated into the media plates and incubated into the incubator (Navyug bacteriological incubator) at 37°C, and the plate was observed for further analysis after 24-48 h.

Identification of Microorganisms

Quadrant streaking

Quadrant streaking was used in this study, which is one of the most extensively utilized streaking methods for gathering an isolated colony. Isolating a single colony or species from a mixed culture is favorable. There are three sorts of streaking patterns: quadrant, continuous, and radiant. A small inoculum was positioned on the first quadrant of an agar medium and then expanded across the three remaining quadrants using the quadrant streaking method. Microbial colonies were most common in the 3rd and 4th quadrants.

Gram staining technique

Gram staining was performed to segregate bacterial species into two groups: gram +ve bacteria and gram -ve bacteria as per standard protocol [18].

Biochemical tests

A battery of biochemical tests were used as a confirmatory test to identify the microorganisms.

The Catalase Test

This method was used to determine which species produce the enzyme called catalase. This enzyme detoxifies hydrogen peroxide by converting it to water and oxygen gas. The formation of oxygen gas bubbles plainly demonstrates a positive catalase result.

Tube Method

The test tubes were filled halfway with a 2 mL solution containing hydrogen peroxide. A sterile loop rod was used to select colonies of the 18 to 24-hour test organism and immersed them in the hydrogen peroxide solution. The bubble production indicated a positive outcome.

Slide Method

The Sterile loop was used to transfer the small amount of colony growth on sterile glass slide. A drop of 3 percent H₂O₂ was been poured on to the sterilize glass slide. Evolution of oxygen bubbles signifies the positive result.





Sandhya Khunger et al.,

Oxidase Test

Oxidase Disc Test

In aerobic respiration, the oxidase test identifies the existence of the cytochrome terminal enzyme system. One filter paper was taken to dry after soaking it in 1 percent Reagent for Kovács oxidase. Sterile loop being used, a well-isolated colony was selected from a fresh (24-hour culture) microbial plate. Color variations were noted.

Bile Esculin Test

The bile-esculin test was used in the present study that utilizes esculin hydrolysis to differentiate streptococci & group D streptococci from non-group D viridians streptococci.

Species Level Identification (VITEK 2 CARDS)

The VITEK 2 is a microbiology system that uses for species level identification [19]. The system is available in three versions (VITEK 2 small, VITEK 2 XL, and VITEK 2 X), each with its own level of capabilities and technology as shown in Figure 1 & 2.

Results

Observational study

These are the responses for those clients as a result as shown in Figure 3. According to responses, 97.8% of those who use cosmetics are female, and the remaining 3.2% are men. [Gender: 97% Female 3% Male. Age: 15-25 are 78%; 25-35 are 18%. Do you put makeup daily? : 93.4% no, 7% yes, 3% sometimes. Do you carry personal cosmetics with you in the parlor or you use their products? 37.4% do not bring personal cosmetics, 24.2% brings personal cosmetics rest 38.5% uses both. Do you share your makeup with others? : 54.9% individual did not share their cosmetics rest 45.1% shares their cosmetic with others. How often you visit to parlor? : 40.7% visit parlor every six months, 33% visit every month and rest 23% visit every week.] According to the responses females use more cosmetics as compare to mens, and 54.9% people do not share their cosmetic products with other people, 45.1% people do share their products which is a big concern. 23% people visit parlor every week and 37.4% people uses parlor's product which is again a matter of concern. All the isolates gave different results for gram staining, catalase test, Oxidase test and Bile esculin test (Table 2).

Bacterial Growth & Sample Analysis

After 24h of incubation, wide variety of colonies appeared on blood agar plates as shown in Fig 4. On BVY1, grey color small oval shaped colonies appeared, on BVY2, sand color colonies appeared, BVY3 showed white color colonies. In Fig 5, Lipstick sample on LUY3 grey color colonies appeared, LUY4 showed small oval shapes colonies in white color, and on LUY5, transparent white some sort of grey color colonies appeared. In the Fig 6, Mascara sample MUY1 showed yellow colonies, MUY2 showed mixed growth, which could not be determined clearly, MUY3 showed mucoid colonies with dark grey color, MUY4 showed grey color colonies and white colonies oval in shape were appeared in MUY5. Fig 7 showed growth of foundation samples in sand color colonies in FUY1, grey color colonies appeared in FUY2, light yellow color colonies were appeared in FUY4, and whitish color colonies were seen in FUY5. In Fig 8, fungus growths appeared in some samples of lipstick, Foundation, Mascara and Blush. In the Fig 9, it was gram positive cocci shape bacteria, catalase positive and oxidase negative, so this confirmed that the blush sample (BVY4) was contaminated by Staphylococcus hominis bacteria.

DISCUSSION

The results revealed harmful bacteria in used items at various levels, indicating user infection while using cosmetic products. The presence of potentially harmful microorganisms as an example E.coli, Pseudomonas aeruginosa, Bacillus cereus and Staphylococcus aureus is a major source of concern. When such germs are introduced near the eyes or mouth, they may pose severe risks of illness. Other research has discovered potentially dangerous microbes in beauty items, including Candida, S. aureus, and E.coli [20]. Products from beauty parlor frequently lack sanitary conditions and are exposed to the outdoors as well as visitors who are permitted to handle and test the product. As a





Sandhya Khunger et al.,

result of increased use and strain on cosmetic preservatives, sharing makeup greatly increases the level of contamination seen in sharing items, which may involve an infection by bacteria, fungi, and yeast. We found *P. aeruginosa*, *Staphylococcus hominis*, *Staphylococcus epidermidis*, and *Bacillus cereus* in foundation, lipstick, blush, and mascara. They are extremely contagious and can result in life-threatening infections, particularly in immune compromised individuals. Even though the disease can be prevented, improper handling of items and lack of cleanliness can lead to scrapes or bruises on the skin that become infected. *S. aureus* and *S. epidermidis* are two examples of the skin-symbiotic *Staphylococcus* species [2, 21]. In the current study, the fungus was also discovered on the SDA plate (Fig. 8). The greatest proportion of bacteria was detected in skincare products, particularly lipstick and foundation, with more than a quarter infected with Gram-positive viral pathogens like; *S. hominis*, *S. epidermis*, and *B. cereus* [21, 22]. All cosmetic products are produced in highly regulated environments to limit microbial content and growth during usage. The preservation system's defense limits the product's lifespan, and the product label makes this information clear [16]. The majority of product lines have an expiration date of 3–12 months. More thorough studies are required to ensure better user compliance, according to the microbiological study that revealed the phases and recurrence of toxins in used products [23]. Seventy to eighty percent of the chemicals used have been found tainted with bacteria [17]. Poor hand hygiene can cause used objects to become contaminated with bacteria like *S. aureus* and *B. cereus* [24]. All product categories had fungus contamination; however, the foundation, lipstick, and mascara had the greatest rates. Additional guidance and instruction are necessary. Apart from the the cosmetics and makeup items, there are many reports of harmful bacteria from environmental samples like; water, salads and meat, which suggested the environment as the reservoir of harmful pathogenic bacteria [25-30]. Some cosmetic items even can cause the ocular infections like endophthalmitis [31]. Antimicrobial resistance is associated with such harmful bacteria which can be difficult to treat [32]. Routine surveillance programs are highly suggested to monitor the bacterial prevalence in the community including different household and cosmetic items.

CONCLUSIONS

The isolation and identification of microorganisms in shared cosmetic goods has revealed important information about the potential health concerns linked with such practices. The study discovered a variety of microbes, including bacteria & fungi that are typically found in shared cosmetics. The research results emphasize the need of not sharing cosmetics in order to prevent the spread of hazardous germs. Shared cosmetics foster microbial development and can result in skin infections, eye irritations, and other health problems, especially when they come into touch with mucous membranes or vulnerable skin. To protect consumer health and well-being, it is critical to raise awareness about the risks of sharing cosmetics and promote responsible cosmetic usage practices. Consumers should be informed on the importance of personal cosmetic hygiene and the need to avoid using cosmetics near sensitive regions. *S. hominis* was discovered in abundance following species level detection followed by *Bacillus cereus*. *S. hominis* is commonly found on the human body and is usually harmless; however, in individuals with unnaturally weakened immune systems, can lead to infection on rare occasions.

Funding

Authors received no funding for this study.

ACKNOWLEDGEMENTS

We thank Shree Guru Gobind Singh Tricentenary University, Gurugram India for providing the institutional facilities for carrying out the present study.

Conflicts of Interest

Authors declare no conflict of interests.

REFERENCES



**Sandhya Khunger et al.,**

1. Costa EF, Magalhaes WV, Di Stasi LC. Recent Advances in Herbal-Derived Products with Skin Anti-Aging Properties and Cosmetic Applications. *Molecules*. 2022;27(21). doi: 10.3390/molecules27217518.
2. Almukainzi M, Alotaibi L, Abdulwahab A, Albukhary N, El Mahdy AM. Quality and safety investigation of commonly used topical cosmetic preparations. *Sci Rep*. 2022;12(1):18299. doi: 10.1038/s41598-022-21771-7.
3. Wan Mohamed Radzi CWJ, Nordin FNM. Status of cosmetic safety in Malaysia market: Mercury contamination in selected skin whitening products. *J Cosmet Dermatol*. 2022;21(12):6875-82. doi: 10.1111/jocd.15429.
4. Anelich LE, Korsten L. Survey of micro-organisms associated with spoilage of cosmetic creams manufactured in South Africa. *Int J Cosmet Sci*. 1996;18(1):25-40. doi: 10.1111/j.1467-2494.1996.tb00133.x.
5. Mohammed AH, Blebil A, Dujaili J, Hassan BAR. Perception and attitude of adults toward cosmetic products amid COVID-19 pandemic in Malaysia. *J Cosmet Dermatol*. 2021;20(7):1992-2000. doi: 10.1111/jocd.14147.
6. Gupta V, Mohapatra S, Mishra H, Farooq U, Kumar K, Ansari MJ, et al. Nanotechnology in Cosmetics and Cosmeceuticals-A Review of Latest Advancements. *Gels*. 2022;8(3). doi: 10.3390/gels8030173.
7. Zalecki P, Twardowska J, Nowicka D, Andrzejewski W. Effectiveness of the Disinfection of Reusable Make-Up Applicators-Initial Experiences. *J Cosmet Sci*. 2021;72(2):163-71.
8. Noor AI, Rabih WM, Alsaedi AA, Al-Otaibi MS, Alzein MS, Alqireawi ZM, et al. Isolation and identification of microorganisms in selected cosmetic products tester. *African Journal of Microbiology Research*. 2020;14(9):536-40. doi: 10.5897/AJMR2020.9399.
9. Halla N, Fernandes IP, Heleno SA, Costa P, Boucherit-Otmani Z, Boucherit K, et al. Cosmetics Preservation: A Review on Present Strategies. *Molecules*. 2018;23(7). doi: 10.3390/molecules23071571.
10. Bouslimani A, da Silva R, Kosciolk T, Janssen S, Callewaert C, Amir A, et al. The impact of skin care products on skin chemistry and microbiome dynamics. *BMC Biol*. 2019;17(1):47. doi: 10.1186/s12915-019-0660-6.
11. Fourniere M, Latire T, Souak D, Feuilloley MGJ, Bedoux G. Staphylococcus epidermidis and Cutibacterium acnes: Two Major Sentinels of Skin Microbiota and the Influence of Cosmetics. *Microorganisms*. 2020;8(11). doi: 10.3390/microorganisms8111752.
12. Jairoun AA, Al-Hemyari SS, Shahwan M, El-Dahiyat F, Bisgwa J, Jamshed S, et al. Development and Delphi validation of instrument for the preparation of a GMP audit of a cosmetic contract manufacturer in the UAE. *Sci Rep*. 2022;12(1):11265. doi: 10.1038/s41598-022-14457-7.
13. Dini I, Laneri S. Nutricosmetics: A brief overview. *Phytother Res*. 2019;33(12):3054-63. doi: 10.1002/ptr.6494.
14. Sharmeen JB, Mahomoodally FM, Zengin G, Maggi F. Essential Oils as Natural Sources of Fragrance Compounds for Cosmetics and Cosmeceuticals. *Molecules*. 2021;26(3). doi: 10.3390/molecules26030666.
15. Kim HW, Seok YS, Cho TJ, Rhee MS. Risk factors influencing contamination of customized cosmetics made on-the-spot: Evidence from the national pilot project for public health. *Sci Rep*. 2020;10(1):1561. doi: 10.1038/s41598-020-57978-9.
16. Rathee P, Sehrawat R, Khatkar A, Akkol EK, Khatkar S, Redhu N, et al. Polyphenols: Natural Preservatives with Promising Applications in Food, Cosmetics and Pharma Industries; Problems and Toxicity Associated with Synthetic Preservatives; Impact of Misleading Advertisements; Recent Trends in Preservation and Legislation. *Materials (Basel)*. 2023;16(13). doi: 10.3390/ma16134793.
17. Dadashi L, Dehghanzadeh R. Investigating incidence of bacterial and fungal contamination in shared cosmetic kits available in the women beauty salons. *Health Promot Perspect*. 2016;6(3):159-63. doi: 10.15171/hpp.2016.25.
18. Kumar S, Singhal L, Ray P, Gautam V. In vitro and in vivo fitness of clinical isolates of carbapenem-resistant and -susceptible *Acinetobacter baumannii*. *Indian J Med Microbiol*. 2020;38(1):52-7. doi: 10.4103/ijmm.IJMM_19_468.
19. Kim SY, Park SY, Jin JE, Hong KS, Kim DJ, Kim YK, et al. Comparing the VITEK 2 ANC card, species-specific PCR, and MALDI-TOF mass spectrometry methods for identification of lactic acid bacteria. *J Food Sci*. 2022;87(11):5099-106. doi: 10.1111/1750-3841.16343.
20. Brasch J, Becker D, Aberer W, Bircher A, Kränke B, Jung K, et al. Guideline contact dermatitis. *Allergo Journal International*. 2014;23(126-138). doi: 10.1007/s40629-014-0013-5.
21. Zhang W, Wang X, Zhao L, Gu Y, Chen Y, Liu N, et al. Effect of leave-on cosmetic antimicrobial preservatives on healthy skin resident *Staphylococcus epidermidis*. *J Cosmet Dermatol*. 2023;22(7):2115-21. doi: 10.1111/jocd.15690.





Sandhya Khunger et al.,

22. Yossa N, Huang S, Canida T, Binet R, Macarisin D, Bell R, et al. qPCR detection of viable Bacillus cereus group cells in cosmetic products. *Sci Rep.* 2023;13(1):4477. doi: 10.1038/s41598-023-31128-3.
23. Akhtar A, Kazi TG, Afridi HI, Khan M. Human exposure to toxic elements through facial cosmetic products: Dermal risk assessment. *Regulatory Toxicology and Pharmacology.* 2022;131(105145). doi: 10.1016/j.yrtph.2022.105145.
24. Burton M, Cobb E, Donachie P, Judah G, Curtis V, Schmidt WP. The effect of handwashing with water or soap on bacterial contamination of hands. *Int J Environ Res Public Health.* 2011;8(1):97-104. doi: 10.3390/ijerph8010097.
25. Kumar S, Anwer R, Sehrawat A, Yadav M, Sehrawat N. Assessment of Bacterial Pathogens in Drinking Water: a Serious Safety Concern. *Current Pharmacology Reports.* 2021;7:206-12. doi: 10.1007/s40495-021-00263-8.
26. Kumar S, Anwer R, Sehrawat A, Sehrawat N, Yadav M, Sharma AK. Isolation and characterization of pathogenic bacteria from drinking water in North India. *International Journal of Environmental Science and Technology.* 2022;19:12605–10. doi: 10.1007/s13762-021-03774-5.
27. Kumar S, Anwer R, Yadav M, Sehrawat N, Kumar V, Sharma AK. Isolation and characterization of Acinetobacter baumannii from chicken meat samples in north India. *Asian Journal of Biological and Life Sciences.* 2021;10(2):462-8. doi: 10.5530/ajbls.2021.10.61. .
28. Alrehaili J, Almarri FK, Kumar S, Mustafa S, Alshehri H, Haque S, et al. Molecular Characterization of Microbial Quality of Ready-to-eat Salads using Multi-locus Sequence Typing. *Journal of Pure & Applied Microbiology,.* 2023;17(2):1-11. doi: 10.22207/JPAM.17.2.10.
29. Kumar S, Yadav M, Devi A, Uniyal M, Kumar V, Sehrawat N, et al. Assessment of Pathogenic Micro-organisms Associated with Vegetable Salads. *Asian Journal of Biological and Life Sciences.* 2022;11(1):1-7. doi: 10.5530/ajbls.2022.11.1.
30. Kumar S, Yadav M, Anwer R, Sehrawat N, Devi T, Sharma AK. Isolation and Characterization of E. coli and Comamonas kerstersii from Chicken Litter Samples from North India. *Environment and Ecology.* 2022;40(4B):2476-81.
31. Sharma SP, Bansal R, Kumar S. Endophthalmitis: Types and Recent Trends in Diagnosis. *Current Pharmacology Reports.* 2022;8:106-11. doi: 10.1007/s40495-021-00278-1. .
32. Kumar S, Chaudhary M, Yadav M, Kumar V. Global Surveillance Programs on Antimicrobial Resistance. In: Panwar, H., Sharma, C., Lichtfouse, E. (eds). *Sustainable Agriculture Reviews* Springer, Cham 2020;46:33-58. doi: 10.1007/978-3-030-53024-2_2.

Table1: Showing sample categories with the sample size (n=40), includes lipstick, foundation, mascara and blush respectively. (LVY=Lipstick Vandana Yadav) (BVY=Blush Vandana Yadav) (FVY=Foundation Vandana Yadav) (MVY=Mascara Vandana Yadav)

PRODUCTS	CATEGORIES	SAMPLES
1. Lipstick (LVY)	a) Sealed (used as a control) b) Parlors (shared products)	5 Samples Each
2. Foundation (FVY)	a) Sealed (used as a control) b) Parlors (shared products)	5 Samples Each
3. Mascara (MVY)	a) Sealed (used as a control) b) Parlors (shared products)	5 Samples Each
4. Blush (BVY)	a) Sealed (used as a control) b) Parlors (shared products)	5 Samples Each

Table 2. Shows all the gram staining, Catalase test, Oxidase test and Bile esculin test results of all the samples which are Lipstick (LVY), Blush (BVY), Foundation (FVY) and Mascara (MVY).

Sample ID	Gram Stain	Microscopic Observation	Catalase Test	Oxidase Test	Bile Esculin Test
LVY-1	Positive	Cocci	+	+	-





Sandhya Khunger et al.,

LVY-2	Positive	Cocci	+	+	-
LVY-3	Negative	Cocci	-	+	+
LVY-4	Positive	Long Rods	+	+	-
LVY-5	Positive	Cocci	+	-	+
FVY-1	Positive	Rods in Chain	+	+	-
FVY-2	Positive	Long Rods	+	+	-
FVY-3	Positive	Rods	+	+	-
FVY-4	Positive	Cocci in Clusters	-	+	-
FVY-5	Positive	Cocci	+	+	-
MVY-1	Negative	Rods	+	+	-
MVY-2	-	-	-	+	-
MVY-3	Positive	Rods	-	+	-
MVY-4	Negative	Cocci	-	+	-
MVY-5	Positive	Rods	+	+	-
BVY-1	Positive	Rods in Chain	+	-	-
BVY-2	Positive	Cocci	-	+	-
BVY-3	Negative	Rods	+	-	-
BVY-4	Positive	Cocci	+	-	-
BVY-5	Positive	Rods	+	+	+

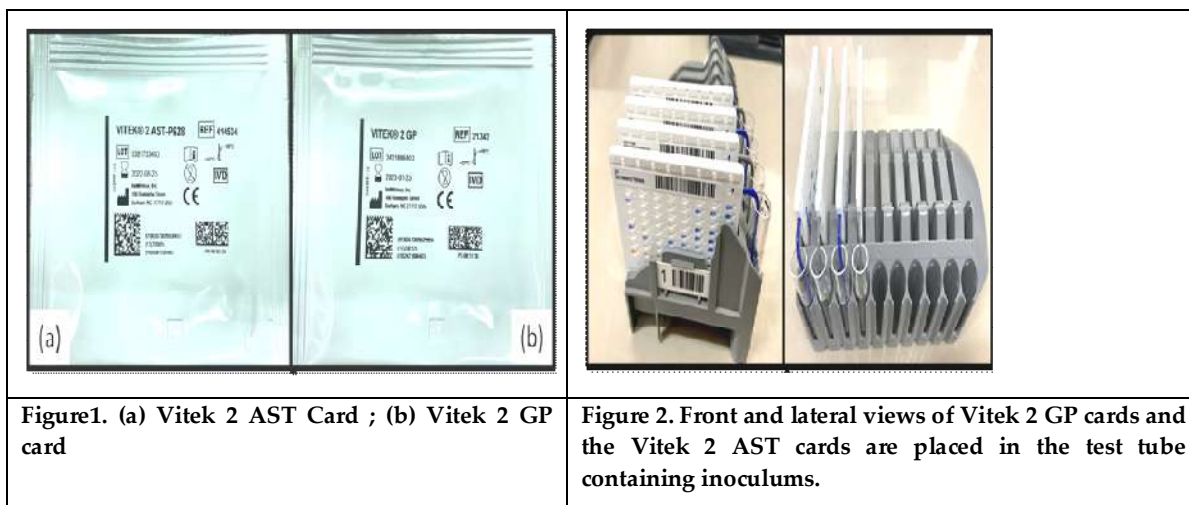


Figure1. (a) Vitek 2 AST Card ; (b) Vitek 2 GP card

Figure 2. Front and lateral views of Vitek 2 GP cards and the Vitek 2 AST cards are placed in the test tube containing inoculum.





Sandhya Khunger et al.,

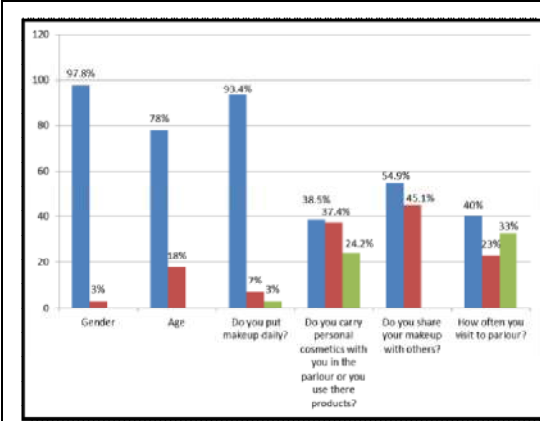


Figure 3. The graphical presentation of the questionnaire showing general awareness about cosmetic to randomly selected 100 individuals.

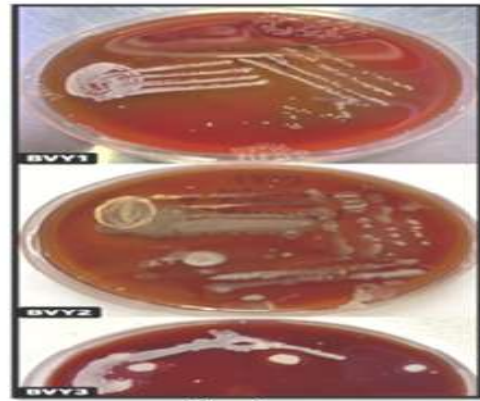


Fig. 4

Figure 4. Growth of Blush samples inoculated on to the blood agar plate



Figure 5. Growth of Lipstick samples inoculated on to the blood agar plate.

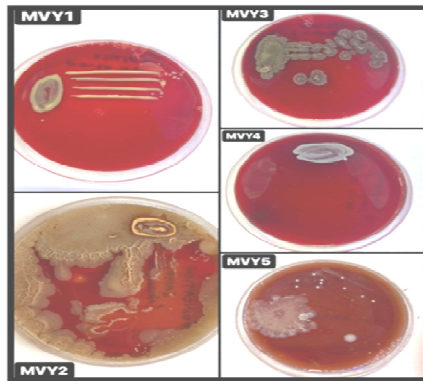


Fig. 6

Figure 6. Growth of Mascara samples inoculated on to the blood agar plate.

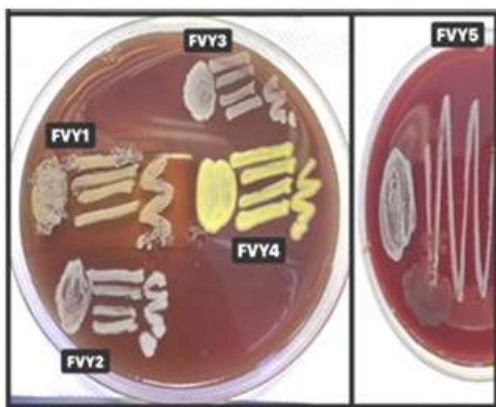


Figure 7. Growth of Foundation samples

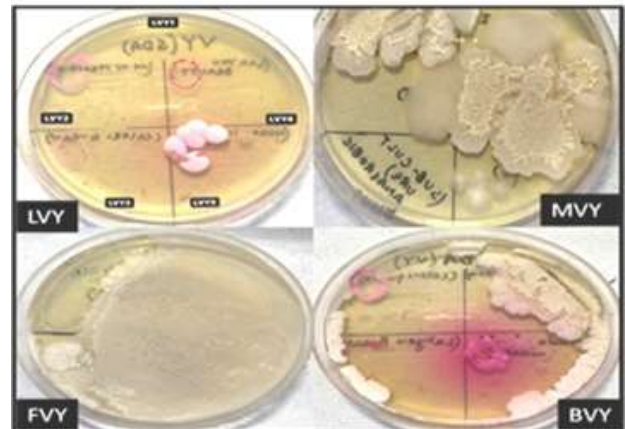
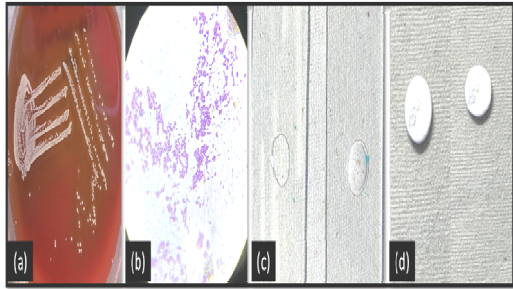


Figure 8. Growth of four samples Lipstick (LVY),





Sandhya Khunger et al.,

inoculated on the blood agar plates	Mascara (MVY), Foundation (FVY) & the Blush (BVY) samples that they were inoculated on to the SDA plates.
	
<p>Figure 9. (a) Growth of blush sample (BVY4) inoculated on to the blood agar (b) Gram staining showed appearance of Gram +ve bacteria as purple colored colonies (c) Catalase positive Test (d) Oxidase negative Test.</p>	





Anticonvulsant Activity of *Tectona grandis* Linn. Leaf Buds in Zebrafish Model of Epilepsy

Chaithra S R¹, Salini P Nair¹, Chaithanya S R², Bijesh Vatakkeel^{3*} and Nagashree K S^{4*}

¹Research Scholar, Department of Pharmacology, JSS College of Pharmacy, JSSAHER, Mysuru, Karnataka, India.

²PG Student, Department of Surgery, Assam Medical College, (Affiliated to Srimanta Sankaradeva University of Health Sciences) Dibrugarh, Assam, India.

³Lecturer, Department of Pharmacology, College of Pharmaceutical Sciences, Govt. Medical College, (Affiliated to Kerala University of Health Sciences) Kannur, Kerala, India.

⁴Lecturer, Department of Pharmacology, JSS College of Pharmacy, JSSAHER, Mysuru, Karnataka, India.

Received: 05 Sep 2023

Revised: 10 Nov 2024

Accepted: 27 Dec 2023

*Address for Correspondence

Bijesh Vatakkeel

Lecturer,
Department of Pharmacology,
College of Pharmaceutical Sciences,
Govt. Medical College,
(Affiliated to Kerala University of Health Sciences)
Kannur, Kerala, India.

Nagashree K S

Lecturer,
Department of Pharmacology,
JSS College of Pharmacy, JSSAHER,
Mysuru, Karnataka, India.



This is an Open Access Journal / article distributed under the terms of the **Creative Commons Attribution License** (CC BY-NC-ND 3.0) which permits unrestricted use, distribution, and reproduction in any medium, provided the original work is properly cited. All rights reserved.

ABSTRACT

Transient pentylentetrazol (PTZ) treatment on Zebrafish, is a widely accepted and promising alternative model. Zebra fish model proven to be a rising model for epilepsy by Baraban et al on 2005. The purpose of the study is to " evaluate the antiepileptic activity of hydro-alcoholic extract of leaf buds of *Tectona grandis*. Linn" using Zebra fish model. The leaf buds were extracted using methanol and water and phytochemical analysis was done, *in-vitro* anti-oxidant study was done by using DPPH and ABTS assay and *in-vivo* study was done by using PTZ induced epilepsy in Zebrafish (*Danio rerio*) to determine the antiepileptic activity of the extract. The extract was evaluated to determine the effect on brain GABA and MDA to determine the possible mechanism of action. The result from the phytochemical studies shows that the hydro-alcoholic extract of leaf buds contains glycosides, phenolic compounds, coumarins, and flavonoids. The antioxidant activity of leaf bud extract was studied against DPPH and ABTS radical assays using ascorbic acid as standard (200µg/ml). The results of both antioxidant assays (DPPH- 75.53% and ABTS 74.32% activity) shows antioxidant activity of the extract. The results of the *In-vivo* study reveal that the hydro-alcoholic extract leaf buds of *Tectona grandis*. Linn (100 & 200 mg/L) shows significant dose-dependent anticonvulsant activity. The study shows that leaf bud extract could have a



**Chaithra et al.,**

direct modification on GABA production and lipid peroxidation (MDA) in the brain. All these results were statistically evaluated using Graph pad prism software 8.

Keywords: Epilepsy, *Tectona grandis*. Linn, hydro-alcoholic extract, leaf buds, antioxidants, antiepileptic activity, MDA, GABA.

INTRODUCTION

Epilepsy is a neurological disorder resulting from a recurrent spontaneous and abnormal discharge of a group of neurons in the brain and as a result seizure occurrence in patients. A seizure is a condition where there is a rapid firing of neurons (1). Anti-epileptic medicines (AEDs) are the first line of treatment for epilepsy; they are 60% effective at preventing seizures in epilepsy patients. There are various AEDs on the market that act by either inhibiting excitatory mechanisms or enhancing inhibitory ones and have a variety of molecular targets. Even while AEDs are successful in two thirds of patients, some patients are still unable to control their seizures. As a result, patients will develop drug-resistant epilepsy(2). Recurrent seizure sufferers are at risk for a wide range of medical, psychological, and social morbidities, regardless of the cause. Psychiatric and psychologic complications are common in epilepsy and it will affect the daily living of epilepsy patients (3,4). Incidence studies of epilepsy revealed that about 61.4 per 100,000 people in a year affected by epilepsy. Depending on etiological factors and local distribution of risk, prevalence of epilepsy differs significantly among countries (5). In India more than 10 million people are with epilepsy. The prevalence of epilepsy in urban population is 0.6% which is less compared to rural areas the prevalence is 1.9%. Over all prevalence based on various studies in India is 5.59-10 per 1000(6). Plant *Tectona grandis*. Linn is a most commonly available plant. According to previous studies, the bark is used as a depurative, astringent, treating constipation, and as an anthelmintic(7). The oil extract of wood is used to relieve headaches, burning pains, and biliousness. Roots are useful in urine retention and anuria. Flowers can use to treat bronchitis and act as an acrid, for treating urinary discharge(8). In the Unani system of medicine, flower oil extract is used for hair growth and used for scabies (9). The plant shows antioxidant activity, protect from free radicals. (10).

flavonoids show a broad spectrum of biological activities by binding with specific molecular targets and also show antioxidant properties. These biologically active molecule act on CNS and in the benzodiazepine receptor it acts as a ligand (11). Diniz TC et al, reported the antiepileptic activity of flavonoids by modulating the GABA-Cl channel. In neurodegenerative diseases also flavonoids show modulating action, this is mainly because of the phenolic nature of these compounds. In CNS they can disrupt the cellular oxidative process (12). Flavonoids in different classes inhibit certain enzymes that act on signal transduction pathways by either phosphorylating or dephosphorylating the critical proteins (13). The study aims to establish the antiepileptic activity of leaf bud extract of *Tectona grandis*. Linn. (Family: Verbenaceae). It is a popular plant that shows various medicinal properties. In Ayurveda, it is used as a cooling, laxative, and sedative. In the Unani system of medicine, it is used for pain and burning sensation, trouble related to the liver, headache, and anthelmintic activity (14,15). Thus, it is necessary to investigate the antiepileptic activity of highly efficacious as well as safe drugs in terms of drug-related toxicity.

MATERIALS AND METHODS

Collection and identification of plant material

The leaf buds of *Tectona grandis*. Linn were collected from Pariyaram, Kannur district, Kerala (India) in November 2019 authenticated by Dr. Abdussalam, a taxonomist from the Department of PG Studies and Research in Botany, Sir Sayed College, Taliparamba, Kannur, Kerala, India. A herbarium specimen of the same was prepared and submitted to the Department of PG Studies and Research in Botany, Sir Sayed College, Taliparamba, Kannur, Kerala, India.





Chaithra et al.,

Extraction method

100 grams of the air-dried powdered leaf buds of *Tectona grandis*. Linn was weighed and subjected to successive maceration with methanol and water as solvents (7:3). For 3 days placed the solution at room temperature until the soluble material disintegrated, there was constant stirring. Following pressing of the marc and straining of the combination, the resulting liquid is mixed and purified by decantation (16).

Phytochemical parameters detection and screening

Hydro alcoholic extract of *Tectona grandis*. Linn analyzed to determine the presence of phytochemical constituents like flavonoids, tannins, saponins, cardiac glycosides, alkaloids and phenolic compounds with standard qualitative methods.

IN VITRO ANTIOXIDANT ACTIVITY

DPPH (2,2-diphenyl-1-picryl hydrazyl) scavenging activity

The radical-scavenging capacity of TG. Linn was examined using a DPPH assay. At 517 nm, a decrease in DPPH solution absorption was seen after the addition of an antioxidant. Ascorbic acid (10 mg/ml DMSO) serves as the reference substance. 1, 1-diphenyl-2-picryl hydrazyl is a free stable free radical with red color but after scavenging it changes to yellow color. To show free radical scavenging activity DPPH assay uses this character. Take the plant extract and add 20µl of DMSO and 0.1 mM DPPH solution (1.48ml) to prepare different concentration of extract. Place the mixture 20 minutes in an isolated dark room temperature. The absorbance at 517nm was measured after 20 minutes. Control used for this was 3ml of DPPH (17).

$$\text{Percentage inhibition} = \frac{\text{control} - \text{test}}{\text{control}} \times 100$$

ABTS⁺ scavenging activity

Chemically ABTS is 2, 2-azino-bis (3-ethylbenzothiazoline-6, 6-sulphonic acid). At 734 nm, ABTS is used to determine the test compound's ability to reduce free radicals. The first step is preparation of ABTS⁺ radical cation, 2mM ABTS was prepared by adding in 0.548g in 50 ml of distilled water. 70mM potassium per-sulphate prepared by adding 0.0189 g potassium per-sulphate dissolved in 1ml of distilled water. After 2hrs from these above prepared mixtures take 50ml of ABTS solution and 200µl of potassium per-sulphate, and the ABTS radical cation is synthesized. Then take different concentrations of the extract and add ABTS radical cation (0.3ml) and Phosphate buffer (1.7ml) with pH of 7.4. for control group instead for alcoholic extract methanol and aqueous extract water is used. And at 734 nm the absorbance was measured. Repeat the experiment 3 times and find out the absorbance (18).

$$\text{Percentage inhibition} = \frac{\text{Control} - \text{Test}}{\text{Control}} \times 100$$

IN-VIVO ANTIEPILEPTIC ACTIVITY

Animals

Zebrafish (*Danio rerio*) collected and must be held in the laboratory for at least 12 days for acclimatization. Before testing, they must be kept in water for at least 7 days, and only under the following circumstances are they allowed to be used in tests. Light and dark cycle of 12 hours used, and kept in a temperature condition of 28°C ± 2°C, with 80 % of air saturation. Fishes were feeded 2 times a day and Pellets were purchased from the neighbourhood aquarium retailer Kannur.

Grouping of fishes

The fishes were divided into 5 groups. Tank method was used for dose administration. Group I were treated with normal control (Normal saline), Group II were treated with PTZ (6mM) as Toxic control (Wong et al. (2010), Group III were treated with PTZ and standard drug (Diazepam 10µm), and group IV & V were treated with higher and lower dose of extract (200&100mg/L). Prior to PTZ exposure, native fishes are pre-treated by immersion for 1hrs in a chamber containing standard drug, higher & lower doses of extract dissolved in deionized water. Monitored continuously during pre-treatment group. Following pre-treatment period, fishes were transferred to tank, containing PTZ (induce generalized seizure). Behavior was continuously monitored. (19,20).





Chaithra et al.,

BIOCHEMICAL EVALUATION IN BRAIN TISSUE

All the animals were sacrificed after 7 days and brain homogenate was prepared to analyze parameters like MDA and GABA (21–23).

Preparation of homogenate

10% brain homogenate was prepared in 0.1 M phosphate buffer (pH 7.4). Centrifuged for 15 minutes (3000rpm), supernatant was used to estimate GABA and MDA levels.

Estimation of brain Malondialdehyde (MDA)

Malondialdehyde (MDA) dialdehyde have 3 carbons and a highly reactive compound. MDA is a byproduct produced during prostaglandin synthesis and poly unsaturated fatty acid peroxidation. Functional groups like RNA, DNA, lipoproteins, proteins are MDA combined with. Hiroshi ohkawa et al identified the indicator action of malondialdehyde in lipid peroxidation. Lipid peroxidation was detected by determination of MDA production determined by method of Hiroshi ohkawa.et al (24).

Estimation of GABA by spectrophotometry

Gamma amino butyric acid (GABA) was determined from whole brain. First the brain isolated and immediately placed in homogenization tube consist of 5ml hydrochloric acid (0.01M). And followed method used by Herrera-Calderon O et al.(25).

Statistical analysis

All the result shown as Mean \pm SEM. The results were analyzed for statistical significance by one-way analysis of variance (ANOVA) followed by multiple comparison using Dunnett's test in graph pad prism software (version 8). Statistical multiple comparisons were done concerning normal group, control group and standard group. P values less than 0.05 ($P < 0.05$) were found to be statistically significant (26).

RESULTS

The percentage yield of hydro alcoholic extract of *Tectona grandis*. Linn after solvent extraction was estimated and the result showed a yield of 12.23 %w/w. And phytochemical parameters like loss on drying, total ash content, water soluble ash, acid soluble ash and extractive value of hydro alcoholic extract was determined. And extractive value was found to be 27.7% w/w (Table 3).

Phytochemical screening

Phytochemical screening of the leaf bud extract was done and results are given in table 4. Results shows the presence of flavonoids, saponins, carbohydrates, tannins etc.

IN VITRO ANTI-OXIDANT ACTIVITY**DPPH scavenging assay**

In DPPH scavenging assay it is observed that the hydro-alcoholic extract of *Tectona grandis*. Linn have dose dependent increase in DPPH scavenging activity. The 200 μ g/ml Ascorbic acid (Standard) showed the maximum activity of 79.59%. Methanol extract showed maximum activity of 75.53%. (Table:5)

b. ABTS⁺ Scavenging activity

In ABTS⁺ assay it is observed that leaf bud extract of *Tectona grandis*. Linn have dose dependent increase in the ABTS⁺ radical scavenging activity. The 200 μ g/ml Ascorbic acid (Standard) showed the maximum activity of 90.46 %. Hydro-alcoholic extract showed maximum activity of 74.32 % (Table 6).





Chaithra et al.,

IN-VIVO ANTIEPILEPTIC ACTIVITY

PTZ - Induced convulsions

The anticonvulsant activity of leaf bud extract of *Tectona grandis*. Linn showed a significant decrease in onset of action and duration of action, compared to standard drug diazepam and control pentylenetetrazol. The percentage protection of leaf bud extract of TG at higher dose was found to be 41.57 and diazepam was found 77.89, which shows that at higher concentration the leaf bud extract of TG shows good percentage protection when compared with standard drug (diazepam). The results of onset of action and duration of action and percentage protection are given in Table 7 (Figure 5). Values are Mean \pm SEM (n = 6). * indicates P < 0.05, ** indicates P < 0.001 and *** indicates P < 0.0001 as compared to the control group using one-way ANOVA followed by multiple comparison using Dunnett's test.

Biochemical evaluation in brain tissue

The effect of hydro-alcoholic extract in the activity of MDA and GABA was assessed and the results were shown in the given table 8. Administration of PTZ significantly raised MDA concentration and attenuated the GABA level in control group as compared to other treatment group. However, treatment with standard, hydro-alcoholic extract 200mg/kg and 400mg/kg significantly reduced the MDA concentration and also enhances GABA (Table 9). Values are expressed as mean \pm SEM (n=6), * indicates P value <0.001, **** indicates P <0.0001, *** indicates P < 0.01 and ** indicates P < 0.05, a indicates Normal control Vs Toxic control, Standard, Lower dose, Higher dose, b indicates Toxic control Vs Standard, Lower dose, Higher dose, c indicates Standard Vs Lower dose, higher dose.

DISCUSSION

In the current study, we evaluated and confirmed the antiepileptic activity of *Tectona grandis*. Linn. *Tectona grandis*. Linn leaf buds are collected and shade dried. The extract was prepared by maceration method. The result from preliminary phytochemical analysis showed the hydro- alcoholic extract of *Tectona grandis*. Linn leaf buds contain flavonoids, phenols, coumarins, glycosides, and tannins. Different factor responsible for the hyper excitability of neurons, receptor biochemical modifications, gene expression, secondary messaging system modulation, number, biophysical properties, distribution, and type of ion channels in the neuronal membrane, changes in extracellular ion concentrations. The major reason considered to be responsible for epilepsy is neurotransmitter imbalance between excitatory and inhibitory. The development of seizure in epilepsy patients affects the antioxidant defense mechanism in brain and activate the free radicals leads to induction of stress. Cell communication and defense mechanism in human are taking place in presence of reactive oxygen species. But even though it is useful excess amount of ROS accumulation in cell can cause diseases due to changes in biochemical reactions. Natural antioxidants are helpful for the prevention of these ROSs. So, such disease conditions instead of synthetic products we can depend on natural products. Free radicals and seizure are connected through multiple mechanisms. But the seizure induced by free radical are mainly by direct inactivation of glutamine synthase.

The amount of GABA in the cortex of the brain decreases as a result of oxygen free radicals' suppression of the enzyme glutamate decarboxylase, which leads to the commencement of oxygen-induced seizures in animals (1). It has been observed that the available AEDs are unable to control seizures effectively in 25% of the patients. These drugs are associated with different side effects including chronic toxicity, teratogenicity etc. because of these reasons, so it is necessary to look for an alternative medicine with less side effects, affordable and conventional mainly medicinal plants. Studies on medicinal herbs having free radical scavenging activity and antioxidant activity shows that the presence of active constituents likes flavonoids, coumarins, tannins, and phenolic-compounds show antioxidant activity(20). As the most likely culprit causing the neural alterations mediating the behavioural abnormalities in neurodegenerative illnesses, free radicals have been proposed as the culprit. In the rodent epilepsy model, a number of studies have shown that antioxidants are helpful. Although oxygen is essential for aerobic biological activities, it can also be subject to electron transfer reactions that result in the production of extremely



**Chaithra et al.,**

reactive oxygen free radicals such as superoxide, anion radicals, hydrogen peroxide, or hydroxyl radicals. As a result of these free radicals, the brain is particularly vulnerable to oxidative injury. One of the common and widely used screening methods for epilepsy is using a fish model and PTZ as an inducing agent (Ben Hur M. Mussulini et al). PTZ is a GABA-A receptor agonist; it can suppress the inhibitory neurotransmission and enhance the excitatory neurons and leads to development of seizure. In this study diazepam is used as a standard, diazepam produced its effects by opening of GABA mediated opening of chloride channel on GABA_A receptor leading to more chloride ion entering the neuron which in turn decreases the neuronal activity in the brain. In the present study diazepam is shown to antagonize the seizure induced by PTZ (19). In this study the antiepileptic activity of *Tectona grandis* Linn leaf bud extract was evaluated using Zebrafish. The extract was subjected to screen *In-vivo* antiepileptic activity against PTZ induced convulsions in Zebrafish. PTZ method is a valid model for the study of generalized myoclonic seizures (Absence seizure). It was found that the hydro-alcoholic extract of *Tectona grandis* Linn leaf bud on PTZ induced Zebrafish significantly reduced the duration of convulsion ($P < 0.0001$) and delayed the onset of convulsions ($P < 0.001$). PTZ induces epilepsy by activating NMDA glutamate receptor and stimulates the calcium ion entry to nerve cells. NMDA receptor activation is involved in the PTZ induced seizure generation. The result from the phytochemical screening showed hydro-alcoholic extract of *Tectona grandis* Linn contains flavonoids, coumarins, poly phenols and glycosides. These compounds possess antioxidant activity; hence these compounds reduce stress involved during experiments and thereby giving protection to neurons. Most of the flavonoids can bind on GABA receptor because they act as benzodiazepine and can modulate the GABA receptor and activate chloride channel in animal model. Flavonoids show neuroprotective activity by modulating GABA receptor and decrease the glutamergic transmission. In this study the activity of *Tectona grandis* Linn leaf bud extract may attribute to the presence of above-mentioned phytochemical constituents.

We mainly focused on flavonoids, one of the phytochemicals present in *Tectona grandis*. Background studies (Jae Young Kwon et al) state that flavonoids potentiate GABA induced currents in native GABA_A receptors expressed in cortical neurons and also to selectively modulate GABA_A receptor subtype (12). Moreover flavonoids block NMDA receptors in a concentration dependent manner. Terpenoids act on NMDA receptor and block the receptor and on GABA_A receptor it shows positive modulation property. The extract is also shown to delay the latency of PTZ induced seizure suggesting that the extract exhibits anticonvulsant effect. Probably by GABA receptor by opening chloride channel. Administration of single or repeated dose of PTZ reduces the GABA function, it is mainly through the selective blocker action on chloride ionophore complex to GABA-A receptor (23). In this study we demonstrated that the more concentration of free radical scavengers is in the hydro-alcoholic extract. Compared to other organs in human brain needs more oxygen for its proper functions. The presence of high poly unsaturated fatty acids in brain is prone to lipid peroxidation (27). Majority of neuronal problems involve oxidative stress as pathogenesis. It includes neurodegenerative diseases like Parkinson's, Alzheimer's, and other diseases like epilepsy etc (28). This study states that the leaf bud extract could have a direct modification on GABA production, protect from MDA developed in brain. GABA level was decreased in PTZ induced mice. This level was significantly increased ($P < 0.001$) when hydro-alcoholic extract of leaf buds was given. PTZ produced neuronal damage can be prevented by the extract by inhibiting MDA on brain and protect the neurons.

CONCLUSION

The results of the study indicate that the hydro-alcoholic extract of leaf buds of *Tectona grandis* Linn possess promising antiepileptic activity as well as antioxidant activity. These activities may be due to the strong occurrence of flavonoids, tannins, steroids, phenols, terpenoids and other phytochemical constituents present in the leaves. However, these findings will encourage future studies to investigate the phytochemical constituent responsible for the antiepileptic activity, and the mechanism of its action will help to find out the potency of *Tectona grandis* Linn leaf buds as a potent antiepileptic agent with fewer side effects.





ACKNOWLEDGEMENT

Authors would like to thank Kerala State Council for Science and Technology for funding and College of Pharmaceutical Sciences, Govt. Medical College, Kannur, Kerala for the facility provided.

FUNDING

Kerala State Council for Science and Technology (01611/SPS 64/2019/KSCSTE).

ABBREVIATIONS

TG (*Tectona grandis*),

DPPH (2,2-diphenyl-1-picryl hydrazyl),

ABTS (2, 2-azino-bis (3-ethylbenzothiazoline-6, 6-sulphonic acid)),

PTZ (Pentylentetrazol),

GABA (Gamma amino butyric acid),

MDA (Malondialdehyde),

NMDA (N-Methyl-D-aspartic acid),

AED (Antiepileptic drugs).

REFERENCES

1. DiPiro, Joseph, Talbert, Robert, Yee, Gary. *Pharmacotherapy Pathophysiologic Approach*. 2005.
2. Löscher W, Klitgaard H, Twyman RE, Schmidt D. New avenues for anti-epileptic drug discovery and development. Vol. 12, *Nature Reviews Drug Discovery*. 2013. p. 757–76.
3. Steiger BK, Jokeit H. Why epilepsy challenges social life. Vol. 44, *Seizure*. W.B. Saunders Ltd; 2017. p. 1948.
4. Xue-Ping W, Hai-Jiao W, Li-Na Z, Xu D, Ling L. Risk factors for drug-resistant epilepsy: A systematic review and meta-analysis. Vol. 98, *Medicine (United States)*. Lippincott Williams and Wilkins; 2019.
5. Beghi E. The Epidemiology of Epilepsy. Vol. 54, *Neuroepidemiology*. S. Karger AG; 2020. p. 185–91.
6. Amudhan S, Gururaj G, Satishchandra P. Epilepsy in India I: Epidemiology and public health. Vol. 18, *Annals of Indian Academy of Neurology*. Wolters Kluwer Medknow Publications; 2015. p. 263–77.
7. Kumar D, Bag A, Karimulla S. Anti-seizure activity of methanol extract of *tectona grandis* l. on maximal electroshock induced seizure in albino wistar rats. Available from: www.ijepjournal.com
8. Bitchagno GTM, Sama Fonkeng L, Kopa TK, Tala MF, KamdemWabo H, Tume CB, et al. Antibacterial activity of ethanolic extract and compounds from fruits of *Tectona grandis* (Verbenaceae). *BMC Complement Altern Med*. 2015 Aug 6;15(1).
9. Wikipedia. Teak.
10. Cd P, Ys A, Pa P, Vv P, Pr M. Patil C D et al Free radicals, epilepsy and anti-oxidant: an overview [Internet]. *IRJP*. Available from: <http://www.irjponline.com>
11. Citraro R, Navarra M, Leo A, Di Paola ED, Santangelo E, Lippiello P, et al. The anticonvulsant activity of a flavonoid-rich extract from orange juice involves both NMDA and GABA-benzodiazepine receptor complexes. *Molecules*. 2016 Sep 1;21(9).
12. Diniz TC, Silva JC, Lima-Saraiva SRG De, Ribeiro FPRDA, Pacheco AGM, De Freitas RM, et al. The role of flavonoids on oxidative stress in epilepsy. Vol. 2015, *Oxidative Medicine and Cellular Longevity*. Hindawi Publishing Corporation; 2015.
13. Orhan N, DeliormanOrhan D, Aslan M, Ükürolu M, Orhan IE. UPLC-TOF-MS analysis of *Galiumspurium* towards its neuroprotective and anticonvulsant activities. *J Ethnopharmacol*. 2012 May 7;141(1):220–7.
14. Srivastav N SSJVTBK. Anticonvulsant activity of root extract of *Valerianajatumansii* Linn in experimental rats. *IJSSR*. 2016;2(2):121-6.





Chaithra et al.,

15. *Passiflora quadrangularis*. Germplasm Resources Information Network (GRIN). Agricultural Research Service (ARS). United States Department of Agriculture (USDA). 2013. p. 1–13.
16. A Review on the Extraction Methods Use in Medicinal Plants, Principle, Strength and Limitation. *Med Aromat Plants* (Los Angel). 2015;04(03).
17. Marsden S. Blois. Antioxidant Determinations by the Use of a Stable Free Radical. *Nature*. 1958;181:1199–200.
18. Grujić SM, Stojanović GS, Mitić VD, Stankov-Jovanović V, Džamić AM, Alimpić AZ, et al. Evaluation of antioxidant activity of *Melittis melissophyllum* L. extracts. *Arch Biol Sci*. 2014;66(4):1401–10.
19. Mussulini BHM, Leite CE, Zenki KC, Moro L, Baggio S, Rico EP, et al. Seizures Induced by Pentylentetrazole in the Adult Zebrafish: A Detailed Behavioral Characterization. *PLoS One*. 2013 Jan 21;8(1).
20. Kundap UP, Kumari Y, Othman I, Shaikh MF. Zebrafish as a model for epilepsy-induced cognitive dysfunction: A pharmacological, biochemical and behavioral approach. *Front Pharmacol*. 2017 Aug 3;8(AUG).
21. Bhosle V. Anticonvulsant and antioxidant activity of aqueous leaves extract of *Desmodium triflorum* in mice against pentylentetrazole and maximal electroshock induced convulsion. *Revista Brasileira de Farmacognosia*. 2013;23(4):692–8.
22. Singh J, Sood S, Muthuraman A. In-vitro evaluation of bioactive compounds, anti-oxidant, lipid peroxidation and lipoxygenase inhibitory potential of Citrus karna L. peel extract. *J Food Sci Technol*. 2014 Jan;51(1):67–74.
23. Kumar A S GR. Effect of *Guettarda speciosa* extracts on antioxidant enzymes levels in rats brain after induction of seizures by MES and PTZ. *JNat Prod*. 2010;80–5.
24. Okhawa H ONYK. Assay for lipid peroxidation in animals' tissue by thiobarbituric acid reaction. *Annals of Biochemistry*. *Annals of Biochemistry*. 1979;9(5):351–8.
25. Herrera-Calderon O, Santiváñez-Acosta R, Pari-Olarte B, Enciso-Roca E, Campos Montes VM, Luis Arroyo Acevedo J. Anticonvulsant effect of ethanolic extract of *Cyperus articulatus* L. leaves on pentylentetrazol induced seizure in mice. *J Tradit Complement Med*. 2018 Jan 1;8(1):95–9.
26. Article O, Atif M, Rahman SA, Ahmed MI, Baquer Mahmood S, Azharuddin M. Anticataract Potential of *Barleria Prionitis*: In vivo study.
27. Rink C, Khanna Abstract S. Significance of Brain Tissue Oxygenation and the Arachidonic Acid Cascade in Stroke [Internet]. Available from: www.liebertonline.com=ars.
28. Ghosh N, Das A, Chaffee S, Roy S, Sen CK. Reactive oxygen species, oxidative damage and cell death. In: *Immunity and Inflammation in Health and Disease: Emerging Roles of Nutraceuticals and Functional Foods in Immune Support*. Elsevier; 2017. p. 45–55.

Table No 1: List of chemicals.

SL. NO	Chemicals	Suppliers/Manufactures
1	Methanol	Kanton Laboratories, Kannur, India
2	Phenytoin	Abbott Healthcare, Pvt. Ltd, India
3	PTZ	Laboratory equipment stores, Cochin
4	Diazepam	Ranbaxy laboratories, Mumbai
5	Ascorbic acid	Yarrow chemical products, Mumbai
6	DPPH	Yarrow chemical products, Mumbai

Table No 2: Grouping of experimental animals for PTZ induced convulsion

Sl.no	Group	No. of animals	Dose	Treatment
1	Normal	6	-	Vehicle
2	Control	6	6mM	PTZ Treated
3	Standard	6	10µm	PTZ treated + Diazepam treated group
4	HATG(LD)	6	36mg/L	PTZ treated + treated group
5	HATG(HD)	6	72mg/L	PTZ treated + treated group





Chaithra et al.,

Table 3: Phytochemical parameters.

SL.NO	Parameters	Values (%w/w)
1	Loss on drying	8.3
2	Total ash content	12.52
3	Water soluble ash	9.7
4	Acid soluble Ash	3.23
5	Extractive value methanol-aqueous soluble extract	27.7

Table 4: Phytochemical screening result

SL.NO	Phytochemical tested	Methods used	Methanol-water extract
1	Alkaloids	Mayer's test	+
		Wagners test	+
2	Carbohydrates	Molisch's test	+
		Fehling's test	+
3	Steroids	Salkowski's test	+
4	Saponins	Foam test	+
		Haemolysis Test	+
5	Triterpenoids	Noller's test	+
6	Tannins and phenolic compounds	With dilute ferric chloride	+
		With lead acetate	+
7	Flavanoids	Ammonia test	+
		Shinoda's test	-
8	Glycosides	Borntrager's test	+
		Keller-Killani Test	+
		Legal's test	-

Table 5: DPPH free radical scavenging activity of *Tectona grandis*. Linn.

Sl. No	Groups	Concentration (µg/ml)	Percentage of scavenging (%)	IC ₅₀ (µg/ml)
1	Control			
2	Standard (Ascorbic acid)	12.5	60.07	12.377
		25	62.73	
		50	66.53	
		100	74.27	
		200	79.59	
3	Test	12.5	47.90	17.149
		25	52.34	
		50	59.18	
		100	70.49	
		200	75.53	





Chaithra et al.,

Table 6: ABTS⁺ scavenging assay of *Tectona grandis*. Linn

Sl. No	Groups	Concentration (µg/ml)	Percentage of scavenging (%)	IC ₅₀
1	Control			
2	Standard	12.5	45.84	16.219
		25	61.11	
		50	82.39	
		100	87.52	
		200	90.46	
3	Test	12.5	33.23	26.973
		25	44.24	
		50	64.78	
		100	70.65	
		200	74.32	

Table 7: Effect of *Tectona grandis*. Linn leaf bud extract on PTZ induced convulsions.

Antiepileptic Tests	Normal	Control	Standard	HAETG (Lower dose)	HAETG (Higher dose)
Onset of Convulsion (Sec)	-	262.85±0.1687 a*	642.94±0.3705 a*b****	432.3±0.2981 a*b****c*	522.5±0.4731 a*b****c***
Duration of Convulsion (Sec)	-	522.54±0.2213 a*	114.50±0.1811 a*b****	323.40±0.1883 a*b****c*	305.32±0.2173 a*b****c***
Percentage of Protection (%)	-	-	77.89	38.11	41.57




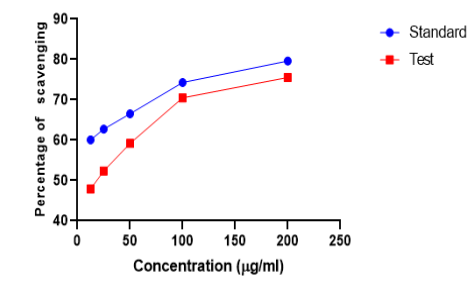
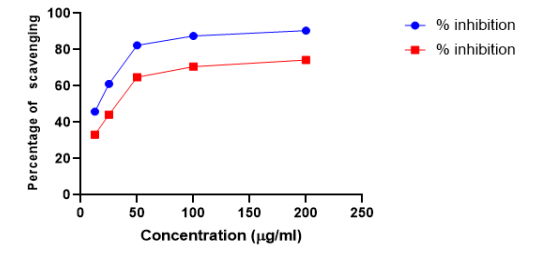
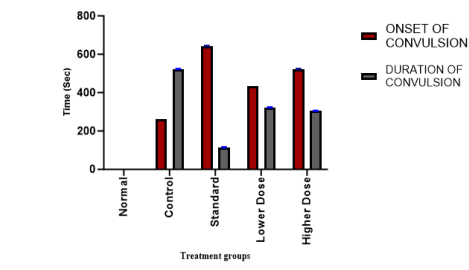
Table 8: Estimation of brain GABA and MDA on Pentylene tetrazol induced convulsion

Groups	Normal	Control	Standard	Lower Dose	Higher Dose
GABA (ng/g of brain tissue)	85.66±0.421	22.81±0.600 a*	80.11±0.307 a** b*	42.81±1.400 a*** b*** c**	72.67±1.174 a** b**** c**
MDA (nmoles/mg of brain tissue)	2.612±0.076	9.421±0.028 a*	3.183±0.059 a** b*	6.442±0.084 a**** b**** c***	3.870±0.080 a** b** c**





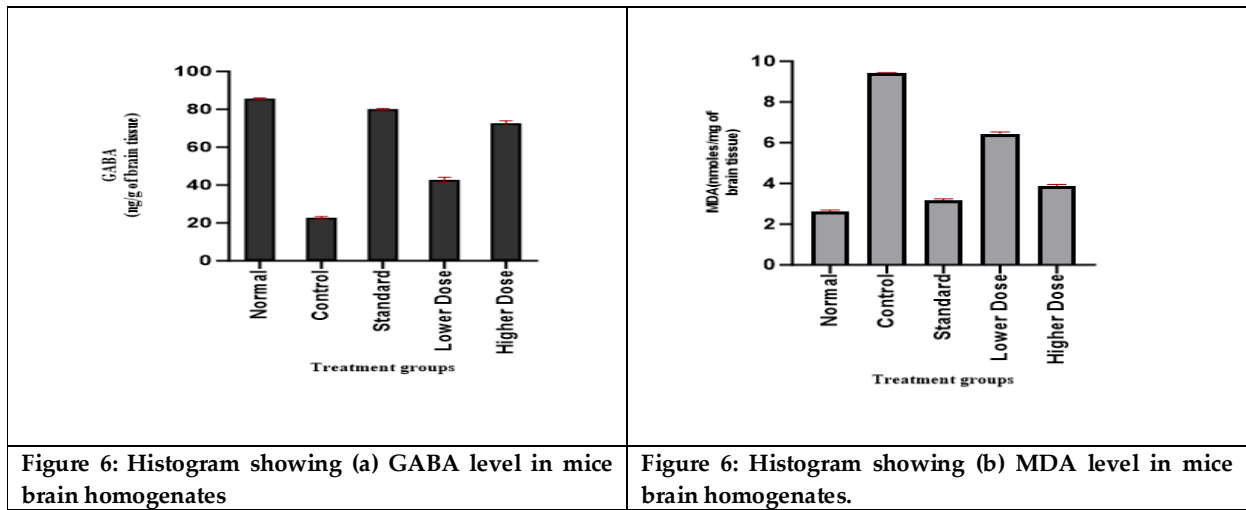
Chaithra et al.,

	
<p align="center">Figure 1: <i>Tectona grandis</i> Linn plant</p>	<p align="center">Figure 2: <i>Tectona grandis</i>. Linn leaf buds</p>
	<p align="center">DPPH scavenging activity of <i>Tectona grandis</i>. Linn</p> 
<p align="center">Fig 3: Zebrafish</p>	<p align="center">Figure 4 :<i>In vitro</i> determination of antioxidant activity of <i>Tectona grandis</i>. Linn by DPPH scavenging activity.</p>
<p align="center">ABTS + Scavenging assay of <i>Tectona grandis</i>.Linn</p> 	
<p>Figure 5: <i>In vitro</i> determination of anti-oxidant activity of <i>Tectona grandis</i>. Linn by ABTS+ scavenging assay.</p>	<p>Figure 6: Effect of <i>Tectona grandis</i>. Linn onset of convulsions and duration of convulsions.</p>





Chaithra et al.,





Advancements in Facial Emotion Recognition: A Comprehensive Review

R.V.V.Muralikrishna¹, I.V.S Venugopal², Srinu Bevara² and Vasudeva Bevara^{3*}

¹Associate Professor, Department of Information Technology, Gayatri Vidya Parishad College of Engineering (Autonomous), (Affiliated to Andhra University), Visakhapatnam, Andhra Pradesh, India.

²Assistant Professor, Department of Information Technology, Gayatri Vidya Parishad College of Engineering (Autonomous), (Affiliated to Andhra University), Visakhapatnam, Andhra Pradesh, India.

³Assistant Professor, Department of Electronics and Communication Engineering, Malla Reddy Engineering College, (Affiliated to Jawaharlal Nehru Technological University Hyderabad), Visakhapatnam, Andhra Pradesh, India.

Received: 09 Sep 2023

Revised: 12 Nov 2023

Accepted: 29 Dec 2023

*Address for Correspondence

Vasudeva Bevara

Assistant Professor,

Department of Electronics and Communication Engineering,

Malla Reddy Engineering College,

(Affiliated to Jawaharlal Nehru Technological University Hyderabad),

Visakhapatnam, Andhra Pradesh, India.

Email: bevaravasudeva@gmail.com



This is an Open Access Journal / article distributed under the terms of the **Creative Commons Attribution License** (CC BY-NC-ND 3.0) which permits unrestricted use, distribution, and reproduction in any medium, provided the original work is properly cited. All rights reserved.

ABSTRACT

The field of face expression analysis has witnessed significant progress in recent times, fueled by advancements in computer vision, deep learning, and affective computing. This abstract highlights the most recent developments in this domain. Researchers have devised sophisticated algorithms that can accurately recognize and interpret facial expressions, allowing for better understanding of human emotions and intentions. State-of-the-art models employ convolutional neural networks (CNNs) and recurrent neural networks (RNNs) to capture intricate facial features and temporal dynamics. Transfer learning and data augmentation techniques have been instrumental in training models with limited labelled data, thus improving generalisation and real-world applicability. Furthermore, the integration of multi-modal cues, such as audio and body language, has demonstrated enhanced emotion recognition accuracy. The deployment of edge computing and lightweight architectures has facilitated real-time face expression analysis on resource-constrained devices. Despite these advances, challenges remain, such as handling individual differences, occlusions, and privacy concerns. Continued research in face expression analysis promises to revolutionize applications across diverse domains, including human-computer interaction, mental health, and social robotics.

Keywords: Index Terms—Massive MIMO, OFDM, sparse, Compressive Sensing



**Muralikrishna et al.,**

INTRODUCTION

Face expression analysis, a branch of computer vision and affective computing, has witnessed significant progress in recent years. The ability to recognize and interpret human emotions from facial cues has important implications in various domains, such as human-computer interaction, healthcare, marketing, social robotics, and more. Understanding emotions conveyed through facial expressions can improve user experiences, mental health diagnostics, and the design of empathetic artificial intelligence systems[1],[2]. Traditionally, face expression analysis relied on handcrafted features and rule-based algorithms, but these approaches had limited capacity to handle the complexities of facial expressions across diverse populations and variations in lighting, pose, and occlusions. However, with the emergence of deep learning and its impressive capabilities in feature learning, this field has experienced a significant paradigm shift. The most recent advances in face expression analysis have been largely driven by the success of convolutional neural networks(CNNs)and recurrent neural networks(RNNs). CNNs are proficient in extracting hierarchical representations from raw image data, allowing them to identify essential facial features and patterns. On the other hand, RNNs are effective in capturing temporal dynamics, which are crucial for recognizing the dynamic nature of facial expressions overtime. One of the key factors contributing to the success of deep learning models in this domain is the availability of large-scale annotated datasets.

Datasets such as the Facial Expression Recognition Challenge (FERC) and the Extended Cohn-Kanade (CK+) data base have played a vital role in training and evaluating facial expression analysis models. These datasets encompass a wide range of facial expressions, making the trained models more robust and generalizable. Transfer learning has also been leveraged to further improve the performance of facial expression analysis models, especially when data is limited. By pre training on vast data sets like Image Net and fine-tuning on smaller expression datasets, models can effectively learn transferable facial features, thus reducing the need for extensive labelled data. In addition to single-modal analysis using only facial images, recent research has explored multi modal approaches that integrate multiple sources of information. This includes incorporating audio, body language, and context to enhance emotion recognition accuracy. Multimodal fusion techniques, such as early fusion and late fusion, have been employed to effectively combine different modalities and leverage their complementary information. Furthermore, the deployment of edge computing and light weight architectures has enabled real-time face expression analysis on resource-constrained devices, such as smart phones and wearables. This development opens up opportunities for various applications, such as emotion-aware mobile applications, smart healthcare systems, and emotion-sensing wearables. Despite there markable progress, several challenges remaining face expression analysis.

One significant challenge is handling individual differences, as people express emotions uniquely based on factors like culture, gender, and personality. Development models that can generalise across diverse populations remains a key area of research. Moreover, dealing with occlusions, pose variations, and subtle expressions presents another obstacle. Improving the robustness of models to handle these real-world scenarios is critical for practical applications. Privacy concerns are also paramount, especially in applications that involve facial expression analysis in public spaces. Addressing privacy issues and ensuring ethical considerations are adhered to in the deployment of facial expression analysis technologies is essential to gain public acceptance and trust. In this review paper, we aim to provide an in-depth exploration of the most recent advances in face expression analysis. We will survey cutting-edge methodologies, architectures, and datasets used in emotion recognition from facial expressions. Additionally, we will discuss the challenges and limitations that researchers are actively working to overcome, as well as potential future directions in this evolving field. By understanding and harnessing these advancements, we can pave the way form or sophisticated and empathetic human-computer interactions and transformative applications in health care, mental wellness, and beyond.

APPLICATIONS

The most recent advances in face expression analysis have opened up a plethora of applications across various





Muralikrishna et al.,

industries and fields. Some of the key applications include

Human-Computer Interaction: Emotion-aware interfaces can enhance human-computer interaction by enabling systems to adapt their responses based on the user's emotional state. This can lead to more personalized and empathetic interactions, improving user experiences in applications like virtual assistants, video games, and online education platforms.

Healthcare and Mental Health: Facial expression analysis can aid in mental health diagnostics and monitoring. It can assist in identifying and tracking emotional states in patients, providing valuable insights to healthcare professionals for early intervention and personalized treatment plans.

Marketing and Advertising: Emotion recognition can be employed in market research to gauge consumers' emotional responses to products and advertisements. This data can inform marketing strategies, enabling companies to create more emotionally resonant and effective campaigns.

Social Robotics: Emotion-aware robots can better understand and respond to human emotions, making them more engaging companions and assistants in various settings, such as elder care, education, and entertainment.

Security and Surveillance: Facial expression analysis can be integrated into surveillance systems to detect suspicious or unusual behavior, aiding in security applications like airport screening and public safety.

Human-Emotion Analysis in Virtual Environments: In virtual reality applications, facial expression analysis can enable avatars and virtual characters to mimic users' emotional expressions, enhancing the sense of presence and realism in virtual environments.

Automotive Industry: Emotion recognition systems in vehicles can monitor the driver's emotional state to enhance safety. For example, if a system detects signs of drowsiness or distraction, it can issue warnings or take corrective actions to prevent accidents.

Education: In the context of e-learning, facial expression analysis can gauge students' engagement and emotional responses to the learning material. This data can help educators optimize course content and teaching methods.

As these applications continue to evolve, researchers and developers must also address ethical considerations, privacy concerns, and potential biases associated with face expression analysis technologies. Nevertheless, the advancements in this field hold great promise in transforming human-computer interactions and enhancing various aspects of our daily lives.

PARAMETERIZATION OF THE FACE

Based on muscular activities, the numerous face behaviours and motions can be parameterized. The different facial expressions can thus be represented by this set of parameters.

There have only been two significant attempts to create these parameter sets thus far, both of which were successful:

- Ekman and Friesen created the Facial Action Coding System (FACS) in 1977 [3], and
- The MPEG-4 Synthetic/Natural Hybrid Coding (SNHC) standard, published in 1998, includes the Facial Animation Parameters (FAPs) [4].

Facial Action Coding System

The Facial Action Coding System (FACS) is a comprehensive and widely used tool for objectively describing facial expressions. Developed by Paul Ekman and Wallace V. Friesen in the 1970s, FACS provides a standardized method to analyze and categorize facial muscle movements, known as action units (AUs). Each AU corresponds to a specific facial muscle or group of muscles and represents a distinct facial expression. FACS enables researchers, psychologists, and computer scientists to break down complex facial expressions into their constituent AUs, allowing for a detailed and systematic analysis of emotional expressions, micro expressions, and subtle changes in facial behavior. By assigning numerical codes to AUs, FACS ensures precision and consistency in describing facial expressions across different observers. FACS has found applications in various fields, including psychology, human-computer interaction, emotion research, and forensic science. It has been instrumental in studying emotions, social communication, and nonverbal behavior, contributing to a deeper understanding of human emotions and expressions. Additionally, FACS serves as a foundation for developing computer-based facial expression analysis systems and emotion recognition algorithms.





Muralikrishna et al.,

The Facial Animation Parameters (FAPs)

Facial Animation Parameters (FAPs) are a set of numerical values used to control and manipulate facial expressions in computer graphics and animation. They serve as the building blocks for creating lifelike and expressive digital characters. FAPs represent specific movements and deformations of facial features, such as raising eyebrows, smiling, or blinking. These parameters are often based on the analysis of real human facial movements, allowing animators to achieve a high level of realism in virtual characters. FAPs are widely utilized in various applications, including video games, movies, virtual reality, and augmented reality, enhancing the emotional and interactive aspects of digital content.

FACIAL EXPRESSION RECOGNITION

Pre-processing, deep feature learning and deep feature classification are the three main phases of autonomous deep FER described in this section. According to the cited articles, we briefly summarise the frequently used algorithms for each step and recommend existing state-of-the-art best practice implementations. Different techniques of Facial expression recognition. are shown in below.

A. Pre-Processing

In unconstrained circumstances, variations that are unrelated to facial expressions, such as various backgrounds, illuminations, and head positions, are fairly common. As a result, pre-processing is frequently required before training the deep neural network to learn meaningful features, in order to align and normalize the visual semantic information communicated by the face.

1) Face Acquisition: Face Acquisition is a technique for improving face recognition accuracy. It's a normalized approach that outputs the image with the face centered on it, rotated such that the line connecting the centers of two eyes is parallel to the horizontal line, and resizes the faces to the same scale. The first step is to detect the face, after which background and non-facial elements are removed. The Viola- Jones (V&J) face detector [5] is a well-known and commonly used implementation for recognizing near-frontal faces. It is reliable and computationally simple.

2) Face Normalization: Variations in illumination and head positions can cause significant picture shifts, lowering FER performance. To address these differences, we present two common face normalizing methods: illumination normalization and posture normalization.

3) Data Augmentation: To achieve generalizability to a specific recognition task, deep neural networks require enough training data. However, most publicly accessible FER databases lack a significant number of images for training. As a result, data augmentation is an important stage in deep FER. On-the-fly data augmentation and offline data augmentation are the two types of data augmentation methods. To avoid overfitting, deep learning toolkits usually include on-the-fly data augmentation. Offline data augmentation methods have been created to increase the size and diversity of data. Random perturbations and transforms, such as rotation, shifting, skew, scaling, noise, contrast, and color jittering, are among the most commonly utilized operations.

4) Face Segmentation: In face image analysis, face segmentation is a fundamental task. Facial segmentation is the process of segmenting a face image into various parts using a computer-based method. Semantic face segmentation enables a computer to comprehend the contents of a facial image down to the pixel level. As a result, a variety of complicated features are used for semantic face segmentation. Robust face segmentation output is used in various computer vision applications, both expressively and exhaustively. Many face analysis tasks, such as facial emotion recognition, head pose estimation, facial landmark identification, sentiment analysis, and so on,

B. Feature Extraction

In the FER system, the feature extraction technique comes next. The technique of discovering and displaying positive features of concern inside an image for further processing is known as feature extraction. Computer vision feature





Muralikrishna et al.,

extraction is an important stage in image processing because it recognises the shift from visual to implicit data depiction. Following that, the classifier may utilise this data visualization as an input. Texture-based techniques, edge-based methods, global and local feature-based methods, geometric feature based methods, and patch-based approaches are the five different types of feature extraction methods.

1) Texture-based techniques: The descriptors which extract the features based on the texture feature-based methods are described. The Gabor filter with the magnitude feature confines the information about the organization of the face image [6]– [8]. Local Binary Pattern (LBP) is also a texture descriptor and it can be used for feature extraction [9]. Weber Local Descriptor (WLD) is a feature extraction technique that extracts the high discriminant texture features from the segmented face images [10]. Discrete Contourlet Transform (DCT) extracts the texture features which can be performed by decomposition with two stages [11]. Both VTB and moments descriptors are effective on spatiotemporal planes.

2) Edge-based methods: The descriptors which extract the features based on the edge based methods are described as follows. Line Edge Map (LEM) descriptor is a facial expression descriptor which improves the geometrical structural features by using the dynamic two strip algorithm (Dyn2S) [22]. Histogram of Oriented Gradients (HOG) is a window supported feature descriptor which uses the gradient filter [23]. Graphics processing unit based Active Shape Model (GASM) is the feature extraction method which can be performed with edge detection, enhancement, tone mapping and local appearance model matching [24].

3) Global and local feature-based approaches: The following are the descriptors for extracting features using global and local feature-based approaches. For feature extraction, the Principal Component Analysis (PCA) approach is applied. The global and low-dimensional characteristics are extracted. Independent Component Analysis (ICA) is another feature extraction approach that uses multichannel observations to identify local characteristics [25]. Stepwise Linear Discriminant Analysis (SWLDA) is a feature extraction approach that uses backward and forward regression models to extract localised features. The F-test values for both regression models are computed based on the class labels.

4) Geometric feature-based methods: The extracted geometric features are mean, entropy and standard deviation. Addition to these geometrical features energy, kurtosis are extracted by using three stage steerable pyramid representation [26]. Local Curvelet Transform (LCT) is a feature descriptor which extracts the geometric features which depends on wrapping mechanism.

5) Patch-based approaches: The following are the descriptors for extracting features using patch-based approaches. Depending on the distance characteristics, facial movement features are retrieved as patches. These are accomplished through the use of two processes: patch extraction and patch matching. Translation of extracted patches into distance characteristics is used to accomplish patch matching. [27]

Facial Expression Classification

The final step of FER is to classify the given image into one of the basic emotion categories after learning the deep information. Unlike standard approaches, which separate the feature extraction and feature classification steps, deep networks may execute FER from start to finish. To manage the back-propagation error, a loss layer is added to the end of the network; then, the network can directly output the prediction probability of each sample. The most often employed function in CNN is soft-max loss, which minimizes the cross-entropy between the estimated class probabilities and the found-truth distribution. Alternatively, the use of a linear support vector machine (SVM) [28] for end-to-end training, which reduces margin-based loss rather than cross-entropy, was demonstrated to be beneficial. Similarly, the adaptability of deep neural forests was examined. which uses NFs [29] to replace the soft-max loss and achieves competitive FER performance.

DIFFERENT FER TECHNIQUES



**Muralikrishna et al.,**

The Facial Emotion Recognition has been held for last few years. There are many state-of-the-art facial expression recognition methods break the records of every year, and some techniques are shown in table-1.

CONCLUSION

this journal paper explored the most recent advances in face expression analysis, highlighting the significant progress made in this field. Cutting-edge technologies, such as deep learning and computer vision algorithms, have revolutionized the way facial expressions are detected, recognized, and analyzed. These advancements have led to more accurate and robust systems, capable of handling complex real-world scenarios with varying lighting conditions and facial occlusions. The integration of multimodal data, including audio and physiological signals, has further enriched the analysis of facial expressions, providing a more comprehensive understanding of emotional states. Moreover, the development of large-scale facial expression databases and benchmarks has facilitated rigorous evaluations and comparisons of different approaches. Despite the remarkable achievements, challenges remain, such as addressing biases in training data and ensuring the ethical use of facial expression analysis technology. As research in this field continues to progress, we anticipate even more sophisticated and socially responsible applications in various domains, including human-computer interaction, psychology, healthcare, and entertainment. The future is promising, as face expression analysis continues to unfold its potential in understanding human emotions and behavior.

REFERENCES

1. V. Bevara and P. K. Sanki, "A new fast and efficient 2-d median filter architecture," *Sādhanā*, vol. 45, no. 1, p. 192, 2020.
2. V. Bevara, S. Alihussain, P. Prasad, and P. K. Sanki, "Design of an efficient qca-based median filter with energy dissipation analysis," *The Journal of Supercomputing*, vol. 79, no. 3, pp. 2984–3004, 2023.
3. P. Ekman, "Wv friesland, manual for the facial action coding system," 1977.
4. M. Video, "Snhc," "text of iso/iec fdis 14 496-3: Audio," Atlantic City MPEG Mtg, 1998.
5. P. Viola and M. Jones, "Rapid object detection using a boosted cascade of simple features," in *Proceedings of the 2001 IEEE computer society conference on computer vision and pattern recognition. CVPR 2001*, vol. 1. Ieee, 2001, pp. I-I.
6. S. Bashyal and G. K. Venayagamoorthy, "Recognition of facial expressions using gabor wavelets and learning vector quantization," *Engineering Applications of Artificial Intelligence*, vol. 21, no. 7, pp. 1056–1064, 2008.
7. E. Owusu, Y. Zhan, and Q. R. Mao, "A neural-adaboost based facial expression recognition system," *Expert Systems with Applications*, vol. 41, no. 7, pp. 3383–3390, 2014.
8. A. Hernandez-Matamoros, A. Bonarini, E. Escamilla-Hernandez, M. Nakano-Miyatake, and H. Perez-Meana, "Facial expression recognition with automatic segmentation of face regions using a fuzzy based classification approach," *Knowledge-Based Systems*, vol. 110, pp. 1–14, 2016.
9. S. Happy and A. Routray, "Automatic facial expression recognition using features of salient facial patches," *IEEE transactions on Affective Computing*, vol. 6, no. 1, pp. 1–12, 2014.
10. M. J. Cossetin, J. C. Nievola, and A. L. Koerich, "Facial expression recognition using a pairwise feature selection and classification approach," in *2016 International Joint Conference on Neural Networks (IJCNN)*. IEEE, 2016, pp. 5149–5155.
11. S. Biswas and J. Sil, "An efficient expression recognition method using contourlet transform," in *Proceedings of the 2nd International Conference on Perception and Machine Intelligence*, 2015, pp. 167–174.
12. P. S. Aleksic and A. K. Katsaggelos, "Automatic facial expression recognition using facial animation parameters and multistream hmms," *IEEE Transactions on Information Forensics and Security*, vol. 1, no. 1, pp. 3–11, 2006.
13. M. Pantic and I. Patras, "Dynamics of facial expression: recognition of facial actions and their temporal segments from face profile image sequences," *IEEE Transactions on Systems, Man, and Cybernetics, Part B (Cybernetics)*, vol. 36, no. 2, pp. 433–449, 2006.





Muralikrishna et al.,

14. N. Sebe, M. S. Lew, Y. Sun, I. Cohen, T. Gevers, and T. S. Huang, "Authentic facial expression analysis," *Image and Vision Computing*, vol. 25, no. 12, pp. 1856–1863, 2007.
15. I. Kotsia and I. Pitas, "Multimedia applications-facial expression recognition in image sequences using geometric deformation features and support vector machines," *IEEE Transactions on Image Processing*, vol. 16, no. 1, p. 172, 2007.
16. J. Wang and L. Yin, "Static topographic modeling for facial expression recognition and analysis," *Computer Vision and Image Understanding*, vol. 108, no. 1-2, pp. 19–34, 2007.
17. F. Dornaika and F. Davoine, "Simultaneous facial action tracking and expression recognition in the presence of head motion," *International Journal of Computer Vision*, vol. 76, pp. 257–281, 2008.
18. G. Hegde, M. Seetha, and N. Hegde, "Kernel locality preserving symmetrical weighted fisher discriminant analysis based subspace approach for expression recognition," *Engineering science and technology, an international journal*, vol. 19, no. 3, pp. 1321–1333, 2016.
19. M. Guo, X. Hou, Y. Ma, and X. Wu, "Facial expression recognition using elbp based on covariance matrix transform in klt," *Multimedia Tools and Applications*, vol. 76, no. 2, pp. 2995–3010, 2017.
20. H.-H. Tsai and Y.-C. Chang, "Facial expression recognition using a combination of multiple facial features and support vector machine," *Soft Computing*, vol. 22, no. 13, pp. 4389–4405, 2018.
21. S. Nigam, R. Singh, and A. Misra, "Efficient facial expression recognition using histogram of oriented gradients in wavelet domain," *Multimedia tools and applications*, vol. 77, no. 21, pp. 28 725–28 747, 2018.
22. Y. Gao, M. K. Leung, S. C. Hui, and M. W. Tananda, "Facial expression recognition from line-based caricatures," *IEEE Transactions on Systems, Man, and Cybernetics-Part A: Systems and Humans*, vol. 33, no. 3, pp. 407–412, 2003.
23. M. Dahmane and J. Meunier, "Prototype-based modeling for facial expression analysis," *IEEE Transactions on Multimedia*, vol. 16, no. 6, pp. 1574–1584, 2014.
24. M. Song, D. Tao, Z. Liu, X. Li, and M. Zhou, "Image ratio features for facial expression recognition application," *IEEE Transactions on Systems, Man, and Cybernetics, Part B (Cybernetics)*, vol. 40, no. 3, pp. 779–788, 2009.
25. M. H. Siddiqi, R. Ali, A. Sattar, A. M. Khan, and S. Lee, "Depth camerabased facial expression recognition system using multilayer scheme," *IETE Technical Review*, vol. 31, no. 4, pp. 277–286, 2014.
26. H. Mahersia and K. Hamrouni, "Using multiple steerable filters and bayesian regularization for facial expression recognition," *Engineering Applications of Artificial Intelligence*, vol. 38, pp. 190–202, 2015.
27. L. Zhang and D. Tjondronegoro, "Facial expression recognition using facial movement features," *IEEE transactions on affective computing*, vol. 2, no. 4, pp. 219–229, 2011.
28. A. Dapogny and K. Bailly, "Investigating deep neural forests for facial expression recognition," in *2018 13th IEEE International Conference on Automatic Face & Gesture Recognition (FG 2018)*. IEEE, 2018, pp. 629–633.
29. P. Kotschieder, M. Fiterau, A. Criminisi, and S. R. Buló, "Deep neural decision forests," in *Proceedings of the IEEE international conference on computer vision*, 2015, pp. 1467–1475.

Table I Machine Learning based for Techniques

Author, Year	Feature Extraction Method	Classification Method	Dataset	Size of Sample	Performance	Pros & Cons
Aldhbi et al. (2006) [12]	MPEG-4 FAFN	HMM & MS-HMM	Cohn-Kanade	subjects-90 recordings-284	HMM: 55.1% MS-HMM: 93.66%	+ performance improved - reduce the dimensionality of the features
Dario et al. (2006) [13]	Mid level parameters	Ek	MMI	1500 samples of both static and profile views	85.6%	+ Automatic segmentation of input video into facial expressions - Testing not performed on video data and
Sobe et al. (2007) [14]	FBVD	Bayesian net, SVM	Cohn-Kanade	53 subjects	Cohn-Kanade: 72.60% to 95.00% FER: 80.77% to 95.37% kNN: 93.57%	+ Recognizes spontaneous expressions - Requires several classifiers
Kozia et al. (2007) [15]	Geometric displacement of Chebik nodes	Multiple SVM	Cohn-Kanade	Whole FER	90.7%	+ Very high recognition rates have been shown - Low efficiency
Wang et al. (2007) [16]	Topographic context	QDC, LDA, SVC and NB	MMI & Cohn-Kanade	53 subjects, 4 images per subject	QDC: 92.79% LDA: 82.68%	+ High Accuracy - Different intensities of facial expressions
Dornika et al. (2008) [17]	Candid face model	stochastic approach	Created own data	1600 frame test	95%	+ Good efficiency, recognition rate and consistency - The video sequences contained posed expressions.
Hegde et al. (2016) [18]	Reinif GP	Euclidean distance (ED)	SVM	59 subjects	97.14% 93.94% 93.33%	+ Improves the recognition efficiency + Accuracy rate for FER dataset - Computation cost is high
Guo et al. (2017) [19]	Normalization	E-ELBP	SVM	JAFFE, CK	93.9% 92.3%	+ simple and fast calculated - Low Accuracy
Cheng (2018) [20]	Face detection	DCT, GP	SVM	-	Not Specified	+ Very High Accuracy - Consider 32 Features
Nigam et al. (2018) [21]	Cropping, Normalization	DWT, FFC	SVM	59 subjects	CR: 93.9% A: 77.21, 43% MR: 75%	+ Dynamic facial expressions recognition for live videos - Low Accuracy





Formulation and Evaluation of Herbal Lipsticks using Turmeric and Beetroot Extracts as Natural Colorants

Piyali Khamkat^{*1}, Ankan Pandey², Sayandip Biswas² and Vivek Barik¹

¹Associate Professor, Department of Pharmaceutical Technology, Brainware University, Barasat, Kolkata, India.

²Undergraduate Student, Department of Pharmaceutical Technology, Brainware University, Barasat, Kolkata, India.

Received: 16 Sep 2023

Revised: 17 Nov 2023

Accepted: 27 Dec 2023

*Address for Correspondence

Piyali Khamkat

Associate Professor,
Department of Pharmaceutical Technology,
Brainware University,
Barasat, Kolkata, India.
Email: piyalikhamkat95@gmail.com



This is an Open Access Journal / article distributed under the terms of the **Creative Commons Attribution License** (CC BY-NC-ND 3.0) which permits unrestricted use, distribution, and reproduction in any medium, provided the original work is properly cited. All rights reserved.

ABSTRACT

Cosmetics are the substance used to alter the appearance or fragrances of the human body. Coloring skin particularly the skin of face and lips is an ancient practice going back to prehistoric period. Cosmetics have been incredibly in demand since historical time till day. One of the most popular cosmetics used to accentuate the attractiveness of lips and add glitz to makeup is lipstick. To meet women's desires, lipstick is marketed in hundreds of different color tones. Continuous use of synthetic colors in lipstick may cause serious adverse effects like lip irritation, lip discoloration, lip cancer etc. The adverse effect can be reduced by using natural color extracts from different natural sources. An Attempt was also made to evaluate the formulated herbal lipstick. Due to various adverse effects of available synthetic preparation the present work was conceived by us to formulate herbal lipsticks having minimal or no side effects. Our goal was to create and test herbal lipstick with natural edible colorants such as turmeric and beet root extracted colour. A variety of natural materials such as bees wax, coconut oil, almond oil, and essential oil have been used as excipients for the study. Different evaluation parameters for herbal lipsticks were performed like colour, texture, pH, melting point, softening point, skin irritation test, and perfume stability, as well as compared to a commercially available standard formulation. The development and evaluation of herbal lipsticks using natural materials with minimal adverse effects and beneficial therapeutic effects are part of this study.

Keywords: Cosmetics, Herbal lipsticks, Turmeric, Beetroot, Almond Oil, Evaluation, commercial.





Piyali Khamkat et al.,

INTRODUCTION

Ayurveda, in particular Charaka Sahita, emphasizes herbal cosmetics and personal care products that improve the appearance of the human body with things like eyeliners, eye creams, and lotions. However, current lip care products not only emphasize aesthetic value but also preferably have added medicinal value to the lips of consumers. If we look at the history of lipsticks, over 3,500 years in the ancient cities of Babylon, humans crushed and smeared semi-precious stones on their lips as lipstick and also ladies in the Indus Valley civilization used to apply red color on their lips. Egyptian queen Cleopatra made her own lipstick from carmine beetles and pestle which worked with pestle gave a strong red color pigment [1]. In the 10th century, lipsticks became quite popular in England under the rule of Queen Elizabeth. The term "cosmetics," which derives from the Greek "kosmtikos," refers to products that are used to wash, treat skin conditions, hide flaws, and enhance appearance. Herbal cosmetics, such as lipsticks, are created using a variety of components to offer various advantages. Waxes, oils, pigments, dyes, alcohol, aroma, preservatives, antioxidants, colours, and surfactants are all present in lipstick without doing any harm or having any negative side effects. They are well-liked cosmetic products that come in a variety of looks, patterns, and packaging. Nowadays herbal products are in great demand and claim to have no side effects. Herbal cosmetics have grown over synthetic agents [2,3]. This study includes preparation and evaluation of herbal lipsticks with the help of natural products like beetroot and turmeric extracts with their beneficial beautifying effects and minimum side effects.

Ideal Characteristics of Lipsticks

Ideal lipstick should cover lips adequately, last long, soften lips. It must be non-toxic, stable, not dry on storage, and non-irritant.

ADVANTAGES

Lipsticks can instantly make everyone feel more beautiful, with hydration additives like vitamin E. Sun protection is crucial for sensitive lips, but many people leave them unprotected. Lipstick makers now include sun protection chemicals in their formulations to protect them from the elements and aging effects.

DISADVANTAGES

Heavy Metal music-influenced lipsticks contain high levels of chromium, cadmium, and magnesium, which can lead to infections, organ damage, kidney failure, and renal failure. Lead, a neurotoxin, can harm the nervous system and brain, causing hormone imbalance and infertility. Mineral oil with formaldehyde, a carcinogen, and mineral oil helps close pores, further contributing to the negative effects of lipsticks [4,5].

MATERIALS AND METHODS

Materials

Beet root and Turmeric were purchased from a reliable store at the neighborhood market of Barasat, Kolkata, 700125. In the preparation of herbal lipsticks Emulsifying wax (manufactured by Otto chemie Pvt Ltd), almond oil (manufactured by Hamdard Laboratories), Coconut oil (manufactured by Shalimar), Castor oil (manufactured by Mekasa Products Pvt Ltd), Rose oil (manufactured by BMV fragrances Pvt Ltd) were obtained from Brainware University, Barasat.

Instruments

Electronic balance manufactured by Mettler Toledo ME204, pH meter manufactured by Mettler Toledo, Hot plate stirrer manufactured by Remi, Water bath manufactured by Vinayak Enterprise, lipstick mould manufactured by A.D.S laboratory was used to manufacture herbal lipsticks using beetroot and turmeric extracts.

Formulations

Different formulations (F1 to F5) of herbal lipsticks using beetroot and turmeric extracts with excipients are shown in Table 1.

Extraction of Beet root

Beet root contains betanin, which is a great option for a natural coloring agent. At first, peeled the beetroot and cut it into uniform-sized fine slices. Spread it over a butter paper, cover it with a fine mesh and allow it to shade dry for a





Piyali Khamkat et al.,

day. Dry the sample to remove moisture. Took the dried beetroot and ground it into a fine powder. Passed the powdered material through a fine sieve. Checked for any grainy particles. Sieved it again if required. Weighed the amount of powder and packed it for lipstick preparation. The major compound betanin, a class of compounds called betacyanin is responsible for the coloration of dark red color [6,7].

Extraction of Turmeric

Peeled the turmeric and washed it properly to extract curcumin, the coloring agent from turmeric. then grated the turmeric properly. After equally grating the peeled turmeric, a fine muslin cloth was used to strain the mixture to separate the juice from the seeds. The juice was taken out of the beaker and placed in storage for later use. Dry the sample to remove moisture. Sieved it again if required. Weighed the amount of powder and packed it for lipstick preparation. Mainly curcumin, a diarylheptanoid from curcuminoids group responsible for the yellow colour [8].

Preparation of herbal lipsticks containing beetroot and turmeric extract

Weighing all the required ingredients for the preparation of herbal lipsticks. At first, emulsifying wax was melted in a beaker at 70°C on a hot plate. Similarly, almond oil, castor oil and coconut oil, were taken in another beaker and melted at 70°C on a hot plate. Then the oil phase was added to the wax at the same temperature. The relevant colored pigment was added. The mixture was cooled to 40°C. Then 1-2 drops of rose oil were given as a flavoring agent for good fragrance. The molten material was poured into the moulds for lipstick preparation. After solidifying, it was taken out of the moulds and put inside the lipstick case. Here, Figure 1 and Figure 2 represented the procedure of lipstick preparation using beetroot and turmeric extract. Emulsifying wax was added as thickening agent, lubricating agent, and waterproofing agent. The use of castor oil was humectant and moisturizer. As hydrating agent, moisturizing agent and rejuvenate coconut oil and almond oil were added to the formulations [9,10].

Evaluation of Herbal Lipsticks containing Beetroot and Turmeric extract

Organoleptic characteristics

Organoleptic properties like colour, odour, shape, size and texture of herbal lipsticks were determined. Natural lip colours contain betanin and curcumin that apply colour to the lips in a precise and controlled manner for beautifying the lips.

Surface anomalies

This was studied for the surface defects, such as no formation of crystals on surfaces, no contamination by moulds, fungi etc [11].

Skin irritation test

Apply the lipstick on the skin for 10min and observe.

Spreadability test

It was tested by repeatedly applying the lipstick onto the glass slide to observe the uniformity in the formulation of the protective layer and whether the stick fragmented, deformed, or broke during application [12].

Identification tests of natural colorants

Turmeric identification test

The melting point of curcumin, an orange-yellow crystalline powder, is 183°C. Concentric sulphuric acid was added to the extract; as it dissolved, it turned yellow and with the addition of NaOH, it turned a deep brown colour.

Beet root identification test

Adding a few drops of diethyl ether to the extract containing betanin gave a violet hue that eventually turned yellow [13,14].

Melting Point

Determination of melting point is important as it is an indication of the limit of safe storage. The melting point of prepared lipstick was determined by capillary tube method. Take both ends open glass capillary tubes and introduce a required amount of lipsticks into each capillary tube. At the specific temperature the lipsticks melted completely in capillary tube was taken as the melting point. The above procedure was done about 3 times and the melting point ratio was observed in all formulation.

Solubility test





Piyali Khamkat *et al.*,

The herbal lipstick formulation was diluted in several solvents like water, ethanol, methanol to test its solubility [15].

pH determination

The pH of formulated herbal lipstick was determined using both pH paper and pH meter to get accurate result.

Breaking point

Breaking point is done to determine the strength of lipstick. The lipstick was positioned in a socket horizontally. The breaking point was determined by progressively increasing the weight by a certain amount (10 grams) every 30 seconds; this weight was regarded to be the breaking point [12, 13].

Force of application

A piece of coarse brown paper was kept on a shadowgraph balance and lipstick was applied at 45° angle to cover a 1 sq. Inch area until fully covered. The pressure reading is an indication of the force of application.

Aging stability

For 1 hour, the product was kept at 40°C. Numerous criteria were noticed, including bleeding, surface crystallization, and ease of application.

Perfume Stability study

The formulation of herbal lipstick was stored in standard storage conditions of cool temperature. It was tested for its fragrance after 60 days to check the stability [14, 15].

Stability Study

A stability study was conducted to examine the formulation's stability profile at 30±2°C and 75± 5% RH (minimum study period: at least two months) [16].

RESULTS

Organoleptic characteristics

Among all, in this study the main organoleptic property is color. Formulations such as F3, F4, and F5 showed better coloring properties. All formulations have smooth textures with sweet smells. As F1 contains no color, it is colorless shown in Table 2.

Skin irritation test

Table 2 represents the result of skin irritation test as there are no skin irritation properties present in the formulations.

Surface anomalies and Spreadability

All formulations have no flaws on the surface and have good spreadability which is shown in the Table 2.

Identification tests of natural colorants

The result of the identification test showed yellow and brown color for curcumin on the addition of concentrated sulphuric acid and NaOH respectively. Also, the violet color confirms the presence of betanin in beetroot on the addition of diethyl ether.

Melting Point

In the study of melting point determination, it can be concluded that F1, F2, and F4 showed better results mentioned in Table 3.

Solubility

All the formulations are very slightly soluble in aqueous medium but they are soluble in both ethanol and methanol.

pH determination

All formulations are in a range near to neutral pH from that F5 showed slightly acidic.

Force of application and Aging stability

All the formulation responses in the good result of the force of application and aging stability mentioned in Table 3.

Perfume

Perfume stability study showed better results for all the formulations represented in Table 3.

Stability study

The results of the stability study depending on some parameters are shown in Table 4 at 30±2°C and 75± 5% RH (minimum study period: at least two months).





Piyali Khamkat et al.,

DISCUSSION

Formulation and evaluation of herbal lipsticks containing natural colorants were done in an effort to bravely create a lipstick employing herbal materials while minimizing the adverse effects caused by the synthetic ones that were already available. The comprised formulation 2 to formulation 5 Herbal lipsticks that contain a colouring component that was produced from turmeric and beetroot extract were created using a variety of natural substances. According to the findings of the current study, herbal formulations are preferable options with less adverse effects, yet thorough clinical trials may be needed to assess the formulation for more efficacy. Skin irritation has not been a result of any of the formulations. No formulation had surface abnormalities. Both formulations had good aging stability. Among all the formulations F2 and F4 showed better results. A stability study has been done with the better formulation (F2). It can be said that herbal formulation can be a better formulation of synthetic lipsticks.

CONCLUSION

Herbal lipsticks were developed as a result of women's rising usage of cosmetics in recent years. In comparison to synthetic lipsticks, it has been discovered that these lipsticks derived from natural substances like emulsifying wax, castor oil, coconut oil, almond oil, beetroot, turmeric extract, and rose oil have less adverse effects. They also support blood circulation improvement, skin elasticity maintenance, dirt removal, and lip rejuvenation. Regular use of natural lips enhances texture and color and protects against abrasive environments and pollutants. Among all the formulations F2 and F4 showed better results and a stability study has been done for F2. It can be concluded that F2 and F4 formulations can be a better alternative to synthetic lipsticks having adverse effects.

ACKNOWLEDGMENTS

The authors are thankful the Department of Pharmaceutical Technology, Brainware University for the infrastructure, constant motivation, and encouragement for the research.

REFERENCES

1. Kaul S, Dwivedi S. Indigenous ayurvedic knowledge of some species in the treatment of human disease and disorders. *Inter J Pharm and Life Sci.* 2010; 1 (1): 44-49.
2. Gediya SK, Mistry RB, Patel UK, Blessy M, Jain HN. Herbal plants: used as cosmetics. *J Nat Prod Plant Resour.* 2011; 1: 24-32.
3. Aher AA, Bairagi SM, Kadaskar PT, Desai SS, Nimase PK. Formulation and evaluation of herbal lipstick from colour pigments of *Bixa orellana* (bixaceae) seeds. *Inter J Pharm Pharm Sci.* 2012; 4(5): 357-359.
4. Kaju M, Vishwasra S, Singh S. Review on Natural Lip Balm. *Int J Res Cosmet Sci.* 2015; 5(1): 1-7.
5. Asseervatham SB, Sasikumar JM, Kumar D. Studies on In-vitro free radical scavenging activity of *Bixa Orellana* L. bark extract. *Inter J Pharm Pharm Sci.* 2012; 4(2):719-726.
6. Shaikh MA, Pathan UA, Patil G. Design and Evaluation of Herbal Lip Balm by using Beet Root. *Int J Innov Sci Res Technol.* 2023;8(5): 2210-2212.
7. Khamkat P, Ghosh A, Mukherjee S. Transfersomes: An Innovative Vesicular Carrier for Boosted Transdermal Delivery System. *Res J Pharm Technol.* 2022; 15 (6): 2793-2800. doi-10.52711/0974-360X.2022.00467
8. Joshi LS, Pawar HA. Herbal Cosmetics and Cosmeceuticals: An Overview. *Nat Prod Chem Res.* 2015; 3:170. doi-10.4172/2329-6836.1000170
9. Lilwani S, Nair V. Extraction and Isolation of Lycopene Form Various Natural Sources. *J biotechnol. Biochem.* 2015; 1(5): 49-51.





10. Ghosh A, Khamkat P. Herbosome: A New Era of Lipid Based Drug Delivery System. J Sci Eng Appl Sci. 2021;7(3):126-40.
11. Larsson SC, Bergkvist L, Naslund I, Rutegard J, Walk A. Vitamin A, retinol, and carotenoids and the risk of gastric cancer: a prospective cohort study. Am J Clin Nutr. 2007; 85(2): 497-503.doi-10.1093/ajcn/85.2.497
12. Sudha Rani G, Pooja G, Harshavardhan V, Vamshi Madhav B, Pallavi B. Formulation and Evaluation of Herbal Lipstick from Beetroot (Beta vulgaris) Extract. Res. J. Pharmacognosy and Phytochem. 2019; 11(3):197-201. doi-10.5958/0975-4385.2019.00034.7
13. Kurthika SV, RamSS, Ahmed SA, Sadiq S, Mallick SD, Sree TR. Formulation and evaluation of natural lipstick from colored pigments of beta vulgaris taproot. J Pharm and Pharm Sci. 2014; 3(3): 65-71.
14. Sabu S, Vismaya A, Chithira CS, Sasi S, Murali V, Bhagyalakshmi, A.S., Mahesh A., Formulation and Evaluation of Herbal Lipsticks by Using Beta vulgaris. Int J Pharm Sci Rev Res. 2022; 75(1): 98-102. doi-10.47583/ijpsrr.2022.v75i01.017
15. Kadian R, Parle M. Therapeutic potential and phytopharmacology of tulsii. Int of Pharm. & Life Sci. 2012;3(7):1858–1867.
16. DeshmukhS, ChavanM, SutarM, Singh S. Preparation and Evaluation of Natural Lipsticks from Bixa Orellana Seeds. Int J Pharm Bio Sci. 2013;4(3):139-144.

Table 1: Different formulations of herbal lipsticks using beetroot and turmeric extracts

Formulations	Ingredients (quantity)						
	Emulsifying wax(gm)	Coconut oil(ml)	Castor oil(ml)	Almond oil(ml)	Turmeric extract(gm)	Beet Root extract(gm)	Rose oil
F1	10	5	5	--	--	--	1-2 drops
F2	10	5	--	5	1	--	1-2 drops
F3	10	4.5	4.5	--	--	3	1-2 drops
F4	10	5	--	5	2	--	1-2 drops





Piyali Khamkat et al.,

F5	9	4	4	--	--	3	1-2 drops
----	---	---	---	----	----	---	-----------

Table 2: Organoleptic parameters of formulated Herbal Lipsticks containing beetroot and turmeric as natural colorant

Organoleptic parameters	Inference				
	F1	F2	F3	F4	F5
Colour	Slight white	Yellowish	Betanin or beet red	Yellowish	Beet red
Texture	Smooth	Smooth	Smooth	Smooth	Smooth
Skin irritation	No	No	No	No	No
Surface Anomalies	No Flaws	No Flaws	Errorless	No Flaws	No flaws
Spreadability	Good	Good	Good	Good	Good

Table 3: Physical parameters determination of formulated Herbal Lipsticks with natural colorants

Evaluation parameters	Inference				
	F1	F2	F3	F4	F5
Melting point	73°C	70°C	67°C	70°C	65°C
Solubility	Soluble in ethanol and methanol	Soluble in ethanol and methanol	Soluble in ethanol and methanol	Soluble in ethanol and methanol	Soluble in ethanol and methanol
pH	6.9±0.2	6.7±0.2	6.3±0.2	6.4±0.2	6.0±0.2
Force of Application	Good	Good	Effortless	Good	Good
Aging stability	Soft	Soft	Soft	Soft	Soft
Perfume	Good	Good	Good	Good	Good

Table 4: Stability study of formulated Herbal Lipsticks containing natural colorants

Time period	Inference			
	Melting point	pH	Skin irritation	Perfume Stability





Piyali Khamkat et al.,

Day 1	70°C	6.7±0.2	No	smelling
Day 60	71°C	6.7±0.2	No	smelling

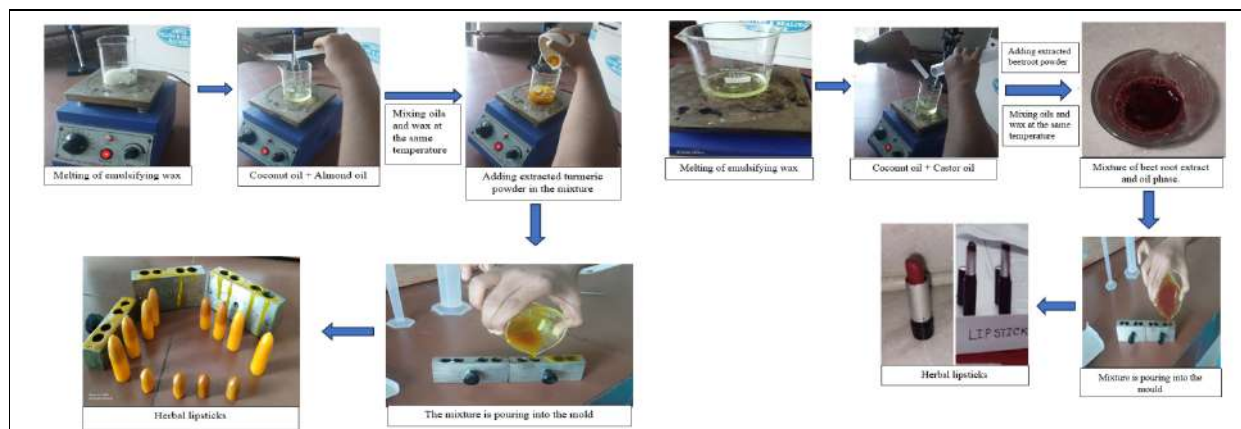


Figure 7: Herbal lipstick formulation steps with turmeric extract

Figure 8: Herbal lipstick formulation steps with beetroot extract



Figure 3: Melting point determination of herbal lipsticks containing natural colorants



Figure 4: Solubility and pH determination of herbal lipsticks containing natural colorants





Study on Performance of Concrete Using Sugarcane Bagasse Ash and Coal Bottom Ash

J.Rex¹ and K.Lakshmi Bhavani^{2*}

¹Associate Professor, Department of Civil Engineering, Malla Reddy Engineering College, Hyderabad, Telangana, India.

²PG Scholar, Department of Civil Engineering, Malla Reddy Engineering College, Hyderabad, Telangana, India.

Received: 18 Oct 2023

Revised: 25 Oct 2023

Accepted: 31 Oct 2023

*Address for Correspondence

K.Lakshmi Bhavani

PG Scholar,

Department of Civil Engineering,

Malla Reddy Engineering College,

Hyderabad, Telangana, India.

E mail: bhavani.mrec@gmail.com



This is an Open Access Journal / article distributed under the terms of the **Creative Commons Attribution License** (CC BY-NC-ND 3.0) which permits unrestricted use, distribution, and reproduction in any medium, provided the original work is properly cited. All rights reserved.

ABSTRACT

Conservation of the natural resources, reduction of the environmental contamination, and the effective use of waste materials are the critical goals for sustainable development. These goals can be met in concrete construction by partially replacing cement and aggregates with the agro waste like sugarcane bagasse ash and rice husk ash, as well as industrial waste like copper slag, steel slag, fly ash, and coal bottom ash, to mention a few. The major goal of this study is to see how using sugarcane bagasse ashCBA as a partial substitute for cement in concrete and coal bottom ashCBA as a partial substitute for fine aggregates influenced the final product. Its primary focus has been on concrete qualities such as strength and durability. The heat stability of all concrete combinations will have been evaluated in this investigation when subjected to higher temperatures. Twenty-five different concrete mixes were created, each with a different amount of SCBA (0%, 5%, 10%, 15%, and 20%) replaced with cement and a different amount of CBA (0%, 10%, 20%, 30%, and 40%) replaced with fine aggregates. The water-to-cement ratio was fixed at 0.55 in each batch. Concrete's durability was evaluated immediately after it was prepared, while its compressive strength was evaluated 14, 28, and 90 days afterwards. Based on test results, a blend of 10% SCBA and 10% CBA was determined to be the optimal solution. According to the findings of this study, the addition of SCBA and CBA to concrete has no effect on its thermal qualities.

Keywords: Compressive strength, Coal bottom ash, Elevated Temperature, Sugarcane bagasse ash, Workability.



**Rex and Lakshmi Bhavani**

INTRODUCTION

Concrete is the most widely used construction material in the world, because the material's remarkable mechanical properties as well as its long-lasting properties. At the moment, aggregates, which are essential in the production of concrete, are in limited supply, and the method by which cement is produced is one of the factors contributing to the deterioration of the environment. The cement industries are responsible for the significant portion of the greenhouse gas emissions that are contributing to the warming of the planet as a result of global warming. These emissions are caused by the burning of fuel in the cement kiln and the use of electricity in the grinding of the clinker. Cement production accounts for approximately 5% of total CO₂ emissions worldwide. The garbage that is produced from a wide range of agricultural goods is referred to as "agrowaste," which is an acronym for agricultural waste. A wide range of goods are produced by agriculture, but bagasse, the byproduct of processing sugarcane, wheat husk and straw, groundnut shell, and rice husk, the byproduct of processing paddy, is one of the most notable. As a consequence of this, it is of the utmost significance to discover viable substitutes not just for cement but also for aggregates that are obtained from natural sources. Aside from this, the principal contributor to a wide variety of environmental challenges and issues is the unabated growth of garbage from agricultural and industrial practices. If the wastes at issue are employed in the construction of concrete structures, then maybe these difficulties and burdens can be addressed to some degree. The garbage that is produced from a wide range of agricultural goods is referred to as "agrowaste," which is an acronym for agricultural waste. At the present time, the husk of rice, bagasse, the shell of crushed nuts, and several other forms of waste are all being used in some capacity as a fuel for the generation of power. As a result of this usage, ash is created, which adds to the difficulty of disposing of the material. Because of the chemical make-up of the ash, the wastes have been repurposed into useful components that may be included in the production of concrete. In addition to this, the waste has been changed into valuable resources. According to the results of a number of studies, the ash that is left over following the processing of sugarcane bagasse may also be used as a pozzolan in concrete. This comes on top of the agrowaste ashes that were discussed before. There have been a significant increase in the quantity of waste and by-products generated by a wide variety of enterprises over the course of the last few decades. This expansion has occurred at an alarming rate. It should not come as a surprise that this leads to a plethora of environmental issues and raises the possibility of pollution of natural resources that are important to human existence, such as water, air, and soil. In fact, it should come as no surprise at all. Getting rid of these wastes and byproducts in a way that is considered to be acceptable poses a major financial and logistical strain on every country. When it comes to some kinds of industrial waste, the expense of getting rid of it in a safe way might be rather significant. In addition, there is a dearth of disposal sites that are appropriate for the management of such wastes in an acceptable way without having a detrimental effect on the ecology in the surrounding area. Therefore, scientists from all over the world are focusing their efforts on discovering techniques to make use of these wastes in a manner that will limit the negative repercussions of doing so.

MATERIALS AND METHODS

Cement

Cement serves as a binder, connecting the various elements of the construction together into a cohesive whole. It is able to maintain its cohesion and adhesiveness even when exposed to water, two of its defining qualities. The pure form of this substance may be obtained while burning a mixture of calcareous & argillaceous materials. Clinker is the end product that is created when this mixture is fused in a kiln at temperatures above 1,450 degrees Celsius, after receiving the appropriate treatment, and after being heated to almost the same temperature. Cement serves as a binder, connecting the various elements of the construction together into a cohesive whole. It is able to maintain its cohesion and adhesiveness even when exposed to water, two of its defining qualities. Clinker is the end product that is created when this mixture is fused in a kiln at temperatures above 1,450 degrees Celsius, after receiving the appropriate treatment, and after being heated to almost the same temperature. The production of cement begins with the cooling of clinker, followed by the addition of a trace amount of gypsum, and last, the pulverisation of the mixture. Cements used in construction can be classified as hydraulic or non-hydraulic, with the distinction based on



**Rex and Lakshmi Bhavani**

the cement's ability to harden when exposed to water in the environment. Hydraulic cements have a greater capacity for this, while non-hydraulic cements have a lower capacity. Mineral hydrates are the products that come about as a direct result of the chemical process. Mineral hydrates are very stable in water and resistant to chemical attack due to the fact that they do not have a high degree of water solubility.

Aggregates

When it comes to the components that go into manufacturing concrete, the aggregates are by far the most significant. It is impossible to declare the investigation of concrete to be finished until both the width and depth of aggregates have been researched. The great majority of natural aggregates are derived from bed rocks, which may be classified as either igneous rocks, sedimentary rocks, or metamorphic rocks. Igneous rocks make up the bulk of the earth's crust. As a consequence of this, aggregates may also be divided into coarse aggregates and fine aggregates according to the size of the particles that make them up. These two types of aggregates are referred to as coarse aggregates and fine aggregates, respectively. Both the aggregate's size and its weight may be employed as determinants in the classification of the aggregate. The normal weight category refers to aggregates that have an average mass. To have a better grasp on concrete, one must first get familiar with the many ways in which it may be categorised according to the sizes of the components that make it up. Only then can one hope to achieve this goal.

Coarse aggregates

A BIS sieve with a particle size of 4.75 millimetres or greater is used to identify coarse aggregates. The shape of the coarse particles in concrete is a vital attribute to take into consideration because of the impact it has on both the workability and the strength properties of the material. Two factors that have a significant influence on the form that the aggregate takes are the type of crusher that is employed and the reduction ratio. Additionally, the Graded Coarse aggregate is distinguished by its nominal size, which varies from 40 millimetres to 20 millimetres, 16 millimetres, and 10 millimetres, respectively. These dimensions are found in the range of the aggregate. Crushed stone aggregates with nominal sizes of 10 millimetres and 20 millimetres were used for the whole of the experimental inquiry in a ratio of 50:50. The nominal size refers to the largest dimension of the aggregates. After being washed to remove any traces of dirt and dust, the aggregates were allowed to dry until they reached a condition in which they were surface dry. Uncrushed stone that was produced by the natural crumbling of rock is known as gravel. Crushed gravel or stone is created when larger rocks, such as stone or gravel, are broken up into tiny pieces. When gravel or stone is created as a result of mixing the two previously mentioned components, only a fraction of it has been crushed.

Fine aggregates

Aggregates most and is passes 4.75-mm BIS Sieve were known as Fine aggregates. Depending on their size, fine aggregates may either be classed as coarse aggregates, medium aggregates, or fine aggregates. The distribution of the particle sizes is used to categorise fine aggregates into one of four distinct grading zones, as stated in the BIS: 383-1970 standard. Each of these zones has a unique designation. The grading zones get increasingly more detailed, beginning with grading zone I and continuing all the way up to grading zone IV. For the purpose of this specific experiment, sand that is suitable for zone II was used.

Sugarcane bagasse ash

Ash from the sugarcane bagasse was formed whenever bagasse is used again after having been employed before as the biomass fuel in boiler, this usage results in the production of ash. Bagasse ash was a common name for this ash. Ash produced as a byproduct of an operation by burning of the bagasse at a temperature that is controlled and also maintained throughout the process. This ash is gathered from the boiler of the sugar mill specifically for a purpose of carrying out this experiment, which may be seen in Figure 2.1. It is possible to get to the sugar mill that is located in the hamlet of Shiv Shakthi sugar mills near my college.



**Rex and Lakshmi Bhavani****Tests Conducted****Workability of concrete as per BIS: 1199-1959**

Workability is one of the most important properties of concrete since it not only affects the strength and durability of hardened concrete, but it also influences the cost of labour because it affects the amount of time it takes to work w/ the concrete. Concrete's workability is one of the most important characteristics to consider. The many ways that workability may be examined have been categorised in accordance with the different sorts of flows that are produced when the tests are being carried out. The slump test was used in this investigation so that the level of workability could be determined. This experiment's goal is to scientifically study how workable freshly mixed concrete is, and its design reflects that goal.

Compressive strength of concrete as per BIS: 516-1959

Before being added to the appropriate batches, the amounts of the Cement, the Coarse aggregates (20 mm and 10 mm), Fine aggregates, Bagasse ash, Coal bottom ash, and Water were each given their own individual weightings. The compressive strength of concrete is evaluated using cubes of concrete with dimensions of 150 millimetres on each side, 150 millimetres long, and 150 millimetres high. These dimensions were employed in the test. Fine aggregates were the smallest aggregate size. The first portion of the process included dry mixing the cement and bagasse ash together, and the second part involved mixing the fine aggregates and coal bottom ash together in a consistent manner. Both parts of the process were carried out in sequence. The coarse aggregates were adequately mixed in order to ensure that they would have a uniform distribution throughout the whole batch. This was done so that there would be uniformity. After the water was added to the mixture, the components were carefully combined with the assistance of a mechanical mixer during the course of the ensuing three to four minutes. Washing and then oiling the cube moulds was the first step in the process of getting them ready for use. This process was repeated until the desired level of density was achieved. This continued until the concrete had reached its final cured state. Figure 3.4 indicates that the final specimens were given a full day to acclimate to their surroundings and harden before being inspected. This was done in order to ensure accurate results. The specimens were withdrawn from the moulds, subjected to a comprehensive examination, and then cast once again for a period of twenty-four hours. These were added to the water tank in the laboratory, which had already been stocked with drinkable water, and the tank was brought up to its maximum capacity once again. At the ages of 14, 28, and 90 days, samples are obtained from tank in which they were being healed to analyse their progress.

Compressive strength of concrete as per BIS: 516-1959

In addition to this, the compressive strength of concrete was tested throughout a broad variety of temperature conditions. This called for the use of cubes that had dimensions of 10 centimetres on a side, 10 centimetres on a side, and 10 centimetres on a side, respectively. Before undertaking the heating process, each cube was put through a curing phase that lasted for a total of 28 days. This was done so that the cubes would be ready for the next step. After the concrete cubes had acquired the necessary degree of hardness, they were moved into the muffle furnace in the manner. This was done so that a temperature distribution could be provided that was uniform throughout the board. After that, the heat was turned off in the furnace, and the samples were left alone to gradually return to room temperature on their own. Compression tests on each and every cooled specimen were carried out with the assistance of the universal testing machine (UTM).

RESULTS AND DISCUSSION

This chapter examines the results that were received from tests that were carried out on a variety of study materials that were used in earlier chapters. These tests were utilised in earlier chapters. The efficiency of a variety of distinct mixes, each of which has a different percentage of SCBA and CBA, is investigated. These mixtures each have their own unique ratios.



**Rex and Lakshmi Bhavani****Properties of Cement**

For the sake of this specific experiment, OPC grade 43 was used. The physical qualities of the cement, which were found by carrying out the appropriate tests and are indicated in the table, are detailed in Table 3.1.

Properties of sugarcane bagasse ash

The boiler of the sugar mill in the hamlet of which was located in Hyderabad near to my college, was the source of ash that were used in this procedure. India is the location where this specific method was carried out.

Properties of Coal bottom ash

The ash was obtained from Kothagudem Thermal Plant, the physical properties of CBA are given in Table 3.3.

Testing of Concrete

In this investigation, the compressive strength of the mixtures was tested after 28 days of curing using the cubes, and the compressive strength of the specimens was examined after 14, 28, and 90 days of curing using the cubes. Both of these evaluations were carried out using the cubes. This research was conducted with the intention of determining the influence that varying temperature ranges have on the compressive strength of all combinations. In addition, in order to assess the effects of SCBA and CBA on concrete, the test specimens were subjected to a battery of examinations after 14, 28, and 90 days had passed since the start of the curing process. A total of 24 unique mixes were created, one of which was used as a control. These mixes were prepared in addition to the mix that acted as the control. Different replacement levels of SCBA were used in order to replace the cement (zero percent, five percent, ten percent, fifteen percent, and twenty percent), while various replacement levels of CBA were utilised in order to replace the fine aggregates (0 percent, 10 percent, 20 percent, 30 percent, and 40 percent). The ratio of water to cement, often known as w/c and abbreviated as 0.55, was maintained throughout each and every one of the many possible combinations. For the sake of this investigation, 225 one-of-a-kind examples of cubes with side lengths of 150 millimetres and the same number of examples of cubes with side lengths of 100 millimetres were deemed to be components of the cubes. You may find a listing of the titles of the various mixes, as well as the percentages of the various components that go into each mix.

Workability of Concrete

The only method to get the ideal level of concrete strength is to use freshly mixed concrete that has the appropriate amount of slump value. During the course of this investigation, the slump of every possible combination was evaluated to see how straightforwardly it might be performed. The slump values for every conceivable combination are taken and a graphical representation of those values may be seen in Figure 3.1. The findings make it possible to draw the conclusion that the quality of the concrete mixes decreased as the proportion of SCBA and CBA that were included within them increased. Given the facts, one may draw this conclusion with some justification. When CBA was used to replace forty percent of the fine aggregates and SCBA was used to replace twenty percent of the cement, the slump values dropped from 110 millimetres to 45 millimetres, resulting in a significant reduction. It is probable that the increased water absorption is due to the porous nature of the particles that make up CBA. This would explain why CBA has such a high water absorption rate.

Compressive Strength of the Concrete

After mixing, Compressive strength of each of the concrete mixes are evaluated once again at 14, 28, and 90 days after the first evaluation. Below tables, display the findings of the average compressive strength as well the percent loss or increase in the compressive strength. The presence of any of these waste elements had an impact on compressive strength of the concrete after 14, 28, and 90 days of curing, respectively. According to the information that is shown in the table, it is glaringly evident that an increase in the quantity of SCBA does not result in a change in the pace at which the compressive strength of concrete mixes increases (up to 15 percent). The concrete that had a replacement level of 5 percent, 10 percent, or 15 percent SCBA gained 2.5 percent, 4.2 percent, or 1.6 percent of its strength, respectively. It is quite likely that the improved strength is the result of the lower particle size of the SCBA,



**Rex and Lakshmi Bhavani**

which results in a filler effect. It would make sense for the SCBA's rise in power to be explained in this way. The concrete that was made by including bottom ash into the production process has a strength that is lower than that of the concrete that was used as a reference. This occurs as a result of the porous nature of bottom ash, which allows it to take in a greater quantity of water than the reference concrete does. Compressive strength tends to decrease with increasing degrees of CBA replacement by fine particles, and this trend is seen to increase. There was never any indication that the substance's potency was becoming stronger during the whole of the period that it was being matured. The compressive strength of concrete changes substantially depending on the proportion of CBA that is used as fine aggregate. This could range from 10% to 40% of the total aggregate. In the table, you'll get an indication of the range of probable percentages. When compared to the concrete that acted as the control, the concrete that was left to cure for 14 days showed that the aggregates had become 2.3 percent, 5.1 percent, 6.9 percent, and 9.3 percent looser. The pattern was the same whether the curing period was 28 days or 90 days, and it was the same regardless of the amount of curing time.

Compressive Strength of Concrete at Elevated Temperature

Both SCBA and CBA concrete combinations exhibited a tendency that was practically exactly the same as what was noticed in the other mixture. The concrete that included 10 percent SCBA and 30 percent CBA exhibited the largest loss in strength after it was heated to 150 degrees Celsius. This loss in strength was roughly 12.9 percent of the concrete's strength before it was heated. When heated to 150 degrees Celsius, the concrete that included 5% SCBA and 0% CBA exhibited the least loss in strength. This concrete's strength after heating was around 7.6% of its strength before it was heated. The concrete that included 5 percent SCBA and 10 percent CBA saw the largest loss in strength when it was heated to 300 degrees Celsius. This loss in strength was roughly 22.1 percent of the concrete's strength before it was heated. In contrast, concrete that included 10 percent SCBA and 10 percent CBA showed the least loss in strength when heated to 300 degrees Celsius. Specifically, this kind of concrete lost roughly 17.1 percent of its strength when compared to its strength before heating. The specimens' compressive strength was observed to significantly diminish after being heated to a temperature of 600 degrees Celsius. The combination that contains 5% SCBA and 0% CBA exhibits the highest drop in compressive strength out of all the mixes.

CONCLUSIONS

In this research, Workability qualities, the strength characteristics, and thermal stability of concrete containing SCBA and CBA were studied. Each of the 25-concrete mixes that are created had a water –cement ratio of 0.55. This was accomplished by substituting SCBA for cement at a rate of 0 to 20 percent with an increase of 5 percent and coal bottom ash for fine aggregates at a rate of 0 to 40 percent with an increment of 10 percent. For the purpose of determining how SCBA and CBA contribute to compressive strength, 225 cubes measuring 15 centimetres on a side, 15 centimetres on a face, and 15 centimetres on a side were produced using varied percentages of SCBA and CBA. To further investigate the impact that increased temperature had on the compressive strength of each mixture, identical numbers of cubes measuring 10 cm by 10 cm by 10 cm were also created. The findings of a compressive strength test performed on specimens comprised of cubes of 150 millimetres in size were also subjected to statistical analysis. Based on the experimental investigations, it is possible to draw the following conclusions:

- As the SCBA and CBA content of concrete rises, the material becomes more difficult to work with. The slump value was reduced from 110 millimetres to 45 millimetres due to the addition of 40% CBA and 20% SCBA.
- At each and every curing age, a rise in the amount of SCBA in the concrete results in a greater compressive strength. When 10 percent of the SCBA is replaced, the compressive strength improves to its highest level; however, once this threshold is passed, the strength begins to decrease. When just 20 percent of the SCBA is replaced, there is a considerable drop in the material's compressive strength.
- SCBA can be used to replace up to 15% of the cement, and CBA can be used to replace up to 10% of the fine aggregates. Both of these substitutions are possible. It is advised that a mix of 10% SCBA and 10% CBA be used in order to achieve increased strength while maintaining an appropriate level of workability.





Rex and Lakshmi Bhavani

- During the heating process, the contribution of SCBA and CBA does not alter the attributes of strength that are possessed by concrete. When heated to a greater temperature, the strength of any and all concrete mixtures will decrease.
- Up to 150 degrees Celsius, there were only a little decrease in strength. The strength decreases by 7.1 to 12.9 percent at temperatures between 71 and 12.9 degrees Celsius, and by 22 percent at temperatures above 300 degrees Celsius.
- At a 600 degrees Celsius temperature, the material begins to seriously degrade. The concrete loses about half of its initial strength after being exposed to water.
- These all benefits also include possible savings in energy consumption.

REFERENCES

1. Aggarwal P, Aggarwal Y and Gupta S M (2007) Effect of bottom ash as replacement of fine aggregates in concrete. Asian J Civil Eng 8
2. Andrade LB, Rocha JC and Cheriaf M(2009) Influence of coal bottom ash as fine aggregate on fresh properties of concrete Constr Build Mater
3. Bajare D, Bumanis G and Upeniece L (2013) Coal Combustion Bottom Ash as Microfiller with Pozzolanic Properties for Traditional Concrete. Procedia Eng 57:149–58.
4. Behnood A and Ghandehari M (2009) Comparison of compressive and splitting tensile strength of high-strength concrete with and without polypropylene fibers heated to high temperatures. Fire Saf J 44:1015-22.
5. BIS: 10262-2009: Recommended guidelines for concrete mix design, Bureau of Indian Standard, New Delhi-2004.
6. BIS: 1199-1959 (Reaffirmed 2004): Methods of Sampling and Analysis of Concrete, Bureau of Indian Standard, New Delhi-1999.
7. BIS: 2386 (Part I)-1963 (Reaffirmed 2002): Methods of Test for Aggregates for Concrete, Bureau of Indian Standard, New Delhi-1963.
8. BIS: 383-1970 (Reaffirmed 2002): Specification for Coarse and Fine Aggregates from Natural Sources for Concrete, Bureau of Indian Standard, New Delhi-1997.
9. BIS: 4031 (Part 4, 5&6)-1988: Methods of Physical Tests for Hydraulic Cement, Bureau of Indian Standard, New Delhi -1988.
10. BIS: 456-2000 (Reaffirmed 2005): Code of practice plain and reinforced concrete, Bureau of Indian Standard, New Delhi-2000.
11. BIS: 5161959 (Reaffirmed 2004): Method soft tests for strength of concrete, Bureau of Indian Standard, New Delhi-2004.
12. BIS: 8112-2013: Specification for 43 grade Ordinary Portland Cement, Bureau of Indian Standard, New Delhi-2005.
13. Bishr HAM (2008) Effect of Elevated Temperature on the Concrete Compressive Strength.
14. Chusilp N, Jaturapitakkul C and Kiattikomol K (2009) Utilization of bagasse ash as pozzolanic material in concrete. Constr Build Mater 23:3352–58.
15. Cordeiro G C, Filho R D T and Fairbairn E M R (2010) Ultrafine sugarcane bagasse ash: High potential pozzolanic material for tropical countries. IBRA CON Struct and Mater 3(1):50-67.
16. Cordeiro GC, Filho RDT, Tavares L M and Fairbairn EMR (2008) Pozzolanic activity and filler effect of sugarcane bagasse ash in Portland cement and lime mortars. Cem Concr Compos 30:410–18.





Rex and Lakshmi Bhavani

Table 3.1: Properties of Cement

Sr. No.	Characteristics	Value Obtained experimentally	Values specified by BIS: 8112-2013
1.	Specific Gravity	3.15	-
2.	Standard consistency	31%	-
3.	Initial Setting time	135 minutes	30 minutes (minimum)
4.	Final Setting time	220 minutes	600 minutes (maximum)
5.	Compressive Strength		
	3 days	25.54 N/mm ²	23 N/mm ²
	7 days	36.12 N/mm ²	33 N/mm ²
	28 days	49.53 N/mm ²	43 N/mm ²

Table 3.2: Chemical properties of SCBA

Sr. No.	Chemical component	% of Chemical component
1.	SiO ₂	78.340%
2.	Fe ₂ O ₃	3.610%
3.	Al ₂ O ₃	8.550%
4.	CaO	2.150%
5.	Na ₂ O	0.120%
6.	K ₂ O	3.460%
7.	Ignition loss	0.420%

Table 3.3: Physical properties of CBA

Colour	Grayish or Shiny Black
Particles shape and texture	Spherical, irregular and porous
Specific Gravity	1.78
Water Absorption	9.64%





Rex and Lakshmi Bhavani

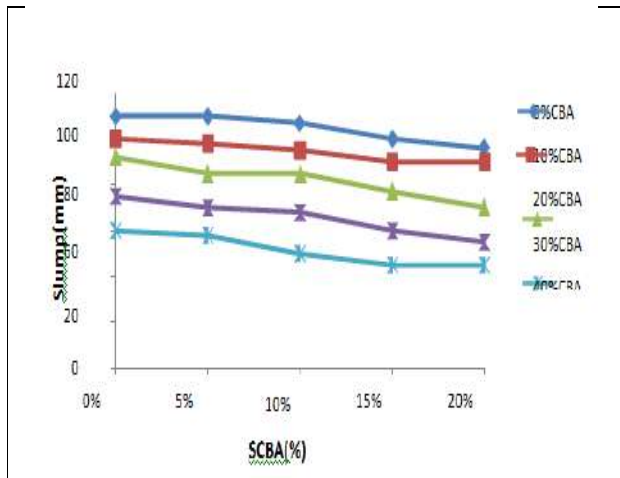


Figure 3.1: Slump values of the concrete w/c different replacements of SCBA and CBA

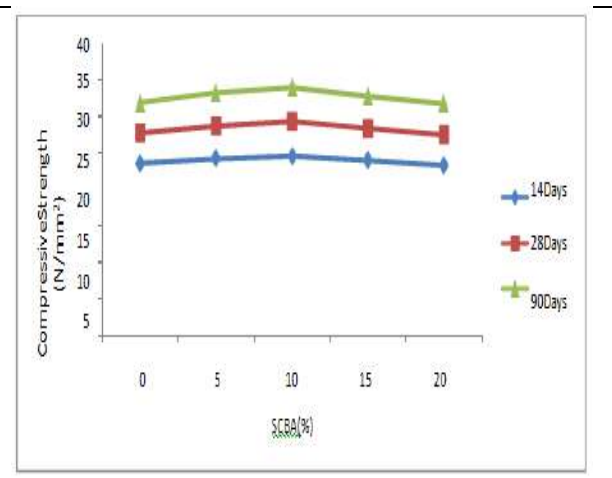


Figure 3.2: The concrete cubes compressive strength with different replacement levels of cement with SCBA for 0% CBA

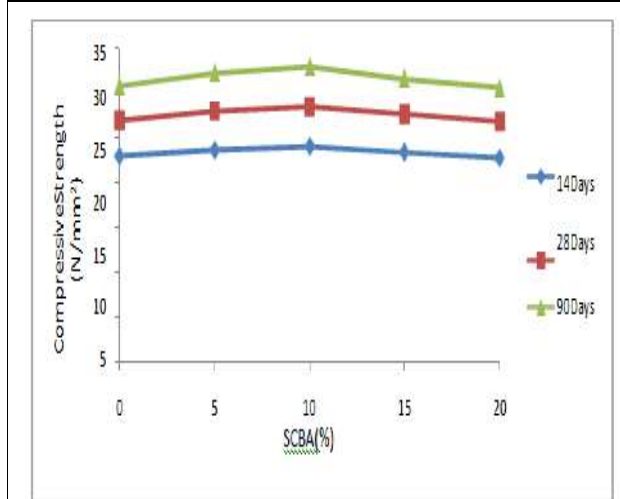


Figure 3.3: The concrete cubes compressive strength with different replacement levels of cement with SCBA for 10% CBA

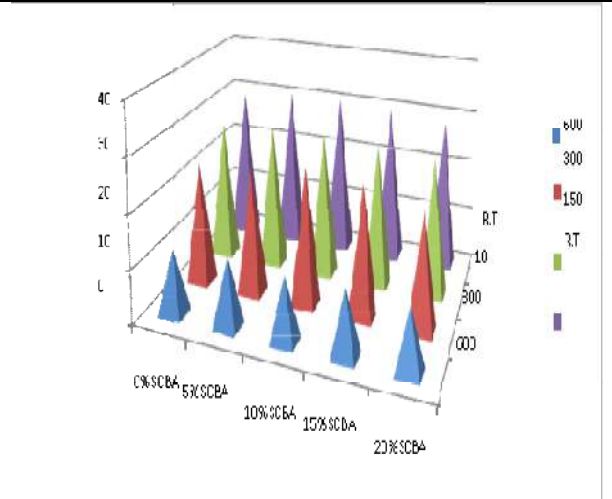


Figure 3.4: The concrete cube compressive strength at different temperature ranges with different replacement levels of cement with SCBA and 10% CBA





R-Norm Information Measure for HFSs and its Application in Decision Making Process

Alisha Aggarwal*, Gurdas Ram and Satish Kumar

Department of Mathematics, Maharishi Markandeshwar (Deemed to be University), Mullana- Ambala, Haryana, India.

Received: 30 Dec 2023

Revised: 09 Jan 2024

Accepted: 12 Jan 2024

*Address for Correspondence

Alisha Aggarwal*

Department of Mathematics,
Maharishi Markandeshwar (Deemed to be University),
Mullana- Ambala, Haryana, India.
E.Mail: aggarwalalisha95@gmail.com,



This is an Open Access Journal / article distributed under the terms of the **Creative Commons Attribution License** (CC BY-NC-ND 3.0) which permits unrestricted use, distribution, and reproduction in any medium, provided the original work is properly cited. All rights reserved.

ABSTRACT

In various situations of life, when we are in a fix about the selection of most suitable alternative among various alternatives, hesitant fuzzy set theory plays a vital role. In this paper, we proposed a new fuzzy entropy measure in the setting of hesitant fuzzy set (HFS) theory dealing with the subject of R-norm information measure. The proposed measure satisfies the priori definition of HFSs and also inspects its properties. Compared to already present entropy measures in literary work, various instances are given to illustrate the effectiveness of R- norm information measure. One of the most critical factors that influences a decision-making process is attribute weights. It aims to provide a clear understanding of its application and its tendencies.

Keywords : R-norm information measure, Entropy, Hesitant fuzzy set, Prospect theory, Multi-attribute decision-making.

INTRODUCTION

In our day to day life we try to find finest alternatives among the set of alternatives to reach a desired result. A lot of real world problems related to commercial and technical fields that are very complicated happen in our life. These problems contain a lot of uncertainty and vagueness. Sometimes even a simple problem becomes too complex because of uncertainty and hesitancy. Uncertainty is realized in various terms like randomness, fuzziness and incompleteness etc. [21] 1st proposed fuzzy theory to tackle the problems of uncertainty in various fields. But it has some boundaries to tackle ambiguous information. So conventional FS present few constraints. To tackle this situation different extensions of fuzzy set has been introduced, like intuitionistic [1], IVIFS [4, 15], the type-2 fuzzy set [5] and so on. [3] explained R-Norm IM of probability distribution. Further, [2] conduct a research on information measure of FSs and provide several means for fuzzy entropy. But, In many complicated situations, people hesitate to





Alisha Aggarwal et al.,

take a final decision and it becomes tough to approach the final agreement. To tackle these circumstances, Torra [14] and Xia and Xu [17, 18] defined new extension, known as hesitant fuzzy sets (HFSs). A little while back, a good number of researchers were fascinated by HFSs, so they gave different innovative ideas in the literature for eg. distance measures, similarity measures, entropy measures and decision making methods to cope with HFS. [19] and [20] reviewed types of HFSs and gave detailed sequence of distance measure, closeness and entropy for HFEs. When experts are in a fix to take some decision HFS proves to be a simple and fruitful mechanism. For eg. when two experts are of different opinion about assigning the membership degree of an alternative for a criterion, as one expert allocates value 0.4, another allocates value 0.9, then this membership degree will be described by the HFE {0.4, 0.9}, that explains vague information of experts choice. So it becomes essential to describe the uncertainty level related to HFE {0.4, 0.9} in proper way. Luca and Termini's development of fuzzy entropy opened the way for future research. They introduce a new fuzzy entropy corresponding to the Shannon entropy. Torra introduced the concept of HFE, specified as list of possible values. Hooda [8, 9, 10] proposed the R-norm information measure for fuzzy entropy. In spite of many researches being made in the field of HFSs yet much work is required on the entropy of HFSs. That's the reason that many researchers were encouraged to work on the entropy measure for HFSs. A more relevant method of entropy measure for HFSs was devised by [16]. Farhadinia [7, 6] calculated the IM for HFSs and IV HFSs. In the mean time, the already present entropy measures of HFSs in [6], [19] and Weital [16] require to assemble the maximum or minimum value that would equalize lengths of large and shorter HFSs. That will wipe out basic data and that is opposite of specific mindset of experts. That's the reason we must formulate another entropy measure to deal with such limitations. In our present work, we formulated another parametric(R-norm) IM inspired by Chungfeng Suo et al. [13]. Hypothesis of HFSs and its approach is broadly executed in MADM. To achieve a goal, MADM problem is defined as opting appropriate alternative from given alternative(s). Each alternative contains various criteria. MADM procedure comprises making decisions in a situation having multiple homogeneous options and identifying ideal choices. Attribute weighting has a vital role when we make a decision. In recent times, MADM theory and mechanism is being applied in fields like management Science and modern decision science. So, a great deal of measures to make a decision were proposed based on day to day life problems. TOPSIS, TODIM are popular approaches towards MADM. These methods mostly merge near ideal options with HFSs to make a preferable choice. Different decision makers have their own priorities according to risk preference while choosing an ideal option. Taking into consideration the risk priority of people, here in paper that is based on R-norm information measure(IM) a new mode that merges TOPSIS with prospect theory(PT) has been introduced. Following is the order of paper: Section 1 presents the introduction about the HFSs. Sect. 2, includes the definitions, basic concepts, properties of HFSs and already present entropy measures of HFSs. And a brief description of R-norm IM for fuzzy sets(FSS) is given. In sect. 3 another R-norm IM for HFSs introduced and validated it. In Sect. 4 The validity of the proposed measure is confirmed by contrasting its result with several current measures. Sect. 5 comprises PT merged with TOPSIS by using the proposed IM in decision-making. In sect.6 a practical application is introduced to indicate the appropriateness of this novel decision-making method. At last, conclusion is settled in sect. 7.

Preliminaries

Definition of HFSs

Definition [14,17,18] Let U be a finite discourse set, and HFSs M is defined on U in terms of function $h_M: U \rightarrow P(I)$, and $h_M \neq \phi$ and finite set for any $u \in U$.

Generally, a hesitant fuzzy set is represented by $M = \{(u, h_M(u)) | u \in U\}$

Here $P(I)$ represents power set of $[0,1]$, $h_M(u)$ represents hesitant fuzzy element (HFE).

$h_M(u) = \{\alpha^1, \alpha^2, \dots, \alpha^{t_u}\}$, where $\alpha^m \in [0,1]$, $m = 1, 2, \dots, t_u$ and t_u represents the no. of elements in $h_M(u)$. $HFS(U)$ denotes the collection of all HFSs on set U .

Properties of HFSs

Here we give brief description of few preceptions and theorems related to hesitant fuzzy sets, See Refs.[14, 17]





Alisha Aggarwal et al.,

Definition 2.2.1 [17,18] For a $HFEh_M(u)$,

$$s(h_M(u)) = \frac{1}{t_u} \sum_{m=1}^{t_u} (\alpha^m) \text{ represents score function of } h_M(u). \text{ Where, } \alpha^m \in h_M(u)$$

General properties on HFS(U) as follow:

Let $M = \{ \langle u, h_M(u) \rangle | u \in U \}$ and $N = \{ \langle u, h_N(u) \rangle | u \in U \}$ are two HFSs on set U , then:

(i)Compliment: $M^c = \{ \langle u, h_{M^c}(u) \rangle | u \in U \}$, where $h_{M^c}(u) = \{ 1 - \alpha | \alpha \in h_M(u) \}$. follow references [17,18,8].

(ii)Union: $M \cup N = \{ \langle u, h_{M \cup N}(u) \rangle | u \in U \}$, where:

$$h_{M \cup N}(u) =$$

- (a) $h_M(u)$, if $s(h_M(u)) > s(h_N(u))$ or $h_M(u) = h_N(u)$;
- (b) $s(h_M(u))$, if $s(h_M(u)) = s(h_N(u))$ or $h_M(u) \neq h_N(u)$;
- (c) $h_N(u)$, if $s(h_M(u)) < s(h_N(u))$

(iii)Intersection: $M \cap N = \{ \langle u, h_{M \cap N}(u) \rangle | u \in U \}$, where:

$$h_{M \cap N}(u) =$$

- (a) $h_M(u)$, if $s(h_M(u)) < s(h_N(u))$ or $h_M(u) = h_N(u)$;
- (b) $s(h_M(u))$, if $s(h_M(u)) = s(h_N(u))$ or $h_M(u) \neq h_N(u)$;
- (c) $h_N(u)$, if $s(h_M(u)) > s(h_N(u))$

(iv)Linear: $\lambda M = \{ \langle u, \lambda h_M(u) \rangle | u \in U \}$, where $\lambda h_M(u) = \{ 1 - (1 - \alpha)^\lambda | \alpha \in h_M(u) \}$, where λ is a positive number. follow Refs.[9,10,11]

Definition 2.2.2 Let $\tilde{H}, H \in HFSs$, where

$$\tilde{H} = \{ \langle u_i, \{ \tilde{\alpha}_i^m | m = 1, 2, \dots, t_i \} \rangle \} \text{ and } H = \{ \langle u_i, \{ \alpha_i^m | m = 1, 2, \dots, t_i \} \rangle \},$$

\tilde{H} represents sharpen version of H . Conditions of sharpened version are :

$$\tilde{\alpha}_i^m \leq \alpha_i^m \text{ if } \alpha_i^m \leq 0.5$$

and

$$\tilde{\alpha}_i^m \geq \alpha_i^m \text{ if } \alpha_i^m \geq 0.5$$

Here , $1 \leq m \leq t_i$; $1 \leq i \leq n$; and t_i represents no. of elements in $h_H(u_i), h_H(u_i)$

Definition 2.2.3 [17,18] Let $M, N \in HFS(U)$, hesitant normalized hamming distance between M and N is given below:

$$d_{hnh}(M, N) = \frac{1}{n} \sum_{i=1}^n \left[\frac{1}{t_{u_i}} \sum_{j=1}^{t_{u_i}} |h_M^{\sigma(j)}(u_i) - h_N^{\sigma(j)}(u_i)| \right] \tag{1}$$

where $h_M^{\sigma(j)}(u_i)$ and $h_N^{\sigma(j)}(u_i)$ represents j th largest values in $h_M(u_i)$ and $h_N(u_i)$, respectively and $t_{u_i} = \max\{t(h_M(u_i)), t(h_N(u_i))\}$ for each $u_i \in U$ being $t(h_M(u_i))$ and $t(h_N(u_i))$ the number of values of $h_M(u_i)$ and $h_N(u_i)$.

Some existing entropies for HFSs

To get various informations, measures like entropy and cross-entropy have been defined. Entropy measures fuzziness, whereas cross-entropy measures discrimination of information. That is why, entropy of HFSs is broadly researched, for instance Xu and Xia [19]:

$$E_{uu}^1(h) = \frac{1}{t(\sqrt{2}-1)} \sum_{m=1}^t \left[\sin \frac{\pi(\alpha^m + \alpha^{t-m+1})}{4} + \sin \frac{\pi(2 - \alpha^m - \alpha^{t-m+1})}{4} - 1 \right]; \tag{2}$$





Alisha Aggarwal et al.,

$$E_{uu}^2(h) = \frac{1}{t(\sqrt{2}-1)} \sum_{m=1}^t \left[\cos \frac{\pi(\alpha^m + \alpha^{t-m+1})}{4} + \cos \frac{\pi(2-\alpha^m - \alpha^{t-m+1})}{4} - 1 \right]; \tag{3}$$

$$E_{uu}^3(h) = -\frac{1}{t \ln 2} \sum_{m=1}^t \left[\frac{\alpha^m + \alpha^{t-m+1}}{2} \ln \frac{\alpha^m + \alpha^{t-m+1}}{2} + \frac{2 - \alpha^m - \alpha^{t-m+1}}{2} \ln \frac{2 - \alpha^m - \alpha^{t-m+1}}{2} \right] \tag{4}$$

$$E_{uu}^4(h) = \frac{1}{t[2^{(q-1)} - 1]} \sum_{m=1}^t \left\{ \left[\left(\frac{\alpha^m + \alpha^{t-m+1}}{2} \right)^p + \left(\frac{2 - \alpha^m - \alpha^{t-m+1}}{2} \right)^p \right]^q - 1 \right\}, \tag{5}$$

Here, h represents HFE; $\alpha^m \in h$ and t represents number of elements in h .
 From Eq.(2)-(5) entropies defined on HFEs can not fully respond in contrast to entropies of HFSs. Because HFSs consist more than one HFE. Then according to references[7] and [6] existing entropy definition and formulated distance-based entropy of HFS as mentioned below:

$$E_{bf}(M) = 1 - \frac{2}{n} \sum_{i=1}^n \left[\frac{1}{t} \sum_{m=1}^t |\alpha_i^m - 0.5| \right] \tag{6}$$

where $M \in HFS(U)$

Instead of this, entropy of HFEs depends upon score function (φ), deviation function (ζ) given by [16] as follows:

$$E_{cw1}(h) = \frac{1 - |1 - 2\varphi(h)| + \zeta(h)}{1 + \zeta(h)} \tag{7}$$

$$E_{cw2}(h) = \frac{1 - |\cos(\varphi(h)\pi)| + \zeta(h)}{1 + \zeta(h)} \tag{8}$$

$$E_{cw3}(h) = \frac{\sin(\varphi(h)\pi) + \zeta(h)}{1 + \zeta(h)} \tag{9}$$

$$E_{cw4}(h) = \frac{1 - 4(\varphi(h) - 0.5)^2 + \zeta(h)}{1 + \zeta(h)} \tag{10}$$

where, h represents HFE.

Currently, Z. Hussain [1] give a new method based on Hausdorff metric to calculate entropy for HFSs.

Let $M = \{ \langle u_i, h_M(u_i) \rangle | u_i \in U \}$ and $M^c = \{ \langle u_i, h_{M^c}(u_i) \rangle | u_i \in U \}$.

entropy measure defined as follow:

$$E_h(M) = 1 - \frac{1}{n} \sum_{i=1}^n \max \left(\max_k \{ \min_m \| \alpha^m - \rho^k \| \}, \max_k \{ \min_m \| \alpha^m - \rho^k \| \} \right) \tag{11}$$

where $\rho^k = 1 - \alpha^k$; $\alpha^m \in h_M(u_i)$; $\rho^k \in h_{M^c}(u_i)$; $1 \leq m, k \leq t_i \forall i$
 and t_i represents number of elements of $h_M(u_i)$ and $h_{M^c}(u_i)$.

R-Norm IM for FSs

$\delta_n = \{ P = (p_1, p_2, \dots, p_n), \sum_{i=1}^n p_i = 1, 0 \leq p_i \leq 1 \forall i \}$ is a set of all probability distributions connected to discrete random variable U taking finite values u_1, u_2, \dots, u_n .

[3] generalized Shannon entropy [12] in terms of R-norm information as below:

$$H_R(P) = \frac{R}{R-1} \left[1 - \left(\sum_{i=1}^n p_i^R \right)^{\frac{1}{R}} \right], R > 0, R \neq 1$$

Afterwards, R-norm IM extended to various situations by researchers, such as Hooda [10],[8],[9] proposed the following fuzzy entropy:





Alisha Aggarwal et al.,

$$H_R(M) = \frac{R}{n(R-1)} \sum_{i=1}^n \{1 - [(\mu_M(u_i))^R + (1 - \mu_M(u_i))^R]^{\frac{1}{R}}\}; R > 0, R \neq 1.$$

Further, corresponding to previous entropy postulation, we will give new fuzzy entropy measure for HFSs.

Definition of Entropy for HFSs

Definition Let $M \in HFS(U)$, then $H(M)$, where $H : HFS(U) \rightarrow R^+$, is called an entropy of hesitant fuzzy set M if $H(M)$ satisfies following properties.

- (H₁) Sharpness : $H(M)$ is minimum iff M is a crisp set, ie $\mu_M(u_i) = 0$ or $1 \forall i$
- (H₂) maximality : $H(M)$ is maximum iff M is a most FS set, ie $\mu_M(u_i) = \frac{1}{2} \forall i$
- (H₃) Symmetric : If M^c is complement of M then $H(M) = H(M^c)$
- (H₄) Resolution : $H(M) \geq H(\tilde{M})$ where \tilde{M} is sharpened version of M .

Proposed R-norm information measure for HF's is in next section.

Parametric information measure for HFSs

Let $M \in HFS(U)$, where $M = \{(u_i, h_M(u_i)) | u_i \in U\}$

$$HH_R(M) = \frac{R}{n(R-1)} \left[n - \sum_{i=1}^n \left(\frac{1}{t_i} \sum_{m=1}^{t_i} [(\alpha_i^m)^R + (1 - \alpha_i^m)^R]^{\frac{1}{R}} \right) \right] \quad (12)$$

Where $R > 1$ or $0 < R < 1$; $\alpha_i^m \in h_M(u_i)$; $m = 1, 2, \dots, t_i$; $\forall i, t_i$ represents no. of elements in $h_M(u_i)$.

Theorem 3.1 Prove that measure given in Eq.(12) is a valid entropy of HFSs.

Proof **(i)Sharpness** :From Eq.(12), it is clear that $\alpha_i^m \geq 0$. If $\alpha_i^m = 0$ or 1 then $HH_R(M) = 0$

Derivative of Eq.(12) w.r.t. α_i^m is

$$\frac{\partial HH_R(M)}{\partial \alpha_i^m} = \frac{R}{n t_i (R-1)} (-W) \quad (13)$$

Where $W = \left(\frac{1}{t_i} \sum_{m=1}^{t_i} [(\alpha_i^m)^R + (1 - \alpha_i^m)^R]^{\frac{1}{R}} \right)^{R-1} [(\alpha_i^m)^{R-1} - (1 - \alpha_i^m)^{R-1}]$

$\forall R > 1$ or $0 < R < 1$, also $\frac{\partial HH_R(M)}{\partial \alpha_i^m} > 0$ in $(0, 0.5)$, so $HH_R(M)$ is monotone increasing w.r.t. α_i^m on $(0, 0.5)$ and $\frac{\partial HH_R(M)}{\partial \alpha_i^m} < 0$ in $(0.5, 1)$, so $HH_R(M)$ is monotone decreasing w.r.t. α_i^m on $(0.5, 1)$.so, $HH_R(M) = 0$ if and only if $\alpha_i^m = 0$ or 1 .

(ii) Maximality: Take second-order mixed partial derivative of Eq.(12) w.r.t. α_i^m and $\alpha_i^k \forall i; m, k = 1, 2, \dots, t$ and $m \neq k$

Second order partial derivative w.r.t α_i^m as follow :

$$\frac{\partial^2 HH_R(M)}{(\partial \alpha_i^m)^2} = \frac{R}{t_i n (R-1)} (D_1 + D_2) \quad (14)$$

Where

$$D_1 = \frac{1-R}{t_i} \left(\frac{1}{t_i} \sum_{m=1}^{t_i} [(\alpha_i^m)^R + (1 - \alpha_i^m)^R]^{\frac{1}{R}-2} [(\alpha_i^m)^{R-1} - (1 - \alpha_i^m)^{R-1}] \right)^2;$$

$$D_2 = -(R-1) \left(\frac{1}{t_i} \sum_{m=1}^{t_i} [(\alpha_i^m)^R + (1 - \alpha_i^m)^R]^{\frac{1}{R}-1} [(\alpha_i^m)^{R-2} + (1 - \alpha_i^m)^{R-2}] \right);$$

When $\alpha_i^m = 0.5 \forall i; m = 1, 2, 3, \dots, t_i$, we get $D_1 = 0$





Alisha Aggarwal et al.,

Now we check the value of D_2 when $\alpha_i^m = 0.5$

Case 1: When $R > 1$ then $D_2 < 0$ then $\frac{\partial^2 HH_R(M)}{(\partial \alpha_i^m)^2} < 0$;

Case 2: When $0 < R < 1$ then $D_2 > 0$ then $\frac{\partial^2 HH_R(M)}{(\partial \alpha_i^m)^2} < 0$;

Computing second order mixed partial derivative of Eq. (12) w.r.t α_i^m and α_i^k as follow:

$$\frac{\partial^2 HH_R(M)}{\partial \alpha_i^m \partial \alpha_i^k} = \frac{R}{nt_i^2(R-1)} (-T) \tag{15}$$

where

$$T = (1-R) \left(\frac{1}{t_i} \sum_{m=1}^{t_i} [(\alpha_i^m)^R + (1 - \alpha_i^m)^R] \right)^{\frac{1}{R-2}} [(\alpha_i^m)^{R-1} - (1 - \alpha_i^m)^{R-1}] [(\alpha_i^k)^{R-1} - (1 - \alpha_i^k)^{R-1}]$$

Clearly when $\alpha_i^m = \alpha_i^k = 0.5 \forall i ; m, k = 1, 2, \dots, t_i$, we get $\frac{\partial^2 HH_R(M)}{\partial \alpha_i^m \partial \alpha_i^k} = 0$.

Hessian fuzzy matrix of $HH_R(M)$ is :

$$H(HH_R(M_0)) = \begin{bmatrix} HH_R(M_0)_{11} & 0 & \dots & 0 \\ 0 & HH_R(M_0)_{22} & \dots & 0 \\ \vdots & \vdots & \ddots & \vdots \\ 0 & 0 & \dots & HH_R(M_0)_{t_i t_i} \end{bmatrix}$$

We denote $M_0 = \{ \langle u_i, \{0.5\} \rangle \mid u_i \in U \forall i \}$

and $HH_R(M_0)_{mm} = \frac{\partial^2 HH_R(M_0)}{(\partial \alpha_i^m)^2} \forall m = 1, 2, \dots, t_i$.

The Hessian matrix of $H(HH_R(M_0))$ is -ve definite, so we obtain $HH_R(M_0)$ the maximum of $HH_R(M)$.

(iii) **Symmetric:** $HH_R(M) = HH_R(M^c)$, obvious from the definition of entropy.

(iv) **Resolution :** From Eq. (13)

For $R > 1$ or $0 < R < 1$, $\frac{\partial^2 HH_R(M)}{\partial \alpha_i^m \partial \alpha_i^k} > 0$ in $(0, 0.5)$ therefore $HH_R(M)$ is monotonically increasing in interval $(0, 0.5)$; For any $R > 1$ or $0 < R < 1$, $\frac{\partial^2 HH_R(M)}{\partial \alpha_i^m \partial \alpha_i^k} < 0$ in $(0.5, 1)$. Therefore $HH_R(M)$ is monotonically decreasing in interval $(0.5, 1)$. Then :

$$\tilde{\alpha}^m \leq \alpha^m < 0.5 \Rightarrow HH_R(\tilde{M}) \leq HH_R(M)$$

$$\tilde{\alpha}^m \geq \alpha^m > 0.5 \Rightarrow HH_R(\tilde{M}) \leq HH_R(M)$$

Hence $HH_R(\tilde{M}) \leq HH_R(M)$. Therefore $HH_R(M)$ is valid entropy of HFSs.

Numerical Examples

Here we compare our formulated entropy measure with existing entropies by giving some examples using Eq. (2) – (5), Eq. (7) – (10) and Eq. (11)

Example 4.1 Let $M, N \in HFS(U)$, for a single set $U = \{u\}$ where $M = \{ \langle u, \{0.3002, 0.4265, 0.4737\} \rangle \}$ and $N = \{ \langle u, \{0.5045, 0.6270, 0.6677\} \rangle \}$

It is clear from Table 1. that the entropies $E_{uu}^1, E_{uu}^2, E_{uu}^3$ and E_{uu}^4 of HFSs M and N are clearly same. But our IM of HH_R has ability of differentiating entropy of HFSs M and N . That's why new entropy measure is more suitable in contrast to entropy measures given by [19] and [6,7].

Example 4.2 Let $M, N \in HFS(U)$, for a single set $U = \{u\}$ where $M = \{ \langle u, \{0.185, 0.330, 0.685\} \rangle \}$ and $N = \{ \langle u, \{0.200, 0.300, 0.700\} \rangle \}$





Alisha Aggarwal et al.,

It is clear from Table 2 that [16] not able to differentiate the entropy of two different sets, this happens because entropies of $E_{cw1}, E_{cw2}, E_{cw3}$ and E_{cw4} defined in [16] having score function, deviation function of M, N are same. So, in such situation, IM HH_R is more appropriate.

Example 4.3 Let $M, N \in HFS(U)$, for a set $U = \{u_1, u_2, u_3\}$ where
 $M = \{\langle u_1, \{0.1, 0.3, 0.7\} \rangle, \langle u_2, \{0.5, 0.8\} \rangle, \langle u_3, \{0.2, 0.5, 0.6, 0.7\} \rangle\}$
 $N = \{\langle u_1, \{0.3, 0.7, 0.9\} \rangle, \langle u_2, \{0.3, 0.6\} \rangle, \langle u_3, \{0.3, 0.4, 0.5, 0.8\} \rangle\}$
 We computed $E_{bf}(M) = E_{bf}(N) = 0.6222$ and $HH_R(M) = 0.3542$ and $HH_R(N) = 0.3761$. It shows entropies of M and N under E_{bf} are same. But our information measure HH_R is able to differentiate between the entropy of two different HFSs.

Example 4.4 Let $M, N \in HFS(U)$, for a set $U = \{u_1, u_2\}$ where
 $M = \{\langle u_1, \{0.485, 0.497, 0.503\} \rangle, \langle u_2, \{0.492, 0.499, 0.510\} \rangle\}$
 $N = \{\langle u_1, \{0.497, 0.502, 0.515\} \rangle, \langle u_2, \{0.490, 0.508\} \rangle\}$
 We computed $E_h(M) = E_h(N) = 0.975$ and $HH_R(M) = 0.5403$ and $HH_R(N) = 0.5402$. It is note worthy that entropies of M and N are alike using entropy E_h . But entropy HH_R for M and N is different. Reason behind minor difference in entropy between M and N is that M and N sets are closely related. Hence It shows that the R - norm IM is more suitable.

Techniques of MADM

MADM problems are related to discrete choice space when there are various alternatives which are predetermined. It is used to opt most suitable alternative out of different alternative(s). MADM procedure comprises making decisions in a situation having multiple homogeneous options and identifying ideal choices. Attribute weight has a vital role when we make a decision. In recent times, MADM theory and mechanism is being applied in fields like management science and modern decision science. Suppose $S = \{A_1, A_2, \dots, A_n\}$, $Q = \{Q_1, Q_2, \dots, Q_n\}$ where A_i 's are alternatives and Q_j are attributes. $\forall 1 \leq i \leq n, 1 \leq j \leq T$. Assessed values of w.r.t is $(1, 2, \dots)$, where

Let (w_1, w_2, \dots) , where w_j are weight of attributes and $0 \leq w_j \leq 1; \sum_{j=1}^T w_j = 1$

When we take decision it becomes difficult to select the the perfect alternative. That's why we require a satisfactory alternative to take decision. For opting the feasible result to handle MADM problems, we formulated a new model, which connects PT with TOPSIS. To determine the weight of an attribute IM is applied.

Steps to compute the attribute weights are given below :

Step 1 Forming HFD matrix:

$$D = \begin{bmatrix} 11 & 12 & \dots & 1 \\ 21 & 22 & \dots & 2 \\ \vdots & \vdots & \dots & \vdots \\ 1 & 2 & \dots & \end{bmatrix}$$

Where rows represents value of attributes corresponding to alternatives and column represents value of attribute of different alternative.

Step 2 Computing attributes weight by using information measure :

$$= \frac{|1-1|}{\sum_{i=1}^n (1-1)} \tag{13}$$

here $= \frac{1}{n} \sum_{i=1}^n HH_R(s_{ij}), j = 1, 2, \dots, T$.

It is notable that, value of IM HH_R may be > 1 , so by adding absolute value, we make sure that weight lies between 0 to 1.





Alisha Aggarwal et al.,

Step 3 Under mentioned method is used to change hesitant fuzzy matrix to HFB matrix.

Assume if s_{ij} is a benefit attribute, then $\bar{s}_{ij} = s_{ij}$ if s_{ij} is cost attribute, then $\bar{s}_{ij} = s_{ij}^c$.

HFB matrix is given below :

$$\bar{D} = \begin{bmatrix} \bar{s}_{11} & \bar{s}_{12} & \dots & \bar{s}_{1T} \\ \bar{s}_{21} & \bar{s}_{22} & \dots & \bar{s}_{2T} \\ \vdots & \vdots & \dots & \vdots \\ \bar{s}_{n1} & \bar{s}_{n2} & \dots & \bar{s}_{nT} \end{bmatrix}$$

where $\bar{s}_{ij} = \{\bar{\alpha}_{ij}^1, \bar{\alpha}_{ij}^2, \dots, \bar{\alpha}_{ij}^{t_{ij}}\}$

Step 4Forming of weighted HFB matrix:

$$\begin{bmatrix} \bar{s}_{11} & \bar{s}_{12} & \dots & \bar{s}_{1T} \\ \bar{s}_{21} & \bar{s}_{22} & \dots & \bar{s}_{2T} \\ \vdots & \vdots & \dots & \vdots \\ \bar{s}_{n1} & \bar{s}_{n2} & \dots & \bar{s}_{nT} \end{bmatrix} \begin{bmatrix} w_1 & 0 & \dots & 0 \\ 0 & w_2 & \dots & 0 \\ \vdots & \vdots & \dots & \vdots \\ 0 & 0 & \dots & w_T \end{bmatrix} = \begin{bmatrix} \tilde{s}_{11} & \tilde{s}_{12} & \dots & \tilde{s}_{1T} \\ \tilde{s}_{21} & \tilde{s}_{22} & \dots & \tilde{s}_{2T} \\ \vdots & \vdots & \dots & \vdots \\ \tilde{s}_{n1} & \tilde{s}_{n2} & \dots & \tilde{s}_{nT} \end{bmatrix}$$

Step 5From step 4, we obtain Hesitant fuzzy PI solution S^+ and NI solution S^- as follow:

$$S^+ = \{s_1^+, s_2^+, \dots, s_T^+\}, \tag{14}$$

$$S^- = \{s_1^-, s_2^-, \dots, s_T^-\}, \tag{15}$$

where $s_j^+ = \{\max_i^n(\max_m^{t_{ij}} \tilde{\alpha}_{ij}^m)\}$, $s_j^- = \{\min_i^n(\min_m^{t_{ij}} \tilde{\alpha}_{ij}^m)\}$, $\tilde{s}_{ij} = \{\tilde{\alpha}_{ij}^1, \tilde{\alpha}_{ij}^2, \dots, \tilde{\alpha}_{ij}^{t_{ij}}\}$, t_{ij} represents no. of elements in \tilde{s}_{ij} , $1 \leq i \leq n; 1 \leq j \leq T$.

Step 6 Distance b/w each alternative to PI solution S^+ of (14) and to NI solution S^- of (15) using Eq.(1) is given below:

$$J_i^+ = d_H(A_i, S^+), \tag{16}$$

$$J_i^- = d_H(A_i, S^-) \tag{17}$$

where $1 \leq i \leq n$.

Step 7 Depends upon PT, if PI solution is considered as a source, each alternative will lose according to PI solution. Inversely, if NI solution is considered as source, each alternative is beneficial, i.e.:

$$v^-(J_i^+) = -\theta(J_i^+)^{\beta}, \tag{18}$$

$$v^+(J_i^-) = (J_i^-)^{\gamma}, \tag{19}$$

where β, γ are risk attitude coefficients where $\beta, \gamma < 1$, θ is loss cautious coefficient where $\theta > 1$. Often we take $\beta = \gamma = 0.92, \theta = 2.33$.

Step 8 Using Eqs.(18)-(19), J_i is calculated as follow:

$$J_i = \frac{|v^+(J_i^-)|}{|v^-(J_i^+)|}$$

where J_i denotes the ratio of benefits to losses and $J_i \in [0,1], 1 \leq i \leq n$.

Alternative's ranking relies upon J_i value size. Preference sequence of alternative A_i improved by a greater value of $J_i, \forall i$

Application of proposed entropy in MADM problem

Here, we give the application of MADM in reference [19] to display the efficacy of IM HH_R to decide criteria weights.





Alisha Aggarwal et al.,

Here, we take the example of industry, who wants to select the best supplier to invest its money to buy infrastructure. For this purpose, quotations of four suppliers are taken, namely A_1 , A_2 , A_3 and A_4 . To opt the best supplier, four assessment attributes Q_1 , Q_2 , Q_3 and Q_4 are taken into account that are quality of material, dealing attitude, work completion and cost price respectively. Here Q_1 , Q_2 and Q_3 are benefit attributes Q_4 is cost attribute. The assessment given by experts are depicted by means of HFSs, as shown in Table 3. Using formulas (12) and (16), entropy weight of the HFSs is computed. While the IM values calculating by HH_R afterwards transformed to weight, which are computed by using step 2. Weight of attributes are: $w_1 = .2439$, $w_2 = .2585$, $w_3 = .2269$, $w_4 = .2707$.

In accordance with technique connecting TOPSIS to PT described in Sect.5, cost attributes Q_4 are converted to benefit attributes. PI solution S^+ , NI solution S^- are calculated below:

$$S^+ = \{0.37, 0.38, 0.27, 0.40\}$$

$$S^- = \{0.04, 0.04, 0.06, 0.04\}$$

It is depicted through Table 6 that distance b/w each alternative to the +ve and -ve ideal sol. respectively are computed according to Eq. (19) and (20). Now using Eq. (21) and (22), we attain the -ve prospect value and +ve prospect value respectively. However, the proportion of benefits to losses of the alternatives is computed as depicted in Table 7 and Table 8. The alternatives can be analysed by using value of $f_i (i=1,2,3,4)$ in Table 8: $A_4 > A_2 > A_1 > A_3$. So, the perfect investment alternative is A_4 . It is note worthy that above analysis is w.r.t. parameter $R=4$. Now we need to examine if different values of the parameters affect the ranking of alternatives. Table 9 shows that alternative's ranking is still $A_4 > A_2 > A_1 > A_3$. Moreover, we notice, though the attributes weights changes according to the value of parameter R , Even the alternative's ranking behaves consistently. Now, we execute compatibility of above-said entropy measure, contrasting it with already present entropy measures given by [19]; [16]. For more details refer Table 10. Comparison of results acquired by existing entropy measures, gives that A_4 is the best supplier and A_3 is the last aspirant. In short, entropy measures, E_{cw1} , E_{cw3} and E_{cw4} are found to be less effective contrasting with other measures. However, ranking outcomes computed by E^{1uu} , E^{2uu} , E^{3uu} and E_{cw2} are identical to the entropy measures formulated by our technique. Finally, It indicates the entropy we formulated is a feasible measure.

CONCLUSION

When decision-makers hesitate among numerous values to represent the uncertain information, in that situation HFS, whose membership is denoted through certain principles seems much convenient. As HFS consist the ability to illustrate unpredictable information, So in present work, we formulated a entropy measure i.e R-norm information measure for HFSs. The new entropy measure not only demonstrate the details about attributes as well as explains unbiased thinking of experts. Further, by using numerical examples, the new entropy measure has been compared with other existing entropy measures and outcomes show that proposed entropy measure is very effective and consistent. Besides this usage of proposed information measure in decision making (MADM) given through real life examples connecting PT with TOPSIS to get superb alternative. In the times to come, we shall explore the new entropy on HFSs and its operational properties.

REFERENCES

1. Krassimir T Atanassov and Krassimir T Atanassov. *Intuitionistic fuzzy sets*. Springer, 1999.
2. Dinabandhu Bhandari and Nikhil R Pal. Some new information measures for fuzzy sets. *Information Sciences*, 67(3):209-228, 1993.
3. Dick E Boeke and Jan CA Van der Lubbe. The r-norm information measure. *Information and control*, 45(2):136-155, 1980.





Alisha Aggarwal et al.,

4. H Bustince, Javier Fernandez, Anna Kolesarova, and Radhko Mesiar. Generation of linear orders for intervals by means of aggregation functions. *Fuzzy Sets and Systems*, 220:69-77, 2013.
5. Didier Dubois, Walenty Ostasiewicz, and Henri Prade. Fuzzy Sets: history and basic notions. *Fundamentals of fuzzy sets*, page 21-124, 2000.
6. Bahram Farhadinia. Information measures for hesitant fuzzy sets and interval- valued hesitant fuzzy sets. *Information Sciences*, 240:129-144,2013.
7. Bahram Farhadinia. A novel method of ranking hesitant fuzzy values for multiple attribute decision- making problems. *International Journal of Intelligent Systems*, 28(8):752-767, 2013.
8. DS Hooda. On generalized measures of fuzzy entropy. *Mathematica Slovaca*, 54(3):315-325, 2004.
9. DS Hooda and DK Sharma. Generalizrd r-norm information measures. *Journal of Appl. Math, Statistics & informatics (JAMSI)*, 4(2):153-168, 2008.
10. DS Hooda and RK Tuteja. Two generalized measures of “useful” information. *Information Sciences*, 23(1):11-24, 1981.
11. Zahid Hussain and Miin-Shen Yang. Entropy for hesitant fuzzy sets based on hausdorff 20:2517-2533, 2018.
12. Claude E Shannon. A mathematical theory of communication (part i and ii). *Bell System technical journal*, 27:379-423, 1948.
13. Chungfeng Suo, Yongming Li, and Zhihui Li. An (r, s)-norm information measure for hesitant fuzzy sets and its application in decision- making. *Computational and Applied Mathematics*, 39:1-19, 2020.
14. Vicene Torra. Hesitant fuzzy sets. *International journal of intelligent systems*, 25(6):529-539, 2010.
15. I Burhan Turksen. Interval valued fuzzy sets based on normal forms. *Fuzzy sets and systems*, 20(2):191-210, 1986.
16. Cuiping Wei, Feifei Yan, and Rosa MRodriguez. Entropy measures for hesitant fuzzy sets and their application in multi- criteria decision-making. *Journal of Intelligent & Fuzzy Systems*, 31(1):673-685, 2016.
17. Meimei Xia and Zeshui Xu, Hesitant fuzzy information aggregation in decision making. *International journal of approximate reasoning* , 52(3):395-407, 2011.
18. Zeshui Xu and Meimei Xia. Distance and similarity measures for hesitant fuzzy sets. *Information Sciences*, 181(11):2128-2138, 2011.
19. Zeshui Xu and Meimei Xia. Hesitant fuzzy entropy and cross-entropy and their use in multiattribute decision- making. *International Journal of Intelligent Systems*, 27(9):799-822, 2012.
20. Zeshui Xu and Xiaolu Zhang. Hesitant fuzzy multi-attribute decision making based on topsis with incomplete weight information. *Knowledge- Based Systems*, 52:53-64, 2013.
21. L Zadeh. Fuzzy sets. *Inform Control*, 8:338-353, 1965.

Table 1: Effect of entropies on HFSs

HFSs	E_{uu}^1	E_{uu}^2	E_{uu}^3	E_{uu}^4	$HH_{R=4}$
M	0.9567	0.9567	0.9567	0.9567	0.7700
N	0.9567	0.9567	0.9700	0.9792	0.5187

Table 2: Effect of entropies on HFSs

HFSs	E_{cw1}	E_{cw2}	E_{cw3}	E_{cw4}	$HH_{R=4}$
M	0.8500	0.7682	0.9633	0.9700	0.6293
N	0.8500	0.7682	0.9633	0.9700	0.6171





Alisha Aggarwal et al.,

Table 3: HFD matrix D

A ₁	{.25, .45, .75, .85}	{.15, .35, .45, .55}	{.25, .35, .55, .65}	{.15, .45, .65, .75}
A ₂	{.25, .45, .65, .75}	{.25, .35, .65, .75}	{.25, .45, .55, .65}	{.15, .25, .45, .85}
A ₃	{.15, .25, .45, .55}	{.15, .25, .75, .85}	{.25, .45, .65, .75}	{.35, .55, .75, .85}
A ₄	{.35, .45, .55, .65}	{.35, .45, .55, .65}	{.45, .55, .65, .75}	{.15, .25, .65, .75}

Table 4: HFB matrix D

	Q ₁	Q ₂	Q ₃	Q ₄
A ₁	{.25, .45, .75, .85}	{.15, .35, .45, .55}	{.25, .35, .55, .65}	{.25, .35, .55, .85}
A ₂	{.25, .45, .65, .75}	{.25, .35, .65, .75}	{.25, .45, .55, .65}	{.15, .55, .75, .85}
A ₃	{.15, .25, .45, .55}	{.15, .25, .75, .85}	{.25, .45, .55, .75}	{.15, .25, .45, .65}
A ₄	{.35, .45, .55, .65}	{.35, .45, .55, .85}	{.45, .55, .65, .75}	{.25, .35, .75, .85}

Table 5: Weighted HFB matrix D

	Q ₁	Q ₂	Q ₃	Q ₄
A ₁	{.07, .14, .29, .37}	{.04, .10, .14, .18}	{.06, .09, .18, .21}	{.07, .11, .19, .40}
A ₂	{.07, .14, .23, .29}	{.07, .10, .23, .29}	{.06, .13, .18, .21}	{.04, .19, .31, .40}
A ₃	{.04, .07, .14, .18}	{.04, .07, .29, .38}	{.06, .13, .18, .27}	{.04, .07, .15, .25}
A ₄	{.10, .14, .18, .23}	{.10, .14, .18, .38}	{.13, .18, .21, .27}	{.07, .11, .31, .40}





Modelling of Parallel Queuing Model with Time Independent Service

Neha Gupta^{1*}, Deepak Gupta² and Vandana Saini

¹Research Scholar in Mathematics, Maharishi Markandeshwar (Deemed to be University), Mullana, Haryana, India

²Prof & Head, Department of Mathematics, Maharishi Markandeshwar (Deemed to be University), Mullana, Haryana, India

³Assistant Professor, Department of Mathematics Govt. College Naraingarh (Ambala), Haryana, India.

Received: 30 Dec 2023

Revised: 09 Jan 2024

Accepted: 12 Jan 2024

*Address for Correspondence

Neha Gupta

Research Scholar in Mathematics,
Maharishi Markandeshwar (Deemed to be University),
Mullana, Haryana, India.
E.Mail.: nehagupta170194@gmail.



This is an Open Access Journal / article distributed under the terms of the **Creative Commons Attribution License** (CC BY-NC-ND 3.0) which permits unrestricted use, distribution, and reproduction in any medium, provided the original work is properly cited. All rights reserved.

ABSTRACT

The present paper deals with development of a complex queue network model consisting of parallel and serial service channels. The model consists of three servers. The first server is commonly connected to other two server, both of which are parallel and contain parallel sub servers. The concept of generating function technique, laws of calculus and differential difference equations are used to analyzed the model. The system accomplishment measures such as average number of customers in each queue, the average waiting time of a customer in each queue, utility of service station, the variance of the content of queue are derived. Behavioral analysis of the model and numerical illustration informed that time independent service rates have remarkable effect on performance measures. The model has many applications in real life problems.

Keywords: Parallel server, Generating function technique, performance measures, Transient behaviour, Arrival rate.

INTRODUCTION

In the development of queueing theory many observers give their effort in the field of queueing theory. Jackson R.R.P (1954) designed the queueing system with phase type service. Maggu (1970) proposed the bi-tandem idea in queueing with importance in manufacturing. V.W. Mak (1990) et.al.an precise and mathematical method for anticipate the execution of a class of parallel programmatic management running on coincident system is described. T Kelly et.al (2008)implement operational research to the obstacle in compassionate and predicting application-level





Neha Gupta et al.,

performance in parallel servers. Deepak Gupta(2011) et.al analyzed a complex queue network model in which two systems containing biserial and parallel service channel is joined in series with common service channel. A.V.S Suhasini(2013) et.al developed a model containing parallel and serial service channel with time dependent bulk arrival. Deepak Gupta et.al(2020) developed a model to analyze steady state behavioral consisting of biserial and serial service channel with batch arrival take place at biserial service channels. Deepak Gupta(2021) et.al analyzed a model to find various queue characteristics containing biserial and parallel service channels with bulk arrival. N. Gupta (2022) et.al studied a model containing two service channels linked with common server with bulk arrival to find different queue characteristics. Heng Qing Ye (2023) et.al develop a model to establish the diffusion limit to optimize the expected queue length. JD Aparajitha, K Srinivasa Rao(2023)et.al. developed a model to analyze the parallel and series organization queueing model with time dependent facility. The present paper deals with a development of a model consisting of three servers s_1, s_2 and s_3 in which s_1 is connected in series with two parallel service channels s_2 and s_3 and this model is different from another models in the way that here arrival take place at single server instead of two or more server. Vandana Saini et.al(2023) developed a complex biserial queue network connected to a common server with feedback and batch arrival.

MODEL DESCRIPTION

The model consisting of three service channels s_1, s_2 and s_3 in which service channel s_2 and s_3 are parallel. The service channels s_2 consists of subservice channel s_{21}, s_{22} and service channel s_3 consist of subservice channel s_{31}, s_{32} . The service channel s_1 is linked in series with two parallel service channels s_2 and s_3 . The customers come in the front of service channel s_1 with poisson arrival rate λ_1 and after taking service will either go to service channel s_2 or s_3 with the probability α and β such that $\alpha + \beta = 1$. Now if the customer take service from service channel s_2 , further has two options i.e either will move to subservice channel s_{21} or s_{22} with the probability α_1, α_2 such that $\alpha_1 + \alpha_2 = 1$. Now if the customer take service from service channel s_3 , further has two options i.e either will move to subservice channel s_{31} or s_{32} with the probability β_1 and β_2 such that $\beta_1 + \beta_2 = 1$ and $\alpha\alpha_1 + \alpha\alpha_2 + \beta\beta_1 + \beta\beta_2 = 1$. After completion of service, customer leave the system.

Number of customers	q_1	q_2	q_3	q_4	q_5
Service Channels	s_1	s_{21}	s_{22}	s_{31}	s_{32}
Service rate	μ_1	μ_2	μ_3	μ_4	μ_5
Arrival rate	λ_1				
Probability of customer moving from one service channel to another service channel.	$s_1 \rightarrow s_2 \alpha$ $s_1 \rightarrow s_{21} \alpha_1$ $s_1 \rightarrow s_{22} \alpha_2$	$s_1 \rightarrow s_3 \beta$ $s_1 \rightarrow s_{31} \beta_1$ $s_1 \rightarrow s_{32} \beta_2$			

NOTATION MATHEMATICAL MODEL FORMULATION

Let us suppose that $P_{q_1, q_2, q_3, q_4, q_5}$ denote the joint probability of customers q_1, q_2, q_3, q_4, q_5 in front of the service channels $s_1, s_{21}, s_{22}, s_{31}, s_{32}$, respectively, where $q_1, q_2, q_3, q_4, q_5 \geq 0$.

The differential difference equation of queue network model in transient state is as follows:

For $q_1 > 0, q_2 > 0, q_3 > 0, q_4 > 0, q_5 > 0$





Neha Gupta et al.,

$$P_{q_1, q_2, q_3, q_4, q_5}(t) = -(\lambda_1 + \mu_1 + \mu_2 + \mu_3 + \mu_4 + \mu_5)P_{q_1, q_2, q_3, q_4, q_5}(t) + \lambda_1 P_{q_1-1, q_2, q_3, q_4, q_5}(t) + \mu_1 \alpha_1 P_{q_1+1, q_2-1, q_3, q_4, q_5}(t) + \mu_1 \alpha_2 P_{q_1+1, q_2, q_3-1, q_4, q_5}(t) + \mu_1 \beta_1 P_{q_1+1, q_2, q_3, q_4-1, q_5}(t) + \mu_1 \beta_2 P_{q_1+1, q_2, q_3, q_4, q_5-1}(t) + \mu_2 P_{q_1, q_2+1, q_3, q_4, q_5}(t) + \mu_3 P_{q_1, q_2, q_3+1, q_4, q_5}(t) + \mu_4 P_{q_1, q_2, q_3, q_4+1, q_5}(t) + \mu_5 P_{q_1, q_2, q_3, q_4, q_5+1}(t)$$

The differential difference equation of queue network model when t approaches to infinity is

For $q_1 > 0, q_2 > 0, q_3 > 0, q_4 > 0, q_5 > 0$

$$(\lambda_1 + \mu_1 + \mu_2 + \mu_3 + \mu_4 + \mu_5)P_{q_1, q_2, q_3, q_4, q_5} = \lambda_1 P_{q_1-1, q_2, q_3, q_4, q_5} + \mu_1 \alpha_1 P_{q_1+1, q_2-1, q_3, q_4, q_5} + \mu_1 \alpha_2 P_{q_1+1, q_2, q_3-1, q_4, q_5} + \mu_1 \beta_1 P_{q_1+1, q_2, q_3, q_4-1, q_5} + \mu_1 \beta_2 P_{q_1+1, q_2, q_3, q_4, q_5-1} + \mu_2 P_{q_1, q_2+1, q_3, q_4, q_5} + \mu_3 P_{q_1, q_2, q_3+1, q_4, q_5} + \mu_4 P_{q_1, q_2, q_3, q_4+1, q_5} + \mu_5 P_{q_1, q_2, q_3, q_4, q_5+1}$$

By taking into account all the possible combination of different values of q_1, q_2, q_3, q_4, q_5 ,

(32) equations are obtained.

In order to find the solution of System of steady state equations (1) to (32) we implement here generating function technique. The generating function is defined as:

$$H(X, Y, Z, R, S) = \sum_{q_1=0}^{\infty} \sum_{q_2=0}^{\infty} \sum_{q_3=0}^{\infty} \sum_{q_4=0}^{\infty} \sum_{q_5=0}^{\infty} P_{q_1, q_2, q_3, q_4, q_5} X^{q_1} Y^{q_2} Z^{q_3} R^{q_4} S^{q_5}$$

Also for solving we define partial generating function as

$$H_{q_2, q_3, q_4, q_5}(X) = \sum_{q_1=0}^{\infty} P_{q_1, q_2, q_3, q_4, q_5} X^{q_1}$$

$$H_{q_3, q_4, q_5}(X, Y) = \sum_{q_2=0}^{\infty} H_{q_2, q_3, q_4, q_5}(X) Y^{q_2}$$

$$H_{q_4, q_5}(X, Y, Z) = \sum_{q_3=0}^{\infty} H_{q_3, q_4, q_5}(X, Y) Z^{q_3}$$

$$H_{q_5}(X, Y, Z, R) = \sum_{q_4=0}^{\infty} H_{q_4, q_5}(X, Y, Z) R^{q_4}$$

$$H(X, Y, Z, R, S) = \sum_{q_5=0}^{\infty} H_{q_5}(X, Y, Z, R) S^{q_5} \tag{A'}$$

After simplifying equations(1-48) by using generating function technique and law of calculus ,we get

$$H(X, Y, Z, R, S) = \frac{\mu_1(1 - \frac{Y\alpha_1}{X} - \frac{\alpha_2 Z}{X} - \frac{\beta_1 R}{X} - \frac{\beta_2 S}{X})H_0(Y, Z, R, S) + \mu_2(1 - \frac{S}{Y})H_0(X, Z, R, S) + \mu_3(1 - \frac{S}{Z})H_0(X, Y, R, S) + \mu_4(1 - \frac{S}{R})H_0(X, Y, Z, S) + \mu_5(1 - \frac{1}{S})H_0(X, Y, Z, R)}{\lambda_1((1-X)^{b_1}) + \mu_1((1 - \frac{Y\alpha_1}{X} - \frac{\alpha_2 Z}{X} - \frac{\beta_1 R}{X} - \frac{\beta_2 S}{X}) + \mu_2(1 - \frac{S}{Y}) + \mu_3(1 - \frac{S}{Z}) + \mu_4(1 - \frac{S}{R}) + \mu_5(1 - \frac{1}{S}))} \tag{I}$$

$X=Y=Z=R=S=1$ and $H(1,1,1,1,1)=1$

For convenience we define: $H_0(Y, Z, R, S) = H_1$;

$H_0(X, Z, R, S) = H_2$

$H_0(X, Y, R, S) = H_3$

$H_0(X, Y, Z, S) = H_4$;

$H_0(X, Y, Z, R) = H_5$;

The equation (I) reduces to determinant form $\frac{0}{0}$, therefore by using L'Hospital rule for limits the following results are obtained from equation (I) and by using the value of H_1, H_2, H_3, H_4, H_5 .

- a) When $Y=Z=R=S=1$ and taking X approaches to 1, we get $\mu_1 H_1 = -\lambda_1 + \mu_1$
- b) When $X=Z=R=S=1$ and taking Y approaches to 1, we get $\mu_2 H_2 - \mu_1 \alpha_1 H_1 = \mu_2 - \mu_1 \alpha_1$
- c) When $Y=X=R=S=1$ and taking Z approaches to 1, we get $\mu_3 H_3 - \mu_1 \alpha_2 H_1 = \mu_3 - \mu_1 \alpha_2$
- d) When $Y=X=Z=S=1$ and taking R approaches to 1, we get $\mu_4 H_4 - \mu_1 \beta_1 H_1 = \mu_4 - \mu_1 \beta_1$
- e) When $Y=X=Z=R=1$ and taking S approaches to 1, we get $\mu_5 H_5 - \mu_1 \beta_2 H_1 = \mu_5 - \mu_1 \beta_2$ on solving these equations for H_1, H_2, H_3, H_4, H_5 , we get





Neha Gupta et al.,

$$H_1 = 1 - \frac{\lambda_1}{\mu_1} = 1 - \rho_1$$

$$H_2 = 1 - \frac{\lambda_1}{\mu_2} \alpha \alpha_1 = 1 - \rho_2$$

$$H_3 = 1 - \frac{\lambda_1}{\mu_3} \alpha \alpha_2 = 1 - \rho_3$$

$$H_4 = 1 - \frac{\lambda_1}{\mu_4} \beta \beta_1 = 1 - \rho_4$$

$$H_5 = 1 - \frac{\lambda_1}{\mu_5} \beta \beta_2 = 1 - \rho_5$$

Therefore,

$$P_{c_1, c_2, c_3, c_4, c_5} = \rho_1^{n_1} \rho_2^{n_2} \rho_3^{n_3} \rho_4^{n_4} \rho_5^{n_5} (1 - \rho_1)(1 - \rho_2)(1 - \rho_3)(1 - \rho_4)(1 - \rho_5)$$

The solution in steady state exist if $\rho_1 \rho_2 \rho_3 \rho_4 \rho_5 < 1$ is satisfied.

QUEUE CHARACTERISTICS

Mean queue length $L = L_{q_1} + L_{q_2} + L_{q_3} + L_{q_4} + L_{q_5}$

Where

$$L_{q_1} = \frac{\rho_1}{1 - \rho_1} = \frac{\lambda_1}{\mu_1 - \lambda_1}$$

$$L_{q_2} = \frac{\rho_2}{1 - \rho_2} = \frac{\lambda_1 \alpha \alpha_1}{\mu_2 - \lambda_1 \alpha \alpha_1}$$

$$L_{q_3} = \frac{\rho_3}{1 - \rho_3} = \frac{\lambda_1 \alpha \alpha_2}{\mu_3 - \lambda_1 \alpha \alpha_2}$$

$$L_{q_4} = \frac{\rho_4}{1 - \rho_4} = \frac{\lambda_1 \beta \beta_1}{\mu_4 - \lambda_1 \beta \beta_1}$$

$$L_{q_5} = \frac{\rho_5}{1 - \rho_5} = \frac{\lambda_1 \beta \beta_2}{\mu_5 - \lambda_1 \beta \beta_2}$$

The average no. of customers (mean queue length) is given by

$$L = L_{q_1} + L_{q_2} + L_{q_3} + L_{q_4} + L_{q_5}$$

$$= \frac{\lambda_1}{\mu_1 - \lambda_1} + \frac{\lambda_1 \alpha \alpha_1}{\mu_2 - \lambda_1 \alpha \alpha_1} + \frac{\lambda_1 \alpha \alpha_2}{\mu_3 - \lambda_1 \alpha \alpha_2} + \frac{\lambda_1 \beta \beta_1}{\mu_4 - \lambda_1 \beta \beta_1} + \frac{\lambda_1 \beta \beta_2}{\mu_5 - \lambda_1 \beta \beta_2}$$

Now, variance of queue

$$V = \frac{\rho_1}{(1 - \rho_1)^2} + \frac{\rho_2}{(1 - \rho_2)^2} + \frac{\rho_3}{(1 - \rho_3)^2} + \frac{\rho_4}{(1 - \rho_4)^2} + \frac{\rho_5}{(1 - \rho_5)^2}$$

$$= \frac{\lambda_1 \mu_1}{(\mu_1 - \lambda_1)^2} + \frac{\lambda_1 \alpha \alpha_1 \mu_2}{(\mu_2 - \lambda_1 \alpha \alpha_1)^2} + \frac{\lambda_1 \alpha \alpha_2 \mu_3}{(\mu_3 - \lambda_1 \alpha \alpha_2)^2} + \frac{\lambda_1 \beta \beta_1 \mu_4}{(\mu_4 - \lambda_1 \beta \beta_1)^2} + \frac{\lambda_1 \beta \beta_2 \mu_5}{(\mu_5 - \lambda_1 \beta \beta_2)^2}$$

NUMERICAL ILLUSTRATION

The numerical is carried out to test the efficiency of the algorithm

The numerical is carried out to test the efficiency of the algorithm

Sr.no.	Average service rate	Average arrival rate	Batch size	Probabilities
1	$\mu_1 = 18$	$\lambda_1 = 4$	$b_1 = 4$	$\alpha = 0.6$
2	$\mu_2 = 11$			$\beta = 0.4$
3	$\mu_3 = 20$			$\alpha_1 = 0.3$
4	$\mu_4 = 9$			$\beta_1 = 0.2$
5	$\mu_5 = 9$			$\alpha_2 = 0.7$
				$\beta_2 = 0.8$

Find average queue length, variance and waiting time for customers.

$$\rho_1 = \frac{\lambda_1}{\mu_1} = 0.2$$





Neha Gupta et al.,

$$Q_2 = \frac{\lambda_1}{\mu_2} \alpha \alpha_1 = \frac{4(0.18)}{11} = 4(0.016) = 0.064$$

$$Q_3 = \frac{\lambda_1}{\mu_3} \alpha \alpha_2 = \frac{4(0.42)}{20} = 4(0.021) = 0.084$$

$$Q_4 = \frac{\lambda_1}{\mu_4} \beta \beta_1 = \frac{4(0.08)}{9} = 4(0.008) = 0.0355$$

$$Q_5 = \frac{\lambda_1}{\mu_5} \beta \beta_2 = \frac{4(0.32)}{9} = 4(0.035) = 0.142 \text{ where } \alpha \alpha_1 + \alpha \alpha_2 + \beta \beta_1 + \beta \beta_2 = 1$$

Therefore on solving , we get mean queue length as :

$$\begin{aligned} L &= L_{q_1} + L_{q_2} + L_{q_3} + L_{q_4} + L_{q_5} \\ &= \frac{\lambda_1}{\mu_1 - \lambda_1} + \frac{\lambda_1 \alpha \alpha_1}{\mu_2 - \lambda_1 \alpha \alpha_1} + \frac{\lambda_1 \alpha \alpha_2}{\mu_3 - \lambda_1 \alpha \alpha_2} + \frac{\lambda_1 \beta \beta_1}{\mu_4 - \lambda_1 \beta \beta_1} + \frac{\lambda_1 \beta \beta_2}{\mu_5 - \lambda_1 \beta \beta_2} \\ &= 0.25 + 0.0695 + 0.0917 + 0.0362 + 0.165 \\ &= 0.6124 \end{aligned}$$

Now, variance of queue

$$\begin{aligned} V &= \frac{Q_1}{(1-Q_1)^2} + \frac{Q_2}{(1-Q_2)^2} + \frac{Q_3}{(1-Q_3)^2} + \frac{Q_4}{(1-Q_4)^2} + \frac{Q_5}{(1-Q_5)^2} \\ &= 0.3125 + 0.0743 + 0.1001 + 0.0371 + 0.192 \\ &= 0.7162 \end{aligned}$$

Average waiting time for customers

$$E(W) = \frac{L}{\lambda_1} = 0.1531$$

BEHAVIOUR ANALYSIS OF THE MODEL

In this section we will discuss the behavior of partial queue length and average queue length with the change of service rates and arrival rates in following manner:

- (i) Behaviour of $L, L_{q_1}, L_{q_2}, L_{q_3}, L_{q_4}, L_{q_5}$ for different values of λ_1 .
- (ii) Behaviour of $L, L_{q_1}, L_{q_2}, L_{q_3}, L_{q_4}, L_{q_5}$ for different values of $\mu_1, \mu_2, \mu_3, \mu_4, \mu_5$.
- (iii) Graphical analysis of partial queue lengths and mean queue length of the system for different λ_1 and $\mu_1, \mu_2, \mu_3, \mu_4, \mu_5$.

RESULT AND DISCUSSION

From Table 1 and figure 2 and we observe that as arrival rate at server s_1 increases ,the partial queue length increases slowly almost with same rate. From table 2 and figure 3,4,5,6,7 and 8 we observe that as service rate at server $s_{11}, s_{21}, s_{22}, s_{31}$ and s_{32} increases the mean queue length decreases slowly with constant rate.

CONCLUSION

The present paper develops a linkage between serial server and parallel services channels. While analyzing the model we observe that as arrival rate increases ,the partial queue length increases slowly but mean queue length increases fastly. Also as service rate increase the mean queue length decreases. This observation helps in manufacturing a system and to redesign the system to minimize the congestion and to increase customer satisfaction level.





Neha Gupta et al.,

REFERENCES

1. Jackson R.R.P(1954), "Random Queuing Process with Phase Service", J.Roy .Statist.Soc.B, Vol.18.
2. Finch, P.D. (1959) "Cyclic queues with feedback" J. Roy state soc, Ser.B Vol No.21, pp.153-157.
3. Maggu, (1970) ,"Phase type service queues with two servers in biseries", Journal of Operational Research Society of Japan, vol.13, no.
4. Mak, V. W., & Lundstrom, S. F. (1990). Predicting performance of parallel computations. IEEE Transactions on Parallel & Distributed Systems, 1(03), 257-270.
5. Kelly, T., Shen, K., Zhang, A., & Stewart, C. (2008, September). Operational analysis of parallel servers. In 2008 IEEE International Symposium on Modeling, Analysis and Simulation of Computers and Telecommunication Systems (pp. 1-10). IEEE.
6. Gupta, D., Sharma, S., & Gulati, N. (2011). On steady state behaviour of a network queuing model with biserial and parallel channels linked with a common server. Computer engineering and intelligent systems, 2(3), 11-22.
7. Suhasini, A. V. S., Rao, K. S., & Reddy, P. R. S. (2013). On parallel and series non homogeneous bulk arrival queuing model. Opsearch, 50, 521-547.
8. Gupta, R., & Gupta, D. (2020). Analysis of Steady State Behaviour of Biserial and Parallel Queue Network Model with Batch Arrival. Journal of Computational and Theoretical Nanoscience, 17(11), 5032-5036.
9. Gupta, D., & Gupta, R. (2021). Time independent analysis of biserial and parallel queuing models with batch arrival. Arya Bhatta Journal of Mathematics and Informatics, 13(1), 83-90.
10. Gupta, N., Gupta, D., & Gupta, R. (2022). Analysis of queue network system with bulk arrival. Arya Bhatta Journal of Mathematics and Informatics, 14(2), 209-216.
11. Ye, H. Q. (2023). Optimal Routing to Parallel Servers in Heavy Traffic. Operations Research
12. Aparajitha, J. D., & Srinivasa Rao, K. (2023). Parallel and series queueing model with state and time dependent service. OPSEARCH, 1-33.
13. Saini, V., Gupta, D., & Tripathi, A. K. (2023). Modeling and Analytical Study of a Complex Bi-Serial Queue Network Connected to a Common Server with Feedback and Batch Arrival. Arya Bhatta Journal of Mathematics and Informatics, 15(1), 67-78.

TABLE 1 : Partial queue length , mean queue length of the system with respect to λ_1

λ_1	L_{q_1}	L_{q_2}	L_{q_3}	L_{q_4}	L_{q_5}	L
4	0.28	0.0695	0.0917	0.0362	0.165	0.6424
4.2	0.298	0.072	0.096	0.0387	0.1723	0.677
4.4	0.315	0.075	0.1018	0.0407	0.1820	0.7145
4.6	0.333	0.0794	0.1069	0.0425	0.1918	0.7506
4.8	0.351	0.083	0.1120	0.044	0.2019	0.7919

TABLE 2 : Mean queue length of the system with respect to $\mu_1, \mu_2, \mu_3, \mu_4, \mu_5$ Type equation here.

μ_1	L	μ_2	L	μ_3	L	μ_4	L	μ_5	L
18	0.6424	11	0.6424	20	0.6424	9	0.6424	9	0.6424
18.5	0.6374	11.5	0.6389	20.5	0.6337	9.5	0.6403	9.5	0.6314
19	0.6274	12	0.6367	21	0.6367	10	0.6393	10	0.6234
19.5	0.6194	12.5	0.634	21.5	0.6352	10.5	0.6362	10.5	0.6144
20	0.6124	13	0.6309	22	0.6329	11	0.6352	11	0.6084





Neha Gupta et al.,

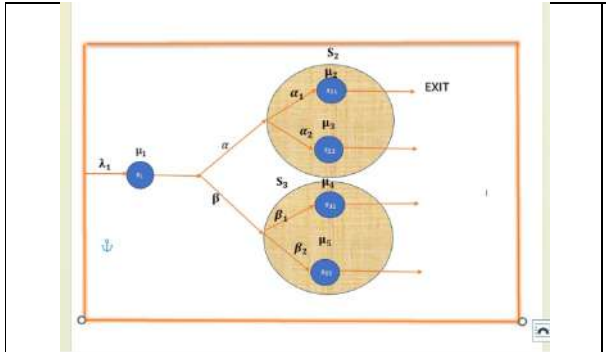


FIGURE 1 : QUEUE NETWORK MODEL

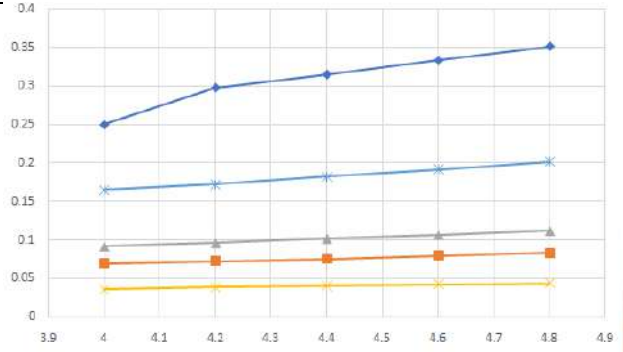


FIGURE 2 : $L_{q1}, L_{q2}, L_{q3}, L_{q4}, L_{q5}$ VS. λ_1

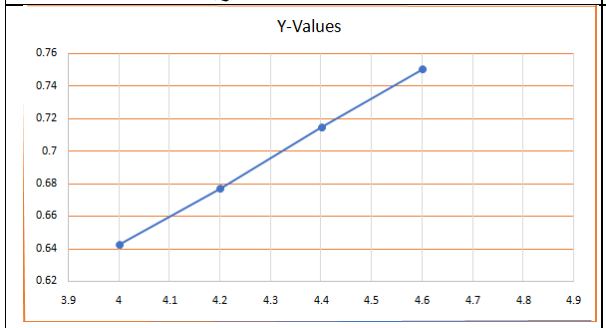


FIGURE 3: L VS. λ_1

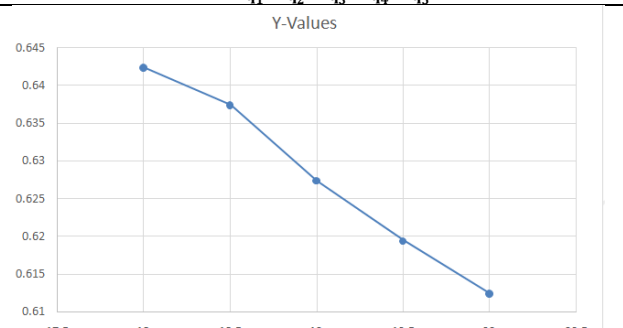


FIGURE 4 : L VS. μ_1

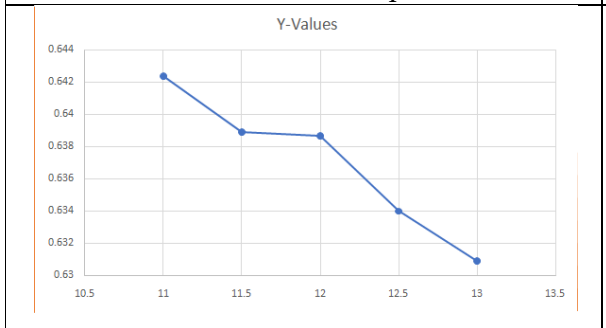


FIGURE 5: L VS. μ_2

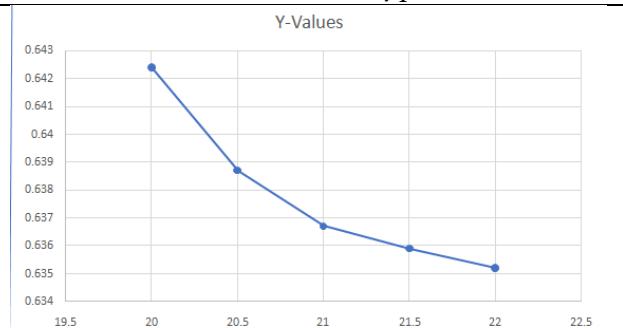


FIGURE 6: L VS μ_3

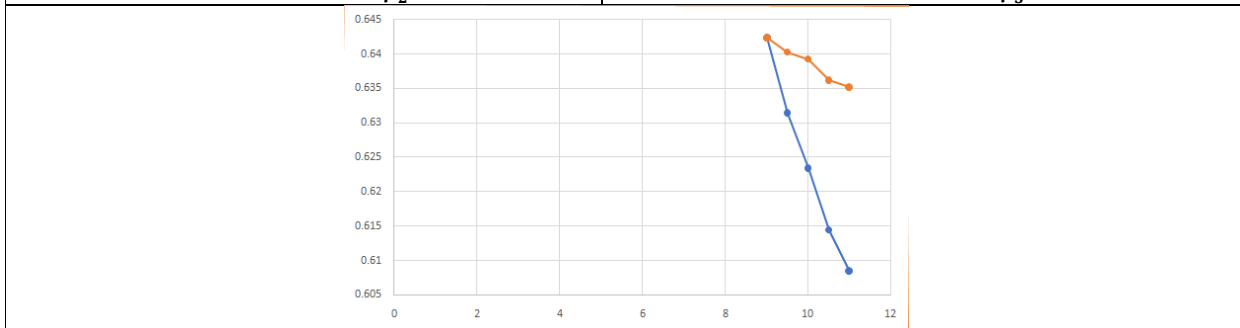


FIGURE 7: L VS. μ_4 and μ_5





Narcissism or Simply the Love of Self: A Social Problem of Personality

Rupali Yadav^{1*} and Kalpana Randhawa²

¹Rehabilitation Psychologist and Psychotherapist (RCI) Mental health and wellbeing support services
PhD Scholar: Clinical Psychology Department of Psychology Suresh Gyan Vihar University Jaipur,
Rajasthan, India.

²Assistant Professor, Department of Psychology, Suresh Gyan Vihar University Jaipur, Rajasthan, India.

Received: 30 Dec 2023

Revised: 09 Jan 2024

Accepted: 07 Jan 2024

*Address for Correspondence

Rupali Yadav

Rehabilitation Psychologist and Psychotherapist (RCI)

Mental health and wellbeing support services

PhD Scholar: Clinical Psychology

Department of Psychology

Suresh Gyan Vihar University

Jaipur, Rajasthan, India.

Email: Psychologistrupali@gmail.com



This is an Open Access Journal / article distributed under the terms of the **Creative Commons Attribution License** (CC BY-NC-ND 3.0) which permits unrestricted use, distribution, and reproduction in any medium, provided the original work is properly cited. All rights reserved.

ABSTRACT

Narcissism characterized by an inflated sense of self-importance, a need for admiration and a lack of empathy is a social problem of personality with wide-ranging implications. This paper provides an overview of narcissism, exploring different theoretical perspectives and models that explain its development and maintenance. It examines previous research on the prevalence and manifestations of narcissism in various social contexts, highlighting the impact on relationships and the dynamics of narcissistic abuse. The paper also discusses the broader societal implications of narcissism, such as its influence on social media, politics, leadership, and organizational environments. Interventions and prevention strategies at both individual and societal levels including therapeutic approaches, education and awareness campaigns. Ethical considerations and challenges in studying and addressing narcissism are acknowledged. The implications of narcissism as a social problem underscore the need for further research to fill gaps in understanding and develop effective interventions. Recognizing narcissism and implementing evidence-based strategies can promote healthier relationships, mental well-being and the cultivation of a more empathetic society.

Keywords: Narcissism, Social problem, Personality, Relationships, Narcissistic abuse, Societal implications, Social media, Leadership, Empathy, Ethical considerations





Rupali Yadav and Kalpana Randhawa

INTRODUCTION

Narcissism in psychological terms refers to a personality trait characterized by an excessive preoccupation with oneself, a grandiose sense of self-importance, a constant need for admiration, and a lack of empathy for others. While some level of self-love and self-esteem is healthy and important for personal well-being, narcissism becomes problematic when it reaches extreme levels and interferes with one's relationships and functioning in society. Narcissism can indeed be considered a social problem when it leads to negative consequences for individuals and those around them. Here are a few reasons why narcissism can be problematic:

1. **Interpersonal Difficulties:** Narcissists often have difficulty forming and maintaining healthy relationships. Their self-centeredness and lack of empathy can strain relationships, as they tend to exploit others for their own gain, lack genuine emotional connection, and engage in manipulative behaviours. They may exploit and manipulate others to fulfil their own desires, resulting in strained and dysfunctional relationships.
2. **Lack of Empathy:** Narcissists typically have limited capacity for empathy, making it challenging for them to understand and relate to the experiences and feelings of others. This can lead to a lack of compassion and disregard for the needs and well-being of those around them.
3. **Entitlement and Exploitation:** Narcissists often have a sense of entitlement, believing they deserve special treatment and attention. They may exploit others to fulfil their own needs, taking advantage of people's kindness, resources, or vulnerabilities. The excessive need for admiration and attention often leaves narcissists vulnerable to emotional distress. They rely heavily on external validation, and any perceived criticism or failure can lead to feelings of inadequacy and emotional instability. This can negatively impact their mental health and overall well-being.
4. **Disruptive Behaviour:** Extreme narcissistic traits can lead to disruptive behaviour in various social contexts. Narcissists may seek constant validation and attention, dominate conversations, or engage in attention-seeking behaviours that disrupt group dynamics. Narcissistic behaviours can disrupt social harmony and interpersonal dynamics. In group settings, narcissists may dominate conversations, seek constant attention and validation, and disregard the contributions and perspectives of others. This disrupts cooperation, collaboration, and the overall functioning of social groups.
5. **Impact on Mental Health:** Narcissism can also be detrimental to the mental health of individuals who possess narcissistic traits. They may experience difficulties in their personal and professional lives, leading to chronic stress, dissatisfaction, and potentially other mental health issues.
6. It's worth noting that not all individuals who display some narcissistic traits meet the criteria for Narcissistic Personality Disorder (NPD), which is a diagnosed mental health condition. However, when narcissistic traits become pervasive, persistent, and significantly impair an individual's functioning, they may warrant clinical attention.
7. **Disruption of Social Harmony:** Addressing the social problem of narcissism involves promoting empathy, emotional intelligence, and healthy self-esteem in society. Encouraging genuine connections, fostering understanding, and promoting the importance of empathy and compassion can help mitigate the negative impact of narcissism on individuals and communities. Narcissistic behaviours can disrupt social harmony and interpersonal dynamics. In group settings, narcissists may dominate conversations, seek constant attention and validation, and disregard the contributions and perspectives of others. This disrupts cooperation, collaboration, and the overall functioning of social groups.
8. **Impact on Emotional Well-being :** Narcissists may exploit and manipulate others to fulfil their own desires. They often seek out relationships or positions that provide them with status, power, or resources, disregarding the well-being of those they interact with. This can lead to a breakdown of trust and integrity within social contexts.
9. **Societal Institutions:** Narcissistic traits can also have implications for societal institutions such as the workplace, education, and politics. In these settings, narcissistic individuals may prioritize personal gain over collective goals, engage in self-promotion and self-aggrandizement, and engage in unethical or harmful behaviours to maintain their inflated self-image.



**Rupali Yadav and Kalpana Randhawa**

The relevance of narcissism as a social problem lies in its impact on interpersonal relationships, societal dynamics and overall well-being. Understanding and addressing narcissism as a social problem is crucial for promoting healthy interpersonal relationships, fostering cooperation, and maintaining social harmony. It involves promoting empathy, emotional intelligence and self-awareness in individuals as well as developing interventions and strategies that mitigate the negative impact of narcissistic behaviours on both individuals and society as a whole.

Objective of the study

The objective of this research paper is to examine the influence of narcissism as a social problem on interpersonal relationships and societal dynamics. It aims to explore the detrimental effects of narcissistic behaviours, including the disruption of social harmony, exploitation of others, and emotional consequences for both narcissistic individuals and those around them. Additionally, the paper seeks to identify and discuss potential interventions and strategies that can be implemented to address the negative consequences of narcissism, promote healthier relationships, and mitigate its impact on society.

Studying Narcissism and its impact on individuals and society is essential for several reasons:

1. **Social and Psychological Well-being:** Understanding narcissism helps us comprehend the factors that contribute to social dysfunction and interpersonal conflicts. By investigating its impact on individuals' emotional well-being, self-esteem and mental health, we can develop interventions to promote healthier relationships and overall social harmony.
2. **Relationship Dynamics:** Narcissistic behaviours can profoundly affect interpersonal relationships. By studying narcissism, we gain insights into how these behaviours disrupt communication, create power imbalances, and hinder the formation of genuine connections. This knowledge can assist in developing strategies for fostering healthier relationship dynamics.
3. **Work and Organizational Environments:** Narcissistic traits can have a significant influence on workplaces and organizational structures. Researching narcissism helps us understand its effects on teamwork, leadership dynamics, and organizational culture. By recognizing and addressing narcissistic tendencies, organizations can foster a more positive and productive work environment.
4. **Impact on Society:** Narcissism can extend beyond individual relationships and permeate society as a whole. Examining its influence on societal institutions, such as politics, media, and education, helps us understand how narcissistic behaviours impact collective decision-making, social cohesion, and the functioning of these institutions. This knowledge can inform interventions to promote ethical and responsible societal participation.
5. **Prevention and Intervention:** By studying narcissism, we can identify risk factors and early signs that may contribute to its development. This knowledge enables the development of prevention strategies and interventions aimed at mitigating the negative consequences of narcissism on individuals and society. It also helps mental health professionals, educators, and policymakers provide appropriate support and resources.
6. **Cultural and Societal Trends:** Societal trends, such as the rise of social media and celebrity culture, may contribute to the prevalence and reinforcement of narcissistic tendencies. Researching narcissism allows us to examine the complex interplay between cultural factors and individual psychology, enhancing our understanding of broader societal shifts and their impact on social dynamics.

In summary, studying narcissism and its impact on individuals and society is crucial for promoting healthier relationships, preventing social dysfunction, and fostering a more harmonious and empathetic society. By gaining insights into the causes and consequences of narcissistic behaviours, we can develop effective strategies to address this social problem and enhance overall well-being for individuals and communities.

Different theoretical perspectives and models of narcissism :

Various theoretical perspectives and models have been proposed to understand and explain narcissism. Here are some of the prominent ones:

1. **Psychodynamic Perspective:** The psychodynamic perspective, influenced by Freudian theory, views narcissism as stemming from early childhood experiences. According to this perspective, narcissism arises as a result of



**Rupali Yadav and Kalpana Randhawa**

- unresolved conflicts during the developmental stages, particularly related to issues of self-worth and inadequate parental nurturing. It suggests that narcissism develops as a defence mechanism to protect a fragile self-esteem.
2. **Object Relations Theory:** Object relations theory, building upon the psychodynamic perspective, emphasizes the role of early relationships in the development of narcissism. It suggests that narcissism arises when individuals have difficulty integrating a positive and realistic sense of self and others. Individuals with narcissistic traits may have experienced disruptions in early relationships, leading to an exaggerated focus on self and an inability to empathize with others.
 3. **Social-Cognitive Perspective:** The social-cognitive perspective emphasizes the role of cognitive processes and social influences in the development of narcissism. It suggests that narcissistic individuals have distorted self-perceptions and engage in cognitive biases, such as an inflated sense of self-worth and a tendency to seek validation from others. This perspective also highlights the influence of cultural and societal factors on the formation and reinforcement of narcissistic tendencies.
 4. **Trait Perspective:** The trait perspective focuses on identifying specific personality traits associated with narcissism. The most widely used model is the Five-Factor Model (FFM), which suggests that narcissism is related to high extraversion (particularly assertiveness and dominance), low agreeableness (lack of empathy and concern for others), and low emotional stability (high levels of emotional volatility and insecurity).
 5. **Vulnerability Model:** The vulnerability model of narcissism proposes that there are two subtypes of narcissism: grandiose and vulnerable. The grandiose subtype is characterized by an exaggerated sense of superiority and dominance, while the vulnerable subtype reflects underlying feelings of insecurity, fragility, and hypersensitivity to criticism. This model suggests that vulnerable narcissism may be associated with more negative outcomes, such as psychological distress and internalizing problems.
 6. **Adaptive and Maladaptive Models:** Some models differentiate between adaptive and maladaptive narcissism. Adaptive narcissism refers to healthy levels of self-esteem, self-confidence, and assertiveness, which are associated with positive outcomes. Maladaptive narcissism, on the other hand, describes the excessive and dysfunctional aspects of narcissism that are associated with negative consequences for both the individual and others.

It is important to note that these theoretical perspectives and models are not mutually exclusive, and researchers often integrate different approaches to gain a comprehensive understanding of narcissism. Each perspective provides a unique lens through which narcissism can be explored, shedding light on different aspects of its development, manifestations, and impact on individuals and society.

Previous studies on the prevalence and manifestations of narcissism in various social contexts:

Analysing previous studies on the prevalence and manifestations of narcissism in various social contexts reveals valuable insights into the extent and impact of narcissistic traits. Here are some key findings from previous research:

1. **Prevalence of Narcissism:** Studies have consistently found that narcissism exists on a continuum, ranging from normal levels of self-confidence and self-esteem to extreme narcissistic traits. Prevalence rates vary across populations, but research suggests that narcissistic traits are relatively common in Western societies.
2. **Gender Differences:** Research has indicated that men tend to display higher levels of grandiose narcissism, characterized by dominance and a desire for power, while women often exhibit higher levels of vulnerable narcissism, associated with feelings of insecurity and self-consciousness.
3. **Social Media and Narcissism:** Several studies have explored the relationship between social media use and narcissism. Findings suggest that individuals with higher narcissistic traits tend to engage in more self-promotion, seek validation through likes and comments, and exhibit higher levels of social media addiction.
4. **Narcissism in Romantic Relationships:** Research indicates that narcissistic individuals may struggle with forming and maintaining satisfying romantic relationships. They often prioritize their own needs, lack empathy for their partners, and engage in manipulative behaviours, leading to relationship dissatisfaction and instability.



**Rupali Yadav and Kalpana Randhawa**

5. Narcissism in the Workplace: Narcissistic traits can impact work environments. Studies have shown that narcissistic individuals are more likely to engage in self-promotion, exploit others for personal gain, and display aggressive or unethical behaviours. This can create a toxic work climate, hinder teamwork, and negatively impact job performance.
6. Narcissism and Leadership: Narcissism is often associated with leadership positions, as individuals with grandiose narcissistic traits may seek out positions of power and influence. However, research suggests that narcissistic leadership can be detrimental, leading to poor decision-making, lack of collaboration, and lower team performance.
7. Parenting and Narcissism: The role of parenting in the development of narcissism has been explored. Overly indulgent or neglectful parenting styles, where children are either excessively praised or neglected, have been associated with the development of narcissistic traits in individuals.
8. Cultural Differences: Studies examining narcissism across cultures have found variations in the prevalence and manifestation of narcissistic traits. Individualistic cultures tend to exhibit higher levels of grandiose narcissism, while collectivistic cultures may display more modesty and communal orientation.

It is important to note that these findings represent a broad overview of research on narcissism in various social contexts. The field of narcissism research is dynamic and further studies continue to shed light on the nuanced manifestations and implications of narcissistic traits in different social settings.

LITERATURE REVIEW

Campbell and Foster (2007): This study provides an overview of the narcissistic self, presenting the background of narcissism research, an extended agency model, and addressing ongoing controversies in the field. Miller and Campbell (2010): The researchers argue for the inclusion of a grandiose narcissism measure in the personality disorders section of the DSM, highlighting the importance of assessing narcissistic traits for diagnostic purposes. Dufner et al. (2013): This study explores the relationship between narcissism and short-term mate appeal, investigating whether narcissistic individuals are perceived as more attractive to potential partners. Vater et al. (2018): The researchers distinguish between narcissistic admiration and narcissistic rivalry, investigating the bright and dark sides of narcissism and their respective impacts on social dynamics.

Barry et al. (2007): The study focuses on the development and psychometric properties of the Child Psychopathy Scale, aiming to measure psychopathic traits in children, including aspects related to narcissism. Grijalva et al. (2015): This meta-analytic review examines gender differences in narcissism, summarizing findings from multiple studies and highlighting variations in narcissistic traits between males and females. Back et al. (2013): The study examines the distinction between narcissistic admiration and narcissistic rivalry, highlighting the positive and negative aspects of narcissism and their associations with psychological well-being.

Zeigler-Hill and Wallace (2011): This research explores the non-equivalence of narcissistic admiration (positive admiration from others) and narcissistic rivalry (competitive envy), and their associations with psychological health and functioning. Campbell and Buffardi (2008): The researchers investigate a two-factor model of the Narcissistic Personality Inventory (NPI), assessing the multidimensionality of narcissism and examining the factors related to grandiosity and entitlement. Ackerman et al. (2011): The study critically examines the Narcissistic Personality Inventory (NPI) and investigates what the inventory truly measures, highlighting the need for a more nuanced understanding of the construct and its assessment. Jonason et al. (2019): This research examines the psychosocial costs associated with the Dark Triad traits, including narcissism, in three countries. It explores the negative outcomes and consequences related to the Dark Triad personality traits. Pincus et al. (2009): The researchers develop and validate the Pathological Narcissism Inventory (PNI), a measurement tool specifically designed to assess pathological narcissism and its related features.



**Rupali Yadav and Kalpana Randhawa****Theoretical Framework**

One theoretical framework that explains the development and maintenance of narcissistic traits is the psychodynamic perspective which draws on Freudian theory and psychodynamic principles. According to this perspective, the development of narcissism is influenced by early childhood experiences and unresolved conflicts. The psychodynamic framework suggests that narcissistic traits may develop as a defence mechanism in response to certain experiences during the developmental stages, particularly related to issues of self-worth and inadequate parental nurturing. Here are the key components of the theoretical framework:

1. **Early Childhood Experiences:** The psychodynamic perspective posits that narcissism may arise from early childhood experiences, such as inconsistent or excessive parental admiration or neglect. These experiences can shape the individual's sense of self and self-worth.
2. **Narcissistic Injury:** Narcissistic traits can develop as a response to narcissistic injury, which refers to experiences that threaten or undermine the individual's self-esteem or self-image. These injuries can occur through perceived criticism, rejection, or experiences of shame or humiliation.
3. **Defence Mechanisms:** Narcissistic traits are seen as defence mechanisms that serve to protect the individual from the pain of narcissistic injury. For example, the development of grandiosity and feelings of superiority may help individuals defend against feelings of inferiority or inadequacy.
4. **Unconscious Processes:** The psychodynamic framework highlights the role of unconscious processes in the development and maintenance of narcissistic traits. Unconscious motivations and desires may drive the individual's need for admiration, attention, and validation.
5. **Object Relations:** Object relations theory, a component of the psychodynamic perspective, emphasizes the impact of early relationships on the development of narcissism. It suggests that disruptions or failures in early relationships may contribute to difficulties in forming healthy self-identity and interpersonal connections.

It is important to note that the psychodynamic perspective is one among several theoretical frameworks used to explain narcissism. Other perspectives, such as social-cognitive, evolutionary, or trait-based models, provide additional insights into the development and maintenance of narcissistic traits. These frameworks consider factors such as cognitive processes, social influences, cultural values, and individual differences. An integrative approach that considers multiple perspectives can provide a more comprehensive understanding of narcissism.

Prominent Theories

Three prominent theories that help explain narcissism are : psychoanalytic theory, social-cognitive theory, and evolutionary theory.

1. **Psychoanalytic Theory:** Psychoanalytic theory, influenced by the work of Sigmund Freud, provides insights into the development of narcissism. According to this theory, narcissism arises from unresolved conflicts during early childhood development, particularly related to the formation of self-identity and the development of the ego.

Some key points of the psychoanalytic perspective on narcissism include:

- **Narcissism as a Defence Mechanism:** Narcissism is viewed as a defence mechanism that individuals employ to protect themselves from underlying feelings of insecurity and vulnerability. The grandiose self-image and exaggerated sense of self-importance serve as a defence against feelings of inferiority and low self-esteem.
- **Narcissistic Supply:** Narcissists seek constant admiration and validation from others, known as narcissistic supply, to maintain their fragile self-esteem. They rely on external sources to affirm their self-worth and may react strongly to any perceived threats to their inflated self-image.





Rupali Yadav and Kalpana Randhawa

- Narcissistic Injury and Rage: Narcissistic individuals are highly sensitive to criticism or perceived threats to their self-esteem, and they may react with intense anger or rage when their grandiose self-image is challenged or undermined.
2. Social-Cognitive Theory: Social-cognitive theories of narcissism emphasize cognitive processes and social influences in the development and maintenance of narcissistic traits.

Key elements of the social-cognitive perspective include:

- Cognitive Biases: Narcissists often exhibit cognitive biases that enhance their self-perception, such as self-serving bias and selective attention to positive self-related information. They may have an inflated view of their abilities, achievements and attractiveness.
 - Social Reinforcement: Narcissistic behaviours can be reinforced by the social environment, particularly in contexts that prioritize individualism, competition, and self-promotion. Social media platforms, for example, can amplify narcissistic tendencies by providing opportunities for self-aggrandizement and seeking validation through likes, comments and followers.
 - Impaired Empathy: Narcissists often display a lack of empathy for others, focusing primarily on their own needs and desires. This diminished empathy contributes to difficulties in forming and maintaining healthy relationships.
3. Evolutionary Theory: Evolutionary theories propose that narcissistic traits may have adaptive functions in certain contexts. These theories suggest that narcissistic behaviours evolved as strategies to enhance reproductive success and survival.

Key aspects of evolutionary theory on narcissism include:

- Mate Attraction and Reproductive Success: Narcissistic traits, such as confidence, self-assuredness, and self-promotion, may be attractive to potential mates and enhance an individual's chances of reproductive success. Narcissistic individuals may display qualities that are valued in short-term mating contexts.
- Dominance and Status Seeking: Narcissistic individuals may strive for dominance and seek high social status, which historically provided access to resources, mating opportunities, and social influence. The pursuit of dominance and status can be driven by evolutionary pressures for reproductive advantage.
- Trade-Offs and Costs: Evolutionary theories also acknowledge potential costs associated with narcissism, such as impairments in empathy, relationship quality, and cooperation. While certain narcissistic traits may confer advantages in specific contexts, they can also have detrimental effects on social relationships and overall well-being.

It's important to note that these theories offer different perspectives on the development and maintenance of narcissism. Each theory provides insights into different aspects of narcissism, including its psychological origins, cognitive processes, social dynamics, and evolutionary roots. Combining these theories and considering their interactions can contribute to a more comprehensive understanding of narcissism.

Cultural and social factors

It plays a significant role in the emergence of narcissistic tendencies. These factors shape individuals' beliefs, values, and behaviours, influencing the development and expression of narcissism. Here are some ways in which cultural and social factors contribute to the emergence of narcissistic tendencies:

1. Individualistic Cultures: Cultures that emphasize individualism, such as Western cultures, tend to promote self-expression, personal achievement, and self-enhancement. In these cultures, there is a greater emphasis on standing out, being unique, and pursuing personal goals, which can contribute to the development of narcissistic tendencies.



**Rupali Yadav and Kalpana Randhawa**

2. **Celebrity Culture and Media Influence:** The rise of celebrity culture and the pervasive influence of media, including social media platforms, can contribute to the emergence of narcissistic tendencies. The constant exposure to carefully curated images of success, wealth, and beauty may lead individuals to prioritize self-presentation, self-promotion, and the pursuit of attention and admiration.
3. **Parenting and Child-Rearing Practices:** Parenting styles that overemphasize the importance of self-esteem and self-worth, while neglecting the development of empathy and perspective-taking, can contribute to the emergence of narcissistic tendencies. Overly indulgent parenting or excessively praising children for their accomplishments without teaching the value of empathy and consideration for others can foster an inflated sense of self-importance.
4. **Cultural Values of Materialism and Success:** Cultures that prioritize material wealth and external markers of success may encourage narcissistic tendencies. The pursuit of wealth, fame, and social status can lead individuals to focus on self-promotion, self-aggrandizement, and the acquisition of possessions as symbols of success and self-worth.
5. **Social Comparison and Competition:** In competitive social environments, individuals may feel the need to constantly compare themselves to others and strive for superiority. This competitive mindset can fuel narcissistic tendencies as individuals seek validation, recognition, and a sense of superiority over others.
6. **Technological Advancements and Social Media:** The advent of technology and social media platforms has provided new avenues for self-presentation, self-promotion, and seeking attention and validation. Social media platforms often encourage self-focused behaviours, such as sharing glamorous or exaggerated representations of one's life, accumulating followers, and seeking affirmation through likes and comments.

It is important to note that cultural and social factors interact with individual characteristics and other psychological processes, contributing to the emergence of narcissistic tendencies. Understanding these factors helps us comprehend the contextual influences that shape the development and expression of narcissism in different societies and social contexts.

Narcissism and Interpersonal Relationships:

Narcissism can have a significant impact on various types of relationships, including romantic, familial, and friendships. The presence of narcissistic traits can lead to unique challenges and consequences for individuals involved with narcissistic individuals. Additionally, the dynamics of narcissistic abuse can have detrimental effects on victims.

Let's explore these aspects in more detail:

1. Impact on Relationships:

- **Romantic Relationships:** Narcissistic individuals often prioritize their own needs, seek constant admiration, and lack empathy for their partners. They may engage in manipulative tactics, exploit their partners, and have difficulty maintaining healthy emotional connections. This can result in relationship dissatisfaction, emotional abuse, and frequent power struggles.
- **Familial Relationships:** In familial relationships, narcissistic individuals may exhibit self-centred behaviours, disregard the needs and boundaries of family members, and seek to maintain control and superiority. This can lead to strained relationships, emotional manipulation, and a lack of emotional support within the family unit.
- **Friendships:** Narcissistic individuals may form superficial friendships that primarily serve their own needs. They may seek friends who provide constant admiration, validation, or serve as an audience for their grandiose narratives. These friendships often lack mutuality and genuine emotional connection.

2. Challenges and Consequences:

- **Emotional Manipulation:** Narcissistic individuals often employ emotional manipulation tactics to control and exploit others. They may gaslight, belittle, or invalidate the emotions and experiences of their partners or loved ones, causing confusion, self-doubt, and emotional distress.



**Rupali Yadav and Kalpana Randhawa**

- Lack of Empathy: Narcissistic individuals struggle with empathizing with others and understanding their emotional experiences. This lack of empathy can lead to dismissive and insensitive responses to the emotions and needs of those around them, resulting in emotional neglect and strained relationships.
- Power Imbalance: Narcissistic individuals tend to seek power and control in relationships, leading to imbalanced dynamics. They may exert dominance, engage in manipulation, and devalue their partners or loved ones, perpetuating an unequal distribution of power and undermining the well-being of the other individuals involved.

3. Dynamics of Narcissistic Abuse:

- Narcissistic Abuse: Narcissistic abuse refers to the pattern of manipulative and exploitative behaviors employed by narcissistic individuals to control and dominate their victims. This can include emotional, psychological, and sometimes physical abuse. Victims often experience a cycle of idealization, devaluation, and discard, leaving them emotionally drained, traumatized, and with a diminished sense of self-worth.
- Psychological Effects: Victims of narcissistic abuse may experience a range of psychological effects, including depression, anxiety, post-traumatic stress disorder (PTSD), low self-esteem, and difficulty trusting others. The constant invalidation, gaslighting, and emotional manipulation inflicted by the narcissistic abuser can lead to significant psychological harm.
- Recovery and Healing: Recovering from narcissistic abuse often involves establishing boundaries, seeking support from trusted individuals or therapists, and rebuilding one's self-esteem and sense of identity. Healing from the effects of narcissistic abuse can be a long and challenging process, requiring self-care, self-reflection, and self-compassion.

It is important to recognize the signs of narcissistic behaviours and prioritize one's well-being in relationships. Seeking professional support and surrounding oneself with a strong support system can be crucial for individuals dealing with narcissistic individuals or recovering from narcissistic abuse.

Narcissism and Society

Narcissism has broader societal implications that extend beyond individual relationships. Its influence can be observed in various domains, including social media, politics, leadership and organizational environments. Let's explore these aspects in more detail:

1. Social Media:

- Self-Promotion and Validation: Social media platforms provide opportunities for narcissistic individuals to engage in self-promotion, seeking validation, admiration, and attention from others. The curated self-presentations and the pursuit of likes, followers, and comments can exacerbate narcissistic tendencies.
- Comparison and Envy: Social media can fuel narcissistic behaviors by fostering constant comparison to others. The highlight reel nature of social media can lead to feelings of envy, as individuals showcase their seemingly perfect lives, achievements, and possessions. This can contribute to a culture of materialism and self-centeredness.
- Reinforcement of Narcissistic Traits: Social media platforms can reinforce and amplify narcissistic traits, as individuals receive positive reinforcement and validation for attention-seeking behaviors. This can further solidify and intensify narcissistic tendencies, perpetuating a self-focused and self-enhancement-oriented mindset.

2. Politics and Leadership:

- Charismatic Leadership: Narcissistic traits can be associated with charismatic leadership styles, as narcissistic individuals may possess strong self-confidence, persuasive abilities, and a desire for power and influence. However, this form of leadership can be detrimental, as it often prioritizes self-interest over collective well-being and fails to consider diverse perspectives.



**Rupali Yadav and Kalpana Randhawa**

- **Authoritarianism and Manipulation:** Narcissistic leaders may exhibit authoritarian tendencies, seeking to dominate and control others. They may use manipulation, exploitation, and a disregard for democratic processes to maintain power and influence, potentially undermining democratic values and the well-being of society.
 - **Lack of Empathy and Collaboration:** Narcissistic leaders often lack empathy and struggle to collaborate effectively. They may prioritize their own interests, ignore the needs of others, and engage in adversarial approaches, which can hinder cooperation and problem-solving in societal contexts.
3. **Organizational Environments and Collective Well-being:**
- **Toxic Work Culture:** Narcissistic traits in organizational settings can contribute to toxic work environments. Narcissistic individuals may engage in self-promotion, exploit others, and prioritize personal gain over collective success. This can lead to a lack of collaboration, reduced morale, and decreased job satisfaction.
 - **Negative Effects on Team Dynamics:** Narcissistic behaviors can disrupt team dynamics, hindering effective communication, cooperation, and trust. The focus on personal achievements and self-enhancement can create unhealthy competition and undermine collective goals and well-being.
 - **Ethical Concerns:** Narcissistic individuals may engage in unethical behaviors, such as lying, manipulation, and exploiting others for personal gain. This can have damaging consequences for organizational ethics and the overall integrity of the workplace.

Addressing the societal implications of narcissism requires a collective effort, including promoting self-awareness, encouraging empathy and collaboration, and fostering a culture that values collective well-being over individualistic pursuits. Building ethical frameworks, promoting inclusive leadership styles, and encouraging responsible use of social media are important steps in mitigating the negative impact of narcissism on society.

Psychological and Emotional Consequences:

Individuals with narcissistic traits may experience various psychological and emotional consequences, which can impact their mental health, self-esteem, and overall well-being. Comorbidity with other mental health disorders such as depression or antisocial personality disorder is also commonly observed.

Let's explore these aspects in more detail:

1. Psychological and Emotional Effects:

- **Fragile Self-Esteem:** Despite their grandiose self-image, individuals with narcissistic traits often have fragile self-esteem that is vulnerable to external validation. They may rely heavily on others' admiration and approval to maintain their sense of self-worth, leading to feelings of insecurity and anxiety.
- **Emotional Vulnerability:** Underneath their defensive grandiosity, individuals with narcissistic traits can experience emotional vulnerability. They may struggle with regulating emotions and have difficulty tolerating criticism or rejection, which can lead to intense emotional reactions such as anger, shame, or feelings of emptiness.
- **Lack of Authentic Relationships:** Narcissistic individuals often have shallow and transactional relationships, lacking genuine emotional intimacy and connection. This can contribute to feelings of loneliness, as their relationships primarily serve to fulfil their own needs for admiration, rather than fostering mutual emotional support.

2. Impact on Mental Health and Self-Esteem:

- **Depression and Anxiety:** Narcissistic individuals may experience higher rates of depression and anxiety. The discrepancy between their grandiose self-image and the realities of life, along with difficulties in maintaining the desired level of admiration, can lead to depressive symptoms and increased vulnerability to anxiety.
- **Low Self-Esteem and Identity Issues:** Paradoxically, individuals with narcissistic traits may have low self-esteem at their core. Their self-worth is contingent on external validation, making them highly susceptible to fluctuations in self-esteem and experiencing a fragile sense of identity.



**Rupali Yadav and Kalpana Randhawa**

- **Dysfunctional Coping Mechanisms:** Narcissistic individuals may employ maladaptive coping mechanisms, such as denial, blaming others, or engaging in self-destructive behaviours, to protect their grandiose self-image and avoid confronting underlying insecurities or emotional pain.
3. **Comorbidity with Other Mental Health Disorders:**
- **Depression:** Narcissistic traits can coexist with depression, as the dissonance between their inflated self-image and the realities of life can lead to feelings of worthlessness, hopelessness, and loss of interest in previously enjoyed activities.
 - **Antisocial Personality Disorder:** Narcissistic traits can also be comorbid with antisocial personality disorder. The combination of grandiosity, lack of empathy, and disregard for social norms can contribute to a range of antisocial behaviours such as manipulation, exploitation, and a disregard for the rights of others.
 - **Borderline Personality Disorder:** Some individuals with narcissistic traits may also exhibit features of borderline personality disorder. This co-occurrence can manifest as unstable self-identity, emotional dysregulation, and intense fear of abandonment.

It's important to note that not all individuals with narcissistic traits will meet the criteria for a specific mental health diagnosis, but they may still experience significant psychological and emotional challenges. Seeking professional help, such as therapy or counselling, can be beneficial in addressing these issues and promoting healthier psychological functioning and well-being.

Intervention and Prevention Strategies:

Addressing narcissism at both individual and societal levels requires a multifaceted approach. Here are potential interventions and strategies that can be implemented:

1. Individual-Level Interventions:

- **Psychotherapy:** Therapeutic approaches, such as cognitive-behavioural therapy (CBT) and psychodynamic therapy, can be effective in treating narcissistic traits. CBT can help individuals identify and modify maladaptive thought patterns and behaviours, while psychodynamic therapy can explore underlying emotional conflicts and facilitate personal growth and self-awareness.
- **Empathy and Emotional Intelligence Training:** Individuals with narcissistic traits can benefit from interventions that enhance empathy and emotional intelligence. Training programs and interventions focused on perspective-taking, recognizing emotions, and understanding the impact of one's behaviour on others can promote healthier interpersonal relationships.
- **Self-Reflection and Self-Compassion:** Encouraging individuals with narcissistic traits to engage in self-reflection, introspection, and self-compassion can help foster a more realistic self-image, build self-esteem based on internal validation, and develop a genuine sense of empathy toward others.

2. Societal-Level Interventions:

- **Education and Awareness:** Promoting education and awareness about narcissism can help individuals recognize and understand narcissistic traits, both in themselves and others. Educational programs in schools, workplaces, and communities can provide information about healthy relationships, emotional intelligence, and the potential consequences of narcissistic behaviours.
- **Promoting Emotional Intelligence in Education:** Incorporating emotional intelligence training into educational curricula can help develop skills in self-awareness, self-regulation, empathy, and effective communication. These skills can foster healthier interpersonal dynamics and mitigate the development of narcissistic traits.
- **Media Literacy and Responsible Social Media Use:** Encouraging media literacy skills can help individuals critically evaluate media messages and reduce the impact of idealized portrayals on self-esteem. Promoting



**Rupali Yadav and Kalpana Randhawa**

responsible social media use, emphasizing authentic connections over self-promotion, and raising awareness about the potential negative consequences of excessive social media engagement can also be beneficial.

- **Fostering a Culture of Empathy and Collaboration:** Creating a societal culture that values empathy, collaboration, and mutual respect can help counteract narcissistic tendencies. This can involve promoting prosocial behaviours, encouraging cooperative problem-solving, and nurturing an environment that supports emotional well-being and positive interpersonal relationships.

It is important to note that addressing narcissism requires a comprehensive and long-term approach. Combining individual-level interventions with societal-level strategies can contribute to a healthier and more empathetic society. Collaboration among mental health professionals, educators, policymakers, and community leaders is crucial in implementing and sustaining effective interventions and prevention strategies.

Future Directions

While research on narcissism has advanced significantly, there are still gaps that warrant further exploration. Here are some areas for future study:

1. **Longitudinal Studies:** Conducting longitudinal research to examine the developmental trajectory of narcissism would provide valuable insights into its stability, change, and potential predictors over time. Longitudinal studies can shed light on the factors that contribute to the emergence and maintenance of narcissistic traits.
2. **Cultural and Cross-Cultural Perspectives:** Further investigation into the cultural and cross-cultural variations in narcissism is needed. Understanding how cultural values, norms, and societal contexts shape the expression and consequences of narcissism can enhance our understanding of this phenomenon.
3. **Comorbidity and Clinical Interventions:** Exploring the comorbidity of narcissism with other mental health disorders, such as depression, anxiety, or personality disorders, can help identify shared risk factors and inform targeted treatment approaches. Additionally, developing effective interventions specifically tailored for individuals with narcissistic traits is an important area for future research.
4. **Digital Age and Technology:** Given the pervasive influence of technology and social media, there is a need to investigate the implications of digital platforms on the development and expression of narcissism. Research could explore how social media use, online interactions, and virtual self-presentation contribute to narcissistic tendencies and their impact on individuals and society.
5. **Mechanisms and Neural Correlates:** Investigating the underlying mechanisms and neural correlates of narcissism can provide insights into the cognitive, affective, and neural processes associated with narcissistic traits. Understanding these mechanisms can help identify potential targets for intervention and inform treatment strategies.

Challenges and Ethical Considerations:

Studying and addressing narcissism present certain challenges and ethical considerations:

1. **Self-Reporting Bias:** Narcissistic individuals may be prone to self-enhancement bias, making it challenging to obtain accurate self-reports and objective data. Researchers must account for this bias when designing studies and interpreting results.
2. **Diagnostic Complexity:** Defining and diagnosing narcissism can be complex, as it encompasses a spectrum of traits and can be challenging to distinguish from other personality disorders. Developing reliable and valid assessment tools and diagnostic criteria is crucial for advancing research in this area.
3. **Potential Harm to Participants:** Studying narcissism, particularly in vulnerable populations, may involve exploring sensitive and potentially distressing topics. Researchers must ensure participant well-being, informed consent, and minimize any potential harm or distress caused by the research process.
4. **Confidentiality and Privacy:** Maintaining participant confidentiality and privacy is essential, particularly in studies that involve self-disclosure or sensitive information. Researchers must adhere to ethical guidelines and protect participant identities and data.





Rupali Yadav and Kalpana Randhawa

5. Stigma and Labelling: Research on narcissism should be conducted in a way that avoids stigmatizing individuals with narcissistic traits. Sensitivity to the potential impact of labelling and the public perception of narcissism is important to ensure ethical treatment of individuals involved in research and in the dissemination of findings. Addressing these challenges and ethical considerations requires researchers to prioritize participant well-being, maintain scientific rigor, and engage in responsible dissemination of findings to ensure the ethical advancement of knowledge in the field of narcissism.

CONCLUSION

In conclusion, this paper has provided an overview of narcissism as a social problem of personality. It discussed different theoretical perspectives and models of narcissism, analysed previous studies on the prevalence and manifestations of narcissism in various social contexts and reviewed recent research on the topic.

Key findings and arguments presented in the paper include:

1. Narcissism is a complex personality trait characterized by an inflated sense of self-importance, a need for admiration, and a lack of empathy.
2. Theoretical perspectives such as psychoanalytic, social-cognitive, and evolutionary theories offer insights into the development and maintenance of narcissistic traits.
3. Narcissism can have a significant impact on various types of relationships, including romantic, familial, and friendships, leading to challenges and consequences for individuals involved with narcissistic individuals.
4. The dynamics of narcissistic abuse can have detrimental effects on victims, including emotional distress, diminished self-worth, and post-traumatic symptoms.
5. Narcissism has broader societal implications, such as its influence on social media, politics, leadership, and organizational environments, which can affect collective well-being.
6. Interventions and prevention strategies at both individual and societal levels, such as therapy, empathy training, education, and promoting responsible social media use, can address narcissism and its impact.

The implications of narcissism as a social problem highlight the importance of understanding and addressing narcissistic traits for the well-being of individuals and society. Further research is needed to fill gaps in our understanding, including longitudinal studies, cross-cultural investigations, and exploring the impact of technology. It is crucial to develop effective interventions, considering the challenges and ethical considerations involved in studying and addressing narcissism.

Overall, recognizing narcissism as a social problem and implementing evidence-based strategies can contribute to healthier relationships, improved mental health, and the cultivation of a more empathetic and compassionate society. Continued research and intervention efforts are necessary to advance our knowledge, promote prevention and support individuals affected by narcissism.

REFERENCES

1. Campbell, W. K., & Foster, J. D. (2007). The Narcissistic Self: Background, an Extended Agency Model, and Ongoing Controversies. In R. W. Robins, R. C. Fraley, & R. F. Krueger (Eds.), *Handbook of Research Methods in Personality Psychology* (pp. 97-108). Guilford Press.
2. Miller, J. D., & Campbell, W. K. (2010). The Case for a Grandiose Narcissism Measure in the Personality Disorders Section of the DSM. *Clinical Psychology Review, 30*(6), 787-797.
3. Dufner, M., Rauthmann, J. F., Czarna, A. Z., & Denissen, J. J. A. (2013). Are Narcissists Sexy? Zeroing in on the Effect of Narcissism on Short-Term Mate Appeal. *Personality and Social Psychology Bulletin, 39*(7), 870-882.
4. Vater, A., Ritter, K., Schröder-Abé, M., Schütz, A., & Lammers, C. (2018). Narcissistic Admiration and Rivalry: Disentangling the Bright and Dark Sides of Narcissism. *Journal of Personality and Social Psychology, 114*(6), 1011-1031.





Rupali Yadav and Kalpana Randhawa

5. Barry, C. T., Frick, P. J., Adler, K. K., & Grafeman, S. J. (2007). The Child Psychopathy Scale: Measurement Development and Psychometric Properties. *Journal of Clinical Child and Adolescent Psychology*, 36(3), 389-404.
6. Grijalva, E., Newman, D. A., Tay, L., Donnellan, M. B., Harms, P. D., Robins, R. W., & Yan, T. (2015). Gender Differences in Narcissism: A Meta-analytic Review. *Psychological Bulletin*, 141(2), 261-310.
7. Back, M. D., Küfner, A. C. P., Dufner, M., Gerlach, T. M., Rauthmann, J. F., & Denissen, J. J. A. (2013). Narcissistic admiration and rivalry: Disentangling the bright and dark sides of narcissism. *Journal of Personality and Social Psychology*, 105(6), 1013-1037.
8. Zeigler-Hill, V., & Wallace, M. T. (2011). Narcissism and the Non-equivalence of Narcissistic Admiration and Rivalry: Associations with Psychological Health. *Journal of Research in Personality*, 45(5), 451-462.
9. Campbell, W. K., & Buffardi, L. E. (2008). The Narcissistic Personality Inventory: Testing a Two-Factor Model. *Journal of Research in Personality*, 42(6), 1397-1406.
10. Ackerman, R. A., Witt, E. A., Donnellan, M. B., Trzesniewski, K. H., Robins, R. W., & Kashy, D. A. (2011). What Does the Narcissistic Personality Inventory Really Measure? *Assessment*, 18(1), 67-87.
11. Jonason, P. K., Li, N. P., & Czarna, A. Z. (2019). Quick and Dirty: Some Psychosocial Costs Associated with the Dark Triad in Three Countries. *Evolutionary Psychological Science*, 5(3), 233-244.
12. Pincus, A. L., Ansell, E. B., Pimentel, C. A., Cain, N. M., Wright, A. G. C., & Levy, K. N. (2009). Initial Construction and Validation of the Pathological Narcissism Inventory. *Psychological Assessment*, 21(3), 365-379.





Generalization of λ - \mathcal{J} -Closed Sets

A. Jenifer Grena¹ and P. Periyasamy^{2*}

¹Research Scholar, “Reg. No: 18232102092014, Department of Mathematics, Kamaraj College, Thoothukudi (Affiliated to Manonmaniam Sundaranar University, Abishekapatti, Tirunelveli), Tamil Nadu, India.

²Assistant Professor, Department of Mathematics, Kamaraj College, Thoothukudi (Affiliated to Manonmaniam Sundaranar University, Abishekapatti, Tirunelveli) Tamil Nadu, India.

Received: 30 July 2023

Revised: 09 Nov 2023

Accepted: 22 Jan 2024

*Address for Correspondence

P. Periyasamy

Assistant Professor,

Department of Mathematics,

Kamaraj College, Thoothukudi (Affiliated to Manonmaniam Sundaranar University,

Abishekapatti, Tirunelveli) Tamil Nadu, India.

E-mail: periyasamyvpp@gmail.com.”



This is an Open Access Journal / article distributed under the terms of the **Creative Commons Attribution License** (CC BY-NC-ND 3.0) which permits unrestricted use, distribution, and reproduction in any medium, provided the original work is properly cited. All rights reserved.

ABSTRACT

This article introduces and explores the idea of generalized λ - \mathcal{J} -closed set and λ -generalized \mathcal{J} -closed sets using open sets and λ -open sets. Additionally, look at some of its fundamental characteristics and characterization in ideal topological spaces.

Keywords: ideal topological space, generalized λ - \mathcal{J} -closed, λ -generalized λ - \mathcal{J} -closed.

INTRODUCTION

In 1930 [7], [12] Kuratowski, vaidyananthasawamy was introduced by ideal topological spaces. A λ -set [9] M which the intersection of all open sets containing M . Caldas, Saied Jafari and Govindappa Navalagi [4] further studied the concept of λ -closed sets in topological spaces. In 2008 Caldas, M, S. Jafari and T. Noiri [4] introduced Λ -generalized closed sets ($\Lambda g, g\Lambda$) in topological spaces. Recently P. Periyasamy, A. Jenifer Grena [11] introduced the concept of λ - \mathcal{J} -closed sets in ideal topological spaces using λ -set and $*$ -closed set. This article's objective is to introduce and explore the idea of generalized λ - \mathcal{J} -closed sets and generalized λ - \mathcal{J} -open sets as a generalizations of λ - \mathcal{J} -closed sets.

Definition 1.1. (i) λ - \mathcal{J} - \mathcal{C} set [11] if $M = G \cap D$ where G is λ -set and D is $*$ -closed set in (X, τ, \mathcal{J}) . Its complement is λ - \mathcal{J} - \mathcal{O} set.

(ii) λ - \mathcal{J} -interior [11] of M if $\exists a \lambda$ - \mathcal{J} - (p) , \mathcal{O} such that $\mathcal{O} \subseteq M$.

Also λ - \mathcal{J} - (p) (resp. λ - \mathcal{J} - $\mathcal{C}(p)$) is the λ - \mathcal{J} - \mathcal{O} (resp. λ - \mathcal{J} - \mathcal{C}) sets containing p .





Jenifer Grena and Periyasamy

Definition 1.2.[11] Let M be a subset of an ITS (X, τ, \mathcal{J}) . If $\mathcal{O} \cap M \neq \emptyset$ for every $\lambda\text{-}\mathcal{J}\text{-}(\mathcal{p}), \mathcal{O}$ then \mathcal{p} is known as a $\lambda\text{-}\mathcal{J}\text{-}$ Limit point of M or $\lambda\text{-}\mathcal{J}\text{-LP}(M)$. $cl_{\lambda\text{-}\mathcal{J}}(M)$ is determined by the collection of all such points. That is $cl_{\lambda\text{-}\mathcal{J}}(M) = \{\mathcal{p} \in X / \mathcal{O} \cap M \neq \emptyset, \text{ for every } \lambda\text{-}\mathcal{J}\text{-}(\mathcal{p}), \mathcal{O}\}$.

Lemma 1.3. [11] For the subsets M, L and $M_t (t \in \mathcal{S})$ of an ITS (X, τ, \mathcal{J}) . Then,

- (i) $M \subseteq cl_{\lambda\text{-}\mathcal{J}}(M) \subseteq cl(M)$.
- (ii) $M \subseteq L$, then $cl_{\lambda\text{-}\mathcal{J}}(M) \subseteq cl_{\lambda\text{-}\mathcal{J}}(L)$.
- (iii) $cl_{\lambda\text{-}\mathcal{J}}(M) = \cap \{F \in \lambda\text{-}\mathcal{J}\text{-}\mathcal{C}(X, \tau, \mathcal{J}) / M \subseteq F\}$.
- (iv) If M_t is $\lambda\text{-}\mathcal{J}\text{-}\mathcal{C}$ set for each $t \in \mathcal{S}$, then $\cap_{t \in \mathcal{S}} M_t$ is $\lambda\text{-}\mathcal{J}\text{-}\mathcal{C}$ set.
- (v) If M_t is $\lambda\text{-}\mathcal{J}\text{-}\mathcal{O}$ set for each $t \in \mathcal{S}$, then $\cup_{t \in \mathcal{S}} M_t$ is $\lambda\text{-}\mathcal{J}\text{-}\mathcal{O}$ set.
- (vi) $cl_{\lambda\text{-}\mathcal{J}}(M)$ is $\lambda\text{-}\mathcal{J}\text{-}\mathcal{C}$ set.

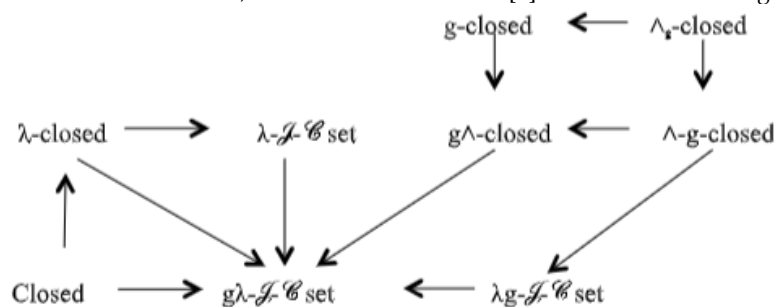
Generalized $\lambda\text{-}\mathcal{J}\text{-}\mathcal{C}$ Sets.

Definition 2.1. A subset M of an ideal topological spaces (briefly, ITS) (X, τ, \mathcal{J}) is called a generalized $\lambda\text{-}\mathcal{J}\text{-}$ closed (resp., $\lambda\text{-}$ generalized $\lambda\text{-}\mathcal{J}\text{-}$ closed) briefly $g\lambda\text{-}\mathcal{J}\text{-}\mathcal{C}$ set (resp., $\lambda g\text{-}\mathcal{J}\text{-}\mathcal{C}$ set) if $cl_{\lambda\text{-}\mathcal{J}}(M) \subseteq \mathcal{O}$, whenever $M \subseteq \mathcal{O}$ and \mathcal{O} is open (resp., \mathcal{O} is $\lambda\text{-}$ open) set.

Remark 2.2.(i) All $\lambda\text{-}\mathcal{J}\text{-}\mathcal{C}$ is $g\lambda\text{-}\mathcal{J}\text{-}\mathcal{C}$.

- (ii) Every $\lambda g\text{-}\mathcal{J}\text{-}\mathcal{C}$ is $g\lambda\text{-}\mathcal{J}\text{-}\mathcal{C}$.
- (iii) Every $\lambda\text{-}$ closed is $g\lambda\text{-}\mathcal{J}\text{-}\mathcal{C}$.
- (iv) Every closed is $g\lambda\text{-}\mathcal{J}\text{-}\mathcal{C}$.
- (v) Every $\lambda\text{-}$ closed is $\lambda\text{-}\mathcal{J}\text{-}\mathcal{C}$.
- (vi) Every $g\lambda\text{-}$ closed is $g\lambda\text{-}\mathcal{J}\text{-}\mathcal{C}$.
- (vii) Every $\wedge\text{-}g\text{-}$ closed is $\lambda g\text{-}\mathcal{J}\text{-}\mathcal{C}$.
- (viii) Every $g\text{-}$ closed is $g\lambda\text{-}\mathcal{J}\text{-}\mathcal{C}$.
- (ix) Every $\wedge_g\text{-}$ closed is $g\lambda\text{-}\mathcal{J}\text{-}\mathcal{C}$.
- (x) Every $\wedge_g\text{-}$ closed is $\lambda g\text{-}\mathcal{J}\text{-}\mathcal{C}$.

From the Definition 2.1, Remark 2.2 & Remark 2.2 [4] refers to the following Diagram.



The following Example 2.3, is an evidence of the lack of converse of Remark 2.2

Example 2.3. If $X = \{3,5,7,9\}$, $\tau = \{X, \emptyset, \{3\}, \{5\}, \{3,5\}, \{3,5,9\}\}$ and $\mathcal{J} = \{\emptyset, \{3\}\}$. Then $\lambda\text{-}\mathcal{J}\text{-}\mathcal{C}(X) = \{X, \emptyset, \{3\}, \{5\}, \{7\}, \{9\}, \{3,5\}, \{3,7\}, \{3,9\}, \{5,9\}, \{7,9\}, \{3,5,9\}, \{3,7,9\}, \{5,7,9\}\}$, $\lambda\text{-}\mathcal{C}(X) = \{X, \emptyset, \{3\}, \{5\}, \{7\}, \{3,5\}, \{5,9\}, \{7,9\}, \{3,7,9\}, \{3,7,9\}, \{3,7,9\}, \{5,7,9\}\}$, $\mathcal{C}(X) = \{X, \emptyset, \{5,7,9\}, \{3,7,9\}, \{7,9\}, \{7\}\}$, $g\text{-}\mathcal{C}(X) = \{X, \emptyset, \{7\}, \{7,9\}, \{3,7,9\}, \{5,7,9\}\}$, $\wedge\text{-}g\mathcal{C}(X) = \{X, \emptyset, \{3\}, \{5\}, \{7\}, \{9\}, \{3,5\}, \{5,9\}, \{3,9\}, \{7,9\}, \{3,7,9\}, \{3,5,9\}, \{5,7,9\}\}$, $\wedge_g\mathcal{C}(X) = \{X, \emptyset, \{3\}, \{5\}, \{7\}, \{3,5\}, \{7,9\}, \{3,5,9\}, \{3,7,9\}, \{5,7,9\}\}$, $g\wedge\mathcal{C}(X) = \{X, \emptyset, \{3\}, \{7\}, \{7,9\}, \{3,7,9\}, \{5,7,9\}\}$, $g\lambda\text{-}\mathcal{J}\text{-}\mathcal{C}(X) = \{X, \emptyset, \{3\}, \{7\}, \{5,7\}, \{3,7\}, \{7,9\}, \{3,7,9\}, \{5,7,9\}, \{3,5,7\}\}$ and $\lambda g\text{-}\mathcal{J}\text{-}\mathcal{C}(X) = \{X, \emptyset, \{3\}, \{5\}, \{7\}, \{9\}, \{3,5\}, \{3,9\}, \{5,9\}, \{7,9\}, \{3,7,9\}, \{3,5,9\}, \{5,7,9\}\}$. Here $\{5,7\}$ is $g\lambda\text{-}\mathcal{J}\text{-}\mathcal{C}$ but not $\lambda\text{-}\mathcal{J}\text{-}\mathcal{C}$ and $\lambda\text{-}$ closed, $\{3,5,7\}$ is $g\wedge$ closed but not $\lambda g\text{-}\mathcal{J}\text{-}\mathcal{C}$ set, $\{3,7,9\}$ is $g\lambda\text{-}\mathcal{J}\text{-}\mathcal{C}$ but not open set, $\{9\}$ is $\lambda\text{-}\mathcal{J}\text{-}\mathcal{C}$ but not $\lambda\text{-}$ closed set, $\{3,7\}$ is $g\lambda\text{-}$





Jenifer Grena and Periyasamy

J - \mathcal{C} but not $g\wedge$ -closed set, $\{3,9\}$ is λg - J - \mathcal{C} but not \wedge - g -closed set, $\{3,7\}$ is $g\lambda$ - J - \mathcal{C} but not g -closed set, $\{5,7\}$ is $g\lambda$ - J - \mathcal{C} but not $\wedge g$ -closed set and $\{3,7,9\}$ is λg - J - \mathcal{C} but not $\wedge g$ -closed set.

Theorem 2.4. The union of two $g\lambda$ - J - (resp., λg - J - \mathcal{C}) sets is $g\lambda$ - J - \mathcal{C} (resp., λg - J - \mathcal{C}) sets.

Proof. Let $M \cup L \subseteq \mathcal{O}$ then $M \subseteq \mathcal{O}$ & $L \subseteq \mathcal{O}$ where \mathcal{O} is open. Since M & L are $g\lambda$ - J - \mathcal{C} (resp., λg - J - \mathcal{C}) set then $cl_{\lambda-J}(M) \subseteq \mathcal{O}$ and $cl_{\lambda-J}(L) \subseteq \mathcal{O}$. Therefore $cl_{\lambda-J}(M \cup L) = cl_{\lambda-J}(M) \cup cl_{\lambda-J}(L) \subseteq \mathcal{O}$. Hence, $(M \cup L)$ is $g\lambda$ - J - \mathcal{C} (resp., λg - J - \mathcal{C}) set.

The intersection of two $g\lambda$ - J - \mathcal{C} sets may not be $g\lambda$ - J - \mathcal{C} . If $X = \{3, 5, 7, 9\}$, $\tau = \{X, \emptyset, \{3\}, \{5\}, \{3,5\}, \{3,5,9\}\}$ and $J = \{\emptyset, \{3\}\}$ then $g\lambda$ - J - \mathcal{C} sets are $\{X, \emptyset, \{3\}, \{7\}, \{3,7\}, \{7,9\}, \{3,5,7\}, \{3,7,9\}, \{5,7,9\}\}$ and λg - J - \mathcal{C} sets are $\{X, \emptyset, \{3\}, \{5\}, \{7\}, \{9\}, \{3,5\}, \{3,9\}, \{5,9\}, \{7,9\}, \{3,5,7\}, \{3,7,9\}, \{5,7,9\}\}$. Let $M = \{5,7,9\}$ and $L = \{3,5,7\}$ are two $g\lambda$ - J - \mathcal{C} set then $M \cap L = \{5,7\}$ is not a $g\lambda$ - J - \mathcal{C} set. If $M = \{3,7,9\}$ and $L = \{3,5,7\}$ are two λg - J - \mathcal{C} set then $M \cap L = \{3,7\}$ is not λg - J - \mathcal{C} set.

Theorem 2.5. In an ITS $M \subseteq X$. Then $cl_{\lambda-J}(M) = \{p \in X / \mathcal{O} \cap M \neq \emptyset, \text{ for every } \lambda$ - J - $\mathcal{O}\}$ is closed.

Proof. Let $p \in cl_{\lambda-J}(M)$ such that $\mathcal{O} \cap cl_{\lambda-J}(M) \neq \emptyset$ for every open set \mathcal{O} containing p . Then $q \in \mathcal{O} \cap cl_{\lambda-J}(M)$. Therefore, $q \in \mathcal{O}$ and $q \in cl_{\lambda-J}(M)$. Since $\mathcal{O} \cap M \neq \emptyset$ where \mathcal{O} is λ - J - \mathcal{O} set, $q \in cl_{\lambda-J}(M)$. Therefore $cl_{\lambda-J}(M) \subseteq cl_{\lambda-J}(M)$. Let $p \in cl_{\lambda-J}(M)$. Then $\mathcal{O} \cap M \neq \emptyset$ for every λ - J - \mathcal{O} . Therefore $\mathcal{O} \cap cl_{\lambda-J}(M) \neq \emptyset$, for every open set \mathcal{O} containing p . Hence $cl_{\lambda-J}(M) \subseteq cl_{\lambda-J}(M)$.

Theorem 2.6. A subset M of an ITS is $g\lambda$ - J - \mathcal{C} set iff \emptyset is the only closed set $incl_{\lambda-J}(M) - M$.

Proof. Necessity condition: Assume that M is $g\lambda$ - J - \mathcal{C} set. Let L be a closed subset of $incl_{\lambda-J}(M) - M$. Then $M \subseteq L^c$. Since M is $g\lambda$ - J - \mathcal{C} set, we have $cl_{\lambda-J}(M) \subseteq L^c$. Consequently, $L \subseteq [cl_{\lambda-J}(M)]^c$. Therefore, $M \subseteq cl_{\lambda-J}(M) \cap [cl_{\lambda-J}(M)]^c = \emptyset$. Hence, $L = \emptyset$.

Sufficiency condition: Assume that \emptyset is the only closed set $incl_{\lambda-J}(M) - M$. Since $M \subseteq \mathcal{O}$ and \mathcal{O} be open set. If $cl_{\lambda-J}(M) \not\subseteq \mathcal{O}$, then $cl_{\lambda-J}(M) \cap \mathcal{O}^c$ is a nonempty closed subset of $incl_{\lambda-J}(M) - M$. Hence M is $g\lambda$ - J - \mathcal{C} set.

Corollary 2.7. A subset M of an ITS is λg - J - \mathcal{C} set iff \emptyset is the only closed set $incl_{\lambda}(M) - M$.

Theorem 2.8. For the subsets M and L of an ITS (X, τ, J) . If M is $g\lambda$ - J - \mathcal{C} set and $M \subseteq L \subseteq cl_{\lambda-J}(M)$, then L is $g\lambda$ - J - \mathcal{C} set.

Proof. Let $M \subseteq L$. Then $cl_{\lambda-J}(L) \subseteq cl_{\lambda-J}(M)$. Hence $cl_{\lambda-J}(L) - L \subseteq cl_{\lambda-J}(M) - M$. By Theorem 2.6, \emptyset is the only closed set $incl_{\lambda-J}(L) - L$. Therefore, again by Theorem 2.6, L is $g\lambda$ - J - \mathcal{C} set.

Theorem 2.9. A subset M of an ITS is open set (resp., λ -open) and $g\lambda$ - J - (resp., λg - J - \mathcal{C}) then M is λ - J - \mathcal{C} set.

Proof. Since M is open set (resp., λ -open) and $g\lambda$ - J - \mathcal{C} set (resp., λg - J - \mathcal{C} set), $cl_{\lambda-J}(M) \subseteq M$ and hence M is λ - J - \mathcal{C} set.

Theorem 2.10. In an ITS. For each $p \in X$, either $\{p\}$ is $g\lambda$ - J - (resp., λg - J - \mathcal{C}) set or λ - J - \mathcal{C} .

Proof. Suppose X is the only λ - J - \mathcal{O} set such that $\{p\} \subseteq X$. If $\{p\}$ is not λ - J - \mathcal{C} set. Therefore, $cl_{\lambda-J}(\{p\}^c) \subseteq X$ and so $\{p\}^c$ is $g\lambda$ - J - \mathcal{C} (resp., λg - J - \mathcal{C}) set.

A subset M of an ITS is said to be λ - J - \mathcal{O} set and its complement is $g\lambda$ - J - \mathcal{C} . It is clear that, every open set in X is $g\lambda$ - J - \mathcal{O} in X but not conversely. If $X = \{3, 5, 7, 9\}$, $\tau = \{X, \emptyset, \{3\}, \{5\}, \{3,5\}, \{3,5,9\}\}$ and $J = \{\emptyset, \{3\}\}$. Then λ - J - \mathcal{O} sets are $\{X, \emptyset, \{3\}, \{5\}, \{7\}, \{3,5\}, \{3,7\}, \{5,7\}, \{5,9\}, \{7,9\}, \{3,5,7\}, \{3,5,9\}, \{3,7,9\}, \{5,7,9\}\}$. If $M = \{7\}$ is λ - J - \mathcal{O} but not open set.

Theorem 2.11. An ITS $g\lambda$ - J - \mathcal{O} in X iff $F \subseteq int_{\lambda}(M)$ whenever F is closed in X and $F \subseteq M$.

Proof. Assume that $F \subseteq int_{\lambda}(M)$ whenever F is closed and $F \subseteq M$. $M^c \subseteq F^c$, where F^c is open. Since $(int_{\lambda}(M))^c \subseteq F^c$, $cl_{\lambda-J}(M^c) \subseteq F^c$. Hence M^c is $g\lambda$ - J - \mathcal{C} set. Hence M is $g\lambda$ - J - \mathcal{O} set. Conversely, Let M be $g\lambda$ - J - \mathcal{O} set. Then M^c is $g\lambda$ - J - \mathcal{C} set. Also let F be a closed set contained in M . Then F^c is open. Thus $M^c \subseteq F^c$, $cl_{\lambda-J}(M^c) \subseteq F^c$. This implies that $F \subseteq (cl_{\lambda-J}(M^c))^c = int_{\lambda}(M)$. Hence $F \subseteq int_{\lambda}(M)$.

Theorem 2.12. A subset M of an ITS is $g\lambda$ - J - \mathcal{O} set then $\mathcal{O} = X$, whenever \mathcal{O} is open and $int_{\lambda}(M) \cup M^c \subseteq \mathcal{O}$.

Proof. Let M be a $g\lambda$ - J - \mathcal{O} and \mathcal{O} is open set, $int_{\lambda}(M) \cup M^c \subseteq \mathcal{O}$. Then $\mathcal{O}^c \subseteq (int_{\lambda}(M))^c \cap (M^c)^c = (int_{\lambda}(M))^c - M^c = cl_{\lambda-J}(M^c) - M^c$. Since M^c is $g\lambda$ - J - \mathcal{C} set, $\mathcal{O}^c = \emptyset$, by Theorem 2.6. Therefore, $X = \mathcal{O}$.





Jenifer Grena and Periyasamy

Theorem 2.13. For the subset M and L of an ITS (X, τ, J) . If $\text{int}_\lambda(M) \subseteq L \subseteq M$ and M is $g\lambda$ - J - \mathcal{O} in X , then L is $g\lambda$ - J - \mathcal{O} in X .

Proof. Suppose that $\text{int}_\lambda(M) \subseteq L \subseteq M$ and M is $g\lambda$ - J - \mathcal{O} in X . Then $M^c \subseteq L^c \subseteq \text{cl}_\lambda(M^c)$ and M^c is $g\lambda$ - J - \mathcal{C} . By Theorem 2.8, L is $g\lambda$ - J - \mathcal{O} in X .

Theorem 2.14. A subset M of an ITS is $g\lambda$ - J - \mathcal{C} iff $\text{cl}_\lambda(M) - M$ is $g\lambda$ - J - \mathcal{O} in X .

Proof. Necessity: Assume that M is $g\lambda$ - J - \mathcal{C} set. Let $F \subseteq \text{cl}_\lambda(M) - M$ where F is closed. By Theorem 2.6, $F = \emptyset$. Therefore $F \subseteq \text{int}_\lambda(\text{cl}_\lambda(M) - M)$ and by Theorem 2.11, $\text{cl}_\lambda(M) - M$ is $g\lambda$ - J - \mathcal{O} in X .

Sufficiency: Let $M \subseteq \mathcal{O}$ where \mathcal{O} is a open set. Then $\text{cl}_\lambda(M) \cap \mathcal{O}^c = \text{cl}_{\lambda-J}(M) - M$. Since $\text{cl}_{\lambda-J}(M) \cap \mathcal{O}^c$ is closed set and $\text{cl}_{\lambda-J}(M) - M$ is $g\lambda$ - J - \mathcal{O} set, we have $\text{cl}_{\lambda-J}(M) \cap \mathcal{O}^c \subseteq \text{int}_{\lambda-J}(\text{cl}_{\lambda-J}(M) - M) = \emptyset$. Hence M is $g\lambda$ - J - \mathcal{C} set.

Theorem 2.15. In an ITS (X, τ, J) , then the statements given below are equivalent $M \subseteq X$.

(i) M is $g\lambda$ - J - \mathcal{C} set.

(ii) \emptyset is the only closed set in $\text{cl}_\lambda(M) - M$.

(iii) $\text{cl}_\lambda(M) - M$ is $g\lambda$ - J - \mathcal{O} set.

Proof. This follows from Theorem 2.6 & 2.14.

Theorem 2.16. A subset M of an ITS is $g\lambda$ - J - \mathcal{C} set then $\text{cl}(\{p\}) \cap M \neq \emptyset$ for every $p \in \text{cl}_{\lambda-J}(M)$.

Proof. Suppose that $\text{cl}(\{p\}) \cap M = \emptyset$ for some $p \in \text{cl}_{\lambda-J}(M)$. Then $X - \text{cl}(\{p\})$ is an open set containing M . Moreover, $p \in \text{cl}_\lambda(M) - (X - \text{cl}(\{p\}))$. Hence $\text{cl}_\lambda(M) \not\subseteq X - \text{cl}(\{p\})$. Therefore, M is not $g\lambda$ - J - \mathcal{C} set.

Theorem 2.17. A subset M of an ITS is $g\lambda$ - J - \mathcal{C} set if $M \subseteq Y \subseteq X$ then M is $g\lambda$ - J - \mathcal{C} relative to Y .

Proof. Given that $M \subseteq Y \subseteq X$ & M is $g\lambda$ - J - \mathcal{C} set in X . Assume that $M \subseteq Y \cap \mathcal{O}$, where \mathcal{O} is open. Since M is $g\lambda$ - J - \mathcal{C} , $M \subseteq \mathcal{O}$. This implies $\text{cl}_\lambda(M) \subseteq \mathcal{O}$. It follows that $Y \cap \text{cl}_\lambda(M) \subseteq Y \cap \mathcal{O}$. Hence M is $g\lambda$ - J - \mathcal{C} relative to Y .

REFERENCES

1. Arenas. F. G, J. Dontchev, M. Ganster, On λ -sets and Dual Generalized Continuity, **Q & A Gen. Topology**, 15, 3-13, 1997.
2. Caldas, Saied Jafari and Govindappa Navalagi, "More on λ -closed Sets in Ideal Topological Spaces., Revisit Columbian de Mathematics Volume 41(2007)2, Paginas 355-369.
3. Caldas, M., And Jafari, S. On Some Low Separation Axioms Via λ -open and λ -closure Operator. *Rend. Circ. Mat. Di Palermo* 54, 2(2005), 195-208.
4. Caldas M, S. Jafari and T. Noiri, On Λ -Generalized Closed Sets in topological spaces, *Acta. Math. Hunger.*, 118(4)(2008), 337-343.
5. Ganster and I. L. Reilly, Locally Closed sets and LC-Continuous functions, *International J. Math. Sci.*, 12(1989), 417-424.
6. Jankovic. D and T. R. Hamlett, New topologies from old via ideals, *Amer. Monthly*, 97(4)(1990), 295-310.
7. Kuratowski. K, *Topology*, Vol. 1. New York. Academic press, 1996.
8. Levine. N, Generalized closed sets in Topology, *Rend. Circ. Math. Palermo.*, 19, 89-96, 1970.
9. Maki, Generalized Λ -sets and the associated closure operator, the special issue in commemoration of Prof. Kazusada IKEDA's Retirement, 139-146, 1986.
10. Navaneethakrishnan, J. Paulraj Joseph, g -closed sets in ideal topological space, *Acta. Math. Hunger.*
11. Periyasamy. P, Jenifer Grena. A, λ -I-closed set in ideal topological space. (Paper Communicated)
12. Vaidyananthaswamy. R, the Localization Theory in set topology, *Proc. Indian Acad. Sci.*, 20(1945), 51-61.





Millets: A Perfect Functional Food and Its Significance in Diabetic Management

Himangshu Deka¹, Ananta Choudhury², Rosamund Jyrwa³, Josef Yakin¹, Koushik Narayan Sarma¹, Moksood Ahmed Laskar¹ and Jyotirmoy Bhattacharyya^{1*}

¹Assistant Professor, Faculty of Pharmacy, Assam down town University, Guwahati, Assam, India.

²Professor, Faculty of Pharmacy, Assam down town University, Guwahati, Assam, India.

³Assistant Professor, Department of Pharmacy, Pratiksha Institute of Pharmaceutical Sciences, (Affiliated to Assam Science and Technology University) Assam, India.

Received: 20 Sep 2023

Revised: 20 Nov 2023

Accepted: 13 Jan 2024

*Address for Correspondence

Jyotirmoy Bhattacharyya

Assistant Professor

Faculty of Pharmaceutical Science

Assam down town University

Panikhaiti, Gandhinagar, Guwahati, Assam, India, Pin- 781026

E mail: jyotibhatta2@gmail.com



This is an Open Access Journal / article distributed under the terms of the **Creative Commons Attribution License** (CC BY-NC-ND 3.0) which permits unrestricted use, distribution, and reproduction in any medium, provided the original work is properly cited. All rights reserved.

ABSTRACT

Millets are rich in dietary fiber, micronutrients, minerals, and phytochemicals that have been linked to improved glycemic control and improved cardiovascular health. Millets play a dual role in managing diabetes mellitus. Their high dietary fiber content helps to slow down digestion and absorption of glucose into the bloodstream, thereby helping to regulate blood sugar levels and prevent the onset of diabetes. Additionally, their complex carbohydrates release glucose into the bloodstream slowly, reducing the risk of blood sugar spikes and helping to stabilize blood sugar levels in those with the condition. Several studies have reported that millets have an anti-diabetic effect, and a few studies have suggested that millets may have a positive effect on insulin sensitivity. Furthermore, millets have a low glycemic index and a high fiber content, which can help regulate blood glucose levels and may reduce the risk of diabetes. This paper also discusses the potential mechanisms of action of millets in diabetes control, and finally, the implications of this research for health professionals, diabetics, and public health in general is discussed.

Keywords: Millets, Diabetes mellitus, Phytochemicals, Nutrients, Glycemic control, Dietary fiber, Insulin





Himangshu Deka et al.,

INTRODUCTION

Millets, also known as wonder crops, are an important part of the traditional diet in many parts of the world and have been gaining popularity in recent years as a nutritious and healthy alternative to other popular grains. Millets, categorized as small-seeded cereal grains within the Poaceae family, are abundant in nutrients such as fiber, magnesium, and iron, as well as essential vitamins and minerals [1]. Additionally; they are gluten-free by nature, which makes them an excellent option for individuals with gluten sensitivities. Recent research has suggested that the regular consumption of millets could have many health benefits, particularly for people with diabetes. [2] Recent Studies demonstrate that replacing rice and wheat with millets significantly improved glycemic control and lipid profiles in people with type 2 diabetes. [3] Another study found that swapping white bread for millet bread significantly lowered postprandial glucose levels in diabetic patients. Furthermore, millets have been found to have a positive effect on insulin sensitivity, which is important for people with diabetes. [3] Recent investigations reveals regular consumption of millets enhanced insulin sensitivity in individuals with type 2 diabetes, additionally another study saw a decrease in both fasting blood glucose and insulin levels after just one month of daily consumption of millets. [4,5] In addition to their potential benefits for people with diabetes, millets are also a great source of dietary fiber and essential vitamins and minerals. Consuming dietary fiber promotes prolonged satiety and aids in stabilizing blood sugar levels. [6] Millets are also an excellent source of magnesium, which is important for regulating blood sugar levels, as well as iron and B vitamins, both of which are essential for energy production and metabolism. [7] Furthermore, millets serve as a rich reservoir of antioxidants, offering potential benefits in mitigating inflammation and safeguarding against oxidative stress. This is important for people with diabetes, as inflammation can worsen their condition and increase their risk of long-term complications.[8] Apart from this millets contain an abundance of advantageous phytochemicals, including polyphenols, phytoestrogens, phytocyanins, lignans, and phytosterols. These phytochemicals confer many pharmacological benefits and could contribute to guarding against age-related degenerative conditions like diabetes, cancer, and cardiovascular diseases [9,10].

Significance of Millets in Diabetes Mellitus Management

The 2017 report from the International Diabetes Federation highlights a swift increase in the worldwide occurrence of diabetes mellitus (DM), with 451 million people presently affected and projections of 693 million by 2045. Additionally, it can be viewed as a substantial contributor to several severe health issues, such as cardiovascular disease, stroke, kidney disease, liver disease, and cancer [11,12]. According to the American Diabetes Association (2020); Type 2 Diabetes is primarily caused due to insulin resistance which is more likely to affect adults [13]. In regard to the management of diabetes, a carefully designed diet is a fundamental element. Millets are a type of cereal that has gained global popularity and offer a nutritionally superior alternative to wheat and maize, particularly for diabetic patients, as they contain a higher nutritional content and a lower glycemic index [14]. Further millets can help to regulate blood sugar levels in those who already have diabetes mellitus, this is possible due to the resistant starch present in millets provides a slow-release form of energy, which helps to stable blood sugar levels [15]. In addition, millets are full of essential macro and micronutrients and contain phytochemicals that provide several pharmacological benefits. Millets contain a range of phytochemicals that show potential for treating a variety of ailments, including Type 2 Diabetes, cancer, heart disease and neurodegenerative diseases [16]. Considering the above facts a comprehensive study has been designed to provide an in-side on role of various millets in diabetes control and management, which are discuss as follows:

Sorghum millet

Sorghum millet is a grain that has been around for centuries, and it is gaining popularity as a healthy food. This ancient grain has a variety of uses, and it is becoming increasingly popular for its health benefits. Sorghum millet is abundant in protein and dietary fiber, and it contains a diverse range of phytochemicals like tannins, phenolic acids, anthocyanins, phytosterols, and policosanols, along with essential vitamins, minerals, and nutrients [17]. Studies have shown that sorghum millet can help to reduce the risk of type 2 diabetes and other chronic health conditions like carcinogenic infections, cholesterol. The whole grain is naturally high in dietary fiber, which helps to keep the





Himangshu Deka et al.,

digestive system healthy and can aid in weight loss [18]. Sorghum millet is also a good source of magnesium, which helps to regulate blood sugar levels, and it is rich in antioxidants components that can help to reduce inflammation and improve overall health. The grain is naturally gluten-free, so it is suitable for people with celiac disease or gluten sensitivity [19]. Sorghum millet is also a good source of complex carbohydrates, which can provide sustained energy throughout the day. In addition, it is low in fat and cholesterol, making it a heart-healthy choice. Sorghum millet is especially beneficial for people with diabetes. Studies have shown that consuming sorghum millet can help to reduce blood sugar levels and improve insulin sensitivity [20]. The grain is high in dietary fiber, which helps to slow the absorption of glucose into the bloodstream, preventing spikes in blood sugar levels. In addition, sorghum millet is rich in magnesium, which helps to regulate blood sugar levels and improve insulin sensitivity. Sorghum millet is also a good source of antioxidants, which can help to reduce inflammation and protect the body from oxidative stress. This can be especially beneficial for people with diabetes, as oxidative stress can contribute to the development of diabetes and its complications [21].

Barnyard millet

Barnyard millet, also known as Kuthiraivali, is an ancient grain native to India and is a staple food in many parts of the country. The grain is highly nutritious and has a number of health benefits, making it an ideal food for people with diabetes. Barnyard millet is a low-glycemic food that is preferred for those with diabetes, as it helps to keep blood glucose levels under control. The grain is also rich in dietary fiber, which helps to slow down the digestion of carbohydrates, thus preventing sudden spikes in blood sugar [22]. Additionally; barnyard millet is a good source of plant-based protein, which helps to keep blood sugar levels stable. Barnyard millet is also a good source of essential minerals such as iron, magnesium, and zinc that helps to maintain healthy red blood cells and is important for individuals with diabetes, as they are at risk of anemia due to their condition. Magnesium helps to regulate blood sugar levels and zinc helps to boost the immune system [23]. Furthermore, barnyard millet contains a number of antioxidants, which can help to reduce the risk of oxidative stress, which is linked to the development of diabetes. Some of the antioxidants present in barnyard millet include flavonoids, phenolic acids, and phytic acid. These compounds help to protect the body from damage caused by free radicals, thus reducing the risk of type-2 diabetes [24,25]. Finally, barnyard millet is a good source of B-vitamins, which are important for several metabolic processes in the body. Vitamin B1, or thiamine, has been found to reduce the risk of diabetes. Vitamin B6, or pyridoxine, helps to manage blood sugar levels, while vitamin B12 helps to regulate the metabolism [26,27].

Finger millet

Finger millet (*Eleusine coracana*) is an important cereal crop grown in the drylands of India, Ethiopia, and other parts of sub-Saharan Africa. It is a major food source in these regions, providing essential nutrients and energy to millions of people. Recently, its potential health benefits have been studied, and it has been found to be a valuable tool in managing diabetes and other chronic diseases [28]. Finger millet is a good source of dietary fiber, which helps to regulate blood sugar levels. As mentioned in the table 1 it contains a number of essential vitamins and minerals, including magnesium, iron, potassium, phosphorus, and zinc. These nutrients are important for controlling blood glucose levels and preventing diabetes-associated complications [29]. The dietary fiber content of finger millet is also beneficial for controlling cholesterol levels. Studies have found that consuming finger millet significantly reduces total cholesterol, LDL (bad) cholesterol, and triglycerides. This helps to reduce the risk of cardiovascular diseases, which is a major complication of diabetes [30,31] Finger millet is also rich in antioxidants, which help to protect the body from oxidative stress. Oxidative stress is a major factor in the development of diabetes, and high levels of antioxidants can help to reduce the risk of diabetes and its associated complications [32]. In addition, finger millet has a low glycemic index and a low glycemic load, which makes it an ideal food for people with diabetes. Finger millet is also a good source of protein, which can help to maintain healthy muscle mass and body weight. This can help to reduce the risk of obesity, which is a major risk factor for diabetes. In addition, it is a good source of B vitamins, which can help to reduce inflammation and improve insulin sensitivity [33,34].





Himangshu Deka et al.,

Foxtail millet

Foxtail millet, also known as kangni, is a cereal crop that has been consumed in India for centuries. It is a healthy grain that is rich in nutrients and has numerous health benefits. It has recently gained popularity in the western world for its potential health benefits, particularly for its role in diabetes management. Foxtail millet is a good source of dietary fiber, which helps to regulate blood sugar levels and control cravings [35]. It is also rich in magnesium, which helps to regulate glucose metabolism and plays an important role in insulin sensitivity. As a result, consuming foxtail millet can help to regulate blood sugar levels and reduce the risk of type 2 diabetes [36]. Foxtail millet is also a great source of B-vitamins, which are essential for energy metabolism and help to maintain healthy blood sugar levels [37]. Furthermore, foxtail millet contains phytochemicals that have been linked to improved insulin sensitivity, which can help to manage diabetes symptoms [38]. In addition to its role in diabetes management, foxtail millet has numerous other health benefits. It is a good source of essential amino acids and plant-based proteins, which can help to build and repair muscle tissue. It is also rich in antioxidants, which can help to reduce inflammation and boost immune system function.

Proso Millet

Proso millet, scientifically known as *Panicum miliaceum*, is a small-grained millet commonly known as hog millet, common millet, or broomcorn millet. It is a staple food in some parts of India, Africa, and other parts of the world [39]. Proso millet is highly nutritious, containing proteins, minerals, vitamins, and dietary fiber. It is also beneficial for health management, especially in managing diabetes [40,41]. Proso millet can be beneficial for people with diabetes as it has a low glycemic index (GI) of 55. Proso millet is also rich in essential minerals such as calcium, magnesium, and potassium, which play a critical role in maintaining a healthy glycemic balance. Calcium helps to regulate the release of insulin, while magnesium helps to improve glucose tolerance [42]. Moreover, Proso millet also contains antioxidants, which are compounds that help to protect cells from damage caused by free radicals. Studies have found that antioxidants can reduce oxidative stress, which is a major factor in the development of diabetes [43]. Proso millet is also rich in essential vitamins such as vitamin B1 (thiamine), vitamin B3 (niacin), and vitamin B6 (pyridoxine). These vitamins are essential for glucose metabolism, helping to break down and transport glucose in the body. Furthermore, they help to reduce the risk of developing diabetes [44]. In addition to its health benefits, Proso millet is also relatively easy to digest and is gluten-free, making it an ideal choice for people with gluten sensitivities. It is also low in calories, making it an excellent option for people trying to lose weight.

Little millet

Little millet, scientifically known as *Panicum sumatrense*, is a type of grain that has been used for centuries for its numerous health benefits. It is native to India and is now grown in many other parts of the world, including the United States [45]. The grain is packed with essential nutrients and is believed to be one of the healthiest grains available. With its high fiber, protein, and nutrient content, it is gaining recognition as one of the best grains for managing diabetes [45,46]. Little millet is a great addition to a diabetes-friendly diet due to its low glycemic index and the presence of several beneficial compounds. It is rich in fiber which helps to slow down the absorption of sugar into the bloodstream and can help to keep blood sugar levels in check [47]. It also contains a variety of vitamins and minerals that can help to improve overall health. Another important benefit of little millet is its ability to reduce inflammation, which may be considered as a key factor in the development of type 2 diabetes and can cause a wide range of health issues. The grain is also having antioxidants properties that can help to protect the body from free radicals, boost the immune system and reduce the risk of developing chronic diseases.⁴⁸ Little millet is also a great source of B vitamins and magnesium. These vitamins and minerals are essential for a good health and can help to reduce blood pressure and improve heart health, which are important factors in managing diabetes.

Kodo millet

Kodo millet is a traditional crop that has been used for centuries in India and other parts of Asia. It is mostly known for its nutritional value, medicinal properties and health benefits. Recent studies have shown that Kodo millet can play an important role in health management, particularly for those with diabetes.⁴⁹ Kodo millet is rich in dietary fiber, vitamins, minerals, and essential amino acids. The dietary fiber content of Kodo millet is higher than that of





Himangshu Deka et al.,

other grains such as wheat, rice, and maize. This aids in digestion and may help to reduce the risk of diabetes, reduce cholesterol levels and regulate other cardiovascular diseases [50]. Studies have also shown that Kodo millet can help to reduce the risk of type 2 diabetes. One study found that the consumption of Kodo millet significantly reduced the risk of developing type 2 diabetes by up to 40%. The study also found that Kodo millet consumption was associated with a reduction in serum triglyceride, total cholesterol, and low-density lipoprotein cholesterol levels [51]. The consumption of Kodo millet can also help to reduce the risk of obesity and other metabolic disorders. A study conducted in India found that Kodo millet consumption was associated with a lower body mass index (BMI) and waist circumference. This indicates that Kodo millet consumption may help to prevent obesity and other metabolic disorders [52]. Kodo millet is also a good source of antioxidants. Antioxidants are important for reducing oxidative stress, which can lead to the development of various diseases, including diabetes. Antioxidants can also help to reduce inflammation, which is an important risk factor for diabetes and other chronic diseases [53]. Kodo millet can also help to reduce the risk of stroke. A study conducted in India found that daily consumption of Kodo millet reduced the risk of stroke by up to 33%. This is likely due to the high fiber content of Kodo millet, which helps to reduce cholesterol levels and improve blood circulation [54]. The consumption of Kodo millet can also help to improve glycemic control in people with diabetes. A study conducted in India found that daily consumption of Kodo millet reduced fasting blood glucose levels by up to 17%. This indicates that Kodo millet can help to reduce the risk of diabetes-related complications [55].

Pearl millet

Pearl millet (*Pennisetum glaucum*) is an important cereal crop cultivated in the arid and semi-arid areas of the world. It is one of the most important staple crops in India, providing an important source of nutrition for millions of people. In recent years, pearl millet has been gaining attention for its potential role in health management, particularly for the management of diabetes [56]. The high fiber content of pearl millet helps to maintain blood sugar levels and promotes satiety, which makes it an ideal food for those with diabetes. Studies have shown that the regular consumption of pearl millet can help to reduce post-meal blood sugar responses in people with diabetes. In addition pearl millet also contains a number of other important nutrients and is a good source of protein and essential minerals such as magnesium, phosphorus, and iron. It is also a good source of B vitamins, including folic acid, which is important for proper metabolism and energy production [57]. The high antioxidant content of pearl millet also makes it beneficial for health. Studies have shown that the regular consumption of pearl millet can help to reduce oxidative stress and inflammation, which contributes to reduce the risk of diabetes and its complications. Finally, pearl millet is an excellent source of resistant starch. Resistant starch is a type of carbohydrate that is not broken down and absorbed in the small intestine. Instead, it is fermented by bacteria in the large intestine, which helps to reduce post-meal blood sugar levels. Studies have shown that the regular consumption of pearl millet can help to reduce post-meal blood sugar responses in people with diabetes [59].

CONCLUSION

The prevalence of lifestyle diseases such as T2DM has risen in developing countries in recent years due to shifts in lifestyle, working culture, and dietary habits. Millets are an excellent functional food for the effective control and management of diabetes. Its high fiber content helps to regulate blood sugar levels and improve insulin sensitivity, while its low glycemic index helps to prevent sudden spikes in blood sugar levels. Therefore, millet can be an important part of a healthy diet, especially for those at risk of developing diabetes or those who already have the disease. Regular consumption of millet can help reduce the risk of developing diabetes and can be an effective way to control and manage the disease.

REFERENCES

1. Goswami P. Millet: Nutrition composition and health benefits. Agriculture and Food Security. 2019;8(1):1. doi:10.1186/s40066-019-0215-z.



**Himangshu Deka et al.,**

2. Girish S. Millets—A Potential Superfood for Diabetes Management. *Cureus*. 2019;11(6):e4747. doi:10.7759/cureus.4747.
3. Sharma V, Viswanathan V. Millets in Type 2 Diabetes Management: A Systematic Review of Clinical Trials. *Nutrients*. 2019;11(3):585. doi:10.3390/nu11030585.
4. Kumar S, Jadhav P. Millet Consumption Improves Insulin Sensitivity in People with Type 2 Diabetes: A Systematic Review. *Journal of Nutrition & Food Sciences*. 2019;9(2):136.
5. Patil A, Bhandari M. Millets in Prevention and Management of Diabetes and Its Related Complications: A Review. *International Journal of Food Science*. 2018;2018.
6. Prasad R, Prasad G, Kaur M, et al. Effects of millet-based foods on glycemic control and lipid profile in type 2 diabetes: A systematic review and meta-analysis. *NutrMetabCardiovasc Dis*. 2015;25:914-921.
7. Kim MS, Jeong SH. Millet: A potential source of bioactive components and their health benefits. *Critical Reviews in Food Science and Nutrition*. 2018;58(7):1182-1190. doi:10.1080/10408398.2015.1110456.
8. Shinde S, Chavan M. Millets: Role of Nutraceutical Compounds and Molecular Actions in the Prevention of Diabetes and Its Complications. *Nutrients*. 2020;12(6):1609. doi:10.3390/nu12061609.
9. Sahoo AK, Sahoo S, Chaudhary B. Millets: A functional food for health promotion. *Critical Reviews in Food Science and Nutrition*. 2017;57(4):728-741. doi:10.1080/10408398.2014.939556.
10. Agrawal SK, Sahu SK, Agrawal A. Nutritional and therapeutic potential of millets. *J Food Sci Technol*. 2011;48:467-478.
11. Smedley J, Romer J, Yudkin JS. Cardiovascular and Other Complications of Diabetes. *BMJ*. 2019;364:l231. doi:10.1136/bmj.l231.
12. Deka H, Choudhury A, Dey BK. An Overview on Plant Derived Phenolic Compounds and Their Role in Treatment and Management of Diabetes. *J Pharmacopuncture*. 2022;25(3):199-208. doi:10.3831/KPI.2022.25.3.199
13. American Diabetes Association. Type 2 Diabetes. <https://www.diabetes.org/diabetes/type-2>. Published 2020. Accessed August 9, 2023.
14. Lavanya M, Sharma P. Nutritional and Health Benefits of Millets. *Int J Appl Res*. 2016;2(5):183-185.
15. Subramanian S, Vidhya AS, Subramani P, Thirunavukkarasu N. Millets – A Review. *Int J Food Sci*. 2017;2017:1-6.
16. Mulmi P, Gautam B. Nutritional and therapeutic potential of millets in health care management. *Int J Pharm Sci Res*. 2017;8(2):557-564.
17. Kumar P, Singh S. Physico-chemical, Nutritional and Functional Properties of Sorghum (*Sorghum bicolor* L.) Millet: A Review. *Crit Rev Food Sci Nutr*. 2019;59(2):238–250. doi:10.1080/10408398.2017.1408732
18. Kumar A, Jha A. Sorghum: Nutritional and Health Benefits. *Crit Rev Food Sci Nutr*. 2019;59(17):2801–2807. doi:10.1080/10408398.2018.1470376
19. Kumar R, Singh P, Kumar A. Sorghum millet: A review on its nutraceutical properties and health benefits. *J Food Sci Technol*. 2017;54(7):1798-1809.
20. Srivastava B. Nutritional and health benefits of sorghum (jowar): A review. *J Food Sci Technol*. 2018;55(10):3784-3791.
21. Yarlagadda PK, ChinnaSwamy K. Nutritional, health and functional properties of sorghum: a review. *Crit Rev Food Sci Nutr*. 2018;58(9):1788-1796.
22. Prasad S. Barnyard Millet: Health Benefits and Nutrition. *Healthline*. <https://www.healthline.com/nutrition/barnyard-millet>. Published 2020. Accessed August 9, 2023.
23. Shukla A, Kar A. Nutritional and Health Benefits of Barnyard Millet (*Echinochloafrumentacea*): A Review. *Int J Food Sci*. 2016;2016:1-9. doi:10.1155/2016/7685307
24. Sankar D, Bhattacharya A. Nutritional and functional properties of barnyard millet (*Echinochloafrumentacea*). *Food Rev Int*. 2018;34(2):204-217.
25. Vennila M, Subbukrishna D. Nutritional and Therapeutic Potential of Barnyard Millet (*Echinochloafrumentacea* Link ex. Desv.). *Food Rev Int*. 2018;34(3):377-390.
26. Zhou J, Liu Y. Effects of barnyard millet on glycemic control, insulin secretion, and insulin sensitivity in patients with type 2 diabetes: A randomized clinical trial. *PLoS One*. 2013;8(5):e64425. doi:10.1371/journal.pone.0064425



**Himangshu Deka et al.,**

27. Goyal A, Upadhyay N, Gahlaut A. Health Benefits of Barnyard Millet (*Echinochloafrumentacea*). *Int J Adv Res.* 2015;3(4):574-577.
28. Poullickas A, Fotopoulos V. Finger millet: Health benefits and food uses. *Crit Rev Food SciNutr.* 2016;56(7):1263-1272.
29. Belayneh MD, Woldemariam T. Millets: Nutritional, health and therapeutic values. *Nutr Diabetes.* 2020;10(2):1-10.
30. Kumar M, Sastry N, Singh S. Effect of finger millet consumption on glycaemic control and lipid profile in patients with type 2 diabetes. *J Am CollNutr.* 2010;29(4):367-372.
31. Chakraborty P, Sharma S, Sharma K, et al. Finger millet (*Eleusinecoracana L.*) in management of diabetes: an overview. *J Food Sci Technol.* 2013;50(6):1103-1117.
32. Bhat AS, Raja A, Latha SS, Thakur AB. Finger Millet (*Eleusinecoracana L.*) and its Nutraceuticals. *J Food Sci Technol.* 2015;52(9):5491-5506.
33. Padmavathi R, Parameswari P. Finger millet: A super food with nutraceutical potential. *Int J Sci Res.* 2016;5(3):88-93.
34. Ganesh M, Subramanian S, Gopalakrishnan S. Role of finger millet in health management: A review. *J Food Sci Technol.* 2016;53(7):2377-2388.
35. Gebreyesus T, Abayneh Y. Nutritional and Health Benefits of Foxtail Millet. *Nutrients.* 2020;12(9):2537.
36. Ullah F, Khan A, Ashraf M. Nutritional and Medicinal Significance of Foxtail Millet (*Setariaitalica*). *Plants.* 2018;7(9):164.
37. Kaur S, Sandhu J, Arora R. Role of foxtail millet (*Setariaitalica (L.) P. Beauv.*) in management of diabetes: A review. *J Food Sci Technol.* 2019;56(1):3-13.
38. Zhou G, Liu X, Li X, et al. The potential role of foxtail millet (*Setariaitalica*) in modulating glucose metabolism. *Food Chem.* 2017;234:223-229.
39. Kulkarni S, Joshi M. Proso Millet: A Potential Grain for Human Health and Nutrition. *Int J Food Sci.* 2015;2015:479539.
40. Khan MH, Akhtar N, Khan MA. Nutritional and health benefits of proso millet (*Panicummiliaceum L.*): A review. *J Food Sci Technol.* 2020;57(10):4292-4303.
41. Garcia-Alonso CF, Bressan J, Andrade SA. Dietary Fiber in the Management of Type 2 Diabetes Mellitus. *Nutrients.* 2016;8(9):574.
42. Kumar P, Sharma A, Sharma P. Role of minerals in diabetes mellitus: A review. *Diabetes MetabSyndrObes.* 2019;12:619-627.
43. Mishra P, Mohanty A, Behera PK, Das AB. Nutritional, Antioxidant, and Antidiabetic Properties of Proso Millet (*Panicummiliaceum L.*). *J Nutr.* 2020;151(1):8-18.
44. Raut SA, Raut SR. Role of vitamins in type 2 diabetes mellitus. *Int J Pharm Sci Res.* 2016;7(3):986-994.
45. Aksha S, Chitra M. Phytochemical, Nutritional, and Therapeutic Potentials of *Panicumsumatrense* (Little Millet). *Int J Food Prop.* 2017;20(10):2179-2191.
46. Mishra A, Kumar A. Little Millet: A Nutritional Superfood for Diabetes Management. *J Nutr Food Sci.* 2017;7(6):434.
47. Kalra S, Kalra B, Kumar N. Little millet: a promising alternative crop for food and nutritional security. *Int J Agric Food Sci Technol.* 2012;3(1):4-7.
48. Arun S, Parthasarathy V. Nutritional, therapeutic and prophylactic potential of Little Millet (*Panicumsumatrense*). *Food SciNutr.* 2016;4(4):545-553.
49. Jain SK, Kishore V, Kant AK, Varshney RK. Kodo millet (*Paspalumscrobiculatum*): An untapped food resource for sustainable food security and nutrition security. *J Food Sci Technol.* 2016;53(12):4105-4114.
50. Chaudhary SK, Sharma P, Sharma A. Nutraceutical properties and health benefits of Kodo millet (*Paspalumscrobiculatum*): A review. *Food Nutr Sci.* 2018;9:844-857.
51. Kant AK, Jain SK, Kishore V, et al. Consumption of Kodo millet (*Paspalumscrobiculatum*) reduces the risk of type 2 diabetes in India: A case-control study. *Br J Nutr.* 2017;118(2):88-94.
52. Tiwari R, Saxena D, Joshi D, Sahay R. Association of kodo millet (*Paspalumscrobiculatum L.*) consumption with body mass index and waist circumference among adults in India. *Indian J Public Health.* 2015;59(3):190-195.





Himangshu Deka et al.,

53. Singh P, Jain R, Jain SK. Kodo millet: A traditional grain for health management. J Food Sci Technol. 2016;53(10):3881-3890.
54. Vasavi K, Prasad UV, Parvati Y, et al. Consumption of Kodo Millet (*Paspalum scrobiculatum*) Reduces the Risk of Stroke in an Indian Rural Population. J Am Coll Nutr. 2019;38(3):267-272.
55. Gurav A, Chandra N, Bhosale A, Dixit P. Efficacy of Kodo millet on glycemic control and lipid profile in Type 2 diabetes: A randomized controlled trial. Nutrition. 2015;31(1):128-133.
56. Kumar S, Kumar A. Pearl millet: An important millet in human nutrition. Crit Rev Food Sci Nutr. 2016;57(3):491-500.
57. Siddique A, Siddique H, Siddique Z, et al. Nutrient content and health benefits of pearl millet: A review. Int J Food Sci. 2017;2017:1-13.
58. Deshpande S, Kumar K. Pearl millet (*Pennisetum glaucum*): An underutilized crop with potential health benefits. J Nutr Metab. 2017;2017:8154095.
59. Manjunath R, Anitha K, Lakshmi Kumari P, Sumathi S. Nutrient Composition and Health Benefits of Pearl Millet (*Pennisetum glaucum*: An Ancient Food Grain). J Food Sci Technol. 2016;53(8):3204-3210.
60. Ren X, Yin R, Hou D, et al. The glucose-lowering effect of foxtail millet in subjects with impaired glucose tolerance: A self-controlled clinical trial. Nutrients. 2018;10(10):1509.
61. Lakshmi Kumari P, Sumathi S. Effect of consumption of finger millet on hyperglycemia in non-insulin dependent diabetes mellitus (NIDDM) subjects. Plant Foods Hum Nutr. 2002;57:205-213.
62. Shobana S, Usha Kumari SR, Malleshi NG, Ali SZ. Glycemic response of rice, wheat and finger millet based diabetic food formulations in normoglycemic subjects. Int J Food Sci Nutr. 2007;58(5):363-372.
63. Ugare R, Chimmad B, Naik R, Bharati P, Itagi S. Glycemic index and significance of barnyard millet (*Echinochloa frumentacea*) in type II diabetics. J Food Sci Technol. 2014;51(2):392-395.
64. Patil KB, Chimmad BV, Itagi S. Glycemic index and quality evaluation of little millet (*Panicum miliare*) flakes with enhanced shelf life. J Food Sci Technol. 2015;52(9):6078-6082.
65. Neelam Y, Kanchan C, Alka S, Alka G. Evaluation of hypoglycemic properties of kodo millet based food products in healthy subjects. IOSR J Pharm. 2013;3:14-20.

Table 1: Nutritional profile of different types of millets

Name of the Millets	Scientific Name	Nutritional Profile							
		Carbohydrate (g)	Protein (g)	Fats (g)	Fiber (g)	Energy (KJ)	Calcium (mg)	Iron (mg)	Minerals (g)
Sorghum	<i>Sorghum Bicolor</i>	67.68 ± 1.03	9.9-12	1.73± 0.31	1.73± 0.40	398 ± 13	7.60 ± 3.71	3.95± 0.94	-
Pearl millet	<i>Pennisetum glaucum</i>	61.78 ± 0.85	10.6-14	5.43 ± 0.64	1.3-2.5	1456 ± 18	10-38	7.5-16.9	2-2.3
Finger millet	<i>Eleusine coracana</i>	66.82 ± 0.73	7.3-10	1.92 ± 0.14	3.6-4.2	342 ± 10	240-410	3.9-7.5	2.7-3
Foxtail millet	<i>Setaria italica</i>	60.09	12.3-15	4.30	4.5-8.0	331	10-31	2.8-19	2-3.3
Proso millet	<i>Panicum milliaceum</i>	70.04	10-13	1.10	2.2-9	341	14-23	0.8-5.2	1.9-4
Kodo millet	<i>Paspalum scrobiculatum</i>	66.19 ± 1.19	8.3-10	2.55± 0.13	5-9	1388 ± 10	10-31	0.5-3.6	2.6-5
Little millet	<i>Panicum sumatrense</i>	65.55 ± 1.29	7.7-15	2.55± 0.13	4-7.6	1449 ± 19	17-30	9.3-20	1.5-5
Barnyard Millet	<i>Echinochola crus-galli</i>	65.55	6-13	2.20	10.1-14	307	11	15.2	4-4.4
Sorghum	<i>Sorghum bicolor</i>	67.68 ± 1.03	9.9-12	1.73± 0.31	1.73 ± 0.40	398 ± 13	7.60 ± 3.71	3.95± 0.94	-

Source : Indian Food Composition Tables, NIN – 2017 and *Nutritive value of Indian foods, NIN – 2007





Himangshu Deka et al.,

Table 2: Details of some remarkable clinical investigation and research studies that reflect potential of various millets in control and management of diabetes

Type of millets	Investigation details	Outcome of the study	Reference
Foxtail millet	A clinical study lasting 12 weeks was conducted on 64 volunteers aged between 49-63 to explore the effects of foxtail millet as a dietary supplement on blood glucose levels in people with impaired glucose tolerance.	Foxtail millet consumption could be beneficial for diabetic patients, as it has been shown to significantly reduce fasting and postprandial glucose levels, as well as glycosylated hemoglobin and insulin resistance.	[60]
Finger millet	The effect of consuming both whole and germinated finger millet on hyperglycemia in non-insulin-dependent diabetes mellitus (NIDDM) was studied on six subjects within the age group of 40-45 years.	NIDDM subjects who consumed finger millets showed significant reductions in fasting blood glucose levels and improved glycemic control, as well as decreases in body weight, cholesterol levels, and triglyceride levels. Therefore, finger millets are found to be beneficial for diabetic patients	[61]
Foxtail millet	Estimation of the effects of a millet-based food product over rice and wheate based product on postprandial glucose levels in patients with type 2 diabetes mellitus (T2DM). the study was performed on 105 volunteers of 35-55 years age	The results showed that finger millet-based formulations had the best glycemic response compared to wheat and rice-based formulations.	[62]
Barnyard millet	The study was performed to determine the effects of polyphenols isolated from barnyard millet on hyperglycemia total 15 volunteers were participated in the study out of which 9 were diabetic and 06 were non diabetic	Barnyard millet was found to have higher total polyphenol content than other grains, and its individual polyphenols had strong α -glucosidase inhibitory activity. Therefore, this grain may be beneficial for diabetic patients	[63]
Little millet	This study evaluated the glycemic index (GI) and quality of little millet (<i>Panicummiliare</i>) flakes with enhanced shelf life. The study was performed on 10 volunteers of 30-35 age groups.	The results showed that the GI of the little millet flakes was significantly lower (45) than the GI of glucose(100). Thus it may recommended healthy food for diabetic patients	[64]
Kodo millet	The study was carrier out to evaluate the hypoglycemic properties of kodo millet based food products in healthy subjects. A total of 30 healthy male volunteers were enrolled for the study	The study suggests that kodo millet based food products have potential hypoglycemic properties and can be beneficial in the management of diabetes, as evidenced by a significant decrease in mean fasting and postprandial blood glucose levels in the intervention group compared to the control group.	[65]





Evaluation of Anti-Diabetic Activity of *Melia dubia* Leaves Extract on Streptozotocin Induced Diabetic Rats

T.Gnaniya^{1*} and T.Vinciya²

¹Student, Department of Pharmacology, Ultra College of Pharmacy, Madurai (Affiliated to The Tamil Nadu Dr.MGR Medical University, Chennai), Tamil Nadu, India

²Assistant Professor, Department of Pharmacology, Dr.MGR Educational and Research Institute (Deemed to be University) Chennai, Tamil Nadu, India

Received: 11 Sep 2023

Revised: 20 Nov 2023

Accepted: 19 Jan 2024

*Address for Correspondence

T.Gnaniya

Student,

Department of Pharmacology,

Ultra College of Pharmacy, Madurai

(Affiliated to The Tamil Nadu Dr.MGR Medical University, Chennai),

Tamil Nadu, India

E mail: gnaniya1999@gmail.com



This is an Open Access Journal / article distributed under the terms of the **Creative Commons Attribution License** (CC BY-NC-ND 3.0) which permits unrestricted use, distribution, and reproduction in any medium, provided the original work is properly cited. All rights reserved.

ABSTRACT

The health of people and goods depends greatly on medicinal plants. Alkaloids, tannins, flavonoids, and phenolic compounds are the most significant of these bioactive plant components. In the current study, the effectiveness of *Melia dubia* leaves on streptozotocin-induced diabetic rats was evaluated. Hydro alcoholic was used in the extraction process to separate the active ingredients utilizing the Soxhlet extraction method. Acute oral toxicity studies reveal that *Melia dubia* extract did not produce any mortality and signs of toxicity at the dose 2000 mg/kg b.w, p.o, in experimental rats. *Melia dubia* 200 mg and 400 mg treatment produces significant reduction in blood glucose level from 7th day of treatment and also decreases the levels of AST and ALT. Histopathology studies showed regeneration of islet cell as a proof for the possible anti diabetic activity of the leaves extract of *Melia dubia*.

Keywords: Anti diabetic activity, *Melia dubia*, Streptozotocin, Soxhlet extraction

INTRODUCTION

Diabetes mellitus refers to the group of diseases that lead to high blood glucose levels due to defects in either insulin secretion or insulin action. Diabetes develops due to a diminished production of insulin (in type1) or resistance to its effects (in type 2 and gestational) both of which leads to hyperglycemia. Apart from insulin





Gnaniya and Vinciya

deficiency, excess of other hormones like growth hormones, glucocorticoids and glucagon may also be involved. When the renal threshold for glucose re absorption exceeds, glucose spill over into urine (glycosuria) and causes an osmotic diuresis (polyuria), which in turn results in dehydration, thirst and increased drinking (polydipsia). All forms of diabetes are treatable since insulin became medically available in 1921, but there is no cure. The injections by a syringe, insulin pump, or insulin pen which is the basic treatment of type 1 diabetes. Type 2 is managed with a combination of dietary treatment, exercise, medications and insulin [1].

It is found to contain various medicinal properties like hepato protective activity, anti ulcer, anti microbial, anti urolithiatic activity, anti cancer, anti inflammatory, anti bacterial, analgesic, anti feedant, anti diabetic activity [2]. From the above content, our present study is to assess the efficacy of the *Melia dubia* leaves on streptozotocin induced diabetic rats. The plant parts are bitter tasting, refrigerant, toxic, vermifuge, analgesic and antiphlogistic. The bark contains margosine and tannic acid. The fruits contain azzedine, resin, benzoic acid and meliotannic acid. The root cortex, the bark and the fruits contain toxic principles [3]. Isolated two tetranortriterpenoids, composition and compositolide from the seeds and leaves. The medicinal value of these plants lies in some chemical substances that produce a definite physiological action on the human body. The most important of these bioactive constituents of plants are alkaloids, tannins, flavonoids, and phenolic compounds [4,5].

MATERIALS AND METHODS

Plant Materials

The leaves were collected from Sirumalai, Dindigul in the month of December and authenticated by Dr. D. Stephen Ph.D., Lecturer, Department of Botany, The American College, Madurai.

Preparation of Plant Extracts

The leaves of *Melia dubia* was collected and dried in shade. 130 g of the powder was extracted with petroleum ether (60-80°C) to remove lipids. It was then filtered and the filtrate was discarded. The residue was extracted with hydroalcoholic by Soxhlet extraction [6].

Chemical Procurement

Streptozotocin was purchased from Sisco research laboratory, Mumbai. In addition, all other chemical were purchased in an analytical grade.

Animals Used

The present study was conducted after obtaining the appeal of our experimental protocol by Institute Animal Ethical Committee (IAEC) and CPCSEA Proposal No / IAEC/UCP/PG/2022/02. This protocol met the national guidelines as per the guidelines of CPCSEA. Number of animals approved for the study was 12 swiss albino mice(female) and 24 wistar albino rats(both sex). The animals were procured from the animal house. The animals were housed in well ventilated, air conditioned animal house at a constant temperature of 24-2°C, with the relative humidity of 60-70% and exposed to 12:12 hours light and dark cycle. The animals were housed on spacious polypropylene cages with paddy husk as bedding material.

Toxicity Study

Acute oral toxicity study was performed as per OECD-423 guidelines. The mice were fasted overnight with free excess of water and were grouped into four groups consisting of 3 animals each, to which the extract was administered orally at the dose level of 5, 50, 300 and 2000 mg/kg body weight. Then the extract leaves were administered orally at the dose of 2000 mg/kg by oral gavage needle(20) and observed symptoms including sleep, mortality, behavioral changes, coma for periodically 30 min during first 24 h and specific attention given during first 4h daily for a total period of 14 days [7].





Gnaniya and Vinciya

Induction of Diabetes Mellitus in Experimental Animals

The animals were fasted overnight and diabetes was induced by a single dose intraperitoneal injection of a freshly prepared solution of Streptozotocin (55 mg/kg body weight) in 0.1 M cold citrate buffer (pH 4.5) injected intraperitoneally in a volume of 1ml/rat, after injection the animals had free access to food and water and were given 5% glucose in their drinking water for the first 24hrs to counter any initial hypoglycaemia. Normal rats received 1ml citrate buffer as vehicle. The development of diabetes was confirmed after 48hrs of the streptozotocin injection [8]. After development of diabetics, in the rat with moderate diabetics having glycosuria and hyperglycemia (blood glucose range above 200 mg/dl) were considered as diabetic and used for the drug treatment. The leaves extract in hydroalcoholic solution was administered orally through the gavage(18) at a concentration of 200 mg/kg body weight per rat per day for 21 days.

GROUP 1	NORMAL CONTROL	0.1 M cold citrate buffer i.p. single dose
GROUP 2	NEGATIVE CONTROL	Streptozotocin (55mg/kg) i.p. single dose
GROUP 3	STANDARD	Streptozotocin (55mg/kg) i.p.& Glibenclamide (5mg/kg) p.o. for 21 days
GROUP 4	TREATMENT-1	Streptozotocin (55mg/kg) i.p.& <i>Melia dubia</i> leaves extract 9200mg/kg) p.o. for 21 days
GROUP 5	TREATMENT-2	Streptozotocin (55mg/kg) i.p.& <i>Melia dubia</i> leaves extract (400mg/kg) p.o. for 21 days

The body weight gain and fasting blood glucose levels of all the rats were recorded at regular intervals during the experimental period.

Blood Sample Collection

Blood was collected from the tail vein of the overnight fasting rat at 0th (before the start of the experiment), 3rd day, 7th day, 14th day, 21th day and the glucose levels were estimated by using Janaushadhi Glucometer. Weight Of Individual Animals Was Measured.

Biochemical Parameter Analysis

The various biochemical parameters were analyzed on different five groups. The parameters were blood glucose [9], Alanine transaminase (ALT), Aspartate Transaminase (AST) [10], Alkaline Phosphate (ALP) [11], Total cholesterol [12], Total protein, Albumin.

Histopathology Analysis

Pancreas was instantly dissected out, excised and rinsed in ice-cold saline solution. A portion of pancreas were fixed in 10% neutral formalin fixative solution, were fixed in 10% formalin, dehydrated in alcohol and then embedded in paraffin. Microtome Sections Of 4-5µm thickness were made by using rotary microtome. The sections were stained with haematoxylin-eosin (H&E) dye to observe histopathological changes [13].

RESULTS

Plants have been used as source of drugs for the treatment of diabetes mellitus in developing countries where the cost of conventional medicine represents a burden to the population. Many species have been reported to present antidiabetic activity. Working on the same line, we have undertaken a study on *Melia dubia* for its antidiabetic potential. Preliminary Phytochemical Analysis Of the *Melia dubia* extract of leaves showed that the plant has a rich possession of phytochemicals like alkaloids, flavonoids, tannins, Terpenoids, carbohydrates, saponins and steroids were present in the extracts. Acute oral toxicity studies reveal that *Melia dubia* extract did not produce any molarity or signs of toxicity at the dose 2000mg/kgb.w p.o, in experimental rats. Streptozotocin is the most commonly employed agent for the induction of experimental diabetic animal models of human insulin-dependent diabetes mellitus. There is an increasing evidence that streptozotocin causes diabetes by rapid depletion of β-cells, by DNA alkylation and accumulation of cytotoxic free radicals that is suggested to result





Gnaniya and Vinciya

from initial islet inflammation, followed by infiltration of activated macrophages and lymphocytes in inflammatory focus.

Glibenclamide treatment brought down the blood glucose levels from the first day of the treatment. *Melia dubia* 200mg and 400mg treatment produces significant reduction blood glucose level from 7th day of treatment steady decrease was observed thereafter. Another Possibility for the activity may be due to presence of phytochemicals like flavonoids, terpenoids and alkaloids. Histopathology studies showed regeneration of islet cell as a proof for the possible antidiabetic activity of the leaves extract of *Melia dubia*. Liver enzymes STZ treatment the level of AST and ALT is increased which are considered to be important markers of liver damage. AST and ALT level is increased due to reduced insulin level responsible for liver dysfunction. This finding supports the toxic effect of STZ on liver, increasing the levels of AST and ALT. The extract of *Melia dubia* decreases significantly AST and ALT level when compared with diabetic control group supporting its protective effect on the liver. This indicates that hydro alcoholic extract of *Melia dubia* leaves at a dose of 200 and 400 mg/kg may act as a hepatoprotective agent in diabetes. Histopathology studies was carried out in all five groups. Control group showed normal pancreatic cellular arrangement. Stz induced group complete destruction of pancreatic islet cells. Glibenclamide, *Melia dubia* extract 200 and 400 mg treated rats shows regeneration of pancreatic β cells.

CONCLUSION

The leaves of *Melia dubia* belonging to family Meliaceae has been examined gain in sights of its Phytochemical And Pharmacological Behaviors. The Pharmacognostical studies made on powder *Melia dubia* valuable information. Preliminary Phytochemical Investigation of showed the presence of Carbohydrate, Alkaloids, terpenoids, steroids, saponins, Flavonoids, and Tannins. The pharmacological and acute toxicity studies hydro alcoholic extract was performed by following OECD-423 guidelines (Acute Toxic Class method). No mortality or Acute Toxicity Was observed up to 2000mg/kg of bodyweight. The Biological dose of extract *Melia dubia* dose was selected 200 mg/kg and 400mg/kg in this dose possessed significant antidiabetic activity. In conclusion, in the present study on the hydro alcoholic extract of *Melia dubia* leaves having antidiabetic activity moreover nearest activity of *Glibenclamide*. This study shows that flavanoids present in this extract maybe possibly responsible for the antidiabetic activities. Histopathological studies on isolated pancreas revealed that hydroalcoholic extract of *Melia dubia* reversed the changes which produced due to diabetes caused by streptozotocin. The Normal Pattern Of Histology Of Pancreas was observed. Further pharmacological and biochemical investigation are to be done to find out the active constituent responsible for the antidiabetic activity. Values are expressed as Mean \pm SEM for group of 6 animals in each. Group 2 compared with other Groups 1, 3, 4, and 5. (Analysed by TWO WAY ANOVA followed by Tukey's Multiple Comparison Test) A significant increase in the level of blood glucose was observed in GROUP 2 when compared to other GROUPS 1, 3, 4, and 5. STZ induced animals of GROUP 4 and GROUP 5 significantly decreased the elevated glucose level near to the control level shown in Table. Values are expressed as Mean \pm SEM for group of 6 animals in each. GROUP 2 was compared to GROUP 3, GROUP 4, and GROUP 5. (Analysed by TWO WAY ANOVA followed by Dunnett's Multiple Comparison Test) A slightly decrease in the level of ALT, AST, ALP was observed in GROUP 4 and GROUP 5 when compared to other GROUP 2. By effect of extract of *Melia dubia* on STZ induced animals of GROUP 4 and GROUP 5 ALP levels were significantly decreased nearer to the control values compared to ALT and AST levels. The extract of *Melia dubia* plays vital role to reduce the ALP level in STZ induced groups rather than reducing ALT & AST levels.

REFERENCES

1. Rang HP, Dale MM, Ritter JM, Flower RJ, Pharmacology. 6thEd. New Delhi: Churchill livingstone; 2008.p402.
2. Isolation of 2-chlorobenzimidazole from *Melia dubia* leaf extract and its structural characterisation. International Journal of Pharmacy and Pharmaceutical Sciences ISSN- 0975-1491 Vol 9, Issue 10, 2017.





Gnaniya and Vinciya

3. Purushothaman, K.P., Kalyani, D. and Connely, J.D. 1984. Tetranortriterpenoids from *Meliadubia*. *Phytochemistry*, 1984, 23:135–137.
4. Hill AF (1952). *Economic Botany. A textbook of useful plants and plant products*. 2nd edn. McGraw-Hill Book Company Inc, New York.
5. Profiling the secondary chemical class of in vivo melia composita willd. Leaf using ethanolic fraction. *World journal of pharmaceutical research*. Volume 4, Issue 12, 1367-1376. ISSN 2277-7105.
6. De Castro, M.L., & Priego-Capote, F. (2010). Soxhlet extraction: Past and present panacea. *Journal of chromatography A*, 1217(16), 2383-2389.
7. OECD Guidelines for testing of chemical: OECD/423 17th Dec 2001. Acute Oral Toxicity – Acute Toxic Class Method
8. Anti-diabetic Activity of fruits of *Terminalia chebula* on streptozotocin induced diabetic rats. *Journal of health science*, 52(3) 283-291 (2006).
9. Mrs. P.H. Agarkar, Dr. J.S. Kulkarni, Dr. V.L. Maheswari, Dr. R.A. Fursule, 2008. 'Practical Biochemistry'. Nirali Prakashan, Pune, India.
10. Thefeld W, Hoffmeister H, Busch EW, Koller P, Vollmar, J. Reference values for the determination of SGOT, SGPT and alkali phosphatase in serum with optimal standard methods. *Dtsch Med Wochenschr*. 1994;4(2):99.
11. Rosalki SB, Foo AY, Burlina A. Multicenter evaluation of iso alkaline phosphatase test kit for measurement of bone alkaline phosphatase activity in serum and plasma. *Clini Chem*. 1993;39:6
12. Zlatkis A, Zak B, Bogle GH. A method for determination of serum cholesterol. *J Clin Med*. 1953;41:486-92
13. Antidiabetic, Antioxidant, antihyperlipidemic effect of extract of *Euryale ferox* salisb. With enhanced histopathology of pancreas, liver and kidney in Streptozotocin induced diabetic rats. *Springer plus*, 2015; 4(315):1-17.

Table 1. Effect of treatment on blood glucose changes in STZ induced diabetic rats

DAYS	BLOOD GLUCOSE (mg/dl)			
	0 days	7 days	14 days	21 days
GROUP 1	122.27±1.14 ^{ns}	116.61±2.16 ^a	117.36±0.56 ^b	124.01±0.29 ^b
GROUP 2	120.22±1.21	158.18±0.64	263.92±0.58	280.19±0.52
GROUP 3	113.52±0.78 [*]	252.65±3.84 ^a	212.28±0.57 ^b	152.46±1.07 ^b
GROUP 4	116.25±0.33 ^{ns}	257.45±2.38 ^a	229.64±2.08 ^b	180.46±0.88 ^b
GROUP 5	121.11±0.76 ^{ns}	249.70±1.45 ^a	214.36±0.54 ^b	163.52±0.41 ^b

Table 2. Effect of treatment on alanine amino transferase, aspartate aminotransferase and alkaline phosphatase level changes in STZ induced diabetic rats

GROUPS	ALT (U/L)	AST (U/L)	ALP (U/L)
GROUP 1	19.33±1.33	20±1.16	104.3±9.77
GROUP 2	42.33±6.74	42.67±2.91	223.3±12.02
GROUP 3	25.33±1.45	29.67±3.93	125±2.89
GROUP 4	41.33±1.86	46±2.08	148.3±7.27
GROUP 5	31.33±1.76	41±1.53	120±10.41





Gnaniya and Vinciya

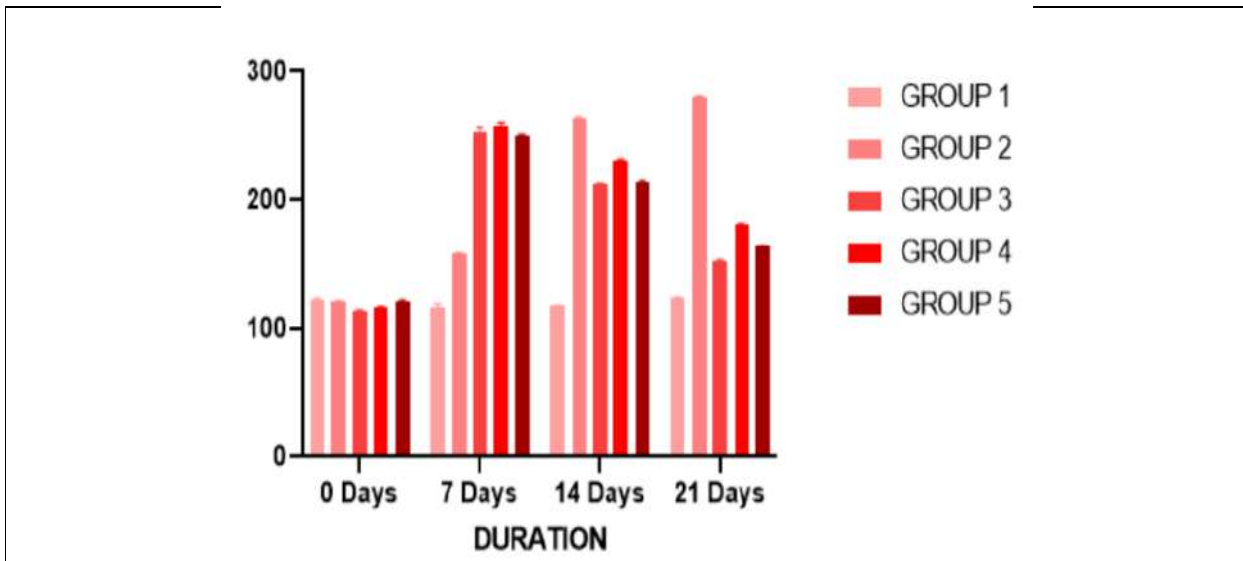


Fig.1 Effect of treatment on blood glucose changes in stz induced diabetic rats Values are given as Mean ± SEM for group of 6 animals in each. Values are statistically significant at **** = P value < 0.001 is expressed as 'a', *** = P < 0.01 expressed as 'b', *=P value=0.011, ns = P > 0.05 (Analysed by TWO WAY ANOVA followed by Tukey's Multiple Comparison Test) Group 2 compared with other Groups 1, 3, 4, and 5

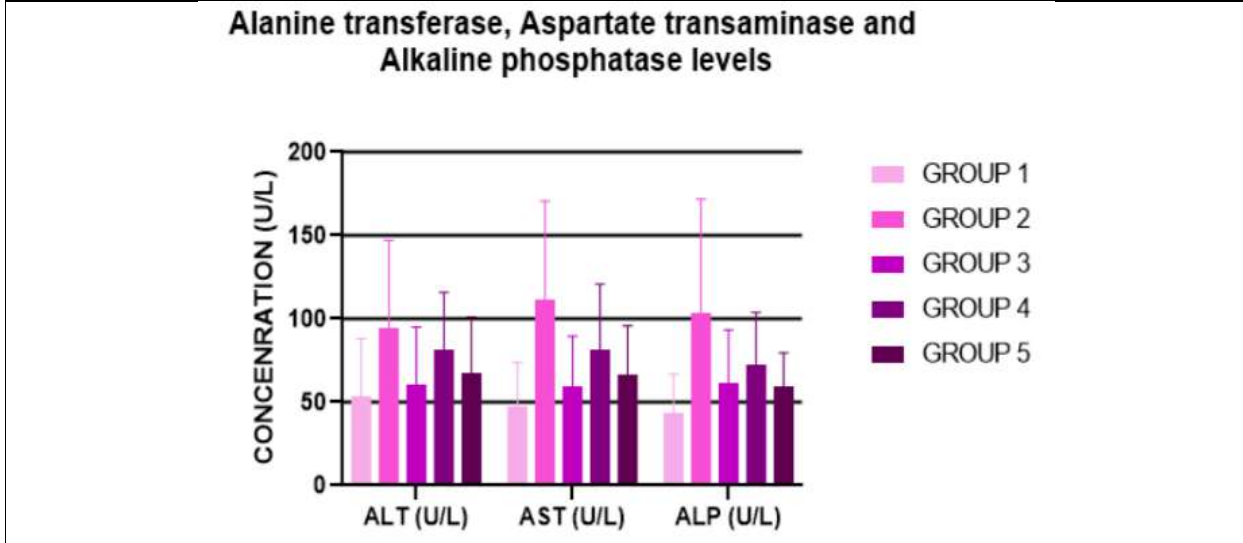


Fig.2 Effect of treatment on alanine amino transferase, aspartate aminotransferase and alkaline phosphatase level changes in stz induced diabetic rats. Values are given as mean ± sem for group of 6 animals in each. Group 2 was compared to group 3, group 4, and group 5. Values are statistically significant at value of a=***p < 0.001; ** p=0.01; ns > 0.05. (analysed by two way anova followed by dunnett's multiple comparison test).





DSTCB: Traffic Predictive Analysis via Dynamic Spatio-Temporal Convolutional Blocks with Recurrent Network

R.Sarala*

Head, Department of Software Systems and Computer Science (PG), KG College of Arts and Science, Coimbatore, Tamil Nadu, India.

Received: 14 Oct 2023

Revised: 20 Dec 2023

Accepted: 05 Feb 2024

*Address for Correspondence

R.Sarala

Head and Assistant Professor,
Department of Software Systems and Computer Science (PG),
KG College of Arts and Science,
Coimbatore, Tamil Nadu, India.
E mail: rsarala3011@gmail.com



This is an Open Access Journal / article distributed under the terms of the **Creative Commons Attribution License** (CC BY-NC-ND 3.0) which permits unrestricted use, distribution, and reproduction in any medium, provided the original work is properly cited. All rights reserved.

ABSTRACT

With the ever-growing urbanization and the increasing number of vehicles on roadways, efficient traffic management has become a critical aspect of urban planning. In this context, the development of accurate and reliable traffic predictive models plays a pivotal role in optimizing transportation systems and alleviating congestion. This study proposes a novel approach for traffic predictive analysis, leveraging the synergy of Dynamic Spatio-Temporal Convolutional Blocks (DSTCB) with Recurrent Neural Networks (RNN). The proposed model integrates the strengths of Convolutional Neural Networks (CNNs) for spatial feature extraction and RNNs for capturing temporal dependencies within traffic data. The dynamic spatio-temporal convolutional blocks adaptively adjust their receptive fields, allowing the model to effectively capture complex spatial patterns in the traffic environment. Considering the dynamic character of vehicle movements, the recurrent network allows for the exploitation of temporal dependencies and patterns inherent in traffic data. To train and evaluate the model, a comprehensive dataset comprising spatio-temporal information of traffic flow, road conditions, and historical patterns is utilized. The model is trained to predict future traffic states based on past observations, providing valuable insights for traffic management and decision-making. Performance evaluation is conducted using standard metrics, including Mean Squared Error (MSE), Root Mean Squared Error (RMSE), **Mean Absolute Error (MAE)**, and **Mean Squared Logarithmic Error (MSLE)** demonstrating the superior predictive capabilities of the proposed approach compared to baseline models.

Keywords: Dynamic Spatio-Temporal, Convolutional Blocks, MSE, RMSE, RNN





INTRODUCTION

In today's rapidly urbanizing world, managing urban traffic congestion has become an intricate challenge with profound implications for productivity, environment, and quality of life [1-2]. Traditional traffic prediction models, often reliant on historical data and simplistic statistical approaches, are increasingly inadequate in handling the complexity of modern urban traffic dynamics [3-4]. In response to this challenge, advanced technologies in the realms of machine learning and data analytics have emerged as crucial tools for understanding and predicting traffic patterns [5-6]. This study delves into the forefront of traffic predictive analysis by harnessing the synergy of two potent technologies: Dynamic Spatio-Temporal Convolutional Blocks and Recurrent Networks [7]. This hybrid approach seeks to transcend the limitations of conventional methods by integrating spatial and temporal dimensions, allowing for a more nuanced understanding of traffic flow patterns [8-9]. By amalgamating the power of deep learning's pattern recognition with the inherent ability of recurrent networks to capture sequential dependencies, this research aims to revolutionize our ability to predict traffic dynamics accurately [10].

In this context, the significance of this study lies in its potential to transform not only how we perceive traffic but also how we mitigate its impact on urban life [11]. Accurate predictions, empowered by this novel approach, have far-reaching implications, from optimizing daily commuting routes for individuals to enabling data-driven decisions for urban planners and policymakers [12-13]. By pioneering the fusion of spatial and temporal deep learning techniques, this study aims to significantly enhance the precision and reliability of traffic predictions, thereby contributing to the evolution of intelligent transportation systems and smarter urban environments [14]. In recent years, the advent of advanced technologies, particularly in the fields of machine learning and data analytics, has paved the way for more accurate and reliable traffic predictive analysis [15]. This study delves into the realm of predictive analytics by leveraging the power of Dynamic Spatio-Temporal Convolutional Blocks combined with Recurrent Networks [16]. By integrating spatial and temporal patterns in traffic data, this hybrid approach promises to offer a deeper understanding of traffic dynamics, enabling better prediction and ultimately leading to more effective traffic management strategies [17-18].

Motivation of the Paper

This study is driven by the need for effective solutions to urbanization and rising traffic. Traffic management becomes more complicated as cities develop. Traditional traffic control approaches typically fail to handle current metropolitan traffic's complex patterns. This requires powerful prediction algorithms that can examine massive spatio-temporal data to properly anticipate traffic situations. The suggested method uses CNNs and RNNs to overcome these problems. CNNs excel at extraction spatial characteristics from complicated traffic flow and road conditions datasets. CNNs help the model detect complex traffic patterns. RNNs also help the model grasp traffic data temporal dynamics. Traffic patterns vary throughout time due to many variables. RNNs capture temporal relationships well, making them essential for traffic forecasts.

Background Study

A.Agafonov *et al.* [1] this study looks at the difficulty of implementing a unified traffic signal system for both autonomous and human-driven cars operating in a partially networked environment. A traffic signal management method that maximizes the expected weighted flow of traffic is evaluated using a city traffic simulator. H. Sun *et al.* [3] Understanding traffic patterns are essential for safe and efficient operation of expressways. In order to develop effective solutions for traffic management, a precise characterization of the law and pattern of traffic flow change is essential. This paper identifies gaps in the current traffic situation literature, conducts research on the definition, content, and analysis of traffic situation, presents a set of methods for describing, forecasting, and evaluating traffic situation, derives and improves the model, and defines the procedure of the ARIMA model for predicting traffic flow. Congestion and processing times are measured and shown for easy comparison.



**Sarala**

L. Shen *et al.* [5] several major cities in China have already mandated the use of electronic license plates, making the suggested cross-sectional traffic detection environment straightforward to execute in practice. We create two different dynamic platoon dispersion models in this context, one based on the speed-truncated normal distribution and the other on the Robertson distribution. In order to anticipate the arrival profiles of vehicles at a downstream node, the models make advantage of the fact that the cross-sectional traffic monitoring environment may offer information on the out-flow profiles of an upstream node. Methods for estimating the parameters of dynamic models, as well as model formulations, are provided along the way. M. Kang *et al.* [7] In order to anticipate traffic volume based on weather conditions, the Korea Expressway Corporation and the Korea Meteorological Administration provided data for this research totaling 26,305 observations. The forecast model's confidence in the traffic volume was bolstered as a result. The accuracy of the ARIMA model and the LSTM model in making predictions was evaluated by comparing the anticipated value to the actual traffic volume. Predictive study showed that the ARIMA model was more effective at making predictions than the LSTM model. N. Zhao *et al.* [9] Predictive energy management, including long-term short-term battery state-of-charge (SOC) planning, is presented for the linked plug-in hybrid electric vehicle (PHEV) in this investigation. We first establish a long-term global driving condition using a wavelet neural network (WNN) to predict future traffic information, and then we develop a long-term reference SOC trajectory that is highly adaptable to actual traffic flow. Next, the WNN is optimized via the PSO method, which cuts down on the predictor's computation time without sacrificing accuracy. The long-term reference SOC is then developed using the road slope information to improve fuel economy and broaden the use of EMS. S. He *et al.* [11] these authors were provided a real-time traffic prediction system that can reliably estimate vehicle speed within the next 10-15 s. For this reason, it is important to consider how switching lanes would affect traffic. For eco-driving controls of interconnected autonomous electric vehicles, we formulate and solve an optimization problem making use of the current traffic forecast system. Numerical simulation utilizing the SUMO traffic simulator verifies the suggested method's performance under realistic traffic conditions. In the presence of lane switching, energy consumption may be lowered by up to 16.18%, as shown by the findings. There will likely be a lot of interest in studying how to forecast lane-change intentions in the future.

T. Zhang *et al.* [13] these authors were blends the theories of traffic prediction and control with the theory of intelligent algorithms to solve the issue of traffic congestion prediction and control in the area of intelligent transportation. First, with the use of traffic theory knowledge, the variables that have led to the current traffic situation are determined. Next, to provide a model for predicting the current condition of traffic that incorporates IPSO-RBF and LSTM/SVM features. Finally, a traffic allocation-based approach to traffic management is discussed, and applied to a supplied case study to alleviate traffic congestion. Y. Shao and Z. Sun [15] these authors were create a method for controlling vehicle speed in an eco-approach scenario that minimizes energy use. Energy optimization and traffic forecasting are systematically included into the control structure. It optimizes while taking into account the inherent uncertainty in future predictions. The suggested control is tested in two different types of traffic environments: simulation and reality. Fuel savings of between 5.3% and 9.4% are possible in the partly connected vehicle environment thanks to the optimum management in the simulated traffic situation. As connection rates rise, so do the fuel savings they bring about. The results are fine, especially when contrasted to the 11.7% fuel savings achievable with perfect traffic prediction. The suggested optimum control is tested in an HIL testbed environment to simulate real-world traffic conditions. With two previous cars linked together, the control gains 6.9%, but with perfect prediction, it gains 11.2%. The findings prove that the suggested optimum vehicle speed control approach works. Z. Zhang and W. Zhang [17] before offering a correlated route computation model that accounts for the non-uniformity of route traffic flow, we define correlated routes, correlated route chains, and correlated route sets, and describe the circumstances under which they emerge. Second, we utilize SOM_DI to figure out which classes of traffic states are relevant for particular loop detectors along a given route chain. In conclusion, we advocate adopting the STFS_SVR method for predicting travel times along correlated route chains.

Problem Definition

Dynamic Spatio-Temporal Convolutional Blocks (DSTCB) and Recurrent Neural Networks (RNN) for traffic prediction analysis improve urban traffic management. This model addresses traffic data's complexity by using





Sarala

CNNs for spatial feature extraction and RNNs for temporal dependency. The adjustable receptive fields of DSTCB allow the model to detect complex spatial patterns in metropolitan areas with different traffic circumstances. Comprehensive spatio-temporal data exposes the model to real-world complications. This research analysis shows the approach's higher prediction power using MSE and RMSE. To strengthen the study, specify a particular issue setting and highlight practical applications to emphasize your research's relevance and influence in improving transportation systems and reducing urban congestion.

MATERIALS AND METHODS

In this section, we provide a comprehensive overview of the materials used and the methodologies employed in our study, aimed at developing an innovative traffic predictive model. The urban landscape is rapidly evolving, marked by an increasing number of vehicles and the consequent challenges of congestion and efficient traffic management. Addressing these challenges necessitates advanced computational techniques that can leverage the complexities of spatio-temporal traffic data. Our approach combines the power of Dynamic Spatio-Temporal Convolutional Blocks (DSTCB) and Recurrent Neural Networks (RNN) to capture both spatial patterns and temporal dependencies within traffic data.

Dynamic Spatio-Temporal Convolutional Blocks

Data skew, or the problem of non-uniform data distribution, is a key performance barrier in real-world distributed systems. Since the existing work on skew mitigation is property-agnostic, it is typically insufficient for distributed spatio-temporal stream processing. Due to the dynamic nature of the geographical and temporal information load, SPEAR offers a GeoHash-based partitioning approach. SPEAR suggests new kinds of distributed data for dealing with unbounded data streams that span both space and time. Are all examples of standard definitions of spatial dimensions that use two or more axes in a particular system. The incorporation of time creates

$$ST(\text{SpatialDim}_{(x,y)}, t) \text{ ----- (1)}$$

$$\text{StreamingST}_{(n)} = ST^i(\text{SpatialDim}_{(x_i,y_i)}, t_i) | i \in [1, n] \text{ ----- (2)}$$

It contains all Spatio-Temporal (ST) occurrences in the data up to time t_n . Not being able to tell the difference between still and moving query objects is a major limitation of traditional spatial and spatio-temporal inquiries and techniques. If the query object is moved or modified in any way, the query must be reissued, either by the user or the system. SPEAR is able to perform Spatio-Temporal Range and Nearest Neighbor inquiries on both static and dynamic query objects since it is based on the suggested streaming data types. Streams of continuity are used to characterize the objects in motion. However, in a distributed setting, data streams are often split up across parallel workers. In its place, we suggest defining dynamic query objects as unbounded streams that are replicated across all distributed workers. Instances of dynamic query objects may be stored in such streams and coupled with the data stream in parallel on geographically dispersed workers.

Recurrent Neural Network

Repeated connections between the buried layer's M units are shown in Figure 2. It is possible that network speed and stability may be enhanced if hidden units were initially assigned non-zero values. What we may term the system's "memory" or "state space" is really the hidden layer.

$$h_t = f_h(o_t) \text{ ----- (3)}$$

Where

$$o_t = W_{IH}x_t + W_{HH}h_{t-1} + b_h \text{ ----- (4)}$$

$f_h(o_t)$ is the activation function for the hidden layer, while b_h is the bias vector for the hidden units. The inferred units' hidden layer is linked to the layer of outputs by weighted connections WHO. The P-units of the output layer may be calculated using the formula $y_t = (y_1, y_2, \dots, y_p)$.

$$y_t = f_o(W_{HO}h_t + b_o) \text{ ----- (5)}$$





Sarala

Separating the activation function $f_o(W)$ from the bias vector b_o in the output layer is crucial. Due to the regularity with which input-target pairs occur, the aforementioned actions are carried out again and over again for $t = (1, \dots, T)$. From these two definitions, it is evident that an RNN is constructed using a system of nonlinear state equations that can be solved in a sequential fashion. Each timestep, the hidden states use the input vector to create an estimate of the future output vector. In an RNN, a straightforward nonlinear activation function is built into each individual node. In the end, a basic model may be able to effectively reproduce complex dynamics with enough time and effort.

Activation Function

Multiple linear hidden layers may accomplish the same goal as a single linear hidden layer in linear networks. What distinguishes nonlinear functions from their linear counterparts is their capacity to have nonlinear boundaries established. RNNs are useful for learning input-target links because of the nonlinearity in one or more successive hidden layers. Typical activation functions are seen in Figure 2. Studies of activation functions including the sigmoid, *tanh*, and rectified linear unit (ReLU) have increased in popularity recently. The "sigmoid" is a well-liked choice since it restricts the range of feasible real numbers. It is common practice to employ a cross-entropy loss function with this activation function when training the output layer of a classification model. The "*tanh*" and "sigmoid" activation functions are defined below:

$$\tanh(x) = \frac{e^{2x} - 1}{e^{2x} + 1} \text{ ----- (6)}$$

And

$$\sigma(x) = \frac{1}{1 + e^{-x}} \text{ ----- (7)}$$

An example of a scaled "sigmoid" activation function is the "*tanh*" activation function.

$$\sigma(x) = \frac{\tanh(\frac{x}{2}) + 1}{2} \text{ ----- (8)}$$

Another common activation function is ReLU, which is defined as where x is any positive number.

$$y(x) = \max(x, 0). \text{ ----- (9)}$$

The particulars of the circumstance and the facts at hand strongly influence the activation function that is selected in the end. The name "sigmoid" is appropriate, for example, for networks whose outputs fall within that range. However, when the neuron is rapidly saturated by "*tanh*" and "sigmoid" activation functions, the gradient disappears. While "*tanh*" does assist, the "sigmoid" function's non-zero centered output might cause the weight gradient updates to behave in an unpredictable manner. When compared to the "sigmoid" or "*tanh*" activation functions, the ReLU activation function produces sparser gradients and greatly speeds up the convergence of stochastic gradient descent (SGD). Setting the activation threshold to 0 makes ReLU computationally efficient. However, if the weight matrix forms during training, the neuron may become inactive since ReLU is not resistant against a significant gradient flow.

Convolutional Neural Networks

The number of trainable features included in each filter used on each layer is what is meant by "parameters." The training procedure weights are learned in a certain manner is determined by the parameters. When it comes to improving the network's efficiency, weights are crucial. Back propagation is a training procedure used to alter the weights of the Weight Matrices, which contribute to the network's prediction ability. CNN is composed of a series of levels, as we've already established. Parameter counts change between layers. There are no trainable parameters in the Input Layer since it just receives the raw data. The model is taught using weight matrices in the Convolutional Layer, the second layer. Here's how to figure out how many parameters this layer, P, has,

$$P = [(m * n * d) + 1 * k] \text{ ----- (10)}$$

where m represents the width of the input, n represents the height, d represents the number of filters in the previous layer, and k represents the number of filters in the current layer. The Pooling Layer, the third layer, just aids in dimensionality reduction and does not involve any learning, hence its parameters are not trainable. Since all neurons





Sarala

in the last layer are linked to all neurons in the preceding layer, there is a maximum number of learnable parameters in this fully-connected layer. This layer's parameter count, P , may be found by using the formula:

$$P = [(N_c * N_p) + (1 * N_c)] \text{----- (11)}$$

Where N_c represents the total number of neurons in the active layer and N_p represents the total number of neurons in the prior layer. The model's efficiency is improved with the use of these adaptable neurons' weights and the Back propagation technique.

RESULTS AND DISCUSSION

In this section, we present the results of our study and engage in a comprehensive discussion of their implications. The findings discussed herein are the culmination of rigorous methodologies and analyses undertaken in our research endeavor. Through a meticulous exploration of the data, we have unearthed significant insights that shed light on traffic predictive analysis. Table 1 shows the existing methods with the proposed Dynamic Spatio-Temporal Convolutional Blocks, it is evident that the proposed approach significantly outperforms the existing techniques in terms of classification performance metrics such as accuracy, precision, recall, and F-measure. The existing methods, including CNN, SVM, and particle swarm optimization, achieved relatively high scores, with accuracy ranging from 93.11% to 95.21%, precision ranging from 94.21% to 95.61%, recall ranging from 95.14% to 96.35%, and F-measure ranging from 95.87% to 96.21%. In contrast, the proposed Dynamic Spatio-Temporal Convolutional Blocks demonstrated exceptional performance, achieving an accuracy of 98.99%, precision of 98.32%, recall of 99.21%, and F-measure of 99.55%. These results indicate that the proposed approach not only provides significantly higher accuracy but also excels in precision, recall, and F-measure, showcasing its effectiveness in accurately classifying instances, minimizing false positives and false negatives, and achieving a balance between precision and recall. The proposed method's superior performance suggests its potential for applications where high accuracy and reliable classification are crucial, making it a robust choice for the specific classification task at hand. The figure 3 shows performance metrics comparison chart the x axis shows metrics and the y axis shows values. Table 2 shows the existing methods with the proposed approach, it is evident that the proposed Dynamic Spatio-Temporal Convolutional Blocks have significantly outperformed the existing techniques in terms of Mean Squared Error (MSE), Root Mean Squared Error (RMSE), Mean Absolute Error (MAE), and Mean Squared Logarithmic Error (MSLE). The existing methods, including deep learning, Support Vector Machine (SVM), and particle swarm optimization, demonstrated higher error metrics, with MSE values ranging from 14.35 to 16.31, RMSE values ranging from 15.42 to 17.61, MAE values ranging from 14.32 to 17.20, and MSLE values ranging from 15.01 to 16.21. In contrast, the proposed Dynamic Spatio-Temporal Convolutional Blocks achieved substantially lower error metrics, with MSE at 9.21, RMSE at 9.41, MAE at 8.54, and MSLE at 8.31. These results signify the superior performance of the proposed approach, suggesting its effectiveness in capturing complex spatio-temporal patterns and making accurate predictions, making it a promising solution for the specific problem at hand. The figure 3 shows error rate comparison chart the x axis shows metrics and th y axis shows values.

CONCLUSION

In summary, our research pioneers a novel method to traffic prediction by combining the adaptive capabilities of Dynamic Spatio-Temporal Convolutional Blocks (DSTCB) with the sequential learning capabilities of Recurrent Neural Networks (RNN). Our model represents a significant leap in comprehending complicated urban traffic patterns by combining Convolutional Neural Networks (CNNs) for spatial feature extraction and RNNs for capturing temporal connections. The dynamic spatio-temporal convolutional blocks exhibit exceptional plasticity, allowing for nuanced analysis of spatial complexities, whilst recurrent neural networks successfully exploit dynamic vehicular motions, resulting in exact forecasts of future traffic situations. A rigorous test against conventional measures confirms our approach's outstanding predictive power, emphasizing its potential to change traffic management. By delivering actionable data to decision-makers, our methodology not only improves traffic flow and reduces congestion, but it also represents a crucial step toward creating smarter, more efficient cities in the future.





REFERENCES

1. A.Agafonov, A. Yumaganov and V. Myasnikov, "Efficiency of Adaptive Traffic Signal Control in a Partially Connected Vehicle Environment," 2023 IX International Conference on Information Technology and Nanotechnology (ITNT), Samara, Russian Federation, 2023, pp. 1-4, doi: 10.1109/ITNT57377.2023.10139039.
2. D. Lee, S. Tak and S. Kim, "Development of Reinforcement Learning-Based Traffic Predictive Route Guidance Algorithm Under Uncertain Traffic Environment," in IEEE Access, vol. 10, pp. 58623-58634, 2022, doi: 10.1109/ACCESS.2022.3179383.
3. H. Sun, Q. Huang, Y. Wei and Z. Liang, "Analysis and Exploration of Expressway Traffic Situation," 2022 IEEE 7th International Conference on Intelligent Transportation Engineering (ICITE), Beijing, China, 2022, pp. 1-6, doi: 10.1109/ICITE56321.2022.10101398.
4. L. Chen, F. Yang, Q. Xing, S. Wu, R. Wang and J. Chen, "Spatial-Temporal Distribution Prediction of Charging Load for Electric Vehicles Based on Dynamic Traffic Information," 2020 IEEE 4th Conference on Energy Internet and Energy System Integration (EI2), Wuhan, China, 2020, pp. 1269-1274, doi: 10.1109/EI250167.2020.9347194.
5. L. Shen, R. Liu, Z. Yao, W. Wu and H. Yang, "Development of Dynamic Platoon Dispersion Models for Predictive Traffic Signal Control," in IEEE Transactions on Intelligent Transportation Systems, vol. 20, no. 2, pp. 431-440, Feb. 2019, doi: 10.1109/TITS.2018.2815182.
6. M. F. Fathurrahman, H. Y. Sutarto and I. Semanjski, "Urban Network Traffic Analysis, Data Imputation, and Flow Prediction based on Probabilistic PCA Model of Traffic Volume Data," 2021 8th International Conference on Advanced Informatics: Concepts, Theory and Applications (ICAICTA), Bandung, Indonesia, 2021, pp. 1-6, doi: 10.1109/ICAICTA53211.2021.9640284.
7. M. Kang, H. Park, C. Han and G. Gim, "Analysis of the Predictive Power of Highway Traffic Flow with Weather Conditions," 2022 IEEE/ACIS 7th International Conference on Big Data, Cloud Computing, and Data Science (BCD), Danang, Vietnam, 2022, pp. 45-49, doi: 10.1109/BCD54882.2022.9900728.
8. N. Lyu, J. Wen, Z. Duan and C. Wu, "Vehicle Trajectory Prediction and Cut-In Collision Warning Model in a Connected Vehicle Environment," in IEEE Transactions on Intelligent Transportation Systems, vol. 23, no. 2, pp. 966-981, Feb. 2022, doi: 10.1109/TITS.2020.3019050.
9. N. Zhao, F. Zhang, Y. Yang, S. Coskun, X. Lin and X. Hu, "Dynamic Traffic Prediction-Based Energy Management of Connected Plug-In Hybrid Electric Vehicles with Long Short-Term State of Charge Planning," in IEEE Transactions on Vehicular Technology, vol. 72, no. 5, pp. 5833-5846, May 2023, doi: 10.1109/TVT.2022.3229700.
10. S. Anveshrihaa and K. Lavanya, "Real-Time Vehicle Traffic Analysis using Long Short Term Memory Networks in Apache Spark," 2020 International Conference on Emerging Trends in Information Technology and Engineering (ic-ETITE), Vellore, India, 2020, pp. 1-5, doi: 10.1109/ic-ETITE47903.2020.97.
11. S. He, S. Wang, Y. Shao, Z. Sun and M. W. Levin, "Real-Time Traffic Prediction Considering Lane Changing Maneuvers with Application to Eco-Driving Control of Electric Vehicles," 2023 IEEE Intelligent Vehicles Symposium (IV), Anchorage, AK, USA, 2023, pp. 1-7, doi: 10.1109/IV55152.2023.10186645.
12. S. Subhashini and R. Maruthi, "A Predictive Model for Road Traffic Data Analysis and Visualization to Detect Accident Zones," 2023 9th International Conference on Advanced Computing and Communication Systems (ICACCS), Coimbatore, India, 2023, pp. 1227-1231, doi: 10.1109/ICACCS57279.2023.10112862.
13. T. Zhang, J. Xu, S. Cong, C. Qu and W. Zhao, "A Hybrid Method of Traffic Congestion Prediction and Control," in IEEE Access, vol. 11, pp. 36471-36491, 2023, doi: 10.1109/ACCESS.2023.3266291.
14. Y. -C. Lai, S. -Y. Chen, S. -F. Wang and B. -S. Lin, "A Weather-Based Traffic Prediction System Using Big Data Techniques," 2022 12th International Conference on Advanced Computer Information Technologies (ACIT), Ruzomberok, Slovakia, 2022, pp. 379-383, doi: 10.1109/ACIT54803.2022.9913125.
15. Y. Shao and Z. Sun, "Eco-Approach With Traffic Prediction and Experimental Validation for Connected and Autonomous Vehicles," in IEEE Transactions on Intelligent Transportation Systems, vol. 22, no. 3, pp. 1562-1572, March 2021, doi: 10.1109/TITS.2020.2972198.





Sarala

16. Y. Zhang, Y. Zhou, H. Lu and H. Fujita, "Spark Cloud-Based Parallel Computing for Traffic Network Flow Predictive Control Using Non-Analytical Predictive Model," in IEEE Transactions on Intelligent Transportation Systems, vol. 23, no. 7, pp. 7708-7720, July 2022, doi: 10.1109/TITS.2021.3071862.
17. Z. Zhang and W. Zhang, "Traffic pattern analysis and traffic state prediction of urban traffic road network based on correlated routes," 2020 39th Chinese Control Conference (CCC), Shenyang, China, 2020, pp. 5654-5659, doi: 10.23919/CCC50068.2020.9189082.
18. Z. Zhang, D. Yao, F. Wu and J. Shen, "Real-time Vehicle Velocity Prediction Strategy under Highway Vehicle-to-vehicle Environment," 2022 IEEE Transportation Electrification Conference and Expo, Asia-Pacific (ITEC Asia-Pacific), Haining, China, 2022, pp. 1-5, doi: 10.1109/ITECAsia-Pacific56316.2022.9941847.

Table 1: Performance metrics comparison

	Algorithm	Accuracy	Precision	Recall	F-measure
Existing methods	CNN	93.11	94.21	95.67	95.94
	SVM	94.52	94.65	95.14	95.87
	particle swarm optimization	95.21	95.61	96.35	96.21
Proposed methods	Dynamic Spatio-Temporal Convolutional Blocks	98.99	98.32	99.21	99.55

Table 2: Error rate comparison table

	Algorithm	MSE	RMSE	MAE	MSLE
Existing methods	deep learning	16.31	17.61	17.20	16.21
	SVM	15.92	17.29	17.01	16.12
	particle swarm optimization	14.35	15.42	14.32	15.01
Proposed methods	Dynamic Spatio-Temporal Convolutional Blocks	9.21	9.41	8.54	8.31

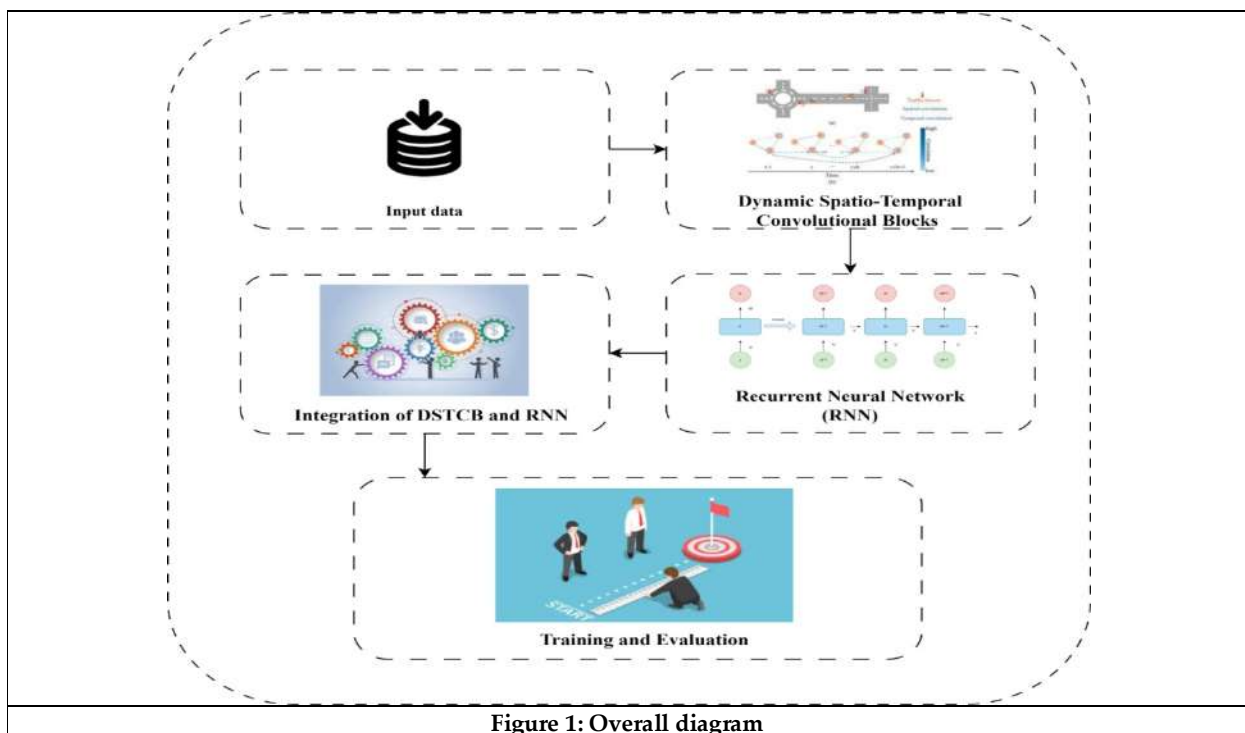


Figure 1: Overall diagram





Sarala

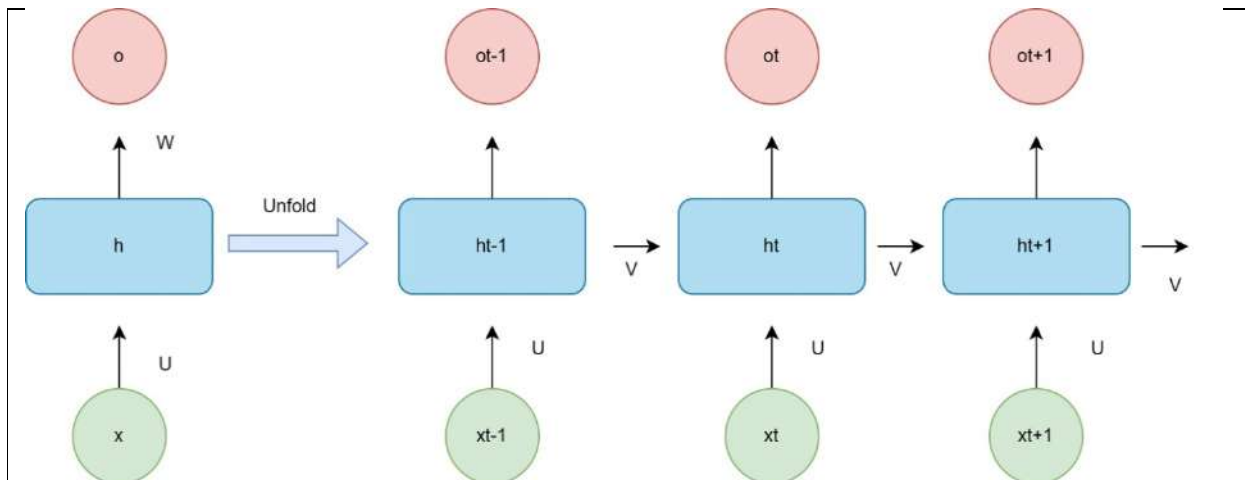


Figure 2: Recurrent Neural Network architecture

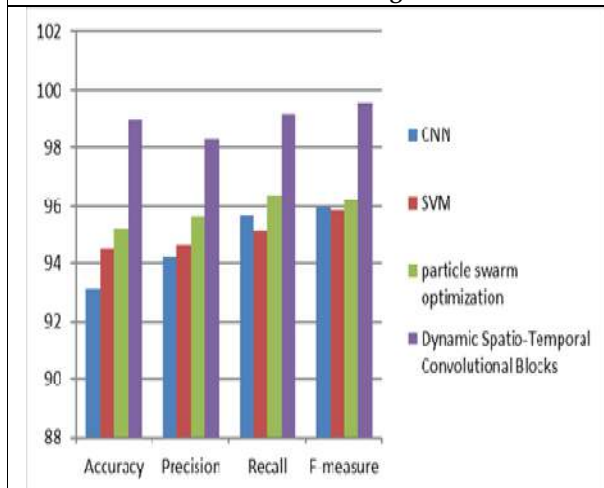


Figure 3: Performance metrics comparison chart

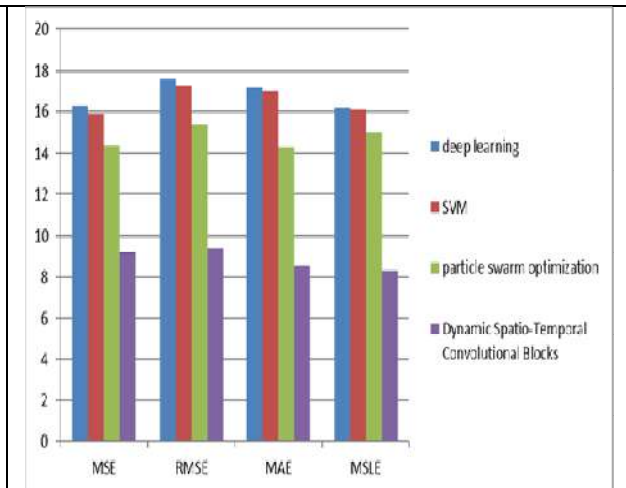


Figure 3: Error rate comparison chart





Clinical uses and Application of *Cocos nucifera* in Dentistry: A Narrative Review

Lakshmi Thribhuvan^{1*}, M. S. Saravanakumar², Priyanka Lekhwani³ and Karan Bharvada⁴

¹Assistant Professor, Department of Pediatric and Preventive Dentistry. Dr. D. Y. Patil Dental College and Hospital, (Affiliated to Dr.D.Y.Patil Vidyapeeth) Pune, Maharashtra, India.

²Professor and HoD, Department of Pediatric and Preventive Dentistry, Sri Venkateshwara Dental College (Affiliated to Dr.MGR Medical University), Chennai, Tamil Nadu, India.

³Assistant Professor, Department of Pediatric and Preventive Dentistry. Dr.D.Y.Patil Dental College and Hospital (Affiliated to Dr.D.Y.Patil Vidyapeeth) Pune, Maharashtra, India.

⁴Assistant Professor, Department of Prosthodontics Crown and Bridge, Mahatma Gandhi Dental College and Hospital (Affiliated to Mahatma Gandhi University of Medical Sciences and Technology) Jaipur, Rajasthan, India.

Received: 30 Dec 2023

Revised: 09 Jan 2024

Accepted: 12 Jan 2024

*Address for Correspondence

Lakshmi Thribhuvan

Assistant Professor,

Department of Pediatric and Preventive Dentistry.

Dr. D. Y. Patil Dental College and Hospital, (Affiliated to Dr.D.Y.Patil Vidyapeeth)

Pune, Maharashtra, India.



This is an Open Access Journal / article distributed under the terms of the **Creative Commons Attribution License** (CC BY-NC-ND 3.0) which permits unrestricted use, distribution, and reproduction in any medium, provided the original work is properly cited. All rights reserved.

ABSTRACT

Oral health continues to be one of the most uprising dental concerns in today's world. Dental caries and other associated oral diseases still continue to remain one of the globally advancing concerns irrespective of region, population or gender. The uphill rise in the available dental services and lack of dental insurance schemes in developing countries continually refrain the dependent population from availing any of these advised dental health services thereby prioritizing their other health care needs. However with due consideration with the existent treatment modalities with advanced technologies the amount of toxicity still persist in par with the advantageous effects. Researchers taking in to considerations all these aspects of hence continue to expand their studies to naturally available product and remedies. These would thereby enhance and counteract available side effects of existing commercially available dental products and thereby counteract the unbearable financial constraints up to greater effects. *Cocos nucifera* or coconut has been studied to have high medicinal values is a common herb found along Indian tropical land. Coconut have been investigated to possess high medicinal value which has been found to be beneficial to the general health of the individual, hence this review will evaluate the profound applications of *Cocos nucifera* in dentistry.

Keywords: Oral health, Herbal, *Cocos nucifera*, Dentistry, Pediatric Patients





Lakshmi Thribhuvan et al.,

INTRODUCTION

Dental health is considered as one of the most significant arena which presumably determines the general health of the affected individual. An ultimate depletion of the predefined oral health greatly affects the estimated life quality as it entraps and continues to remain as an obstacle untimely testifying the patient's daily routine which encompassed speech, mastication and esthetics confining to the individual.[1,2] Diseases of the oral cavity ensembles as one of the most ravishly propagating public health concerns considerably affecting the ultimatum of mankind in all possible reasons and concerns. Dental treatment prevails to continue as one of the sought out speciality with highly anticipated and expected financial burden.[3] The burdened difficulty in availing these needed dental services still continue to persist and remain inaccessible for population and communities of people especially those belonging to underprivileged more oftenly from developing countries. The commonly available dental products due to its evidenced antimicrobial properties are being widely into routine utilization due to its considerably higher and value added beneficial effects still exhibits to possess several side effects though outlining their needed effects including severe burning sensation, mucosal irritation, unpleasant taste, ulcers etc.[4,5]

Hence to provide with most viable and sustainable alternatives which would be considerably harmless, less expensive and more reliable than the routinely available dental treatment modalities for the widely existing dental problems with naturally available more permissible options.[6] These available constraints led to the spacely utilization of naturally available herbal derivatives in constant and multiple combinations which have been evidenced to provide with a more appropriate and comparatively safe cure for the existing and prevailing dental conditions requiring an utmost treatment.[7] Newer evidence based research lining up in the field of Herbal Medicine have inadvertently reestablished the undeniable fact that the naturally inherent constituents within these medicinal plants and shrubs would undoubtedly alter in providing a minimalistic risk involved treatment protocol with negligible or concisely nil specified adverse reactions on its consumption.[8,9] Consistent use of these proven natural derivatives not only provides a highly reasonable and acceptable treatment modalities but also emphasizes on sustained preventive strategies in a scheduled manner with respect to definitive oral health care needs.[10,11]

Hence recently specified and researched experimental studies have proven that these naturally available products including herbal and other plant extracts exhibit highly specific properties which contributes to maintenance of the deteriorating oral health.[12] These naturally available plants also produce useful biproducts which can be added up in the preparation of ideal and novel beneficiary medicaments and alternatives which could provide with a subsidiary alliance in dental health maintenance. The realistic approach with evidence based results also claim that dental care products with natural plant extracts are considered as the new advent due to their implacably minimal adverse reactions, financial reasonability and ease of accessibility.[13] Several herbal products are in the long line run in dentistry which include tulsi, curcumin, aloe vera, mint and rose mary.[14] The research work and the related literature thereby establishes the determining fact that these available plant extracts have remarkable inhibitory effects thereby preventing the occurrence of dental caries and periodontal diseases. In addition to these available cures for dental diseases these plant derivatives have one of the major added benefits of confinely being sugar free and alcohol free which makes these as one of the most opted alternatives.[15] *Cocos nucifera* is considered as "a functional which had already found its wide application in medicine. This review will discuss in detail about the dental implications of *Cocos nucifera*, widely grown tree in Indian subcontinent which has proven its undeniable medicinal properties.[16,17]

***Cocos nucifera*(Coconut)**

Cocos nucifera, coconut palm belongs to the family of *Arecaceae*. Coconut is defined botanically as highly nutritious one seeded fruit which is predominantly rich in fibers, vitamins and essential minerals. The scientific classification of *cocos nucifera* is given in Table.1 and their common names are explained in Table.2 Coconut palms are abundantly found across the globe with the occurrence of main vegetation along the tropical regions of Asian and African





Lakshmi Thribhuvan et al.,

subcontinents namely India, Sri Lanka, Brazil etc [18]. The coconut thus forms one of the most important constituent of the staple diet in these regions which paves to provide majority of the nutrient content. The Coconut fruit is considered as the most functional food which is primarily composed of three main layers namely exocarp or outer layer, the mesocarp (fleshy, middle layer), and the endocarp (hard, woody).[5]The husk of the coconut is hecce formed by exocarp and mesocarp.[19,20] Coconut oil is considered to be one of the most abundant sources of evidently available saturated fats. It is a prime reservoir of nearly 90% of the available fatty acids.[21]These available fatty acids predominantly constitutes of medium chain fatty acids. Lauric acid is the prime constituent of these which makes up nearly 50-60% of coconut oil.[21, 22] Studies conducted by Longo et al stated thatlauric acid has been found to be predominantly effective in killing oral pathogens including E. coli and Candida species.[23]Coconut water is composed of various beneficial aminoacids, nutrients and minerals in un defineable levels. Another important constituent is Caprylic acid which nearly contributes to 10% and is found to be effective against candida thereby defining its strong antifungal along with its persistent antiviral properties.[24]Coconut oil is also composed of several other essential oils and aminoacids including palmitic acid, oleic acid, linoleic acid and stearic acid which have been substantially proven to be highly essential in promoting several health benefits of lowering cholesterol levels and as effective antioxidant.[25] Apart from these the coconut fruit is also assumed to possess Vitamin E in large quantities. Hence coconut is estimated by recent studies to exemplary contribute and reasonably enhance the individuals quality of life with added dental along with these evident health effects.

BOTANICAL and BIOLOGICAL PROPERTIES

Cocos nucifera consists of an even, pier layered, greyish brown trunk with a mean diameter of 30-40cm outdid with coronet of leaves. They may appear as tall and dwarf varieties depending on its existential height variances.[25]The main trunk appears to be slender and proceeds to have a broader anatomy towards the base. The leaves appears to be schematically ordered in plumage manner about 4-7m in length and 1-1.5m in width. The leaf plumage appears to extend to 1-2cm in length. The inflorescence possess both male and female flower domains which appear as bright yellow congregate forming pirogue shaped tunica among its leaves.[25,26]Male domain blossoms are comparatively tiny and numerous whereas female flower domains are minimalistic, nearly 25mm in diameter and most often remains to be mislaid in most of the scenarios. The coconut fruit is ovoid making up about 5cm in length and 3cm in width composed of husk which is fibrous in consistency encapsulating the spherical nut with an approximate diameter of 2-2.5cm and nearly 3-4cm in length.[26]The coconut "Eyes" are three recessed holes of soft tissue are found along one of the nut corners. The hard shell is encompassed with white slimy and fleshy layer avidly known as the "meat" which is consumed for its nutritional benefits. The inner portion of the coconut nut is nearly filled with so called "coconut milk."The Coconut water is considered as an evidently available suspension of endosperm. It appears to be one of the most consumable drinks throughout the world as it compensates to provide all the necessary elements for the human body.[26] Coconut water is composed of essential nutrients, vitamins, proteins, minerals and antioxidants.[27]Apart from this coconut water is considered as in inevitable immunity enhancer due to the presence of all these essential elements.[27]

CHEMICAL CONSTITUENTS IN COCONUT

Lauric acid is one of the major essential constituent present in coconut fruit. It constitutes to nearly 50% of the coconut oil which contribute it into making it as one of the most strong and reliable antimicrobial agent.[25] The second major component id Myristic acid which constitutes to 20% and is now a widely acceptable utility in food industry as a flavoring agent. Caprylic, Capric and Caproic acid present in the coconut contributing to a total of 10% acts as susceptible antifungal agent and is proven to be efficiently active against Candida albicans and also can continue to serve as ideal antimicrobial agents.[25] Palmitic acid and Oleic acid present in coconut is considered as a strong antioxidant and aids in cholesterol reduction. Linoleic acid being one of the minimalistic component present in coconut has been recorded to act as a strong immune activator in children as well as one of the most potentially strong antioxidant available.[26]





Lakshmi Thribhuvan et al.,

APPLICATIONS IN DENTISTRY ANTIMICROBIAL PROPERTIES

Coconut is composed of Monolaurin in addition to other existent medium chain fatty acids which is assumed to possess with the capacitance of activity against microbial cell constituents resulting in cellular disruption and function accordingly. Monolaurin along with other desirable fatty acids has an immense role in deactivation and alteration process of existing bacterial pathogens in particularly S mutans which play a significant role in early childhood caries.[28] Lavine et al in his studies has detailed that the lauric acid in coconut oil has definitive antimicrobial activity against Streptococcus mutans which appeared to be higher than that of chlorhexidine which appeared to be higher than chlorhexidine.[29] Kaushik et al also made significant contributions through their studies stating that virgin coconut oil causes rapid and highly significant reduction in growth of S.mutans thereby displaying its antibacterial potentials.[30] Candida is one of the most common commensal of the oral cavity which appears to range to about 20-40% in healthy oral cavity. Apart from this coconut oil has also been estimated to have considerable activity against Candida species which also defines its antifungal effect. Ghasempour et al have stated through his studies that C. albicans can at ease combine and interact resulting in dissolution of hydroxyapatite crystals thereby rendering nearly 20 fold reactivity rates making it an ideal antifungal agent.[31] Tjin et al has clearly specified that the caproic acid present in virgin coconut oil has well defined static effects against candidal species in addition to the presence of lauric acid.[32] Chiaw et al in his experimental studies have determined that Capric acid present in virgin coconut oil possess substantially evident antiviral and anti fungal properties against oral pathogens thereby preventing their adhesion.[33] These antibacterial and antifungal effects of virgin coconut oil is mainly enhanced due to the monolaurin and lauric acid content within it which results in alteration of bacterial cell wall contents thereby causing active disruption and inactivation of bacterial cell wall components along with inhibition of candidal species and restricting their unwarranted growth within the oral cavity.

STORAGE MEDIUM

Coconut water forms the liquid endosperm of coconut drupe. This water is highly supplemented with pooling of several essential vitamins, nutrients and amino acids. Coconut water is cohesively considered as one of the most substantial hydrolyzing constituent which is supplemented with all the required nutrients. However studies conducted by Gopikrishna et al. on coconut water has definitely claimed the fact that it continues to serve as an ideal storage medium which has highest potential in maintaining the viability of periodontal ligament cells in par with other available storage medias.[34] Coconut water has been studied thoroughly on its highly efficient nature regarding the comparable osmolality, composition and easy acceptance and predominant ability for the maintenance of viability of periodontal ligament which makes it to be considered as an ideal storage medium for avulsed teeth.[35] However the main disadvantage regarding the consideration of coconut water as an ideal medium for avulsion was that Moreira-Neto et al observed that coconut water which had an acidic pH of 4.1 was undeniably claimed to cause devastating and deleterious effects on persistent metabolism of cells and hence stated that coconut water has comparatively moderate capacitance in maintaining periodontal cell viability when in comparison to milk.[36]

ORAL HEALTH ENHANCEMENT IN CHILDREN WITH AUTISM

Oral health care needs have always been prime concern for children, however the concern still appears to be more consistent and demandable in those with special health care needs. Research studies conducted on the efficiency of available agents of coconut oil and palm kernel oil have been identified to reasonably prevent and maintain the oral health of children with special health care needs.[37] Studies conducted by Thaweboon et al has established the fact that coconut oil has high rate of inhibition against Streptococcus mutans and has thus found extend its high oral health care maintenance rate in children with special health care needs when in comparison to corn oil, palm oil, bran oil, sunflower oil and sesame oil.[38]

VIRGIN COCONUT OIL AS MOUTHWASH

The requisites of an ideal plaque agent regarding its justifiable and systematic daily utilization in children were that it should not cause any unwanted interference with normal persistent biota of the oral environment, should be



**Lakshmi Thribhuvan et al.,**

compatible to the oral mucosa in relation to the expected primary concerns that it should be ideally non irritant and non toxic if devoured by children along with being sugarless and non alcohol containing constituent.[38] Peedikayil et al. in his experimental in study critically compared the existent antibacterial activity of chlorehexidine and coconut oil against *Streptococcus mutans* and concluded that coconut oil can be ideally utilized as a swishing mouth wash agent as it reduced the *Streptococcus mutans* count in ratio comparable to that of chlorhexidine. [39]

TRADITIONAL OIL PULLING

The practice of oil pulling is a traditional treatment modality evolved in Ayurvedic treatment practice involving the method of cleansing the oral cavity with a tablespoon of coconut oil for a period of twenty minutes. After 20 minutes of complete swishing of the oral cavity with coconut oil the patient is then advised to expectorate the oil and brush accordingly. Due to the swishing motion within the oral cavity, it prevents accumulation of any food debris or microorganisms around the teeth, gingiva and other associated oral structures as in due to the created inverted pressure within the oral cavity.[40]

CONCLUSION

Dental diseases have always been a serious concern, though there exists large number of synthetically synthesized products these still possess side effects of toxicity to surrounding tissues. Traditional medicine seems to be one of the most affordable emerging treatment trends as it seems to find a validated solution which appears to be non-toxic to both surrounding tissues as well as environment. *Cocos Nucifera* is a common tropical tree found in Indian sub-continent which has already been proven to provide ultimate medicinal uses along with substantiated and beneficial health effects. *Cocos nucifera* presents with highly appreciable health benefits and it is high biocompatibility thereby requires the need for more research and analytical studies on its avid applications in dentistry and the need for procurement of more dental products with the alternative and superficial beneficial effects of coconut.

REFERENCES

1. Adkins, S.W., M. Foale and Y.M.S. Samosir. (Eds.). Coconut revival – new possibilities for the ‘tree of life’. Proceedings of the International Coconut Forum held in Cairns, Australia, 22–24 November 2005. ACIAR Proceedings 2006, 125.
2. Nevin KG, Rajamohan T., Beneficial effects of virgin coconut oil on lipid parameters and in vitro LDL oxidation. *Clinical Biochemistry*. 2004, 37(9):830-835.
3. Andrade AM, Passos PRA, Marques LGC, Oliveira LB, Vidaurre GB, Roch JDS. Pirólise de resíduos do coco-da-baía (*Cocos nucifera* Linn) e análise do carvão vegetal. *Rev Árvore* 2004; 28: 707–714.
4. Esquenazi MD, Wigg MM, Miranda, Rodrigues HM, Tostes JBF, Rozental S, et al. Antimicrobial and antiviral activities of polyphenolics from *Cocos nucifera* Linn. (*Palmae*) husk fiber extract. *Res Microbiol* 2002; 153: 647–652, doi: 10.1016/S0923-2508(02)01377-3
5. Al-Adhroey AH, Nor ZM, Al-Mekhlafi HM, Amran AA, Mahmud R. Evaluation of the use of *Cocos nucifera* as antimalarial remedy in Malaysian folk medicine. *J Ethnopharmacol* 2011; 134: 988–991, doi: 10.1016/j.jep.2011.01.026
6. Solangih A, Iqbal ZA. Chemical composition of meat (kernel) and nut water of major coconut (*Cocos nucifera* L.) cultivars at coastal area of Pakistan. *Pak. Am J Bot* 2011; 43: 357–363
7. Singla RK, Jaiswal N, Bhat GV, Jagani H. Antioxidant and antimicrobial activities of *Cocos nucifera* Linn. (*Arecaceae*) endocarp extracts. *Indo Global J Pharm Sci* 2011; 1: 354–361.
8. Tjin LD, Setiawan AS, & Rachmawati E. Exposure Time of Virgin Coconut Oil Against Oral *Candida Albicans*. *Padjajaran J Dent* 2016;28:89-94
9. Verma V, Bhardwaj A, Rathi S, Raja R.B. Potential antimicrobial agent from *Cocos nucifera* mesocarp extract. *Int Res J Biol Sci* 2012; 1: 48–54.





Lakshmi Thribhuvan et al.,

10. Akinyele TA, Okoh OO, Akinpelu DA, Okoh AI. In-vitro antibacterial properties of crude aqueous and n-hexane extracts of the husk of *Cocos nucifera*. *Molecules* 2011; 16: 2135–2145, doi: 10.3390/molecules16032135.
11. Seneviratne KN, Dissanayake DMS. Variation of phenolic content in coconut oil extracted by two conventional methods. *Inter J Food Sci Technol* 2008; 43: 597–602.
12. Seneviratne KN, Dissanayake DMS. Variation of phenolic content in coconut oil extracted by two conventional methods. *Inter J Food Sci Technol* 2008; 43: 597–602
13. Santos JL, Bispo VS, Filho AB, Pinto IF, Dantas LS, Vasconcelos DF, et al. Evaluation of chemical constituents and antioxidant activity of coconut water (*Cocos nucifera* L.) and caffeic acid in cell culture. *An Acad Bras Cienc* 2013; 85: 1235–1247,
14. Erosa FE, Gamboa-León MR, Lecher JG, Arroyo-Serralta GA, Zizumbo-Villareal D, Oropeza-Salín C, et al. Major components from the epicuticular wax of *Cocos nucifera*. *Rev Soci Química México* 2002; 46: 247–250
15. Singla RK, Jaiswal N, Bhat GV, Jagani H. Antioxidant and antimicrobial activities of *Cocos nucifera* Linn. (*Arecaceae*) endocarp extracts. *Indo Global J Pharm Sci* 2011; 1: 354–361.
16. Mathew, Minne T. "Coconut and Coconut Oil." *Comp. Nanda Kumar. Ed. Sana John. Coconut Insights 1* (Sept. 2007): n. pag. Coconut Developmental Board. Coconut Developmental Board, Sept. 2007. Web. 27 July 2013.
17. Gupta, Shewta. "Coconut Palm (tree)." *Encyclopedia Britannica Online. Encyclopedia Britannica, 2013. Web. 30 July 2013.*
18. Perera, L. Suriya A.C.N. Perera, C. K. B. and Hugh C. H., "Chapter 12 – Coconut". In Johann Vollmann and Istvan Rajcan (Eds.). *Oil Crops. Springer, 2009, pp. 370–372.*
19. Silva RR, Oliveira e Silva, Fontes HR, Alviano CS, Fernandes PD, Alviano DS. Anti-inflammatory, antioxidant, and antimicrobial activities of *Cocos nucifera* var. *typica*. *BMC Complement Altern Med* 2013; 13: 107
20. Esquenazi MD, Wigg MM, Miranda, Rodrigues HM, Tostes JBF, Rozental S, et al. Antimicrobial and antiviral activities of polyphenolics from *Cocos nucifera* Linn. (*Palmae*) husk fiber extract. *Res Microbiol* 2002; 153: 647–652, doi: 10.1016/S0923-2508(02)01377-3
21. Arlee R, Suanphairoch S, Pakdeechanuan P. Differences in chemical components and antioxidant-related substances in virgin coconut oil from coconut hybrids and their parentes. *Int Food Res J* 2013; 20: 2103–2109
22. Debmandal M, Mandal S: Coconut (*Cocos nucifera* L.: *Arecaceae*): in health promotion and disease prevention. *Asian Pacific J Trop Medic*; 4 (3):241- 247, 2001
23. Longo, Natasha. "Antibacterial Action of Coconut Oil Combats Tooth Decay When Consumed." *Antibacterial Action of Coconut Oil Combats Tooth Decay When Consumed. PreventDisease.com, 3 Sept. 2012. Web. 25 July 2013.*
24. Pehowick DJ, Gomes AV, Branes JA: Fatty acid composition and possible health effects of coconut constituents. *West Indian Med*; 49: 128-133,2000
25. Gayatri A, Fauziah EVA, & Suharsini M. Antibacterial Effect of Virgin Coconut Oil on the Viability of Chromogenic Bacteria That Causes Dental Black Stain in Children. *Int J Appl Pharm* 2017;9:83-6.
26. Biofilm M, Lee J, & Jo Y. Antimicrobial Effect of a Lauric Acid on *Streptococcus*. 2016;60-5.
27. Dyyrit FM: Properties of Lauric acid and their significance in coconut oil. *J Am Oil Chemists Soc*; 92: 1-15, 2015.
28. Seleem D, Chen E, Benso B, Pardi V, & Murata RM. In Vitro Evaluation of Antifungal Activity of Monolaurin Against *Candida Albicans* Biofilms. *PeerJ* 2016;4:e2148
29. Lavine P, Fauziah E, Rizal MF, & Budiardjo SB. Antibacterial Effect of Virgin Coconut Oil on the Viability of Chromogenic Bacteria That Causes Dental Black Stain in Children. *Int J Appl Pharm* 2017;9:83-6.
30. Kaushik M, Reddy P, Sharma R, Udameshi P, Mehra N, Marwaha A. The Effect Of Coconut Oil Pulling on *Streptococcus Mutans* Count in Saliva in Comparison with Chlorhexidine Mouthwash. *J Contemp Dent Pract* 2016;17:38-41.
31. Ghasempour M, Sefidgar A, Eyzadian H, Gharakhani S. Prevalence of *Candida albicans* in dental plaque and caries lesion of early childhood caries (ECC) according to sampling site. *Casp J Intern Med* 2011; 2: 304-308.
32. Tjin LD, Setiawan AS, & Rachmawati E. Exposure Time of Virgin Coconut Oil Against Oral *Candida Albicans*. *Padjajaran J Dent* 2016;28:89-94
33. Chiaw MS, Hip SY, & Lai CM. Commercial Virgin Coconut Oil: Assessment of Antimicrobial Potential. *Asian J Food Agro-Industry* 2010;3:567-79.





Lakshmi Thribhuvan et al.,

34. Gopikrishna V, Baweja PS, Venkateshbabu N, Thomas T, Kandaswamy D. Comparison of coconut water, propolis, HBSS, and Milk on PDL cell survival. J Endod 2008 May;34(5): 587-589.
35. Layug ML, Barrett EJ, Kenny DJ. Interim storage of avulsed permanent teeth. J Can Dent Assoc 1998 May;64(5):357-369.
36. Moreira-Neto JJ, Gondim JO, Raddi MS, Pansani CA. Viability of human fibroblasts in coconut water as a storage medium. International endodontic journal. 2009 Sep;42(9):827-30.
37. Nagao K, Yanagita T. Medium-chain fatty acids: Functional lipids for the prevention and treatment of the metabolic syndrome. Pharmacol Res 2010; 61:208-12.
38. Thaweboon S, Nakaparksin J, Thaweboon B. Effect of oil-pulling on oral microorganisms in biofilm models. Asia J Public Health 2011; 2:62-6.
39. Subramaniam P, Nandan N. Effect of xylitol, sodium fluoride and triclosan containing mouth rinse on Streptococcus mutans. Contemp Clin Dent 2011;2(4):287–290.
40. Athlone Institute of Technology. 2012 Press Releases. - Athlone Institute of Technology. N.p., 3 Sept. 2012. Web. 30 July 2013.

Table 1. Scientific Classification.[18]

Kingdom	Plantae
Phylum	Magnoliophyta
Class	<u>Liliopsida</u>
Subclass	Arecidae
Order	<u>Arecales</u>
Family	<u>Arecaceae</u>
Genus	Cocos
Subject	Cocos nucifera Linnaeus

Table 2. Local Names.[19]

Bengali	narikel
English	coconut palm,coconut
French	coco
German	kokospalme
Indonesian	kelapa
Italian	cocco
Tamil	(tennai-maram

APPLICATIONS IN MEDICINE.[26]

PARTS OF COCONUT	PREPARATION	MEDICINAL USES
Coconut shell	Tea	Diarrhea, Amenorrhea, Venereal diseases
	Extract	Antipyretic, kidney inflammation, gonorrhea treatment, Urogenital inflammation
	Cream	Amenorrhea, dysmenorrhea, Diabetes, Asthma, Abscesses, Dermatitis
Root	Tea	<u>Diarrhoea</u>
Coconut Pulp	Oil	Antipyretic, diarrhea, hair loss, wound healing
	Milk	Diarrhoea, NSAID associated antiulcer
	Pulp	Relief to rashes caused by HIV-AIDS
	Water	Fever, Malaria, Renal diseases, changes in the menstrual cycle





Synthesis, Characterization and Catalytic Activity of Heterogeneous MoO₂(VI), Ni(II), and UO₂(VI) Complexes

Amit Kumar¹ and Praveen Kumar Gupta^{2*}

¹Assistant Professor, Department of Chemistry, Indira Gandhi National College, Ladwa, Affiliated to Kurukshetra University, Kurukshetra, Haryana, India.

²Professor, Department of Chemistry, Maharishi Markandeshwar (Deemed to be University), Mullana, Ambala, Haryana, India.

Received: 30 Sep 2023

Revised: 20 Nov 2023

Accepted: 19 Jan 2024

*Address for Correspondence

Praveen Kumar Gupta

Professor,

Department of Chemistry,

Maharishi Markandeshwar (Deemed to be University),

Mullana, Ambala, Haryana, India.

Email: parveen.gupta@mmumullana.org



This is an Open Access Journal / article distributed under the terms of the **Creative Commons Attribution License** (CC BY-NC-ND 3.0) which permits unrestricted use, distribution, and reproduction in any medium, provided the original work is properly cited. All rights reserved.

ABSTRACT

We have successfully synthesized novel mixed ligand precursor, PSCH₂-L'H₂, supported on polystyrene resin, along with their coordination complexes involving Mo(VI), Ni(II), and U(VI). The PSCH₂-L'H₂ compounds were prepared by reacting chloromethylated polystyrene crosslinked with divinylbenzene(PSCH₂-Cl) with ligand precursor (L'H₂) derived from propylenediamine, 3-formylsalicylic acid and acetylacetone. Subsequently, the coordination complexes were formed by reacting PSCH₂-L'H₂ with the respective metal salts in dimethylformamide. Characterization of these compounds was conducted using elemental analyses, infrared spectroscopy (IR), diffused reflectance spectroscopy, and magnetic susceptibility measurements. The observed shifts in the vibrational frequencies of the C–O (phenolic), C=N (azomethine), and C–O (enolic) groups suggest the NNOO donor behavior exhibited by PSCH₂-L'H₂. Specifically, the polystyrene-supported Ni(II) complex adopts a square planar geometry, while the MoO₂(VI) and UO₂(VI) complexes adopt octahedral geometries. Importantly, all the synthesized PSCH₂-L'M complexes (where M = MoO₂, Ni, and UO₂) exhibit diamagnetic properties. The catalytic activities of these heterogeneous complexes were investigated for the decomposition of hydrogen peroxide. Ni(II) and Mo(VI) complexes were found to be effective in the catalytic decomposition of hydrogen peroxide.

Keywords: Polymer support, Chloromethylated Polystyrene, metal complexes, mixed Schiff base, diffused reflectance spectra, catalytic activity



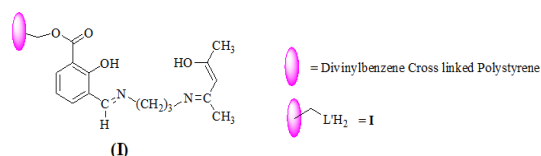


Amit Kumar and Praveen Kumar Gupta

INTRODUCTION

The immobilization of transition metal ions onto polymer supports presents an efficient pathway for the synthesis of immobilized coordination complexes, a versatile class of materials with a multitude of practical applications. These chelating resins find wide-ranging utility in diverse fields, including catalysis[1–4]. For instance, the employment of Fe(III) anchored to a polystyrene-supported complex has demonstrated remarkable efficacy in facilitating the epoxidation of cis-cyclooctene and styrene in the presence of tert-butylhydroperoxide, exemplifying their significance as catalysts. Moreover, they have been crucial in the area of metal ion separation processes[5–8]. Notably, chelating polystyrene divinylbenzene-based resins incorporating quinaldinic acid amide groups have proven invaluable in the quantitative separation of Pd(II) and Pt(IV) ions. Additionally, these resins have made substantial contributions to the field of chromatography[9–11]. For instance, the utilization of immobilized Pd(II) on phosphine sulfide-derivatized polystyrene serves as an effective chromatographic material for selectively adsorbing amino acids. Given that the stability of coordination compounds is known to enhance with an increasing number of chelate rings, there is a compelling interest in the immobilization of multidentate ligands within polymer matrices.

The synthesis of crosslinked polystyrene-bound tetradentate ligands, including but not limited to iminobis(propylenesalicylideneimine)[12,13],tetrathiol[14],2,2'-(diimino-1,2-ethane-diylbis(1,2[ethanediylnitrilomethylidyne])di-phenol[15],salen[16],tetraazomacrocyclics[17,18],andN,N'-ethylenemono(3-carboxysalicylideneimine) mono(salicylideneimine)[19], has been explored to address this intriguing research endeavor This chapter explores the process of immobilizing mixed Schiff bases, specifically PSCH₂-L'H₂(I), synthesized from propylenediamine, 3-formylsalicylic acid and acetylacetone onto a polystyrene matrix. These immobilized mixed Schiff bases on polystyrene serve as a platform for the fabrication of polystyrene-supported coordination complexes encompassing dioxomolybdenum(VI), nickel(II), and dioxouranium(VI). Further the immobilized complexes act as effective catalyst for the decomposition of hydrogen peroxide.



EXPERIMENTAL

Materials

We employed chloromethylated polystyrene cross-linked with 1% divinylbenzene beads (PS-Cl), sourced from Sigma Chemical Co. (USA), with a chlorine content of approximately 1.17 mmol per gram. For our syntheses, we also utilized nickel acetate tetrahydrate, dioxouranium(VI) acetate tetrahydrate, 30% hydrogen peroxide, acetylacetone, and propylenediamine from CDH. The synthesis of bis(acetylacetonato)dioxomolybdenum(VI) followed the procedure outlined by G. J. Chen, J. W. McDonald, and W. E. Newton. Furthermore, the preparation of 3-formyl salicylic acid was based on the method reported by J.C. Duff. All solvents employed underwent drying using molecular sieves prior to use.

Analytical Procedures and Physical Assessments

The analysis of metal content and the examination of FTIR and diffused reflectance spectra for the coordination complexes anchored to polystyrene were conducted following the methodologies detailed in our previously published works⁵.

Preparation of Ligand Precursor, L'H₂(I)

An ethanolic solution consisting of 3-formylsalicylic acid (2.32 g, 20 mmol) in 30 ml of ethanol was combined with another ethanolic solution containing acetylacetone (2.0 g, 20 mmol) in 30 ml of ethanol. This mixture was carefully



**Amit Kumar and Praveen Kumar Gupta**

placed in an ice bath for 30 minutes. Subsequently, an ethanolic solution of propylenediamine (1.48 g, 20 mmol) was gradually introduced into the aforementioned mixture with continuous stirring. The resulting blend was then heated under reflux for 45 minutes and subsequently cooled in an ice bath. Yellow precipitates formed and were separated by suction filtration, followed by multiple washes with ethanol. The isolated precipitates were ultimately dried under vacuum conditions at room temperature, yielding an 80% product

Preparation of Polystyrene-anchored ligand, PSCH₂-L'H₂(I)

Chloromethylated polystyrene (2.0 g) was suspended in 30 ml of DMF for a duration of 45 minutes. Following this, a DMF solution (60 ml) containing L'H₂ (1.72 g, 5.64 mmol) was introduced into the suspension. The ensuing mixture was heated under reflux for a period of 8 hours, with continuous magnetic stirring, in the presence of ethyl acetate (100 ml) and triethylamine (3 ml). After completion of the reflux, the mixture was allowed to cool to room temperature. The resulting yellow-colored products were isolated through suction filtration, subjected to thorough washing with DMF, ethyl acetate, ethanol, methanol, and petroleum ether, and finally, dried under vacuum conditions at room temperature.

Procedure for Preparing Polystyrene-Supported Ni(II) and UO₂(VI) Complexes

1.0 g of polystyrene-anchored ligand(I) was suspended in 25 ml of DMF for a period of 1 hour. Following this suspension, an appropriate metal acetate (1.88 mmol) in DMF solution (50-80 ml) was introduced. The resulting mixture underwent reflux for 8 hours under constant magnetic stirring. After cooling to room temperature, the products were separated by suction filtration and thoroughly washed with DMF, methanol, ethanol and acetone multiple times. The compounds were subsequently dried using the aforementioned procedure.

Procedure for Preparation of Polystyrene-Supported MoO₂(VI) Complexes

1.0 g of polystyrene-anchored ligand, I, equivalent to 0.94 mmol, was introduced into a 30 ml DMF suspension, allowing it to stand for 1 hour. Subsequently, a DMF solution (50 ml) containing bis (acetylacetonato) dioxomolybdenum(0.62 g, 1.88 mmol) was carefully added to the suspension. The mixture was subjected to reflux for a duration of 5 hours under constant magnetic stirring and then gradually cooled to room temperature. The resulting compounds were isolated via suction filtration and meticulously cleansed with DMF, ethanol, methanol and acetone. The compounds were then subjected to the aforementioned drying procedure

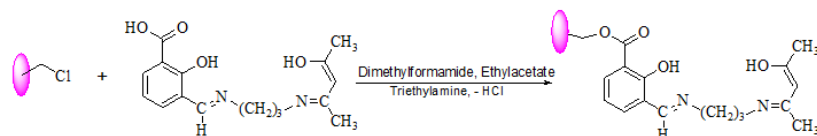
RESULTS AND DISCUSSION

The synthesis of polystyrene-anchored ligand (I) involved the reaction between chloromethylated polystyrene (PSCH₂-Cl) and mixed Schiff base (L'H₂) at a ratio of 1:3, respectively, within a DMF medium. The reaction was allowed to proceed for a duration of 8 hours, maintaining the PSCH₂-Cl to Schiff base ratio at 1:3. When the reaction time fell below 8 hours or when the ratio kept 1<3, the resulting polystyrene-anchored Schiff bases consistently retained unreacted CH₂Cl groups. Notably, this polystyrene-anchored ligand exhibit insolubility in both aqueous and non-aqueous solvents. Nevertheless, they exhibit substantial swelling behavior when exposed to DMF. For this investigation, DMF was selected as the solvent of choice due to its elevated dielectric constant and its capacity to dissolve a wide array of metal salts and metal complexes. We choose chloromethylated polystyrene cross linked with only 1% divinylbenzene for this study because a higher degree of cross linking can diminish the metal-binding capacity of I. Chloromethylated polystyrene (PSCH₂-Cl) exhibits a white color, while the resulting Schiff base (I) is pale yellow. During the course of the reaction, the white color of PSCH₂-Cl gradually transitions to pale yellow. Remarkably, the color of the polystyrene-anchored Schiff bases remains consistent, showing no observable change even after extensive washing with DMF, ethyl acetate, ethanol, and methanol. The synthesis of polystyrene-anchored Schiff bases (PSCH₂-L'H₂) (I) and their subsequent coordination compounds is presented in accordance with Scheme 1.

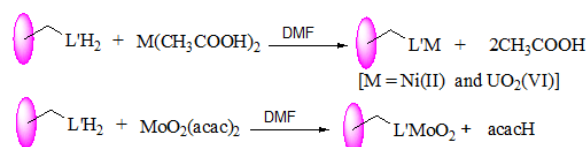




Amit Kumar and Praveen Kumar Gupta



Scheme 1



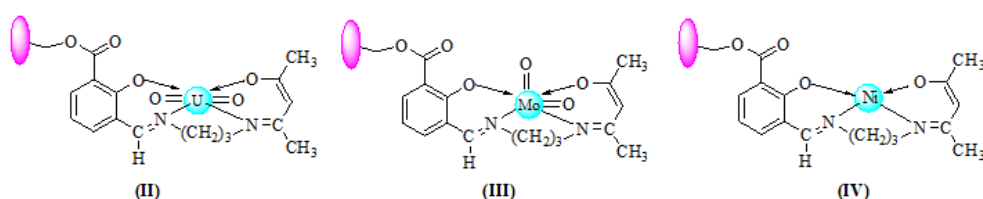
The syntheses of polystyrene-anchored coordination complexes were conducted using a 1:2 molar ratio of polystyrene-anchored ligand to metal salt/metal complex. The resulting polystyrene-anchored coordination complexes exhibit various colors, including yellow-green, yellow, or orange, depending on the specific metal salts employed. Notably, the coloration of these compounds remains unaffected even after undergoing extensive washing procedures involving DMF, ethanol, methanol, and acetone. Characterized by a 1:1 metal-to-ligand stoichiometry (as outlined in Table 1), these polystyrene-anchored coordination complexes display a variable percent reaction conversion ranging from 37.9% to 92.5% (see Table 1). Interestingly, there appears to be no discernible correlation between the percent reaction conversion and the size of the metal ion. The metal binding capacity of the resins ranges from 0.26 mmol to 0.67 mmol of metal per gram of resin (as detailed in Table 1). Importantly, the metal ions within the polystyrene-anchored complexes can be easily stripped away using dilute acid treatments. The infrared spectra of polystyrene-anchored ligand (PSCH2-L'H2(I)) and their respective coordination complexes are documented in Table 2. In the case of 3-formylsalicylic acid, a characteristic $\nu(\text{C}=\text{O})(\text{COOH})$ stretch appears at 1660 cm^{-1} . For L'H2, this particular band emerges at 1670 cm^{-1} . However, upon the formation of PSCH2-L'H2, two new bands at 1730 and 1640 cm^{-1} , respectively, manifest themselves. The former band corresponds to $\nu(\text{C}=\text{O})(\text{ester})$, while the latter can be attributed to $\nu(\text{C}=\text{N})(\text{azomethine})$ and/or $\nu(\text{C}=\text{O})(\text{ketone})$ vibrations from the acetylacetonate moiety. Notably, the positive shift of the band from 1670 to 1730 cm^{-1} signifies the establishment of a covalent bond between PSCH2-Cl and L'H2. In the case of the polystyrene-anchored coordination complexes, a band at approximately 1730 cm^{-1} is observed, indicating the absence of $\nu(\text{C}=\text{O})(\text{ester})$ from I. However, the band located at 1630 cm^{-1} within I exhibits a noticeable downward shift in energy by approximately $15\text{--}25\text{ cm}^{-1}$ upon coordination. This negative shift signifies the active participation of the azomethine N atom in the coordination process. Furthermore, it is evident that PSCH2-L'H2 primarily exist in the keto form, as indicated by the disappearance of the $\nu(\text{C}=\text{O})$ stretch characteristic of I upon complexation. Additionally, the coordination compounds manifest a novel band within the range of $1220\text{--}1230\text{ cm}^{-1}$, attributed to the $\nu(\text{C}=\text{O})(\text{enolic})$ stretch.

The presence of this band unequivocally suggests that a tautomeric shift occurs in I upon complexation. Moreover, the $\nu(\text{C}=\text{O})(\text{phenolic})$ stretch, originally at 1530 cm^{-1} in I, undergoes a minor upward shift of $\leq 10\text{ cm}^{-1}$ in the coordination complexes. This positive shift implies the active involvement of the phenolic oxygen atom in coordination. Notably, the infrared data dismisses the possibility of a dimetallic structure, as the $\nu(\text{C}=\text{O})(\text{phenolic})$ stretch would be expected to shift to higher energy by $>10\text{ cm}^{-1}$ in such cases. Furthermore, the absence of $\nu(\text{O}=\text{H})$ signals in the coordination complexes suggests the deprotonation of the phenolic hydroxyl group. These findings collectively support the ONNO donor behavior exhibited by the polystyrene-supported ligand. The polystyrene-anchored dioxo-uranium(VI) complexes exhibit a prominent band at 905 cm^{-1} , which can be attributed to the $\nu(\text{O}=\text{U}=\text{O})$ stretch, indicative of the trans-UO₂ structural configuration(II). The force constant values ($f(\text{U}=\text{O})$) within the range of $6.66\text{--}6.81\text{ mdyne/\AA}$ align closely with the reported range ($6.58\text{--}7.03\text{ mdyne/\AA}$) commonly observed for dioxouranium(VI) complexes. The U–O bond distance (RU–O) measures at 1.74 \AA , a value well within the typical range ($1.60\text{--}1.92\text{ \AA}$) associated with dioxouranium(VI) complexes[22]. For the dioxo-molybdenum(VI) compounds, distinctive $\nu(\text{O}=\text{Mo}=\text{O})$ and $\nu(\text{O}=\text{Mo}=\text{O})$ stretches are evident at 915 cm^{-1} and 935 cm^{-1} , respectively. These



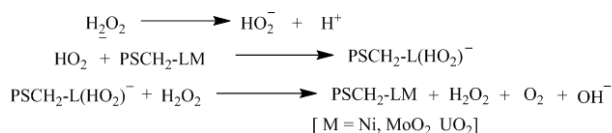


bands fall within the customary ranges of 892–964 and 840–925 cm^{-1} , respectively, often observed for $\text{MoO}_2(\text{VI})$ coordination complexes[22]. The IR data convincingly support the presence of the *cis*- MoO_2 structure (III), as these compounds do not exhibit characteristics associated with oligomeric structures featuring $\bullet\bullet\bullet\text{Mo}=\text{O}\bullet\bullet\bullet\text{Mo}=\text{O}\bullet\bullet\bullet$ interactions. The absence of such oligomeric structures is attributed to the polymer backbone, which occupies the space between adjacent metal centers in the polystyrene-anchored coordination complexes. The diffused reflectance spectroscopic data for the polystyrene-anchored coordination complexes have been meticulously tabulated in Table 2. In the case of polystyrene-anchored nickel(II) complexes, two distinctive bands emerge at 20110 cm^{-1} (②) and 24810 cm^{-1} (③). These bands correspond to the $1\text{A}_{1g} \rightarrow 1\text{A}_{2g}$ and $1\text{A}_{1g} \rightarrow 1\text{B}_{1g}$ transitions, respectively, within a square planar geometry (IV)[23]. Additionally, a relatively weaker band at 12560 cm^{-1} (①) is observed, which can be attributed to the spin-forbidden $1\text{A}_{1g} \rightarrow 3\text{A}_{2g}$ transition[23].



CATALYTIC ACTIVITY

The catalytic activity of the polymer bound metal complexes were evaluated for the decomposition of H_2O_2 . Out of three complexes, the catalytic activity decreased in the order: nickel(II) > dioxomolybdenum(VI) > dioxouranium(VI). The variation in reactivity may be explained by their coordination geometry. In case of dioxomolybdenum(VI), the accessibility of H_2O_2 to their coordination site is less, making its catalytic activity much less. The catalytic decomposition of hydrogen peroxide by polymer supported complexes can be schematically represented as



CONCLUSION

Polystyrene-supported $\text{MoO}_2(\text{VI})$, $\text{Ni}(\text{II})$, and $\text{UO}_2(\text{VI})$ complexes have been synthesized and finally characterized by different spectroscopic techniques. Ni complex exhibits square planar geometry, while the molybdenum and uranium complexes were found to have octahedral geometries. Magnetic data reveals that all the complexes exhibit diamagnetic properties. The catalytic activities of these complexes shows that, Ni and Mo complexes were effective in the catalytic decomposition of hydrogen peroxide and follow the order: $\text{Ni}(\text{II}) > \text{MoO}_2(\text{VI}) > \text{UO}_2(\text{VI})$.

ACKNOWLEDGMENT

The authors are thankful to the Maharishi Markandeshwar (Deemed to be University), Mullana, Haryana, India.

CONFLICT OF INTEREST

The authors declare that they have no conflict of interest.

REFERENCES

1. Maurya A, Kesharwani N, Kachhap P, Mishra V K, Chaudhary N, Haldar C. Polymer-anchored mononuclear and binuclear Cu II Schiff-base complexes: Impact of heterogenization on liquid phase catalytic oxidation of a series of alkenes. Applied Organometallic Chemistry 2019; e5094:1-23. doi:10.1002/aoc.5094.



**Amit Kumar and Praveen Kumar Gupta**

2. Gupta K C, Sutar A K. Catalytic activities of Schiff base transition metal complexes. *Coordination Chemistry Reviews* 2008; 252(12-14): 1420–1450. doi:10.1016/j.ccr.2007.09.005.
3. Maurya M R, Saini P, Haldar C, Chandrakar A K, Chand S. Oxidation of styrene and cyclohexene with TBHP catalyzed by copper(II) complex encapsulated in zeolite-Y. *Journal of Coordination Chemistry* 2012; 65(16): 2903–2918. doi:10.1080/00958972.2012.706281.
4. Islam S M, Molla R A, Roy A S, Ghosh K. Polymer supported Pd catalyzed thioester synthesis via carbonylation of aryl halides under phosphine free conditions. *RSC Adv* 2014; 4(50): 26181–26192. doi:10.1039/c4ra03338h.
5. Kumar A, Kumar D, Gupta P K, Dass D. *Rasayan Journal of Chemistry*, 2019; 12(2): 577. doi:10.31788/RJC.2019.1225081.
6. Kumagai H, Yokoyama T, Suzuki T M, Suzuki T. Liquid chromatographic selectivity and retention behavior of rare-earth elements on a chelating resin having a propylenediaminetetraacetate type functional group. *The Analyst*, 1999; 124(11); 1595–1597. doi:10.1039/a905070a.
7. Das N, Das J, *Indian J. Chem.* 1989; 28A: 150.
8. Das D, Das AK, Sinha C, *Talanta*, 1999; 48: 1013.
9. G. Marques, J. L. Bourdelande and M. Valiente, *React. Funct. Polym.*, 41 (1999) 77.
10. Fiestel J, Popov G, Schwachulla G, *Plast. Kautsch.* 1983; 30; 496; Samsarzadeh MA, Hudgin DE, *J. Polym. Sci. Part C, Polym. Lett.* 1986; 24: 541.
11. Kumagai H, Inoue Y, Yokoyama T, Suzuki TM, Suzuki T. Chromatographic Selectivity of Rare Earth Elements on Iminodiacetate-Type Chelating Resins Having Spacer Arms of Different Lengths: Importance of Steric Flexibility of Functional Group in a Polymer Chelating Resin. *Analytical Chemistry*. 1998; 70(19): 4070–4073. doi:10.1021/a980334v.
12. Akelah A, Masoud, Kandil SS, *Indian J. Chem.* 1986; 25A: 918.
13. Wohrle D, Bohlon H, *Macromol. Chem.* 1989; 187: 20.
14. Nishizawa M, Yokoyama T, Kimura T, Suzuki TM. Preparation and metal-adsorption properties of polystyrene resins functionalized with multidentate ligands having nitrogen and sulfur donor sets. *Polyhedron* (1986); 5(12): 2047–2049. doi:10.1016/s0277-5387(00)87136-3.
15. Syamal A, Singh MM, *Indian J. Chem.* 1998; 37A: 350.
16. Reger TS, Janda KD, Polymer-Supported (Salen)Mn Catalysts for Asymmetric Epoxidation: A Comparison between Soluble and Insoluble Matrices. *Journal of the American Chemical Society*, 2000; 122(29): 6929–6934. doi:10.1021/ja000692r.
17. Nakajima Y, Fujiwara M, Matshushite T, Shono LT, *Polyhedron*, 1986; 5 ;1601.
18. Matsushita T, Sakiyama J, Fujiwara M, Shono T. Synthesis of Copper(II) Selective Chelating Resin Bearing a Tetraaza Macrocyclic Schiff Base Ligand. *Chemistry Letters* 1988; 17(10): 1577–1580. doi:10.1246/cl.1988.1577.
19. Syamal A, Singh MM, Kumar D, Syntheses and characterization of a chelating resin containing ONNO donor quadridentate Schiff base and its coordination complexes with copper(II), nickel(II), cobalt(II), iron(III), zinc(II), cadmium(II), molybdenum(VI) and uranium(VI). *Reactive and Functional Polymers*, 1999; 39(1): 27–35. doi:10.1016/s1381-5148(97)00161-2.
20. D. Dolphin and A. Wick, "Tabulation of Infrared Spectral Data", Wiley Interscience, New York, 1977, pp. 303, 304.
21. Syamal A, Singh MM, Novel polystyrene-anchored copper(II), nickel(II), cobalt(II), iron(III), zinc(II), cadmium(II), zirconium(IV), molybdenum(V), molybdenum(VI) and uranium(VI) complexes of the chelating resin containing the Schiff base derived from salicylaldehyde and 1-amino-2-naphthol-4-sulphonic acid. *Reactive Polymers*; 1993; 21(3): 49–158. doi:10.1016/0923-1137(93)90117-x
22. Kumar D, Gupta P.K, Syamal A, Syntheses and structural studies on coordination compounds of polystyrene anchored Schiff base with some metal ions. *Journal Chilean Chemical. Society*, 59, N° 1 (2014)2260.
23. Lever ABP, *Inorganic electronic spectroscopy*, Elsevier, Amsterdam, 2nd Edn, 1984.





Amit Kumar and Praveen Kumar Gupta

Table1. Characteristics and Analytical Information for Coordination Complexes Immobilized on Polystyrene

Polystyrene-anchored Complexes	Colour	Found (Calcd.) (%)	Metal-binding capacity ($\times 10^{-2}$) (mmol/g of resin)	Percent conversion
PSCH ₂ -L'Ni	Yellowish green	3.8 (4.20)	66.5	92.5
PSCH ₂ -L'MoO ₂	Yellow	2.6 (6.57)	26.1	37.9
PSCH ₂ -L'UO ₂	Orange	11.8 (14.76)	48.6	77.9

Table 2. Infrared and Diffused Reflectance Spectroscopic Analyses of Polystyrene-Anchored Ligand and Its Complexes

Polystyrene-anchored ligand/complexes	$\nu(\text{C}=\text{N})$	$\nu(\text{C}-\text{O})$ (phenolic)	$\nu(\text{C}-\text{O})$ (enolic)	$\nu_{\text{sy}}(\text{O}=\text{M}=\text{O})$	$\nu_{\text{asy}}(\text{O}=\text{M}=\text{O})$	$\nu_{\text{max}}(\text{cm}^{-1})$
PSCH ₂ -L'H ₂	1630	1530				
PSCH ₂ -L'Ni	1615	1540	1220			12560 20110 24810
PSCH ₂ -L'MoO ₂	1605	1535	1220	915	935	
PSCH ₂ -L'UO ₂	1610	1540	1230		905	





An Integrated Framework for Examining the Infectious Diseases using Fuzzy ELECTRE I Method combined with Modified Chang's Rule

S. Sujitha^{1*} and G. Sivakumar²

¹Research Scholar, Department of Mathematics, A.V.V.M Sri Pushpam college, Thanjavur (Dt.), (Affiliated to Bharathidasan University, Tiruchirappalli) Tamil Nadu - 613503, India.

²Assistant Professor, Department of Mathematics, A.V.V.M Sri Pushpam College, Thanjavur (Dt.), (Affiliated to Bharathidasan University, Tiruchirappalli) Tamil Nadu - 613503, India.

Received: 02 Oct 2023

Revised: 04 Dec 2023

Accepted: 19 Jan 2024

*Address for Correspondence

S. Sujitha

Research Scholar,
Department of Mathematics,
A.V.V.M Sri Pushpam college,
Thanjavur (Dt.),
Tamilnadu - 613503, India.
Email: sujitha8991@gmail.com



This is an Open Access Journal / article distributed under the terms of the **Creative Commons Attribution License** (CC BY-NC-ND 3.0) which permits unrestricted use, distribution, and reproduction in any medium, provided the original work is properly cited. All rights reserved.

ABSTRACT

The decision-making process is used to choose the best solutions based on a variety of criteria for the specific problem. Medical diagnosis is the process of determining a patient's illness or condition based on disease symptoms or indications. In two sets of criteria and alternatives in this research, the number of kids with the illness and the number of kids with signs are mentioned. By combining the two sets of criteria and alternatives with the calculated CRITIC (Criteria Importance Through Inter-Criteria Correlation) weight, the fuzzy ELECTRE I (Elimination and Choice Translating Reality) method is used to determine the priority of the child's selection for treatment. Using a modified version of Chang's method, the minimum degree of possibility for each criterion over the other for combining the sets is determined. Also, the comparison analysis shows that the more trustworthy and accurate diagnostic approach is the one where the fuzzy concordance selects the maximum weight qualifier. Using the aforementioned two sets of criteria and diseases, this study provides indication and determines that a certain child is affected by a particular disease with a different symptom.

Keywords: Fuzzy ELECTRE I, Fuzzy modified Chang's, Fuzzy Concordance, Degree of possibility.





INTRODUCTION

The decision-making process is used to pick the best solution based on a variety of criteria for the specific problem. Medical diagnosis refers to the manner of determining a patient's ailment or condition through the signs or indicators of the disease. The Fuzzy ELECTRE I (Elimination and Choice Translating Reality) method is used in this paper to combine two sets of criteria and alternatives with the obtained CRITIC weight in order to determine the priority of the kid's selection for treatment. With regard to the number of children, diseases, and diseases with symptoms utilizing linguistic variables, two sets of criteria and alternatives are provided. We used a multi-criteria decision-making (MCDM) process as our access. MCDM is used to address risk assessment situations with numerous criteria in order to determine the best alternatives. AHP (Satty 1980), PROMETHEE (Brans *et al.* 1986), TOPSIS (Hwang and Yoon 1981), and VIKOR (Opricovic and Tzeng 2004) are often used to solve MCDM. Since Bellman and Zadeh initially proposed fuzzy decision-making in 1970, it has developed into an exciting field of research for practitioners. A serious outranking method is used for a rate at a set of options in the ELECTRE method, and its derivatives play a key and significant role in this class of MCDM approaches. The ELECTRE method and its derivatives play a key and significant role in this class of MCDM approaches. The ELECTRE method was first proposed by Benayoun *et al.* in 1966. Later, it was known as ELECTRE I. Many iterations of ELECTRE I, II, III, IV, and TRI. Hatami-Marbini and Tavana proposed an alternative fuzzy outranking method in 2011 by expanding the ELECTRE I strategy to take into account the vague, ambiguous, and linguistic assessments provided by a group of decision makers [9]. For the purpose of choosing a supplier to aid in an organisation's efforts to construct strategies and a supply chain, Sevкли developed the fuzzy ELECTRE technique [11]. A fuzzy ELECTRE application was created by Asghari *et al.* to evaluate five distinct mobile payment models according to seven different criteria [1]. Kheirkhah and Dehghani use the fuzzy ELECTRE approach to assess the quality of public transportation [10]. By utilising the ELECTRE I approach for Atanassov's intuitionistic fuzzy sets model, Xu and Shen created a method for MCDM issues [12]. In medical diagnosis, Adlassning KP represented fuzzy set theory [2]. In their method of medical diagnosis, Akram *et al.* used bipolar fuzzy TOPSIS and bipolar fuzzy ELECTRE I [3]. Fuzzy soft set theory applied to medical diagnosis using fuzzy arithmetic operations represents Celik Y Yamak S [5]. In order to conduct a study based on the Fuzzy ELECTRE method and evaluate the service quality of three international airports in the Sicilia region, Chen and Xu integrated the ELECTRE II approach with imprecise fuzzy logic [8]. Fuzzy ELECTRE I is a method developed by Aytac E for assessing catering company alternatives [4]. They then provided specific recommendations. Chang proposed a method that makes use of triangular fuzzy numbers for the fuzzy AHP pair-wise comparison scale and extent analysis for the pair-wise comparisons of synthetic extent values [6,7]. Medical diagnosis is the process of determining an illness based on its indicators and symptoms. Numerous theories related to medical diagnosis have been proposed in the past, including rough set theory (Paszek and Wakulicz Deja 2007), SST (Celik and Yamak 2013), and fuzzy set theory (Adlassning 1986). Using MCDM approaches, Children's medical data can be evaluated in a diagnostic medical system. We present some medical diagnosis applications that use fuzzy ELECTRE I with a modified Chang's method in this paper. We then used them in real-life scenarios. These suggested techniques indicate the effectiveness and feasibility of the diagnostic process.

Methodology for ELECTRE I

Assume an MCDM situation where the alternatives are $\{K_1, K_2, \dots, K_m\}$ and the criterion set is $\{A_1, A_2, \dots, A_l\}$. Consider a decision maker is in authority of evaluating l alternatives $A_i, i=1, 2, \dots, l$ under each of k attributes, $K_j, j=1, 2, \dots, m$. m attributes are chosen based on the inquiry of Decision Makers. Suppose that the weights given to the criterion are also fuzzier than the appropriateness ratings given to each alternative with regard to the m-criteria.

(i) Each alternative is evaluated with respect to k criteria. A decision matrix is constructed when all the values assigned to the alternatives in relation to each criterion are combined.

$$X = [x_{ij}]_{l \times m} = \begin{bmatrix} x_{11}, x_{12} & \cdots & x_{1m} \\ \vdots & \ddots & \vdots \\ x_{l1}, x_{l2} & \cdots & x_{lm} \end{bmatrix} \quad (1)$$





Sujitha and Sivakumar

(ii)The weights are assigned by applying the CRITIC method to each criterion and also satisfying the condition of normality.

(iii)The decision matrix to weight vector is multiplied as described above to generate a fuzzy weight decision matrix.

$$X \otimes W = [\omega_{ij}]_{l \times m} = \begin{bmatrix} \omega_{11} & \dots & \omega_{1m} \\ \vdots & \ddots & \vdots \\ \omega_{l1} & \dots & \omega_{lm} \end{bmatrix} \tag{2}$$

(iv)Since alternative evaluations are expressed using fuzzy sets, component priority impacts way concordance is defined. The concordance sets are now defined.

The fuzzy concordance indices are calculated as follow $C_{ab} = \sum_{j \in ab} w_j$.As a result, the fuzzy concordance matrix can be formed using the following method.

$$C = \begin{bmatrix} - & c_{12} & \dots & c_{1r} \\ \vdots & \ddots & \ddots & \vdots \\ c_{r1} & \dots & \dots & - \end{bmatrix} \tag{3}$$

\mathcal{A} 's is the aggregate of all components in each row and \mathcal{K} 's are aggregate of all components in each column. \mathcal{A} 's, \mathcal{K} 's and $\sum \mathcal{A}_i = \sum \mathcal{K}_i$. ($\sum \mathcal{A}$'s $\sum \mathcal{K}$'s) have to be considered for future evaluate of modified Chang's method

(v) After slight modifications of the limits in the Chang's method, we will have to select the minimum possibilities of the normalized weight vectors as follows.

(vi) The value of fuzzy synthetic extent with respect to the i^{th} object is represented as, $\mathcal{A}_i = \sum_{j=1}^m C_{g_i}^j \otimes [\sum_{i=1}^n \sum_{j=1}^m C_{g_i}]^{-1}$ in vertical manner and fuzzy addition operation of m extent analysis values can be performed particular matrix such that $\sum_{j=1}^m C_{g_i}^j = (\sum_{j=1}^m \alpha_j, \sum_{j=1}^m \beta_j, \sum_{j=1}^m \gamma_j)$ to obtain $\sum_{j=1}^m C_{g_i}^j$ ($j= 1,2,\dots,m$) values such that $\sum_{i=1}^n \sum_{j=1}^m C_{g_i}^j = (\sum_{i=1}^n \alpha_i, \sum_{i=1}^n \beta_i, \sum_{i=1}^n \gamma_i)$ are performed to obtain $[\sum_{i=1}^n \sum_{j=1}^m C_{g_i}^j]^{-1}$, the inverse of the \mathcal{A}_i determined vector can be expressed as follows.

$$[\sum_{i=1}^n \sum_{j=1}^m C_{g_i}^j]^{-1} = (\frac{1}{\sum_{i=1}^n \alpha_i}, \frac{1}{\sum_{i=1}^n \beta_i}, \frac{1}{\sum_{i=1}^n \gamma_i}) \tag{4}$$

(vii) The degree of possibility of $\mathcal{A}_2 = (\alpha_2, \beta_2, \gamma_2) \geq \mathcal{A}_1 = (\alpha_1, \beta_1, \gamma_1)$ is defined as $E(\mathcal{A}_2 \geq \mathcal{A}_1) = \sup_{y \geq x} [\min \mu_{\alpha_1}(x), \mu_{\alpha_2}(y)]$. When a pair (x,y) exists such that $y \geq x$ and $\mu_{\alpha_1}(x) = \mu_{\alpha_2}(y)$, then we have $E(\mathcal{A}_2 \geq \mathcal{A}_1) = 1$. Since \mathcal{A}_1 and \mathcal{A}_2 are convex fuzzy numbers. We have that $E(\mathcal{A}_2 \geq \mathcal{A}_1) = 1$ iff $\alpha_2 \geq \alpha_1, E(\mathcal{A}_2 \geq \mathcal{A}_1) = \text{hgt}(\alpha_1 \cap \alpha_2) = \mu_{\alpha_2}(d)$. Where d is the ordinate of the highest point where $\mu_{\alpha_1}(d)$ and $\mu_{\alpha_2}(d)$. Additionally, the equivalent form of theafore mentioned equation is as follows.

$$E(\mathcal{A}_2 \geq \mathcal{A}_1) = \text{hgt}(\alpha_1 \cap \alpha_2) = \mu_{\alpha_2}(d) = \begin{cases} 1, & \text{if } \beta_2 \geq \beta_1 \\ 0, & \text{if } \alpha_1 \geq \gamma_2 \\ \frac{\alpha_1 + \gamma_2}{(\beta_2 + \gamma_2) + (\beta_1 + \alpha_1)}, & \text{otherwise} \end{cases} \tag{5}$$

(viii)The degree possibility for an i^{th} convex fuzzy number to be higher than k convex fuzzy numbers $\mathcal{A}_i(i=1,2,\dots,k)$ can be defined from acquiring $k(k=1,2,\dots,n)$ convex fuzzy numbers. $E(\mathcal{A}_i \geq \mathcal{A}_k) = E(\mathcal{A}_i \geq \mathcal{A}_1)$ and $E(\mathcal{A}_i \geq \mathcal{A}_2) \dots E(\mathcal{A}_i \geq \mathcal{A}_k) = E(\mathcal{A}_i \geq \mathcal{A}_1, \mathcal{A}_2, \mathcal{A}_3, \dots, \mathcal{A}_k)$ with $i \neq k = \min_v(\mathcal{A}_k \geq \mathcal{A}_i)$

Assume that $e'(\mathcal{A}_i) = \min(\mathcal{A}_i \geq \mathcal{A}_k)$; for $k=1,2,\dots,n; k \neq i$. (6)

The weight vector is given by $w^1 = (e'(\mathcal{A}_1), e'(\mathcal{A}_2), e'(\mathcal{A}_3), \dots, e'(\mathcal{A}_n))^T$. Where $\mathcal{A}_i(i=1,2,\dots,n)$ are n elements.

(ix) The normalized weight vectors are obtained by normalizing

$w = (e(\mathcal{A}_1), e(\mathcal{A}_2), \dots, e(\mathcal{A}_n))^T$. Where is w a nonfuzzy number that indicates the preference of one alternative or set of qualities over another. So, we are left with the basic weight vector-based fuzzy decision model.

(x) Similarly, we follow the step in horizontal manner using (vi),(vii),(viii) for

$$\mathcal{K}_i = \sum_{j=1}^m C_{g_i}^j \otimes [\sum_{i=1}^n \sum_{j=1}^m C_{g_i}]^{-1} \text{also.} \tag{7}$$

(xi) Add up the relative importance of the various decision-making factors to get an overall assessment of the choices. The best option is ultimately determined by the alternative with the largest weight.

In this study, we demonstrate the use of fuzzy ELECTRE I with the Modified Chang's approach in the context of medical diagnostics. After that, we applied them in real-life situations. These suggested methods demonstrate the value and applicability of the diagnostic process.





Sujitha and Sivakumar

Numerical Example

Kids admitted to the hospital with different diseases have symptoms of the disease. Every child is monitored for diseases such as \mathcal{A}_1 = pertussis, \mathcal{A}_2 = sinusitis, \mathcal{A}_3 = pneumonia, \mathcal{A}_4 =diarrhea, with symptoms such as ζ_1 = fever, ζ_2 = cough, ζ_3 = headache, ζ_4 = body pain, and ζ_5 = vomiting. Every child has to be associated with five symptoms, and every symptom has to be associated with four diseases. Every association is calculated using linguistic variables. Our problem is to propose that the children have been affected by a particular disease. Consider the MCDM problem, where a set of alternatives $\mathcal{A}_1, \mathcal{A}_2, \mathcal{A}_3, \mathcal{A}_4$, and a set of criteria $\mathcal{K}_1, \mathcal{K}_2, \mathcal{K}_3, \mathcal{K}_4$. Where alternatives \mathcal{A}_1 = pertussis, \mathcal{A}_2 =sinusitis, \mathcal{A}_3 =pneumonia, \mathcal{A}_4 = diarrhea, and criteria \mathcal{K}_1 =kid 1, \mathcal{K}_2 = kid 2, \mathcal{K}_3 = kid 3, and \mathcal{K}_4 = kid 4. The above problem can be solved by using fuzzy ELECTRE I with Modified Chang's method in fuzzy set theory.

The normalizing values of the fuzzy for the children are described in the following part of Table 2. Weight is determined using the CRITIC technique. ((0.346,0.365,0.355), (0.191,0.205,0.211), (0.243,0.199,0.167), (0.219,0.228,0.266)) The following table 3 provides the weighted fuzzy decision matrix. Using eqn (3), a fuzzy concordance set is utilized to arrive at the relationships between different alternatives that outrank one another.

The minimum level of superiority of each criterion over the others is calculated. The fuzzy concordance of the criteria is improved as a result.

(i.e) The degree of possibility using eqn (6) and (7)

$$e'(\mathcal{A}_1) = \min(A_1 \geq A_2, A_3, A_4) = (1, 1, 0.499489) = 0.499489,$$

$$e'(\mathcal{A}_2) = 0.361725, e'(\mathcal{A}_3) = 0.282952, e'(\mathcal{A}_4) = 1$$

$$e'(\mathcal{K}_1) = 0.50561, e'(\mathcal{K}_2) = 0.505102, e'(\mathcal{K}_3) = 1, e'(\mathcal{K}_4) = 0.492453$$

The criteria's normalized weight vector is calculated as

$$w_{\mathcal{A}} = (0.20198, 0.201785, 0.39949, 0.19673),$$

$$w_{\mathcal{K}} = (0.23295, 0.168697, 0.131964, 0.466384)$$

CONCLUSION

The fuzzy ELECTRE I with the Modified Chang's Method, a multiple-criteria decision-making technique, is introduced in this study. To demonstrate how simple and adaptable the suggested solution is to implement, a step-by-step methodology is used. It was validated using real-world problems, and the answers were evaluated based on the technique. The difficulty of the aforementioned application is to ascertain, based on the symptoms of the condition, whether a specific kid is suffering from it. Any condition with similar symptoms in children may be treated using this method. The solution obtained by combining fuzzy ELECTRE I with Modified Chang's methodologies establishes the most effective method of evaluating the approaches' decision indicator correctness. We intend to integrate fuzzy ELECTRE II and fuzzy AHP MCDM approaches as part of our study's expanded focus.

REFERENCES

1. Asgari, F., Amidian, A.A., Mohammadi, J., Rabiee, H.R.(2010). "A Fuzzy ELECTRE Approach for Evaluation Mobile Payment Business Models", International Conference on Management of e-Commerce and e-Government, 351-355.
2. Adlassnig KP (1986) Fuzzy set theory in medical diagnosis. IEEE Trans Syst Man Cybern 16(2):260-265
3. Akram, M.; Shumaiz; Arshad, M Bipolar fuzzy TOPSIS and Bipolar fuzzy ELECTRE –I method to diagnosis.
4. Aytac E., Tus Isik A, Kundakci N (2011) Fuzzy ELECTRE I method for evaluating catering firm alternatives. Ege Akad Rev 11: 125-134.
5. Celik Y Yamak S (2013) Fuzzy soft set theory applied to medical diagnosis using fuzzy arithmetic operations. J Inequal Appl 1:82
6. Chang, D.Y. Applications of the extent analysis method of fuzzy AHP. European Journal of Operational Research. 95(3), 649-655, 1996.
7. Chang, D.Y, Extent analysis and synthetic decision. Optimization Techniques and Application. 1, 352-355, 1992.





Sujitha and Sivakumar

8. Chen, N., Xu, Z. (2015) "Hesitant Fuzzy ELECTRE II Approach: A New Way to Handle 4 Multi Criteria Decision Making Problem", Information Science, 292-20,175-197.
9. Hatami, A., Tavana, M.(2011). "An Extension of the ELECTRE I Method for Group Decision Making Under a Fuzzy Environment", omega,39,373-386.
10. Kheirkhah, A. S., Deghani, A. (2013). " The Group Fuzzy ELECTRE Method to Evaluate the quality of public Transportation Service", International Journal of Engineering Mathematics and Computer Sciences,1,3.
11. Sevkli, M. (2010). " Application of Fuzzy ELECTRE Method For Supplier Selection", International Journal of the Production Research, 48:12, 2292-3405
12. Xu, M., Chen, T. (2014). " A New Outranking Choice Method for Group Decision Making under Atanassov's Interval Valued Intuitionistic Fuzzy Environment", Knowledge B

Table 1: The linguistic values for the table below's linguistic variable.

Linguistic Variables	Linguistic Values	Linguistic Variables	Linguistic Values
Mild(M_i)	(0,0.2,0.4)	Severe(S)	(0.8,0.9,1)
Moderate Mild (M_m)	(0.2,0.4,0.6)	Moderate Severe(M_s)	(0.7,0.8,0.9)
Moderate Severe (M_s)	(0.4,0.6,0.8)	Moderate(M_o)	(0.5,0.6,0.7)
Severe(S)	(0.6,0.8,1)	Moderate Mild(M_m)	(0.3,0.4,0.5)
		Mild (M_i)	(0.1,0.2,0.3)

Table 2: Normalized fuzzy decision matrix

	\mathcal{A}_1	\mathcal{A}_2	\mathcal{A}_3	\mathcal{A}_4
\mathcal{K}_1	(0.543,0.673,0.804)	(0.667,0.833,1)	(0.667,0.833,1)	(0.571,0.690,0.809)
\mathcal{K}_2	(0.608,0.760,0.913)	(0.667,0.833,1)	(0.691,0.833,0.976)	(0.69,0.785,0.976)
\mathcal{K}_3	(0.695,0.847,1)	(0.690,0.833,0.881)	(0.619,0.785,0.952)	(0.667,0.833,1)
\mathcal{K}_4	(0.543,0.673,0.804)	(0.595,0.738,0.881)	(0.642,0.785,0.923)	(0.619,0.785,0.952)

Table 3: Weighted fuzzy decision matrix

	\mathcal{A}_1	\mathcal{A}_2	\mathcal{A}_3	\mathcal{A}_4
\mathcal{K}_1	(0.188,0.246,0.286)	(0.127,0.1717,0.211)	(0.162,0.166,0.167)	(0.125,0.157,0.215)
\mathcal{K}_2	(0.210,0.278,0.3242)	(0.127,0.171,0.210)	(0.167,0.166,0.167)	(0.151,0.179,0.259)
\mathcal{K}_3	(0.241,0.310,0.355)	(0.132,0.171,0.205)	(0.150,0.156,0.159)	(0.146,0.190,0.266)
\mathcal{K}_4	(0.188,0.246,0.286)	(0.113,0.151,0.185)	(0.1561,0.156,0.155)	(0.135,0.179,0.253)

Table 4: Fuzzy Concordance sets

	\mathcal{A}_1	\mathcal{A}_2	\mathcal{A}_3	\mathcal{A}_4
\mathcal{K}_1	-	(0.434,0.405,0.378)	(0.434,0.405,0.378)	(0.780,0.771,0.733)
\mathcal{K}_2	(0.756,0.800,0.832)	-	(0.434,0.405,0.378)	(1,1,1)
\mathcal{K}_3	(0.756,0.800,0.832)	(0.756,0.800,0.832)	-	(0.756,0.800,0.832)
\mathcal{K}_4	(0.565,0.594,0.621)	(0.219,0.228,0.266)	(0.243,0.199,0.167)	-

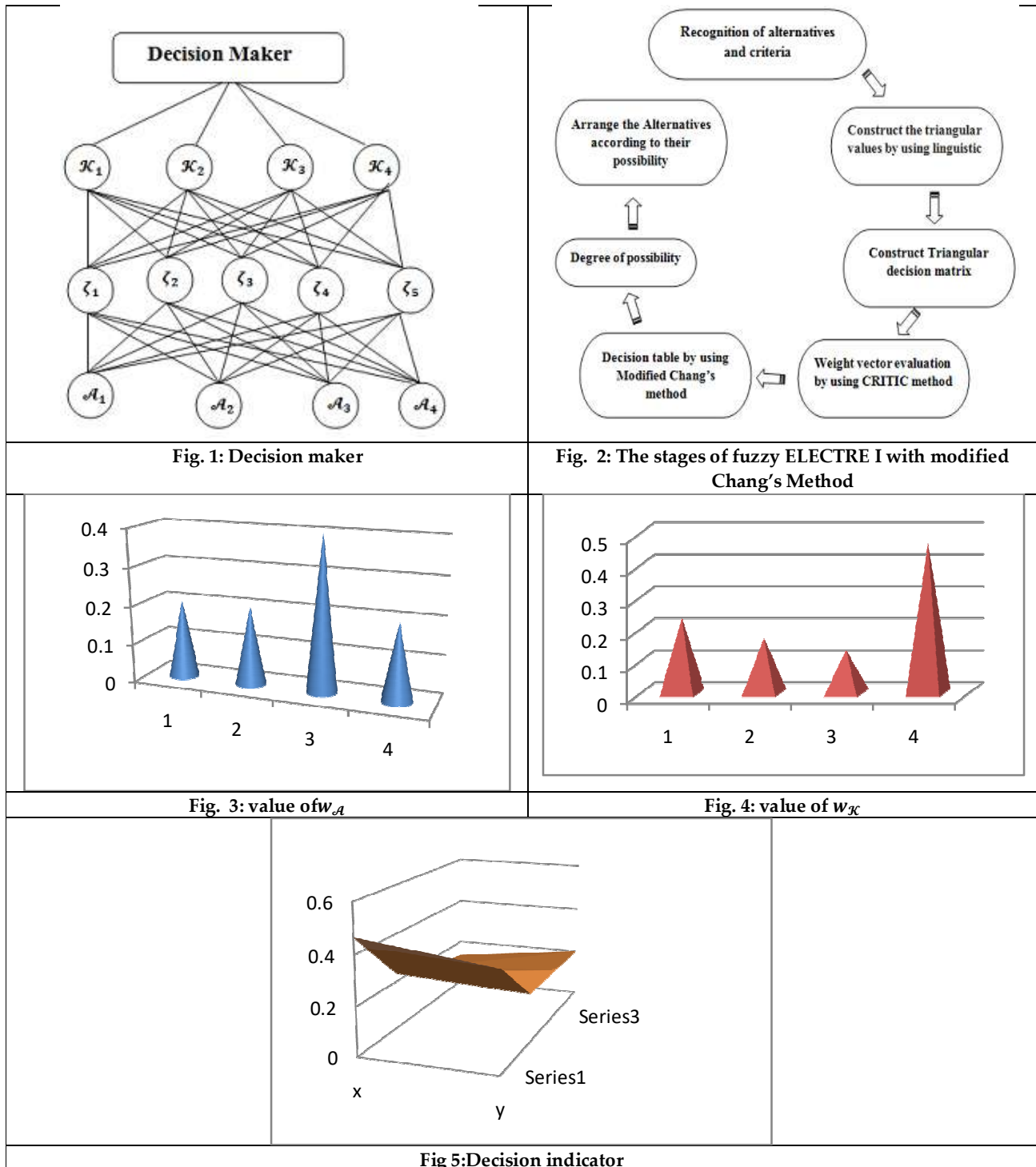
Table 5: Ranking

$w_{\mathcal{A}}$	$w_{\mathcal{K}}$	Ranking
0.39949	0.466384	1
0.20198	0.23295	2
0.201785	0.168697	3
0.19673	0.131964	4





Sujitha and Sivakumar





Bioremediation of Herbicides from Soil

Tuhin Subhra Ghosh, Buddhadev Mallick and Sukanta Rana*

Assistant Professor, Department of Zoology, Searsole Rajbari, Paschim Bardhaman, (Affiliated to Kazi Nazrul University) West Bengal, India.

Received: 28 Sep 2023

Revised: 20 Nov 2023

Accepted: 25 Jan 2024

*Address for Correspondence

Sukanta Rana

Assistant Professor,
Department of Zoology,
Searsole Rajbari, Paschim Bardhaman,
(Affiliated to Kazi Nazrul University)
West Bengal, India.
Email: sukanta_rana@rediffmail.com



This is an Open Access Journal / article distributed under the terms of the **Creative Commons Attribution License** (CC BY-NC-ND 3.0) which permits unrestricted use, distribution, and reproduction in any medium, provided the original work is properly cited. All rights reserved.

ABSTRACT

Extensive application of herbicides in intensive agriculture contaminates the soil severely, resulting in adverse changes in soil structure, and microbial density and diversity. The soil is decontaminated by applying soil microbes, soil enzymes, micro algae, rhizospheres, macrophytes, nano particle-microbes, and earthworms. Fungi can degrade a wide range of herbicides owing of its low substrate specificity and are more potential degrader than bacteria. Bacterial consortia and fungi-bacterial consortia completely mineralize the herbicides through the synergistic use of metabolites as nutrient sources. Filamentous fungi allow bacteria to disperse along mycelia and thus improve herbicide degradation. The symbiotic species in consortia rarely release toxic metabolites. Microbial consortia degrade herbicide residues efficiently and fast. Application of immobilization technology in microbial consortia improves herbicide remediation efficiency. Microbial consortium and nanoparticle-microbes are more potential methods for absolute remediation of herbicides. New fungal-bacteria consortia and combination of Cu, Fe, C nanoparticles with fungal-bacteria consortia and their remediation efficiency will be studied in future.

Keywords: Herbicides, Remediation, Microbes, Consortia, Cometabolism, Rhizosphere, Macrophytes, Earthworms





Tuhin Subhra Ghosh et al.,

INTRODUCTION

Weed management by applying herbicides is an integrated part of modern agricultural practices for optimizing plant growth and crop yield. In 2021, global herbicide consumption reached 1732.3 thousand metric tons (~ 50%), whereas fungicides-bactericides and insecticides were used at 816.38 (~23%) and 757.54 (~21%) thousand metric tons respectively[1]. Glyphosate, the most intensively used herbicide, is applied at 600-750 thousand tons annually worldwide and is projected to reach 740-920 thousand tons annually by 2025[2]. For decades, atrazine is used extensively worldwide to control pre- and post-emergence grasses and broadleaf weeds. The use of dicamba in US agriculture rose from 36×10^5 kg in 2016 to 140×10^5 kg in 2019[3]. The root growth inhibiting pre-emergence herbicide, trifluralin, is used as much as 4400 tons annually worldwide for controlling annual grasses and broadleaf weeds in crops mainly cotton, alfalfa, and soybean[4]. Interestingly, about 1% of herbicides after application are utilized by plants and remaining 99% are accumulated in soil and surface water and contaminate it[5].

This practice changes the soil microbial community negatively, enhances the production of toxic metabolites through partial biodegradation, and interferes with the biogeochemical cycle and fertility of the soil. Microbial degradation metabolites are persistent in soil and are accumulated and magnified in food chain[6]. Especially, non-target soil microbes are severely damaged via oxidative stress mechanism[6]. Foliar application of sulfonylurea decreases the abundance the fast-growing bacteria on winter wheat soil[7]. A High dose of either bensulfuron-methyl-butachlor or quinchlorac in paddy soil suppresses soil urease activity [8]. Soil urease activity can be affected by herbicide types, concentration and application time[9]. Preemergence herbicides are more harmful to soil than the post emergence herbicides due to absolute exposure to soil[10]. The objective of the study is to discuss the different bioremediation approaches, methods, and living organisms involved in the removal of herbicides from contaminated soil, as well as to find out clues for further study and recommendation.

IN SITU AND EX SITU BIOREMEDIATION APPROACH

In-situ bio remediation of herbicides is performed by, natural attenuation, bio stimulation, bio augmentation, bio sparging and rhizofiltration[11],[12],[13],[14],[15]. In this process the soil environment is modified by supplying various forms of rate-limiting nutrients and electron acceptors such as phosphorus, oxygen, nitrogen, carbon, etc. for the stimulation of the existing microbes to be capable of bioremediation[13]. The efficiency of the bioremediation of contaminated soils is multiplied by coupling bio augmentation and bio stimulation treatments[14]. Ex-situ bioremediation involves excavation of the contaminated soil and sediment or groundwater pumping. Land farming, composting, and bio piles are well accepted methods for herbicide bioremediation. The excavated contaminated soil, sediment, and sludge are spread over a prepared bed and are tillage periodically for aeration and mixing and the contaminants are decomposed^[13]. The land farming and composting techniques are combined in the *biopiles*, which are equipped with a piping system that permits the aeration of the piles of contaminated soil[16].

BIOREMEDIATION STRATEGIES

Bioremediation strategies are the best technologies for herbicides removal from contaminated soil because of its transformation, degradation and mineralization with high efficacy. Microbial, enzymatic, phyto-, nano particle and vermin- remediation are more popular recently as eco-techs. Synergy of biological techniques with physical and chemical techniques maximizes the removal capacity and efficiency[17]. Microbial consortia degrade herbicides better than single species because of complementary metabolism among members[6]but any single species of the consortium of *Comamonas testosteroni*, *Hyphomicrobium sulfonivorans* and *Variovorax* spp. in biofilms in soil is not able to degrade linuron[18]. Glyphosate is degraded by microbial consortium containing 19 bacterial species and five fungal species[6]. Phenoxy herbicides are efficiently removed by phyto- and rhizo-remediation methods[19]. Microbial augmentation and bio-stimulation in contaminated soil improve decontamination. Introduction of omics-based technologies promotes microbial remediation by altering microbial community in soil.



**Tuhin Subhra Ghosh et al.,**

Microorganisms consume pesticides as nutrient sources and metabolically convert them into degraded products or minerals under the catalysis of hydrolases, peroxidases and oxygenases, and the rate of degradation is proportional to the concentration of contaminants[20].

Bacterial remediation

In soil, bacteria metabolically degrade herbicides into less toxic or no toxic compounds. Each bacterium has a particular degradative process for a specific herbicide. A number of bacteria are involved in transformation, degradation and mineralization processes (Table-1). The degradation potency of bacterial consortium is higher than a single bacterium due to complementary use of metabolites[56],[57]. *Acinetobacter baumannii* DT transforms Propanil to 3,4-dichloroaniline via the ortho-cleavage pathway for C and N[52](Table-1).

Enzyme remediation soil

Soil enzymes – oxygenase, laccase, lipase, esterase, cellulase etc. secreted by bacteria catalyze oxidation-reduction and hydrolytic reactions utilizing herbicides as substrates and degrade it [58]. Oxidation-reduction is the first step of herbicide degradation catalyzed by oxygenase and laccase cleaves aromatic ring. Lipase, esterase and cellulase catalyze hydrolytic reaction and degrade herbicides[59],[60]. Nitro reductase catalyzes reductive transformation of nitroaromatic and nitrohetero cyclic herbicides.

Mineralization and remediation

The mineralization is the final step of metabolites degradation of herbicides into CO₂, minerals and H₂O by bacterial enzymes. The indigenous bacteria *Ammoniphilus* sp. JF and *Bacillus altitudinis* A16 mineralize the Butachlor for carbon requirement[24],[25](Table-1). The rate of mineralization is influenced by the concentration of microbial community[61], bacterial species, soil characteristics and type of herbicides[16].

Cometabolism and remediation

Cometabolism is one of the most appreciated strategies for herbicide removal from soil due to its higher sensitivity and higher efficacy. It is used to degrade the most recalcitrant herbicides, like atrazine, and even trace concentrations in soil. Indigenous bacteria are stimulated for the degradation and propagation without depending on the contaminant for carbon or energy, resulting in an enhancement in the remediation of herbicides. The simultaneous catabolism is catalyzed by hydrolytic enzymes (esterases, amidases, and nitrilases), transferases (glutathione S-transferase and glucosyl transferases), oxidases (cytochrome P-450s and peroxidase), and reductases (nitroreductases and reductive dehalogenases). The herbicide, diuron used widely in a variety of agricultural and non-agricultural crops is degraded by a number of bacteria in soil namely *Micrococcus* sp. PS-1[62], *Bacillus cereus*, *Vagococcusfluvialis*, *Burkholderiaambifaria*, *Bacillus*spp.[34], *Arthrobacter* sp. BS2, *Arthrobacter* sp. BS1, SED1[63], *Bacillus licheniformis* SDS12[35], *Stenotrophomonas rhizophila* CASB3[36], *Pseudomonas aeruginosa* FN[37], *Bacillus pseudomycoides* D/T, *Bacillus simplex/Bacillus muralis* D/N[38]. *Rhodococcus* sp. B2 remediates pretilachlor by using bifunctional P450 family oxygenase which catalyzes O-dealkylation and N-dealkoxymethylation reaction[28],[29]. A novel bacterial strain, *Proteini clasticum sediminis* BAD-10^T anaerobically degrades and detoxifies chloroacetamide herbicides (alachlor, acetochlor, propisochlor, butachlor, pretilachlor and metolachlorin) in anoxic environments such as subsoil, wetland sediment[64].

The bacteria, *Sphingobium* sp. strain MEA3-1 utilizes 2-methyl-6-ethylaniline (MEA) (metabolic intermediate of chloroacetanilide herbicides) as a sole source of carbon and energy[65]. *Sphingobiumbaderi* DE-13 synthesizes two-component flavoprotein monooxygenase system which catalyzes the hydroxylation of two common metabolites of chloroacetanilide, i.e., 2-methyl-6-ethylaniline (MEA) and 2,6-diethylaniline (DEA) using NADH and flavin mononucleotide (FMN)[31]. The enzyme hydrolase (ChIH) of *Rhodococcus* sp. Strain B1 catalyzes N-dealkylation of chloroacetamide herbicides (e.g.,alachlor, acetachlor, butachlor, pretilachlor) generating butoxymethanol and 2-chloro-N-(2,6-dimethylphenyl)-acetamide[66]. Pourbabaei et al, 2020[27] isolate *Pseudomonas aeruginosa* strain PK that can dissipate butachlor (100 µg/mL) in an M9 liquid medium within 0.5 ± 0.03 -1 day. Chlorimuron-ethyl (a sulfonylurea herbicide) is degraded by *Rhodococcus* sp. D310-1 with 88.95% efficiency and produces eight





Tuhin Subhra Ghosh et al.,

biodegradation products, such as 2-amino-4-chloro-6-methoxypyrimidine, ethyl 2-sulfamoyl benzoate, 2-sulfamoyl benzoic acid, o-benzoic sulfimide, 2-[(4-chloro-6-methoxy-2-pyrimidinyl) sulfamoyl] benzoic acid, ethyl 2-carbonyl sulfamoyl benzoate, ethyl 2-benzenesulfonyl isocyanate benzoate, and N,N-2(ethyl formate) benzene sulfonylurea[41]. Carles et al, 2018[67] isolated *Plectosphaerella cucumerina* AR1 nicosulfuron-degrading fungal strain which functions by the co-metabolic process following first-order model dissipation, leading to the production of two major metabolites: 2-amino-4,6-dimethoxypyrimidine (ADMP) and 2-(aminosulfonyl)- N,N-dimethyl-3-pyridinecarboxamide (ASDM) in a wood grown biofilms enabling 97% rate of dissipation within 21 d at pH 6.40 ± 0.36 . The *Enterobacter ludwigii* sp. CE-11 is a promising bacterial resource for the biodegradation and detoxification of chlorimuron-ethyl into 2-amino-4-chloro-6-methoxypyrimidine and an intermediate product by the cleavage of the sulfonylurea bridge, and then transformed into saccharin via hydrolysis and amidation at pH 7.0 and temperatures 20–40 °C [68]. The acetochlor degrader *Pseudomonas aeruginosa* strain JD115 grows optimally at a pH value of 7.0 and a temperature of 37°C, which enhance the degradation rate of acetochlor up to 95.4% in the presence of 50 mg acetochlor l(-1) [69]. The Mixed Bacteria of *Klebsiella variicola* Strain FH-1 and *Arthrobacter* sp. NJ-1 involves biodegradation of atrazine at a rate of 85.6% with initial concentration of 50 mg/L, neutral or weakly alkaline pH value, 30°C [21]. Up to now, regarding nicosulfuron-biodegradation, nine bacterial strains, namely *Oceanisphaerapsychrotolerans* LAM-WHMZC [70], *Bacillus subtilis* YB1 [71], *Ochrobactrum* sp. ZWS16 [72], *Rhodopseudomonas* sp. J5-2 [73], *Alcaligenes faecalis* ZWS11 [44], *Klebsiella* sp. Y1 [45], *Serratia marcescens* N80 [46], *Pseudomonas fluorescens* SG-1 [47] and *Pseudomonas nitroreducens* strain NSA02 [48]) have been screened.

Chryseobacterium sp. Y16C is an efficient degrader that can completely degrade glyphosate by a novel gene (goW) product,[50]. The glyphosate and its major metabolite amino methyl phosphonic acid (AMPA) are completely degraded by a novel strain of *Stenotrophomonas acidaminiphila* Y4B with a degradation efficiency of more than 98% within 72 h (50 mg L⁻¹) [51]. Till now, various aerobic chloroacetamide herbicide-degrading bacterial strains, e.g., *Rhodococcus* sp. B1,[66] *Rhodococcus* sp. T31, *Pseudomonas oleovorans* LCa2[74], *Sphingobiumquisquiliarum* DC2[75], *Sphingomonas wittichii* DC6[76], *Sphingobium baderi* DE-13[31], *Sphingobium* sp. MEA3-1[65], *Paracoccus* sp. FL Y8[73], *Pseudomonasaeruginosa* JD115[69], *Catelli bacterium caeni* DCA-1[77], *Stenotrophomonas acidaminiphila* JS-1[78], *anthomonas axonopodi*[79], *Acinetobacter baumannii* DT[52], *Rhodopseudomonas marshes*[80], *Bacillus altitudinis* A16[25] and *Pseudomonas putid* [26], have been isolated and characterized for herbicide degradation. The bacteria, *Talaromyces flavus* LZM1 can degrades 100% of the initially added nicosulfuron (100 mg L⁻¹) within 5 days at optimum condition pH 6.1, 29 °C, and also highly capable in degrading tribenuron methyl, chlorsulfuron, bensulfuron methyl, ethametsulfuron methyl, cinosulfuron, and rimsulfuron[81]. The bacterial isolate, *Ochrobactrum* sp. ZWS16 is capable of 99.5% biodegradation of 50 mg thifensulfuron-methyl at 40°C over 10 days, and it also degrades nicosulfuron, tribenuron-methyl, pyrazosulfuron-ethyl, metsulfuron-methyl and triasulfuron[42].

Mycoremediation

Mycoremediation is the most suitable and cheap green-tech for herbicide cleanup from soil owing to their robust morphology and diverse metabolic capacity. Fungi (Table-2) secrete catalases, laccase, peroxidases, and cytochrome P450 mono oxygenase in soil and catalyze a wide range of degrading reactions due to its low substrate specificity. Xyloxylation, alkylation, acylation, and nitrosylation during catabolism facilitate the mineralization of pesticides. Fungi-bacteria consortium receives easier and more accessible forms of pesticide metabolites from fungi[95]. Filamentous fungi are advantageous in situations of low concentration and large dispersion of contaminant due to their inherent translocation capabilities through mycelium-hyphae networks in the soil[96]. The fungal mycelium with penetration capacity can act as an adjuvant to bacterial degradation by breaking physical barriers in air-soil interfaces [97],[98], or allowing bacteria to disperse along fungal mycelium[99]. The white-rot fungi generate high levels of extracellular ligninolytic enzymes, intracellular cytochrome P450 monooxygenases, and antioxidant enzymes to potentially degrade diuron [84] (Table-2). The white rot fungi produce oxidative and extracellular ligninolytic enzymes such as lignin peroxidase, manganese peroxidase, versatile peroxidase, and laccase for the purposes of pesticide bioremediation [100]. *Bjerkandera adusta* removes atrazine at a 92% level [82]. In agricultural wastewater, the herbicides diuron and bentazon are removed by *Trametes versicolor* [87]. *Neurospora intermedia* DP8-1[86], *Trametes versicolor* K-41[84], *Pluteus cubensis* SXS 320, and *Pycnoporus sanguineus* MCA 16[85] are capable of



**Tuhin Subhra Ghosh et al.,**

diuron degradation. The fungus *Aspergillus ficuum* AJN2 is a potential strain that can degrade 73% of pretilachlor and 70% of its major metabolite PME (2-methyl-6-ethylalanine) within 15 days[88]. This mycogradation of pretilachlor and its major metabolite is based on the activity of the ligninolytic enzyme lignin peroxidase [88]. *Penicillium oxalicum* YC-WM1 is a potential degrader for nicosulfuron[89](Table-2). *Paecilomycesmarquandii*, a soil microscopic fungus, converts alachlor via N-acetyl oxidation into mono-, di-, and tri-hydroxylated byproducts [101]. *Alternaria alternata* hydrolyzes the pyrazosulfuron-ethyl by 86.9% within 60 days of exposure to soil[92] (Table-2).

Consortium-based remediation

It has been confirmed that the biodegradation of herbicides is more efficient and faster in a mixed microbial population compared to a single strain [102][103]. In a microbial consortium, the complementary catabolism between synergistic species rarely releases harmful intermediates [104] [105]. The consortium with *Bacillus*, *Phyllobacterium*, *Pseudomonas*, *Rhodococcus* and *Variovorax* degrades azimsulfuron[6]. Several microbial consortia in soil engaged in mineralization of different herbicides are enlisted with efficiencies in Table -3. *Variovorax* sp. WDL1 obtains carbon and nutrients by consuming the metabolites of linuron from *Comamonastestosteroni* WDL7 and/or *Hyphomicrobiumsulfonivorans* WDL6[111]. The bacterial consortium composing *Sphingobiumquisquiliarum* strain DC-2 and *Sphingobiumbaderi* strain DE-13 completely mineralize the acetachlor through transitory intermediates 2-chloro-N-(2-methyl-6-ethylphenyl) acetamide to 2-methyl-6-ethylaniline to 2-methyl-6-ethylaminophenol to 2-methyl-6-ethylbenzoquinoneimine[75]. The symbiotic association of *Chenggangzhangellamethanolivorans* CHL1 (-ve) and *Arthrobacter* sp. ART1 (+ve) is capable of remediating the combined contamination of chlorimuron-ethyl and atrazine in soils[112]. The bio remedial efficiency of atrazine (20 mg/kg) is enhanced by 98.23% in soil with the half-life shortened from 19.80 to 7.96 days by using the immobilized bacterial mixture of *Arthrobacter* sp. NJ-1 and *Klebsiella variicola* strain FH-1 on sodium alginate-CaCl₂ at pH 9 and 30°C [68]. A mixed bacterial culture of *Pseudomonas* sp. But2 (a butachlor-degrading strain) and *Acinetobacter baumannii* DT (a propanil-degrading strain), performs a higher rate of biodegradation of both butachlor and propanil in contaminated liquid media and soil [39]. A synthetic microbial consortium system (SMCs) is constructed through immobilization technology by non-living or living composite materials that synergistically maximize the acetochlor degradation efficiency up to 97.81% [30].

Rhizoremediation

Root-microbe association is a highly effective strategy for soil herbicide removal. Rhizospheral microorganisms exert their degradative capacities and decontaminate the soil[113]. Rhizosphere enhanced microbial mineralization of 2,4-D is significantly greater in monocot rhizosphere soil than in dicot rhizosphere soil^[114]. In the cucumber rhizosphere, the root exudates containing citric acid and fumaric acid enhance the colonization of *Hansschlegeliazhihuaiae* S113 (2.14×10^5 cells per gram of root), which increases the rate of bioremediation of chlorimuron-ethyl soil to ensure crop safety and improved growth[115]. The proper selection of appropriate plant-microbe combinations optimizes rhizoremediation.

Phytoremediation

Phytoremediation is an in-situ, emerging and cost-effective eco-tech for herbicide remediation from soil. It reduces contaminants through leaching, soil aeration, phyto degradation, phyto volatilization, evapo transpiration, and rhizoremediation[116]. The efficient elimination of soil contaminants involves the choice of suitable plant species and cultivars that mainly take into account plant growth rate, high biomass production, capability for contaminant accumulation, and tolerance to higher xenobiotic concentrations[117],[118]. The green manure species *Mucuna pruriens* and *Pennisetum glaucum* are capable to remove tebutiuron herbicide from soil[119]. Peanut (*Arachis hypogaea*) and sorghum (*Sorghum bicolor*) can remediate tebutiuron by 76% and 45%, respectively (Conciani et al 2023[120]). The aquatic macrophytes *Pistia stratiotes* and *Eichhornia crassipes* reduced the concentration of clomazone herbicide through dissipation, with a reduction of 90% and 99.0%, respectively (Alencar et al 2020[121]). The efficiency of atrazine removal by *Salvinia biloba* from the contaminated water (5 mg L^{-1}) over 21 days of exposure is ~ 30%[122].



Tuhin Subhra Ghosh *et al.*,**Microalgal remediation**

Many microalgae are capable in herbicide remediation from contaminated soil (Table-4). It can be done through cell wall adsorption, cellular absorption and accumulation or degradation by microalgae. The biosorption capabilities of the microalgae are higher due to the carbohydrate structure of the cell wall [123],[124]. In addition, the binding of herbicides depends on some molecular sites, such as proteins or some lipids containing functional groups such as amino, hydroxyl, carboxyl, and sulfate[125],[126]. The removal and adsorption of herbicides are affected by the structure of the herbicide, temperature, pH, salinity, nutrients, and light quality and [127]. The uptake capacity of herbicide also depends on algal surface area, cellular biovolume, species-specific sensitivity, and the concentration of herbicide (atrazine) in the solution[128]. The microalgae perform this energy-dependent transfer of herbicide components across the cell membrane for metabolic bioaccumulation [129],[130],[131]. Microalgae degrade herbicides into smaller molecules by enzyme metabolism under the catalysis of hydrolase, phosphatase, phosphotriesterase, oxygenase, esterase, transferase, and oxidoreductases, that functions as a nutrition supplement in microalgal growth [132],[133],[134].

Nanotechnology-based approach

Currently, the integration of nano particles to microorganism enhances the pesticide remediation from soil[145]. Thenano particles of silica adsorb pesticides and mediate their degradation via immobilization of degrading exogenous enzymes in soil e.g., organophosphate hydrolase, carboxy-esterase, and laccases and bacterial cells that can produce recombinant enzymes [146].

Vermiremediation

Earthworm stimulates microbial proliferation in soil and thus increases the biodegradation capacity of soil. The degradation of contaminants takes place through gastro-intestinal secretion of detoxifying enzyme[147]. The red earthworm species *Eisenia foetida* and *Amyntas robustus* remove atrazine by 89.6% and 89.8% correspondingly within 28 days[148]. Earthworms promote the degradation of the highly toxic acetochlor S-enantiomer by stimulating indigenous soil microbiota (i.e., *Lysobacter*, *Kaistobacter*, *Flavobacterium*, *Arenimonas*, and *Aquicel*) in repeatedly treated soil [149]. The degradation rate of acetochlor by *Eisenia fetida* increases by 62.3% and 9.7% compared to sterile and natural soil[150]. *Eisenia fetida* stimulates the degradation of metolachlor mostly by enhancing the fungal degraders like order *Sordariales*, *Microascales*, *Hypocreales*, and *Mortierellales*, and the possible bacteria genus *Rubritalea*, and strengthen the community structure and relationships between these primary fungi [151]. The tropical indigenous earthworms (*Alma millsoni*, *Eudriluseugeniae*, and *Libyodrilus violaceus*) are capable of degrading of glyphosate-based herbicides in soil within 8 weeks [152].

FACTORS AFFECTING BIODEGRADATION OF HERBICIDES

The bioremediation kinetics of herbicides is influenced by several bio-physico-chemical factors in soil. The microbial degradation of herbicide is regulated by factors including the number and type of microbes, metabolic activity of microbes, capacity of environmental stress resistance of microbes, chemical structure and concentration of the processed contaminants, and intrinsic soil environmental factors such as pH, temperature, water availability, light, salinity, nutrients availability, and oxygen and carbon dioxide concentration[153],[154]. The **biodegradation rate and persistence are influenced by even minor structural differences between phenylurea herbicides [155]. The polar groups of the pesticides are the sites of microbial attack[156]. Microorganisms can degrade only a dissolved part of the pesticides[157], and the water solubility of herbicides depends on temperature, pH, polarity, hydrogen bonding, and molecular size [158].** Herbicide molecules are adsorbed on the soil particles physically by Van der Waals forces or chemically by electrostatic interactions, and the process is described by adsorption isotherms[159],[160],[161]. The adsorption process influenced by various parameters, such as soil organic matter content, clay content, clay mineralogy, and pH. Water-less conditions are responsible for decreasing microbial activity, a declining number of microbes, and a loss of mobility for mobile degraders[162]. Therefore, higher soil moisture contents may lead to higher mineralization rates by enhancing growth, activity, the spread of degraders, and mass transfer[163]. Although high soil water contents limit microbial growth and oxygen transfer rates, this leads to a lower rate of mineralization. At -0.015 MPa, optimum mineralization has been obtained[164].





Tuhin Subhra Ghosh et al.,

Increasing the soil organic matter content increases the adsorption of pesticides to soil particles, leading to a decrease in the amount of pesticides available in the soil solution [165],[166]. Microbial growth and activity are enhanced through a higher turnover of soil organic matter [167]. The various soil organic amendments and bio processed materials including compost, manure, sludge, bio char, etc. stimulate the indigenous soil microbial activity and therefore improve the degradation and mineralization of herbicides applied in soil[168], [169]. Soil pH affects the soil sorption of herbicides and provides a strong selective influence on soil microbial communities [170],[171]. The enzymatic activity of microorganisms is influenced by soil temperature fluctuation. The range of optimum temperature for maximum microbial degradation is 20°C to 40°C [172]. The solubility, conformational stability, and rate of hydrolysis of pesticides depend on soil temperature. The presence of a few key microbial species is essential for herbicide degradation in soil but the species density, diversity and community size increases with the rise of pesticide quantity in soil[173]. The degradation of herbicides depends on the presence of other pollutants that can compete for adsorption sites and the accessibility of nutrients and cofactors essential for microbial growth and activity[174]. Immobilization of free microbial cells in a particular structural area composed of carrier materials that enhance the remediation of polluted environments, relative stability, and reusability[175]. The efficient microbial activity, growth, metabolism, and proliferation at the contaminated sites in soil require[176] in sufficient amount which allow the microbe to create enzymes for further break down of contaminants during microbial bio transformation[177]. The soil microbial transformation of herbicides is significantly increased by the addition of various forms of nitrogen (N), phosphorous (P), sodium (Na), and magnesium[178].

CONCLUSIONS

Herbicides residues from contaminated soil can be degraded by soil bacteria, soil enzymes, bacterial co-metabolism, bacterial consortia, fungus, fungus-bacteria consortia, microalgae, nanoparticle-microbes, rhizospheres, macrophytes, and earthworms without deteriorating soil structure, environment, and fertility but no method is capable of absolute remediation of herbicides from contaminated soil. Bacterial co-metabolism, microbial consortia, and nano particle-microbes are more promising green-techs owing to their excellent remediation efficacies. Fungal-bacteria consortia strategy will be emphasized more due to better degrading capability of fungi than bacteria and better mineralizing efficiency of fungal-bacterial consortia than bacterial consortia. New fungal-bacteria consortia and their herbicide removal efficacy will be studied. Integration of Cu, Fe, C and SiO₂- nanoparticles to fungi-bacteria consortia and their remediation efficiency will be investigated further. We need omics-based technological study to improve microbial remediation efficiency.

ACKNOWLEDGEMENT

The authors are grateful to Raniganj Girls' College for technical and moral support.

REFERENCES

1. Statista, 2023. Global pesticide use 2021.<https://www.statista.com/statistitype/#:~:text=In%202021%2C%20herbicide%20consumption%20worldwide,to%203.53%20million%20metric%20tons>.
2. Maggi F, Cecilia D, Tang FHM, McBratney A. The global environmental hazard of glyphosate use. *Sci of The Total Environ* 2020;717:137167.
3. USGS, 2021. Estimated Agricultural use for Dicamba, 2019.https://water.usgs.gov/nawqa/pnsp/usage/maps/show_map.php?year=2019&map=DICAMBA&hilo=LColeman NV, Rich DJ, Tang FHM, Vervoort RW, Maggi F. Biodegradation and Abiotic Degradation of Trifluralin: A Commonly Used Herbicide with a Poorly Understood Environmental Fate. Environ Sci Technol 2020;54:10399-10410.
4. Bernardes MFF, Pazin M, Pereira LC, Dorta DJ. Impact of Pesticides on Environmental and Human Health. In: Cristina A, Scola G, editors. *Toxicology Studies—Cells, Drugs and Environment*. London :IntechOpen; 2015.p. 195–233.





Tuhin Subhra Ghosh et al.,

5. Pileggi M, Pileggi SAV, Sadowsky MJ. Herbicides bioremediation: from strains to bacteria communities. *Heliyon* 2020;6:e05767.
6. Bezuglova OS, Gorovtsov AV, Polienko EA, et al. Effect of humic preparation on winter wheat productivity and rhizosphere microbial community under herbicide-induced stress. *J Soils Sediments* 2019;19:2665-2675.
7. Xie ZJ, Li HL, Xu CX, Zhang Q, Liu GR. Effects of two kinds of herbicides on paddy soil ecology and growth of succeeding crops. *Acta Pedologica Sinica* 2014;51:880–887.
8. Kumari JA, Rao PC, Madhavi M, Padmaja G. Effect of herbicides on the activity of soil enzymes urease in maize crop. *Indian J of Agric Res* 2018;52:300-304.
9. Chen J, Yang W, Li J, Anwar S, Wang K, yang Z. Effects of Herbicides on the Microbial Community and Urease Activity in the Rhizosphere Soil of Maize at Maturity Stage. *J Sens* 2021;2021: 11.
10. Sharma I. Bioremediation Techniques for Polluted Environment: Concept, Advantages, Limitations, and Prospects. In: Murillo-Tovar MA, Saldarriaga-Norena H, Saeid A, editors. *Trace Metals in the Environment- New approaches and recent Advances*. IntechOpen 2020.
11. Raper E, Stephenson T, Anderson DR, Fisher R, Soares A. Industrial wastewater treatment through bioaugmentation. *Process Safety and Environ Protect* 2018;118:178-187.
12. Varshney K. Bioremediation of pesticide waste at contaminated sites. *J of Emerging Technol and Innovat Res* 2019;6:128-134.
13. Villaverde J, Rubio-Bellido M, Lara-Moreno A, Merchan F, Morillo E. Combined use of microbial consortia isolated from different agricultural soils and cyclodextrin as a bioremediation technique for herbicide contaminated soils. *Chemosphere*. 2018;193:118-125.
14. Ashraf S, Ali Q, Zahir ZA, Ashraf S, Asghar HN. Phytoremediation: Environmentally sustainable way for reclamation of heavy metal polluted soils. *Ecotoxicol Environ Saf* 2019; 174: 714-727.
15. Raffa CM, Chiampo F. Bioremediation of Agricultural Soils Polluted with Pesticides: A Review. *Bioengineering* 2021;8:92.
16. Hu F-Y, An J, Wang B-Y, Xu M-K, Zhang H-W, Wei S-H. Research Progress on the Remediation Technology of Herbicide Contaminated in Agricultural Soils. *Huan Jing Ke Xue* 2023; 44:2384-2394.
17. Flemming H-C, Wingender J, Szewzyk U, Steinberg P, Rice SA, Kjelleberg S. Biofilm: an emergent form of bacterial life. *Nat Rev Microbiol* 2016; 14: 563 – 575.
18. Urbaniak M, Mierzejewska E. Biological Remediation of Phenoxy Herbicide-Contaminated Environments. In: Saldarriaga-Norena H, Murillo-Tovar MA, Farooq R, Dongre R, Riaz S, editors. *Environmental Chemistry and Recent Pollution Control Approaches*. Open access Peer-Reviewed; 2019.
19. Khajezadeh M; Abbaszadeh-Goudarzi K, Pourghadamyari H, Kafilzadeh F. A newly isolated *Streptomyces rimosus* strain capable of degrading deltamethrin as a pesticide in agricultural soil. *J Basic Microbiol* 2020;60:435–443.
20. Gao N, Zhang J, Pan Z, Zhao X, Ma X, Zhang H. Biodegradation of Atrazine by Mixed Bacteria of *Klebsiella variicola* Strain FH-1 and *Arthrobacter* sp. NJ-1. *Bull Environ Contam Toxicol* 2020; 105: 481–489.
21. Zhao Y, Li X, Li Y, Bao H, Nan J, Xu G. Rapid biodegradation of atrazine by a novel *Paenarthrobacter ureafaciens* ZY and its effects on soil native community dynamic. *Front Microbiol* 2022; 13: 1103168.
22. Li H, Wang Y, Fu J, Hu S, Qu J. Degradation of acetochlor and beneficial effect of phosphate-solubilizing *Bacillus* sp. ACD-9 on maize seedlings. *3 Biotech* 2020; 10: 67.
23. Singh J, Nandabalan NY. Prospecting *Ammoniphilus* sp. JF isolated from agricultural fields for butachlor degradation. *3 Biotech*. 2018;8:164.
24. Kaur R, Goyal D. Biodegradation of Butachlor by *Bacillus altitudinis* and Identification of Metabolites. *Curr Microbiol* 2020;77:2602-2612.
25. Mohanty SS, Jena HM. Degradation kinetics and mechanistic study on herbicide bioremediation using hyper butachlor-tolerant *Pseudomonas putida* G3. *Process Saf Environ* 2019;125:172-181.
26. Pourbabaee AA, Khoshhal NE, Torabi E, Farahbakhsh M. Dissipation of butachlor by a new strain of *Pseudomonas* sp. isolated from paddy soils. *Pollution*, 2020;6:627-635.





27. Liu H, Yuan M, Liu Am, Ren L, ZhuGp, Sun Ln. A bifunctional enzyme belonging to cytochrome P450 family involved in the O-dealkylation and N-dealkoxymethylation toward chloroacetanilide herbicides in *Rhodococcus* sp. B2. *Microb Cell Fact* 2021;61.
28. Chen Q, Wang C-H, Deng S-K, Wu Y-D, Li Y, Yao L, et al. A novel three-component Rieske non-heme iron oxygenase (RHO) system catalyzing the N-dealkylation of chloroacetanilide herbicides in sphingomonads DC-6 and DC-2. *Appl Environ Microbiol* 2014; 80.
29. Liu J, Bao Y, Zhang X, Zhao S, Qiu J, Li N, et al. Anaerobic biodegradation and detoxification of chloroacetamide herbicides by a novel *Proteiniclasticum sediminis* BAD-10T. *Environ Res* 2022;209:112859.
30. Cheng M, Meng Q, Yang Y, Chu C, Chen Q, Li Y, et al. The Two-Component Monooxygenase MeaXY Initiates the Downstream Pathway of Chloroacetanilide Herbicide Catabolism in Sphingomonads. *Appl Environ Microbiol* 2017; 83:e03241-16.
31. Pujar NK, Laad S, Premakshi HG, Pattar SV, Mirjankar M, Kamanavalli CM. Biodegradation of phenmedipham by novel *Ochrobactrum anthropi* NC-1. *3 Biotech* 2019;9:1–10.
32. Alba LM, Esmeralda M, Jaime V. Enhanced Biodegradation of Phenylurea Herbicides by *Ochrobactrum anthropi* CD3 Assessment of Its Feasibility in Diuron-Contaminated Soils. *Int J Environ Res Public Health* 2022; 19:1365.
33. Ngigi A, Getenga Z, Boga H, Ndalut P. Biodegradation of phenylurea herbicide diuron by microorganisms from long-term-treated sugarcane-cultivated soils in Kenya. *Toxicol and Environ Chem* 2011;93:1623–35
34. Singh AK, Singla P. Biodegradation of diuron by endophytic *Bacillus licheniformis* strain SDS12 and its application in reducing diuron toxicity for green algae. *Environ Sci Pollut Res* 2019;26:26972–26981.
35. Silambarasan S, Logeswari P, Ruiz A, Cornejo P, Kannan VR. Influence of plant beneficial *Stenotrophomonas rhizophila* strain CASB3 on the degradation of diuron-contaminated saline soil and improvement of *Lactuca sativa* growth. *Environ Sci Pollut Res* 2020;27:35195–35207.
36. Grgić, DK, Bulatović VO, Cvetnić M, Vučinić ŽD, Domanovac MV, Markić M, et al. Biodegradation kinetics of diuron by *Pseudomonas aeruginosa* FN and optimization of biodegradation using response surface methodology. *Water Environ J* 2020;34:61–73.
37. Muendo BM, Shikuku VO, Lalah JO, Getenga ZM, Wandiga SO, Rothballer M. Enhanced degradation of diuron by two *Bacillus* species isolated from diuron contaminated sugarcane and pineapple-cultivated soils in Kenya. *Appl Soil Ecol* 2021;157:103721.
38. Duc HD. Degradation of isoproturon in vitro by a mix of bacterial strains isolated from arable soil. *Can J Microbiol* 2022; 68:605-613.
39. Zhu J, Zhao Y, Li X, Wu L, Fu LI, Yang N, et al. Isolation of 2 simazine-degrading bacteria and development of a microbial agent for bioremediation of simazine pollution. *An Acad Bras Cienc* 2021;93:e20210373.
40. Li C, Zang H, Yu Q, TongyangLv, Cheng Yi, Cheng X, et al. Biodegradation of chlorimuron-ethyl and the associated degradation pathway by *Rhodococcus* sp. D310-1. *Environ Sci and Pollut Res* 2016;23.
41. Zhao W, Xu L, Li D, Li X, Wang C, Zheng M, et al. Biodegradation of thifensulfuron-methyl by *Ochrobactrum* sp. in liquid medium and soil *Biotechnol Lett* 2015;37:1385–1392.
42. Qing-yun M, Xu J, Qing-qing L, Jin-long S, Yi-qing Z, Zhi-yong R. Isolation and Identification of Nicosulfuron Degrading Strain *Chryseobacterium* sp. LAM-M5 and Study on Its Degradation Pathway. *Biotechnol Bulletin* 2022; 38: 113-122.
43. Zhao W, Wang C, Xu L, Zhao C, Liang H, Qiu L.. Biodegradation of nicosulfuron by a novel *Alcaligenes faecalis* strain ZWS11. *J Environ Sci.* 2015;35:151–162.
44. Wang L, Zhang X, Li Y. Degradation of nicosulfuron by a novel isolated bacterial strain *Klebsiella* sp. Y1: condition optimization, kinetics and degradation pathway. *Water Sci Technol* 2016;73:2896–2903.
45. Zhang H, Mu W, Hou Z, Wu X, Zhao W, Zhang X, et al. Biodegradation of nicosulfuron by the bacterium *Serratia marcescens* N80, *J of Environ Sci and Health Part B* 2012;47:153-160.
46. Carles L, Joly M, Bonnemoy F, Leremboure M, Batisson I, Besse-Hoggan P. Identification of sulfonylurea biodegradation pathways enabled by a novel nicosulfuron-transforming strain *Pseudomonas fluorescens* SG-1: toxicity assessment and effect of formulation. *J Hazard Mater* 2017; 324: 184–193.





Tuhin Subhra Ghosh et al.,

47. Zhao H, Zhu J, Liu S, Zhou X. Kinetics study of nicosulfuron degradation by a *Pseudomonas nitroreducens* strain NSA02. *Biodegradation* 2018;29:271–283.
48. Xu J, Li X, Xu Y, Qiu L, Pan C. Biodegradation of pyrazosulfuron-ethyl by three strains of bacteria isolated from contaminated soils. *Chemosphere* 2009;74:682–687.
49. Zhang W, Wen-Juan C, Shao-Fang C, Qiqi L, Jiayi L, Pankaj B, et al. Cellular Response and Molecular Mechanism of Glyphosate Degradation by *Chryseobacterium* sp. Y16C. *J of Agri and Food Chem* 2023;71.
50. Li J, Wen-Juan C, Zhang W, Zhang Y, Lei Q, Wu S, et al. Effects of Free or Immobilized Bacterium *Stenotrophomonas acidaminiphila* Y4B on Glyphosate Degradation Performance and Indigenous Microbial Community Structure. *J of Agric and Food Chem* 2022;70.
51. Oanh NT, Duc HD, Ngoc DTH, Thuy NTD, Hiep NH, Van Hung N. Biodegradation of propanil by *Acinetobacter baumannii* DT in a biofilm-batch reactor and effects of butachlor on the degradation process. *FEMS Microbiol Lett* 2020;367:fnaa005.
52. Jindakaraked M, Khan E, Kajitvichyanukul P. Biodegradation Capabilities of Paraquat-Degrading Bacteria Immobilized on Nanoceramics. *Toxics*.2023; 11:638.
53. Fang H, Xu T, Cao D, Cheng L, Yu Y. Characterization and genome functional analysis of a novel metamitron-degrading strain *Rhodococcus* sp. MET via both triazinone and phenyl rings cleavage. *Sci Rep* 2016; 6: 32339.
54. Ni H, Yao L, Li N, Cao Q, Da C, Zhang J, et al. Biodegradation of pendimethalin by *Bacillus subtilis* Y3. *Appl Environ Microbiol* 2016;82:7052–7062.
55. Doolotkeldieva T, Bobusheva S, Konurbaeva M. The Improving Conditions for the Aerobic Bacteria Performing the Degradation of Obsolete Pesticides in Polluted Soils. *Air Soil Water Res* 2021; 14.
56. Jariyal M, Jindal V, Mandal K, Gupta VK, Singh B. Bioremediation of organophosphorus pesticide phorate in soil by microbial consortia. *Ecotoxicol Environ Saf* 2018 ;159: 310–316.
57. Scott C, Pandey G, Hartley CJ, Jackson CJ, Cheesman MJ, Taylor MC, et al. The enzymatic basis for pesticide bioremediation. *Indian J Microbiol* 2008;48:65–79.
58. Lin Z, Pang S, Zhang W, Mishra S, Bhatt P, Chen S. Degradation of acephate and its intermediate methamidophos: mechanisms and biochemical pathways. *Front Microbiol* 2020;11:2045.
59. Mishra S, Zhang W, Lin Z, Pang S, Huang Y, Bhatt P, et al. Carbofuran toxicity and its microbial degradation in contaminated environments. *Chemosphere* 2020;259:127429.
60. De Souza AJ, De Andrade PAM, De Araújo PAP, Andreote FD, Tornisielo VL, Regitano JB. The depleted mineralization of the fungicide chlorothalonil derived from loss in soil microbial diversity. *Sci Rep* 2017; 7: 14646.
61. Sharma P, Chopra A, Cameotra SS, Suri CR. Efficient biotransformation of herbicide diuron by bacterial strain *Micrococcus* sp. PS-1. *Biodegradation* 2010;21:979–987.
62. Devers-Lamrani M, Pesce S, Rouard N, Martin-Laurent F. Evidence for cooperative mineralization of diuron by *Arthrobacter* sp. BS2 and *Achromobacter* sp. SP1 isolated from a mixed culture enriched from diuron exposed environments. *Chemosphere* 2014; 117: 208–215.
63. Liu J, Zhou X, Wang T, Fan L, Liu S, Wu N, et al. Construction and comparison of synthetic microbial consortium system (SMCs) by non-living or living materials immobilization and application in acetochlor degradation. *J Hazard Mater* 2022;438:129460.
64. Dong W, Chen Q, Hou Y, Li S, Zhuang K, Huang F, et al. Metabolic pathway involved in 2-methyl-6-ethylaniline degradation by *Sphingobium* sp. strain MEA3-1 and cloning of the novel flavin-dependent monooxygenase system meaBA. *Appl Environ Microbiol* 2015; 81:8254–64.
65. Liu HM, Cao L, Lu P, Ni H, Li YX, Yan X, et al. Biodegradation of Butachlor by *Rhodococcus* sp. Strain B1 and Purification of Its Hydrolase (ChlH) Responsible for N-Dealkylation of Chloroacetamide Herbicides. *J of Agric and Food Chem* 2012;60:12238–12244.
66. Carles L, Rossi F, Besse-Hoggan P, Blavignac C, Lerembouere M, Artigas J, Batisson I. Nicosulfuron Degradation by an Ascomycete Fungus Isolated From Submerged Alnus Leaf Litter. *Front Microbiol* 2018; 9 :3167.





Tuhin Subhra Ghosh et al.,

67. Pan Z, Wu Y, Zhai Q, Tang Y, Liu X, Xu X, et al. Immobilization of bacterial mixture of *Klebsiella variicola* FH-1 and *Arthrobacter* sp. NJ-1 enhances the bioremediation of atrazine-polluted soil environments. *Front Microbiol* 2023;14:1056264.
68. Luo W, Gu Q, Chen W, Zhu X, Duan Z, Yu X. Biodegradation of acetochlor by a newly isolated *Pseudomonas* strain. *Appl Biochem Biotechnol* 2015;176:636-44.
69. Zhou S, Song J, Dong W, Mu Y, Zhang Q, Fan Z, et al. Nicosulfuron biodegradation by a novel cold-adapted strain *Oceanisphaera psychrotolerans* LAM-WHM-ZC. *J Agric Food Chem* 2017;65:10243–10249.
70. Lu XH, Kang ZH, Tao B, Wang YN, Dong JG, Zhang JL. Degradation of nicosulfuron by *Bacillus subtilis* YB1 and *Aspergillus niger* YF1. *Appl. Biochem. Microbiol* 2012;48:460–466.
71. Zhao W, Xu L, Li D, Li X, Wang C, Zheng M, et al. Biodegradation of thifensulfuron-methyl by *Ochrobactrum* sp. in liquid medium and soil. *Biotechnol Lett* 2015;37:1385-92.
72. Zhang J, Zheng JW, Liang B, Wang CH, Cai S, Ni YY, et al. Biodegradation of chloroacetamide herbicides by *Paracoccus* sp. FLY-8 in vitro. *J. Agric Food Chem* 2011;59:4614-4621.
73. Xu J, Qiu X, Dai J, Cao H, Yang M, Zhang J, et al. Isolation and characterization of a *Pseudomonas oleovorans* degrading the chloroacetamide herbicide acetochlor. *Biodegradation* 2006;17:219-25.
74. Li Y, Chen Q, Wang CH, Cai S, He J, Huang X, et al. Degradation of acetochlor by consortium of two bacterial strains and cloning of a novel amidase gene involved in acetochlor-degrading pathway. *Bioresour Technol* 2013;148:628-31.
75. Cheng M, Yan X, He J, Qiu J, Chen Q. Comparative genome analysis reveals the evolution of chloroacetanilide herbicide mineralization in *Sphingomonas wittichii* DC-6. *Arch Microbiol* 2019; 201: 907–918.
76. Zheng J, Li R, Zhu J, Zhang J, He J, Li S, et al. Degradation of the chloroacetamide herbicide butachlor by *Catellibacterium caenisp.* nov DCA-1T. *Int Biodeterior Biodegradation* 2012; 73:16-22.
77. Dwivedi S, Singh BR, Al-Khedhairi AA, Alarifi S, Musarrat J. Isolation and characterization of butachlor-catabolizing bacterial strain *Stenotrophomonas acidaminiphila* JS-1 from soil and assessment of its biodegradation potential. *Lett Appl Microbiol* 2010; 51: 54-60.
78. Ahmad KS. Environmental contaminant 2-chloro-N-(2,6-diethylphenyl)-N-(methoxymethyl) acetamide remediation via *Xanthomonas axonopodis* and *Aspergillus niger*. *Environ Res* 2020; 182 :109117.
79. Wu P, Xie L, Li J, Yang W, Han Z, Wu X, et al. The removal of butachlor from soil by wastewater-derived *Rhodospseudomonas marshes*. *Soil Use and Manage* 2020;00:1-4.
80. Song J, Gu J, Zhai Y, Wu W, Wang H, Ruan Z, et al. Biodegradation of nicosulfuron by a *Talaromyces flavus* LZM1. *Bioresour Technol* 2013;140:243–248.
81. Dhiman N, Jasrotia T, Sharma P, Negi S, Chaudhary S, Kumar R, et al. Immobilization interaction between xenobiotic and *Bjerkandera adusta* for the biodegradation of atrazine. *Chemosphere* 2020; 257: 127060.
82. Da Silva C-M J, Brugnari T, Sá-Nakanishi AB, Castoldi R, De Souza CG, Bracht A, et al. Evaluation of diuron tolerance and biotransformation by the white-rot fungus *Ganoderma lucidum*. *Fungal Biol* 2018; 122: 471–478.
83. Mori T, Sudo S, Kawagishi H, Hirai H. Biodegradation of diuron in artificially contaminated water and seawater by wood colonized with the whiterot fungus *Trametes versicolor*. *J Wood Sci* 2018;64:690–696.
84. Henn C, Arakaki RM, Monteiro DA, Boscolo M, da Silva R, Gomes E. Degradation of the organochlorinated herbicide diuron by rainforest basidiomycetes. *Biomed Res Int* 2020: 5324391.
85. Wang Y, Li H, Feng G, Du L, Zeng D. Biodegradation of diuron by an endophytic fungus *Neurospora intermedia* DP8-1 isolated from sugarcane and its potential for remediating diuron-contaminated soils. *PLoS One* 2017;12:e0182556.
86. Beltrán-Flores E, Sarrà M, Blánquez P. Pesticide bioremediation by *Trametes versicolor*: Application in a fixed-bed reactor, sorption contribution and bioregeneration. *Sci. Total Environ* 2021; 794: 148386.
87. Kwatra N, Abraham J. Mycoremediation of pretilachlor and its metabolite by *Aspergillus ficuum*. *J Environ Sci Health B* 2023;58:489-499.
88. Feng W, Wei Z, Song J, Qin Q, Yu K, Li G, et al. Hydrolysis of nicosulfuron under acidic environment caused by oxalate secretion of a novel *Penicillium oxalicum* strain YC-WM1. *Sci Rep* 2017; 7:647.
89. Chang X, Liang J, Sun Y, Zhao L, Zhou B, Li X, Li Y. Isolation, Degradation Performance and Field Application of the Metolachlor-Degrading Fungus *Penicillium oxalicum* MET-F-1, *Appl Sci* 2020; 10: 8556.



Tuhin Subhra Ghosh *et al.*,

90. Han Y, Tang Z, Bao H, Wu D, Deng X, Guo G, Ye BC, Dai B. Degradation of pendimethalin by the yeast YC2 and determination of its two main metabolites. *RSC Adv* 2019;9:491-497.
91. Sondhia S, Waseem U. Degradation of pyrazosulfuron-ethyl in the agricultural soil by *Alternaria alternata*. *Indian J of Weed Sci* 2019;51:402-406.
92. Correa LO, Bezerra AFM, Honorato LRS, Cortez ACA, Souza JVB, Souza ES. Amazonian soil fungi are efficient degraders of glyphosate herbicide; novel isolates of *Penicillium*, *Aspergillus*, and *Trichoderma*, *Braz J Biol* 2023; 83.
93. Nguyen TLA, Dao ATN, Dang HTC, Koekkoek J, Brouwer A, de Boer TE, *et al.* Degradation of 2,4-dichlorophenoxyacetic acid (2,4-D) and 2,4,5-trichlorophenoxyacetic acid (2,4,5-T) by fungi originating from Vietnam. *Biodegradation* 2022;33:301-316.
94. Purnomo AS, Sariwati A, Kamei I. Synergistic interaction of a consortium of the brown-rot fungus *Fomitopsis pinicola* and the bacterium *Ralstonia pickettii* for DDT biodegradation. *Heliyon* 2020;6.
95. Ingham E, Griffiths R, Cromack K, Entry J. Comparison of direct vs fumigation incubation microbial biomass estimates from ectomycorrhizal mat and non-mat soils. *Soil Biol Biochem* 1991; 23: 465-471.
96. Kohlmeier S, Smits THM, Ford RM, Keel C, Harms H, Wick LY. Taking the fungal highway: Mobilization of pollutant-degrading bacteria by fungi. *Environ Sci Technol* 2005;39:4640-4646.
97. Wick LY, Remer R, Würz B, Reichenbach J, Braun S, Schäfer F, *et al.* Effect of fungal hyphae on the access of bacteria to phenanthrene in soil. *Environ Sci Technol* 2007;41:500-505.
98. Junier P, Cailleau G, Palmieri I, Vallotton C, Trautschold OC, Junier T, *et al.* Democratization of fungal highway columns as a tool to investigate bacteria associated with soil fungi. *FEMS Microbiol Ecol* 2021;97: fiab003.
99. Zhuo R., Fan F. A comprehensive insight into the application of white rot fungi and their lignocellulolytic enzymes in the removal of organic pollutants. *Sci. Total Environ.* 2021;778:146132.
100. Słaba M, Szewczyk R, Piątek MA, Długoński J. Alachlor oxidation by the filamentous fungus *Paecilomyces marquandii*, *J of Hazard Mater* 2013;26:443-450.
101. Kim NH, Kim DU, Kim I, Ka JO. Syntrophic biodegradation of butachlor by *Mycobacterium* sp. J7A and *Sphingobium* sp. J7B isolated from rice paddy soil. *FEMS Microbiol Lett* 2013; 344:114-120.
102. Torabi E, Talebi K., Pourbabaei A, Ahmadzadeh M. Diazinon dissipation in pesticide-contaminated paddy soil: kinetic modeling and isolation of a degrading mixed bacterial culture. *Environ Sci Pollut Res* 2017;24:4117-4133.
103. Zhang L, Hang P, Hu Q, Chen XL, Zhou XY, Chen K, *et al.* Degradation of phenylurea herbicides by a novel bacterial consortium containing synergistically catabolic species and functionally complementary hydrolases. *J. Agric Food Chem* 2018;66:12479-12489.
104. Zhang L, Hang P, Zhou X, Dai C, He Z, Jiang j, Mineralization of the herbicide swep by a two-strain consortium and characterization of a new amidase for hydrolyzing swep. *MicrobCell Fact* 2020;19:4.
105. Hou Y, Dong W, Wang F, Li J, Shen W, Li Y, Cui Z. Degradation of acetochlor by a bacterial consortium of *Rhodococcus* sp. T3-1, *Delftia* sp. T3-6 and *Sphingobium* sp. MEA3-1. *Lett Appl Microbiol* 2014;59:35-42.
106. Ellegaard-Jensen L, Knudsen BE, Johansen A, Albers CN, Aamand J, Rosendahl S. (2014). Fungal-bacterial consortia increase diuron degradation in water-unsaturated systems. *Sci Total Environ* 2014;466-467: 699-705.
107. Villaverde J, Rubio-Bellido M, Merchán F, Morillo E. Bioremediation of diuron contaminated soils by a novel degrading microbial consortium. *J Environ Manage* 2016;188:379-386.
108. Sørensen SR, Ronen Z, Aamand J. Growth in coculture stimulates metabolism of the phenylurea herbicide isoproturon by *Sphingomonas* sp. Strain SRS2. *Appl Environ Microbiol* 2002;68:3478-3485.
109. Anwar S, Wahla AQ, Ali T, Khaliq S, Imran A, Tawab A, Afzal M, Iqbal S. Biodegradation and Subsequent Toxicity Reduction of Co-contaminants Tribenuron Methyl and Metsulfuron Methyl by a Bacterial Consortium B2R. *ACS Omega* 2022;7:19816-19827.
110. Albers P, Weytjens B, De Mot R, Marchal K, Springael D. Molecular processes underlying synergistic linuron mineralization in a triplespecies bacterial consortium biofilm revealed by differential transcriptomics. *Microbiologyopen* 2018;7:e559.
111. Wang J, Li X, Li X, Wang H, Su Z, Wang X, *et al.* Dynamic changes in microbial communities during the bioremediation of herbicide (chlorimuron-ethyl and atrazine) contaminated soils by combined degrading bacteria. *PLoS One* 2018;13:e0194753.
112. Glick BR. Using soil bacteria to facilitate phytoremediation. *Biotechnol Adv* 2010;28:367-374.



Tuhin Subhra Ghosh *et al.*,

113. Boyle JJ, Shann JR. Biodegradation of phenol, 2,4-DCP, 2,4-D, and 2,4,5-T in field-collected rhizosphere and nonrhizosphere soils. *J Environ Qual* 1995;24:782.
114. Zhang H, Chen F, Zhao H, Lu J, Zhao M, Hong Q, *et al.* Colonization on cucumber root and enhancement of chlorimuron-ethyl degradation in rhizosphere by *Hansschlegeliazhihuaiae* S113 and root exudates. *J of Agric and Food Chem* 2018;66:4584-459.
115. Chang SW, Lee SJ, Je CH. (2005). Phytoremediation of atrazine by poplar trees: Toxicity, uptake, and transformation. *J. Environ. Sci. Health*.2005; 40: 801–811.
116. Chang SW, Lee SJ, Je CH. (2005). Phytoremediation of atrazine by poplar trees: Toxicity, uptake, and transformation. *J. Environ. Sci. Health*.2005;40:801–811.
117. Siwek M. Biologicznesposobyoczyszczaniaśrodowiska—fitoremediacja. *WiadomościBotaniczne*. 2008;52:23-28
118. Posmyk K, Urbaniak M. Fitoremediacja jako alternatywna metoda oczyszczania środowiska. *Aura*. 2014;7:10-12
119. Ferreira LC, Moreira BRA, Montagnolli RN, Prado EP, Viana RS, Tomaz RS, *et al.* Green Manure Species for Phytoremediation of Soil With Tebuthiuron and Vinasse. *FrontBioengBiotechnol* 2021;8:613642.
120. **Conciani P A, Mendes KF, de Sousa RN, Ribeiro AP, Pimpinato RF, Tornisielo VL.** (2023) Peanut and sorghum are excellent phytoremediators of ¹⁴C-tebuthiuron in herbicide-contaminated soil. *Adv Weed Sci* 2023;41.
121. Alencar BTB, Ribeiro VHV, Cabral CM, dos Santos NMC, Ferreira EA, Francino DMT, *et al.* Use of macrophytes to reduce the contamination of water resources by pesticides. *Ecol Indic* 2020;109:105785.
122. Loureiro DB, Lario LD, Herrero MS, Salvatierra LM, Novo LAB, Pérez LM. Potential of *Salvinia biloba* Raddi for removing atrazine and carbendazim from aquatic environments. *Environ Sci and Pollut Res* 2022;30:22089–22099.
123. Sutherland DL, Ralph PJ. Microalgal Bioremediation of Emerging Contaminants—Opportunities and Challenges. *Water Res* 2019;164:114921.
124. Mustafa S, Bhatti N, Maqbool M. Microalgae Biosorption, Bioaccumulation and Biodegradation Efficiency for the Remediation of Wastewater and Carbon Dioxide Mitigation: Prospects, Challenges and Opportunities. *J Water Process Eng* 2021;41:2214–7144.
125. Komárek M, Cadková E, Chrástný V, Bordas F, Bollinger JC. Contamination of Vineyard Soils with Fungicides: A Review of Environmental and Toxicological Aspects. *Environ Int* 2010;36:138–151.
126. Sakurai T, Aoki M, Ju X, Ueda T, Nakamura Y, Fujiwara S, *et al.* Profiling of Lipid and Glycogen Accumulations Under Different Growth Conditions in the Sulfothermophilic Red Alga *Galdieriasulphuraria*. *Bioresour Technol* 2016;200:861-866.
127. Nie J, Sun Y, Zhou Y, Kumar M, Usman M, Li J, Shao, *et al.* Bioremediation of Water Containing Pesticides By Microalgae: Mechanisms, Methods, and Prospects For Future Research *Sci Total Environ* 2020;707:136080.
128. Weiner JA, DeLorenzo ME, Fulton MH. Relationship between uptake capacity and differential toxicity of the herbicide atrazine in selected microalgal species. *AquatToxicol* 2004;68:121-128.
129. Ghasemi Y, Rasoul-Amini S, Fotooh-Abadi E. The Biotransformation, Biodegradation, and Bioremediation of Organic Compounds by Microalgae. *J Phycol* 2011;47: 969–980.
130. Velásquez L, Dussan J. Biosorption and Bioaccumulation of Heavy Metals on Dead and Living Biomass of *Bacillus sphaericus*. *J Hazard Mater* 2009;167:713–716.
131. Bilal M, Rasheed T, Sosa-Hernández JE, Raza A, Nabeel F, Iqbal HMN. Biosorption: An Interplay between Marine Algae and Potentially Toxic Elements—A Review. *Mar Drugs* 2018;16:65.
132. Kabra AN, Ji MK, Choi J, Kim JR, Govindwar SP, Jeon BH. Toxicity of Atrazine and Its Bioaccumulation and Biodegradation in a Green Microalga, *Chlamydomonas mexicana*. *Environ Sci Pollut Res* 2014;21:12270–12278.
133. Swackhamer DL, Skoglund RS. Bioaccumulation of PCBs by Algae: Kinetics Versus Equilibrium. *Environ Toxicol Chem* 1993;12:831–838.
134. Pérez-Legaspi IA, Ortega-Clemente LA, Moha-León JD, Ríos-Leal E, Gutiérrez SCR, Rubio-Franchini I. Effect of the Pesticide Lindane on the Biomass of the Microalgae *Nannochlorisoculata*. *J Environ Sci Health Part B* 2015;51:103–106.
135. González-Barreiro O, Rioboo C, Herrero C, Cid A. Removal of triazine herbicides from freshwater systems using photosynthetic microorganisms, *Environ Pollut* 2006;144:266-271.





Tuhin Subhra Ghosh et al.,

136. Hussein MH, Abdullah AM, Badr El, Din NI, MishaqaESI .Biosorption Potential of the Micro chlorophyte *Chlorella vulgaris* for Some Pesticides. J Fertil Pestic2017;8:1–5.
137. Philippat C, Barkoski J, Tancredi DJ, Elms B, Barr DB, Ozonoff S, et al. Prenatal Exposure to Organophosphate Pesticides and Risk of Autism Spectrum Disorders and Other Non-Typical Development at 3 Years in a High-Risk Cohort. Int J Hyg Environ Health 2018;221:548–555.
138. Wang L, Xiao H, He N, Sun D, Duan S. Biosorption and Biodegradation of the Environmental Hormone Nonylphenol By Four Marine Microalgae. Sci Rep 2019;9:5277.
139. Encarnaçao T, Santos D, Ferreira S, Valente AJM, Pereira JC, Campos MG, Burrows HD, Pais AACC. Removal of Imidacloprid from Water by Microalgae *Nannochloropsis* sp. and Its Determination by a Validated RP-HPLC Method. Bull. Environ. Contam. Toxicol. 2021;107:31–139.
140. Ni Y, Lai J, Wan J, Chen L. Photosynthetic Responses and Accumulation of Mesotrione in Two Freshwater Algae. Environ. Sci Process Impacts 2014;16:2288–2294.
141. Cai X, Liu W, Jin M, Lin K. Relation of diclofop-methyl toxicity and degradation in algae cultures. Environ Toxol Chem 2007;26:970-975.
142. Li H, Yuan Y, Shen C, Wen Y, Liu H. Enantioselectivity in toxicity and degradation of dichlorprop-methyl in algal cultures. J of Environ Sci and Health - Part B Pesticides, Food Contami and Agric Wastes 2008;43:288-292.
143. Salman JM, Abdul-Adel E. Potential use of cyanophyta species *Oscillatoria limnetica* in bioremediation of organophosphorus herbicide glyphosate. Mesop environ J 2015;1:15-26.
144. Wonguttisin P, Supo C, Suwannarach N, Honda Y, Nakazawa T, Kumla J, Lumyong S, Khanongnuch C. Filamentous fungi with high paraquat-degrading activity isolated from contaminated agricultural soils in northern Thailand. Lett Appl Microbiol2021;72:467-475.
145. Zanatta MBT, de Oliveira ML, Souza LRR. Nano-phytoremediation: The Successful Combination of Nanotechnology and Phytoremediation. In: Newman L, Ansari AA, Gill SS, Naem M, Gill R, editors. Phytoremediation. Switzerland AG: Springer Cham; 2023. P. 443–462.
146. BapatG, Labade C, Chaudhuri A, ZinzardeS. Silica nanoparticle based techniques for extraction, detection and degradation of pesticides. Adv Colloid Interface Sci 2016;237:1-14.
147. Morillo E, Villaverde J. Advanced technologies for the remediation of pesticide contaminated soils. Sci Total Environ 2017;586:576–597.
148. LinZ, Zhen Z, Liang Y, Li J, Yang J, Zhong L, et al. Changes in atrazine speciation and the degradation pathway in red soil during the vermiremediation process. J of Hazard Mater2019;364:710-719.
149. HanL, Fang K, Liu Y, Fang J, Wang F, Wang X. Earthworms accelerated the degradation of the highly toxic acetochlor S-enantiomer by stimulating soil microbiota in repeatedly treated soils, J Hazard Mater 2021;420:126669.
150. HaoY, Zhao L, Sun Y, Li X, Weng L, Xu H, LiY. Enhancement effect of earthworm (*Eisenia fetida*) on acetochlor biodegradation in soil and possible mechanisms. EnvironmPollut2018; 242 Part A: 728-737.
151. Sun Y, ZhaoL, Li X, Hao Y, Xu H, Weng L, et al. Stimulation of earthworms (*Eisenia fetida*) on soil microbial communities to promote metolachlor degradation. Environ Pollut2019;248:219-228.
152. Owagboriaye F, Dedeke G, Bamidele J, Aladesida A, Isibor P, Feyisola R, et al. Biochemical response and vermiremediation assessment of three earthworm species (*Alma millsoni*, *Eudriluseugeniae* and *Libyodrilus violaceus*) in soil contaminated with a glyphosate-based herbicide. EcolIndicators 2019;108:1056789.
153. Aislabie J, Lloyd-Jones G. A review of bacterial degradation of pesticides. Aust J Soil Res 1995; 33: 925–942.
154. Huang Y, Xiao L, Li F, Xiao M, Lin D, Long X, Wu Z. Microbial degradation of pesticide residues and an emphasis on the degradation of cypermethrin and 3-phenoxy benzoic acid: A review. Mol2018;23:2313.
155. Hussain S, Arshad M, Springael D, Sørensen SR, Bending GD, Devers-Lamrani M, Maqbool Z, Martin-Laurent F. 2015. Abiotic and biotic processes governing the fate of Phenylurea herbicides in soils: A review. Crit Rev Environ Sci Technol2015;45:1947–1998.
156. Pal R, Chakrabarti K, Chakraborty A, Chowdhury A. Degradation and Effects of Pesticides on Soil Microbiological Parameters-A Review. Int J of Agric Res2006;1:240–258. doi:10.3923/ijar.2006.240.258.



Tuhin Subhra Ghosh *et al.*,

157. Jaiswal DK, Verma JP, Yadav J. 2017. Microbe induced degradation of pesticides in agricultural soils. *Environ Sci Eng (Subser: Environ Sci)*2016;167–189.
158. Zacharia, Tano J. Identity, Physical and Chemical Properties of Pesticides. In: Stoytcheva M, editor. *Pesticides in the Modern World - Trends in Pesticides Analysis*. IntechOpen 2011.
159. Konda LN, Czinkota I, Füleky G, Morovján G. Modeling of Single-Step and Multistep Adsorption Isotherms of Organic Pesticides on Soil. *J Agric Food Chem* 2002;50:7326–7331.
160. Yu YL, Wu XM, Li SN, Fang H., Zhan HY, Yu JQ. An exploration of the relationship between adsorption and bioavailability of pesticides in soil to earthworm. *Environ Pollut*2006;141:428–433.
161. Alfonso LF, Germán GV, del Carmen PCM, Hossein G. Adsorption of organophosphorus pesticides in tropical soils: The case of karst landscape of northwestern Yucatan. *Chemosphere* 2017;166:292–299.
162. Han SO, New PB. Effect of water availability on degradation of 2, 4-dichlorophenoxyacetic acid (2, 4-d) by soil microorganisms. *Soil Biol Biochem*1994;26:1689–1697.
163. Monard C, McHergui C, Nunan N, Martin-Laurent F, Vieublé-Gonod L. Impact of soil matrix potential on the fine-scale spatial distribution and activity of specific microbial degrader communities. *FEMS Microbiol Ecol*2012;81:673–683.
164. Schroll R, Becher HH, Dörfler U, Gayler S, Grundmann S, Hartmann HP, *et al.* Quantifying the effect of soil moisture on the aerobic microbial mineralization of selected pesticides in different soils. *Environ Sci and Technol*2006;40:3305–3312.
165. Li K, Liu W, Xu D, Lee S. Influence of organic matter and pH on bentazone sorption in soils. *J of Agric and Food Chem*2003;51:5362–5366.
166. Rodríguez-Cruz MS, Jones JE, Bending GD. Field-scale study of the variability in pesticide biodegradation with soil depth and its relationship with soil characteristics. *Soil Biol and Biochem*2006;38:2910–2918.
167. Pagel H, Ingwersen J, Poll C, Kandeler E, Streck T. Micro-scale modeling of pesticide degradation coupled to carbon turnover in the detritusphere: Model description and sensitivity analysis. *Biogeochemistry*2014;117:185–204.
168. Kanissery RG, Sims GK. Biostimulation for the enhanced degradation of herbicides in soil. *Appl Environ Soil Sci* 2011;2011:843450.
169. He L, Fan S, Müller K, Hu G, Huang H, *et al.* Biochar reduces the bioavailability of di-(2-ethylhexyl) phthalate in soil. *Chemosphere* 2016; 142: 24-27.
170. Lauber CL, Hamady M, Knight R, Fierer N. Pyrosequencing-based assessment of soil pH as a predictor of soil bacterial community structure at the continental scale. *Appl and Environ Microbiol*2009;75:5111–5120.
171. Franco A, Wenjing FU, Trapp S. Influence of soil pH on the sorption of ionizable chemicals: Modeling advances. *Environ Toxicol Chem*2009;28:458–464.
172. Singh S, Gupta A, Waswani H, Prasad M, Ranjan R. Impact of pesticides on the ecosystem. In: Naeem M, Bremont JFJ, Ansari AA, Gill SS editors. *Agrochemicals in Soil and Environment*. Singapore: Springer; 2022. P. 157-181.
173. Bazhanov DP, Li C, Li H, Li J, Zhang X, Chen X, Yang H. 2016. Occurrence, diversity and community structure of culturable atrazine degraders in industrial and agricultural soils exposed to the herbicide in Shandong Province, P.R. China. *BMC Microbiol*2016;16:1–21.
174. Haws NW, Ball WP, Bouwer EJ. Modeling and interpreting bioavailability of organic contaminant mixtures in subsurface environments. *J Contam Hydrol*2006;82:255-292.
175. Zhou GT, Xia X, Wang H, Li LQ, Wang GJ, Zheng SX, *et al.* Immobilization of Lead by *Alishewanella* sp. WH16-1 in pot experiments of Pb-contaminated paddy soil. *Water Air Soil Pollut*2016;227:339.
176. Kumar V, Shahi SK, Singh S. Bioremediation: An Eco-sustainable Approach for Restoration of Contaminated Sites. In: Singh J, Sharma D, Kumar G, Sharma N, editors. *Microbial Bioprospecting for Sustainable Development*. Singapore: Springer Nature; 2018. P. 115-136.
177. Van Deuren J, Lloyd T, Chetry S, Liou R, Peck J. Remediation Technologies Screening Matrix and Reference Guide., Report by Platinum International, Inc. for US Army Environmental Center. 2002, Report No. SFIM-AEC-ET-CR-97053. <http://www.frtr.gov/matrix2/section1/toc.html>.





Tuhin Subhra Ghosh et al.,

178. De Liphthay JR, Sørensen SR, Aamand J. Effect of herbicide concentration and organic and inorganic nutrient amendment on the mineralization of mecoprop, 2,4-D and 2,4,5-T in soil and aquifer samples. Environ Pollut2007;148:83-93.

Table 1: Different herbicides and their remediation with efficiencies by bacteria.

Herbicides	Strains of bacteria	Efficiency and optimum conditions	Metabolites	References
Atrazine (triazine)	<i>Klebsiella variicola</i> FH-1, <i>Arthrobacter</i> sp. NJ-1	85.6%, 50 mg/L, pH ≥ 7, 30°C	-	[21]
	<i>Paenarthrobacter ureafaciens</i> sZY	12.5 mg/L/h, 10 0 mg/L, pH 7, 30°C	-	[22]
Acetochlor (chloroacetanilide)	<i>Bacillus</i> sp. ACD-9	> 60%, 30 mg/L, 2d, pH6, 42°C,	2-chloro-N-(2-methyl- 6-ethylphenyl) acetamide	[23]
Butachlor(chloroacet anilide)	<i>Ammoniphilus</i> sp. JF	100%, 100 mg/L, 24h, 30°C	1,2- benzenedicarboxylic acid, bis(2- methylpropyl) ester and 2,4-bis(1,1- dimethylethyl)-phenol	[24]
	<i>Bacillus altitudinis</i> A16	90%, 50 mg/L, 5d	(N-(butoxymethyl)-N- (2-chloroethyl)-2,6- diethylaniline, (N- (butoxymethyl)-2- chloro-N-(2- ethylphenyl) acetamide, N- (butoxymethyl)-2,6- diethyl-N- propylaniline, 2- chloro-N-(2,6- diethylphenyl) acetamide and 2,6- diethylaniline)	[25]
	<i>Pseudomonas putida</i> G3	2.74 mg/L/ h	2-chloro-N-(2,6- diethylphenyl)-N- hydroxymethylacetam ide, 2-chloro-N-(2,6- diethylphenyl) acetamide and 2,6- diethylaniline	[26]
	<i>Pseudomonas aeruginosa</i> PK	95%, 100 µg/mL,5d	-	[27]
Pretilachlor(chloroac etanilide)	<i>Rhodococcus</i> sp. B2	86.1%,50 mg/L, 5d, pH 6.98, 30.1°C	N-hydroxyethyl-2- chloro-N-(2, 6-diethyl- phenyl)-acetamide	[28], [29]



Tuhin Subhra Ghosh *et al.*,

Alachlor, acetochlor, propisochlor, butachlor, pretilachlor and metolachlorin. (chloroacetamide)	<i>Proteiniclasticumsediminis</i> BAD-10 ^T	37 °C, pH 7.0–7.5	2-ethyl-6-methyl- <i>N</i> -(ethoxymethyl)-acetanilide (EMEMA), <i>N</i> -(2-methyl-6-ethylphenyl)-acetamide (MEPA), <i>N</i> -2-ethylphenyl acetamide and 2-ethyl- <i>N</i> -carboxyl aniline	[30]
Chloroacetanilide	<i>Sphingobiumbaderi</i> DE-13	-	2-methyl-6-ethylaniline (MEA) and 2,6-diethylaniline (DEA)	[31]
Phenmedipham (carbamate)	<i>Ochrobactrumanthropi</i> NC-1	98.5%, 2 mM, 168h, pH 7.0, 30–35 °C	<i>m</i> -aminophenol, methyl- <i>N</i> -(3-hydroxyphenyl) carbamate, <i>m</i> -toluidine	[32]
Diuron, linuron, chlorotoluron, fluometuron phenylurea)	<i>Ochrobactrumanthropi</i> CD3	99%, 10 mg/L, 20d, 30 °C	<i>N</i> -(3,4-dichlorophenyl)urea, <i>N</i> -(3,4-dichlorophenyl)- <i>N</i> -methylurea and 3,4-dichloroaniline.	[33]
Diuron (phenylurea)	<i>Bacillus cereus</i> , <i>Vagococcus fluvialis</i> , <i>Burkholderia ambifaria</i> , <i>Bacillus</i> spp. (cooperative mineralization)	58–74%, 40 mg/L, 35d	3,4-dichloroaniline and the demethylated metabolite <i>N</i> -(3,4-dichlorophenyl)- <i>N</i> -methylurea	[34]
	<i>Bacillus licheniformis</i> SDS12	85.60 ± 1.36%, 50 ppm	3, 4-dichloroaniline	[35]
	<i>Stenotrophomonas rhizophila</i> CASB3	94%, 50 mg/kg, 42d	Complete degradation	[36]
	<i>Pseudomonas aeruginosa</i> FN	0.5 mg/L, 25°C	3,4-dichloroanilines	[37]
	<i>Bacillus pseudomycooides</i> D/T, <i>Bacillus simplex</i> / <i>Bacillus muralis</i> D/N (cooperative mineralization)	86.2%, 5 mg/g	<i>N</i> -(3,4-dichlorophenyl)- <i>N</i> -methylurea and 3,4-dichloroaniline	[38]
Isoproturon (phenylureas)	<i>Sphingomonas</i> sp. ISP1, <i>Arthrobacter</i> sp.SP2, <i>Acinetobacterbaumannii</i> 4IA, & <i>Pseudomonas</i> sp. ISP3	51%, 100 mg/L, 10d	3-(4-isopropylphenyl)-1-methylurea, 3-(4-isopropylphenyl)-urea, 4-isopropylaniline, and 4-toluidine	[39]
Simazine	<i>Bacillus licheniformis</i> SIMA-N5,	SIMA-N9 (98%)	-	[40]



Tuhin Subhra Ghosh *et al.*,

(triazine)	<i>Bacillus altitudinis</i> SIMA-N9	andSIMA-N5 94% of 5 mg/L in 5 days		
Chlorimuron-ethyl (sulfonylurea)	<i>Rhodococcus</i> sp. D310-1	88.95%	2-amino-4-chloro-6-methoxypyrimidine, ethyl 2-sulfamoyl benzoate, 2-sulfamoyl benzoic acid, o-benzoic sulfimide, 2-[(4-chloro-6-methoxy-2-pyrimidinyl) sulfamoyl] benzoic acid, ethyl 2-carbonyl sulfamoyl benzoate, ethyl 2-benzenesulfonyl isocyanate benzoate, and N,N-2(ethyl formate) benzene sulfonylurea	[41]
Thifensulfuron-methyl (sulfonylurea)	<i>Ochrobactrum</i> sp. ZWS16	99.5 %, 50 mg/L, 40°C, 10d	Methyl 3-(N-carbamoylsulfamoyl) thiophene-2-carboxylate and 3-[(formimidoylamino-hydroxy-methyl)-sulfamoyl]-thiophene-2-carboxylic acid	[42]
Nicosulfuron (sulfonylurea)	<i>Chryseobacterium lacus</i> LAM-M5	92.39%,50 mg/L,7d	-	[43]
	<i>Alcaligenesfaecalis</i> ZWS11	80.56%, 500 mg/L, pH 7, 30°C	2-aminosulfonyl-N, N-dimethylnicotinamide (M1), 4, 6-dihydroxypyrimidine (M2), 2-amino-4, 6-dimethoxypyrimidine (M3) and 2-(1-(4,6-dimethoxy-pyrimidin-2-yl)-ureido)-N,N-dimethyl-nicotinamide (M4)	[44]
	<i>Klebsiella</i> sp. Y1	pH 7.0, 35 °C	2-amino-4,6-dimethoxypyrimidine	[45]
	<i>Serratiamarcescens</i> N80	93.6%, 10 mg/L, 96 h	-	[46]
	<i>Pseudomonas fluorescens</i> SG-1	77.5%,1 mM, 28 °C, ≤1d	2-(aminosulfonyl)-N,N-dimethyl-3-	[47]





Tuhin Subhra Ghosh et al.,

			pyridinecarboxamide and (2-amino-4,6-dimethoxypyrimidine)	
	<i>Pseudomonas nitroreducens</i> NSA02	100 mg/L, pH7, 30°C	-	[48]
Pyrazosulfuron-ethyl (<i>sulfonylurea</i>)	<i>Pseudomonas</i> sp. D66, <i>Pseudomonas</i> sp.D61, <i>Bacillus</i> sp. D713	85.9%, 90 mg/L, low pH, 28°C	5-(N-(4,6-dimethoxypyrimidin-2-ylcarbamoyl)sulfamoyl)-1-methyl-1H-pyrazole-4-carboxylic acid	[49]
Glyphosate (glycine derivative)	<i>Chryseobacterium</i> sp. Y16C	100%, 400 mg/L, ≤ 4d	Minomethylphosphonic acid	[50]
	<i>Stenotrophomonas acidaminiphila</i> Y4B	98%, 50 mg/L, ≤72 h	Aminomethylphosphonic acid (AMPA)	[51]
Propanil (anilide)	<i>Acinetobacter baumannii</i> DT	99.9%, 0.027±0.003 mM/h	3,4-dichloroaniline	[52]
Paraquat (bipyridylum)	<i>Pseudomonas putida</i> TISTR 1522 and <i>Bacillus subtilis</i> TISTR 1248	68% and 52% 10 mg/L, pH 7, 28°C, 24 h	Monoquat and 4-carboxy-1-methylpyridinium	[53]
Metamitron (triazinones)	<i>Rhodococcus</i> sp. MET	74.7%, 10 mg/L, pH 9, 20°C, 9 h	-(3-hydrazinyl-2-ethyl)-hydrazono-2-phenylacetic acid, 3-methyl-4-amino-6-(2-hydroxy-muconic acid)-1,2,4-triazine-5(4H)	[54]
Pendimethalin (<i>dinitroaniline</i>)	<i>Bacillus subtilis</i> Y3	99.5%, 100 mg/L, pH 7.5, ≤ 2.5d, 30°C	6-aminopendimethalin, 5-amino-2-methyl-3-nitroso-4-(pentan-3-ylamino) benzoic acid, and 8-amino-2-ethyl-5-(hydroxymethyl)-1,2-dihydroquinoxaline-6-carboxylic acid	[55]

Table 2: Different herbicides and their remediation with efficiencies by fungi.

Herbicides	Strains of fungi	Efficiencies & optimum condition	Intermediates / enzymes	References
Atrazine (triazine)	<i>Bjerkandera adusta</i>	92%, 25-100 ppm, pH 2-8,	-	[82]





Tuhin Subhra Ghosh et al.,

		16-32°C		
Diuron (phenylurea)	<i>Ganodermalucidum</i>	>50%, 3.5 mg/mL, 28°C, 25d	N-(3,4-dichlorophenyl)-N-methylurea (DCPMU) and 3,4-dichlorophenylurea (DCPU)	[83]
	<i>Trametesversicolor</i> K-41	98.7%, 1.0 µM, ≤ 14d	1-(3,4-dichlorophenyl)-3-methylurea and 1-(3,4-dichlorophenyl)urea	[84]
	<i>Pluteuscubensis</i> SXS 320 and <i>Pycnoporussanguineus</i> MCA 16	25mg/L	1-(3,4-dichlorophenylurea , 3-(3-chlorophenyl)-1,1-dimethylurea	[85]
	<i>Neurosporaintermedia</i> DP8-1	98.42%, 50 mg/L, 3d	N-(3,4-dichlorophenyl)-urea and N-(3,4-dichlorophenyl)-N-methylurea	[86]
Diuron (phenylurea) and Bentazon (benzothiadiazinone)	<i>Trametesversicolor</i>	~93%, 10 ppm, pH 4.5, 1-3d	-	[87]
Pretilachlor (chloroacetanilide)	<i>Aspergillusficuum</i> AJN2	79%, ≤15d	2-methyl-6-ethylalanine	[88]
Nicosulfuron (sulfonylurea)	<i>Plectospherellacucumerin</i> a AR1	97%, 10 g/L, pH 6.5, 28°C, ≤ 21d	2-amino-4,6-dimethoxypyrimidine and 2-(aminosulfonyl)-N,N-dimethyl-3-pyridinecarboxamide	[67]
	<i>Penicilliumoxalicum</i> YC-WM1	100%, 100 mg/L, pH 5-8, 33°C, 6d	Aminopyrimidine and Pyridylsulfonamide	[89]
Metolachlor (chloroacetamide)	<i>Penicilliumoxalicum</i> MET-F-1	75%, 50 mg/L, pH 6.5, 25°C, 72h	2-[2-Ethyl-N-(1-methoxypropan-2-yl)-6-methylanilino]-2-oxoacetic acid, 2-Hydroxy-N-(2-ethyl-6-methylphenyl)-N-(2-methoxy-1-methylethyl)acetamide, N-(2-ethyl-6-methylphenyl)-N-(1-methoxypropan-2-yl)acetamide	[90]
Pendimethalin(Dinitroaniline)	<i>Clavisporalunitaniae</i> (Yeast YC2)	74%, 200 mg/L, 8d	1,2-dimethyl-3,5-dinitro-4-N(buta-1,3-dien-2-yl)-dinitrobenzamine-N-oxide and 1,2-dimethyl-3,5-dinitro-4-N(prop-1-en-2-yl)-dinitrobenzamine-N-	[91]





Tuhin Subhra Ghosh et al.,

			oxide	
Pyrazosulfuronethyl	<i>Alternaria alternate</i>	86.9%, 8 mg/kg, 60d	dimethoxypyrimidin-2-ylcarbonyl amine; amino sulfonyl,1-H pyrazole carboxylic acid and 4,6-dimethoxypyrimidin-2-amine (IV)	[92]
Glyphosate (glycine derivative)	<i>Penicillium</i> 4A21	60%, 2.35 g/L, pH 6,25 °C, ≤ 14d	sarcosine and aminomethylphosphonic acid	[93]
2,4-dichlorophenoxyacetic acid and 2,4,5-trichlorophenoxyacetic acid	<i>Rigidoporus</i> sp. FMD21	2,4-D, 200 mg/L and 2,4,5-T 100mg/L, pH 7,30 °C,200 rpm , 16d	Enzymes: Laccase, cytochromes P450-type	[94]

Table 3: Herbicides and their remediation by microbial consortia with efficiencies.

Herbicides	Consortium	Efficiencies & conditions	Cooperative metabolism	References
Acetochlor and butachlor (chloroacetamide)	<i>Rhodococcus</i> sp. T3-1, <i>Delftia</i> sp. T3-6, <i>Sphingobium</i> sp. MEA3-1	100 mg/L, ≤ 6d	Acetochlor to 2'-methyl-6'-ethyl-2-chloroacetanilide (CMEPA) by <i>Rhodococcus</i> sp. T3-1, CMEPA to 2-methyl-6-ethyl aniline (MEA) by <i>Delftia</i> sp.T3-6 and MEA by <i>Sphingobium</i> sp.MEA3-1	[106]
Alachlor (chloroacetamide)	<i>Aspergillusflavus</i> , <i>Penicilliumchrysogenum</i> , <i>Aspergillusniger</i> and <i>Xanthomonasaxonopodis</i>	≤ 82.1%, 10 mg/L, 35 d	1-chloroacetyl, 2,3- dihydro-7 ethylindole, 7 ethylindole, 7-ethyl-3-methyl-2-methoxy-2,3-dihydroindole, N- (2,6-diethylphenyl)-methyleneamine and 7-Ethyl-N-methylindole	[79]
Swep (carbamate)	<i>Comamonas</i> sp. SWP-3 and <i>Alicyclophilus</i> sp. PH-34	30 mg/L, 30 °C, 5d	<i>Comamonas</i> sp. SWP-3 transform Swep to 3,4-dichloroaniline (3,4-DCA), then <i>Alicyclophilus</i> sp. PH-34 mineralize 3,4-DCA.	[105]
Butachlor (chloroacetanilide)	<i>Mycobacterium</i> sp. J7A and <i>Sphingobium</i> sp. J7B	100 µg/mL, 28°C ≤ 24 h	J7A degrade butachlor to 2-chloro-N-(2,6-diethylphenyl) acetamide (CDEPA), then J7B completely degrade through 2,6-diethylaniline (DEA)	[102]
	Bacteria (<i>Sphingomonas</i> sp., <i>Variovorax</i> sp., and <i>A. globiformis</i>) and fungi	-	-	[107]





Tuhin Subhra Ghosh et al.,

	(<i>Mortierella</i> sp. LEJ702 and LEJ703)			
	<i>Arthrobactersulphonivorans</i> , <i>Varioovorax soli</i> , and <i>Advenella</i> sp. JRO	98.8%, within a few days	-	[108]
Isoproturon	<i>Sphingomonas</i> sp. SRS2 and <i>Sphingomonas</i> sp. SRS1	-	SRS2- SRS1 mutual cooperation: Isoproturon / metabolites [3-(4-isopropylphenyl)-1-methylurea, 3-(4-isopropylphenyl)-urea, or 4-isopropyl-aniline] → CO ₂	[109]
Tribenuron methyl (TMB) and metsulfuron methyl (MET) (sulfonylurea)	<i>Bacillus cereus</i> SU-1, <i>Bacillus velezensis</i> OS-2, and <i>Rhodococcusrhodochrous</i> AQ1	TMB - 94.8%, MET - 80.4%, 2.5mg/L, pH 7, 37°C	Co-metabolism of the co-contaminats	[110]

Table 4: Herbicides and their remediation by microalgae with efficiency.

Herbicides	Species of algae	Mode of action	Concentration of pesticides Tested	Removal efficiency (%)	References
	<i>Chlamydomonasmexicana</i>	Biodegradation	10 µg/L	36	[129]
	<i>Isochrysisgalbana</i> , <i>Dunaliellatertiolecta</i> , <i>Phaeodactylumtricornutum</i> , <i>P. subcapitata</i> , and <i>Synechococcus</i> sp.	Bioaccumulation	44–91 µg/L	-	[128]
Atrazine (Triazine)	<i>C. vulgaris</i>	Bioaccumulation	0.75 µM/L	83%	[135]
Terbutryn (Triazine)	<i>C. vulgaris</i>		0.75 µM	93%	
Atrazine, Molinate, Simazine, Isoproturon, Propanil, Pendimethali, Metoalcholar	<i>Chlorella vulgaris</i>	Biosorption	10 µg/l	87% to 96.5%	[136]
Fluroxypyr (pyridinomy acid)	<i>Chlamydomonasreinhardtii</i>	Biodegradation	0.5 mg/L	57%	[137]
Isoproturon (phenylureas)	<i>Chlamydomonasreinhardtii</i>	Bioaccumulation, Biodegradation	50 mg/L	15.1%	[138]





Tuhin Subhra Ghosh et al.,

Mesotrione	<i>Scenedesmusquadricauda</i>	Biodegradation	5 mg/L	15.2%	[139]
Prometryne (triazine)	<i>Chlamydomonasreinhardtii</i>	Biodegradation	7.5 µg/L	32%	[140]
Diclofop-methyl (DM) (aryloxyphenoxypropionate)	<i>Chlorella vulgaris</i> <i>C. pyrenoidosa</i> <i>Scenedesmusobliquus</i>	Biodegradation	-	-	[141]
Dichlorprop-methyl (2,4-DCPPM) (chlorophenoxy)	<i>Chlorella pyrenoidosa</i> , <i>C. vulgaris</i> <i>Scenedesmusobliquus</i>	Biodegradation	-	-	[142]
Glyphosate (glycine derivative)	<i>Oscillatorialimnetica</i>	Bioaccumulation	After 35 days at 20 mg/l	99.9%	[143]
Paraquat (bipyridylium)	<i>Aspergillustamarii</i> PRPY-2 and <i>Cunninghamella</i> sp. PFCM-1	Biosorption	-	80% and 68%	[144]





Change of Equitable Color Class Domination Number after the Node Removal in Graphs

A. Esakkimuthu^{1*} and S. Mari Selvam²

¹Assistant Professor, PG and Research Department of Mathematics, Kamaraj College, Thoothukudi, (Affiliated to Manonmaniam Sundaranar University, Tirunelveli) Tamil nadu, India.

²Research Scholar, Reg. No: 21212102091009, PG and Research Department of Mathematics, Kamaraj College, Thoothukudi, (Affiliated to Manonmaniam Sundaranar University, Tirunelveli) Tamil nadu, India.

Received: 08 Sep 2023

Revised: 18 Sep 2023

Accepted: 29 Dec 2023

*Address for Correspondence

A. Esakkimuthu

Assistant Professor, PG and Research
Department of Mathematics,
Kamaraj College, Thoothukudi,
(Affiliated to Manonmaniam Sundaranar University, Tirunelveli)
Tamil Nadu, India.
Email: esakkimsu005@yahoo.com



This is an Open Access Journal / article distributed under the terms of the **Creative Commons Attribution License** (CC BY-NC-ND 3.0) which permits unrestricted use, distribution, and reproduction in any medium, provided the original work is properly cited. All rights reserved.

ABSTRACT

Let $G = (V, E)$ be a connected graph. Assume a group CC containing colors. Let $\tau : V(G) \rightarrow CC$ be an equitable colorable function. A dominating subset S of V is called an equitable color class dominating set if the number of dominating nodes in each color class is equal. The least possible cardinality of an equitable color class dominating set of G is called the equitable color class domination number itself. It is indicated by $\gamma_{ECC}(G)$. In this paper, we study the change of ECC Domination number after node removal.

Keywords: Dominating Set, Equitable Coloring, Color Class (CC), Equitable Color Class (ECC), Equitable Color Class Dominating Set, Node Removal.

INTRODUCTION

The study of the effect of removing a node on any graph theoretic parameter has interesting applications in the network context. That is, analyzing the removal of a node is more vital as an important consideration in the topological design of a network is fault tolerance. The behavior of a network in the presence of a fault can be analyzed by determining the effect that removing a node (processor failure) from its underlying graph G has on the fault-tolerance criterion. A detailed study of changing and unchanging domination is given in Chapter 5 of Haynes





Esakkimuthu and Mari Selvam

et. al [6]. Further, The semi-expository paper by Carrington et. al. [2] surveyed the problems of characterizing the graphs G into three classes based on node removal. If a node is deleted, the value of γ may increase or decrease or remain unaltered. Therefore the node set V can be partitioned into the subsets V^-, V^0 and V^+ where

$$\begin{aligned} V^0 &= \{v \in V : \gamma(G - v) = \gamma(G)\} \\ V^+ &= \{v \in V : \gamma(G - v) > \gamma(G)\} \\ V^- &= \{v \in V : \gamma(G - v) < \gamma(G)\} \end{aligned}$$

Several results on nodes and links belonging to the above subsets are given in [6]. In this chapter, we initiate a similar study corresponding to the equitable color class domination number of a graph.

DEFINITIONS AND NOTATIONS

Definition

[5] In a graph $G = (V, E)$, a subset S of nodes is a dominating set if every node in $V - S$ is adjacent to some node in S . The least possible cardinality of the dominating set of G is called its domination number and it is indicated by $\gamma(G)$.

Definition

[8] In a graph G , adjacent nodes don't or do in the same color is known as proper coloring. The least possible number of colors used to color a graph G is known as its chromatic number and it is indicated by $\chi(G)$.

Definition

A subset of nodes ordained to the same color is known as a color class.

Definition

[8] In a graph, adjacent nodes don't have the same color, and the difference between the cardinality of color classes is ≤ 1 is called an equitable coloring graph. The least possible number of colors used to equitably color a graph G is known as its equitable chromatic number and it's indicated by $\chi_E(G)$.

Notation

Let X be any real number. Then $\lfloor X \rfloor$ indicates the greatest integer $\leq X$ and $\lceil X \rceil$ indicates the smallest integer $\geq X$.

Notation

If a, b be the integers and $n > 0$ then $a \equiv b \pmod{n}$ indicates $n \mid a - b$.

PRIMARY RESULTS

Definition

[4] Let $G = (V, E)$ be a connected graph. Assume a group CC containing colors. Let $\tau: V(G) \rightarrow CC$ be an equitably colorable function. A dominating subset S of V is called an equitable color class dominating set if the number of dominating nodes in each color class is equal. The least possible cardinality of an equitable color class dominating set of G is the equitable color class domination number itself. It is indicated by $\gamma_{ECC}(G)$.

Theorem

[3] If $G = (V, E)$ be a connected graph then $\gamma_{ECC}(G) = k \chi_E$ where $k \in \mathbb{N}$ and χ_E be the equitable chromatic number of G .

Proof

let $G = (V, E)$ be a connected graph and $v_1, v_2, v_3, \dots, v_n$ be the nodes of G . The equitable chromatic number of G is χ_E . Let $\tau: V(G) \rightarrow CC$ be an equitably colorable function where $CC = \{1, 2, 3, 4, \dots, \chi_E\}$. Choose dominating nodes like a pair of χ_E number of different color nodes. So, the number of dominating nodes in each color class is equal. Let k be the minimum number of pairs to dominate a graph G . Hence, the equitable color class domination number of a graph G is $k \chi_E$ where $k \in \mathbb{N}$.





Esakkimuthu and Mari Selvam

Example

A simple example of finding γ_{ECC} of a general graph G . χ_E of the general graph G is 3 and chosen dominating nodes in each color class are equal and one, $\gamma_{ECC}(G) = 3$.

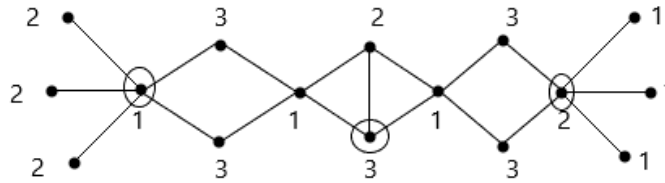


Fig.1

NODE REMOVAL

We observe that the ECC domination number $\gamma_{ECC}(G)$ of a graph G may increase or decrease or remain unchanged when a node is removed from G . Depending on the ECC domination number of the graph G after removing the node, the node set $V(G)$ is partitioned into three subsets V_{ECC}^-, V_{ECC}^0 and V_{ECC}^+ as follows.

$$V_{ECC}^0 = \{v \in V : \gamma_{ECC}(G - v) = \gamma_{ECC}(G)\}$$

$$V_{ECC}^+ = \{v \in V : \gamma_{ECC}(G - v) > \gamma_{ECC}(G)\}$$

$$V_{ECC}^- = \{v \in V : \gamma_{ECC}(G - v) < \gamma_{ECC}(G)\}$$

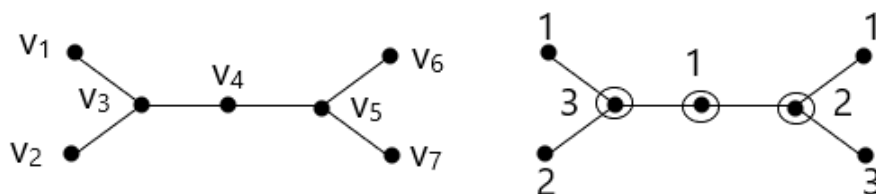
In this section, we investigate the properties of the above sets.

Example

- Let K_n be the complete graph with n nodes and $\gamma_{ECC}(K_n) = n$. After the removal of the node, it becomes the complete graph with $n - 1$ nodes and also $\gamma_{ECC}(K_{n-1}) = n - 1$. Implies $\gamma_{ECC}(K_n - v) = \gamma_{ECC}(K_n) - 1$. The value of γ_{ECC} is decreasing by 1 for each node removal. Hence, $V(K_n) = V_{ECC}^-(K_n)$.
- (ii) For the star graph $S_{1,n}$ with $n(v_r : 1 \leq r \leq n)$ pendant nodes and one (v) center node, $\gamma_{ECC}(S_{1,n}) = 1 + \lceil \frac{n}{2} \rceil$. After the removal of the center node, the graph becomes a completely disconnected graph with n nodes. So, the graph needs n dominating node to dominate the completely disconnected graph. Therefore, $\gamma_{ECC}(S_{1,n} - v) = n > 1 + \lceil \frac{n}{2} \rceil$. Now, removal of the pendant node. It becomes the star graph with $n - 1$ pendant nodes. if n is even, we know that $\lceil \frac{n}{2} \rceil = \lceil \frac{n-1}{2} \rceil$. Therefore, $\gamma_{ECC}(S_{1,n} - v_r) = \gamma_{ECC}(S_{1,n-1}) = 1 + \lceil \frac{n-1}{2} \rceil = 1 + \lceil \frac{n}{2} \rceil = \gamma_{ECC}(S_{1,n})$. If n is odd, we know that $\lceil \frac{n-1}{2} \rceil = \lceil \frac{n}{2} \rceil - 1$. Therefore, $\gamma_{ECC}(S_{1,n} - v_r) = \gamma_{ECC}(S_{1,n-1}) = 1 + \lceil \frac{n-1}{2} \rceil = \lceil \frac{n}{2} \rceil = \gamma_{ECC}(S_{1,n}) - 1$. Hence, $v \in V_{ECC}^+$ and $v_r \in \begin{cases} V_{ECC}^- & \text{if } n \text{ is odd} \\ V_{ECC}^0 & \text{if } n \text{ is even} \end{cases}$.

Remark

There is a graph for which all the sets V_{ECC}^-, V_{ECC}^0 and V_{ECC}^+ are non-empty. Shown in Fig. 1. is a general graph G and $V(G) = \{v_1, v_2, v_3, v_4, v_5, v_6, v_7\}$. $\chi_E(G) = 3$. ECC Dominating set = $\{v_3, v_4, v_5\}$ and $\gamma_{ECC}(G) = 3$.



Now determine the node removal sets using Figure 2.

$$\gamma_{ECC}(G - v_1) = 3 = \gamma_{ECC}(G)$$

$$\gamma_{ECC}(G - v_2) = 3 = \gamma_{ECC}(G)$$

$$\gamma_{ECC}(G - v_3) = 6 > \gamma_{ECC}(G)$$

$$\gamma_{ECC}(G - v_4) = 2 < \gamma_{ECC}(G)$$





Esakkimuthu and Mari Selvam

$$\begin{aligned} \gamma_{ECC}(G - v_5) &= 6 > \gamma_{ECC}(G) \\ \gamma_{ECC}(G - v_6) &= 3 = \gamma_{ECC}(G) \\ \gamma_{ECC}(G - v_7) &= 3 = \gamma_{ECC}(G) \end{aligned}$$

Now conclude that $V_{ECC}^0 = \{v_1, v_2, v_6, v_7\}$, $V_{ECC}^+ = \{v_3, v_5\}$ and $V_{ECC}^- = \{v_4\}$. Hence, all the sets V_{ECC}^- , V_{ECC}^0 and V_{ECC}^+ are non-empty.

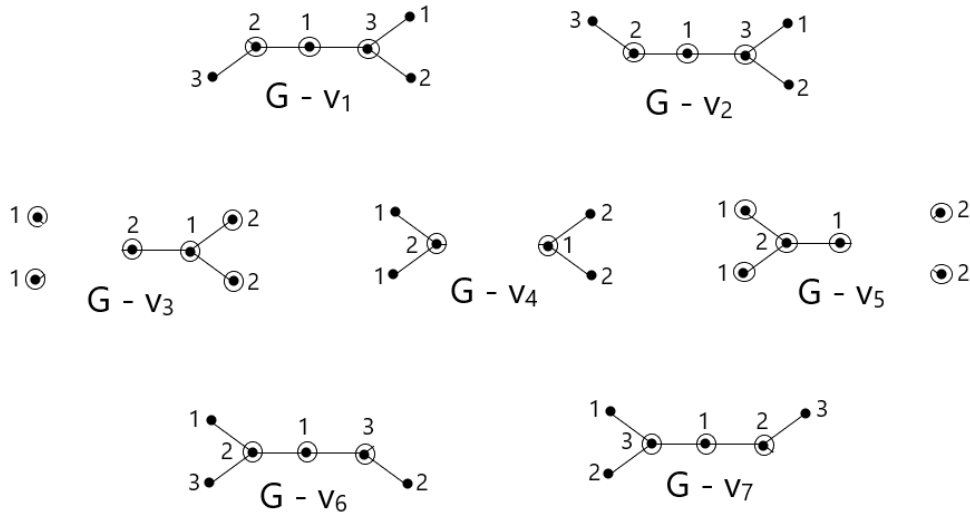


Fig.3.

Theorem

For the path graph $n > 1$, $P_n = (v_1, v_2, \dots, v_n)$ on n nodes, we have $1 \leq r \leq n$,

$$\gamma_{ECC}(P_n - v_r) = \begin{cases} \gamma_{ECC}(P_n) - 2 & \text{if } v_r \in V_{ECC}^- \\ \gamma_{ECC}(P_n) & \text{if } v_r \in V_{ECC}^0 \\ \gamma_{ECC}(P_n) + 2 & \text{if } v_r \in V_{ECC}^+ \end{cases}$$

1. If $n \equiv 1 \pmod{6}$

$$v_r \in \begin{cases} V_{ECC}^- & \text{if } r = 3i + 1, i = \{0, 1, \dots, \frac{n-1}{3}\} \\ V_{ECC}^0 & \text{otherwise} \end{cases}$$
2. If $n \equiv 0 \pmod{6}$

$$v_r \in \begin{cases} V_{ECC}^+ & \text{if } r = 3i - 1, i = \{1, 2, \dots, \frac{n}{3}\} \\ V_{ECC}^0 & \text{otherwise} \end{cases}$$
3. If $n \equiv -1 \pmod{6}$

$$v_r \in \begin{cases} V_{ECC}^+ & \text{if } r = 2, n - 1 \\ V_{ECC}^0 & \text{otherwise} \end{cases}$$
4. Otherwise, $V(P_n) = V_{ECC}^0$

Proof

let P_n be the path graph, $V(G) = \{v_r : 1 \leq r \leq n\}$ and $E(G) = \{v_r v_{r+1} : 1 \leq r \leq n - 1\}$. $\chi_E(P_n) = 2$ and $\gamma_{ECC}(P_n) = 2 \lceil \frac{n}{6} \rceil$.

Case

If $n \equiv 1 \pmod{6}$





Esakkimuthu and Mari Selvam

Let $n = 6k + 1$ for some positive integer k .

If $r = 3i + 1, i = \{0, 1, \dots, \frac{n-1}{3}\}$

Now removal of the node v_r when $r = 1, n$ the path is connected and has $6k$ nodes so, it has $2k$ dominating nodes. Otherwise, the path is divided into two paths with $3t$ nodes and $n - 1 - 3t$ nodes where $1 \leq t < \frac{n-1}{3}$. In this case, the two paths are having a number of nodes that are multiple of 3 and a total of $6k$ nodes. So, it has $\lceil \frac{3t}{3} \rceil$ and $\lceil \frac{n-1-3t}{3} \rceil$ dominating nodes respectively. For the maximum value of $t, \gamma(3t) + \gamma(n - 1 - 3t) = \frac{n-1}{3} - 1 + 1 = \frac{n-1}{3} = 2(\frac{n-1}{6}) = 2 \lceil \frac{n}{6} \rceil - 2$. Therefore, $\gamma_{ECC}(P_n)$ is decreased by 2 values. Hence, $v_r \in V_{ECC}^-$.

Otherwise,

Now removal of the node $v_r (r \neq 2, n - 1)$ then the path is divided into two paths with t nodes and $n - 1 - t$ nodes where $3 \leq t \leq n - 2$ and $t \neq 1 \pmod{3}$. So, it has $2 \lceil \frac{t}{6} \rceil$ and $2 \lceil \frac{n-1-t}{6} \rceil$ dominating nodes. For the maximum value of $t, \gamma_{ECC}(t) + \gamma_{ECC}(n - 1 - t) = 2 \lceil \frac{n-2}{6} \rceil + 2 = 2 \lceil \frac{n}{6} \rceil - 2 + 2 = 2 \lceil \frac{n}{6} \rceil$. If $r = 2, n - 1$ then the path is divided into an isolated node and a path with $n - 2$ nodes. So, it has 1 and $2 \lceil \frac{n-2}{6} \rceil + 1$ dominating nodes. Implies, total nodes is $2 \lceil \frac{n-2}{6} \rceil + 2 = 2 \lceil \frac{n}{6} \rceil - 2 + 2 = 2 \lceil \frac{n}{6} \rceil$. Therefore, $\gamma_{ECC}(P_n)$ remains unaltered. Hence, $v_r \in V_{ECC}^0$.

Case

If $n \equiv 0 \pmod{6}$

Let $n = 6k$ for some positive integer k .

If $r = 3i - 1, i = \{1, 2, \dots, \frac{n}{3}\}$

Now removal of the node v_r when $i = 1$ or $\frac{n}{3}$ the path is divided into an isolated node and a path with $n - 2$ nodes. So, it has 1 and $2 \lceil \frac{n-2}{6} \rceil + 1$ dominating nodes. Implies, total nodes is $2 \lceil \frac{n-2}{6} \rceil + 2 = 2 \lceil \frac{n}{6} \rceil + 2$. Otherwise, the path is divided into two paths with $3t + 1$ nodes and $n - 3t - 2$ nodes where $1 \leq t \leq \frac{n}{3} - 2$. So, it has $2 \lceil \frac{3t+1}{6} \rceil$ and $2 \lceil \frac{n-3t-2}{6} \rceil$ dominating nodes. For the maximum value of $t, \gamma_{ECC}(3t + 1) + \gamma_{ECC}(n - 3t - 2) = 2 \lceil \frac{n-5}{6} \rceil + 2 = 2 \lceil \frac{n}{6} \rceil + 2$. Therefore, $\gamma_{ECC}(P_n)$ is increased by 2. Hence, $v_r \in V_{ECC}^+$. Otherwise, Now removal of the node $v_r (r \neq 3i - 1, i = \{1, 2, \dots, \frac{n}{3}\})$ then the path is divided into two paths with t nodes and $n - 1 - t$ nodes where $0 \leq t \leq n - 1$ and $t \neq 1 \pmod{3}$. So, it has $2 \lceil \frac{t}{6} \rceil$ and $2 \lceil \frac{n-1-t}{6} \rceil$ dominating nodes. For the maximum value of $t, \gamma_{ECC}(t) + \gamma_{ECC}(n - 1 - t) = 2 \lceil \frac{n-1}{6} \rceil + 0 = 2 \lceil \frac{n}{6} \rceil$. Therefore, $\gamma_{ECC}(P_n)$ remains unaltered. Hence, $v_r \in V_{ECC}^0$.

Case

If $n \equiv -1 \pmod{6}$

Let $n = 6k - 1$ for some positive integer k .

If $r = 2, n - 1$

Now removal of the node v_r the path is divided into an isolated node and a path with $n - 2$ nodes. So, it has 1 and $2 \lceil \frac{n-2}{6} \rceil + 1$ dominating nodes. Implies, total nodes is $2 \lceil \frac{n-2}{6} \rceil + 2 = 2 \lceil \frac{n}{6} \rceil + 2$. Therefore, $\gamma_{ECC}(P_n)$ is increased by 2. Hence, $v_r \in V_{ECC}^+$. Otherwise, Now removal of the node $v_r (r = 1, n)$ then the path is connected and has $n - 1$ nodes and it has $2 \lceil \frac{n-1}{6} \rceil$ dominating nodes. Implies, $2 \lceil \frac{n}{6} \rceil$. Otherwise, the path is divided into two paths with t nodes and $n - 1 - t$ nodes where $2 \leq t \leq n - 3$. So, it has $\lceil \frac{t}{3} \rceil$ and $\lceil \frac{n-1-t}{3} \rceil$ dominating nodes respectively. For the maximum value of $t, \gamma(t) + \gamma(n - 1 - t) = \lceil \frac{n-3}{3} \rceil + 1 = 2 \lceil \frac{n}{6} \rceil - 1 + 1 = 2 \lceil \frac{n}{6} \rceil$. Therefore, γ_{ECC} has remained unaltered. Hence, $v_r \in V_{ECC}^0$.

Case 4

Otherwise Now removal of the node $V(P_n)$ the path is divided into two paths with t nodes and $n - 1 - t$ nodes where $0 \leq t \leq n - 1$.





Esakkimuthu and Mari Selvam

Subcase

When $t = 0$ or $n - 1$ only one path remains and it has $n - 1$ nodes. So, it has $2 \lceil \frac{n-1}{6} \rceil = 2 \lceil \frac{n}{6} \rceil$ dominating nodes.

Subcase

When $t = 1$ or $n - 2$ the path is divided into one path with $n - 2$ nodes and one isolated node.

If $n \equiv 2 \pmod{6}$, it has $2 \lceil \frac{n-2}{6} \rceil + 1$ and 1 dominating node respectively. Implies, the total number of dominating nodes = $2 \lceil \frac{n}{6} \rceil - 2 + 2 = 2 \lceil \frac{n}{6} \rceil$ dominating nodes. Otherwise, it has $\lceil \frac{n-2}{3} \rceil$ and 1 dominating node respectively. Implies, the total number of dominating nodes = $2 \lceil \frac{n}{6} \rceil - 1 + 1 = 2 \lceil \frac{n}{6} \rceil$ dominating nodes.

Subcase

When $2 \leq t \leq n - 3$,

If $n \equiv -2 \pmod{6}$ the two paths have $\lceil \frac{t}{3} \rceil$ and $\lceil \frac{n-1-t}{3} \rceil$ dominating nodes. For the maximum value of t , $\gamma(t) + \gamma(n - 1 - t) = \lceil \frac{n-3}{3} \rceil + 1 = 2 \lceil \frac{n}{6} \rceil - 1 + 1 = 2 \lceil \frac{n}{6} \rceil$. Otherwise, the two paths have $2 \lceil \frac{t}{6} \rceil$ and $2 \lceil \frac{n-1-t}{6} \rceil$ dominating nodes. For the maximum value of t , $\gamma_{ECC}(t) + \gamma_{ECC}(n - 1 - t) = 2 \lceil \frac{n-3}{6} \rceil + 2 = 2 \lceil \frac{n}{6} \rceil - 2 + 2 = 2 \lceil \frac{n}{6} \rceil$. Therefore, $\gamma_{ECC}(P_n)$ remains unaltered. Hence, $V(P_n) = V_{ECC}^0$.

Theorem

For the cycle graph $n > 2$, $C_n = (v_1, v_2, \dots, v_n)$ on n nodes, we have $1 \leq r \leq n$, $1 \leq t \leq 3$, $\gamma_{ECC}(C_n - v_r) =$

$$\begin{cases} \gamma_{ECC}(C_n) - t & \text{if } V = V_{ECC}^- \\ \gamma_{ECC}(C_n) & \text{if } V = V_{ECC}^0 \\ \gamma_{ECC}(C_n) + 1 & \text{if } V = V_{ECC}^+ \end{cases}$$

1. If n is even, $V = V_{ECC}^0$
2. If n is odd and
 - i. If $n \equiv -3, -1 \pmod{18}$, $V = V_{ECC}^0$
 - ii. If $n \equiv 0 \pmod{9}$, $V = V_{ECC}^+$
 - iii. If $n \equiv 3, 5, 7 \pmod{18}$, $V = V_{ECC}^-$ and $t = 1$
 - iv. If $n \equiv -7, -5 \pmod{18}$, $V = V_{ECC}^-$ and $t = 2$
 - v. If $n \equiv 1 \pmod{18}$, $V = V_{ECC}^-$ and $t = 3$

Proof

let C_n be the cycle graph, $V(G) = \{v_r : 1 \leq r \leq n\}$ and $E(G) = \{v_r v_{r+1}, v_n v_1 : 1 \leq r \leq n - 1\}$. $\chi_E(C_n) = \begin{cases} 2 & \text{if } n \text{ is even} \\ 3 & \text{if } n \text{ is odd} \end{cases}$ and $\gamma_{ECC}(C_n) = \begin{cases} 2 \lceil \frac{n}{6} \rceil & \text{if } n \text{ is even} \\ 3 \lceil \frac{n}{9} \rceil & \text{if } n \text{ is odd} \end{cases}$. Now removal of the vertex $V(C_n)$ the cycle is changed to a path with $n - 1$ nodes.

Case

n is even When n is even $\gamma_{ECC}(C_n) = \gamma_{ECC}(P_n)$ and $\gamma_{ECC}(P_n) = \gamma_{ECC}(P_{n-1})$ which implies $\gamma_{ECC}(C_n) = \gamma_{ECC}(P_{n-1})$. Therefore, $\gamma_{ECC}(C_n - v_r)$ remains unaltered. Hence, $V(C_n) = V_{ECC}^0$.

Case

n is odd When n is odd, after the removal of one node in an odd cycle it becomes an even path.

Sub Case

$n \equiv -3, -1 \pmod{18}$ Let $n = 18k - 3$ and $18k - 1$, k be a natural number. When $n \equiv -3, -1 \pmod{18}$, $\gamma_{ECC}(C_n) = \gamma_{ECC}(P_n)$ and $\gamma_{ECC}(P_n) = \gamma_{ECC}(P_{n-1})$ which implies $\gamma_{ECC}(C_n) = \gamma_{ECC}(P_{n-1})$. Therefore, $\gamma_{ECC}(C_n - v_r)$ remains unaltered. Hence, $V(C_n) = V_{ECC}^0$.





Esakkimuthu and Mari Selvam

Sub Case

$n \equiv 0 \pmod{9}$ Let $n = 9k$, k be a natural number. When $n \equiv 0 \pmod{9}$, $\gamma_{ECC}(C_n) = \gamma_{ECC}(P_n) - 1$ and $\gamma_{ECC}(P_n) = \gamma_{ECC}(P_{n-1})$ which implies $\gamma_{ECC}(C_n) = \gamma_{ECC}(P_{n-1}) - 1$. Therefore, $\gamma_{ECC}(C_n - v_r)$ is increased by 1. Hence, $V(C_n) = V_{ECC}^+$.

Sub Case

$n \equiv 3,5,7 \pmod{18}$ Let $n = 18k + 3, 18k + 5$ and $18k + 7$, k be a whole number. When $n \equiv 3,5 \pmod{18}$, $\gamma_{ECC}(C_n) = \gamma_{ECC}(P_n) + 1$ and $\gamma_{ECC}(P_n) = \gamma_{ECC}(P_{n-1})$ which implies $\gamma_{ECC}(C_n) = \gamma_{ECC}(P_{n-1}) + 1$. When $n \equiv 7 \pmod{18}$, $\gamma_{ECC}(C_n) = \gamma_{ECC}(P_n) - 1$ and $\gamma_{ECC}(P_n) = \gamma_{ECC}(P_{n-1}) + 2$ which implies $\gamma_{ECC}(C_n) = \gamma_{ECC}(P_{n-1}) + 1$. Therefore, $\gamma_{ECC}(C_n - v_r)$ is decreased by 1. Hence, $V(C_n) = V_{ECC}^-$.

Sub Case

$n \equiv -7, -5 \pmod{18}$ Let $n = 18k - 7$ and $18k - 5$, k be a natural number. When $n \equiv -7 \pmod{18}$, $\gamma_{ECC}(C_n) = \gamma_{ECC}(P_n) + 2$ and $\gamma_{ECC}(P_n) = \gamma_{ECC}(P_{n-1})$ which implies $\gamma_{ECC}(C_n) = \gamma_{ECC}(P_{n-1}) + 2$. When $n \equiv -5 \pmod{18}$, $\gamma_{ECC}(C_n) = \gamma_{ECC}(P_n)$ and $\gamma_{ECC}(P_n) = \gamma_{ECC}(P_{n-1}) + 2$ which implies $\gamma_{ECC}(C_n) = \gamma_{ECC}(P_{n-1}) + 2$. Therefore, $\gamma_{ECC}(C_n - v_r)$ is decreased by 2. Hence, $V(C_n) = V_{ECC}^-$.

Sub Case

$n \equiv 1 \pmod{18}$ Let $n = 18k + 1$, k be a natural number. When $n \equiv 1 \pmod{18}$, $\gamma_{ECC}(C_n) = \gamma_{ECC}(P_n) + 1$ and $\gamma_{ECC}(P_n) = \gamma_{ECC}(P_{n-1}) + 2$ which implies $\gamma_{ECC}(C_n) = \gamma_{ECC}(P_{n-1}) + 3$. Therefore, $\gamma_{ECC}(C_n - v_r)$ is decreased by 3. Hence, $V(C_n) = V_{ECC}^-$.

CONCLUSION

The study of the effect of the removal of a node in any graph theoretic parameter has interesting applications in the context of the network. In this paper, a similar study has been initiated concerning the Equitable Color Class Domination number for a graph G .

REFERENCES

1. S. Balamurugan, Changing and Unchanging Isolate Domination: Edge Removal, Discrete Mathematics, Algorithms and Applications, Vol. 09, No. 01, 1750003 (2017).
2. J.R. Carrington, F. Harary, and T.W. Haynes, Changing and Unchanging The Domination Number of a Graph, J. Combin. Math. Combin. Comput., 9(1991), 57-63.
3. A.Esakkimuthu and S.MariSelvam, Equitable Color Class Domination Number of Some Cycle Related graphs, International Journal of Research and Analytical Reviews (IJRAR), Volume 9, Issue 4, December 2022.
4. A.Esakkimuthu and S.MariSelvam, Equitable Color Class Domination Number of Some Special Graphs and Some Derived Path Graphs, Journal of Emerging Technologies and Innovative Research (JETIR), Volume 9, Issue 12, December 2022.
5. T. W. Haynes, S. T. Hedetniemi and P. J. Slater, Domination in Graphs-Advanced Topics, New York: Dekker, 1998.
6. T.W. Haynes, S.T. Hedetniemi and P.J. Slater, Fundamentals of Domination in Graphs, Marcel Dekker, New York (1998).
7. S. T. Hedetniemi and R. C. Laskar, Topics on domination, North Holland 1991.
8. K.W. Lih, The Equitable Coloring of Graphs, Handbook of Combinatorial Optimization, 1998, (pp. 2015-2038).
9. Sahul Hamid and S. Balamurugan, Critical and Stable Isolate Domination, Discrete Mathematics, Algorithms and Applications, Vol. 07, No. 02, 1550010 (2015).





Propensity of Amino Acid Residues for Secondary Structural Elements of All Beta Protein of Ribovirus based on Deviation Parameter Value

P.Thenmozhi Kanaga^{1*} and S.Arul Mugilan²

¹Research Scholar (Reg. No. 21111062132005), Department of Physics, Kamarajar Government Arts College, Surandai 627859 (Affiliated to Manonmaniam Sundaranar University, Abishekapatti, Tirunelveli 627012, India.

²Assistant Professor, Department of Physics, Kamarajar Government Arts College, Surandai 627859 (Affiliated to Manonmaniam Sundaranar University, Abishekapatti, Tirunelveli 627012, India.

Received: 26 Aug 2023

Revised: 20 Nov 2023

Accepted: 19 Jan 2024

*Address for Correspondence

P.Thenmozhi Kanaga

Research Scholar (Reg. No. 21111062132005),

Department of Physics,

Kamarajar Government Arts College,

Surandai 627859 (Affiliated to Manonmaniam Sundaranar University),

Abishekapatti, Tirunelveli 627012, India.

Email: thenmozhikanaga@gmail.com



This is an Open Access Journal / article distributed under the terms of the **Creative Commons Attribution License** (CC BY-NC-ND 3.0) which permits unrestricted use, distribution, and reproduction in any medium, provided the original work is properly cited. All rights reserved.

ABSTRACT

Numerous studies have been performed to determine the propensity of amino acid residues for secondary structural elements. The propensity of amino acids is crucial in bioinformatics. Certain amino acid residues are more prevalent in secondary structural elements; this tendency is known as propensity. Other researchers explain the α -helix, β -sheet and random structure amino acid propensity. Here, based on the deviation parameter values, we establish the propensity for secondary structure elements including α -helix, β -sheet 3/10 alpha-helix, pi-helix, isolated beta-bridge, beta-turn, bend and random structure in 3148 all beta-proteins of ribovirus. Additionally, this information will be helpful to experimental biologists who need to make accurate predictions about protein structure, molecular modeling, and the development of drugs.

Keywords: Amino acid propensity, Deviation parameter, Secondary structure of protein



**Thenmozhi Kanaga and Arul Mugilan**

INTRODUCTION

A protein's structure is mostly composed of lengthy chains of amino acids. The structure of proteins is organized into four levels: primary, secondary, tertiary, and quaternary structure. Only the amino acid sequence, which is organized in the polypeptide chain, makes up a protein's primary structure. The term "secondary structure of proteins" refers to periodic conformations that occur repeatedly in chains of polypeptide. The tertiary structure of a protein is formed when a protein is folded from its secondary structures into a stable three-dimensional structure. The quaternary structure is created by the spatial arrangement of the multiple tertiary structures. Comparing all protein structures secondary structures serve an important role in bioinformatics [1, 2]. Protein secondary structures can be classified into three general states: helix (H), strand (E), and coil (C). The DSSP algorithm suggested converting the three main states into eight states to provide a more precise characterization of the secondary structures: 3/10 helix (G), alpha-helix (H), pi-helix (I), beta-strand (E), bridge (B), turn (T), bend (S), and others (C). Several studies have been undertaken to better understand the propensity of secondary structural elements. Through statistical study of three-dimensional structures, experimental investigation of the alpha-helix or beta-sheet composition of peptides, and experimental evaluation of the thermodynamic stability of mutant proteins, the propensities have been estimated [3-5]. Chou and Fasman examined each amino acid's frequency of occurrence and structural propensity in the secondary structures of 15 proteins, accounting for a total of 2473 amino acid residues.

They published their results in 1974 [6]. Despite the fact that Richardson et al. and Engel et al. showed that amino acid propensities vary depending on amino acids for different positions of the alpha-helix, the acquired propensities for alpha-helix are consistent throughout investigations, with the pair-wise correlation coefficient (R) often being >0.8 [7,8]. The IgG-binding domain of protein G includes four antiparallel strands, and Minor and Kim showed that the beta-sheet propensity examined at the center strand differed significantly from that measured at an edge strand [9]. The secondary structure propensities for four protein structural classes: "all- α ", "all- β ", " α/β ", and " $\alpha + \beta$ " were estimated by Jiang et al. and Costantini et al. They showed that these structural groups affected the tendency for beta-sheets [10, 11]. After 40 years, Mehmet can evaluate the conformational parameters of amino acids in helical, beta-sheet random coil regions [12]. S A Mugilan and K Veluraja developed deviation parameters for amino acid singlets, doublets, and triplets from three-dimensional protein structures in order to predict secondary structure from amino acid sequences [13]. In this study, we focused on preferred and non-preferred amino acid residues for the secondary structural elements ribovirus of all beta protein. However, the majority of techniques anticipate just the secondary structure elements of the alpha-helix and beta-sheet. However, our method is also applicable to the other structural elements, notably alpha-helix beta-sheet, bend, beta-turn, isolated beta-bridge, 3/10-helix, pi-helix and the random structure.

MATERIALS AND METHODS

Data collection

In the course of the investigation, I employed 3458 all beta proteins from the Protein Data Bank (PDB). The DSSP files from the DSSP data base are extracted for the associated PDB IDs. The DSSP database contains 3148 DSSP files out of 3458 total. The DSSP file comprises detailed information about all beta proteins. We need the total amount of amino acid residues for secondary structural elements such as alpha-helix, beta-sheet, beta-turn, bend, 3/10-helix, pi-helix, isolated-beta bridge, and random structure for our analysis. By utilizing the Python program, the amino acid residues are extracted from the DSSP file. We determine the frequency of occurrence, as well as the observed and expected values. The deviation parameter value for the 20 amino acid residues has been determined using the observed and expected values. Within the secondary structure elements, the deviation parameter values are then normalized. The graph depicts the relationship between amino acid residues and the deviation parameter value. We may deduce the preferred and undesirable amino acid residues for all beta proteins' secondary structural elements from the graph. The frequency of occurrence of 20 amino acids can be calculated using the following equation [13, 14]





Thenmozhi Kanaga and Arul Mugilan

$$P(X) = \frac{\sum_{i=1}^n N_i(X)}{\sum_{i=1}^n Y_i}$$

Here, X represents individual amino acid residues. $N_i(X)$ is the number of counts for X in the i^{th} protein, Y_i is the total number of amino acid residues in the i^{th} protein, and n is the total number of proteins considered (3148). Based on the frequency of occurrence of amino acid residues, one can calculate the expected number of these units (for each structural elements) as follows:

$$C_{\text{exp}}(X) = P(X) \sum S_i$$

Here S_i represent the total number of particular entity (X) in a particular structural element in protein i.

The deviation parameters for the secondary structural elements are calculated according to the formula [13,14]

$$\text{Deviation parameter} = \frac{\text{Observed} - \text{Expected}}{\text{Expected}} \times 100$$

The deviation parameter values are then normalized using the following formula [15].

$$N = \frac{X - \text{Minimum}}{\text{Maximum} - \text{Minimum}}$$

The deviation parameter value is used to determine the propensity of amino acid residues for the secondary structural elements.

RESULT

The distribution of amino acids for all beta proteins of ribovirus secondary structural elements is shown in Table1. Based on Table 1, we can infer that the beta-sheet has more amino acid residues than the other secondary structural elements. Table2 displays the deviation parameter value for the secondary structural elements. Glu (Alpha-helix), Val (Beta-sheet), Gly (Beta-turn), Cys (Bend), His (3/10-helix), Ala (Pi-helix), His (Isolated beta-bridge), and Pro (random structure) had the highest deviation parameter value. Pro (Alpha-helix, Beta-sheet, Pi-helix), Trp (Beta-turn, Bend), Cys, (3/10-helix), Ile (Random Structure), and Gly (Isolated beta-bridge) all contributed to the value of the minimum deviation parameter. The values of the amino acid residue deviation parameters deviate slightly from previously published data [13].

Graphical representation

The plot is drawn between amino acid residues and the deviation parameter value. From the graph, the amino acid residue distribution of all beta proteins ribovirus can be seen. The preference of the amino acid residue over secondary structural elements is conveyed by the value +1. The number -1 indicates that it is not favored. According to this graph1, the amino acid Glu is more excited in the area on the positive side. Consequently, it is the alpha-helix's most important amino acid residue. Pro is also more enthusiastic about the negative aspects of things. They are the least important amino acid residue. Graph 2 Val is more enthusiastic about positive aspects. As a result, it is more important for beta-sheet amino acid residues. Similarly, Pro is more excited on the negative side. They are the amino acid residues that are least necessary. The amino acid Gly is more excited on the positive side region of the graph 3. As a result; it is a more crucial amino acid residue for the beta-turn. Val is also more excited on the negative side region. They are the least crucial amino acid residue. Graph 4 shows that the amino acid Cys is more excited in the positive side region. Consequently, it is a more crucial amino acid residue for the bend structure. Even on the negative side, Val is more excited. They are the least significant amino acid residue. In accordance with the graph 5, the amino acid His is more activated on the positive side. As therefore, the 3/10-helix has more significant amino acid residues. Cys is also more excited in the negative side region. They are the least abundant amino acid residue. From the graph 6, the amino acid Ala is excited more in the positive side region. So it is more significant amino acid residues for pi-helix. On the other hand, Pro is more excited on the negative side region. They are least significant amino acid residue. From the graph 7, the amino acid His is excited more in the positive side region. So it is more significant amino acid residues for Isolated Beta Bridge. Gly is also more excited in the negative side region. They are least significant amino acid residue. From the graph 8, the amino acid Pro is excited more in the positive side region. So it is more significant amino acid residues for random structure. Similarly, Ile is more aroused in the negative side



**Thenmozhi Kanaga and Arul Mugilan**

region. They are least significant amino acid residue. There are small differences between the preferential and non-preferred amino acid residues from the earlier analysis. [16-28].

DISCUSSION

The distribution of amino acid residues, frequency of occurrence, and deviation parameter value were determined based on these observations. According to the distribution, the beta sheet has more amino acid residues than the other secondary structural elements. The value of the deviation parameter represents the result of favored and non-preferred amino acid residues in secondary structural elements. Experimental biologists can make use of the abovementioned information for structure prediction, molecular modeling, and medication development.

ACKNOWLEDGMENT

We would like to acknowledge my professor, Dr. S.Arul Mugilan, for his support with this work.

REFERENCES

1. Gromiha MM. Proteins protein bioinformatics from sequence to function. *Protein* 2010; 1-27.
2. Tomasz Smolarczyk, Irena Roterman-Konieczna and Katarzyna Stapor. Protein Secondary Structure Prediction: A Review of Progress and Directions. *Curr. Bioinform* 2020; 15:90-107.
3. Kabsch W, Sander. Dictionary of protein secondary structure: pattern recognition of hydrogen-bonded and geometrical features. *Biopolymers* 1983;22(12): 2577-637.
4. Juliette Martin, Guillaume Letellier, Antoine Marin, Jean-François Taly, Alexandre G De Brevern And Jean-François Gibrat. Protein secondary structure assignment revisited: a detailed analysis of different assignment methods. *BMC Struct. Biol* 2005; 5:17.
5. Frishman D, Argos P. Knowledge-based protein secondary structure assignment. *Proteins* 1995;23(4): 566-579.
6. Chou, P.Y, Fasman, G.D. Conformational parameters for amino acids in helical, beta-sheet, and random coil regions calculated from proteins. *Biochem* 1974; 13: 211-222.
7. Richardson JS, Richardson DC. Amino acid preferences for specific locations at the ends of alpha helices. *Sci.* 1988; 240(4859):1648-1652.
8. Engel DE, DeGrado WF. Amino acid propensities are position-dependent throughout the length of alpha-helices. *J Mol Biol* 2004; 337(5):1195-1205.
9. Minor DL Jr, Kim PS. Measurement of the beta-sheet-forming propensities of amino acids. *Nature* 1994; 367(6464):660-663.
10. Jiang B, Guo T, Peng L, Sun Z. Folding Type-Specific Secondary Structure Propensities of Amino Acids, Derived from Alpha-Helical, Beta-Sheet, a/b, and a + b Proteins of Known Structures. *Biopolymers* 1998; 45:35-49.
11. Costantini S, Colonna G, Facchiano AM. Amino acid propensities for secondary structures are influenced by the protein structural class. *Biochem Biophys Res Commun* 2006; 342(2):441-451.
12. Mehmet Can. Conformational Parameters for Amino Acids in Helical, Beta-sheet and Random Coil Regions Calculated from Proteins: After 40 Years. *SEJSC* 2015; 4:1-6.
13. Mugilan S.A, Veluraja. Generation of deviation parameters for amino acid singlets, doublets and triplets from three-dimensional structures of proteins and its implications for secondary structure prediction from amino acid sequences. *Indian Acad. Sci* 2000;25:81-91.
14. Arul Mugilan, Sherlyn Jemimah and Preethi Jennifer. Novel Method of Protein Structure Prediction (NPSPM) based on Short Range Interactions between Amino acids. *Trends in Bioinformatics* 2014;7(1):1-6.
15. Fodje MN, Al-Karadaghi S. Occurrence, conformational features and amino acid propensities for the pi-helix. *Protein Eng* 2002;15(5): 353-358.
16. Chou, P.Y, Fasman, G.D. Prediction of protein conformation. *Biochem* 1974; 13: 222-245.





Thenmozhi Kanaga and Arul Mugilan

17. Chou PY, Fasman GD. Prediction of the secondary structure of proteins from their amino acid sequence. *Adv Enzymol Relat Areas Mol Biol* 1978; 47:45–148.
18. Kazuo Fujiwara, Hiromi Toda and Masamichi Ikeguchi. Dependence of α -helical and β -sheet amino acid propensities on the overall protein folds type. *BMC Struct. Biol* 2012;12:18.
19. Jane S, Richardson and David C, Richardson. Amino Acid Preferences for Specific Locations at the Ends of Alpha Helices. *Science* 1988; 240:1648-1652.
20. Susan Costantini , Giovanni Colonna, Angelo M. Facchiano . PreSSAPro: A software for the prediction of secondary structure by amino acid properties. *Comput. Biol. Chem* 2007;31:389–392.
21. O'Neil KT, DeGrado WF. A thermodynamic scale for the helix-forming tendencies of the commonly occurring amino acids. *Science* 1990;250(4981):646–651.
22. Anton V, Persikov, John A. M, Ramshaw, Alan Kirkpatrick and Barbara Brodsky. Amino Acid Propensities for the Collagen Triple-Helix. *Biochem* 2000;39:14960-14967.
23. Pal D, Chakrabarti P. Beta-sheet propensity and its correlation with parameters based on conformation. *Acta Crystallogr D: Biol Crystallogr* 2000; 56:589–594.
24. Bhattacharjee N, Biswas P. Position-specific propensities of amino acids in the beta-strand. *BMC Struct Biol* 2010;10:29.
25. Susan Costantini ,Giovanni Colonna ,Angelo M. Facchiano. Amino acid propensities for secondary structures are influenced by the protein structural class. *BBRC* 2006; 342 :441–451.
26. Patrice Koehl and Michael Levitt. Structure-based conformational preferences of amino acids. *Comput Biol Chem* 1999 ;96 (22): 12524-12529.
27. Michael Gromiha M, Makiko Suwa. Influence of amino acid properties for discriminating outer membrane proteins at better accuracy. *BBA* 2006;1764:1493–1497.
28. Michael Gromiha M, Makiko Suwa. Variation of amino acid properties in all-beta globular and outer membrane protein structures. *Int. J. Biol. Macromol* 2003;32:93–98.

Table1: Distribution of amino acid residues for secondary structural elements

AA	Total number of amino acids	Alpha - helix	Beta-sheet	Beta-turn	Ben d	3/10-helix	Pi-helix	Isolated beta-bridge	Random structure
A	125801	18383	43411	10510	1462 5	3257	379	1572	33664
R	92351	14814	28739	8336	9792	2938	30	2189	25513
N	122242	17025	22294	22082	1988 5	3975	100	1457	35424
D	101603	14939	17703	13699	1773 2	5075	37	1059	31359
C	19151	1372	6508	2979	4108	143	6	422	3613
E	104875	22095	30256	10209	1273 2	3827	200	946	24610
Q	86960	14927	31283	7106	9437	2680	64	1207	20256
G	178650	7012	39452	49090	3559 3	2697	319	1371	43116
H	44876	4270	20336	2202	4793	2587	3	1847	8838
I	125622	15580	70777	5553	6842	2117	246	4379	20128
L	163067	34109	72599	9013	9829	3683	164	2991	30679
K	111668	15602	40291	9790	1775 3	2738	24	1752	23718
M	39746	6614	17046	2254	2204	1139	28	441	10020





Thenmozhi Kanaga and Arul Mugilan

F	78198	5463	39831	4639	5018	2266	233	2439	18309
P	108844	2783	16174	16314	1515 8	3463	1	1011	53940
S	162955	13284	50866	17953	2327 4	6714	83	3029	47752
T	208263	13481	61863	13470	1657 1	2873	87	4130	95788
W	40092	4948	18222	2370	5230	736	15	1451	7120
Y	78455	9658	40345	4164	5961	1805	120	1979	14423
V	146139	15770	85504	3872	7518	2345	54	4145	26931
Total	2139558	252129	753500	21560 5	2440 55	57058	2193	39817	575201

Table2: Deviation parameter value for secondary structural elements

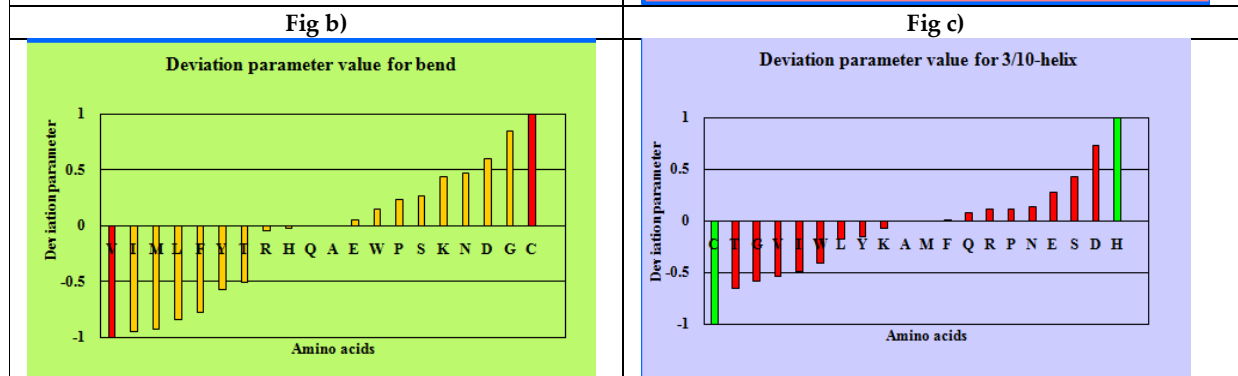
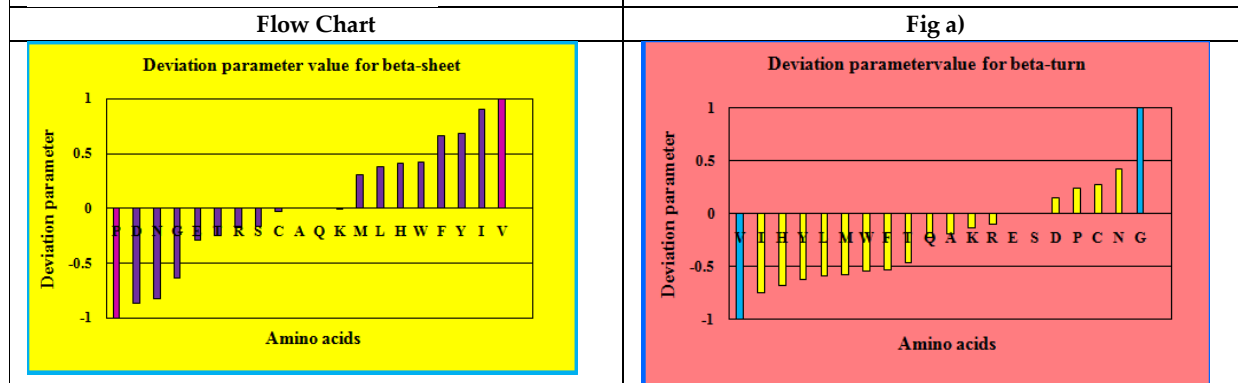
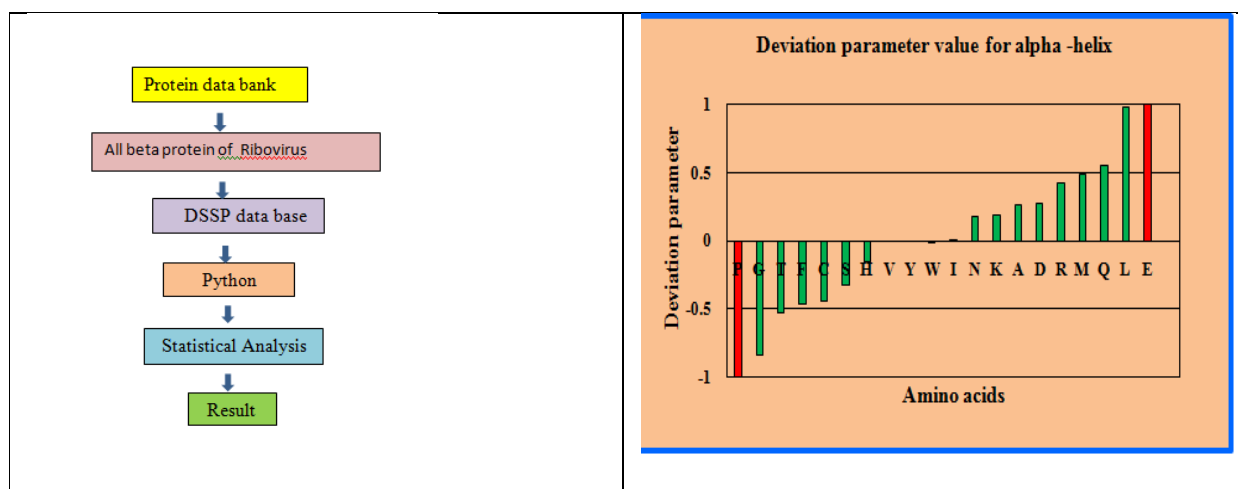
A	Alpha-helix	Beta-sheet	Beta-turn	Bend	3/10-helix	Pi-helix	Isolated beta-bridge	Random structure
A	0.262914	0	-0.19478	0	0	1	-0.5582	0
R	-0.44048	-0.02673	0.27569	1	-1	- 0.69483	0.103376	-0.7352
N	0.273253	-0.86951	0.14979	0.59304 8	0.734452	- 0.64379	-0.74814	0.14765
D	1	-0.28797	0	0.05238 3	0.270227	0.25452	-0.87667	-0.30676
C	-0.46209	0.663958	-0.53664	- 0.77703	0.011064	0.97769 7	0.532624	-0.31164
E	-0.83385	-0.63235	1	0.84455 5	-0.58587	0.17265 6	-1	-0.24452
Q	-0.15496	0.41456	-0.68139	- 0.03006	1	- 0.94214	1	-0.65804
G	0.01051	0.903818	-0.75005	- 0.94707	-0.49058	0.28905 7	0.704634	-1
H	0.189722	0.00475	-0.13654	0.43485 8	-0.07442	- 0.79355	-0.26559	-0.51411
I	0.982784	0.37928	-0.59384	- 0.84527	-0.17936	0	-0.02252	-0.74005
L	0.494471	0.306786	-0.57353	- 0.92978	0	-0.3023	-0.68652	-0.14433
K	0.184643	-0.82808	0.4281	0.47240 5	0.133163	- 0.18832	-0.61106	0.061669
M	-1	-1	0.241251	0.23418 1	0.108973	-1	-0.85209	1
F	0.554383	0	-0.22059	0	0.074568	- 0.27069	-0.43138	-0.32283
P	0.425995	-0.17245	-0.09993	- 0.04364	0.108877	- 0.68324	0.181569	0
S	-0.32051	-0.1676	0	0.27042 7	0.43271	-0.4981	0	0.076498





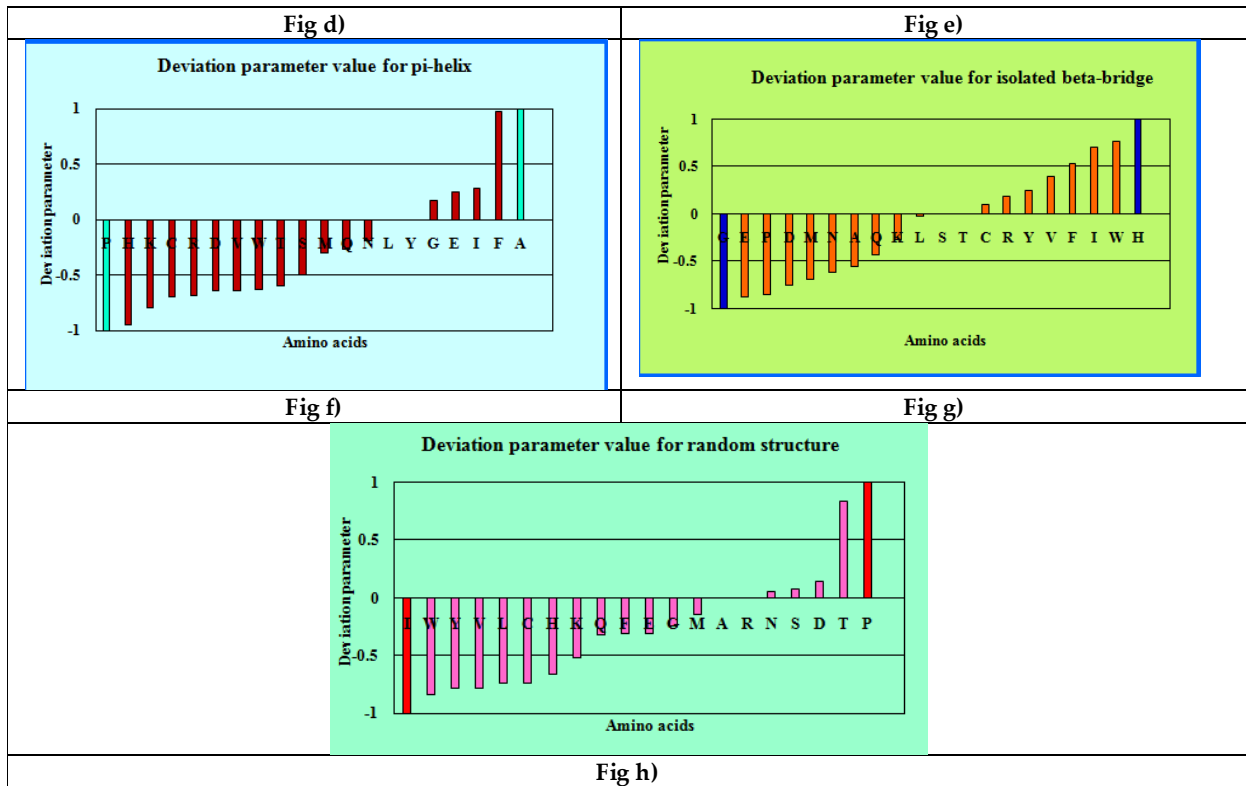
Thenmozhi Kanaga and Arul Mugilan

T	-0.5244	-0.24447	-0.46107	-	-0.65651	-	0	0.837518
W	0	1	-1	-1	-0.53431	-	0.400087	-0.77595
Y	0.003582	0.420528	-0.5396	0.14447 7	-0.40885	-	0.767147	-0.83827
V	0	0.685627	-0.62484	-	-0.1565	0	0.252915	-0.7801





Thenmozhi Kanaga and Arul Mugilan





Effectiveness of Blood Flow Restriction Training Exercise on Physical Function and Muscle Strength in Subjects with Osteoarthritis of Knee: A Systemic Review

Sandipkumar Parekh^{1*}, Drashti Jani², Hiral Parmar³ and Mehul Jadav⁴

¹Professor, Parul Institute of Physiotherapy and Research, Parul University, Vadodara, Gujarat, India.

²Clinical Therapist, Parul Institute of Physiotherapy and Research, Parul University, Vadodara, Gujarat, India.

³Assistant Professor, Balaji College Physiotherapy, Vadodara, Gujarat, India.

⁴Principal and Professor, Parul Institute of Physiotherapy and Research, Parul University, Vadodara, Gujarat, India.

Received: 13 Apr 2023

Revised: 18 Dec 2023

Accepted: 20 Jan 2024

*Address for Correspondence

Sandipkumar Parekh

Professor,

Parul Institute of Physiotherapy and Research,

Parul University,

Vadodara, Gujarat, India.

Email: sandip.parekh28008@paruluniversity.ac.in,



This is an Open Access Journal / article distributed under the terms of the **Creative Commons Attribution License** (CC BY-NC-ND 3.0) which permits unrestricted use, distribution, and reproduction in any medium, provided the original work is properly cited. All rights reserved.

ABSTRACT

Osteoarthritis is commonest musculoskeletal disorders. OA is most common cause of disability among persons over 60 years of age. It affecting 30-50% of the population. There are many therapies for treatment of osteoarthritis of knee joint but blood flow restriction is effective in treatment of knee osteoarthritis. Resistance training is beneficial for musculoskeletal function, cardiovascular function, psychological health, functional status. Resistance training is very effective in improving strength of quadriceps in OA knee. There is various therapy available for treatment of osteoarthritis of knee and BFR is one of them which useful in improving muscle strength and reducing pain. In patients with osteoarthritis of knee patients will have low risk factors if they have more strength in quadriceps muscles. Many studies suggest that BFR is effective this review is done to find out its effectiveness. Objectives: To identification, evaluation and summarization of blood flow restriction training on elder people with osteoarthritis on pain, physical function and muscle strength. Google scholar, Pubmed, concrane library, PEDro until 2020 This systemic review was done with using prizma guidelines. The keywords were used BFR, Resistance training, Physical therapy, Osteoarthritis knee. The article was evaluated with pedro scale. This Review registered in PROSPERO(CRD42021291792).After searching non randomized control trial journal were excluded. Then, the level of evidence was re-evaluated with the help of Pedro scale. Total 8 articles were included. All but 4 studies observed a significant increase in

69698





Sandipkumar Parekh *et al.*,

muscle strength and physical function following treatment. Published limited data show BFRT to be safe and effective in improving quadriceps muscle strength in patients with weakness with people with knee osteoarthritis and reducing pain.

Keywords: treatment, BFRT, people, studies, osteoarthritis

INTRODUCTION

Osteoarthritis is most common musculoskeletal disease which causes disability in persons. OA is most common cause of disability in over 60 years of age. Which affects 30-50% of the population. (1) OA in older adults' responsible for OA to decrease physical function. Many studies have concluded that people with knee OA have weak quadriceps muscles. So, strengthening knee extensors muscle is mandatory for reduction of pain and disability in patients with risk factor of osteoarthritis knee. (2) Resistance training is effective in improvement in musculoskeletal function, cardiovascular function, psychological health, functional status. Resistance training is very effective in improving strength of quadriceps in OA knee. (3) Blood Flow Restriction (BFR) training: BFR is also known as KAATSU training. BFR training was originated 50years ago in Japan. (4) The BFR is done by applying a pneumatic cuff or elastic bands to the most proximal part of the muscle. The training can be performed with low loads, around 10–30% of the maximum resistance. (5) BFR will only partially restricts blood flow and reduces the venous return and maintaining free arterial flow. (10) The exact mechanisms that promote gain in strength and hypertrophy remain unknown. But with arterial blood flow restriction there will be activation of muscles, increasing growth hormones and also increasing in metabolites lactate. And with the venous blood flow restriction there will be increase in metabolite stress, and reduction of stroke volume. (6)

BFR resistance training is beneficial for increasing skeletal muscle strength in some older adults, those who're with risk factors for knee OA. American College of Sport Medicine (ACSM) guidelines for strength training with older people recommend loads above 60% of 1 repetition maximum (1-RM) with frequency of 2–3 times per week, 1–3 sets of 8 to 12 repetitions. (7) High intensity resistance training can be performed with 70–85% 1RM resistance. (8) In OA patients muscle strength training is best intervention therapy to improve mobility in older people with sarcopenia. (9) Resistance exercise is program provides more muscle strength when we apply it with BFR. (10) Loenneke *et al.* has concluded that BFR combined with several types of exercise resulted about improvement in muscle strength and physical function. (11) There are various therapy available for treatment of osteoarthritis of knee and BFR is one of them which useful in improving muscle strength and reducing pain. In patients with osteoarthritis of knee patients will have low risk factors if they have more strength in quadriceps muscles. Many studies suggest that BFR is effective this review is done to find out its effectiveness.

Purpose

The main purpose of the study is to provide elaborated, studies in one document. Purpose of systemic review is to for supremacy health care decisions, production of primary research design. And the need of this study is for identification, evaluation and summarization of blood flow restriction training on elder people with osteoarthritis on pain, physical function and muscle strength.

Search strategy

The search strategy and reporting of this systematic review adhered to the PRISMA guidelines (Moher, Liberati, Tetzlaff, & Altman, 2009) and followed recommendations of the Cochrane Handbook for Systematic Reviews (Higgins & Green, 2011). The protocol of the review was prospectively registered in PROSPERO, submitted online in DECEMBER 2021 (CRD42021291792).





Sandipkumar Parekh *et al.*,

Study Inclusion and Exclusion Criteria

Articles were included if they fulfilled the following criteria: (1) written in English; (2) Treatment given for at least 4 weeks or more with proper method followed. (3) Physical function and pain results were reported pre- and post-treatment. Articles that have poor quality PEDro were Excluded. Systematic reviews and meta-analyses were also excluded, as the authors wanted to develop their own interpretations of the available data, and full article is not available that was also excluded.

Study Selection

One author ensured that all selected studies met the minimum requirements for inclusion. The author then conferred with another author to confirm inclusion and appropriateness of each article.

Data Extraction

One author abstracted information from the selected articles. The extracted information included study population, treatment utilized, duration of the treatment, length of time until follow-up measurements, and measured outcomes.

Data Synthesis

After searching journals, non-RCT articles were first excluded. Then, the level of evidence was further evaluated by using the PEDro scale (<http://www.pedro.org.au/>). If not found in the PEDro database, the article was evaluated by 2 reviewers who had completed the PEDro scale training tutorial. In case of score disagreement or other problems, a group discussion was used to decide whether to include or exclude an article from this study. The authors used the PEDro scale to assess the methodological quality of all studies included in the current review. The PEDro scale evaluates for 11 criteria to determine the methodological quality of a study. PEDro scores range from 0 = poor to 10 = high. The authors recognize that the PEDro scale is intended to be used solely for randomized control trials. Three authors independently scored each study included in the current review and then conferred with one another, discussed any disparities in the scores, and reached a consensus on each item included in the PEDro scale. Following data abstraction and methodological quality assessments, all authors compiled the findings of the included studies to form a comprehensive synthesis and interpretation of the data. The full text of all included RCT articles was reviewed. The following questions were investigated. All included RCT articles were summarized and analyzed with descriptive statistics. The author, publication year, subjects, intervention, exercise type, and outcome measures of all included articles were extracted by 2 reviewers. A third reviewer validated the data using a predefined form. If the reviewers had different opinions related to article selection, data extraction, or quality assessment, a consensus was achieved through discussion.

RESULTS

Search Results The initial search of the electronic databases resulted in 2253 articles available for review. Duplicate articles were removed, and 1348 titles and abstracts were reviewed. Review of the 1068 titles and abstracts resulted in 378 articles being removed. 200 additional articles were excluded following full-text review. The reference list of each remaining article was reviewed, and an additional article 38 were identified. The inability to abstract the necessary data from certain articles or through correspondence with the articles authors resulted in articles being removed. After those 19 articles found and some were not meeting inclusion criteria of review. In total, 4 articles were included in the current review. The Figure shows a flow chart of the article search results and data abstraction. **Table 1** presents the quality of included studies. The mean Pedro score of included articles was 7 with a range of 7–8. All studies were randomized (100%), conducted concealed allocation (100%), and had baseline comparability (100%). All studies were analyzed between-group comparisons, with reported point estimates and variability (100%). (17)(18)(19) **Table 3** Provides the summarized information (including author, experimental design, participants, intervention, comparison, and outcome measures) for each RCT article. The ages of the experimental subjects ranged from 50-70 years of age. For all other articles, the experimental and control groups showed a similar age distribution.





Sandipkumar Parekh et al.,

Supervised BFR intervention was included in most of the RCT articles, and the RCT BFR programs lasted for 1 hour each time, 1–4 times per week for 6–12 weeks.

DISCUSSION

The current systematic review shows a comprehensive review of blood flow restriction therapy and their effects on pain reduction, muscular performance, and muscle function. Evidence supports the use of BFR therapies to improve physical function in osteoarthritis of knee. The data shows that BFRT to be safe and potentially effective in improving quadriceps strength in patients with knee-related weakness. There were no complications related to BFRT. Improvements in study design and refinements in protocols related to cuff pressure and exercise dosage and duration are required to further advance our knowledge of this treatment option. The low-resistance load of 30% 1 RM used in studies was effective in improving quadriceps strength. BFRT does not enhance the key clinical outcomes of pain and disability relative to regular high intensity resistance training. These findings are also relatively consistent with the most promising results reported for BFRT in other painful musculoskeletal conditions. For example, Giles et al. (2017) (Giles et al., 2017) which was included within two of the systematic reviews (Cuyul-Vasquez et al., 2020; Van Cant et al., 2020) on painful knee conditions, but not in the current review reported that 'pain with daily activities' improved significantly more for people with patellofemoral pain using BFRT than those undergoing only traditional RT. However, this additional benefit was only evident immediately post-intervention at eight weeks, and was no longer evident at six months. Secondly, and arguably more importantly, pain with daily activities was not a primary outcome in that RCT, with neither the two primary outcomes (worst pain, and pain-related function) nor any other secondary outcomes demonstrating significant benefits for the BFRT group. Our findings are also consistent with Ladlow et al. (2018) (Ladlow et al., 2018) who reported no significant benefit of BFRT over conventional RT among people with lower limb musculoskeletal pain. We are aware of no other RCTs demonstrating a sustained (e.g., at least 4 weeks) clinical benefit on pain or disability for BFRT, over and above the benefit of exercise, among people with painful musculoskeletal conditions.

CONCLUSION

Published limited data show BFRT to be safe and p effective in improving quadriceps muscle strength in patients with weakness with people with knee osteoarthritis and reducing pain. The use of short-duration vascular occlusion and light-load resistance exercises appears in arthritic knees. This treatment option requires further investigation to refine protocols related to cuff pressure and exercise dosage and duration.

REFERENCES

1. Zhang Y, Jordan JM. Epidemiology of osteoarthritis. Clinics in geriatric medicine. 2010 Aug 1;26(3):355-69.
2. Alnahdi AH, Zeni JA, Snyder-Mackler L. Muscle impairments in patients with knee osteoarthritis. Sports health. 2012 Jul;4(4):284-92.
3. Pollock ML, Franklin BA, Balady GJ, Chaitman BL, Fleg JL, Fletcher B, Limacher M, Piña IL, Stein RA, Williams M, Bazzarre T. Resistance exercise in individuals with and without cardiovascular disease: benefits, rationale, safety, and prescription an advisory from the committee on exercise, rehabilitation, and prevention, council on clinical cardiology, American Heart Association. Circulation. 2000 Feb 22;101(7):828-33.
4. Sato Y. The history and future of KAATSU training. International Journal of KAATSU Training Research. 2005;1(1):1-5.
5. Patterson SD, Hughes L, Warmington S, Burr J, Scott BR, Owens J, Abe T, Nielsen JL, Libardi CA, Laurentino G, Neto GR. Blood flow restriction exercise: considerations of methodology, application, and safety. Frontiers in physiology. 2019:533.





Sandipkumar Parekh et al.,

6. Pearson SJ, Hussain SR. A review on the mechanisms of blood-flow restriction resistance training-induced muscle hypertrophy. *Sports medicine*. 2015 Feb;45(2):187-200.)
7. Kraemer WJ, Adams K, Cafarelli E, Dudley GA, Dooly C, Feigenbaum MS, Fleck SJ, Franklin B, Fry AC, Hoffman JR, Newton RU. American College of Sports Medicine position stand. Progression models in resistance training for healthy adults. *Medicine and science in sports and exercise*. 2002 Feb 1;34(2):364-80.)
8. Kraemer WJ, Adams K, Cafarelli E, Dudley GA, Dooly C, Feigenbaum MS, Fleck SJ, Franklin B, Fry AC, Hoffman JR, Newton RU, Potteiger J, Stone MH, Ratamess NA, Triplett-McBride T, American College of Sports Medicine.
9. Vikberg S, Sörlén N, Brandén L, Johansson J, Nordström A, Hult A, Nordström P. Effects of resistance training on functional strength and muscle mass in 70-year-old individuals with pre-sarcopenia: a randomized controlled trial. *Journal of the American Medical Directors Association*. 2019 Jan 1;20(1):28-34.)
10. Slys J, Stultz J, Burr JF. The efficacy of blood flow restricted exercise: A systematic review & meta-analysis. *Journal of science and medicine in sport*. 2016 Aug 1;19(8):669-75.)
11. Loenneke JP, Wilson JM, Wilson GJ, Pujol TJ, Bemben MG. Potential safety issues with blood flow restriction training. *Scandinavian journal of medicine & science in sports*. 2011 Aug;21(4):510-8.)

Table 1. PEDro score for included studies (n = 4)

	Mikhail Santos Cerqueira	Rodrigo brancoferraz	Sara A harper at al.	Mai m a Abdallah
Eligibility	Y	Y	Y	Y
Random allocation	Y	Y	Y	Y
Concealed allocation	Y	N	N	Y
Baseline comparability	Y	Y	Y	Y
Blind subjects	Y	Y	Y	Y
Blind therapists	N	N	N	N
Blind assessors	N	Y	Y	N
Adequate follow-up	Y	Y	Y	Y
Intention-to-treat analysis	Y	Y	Y	Y
Between-group comparisons	Y	Y	Y	Y
Point estimates and variability	Y	Y	Y	Y
Total score (0–10)	7	7	7	7

PEDro: Physiotherapy Evidence Database; Y: yes; N: no

Title	Author	Design	Participant Number Age=mean=SD	Intervention	Exercise mode (frequency/intensity)	Outcome measures
Effects of blood flow restriction exercise with very low load and low volume in	Mikhail Santos Cerqueira ¹ , WouberHéricksen de Brito Vieira	two-arm randomized placebo-controlled trial	50 or above	Group 1: high-intensity resistance exercise Group 2: Blood flow	2 sessions per week for 12 weeks	Primary outcome:VAS, 30-s chair stand test Secondary outcome:





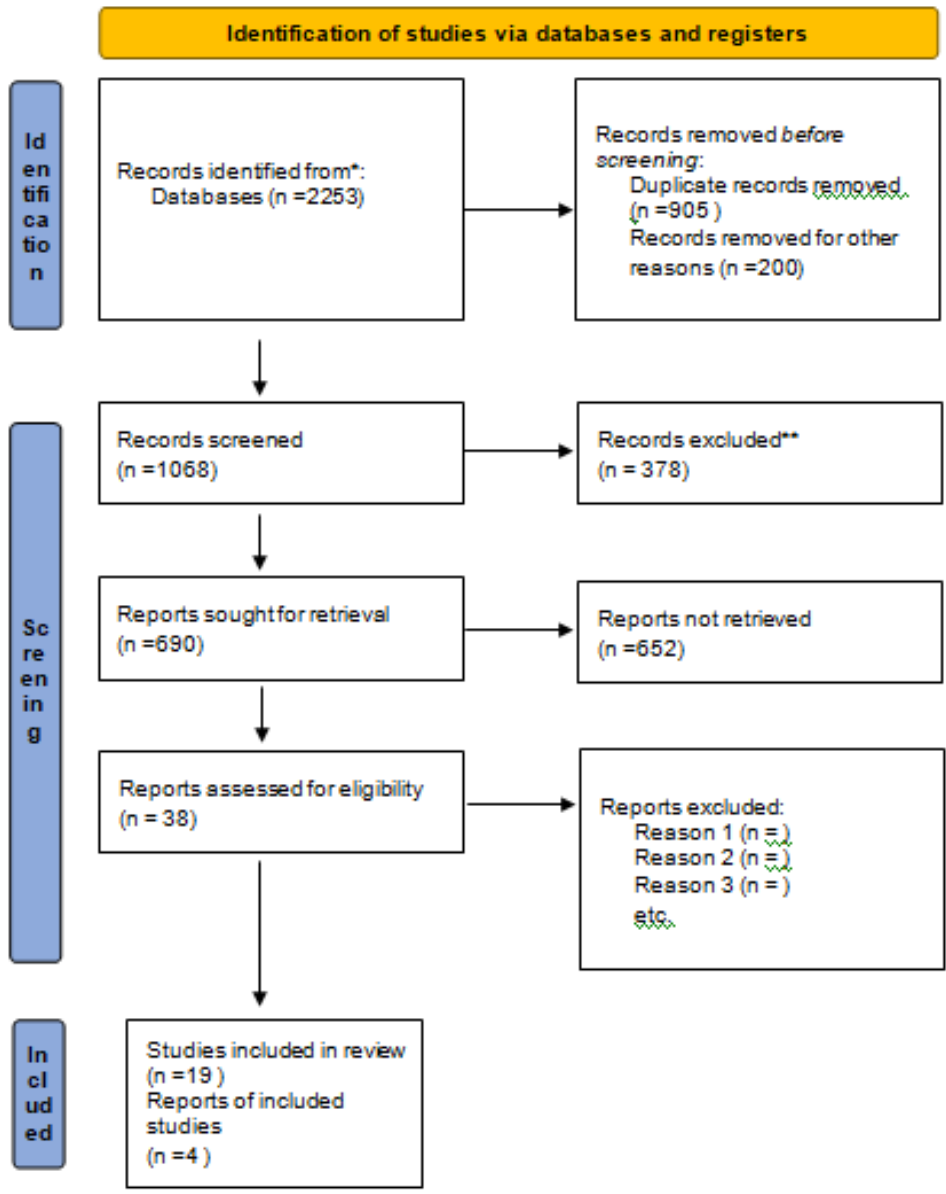
Sandipkumar Parekh et al.,

patients with knee osteoarthritis: protocol for a randomized trial				restriction exercise		SF-36 questionnaire
Benefits of resistance training with blood flow restriction in knee osteoarthritis	Rodrigo brancoferraz	Randomized control trial	50 to 60 years	Low intensity resistance training, partial blood flow restriction +high intensity resistance training		
Blood flow restriction resistance exercise for older adults with knee osteoarthritis: A pilot RCT	Sara A harper at al.	A pilot RCT	>60	Low load resistance training with BFR And Moderate intensity resistance training		
Effect of low load resistance blood flow restriction training on knee osteoarthritis	Mai m a Abdallah	RCT	40-60	Conventional High load resistance training and low load resistance training with BFR	3 sessions per 4 weeks, total 12 sessions	Time up go test VAS





Sandipkumar Parekh *et al.*,





Study on Cognitive Abilities in Mental Development and Proficiency in Mathematics among Students Studying at Secondary Level

V. Ramesh^{1*}, M. Sanmuga Revathi² and A.Sankar³

¹Research Scholar, Department of Education, Alagappa University, Karaikudi, Tamil Nadu, India

²Assistant Professor, Department of Education, Alagappa University, Karaikudi, Tamil Nadu, India

³Director, Department of Physical Education, Kongu Arts and Science College, (Affiliated to Bharathiar University), Coimbatore, Tamil Nadu, India

Received: 29 Sep 2023

Revised: 16 Nov 2023

Accepted: 10 Jan 2024

*Address for Correspondence

V. Ramesh,

Research Scholar,

Department of Education,

Alagappa University,

Karaikudi, Tamil Nadu, India

Email:rameshshyuvraj@gmail.com



This is an Open Access Journal / article distributed under the terms of the **Creative Commons Attribution License** (CC BY-NC-ND 3.0) which permits unrestricted use, distribution, and reproduction in any medium, provided the original work is properly cited. All rights reserved.

ABSTRACT

Education is a process of human empowerment for the achievement of better and high quality of life. As with literacy in the 20th century mathematical calculations and numeracy skills will be needed for everybody in the 21st century. An individual who do not acquire basic competencies in mathematics before leaving secondary school level will be disadvantaged in the work place of the 21st century and in their ability to function in many new routine day to day activities. Especially cognitive abilities like thinking, reasoning, memory, attitude, towards perception, decision making, etc., are some of the variables, necessary for proficiency in mathematics.

Keywords: cognitive, ability, mathematics, proficiency.

INTRODUCTION

Mathematics is the science that deals with the logic of shape, quantity, and arrangement, Mathematics is all around us, in everything we do. Mathematics is a science of numbers, magnitude, space, geometrical figures and algebraic expressions. Achievement in mathematics signifies that an individual have an ability to deal with numbers, solve difficult mathematical problems have an understanding of geometrical figures and their constructions. A high achiever in mathematics has excellent computational and interpretation skills.

Mathematical performance is made up of a number of components such as basic knowledge of numbers, memory for arithmetical facts, understanding of mathematical concepts and ability to follow problem solving procedure (Dowker

69705

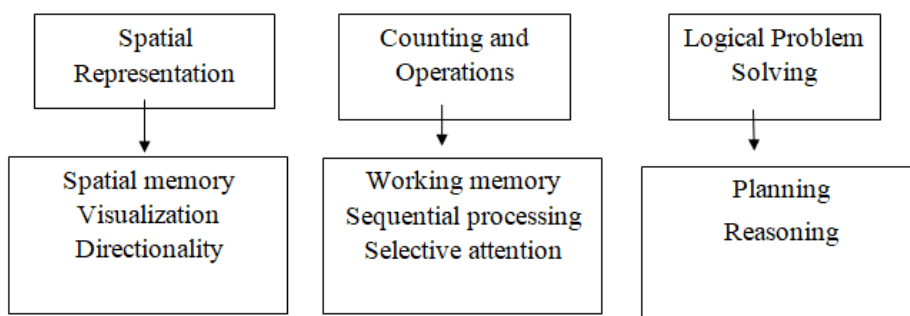




Ramesh et al.,

1998). These elementary arithmetic skills increase over time (Siegler1988). In the beginning, at a basic level, children start by using fingers or other concrete references to help them with the counting process. From these simple strategies, children move on to auditory counting starting with the addition process and counting up to the subtraction process through experience and improvements in working memory children are better able to mentally keep the counting process and thus gradually abandon the use of manipulative and fingers for verbal counting (Gearg, 2006). The cognitive process associated to the measurement process implies the subdivision of continuous quantities (such as length) in order to make them countable and comparable. Hence measurement skills are complex, cognitive processes associated with both number and arithmetic operations (Clements and Sarama, 2009).

Cognitive processes Associated with mathematics



SPATIAL MEMORY

This refers to the ability to remember those that are in space and their relationship with other objects in space. This understanding provides the foundation on which problems in space can be solved.

VISUALIZATION

The ability to visualize a problem that are considered to visualize alternative solutions contributes substantially to the understanding of the problem. In learning, transformations in geometry, for example, interpreting the difference between a translation (Sliding an object along a straight line), a rotation turning an object, around a point and a reflection (mirror image) is greatly aided by the visualization skills.

DIRECTIONALITY

The ability to distinguish left and right, of course, is more than about math. It comes in handy when trying shoes, reading a map or a chart and in executing a football or basketball play. It is critical in chemistry (Where two molecules may differ only in the orientation of the atoms (the technical term is “enantiomer”), but have two completely different uses like one drug used to treat tuberculosis whose enantiomer causes blindness. When it comes to counting and numerical operations they are again dependent for math success on some foundational cognitive skills, such as sequential processing and selective attention and on executive functions (the directive capacities of our minds) such as working memory.

WORKING MEMORY

Working memory refers to the ability to hold information in the minds while manipulating it. Working capacity is highly correlated with reading comprehension, with math performance, and with many other academic and non-academic outcomes. Working memory serves math process from the very simple (for example, keeping track of which applies in the basket have counted and which we haven't) to the most complex reasoning and mental simulations that are performed when calculating statistics or manipulating derivatives in calculus.



**Ramesh et al.,****SEQUENTIAL PROCESSING**

Counting of course is all about sequences so once again cognitive skills contribute crucially at even the most elementary stages of math. To manipulate and calculate, the sequence of steps, to solve problem must be observed. A concrete example is the concept of order of operations and the different result that comes from $(6+5) \times 2$ and from $6+(5 \times 2)$.

SELECTIVE ATTENTION

When there is good selective attention, it will be easy to screen out the irrelevant parts of a complex problem and isolate the pertinent facts that are needed to concentrate on. Finally, mathematics is problem solving there are other types of problem solving, of course, but problems with numbers almost always call for mathematical thinking and logic. In the discussion above, it is already highlighted some of the cognitive skills that are used problem solving but higher order cognitive processes are often required to be successful in mathematics and to be started with planning.

PLANNING

Planning is a fundamental cognitive skill that forms part of our executive functions. Planning can be defined as ability to “think about the future” or mentally anticipate the right way to carry-out a task or reach a specific goal. Planning is the mental process that allows us to choose the necessary actions to reach a goal, decide the right order, assign each task to the proper cognitive resources, and establish a plan of action. Good planning is in evidence that is considered alternative approaches to a problem, map out the sequence of steps in advance, and then carry them out efficiently and accurately.

REASONING

It is defined as reorganizing and combining in new ways the ideas and experiences to solve a problem which confronts us, so reasoning is a tool in problem solving which is related to cognitive psychology. The word reasoning is used to describe the mental recognition of cause and effect relationship. One makes one’s previous knowledge and experience in reasoning.

STATEMENT OF THE PROBLEM

A study on cognitive abilities in mental development and proficiency in mathematics among students studying at secondary level.

OBJECTIVES OF THE STUDY

1. To identify the cognitive abilities in mental development and proficiency in mathematics among students studying at secondary level.
2. To find out the level of cognitive abilities in mental development and proficiency in mathematics among students studying at secondary level
3. To find out the significant difference between the group of Demographic variable such sex and their cognitive abilities and mental development and proficiency in mathematics among students studying at secondary level.

HYPOTHESES OF THE STUDY

1. The level of cognitive abilities in mental development and proficiency in mathematics studying at secondary level is found at average level.
2. There exists significant difference between different groups of Demographic variables such sex (Boys and Girls) their cognitive abilities in mental development and proficiency in mathematics among students studying at secondary level .





Ramesh et al.,

METHODOLOGY

The investigator preferred normative survey method to collect the data from the secondary school students in and around Pudukkottai district in order to identify their cognitive abilities in mental development and proficiency in mathematics among students studying at secondary level.

Tool Used

The investigator himself developed a questionnaire on cognitive abilities in mental development and proficiency in mathematics among students studying at secondary level.

DATA ANALYSIS

After collecting data, all the responses of the students were entered in a table. The score were given to each and every items of the questionnaire. All the scores were converted into percentages, in order to identify the cognitive abilities in mental development and proficiency in mathematics among students studying at secondary level. The following tables shows the correlation, means, SD, t-Value and level of significance table.

EDUCATIONAL IMPLICATIONS

- The level of cognitive abilities in mental development and proficiency in maths among girls is higher than boys studying at secondary level.
- The level of Cognitive abilities in mental development and proficiency in maths students are very strong at secondary level.

LIMITATIONS OF THE STUDY

The present study suffers from the following limitations

- The study is confined to the area in and around Pudukkottai District.
- The size of the sample was not very large.
- The study is administered only for the maths students studying in secondary schools.
- The aim of study was only to cognitive abilities in mental development and proficiency in mathematics studying at secondary school students.

SUGGESTIONS

- The special programmes or trainings may be conducted to enrich cognitive abilities in mental development and proficiency in mathematics studying at secondary level.
- Talent exams, Project work may be assigned at individual level to promote their cognitive abilities.

REFERENCES

1. Borghans L., Angela L. D., James J. H., Bas T. W. (2008). The economics and psychology of personality traits. *J. Hum. Resour.* 45 640–654. 10.1111/j.0042-7092.2007.00700.x [CrossRef] [Google Scholar]
2. Cao L. R., Cao X. H. (2004). The effects of time management tendencies, cognitive styles, and meta-concern levels on academic achievement of high school students. *Chin. J. Ergon.* 10 13–15. 10.3969/j.issn.1006-8309.2004.03.005 [CrossRef] [Google Scholar]
3. Claessens B. C., Eerde W. V., Rutte C. G., Roe R. A. (2007). A review of the time management literature. *Pers. Rev.* 36 255–276. 10.1108/00483480710726136 [CrossRef] [Google Scholar]
4. Claessens B. C., Eerde W. V., Rutte C. G., Roe R. A. (2010). Planning behavior and perceived control of time at work. *J. Organ. Behav.* 25 937–950. 10.2307/4093778 [CrossRef] [Google Scholar]
5. Dai Y. (2013). *A Correlation Study of Junior High School Students' Learning Self-Control, Emotional Stability and Academic Achievement*. Nanchang: Jiangxi Normal University. [Google Scholar]





Ramesh et al.,

6. David F. L. (2005). The role of nonverbal ability tests in identifying academically gifted students: an aptitude perspective. *Gift. Child Q.* 2:409. 10.1177/001698620504900203 [CrossRef] [Google Scholar]
7. Deary I. J., Steve S., Pauline S., Cres F. (2006). Intelligence and educational achievement. *Intelligence* 35 13–21. [Google Scholar]
8. Dickson W. P. (1981). *Childrens Oral Communication Skills*. New York, NY: Academic Press. [Google Scholar]
9. Duckworth A. L., Seligman M. (2010). Self-discipline outdoes IQ in predicting academic achievement of adolescents. *Psychol. Sci.* 16 939–944. 10.1111/j.1467-9280.2005.01641.x [PubMed] [CrossRef] [Google Scholar]
10. Edwards J. R., Lambert L. S. (2007). Methods for integrating moderation and mediation: a general analytical framework using moderated path analysis. *Psycholo Methods* 12 1–22. 10.1037/1082-989X.12.1.1 [PubMed] [CrossRef] [Google Scholar]
11. Fang A. R., Wang H. P. (2003). A comparative study of study time management between academically gifted students and academically disadvantaged students. *Prim. Second. School. Abroad* 4 45–49. 10.3969/j.issn.1007-8495.2003.04.005 [CrossRef] [Google Scholar]
12. Formazin M., Schroeders U., Kller O., Wilhelm O., Westmeyer H. (2011). Studierendenauswahlimfachpsychologie. *Psychol. Rundschau* 62 221–236. 10.1026/0033-3042/a000093 [CrossRef] [Google Scholar]
13. Grass J., Strobel A., Strobel A. (2017). Cognitive investments in academic success: the role of need for cognition at University. *Front. Psychol.* 8:790. 10.3389/fpsyg.2017.00790 [PMC free article] [PubMed] [CrossRef] [Google Scholar]
14. Heckman J. J., Humphries J. E., Veramendi G. (2018). Returns to education: the causal effects of education on earnings, health, and smoking. *J. Polit. Econ.* 126 S197–S246. 10.1086/698760 [PMC free article] [PubMed] [CrossRef] [Google Scholar]
15. Hu X. D. (2017). The principles and paths of the core competence of chinese in the college entrance examination. *J. China Exam.* 7 58–65. 10.19360/j.cnki.11-3303/g4.2017.07.012 [CrossRef] [Google Scholar]
16. Huang X. T., Zhang Z. J. (2001). Development of the adolescent time management tendency scale. *Acta Psychol. Sin.* 4 338–343. [Google Scholar]
17. Ian J. D., Steve S., Pauline S., Cres F. (2006). Intelligence and educational achievement. *Intelligence* 35 13–21. 10.1016/j.intell.2006.02.001 [CrossRef] [Google Scholar]
18. James J. H., Jora S., Sergio U. (2006). The effects of cognitive and noncognitive abilities on labor market outcomes and social behavior. *NBER Work. Pap.* 24 411–482. 10.1086/504455 [CrossRef] [Google Scholar]
19. Kuncel N. R., Hezlett S. A., Ones D. S. (2004). Academic Achievement, career potential, creativity, and job performance: can one construct predict them all? *J. Personal. Soc. Psychol.* 86 148–161. 10.1037/0022-3514.86.1.148 [PubMed] [CrossRef] [Google Scholar]
20. Li C., Wang N. X., Li Q. F. (2016). Advances in research related to time management tendencies of undergraduate nursing students. *Chin. Gen. Prac. Nurs.* 14 1641–1643. 10.3969/j.issn.1674-4748.2016.16.007 [CrossRef] [Google Scholar]
21. Li T., Zhang W. T. (2015). International trends in the study of personality economics. *Econ. Perspect.* 8 128–143. [Google Scholar]
22. Li X. Y. (1999). Cognitive theory of PTSD and cognitive-behavioral therapy. *Chin. J. Clin. Psychol.* 7 125–128. [Google Scholar]
23. Liang X. L., He J., Liu P. P. (2020). The influence of cognitive ability on academic achievement of junior middle school students: a mediated moderation model. *Psychol. Dev. Educ.* 36 449–461. 10.16187/j.cnki.issn1001-4918.2020.04.08 [CrossRef] [Google Scholar]
24. Lin C. D., Wo J. Z., Liu H. J. (2003). An EEG study on the intelligence development of primary and middle school students. *Stud. Psychol. Behav.* 1 5–10. [Google Scholar]
25. Lin H. P. (2021). Comprehensively promote the reform of the college entrance examination content to help build a high-quality education system. *J. China Exam.* 1 1–7. 10.19360/j.cnki.11-3303/g4.2021.01.001 [CrossRef] [Google Scholar]
26. Liu J., Wang H. L. (2000). Application of information processing learning theory in educational technology. *Inserv. Educ. Train. Sch. Teach.* 12 51–52. [Google Scholar]





Ramesh et al.,

27. Liu L. J. (2020). On the cultivation of students' self-discipline ability. *J. Dalian Educ. Univ.* 2 52–53. [Google Scholar]
28. Liu S., Wei W., Chen Y., Hugo P., Zhao J. (2021). Visual–spatial ability predicts academic achievement through arithmetic and reading abilities. *Front. Psychol.* 11:591308. 10.3389/fpsyg.2020.591308 [PMC free article] [PubMed] [CrossRef] [Google Scholar]
29. Liu X. J. (2019). *Analysis of Factors Affecting High School Students' College Entrance Examination Results*. Hunan: Hunan University. [Google Scholar]
30. Liu Y. (1988). On the cultivation of thinking conversion ability in middle school mathematics teaching. *J. Yangzhou Univ.* 3 110–114. 10.19411/j.1007-824x.1988.03.021 [CrossRef] [Google Scholar]
31. Macan T. H. (1994). Time management: test of a process model. *J. Appl. Psychol.* 79 381–391. 10.1037/0021-9010.79.3.381 [CrossRef] [Google Scholar]
32. Carmichael, L.(Ed.), *Manual of Child Psychology*, John Wiley, New York, 1946.
33. Crow., L.D. and Crow, Alice, *Child Psychology*, Barney & Noble, New York, 1969.
34. Harlock and Schewartz, quoted by KuppSwany, B., *Advanced Educational Psychology*, Delhi University Publication, 1964.
35. Marry, F.K. and Marray, R.V., *From infancy to adolescence*, Harpers & Brothers, New York, 1940.
36. Sorenron, Herbert, *Psychology in Education*, MC Graw-Hill, New York, 1948.
37. George, J.Mouley, *Psychology of Effective Teaching*, New York, Holt, Rinehart and Winston, 1968.
38. James, William, *Psychology, Briefer Course*, London, Collier Ltd., 1969, (7th Print).
39. Crow, L.D. and Crow A., *Child Psychology* New York, Barney and Noble, 1969.

Table I Shows the Distribution of Boys secondary school students percentage scores and their cognitive abilities in mental development and proficiency in mathematics among students studying at secondary level.

S.No	Category	Cognitive ability
1	Boys	95%

Table II Shows that Distribution of Girls secondary school students percentage scores and their Cognitive abilities in mental development and proficiency in mathematics among students studying at secondary level.

S.No	Category	Cognitive ability
1	Girls	98%

Table III Shows the mean, SD, t-Value and level of significance between boys and girls.

Students	Mean	SD	T-Value	Level of significance
Boys	21.86	37.4	1.77	Not Significant
Girls	22.66	3.21		

Table IV Shows the mean, SD, t-Value and level of significance between boys and girls.

Students	Mean	SD	t-Value	Level of significance
Boys	22.50	3.45	0.702	Not Significant
Girls	22.17	3.76		





Analysis of Pentagonal Neutrosophic Replacement Problem

Hema. R¹ and Rajeshwari .S^{2,3}*

¹Assistant Professor, Department of Mathematics, Annamalai University, Annamalai nagar – 608002 (Deputed to Government Arts and Science College, Nagercoil – 629004), Tamil Nadu, India

²Research Scholar, Annamalai University, Annamalai nagar– 608002 Tamil Nadu, India

³Assistant Professor, Department of Mathematics, Mohamed Sathak AJ College of Engineering, Chennai, Tamil Nadu, India.

Received: 30 Oct 2023

Revised: 25 Oct 2023

Accepted: 08 Jan 2024

*Address for Correspondence

Rajeshwari .S

Research Scholar,

Annamalai University,

Annamalai nagar– 608002,

Tamil Nadu, India

Email: srajeshwarimphil1988@gmail.com



This is an Open Access Journal / article distributed under the terms of the **Creative Commons Attribution License** (CC BY-NC-ND 3.0) which permits unrestricted use, distribution, and reproduction in any medium, provided the original work is properly cited. All rights reserved.

ABSTRACT

In our busy real life we are facing a situation of replacement. The situation of replacement arises to overcome sudden failures and also to improve the efficiencies of Machines. Replacement is the main aspect to run our activities/work smoothly and economically. In this paper we are going to analyze such a case, using accuracy function and removal area method to solve pentagonal neutrosophic replacement problem. And also we are going to compare the results to get the minimum cost of replacement.

Keywords: Pentagonal neutrosophic number, Replacement problem, Removal area method, Accuracy function.

INTRODUCTION

In replacement theory we are dealing with two types of failures namely Gradual failure and Sudden failure. Gradual failure is progressive, because as the life of an item increases, its efficiency gets deteriorates. This results, 1. Poor resale value 2. Poor output 3. Expenditure is high for cost of operating. On the other hand sudden failure occurs after a period of use and that period is not constant. It follows a probability distribution which might be random, progressive or retrogressive. The sudden failure mechanism can be treated by, 1. the item will be replaced when it fails 2. Individual preventive replacement 3. Common preventive replacement. Our task is to find the age of replacement of such items under two cases.

1. Maintenance cost increases with time and value of money is not changed.
2. Maintenance cost increases with time and value of money changes with time.





Hema and Rajeshwari

In 1965, Lofti. Zadeh first dealt the problems of fuzzy nature [17]. In 1995 the idea of neutrosophy, introduced by Smarandache [14]. Many researchers developed triangular, trapezoidal, pentagonal, octagonal neutrosophic numbers and discussed their properties and applications. Bellman [5] developed RP as a dynamic programming. Fuzzy replacement problem with change in money value along with time is introduced by Pranab Biswas and Surapati Pramanik [13]. So here in this paper we will analyze the pentagonal neutrosophic replacement problem by using accuracy function method and Removal area Method to arrive the optimal cost of replacement.

2. Preliminaries

In this section, we recall the basic definitions of Neutrosophic set, Single valued Neutrosophic set, Pentagonal neutrosophic number.

Definition 2.1 Neutrosophic set [6]: "Let U be an universe of discourse then the neutrosophic set A is an object having the form $A = \{ \langle x: T_A(x), I_A(x), F_A(x) \rangle, x \in U \}$, where the functions T, I, F: $U \rightarrow]0,1+[$ define respectively the degree of membership, the degree of indeterminacy, and the degree of non-membership of the element $x \in U$ to the set A with the condition.

$$0 \leq T_A(x) + I_A(x) + F_A(x) \leq 3$$

From philosophical point of view, the neutrosophic set takes the value from real standard or non-standard subsets of $]0,1+[$. [So instead of $]0,1+[$ we need to take the interval [0,1] for technical applications, because $]0,1+[$ will be difficult to apply in the real applications such as in scientific and engineering problems".

Definition 2.2: Single-Valued Neutrosophic Set [3]: "A Neutrosophic set in the definition 2.2 is said to be a single-valued Neutrosophic Set if x is a single-valued independent variable. $\tilde{S}A = \{ \langle x; [T_{\tilde{S}A}(x), I_{\tilde{S}A}(x), F_{\tilde{S}A}(x)] \rangle : x \in X \}$, where $T_{\tilde{S}A}(x), I_{\tilde{S}A}(x), F_{\tilde{S}A}(x)$ denoted the concept of accuracy, indeterminacy and falsity memberships function respectively".

Definition 2.3: Single-Valued Pentagonal Neutrosophic Number [3]: "A Single-Valued Pentagonal Neutrosophic Number (\tilde{S}) is defined as and described as

$\tilde{S} = \{ [(g^1, h^1, i^1, j^1, k^1): \rho], [(g^2, h^2, i^2, j^2, k^2): \sigma], [(g^3, h, i^3, j^3, k^3): \omega], \}$, where $\rho, \sigma, \omega \in [0,1]$. The accuracy membership function ($\theta_{\tilde{S}}$): $\mathbb{R} \rightarrow [0, \rho]$, the indeterminacy membership function ($\phi_{\tilde{S}}$): $\mathbb{R} \rightarrow [\sigma, 1]$ and the falsity membership function ($\psi_{\tilde{S}}$): $\mathbb{R} \rightarrow [0, \rho]$ are given as:

$$\theta_{\tilde{S}}(x) = \begin{cases} \theta_{\tilde{S}T_1}(x)g^1 \leq x \leq h^1 \\ \theta_{\tilde{S}T_2}(x)h^1 \leq x \leq i^1 \\ p & x = i^1 \\ \theta_{\tilde{S}T_2}(x)i^1 \leq x \leq j^1 \\ \theta_{\tilde{S}T_1}(x)j^1 \leq x \leq k^1 \\ 0 & \text{otherwise} \end{cases}, \quad \phi_{\tilde{S}}(x) = \begin{cases} \phi_{\tilde{S}T_1}(x)g^2 \leq x \leq h^2 \\ \phi_{\tilde{S}T_2}(x)h^2 \leq x \leq i^1 \\ \sigma & x = i^2 \\ \phi_{\tilde{S}T_2}(x)i^2 \leq x \leq j^2 \\ \phi_{\tilde{S}T_2}(x)j^2 \leq x \leq k^2 \\ 1 & \text{otherwise} \end{cases}$$

$$\psi_{\tilde{S}}(x) = \begin{cases} \psi_{\tilde{S}T_1}(x)g^3 \leq x \leq h^3 \\ \psi_{\tilde{S}T_2}(x)h^3 \leq x \leq i^3 \\ \omega & x = i^3 \\ \psi_{\tilde{S}T_2}(x)i^3 \leq x \leq j^3 \\ \psi_{\tilde{S}T_1}(x)j^3 \leq x \leq k^3 \\ 1 & \text{otherwise} \end{cases}$$



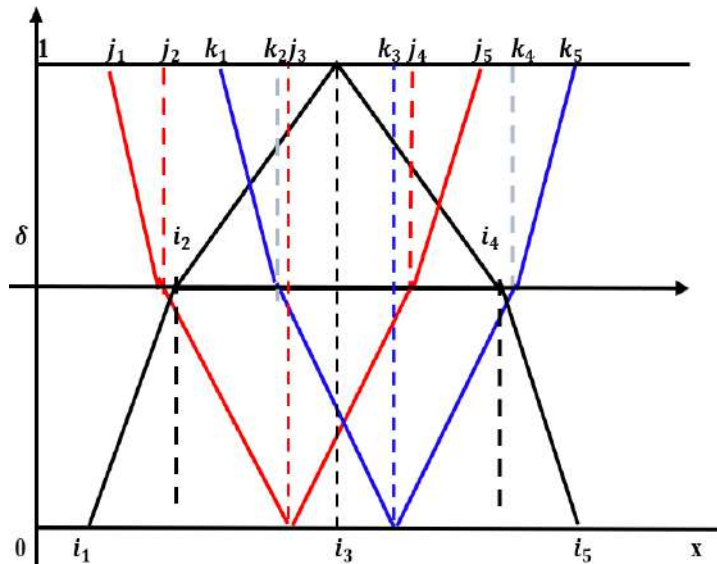


Hema and Rajeshwari

Definition 2.4 Removal area Method for De-Neutrosophication of linear PNN [2]:

Suppose, we consider a linear pentagonal neutrosophic number as follows

$$\tilde{A}_{Blineu} = (i_1, i_2, i_3, i_4, i_5; j_1, j_2, j_3, j_4, j_5; k_1, k_2, k_3, k_4, k_5)$$



The De-neutrosophication value of a linear pentagonal neutrosophic number as,

$$A_{Neu}(\widetilde{D_{Pen}}, s) = \frac{A_{Neu}(\check{P}, s) + A_{Neu}(\check{Q}, s) + A_{Neu}(\check{R}, s)}{2}$$

For s = 0,

$$A_{Neu}(\check{P}, 0) = \frac{\frac{(i_1+i_2)\delta}{2} + \frac{(i_2+i_3)(1-\delta)}{2} + \frac{(i_4+i_5)\delta}{2} + \frac{(i_3+i_4)(1-\delta)}{2}}{2}$$

$$A_{Neu}(\check{Q}, 0) = \frac{\frac{(j_1+j_2)(1-\delta)}{2} + \frac{(j_2+j_3)\delta}{2} + \frac{(j_3+j_4)\delta}{2} + \frac{(j_4+j_5)(1-\delta)}{2}}{2}$$

$$A_{Neu}(\check{R}, 0) = \frac{\frac{(k_1+k_2)(1-\delta)}{2} + \frac{(k_2+k_3)\delta}{2} + \frac{(k_3+k_4)\delta}{2} + \frac{(k_4+k_5)(1-\delta)}{2}}{2}$$

$$A_{Neu}(\widetilde{D_{Pen}}, 0) = \frac{(i_1+i_2+i_4+i_5+j_2+2j_3+j_4+k_2+2k_3+k_4)\delta + (i_2+2i_3+i_4+j_1+j_2+j_4+j_5+k_1+k_2+k_4+k_5)(1-\delta)}{12}$$





Hema and Rajeshwari

Definition 2.5 Accuracy Function Method

Consider a linear pentagonal neutrosophic number as follows

$$\tilde{A}_{Bineu} = (i_1, i_2, i_3, i_4, i_5; j_1, j_2, j_3, j_4, j_5; k_1, k_2, k_3, k_4, k_5)$$

Then,

$$D^{T_{NP_N}} = \left(\frac{i_1 + i_2 + i_3 + i_4 + i_5}{5} \right),$$

$$D^{I_{NP_N}} = \left(\frac{j_1 + j_2 + j_3 + j_4 + j_5}{5} \right),$$

$$D^{F_{NP_N}} = \left(\frac{k_1 + k_2 + k_3 + k_4 + k_5}{5} \right)$$

$$D_{NP_N} = \left\{ \frac{i_1 + i_2 + i_3 + i_4 + i_5}{5}, \frac{j_1 + j_2 + j_3 + j_4 + j_5}{5}, \frac{k_1 + k_2 + k_3 + k_4 + k_5}{5} \right\}$$

$$D_{NP_F} = \frac{D^{T_{NP_N}} + D^{I_{NP_N}} + D^{F_{NP_N}}}{3}$$

Where,

- $D^{T_{NP_N}}, D^{I_{NP_N}}, D^{F_{NP_N}}$ represent the de-neutrosophication of trueness, Indeterminacy, falseness of Pentagonal Neutrosophic number into neutrosophic respectively.
- D_{NP_N} represents the de-neutrosophication of Pentagonal neutrosophic number into neutrosophic number.
- D_{NP_F} represents the de-neutrosophication of Pentagonal neutrosophic number into Fuzzy number.

Replacement Model

Case-1: To find the Replacement cost when maintenance cost increases with time and money value is constant.

Let C be the capital cost of the item

S be the scrap value after the time 't'

f_t be the maintenance cost during the time 't'

Total cost = Capital cost – Scrap value + maintenance cost

Total cost = $C - S + \sum_{t=1}^n f_t$ [if t is discrete]

Average cost A (n) = $\frac{C-S}{n} + \frac{1}{n} \sum_{t=1}^n f_t$ ----- (1)

A (n+1) = $\frac{C-S}{n+1} + \frac{1}{n+1} \sum_{t=1}^{n+1} f_t$

A (n) will be minimum for the value of n, if

$A (n+1) \geq A (n) \leq A (n-1)$

$A (n+1) - A (n) = \frac{1}{n+1} [f_{n+1} - A(n)]$

$\therefore A (n+1) \geq A (n)$

$\Rightarrow f_{n+1} \geq A(n)$ ----- (2)

Similarly $A (n) \leq A (n - 1) \Rightarrow f_n \leq A (n-1)$ ----- (3)

From (2) & (3), we conclude,

1. There is no need to replace the item if the next year operating cost is less than the previous year operating cost.





Hema and Rajeshwari

2. If the next year operating cost is greater than previous year operating cost then replace the item.

Procedure to solve Pentagonal Neutrosophic replacement problem

- If t is a discrete variable,

$$A(n) = \frac{C-S}{n} + \frac{1}{n} \sum_{t=1}^n f_t$$

- Convert the PNN into crisp by using Removal area method and Accuracy function
- Compute T, T_A
- Examine at what period T_A reaches its minimum value, which give the replacement period.

ILLUSTRATION 1:

An Electro mechanical equipment cost Rs.60000 and the owner estimates the operating cost as follows.

AGE	OPERATING COST IN PENTAGONAL (100`S) NEUTROPHIC NUMBER
1	(10 , 20 , 15 , 40 , 35 ; 15 , 20 , 45 , 60 , 20 ; 25 , 30 , 42 , 33 , 40)
2	(12 , 8 , 15 , 20 , 30 ; 16 , 35 , 40 , 20 , 25 ; 15 , 20 , 18 , 26 , 40)
3	(30 , 40 , 10 , 18 , 16 ; 14 , 18 , 25 , 42 , 33 ; 16 , 28 , 42 , 30 , 20)
4	(10 , 20 , 15 , 35 , 40 ; 15 , 35 , 5 , 45 , 25 ; 25 , 20 , 30 , 40 , 60)
5	(5 , 10 , 25 , 40 , 35 ; 25 , 35 , 40 , 20 , 25 ; 22 , 40 , 60 , 80 , 25)

Resale value decreases by 10% of buying price each year. Estimate the best replacement policy?

Solution:

SL. No.	DE-NEUTROPHICATION OF OPERATING COST USING REMOVAL AREA METHOD (100`S)	DE-NEUTROPHICATION VALUE USING ACCURACY FUNCTION(100`S)
1	31.45	30.00
2	22.58	22.66
3	26.45	25.46
4	27.70	28.00
5	34.87.	32.40

REMOVAL AREA METHOD:

YEAR	f_t	$\sum f_t$	S	C - S	T	T_A
1	3145	3145	54000	6000	9145	9145
2	2258	5403	48000	12000	17403	8701.5
3	2645	8048	42000	18000	26048	8682.6
4	2770	10818	36000	24000	34818	8704.5
5	3487	14305	30000	30000	44305	8861

The average cost reaches its minimum value at the end of 3rd year. So the optimal replacement period is at the end of 3rd year with the average cost of Rs.8682.6

ACCURACY FUNCTION METHOD

YEAR	f_t	$\sum f_t$	S	C - S	T	T_A
1	3000	3000	54000	6000	9000	9000
2	2266	5266	48000	12000	17266	8633





Hema and Rajeshwari

3	2546	7812	42000	18000	25812	8604
4	2800	10612	36000	24000	34612	8653
5	3240	13852	30000	30000	43852	8770

The average cost reaches its minimum value at the end of 3rd year. So the optimal replacement period is at the end of 3rd year with the average cost of Rs.8604.

- Pentagonal Neutrosophic replacement problem has been solved using De-neutrosophication technique of removal area method and accuracy function method.
- In both the method the optimal replacement period is at the end of 3rd year. But Accuracy function Method provides least average cost than removal area method.
- Accuracy function method yields best result.

Case-2: Replacement of an item whose maintenance cost increases with time and value of money changes with time

Let \tilde{C} be the cost of the item

$\tilde{C}_1, \tilde{C}_2, \dots, \tilde{C}_n$ be the maintenance lost for n years n = 1, 2, respectively.

Present value of maintenance costs are $\tilde{C}_1 r, \tilde{C}_2 r^2, \dots, \tilde{C}_n r^{n-1}$ where r is discount rate.

The present value of the total expenditure of the item for n years is

$$P(n) = \tilde{C} + \sum_{k=1}^n \tilde{C}_k r^{k-1} \quad \text{----- (1)}$$

If the item is replaced after 'n' years, the new item starts its operation from (n + 1)th year.

∴ The present value of this machine is,
 $(\tilde{C} + \tilde{C}_1)r^n + \tilde{C}_2 r^{n+1} + \dots + \tilde{C}_n r^{2n-1}$ for n+1, n+2, , 2n years

$$\therefore \tilde{C}(n) = \tilde{C} + \sum_{k=1}^n \tilde{C}_k r^{k-1} + r^n [\tilde{C} + \sum_{k=1}^n \tilde{C}_k r^{k-1}] + r^{2n} [\tilde{C} + \sum_{k=1}^n \tilde{C}_k r^{k-1}] + \dots$$

$$\tilde{C}(n) = \frac{\tilde{C} + \sum_{k=1}^n \tilde{C}_k r^{k-1}}{1-r^n} = \frac{P(n)}{1-r^n} \quad \text{----- (2)}$$

$\tilde{C}(n)$ will be minimum if
 $\Delta \tilde{C}(n-1) < 0 < \Delta \tilde{C}(n)$ where $\Delta \tilde{C}(n) = \tilde{C}(n+1) - \tilde{C}(n)$

$$\tilde{C}_{n+1} > \frac{\tilde{C} + \sum_{k=1}^n \tilde{C}_k r^{k-1}}{1+r+r^2+\dots+r^{n-1}} \text{ and}$$

$$\tilde{C}_n < \frac{\tilde{C} + \sum_{k=1}^{n-1} \tilde{C}_k r^{k-1}}{1+r+r^2+\dots+r^{n-2}} \quad \text{----- (4)}$$

i.e. $\tilde{C}_{n+1} < R(n)$ and $\tilde{C}_n < R_{n-1}$

where $R(n) = \frac{\tilde{C} + \sum_{k=1}^n \tilde{C}_k r^{k-1}}{1+r+r^2+\dots+r^{n-1}}$ = Weighted average cost for n years

From (4) we conclude,

1. Replacement is preferred when the operating cost of next year is greater than





Hema and Rajeshwari

Operating cost of previous year.

2. Replacement is not preferred, if the operating cost of next year is less than Operating cost of previous year.

ILLUSTRATION 2 :

The cost of a machine is Rs.5,000 the maintenance and operating costs are PNN and it is zero for the first year and for every year increased by (8, 10, 25, 40, 35 ; 25, 35, 40, 20, 25 ; 22, 40, 60, 80, 25) mentioned in 10's. If the money value is 10% worth every year, find the best period of replacement.

Solution

$$\begin{aligned}
 \text{PV factor at the end of the first year} &= \frac{1}{1+r} \\
 &= \frac{1}{1+0.1} \\
 &= 0.9091
 \end{aligned}$$

On De-neutrosophication of operating cost, using removal area method,

$$\begin{aligned}
 (8, 10, 25, 40, 35 ; 25, 35, 40, 20, 25 ; 22, 40, 60, 80, 25) &\text{ (in } 10\text{'s)} \\
 &= 35 \text{ (in } 10\text{'s)} \\
 &= 350
 \end{aligned}$$

REMOVAL AREA METHOD

Year	Maintenance Cost	PVF	PV Of Maintenance Cost	Total PV	CPVF	Weighted Cost
1	0	1.000	0	5000	1.000	5000
2	350	0.9091	318.18	5318.18	1.9091	2785.7
3	700	0.8264	578.48	5896.66	2.7355	2155.6
4	1050	0.7513	788.86	6685.52	3.4868	1917.37
5	1400	0.6830	956.2	7641.72	4.1698	1832.63
6	1750	0.6209	1086.57	8782.29	4.7907	1821.92
7	2100	0.5645	1185.45	9913.74	5.3552	1851.2

The machine should be replace at the end of 6th year, because it reaches its minimum at the end of 6th year with the average cost of Rs.1821.92

ACCURACY FUNCTION METHOD

Year	Maintenance Cost	PVF	PV Of Maintenance Cost	Total PV	CPVF	Weighted Cost
1		1.000	0	5000	1.000	5000
2	327	0.9091	297.2	5297.2	1.9091	2774.7
3	654	0.8264	540.46	5837.6	2.7355	2134
4	981	0.7513	737.02	6574.68	3.4868	1885.59
5	1308	0.6830	893.3	7467.98	4.1698	1790.9
6	1635	0.6209	1015.17	8483.15	4.7907	1770.75
7	1962	0.5645	1107.5	9590.65	5.3552	1790.90

The Optimal replacement period is at the end of 6th year with the average cost of 1770.75, which is less than the average cost yield by Removal area Method.

- Accuracy function Method provides Optimal Solution.





Hema and Rajeshwari

CONCLUSION

In this paper we have considered the operating cost/maintenance cost as an imprecise case say, pentagonal neutrosophic number. The removal area method as well as Accuracy function Method has been applied to change the PNN into crisp. The Pentagonal Neutrosophic Replacement Problem has been solved for the optimal replacement period in both the cases 1.maintenance cost increases with time and money value remains constant 2.maintenance cost increases with time and value of money changes. On comparing the results in both the cases Accuracy function gives the optimal result than Removal area method.

REFERENCES

1. Arithmetic and Geometric Operators of Pentagonal Neutrosophic Number and its Application in Mobile Communication Based MCGDM Problem"; A Chakraborty, B Banik, S Mondal and S Alam; Neutrosophic Sets and System, Vol 32, p.p-61-79.
2. AvishekChakraborty, ShreyashreeMondal, Said Broumi, "De-Neutrosophication Technique of Pentagonal Neutrosophic Number and Application in Minimal Spanning Tree", Neutrosophic Sets and Systems, Vol.29, 2019.
3. AvishekChakraborty 1, 3, Said Broumi2* and Prem Kumar Singh4,"Some properties of Pentagonal Neutrosophic Numbers and its Applications in Transportation Problem Environment", Neutrosophic Sets and Systems, Vol.28, 2019.
4. Atanassov, K. (1986). "Intuitionistic fuzzy sets". Fuzzy Sets and Systems 20 87-96.
5. Bellman, R.E., 1955. Equipment replacement policy. SIAM Journal Applied Mathematics 3,133-136.
6. S.Broumi and F. Smarandache, "Intuitionistic Neutrosophic Soft Set", Journal of Information and Computing Science, England, UK , ISSN 1746-7659,Vol. 8, No. 2, (2013), pp.130-140.
7. A.Chakraborty, S.P Mondal, A.Ahmadian, N.Senu, D.Dey, S.Alam, S.Salahshour, "The Pentagonal Fuzzy Number: Its Different Representations, Properties, Ranking, Defuzzification and Application in Game Problem", Symmetry,Vol-11(2), 248; doi:10.3390/sym11020248.
8. Chakraborty, A., Mondal, S. P., Alam, S., &Mahata, A. (2020). Cylindrical neutrosophic single-valued number and its application in networking problem, multi-criterion group decision-making problem and graph theory. *CAAI Transactions on Intelligence Technology*, 5(2), 68-77.
9. Chakraborty, A., Mondal, S.P., Alam, S., Dey, A., Classification of trapezoidal bipolar neutrosophic number, de-bipolarization technique and its execution in cloud service-based MCGDM problem. *Complex Intell. Syst.* 7, 145–162 (2021). <https://doi.org/10.1007/s40747-020-00170-3>.
10. Das, S.K., Chakraborty, A. "A new approach to evaluate linear programming problem in pentagonal neutrosophic environment". *Complex Intell. Syst.* 7, 101–110 (2021). <https://doi.org/10.1007/s40747-020-00181-0>
11. P. Kannagi, G. Uthra, "Group Replacement Strategy under Fuzzy Methods", *International Journal of Engineering and Advanced Technology (IJEAT)* ISSN: 2249 – 8958, Volume-9 Issue-155, December, 2019.
12. Pranab Biswas and SurapatiPramanik, "Application of Fuzzy Ranking Method to Determine the Replacement Time for FuzzyReplacement Problem". *International Journal of Computer Applications (0975- 8887)* Volume 25 - No11,July 2011
13. Pranab Biswas and SurapatiPramanik, "Fuzzy Approach to Replacement Problem with Value of Money Changes Time", *International Journal of Computer Application*, 30(10)(2011),28-33.
14. Smarandache, F. (1999). "A Unifying Field in Logics. Neutrosophy: Neutrosophic Probability, Set and Logic". Rehoboth: American Research Press.
15. T S Haque, A Chakraborty, S Mondal and S. Alam, "A New Approach to Solve Multi-Criteria Group Decision Making Problems by Exponential Operational Law in Generalised Spherical Fuzzy Environment"; *CAAI Transactions on Intelligence Technology*, Vol-5(2), pp: 106-114, DOI: 10.1049/trit.2019.0078, 2020.
16. G.Uthra, K.Thangavelu and P.Kannagi, "Optimal Solution of an Intuitionistic Fuzzy Replacement Problem". *IJPAM* Volume 119 No. 9 2018, 223-231.
17. Zadeh, L. (1965). "Fuzzy sets", *Inform and Control* (8) 338-353.





Evaluation of *In vitro* Antiurolithiatic Activity of Ethanolic Extract of *Phaseolus vulgaris* Linn

T. Vinciya^{1*} and A.M. Janani²

¹Assistant Professor, Department of Pharmacology, Dr. M.G.R Educational and Research Institute (Deemed to be University), Chennai, Tamil Nadu, India.

²Assistant Professor, Department of Pharmacology, Dr. M.G.R Educational and Research Institute (Deemed to be University), Chennai, Tamil Nadu, India.

Received: 26 Sep 2023

Revised: 20 Nov 2023

Accepted: 22 Jan 2024

*Address for Correspondence

T. Vinciya

Assistant Professor,

Department of Pharmacology,

Dr. M.G.R Educational and Research Institute (Deemed to be University),

Chennai, Tamil Nadu, India.

Email: veenusvinciya1995@gmail.com



This is an Open Access Journal / article distributed under the terms of the **Creative Commons Attribution License** (CC BY-NC-ND 3.0) which permits unrestricted use, distribution, and reproduction in any medium, provided the original work is properly cited. All rights reserved.

ABSTRACT

To evaluate *in vitro* antiurolithiatic activities of *Phaseolus vulgaris* Linn. The Seeds of Ethanolic extract of *Phaseolus vulgaris* Linn was prepared and arranged in the three different concentrations (10mg/ml, 20mg/ml, and 30mg/ml). *In vitro* antiurolithiatic activity of Ethanolic extract of *Phaseolus vulgaris* Linn through turbidometric and titrimetric method was tested in terms of inhibition of calcium oxalate by nucleation and aggregation and dissolution of calcium oxalate, using the standard drug. Standard drug has high percentage inhibition and dissolution ability and thus Ethanolic extract of *Phaseolus vulgaris* Linn also have a good percentage inhibition and dissolution ability was comparable to standard drug. The study concludes that the Ethanolic extract of *Phaseolus vulgaris* Linn have inhibitory effect on calcium oxalate for nucleation and aggregation assay. It also showed good dissolution of calcium oxalate crystals, so this extract has the good protection against Urolithiasis activity.

Keywords: Antiurolithiatic, Ethanolic, *Phaseolus vulgaris* Linn, Nucleation, Aggregation, Dissolution

INTRODUCTION

The term 'Urolithiasis' comes from the Greek word, ouron means urine and lithos means "stone". Urolithiasis is a condition in which the crystals of stone or formation of calcifications present in the urinary system, mainly in the kidneys or ureters and may also affect the bladder or urethra. Kidney stones are related to an increased risk of chronic kidney diseases, end-stage kidney failure, cardiovascular diseases, diabetes, and hypertension. It has been suggested that urinary calculus could also be a systemic disorder linked to the metabolic syndrome. Urolithiasis is the formation of uneven calculi, or the condition which called as urinary calculi is synonymous with the term

69719



**Vinciya and Janani**

urolithiasis, stones, or crystals. These uneven urinary calculi are produced by deposition of polycrystalline aggregates composed of various amounts of crystalloid and organic matrix. Calculi was in different in size and shape which found anywhere within the tract from kidney to the bladder. Risk factors for crystallization is the level of urinary saturation with estimation to the stone forming constituents like calcium, phosphorus, uric acid, oxalate, cystine, and low urine volume. The mechanism of kidney stone formation involves urinary super saturation, crystal nucleation, crystal growth, and crystal aggregation. *Phaseolus vulgaris*, also known as kidney beans, called Raajmah in India, is a common Indian dish. The seeds of *P. vulgaris* are gaining increasing attention as a functional or nutraceutical food, due to its rich variety of phyto chemicals such as proteins, amino acids, complex carbohydrates, dietary fibers, oligosaccharides, phenols, saponins, flavonoids, alkaloids, and tannins, with potential health benefits. The seeds were claimed to possess diuretic activity and were commonly used in water retention treatment in pregnant women. Studies indicate that seeds of *P. vulgaris* were found to have activities such as enhancement of the bifidogenic, antioxidant, antimutagenic, anticarcinogenic, and antihyperglycemic effects. Our study demonstrated in vitro antiurolithiatic activity of ethanolic seed extract of *P. vulgaris* on CaOx crystallization.

MATERIALS AND METHODS**Collection of plants**

Dried Seeds was collected from the local area around Madurai District, Tamil Nadu (India), in the month of November. . The seeds were coarsely powdered and used for extraction.

Preparation of Ethanolic Seed Extract of Phaseolus Vulgaris

The seed powder (200 g) was macerated with 95% ethanol (1 L) for 24 h at room temperature followed by Soxhlet extraction for 6 h. The extract was concentrated under reduced pressure, and the obtained semisolid mass was stored in an airtight container in a refrigerator.

IN VITRO ANTIUROLITHIASIS STUDIES**Turbidometric method:**

The in vitro anti-urolithiatic activity of the ethanolic extracts was test in terms of inhibition of calcium oxalate nucleation and aggregation in the presence of inhibitors (standard drug and plant extracts) and absence of inhibitors. A UV/Visible spectrophotometer was employed to measure the turbidity changes in each assay. Three different concentrations (10mg/ml, 20mg/ml, and 30mg/ml) of the ethanolic extracts were test in each assay.

Nucleation assay

Solutions of calcium chloride and sodium oxalate were prepared at the concentrations of 5 mmol/L and 7.5 mmol/L respectively in a buffer solution containing Tris 0.05 mol/L and NaCl 0.15 mol/L at pH 6.5. 950 µL of calcium chloride solution was mixed with 100 µL of ethanolic extract at different concentrations (10mg/ml, 20mg/ml and 30mg/ml). Crystallization was formed by adding 950 µL of sodium oxalate solution and the temperature was maintained at 37°C. The optical density of the solution was detected at 620 nm. The rate of nucleation was estimated by comparing the induction time in the presence of the plant extract with that of control. Standard (Cystone) were used as the standard solution. The rate of nucleation was estimated by comparing the induction time in the presence of Standard with that of the control. Percentage inhibition of nucleation was calculated using this following formula below:

$$\% \text{ Inhibition of nucleation} = [(C-S)/C] \times 100$$

Where,

C is the turbidity without extract and

S is the turbidity with extract

Aggregation assay

The ethanolic extract of *Phaseolus vulgaris* influence on calcium oxalate (CaOx) crystal aggregation was resolved through the assay. Calcium oxalate crystals were formed by mixing calcium chloride and sodium oxalate at 50



**Vinciya and Janani**

mmol/L. Both mixers were equilibrated to 60°C in a water bath for 1 h and then cooled to 37°C overnight. The CaOx crystals were harvested by centrifugation and then evaporated at 37°C. The Calcium oxalate crystals were used at a concentration of 0.8 mg/ml, buffered solutions with Tris 0.05 mol/L and NaCl 0.15 mol/L at pH 6.5. The experiments were conducted in the absence and presence of the ethanolic extract after stopping stirring. Standard drugs were used as drug standard solution. The rate of aggregation was estimated using the formula given below:

$$Ir = (1 - (\text{Turbidity sample} / \text{Turbidity control})) \times 100$$

Where, Ir is the percentage aggregation inhibition rate

Titrimetric method

This method was used to evaluate the activity of the ethanolic extracts in dissolving the already formed stones in the kidneys.

Step 1

Preparation of calcium oxalate crystals Solution of Calcium chloride dihydrate which was dissolved in distilled water and Sodium oxalate was dissolved in 10 ml of 2N H₂SO₄, sufficient quantity was allowed to react in a beaker. The resulting precipitate of calcium oxalate which was freed from traces of Sulphuric acid by washing with ammonia solution. Then again it was washed with distilled water and dried at a temperature of 60°C for 4 hours.

Step 2

Preparation of the semi permeable membrane from farm eggs. The semi permeable egg membranes lie in between the outer calcified shell and the inner contents like albumin & yolk. The preparation included the following steps: Apex of eggs was punctured by a glass rod in order to squeeze out the whole inner content. Empty eggs were washed thoroughly with water and placed in a beaker containing 2M HCl solution for an overnight, which caused complete decalcification. Then, the semi permeable egg membranes were washed thoroughly with distilled water, placed in ammonia solution for neutralization of acid traces in the moistened condition for a while and was rinsed with distilled water. Finally, the semi permeable egg membranes were stored in 2% ammonia until used.

Step 3

Estimation of Calcium oxalate by Titrimetry Weighed exactly 1 mg of the calcium oxalate and three different concentrations (10mg/ml, 20mg/ml, 30mg/ml) of ethanolic extract and standard drug were packed in semi-permeable membrane by suturing. They were allowed to suspend in a conical flask containing 100 ml 0.1 M TRIS buffer solution. One group served as negative control (containing only 1 mg of calcium oxalate). Standard was used as a positive control. Conical flask of all groups will be placed in an incubator pre heated to 37°C for 6 hours. Contents of semi-permeable egg membrane from each group will be removed into a test tube. Added 2 ml of 1 N H₂SO₄ and titrated with 0.9494 N KMnO₄ till a light pinkish colour end point obtained. 1ml of 0.9494 N KMnO₄ equivalent to 0.1898 mg of Calcium.

Group I 1ml of CaOx (1mg/ml) + 1ml of distilled water,

Group II 1ml of CaOx (1mg/ml) + 1ml of Standard solution,

Group III 1ml of CaOx (1mg/ml) + 1ml of ethanolic extract of *Phaseolus vulgaris*.

RESULTS AND DISCUSSION**IN VITRO ANTIUROLITHIASIS STUDIES**

Turbidimetry method Nucleation Assay Addition of Sodium oxalate solution in the reaction mixture of Calcium chloride resulted in the formation of numerous Calcium oxalate crystals. The three different concentrations (10mg/ml, 20mg/ml, 30mg/ml) of Ethanol extract and Standard in the reaction mixture produced a percent reduction of calcium oxalate in nucleation. The highest percentage inhibition was obtained from Standard drug at a concentration of 30mg/ml. Percent reduction in size of Calcium oxalate crystals produced by ethanolic extract of *Phaseolus vulgaris* was comparable to that produced by Standard. The results were shown in the Table 1 and Graph 1. Aggregation Assay In the aggregation assay, three different concentrations (10mg/ml, 20mg/ml, 30mg/ml) of Ethanol extract and Standard produced a percent reduction of calcium oxalate. The highest percentage aggregation inhibition was obtained from Standard at a concentration of 30mg/ml. The percentage inhibition of Ethanolic extract of *Phaseolus*





Vinciya and Janani

vulgaris at the concentration of 30mg/ml slightly close to Standard. So, the percent reduction in aggregation produced by Ethanolic extract of *Phaseolus vulgaris* was comparable to that of Standard. The results were shown in the Table 2 and Graph 2. Titrimetry method In dissolution study, the Negative control shows zero dissolution. The three different concentrations (10mg/ml, 20mg/ml, 30mg/ml) of Ethanol extract and Standard of test drugs in the semi permeable membrane produced a dissolution of calcium oxalate. The results finding revealed that Standard drug has high dissolution ability, and thus Ethanolic extract of *Phaseolus vulgaris* also have a good dissolution ability comparable to Standard. The results were shown in the Table 3 and Graph 3.

CONCLUSION

From this study we conclude that the ethanolic extract of *Phaseolus vulgaris* through turbidometric and titrimetric method showed leading inhibition of all phases of calcium oxalate crystallization which include nucleation and aggregation. It also showed good dissolution ability of calcium oxalate crystal. Further conclusion of present study of ethanolic extract of the plant *Phaseolus vulgaris* produce better protection against for urolithiasis activity.

REFERENCES

1. Natarajan P, Balamurugan K, Annapandian V M, Thirupathi M, and Edwin Jose1, Preclinical Evaluation of antiurolithiatic activity of Pistia stratiotes On Sodium Oxalate Induced Urolithiasis, Research Journal of Pharmaceutical, Biological and Chemical Sciences, 2022; 13(1):201-206
2. Manjula K, Pazhanichami K, Rajendran K, Kumaran S, Eevera T. Herbal remedy for urinary stones. Vegetables and human health, Scientific Publishers, 2015: 457-458
3. Alelign, T. and Petros, B. Kidney stone disease: an update on current concepts. Advances in urology, 2018: 1 : 1-12
4. Khan, F., Haider, M.F., Singh, M.K., Sharma, P., Kumar, T. and Neda, E.N. A comprehensive review on kidney stones, its diagnosis and treatment with allopathic and ayurvedic medicines. International Urology and Nephrology, 2019; 7(4): 69-74.
5. Basavaraj, D.R., Biyani, C.S., Browning, A.J. and Cartledge, J.J. The role of urinary kidney stone inhibitors and promoters in the pathogenesis of calcium containing renal stones. EAUEBU update series, 2007; 5(3): 126-136.
6. Pak CY. Prevention and treatment of kidney stones. Role of medical prevention. J Urol 1989;141:798-801.
7. Tang X, Lieske JC. Acute and chronic kidney injury in nephrolithiasis. Curr Opin Nephrol Hypertens 2014;23:385-90.
8. Barros ME, Lima R, Mercuri LP, Matos JR, Schor N, Boim MA, et al. Effect of extract of Phyllanthus niruri on crystal deposition in experimental urolithiasis. Urol Res 2006;34:351-7
9. Niharika, M., Suchitha, N., Akhila, S., Himabindhu, J. and Ramanjaneyulu, K., 2018. Evaluation of in vitro antiurolithiatic activity of Gossypium herbaceum. Journal of Pharmaceutical Sciences and Research, 2018; 10(5): 1236- 1237.
10. Ganeshiah, K. N., UAS, Bangalore, India. Kailash, B. R., ATREE, Bangalore, India. Royal Norwegian Embassy grants. Indian Bio resource Information Network (IBIN), Department of Biotechnology, New Delhi, India. 2021; 127- 132

Table 1: Result of Ethanolic Extract of *Phaseolus vulgaris* on Nucleation Assay

Sample Types	Concentration	% inhibition of Nucleation
Ethanol Extract	10mg/ml	6.21
	20mg/ml	14.32
	30mg/ml	22.14
Standard	10mg/ml	6.11
	20mg/ml	14.21
	30mg/ml	24.31





Vinciya and Janani

Table 2: Result of Ethanolic Extract of *Phaseolus vulgaris* on Aggregation Assay

Sample Types	Concentration	% inhibition of Aggregation
Ethanolic Extract	10mg/ml	27.21
	20mg/ml	31.32
	30mg/ml	42.14
Standard	10mg/ml	31.11
	20mg/ml	37.21
	30mg/ml	42.31

Table 3: Result of Ethanolic Extract of *Phaseolus vulgaris* on Dissolution study

Sample Types	Concentration	% inhibition of Dissolution
Ethanolic Extract	10mg/ml	22.21
	20mg/ml	41.32
	30mg/ml	46.14
Standard	10mg/ml	31.11
	20mg/ml	47.21
	30mg/ml	52.31

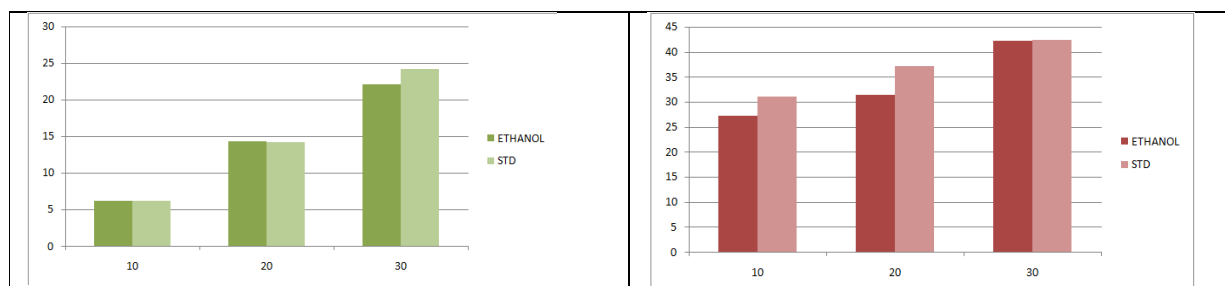


Fig:1 Result of Ethanolic Extract of *Phaseolus vulgaris* on Nucleation Assay

Fig 2: Result of Ethanolic Extract of *Phaseolus vulgaris* on Aggregation Assay

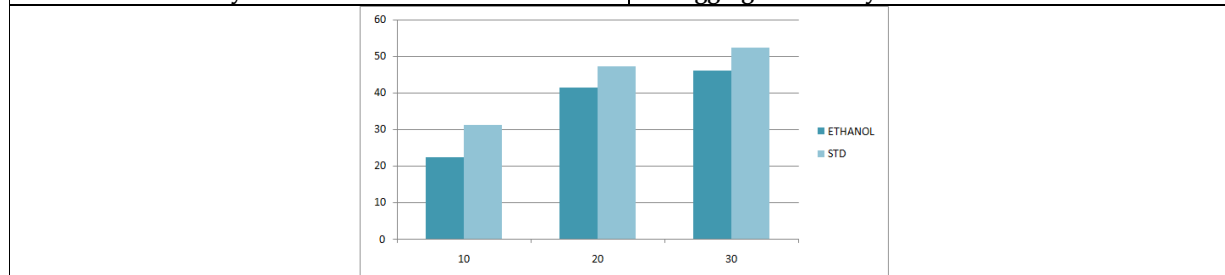


Fig 3: Result of Ethanolic Extract of *Phaseolus vulgaris* on Dissolution study





Research on Quick Bills: Web based Billing Software

Ritam Podder¹, Tulika Paul¹, Shreya Bose¹, Gourav Shaw¹, Susmita Das¹, Sk Asfaq Ahamed², Indranil Sarkar³, Sandip Roy^{4*} and Rajesh Bose⁴

¹Student, Department of Computational Sciences, Brainware University, West Bengal, India

²Student, Department of Computer Science and Engineering, JIS University, West Bengal, India

³Assistant Professor, Department of Computer Applications, Guru Nanak Institute of Technology, West Bengal, India

⁴Professor, Department of Computer Science and Engineering, JIS University, West Bengal, India

Received: 13 Oct 2023

Revised: 20 Nov 2023

Accepted: 05 Feb 2024

*Address for Correspondence

Sandip Roy

Professor,

Department of CSE

JIS University,

West Bengal, India



This is an Open Access Journal / article distributed under the terms of the **Creative Commons Attribution License** (CC BY-NC-ND 3.0) which permits unrestricted use, distribution, and reproduction in any medium, provided the original work is properly cited. All rights reserved.

ABSTRACT

This article designs a billing system for online non-E-Commerce business management. Our application is fully customizable for clients. This billing solution lets our client work from home or anywhere with a stable internet connection. A basic system that lets them open panels and administer the business online is all they need. Admin can access all panels and view daily progress reports and a complete work history. By managing a major firm autonomously, they can track their operations. Our application has stock, user, and admin panels. The goal is to automate its manual system with computerized hardware and comprehensive computer software to save essential data and information for a longer time with easy access and change. They can track staff activity. The business owners can give their employees IDs and passwords to the web-application. Employees can only access their allocated modules; all others are hidden. If an employee misbehaves, they can sum up their work by expense. The project focuses on managing for performance and client service. The administrator can use this Node JS app anytime, anywhere. Clients might upload it to any cloud server. The online billing system streamlines the manual system by using computerized hardware and robust software to meet their needs and store vital data and information for extended periods with easy access and manipulation. The necessary hardware and software are easily accessible. We want our clients to run their businesses more easily and profitably. With a few mouse clicks, they can access every part of their business from home or on vacation.

Keywords: billing system, non-E-commerce business, Node JS-built application, EDI, AWS.



**Ritam Podder et al.,**

INTRODUCTION

Billing software helps businesses send and receive payments from clients and partners. Billing software improves efficiency and reduces errors by automating document preparation and other repetitive tasks. It streamlines customer product and service monitoring, invoice production and communication, and payment processing. This article discusses business-specific billing software. Custom invoices let you customize and brand invoices. Companies and individuals bill for goods and services. Designed to produce product and service invoices. The billing process is chaotic due to changing client expectations, real-time transactions, and remote activities. The underlying causes can vary, ranging from an assortment of inadequate tools that fail to address the challenges faced by your finance team, to outdated software solutions that hinder business growth [1]. All your billing issues can be solved with tailored billing software. Merchants previously tracked sales and inventory using laborious ledger entries. Bills are useful for expense control, strategic spending, and business improvement beyond transaction tracking. Technology made manual bill management digital. Initially, a basic billing management system was introduced where software was utilized on computers to generate and print bills [2]. Only authorized administrators could record purchases, update personnel information, and change prices in databases. Databases sorted and ordered items. Specialized software tracks time and bills and updates customers on their purchases. Billing software tracks project or client spending, personnel hours, and product quantities [3]. Bills capture consumer purchases. It helps keep corporate records and track valuable acquisitions. Bill production, analysis, and printing must be streamlined with a billing system. [1] Medieval merchants kept handmade records of sales and goods, which led to billing systems. Bills enable firms to monitor spending, allocate resources, and drive improvement beyond transactional paperwork.

Technology transformed paper-based bill management into digital systems. Computer-generated and printed bills were first offered with basic billing management software. The system simply allowed administrators to record and charge acquired products, manage personnel data, and change prices using database operations. For effective organization, the database categorized goods. [2] This software tracks time and bills and updates customers on their purchases. Billing software could track labor hours, product quantities, and project or customer expenses. [3] Most billing software applications can create billing reports. These reports can display information such as hours worked, expenses incurred, how much to bill customers, and which customers owe how much money for which goods, total investment, and total income of the month. Few examples of billing management systems are: -

- i) Sage Timeslips
- ii) Intuit QuickBooks Time
- iii) Billing Tracker and kBilling [3]

This program lets you customize non-linear workflows and analytics to meet your needs. Your product offers, pricing methods, and client preferences may necessitate additional billing capabilities. A flexible billing solution is needed to handle monthly, semi-annual, annual, or bespoke payment schedules. Customized invoices that include all relevant details and can be updated periodically are needed for every firm. The app creates party and amount master data and allows offline or online backups. Data extraction for tax return filing and other uses is simplified, assuring GST compliance. The system generates reports on several topics, saving time and money and improving analysis. Online payments and reconciliation are simplified by barcode functionality. Automated bill and invoice production uses pre-existing formats and client data to process invoices faster and personalize them easily, saving time and money.

After installing the software, unauthorized use or inaccurate billing can be prevented. Invoicing responsibility is also ensured. Billing systems automate the documenting of products and services, reducing errors and overheads in accounting and report preparation. Online invoicing streamline payments and allow complete traceability. For single-transaction transactions, bills are usually used for documentation. Because bills focus on prices and taxes, they are shorter and less thorough than invoices. This is frequent in restaurants, pharmacies, beauty salons, and other in-person retailers. Credit-based or recurring product sales often require invoices. Businesses use invoices instead of



**Ritam Podder et al.,**

bills when customers don't pay immediately. Payment terms, due dates, contact information, detailed product descriptions, and more are included in invoices. Modern automated companies where computers execute instructions require good coordination between people, things, and computers.

Related Work**Motivating Examples**

Internet usage and proliferation have led to many electronic applications. Electronic commerce is useful for individuals, businesses, retail, and bulk suppliers. Electronic commerce allows shoppers and bankers to shop and transact 24/7, without vacations. It avoids intermediaries, physical inventory, and more. E-commerce also lets shoppers compare products within a range, evaluate their features and performance, and make informed choices. E-commerce has created new financial needs that traditional payment systems struggle to meet. Given this, all parties are actively studying electronic payment systems and tackling digital currency and e-payment concerns.

EFT was one of the first kinds of e-commerce. It enabled secure and efficient financial institution fund transfers. Later, EDI was developed to facilitate inter-business transactions. Early EDI systems used sophisticated, expensive networks to construct and maintain. The widespread adoption of EDI fell short. However, Internet technologies and sophisticated cryptography allowed e-commerce across the public network—the Internet. The World Wide Web hastened this development. The WWW accelerated e-commerce and broadened its applications [4]. E-commerce includes several activities, including investor relations websites. Information technology is used to improve communication and transactions with all organization stakeholders. Customers, suppliers, regulators, financial institutions, managers, employees, and the public are stakeholders. E-commerce is a major commercial transformation that requires a strategic approach to capitalize on new Internet technology. Corporate and e-commerce strategies must be aligned. In general, e-commerce improves organizational effectiveness through computer networks.

By adopting e-commerce, companies can boost profits, market share, customer service, and product delivery. E-commerce includes all electronic contacts between an organization and its stakeholders—those who shape the organization's destiny. [5]. Certainly! The four buyer-seller e-commerce application categories are summarized here:

A. B2C: Buyers are consumers and sellers are businesses in this sort of e-commerce. Electronic retailing or consumer-oriented e-commerce mimics traditional retailing. Smaller payments, short relationships, and lesser transaction volumes characterize B2C transactions.

B. Business-to-Business (B2B): B2B e-commerce includes two businesses, not individuals. Both vendor and buyer are businesses. B2B e-commerce has high volumes of goods traded, pre-existing agreements or contracts, and more authorization, taxation, documentation, and information exchange than B2C.

C. Consumer-to-Consumer (C2C): Sellers and buyers are consumers. C2C e-commerce benefits from online auctions. C2C transactions include people buying and selling goods and services.

D. Consumer-to-Business (C2B): C2B e-commerce is growing. Customer needs for a product or service are sent to an e-commerce site in this application. E-commerce sites search the Internet for websites that meet these parameters and return the results to customers.

These four categories help explain e-commerce applications based on buyer-seller relationships [6].

Online Billing Software

Corporate law departments are rapidly adopting online billing. Recent surveys show that 15% of these agencies require electronic bills from their law firms and 15% are contemplating it. Corporate clients have likely requested more electronic bill submission from law firms. Lawyers must choose electronic billing and matter management systems carefully since they might have beneficial or negative effects. Electronic billing is not new; some consumers have been paying their bills online after getting paper invoices by mail. Electronic bill presentment is new to electronic billing [4]. Billers post consumers' statements online for viewing and electronic payments. Phone and utility companies are shifting their focus to bill presentment and payment services as the internet grows. This solution turns billing centers into revenue centers and personalizes services. Cross-selling ads are possible since





Ritam Podder et al.,

billers and payers can communicate directly. It also decreases paper-based billing costs, allowing customers to receive and pay bills on their computers [5].

Computers generated and printed invoices, and only the administrator could use database operations to record and invoice purchased items, personnel details, and pricing changes. The software was created to manage time, billing, and customer communications. Billing software tracks labor hours, product sales, and project or client expenses [6]. Most billing software can generate detailed reports. These reports can contain hours worked, expenses, client billing, outstanding balances, total investments, and monthly income. Billing software organizes and manages products in a database.

MATERIALS AND METHODS

System Flow

In software engineering, a system flow diagram shows data flow. In multiple steps, the diagram shows where the system receives input and outputs. The flowchart illustrates the steps as boxes with arrows arranging them. A model for solving the problem is shown below. Process and program analysis, design, documentation, and control use flowcharts [7]. In 1921, Frank and Lillian Gilbreth presented "Process Diagrams: First Steps in Finding the One Best Way to Do a Job," which introduced the flow process chart [8]. Art Spinanger, a 1944 Mogensen graduate, designed Procter and Gamble's Intentional Methods Change Program with the tools. Another 1944 graduate, Ben S. Graham, director of Formcraft Engineering at Standard Register Industrial, created a multi-flow process diagram to show various documents and their interactions [9]. ASME established "ASME Standard: Operation and Flow Process Charts" in 1947 using Gilbreth's symbols [10]. In 1949, Douglas Hartree explained that Herman Goldstine and John von Neumann invented the computer program flowchart [11]. IBM developers confirmed its modern description [12]. in von Neumann's Collected Works [13]. Goldstein and von Neumann's unpublished report "Planning and Coding Problems for an Electronic Computing Instrument, Part II, Volume 1" (1947) contains their original programming flowcharts [14]. Build a Customize Online Billing Software app. Admin, Stock, and User Panels make up this software. Our idea mimics a business's computerized application handling. The stock can manage the warehouse, store stock information, produce barcodes, bills, transit bills, and purchase products. Create receipts, analyze credit card history, and add charges and refunds. The admin should have access to stock, users, cash, sale, refund, transit, and purchase records, and an account summary. The administrator can hire stock and user managers [15]. The admin can access all his assets.

- We customize online billing software to meet client needs. Our software has three panels:
- The customer can handle everything in the Master Admin Panel, including stock and user panels. They can choose who handles the stock panel and the user panel and relocate personnel across stores. The financial statement shows how many assets have ledgers, credit, refund, transportation, purchase, and spending history, and invoices. Stock records allow them to verify product quality. They can see all worker work information. Each product's cost can be estimated [16].
- The Stock Panel enables clients to manage their warehouse and stored items. Clients can order and track products with invoices to identify missing items. They can produce bills and barcodes for huge orders. They can also track how many products are shipped to which locations and how many are in stock across numerous branches. They can also set product prices, including discounts. All business assets are under their control. Customers may have different commodities to manage, hence the stock panel menu is adjustable. We can develop panel menus according client want [17,18].
- Store/Shop Panel: Cashier calculates product pricing and generates receipts for buyers. Products are priced from the stock panel, with discounts if available. The cashier must select the product or its unique number to generate the name and quantity of each good, and our system will add up the amount to generate a receipt for the buyer. GST can also be chosen by bill amount. GST types are GSTR1, GSTR2, and GSTR3B. Creditors and Debtors modules track customers' payment statements. They can record expenses and refunds.





Ritam Podder et al.,

Proposed Design

To develop Customise Online Billing Software app. This software has Admin, Stock, and User Panels. Our project largely replicates a business's computerized application handling. The stock can manage warehouse and store information, create barcodes, bills, transit bills, and purchase things. Users can produce receipts, analyse credit card history, and add charges and refunds. Stock, users, cash, sale, refund, transportation, and purchase records, and a complete account summary should be available to the admin. Administrators can hire stock and user managers. All assets are accessible to Admin. The administrator can use this Node JS app anytime, anywhere. The AWS upload occurred. The online billing system automates the manual system with computerized hardware and comprehensive software, meeting their needs and allowing them to store their important data and information for a longer time with easy access and manipulation. The essential hardware and software are easily available and easy to use. We want our clients to run their businesses more easily and profitably. With a few mouse clicks, they can access every part of their business from home or on vacation. Online billing software is customizable software where we will create the software as per client's requirements. Our software consists of three panels – Master Admin, Stock, and User.

Master Admin Panel

An admin panel lets application, website, or IT system administrators manage platform aspects. They can adjust settings, control access, change content, and manage system functions. Administrators can check the platform's status and complete their duties through the admin panel. Besides technological and administrative tasks, admin panels aid corporate operations. The panel lets administrators manage client accounts, handle enquiries, and process transactions. The admin panel lets administrators handle many technical and operational platform duties. Fig. 3 shows Admin Panel Data Flow Diagram.

1. **Authentication/Admin Login:** This page requires the admin to connect with their admin-provided username and password. The admin must provide their username and password to login to this page. The admin can view the password field's actual value by clicking the show me check box, which may help them login to the Admin Panel.
2. **Warehouse Manager:** Here, admins can quickly add warehouses. You can search any warehouse using the search box and get an Excel, PDF, or CSV list of all warehouses to print.
3. **Store Manager:** Admins can easily add stores here. You can search any store using the search box and get an Excel, PDF, or CSV list of all warehouses to print.
4. **Product Manager:** The Product Managers page lets users manage company names, product sizes, and other data.
5. **How to add Company Product and manage all company names?**
 - a. Click Add Company to launch the Add Company form and add your company info. Add n firm names at once here.
 - b. Clicking Company manager opens a modal where you can simply display the company names you added. This modal lets you search and erase corporate info.
6. **How to add Product size and manages all those data?**
 - a. Click on Add Product size then open a product size modal. Here you can upload your product size data through that forum.
 - b. After clicking Product Size Manager, a modal will appear where you can search and delete product size data.
7. **How to Add Product and manage all those data?**
 - a. Click Add product to easily add multiple products, including company and product size, and find all the product details you successfully entered on your system in the mother table of this page. You can also search your system and add profit details.
 - b. You can search your product by the given search box and you able to delete a particular product data by clicking trash button.
8. **Cost Manager:** Here, the admin may easily add the detailed cost of every product, modify product data, and search for product costs using the search box.
9. **Agent Manager:** This page was under maintenance.





Ritam Podder et al.,

10. **System History:** From this page here will show the user and the admin what did the work and when through a list and can search any work details through the search box.
11. **Support Section:** From this section, if any problem creates using the software, then you can contact the developers of this software.
12. **Employee Manager:** From this section, admin can easily add, edit, and remove the employees' details.
13. **Add Stock Manager:** From this page admin can create the accounts of stock managers and can remove also.
14. **Add Store Manager:** From this page admin can create the accounts of store managers and can remove also. The admin can be able to transfer the managers for one shop to another shop.
15. **Quality Product Stock:** This page will show the list of quality products with proper product worth details.
16. **Quality Product Transfer History:** Here the admin can be able to transfer the product details from one shop to another.
17. **Damage Product Stock:** This page was under maintenance.
18. **Damage Product Transfer History:** This page was under maintenance.
19. **Assets:** Here you can get the total product value based on its basic pricing and the all-product list of a warehouse and store. Also, can create a PDF.
20. **Ledger:** All data will be displayed professionally on this page. Admins can download Excel, PDF, and CSV files and make photocopies.
21. **Cash History:** This page will show all the receipts which are paid in cash and can get Excel, PDF, and CSV file of it and can get print out of it.
22. **Bank History:** This page was under maintenance.
23. **Journal:** This page was under maintenance.
24. **Sale History:** This page lists sold items. If desired, admin can download Excel, PDF, and CSV files and make photocopies.
25. **Credit Pay History:** This page displays all credited receipts. Admins can download Excel, PDF, and CSV files and make photocopies.
26. **All Involves:** This page lists sold products. Admins can download Excel, PDF, and CSV files and make photocopies.
27. **Refund History:** This page will show the list of all refunds. Admin can be able to download Excel, PDF, CSV files of it and they can also be able to generate photocopy of it, if they want.
28. **Wholesale Account History:** This page was under maintenance.
29. **Transit History:** This page displays transport transmits reports. Admins can download Excel, PDF, and CSV files and make photocopies.
30. **Purchase History:** Complete purchase details are on this page. Admins can download Excel, PDF, and CSV files and make photocopies.
31. **Expenses History:** This page will show all the list of expenses. Admin can be able to download Excel, PDF, CSV files of it and they can also be able to generate photocopy of it, if they want.
32. **Total Account Summary:** The money transfer details will appear here. Admins can download Excel, PDF, and CSV files and make photocopies.
33. **Edit Account:** The form on this page lets admins change their passwords. Show the alert box if the strong password criteria cannot be met.

Stock Panel

Users must provide their administrator-issued ID and password to access the stock panel. This panel manages warehouses and their contents. Fig. 5 shows Stock Panel Dataflow Diagram.

1. **Authentication/User Login:** The stock manager must login using their admin-provided username and password on this page. Portal managers must enter their username and password to login in this panel. By clicking the show, me check box, the portal manager can view the password field's actual value, which may help stock managers login.
2. **Home Page:** The Home page of this stock panel lists all page shortcut buttons. Users can easily jump to the pages they need to finish their work swiftly.





Ritam Podder et al.,

3. **Product Manager:** The Product Managers page lets users manage company names, product sizes, and other data.
4. **How to add Company Product and manage all company names?**
 - a. Click Add Company to launch the Add Company form and add your company info. Add n firm names at once here.
 - b. Clicking Company manager opens a modal where you can simply display the company names you added. This modal lets you search and erase corporate info.
5. **How to add Product size and manages all those data?**
 - a. Add Product size opens a product size modal. This topic lets you upload product size data.
 - b. You may search and delete product size details in the Product Size Manager modal after clicking on it.
6. **How to Add Product and manage all those data?**
 - a. Click Add product to add many products at once, including company and product size, then search your system from the mother table of this page to see all the product details you entered.
 - b. Search for your product in the search window and delete it by clicking trash.
7. **Existing Warehouse Stock:** Search for your product in the search window and delete it by clicking trash.
8. **Existing Damage Product Stock:** This Page was under maintenance.
9. **Transfer Damage Product to shop:** This page was under maintenance.
10. **Transit Manager:** Search for your product in the search window and delete it by clicking trash.
11. **Purchase Product:** The things you buy from your firm are promptly added to your warehouse after you submit your purchase form.
12. **Purchase Product History:** Here you can easily find out the purchase history of each purchase report and you can generate a receipt from this page.
13. **Transfer Products:** You may quickly transfer products between warehouses and storefronts from this section. You may also view all warehouse and shop product data in one place. Choose your products to search.
14. **Barcode Generation:** Here you can create your own product barcode and easily print them in a very well.
15. **Assets:** You may obtain the total product worth as a basic price of a warehouse's products, as well as its product list and generate a PDF file.

Store/Shop Panel

Using this technique, the cashier calculates prices and issues receipts. Product prices are based on stock panel data, including discounts. The cashier must choose the product or enter its number to print a receipt. The system will then get the product name and quantity and calculate the total cost. Fig. 7 shows Store/Shop Panel Data Flow Diagram.

1. **Receipt Generator:** Users can quickly add and remove products from their carts here. The user can quickly retrieve the product payment receipt from here, with full and credit payment options. A PDF receipt will be sent after payment.
2. **Damage Product Receipt:** This page was under maintenance.
3. **Receipt History:** From this page you will find the list of all receipts and you can search any receipt through the search box.
4. **Credit Pay History:** From this page you will find the list of all credited receipts and you can search any receipt through the search box.
5. **Add Expenses:** Here the user can add all the expenses of the shop for help the all-total calculation.
6. **Make Refund:** From this section, if any product will return, then there will make sure for refund the products.
7. **Refund History:** From this page you will find the list of all refunds and you can search any refund story through the search box.
8. **Edit Accounts:** Here the user can easily update their password with the form of this page. And show the alert box if the criteria cannot be fulfilled you make a password.



**Ritam Podder et al.,****Future Scope**

In a nutshell, it can be summarized that the future scope of the project circles around maintaining information regarding:

- Damage Product Management with Cost
- Agent Commission
- Insert expiry date of products

The above points represent improvements that can be made to increase the usability and usability of this project. Today it can be seen that trading is versatile, that means there is scope to introduce a way to maintain the online invoicing system. Enhancements can be made to preserve all panels.

We have left all options open so that if there is any future user request to improve the system, it can be implemented. Finally, we would like to thank everyone who directly or indirectly participated in the development of the system. We hope that the project will fulfil the purpose for which it is developed here, based on the success of the process.

CONCLUSION

Our research is just a modest venture to meet their project work management needs. This package proves to be a powerful package that fulfils all the requirements of running a business. The goal of software planning is to provide a framework that allows management to make reasonable estimates made within a limited time frame at the beginning of a software project and should be updated regularly as the project progresses.

At the end it is concluded that our application can be completely customize based on client's requirement. They can generate professional ledger. Our application can do cost estimation, manage stock with transit and generate barcodes. It is useful for multi-branch and keeps data backups with all transaction history.

ACKNOWLEDGMENTS

We express our heartfelt gratitude to all those individuals with whom we have had the privilege of collaborating on this project. Every member of our team has offered invaluable personal and professional guidance, imparting profound knowledge about scientific research and life as a whole.

REFERENCES

1. S.Hasan, "POS System (Shoe Retail System) Documentation", November 2015.
2. M. Takavingofa, "Manzlee Retail Management System", Great Zimbabwe University, May 2006,
3. P.Chatterjee, R.Bose, S. Banerjee, S. Roy, Enhancing Data Security of Cloud Based LMS. Wireless Personal Communications. 2023 May;130(2):1123-39.
4. T. Rob, "Choosing an E-Billing System", published in I L T A, December, 2005.
5. Assimakopoulos NA, Riggas AN, Kotsimpos GK. A systemic approach for an open internet billing system. Department of Informatics, University of Piraeu. 2015.
6. R. Bose, H. Mondal, I. Sarkar, S. Roy, "Design of smart inventory management system for construction sector based on IoT and cloud computing", e-Prime-Advances in Electrical Engineering, Electronics and Energy, 2022 Jan 1; 2:100051.
7. B. Mukhopadhyay, R. Bose, S. Roy, R. Dutta, H. Mondal, "IMPLEMENTATION OF BARCODES IN COMMERCIAL AND TECHNICAL ASPECTS", Shodhsamhita Journal, 2021, 8 (9), 107-110.
8. Frank Bunker Gilbreth, Lillian Moller Gilbreth (1921) "Process Charts" (PDF). Archived from the original on 2015-05-09. Retrieved 2016-05-06. American Society of Mechanical Engineers.
9. Graham, Ben S. Jr. (10 June 1996). "People come first". Keynote Address at Workflow Canada, 1996 Jun 10.
10. American Society of Mechanical Engineers (1947) ASME standard; operation and flow process charts. New York, 1947. (online version).





Ritam Podder et al.,

11. Hartree DR. *Calculating instruments and machines*. Cambridge University Press; 2012 Sep 27, p.112.
12. Bashe CJ, Johnson LR, Palmer JH, Pugh EW, editors. *IBM's early computers*. MIT press; 1986 May 19.
13. Goldstine, Herman, *The Computer from Pascal to Von Neumann*. Princeton University Press, 1972, pp.266–267. ISBN 0-691-08104-2.
14. Taub, Abraham, *John von Neumann Collected Works*, Macmillan, 1963, Vol. 5, pp. 80–151.
15. S. Singh, "Emergence of Payment Systems In The Age of Electronic Commerce: The State of Art ", *Global Journal of International Business Research*, 2009, Vol, 2, No, 2.
16. T.R. Watson, B. Pierre, P.F. Leyland and Z.M. George, "ElectronicCommerce:The Strategic Perspective", Creative Commons Attribution 3.0 License, 2007.
17. A.R.A. Media, "Design and Implementation of SET Enabled E-commerce System", In a computer and software engineering department of the University of AL-mustansiriya, 2005.
18. S.K. Nayak, A. Dutta, S. Bhowmick, S. Ghosh, S.K. Jha, R. Bose, S. Roy, "Implementing an Structural Prototype of Emergency Services in Web-Application", *International Journal Of Engineering And Computer Science*, 2021 Aug;10(8).

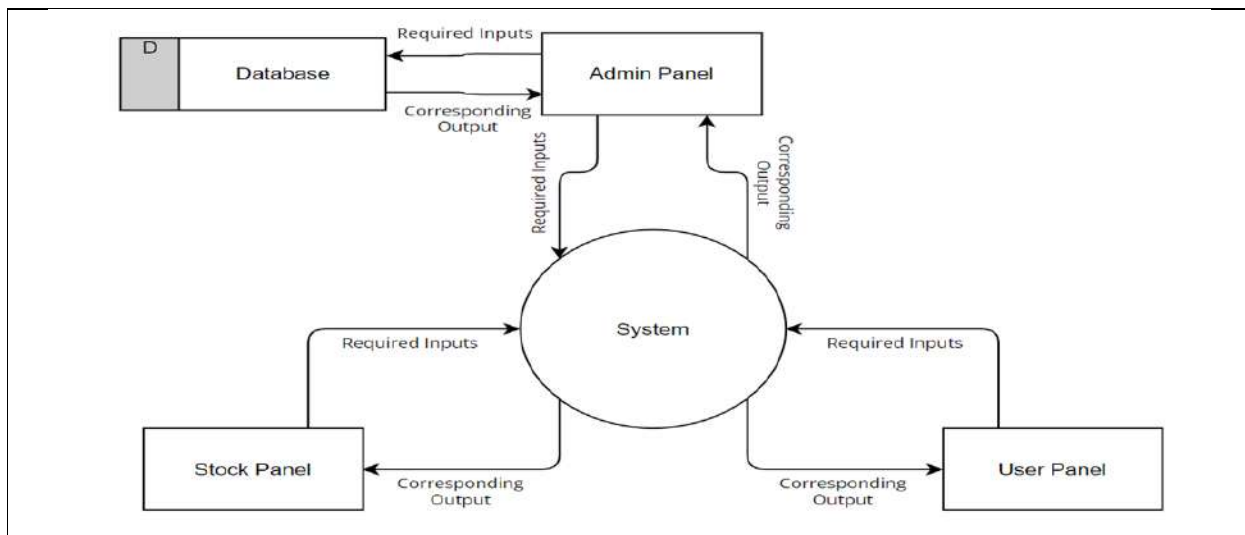


Fig.1. System Outlook *In every panel the account user can change their password

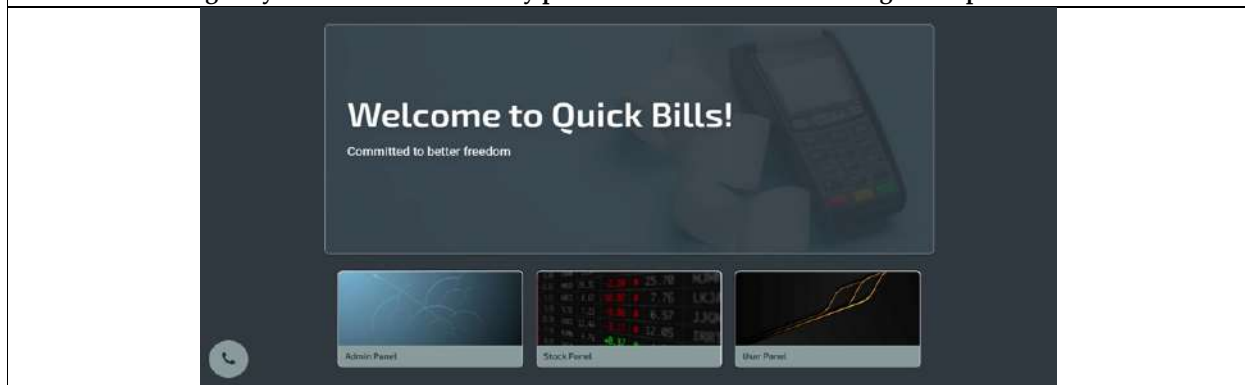


Fig. 2. Software Outlook





Ritam Podder et al.,

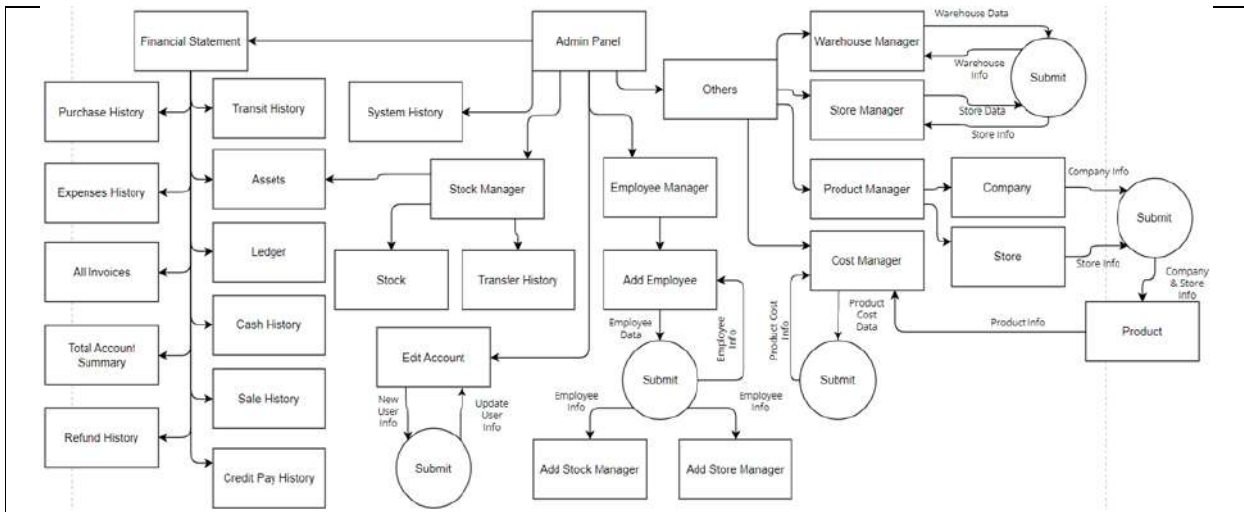


Fig. 3. DFD Level 1 of Master Admin

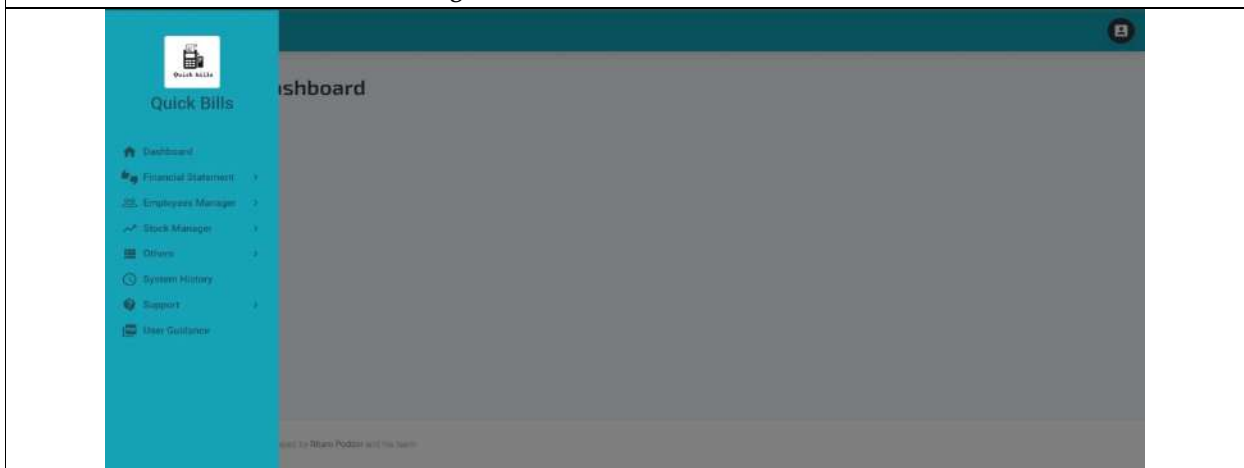


Fig. 4. Outlook of Master Admin Panel

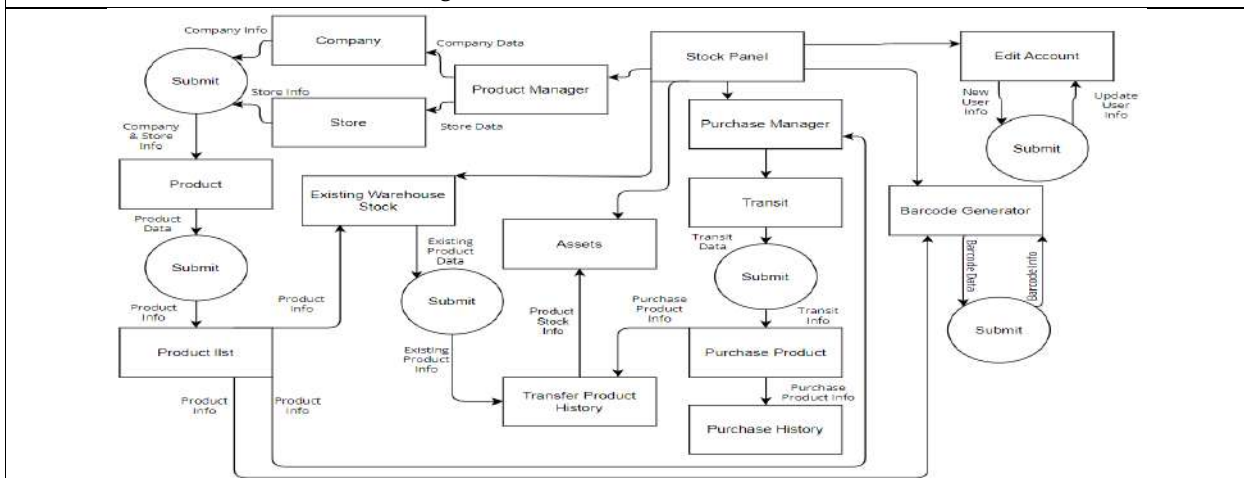


Fig.5. DFD Level 1 of Stock Panel





Ritam Podder et al.,

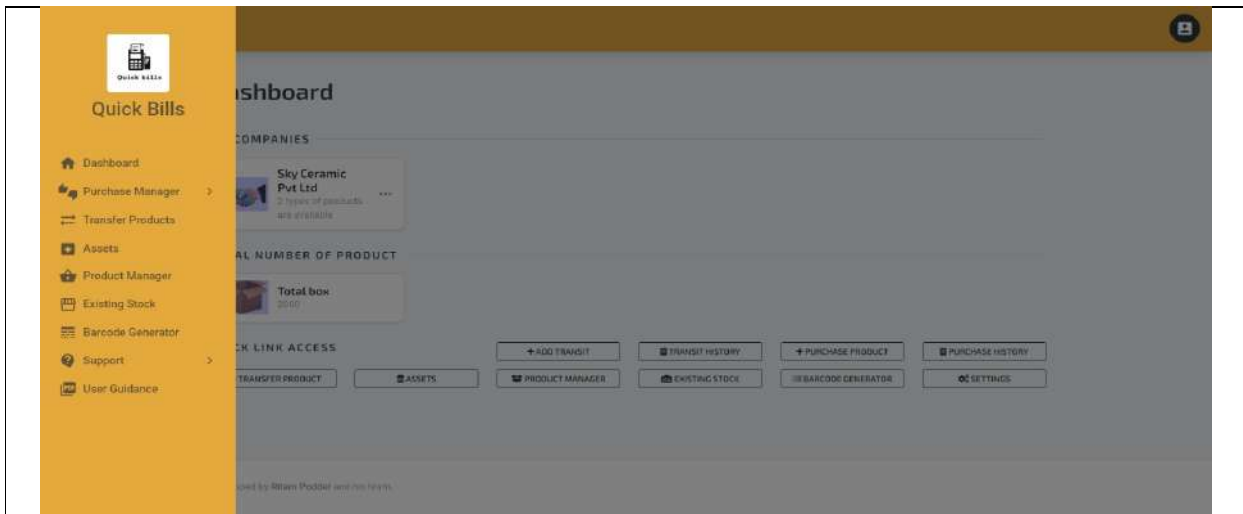


Fig. 6. Outlook of Stock Panel

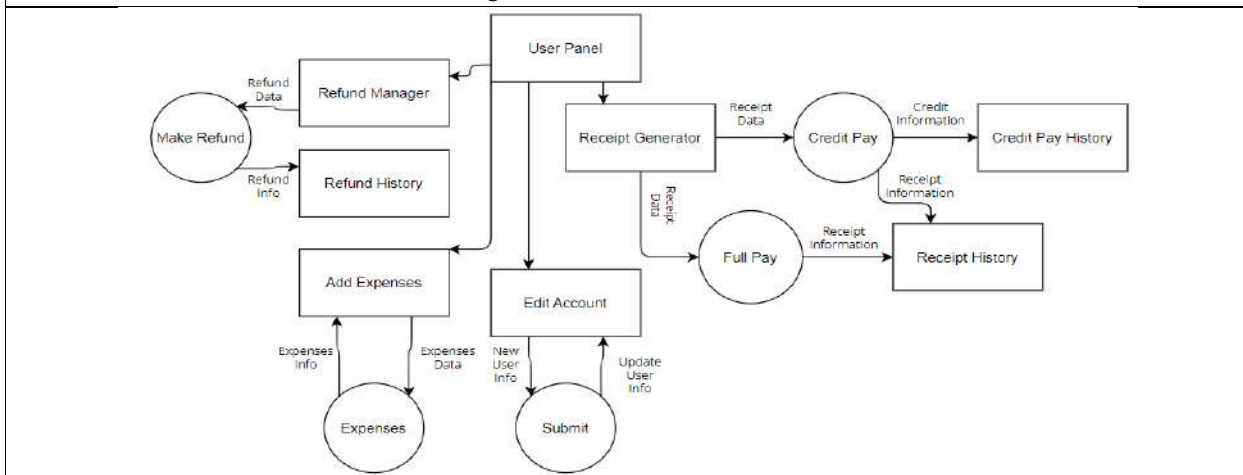


Fig. 7. DFD Level 1 of Store/Shop Panel

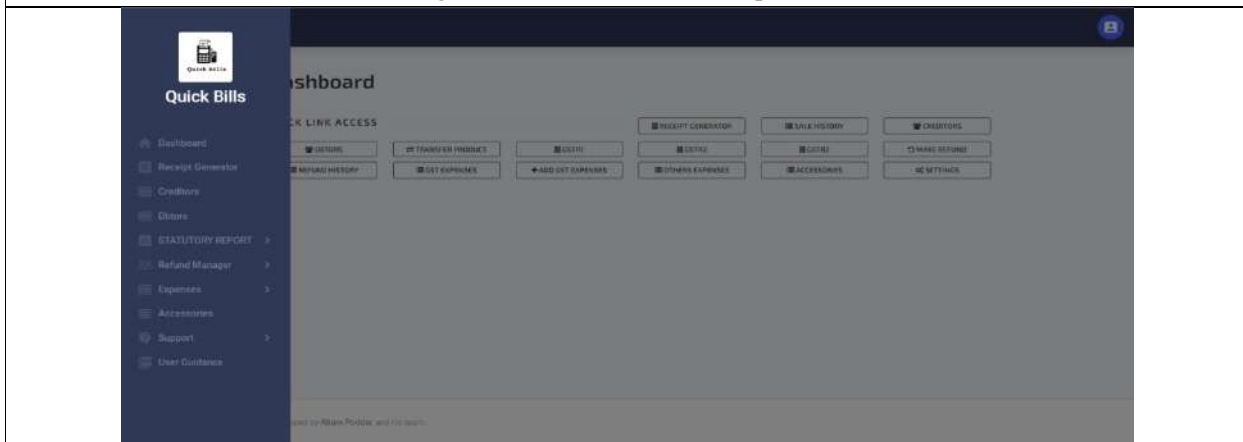


Fig. 8. Outlook of Store/Shop Panel





Neutrosophic Pre Star Generalized b-Closed Set in Neutrosophic Topological Spaces

I.Aruna Glory Sudha^{1*} and S. Zion Chella Ruth²

¹Research Scholar, (Reg. Number: 21212152092002), Department of Mathematics, Nazareth Margoschis College, at Pillaiyanmanai, Nazareth (Affiliated to Manonmaniam Sundaranar University, Abishekapatti, Tirunelveli) Tamil Nadu, India.

²Assistant Professor, Department of Mathematics, Nazareth Margoschis College at Pillaiyanmanai, Nazareth (Affiliated to Manonmaniam Sundaranar University, Abishekapatti, Tirunelveli) Tamil Nadu, India.

Received: 10 Oct 2023

Revised: 18 Nov 2023

Accepted: 19 Jan 2024

*Address for Correspondence

I. Aruna Glory Sudha

Research Scholar, (Reg. Number: 21212152092002),

Department of Mathematics,

Nazareth Margoschis College, at Pillaiyanmanai,

Nazareth (Affiliated to Manonmaniam Sundaranar University, Abishekapatti, Tirunelveli)

Tamil Nadu, India.

Email: sudhaagers@gmail.com



This is an Open Access Journal / article distributed under the terms of the **Creative Commons Attribution License** (CC BY-NC-ND 3.0) which permits unrestricted use, distribution, and reproduction in any medium, provided the original work is properly cited. All rights reserved.

ABSTRACT

In this paper, we introduce a new class of sets called neutrosophic pre star generalized b-closed sets in neutrosophic topological spaces (briefly Np^*gb -closed set). Also we discuss some of their properties

Keywords: Np^*gb -closed set, Np^*gb - open set.

1. INTRODUCTION

In 1970[13], Levine introduced the concept of generalized closed set and discussed the properties of sets, closed and open maps, compactness, normal and separation axioms. Later in 1996 Andrić [2,3] gave a new type of generalized closed set in topological space called b closed sets. The investigation on generalization of closed set has led to significant contribution to the theory of separation axiom, generalization of continuity and covering properties. A.A. Omari and M.S.M. Noorani [1] made an analytical study and gave the concepts of generalized b closed sets in topological spaces. Many real life problems in Business, Finance, Medical Sciences, Engineering and Social Sciences deal with uncertainties. There are difficulties in solving the uncertainties in these data by traditional mathematical models. To overcome these difficulties many authors have introduced many sets which deals with inconsistent data. Some of these approaches are fuzzy sets [29], Intuitionistic fuzzy sets [7], Neutrosophic sets [24] and so on which can be treated as mathematical tools to avert obstacles dealing with ambiguous data. The introduction of the idea of

69735





Aruna Glory Sudha and Zion Chella Ruth

fuzzy set was introduced in the year 1965 by Zadeh[29]. He proposed that each element in a fuzzy set has a degree of membership. Thereafter the paper of Chang(1968)[10] paved way for the subsequent tremendous growth of the numerous fuzzy topological concepts. Following this idea K.Atanassov[6,7,8] in 1983 introduced the idea of intuitionistic fuzzy set on a universe X as a generalization of fuzzy set. Here besides the degree of membership a degree of non-membership for each element is also defined. The topological framework of intuitionistic fuzzy set introduced by D. Coker [12]. The neutrosophic set was initiated by Smarandache and he explained that neutrosophic set is a generalization of intuitionistic fuzzy set. Smarandache[23,24] originally gave the definition of a neutrosophic set and neutrosophic logic. The neutrosophic logic is a formal frame trying to measure the truth, indeterminacy and falsehood. In 2012 Salama,Alblowi [25,26] introduced the concept of neutrosophic topological space. In 2016 concept of neutrosophic semi-open sets in neutrosophic topological space by introduced P.Ishwarya and K.Bageerathi[13]. In 2017 V.VenkateswaraRao and Y. SrinivasaRao[28] introduced the concept of neutrosophic pre-open sets and neutrosophic pre-closed in neutrosophic topological spaces.In 2018Dhavaselan R and JafariS[11] initiated the idea of Generalizedneutrosophic closed set,In 2018 the idea of neutrosophic generalized b-closed sets in neutrosophic topological spaces introduced by C.Maheswari, M.Sathyabama and S.Chandrasekar[17].In this paper, a new class of closed set called neutrosophic pre star generalized b-closed set is introduced to prove that the class forms a neutrosophic topology. The notion of pre star generalized b-closed set and its different characterizations are given in this paper. Throughout this paper (X, τ_N) and (Y, σ_N) represent the non-empty neutrosophic topological spaces on which no separation axioms are assumed, unless otherwise mentioned.

2. Preliminaries

Before entering into our work we recall the following definitions.

Definition 2.1 [19]

A subset A of a topological space (X, τ) is called a preopen set if $A \subseteq \text{int}(\text{cl}(A))$ and pre-closed set if $\text{cl}(\text{int}(A)) \subseteq A$.

Definition 2.2 [12]

A subset A of a topological space (X, τ) is called a semiopen set if $A \subseteq \text{cl}(\text{int}(A))$ and semi closed set if $\text{int}(\text{cl}(A)) \subseteq A$.

Definition 2.3 [20]

A subset A of a topological space (X, τ) is called an α -open set if $A \subseteq \text{int}(\text{cl}(\text{int}(A)))$ and an α -closed set if $\text{cl}(\text{int}(\text{cl}(A))) \subseteq A$.

Definition 2.4 [2]

A subset A of a topological space (X, τ) is called a b-open set if $A \subseteq \text{cl}(\text{int}(A)) \cup \text{int}(\text{cl}(A))$ and b-closed set if $\text{cl}(\text{int}(A)) \cup \text{int}(\text{cl}(A)) \subseteq A$.

Definition 2.5 [1]

A subset A of a topological space (X, τ) is called a generalized b-closed set (simply gb-closed) if $\text{bcl}(A) \subseteq U$, whenever $A \subseteq U$ and U is open in X .

Definition 2.6 [15]

A subset A of a topological space (X, τ) is called a generalized closed set(briefly g-closed) if $\text{cl}(A) \subseteq U$, whenever $A \subseteq U$ and U is open in X .

Definition 2.7 [9]

A subset A of a topological space (X, τ) is called a semigeneralized closed set, (briefly sg-closed) if $\text{scl}(A) \subseteq U$, whenever $A \subseteq U$, U is semi-open in (X, τ) .

Definition 2.8 [27]

A subset A of a topological space (X, τ) is called a generalized* closed set(briefly g*-closed) if $\text{cl}(A) \subseteq U$, whenever $A \subseteq U$ and U is g-open in X .

Definition 2.9 [18]

A subset A of a topological space (X, τ) is called a generalized pre-closed set(briefly gp-closed) if $\text{pcl}(A) \subseteq U$, whenever $A \subseteq U$ and U is g-open in X .

Definition 2.10 [22].

Let a subset A of a topological space (X, τ) , is called a pre generalized b- closed set (briefly pgbclosed) if $\text{bcl}(A) \subseteq U$ whenever $A \subseteq U$ and U is pre open in X .





Aruna Glory Sudha and Zion Chella Ruth

Definition 2.11 [1]

A subset A of a topological space (X, τ) is called a generalized b -closed set (briefly gb - closed) if $bcl(A) \subseteq U$ whenever $A \subseteq U$ and U is open in X .

Definition 2.12. [21]

Let a subset A of a topological space (X, τ) , is called a pre-generalized closed set (briefly pg - closed) if $pcl(A) \subseteq U$ whenever $A \subseteq U$ and U is pre-open in X .

Definition 2.13 [14]

A subset A of a topological space (X, τ) is called a semi generalized b - closed set (briefly sgb - closed) if $bcl(A) \subseteq U$ whenever $A \subseteq U$ and U is semi open in X .

Definition 2.14[4]. Let (X, τ) be a topological space. A subset A of the space X is said to be pre^* -open if $A \subseteq \text{int}^*(cl(A))$ and pre^* -closed if $cl^*(\text{int}(A)) \subseteq A$.

Definition 2.15[4]

A subset A of a topological space (X, τ) is called a pre^* generalized b -closed set (briefly, p^*gb -closed) if $bcl(A) \subseteq U$ whenever $A \subseteq U$ and U is pre^* -open in (X, τ) .

Definition 2.16 [24]

Let X be a non empty set. A neutrosophic set (NS for short) A is an object having the form $A = \langle x, A^1, A^2, A^3 \rangle$ where A^1, A^2, A^3 represent the degree of membership, the degree of indeterminacy and the degree of non-membership respectively of each element $x \in X$ of the set A .

Definition 2.17[24]

Let X be a non empty set, $A = \langle x, A^1, A^2, A^3 \rangle$ and $B = \langle x, B^1, B^2, B^3 \rangle$ be neutrosophic sets on X , and let $\{A_i : i \in J\}$ be an arbitrary family of neutrosophic sets in X , where $A^i = \langle x, A^1, A^2, A^3 \rangle$

- (i) $A \subseteq B$ if and only if $A^1 \leq B^1, A^2 \leq B^2$ and $A^3 \geq B^3$
- (ii) $A = B$ if and only if $A \subseteq B$ and $B \subseteq A$.
- (iii) $A^c = \langle x, A^3, A^2, A^1 \rangle$
- (iv) $A \cap B = \langle x, A^1 \wedge B^1, A^2 \wedge B^2, A^3 \vee B^3 \rangle$
- (v) $A \cup B = \langle x, A^1 \vee B^1, A^2 \vee B^2, A^3 \wedge B^3 \rangle$
- (vi) $\cup A_i = \langle x, \vee A_i^1, \vee A_i^2, \wedge A_i^3 \rangle$
- (vii) $\cap A_i = \langle x, \wedge A_i^1, \wedge A_i^2, \vee A_i^3 \rangle$
- (viii) $A \setminus B = A \cap \overline{B}$.
- (ix) $0_N = \langle x, 0, 0, 1 \rangle; 1_N = \langle x, 1, 1, 0 \rangle$.

Definition 2.18[25]

A neutrosophic topology (NT for short) on a nonempty set X is a family τ of neutrosophic set in X satisfying the following axioms:

- (i) $0_N, 1_N \in \tau$.
- (ii) $G_1 \cap G_2 \in \tau$ for any $G_1, G_2 \in \tau$.
- (iii) $\cup G_i \in \tau$ for any arbitrary family $\{G_i : i \in J\} \subseteq \tau$.

In this case the pair (X, τ) is called a Neutrosophic topological space (NTS for short) and any Neutrosophic set in τ is called a Neutrosophic open set (NOS for short) in X . The complement A of a Neutrosophic open set A is called a Neutrosophic closed set (NCS for short) in X .

Definition 2.19[27]

Let (X, τ) be a neutrosophic topological space and $A = \langle X, A_1, A_2, A_3 \rangle$ be a set in X . Then the closure and interior of A are defined by

$Ncl(A) = \cap \{K : K \text{ is a neutrosophic closed set in } X \text{ and } A \subseteq K\},$
 $Nint(A) = \cup \{G : G \text{ is a neutrosophic open set in } X \text{ and } G \subseteq A\}.$

It can be also shown that $Ncl(A)$ is a neutrosophic closed set and $Nint(A)$ is a neutrosophic open set in X , and A is a neutrosophic closed set in X iff $Ncl(A) = A$; and A is a neutrosophic open set in X iff $Nint(A) = A$.



**Definition 2.20**

A subset A of a neutrosophic topological space (X, τ_N) is said to be,

- (i) A neutrosophic pre-open[26] set if $A \subseteq \text{Nint}(\text{Ncl}(A))$ and neutrosophic pre-closed set if $\text{Ncl}(\text{Nint}(A)) \subseteq A$.
- (ii) A neutrosophic α -open[26] set if $A \subseteq \text{Nint}(\text{Ncl}(\text{Nint}(A)))$ and neutrosophic α -closed set if $\text{Ncl}(\text{Nint}(\text{Ncl}(A))) \subseteq A$.
- (iii) neutrosophic semi-open[11] set $A \subseteq \text{Ncl}(\text{Nint}(A))$ and neutrosophic semi-closed set if $\text{Nint}(\text{Ncl}(A)) \subseteq A$.
- (iv) neutrosophic b-open set[9] if $A \subseteq \text{Ncl}(\text{Nint}(A)) \cup \text{Nint}(\text{Ncl}(A))$ and neutrosophic b-closed set $\text{Ncl}(\text{Nint}(A)) \cup \text{Nint}(\text{Ncl}(A)) \subseteq A$.

Definition 2.21:

A subset A of a neutrosophic topological space (X, τ_N) is said to be,

- (i) Neutrosophic generalized closed[9] set if $\text{Ncl}(A) \subseteq U$ whenever $A \subseteq U$ and U is neutrosophic open set in (X, τ_N)
- (ii) Neutrosophic generalized b- closed[15] set if $\text{Nbcl}(A) \subseteq U$ whenever $A \subseteq U$ and U is neutrosophic open set in (X, τ_N)

3. Neutrosophic pre star generalized b -closed sets

In this section, we introduce neutrosophic pre star generalized b - closed set and investigate some of its properties.

Definition 3.1

A subset A of a neutrosophic topological space (X, τ_N) , is called neutrosophic generalized pre- closed set (briefly Ngp-closed set) if $\text{Npcl}(A) \subseteq U$ whenever $A \subseteq U$ and U is neutrosophic pre-open in X .

Definition 3.2

A subset A of a neutrosophic topological space (X, τ_N) , is called neutrosophic generalized semipre- closed set (briefly Ngsp-closed set) if $\text{Nspcl}(A) \subseteq U$ whenever $A \subseteq U$ and U is neutrosophic open in X .

Definition 3.3

A subset A of a neutrosophic topological space (X, τ_N) , is called neutrosophic generalized α - closed set (briefly Ng α -closed set) if $\text{N}\alpha\text{cl}(A) \subseteq U$ whenever $A \subseteq U$ and U is neutrosophic α -open in X .

Definition 3.4

A subset A of a neutrosophic topological space (X, τ_N) , is called neutrosophic pre star generalized b- closed set (briefly Np*gb-closed set) if $\text{Nbcl}(A) \subseteq U$ whenever $A \subseteq U$ and U is neutrosophic pre*-open in X .

Theorem 3.5

Every neutrosophic closed set is Np*gb -closed.

Proof

Let A be any neutrosophic closed set in X such that $A \subseteq U$, where U is neutrosophic pre*- open containing A . Since $\text{Nbcl}(A) \subseteq \text{Ncl}(A) = A$. Therefore $\text{Nbcl}(A) \subseteq U$. Hence A is p*gb -closed set in X .

Remark 3.6

The converse of above theorem need not be true as seen from the following example.

Example 3.7: Let $X = \{x_1, x_2\}$ and define $\tau_N = \{0_N, 1_N, A\}$ be a neutrosophic topology on X . Here $A = \{\langle x_1, 0.5, 0.3, 0.2 \rangle, \langle x_2, 0.6, 0.4, 0.2 \rangle\}$. Then the neutrosophic set $M = \{\langle x_1, 0.4, 0.5, 0.6 \rangle, \langle x_2, 0.6, 0.5, 0.3 \rangle\}$ is a Np*gb –closed but not a neutrosophic closed set in X . Since $\text{Ncl}(M) \neq M$.

Theorem 3.8

Every neutrosophic g - closed set is Np*gb -closed set.

Proof

Let A be any neutrosophic g - closed set in X and U be any neutrosophic pre star open set containing A . Then $\text{Nbcl}(A) \subseteq \text{Ncl}(A) \subseteq U$. Therefore $\text{Nbcl}(A) \subseteq U$. Hence A is Np*gb –closed set.

Remark 3.9

The converse of above theorem need not be true as seen from the following example





Aruna Glory Sudha and Zion Chella Ruth

Example 3.10: Let $X = \{x_1, x_2\}$ and define $\tau_N = \{0_N, 1_N, A\}$ be a neutrosophic topology on X . Here $A = \{\langle x_1, 0.5, 0.3, 0.2 \rangle, \langle x_2, 0.6, 0.4, 0.2 \rangle\}$. Then the neutrosophic set $M = \{\langle x_1, 0.4, 0.5, 0.6 \rangle, \langle x_2, 0.6, 0.5, 0.3 \rangle\}$ is a Np^*gb -closed but not a neutrosophic g -closed set in X .

Theorem 3.11

Every neutrosophic semi closed set is Np^*gb -closed set.

Proof: Let A be any neutrosophic semi closed set in X and U be any neutrosophic pre star open set containing A . Since A is neutrosophic semi closed set, $Nbcl(A) \subseteq Nscl(A) \subseteq U$. Therefore $Nbcl(A) \subseteq U$. Hence A is Np^*gb closed set.

Remark 3.12

The converse of above theorem need not be true as seen from the following example

Example 3.13

Let $X = \{x_1, x_2\}$ and define $\tau_N = \{0_N, 1_N, A\}$ be a neutrosophic topology on X . Here $A = \{\langle x_1, 0.5, 0.3, 0.2 \rangle, \langle x_2, 0.6, 0.4, 0.2 \rangle\}$. Then the neutrosophic set $M = \{\langle x_1, 0.4, 0.5, 0.6 \rangle, \langle x_2, 0.6, 0.5, 0.3 \rangle\}$ is a Np^*gb -closed but not a neutrosophic semi-closed set in X . Since $M \not\subseteq Ncl(Nint(M)) = 0_N$

Theorem 3.14

Every neutrosophic α -closed set is Np^*gb -closed set.

Proof: Let A be any neutrosophic α -closed set in X and U be any neutrosophic pre star open set containing A . Since A is neutrosophic α -closed, $Nbcl(A) \subseteq N\alpha cl(A) \subseteq U$. Therefore $Nbcl(A) \subseteq U$. Hence A is Np^*gb -closed set.

Remark 3.15

The converse of above theorem need not be true as seen from the following example.

Example 3.16

Let $X = \{x_1, x_2\}$ and define $\tau_N = \{0_N, 1_N, A\}$ be a neutrosophic topology on X . Here $A = \{\langle x_1, 0.5, 0.3, 0.2 \rangle, \langle x_2, 0.6, 0.4, 0.2 \rangle\}$. Then the neutrosophic set $M = \{\langle x_1, 0.4, 0.5, 0.6 \rangle, \langle x_2, 0.6, 0.5, 0.3 \rangle\}$ is a Np^*gb -closed but not a neutrosophic α -closed set in X . Since $M \not\subseteq Nint(Ncl(Nint(M))) = 0_N$

Theorem 3.17

Every neutrosophic pre - closed set is Np^*gb -closed set.

Proof

Let A be any neutrosophic pre -closed set in X and U be any neutrosophic pre star open set containing A . Since every A neutrosophic pre closed set, $Nbcl(A) \subseteq Npcl(A) \subseteq U$. Therefore $Nbcl(A) \subseteq U$. Hence A is Np^*gb -closed set.

Remark 3.18

The converse of above theorem need not be true as seen from the following example.

Example 3.19

Let $X = \{x_1, x_2\}$ and define $\tau_N = \{0_N, 1_N, A\}$ be a neutrosophic topology on X . Here $A = \{\langle x_1, 0.2, 0.8, 0.6 \rangle, \langle x_2, 0.1, 0.7, 0.8 \rangle\}$. Then the neutrosophic set $M = \{\langle x_1, 0.5, 0.3, 0.5 \rangle, \langle x_2, 0.6, 0.4, 0.7 \rangle\}$ is a Np^*gb -closed but not a neutrosophic pre-closed set in X . Since $M \not\subseteq Nint(Ncl(M)) = 0_N$

Theorem 3.20

Every Nag -closed set is Np^*gb -closed set.

Proof

Let A be Nag -closed set in X and U be any neutrosophic open set containing A . Since every neutrosophic open set is Nag -open sets, we have $Nbcl(A) \subseteq N\alpha cl(A) \subseteq U$. Therefore $Nbcl(A) \subseteq U$. Hence A is Np^*gb -closed set.

Remark 3.21: The converse of above theorem need not be true as seen from the following example.

Example 3.22

Let $X = \{x_1, x_2\}$ and define $\tau_N = \{0_N, 1_N, A\}$ be a neutrosophic topology on X . Here $A = \{\langle x_1, 0.5, 0.3, 0.2 \rangle, \langle x_2, 0.6, 0.4, 0.2 \rangle\}$. Then the neutrosophic set $M = \{\langle x_1, 0.4, 0.5, 0.6 \rangle, \langle x_2, 0.6, 0.5, 0.3 \rangle\}$ is a Np^*gb -closed but not a neutrosophic Nag -closed set in X .





Aruna Glory Sudha and Zion Chella Ruth

Theorem 3.23

Every Np^*gb - closed set is $Ngsp$ - closed set.

Proof

Let A be any Np^*gb -closed set such that U be any neutrosophic open set containing A . Since every neutrosophic open set is Npg -open, we have $Nbcl(A) \subseteq Nspcl(A) \subseteq U$. Therefore $Nbcl(A) \subseteq U$. Hence A is $Ngsp$ -closed set.

Remark 3.24

The converse of above theorem need not be true as seen from the following example.

Example 3.25: Let $X = \{x_1, x_2\}$ and define $\tau_N = \{0_N, 1_N, A\}$ be a neutrosophic topology on X . Here $A = \{\langle x_1, 0.4, 0.5, 0.6 \rangle, \langle x_2, 0.6, 0.5, 0.3 \rangle\}$. Then the neutrosophic set $M = \{\langle x_1, 0.2, 0.7, 0.5 \rangle, \langle x_2, 0.2, 0.6, 0.6 \rangle\}$ is a $Ngsp$ -closed but not a Np^*gb -closed set in X .

Theorem 3.26

Every Np^*gb - closed set is Ngb - closed set.

Proof

Let A be any Np^*gb -closed set in X such that U be any neutrosophic open set containing A . Since every neutrosophic open set is Npg open, we have $Nbcl(A) \subseteq U$. Hence A is gb -closed set.

Remark 3.27

The converse of above theorem need not be true as seen from the following example.

Example 3.28: Let $X = \{x_1, x_2\}$ and define $\tau_N = \{0_N, 1_N, A\}$ be a neutrosophic topology on X . Here $A = \{\langle x_1, 0.4, 0.5, 0.6 \rangle, \langle x_2, 0.6, 0.5, 0.3 \rangle\}$. Then the neutrosophic set $M = \{\langle x_1, 0.2, 0.7, 0.5 \rangle, \langle x_2, 0.2, 0.6, 0.6 \rangle\}$ is a Ngb -closed but not a Np^*gb -closed set in X .

Theorem 3.29

Every Npg - closed set is Np^*gb - closed set.

Proof

Let A be any Npg -closed set in X such that U be any neutrosophic pre star open set containing A . Since every neutrosophic pre open set is Npg open, we have $Nbcl(A) \subseteq Npcl(A) \subseteq U$. Therefore $Nbcl(A) \subseteq U$. Hence A is Np^*gb -closed set.

Remark 3.30

The converse of above theorem need not be true as seen from the following example.

Example 3.31

Let $X = \{x_1, x_2\}$ and define $\tau_N = \{0_N, 1_N, A\}$ be a neutrosophic topology on X . Here $A = \{\langle x_1, 0.2, 0.8, 0.6 \rangle, \langle x_2, 0.1, 0.7, 0.8 \rangle\}$. Then the neutrosophic set $M = \{\langle x_1, 0.5, 0.3, 0.5 \rangle, \langle x_2, 0.6, 0.4, 0.7 \rangle\}$ is a Np^*gb -closed but not a Npg -closed set in X .

Remark 3.32

From the above theorems and examples we have the following implications

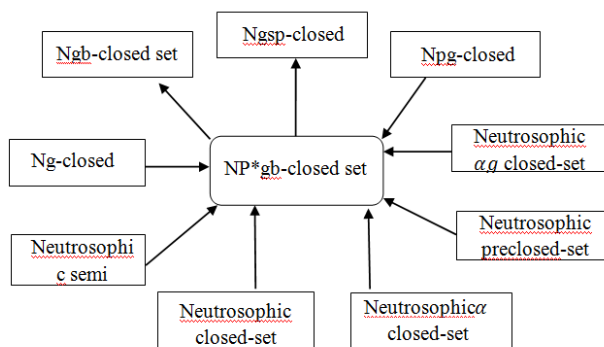


Fig.1. NP^*gb -closed set





Aruna Glory Sudha and Zion Chella Ruth

4. Characteristics of Np^*gb -Closed Sets

Theorem 4.1

If a set A is Np^*gb -closed set then $Nbcl(A) - A$ contains no non empty pre star closed set.

Proof: Let F be a pre star closed set in X such that $F \subseteq Nbcl(A) - A$. Then $A \subseteq X - F$. Since A is Np^*gb -closed set and $X - F$ is neutrosophic pre star open then $Nbcl(A) \subseteq X - F$. (i.e) $F \subseteq X - Nbcl(A)$. So $F \subseteq (X - Nbcl(A)) \cap (Nbcl(A) - A)$. Therefore $F = \emptyset$.

Theorem 4.2

If A is Np^*gb -closed set in X and $A \subseteq B \subseteq Nbcl(A)$. Then B is Np^*gb - closed set in X .

Proof

Since $B \subseteq Nbcl(A)$, we have $Nbcl(B) \subseteq Nbcl(A)$ then $Nbcl(B) - B \subseteq Nbcl(A) - A$. By Theorem 4.1, $Nbcl(A) - A$ contains no non empty neutrosophic pre star closed set. Hence $Nbcl(B) - B$ contains no non empty neutrosophic pre star closed set. Therefore B is Np^*gb -closed set in X .

Theorem 4.3

If $A \subseteq Y \subseteq X$ and suppose that A is Np^*gb closed set in X then A is Np^*gb - closed set relative to Y .

Proof

Given that $A \subseteq Y \subseteq X$ and A is Np^*gb -closed set in X . To prove that A is Np^*gb - closed set relative to Y . Let us assume that $A \subseteq Y \cap U$, where U is neutrosophic pre star- open in X . Since A is Np^*gb - closed set, $A \subseteq U$ implies $Nbcl(A) \subseteq U$. It follows that $Y \cap Nbcl(A) \subseteq Y \cap U$. That is A is Np^*gb - closed set relative to Y .

Theorem 4.4

If A is both Np^* open and Np^*gb - closed set in X , then A is neutrosophic b closed set.

Proof

Since A is Np^* open and Np^*gb closed in X , $Nbcl(A) \subseteq A$. But $A \subseteq Nbcl(A)$. Therefore $A = Nbcl(A)$. Hence neutrosophic A is b closed set.

Theorem 4.5

For x in X , then the set $X - \{x\}$ is a Np^*gb -closed set or Np^* -open.

Proof

Suppose that $X - \{x\}$ is not Np^* open, then X is the only Np^* open set containing $X - \{x\}$. (i.e.) $Nbcl(X - \{x\}) \subseteq X$. Then $X - \{x\}$ is Np^*gb -closed in X .

Theorem 4.6

If A and B are Np^*gb -closed sets in a space X . Then $A \cup B$ is also Np^*gb -open set in X .

Proof

If A and B are Np^*gb - closed sets in a space X . U be any Np^* open set containing A and B . Therefore $Nbcl(A) \subseteq U$, $Nbcl(B) \subseteq U$. Since $A \subseteq U$, $B \subseteq U$ then $A \cup B \subseteq U$. Hence $Nbcl(A \cup B) = Nbcl(A) \cup Nbcl(B) \subseteq U$. Therefore $A \cup B$ is Np^*gb closed set in X .

5. NeutrosophicPre Star Generalized b-Open Sets

In this section, we introduce neutrosophic pre star generalized b-open sets (briefly Np^*gb -open) in neutrosophic topological spaces by using the notions of Np^*gb -open sets and study some of their properties.

Definition 5.1

A subset A of a neutrosophic topological space (X, τ_N) , is called neutrosophic pre star generalized b- open set (briefly Np^*gb -open set) if A^c is Np^*gb -closed in X . We denote the family of all Np^*gb -open sets in X by Np^*gb - $O(X)$.

Theorem 5.2

If A and B are Np^*gb -open sets in a space X . Then $A \cap B$ is also Np^*gb -open set in X .





Aruna Glory Sudha and Zion Chella Ruth

Proof: If A and B are Np^*gb -open sets in a space X . Then A^c and B^c are Np^*gb -closed sets in a space X . By Theorem 4.6 $A \cup B^c$ is also Np^*gb -closed set in X . (i.e.) $A \cup B^c = (A \cap B)^c$ is a Np^*gb -closed set in X . Therefore $A \cap B$ Np^*gb -open set in X .

Theorem 5.3

If $Nint(B) \subseteq B \subseteq A$ and if A is Np^*gb -open in X , then B is Np^*gb -open in X .

Proof

Suppose that $Nint(B) \subseteq B \subseteq A$ and A is Np^*gb -open in X then $A^c \subseteq B^c \subseteq Ncl(A^c)$. Since A^c is Np^*gb -closed in X , by Theorem 4.2 B^c is Np^*gb closed set. Therefore B is Np^*gb -open in X .

REFERENCES

1. Ahmad Al-Omari and Mohd. Salmi Md. Noorani, On Generalized b-closed sets, Bull.Malays. Math. Sci. Soc(2) 32(1) (2009), 19-30
2. D.Andrijevic, Semi-pre open sets, Mat.Vesnik 38(1)1986,24-32.
3. D.Andrijevic, b-open sets, Mat.Vesink, 48 (1996), 59-64.
4. I. Aruna Glory Sudha, S. Zion Chella Ruth, More on p^*gb -Closed Sets in Topological Spaces, International Journal of Mathematical Archive, 14(1), 2023, 10-14, ISSN NO: 2229-5046.
5. I. Aruna Glory Sudha, S. Zion Chella Ruth, Normal spaces associated with P^*Gb -Open Sets, Journal of Namibian studies, 35 S1 (2023): 3357-3368 ISSN: 2197-5523.
6. K. Atanassov, Intuitionistic fuzzy sets, in V.Sgurev, ed., VII ITKRS session, sofia (June 1983 central Sci. and Tech. Library, Bulg, Academy of sciences (1984)).
7. K. Atanassov, Intuitionistic fuzzy sets, Fuzzy sets and systems 20(1986) 81-86.
8. K.Atanassov, Review and new result on intuitionistic fuzzy sets, preprint Im-MFAIS-1-88, Sofia, 1988.
9. P.Bhattacharya and B.K.Lahiri, Semi-generalized closed sets on topology, Indian J.Maths 29 (3) (1987) 375-382.
10. C.L. Chang, Fuzzy Topological Spaces, J. Math. Anal Appl.,24 (1968), 182-1 90.
11. Dhavaselan R and Jafari S ,Generalized neutrosophic closed set, New trends in neutrosophic theory and applications II pp 261-273.
12. Dogan Coker, An introduction to Intuitionistic fuzzy topological spaces, Fuzzy sets and systems, 88, 81-89 (1997).
13. P.Ishwarya and K.Bageerathi, On Neutrosophic semi-open sets in Neutrosophic topological spaces, International Journal of Mathematics Trends and Technology, Vol 37(3), 214-223(2016).
14. D. Iyappan & N.Nagaveni, On semi generalized b-closed set, Nat. Sem. On Mat & Comp.Sci, Jan (2010), Proc.6
15. N.Levine, Generalized closed sets in topology, Tend Circ., Mat. Palermo (2) 19 (1970), 89-96.
16. N.Levine, Semi-open sets and semi-continuity in topological spaces, Amer. Math. Monthly 70 (1963)), 36-41.
17. C.Maheswari, M.Sathyabama and S.Chandrasekar , Neutrosophic generalized b-closed sets in neutrosophic topological spaces, International conference on applied and computational mathematics,(2018),1-7.
18. H.Maki, R.J.Umehara and T.Noiri, Every topological space is pre-T 1/2 , Mem. Fac. Sci. Kochi. Univ. Ser. A. Math. 17(1996), 33- 42
19. A.S.MashorAbd.El-Monsef.M.E and Ei-Deeb.S.N., On Pre continuous and weak precontinuous mapping, Proc.Math.,Phys.Soc.Egypt, 53 (1982), 47-53.
20. O.Njastad, On some classes of nearly open sets, Pacific J Math.,15(1965), 961-970.
21. J. H. Park, Y. B. Park and B. Y. Lee, On gp-closed sets and gp-continuous functions, Indian J. Pure Appl. Math., 33(1) (2002), 3- 12.
22. S. Sekar and R. Brindha , On Pre Generalized b-Closed Set In Topological Spaces International Journal of Pure and Applied Maths.,Volume 111 No.4 2016, 577-586
23. Florentin Smarandache, neutrosophy and neutrosophic Logic, First International conference on neutrosophy, Neutrosophic Logic, set, probability and statistics university of New mexico, Gallup NM 87301, USA(2002).
24. F. Smarandache. A Unifying Field in Logics: Neutrosophic Logic. Neutrosophy, Neutrosophic Set, Neutrosophic Probability, American Research Press, Rehoboth, NM (1999).





Aruna Glory Sudha and Zion Chella Ruth

25. A.A. Salama, S.A. AL-Blowi, Neutrosophic Set and Neutrosophic Topological Spaces, IOSR Journal of Math., 3 (2012), 31-35.
26. A. A. Salama, S. A. Alblowi, Generalized Neutrosophic Set and Generalized Neutrosophic Topological Spaces, Comp. Sci. Engg., 2 (2012), 129-132.
27. Veerakumar .M.K.R.S., Between closed sets and g-closed sets, Mem.Fac.Sci.Kochi.Univ.Ser.A, Math, 21 (2000), 1-19.
28. V. Venkateswara Rao and Y. Srinivasa Rao, Neutrosophic Pre-open Sets and Pre-closed Sets in Neutrosophic Topology, International Journal of ChemTech Research, Vol.10 No.10, pp: 449-458, 2017.
29. L.A. Zadeh, Fuzzy sets, Information and control 8(1965) 338-353.





Effect of Thoracic Load Carriage on Heart Rate and Maximum Oxygen Uptake (VO₂ max) by Six Minute Walk Test in School Going Students

Shivani Sutaria¹ and Sweety Shah²

¹Assistant Professor, Department of Physiotherapy, Mahatma Gandhi Physiotherapy College (Affiliated with Gujarat University), Ahmadabad, Gujarat, India.

²Lecturer, Department of Physiotherapy, VSGH Hospital, Ahmadabad, Gujarat India.

Received: 11 Sep 2023

Revised: 12 Dec 2023

Accepted: 31 Jan 2024

*Address for Correspondence

Shivani Sutaria

Assistant Professor,

Department of Physiotherapy,

Mahatma Gandhi Physiotherapy College (Affiliated with Gujarat University),

Ahmadabad, Gujarat, India.

Email: sutariashivani@gmail.com



This is an Open Access Journal / article distributed under the terms of the **Creative Commons Attribution License** (CC BY-NC-ND 3.0) which permits unrestricted use, distribution, and reproduction in any medium, provided the original work is properly cited. All rights reserved.

ABSTRACT

Present study was designed to determine the effect of thoracic load carriage on heart rate and maximum oxygen uptake (VO₂max) by six minute walk test in school going students. A total 30 normal healthy school going students with age group of 12-17 years both girls and boys were included in the study. Six minute walk test was conducted with different backpack load carriage of 0%, 5%, 10%, and 15% of body mass with one trial for one load condition each day. Pre and post heart rate and VO₂max was measured. Non parametric Kruskal Wallis test was used which shows statistical significance association between 0% VS 15%, 5% VS 15%, 10% VS 15% for heart rate and between 0% VS 10%, 0% VS 15%, 5% VS 15% for VO₂max. So Post. hoc analysis was done. In Post.hoc analysis, HR changes was most significant between 0% VS 15% (p< 0.001), 5%VS 15% (p< 0.047) compared to 0% VS 5%, 0% VS 10% and 10% VS 15%. VO₂maxchanges was most significant between 0% VS 15% (p< 0.004) compared to 0% VS 5%, 0%VS 10% and 5% VS 15% , 10% VS 15%. Study concluded that load of maximum 5% and 10% body weight can be consider the ideal body weight to be carried by school going students.

Keywords: heart rate, maximum oxygen uptake, school going students, backpack, six minute walk test



**Shivani Sutaria and Sweety Shah**

INTRODUCTION

Children's physical fitness has long been a source of great interest to teachers, parents, physicians, clinicians, and researchers. Focus is frequently placed on improving presumably low fitness levels of children to enhance scores on fitness tests, to improve athletic performance, and to benefit the child's long- and short-term health.[1] Reports of Europe and Asia have found that many students carry weight of more than 10% and in some cases even up to 20% of their body weight.[2] According to data released by Ministry of Human Resource Development in 2014 approximately 223 million students in India need a backpack to take away items to and from school every day.[3] The ideal load carrying system would be one that does not disturb the body's natural posture, balance, and movements. The load must be dispersed onto skeletal structure in a balanced way and should not put strain on body in any direction.[4] A National Advisory Committee popularly known as Yash Pal Communittee, in July 1993, said that as far as physical load of the school bag is concerned, the situation has become worse over the past few years.[5] Carrying heavy loads in a backpack can induce increased physical stress and cause discomfort and pain.[6] Carrying heavy loads close to the trunk affects pulmonary function since the backpack system opposes the expansion of the chest wall during inspiration.[7] Additionally, increased oxygen consumption and energy cost have been observed when carrying heavy loads in backpacks compared with no backpack conditions.[6]

Physiological studies have consistently shown that heart rate and oxygen consumption increase as load mass increases during short term load carriage.[8] VO_{2max} is the product of maximal CO (L/ min) and maximal atrio venous oxygen difference (mL.O₂/ L Blood). Exercise professionals often rely on sub-maximal exercise tests to assess Cardio Respiratory Fitness (CRF) because maximal exercise testing is not always feasible in the health/fitness setting. The basic aim of sub-maximal exercise testing is to determine the HR response to one or more sub-maximal work rates and use the results to predict VO_{2max} . [9] So, most of load carriage studies have focused on the metabolic, biomechanical and subjective perceptual changes associated with load weight, walking speed, gradient, terrain and other factors as well as medical hazards and performance limitations. Many authors in the past have studied the effect of carrying load on different electromyography and pathological, biomechanical and physiological parameters in adults. Most of these studies have focused on soldiers and hikers with the purposes of improving the techniques of load carriage.[10] So the aim of the study is to see the effect of carrying backpack on heart rate and maximum oxygen consumption among school going students.

MATERIALS AND METHODS

An experimental study was conducted among 30 normal healthy school going students with age group of 12-17 years including both girl and boy and willing to participate were included in the study, students participating in any formal training or organized sports, with neurological, cardiovascular, or musculoskeletal problems were excluded from the study. Materials used in this study was 22m course of walking, two small plastic bottles to mark the lap boundaries, data collection sheath, consent form, books or weight cuff for load as required, backpack as recommended, stop watch or timer, measurement scale for floor measurement, chair, weighing machine. Ethical approval was obtained for study by Institutional Review Board (IRB) .Assent of student was taken regarding their participation in the study. Consent of parents was taken regarding their participation in the study. Consent of principal was taken to allow me to conduct the study in their school and also to allow students to participate in the study. Participant were selected according to inclusion and exclusion criteria. Participant were made to understand the nature and procedure.

Backpack

A school backpack with two pads and wide strap on the shoulder, which has been recommended by the American Occupational Therapy Association was used in this study. The backpack was carried suspended from both shoulders of the subject, placed on the trunk, which the subject will feel most comfortable and stable.⁴ The backpacks was fill



**Shivani Sutaria and Sweety Shah**

with books and weight cuffs so that they weighed (empty, 5, 10, 15% of body weight). Basic demographic detail in the form of age, gender was obtained self-report. Height was obtained using a wall-mounted measuring tape. Weight was obtained using calibrated digital scales. Body mass index (BMI) was calculated using the height and weight values. Subject was asked to perform the six min walk test with different backpack load carriage. Test with different backpack load carriage of 0%, 5%, 10%, and 15% of body mass was arranged on four different days with one trial for one load condition each day in order to eliminate the possible interference factors such as fatigue and adaptation. Heart rate was calculated initially and after completion of test by taking the radial pulse manually. Maximum oxygen uptake (VO₂max) was calculated after completion of test using the following formula.

PREDICTED VO₂max: VO₂PEAK = 0.03 × DISTANCE(m) + 3.98¹¹ Four different values of Heart rate and VO₂max obtained by the carriage of different loads was compared by application of appropriate statistical test.

RESULT

In this study, Statistical analysis was done using SPSS version 20 and excel 2007. The level of significance was kept at < 0.05 with 95% confidence interval. As the data did not follow the normal distribution according to Shapiro-Wilk test, Kruskal Wallis test was used to determine the effect of 0%, 5%, 10%, & 15% of backpack load carriage on HR and VO₂max. Results by application of Kruskal Wallis shows statistical significance association between 0% VS 15%, 5% VS 15%, 10% VS 15% for heart rate and between 0% VS 10%, 0% VS 15%, 5% VS 15% for VO₂max, So Post.hoc analysis was done. In Post.hoc analysis, HR changes was most significant between 0% VS 15% (p < 0.001), 5% VS 15% (p < 0.047) compared to 0% VS 5%, 0% VS 10% and 10% VS 15%. VO₂max changes was most significant between 0% VS 15% (p < 0.004) compared to 0% VS 5%, 0% VS 10% and 5% VS 15%, 10% VS 15%. (Table no. 3) Above result shows that effect on HR by carrying load of 15% of body weight produces significant change compared to 5% and 10%. The effect on VO₂max by carrying load of 15% body weight produces significant changes compared to 5% and 10%. Hence, load of maximum 5% and 10% body weight can be consider the ideal body weight to be carried by school going students. Detail of demographic detail (table 1) mean and SD of HR and VO₂max of different loads is shown in table 2, mean of heart rate for different load presented in graph 1, mean of VO₂max for different load presented in graph 2, Statistical results obtained for HR and VO₂max with different percentage of load carriage (table 3).

DISCUSSION

The present study conducted with the aim to determine the effect of thoracic load carriage on heart rate and maximum oxygen uptake (VO₂max) by six minute walk test in school going students. Total 30 students were enrolled in the study according to inclusion criteria. Students was asked to perform the six min walk test with different backpack load carriage. Test with different backpack load carriage of 0%, 5%, 10%, and 15% of body mass was arranged on four different days with one trial for one load condition each day. The three different aspects of the result was present in the study

1. With increase in the load carriage there is decrease in the maximum oxygen uptake (VO₂max).
2. With increase in the load carriage, there is increase in the heart rate.
3. Ideal 5-10% body weight should be carried by school going students

The present study shows that there is significant increase in the heart rate while carrying load carriage from 0% to 15% of body weight. As heart rate increases in a linear fashion with the work rate and oxygen uptake during dynamic exercise. The increase in HR during exercise occur primarily at the expense of diastole (filling time), rather than systole. Thus, at high exercise intensities, diastolic time may be so short as to preclude adequate ventricular filling.¹⁵ Siddhartha Sen and Ajita (2016), further supports these result by showing that significant increase in heart rate and RPE with right side pack, with left side pack and with back pack after treadmill walking in 105 collegiate students. He suggested that significant increase in heart rate is due to increase in cardiac output during static contraction is mainly directed towards peripheral parts of the body and only a small part is supplied to



**Shivani Sutaria and Sweety Shah**

myocardium.[12] The present study shows that with increase in load carriage from 0% to 15%, there is decrease in maximum oxygen consumption. As load carriage increases there is overall increase in weight i.e (BM + weight) and as VO₂max is calculated in ml/kg/min, this increase in load carriage justify decrease in VO₂max. Also with increase in load carriage there is increase in activity of the muscle, assumed that there is greater compression of arteries underlying muscles which further reduces the blood flow to periphery thus decreased maximum oxygen uptake. Aparna Kondapalli et al (2019), in her study showed statistically significant higher level of VO₂max in normal weight girls when compared to overweight girls and overweight girls shows a better VO₂max than obese girls. The decrease in VO₂max with greater BMI is because the mitochondrial oxidative enzyme activity is very less in obese people as the number of mitochondria and their function is limited in the skeletal muscles of overweight and obese individual. Whereas the glycolytic enzymes that is the phosphor fructokinase and aglycerol phosphate activity is more in obesity and type 2 diabetes.[13] Ideally 5-10% backpack weight is safe to use by school going students as it put lesser stress on cardio-respiratory functions as with 15% backpack load carriage significantly increases the heart rate and decreases the maximum oxygen consumption. S.O. Ismaila et al, 2018, determine the safe weight of backpack for male and female secondary school students in Ibadan, Southwestern Nigeria as 2.87 kg (5.18% of body weight) and 2.53 kg (4.91% of body weight) respectively.[14] Thus in the present study, it is seen that with increase in load carriage, there is increase in HR and decrease in VO₂max. So on the basis of that ideally 0-5% body weight should be carried by school going students. Limitation of the study is small sample size, age criteria is restricted to small range, gender distribution was not done, the study was done on only two cardio-respiratory parameter while it can be affected by other parameters also such as blood pressure, respiratory rate, rate of perceived exertion, etc which are not included in the study. effect of BMI was not considered. Future recommendation is comparison of heart rate and maximum oxygen uptake can be made between each groups for different percentage of load carriage in school going students and in adults, other outcome measure can be studied, consider BMI - variable. Clinical implication of study is optimal weight of backpack according to body weight can be suggested so that it induces minimal cardiovascular responses.

CONCLUSION

The present study shows significant change in cardio-respiratory parameters- heart rate and maximum oxygen uptake while carrying backpack load of 15% of body weight, but no significant change while carrying load of 5% and 10% body weight. Thus the present study accept the experimental hypothesis and reject the null hypothesis. Hence , load of 5% and 10% body weight can be consider the ideal body weight to be carried by school going students.

ACKNOWLEDGEMENT

Authors are thankful to Dr. Pankaj Patel (Former dean) and Dr. Pratik Patel (Current dean), NHL Municipal Medical College for giving me an opportunity to do this study. Thanking to Dr. Nehal Shah, I/C Principal, S.B.B. College of Physiotherapy, V.S. General Hospital for providing me all facilities for my work, without which it would not have been possible to complete this project. Heartfelt thanks to all the principals of school and students who participated in the study

REFERENCES

1. V. Gregory Payne and James R. Morrow, Jr. Exercise and V₀₂max in Children: A Meta-Analysis. Research Quarterly for Exercise and Sport,1993.Vol. 64, No.3, pp.305- 313.
2. Jing Xian Li and Youlian Hong. Changes of trunk position and breathing pattern in children walking under conditions of load carriage. Biomechanics Symposia, 2001.
3. MHRD. <http://mhrd.gov.in/>. Department of School Education and Literacy/AR2013-14.pdf 2013.
4. Grimmer, K., Dansie, B., Milanese, S., Pirunsan, U., Trott, P.: Adolescent standing postural response to backpack loads: a randomised controlled experimental study. BMC Musculoskeletal. Disorder,2002.3(1),10.





Shivani Sutaria and Sweety Shah

5. Yashpal communitte. A National Advisory Committee. July 1993.
6. Samira Golriza, Jeremiah J. Peifferb, Bruce F. Walkera, K. Bo Foremanc and Jeffrey J. Hebert. The effect of backpack load placement on physiological and self-reported measures of exertion. IOS Press ,2018. 1051-9815/18/\$35.00.
7. D.H.K. Chow, J.M.L Ting, M.H. Prope, A,Lai. Effect of backpack load placement on pulmonary capacities of normal schoolchildren during upright stance. International Journal of Industrial Ergonomics 39, 2009. 703–707.
8. Katrina M. Simpson, Bridget J. Munro, Julie R. Steele. Effect of load mass on posture, heart rate and subjective responses of recreational female hikers to prolonged load carriage. Applied Ergonomics 42, 2011. 403-410.
9. Wolters Kluwer. ACSM’s Guidelines for exercise testing and prescription ,7th edition.
10. H. Daneshmandi · F. Rahmani-Nia · S.H. Hosseini. Effect of carrying school backpacks on cardio-respiratory changes in adolescent students. Sport Sci Health 2008. 4:7–14.
11. Lawrence P. Cahalin, Michael A. Mathier, Marc J. Semigran, G. The Six-Minute Walk Test Predicts Peak Oxygen Uptake and Survival in Patients With Advanced Heart Failure. American College of Chest Physicians 1996.110;325-332.
12. Siddhartha Sen and Ajita . Influence of carrying loads on rating of perceived exertion and heart rate during walking. Journal of Ergonomics,2016. DOI: 10.4172/2165-7556. 1000176.
13. Aparna Kondapalli, Dr. Ganpat Devpura. Cardio respiratory Fitness among Normal and overweight and obese adolescent girls of Hyderabad. International journal of health science and research,2019. 2249-9571.
14. Salami O. Ismaila, Kolawole T. Oriolowo. Determination of Safe Mass of Backpack for Students in Tertiary Institutions. International Conference on Industrial Engineering and Operations Management Dubai, United Arab Emirates (UAE), March 3 – 5, 2015.

Table 1: Demographic Details

Number of subject	30
Age	12-17 years
Male	12
female	18

Table 2: Mean and SD of HR and VO2max of different loads

LOAD CARRIAGE)	HR(mean ± SD)	VO2max (mean ± SD)
0%	106.03 ± 21.07	16.76 ± 2.831
5%	109.23 ± 17.07	15.99 ± 3.519
10%	111.7 ± 17.20	15.38 ± 4.273
15%	121.6 ± 16.00	14.24 ± 4.533

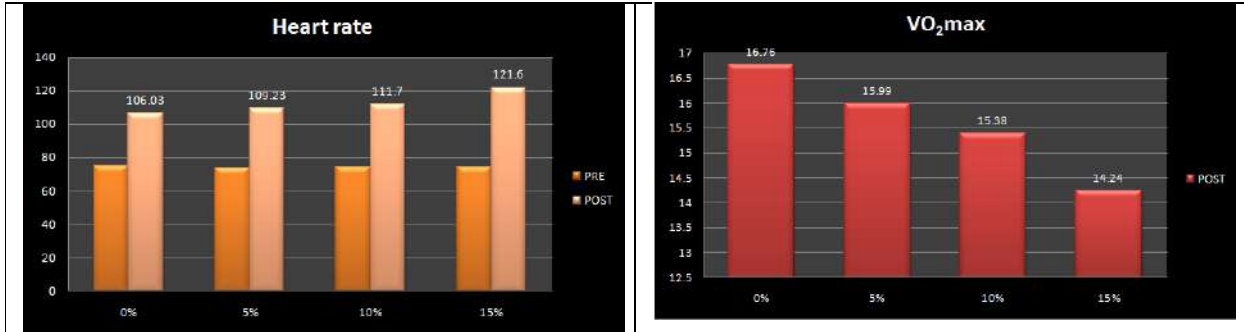
Table 3: Statistical results obtained for HR and VO2max with different Percentage of load carriage

LOAD CARRIAGE	HR (significant)	VO2max (significant)
Between 0% & 5%	Non significant (p>0.293)	Non significant (p>0.191)
Between 0% & 10%	Non significant (p>0.099)	Significant (p<0.022)
Between 0% & 15%	Significant (p<0.001)	Significant (p<0.002)
Between 5% & 10%	Non significant (p>0.684)	Non significant (p>0.231)
Between 5% & 15%	Significant (p<0.007)	Significant (p <0.021)
Between 10% & 15%	Significant (p<0.017)	Non significant (p>0.186)





Shivani Sutaria and Sweety Shah



Graph 1: Mean of heart rate for different load

Graph 2: Mean of VO₂max for different load





An Analysis of Issues Concerning Health and Reproductive Rights of Women in India

Rakhi Sharma¹ and Maryam Ishrat Beg^{2*}

¹Ph.D. Scholar, Faculty of Law, School of Law, Manipal University Jaipur, Jaipur, Rajasthan, India.

²Associate Professor, Faculty of Law, Manipal University Jaipur, Jaipur, Rajasthan, India

Received: 02 Dec 2023

Revised: 28 Dec 2023

Accepted: 06 Feb 2024

*Address for Correspondence

Maryam Ishrat Beg

Associate Professor,

Faculty of Law,

Manipal University Jaipur ,

Jaipur, Rajasthan, India



This is an Open Access Journal / article distributed under the terms of the **Creative Commons Attribution License** (CC BY-NC-ND 3.0) which permits unrestricted use, distribution, and reproduction in any medium, provided the original work is properly cited. All rights reserved.

ABSTRACT

India has seen a decrease in the rights women had, to their resurgence as super-women. It is often difficult for women to participate in the nationalist movements due to their commitment to the domestic household. The recognition of females' rights in the country is still quite low. The few women who do get recognition are only being thought of around issues such as child marriage, female feticide, and menstruation. In the meantime, it's important to also support their reproductive rights. "Political parties have committed to requiring marriage registration, prohibit child marriage and include marital rape as an offence. "The Pre-conception and Pre-Natal Diagnostic Techniques (Prohibition of Sex Selection) Act (PCPNDT)" provides reproductive health services to women across India". The study also contrasts the American and Indian judicial stances and government policies. Legal problems related to reproductive autonomy, such as abortion and forced sterilization, are examined from the perspective of both nations, despite the obvious differences in social and cultural norms.

Keywords: Women Rights, Health Rights, Reproductive Rights, India, U.S.

INTRODUCTION

Everywhere in the globe, people have the fundamental right to obtain treatment for reproductive health. To be in a state of sexual and reproductive health (SRH) is to be in a complete status of "the reproductive system and all of its roles in promoting social, mental, and physical health; it encompasses more than just the absence of illness or disability". "Health and Reproductive Rights have been gradually recognized as human rights since the 1968 Declaration on the "International Conference on Human Rights and the 1994 International Conference on Population and Development". The ICESCR and the CEDAW also emphasize the importance of reproductive rights in

69750



**Rakhi Sharma and Maryam Ishrat Beg**

achieving women's human rights. The SDGs and MDGs also cater to various objectives that discuss reproductive rights both directly and indirectly". The SDGs and MDGs both support the idea of reproductive rights. India, who is a signatory to these of the covenants and also the conventions, must ensure that they implement these mandates in their policies and the laws. When reviewing national law and policy regarding RHRs, it is evident that there are immense compliance issues as well as heaps of irrelevancies [1]. The right to reproductive healthcare and the fundamental right to self-determination over one's reproductive process of the developing body of international law concerning reproductive rights. Human rights that are inextricably linked to the defense of reproductive freedom are as follows: For women and girls, this means having the following rights guaranteed to them:

"the right to health, reproductive health, and family planning;"

"the right to life, liberty, and security;"

"the right to determine the number and spacing of children;" and

"the right to equality in marriage and consent to marriage;"

Women Health Condition in India

Women's health basically refers to the a specialty of medicine that concentrates on the management of illnesses and ailments, and well-being in women. Health contributes to occupational success, economic growth. In India, women confront health inequities that may be addressed with better medical treatment. Increasing access to these services and expenditure would boost economic output in India. The health of Indian women is another area that might be studied by looking at a variety of indicators. Different communities have different challenges, which is why it is important to understand the starting point for tackling them. In order to sufficiently improve the health condition of women in country India, it is necessary to analyze more than just one dimension of wellbeing. Women in India are facing many health problems which are affecting the quality of the economy. By improving their healthcare, women can have higher savings and investment, as well as more qualified human resources [2]. This is because Indian women have more obstacles in urban public spaces, which obstructs their access to different services. The number of women participating in economic and societal activities is less than that of men. This leads to bad access to healthcare, where marginalized women have worse conditions than other groups. Women on their periods do not know the happenings of their bodies, which creates so many misconceptions about female reproductive health.

The discomfort that women go through during their period has a strong impact on both the physical and also the mental health of women. Menstrual cramps can cause discomfort. Sexuality, which deals with female issues like dryness and irritation in a female body, is not discussed or dealt with because it's taboo. We need to move beyond hesitations and stigmatization to think seriously about feminine health and wellness. We need to embrace the idea that these are important issues with major consequences. People's ability to function in society and contribute to the global economy depends on their sexual and reproductive health. Governmental commitment to SRHR is discussed in more detail through international accords. However, there have been barriers to progress such as a lack of resources and insufficient political will.

Sexual And Reproductive Health Right

"Human rights pertaining to sexuality and reproduction, such as civil, political, economic, social, and cultural rights, are collectively referred to as SRHR". It's important that both women and men have the same rights when it comes to sexual health and reproduction. The right to formulate and decide one's own choices regarding sexual reproductive health is available to all, including the children and also the adolescents. "It is crucial to universal health coverage because it includes the lack of diseases, as well as physical, mental, emotional, and social well-being" [3].

The physical, mental, emotional, and social dimensions of health all have a role in sexual and reproductive functioning. It's more than simply the absence of sickness. Respect for people's autonomy in sexual and reproductive matters is crucial to achieving sexual and reproductive health. Human rights that are foundational to one's survival and flourishing are the rights upon which these others are based. decide if you want to have a child or children and how many you will have. All autonomous beings should have access to information and support both during their lifetime and after death. Recent events of the rape cases across the country have also led to the public protests, people



**Rakhi Sharma and Maryam Ishrat Beg**

demanding better laws and stricter enforcement, and public discussions about sexual violence in India. Population control in India is alarming. The problem could be solved through addressing the concerns of women. 78% of abortions had taken occur outside of clinics, and 30 million married women lack access to contraception. Sexual violence towards girls and women is a violent act of discrimination. It has serious physical, the emotional, the mental and also the social consequences. A range of people outside the traditional gender binary are also vulnerable to discrimination, so they need to be included in definitions of sexual violence [4].

Reproductive Rights of Women**Reproductive Rights Include**

The freedom to start a family, end a pregnancy, have access to reproductive health care, and learn about sex education in public schools. Women have the right to be proactively informed about reproductive health care strategies, plan for family size and time, and control their bodies without judgment.

Reproductive Rights of Women in India in Present Scenario

Despite having legal frameworks in place and socially progressive policies, India continues to experience significant barriers related to reproduction. "This includes inadequate health care together with the rejection of women's power to make decisions".

Typically, women's rights are not promoted in the law. The law is set up to look only at the population, rather than anything else. It limits reproductive choices and sometimes even takes away what little choice a woman might have.

"Judicial Recognition of Reproductive Rights as Fundamental and Human Rights"

"A number of state high courts and the Indian Supreme Court have rendered rulings that assert women's and girls' rights to reproductive healthcare. International human rights law obligates Indian states to provide maternal health care, to guarantee access to the full range of contraceptive methods, and to avoid child marriage". According to U.N., human rights issues include maternal mortality, lack of access to contraceptives and substandard sterilization. *Puttaswamy v. Union of India* recognized the constitutional rights of women.

International Framework on the Right To Reproduce

As stated in the preamble of the WHO constitution, everyone, no matter where they live, has the right to the highest degree of health that is physically and mentally attainable. The term "health" refers to a person's physical, mental, and social well-being. It also includes the availability of reproductive medical services for females. The importance of women's health and the freedom to get medical treatment is amplified when one considers the biological makeup of women and their capacity to have children. In accordance with Article 16(1) of the Universal Declaration of Human Rights, which was adopted in 1948, all individuals who have reached the age of majority are entitled to the freedom to marry and have a family, regardless of their race, nationality, or religion. Before, during, and after a marriage, they are afforded the same legal protections as one another. Articles 11, 12, and 14 of the 1979 Convention on the Elimination of All Forms of Discrimination against Women require countries to take actions aimed at eliminating gender-based discrimination within the healthcare sector. This is done to ensure that all Women have the ability to obtain information, counseling, and services pertaining to family planning on equal terms with men. According to the provisions of Article 12 everyone has the right to the highest attainable standard of physical and mental health." which was ratified in 1966, every individual has the right to the highest attainable level of both bodily and mental well-being.

Comparison of Reproductive Rights in India and U.S.

In India, the debate surrounding reproductive rights has been pushed to the forefront of contemporary legal discussion following some recent developments, which reflect the same underlying jurisprudential conflict, as is seen in the context of the United States. Unfortunately, the issues underlying the reproductive rights debate have not received sufficient focus by Indian courts. In contrast, debates on reproductive choices have a long history in the western world, especially in the U.S., which provides the best comparative standard for assessing the Indian situation, as opposed to other countries. This is because of the raging public debate over reproductive rights in the U.S. and its relatively advanced constitutional jurisprudence and legal argumentation on the issue. Further, the fact



**Rakhi Sharma and Maryam Ishrat Beg**

that Indian courts have often looked towards American constitutional jurisprudence for inspiration in interpreting the Indian Constitution legitimizes the comparison. An analysis of the U.S. position on reproductive rights will, therefore, help in understanding the contours of the debate surrounding this issue, both in the realm of State policy, as well as in constitutional and judicial approaches.

A State Policy in the U.S.

With a woman's agreement, abortion is legal in the United States. The only time this was tolerated was before the 'Quickening' stage. The research on abortion regulations in the United States shows that "lobbying of strong religious groups" has been the primary inspiration for State involvement. As a result of the state's interference, unrestricted abortion is now illegal in many places, despite the fact that it poses serious risks to the lives of both the mother and the unborn child.

State Policy in India

Abortion is considered a crime under Indian law according to Section 312 of the "Indian Penal Code 1860". In addition, in 1971, Parliament approved the "Medical Termination of Pregnancy Act" (abbreviated "M.T.P. Act"). Abortion is legal in India thanks to this law, which overrides the restrictive provisions of "Section 312 of the Indian Penal Code". In circumstances when the continuation of the pregnancy would result in "grave injury to mental and physical health," however, abortion is legal.

CONCLUSION and Recommendation

The social environment that influences women's reproductive behavior strongly shapes Indian culture. A woman's desire to have a family may conflict with her legal right to choose whether or not to have children. These contrasting situations arise not just in the home, but also in the more institutionalized ways in which policies are formulated and services are provided. Women and girls in India believe that the regulations and frameworks in place do not fully protect their reproductive rights, despite the fact that abortion and contraception are now legal. Reproductive autonomy is essential for women. We should promote this not just to ensure the continued success of our economy but also to offer women and girls with the opportunity to shed restrictive gender norms. Judiciary or legislative action is required to resolve the many ambiguities in the law. It is still not quite clear where issues like reproductive rights and the far more basic right to privacy stand in the Constitution. The need to educate lawmakers and judges on the need of respecting individual autonomy in matters of reproduction is very important. The development of reproductive rights in the United States offers important lessons for India's policymakers and courts in this area. The difficulty is in taking on board the motivation behind reproductive rights recognition and using it to address the social and legal issues that are specific to India

REFERENCES

1. Hina Ilyas, in her work titled "Reproductive Rights of Women: A Path to Achieving Gender Equality" published on October 15, 2015, discusses the importance of reproductive rights for women as a means to establish gender justice. This source was accessed via SSRN on August 11, 2023.
2. Sarthak Garg and Keshav Gaur discuss the ethical and practical considerations surrounding women's reproductive rights in their paper titled "Reproduction Rights of Women: Ethical or Feasible Aspects of Surrogate Motherhood," which was published on November 20, 2012. You can access the paper on SSRN at the following link: <https://ssrn.com/abstract=2178623>. (Retrieved on August 15, 2023).
3. Devpriya Banerjee, "The K. S. Puttaswamy Judgement and its Pivotal Role in Reproductive Rights (January 11, 2023). Available at SSRN: <https://ssrn.com/abstract=4322166>" (Retrieved on August 11, 2023).
4. Nivedita Menon, The Impossibility of 'Justice': Female Foeticide and Feminist.





Rakhi Sharma and Maryam Ishrat Beg

5. "Reproductive and Sexual Rights of Women in India. (n.d.). Drishti IAS. Retrieved from <https://www.drishtias.com/daily-updates/daily-news-editorials/reproductive-and-sexual-rights-of-women-in-india>"
6. "Ramakrishnan, L. 2017. Interview for NHRC Study on Sexual Health and Well-being. In person. Chennai".
7. "Wikipedia contributors. (2022, July 15). Women's health in India.
8. "Wikipedia contributors. (2022, July 15). Women's health in India.
9. Javed v. State of Haryana, A.I.R. 2003 S.C. 3057





Impact of High-Intensity Training on Stress Biomarker Salivary Amylase on Moderate Trained Athletes: An Experimental Study

Jamil Ahmad Butt^{1*}, Jai Prakash Bhukar², Ramgopal Nitharwal³

¹Research Scholar, Department of Physical Education and Sports, Central University of Haryana, Mahendragarh, Haryana, India.

²Professor, Department of Physical Education and sports, Central University of Haryana, Mahendragarh, Haryana, India.

³Assistant Professor, Department of Biotechnology, Central University of Haryana, Mahendragarh, Haryana, India.

Received: 09 Sep 2023

Revised: 10 Nov 2023

Accepted: 29 Dec 2023

*Address for Correspondence

Jamil Ahmad Butt

Research Scholar,

Department of Physical Education and Sports,

Central University of Haryana, Mahendragarh, Haryana, India.

E mail: bhatjameel50@gmail.com



This is an Open Access Journal / article distributed under the terms of the **Creative Commons Attribution License** (CC BY-NC-ND 3.0) which permits unrestricted use, distribution, and reproduction in any medium, provided the original work is properly cited. All rights reserved.

ABSTRACT

The purpose of the study is to explore whether high-intensity exercise on selected moderately trained athletes can cause a substantial increase in stress, analysed with the stress biomarker tool i.e., Salivary Alpha-amylase (SAA) which occurs as a significant cause in response to physiological stress. The exercise protocol was identical for using high aerobic intensity exercise in which the pulse rate was measured and expressed as a percentage of peaked pulse rate (PPR >85%) during 30 minutes of the six moderately trained athletes between the age group of 18-22 years held at the sports complex, Central University of Haryana, Mahendergrah (India). Saliva was collected in the morning session in Eppendorf tubes pre-exercise, and post-exercise and stored at freeze temperature for two hours, then analysed at Laboratory. Eppendorf Tubes were marked in pairs and coded as A1 A2, B1 B2, C1 C2, D1 D2, E1 E2, F1 F2. Exercise was significant for salivary alpha-amylase with different values between pre-exercise (0.927, 0.365, 0.514, 0.413, 0.617, 0.424) and post-exercise (0.409, 0.287, 0.373, 0.317, 0.438, 0.298) for the selected athletes. The result shows a significant difference in salivary alpha-amylase before and after the activity. Before exercise, it was found low and after the activity, it was high in concentration. Further study is necessary to consider whether amylase levels could be employed in place of other sorts of uncomfortable conditions, heart rate or VO₂ measurements. To assess potential hormonal changes in an active group, more amylase during exercise should be collected in future studies.

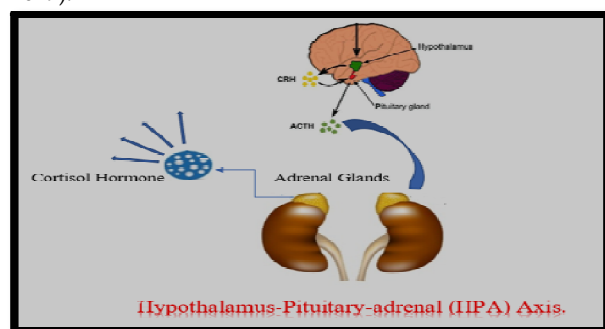
Keywords: Salivary-amylase, Exercises, Athletes, Pulse Rate.



Jamil Ahmad Butt *et al.*,

INTRODUCTION

Pre-exercise (anticipatory), during-exercise, and post-exercise stress responses in human beings have all been investigated by researchers. It has been shown that salivary cortisol and salivary alpha-amylase (SAA) react to an exercise situation. This response presumably results from the hypothalamic-pituitary-adrenal (HPA) and sympathoadrenal medullary system (SMS) axis being activated (Backes, T. P *et al.*, 2015). Salivary alpha-amylase is an enzyme that is produced and secreted by the salivary glands in the mouth. It plays an important role in the digestion of carbohydrates by breaking down starches and glycogen into smaller sugars, such as maltose and glucose. Salivary alpha-amylase is also sometimes called ptyalin in the humans and various other mammals of digestive system. It is an endo-enzyme, meaning that it breaks down carbohydrates to split the interior bonds between the sugar molecules. This is different from exon-enzymes, which breaks down carbohydrates by splitting the bonds at the end of the sugar molecules. In addition to its role in digestion, SAA has also been identified as stress biomarker. When the body is under stress, the sympathetic nervous system is activated, leading to an increase in salivary alpha-amylase production. Measuring the levels of salivary alpha-amylase that provides the information about the body's stress response (Hensten, & Jacobsen, (2019). The HPA, an axis with your brain secretes cortisol from the adrenal gland. HPA releases different hormones and Corticotropin Release Hormone (CRH) to stimulate the anterior pituitary gland which releases Adrenocorticotropin Hormone (ACTH) to energize the adrenal gland with stress response. About 90% of stress response is attached to proteins and 10% is free cortisol that is biologically active and creates negative feedback and triggers HPA while secretion of CRH and ACTH takes place (Kandhalu, P. (2013). The HPA axis is activated when a situation is perceived as stressful, causing neurons in the hypothalamus, a brain region referred to as the "master gland," to release the hormone known as CRH. The pituitary gland, which is also found in the brain, produces the Adrenocorticotropin Hormone in response to the release of CRH. The adrenal glands are located above the kidneys, and when the pituitary gland secretes ACTH, that travels through the blood and activates the release of the so-called "Stress Hormones". In the short term, activation of the HPA axis is adaptive, but persistent or long-term stimulation can be harmful to health and cause an improper functioning of the negative feedback mechanism. To be more precise, extended exposure to stressors seems to detach cortisol from its capacity to prevent ongoing CRH and ACTH release, which results in an excess of cortisol. Chronic health issues, psychological diseases, issues with memory, learning and attention are all linked to cortisol elevations (Piazza, J. R., *et al.* (2010). The daily functioning of rodents depends on the steroid hormones known as glucocorticoids (Timmermans,*et al.*, 2019).



Exercise is a voyage that promotes mood, happiness, and helps to demonstrate that exercise referral programmes create a sense of social inclusion as well as proficiency in tasks for people with depression (Cripps, F. (2008). Evidence shows that exercise increases the level of different hormones which are beneficial for the body like dopamine, a neuromodulator molecule that constitutes about 80% of catecholamine content in the brain which decreases stress and depression, serotonin that helps positively impact mood, sleep, social behaviour, digestion, appetite, memory, blood clotting and sexual functioning, testosterone is a sex hormone that is boosted by regular exercise which helps an individual to regulate his sex drive, muscle mass, and strength, production of sperm and RBCs count (Basso, *et al.*, 2017; Bhattacharya, *et al.*, 2023). Oestrogen is a sex hormone produced primarily by the





Jamil Ahmad Butt *et al.*,

ovaries and testes in males to regulate the growth and maturity of the human reproduction system (Basso, *et al.*, 2017). The study shows that three hours of moderate exercise per week helps to reduce the circulation of oestrogen used in post-menopausal women (Fred Hutch 2004). According to Petty, "In today's fast-paced Technology driven society, everybody is in need to fix up some time for exercise. As it is a productive outlet which stimulates the feel-good transmitters that help to boost overall well-being." An exercise physiologist Hahn's Petty recommends that "exercise is to enhance the quality of life and helps to regulate the hormonal imbalances". However, an exerciser performer needs moderate to high-intensity exercises to make a significant change in cortisol response that is up to 80% of his or her capacity that stimulates exercise to provoke the hormonal glands (Hill, E. E., *et al.*, 2008). Biofluids like blood or saliva can be used to measure the biomarkers of these stress hormonal activation. Most of the proteins found in saliva, a vital biological fluid that contains a wide variety of proteins, may be appropriate as biomarkers of health status. As proteins make up around 30% of blood, saliva also contains proteins. Due to its quickness, simple, non-invasive, and stress-free collection, saliva is particularly helpful in stress studies. Numerous studies have shown that biologically it is very useful for stress monitoring with a saliva sample. The two stress biomarkers that have been identified the most, are cortisol and salivary alpha-amylase (Tecles, F., *et al.*, 2014). Making an effort to reduce stress at workplace that may help educators to deal with continuous stress and ultimately affect health outcomes. Different ways that people experience stress can have a detrimental effect on their physical and mental well-being. Evidence suggests that stress-reduction practices including meditation, yoga, and aerobic exercise can reduce stress. These practices are frequently linked to positive health consequences (Wagner, & Pearcey, 2022). The purpose of this study is to examine the athletes who are engaged in moderate types of activities, when put under a hard training zone continuously for 30 minutes high intensity training will significantly raise the level of salivary amylase concentrations. The study further examines the pulse rate and VO₂ max. while performing the activities. Existing theory suggests that moderately trained athletes may be put under stressful conditions when they are put under hard training doses.

Limitations of the Study

There are a few limitations to this study. While the small sample size makes it difficult to generalise the findings, the authors believe that since this was a preliminary investigation, the limited subject pool nevertheless supplied significant information for future research. Second, during the training, heart rate monitors were not used by the athletes but were measured pulse rate with the help of finger tips. Third, the estimation of the athletes' travel distance was not shown but was considered as pulse beats during the training. Heart rate and information on the distance travelled could be used to determine the training load more precisely and to confirm the load determined by biomarkers. Future research should include a local positioning device that also monitors heart rate while assessing biomarker stress. Fourth, it is difficult to determine whether the Salivary amylase concentration was caused solely by general physical effort and also by the psychological stresses of competition. When paired with biomarkers, a measure like the value or concentration of salivary amylase with the help of spectrophotometer, which characterises the acute state of psychological stress, may provide new information regarding acute stress and should be taken into consideration in future studies.

MATERIAL AND METHODS

Subjects

The present study was experimental and analysed the salivary amylase activity of selected athletes before and after the physical training. Total six athletes were selected 18–22-year-old (19.1 ± 2.4 years, 171.2 ± 3.4 cm, 62.0 ± 4.2 kg) Central University of Haryana (India) at Mahendragarh, male bachelor's degree students were subjects for this study. Subjects were recruited within the campus, who were performed (moderate) training session.

Study Design

The athletes were free from injuries or illness and continuing their training as per schedule during the academic session. The subjects were told to undergo excessive physical activity during last 30 minutes form (65% to 90% VO_{2max}).





Jamil Ahmad Butt *et al.*,

can cause substantial increase in stress upon the salivary alpha-amylase which occurs a significant cause in response to physiological stress. Saliva obtained in Eppendorf tubes approximately 2 ml from the participants before and after the activity at morning session and put immediately in the refrigerator at freezing temperature for two hours, then analysed at Laboratory. Tubes were marked in pairs and coded as A₁ A₂, B₁ B₂, C₁ C₂, D₁ D₂, E₁ E₂, F₁ F₂. Exercise was significant for SAA with different values between pre-exercise (0.927, 0.365, 0.514, 0.413, 0.617, 0.424) and post exercise (0.409, 0.287, 0.373, 0.317, 0.438, 0.298) for the selected athletes. All the procedures were reviewed and discussed by an institutional experts committee. The assessment procedures to check the salivary alpha-amylase activity of the selected group. Subjects were familiar with the test before and after the activity. The participants were continuously engaged during the academic year from February to May 2023. Physical activity modulates the stress response while an individual is engaged in training.

Measurements & Instruments (Salivary amylase activity)

1. Potassium iodide and iodine solution: Put 2 g of potassium iodide into a beaker with 100 mL of water. Iodine, 1.3 g in weight, is added to the same beaker. A few millilitres of pure water were added, and the iodine was dissolved after a short while of swirling. Transferred the iodine solution to a 1 L glass beaker, being careful to rinse the volumetric flask completely with distilled water before doing so. Added distilled water to the solution until it reached the 1 L mark.
2. Phosphate buffer saline (PBS): Mixed the tablets with the right amount of water to dissolve them.
3. A 100-mL conical flask filled with 50 mL of nearly boiling water and 1.0 g of soluble starch will make a 1% starch solution. Before using, stir to dissolve and let cool.

The Fig. 2 displays the change in salivary biomarker concentration before and after physical activity according to the players' coding/position. The values are inversely proportional to stress biomarkers (SAA). High values indicate a decrease in stress response and low values indicate an increase in stress response.

RESULTS

Statistical evaluation of the changes in the concentration of salivary amylase before and after the exercise. The data was analysed using SPSS-26 and paired t-test was employed for the analysis of the data. The p-value i.e., significant value is 0.039 which is less than 0.05 reveals that the p value is significant and the null hypothesis can be rejected. It concludes that there is significant difference between the means of pre-test and post-test. Table 1. shows the significant difference during the training program implemented to the subjects showed an effect in the stress biomarkers salivary alpha-amylase level among the subjects resulting in the increase of stress biomarkers salivary alpha-amylase concentration after the activities. The result shows the significant difference in salivary alpha-amylase before and after the activity. Prior to exercise it was found low and after the activity it was high in concentration.

DISCUSSION

The goal of the study was to determine how intensive (high) exercises affected the stress biomarker salivary alpha-amylase in athletes who are also engaged in moderate type of activities and to establish whether exercise intensity results in an increase of salivary-amylase concentration by examining the effect of high exercise intensity on the HPA axis's stress response to 30 minutes of high intensity exercises of 65% and 90% of VO₂max and PPR. The results accepted to the idea that exercise of moderate to high intensity (65–90%) will cause appreciable rises in salivary-amylase levels in the saliva. The main findings of this study are the acute salivary amylase response of specific athletes following an acute workout. Theory suggests that, low intensity (up to 40%) exercise does not lead to any appreciable rises in stress biomarkers of the subject (Hill, E. E., *et al.*, 2008). Acute stress hormone responses were not observed in any of these endurance competitions lasting six hours or longer, but recent studies have also noted significant increases in stress hormones during triathlon competitions, wrestling matches, weightlifting competitions women's handball and volleyball matches. This is because to the fact that soccer is an activity that calls for high levels of aerobic and anaerobic skills. A typical male athlete travels 10 km in total in 90 minutes, or 6.6 km per hour while





Jamil Ahmad Butt et al.,

sprinting once every 30 to 90 seconds. Soccer matches last 90 minutes, making them longer than many other sports in terms of the physiological demands than place on athletes (Haneishi, *et al*, 2007). Players that played for longer periods of time indicated a greater Cortisol response. Physical contact during the game directly influenced the Cortisol response, with players in contact positions showing a greater Cortisol response than those in non-contact positions (Foretić, *et al*, 2022). Salivary amylase secretion was lower immediately before pre-exercise than it was following post-exercise, which may have been brought by psychological stress from anticipation. It is common knowledge that in order to increase their capacity for performance, athletes must engage in a significant number of workouts at different levels of effort. Exercise stresses the body, causing various hormonal changes (Hackney, & Viru, 1999). One of the study involved participants were 10 men and women, ages 18 to 32, who had no physical restrictions related to their hearts, lungs, or musculoskeletal systems. Saliva was collected before, after, and 20 minutes after the jumping session as part of the participants' engagement in a treadmill maximum exertion test (GXT). Results showed that salivary amylase levels had significantly increased from resting values (Allen, S. (2014).

CONCLUSION

The findings of the current study results that increasing stress produces the increase in salivary-amylase concentrations, therefore it provides support for the theory that exercise from moderate to high intensity among the normal trained athletes can cause substantial increases in salivary amylase. During the high intensity exercise, the hypothalamus releases SAA enzyme to pituitary and then adrenal axis which puts the body under stressful conditions that disturbs the homeostasis of the athlete. This study allows for the possibility of employing these markers to assess the physiological stress that athletes' experience while participating in various sports. The scenario of the present study undoubtedly illustrates a pertinent usage of salivary biomarkers in sports sciences. The study also inspires more research into how a psychologically based training regimen affects different category athlete's ability to perform at their best while avoiding exhaustion and maintaining their physical and mental health. Further study is necessary to consider whether amylase levels could be employed in place of other sorts of uncomfortable conditions, heart rate or VO₂ measurements. To assess potential hormonal changes in an active group, more amylase during exercise should be collected in future studies. This study can also help to distinguish the stress among the competitive sports performers for those researchers who often use "questionnaire type" research.

REFERENCES

1. Allen, S. (2014). Salivary Alpha-Amylase as an Indicator of Body Stress Following an Acute Session of Repetitive Jumping.
2. Backes, T. P., Horvath, P. J., & Kazial, K. A. (2015). Salivary alpha amylase and salivary cortisol response to fluid consumption in exercising athletes. *Biology of Sport*, 32(4), 275-280.
3. Basso, J. C., & Suzuki, W. A. (2017). The effects of acute exercise on mood, cognition, neurophysiology, and neurochemical pathways: A review. *Brain Plasticity*, 2(2), 127-152.
4. Bhattacharya, P., Chatterjee, S., & Roy, D. (2023). Impact of exercise on brain neurochemicals: a comprehensive review. *Sport Sciences for Health*, 1-48.
5. Cripps, F. (2008). Exercise your mind: Physical activity as a therapeutic technique for depression. *International journal of therapy and rehabilitation*, 15(10), 460-465.
6. Foretić, N., Nikolovski, Z., Marić, D., Perić, R., & Sekulić, D. (2022). Analysis of the associations between salivary cortisol-, alpha-amylase-, and testosterone-responsiveness with the physical contact nature of team handball: a preliminary analysis. *The Journal of Sports Medicine and Physical Fitness*, 27.
7. Hackney, A. C., & Viru, A. (1999). Twenty-four-hour cortisol response to multiple daily exercise sessions of moderate and high intensity. *Clinical physiology (Oxford, England)*, 19(2), 178-182.
8. Haneishi, K., Fry, A. C., Moore, C. A., Schilling, B. K., Li, Y., & Fry, M. D. (2007). Cortisol and stress responses during a game and practice in female collegiate soccer players. *The Journal of Strength & Conditioning Research*, 21(2), 583-588.





Jamil Ahmad Butt et al.,

9. Hensten, A., & Jacobsen, N. (2019). Salivary alpha amylase as a stress biomarker. *OSP J Dent Sci*, 1(1), 1-6.
10. Hill, E. E., Zack, E., Battaglini, C., Viru, M., Viru, A., & Hackney, A. C. (2008). Exercise and circulating cortisol levels: the intensity threshold effect. *Journal of endocrinological investigation*, 31, 587-591.
11. Kandhalu, P. (2013). Effects of cortisol on physical and psychological aspects of the body and effective ways by which one can reduce stress. *Berkeley Scientific Journal*, 18(1).
12. Piazza, J. R., Almeida, D. M., Dmitrieva, N. O., & Klein, L. C. (2010). Frontiers in the use of biomarkers of health in research on stress and aging. *Journals of Gerontology Series B: Psychological Sciences and Social Sciences*, 65(5), 513-525.
13. Tecdes, F., Fuentes-Rubio, M., Tvarijonaviciute, A., Martínez-Subiela, S., Fatjó, J., & Cerón, J. J. (2014). Assessment of stress associated with an oral public speech in veterinary students by salivary biomarkers. *Journal of veterinary medical education*, 41(1), 37-43.
14. Timmermans, S., Souffriau, J., & Libert, C. (2019). A general introduction to glucocorticoid biology. *Frontiers in immunology*, 10, 1545.
15. Wagner, D., & Pearcey, S. M. (2022). Perceived stress and salivary biomarkers in educators: comparison among three stress reduction activities. *Health Psychology and Behavioral Medicine*, 10(1), 617-631.

	Mean	N	SD	SE
Pre-Test Measurement of Salivary Amylase	0.54183	6	0.20966	0.0856
Post-Test Measurement of Salivary Amylase	0.35367	6	0.06235	0.02545

	Paired Differences					t-value	d f	Sig.
	Mean	SD	SE	95% Confidence Interval of the Difference				
				Lower	Upper			
Pre-Test and Post-Test	0.18817	0.16593	0.06774	0.01404	0.3623	2.778	5	0.039

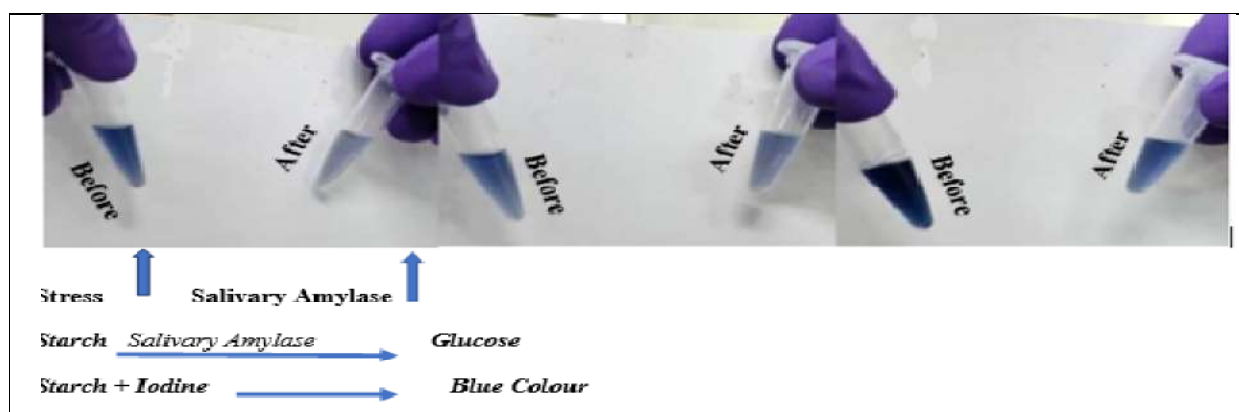


Fig.1 shows (Some Visuals of Stress incitement) the functional activity of the salivary amylase enzyme that breaks down the starch into glucose which appears in blue colour with iodine solution. Hence the more enzyme found in saliva, seems less in blue colour which shows higher amount of amylase enzyme and high dark blue colour indicates low amount of amylase enzyme in the sample.





Jamil Ahmad Butt et al.,

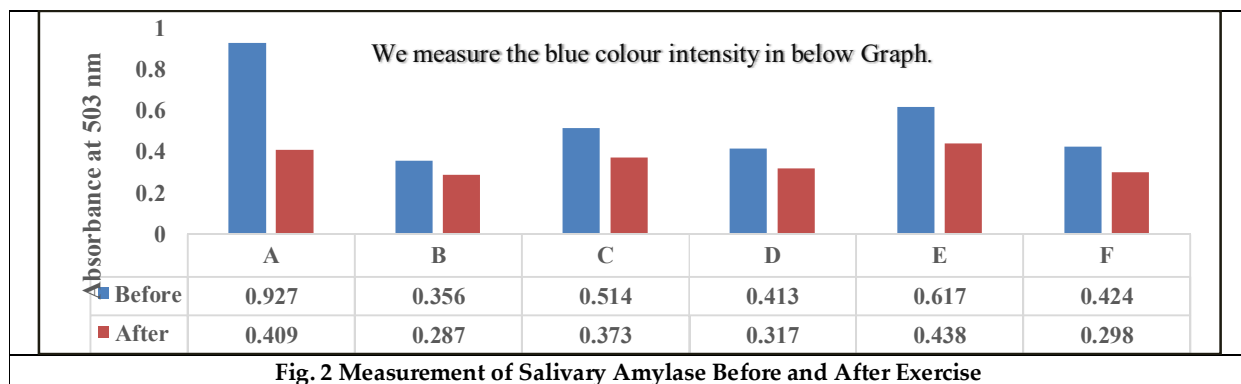


Fig. 2 Measurement of Salivary Amylase Before and After Exercise





Distribution of Marine Macro Algae and Hydrological Studies in Muttom Coast of Kanniyakumari District

Juwairiya Nasreen.J^{1*}, Ramisha.S², Iren Amutha.A³, Mathevan Pillai.M⁴, Shasheela.P⁵ and Natchathiram P⁶

¹Research Scholar, Reg No: 21113152262014, Department of Botany, S.T. Hindu College, Nagercoil (Affiliated to Manonmaniam Sundaranar University, Abishekapatti, Tirunelveli)Tamil Nadu, India.

²Research Scholar, Reg No: 21213152262015, Department of Botany, S.T. Hindu College, Nagercoil (Affiliated to Manonmaniam Sundaranar University, Abishekapatti, Tirunelveli)Tamil Nadu, India.

³Assistant Professor, Department of Botany, Women's Christian College, Nagercoil (Affiliated to Manonmaniam Sundaranar University, Abishekapatti, Tirunelveli)Tamil Nadu, India.

⁴Associate Professor and Head, Department of Botany and Research Centre, S.T. Hindu College, Nagercoil (Affiliated to Manonmaniam Sundaranar University, Abishekapatti, Tirunelveli)Tamil Nadu, India.

⁵Research Scholar, Reg No: 21213152262014, Department of Botany, S.T. Hindu College, Nagercoil (Affiliated to Manonmaniam Sundaranar University, Abishekapatti, Tirunelveli)Tamil Nadu, India.

⁶Research Scholar, Reg No: 20213152262011 Department of Botany, S.T. Hindu College, Nagercoil (Affiliated to Manonmaniam Sundaranar University, Abishekapatti, Tirunelveli)Tamil Nadu, India.

Received: 03 Oct 2023

Revised: 20 Dec 2023

Accepted: 22 Jan 2024

*Address for Correspondence

Juwairiya Nasreen.J

Research Scholar,

Reg No: 21113152262014,

Department of Botany,

S.T. Hindu College, Nagercoil

(Affiliated to Manonmaniam Sundaranar University, Abishekapatti, Tirunelveli)

Tamil Nadu, India.

Email: juwairiyagj@gmail.com



This is an Open Access Journal / article distributed under the terms of the **Creative Commons Attribution License** (CC BY-NC-ND 3.0) which permits unrestricted use, distribution, and reproduction in any medium, provided the original work is properly cited. All rights reserved.

ABSTRACT

Seaweeds are multi cellular macroalgae which are abundant in intertidal zones of coastal environments. The study was conducted at Muttom coast from October 2016 to March 2017. During the study period, a total of 20 seaweeds belonging to Chlorophyta (5 species), Phaeophyta (5 species) and Rhodophyta (10 species) were collected and identified. Rhodophyta shows dominance during the study period. Besides, hydrological parameters such as temperature, salinity, pH, total dissolved oxygen, electrical conductivity and BOD were determined.

Keywords: Macroalgae, Muttom Coast, Seaweeds, Chlorophyta, Phaeophyta, Rhodophyta.



Juwairiya Nasreen *et al.*,

INTRODUCTION

Macroscopic marine algae, popularly known as seaweeds, constitute one of the important living resources of the ocean. They were found attached to the bottom, in relatively shallow coastal water areas up to 180-meter depth, on solid substrate such as rocks, dead corals, pebbles etc., The seaweed flora of India is highly diversified and comprises mostly of tropical species, in all, 271 genera and 1153 species of marine algae which include forms and varieties [1]. The coast is extensively used and densely inhabited in many regions, and under great pressure worldwide. Macroalgae dominate the vegetation in the intertidal and the euphotic zone, and consequently, their occurrence and abundance may be strongly affected by anthropogenic activity. Reports of conspicuous changes in macroalgal composition and abundances are due to anthropogenic impacts such as nutrient enrichment [2]. Sea temperature and salinity are usually the main physical factors which determine regional and local distributions of macroalgae in euphotic coastal waters. Seaweeds are the only source for the production of phyto chemicals such as agar, alginate and carrageenan. In India, algae and alginate are manufactured from the seaweeds exploited from the natural seaweed beds, particularly from Tamil Nadu coast. Seaweeds are not only high ecological, but also of great economic importance. Dried thalli are directly used as human and animal food and also as fertilizer. Seaweed makes a substantial contribution to marine primary production and provide habitat for near shore benthic communities [3]. Marine algae have been explored as a resource for treating various medical conditions due to their antihypertensive, antioxidant, antibiotic and anti-inflammatory properties [4]. The macroalgal community serves as a valuable bio indicator, because macroalgal species respond rapidly to environmental changes in the coastal ecosystem [5]. Algae are naturally abundant, mostly autotrophic, found in all kinds of aquatic bodies, with different environmental conditions.

MATERIALS AND METHODS

The study was carried out for the period of six months from October 2016 to March 2017 at Muttom Coast in South west coast of India. Seaweeds and sea water was collected for each month. Seaweeds were collected by hand picking and kept in polythene bags and transported to the laboratory for further identification. The collected seaweeds were carefully analyzed to study its distribution, morphology and abundance. Seawater samples were carefully taken to the laboratory for investigation. Hydrological parameters such as Temperature, pH, total dissolved oxygen and electrical conductivity were determined using standard methods.

RESULTS AND DISCUSSION

Seaweeds are one of the most important marine living resources in the world. They play a key role in coastal diversity. In the recent years, attention was focused on the biodiversity of marine algal populations at different regions of east and west coasts of India [6]. Water is a great concern of biologist and environmentalist. The studies about the variation in the hydrological parameters are very important factor. The environmental parameters differ with seasonal periods and changes in ecological conditions can influence the synthesis of nutrients in seaweeds. Temperature regulates the biogeochemical activities of the marine environment. The water temperature ranged between minimum value was 25.1°C and maximum value was 27.6°C. This result supports the findings of [7] Pillai and Prabhavathy, 2012. Hydrogen ion Concentration (pH) is closely related to free CO₂. During the study period, the pH varied from minimum value (7.11) and maximum value 7.81. The maximum pH was observed in the month of March. The elevated pH level in the summer might be due to the water evaporation and high salt accumulation in Palk strait [8],[9] Prabu *et al.*, 2008 also recorded a variation in pH in the Muttom coastal waters. Salinity showed fluctuations between months and different sites. The maximum salinity recorded in the month of March and minimum was in December. The salinity values showed a general downstream increase towards sea in the study station was due to the influence of seawater entry or seepage from the sea. Higher salinity observed during the non-monsoon season was due to the influence of higher solar radiation and the domination of adjacent neritic water into



**Juwairiya Nasreen et al.,**

the study area with the decrease in fresh water flow [9]. During the study period, salinity positively correlated with the temperature. Dissolved oxygen is required for many physical and biological processes prevailing in salt water. DO was found maximum (6.33) in the month of December and minimum (5.65) in the month of March. The low concentration of dissolved oxygen in non-monsoon season was attributed to increase in the temperature and salinity of water as observed in the Manakudy estuary [10]. Electrical conductivity varied from minimum (7.24) to maximum (7.24). Electrical Conductivity more during the month of March. [11] Sharma (1986) reported that during non-monsoon months electrical conductivity showed an increasing trend with increase in ambient temperature. Biological Oxygen Demand is dissolved oxygen required by microorganism for aerobic decomposition of organic matter present in water. BOD is found maximum (0.82) in the month of March and minimum (0.60) in the month of December. High temperature does play an important role by increasing rate of oxidation. The high BOD content during summer may be due to the high rate of organic decomposition, influenced by high temperature [12]. The clear differences in the responses of macroalgal species groups to the environmental factors were observed in the present study. The red algal species showed the high degree of correlation with the maximum temperature gradient. The brown algae showed some positive response to the higher temperature in the study area but less than the red algae this accordance with the red algae generally having higher affinity to warm water compared brown algae. During the study period, a total of 20 seaweeds belonging to Chlorophyta, Phaeophyta and Rhodophyta were collected were collected. The percentage contribution was Chlorophyta (25%), Phaeophyta (25%) and Rhodophyta (50%). The distribution, morphology and the seasonal variation of seaweeds along with the hydro biological parameters were considered and related to the algal distribution. The distribution of species varied between months. Along the south most coast of India the littoral and sublittoral rocky areas supports a good of different seaweeds especially green, brown and red seaweeds.

ACKNOWLEDGEMENT

The author wishes to thank Manonmanium Sundaranar University, Abishekapatti, Tirunelveli-627 012, Tamil Nadu, India.

REFERENCES

1. V.Krishnamurthy, *Anonymous seaweed: Wonder plants of the sea*. Aquaculture foundation of India. pp 30, 2005.
2. DLiu, J. K. Keesing, P. He, Z. Wang, Y. Shi and Y. Wang. "The world's largest macroalgal bloom in the Yellow Sea, China: formation and implications". *Estuar Coast Shelf Sci.*, 129:2-10, 2013.
3. S.L. Williams and J. E. Smith. "A Global Review of the Distribution, Taxonomy and Impacts of Introduced Seaweeds". *The Annual Review of Ecology, Evolution and Systematics*, 38: 327-59. 2007.
4. M. S Tierney, A. K. Croft and M. Hayes. "A review of antihypertensive and antioxidant activities in macroalgae". *Bot. Mar.*, 53: 387-408, 2010.
5. M. S. Tribollet, and P. S. Vroom. "Temporal and Spatial comparison of the relative abundance of macroalgae across the Marina Archipelago between 2003 and 2005". *Phycologia.*, 46: 187-197, 2007.
6. J. Rath. and S. P. Adhikary. "Distribution of Marine macroalgae at different salinity gradients in Chilika Lake, India". *J. Mar. Sci.*, 34 (2): 237-241, 2005.
7. M. Pillai. and H. Prabavathy. "Studies on Physiochemical characteristics and distribution of intertidal diatoms associated with sediments at Chankuthurai coast, Kanyakumari District, Tamil Nadu". *Seaweed Res. Utilin.*, 34(1&2): 182-190, 2012.
8. V.Srinivasan, U. Natesan and A. Parthasarathy. "Seasonal Variability of coastal water quality in Bay of Bengal and Palk Strait, Tamilnadu, Southeast coast of India". *Int. J. Braz. Arch. Biol. Technol.*, 56(5): 875-884, 2013.
9. A.V Prabh, M. Rajkumar and P. Perumal. "Seasonal variations in Physico- Chemical Characteristics of Pitchavaram mangroves, Southeast coast of India". *J. Environ. Biol.*, 29(3): 945-950, 2008.
10. M. Sukumaran. *Studies on Microbiol ecology in Manakudy estuary, South India*. Ph.D. thesis, University of Kerala. pp. 13, 2001





Juwairiya Nasreen et al.,

11. R. C. Sharma. "Effect of Physico-Chemical factors on benthic fauna of Bhagirathi River, Garhwal Himalaya". *Indian. J. Ecol.*, 13: 133-137, 1986.
12. L. R Bhatt, R. P. Lacoul, H. D. Lekhak and P. K. Jho. "Physico chemical characteristics and phytoplanktons of Taulaha Lake, Kathmandu". *Poll. Res.*, 18(4): 353-358,1999.

Table 1: Physico-chemical parameters recording in the experimental station during October 2016-March 2017

Parameters	October	November	December	January	February	March
Temperature	25.7±0.52	26.3±0.08	25.1±0.12	26.2±0.40	27.2±0.61	27.6±0.16
pH	7.25±0.16	7.53±0.12	7.11±0.08	7.36±0.07	7.49±0.64	7.81±0.06
Salinity	29.8±0.33	32.4±0.16	30.1±0.04	33.2±0.36	34.6±0.36	35.7±0.08
TDS	30.3±0.21	31.5±0.40	32.4±0.21	32.9±0.16	33.4±0.40	35.9±0.24
Electrical conductivity	5.05±0.81	5.16±0.23	5.23±0.36	5.77±0.21	6.09±0.12	7.24±0.40
DO	6.21±0.56	6.27±0.28	6.33±0.65	6.11±0.89	5.94±0.46	5.65±0.35
BOD	0.64±0.03	0.63±0.02	0.60±0.02	0.67±0.10	0.74±0.01	0.82±0.08

Table 2: Distribution of Seaweeds in Muttom

S.No	Name of the Macroalgae	Months					
		October	November	December	January	February	March
Chlorophyta							
1.	<i>Bryopsis plumosa</i>	-	+	+	-	-	-
2.	<i>Caulerpa peltata</i>		++	+	-	-	-
3.	<i>Chaetomorpha antennina</i>	++	+++	++	-	+	+
4.	<i>Ulva fasciata</i>	++	+	-	+	-	+
5.	<i>Ulva lactuca</i>	+++	++				
Phaeophyta							
1.	<i>Ectocarpus simpliciusculus</i>	+	++	+	++	-	-
2.	<i>Padina gymnospora</i>	-	+	-	-	-	+
3.	<i>Sargassum linearifolium</i>	-	-	-	-	+	-
4.	<i>Sargassum wightii</i>	+	-	+	++	-	-
5.	<i>Sargassum spp</i>	+	-	+	+	-	-
Rhodophyta							
1.	<i>Corallina berteroi</i>	-	+	-	-	-	-
2.	<i>Gelidium pusillum</i>	+	++	-	+	-	-
3.	<i>Gracilariacorticata</i>	+++	+++	+	++	+	+
4.	<i>Gracilaria corticata. var. cylindrica</i>	-	-	-	+++	++	+
5.	<i>Gracilaria edulis</i>	-	+	-	-	-	-
6.	<i>Grateloupialithophila</i>	-	-	-	+	-	-
7.	<i>Laurencia obtusa</i>	-	+	-	+++	-	-
8.	<i>Hypneanuscififormis</i>	-	+	-	++	-	+













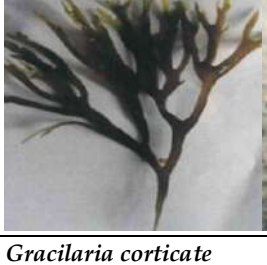







Juwairiya Nasreen et al.,

9.	<i>Hypneavalentiae</i>	++	+	-	-	-	+
10.	<i>Spyridiahypnoides</i>	-	++	-	++	-	+





(+++ Abundant; ++ Common; + Rare; - Absent.)

			
<i>Bryopsis plumosa</i>	<i>Caulerpa peltata</i>	<i>Chaetomorpha antennina</i>	<i>Ulva fasciata</i>
			
<i>Ulva lactuca</i>	<i>Ectocarpus simpliciusculus</i>	<i>Padina gymnospora</i>	<i>Sargassum linearifolium</i>
			
<i>Sargassum wightii</i>	<i>Sargassum spp</i>	<i>Corallina berteroi</i>	<i>Gelidium pusillum</i>
			
<i>Gracilaria corticate</i>	<i>Gracilaria corticata</i>	<i>Gracilaria edulis cylindrica</i>	<i>Grateloupia lithophila var.</i>





Juwairiya Nasreen et al.,

			
<i>Laurencia obtuse</i>	<i>Hypnea musciformis</i>	<i>Hypnea valentiae</i>	<i>Spyridia hypnoides</i>





Synthesis and Characterization of Escin Gold Nanoparticles: Evaluation of its *In vitro* Antioxidant Properties

K.Amali¹, A. Justin Thenmozhi^{2,3*} and T. Manivasagam³

¹Research Scholar, Department of Biochemistry and Biotechnology, Faculty of Science, Annamalai University, Annamalai Nagar, Tamil Nadu, India

²Assistant Professor, Department of Biochemistry, School of Biological Sciences, Madurai Kamaraj University, Madurai, Tamilnadu, India.

³Assistant Professor, Department of Biochemistry and Biotechnology, Annamalai University, Annamalainagar, Tamilnadu, India.

Received: 29 Sep 2023

Revised: 20 Nov 2023

Accepted: 30 Jan 2024

*Address for Correspondence

A. Justin Thenmozhi

Assistant Professor,
Department of Biochemistry,
Madurai Kamaraj University,
Madurai, Tamil Nadu, India.
E mail: justinthenmozhi@rediffmail.com



This is an Open Access Journal / article distributed under the terms of the **Creative Commons Attribution License** (CC BY-NC-ND 3.0) which permits unrestricted use, distribution, and reproduction in any medium, provided the original work is properly cited. All rights reserved.

ABSTRACT

Nanotechnology is an emerging field that have wide applications from cosmetics to medicine. Gold nanoparticles (AuNps) are reported be inert in nature and antioxidant functions of gold may results in several pharmaceutical properties. The aim of the present study is to analyse the synergetic antioxidant effect of gold nanoparticles with the natural antioxidant escin. AuNps-escin synthesis was confirmed by UV-Vis spectroscopy, X-ray diffraction (XRD), Dynamic light scattering (DLS), Fourier transform infrared spectroscopy (FT-IR), scanning electron microscopy (SEM) and transmission electron microscopy (TEM) methods. *In vitro* antioxidant assays were studied to compare the reactive oxygen species, scavenging activity of green synthesized AuNps-esc with standard ascorbic acid (AA) and escin. AuNps-esc possesses enhanced and dose-dependent antioxidant activities than the AA and escin alone treated groups. In conclusion, the enhanced antioxidant effect of AuNps-esc as compared to escin alone treatment is owing to the synergistic effect of escin with AuNps.

Keywords: AuCl₃, escin, AuNPs-escin, characterization, ascorbic acid, biochemical assays





INTRODUCTION

Nanotechnology has created many revolutions in the medicinal field and enhanced the development of a new field of interest called as nanomedicine, leading to the improvement of drugs with improved bioavailability, lowered toxicity and side effects [1]. Metallic nanoparticles particularly bio-reduced gold and silver nanoparticles are having key advantage in biomedical applications [2]. The gold nanoparticles (AuNPs) are reported to have simple in synthesis and characterization, surface adaptation, reduced toxicity, tunable surface plasmon resonance, steadiness and bioavailability with antimicrobial, wound-healing and antioxidant properties when coupled with natural phytochemicals [3]. Gold nanoparticles (AuNPs) are reported to be inert in nature and antioxidant functions of gold may result in several pharmaceutical properties.

Reactive oxygen species (ROS) are considered as the vital player in the regulation of several cellular events. But their accumulation in the biological system could lead to oxidative stress and thus eradicate the cellular homeostasis [4]. Antioxidant consumption has been linked with reducing DNA damage, malignancy, cellular injury and diminished the occurrence of oxidative stress mediated degenerative disorders such as cancer, heart diseases, Parkinson's disease, Alzheimer's disease etc [5]. Few antioxidants like glutathione and uric acid are endogenous, whereas, most of them are exogenous in nature i.e., obtaining from the diet [6]. Previous studies have emphasized the prominence of dietary intake of secondary metabolites that are ubiquitously exist in vegetables and fruits lowering the manifestations of several diseases [7].

Aesculus hippocastanum (horse chestnut) is mainly used as a traditional medicine from ancient times [8] and now also used to treat the varicose veins, hematoma, hemorrhoids, and venous congestion [9, 10]. *A. hippocastanum* extract is a potent scavenger of ROS, and reported to have strong (20 times) antioxidant activity against superoxide radical as compared to ascorbic acid [9]. Escin is the main constituent in horse chestnut and accounting for utmost of its pharmacological properties. The antioxidant activities mainly depend on the presence of hydroxyl groups i.e., enhancing hydrogen-donating and ion-chelating capability [11]. Investigators have achieved innovation in the experimental studies by using two or more antioxidant agents simultaneously for treating the disease [12]. The synergistic/additive role of their components may enhance the therapeutic effect [13]. Hence, aim of the present study is to synthesise and characterize the escin gold nanoparticles and analysing the synergetic antioxidant effect of green synthesised escin gold nanoparticles with natural antioxidant escin.

MATERIALS AND METHODS

Chemicals

β escin and AuCl_3 were procured from Sigma Aldrich, USA. DPPH (1,1-diphenyl-2-picryl hydrazyl) reagent, methanol, ascorbic acid (AA), potassium persulphate, 2,2'-Azino bis-3 ethylbenzotiazole 6 sulphonic acid (ABTS), 2,2'-ferric chloride, EDTA, 2-deoxyribose, hydrogen peroxide, thiobarbituric acid, trichloro acetic acid, potassium ferricyanide, NADH, nitroblue tetrazolium, PMS, phosphate buffer saline and potassium ferricyanide were procured from Hi-media, Bangalore. All other used chemicals were of analytical grade.

Green synthesis of AuNp-esc

The AuNp-esc was synthesized by mixing 20 ml of 0.1% escin in 1mM AuCl_3 [14]. The mixture solution is then kept under the direct sun light for one hour. During the incubation period, the above said colourless solution was first turned to dark brown and then into purple colour. For the complete reduction of AuCl_3 to AuNPs, the solution was kept at room temperature for 2 days and was monitored by spectrophotometrically. Finally the suspension was centrifuged (12,000 rpm for 20 min) to attain the pellets for characterization studies.

Characterization of AuNp-esc

UV spectroscopy





Amali et al.,

The synthesis of AuNps-esc were monitored by UV spectroscopy (Lamda 365 model- Perkin Elmer UV spectrum) in the range 400-700nm. The distilled water was used as blank solution.

Dynamic light scattering (DLS) method

The size, molecular weight, diffusion constant and interaction length of the particles were measured by DLS [15]. The size of AuNps-esc particle was measured by normal hydrodynamic size and with the minimal polydispersity index.

X-ray diffraction (XRD) analysis

The XRD analysis was done by an X-ray diffractometer at 30 mA and 40 kV.

FTIR Analysis

The AuNp-esc was analysed in FTIR range (400-4000 cm^{-1}) to study the interaction between escin and AuNps.

Scanning Electron Microscope

Freeze dried sample was performed by mounting nanoparticles on specimen slide with double side adhesive and coated with platinum in sputter for examination (JEOL-JSM-5610LV with INCA EDS) [16].

Transmission Electron Microscope

The sample was sonicated for 5 mins. AuNp-esc samples were applied on carbon layered copper grids and the solvent was evaporated by Infra light (30 mins). TEM analysis was carried out by the protocol according to [14].

In vitro antioxidant assay**ABTS scavenging test**

In this method, 25, 50 μl and 100 μl of standard AA, escin and AuNps-esc were added with ABTS reagents containing 2.5 mM potassium persulphate and preserved in the dark place (12 h) to prevent the incomplete oxidation. Water was used as blank and absorbance was read at 734 nm [17].

Scavenging assay (%) = Control OD- test OD/control OD $\times 100$

DPPH scavenging analysis

The reaction solutions (3 ml) containing 1ml of DPPH (dissolved in methanol), various concentrations (25, 50 μl and 100 μl) of samples AA, escin and AuNps-esc were diluted to 3 ml. Then tubes were kept in dark place for 30 mins and was measured spectroscopically (517 nm) [18].

Free radical scavenging activity (%) = Control OD- test OD/control OD $\times 100$

Hydroxyl radical scavenging analysis

Incubation mixture consists of 0.1 ml of potassium per sulphate buffer (100mM), 0.2 ml of ferric chloride (500mM), 0.1ml of EDTA (1mM), 2-deoxyribose (10mM), several concentrations (25, 50 μl and 100 μl) of AA, escin and AuNps-esc and 0.1 ml of H_2O_2 . Then it was mixed and kept at room temperature for 1 h and added with 1ml of TBA and TCA. The reaction mixture was placed in boiling water bath (30 mins) and OD was read (535nm) [19]. The percentage scavenging activity was calculated as follows

Scavenging activity (%) = Control OD- test OD/control OD $\times 100$

Metal chelation activity

Varying concentrations of AA, escin and esc-AuNps (25, 50 and 100 μl) in double distilled water was mixed with 50 μl of 2 mM ferrous chloride and 200 μl of 5 mM ferrozine solution. The solution was mixed thoroughly and incubated in dark at room temperature for 10 min. The absorbance was read at 562 nm [20]. The percentage chelating activity was calculated as shown below: Scavenging activity (%) = Control OD- test OD/control OD $\times 100$

Super oxide anion scavenging activity

The reaction mixture consists of 1ml of NADH (100mM), 1ml of nitroblue tetrazolium (100mM) and varying volumes of AA, escin and esc-AuNps (25, 50 μl and 100 μl) were added with 100 μl of PMS. It was incubated at 37°C for 15 minutes followed by the measuring absorbance at 560nm spectrophotometrically [21].

Scavenging activity (%) = Control OD- test OD/control OD $\times 100$





Amali et al.,

Data analysis

All data were expressed as the mean±standard error (SEM) of the six numbers of experiments. The statistical significance was calculated by one-way analysis of variance using SPSS version 15.0 and the individual comparisons were obtained by Duncan's Multiple Range Test (DMRT). A value of $p < 0.05$ was considered to indicate a significant difference between groups and the values sharing a common alphabet do not differ significantly with each other.

RESULTS**Visual Observation**

In the present experiment, Figure 1 depicts escin solutions before (A) and after reaction with Au⁺ ions (B). After the addition of AuCl₃ to the escin solution, the colourless mixture turned to dark brown and then into purple colour. The colour remains unchanged even after the incubation period of 2 days.

UV-Visible Spectral Analysis

The light absorption pattern of the AuNp-esc was monitored in the series of 400–700 nm using a UV-visible spectrophotometer. The UV-visible spectra recorded at 2 h after introducing gold ions into the flask containing the escin resulted in the spectrum of increasing intensity (Figure 2) at around 537 nm.

DLS analysis

The results of DLS showed the hydrodynamic size particle of AuNps-esc is 60.1nm (Figure 3).

XRD analysis

In escin AuNps peaks were noticed at 37.6°, 43.7°, 64.0° and 76.8°. The first peak is more intense than the other three. The polydispersity value between 0.05-0.7 the obtained results supports the size of the particle (Figure 4).

FTIR analysis

To determine the occurrence of different functional groups of AuNps-esc, Perkin- Elmer FTIR spectrum was used. It was determined that the vibrations at 3434 ^{cm-1}/ 3644 ^{cm-1} arising peaks of AuNps-esc corresponds to -OH group in saponin structure. This is also strengthen the studies of seed extract of beta escin (triterpanoid) contains -OH group due to stretching -OH in the peaks obtained (Figure 5).

SEM analysis

SEM image of AuNps-esc can be envisaged in Figure 6. The SEM images displayed the aggregation of reduced gold. Based on SEM images, AuNps-esc presented the occurrence of polydispersity rectangular particles and the particle size range from 74 nm to 105 nm respectively.

TEM analysis

TEM images of gold nanoparticles formed with the escin are shown in Figure 7. The synthesized AuNPs were of spherical or almost spherical shape and polydispersity with approximately diameter of 20 nm. The ring-like pattern with bright circular spots corresponding to Bragg's planes confirmed the polycrystalline structure of gold nanoparticles.

In vitro antioxidant assays

The results of the present study indicated the free radical scavenging activity of green synthesized AuNps-esc as compared to standard AA and escin. The antioxidant (superoxide anion scavenging - Figure 8A, hydroxyl radicals scavenging- Figure 8B, ABTS radical scavenging- Figure 8C, DPPH radical scavenging - Figure 8D and metal chelating - Figure 8E activities of AuNps-esc possesses more significant and dose-dependent inhibition than AA and escin alone treated groups. In all above said assays, esc exhibited potent antioxidant and metal chelating activities than AA treated groups.

DISCUSSION

The conversion of colourless solution to brown and then to purple colour endorses the reduction of Au³⁺ to Au⁰ for the synthesis of AuNps-esc. Colour change is the clear indication of AuNps synthesis, which occurs due to the reduction of gold ions and excitation of surface plasmon vibrations in the nanoparticles [22]. Upon filtration, the





Amali et al.,

colour remains unchanged even after the incubation period of 2 days demonstrating that newly synthesized AuNPs are well dispersed and did not aggregated (Fig.1). The UV–visible spectrophotometer analysis exhibited a peak at 540 nm absorbance (Fig. 2), indicating the formation of more gold nanoparticles in the solution. In general, AuNPs show a precise plasmon peak (500-580 nm), which is used to find the synthesis of gold nanoparticles [23]. DLS measurements exhibited that the particle size of AuNPs-esc were found in the range of 10-1000 nm, however, the maximum percentage of particles are found in the size of 60.1 nm. In XRD studies, AuNPs-esc peaks were noticed at 37.6°, 43.7°, 64.0° and 76.8°. The first peak is more intense than the other three. The XRD analysis of leaf extracts of *Aesculus hippocastanum* showed a peak found at 38° and indicated that β -escin as the active compound [24]. The slight difference found in the present experiment may be owed to the occurrence of pure compound, β -escin.

FTIR spectrum showed unique functional groups in their respective peaks range. The region between 3644 – 3420 cm^{-1} relates to –OH vibrations. Weaker peak at 2927 indicated the asymmetric stretching of methylene group(C-H). Clear band in 1637 can be related to form primary amine groups in the NH bend. Sharp and clear IR band is formed at 1384 represented C-N stretching vibration of aliphatic amines. These signals can be correlated to the plenitude functional compound present in escin. In SEM images, AuNPs-esc showed the presence of polydispersity rectangular particles due to the bio reduction of gold ions and the average size of the particle was from 10 to 200 nm range. However nanoparticles were aggregated and tough to differentiate shape from one another due to presence of some additional polymeric compounds that kept NPs closely linked each other. The pH, temperature and oxidation state of the gold displayed a key role in the formation of the uncontrolled sized and shaped nanoparticles [25]. The synthesized AuNPs were having spherical or near-spherical shape with an average diameter of 20 nm. AuNPs encapsulated by several organic biomolecules. Singh et al [26] reported a similar geometry of synthesized gold nanoparticles using natural precursor clove. The difference found in particles size as calculated by DLS, SEM and TEM may be owing to the difference in detection methods and principles.

Reactive oxygen species (ROS) are involved in the cause and progression of chronic diseases including neurodegenerative diseases [27]. Administration of gold nanoparticles have been improved the biocompatibility of natural products [28]. The 2, 2-diphenylpicrylhydrazyl (DPPH) assays is a commonly used for the evaluation of antioxidant properties of compounds. DPPH radical itself contains an unpaired electron that is accountable for deep purple colour. If this compound receives an electron from an antioxidant, DPPH is decolorized, which can be quantified by alterations in optical density. ABTS assay is mainly established on inhibition of the ABTS radical cation synthesis. ABTS is substrate for peroxidase, and if it is oxidized to form a metastable radical cation in the presence of H_2O_2 with altered absorption spectrum. DPPH is the main radical scavenger while ABTS is involved in Hydrogen atom transfer and Single electron transfer. Hydroxyl radical is a strong ROS induces cellular damage by disturbing plasma membrane. The metal chelating assay measures the chelating capacity of AUNPs-esc nanoparticles for ferrous ions which was indicated by colour change [29]. Nanoparticles can scavenge superoxide anion (most toxic form of ROS) as that of the function of superoxide dismutase in biological systems [30]. Metal NPs are having the capability to eliminate superoxide ions by altering the surface electronic states at large surface area to volume ratio. In this study, it was observed that the scavenging ability of AUNPs-esc against various ROS is increased in a dose dependent way as comparison with escin alone.

CONCLUSION

Herein, we have reported the green synthesis of AuNPs from escin and confirmed the synthesis of gold nanoparticles by using UV-visible spectroscopy, XRD, DLS analysis, and FT-IR techniques. Further, the size, shape and characterization of the synthesized AuNPs-esc were analysed by SEM and TEM. The promising free radical scavenging activities of phyto-engineered gold nanoparticles are mainly owing to the synergetic effect of antioxidant capacity of escin with chemically inert nature and antioxidant properties of gold. Further, It is suggested that the synthesised AuNPs-esc may be investigated in *in vivo* models for their potential therapeutic applications.





Amali et al.,

REFERENCES

1. Ventola CL. The nanomedicine revolution: part 2: current and future clinical applications: P T. 2012 Oct; 37(10):582-91.37:582-91.
2. Mody V, Siwale R, Singh A, Mody H. Introduction to metallic nanoparticles: J Pharm Bioall Sci 2010; 2:282-9.
3. Boomi P, Ganesan R, Prabu Poorani G, Jegatheeswaran S, Balakumar C, Gurumallesh Prabu H, Anand K, Marimuthu Prabhu N, Jeyakanthan J, Saravanan M. Phyto-Engineered Gold Nanoparticles (AuNPs) with potential antibacterial, antioxidant, and wound healing activities under in vitro and in vivo Conditions: Int J Nanomedicine 2020;15:7553-7568.
4. Richardson. C, Yan .SC. Vestal Oxidative stress, bone marrow failure and genome instability in hematopoietic stem cells: Int. J. Mol. Sci., 16 (2) (2015), pp. 2366-2385.
5. Joanne L, Watters, Jessie A, Satia, Larry K, James AS, Jane C, Schroeder, Boyd RS. Associations of antioxidant nutrients and oxidative DNA damage in healthy African-American and white adults: Cancer Epidemiol Biomarkers Prev 2007; 16:1428–1436
6. Mohamad IK, Giridhar P. Dietary antioxidants: the insurer of health: Everyman’s science 2011; XLVI, p 4.
7. Patricia IM, Mario SO, Olov S, Esther LP. In: V Rao (ed) Phytochemical studies of fractions and phytochemicals: a global perspective of their role in nutrition and Health. In Tech 2012; ISBN 978-953-51-0296-0.
8. Sirtori CR. Aescin: pharmacology, pharmacokinetics and therapeutic profile: Pharmacol Res 2001; 44: 183-193.
9. Masaki H, Sakaki S, Atsumi T, Sakurai H. Active-oxygen scavenging activity of plant extracts. Biol Pharm Bull 1995; 18: 162-166.
10. Carrasco OF, Vidrio H. Endothelium protectant and contractile effects of the antivaricose principle escin in rat aorta: Vascul Pharmacol 2007; 47: 68-73.
11. Vašková J, Fejčáková A, Mojžišová G, Vaško L, Patlevič P. Antioxidant potential of *Aesculus hippocastanum* extract and escin against reactive oxygen and nitrogen species: Eur Rev Med Pharmacol Sci 2015;19(5):879-86.
12. Jennifer F. Compounds present in *Vernonanthura Patens* with antifungal Bioactivity and Potential as Antineoplastic: managing hypertension using combination therapy. Am Fam Physician 2008; 77(9):1279–1286.
13. Kawabata S, Gills JJ, Mercado-Matos JR, LoPiccolo J, Wilson W III, Hollander MC, Dennis PA. Synergistic effects of nelfinavir and bortezomib on proteotoxic death of NSCLC and multiple myeloma cells: Cell Death Dis 2012; 3:e353.
14. Bhanuvalli R. Shamprasad, Sivakumar Keerthana, Sengan Megarajan, Robert Lotha, Sivasubramanian Aravind, Anbazhagan Veerappan,. Photosynthesized escin stabilized gold nanoparticles exhibit antidiabetic activity in L6 rat skeletal muscle cells: Materials Letters 2019; Volume 241, Pages 198-201, ISSN 0167-577X.
15. Youngil Lee1, Jun-rak Choi1, Kwi Jong Lee1, Nathan E Stott1, and Donghoon Kim1. Large-scale synthesis of copper nanoparticles by chemically controlled reduction for applications of inkjet-printed electronics. IOP Publishing Ltd. Nanotechnology 2008; 19 415604.
16. Aritonang HF, Koleangan H, and Wuntu AD. Synthesis of silver nanoparticles using aqueous extract of medicinal plants' (*Impatiens balsamina* and *Lantana camara*) fresh leaves and analysis of antimicrobial activity: International Journal of Microbiology 2019.
17. Wolfenden BS, and Willson RL. Radical-cations as reference chromogens in kinetic studies of one-electron transfer reactions: pulse radiolysis studies of 2, 2'-azinobis-(3-ethylbenzthiazoline-6-sulphonate): Journal of the Chemical Society 1982; Perkin Transactions., 2 805-12.
18. Brand-Williams W, Cuvelier ME, and Berset CL. Use of a free radical method to evaluate antioxidant activity: LWT-Food science and Technology 1995; 28 25-30
19. Halliwell B, Gutteridge JM, and Aruoma OI. The deoxyribose method: a simple “test-tube” assay for determination of rate constants for reactions of hydroxyl radicals: Analytical Biochemistry 1987; 165 215-9.
20. Soler-Rivas C, Espín JC, and Wichers HJ. An easy and fast test to compare total free radical scavenger capacity of foodstuffs. Phytochemical Analysis: An International Journal of Plant Chemical and Biochemical Techniques 2000; 11 330-38.





Amali et al.,

21. Nishimaki N, Matsusaka Y, and Doi Y. On the FB centers in alkali halides: Journal of the Physical Society of Japan 1972; 33 424-9.
22. Rahi DK, and Parmar AS. Mycosynthesis of silver nanoparticles by an endophytic *Penicillium* species of Aloe vera root, evaluation of their antibacterial and antibiotic enhancing activity: International Journal of Nanomaterials Biostructures 2014; 46 51
23. Elyahb Allie Kwizera, Elise Chaffin, Xiao Shen, Jingyi Chen, Qiang Zou, Zhiming Wu, Zheng Gai, Saheel Bhana, Ryan O'Connor, Lijia Wang, Hitesh Adhikari, Sanjay R. Mishra, Yongmei Wang, and Xiaohua Huang. Size- and Shape-Controlled Synthesis and Properties of Magnetic-Plasmonic Core-Shell Nanoparticles: The Journal of Physical Chemistry C. 120 2016; 10530-46.
24. Kup Aylikci N. Semi-empirical determination of $K\alpha_{1, 2}$, $K\beta_{1, 3}$, and $K\beta_{2, 4}$ X-ray natural line widths for various elements between $29 \leq Z \leq 74$ at 123.6 keV: Spectroscopy Letters 2019; 52 346-55.
25. Anuradha J, Abbasi T, and Abbasi SA. An eco-friendly method of synthesizing gold nanoparticles using an otherwise worthless weed pistia (*Pistia stratiotes* L.): Journal of Advanced Research 2015; 6 711-20.
26. Singh AK, Talat M, Singh DP, and Srivastava. Biosynthesis of gold and silver nanoparticles by natural precursor clove and their functionalization with amine group: Journal of Nanoparticle Research 2010; 12 1667-75
27. Jomova K, and Valko M. Advances in metal-induced oxidative stress and human disease: Toxicology 2011; 283 65-87.
28. Yamada M, Foote, and Prow TW. Therapeutic gold, silver, and platinum nanoparticles Wiley Interdisciplinary Reviews: Nanomedicine and Nanobiotechnology 2015; 2015 3 428-45.
29. Inbathamizh L, Ponnu TM, and Mary EJ. In vitro evaluation of antioxidant and anticancer potential of *Morinda pubescens* synthesized silver nanoparticles: Journal of Pharmacy Research 2013; 6 32-8
30. Fukai T, and Ushio-Fukai M. Superoxide dismutases: role in redox signaling, vascular function, and diseases: Antioxidants & Redox Signal 2011; 15 1583-606.

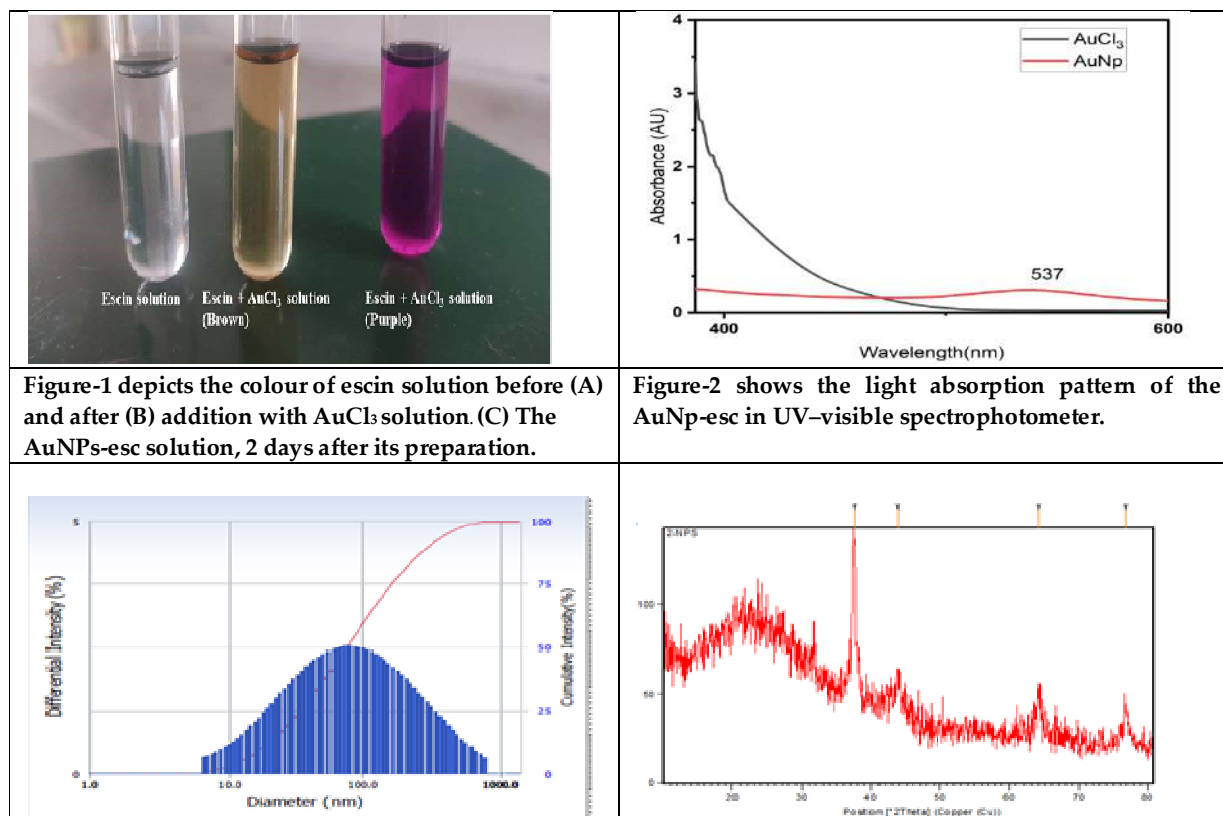


Figure-1 depicts the colour of escin solution before (A) and after (B) addition with $AuCl_3$ solution. (C) The AuNPs-esc solution, 2 days after its preparation.

Figure-2 shows the light absorption pattern of the AuNp-esc in UV-visible spectrophotometer.





Amali et al.,

Figure-3 indicates the DLS analysis of AuNps-esc

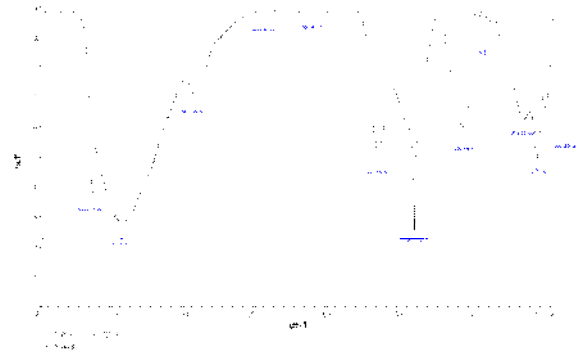


Figure-4 shows the XRD analysis of AuNps-esc

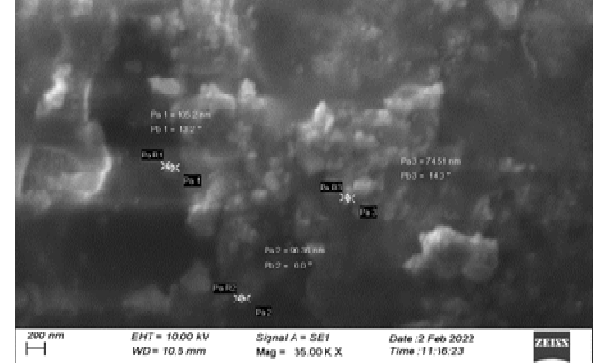


Figure-5 depicts the FT-IR studies of AuNps-esc

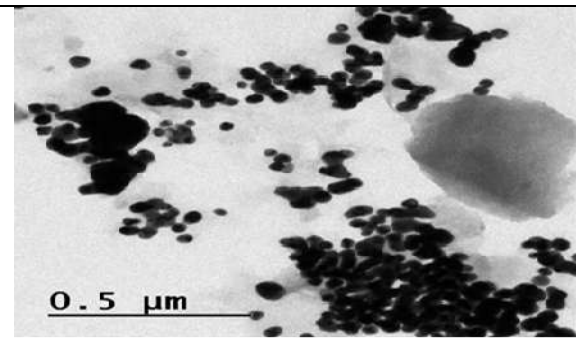


Figure-6 shows the shape and size analysis of AuNps-esc by SEM

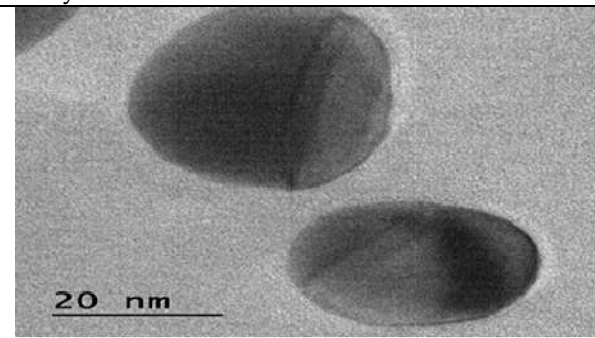
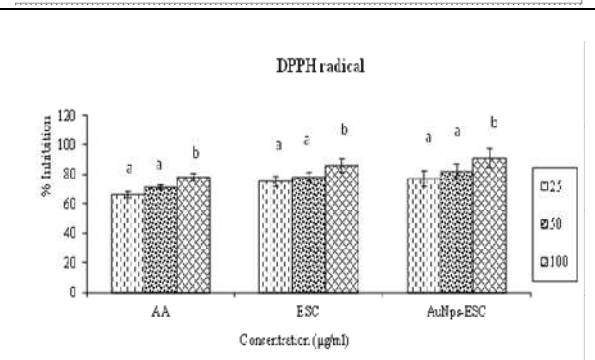
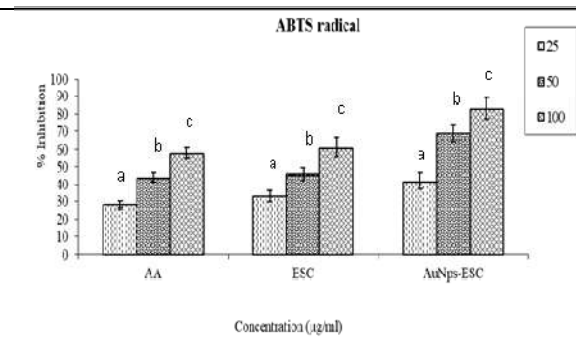
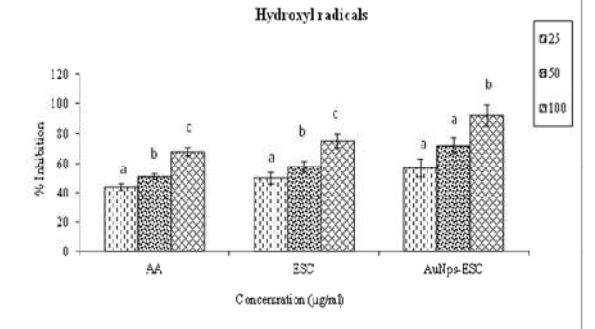
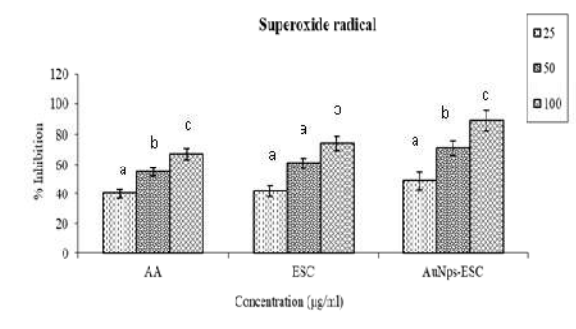


Figure-7 (A & B) shows the shape and size analysis of AuNps-esc by TEM





Amali et al.,

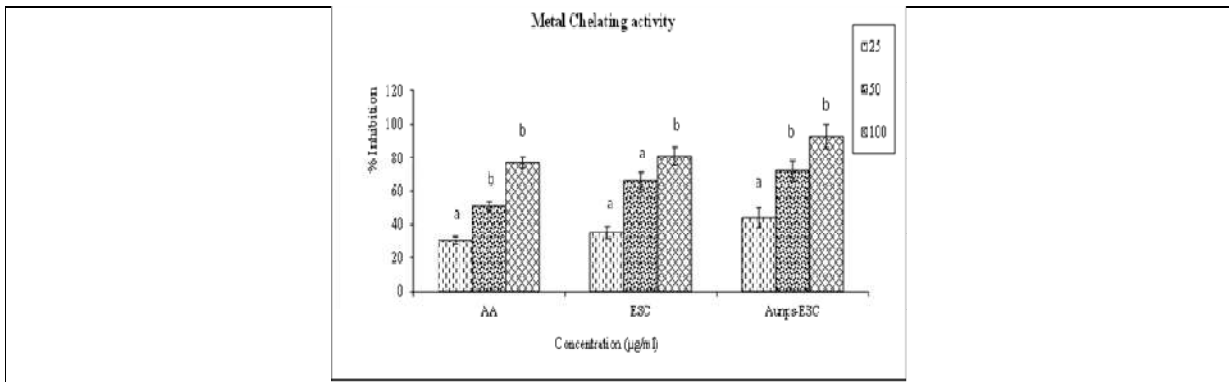


Figure-8 (A, B, C, D & E) depicts the antioxidant and metal chelating activities of AuNps- esc.





Method Development and Validation for the Simultaneous Estimation of Cefpodoxime Proxetil and Azithromycin in Bulk and Tablet Dosage form by RP-HPLC

Haritha Pavani Kondeti^{1*}, Venkata Rao Vutla², Rihana Syed¹, Vidyadhara Suryadevara²

¹Assistant Professor, Department of Pharmaceutical Analysis, Chebrolu Hanumaiah Institute of Pharmaceutical Sciences, Guntur, Andhra Pradesh, India.

²Professor and HoD, Department of Pharmaceutics, Chebrolu Hanumaiah Institute of Pharmaceutical Sciences, Chowdavaram, Guntur, Andhra Pradesh, India.

Received: 27 Oct 2023

Revised: 20 Dec 2023

Accepted: 31 Jan 2024

*Address for Correspondence

Haritha Pavani Kondeti

Assistant Professor,
Department of Pharmaceutical Analysis,
Chebrolu Hanumaiah Institute of Pharmaceutical Sciences,
Guntur, Andhra Pradesh, India.
Email: prahasa11816@gmail.com



This is an Open Access Journal / article distributed under the terms of the **Creative Commons Attribution License** (CC BY-NC-ND 3.0) which permits unrestricted use, distribution, and reproduction in any medium, provided the original work is properly cited. All rights reserved.

ABSTRACT

In simultaneous RP-HPLC method development, Waters HPLC with PDA detector and column used is Kromasil, C8, 250 × 4.6 mm, 5 μ . Injection volume of 10 μ l is injected and eluted with the mobile phase selected after optimization was mixed Methanol & Buffer (Sodium dihydrogen phosphate) in the ratio of 50:50 was found to be ideal. The flow rate was found to be optimized at 1.2 ml/min. Detection was carried out at 260 nm. Quantitation was done by external standard method with the above mentioned optimized chromatographic condition. This system produced symmetric peak shape, good resolution and reasonable retention times of Cefpodoxime Proxetil and Azithromycin were found to be 2.77 and 5.57 minutes respectively. The Cefpodoxime Proxetil and Azithromycin showed linearity in the range of 20ppm to 80ppm. The slope, intercept and correlation coefficient(s) were found to be 15655, 11860 & 0.99 for Cefpodoxime proxetil and 44258, 5996 & 0.99 respectively for Azithromycin which indicates excellent correlation between response factor Vs concentration of standard solutions.

Keywords: Cefpodoxime proxetil, Azithromycin, RP-HPLC





INTRODUCTION

In liquid chromatography, the solute retention is governed by the solute distribution factor, which reflects the different interactions of the solute – stationary phase, solute – mobile phase and the mobile phase – stationary phase. The primary objective in selection and optimization of mobile phase is to achieve optimum separation of all the individual impurities and degradants from each other and from analytic peak. For a given stationary phase, the retention of the given solute depends directly upon the mobile phase, the nature, and the composition of which must be judiciously selected to get appropriate and required solute retention. The mobile must be adapted in terms of elution strength (solute retention) and solvent selectivity (solute separation). Cefpodoxime Proxetil is an oral, third generation cephalosporin antibiotic. It is used to treat a wide variety of bacterial infections. Cefpodoxime works by stopping the growth of bacteria. It is active against most gram positive and gram-negative microorganisms. It is commonly used to treat acute otitis media, pharyngitis, sinusitis, and gonorrhoea. Cefpodoxime proxetil is a prodrug. Its active metabolite is cefpodoxime. It is marketed under the trade names Cefpo, Vantin and Otreon.

Azithromycin is a semi-synthetic antibiotic useful for the treatment of bacterial infections belonging to the class of macrolide antibiotics. It works by stopping the growth of bacteria. Azithromycin is used to treat certain bacterial infections such as bronchitis, pneumonia, pharyngitis, gastrointestinal infections etc. It is derived from erythromycin, with a methyl substituted nitrogen atom incorporated into the lactone ring. Azithromycin is more potent against certain bacterial species than erythromycin. It is marketed under the trade names zithrox, zithromax etc., Extensive literature review was conducted and an attempt was made to develop an unambiguous, valid method for the simultaneous estimation of Cefpodoxime and Azithromycin. Few of spectroscopic, chromatographic, and other analytical methods have been reported for the estimation of Cefpodoxime and Azithromycin individually and or along with drug combinations in pharmaceutical preparations. The aim of this study is to develop and validate a new simple, accurate and economic stability-indicating HPLC method with less runtime, which would be able to separate and quantify a combination of Cefpodoxime and Azithromycin in a single run. The developed method was validated as per ICH guidelines and can be applied lucratively to quality control purposes.

MATERIALS AND METHODS

Preparation of Standard solution

Standard stock solution of Cefpodoxime and Azithromycin was prepared by dissolving 200 mg of Cefpodoxime and 250 mg of Azithromycin in 100 ml of diluent. From this transfer 4 ml of stock solution into 100 ml volumetric flask and make up the volume with diluent (80 and 100 ppm respectively). From this solution transfer 1 ml into 10 ml volumetric flask and made up to the volume with diluent (8 and 10 ppm respectively).

Preparation of Sample solution

Weigh 10 tablets and crush into fine powder and accurately transfer equivalent to 200 mg of Cefpodoxime and 250 mg of Azithromycin into 100 ml volumetric flask, add 50 ml of diluent, sonicate for 15 minutes with occasional stirring, and make up to the volume with diluent. Then pipette out 4 ml of stock solution and transfer into 100 ml volumetric flask and make up to the volume with diluent.

METHOD VALIDATION

The developed and optimized RP-HPLC method was validated according to international conference on harmonization (ICH) guidelines Q2(R1) in order to determine the system suitability, linearity, limit of detection (LOD), limit of quantification (LOQ), precision, accuracy, ruggedness and robustness.

System suitability

System suitability parameters were evaluated to verify system performance. 10 µL of standard solution was injected five times into the chromatograph, and the chromatograms were recorded. Parameters such as number of theoretical plates and peak tailing were determined.

Specificity

The specificity of the analytical method was established by injecting the solutions of diluent (blank), placebo, working standards and sample solution individually to investigate interference from the representative peaks.





Haritha Pavani Kondeti *et al.*,

Precision

Repeatability/method precision was performed by injecting six replicates of same concentrations of cefpodoxime and azithromycin, calculated % assay and %RSD for each compound. Reproducibility/Ruggedness/Intermediate precision was performed using different analysts and a different instrument in the same laboratory.

Accuracy

Accuracy of the proposed method was determined using recovery studies by spiking method. The recovery studies were carried out by adding known amounts (50%, 100% and 150%) of the working standard solutions of cefpodoxime and azithromycin to the pre-analyzed sample. The solutions were prepared in triplicates to determine the accuracy.

Linearity

Linearity was evaluated by analyzing different concentrations of the standard solutions of cefpodoxime and azithromycin. Six working standard solutions ranging between 4 μ g/mL-12 μ g/mL for cefpodoxime, 5 μ g/mL - 15 μ g/mL for azithromycin were prepared and injected. The response was a linear function of concentration over peak area and were subjected to linear least-squares regression analysis to calculate the calibration equation and correlation coefficient.

Limit of detection and Limit of quantification

Limit of detection (LoD) and limit of quantification (LoQ) of cefpodoxime and azithromycin were determined by calibration curve method. Solutions of cefpodoxime and azithromycin were prepared in linearity range and injected (n = 3).

Robustness

To examine the robustness of the developed method, experimental conditions were deliberately changed, resolution, tailing factor, and theoretical plates of cefpodoxime and azithromycin peaks were evaluated. To study the outcome of the flow rate on the developed method, it was changed \pm 0.1mL/minute. The effect of column temperature on the developed method was studied at \pm 5 $^{\circ}$ C and the mobile phase composition was changed \pm 5% from the initial composition of the organic phase. In all the above varied conditions, the aqueous component of the mobile phase was held constant.

RESULTS AND DISCUSSION

System Suitability

From the results in table 2, the column efficiency for cefpodoxime and azithromycin peaks was identified from the theoretical plate count which is more than 3000, tailing factor less than 2.0, %RSD was found to be less than 2.0%. The resolution of the peaks of cefpodoxime and azithromycin were also found to be within the limits.

Specificity

From the obtained chromatograms in figures 3 to 5 it can be inferred that there were no co-eluting peaks at the retention time of cefpodoxime and azithromycin which shows that peak of analyze was pure and the excipients in the formulation did not interfere with the analyze of interest.

Accuracy

From the results in table 4, the % recovery for cefpodoxime and azithromycin found to be in the range of 98 –102% and the % RSD for cefpodoxime and azithromycin is less than 2%. Hence the proposed method was accurate.

Precision

From the results in table2, % Assay for cefpodoxime and azithromycin was found to be in the range of 98 – 102%, and the % RSD for cefpodoxime and azithromycin to be within 2%. Hence the method is precise, reproducible and rugged for 48 hours' study.

Linearity

Linearity was evaluated by analyzing different concentrations. From the results tabulated in table 5, it is inferred that the correlation coefficient was greater than 0.999. The slope and y-intercept values were also provided, which confirmed good linearity between peak areas and concentration.

LoD and LoQ



**Haritha Pavani Kondeti et al.,**

The Limit of Detection and Limit of Quantification of cefpodoxime and azithromycin were calculated by using following equations (ICH, Q2 (R1)) and the LoD and LoQ values are reported in table 5. These $LOD = 3.3 \times \sigma/S$ and $LOQ = 10 \times \sigma/S$ Where σ = the standard deviation of the response and S = slope of the calibration curve.

Robustness

From the results in table 7, it is evident that the system suitability parameters such as resolution, RSD, tailing factor, and the theoretical plate count of cefpodoxime and azithromycin remained unaffected by deliberate changes. The results were presented along with the system suitability parameters of optimized conditions. Thus, the method was found to be robust with respect to variability in applied conditions.

Assay for Formulation**Preparation of Standard Solution**

Weigh accurately 200 mg of Cefpodoxime Proxetil and 250 mg of Azithromycin and dissolve in 100 ml of diluent. From this transfer, 4 ml into 100 ml volumetric flask and make up the volume with diluent to make 80 and 100 ppm solution respectively. From this solution transfer 1 ml into 10 ml volumetric flask and make up to the volume with diluent to make 8 and 10 ppm solution respectively.

Preparation of Sample Solution

Gudcef- AZ tablets; claimed to contain 200 mg of Cefpodoxime proxetil and 250 mg of Azithromycin was used in analysis. A total of 20 tablets were accurately weighed and powdered in a mortar. An amount equivalent to 200 mg of Cefpodoxime proxetil and 250 mg of Azithromycin was taken and dissolved in some number of diluents and sonicated for 20 min and made up to 100 ml in 100 ml volumetric flask. The solution was transferred through a Whatmann No.1 filter paper. Further 4 ml of the above solution was pipetted out into a 100 ml volumetric flask and the volume was made up to 100 ml with diluent.

Procedure

The prepared standard and sample solutions were injected into HPLC by setting the optimized chromatographic conditions. The peak areas of standard and sample were determined. These values are substituted in the following formula to get the percentage purity of formulation.

CONCLUSION

The chromatographic method for the simultaneous estimation of Cefpodoxime Proxetil and Azithromycin was developed and was validated according to ICH guidelines. The method was found to be economical as the mobile phase composition involves more aqueous phase and less run time on C8 column when compared to the existing methods in literature. It was also found to be rapid, simple, specific, sensitive, precise, accurate and reliable that can effectively apply for routine analysis in research institutions, quality control department of industries and approved testing laboratories.

ACKNOWLEDGMENTS

The authors wish to thank the Department of Pharmaceutical Analysis, Chebrolu Hanumaiah Institute of Pharmaceutical Sciences Guntur for their constant support to complete this work. The authors wish to acknowledge the management of Spectrum Pharma Ltd. Hyderabad for providing the samples for their research. They would also like to thank colleagues in bulk manufacturers for providing chemicals and standards for research work. They would also like to thank colleagues in bulk manufacturers for providing chemicals and standards for research work.

Conflicts of Interest

The authors declare that they have no conflict of interest.





Haritha Pavani Kondeti et al.,

REFERENCES

1. Nieman & Timothy A; Skoog, Douglas A; Holler, F. James (1998). "Principles of Instrumental Analysis". Pacific Grove, CA: Brooks/Cole. ISBN 0-03-002078-6. James Robinson W, Marcel Dekker. Undergraduate Instrumental Analysis. 5th edition, 1997, pg no. 584-589.
2. N.Ravindra Kamble : "Development of RP-HPLC method for the determination of Azithromycin and Levo floxacin in Pharmaceutical dosage form," 'IJPS', April 2015, Article No-27, pg. no.162-165.
3. Narendra. N: "Development of RP-HPLC method for the simultaneous estimation of Cefixime and Azithromycin in pharmaceutical dosage form." 'Asian Journal of Pharmaceutical Sciences', Vol-2, 2014, pg.no186-196.
4. P.D.Sethi, "HPLC Quantitative Analysis of Pharmaceutical Formulations," 1st edition, CBS Publishers, 2001, pg.no.69-70.
5. Pesek, J. J; et al., S. J. (2005). "Synthesis and Characterization of chemically bonded stationary phases on hydride surfaces by hydrosilation of alkynes and dienes." 'Journal of Separation Science' 28 (18):2437.
6. P. D. Sethi, "HPLC Quantitative Analysis of Pharmaceutical Formulations", CBS Publisher and Distributor, New Delhi, 1996, pg no5.
7. Pillai A, et al., "Process validation techniques". 'Indian J. Pharm. Sci'. 2001: pg.no.420-421.
8. Patel C, et al., "Validation of analytical methods for pharmaceutical analysis". 'Indian J. Pharm. Sci'. 2002; 64: pg.no.362-366.
9. Prashanth. D. Ghode : "Development of stability indicating RP-HPLC method for the determination of Azithromycin and Ofloxacin in tablet dosage form." 'IJCSR', 2015 Vol-1, pg. no.169-174.
10. R.Senthil : "Development of RP-HPLC method for the simultaneous determination of Azithromycin and Ambroxol Hydrochloride in tablet dosage form." 'IJPRBS', 2012, Vol-1, pg. no.167-178.
11. Rakes, Kotkar.P: "Development of RP-HPLC method for the simultaneous estimation of Cefpodoxime Proxetil and Ambroxol hydrochloride in tablet dosage form." 'IJRPBS', Feb 2007, ISSN2229-3701.

Table 1: HPLC parameters for Optimized method

Parameters	Description
Stationary phase (Column)	Kromasil, 250×4.6 mm, 5μ, C8
Mobile phase-A	Buffer (Sodium dihydrogen phosphate)
Mobile phase-B	Methanol
Elution mode	Isocratic
Mobile phase ratio	50:50
Flow rate	1.0 ml/min
Detection wavelength	260
Detector used	PDA
Column Oven temperature	30°C
Injection volume	10 μl
Run time	9 min

Table 2: System suitability Parameters

Parameters	Cefpodoxime proxetil	Azithromycin	Acceptance Criteria
Retention time	2.8516	6.3464	—
No. of theoretical plates	8296.6	8051.4	NLT 3000
% RSD of Peak area	0.6	0.4	NMT 2.0
Resolution		3.701	NLT 2.0
Tailing	1.26	1.154	NMT 2
Area (Avg)	1557810	4413654	-





Table 3: Accuracy for Cefpodoxime Proxetil

Drug name	Conc. (%)	Amount spiked (µg/mL)	Amount recovered (µg/mL)	% recovery	Statistical parameters
Cefpodoxime	50	4	3.97	99.25	Mean %: 99.77 SD: 0.82 %RSD: 0.8
	100	8	8.02	99.45	
	150	12	11.99	100.22	
Azithromycin	50	5	5.04	100.50	Mean %: 100.27 SD: 1.09 %RSD: 1.09
	100	10	10.04	100.52	
	150	15	14.98	99.90	

Table 4: Precision data

S.NO	RT	Peak Areas	RT	Peak Areas
	Cefpodoxime		Azithromycin	
1	2.842	1557836	6.180	4415727
2	2.842	1551959	6.208	4414361
3	2.840	1559759	6.171	4411495
4	2.839	1551207	6.109	4418735
5	2.831	1554959	6.077	4414565
6	2.823	1552213	5.993	4416842
Mean	2.836	1554655.5	6.123	4415287.5
SD	0.00762	3503.7829	0.07998	2640.01
% RSD	0.26	0.22	1.30	0.05

Table 5: Linearity data of Cefpodoxime and Azithromycin

S.NO	LDP		SFB	
	Concentration (µg/mL)	Peak area*	Concentration (µg/mL)	Peak area*
1	4	778955	5	2206710
2	6	1168348	7.5	3310719
3	8	1517027	10	4413635
4	10	1947946	12.5	5547067
5	12	2336066	15	6620752
	Regression equation y = 38938x + 38152 R ² = 0.999		Regression equation y = 73499x + 6964.2 R ² = 0.9992	

Table 6: LoD and LoQ data

Drug name	LoD (µg/mL)	LoQ (µg/mL)
cefpodoxime	0.123	0.408
azithromycin	0.109	0.365

Table 6: Robustness data

Parameters		System Suitability Parameters		
		RT	Theoretical Plates	Peak Tailing
Optimized method	cefpodoxime	2.839	17053	1.10
	azithromycin	6.075	10841	1.07
	cefpodoxime	2.541	15685	1.10





Flow rate (1.1 mL/min)	azithromycin	6.283	9851	1.07
Flow rate (0.9 mL/min)	cefepodoxime	2.684	18129	1.11
	azithromycin	6.17	12683	1.07
Mobile phase composition Buffer: Methanol (48:52)	cefepodoxime	2.572	17367	1.06
	azithromycin	6.160	12028	1.04
Mobile phase composition Buffer: Methanol (52:48)	cefepodoxime	2.586	16823	1.09
	azithromycin	6.258	10970	1.07

Sample taken	Cefepodoxime			Azithromycin		
	RT	Peak Area	% Assay	RT	Peak Area	% Assay
Standard	2.872	1554049	99.82	6.602	4417925	101.21
Sample	2.780	1569366	99.98	5.577	4474756	100.52

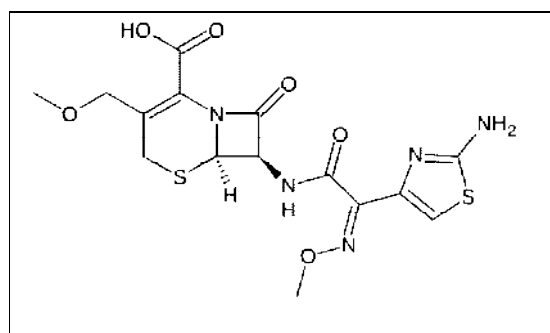


Fig.1: Structure of Cefepodoxime proxetil

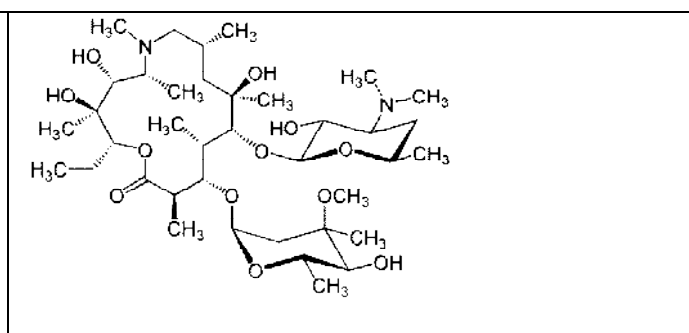


Fig.2: Structure of Azithromycin

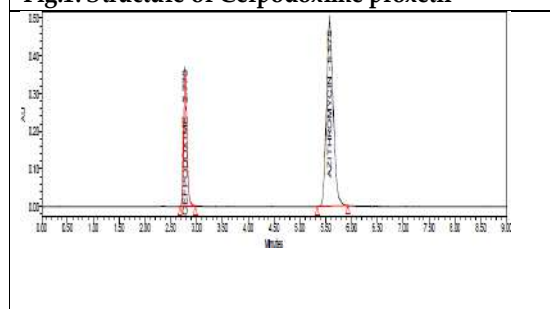


Fig. 3. Typical chromatogram of mixture of cefepodoxime and azithromycin

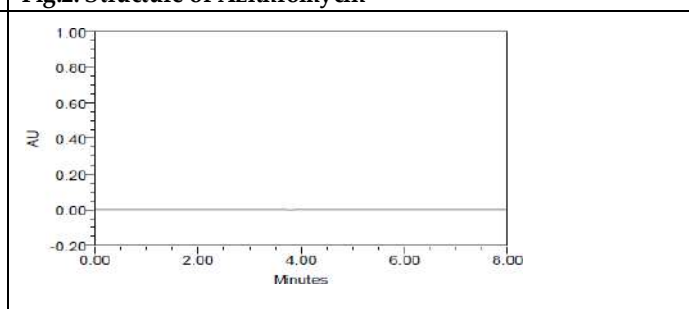


Fig. 4. Chromatogram of blank

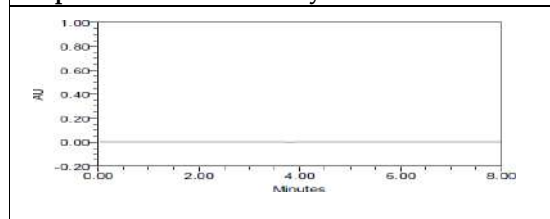


Fig. 5. Chromatogram of placebo

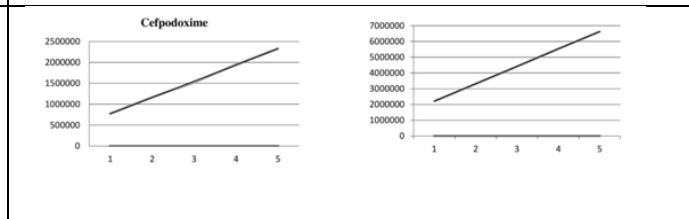


Fig 6 :Linearity plots of Cefepodoxime and Azithromycin





Multivariate Time Series Forecasting for Water Quality Prediction using ML and DL Models

D.Venkata Vara Prasad¹, Lokeswari Y Venkataramana^{2*}, V. Balasubramanian² and Divya K³

¹Professor, Department of Computer Science and Engineering, Sri Sivasubramaniya Nadar (SSN) College of Engineering, Chennai, Tamil Nadu, India

²Associate Professor, Department of Computer Science and Engineering, Sri Sivasubramaniya Nadar (SSN) College of Engineering, Chennai, Tamil Nadu, India.

³Software Developer, HCL Technologies Ltd, Chennai, Tamil Nadu, India.

Received: 24 July 2023

Revised: 08 Nov 2023

Accepted: 31 Jan 2024

*Address for Correspondence

Lokeswari Y Venkataramana

Associate Professor,

Department of Computer Science and Engineering,

Sri Sivasubramaniya Nadar (SSN) College of Engineering,

Chennai, Tamil Nadu, India.

Email: lokeswariyv@ssn.edu.in



This is an Open Access Journal / article distributed under the terms of the **Creative Commons Attribution License** (CC BY-NC-ND 3.0) which permits unrestricted use, distribution, and reproduction in any medium, provided the original work is properly cited. All rights reserved.

ABSTRACT

With the discharge of untreated industrial effluents, sewage, and domestic wastewater, together with agricultural runoff and untreated wastewater, water bodies including rivers, lakes, and ponds have been contaminated, which has an impact on groundwater. The quality of the water that is consumed directly impacts the health of any living thing; drinking unclean water increases the risk of cholera and other water-borne illnesses like diarrhoea and has an impact on child mortality. To address these issues, we will use multiple Machine Learning (ML) and Deep Learning (DL) models, including Ada Boost Regressor, Long-Short Term Memory, Random Forest Regressor, XGBoost, Convolutional Neural Network, and Gated Recurrent Units. It will be trained using multivariate time series, which have multiple time-dependent variables and each variable's ability to forecast water quality depends not only on its past values but also on other variables. To determine which models are most appropriate, the accuracy, precision, and recall of the water quality so acquired from each model are compared and assessed. As a result, this effort aids in assessing the efficiency of the models that can be applied to future predictions.

Keywords: Multivariate time series, Convolutional Neural Network, Ada Boost Regressor, Random Forest Regressor, Long- Short Term Memory, XGBoost, and Gated Recurrent Units.





Venkata Vara Prasad et al.,

INTRODUCTION

All life depends on water, which makes up 71% of the surface of the Earth. Drinking water is becoming increasingly scarce as a result of pollution brought on by urbanisation and industrialisation. Water contamination has gotten progressively worse with the economy's rapid growth and the city's quick urbanisation. Public health and the environment are directly impacted by water quality. Health problems might result from drinking contaminated water. So, before drinking, it's crucial to evaluate the water's quality.

Groundwater contamination generally happens in places with high population densities. It is crucial to evaluate several aspects of water quality in order to decrease the amount of contamination that occurs in different water bodies. To lessen the prevalence of water-borne diseases, it can be helpful to predict water quality indicators a few steps in advance. As a result, it is important to assess the quality of water before drinking it.

The current methods that are developed require a lot of labor and are time-consuming need an alternative automated technology to predict the quality of water. The proposed work aims to perform water quality prediction of well water data in the Chengalpattu district of Tamil Na^odu. And perform analysis and comparison between machine learning and deep learning and predict the maximum accuracy.

To date, a number of machine learning and deep learning algorithms have been developed to forecast the quality of water, but they have not been shown to be sufficiently accurate. Additionally, the parameters examined were insufficient. They were unable to manage the distorted and multidimensional datasets. The existing models did not meet the requirements; hence the work uses machine learning and deep learning techniques.

The prediction of water quality is challenging since it is nonlinear. However, the use of various deep learning and machine learning approaches has grown to be a potent source for prediction. These methods aid in the prediction of future behaviour by using past data on the water quality to train machine learning and deep learning algorithms.

The ML and DL models such as LSTM, Ada Boost Regressor, XG Boost, CNN, Random Forest Regressor and GRU are used for prediction. These models are well suited for time series and high dimensional data. The parameters considered are given in [19]. Based on the predicted values from these models, the results of the ML and DL models were compared to find the most suitable model. Muharemi et al. [17] addressed a recently created time-series data-based water quality prediction system.

Logistic regression SVMs, linear discriminant analysis (LDA), artificial neural networks (ANN), deep neural networks (DNN), long short-term memories (LSTM), and recurrent neural networks were all included in it (RNN). They determined the following variables: flow rate, time, TUR, pH, EC, water temperature, Cl, and redox ClO₂.

Support Vector Machines (SVM), Deep Neural Networks, Neural Networks (NN), and k-Nearest Neighbors (kNN) are the four machine learning techniques used in Shafi et al. [24] to predict the quality of the water. Twenty five characteristics have been incorporated as input parameters for single feed-forward neural networks used to classify water quality [1]. Varalakshmi et al. demonstrated the application of Naive Bayesian model to calculate the quality of drinking water [27]. The model took into account variables including TDS, pH, nitrate-nitrogen, hardness, and chloride. As a result, their model was designed to evaluate the water's quality by taking drinking water standards into account and computing the posterior probability. Rankovi et al. [21] used the ANN model to measure the dissolved oxygen (DO). An ANN model was used by Gazzaz et al. [11] to estimate the WQI, and the Internet of Things (IOT) technology was used to gather the dataset from water resources. As an alternative, ML models were used to predict the quality of the Tireh River in southwest Iran. They took into account variables including K, Na, and Mg as well as DO, CoD, BoD, EC, pH and temperature [12].

To anticipate the chemical oxygen requirement, Abyaneh et al. [30] has used machine learning techniques like ANN and regression (COD). Sakizadeh et al. [22] estimated the water quality index using ANN and Bayesian





Venkata Vara Prasad et al.,

regularisation (WQI). However, the prediction and categorization of water quality were done using the radial-basis-function (RBF), a form of ANN model [29]. By taking into account the variables of pH, temperature, total dissolved solids (TDS), and turbidity, Ahmed et al. [2] suggested a new technique. The quality of Rawal Lake Water was predicted using 15 supervised machine learning algorithms.

PROPOSED SYSTEM

Raw data

The information was gathered from numerous wells in Tamil Nadu's Chengalpattu area. It contains water statistics for more than 28 years in a row (1992 to 2020). The dataset includes 13 parameters, including PH, TDS, Turbidity, Phosphate, Nitrate, Iron, COD, Chloride, Sulfite, Potassium, Flouride, Calcium, and Sodium, and has roughly 10,248 entries.

Data preparation

The act of converting raw data into the extremely precise format needed by machine learning and deep learning algorithms in order for them to provide insightful results is known as data preparation. Clean, well-curated data are produced through effective data preparation, and this in turn delivers more accurate, useful model results.

1. Handling missing values: Projecting the intensity of image data pixels to a predetermined range is the process of intensity normalisation. The anatomies are represented by pixel values in the range of 1 to the entire number of anatomies when it is applied to the ground truth mask label.
2. Data Scaling: To ensure that the range of values in numerical data is uniform, data scaling is performed. The dataset can be normalised to make it simpler to improve model accuracy. Scaling is frequently done using normalisation.
3. Date transformation: In order to facilitate time series analysis, the date property is translated into the index row. The date attribute is changed to the format dd/mm/yyyy.
4. Water Quality Index Calculation: A straightforward indicator of water quality can be provided by the WQI, which is calculated based on thirteen parameters including Potassium, pH, Nitrate, Calcium, SAR, Magnesium, Sodium, SAR, Potassium, TDS, Chloride, Sulfate, Fluoride, Alkalinity, HAR. [3].

The quality rating scale is found by using the formula

$$Q_i = (C_i / S_i) * 100$$

Where,

C_i is the concentration of each parameter

S_i is the desirable or permissible range

Then, the water quality index is found by

$$WQI = \sum (W_i * Q_i) / n$$

Where,

W_i is the weight assigned to each parameter.

The weights assigned to each parameter are shown in table I and the permissible limits in Table II.

Multivariate Time Series Forecast Data

In order to forecast time series, historical data must be fitted, and future data must be predicted using the fit. A multivariate time series consists of multiple time-dependent variables, each of which is reliant on a number of other factors in addition to past values. Using many input features, we can forecast the demand for water quality using multivariate time series analysis. Multiple variable histories are gathered as input for the analysis in multivariate time series forecasting. Reading the parameter begins the workflow. read csv function on a csv file. It is necessary to structure the preparation of the water quality dataset for the machine learning and deep learning models as a supervised learning issue and to normalise the input variables. The goal of the challenge is to forecast the water



**Venkata Vara Prasad et al.,**

quality for the current day (t) using supervised learning and more than one day's worth of parameter measurements. using the input of the water quality index at earlier time steps. The dataset is then turned into a supervised learning problem in the following stage, after which all features have been normalised. Then, the variables for the expected hour (t) are deleted.

Converting Time Series Problem to Supervised Learning Problem

A time index is used to rank a set of numbers as a time series. In order for an algorithm to learn how to anticipate the output patterns from the input patterns, a supervised learning issue consists of input patterns (X) and output patterns (y). Here, the output is the water quality index for the current day, with input patterns being parameters from the day before. The Pandas shift() function is a crucial tool for converting time series data into a supervised learning issue. The shift() function creates duplicates of columns that are pushed forward (rows of NaN values are added to the front) or pulled back, given a DataFrame (rows of NaN values added to the end). For a time series dataset in a supervised learning format, this behaviour is necessary to generate columns of lag observations as well as columns of prediction observations. In the language of time series forecasting, forecasts are made using prior observations (t-1, t-n) and the current time (t), as well as the future times (t+1, t+n).

Model Building

By developing multiple Machine Learning and Deep Learning models, the water quality is predicted. The following is a list of the model construction algorithms:

Model Building

Building numerous ML and DL models allows for the prediction of water quality. Here is a list of the modelling algorithms used:

1. Machine Learning Algorithms

- Ada Boost Regressor
- Random Boost Regressor
- XGBoost Regressor

Deep Learning Algorithms

- Convolutional neural network
- Long short-term memory
- Gated recurrent units

Model Evaluation

Many works have been done to evaluate time series forecasting challenges. One such endeavour, [26], involves gene expression forecasting. Data on time series gene expression is frequently utilised to investigate a variety of dynamic biological processes. They assessed gene prediction in this work by framing it as a classification challenge. and categorise the output expected values. In our work, evaluation is conducted using a similar methodology. Due to the lack of explicit train and test splits in the data set, the models are assessed using k-fold cross validation.

k-Fold Cross Validation:: The model is assessed using k-Fold cross validation utilising various subsets of the data set as the validation set. The data set has been split into ten portions using 10-folds. One portion of each fold is used to create the model, and the other portion is utilised to test the model that has been created. By determining the average performance metrics across all splits, the performance of the model is assessed. By taking into account the output range, the class labels were divided into 10 and 20 classes for the purpose of calculating performance. In the beginning, the output values are classified into distinct classes based on the range in which they fall.

By dividing the values in the range of 10, the original labels are also divided into 10 classes. By dividing the values in the range of 5, the original labels are separated into 20 classes as well. As a result, the model's performance is





Venkata Vara Prasad *et al.*,

assessed using performance measures, and the evaluation is conducted as a classification issue. And the best model for these data is chosen.

Machine Learning Algorithms

By dividing the values in the range of 10, the original labels are also divided into 10 classes. By dividing the values in the range of 5, the original labels are separated into 20 classes as well. As a result, the model's performance is assessed using performance measures, and the evaluation is conducted as a classification issue. And the best model for these data is chosen.

Ada Boost Regressor: Adaptive Boosting is an ensemble of numerous weak learner decision trees, which perform marginally better than random guessing. However, because the AdaBoost algorithm is adaptive, it transfers the gradient from earlier trees to later trees to reduce the error of the earlier tree. As a result, this continual learning of trees at each stage develops a strong learner. The weighted average of the forecasts made by each tree serves as the final prediction

Random Forest Regressor: Numerous different decision trees acting as an ensemble make up the random forest. It uses sampling to break up the total dataset into smaller subgroups, trains each member using a decision tree, and then merges the results. The class with the most votes become the prediction made by our model. Each tree in the random forest emits a class prediction.

XGBoost: The gradient boosting framework is used in the decision tree-based ensemble machine learning technique XGBoost. Recently, competitions on Kaggle for structured or tabular data and applied machine learning have been dominated by an algorithm. XGBoost is used to create gradient boosted decision trees quickly and efficiently.

Deep Learning Algorithms

Deep learning algorithms such as LSTM, GRU and CNN are used.

1. *Convolutional Neural Network:* By utilizing CNNs' ability to automatically learn and extract characteristics from the raw input data, time series forecasting problems can be resolved. A CNN model can read and interpret a set of data as a one-dimensional image in order to extract the most crucial details. In time series classification tasks, this CNN capability has proven to be useful.
2. *Long-Short Term Memory:* A special kind of RNNs that may learn long-term dependencies are known as "LSTMs," or Long Short Term Memory Networks. They are currently widely employed and deliver outstanding results when used to address a variety of problems. With LSTMs, the problem of long-term dependency is expressly avoided. They don't have a hard time picking up new material; in fact, it's almost like it comes naturally to them to retain it for a long time.
3. *Gated Recurrent Units:* Unlike LSTM, GRU just has three gates and doesn't monitor the internal state of the cell. The hidden state of the gated recurrent unit contains the information that is stored in the internal cell state of an LSTM recurrent unit. This set of data is sent to the following Gated Recurrent Unit.

RESULTS AND DISCUSSIONS

Model Evaluation Metrics

The performance of the models can be measured using accuracy, precision and recall.

1. *Accuracy:* The percentage of predictions made correctly by the model is its accuracy. It is a crucial indicator that is used to assess how well the model is working. It measures the proportion of accurate predictions to all predictions. The accuracy formula is as follows:





Accuracy = $(TN+TP) / (TN+TP+FN+FP)$

2. *Precision*: In situations where the classes are highly unbalanced, precision is a valuable indicator of prediction success. The proportion of your results that are pertinent is referred to as precision. In other words, precision measures how many samples out of the total that the model accurately predicted. The precision formula is as follows:

Precision = $TP / (TP + FP)$

3. *Recall*: The percentage of Positive samples that were correctly identified as Positive relative to the total number of Positive samples is how the recall is calculated.

Recall = $TP / (TP + FN)$

Accuracy of machine learning algorithms

Figure 1 displays a comparison of the machine learning models' accuracy. When 10 samples are taken into account, it is seen that the ML algorithms have achieved improved accuracy. The XGBoost method was determined to have the best accuracy of all the algorithms, at 89.2

Precision of machine learning algorithms

When comparing the calculated accuracy of each model, as shown in Figure 2, Ten classes are found to have superior precision. The XGBoost method was determined to have the highest precision of all the algorithms, at 75.8

Recall of machine learning algorithms

Upon evaluating the calculated accuracy of each model, as shown in Figure 3. Ten classes are found to have superior precision. The XGBoost method was found to have the highest recall of all the algorithms, at 74.8 percent.

Accuracy of Deep learning algorithms

Figure 4 displays a comparison of the deep learning models' accuracy. When 10 classes are taken into account, it is seen that DL algorithms have achieved greater accuracy. The GRU algorithm was determined to have the best accuracy of 94.8 percent among all the algorithms.

Precision of Deep learning algorithms

Fig. 5 displays a comparison of the deep learning models' accuracy. When 10 classes are taken into account, it is seen that DL algorithms have achieved greater accuracy. The GRU algorithm was found to have the greatest accuracy of 93.4 percent among all the algorithms.

Recall of Deep learning algorithms

Figure 6 displays a comparison of the recall of the deep learning models. When 10 classes are taken into account, it is seen that deep learning algorithms have provided improved recall. Fig. 7 shows how accuracy, precision, and recall are compared. The examination and comparison of every algorithm revealed that GRU had the highest precision, accuracy, and recall of any deep learning model. So the model of deep learning GRU was identified as the most appropriate algorithm for our dataset is employed for the future year's forecast of water quality. The present project is contrasted with the existing systemaldhyani2020water. And it was found that the proposed method had an accuracy of 94.8 percent, outperforming the existing system. The existing system used 3 GRU layers (128,64,32). And activation function of tanh. And a dropout layer of 0.1. When the proposed model is fine-tuned by reducing the number of layers, this creates a better impact on the model. The model performed with better efficiency. Adding layers unnecessarily to the model can increase the number of parameters. You can extract more features by adding more layers. False positives and other problems can result from overfitting. As a result, the suggested method can be considered as the best DL algorithm for analyzing quality of water.





Venkata Vara Prasad et al.,

CONCLUSION

The Ada Boost Regressor, XGBoost, Random Forest Regressor, LSTM, GRU, and CNN are among the machine learning and deep learning models that were utilized for training and testing. The deep learning models outperformed the machine learning models in terms of performance. GRU demonstrated a noteworthy performance with a 94.8 percent accuracy rate. The model serves as the foundation for forecasting water quality for the following three years. By gathering the most recent samples of water from the well, GRU was used to estimate the water quality of the Chengalpattu well for the upcoming three years (2020–2022). The model was given the parameters of the water, and it projected that the water's quality would be "not drinkable." It is observed that the water is not suitable for drinking based on results of the ML and DL models.

REFERENCES

1. Ahmad, Z., Rahim, N.A., Bahadori, A. and Zhang, J. (2017). Improving water quality index prediction in Perak River basin Malaysia through a combination of multiple neural networks. vol.1, 15:79-87.
2. Ahmed U., Mumtaz R., Anwar H., Shah A.A., Irfan R., and Garcia Nieto
3. J. (2019). Efficient water quality prediction using supervised machine learning. *Water*. vol. 11, 11:2210-2218.
4. Aldhyani, T.H., Al-Yaari, M., Alkahtani, H. and Maashi, M., . (2020). Water quality prediction using artificial intelligence algorithms *Applied Bionics and Biomechanics* .vol 2020.
5. Barrera-Animas A.Y., Oyedele L.O., Bilal M., Akinosho T.D., Delgado J.M.D., and Akanbi L.A. (2022). Rainfall prediction: A comparative analysis of modern machine learning algorithms for time-series forecasting. *Machine Learning with Applications*. vol. 7:100204-100208.
6. Schonlau, M. and Zou, R.Y., . (2020) .Random forests *The Stata Journal*
7. . vol. 20, 1:3-29. Springer.
8. Chen E., and He X.J. (2019). Crude oil price prediction with decision tree based regression approach. *Journal of International Technology and Information Management*, vol. 27, 4:2–16.
9. Chao, Z., Pu, F., Yin, Y., Han, B. and Chen, X. (2018). Research on real-time local rainfall prediction based on MEMS sensors. *Journal of Sensors*. vol. 2018:1021-27.
10. Džeroski S., Demšar D., and Grbovic J. (2000). Predicting chemical parameters of river water quality from bioindicator data. *Applied Intelligence*. vol. 13, 1:7–17.
11. Freund, Y. and Schapire, R.E., . (1997).A decision-theoretic generalization of on-line learning and an application to boosting. *Journal of computer and system sciences* . vol. 55, 119-139.
12. Friedman, J.H., . (2001).Greedy function approximation: a gradient boosting machine *Annals of statistics* . pp. 1189–1232.
13. Gazzaz, N.M., Yusoff, M.K., Aris, A.Z., Juahir, H. and Ramli, M.F. (2012). Artificial neural network modeling of the water quality index for Kinta River (Malaysia) using water quality variables as predictors. *Marine pollution bulletin*. vol. 64, 11:2409-2420.
14. Haghbi A.H., Nasrolahi A.H., and Parsaie A. (2018). Water quality prediction using machine learning methods. *Water Quality Research Journal*. vol. 53, 1:3–13.
15. James, G., Witten, D., Hastie, T. and Tibshirani, R., . (2013).An introduction to statistical learning. vol. 112, 109-129.Springer.
16. Khan Y., and See C.S. (2016). Predicting and analyzing water quality using machine learning: a comprehensive model. In proceedings of *Long Island Systems, Applications and Technology Conference*. April 29. pp. 1-6. IEEE.
17. Lee, J.H., Lee, J.Y., Lee, M.H., Lee, M.Y., Kim, Y.W., Hyung, J.S., Kim, K.B., Cha, Y.K. and Koo, J.Y. (2022). Development of a short-term water quality prediction model for urban rivers using real-time water quality data. *IWA Publishing*. vol 22, 4082-4097.
18. Lu H., and Ma X. (2020). Hybrid decision tree-based machine learning models for short-term water quality prediction. *Chemosphere*. vol. 249:126169-126179.





Venkata Vara Prasad et al.,

19. Muharemi F., Logofatu D., and Leon F. (2019). Machine learning approaches for anomaly detection of water quality on a real-world dataset. *Journal of Information and Telecommunication*. vol. 3, 3:294–307.
20. Poornima S., and Pushpalatha M. (2019). Prediction of rainfall using intensified lstm based recurrent neural network with weighted linear units. *Atmosphere*. vol. 10, 11:668-703.
21. Prasad D., Vara V., Venkataramana L.Y., Kumar P.S., Prasannamedha G., Soumya K., and Poornima A. (2021). Prediction on water quality of a lake in Chennai, India using machine learning algorithms. *Desalination And Water Treatment*. vol. 218:44–51.
22. Prasad D., Vara V., Venkataramana L.Y., Kumar P.S., Prasannamedha G., Soumya K., and Poornima A. (2020). Water quality analysis in a lake using deep learning methodology: prediction and validation. *International Journal of Environmental Analytical Chemistry*. vol. 4:25-28.
23. Rankovic, V., Radulovic, J., Radojevic, I., Ostojic, A. and Comic, L. (2010). Neural network modeling of dissolved oxygen in the Gruz'a reservoir, Serbia. *Ecological Modelling*. vol. 221, 8:1239-1244.
24. Sakizadeh, M.(2016). Artificial intelligence for the prediction of water quality index in groundwater systems. *Modeling Earth Systems and Environment*. vol. 2, 1:1-9.
25. Shafi, U., Mumtaz, R., Anwar, H., Qamar, A.M. and Khurshid, H. (2018). Surface water pollution detection using internet of things. In proceedings 15th International Conference on Smart Cities: Improving Quality of Life Using ICT & IoT (HONET-ICT). October 8. pp. 92-96. IEEE.
26. Singha S., Pasupuleti S., Singha S.S., Singh R., and Kumar S. (2021). Prediction of groundwater quality using efficient machine learning technique. *Chemosphere*. vol. 276:130265–67.
27. Solanki A., Agrawal H., and Khare K. (2015). Predictive analysis of water quality parameters using deep learning. *International Journal of Computer Applications*. vol. 125, 9:0975–8887.
28. Tripto, N.I., Kabir, M., Bayzid, M.S. and Rahman, A., (2020). Evaluation of classification and forecasting methods on time series gene expression data *Plos one*. vol 15, 11: p.e0241686.
29. Varalakshmi P., Vandhana S., and Vishali S. (2017). Prediction of water quality using naive bayesian algorithm. In proceedings of Eighth International Conference on Advanced Computing. January 19. pp. 224–229. IEEE.
30. Xiang Y., and Jiang L. (2009). Water quality prediction using ls-svm and particle swarm optimization. *International workshop on Knowledge Discovery and Data Mining*. pp. 900–904. IEEE.
31. Yesilnacar, M.I., Sahinkaya, E., Naz, M. and Ozkaya, B.(2008). Neural network prediction of nitrate in groundwater of Harran Plain, Turkey. *Environmental Geology* . vol. 56, 1:19-25.
32. Zare H. (2014). Evaluation of multivariate linear regression and artificial neural networks in prediction of water quality parameters. *Journal of Environmental Health Science and Engineering*. vol. 12, 1:1–8.

Table 1 - Weights Assigned To Each Parameter

Chemical Parameter	Weights
TDS- Total Dissolved Solids	5
NO ₂ +NO ₃ - Nitrate	3
Ca- Calcium	4
Mg - Magnesium	3
Na - Sodium	5
K - Potassium	2
Cl -Chloride	5
So ₄ - Sulfate	3
F - Fluoride	2
CO ₃ + HCO ₃ (Alkalinity)	4
pH- power of hydrogen	4
HAR Total- Total Hardness	2
SAR - Sodium Adsorption Ratio	1
	Total = 43





Venkata Vara Prasad et al.,

Table 2- Permissible Limits

Chemical Parameter	Permissible Limit
TDS- Total Dissolved Solids	5000
NO ₂ +NO ₃ -	100
Ca- Calcium	200
Mg - Magnesium	100
Na - Sodium	2
K - Potassium	11
Cl -Chloride	1000
So ₄ - Sulfate	400
F - Fluoride	1 - 1.5
CO ₃ + HCO ₃ (Alkalinity)	600
pH- power of hydrogen	6.5-8.5
HAR Total- Total Hardness	300
SAR - Sodium Adsorption Ratio	10

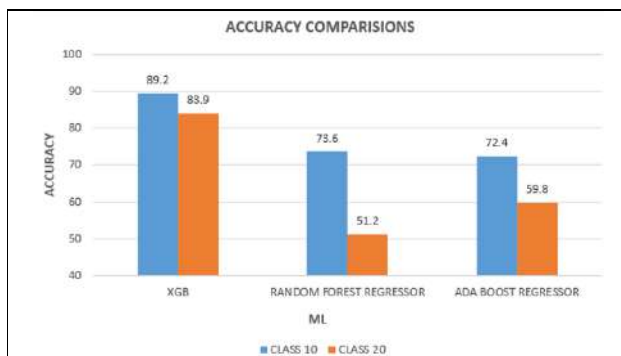


Fig. 1. Accuracy of ML models

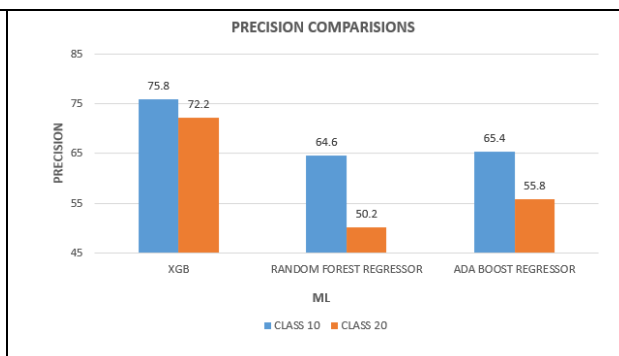


Fig. 2. Precision of ML models

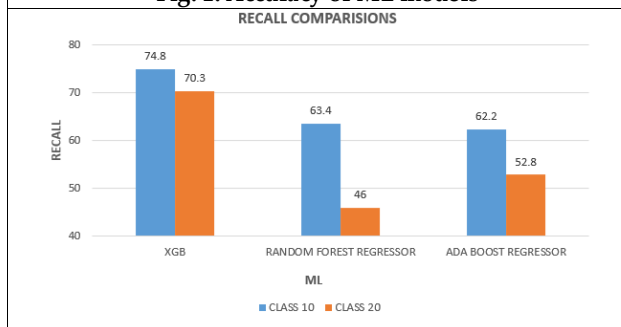


Fig. 3. Recall of ML models

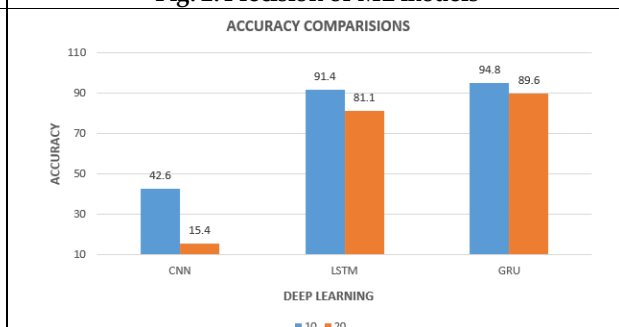


Fig. 4. Accuracy of DL models





Venkata Vara Prasad et al.,

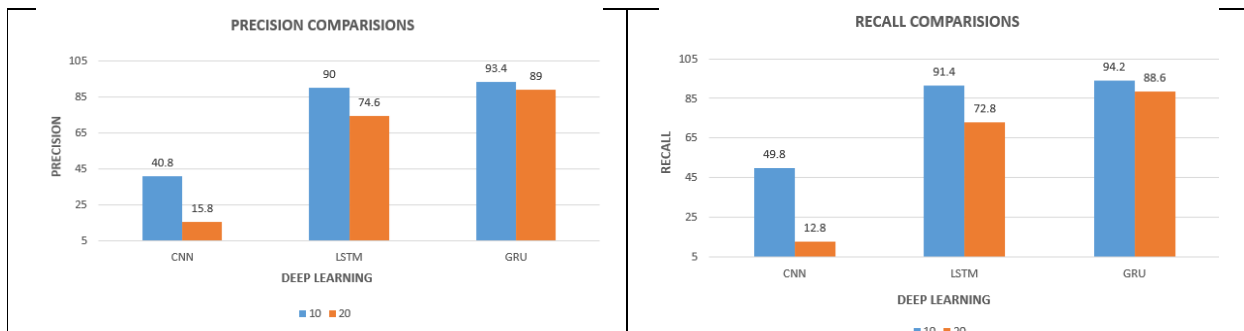


Fig. 5. Precision of DL models

Fig. 6. Recall of DL models

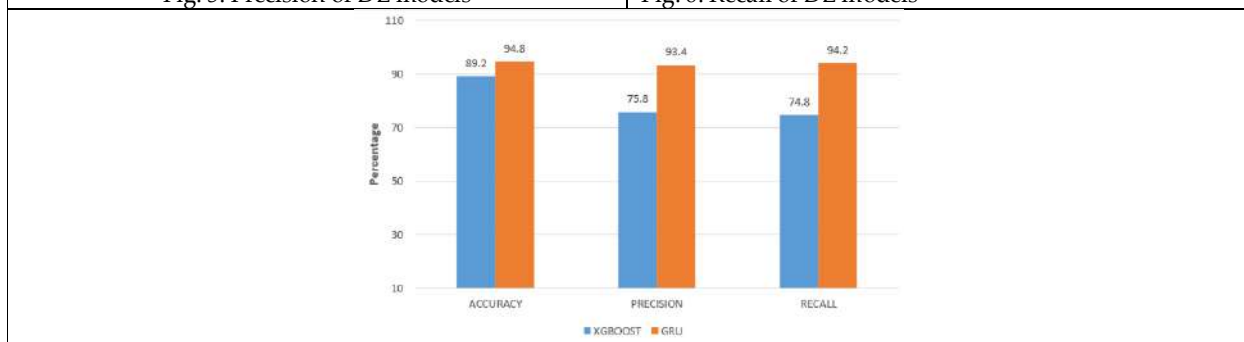


Fig. 7. Comparison of Accuracy, Precision and Recall

	<p>Dr. D. Venkata vara Prasad is a Professor in the Department of Computer Science and Engineering, SSN College of Engineering, Chennai. He has more than 20 years of teaching and research experience. His PhD work is on “Chip area minimization using interconnect length optimization”. His area of research is Computer Architecture and GPU Computing. He is a member of IEEE and also a Life member of CSI and ISTE. He is a Principal Investigator for SSN-nVIDIA GPU Education/Research Center.</p>
	<p>Dr. Lokeswari Venkataramana is an Associate Professor in the Department of Computer Science and Engineering, SSN College of Engineering, Chennai. She has 2 years of industrial experience at Cognizant Technology Solutions Pvt. Ltd. Her area of interest includes Parallel Data Mining for massive data, Databases, Distributed Systems, Computational Biology and Cloud Computing.</p>
	<p>Dr. V. Balasubramanian is currently working as Associate Professor in department of CSE, SSN College of Engineering, Chennai. He has 25 years of teaching and research experience. He received his B.E. in Electronics and Communication from the University of Madras, in the year 1997 and M.E. degree in Computer Science and Engineering from College of Engineering, Guindy, Anna University, Chennai, in the year 2002. He received his Ph.D from the College of Engineering, Guindy, Anna University. He has published 20 papers in the National, International Conferences and Journals. He has authored five books: Theory of Computation, Computer Networks, Computer Architecture, Design and Analysis of Algorithms and Artificial Intelligence. He is a Senior member of IEEE, Senior Member of ACM and a Life member of Computer Society of India (CSI), and Indian Society for Technical Education (ISTE). Areas of Research include Cloud Computing, Security and Privacy, Blockchain.</p>





Venkata Vara Prasad et al.,



Kandikattu Divya is currently working as software Engineer at HCL Technologies Ltd. She has completed her bachelors and master's degree from Anna University, Chennai.





Comparative Analysis of *Bacopa monnieri* and *Withania somnifera* in *Drosophila melanogaster* Neurodegeneration Models: Memory, Locomotion, Fertility, and Lifespan

Cynthia Irene Kasi^{1*}, J.Sowmya², K.V.Meghana² and Shivakumar K.S²

¹Assistant Professor, Department of Life Sciences, Indian Academy Degree College (Affiliated to North University) Bangalore, Karnataka, India

²M.Sc. Student, Department of Life Sciences, Indian Academy Degree College (Affiliated to North University), Bangalore, Karnataka, India

Received: 30 Sep 2023

Revised: 20 Nov 2023

Accepted: 13 Jan 2024

*Address for Correspondence

Cynthia Irene Kasi

Assistant Professor,

Department of Life Sciences,

Indian Academy Degree College (Affiliated to North University)

Bangalore, Karnataka, India

E mail: cynthia_genetics_iadca@indianacademy.edu.in



This is an Open Access Journal / article distributed under the terms of the **Creative Commons Attribution License** (CC BY-NC-ND 3.0) which permits unrestricted use, distribution, and reproduction in any medium, provided the original work is properly cited. All rights reserved.

ABSTRACT

This study delves into the manifestation of neurodegeneration-like symptoms in *Drosophila melanogaster*, particularly focusing on memory and locomotion impairments, as well as decline in fertility and reduced lifespan. It also explores the potential for mitigating these symptoms through treatment with *Bacopa monnieri* and *Withania somnifera*. To investigate potential variations in neurodegenerative responses and therapeutic effectiveness, we conducted a comparative analysis between *Drosophila* Oregon K-Type and hybrid fly strains. *Drosophila melanogaster*, a widely recognized model organism, serves as a valuable platform for probing neurodegenerative mechanisms. We induced neurodegeneration-like symptoms by exposing flies to paraquat herbicide, replicating oxidative stress conditions. Subsequently, we assessed memory and locomotion deficits as behavioural indicators of neurodegeneration. Additionally, our observations revealed a substantial decrease in fertility and a shortened lifespan among Paraquat-exposed flies in comparison to the control group. These findings underscore the detrimental impact of Paraquat on both reproductive and aging processes in *Drosophila melanogaster*. Our research findings have revealed significant impairments in memory and locomotion in *Drosophila* flies exposed to paraquat, mirroring symptoms commonly associated with neurodegenerative diseases. Specifically, we observed a reduction in memory index from 100% to -26.5% and a decrease in locomotion from 100% to 45.5%. Furthermore, these exposed flies exhibited diminished fertility, decreasing from 100% to 72%, and a shortened lifespan, declining from 100% to 86%. However, the administration of *Bacopa monnieri* and *Withania somnifera* extracts showed promising potential for alleviating these symptoms. In the case of

69795





Cynthia Irene Kasi et al.,

Brahmi-treated flies, we observed an increase in locomotion from 45.5% to 81%, an improvement in memory from -26.5% to 50%, an increase in fertility from 72% to 82.5%, and an extension of lifespan from 86% to 91%. On the other hand, Ashwagandha-treated flies displayed an increase in locomotion from 45.5% to 63.5%, an enhancement in memory from -26.5% to 26.5%, a slight improvement in fertility from 72% to 77.5%, and a modest extension of lifespan from 86% to 92.5%. Treatment with these herbal supplements not only led to improved performance in memory and locomotion assessments but also had adverse effects on fertility and longevity, shedding light on their neuroprotective and neurorestorative qualities.

Keywords: Neurodegeneration, *Drosophila melanogaster*, Memory impairment, Locomotion deficits, Fertility, Lifespan, Paraquat herbicide, *Bacopa monnieri*, *Withania somnifera*,

INTRODUCTION

Neurodegeneration is a complex and debilitating process characterized by the gradual loss of structure and function of neurons in the central nervous system (CNS) or peripheral nervous system (PNS). This complex process lies at the heart of various debilitating disorders, including Alzheimer's disease, Parkinson's disease, Huntington's disease, and amyotrophic lateral sclerosis (ALS), among others. These disorders collectively pose a significant global health challenge, as they not only impact the quality of life for affected individuals but also place a substantial burden on healthcare systems and society at large [1]. Neurodegenerative disorders exert wide-ranging consequences, impacting facets such as cognition, motor function, and overall quality of life. Patients with these conditions often grapple with cognitive decline, memory deficits, motor impairments, and behavioural alterations. With a growing aging population worldwide, there is an escalating prevalence of these disorders, underscoring the urgency of comprehending their underlying mechanisms and devising effective interventions [2]. Moreover, the toxic nature of neurodegeneration disrupts cellular processes, leading to oxidative stress and a significant reduction in overall survival rates. In parallel, fertility and longevity represent crucial components of an organism's life history traits, closely intertwined with its overall fitness. Disruptions in these traits can carry profound ecological and evolutionary implications [3].

To comprehend the intricate mechanisms underlying these conditions and to develop effective therapeutic strategies, research has often relied on model organisms. One such valuable model organism that has significantly contributed to our understanding of neurodegeneration is *Drosophila melanogaster*, commonly known as the fruit fly. It has been extensively employed in scientific research since the early 20th century [4]. Despite its seemingly distant evolutionary relationship with humans, the fruit fly shares a surprising degree of genetic and molecular homology with humans. Approximately 75% of human disease-related genes have functional homologs in the fly genome, making it an ideal model for investigating the molecular underpinnings of various diseases, including neurodegenerative disorders. Moreover, the fly's short generation time and prolific reproduction enable rapid genetic manipulation and screening of potential therapeutic targets [5]. Indeed, within the realm of *Drosophila* research, there exist various strains, and among them are the Oregon K flies and hybrid flies. The Oregon K strain, notable for its genetic stability and well-documented genome, provides researchers with a reliable foundation for studying *Drosophila* biology. In contrast, hybrid flies, produced by combining different genetic backgrounds, offer a unique opportunity to explore the impact of genetic diversity on various phenotypic traits, including responses to environmental stressors and therapeutic interventions [6].

Herbicides, such as paraquat, have been implicated in playing a role in neurodegeneration due to their capacity to induce oxidative stress and disrupt cellular homeostasis. These chemicals, designed to eliminate unwanted plant growth, can inadvertently impact neural tissues when exposure occurs. Paraquat, for instance, generates reactive





Cynthia Irene Kasi et al.,

oxygen species (ROS) within cells, leading to oxidative damage and triggering inflammatory responses. Over time, this oxidative stress and inflammation can contribute to neuronal dysfunction and degeneration, potentially resembling aspects of neurodegenerative diseases [7]. The urgency to find novel therapeutic strategies has prompted exploration into the potential of herbal remedies, such as *Withania somnifera* (Ashwagandha) and *Bacopa monnieri* (Brahmi), as neuroprotective agents. Ashwagandha contains bioactive compounds known as withanolides (steroids), which exhibit antioxidant and anti-inflammatory properties. These withanolides have been studied for their ability to protect neurons from oxidative stress and inflammation, which are common factors in neurodegenerative diseases. *Bacopa monnieri*, on the other hand, contains compounds called bacosides (saponins). These bacosides have been investigated for their role in supporting neuronal growth and survival, enhancing synaptic plasticity (crucial for memory and learning), and reducing oxidative damage and inflammation in the brain. Their neuroprotective properties make them attractive candidates for further research and development of treatments for neurodegenerative diseases [8].

METHODOLOGY

Culturing Oregon-K and Hybrid *Drosophila melanogaster* flies

The Oregon-K wild type strain of *Drosophila* was sourced from the *Drosophila* Stock Center in Mysuru. Additionally, A population of *Drosophila* flies, which had naturally evolved into hybrid flies, was collected from our in-house breeding program. A culture medium was prepared for *Drosophila* culture by homogenizing semolina (suji rava), jaggery, distilled water, and Agar agar. Subsequent to medium formulation, propionic acid was introduced, and the resulting mixture was aseptically transferred into glass containers. Following this, a controlled dispersion of yeast granules was evenly applied to the medium's surface, facilitating desiccation under sterile conditions. Upon complete drying, *Drosophila* flies were introduced into the cultured environment [9].

Standardizing Paraquat Dosage For Inducing Neurodegeneration Like Symptoms In Flies

A 24% paraquat solution was employed to prepare five distinct concentrations by adding precise volumes of 107, 160, 214, 267, and 327 microliters of this solution into separate glass tubes Each test tube was subsequently brought to a final volume of 10 ml by the addition of distilled water. Concurrently, in a separate test tube, 1g of sucrose was dissolved in 10 ml of water. [Refer Fig:8] To facilitate our experiments, glass tubes were prepared, and Whatman filter paper was custom-cut to fit the bases of these tubes. Subsequently, a precise volume of 75 microliters of the sucrose solution was pipetted into all tubes, followed by the addition of 75 microliters of each paraquat concentration into their respective tubes. The tubes were then securely sealed with cotton plugs and allowed to air-dry for a duration of 10 minutes. [Refer Fig:9&10] Subsequently, 25 *Drosophila* flies were introduced into each glass tube previously exposed to paraquat, enabling them to inhale the substance over a 48-hour period. Following this interval, the number of deceased flies in each tube was assessed. The tube with the lowest number of deceased flies was selected as the reference for determining the paraquat dosage required to induce neurodegeneration-like symptoms in *Drosophila*. This process was meticulously repeated for three separate trials. The selection of a higher paraquat concentration was deemed impractical, as it could potentially result in premature fly mortality, precluding the observation and study of other neurodegenerative symptoms [10].

Exploring Medicinal Plant-Based Interventions For Neurodegenerative Disorders In *Drosophila melanogaster* Plant Extraction

Dried whole plant specimens were subjected to desiccation in a hot air oven for a period of 24 hours. Subsequently, the desiccated plant material was finely powdered using a mechanical grinder. The powdered plant material was then immersed in a methanol solution in a ratio of 3:1 (methanol to plant material) and placed within a shaker incubator for a duration of 48 hours. Following this extraction period, the methanol-extract was subjected to centrifugation at a speed of 4,500 RPM for a duration of 15 minutes. This centrifugation process was repeated three times to ensure thorough separation of the supernatant from any particulate matter. The resulting supernatant, which contained the extracted compounds, was carefully collected.



**Cynthia Irene Kasi et al.,**

To obtain a purified sample, the collected supernatant was subsequently passed through a Whatman filter paper, effectively removing any residual solid particles and obtaining a refined, liquid sample [11]. [Refer fig:11]

Phytochemical Tests

Alkaloid Test: The crude extract was treated with a 1% HCL solution, followed by the addition of Mayer's reagent, resulting in the formation of a reddish-brown precipitate.

Saponins test: The crude extract was vigorously mixed with distilled water, resulting in the formation of a stable foam [12].

Carbohydrates test: The crude extract was combined with Benedict's reagent and gently heated in a water bath, leading to the development of a green colouration [13].

Phenol test: The crude extract was combined with distilled water, and a few drops of FeCl₃ were added, resulting in the formation of a green colour [14].

Flavonoids test: The crude extract was mixed with a FeCl₃ solution, resulting in the formation of a dark blue/black colouration [15].

Steroids test: The crude extract was mixed with chloroform, and a few drops of concentrated H₂SO₄ were added, leading to the development of a reddish-brown coloration.[16]

Infusing Plant Extracts In Drosophila Culture Media

Plant extracts were formulated at six discrete concentrations: 0.1%, 0.25%, 0.5%, 0.75%, 1% and 1.25%. These extracts were then methodically incorporated into separate bottles by blending them with the culture media, with each concentration being allocated to its dedicated bottle.

Standardising The Optimal Dosage Of Medicinal Plants For Neuroprotection

Herbicide-induced neurodegeneration Drosophila flies were systematically collected and subsequently transferred into glass bottles containing culture media infused with medicinal plant extracts. In each bottle, a standardized population of 15 flies was introduced, and they were allowed to consume the extract-infused media over a period of 7 days. Following this incubation period, the number of deceased flies was meticulously counted for each bottle across various concentrations of the medicinal plant extracts. This comprehensive process was executed with precision across three independent trials to ensure the robustness of the findings. Subsequently, the average death percentage resulting from these three trials was calculated for each concentration. Through this rigorous analysis, the concentration demonstrating the lowest average death percentage was identified and selected as the optimal dose for conferring neuroprotection in the experimental model [17].

T-Maze Assay

Constructed an in-house T-Maze apparatus for our experiments and implemented a rigorous cleaning protocol to ensure that the apparatus is thoroughly cleansed before each trial, effectively eliminating any lingering odors or cues.[Refer Fig: 12] Cold-anesthetized Drosophila underwent three training trials where they associated a sweet odor (mango with jaggery) with an electric shock paired with a clove scent. [Refer Fig: 13,14] After a one-hour rest, the same odors were presented in a testing phase. After a 2-minute period, two of the pipes or tubes were removed, and counted the number of flies in each tube to determine how many of them chose the tube with the sweet odor and how many chose the tube with the clove odor, and their preferences for the conditioned odors were quantified to calculate memory retention percentages, informing conclusions about odor preference and memory [18].

Fertility and Longevity Analysis

The fertility and longevity analysis were performed on Drosophila strains by exposing 20 hybrid fly pupae (10 male and 10 female) to 75 microlitre of 160 microlitre paraquat concentration and 20 Oregon k fly pupae (10 male and 10 female) to 75 microlitre of 160 microlitre paraquat concentration, along with 75 microlitre of 10% sucrose solution for 24 hours. During this period, male and females were distinguished by the presence or absence of sex comb. [Refer Fig:15,16]





Cynthia Irene Kasi et al.,

Following the 24-hour exposure, the flies were transferred to a growth medium. In fertility analysis the emergence of adult flies from the pupa stage was observed whereas in longevity analysis the number of deceased flies were recorded each day [19,20].

Climbing Assay

In the climbing assay, two glass tubes, marked with an 8 cm line from the bottom, were employed. A timer was positioned between these tubes. [Refer Fig: 17] Flies within a vial were held vertically at the bottom, and the timer was initiated while gently tapping the flies downwards, prompting them to descend to the vial's base. The time taken for the flies to ascend above the designated 8cm line was closely monitored and recorded. A predefined time range of 5 seconds was established as the criterion for successful ascent. This procedure was repeated for three separate trials to ensure accuracy and consistency in the assessment [21].

RESULTS

The Optimal Paraquat Dosage For Neurodegeneration Induction In Flies

The study's findings indicate that a paraquat dosage of 107 microliters was effective in inducing neurodegeneration in 'OK' flies, yielding the highest observed survival rate of 84% among all tested concentrations. Conversely, in the case of hybrid *Drosophila* flies, the highest survival rate of 87% was observed with a dosage of 160 microliters of paraquat. These results suggest that 160 microliters is the optimal dosage for inducing neurodegeneration in hybrid flies. [Refer Fig: 1]

Phytochemical Screening

Phytochemical analyses revealed that both plants contain a range of bioactive compounds including alkaloids, saponins, steroids, phenols, and carbohydrates. Notably, flavonoids were absent in Ashwagandha but present in Brahmi. [Refer Table: 1]

The Optimal Dosage Of Medicinal Plants For Neuroprotection

After conducting a thorough analysis of fly mortality across different concentration levels, it was observed that the 1% concentration of plant extract-infused media consistently had the lowest number of deceased flies. A similar outcome was observed at the 1.25% concentration; however, flies in this group exhibited reduced activity compared to those in the 1% group. Consequently, based on these findings, the selected dosage of plant extract for administering to neurodegenerative fruit flies to promote neuroprotection has been established as 1%. Upon comparative analysis, it was observed that the culture bottle containing media infused with Brahmi plant extract exhibited a lower mortality rate in both types of fruit flies when contrasted with the culture containing Ashwagandha extract. Consequently, it can be deduced that Brahmi extract demonstrates a higher efficacy in terms of survival rates. [Refer Fig:2,3]

T-Maze Assay

OK and Hybrid flies exhibited varying memory index values in response to different conditions, with control flies generally showing a preference for positive reinforcement, while paraquat-induced flies displayed a preference for negative reinforcement that reversed upon treatment in the T-maze. Upon scrutinizing the data, it becomes apparent that 'OK' flies display enhanced memory retention as evidenced by the memory index when compared to hybrid flies. However, when examining the manifestation of neurodegeneration-like symptoms, hybrid flies exhibit greater resilience compared to 'OK' flies. Additionally, flies that consumed media infused with Brahmi displayed notably better memory performance in contrast to those exposed to Ashwagandha. [Refer Fig:4]





Cynthia Irene Kasi et al.,

Fertility And Longevity Analysis

The results showed that hybrid flies exhibited a higher fertility rate and had a notably longer lifespan compared to Oregon k flies. *Bacopa monnieri* demonstrates superior therapeutic effects compared to *Withania somnifera* in ameliorating the declines in fertility and lifespan induced by Paraquat exposure. [Refer Fig:5,6]

Climbing Assay

The results indicate that neurodegeneration-induced flies exhibit diminished climbing abilities. However, the application of medicinal plant treatments, specifically Brahmi and Ashwagandha, exerts a beneficial influence, enhancing the climbing performance of both hybrid and 'OK' flies within the specified experimental conditions. When analyzing the climbing index with respect to the graph, it becomes evident that hybrid flies exhibit a higher climbing percentage in comparison to 'OK' flies. Furthermore, a comparison between Ashwagandha and Brahmi-infused media reveals that flies exposed to Brahmi exhibit a notably higher climbing percentage as opposed to those exposed to Ashwagandha. [Refer fig: 7]

DISCUSSION

This study had two primary objectives: firstly, to determine the optimal dosage of paraquat capable of inducing neurodegeneration-like symptoms in *Drosophila* flies, and secondly, to investigate the therapeutic potential of treatments involving Brahmi and Ashwagandha extracts. The comparative analysis of *Withania somnifera* (Ashwagandha) and *Bacopa monnieri* (Brahmi) for neuroprotection in a neurodegenerative *Drosophila* model provided valuable insights into the potential benefits of these herbal interventions. Phytochemical analyses revealed the presence of various bioactive compounds, including alkaloids, saponins, glycosides, steroids, phenols, and carbohydrates, in both Brahmi and Ashwagandha extracts. Interestingly, Brahmi contained flavonoids, a class of compounds absent in Ashwagandha. Survival analysis, conducted with varying concentrations of plant extracts infused in the media, yielded a significant finding: a 1% concentration of both Ashwagandha and Brahmi extracts led to a substantial reduction in mortality rates among neurodegenerative flies. This suggests the potential of both plants for neuroprotection, with the possibility that higher concentrations may offer increased effectiveness. Subsequent evaluations included memory and locomotion assessments using T-maze and climbing assays, along with fertility and longevity assays. Notably, in both the OK and hybrid fly groups, we observed a reduction in memory index from 100% to -10% (OK) and from 100% to -43% (hybrid), accompanied by a decrease in locomotion from 100% to 40% (OK) and from 100% to 51% (hybrid). Furthermore, these exposed flies exhibited diminished fertility, decreasing from 100% to 69% (OK) and from 100% to 75% (hybrid), along with a shortened lifespan, declining from 100% to 84% (OK) and from 100% to 88% (hybrid).

However, the administration of *Bacopa monnieri* and *Withania somnifera* extracts showed promising potential for alleviating these symptoms. In the case of Brahmi-treated flies, we observed an increase in locomotion from 40% to 80% (OK) and from 51% to 82% (hybrid), an improvement in memory from -10% to 57% (OK) and from -43% to 43% (hybrid), an increase in fertility from 69% to 80% (OK) and from 75% to 85% (hybrid), and an extension of lifespan from 84% to 88% (OK) and from 88% to 92% (hybrid). Conversely, Ashwagandha-treated flies displayed an increase in locomotion from 40% to 60% (OK) and from 51% to 67% (hybrid), an enhancement in memory from -10% to 43% (OK) and from -43% to 10% (hybrid), a slight improvement in fertility from 69% to 75% (OK) and from 75% to 80% (hybrid), and a modest extension of lifespan from 84% to 86% (OK) and from 88% to 90% (hybrid). Noteworthy differences were observed between hybrid flies and the Oregon K (OK) *Drosophila* strain. Hybrid flies exhibited superior locomotion abilities, while the OK strain displayed better memory function. Additionally, hybrid flies demonstrated higher fertility rates and longer lifespans compared to Oregon K flies, emphasizing the role of genetic variability in neurodegenerative responses. Furthermore, neurodegeneration induction via paraquat significantly impaired memory, locomotion, fertility, and lifespan in both fly groups, indicating the effectiveness of the model in simulating neurodegenerative conditions. Remarkably, Brahmi-treated flies exhibited more substantial improvements in memory, climbing abilities, fertility, and lifespan when compared to Ashwagandha-treated flies,





Cynthia Irene Kasi et al.,

suggesting Brahmi's potential neuroprotective properties. The reversal of neurodegenerative symptoms in response to these plant treatments underscores their therapeutic potential in mitigating the effects of neurodegeneration. This study opens avenues for further research in the field of herbal remedies for neurodegenerative diseases, where in-depth investigations are warranted to better understand the mechanisms underlying these observed effects.

REFERENCES

1. Gitler AD, Dhillon P, Shorter J. Neurodegenerative disease: models, mechanisms, and a new hope. *Dis Model Mech*. 2017 May 1;10(5):499-502
2. Lamptey RNL, Chaulagain B, Trivedi R, Gothwal A, Layek B, Singh J. A Review of the Common Neurodegenerative Disorders: Current Therapeutic Approaches and the Potential Role of Nanotherapeutics. *Int J Mol Sci*. 2022 Feb 6;23(3):1851
3. Singh A, Kukreti R, Saso L, Kukreti S. Oxidative Stress: A Key Modulator in Neurodegenerative Diseases. *Molecules*. 2019 Apr 22;24(8):1583
4. Bolus H, Crocker K, Boekhoff-Falk G, Chtarbanova S. Modeling Neurodegenerative Disorders in *Drosophila melanogaster*. *Int J Mol Sci*. 2020 Apr 26;21(9):3055.
5. Lu B, Vogel H. *Drosophila* models of neurodegenerative diseases. *Annu Rev Pathol*. 2009; 4:315-42.
6. Sigris-Flores SC, Castañeda-Partida L, Campos-Aguilar M, Santos-Cruz LF, Miranda-Gutierrez A, Gallardo-Ortiz IA, Villalobos-Molina R, Dueñas-García IE, Heres-Pulido ME, Piedra-Ibarra E, Rosales-García VH, Jimenez-Flores R, Ponciano-Gómez A. Variation in resistance to oxidative stress in Oregon-(R)R-flare and Canton-S strains of *Drosophila melanogaster*. *Toxicol Res (Camb)*. 2021 Jul 22;10(4):817-823
7. Huang Y, Zhan H, Bhatt P, Chen S. Paraquat Degradation from Contaminated Environments: Current Achievements and Perspectives. *Front Microbiol*. 2019 Aug 2; 10:1754
8. Simpson T, Pase M, Stough C. Bacopa monnieri as an Antioxidant Therapy to Reduce Oxidative Stress in the Aging Brain. *Evid Based Complement Alternat Med*. 2015; 2015:615384.
9. Ashburner M, Roote J. Culture of *Drosophila*: the laboratory setup. *CSH Protoc*. 2007 Mar 1;2007: pdb.ip34
10. Rzezniczak TZ, Douglas LA, Watterson JH, Merritt TJ. Paraquat administration in *Drosophila* for use in metabolic studies of oxidative stress. *Anal Biochem*. 2011 Dec 15;419(2):345-7
11. Paras Jain, Hanuman Prasad Sharma. Phytochemical analysis of Bacopa monnieri (L.) Wettst. and their anti-fungal activities. January 2017 DOI:10.13140/RG.2.2.17307.46882
12. Swati Nandi Chakraborty. Estimation of phytochemical characteristics and antioxidant property of secondary metabolites of a memory enhancing medicinal herb bacopa monnieri of east kolkata wetland. DOI:10.13040/IJPSR.0975-8232.11(6).2860-67
13. Jyothiprabha and P.Venkatachalam. Preliminary Phytochemical Screening of Different Solvent V Extracts of Selected Indian Spices. doi: <http://dx.doi.org/10.20546/ijcmas.2016.502.013>
14. Solihah, M.A., Wan Rosli, W.I. and Nurhanan, A.R. Phytochemicals screening and total phenolic content of Malaysian Zea mays hair extracts. 19(4): 1533-1538 (2012)
15. Usman H, Abdulrahman F, Usman A. Qualitative phytochemical screening and in vitro antimicrobial effects of methanol stem bark extract of Ficus thonningii (Moraceae). *Afr J Tradit Complement Altern Med*. 2009 May 7;6(3):289-95.
16. Nath, m., chakravorty, m. & chowdhury, s. Liebermann-burchard reaction for steroids. *Nature* 157, 103–104 (1946).
17. Sanjana Parise. The Effect of Ayurvedic Plant Extracts-- Mucuna pruriens and Brassica oleracea--on the Delay of Motor Symptoms in PINK1 *Drosophila melanogaster*: A Model of Parkinson's Disease.
18. Coxa, R.; Martin, F.; Calvin-Cejudo, L.; Gomez-Diaz, C.; Alcorta, E. Validation of an Optogenetic Approach to the Study of Olfactory Behavior in the T-Maze of *Drosophila melanogaster* Adults. *Insects* 2022, 13, 662. <https://doi.org/10.3390/insects13080662>





Cynthia Irene Kasi et al.,

19. Rahman, M.M., Noman, M.A.A., Hossain, M.W. et al. Curcuma longa L. Prevents the Loss of β -Tubulin in the Brain and Maintains Healthy Aging in *Drosophila melanogaster*. *Mol Neurobiol* **59**, 1819–1835 (2022).
20. Silu Lin, Ido Pen, Judith Korb, Effect of food restriction on survival and reproduction of a termite, *Journal of Evolutionary Biology*, 10.1111/jeb.14154, **36**, 3, (542-549), (2023)
21. Madabattula ST, Strautman JC, Bysice AM, O'Sullivan JA, Androschuk A, Rosenfelt C, Doucet K, Rouleau G, Bolduc F. Quantitative Analysis of Climbing Defects in a *Drosophila* Model of Neurodegenerative Disorders. *J Vis Exp*. 2015 Jun 13;(100):e52741

Table 1: Phytochemical investigations of the methanol extract of Brahmi and Ashwagandha

Bioactive compounds	Ashwagandha	Brahmi
Alkaloids	+	+
Saponins	+	+
Carbohydrates	+	+
Flavonoids	-	+
Steroids	+	+
Phenols	+	+

+ = Positive, - = Negative

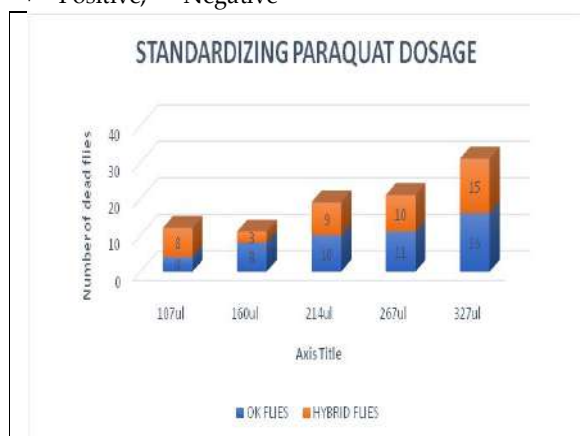


Fig1: Graphical Depiction of Comparative Analysis: Mortality Rates in OK vs. Hybrid Flies

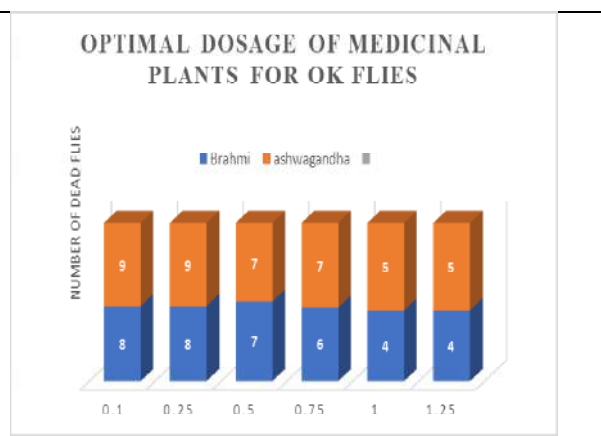


Fig2: Graphical Depiction of Comparative Analysis: Mortality Rates in 'Brahmi' vs. Ashwagandha for Ok Flies

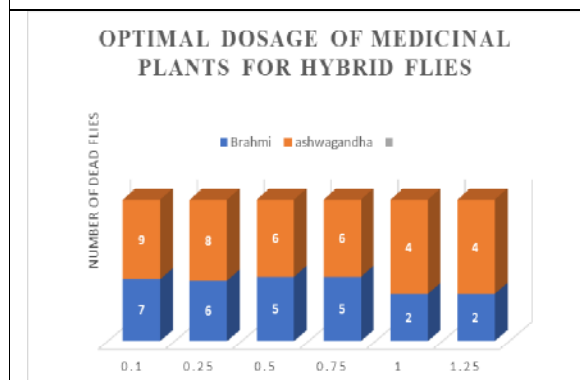


Fig3: Graphical Depiction of Comparative Analysis: Mortality Rates in 'Brahmi' vs. Ashwagandha for Hybrid Flies

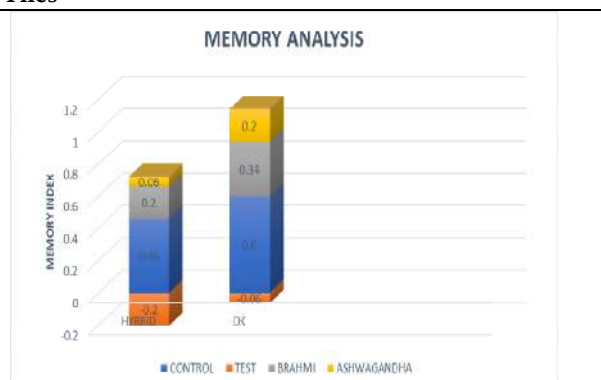


Fig4: Graphical Depiction of Comparative Analysis: Memory Index in Hybrid vs. OK Flies





Cynthia Irene Kasi et al.,

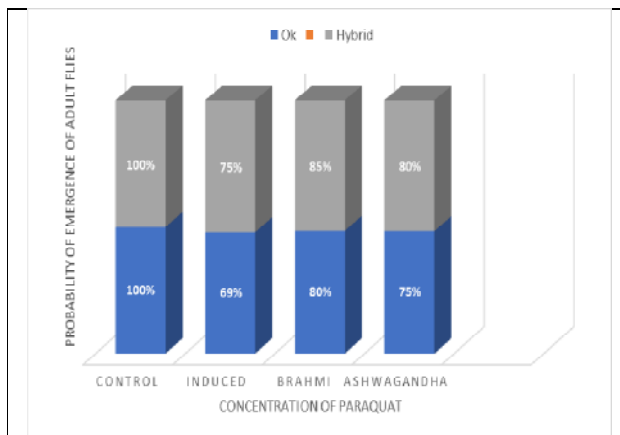


Fig5: Graphical Depiction of Comparative Analysis: Fertility analysis in OK vs. Hybrid Flies

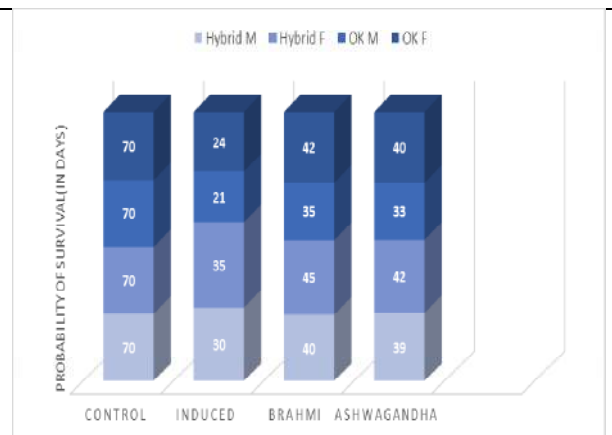


Fig6: Graphical Depiction of Comparative Analysis: Longevity analysis in OK vs. Hybrid Flies

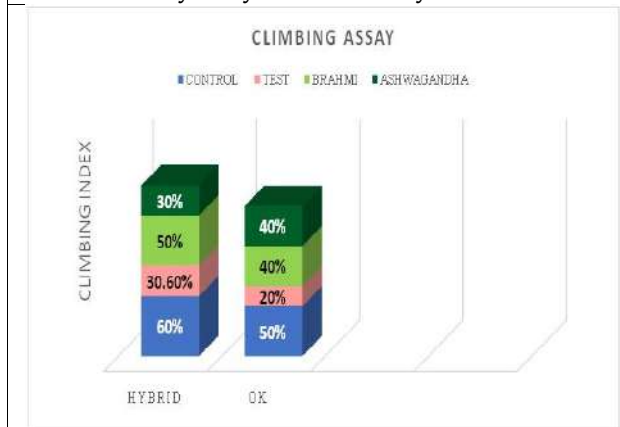


Fig7: Graphical Depiction of Comparative Analysis: Climbing Assay in Hybrid vs. OK Flies



Fig 8: five distinct concentrations of paraquat



Fig 9,10: Pipetting paraquat and sucrose into all tubes for both fly varieties and 10% sucrose



Fig11: Brahmi and Ashwagandha plant extracts





Cynthia Irene Kasi et al.,

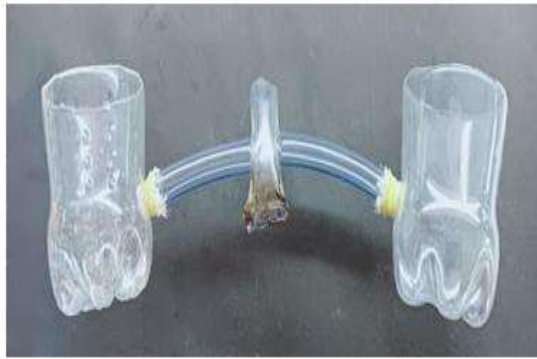


Fig 12: Homemade T-MAZE apparatus



Fig13: Conditioned stimulus



Fig14: Unconditioned stimulus

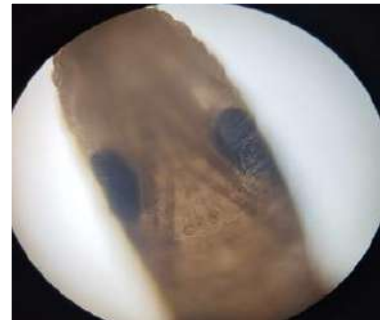


Fig15: Absence of sex comb Magnification:10x



Fig16: Presence of sex comb Magnification:10x



Fig17: Apparatus setup for climbing assay`





Cynthia Irene Kasi et al.,



Fig18: Culturing neurodegenerated flies in 1% plant extract infused media





A Concise Insight on Nanoemulgel Formulation an Overview towards its Development

Supriya Huljute Ravindra^{1*}, Rutuja Bhangare Gorakshnath¹, Shruti Burad Hanumant¹, Shashikant Dhole Nivrutti² and Nilesh Kulkarni Shrikant³

¹M.Pharam Student, Department of Pharmaceutics, PES Modern College of Pharmacy (For Ladies), Moshi, Pune, Maharashtra, India.

²Principal and Professor, Department of Pharmaceutics, PES Modern College of Pharmacy (For Ladies) Moshi, Pune, Maharashtra, India.

³Associate Professor, Department of Pharmaceutics, PES Modern College of Pharmacy (For Ladies) Moshi, Pune, Maharashtra, India.

Received: 07 Aug 2023

Revised: 22 Nov 2023

Accepted: 05 Feb 2024

*Address for Correspondence

Supriya Huljute Ravindra

M.Pharam Student,
Department of Pharmaceutics,
PES Modern College of Pharmacy (For Ladies),
Moshi, Pune, Maharashtra, India.
Email: supriyahuljute816@gmail.com



This is an Open Access Journal / article distributed under the terms of the **Creative Commons Attribution License (CC BY-NC-ND 3.0)** which permits unrestricted use, distribution, and reproduction in any medium, provided the original work is properly cited. All rights reserved.

ABSTRACT

About 40 to 70% of drugs in the pharmaceutical industry are among those with poor- water solubility because they are largely produced through synthetic chemistry. The formulation researcher must stay updated out, it resolves significant problems such limiting the use of lipophilic medications, low oral bio availability and fluctuations in absorption. To improve the efficacy of the hydrophobic drug, nanoemulsion delivery system has been developed. Its non-greasy texture and spread ability improve patient compliance at the same time. The main purpose of current dosage form is on developing particle carrier systems like solid-lipid nano particles, liposomes, self-emulsifying formulations, macro emulsions, and Nanoemulsions, etc. Nanoemulgel have priority for distribution of drug to a specific skin target. By creating nanoemulgel, it is possible to enhance the permeation rate and regulate the skin drug delivery. Topical nanoemulgel preparation can be supplied in the form of anti-acne, anti-fungal, anti-periodontitis, anti-parkinson's and other medications. In the most comprehensive review, the stages of drug development for topical targeted Nano emulgel delivery are highlighted. Review covers several preparation techniques, literature survey of topical drugs and evaluation of topical nanoemulgel drug delivery system.

Keywords: Nanoemulgel, Bio availability, Topical targeted, Lipophilic, Permeation rate.





Supriya Huljute Ravindra et al.,

INTRODUCTION

In pharmaceutical industry since about 40 to 70% of new chemical entities have a hydrophobic nature and they are prohibited from pipeline development because of their poor solubility, low permeability or both may contribute to low bioavailability. [1,2] Unfortunately, more than half of these drugs are classified as BCS [bio pharmaceuticals classification system] class II and IV and drug delivery of these poorly water drug is challenging. Hence, to overcome this poorly water-soluble drug problem/challenge, the novel drug delivery system is developed.[1] To improve the efficacy of the hydrophobic drug nanoemulsion delivery system has been developed. However, in this study we created a nano emulsion based nanocarriers, which we subsequently transformed into agel-based form.[3]In terms of controlled and homogeneous droplet size distribution, nanoemulsion produced by high-energy emulsification techniques, such as high-pressure homogenizers and high-shear motionless mixers, which offer various industrial advantages.[4] As a result, nanoemulgel can be produced by incorporating nanoemulsion into a gel matrix. They have a higher ability to penetrate more deeper in the skin[5]. Because of its effectiveness for drug delivery to skin, nanoemulgel is one of the suitable candidates. Both nano emulsion and gel base are dual characteristics.[6] The benefits of using gels for dermatologically include thixotropic, greaseless, easily soluble. characteristics like emollient, non-staining, spreadable, readily removed water-soluble suitable for a variety of excipients miscible.[7] In order to treat a condition, transdermal preparation is applied directly to the skin or nasal membrane. This bypassing of the first pass impact results in systemic/localized effect and lower risks of adverse effects.[8,9]

Physiology of human skin

Mostly topical treatments are designed to be used on the skin [fig1]. About one-third of the blood that circulates through the adult's body and receives passage through the skin, which has a surface area of about 2msquare. Every square centimetre of human skin is estimated to have between 200 and 300 sweat ducts and between 40 and 70 hair follicles. The pH range of the skin is 4 to 5.6 secreted fatty acids and sweat from sebum the skin's surface pH can be affected. Three separate layers of tissue can be thought of as being present in the skin. They are epidermis, dermis, subcutaneous connective tissue. When the gelling components is present in the aqueous phase, a conventional emulsion changes into a nanoemulgel. Nanoemulgel has many advantages for dermatological applications, including being thixotropic, greaseless, easily spreadable, quickly removable, emollient, greaseless, easily spreadable, quickly removable, emollient, non-staining, water-soluble, extended shelf life, bio friendly, translucent, and appealing appearance. The unbroken stratum corneum, sweat ducts, or sebaceous follicles are the three entry points for molecules into skin. Its capacity to penetrate this outer layer restricts percutaneous absorption. The development of a concentration gradient, which acts as a propellant for the release of the drug from the vehicle [partition coefficient]drug diffusion, and migration of the drug across the skin.[3,10] Different pathways involved in the skin permeation of nanoemulgel, nanoemulsion and nano micelles. Figure -1 is given below[skin penetration pathways]

Factors to be consider for preparing a topical formulation

1. The penetration of the active components and its efficiency are increased by the vehicle effect of an occlusive vehicle. There is a chance that the vehicle will have cooling, drying, emollient, or protective characteristics.
2. Choose the proper lesions-specific preparation for instance, avoid using greasy ointments in acute weepy dermatitis.
3. Select a technique for pepping that is suitable for the environment. Use gel or lotion on hairy areas.
4. Ointments and creams without alcohol frequently have lower potential for causing irritation or hypersensitivity, whereas gels do. If you are allergic to emulsifiers or preservatives, ointments are not for you. [11]

ADVANTAGES OF NANOEMULGEL OVER CONVENTIONAL GEL

1. Drugs which are lipophilic and poorly soluble are known to be delivered more effectively by using nanoemulgel formulation. E.g lacidipine[12].



**Supriya Huljute Ravindra et al.,**

2. By extending the effects of drugs with shorter half-life, nanoemulgel improves in controlling the release of drugs.
3. It shows excellent stability, increased drug release and robust antibacterial activity. E.g ketorolac [13]
4. Avoid problems associated with gastrointestinal absorption. E.g luliconazole [14]
5. Increased compliance and prevention of first pass metabolism. E.g.Ropinirole.
6. Nanoemulgel formulation is a potential alternative to traditional oral drug delivery system to improve its bioavailability and penetration rate.eg voriconazole [15].
7. Nanoemulgel technique improves the skin permeability and storage stability. E.g retinyl palmitate[16].
8. The Nanoemulgel shows synergistic effect against vaginal candidiasis. E.g.Teatree oil combined with intraconazole [17]
9. Nanoemulgel shows non-sticky nature, greater spread ability, which improves patient compliance compared to conventional gel formulation.[18]
10. nanoemulgel increases the solubility and permeability of the drug via skin and prevents hairloss as compared to marketed conventional gel. E.g.minoxidil. [19]
11. It is suitable and acceptable for self-medication.[20]

DISADVANTAGES OF CONVENTIONAL GEL

1. Skin irritation is produced on by contact with dermatitis.
2. In conventional gel drugs have limited skin absorption.
3. In conventional gel large particle size of formulation is difficult to absorb through the skin.[21]
4. Conventional gel suffers from low spread ability, low viscosity and poor skin retention issue.[22]

DRUG SELECTION CRITERIA

The transdermal drug delivery system (TDDS) uses for numerous pharmacological substances through the skin for a long time, especially poorly water-soluble drugs and those with a narrow therapeutic window pharmacological index[23,24] the bioactive materials can go through TDDS in the skin layer in order to reach the blood supply. The ingested medication is subsequently carried throughout the body via the bloodstream. The many dose forms used in TDDS include transdermal patches, gel, emulgel, and nanoemulgel. The dual nature of nanoemulgel makes it a prospective TDDS. The existence of a gel basis and a nanosized emulsion integrated onto a single composition. Nanoemulgel can effectively distribute both hydrophilic and lipophilic pharmaceuticals, unlike hydrogels, which have difficulty delivering lipophilic drugs.[25] For transdermal delivery, a pharmaceutically modified form of nanoemulsion with the addition of an appropriate gelling agent may be a superior option for BCS class II and IV drugs.[26] For BCS class II and IV drugs, the nanoemulgel is a more effective carrier system, according to the BCS classification formulation selection is standards. The intensively metabolized class II drugs are a suitable option for nanoemulgel formulation because it reduces the side effect of the first pass metabolism even if nanoemulgel is a more effective carrier system for BCS class IV pharmaceuticals in order to boost solubility and permeability.[27] Biopharmaceuticals classification system shows the different classes related to solubility and permeability from that we can easily divide and select a drug for making new formulation Nanoemulgel improves the solubility of poorly water-soluble drugs. In biopharmaceuticals classification system, the nanoemulgel mostly focuses on the class and II and class IV drugs in that class the solubility of drugs is poor but has high permeability so the permeation through the skin is good. Hence, due to this it can be used for topical preparation of nanoemulgel.[28] Table -1 is given below.

SELECTION OF EXCIPIENTS**Excipients selection criteria [29,30]**

This is our major objectives while creating this nanoemulgel for topical application were to prevent irritation and reduces skin sensitivity. The drugs must have a higher solubility in the oil phase in order to retain solubility throughout the nanoemulsion. To prepare a stable nanoemulsion, the hydrophile-lipophile balance [HLB] value of the surfactant must be more than 10. Surfactant and co-surfactant with greater and lower HLB values were taken into consideration for admixing in order to maintain a stable nanoemulsion.





Supriya Huljute Ravindra *et al.*,

The ability of the formulation to contain a significant amount of a poorly soluble drugs effects the choice of excipients as well excipients should solubilize the lipophilic drugs as much as feasible in order to lower the amount of drugs product required to deliver an ideal therapeutic dose of the drug in an emulsified state.[31] It is essential that oil in the nano emulsion have a high ability to solubilize the drugs. The surfactants are safe, bio compatible, and less toxic and they form micelles at low concentration. They all have HLB larger than 12, and they are all thought to be safe the selection method may be guided by the surfactant's miscibility with oil. [32] Table -2 is given below.

Important components of nanoemulgel preparation

Aqueous phase For the aqueous phase of the emulsion, aqueous solvents are necessary. The two most common aqueous solvents in use presently are water and alcohol.

Oils Minerals oils, either alone or in combination with soft paraffin or hard paraffin are commonly employed as the drug's carrier and their occlusive and sensory properties in topically administered emulsion. Non biodegradable minerals and castor oils which have a local laxative effect are often used in oral preparations as are fish liver oils or different fixed vegetable oils [E.g, arachis oil, cottonseed oil, and maize oil] as nutritional supplements.

Emulsifiers Emulsifying substances are used to improve emulsification throughout the production process and preserve stability during a shelf life that range from a few days to month or years for commercial preparations. Sodium stearate, polyethylene sorbitan monooleate [span 80] polyoxyethylene sorbitan monooleate [tween 80] stearic acid, etc are some examples.

Gelling agent Gelling agents can also be used as thickening agents to improve the consistency of any dosage form. Carbopol-934, poloxamer-407, sodium CMC and more examples. [33]

Preservatives By shielding the formulation from microbial attack, they extend the shelf of the product. Among the often-employed preservatives are methyl paraben, propyl paraben, benzalkonium chloride, benzoic acid, etc.

Antioxidants They protect against oxidation-induced components deterioration. Ascorbyl palmitate, butylated hydroxyl toluene, and butylated hydroxyl anisole are all effective are utilized.

Humectants These substance are used to prevent moisture loss .propylene glycol and glycerine are some example which is utilized.[34]

Surfactants The stabilization of the nanoemulsion system depends on the application of surfactants. In this system, surfactants of the anionic, cationic and non-ionic types were utilized. The right choice of surfactants becomes essential in achieving a stable delivery system because of their various chemical properties. Surfactants with a respectable HLB value are necessary for the development of a nanoemulsion. Some commonly used surfactants are tween-80, tween 40, tween 20, span20, span 80 etc[35].

Co-surfactants In order to create a stable nanoemulsion, cosurfactants plays a crucial role in lowering the polarity of surfactant. Many other cosurfactants, such as alcohols with short to medium chains, act at the surfactant interface [c3-c8] these are beneficial for improving oil's penetrability and obtaining a stable formulation some commonly used co-surfactants are Transcutol, glycerol, propylene glycol, ethanol, Propanol etc [20].

MANUFACTURING OF NANOEMULGEL

A developed nanoemulsion is combined with an appropriate gel base during the multi-step process that creates nanoemulgel. Therefore, we will first discuss how to formulate and produced nanoemulsions before preparing gel bases.

PREPARATION OF NANOEMULSION

A significant quantity of energy, a surfactant or both are required for the formation of nanoemulsion since they are a non-equilibrium system of structured liquids. To create a nanoemulsion, either high-or-low-energy technique can be used. The temperature, phase inversion, phase transition, and self-emulsification methods make up the low energy method. Mechanical devices can be utilized to generate high disruptive forces in the high energy approach to separate the oil and water phases and produce nano droplets. For this, high pressure homogenizers, micro fluidized and ultra sonicators are utilized[30,36]

METHODS FOR PREPARATION OF NANOEMULSION

High energy methods

Since the normal range of nanoemulsion droplets sizes is between 5 to 500nm, achieving this size requires a lot of mechanical energy.

High-pressure homogenization



**Supriya Huljute Ravindra et al.,**

Several methods are used in high-pressure homogenization to achieve the required particles size. The techniques, which are frequently applied at pressure between 500 to 5000 psi, include hydraulic shear, cavitation and severe turbulence. Transferring the surfactant and co-surfactant into orifices allows for future dilution. The liquids can be passed through the homogenizer repeatedly throughout this process to unify them and reduce the size of the droplets to 1-10nm. This method works effectively for nanoemulsion with a 20% oil content because a large percentage of oil in the formulation significantly reduce the method's productivity. The high energy method is one of most popular method for preparing nanoemulsion.[37].Table -3 is given below.

Ultrasound generation

By using a probe sonicator, this technique transforms the coarse emulsion into the appropriate nanosized emulsion droplets. High-sonication sound waves with a frequency of at least 20khz are produced by the probe sonicator. The strong sound waves disperse the thick emulsion into tiny, thin droplets known as nanoparticles[5-500nm].It is possible to reduce the size to desired levels using a variety of probe types with different diameters. Table -4 is given below.

Low energy methods

In this technique due to the inclusion of high energy during the manufacturing process low-energy emulsification techniques, such as spontaneous method and phase inversion method, are shown to superior than high energy emulsification technique.[46] A consistent mixture of a selected oil and surfactant and co-surfactant (Smix) mixture phase was produced by utilizing a vortex mixer and a low-energy emulsification technique in the right proportions. Purified water was immediately added as a continuous phase after properly combining the oil and (Smix) and the system was vortexed until an emulsion that was transparent, clear, and isotropic was obtained of thermodynamic stability of the final formulation. [47].Table -5 is given below.

Phase inversion technique

In phase inversion technique based on variables like temperature, the chemical environment of the components, including pH, ionic strength, and numerous physicochemical properties of the component sutilized phase inversion procedures are used to create kinetically stable nanoemulsion. Water in oil(w/o) or oil in water (o/w) emulsion are converted into one another throughout the emulsion production process. PIT (transitional-phase inversion) can be quickly cooled to produced nanosized emulsion droplets and the necessary polydispersity index. The formulation of the thermo sensitive drugs may be at risk because the high temperature is a crucial components of the process. Regarding the phase inversion composition (PIC) method, the temperature is held constant and composition change is permitted during the inversion process. For the formulation, the most preferred pseudo-ternary phase diagram approach is utilized for nanoemulsion formulation.[49].

Spontaneous emulsification method

It involves two liquids phases, one of which is aqueous and the other is organic and is one of the most practical techniques for creating nanoemulsions on a lab and commercial scale. It involves two liquids phases, one is aqueous and the other is organic, and it is one of the most practical techniques for creating nanoemulsion in both the laboratory and on an industrial scale. The organic or oil phase contains components like caproyl 90 or any comparable substance, such as acetone, ethyl methyl ketone, etc. in which the medication is pre-solubilized. The aqueous phase is composed of a hydrophilic surfactant of various categories, such as tween, span, etc. When the organic phase is gently introduced to the aqueous phase and then evaporated, the spontaneous creation of nanoemulsion is accomplished. The procedure can benefit from gentle stirring with the aid of a magnetic stirrer, which produces small convection currents beneficial in the distribution of oil droplets in the bulk solvents[48,50].Table -6 is given below.

PREPARATION OF NANOEMULGEL OR INCORPORATION OF GELLING AGENT IN NANOEMULSION:**Methods of preparation of nanoemulgel:[55,56]**

Step-1: Preparation of emulsion

Depending on whether an oil in water or a water in oil emulsion is formulated.

Step-2: Formation of gel base

By adding suitable gelling agent. Example- carbopol 940.

Step-3: Addition of emulsion into gel base:



**Supriya Huljute Ravindra et al.,**

Finally, the formulated emulsion is mixed with gel base to create a nanoemulgel [55]. Figure -2 is given below. [Diagram indicates the preparation of nanoemulgel]

Preparation of gel phase

By dispersing polymer in purified water while continuously stirring at a reasonable speed with a mechanical shaker, the gel phase in the formulation is created. The pH was then corrected to 6-6.5 using triethanolamine [TEA]. Emulsion's oil phase is made by dissolving an emulsifier, such as span 20, in the oil phase, which is made up to light liquid paraffin.

Aqueous phase preparation

To prepare the aqueous phase, emulsifier like tween 20 are dissolved in distilled water.

Drug solution preparation

The drug is dissolved in ethanol[56].

CHARACTERIZATION OF TOPICAL NANOEMULGEL**Measurement of pH**

A pH meter was used to measure the pH of different topical preparation, which ranged from to 6.1 g of gel is dissolved in 10 ml of water for testing purposes using digital pHmeter. To prevent errors, the pH of each formulation is performed three times.

Globule size

To measure this parameter, 1.0gm of gel was dissolved in water, agitated to obtain dispersion, and then sample was injected in to the photocell of Malvern Zetasizer.

Swelling index

10ml of 0.1NNAOH solutions are added to porous aluminium foil that has been coated with 1 gram of topical nanoemulgel that has been manufactured. Sample taken periodically; weight recorded until no weight change is observed: $\text{swelling index (SW)\%} = \frac{wt - wo}{wo} * 100$

Where wo=original weight of the nanoemulgel and (sw)%= percentage of swelling

Wt.= weight of the nanoemulgel at time t with swelling.

Measurement of bioadhesive strength

Bioadhesive strength measurement on each arm of the equipment, a glass slide was situated between two other glass plates. A single plate is used to add weight. Between two slides containing rate skin fragment (hairless) precisely 1 gm of nanoemulgel is positioned. Placing pressure on a single glass slide can lead to the removal of the sandwich of two slides. Weight gain is added on at a rate of 200 mg per minute until the skin surface separates. Bio adhesive strength was determined by the weight required to separate the nanoemulgel from the skin. It is calculated the equation shown below:

Bio adhesive strength = w/a where w is needed weight (in gm) and a is the area (in cm^2) [57]

Test for skin irritation

The preparation is applied to a rat's shaven skin and may unfavourable effects such as a change in skin colour or morphology should be monitored for up to 24 hours. The study can employ the entire set of 8 rats. The test is considered successful if no irritation happens. The trial should be repeated if the skin irritation symptoms appear in more than two animals[58].

Physical characteristics

The colour, homogeneity, consistency and phase separation of the topical emulgel formulation were Visualized [59].

Rheological studies

Using a cone and plate viscometer, the viscosity of the various emulgel formulations assessed at 25°C with spindle count of 62 and connected to a water bath with a thermostat [60].

CHARACTERISTICS OF NANOEMULGEL**Stability studies**

The prepared nanoemulgel were placed in aluminium collapsible tubes (5g) and stability tests were conducted on them for three months at 50°C/25%RH, 30°C/65%RH and 4°C/75%RH. At intervals of 15 days samples were taken out and examined for their physical characteristics, pH, rheological characteristics, drug contents and drugs release profiles. [61]





Supriya Huljute Ravindra et al.,

Determining the drug content

Mix 1 g of nanoemulgel with the appropriate solvent. To get a clear answer filter it. Utilize an ultraviolet UV spectrophotometer to ascertain its absorption. The same solvent is used to prepare the drug standard formulation. By including the value of absorbance in the standard plot, concentration and drug content can be estimated [62].

Drug content = (concentration × dilution factor × volume taken) × conversion

Surface morphology

To visualize the size, shape, and structure of nanoemulgel, TEM (transmission electron microscope) and SEM (scanning electron microscope) description were derived. These techniques are used to observe the morphological parameters such as size, shape, crystallinity and surface topography of a plain drug and formulated nanoemulgel. Any variation in crystallization state of developed nanoemulgel can be easily detected through microscopic studies [63].

FTIR: (Fourier transform infrared spectroscopy)

Fourier transform infrared spectroscopy is utilized to identify any functional groups that may be present in the structure. Quantitative FTIR is used to measure the interaction with excipients and any alteration to the formulation of the generated nanoemulgel. [64].

Particle size analysis and zeta potential

Using either the photon correlation spectroscopy technique or the dynamic light scattering approach, the particle size of the synthesized nanoemulgel is determined. Ionized water is used to dilute the produced nanoemulgel (1:1000) before measuring the particle size and Zeta sizer (ZS 90, Malvern instrument inc. UK) is used to calculate the zeta potential for nanoemulgel utilizing an electrophoretic light scattering technique [65,59].

Drug loading efficiency

Efficiency of nanoemulgel within the formulated nanoemulsion. Entrapment of nanoemulgel within the nanoemulsion formulation is successfully trapped is known as drug loading efficiency. The concentration of the drug were determined by using a UV-Visible spectrophotometer at, λ_{max} 299 nm. Entrapment is calculated by -[leflunamide]

$$\text{Entrapment efficiency} = \frac{\text{Actual drug content}}{\text{Theoretical drug content}} \times 100$$

SPECIALIZED CHARACTERIZATION

Permeation data analysis:

When compared to conventional gel, nano emulsions and the nano emulgel formulation had significantly higher steady-state flux (JSS), permeability coefficient (KP), and enhancement ratio (ER) permeability parameters. This is due to the size of the drug-loaded globules being reduced by nano emulsions and nanoemulgel. When compared to conventional gel, nanoemulgel exhibits steady state flux, permeability coefficient, and enhancement ratio.

Skin irritancy test

Male Swiss albino mice weighing 25–30g were used for the skin irritancy test. Standard laboratory settings, including temperature (25°C) and relative humidity (55%) were used to maintain the animals. The animals were kept in polypropylene cages with six individuals per cage and had unlimited access to a normal laboratory feed (Lipton feed, India). The mice's left ear received a single dose of the nanoemulgel, while their right ear served as a control. Six days' worth of erythema development were observed.

Studies on in-vitro skin permeation

Rat abdomen skin was used for in-vitro skin permeation tests on a Franz diffusion cell with a 3.14 cm² effective diffusion area and a 25 ml receiver chamber capacity. The abdomen region's rat skin was completely removed, and any remaining hairs were clipped off with an electric clipper. Surgery was used to remove the subcutaneous tissue, and fat clinging to the dermis was removed by wiping it with isopropyl alcohol. After being thoroughly cleaned, the skin was rinsed with distilled water and kept at -21°C until usage. The skin was warmed to room temperature before being put in the Franz diffusion cell so that the stratum corneum side faced the donor compartment and the dermal side faced the receiver compartment.

In-vivo research model

The Institutional Animal Ethics Committee granted permission to conduct in-vivo investigations, with approval number. MRCP/CPCSEA/IAEC/2016-17/PECU/02 and their criteria were adhered to throughout the experiments. The carrageenan-induced hind paw Edema method, created by Winter et al. 19 in Wistar rats, was used to assess





Supriya Huljute Ravindra *et al.*,

the anti-inflammatory and sustaining activities of the optimized formulations. Young male Wistar rats weighing 180–220 g was randomly assigned to one of three groups, each of which contained six rats: control, nanoemulgel, and conventional gel. The animals were housed in typical lab settings with a temperature of 25°C and a relative humidity of 55% and 5%. Six animals were kept in each polypropylene cage, and they were given free access to a normal laboratory meal (Lipton's feed) as well as unlimited amounts of water. Based on the predicted doses for the rats. All animals (aside from those in the control group) had their abdomen regions shaved and applied with either nanoemulsion gel and regular conventional gel formulations 30 minutes prior to receiving a sub planter injection of carrageenan into their right paws. By injecting 0.1 ml of a homogenous 1% (m/m) carrageenan suspension in distilled water, paw Edema was generated. Using a digital plethysmometer 20, the paw volume was measured at 1, 2, 3, 6, and 12 hours after injection. Periodically, the quantity of paw Edema was measured and expressed as a percentage of the original hind paw volume. Each formulation-treated group's percentage suppression of the Edema it created was calculated in comparison to the corresponding control group and anti-inflammatory activity results were compared. Using these equations [66]. Edema rate (e%) = $\frac{vt - vo}{vo} * 100$ (3) Inhibition rate (i%) = $\frac{ec - et}{ec} * 100$ (4) Where ec is the Edema rate of the control group and et is the Edema rate of the treated group, vo is the mean paw volume prior to CFA injection (in millilitres) and vt is the mean paw volume following CFA injection (in millilitres).[66]

DIFFUSION MECHANISM OF TRANSDERMAL DRUG DELIVERY SYSTEM.

When a Transdermal drug delivery is applied to the skin, it diffuses to the stratum corneum, the skin's outermost layer then moves through the deeper epidermis and dermis. The drugs can enter the skin through three different channels. Through the appendages is the initial route. The stratum corneum barrier will be bypassed by the drug molecules making their "first cut" into the sweat gland. If the drug molecules are not delivered through the "first cut," they typically remain in the stratum corneum's bilayered lipids, where they can then be transported either through the transcellular or paracellular routes into the deeper layers of the skin, such as the subcutaneous layer. According to the para cellular pathway, the solutes pass through the junction between the cell. The stratum corneum, a very fatty layer, must be traversed by the topical drug molecules when they transit via the paracellular route. However, they must do so between the cells. The trans cellular pathway, on the other hand, may be used by the molecules of topical drugs. Molecules can travel across the cell using this route. The medicine is delivered into the bilayered lipid cells that make up the stratum corneum via the trans cellular pathway. Drug molecules will diffuse through these bilayered lipids into deeper areas of the skin since the stratum corneum contains a water-soluble environment inside of them. The keratin, which is one of the skin's components found in the stratum corneum, may bond to the molecules of topical drugs as they travel through the skin.[67]

CONCLUSION

Nanoemulgel is a nanoemulsion-based system by incorporated a gelling agent that provides the three-dimensional structure system. It gives mollient, non-staining, spreadable and readily removed water-soluble effect. Nanoemulgel is an incredibly effective delivery method for hydrophobic drugs. It is a powerful alternative delivery strategy for the treatment of many diseases because of the high drug loading provided by increased in solubilizing efficacy, improved bioavailability provided by better permeability and ability to regulate drug release.

Conflict of interest

The authors declare they have no conflict of interest.

REFERENCES

1. Bhavna Dhawan, Geeta Aggarwal, SL Harikumar. Enhanced transdermal permeability of piroxicam through novel nanoemulgel formulation. International Journal of Pharmaceutical Investigation 2014; Vol 4 (2):65–76.
2. Baboota S, Al-Azaki A, Kohli K, Ali J, Dixit N, Shakeel F. Development and evaluation of a micro emulsion formulation for transdermal delivery of terbinafine. PDA J Pharm Sci Technology 2007;61(4):276-85.





Supriya Huljute Ravindra et al.,

3. Chandra Prabha, Pankaj Kumar. Emulsion based gel technique: A novel approach for Topical drug delivery system. *Journal of Pharmaceutical Advanced Research*2022;5(5):1512-1523.
4. Asiya Mahtab, Mohammed Anwar, Neha Mallick, Zrien Naz, Gaurav K. Jain, and Farhan J Ahmad. Transungual Delivery of Ketoconazole Nanoemulgel for the Effective Management of Onychomycosis. *AAPS Pharmaceutical Science Technology*2016;Vol.17(No.6):1477-1490.
5. S. Panwar, S. Gandhi, A. Sharma, N. Upadhyay, M. Bairagi, S. Gujar, G. N. Darwhekar, D. K. Jain. Emulgel: A Review. *Asian Journal of Pharmacy and Life Science*2011;Vol.1(3):333-343.
6. Manasi Nikam, Pavithra Yendapalli, Ravichandra VD, Vaishnavi Pai. Formulation And Evaluation Of Topical Nanoemulgel Of Moringa Oleifera Leaves Extract. *Zeichen Journal*2022;Vol.8(8):504-513.
7. P Vijaya Bhanu, V Shanmugam and P K Lakshmi. Development And Optimization of Novel Diclofenac Emulgel for Topical Drug Delivery. *Pharmacie Globale International Journal of Comprehensive Pharmacy*2011; Vol.02(09):1-4.
8. Hina Javed, Syed Nisar Hussain Shah, and Furqan Muhammad Iqbal. Formulation Development and Evaluation of Diphenhydramine Nasal Nano-Emulgel. *American Association of Pharmaceutical Scientists*2018;19(4):1730-1743.
9. Cho C-W, Choi J-S, Shin S-C. Development of the ambroxol gels for enhanced transdermal delivery. *Drug Development and Industrial Pharmacy*2008;34(3):330-335.
10. Tanaji DN. Emulgel: A comprehensive review for topical delivery of hydrophobic drugs. *Asian Journal Pharmaceutics*2018;12(2):382-393.
11. Hasan S, Bhandari S, Sharma A, Garg P. Emulgel: A review. *Asian Journal Pharmaceutical Research* 2021;11(4):263-268.
12. Padmadevi Chellapa, Aref T. Mohamed, Eseldin I. Keleb, Assad Elmahgoubi, Ahmad M. Eid, Yosef S. Issa, Nagib A. Elmarzugi. Nanoemulsion and Nanoemulgel as a Topical Formulation. *IOSR Journal of Pharmacy*2015; Vol.5(10):43-47.
13. Ajazuddin, Amit Alexander, Ajita Khichariyas, Saurabh Gupta, Ravish J. Patel, Tapan Kumar Giri, Dulal Krishna Tripathi. Recent expansions in an emergent novel drug delivery technology. *Journal of Controlled Release*, 2013, 1-11.
14. Sonia Paliwal, Kanak Pandey, Himanshu Joshi, Gurleen Kaur, Nawaz Akbar. An overview of nanoemulgel as a nanocarrier drug delivery. *Journal of medical pharmaceutical and allied sciences*2022;Vol.2(2):235-238.
15. Nitin Prabhakar Ambhore, Panchaxari Mallapa Dandagi, Anand Panchaxari Gadad, Paresh Mandora. Formulation and Characterization of Tapentadol Loaded Emulgel for Topical Application 2017; Vol 51(4):525-535.
16. Mohammed S. Algahtani, Mohammad Zaki Ahmad and Javed Ahmad. Nanoemulgel for Improved Topical Delivery of Retinyl Palmitate: Formulation Design and Stability Evaluation. *Nanomaterials*2020;10(5):1-18.
17. Iqbal Z, Manzoor N, Mirza MN, Ahmad S, Talegaonkar S. Development of a novel synergistic thermosensitive gel for vaginal candidiasis: An in vitro, in vivo evaluation. *Colloids Surfaces B Biointerfaces*2012;(103):275-282.
18. Chellapa P, Mohamed AT, Keleb EI, Elmahgoubi A, Eid AM, Issa YS, et al. Nanoemulsion and nanoemulgel as a topical formulation. *IOSR Journal of Pharmacy*2015;(5):43-47.
19. Eman Abd, Heather A. E. Benson, Michael S. Roberts and Jeffrey E. Grice. Minoxidil Skin Delivery from Nanoemulsion Formulations Containing Eucalyptol or Oleic Acid: Enhanced Diffusivity and Follicular Targeting. *Pharmaceutics* 2018; 10(19):1-12.
20. V. Harshitha, M. Venkata Swamy, D. Prasanna Kumar, K. Sai Rani, A. Trinat. Nanoemulgel: A Process Promising in Drug Delivery System. *Research Journal Pharmaceutical Dosage form and Technology*2020;12(2):125-130.
21. G. Sushma, T. Pravalika, B. Renu Sri, P. Priyanaka, Dr. P. Vishnu Priya, Dr. J.V.C Sharma. Emulgels- A Novel Approach for Topical Drug Delivery. *International Journal of Pharmaceutical Sciences Review and Research*2021;67(1):142-147.
22. Mou D, Chen H, Du, Mao C, Wan J, Xu H, et al. Hydrogel-thickened nanoemulsion system for topical delivery of lipophilic drugs. *International Journal Pharmaceutics*2008;353:270-276.



Supriya Huljute Ravindra *et al.*,

23. M.R. Prausnitz, R. Langer. Transdermal drug delivery. *Nature Biotechnology* 2008; 26(11):1261–1268.
24. P. van Hoogevest, X. Liu, A. Fahr. Drug delivery strategies for poorly water-soluble drugs: the industrial perspective. *Expert Opinion Drug Delivery* 2011; 8(11):1481-1500.
25. Marwa H. Abdallah, Amr S. Abu Lila, Rahamat Unissa A, Heba S. Elsewedy, Hanaa A. Elghamry, Mahmoud S. Soliman. Preparation, Characterization and Evaluation Of Anti-Inflammatory And Anti-Nociceptive Effects Of Brucine-Loaded Nanoemulgel. *Colloids And Surfaces B: Biointerfaces* 2021; Vol.205:1-8.
26. Kumar Anand, Subhabrata Ray, Mahfoozur Rahman, Adil Shaharyar, Rudranil Bhowmik Rammohan Bera and Sanmoy Karmakar. Nano-emulgel: Emerging as a Smarter Topical Lipidic Emulsion-based Nanocarrier for Skin Healthcare Applications. *Recent Patents on Anti-Infective Drug Discovery* 2019; Vol.14:1-14.
27. Poovi Ganesan, Damodharan Narayanasamy. Lipid nanoparticles: A challenging approach for oral delivery of BCS Class-II drugs. *Future Journal of Pharmaceutical Science* 2018; 1-15.
28. Brijesh Ojha, Vineet Kumar Jain, Surabhi Gupta, Sushama Talegaonkar, Keerti Jain. Nanoemulgel: a promising novel formulation for treatment of skin ailments. *Polymer Bulletin* 2021; Issue(7):1-25.
29. Ankha Bhattacharya, Bhupendra G Prajapat. Formulation And Optimization of Celecoxib Nanoemulgel. *Asian Journal of Pharmaceutical and Clinical Research* 2017; Vol10(8):353-365.
30. Shakeel F, Baboota S, Ahuja A, Ali J, Aqil M, Shafiq S. Nanoemulsion as vehicles for transdermal delivery of Aceclofenac. *AAPS Pharmaceutical Science Technology* 2007; 8(4):1-9.
31. Vivek Verma, T S Easwari. A Novel Approach of Leflunomide Nanoemulgel for Topical Drug Delivery System. *International Journal of Pharmaceutical Investigation* 2022; Vol12 (2):1-5.
32. Azeem A, Rizwan M, Ahmad FJ, Iqbal Z, Khar RK, Aqil M, et al. Nanoemulsion components screening and selection: A technical note. *AAPS Pharmaceutical Science Technology* 2009; Vol.10:69-76.
33. Sharma Bhavesh R, Chainesh N. Shah. Nanoemulgel: A Comprehensive review on the recent advances in topical drug delivery. *An International Journal of pharmaceuticals Science* 2016; 7(2):346-35.
34. Pinaki Sengupta, Bappaditya Chatterjee. Potential and future scope of nanoemulgel formulation for topical delivery of lipophilic drugs. *International Journal of Pharmaceutic* 2017; 526(1-2):353–365.
35. Vats S, Saxena C, Easwari TS, Shukla VK. Emulsion Based Gel Technique: Novel Approach for Enhancing Topical Drug Delivery of Hydrophobic Drugs. *International Journal for Pharmaceutical Research Scholar* 2014; 3(2):2277-7873.
36. Lovelyn C, Anthony A. Attama. Current State of Nanoemulsions in Drug Delivery. *Journal of Biomaterials and Nanobiotechnology* 2011; 2(5):626–639.
37. R. Neslihan Gursoy, S. Benita. Self-emulsifying drug delivery systems (SEDDS) for improved oral delivery of lipophilic drugs. *Biomedicine & Pharmacotherapy* 2004; 58:173-182.
38. Nabil A. Alhakamy, Shadab Md. Md Shoaib Alam, Rasheed A. Shaik, Javed Ahmad, Abrar Ahmad, Hussam I. Kutbi, Ahmad O. Noor, Alaa Bagalagel, Douha F. Bannan, Bapi Gorain and Ponnurengam Malliappan Sivakumar. Development, Optimization, and Evaluation of Luliconazole Nanoemulgel for the Treatment of Fungal Infection. *Journal of Chemistry*; 2021:1-13.
39. Mohammed S. Algahtani, Mohammad Zaki Ahmad, Ibrahim Ahmed Shaikh, Basel A. Abdel-Wahab, Ihab Hamed Nourein and Javed Ahmad. Thymoquinone Loaded Topical Nanoemulgel for Wound Healing: Formulation Design and In-Vivo Evaluation. *Molecules* 2021; 26:16.
40. Md. Shoaib Alam, Mohammed S Algahtani, Javed Ahmad, Kanchan Kohli, Sheikh Shafiq-un-Nabi, Musarrat Husain Warsi and Mohammad Zaki Ahmad. Formulation design and evaluation of aceclofenac nanogel for topical application. *Therapeutic Delivery* 2020; 11(12):767–778.
41. Nidhi Srivastava, Dinesh Kumar Patel, Vineet Kumar Rai, Anirban Pal, Narayan Prasad Yadav. Development of emulgel formulation for vaginal candidiasis, Pharmaceutical characterization. In vitro and in vivo evaluation. *Journal of Drug Delivery Science and Technology* 2018; vol 48:409-498.
42. Swati Talele, Preetam Nikam, Braja Ghosh, Chaitali Deore, Ashwini Jaybhav, Anil Jadhav. A Research Article on Nanogel as Topical Promising Drug Delivery for Diclofenac sodium. *Indian Journal of Pharmaceutical Education and Research* 2017; Vol 51(4):580-587.



**Supriya Huljute Ravindra et al.,**

43. Sanjeev Rambharose, Rahul S. Kalhapure, ThirumalaGovender. Nanoemulgel using a bicephalous heterolipid as a novel approach to enhance transdermal permeation of tenofovir. *Colloids and Surfaces B: Biointerfaces* 2017; vol 154:221-227.
44. Neelam Datt, Rajasekhar Reddy Poonuru, Pankaj K. Yadav. Development and characterization of griseofulvin loaded nanostructured lipid carrier gel for treating dermatophytosis. *Food Hydrocolloids for Health* 2022; (2):1-15.
45. Abimanyu Sugumaran, Vishali Mathialagan. Topical Delivery of Methocarbamol Loaded Nanoemulgel - in-vitro Characterization. *Indian Journal of Pharmaceutical Education and Research* 2022; Vol 55I(4):1-10.
46. Hira Choudhury, Bapi Gorain, Manisha Pandey, Lipika Alok Chatterjee, Pinaki Sengupta, Arindam Das, Nagashekhar Molugulu, Prashant Kesharwani. Recent update on nanoemulgel as topical drug delivery system. *Journal of Pharmaceutical Sciences* 2017:1-44.
47. Yuvraj Singh, Jaya Gopal Meher, Kavita Raval, Farooq Ali Khan, Mohini Chaurasia, Nitin K. Jain, Manish K. Chourasia. Nanoemulsion, Concepts, development and applications in drug delivery. *Journal of controlled release* 2017; 252:28-49.
48. Garg A, Gautam A, Ahmad J, Jain K, Komath S, Bano M. Topical nano-emulgel for skin disorders: Formulation approach and characterization. *Recent Patents on Anti-Infective Drug Discover* 2018; 14:1-13.
49. P. Fernandez, V. André, J. Rieger, A. Kühnle. Nano-emulsion formation by emulsion phase inversion. *Colloids and Surfaces A: Physicochemical and Engineering Aspects* 2004; vol 251 (1-3):53-58.
50. K. Bouchemal, S. Briançon, E. Perrier, H. Fessi. Nano-emulsion formulation using spontaneous emulsification: solvent, oil and surfactant optimisation. *International journal of pharmaceutics* 2004; vol 280(1-2):241-251.
51. Amanpreet Kaur, Sameer S, Katiyar, Varun Kushwah, Sanyog Jain. Nanoemulsion loaded gel for topical delivery of clobetasol propionate and Calcipotriol psoriasis. *Nanomedicine, Nanotechnology, Biology, and Medicine* 2017; 13(4):1473-1482.
52. Eileen Yeo, Clement Jia Yew Chieng, Hira Choudhury b, Manisha Pandey, Bapi Gorain. Tocotrienols-rich naringenin nanoemulgel for the management of diabetic wound: Fabrication, characterization and comparative in vitro evaluations. *Current Research in Pharmacology and Drug Discovery* 2021; (2):1-10.
53. Soliman Mohammadi-Samani, Pedram Masoumzadeh, Parisa Ghasemiyeh, and Shohreh Alipour. Oxybutynin-Nanoemulgel Formulation as a Successful Skin Permeation Strategy: In-vitro and Ex-vivo Evaluation. *Frontier in Material* 2022; vol(9):1-11.
54. Rachit Khullar, Deepinder Kumar, Nimrata Seth, Seema Saini. Formulation and evaluation of mefenamic acid emulgel for topical delivery. *Saudi Pharmaceutical Journal* 2012; 20:63-67.
55. Prahudas Papagari, Anie Vijetha. A Review on Emulgel: As a Novel Topical Drug Delivery System. *Research & Reviews: Journal of Pharmaceutics and Nanotechnology* 2021; Volume 9(1):25-32.
56. Sunil Kumar Yadav, Manoj Kumar Mishra, Anupama Tiwari, Ashutosh Shukla. Emulgel: A New Approach for Enhanced Topical Drug Delivery. *International Journal of Current Pharmaceutical Research* 2016; Vol 9(1):15-19.
57. Malay N Jivani, Chandresh P Patel and Bhupendra G Prajapati. Nanoemulgel Innovative Approach for Topical Gel Based Formulation. *Research and Reviews on Healthcare: Open Access Journal* 2018; Vol 1(2):18-23.
58. G. Sushma, T. Pravalika, B. Renu Sri, P. Priyanaka, Dr. P. Vishnu Priya, Dr. J.V.C Sharm. Emulgels- A Novel Approach for Topical Drug Delivery. *International Journal of Pharmaceutical Sciences Review and Research* 2021; 67(1):142-147.
59. Mengesha M. Preparation, characterization and optimization of oromucosal clotrimazole emulgel formulation. *Jesuit historical institute in Africa* 2015.
60. S. B. Kute and R.B. Saudaga. Emulsified gel A Novel approach for delivery of hydrophobic drugs: An overview. *Journal of Advanced Pharmacy Education & Research* 2013; Vol 3(4):368-376.
61. Jadhav CM, Kate V, Payghan SA. Formulation and evaluation of antifungal non-aqueous microemulsion for topical drug delivery of griseofulvin. *Inventi Impact Pharmaceutical Technology* 2015; vol 2015(1):38-50.



Supriya Huljute Ravindra *et al.*,

62. Anil R. Phad, Nandgude Tanaji Dilip, R. Sundara Ganapathy. Emulgel: A Comprehensive Review for Topical Delivery of Hydrophobic Drugs. *Asian Journal of Pharmaceutics* 2018;12 (2):1-12.
63. Prashant Sahu, Sushil K. Kashaw, Samaresh Sau, Varun Kushwah, Sanyog Jain, Ram K. Agrawal, Arun K. Iyer. pH triggered and charge attracted nanogel for simultaneous evaluation of penetration and toxicity against skin cancer: In-vitro and ex-vivo study. *International Journal of Biological Macromolecules* 2019;1-34.
64. Chakraborty M, Dasgupta S, Bose P, Misra A, Kumar Mandal T, Mitra M, *et al.* Layered double hydroxide: inorganic-organic conjugate nanocarrier for methotrexate. *Journal of physics and Chemistry Solids* 2011;72:779–83.
65. Prasetyo BE, Karsono, Maruhawa SM, Laila L. Formulation and physical evaluation of castor oil based nanoemulsion for diclofenac sodium delivery system. *Research Journal of Pharmacy and Technology* 2018;11(9):3861–3865.
66. Vikram V.B.K. Mishra, S. B. Bhanja, B. B Panigrahi. Development and Evaluation of Nanoemulsion gel for transdermal delivery of Valdecoxib. *Research Journal Pharmaceutics and Technology* 2019;12(2):600-610.
67. Gandhi K, Monika AD, Kalra T, Singh K. Transdermal drug delivery -A review. *International Journal of Research in Pharmaceutical Sciences* 2012;3(3):379-388.
68. Kamarza Mulia, Rosalia M.A. Ramadhan, and Elsa A. Krisanti. Formulation and characterization of nanoemulgel mangosteen extract in virgin coconut oil for topical formulation. *MATEC Web of Conferences* 2018;Vol156:1-7.
69. M. Rahil G. Bhura, Khushboo A. Bhagat and Samir K. Shah. Formulation and evaluation of topical emulgel of adapalene. *World Journal of Pharmaceutical Sciences* 2015; 3(4):1013-1024.
70. Mehreen Bashir, Junaid Ahmad, Muhammad Asif, Salah-Ud-Din Khan, Muhammad Irfan, Asim Y Ibrahim, Sajid Asghar, Ikram Ullah Khan, Muhammad Shahid Iqbal, Abdul Haseeb, Syed Haroon Khalid, Mohammed AS Abourehab. Nanoemulgel an Innovative Carrier for Diflunisal Topical Delivery with Profound Anti-Inflammatory Effect: in vitro and in vivo Evaluation. *International Journal of Nanomedicine* 2021;(16):1457–1472.
71. Magdy I. Mohamed. Optimization of Chlorphenesin Emulgel Formulation. *The AAPS Journal* 2004;6(3):1-7.
72. Mohamed A. Morsy, Rania G. Abdel-Latif, Anroop B. Nair, Katharigatta N. Venugopala Amira F. Ahmed, Heba S. Elsewedy and Tamer M. Shehata. Preparation and Evaluation of Atorvastatin-Loaded Nanoemulgel on Wound-Healing Efficacy. *Pharmaceutic* 2019;11(609):1-15.
73. M. Srivastava, K. Kohli, and M. Ali. Formulation development of novel in situ nanoemulgel of ketoprofen for the treatment of periodontitis. *Drug Delivery* 2014;1-13.
74. Noha S. El-Salamouni, Mai M. Ali, Sheeren A. Abd El-Hady, Lamia S. Kandil, Gihan A. El Batouti and Ragwa M. Farid. Evaluation of chamomile oil and nanoemulgels as a promising treatment option for atopic dermatitis induced in rats. *Expert Opinion on Drug Delivery* 2020;17(1):111-122.
75. Deepak Kumar Upadhyay and Amit Sharma and Navjot Kaur and Ghanshyam Das Gupta and Raj Kumar Narang and Vineet Kumar Rai, Nanoemulgel for Efficient Topical Delivery of Finasteride Against Androgenic Alopecia, *Journal of Pharmaceutical Innovation* 2020;(16):735-746.
76. Yujuan Mao, Xiaolan Chen, Bohui Xu, Yan Shen, Zixuan Ye, Birendra Chaurasiya, Li Liu, Yi Li, Xiaoling Xing and Daquan Chen. Eprinomectin nanoemulgel for transdermal delivery against endoparasites and ectoparasites: preparation, in vitro and in vivo evaluation. *Drug delivery* 2019;Vol.26(1):1104–1114.
77. Disha Nailwal, Himansu Chopra, Alankar Shrivastav, Dr. Yusra Ahmad. Formulation and Evaluation of Vegetable Oil Based Emulgel of Fluconazole. *Journal of Drug Delivery and Therapeutics* 2019;9(4):415-418.
78. Nafiu Aminu, Siok-Yee Chan, Mun-Fei Yam, Seok-Ming Toh. A dual-action chitosan-based nanogel system of triclosan and flurbiprofen for localised treatment of periodontitis. *International Journal of Pharmaceutics* 2019;570:1-30.
79. Rabab Kamel, Nahla A. El-Wakil, AbdelFattah A, Abdelkhalek, Nermeen A. Elkasabgy. Topical cellulose nanocrystals-stabilized nanoemulgel loaded with ciprofloxacin HCl with enhanced antibacterial activity and tissue regenerative properties. *Journal of Drug Delivery Science and Technology* 2021;1-29.





Supriya Huljute Ravindra et al.,

80. Yehia I. Khalil, Abeer H. Khasraghi, and Entidhar J. Mohammed. Preparation and Evaluation of Physical and Rheological Properties of Clotrimazole Emulgel. *Iraqi Journal Pharmaceutics Science* 2011; Vol.20(2):19-27.
81. Wael H. Mohammed, Widad K. Ali, Mohammed J Al-Awady. Evaluation of in vitro drug release kinetics and antibacterial activity of vancomycin HCl-loaded nanogel for topical application. *Journal of Pharmaceutical Science & Research* 2018; Vol.10(11):2747-2756.
82. Richa Vartak, Suvidha Menon, Manali Patki, Blase Billack, Ketan Patel. Ebselen nanoemulgel for the treatment of topical fungal infection. *European Journal of Pharmaceutical Sciences* 2020; 148:1-10.
83. Lydia Thomas, Foziyah Zakira, Mohd. Aamir Mirza, Md. Khalid Anwer, Farhan Jalees Ahmad, Zeenat Iqbal. Development of Curcumin loaded chitosan polymer based nanoemulsion gel: In vitro, ex vivo evaluation and in vivo wound healing studies. *International Journal of Biological Macromolecules* 2017; 101:569-579.
84. Ahmad M. Eid and Mohammed Hawash. Biological evaluation of Safrole oil and Safrole oil Nanoemulgel as antioxidant, antidiabetic, antibacterial, antifungal and anticancer, *BMC Complementary Medicine and Therapies*. Eid and Hawash *BMC Complementary Medicine and Therapies* 2021; 21(1):1-12.
85. Ahmad M. Eid, Nidal Jaradat, Linda Issa, Aya Abu-Hasan, Nada Salah, Mohamad Dalal, Ahmed Mousa, Abdalrazizq Zarour. Evaluation of anticancer, antimicrobial, and antioxidant activities of rosemary (*Rosmarinus Officinalis*) essential oil and its Nanoemulgel. *European journal of Integrative Medicine* 2022; vol 55:1-7.
86. Iluska Martins Pinheiro, Ivana Pereira Santos Carvalho, Jose Alves Terceiro Neto, Glauca Lals Nunes Lopes, Elvilene de Sousa Coelho, Enoque Pereira Costa Sobrinho-Junior, Michel Mualem de Moraes Alves, Fernando Aecio de Amorim Carvalho, and Andre Luls Menezes Carvalho. Amphoteracin B-Loaded Emulgel: Effect of Chemical Enhancers on the Release Profile and Antileishmanial Activity In Vitro. *AAPS Pharm Science Technology* 2019; 20(3):122.
87. Gururaj C Aithal, Usha Yogendra Nayak, Chetan Mehta, Reema Narayan, Pratibha Gopalkrishna, Sudharshan Pandiyan, Sanjay Garg. Localized In situ nanoemulgel drug delivery system of Quercetin for Periodontitis: Development and Computational Simulation. *Molecules* 2018; 23(6):1-15
88. Singh Bhuwanesh Pratap, Kumar Brajesh, Jain S.K, Shafaat Kausar. Development and Characterization of A Nanoemulsion Gel formulation for Transdermal delivery of Carvedilol. *International Journal of Drug Development & Research* 2012; Vol.4(1):151-161.
89. Harwansh RK, Mukherjee PK, Bahadur S, Biswas R. Enhanced permeability of ferulic acid loaded nanoemulsion based gel through skin against UVA mediated oxidative stress. *Life Science* 2015; 14:202-11.
90. Wais M, Samad A, Nazish I, Khale A, Aquil M, Khan M. Formulation development ex-vivo and in -vitro evaluation of nanoemulsion. *International Journal of Pharmacy and Pharmaceutical Science* 2013; vol.5:747-754.
91. Anju KP, Shripathy D, Shabaraya AR. Antifungal Topical Nanoemulgel Containing Miconazole Nitrate. *International Journal of Health Sciences and Research* 2021; Vol.11(11):208-229.
92. Made Laksmi Dewi Dhyaksa and Mahdi Jufri. Formulation and physical stability study of nanoemulsion gel (nanoemulgel) containing Belimbing wuluh (*Averrhoa Bilimbi* L.) Ethanolic extract. *World Journal of Pharmaceutical and Life Science* 2021; vol 7(3):11-19.
93. Anayanti Arianto, Desi Yet Lie, Sumaiyah Sumaiyah, Hakim Bangun. Preparation and Evaluation of Nanoemulgels Containing a Combination of Grape Seed Oil and Anisotriazine as Sunscreen. *Open Access Macedonian Journal of Medical Sciences* 2020; 14,8(B):994-999.
94. V. Naga Sravan Kumar Varma, P.V. Maheshwari, M. Navya, Sharath Chandra Reddy, H.G. Shivakumar, D.V. Gowd. Calcipotriol delivery into the skin as emulgel for effective permeation *Saudi Pharmaceutical Journal* 2014; 22 (6):591-599.
95. Venkateswara Rao, S, Vijaya Sri, P. and Padmalatha, K. Formulation and evaluation of oxiconazole emulgel for topical drug delivery. *International Journal of Current Research* 2017; Vol.9(10):58876-58878.
96. Yan Shen, Xiang Ling, Weiwei Jiang, Shuang Du, Yang Lu, and Jiasheng Tu. Formulation and evaluation of Cyclosporin A emulgel for ocular delivery. *Drug Delivery* 2015; 22(7):1-7.





Supriya Huljute Ravindra et al.,

97. Radhika PR, Guruprasad S. Nanoemulsion based emulgel formulation of liophilic drug for topical delivery. *International Journal of Pharmaceutical Technology Research* 2016;(9):210-223.
98. Chin LY, Tan JYP, Choudhury H, Pandey M, Sisinthy SP, Gorain B. Development and optimization of chitosan coated nanoemulgel of telmisartan for intranasal delivery : A comparative study. *Journal of Drug Delivery Science and Technology* 2021;62:1-12.
99. Elmataeeshy ME, Sokar MS, Bahey-EL-Din M, Shaker DS. Enhanced transdermal permeability of terbinafine through novel emulgel formulation; development, in vitro and in vivo characterization. *Future Journal of Pharmaceutical Science* 2018;4(1):18-28.
100. Aman RM, Hashim IA, Meshali MM. Novel clove essential oil nanoemulgel tailored by Taguchi's model and scaffold-based nanofibers: Phytopharmaceutical with promising potential as cyclooxygenase-2 inhibitors in external inflammation. *International Journal of Nanomedicine* 2020;(15):2171-2195.
101. Narang RS, Srivastava S, Ali J, Baboota S, Singh B, Kahlon SS, Dogra A, Narang JK. Formulation and In vitro Evaluation of Fluconazole Loaded Nanoemulgel against *Candida albicans*. *European Journal of Molecular & Clinical Medicine* 2018;Volume 05(01):298-306.

Table 1: BCS Classification

BCS class	Solubility	Permeability
Class I	High	High
Class II	Low	High
Class III	High	Low
Class IV	Low	Low

Table 2 - surfactants and co-surfactants with their respective HLB values [hydrophilic-lipophilic balance]

Surfactants	HLB value	Co-surfactants	HLB value
Tween 20	16.72	Span 20	8.6
Pluronic f-68	29	PEG 400	13.0
Tween 80	15.0	Transcutol HP	4
Triethanolamine	34	Span 80	4.3

Table 3- literature for nanoemulgel prepared using high-pressure homogenization method.

Drugs	Excipients	Outcome	Ref
Luliconazole	Carbopol 934, Tween20, PEG 200	Effective approach for localized delivery of luliconazole safely with improved its efficacy.	[38]
Thymoquinone	Oleic acid, castor oil Isopropyl myristate, PEG 400, Tween 20, Tween 80, Solutol HS, sesame oil	Thymoquinone nanoemulgel accelerates the process of wound healing.	[39]
Aceclofenac	Carbopol 940, labrafil, triacetin, tween80, cremophor EL	Excellent skin permeation compared to the marketed sample	[40]
Mentha essential oil	Carbopol 94, triethanolamine, tween 80, species of candida.	It shows sustained release and possess antifungal activity	[41]



Supriya Huljute Ravindra *et al.*,**Table 4- Literature for nanoemulgel prepared using ultra sonification method**

Drugs	Excipients	Outcome	Ref
Diclofenac sodium	Carbopol 940, Glycerol, Tween 80, triethanolamine.	Diclofenac sodium shows better flux enhancement with propylene glycol as permeation enhancer.	[42]
Tenofovir	Solutol HS, PEG 400, triethylamine, hydroxypropyl methyl cellulose (HPMC)	First study to report formulation using a nano drug delivery system and potential to revolutionize HIV/AIDS treatment.	[43]
Griseofulvin	Tween80, Pluronic F68, carbopol940	Enhancement of antifungal and efficacy and used for treatment of superficial infection like ringworm and tenia pedis	[44]
Methocarbamol	Acconon oil, tween80, carbapol934, triethanolamine, sodium benzoate.	Shows slower release and lower size of droplets compared to conventional formulation due to presence of surfactant, hydrogel and acconon oil.	[45]

Table 5 - Literature for nanoemulgel prepared using low energy method

Drugs	Excipients	Outcome	Ref
Retinyl palmitate	Kolliphor® HS, tween 20, triethanolamine, glycerol, caproyl90, captex®355, capmul®	Improvement in UV and storage stability with better skin permeability having nanoemulsion droplet dimension <50nm.	[16]
Thymol	Isopropyl myristate, tween80, tween 20, cremophore EL, and rh, (polyethylene glycol) PEG 400, carbopol 940.	Formulation improved antimicrobial efficacy against Propionibacterium acnes and have good biopharmaceutic characteristics of topical application.	[48]

Table 6 -Literature for nanoemulgel prepared using spontaneous emulsification method

Drugs	Excipients	Outcome	Ref
Clobetasol propionate and caciprotiol.	Pluronic f-68, tween®20, capmul®, captex®355, sodium dodecyl sulfate, tween80, labrafil 1944 cs, cremophor RH 40.	Developed nanoemulsion base gel shows higher anti-psoriatic activity and negligible skin irritation with increased penetration into the skin.	[51]
Tocotrienols-rich naringenin	Capryol90, tocotrienols, Solutol HS15, transcuto-p	It is thermodynamically stable with good spreadability in promising wound management associated with diabetes complications.	[52]
Oxybutynin	Sodium alginate, hydro propyl methyl cellulose (HPMC), tween 80, span 20, carboxy methyl cellulose (CMC), potassium chloride.	It shows sustained release property and effective skin permeation ability.	[53]
Mefenamic acid	Labrafac WL 1349, labrasol, Transcutol P, tween 20, tween 80, labrafil M.	It shows higher penetration, better skin retention and permeability for treatment of rheumatoid arthritis.	[54]

Table 7 – Literature survey of topical drugs used for nanoemulgel

Drugs	Excipients	Method of preparation	Result	Ref
Tapentadol	Liquid paraffin, tween 20, peg 400, Carbopol 940 NF Carbopol 934 NF	Aqueous titration method	It enhance solubility, bioavailability of poorly soluble drug and a potential	[15]





Supriya Huljute Ravindra et al.,

			alternative to oral drug delivery system.	
Mangosteen extract	Tween 80, Span 80, virgin coconut oil, xanthan gum.	High-speed homogenization method	Have better skin penetration result by penetrating more than 95% in the skin layer and study revealed that VCO-mangosteen nanoemulgel is prospective topical formulation	[68]
Adapalene	Carbopol 934, soyabean oil, tween 80, glycerine, isopropyl alcohol.	Incorporation of emulsion into the gel method.	It shows fast release of drug and increases in permeability across membrane which emerged interesting topical drug delivery system.	[69]
Diflunisal	Carboxymethylcellulose sodium (CMC-Na), xanthan gum, sodium alginate (Na-ALG), sunflower oil, sandalwood oil, olive oil, propylene glycol, tween 20, span 20 etc.	Aqueous titration method.	It shows enhancement in the solubility for better skin permeation and topical anti-inflammatory activity.	[70]
Chlorphenesin	Hydroxypropyl methyl cellulose, carbopol934, triethanolamine, tween 20, ethyl alcohol.	Incorporation of emulsion into the gel method.	It shows highest drug release and antifungal activity.	[71]
Atorvastatin	Carboxymethyl cellulose (CMC), tween80, propylene glycol.	High pressure homogenizer method,	It shows greater retention and highest wound healing power for topical application.	[72]
Ketoprofen	Labrasol, labrafac, transcuto HP, cremophor EL triacetin, Tween 80 PEG 400.	Aqueous titration method.	It shows sustained release and significantly lower in vitro toxicity and nano size suggests nanoemulgel intra-pocket delivery and to treat periodontitis.	[73]
Chamomile oil	Propylene glycol, Tween 20, Tween 80, hydro propyl methyl cellulose (HPMC)4000 cp.	High pressure homogenizer method.	It explores an effective in treatment of Atopic dermatitis with developed chamomile emulgel having nanometre size shows stability for topical application	[74]
Finasteride	Vitamin oil, cholesterol, lecithin, Acetonitrile.	High-speed homogenization method	It ensures longer duration on skin with slower permeation and higher efficacy against Alopecia.	[75]
Eprinomectin	Carbomer 940, tween80, labrasol, acetonitrile	High-pressure homogenizer	It retains for prolonged period of time and hydrogel matrix to trap nanosized for treatment of endo-and ectoparasites.	[76]
Fluconazole	Span 20, tween 80, carbopol 940,	Incorporation of	Vegetable oil based emulgel	[77]



Supriya Huljute Ravindra *et al.*,

	triethanolamine, liquid paraffin.	emulsion into the gel method	acts as stable and effective compared to liquid paraffin based emulgel for topical delivery.	
Triclosan and flurbiprofen	Acetonitrile, methanol, citric acid, acetone, citric acid, potassium bromide.	Incorporation of emulsion into the gel method	Improved release of poorly water-soluble drugs and increased solubility of such drugs and dual action of triclosan and flurbiprofen loaded nanoemulgel for effective treatment of periodontitis.	[78]
Ciprofloxacin HCL	Linoleic acid, spray-dried cellulose nanocrystals, sodium chloride, potassium dihydrogen carbopol 934, span 20, o phosphate, pseudomonas aeruginosa.	Incorporation of emulsion into the gel method.	The formulation shows safe, biocompatible and promising approach for injured skin care with antibacterial activity.	[79]
Clotrimazole	Carbopol 934, Span20, potassium dihydrogen phosphate, methyl paraben, ethanol, propyl paraben, triethanolamine tween 20.	Incorporation of emulsion into the gel method.	It shows greater drug release than conventional Creams and gel.	[80]
Vancomycin HCL	Carbopol Aqua SF1, Xanthum gum, HPMC-K100M., carboxymethyl cellulose, Carbopol 974P, Disodium hydrogen.	Preparation of vancomycin loaded nanogel. .	It enhances the antibacterial activities of others antibiotics by encapsulating it into the nanogel topical formulation.	[81]
Ebselen	Dimethylacetamide, Kolliphore® ELP, Tween 80, captex®300, Soluplus®, poloxamer®, Carbopol®, candida albicans.	Incorporation of Emulsion into the gel method.	It increases the solubility and efficacy by incorporating it into the gel formulation and use in treatment of candidiasis.	[82]
Curcumin	Labrafac PG, Triacetin, Tween 80, PEG400,	Incorporation of emulsion into the gel method.	It enhances the solubilization of curcumin and shows higher permeation rate through skin for the treatment of wound healing.	[83]
Safrole oil	Carbopol 940, Dimethyl sulfoxide, span, Tween, Diphenyl-1-picrylhydrazyl [DPPH].	Self-emulsifying technique.	It shows higher stability and shows greater activity against different microbial species.	[84]
Rosemary oil	Tween 80, Span 80, carbopol 940, Dimethyl sulfoxide.	Self-emulsifying technique	It shows higher activity on cancer cell line and greater bioactive property than crude oil.	[85]
Amphotericin B	Sefsol, oil, Tween80, Transcutol-p Carbopol gel.	Slow spontaneous emulsification method.	It shows greater penetration, low skin irritation, high-drug loading capacity, and use to treat skin fungal infection.	[86]
Piroxicam	Carbopol 934, Tween 80, Oleic acid, Ethanol, Labrasol.	Aqueous titration method.	It Shows higher permeation rate and less drug retain significantly shows	[1]



Supriya Huljute Ravindra *et al.*,

			nanoemulgel as better alternative to conventional gel.	
Quercetin	Carbopol, cinnamon oil Tween 80, Carbitol®, poloxamer	Spontaneous emulsification method.	It increases the solubility and bioavailability of quercetin drug and shows potent antimicrobial and anti-inflammatory agent for the treatment of periodontitis disease in controlled-release manner.	[87]
Carvedilol	Oleic acid, Tween 20, Carbitol, Carbopol 934, isopropyl myristate (IPM),	Aqueous titration method	It enhances the water solubility as well as bioavailability of carvedilol and have sustained and Greater absorption by overcoming the barrier of drug penetration into the skin.	[88]
Ferulic Acid	Isosteryl isostearate Labrasol Plurol Isostearique, Carbopol 940.	Spontaneous nano-emulsification method	It enhances the permeability and bioavailability of drug by increasing its solubility through the nanoemulsion (NE) and shows maximum antioxidant activity against UVA induced oxidative stress in rat.	[89]
Glibenclamide	Labrafac, Triacetin Tween80, Diethylene glycol Monoethyl Ether, Carbopol 934	Incorporation of emulsion into the gel method.	The current results demonstrate that Glibenclamide nanoemulsion gel for transdermal systems demonstrated better management of hyperglycemia and more effectively cured the consequences of diabetes mellitus than oral Glibenclamide treatment in Wistar rats.	[90]
Miconazole Nitrate	Span 80, Tween 80, propylene glycol sunflower oil, Carbopol 934	High pressure homogenization technique.	The formulation of miconazole nitrate nanoemulgel is a potential technique for the topical delivery of medications as well as a different way to administer drugs that are hydrophobic in nature basis for soluble gels.	[91]
Belimbing	Carbopol 940, Tween 80, Span 20,	High pressure	It is believed to prevent the	[92]



Supriya Huljute Ravindra *et al.*,

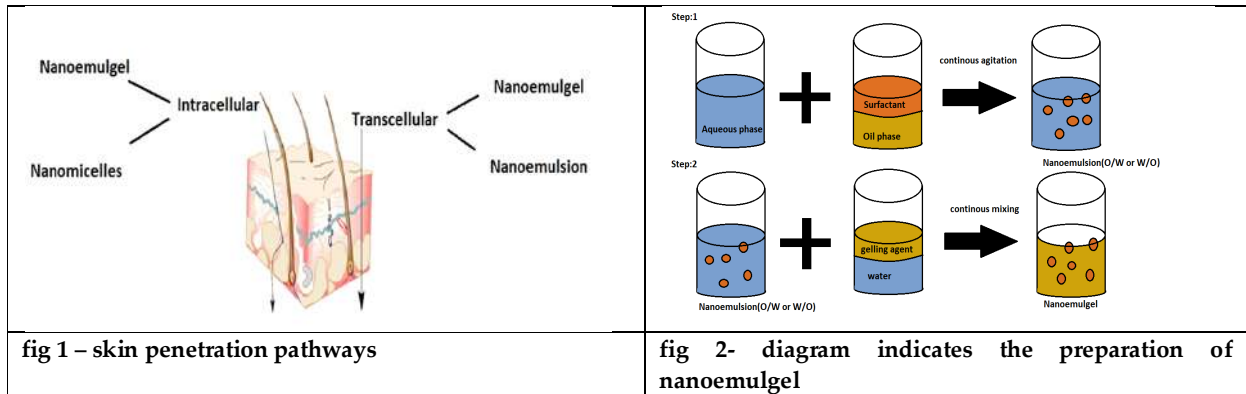
wuluh (Averrhoa bilimbi L.)	Propylene glycol, Isopropyl myristate, Triethanolamine, Methylparaben, Propylparaben, Butylated hydroxytoluene, EDTA, Methanol, Acorbic acid, and DPPH (2,2-diphenyl-1-picryl hydrazil)	homogenizer method	photoaging process. To create a nanoemulgel with strong physical stability and antioxidant activity, the formula is not ideal.	
Grape Seed Oil and Anisotriazine	Carbopol 940, Tween 80, sorbitol methylparaben, propylparaben, Span 80, propylene glycol, glycerol, ethanol, triethanolamine (TEA)	High-energy emulsification method	The sunscreen nanoemulgel made of grape seed oil and anisotriazine is more stable.	[93]
Calcipotriol	Isopropyl alcohol and polyethylene glycol, Cocoyl caprylocaprate (Kollcream3C), Cetostearyl Ether, Kolliphor CS, carbopol	Preparation of gel base to load it into nanoemulsion formulation.	Nanoemulgel shows significantly improvement in delivery of a hydrophobic drugs.	[94]
Oxiconazole	Carbopol934, liquid paraffin Tween-80 Span-80, Tri Ethanol Amine (TEA)	Preparation of gel base to incorporated into gel form.	Nanoemulgel shows better drug release as compared other conventional gel and creams.	[95]
Cyclosporin A	Lubrizol, Poloxamer188, Castor oil	Incorporation of emulsion into the gel method	Nanoemulgel higher drug release which turns to improves its bioavailability of topical dosage form.	[96]
Flurbiprofen	Turpentine oil, castor oil, Eucalyptus oil, propylene glycol (PG), and Carbopol-934, Tween 20, Tween 40, Tween 80, and isopropyl myristate (IPM)	High pressure homogenizer	It shown increase in the solubility and bioavailability of drug.	[97]
Telmisertan	Sefsol 218 and oleic acid (oil mix), Tween 20, Capryol 90, Labrafac, Labrafil 2125, Labrafil 1944,Lauroglycols, Transcutol HP, Solutol HS-15	Aqueous titration method	It shows the sustained release and improved mucoadhesive property. It is an alternative approach for the treatment of dementia for direct nose-to-brain delivery with effective penetration.	[98]
Terbinafine	Peceoloil, Propylene glycol, Tween 80 and Propanol Cremophor RH40® castor oil, Maisine35-1® (Glycerol monolinoleate), Caproyl90® (propyleneglycol monocaprylate), Labrafil Transcutol Carbopol 940 Terbinafine	High pressure homogenizer method	It shows improve in its solubility with highest permeability and shows antifungal activity to treat Candida infection.	[99]
clove essential oil	Polyoxyethylene (20) sorbitan monooleate (tween 80®) croton oil, Labrasol, Dimethyl sulfoxide (DMSO)	Incorporation of emulsion into the gel method	It introduced the phytomedicine field as promising topical delivery systems for effective treatment of inflammatory diseases	[100]





Supriya Huljute Ravindra et al.,

Fluconazole	Clove oil, Carbopol 934, Tween 20 Candida albicans.	Aqueous phase titration method	fluconazole loaded nanoemulgel shows fungicidal activity against Candida albicans and have higher zone of inhibition.	[101]
-------------	--	-----------------------------------	---	-------





***In vitro* Enzyme Inhibitory Activity of *Volvariella volvacea* (Paddy Straw Mushroom) to establish Its Antidiabetic Potential**

Amit Roy¹, Pushpa P. Gupta^{*1}, Shashikant Chandrakar², Poonam Sahu², Neeta Gupta³, Akhilesh Sahu¹, Dhanesh Sahu¹

¹Chhatrapati Shivaji Institute of Pharmacy, Durg (C.G)

²Columbia Institute of Pharmacy, Raipur (C.G)

³Govt. E. Raghavendra Rao P.G Science College, Bilaspur (C.G)

Received: 29 Sep 2023

Revised: 13 Nov 2023

Accepted: 09 Jan 2024

***Address for Correspondence**

Pushpa P. Gupta

Professor

Department of Pharmacology

Chhatrapati Shivaji

Institute of Pharmacy,

Durg, Chhattisgarh, India -491001

Email: pushpaprasad81@gmail.com



This is an Open Access Journal / article distributed under the terms of the **Creative Commons Attribution License** (CC BY-NC-ND 3.0) which permits unrestricted use, distribution, and reproduction in any medium, provided the original work is properly cited. All rights reserved.

ABSTRACT

The enzymes α -amylase and α -glucosidase amplify postprandial blood glucose in patients of diabetes, while dipeptidyl peptidase IV inhibits the polypeptides that regulate insulin secretion. Inhibition of these enzymes can help in controlling diabetes. The mushroom *Volvariella volvacea* was selected for the study to determine its inhibitory activity of these enzymes as this mushroom had already shown in-vitro antidiabetic activity in a previous study. The IC₅₀ values of LE and ODE of *V. volvacea* and reference drug acarbose were found to be 28.11, 54.10 and 20.24 μ g/ml respectively for α -amylase enzyme inhibition. While for α -glucosidase inhibition IC₅₀ values of LE and ODE of *V. volvacea* and reference drug acarbose were 22.04, 40.93 and 26.21 μ g/ml respectively. The IC₅₀ value in inhibition of DPP-IV enzyme were 34.24 μ g/ml for the reference drug sitagliptin while IC₅₀ value of LE and ODE of *V. volvacea* was found to be 49.09 μ g/ml and 76.08 μ g/ml, respectively. The result suggests both the extracts exhibited significant α -amylase and α -glucosidase inhibitory action, but not very promising DPP-IV enzyme inhibition. The LE of *V. volvacea* is more active compared to ODE in vitro enzyme inhibitory activity assays. The study concludes that the more polar fraction of the mushroom constituents is accountable for its activities.

Keywords: Diabetes, α -amylase, α -glucosidase, DPP-IV, *V. volvacea*, enzyme inhibitory activity.



**Amit Roy et al.,**

INTRODUCTION

Hyperglycaemia or diabetes is a condition that is due to inactivity of insulin or deficiency in secretion of insulin. In some cases both the condition may occur. The second condition where the ailment is not dependent on insulin is called diabetes mellitus (DM). It is also termed as type 2 diabetes. In this condition there might be unusual glucose tolerance as well as resistance to insulin [1, 2]. Medically diabetes is a disorder caused in metabolism of endocrine system [3]. In this glucose metabolism is not proper and it affects balance of cellular metabolism of lipid and carbohydrate [4]. It is a very complex disease that is the major cause for disorder in metabolism of fat, carbohydrate as well as protein. The defective metabolisms later results in micro as well as macro changes in vascular system and thereafter secondary problems arises [3]. It further results in a condition called postprandial hyperglycaemia, which is the reason for type 2 diabetes that is not dependent on insulin [5]. Postprandial hyperglycaemia results in the higher glycation end product formation. These products promote aging and other diabetic problems [6]. When hyperglycaemia becomes chronic it manifests into damage in long-term and in number of organs. Those are failure or functional problems of, nerves, kidneys, eyes, cardiovascular ailments, strokes, serious wounds and even blindness [1]. One of the significant approaches in therapy and management of hyperglycaemia is to control glucose level in blood by decreasing glucose production and also its absorption in gastrointestinal system [7,8].

In our system digestive enzymes, such as α - amylase as well as α -glucosidase are responsible for catalyzing the hydrolytic cleavage of carbohydrates which in turn produces sugars in blood. In the first step α -amylase breaks down the bonds of glycosides of starch (polysaccharides) to form three main products, which are maltose, maltotriose and limit dextrans. After this step α - glucosidase catalyzes the last step of digestion of starch and disaccharides. The enzyme α amylase is present in saliva as well as in digestive system. The enzyme present in saliva breaks starch and other polysaccharides into dextrin and maltose and where as the pancreatic amylase at random breaks α (1-4) glycoside linkage of amylose to form maltose, or maltotriose and dextrin. On the other hand α - glucosidase is an enzyme that is found in intestinal cell membrane and its function is to hydrolyze polysaccharides [9,11]. If these two enzymes are inhibited, hydrolysis of carbohydrate will go down and this will help to control sudden increase in postprandial glucose levels in blood after a carbohydrate diet. This strategy can play an important role in management of glucose levels in blood [12]. There are other factors also that play very important role in the progress of DM. Deficiency or resistance of incretin is also an important factor [13]. Two polypeptides are said to be major incretin, one of them is glucagon like peptide-1 or GLP-1, and the other is glucose dependent and insulinotropic in nature or GIP. These two are secreted in the gastrointestinal tract. They are secreted as soon as a meal is ingested [14]. These two have the ability to increase secretion of insulin that is dependent to glucose there by the secretion of glucagon is suppressed [15]. There is a very complex relation of GIP and glucagon.

GIP in fact works like hormone and increases glucagon response during hypoglycaemia, while it enhances the rate of secretion of insulin during hyperglycaemia and this helps in stabilizing glucose in DM [16]. There is an “incretin effect, when there is resistance or deficiency of incretin. The effect is defined as magnification of secretion of insulin after an oral load of glucose when compared to response of insulin seen when same glycemic level is attained when an intravenous glucose infusion is given [17]. The lives of both, GLP-1 as well as GIP is short as they are quickly broken down by an enzyme dipeptidyl peptidase IV or DPP4. DPP4 is an enzyme that is present in almost all the tissues. This is present in soluble form in cell membranes as well as in plasma [18]. This enzyme DPP4 is a glycoprotein and it cuts down the N-terminal dipeptides from a wide range of substrates. They include the growth factors, cytokines, neuro-peptides, and also from incretin hormones. The effect of DPP4 is very significant in disease like diabetes, cancer, inflammation as well as in obesity. The two incretin hormones GIP and GLP-1 are the major key in regulating postprandial insulin secretion, therefore in recent years DPP4 inhibitors from gliptin family have become very popular for the management of type2 diabetes [19,20,21]. For the management of diabetes as well as controlling blood glucose levels many classes of drugs are available today. They include biguanides, meglitinide, sulfonylureas, non- sulfonylureas, thiazolidinediones, along with different inhibitors of enzymes that play major role in regulation of insulin and sugar in blood [22]. However, most of these are not very specific in their action which is





Amit Roy et al.,

the main cause for their unpleasant side effects like flatulence, diarrhoea, cramping etc [23]. This is why since last few years several researchers have directed their attention towards harnessing the medicinal value of plants for the management of diabetes [24]. Scientists have shown that the phytoconstituents of medicinal plants exhibit a variety of mechanism to manage and control diabetes. Some act on beta cells of pancreas to augment the secretion of insulin, while some of them have insulin like activity and many of them act by modifying the utilization of glucose. Those herbal drugs that modify utilization of glucose have been found to do so by changing the viscosity of contents in gastrointestinal tract which in turn delays gastric emptying or they may delay the absorption of glucose [25]. The delay in glucose absorption affected is by reducing the digestion rate. This is possible when the inhibition of α -amylase enzyme present in intestine. This enzyme is responsible for digestion of polysaccharides in to monosaccharides which are then absorbed. This inhibition causes decreased absorption of glucose and thus postprandial blood glucose level is controlled [26].

Mushrooms are macro fungi belonging to Ascomycetes and Basidiomycetes class. They are fleshy in nature with a distinct fruiting body. They are easily visible by naked eye and they are comfortably picked up by hand [27]. There are about 38,000 mushroom varieties and out of this only 300 varieties are edible. However only 30 of them could be domesticated but only 10 of those species are presently grown commercially [28]. Literature shows that since primitive ages there has been quite extensive use of mushrooms as foods, as flavours in food as well as for medicinal purpose [29]. Mushrooms contain proteins in very high quality, they are also rich in fibres, minerals and vitamins which aids in their easy digestion. A mushroom diet has the potential to control the cholesterol and glucose levels in blood. In traditional folk medicine, several mushroom species and their different products have been used as medicines for many diseases in all over the world for ages [30]. *V. volvacea* or paddy straw mushroom is safe to eat and consumed in many parts of tropical world. The biochemical analysis of this mushroom has shown that it has many phytoconstituents that have application as medicine in number of diseases.

V. volvacea has good nutritional qualities as well as medicinal properties therefore it is an attractive candidate for development of development of drugs and nutraceuticals [31]. It was reported that aqueous ethanolic extract of *V. volvacea* mycelium exhibited significant ferric reducing, lipid peroxidation-inhibiting, hydroxyl radical scavenging and also DPPH radical scavenging property. It also exhibited significant antitumor action on solid and ascites tumours [32]. *V. volvacea* is has been employed in folk and traditional system of medicinal in our country. Reports show that it has anti-tumor, immune modulatory and immunosuppressant properties. It is very rich in protein, vitamins and fibers. It also is good source of carbohydrates (56.8%), and all essential amino acids. It has very little fat (5.7%) but appreciable amounts of unsaturated fatty acids and essential minerals. The reports of investigations of *V. volvacea* show that it possesses several phytochemicals that have significant medicinal properties [33]. It has been reported that hydroalcoholic extract of *V. volvacea* possesses carbohydrates, alkaloids, flavonoids, glycosides, tannins and saponins. It contained significant amounts of phenols and flavonoids. The extracts exhibited noteworthy DPPH and superoxide anion radical scavenging property [34]. Another study with the same extracts have shown significant anti diabetic activity diabetic rat model [35]. *V. volvacea* was therefore selected for further investigation to get an insight into its antidiabetic potential. Study was carried out to find inhibitory action on a few enzymes like DPP-IV, α -glucosidase along with α -amylase.

METHODS

Cultivation and collection of mushroom

V. volvacea spawn were procured as gift from the Agriculture University of Raipur that is situated in the state of Chhattisgarh in India. In the mushroom cultivation centre of Columbia Institute of Pharmacy, Raipur the spawns were grown.





Amit Roy et al.,

Preparation of Material

When the mushroom got completely matured they were harvested. Mushroom was washed to remove all the dirt. The mushroom was dried under sun to remove extra moisture and after that was dried further in shade. The dried mushroom was ground into coarse powder and kept in an air tight container.

Preparation of extracts

Powdered *V. volvacea* (1 Kg) was added to petroleum ether and macerated for one week. Every day the maceration container was shaken for 6 hours in orbital shaker to improve maceration activity. At completion of maceration process the macerated material was subjected to filtration. The filtrate was kept on water bath to dry, while marc was placed in tray drier at 40°C till it completely dried. The dried marc was further extracted with hydroalcoholic mixture (ethanol 70% and water 30%) by maceration at room temperature for ten days; during this period the flasks containing the drug and solvent mixture were kept on rotary shaker for six hours to enhance extraction. After completion of this process the extract was filtered. This hydroalcoholic extract was then divided in two equal parts. The two different parts were dried by different methods. One part was dried by lyophilizing it at -20°C, and the other part was dried in hot tray drier at 50°C. During drying the extracts were weighed periodically and both the processes were carried out till a constant weight of extract was obtained. The lyophilized extract (LE) and the oven dried extract (ODE) were weighed and then stored separately in air tight container in refrigerator.

α -amylase enzyme inhibitory activity [36]

200 μ l of sodium phosphate buffer (0.02 M) was combined with the enzyme α amylase (20 μ l). Different concentrations (20-100 μ g/ml) of LE, ODE, and acarbose were mixed separately to above in different micro test tubes and sealed. These test tubes were kept for incubating them at normal room temperature for about ten mins. After that in every test tube starch (200 μ l) was added separately. The reaction was stopped by addition of DNS reagent (400 μ l) in every test tube thereafter they were heated for 5 minutes in water bath. Lastly test tubes were cooled and distilled water (15 ml) was added in each test tube, respectively. Then absorbance was observed at 540 nm. A control group was also taken in which no extract or drug was added. Percentage inhibition was found by putting the values in the formula given below.

$$\% \text{ Inhibition} = \frac{\text{Abs control} - \text{Abs sample}}{\text{Abs control}} \times 100$$

α -glucosidase enzyme inhibitory activity [36]

The inhibition of α -glucosidase enzyme was calculated by the computing liberated amount of 4-nitrophenol out of p-nitrophenyl α -D glucopyranoside. p-nitrophenyl α -D-glucopyranoside (0.3 ml) 10 mM was mixed with 1.0 ml of potassium phosphate (0.1M, pH: 6.8) followed by addition of α -glucosidase enzyme solution (0.2 ml). 0.2 ml of LE, ODE and acarbose were mixed separately diverse concentrations respectively to above in different micro test tubes. Then water was added to all the test tubes to make their volume up to 1.7 ml. Thereafter the test tubes were kept at 37°C to incubate for 30 min. The reaction was then blocked by the addition of 100 mM sodium carbonate (2.0 ml) in every test tube. The p- nitrophenol that liberated during the reaction time was measured by spectrophotometer at 400 nm. Percentage Inhibition for each was determined by the formula given below.

$$\% \text{ Inhibition} = \frac{\text{Abs control} - \text{Abs sample}}{\text{Abs control}} \times 100$$

α -glucosidase enzyme inhibitory activity [36]

The inhibition of α -glucosidase enzyme was calculated by the computing liberated amount of 4-nitrophenol out of p-nitrophenyl α -D glucopyranoside. p-nitrophenyl α -D-glucopyranoside (0.3 ml) 10 mM was mixed with 1.0 ml of potassium phosphate (0.1M, pH: 6.8) followed by addition of α -glucosidase enzyme solution (0.2 ml). 0.2 ml of LE, ODE and acarbose were mixed separately diverse concentrations respectively to above in different micro test tubes. Then water was added to all the test tubes to make their volume up to 1.7 ml. Thereafter the test tubes were kept at 37°C to incubate for 30 min. The reaction was then blocked by the addition of 100 mM sodium carbonate (2.0 ml) in





Amit Roy et al.,

every test tube. The p-nitrophenol that liberated during the reaction time was measured by spectrophotometer at 400 nm. Percentage Inhibition for each was determined by the formula given below.

$$\% \text{ Inhibition} = \frac{\text{Abs control} - \text{Abs sample}}{\text{Abs control}} \times 100$$

Dipeptidyl peptidase IV (DPP-IV) inhibitory action [36]

Method of DPP-IV enzyme isolation

100mg of tissues taken from goat intestine homogenized in 300 μ l of cold PBS in which 1% Triton X-100 and 100 KIU/ml aprotinin was present. This mixture was centrifuged for 10 min at 100 rpm. Supernatant liquid was decanted into eppendorf tubes, and were subjected to centrifugation again at 20,000 rpm for 10 min at 4°C. Tris-HCl buffer at pH 8.0 measuring 0.1 M/L was taken and DPP-IV was suspended into it. 25 μ L of LE and ODE was prepared separately in which equal volumes of substrate, Gly- Pro- p-nitroanilide measuring 1.6 mM, was added. These mixtures were thereafter incubated for 10 minutes at 37°C. There after DPP-IV at concentration of 0.01 U/mL and measuring 50 μ L was mixed with 0.1 M/L of Tris-HCl buffer which had a pH of 8.0. This mixture was made for all the test tubes and mixed in to every test tube respectively. The test tubes were kept again for incubation for 60 minutes 37° C. After 60 minutes reaction was stopped by the adding in every test tube of sodium acetate buffer at concentration of 1 M/L, at pH of 4.0 and measuring 100 μ L. The liberated hydrolysis product, p-nitroanilide, was measured by spectrophotometer at 405nm.

$$\% \text{ Inhibition} = \frac{\text{Abs control} - \text{Abs sample}}{\text{Abs control}} \times 100$$

RESULT AND DISCUSSION

The strategy to inhibit digestive enzymes like α -amylase, α -glucosidase as well as DPP-IV is believed to be successful process to manage diabetes. The phytoconstituents from medicinal plants are very promising as they are well tolerated and have little side effects when compared with synthetic oral hypoglycaemic drugs available in market today [37, 38, 39, 40]. This study was based on study of bioactive principles of *V. volvacea* for management of type 2 diabetes. DM at one point of time was considered as maturity onset diabetes. However increase in obesity has resulted in increased risk of this disease in childhood [41]. The treatment in this disease is to maintain levels of blood glucose and prevent the progress of other disorders associated with it [42]. Inhibitory activity of LE and ODE of *V. volvacea* on α -amylase enzyme Both extracts LE along with ODE significantly inhibited α -amylase enzyme in generation of maltose in a concentration-related manner. The calculated IC₅₀ values were 28.11 μ g/ml and 54.10 μ g/ml respectively for inhibitory activity of α -amylase enzyme (Table 1) (Fig 1-2) for the extracts. Inhibitory activity of standard drug acarbose was found to be 50% at 20.24 μ g/ml (Table 1, Fig 3). The α -amylase enzyme aids hydrolysis of α bandings in polysaccharides present in starch along with glycogen, maltose, and glucose [43]. This is the chief type of amylase that exists in all the mammals including humans and its inhibition is very significant for managing diabetes and controlling blood sugar levels [44]. *V. volvacea* extracts ODE as well as LE along with reference drug acarbose presented concentration dependant α -glucosidase inhibitory action (Table 2).

Extracts LE as well as ODE showed 50% inhibition of α -glucosidase at 22.04 μ g/ml and 40.93 μ g /ml respectively (Fig 4-5), while reference Acarbose displayed 50% inhibition at 26.21 μ g/ml (Fig.6). Enzyme α -glucosidase is present in the small intestine at its brush end and it acts upon α (1– 4) bonds [45, 46, 47, 48,49]. It breaks down starch as well as disaccharides to glucose and the enzyme maltase decomposes maltose. However main function of α -glucosidase is to bring about hydrolytic cleavage of incurable non reducing (1–4) attached α -glucose that releases lonely α - glucose molecule, hence its inhibition is a key step in regulation of blood glucose and management of DM [50]. Table 3 shows activity of LE and ODE and reference drug sitagliptin on inhibition of DPP-I enzyme. The LE and ODE exhibited 50% inhibitory activity of DPP-IV enzyme at 49.09 μ g/ml and 76.08 μ g/ml, respectively (Fig 7-8). However the reference drug sitagliptin 34.24 μ g/ml showed 50% inhibition on DPP-IV (Fig 9). DPP-IV as an enzyme was discovered in 1966





Amit Roy et al.,

as glycyloprolyl β -naphthylamidase. It was later found that it could release glycyloprolin that is responsible to produce β -naphthylamine that can be detected by colorimetric methods. Enzyme DPP-IV is a group of serine proteases that is there in high amount in the luminal membrane of intestinal epithelial cells. The enzyme DPP-IV works very fast and breaks incretin hormones that play a major role in maintenance of glucose level [51, 52, 53]. The inhibitors of DPP-4 increases body's capability to manage glucose in blood by enhancing levels of hormone incretin in human system. The mechanism of action of drugs of this class is dissimilar to other type of oral hypoglycaemics. The drugs of this class maintain blood glucose by activating secretion of insulin from pancreas and sending signals to decrease glucose production to liver. Inhibitors of DPP-4 have exhibited in present diabetes management and also lowered threat of hypoglycaemia along with no effect on weight of body as reported in several vitro studies. These drugs have also reported to show renewal of pancreatic beta-cells [54].

CONCLUSION

The IC₅₀ values of LE and ODE of *V. volvacea* was and reference drug acarbose were found to be 28.11, 54.10 and 20.24 μ g/ml respectively for α -amylase enzyme inhibition. While for α -glucosidase inhibition IC₅₀ values of LE and ODE of *V. volvacea* was and reference drug acarbose were 22.04, 40.93 and 26.21 μ g/ml respectively. The IC₅₀ value in inhibition of DPP-IV enzyme were 34.24 μ g/ml for the reference drug sitagliptin while IC₅₀ value of LE and ODE of *V. volvacea* was found to be 49.09 μ g/ml and 76.08 μ g/ml, respectively. The result suggests that DPP-IV inhibitory action of ODE and LE was not very significant as compared to their α -amylase and α -glucosidase inhibitory action. The study however shows that *V. volvacea* possesses significant enzyme inhibitory activities and the extracts possess excellent hypoglycaemic and antidiabetic potential. The results have shown that LE of *V. volvacea* is more active compared to ODE in vitro enzyme inhibitory activity assays. The study concludes that the more polar fraction of the mushroom constituents is accountable for its activities. It is required to carry further studies on this species so that it can be incorporated in nutraceuticals or as food supplement for management of diabetes.

ACKNOWLEDGEMENT

Authors would like to show their deep gratitude towards the Management of Columbia Institute of Pharmacy, Raipur, Chhattisgarh, India for providing all the necessary equipment and facilities to carry out this research activity.

CONFLICT OF INTEREST

The authors of this article proclaim that there is no conflict of interest in regards to this research work and publication of the article.

REFERENCES

1. American Diabetes Association. Diagnosis and classification of diabetes mellitus. Diabetes Care 29 Suppl. 2006; 1:S43-S48.
2. King H, Aubert RE, Herman WH. Global burden of diabetes, 1995-2025: prevalence, numerical estimates and projections. Diabetes care. 1998; 21(9):1414-1431.
3. American Diabetes Association. Diagnosis and classification of diabetes mellitus. Diabetes Care 37 Suppl. 2014; 1:S81-S90.
4. Henriksen EJ, Diamond-Stanic MK, Marchionne EM. Oxidative stress and the etiology of insulin resistance and type 2 diabetes. Free Radic. Biol. Med. 2011; 51: 993-999.
5. Gruenwald J, Freder J, Armbruester N. Cinnamon and health. Crit. Rev. Food Sci. Nutr. 2010; 50(9): 822-834.
6. Tiwari AK, Swapna M, Ayesha SB, Zehra A, Agawane SB, Madhusudana K. Identification of proglycemic and antihyperglycemic activity in antioxidant rich fraction of some common food grains. Int. Food Res. J. 2011; 18(3): 915-923.
7. Nathan DM, Buse JB, Davidson MB, Ferrannini E, Holman RR, Sherwin R, Zinman B. Medical management of

69831





Amit Roy et al.,

- hyperglycemia in Type 2 diabetes: A consensus algorithm for the initiation and adjustment of therapy. *Diabetes care*. 2009; 32(1):193–203.
8. Rines AK, Sharabi K, Tavares CDJ, Puigserver P. Targeting hepatic glucose metabolism in the treatment of type 2 diabetes. *Nat. Rev. Drug Discov*. 2016; 15(11): 786-804.
 9. Ghosh S, More P, Derle A, Patil AB, Markad P, Asok A, Kumbhar N, Shaikh ML, Ramanamurthy B, Shinde VS, Dhavale DD, Chopade BA. Diosgenin from *Dioscorea bulbifera*: novel hit for treatment of type II diabetes mellitus with inhibitory activity against α -amylase and α -glucosidase. *PlosOne*. 2014; 12(9): e106039.
 10. Robyt JF. Starch: structure, properties chemistry and enzymology. ed. by Fraser-Reid BO, Tatsuta K, Thiem J. *Glycoscience*. Berlin, Heidelberg Springer. 2008; 1437-1472.
 11. Manohar V, Talpur A, Echard BW, Lieberman S, Preuss HG. Effects of a water soluble extract of maitake mushrooms on circulating glucose insulin concentrations in mice. *Diabetes Obes. Metab*. 2002; 4(1) :43-48.
 12. Ahamad J, Naquvi KJ, Mir SR, Ali M, Shuaib M. Review on role of natural alpha- glucosidase inhibitors for management of diabetes mellitus. *Int. J. Biomed. Res*. 2011; 2(6): 374-380.
 13. DeFronzo RA. From the triumvirate to the ominous octet: a new paradigm for the treatment of type 2 diabetes mellitus. *Diabetes*. 2009; 58(4):773–795.
 14. Godoy-Matos AF. The role of glucagon on type 2 diabetes at a glance. *Diabetol. metab. Syndr*. 2014; 6(1): 91.
 15. DeaconCF, Mannucci E, Ahr'en B. Glycaemic efficacy of glucagon-like peptide-1 receptor agonists and dipeptidyl peptidase-4 inhibitors as add-on therapy to metformin in subjects with type 2 diabetes—a review and meta analysis. *Diabetes Obes. Metab*. 2012; 14(8): 762–767.
 16. Christensen MB, Calanna S, Holst JJ, Vilsboll T, Knop FK. Glucose-dependent insulinotropic polypeptide: blood glucose stabilizing effects in patients with type 2 diabetes. *J. Clin. Endocrinol. Metab*. 2014; 99 (3): E418–E426.
 17. Cernea S and Raz I. Therapy in the early stage: incretins. *Diabetes Care* 34 Suppl. 2011; 2(2): S264–S271.
 18. Holst JJ. On the physiology of GIP and GLP-1. *Horm. Metab. Res*. 2004 36(11-12): 747–754.
 19. Capuano A, Sportiello L, Maiorino MI, Rossi F, Giugliano D, Esposito K. Dipeptidyl peptidase-4 inhibitors in type 2 diabetes therapy--focus on alogliptin. *Drug Des Devel Ther*. 2013; 7:989–1001 .
 20. Scheen AJ. A review of gliptins in 2011. *Expert Opin. Pharmacother*. 2012; 13: 81-99.
 21. Nabeno M, Akahoshi F, Kishida H, Miyaguchi I, Tanaka Y, Ishii S, Kadowaki T. A comparative study of the binding modes of recently launched dipeptidyl peptidase IV inhibitors in the active site. *Biochem. Biophys. Res. Commun*. 2013; 434(2):191–6.
 22. Chaudhury A, Duvoor C, Dendi VSR, Kraleti S, Chada A, Ravilla R, Marco A, Shekhawat NS, Montales MT, Kuriakose K, Sasapu A, Beebe A, Patil, Musham CK, Lohani GP, Mirza W. Clinical review of antidiabetic drugs: implications for type 2 diabetes mellitus management. *Front Endocrinol* 8(6): 1-12 (2017).
 23. Hsieh SH, Shih KC, Chou CW, Chu CH. Evaluation of the efficacy and tolerability of miglitol in Chinese patients with type 2 diabetes mellitus inadequately controlled by diet and sulfonylureas. *Acta Diabetol* 48(1): 71–77 (2011).
 24. Ali H, Houghton PJ, Soumyanath A. α -Amylase inhibitory activity of some Malaysian plants used to treat diabetes; with particular reference to *Phyllanthus amarus*. *J Ethnopharmacol* 107(3):449–455 (2006).
 25. Wadkar KA, Magdum CS, Patil SS, Naikwade NS. Anti-diabetic potential and Indian medicinal plants. *J. herb. med. toxicol*. 2(1): 45–50 (2008).
 26. Karthic K, Kirthiram KS, Sadasivam S, Thayumanavan B, Palvannan T. Identification of α amylase inhibitors from *Syzygium cumini* Linn seeds. *Indian J. Exp. Biol*. 46(9): 677–680 (2008).
 27. Isikhuemhen OS and Okhuoya JA. Cultivation of *Pleurotus tuber regium* (Fr) Singer for production of edible sclerotia on agricultural wastes. *Mushroom Biology and Mushroom Products*. ed. Royese (ed) Penn State Univ (1996).
 28. Narayanasamy P, Suganthavel P, Sabari P, Divya D, Vanchinathan J, Kumar M. Cultivation of mushroom (*Pleurotus florida*) by using two different agricultural wastes in laboratory condition. *Internet J. Microbiol*. 2008; 7(2):1-4.
 29. Oei P. *Mushroom cultivation, appropriate technology for mushroom growers*. 3rd edn. Backhugs Publishers, Leiden The Netherlands. 2003.





Amit Roy et al.,

30. Jones S, Janardhanan KK. Antioxidant and antitumor activity of *Ganoderma lucidum* (Cart. Fr.) P. Karst. - Reishi (Aphyllophoromycetidae) from South India. *Int. J. Med. Mushrooms*. 2000; 2:195-200.
31. Roy A, Prasad P, Gupta N. *Volvariella volvacea*: A Macrofungus Having Nutritional and Health Potential. *Asian J. Pharm.* 2014; 4(2):110-113.
32. Mathew J, Sudheesh Np, Rony KA, Janardhanan KK. Antioxidant and antitumor activities of cultured mycelium of culinary-medicinal paddy straw mushroom *Volvariella volvacea* (Bull.: Fr.) Singer (Agaricomycetidae). *Int. J. Med. Mushrooms*. 2008; 10(2):139-148.
33. Morris HJ, Llauradó G, Beltrán Y, Lebeque Y, Bermúdez RC, García N, Gaime-Perraud I, Moukha S. The Use of Mushrooms in the Development of Functional Foods, Drugs, and Nutraceuticals: Functional Food Properties and Applications, *Wild Plants, Mushrooms and Nuts*, ed. by Ferreira ICFR, Morales P, Barros L. Wiley Blackwell. 2016; 123-157.
34. Roy A, Prasad P. Determination of physicochemical, phytochemical and antioxidant activity of *Volvariella volvacea*. *Am. j. PharmTech res.* 2016; 6(2): 641-654.
35. Gupta PP, Chandrakar S, Roy A, Verma S, Gupta N, Sahu RK. Assessment of antidiabetic activity of hydroalcoholic extract of *Volvariella volvacea*. *Eur. J. Mol. Clin. Med.* 2021; 8(3): 1499- 1509.
36. Roy A, Prasad P, Assessment of mechanism of action of antidiabetic activity of *Calocybe indica* by enzyme inhibitory activity. *Biosci. Biotechnol. Res. Asia*. 13(4): 2117-2123 (2016).
37. Tadera K, Minami Y, Takamatsu K, Matsuoka T. Inhibition of alpha-glucosidase and alpha-amylase by flavonoids. *J. Nutr. Sci. Vitaminol.* 2006; 52(2): 149-153.
38. Borde MK, Mohanty IR, Suman RK, Desmukh Y. Dipeptidyl peptidase-IV inhibitory activities of medicinal plants: *Terminalia arjuna*, *Commiphora mukul*, *Gymnema sylvestre*, *Morinda citrifolia*, *Embllica officinalis*. *Asian J Pharm Clin Res.* 2016; 9(3): 180-182.
39. Osadebe PO, Odoh EU, Uzor PF. Natural Products as Potential Sources of Antidiabetic Drugs. *Br. J. Pharm. Res.* 2014(17): 2075-2095.
40. Blahova J, Martiniakova M, Babikova M, Kovacova V, Mondockova V, Omelka R. Pharmaceutical Drugs and Natural Therapeutic Products for the Treatment of Type 2 Diabetes Mellitus. *Pharmaceuticals*. 2021; 14(8): 806.
41. Urrutia-Rojas X and Menchaca J. Prevalence of Risk for Type 2 Diabetes in School Children. *Journal of School Health*. 2006; 76(5): 189-194.
42. Martín-Timón I, Sevillano-Collantes C, Segura-Galindo A, Cañizo-Gómez FJ. Type 2 diabetes and cardiovascular disease: Have all risk factors the same strength?. *World Journal of Diabetes*. 2014; 5(4): 444-470.
43. Janecek S, Svensson B, MacGregor EA. α -Amylase: an enzyme specificity found in various families of glycoside hydrolases. *Cell. Mol. Life Sci.* 2013; 71(7): 1149-1170.
44. Butterworth PJ, Warren FJ, Ellis PR. Human α -amylase and starch digestion: An interesting marriage. *Starch/Starke*. 2011; 63: 395-405.
45. Shinde J, Taldone T, Barletta M, Kunaparaju N, Hu B, Kumar A, Placido J, Zito SW. Alpha-glucosidase inhibitory activity of *Syzygium cumini* (Linn.) Skeels seed kernel in vitro and in Goto-Kakizaki (GK) rats. *Carbohydrate Research* 343(7): 1278–1281 (2008).
46. Assefa ST, Yang EY, Chae SY, Song M, Lee J, Cho MC, Jang S. Alpha glucosidase inhibitory activities of plants with focus on common vegetables. *Plants*. 2020; 9(2): 1-17.
47. Hossain U, Das AK, Ghosh S, Sil PC. An overview on the role of bioactive α - glucosidase inhibitors in ameliorating diabetic complications. *Food Chem. Toxicol.* 2020; 145: 111738.
48. Oh J, Jo SH, Kim JS, Ha KS, Lee JY, Choi HY, Yu SY, Kwon YI, Kim YC. Selected tea and tea pomace extracts inhibit intestinal α -glucosidase activity in vitro and postprandial hyperglycemia in vivo *jangbae*. *Int. J. Mol. Sci.* 2015; 16(4): 8811-8825.
49. Wen H, Tang B, Stewart AJ, Tao Y, Shao Y, Cui Y, Yue H, Pei J, Liu Z, Mei Z, Yu R, Jiang L. Erythritol Attenuates Postprandial Blood Glucose by Inhibiting α -Glucosidase. *J Agric Food Chem.* 2018; 66(6): 1401-1407.
50. Kumar S, Narwal S, Kumar V, Prakash O. α -glucosidase inhibitors from plants: A natural approach to treat diabetes. *Pharmacognosy Reviews*. 2011; 5(9): 19-29.
51. Riyanti S, Sugandha AG, Sukandari EY. Dipeptidyl peptidase-iv inhibitory activity of some indonesian medicinal plants. *Asian J. Pharm. Clin. Res.* 2016; 9(2): 375-377.





Amit Roy et al.,

52. Singh AK, Yadav D, Sharma N, Jin J., Dipeptidyl peptidase (DPP)-IV inhibitors with antioxidant potential isolated from natural sources: A novel approach for the management of diabetes. *Pharmaceuticals*. 2021; 14(6): 586.
53. Mulvihill EE and Drucker DJ. Pharmacology, Physiology, and Mechanisms of Action of Dipeptidyl Peptidase-4 Inhibitors. *Endocrine Reviews*. 2014; 35(6):992-1019.
54. Barnett A. DPP-4 inhibitors and their potential role in the management of type 2 diabetes. *Int. J. Clin. Pract.* 2006; 60(11):1454-70.

Table 1: Inhibition values of alpha-amylase by reference drug Acarbose and extracts LE and ODE of *V. voluacea*

Concentration (µg/ml)	% inhibition by LE	IC ₅₀ (µg/ml) LE	% inhibition by ODE	IC ₅₀ (µg/ml) ODE	% inhibition by Acarbose	IC ₅₀ (µg/ml) Acarbose
20	37.26±0.49	28.11	23.14±0.26	54.10	49.35±0.31	20.24
40	62.52±0.37		36.47±0.47		75.52±0.52	
60	89.67±0.52		52.36±0.92		93.81±0.94	
80	102.42±0.67		76.13±0.34		116.32±0.47	
100	116.92±0.85		86.41±0.18		138.73±0.18	

Values are mean ± SEM of three determinations

Table 2: Inhibition values of α-glucosidase by reference drug Acarbose and extracts LE and ODE of *V. voluacea*

Concentration (µg/ml)	% inhibition by LE	IC ₅₀ (µg/ml) LE	% inhibition by ODE	IC ₅₀ (µg/ml) ODE	% inhibition by Acarbose	IC ₅₀ (µg/ml) Acarbose
20	45.36±0.62	22.04	27.91±0.53	40.93	41.32±0.29	26.21
40	70.41±0.17		48.73±0.42		68.53±0.38	
60	93.58±0.73		70.16±0.94		86.39±0.42	
80	114.74±0.51		92.53±0.38		112.48±0.93	
100	131.54±0.34		105.18±0.42		132.61±0.71	

Values are mean ± SEM of three determinations



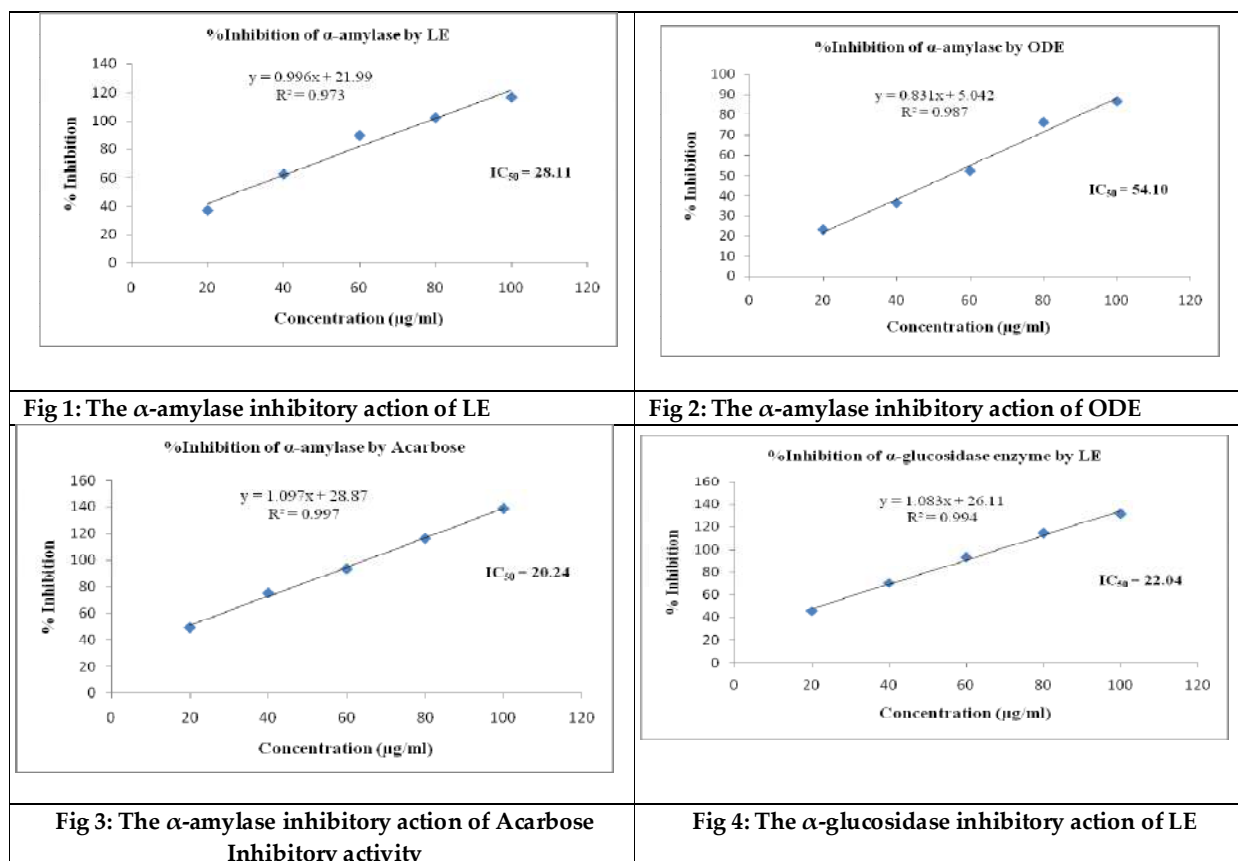


Amit Roy et al.,

Table 3: Inhibition values of DPP-IV by reference drug Sitagliptin and extracts LE and ODE of *V. voluacea*

Concentration (µg/ml)	% inhibition by LE	IC ₅₀ (µg/ml) LE	% inhibition by ODE	IC ₅₀ (µg/ml) ODE	% inhibition by Acarbose	IC ₅₀ (µg/ml) sitagliptin
20	28.19±0.78	49.09	17.62±0.65	76.08	35.47±0.84	34.24
40	40.65±0.52		26.83±0.42		58.68±0.53	
60	54.38±0.91		38.17±0.39		72.15±0.76	
80	77.82±0.58		51.59±0.58		96.54±0.24	
100	96.14±0.27		65.32±0.19		118.62±0.39	

Values are mean ± SEM of three determinations





Amit Roy et al.,

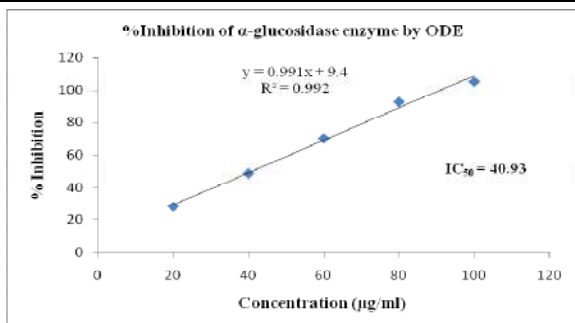


Fig 5: The α -glucosidase inhibitory action of LE ODE

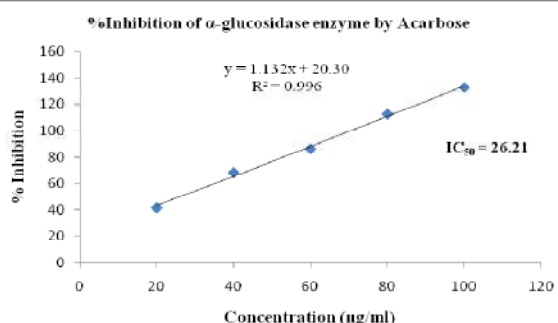


Fig 6: The α -glucosidase inhibitory action of Acarbose
Inhibitory activity of LE and ODE of *V. Volvacea* on DPP-IV enzyme

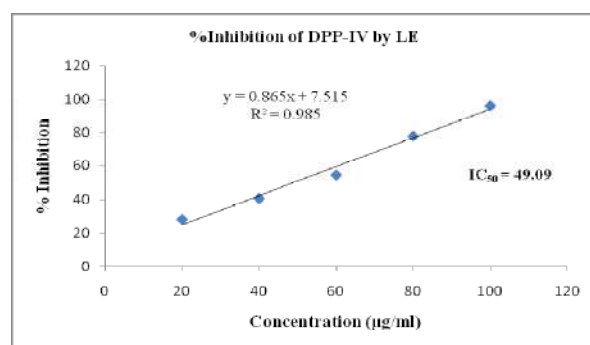


Fig 7: The DPP-IV inhibitory action of LE

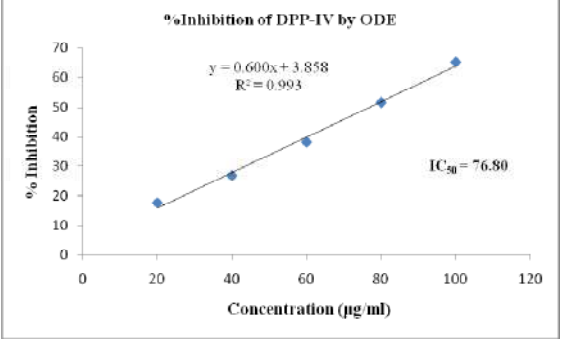


Fig 8: The DPP-IV inhibitory action of ODE

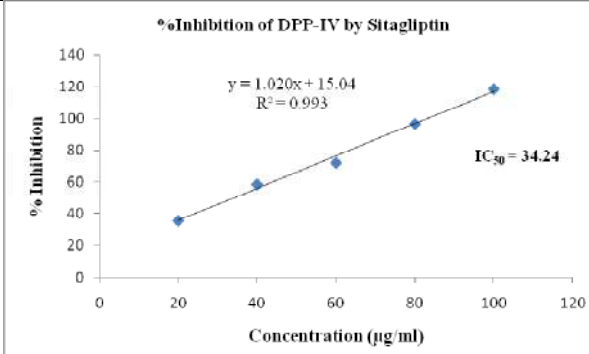


Fig 9: The DPP-IV inhibitory action of sitagliptin





Review on Siddha Herbal Medicine Oma Chooranam (*Tachyspermum Ammi* Powder)

Bharathy K^{1*} and Lakshmi Kantham T²

¹PG Scholar, Department of Maruthuvam, National institute of Siddha, Tambaram Sanatorium, Chennai, Tamil Nadu, India.

²Associate Professor, Head of the Department (i/c), Department of Maruthuvam, National institute of Siddha, Tambaram Sanatorium, Chennai, Tamil Nadu, India

Received: 20 Sep 2023

Revised: 20 Nov 2023

Accepted: 18 Jan 2024

*Address for Correspondence

Bharathy K,

PG Scholar,

Department of Maruthuvam,

National institute of Siddha,

Chennai - 47

Email: bharathyk30@gmail.com



This is an Open Access Journal / article distributed under the terms of the **Creative Commons Attribution License** (CC BY-NC-ND 3.0) which permits unrestricted use, distribution, and reproduction in any medium, provided the original work is properly cited. All rights reserved.

ABSTRACT

Siddha medicine classifies the diseases Mainly On the basis of derangement of 3 major humors namely vatham, pitham and kabam. One such classification is moolam. There are 21 types of moola m mentioned in Yugi Vaithiya Chinthamani-800. There are many formulations in siddha system of medicine for treating moolam. One among them is Oma chooranam -Tachyspermum ammi powder. This review aims to explore about siddha medicine Oma chooranam for the treatment of moolam (Internal hemorrhoids).Oma chooranamis a single herbal formulation. This review paper discusses about the ingredient of the siddha herbal medicine Oma chooranam and its pharmacological action, medicinal uses and its scientific review mentioned in various research studies. Based on results of the review, Oma chooranam is having the potency of relieving the symptoms of moolam (Internal hemorrhoids).

Keywords: oma chooranam, Internal Hemorrhoids, Moolam, siddha, Tachyspermum ammi

INTRODUCTION

Hemorrhoid disease is the gastrointestinal diagnosis which takes fourth leading position in outpatient diagnosis worldwide. It arises from congestion of the internal and/or external venous plexuses around the anal canal. It has muscular mass specifically like tuber in anal region[1]. Classification Of Diseases Is mainly based on derangement of 3 major humors namely vatham, pitham and kabam. There are 4448 diseases. One among them is moolam. There are 21 types of Moolam Mentioned In Yugi Vaithiya Chinthamani-800 [2]. It occurs due aggravated Vatham and



**Bharathy and Lakshmi kantham**

Pithamhumors. Its general symptoms are Constipation, difficult defecation, hard stools which cause discharge of blood from the fleshy growths– T.V Sambasivam pillai Agaraathi[3]. In siddha system of medicine, many formulations are prescribed for -the management *moolam*. The drug *oma chooranam* is indicated for Internal hemorrhoids. It contains *Omam* (*Tachyspermum ammi* Hook.f). The drug is having Anti hemorrhoidal[6], Anti – inflammatory[4], laxative[5]activities which makes it a good option for the management of *moolam*. This article reviews the pharmacological action, medicinal uses of siddha formulation *oma chooranam* which is mentioned in The *Siddha Pharmacopoea of India Part 1 Vol 2*[7].

MATERIALS AND METHODS**Standard Operating Procedure for Omachooranam****Required Raw Drug**

Omam (*Tachyspermum ammi*.L.)

Purification of Raw Drug

Soak *omam* in lime water and dry it[8]

Method of Preparation

Step 1 : Saute *Omam* for 7 times and remove the dust

Step 2 : *Omam* is then powdered and filtered [7]

**RESULT**

Name of the drug: “Oma Chooranam”

Omam



Bharathy and Lakshmi kantham

Botanical name : Trachyspermum ammi.L.

Synonyms: Asamotham, Thippiyam^[9]

Taxonomic Classification^[10]:

Kingdom: Plantae-

Division: Magnoliophyta

Class: Magnoliopsida

Order: Apiales

Family: Apiaceae

Genus: Tachyspermum

Species: ammi

Parts Used: Seed

Habitat:^[27]

Omam belongs to 'Apiaceae' family. It grows well in temperate areas all over the world .It is an annual herbaceous plant and has fruits or seeds which are greyish brown in colour. It is an annual, erect, branched, minutely pubescent plant which grow until 90 cm.

Description:^[7]

Fruit, a cremocarp, entire or separated into mericarps in the bulk drug which is greyish brown in colour, ovoid in shape, compressed with 2 mm long and 1 mm wide. It has protuberances which are pale in colour with 5 pale coloured primary ridges; each of the 2 mericarps contain 5 ridges; It smells like thymol and has pungent taste.

Organoleptic Characters:

Taste : Acrid

Character: Heat

Division : Acrid

Action:^[9]

- Carminative
- Antiseptic
- Anti spasmodic
- Stimulant
- Sialogogue
- Tonic
- Stomachic

Powder: Oily, greyish-brown; shows fragments of epidermis with papillae, yellow brownish septate vittae in surface view.It contain oil globules and endosperm cells arranges in groups.

General Characteristics of Omam:^[9]

சீதசுரங்காசஞ்செரியாமந்தம்பொருமல்

பேதியிரைச்சல்கடுப்புபேராமம்-ஓதிருமல்

பல்லொடுபல்லுமம்பகமிவைநோயென்செயுமோ?

சொல்லொடுபோம்ஓமெனச்சொல்.

- *Padharthaguna chinthamani*

Medicinal Uses:

- Increases appetite
- Indigestion



**Bharathy and Lakshmi kantham**

- Fever due to chills
- *Kabha* diseases
- Diarrhea
- Hemorrhoids
- Flatulence

Scientific Review**Phytochemical Constituents**

- Tannins, Saponins, Cardiac glycosides, Flavonoids, Alkaloids[11]
- Fibre(11.9%), saponins, carbohydrates(38.6%), moisture content(8.9%), protein(15.4%),fat(18.1%), flavone, tannins, glycosides and mineral matter (7.1%) containing iron, calcium, phosphorous and nicotinic acid[12].
- The fruits of *Omam* yields 2% to 4% essential oil which is brown in colour.
- 35% to 60% thymol is its essential constituent [13]
- Many components comprising α -thujene, styrene, α -phyllanderene, β – pinene, terpinene-4-ol, carvacrol, sabinene, γ -terpinene, p-cymene, α -pinene, thymol, β – phyllanderene, and δ -3-carene were found through GLC and GC-MS analysis [14]
- 6-O- β -glucopyranosyl oxy thymol have been found in fruits. Two new glycosyl constituents namely 6-hydroxy carvacrol 2-O- β -D-glucopyranoside and 3,5-dihydroxytoluene 3-O- β -D-galactopyranoside were identified[15]
- Chauhan *et. al.*, Am. J. PharmTech Res. 2012; 2(4) ISSN: 2249-3387 333 www.ajptr.com ← Fruits of ajwain contain various minerals like cadmium, calcium, copper, iron, aluminium, and lithium whereas nitrates and nitrite were not detected in Ajowan fruit[16]
- The fruits afforded riboflavin, nicotinic acid, manganese, calcium, chromium, cobalt, thiamine, copper, iodine, carotene, iron, phosphorus and zinc [17]

Pharmacological Activities**1. Cytoprotective, Anti-secretory, Anti-ulcer-Gastroprotective [18]**

Extract of *Trachyspermum ammi* fruit produced a decrease in the ulcer index indicated by increase in percentage protection from ulcers.

2. Anti bacterial activity[20]

A maximum zone of inhibition was found in the methanolic extract.

3. Anti oxidant activity[18]

Recent reports show a highly positive relationship between total phenols and antioxidant activity.

4. Anti-hemorrhoidal activity[6]

Tachyspermum ammi exerts anti-hemorrhoid and anti-diarrheal activity.

5. Anti-inflammatory activity[4]

Tachyspermum ammi exerts anti-inflammatory activity.

6. Anti cancer activity[19]

The possible mechanism of its anti-cancer activity may be by apoptosis which is induced by DNA fragmentation. It might be due to active phytochemicals such as alkaloids, phenols and flavonoids found in the extracts.

7. Hepatoprotective activity[22]

It exhibits preventive effects against CCl₄-induced prolongation of pentobarbital sleeping time as well as equilibrating the level of Aminotransferases (AST and ALT), Alkaline Phosphatase (ALP), hepatic enzymes, and during liver damage.

8. Anti hyperlipidemic activity[21]

Tachyspermum ammi exerts anti-hyperlipidemic activity.





DISCUSSION

According to review of literature of *Oma chooranam*, the following contents were reviewed-parts used, morphology family, pharmacological actions, indications for which it is prescribed. *Omam* is having carminative and anti spasmodic activity which helps in the treatment of *moolam*. The laxative action of the drug helps in relieving constipation. *Oma chooranam* is having anti-hemorrhoidal activity which indicates that it is effective in treatment of hemorrhoids. Anti hyperlipidemic action of *omam* makes it a good option in the treatment of dyslipidemia. It can also be used in treating liver diseases since the drug is having hepatoprotective activity.

CONCLUSION

Based on various *siddha* texts, the ingredient of *Oma chooranam* are commonly used in treating the various diseases. The pharmacological activities of ingredient are hepatoprotective, Anti-inflammatory, Antioxidant, Anti cancer activity, Cytoprotective, Anti-secretory, Anti-ulcer-Gastroprotective, Antihypertensive, antispasmodic and broncho-dilating activity. Therefore the medicine could be very effective in the management of *Moolam*(Internal hemorrhoids). The availability of the drug is easy, single drug, safe to administer, minimal sources are required and is cost effective. Further clinical studies has to be carried out for exploring this *siddha* medicine.

ACKNOWLEDGEMENTS

Authors wish to express their gratitude to all the faculties of National institute of Siddha for their support.

Competing Interests

There is no conflict of interest among the authors.

Funding

No funding was received for the entire study.

REFERENCES

1. Niranjana Agarwal *et.al.*, The association of Colon & Rectal surgeons of India (ACRSI) practice Guidelines for the management of Hemorrhoids. Indian Journal of Surgery 2017 ;79(1):58-61.
2. Yugi vaithiya sinthamani by Sage Yugi, second edition 2005, published by Indian medicine Homoeopathy department, Arumbakkam, Chennai-106, page no :208,211-213.
3. Tamil-English dictionary by T.V. Sambasivam pillai, Vol 5, Government of Tamilnadu, page no : 895.
4. Aslam A, Nokhala A, Peerzada S, Ahmed S, Khan T, Siddiqui MJ. Evaluation and Comparison of *Trachyspermum ammi* Seed Extract for Its Anti-inflammatory Effect. J Pharm Bio allied Sci. 2020 Nov;12(Suppl2):S777-S780. doi:10.4103/jpbs.JPBS_243_19. Epub 2020 Nov 5. PMID:33828377; PMCID:PMC8021059.
5. Husain N, Pandey B, Trak TH, Chauhan D. MEDICINAL VIRTUES AND PHYTOCHEMICAL CONSTITUENTS OF SOME OF THE IMPORTANT INDIAN SPICES.
6. Dwivedi SN, Mishra RP, Alava S. Phytochemistry, Pharmacological studies and Traditional benefits of *Trachyspermum ammi* (Linn.) Sprague. International journal of pharmacy & life sciences. 2012 May 1;3(5). The *siddha* pharmacopoeia of India Part-1 Volume II, First edition page no.97-98, published by the controller of publications civil lines, Delhi-110054, on behalf of Government of India Dept of Ayurveda, Yoga AND Naturopathy, *siddha* and homeopathy (AYUSH, Indian red cross society building, red cross road, New Delhi-110001



**Bharathy and Lakshmi kantham**

7. C.kannusamipillai,chikicharathna Deepam(Vaithiya nool),B.Rathinanayakkar and sons,1st edition 2007,page no.29,30.
8. Vaidhya Rathnam Ka.sa.Murugesu Mudhaliyar, Gunapaadam Mooligai vaguppu; Edition 2006; Page no: (173-174, 514-515, 376, 519,127-128) Damodar K, Bhogineri S, Ramanjaneyulu B. Phytochemical screening, quantitative estimation of total phenolic, flavanoids and antimicrobial evaluation of *Trachyspermum ammi*. Journal of Atoms and molecules. 2011 Nov 1;1(1):1.
9. Kaur GJ, Arora DS. Antibacterial and phytochemical screening of *Anethum graveolens*, *Foeniculum vulgare* and *Trachyspermum ammi*. BMC complementary and alternative medicine. 2009 Dec;9(1):1-0.
10. Pruthi JS. Spices and Condiments. 4th edition; National Book trust, New Delhi; 1992.
11. Anonymous. The Wealth of India, A Dictionary of Indian Raw Materials and Industrial Products Publications and Information Directorate. New Delhi CSIR; 2003; 10: 267-272.
12. Mohagheghzadeh A, Faridi P, Ghasemi Y. *Carum copticum* Benth. & Hook. Essential oil chemotypes. Food Chemistry 2007; 100: 1217–1219. 9.
13. Gang SK, Sharma ND, Gupta SR. A phenolic glucoside from the seeds of *Carum copticum*. Phytochemistry 1980; 19: 2215-2216.
14. Yahara S, Sakamoto C, Nohara T, Niiho Y, Nakajima Y, Ito H. Thymoquinol 5-O-beta-dglucopyranoside, kaempferol 3-O-beta-rutinoside and protocatechuic acid from fruit of *Scisandra chinensis*. Shoyakugaku Zasshi 1993; 47 (4): 420-422.
15. Ishikawa T, Segal Y, Kitajima J. Water-Soluble Constituents of Ajowan. Chem Pharm Bull 2001; 49 (7): 840-844.
16. Ramaswamy S, Sengottuvelu S, Sherief SH, Jaikumar S, Saravanan R, Prasadkumar C, Sivakumar T. *Trachyspermum ammi* fruit. International Journal of Pharma and Bio Sciences. 2010;1(1).
17. Bashyal SA, Guha AV. Evaluation of *Trachyspermum ammi* seeds for antimicrobial activity and phytochemical analysis. Evaluation. 2018;11(5):148-222.
18. Chatterjee S, Goswami N, Bhatnagar P. Estimation of Phenolic Components and in vitro Antioxidant Activity of Fennel (*Foeniculum vulgare*) and Ajwain (*Trachyspermum ammi*) seeds. Advances in Bioresearch. 2012 Jun;3(2):109-18.
19. Ramya N, Priyadarshini XX, Prakash R, Dhivya R. Anti-cancer activity of *Trachyspermum ammi* against MCF7 cell lines mediates by p53 and Bcl-2 mRNA levels. J Phytopharmacol. 2017;6(2):78-83.
20. Saraswat, N., N. Sachan, and P. Chandra, A review on ethnobotanical, phytochemical, pharmacological and traditional aspects of indigenous Indian herb *Trachyspermum ammi* (L). Current Traditional Medicine, 2020. 6 (3): p. 172-187.
21. Saleem U, Riaz S, Ahmad B, Saleem M. Pharmacological Screening of *Trachyspermum ammi* for Antihyperlipidemic Activity in Triton X-100 Induced Hyperlipidemia Rat Model. Pharmacognosy Res. 2017 Dec;9(Suppl 1):S34-S40. doi: 10.4103/pr.pr_37_17. PMID: 29333040; PMCID: PMC5757323.
22. Chauhan B, Kumar G, Ali M. A review on phytochemical constituents and activities of *Trachyspermum ammi* (L.) Sprague fruits. AJPTR. 2012;2(4):329-40.





Physiotherapy and Dry Needling Management on Tic Douloureux- A Case Report

S.Jeyakumar¹, Rajasekar² and S .Senthil kumar³

¹Post-Doctoral Fellow, Department of Physiotherapy, Srinivas University, Mangalore, Karnataka, India.

²Dean and Professor, Department of Physiotherapy, Srinivas University, Mangalore, Karnataka, India.

³Professor, Department of Physiotherapy, School of Health Sciences, Gardern City University, Bangalore, Karnataka, India.

Received: 07 Sep 2023

Revised: 10 Nov 2023

Accepted: 05 Feb 2024

*Address for Correspondence

S.Jeyakumar

Post-Doctoral Fellow,

Department of Physiotherapy,

Srinivas University,

Mangalore, Karnataka, India.



This is an Open Access Journal / article distributed under the terms of the **Creative Commons Attribution License** (CC BY-NC-ND 3.0) which permits unrestricted use, distribution, and reproduction in any medium, provided the original work is properly cited. All rights reserved.

ABSTRACT

Trigeminal neuralgia, commonly referred to as ticdouloureux (TD), is a paroxysmal kind of intense, piercing, stabbing pain that resembles an electric shock and typically affects the second and third regions of the face on one side. Characterized by seizures. TD is sometimes referred to medically as "the worst pain known to mankind" and "a suicidal disorder." Triggered by chewing, talking, cold wind, and touching the trigger site. In most cases, The TD patients who were partially responsive or refractory to pharmacotherapy underwent surgery to relieve pain. Few studies reported on the role of physical therapy in Ticdouloureux disease. This study aims to discuss a 51 years old female had determine the effect of physical therapy treatment on pain in trigeminal neuralgia. The patient is treated with 20 minutes of transcutaneous electrical nerve stimulation, 10 minutes of relaxation techniques (deep breathing exercises), 10 minutes of hot wet trapezius pack, neck isometric exercise , 5 times per side with dry needling technique done on or ofacial muscle. the Duration of study 4 weeks analzed with Visual Analogue Scale (VAS) and Short-Term Pain Inventory-Faceand18-Item Questionnaire .Pain was significantly reduced on the VAS and on the Short-Term Pain Inventory-Faceand 18 item questionnaire. The results of the study showed that continuous his use of dry needling technique ,TENS, are laxation technique, hot wet wraps to the trapezius muscles, and isometric neck training reduced pain in trigeminal neuralgia

Keywords: tic douloureux; Visual analog scale; Brief pain inventory-facial, dry needling





Jeyakumar et al.,

INTRODUCTION

For centuries, ticdouloureux (TD) has been mentioned in medical literature. Writings by the Arab physician Jujani in the eleventh century A.D. and Aretaeus of Cappadocia in the second century A.D. both make reference to unilateral face pain that results in facial spasms. The international Association for the study of pain defined Trigeminal neuralgia as “sudden, usually unilateral, severe, brief, stabbing, recurrent pains in the distribution of one or more branches of the fifth cranial nerve” (Merskey & Bogduk 1994). People often called it as Tri facial neuralgia, or Trigeminal Neuralgia”. Medical Science sometimes calls TD “the worst pain known to mankind and “the suicide disorder” because of the significant numbers of people taking their own lives when they cannot find effective treatments. The pain involves the second (maxillary) or third (mandible) divisions more often than the first (ophthalmic); it rarely occur bilaterally and never simultaneously on each side, occasionally more than one division is involved. Paroxysmal seizures last from seconds to minutes [1, 2]. people involved. Paroxysmal seizures last from seconds to minutes [1, 2]. This disorder usually affects older women over the age of 35 and occurs mainly on the right side of the face. Chewing, talking, washing your face, brushing your teeth, a cold breeze, or touching certain “trigger points” such as your upper lip or gums can all trigger a bout of pain. Its etiology is also a mystery today.

Periodontal disease, traumatic occlusion, nerve degeneration of deciduous teeth, circulatory disturbance in the trigeminal ganglion, multiple sclerosis, compression of dilated tortuous arteries near the trigeminal ganglion, brain relaxation associated with aging, idiopathic diseases, etc. It will be considered. It has long been pointed out as a cause [1,2]. According to the practice parameters recommended by the Quality Standards Subcommittee of the American Academy of Neurology and the Quality Standards Subcommittee of the European Union of Neurological Societies, the following should be provided for pain management in patients with FD: Carbamazepine, oxcarbazepine, baclofen, lamotrigine and pimozide should be considered [3] . Early surgical therapy, 4,444 percutaneous Gassel ganglion surgeries, gamma knife, and his 4,444 micro vascular decompressions are considered for the 4,444 of her FD patients who do not respond to medical therapy. All of these have positive and negative effects and negative effects. Physiotherapy promotes, maintains, and restores the physical, psychological, and social wellbeing of an individual by the use of different techniques. Physiotherapy Management will also aim at reducing pain and improve the ability to carry on with the activities of daily living (ADLs)[4][5]

Case report methodology

The study was conducted in a 51-year-old female patient referred from the Department of Dentistry and to Department of Neuro physiotherapy, Gardern City University, Bangalore, Karnataka. MRI report, dental and neurological examination were normal. The study included patients who were receiving treatment and had intolerance to drugs. Written informed consent was obtained from the participant. Psychiatric disorders, behavioral disorders, anxiety, agitation, and depression are most commonly associated with pain. patient was unaware of their symptoms. Education about the anatomy of the affected body part and the pathophysiology of pain can help patients better understand the nature of the problem, reduce anxiety, and increase compliance and participation in physical therapy treatment. increase. Therefore, patient information was provided prior to treatment [4,5].

The following therapeutic aspects are central to pain management in TD

Patients receive continuous trans cutaneous electrical nerve stimulation (TENS) [Gymna Uniphy Phyaaction Guide E] 250Hz, 120 u, z 20 minutes Treated with pulses. Treat the affected nerve5 days a week for 4 weeks. One electrode was placed just in front of the ear and another at the terminal of each nerve. However, placement was adjusted for pain transmission and efficacy as needed [6-10]. Positive Measures – Exercise In severe intractable pain, two causes of disability may be identified. One is the primary disorder due to a documented organic pathology and the other is the secondary disorder (such as inactivity and general) resulting from the physical and emotional consequences of the painful experience. Psycho physiological, state deterioration). Poor conditioning results in decreased muscle strength and endurance, increased joint stiffness and postural distortion. These deficits independently contribute to the perception of pain and the inability to





Jeyakumar et al.,

perform functional activities. TD Patients may experience a gradual decrease in neck movement as they perceive the severity of their pain. Maintaining a fixed posture causes spasms in the neck and trapezius muscles, reducing muscle strength and neck mobility. This has also been observed in our patients [5]. Therefore, a hot, moist pack was applied to the neck and trapezius muscles for 10 minutes to reduce muscle spasm. Isometric neck movements were performed with 5 repetitions each of lateral and free neck movements (neck flexion, neck extension, and lateral flexions). Components of Self-Management Techniques relaxation techniques including deep breathing exercises were performed for 10 minutes. The patient was asked to engage in pleasurable activities instead of sitting, such as distraction techniques, which is ideal for keeping them from thinking about distressing situations.

Desensitization Program and Dry Acupuncture

To reduce hypersensitivity, after her 3-minute dry acupuncture of the masticatory muscles, the patient was asked to cover the affected side with a soft cloth or cotton pad for 15 minutes daily. was requested to Habituation of the nervous system to facilitate constant afferent input [13].

Note

Patients should be instructed not to use cold water for drinking or washing the face, to wear a scarf to protect the face from the cold environment, to avoid eating hard foods, and to avoid food from the unaffected side. They were asked to avoid chewing [4].

Outcome Measures

Visual Analogue Scale (VAS): Used to assess pain at the start of the intervention and after her 4 weeks of intervention. This is a 0-10 rating scale.

Brief pain inventory (BPI) – Facial

The BPI- Facial is a 3 factor, 18 items questionnaire that is commonly used to assess 2 factors of chronic pain: pain intensity and interference (that is, how pain interferes with the patient's general activity and function). The pain intensity factor is elucidated by questions about a patient's worst, least, average, and current level of pain. For the interference factor, the BPI includes items that assess how pain interferes with a patient's general activity, mood, walking ability, and normal work, relationships with other people, sleep, and enjoyment of life. These 7 interference items are referred to as "interference with general activities". The additional 7 facial interference items include eating a meal, touching one's face (including grooming), brushing or flossing one's teeth, smiling or laughing, talking, opening one's mouth widely, and eating hard foods such as apples. Its reliability and validity has been documented by various authors [16]. Pre and post interventional assessment of this scale was also used.

DISCUSSION

The results of this study showed that the VAS score and BPI facial score decreased significantly after 4 weeks of intervention. The significant reduction in VAS score may be attributed to the effects of dry needling acupuncture and physical therapy. The impulse inhibits pain signals to the brain by presynaptic inhibition of noxious information in afferent C-fibers. This mechanism is based on the gate control theory proposed by Melzack and Wall. Second, by stimulating the higher center, it releases endogenous opioids that have descending inhibitory effects in the dorsal horn and bind to receptors on nociceptive afferent neurons, inhibiting the release of substance P. There is also [13]. Also, Wolf et al. showed that peripheral electrical stimulation can also stimulate naloxone-dependent anti-nociceptive mechanisms. H. The endogenous opioid system acts at both spinal and supraspinal levels [5, 18]. A significant decrease in the GDP facial scale indicates that there was improvement in functional activity, quality of life, and physical and emotional functioning. Use of additional therapies such as B. Applying hot, moist packs to relieve muscle spasm involves the direct effects of heat primarily on muscle spindles and sensory nerve conduction. This reduces neuronal activity in the secondary terminals and increases activity in the primary terminals and the Golgi tendon organ, producing an overall inhibitory effect on the motor neuron pool, leading to a vicious pain-spasm-pain cycle. cut off [5,9,10].





Jeyakumar et al.,

Neck isometric exercises and dry needling improve neck muscle pain and endurance, and reduce the effects of prolonged neck posture in the same position. The analgesic effects of exercise are generally attributed to the production of beta-endorphins during exercise [12]. Obvious limitations of this study included the study design itself in a case report format, limited generalization of the concept to others with similar problems, and a short follow-up period. It was a short period of 4 weeks. It is therefore recommended to conduct a similar study in a large sampling with long-term follow-up.[16]

CONCLUSION

The results of this study highlight the role of physical therapy in : Tic douloureux disease as an educator, counselor, motivator, analgesic, and in reducing disability. The results of the study showed that continuous his use of dry needling technique ,TENS, are laxation technique, hot wet wrapsto the trapezius muscles, and isometric neck training reduced pain in tic douloureux disease

REFERENCES

1. Shafer WG, Hine MK, Levy BM (1983) A textbook of oral pathology. Fourth Edition. Philadelphia: W.B. Saunders Co. Diseases of the nerves and muscles: 854-856.
2. Beal MF, Hauser SL (2008) Harrison's Principles of Internal Medicine. Trigeminal neuralgia, Bell's palsy and other cranial nerve disorder. (7thedn), McGraw Hill Co, New York, USA, 2: 583-584.
3. Gronseth G, Cruccu G, Alksne J, Argoff C, Brainin M, et al. (2008) Practice Parameter: the diagnostic evaluation and treatment of trigeminal Neuralgia (an evidence-based review): report of the quality standard subcommittee of the American Academy of Neurology and the European Federation of Neurological Societies. *Neurology* 71: 1183-1190.
4. Zakrzewska JM, Lopez BC (2006) Wall and Melzack: Textbook of Pain. 5th. Elsevier Science.
5. Harriet Wittink, Theresa Hoskins Michel, Lisa Janice Cohen (2002) Chapter 7 Pain Rehabilitation. In: Physical Therapy Treatment, Textbook of Chronic Pain Management for Physical Therapists. (2ndedn), Elsevier Science.
6. Long DM, Hagfors N (1975) Electrical stimulation in the nervous system: the status of electrical stimulation of the nervous system for relief of pain. *Pain* 1: 109-123.
7. Bates JA, Nathan PW (1980) Trans cutaneous electrical nerve stimulation for chronic pain. *Anaesthesia* 35: 817-822.
8. Wall PD, Sweet WH (1967) Temporary abolition of pain in man. *Science* 155: 108-109.
9. Oncel M, Sencan S, Yildiz H, Kurt N (2002) Trans cutaneous electric nerve stimulation for pain management in patients with uncomplicated minor rib fractures. *Eur J Cardiothoracic Surg* 22: 13-17.
10. Charman RA (2000) Complementary therapies for physical therapists. Butterworth-Heinemann. 13. Theresa Hoskins Michel (2002) Chapter 15 Neuropathic pain. In: Chronic Pain Management for Physical Therapist. (2ndedn), Elsevier Science.
11. Hayes MH, Patterson DG (1921) Experimental development of the graphic rating method. *Psychological Bulletin* 18: 98-99. 15. Freyd M (1923) The graphic rating scale. *J Educational Psychol* 14: 83-102. 16. Lee JYK, Chen HI, Urban C, Hojat BSA, Church EBA, et al. (2010) Development of and psychometric testing for the Brief Pain Inventory-Facial in patients with facial pain syndromes Clinical article. *J Neurosurgery* 113: 516-523.
12. Melzack R, Wall PD (1965) Pain mechanisms: A new Theory. *Science* 150: 971-978. 18. Basbaum AI, Fields HL (1984) Endogenous pain control mechanisms: Review and hypothesis. *Ann Neurol* 7: 309-338.
13. Allen RJ (2006) Physical agents used in the management of chronic pain by Physical Therapists. *Phys Med Rehabil Clin N Am* 17: 315-345. 20. Lum LC (1975) Hyperventilation: the tip of iceberg. *J Psychosomatic Res* 19: 375-383.
14. Chaitow L (2004) Breathing pattern disorders, motor control and low back pain. *J Osteo Med* 7: 34-41.
15. Mehling WE, Hamel KA, Acree M, Byl N, Hecht FM (2005) Randomized, controlled trial of breath therapy for patients with chronic low back pain. *Altern Ther Ther Health Med J* 11: 44-52.

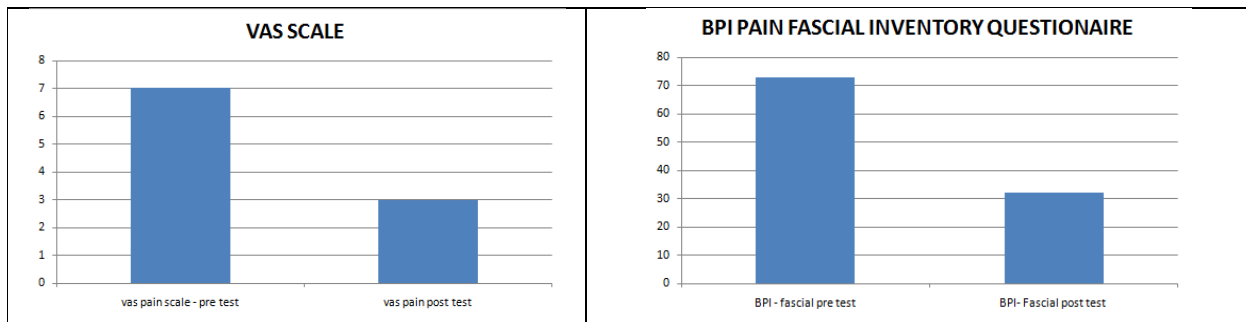




Jeyakumar et al.,

16. Andrew Sukiennik, Harriet Wittink. (2002) Chapter 3 Patho physiology of Pain. In: A Primer, Textbook of Chronic Pain Management for Physical Therapist. (2ndedn), Elsevier Science

OUTCOME MEASURES	PRE TEST	POST TEST
VAS SCALE	7	3
BPI PAIN FASCIAL INVENTORY QUESTIONAIRE	70	32





Identification of Soil Erosion - Susceptible Areas using AHP Model: A Case Study of Lower Vellar Watershed, Tamil Nadu, India

Arun Shourie.R¹* and Ezhisavallabi.K

¹Research Scholar, Department of Civil Engineering, Annamalai University, Annamalai Nagar, Tamil Nadu, India

²Associate Professor, Department of Civil Engineering, Annamalai University, Annamalai Nagar, Tamil Nadu, India

Received: 15 Oct 2023

Revised: 12 Dec 2023

Accepted: 30 Jan 2024

*Address for Correspondence

Arun Shourie.R

Research Scholar,

Department of Civil Engineering,

Annamalai University,

Annamalai Nagar, Tamil Nadu, India



This is an Open Access Journal / article distributed under the terms of the **Creative Commons Attribution License** (CC BY-NC-ND 3.0) which permits unrestricted use, distribution, and reproduction in any medium, provided the original work is properly cited. All rights reserved.

ABSTRACT

Being a natural process that disintegrates ecosystems, landscapes and sustainability of water maximizes risks. Soil Erosion has been adversely affected by Natural resources, methods of agriculture, ecological balance, and the quality of the environment. The research study encompasses the Analytic Hierarchy Process (AHP), it's a machine learning approach built around the use of geographic information systems that incorporate the study of the Lower Vellar River Watershed, Tamil Nadu, India. The research findings experimented with the GIS-based on Analytical Hierarchy Process (AHP) and weighted sum method (WSM) to extract ten factors (topographical derivatives, LULC, soil, drainage density, Mean Annual rainfall, lithology, and NDWI of an area) via datasets of precipitation, geological maps, soil maps, and satellite images. The (ten*ten) decision matrix of the AHP model stipulated the weights for every element that contribute to erosion, adhering to each of their distinct priorities from Low to High as the following factors: Elevation (12.07%), Rainfall erosivity (RE) (13.78%), Rainfall (13.45%), slope (9.90%), soil type and drainage density (9.32%), Land use land cover (LULC) (6.59%), Normalized difference water Index (NDWI) (5.59%). The analysis indicates that 26% of the region as a whole is extremely vulnerable to soil erosion, demonstrating an amount of high and extremely highly vulnerable zones, which encompass 460 km² and 390.8 km² (24%) of the land, respectively. Management techniques that prevent soil erosion in agricultural watersheds play a role when it comes to environmentally friendly land-use planning.

Keywords: Analytical Hierarchy Process, GIS, Preference matrix combinations, Weighted sum method, Vulnerable zone of erosion



**Arun Shourie and Ezhisaivallabi**

INTRODUCTION

In addition to obvious off-site effects like sediment build-up, eutrophication of streams, and increased flooding, Soil deterioration, which is a widespread issue, has an extensive number of adverse ecological impacts, including land degradation and fertility loss. Asia has the highest rate of erosion of any continent in the world, at about 74 tons per acre each year. In accordance with (Wei et al., 2007), Soil erosion is a significant contributor to soil degradation and poses a substantial risk to both natural ecosystems and communities that depend on local resources are frequently exposed to dangerous geological and meteorological risks. Soil erosion is a common occurrence in agricultural watersheds, which reduces the effectiveness of land use (Amiri et al., 2019). Soil erosion rates around the world are 10 to 40 times greater than soil formation rates, posing a risk to environmental quality and food preservation. According to Pimentel et al. (2006), Soil erosion can have significant environmental and economic impacts, particularly in agricultural areas where intensive farming practices, such as tillage, can accelerate the process. When soil is eroded, it can end up in nearby waterways, which can lead to increased sedimentation and nutrient pollution, affecting aquatic ecosystems and posing a risk to human health. By using pesticides, which prevent biological activities including plant development, microbial activity which breaks down soil-forming processes can be concluded. Due to centuries of cultural soil exploitation, organic matter, and soil nutrients have decreased in numerous regions across the globe (Cerda et al., 2017). Tillage can increase soil bulk density initially but may lead to compaction over time. Furrowing can temporarily reduce soil densification by creating channels for water and roots.

However, both practices need to be carefully managed to avoid long-term negative effects on soil health. Combining tillage with biocide sprays can further exacerbate soil erosion and deterioration due to the disruption of natural processes. It's important to consider sustainable soil management practices that minimize soil disturbance and promote soil conservation to maintain long-term soil health. Tillage can initially improve soil bulk density but can eventually contribute to compaction. Furrowing can minimize soil densification momentarily by providing pathways for water and roots. However, both practices must be properly regulated to practices, nevertheless, need to be properly regulated in order to avoid long-term harmful consequences on soil health. Combining tillage with antimicrobial applications may accelerate soil deterioration by disrupting with natural processes. To ensure long-term soil health, it is crucial to consider sustainable soil management practices that reduce soil disturbance while promoting soil conservation. Herbicides affect soil structure and cause compaction because they consume fewer organic materials. According to (Chen et al., 2001), the most important predictor of soil erosion exposure is the utilization of land, vegetative cover (LULC), which will potentially reduce or increase sediment yields and runoff from the surface rates. Inequitable land use patterns and an array of flora, according to (Siriwardena et al., 2006), have significant effects on the watershed responses of streams. In addition to enhancing soil attributes that lessen soil degradation, the management of LULC impacts the quality and durability of plants (Kosmas et al., 2000). Rapid soil erosion harms topsoil, diminishing soil quality, boosting floods, tampering with harvesting, and jeopardizing the stability of neighbourhood's and areas (Lal et al., 2001).

Dams and reservoirs may eventually lose their ability to perform as intended due to severe soil erosion. Numerous methodologies have been suggested for evaluating soil erosion at various sizes, which vary from local to regional to global (Poesen et al., 2003). Physical and empirical models have primarily been utilized to analyze soil erosion rates at various geographical scales. It is difficult to offer quantitatively accurate estimates of soil erosion due to the complexity of soil erosion, which is influenced by environmental factors such as land surface and soil parameters (Park et al., 2011). Different equations have been developed to address the issue of spatially specific quantified predictions in order to enhance statistical modelling (Rahmati et al., 2017). Assessment methods can be made better with the use of aerial photographs and incredibly high-resolution satellite images (Kropacek et al., 2016). The Arc GIS and ERDAS environments, a raster-based weighted linear combination (WLC) tackle concerning six soil deterioration driving variables was employed. RUSLE is used to quantify the WLC-generated raster-based qualitative spatial erosion susceptible model (Swadas pal et al., 2016). In this work, the effects of an AHP knowledge-based model were investigated for a catchment that is used for agriculture in the Lower Vellar River Watershed.



**Arun Shourie and Ezhisaivallabi**

Because the Lower Vellar River Watershed has never had soil erosion resistance research and mapping, the results are beneficial for planners and policymakers who look for to preserve and manage soil resources.

Study Area

Vellar River is one of the numerous ephemeral rivers and it is located in the Cuddalore district in the coastal region of Tamil Nadu. The Lower Vellar River Watershed lies in the Eastern Deltaic Plain of the Vellar Basin as well as faces the Bay of Bengal. The Lower Vellar River Watershed covers a span of 20 blocks in five districts such as Cuddalore, Kallakurichi, Ariyalur, Perambalur and Salem. The boundary area of the Lower Vellar watershed is 1754 km² and its longitude and latitude extend from 78° 30'00" E - 79° 46'6" E and 11° 30'10" N - 11° 42' 16" N, as shown in Figure 1. The Vellar River turns right at the Anaivari Odai inflow point and flows for about 15 km in a southerly direction, passing through the Sethiathope Regulator Comes Bridge before finally emptying into the Bay of Bengal close to Porto-Novo in the Cuddalore District. The Perumal Tank is connected to the lower Vellar River watershed to the east by the Bay of Bengal. Agriculture has been noted to be one of the main pursuits of the local populace in the watershed. It frequently suffers effects from extreme weather, particularly in coastal locations, such as flooding. When a low-pressure system forms in the Bay of Bengal, rain falls more heavily along the coastline (normal coastal rainfall ranges from 930 to 1500 mm). The north-eastern monsoon causes catastrophic floods in nearly all of these three coastal taluks. It has a pleasant tropical environment all year long, with summer temperatures often ranging between 26 and 38 ° C and winter temperatures typically falling between 21 and 29 ° C.

MATERIALS AND METHODS

The study assessed the Soil erosion hazard in the Lower Vellar Watershed using a variety of datasets and methodologically sequential procedures. The goal of the current study is to develop a framework for the Analytical Hierarchy Process (AHP) Model using ArcGIS 10.8.1, remote sensing, and GIS. The model's formulation encompasses the ten Soil Erosion-influencing physical variables, such consist Digital Elevation Model, Slope, Rainfall Erosivity, Precipitation, Drainage Density, LULC, NDWI, Soil Type, Aspect and Lithology. Also, here Raw Data are tabulated in Table 1 as follows below. In accordance with the provided information, a map of soil erosion vulnerability zones is created to illustrate the places where soil erosion was exceptionally high, very high, moderately elevated, low, and extremely low.

METHODS

A number of steps were taken in this study to prepare the Soil erosion susceptibility zone, including expressing the complicated problem, constructing an AHP model-based hierarchical framework for the adopted requirements, conducting a comparison by pair using a matrix approach for the assigned influencing elements (binary comparison), determining goals and establishing the corresponding weights for all variables, forecasting parallelism values for the evaluations, and discussing what emerged. More information on the elements that should be evaluated while using MCDM for figuring out the relative importance (or priorities) of each element in order to accomplish a meaningful outcome is provided below. An AHP model based on the MCDM was used to quantify the weighting of 10 specified erosion-beginning variables in order to forecast the potential for particular substances to be included in the Soil erosion susceptibility zone. The aforementioned contributing elements were divided up further into sub-classes in order to compute their relative weights.

Analytical Hierarchy Process (AHP) model

AHP was initially employed in multi-criteria decision-making by Saaty et al., (1980). The AHP is a tool for supporting decisions. It employs a multi-level hierarchical structure of goals, standards, sub-standards, and choices to address complicated decision-making challenges. It establishes the relative importance of several elements for Soil-Suspectable zones (SSZ) and their weights. Each theme layer has been prepared using the AHP model. By segmenting the currently available thematic maps into five vulnerability categories, an AHP-based Pair-by-Pair





Arun Shourie and Ezhisaivallabi

comparison matrix of the different above-mentioned components are constructed. If the mathematical frameworks are used to compare the ten distinct elements with different weights, the ten parameters are graded on an absolute number scale from one through nine (Table 2). Each matrix element's size attributes, ranging from smaller to larger, can be obtained by dividing each element by the sum of its columns. However, the row averages are calculated in order to derive the priority vector.

Consistency ratio

To perform adjustments to the created Pair- matrices and their corresponding weighting scheme, apply the following equation (Saaty et al., 1980): A consistency ratio (CR) evaluation of the data was used, with a value of less than 0.1 being regarded as acceptable. The consistency of the resulting eigen vector-matrices following the index below found in the current inquiry is 0.093, which supports the assertion that the set of alternatives n assessed is appropriate.

$$CR = \frac{CI}{RI} \quad \text{Eq.1}$$

CI is computed using Eq.2

$$CI = \frac{\lambda_{max} - n}{n-1} \quad \text{Eq.2}$$

CR, CI, and RI are acronyms for consistency proportion, consistency index, and random index, respectively. Maximum is the comparison matrix's principal eigenvalue, where n is the number of matrix components or elements. RI indicates the consistency of the pair-by-pair matrix, which is shown in Table 4 and produced at random. Many AHP-related parameters influence the values in the table. The determined RI for the study, based on the 10 criteria, is thus 1.49.

$$FVI = \sum^n W_i * R_i \quad \text{Eq.3}$$

where RI represents the rating class and WI indicates the specific values for each parameter's erosion conditioning. Finally, the resulting SSZ was categorized into five categories using natural breaks: very low, low, moderate, high, and very high (Rocha et al. 2020).

Weighted Sum Method (WSM)

For WSM implementation, all requirements were prioritized into five groups: shallow, low, moderate, substantial, and exceptionally high (Table 7). The classes of data spectrum associated with every grid layer were defined in the succeeding reclassification. An accumulation of data has been divided into "natural" classes using ArcGIS and the natural break classification method. Five priority classifications were used, which were chosen based on the available research. Ratings for the course's qualitative relevance for erosion within each stratum ranged from extremely high (5) to extremely low (1). The functional connection between every statistic and its related classes was employed to rank each metric and its associated classes. Cells bringing a higher risk of soil erosion obtained higher scale values, whereas cells with a lower likelihood of erosion earned lower scale values. Finally, a WSM was implemented for determining the pixel-level degree of soil erosion. Each parameter was multiplied by its associated weight to create the soil severity index once all the layers had been summed up in the WSM.

$$SES = E_{Lw} * E_{Lwj} + S_{Lw} * S_{Lwj} + A_{Sw} * A_{Swj} + S_{Ow} * S_{Owj} + LU_{LCw} * LU_{LCwj} + DD_w * DD_{wj} + P_{Ew} * P_{Ewj} + R_{Ew} * R_{Ewj} + L_{Iw} * L_{Iwj} + NDWI_w * NDWI_{wj} \quad \text{Eq.4}$$

where SES displays the areas with the most severe soil erosion. The layers of Digital Elevation Model Slope Map, Aspect of Map, Soil Map, Land use/Land cover, Drainage Density, Precipitation, Rainfall Erosivity, Lithology, and NDWI are represented by the letters E_L , S_L , A_S , S_O , L_U , P_E , D_D , R_E , L_I , and $NDWI$. W and W_j stand for the weight of a layer and a specific parameter, respectively.

RESULTS AND DISCUSSION

Based on knowledge of the subject substance, experience with the area substance, and the Lower Vellar Watershed, eight factors that have an effect (Elevation, Slope, Aspect, Soil, LULC, Drainage Density, Precipitation, Rainfall



**Arun Shourie and Ezhisaivallabi**

Erosivity, Lithology, and NDWI) were identified for research based on a scrutiny of the data obtained through a survey of the prior studies. The aforementioned traits have been selected based on their knowledge of the place of residence, previous exposure to the area, and comprehension of the collected data. The requirements for each of the ten parameters, along with the techniques that resulted in them, are presented below.

Elevation (E_L)

Elevation is a significant factor in influencing the degree of erosion due to its impacts on soil moisture and water balance, erosional and depositional processes, the quantity of organic material in the soil, vegetation, and specific species that create cultivated plants and wild flora. The Shuttle radar topography mission DEM elevation layer has been classified for use as an input in the overlay analysis (Figure 3). The elevation of the research site ranges from 0 to 170 meters.

Slope (S_L)

Slope angles influence the rate of infiltration and runoff velocity. Steep slopes have higher rates of erosion than low-angle slopes with high infiltration rates. The gradient map in degrees was constructed in Arc GIS using the Shuttle radar topography mission DEM for the research location to examine the gradient's influence on erosion (Figure 4).

Aspect (A_s)

An aspect is a significant feature in erosion since it may be used to figure out the slope's direction. Slopes facing north, for example, are less likely to deteriorate than slopes facing south. Flat, north, northeast, east, southeast, south, west, southwest, and northwest are the nine slope directions as shown in the (Figure 5).

Soil (S_o)

Texture, biological content, foundational substance, porosity, structure, and permeability all have an immediate effect on the capacity of soil to resist erosion. The sort of soil and the texture of the soil are two major aspects that impact an area's ability to retain water and its characteristics for surface infiltration. The research area consisted of five unique soil grades. The final map was categorized based on infiltration capacity, with each type of soil given a distinct weight. The Lower Vellar River comprises a combination of clay loam, clay loam, gravelly loam, and sand and clay dirt, but the rest of the research area includes a mix of soil types (Figure 7).

LULC (L_u)

Land use and cover are the primary determinants of how an individual area's landscape changes. The Landsat-8 LULC map was obtained using supervised classification and organized into eleven groups before being reclassified based on weights into seven classes. Class one agricultural land, for example, has an area of 1508.363 km², class two urban/built-up area has an area of 58.279 km², class three forest land has an area of 31.876 km², class fourth mangrove forest has an area of 8.568 km², class fifth river has an area of 59.266 km², and class sixth water bodies has an area of 87.677 km². The study revealed that classes six and one are the least likely to undergo erosion, but classes three, four, five, seven, and two are estimated to be the most probable.

Precipitation (P_e)

The most striking feature of this is that, despite the coastal regions receiving adequate rainfall from both the northeast and southwest monsoons, the northeast monsoon season (October to December) is thought to be rainier than the southwest monsoon. The precipitation for the rainfall distribution map was created using the Inverse Distance Weighted (IDW) Spatial Analyst tool in Arc GIS 10.8.1. This tool makes use of precipitation information from all rain gauge stations. The rainfall data covers the 31-year period from 1991 to 2022. Rainfall information was collected from the Indian Meteorological Department (IMD). Five classifications are distinguished, as shown in Figure 11.



**Arun Shourie and Ezhisaivallabi****Drainage Density (D_D)**

By eroding sediment deposits, conveying them to water bodies, and depositing them there, the drainage network is an important factor that influences erosion in hilly environments. There are more streams in densely populated places, which increases the likelihood of soil erosion. The DEM was used to outline the drainage system (Figure 6).

Rainfall erosivity (R_E)

The potential for rainfall to contribute to soil erosion from hill slopes owing to water action is characterized as this influencing component. The volume, degree, and rhythm of precipitation all have an influence on erosion. Because high-quality meteorological records for the region were unavailable, computing these figures was seen as an extremely difficult undertaking. In these conditions, a number of empirical models were used to quantify the amount of rainfall based on daily precipitation data, and Figure 12 shows how the link was created by analyzing the precipitation erosivity factor.

Lithology (L_i)

The lithological location is critical in regulating erosional processes. These lithological characteristics of floodplain undulations, gradients, soil types, natural resources, and layers are all unique. The lithofacies shown in Figure 8 were created by the Geological Survey of India using Bhukosh data.

Normalized Difference Water Index (ND_{wi})

This indicates the vegetation's water content, which is defined as the ratio of the erosion severity to the water flow, offered that the frequency of flow is adequate for a given region. This is frequently the result of regional soil and climatic conditions, which govern water availability. Figure 10 was constructed by computing the ratios of the green and Near-infrared red bands in operation land imagery from satellites.

Soil Erosion Susceptibility Classes

From Figure 13 shows the final map showing Lower Vellar watershed susceptibility to soil erosion created using a GIS-based methodology. The resultant layer was categorized into five groups based on the level of intensity of the soil erosion: very low, low, medium, high, and very high. 12.54% (220 km²) and 15.9% (280 km²) of the region have been shown to have extremely modest to low levels of erosion severity. These areas were generally found in valley bottoms, where agriculture and built-up areas predominate. The Lower Vellar River basin has elevations ranging from 0 to 170 meters. Meanwhile, because soil susceptibility to erosion agents is intricately linked to its chemical, biological, and physical properties, the poor results might be explained by the surface roughness of the soil, which is absolutely smooth loamy to loam at lower elevations. Silt, extremely fine sand, and some clayey soils are more erodible than sand, sandy loam, and loamy soils in general because of a degree of forest cover, 21.32% (374 km²) of the region was identified as somewhat susceptible. Despite falling in the intermediate concentrations class because trees cover the majority of the forest area, the forest offers substantial defense against losses through soil erosion and surface runoff. A total of 50.16% (880 km²) of the area was very prone to erosion, which includes high and extremely high-prone zones. This results from the low height and slope of the land. This region is very susceptible to natural calamities, especially floods during the northeast monsoon (October to December), which is the season when floods are most common in this area. Since GIS tools are so time- and money-effective, planners from all over the world have recently emphasized the importance of using them when making decisions in erosion-prone zones. The accuracy of the AHP method depends on the provided weights. The most important discovery, however, was that different researchers' weights and rankings of numerous factors in their studies varied significantly.

CONCLUSION

In order to determine how susceptible various places are to natural disasters, the current study identified Erosion Susceptibility zones as a crucial first step. The Lower Vellar Watershed's erosion susceptibility assessment was carried out using the most efficient and frequently utilized methodology, the MCDM-based AHP model approach.



**Arun Shourie and Ezhisaivallabi**

Since they were less expensive and time-consuming, the research used the analytical hierarchy process (AHP) and GIS methodologies. Elevation, slope, rainfall, Land use/Landover, NDWI, Rainfall, Rainfall erosivity, aspect, lithology, drainage density, and soil type map are just a few of the integrated variables available on ArcGIS Software. As a result, an erosion vulnerability map was created, revealing that 26% of the whole research region has suffered very high, 23% high, 21% moderate, and 15% low erosion levels. In the southernmost part of the study area, these regions are typically located along the coastline. Furthermore, it was found that 26% of the 1754 km² area was likely to experience high levels of erosion. The strategy that was employed yielded data indicating that it's a very efficient and rapid way to evaluate the qualitative characteristics of erosion Vulnerability throughout an enormous area. Planners and politicians can use this methodology in order to implement appropriate conservation measures. The current study makes a substantial contribution to giving authorities and decision-makers a useful forecast for adopting appropriate strategies to reduce possible damages that may result from soil erosion in the Lower Vellar Watershed. Examining current scientific management techniques and creating appropriate, conservative catchment-level procedures are prerequisites for minimizing the magnitude of soil loss. Among the conservation methods provided are urban tree planting, excessive overgrazing management, contour agricultural activities, water conservation systems, flood and erosion prevention strategies, and runoff water collecting system design. Since slope orientation is a macro component or integrating component in the entire erosion process, it is critical to include it while establishing management approaches. In order to reduce soil disturbance on agricultural land, no-till (NT) practices, which entail planting straight to stubble following the previous harvest without cultivating or other cultivating practices typical of traditional agriculture (CT), can be utilized. In comparison with conventional farming, NT practice reduces agricultural labor while also having environmental benefits, such as beneficial erosion risk mitigation due to enhanced structure of the soil and stable plant cover. The practices stated will improve crop yield and soil health in addition to reducing soil loss, thus enhancing local residents' quality of life. Assessments of the susceptibility to soil erosion will always be unreliable because of the inherent uncertainty in the conditioning factors. There may be certain restrictions on the subjectivity of expert evaluation. As a result, in the future, a soft approach or machine learning algorithm may be considered with other crucial conditioning components such as geographical differences in precipitation distribution and periodicity in conjunction with climate change.

REFERENCES

1. Agnihotri, D.; Kumar, T.; Jhariya, D. Intelligent vulnerability prediction of soil erosion hazard in semi-arid and humid region. *Environ. Dev. Sustain.* 2021, 23, pp2524–2551.
2. Al-Rahbi, A.K.H.; Abushammala, M.F.; Qazi, W.A. Application of the analytic hierarchy process for management of soil erosion in Oman. *Int. J. Anal. Hierarchy Process.* 2020, 12, pp 104–116.
3. Aslam, B.; Maqsoom, A.; Alaloul, W.S.; Musarat, M.A.; Jabbar, T.; Zafar, A. Soil erosion susceptibility mapping using a GIS-based multi-criteria decision approach: Case of district Chitral, Pakistan. *Ain Shams Eng. J.* 2021, 12, pp1637–1649.
4. Bosco, C.; de Rigo, D.; Dewitte, O.; Poesen, J.; Panagos, P. Modelling soil erosion at European scale: Towards harmonization and reproducibility. *Nat. Hazards Earth Syst. Sci.* 2015, 15, pp225–245.
5. Borrelli, P.; Paustian, K.; Panagos, P.; Jones, A.; Schütt, B.; Lugato, E. Effect of good agricultural and environmental conditions on erosion and soil organic carbon balance: A national case study. *Land Use Policy* 2016, 50, pp408–421.
6. Boardman, J.; Poesen, J.; Evans, M. Slopes: Soil erosion. *Geol. Soc. Lond. Mem.* 2022, 58, pp 241–255.
7. Borrelli, P.; Robinson, D.A.; Panagos, P.; Lugato, E.; Yang, J.E.; Alewell, C.; Ballabio, C. Land use and climate change impacts on global soil erosion by water (2015–2070). *Proc. Natl. Acad. Sci. USA* 2020, 117, pp21994–22001.
8. Cerdà, A.; Borja, M.E.L.; Úbeda, X.; Martínez-Murillo, J.F.; Keesstra, S. *Pinus halepensis* M. versus *Quercus ilex* subsp. *Rotundifolia* L. runoff and soil erosion at pedon scale under natural rainfall in Eastern Spain three decades after a forest fire. *For. Ecol. Manag.* 2008, 400, pp 447–456.
9. Chen, S.; Liu, W.; Bai, Y.; Luo, X.; Li, H.; Zha, X. Evaluation of watershed soil erosion hazard using





Arun Shourie and Ezhisaivallabi

- combination weight and GIS: A case study from eroded soil in Southern China. *Nat. Hazards* 2021, 109, pp1603–1628.
10. Choi, J.K.; Kim, K.D.; Lee, S.; Won, J.S. Application of a fuzzy operator to susceptibility estimations of coal mine subsidence in Taebaek City, Korea. *Environ. Earth Sci.* 2010, 59, pp1009–1022.
 11. Comino, J.R.; Iserloh, T.; Lassu, T.; Cerdà, A.; Keestra, S.D.; Prosdoci, M.; Ries, J.B. Quantitative comparison of initial soil erosion processes and runoff generation in Spanish and German vineyards. *Sci. Total Environ.* 2016, 565, pp1165–1174.
 12. Dorje Dawa et.al., Identifying Potential Erosion-Prone Areas in the Indian Himalayan Region Using the Revised Universal Soil Loss Equation (RUSLE), *Asian Journal of Water, Environment and Pollution*, Vol. 18, No. 1 (2021), pp. 15-23.
 13. Eltner, A.; Mulso, C.; Maas, H.G. Quantitative measurement of soil erosion from TLS and UAV data. *Int. Arch. Photogramm. Remote Sens. Spat. Inf. Sci.* 2013, 40, pp4–6.
 14. García-Ruiz, J.M.; Beguería, S.; Nadal-Romero, E.; González-Hidalgo, J.C.; Lana-Renault, N.; Sanjuán, Y. A meta-analysis of soil erosion rates across the world. *Geomorphology* 2015, 239, pp160–173.
 15. Kim, K.D.; Lee, S.; Oh, H.J.; Choi, J.K.; Won, J.S. Assessment of ground subsidence hazard near an abandoned underground coalmine using GIS. *Environ. Geol.* 2006, 50, pp1183–1191.
 16. Kundu, S.; Khare, D.; Mondal, A. Landuse change impact on sub-watersheds prioritization by analytical hierarchy process (AHP). *Ecol. Inform.* 2017, 42, pp100–113
 17. Lee, S.; Oh, H.J.; Kim, K.D. Statistical spatial modeling of ground subsidence hazard near an abandoned underground coal mine. *Disaster Adv.* 2010, 3, pp11–12.
 18. Lal Chand Malav et.al, “Mapping of Land degradation vulnerability in the semi – Arid watershed of Rajasthan, India Sustainability 2022, 14, 10198.
 19. Mushtaq, F.; Lala, M.G.N.; Wadood, A. Estimation of soil erosion risk in upper catchment of Wular Lake, Jammu & Kashmir using RUSLE model. *Int. J. Adv. Res. Sci. Eng.* 2018, 7, pp1828–1839.
 20. Ni, J.R.; Li, X.X.; Borthwick, A.G.L. Soil erosion assessment based on minimum polygons in the Yellow River basin, China. *Geomorphology* 2008, 93, pp233–252.
 21. Ouyang, W.; Hao, F.; Skidmore, A.K.; Toxopeus, A.G. Soil erosion and sediment yield and their relationships with vegetation cover in upper stream of the Yellow River. *Sci. Total Environ.* 2010, 409, pp 396–403.
 22. Oh, H.J.; Lee, S. Integration of ground subsidence hazard maps of abandoned coal mines in Samcheok, Korea. *Int. J. Coal Geol.* 2011, 86, pp58–72
 23. Polidori, L.; El Hage, M. Digital elevation model quality assessment methods: A critical review. *Remote Sens.* 2020, 12, pp3522.
 24. Prasuhn, V.; Liniger, H.; Gisler, S.; Herweg, K.; Candinas, A.; Clément, J.P. A high-resolution soil erosion risk map of Switzerland as strategic policy support system. *Land Use Policy* 2013, 32, pp281–291.
 25. Pradeep, G.S.; Krishnan, M.N.; Vijith, H. Identification of critical soil erosion prone areas and annual average soil loss in an upland agricultural watershed of Western Ghats, using analytical hierarchy process (AHP) and RUSLE techniques. *Arab. J. Geosci.* 2015, 8, pp3697–3711.
 26. Pramanik, M.K. Site suitability analysis for agricultural land use of Darjeeling district using AHP and GIS techniques. *Model. Earth Syst. Environ.* 2016, 2, pp1–22.
 27. Pradhan, B.; Lee, S. Utilization of optical remote sensing data and GIS tools for regional landslide hazard analysis by using an artificial neural network model. *Earth Sci. Front.* 2007, 14, pp 143–152.
 28. Rahman, M.R.; Shi, Z.H.; Chongfa, C. Soil erosion hazard evaluation—An integrated use of remote sensing, GIS and statistical approaches with biophysical parameters towards management strategies. *Ecol. Model.* 2009, 220, pp1724–1734.
 29. Raymo, M.E.; Ruddiman, W.F. Tectonic forcing of late Cenozoic climate. *Nature* 1992, 359, pp117–122.
 30. Sandeep, P.; Reddy, G.O.; Jegankumar, R.; Kumar, K.A. Modeling and assessment of land degradation vulnerability in semi-arid ecosystem of Southern India using temporal satellite data, AHP and GIS. *Environ. Model. Assess.* 2021, 26, pp143–154.
 31. Saini, S.S.; Jangra, R.; Kaushik, S.P. Vulnerability assessment of soil erosion using geospatial techniques-A





Arun Shourie and Ezhisaivallabi

- pilot study of uppercatchment of Markanda river. *Int. J. Adv. Remote Sens. GIS Geogr.* 2015, 2, pp 9–21.
32. Singh, G.; Singh, R.M.; Singh, S.; Kumar, A.R.S.; Jaiswal, R.K.; Chandola, V.K.; Nema, A.K. Multi-criteria analytical hierarchical process based decision support system for critical watershed prioritization of Andhiyarkhore catchment. *Indian J. Soil Conserv.* 2019, 47, pp 263–272.
33. Singh, G.; Babu, R.; Narain, P.; Bhushan, L.S.; Abrol, I.P. Soil erosion rates in India. *J. Soil Water Conserv.* 1992, 47, pp 97–99.
34. Stoddart, D.R. World erosion and sedimentation. In *Introduction to Fluvial Processes*; Routledge: Oxfordshire, UK, 2019; pp. 8–29.
35. Swades Pal, Identification of soil erosion vulnerable areas in Chandrabhagariver basin: a multi-criteria decision approach, *Model. Earth Syst. Environ.* (2016) *Model. Earth Syst. Environ.* (2016) Vol 5, pp 1-11.
36. Tirkey, A.S.; Pandey, A.C.; Nathawat, M.S. Use of satellite data, GIS and RUSLE for estimation of average annual soil loss in Daltonganj watershed of Jharkhand (India). *J. Remote Sens. Technol.* 2013, 1, pp20–30.
37. Veihe, A.; Rey, J.; Quinton, J.N.; Strauss, P.; Sancho, F.M.; Somarriba, M. Modelling of event-based soil erosion in Costa Rica, Nicaragua and Mexico: Evaluation of the EUROSEM model. *Catena* 2001, 44, pp187–203.
38. Yüksel, A.; Akay, A.E.; Gundogan, R.; Reis, M.; Cetiner, M. Application of GeoWEPP for determining sediment yield and runoff in the Orcan Creek watershed in Kahramanmaras, Turkey. *Sensors* 2008, 8, pp1222–1236.
39. Yilmaz, I. A case study from Koyulhisar (Sivas-Turkey) for landslide susceptibility mapping by artificial neural networks. *Bull. Eng. Geol. Environ.* 2009, 68, pp297–306.
40. Wu, Q.; Wang, M. A framework for risk assessment on soil erosion by water using an integrated and systematic approach. *J. Hydrol.* 2007, 337, pp11–21.

Table 1 Raw Data utilized in the Research

Sl. No	Datasets	Description	Source	Resolution/scale
1	Elevation (DEM)	SRTM (DEM)	USGS earth explorer https://earthexplorer.usgs.gov/	30 m
2	Landsat Data Continuity Mission -8	Downloaded	USGS earth explorer https://earthexplorer.usgs.gov/	30 m
3	Soil	Digitally preserved the soil map	FAO Soil Data Base on Worldwide. (https://www.fao.org/)	
4	Rainfall	Cuddalore District. Using (IDW)	Indian Meteorological Department (IMD) https://www.imdpune.gov.in/ Institute of Water Studies (IWS)	mm
5	Slope	Derived from Elevation	USGS Earth Explorer https://earthexplorer.usgs.gov/	30 m
6	NDWI	LANDSAT-8 Images	USGS Earth Explorer https://earthexplorer.usgs.gov/	30 m
7	Rainfall erosivity	Based on the Rainfall Factor	Indian Meteorological Department (IMD) https://www.imdpune.gov.in/ Institute of Water Studies (IWS)	mm
8	Aspect	Derived From Elevation	USGS Earth Explorer https://earthexplorer.usgs.gov/	30m





Arun Shourie and Ezhisaivallabi

9	Drainage density	Derived From Elevation	USGS earth explorer https://earthexplorer.usgs.gov/	30 m
10	Lithology	Downloaded as Polygon	Geological Survey of India https://bhukosh.gsi.gov.in/Bhukosh/Public	-

Table 2 Weights for the Pair-Wise Comparison Scale are based on the AHP Scale

Rating of Numerical	Preference of Verbal Judgements
1	Both are advised
2	Identical to fairly
3	Mostly favored
4	Slightly to fiercely
5	Most likely preferable
6	Strongly to diverge Strongly
7	Significantly preferred
8	Incredibly strongly to extremely firmly
9	Exceptionally preferred

Table 3 Comparison of Ten-by-Ten Preference Matrix Combinations

Parameters	Rainfall erosivity	Elevation	Slope	Precipitation	LULC	Lithology	NDWI	Aspect	Drainage Density	Soil Type
Rainfall erosivity	1.0	1.0	1.0	1.0	3.0	5.0	1.0	3.0	1.0	1.0
Elevation	1.0	1.0	1.0	1.0	2.0	3.0	1.0	3.0	1.0	1.0
Slope	1.0	1.0	1.0	1.0	3.0	1.0	1/2	1.0	1.0	1.0
Precipitation	1.0	1.0	1.0	1.0	3.0	2.0	2.0	3.0	1.0	1.0
LULC	1/3	1/2	1/3	1/3	1.0	1.0	1/3	3.0	1.0	1.0
Lithology	15	1/3	1.0	1/2	1.0	1.0	1/5	1.0	1.0	1.0
NDWI	1.0	1.0	2.0	1/2	3.0	5.0	1.0	3.0	1.0	1.0
Aspect	1/3	1/3	1.0	1/3	1/3	1.0	1/3	1.0	1.0	1.0
Drainage Density	1.0	1.0	1.0	1.0	1.0	1.0	1.0	1.0	1.0	1.0
Soil Type	1.0	1.0	1.0	1.0	1.0	1.0	1.0	1.0	1.0	1.0
Sum	7.9	8.2	10.3	7.7	18.3	21.0	8.4	20.0	10.0	10.0

Table 4 Random Index (RI) Value

Size of Matrix (n)	1	2	3	4	5	6	7	8	9	10
Random Index (RI)	0	0	0.58	0.9	1.12	1.24	1.32	1.41	1.45	1.49





Arun Shourie and Ezhisaivallabi

Table 5 Pair-wise Comparison Matrix

Class	Rainfall Erosivity	Elevation	Slope	Rainfall	LULC	Lithology	NDWI	Aspect	Drainage Density	Soil Type	Weight	Weight in Percentage
Rainfall Erosivity	0.13	0.12	0.10	0.13	0.16	0.24	0.12	0.15	0.10	0.10	0.14	13.78
Elevation	0.13	0.12	0.10	0.13	0.11	0.14	0.12	0.15	0.10	0.10	0.12	12.07
Slope	0.13	0.12	0.10	0.13	0.16	0.05	0.06	0.05	0.10	0.10	0.10	9.90
Rainfall	0.13	0.12	0.10	0.13	0.16	0.10	0.24	0.15	0.10	0.10	0.13	13.45
LULC	0.04	0.06	0.03	0.04	0.05	0.05	0.04	0.15	0.10	0.10	0.07	6.62
Lithology	0.03	0.04	0.10	0.07	0.05	0.05	0.02	0.05	0.10	0.10	0.06	5.87
NDWI	0.13	0.12	0.19	0.07	0.16	0.24	0.12	0.15	0.10	0.10	0.14	14.08
Aspect	0.04	0.04	0.10	0.04	0.02	0.05	0.04	0.05	0.10	0.10	0.06	5.59
Drainage Density	0.13	0.12	0.10	0.13	0.05	0.05	0.12	0.05	0.10	0.10	0.09	9.32
Soil Type	0.13	0.12	0.10	0.13	0.05	0.05	0.12	0.05	0.10	0.10	0.09	9.32
Sum	1.00	1.00	1.00	1.00	1.00	1.00	1.00	1.00	1.00	1.00	1.00	100.00

Table 6 Data Sources and Strategies Used in Thematic Layer Preparation

S. No.	Parameter	Data Source	Strategies
1	E _L	SRTM DEM	30 × 30 m Elevation
2	S _L	Digital Elevation model	$\tan \theta = \frac{N * i}{636.6}$ N = No of contour cutting i = Contour interval
3	A _s	Digital Elevation model	$As(p,q) = 1 - \sqrt{2} \frac{b}{k\theta} \sqrt{1 + q + q^2 / (1 - p + q)}$
4	SO	SLUSI	Digitization
5	LULC	Landsat-8	Digitization
6	Precipitation	IMD and IWS Climate Data	IDW METHOD in ArcGIS Tool
7	DD	Digital Elevation model	Spatial Analysis Tool
8	RE	Indian metrological department	RE = 79 + 0.363R
9	LJ	Bhukosh	Clipping the polygon area
10	NDWI	LANDSAT	$NDWI = \frac{(Green - NIR)}{(Green + NIR)}$

Layers of Thematic	Units	Class	Vulnerability Class Scale	Vulnerability Class Gradings
Rainfall Erosivity	MJ.mm/ha.h.yr	420-470	Very minimal	1
		480-510	Low	2
		520-540	Moderate	3
		550-570	High	4
		580-610	Extremely Elevated	5
Elevation	m	0-28	Extremely Elevated	5
		29-55	High	4
		56-79	Moderate	3





Arun Shourie and Ezhisaivallabi

		80-110	Low	2
		120-170	Very minimal	1
		0.36-0.66	High	4
		0.67-1	Moderate	3
		1.1-1.5	Low	2
		1.6-3.9	Very minimal	1
Precipitation	mm/year	930-1000	Very minimal	1
		1100-1200	Low	2
		1200-1300	Moderate	3
		1300-1400	High	4
		1400-1500	Extremely Elevated	5
LULC	Level	Water bodies & River	Extremely Elevated	5
		Agricultural Land	High	4
		Build up Rural & Urban	Moderate	3
		Forest	Low	2
		Mangroves Forest	Very minimal	1
NDWI	Level	-0.4799 – 0.23052	Extremely Elevated	5
		-0.23052 – 0.067	High	4
		-0.067-0.1316	Moderate	3
		0.1317-0.3	Low	2
		0.300-0.6	Very minimal	1
Lithology	Level	Archean-Proterozoic	Extremely Elevated	5
		Quaternary	High	4
		Miocence	Moderate	3
		Late Cretaceous	Low	2
		Late Cretaceous & Miocence	Very minimal	1
Aspect	Level	North	Extremely Elevated	5
		Northwest	High	4
		West	Moderate	3
		South	Low	2
		Southwest	Very minimal	1
Drainage Density	km/km ²	<1	Very minimal	1
		0.37-0.71	Low	2
		0.72-1.10	Moderate	3
		1.20-1.40	High	4
		>2	Extremely	5





Arun Shourie and Ezhisaivallabi

			Elevated	
Soil Type	Level	Clay Loam	Extremely Elevated	5
		Clay	High	4
		Sandy Loam	Moderate	3
		Loam	Low	2
		Sandy Clay Loam	Very minimal	1

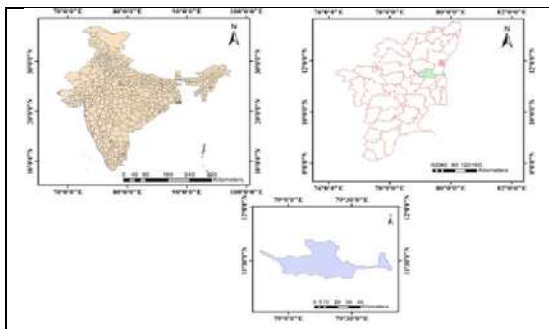


Figure 1 Study area map of Lower Vellar Watershed

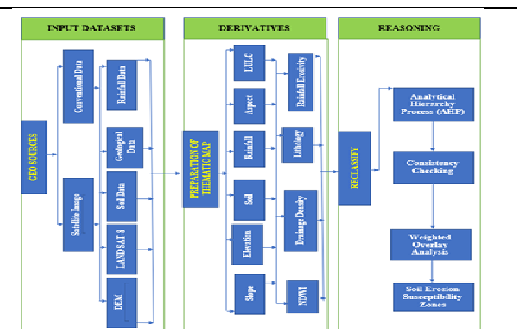


Figure 2 Flow chart of Methodology

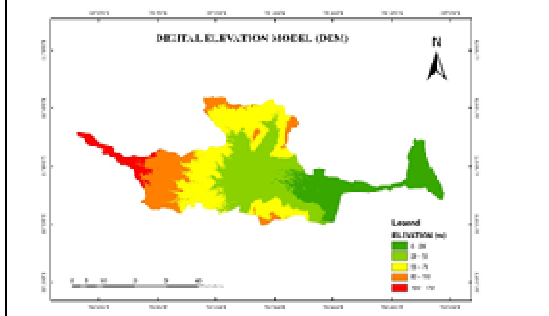


Figure 3 DEM of Lower Vellar Watershed

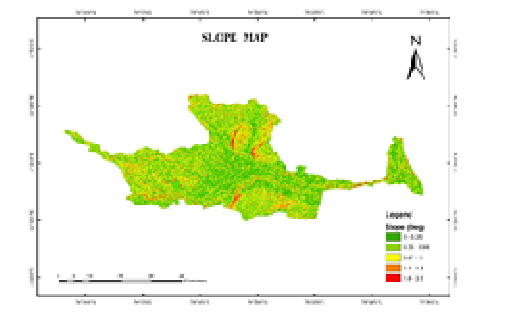


Figure 4 Slope of Lower Vellar Watershed

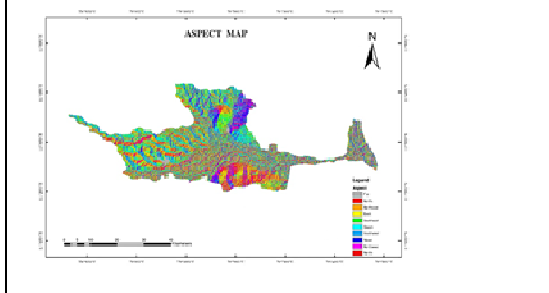


Figure 5 Aspect of Lower Vellar Watershed

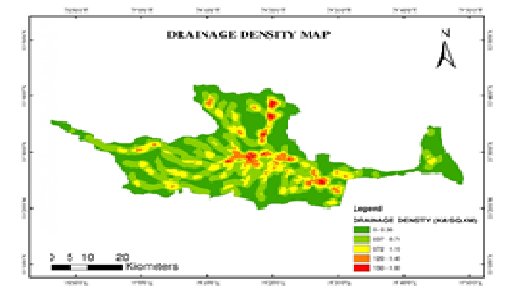


Figure 6 Drainage Density of Lower Vellar Watershed





Arun Shourie and Ezhisaivallabi

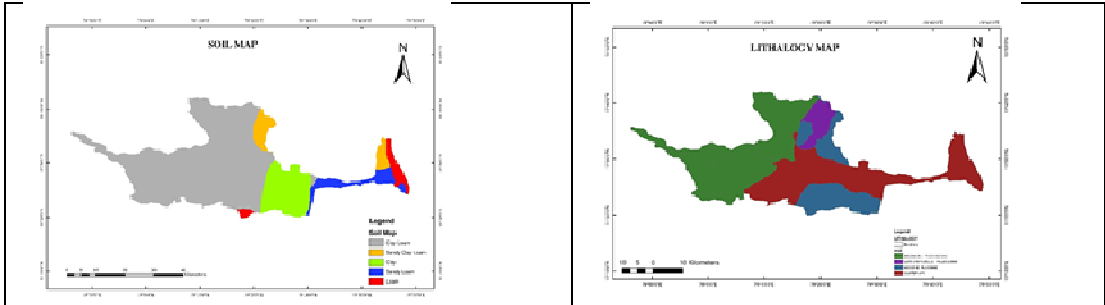


Figure 7 Soil Map of Lower Vellar Watershed

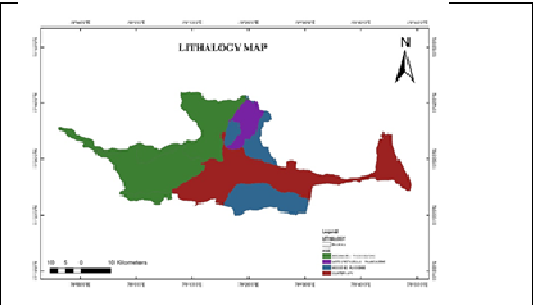


Figure 8 Lithology Map of Lower Vellar Watershed

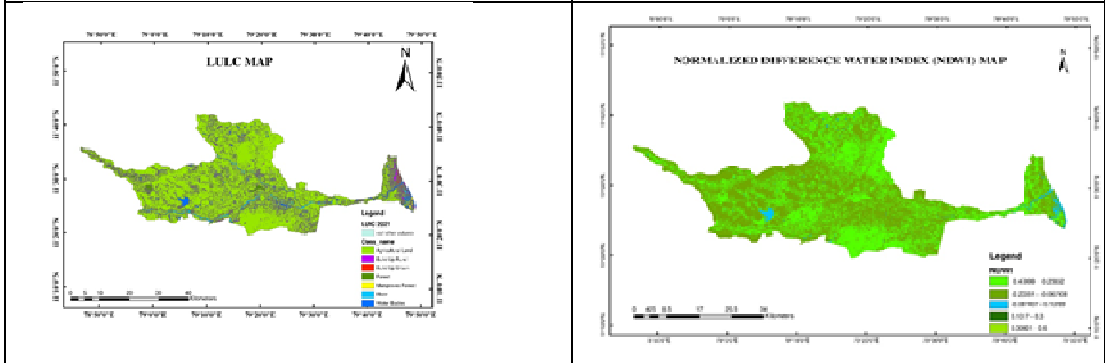


Figure 9 LULC Map of Lower Vellar Watershed

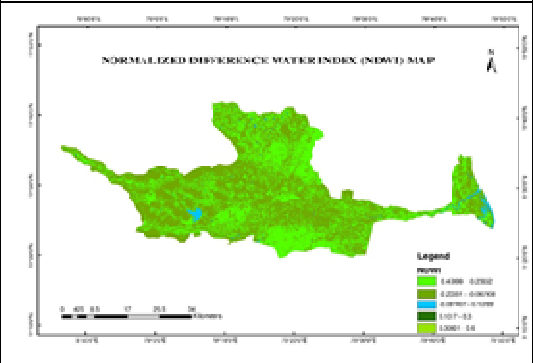


Figure 10 NDWI Map of Lower Vellar Watershed

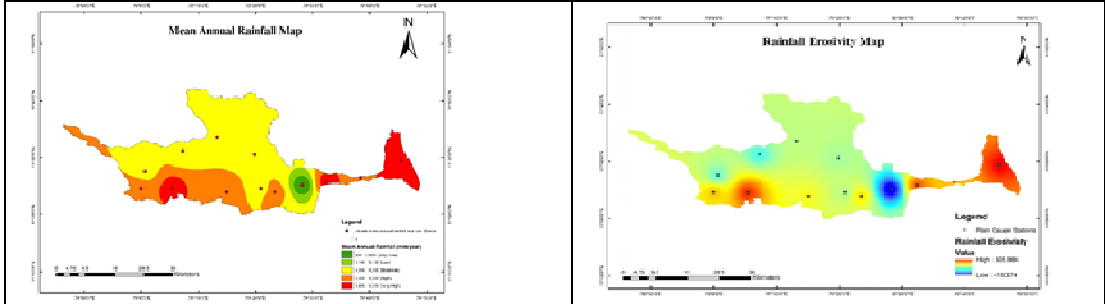


Figure 11 Mean Annual Rainfall Map of Lower Vellar Watershed

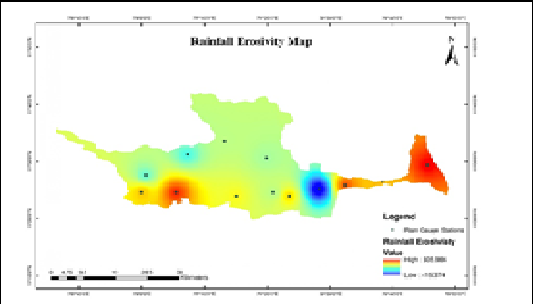


Figure 12 Rainfall Erosivity of Lower Vellar Watershed

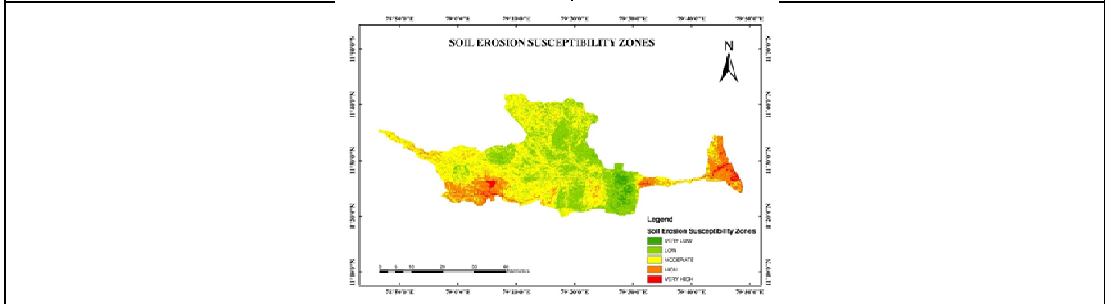


Figure 13 Soil Erosion Susceptibility Zones of Lower Vellar Watershed





A Review on Primary and Novel Approaches of Colon Targeted Drug Delivery Systems

Bhavani Ummuri¹, Y. Srinivasa Rao², S. Satyalakshmi³ and Ketha Srilekhya^{1*}

¹Assistant Professor, Department of Pharmaceutics, Vignan Institute of Pharmaceutical Technology, Visakhapatnam (Affiliated to JNTUGV), Andhra Pradesh, India.

²Professor, Department of Pharmaceutics, Vignan Institute of Pharmaceutical Technology, Visakhapatnam (Affiliated to JNTUGV), Andhra Pradesh, India.

³Assistant Professor, Department of Pharmaceutics, Vignan Institute of Pharmaceutical Technology, Visakhapatnam (Affiliated to JNTUGV), Andhra Pradesh, India.

Received: 02 Sep 2023

Revised: 10 Nov 2023

Accepted: 02 Jan 2024

*Address for Correspondence

Ketha Srilekhya

Assistant Professor,

Department of Pharmaceutics,

Vignan Institute of Pharmaceutical Technology,

Visakhapatnam (Affiliated to JNTUGV),

Andhra Pradesh, India.

Email: srilekhyaketha20@gmail.com



This is an Open Access Journal / article distributed under the terms of the **Creative Commons Attribution License** (CC BY-NC-ND 3.0) which permits unrestricted use, distribution, and reproduction in any medium, provided the original work is properly cited. All rights reserved.

ABSTRACT

Oral administration of different dosage forms is the most common form of administration due to greater patient compliance and flexibility. Targeted drug delivery system is the system in which the dosage form is modified to deliver the drug at the target region or at the disease region. Colon targeted drug delivery systems have received a lot of attention as potential carriers for the local treatment of colonic diseases with fewer systemic side effects, as well as for the improved oral delivery of various therapeutics susceptible to acidic and enzymatic degradation in the upper GI tract. The worldwide pharmaceutical market for biologics has expanded in recent years, and rising demand for a more patient-friendly drug administration system emphasises the relevance of colonic drug delivery as a noninvasive delivery method for macromolecules. Colon-targeted macromolecule drug delivery systems can give therapeutic advantages such as improved patient compliance and cheaper costs. As a result, many ways have been investigated to obtain more efficient colonic drug administration for local or systemic pharmacological effects, including pH-dependent systems, enzyme-triggered systems, receptor-mediated systems, and magnetically-driven systems. Recent advances in diverse techniques for creating colon targeted drug delivery systems and their pharmaceutical applications are reviewed in this review, with a focus on formulation technology.

Keywords: Colon specific drug delivery, Formulation approaches, Novel approaches, Biodegradable polymers.



Ketha Srilekhya *et al.*,

INTRODUCTION

Targeted drug administration into the colon is extremely desirable for the local treatment of a range of bowel disorders such as ulcerative colitis, Crohn's disease, amebiasis, colonic malignancy, local therapy of colonic pathologies, and systemic protein and peptide drug delivery [1, 2]. The colon specific drug delivery system (CDDS) should be capable of protecting the drug en route to the colon, which means that drug release and absorption should not occur in the stomach or small intestine, and the bioactive agent should not be degraded in either dissolution site, but only released and absorbed once the system reaches the colon [3]. The colon is thought to be a suitable absorption site for peptides and protein drugs due to the following factors: (i) less diversity and intensity of digestive enzymes, (ii) comparative proteolytic activity of colon mucosa is much lower than that observed in the small intestine, thus CDDS protects peptide drugs from hydrolysis and enzymatic degradation in the duodenum and jejunum, and eventually releases the drug into the ileum or colon, resulting in greater systemic availability (4). Furthermore, it was preferable because of less discomfort, a lower risk of cross-infection, needlestick injuries, patient acceptability, and convenience of administration. Oral medication delivery methods account for over half of all drug delivery systems on the market [5]. Aside from these benefits, the oral route is not appropriate for the administration of medications for lower gastrointestinal (GI) illnesses; this is owing to their release at the upper GI tract (stomach, small intestine), which further reduces drug accessibility at the lower GI tract [6]. To address this issue, colon-specific medicine delivery devices have been extensively researched during the last two decades. A colonic delivery is defined as the correct delivery of medications into the lower GI tract (by avoiding drug release in the upper GIT, which happens largely in the large intestine) (i.e. colon) [7]. Rectal administration is another method for colon targeting, although it is less pleasant and makes reaching the colon more challenging. Traditional dosage forms employed in the prevention of colon disorders (ulcerative colitis, Crohn's disease, and amoebiasis) are failing because an insufficient quantity of medicine reaches the site of action. The traditional dose form allows the medicine to be absorbed from the upper section of the GIT, i.e., the stomach [8]. The action of traditional dose forms has a significant disadvantage for colonic localised distribution. Thus, for effective and safe therapy, the medicine must be protected from the upper hostile environment [9].

Advantages of CDDS over Conventional Drug Delivery

Glucocorticoids and other anti-inflammatory medications are being used to treat chronic colitis, namely ulcerative colitis and Crohn's disease. Oral and intravenous use of glucocorticoids, including dexamethasone and methyl prednisolone, causes systemic adverse effects such as adreno suppression, immune suppression, cushinoid symptoms, and bone resorption. Thus, medication delivery to the colon selectively might not only minimise the needed dose but also the systemic negative effects induced by large doses [10, 11].

Criteria for Selection of Drug for CDDS

Drugs with low absorption from the stomach or intestine, such as peptides, that are used to treat IBD, ulcerative colitis, diarrhoea, and colon cancer, are suitable candidates for local colon administration. Another aspect that impacts CDDS is the carrier. The choice of carrier for certain pharmaceuticals is determined by the physicochemical characteristics of the substance as well as the ailment for which the system is intended [12]. The chemical composition, stability, and partition coefficient of the medication, as well as the type of absorption enhancer used, all have an impact on carrier selection. Furthermore, the drug carrier of choice is determined by the functional groups of the drug molecule [13]. Aniline or nitro groups on a medicine, for example, might be used to make an azo link with another benzene group. Carriers including additives such as polymers (which can be used as matrices, hydro gels, or coating agents) may have an influence on the release properties and efficacy of the systems [14].

Formulation Approaches for Colon Targeted Drug Delivery

pH Dependent Drug Delivery Systems:

Because the colon has a higher pH than the upper GI tract, it can be employed as a targeting method for colonic medication delivery. As a result, a pH-dependent polymer such as cellulose acetate phthalates (CAP),





Ketha Srilekhya *et al.*,

hydroxypropyl methyl-cellulose phthalate (HPMCP) 50 and 55, and copolymers of methacrylic acid and methyl methacrylate are used to create a colon-targeted drug delivery system [15, 16]. The ideal polymer should be able to tolerate the low pH of the stomach and proximal small intestine while being dissolved by the terminal ileum and colon. As a result, drug delivery systems coated with pH-dependent polymers with a solubility threshold of pH 6.0-7.0 should delay drug breakdown and avoid premature drug release in the upper GI tract before reaching colonic locations [17]. However, due to substantial inter- and intra-subject variability in crucial factors such as pH, fluid volumes, GI transit durations, and motility, this pH-dependent device has showed significant variability in drug release and failure in vivo [18]. Furthermore, nutrition, illness status, water consumption, and microbial metabolism can all drastically affect GI tract pH ranges. Patients with ulcerative colitis, for example, have higher acidic intestinal pH than healthy people, resulting in inadequate medication release from enteric coated systems at the target location [19, 20]. To circumvent this restriction of pH-dependent delivery systems, attempts have been made to combine pH-dependent delivery systems with other delivery systems such as time-dependent systems and enzyme-triggered systems. Eudragit® S, for example, was combined with high-amylose maize starch for the integration of pH-dependent and colonic microbial degrading processes [21]. Eudracol® is another example of a multi-unit technology that provides delayed and consistent medication release to the colon. This technique is based on covering the pellet with Eudragit® RL/RS and Eudragit® FS 30D, which provides pH- and time-dependent drug release in the colon [22].

Polymer-Based Nano-/Micro-Particles

Many studies have shown that pH-dependent polymeric nanoparticles are successful as colonic drug delivery vehicles. Mutalik *et al* [23]. developed a new pH-sensitive hydrolyzed polyacrylamide-grafted-xanthan gum (PAAm-g-XG) for colon-targeted administration of curcumin nanoparticles. The amount of medication released from PAAm-g-XG-modified nanoparticles was small under acidic circumstances (pH 1.2 and 4.5), but it was quicker and greater at pH 7.2 [24, 25]. As a result, the nanoparticles were efficient in reducing intestinal inflammation and promoting weight reduction in IBD rat models. Furthermore, a mixed combination of two separate pH-sensitive polymers can be utilised to modulate the rate of medication release. Sahu and Pandey created HBsAg-loaded nanoparticles for successful colonic immunisation by combining Eudragit® L100 and Eudragit® S100, proving the effective dispersion of nanoparticles at the colon as well as the increased immune response [26].

Lipid-Based Formulations

Liposomes are a very effective medication delivery mechanism made up of double-layered phospholipids. Liposomes are biodegradable, biocompatible, and may contain both hydrophilic and lipophilic medicines. Liposome surfaces can be coated with pH-dependent polymers to prevent liposome disintegration under acidic circumstances, as well as ligands to increase site-specificity. Zhao *et al.*, for example, created colon-targeted liposomal formulations for sorafenib by covering anionic liposome surfaces with glycol chitosan and pH-dependent Eudragit® S100. These liposomes demonstrated good stability at acidic and neutral pHs with negligible drug leakage, increasing sorafenib systemic exposure in rats [27]. SMEDDS offer enormous potential for improving the oral bioavailability of many hydrophobic medicines, which might be beneficial in the design of colon-targeted drug delivery systems [28-30].

Tablets and Capsules

Despite the fact that, there are few commercially available products like film coated tablets or capsules can be used to deliver drugs to the colon. This technique is suitable to both macromolecules and low molecular weight synthesised medicines. Crowe *et al.* have created Eudragit L100-coated tablets for the colonic administration of a new anti-tumor necrosis factor domain antibody (V565). This tablet demonstrated sustained drug release at pH 6, but no drug release over a 2-hour acidic incubation period. In vivo monkey studies also indicated the persistent release of V565 in the colon for topical IBD therapy [31]. Furthermore, the pH-dependent system's site-specific drug release is influenced by variations in GI fluid composition, eating state, and GI transit duration. As a result, ongoing attempts have been made to increase targeting efficacy using multi-unit formulations based on the combination of several mechanism-based systems with pH-dependent coating [32]. Park *et al.*, for example, created a bisacodyl-loaded multi-unit tablet by coating it with various pH-dependent polymers (Eudragit S and Eudragit L) and time-dependent polymers





Ketha Srilekhya et al.,

(Eudragit RS) [33]. Because it is resistant to low pH settings, zein is a possible carrier for controlled-release solid dispersion systems delivering poorly water soluble medicines to the colon. A single-layer film coating of tablets employing biopolymer Zein in conjunction with Kollicoat® MAE 100P recently demonstrated strong potential to inhibit drug release in the upper GI tract for delayed drug release in the colon [34]. The coating component ratio and coating layer thickness both have an impact on the performance of coated tablets for colonic medication administration [35]. New coating technology has been intensively pursued in recent years to increase the targeting efficacy of pH-dependent delivery systems [36]. ColoPulse technology, for example, is a revolutionary pH sensitive coating technique that includes a super-disintegrant into the coating matrix to expedite disintegration at the target spot [37].

Enzyme-Sensitive Drug Delivery Systems

Polysaccharide-Based Systems

Because of the sudden rise in microbiota and the related enzyme activity in the lower GI tract, crobiota-activated delivery methods have showed promise in colon-targeted medication delivery. These methods rely on colonic bacteria's particular enzyme activity and polymers degradable by colonic microorganisms. Polysaccharides, in particular, pectin, guar gum, inulin, and chitosan, have been employed in colon-targeted drug delivery systems because they may keep their integrity in the upper GI tract while being metabolised by colonic bacteria to release the entrapped medication [38]. Rides can improve medication intake by allowing for extended contact between the mucosal surface and drug delivery carriers. Polysaccharide-based delivery methods provide additional advantages such as large-scale availability, cheap cost, low toxicity and immunogenicity, good biocompatibility, and biodegradability [39]. Furthermore, the limited solubility of most organic solvents restricts hydrophilicity and high water solubility of polysaccharides may promote early and undesired medication release in the upper GI tract, As a result, cross-linking agents are frequently utilised to address this problem [40]. Furthermore, the absence of the propensity of polysaccharides to form films, as well as their swelling and solubility, restricts their use for colonic medication administration [41].

Phloral® Technology

Ibekwe et al. described a revolutionary colonic coating technique that combined pH-dependent and bacterially-activated systems in a single layer matrix film. Eudragit S and biodegradable polysaccharide were used to film-coat the tablets. A gamma scintigraphy research in human volunteers demonstrated that these tablets disintegrated consistently in the colon independent of eating state, implying that this dual-mechanism coating may overcome the limitations of single trigger systems and improve colonic medication targeting [42]. Even if the pH-dependent polymer's dissolving threshold is not achieved, the enzyme-sensitive component is digested independently by enzymes released by intestinal microbiota. The incorporation of this fail-safe mechanism overcomes the constraints of traditional pH-dependent systems. In clinical tests, this new technique has been proven for consistent medication release with little intra-subject variability in patients and healthy participants [43, 44].

Ligand/Receptor-Mediated Drug Delivery System

For a more effective local therapy of colonic illness with less hazardous side effects, ligand/receptor-mediated systems that improve target specificity through the interaction of targeted ligands on the carrier surface and particular receptors expressed at disease locations have been investigated. Various ligands (e.g., antibodies, peptides, folic acid, and hyaluronic acids) can be used to create ligand/receptor-mediated systems based on the functional expression patterns of certain receptors/proteins at target cells or organs [45].

Folic Acid

Because the folate receptor is over expressed in many forms of cancer, folic acid, a water-soluble vitamin, is a tumor-selective targeting ligand. Numerous studies have shown that nano particles coated with folic acid can improve tumor-selective medication absorption [46]. Xiong et al., for example, demonstrated that folic acid-conjugated liposomes increased daunorubicin anti-cancer effectiveness by enhancing folate receptor-mediated drug absorption [47]. Zhang et al. have previously studied a folate-modified self-micro emulsifying drug delivery system (FSMEDDS)





Ketha Srilekhya *et al.*,

using curcumin to improve drug solubility and transport to the colon. Their findings demonstrated that an FSMEDDS could efficiently enter the colon and promptly release its pharmacological payload. Furthermore, the FSMEDDS formulation may aggressively target tumour cells over expressing folate receptors, indicating that an FSMEDDS could be a suitable carrier for curcumin delivery in the colon [48].

Hyaluronic Acid

Hyaluronic acid (HA) is a natural polysaccharide composed of d-glucuronic acid disaccharide units and N-acetyl-d-glucosamine. Because HA has a high affinity for the CD44 receptor, which is over expressed in many malignancies, HA-conjugated drug delivery systems have been investigated for target-specific drug administration. For example, earlier research have studied the effectiveness of HA-modified mesoporous silica nano particles targeting the CD44-overexpressing cancer cells [49]. Vafaei et colleagues created self-assembled HA nano particles as budesonide colonic carriers for targeting inflamed intestinal mucosa. Budesonide-loaded HA nano particles were taken up more readily by inflammatory cells over-expressing CD44 receptors, resulting in a reduction in IL-8 and TNF- production in an inflamed cell model. As a result, HA-conjugated nano particles promise to be an appealing targeted drug delivery strategy for the treatment of IBD [50].

Peptides

Peptide is gaining popularity as a possible ligand for targeted medication delivery. Peptides have several advantages, including biocompatibility, low cost, chemical variety, and stimulus responsiveness. Furthermore, peptide ligands have substantially better binding affinity and specificity than small molecule ligands due to their wide binding surfaces with receptors [51, 52]. Ren et al., for example, evaluated the use of a synthetic 12-residue peptide (TWYKIAFQRNRK, TK peptide) for colon-specific medication delivery. TK has a strong affinity for integrin $\alpha 6 \beta 1$, a subtype of integrin that is over expressed in human colon cancer cells. As a result, as a targeting ligand, the TK peptide was coupled to doxorubicin-loaded PEG-PLA micelles. This TK-conjugated micelle had much higher cytotoxicity and penetrated tumour spheroids more efficiently, indicating that TK peptide is a potential targeting ligand for colon-targeted treatment [53]. The results from in vitro and in vivo evaluation suggest that CS-CPP NPs may be an effective colon-specific drug delivery system to improve the oral absorption of proteins and peptides.

Magnetically-Driven Drug Delivery System

Magnetic micro carriers, which include magnetic microspheres, magnetic nano particles, magnetic liposomes, and magnetic emulsions, are new formulations for controlled and targeted medication delivery. Grifantini et al developed two different novel drug delivery systems with magnetic properties to improve the targeted treatment of colorectal cancer by mAb198.3 (a FAT1-specific monoclonal antibody), where mAb198.3 was directly bound to super-paramagnetic nano particles or embedded into human erythrocyte-based magnetised carriers. Both approaches were shown to be extremely successful at targeting colon cancer cells and preventing cancer development at much lower antibody concentrations [54]. This nano device was made up of hydrocortisone-loaded magnetic mesoporous silica micro particles. The drug-loaded nano particles' outer surface was functionalized with a bulky azo derivative containing urea moieties. The nano devices remained capped at neutral pHs, however the addition of sodium dithionite caused a considerable payload release because it weakened the azo bonds in the capping joint. They also saw greater effectiveness in rats wearing magnetic belts, especially when a magnetic field was administered externally to extend the retention period in the areas of interest [55]. This study found that using a magnetic belt improves therapeutic effectiveness in the treatment of IBD by increasing drug retention time in the colon. Kono et al. have created magnetically-directed cell delivery systems using RAW264 murine macrophage-like cells and super paramagnetic iron oxide nano particles (SPIONs) and plasmid DNA (pDNA) [56].

Newly Developed Approaches for CDDS

Pressure Controlled Drug-Delivery Systems

The colon experiences higher pressures than the small intestine due to peristalsis. Takaya et al. created water-insoluble pressure-controlled colon-delivery capsules out of ethyl cellulose. Drug release happens in such systems as a result of pressure in the colon's lumen causing the breakdown of a water-insoluble polymer capsule. The thickness





Ketha Srilekhya *et al.*,

of the ethyl cellulose membrane is the most essential element in formulation disintegration. The mechanism appeared to be affected by capsule size and density as well. The viscosity of luminal material is greater in the colon than in the small intestine due to re absorption of water from the colon. As a result, it has been determined that medication breakdown in the colon may provide a challenge for colon-specific oral drug delivery systems. The medicine is in liquid form in pressure controlled ethyl cellulose single unit capsules [57].

Novel Colon Targeted Delivery System

CODESTM is a one-of-a-kind CDDS technology that was created to circumvent the inherent issues that come with pH or time-dependent systems. CODESTM is a hybrid of pH-dependent and microbially induced CDDS. It was created by employing a novel method incorporating lactulose, which serves as a trigger for site-specific drug release in the colon. The system comprises of a typical lactulose tablet core that is over coated with an acid soluble substance, Eudragit E, and then over coated with an enteric material, Eudragit L.

Osmotic Controlled Drug Delivery (ORDS-CT)

The OROS-CT (Alza company) can be used to focus drugs locally to the colon for illness therapy or to achieve systemic absorption that would otherwise be impossible [58]. OROSCT systems can be as simple as a single osmotic unit or as complex as 5-6 push-pull units, each 4 mm in diameter and enclosed within a hard gelatin capsule. Each bilayer push pull unit is made up of an osmotic push layer and a drug layer that are both enclosed by a semi permeable membrane. Next to the drug layer, a hole is bored through the membrane. The gelatin capsule holding the push-pull units melts immediately after the OROSCT is eaten. Each push-pull unit is prevented from absorbing water in the acidic aqueous environment of the stomach due to its drug-impermeable enteric coating, and hence no medicine is administered [59].

CONCLUSION

The colonic area of the GIT has grown in importance as a location for medication administration and absorption. In terms of both local and systemic therapy, CDDS provides significant therapeutic benefits to patients. Systems that use natural materials destroyed by intestinal bacterial enzymes are more likely to achieve colon specificity. Given the sophistication of colon-specific drug delivery systems and the uncertainty of current dissolution methods in establishing possible in-vitro/in-vivo correlations, pharmaceutical scientists face challenges in developing and validating a dissolution method that incorporates physiological features of the colon while also being applicable in an industry setting for CDDS evaluation.

ACKNOWLEDGEMENT

We are thankful to the management of VIPT for providing support to carry out this work.

REFERENCES

1. Philip AK, Dabas S, Pathak K. Optimized prodrug approach: a means for achieving enhanced anti-inflammatory potential in experimentally induced colitis. *J Drug Target* 2009 Apr;17(3):235-241.
2. Oluwatoyin AO, John TF. In vitro evaluation of khaya and albizia gums as compression coating for drug targeting to the colon. *J Pharm Pharmacol* 2005;57:63-168.
3. Akala EO, Elekwachi O, Chase V, Johnson H, Lazarre M, Scott K. Organic redox-initiated polymerization process for the fabrication of hydrogels for colon-specific drug delivery. *Drug Dev Ind Pharm* 2003 Apr;29(4):375-386
4. Chourasia MK, Jain SK. Pharmaceutical approaches to colon targeted drug delivery systems. *J Pharm Pharm Sci* 2003 Jan-Apr;6(1):33-66.
5. Bhalersao SD and Mahaparale PR: Different approaches to colon drug delivery systems. *International Journal of Research and Reviews in Applied Sciences* 2012; 2(3): 529-549.



**Ketha Srilekhya et al.,**

6. Asija R, Chaudhari B and Aseeja S: Oral colon targeted drug delivery system: current and novel perspectives. *Journal of Pharmaceutical and Scientific Innovation* 2012; 1(5): 6-12.
7. Mehta TJ, Patel AD, Patel MR and Patel NM: Need for colon-specific drug delivery system: primary and novel approaches. *International Journal of Pharmaceutical Research and Development* 2011; 3(1): 134-15.
8. Jawalkoti SP, Jadhav PD, Mane SV and Khade MM: Colon targeted drug delivery system. *International Journal of Pharmaceutical Research and Bioscience* 2013; 2(2): 122-136.
9. Patel A, Bhatt N, Patel KR, Patel NM and Patel MR: Colon targeted drug delivery system. *Journal of Pharmaceutical and Biosciences* 2011; 1(1): 37-49.
10. Kulkarni SK. Pharmacology of gastro-intestinal tract (GIT). In: Kulkarni SK. editor, *Handbook of experimental pharmacology*. New Delhi: Vallabh Prakashan; 1999; 148-150.
11. McLeod AD, Friend DR, Tozer TN. Gluco corticoid-dextran conjugates as potential prodrugs for colon-specific delivery: hydrolysis in rat gastrointestinal tract contents. *J Pharm Sci* 1994 Sep;83(9):1284-1288.
12. Vyas SP, Khar RK. Gastroretentive systems. In: Vyas SP, Khar RK, editors. *Controlled drug delivery: concepts and advances*. New Delhi: Vallabh Prakashan, 2005; 218-253.
13. Friend DR, Chang GW. A colon-specific drug-delivery system based on drug glycosides and the glycosidases of colonic bacteria. *J Med Chem* 1984 Mar;27(3):261-266
14. Vyas SP, Khar RK. Gastroretentive systems. In: Vyas SP, Khar RK, editors. *Controlled drug delivery: concepts and advances*. New Delhi: Vallabh Prakashan, 2005; 218-253.
15. Newton, A.; Prabakaran, L.; Jayaveera, K. Pectin-HPMC E15LV vs. pH sensitive polymer coating films for delayed drug delivery to colon: A comparison of two dissolution models to assess colonic targeting performance in-vitro. *Int. J. Appl. Res. Nat. Prod.* 2012, 5, 1-16.
16. Nidhi; Rashid, M.; Kaur, V.; Hallan, S.S.; Sharma, S.; Mishra, N. Microparticles as controlled drug delivery carrier for the treatment of ulcerative colitis: A brief review. *Saudi Pharm. J.* 2016, 24, 458-472.
17. Maroni, A.; Zema, L.; Loreti, G.; Palugan, L.; Gazzaniga, A. Film coatings for oral pulsatile release. *Int. J. Pharm.* 2013, 457, 362-371. [CrossRef] [PubMed]
18. Maroni, A.; Moutaharrik, S.; Zema, L.; Gazzaniga, A. Enteric coatings for colonic drug delivery: State of the art. *Expert Opin. Drug Deliv.* 2017, 14, 1027-1029.
19. Maroni, A.; Moutaharrik, S.; Zema, L.; Gazzaniga, A. Enteric coatings for colonic drug delivery: State of the art. *Expert Opin. Drug Deliv.* 2017, 14, 1027-1029.
20. Bak, A.; Ashford, M.; Brayden, D.J. Local delivery of macromolecules to treat diseases associated with the colon. *Adv. Drug Deliv. Rev.* 2018, 136-137, 2-27
21. Ibekwe, V.C.; Khela, M.K.; Evans, D.F.; Basit, A.W. A new concept in colonic drug targeting: A combined pH-responsive and bacterially-triggered drug delivery technology. *Aliment. Pharmacol. Ther.* 2008, 28, 911-916
22. Patel, M.M. Cutting-edge technologies in colon-targeted drug delivery systems. *Expert Opin. Drug Deliv.* 2011, 8, 1247-1258
23. Zeeshan, M.; Ali, H.; Khan, S.; Khan, S.A.; Weigmann, B. Advances in orally-delivered pH-sensitive nanocarrier systems; an optimistic approach for the treatment of inflammatory bowel disease. *Int. J. Pharm.* 2019, 558, 201-214.
24. Ma, X.; Williams, R.O. Polymeric nanomedicines for poorly soluble drugs in oral delivery systems: An update. *J. Pharm. Investig.* 2018, 48, 61-75.
25. Mutalik, S.; Suthar, N.A.; Managuli, R.S.; Shetty, P.K.; Avadhani, K.; Kalthur, G.; Kulkarni, R.V.; Thomas, R. Development and performance evaluation of novel nanoparticles of a grafted copolymer loaded with curcumin. *Int. J. Biol. Macromol.* 2016, 86, 709-720
26. Sahu, K.K.; Pandey, R.S. Development and characterization of HBsAg-loaded Eudragit nanoparticles for effective colonic immunization. *Pharm. Dev. Technol.* 2019, 24, 166-175.
27. Zhao, M.; Lee, S.H.; Song, J.G.; Kim, H.Y.; Han, H.K. Enhanced oral absorption of sorafenib via the layer-by-layer deposition of a pH-sensitive polymer and glycol chitosan on the liposome. *Int. J. Pharm.* 2018, 544, 14-20.
28. Madhav, K.V.; Kishan, V. Self microemulsifying particles of loratadine for improved oral bioavailability: Preparation, characterization and in vivo evaluation. *J. Pharm. Investig.* 2018, 48, 497-508.



**Ketha Srilekhya et al.,**

29. Ahsan, M.N.; Verma, P.R.P. Enhancement of in vitro dissolution and pharmacodynamic potential of olanzapine using solid SNEDDS. *J. Pharm. Investig.* 2018, 48, 269–278.
30. Zhang, L.; Zhu, W.; Yang, C.; Guo, H.; Yu, A.; Ji, J.; Gao, Y.; Sun, M.; Zhai, G. A novel folate-modified self-microemulsifying drug delivery system of curcumin for colon targeting. *Int. J. Nanomed.* 2012, 7, 151–162.
31. Crowe, J.S.; Roberts, K.J.; Carlton, T.M.; Maggiore, L.; Cubitt, M.F.; Ray, K.P.; Donnelly, M.C.; Wahlich, J.C.; Humphreys, J.I.; Robinson, J.R.; et al. Oral delivery of the anti-tumor necrosis factor alpha domain antibody, V565, results in high intestinal and fecal concentrations with minimal systemic exposure in cynomolgus monkeys. *Drug Dev. Ind. Pharm.* 2019, 45, 387–394.
32. Lin, C.; Ng, H.L.; Pan, W.; Chen, H.; Zhang, G.; Bian, Z.; Lu, A.; Yang, Z. Exploring different strategies for efficient delivery of colorectal cancer therapy. *Int. J. Mol. Sci.* 2015, 16, 26936–26952.
33. Park, H.J.; Jung, H.J.; Ho, M.J.; Lee, D.R.; Cho, H.R.; Choi, Y.S.; Jun, J.; Son, M.; Kang, M.J. Colon-targeted delivery of solubilized bisacodyl by doubly enteric-coated multiple-unit tablet. *Eur. J. Pharm.* 2017, 102, 172–179.
34. Nguyen, M.N.U.; Vo, T.V.; Tran, P.H.L.; Tran, T.T.D. Zein-based solid dispersion for potential application in targeted delivery. *J. Pharm. Investig.* 2017, 47, 357–364. [CrossRef]
35. Nguyen, M.N.U.; Tran, P.H.L.; Tran, T.T.D. A single-layer film coating for colon-targeted oral delivery. *Int. J. Pharm.* 2019, 559, 402–409.
36. Maurer, J.M.; Schellekens, R.C.; van Rieke, H.M.; Wanke, C.; Iordanov, V.; Stellaard, F.; Wutzke, K.D.; Dijkstra, G.; van der Zee, M.; Woerdenbag, H.J.; et al. Gastrointestinal pH and transit time profiling in healthy volunteers using the IntelliCap system confirms ileo-colonic release of ColoPulse tablets. *PLoS ONE* 2015, 10, e0129076.
37. Gareb, B.; Dijkstra, G.; Kosterink, J.G.W.; Frijlink, H.W. Development of novel zero-order release budesonide tablets for the treatment of ileo-colonic inflammatory bowel disease and comparison with formulations currently used in clinical practice. *Int. J. Pharm.* 2019, 554, 366–375.
38. Kotla, N.G.; Rana, S.; Sivaraman, G.; Sunnapu, O.; Vemula, P.K.; Pandit, A.; Rochev, Y. Bioresponsive drug delivery systems in intestinal inflammation: State-of-the-art and future perspectives. *Adv. Drug Deliv. Rev.* 2019, 146, 248–266.
39. Barclay, T.G.; Day, C.M.; Petrovsky, N.; Garg, S. Review of polysaccharide particle-based functional drug delivery. *Carbohydr. Polym.* 2019, 221, 94–112.
40. Jain, V.; Shukla, N.; Mahajan, S. Polysaccharides in colon specific drug delivery. *J. Transl. Sci.* 2015, 1, 3–11.
41. Wen, Y.; Oh, J.K. Recent strategies to develop polysaccharide-based nanomaterials for biomedical applications. *Macromol. Rapid. Commun.* 2014, 35, 1819–1832.
42. Ibekwe, V.C.; Khela, M.K.; Evans, D.F.; Basit, A.W. A new concept in colonic drug targeting: A combined pH-responsive and bacterially-triggered drug delivery technology. *Aliment. Pharmacol. Ther.* 2008, 28, 911–916.
43. Ranmal, S.R.; Yadav, V.; Basit, A.W. Targeting the end goal: Opportunities & innovations in colonic drug delivery. *ONdrugDelivery Mag.* 2017, 77, 22–26.
44. D'Haens, G.R.; Snadborn, W.J.; Zou, G.; Stitt, L.W.; Rutgeerts, P.J.; Gilgen, D.; Jairath, V.; Hindryckx, P.; Shackelton, L.M.; Vandervoort, M.K.; et al. Randomised non-inferiority trial: 1600 mg versus 400 mg tablets of mesalazine for the treatment of mild-to-moderate ulcerative colitis. *Aliment. Pharmacol. Ther.* 2017, 46, 292–302.
45. Si, X.Y.; Merlin, D.; Xiao, B. Recent advances in orally administered cell-specific nanotherapeutics for inflammatory bowel disease. *World J. Gastroenterol.* 2016, 22, 7718–7726.
46. Shia, J.; Klimstra, D.S.; Nitzkorski, J.R.; Low, P.S.; Gonen, M.; Landmann, R.; Weiser, M.R.; Franklin, W.A.; Prendergast, F.G.; Murphy, L.; et al. Immunohistochemical expression of folate receptor alpha in colorectal carcinoma: Patterns and biological significance. *Hum. Pathol.* 2008, 39, 498–505.
47. Xiong, S.; Yu, B.; Wu, J.; Li, H.; Lee, R.J. Preparation, therapeutic efficacy and intratumoral localization of targeted daunorubicin liposomes conjugating folate-PEG-CHEMS. *Biomed. Pharmacother.* 2011, 65, 2–8.
48. Zhang, L.; Zhu, W.; Yang, C.; Guo, H.; Yu, A.; Ji, J.; Gao, Y.; Sun, M.; Zhai, G. A novel folate-modified self-microemulsifying drug delivery system of curcumin for colon targeting. *Int. J. Nanomed.* 2012, 7, 151–162.
49. Vafaei, S.Y.; Esmaili, M.; Amini, M.; Atyabi, F.; Ostad, S.N.; Dinarvand, R. Self assembled hyaluronic acid nanoparticles as a potential carrier for targeting the inflamed intestinal mucosa. *Carbohydr. Polym.* 2016, 144, 371–381.





Ketha Srilekhya et al.,

50. Ghosh, D.; Peng, X.; Leal, J.; Mohanty, R. Peptides as drug delivery vehicles across biological barriers. *J. Pharm. Investig.* 2018, 48, 89–111.

51. Jiang, Z.; Guan, J.; Qian, J.; Zhan, C. Peptide ligand-mediated targeted drug delivery of nanomedicines. *Biomater. Sci.* 2019, 7, 461–471.

52. Al-azzawi, S.; Masheta, D. Designing a drug delivery system for improved tumor treatment and targeting by functionalization of a cell-penetrating peptide. *J. Pharm. Investig.* 2019, 49, 643–654.

53. Ren, Y.; Mu, Y.; Song, Y.; Xie, J.; Yu, H.; Gao, S.; Li, S.; Peng, H.; Zhou, Y.; Lu, W. A new peptide ligand for colon cancer targeted delivery of micelles. *Drug Deliv.* 2016, 23, 1763–1772

54. Grifantini, R.; Taranta, M.; Gherardini, L.; Naldi, I.; Parri, M.; Grandi, A.; Giannetti, A.; Tombelli, S.; Lucarini, G.; Ricotti, L.; et al. Magnetically driven drug delivery systems improving targeted immunotherapy for colon-rectal cancer. *J. Control. Release* 2018, 280, 76–86.

55. Teruel, A.H.; Pérez-Esteve, É.; González-Álvarez, I.; González-Álvarez, M.; Costero, A.M.; Ferri, D.; Parra, M.; Gaviña, P.; Merino, V.; Martínez-Mañez, R.; et al. Smart gated magnetic silica mesoporous particles for targeted colon drug delivery: New approaches for inflammatory bowel diseases treatment. *J. Control. Release* 2018, 281, 58–69

56. Kono, Y.; Gogatsubo, S.; Ohba, T.; Fujita, T. Enhanced macrophage delivery to the colon using magnetic lipoplexes with a magnetic field. *Drug Deliv.* 2019, 26, 935–943.

57. Hay DJ, Sharma H, Irving MH. Spread of steroid-containing foam after intrarectal administration. *Br Med J* 1979 Jun;1(6180):1751-1753

58. Theeuwes F, Guittard G, Wong P. Delivery of drugs to colon by oral dosage forms. U. S. Patent, 4904474

59. Swanson D, Barclay B, Wong P, Theeuwes F. Nifedipine gastrointestinal therapeutics system. *Am J Med* 1987;8(6):3 .

Table 1: Colon targeting diseases, drugs and sites

Target Sites	Disease conditions	Drug and active agents
Topical action	Inflammatory Bowel diseases, Irritable bowel disease and Crohn’s disease, Chronic pancreatitis	Hydrocortisone, Budesonide, Prednisolone, Sulfasalazine Olsalazine, Mesalazine Balsalazide.
Local action	Pancreatotomy and cystic fibrosis, Colorectal cancer	Digestive enzyme Supplements 5-Flourouracil,
Systemic action	To prevent gastric irritation To prevent first pass metabolism of orally ingested drugs Oral delivery of peptides Oral delivery of vaccines	NSAIDS Steroids Insulin Typhoid

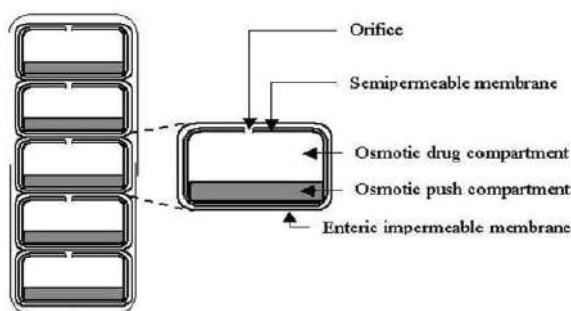


Fig 1: Cross Section of oros-ct colon targeted drug delivery system





Modelling $M^x/G/1$ Queueing System with Optional Second Service under Disaster and Repairs with Non Terminating Vacation

S.Jeyakumar¹ and B.Logapriya^{2*}

¹Assistant Professor, Department of Mathematics, Government Arts College,(Affiliated to Bharathiar University) Coimbatore, Tamil Nadu, India.

²Assistant Professor, Department of Science and Humanities, Sri Krishna College of Engineering and Technology (Affiliated to Anna University) Coimbatore, Tamil Nadu, India

Received: 16 Sep 2023

Revised: 20 Oct 2023

Accepted: 27 Dec 2023

*Address for Correspondence

B.Logapriya

Assistant Professor,
Department of Science and Humanities,
Sri Krishna College of Engineering and Technology
(Affiliated to Anna University)
Coimbatore, Tamil Nadu, India
Email: logapriyab@skcet.ac.in



This is an Open Access Journal / article distributed under the terms of the **Creative Commons Attribution License** (CC BY-NC-ND 3.0) which permits unrestricted use, distribution, and reproduction in any medium, provided the original work is properly cited. All rights reserved.

ABSTRACT

In this article, the disaster in queueing system with second optional service is considered. Arriving customer of this system will receive the essential service and optional second service on request. If the system is interrupted by the disaster, the server initiates the repair period making all the customer leave the system immediately. The server is not idly waiting for customer to serve. The disaster cannot happen when server is under vacation or in repair period. The above queueing system is analysed using supplementary variable technique to obtain the probability generating function for various parameters and effects of parameters are explained graphically with numerical illustrations.

Keywords: Supplementary variable technique, Second optional service, Disaster, Repairs, Non-terminating vacation.

INTRODUCTION

Disaster is a sudden happening which collapses entire working environment. Many researchers have studied disaster in different names as negative arrivals, queue flushing and few more like catastrophes. Disaster can be seen in manufacturing systems, communication systems, production units which may lead to huge loss. As disaster removes all customers immediately from the system, it is extensively modeled by many researchers. The concept of disaster in Queueing models were introduced by Towsley and Tripathi in analysing the distributed data base system





Logapriya and Jeyakumar

that undergoes failure. Arumuganathan R and Jeyakumar S [1] studied steady state analysis of a bulk queue with multiple vacations, setup times with N-policy and closedown times. Bu, Q., & Liu, L. [2] analyzed M/G/1 clearing queueing system with setup time and multiple vacations for an unreliable server. Chakravarthy S.R [3] analyzed a disaster Queue with Markovian arrivals and impatient customers. Chang, F. M., Liu, T. H., & Ke, J. C. [4] studied an unreliable-server retrial queue with customer feedback and impatience. Choudhury, G., & Kalita, C. [5] analyzed M/G/1 queue with two types of general heterogeneous service and optional repeated service subject to server's breakdown and delayed repair. George C. Mytalis, Michael A. Zazanis [6] studied $M^X/G/1$ queueing system with disasters and repairs under MAV policy. George C. Mytalis & Michael A. Zazanis [7] analyzed Bernoulli feedback queues subject to disasters: a system with batch Poisson arrivals under a multiple vacation policy. Jain, M., & Singh, M. [8] analyzed markov queueing model with feedback, discouragement and disaster. Jeyakumar S and Senthilnathan B [9] Modelled and analysed $M^X/G(a, b)/1$ queue with multiple vacation, setup time, closedown time server breakdown without interruptions. Jiang T, Liu L [10] analysed G1/M/1 queue in a multi-phase service environment with disaster and working breakdowns. Jingjing Y.E, Liu Liwei and Jiang Tao [11] analysed single server queue with disasters and repairs under Bernoulli vacation schedule. Kim B.K and Lee D.H [12] modelled and analysed M/G/1 Queue with disasters and working Breakdowns. Lakshmi Priya M, Janani B [13] studied single server queue with disasters and repairs under Bernoulli working vacation schedule.

Mian Zhang and Shan Gao [14] studied the disasters queue with working breakdowns and impatient customers. Nitin Kumar, Farida P. Barbhuiya and Umesh C. Gupta [15] analysed Geometric catastrophe model with discrete-time batch renewal arrival process. Park H.M, Yang W.S, Chae K.C [16] analysed G1/Geo/1 Queue with disaster. Rajadurai, P., Saravanarajan, M. C., & Chandrasekaran, V. M [17] studied M/G/1 feedback retrial queue with subject to server breakdown and repair under multiple working vacation policy. Shan Gao, Jinting Wang and Tien Van Do [18] analysed discrete-time repairable queue with disasters and working breakdowns. Sudhesh R and Sebasthi Priya R [19] analysed discrete-time Geo/Geo/1 queue with feedback, repair and disaster. Li, K., & Wang, J. [20] analysed Equilibrium balking strategies in the single server retrial queue with constant retrial rate and catastrophes. The above literature survey motivated me to model and analyse the queue with disaster and repairs under non-terminating vacation in $M^X/G/1$. The above model can be identified in management system where as it also be seen in small scale industries with single server system. When the server is engaged in packing (essential service) in manufacturing units. The server may also engage in darning (technique to repair holes or worn areas, it is done manually in hand) it is optional service, as this may not require for all fabric which is under packing. When server completes packing, he may move to another work or goes for vacation which is considered as vacation from current packing. He may not wait idly for garments (customer) for packing. He may return back to work only if garments are ready for packing. Based such scenario the above queue is modeled and analysed.

MATHEMATICAL MODEL

In a compound Poisson process, a batch of customers with the parameters $\lambda, \lambda > 0$ joins the system. With the first order probability $\lambda c_i dt$, the batch of i customers join the system in the short duration of time $(t, t + dt)$. Each and every customer who arrives at the system is provided with first essential service under first come, first serve discipline. $E(C)$ is the mean batch size. Arriving customer is served one by one in the batch. Let $\mu_1(x) = \frac{S_1'(x)}{1-S_1(x)}$ be the hazard rate function of the first essential service with $S_1^*(s) = \int_0^\infty e^{-sx} dS_1(x)$, where S_1 is the general distribution function with the corresponding density function S_1' and mean $E(S_1)$. When the first essential service to the customer is completed, the customer may opt for optional service with the probability 's' or leave the system with the probability $1 - s$. Let $\mu_2(x) = \frac{S_2'(x)}{1-S_2(x)}$ be the hazard rate function of the second optional service with $S_2^*(s) = \int_0^\infty e^{-sx} dS_2(x)$, where S_2 is the general distribution function with the corresponding density function S_2' and mean $E(S_2)$. Once the server completes his essential and optional service to the customer, the server may take vacation. The vacation terminates only when the customers arrive at the system. Let $v(x) = \frac{L'(x)}{1-L(x)}$ be the hazard rate function of the





Logapriya and Jeyakumar

vacation with $L^*(s) = \int_0^\infty e^{-sx} dL(x)$, where L is the general distribution function with the corresponding density function L' and mean $E(L)$. Finally, disaster is assumed to happen in the system during first essential service, since second optional service is the manual service. With rate of the disaster δ , it removes all the customers including one is been served from the system and the system is immediately moved to repair period. Let $r(x) = \frac{R'(x)}{1-R(x)}$ be the hazard rate function of the repair period with $R^*(s) = \int_0^\infty e^{-sx} dR(x)$, where R is the general distribution function with density function R' and mean $E(R)$. The customers who arrive during repair time may wait in queue. Fig.1

NOTATIONS AND ABBREVIATIONS

At time t , let the system size be N_t . Let $S_{i,t}, i = 1,2$ and $L_{j,t}, j = 1,2, \dots$ be introduced as supplementary variables to obtain a Markov process. $\{N_t, \Omega(t), S_{i,t}, R_t, L_{j,t}, t \geq 0\}$. Limiting probabilities are defined to derive Kolmogorov Chapman equation as,

$$P_n^{(e)}(x) = \lim_{t \rightarrow \infty} \{N_t = n, \Omega(t) = 1, x < S_{1,t} < x + dt\}, n \geq 1$$

$$P_n^{(o)}(x) = \lim_{t \rightarrow \infty} \{N_t = n, \Omega(t) = 2, x < S_{2,t} < x + dt\}, n \geq 1$$

$$R_n(x) = \lim_{t \rightarrow \infty} \{N_t = n, \Omega(t) = 3, x < R_t < x + dt\}, n \geq 1$$

$$L_{j,n}(x) = \lim_{t \rightarrow \infty} \{N_t = n, \Omega(t) = 4, x < L_{j,t} < x + dt\}, n \geq 1, j = 1,2,3, \dots$$

STEADY STATE DIFFERENTIAL EQUATIONS USING SUPPLEMENTARY VARIABLE TECHNIQUE

Governing equations for various states of the system are framed for $n > 0$,
 $0 =$

$$\sum_{j=1}^\infty (1 - b_j) \int_0^\infty L_{j,0}(x) v(x) dx + (1 - b_0) \left(\int_0^\infty P_1^{(o)}(x) \mu_2(x) dx + (1 - s) \int_0^\infty P_0^{(e)}(x) \mu_1(x) dx + \int_0^\infty R_0(x) r(x) dx \right) \tag{1}$$

$$\left(\frac{d}{dx} + \lambda + \mu_1(x) + \delta \right) P_n^{(e)}(x) = \lambda \sum_{i=1}^{n-1} C_i P_{n-i}^{(e)}(x), n \geq 1 \tag{2}$$

$$\left(\frac{d}{dx} + \lambda + \mu_2(x) \right) P_n^{(o)}(x) = \lambda \sum_{i=1}^{n-1} C_i P_{n-i}^{(o)}(x), n \geq 1 \tag{3}$$

$$\left(\frac{d}{dx} + \lambda + r(x) \right) R_n(x) = \lambda \sum_{i=1}^{n-1} C_i R_{n-i}^{(o)}(x), n \geq 1 \tag{4}$$

$$\left(\frac{d}{dx} + \lambda + r(x) \right) R_0(x) = 0, n = 1 \tag{5}$$

$$\left(\frac{d}{dx} + \lambda + v(x) \right) L_{j,n}(x) = \lambda \sum_{i=1}^{n-1} C_i L_{j,n-i}(x), n \geq 1, j = 1,2, \dots \tag{6}$$

$$\left(\frac{d}{dx} + \lambda + v(x) \right) L_{j,0}(x) = 0, n = 1, j = 1,2, \dots \tag{7}$$

The above equations are solved with the boundary conditions:

$$P_n^{(e)}(0) = \sum_{j=1}^\infty \int_0^\infty L_{j,n}(x) v(x) dx + \int_0^\infty P_{n+1}^{(o)}(x) \mu_2(x) dx + (1 - s) \int_0^\infty P_{n+1}^{(e)}(x) \mu_1(x) dx + \int_0^\infty R_n(x) r(x) dx, n \geq 1 \tag{8}$$

$$P_n^{(o)}(0) = s \int_0^\infty P_n^{(e)}(x) \mu_1(x) dx, n \geq 0 \tag{9}$$

$$R_0(0) = \delta \sum_{n=1}^\infty \int_0^\infty P_n^{(e)}(x) dx \tag{10}$$

$$L_{1,0}(0) = b_0 \left(\int_0^\infty P_1^{(o)}(x) \mu_2(x) dx + (1 - s) \int_0^\infty P_1^{(e)}(x) \mu_1(x) dx + \int_0^\infty R_0(x) r(x) dx \right) \tag{11}$$

$$L_{j,0}(0) = b_{j-1} \int_0^\infty L_{j-1,0}(x) v(x) dx, j = 2,3, \dots \tag{12}$$





Logapriya and Jeyakumar

PROBABILITY GENERATING FUNCTIONS

To obtain PGF, we define probability generating functions as,

$$P^{(e)}(x, z) = \sum_{n=1}^{\infty} P_n^{(e)}(x)z^n, P_n^{(e)}(z) = \sum_{n=1}^{\infty} P_n^{(e)}z^n \tag{13}$$

$$P^{(o)}(x, z) = \sum_{n=1}^{\infty} P_n^{(o)}(x)z^n, P_n^{(o)}(z) = \sum_{n=1}^{\infty} P_n^{(o)}z^n \tag{14}$$

$$L_j(x, z) = \sum_{n=0}^{\infty} L_{j,n}(x)z^n, L_j(z) = \sum_{n=0}^{\infty} L_{j,n}z^n \tag{15}$$

$$R(x, z) = \sum_{n=0}^{\infty} R_n(x)z^n, R(z) = \sum_{n=0}^{\infty} R_nz^n \tag{16}$$

$$C(z) = \sum_{i=1}^{\infty} C_i z^i \tag{17}$$

Now by multiplying the equations (2 – 11) with certain powers of z and summing it over n , we obtain PDE's on solving those equations

$$P^{(e)}(x, z) = P^{(e)}(0, z)(1 - S_1(x))e^{-(\lambda+\delta-\lambda C(z))x} \tag{18}$$

$$P^{(o)}(x, z) = P^{(o)}(0, z)(1 - S_2(x))e^{-(\lambda-\lambda C(z))x} \tag{19}$$

$$R(x, z) = R(0, z)(1 - R(x))e^{-(\lambda-\lambda C(z))x} \tag{20}$$

$$L_j(x, z) = L_{j,0}(z)(1 - L(x))e^{-(\lambda-\lambda C(z))x} \tag{21}$$

$$R_0(x) = R_0(0)(1 - R(x)) \tag{22}$$

$$L_{j,0}(x) = L_{j,0}(0)(1 - L(x))e^{-\lambda x}, j = 1, 2, 3.. \tag{23}$$

To evaluate the value of equation shazard rates are multiplied and the equations are integrated to obtain:

$$\int_0^{\infty} P^{(e)}(x, z)\mu_1(x)dx = P^{(e)}(0, z)S_1^*(\lambda + \delta - \lambda C(z)) \tag{24}$$

$$\int_0^{\infty} P^{(o)}(x, z)\mu_2(x)dx = P^{(o)}(0, z)S_2^*(\lambda - \lambda C(z)) \tag{25}$$

$$\int_0^{\infty} R(x, z)r(x)dx = R(0, z)R^*(\lambda - \lambda C(z)) \tag{26}$$

$$\int_0^{\infty} L_j(x, z)v(x)dx = L_{j,0}(z)L^*(\lambda - \lambda C(z)) \tag{27}$$

On multiplying $r(x)$ and $v(x)$ and integrating the equation (22-23) becomes,

$$\int_0^{\infty} R_0(x)r(x)dx = R_0(0)R^*(\lambda)$$

$$\int_0^{\infty} L_{j,0}(x)v(x)dx = L_{j,0}(0)L^*(\lambda)$$

When j^{th} vacation begins immediately after the disaster and when the repair time starts after the disaster, the system is empty without customers, therefore

$$L_j(0, z) = L_{j,0}(0)$$

$$R(0, z) = R_0(0)$$

PGF OF QUEUE SIZE DISTRIBUTION FOR VARIOUS STATES

The explicit expressions of pgf's of size of the system, in different states are obtained as,

$$P^{(e)}(0, z) = \frac{z \left(\delta P^{(e)}(1)R^*(A_z) - \frac{v_1}{1-\beta}(1-L^*(A_z)) \right)}{z - S_1^*(A_z + \delta)((1-s) + s.S_2^*(A_z))} \tag{28}$$

Where $A_z = \lambda - \lambda C(z)$ and $\beta = L^*(\lambda)$

If possible, using Rouché's theorem, let $z = z_{\theta}$ be the unique solution of $z = S_1^*(A_z + \delta)((1 - s) + s.S_2^*(A_z))$. In that case equality becomes, $\frac{v_1}{1-\beta}(1 - L^*(A_{z_{\theta}})) = \delta P^{(e)}(1)R^*(A_{z_{\theta}})$.

RESULTS

The PGF of size of the system at epoch of essential service to the customer is given as

$$P^{(e)}(z) = \frac{\frac{z v_1}{1-\beta} (\pi R^*(A_z) - (1 - L^*(A_z)))}{z - S_1^*(A_z + \delta)((1-s) + s.S_2^*(A_z))} \left(\frac{1 - S_1^*(A_z + \delta)}{A_z + \delta} \right) \tag{29}$$

The PGF of size of the system at epoch of optional second service to the customer is given as

$$P^{(o)}(z) = \frac{\frac{z s v_1}{1-\beta} (\pi R^*(A_z) - (1 - L^*(A_z)))}{z - S_1^*(A_z + \delta)((1-s) + s.S_2^*(A_z))} \left(\frac{(S_1^*(A_z + \delta))(1 - S_2^*(A_z))}{A_z} \right) \tag{30}$$





Logapriya and Jeyakumar

The PGF of size of the system at epoch under repair is given as

$$R(z) = \frac{\frac{\pi v_1(1-R^*(A_z))}{1-\beta}}{A_z} \tag{31}$$

The PGF of size of the system at epoch of under vacation is given as

$$L(z) = \frac{\frac{v_1(1-L^*(A_z))}{1-\beta}}{A_z} \tag{32}$$

Using the normalizing condition at $z = 1$,

$$\frac{v_1}{1-\beta} = \left(\frac{\pi}{\delta} + \frac{s\pi S_1^*(\delta)E(S_2)}{1-S_1^*(\delta)} + \pi E(R) + E(L) \right)^{-1} \tag{33}$$

Finally, the total probability generating function of queue size $X(z)$ is obtained at arbitrary epoch as,

$$X(z) = \left(\frac{\pi}{\delta} + \frac{s\pi S_1^*(\delta)E(S_2)}{1-S_1^*(\delta)} + \pi E(R) + E(L) \right)^{-1} \left(\frac{\pi(1-R^*(A_z))}{A_z} + \frac{(1-L^*(A_z))}{A_z} + \frac{z(\pi R^*(A_z) - (1-L^*(A_z)))}{z - S_1^*(A_z + \delta)((1-s) + s.S_2^*(A_z))} \left(\frac{(1-S_1^*(A_z + \delta))}{A_z + \delta} + \left(\frac{s(S_1^*(A_z + \delta))(1-S_2^*(A_z))}{A_z} \right) \right) \right) \tag{34}$$

Also, due disaster the PGF of total number of customers removed from the system is given as

$$X_d(z) = \frac{z\delta(\pi R^*(A_z) - (1-L^*(A_z)))}{\pi(z - S_1^*(A_z + \delta)((1-s) + s.S_2^*(A_z))} \left(\frac{1-S_1^*(A_z + \delta)}{A_z + \delta} \right) \tag{35}$$

PERFORMANCE MEASURES

(i) Expected queue length ($E(Q_L)$) and waiting time ($E(W_T)$):

$$E(Q_L) = E(c) \left(\frac{\frac{\pi}{\delta} + \frac{s\pi S_1^*(\delta)E(S_2)}{1-S_1^*(\delta)}}{\pi E(R) + E(L)} \right)^{-1} \left(\frac{S_b + S_b\delta}{S_c} \left(\frac{\pi S_1^*(\delta)}{\delta E(c)} \left(\frac{-1}{2} - \frac{\lambda s}{2} S_2^{*''}(0) \right) + S_b s S_1^*(\delta) E(S_2) - \frac{s\pi E(S_2)}{S_c} \left(\frac{S_1^*(\delta)}{E(c)} \right)^2 + \lambda S_1^{*'}(\delta) \right) \right) \tag{36}$$

Where,

$$S_c = 1 - S_1^*(\delta), S_b = \frac{\lambda\pi}{\delta} + \lambda\pi E(R) + \lambda E(L), S_b\delta = \frac{\lambda}{2} (\pi E(R^2) + E(L^2))$$

let $S_2^{*'}(0), R^{*'}(0), L^{*'}(0)$ are the mean time; $S_2^{*''}(0), R^{*''}(0), L^{*''}(0)$ be the second moment. Using little's formula, the expected waiting time is calculated as





Logapriya and Jeyakumar

$$E(W_T) = \frac{\left(\frac{\pi}{\delta} + \frac{s\pi S_1^*(\delta)E(S_2)}{1-S_1^*(\delta)}\right)^{-1}}{\beta + \pi E(R) + E(L)} \left(S_b + S_{b\delta} + \frac{1}{S_c} \left(\begin{aligned} &\pi S_1^*(\delta) \left(\frac{-1}{\delta E(c)} - \frac{\lambda s}{2} S_2^{*''}(0) \right) \\ &+ S_b s S_1^*(\delta) E(S_2) \\ &- \frac{s\pi E(S_2)}{S_c} \left(\frac{(S_1^*(\delta))^2}{E(c)} + \lambda S_1^*(\delta) \right) \end{aligned} \right) \right) \tag{37}$$

NUMERICAL ILLUSTRATION

The queue size distribution for various states are computed using numerical technique. Service time, repair time and vacation time are assumed to be in exponential parameter μ, r, v respectively. The arrival rate is λ with service rate $\mu_1 = 5$ and $\mu_2 = 6$. Whereas disaster may take place with rate δ . Expected queue length and expected waiting time are computed and tabulated below with assumption of arrival and vacation as single: Table 1, Fig.2 From table 1 and figure 2, it is observed that when probability of second optional service increases then the queue length and expected waiting time increases. Table 2, Fig.3 From table 2 and figure 3, it is observed that when arrival rate increases then expected waiting time and expected queue length of the server increases. Table 3, Fig.4 From table 3 and figure 4, it is observed that expected queue length and expected waiting time decreases as the disaster rate increases.

CONCLUSIONS

In this paper, $M^X/G/1$ Queue with the second optional service with non-terminating vacation is taken into consideration for disaster and repairs. We derive the queue size distributions for various steady-states with quality metrics and special cases using the supplementary variable technique. Additionally, we've provided numerical examples to illustrate the approach and demonstrate how disasters affect waiting times and queue length with the second optional service. From the numerical illustration, it is observed that when arrival rate and probability for second optional service increases, the queue length of the system and waiting time of the customer increases as well as when disaster rate increases the queue length of the system and waiting time of the customer decreases.

REFERENCES

1. Arumuganathan R and Jeyakumar S (2006), "Steady state analysis of a bulk queue with multiple vacations, setup times with N-policy and closedown times", Applied Mathematical Modelling 29,972 – 986.
2. Bu, Q., & Liu, L. (2019), "An M/G/1 clearing queueing system with setup time and multiple vacations for an unreliable server", Communications in Statistics - Theory and Methods, 48(11),2810-2826.
3. Chakravarthy S.R (2009), "A disaster Queue with Markovian arrivals and impatient customers", Applied Mathematics and Computations 214,48-59.
4. Chang, F. M., Liu, T. H., & Ke, J. C. (2018), "On an unreliable-server retrial queue with customer feedback and impatience", Applied Mathematical Modelling, 55, 171–182.
5. Choudhury, G., & Kalita, C. (2018), "An M/G/1 queue with two types of general heterogeneous service and optional repeated service subject to server's breakdown and delayed repair", Quality Technology & Quantitative Management, 15(5), 622–654.
6. George C.Mytalas, Michael A.Zazanis (2015), "An $M^X/G/1$ queueing system with disasters and repairs under MAV policy", Naval Research Logistics 62, 171-189.
7. George C. Mytalas & Michael A. Zazanis (2023), "Performance analysis for Bernoulli feedback queues subject to disasters: a system with batch Poisson arrivals under a multiple vacation policy", Quality Technology & Quantitative Management, 20:1, 113-146.
8. Jain, M., & Singh, M. (2020), "Transient analysis of a Markov queueing model with feedback, discouragement and disaster", International Journal of Applied and Computational Mathematics, 6 (2): 1-14.
9. Jeyakumar S and Senthilnathan B. (2015), "Modelling and analysis of a $M^X/G(a,b)/1$ queue with multiple vacation, setup time, closedown time server breakdown without interruptions", International Journal of Operational research 1, 114 – 139.





Logapriya and Jeyakumar

10. Jiang T, Liu L (2015), "The G1/M/1 queue in a multi-phase service environment with disaster and working breakdowns", International Journal of Computer Mathematics 94, 707-726.
11. Jingjing Y.E, Liu Liwei and Jiang Tao (2016), "Analysis of a single server queue with disasters and repairs under Bernoulli vacation schedule", Journal of Systems Science and Information 4, 547-559.
12. Kim B.K and Lee D.H (2014), "The M/G/1 Queue with disasters and working Breakdowns", Applied Mathematical Modeling 38, 1788-1798.
13. Lakshmi Priya M, Janani B (2021), "Transient Analysis of a Single Server Queue with Disasters and Repairs under Bernoulli Working Vacation Schedule", Journal of mathematical and Computational Science, 11, 312-329.
14. Mian Zhang and Shan Gao (2020), "The Disasters Queue with Working breakdowns and Impatient customers", RAIRO Operations Research, 54, 815–825.
15. Nitin Kumar, Farida P. Barbhuiya and Umesh C. Gupta (2020), "Analysis of a Geometric Catastrophe Model with Discrete-Time Batch Renewal Arrival Process", RAIRO Operations Research 54, 1249–1268.
16. Park H.M, Yang W.S, Chae K.C (2009), "Analysis of the G1/Geo/1 Queue with disaster", Stochastic Analysis and Applications 28, 44-53.
17. Rajadurai, P., Saravananarajan, M. C., & Chandrasekaran, V. M. (2018), "A study on M/G/1 feedback retrial queue with subject to server breakdown and repair under multiple working vacation policy. Alexandria Engineering Journal", 57(2), 947–962.
18. Shan Gao, Jinting Wang and Tien Van Do (2019), "Analysis of a Discrete-Time Repairable Queue with Disasters and Working Breakdowns", RAIRO Operations Research, 53, 1197–1216.
19. Sudhesh R and Sebasthi Priya R (2017), "An Analysis of Discrete-Time Geo/Geo/1 Queue with Feedback, Repair and Disaster", International Journal of Operational Research, 35, 37–53.
20. Li, K., & Wang, J. (2020), "Equilibrium balking strategies in the single server retrial queue with constant retrial rate and catastrophes" Quality Technology & Quantitative Management, 18(2), 156–178.

Table 1: Performance measures with $\lambda = 0.9$ and $\delta = 5$

<i>s</i>	$E(Q_L)$	$E(W_T)$
1	0.9997	1.1108
2	1.0402	1.557
3	1.0769	1.1965
4	1.1103	1.2337
5	1.1409	1.2678

Table 2: Performance measures with $s = 3$ and $\delta = 2$

λ	$E(Q_L)$	$E(W_T)$
0.1	0.0667	0.6675
0.3	0.2123	0.7075
0.5	0.3994	0.7386
0.7	0.5346	0.7638
0.9	0.7057	0.7842

Table 3: Performance measures with $\lambda = 4$ and $s = 5$

δ	$E(Q_L)$	$E(W_T)$
1	4.1978	1.0495
1.5	3.8228	0.9557
2	3.6773	0.9193
2.5	3.6182	0.9046
3	3.5987	0.8997





Logapriya and Jeyakumar

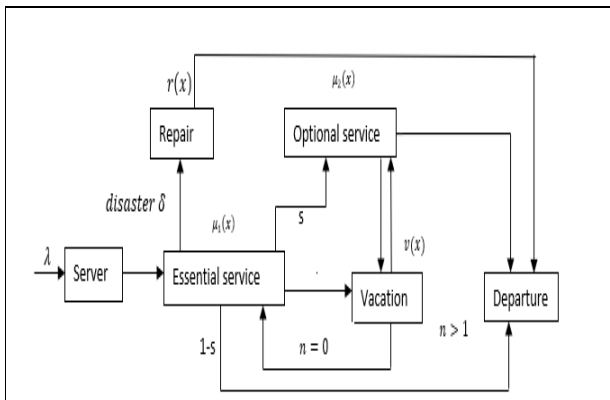


Figure 1: Schematic diagram of the queueing model

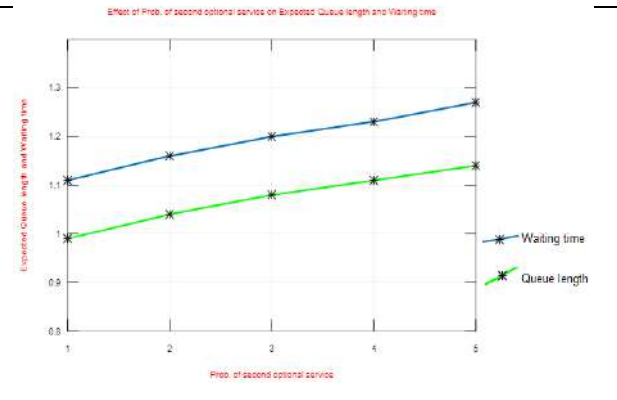


Figure 2: Second optional service versus queue length and waiting time

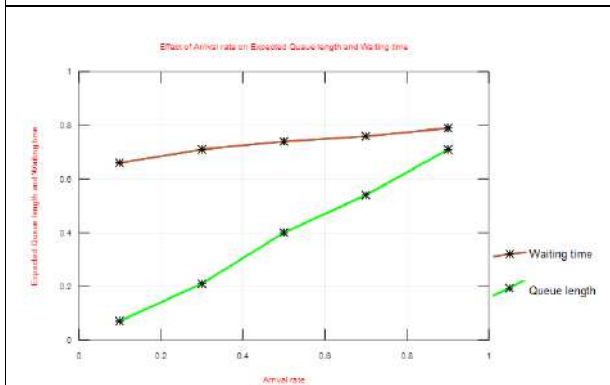


Figure 3: Effect of arrival rate on queue length and waiting time

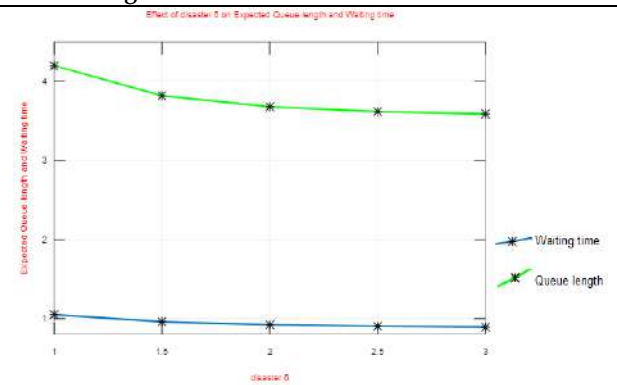


Figure 4: Effect of disaster on queue length and waiting time





Biodegradation of Hydrocarbon by Fungal Isolates from Oil Contaminated Soils

Thilagavathi .C^{1*}, Hemalatha .M², Thevasundari S¹, Abirami. P³ and Rajeswari B⁴

¹Assistant Professor, Department of Botany, Seethalakshmi Ramaswami College (Affiliated to Bharathidasan University) Tiruchirapalli, Tamil Nadu, India.

²Associate Professor, Department of Botany, Seethalakshmi Ramaswami College (Affiliated to Bharathidasan University) Tiruchirapalli, Tamil Nadu, India.

³Assistant Professor, Department of Botany, Seethalakshmi achi College for women, Pallathur, Sivagangai (Affiliated to Alagappa University, Karaikkudi) Tamil Nadu, India.

⁴Associate Professor, Department of Science and Humanities, Kurinji College of Engineering and Technology, Manapparai, Tiruchirapalli (Affiliated to Anna University, Chennai) Tamil Nadu, India.

Received: 25 Aug 2023

Revised: 20 Nov 2023

Accepted: 22 Jan 2024

*Address for Correspondence

Thilagavathi .C

Assistant Professor,

Department of Botany,

Seethalakshmi Ramaswami College (Affiliated to Bharathidasan University)

Tiruchirapalli, Tamil Nadu, India.

Email: thilagabot@gmail.com



This is an Open Access Journal / article distributed under the terms of the **Creative Commons Attribution License** (CC BY-NC-ND 3.0) which permits unrestricted use, distribution, and reproduction in any medium, provided the original work is properly cited. All rights reserved.

ABSTRACT

The process of bioremediation is an ever-evolving technique for the elimination and decomposition of many environmental contaminants, including those produced by the petroleum industry. Because of their diverse metabolic capabilities, microorganisms are used to detoxify or remove pollutants. Furthermore, bioremediation technology is thought to be non-intrusive and inexpensive. Hydrocarbons degrade very slowly in ecosystems exposed to extremely low temperatures. Temperature typically increases the rate of biodegradation. In this study, the main degrading organisms are fungi and bacteria, with fungi playing a larger role in freshwater and terrestrial ecosystems than bacteria does in marine ecosystems. The current study concluded that the presence of heavy metals in oil-contaminated soil demonstrated that oil contamination significantly increased heavy metal concentrations such as zinc and chromium.

Keywords: biodegradation, hydrocarbon, fungal isolates, oil, contaminated soils



**Thilagavathi et al.,**

INTRODUCTION

The most common environmental issue is pollution brought on by petroleum and its byproducts[1]. Global attention is being paid to the release of crude oil into the environment due to oil spills. Numerous accidents can pollute soil, which is why numerous methods are being developed to clean up petroleum-contaminated soil[2]. One of the main categories of these contaminants is polycyclic aromatic hydrocarbons (PAH)[3]. A diverse class of organic compounds known as PAH is made up of two or more aromatic rings in different structural arrangements. Because they are benzene derivatives, PAH are thermodynamically stable[4]. Additionally, due to their strong hydrophobicity and low water solubility, these chemicals have a tendency to stick to particle surfaces like soil, which results in greater persistency under natural circumstances[5]. Many industrial sites have high concentrations of PAH, especially those connected to the oil, gas, and wood preservation industries. The traditional methods for cleaning up polluted soil involve either excavating the polluted soil and disposing of it in a secure landfill or simply capping and containing the polluted areas of a site[6]. However, these techniques do have some limitations. Compared to chemical and physical treatments, biological ones are more effective and less expensive[7].

In terms of biological treatment, microorganisms that can convert petroleum hydrocarbons into less toxic compounds are used in the bioremediation technology to break down crude oil in soil matrix[8]. However, two key characteristics of high molecular weight hydrocarbons that restrict their accessibility to microorganisms are their low solubility and adsorption. In this situation, the inclusion of a bio surfactant improves the solubility and elimination of these contaminants, enhancing the rate of oil biodegradation. Bio surfactants are metabolic byproducts of bacteria and fungi and are categorized according to their microbial origin or chemical make-up[9]. These bio molecules are primarily produced by the aerobic growth of microorganisms in aqueous phase with carbon sources such as carbohydrates, hydrocarbons, or a combination of them. The majority of bio surfactants, which range in size from small fat acids to substantial polymeric structures, are neutral or anionic[10]. The microbiology of hydrocarbon degradation will be a developing area of study once microbiological techniques can be used in the decontamination processes[11]. The ability to grow on petroleum hydrocarbons has been cultivated in fungi. The two filamentous fungi most frequently isolated from soil are *Trichoderma* and *Mortierella spp*[12]. This common practice to isolate *Aspergillus* and *Penicillium* species from terrestrial and aquatic environments. Cytochrome P-450s are mixed-function oxidases (mono oxygenases), descended from a super family of genes, and they play a key role in a number of environmental biotransformations as well as the degradation of petroleum[13].

The function of P-450 involves both activation and detoxification. Fungal mono oxygenases resemble mammalian cytochromes more than they do bacterial ones. Biodegradation of Hydrocarbons in the Environment by Bacteria, Fungi, and other microorganisms is primarily carried out by bacteria and fungi[14]. Although common in terrestrial and aquatic ecosystems, the percentage of the total heterotrophic community made up of bacteria and fungi that use hydrocarbons is highly variable, with reported frequencies for soil fungi ranging from 6% to 82%, for soil bacteria from 0.13% to 50%, and for marine bacteria from 0.003% to 100%. In order to break down complex mixtures of hydrocarbons like crude oil in soil, freshwater, and marine environments, it takes assemblages of mixed populations with generally broad enzymatic capacities. Individual organisms can only break down a finite range of hydrocarbon substrates. Many different bacterial and fungal genera are capable of utilizing and degrading hydrocarbon substrates[15]. Ecosystems exposed to extremely low temperatures degrade hydrocarbons very slowly. Biodegradation rates typically increase with increasing temperature. In this study, fungi and bacteria are the main degrading organisms, with fungi playing a larger role in freshwater and terrestrial ecosystems than bacteria does in marine ecosystems. The investigation take place with the following goals in mind while keeping the aforementioned details in mind.

1. To isolate the bacteria and fungi from oil contaminated sites.
2. To identify the bacteria and fungus.
3. To estimate the physicochemical analysis of contaminated soil.
4. To estimate the heavy metals such as Chromium and Zinc in the sample.





Thilagavathi et al.,

5. To know the degradation ability of the bacteria and fungus.

MATERIALS AND METHODS

The soil samples used in this study have been collected from Thanjavur, Tamil Nadu, India, which has oil-contaminated sites. The samples were taken 5 cm or less below the soil's surface. The collected soil samples are hand-selected, air-dried, and brought to the lab in sterilized polythene bags. They are then placed in a deep freezer for later use. In order to isolate bacteria and fungus, soil samples are used. Additionally, the soil sample is powdered and air dried to pass through a 2mm sieve. The ground up soil is gathered, sealed in a plastic bag, and kept at 4°C until needed. Then, using a glass rod to stir, 20g of soil powder is combined with 40 ml of distilled water. The pH was measured using a pH meter (Elico Instruments, India) after it was left undisturbed for 15 minutes. PH 4.0 and pH 9.2 buffer solutions were used for standardization. Similarly, a conductivity meter is used to gauge the soil suspension's electrical conductivity. The suspension was made by combining 20 grammes of soil with 100 mm of distilled water, stirring it for an hour in a shaker, and measuring the conductivity with an electronic digital conductivity meter (Elico Instruments, India). Additionally, the rapid titration method has been used to determine the amount of soil organic matter. In a 500 ml conical flask, one gramme of finely sieved dry soil was added along with 190 ml of 1 N $K_2Cr_2O_7$.

The 20 ml of concentrated H_3BO_4 was added after thorough mixing, and the mixture was left undisturbed for 30 minutes at room temperature ($27 \pm ^\circ C$). Indicator diphenylamine (0.4%), 10ml of 80% ortho-phosphoric acid, and 200ml of water were added after it had been diluted. The answer took on a dark blue hue. Upon titration with 0.5 N ferrous sulphate solutions, it turned green. Equation 1 is used to determine the amount of organic matter in the soil.

$$\text{Organic matter (\%)} = B - S \times 0.003 \times 1.74 \times 100 \quad \text{-----} \quad (1)$$

Where, 'B' is volume of $FeSO_4$ used for blank titration, 'S' is volume of $K_2Cr_2O_7$ used for sample titration, 'W' is weight of the soil sample in gram, 1.724 is conversion factor from organic carbon to organic matter. In order to isolate bacteria, 100 mg of the soil sample is put in a 250 ml conical flask with 90 ml of sterile, distilled water. The flask was shaken on an electric shaker to get a homogenous suspension and transferring serially 10ml of the water suspension to 90ml of sterile distilled water made different dilutions viz., $10^{-1}, 10^{-2}, 10^{-3}, 10^{-4}$ and 10^{-5} . One ml of 10^{-5} dilution is plated in Petri dishes containing nutrient agar medium. Composition of nutrient agar medium is tabulated in Table 1. The medium's pH has been raised to 7. The inoculated plates were incubated at $25 \pm 2^\circ C$ for one or two days, and bacteria that began to appear on the medium were removed, mounted on a clean slide, stained with crystal violet, Gram's iodine, and safran in, and then examined under a microscope. Based on the characteristics of the colony, the bacteria were identified. A 250 ml conical flask containing 90 ml of sterile distilled water was used to hold 10 ml of the water sample for the fungi isolation process. The flask was shaken on an electric shaker to get a homogenous suspension and transferring serially 10ml the water suspension and to 90ml of sterile distilled water made different dilutions viz., $10^{-1}, 10^{-2}, 10^{-3}, 10^{-4}$, and 10^{-5} . One ml of 10^{-5} dilution was plated in petri dishes containing Potato Dextrose Agar medium (PDA). The composition PDA medium is tabulated in Table 2. The medium's pH has been raised to 5.6. To stop bacterial growth, streptomycin sulphate (100 mg-1), was added to the media. The plates were incubated at $25^\circ C$ for five days, and fungi that appeared on the medium were mounted over a clear slide and observed under a microscope after being stained with lacto phenol cotton blue stain

RESULT AND DISCUSSIONS

Most of the waste and chemicals used in today's industrial society end up in the soil, whether on purpose or by accident. The contamination of soil and groundwater by petroleum mineral oil and goods made from mineral oil is one of the most frequent sources of pollution. Common analytical methods used to assess petroleum product contamination include determining hydrocarbon fractions, total hydrocarbon content, and heavy metal contents. Heavy metals and hydrocarbons are two examples of toxic materials that are bad for human health. In this study, local microbes like bacteria and fungi degraded heavy metals. Table 3 lists the physico-chemical characteristics of the

69881



**Thilagavathi et al.,**

soil sample from the study sites. The chosen soil sample has a pH of 9.5 and an electrical conductivity of 0.45. The total amount of nitrogen in the study site is 76.5 mg/g, followed by phosphorus at 9.5 mg/g and potassium at 60.5 mg/g as measured in the soil samples. Micronutrients like zinc, copper, iron, and manganese are present in the soil sample in a moderate amount. Bacterial isolates are isolated from soil using serial dilution techniques. The isolated bacteria are then identified using a variety of biochemical tests, as shown in Table 4. The soil sample contains 5 species of bacteria, including *Pseudomonas putida*, *P. fluorescens*, *Klebsiella pneumonia*, *Escherichia coli*, and *Micrococcus sp.* *Pseudomonas* dominated this genus with two species. Furthermore, 9 fungi species from 6 genera have been identified in the effluent. *Aspergillus* is the dominant genus, with three species including *A. niger*, *A. flavus*, and *A. terreus*. *Penicillium*, *Trichoderma*, and *Rhizobus* are the only remaining genera with a single species. Furthermore, the effluent is initially tested for heavy metals such as chromium (Cr) and zinc (Zn). *Aspergillus niger*, *Aspergillus flavus*, *Aspergillus terreus*, *Trichoderma viride*, *Rhizobus sp.*, and *Penicillium sp.* are found in the samples. Among the heavy metals tested, chromium had the highest concentration (0.47mg l⁻¹) followed by zinc (0.24mg l⁻¹). The amounts of heavy metals Cr and Zn are estimated in the control (un inoculated sample) and *Pseudomonas* and *Aspergillus* inoculated (50g and 100g) soil sample on 20th day. *Pseudomonas* treated soil showed a maximum removal of Cr and Zn when compared to *Aspergillus* treated soil. In the general maximum amount of heavy metals (Cr and Zn) removal was observed in the effluent treated with 100 mg of organisms. Generally the heavy metal was maximum removal by the *Pseudomonas sp.* The level of heavy metals in soil treated with different concentration (50 and 100 g) of organism is tabulated in Table 5.

CONCLUSIONS

Soil samples were used to isolate local microbes such as bacteria and fungus. To treat these microbes, chromium and zinc-contaminated soil was used. The current study concluded that the presence of heavy metals in oil-contaminated soil demonstrated that oil contamination significantly increased heavy metal concentrations such as zinc and chromium. This study demonstrated the ability of bacterial and fungal species, such as *P. putida* and *A. niger*, to bioaccumulate heavy metals that pose health risks when consumed by humans and their animals. The study also revealed that Cr and Zn were present in higher concentrations than other metals, and that waste-lubricating pollution indicated that metal levels rose as oil dosage increased. Since Cr was the primary issue identified by this study, this contaminant has the potential to be carcinogenic, whereas Cr has been demonstrated to have mutagenic potential and is a major environmental concern to the regulatory agencies in terms of surface and underground water pollution and issues relating to the food chain. Preventing oil spills or leaks should be the top priority because there is no general method that can be used to remove all of the oil from contaminated sites. To reduce potential environmental effects, action should be taken right away if there are oil spills or leaks.

REFERENCES

1. Truskewycz, A., Gundry, T. D., Khudur, L. S., Kolobaric, A., Taha, M., Aburto-Medina, A., Ball, A. S., & Shahsavari, E. (2019). Petroleum hydrocarbon contamination in terrestrial ecosystems—fate and microbial responses. *Molecules*, 24(18). <https://doi.org/10.3390/molecules24183400>
2. Verla, A. W., Enyoh, C. E., Verla, E. N., & Nwarnorh, K. O. (2019). Microplastic-toxic chemical interaction: a review study on quantified levels, mechanism and implication. *SN Applied Sciences*, 1(11). <https://doi.org/10.1007/s42452-019-1352-0>
3. Elkarrach, K., Atia, F., Omor, A., Laidi, O., Biyada, S., Benmelih, M., & Merzouki, M. (2022). Biological versus Physicochemical Technologies for Industrial Sewage Treatment: Which Is the Most Efficient and Inexpensive? *Sewage - Recent Advances, New Perspectives and Applications*. <https://doi.org/10.5772/intechopen.100325>
4. Pardhi, D. S., Panchal, R. R., Raval, V. H., Joshi, R. G., Poczai, P., Almalki, W. H., & Rajput, K. N. (2022). Microbial surfactants: A journey from fundamentals to recent advances. *Frontiers in Microbiology*, 13. <https://doi.org/10.3389/fmicb.2022.982603>





Thilagavathi et al.,

5. Abdel-Shafy, H. I., & Mansour, M. S. M. (2016). A review on polycyclic aromatic hydrocarbons: Source, environmental impact, effect on human health and remediation. *Egyptian Journal of Petroleum*, 25(1), 107–123. <https://doi.org/10.1016/j.ejpe.2015.03.011>
6. Chukwunonso Ossai, I., Shahul Hamid, F., & Hassan, A. (2022). Biological Treatments for Petroleum Hydrocarbon Pollutions: The Eco-Friendly Technologies. *Hazardous Waste Management*. <https://doi.org/10.5772/intechopen.102053>
7. Sattar, S., Hussain, R., Shah, S. M., Bibi, S., Ahmad, S. R., Shahzad, A., Zamir, A., Rauf, Z., Noshad, A., & Ahmad, L. (2022). Composition, impacts, and removal of liquid petroleum waste through bioremediation as an alternative clean-up technology: A review. *Heliyon*, 8(10), e11101. <https://doi.org/10.1016/j.heliyon.2022.e11101>
8. Titaley, I. A., Walden, D. M., Dorn, S. E., Ogba, O. M., Massey Simonich, S. L., & Cheong, P. H. Y. (2019). Evaluating Computational and Structural Approaches to Predict Transformation Products of Polycyclic Aromatic Hydrocarbons. *Environmental Science and Technology*, 53(3), 1595–1607. <https://doi.org/10.1021/acs.est.8b05198>
9. Patel, A. B., Shaikh, S., Jain, K. R., Desai, C., & Madamwar, D. (2020). Polycyclic Aromatic Hydrocarbons: Sources, Toxicity, and Remediation Approaches. *Frontiers in Microbiology*, 11. <https://doi.org/10.3389/fmicb.2020.562813>
10. Santos, D. K. F., Rufino, R. D., Luna, J. M., Santos, V. A., & Sarubbo, L. A. (2016). Bio surfactants: Multifunctional bio molecules of the 21st century. *International Journal of Molecular Sciences*, 17(3). <https://doi.org/10.3390/ijms17030401>
11. Das, N., Das, A., Das, S., Bhatawadekar, V., Pandey, P., Choure, K., Damare, S., & Pandey, P. (2023). Petroleum Hydrocarbon Catabolic Pathways as Targets for Metabolic Engineering Strategies for Enhanced Bioremediation of Crude-Oil-Contaminated Environments. *Fermentation*, 9(2). <https://doi.org/10.3390/fermentation9020196>
12. Tyśkiewicz, R., Nowak, A., Ozimek, E., & Jaroszuk-Ścisiel, J. (2022). Trichoderma: The Current Status of Its Application in Agriculture for the Biocontrol of Fungal Phyto pathogens and Stimulation of Plant Growth. *International Journal of Molecular Sciences*, 23(4). <https://doi.org/10.3390/ijms23042329>
13. Permana, D., Niesel, K., Ford, M. J., & Ichinose, H. (2022). Latent Functions and Applications of Cytochrome P450 Mono oxygenases from *Thamnidium elegans*: A Novel Biocatalyst for 14 α -Hydroxylation of Testosterone. *ACS Omega*, 7(16), 13932–13941. <https://doi.org/10.1021/acsomega.2c00430>
14. Dell' Anno, F., Rastelli, E., Sansone, C., Dell' Anno, A., Brunet, C., & Ianora, A. (2021). Bacteria, fungi and microalgae for the bioremediation of marine sediments contaminated by petroleum hydrocarbons in the omics era. *Microorganisms*, 9(8). <https://doi.org/10.3390/microorganisms9081695>
15. Heras-Martínez, H. M., Muñoz-Castellanos, L. N., Bugarin, A., Ramos-Sánchez, V. H., Ochoa, I. S., & Chávez-Flores, D. (2022). Biodegradation of Polycyclic Aromatic Hydrocarbons by *Acremonium* sp. ACTIVITY. *Revista Internacional de Contaminación Ambiental*, 38, 261–269. <https://doi.org/10.20937/RICA.54462>

Table 1 Composition of nutrient agar medium

Peptone (g)	Beef Extract (g)	NaCl (g)	Agar (g)	Distilled water (ml)
5	3	5	15	1000

Table 2 Composition PDA medium

Potato (g)	Dextrose (g)	Agar (g)	Distilled water (ml)
250	20	15	1000

Table 3 Physico-chemical analysis of oil contaminated soil

pH	Ec (dsm-1)	Organic matter (%)	Nitrogen(mg/g)	Potassium(mg/g)
9.5	0.45	0.56	76.5	60.5
Phosphorus(mg/g)	Zinc(ppm)	Chromium(ppm)	Iron(ppm)	Manganese(ppm)
9.5	1.04	0.45	1.82	6.96





Thilagavathi et al.,

Table 4 Biochemical characterization of isolated bacteria

Sl.no	Biochemical characterization	<i>P.flourescence</i>	<i>P.putida</i>	<i>K.pneumonia</i>	<i>E.coli</i>	<i>Micrococcus sp.,</i>
1	MaeConkeyagar test	+	+	+	-	-
2	Indole test	-	-	-	+	-
3	Methylred test	+	-	-	+	+
4	VogesProska uertest	+	+	+	-	+
5	Citrate utilization test	-	-	-	-	-
6	Starch hydrolysis test	+	+	+	-	+
7	Urea hydrolysis test	-	+	+	-	-
8	Nitrate reduction test	-	-	-	+	+
9	H ₂ S production test	+	-	-	-	-
10	Cytochrome oxidasetest	+	+	+	+	-
11	Catalasetest	-	-	-	+	-

Table 5 Level of heavy metals in soil treated with different concentration of organism

Sl.No	Heavy metals	Control	Treated soil			
			<i>P.pudita</i>		<i>A.niger</i>	
			50g	100g	50g	100g
1	Chromium	0.45	0.17	0.13	0.24	0.20
2	Zinc	0.22	0.15	0.10	0.19	0.16





A Review on Nano Emulgels

Ketha Srilekha¹, Y.Srinivasa Rao², S.Satyalakshmi³ and Bhavani Ummuri^{1*}

¹Assistant Professor, Department of Pharmaceutics, Vignan Institute of Pharmaceutical Technology, (Affiliated to JNTUGV), Visakhapatnam, Andhra Pradesh, India.

²Professor, Department of Pharmaceutics, Vignan Institute of Pharmaceutical Technology, (Affiliated to JNTUGV), Visakhapatnam, Andhra Pradesh, India.

³Associate Professor, Department of Pharmaceutics, Vignan Institute of Pharmaceutical Technology, (Affiliated to JNTUGV), Visakhapatnam, Andhra Pradesh, India.

Received: 08 Sep 2023

Revised: 03 Nov 2023

Accepted: 04 Jan 2024

*Address for Correspondence

Bhavani Ummuri

Assistant Professor,
Department of Pharmaceutics,
Vignan Institute of Pharmaceutical Technology,
(Affiliated to JNTUGV),
Visakhapatnam, Andhra Pradesh, India.
Email: bhavaniummuri31@gmail.com



This is an Open Access Journal / article distributed under the terms of the **Creative Commons Attribution License** (CC BY-NC-ND 3.0) which permits unrestricted use, distribution, and reproduction in any medium, provided the original work is properly cited. All rights reserved.

ABSTRACT

Most anti-inflammatory medications possess hydrophobicity which has the drawback of causing low permeability and unpredictable bioavailability. This problem can be conquered by novel drug delivery systems called nanoemulsions (NEGs) that are designed to increase the solubility and permeability characteristics of medicines across biological membranes. Permeability is mainly improved by the nano-sized droplets in the nanoemulsion which is composed of surfactants and co-surfactants that act as permeation enhancers, increase the formulation's ability to penetrate. Hydrogel component of NEG plays a significant role in enhancing the formulation's viscosity and spread ability which makes it perfect for topical administration. Additionally, anti-inflammatory oils with synergistic effects with the active moiety are used as oil phases in the creation of the nanoemulsion, enhancing its overall therapeutic profile. The most commonly used oils in the preparation of nanoemulsion are eucalyptus oil, emu oil, and clove oil. As a result, hydrophobic medicines are developed that have improved pharmacokinetic and pharmacodynamic properties while also preventing systemic negative effects in those with external inflammatory illnesses. Many inflammatory disorders, including dermatitis, psoriasis, rheumatoid arthritis, osteoarthritis are treated by nanoemulsions which possess effective spread ability, simplicity of application, non-invasive administration, and subsequent ability to achieve patient compliance. Use of high energy approaches during the creation of nanoemulsion technique will be associated with issues like scalability and thermodynamic instability that limit the large-scale practical application of NEG, these problems can be overcome by the development of an alternative nanoemulsification technique. This review mainly deals with potential relevance of using nanoemulsions

69885





Ketha Srilekhya *et al.*,

in a topical delivery system for anti-inflammatory medications, taking into account the possible advantages and long-term benefits of NEGs.

Keywords: Nanoemulsion; Nanoemulgel; Pharmacokinetics; Anti inflammatory.

INTRODUCTION

Nanoemulgels (NEGs) are created by incorporating Oil/water or water/oil nanosized emulsions into a gel-based system. NEGs transform nanoemulsions into a more stable, non-greasy, and thicker system [01] by the addition of a suitable gelling agent used in the manufacture of the gel base. Nanoemulsions often associated with the problems like poor viscosity, spread ability, skin retention and are non scalable [02,03], on other hand Gels are lacking the ability to absorb hydrophobic molecules [04]. This drawback of both components can be fixed by A new method employing NEGs. These allow the lipid-soluble medicines to be solubilized in the oil phase of the nanoemulsion, which is mixed with the gel to create a NEG. This increases the viscosity of the nanoemulsion while also enabling the incorporation of the lipophilic drug into a hydrogel [05]. Medications are protected from enzymatic and hydrolytic deterioration by the components of NEGs nanoemulsion. Gel components stabilizes the system's thermodynamics by reducing surface and interfacial tension and raising viscosity and spread ability [06]. Because the distribution of nanoemulsion droplets covers a broad surface area on the skin, lipophilic chemicals are easily formed into NEs, which can increase the permeability of medications so that they can pass through the layers of skin. As a result, the pharmacokinetic and pharmacodynamic properties of lipophilic medicines have been significantly improved [07]. NEG formulations were successful in gaining patient compliance by overcoming the Patient noncompliance caused by drawbacks of conventional topical formulations, such as hygroscopic powders, unstable creams (such as phase inversion or breakdown in their formulations), rancid components in ointments, sticky lotions, etc. [07,08].

Nanoemulgel development has gained attention recently this is because of its unique properties like site specificity, continuous delivery, two-step drug release (first from the nanoemulsion, then from the gel), and a decrease in dose and dosing frequency. The overall efficacy of drug delivery via the topical route is enhanced as a result. NEGs have higher drug loading efficiency as they do not have drug leaching and drug degradation issues which is seen in case of niosomes and liposomes. Drug release of short half life drugs can be prolonged by converting them into of NEGs have the capacity to regulate drug release for a protracted length of time. Concentration gradient and Skin permeability of drugs is enhanced because of their increased ability to stick to the skin and their larger drug solubilizing ability,. Additionally, because of their noninvasive administration and ability to avoid GI side effects, they have simple applications and high safety and therapeutic profiles, which ultimately improve patient compliance. NEGs are used as a carrier system in the treatment of a variety of inflammatory skin disorders, including osteoarthritis- and rheumatoid arthritis-related inflammation, acne-related fungal infections, pimples, and psoriasis. According to the literature, nanoemulgels can be delivered intravenously, orally, vaginally, or through the nose to treat both local and systemic conditions such baldness, periodontitis, and Parkinson's [08].

Nanoemulgels in Topical Delivery for Anti-Inflammatory Drugs

Anti-inflammatory medications demonstrate their effectiveness at various points during the inflammatory cascade (Figure 1). Arachidonic acid, the precursor of inflammatory mediators such prostaglandins and leukotrienes, is produced by the phospholipase enzyme, which is inhibited by gluco corticoids [09,10]. Inhibiting cyclo oxygenase 1 (COX1) and cyclo oxygenase 2 (COX2) is the main mechanism by which NSAIDs work to reduce the production of prostaglandins, which are the molecules that cause inflammation [11]. Curcumin and quercetin are two examples of natural anti-inflammatory compounds that have been shown to have COX and lipoxygenase (LOX) inhibition activities [12,13]. Topical delivery is a great strategy for treating external inflammatory conditions because, by choosing this route, we can avoid the GI barriers of intestinal transit time, gastric emptying time, enzyme presence, and pH changes in addition to first-pass metabolism [14,15]. In addition to reducing the danger of systemic side



**Ketha Srilekha et al.,**

effects including GI bleeding and peptic ulcers, topical NSAID administration offers the advantage of enhancing the delivery of local medications to the injured tissues [16]. Additionally, the formulation's oil phase can be carefully chosen to contain oils with anti-inflammatory qualities, which can work in concert to improve the desired results. By increasing the permeability and diffusibility of the NEG by using the proper permeation enhancers, the nanosized globules of the selected NE increase its efficacy [06]. Additionally, the stratum corneum (SC)'s tight construction can breach due to a high water content in the gel, allowing the active chemicals to easily penetrate the skin [17]. The medication in the NE travels from the internal phase (Nanoemulsion) to the exterior phase (gel) before reaching the skin's surface, acting as a drug reservoir for topical delivery. Oily globules that are administered topically first break free from the hydrogel and then penetrate deeply into the SC of the skin, delivering the drug moiety [18].

Mechanistic Approach of Nanoemulgel Delivery Via Topical Route

The most effective barrier for controlling the entry and penetration of topically administered medicines is thought to be the stratum corneum. When the subcutaneous (SC) layer is compromised by skin conditions or penetration enhancers, tight junctions function as a secondary barrier [19][20]. Three pathways—para cellular, trans cellular, and transappendageal—are used by the drug molecule to enter cells (Figure 1). The para cellular route, which involves the medication passing via the lipid milieu in between the corneocytes, is the main mechanism by which substances permeate skin. Small lipophilic molecules (molecular mass 500 Dalton) can circumvent the tight lipid connections between the cells to travel along this channel [21]. The SC's direct access to the inner layers of the epidermis and, perhaps, the dermis at the bottom is made possible through the trans cellular pathway. Up to 20 lipid lamellae separate each of these cells, and a molecule travelling through the trans cellular pathway must partition into and diffuse through corneocytes in order to cross corneocytes. As a result, the medicine or carrier must possess both hydrophilic and hydrophobic qualities in order to cross the trans cellular pathway. The trans cellular pathway permits small hydrophilic or mildly lipophilic substances (log p between 1-3) to pass across the epidermis while inhibiting the permeability of highly lipophilic molecules [22]. Compounds are transported along sweat glands, hair follicles, and the sebaceous glands that accompany them via the trans appendageal route. It is well acknowledged that the appendages' (hair follicles and associated glands) contribution to epidermal permeation is frequently negligible because they only account for a small proportion of the skin (e.g., only around 0.1% of the forearm skin) [23]. NEGs improve drug penetration since they can use all three routes to pass through the epidermis. Oils, surfactants alone or in conjunction with a cosurfactant, which works as a natural enhancer of permeation and a gelling ingredient that helps increase permeability by improving the formulation's adhesion to the skin, make up the formulation.

Advantages of Emulgels [24,25,26]

As topical agent

The majority of topical dermatological formulations, such as creams and ointments, have the drawbacks of having a low spreading coefficient, being sticky, and requiring rubbing during administration. These restrictions are removed in gel formulation, however despite their many benefits, gels have a significant restriction in the distribution of hydrophobic medications. Emulgels have thus been extremely helpful in delivering hydrophobic medications topically and giving them the benefits of gel composition.

Stability

Compared to emulgels, several other topical preparations exhibit less stability. Creams exhibit phase inversion, ointments exhibit rancidity from their oily foundation, and powders have a hygroscopic tendency.

Better than other vesicular techniques

Other vesicular procedures for topical preparation, such as niosomes and liposomes, have limited loading capacity because vesicular features cause leakage and because their small size results in lower trapping efficiency. While gels exhibit superior loading capacity as a result of their extensive polymeric three-dimensional structure.





Ketha Srilekhya *et al.*,

Simple production

Emulgels can be made quickly and easily without the use of specialised equipment, which lowers the cost of its formulation.

Controlled release

Emulgels function as a dual control preparation, making them ideal for releasing medications with brief half-lives.

No intensive sonication

Niosomes required sonication during manufacture, which could cause drug degradation and leakage. This contrasts with the production of vesicular molecules like liposomes. In the formation of emulgels, this is not necessary. Emulgels enhance patient compliance since patients can self-apply them and stop using the drug as needed. Emulgels also bypass first pass metabolism and offer targeted medication administration. Negative aspects [26].

Disadvantages

Emulgels for medication delivery have a number of benefits but also some drawbacks, such as:

1. Drugs with large particle sizes do not readily penetrate the skin.
2. Some medications exhibit low skin permeability
3. Emulgel formulation could result in bubble formation.

Potent Components for Nanoemulgel Formulation

Nano emulgel is a combination of two distinct systems namely a nano emulsion and a gel system. Oil-in-water or water-in-oil nano emulsions can be used as a delivery system for drugs. It consists of an oil phase, an aqueous phase, a surfactant, and occasionally a co surfactant in both situations. This section provides an overview of the primary components of nano emulgel formulation that are most frequently employed.

Formulation Technique of Nanoemulgel

Nanoemulgel is prepared by combining Nanoemulsion and gel together. When making nanoemulgel, the nanoemulsion and gel must be made separately. Nanoemulsions might be of two types the o/w or w/o . Nanoemulsion can be created Either by high-energy or low-energy emulsification techniques [27,28]. Whenever the high-energy emulsification technique is used, external energy will cause the oil phase to break down and create nanosized droplets in the aqueous phase. Additionally, it might employ high-pressure homogenization and ultrasonic emulsification techniques. The solvent displacement method, phase inversion temperature method, and low-energy emulsification procedures are all applicable [29]. Ultimately, the chosen surfactant and co-surfactant are dissolved in the appropriate aqueous or oil phase, depending on the situation. The active ingredient will then be heated and combined in the appropriate phase. The nanoemulsion is then created by progressively adding one phase to another while stirring continuously until the entire mixture reaches room temperature [30]. Every herbal medicine's nanoemulgel formulation has a nanoemulsion that is disseminated in the gel phase. Nanoemulsions are converted into gels by the aid of various thickening agents like carbopol 934, carbopol 940, and hydroxypropyl methyl cellulose (HPMC), they not only help in gel formation but also increase the thickness of the formulation for better spread ability and may interact with the surfactant to modify the viscosity of the formulation as needed [31]. Triethylamine was also used to adjust pH [32]. In order to improve skin penetration, this composition formulation exhibits a dual release control system [33]. By lowering the emulsion's surface and interfacial tension as well as its transport characteristics, the gelling phase stabilizes the formulation.

Rationale behind use of Emulgel

Dosage forms like Ointments, creams, lotions, and other frequently used topical formulations are often associated with a number of disadvantages, including stickiness that might irritate patients when applied, a reduced coefficient of spreading, and the requirement for rubbing while applying. Additionally, they are having stability issues. The usage of transparent gels has grown in both pharmaceutical and cosmetic preparations due to the aforementioned



**Ketha Srilekhya et al.,**

drawbacks of the vast group of semisolid preparations. The surface tension between the colloid gel and the macromolecular fibre network produced by the little quantity of gelling material present immobilizes the colloid gel, which is typically 99% liquid. Currently, more than 40% of therapeutically effective chemicals are hydrophobic, and gel's ability to handle these substances is severely constrained. A technique that can successfully include and deliver a therapeutic hydrophobic moiety with increased solubility and penetrability through the skin is the emulsion-based gel. Due to the emulgel's high penetration of soft tissues, it can also result in a significant improvement in the pharmacological activity and a decrease in the drug's dose[32]. In recent years, there has been a lot of interest in the usage of new polymers with intricate roles as thickeners and emulsifiers. By lowering surface and interfacial stress and raising aqueous phase viscosity, these chemicals' capacity to gel enables the production of stable emulsions and creams[34,35].

Formulation Considerations

It is crucial to assess topical emulgel for its non-toxic, non-irritating, non-comedo genic, and non-sensitizing features when developing the product. Furthermore, it is crucial to create an emulgel that is both aesthetically pleasing and biocompatible. The formulation excipients utilized are primarily responsible for the aforementioned emulgel characteristics. As a result, the formulation issues become crucial in the emulgel[36–41].

Drug

The drug's characteristics have the biggest impact on how well it absorbs into the skin. Drugs must have certain physical, chemical, and biological characteristics in order to be formulated into emulgel for topical or trans dermal use. The ideal drug candidate for emulgel formulation should have a high pKa value, a half-life ($t_{1/2}$) of less than 10 hours, a molecular mass of 500 daltons or less, a low molecular size, a low partition coefficient ($\log P$) value of 0.8 to 5, and low polarity. A non-irritating medication candidate should also have a skin permeability coefficient of at least 0.510-3 cm/h [42].

Vehicle

Vehicle plays a crucial role in the emulgel's formulation as it is a part of how well the medication is absorbed through the skin. The vehicle used to prepare the emulgel should have qualities such effective drug deposition with even distribution on the skin, drug delivery and release at the surgical site, and maintaining a therapeutic level in the target tissue for an adequate amount of time. It should also be suitable with the patient's skin[42].

Aqueous component

This makes up the emulsion's aqueous phase. This aqueous phase is in charge of converting the emulsion form into the emulgel when the gelling agent is present. Water and alcohols are two commonly used watery materials[43].

Oils

The main component of the emulgel is an emulsion. The final use of emulgel is mostly related to the choice of type and quantity of oil as one of the phases of the emulsion. Oil phase influences the viscosity, permeability, and stability of the emulsion. The oil must be pure and free of undesirable and un saponifiable components, such as free radicals, peroxides, sterols, and polymers, during the selection of oil phase. Unstable formulations often occur as a result of deterioration of oil phase that contains undesirable elements [44,43]. For topically applied emulsions, mineral oils are frequently utilized as the carrier as well as for their occlusive and sensory qualities, either alone or combined with soft or hard paraffin. Widely used oils in oral preparations include non-biodegradable mineral and castor oils, which have a local laxative effect. As nutritional supplements, fish liver oils or various fixed oils of vegetable origin (such as arachis, cotton, and maize oils) are used [44].

Emulsifiers

Emulgel is an emulsion that has been gelled using the proper gelling agent. Unstable emulsions are stabilized thermo dynamically by means of a proper amount of emulsifying agents. The emulsifying agents are primarily responsible for lowering the interfacial tension, which increases the emulsion's stability. The chosen emulsifying agent needs to





Ketha Srilekhya et al.,

produce stable emulsions and have a satisfactory Hydrophilic-Lipophilic Balance (HLB). Stability of emulsion is mainly related to the type and quantity of emulsifying agent added to it. In general emulsifying agents with HLB of less than 8 are used to prepare w/o type emulsion and o/w type emulsion is prepared by using emulsifying agents with HLB of more than 8[44]. Emulsifying agents aid in emulsification during manufacture as well as to preserve stability during shelf life. The following substances are frequently employed as emulsifiers: polyethylene glycol 40 stearate, sorbitan monooleate (Span 80), polyoxyethylene sorbitan monooleate (Tween 80), stearic acid, and sodium stearate[42,44].

Gelling agents

Gelling (cross-linking) agents are crucial components of the emulgel needed to create a thixotropic system. They are primarily used as a thickening agent to improve the quality and texture of the dosage form. The stability and drug release of emulgel are significantly influenced by the type of gelling agent used and its concentration. For instance, it has been noted that emulgels prepared with carbopol polymers release drugs less effectively than those made with hydroxypropyl methyl cellulose (HPMC), a gelling agent[45]. Numerous studies have shown that the concentration of the gelling agent and the medicine release from the emulgel also have an inversely proportional relationship. Combining gelling agents was also reported to increase the stability of emulgel[46].

Penetration enhancers

Trans dermal administration of the medication has been improved by the addition of substances called as penetration enhancers. Medicine penetration from emulgel depends on the type and concentration of the penetration enhancer. To improve the trans dermal distribution of the medicine, it is therefore necessary to optimize the kind and concentration of these agents. Low irritancy, low toxicity, and improved penetrability should be characteristics of the penetration enhancers employed in the emulgel. Penetration enhancers act by various methods, such as momentarily rupturing the skin barrier, fluidizing the lipid channels between corneocytes, modifying the partitioning of the drug into skin structures, etc., [44]. Some of the commonly used penetration enhancers are Oleic acid, lecithin, isopropyl myristate, linoleic acid, clove oil, menthol, eucalyptus oil, MyrjTM, Transcutol® P, cineol, etc. [22].

Methods of Preparation

Three steps make up the straightforward process for making emulgel. The creation of the emulsion and gel basis separately, followed by the inclusion of the emulsion into the gel base to create the emulgel, are the first two phases. Figure 2 depicts the basic steps in the emulgel preparation. In the earliest stages of the emulsion formulation, distilled water is mixed with hydrophilic surfactants or emulsifying agents like Tween 20 to create the aqueous phase. Span 20 or another emulsifying agent, such as lipophilic surfactants, are similarly dissolved into oil (liquid paraffin) to prepare the oil phase. An emulsion is created by heating the aqueous and oil phases separately to a temperature between 70° and 80° before combining the two phases while stirring continuously. Gel phase preparation involves scattering gelling chemicals into distilled water, such as carbopol or HPMC. In order to create emulgel, the emulsion and gel phases are finally combined in a 1:1 ratio while being gently stirred[47]. Another method for creating emulgels has been published. It comprises multiple processes, including neutralizing the polymer after it has been dispersed in the aqueous phase and emulsifying the oil phase. The polymer is first dissolved in deionized water and continuously swirled at room temperature for the appropriate amount of time and speed. The subsequent addition of sodium hydroxide (NaOH) solution neutralizes the resulting dispersion and causes the polymer chains in the dispersion to contract, resulting in the development of a stable gel. The gel is subsequently kept at 4 degrees for 24 hours, which completes the hydration of polymer gels. In order to create emulgel, the oil phase is lastly introduced to the polymer gel while being continuously stirred.

Evaluation of Emulgel

Physical appearance

Characteristics of gel like Colour, homogeneity and consistency are checked visually. The resulting gellified emulsion's 1% aqueous solution's pH values are determined using a pH meter (Digital pH meter 115 pm)[48–50].





Ketha Srilekhya et al.,

Spreading coefficient

The device recommended by Mutimer is used to calculate the spreading coefficient. It is made up of a wooden block with a pulley attached to one end. The 'Slip' and 'Drag' properties of the emulgel are used to calculate the spreading coefficient. On the wooden block is fastened a ground glass slide. On this ground slide, extra emulgel (approximately 2 g) is used for the investigation. Then, a second glass slide with the same dimensions as the fixed ground slide is placed in between this one and the emulgel preparation. There is a hook included with the second glass slide. To remove air and create a consistent emulgel coating between the two slides, a weight of 500 mg is placed on top of them for five minutes. The weight that has been measured is added to the pan that is hooked to the pulley. The top slide's time (s) to travel a distance of 5 cm is noted. A better spreading coefficient is indicated by a shorter interval [48–50]. It is determined via the formula below.

$S=M \times L / T$ Where, M=Weight tied to upper slide; L=Length of glass slides and T=Time taken to separate the slides.

In vitro release study

For drug release research, Franz diffusion cells are employed. 200 mg of the gelatinized emulsion are equally placed to the egg membrane's surface. Between the donor and the receptor chambers of the diffusion cell, the egg membrane is pinched. To solubilize the medication, a freshly made solution of Phosphate Buffered Saline (PBS) (pH 5.5) is poured into the receptor chamber. A magnetic stirrer is used to stir the receptor chamber. After the necessary dilutions, the samples (1.0 ml aliquots) are collected at a reasonable interval and subjected to a UV visible Spectrophotometer analysis to determine their drug concentration. As a function of time, the total amount of medication released through the egg membrane is calculated [48–50].

Antimicrobial assay

The antimicrobial assay uses microorganisms to estimate antimicrobial agents both qualitatively and quantitatively. This test can be run using the agar well diffusion method or the ditch plate method. In the agar well diffusion technique, sterile nutrient agar medium is first used to make the agar plates. Following that, these plates are inoculated with a particular amount of a 24 hour broth culture. The 8 mm-diameter cavities are then created on the agar plates using a sterile borer. The test formulations are then added into each cavity separately (fixed volume). Finally, the diameter of the zone of inhibition in mm is determined after each plate has been incubated for 24 to 48 hours at 37° [46]. When using the ditch plate approach, the test formulation is first deposited in the prepared ditch in the plate containing media. The fresh culture loop is then streaked at a right angle from the ditch to the plate's edge across the agar. The plates are then incubated at 25° for 18 to 24 hours, after which the percentage of inhibition is calculated [51]. % Inhibition = $L_2 / L_1 \times 100$

Where, L_1 =Total length of the streaked culture and L_2 =Length of inhibition

Skin irritation test

Studies on skin irritation are carried out both in vitro and in vivo. The main goal of this study is to assess how well the emulgel's ingredients tolerate being applied topically. Hen's Egg- Chorioallantoic Membrane (HET-CAM), a suggested test by the Organization for Economic Co-operation and Development (OECD), is used in the in vitro skin irritation study. This method uses recently laid hen eggs containing fully grown chick embryos, and it studies the irritating behaviour of test formulation on chick embryo [52]. On the other hand, a number of studies noted that the in vivo skin irritation test was carried out on rabbits or rats. Before the investigation begins, the rat or rabbit's (4 cm²) skin is shaved. The created emulgel formulation (specific dose) is then applied to the animal's skin on the dorsal side, where it has been shaved. Animals are checked for signs of irritation 24 hours later. The animals' skin irritation is documented, and a score is given [46], including any erythema or edoema. Other in vivo animal studies done for emulgel may be relevant to the type of drug added to the emulgel and eventual application of the created system. Anti-inflammatory, anti-fungal, and other potential tests may be included of this procedure [46].





Ketha Srilekhya *et al.*,

Pharmacokinetic study

For those emulgel formulations that exhibit systemic absorption upon trans dermal administration, the pharmacokinetic investigation is carried out. The major pharmacokinetic parameters, including peak plasma concentration (C_{max}), duration to achieve C_{max} (T_{max}), and total area under the curve (AUC₀₋), are evaluated in animals like rats. Following a particular amount of time following topical administration, a blood sample is taken from the animal via the retro-orbital vein in order to estimate the aforementioned parameters. The samples are then centrifuged for 10 minutes at a temperature of 4° at 15 000 rpm. The separated plasma (100 l) is then combined with 1 ml of acetonitrile to precipitate the proteins. The samples are then centrifuged one more for 5 minutes at 15 000 rpm and 4°, and the supernatant (20 l) is collected. Finally, the sample is analyzed using High-Performance Liquid Chromatography (HPLC)[53].

Stability study

Emulgel's stability research is carried out in accordance with recommendations from the International Council on Harmonisation (ICH). Briefly, aluminium collapsible tubes are used to package the emulgel compositions. The tubes are then kept for three months at various temperatures and relative humidity levels, including 5°, 25°/60%RH, 30°/65% RH, and 40°/75% RH. The formulations are removed from storage after a specific amount of time (15, 30, 60, and 90 d) and can then be tested for physical appearance, viscosity, pH, drug content, in vitro drug release, and other factors[51].

Packaging of Emulgels

According to the Public Assessment Report of Voltaren Emulgel, the packaging of emulgel is typically done in membrane-sealed lacquered aluminium tubes with an inner coating of a phenoxy-epoxy-based lacquer and capped with a propylene screw cap. These lamination tubes combine the advantages of aluminium tubes with their plastic-like look. The latest generation of laminate tubes combines cutting-edge technology to create tubes with the most graphic space possible. Light, air, and moisture cannot be transferred via laminate material. It is made of two layers: shelf-appealing plastic tubes and an aluminium layer that provides integrity. As they offer high gloss protective lacquer, a resistant barrier for products requiring maximum compatibility, as well as flavour and smell protection with decreased absorption, the protective barrier serves a variety of purposes [54].

Tubes made of laminated material

Laminated foil

Laminates made of foil act as a barrier against moisture, air, and light. It lessens the aroma's (flavour and smell) absorption. Additionally, it exhibits aluminium characteristics with a plastic-like appearance.

All laminated plastic

It features a barrier that resists chemicals. It provides a plastic-like appearance and feel and aids in maintaining shape and form. It appears to be both opaque and transparent.

CONCLUSION

It has been determined that topical Nanoemulgels are a more favourable option for a dependable and practical medicine transport system. The gel-like and non-greasy characteristics of the new formulations increase patient compliance, and the absence of oil as a basis enhances medication release. Having more appropriate Spread ability, Based on formulations, issues with conventional emulsions including phase separation and creaming are eliminated. Using nanoemulsion-gel may also offer a more effective and reliable method for the management of drugs that are hydrophobic. Hydrophobic substances make up a large portion of the pills used to treat skin infections. These tablets can be successfully incorporated into the oil portion of the nano emulsion before being distributed as Nanoemulgels and after that, the gel base is mixed. Despite several challenges, nano emulgel has a good possibility of being the primary topical delivery system for lipophilic medications in the future. For topical medications used to treat a wide





Ketha Srilekhya et al.,

range of illnesses, it offers a variety of transport options, including the flexibility to alter drug release as well as high drug loading due to improved solubilizing efficiency. Along with trans dermal administration, it can also be used to administer medication through the ocular, vaginal, dental, and nose-to-brain routes for the treatment of a variety of local and systemic conditions, including alopecia, periodontitis, and Parkinson's disease.

REFERENCES

1. Ojha, B.; Jain, V.K.; Gupta, S.; Talegaonkar, S.; Jain, K. Nanoemulgel: A promising novel formulation for treatment of skin ailments. *Polym. Bull.* 2022, 79, 4441–4465.
2. Rai, V.K.; Sharma, A.; Thakur, A. Quality Control of Nanoemulsion: By PDCA Cycle and 7QC Tools. *Curr. Drug Deliv.* 2021, 18, 1244–1255.
3. Indrati, O.; Martien, R.; Rohman, A.; Nugroho, A.K. Development of Nanoemulsion-based Hydrogel Containing Andrographolide: Physical Properties and Stability Evaluation. *J. Pharm. Bioallied. Sci.* 2020, 12, S816–S820.
4. Kass, L.E.; Nguyen, J. Nanocarrier-hydrogel composite delivery systems for precision drug release. *Wiley Interdiscip. Rev. Nanomed. Nanobiotechnol.* 2022, 14, e1756.
5. Liu, Y.; Weng, P.; Liu, Y.; Wu, Z.; Wang, L.; Liu, L. Citrus pectin research advances: Derived as a biomaterial in the construction and applications of micro/nano-delivery systems. *Food Hydrocoll.* 2022, 133, 107910.
6. Aithal, G.C.; Narayan, R.; Nayak, U.Y. Nanoemulgel: A Promising Phase in Drug Delivery. *Curr. Pharm. Des.* 2020, 26, 279–291.
7. Sengupta, P.; Chatterjee, B. Potential and future scope of nanoemulgel formulation for topical delivery of lipophilic drugs. *Int. J. Pharm.* 2017, 526, 353–365.
8. Nazneen, S.; Juber, A.; Badruddeen; Mohammad Irfan, K.; Usama, A.; Muhammad, A.; Mohammad, A.; Tanmay, U. Nanoemulgel: For Promising Topical and Systemic Delivery. In *Drug Development Life Cycle*; Juber, A., Badruddeen, Mohammad, A., Mohammad Irfan, K., Eds.; IntechOpen: Rijeka, Croatia, 2022; pp. 1–20.
9. Ricciotti, E.; FitzGerald, G.A. Prostaglandins and inflammation. *Arter. Thromb. Vasc. Biol.* 2011, 31, 986–1000.
10. van der Velden, V.H. Glucocorticoids: Mechanisms of action and anti-inflammatory potential in asthma. *Mediat. Inflamm.* 1998, 7, 229–237.
11. Vane, J.R.; Botting, R.M. Anti-inflammatory drugs and their mechanism of action. *Inflamm. Res.* 1998, 47, S78–S87.
12. Li, Y.; Yao, J.; Han, C.; Yang, J.; Chaudhry, M.T.; Wang, S.; Liu, H.; Yin, Y. Quercetin, Inflammation and Immunity. *Nutrients* 2016, 8, 167.
13. Rao, C.V. Regulation of COX and LOX by curcumin. *Adv. Exp. Med. Biol.* 2007, 595, 213–226.
14. Benson, H.A.E.; Grice, J.E.; Mohammed, Y.; Namjoshi, S.; Roberts, M.S. Topical and Transdermal Drug Delivery: From Simple Potions to Smart Technologies. *Curr. Drug Deliv.* 2019, 16, 444–460.
15. Viswanathan, P.; Muralidaran, Y.; Ragavan, G. Chapter 7—Challenges in oral drug delivery: A nano-based strategy to overcome. In *Nanostructures for Oral Medicine*; Andronesco, E., Grumezescu, A.M., Eds.; Elsevier: Amsterdam, The Netherlands, 2017; pp. 173–201.
16. Heyneman, C.A.; Lawless-Liday, C.; Wall, G.C. Oral versus Topical NSAIDs in Rheumatic Diseases. *Drugs* 2000, 60, 555–574.
17. Permawati, M.; Anwar, E.; Arsianti, A.; Bahtiar, A. Anti-inflammatory Activity of Nanoemulgel formulated from *Ageratum conyzoides* (L.) L. and *Oldenlandia corymbosa* L. Extracts in Rats. *J. Nat. Remedies* 2019, 19, 124–134.
18. Mukherjee, P.K.; Harwansh, R.K.; Bhattacharyya, S. Chapter 10—Bioavailability of Herbal Products: Approach Toward Improved Pharmacokinetics. In *Evidence-Based Validation of Herbal Medicine*; Mukherjee, P.K., Ed.; Elsevier: Boston, MA, USA, 2015; pp. 217–245.
19. Gorzelanny, C.; Mess, C.; Schneider, S.W.; Huck, V.; Brandner, J.M. Skin Barriers in Dermal Drug Delivery: Which Barriers Have to Be Overcome and How Can We Measure Them? *Pharmaceutics* 2020, 12, 684.
20. Yu, Y.-Q.; Yang, X.; Wu, X.-F.; Fan, Y.-B. Enhancing Permeation of Drug Molecules Across the Skin via Delivery in Nanocarriers: Novel Strategies for Effective Transdermal Applications. *Front. Bioeng. Biotechnol.* 2021, 9, 646554.



**Ketha Srilekha et al.,**

21. Zoabi, A.; Touitou, E.; Margulis, K. Recent Advances in Nanomaterials for Dermal and Transdermal Applications. *Colloids Interfaces* 2021, 5, 18.
22. Kim, B.; Cho, H.-E.; Moon, S.H.; Ahn, H.-J.; Bae, S.; Cho, H.-D.; An, S. Transdermal delivery systems in cosmetics. *Biomed. Dermatol.* 2020, 4, 10.
23. Wiechers, J.W. The barrier function of the skin in relation to percutaneous absorption of drugs. *Pharm. Weekbl.* 1989, 11, 185–198.
24. Anton N, Vandamme TF. The universality of low-energy nano-emulsification. *International journal of pharmaceutics.* 2009, 377(1-2):142-147.
25. Khullar, Rachit, et al. "Emulgels: a surrogate approach for topically used hydrophobic drugs." *Int J Pharm Bio Sci* 1.3 (2011): 117-28.
26. Kumar, P. M., et al. "Emulgels: a novel approach to topical drug delivery." *Int J Univ Pharm Bio Sci* 2.1 (2013): 134-48.
27. Joshi, Baibhav, et al. "Emulgel: a comprehensive review on the recent advances in topical drug delivery." *Int Res J Pharm* 2.11 (2011): 66-70.
28. Flanagan J, Kortegaard K, Pinder DN, Rades T, Singh H. Solubilisation of soybean oil in microemulsions using various surfactants. *Food hydrocolloids.* 2006, 20(2-3):253-260.
29. Date AA, Desai N, Dixit R, Nagarsenker M. Self-nanoemulsifying drug delivery systems: formulation insights, applications and advances. *Nanomedicine.* 2010, 5(10):1595-1616.
30. Sultana N, Akhtar J, Khan MI, Ahmad U, Arif M, Ahmad M, Upadhyay T. Nanoemulgel: For Promising Topical and Systemic Delivery. in J. Akhtar et al. (eds.), *Drug Development Life Cycle [Working Title]*, IntechOpen, London. 2022. 10.5772/intechopen.103878.
31. Dhawan B, Aggarwal G, Harikumar SL. Enhanced transdermal permeability of piroxicam through novel nanoemulgel formulation. *International journal of pharmaceutical investigation.* 2014, 4(2):65.
32. Sampathi S, Mankala SK, Wankar J, Dodoala S. Nanoemulsion based hydrogel of itraconazole for trans dermal drug delivery. *Journal of Scientific and Industrial Research.* 2015, 74:88-92.
33. Raut BP, Khan SA, Ubhate AA, Ganjiwale RO. A review on herbal nanoemulgel for the treatment of acne vulgaris. *World Journal of Pharmaceutical Research.* 2021, 10(9):487-497.
34. Patel, C., et al. "Microemulsion based gel: A Combination of emulsion and gel." *Journal of drug discovery and therapeutics* 1.6 (2013): 57-61.
35. Panwar, A., et al. "Emulgel: A review." *Asian J Pharm Life Sci* 2231 (2011): 4423.
36. Aher, S. D., et al. "Emulgel: a new dosage form for topical drug delivery." *IJIPLS* 3.3 (2013): 1-10.
37. Alexander, Amit, et al. "Recent expansions in an emergent novel drug delivery technology: Emulgel." *Journal of Controlled Release* 171.2 (2013): 122-132.
38. Pant, Shailaja, et al. "A review on emulgel novel approach for topical drug delivery system." *World journal of pharmacy and pharmaceutical sciences* 4.10 (2015): 1728-1743.
39. Dev, Asish, Reha Chodankar, and Om Shelke. "Emulgels: a novel topical drug delivery system." *Pharmaceutical and biological evaluations* 2.4 (2015): 64-75.
40. Khullar, Rachit, et al. "Formulation and evaluation of mefenamic acid emulgel for topical delivery." *Saudi pharmaceutical journal* 20.1 (2012): 63-67.
41. Mulye, Snehal P., Kiran A. Wadkar, and Manish S. Kondawar. "Formulation development and evaluation of Indomethacin emulgel." *Der pharmacia sinica* 4.5 (2013): 31-45.
42. Charyulu, Narayana Rompicherla, et al. "Emulgel: A boon for enhanced topical drug delivery." *Journal of Young Pharmacists* 13.1 (2021): 76.
43. Anand, Kumar, et al. "Nano-emulgel: emerging as a smarter topical lipidic emulsion-based nanocarrier for skin healthcare applications." *Recent patents on anti-infective drug discovery* 14.1 (2019): 16-35.
44. Alexander, Amit, et al. "Recent expansions in an emergent novel drug delivery technology: Emulgel." *Journal of Controlled Release* 171.2 (2013): 122-132.
45. Mohamed, Magdy I. "Optimization of chlorphenesin emulgel formulation." *The AAPS journal* 6 (2004): 81-87.
46. Shahin, Mostafa, et al. "Novel jojoba oil-based emulsion gel formulations for clotrimazole delivery." *Aaps Pharmscitech* 12 (2011): 239-247.





Ketha Srilekhya et al.,

47. Malavi, S., et al. "Emulgel for improved topical delivery of Tretinoin: Formulation design and characterization." *Annales Pharmaceutiques Françaises*. Vol. 80. No. 2. Elsevier Masson, 2022.
48. Azeem, Adnan, et al. "Nanocarrier for the transdermal delivery of an anti parkinsonian drug." *AAPS PharmSciTech* 10 (2009): 1093-1103.
49. Bolzinger, M-A., et al. "Percutaneous release of caffeine from microemulsion, emulsion and gel dosage forms." *European Journal of Pharmaceutics and Bio pharmaceutics* 68.2 (2008): 446-451.
50. Fini, Adamo, et al. "Control of transdermal permeation of hydrocortisone acetate from hydrophilic and lipophilic formulations." *AAPS PharmSciTech* 9 (2008): 762-768.
51. Tanaji, Dilip Nandgude. "Emulgel: A comprehensive review for topical delivery of hydrophobic drugs." *Asian Journal of Pharmaceutics (AJP)* 12.02 (2018).
52. Sandeep, D. S. "Development, characterization, and in vitro evaluation of aceclofenac emulgel." *Asian Journal of Pharmaceutics (AJP)* 14.03 (2020).
53. Aparna, C., Prathima Srinivas, and K. S. K. R. Patnaik. "Enhanced transdermal permeability of telmisartan by a novel nanoemulsion gel." *Int J Pharm Pharm Sci* 7.4 (2015): 335-42.
54. Bhavesh, S., and C. N. Shah. "Nanoemulgel: a comprehensive review on the recent advances in topical drug delivery." *Pharma Sci Monit* 7.2 (2016): 346-355.

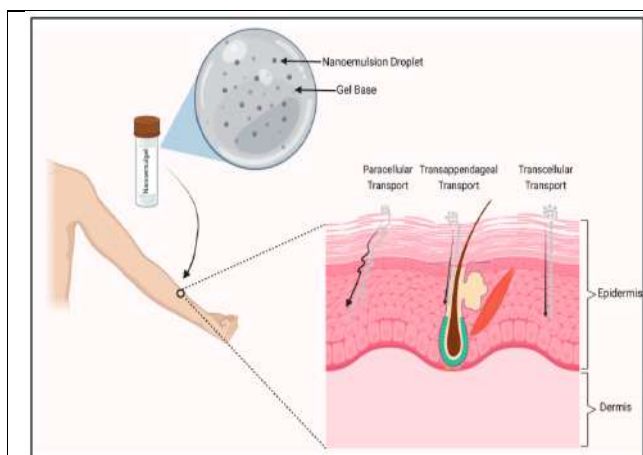


Fig. 1. Mechanistic representation of nanoemulgel delivery via skin.

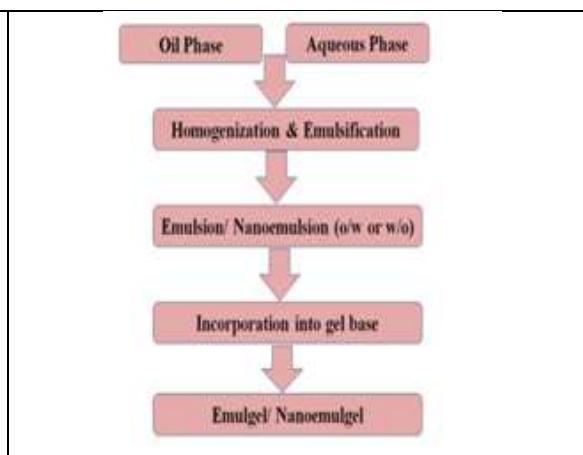


Fig. 2: Fundamental steps in the preparation of emulgel





Correlation between Pes Planus and Osteoarthritis of Knee in Ipsilateral Leg Patients: Cross Sectional Pilot Study

Santosh Kumar Rajak¹, Abhijit Kalita², Abhijit Dutta³ and Pratap Chandra Sarma^{4*}

¹Teaching Associate, Department of Physiotherapy, Assam Women's University, Assam, India

²Associate Dean (i/c), Faculty of Physiotherapy and Rehabilitation, Assam down town University, Panikhaiti, Guwahati, Assam, India.

³Dean, Faculty of Paramedical Sciences, Assam down town University, Panikhaiti, Guwahati, Assam, India.

⁴Chairperson, Faculty of Science and Paramedical Sciences, Assam down town University, Panikhaiti, Guwahati, Assam, India.

Received: 21 Sep 2023

Revised: 10 Nov 2023

Accepted: 05 Jan 2024

*Address for Correspondence

Pratap Chandra Sarma

Chairperson,

Faculty of Science and Paramedical Sciences,

Assam down town University, Panikhaiti,

Guwahati, Assam, India.

Email: drpratapsarma@gmail.com



This is an Open Access Journal / article distributed under the terms of the **Creative Commons Attribution License** (CC BY-NC-ND 3.0) which permits unrestricted use, distribution, and reproduction in any medium, provided the original work is properly cited. All rights reserved.

ABSTRACT

Osteoarthritis (OA) is a chronic degenerative ailment of multi factorial etiology characterized by deprivation of Particular cartilage and many other structural changes. In Indian impact, nearly 80% of population indicates OA among the patient who claimed for knee pain, out of which approximately 20% reported difficulty in daily activities. Pes planus or Flat feet is a condition where the curvature of Medial Longitudinal Arch (MLA) is more flat than normal and entire sole of the foot comes into near complete or complete contact with the ground. As the evidence of OA Knee prevalence in India is well documented, and its most of the risk factors are studied like Age, Obesity, Bone density, while the Pes planus (Flat Feet) is not considered while treating OA Knee. Aim of the study is determine the correlation between Acute OA knee and Pes Planus. Subjects diagnosed as Acute Osteoarthritis of Knee were chosen from specific private clinics of Guwahati, Assam. After diagnosed as Acute Osteoarthritis of knee by the Medical practitioner with radiological evidence, 45 subjects were selected through purposive sampling; 3 drop outs from the study. Later they were assessed for Pes planus through Navicular drop test. (NDT) by a Qualified Physiotherapist. A Spearman's rho is 0.244 which indicates a weak relationship between the variables OA and NDT. The significance (two-tailed) value is 0.119 which concludes that the correlation is statistically weak. These outcomes show that weak association between the subjects suffering from OA





Santosh Kumar Rajak et al.,

knee and Pes Planus. Statistically it indicates no considerable correlation, but it is worth to have further investigation to assess the correlation among the two variables.

Keywords: Flat feet, Navicular drop test ,Osteoarthritis of Knee(OA Knee), Pes planus.

INTRODUCTION

Osteoarthritis (OA) is a chronic degenerative disorder of multifactorial etiology characterized by loss of Particular cartilage, hypertrophy of bone at the margins, sub-chondral sclerosis and range of biochemical and morphological alterations of the synovial membrane and joint capsule. In Indian impact, nearly 80% of cases shows OA among which claimed for knee pain, out of which roughly 20% reported incapability in activities of daily living and around 11% need peculiar care [1] . Approximately 40% population of more than 70 years shows OA, in which nearly 2% have severe knee pain and disability [2] A community based cross sectional study on morbidity pattern of elderly in Rani block, Kamrup [3] Pes planus is a medical condition where the arch of MLA of foot is more flat than normal and entire sole of the foot comes into near complete or complete contact with the ground [4]. The structure and dynamicity of foot arches are essential for functions of foot like shock absorption, body weight transmission and to act as a lever for propelling the body forward during locomotion [5] The feet appear to be flat in infants due to presence of fat. The arches become prominent when the child starts walking and the foot starts bearing the weight [6]. The arches of foot rapidly develop between two to six years and become structurally mature around 12-13 years [7].Prevalence of flat feet is higher in children due to ligament laxity and declines with age. Early shoe wearing in children impairs the development of longitudinal arches [8].Flat foot deformity was classified into three subtypes by Harris RT and Beath T, viz. rigid flat foot, Flexible Flat Foot (FFF) and Flexible Flat Foot With Short Tendo-Achilles (FFF-STA) [9]. FFF is generally asymptomatic while FFF-STA gives rise to pain and functional disability. Rigid flat foot is often symptomatic and associated with tarsal coalitions and reduced range of motion at sub talar joint.

The true prevalence of flat foot is uncertain due to lack of exact clinical or radiographic criteria for defining flat foot [10]. The prevalence of flat feet has been investigated by many researchers in different parts of the world. Higher prevalence (21 to 57%) is reported among children of two to six years which declines (13.4% to 27.6%) in primary school children [11,12]In adult population, it is reported to be approximately 5 to 14% by different researchers [13]. Literature on the prevalence of adult flat foot in Indian population is limited and wherever it is available the methods employed to determine the flat feet, such as Foot print method or Visual Assessment method, are less reliable [14,15].So the present study was undertaken to investigate the prevalence of FFF among adults (46 to 59-year-old) by using NDT which has proven to be more valid. Additionally, the study also aimed to find out the correlation of ND with demographic variables such as Height, Weight and Body Mass Index (BMI) of the individualThe development of foot arch is rapid between 2 and 6 years of age and becomes structurally matured around 12or 13 years of age. A flexible flat foot has an arch that is present in open kinetic chain (non-weight bearing) and lost in closed kinetic chain (weight bearing). A rigid flatfoot has loss of the longitudinal arch height in open and closed kinetic chain, generic classification of flat foot deformities that differentiated between flat feet due to physiological and pathological etiologies. Causes of flat foot can be Congenital flat foot, adult flexible flat foot, posterio tibial tendon dysfunction, tarsal coalition, peroneal spastic flat foot, latrogenic, post traumatic arthritis, charcot foot,neuro muscular flat foot.[16] Foot and ankle specialists agree that flatfoot is a frequently encountered pathology in the adult population.[17]

Evidence suggests that many of the characteristic features of knee OA are related to mechanical loading [18]. Excessive loading of the knee can result from factors that increase compressive and/or shear stress on the tibio femoral (TF) or patella femoral (PF)compartments. Much of the research has focused on the consequences of local kneemal alignment [19,20,21] The association between patellar alignment on magnetic resonance imaging and radiographic manifestations of knee osteoarthritis.[22] However, the foot plays an even more immediate role in





Santosh Kumar Rajak *et al.*,

absorbing the mechanical stresses of ground contact and sculpting the pattern of postural alignment and joint motion at the knee and throughout the lower extremity [23] Despite its central role in lower extremity biomechanics, little is known about the consequences of abnormal foot morphology (planus or cavus) for the risk of knee tissue damage or frequent knee symptoms. Planus foot morphology (“flat-footedness”) has been posited to contribute to both TF [24,25] and preliminary findings suggest that cases of older adults with medial TF OA may differ from age-matched controls in several common clinical indicators of flat-footedness in standing [26]. During most weight bearing activities, the posture and motion of the foot and knee are coupled within a closed kinematic chain. Closed chain coupling may link excessively planus foot morphology to excessive internal rotation of the lower limb [27] The consequences of this rotation are unknown, but it may have effect on mechanical stress across the knee, possibly resulting in increased rotational stress on the load bearing tissues of the TF compartments and increased contact between the articulating surfaces of the lateral patella and the lateral trochlea femoris. As the evidence of OA Knee prevalence in India is well documented, and its most of the risk factors are studied like Age, Obesity, Bone density, while the Pes planus (Flat Feet) is not considered while treating OA Knee. While this study will try to find the correlation between OA Knee and Pes Planus

AIMS AND OBJECTIVES

To Find the Co Relation Between Pes Planus And Oa Knee

METHODOLOGY

It was a cross sectional pilot study in which 45 subjects diagnosed as Acute Osteoarthritis of Knee were included from different private clinics of Guwahati, Assam. After being diagnosed as Osteoarthritis of knee by the Medical practitioner with radiological evidence to assess for the Flexible Flat Feet, they were selected through purposive sampling. Out of 45 subjects 42 were included in the study, 3 subjects dropped out because of unavoidable reasons like leaving out of station, pregnancy during the assessment period and Planned for Surgery. Patients with Deformities in Knee, post-operative cases in lower limb, pregnant women, injury or neuromuscular disorder were excluded from the study at the time of assessment. The study obtained Ethical certificate (Ref. No. IEC/dth/2019/MS/14) from the Institutional ethical committee. Written Informed consent from the participants before undertaking the study. The materials used for the study were custom made index card, ruler, marker pen. The demographic data such as gender, age of each participant were recorded.

Inclusion criteria : Subjects diagnosed as Acute Osteoarthritis of Knee and Positive ND test

Exclusion criteria : Patients with Deformities in Knee

Post-operative cases in lower limb,

Pregnant women, injury or

Neuromuscular disorder

Outcome Measure : Navicular drop test

Source of Data : AdtU OPD, Panikhaiti, Guwahati, Assam

: Active Care, Bhangagharh, Guwahati Assam

PROCEDURE

Each subject was asked to sit in relaxed position with hip and knee flexed at 90 degree and the foot gently placed flat on a firm supporting surface For assessing Pes Planus, the subject was first positioned in relaxed sitting position i.e. non weight bearing position. Using a small rigid ruler, the height of the navicular bone was measured from the floor to the most prominent part of navicular tuberosity when in the neutral talar position. Again the height of the navicular bone was measured in standing position i.e. weight bearing .The difference in measurement is the navicular drop and drop >10mm will be regarded as pes planus. The ND was measured applying Brody Method.

69898





Santosh Kumar Rajak *et al.*,

Each subject was asked to sit in relaxed position with hip and knee flexed at 90 degree and the foot gently placed flat on a firm supporting surface. The observer ensured that the ankle and subtalar joints were placed in neutral position. The height of navicular tuberosity in this position was marked on the index card. The subject was then asked to stand with equal weight on both the feet. Now the new height of Navicular tuberosity was marked on index card . The difference between the marks on the index card (ND) was measured with Vernier caliper. The ND was measured for both feet in each subject.

STATISTICAL ANALYSIS

Correlation between OA Knee and Pes planus was analyzed by Spear man's Correlation test using the SPSS software (version 21) was used to determine the correlation between the OA and pes planus. An adjusted p-value at 0.05 was used to indicate significant difference

RESULT

Participants in the present study were adults from the age group of 46 yrs to 59 yrs. The distribution of Height, Weight , BMI and Navicular drop test values was calculated. [Table 2]. The data was not normally distributed, so we have to express in Median, Mode and Mean. The data of Navicular drop test were assessed with OA Knee patients and it was found that they were weakly associated with each other. A Spearman's rho is 0.244 which indicates a weak relationship between the variables OA and NDT. The significance (two-tailed) value is 0.119 which concludes that the correlation is not statistically significant. While BMI values were also studied and it was found that values (Median, Mode and Mean) were within Normal range, indicative of no relationship of Pes planus and OA Knee. Its observed that out of 42 samples marginal dominance of Women (57. 14 %) over males (42.85 %) was seen [Fig. 3]

DISCUSSION

Pes Planus is a relatively common foot deformity that refers to the loss of the medial longitudinal arch of the foot, resulting in this region of the foot coming closer to the ground or making contact with the contacting ground. It serves as an adaptive support base for the entire body, functions to dissipate the forces of weight bearing and acts to store energy during the gait cycle.[28]Flexible Pes Planus describes a normal arch without bearing weight, which disappears with weight bearing. These results show that weak association between the subjects suffering from OA knee and Pes Planus. Statistically it shows no significant correlation, but it is worth to have further investigation to assess the correlation between the two variables. However this study has its own limitations like sample size and cross sectional study restricts its ability to infer of causation in the observed associations. There is no consensus over standard values of ND among different researchers. Also, the researchers have employed various methods to measure the ND. Brody DM, Muller MJ *et al.*, and Beckett ME *et al.*, have reported the values of 15 mm, 13 mm and 10 mm respectively as the upper limit of range of ND in their study population [31-33]. Very few studies have reported gender wise separate values of ND for right and left foot. The Navicular drop test has found to be more valid and reliable compared to foot print and visual assessment methods applied by other researchers [34,35].

In our study out of 42 OA knee patients, 18 male and 24 female subjects, we found that 14 (33.33 %) of the subjects are suffering from Pes planus in the ipsilateral leg. Our data contradicted with the study done by Yona Kosashvili,Tali Fridman *et. all* in respect to gender distribution. Study done by Yona Kosashvili, Tali Fridman *et. All* reported to have dominance of male over female. However the study was done retrospectively on 97,279 military recruits, which is large sample, but also the recruitment of Males are more in comparison to Females. These findings may have implications for the prevention or treatment of degenerative disease of knee.In a study done byAshok Aenumulapalli *et al.*, Prevalence of Flexible Flat Foot in Adults: A Cross-sectional Study, showed prevalence of 13.6 % .where they took NDT as an outcome measurement to assess the flexibility of the MLA. While Pes Planus is a



**Santosh Kumar Rajak et al.,**

common foot deformity, however getting associated with Osteoarthritis of Ipsilateral Knee still needs to be further analyzed with a larger number of subjects. Another study used the Staheli Arch Index to measure the foot morphology and compared it to knee cartilage damage obtained through MRI imaging around 1,903 subjects. Their findings showed that pes planus feet had 29 % ipsilateral medial tibio femoral cartilage damage on MRI, while there was no association with lateral tibio femoral cartilage damage was a significant finding, however study did not measure the tibio femoral angle, therefore the correlation between pes planus and tibio femoral angle was not determined. Min Zhang, Mao-dan Nie,, Xin-zheng et. all did a study to assess the association between the presence and severity of flatfoot and symptoms of knee OA. Out of 146, 73 patients diagnosed as OA and PP. coexisting flatfoot increased the disability level in patients with knee OA. A study done by I Hetsroni, A Finestone, C Milgrom et.al Titled A prospective biomechanical study of the association between foot pronation and the incidence of anterior knee pain among military recruits in July 2006 where the study suggested no association between Knee pain and pronated foot. In the said study 473 infantry recruits were enrolled. Only 15 % experienced anterior knee pain.

Even though no significant correlation was found between Flexible Pes planus and osteoarthritis of Knee statistically, it's very important and urgent to address the issues clinically and scientifically. Due to limited studies done in the aspect to correlate flexible Pes Planus and Osteoarthritis of Ipsilateral Knee, furthermore studies can be done in a larger sample to identify and reduce the global factors responsible for early degenerative diseases. CM Powers, R Maffucci, S Hampton reported that increased rear foot varus may be a contributing factor in patella femoral pain and should be assessed when evaluating the events at the sub talar joint and the lower extremity. The study was done on 30 female subjects. A small but significant increase in rear foot varus was found in the patella femoral pain group compared with the control group. Fukano M and Fukubayashi have stated that normal values of ND are difficult to establish as ND is influenced by various factors like foot length, age, gender and BMI [36] Milenkovic S et al., stated that in adults, the FFF or Flexible Pes Planus may be considered as normal variant of strong and stable foot instead of deformity resulting from bony or muscular abnormalities [37] and or opinion are very similar with that. This study had its own limitations, like sample size. Small sample size within a cross sectional population might not have reflected an exact reflection of the numbers. In addition more objective method for pes planus may be used in future studies.

CONCLUSION

After statistical analysis of the observed data, it shows a weak correlation between OA Knee and Pes Planus. While looking at the other studies, it's worth to look at a larger sample to verify the relation.

Limitation

Following are some of the limitations that were experienced and seen during the study depending upon the selection criteria, sample size was less.

Authors contribution statement

Santosh Kr. Rajak Carried out the research work as partial fulfillment for completing his structured doctorate of Philosophy (PhD) programme under the supervision of Dr. Pratap Chandra Sarma. He supervised the entire work and helped in designing the methodology. Dr. Abhijit Kalita helped in drafting the manuscript and reviewing the literature. Dr. Abhijit Dutta helped in conceptualizing the study and also helped in data collection.

ACKNOWLEDGEMENT

The authors would like to thank all the study subjects for their participation and duly acknowledge all the clinicians who have helped for collection of samples



Santosh Kumar Rajak *et al.*,**Conflict of interest** none**Funding Source** This study was self-financed.

REFERENCES

1. Hinman RS, Bennel K, Metcalf B, Crossley K. Delayed onset quadriceps activity and altered knee joint kinematics during stair stepping in individuals with knee joint osteoarthritis. *Arch Phys Med Rehabilitation* 2002; 83: 1080 -6.
2. Jain S, Arthritis: Freedom from pain (last accessed on Dec 2011) Available from: <http://www.Completewellbeing.com/article/towards-a-joint-effort,2008>
3. Hakmaosa A, Baruah KK, Hajong S.A community based cross sectional study on morbidity pattern of elderly in Rani block, kamrup (rural)district, Assam. *Indian Journal of Basic and Applied Medical Research* 2014; 3(4): 72 - 79
4. Lovett HW, Dane J. The affections of the arch of the foot commonly classified as flat-foot. *The Journal of Bone & Joint Surgery*. 1896;8(1):78-92.
5. Ker RF, Bennett MB, Bibby SR, Kester RC, Alexander RM. The spring in the arch of the human foot. *Nature*. 1987;325(6100):147-49.
6. Ogon M, Aleksiev AR, Pope MH, Wimmer C, Saltzman CL. Does arch height affect impact loading at the lower back level in running? *Foot & ankle International*. 1999;20(4):263-66
7. Gore AJ, Spencer JP. The newborn foot. *American Family Physician*. 2004;69(4):865-72
8. Bhoir MT. Prevalence of flat foot among 18-25 years old physiotherapy students: cross sectional study. *Indian Journal of Basic and Applied Medical Research*. 2014;3(4):272-78.
9. Rao UB, Joseph B. The influence of foot wears in the prevalence of flat foot- A survey of 2300 children. *The Journal of Bone & Joint Surgery*. 1992;74(4):525- 27.
10. Harris RI, Beath T. Army foot survey. An investigation of foot ailments in Canadian soldiers. Report No.1574 Ottawa, Ontario. National Research Council of Canada. 1947;44:1-268
11. Shih YF, Chen CY, Chen WY, Lin HC. Lower extremity Kinematics in children with and without flexible flatfoot: a comparative study. *BMC Musculoskeletal Disorders*. 2012;13(1):31
12. Shih YF, Chen CY, Chen WY, Lin HC. Lower extremity Kinematics in children with and without flexible flatfoot: a comparative study. *BMC Musculoskeletal Disorders*. 2012;13(1):31.
13. Vittore D, Patella V, Petrera M, Caizzi G, Ranieri M, Putignano P et al. Extensor deficiency: first cause of childhood flexible flat foot. *Orthopaedics*. 2009;32(1):28.
14. Ganapathy A, Sadeesh T, Rao S. Morphometric analysis of foot in young adult individuals. *World Journal of Pharmacy and Pharmaceutical Sciences*. 2015;4(8):980-93.
15. Menz HB. Alternative techniques for the clinical assessment of foot pronation. *Journal of American Podiatric Medical Association*. 1998; 88(3):119-29.
16. Murely GS, Menz HB, Landorf KB. A protocol for classifying normal and flatarched foot posture for research studies using clinical and radiographic measurements. *Journal of Foot and Ankle Research*. 2009;2(1):22
17. Riccio I, Gimigliano F, Gimigliano R, Porpora G, Iolascon G. Rehabilitative treatment in flexible flatfoot: a perspective cohort study. *ChirOrganiMov*. 2009;93(3):101-7.
18. Volpon JB. Footprint analysis during the growth period. *JPediatrOrthop*. 1994;14:83-85.
19. Brandt KD, Dieppe P, Radin E. Etiopathogenesis of osteoarthritis. *Med Clin North Am*. 2009; 93(1):1-24. xv. [PubMed: 19059018]
20. Sharma L, Song J, Felson DT, Cahue S, Shamiyeh E, Dunlop DD. The role of knee alignment in disease progression and functional decline in knee osteoarthritis. *Jama*. 2001; 286(2):188-195. [PubMed: 11448282]
21. Cahue S, Dunlop D, Hayes K, Song J, Torres L, Sharma L. Varus-valgus alignment in the progression of patellofemoral osteoarthritis. *Arthritis Rheum*. 2004; 50(7):2184-2190. [PubMed: 15248216]
22. Kalichman L, Zhang Y, Niu J, Goggins J, Gale D, Zhu Y, et al.





Santosh Kumar Rajak et al.,

23. Structural factors associated with malalignment in knee osteoarthritis: the Boston osteoarthritis knee study. *J Rheumatol.* 2005; 32(11):2192–2199. [PubMed: 16265702].
24. Williams DSML, Hamill J, Buchanan TS. Lower Extremity Kinematic and Kinetic Differences in Runners With High and Low Arches. *Journal of Applied Biomechanics.* 2001; 17(2):153–163.
25. Williams DS 3rd, McClay IS, Hamill J. Arch structure and injury patterns in runners. *Clin Biomech (Bristol, Avon).* 2001; 16(4):341–347 and PF pathology (10, 11), Tiberio D. The effect of excessive subtalar joint pronation on patellofemoral mechanics: a theoretical model. *J Orthop Sports Phys Ther.* 1987; 9:160–165. [PubMed: 18797010]
26. Powers CM. The influence of altered lower-extremity kinematics on patell of emoral joint dysfunction: a theoretical perspective. *J Orthop Sports Phys Ther.* 2003; 33(11):639–646. [PubMed: 14669959]
27. Reilly A, Barker L, Shamley D, Sandall S. Influence of foot characteristics on the site of lower limb osteoarthritis. *Foot Ankle Int.* 2006; 27(3):206–211. [PubMed: 16539904]
28. Nester CJ, Hutchins S, Bowker P. Shank rotation: A measure of rear foot motion during normal walking. *Foot Ankle Int.* 2000; 21(7):578–583. [PubMed: 10919624] 14. Souza TR, Pinto RZ, Trede RG, Kirkwood RN, Fonseca ST. Temporal couplings between rear foot shank complex and hip joint during walking. *Clin Biomech (Bristol, Avon).* 2010; 25(7):745–7.
29. *Pes Planus*, Raj MA, Tafti D, Kiel J, Treasure Island (FL): Stat Pearls Publishing; 2022 Jan
30. Michaudet C, Edenfield KM, Nicolette GW, Carek PJ. Foot and Ankle Conditions : *Pes Planus*. *FP Essent.* 2018 Feb; 465: 18 -23
31. Brody DM. Techniques in the evaluation and treatment of injured runner. *The Orthopaedic Clinics of North America.* 1982;13(3):541-58.
32. Mueller MJ, Host JV, Norton BJ. Navicular drop as a composite measure of excessive pronation. *Journal of the American Podiatric Medical Association.* 1993;83(4):198-202
33. Beckett ME, Massie DL, Bowers KD, Stoll DA. Incidence of Hyper pronation in the ACL Injured knee: A clinical Perspective. *Journal of athletic training.* 1992;27(1):58-62
34. Menz HB. Alternative techniques for the clinical assessment of foot pronation. *Journal of American Podiatric Medical Association.* 1998; 88(3):119-29.
35. [18] Murely GS, Menz HB, Landorf KB. A protocol for classifying normal and flat arched foot posture for research studies using clinical and radiographic measurements. *Journal of Foot and Ankle Research.* 2009;2(1):22
36.] Fukano M, Fukubayashi T. Motion characteristics of the medial and lateral longitudinal arch during landing. *European Journal of Applied Physiology.* 2009;105(3):387-92
37. Milenkovic S, Zivkovic M, Bubanj S. Incidence of flat foot in high school student series: *Physical Education and Sport.* 2011;9(3):275-81

Table 1: Statistical Analysis of Correlations between Osteoarthritis and PesPlanus using Spearman’s Correlation test. Spearman’s rho value indicates a very weak statistical relationship between Osteoarthritis of Knee and Pesplanus in the ipsilateral leg.

Correlations				
			OA	NDT
Spearman's rho	OA	Correlation Coefficient	1.000	.244
		Sig. (2-tailed)	.	.119
		N	42	42
	NDT	Correlation Coefficient	.244	1.000
		Sig. (2-tailed)	.119	.
		N	42	42





Santosh Kumar Rajak et al.,

Table 2: Distribution of Height, Weight, BMI and Navicular drop among study samples.In the selected subjects for the study the BMI values 24.67 (Median), 22.89 (Mode) and 24.67 (Mean) are considered to be in healthy weight range. While Navicular drop (ND) test values were 9.5 (Median), 8 (Mode) and 10.02 (Mean) respectively Subjects studied in the group were among the age group of 46 – 59 yrs. The distribution of Height, Weight, BMI and Navicular Drop values are shared in (Table 2). The data between Navicular drop and Osteoarthritis of Knee was test with Spearman’s Rho test, shown in (Table 1).

	Min.	Median	Mode	Mean	Max.
Height (cms)	147	167.5	162	167.11	186
Weight (Kgs)	32	71.25	72	68.84	92
BMI	14.81	24.67	22.89	24.67	35.94
ND	5	9.5	8	10.02	18

Table 3. Comparison of Prevalence of Flat foot with previous workers.

Researchers	Sample Size	Age	Method Used	Prevalence
Kosashvili et. all	97,279		IDF medical grading	16.1 %
Hefa Alsaleh et. all	30	26yrs (Mean)	Feiss Line Test	66.66 – 76.66%
K Douglas Gross et. All	1903	65 yrs (mean)	SAI (Staheli Arch Index)	22%
In This study	42			33.33



Fig 1. Procedure for measurement of Navicular drop for Samples in the study. (A) Subject in sitting position with Hip and knee at 90 degree flexion with neutral subtalar joint, (B) Initial Mark of Navicular tuberosity, Height of Navicular bone in Sitting Position is marked in a customized card (Non Weight bearing) (C), Revised Mark of Navicular Tuberosity height after Standing (Weight bearing) is marked in customized card used for measuring Navicular height in Navicular drop test.





Santosh Kumar Rajak et al.,

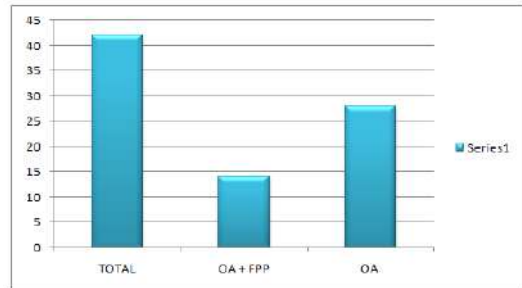
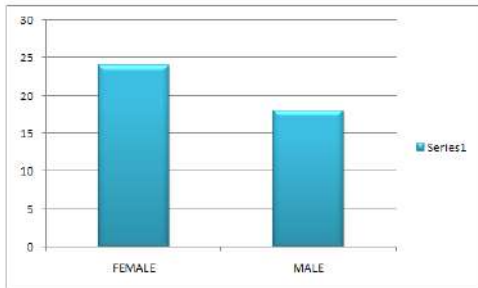


Fig.2. Gender Distribution between the subjects, showing 24 females and 18 males..X axis indicating the gender distribution and Y axis indicating the number of subjects in both gender groups. It's observed that 24 females and 18 males were found in the total sample of 42. It shows the marginal dominance of female (57.14 %) over male (42.85 %).

Fig.3. Distribution of OA of Knee and PesPlanus. It shows the graphical presentation of distribution of subjects in selected and excluded. Total Sample studied were 42, where 14 of them were found to be having Flexible pesplanus in the Ipsilateral leg through Navicular drop test, while 28 individuals were tested negative for Navicular Drop test. Its observed that 33.33 % subjects were tested positive for Navicular drop test while 63.63 % tested negative for Navicular Drop test.





Anti-Rheumatoid Arthritis Activity of Hydro-Ethanollic Extract of *Cassia tora* Seeds in Freund's Complete Adjuvant Induced Arthritis in Rats

Mukesh Lekhak¹, Jyothi Y^{2*}, Dikcha Gupta¹, Syed Sohaila¹ and Yashas R Kumar³

¹Student, Department of Pharmacology, Krupanidhi College of Pharmacy, Bengaluru, (Affiliated to Rajiv Gandhi University of Health Sciences) Karnataka, India.

²Associate Professor, Department of Pharmacology, Krupanidhi College of Pharmacy, Bengaluru (Affiliated to Rajiv Gandhi University of Health Sciences), Karnataka, India.

³Veterinarian, Department of Pharmacology, Krupanidhi College of Pharmacy, Bengaluru (Affiliated to Rajiv Gandhi University of Health Sciences) Karnataka, India.

Received: 26 May 2023

Revised: 17 Nov 2023

Accepted: 13 Jan 2024

*Address for Correspondence

Jyothi Y

Associate Professor,

Department of Pharmacology,

Krupanidhi College of Pharmacy, Bengaluru

(Affiliated to Rajiv Gandhi University of Health Sciences),

Karnataka, India.

E mail: jokiran05@gmail.com



This is an Open Access Journal / article distributed under the terms of the **Creative Commons Attribution License** (CC BY-NC-ND 3.0) which permits unrestricted use, distribution, and reproduction in any medium, provided the original work is properly cited. All rights reserved.

ABSTRACT

In the present study the research work deals with evaluation of anti-rheumatoid arthritis activity of hydro-ethanollic extract of *Cassia tora* seeds in Freund's complete adjuvant induced arthritis in rats. The hydro-ethanollic extract of *Cassia tora* seeds was administered orally at two different doses 800mg/kg and 1600mg/kg for low dose and high dose in rats that were then induced with Complete Freund's Adjuvant (CFA) in sub-plantar surface of the hind paw region and was designated as day 0. Physical parameters like change in body weight, paw volume and grip strength were measured on 0,7,13,17 and 22day and haematological parameters such as RBC, Hb, ESR and total WBC count were measured. The radiology of paw was compared with standard and histopathological studies were also conducted. The study reveals that both 800mg/kg and 1600mg/kg doses of *Cassia tora* seed extract showed significant reduction in paw volume compared to CFA induced group. The treated group showed increased level of RBC and Hb similar to that of the normal group, and the increase in WBC count and ESR was dramatically reduced in the extract treated groups. The extract treated group showed prevention against bony destruction, less swelling of soft tissue along with joint protection compared to arthritic rats by reducing destruction of cartilage. The dose of 1600mg/kg showed reduction in destruction of cartilage and decreased vascularity in the adjacent structures. It is clear from this study that hydro-ethanollic extract of *Cassia tora* seeds showed a powerful anti-rheumatoid arthritis activity.

Keywords: *Cassia tora*, Rheumatoid Arthritis, Complete Freund's adjuvant, anti-rheumatoid.



**Mukesh Lekhak et al.,**

INTRODUCTION

Between 0.3 and 1% of people worldwide are affected by rheumatoid arthritis (RA), a multifactorial autoimmune disease with uncertain cause, usually affects the joints but can also show extra-articularly [1,2]. Rheumatoid arthritis strikes people of all ages, including children, adolescents, as well as the elderly, with women more likely to be affected than men.^[3] Good RA care necessitates a holistic treatment due to its intricacy, which is based on a pathophysiological process that is still partially understood[1]. RA exhibits stages of the pathogenic process, initial symptoms of heat, edema, discomfort, and impaired joint function, and late-stage symptoms of varying degrees of joint stiffness and malformation along with a risk of bone loss and disability[2]. As a common autoimmune disease, rheumatoid arthritis is best studied in animals using immunologically mediated FCA-induced arthritic model[4]. Controlling inflammation, relieving pain, and reducing bone deformity are the basic therapy aims for rheumatoid arthritis. Ibuprofen and naproxen are the most commonly used NSAIDs for relieving pain and swelling [5,6]. The creation of disease-modifying anti-rheumatic drugs (DMARDs), a class to which ordinary synthetic, biologic, and targeted synthetic medications belong, as well as NSAIDs, that have the potential to treat pain and inflammation, produced the most encouraging outcomes [7].

Cassia tora is often referred to as “Sickle senna, Foetid senna, Chakavat and Chakramarda” in India. It belongs to the family Fabaceae and the sub-family caesalpinioideae. It is regarded as a weed in many localities and grows wild in the majority of tropical regions. Its native range is in Nepal, India, Central America, Polynesia, Japan, China and Indonesia widespread from the coast in floodplains, river sides, derelict lands, and barren-land in the plains. Located up to 1400 metres. *Cassia tora* has been reported for analgesic, antipyretic, anticonvulsant, antibacterial, antifungal, anthelmintic, diuretics, laxative, purgative activity and also found to be useful in the treatment of glaucoma, hypertension, skin disease, ringworm, leprosy, flatulence, colic dyspepsia, cough itch[8]. It has been reported in the literature that anthraquinone derivatives like emodin, chryso-obtusin, obtusifolin, physcion, chrysophanol, chryso-obtusin-2-O-beta-D-glucoside and obtusifolin-2-O-beta-D-glucoside has anti rheumatic property[9].

MATERIALS AND METHODS

Cassia tora seeds were brought from Ayush Life Elements, Neemuch, MP. Dr. P.E. Rajasekharan, Principal Scientist, Division of Plant Genetic Resources, verified and authenticated the seeds. It was identified as *Cassia tora* with authentication letter no. PCOL/CT-436/KCP 2021-22.

Plant Extracts Preparation

A 14-day air-drying process was performed on the *Cassia tora* seeds after they were purchased and ground in a blender to a uniform powder. The 500gm of powdered drug was sealed in a Soxhlet device and defatted using pet ether for 6 hrs at 45°C. The defatted material was thoroughly dried to remove any traces of pet ether and extracted the marc using hydro-ethanol (70% ethanol and 30% water) as a solvent till it exhausts completely [10].

Experimental Animals

All investigations employed 150–250gm Wistar albino rats (both sexes); they were procured from the Krupanidhi College of Pharmacy's Central Animal House. 3 rats were housed in each of the polypropylene cages lined with husk, renewed every 24 hr, under a 12-hr light/dark cycle at around 22±2°C with 50% humidity. According to CPCSEA guidelines, rats were fed a regular pellet diet as well as had free access to tap water. The Institutional Animal Ethics Committee gave its approval to the study's protocol with approval number (KCP/IAEC/PCOL/72/2021).

Criteria for Dose Selection

The doses of *Cassia tora* seeds were selected as per the previous toxicity studies conducted and given by oral route [11]. For the current study two doses were selected of which low dose is 800 mg/kg and high dose is 1600 mg/kg.





Mukesh Lekhak et al.,

Experimental Model

Wistar rats were grouped into 5 group consisting 6 rats in each group. Group 1 received normal saline. Group 2 was the control group where rats were induced with CFA (Complete Freund's Adjuvant). Group 3 received a low dose of *cassia tora* extract at 800 mg/kg. Group 4 received a higher dose of *cassia tora* extract at 1600 mg/kg. Lastly, Group 5 was administered the standard treatment, which consisted of Ibuprofen at dose 15 mg/kg.

Freund's Adjuvant Induced Rheumatoid Arthritis In Rat

Animals after 30 min of oral administration of test & standard (Ibuprofen 15 mg/kg body weight) was treated with CFA (0.1ml) in sub-plantar surface of the hind paw region. This was designated as day 0. For a total of 22 days, drug treatment was continued [12].

Evaluation Parameters

Physical Parameters

Body Weight

Lean tissues, which hold the majority of the body's protein, are lost as a result of RA. The animal weight was measured on 0th, 7th, 13th, 17th, 22nd day using weighing balance and body weight of induced group was compared with normal group.

Measurement of Paw volume

The Plethysmometer was used to measure the paw volume. On 0th, 7th, 13th, 17th, 22nd day paw volume was measured and paw volume of induced group was compared with normal group.

Motor Coordination Test

Animals from the same cage were placed in separate lanes on a rod that rotates at 4 rpm and then accelerates to 40 rpm in 300 seconds. Acceleration signalled the start of the trial, which terminated when the animals fell off rod. Timekeeper was paused for the animal when it clung to rod and completed a complete passive spin. Passive rotation was registered, and the animal was then brought back to its own cage. Various trial cut-offs and re-run trial configurations were employed, such as a fourth re-run trial if the animal passively turns (1 or 3 consecutive rotations are allowed) or falls off less than 5 seconds into the trial. 3 trails altogether, with intertribal intervals of 15 minutes, were covered by the same procedure. Animals were weighed at the trail's conclusion [13].

Haematological Parameters

Animals were given diethyl ether anesthesia at the study's conclusion and blood was drawn retro-orbitally into Heparin tubes/ EDTA tubes.

Estimation of RBC using Neubauer's chamber [14].

A sufficient amount of red blood cell dilution solution was poured into a watch glass, and blood was sucked into an RBC pipette by sucking it up to exact 0.5 mark before wiping the tip. Exact 101 marks of RBC dilution solution were sucked up. A suspension of erythrocytes (dilution 1/200) was created by thoroughly mixing blood and liquid. After 5 minutes, a few drops were extracted by holding the pipette vertically and pouring the liquid into counting chamber. 2-3 minutes were given for it to settle. A huge square in the centre and 25 smaller squares were adjusted to light by transitioning to a low power (10x) objective. High power (40x) objective has now been changed. Four of corners and one of centre squares had blood cell counts.

$$\text{Number of RBCs/mm}^3 = \frac{\text{Number of cells counted} \times \text{dilution (200)}}{\text{Area counted (mm}^2) \times \text{depth}}$$





Mukesh Lekhak *et al.*,

Acid Hematin Method For Estimation of Hemoglobin Using Sahli's Hemoglobinometer [15]

After adding N/10 HCL to diluting tube up to mark 20, blood was pipetted into tube up to the 20 mm³ mark, washed the pipette, and after 10 minutes, distilled water was added drop by drop until the colour perfectly matched the standard. The reading which reveals haemoglobin % was then recorded.

Estimation of WBC Using Neubauer's Chamber [14]

In a white blood cell dilution pipette, blood was precisely pipetted out to 0.5 mark. This blood column can't have air bubbles in it. Remaining blood on the pipette's outside was cleaned off to prevent cell transmission to the solution that was diluting it. Drawn diluent fluid to the "11" mark right away, then rotated the pipette between thumb and fingers to mix the sample with diluents. To eliminate air bubbles in the bulb, the pipette held upright. For an equal distribution of cells, pipette's contents were mixed for 3-5 minutes. The capillary end of the pipette discharged an unmixed, mainly cell-free solution (usually 4 drops). The forefinger must be put over the pipette's top (short end) and pipette held at a 45° angle with the tip touching the junction of the cover glass and counting chamber. To fully charge chamber, mixture was run under the cover glass. Allowed cells to settle for about 3 minutes. Observed for even distribution cells under microscope and white cells in each of the four 1 mm² corner spaces were counted including those in the four 1 mm² corner sections.

$$\text{WBC count} = \frac{\text{Cell counted} \times \text{dilution factor (20)}}{\text{Area counted (mm}^2\text{)} \times \text{depth (0.1)}}$$

Platelet Count Determination by Heamocytometry [16]

Fresh blood was manually aliquoted into an Erythrocyte pipette upto the 0.5 point, and afterwards dilution solution was pipetted up to a 101 mark. This mixture took at least 5 minutes. The scoring chamber was charged with fluid after 5 minutes, positioning the pipette vertically allowed the initial drips to be discarded, and fluid was then stored in a wet chamber for 30 minutes to allow the platelets gradually settle. Platelets were enumerated in the full centre 1mm² (erythrocyte counting area) of either flank of the haemocytometer chamber by focusing with a 10x objective on the surface of the chamber, switching to a 40x objective, dimming the light with iris aperture, and lower condenser. It was opted to aggregate the 2 sides.

$$\text{Platelet count/mm}^3 = \text{No. of cells counted} \times \text{dilution factor} / \text{volume } (\mu\text{l})$$

Determination of ESR by Wintrobe Method [17]

ESR is a straightforward, quasi testing method that inferentially assesses the existence of bodily inflammation. Due to a rise in plasma fibrinogen, antibodies, and other acute phase response proteins, it signifies the ability of red blood cells (RBC) to settle more quickly. ESR was determined by Wintrobe method.

Radiographical Analysis

The rats were weighed and Animals used in experiments had their afflicted paws imaged using X-ray technology. The knee joint was selected for the analysis and representative rats from each group were photographed.

Histopathological Examination

Excessive anaesthesia was used to kill all the rats at the conclusion of trial and tibiotarsal joints were collected from each group, washed in ice cold saline. Tibiotarsal joint tissues were then processed for histopathological evaluation after being promptly preserved in 10% buffered neutral formaldehyde solution [13]

Statistical Analysis

The values were illustrated as mean \pm SEM (Standard error of mean). Results were analysed using one way analysis of variance (ANOVA) proceeded by Dunnett's multiple comparison and $p < 0.05$ was regarded as significant.





RESULTS

Plant Extract

Cassia tora seed were air-dried, grounded into a powder, and defatted with petroleum ether. The remaining material was extracted with hydro-ethanol, resulting in a yield of 5.06% w/w.

Effect of *Cassia tora* Seed Extract and Ibuprofen on Body Weight

Complete Freund's adjuvant (CFA) caused significant ($P < 0.05$) decrease in body weight when collated to normal saline treated rats. Treatment with *Cassia tora* seed extract and Ibuprofen showed a change in body weight to near-normal levels significantly ($p < 0.01$). When compared to normal rats, CFA treated (control) rats gained less body weight, which may be because the immunological response was triggered. In high dose treated rats and Ibuprofen treated rats, there was a significant ($p < 0.01$) weight gain when collated with CFA treated rat (Table 1).

Effect of *Cassia tora* Seed Extract and Ibuprofen on Paw Volume

When compared to control rats, Complete Freund's adjuvant (CFA) significantly ($P < 0.001$) enlarged the volume of the paws. Treatments with *Cassia tora* seed extract and Ibuprofen indicated a marked reduction in paw volume to values close to normal. Immunization with sub-plantar injection of CFA produced a larger paw compared to vehicle treated group. The paw volume peaked on day 7 and then gradually decreased over the following days and through the study's conclusion. On treatment with *Cassia tora* seed extract (800mg/kg and 1600mg/kg) a significantly ($p < 0.05$) and dose dependently diminished in paw volume was seen (Table 2).

Effect of *Cassia tora* Seed Extract and Ibuprofen in Fall of Time

Complete Freund's adjuvant (CFA) caused significantly ($p < 0.05$) decline when compared to control rats. Treatment with *Cassia tora* seed extract and Ibuprofen showed increase in fall of time. For the purpose of evaluating motor coordination, the mean fall of time in the rotarod test was calculated. When compared to the group that received vehicle treatment, the fall of time is reduced after CFA administration. Rats treated with *Cassia tora* seed extract (800mg/kg and 1600mg/kg) and Ibuprofen (15mg/kg) markedly increased ($p < 0.05$) fall of time when compared to CFA induced (control) group (Table 3).

Effect of *Cassia tora* seed extract and Ibuprofen on Complete Freund's adjuvant (CFA) induced changes in RBC, WBC, HB, ESR

A significant ($p < 0.01$) reduction in the levels of HB and RBC was observed in the CFA treated when compared with normal rats. Administration of *Cassia tora* seed extract and Ibuprofen to diseased rats RBC and Hb levels returned to normal. The increase in WBC count and ESR was considerably ($p < 0.05$) reduced in the groups that received extract treatment (Table 4).

Histopathological Analysis

The histological analysis of the tibiotarsal joint in the first group revealed the presence of normal synovial lining cells within the cartilage. The second group, the control group showed moderate cartilage cell hyperplasia and distortion of the areolar tissue. These findings indicate that the induction of inflammation through CFA had a significant impact on the joint structure. The third group received a low dose of *cassia tora* at 800 mg/kg. Interestingly, the histological analysis of the tibiotarsal joint in this group demonstrated near normal histology. This suggests that the low dose treatment was able to effectively mitigate the histological changes induced by inflammation, restoring the joint structure to a great extent. The fourth group received a high dose of *cassia tora* at 1600 mg/kg. Strikingly, the histological examination of the tibiotarsal joint in this group showed normal histology. This indicates that the high dose treatment was highly effectively in preventing any adverse histological changes associated with inflammation. Lastly, the fifth group received a standard treatment of Ibuprofen at a dose of 15 mg/kg. The histological analysis of the tibiotarsal joint in this group revealed near normal histology (Fig 1).





Mukesh Lekhak et al.,

Radiographic analysis

According to the X-ray results, animals in the normal group did not exhibit any soft tissue swelling or bone damage. The animals in the control (CFA-induced) group had swollen soft tissues and their joint spaces had shrunk. The *Cassia tora* seed extract treated rats shown prevention against shrinking of joint gap by showing less soft tissue swelling (Fig 2).

DISCUSSION

As a typical autoimmune condition, rheumatoid arthritis is best studied in animals using the immunologically mediated FCA-induced arthritic model. (4) In a model of adjuvant-induced arthritis, inflammatory cells caused rats to experience chronic swelling in a number of joints, as well as bone degeneration and remodelling that are strikingly comparable to the symptoms of rheumatoid arthritis in humans. The current study was initiated to investigate whether hydro-ethanolic extract *Cassia tora* extract could offer anti rheumatoid effect against CFA induced rheumatoid arthritis in rats. The hydro-ethanolic extract of *Cassia tora* seeds was first used for phytochemical studies, which identified the presence of secondary metabolites such as anthraquinone glycosides, flavonoids, proteins, folic acid, saponins, and tannins, among others.

The advancement of a disease's state and how well an anti-inflammatory drug works are both indirectly connected with changes in body weight. The FCA induced (control) rats showed slight gain in body weight, increased paw volume and decreased grip strength as compared with Ibuprofen and *Cassia tora* seed extract treated arthritic rats. In *Cassia tora* seed extract treated and Ibuprofen treated rats, there was a significant weight gain, a significant decrease in paw volume and increased grip strength when compared to Complete Freund's Adjuvant treated rats. When comparing the CFA-treated rats to control rats, a substantial decrease in HB and RBC levels was seen. Administration of *Cassia tora* seed extract and Ibuprofen to diseased rats raised RBC and Hb values to normal levels. The elevation in WBC count and ESR were dramatically mitigated in the extract treated groups. Histopathological studies of the tibiotarsal joints shows destruction of cartilage, erosion of osteoid, inflammatory cells and increased vascularity in adjacent cells in the CFA treated animals. *Cassia tora* seed administered rats exhibited joint protection compared to diseased rats by reducing destruction of cartilage. Rats treated with 800mg/kg and 1600mg/kg showed reduction in destruction of cartilage and decreased vascularity in the adjacent structures. The radiographic characteristics of rat joints in CFA-induced arthritic rats show soft tissue inflammation coupled with shrinking of joint spaces, which presumes the bony ruination in arthritic state. In contrast, the *Cassia tora* seed extract group receiving at both doses of 800mg/kg, 1600mg/kg and Ibuprofen clearly shows substantial protection against bony damage by revealing fewer soft tissue swelling as well as shrinking of joint spaces.

CONCLUSION

In conclusion, present study demonstrated that the treatment with *Cassia tora* seed extract, Ibuprofen significantly potentiated anti-rheumatoid activity against CFA induced rheumatoid-arthritis. The high concentration of anthraquinone glycoside, flavonoids, and polyphenolic components in the extract may be a factor in the antioxidant activity because these compounds are known to have direct antioxidant properties because they include hydroxyl groups, which can act as hydrogen donors. A compound's potential antioxidant activity may be strongly correlated with its capacity for lowering.

REFERENCES

1. Radu A, Bungau S. Management of Rheumatoid Arthritis: An Overview. Cells. 2021;10(11):2857.
2. Sayah A, English JC. Rheumatoid arthritis: A review of the cutaneous manifestations. J Am Acad Dermatol. 2005;53(2):191–209.





Mukesh Lekhak et al.,

3. Küçükdeveci AA. Nonpharmacological treatment in established rheumatoid arthritis. Best Practice & Research Clinical Rheumatology. 2019;33(5):101482.
4. Alfons B. Modes of action of Freund's adjuvants in experimental models of autoimmune diseases. Journal of Leukocyte biology, 2001;70(6):105-9.
5. Kahlenberg JM, Fox DA. Advances in the medical treatment of rheumatoid arthritis. Hand clinics. 2011;41(2).
6. Bullock J, Rizvi SA, Saleh AM, Ahmed SS, Do DP, Ansari RA, Ahmed J. Rheumatoid arthritis: a brief overview of the treatment. Medical Principles and Practice. 2018;27(6):501-7.
7. Radu A, Bungau S. Management of Rheumatoid Arthritis: An Overview. Cells. 2021;10(11):2857.
8. Sarwa K. Phytochemical and Biological Potential of *Cassia tora* Linn. European J Med Plants. 2014;4(8):946–63.
9. Jang D, Lee G, Kim Y, Lee Y, Kim C, Yoo J et al. Anthraquinones from the Seeds of *Cassia tora* with Inhibitory Activity on Protein Glycation and Aldose Reductase. Biological and Pharmaceutical Bulletin. 2007;30(11):2207-10.
10. Patil U, Saraf S, Dixit V. Hypolipidemic activity of seeds of *Cassia tora* Linn. Journal of Ethnopharmacology. 2004;90(2-3):249-52.
11. Cholendra A, Vijayaraghavan R, Babu Y, Mohan SK, Rao SD, Dorababu K, Reddy KK. Acute toxicity studies of *Cassia tora* leaf powder. Int J Pharmacol Res. 2014;4(4):176-81.
12. Rajaram C, Reddy K, Sekhar K. Evaluation of anti-arthritis activity of *Caesalpinia pulcherrima* in Freund's complete adjuvant induced arthritic rat model. Journal of Young Pharmacists. 2015;7(2):128-32.
13. Manjusha C, Vipin K, Pankaj Kumar G, Surender S. Anti- arthritic activity of *Barleriapronitis* Linn. leaves in acute and chronic models in Sprague Dawley rats. Elsevier, 2014; 52(2):199-209.
14. Manual cell counting with Neubauer chamber. Posted on May 14, 2016 by Dhurba Giri in Hematology. [reviewed on 02/01/2020]
15. Balasubramaniam P, Malathi A, Comparative study of hemoglobin by Drabkin's and Sahli's methods. Journal of Postgraduate Medicine. 1992;38(1):8.
16. Nandhini BY, Kumar S, et. al. An improved method for counting platelets. Journal of the American Medical Association, 2018; 80(9): 621-2.
17. www.medicine.mcgill.ca/physio/vlab/bloodlab/esr (reviewed 02/01/2020)

Table 1: Effect of *Cassia tora* seed extract and Ibuprofen on CFA induced changes in body weight on 1st, 7th, 13th, 17th, 22nd day

BODY WEIGHT (gm)	1 st day	7 th day	13 th day	17 th day	22 nd day
NORMAL SALINE	155±1.66	161±1.265	167.66±2.57	174.33±2.389	182.16±2.70
CONTROL (CFA INDUCED)	178.5±2.17	174.8±2.51 ***	168.70±3.70***	169±2.951**	171.3±3.12 ***
LOW DOSE (800mg/kg)	157.8±1.21	165.5±1.455 ^b	174.83±3.515 ^{ns}	185.83±2.372 ^c	179.00±2.633 ^b
HIGH DOSE (1600mg/kg)	151.5±0.9	160.2±1.27 ^b	166.33±2.389 ^{ns}	183.00±2.081 ^b	189.33±1.994 ^a
STANDARD (15mg/kg)	167.7±1.05	185.2±2.738 ^a	190.16±4.512 ^b	199.16±3.534 ^b	208.83±2.441 ^b

Values are plotted as the mean ±SEM, n=6 in each group; analysed by ANOVA followed by Dunnett's test. where, * indicates P<0.05, **p<0.01, *** p<0.001, **** p<0.0001 when control group is compared with normal saline group and ns indicates non-significant, a indicates P<0.05, b p<0.01, c p<0.001, d p<0.0001 when LD, HD and standard group is compared with control group.





Mukesh Lekhak et al.,

Table 2: Effect of *Cassia tora* seed and Ibuprofen on CFA induced change in paw volume on 1st, 7th, 13th, 17th, 22nd day

PAW VOLUME	1 st day	7 th day	13 th day	17 th day	22 nd day
NORMAL SALINE	0.30±0.202	0.33±0.024	0.325±0.03	0.325±0.03	0.316±0.03
CONTROL (CFA INDUCED)	1.20±0.09 0.7	1.38±0.06 ****	1.81±0.09 ****	1.85±0.1 ****	1.717±0.09****
LOW DOSE (800mg/kg)	1.217±0.027	1.41±0.04 ^{ns}	1.2±0.09 ^a	1.1±0.03 ^b	0.935±0.03 ^b
HIGH DOSE (1600mg/kg)	1.4±0.14	1.48±0.06 ^{ns}	1.2±0.057 ^b	1.0±0.04 ^b	0.833±0.04 ^b
STANDARD (15mg/kg)	1.117±0.07	1.2±0.06 ^b	1.03±0.02 ^b	0.91±0.03 ^b	0.817±0.047 ^c

Values are plotted as the mean ±SEM, n=6 in each group; analysed by ANOVA followed by Dunnett's test. where, * Indicates P<0.05, **p<0.01, *** p<0.001, **** p<0.0001 when control group is compared with normal saline group and ns indicates non-significant, a indicates P<0.05, b p<0.01, c p<0.001, d p<0.0001 when LD, HD and standard group is compared with control group.

Table 3: Effect of *Cassia tora* seed extract and Ibuprofen on CFA induced change in fall of time on 1st, 7th, 13th, 17th, 22nd day

FALL OF TIME (Sec.)	1 st day	7 th day	13 th day	17 th day	22 nd day
NORMAL SALINE	81.50±4.32	74.66±6.07	69.66±4.42	74.00±3.12	81.00±4.54
CONTROL (CFA INDUCED)	48.00±4.18	34.33±3.95 ***	26.33±2.48 ***	20.00±2.51 ***	20.33±1.28 ***
LOW DOSE (800mg/kg)	47.33±2.49	48.83±2.98 ^a	46.50±3.11 ^a	46.50±2.63 ^a	50.83±3.06 ^a
HIGH DOSE (1600mg/kg)	52.83±2.07	54.83±2.62 ^b	60.33±2.97 ^b	64.00±2.00 ^b	63.66±2.21 ^b
STANDARD (15mg/kg)	62.00±1.89	63.66±4.7 ^b	67.83±3.07 ^b	72.00±2.87 ^b	79.33±1.43 ^c

Values are plotted as the mean ±SEM, n=6 in each group; analysed by ANOVA followed by Dunnett's test. where, * Indicates P<0.05, **p<0.01, *** p<0.001, **** p<0.0001 when control group is compared with normal saline group and ns indicates non-significant, a indicates P<0.05, b p<0.01, c p<0.001, d p<0.0001 when LD, HD and standard group is compared with control group.

Table 4: Effect of *Cassia tora* seed extract and Ibuprofen on CFA induced change in RBC, WBC, Hb, ESR count

BLOOD PARAMETERS	RBC (10 ⁶ ×µL)	WBC (10 ³ ×µL)	Hb (gm/dl)	ESR (mm/hr)
NORMAL SALINE	7.863±0.347	10.17±0.318	13.18±0.370	2.395±0.51
CONTROL (CFA INDUCED)	3.863±0.462***	23.65±0.657***	6.323±0.858***	18.58±2.85***
LOW DOSE (800mg/kg)	5.693±0.365 ^{ns}	18.07±0.515 ^a	8.032±0.872 ^{ns}	15.34±2.305 ^a
HIGH DOSE (1600mg/kg)	6.493±2.769 ^b	11.76±0.309 ^b	9.417±0.882 ^a	10.73±1.212 ^a
STANDARD (15mg/kg)	6.835±0.498 ^b	11.42±0.254 ^b	10.67±0.693 ^b	8.617±0.276 ^b

Values are plotted as the mean ±SEM, n=6 in each group; analysed by ANOVA followed by Dunnett's test. where, * Indicates P<0.05, **p<0.01, *** p<0.001, **** p<0.0001 when control group is compared with normal saline group and ns indicates non-significant, a indicates P<0.05, b p<0.01, c p<0.001, d p<0.0001 when LD, HD and standard group is compared with control group.





Mukesh Lekhak et al.,

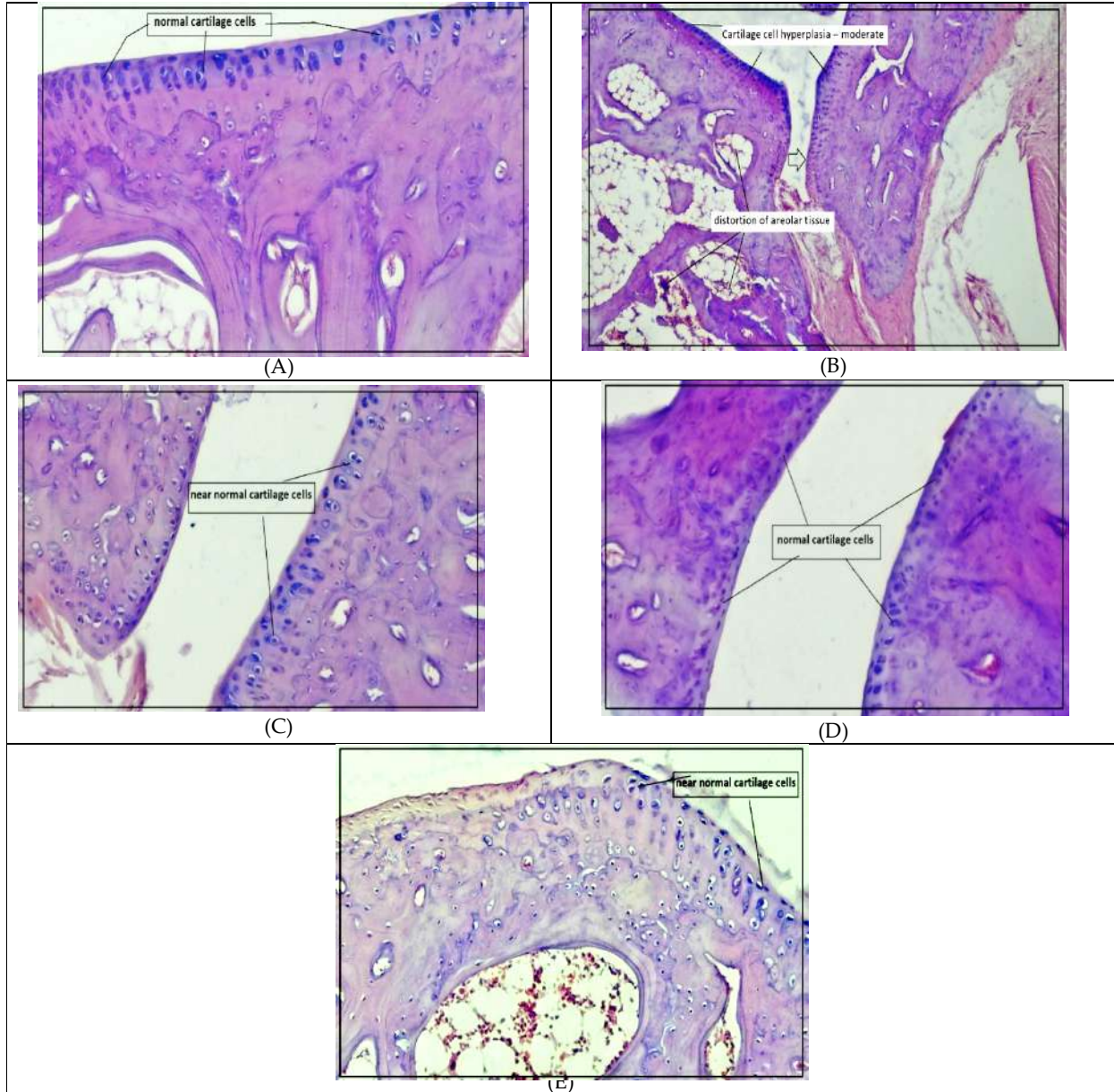


Fig 1: Histopathological images of tibiotarsal joints of all 5 groups

A: Tibiotarsal joint of normal saline group showing normal synovial lining cells (cartilage).

B: Tibiotarsal joint of control (CFA induced) group showing Cartilage cell hyperplasia – moderate and areolar tissue distortion.

C: Tibiotarsal joint of low dose (800mg/kg) showing near normal histology.

D: Tibiotarsal joint of high dose (1600mg/kg) showing normal histology.

E: Tibiotarsal joint of standard (Ibuprofen 15mg/kg) showing near normal histology.





Mukesh Lekhak et al.,

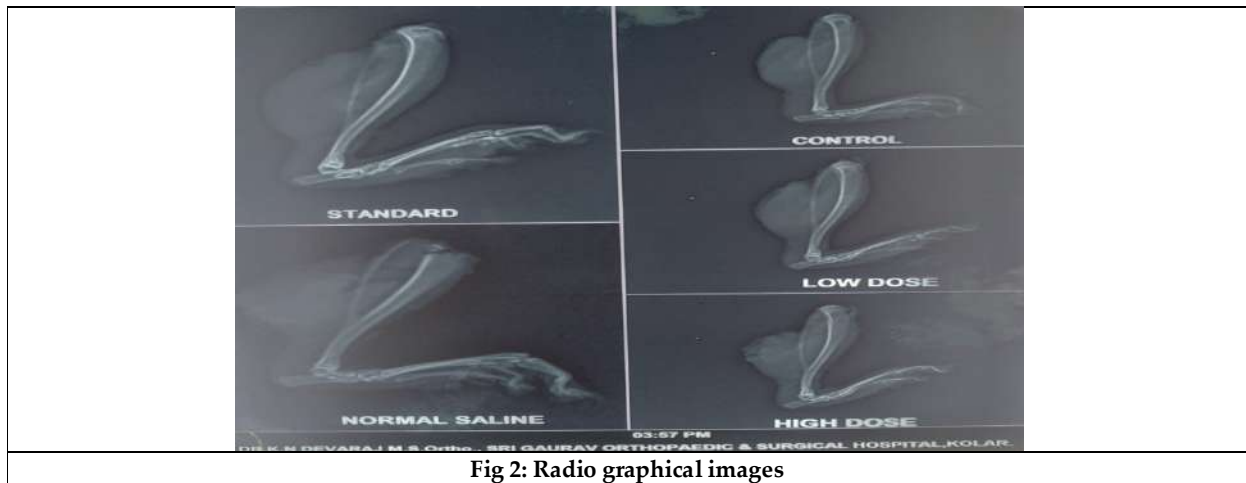


Fig 2: Radio graphical images





Relationship between Isometric Trunk Muscle Strength, Balance, and forward Reaching Ability in Children with Cerebral Palsy

Krishna Variyavwala¹, Drashti Gondalia¹, Jankiben Sagar¹ and Vivek Ramanandi^{2*}

¹Internee, Department of Neurological Physiotherapy, SPB Physiotherapy College, Surat (Affiliated to Veer Narmad South Gujarat University), Gujarat, India

²Associate Professor, Department of Neurological Physiotherapy, SPB Physiotherapy College, Surat (Affiliated to Veer Narmad South Gujarat University), Gujarat, India

Received: 07 Sep 2023

Revised: 14 Nov 2023

Accepted: 13 Jan 2024

*Address for Correspondence

Vivek Ramanandi

Associate Professor,

Department of Neurological Physiotherapy,

SPB Physiotherapy College, Surat

(Affiliated to Veer Narmad South Gujarat University),

Gujarat, India

E mail: vivekramanandi@gmail.com



This is an Open Access Journal / article distributed under the terms of the **Creative Commons Attribution License** (CC BY-NC-ND 3.0) which permits unrestricted use, distribution, and reproduction in any medium, provided the original work is properly cited. All rights reserved.

ABSTRACT

Trunk muscle strength is impaired in children with cerebral palsy thus influencing their functional balance. Forward reaching is an important test and an essential component of daily life activities. However, there is paucity of literature determining the relationship between trunk muscle strength, balance and forward reaching ability in children with CP. The study intends to assess relationship between trunk muscle strength, balance and forward reaching ability in children with cerebral palsy from Surat city. This cross-sectional observation study included 47 children with cerebral palsy from physiotherapy and rehabilitation setups of Surat. Children with CP were assessed using stabilizer pressure biofeedback equipment for muscle strength; pediatric balance scale for balance and forward reach test for reaching ability after signing informed consent from their parents. The data was analysed using Microsoft Excel and SPSS 20.0. The findings are suggestive that there is moderately strong correlation between the isometric trunk muscle strength and balance; the isometric trunk muscle strength and forward reaching ability or balance and forward reaching ability. The study implicates use of trunk control and strength measures in rehabilitation of CP children to improve balance and functional independence.

Keywords: Balance, cerebral palsy, functional reach, physiotherapy, trunk muscle strength.





INTRODUCTION

Cerebral palsy [CP] is one of the commonest causes of motor disability in children with some amount of dysfunction of posture and movement [1]. Because ability to control posture is an integral part of all movements, deficits in the postural control system contribute to the challenges in body structure and function, daily activities, and participation of children with CP [2]. Balance dysfunction associated with impairment in trunk control is usually reported in children with CP who have lower levels in Gross Motor Function Classification System [GMFCS], suggesting probable relationship between trunk control and balance with functional abilities in these children [3]. Children at GMFCS levels IV–V have undeveloped postural control and require contextual modifications to enable opportunities for basic acquisition and practice of head and trunk control [4]. Trunk muscle strength is an important factor influencing the balance in normal individuals as well as in children with CP [5]. The purpose of this study was to find relationship between the isometric trunk muscle strength, balance and forward reaching ability among CP child.

MATERIALS AND METHODS

Study Setting The Study was conducted at various hospital, neuro-rehabilitation centers, and physiotherapy departments in Surat city of Gujarat.

Sample Population Children with CP attending neuro-rehabilitation centers, hospitals, and physiotherapy departments in Surat.

Inclusion Criteria

Children with CP from both genders were included if they fit following criteria-

1. Age of 5 to 15 years of age.
2. GMFCS level I, II and III.
3. Children able to understand the test instruction, able to sit and stand.
4. Parents of child who willingly consents for their child's participation in the study.

Exclusion Criteria

Children with CP were excluded if they fit following criteria-

1. Parents of child not willing for their child's participation in the study
2. Children who prescribed with the botulinum toxin or intrathecal baclofen pump Implantation during last six months.
3. Child who has a history of injury to spine and pelvis, on medication like antiepileptic and anti spastic drugs.
4. Children who have progressive neurological disorder, genetic or metabolic disorder and severe concurrent and illness or diseases not typically associated with CP or other than CP. [e.g., traumatic brain injury or acute pneumonia].

Procedure

Data was collected from various hospitals, neuro rehabilitation centers and physiotherapy departments of Surat. Parents were invited and explained about the study. After that parents who were willing to participate were asked to sign all informed consent form. Children with CP were screened and selected, based on inclusion and exclusion criteria through convenience sampling. Children were assessed for isometric trunk muscle strength using core stabilizer [6]; forward reaching ability by Functional Reach Test [FRT] [7]; and balance by Pediatric Balance Scale [PBS][8]. Results were analysed using SPSS 20.0 and Microsoft Excel for Windows.

RESULTS

The demographic data were analysed using frequency distributions. Correlations between the outcomes were evaluated using Pearson's correlation co-efficient as comparison of baseline data showed normal distribution using Kolmogorov–Smirnov test. Demographic distribution of the subjects in the study sample is shown in table-1. Mean





Krishna Variyavwala *et al.*,

age of the children included in the study was 9.17 ± 2.58 years and most of the children [n=31] were from 5-10 years' age group. It is also evident that most of the children included were diagnosed as diplegic [n=21] or hemiplegic [n=21] type of CP. Table-2 shows the correlation co-efficient values for average core muscle strength [mm Hg], pediatric balance scale score, and average functional reach distance [cm]. Values of correlation coefficients for all the variables considered, showed positive correlation with each other as the values are all greater than 0 [9]. The findings are suggestive that there is moderately strong correlation between the isometric trunk muscle strength and balance; the isometric trunk muscle strength and forward reaching ability; and balance and forward reaching ability.

DISCUSSION

As the studies from Gujarat including CP children and correlating trunk muscle strength and balance in them are not available, the discussion will present unique findings with probable justifications keeping in mind the objectives of the study. Demographics of the participants from the present study are in concurrence with other studies showing that most of the children with CP were primarily diagnosed as diplegic or hemiplegic type of CP [11,12]. Present study shows moderately strong positive correlation between the isometric trunk muscle strength and PBS scores as well as FR distance; which is supported by previous studies [13,14]. Monica *et. al.* [2021]; Lim, Lee, and Lim [2021]; and Kim, An and Yoo [2018] have concluded that trunk control and trunk muscle strength are important factors affecting the balance activities including functional reach activities [3,12,15].

Static, active, and reactive postural control involves complex neural processes coupled with biomechanical and environmental constraints. As postural control during all the movements is integral to daily life activities, deficits in the posture system can contribute to the challenges in body structure and function, daily activities, and participation [4,16]. In addition, impaired trunk control in children with spastic CP is associated with balance dysfunction [3]. It has been documented that, children with CP at GMFCS levels IV–V have under-developed postural control and therefore require contextual modifications to enable opportunities for acquisition and practice of head and trunk control [16]. The reason for the moderately strong correlation found in this study can be attributed to the fact that all the participants belonged to GMFCS levels I, II and III and were all able to sit and stand. The findings in this study indicate that the correlation between the balance and forward reaching ability is moderately strong. Postural trunk control during frontal plane movements is suggested to be more difficult than while performing trunk movements in the sagittal plane [13]. Based on the motor involvement, children in the lower GMFCS level have profound impairment of trunk control affecting forward reaching abilities of child and suggesting that there is relationship between functional abilities and trunk control.

Limitations and Further Recommendations

The sample size covered for the study was smaller when we consider the strength of population of children with CP in India. As only smaller geographical region of Surat city was studied, the sample shall be representative and future study can include more subjects stratified based upon the type, geography, age, and gross motor function levels. It is also recommended to use more stringent outcome to assess trunk muscle strength such as EMG to quantify the strength and make study robust.

REFERENCES

1. Richards CL, Malouin F. Cerebral palsy: definition, assessment, and rehabilitation. Handbook of clinical neurology. 111: Elsevier; 2013. p. 183-95.
2. Saavedra S.L., Goodworth A.D. [2019] Postural Control in Children and Youth with Cerebral Palsy. In: Miller F., Bachrach S., Lennon N., O'Neil M. [eds] Cerebral Palsy. Springer, Cham. https://doi.org/10.1007/978-3-319-50592-3_161-1.
3. Monica S, Nayak A, Joshua AM, Mithra P, Amaravadi SK, Misri Z, Unnikrishnan B. Relationship between Trunk Position Sense and Trunk Control in Children with Spastic Cerebral Palsy: A Cross-Sectional Study. Rehabilitation Research and Practice. 2021 Aug 19;2021.





Krishna Variyavwala et al.,

4. Rose J, Wolff DR, Jones VK, Bloch DA, Oehlert JW, Gamble JG. Postural balance in children with cerebral palsy. *Developmental medicine and child neurology*. 2002 Jan;44[1]:58-63.
5. Glady SR. Cerebral Palsy. In: *Physiotherapy in Neuro-conditions*. India; 2006. p. 233-256.
6. Aggarwal A, Kumar S, Madan R, Kumar R. Relationship among different tests of evaluating low back core stability. *Journal of Musculoskeletal Research*. 2011 Sep 16;14[02]:1250004
7. Gan SM, Tung LC, Tang YH, Wang CH. Psychometric properties of functional balance assessment in children with cerebral palsy. *Neurorehabilitation and neural repair*. 2008 Nov;22[6]:745-53.
8. Franjoine MR, Gunther JS, Taylor MJ. Pediatric balance scale: a modified version of the berg balance scale for the school-age child with mild to moderate motor impairment. *Pediatric physical therapy*. 2003 Jul 1;15[2]:114-28.
9. Schober P, Boer C, Schwarte LA. Correlation coefficients: appropriate use and interpretation. *Anesthesia & Analgesia*. 2018 May 1;126[5]:1763-8.
10. Banerjee TK, Hazra A, Biswas A, Ray J, Roy T, Raut DK, et al. Neurological disorders in children and adolescents. *The Indian Journal of Pediatrics*. 2009;76[2]:139-46.
11. Stanley FJ, Blair E, Alberman E. *Cerebral palsies: epidemiology and causal pathways*: Cambridge University Press; 2000.
12. Lim M, Lee H, Lim H. Correlation between the Korean Version of the Trunk Control Measurement Scale, and the Selective Control Assessment of the Lower Extremity Scores in Children with Cerebral Palsy. *Medicina*. 2021 Jul;57[7]:687.
13. Duarte Nde A, Grecco LA, Franco RC, Zanon N, Oliveira CS. Correlation between Pediatric Balance Scale and Functional Test in Children with Cerebral Palsy. *J Phys Ther Sci*. 2014 Jun;26[6]:849-53. doi: 10.1589/jpts.26.849.
14. Yi SH, Hwang JH, Kim SJ, Kwon JY. Validity of pediatric balance scales in children with spastic cerebral palsy. *Neuropediatrics*. 2012 Dec;43[6]:307-13. doi: 10.1055/s-0032-1327774
15. Kim DH, An DH, Yoo WG. The relationship between trunk control and upper limb function in children with cerebral palsy. *Technology and Health Care*. 2018 Jan 1;26[3]:421-7.
16. Bigongiari A, e Souza FD, Franciulli PM, Neto SE, Araujo RC, Mochizuki L. Anticipatory and compensatory postural adjustments in sitting in children with cerebral palsy. *Human movement science*. 2011 Jun 1;30[3]:648-57.

Table 1: Demographic Details of the Sample Population

Characteristic	Category	Frequency [n]
Age Group [years]	5 to 10	31
	11 to 15	16
Type of CP	Diplegic CP	21
	Hemiplegic CP	18
	Quadriplegic CP	6
	Monoplegic CP	2

Note: CP- Cerebral Palsy

Table 2: Pearson’s Correlation between the Outcome measures

	Isometric Muscle Strength [mm Hg]	PBS Score	FR Distance [cm]
Isometric Muscle Strength [mm Hg]	1.000 ³	0.489 ²	0.457 ²
PBS Score	0.489 ²	1.000 ³	0.566 ²
FR Distance [cm]	0.457 ²	0.566 ²	1.000 ³

Note:

- PBS- Pediatric Balance Scale; FR: Functional reach
- 1- Weak correlation; 2- Moderate correlation; 3- Strong correlation [9]





Preliminary Pollen Analysis of *Ocimum gratissimum* L. and *Ocimum sanctum* L.: Some Observations

Devika KS¹, Anil Kumar VS² and Remya Krishnan^{3*}

^{1&3}Post Graduate Department and Research Centre of Botany, Mahatma Gandhi College, Thiruvananthapuram (Affiliated to Kerala University) Kerala, India.

²Principal, Department of Botany, Govt. College, Kasaragode (Affiliated to Kannur University) Kerala, India

Received: 26 Sep 2023

Revised: 12 Nov 2023

Accepted: 19 Jan 2024

*Address for Correspondence

Remya Krishnan

Post Graduate Department and Research Centre of Botany,
Mahatma Gandhi College,
Thiruvananthapuram,
Kerala, India.

E. mail: drrkbotany2020@gmail.com



This is an Open Access Journal / article distributed under the terms of the **Creative Commons Attribution License** (CC BY-NC-ND 3.0) which permits unrestricted use, distribution, and reproduction in any medium, provided the original work is properly cited. All rights reserved.

ABSTRACT

The members of Lamiaceae are cosmopolitan in distribution and have great importance due to their economic value. In traditional systems of medicine, different parts of *Ocimum* have been recommended for the treatment of various ailments. There is a variation in the production of phytochemicals among different species of *Ocimum*. Therefore, precise characterization such as anatomical, morphological and phytochemical features of promising species of *Ocimum* is felt necessary. Pollen grains are widely used as a tool for taxonomical analysis of flowering plants. Taxonomists have recognized the necessity of pollen morphology in clarifying the classification and differentiating plant groups up to species level or variety level. In this scenario the present study was aimed to compare two *Ocimum* species, *Ocimum gratissimum* L. and *Ocimum sanctum* L. in terms of pollen morphology using light microscopy and scanning electron microscopy (SEM). Both the plant species showed significant variations in morphological characters including variations in pollen morphology even under light microscopy. The pollen types present in *O. gratissimum* showed 2-3 visible colpi and was convex in shape, the mean diameter of the pollen grains were $40 \pm 0.87 \mu\text{m}$. In *O. sanctum* pollen grains were radially symmetrical, or ovate ellipsoidal with number of visible colpi 2-3. Exine ornamentation also showed variations in microscopic level. From the results it can be concluded that, both the studied species shows significant variations at all the studied parameters. Further studies are warranted at molecular level for effective characterization and comparison.

Keywords: *Ocimum*, morphology, acetolysis, SEM, Pollen grains, Colpi, Exine





INTRODUCTION

The *Ocimum* genus, includes many popular herbs known for their aromatic, culinary, medicinal, ornamental, sacred and other aesthetic properties, is varied and complex. Species in this genus are typically herbs, shrubs, or undershrubs and can be either annual or perennial. They are characterized by glandular hairs or glands that secrete fragrant volatile oils. Though their flowers may appear uniform throughout the genus, they serve as critical taxonomic markers for distinguishing between species. This taxonomic complexity in *Ocimum* is attributed to genetic diversity, thought to be influenced by cross-pollination and certain environmental factors (Ashraf *et al.*, 2021). Genetic variations are evident both within and between *Ocimum* species, with noticeable differences in morphology, growth characteristics, reproductive behaviour, and chemical composition. This morphological diversity, however, often leads to confusion in taxonomy (Jehanzeb *et al.*, 2020).

Traditionally, plant taxonomy has relied primarily on comparative morphological and anatomical features for taxon delimitation and identification (Pandey & Misra 2014). Several studies have emphasized the importance of such characteristics in identifying various plant species (Celep *et al.*, 2011 & Kiliç, 2014). For the Lamiaceae family, anatomical characteristics of vegetative organs are crucial for taxon characterization (Kahraman *et al.*, 2010). Features such as the presence and distribution of glandular hairs, stomatal distribution, and other anatomical details offer significant taxonomic information about plants (Celep *et al.*, 2011 and Venkateshappa & Sreenath, 2013) and are instrumental in elucidating phylogenetic relationships within many plant groups (Pandey & Misra, 2014). Pollen characteristics, too, have been widely used in angiosperm taxonomy and are useful in tracing the history of plant groups or species. The morphology of pollen grains, including attributes such as symmetry, shape, apertural pattern, and exine configuration, has been extensively studied and has proven to be a reliable resource for phylogenetic analysis (Sarkar, 2021). Given their taxon-specific yet highly variable characteristics, pollen morphological features offer significant scope for application in plant taxonomy (Sarkar, 2021).

Palyno-morphological characteristics are critical in the taxonomic identification and delimitation of various plant groups (Shah *et al.*, 2019). Several pollen attributes are specifically subjected to intense selective pressures involved in different systematic plant processes, including reproductive activities, pollination, dispersal, and germination. Palynologists utilize these pollen features for plant identification, allowing ecologists and botanists to reconstruct past plant taxa assemblages and identify periods of environmental change (Usma *et al.*, 2020; Gul *et al.*, 2021). The use of both light and scanning electron microscopy (SEM) has demonstrated that there are variations in the pollen morphology and sculpture among the genera from all the tribes within the Rosaceae family. Akinwusi and Illoh (1996) conducted research on the pollen morphology of the *Hibiscus* genus, demonstrating that such studies can provide valuable data for taxonomic classification. Indeed, pollen morphology is a crucial tool for the taxonomic study of angiosperms. The present study undertook a comparative analysis of two *Ocimum* species, *Ocimum gratissimum* L. and *Ocimum sanctum* L. based on pollen morphological attributes, including the structure of the exine. Both light microscopy and Scanning Electron Microscopy (SEM) were utilized to facilitate these examinations.

MATERIALS AND METHODS

Ocimum gratissimum L. and *Ocimum sanctum* L. were selected for the study. *Ocimum sanctum*, typically an aromatic under shrub, or shrub, is distinguished by oil glands that emit a robust aroma. This plant is often cultivated for its medicinal properties and religious importance, especially in many parts of India. When it matures enough to form wood, the plant, which can grow to a height of about 4.5 feet, is commonly transformed into beads for rosaries. Contrastingly, *Ocimum gratissimum*, an aromatic perennial herb, has unique characteristics including an erect, round-quadrangular stem that is highly branched and can be either glabrous or pubescent. The stem becomes woody at the base and the plant's epidermis frequently peels off in strips. The plant's leaves are consistently arranged in opposite pairs and it produces small, hermaphroditic flowers grouped in clusters of 6-10.



Devika KS *et al.*,

METHODOLOGIES

Analysis of pollen grains- Acetolysis and Scanning Electron Microscope

Pollen grains were extracted from fresh samples. To verify the consistency of pollen characteristics within each species, the acetolysis method (Clarke *et al.*, 1979) was applied to two samples each from both sps. Measurements were taken from twenty pollen grains using an ocular micrometer fitted to a Zeiss Photometric microscope, and the mean was determined. The shape category of the pollen grains was primarily decided by the ratio of the equatorial width to the polar length of the pollen grain (P/E). Preparations for scanning electron microscopic studies involved sprinkling the pollen onto specific silver-coated aluminum stubs. These stubs were subsequently coated with gold and observed and photographed using a JEOL T-20 Scanning Electron Microscope. Descriptive terminology was based on the standards set by Moore and Webb (1978) and Punt *et al.* (2007). Size measurements for the pollen grains followed Erdtman's categorization (1971): very small for dimensions less than 10 μm , small for 10–25 μm , medium for 25–50 μm , large for 50–100 μm , very large for 100–200 μm , and huge for dimensions greater than 200 μm .

RESULTS AND DISCUSSION

Pollen Morphology by acetolysis & Scanning electron Microscopic Studies

This study focused on the shape, colpi number, size, and surface characteristics of pollen grains from two *Ocimum* species. The primary features of the pollen can be seen in Fig. 1 a & b. Scanning electron microscopy revealed that the pollen from *O. gratissimum* is more or less globose, with 2-3 visible colpi. These pollen grains are circular in outline, giving them a discoid appearance. Their surface ornamentation is reticulate, featuring prominently raised ridges in an irregular pattern, and the exine surface is punctate. The pollen grains have a length and breadth of approximately $40 \pm 0.87 \mu\text{m}$ (Fig. 2 a, b, c & d). In contrast, the pollen grains of *O. sanctum* are rectangular or ovate elliptical in shape, with a length of approximately $60 \pm 0.87 \mu\text{m}$ and a breadth of about $30 \pm 0.68 \mu\text{m}$. Like *O. gratissimum*, the number of visible colpi ranges from 2-3. The surface ornamentation is also reticulate but features prominently raised ridges in a regular pattern. The exine surface is prominently punctate, and the colpus lacks specific ornamentation in both species. Notably, the punctae in *O. sanctum* appear larger and more conspicuous (Fig. 2 a, b, c & d).

Pollen characteristics have played a considerable role in the taxonomy of angiosperms, and can even be used to trace the history and evolution of plant groups and species (Moore and Webb, 1978). Notably, researchers such as Patel and Datta (1958) and Sowunmi (1973) have extensively explored pollen grain morphology, underlining the importance of pollen architecture in phylogenetic studies. For instance, Akinwusi and Illoh's (1996) research on *Hibiscus* pollen morphology demonstrated how palynology, the study of pollen grains, provides valuable data for genus taxonomy. Similarly, Adedeji (2005) utilized pollen morphology to trace evolutionary relationships among three *Emilia* species. Arogundade & Adedeji (2009) studied the pollen grains of various *Ocimum* species, observing similarities *yet also* significant differences. They found that the pollen grains of all the studied species and variety ranged from spherical to ellipsoid in shape. Acolpate pollen grains were found in all species and the studied variety, while monocolpate and bicolpate pollen grains were occasionally observed in *O. canum* and *O. basilicum*. Notably, pentacolpate pollen grains were found in *O. canum* and *O. gratissimum*, and all the species and the variety had hexacolpate pollen grains. Heptacolpate and octacolpate pollen grains, only observed in *O. canum*, set this species apart from the others.

Furthermore, morphologically distinct pollen grains such as those with a concave shape were found in *O. basilicum*, *O. gratissimum* and *O. basilicum* var. *purpurascens*. Ribbon-like pollens were observed in *O. canum*, *O. gratissimum*, and *O. basilicum* var. *purpurascens*. Tetrazonocolpate pollen grains with four colpi arranged in an equatorial zone were found in *O. gratissimum* and *O. basilicum* var. *purpurascens*, while hexazonocolpate pollen grains with six colpi in an equatorial zone were only observed in *O. canum*. Swapna (2018) conducted research on the pollen characteristics of *Ocimum sanctum*, which aligns with the findings of the present study. According to Erdtman's (1952) classification, pollen grains can be grouped into categories based on their sizes: Perminuta (diameter less than





Devika KS *et al.*,

10µm), Minuta (diameter 10-25µm), Media (diameter 25-50µm), Magna (diameter 50-100µm), Permagna (diameter 100-200µm), and Giganta (diameter greater than 200µm). In line with this categorization, the pollen grains of the *Ocimum* genus can be described as either media (diameter 25-50µm) or magna (diameter 50-100µm). *O. basilicum* var. *purpurascens* and *O. gratissimum* fall under the media group, while *O. canum* and *O. basilicum* fit into the magna category. A similar approach of using pollen grain sizes to categorize species was employed by Akinwusi and Illoh (1996) in their study of *Hibiscus* species in Nigeria. Based on the characteristics of their pollen grains, *O. basilicum* var. *purpurascens* and *O. gratissimum* appear to be more closely related as they share a higher level of similarity compared to *O. basilicum* and *O. canum*.

Walker (1976) and Adedeji (2005) suggest that the number of colpi on pollen grains can serve as an effective tool for tracing evolutionary relationships among the species within a genus. They found that more advanced dicotyledons have a greater number of colpi than the more primitive ones, which tend to have only one colpus (monocolpate) or none at all (acolpate). The scanning electron microscope has been utilized to examine the pollen morphology of the *Rosa sericea* complex, offering essential information for taxonomic identification of the taxa within this complex. There's a notable variability in the pollen sculpture, outline, and aperture among the taxa studied, highlighting the diversity within the *R. sericea* complex (Ullah *et al.*, 2022). Pollen morphology has long been recognized as a valuable tool in taxonomic classification and botanical research, offering insights into plant evolution, ecology, and phylogenetics (Pacini and Franchi, 2020; Ullah *et al.*, 2021).

CONCLUSION

Indeed, pollen morphology plays a critical role in taxonomic classification. The shape, size, and surface patterns of pollen provide unique characteristics that can help to differentiate between plant species (Ragho, 2020). Such pollen features are remarkably consistent within species, which makes them a reliable tool in taxonomic studies. By examining the similarities and differences in pollen features, scientists can construct phylogenetic trees that illustrate the historical lineages and connections between different plant groups. Beyond identification and classification, pollen morphology is also used to understand past environments and climate change. Furthermore, pollen morphology is valuable in agriculture and horticulture, where understanding plant relationships is key for breeding programs. Similarly, in forensic science, the identification of pollen can provide crucial information, as different plants with their specific pollen are found in different geographical locations.

REFERENCES

1. Adedeji O (2005). Pollen morphology of the three species of the genus *Emilia* Cass. (Asteraceae) from Nigeria. *Thaiszia – Journal of Botany* 15: 1 – 9.
2. Akinwusi O and Illoh HC (1996). Pollen grain morphology of some species of *Hibiscus* Linn. *Nigerian Journal of Botany*, 9, 9 – 14.
3. Arogundade B and Adedeji O (2010). Pollen grain morphology of three species and a variety of *Ocimum* Linn. (Lamiaceae) in Southwestern Nigeria, *Journal of Science and Technology*, 29, DOI 10.4314/just.v29i3.50028
4. Ashraf K, Haque MR, Amir M, Ahmad N, Ahmad W, Sultan S, Ali Shah SA, Mahmoud AAMujeeb M and Bin Shafie MF (2021). An overview of phytochemical and biological activities: *Ficus deltoidea* Jack and other *Ficus* spp. *Journal of Pharmacy and Bioallied Sciences*, 13, 11-25.
5. Celep F, Kahraman A and Doğan M (2011). A new taxon of the genus *Salvia* (Lamiaceae) from Turkey. *Plant Ecology and Evolution*, 144(1), 111-114.
6. Clarke GC, Chanda S and Sahay S (1979). Pollen morphology in the genus *Pardoglossum* (Boraginacea) with some observations on heterocolpate pollen. *Review of Palaeobotany and Palynology*, 28(3-4), 301-309.
7. Erdtman G (1952). *Pollen Morphology and Plant Taxonomy—Angiosperms*. Almqvist and Wiksell, Stockholm, 539





Devika KS et al.,

8. Erdtman G (1971). Handbook of Palynology. Morphology – Taxonomy – Ecology. An Introduction to the Study of Pollen Grains and Spores. 486 S., 50 Illustration, 125 Tafeln. Verlag Munksgaard, Copenhagen, 1969. Preis: Leinen D. kr. 180. Journal of Botanical Taxonomy and Geobotany.
9. Gul S, Ahmad M, Zafar M, Bahadur S, Zaman W, Ayaz A, Shuaib M, Butt MA, Ullah F and Saqib S (2021). Palynological characteristics of selected Lamiaceae taxa and its taxonomic significance. Microscopy Research and Technique, 84, 471–479.
10. Jehanzeb S, Zafar M, Ahmad M, Sultana S, Zaman W and Ullah F (2020). Comparative petiole anatomy of tribe Menthae subfamily Nepetoideae, Lamiaceae from Pakistan. Feddes Repert, 131, 163–174.
11. Kahraman A, Celep F and Dogan M. (2010). Anatomy, trichome morphology and palynology of *Salvia chrysophylla* Stapf (Lamiaceae). South African Journal of Botany, 76, 187–195
12. Kılıc O (2014). A morphological study on *Nepeta fissa* C. A. Mey. (Lamiaceae) from Bingöl. (Turkey). Bilecik Şeyh Edebali Üniversitesi Fen Bilimleri Dergisi, 1(1), 59–65.
13. Moore PD and Webb JA (1978). Hodder and Stoughton, London-Sydney- Auckland- Toronto 1978. An illustrated guide to pollen analysis 133 :48.
14. Pacini E and Franchi GG (2020). Pollen biodiversity—Why are pollen grains different despite having the same function? A review. Botanical Journal of the Linnean Society, 193, 141–164.
15. Pandey S and Misra S (2014). Taxonomy of angiosperms. Ane Books. New Delhi. pp. 620. Pei, S. (2005). Ethnobotany and development of new traditional Chinese medicine. Ethnobotany. 17.35-40
16. Patel GI and Datta RM (1958). Pollen grain studies in various types of *Corchorus olitorius* L., *C. capsularis* L. and some other species of *Corchorus*. Grana Palynological, 1, 18 – 24.
17. Punt W, Hoen PP, Blackmore S, Nilsson S, A Le Thomas (2007). Glossary of pollen and spore terminology. Review of Palaeobotany and Palynology, 143(1–2): 1-81.
18. Ragho KS (2020). Role of pollen morphology in taxonomy and detection of adulterations in crude drugs. Journal of Plant Science and Phytopathology, 4, 024-027.
19. Sarkar B (2021). Studies on the pollen morphology of arboreal spermatophytes from Terai and Dooars of West Bengal, India (Doctoral dissertation, University of North Bengal).
20. Shah SN, Ahmad M, Zafar M, Ullah F, Zaman W, Malik K, Rashid N and Gul S (2019). Taxonomic importance of spore morphology in Thelypteridaceae from Northern Pakistan. Microscopy Research and Technique, 82, 1326–1333.
21. Sowunmi MA (1973). Pollen grains of Nigerian Plants. Grana 13: 145 – 186.
22. Swapna S (2018). The morphological diversification of pollen grains of three different species belongs to (Lamiaceae, Asclepiadaceae, Euphorbiaceae). International Journal of Recent Scientific Research, 9(2), 23973-23975
23. Ullah F, Gao Y, Jiao RF and Gao XF (2021). Comparative taxonomic variation in fruits and seeds' surface morphology among populations of alpine *Rosa sericea* complex (Rosaceae). Microscopy Research and Technique, 84, 2337–2350
24. Ullah F, Gao Y-D, Zaman W and Gao X-F (2022). Pollen Morphology of *Rosa sericea* Complex and Their Taxonomic Contribution. Diversity. 14(9), 705. <https://doi.org/10.3390/d14090705>
25. Usma A, Ahmad M, Zafar M, Sultana S, Lubna, Kalsoom N, Zaman W and Ullah F (2020). Micromorphological variations and taxonomic implications of caryopses of some grasses from Pakistan. Wulfenia, 27, 86–96.
26. Venkateshappa S and Sreenath K (2013). Some species of Lamiaceae comparative anatomical studies. Indo American Journal of Pharmaceutical Research, 3(11): 9249-9256.
27. Walker JRI (1976). The control of enzymatic browning in fruit juices by cinnamic acid. Journal of food technology 11,341-345





Devika KS et al.,

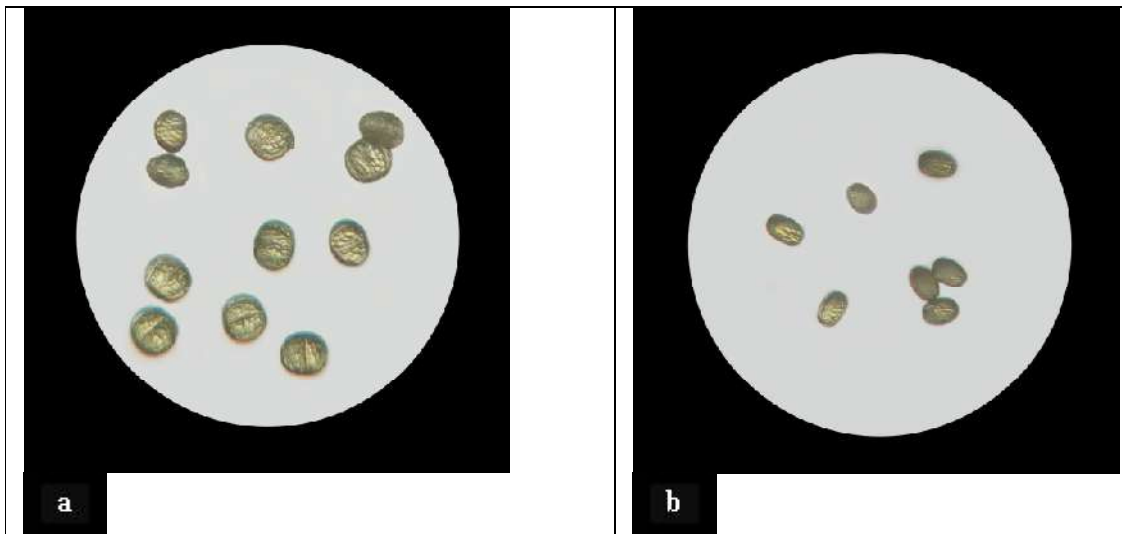


Figure 1 a & b: Acetolysis- Pollen grains of *Ocimum gratissimum* & *Ocimum sanctum*

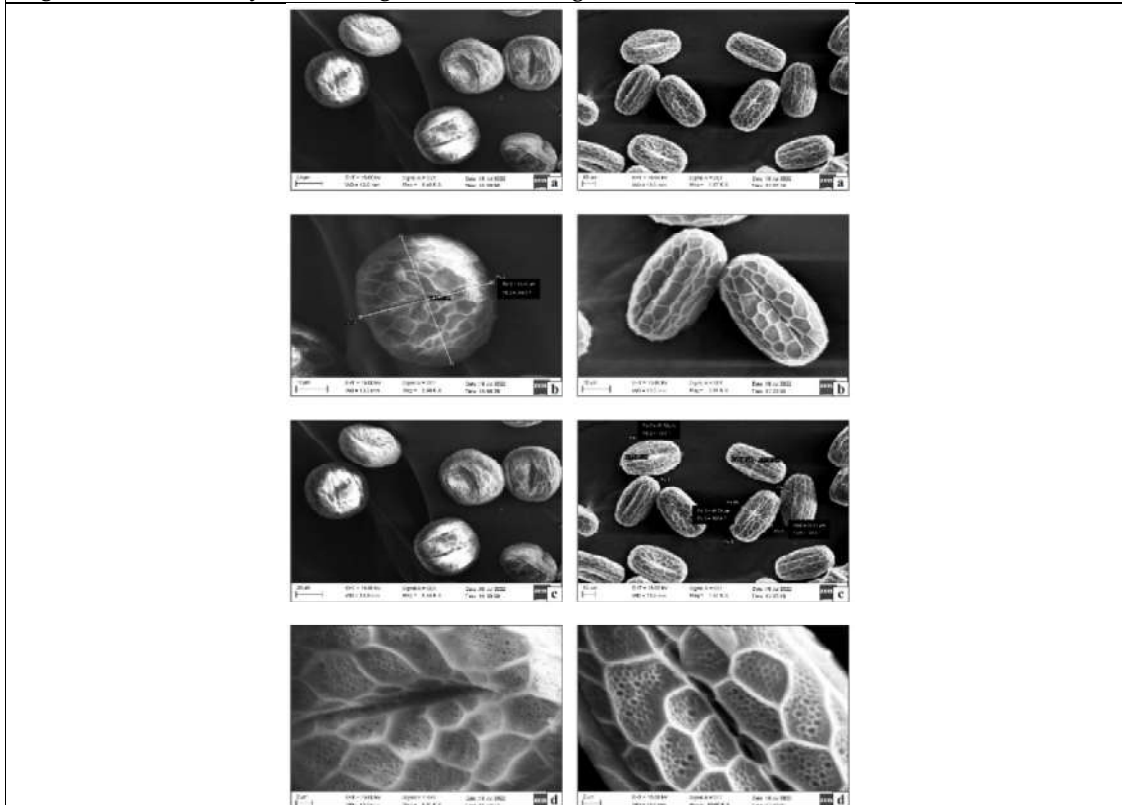


Figure 2 a, b, c & d: SEM analysis – Pollen grains of *Ocimum gratissimum* & *Ocimum sanctum*





Assessment of Torsional Behavior of Fused Deposition Modeling Parts for Different Layer Heights: A Pilot Study

Prasad A Hatwalne^{1*}, S.V Prayagi² and S.V.Bhalerao³

¹Assistant Professor, Department of Mech. Engg., YCCE (Affiliated to RTNMU) Nagpur, Maharashtra, India.

²Professor, Department of Mech. Engg., YCCE (Affiliated to RTNMU) Nagpur, Maharashtra, India.

³Associate Professor, Department of Mech. Engg., JDIET Yavatmal (Affiliated to SGBAU Amaravati) Maharashtra, India.

Received: 10 July 2023

Revised: 09 Jan 2024

Accepted: 19 Jan 2024

*Address for Correspondence

Prasad A Hatwalne

Assistant Professor,

Department of Mech. Engg.,

YCCE (Affiliated to RTNMU)

Nagpur, Maharashtra, India.

Email: hatwalneprasad1@gmail.com



This is an Open Access Journal / article distributed under the terms of the **Creative Commons Attribution License** (CC BY-NC-ND 3.0) which permits unrestricted use, distribution, and reproduction in any medium, provided the original work is properly cited. All rights reserved.

ABSTRACT

Since inception, application areas of Fused deposition modeling are growing in diversity day by day. This is made possible because of development of newer and newer materials and parametric optimization for improved surface finish, improved mechanical properties like tensile, compressive, fatigue, bending etc. These developments of newer materials and mechanical testing of improved parts are finding useful to evaluate the manufacturing capability of FDM process for a particular application which otherwise would have been manufactured by some other conventional manufacturing process. In an attempt to this the torsional behavior of FDM parts under different loading conditions needs to be evaluated thoroughly to estimate the capabilities of FDM parts to sustain the torsional loads. For this a pilot study was conducted in which testing was performed on standard ASTM specimen printed with different a layer height. and obtained values are compared with values of same parts prepared by injection molding. In the result obtained it was observed that injection molded parts were comparatively have greater torsional strength. This study can be very useful as in increasing applications of FDM parts which are subjected to torsional loading like gears, pulleys, stir welding parts, plastic fasteners etc.

Keywords: Fused deposition Modeling (FDM), Parametric Optimization, Torsional strength, layer height, FDM applications.





Prasad A Hatwalne et al.,

INTRODUCTION

Additive manufacturing (AM) is popular manufacturing technology emerged around the 1980s. From the various AM technologies such as Selective laser sintering (SLS), Vat polymerization, powder bed fusion, Laminated object Manufacturing (LOM) etc, the fused deposition modeling (FDM) is the cheapest and very commonly adopted technology amongst all.[1] FDM printer takes the input from the CAD files in stl format. FDM makes use of thermoplastic filaments like Acrylonitrile butadiene styrene (ABS), Nylon, Poly lactic acid (PLA), Pet-G etc which are subjected to temperature sufficient enough to melt the filament. This semi molten filament is extruded from the tip of nozzle. Firstly the contour of outer boundary is laid down followed by rasterizing the internal structures. Likewise number of layers are deposited one over other till complete part is created.[2] The data processing in FDM process is as shown in figure 1. Fused deposition modeling is having lots of advantages like ease of making complex design parts, no need of tooling's like molds, dies etc, combining complex assembly parts, reducing manufacturing lead time.[3]. In spite of this FDM technology has its own challenges too like staircasing effect, dimensional inaccuracy, Anisotropic mechanical properties, Low surface finish etc[4]. FDM technology is widely used in various application like making conceptual/ demonstrative models and prototypes, functional parts like drilling grid in aero plane industry, mandible trays[5], Biomedical ,textiles, acoustics [6]. Even in FDM technology found its application during COVID-19 pandemic in which face shields, face masks, valves, nasopharyngeal swabs, and others were 3 D printed [7] As the material is deposited layer wise, the FDM parts possess anisotropic properties.[8]. Thus the mechanical properties under different loading conditions such as when loaded in tension, compression, fatigue, bending etc are greatly influenced by the FDM process parameters. These parameters includes build orientation, layer height, air gap, Raster angle etc. this process parameters and basic FDM process is as depicted in figure 2. The definition's of various process parameters is as discussed below.

1. Layer height: This is the height of deposited layers. It refers to thickness or thinness of layer.
2. Built orientation: This is inclination of part with respect to depositing platform. This inclination can be vertical (90°), horizontal (flat) 0°, inclined (between 0°-90°)
3. Raster angle: it is angle of deposited road with horizontal measured in a plane of building platform.
4. Raster width: It is width of deposited raster.
5. Air Gap: The space between adjacent deposited beads is called as air gap.[9]

Since last few years many researchers are evaluating the effect of variation of these process parameters on mechanical properties. Few important among that is discussed below. Pritishshubham et al has examined the effect of layer height on the capacity of ABS plastic parts printed by Fused Deposition Modeling process to sustain tensile loads. In their research work they observed that as layer thickness is increased, the parts were able to sustain lower tensile loads [9] The effect of different build orientation (Along X,Y and Z axis) with different values of raster angles ranging between 0° to 90° in the equal step of 30° was studied by AshuGerg et al. the finding reveals that parts printed with X and Y inclination with 60° raster angle gives the maximum tensile strength. Further the post acetone treatment causes the little decrement in mechanical properties of FDM components. [10] Abhinavchadha et al conducted research in which parameters such as depositing surface temperature, layer height and infill pattern such as triangular, honeycomb, rectilinear were varied and its effect on tensile and bending strength were investigated. They concluded that flexural and tensile strength firstly increase and then decreases as the depositing surface temperature increases. With the increment in layer height the increase in tensile and flexural capacity was observed. Triangular and honeycomb infill pattern found to be have greater tensile and flexural strength. [11] From the literature cited following points were observed.

1. Products/applications of FDM is growing in diversity. Instead of just a prototype, focus is towards manufacturing functional parts. Poor mechanical properties is one of the major limitations for applications of FDM process.[12-13]
2. Nature of manufacturing process changes the mechanical properties of plastic part being manufacture. [14]





Prasad A Hatwalne et al.,

Hence these facts were leading to Investigate the behavior of FDM parts under the torsional loads. For this the pilot project was conducted in which effect of alteration in layer height on the torsional characteristics was investigated. The details are as discussed in subsequent sections.

METHODOLOGY ADOPTED

Sample Preparation.

The CAD model of testing specimen as per ASTM-143 standard was prepared in CATIA software. The dimension of specimen is as shown in figure3. The same were printed on FDM printer with material Polylactic Acid (PLA). Three specimens with layer height 0.12mm,0.16mm, 0.20mm were used. The values of controlling factors and fixed parameters are as mentioned in table no 1.

Torsional Testing

After printing the samples ,they were tested for torsional loading as per ASTM standard on torsional testing setup. Parts were hand tightened on grip style chuck so as to avoid the unnecessary compressing of samples at end. At one end samples were fixed and while other end is rotated slowly. Torsional test was monotonic and parts were twisted at rate of 1 degree per sec. Real time values of Angle of twist (in degree) and applied load (Kgf) were recorded. Then for each reading values of stress in shear (T) in Mpa, Shear Modulus (G) rate of shear strain (Y) were estimated.

RESULT AND DISCUSSION

To examine the Influence of alteration of Layer height on torsional strength. the following values were calculated

- 1.stress in shear (T) in Mpa,
- 2.Shear Modulus (G) and
- 3.rate of shear strain (Y) for different values of layer thickness.

The equations used were,

$$\text{For shear stress (T)} = \frac{T D}{2J},$$

Where T is torque measured by torsion load cell, D is gauge diameter, L length , J polar moment of inertia which is given by $J = \pi D^4 /32$

And rate of shear strain (Y),

$$Y = \theta D/2L$$

From the results obtained, it is observed that for layer thickness of 0.16mm maximum values shear stress (20.27 Mpa), Shear Modulus (66.27) and Strain in shear (2.90) are obtained. After comparing these values with the same parts produced by injection molding method, it clearly reveals that layer thickness is having strong influence on the torsional properties of FDM parts.

CONCLUSION

Above presented experimental work was a pilot work conducted to see whether parameters of FDM process influences its torsional behavior or not. For this only one of the input parameter ie. Layer height was varied for three times ie., 0.12mm, 0.16mm and 0.20mm and accordingly three specimens of PLA material were printed using FDM machine and tested on Torsional testing machine. From the results obtained it can be said that torsional strength of FDM parts are greatly influenced by change in layer thickness. Being pilot study experimentation was conducted at small scale that is only for three different heights. For through characterization, complete investigation considering variation of different processing parameters ie, Built orientation, raster angle, air gap etc and its effect on torsional properties needs to be explored. This analysis will be useful for development of functional parts which are subjected to torsional loads like gears, shafts, plastic stir welding parts etc.





REFERENCES

1. R Singh and S Singh, MSJ Hashmi,(2016), Implant Materials and Their Processing Technologies. Reference Module in Materials Science and Materials Engineering;1-21
2. R. Anandkumar, • S. (2018). FDM filaments with unique segmentation since evolution: a critical . Progress in Additive Manufacturing.
3. G. Kaur, R. S. (2021). A review of fused filament fabrication (FFF): Process parameters and their impact on the. Materials Today: Proceedings,.
4. M. Kamaal, M. A. (2020). Effect of FDM process parameters on mechanical properties . Progress in Additive Manufacturing.
5. Alafaghani A., Q. A. (2017). Experimental optimization of fused deposition modeling process parameters: A design for manufacturing approach. Procedia manufacturing, 791-803.
6. Yodo, A. D. (2019). A Systematic Survey of FDM Process Parameter Optimization and Their Influence on. Journal of Manufacturing and material processing.
7. AlbaCano-VicentaMurtaza M.Tambuwala, e. a. (2021). Fused deposition modelling: Current status, methodology, applications and future prospects. Journal Additive Manufacturing.
8. Guilherme Arthur Longhitano, G. B. (2020). The role of 3D printing during COVID 19 pandemic: a review. Progress in Additive Manufacturing.
9. Godfrey C. Onwubolu, Farzad Rayegani (2014)Characterization and Optimization of Mechanical Properties of ABS Parts Manufactured by the Fused Deposition Modelling Process.International Journal of Manufacturing Engineering.
10. Rui Zou, Y. X. (2016). Isotropic and anisotropic elasticity and yielding of 3D printed material. Composites Part B, 506-513.
11. Shubham, P. S. (n.d.). The Influence of Layer Thickness on Mechanical Properties of the 3D Printed ABS Polymer by Fused Deposition Modeling. Key Engineering Materials, , 63-67.
12. AshuGerg,Amitabh Bhattacharya,& Ajay Batish 2015, on surface finish and dimensional accuracy of FDM parts after cold vapour treatment. Materials and Manufacturing Processes 31 (4), 522-529
13. Abhinav Chadha, M. I. (2019). Effect of fused deposition modelling process parameters on mechanical properties of 3D printed parts. World Journal of Engineering, 550-560.
14. Krishna Mohan Agarwal, P. S. (2022). Analyzing the Impact of Print Parameters on Dimensional Variation of ABS. Sensors International.
15. Mst Faujiya Afrose, S. H. (2016). Effects of part build orientations on fatigue behaviour of FDM-processed PLA material. Progress in Additive Manufacturing, 21-28.
16. Jonathan Torres, Matthew Cole etal (2016), An Approach for Mechanical Property optimization of fused deposition with polylactic acid via design of experiments; Rapid prototyping journal 22(2),287-404.

Table No1 : Values of Varying and Fixed parameters.

Varying Parameters			Fixed Parameters		
Parameter	Values	Unit	Parameter	Values	Unit
Layer Thickness	0.12	mm	Raster angle	0	°
	0.16	mm	Layer orientation	0	°
	0.20	mm	Air Gap	0	mm
			Extrusion temperature	215	°C





Prasad A Hatwalne et al.,

Table 2: Calculated Average figures of stress in shear (T) in Mpa, Shear Modulus (G) rate of shear strain (Y)

Sr No	Material	Layer height	stress in shear (T) in Mpa	Shear Modulus (G)	shear strain (Y)
1	PLA plastic	0.12	39.33	0.68	0.4
2		0.16	33.33	0.59	0.4
3		0.20	29	0.50	0.06

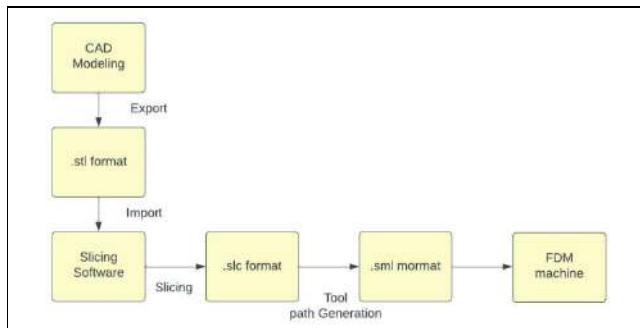


Fig1: Block diagram for processing of data in FDM.

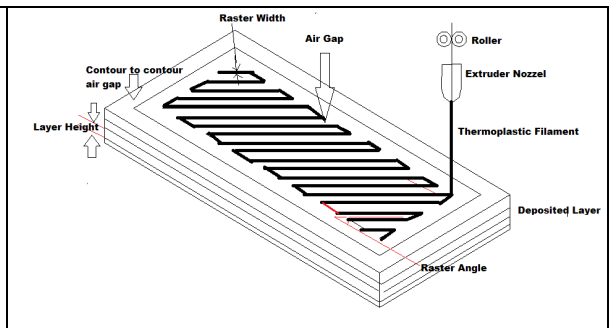


Fig2. FDM Process with parameters

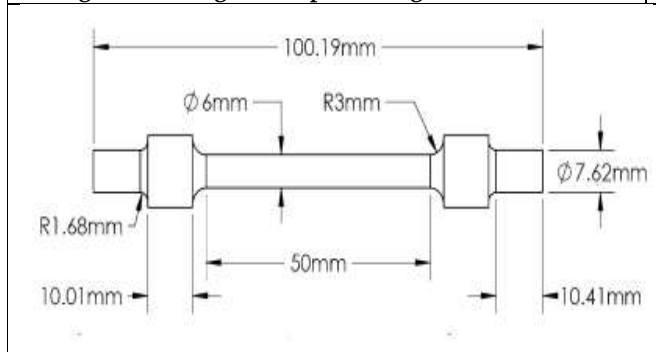


Fig3: Dimensions of torsional specimen[16].



Fig 4: Sample Printed PLA Specimen



Fig5: Twisting of Specimen





Types of Annihilator in \mathcal{LPW} -Algebras

M. Indhumathi^{1*}, K. Jeya Lekshmi² and A. Ibrahim³

¹Assistant Professor and Head, Department of Mathematics, RVS College of Arts and Science, Suler (Affiliated to Bharathiar University), Coimbatore, Tamil Nadu, India.

²Assistant Professor, Department of Mathematics, RVS College of Arts and Science, Suler (Affiliated to Bharathiar University), Coimbatore, Tamil Nadu, India.

³Assistant Professor, P.G. and Research Department of Mathematics, H. H. The Rajah's College, Pudukkottai (Affiliated to Bharathidasan University, Tiruchirappalli) Tamil Nadu, India.

Received: 30 Sep 2023

Revised: 20 Nov 2023

Accepted: 19 Jan 2024

*Address for Correspondence

M. Indhumathi

Assistant Professor and Head,
Department of Mathematics,
RVS College of Arts and Science, Suler
(Affiliated to Bharathiar University),
Coimbatore, Tamil Nadu, India.
Email: indumathi@rvsgroup.com



This is an Open Access Journal / article distributed under the terms of the **Creative Commons Attribution License** (CC BY-NC-ND 3.0) which permits unrestricted use, distribution, and reproduction in any medium, provided the original work is properly cited. All rights reserved.

ABSTRACT

The aim of this paper is to expand the idea of annihilators in \mathcal{LPW} -Algebras. We introduce the definition of annihilators. And also, we introduce the definitions of Normal, $(\rightarrow, \leftrightarrow)$ – Normal and $(\leftrightarrow, \rightarrow)$ – Normal \mathcal{PWI} -ideals. We obtain some characterizations and several basic properties of annihilators. Moreover we investigate the relationship between $\check{f}(\check{S}^{(\rightarrow, \leftrightarrow)})$ and $(\check{f}(\check{S}))^{(\rightarrow, \leftrightarrow)}$ for a homomorphism of \mathcal{LPW} -Algebras.

Keywords: Annihilators, Normal, $(\rightarrow, \leftrightarrow)$ – Normal and $(\leftrightarrow, \rightarrow)$ – Normal \mathcal{PWI} -ideals.

Mathematical Subject classification: 03B05, 03G10, 06B10, 06B75

INTRODUCTION

The concepts of W -algebra was presented by M.Wajsberg[9]. CeterchiRodica[1] introduced the concept of \mathcal{LPW} -Algebras. In our paper [4] we introduced \mathcal{PWI} -ideals and examined its propositions. In this paper, we introduce the concept gradually to a new classes of annihilators. Also, we define Normal, $(\rightarrow, \leftrightarrow)$ – Normal and $(\leftrightarrow, \rightarrow)$ – Normal \mathcal{PWI} -ideals. We discuss some known concept of annihilators and discuss the relationships between $\check{f}(\check{S}^{(\rightarrow, \leftrightarrow)})$ and $(\check{f}(\check{S}))^{(\rightarrow, \leftrightarrow)}$ for a homomorphism of \mathcal{LPW} -Algebras.





Indhumathi et al.,

Main Result

In this section, we define the types of annihilators in \mathcal{LPW} -Algebras and investigate some related properties.

Definition 2.1. Let S be a nonempty subset of \mathcal{LPW} -Algebra T , then the sets

$$S^{(\rightarrow, \leftrightarrow)} = \{x \in T / [a \rightarrow (a \leftrightarrow x)]^- = 0\} \text{ for all } a \in S \tag{1}$$

$$S^{(\leftrightarrow, \rightarrow)} = \{x \in T / [a \leftrightarrow (a \rightarrow x)]^- = 0\} \text{ for all } a \in S \tag{2}$$

$$S^{\leftrightarrow} = S^{(\rightarrow, \leftrightarrow)} \cap S^{(\leftrightarrow, \rightarrow)} \tag{3}$$

are said to be $(\rightarrow, \leftrightarrow)$ – annihilator, then $(\leftrightarrow, \rightarrow)$ – annihilator and the annihilator of S respectively. Obviously $\bar{0} \in S^{(\rightarrow, \leftrightarrow)}$ and $\bar{0} \in S^{(\leftrightarrow, \rightarrow)}$ and hence $\bar{0} \in S^{\leftrightarrow}$.

Example 2.2. Let $T = (\{\bar{0}, \bar{e}, \bar{f}, \bar{g}, \bar{1}\}, -, \sim, \rightarrow, \leftrightarrow)$ be a \mathcal{LPW} -Algebra, which double operations \rightarrow and \leftrightarrow are defined as follows.

Table 1. Complement		Table 2. Implication						Table 3. Complement		Table 4. Implication					
\bar{x}	\bar{x}^-	\rightarrow	$\bar{0}$	\bar{e}	\bar{f}	\bar{g}	$\bar{1}$	\bar{x}	\bar{x}^-	\leftrightarrow	$\bar{0}$	\bar{e}	\bar{f}	\bar{g}	$\bar{1}$
$\bar{0}$	$\bar{1}$	$\bar{0}$	$\bar{1}$	$\bar{1}$	$\bar{1}$	$\bar{1}$	$\bar{1}$	$\bar{0}$	$\bar{1}$	$\bar{0}$	$\bar{1}$	$\bar{1}$	$\bar{1}$	$\bar{1}$	$\bar{1}$
\bar{e}	\bar{f}	\bar{e}	\bar{f}	$\bar{1}$	$\bar{1}$	$\bar{1}$	$\bar{1}$	\bar{e}	\bar{g}	\bar{e}	\bar{g}	$\bar{1}$	$\bar{1}$	$\bar{1}$	$\bar{1}$
\bar{f}	\bar{e}	\bar{f}	\bar{e}	\bar{e}	$\bar{1}$	$\bar{1}$	$\bar{1}$	\bar{f}	\bar{e}	\bar{f}	\bar{e}	\bar{e}	$\bar{1}$	$\bar{1}$	$\bar{1}$
\bar{g}	\bar{e}	\bar{g}	\bar{e}	\bar{e}	\bar{f}	$\bar{1}$	$\bar{1}$	\bar{g}	\bar{f}	\bar{g}	\bar{f}	\bar{e}	\bar{f}	$\bar{1}$	$\bar{1}$
$\bar{1}$	$\bar{0}$	$\bar{1}$	$\bar{0}$	\bar{e}	\bar{f}	\bar{g}	$\bar{1}$	$\bar{1}$	$\bar{0}$	$\bar{1}$	$\bar{0}$	\bar{e}	\bar{f}	\bar{g}	$\bar{1}$

If $S = \{\bar{0}, \bar{e}, \bar{1}\}$, then it can be checked that $S^{(\rightarrow, \leftrightarrow)} = \{\bar{0}\}$ and $S^{(\leftrightarrow, \rightarrow)} = \{\bar{0}, \bar{e}\}$. Therefore $S^{(\rightarrow, \leftrightarrow)} \neq S^{(\leftrightarrow, \rightarrow)}$.

Proposition 2.3. Let S and P be a nonempty subsets of T . If $S \subseteq P$, then $P^{(\rightarrow, \leftrightarrow)} \subseteq S^{(\rightarrow, \leftrightarrow)}$.

In the example 2.2, taking $S = \{\bar{0}, \bar{e}\}$ and $P = \{\bar{0}, \bar{e}, \bar{f}\}$, then it is easily verify that $P^{(\rightarrow, \leftrightarrow)} \subseteq S^{(\rightarrow, \leftrightarrow)}$.

Proposition 2.4. If S is a nonempty subset of T then, $\bar{0} \in S$ iff $S \cap S^{(\rightarrow, \leftrightarrow)} = \{\bar{0}\}$.

Proof: The sufficient part is obviously true and we have to prove the necessary part. Let $\bar{x} \in S \cap S^{(\rightarrow, \leftrightarrow)}$, then by the definition of $(\rightarrow, \leftrightarrow)$ – annihilator, $[a \rightarrow (a \leftrightarrow \bar{x})]^- = \bar{0}$ for all $a \in S$. Since $\bar{x} \in S$, by putting $a = \bar{x}$, we get $[\bar{x} \rightarrow (\bar{x} \leftrightarrow \bar{x})]^- = [\bar{x} \rightarrow \bar{1}]^- = \bar{1}^- = \bar{0}$. Therefore $S \cap S^{(\rightarrow, \leftrightarrow)} = \{\bar{0}\}$ and so, by hypothesis $\bar{0} \in S^{(\rightarrow, \leftrightarrow)}$, the result holds.

Proposition 2.5. Let $\{S_i \mid i \in N\}$ be a family of non-empty subsets of T , then

$$i. \quad \bigcap_{i \in N} S_i^{(\rightarrow, \leftrightarrow)} = \bigcup_{i \in N} S_i^{(\rightarrow, \leftrightarrow)}$$

$$ii. \quad \bigcup_{i \in N} S_i^{(\rightarrow, \leftrightarrow)} \subseteq \bigcap_{i \in N} S_i^{(\rightarrow, \leftrightarrow)}$$

Proof: (i) From proposition 2.3, we get $\bigcup_{i \in N} S_i^{(\rightarrow, \leftrightarrow)} \subseteq \bigcap_{i \in N} S_i^{(\rightarrow, \leftrightarrow)}$. To prove the reverse part, assume that $\bar{x} \in \bigcap_{i \in N} S_i^{(\rightarrow, \leftrightarrow)}$ then $\bar{x} \in S_i^{(\rightarrow, \leftrightarrow)}$ for all $i \in N$, and consequently $[a \rightarrow (a \leftrightarrow \bar{x})]^- = \bar{0}$ for all $a \in S_i$. Hence $[a \rightarrow (a \leftrightarrow \bar{x})]^- = \bar{0}$ for all $a \in \bigcup_{i \in N} S_i$ and so, $\bar{x} \in \bigcup_{i \in N} S_i^{(\rightarrow, \leftrightarrow)}$. Therefore $\bigcap_{i \in N} S_i^{(\rightarrow, \leftrightarrow)} \subseteq \bigcup_{i \in N} S_i^{(\rightarrow, \leftrightarrow)}$ and so (i) holds.

From the proposition 2.3, we get $\bigcup_{i \in N} S_i^{(\rightarrow, \leftrightarrow)} \subseteq \bigcap_{i \in N} S_i^{(\rightarrow, \leftrightarrow)}$. Assume that $\bar{x} \in \bigcup_{i \in N} S_i^{(\rightarrow, \leftrightarrow)}$, thus $\bar{x} \in S_i^{(\rightarrow, \leftrightarrow)}$ for all $i \in N$, and consequently $[a \rightarrow (a \leftrightarrow \bar{x})]^- = \bar{0}$ for all $a \in S_i$ and so, $\bar{x} \in \bigcap_{i \in N} S_i^{(\rightarrow, \leftrightarrow)}$. Hence $\bigcup_{i \in N} S_i^{(\rightarrow, \leftrightarrow)} \subseteq \bigcap_{i \in N} S_i^{(\rightarrow, \leftrightarrow)}$.

Theorem 2.6. Let S be a non-empty subset of T . Then $S^{(\rightarrow, \leftrightarrow)} \cap S^{(\leftrightarrow, \rightarrow)}$ are \mathcal{CCPWJ} -ideal (Completely Closed PWJ-ideal) of T .

Proof: Let $[a \rightarrow (a \leftrightarrow \bar{0})]^- = \bar{0} \in S^{(\rightarrow, \leftrightarrow)}$ and $[a \leftrightarrow (a \rightarrow \bar{0})]^- = \bar{0} \in S^{(\leftrightarrow, \rightarrow)}$ for all $a \in S$. It follows that $\bar{0} \in S^{(\rightarrow, \leftrightarrow)} \cap S^{(\leftrightarrow, \rightarrow)}$. Assume that, $\bar{x}, \bar{y} \leftrightarrow \bar{x} \in S^{(\rightarrow, \leftrightarrow)}$ and $\bar{x}, \bar{y} \rightarrow \bar{x} \in S^{(\leftrightarrow, \rightarrow)}$ for some $\bar{x}, \bar{y} \in T$. Then for all $a \in S$ we have,





Indhumathi et al.,

$$[\ddot{a} \rightarrow (\ddot{a} \leftrightarrow \ddot{x})]^- = \ddot{0} \text{ and } [\ddot{a} \rightarrow (\ddot{a} \leftrightarrow (\ddot{y} \leftrightarrow \ddot{x}))]^- = \ddot{0} \text{ also,}$$

$$[\ddot{a} \leftrightarrow (\ddot{a} \rightarrow \ddot{x})]^- = \ddot{0} \text{ and } [\ddot{a} \leftrightarrow (\ddot{a} \rightarrow (\ddot{y} \rightarrow \ddot{x}))]^- = \ddot{0}$$

Since,

$$[\ddot{a} \rightarrow (\ddot{a} \leftrightarrow (\ddot{y} \leftrightarrow \ddot{x}))]^- = \{[\ddot{a} \rightarrow (\ddot{a} \leftrightarrow (\ddot{y} \leftrightarrow \ddot{x}))]^- \leftrightarrow \ddot{0}\}^- \text{ and}$$

$$[\ddot{a} \leftrightarrow (\ddot{a} \rightarrow (\ddot{y} \rightarrow \ddot{x}))]^- = \{[\ddot{a} \leftrightarrow (\ddot{a} \rightarrow (\ddot{y} \rightarrow \ddot{x}))]^- \rightarrow \ddot{0}\}^-$$

This implies that,

$$\{[\ddot{a} \rightarrow (\ddot{a} \leftrightarrow (\ddot{y} \leftrightarrow \ddot{x}))]^- \leftrightarrow \ddot{0}\}^-, \{[\ddot{a} \leftrightarrow (\ddot{a} \rightarrow (\ddot{y} \rightarrow \ddot{x}))]^- \rightarrow \ddot{0}\}^- \in \mathcal{S}^{(\rightarrow, \leftrightarrow)} \cap \mathcal{S}^{(\leftrightarrow, \rightarrow)} \text{ and } \ddot{y} \in \mathcal{S}. \text{ It follows that,}$$

$$(\ddot{a} \rightarrow \ddot{0})^-, (\ddot{a} \leftrightarrow \ddot{0})^- \in \mathcal{S}^{(\rightarrow, \leftrightarrow)} \cap \mathcal{S}^{(\leftrightarrow, \rightarrow)} \text{ for all } \ddot{a} \in \mathcal{S}.$$

Hence, $\mathcal{S}^{(\rightarrow, \leftrightarrow)} \cap \mathcal{S}^{(\leftrightarrow, \rightarrow)}$ is a \mathcal{CCPWJ} -ideal of \mathcal{T} .

Proposition 2.7. For any non-empty subset \mathcal{S} of \mathcal{T} , $\mathcal{S}^{(\rightarrow, \leftrightarrow)} \subseteq \mathcal{K}(\mathcal{T})$.

Proof: Let $\ddot{x} \in \mathcal{S}^{(\rightarrow, \leftrightarrow)}$ then $[\ddot{a} \rightarrow (\ddot{a} \leftrightarrow \ddot{x})]^- = \ddot{0}$ for all $\ddot{a} \in \mathcal{S}$ and we have,

$$(\ddot{0} \rightarrow \ddot{x})^- = \{[\ddot{a} \rightarrow (\ddot{a} \leftrightarrow \ddot{x})]^- \leftrightarrow \ddot{x}\}^- = \{(\ddot{a} \rightarrow \ddot{x})^- \leftrightarrow (\ddot{a} \leftrightarrow \ddot{x})^-\}^- = \{\ddot{1}\}^- = \ddot{0} \text{ and}$$

so, $\ddot{x} \in \mathcal{K}(\mathcal{T})$. Therefore $\mathcal{S}^{(\rightarrow, \leftrightarrow)} \subseteq \mathcal{K}(\mathcal{T})$.

Theorem 2.8. If \mathcal{S} is a \mathcal{CCPWJ} -ideal of \mathcal{T} , then $\mathcal{S}^{(\rightarrow, \leftrightarrow)}$ is the extended \mathcal{PWJ} -ideal of \mathcal{T} , such that $\mathcal{S} \cap \mathcal{S}^{(\rightarrow, \leftrightarrow)} = \{\ddot{0}\}$ and $\mathcal{S}^{(\rightarrow, \leftrightarrow)} \subseteq \mathcal{K}(\mathcal{T})$.

Proof: From theorem 2.6, $\mathcal{S}^{(\rightarrow, \leftrightarrow)}$ is a \mathcal{CCPWJ} -ideal of \mathcal{T} and by proposition 2.4 $\mathcal{S} \cap \mathcal{S}^{(\rightarrow, \leftrightarrow)} = \{\ddot{0}\}$ also by proposition 2.7 $\mathcal{S}^{(\rightarrow, \leftrightarrow)} \subseteq \mathcal{K}(\mathcal{T})$. Let \mathcal{P} be a \mathcal{CCPWJ} -ideal of \mathcal{T} such that $\mathcal{S} \cap \mathcal{P} = \ddot{0}$ and $\mathcal{P} \subseteq \mathcal{K}(\mathcal{T})$. Let $\ddot{x} \in \mathcal{P}$, then $\ddot{x} \in \mathcal{K}(\mathcal{T})$ implies that $(\ddot{0} \rightarrow \ddot{x})^- = \ddot{0}$ and $(\ddot{0} \leftrightarrow \ddot{x})^- = \ddot{0}$ also by $[\ddot{a} \rightarrow (\ddot{a} \leftrightarrow \ddot{x})]^- \leq \ddot{x} \in \mathcal{P}$ and $[\ddot{a} \leftrightarrow (\ddot{a} \rightarrow \ddot{x})]^- \leq \ddot{x} \in \mathcal{P}$ for all $\ddot{a} \in \mathcal{S}$. Since \mathcal{P} be a \mathcal{CCPWJ} -ideal of \mathcal{T} , we get $[\ddot{a} \rightarrow (\ddot{a} \leftrightarrow \ddot{x})]^- \in \mathcal{P}$ and also $[\ddot{a} \leftrightarrow (\ddot{a} \rightarrow \ddot{x})]^- \in \mathcal{P}$.

On the other hand,

$$\{((\ddot{a} \rightarrow (\ddot{a} \leftrightarrow \ddot{x}))^-)^- \leftrightarrow \ddot{a}\}^- = \{((\ddot{a} \rightarrow \ddot{a})^- \leftrightarrow (\ddot{a} \rightarrow \ddot{x})^-)^- \leftrightarrow \ddot{a}\}^-$$

$$= \{(\ddot{0} \leftrightarrow (\ddot{a} \leftrightarrow \ddot{x})^-)^- \leftrightarrow \ddot{a}\}^-$$

$$= ((\ddot{1})^- \leftrightarrow \ddot{a})^-$$

$$= (\ddot{0} \leftrightarrow \ddot{a})^-$$

$$\{((\ddot{a} \leftrightarrow (\ddot{a} \rightarrow \ddot{x}))^-)^- \rightarrow \ddot{a}\}^- = \{((\ddot{a} \leftrightarrow \ddot{a})^- \rightarrow (\ddot{a} \leftrightarrow \ddot{x})^-)^- \rightarrow \ddot{a}\}^-$$

$$= \{(\ddot{0} \rightarrow (\ddot{a} \leftrightarrow \ddot{x})^-)^- \rightarrow \ddot{a}\}^-$$

$$= ((\ddot{1})^- \rightarrow \ddot{a})^-$$

$$= (\ddot{0} \rightarrow \ddot{a})^-$$

Since, \mathcal{S} is \mathcal{CCPWJ} -ideal of \mathcal{T} , we have $(\ddot{0} \rightarrow \ddot{a})^-$, $(\ddot{0} \leftrightarrow \ddot{a})^- \in \mathcal{S}$ and so,

$\{((\ddot{a} \rightarrow (\ddot{a} \leftrightarrow \ddot{x}))^-)^- \leftrightarrow \ddot{a}\}^-$ and $\{((\ddot{a} \leftrightarrow (\ddot{a} \rightarrow \ddot{x}))^-)^- \rightarrow \ddot{a}\}^- \in \mathcal{S}$. Thus from $\ddot{a} \in \mathcal{S}$, we get $(\ddot{a} \rightarrow (\ddot{a} \leftrightarrow \ddot{x}))^-$, $(\ddot{a} \leftrightarrow (\ddot{a} \rightarrow \ddot{x}))^- \in \mathcal{S}$ and hence,

$\mathcal{S} \cap \mathcal{P} = \{(\ddot{a} \rightarrow (\ddot{a} \leftrightarrow \ddot{x}))^-, (\ddot{a} \leftrightarrow (\ddot{a} \rightarrow \ddot{x}))^-\}$. But $\mathcal{S} \cap \mathcal{P} = \{\ddot{0}\}$. Hence $(\ddot{a} \rightarrow (\ddot{a} \leftrightarrow \ddot{x}))^- = \ddot{0}$ and $(\ddot{a} \leftrightarrow (\ddot{a} \rightarrow \ddot{x}))^- = \ddot{0}$, which implies that $\ddot{x} \in \mathcal{S}^{(\rightarrow, \leftrightarrow)}$. Therefore $\mathcal{P} \subseteq \mathcal{S}^{(\rightarrow, \leftrightarrow)}$. Thus $\mathcal{S}^{(\rightarrow, \leftrightarrow)}$ is the extended \mathcal{PWJ} -ideal of \mathcal{T} .

Proposition 2.9. If \mathcal{S} is a \mathcal{CCPWJ} -ideal of \mathcal{T} , then $\mathcal{S}^{(\rightarrow, \leftrightarrow)} = \mathcal{S}^{(\leftrightarrow, \rightarrow)}$.

Proof: From theorem 2.8, $\mathcal{S}^{(\rightarrow, \leftrightarrow)}$ is a \mathcal{CCPWJ} -ideal with two properties, $\mathcal{S} \cap \mathcal{S}^{(\rightarrow, \leftrightarrow)} = \{\ddot{0}\}$ and $\mathcal{S}^{(\rightarrow, \leftrightarrow)} \subseteq \mathcal{K}(\mathcal{T})$. But, by theorem 2.8, $\mathcal{S}^{(\rightarrow, \leftrightarrow)}$ is the extended \mathcal{PWJ} -ideal of \mathcal{T} such that $\mathcal{S} \cap \mathcal{S}^{(\leftrightarrow, \rightarrow)} = \{\ddot{0}\}$ and $\mathcal{S}^{(\leftrightarrow, \rightarrow)} \subseteq \mathcal{K}(\mathcal{T})$. Therefore $\mathcal{S}^{(\rightarrow, \leftrightarrow)} \subseteq \mathcal{S}^{(\leftrightarrow, \rightarrow)}$. By similar argument, we get $\mathcal{S}^{(\leftrightarrow, \rightarrow)} \subseteq \mathcal{S}^{(\rightarrow, \leftrightarrow)}$ and, Hence $\mathcal{S}^{(\rightarrow, \leftrightarrow)} = \mathcal{S}^{(\leftrightarrow, \rightarrow)}$.

Definition 2.10. Let \mathcal{S} be a \mathcal{PWJ} -ideal of \mathcal{T} , then \mathcal{S} is said a,

$(\rightarrow, \leftrightarrow)$ – Normal if it satisfies for all $\ddot{x}, \ddot{y} \in \mathcal{T}$, then such that, $(\ddot{x} \rightarrow (\ddot{x} \leftrightarrow \ddot{y}))^- \in \mathcal{S}$ implies $(\ddot{y} \rightarrow (\ddot{y} \leftrightarrow \ddot{x}))^- \in \mathcal{S}$.(4)

$(\leftrightarrow, \rightarrow)$ – Normal if it satisfies for all $\ddot{x}, \ddot{y} \in \mathcal{T}$, then such that, $(\ddot{x} \leftrightarrow (\ddot{x} \rightarrow \ddot{y}))^- \in \mathcal{S}$ implies $(\ddot{y} \leftrightarrow (\ddot{y} \rightarrow \ddot{x}))^- \in \mathcal{S}$.

(5) Normal if it is both $(\rightarrow, \leftrightarrow)$ – Normal and $(\leftrightarrow, \rightarrow)$ – Normal. (6)

Example 2.11. Let $\mathcal{T} = (\{\ddot{0}, \ddot{u}, \ddot{v}, \ddot{1}\}, -, \sim, \rightarrow, \leftrightarrow)$ be a \mathcal{LPW} -Algebra, which double operations \rightarrow and \leftrightarrow are defined as follows





Indhumathi et al.,

Table 5. Complement		Table 6. Implication					Table 7. Complement		Table 8. Implication					
\check{x}	\check{x}^-	\rightarrow	$\check{0}$	\check{u}	\check{v}	$\check{1}$	\check{x}	\check{x}^-	\leftrightarrow	$\check{0}$	$\check{1}$	$\check{1}$	$\check{1}$	$\check{1}$
$\check{0}$	$\check{1}$	$\check{0}$	$\check{1}$	$\check{1}$	$\check{1}$	$\check{1}$	$\check{0}$	$\check{1}$	$\check{0}$	$\check{1}$	$\check{1}$	$\check{1}$	$\check{1}$	$\check{1}$
\check{u}	\check{v}	\check{u}	\check{v}	$\check{1}$	$\check{1}$	$\check{1}$	\check{u}	\check{v}	\check{u}	\check{v}	$\check{1}$	$\check{1}$	$\check{1}$	$\check{1}$
\check{v}	\check{u}	\check{v}	\check{u}	\check{u}	$\check{1}$	$\check{1}$	\check{v}	\check{u}	\check{v}	\check{u}	\check{v}	$\check{1}$	$\check{1}$	$\check{1}$
$\check{1}$	$\check{0}$	$\check{1}$	$\check{0}$	\check{u}	\check{v}	$\check{1}$	$\check{1}$	$\check{0}$	$\check{1}$	$\check{0}$	\check{u}	\check{v}	$\check{1}$	$\check{1}$

Consider a \mathcal{PWJ} -ideal $\check{S} = \{\check{0}, \check{u}\}$ of \check{T} , it can be checked that \check{S} is a $(\rightarrow, \leftrightarrow)$ – Normal, but it is not $(\leftrightarrow, \rightarrow)$ – Normal. Since $(\check{u} \leftrightarrow (\check{u} \rightarrow \check{1}))^- = \check{1}^- = \check{0} \in \check{S}$ but $(\check{1} \leftrightarrow (\check{1} \rightarrow \check{u}))^- = (\check{1} \leftrightarrow \check{u})^- = \check{u}^- = \check{v} \notin \check{S}$.

Proposition 2.12. The following are equivalent,

- (i) \check{T} is a \mathcal{LPW} -Algebra
- (ii) There exists a $(\rightarrow, \leftrightarrow)$ – Normal \mathcal{PWJ} -ideal of $\check{T} \subseteq \check{K}(\check{T})$.

Proof: (i) implies (ii)

Let \check{T} be a \mathcal{LPW} -Algebra. Obviously, \check{T} is a $(\rightarrow, \leftrightarrow)$ – Normal \mathcal{PWJ} -ideal of \check{T} and $\check{K}(\check{T}) = \check{T}$. Thus, $\check{T} \subseteq \check{K}(\check{T})$.

(ii) implies (i)

Assume that \check{S} is a $(\rightarrow, \leftrightarrow)$ – Normal \mathcal{PWJ} -ideal of \check{T} contained in $\check{K}(\check{T})$. By the $(\rightarrow, \leftrightarrow)$ – Normality of \check{S} , it follows from $(\check{u} \rightarrow (\check{u} \leftrightarrow \check{1}))^- = \check{0} \in \check{S}$ we get $(\check{1} \rightarrow (\check{1} \leftrightarrow \check{u}))^- \in \check{S}$ and so from $\check{S} \subseteq \check{K}(\check{T})$. We get,

$$[(\check{u} \leftrightarrow (\check{u} \rightarrow (\check{u} \leftrightarrow \check{1})))]^- = [(\check{u} \rightarrow (\check{u} \leftrightarrow (\check{u} \rightarrow \check{1})))]^- = \check{1}^- = \check{0},$$

we obtain $(\check{0} \leftrightarrow \check{u})^- = \check{1}^- = \check{0}$. Therefore \check{T} is a \mathcal{LPW} -Algebra.

Proposition 2.13. Every $(\rightarrow, \leftrightarrow)$ – Normal \mathcal{PWJ} -ideal of \check{T} is \mathcal{CCPWJ} -ideal and contains $\check{M}(\check{T})$.

Proof: Let \check{S} be a $(\rightarrow, \leftrightarrow)$ – Normal \mathcal{PWJ} -ideal of \check{T} and let $\check{u} \in \check{S}$. Since,

$[(\check{u} \rightarrow \check{1}) \leftrightarrow ((\check{u} \rightarrow \check{1}) \leftrightarrow \check{1})]^- = (\check{1} \leftrightarrow \check{1})^- = \check{1}^- = \check{0} \in \check{S}$, it follows from $(\rightarrow, \leftrightarrow)$ – Normality of \check{S} , $[\check{u} \rightarrow (\check{u} \leftrightarrow (\check{u} \rightarrow \check{1}))]^- \in \check{S}$ and so, $(\check{0} \rightarrow \check{u})^- = \check{1}^- = \check{0} \in \check{S}$. This implies that \check{S} is \mathcal{CCPWJ} -ideal. Let $\check{u} \in \check{M}(\check{T})$, then $(\check{1} \rightarrow (\check{1} \leftrightarrow \check{u}))^- = \check{u}$ on the other hand, from $(\check{u} \rightarrow (\check{u} \leftrightarrow \check{1}))^- = \check{0} \in \check{S}$ we get, $(\check{1} \rightarrow (\check{1} \leftrightarrow \check{u}))^- \in \check{S}$. Therefore $\check{u} \in \check{S}$, thus, it contains $\check{M}(\check{T})$.

Corollary 2.14. If \check{S} is a $(\rightarrow, \leftrightarrow)$ – Normal \mathcal{PWJ} -ideal of \check{T} , then $\check{S}^{(\rightarrow, \leftrightarrow)} = \check{S}^{(\leftrightarrow, \rightarrow)} = \check{S}^*$.

Proof: By Proposition 2.13, \check{S} is \mathcal{CCPWJ} -ideal and so by Proposition 2.9 the result holds.

Proposition 2.15. Let \check{S} be a Normal \mathcal{PWJ} -ideal and \check{P} is a \mathcal{PWJ} -ideal of \check{T} , then the following are equivalent.

- (i) $\check{S} \cap \check{P} = \{\check{0}\}$
- (ii) $\check{P} \subseteq \check{S}^{(\rightarrow, \leftrightarrow)}$

Proof: (i) implies (ii)

Suppose that $\check{S} \cap \check{P} = \{\check{0}\}$ and $\check{v} \in \check{P}$, for any $\check{u} \in \check{S}$, we have $(\check{v} \rightarrow (\check{v} \leftrightarrow \check{u}))^- \leq \check{u} \in \check{S}$ and so, $(\check{v} \rightarrow (\check{v} \leftrightarrow \check{u}))^- \in \check{S}$, then since \check{S} is normal, we get $(\check{u} \rightarrow (\check{u} \leftrightarrow \check{v}))^- \in \check{S}$. Similarly, we have $(\check{u} \rightarrow (\check{u} \leftrightarrow \check{v}))^- \leq \check{v} \in \check{P}$ and hence, $(\check{u} \rightarrow (\check{u} \leftrightarrow \check{v}))^- \in \check{S} \cap \check{P} = \{\check{0}\}$ for every $\check{u} \in \check{S}$. This implies $\check{v} \in \check{S}^{(\rightarrow, \leftrightarrow)}$ and $\check{P} \subseteq \check{S}^{(\rightarrow, \leftrightarrow)}$.

(ii) implies (i) Assume that $\check{P} \subseteq \check{S}^{(\rightarrow, \leftrightarrow)}$, obviously, we have $\check{0} \in \check{S} \cap \check{P} \subseteq \check{S} \cap \check{S}^{(\rightarrow, \leftrightarrow)} = \{\check{0}\}$ and so, $\check{S} \cap \check{P} = \{\check{0}\}$.

Proposition 2.16. Let $\{\check{0}\}$ be a $(\rightarrow, \leftrightarrow)$ – Normal \mathcal{PWJ} -ideal of \check{T} and $\check{S} \subseteq \check{T}$, then the following hold,

- (i) $\check{S} \subseteq \check{S}^{(\rightarrow, \leftrightarrow)(\rightarrow, \leftrightarrow)}$





Indhumathi et al.,

(ii) $\mathcal{S}^{(\rightarrow, \leftrightarrow)} = \mathcal{S}^{(\rightarrow, \leftrightarrow)(\rightarrow, \leftrightarrow)(\rightarrow, \leftrightarrow)}$

(iii) $\hat{T} = \hat{T}^{(\rightarrow, \leftrightarrow)(\rightarrow, \leftrightarrow)}$

Proof:

(i) Let $\ddot{u} \in \mathcal{S}$ and $\ddot{v} \in \mathcal{S}^{(\rightarrow, \leftrightarrow)}$ then $(\ddot{a} \rightarrow (\ddot{a} \leftrightarrow \ddot{v})) \sim \ddot{0}$ for all $\ddot{a} \in \mathcal{S}$ and so by putting $\ddot{a} = \ddot{u}$, we get $(\ddot{u} \rightarrow (\ddot{u} \leftrightarrow \ddot{v})) \sim \ddot{0}$, hence by the $(\rightarrow, \leftrightarrow)$ – Normality of $\{\ddot{0}\}$, we conclude $(\ddot{v} \rightarrow (\ddot{v} \leftrightarrow \ddot{u})) \sim \ddot{0}$ this implies $\ddot{u} \in \mathcal{S}^{(\rightarrow, \leftrightarrow)(\rightarrow, \leftrightarrow)}$, therefore $\mathcal{S} \subseteq \mathcal{S}^{(\rightarrow, \leftrightarrow)(\rightarrow, \leftrightarrow)}$.

(ii) by (i), we have $\mathcal{S}^{(\rightarrow, \leftrightarrow)} \subseteq \mathcal{S}^{(\rightarrow, \leftrightarrow)(\rightarrow, \leftrightarrow)(\rightarrow, \leftrightarrow)}$ on the other hand, by Proposition 2.3, It follows from $\mathcal{S} \subseteq \mathcal{S}^{(\rightarrow, \leftrightarrow)(\rightarrow, \leftrightarrow)}$ that $\mathcal{S}^{(\rightarrow, \leftrightarrow)(\rightarrow, \leftrightarrow)(\rightarrow, \leftrightarrow)} \subseteq \mathcal{S}^{(\rightarrow, \leftrightarrow)}$.

Therefore $\mathcal{S}^{(\rightarrow, \leftrightarrow)} = \mathcal{S}^{(\rightarrow, \leftrightarrow)(\rightarrow, \leftrightarrow)(\rightarrow, \leftrightarrow)}$.

(iii) Let $\ddot{u} \in \mathcal{S}$ and $\ddot{v} \in \mathcal{S}^{(\rightarrow, \leftrightarrow)}$ for all $\ddot{u}, \ddot{v} \in \hat{T}$, then from (i) $\mathcal{S} \subseteq \mathcal{S}^{(\rightarrow, \leftrightarrow)}$ for $\mathcal{S} \subseteq \hat{T}$, and $\mathcal{S}^{(\rightarrow, \leftrightarrow)} \subseteq \hat{T}^{(\rightarrow, \leftrightarrow)}$. Similarly, $\mathcal{S}^{(\rightarrow, \leftrightarrow)} \subseteq \mathcal{S}$, therefore $\mathcal{S} = \mathcal{S}^{(\rightarrow, \leftrightarrow)}$ for $\mathcal{S} \subseteq \hat{T}$, and $\mathcal{S}^{(\rightarrow, \leftrightarrow)(\rightarrow, \leftrightarrow)} \subseteq \hat{T}^{(\rightarrow, \leftrightarrow)(\rightarrow, \leftrightarrow)}$. Hence $\hat{T} = \hat{T}^{(\rightarrow, \leftrightarrow)(\rightarrow, \leftrightarrow)}$.

Proposition 2.17. Let $\phi \neq \mathcal{S} \subseteq \hat{T}$ if $\mathcal{S}^{(\rightarrow, \leftrightarrow)} = \hat{T}$, then $\mathcal{S} = \{\ddot{0}\}$.

Proof: Let $\mathcal{S}^{(\rightarrow, \leftrightarrow)} = \hat{T}$ and $\ddot{a} \in \mathcal{S}$, then for all $\ddot{u} \in \hat{T}$, we have $\ddot{u} \in \mathcal{S}^{(\rightarrow, \leftrightarrow)}$ and so, $(\ddot{a} \rightarrow (\ddot{a} \leftrightarrow \ddot{u})) \sim \ddot{0}$ for all $\ddot{a} \in \mathcal{S}$. By putting $\ddot{u} = \ddot{a}$, we get $(\ddot{a} \rightarrow (\ddot{a} \leftrightarrow \ddot{a})) \sim \ddot{0}$.

Therefore $\mathcal{S} = \{\ddot{0}\}$.

Proposition 2.18. Let \mathcal{S} be a Normal \mathcal{PWJ} -ideal of \hat{T} , then $\mathcal{S}^{(\rightarrow, \leftrightarrow)} = \hat{T}$ if and only if $\mathcal{S} = \{\ddot{0}\}$.

Proof: Let $\mathcal{S}^{(\rightarrow, \leftrightarrow)} = \hat{T}$ and $\ddot{a} \in \mathcal{S}$, then for all $\ddot{u} \in \hat{T}$, we have $\ddot{u} \in \mathcal{S}^{(\rightarrow, \leftrightarrow)}$ and so, $(\ddot{a} \rightarrow (\ddot{a} \leftrightarrow \ddot{u})) \sim \ddot{0}$ for all $\ddot{a} \in \mathcal{S}$ by Proposition 2.17, the result holds, conversely, let $\mathcal{S} = \{\ddot{0}\}$ and $\ddot{u} \in \hat{T}$, then $(\ddot{u} \rightarrow (\ddot{u} \leftrightarrow \ddot{1})) \sim \ddot{1} \sim \ddot{0} \in \mathcal{S}$ and so, by the normality of \mathcal{S} , and by putting $\ddot{u} = \ddot{1}$, $(\ddot{1} \rightarrow (\ddot{1} \leftrightarrow \ddot{1})) \sim \ddot{1} \sim \ddot{0}$, this implies $\ddot{u} \in \mathcal{S}^{(\rightarrow, \leftrightarrow)}$ and hence $\hat{T} = \mathcal{S}^{(\rightarrow, \leftrightarrow)}$.

Example 2.19. Consider the \mathcal{PWJ} -ideal $\mathcal{S} = \{\ddot{0}, \ddot{u}, \ddot{1}\}$ in an example 2.11 \mathcal{S} is not normal, since \mathcal{S} is not $(\leftrightarrow, \rightarrow)$ – Normal by example 2.11. A simple investigation shows that $(\ddot{0} \rightarrow (\ddot{0} \leftrightarrow \ddot{1})) \sim \ddot{0}$ and $(\ddot{u} \rightarrow (\ddot{u} \leftrightarrow \ddot{1})) \sim \ddot{0}$ for all $\ddot{1} \in \hat{T}$. Hence $\mathcal{S}^{(\rightarrow, \leftrightarrow)} = \hat{T}$, Similarly, we have $\mathcal{S}^{(\leftrightarrow, \rightarrow)} = \hat{T}$. Therefore $\mathcal{S}^{\leftrightarrow} = \hat{T}$. But $\mathcal{S} \neq \{\ddot{0}\}$.

Proposition 2.20. Let $\check{f}: \hat{X} \rightarrow \hat{Y}$ be a homomorphism and \mathcal{S} is a subset of \hat{T} then, $\check{f}(\mathcal{S}^{(\rightarrow, \leftrightarrow)}) \subseteq (\check{f}(\mathcal{S}))^{(\rightarrow, \leftrightarrow)}$ moreover, if \check{f} is an isomorphism, then $\check{f}(\mathcal{S}^{(\rightarrow, \leftrightarrow)}) = (\check{f}(\mathcal{S}))^{(\rightarrow, \leftrightarrow)}$.

Proof: Let $\check{v} \in \check{f}(\mathcal{S}^{(\rightarrow, \leftrightarrow)})$, then $\check{v} = \check{f}(\ddot{u})$ for some $\ddot{u} \in \mathcal{S}^{(\rightarrow, \leftrightarrow)}$. It follows that $(\ddot{a} \rightarrow (\ddot{a} \leftrightarrow \ddot{u})) \sim \ddot{0}$ for all $\ddot{a} \in \mathcal{S}$ and so, $(\check{f}(\ddot{a}) \rightarrow (\check{f}(\ddot{a}) \leftrightarrow \check{f}(\ddot{u}))) \sim \check{f}(\ddot{0}) = \ddot{0}$ for all

$\check{f}(\ddot{a}) \in \check{f}(\mathcal{S})$. This implies $\check{f}(\ddot{u}) \in (\check{f}(\mathcal{S}))^{(\rightarrow, \leftrightarrow)}$, therefore $\check{f}(\mathcal{S}^{(\rightarrow, \leftrightarrow)}) \subseteq (\check{f}(\mathcal{S}))^{(\rightarrow, \leftrightarrow)}$, to prove $(\check{f}(\mathcal{S}))^{(\rightarrow, \leftrightarrow)} \subseteq \check{f}(\mathcal{S}^{(\rightarrow, \leftrightarrow)})$.

Let $\check{v} \in (\check{f}(\mathcal{S}))^{(\rightarrow, \leftrightarrow)}$. Thus by the on to of \check{f} , we have $(\check{f}(\ddot{a}) \rightarrow (\check{f}(\ddot{a}) \leftrightarrow \check{f}(\ddot{u}))) \sim \check{f}(\ddot{0})$ in which $\check{v} = \check{f}(\ddot{u})$ for some consequently,

$\check{f}((\ddot{a} \rightarrow (\ddot{a} \leftrightarrow \ddot{u}))) \sim \check{f}(\ddot{0})$. It follows that, $(\ddot{a} \rightarrow (\ddot{a} \leftrightarrow \ddot{u})) \sim \check{f}^{-1}(\check{f}(\ddot{0}))$. By the one to one of \check{f} , we have

$\check{f}^{-1}(\check{f}(\ddot{0})) = \ddot{0}$. Thus, $(\ddot{a} \rightarrow (\ddot{a} \leftrightarrow \ddot{u})) \sim \ddot{0}$ for all $\ddot{a} \in \mathcal{S}$ and so $\ddot{u} \in \mathcal{S}^{(\rightarrow, \leftrightarrow)}$. It follows that, $\check{v} = \check{f}(\ddot{u}) \in \check{f}(\mathcal{S}^{(\rightarrow, \leftrightarrow)})$.

Therefore, $(\check{f}(\mathcal{S}))^{(\rightarrow, \leftrightarrow)} \subseteq \check{f}(\mathcal{S}^{(\rightarrow, \leftrightarrow)})$. Hence

$\check{f}(\mathcal{S}^{(\rightarrow, \leftrightarrow)}) = (\check{f}(\mathcal{S}))^{(\rightarrow, \leftrightarrow)}$.

CONCLUSION

In this study, we provide new definitions of annihilators in \mathcal{LPW} -Algebras that are connected to the $(\rightarrow, \leftrightarrow)$ – Normal and $(\leftrightarrow, \rightarrow)$ – Normal \mathcal{PWJ} -ideals, along with appropriate instances. We learn a few characterizations and a few fundamental characteristics of annihilators. We also look into how and for an algebraic homomorphism relate to



**Indhumathi et al.,**

one another. This technique can be further expanded to fuzzy $(\rightarrow, \rightsquigarrow)$ –normal and fuzzy $(\rightsquigarrow, \rightarrow)$ –normal \mathcal{PWI} -ideals for fresh outcomes in our upcoming research.

REFERENCES

1. Ceterchi Rodica, *The Lattice Structure of Pseudo-Wajsberg Algebras*, Journal of Universal Computer Science, 6, 22, 2000.
2. Ceterchi Rodica, *Pseudo-Wajsberg Algebras*, Multi-Valued Logic, 6, 67, 2001.
3. Font, J. M., Rodriguez, A. J., and Torrens, A., *Wajsberg Algebras*, Stochastica, 8, 5, 1984.
4. Ibrahim, A., and Indhumathi, M., *PWI-Ideals of Lattice Pseudo-Wajsberg algebras*, Advances in Theoretical and Applied Mathematics, 13, 1, 2018.
5. Ibrahim, A., and Indhumathi, M., *Classes of p-ideals of Lattice pseudo-Wajsberg Algebras*, International Journal of Research in Advent Technology, 7, 172, 2019.
6. Ibrahim, A., and Indhumathi, M., *Various Types of PWI-Ideals of a Lattice pseudo-Wajsberg Algebras*, Advances in Mathematics, 3, 285, 2019.
7. Ibrahim, A., and Indhumathi, M., *On fuzzy Extended PWI-Ideals of Lattice pseudo-Wajsberg Algebras*, International Journal of Advanced Science and Technology, 29, 1163, 2020.
8. Ibrahim, A., and Indhumathi, M., *On anti-fuzzy EPWI-ideals of lattice pseudo W-algebras*, Malaya Journal of Matematik, 8, 1587, 2020.
9. Wajsberg, M., *Beitrage zum Metaaussagenkalkul I*, Monatshefte fur Mathematik, 42, 221, 1935.





Diversity of Avifauna in Selected Pond in Theni District, Tamil Nadu

Pushpa^{1*} and Arun Nagendran²

¹Assistant Professor, Department of Zoology, Jayaraj Annapackiam College for Women (Autonomous), Periyakulam, Theni, (Affiliated to Mother Teresa Women's University, Kodaikanal) Tamil Nadu, India.

²National Centre of Excellence, Department of Zoology, Thiagarajar College, (Affiliated to Madurai Kamaraj University) Madurai, Tamil Nadu, India.

Received: 04 Sep 2023

Revised: 10 Nov 2023

Accepted: 19 Jan 2024

*Address for Correspondence

Pushpa

Assistant Professor,
Department of Zoology,
Jayaraj Annapackiam College for Women (Autonomous),
Periyakulam, Theni,
(Affiliated to Mother Teresa Women's University, Kodaikanal)
Tamil Nadu, India.
E mail: pushpazoo@annejac.ac.in



This is an Open Access Journal / article distributed under the terms of the **Creative Commons Attribution License** (CC BY-NC-ND 3.0) which permits unrestricted use, distribution, and reproduction in any medium, provided the original work is properly cited. All rights reserved.

ABSTRACT

Wetlands are integral to a healthy environment. Aquatic environments provide critical habitat to a wide variety of bird species which are a part of the balance of nature, indicators of the quality of the environment and are sensitive to habitat change. The present study deals with the species diversity, abundance, and species richness of avian communities in selected ponds in Theni District. The visits were made during early mornings, since activity of birds is at its peak during this time. Total count method was used to cover most of the study area. A total of 34 species of birds belonging to 26 families under 13 orders were recorded. The diversity of the birds were high during the month of September and low in December. The abundance of birds were high during the month of July followed by August and September and low in December. The highest number of species richness were little egret followed by great egret, little grebe and common coot and low were king fisher, jacana and lapwing. The study also revealed that the wetland harbors plenty of resident as well as few migratory birds. Hence this study was taken up to assess the status of wetlands and this site could be protected for wetland birds.

Keywords: Wetlands, Diversity of birds, Abundance, Richness.

INTRODUCTION

Wetlands are the maximum productive environment within the world [15] and provide the transitional hyperlink among aquatic and terrestrial habitats [28]. They have got precise ecological traits, capabilities, and values, 69936



**Pushpa and Arun Nagendran**

occupying approximately 6% of the earth's floor [17] and imparting habitat to a big selection of flowers and fauna three. Wetlands are taken into consideration as resources of biodiversity inside a vicinity or a landscape [9]. The various nature of wetland ecosystems match the range of avifauna. For example, artificial wetlands had been pronounced to captivate distinctive styles of hen species from the ones in natural wetland ecosystems [12]. Such ecosystems are numerous in nature empower the want to apprehend their impact at the avifauna populations [25]. The development of an synthetic wetland region is regarded as a precious measure for the reason that it could provide a brand new habitat for chook groups if all other elements are appropriate [20]. Furthermore, the presence of an artificial wetland habitat has been discovered to supplement its herbal counterpart with the aid of permitting more species to use one-of-a-kind habitats in different situations [14]. Wetlands are still being degraded in lots of components of the world [24]. There may be a want to assess and reveal birds' populations given that their numbers, distribution and sports reflect the environment's quality and status eleven. Because of the great variety of wetlands, fowl version to and use of wetland environments differs substantially from species [5]. breeding, nesting, feeding, or shelter in the course of their breeding cycles [23]. Wetlands may be seen as herbal ecological islands of freshwater habitats encircling by means of terrestrial habitats. Wetlands dispense meals for birds inside the shape of vegetation, vertebrates, and invertebrates thirteen, sixteen. Positive feeders forage for food within the wetland soils, some discover food inside the water column, and some feed at the vertebrates and invertebrates that live on inundate and emergent plant life. Wetlands are the various efficient and fragile ecosystems which deserve special interest due to their biodiversity richness [2,7,27]. Avifauna is a accepted call for chicken species. Birds are feathered, winged, egg-laying vertebrates. They belong to the kingdom "Animalia," Phylum Chordata and sophistication Aves. They have a global distribution, dwelling in and around oceans, rivers, forest and mountains. They may be the most perceptible group inside the animal nation. Their vivid colours, well described songs and calls, and showy shows upload fun to human existence. Many people reap high-quality satisfaction from looking birds and taking note of their stunning songs. Birds are gregarious animals that talk with visible symptoms, calls and songs. They show societal behaviors which includes cooperative breeding and searching, flocking and surround of predators. Birds stay and breed in most terrestrial habitats and on all of the seven main lands. The mixing impact of climate exchange [21] and urbanization [8,23,31,6,24] leading to habitat loss stays one of the maximum hard troubles for conservation of bird diversity.

MATERIALS AND METHODS**Study Area**

Theni is a valley town situated in the Indian state of Tamil Nadu at the foothills of Western Ghats. Meenakshipuram pond is located in Bodinayakkanur which is 14 kilometers from Theni. Periyakulam pond is located in Theni District. Sugar cane, Mango grove, Coconut grove and Paddy fields are located around the Periyakulam pond and the distance from the Meenakshipuram pond is 30 Km and Katroad pond, Sengulathupatti pond, and Kattakamanpatti ponds are also located in Theni District at the distance of nearby 60 Km from the Meenakshipuram pond.

Bird Census

The bird census was taken twice in a month from July to December 2021. The method of total count was employed to survey the bird population. In this method, the blocks were counted using (7X50) pentax binocular and identified using features with the help of field guild [1,11].

Data Analysis**Species Abundance**

Species abundance was measured by (number of water birds in each recorded on the habitat) during the monthly census (Verner, 1985).

Species Diversity

Species diversity was calculated using the Shannon – Weaver index (Shannon Weaver, 1964).

$$H1 = -\sum Pi \times \ln (Pi)$$



**Pushpa and Arun Nagendran**

Where, P_i = The proportions of individuals found in the 1st species

\ln = Log Normal

Species Richness

The richness of bird species was calculated using the margalef (1958) index.

$$R1 = (S - 1) \ln(n)$$

Where,

S = The total number of species

N = The number of individuals

RESULT AND DISCUSSION

The chook variety was high in August and September and minimal for the duration of November and December. This showed that this species is equally allotted in September and low in November and December with lowest equitability. Bird abundance turned into excessive in July accompanied by way of August September. The abundance become very low in November and December because of the migrant chook species in these selected ponds in Theni District. The very best wide variety of species richness have been little grebe, common place coot, Little egret, Indian pond heron, Black winged stilt and Great egret and low have been King fisher, White browed wagtail and Indian robin bird in Meenakshipuram pond. The best number of species richness had been commonplace coot, little grebe, first-rate egret and Black winged stilt and low had been King fisher, Jacana in Katroad pond. The best number of species richness had been little grebe, Little egret, exceptional egret and residence crow and low were King fisher in Periyakulam pond. The very best quantity of species richness have been little egret, brilliant egret, little grebe and not unusual myna and occasional have been Indian roller in Sengulathupatti pond. The very best range of species richness had been Little grebe, Indian pond heron, residence crow and Common coot and low have been grey francolin and White breasted kingfisher in Kattakamanpatti pond because of the supply of prey classes. The equal end result was mentioned as7.

SUMMARY

In a wetland ecosystem this area is important for the breeding and roosting birds and several other taxa of fauna and flora. Wetlands are still being degraded in many parts of the world. Besides human activities such as sewage discharge, throwing of domestic garbage, weed infestation were some of the threats found in the wetland. There is a need to assess and monitor birds' populations since their numbers, distribution and activities reflect the ecosystem's quality and status. So, it may be suggested that drastic steps must be taken to preserve and maintain these types of wetlands and to save the wetland birds.

REFERENCES

1. Ali, S. and Ripley, S.D. (1983). A pictorial guide to the birds of subcontinent. Bombay Natural History Society, Oxford University Press, Mumbai.
2. Barbier E.B., Acreman MC, Knowler D (1997) Economic valuation of wetlands: a guide for policy makers and planners. Ramsar Convention Bureau. Gland, Switzerland.p.127.
3. Buckton, S. (2007). Managing wetlands for sustainable livelihoods at KoshiTappu. *Danphe*16(1): 12–13.
4. Custer, T.W. & R.G. Osborn (1977). Wading birds as biological indicators: 1975 colony survey. United States fish and wildlife Services, Special Scientific Report-Wildlife. No. 206.
5. Dahl TE, Johnson CE (1991). Wetlands status and trends in the conterminous United States, mid-1970's to mid-1980': Washington, D.C., U.S. Fish and Wildlife Service. P.22.





Pushpa and Arun Nagendran

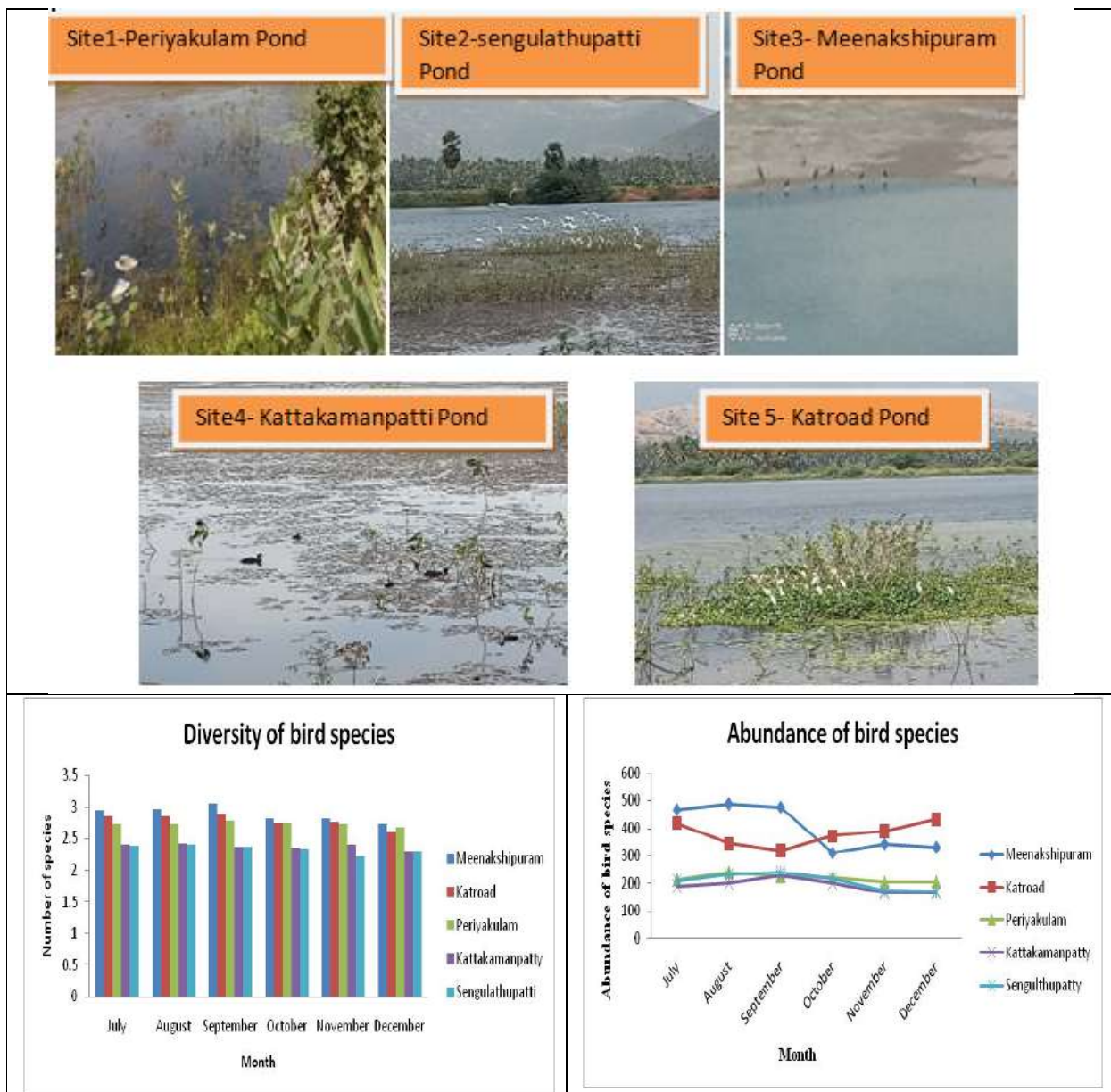
6. Ferenc, M., Sedlacek, O., Fuchs, R., Dinet, M., Fraissinet, M. & D. Storch (2014). Are cities different? Patterns of species richness and beta diversity of urban bird communities and regional species assemblages in Europe. *Global Ecology and Biogeography* 23: 479-489;
7. Geoffrey Soka, (2013). Species diversity and abundance of avifauna in and around Hombolo wetland in general Tanzania. *International journal of biodiversity and conservation*. Vol. 5(11): 782-790.
8. Getzner, M. (2002). Investigating public decisions about protecting wetlands. *Journal of Environmental Management* 64(3): 237-246;
9. Gopal, B. & M. Sah (1993). Conservation and management of rivers in India: case study of the River Yamuna. *Environmental Conservation* 20(3):243-254;
10. Green, A.J. (1996). Analysis of globally threatened Anatidae in relation to threats, distribution, migration patterns, and habitat use. *Conservation Biology* 10(5): 1435-1445;
11. Inskipp, T. (1998) Pocket Guide to the Birds of Indian Subcontinent. Oxford University Press, Mumbai.
12. Ismail A., Rahman F, Zulkifli SZ (2012). Status, Composition and Diversity of Avifauna in the Artificial Putrajaya Wetlands and Comparison with its Two Neighboring Habitats. *Trop. Nat. Hist.* 12(2): 137 – 145.
13. Jaikrishna R (2008). Legislative framework for the protection of wetlands. *J. Environ. Res. Dev.* 2 (3): 498-501.
14. Kloskowi J, Green AJ, Polak M, Bustamante J, Krogulec J (2009). Complementary use of natural and artificial wetlands by water birds wintering in doñana, South-West Spain. *Aquat Conserve. Mar. Fresh W, Ecosyst.* 19:815-826.
15. Knudsen, E., A. Linden, C. Both, N. Jonzen, F. Pulido, N. Saino, W.J. Sutherland, L.A. Bach, T. Coppack, T. Ergon, P. Gienapp, J.A. Gill, O. Gordo, A. Hedenström, E. Lehikoinen, P.P. Marra, A.P. Mller,
16. Kumar, A., J.P. Sat, P.C. Tak & J.R.B. Alfred (2005). Handbook on Indian Wetland Birds and their Conservation. Zoological Survey of India, Kolkata, India, xxvi+468pp.
17. Lameed GA (2011). Species diversity and abundance of wild birds in Dagona-water fowl Sanctuary Borna State, Nigeria. *Afr. J. Environ. Sci. Technol.* 5 (10): 855-866.
18. Maltby, E. & R.E. Turner (1983). Wetlands of the world. *Geographical Magazine* 55: 12-17.
19. McKinney, M.L. (2006). Urbanization as a major cause of biotichomogenization. *Biological Conservation* 127: 247-260; <http://doi.org/10.1016/j.biocon.2005.09.005>
20. Morrison, M.L. (1986). Bird Populations as indicators of environmental change, pp. 429-451. In: Johnston, R. (ed.). *Current Ornithology - Vol. 3*. Springer, Boston, 522pp.
21. Oindo BO, deBy RA, Skidmore AK (2001). Environmental factors influencing bird Species diversity in Kenya. *Afr. J. Ecol.* 39:295-302.
22. Opdam, P. & D. Wascher (2004). Climate change meets habitat fragmentation: linking landscape and biogeographically scale levels in research and conservation. *Biological Conservation* 117: 285-297;
23. Paton, D., F. Romero, J. Cuenca & J.C. Escudero (2012). Tolerance to noise in 91 bird species from 27 urban gardens of Iberian Peninsula. *Landscape and Urban Planning* 104: 1-8;
24. Rayner, L., K. Ikin, M.J. Evans, P. Gibbons, D.B. Lindenmayer & A.D. Manning (2015). Avifauna and urban encroachment in time and space. *Diversity and Distributions* 21: 428-440;
25. Saab V (1999). Importance of spatial scale to habitat use by breeding birds in riparian forests: a hierarchical analysis. *Ecol. Appl.* 9(1): 135-151.
26. Schuyt KD (2005). Economic consequences of wetland degradation for local populations of Africa. *Ecol. Econ.* 53(2): 177-190.
27. Sriharan S, Burgess ND (2012). Protected area gap analysis of important bird areas in Tanzania. *Afr. J. Ecol.* 50:66-76.
28. Surana, R., B.R. Subba & K.P. Limbu (2007). Avian diversity during rehabilitation stage of Chimdi Lake, Sunsari, Nepal. *Our Nature* 5(1): 75-80;
29. Tiner RW (1999) wetland indicators. Lewis, New York, USA. pp.392. UNEP-MAP RAC/SPA (2010). The Mediterranean Sea Biodiversity: state of the ecosystems, pressures, impacts and future priorities. By Bazairi, H., Ben Haj, S., Boero, F., Cebrain, D., De Juan, S., Limam, A., Lleonart, J., Torchia, G., and Rais, C., Ed. RAC/SPA, Tunis. p.100.





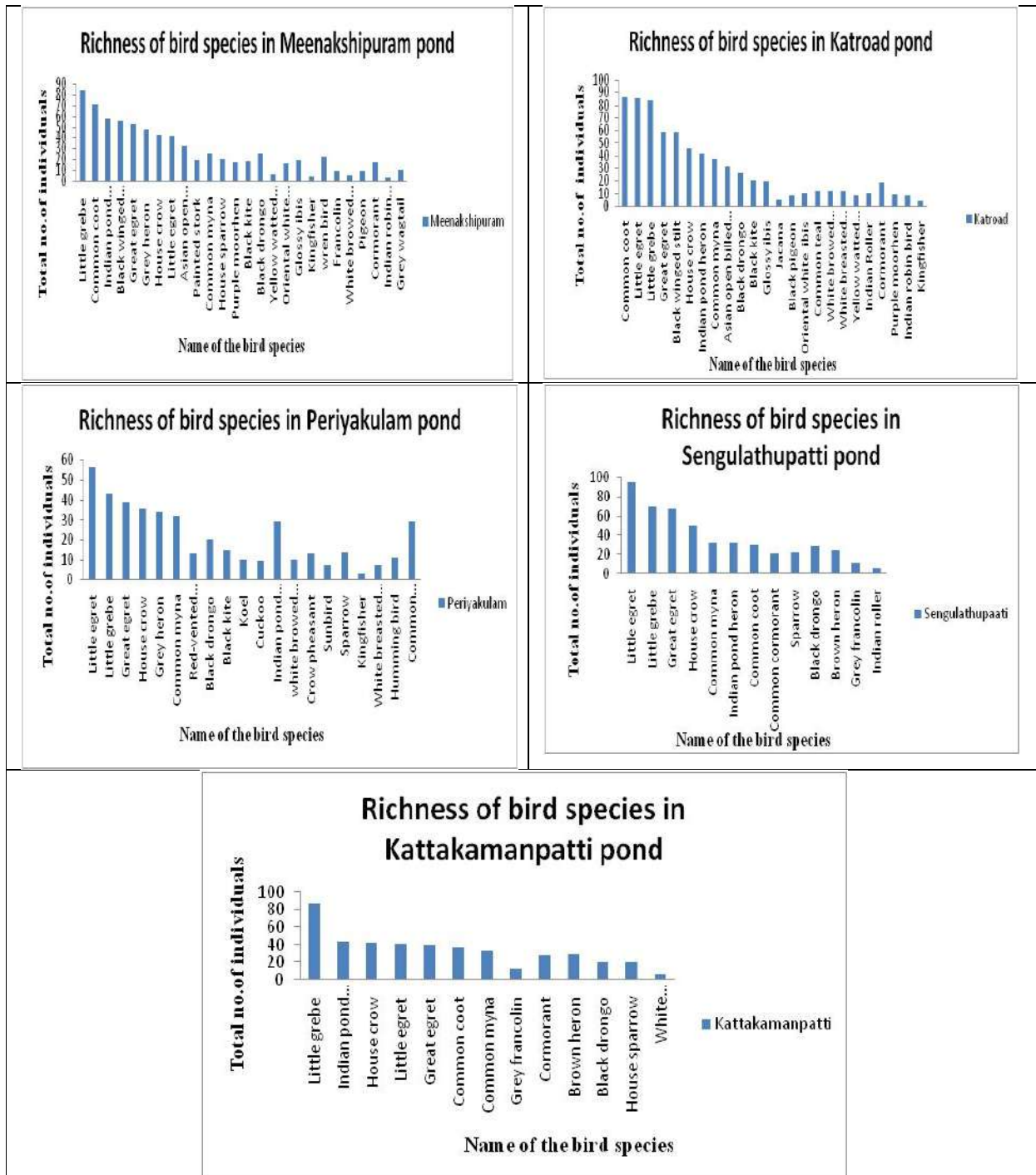
Pushpa and Arun Nagendran

30. Torell, M., A.M. Salamanca & M. Ahmed (2001). Management of wetland resources in the Lower Mekong Basin: issues and future directions. *Naga* 24(3 &4): 4–10.
31. Tschardtke, T., J.M. Tylianakis, T.A. Rand, R.K. Didham & L. Fahrig (2012). Landscape moderation of biodiversity patterns and processes - eight hypotheses. *Biological Reviews* 87(3): 661–685;
32. Zedler J.B. (2003). Wetlands at your service: reducing impacts of agriculture at the watershed scale. *Front. Ecol. Environ.* 1:65-72.
33. Zedler, J.B. & S. Kercher (2005). Wetland resources: status, trends, ecosystem services, and restorability. *Annual Review of Environment and Resources* 30: 39–74; <http://doi.org/10.1146/annurev.energy.30.050504.144248>





Pushpa and Arun Nagendran





Effects of Otago Exercise Versus Otago Exercise Combine with Postural Correction on Balance, Mobility and Fall in Young Old Individual

Viral Gareja^{1*}, Chaitali Shah² and Bhavana Gadhavi³

¹MPT Scholar, Department of Physiotherapy, Parul Institute of Physiotherapy, Vadodara, Gujarat, India.

²Associate Professor, Department of Physiotherapy, Parul Institute of Physiotherapy, Vadodara, Gujarat, India.

³Dean / Principal, Department of Physiotherapy, Parul Institute of Physiotherapy, Vadodara, Gujarat, India.

Received: 10 Oct 2023

Revised: 15 Nov 2023

Accepted: 19 Jan 2024

*Address for Correspondence

Viral Gareja

MPT Scholar,

Department of Physiotherapy,

Parul Institute of Physiotherapy,

Vadodara, Gujarat, India.

Email: viral.k.gareja1111@gmail.com



This is an Open Access Journal / article distributed under the terms of the **Creative Commons Attribution License** (CC BY-NC-ND 3.0) which permits unrestricted use, distribution, and reproduction in any medium, provided the original work is properly cited. All rights reserved.

ABSTRACT

Population declines in older age groups are a main cause of sickness and mortality. Falls in older adults can be caused by a variety of factors, including muscle atrophy, balance issues, poor posture, and visual impairments. neurological disorders of the muscles (such as ataxia, Parkinson's Gait and additional mobility are also factors in the ageing population. Exercises that increase strength and balance can help people move more easily and prevent falls and falls-related injuries. 109 subjects who were meeting inclusion criteria are taken and randomly assigned into two groups. Group A underwent otago exercise program whereas Group B underwent otago exercise with postural correction exercise program for 4 weeks. In this study, Timed up and go test for mobility, Fall efficacy scale for evaluating fear of fall and for static balance Four stage balance test was used. There was statistical significant improvement shown by Wilcoxon Mann Whitney test in shoulder stability and throwing accuracy post intervention ($p < 0.05$). On comparison of pre and post intervention mean difference of closed kinetic upper extremity and throwing accuracy test show significant improvement in shoulder stability (4.04 ± 2.236) and (6.12 ± 2.551), throwing accuracy (1 ± 0.885) and (0.85 ± 0.732) for group A and group B respectively. This study concludes that there was positive effect on balance, mobility and prevention of fall in both the treatment groups. The effect is more significant in the Group B which was treated with Otago Exercise with Postural correction in improving balance and mobility compare to Group A. The fall is prevented in both the groups but there were no significant differences noted between both the groups.



**Viral Gareja et al.,****Keywords:** Otago Exercise, Postural Correction, Balance, Mobility, Young Old Individual

INTRODUCTION

A major factor causing illness and mortality is the population drop in older age groups. 2.8 million people received emergency department treatment for their injuries, with about 800,000 of them ending up in hospitals, despite the varying severity of the injuries. 37.5% of people who reported falling claimed to have experienced at least one fall that required medical treatment or restricted activity for at least a day. Falls are thought to have contributed to 27,000 older people's deaths during the same time period. [1] Men are less likely than women to report falling and getting hurt by the fall. The percentage of older persons who fall increases with age, rising from 26% among those aged 65 to 74 to 29.8% among those aged 75 and older.[1] The aging population is also affected by neurological conditions of the muscles, such as ataxia, Parkinson's gait, and increased mobility. For interventions to be most effective among persons who are at risk for falling, the maximum exercises should have been performed standing up, giving more importance to lower limb muscles, and being structured and gradual in intensity and balance challenge.[2]

Patho physiology of falls

Falls are one of the most common health concerns facing elderly persons today. About one-third of community-dwellers over the age of 65. [3] Fear of falling is common among elderly fallers, and fear of falling has been associated with impaired mobility and decreased functional status.[4] The best predictor of falling is a previous fall. However, falls in older people rarely have a single cause or risk factor. A fall is usually caused by a complex interaction among the following

Intrinsic factors

Age related changes can weaken the systems responsible for maintaining stability and balance, which raises the risk of falling. Depth perception, contrast sensitivity, visual acuity, and dark adaption all deteriorate.

Extrinsic factors

Independently or more importantly by interacting with intrinsic characteristics, environmental influences can raise the risk of falls. Risk is greatest in environments that demand more postural control and movement as well as in environments that are new.

Situational factors

Engaging in specific actions or making certain choices can heighten the likelihood of experiencing falls and injuries related to them. Instances include walking while engaged in conversation or distracted by multitasking, subsequently overlooking potential environmental dangers, hurrying to the restroom, and rushing to answer the phone.

Otago Exercise Program

The Otago Exercise Program (OEP) has been found to effectively decrease the occurrence of falls and enhance balance and mobility among older individuals. This protocol encompasses seventeen strength exercises, balance exercises, and a walking regimen. Participants are instructed to engage in these exercises, followed by a 10-minute rest, three times a week within their local community or home settings. These exercises can be performed individually or in a group setting. Research indicates that individuals who follow the Otago exercise program typically experience a substantial reduction in falls, with a reduction rate ranging from 35% to 40%. The program is administered over a 4-week period, after which participants are provided with self-management strategies.

Timed Up and Go Test

The test is created for the purpose of evaluating and examining mobility, specifically using the timed up and go (TUG) method, which is a straightforward and cost-effective approach to assess fundamental mobility. This

69943





Viral Gareja et al.,

assessment involves everyday movements such as rising from a chair, walking a distance of 3 meters, turning around, returning to the chair, and sitting back down. The timing of the test concludes when the patient is fully seated. By considering the time it takes to complete these tasks and whether or not an assistive device is used, we can determine the individual's risk of falling and their overall mobility. [5]

Fall Efficacy Scale

The objective of this test is to assess the level of fear of falling in a population that is at risk of falling. This test comprises 10 items, each rated on a scale from 1 to 10, where 1 indicates very high confidence, and 10 represents no confidence at all. The items in this scale cover various daily activities, including bathing or showering, reaching for items in cabinets, moving around the house, preparing meals, transitioning in and out of bed, answering the telephone or door, sitting down and standing up from a chair, dressing and undressing, personal grooming, and using the toilet. [6]

Four Stage Balance Test

Static balance is assessed by FOUR STAGE BALANCE TEST. Therapist gives task to maintain that position for 10sec. Four positions are:

1. Stand keeping your feet aside.
2. Place the step of one foot so that it is touching with big toe of the other foot.
3. Tandem stand
4. Stand on one foot and posture will assessed by normal plumb line in lateral, posterior and anterior view.[8]

The time is to be noted for each position. If one position is not held by the patient then you cannot proceed to the next position. With increase in position number the difficulty level also increases. Precautions to be taken to avoid any incident of fall.

METHODS OF DATA COLLECTION

The data for this research is drawn from individuals residing in villages located in close proximity to Parul University. The villages under consideration are Ishwarpura, Limda, Madheli, and Narmadpura, and individuals from these villages will be the participants in the study. The data collection method chosen is a comparative study design employing a closed envelope sampling technique. The study's sample size is determined to be 109 participants, distributed into two groups: Group A comprises 54 participants, while Group B consists of 55 participants. The study's intervention spans a 4-week program, with sessions conducted on three days each week. The primary objective of this study is to assess and compare the effectiveness of two different interventions, seeking to determine which one yields superior results.

INCLUSION CRITERIA

The criteria for participant inclusion in this study have been set up to guarantee that they are suitable for the research and can supply precise data for analysis. The initial requirement is the inclusion of individuals belonging to the elderly population, specifically those aged between 65 and 75 years. Additionally, participants must possess an MMSE score of 24 or higher, signifying their cognitive capability to engage in the study. Moreover, participants must demonstrate their willingness to take part and provide written consent. Both male and female participants will be encompassed within the study. Finally, participants must be proficient in both Hindi and Gujarati languages to ensure that language barriers do not hinder their participation or comprehension of intervention instructions. These inclusion criteria have been established with the goal of ensuring that the study's findings are pertinent to the targeted population and can be used to guide further research and interventions tailored to this demographic.

EXCLUSION CRITERIA

To ensure the safety and accuracy of the study, exclusion criteria have been established to exclude individuals who may be unable to participate fully or who may present a risk to themselves or others during the study period. The



**Viral Gareja et al.,**

first criterion is that individuals with neurological and neuromuscular disorders will be excluded from the study, as these conditions can affect an individual's ability to perform physical tasks and may confound the results of the study. Participants with moderate to severe cardiovascular disorders will also be excluded, as they may be at risk of experiencing complications during the intervention. Individuals suffering from speech and cognitive deficits that could interfere with conducting the research will be excluded from the study as well. Participants with significant hearing or visual impairments will be excluded as these conditions can affect their ability to communicate and participate in the intervention. Lastly, individuals with musculoskeletal disorders will be excluded from the study as these conditions can affect their ability to perform physical tasks and may impact the results of the study.

MATERIAL USED

1. Consent form
2. Paper
3. Stopwatch
4. Measure tape
5. Elastic band
6. Pencil/pen
7. Questionnaire

OUTCOME MEASURES

1. Timed Up and Go Test
2. Fall Efficacy Scale
3. Four Stage Balance Test

RESULT

The graph shows the mean data of outcome measures used in the study i.e Timed up and go for which pre and post treatment score was 13.42 and 8.69, similarly for Fall Efficacy scale the pre and post treatment score was 74.49 and 74.87 respectively and for Four stage Balance scale score was 26.87 and 33.31, Similarly 1.52, 1.42, 3.20, 2.92, 2.46, 2.09 is the Standard Deviation for all the outcome measures respectively in Group A which was treated with Otago Exercise only. The above graph shows the mean data of outcome measures used in the study i.e Timed up and go for which pre and post treatment score was 13.51 and 8.13, similarly for Fall Efficacy scale the pre and post treatment score was 79.51 and 73.34 respectively and for Four stage Balance scale score was 25.85 and 38.68. Similarly 1.50, 0.96, 3.14, 2.72, 3.07, 5.14 in Group B which was treated with Otago Exercise along with Postural Correction. The difference between pre and post treatment in Group A which was treated with Otago Exercise. The data was analyzed with 95% confidence interval. The Timed Up and Go tests shows significant difference between pre and post treatment with the $p < 0.05$ ($p = 0.00$) with mean 4.73 and 1.51 standard deviation. The Fall Efficacy Scale shows significant difference between pre and post treatment with $p < 0.05$ ($p = 0.00$) with 4.62 mean and 1.31 standard deviation. Similarly, in the Four Stage Balance Scale, there is significant difference was found between pre and post treatment with $p < 0.05$ ($p = 0.00$) with 6.26 mean and 3.14 standard deviation. The t value here is positive and > 1.96 which suggest that there is significant variances between the data.

The difference between pre and post treatment in Group B which was treated with Otago Exercise along with Postural Correction. The data was analyzed with 95% confidence interval. The Timed Up and Go test shows significant difference between pre and post treatment with the $p < 0.05$ ($p = 0.00$) with mean 5.38 and 1.70 standard deviation. The Fall Efficacy Scale shows significant difference between pre and post treatment with $p < 0.05$ ($p = 0.00$) with 6.17 mean and 3.88 standard deviation. Similarly, in the Four Stage Balance Scale, there is significant difference was found between pre and post treatment with $p < 0.05$ ($p = 0.00$) with 12.82 mean and 5.38 standard deviation. The t value here is positive and > 1.96 which suggest that there is significant variances between the data. The comparison between the pre and post treatment effects of both the groups. Here the TUG shows significant variances between





Viral Gareja et al.,

Group A and B, with $p=0.02$ ($p<0.05$). This says that Group B shows more improvement compare to Group A on Balance. The Fall Efficacy Scale doesn't show significant no variances which concludes that there is no differences with the scores in FES in both the groups. The Four stage Balance scale also shows significant variances between both the groups post treatment. The $p=0.00$ ($p<0.05$) which highly significant, concludes the effect of treatment is more in Group B compare to Group A. Hence, the above table concludes that the Balance and Mobility is significantly improved more in Group B which was treated with Otago Exercise and Postural Correction compare to Group A which was only treated with Otago Exercise. But there were no significant differences noted in the prevention off all between both the groups.

DICUSSION

Improvement in FES, TUG and FSBS in Group A

The results were analyzed using paired sample t test in group A for pre and post treatment comparison. The means differences were, 4.73, 4.52 and 6.26 respectively in the outcome measure used which was TUG, FES and FSBS. The t test showed significant improvement in all the three outcome measure to assess mobility and balance with a significance p value .00 which is <0.05 which says that there is significant differences between post and pre-treatment. Thus, this statistically says that post treatment there is improvement in mobility and balance after Otago Exercise. The results were supported by previous literatures as well in which was One of the previously conducted study by Leila Ali ali et al, (2022) conducted a study with a title "The Effect and Persistence Of Otago Exercise Program On Balance, Cardiovascular Endurance And Lower Limb Strength In Elderly Women With A History Of Falls" in which randomly, two equal experimental groups of 15 people in Otago and a control group of 30 elderly women between the ages of 60 and 70 years old were divided (15 people). The test group engaged in Otago exercises (8 weeks, 3 sessions per week and 45 minutes per session). Prior to and after 8 weeks of training, as well as one month after training, the subjects' balance, cardiovascular endurance, and lower limb strength were measured using the Y test, the 6-minute walk test, and the 30-second standing-up test. The results revealed that the Otago training group significantly increased the elderly subjects' balance, cardiovascular endurance, and lower limb strength. Otago exercises can therefore be used to lower the risk of falls and enhance postural control in seniors.

Improvement in post treatment in Group B

The group B included Otago exercise along with postural correction. As the movement in correct posture is required for effective movement which increases the effects along with the Otago exercises. The paired t test was used to analyze the comparison between pre and post treatment data for TUG, FES and FSBS respectively. The mean difference between these outcome measures was 5.38, 6.17 12.82 respectively. This result says that there is significant improvement seen in all the outcome measures for mobility and balance. Here, the p value is <0.05 which is statistically significant. The above mentioned statistical analysis shows the improvement with the Otago Exercise and postural correction because, this training programme includes strength, endurance and balance with multi task conditions so that we can stimulate the cognitive and physical abilities focusing on attention. This effects are also seen in one of the study which supports the same results, in which the BBS and short Physical performance battery tests were used in the study for which the conclusion was like eight weeks of multi component exercise training has beneficial effects on balance and physical function and results improved equilibrium and decreasing probability of falling. Thus, practitioner can use this 8 week programme for older individuals. There have been researches which have proven effect of OTTAGO and Postural exercises on FSBT, FET and TUG but very few studies showed the combined effect of postural exercises and OTTAGO combined on FSBT, FET and TUG. Hence the current study has statistically proven that when OTTAGO exercises are combined with Postural exercises, the effect is doubled and the improvement is seen faster and in a much better fashion.



**Viral Gareja et al.,****Comparison between the Ottago exercise group and Ottago and Postural correction group (Between group analysis)**

The independent samples t test was used to compare the means between the two independent data to find the difference between these data and to know the effectiveness of the exercise and which exercise is more effective. The test results show that there is equal variances observed in Timed Up and Go test between Group A and Group B which says there is significant differences between these groups with the significant value 0.01 respectively. Similarly, in Four Stage Balance scale there is equal variances observed with p value 0.00 which is highly significant. Thus if these exercise regimes are incorporated in the day to day life of elderly individual's significant risk off all and post uralim balances can be prevented and hence the rate of comorbidity and disability due to fall in elderly can be minimized and also the level of physical activity can be improved which in turn can give them a better life.

CONCLUSION

In summary, both treatment groups experienced a beneficial impact on balance, mobility, and fall prevention. The effect was notably more pronounced in Group B, which received the Otago Exercise with Postural correction, leading to greater improvements in balance and mobility compared to Group A. While falls were prevented in both groups, no significant differences were observed between them in this regard. Therefore, in the context of geriatric rehabilitation in clinical practice, the implementation of the Otago exercise is recommended to enhance balance and mobility, ultimately boosting patient confidence and aiding in fall prevention.

LIMITATIONANDFURTHERRECOMMENDATIONS

The sample size was limited, potentially resulting in some participants discontinuing the training after the study period. To address this, a more extended, long-term protocol should be devised, and the intervention duration should be prolonged. Additionally, post-intervention outcome measurements did not assess long-term effects, suggesting the need for extended follow-up to evaluate the exercise regimen's enduring impact. Furthermore, since all participants were in good health, the intervention's effects were not analyzed in the context of patients with neurological or musculoskeletal conditions. Therefore, a separate study could be undertaken to investigate the exercise regimen's effects in individuals with such conditions.

INFORMED CONSENT PROCESS

A written and informed consent about enrolment in the study and maintaining adequate privacy and confidentiality were taken from all the participants recruited for the study.

CONFIDENTIALITY ISSUES AND DATA SAFETY

Adequate privacy and confidentiality of participants were also maintained by the researcher.

SOURCE OF FUNDING

This study was not funded by any public, commercial, or not-for-profit agencies.

ETHICAL APPROVAL

Ethical clearance is obtained from ethical committee of institution and institution where the subjects belongs at Parul University of Physiotherapy, Waghodia, Vadodara.

CONFLICT OF INTEREST

None



**Viral Gareja et al.,****CONSENT FOR PUBLICATION**

Prior to the study, participants received information about it. After receiving consent, we maintained proper privacy and confidentiality for all of the study's patients.

AUTHORS CONTRIBUTION

VG: conceptualization, project administration, methodology, reviewing, writing, and editing; methodology, formal analysis, and reviewing; MV: writing, and editing; methodology, formal analysis, and reviewing; CS: reviewing and editing. The final draft of the manuscript has undergone critical review and approval by all authors, who take full responsibility for its content and similarity index.

REFERENCES

1. Cuevas-Trisan R. Balance Problems and Fall Risks in the Elderly. *Phys Med RehabilClin NAM*.2017 Nov;*28*(4):727-737. doi: 10.1016/j.pmr.2017.06.006. PMID: 29031339.
2. Shubert TE, Smith ML, Goto L, Jiang L, Ory MG. Otago Exercise Program in the United States: Comparison of 2 Implementation Models. *Phys Ther*. 2017 Feb 1;*97*(2):187-197. doi:10.2522/ptj.20160236.PMID: 28204770.
3. Yoo HN, Chung E, Lee BH. The Effects of Augmented Reality-based Otago Exercise on Balance, Gait, and Falls Efficacy of Elderly Women. *J PhysTher Sci*. 2013 Jul;*25*(7):797-801.doi:10.1589/jpts.25.797.Epub 2013Aug 20. PMID: 24259856;PMCID: PMC3820389.
4. Cohen, Rajal& Baer, Jason & Ravichandra, Ramyaa & Kral, Daniel & McGowan, Craig &Cacciatore, Tim. (2020). Lighten Up! Postural Instructions Affect Static and Dynamic Balance in Healthy Older Adults. *Innovation in Aging*.4. 10.1093/geroni/igz056.
5. Cohen, Rajal& Baer, Jason & Ravichandra, Ramyaa &Kral, Daniel & McGowan, Craig &Cacciatore, Tim. (2020). Lighten Up! Postural Instructions Affect Static and Dynamic Balance in Healthy Older Adults. *Innovation in Aging*.4. 10.1093/geroni/igz056.
6. Mittaz Hager AG, Mathieu N, Lenoble-Hoskovec C, Swanenburg J, de Bie R, Hilfiker R. Effects of three home-based exercise programmes regarding falls, quality of life and exercise-adherence in older adults at risk of falling: protocol for a randomized controlled trial. *BMCgeriatrics*.2019 Dec;*19*(1):1-1.
7. Leem SH, Kim JH, Lee BH. Effects of Otago exercise combined with action observation training on balance and gaitin the old people. *Journal of exercise rehabilitation*. 2019 Dec;*15*(6):848.
8. Goecke J. Effectiveness of the stepping on program in fall prevention measured by the Four Stage Balance Test (FSBT).
9. Shubert TE, Smith ML, Goto L, Jiang L, Ory MG. Otago Exercise Program in the United States: Comparison of 2 Implementation Models. *PhysTher*. 2017 Feb 1;*97*(2):187-197. doi:10.2522/ptj.20160236.PMID: 28204770.
10. Chan PP, Si Tou JI, Tse MM, Ng SS. Reliability and Validity of the Timed Up and Go Test With a Motor Task in People With Chronic Stroke. *Arch Phys Med Rehabil*.2017Nov;*98*(11):2213-2220.doi:10.1016/j.apmr.2017.03.008.Epub 2017Apr 7. PMID:28392324.
11. Renfro M, Bainbridge DB, Smith ML. Validation of evidence-based fall prevention programs for adults with intellectual and/or developmental disorders: a modified Otago exercise program. *Frontiers in public health*. 2016 Dec 6; *4*:261.
12. Nancy N. Patel, & Shweta Pachpute. (2015). The Effects Of Otago Exercise Programme For Fall Prevention In Elderly People. *International Journal of Physiotherapy*, *2*(4),633-639.





Viral Gareja et al.,

